V 3. At 7: 16/19-23

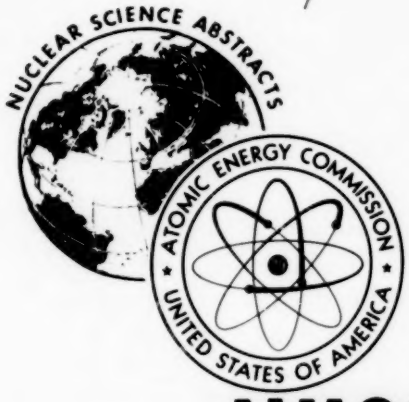

NUCLEAR SCIENCE ABSTRACTS

Volume 19 Number 23

Abstracts 43642–45725

JAN 4 - 1966

December 15, 1965

UNITED STATES ATOMIC ENERGY COMMISSION
Division of Technical Information

MIAMI UNIVERSITY LIBRARY

USAEC DEPOSITORY LIBRARIES

Collections of USAEC reports are maintained in the libraries of the organizations listed below for reference use by the general public. Facilities for making photocopies are available. The USAEC also makes available through these libraries atomic energy reports of countries other than the U. S. that are abstracted in *Nuclear Science Abstracts*.

ALABAMA
Auburn, Auburn University
ARIZONA
Tucson, University of Arizona
ARKANSAS
Fayetteville, University of Arkansas
CALIFORNIA
Berkeley, University of California
Davis, University of California
Los Angeles, University of California
San Diego, Public Library
Stanford, Stanford University
COLORADO
Boulder, University of Colorado
Denver, Public Library
CONNECTICUT
New Haven, Yale University
DELAWARE
Newark, University of Delaware
DISTRICT OF COLUMBIA
Washington, Library of Congress
FLORIDA
Coral Gables, University of Miami
Gainesville, University of Florida
GEORGIA
Atlanta, Georgia Institute of Technology
HAWAII
Honolulu, University of Hawaii
ILLINOIS
Chicago, John Crerar Library
Chicago, University of Chicago
Evanston, Northwestern University
Urbana, University of Illinois
INDIANA
Bloomington, Indiana University
Lafayette, Purdue University
IOWA
Ames, Iowa State University
KANSAS
Manhattan, Kansas State University
KENTUCKY
Lexington, University of Kentucky
Louisville, University of Louisville
LOUISIANA
Baton Rouge, Louisiana State University
New Orleans, Tulane University
MARYLAND
Baltimore, Johns Hopkins University
College Park, University of Maryland
MASSACHUSETTS
Cambridge, Harvard University
Cambridge, Massachusetts Institute of Technology
MICHIGAN
Ann Arbor, University of Michigan
Detroit, Public Library
East Lansing, Michigan State University
MINNESOTA
Minneapolis, University of Minnesota
MISSISSIPPI
State College, Mississippi State University
MISSOURI
Kansas City, Linda Hall Library
Rolla, University of Missouri School of Mines and Metallurgy
St. Louis, Washington University
MONTANA
Bozeman, Montana State College
NEVADA
Las Vegas, Nevada Southern University
Reno, University of Nevada
NEW JERSEY
Princeton, Princeton University
Teaneck, Fairleigh Dickinson University
NEW MEXICO
Albuquerque, University of New Mexico
NEW YORK
Albany, The University of the State of New York
Buffalo, State University of New York at Buffalo
Ithaca, Cornell University
New York, Atomic Industrial Forum, Inc.
New York, Columbia University
New York, New York University
Rochester, University of Rochester
Schenectady, Union College
Syracuse, Syracuse University
Troy, Rensselaer Polytechnic Institute
NORTH CAROLINA
Charlotte, Public Library of Charlotte and Mecklenburg County
Durham, Duke University
Raleigh, North Carolina State College
NORTH DAKOTA
Grand Forks, University of North Dakota
OHIO
Cincinnati, University of Cincinnati
Cleveland, Public Library
OHIO (CONT.)
Columbus, Ohio State University
Toledo, University of Toledo
Youngstown, Youngstown University
OKLAHOMA
Norman, University of Oklahoma
Stillwater, Oklahoma State University
OREGON
Corvallis, Oregon State University
Portland, Reed College
PENNSYLVANIA
Philadelphia, University of Pennsylvania
Pittsburgh, Carnegie Library
University Park, Pennsylvania State University
PUERTO RICO
Rio Piedras, University of Puerto Rico
RHODE ISLAND
Providence, Brown University
SOUTH CAROLINA
Columbia, University of South Carolina
TENNESSEE
Knoxville, University of Tennessee
Memphis, Public Library
Nashville, Joint University Libraries
Oak Ridge, Oak Ridge Institute of Nuclear Studies
TEXAS
Austin, University of Texas
College Station, Texas A & M University
Dallas, Southern Methodist University
Houston, Rice University
Lubbock, Texas Technological College
San Antonio, Public Library
UTAH
Salt Lake City, University of Utah
VIRGINIA
Blacksburg, Virginia Polytechnic Institute
Charlottesville, University of Virginia
Norfolk, Old Dominion College
WASHINGTON
Pullman, Washington State University
Seattle, University of Washington
WEST VIRGINIA
Morgantown, West Virginia University
WISCONSIN
Madison, University of Wisconsin
Milwaukee, Public Library
WYOMING
Laramie, University of Wyoming

Volume 19, Number 23, December 15, 1965

NUCLEAR SCIENCE ABSTRACTS

A semimonthly publication of the USAEC Division of Technical Information, Edward J. Brunenkant, Director.
Published by the USAEC Division of Technical Information Extension, Robert L. Shannon, Extension Manager.

Nuclear Science Abstracts covers the international literature on nuclear science and technology and provides the only comprehensive abstracting and indexing of this body of information. Published twice each month since 1947, *NSA* covers technical reports of the U. S. Atomic Energy Commission and its contractors, technical reports of U. S. Government agencies and other governments, universities, industrial and research organizations, as well as patents, books, and journal literature on a world-wide basis. Nearly 300,000 abstracts have appeared in *NSA* through Volume 18. The subject matter covered in *NSA* is described in issue Number 1 and in TID-4552, *Subject Scope of Nuclear Science Abstracts*, available free from the U. S. Atomic Energy Commission, Division of Technical Information Extension, P. O. Box 62, Oak Ridge, Tennessee 37831.

Abstracts are arranged according to a number of subject categories and subcategories. Definitions of categories appear in issues Number 1 and 13. If the language of the original item is not English, the language will be indicated. Translations are not abstracted where an abstract of the original item has appeared in *NSA*.

INDEXES TO NSA

Corporate author, personal author, subject, and report number indexes appear in each issue and are cumulated quarterly, semiannually, and annually. At the end of Volume 19, report number indexes will be cumulated in two separate publications. Indexes for Vols. 1–15 will be reissued with the latest public availability known at that time. This index will not be reissued. Indexes for Vols. 16–19 will be cumulated as a separate issuance and will be reissued annually to include all volumes beginning with Volume 16.

AVAILABILITY OF PUBLICATIONS ABSTRACTED

The public availability of all U. S. Atomic Energy Commission reports is indicated in the report number indexes. The availability of other reports, when known, is also indicated. The availability of some unnumbered reports is given in the abstract.

Dissertations abstracted in *Dissertation Abstracts* and included in *NSA* are available from University Microfilms, Inc., 315 N. First Street, Ann Arbor, Michigan.

Most of the published literature abstracted in *NSA* is on deposit at the Oak Ridge Institute of Nuclear Studies Library, Oak Ridge, Tennessee, (a USAEC depository library) and is available through interlibrary loan. When requesting papers from this source, it is important that *NSA* volume and abstract number be cited.

HOW TO OBTAIN NUCLEAR SCIENCE ABSTRACTS

NSA is available on an exchange basis to universities, research institutions, industrial firms, and publishers of scientific information. Inquiries should be directed to the U. S. Atomic Energy Commission, Division of Technical Information Extension, P. O. Box 62, Oak Ridge, Tennessee 37831.

Government agencies may obtain *NSA* free of charge.

NSA is available to the general public on a subscription basis from the Superintendent of Documents, U. S. Government Printing Office, Washington, D. C. 20402, as follows:

For the 24 regular issues, $30.00 domestic, $37.00 foreign. A single issue costs $1.75, plus 25 per cent for foreign mailing. Domestic rates apply to the United States, Canada, Mexico, and Central and South American countries except Argentina, Brazil, British and French Guiana, Surinam, and British Honduras. Foreign rates apply to the countries excepted above and to all other countries throughout the world.

For the quarterly, semiannual, and annual indexes, $22.00 domestic, $25.00 foreign.

Multivolume subject and author indexes are available as follows:

Vols. 1–4 (1948–1950) Johnson Reprint Corporation, 111 Fifth Avenue, New York, N. Y. 10003, $30.00.

Vols. 5–10 (1951–1956) Superintendent of Documents, U. S. Government Printing Office, Washington, D. C. 20402, $5.25.

Vols. 11–15, Subjects, Superintendent of Documents, U. S. Government Printing Office, Washington, D. C. 20402, $19.00.

Vols. 11–15, Personal Authors, Superintendent of Documents, U. S. Government Printing Office, Washington, D. C. 20402, $14.25.

Vols. 11–15, Corporate Authors, Superintendent of Documents, U. S. Government Printing Office, Washington, D. C. 20402, $2.50.

Cumulative Report Number Index, Vols. 1–18, is available from the Superintendent of Documents, U. S. Government Printing Office, Washington, D. C. 20402, $5.75.

Annual Indexes are available separately from the U. S. Government Printing Office as follows:

Vol. 16, Subject and Authors, $9.75.
Vol. 17, Subject and Authors, $12.25.
Vol. 18, Subject and Authors, $12.50.

ACKNOWLEDGMENTS

Agreements between the United States Atomic Energy Commission and the following organizations with regard to providing continuing services and specific literature coverage for *Nuclear Science Abstracts* are gratefully acknowledged:

American Institute of Physics; Atomic Energy of Canada Limited; Atomic Energy Research Establishment, United Kingdom; European Atomic Energy Community (EURATOM); Gmelin Institute; International Atomic Energy Agency; Japan Atomic Energy Bureau — Japan Atomic Energy Research Institute; Netherlands Patent Office; Reactor Centrum Nederland.

TABLE OF CONTENTS

Volume 19, Number 23, December 15, 1965

Category	Page
BIOLOGY AND MEDICINE	5441
General	5441
Ecology	5444
Metabolism, Tissue Distribution, and Toxicology	5444
Radiation Effects	5452
Radiation Effects Therapy and Countermeasures	5480
Radiation Hazards and Protection	5483
Radiotherapy and Radiodiagnosis	5484
CHEMISTRY	5494
General	5494
Analytical Procedures	5494
Inorganic and Physical Chemistry	5501
Organic Chemistry	5509
Radiation Chemistry	5510
Radiochemistry	5516
Separation Processes and Procedures	5517
ENGINEERING	5521
General	5521
Applications of Nuclear Explosions	5523
Facilities and Equipment	5524
Heat Transfer and Fluid Flow	5526
Materials Testing	5530
Protective Structures	5530
Space Propulsion	5531
Vacuum Engineering	5533
GEOLOGY AND MINERALOGY	5534
General	5534
Natural Radioactivity and Fallout	5535
Site Survey and Selection	5538
Techniques and Equipment	5538
Thorium and Uranium Minerals	5538
HEALTH AND SAFETY	5540
INSTRUMENTATION	5550
General	5550
Radiation Detection	5553
Radiation Effects	5570
ISOTOPE TECHNOLOGY	5572
General	5572
Industrial Applications	5572
Power Application	5574
Separation and Production	5575
MATHEMATICS AND COMPUTERS	5577
METALS, CERAMICS, AND OTHER MATERIALS	5578
General	5578
Corrosion	5582
Fabrication	5585
Properties and Structure	5589
Radiation Effects	5597
METEOROLOGY	5602
PHYSICS	5605
General	5605
Accelerators	5610
Astrophysics and Cosmology	5614
Atomic Physics	5619
Cosmic Radiation	5623
Criticality Studies	5624
Direct Energy Conversion	5625
Elementary Particles and Radiations	5626
Field Theory and Quantum Mechanics	5640
Geophysics	5643
Low Temperature Physics	5648
Neutron Physics	5651
Nuclear Properties and Reactions	5655
Plasma Physics and Thermonuclear Processes	5670
Shielding	5680
Solid State Physics	5681
REACTOR TECHNOLOGY	5685
General	5685
Auxiliaries and Components	5685
Criticality Studies	5688
Design and Feasibility	5690
Fuels	5690
Power and Power-Breeder Reactors	5692
Process Heat Reactors	5701
Production Reactors	5701
Propulsion and Space	5702
Research and Test Reactors	5705
WASTE DISPOSAL AND PROCESSING	5708
GENERAL AND MISCELLANEOUS	5710
CORPORATE AUTHOR INDEX	INDEX-1
PERSONAL AUTHOR INDEX	INDEX-16
SUBJECT INDEX	INDEX-64
REPORT NUMBER INDEX	INDEX-153

STAFF OF NUCLEAR SCIENCE ABSTRACTS

MANAGING EDITOR

John W. Norris

ASSISTANT MANAGING EDITOR

Donald D. Davis

ASSOCIATE EDITORS

Lawrence T. Whitehead
David E. Bost
Robert C. Kelly
Lee M. Thompson

SUBJECT INDEX EDITOR

Everett J. Hoffman

EVALUATORS

William D. Matheny
John H. Mitchell
Mary H. Newman

ABSTRACTORS

F. S. Armstrong (AECL)
Jane G. Buchanan
D. Lamar Cason
Helen G. Donald
James R. Dulaney
Wells L. Green
Bernard O. Griggs
Mary Catherine Grissom
Fernando J. Hamilton
Phyllis C. Hansen
Thomas F. Heagerty
Carolyn D. Houston
Rose V. Jermain
Betty L. McDowell
Jean F. Peckham
Mona H. Raridon
Julia Redford
Lila B. Smith
Charles E. Stuber
Martha J. Thomas
Anne G. Ward
David C. West
Milton O. Whitson

SUBJECT HEADING SPECIALIST

Robert E. Upchurch

CORPORATE AUTHOR SPECIALIST

Clara L. Fox

DESCRIPTIVE CATALOGING SPECIALIST

J. Paul Meredith

SCHEDULING AND PUBLISHING COORDINATOR

Brainard L. Patton

Communication concerning the editorial policy and content of *NSA* should be addressed to the Managing Editor, *Nuclear Science Abstracts*, AEC Division of Technical Information Extension, P. O. Box 62, Oak Ridge, Tennessee 37831.

Use of funds for printing this publication approved by the Director of the Bureau of the Budget, May 20, 1963

Volume 19, Number 23 December 15, 1965

NUCLEAR SCIENCE ABSTRACTS

BIOLOGY AND MEDICINE

General

43642 (NYO-2280-8) MUTATION RATES AND MUTATIONAL LOADS IN MAN. Yearly Progress Report of Scientific Activity, September 1, 1964–August 31, 1965. Cavalli-Sforza, L. L. (Pavia Univ. (Italy). Istituto di Genetica). Contract AT(30-1)-2280. 12p. Dep. mn; CFSTI $1.00 cy, $0.50 mn.

Progress on mutation studies in man was reported in the following areas: consanguinity, genealogies by record linking of parish book data in the Parma valley, analysis of mutations in hemophilia; computer analyses of human evolution; and simulation of human populations. The highest effects of consanguinity observed were on psychiatric diseases. Record linking in the Parma Valley led to a 70% linkage of deaths to births. Mutation rates were determined for hemophilia A and B by means of classical segregation analysis. Hemophilia B had a lower mutation rate than A. Frequency of hemophilia mutants as a function of age was estimated. The age at birth of the parents of women heterozygous for hemophilia was not a significant factor. Programs were prepared for IBM 7090 analysis of additive trees by least squares, and of minimum evolutionary path, for numerous populations, giving the analysis of selected trees. Programming of artificial population simulation in the Parma Valley was rewritten for IBM 7090 and was used to study the population drift. (H.G.D.)

43643 (TID-22143) EXPERIMENTAL EMBRYOGENESIS AND HISTOGENESIS IN PINUS LAMBERTIANA DOUGL. Progress Report. Berlyn, Graeme P. (Yale Univ., New Haven, Conn.). Apr. 20, 1965. Contract AT(30-1)-1349. 10p. Dep. mn; CFSTI $1.00 cy, $0.50 mn.

Progress is reported on: techniques for culturing hypocotyl tissue slices from dormant embryos; the fluorescent tracing of the movement of dyes and dye-conjugated proteins in pine embryos and tissue slices; medium formulation; quantitative evaluation of the role of the cotyledons in the growth of excised sugar pine embryos and effect of light and dark on the growth of excised embryos; and autoradiographic tracing of ^{14}C-labelled sucrose uptake by sugar pine embryos. Anatomical studies were made of the mature Pinus lambertiana embryo, germination and seedling development, and multiple embryos. (H.G.D.)

43644 (UCD-472-112) THE EFFECTS OF CONTINUED Sr-90 INGESTION DURING THE GROWTH PERIOD OF THE BEAGLE AND ITS RELATION TO Ra-226 TOXICITY. 8th Annual Progress Report. Andersen, A. C. (California Univ., Davis. School of Veterinary Medicine). June 1965. Contract AT(04-3)-472. 178p. Dep. mn; CFSTI $5.00 cy, $1.00 mn.

Separate abstracts were prepared on 15 sections of this report. Other sections discuss the merits of air conditioned dog cages and vitamin stability in prepared dog food storage. (C.H.)

For abstracts of individual sections see: 43645, 43646, 43674–43680, 43725–43727, 43882, 43939, and 45692.

43645 (UCD-472-112, pp 10-22) KENNEL STATUS REPORT—OBSERVATIONS IN AN EXPERIMENTAL BEAGLE COLONY. McKelvie, D. H.; Parcher, J. W. (California Univ., Davis. School of Veterinary Medicine).

A colony of Beagles maintained for chronic experimentation is divided into two groups, with 231 dogs being used for reproduction and special studies, and 447 included in the actual experimental design. Clinical observations are made daily, and routine examinations are conducted biweekly. Some conditions found are normal to a large colony, such as accumulation of ear wax, ocular discharge, and enlarged anal pouches. Environmental effects on mange, dental tartar, and diarrhea are considered. Comparison of growth rates from birth to weaning shows slight differences in body weight among the dose levels of Sr-90-fed dogs, but further statistical analyses will be necessary to determine the significance of the differences. (auth)

43646 (UCD-472-112, pp 23-35) PROCEDURES FOR MAINTAINING AN OUTBRED BEAGLE COLONY. McKelvie, D. H.; Shultz, F. T. (California Univ., Davis. School of Veterinary Medicine).

The maintenance of a large colony of dogs consisting of groups receiving different radionuclide treatments is complicated by factors which may introduce considerable bias into the interpretation of experimental results. These factors are minimized by a carefully planned program of random selection of sires and dams, random assignment to dose levels, and random culling of excess progeny. Environmental variables are controlled by random placement of levels within treatment facilities. (auth)

43647 (UCLA-12-565) SEMIANNUAL PROGRESS REPORT FOR THE PERIOD ENDING JUNE 30, 1965. (California Univ., Los Angeles. Lab. of Nuclear Medicine and Radiation Biology). Contract AT(04-1)-Gen-12. 118p. Dep. Mn; CFSTI $4.00 cy, $0.75 mn.

Separate abstracts were prepared for the six sections of the report. (J.R.D.)

For abstracts of individual sections see: 43648, 43662, 43681, 43682, 43728, and 43883.

43648 (UCLA-12-565, pp 87-96) BIOPHYSICS. (California Univ., Los Angeles. Lab. of Nuclear Medicine and Radiation Biology).

Results of biophysical hematology studies are summarized along with biological and medical work on imaging and scanning. Investigations of radiation effects on Neurospora crassa are reported. (J.R.D.)

43649 (UCRL-16177) CONSTRUCTION OF A GROWTH CURVE FOR MAMMARY FIBROADENOMA IN THE FEMALE RAT. Durbin, Patricia W.; Jeung, Nylan; Williams, Marilyn H.; Arnold, James S. (Lawrence Radiation Lab.,

Univ. of California, Berkeley). June 3, 1965. Contract W-7405-eng-48. 20p. Dep. mn; CFSTI $1.00 cy, $0.50 mn.

An empirical growth curve for mammary fibroadenomata of the female Sprague-Dawley rat was constructed. Fibroadenomata used to construct the growth curve included 25 spontaneous tumors arising in normal controls and 65 radiation-induced tumors. Growth data were obtained both by measurement of external dimensions and from autopsy tumor weight. Tumor growth from 0.42 to 200 g could be represented by three (and possibly four) positive exponentials, each defined over certain limits. The growth pattern of fibroadenomata was highly variable, reflecting the degree of morphological variation both among individual fibroadenomata and within each individual tumor. Growth rates varied so widely that it was not possible to distinguish differences, if such exist, between the growth rate of carcinomata and the average fibroadenoma; the growth of secretory and nonsecretory fibroadenomata; or the growth of spontaneous tumors arising in old rats and radiation-induced tumors in young rats. Neither was it possible to estimate the general growth behavior of a fibroadenoma from scoring tests on a single histological section. Suitability of other mathematical descriptions of tumor growth, particularly the Gompertzian function, to the growth of mammary fibroadenomata is discussed. (24 references.) (C.H.)

43650 (JPRS-31349) PHARMACOLOGY AND TOXICOLOGY, 1962. Translated from Farmakol. i Toksikol., 27: 110-36; 145-6 (Mar.-Apr. 1964). 28p. (TT-65-31846). CFSTI $2.00 cy, $0.50 mn.

A separate abstract was prepared for one article in this journal. Other articles discuss the use of fluorinated hydrocarbons and others as narcotics, the chemical structure and pharmacology of cholinergic substances; the effects of hypotensive preparations on the nervous system; and modern diuretics. (C.H.)

For an abstract of the individual paper see: 43861.

43651 TRITIUM LABELLING OF CELLS IN VITRO. Ahnstroem, G.; Ehrenberg, L.; Rosen, C.-G. (Univ. of Stockholm). Acta Chem. Scand., 19: 964-6(1965).

Alkyl alkanesulfonates tritiated in the alkyl groups could be utilized to introduce tritium into protein molecules. On this basis a rapid and simple method for isotope labeling of living cells was developed. The labeling could be performed under conditions where no harmful effects on the cells accompany the treatment. (auth)

43652 INHALANT ALLERGY TO THE SCREWWORM FLY: PRELIMINARY REPORT. Gibbons, Harry L.; Dille, J. Robert; Cowley, Ray G. (Federal Aviation Agency, Fort Worth, Tex.). Arch. Environ. Health, 10: 424-30 (Mar. 1965).

Following the emergency landing of three light aircraft being used for the aerial dispersal of radio-sterilized screwworm flies (Cochliomyia hominivorax) eradication program, a preliminary survey revealed that ~70% of the flight crew members reported developing mild to severe allergic symptoms, after spending from two weeks to six months in the program. The radio-sterilized screwworm flies are being released in the Southwestern United States to combat multimillion dollar losses to the cattle industry. Up to 100,000,000 flies per week are raised in a plant near Mission, Texas. Fertile adult flies lay eggs which hatch into larvae and then transform into the pupal stage. Sexual sterilization is accomplished 5½ days after entering this stage when canisters containing 25,000 pupae are given a dose of about 8000 R of γ radiation from a ^{60}Co source. The pupae are packaged in boxes of about 400 and placed in holding rooms until they emerge as adults. They are then loaded into aircraft at the plant or trucked in refrigerated vans to other distribution centers. Dispersal is made from 20 light aircraft. Plans for release vary from 200 to 1000 flies/mi^2, depending upon the presence or absence of reported infestations in the area. Persons involved in aerial dissemination of irradiated flies experienced significant allergic manifestations, with near disastrous results in some cases. Symptoms consist of eye irritation, nasal congestion, coughing, wheezing, and shortness of breath. The results of a survey of symptoms, dust analysis, skin testing, and case histories are presented. (TCO)

43653 RADIOMIMETIC EFFECTS OF MONO- AND BI-FUNCTIONAL ALKYLATING COMPOUNDS IN TRITICUM MONOCOCCUM (2X) AND TRITICUM DURUM (4X). Mariani, A.; Sparrman, B. (Universita, Perugia, Italy; Univ. of Stockholm). Atti Assoc. Genet. Ital., 10: 136-49 (1965). (In Italian).

The comparison between mono (BMS and MOEMS) and bifunctional (PDDE and MYLERAN) alkylating compounds at cytological and physiological level was performed on T. monococcum (2×) and T. durum Cappelli (4×). All the chemicals studied induced chromosomal damage, the most active being the bifunctional Myleran and to some degree, the doubly monofunctional PDDE. The aberrations observed were almost exclusively of chromatid type, the rare B″ being very probably isochromatid breaks. The percentage of aberrant anaphases and the number of B′ per cell, considering all the anaphases analyzed, were always higher in T. durum than in T. monococcum. Comparing the results of the two treatments with Myleran on presoaked and dry seeds, it was concluded that presoaking did not enhance the sensitivity at the cytological level. Data obtained on the growth inhibition of root and shoot by the four chemicals showed that T. monococcum was more sensitive than T. durum, but the shoot was more or less depressed than the root, depending on the chemical used. The results also showed that the chemicals most active at the physiological level are also more effective in inducing chromosomal aberrations. A hypothesis to explain the different effects of the chemicals used is discussed in relation to their formula. (auth)

43654 OBSERVATIONS ON AUTOCLAVED, FUMIGATED AND IRRADIATED DIETS FOR BREEDING MICE. Porter, G.; Lane-Petter, W. (Medical Research Council, Carshalton, Eng.). Brit. J. Nutr., 19: 295-305(1965).

Attempts were made to develop an adequate diet, free from common murine pathogens, for pathogen-free animal units. The commercial diets for such units are not always satisfactory; moreover, there is the difficulty of obtaining complete sterility of the diet and the obstacle of preventing contamination of the diet after it leaves the factory. Twelve commercial diets, before and after sterilization by autoclaving, fumigation, or irradiation, were studied for their effects on the breeding performance of inbred strains of mice. Breeding time, litter size, preweaning loss, numbers weaned, and weaning weight of the young were recorded. It was shown that one commercial diet (F.F.G.) was superior to the other diets tested, and that this diet, when autoclaved, supported reproduction, lactation, and growth better than did the other two autoclaved diets. Irradiation and fumigation were both found to be acceptable methods of sterilization, and fumigation used in the prescribed manner did not give rise to toxicity. The breeding performance of CBA mice on F.F.G. diet sterilized by three methods, i.e. autoclaved by steam, fumigated by ethylene oxide, and sterilized by γ irradiation at 2.5 Mrad, showed that the autoclaved diet gave the best results. The number of prenatal days was less with this diet than with the other two, and the other relevant criteria showed the superiority of autoclaved over ethylene oxide-treated or γ-irradiated F.F.G. diet. The physical properties of a diet had an important bearing on its efficiency. A difference was evident between hardness of a cube and what is described as gnaw-ability. A hard gnawable cube was acceptable to most mice and rats, but an equally hard ungnawable one is unacceptable. (BBB)

43655 A MORTALITY STUDY OF PRIMARY TUMOURS OF BONE IN CANADA. Phillips, A. J. (National Cancer Inst. of Canada, Toronto). Can. Med. Assoc. J., 92: 391-3(Feb. 20, 1965).

A five-year study was undertaken to determine the incidence of primary bone cancer in Canada to assess the effects of subsequent increases in background radiation, should such occur. For each Provincial Department of

Health, records were extracted of all deaths assigned to malignant tumors of bone from 1956 to 1960. In all, 827 cases were investigated and reports were received on 674 cases (81.5%). Confirmation of a primary bone cancer was received for 437 cases (52.8%), while in 237 cases (28.7%) the neoplasm actually arose in sites other than bone. The method of verification of the tumor is shown. Of the 437 cases, 77.1% were pathologically proved and 15.8% were based on radiological evidence. Only 6.4% were diagnosed by clinical examination alone. The annual mortality rate is 6.3 per million population, 7.7 for males and 4.8 for females. Osteosarcoma was the most common type of tumor and accounted for 58% of all confirmed cases; 61% of the tumors occurred in males. The United Nations Scientific Committee on the Effects of Atomic Radiation has estimated, on the assumption that the natural annual incidence of bone tumors is five to 10 cases per million population and that 10% could be attributable to natural radioactivity, that on the basis of 9 rem per 70-year human lifetime, four to eight cases would be added for each additional rem in 70 years. The accuracy of this estimate is dependent largely upon a reliable measure of the incidence of bone tumors, which the present data supplies. (BBB)

43656 MUTATIONS AND CROP IMPROVEMENT. I. INTRODUCTORY COMMENTS. Gustafsson, Ake; Gadd, Ivar (International Atomic Energy Agency, Vienna; Royal Coll. of Forestry, Stockholm). Hereditas, 53: 12-14(1965).

A series of papers on mutations and crop improvements was prepared as a literature survey and analysis anticipatory to the preparation of a manual for IAEA. Separate abstracts were prepared for the papers included. (H.G.D.)

For abstracts of individual papers see: 43776–43779.

43657 ERYTHROCYTE CHIMERISM AND ACQUIRED IMMUNOLOGIC TOLERANCE. Wilson, W. E. C.; Talmage, David W. (Univ. of Colorado, Denver). J. Immunol., 94: 150-6(Jan. 1965).

Results are reported of tolerance induced in C57BL/6 and DBA/2 mice as a consequence of injection, in the neonatal period, with spleen and bone marrow cells from the adult hybrid $B_6D_2F_1$ mice. Recipients, which accepted skin grafts from the reciprocal parent strain for prolonged periods, were found to be erythrocyte chimeras, as demonstrated by a fluorescent antibody technique, which identified allogenic erythrocytes in the peripheral circulation. The minor population of fluorescent erythrocytes was believed to be the progeny of the $B_6D_2F_1$ cells. To insure that the cells identified had not persisted from the initial injection, the mice were studied for chimerism only after an interval of three times the life span of the mouse erythrocyte. The results therefore indicate that the mature erythrocytes with $B_6D_2F_1$ antigenic specificity were derived from well-established precursor cells capable of self-perpetuation by asymmetric division. DBA/2 mice, which were rendered tolerant of C57BL/6 skin by injection with $B_6D_2F_1$ spleen and bone marrow cells that had been maintained in vitro for 24 hr, were also erythrocyte chimeras, indicating that a culture period of 24 hr does not irreversibly damage the erythrocyte precursor cells in the suspension. Although this study demonstrated only erythrocytes of donor origin, donor leukocytes probably persisted as well as reported earlier in studies of irradiation-induced erythrocyte chimeras, where the presence of donor-type polymorphonuclear leukocytes and lymphocytes was demonstrated. The stem cells in the inoculum which was introduced shortly after birth apparently established themselves permanently in the recipient's hematopoietic organs. (TCO)

43658 IMMUNOLOGIC STUDIES OF OCTAPEPTIDES. II. PRODUCTION AND DETECTION OF ANTIBODIES TO OXYTOCIN. Gilliland, Paul F.; Prout, Thaddeus E. (Johns Hopkins Univ. School of Medicine, Baltimore). Metab. Clin. Exptl., 14: 918-23(Aug. 1965).

Prior to development of a radioimmunoassay method, synthetic oxytocin was successfully used, without conjugation to another particle, to produce antibodies in the rabbit. The antibody produced is relatively specific for oxytocin and does not appear to react with 8-lysine vasopressin. The inhibition of the reaction between the antioxytocin antibody and radio-oxytocin by unlabeled oxytocin in serum suggests that assay of endogenous octapeptides by this method will be possible. Thus, serum obtained from rabbits prior to immunization was incubated with or without unlabeled synthetic oxytocin, and labeled oxytocin was then added. Electrophoresis of these mixtures was carried out on agar and radioautographs were produced. These radioautographs demonstrated that most of the radioactivity in pre-immunization serum is associated with the proteins that have migrated toward the anode. When serum obtained from rabbits 28 weeks after beginning immunization was treated in the same manner as the pre-immunization serum, there was a marked increase in the radioactivity that migrated toward the cathode and this radioactivity is associated with the γ-globulins. The specificity of this reaction was also demonstrated. The amount of radioiodinated oxytocin associated with the γ-globulins in the postimmunization serum decreased with increasing quantities of unlabeled oxytocin. This is the first evidence that antibodies could be produced to octapeptides without conjugation to a larger particle. Immunoelectrophoretograms of pre- and post-immunization serum incubated with oxytocin-^{131}I were produced and their autoradiographs examined. The radioactivity in pre-immunization sera was attached predominantly to two proteins: an α-globulin and a β-globulin. No radioactivity is associated with the γ-globulin, and the radio-oxytocin attached to the anodal proteins does not appear to be influenced by prior incubation with unlabeled oxytocin. The autoradiograph of the postimmunization sera shows the radioactivity in association only with γ-globulin. (BBB)

43659 MEASURING RADIOISOTOPES IN BIOMEDICAL SAMPLES. Parr, Robert M. (International Atomic Energy Agency, Vienna). Nucleonics, 23: No. 9, 56-60; 62 (Sept. 1965).

Gamma spectrometry, computer applications, semiconductor detectors, thin-layer chromatography, liquid-scintillation counting, radioactivity standardization, and activation analysis for measuring radioisotopes in biological and medical samples were discussed at the IAEA symposium, in Vienna, May 24 to 28, 1965. Applications in health physics were also considered. (M.C.G.)

43660 APPARATUS FOR THE DETERMINATION OF THE VOLUME OR AGE OF A LIQUID USING RADIATION DILUTION TECHNIQUES. (to Ames Lab-Tek Inc.). British Patent 1,001,875. Aug. 18, 1965. Priority date Oct. 10, 1960, United States.

The described apparatus for the determination of liquid volume by radioactivity dilution techniques is particularly applicable to the measurement of circulating blood volume. The apparatus includes a housing adapted to receive radioactive samples at first and second spaced positions within the housing, a radiation detector mounted within the housing at each of the spaced positions that generates output pulses in response to radiation from the corresponding sample, and an electrical circuit simultaneously responsive to the pulses generated at the detectors. Detailed description of the electrical circuitry is included. Provision is also made for modifying the apparatus to receive a third sample at a position in the housing spaced from the first and second sample positions and midway between them. This modification enables successive measurements of dose activity and sample activity and for the simultaneous counting of the value of dose activity by two space detectors with the dose positioned between them, substantially reducing the effects of errors in dose positioning. (B.L.M.)

43661 APPARATUS FOR DETECTING RADIATION. (to Ames Lab-Tek Inc.). British Patent 1,001,876. Aug. 18, 1965. Priority date Oct. 10, 1960, United States.

An apparatus is described for the detection of radiation, particularly for the determination of liquid volume by radioactivity dilution techniques and especially for the measurement of circulating blood volume. The apparatus includes a

radiation-shielding housing having wall means defining a predetermined viewing area, a radiation detector located adjacent to the viewing area, a sample receptacle, and means for positioning the sample receptacle in the sample position within the viewing area so that the receptacle extends across the view area. The receptacle is provided with an opening for the introduction of samples and is of generally cylindrical tubular shape. The detector includes a radiation-responsive element surrounding the portion of the receptacle having the predetermined volume exposed to the viewing area. When a radioactive sample fills the portion of the receptacle within the viewing area, a predetermined volume of the sample is exposed to view by the detector; and upon subsequent positioning in the sample position of an identical receptacle containing a second sample filling the portion within the viewing area, the same predetermined volume of the sample is exposed to view by the detector irrespective of any difference in the total volumes of the two samples. (B.L.M.)

Ecology

43662 (UCLA-12-565, pp 97-128) ENVIRONMENTAL RADIATION. (California Univ., Los Angeles. Lab. of Nuclear Medicine and Radiation Biology).

Vegetation and animal studies at the Nevada Test Site (NTS) are described along with radiation effects studies. Environmental measurements are reported, and a vascular plant inventory was made. Rodent energy requirements are being investigated. Studies of radiation effects on mice are reported, along with those on NTS animal populations. Investigations are reported on ^{137}Cs distribution on the NTS farm, fallout uptake by desert shrubs, nuclear excavation effects on soil and vegetation, gamma radiation effects on desert shrubs, irradiation of plants in NTS rock valley, radionuclide food-chain kinetics from Sedan fallout, solubility of radionuclides in reactor-activated soils, Be effects in soils and plants, CO_2 effects in bean roots, and radiation effects on lizards. (J.R.D.)

43663 ECOLOGICAL IMPLICATIONS OF FALLOUT RADIOACTIVITY ACCUMULATED BY MOLLUSCS. Schelske, Claire L. (Bureau of Commercial Fisheries, Beaufort, N. C.). 21p. (CONF-641219-1). Gmelin, AED-CONF-64-272-3.

From American Association for the Advancement of Science, 131th Annual Meeting, Montreal.

Existing levels of radioactivity were measured in the estuarine environment for the purposes of establishing base lines for future comparisons of radioactivity in estuarine organisms and for determining ecological and biological relationships in situ. Four species of lamellibranch mollusks collected near Beaufort, North Carolina were studied: marsh mussels, Modiolus demissus; hard clams, Mercenaria mercenaria; American oysters, Crassostrea virginica; and bay scallops, Aequipecten irradians. Only gamma emitters were measured because existing quantities of radioactivity in estuarine organisms are small making it difficult and time consuming to prepare samples for analysis of beta activity. Both clams and marsh mussels contained relatively large quantities of ^{144}Ce and ^{106}Ru. Although oysters also accumulated these nuclides, they were biological indicators for ^{65}Zn. Scallops contained more gamma activity than the other mollusks and were indicators for ^{54}Mn, approximately 60% of the total counts in the spectrum being due to the nuclide. In addition to the radionuclides for which mollusks served as indicators ^{95}Zr-^{95}Nb were also found in the environment. Results show differences among the gamma spectra of filter feeders in what might be considered one trophic level, differences possibly being attributable to selective feeding. Results suggest that the distribution of environmental radioactivity in organisms may be used to distinguish ecological niches among organisms having similar feeding mechanisms. (H.G.D.)

Metabolism, Tissue Distribution, and Toxicology

Refer also to abstract 44269.

43664 (BNL-9337) GALVANI, VOLTA AND BIOELECTRICITY. Alexander Forbes Lecture, Marine Biological Laboratory, Woods Hole, Massachusetts, July 9, 1965. Nims, Leslie F. (Brookhaven National Lab., Upton, N. Y.). Contract AT(30-2)-Gen-16. 35p. Dep. mn; CFSTI $2.00 cy, $0.50 mn.

Developments in the field of bioelectricity since the studies of Galvani in 1794 are reviewed, with emphasis on the development of the voltaic pile, or galvanic cell, by Volta, and the formulation of the concept of a hypothetical difference in electrical potential across a membrane. It is stressed that in theoretical electrophysiology, account must be taken of the fact that equilibrium between phases separated by a membrane is the exception rather than the rule in biological systems; that a fundamental observation of bioelectricity is that electric currents flow; that the electric currents of interest are quasi-direct, or steady state currents in closed electrical circuits; and that there are no metallic electrodes or electrochemical reactions. Equations are presented that illustrate the thermodynamics of irreversible processes for material transfer across a membrane of constant thickness in which there is a difference in the chemical potential of neutral molecules or a difference in electrochemical potential of an ion between two homogeneous phases in contact with the barrier. A unit transfer system in a Sollner ring system is cited as an example, in which the system is regarded as two unit transfer systems containing barriers of different properties arranged in an electrical circuit. Applications of the theories discussed to the thermodynamics of material transfer across biological membranes are developed. (C.H.)

43665 (BNL-9338) MATERIAL TRANSFER, MEMBRANES AND METABOLISM. Alexander Forbes Lecture, Marine Biological Lab., Woods Hole, Massachusetts, July 8, 1965. Nims, Leslie F. (Brookhaven National Lab., Upton, N. Y.). Contract AT(30-2)-Gen-16. 56p. Dep. mn; CFSTI $3.00 cy, $0.50 mn.

Thermodynamic principles involved in the transfer of ions across membranes are discussed on the basis of their applicability in studies of the flow of nutrients and excrements into and out of a biological system. It is pointed out that all living systems operate as open systems for the major fraction of their life span. The point is stressed that the motion of material substances through biological barriers appears to obey the same basic laws as the motion of proteins in a centrifuge, the sedimentation of cells in a test tube, or the motion of satellites in the atmospheric barrier. Theories of material transfer are developed by means of mathematical relations that apply physical-chemical concepts to biological processes. The details of the molecular traffic occurring in all biological barriers will be of interest to the experimentalist in that they lead to formal relations between metabolism and ion distribution patterns verifiable by experiment, and in some instances a quantitative prediction of the behavior of particular membranes. Applications of the theories in explaining the results of radioisotope tracer studies of membrane transfer are discussed briefly. (52 references.) (C.H.)

43666 (BNL-9406) TRANSFER RATES OF GAMMA GLOBULIN BETWEEN CEREBROSPINAL FLUID AND BLOOD PLASMA IN MULTIPLE SCLEROSIS. Lippincott, Stuart W.; Korman, Samuel; Lax, Louis C.; Corcoran, Cornelia (Brookhaven National Lab., Upton, N. Y.). [1965]. Contract AT-30-2-GEN-16. 22p. (CONF-650647-1). Dep. mn; CFSTI $1.00 cy, $0.50 mn.

From Society of Nuclear Medicine, 12th Annual Meeting, Bal Harbour, Fla.

Iodine-131-labeled gamma globulin was injected both intravenously and intratheccally into patients with multiple sclerosis with subsequent sampling of blood and cerebrospinal fluid. Specific activity versus time curves were constructed from the data obtained from these samples. The transfer rate of gamma globulin from the cerebrospinal fluid to the blood plasma was 11.6 times as rapid as from the blood plasma to the cerebrospinal fluid compartment. The average time a molecule of gamma globulin spent in the cerebrospinal fluid compartment was 17.3 hours whereas in the blood plasma compartment it was 72.4 hours. The gamma globulin in the cerebrospinal fluid compartment was found to be replaced 4.2 times as fast as it was in the blood plasma compartment. (auth)

43667 (EUR–1890.f) BASES EXPERIMENTALES D'UNE INTERPRETATION QUANTITATIVE DU RENOGRAMME. (Experimental Basis of the Quantitative Interpretation of the Renogram). Colin, F.; Mercenier, P.; Kornitzer, F.; Cleempoel, H. (Brussels Univ. (Belgium)). 1964. 13p. (CONF-640808-2). Dep. mn.

From European Congress on Cardiology, Prague.

The renogram and the evolution of the activity in the arterial and venous renal blood and in the urine sampled in the urethra after intravenous injection of hippuran was studied on the exposed kidney of the dog. The examination of these different data made it possible to reject the classical interpretation of the theory of compartments. The morphology of the renogram can be explained only beginning with the propagation of the isotope in the dead space of the kidney. This propagation introduces at the same time a delay between the phenomona of uptake and elimination and a deformation of the uptake curve by the renal cavities. The respective importance of these two factors is studied. (tr-auth)

43668 (HW-SA–3618) AN INSTRUMENT FOR THE AUTOMATIC REGULATION OF INHALED AEROSOLS. Brown, D. P.; Porter, N. S. (General Electric Co., Richland, Wash. Hanford Atomic Products Operation). Sept. 25, 1964. Contract AT(45-1)-1350. 9p. Dep. mn; CFSTI $1.00 cy, $0.50 mn.

Beagle dogs were exposed to ^{59}Fe during inhalation experiments at the Hanford Biology Inhalation Toxicology Laboratory. Subsequently, the animals were caused to inhale cigarette smoke in an effort to discover a possible relationship between smoking and the clearance rate of the isotope from the lungs. The smoking routine was conducted manually by a technician on a regular daily basis. Standardization of the smoking process would provide a more consistent and uniform application of smoke and provide more effective control for such a laboratory experiment. It was desired to duplicate the smoking process of man as closely as possible with air inhaled through the nose and smoke through the mouth. An instrument to control the number of fresh-air breaths for each smoke-filled breath was developed to aid in the experimental investigations. (auth)

43669 (NP-15159) STUDIES ON UPTAKE OF RADIOISOTOPES BY EDIBLE MARINE PRODUCTS. Progress Reports, 1960-1962. Hiyama, Yoshio (Tokyo Univ. (Japan)). IAEA Contract No. 20R/RB. 51p. Dep. mn.

The concentration factors, defined as ratio of concentration of radionuclide in tissue or organ of marine organisms to that in water where these are living, of several radionuclides (^{131}I, ^{60}Co, ^{106}Ru, ^{144}Ce, ^{65}Zn, ^{115m}Cd, ^{134}Cs, and ^{89}Sr) were determined for representative edible marine organisms including fish, shell fish, crustacea, sea-urchins, and algae. Rate of up-take, or time to reach equilibrium, were found to vary according to the kind of radionuclide, kind of marine organisms, age of the organism, and temperature of the water. Concentration factors in equilbrium were found to vary according to the kind of tissue or organ of organism, the kind of organisms, and the kind of radionuclide, but were not affected by water temperature and the concentration of radionuclide in water. Existence of carrier in sea water reduced the concentration factors in some degree for ^{131}I, ^{60}Co, ^{65}Zn, and ^{115m}Cd, but not for ^{134}Cs and ^{89}Sr. In case of Fe uptake by seaweeds, the existence of light affected the concentration factor. The forms of radionuclides in sea-water affected the up-take, especially the particulate or colloid form. Difference of concentration factor obtained by rearing experiment in equilibrium from that by ingestion or injection experiment is not remarkable for the nuclides tested. The destination of radionuclides (critical organs) in the body is similar in any method. It is concluded that the concentration factors of edible marine organisms for radionuclides are the keys to the evaluation of hazards caused by radioactive contamination of sea-water. (auth)

43670 (NP–15310, pp 36-47) FURTHER STUDIES ON THE MECHANISM OF ACTION OF 2-MERCAPTOETHYLAMINE. Yam, Kei-Ming; DuBois, Kenneth P. (USAF Radiation Lab., Univ. of Chicago, Ill.).

A hexobarbital metabolizing reaction system was developed which requires the following factors as the optimal conditions for the metabolism of 0.6 μM of hexobarbital in a period of 30 minutes: 30 mgm. of liver tissue (prepared as a 20% homogenate in isotonic KCl and 0.25% nicotinamide solution), 1.3 μM TPN, 3 μM of glucose-6-phosphate, 30 μM of $MgCl_2 \cdot 6\,H_2O$, 20 μM of potassium phosphate buffer (pH = 7.4), and distilled water to a final volume of 0.8 ml. A sex difference was observed in the metabolism of hexobarbital in the rat with the female exhibiting much lower enzyme activity. At concentrations comparable to the radioprotective dose, MEA produced about 23% inhibition of metabolism of hexobarbital. (auth)

43671 (PG-Report–662) METABOLISM OF RADIOACTIVE STRONTIUM IN RAT. PART I. THE WHOLE-BODY RETENTION AND TISSUE DISTRIBUTION CHARACTERISTICS OF ^{85}Sr. PART II. ATTEMPTS TO INFLUENCE ELIMINATION BY PHYSIOLOGICAL AND OTHER PROCEDURES. Bates, T. H.; Dymond, B.; Chapman, I. V.; Smith, H. (Production Group, United Kingdom Atomic Energy Authority, Annon (Scotland)). 1965. 28p. Dep.; BIS $1.60; HMSO 8s.

A satisfactory method of whole-body counting of ^{85}Sr in small experimental animals was devised along with methods for analysis of excreta and tissues. Use of rats of bodyweight between 150 and 200 g is convenient and ensures reproducible body retention characteristics. Analysis of tissues from animals sacrificed at intervals following administration of ^{85}Sr shows a rapid clearance from soft tissues and uptake into bone tissue in a matter of hours. This underlines the need for early therapy if attempts at removal are to be simple and effective. Any alternative approach will necessarily involve modification of basic physiological parameters affecting bone metabolism. Distribution in tissues over a 48 hour period was analysed in more detail than has been reported hitherto. There is evidence that skin should be regarded as a separate compartment. Movement of ^{85}Sr along the gastrointestinal tract was studied and it transpires that little absorption occurs in caecum or colon. (auth)

43672 (TID–22131) RADIUM AND MESOTHORIUM POISONING DOSIMETRY AND INSTRUMENTATION TECHNIQUES IN APPLIED RADIOACTIVITY. Comprehensive Report of Over-all Activities, 1950–1965. (Massachusetts Inst. of Tech., Cambridge. Dept. of Physics). Contract AT(30-1)-952. 47p. Dep. mn; CFSTI $2.00 cy, $0.50 mn.

A review is presented of a 15-year investigation of Ra and ^{228}Ra poisoning in human beings. The investigation consisted of identification and location of cases; measurements of the body burdens of radioactivity in 428 cases; compilation of personal and medical histories, with a complete series of x rays; and proper interpretation, compilation, storage, and distribution of case records. A large NaI scintillation detector in a shielded room was used for whole-body counting and Rn in exhaled breath was also measured. Sufficient data was accumulated for preliminary statistical studies of dose-response relationships for a number of health factors. Related studies included chromosome studies in the red blood cells of persons with Ra poisoning, the metabolism of Ca in Ra in man

and experimental animals; fundamental studies of the properties of nuclei and of the interactions of radiations with matter, and the development of new types of counters and electronic instrumentation. (157 references) (C.H.)

43673 (TID-22147) ACUTE DEPLETION OF CALCIUM, PHOSPHORUS, AND STRONTIUM FROM THE BOVINE CALF BY HEMODIALYSIS (thesis). Downey, Harry Fred (Maryland Univ., College Park). 1964. Contract AT-40-1-GEN-33. 134p. Dep. mn; CFSTI $4.00 cy, $1.00 mn.

An artificial kidney and radioisotopes were used to study electrolyte hemodialysis in dairy cattle. Two randomized 3 × 3 complete block design experiments were conducted simultaneously to investigate the effects of acute depletion of calcium, phosphorus, and strontium by hemodialysis from 200 lb, 100-day-old Hereford and Holstein calves. The calves were intravenously dosed with ^{45}Ca, ^{32}P, and ^{89}Sr at 48, 96, or 144 hr predialysis and with ^{85}Sr at 4, 14, and 24 hr predialysis. Dialysis was continued until the animal died or in two cases was terminated at the end of 12 hr. Dialysis survival time ranged from 7.1 to 28.7 hr. No obvious reasons for the inability of some animals to withstand long periods of dialysis were apparent. The young bovine was able to mobilize reserve calcium and phosphorus during 12 hr of dialysis to maintain the plasma concentrations of these elements within 74% of predialysis concentrations. The depletion of ^{45}Ca, ^{89}Sr, and ^{85}Sr (^{32}P depletion was not measured) decreased ($P < .01$) as the interval between dosing and the initiation of dialysis increased. Twelve hours of dialysis depleted 13.5, 4.2, and 2.5% of the ^{85}Sr dosed 4, 14, and 24 hr predialysis. The plasma concentrations of all isotopes declined ($P < .01$) during dialysis. Rib epiphyseal ^{89}Sr, but not ^{45}Ca, appeared to be always in equilibrium with the plasma. Calcium-45 was the only isotope significantly depleted ($P < .05$) from the rib samples during dialysis. It was suggested that ^{45}Ca was preferentially incorporated in the bone crystals and then released during mobilization. (180 references.) (auth)

43674 (UCD-472-112, pp 36-43) CLINICAL BLOOD CHEMISTRY STUDIES IN BEAGLES. McKelvie, D. H.; Powers, S.; McKim, F. (California Univ., Davis. School of Veterinary Medicine).

Blood chemistry studies on all experimental Beagles are continuing on a 120-day schedule. All samples are analyzed by microtechniques that allow eleven or more tests on as little as 1 ml. of serum. Preliminary analyses were made of sera from two female Beagles to determine the effects on chemistry values of storage, either refrigerated or quick-frozen. Glucose values decreased rapidly from 95 mg% in six weeks under refrigeration, whereas frozen samples retained approximately 85% of the value in a comparable period. Cholesterol values decreased 30% when refrigerated and 20% when frozen. A survey of the serum chemistry values of 32 females in anestrus to determine the difference in sera samples immediately after feeding and after 24 hours of starvation showed 17% higher BUN, 52% higher uric acid, 18% higher phosphorus, and 19% increase in α 1 and γ globulins in dogs starved for a 24-hour period. In addition, the white blood count was elevated 16%. A serum test showed that 10-year-old Beagles had 50% higher glucose (156 mg%) and a 100% higher bilirubin (.38 mg%) concentration than one-year-old Beagles. A large number of samples are being analyzed by an IBM 7040 computer. (auth)

43675 (UCD-472-112, pp 73-7) QUALITY CONTROL OF ^{90}Sr CONTAINING FOOD. Della Rosa, R. J.; Nix, N.; Wittmier, J.; Santos, A.; Abrahams, C. (California Univ., Davis. School of Veterinary Medicine).

The quality control of Sr-90, Ca, and P content in six dietary dose levels, for the continuous feeding of Sr-90 containing food to more than 200 Beagles, has been satisfactorily maintained to within 10 percent of prescribed values. (auth)

43676 (UCD-472-112, pp 80-5) DISCRIMINATION IN BEAGLE PUPPIES: THE EFFECT OF EXTENDED NURSING ON THE DEPOSITION AND RETENTION OF STRONTIUM IN BONE AND TEETH. Della Rosa, R. J.; Wolf, H.; Calvert, S. (California Univ., Davis. School of Veterinary Medicine).

The effect of extended nursing on calcium-strontium discrimination in Beagle puppies was determined using esbilac, a milk replacement. When the nursing period was extended from 38 to 70 days, there was almost equal absorption of both elements, and a near-lack of discrimination. An OR value bone/diet of about 1 was obtained at 70 days of age. The absence of discrimination may be attributed to the nature of the milk diet rather than some other mechanism. (auth)

43677 (UCD-472-112, pp 86-96) THE ABSORPTION AND DEPOSITION OF ^{85}Sr AND ^{47}Ca FROM LIGATED INTESTINAL SEGMENTS OF ADULT BEAGLES. Della Rosa, R. J.; Wolf, H. (California Univ., Davis. School of Veterinary Medicine).

The differential transfer of Sr-85 and Ca-47 from the duodenal, jejunal, and ileal segments of the intestinal tract of Beagles to plasma, and their subsequent deposition in bone was studied under conditions of fasting and in the presence of test meals. In the fasting dog, both alkaline earths were transported equally across the intestinal membrane to plasma. Effective discrimination occurred only in the presence of a test meal. Further changes in the Sr/Ca of plasma relative to bone was attributable to preferential excretion of strontium by the kidney. The data indicate that gastrointestinal absorption of strontium and calcium was by way of their ionic forms. (auth)

43678 (UCD-472-112, pp 97-108) RADIUM METABOLISM BY BEAGLES FOLLOWING SINGLE AND MULTIPLE INJECTIONS—A PRELIMINARY REPORT. Goldman, M.; Della Rosa, R. J.; Stone, J. M.; Young, L. G.; Wolf, H. (California Univ., Davis. School of Veterinary Medicine).

Ra-226 uptake and retention was measured in four adult Beagles by total-body counting and excreta analysis following single and fractionated doses. Two of the dogs received four ~0.9 μC injections of Ra-226 at 14-day intervals, and the other two received the ~3.5 μC in a single injection. The Ra-226 body burdens were estimated by the difference between the injected dose and the cumulative excreta, and were compared to the γ ray emission from each dog. Based on excreta analysis, the dogs appeared to retain an average of 31% of the injected dose 72 days after the first injection. With increasing burden time, the radon to radium ratio reached a maximum of approximately 11% at sacrifice for the single injected dose and was about 6 to 10% for the dogs receiving the fractionated dose. (auth)

43679 (UCD-472-112, pp 109-19) ^{90}Sr UPTAKE AND RETENTION PATTERNS IN UNIFORMLY LABELED BEAGLES. Goldman, Marvin; Powell, T. J.; Young, L. G. (California Univ., Davis. School of Veterinary Medicine).

Patterns of individual skeletal growth have been studied in Beagles reared on Sr-90 containing diets for their first 18 months of life. A measure of skeletal growth rate, based on the age at which 50% of the maximum body burden is achieved, suggests that the female reaches this level at about 104 days of age compared to males at 124 days, although the range in individual values demonstrates considerable overlap. In females from 1.5 to 3.5 years old, the rate of Sr-90 loss appears to increase with delay in rate of initial burden acquisition; in males this is less apparent. An increased rate of loss of body burden with increasing dose rate up to two years following labeling, may be a physiological reaction to skeletal irradiation during immaturity. (auth)

43680 (UCD-472-112, pp 148-74) STATUS OF EXPERIMENTAL ^{90}Sr-^{226}Ra BEAGLE COLONY AS OF 31 JANUARY 1965. (California Univ., Davis. School of Veterinary Medicine).

The status of an experimental dog colony used in long-term experiments on the effects of ^{90}Sr or ^{226}Ra is reviewed. (C.H.)

43681 (UCLA-12-565, pp 17-31) BIOCHEMISTRY. (California Univ., Los Angeles. Lab. of Nuclear Medicine and Radiation Biology).

Progress is reported in investigations on cofactor requirements for the alpha oxidation of long-chain fatty acids, synthesis of 15-hexadecanoic acid-1-^{14}C and its metabolism in rats, semibromination of linoleic acid, mechanism radioinduced decarboxylation of saturated fatty acids, metabolic energy sources for beating activity, myosin synthesis in cultured heart cells, effects of lipids on beating rat heart cells, role of lipids in growth and membrane functions, enzyme levels in beating rat heart cells, and wax esters in coelacanth fish. (J.R.D.)

43682 (UCLA-12-565, pp 33-57) RADIOBIOLOGY. (California Univ., Los Angeles. Lab. of Nuclear Medicine and Radiation Biology).

Progress is reported in investigations of gamma-irradiation of ice-cold thymine and thymine dimers, radiation effects on aqueous thymine, radiation effects on polynucleotides, electromicroscopy of RNA in cytoplasm, soluble RNA in estrogenized chickens, hemoglobin synthesis in Avian red cell nuclei, radiation effects on myelin in rats, radiation effects on enzyme activity in brains, enzyme activity in livers of estrogenized chickens, protein synthesis in irradiated rat brains, DNA synthesis during cell cycle in Stentor Coeruleus, RNA synthesis in Stentor Coeruleus, respiration of red cells in chickens, enzyme reactions involving substrate complexes, radiation effects on Pinus Thunbergii, effects of plethora on irradiated mice, and relations of spleen nodules to stem cell kinetics in irradiated animals. (J.R.D.)

43683 AUTORADIOGRAPHY OF THE THYROID GLAND. Lupulescu, A.; Merculiev, E.; Nicolae, M. (Inst. of Endocrinology, Bucharest). Acta Anat., 57: 37-51(1964).

Localization and distribution of ^{131}I was studied with the aid of autoradiography in control rats and rats with goiter induced by iodine deficiency, methylthiouracil, administration of thyrotropic hormone (TSH), hypophysectomy, or hypothalamic lesions. These data were interpreted in terms of dynamics of the synthesis and release of thyroid hormones. In autoradiographs of control rats 1 hr after injection of ^{131}I the protein-bound radioiodine had entered most of the follicles and localized almost entirely in the colloid in a homogeneous mass. In the center of the gland clear zones were seen into which the radioiodine failed to penetrate and which were represented by nonfunctional microfollicles. On the other hand, all follicles contained protein-bound radioiodine after 6 hr. The accumulation was more intense in microfollicles and almost exclusively in the follicular colloid. After administration of TSH, massive accumulation of protein-bound radioiodine was noted in the lumen of the follicles. The isotope was almost entirely deposited in the colloid and homogeneously so. Decreased accumulation of protein-bound ^{131}I in the thyroid follicles was observed in hypophysectomized rats. Hypothalamic lesions likewise altered protein-bound ^{131}I accumulation in the thyroid tissues in relation to the site of the lesion. In contrast, the lesions in the extrapyramidal system (globus pallidum) enhanced radioiodine accumulation, as observed in most follicles after 1 hr, in the colloid. (TCO)

43684 RETENTION OF RADIOACTIVE PHOSPHORUS IN THE BODY OF THE HUMAN LOUSE (PEDICULUS HUMANUS L., ANOPLURA). Piotrowski, Feliks; Rudnicki, Tadeusz. Acta Physiol. Polon., 16: 435-9(1965). (In Polish).

Retention of radioactive phosphorus in the body louse was investigated. It was found that the mean effective half time of ^{32}P was 2.2 days. Excretion of ^{32}P takes place in the phases: in first with the turnover rate $k_1 = 0.2$, and in the second with $k_2 = 0.02$. The method employed permits labeling of body lice for a period of 1-2 weeks. (auth)

43685 METABOLISM AND TRANSPORT OF ORGANIC SUBSTANCES IN THE PHLOEM. Kursanov, A. L. (Inst. of Plant Physiology, Moscow). Advan. Botan. Res., 1: 209-78(1963).

Studies utilizing ^{14}C-labeled metabolites, as well as D_2O and T_2O, are reviewed. (BBB)

43686 PHYSICO-CHEMICAL AND BIOLOGICAL ALTERATIONS INDUCED BY GAMMA IRRADIATION OF ^{131}I-LABELLED RABBIT SERUM γ-GLOBULIN. Bocci, V. (Istituto di Fisiologia Generale dell'Universita, Italy). Arch. Fisiol., 62: 292-312(Dec. 30, 1963).

The purposes of this report were to ascertain the catabolism in rabbits of homologous ^{131}I-γ-globulins (RSIGG) irradiated with γ rays in the presence of oxygen and to show that heavily irradiated 6.6S RSIGG have rates of metabolic decay and intra-extravascular distribution volumes resembling those of intact γ-macroglobulins. Cold precipitation of the RSIGG was carried out with 10% trichloroacetic acid (TCA), and ^{131}I-TCA soluble radioactivity was expressed as a percentage of the original radioactivity. In vitro γ irradiation of the RSIGG, in neutral glass bottles (4.5 mg/ml in 0.1M phosphate buffer, pH 7.0) was performed at 20°C in aerobic conditions with a ^{60}Co source. The dose rate was 139 kR/hr and the RSIGG samples received doses of 125, 250, and 500 kR. After labeling no more than 1.6% of the radioactivity was soluble in 10% TCA, but following γ irradiation it increased to a max of 45%. An observed small increase of TCA-soluble radioactivity in the control RSIGG was likely due to selfirradiation. The 500-kR irradiated RSIGG could be hydrolysed by papain to an extent of 44%, whereas only 6.7% TCA-soluble radioactivity derived from normal RSIGG. Proteolysis of irradiated RSIGG by papain was almost directly proportional to the irradiation dose. A comparison between the absorption spectra of normal and irradiated RSIGG showed an increase in optical density roughly proportional to the dose most evident in the region of wavelengths from 2400 to 2510 Å. The electrophoretic patterns of RSIGG subjected to 125, 250, and 500 kR showed an increase of fast-moving (towards the anode) components which were absent in the original protein. New fast moving components obtained after exposure of RSIGG to 500 kR had in part the electrophoretic mobility of serum β-globulins, as well as fibrinogen or of fast γ-globulins. Up to 18% of the 500-kR irradiated RSIGG was taken up by rat liver within 15 min after injection in rats, whereas normal RSIGG gave no more than 3% retention; a totally heat denatured RSIGG gave about 86% retention. When injected into rabbits, irradiated RSIGG was catabolized more rapidly than the nonirradiated protein, the effect being proportional to the dose. After about 9 hr following the injection the 500-kR RSIGG exhibited up to 37.0% of nonprecipitable plasma radioactivity whereas the control gave only 3.6% of unbound radioactivity. Daily urinary excretion of radioiodide, 24 hr after injection in rabbits of 125, 250, and 500 kR irradiated samples was 39.5, 58.3, and 70.1% of dose respectively in comparison to 30.6% of normal RSIGG. Thus irradiated protein was more susceptible to rapid metabolic degradation in vivo and the extent of alteration was a direct function of the radiation dose. (BBB)

43687 POLARIZING MICROSCOPY OF ABNORMAL DENTINE PRODUCED BY INJECTIONS OF STRONTIUM OR FLUORIDE. Grady, J. E.; Yaeger, J. A. (Univ. of Illinois, Chicago). Arch. Oral Biol., 10: 175-8(Jan.-Feb. 1965).

Birefringent changes in the hypomineralized zones in dentin were studied in rats injected with NaF or $SrCl_2$ and sacrificed 5 to 7 days later. Transverse ground sections of incisors were prepared, radiographed, and photographed in a polarizing microscope. After demineralization, the same sections were again photographed in the polarizing microscopy. A difference was seen in orientation of collagen in the hypomineralized zones induced by both F and Sr. In polarizing microscopy, normal dentine was brightest when the hypomineralized zone was dark, and the hypomineralized dentine was brightest when the normal dentine was dark. The change in orientation was about 45° (range 31 to 57°). The hypomineralized zone appeared narrower in the polarizing microscope than the microradiographs indicated, probably because the collagen fibrils do not make a sharp

angle bend, but rather follow an S-shaped course in going from one normal zone of dentin through the hypomineralized to the remaining normal mineralized dentin. Birefringence is produced by the preferential organization of fibrils in the tissue (form birefringence) and by the alignment of chemical bonds within a substance (intrinsic birefringence). The birefringence of dentin, either mineralized or demineralized, is predominantly due to the presence of oriented collagen fibrils. A change in collagen fibril orientation because of F or Sr, with or without a change in macromolecular organization, could result from decreased aggregation of ground substance. Collagen fibrils become oriented along lines of stress in the medium in which they develop. Decreased aggregation of ground substance in the hypomineralized component may result in abnormal orientation of lines of stress, and, therefore, abnormal orientation of developing collagen fibrils. (BBB)

43688 THE EFFECT OF Sr^{2+} ON SWELLING AND ATP-LINKED CONTRACTION OF MITOCHONDRIA. Caplan, Arnold I.; Carafoli, Ernesto (Johns Hopkins Univ., Baltimore). Biochim. Biophys. Acta, 104: 317-29 (July 8, 1965).

Although Sr^{2+} and Ca^{2+} are actively accumulated by rat-liver mitochondria during respiration by a common mechanism, Ca^{2+} is a very potent swelling agent at low concentrations, whereas Sr^{2+} shows no swelling activity. In fact, Sr^{2+} protects mitochondria against spontaneous swelling or that induced by Ca^{2+}, thyroxine, oleate, or phosphate. The protective action of Sr^{2+} in some respects resembles that of bovine serum albumin, and in other respects that of Mg^{2+}. When Sr^{2+} protects mitochondria against swelling caused by phosphate, some Sr^{2+} is accumulated from the medium. Sr^{2+} supports maximum contraction of swollen mitochondria induced by ATP. Sr^{2+} may completely replace both Mg^{2+} and bovine serum albumin in supporting ATP-linked reversal of Ca^{2+}-induced swelling. Sr^{2+} also prevents reswelling at ATP-contracted mitochondria. When Sr^{2+} is added to Ca^{2+}-swollen mitochondria together with ATP, contraction is accompanied by accumulation of Sr^{2+}, and by inhibition of Ca^{2+} accumulation; no reswelling then occurs. The production of U factor or free fatty acids, which is accelerated by Ca^{2+}, is not influenced by Sr^{2+}. However, Sr^{2+} does appear to block the normal swelling action of free fatty acids. Sr^{2+} thus differs sharply from Ca^{2+} in its action on the structural state of mitochondria, although active uptake of both ions shows the same stoichiometric relationship to respiration. Sr^{2+} depresses the resting and the Ca^{2+}-stimulated ATPase activity of rat-liver mitochondria. It also inhibits the Mg^{2+}-stimulated ATPase activity of aged rat-liver-mitochondrial preparations. The $^{32}P_i$–ATP exchange activity was also found to be very markedly inhibited by Sr^{2+}. (auth)

43689 THE RETENTION OF ^{131}I IN THE BLOOD PLASMA OF MOLYBDATE-FED RABBITS. Robinson, G. A.; Riddell, Patricia E.; McCarter, Anne (Ontario Veterinary Coll., Guelph). Can. J. Physiol. Pharmacol., 43: 723-30(Sept. 1965).

The initial rate of uptake of ^{131}I by the thyroids of 44 molybdate-fed rabbits, as determined by in vivo counting, was slightly less than for 34 control rabbits. Thirty to sixty hours after ^{131}I injection, thyroidal ^{131}I levels were approximately equal in the two groups. Thoracic counting rates decreased more slowly in molybdate-fed rabbits, resulting by 72 hours in ^{131}I levels 3 to 35 times those of the control rabbits. Differences in the ^{131}I concentrations of protein-free plasma supernatants were of the same magnitude as for thoracic counts. The greater the effect of molybdate on the individual rabbit, the greater the ^{131}I retention in the plasma. For example, the product moment correlation coefficient for supernatant ^{131}I concentrations at 72 hours against hemoglobin concentrations for the 27 surviving molybdate-fed rabbits in one grouping of experiments was –0.77. Protein-free supernatant containing ^{131}I was chromatographed on plates coated with silica gel in 1:4:5 dioxane–butan-1-ol–2 N NH_3 (aqueous). A single ^{131}I band was found and tentatively identified as iodide by comparison with plates treated with iodide-127. (auth)

43690 COMBINATION OF RADIOACTIVE GAMMA AMINOBUTYRIC ACID IN THE CEREBRAL TISSUE OF THE RAT IN VITRO. Boulanger, Paul; Biserte, Gerard; Davril, Monique (Institut de Recherches sur le Cancer, Lille). Compt. Rend., 260: 5918-19(May 31, 1965). (In French).

When the cerebral tissue of the rat was incubated in vitro with γ-aminobutyric-1-^{14}C acid, the radioactivity was found in the CO_2 released (17 to 31%), in the aspartic acid (5.6 to 13.4%), and in low proportion in the glutamic acid, alanine, and β-alanine. A part of the γ-aminobutyrate, of variable importance according to the length of the experiment (48.4 to 73.3%), was not transformed; a small fraction existed in a combined form with behavior identical to that of the pantothenic and homopantothenic acids. (tr-auth)

43691 THE RADIOIODINE METABOLISM IN PATIENTS AFFECTED BY A SIMPLE SPORADIC GOITER. Giustina, G.; Bevacqua, V.; Cantalamessa, L.; Lo Deserto, A.; Ripamonti, A.; Valentini, L. (Universita, Milan). Folia Endocrinol. (Rome), 12: No. 1, 44-57(1964). (In Italian).

Radioiodine (^{131}I) metabolism was investigated in 260 patients with normal goiter diffuse or nodular. High thyroidal uptake of ^{131}I with normal or lower than normal levels of $PB^{131}I$ 48 hr/l plasma was detected in almost all patients. High uptake of ^{131}I was depressed by triiodothyronine. Most of the patients with normal uptake of ^{131}I had assumed iodine in the months preceding the radioiodine test. The results are consistent with the hypothesis of absolute or relative iodine deficiency and slow intrathyroidal turnover of radioiodine in simple goiter. The radioiodine metabolism was not different in hot or cold nodular and diffuse goiter; only in subjects with cold nodular goiter the ^{131}I uptake <50% was more frequent than in others. Maximum radioiodine uptake decreased with age in diffuse goiter; also the frequence of diffuse goiter decreased with age. (auth)

43692 METABOLISM OF ^{46}Sc IN MAN. Rosoff, Betty (Veterans Administration Hospital, Hines, Ill.); Spencer, Herta; Cohn, S. H.; Gusmano, E. A. Intern. J. Appl. Radiation Isotopes, 16: 479-85(Aug. 1965).

The metabolism, tissue distribution, and biological turnover of radioactive chelated scandium were determined in man. When administered intravenously as the weak chelate ^{46}Sc NTA (nitrilotriacetate), ^{46}Sc disappeared very slowly from the vascular space; it was excreted principally via the intestine. When ^{46}Sc was administered as the strong chelate of ethylenediaminetetraacetic acid, EDTA, or of diethylenetriaminepentaacetic acid, DTPA, the plasma level of ^{46}Sc decreased rapidly and urinary excretion was high with up to 82% of the dose excreted in 24 hr. The concentration of ^{46}Sc in various tissues determined 5, 6, and 7 months after the administration of ^{46}Sc NTA showed that uptake was highest in the spleen. Evidence is presented, which suggests that the high body retention of ^{46}Sc NTA may be due to the formation of colloidal aggregates and to binding of scandium to proteins. The biological half life of ^{46}Sc NTA determined with the whole body counter and computer analysis was 1300 days in one patient and 1557 days in another. (auth)

43693 THE PARTITION OF CERTAIN MINERAL NUTRIENTS IN THE COLOSTOMIZED LAYING PULLET AND THE DETERMINATION OF FAECAL ENDOGENOUS CALCIUM AND PHOSPHORUS EXCRETION BY AN ISOTOPIC DILUTION METHOD. Brown, W. O.; McCracken, K. J. (Queen's Univ., Belfast). J. Agr. Sci., 64: 305-10 (June 1965).

The urinary and fecal excretion of ^{32}P and ^{45}Ca, as well as that of Na, K, and Mn, was determined in colostomized pullets. Attempts were also made to establish whether the specific activity of egg shell ^{45}Ca as well as that of the blood serum could provide a useful index of the magnitude of the endogenous Ca appearing in the feces. Each bird received 20 μC ^{32}P (as carrier-free orthophosphate) and

10 μC ^{45}Ca (as $CaCl_2$) by intraperitoneal injection, and similar injections daily for seven more days. About 60% of the Ca was absorbed on a diet containing 2.25% Ca and only 34% of the P was absorbed at the dietary level of 0.59%. Sodium excretion in urine was very low, being only about 10% of the intake, but K excretion by the urinary route was 61% of the intake. No Mn was found in the urine and the apparent absorption of 30% agrees with data obtained by other methods in the fowl. Endogenous fecal Ca was estimated at 3% of the total fecal excretion and 10% of the fecal excretion of P. The results obtained using egg shell specific activity of ^{45}Ca rather than blood serum specific activity to determine endogenous fecal output of Ca gave high results. There was a mean retention of sufficient Ca to allow for about 70% egg production without loss of body Ca and the fairly low excretion of P in the urine indicated that a large amount of mobilization from the skeleton was not taking place. The mean figure for the absorption of P from the diet was only about 50% of that obtained for a diet containing a similar level of P but in the inorganic form. A high proportion of the dietary P was supplied by plant materials in which phytate P of lower availability might have accounted for the reduced absorption. (BBB)

43694 TOTAL BODY WATER ESTIMATIONS IN DAIRY CATTLE USING TRITIATED WATER. Aschbacher, P. W. (State Univ., Station Fargo, N. D.); Kamal, T. H.; Cragle, R. G. J. Animal Sci., 24: 430-3 (May 1965).

Tritiated water (TOH) was used with liquid scintillation detection as a method of estimating total body water and rumen-blood plasma equilibrium of water in dairy cows. Four nonpregnant cows were dosed intravenously with 10 mC of TOH per 1000 lb body weight; on the next day blood, urine, and milk samples were taken. A second experiment was conducted using two fistulated, nonlactating Jersey cows, dosed intravenously with 7.5 mC of TOH per 1000 lb body weight. Samples were counted in a liquid scintillation spectrometer at −10°C. The log of T activity in blood plasma, urine, or milk plotted against cumulative water intake resulted in a linear relation for ~5 days after dosing. Linear regressions were fitted to the points observed over the first 5 days and these equations are shown. The slopes of the lines were similar for T activity in blood plasma, urine, and milk on an individual basis. When log of T activity was plotted against time, the slopes of the lines were much greater for the two lactating cows. Biological half-life of TOH was 70 to 75 hr in the two lactating cows vs 120 to 130 hr in the two nonlactating cows. The greater water ingestion and body water estimates from urine and milk data were consistently higher than from plasma data, but the reason for this discrepancy was not apparent. Also determined was the time required for TOH to come to equilibrium between rumen juice and blood plasma when TOH was given intravenously. This equilibrium was reached 3 to 4 hr after intravenous injection of TOH but the results did not indicate clearly the time required for the body pool of TOH to equilibrate with ingested water. However, the time is not more than 4 hr. Body water estimates of 69.8 and 71.9% were obtained for two lactating cows, 69.0 and 67.6% for two nonlactating cows and 56.3 and 56.2% for two fat nonlactating cows. Sampling of blood plasma appeared to be the most satisfactory method for body water determinations with TOH. Urine and milk offered no advantages, and problems were encountered in a simple assay for T in urine. (BBB)

43695 THE FATE OF THORIUM DIOXIDE INJECTED INTO THE PEDAL SINUS OF BULLIA (GASTROPODA: PROSOBRANCHIATA). Brown, A. C.; Brown, Rosalind J. (Univ. of Cape Town). J. Exptl. Biol., 42: 509-19(June 1965).

The removal and ultimate disposal of foreign particles injected into the hemolymph of the sandy-beach snail, Bullia, was studied by using the radio-opaque dye Thorotrast. Particles are removed by phagocytic hemocytes which migrate by various routes to the outside of the body. The main pathway is through the heart wall into the pericardial cavity and via the renopericardial canal into the lumen of the kidney, from which the cells escape into the mantle cavity. The injection of foreign particles stimulates a marked increase in the hemocyte population and also in the mitotic index. The discussion integrates the available evidence and a comparison is made between Bullia and other mollusks. The origin of the macrophages is discussed. (auth)

43696 AUTORADIOGRAPHIC LOCALIZATION OF LIPID- AND WATER-SOLUBLE COMPOUNDS: A NEW APPROACH. Wilske, Kenneth R.; Ross, Russell (Univ. of Washington, Seattle). J. Histochem. Cytochem, 13: 38-43(Jan. 1965).

The method described was devised as a practical means for localizing labeled lipid- or water-soluble compounds such as acetylsalicylic acid and estradiol. It was compared with the usual approaches to tissue preparation for autoradiography. Previous attempts to retain such substances in situ in tissues have often been unsuccessful due to diffusion in the media involved in tissue preparation; and at the interface between the emulsion and the tissue section. Rats were given estradiol-^3H and aspirin-^3H as representatives of lipid-soluble and partially water-soluble compounds. After removal, tissues were quick frozen, frozen-dried, fixed in the vapor phase with osmium tetroxide or paraformaldehyde, and vacuum embedded in Epon. One-μ sections were coated with emulsion and subsequently developed. Discrete localization of the ^3H isotope was seen in autoradiographs. Data are presented to demonstrate the marked solubility of these compounds in the media used for routine fixation and dehydration, in contrast to their insolubility in epoxy resin. Thus cellular localization of numerous compounds by autoradiography, heretofore not possible, is now feasible. It is conceivable that with improvement in the method of freezing, tissues could be used for autoradiographic examination at the electron microscopic level as well. (BBB)

43697 MANGANESE (^{54}Mn) DISTRIBUTION IN SCORBUTIC GUINEA PIGS. Hsu, Jeng M.; Kawin, Bergene (Veterans Administration Hospital, Baltimore). Life Sci., 4: 1241-5(June 1965).

In view of the reported decreased Mn content of organs of scorbutic guinea pig, ^{54}Mn was used to study tissue distribution of Mn in these animals. Scorbutic animals were injected intramuscularly with 1.5 μC of carrier-free ^{54}Mn, and after 3, 18, and 70 hr representative organs were removed from the animals, weighed, and assayed for their ^{54}Mn concentrations. Of the 40% of the administered ^{54}Mn dose that was retained by the normal animals at 18 hr, two-thirds appeared in the feces by the end of the 70 hr interval. In contrast, from the fact that only about half of the ^{54}Mn that was retained by the scorbutic animals in the gastrointestinal tract at 18 hours and was fecally excreted by 70 hr, it is evident that in these animals a smaller total amount of ^{54}Mn was excreted, and also that it was excreted at a possibly slower rate than in normal controls. Prolongation and diminution of Mn excretion may have increased the availability of ^{54}Mn to tissues and organs generally. In addition to an early increased uptake by liver within 3 hr after injection, by 18 or 70 hr there was also enhanced uptake of ^{54}Mn observed in all of the organs studied. There was no pattern in these differences to suggest that it represented either any specificity in uptake between any of the soft tissues or between any of these and bone. The apparent avidity for ^{54}Mn displayed by the organs might relate to a depletion of tissue Mn stores, as was previously reported to be brought about by vitamin C deficiency. As based on the delayed excretion observed here, enhanced deposition might also be ascribed to an increased availability of ^{54}Mn to the organs of the scorbutic animals. (BBB)

43698 BIOLOGICAL PROPERTIES AND RADIOSENSITIVITY OF TUMOURS: DETERMINATION OF THE CELL-CYCLE AND TIME OF SYNTHESIS OF DEOXY-

RIBONUCLEIC ACID USING TRITIATED THYMIDINE AND AUTOPADIOGRAPHY. Goldfeder, Anna (New Uork Univ., New York). Nature, 207: 612-14(Aug. 7, 1965).

The kinetics of two types of tumors with varying growth rates, both indigenous to the same host were compared. Analysis was based on the quantitative autoradiographic estimation of the number of cells incorporating tritiated thymidine as a precursor in DNA synthesis, thus permitting determination of the time the cell spends in the various phases of its cycle. Male mice were implanted with several tiny particles of either epithelial or spindle cell tumor. Each tumor-bearing mouse was injected intraperitoneally with 0.3 cc aqueous solution containing 25 μC of tritiated thymidine. The phase of the cell-cycle was divided as follows: T_G: = post-synthetic, pre-mitotic period from the time of injection of the labeled precursor to the earliest time of appearance of labeled mitotic figures. In the case of the spindle cell tumor, T_G: phase lasted about 1 hr, and in epithelial tumor, about 2.5 hr. The frequency of the labeled mitotic figures rose rapidly after the T_G: period and reached a peak of approximately 76% for spindle cell and about 80% for epithelial tumor. The average time for DNA synthesis (T_s) for the spindle cell tumor was 12 hr and for epithelial tumor 6 hr. The generation time for both tumors was approximately 16 hr. (P.C.H.)

43699 TISSUE DISTRIBUTION OF ^{65}Zn IN TUMOUR TISSUE AND NORMAL TISSUE IN MAN. Rosoff, Betty; Spencer, Herta (Veterans Administration Hospital, Hines, Ill.). Nature, 207: 652-3(Aug. 7, 1965).

Zinc-65 uptake in tumor tissue localized at different sites in the body was determined and compared with that of the corresponding normal tissues. Samples of tumor tissue and of adjacent normal tissue were obtained at autopsy from 9 patients with advanced neoplastic disease at time intervals ranging from 1 to 71 days after injection of a single intravenous dose of $^{65}ZnCl_2$. The results indicate that tumor tissue that is localized in organs that normally have a low concentration of Zn have a similar or a greater ^{65}Zn uptake than the tissue in which the tumor is located. On the other hand, tumor tissue located in organs that normally have a high zinc concentration, for example, the liver and prostate gland, have a lower ^{65}Zn uptake than liver and prostatic tissue uninvolved by tumor. (P.C.H.)

43700 REMOVAL OF RADIONUCLIDES FROM THE BODY. Smith, Hylton; Bates, T. H. (AEA Chapelcross Works, Annan, Eng.). Nature, 207: 799-804(Aug. 21, 1965).

Along with a review on the removal of radioisotopes from the body, studies were made on the removal of ^{85}Sr and ^{239}Pu from rats by chelating agents and other compounds. Special attention is given to removing ^{85}Sr from rat bones. It was concluded that the most fruitful approach is that of combined therapy consisting of early citrate treatment in the presence of carrier strontium, followed by late treatment with sodium salicylate. (P.C.H.)

43701 THE METABOLISM OF CALCIUM, PHOSPHORUS, MAGNESIUM AND STRONTIUM. Widdowson, E. M.; McCance, R. A. (Univ. of Cambridge, Eng.). Pediat. Clin. North Am., 12: 595-614(Ag. 1965).

The supply, transfer, and amounts of calcium, phosphorus, magnesium, and strontium incorporated into the growing organism before birth are discussed; and the supply of these elements in mother's milk, and their absorption, retention, and excretion after birth are also considered. Most of the Sr in the body, like Ca, is in the skeleton, and from the Sr/Ca ratio in bone it has been calculated that the fat-free body tissue of the baby at birth contains about 2 mg/kg of Sr as compared with about 8 mg/kg in the adult. There is thus a greater difference between the newborn and the adult values for Sr than there is for Ca, P, or Mg. The ratio of Sr (mg) to Ca (g) in the bone of infants at birth is about 0.2. The ratio may fall slightly in the first few days but generally it remains the same for the first six months. Since the concentration of Ca in the dry fat-free bone falls during this time, the concentration of Sr must also fall. Then from about six months of age the Sr/Ca ratio begins to rise steeply towards the adult level of about 0.33. The concentration of Sr in serum, is lower on the fetal (0.075 μg/ml) than on the maternal side (0.095) of the placenta at birth. Strontium is transferred atom for atom much less readily than Ca across many biological membrane systems, including the placenta. Meconium contains about as much Mg and Ca in terms of actual weight, a higher Ca/P ratio than bone, and unexpectedly high amounts of Sr. Gradual pile up of Sr in the meconium is the final result of the preferential transmission of Ca across all the biological membranes involved in the maintenance of the mother and the fetus. This is referred to as the discrimination of the organism in favor of Ca and against Sr. Movement of Ca and Sr about the body is considered in terms of their relative rates of transmission across biological membranes and the effect that this has on their over-all metabolism. Calcium appears to be absorbed preferentially, by active transport, in the duodenum of the rat and to be deposited preferentially in bone. The renal clearance of Sr is also three to five times that of Ca, presumably because of preferential reabsorption of Ca in the tubules. Calcium is also preferentially excreted in milk. All these findings show that the developing offspring retains less Sr than a consideration of the ratio of Ca and Sr in its diet and even more in the diet of its mother indicates. (BBB)

43702 RADIAL EXCHANGE OF LABELED WATER IN INTACT MAIZE ROOTS. Woolley, Joseph T. (Univ. of Illinois, Urbana). Plant Physiol., 40: 711-17(July 1965).

Equilibration of maize (Zea mays) roots with tritiated water was compared with theoretical curves for the single cell, sheet, cylinder, and sphere, and was found to follow the cylinder curve. This was interpreted to indicate that the epidermis does not constitute a barrier to the entrance of water. The stele was removed from roots after treatment with tritiated water, and the equilibration of the stele was compared with that of the cortex. This equilibration was not greatly different from the theoretical equilibration to be expected of uniform tissue. It was concluded that the endodermis did not constitute a barrier to the diffusion of water. The apparent diffusion coefficient (D) of tritiated water in maize root at 25° was 5×10^{-6} cm^2 sec^{-1}. D was decreased by metabolic inhibitors, or low-temperature treatment, but it remained unchanged with treatment by dimethyl sulfoxide or 2,4-dichlorophenoxyacetic acid. D increased about 3-fold when the roots were killed with hot water. D for tritiated water in the normal root (~500 μ^2 sec^{-1}) is about one-fifth of the diffusion coefficient of tritiated water in water. If all water movement were confined to the cell walls, these walls would have to occupy about 20% of the root volume for such rapid diffusion to occur, yet the cell walls actually occupy between 3 and 6% of the root volume, estimated microscopically on hand-cut sections. Thus at least 70% of the water movement must involve the cytoplasm in some way. (BBB)

43703 FORCES INVOLVED IN RETENTION AND MOVEMENT OF NON-METABOLIC STRONTIUM IN PHASEOLUS VULGARIS. Emmert, Fred H. (Univ. of Connecticut, Storrs). Plant Soil, 22: 136-42(Feb. 1965).

Investigation was made of nonmetabolic deposition of Sr in the tops of bean plants. Attention was confined to the nonmetabolic fraction since it is believed that upward movement of ions primarily involves this fraction. Uptake solutions accordingly contained 2,4-dinitrophenol (DNP) as a metabolic inhibitor. Root influences were avoided by severing the roots from the plants, and allowing direct access of solution into the stem. Test solutions contained 10^{-3}M DNP, and sufficient $^{89}SrCl_2$ to yield ca 30 cpm/ml after evaporation. Carrier level was 1.0 ppM Sr. Stems of test plants were found to contain an efficient trapping mechanism for nonmetabolic Sr, as shown by buildup of ^{89}Sr for severed plants in which hypocotyls were reduced to various lengths. In all cases, the bulk of radiostrontium was immobilized in the most basal segment of the stem. Only small amounts of it remained in the ascending stream for transport and deposition farther along the plant length. An isotherm was developed for Sr buildup in the hypocotyl-1 sample, indicating that Sr buildup conformed closely to the

Freundlich gas equation. The reversibility of the Sr binding process was investigated with several plants placed in the ^{89}Sr solution 12 hr and then checked for isotope content. Other plants were similarly exposed to the radiosolution, but were then removed to a stable Sr or to water for an additional 12 hr before being checked for radioactivity. No significant change in ^{89}Sr occurred in samples exposed to pure solvent; however, when stable Sr was introduced, an overall shift in an acropetal direction occurred in ^{89}Sr distribution throughout the plant. It is suggested that Sr binding involved electrostatic adsorption to charged sites along the route of upward movement. (BBB)

43704 ^{131}I UPTAKE IN RADIOTHYROIDECTOMIZED CHICKS. Siegel, H. S. (U. S. Dept. of Agriculture Southeastern Poultry Research Lab., Athens, Ga.); Mraz, F. R. Poultry Sci., 44: 785-8(May 1965).

Observations were made on the relation of level and age at the time of initial ^{131}I treatment on subsequent uptake of iodine by the thyroids, muscle, and blood plasma. Single Comb White Leghorns were given varying doses of carrier-free ^{131}I, either as embryos or at one or 14 days posthatch age. The ^{131}I was placed on the inner shell membrane in the embryos or intramuscularly after hatching. At 14 weeks of age, 79 male survivors were given intramuscular injections of 100 μC of carrier-free ^{131}I and after 48 hr ^{131}I content of muscle, plasma, and thyroid was determined. The effects of ionizing radiation from ^{131}I on the thyroid of the embryo and the subsequent effects on other tissues appeared to be age dependent. Reduced thyroid activity, as measured by ability to concentrate iodine, was found at all embryonic ages studied (8 to 16 days) in birds receiving 50 μC per embryo, but only at 16 days in those receiving the 5-μC dosage. In general, as thyroid uptake of ^{131}I decreased, plasma content increased. At one day posthatch, intramuscular doses of as low as 50 μC ^{131}I were sufficient to radically reduce iodine uptake by the thyroid and reduce body weights. Although iodine uptake by the thyroid was significantly reduced by 100- to 200-μC treatments at 14 days of age, body weight depression was not observed until 400 μC was administered. Muscle and plasma uptakes were again generally increased by previous treatment with ^{131}I. The embryo data are compatible with earlier reports that thyroids of chick embryos begin to concentrate significant amounts of ^{131}I by the eighth day. (TCO)

43705 IN VITRO STUDIES OF THE INTERACTIONS OF PuIV WITH BLOOD PROTEINS. Stevens, Walter; Bruenger, Friedrich W.; Stover, Betsy J. (Univ. of Utah, Salt Lake City). Radiation Res., 26: 114-23(Sept. 1965).

The binding of Pu(IV) to bovine albumin, canine α-, β-, and γ-globulin, and blood cells and plasma proteins of beagle hounds was studied in vitro. Basically, all those proteins tested are capable of interacting with PuIV in vitro. Blood cells exhibited a low affinity for Pu(IV). There was no penetration of Pu(IV) through cell membranes, although isolated hemoglobin was able to bind Pu(IV). In plasma, Pu(IV) was associated primarily with the low-molecular-weight proteins consisting of albumin and a globulin, and to a lesser extent with constituents having a molecular weight greater than 200,000. (auth)

43706 IN VIVO AND IN VITRO EXPERIMENTS ON ELIMINATION OF RADIOACTIVE STRONTIUM DEPOSITED IN BONE. Ogawa, Eiichi; Suzuki, Shiro; Tsuzuki, Hiroshi (Gunma Univ., Japan). Radioisotopes (Tokyo), 14: 422-7 (Sept. 1965).

Mice were preliminarily injected with ^{85}Sr and sacrificed after a given time, the femurs were taken out, placed in test tubes and their radioactivity (A_1) was determined in a well-type scintillation counter. Then the femurs were incubated in various media with or without addition of drug, and after a given time, the radioactivity of the medium (A_2) was determined. ^{85}Sr elution rate (%) was computed by $A_2/A_1 \times 100$, and using this the affinity of ^{85}Sr with bone was assessed. Further, effects of various drugs — chelating agents and salts — on elution of ^{85}Sr were investigated. (auth)

43707 THE USE OF ISOTOPES IN PHYSIOLOGICAL CHEMISTRY. Rotzsch, Wolfgang (Karl-Marx-Universitaet, Leipzig). Wiss. Z. Karl-Marx-Univ. Leipzig Math.-Naturw. Reihe, 13: 133-5(1964). (In German).

A table of the stable and radioactive isotopes of the most important elements in biology, with their relative abundances, modes of decomposition, and half lives, — H, C, N, and O — is given. Several of the most useful experiments using radioisotopes are described. The use of ^{131}I in diagnosis of thyroid conditions is described, with note drawn to the distinct iodine metabolism of different species. The determination of biological half lives using isotopic compounds is described; rates of incorporation in embryos and homogenates are compared. The biosynthesis of cholesterol and radiochemical studies of this problem are also mentioned. The amount of trimethylamine and trimethylamine oxide excreted in the urine of the rabbit after peroral dosage is reported; trimethylamine is oxidized to the oxide so that very little free amine is excreted. Use of ^{15}N permits determination of the % of trimethylamine and oxide immediately excreted; on the first 3 days the amount of ^{15}N compounds is 31.5%, 1.1%, and 0.5% of the total N in the amine and the oxide. Labeled betaines are used to study the incorporation of decomposition products in the trimethylamine yield excreted. (BBB)

43708 THE CATALYTIC EFFECT OF THORIUM AND ZIRCONIUM IONS ON THE HYDROLYSIS OF NUCLEOTIDES. Trapmann, Heina; Devani, Muljibhai (Universitaet, Munich). Z. Physiol. Chem., 340: 81-5(1965). (In German).

Thorium and Zr are known to have profound biological effects. Their toxicity can be related to their deposition in certain organs, and to damage to carbohydrate metabolism and other metabolic systems. Data are presented to show that they may affect nucleic acid metabolism. RNA and DNA are dephosphorylated in alkaline medium by Th ions; Zr ions have no measureable activity in this regard. In alkaline medium, in the presence of Th ions, RNA is dephosphorylated more rapidly than DNA. The 3′-nucleotides of adenosine, guanosine, cytidine, and uridine (AMP, GMP, CMP, and UMP) are dephosphorylated by Th and Zr ions, in alkaline and acidic media, much more rapidly than the polynucleotides RNA and DNA. Thorium ions are more active than Zr ions in this effect. The rates of hydrolysis of mononucleotides by Th ions in alkaline medium decrease in the order: AMP > CMP > UMP > GMP; this also applies to an acidic medium after a reaction time of 24 hr. After 6 hr in acid medium the order is: AMP > UMP > CMP > GMP. The more rapid hydrolysis of RNA as compared with DNA may be related to the presence of the OH group on the former. (BBB)

43709 MACROMOLECULE SYNTHESIS IN DEVELOPING SEA URCHIN EGGS. THE EFFECT OF ACTINOMYCIN D AND DEUTERIUM OXIDE (thesis). Cousineau, Gilles Herve. Providence, Brown Univ., 1964. 90p.

The effect of Actinomycin D and deuterium oxide on developing sea urchin eggs was observed. Embryos treated with Actinomycin D showed cell divisions for many hours although the division rates decrease with increasing concentrations of the antibiotic. Fertilized eggs treated with this drug did not differentiate normally. Even with low concentrations of the antibiotic, incorporation of ^{14}C-uracil into RNA was totally suppressed before the blastula stage. DNA synthesis was slightly depressed, the lower rates of thymidine incorporation being due in part to slower cleavage rates. Incorporation of amino acids into protein was not affected by concentrations of actinomycin sufficient to shut down RNA synthesis. Deuteration of fertilized sea urchin eggs produced usefully variant effects, i.e., abrupt switching off of DNA synthesis, depression of RNA turnover, and maintenance of active protein synthesis. Autoradiographic data show that the precursors used to label RNA, DNA, and protein do label these polymers and are incorporated intracellularly. The autoradiograms confirm qualitatively all the ^{14}C-labeling data. (Dissertation Abstr.)

Radiation Effects

Refer also to abstract 44315.

43710 (ABCC-16-64) ACTIVE TUBERCULOSIS IN MALIGNANT DISEASE OF RETICULOENDOTHELIAL ORIGIN, HIROSHIMA, 1949–62. Morrow, Lewis B.; Anderson, Robert E. (Atomic Bomb Casualty Commission, Hiroshima (Japan)). [June 18, 1964]. Contract [AT(49-1)-Gen-72]. 19p. Dep. mn; CFSTI $1.00 cy, $0.50 mn.

The present study demonstrated an increased prevalence of active disseminated tuberculosis in cases of chronic myelogenous leukemia and myelofibrosis autopsied at the Atomic Bomb Casualty Commission during 1949 to 62. No such increase was found in association with acute leukemia or malignant lymphoma. The prevalence of disseminated tuberculosis among the myeloproliferative disorders was directly proportional to the estimated duration of symptoms of the primary hematologic disease and, with the possible exception of therapeutic x ray, was little influenced by antileukemic therapy. There appeared to be no increase in tuberculosis in association with previous steroid or antimetabolite administration; the relationship with alkylating agents was equivocal. Cases of chronic myelogenous leukemia arising in persons within 1400 m of the atomic explosion showed a significantly increased prevalence of disseminated tuberculosis in comparison with cases at 1400 to 9999 m. The implications of the data are discussed in relation to the pathogenesis of tuberculosis in the myeloproliferative disorders. (auth)

43711 (BNL-924) RADIATION AND THE PATTERNS OF NATURE. Woodwell, George M. (Brookhaven National Lab., Upton, N. Y.). Mar. 24, 1965. Contract AT(30-2)-Gen-16. 18p. Dep. mn; CFSTI $1.00 cy, $0.50 mn.

Brookhaven Lecture Series No. 45.

The patterns of radiation effects on natural plant communities are described and the way in which they parallel and help explain the normal patterns of structure, function, and development of these communities is discussed. It is pointed out that most life as we know it has evolved in environments where the total exposures to ionizing radiation have been less than a few tenths of a R per year. Results are reported from two experiments in which an old field and a forest were exposed to γ radiation doses ranging from several thousand R/day within a few meters of the source to near background levels at distances of about 300 m and the zonation of vegetation followed over a 4-yr period. Irradiation produced striking changes in the communities of the early successional stages. Irradiation at 1000 R/day reduced diversity to about 50% that of a non-irradiated field about 2 km distant. The decline in diversity was continuous along the radiation gradient and not marked by any abrupt decline indicating exclusion of several species in a narrow range of exposure rates, but certain species survived exposures of about 2000 R/day. Plants that persisted at high radiation levels were those that grew close to the ground and have small chromosome size. Thus the first year of succession was characterized by a loose array of herbaceous plants, mostly annuals or biennials, of varying life forms and physiologies. It is pointed out that the primary effect of extreme environments, including irradiation, is reduction of diversity. In the case of radiation, the reduction is continuous along the radiation gradient and not characterized by the simultaneous exclusion of more closely associated species. The irradiated forest showed five zones apparent along the radiation gradient including a central zone in which no higher plants survived, a sedge zone containing a few sprouts of the heath-shrub layer, a shrub zone where both blueberries and huckleberries survived, an oak forest zone at exposures below about 40 R/day, and the oak-pine forest in which radiation effects on growth were apparent but there was no change in species composition. The zonation of vegetation reflected the decline in diversity along the gradient, and in contrast to the old field, standing crop in the forest declined at approximately the same rate as diversity. No higher plant indigenous to the forest survived exposure to about 350 R/day in the first year and the 50% diversity point occurred at about 160 R/day. The forest unit as a whole was substantially more radiosensitive than the herb field. (C.H.)

43712 (BNL-9383) RELATIVE BIOLOGICAL EFFECTIVENESS OF DIFFERENT TYPES OF IONIZING RADIATIONS: CYTOGENETIC EFFECTS IN MAIZE. Smith, Harold H. (Brookhaven National Lab., Upton, N. Y.). [1965]. Contract AT-30-2-GEN-16. 4p. (CONF-650814-1). Dep. mn; CFSTI $1.00 cy, $0.50 mn.

From Symposium on Mutational Process, Prague.

The frequency of yg_2 events in leaves grown from irradiated Yg_2/yg_2 maize seeds shows a linear response to dose. Compared with 250 kvp x rays, the approximate relative biological effectiveness (RBE) of monoenergetic neutrons (0.43 to 14.7 Mev) is between 50 and 100, of muons (7 Bev) 0.76, of π^- mesons (8 Bev) 3.2, and of protons (28 Bev) 4.4. These results were considered in terms of dose average linear energy transfer (LET) and whether or not nuclear interactions take place. Application of microdosimetric concepts to this system indicates that the interphase chromosome is broken, to cause a yg_2 event, when a charged particle delivers an energy of approximately 93 kev to a spherical region of the cell nucleus that is approximately 1 micron in diameter but proportional to nuclear size. (auth)

43713 (BNWL-115) A SELECTED LIST OF REFERENCES (1960–MAY 1965) ON SWINE IN BIOMEDICAL RESEARCH. Pekas, J. C.; Bustad, L. K. (Battelle-Northwest, Richland, Wash. Pacific Northwest Lab.). June 1965. Contract AT(45-1)-1830. 145p. Dep. mn; CFSTI $5.00 cy, $1.00 mn.

This bibliography consists of 1509 references on the use of swine in biological and medical research. These references are for articles published in the literature between 1960 and 1965. Author and cross-subject indexes are included. (auth)

43714 (EUR-2438.f) RECHERCHE SUR L'ETUDE DES EFFETS DES RADIATIONS SUR LES FONCTIONS ET L'EQUIPEMENT ENZYMATIQUE DES PLAQUETTES. Rapport Annuel 1963/64. (Research Relating to the Study of Radiation Effects on the Functions and Enzymatic Potential of Platelets. Annual Report, 1963/64). Caen, J. (Association Claude Bernard, Paris (France)). June 1965. 20p. Dep. mn.

After exposure of platelet-rich citrated plasma to x ray doses varying from 50 to 800 R, the following results were obtained: no change in the number of platelets; a few morphological alterations in 2 to 10% of the cells, even after a 50 R dose; the total adhesion of platelets to the glass was retarded; spontaneous platelet aggregation was increased; in the presence of extrinsic ADP, aggregation of the platelets was reduced; and thrombin-treated irradiated platelets released less ADP than non-irradiated platelets. It was concluded that irradiation activates the platelet ATPases, releases intrinsic ADP, and causes spontaneous hyperaggregability; the cells thus damaged by x rays are less sensitive to extrinsic ADP; and they are also less sensitive to thrombin, which normally releases intrinsic ADP, which is found to a less extent after irradiation. (auth)

43715 (HW-SA-3747) DIFFERENTIAL RESPONSES OF GERM CELLS IN FLOUR BEETLES, TRIBOLIUM CASTANEUM HERBST, DUE TO X-RAY DOSE, HYPOTHERMIA, SEX-EXPOSED AND AGE. Erdman, Howard E. (General Electric Co., Richland, Wash. Hanford Atomic Products Operation). [Oct. 12, 1964]. Contract AT(45-1)-1350. 21p. Dep. mn; CFSTI $1.00 cy, $0.50 mn.

Day-old virgin flour beetles, Tribolium castaneum, were x-irradiated with 0, 500, 1,000, 2,000, and 4,000 R. Ten replicates of control, male-, female-, and both-exposed mating combinations were established at 25, 29, and 32°C in 65 to 70 percent relative humidity. Each pair was given

5 g of acclimated food daily for two weeks. The number of fertile pairs and the number of F_1 adults were measured on the day of reproductive onset. Reproductive onset was delayed two to three days in females given 4000 R x-ray doses, but no delay was observed in exposed males. For both-exposed, a progressive delay was induced by 2,000 or 4,000 R. For male- or female-exposed groups irradiated from 29 to 32°C, no modification in reproductive onset was found, but a delay was evident at lower temperatures. The 2,000 or 4,000 R exposures and decreased temperatures synergistically delayed reproductive onset for both-exposed pairs. The number of fertile pairs after 4,000 R were reduced in female-exposed groups more than in male-exposed groups. A saturation effect in both-exposed combinations at 29°C was indicated. X-ray doses of 2,000 R and higher reduced productivity. Males were more productive after 4,000 R than were females. Viability or lethality effects were additive when both sexes of mating combinations were exposed to 2,000 or 4,000 R. The modifications of the three parameters investigated for productivity are discussed from the standpoints of temperature effects, and dose effects on the degree of development, and differentiation of male and female germ cells. The dose-response curves were the multi-hit type, implicating chromosomal aberrations as the cause of altered productivity. (H.S.D.)

43716 (HW-SA-3748) REPRODUCTIVE PERFORMANCE OF X-RAYED SINGLE-SPECIES AND MIXED-SPECIES CULTURES OF TRIBOLIUM CONFUSUM AND T. CASTANEUM REARED AT DIFFERENT TEMPERATURES. **Erdman, Howard E. (General Electric Co., Richland, Wash. Hanford Atomic Products Operation).** [1964]. Contract AT(43-1)-1350. 20p. Dep. mn; CFSTI $1.00 cy, $0.50 mn.

Adult flour beetles, T. confusum and T. castaneum, sexed as pupae and maintained separately for three weeks after adult emergence, were given 0, 1575, or 2625 R of x rays. Single- and mixed-species populations were established and incubated at 25, 29, or 32°C at 65 to 70% relative humidity. Productivity was determined during 10 weeks post-irradiation. Reproductive abilities increased with increased temperature and decreased with increased x-ray exposure for a given temperature. The reproductive fitness of Tribolium castaneum was superior in all environments except at 0 R, 32°C. The frequencies of dominant lethals (which included lethality due to coexistence in mixed-species populations) increased with higher x-ray doses, but temperature and cohabitation influenced their expression within a species. Coexistence was responsible for a considerable reduction of productivity, which was also altered by temperature and x radiation. The rigors of coexistence were lessened at 2625 R exposures (undoubtedly due to reduced population density). Interpretations of dose-response curves on the bases of single-hit and multi-hit radiation phenomena were inferred from similar responses of diverse organisms. Most lethality occurred in the early (eggs to young larvae) part of the life cycle for both species. Species proportions in coexistent populations varied with temperature and x radiation but T. castaneum was consistently superior compared to T. confusum. The greater variability of T. castaneum probably makes it more fit in environments featuring different temperatures and x-radiation exposures plus coexistence. Responses to radiation of single-species populations cannot be used to predict those of mixed-species populations. (auth)

43717 (NASA-CR-303) EFFECT OF WEIGHTLESSNESS AND RADIATION ON THE GROWTH OF THE WHEAT COLEOPTILE FOR THE PURPOSE OF DEFINING AND VERIFYING AN EXPERIMENT SUITABLE FOR USE IN A BIOSATELLITE. **Grey, Stephen; Edwards, Betty F. (Emory Univ., Atlanta, Ga.).** Sept. 1965. 63p. Dep. mn; CFSTI $3.00 cy, $0.75 mn.

The characteristic orientation of the majority of plants is a response to gravity. Almost nothing is known about the response of any living organism to gravitational forces at less than normal gravity. Background experiments are described that were performed in anticipation of studies of the effects of weightlessness and radiation on the growth of wheat seedlings while orbiting the earth in a satellite. The seedlings of Triticum vulgare, a hexaploid hybrid with a chromosome number of 42, were used. The substrate and seed container and methods used for growing seeds, and methods used for fixation of tissues for microscopic study are described. The effects of centrifugation, temperature, and x radiation doses up to 160,000 R plus centrifugation, on growth of both the coleoptile and root of the seedlings were measured. (47 references.) (C.H.)

43718 (NASA-SP-7011(12)) AEROSPACE MEDICINE AND BIOLOGY. A Continuing Bibliography. (National Aeronautics and Space Administration, Washington, D. C. Scientific and Technical Information Div.). June 1965. 107p. CFSTI $1.00 cy, $0.75 mn.

A selection is presented of 335 references to unclassified reports and journal articles introduced into the NASA Information System during May, 1965. The references cover biological, physiological, and environmental effects of space flight in man and related studies in experimental animals. Author, corporate source, and subject indexes are included. (C.H.)

43719 (NASA-SP-7011(13)) AEROSPACE MEDICINE AND BIOLOGY. A Continuing Bibliography. (National Aeronautics and Space Administration, Washington, D. C.). July 1965. 136p. CFSTI $1.00 cy, $1.00 mn.

A selection is presented of 431 references to unclassified reports and journal articles introduced into the NASA Information System during June, 1965. The references cover biological, physiological, psychological, and environmental effects of space flight in man and related studies in experimental animals. Author, corporate source, and subject indexes are included. (C.H.)

43720 (NP-15310, pp 26-35) THE INHIBITORY EFFECT OF X-RADIATION ON THE DEVELOPMENT OF N-DEMETHYLASE ACTIVITY IN THE LIVERS OF YOUNG, MALE RATS. **DuBois, Kenneth P.; Kinoshita, Florence (USAF Radiation Lab., Univ. of Chicago, Ill.).**

A study was carried out to improve the available method for measuring the N-demethylase activity of the livers of rats. A modification of the existing method was developed which constituted a valid, quantitative enzyme assay and was somewhat simplified to facilitate analysis of livers from irradiated animals. The N-demethylase activity of the livers of normal rats was measured and it was found that the activity of the livers of adult males was 4 to 5 times the level in the livers of adult females and weanling males. Weanling male rats (22 days old) were exposed to 400 R and the rate of enzyme development was followed. X irradiation retarded the rate of development of this enzyme system thus providing the same type of effect as was obtained previously in studies on the microsomal desulfuration enzyme and EPN detoxification. (auth)

43721 (ORNL-TM-1217) THE ORNL SPACE BIOLOGY PROGRAM ANNUAL REPORT [FOR] PERIOD ENDING JUNE 30, 1965. **Stapleton, G. E.; Darden, E. B. Jr. (Oak Ridge National Lab., Tenn.).** Sept. 1965. Contract W-7405-eng-26. 19p. Dep. mn; CFSTI $1.00 cy, $0.50 mn.

Work performed in the AEC-NASA Space Biology Program is described. At present the general space radiobiology program supports chiefly high-energy proton studies on several mammalian systems, including cataractagenesis, shortening of life span, and acute lethality. Development of the Oak Ridge Isochronous Cyclotron facility, pertinent dosimetry, and results to date are reported. Results obtained in mock-up experiments in preparation for the Biosatellite A Project are also reported. Participation in the Gemini IV experiment are not covered in this report. (auth)

43722 (TID-22108) EFFECT OF IONIZING RADIATION ON FOREST TREES. ITS GENETIC AND CYTOLOGICAL IMPLICATIONS. Technical Progress Report.

Mergen, Francois (Yale Univ., New Haven, Conn. School of Forestry). July 6, 1965. Contract AT(30-1)-2755. 18p. Dep. mn; CFSTI $1.00 cy, $0.50 mn.

The effects of ionizing radiation on reproductive processes and survival were studied in Pinus rigida and Quercus spp. Progress is reported on studies of low-level chronic gamma radiation on a pitch pine-oak forest (Pinus rigida and Quercus alba); effects of low-level chronic gamma irradiation on a red pine plantation (Pinus resinosa); determination of permanency of radiation damage (Quercus alba and Quercus coccinea); effects of gamma radiation on morphology and cytology of seedlings and on seed production and microsporogenesis in Pinus rigida; and effects of gamma irradiation on Pinus and Quercus germination and seedling growth. (H.G.D.)

43723 (TID-22128) THE EFFECTS OF RADIATIONS ON BIOLOGICAL MOLECULES AND ON CELLS IN TISSUE CULTURE. Annual Progress Report, 1964. (Yale Univ., New Haven, Conn.). Contract AT(30-1)-2653. 18p. Dep. mn; CFSTI $1.00 cy, $0.50 mn.

Progress is reported in studies on the electron spin resonance spectra of x irradiated DNA; the radiosensitivity of mammalian cells in tissue culture, with emphasis on high LET radiations such as accelerated He, Li, B, and C ions, and the identification of a strain of Bacillus subtilis DNA that has an uneven distribution of thymine in the two complementary strands. A list is included of papers published during the period covered by this report. (C.H.)

43724 (TID-22160) THE INFLUENCE OF RADIATION IN ALTERING THE INCIDENCE OF MUTATIONS IN DROSOPHILA. Report on the Terminal Period, 1963-June 30, 1964. Muller, H. J. (Indiana Univ. Foundation, Research Div., Bloomington, Ind.). Aug. 1965. Contract AT(11-1)-195. 8p. Dep. mn; CFSTI $1.00 cy, $0.50 mn.

Progress is reported on the effectiveness of acute vs. chronic exposure to ionizing radiation in producing gene mutations in Drosophila oogonia, the criterion of effect being the frequency of sex-linked lethals. Precisely equal doses of acute and chronic irradiation were attained by using given concentrations of $^{137}CsCl$. When allowances were made for errors, the more highly concentrated solution that delivered a total of about 200 R, resulted in a frequency of sex-linked lethals induced in the oogonia about 1.45 times as high per R. The errors of the sperm-corrected oogonial frequencies obtained at the two widely differing dose-rates were so large that the difference between them was somewhat less than the standard error of that difference. Acute x-ray treatments at 240,000 R/m, proved to have a mutogenicity for oogonia virtually identical with that of the 2.1% for the 4000 R found previously. Mutation frequencies were also determined among ring X-chromosomes in young males from ejaculations into successive females. Results indicated that: sperm fully mature at irradiation were more radiosensitive; when earlier ejaculations were prevented, later ones consisted of sperm mixed in maturity at time of irradiation; when a fertile male failed to utilize the opportunity to ejaculate during the first one or two half-days, it was usually because he did not yet contain enough sperm that were fully mature at the time of irradiation; and no evidence remained for recovery from gene-mutagenesis, or even for structural changes, in sperm when they were held over within Drosophila males. (H.G.D.)

43725 (UCD-472-112, pp 44-9) HEMATOLOGY REPORT. Andersen, A. C.; Gee, W. (California Univ., Davis. School of Veterinary Medicine).

A hematology program is reported to conduct 60-day blood counts on the 585 Beagles. Methods and materials for obtaining and handling these data are described. D4 and D5 ingested ^{90}Sr dose levels continue to show depressed leukocyte values for some 1½ years after treatment stopped. No decrease in erythrocytic elements or thrombocytes was observed in Beagles ^{90}Sr fed to 540 days of age. (auth)

43726 (UCD-472-112, pp 120-5) SKELETAL DOSIMETRY AND THE EXPOSURE STATUS OF THE COLONY. Powell, T. J.; Goldman, M. (California Univ., Davis. School of Veterinary Medicine).

A computational model is presented for evaluating the average skeletal radiation exposure status of a colony of Beagles subject to chronic Sr-90 exposure. Some consideration is given to the accuracy and limitations of the model when applied to an individual dog. The exposure status of the colony is given and, when related to that of several dogs exhibiting radiation pathology, it appears that knowledge of the dose alone is not sufficient to completely assess the radiation risk. Finally, a proposed measure of relative radiation risk is presented. (auth)

43727 (UCD-472-112, pp 126-40) PATHOLOGY REPORT. Andersen, A. C.; McKelvie, D. H. (California Univ., Davis. School of Veterinary Medicine).

During the past year, 158 pre-weaned, post-weaned, and sacrificed (culled) dogs were autopsied. Eighty-two percent of the deaths were pre-weaned with no detectable lesions found in most of the neonatal losses. One case of soft tissue neoplasm (lymphosarcoma) in the highest ^{90}Sr ingestion level caused death at 827 days of age. One case of highly malignant carcinoma of undetermined origin was detected in a 52 day old pup. Evidence of non-fatal pathology was found in about one-third of the experimental Beagles culled on a random basis. (auth)

43728 (UCLA-12-565, pp 59-64) PHARMACOLOGY AND TOXICOLOGY. (California Univ., Los Angeles. Lab. of Nuclear Medicine and Radiation Biology).

Progress is reported in investigations of papaverine derivatives effects on uridine diphosphate spasmogenic actions, pharmacology and toxicology of the rare earth elements, antagonism of uridine diphosphate spasmogenic effects by 3-methylisoquinoline compounds, pharmacology and toxicology of Dy, Ho, and Er chlorides, properties of three indoyl-ethyl-piperazine, adsorption of tryptophan from irradiated rat intestine, and l'methionine functions in irradiated rat intestine. Design of a rat metabolism cage is described. (J.R.D.)

43729 (BNL-tr-12) THE RATE OF SPONTANEOUS AND RADIATION INDUCED CHROMOSOME RE-ARRANGEMENTS IN THE MEDULLA OSSIUM OF MICE OF DIFFERENT AGE. Bocharov, Yu. S.; Savitsky, V. F. (Gosudarstvennyi Komitet po Ispol'zovaniyu Atomnoi Energii SSSR, Moscow. Institut Teoreticheskoi Eksperimental'noi Fiziki). Translated by S. Amoretty (Brookhaven National Lab., Upton, N. Y.). 6p. Dep. mn; CFSTI $1.00 cy, $0.50 mn; JCL $1.10 fs, $0.80 mf.

Male BALB mice of three different ages (the newborn, 2 months, or 10 months) were given 100 rad x-ray doses. Chromosomal aberrations were determined in anaphase or early telophase cells from the medulla ossium or thigh bone. The spontaneous chromosome aberration rate in the medulla ossium cells of mice decreased from birth until the period of puberty and then began to increase again until the tenth month. Changes in the rate of the induced chromosome aberrations occurring after 100 R x-ray doses corresponded to the changes in the rate of the spontaneous aberrations. The observed changes in the percentage of chromosome aberrations were dependent on the difference in their formation rate and had no connection with the process of cell selection. In the ontogenesis of animals, a period of maximal cytogenetical stability of cells exists which corresponds in mammals to the pubescent period. (H.G.D.)

43730 MORPHOGENESIS OF BINUCLEATED ERYTHROPOIETIC CELLS BY THE ACTION OF X RAYS. Rondanelli, G.; Trenta, A.; Magliulo, E.; Vannini, V.; Gerna, G. (Universita, Pavia, Italy). Acta Haematol., 33: 97-109 (1965). (In French).

The formation of binucleated cells has been explained by three mechanisms: (1) amitosis, (2) fusion of two cells, or (3) mitotic arrest. The mechanism of formation of these cells with two nuclei was investigated by morpho-

genetic studies in in vitro experiments on hematopoietic cells exposed to low doses of x rays. Thus basophilic and polychromatophilic erythroblasts of the triton (Molge vulgaris) were irradiated with 12- to 25-R doses of x rays and studied by phase-contrast microphotography and microcinematography. Analysis of the results showed that in irradiated hematopoietic tissue the formation of iso- and aniso-binucleated erythropoietic cells is caused by the failure of cytoplasm to divide and separate daughter nuclei reconstituted by the chromosomes of bi-pluri-centric metaphases and bi-pluri-polar anatelophases. The size of the two nuclei, and the resulting iso- or aniso-nuclearity, is correlated with the number of chromosomes from which each nucleus was reconstituted. Binucleated cells may also result by fusion of the cytoplasm of two neighboring cells previously issuing from a noraml mitosis. Intrinsic mechanisms of the formation of binucleated cells are discussed. Although binucleated cells have been reported to undergo mitosis, in the present experiments this was never observed. Since it is essential that the spindle be completely intact for this to occur, it is possible that x irradiation caused preprophase inhibition in the binucleated cells. (BBB)

43731 METHOD OF ^{3}H-THYMIDINE INCORPORATION IN FRACTIONALLY IRRADIATED BONE MARROW. **Chone, B. (Universitaet, Heidelberg). Acta Haematol., 33: 220-9(Apr. 1965). (In German).**

Comparative study of bone marrow preparations labeled with ^{3}H-thymidine after fractionated partial γ irradiation showed characteristic differences in marking between erythropoiesis and myelopoiesis. The functional cellular impairment resulting from an average single effective dose of 200 to 300 R to the marrow affects erythropoiesis primarily; this is probably due, apart from the increased radiosensitivity on account of the high rate of proliferation, to the particular radiation interval. The undifferentiated matrix represented by reticulum cells is highly resistant to radiation in its reserve of functional capacity. (tr-auth)

43732 STUDIES IN INDUCED MUTATIONS IN PEAS. VI. MUTATIONS IN SEED COLOUR, FLOWER COLOUR, MACULUM COLOUR, POD COLOUR, AND GREY SPOTTING OF LEAVES. **Blixt, Stig (Weibullsholm Plant Breeding Inst., Landskrona, Sweden). Acta Hort. Genet., 20: 95-100(1962).**

A compilation of mutations that have been produced in peas by ionizing radiation and other agents is presented. (BBB)

43733 TOTAL DOSE AND SOME POSTIRRADIATION REACTIONS AT THE CELLULAR LEVEL. **Rudnicki, Tadeusz. Acta Physiol. Polon., 16: 427-33(1965). (In Polish).**

Mitotic activity and structural chromosomal changes in bone marrow cells of the rat due to integral dose were investigated. Integral dose and primary injury at the cellular level were not found to be correlated. The integral dose can only affect the restoration processes after irradiation. (auth)

43734 QUANTITATIVE STUDIES OF INDUCED MUTATIONS IN PEAS. V. CHLOROPHYLL MUTATIONS. **Blixt, Stig (Weibullsholm Plant Breeding Inst., Landskrona, Sweden). Agri. Hort. Genet., 19: 402-47(1961).**

The occurrence of spontaneous as well as induced chlorophyll mutations in peas is reviewed, and nomenclature for chlorophyll mutation types is presented. A list of chlorophyll mutations observed in peas is presented. Different factors influencing the manifestation of chlorophyll deficiencies are considered. Specific mutations, induced by ethyleneimine (EI), ethyleneoxide (EO), N-mustard (M), oxygen (0), neutrons (N), and x rays (R) are listed and discussed. In the Weitor variety, the only one tested with all mutagenic agents, there is no significant difference between mutation cases induced by R, N, or O, nor is the difference between EO- and EI-induced cases significant. In comparing on the one hand R-, N-, and O-induced cases with EI- and EO-induced cases on the other, the difference is seen to be significant. The mean percentage of homozygous recessives obtained for the R-N-O group is 11.57 and for the EI-EO group, 21.21. In the chlorina-type mutation the deficit of homozygous recessives is not of the same magnitude as in the xantha type. If differences exist between varieties or between mutagenic agents used, they are too small to permit statistical evaluation. In the chlorotica type there is a clear difference between the R- and N-induced mutations (19.85% homozygous recessives) on the one hand and EI-, EO-, and O-induced cases, (25.00% homozygous recessives) on the other. A discussion is also given of the possibilities of distinguishing mutations occurring in X_2 from mutations occurring in X_1 but not detected before X_3. Results from irradiation treatments, based entirely on X_2 data, may offer considerable uncertainty. At present, X_3 analysis is therefore required for the correct classification of these mutation types. When only one deviate appears in a large progeny, which is frequent at lower doses of x rays or neutrons, so many plants must be carried on to X_3 to have a reasonable probability of obtaining a segregating family. This involves so many plants that serious problems for the practical handling of the material arise. (BBB)

43735 RESPONSE OF THE LIVER TO TARGET IRRADIATION. **de Mignard, Valentin A.; Patek, Paul R.; Bernick, Sol (Univ. of Southern California, Los Angeles). Am. J. Pathol., 47: 339-51(Sept. 1965).**

A modified technical approach to the study of the effects of irradiation was demonstrated. Correlative morphologic observations using cytologic and histochemical techniques were made on the livers of rats after sublethal target x irradiation. The central portion of the liver received 100 per cent irradiation dosage and the peripheral area 15 to 30 per cent irradiation. By comparison, different cellular responses in these areas suggested differences between the primary and secondary effects of irradiation. The qualitative effects included changes in the parenchymal cells: first, in reorganization of RNA and glycogen, then in the DNA, and finally in lipid distribution. Alterations were also demonstrable in reticuloendothelial cells. Maximal changes occurred at the 600R level and in the central portion of the liver which received 100 per cent of radiation. These changes, however, were transistory in character for the most part and by the sixth post-irradiation week, the cells had returned to normal. A sequential pattern of morphologic events was demonstrated, and the period of radiation reaction was distinguished from the period of tissue regeneration. (auth)

43736 THE EFFECT OF NEAR-ULTRAVIOLET LIGHT ON STAPHYLOCOCCI AND MYCOBACTERIA IN DROPLET NUCLEI. **Cohn, M. L.; Middlebrook, G. (Univ. of Colorado School of Medicine, Denver). Am. Rev. Respirat. Diseases, 91: 880-6(June 1965).**

Effects of near-uv light on staphylococci and on several strains of mycobacteria in droplet nuclei were investigated. Experiments with pigmented and nonpigmented staphylococci, undertaken to ascertain whether pigmentation protects against light, showed that uv light had a decided killing action on both strains. Droplet nuclei containing tubercle bacilli grown both in vitro and in vivo were irradiated with near uv light. Results indicated no statistically significant difference in the effect of near-uv light on tubercle bacilli grown in vivo and in vitro when they were contained in droplet nuclei. Most tubercle bacilli in droplet nuclei subjected to irradiation with near-uv light were irreversibly sterilized and were rendered noninfectious as well as nonculturable. A few tubercle bacilli remained infectious. When single cell suspensions of S. aureus and tubercle bacilli were prepared and irradiated in Pyrex tubes, 20 by 125 mm in size, the light took much longer to produce a lethal effect under these conditions than in droplet nuclei, and a lag period was observed before the sterilizing effect. This was especially true of pigmented strains of bacteria. These observations suggest the use of radiation in the wave length region 320 to 370 mμ for sterilization of staphylococci and mycobacteria in droplet nuclei in the air. (TCO)

43737 THE EFFECT OF NEAR-ULTRAVIOLET LIGHT ON CULTURE MEDIA. Cohn, M. L.; Middlebrook, G. (Univ. of Colorado School of Medicine, Denver). Am. Rev. Respirat. Diseases, 91: 929(June 1965).

A deleterious action of diffuse daylight on the oleic acid albumin agar medium 7H10 was shown by exposure of the medium in glass Petri dishes to indirect sunlight. This resulted in a change in the medium that prevented growth of tubercle bacilli from moderate or small inocula. Media irradiated with near-uv light showed the same deleterious effect. The 7H10 medium used for the isolation of mycobacteria from pathologic specimens contains 1 μg of malachite green per ml. The malachite green is incorporated in the medium to retard contamination by organisms not killed by the usual decontamination procedures used in the isolation of tubercle bacilli. It was shown that the malachite green in the 7H10 medium was not the substance responsible for the lack of growth after irradiation with diffuse daylight, as the toxic effect was present in the medium in the absence of this dye. Since the 7H10 medium contains catalase, hydrogen peroxide probably is not the toxic product. In other experiments, it was observed that amber-colored plastic could protect the 7H10 medium against this toxic action of glass-filtered daylight under the same experimental conditions. Therefore, amber-colored Petri dishes were used to protect the media against the harmful effects of near-uv light. Conventional dishes made of polystyrene colored amber were found suitable, and are recommended for protection of culture media against accidental irradiation by daylight. (BBB)

43738 THOROTRAST DISEASE CONCERNING ONE OBSERVATION. Etienne-Martin, P.; de Girardier, J.; Klepping, Cl.; Aupecle, P.; Guerrin, J.; Dusserre, L. (Universite, Dijon, France). Arch. Maladies App. Digest. Maladies, 50: 547-53(May 1961). (In French).

The late manifestations of prior injections of Thorotrast (ThO_2) are illustrated by a 73-yr-old woman, suffering from venous occlusion in the lower limbs and a hepatosplenic thorotrastosis revealed during examination for cholelithiasis. Deposition of this contrast agent in the tissues was a sequel to a 25-ml dose of Thorotrast, injected 13 yr previously, and was manifested in two clinical aspects. The accidental para-arterial leakage from the injection had led to the formation of an inflammatory process, seen as a granuloma. The second clinical aspect was represented by the fixation in the reticuloendothelial system of Th, whose half-life period is 1.4×10^{10} yr. The liver, spleen, lymph nodes, and bone marrow were particularly affected. The radioactivity of these areas was examined with a Geiger counter during surgery. It was of the order of 7 to 8×10^{-10} R, originating from γ radiation which is of minor importance, compared with α emission, in the Th family. Subsequent radiography was conducted by an injection of diodone for visualization of the biliary tract. An autoradiographic study was accomplished through the visualization of α-particle tracks, sometimes isolated, sometimes together, in the form of multi-branched stars, that reveal the site of emission of the α radiation of the Thorotrast. Because of the elimination of Thorotrast in angiographic investigations, such cases are extremely rare. (BBB)

43739 INTRACELLULAR ENZYME VARIATIONS FROM X RAYS. I. HISTOCHEMISTRY OF PHOSPHATASES IN THE OVARY, VAGINA, KIDNEY, LIVER AND SPLEEN AFTER IRRADIATION AND TREATMENT WITH THIOCTIC ACID. Genazzani, E.; Montemagno, U. (Universita, Naples). Arch. Ostet. Ginecol., 64: 9-34(Jan.-Feb. 1959). (In Italian).

In the rat, a whole-body irradiation by 500-R doses of x rays did not give rise to significant changes of the alkaline and acid phosphatases content of liver, kidney, ovary, and vagina. Only the spleen showed a higher content of alkaline phosphatase. Irradiation by 800 R on the contrary, produced a decrease of the alkaline phosphatase and morphologic changes in the various organs, except in the liver, in which the enzyme appeared to be increased. Acid phosphatase decreased in the liver, kidney, ovary, and vagina and increased in the spleen. Thioctic acid in a dose of 50 mg/kg, administered before irradiation, had no influence on these effects of x rays. The vaginal cytologic cycle did not show changes until the 8th day after a dose of 800 R. (BBB)

43740 STUDIES OF CYTOTOXICITY USING ^{32}P. Forbes, I. J. (Univ. of Adelaide). Australian J. Exptl. Biol. Med. Sci., 41: 255-64(1963).

The method described has general application in the detection of cell damage induced by immunological and other agents, and in the study of the kinetics of antibody action. The principle of the method depends on the fact that ^{32}P passes from cells into normal medium at a rate which is a characteristic of the particular strain of cell. Several types of toxic substance which were investigated caused an increased rate of loss of ^{32}P from cells. Data are presented to demonstrate this principle, to show the sensitivity of the technique when it is used to detect cytotoxicity, and to show the reproducibility of the results obtained with it. Various types of cells were cultured in media containing 2 μC/ml ^{32}P as Na_3PO_4. Since ^{32}P is a pure β emitter with a maximum energy of 1.7 Mev, a scintillation well-type counter was used to measure bremsstrahlung radiation. Using a pulse-height analyser, all energies above 0.01 Mev were detected. Total ^{32}P counts were usually 20 times background. After measuring the total ^{32}P activity the medium was poured off and the cells were washed. The results were expressed as the percentage of the total ^{32}P which had passed from the cells into the medium. The studies showed that ^{32}P passes from cells into a normal medium at a rate which is characteristic of the type of cell, and that the loss is accelerated when cells are damaged. It is, therefore, not necessary, when comparing the effects of substances on the rate of ^{32}P loss, to have identical numbers of cells in the replicate cultures, since the rate of loss is determined by measuring the ratio of ^{32}P in the medium to the total ^{32}P. The correlation of cell numbers with counts of the ^{32}P within the cells was evidence that loss of ^{32}P is due to destruction of cells. Furthermore, microscopic evidence of cell damage was always seen in cultures where ^{32}P loss was accelerated. The ^{32}P which can be precipitated from the medium by trichloroacetic acid (TCA) apparently comes from within the cells as it was only detected in the medium when cells had been visibly damaged. The release of TCA-precipitable ^{32}P was proportional to the total amount of ^{32}P released. Also, with natural rat cytotoxin found in rabbit serum, the ^{32}P release was proportional to the concentration of the toxin in the medium. Other cytotoxic agents were tested: antisera to rat tissues containing heat-stable antibody, NaOH, and mechlorethamine hydrochloride (Mustargen). Each caused an increased rate of ^{32}P loss from appropriate cells. Results with nitrogen mustard showed that in the dosages which were used the cytotoxic effect varied inversely with the concentration of the drug. The technique should be valuable in the study of chemotherapeutic agents. The technique yields results which correspond to those obtained by measuring the acid-insoluble isotope content of the medium, and has advantages of simplicity and accuracy which accompany the performance of multiple determinations. In addition, in the case of minimal damage to cells the release of TCA-insoluble ^{32}P is accompanied by the release of many times more soluble ^{32}P, so that there is a greater margin between the radioactivity of the sample to be counted and the level of background radioactivity. The operations are greatly simplified by counting bremsstrahlung radiations in a well-type scintillation counter from tubes containing monolayers and medium in the first count, and separated medium in the second, instead of measuring the β emission from dried aliquots of lysed cells and medium in planchets. (BBB)

43741 X-RAY-INDUCED PERTURBATIONS IN THE REPLICATION OF THE BACTERIAL CHROMOSOME. Billen, Daniel; Hewitt, Roger; Jorgensen, George (Univ. of Texas, Houston). Biochim. Biophys. Acta, 103: 440-54(July 15, 1965).

Using [^{3}H]thymine or [^{3}H]thymidine as a pre-irradiation label and the thymine analogue 5-bromo-[^{14}C]uracil as a combined density and radioisotopic label for observing post-irradiation DNA synthesis, it was determined that relatively low doses of x rays can induce changes in the normal sequence of chromosome replication in E. coli. Changes were noted at doses of 2000 R or higher, with the effects becoming increasingly manifest with higher doses. DNA synthesis immediately following irradiation occurred in limited regions of the chromosome. Resumption of chromosome replication occurred at a point(s) apparently differing from the original growth point. An early temporal appearance of a second generation of DNA was observed. A portion of the DNA did not appear to participate in post-irradiation chromosomal replication. A feature of the experimental method was that at least 98% of the cellular DNA was recovered in the CsCl gradients. (auth)

43742 SOME STUDIES OF THE INFECTIOUS PROCESS WITH MS_2 BACTERIOPHAGE. Rappaport, Irving (Univ. of Chicago). Biochim. Biophys. Acta, 103: 486-94(July 15, 1965).

Certain aspects of the infection of Escherichia coli K_{12} Hfr AB_{261} with bacteriophage MS_2 were studied. Following adsorption, which could be reversed by dilution, was an eclipse period of 15–17 min duration, after which mature phage made their intracellular appearance. The first bursts occurred 38 min after adsorption at which time approximately 1000 p.f.u. (plaque-forming units) per cell were present intracellularly. The bursts were asynchronous and distributed over a 25-min rise period. A final yield of 2000 p.f.u. per cell was observed. About one-half of the infected cells did not lyse and retained its colony-forming ability. Radiological studies revealed no marked differences between the sensitivity of the virus in vitro to ultraviolet light and the capacity of the irradiated bacteria to synthesize MS_2. The behavior of the infectious centers in the Luria-Latarjet experiments was independent of the multiplicity of infection. Immediately after infection, the sensitivity of the infectious centers to ultraviolet light was greater than that of the free virus. Although resistance gradually increased during the latent period, no high multiplicity was detected. Complete radioresistance failed to occur even prior to lysis. (auth)

43743 EFFECT OF X-IRRADIATION ON PULSE-LABELLING OF RIBONUCLEIC ACID IN SALMONELLA TYPHIMURIUM. Hudnik-Plevnik, Tamara A. (Inst. of Nuclear Science Boris Kidrich, Belgrade). Biochim. Biophys. Acta, 103: 515-16(July 15, 1965).

Salmonella typhimurium bacteria were grown in a complete medium without glucose and irradiated at 22°C. Ten minutes after the addition of glucose at 37°C, the bacteria were exposed to $^{32}PO_4^{3-}$ for 3 min and the RNA was extracted and analyzed. RNA prepared from irradiated cells was different in two respects from the control RNA; there was an increase of incorporated label into RNA of all fractions in the irradiated bacteria. The increase was not uniform in all fractions but was markedly higher in the region corresponding to 23S-16S than in the region corresponding to 14S-10S in the sedimentation profile. (P.C.H.)

43744 BASE COMPOSITION OF MESSENGER RNA OF PSEUDOMONAS EFFUSA IRRADIATED WITH ULTRAVIOLET LIGHT. Nozu, K.; Harada, Y.; Yuasa, S.; Honjo, I. (Osaka Univ.). Biochim. Biophys. Acta, 103: 517-19 (July 15, 1965).

Studies were made on the base composition of messenger RNA in uv irradiated Pseudomonas effusa. The results showed that the ratio of adenosine 3'-monophosphate to guanosine 3'-monophosphate (A/G) in m-RNA was increased by uv irradiation. It is assumed that end-adding adenylate polymerization would occur at the site of thymine dimer in primer DNA in the course of RNA transcription. (P.C.H.)

43745 QUALITATIVE BIOLOGICAL EFFECTS VARIATION AFTER IRRADIATION OF PARTITION TISSUE WITH FAST ELECTRONS OF DIFFERENT ENERGY SPECTRA. Markus, Benno; Killiopoulou, Helena (Universitaet-Hautklenik, Gottinges, Ger.). Biophysik, 2: 263-70(1965). (In German).

The observation of chromosome aberrations in root tip cells of Allium cepa between 0 and 24 hr after irradiation with electrons at 14.2 Mev shows a qualitative effectiveness variation, according to whether the object was irradiated at 5 or 53 mm depth of a plexiglass phantom with 136 R (120 or 130 rad). The effect observed was that there was a single maximum of the aberration frequency at 3 hr after irradiation at 5 mm depth and 2 maxima (at 3 and 9 hr) after irradiation at 53 mm depth. A reversal in the relative effectiveness of both irradiation depths occurs between 6 and 9 hr through the height of the maxima. The effect was explained as the result of the different electron spectra with their differing effects on dividing and quiescent cells. (tr-auth)

43746 RADIATION-INDUCED MUTATIONS IN DIGITALIS LANATA EHRH. Michalski, T. Biul. Inst. Roslin Leczniczych, 9B: 45-51(Mar.-June 1963). (In Polish).

In 1961, 2 lots of dry seeds of the medicinal plant, Digitalis lanata (foxglove), were exposed to γ-irradiation doses of 15,000 and 20,000 r from a ^{60}Co source. Six out of 50 plants grown from seeds that had received the higher radiation dosage differed from other irradiated and unirradiated plants. The mutation effects resulted in retarded development and morphological changes, especially in inflorescence. The mutants produced many more flower shoots than the control plants and the flowers differed in color and form. The flowers were pollinated by bumblebees. The seeds of fertile mutants were diploid. The mutants yielded a distinctly higher crop of the drug, digitalis, than the controls with an increased lanatoside content. Further experiments will be carried out to find the optimum dose for obtaining suitable mutants because the applied radiation doses of 15,000 and 20,000 r were lower than the lethal dose, LD_{50}. (OID)

43747 URIDINE DIPHOSPHATE GLUCOSE PYROPHOSPHORYLASE ACTIVITY IN THE LIVER OF IRRADIATED RATS. Bonsignore, D.; Canonica, C.; Carrai, M.; Lenzerini, L. (CAMEN, Pisa, Italy; Universita, Genoa). Boll. Soc. Ital. Biol. Sper., 40: 1127-30(Sept. 30, 1964). (In Italian).

The uridine diphosphate glucose pyrophosphorylase activity was studied in white rats exposed to whole-body irradiation at 700 r. The techniques used are briefly described and the results are discussed. They show that the irradiation caused an inhibition of the specific pyrophosphorylase polysaccharide activity and the hepatic glucose-6-phosphate-phosphatase activity. The accumulation of glycogen in the liver of rats exposed to acute irradiation can depend in part on an inhibition of the destructive processes and partly on an increase of the synthesis processes. (J.S.R.)

43748 TOTAL-BODY X IRRADIATION AND SUBSEQUENT ADMINISTRATION IN A SINGLE OR REPEATED DOSE OF HEMATOPORPHYRIN: ALTERATIONS OF LETHALITY CURVE IN THE ALBINO MOUSE. Cittadini, G. (Universita, Siena, Italy). Boll. Soc. Ital. Biol. Sper., 41: 366-9(Apr. 15, 1965). (In Italian).

Sixty mice of the NMRI strain, two and one-half months old, were subjected to whole-body irradiation with 200-kv x rays at a dose rate of 46 R/min to total doses of 800 R. They were divided into five groups, which were injected intraperitoneally with distilled water (controls) or with 5, 15, or 45 mg/kg of hematoporphyrin 24-hr postirradiation. The fifth group received 30 mg/kg of the pigment at 24 and again at 48 hr postirradiation. The mean survival times (in hr) of the five groups (controls, 5, 15, 45, and 2×30 mg/kg) were 272, 212, 246, 213, and 205. Statistical analysis of the results showed a significant difference (at the 95% confidence level) between controls and the animals treated with 15, 45, or 2×30 mg/kg of the pigment, showing that hematoporphyrin has a radiosensitizing action in mice. These results resemble those obtained when oxygen tension of the tissues of mice is increased. (BBB)

43749 SOMATIC MUTATION AND CHRONIC DISEASE. Burnet, MacFarlane (Walter and Eliza Hall Inst. of Medical Research, Melbourne). Brit. Med. J., 1: 338-42 (Feb. 6, 1965).

Radioinduced mutations are referred to in a discussion of the possible role of mutations from various causes being responsible for some chronic diseases. (BBB)

43750 VACCINATION AGAINST DICTYOCAULUS FILARIA WITH IRRADIATED LARVAE. Sokolic, A.; Jovanovic, M.; Cuperlovic, K.; Movsesijan, M. (Inst. for the Application of Nuclear Energy in Agriculture, Veterinary Medicine, and Forestry, Zemun, Yugoslavia). Brit. Vet. J., 121: 212-22(May 1965).

The results are reported of laboratory and field work with a radiation vaccine against the sheep lungworm. Larvae were exposed to doses of 20, 40, and 60 kR of x rays or 40 and 60 kR of ^{60}Co γ rays and 2000 larvae from each dose schedule were administered orally, on the fifth postirradiation day, to each animal of one group consisting of two lambs. Controls were treated with nonirradiated infective larvae from the same batch as the irradiated larvae. The animals were slaughtered on the 55th postinfection day and examined. A characteristic feature was the finding of few sexually mature female larvae and few males in the respiratory organs. The total male to female ratio was 1:11.5, compared with 1:1.6 with nonirradiated larvae in control animals. The results of immunity generally showed that in the group of doubly vaccinated lambs, except in the group challenged on the third postvaccinal day, a greater number of resistant animals occurred as compared with singly vaccinated animals; and the number of resistant animals increased with the postvaccinal time. In the doubly vaccinated lambs 38% resisted challenge on the third day after vaccination, 81.8% on the 15th day, and 100% on the 60th day. In singly vaccinated lambs the number of resistant animals increased from 50 to 62.5% from the 60th to the 90th day. With the increase in time between vaccination and challenge it was generally found that there was a decrease of all parameters selected for the assessment of the vaccine, thus indicating the increase of the degree of resistance as compared with the controls. Vaccination resulted in the inhibition of development and retardation of reproduction in the females. This led to a reduction in oögenesis which was evidenced by a marked decrease in larval output, sometimes amounting to a factor of 500, as compared with the corresponding controls. The results obtained by administering larvae irradiated with equal doses of x or γ rays were almost identical. In field tests, vaccination of previously infected animals resulted, in almost all of the experimental flocks, in a decrease in larval output and in the number of infected animals. The postvaccinal decrease of larval numbers in the feces and the number of infected animals is a significant factor from the epidemiological point of view. It gives perspective for eradication of the disease if vaccination is carried on over a period of several years. (BBB)

43751 MUTATION VARIABILITY OF E. COLI K-12 λ UNDER THE INFLUENCE OF NEUTRON IRRADIATION FROM AN IRT-1000 REACTOR. Murav'eva, L. I. Bull. Exptl. Biol. Med. (USSR)(English Transl.), 59: 75-9(1965).

The effect of neutron irradiation on the biological properties of E. coli K-12 λ was studied. A suspension of the bacteria was subjected to neutron irradiation (doses 3000 to 60,000 rad) in an IRT-1000 reactor. Gamma rays made up about 10% of the dose, and some β-radiation from short-lived isotopes was detected; nevertheless, most of the described changes are due to the predominant influence of neutrons. Cultures were prepared from the irradiated suspensions, and the number of colonies was counted to determine the survival percentage. An LD_{50} of 2500 to 3000 rad was determined. Study of preparations made 1 to 1.5 hr after irradiation showed that neutrons cause a number of changes in cell morphology. Sharp intensification of the polymorphism characteristic of E. coli was noted; there were more coccus-shaped, elongated cells than usual. In addition, at doses of 10,000 and 40,000 rad, curved, swollen cells were observed, which stained irregularly. It was concluded that doses of neutrons change cell morphology appreciably in the first few hr after irradiation; furthermore, the degree of change is proportional to the dose. With 10,000- and 20,000-rad doses of neutron irradiation, the frequency of mutations affecting the synthesis of amino acids was slightly greater than the frequency of spontaneous mutations. It is interesting that an increased dose of 30,000 rad did not further increase the frequency of mutations. Mutants, isolated by a special method, were distinguished chiefly by their inability to synthesize hystidine. (ATD)

43752 EARLY EFFECTS OF IRRADIATIONS AT LOW DOSES. Closon, Jacques. Bull. Inform. Assoc. Belge Develop. Pacifique Energie At., 10: No. 55, 3-7(Apr. 1965). (In French).

A bibliographic review is given of the early effects of weak doses. An attempt was made to place the apparent dose threshold for detectable metabolic, histologic, functional, and psychological effects. In the light of the brief review it seems that several conclusions can be made. In man after an acute irradiation at low doses (several Rems) no early effect is detectable except retinal excitation and chromosomic lesions at the level of the leukocytes. Doses of this order, if they are repeated, can modify temporarily the spermatogram. The apparent threshold of doses for hematopoietic tissues and the testicles is very low. It is probably of the same order for the ovaries but there is no precise information on this subject. The apparent dose threshold for endocrine, vascular, or digestive effects appears to be at approximately 25 Rems. (J.S.R.)

43753 BIOLOGICAL INDICATORS TO EVALUATE RADIOACTIVE DAMAGE. THEIR POSSIBILITIES—THEIR MODE OF ACTION. Berger, G.-B. (EURATOM-CEN, Mol, Belg.). Bull. Inform. Assoc. Belge Develop. Pacifique Energie At., No. 56, 3-5(June 1965). (In French).

Three areas in which biological indicators can be used to evaluate radioactive damage are indicated. They are the metabolic system of the organism, the specific role of certain cells very sensitive to radiation, and tests based on the response of the organism to radioactive damage. A list of substances whose concentration in urine is modified after irradiation is given. The necessity of detailed study is emphasized. (J.S.R.)

43754 FORMAL DISCUSSION OF: SOMATIC MUTATIONS AND CARCINOGENESIS. Curtis, Howard J. (Brookhaven National Lab., Upton, N. Y.). Cancer Res., 25: 1305-9(Sept. 1965).

A great deal of evidence is now available indicating that mutations play a dominant role in the aging process. Because carcinogenesis is one facet of the aging process, mutations must play a major role here also. However, carcinogenesis certainly does not consist of the simple induction of a mutation in one cell which confers the property of uncontrolled growth on that cell and its progeny. There must be some general conditions, as well as a specific event, before carcinogenesis can take place. It is postulated that mutations in one form or another are responsible for both conditions. (auth)

43755 CHROMATOGRAPHIC INVESTIGATION OF SOME IMPORTANT SUBSTANCES IN THE AQUEOUS HUMOR OF THE SOUND EYE, AFTER X IRRADIATION, AND IN TRAUMATIC CATARACT. Kubena, K. (Medical Faculty, Golomouc, Czechoslovakia). Cesk. Oftalmol., 20: 324-32(Sept. 1964). (In Czech).

Biochemical studies were made of three successive aqueous humor fractions, aspirated at 30-min intervals, from the rabbit eye, each succeeding sample showing a lower content of organic constituents. Paper chromatography was used to separate and quantitate free amino acids, sugars, and carboxylic acids. In first samples of normal rabbit aqueous humor it was possible to detect a total of 19 amino acids, including taurine, not detected before. In comparison, the second aqueous humor aspirate of the healthy rabbit contained only one quarter to one third of free amino acids as compared with the first, and

the third sample of aqueous humor 50% less than the second. As regards sugars it was possible to identify glucose, fructose, xylose, arabinose, and spots corresponding to disaccharides and trisaccharides. As for carboxylic acids, citric, malic, and lactic acid were found, and in the second samples of aqueous humor spots corresponding to tartaric acid and α-ketoglutaric acid. Also investigated were the free amino acids and sugars and carboxylic acids in rabbit eyes irradiated with 1500 R. A slight increase was seen in amino acids and sugars as compared with controls. The increase found in the amount of lactic acid was marked. In the aqueous humor of eyes with traumatic cataract, as compared with controls, an increase was observed in phenylalanine, valine, and methionine. The amount of glucose was 50% lower as compared with the control eye. The chromatograms showing the different patterns in the three groups are illustrated. (BBB)

43756 THE SENSITIVITY OF THE GONADS TO RADIATION. Zuckerman, Solly (Univ. of Birmingham, Eng.). Clin. Radiol., 16: 1-15(Jan. 1965).

Effects of ionizing radiation on germ cells are reviewed in terms of cell-death, reproductive performance, and mutagenesis as radioresponses. With the exception of one developmental stage, the sensitivity of male germ cells to a given dose of radiation, using cell-death as the criterion, is related to their stage of mitosis or meiosis. The exceptional stage in the male is the primordial germ cell of the late fetal and neonatal animal. Then, the cells are extremely radiosensitive, permanent sterility being achieved by $^1/_{10}$ of the dose required to bring about the same effect in the adult. In the female mammal, susceptibility to radiation-induced cell-death also depends on the developmental stage of the germ cell, although there is also some evidence that sensitivity may at times be also correlated with age. Sensitivity is high during the period oogonia reach their peak of mitotic activity. Radiosensitivity is relatively low during the leptotene, zygotene, and pachytene stages of meiotic prophase, i.e., it decreases between the last premeiotic generation of oogonia and the appearance of primary oocytes. Unlike the male, however, radiosensitivity increases in the female with the onset of the diplotene stage of the prophase, when the oocyte becomes surrounded by a single layer of granulosa cells to form a primary follicle. Primary follicles are extremely sensitive in the rat, mouse, and rabbit, but sensitivity falls off as the follicles develop. Other mammals behave differently; for example, in the guinea pig and the monkey, primary follicles are relatively resistant to x rays, and the oocytes become more radiosensitive as the follicle develops. The doses of ionizing radiation required to kill a given proportion of the total stock of primary follicles also vary enormously between species, probably because the chromosomal configuration of the germ cells at the same follicular stage of development varies widely between species. The decline of reproductive capacity after irradiation depends on the partial or complete destruction of germinal cells, and on the induction of dominant lethals rises sharply between the end of the diplotene stage of the prophase of meiosis and the onset of the maturation division preceding ovulation. Data available from clinical studies on the sensitivity of human testes and ovaries to radiation are also reviewed. (BBB)

43757 THE EFFECT OF IRRADIATION ON THE FUNCTION AND SURVIVAL OF RAT THYROID CELLS. Al-Hindawi, A. Y.; Wilson, G. M. (Univ. of Sheffield, Eng.). Clin. Sci., 28: 555-71(June 1965).

The thyroids of rats were irradiated by ^{131}I in doses of from 5 to 100 μc and the subsequent effect on the function of the gland and on the survival of the thyroid cells was determined at intervals of up to 1 year. The iodide concentrating capacity and the organification of iodine by the thyroid gland were little affected by irradiation. The response to propylthiouracil was decreased as the irradiated glands did not show the noraml increase in weight. This was due to the inhibition of hyperplasia of the cells; hypertrophy was not prevented by irradiation. DNA synthesis was inhibited in the irradiated glands as shown by the decrease in the corporation of ^3H-thymidine into thyroid cells. The persistence of ^3H-DNA was shorter in the irradiated thyroids than in the non-irradiated glands, indicating shortening of the life span of irradiated cells. The inhibition of new cell formation and the shortening of the life span of thyroid cells following ^{131}I irradiation may explain the rising incidence of hypothyroidism several years after radioiodine therapy of thyrotoxicosis. (44 references.) (auth)

43758 STUDIES OF THE LIFE CYCLE OF MAMMALIAN CELLS. Puck, Theodore T. (Univ. of Colorado, Denver). Cold Spring Harbor Symp, Quant. Biol., 29: 167-76(1964).

The method described permits analysis with high resolution of the position in the life cycle of mammalian cells at which various biochemical events occur. Application of this method is described in the determination of the mode of action on the cell life cycle of various chemical and physical agents, including x rays. In a population of randomly dividing cells with a uniform generation time, T, if a specific inhibitor is added which blocks passage of the cells at one specific point in the left cycle, it causes cells to accumulate at the point of block. If this blocking point occurs at the end of mitosis so that cell division is not completed and cells are accumulated in the mitotic phase of the life cycle, it is shown that the accumulation of cells in mitosis is given by the following equation: $\log(1 + N_M) = 0.301/T(T_M + t)$, where N_M is the fraction of the cell population in mitosis; T is the generation time of the culture; T_M is the time required for mitosis; and t is the elapsed time since the addition of inhibitor. The quantity $\log(1 + N_M)$ is called the collection or accumulation function. This equation predicts that for a random culture the accumulation function will consist of a straight line whose slope, 0.301/T, furnishes the value of the generation time. If all of the cells have exactly the same value of T, the accumulation function will be linear until all of the cells are in mitosis, at which time the curve will become horizontal with a discontinuity. This method of life cycle analysis was used to trace the kinetics of the reversible lag produced by small doses of x irradiation. In HeLa cells a change in the collection function was produced by an x irradiation dose of only 9 rad. This does not permanently kill any cells, but temporarily inhibits the cell contingent in the central region of the G2 period. During the first 0.60 hr, the collection function is normal, demonstrating that these cells have not been impeded at all. Thereafter, the curve is flat for the subsequent 0.70 hr, indicating complete cessation of progression toward mitosis. Then the curve again rises and for 0.65 hr thereafter the slope is virtually the same as in the control, indicating that the cells on the other side of the inhibited population are now coming into mitosis without a delay. From that point on until the 3-hr point the slope is greater than normal, indicating that during this period cells which have not been held up in mitosis are being rejoined by those which have recovered from the lag, so producing a slope greater than normal. The fact that after the 3-hr point the radiation-delayed curve and the normal curve coincide demonstrates the completely reversible nature of this particular lag. This lag reflects damage to chromosomes, as demonstrated by the fact that tritiated thymidine (which becomes incorporated only into the DNA of the cell and hence is in a position to irradiate only the cell nucleus, because of the very weak β ray which it emits) also produces a characteristic G2 lag in cells which have incorporated the radioisotope. (BBB)

43759 INFLUENCE OF IONIZING RADIATIONS ON NORMAL VOLUTIN AND VOLUTIN INDUCED BY MEANS OF SULFONAMIDES IN CERTAIN BACTERIA. Christov, G. (Inst. of Oncologic Research, Sofia-Darvenitza, Bulgaria). Compt. Rend. Acad. Bulgare Sci., 18: 169-72 (1965). (In French).

Two species of bacteria, Lactobacterium bulgaricum and Neisseria catarrhalis, after having been cultivated in appropriate media, in some cases containing sulfathiazole,

were irradiated with x rays (180 kv) at a dose rate of 361 R/min. The dose was 5000, 20,000, or 100,000 R. After incubation for 24 hr at 37°C, the bacteria were examined for possible changes in morphology and content of volutin. No such changes were observed. It is believed that the structure of bacteria is not influenced by irradiation doses up to 100,000 R. The volutin contained in the cells was preserved and showed the same sensitivity to staining solutions as before irradiation. The results indicate that the changes in volutin that eventually intervene in the composition of bacterial cells after high-dose irradiation did not appear, either immediately or as a late reaction in the 24 hr that followed irradiation. This result was independent of the known sensitivity of nucleic acids, nucleoproteins, proteins, and other cellular constituents to ionizing radiation. (TCO)

43760 COMPARISONS OF THE PRENATAL AND NEONATAL MORTALITIES INDUCED IN MICE BY THE X IRRADIATION OF THE FETUS ALONE OR OF THE MOTHER ALONE. Duplan, J. F.; Monnot, P. (Universite, Paris). Compt. Rend. Soc. Biol., 159: 17-21 (1965). (In French).

The mortality of newly born mice after irradiation of the mother alone or of the fetus alone on the fifteenth day of gestation with 200 or 400 R x radiation was studied. The results showed that the maternal irradiation has a preponderant effect on the survival of the fetus since irradiation of the mother alone causes a higher mortality than that caused by irradiation of the fetus alone. After a dose of 400 R on the mother, no newly born survive for 10 days. It is assumed that this is due in large part to an intoxication of the fetus by the products of cellular radiolysis liberated in the maternal blood. (J.S.R.)

43761 EFFECT AT A DISTANCE, BY CHORIOALLANTOID GRAFTING, OF SPINAL CORD FRAGMENTS IRRADIATED BY X RAYS, ON THE CULTURE GROWTH OF THE MARROW OF THE GRAFT CARRIER. Denefle, J. P. (Universite de Paris, Orsay, France). Compt. Rend. Soc. Biol., 159: 51-4(1965). (In French).

Lombo-sacral fragments of irradiated chicken embryo were grafted to the chorioallantosis. The spinal cord was exposed in the egg to 1500 R. The effects on the donator, the graft itself, and the graft acceptor were studied. The results showed that the chorioallantoid graft of irradiated medullary fragments produced a degeneration of the culture fibers in the graft carriers. This degeneration is characterized by the coexistence in the same culture of two distinct types of fibers, one of which is normal and the other is totally degenerate. In the cultures of the grafted material the diameters of the fibers are higher than those of the fibers of the cultures from the donators and from the graft receivers. (J.S.R.)

43762 PERMANENT AND TRANSMISSIBLE MODIFICATION OF THE VIRULENCE OF A SOLID ISOLOGOUS TUMOR AFTER X IRRADIATION. Oth, D.; Robert, J.; Rauber, G.; Burg, C. (Faculte des Sciences, Nancy). Compt. Rend. Soc. Biol., 159: 194-7(1965). (In French).

The effects of x irradiation on the tumor itself was investigated by grafting a tumor onto successive generations of mice. The isologous tumor was exposed to a total dose of 4000 R. Immediately after irradiation the animal was sacrificed and the tumor grafted to a new host. The virulence of the tumor was measured by the life span of the host. The graft was carried through five successive generations. The results showed that the average life span of mice grafted with a nonirradiated tumor was 51 days. These results seemed to show permanent decrease in tumor virulence after irradiation, a decrease that seemed to be maintained for at least a year during 5 generations of successive grafts. The mechanism of the phenomenon is discussed. (J.S.R.)

43763 STUDY OF THE GROWTH IN THE CBA MOUSE OF THE J SARCOMA IRRADIATED IN VITRO. Chevalier, P. (Hopital de Baviere, Liege). Compt. Rend. Soc. Biol., 159: 492-5(1965). (In French).

Fragments of J sarcoma were irradiated with doses from 1000 to 8000 R and immediately afterwards were grafted to the animal. The results showed that the percentage of grafts disappearing definitely increased with the dose received. For the grafts established, the stabilization of growth and increase of survival time were also a function of the dose absorbed. At 7000 r, tumor regression was obtained in 100% of the cases. These results are discussed in comparison with the results obtained on the irradiation in vivo. The differences in radiosensitivity are explained by two mechanisms: a larger radioresistance of the graft irradiated in vitro in conditions of anoxia; and an important alteration of the peritumoral vascularization induced by irradiation in vivo. (J.S.R.)

43764 BIOCHEMICAL CHANGES INDUCED BY ULTRAVIOLET LIGHT. Everett, Mark Allen (Univ. of Oklahoma Medical Center, Oklahoma City). Dermatol. Trop. Ecol. Geograph., 3: 97-101(Apr.-June 1964).

This review surveys the specific biochemical events, known to occur following exposure of skin to uv light, which may be manifested by the erythema reaction, actinic degeneration of collagen, systemic uv effects, photopigmentation, and vitamin D formation. The action spectrum for uv effects in organisms resembles the absorption spectrum for nucleic acids, suggesting that the damaging radiation is absorbed in nucleic acids or in similarly absorbing compounds, such as nucleosides, nucleotides, and free bases. Fundamentally, understanding uv effects in the skin depends upon knowledge of chemical changes produced in nucleoproteins by photons of light. The specific changes reported are: disulfide and carbon-sulfur bond fission, isomerization in maleic and fumaric acids, addition of water in pyrimidine nucleotides, especially at the 5–6 bond, dimerization of nucleotides, and attenuation of hydrogen bonding. Extremely large amounts of uv radiation may induce more profound chemical alterations, including the formation of new compounds and polymers, but the amounts of uv required are far more than the quantity experienced under physiologic conditions. Uv exposure may result in the actinic degeneration of collagen, with increase in hexosamine and in mucopolysaccharide-staining material in histologic sections. The long-favored theory that activated histamine or histamine-like precursors within the epidermis are responsible for uv erythema has received little support. Histamine content of human skin does not increase significantly after irradiation. Oxidation of aromatic groups in perivascular proteins plays a key role in the production of erythema by 290 mμ light. Urocanic acid, found principally in the outer epidermis, is one of the most potent uv-absorbing compounds in the skin. Some evidence suggests that photochemical disintegration products of this substance may be fundamental participants in the production of 290-mμ erythema. (BBB)

43765 THE ACCELERATION OF GLYCOLYSIS IN YEAST CELLS BY ULTRAVIOLET LIGHT OF MITOGENETIC INTENSITY. Konev, S. V.; Lyskova, T. I. Dokl. Akad. Nauk BSSR, 9: 190-3(Mar. 1965). (In Russian)

Yeast cells of Saccharomyces cerevisiae in a sugar-wort nutrient solution were irradiated with filtered light from a bactericidal lamp at a light flux of 10^7 to 10^8 quanta cm^{-2} sec^{-1} containing primarily the 254 mμ line of mercury. The concentration of yeast cells in the quartz vessel was 50,000 to 60,000 cells per 1 mm^3 in a layer 3 mm thick at a temperature of 26 to 27°C. The glycolysis rate in the closed vessel was estimated from the time necessary to raise the pressure about 10 cm of water. The results showed that a light flux of 10^6 to 10^8 quanta cm^{-2} sec^{-1} stimulated the glycolysis rate by a factor of 1.5 to 3 compared to the control. At an intensity of 10^7 quanta cm^{-2} sec^{-1} each yeast cell absorbed on the average 1 quantum/sec, or about 300 quanta for the entire exposure time. On estimating the quantum yield of carbon dioxide that is formed, a high value of 10^5 to 10^7 molecules of CO_2/quantum is obtained. This high value indicates the presence of a trigger mechanism in the cell, where a change to one molecule or to a few molecules in a cell starts a reaction in the cell which consists of 10^{14} cells. (TTT)

43766 BLOOD SERUM PROTEINOGRAPHIC CHART DURING CHRONIC X-RAY IRRADIATION. Fomichenko, K. V.; Disko, N. A. (Belorussian State Univ., USSR). Dokl. Akad. Nauk BSSR, 9: 199-201(Mar. 1965). (In Russian).

White rats were given a daily x-ray dose of 40 R on 19 separate days over a period of one month (total dose of 40 × 19 or 760 R). The blood serum proteins were separated by paper electrophoresis. The control animals had a content of 43.7% albumins, 19.6% alpha-globulins, 22.4% beta-globulins, and 13.1% gamma-globulins. The irradiated animals showed no change in the alpha-globulin or beta-globulin fractions. On the other hand, the content of gamma-globulins increased from 13.1% in the controls to 21.7% fifteen days after irradiations, to 30.2% thirty days after irradiation, and was still 29.0% ninety days after irradiation. The albumin content decreased from 43.7% in the controls to 29.1% ninety days after the irradiation. (TTT)

43767 STERILITY OF MALE PLANTS DUE TO PENETRATING RADIATION. Avramenko, B. I.; Ipatev, A. N.; Mushinskaya, L. G.; Savchenko, A. P. (Inst. of Genetics and Cytology, Academy of Sciences, Belorussian SSR). Dokl. Akad. Nauk BSSR, 9: 202-4(Mar. 1965). (In Russian).

Induced male sterility in plants is of interest in the production of hybrid seeds, since removal of the male flowers by hand labor is undesirable. Air-dried seeds of corn, smut, wheat, cucumber, tomato, bean, mustard, radish, cabbage, and others were irradiated with varying doses of ^{60}Co gamma rays. The pollen sterility was determined by staining the pollen with acetocarmine and counting under a microscope. The average % male sterility of cucumber seeds increased with increasing dose from 10.4% in the controls to 18.3% at a dose of 30 kR, and then to 37.0% at a dose of 45 kR. In mustard the sterility increased from zero percent in the controls to 25.7% at a dose of 200 kR. With Chinese cabbage the sterility went from zero percent in the controls to 23.6% at a dose of 200 kR. Winter cress (Barbarea vulgaris R.) showed zero percent for the controls and 22.1% sterility at a dose of 120 kR. The Cruciferae did not show a clear dependence between dose and sterility. At a dose of 9 kR the white bean gave a male sterility of 14.3%, while the Russian black bean showed a sterility of 20.7%. The percent fertile plants decreased in proportion to the irradiation dose. Analogous results were obtained with the irradiation of corn seeds. Different corn varieties show differences in radiation resistance. The results show that pollen sterility is increasing by seed irradiation. Thus, it can be assumed that more hybrid seeds can be produced by planting an irradiated maternal variety with an unirradiated paternal variety. (TTT)

43768 RESTORATION OF MITOTIC ACTIVITY IN THE EPENDYMA OF THE CEREBRAL HEMISPHERES OF X-IRRADIATED RAT EMBRYOS. Val'shtrem, E. A. (Leningrad State Inst. of Pedagogy; Inst. of Experimental Medicine, Academy of Medical Sciences, USSR). Dokl. Akad. Nauk SSSR, 161: 955-7(Apr. 1, 1965). (In Russian).

The author had observed earlier that single whole-body x irradiation of 10-day-old rat embryos with 130 R sharply reduced the number of mitoses in the ependyma of the cerebral hemispheres. Restoration of normal function began on the 14th day of embryogenesis. Brain anomalies which were induced decreased in the 14th to 17th day period. The effects of a 240 R dose on mitosis in the same tissue are described. Mitotic activity in the 10-day-old embryo is normally very intense, especially in the ependyma, with 42.13% of the cells dividing. In the experimental animals 24 hours after irradiation (10th day of embryogenesis), the rate dropped to 11.11%. It increased thereafter and by the 16th day was about the same as in the control, an indication that mitosis had returned to normal. Normalcy had been restored two days earlier (14th day) when the 130 R dose was used, and the lower dose had caused fewer brain anomalies. No brain repair was noted after the 240 R dose. The irreversibility of brain anomalies is apparently not due to a decrease in mitotic activity. (ATD)

43769 CHANGES IN CONCENTRATION OF NUCLEIC ACIDS IN THE GONADS OF LEUCASPIUS DELINEATUS AFTER EXPOSURE TO URANIUM. Telitchenko, M. M.; Chistyakova, T. I. (Moscow State Univ.). Dokl. Akad. Nauk SSSR, 161: 962-3(Apr. 1, 1965). (In Russian).

Earlier histological investigations indicated that uranium seems to injure the gonads of female fishes more than it does those of males. However, visual observations over several generations failed to show that males have greater resistance to uranium than do females. In view of the role of the nucleic acids in the transmission of hereditary information, the authors undertook to investigate the concentration of DNA and RNA in the gonads of fishes (Leucaspius delineatus) chronically exposed to uranium. The gonads of males kept 8 or 15 days in water containing solutions of uranyl nitrate (10 or 25 mg of uranium per liter) showed a marked decrease in the DNA and RNA content (averaging 37% and 22%, respectively). The gonads of the females, on the other hand, did not change significantly in this respect; in fact, the DNA and RNA content increased slightly (DNA by 9% and RNA by 5% on the average). The authors concluded that the testes of Leucaspius delineatus males are not more resistant to uranium than the ovaries of the females. (ATD)

43770 ANALYSIS OF THE DELAYED EFFECTS OF GAMMA RAYS AND 660-Mev PROTONS ON CHROMOSOMES. Khvostova, V. V.; Nevzgodina, L. V.; Dubinin, N. P. (Inst. of Biophysics, Academy of Sciences, USSR). Dokl. Akad. Nauk SSSR, 161: 1219-21(Apr. 11, 1965). (In Russian).

The effect of storage (1 year) of irradiated pea seeds on the number of chromosomal rearrangements in primary rootlets sprouted from these seeds was investigated. Study of the delayed effects of radiation, i.e., the increase of radiation injury during storage, helps clarify the ways in which cells are influenced by different types of radiation. Previous studies showed less delayed effects in seeds irradiated with fast neutrons than in those subjected to gamma and x ray irradiation. It was concluded that neutrons injure chromosomes directly during irradiation, whereas gamma and x rays act, to a great extent, after irradiation, perhaps explained by the presence of long-lived free radicals in the latter case. Two batches of air-dried pea seeds were irradiated with 660-Mev protons (dose 1940 Rad, dose rate 43 Rad/min), and with an identical dose of gamma rays (dose rate 289 Rad/min). Both groups were germinated, and then fixed 2 days, 6 months, and 1 year after irradiation. Seeds were stored at 15 to 20°C in paper packets. As a result of a year's storage of seeds irradiated with gamma rays, the number of cells with chromosomal rearrangements in the meristem of primary rootlets increased 4 to 5 times. But only twice as many aberrant cells were observed in proton-irradiated seeds. According to this index, 660-Mev protons have a weak delayed effect on seeds, i.e., they injure chromosomes mainly at the moment of irradiation. Other studies showed that the RBE of high-energy protons is between that of x rays and neutrons, but somewhat nearer the latter. Thus, the effect of 660-Mev protons is closer to that of radiation with a high linear energy loss than to that of gamma radiation. (ATD)

43771 EFFECTIVENESS OF RECOVERY OF MICE FOLLOWING THEIR EXPOSURE TO 660-Mev PROTONS. Konoplyannikov, A. G.; Kudryashov, Yu. B.; Yarmonenko, S. P. (Moscow State Univ.; Inst. of Industrial Hygiene and Occupational Diseases, Academy of Medical Sciences, USSR). Dokl. Akad. Nauk SSSR, 161: 1448-50(Apr. 21, 1965). (In Russian).

Experiments were conducted to determine the postradiation recovery of animals after irradiation with x rays and 660-Mev protons. The experimental animals were 960 male white mice, weighing 19 to 22 g. They were irradiated with 660-Mev protons on a synchrocyclotron (dose power 300 to 400 Rad/min) and with x rays on a 180-kv unit (dose power 30 Rad/min). The degree of radiation injury was determined by calculating the 50% lethal dose for 30 days

after irradiation. After this preliminary determination, two large groups of mice were irradiated with half the lethal dose (580 to 295 Rad, respectively, for protons and x rays). Two, 6, 13, and 20 days after this primary irradiation, groups of 120 to 150 mice received an additional dose of x rays, and the lethal dose after secondary irradiation was determined. The extent of residual injury (from the first irradiation to the second) was calculated by comparing the two lethal dose values (with single and multiple irradiation). The existence of a period of increased radiation resistance was observed with both proton and x ray irradiation. No statistically reliable differences were found in the length of the period of partial recovery for animals irradiated with protons and x rays, or in the dynamics of recovery in both cases. Previous theories, which postulated the uniformity of the recovery rate and the presence of irreversible components of radiation injury, were disproved. Experiments show that postradiation recovery processes with both 660-Mev protons and hard x rays have a similar nature. This suggests the possibility of extending the principles of radiation therapy and prevention to the field of proton irradiation. (ATD)

43772 HISTOPATHOLOGICAL STUDIES ON TRANSPLANTED EXPERIMENTAL OSTEOGENIC SARCOMA. Horie, Kenya; Makita, Motoo; Sato, Kazuto (Tachikawa Hospital, Tokyo). Gann, 52: 225-32(Sept. 1961).

Osteogenic sarcoma was induced in the tibia of rats by administering various carcinogenic substances in combination with ^{32}P. This sarcoma was successfully transplanted for successive generations (12) into rats of the same strain. The fate of this osteogenic sarcoma during transplantation was followed histologically and observations were made on the effects of various agents such as x radiation, anticancer drugs, prednisolone (Predonin), and aminoacetonitrile (AAN). The effects of x radiation on tumor and normal tissues varied with the dose and the method of radiation. After a single, relatively low dose (250 R) very slight edema only was noted, but definite effects were observed with 1500 R (in 3 daily doses of 500 R each). After irradiation with 2000 R (in 4 daily doses of 500 R each), the animals died the following day. Although tumor degeneration and atrophy were noted histologically they were not conspicuous grossly. Histologically, tumors irradiated with 250 R and showed some dissociation of cells and edematous fluid in the intercellular spaces. Foci of necrosis were not observed. Variation in size of the tumor cells, mononuclear and polynuclear giant cells, and slightly atrophied cells were noted. After 1500-R radiation (in 3 daily doses of 500 R each), intense atrophy and dissociation of tumor cells were noted. The cytoplasm was reduced in amount and the nuclei elongated. Thus atrophy of tumor cells was prominent and appearance of mononuclear and polynuclear giant cells conspicuous. There were also foci of necrosis, which, when compared with those caused by the anticancer drugs, did not have clear-cut margins and merged into ordinary sarcomatous tissue. The necrotic portions in most tumors were converted to hyaline. Similar changes were noted with cytostatic drugs. When Predonin was administered intramuscularly to the sarcomatous animals in 20 daily doses of 50 mg/kg each, growth of the tumor was considerably inhibited. The tumors, compared with the controls, were about one-fifth in size. Also some transplants atrophied and disappeared. Histologically, the tumor cells were elongated and atrophied, but giant cells remained. As the tumor cells atrophied, collagen fibers and silver-staining fibers increased. The necrotic foci were much fewer compared with those of x-irradiated group or those treated with anticancer drugs. Predonin and AAN combined showed almost the same effects as seen in the Predonin group. In the AAN-treated group, the clinical findings in the animals were anorexia, loss of weight, and coarseness of fur. The animals became weak but the tumors continued to grow similarly to controls, and the histological picture did not differ much from that of the controls. (BBB)

43773 THYROID FUNCTION IN THE RAINBOW TROUT (SALMO GAIRDNERI, RICH.). I. BIOCHEMICAL AND HISTOLOGICAL EVIDENCE OF RADIOTHYROIDECTOMY. La Roche, Gilles; Johnson, C. L.; Woodall, A. N. (Univ. of California, Berkeley). Gen. Comp. Endocrinol., 5: 145-59(Apr. 1965).

This report gives biochemical and histological evidence of complete thyroid destruction which is associated with changes in iodine metabolism of rainbow trout. A procedure for radiothyroidectomy in the trout is presented in detail. Investigations of radioiodine turnover and stable iodine distribution furnish adequate evidence of the completeness of radiothyroidectomy when compared with similar studies in intact controls. Stable iodine contents in the thyroid gland of intact controls were ascertained and found to be proportional to the level of ingested iodine. In intact fish thyroidal radioiodine uptakes were shown to be dependent, as in homoiotherms, on the adequacy of dietary iodine. Total serum ^{127}I levels were proportional to the amount of iodine in the diet. Serum protein-bound ^{127}I levels were found to be independent of dietary iodine and of the presence or absence of thyroid tissue. Serum organically bound iodine in thyroidectomized animals is explained by peripheral iodination or iodide binding. Histological examination of serial sections of the thyroid regions, at various times after ^{131}I administration, confirmed the disappearance of thyroid follicles. Results suggest that tyrosine iodination may occur in the absence of thyroid follicles. It is likely that isolated surviving thyroid cells are responsible for continued thyroid hormone synthesis in the absence of follicular epithelium. (BBB)

43774 THE EFFECT OF CLIMATIC CONDITIONS ON CHRONIC IRRADIATION WITH ULTRA-HIGH FREQUENCY ENERGY. Loshak, A. Ya. (Research Inst. of Commercial Air Fleet, Moscow). Gigiena i Sanit., No. 6, 18-22 (June 1965). (In Russian).

Irradiation with ultra-high frequency energy under torrid climatic conditions produced a more frequent and radical functional shift of the organism than in temperate climates. Most sensitive to the combined effect of microwaves and high temperatures is the nervous system in which debilitation processes prevail. Preventive measures are suggested. (tr-auth)

43775 CHANGES OF THE CHOLINESTERASE ACTIVITY IN CHRONIC ADMINISTRATION OF CERTAIN ISOTOPES. Zapolskaya, N. A.; Fedorova, A. V. Gigiena i Sanit., No. 6, 102-4(June 1965). (In Russian).

During chronic exposure to ^{90}Sr and ^{137}Cs changes of the cholinesterase activity were observed; the direction of these changes varied in dependence on reaction time and form of the isotope. At first a sharp increase in the cholinesterase activity was traced, during which the effect of the ^{90}Sr was detected somewhat earlier. Later a temporary decrease of activity during administration of ^{90}Sr and of the normal reaction during daily injections of ^{137}Cs was observed. (tr-auth)

43776 MUTATIONS AND CROP IMPROVEMENT. II. THE GENUS LUPINUS (LEGUMINOSAE). Gustafsson, Ake; Gadd, Ivar (International Atomic Energy Agency, Vienna; Royal Coll. of Forestry, Stockholm). Hereditas, 53: 15-39(1965).

Research reported since 1942 on Lupinus is summarized. Lupinus luteus and angustifolius were changed from the wild state into cultivated plants in the course of 13 years. Strains with valuable mutant genes in the homozygous condition were selected. The starting point for further breeding work was the finding of genes resulting in a profound decrease in alkaloid formation. Mutant genes with discrete phenotypic properties were successively isolated. These were: white seed, soft seed-coat, non-shattering pods, early youth development, rapid growth, glabrous and short-haired pods, resistance to Erysiphe, Fusarium and Glomerella. Specific properties or reactions are generally conditioned by several mutant genes at different gene loci. Most mutant genes are strictly recessive, some are, however, dominant in behavior. Irradiation work has had an introductory character so far. Suitable doses (causing

LD_{50}-survival) are about 15,000 to 20,000 to 25,000 R. Seeds of Lupinus albus and digitatus are less susceptible to irradiation than those of Lupinus luteus and angustifolius. A great proportion of X_2 mutations consists of practically useless types. In Lupinus luteus approximately half of the mutants isolated inhibited chlorophyll formation or caused lethality, sterility or dwarfishness. In Lupinus digitatus the proportion of lethal or semilethal types seemed to be higher, around 80 to 85%. However, some valuable properties such as increased earliness, short hairiness of pods, type of growth, high anthocyanin content were recovered. Some mutants were fully viable and could probably be included in continued breeding work. The population structure of lupine species ranges from almost full self-fertility in Lupinus angustifolius, over a certain amount of spontaneous cross-fertilization in this species and in Lupinus luteus, to a seemingly obligatory cross-fertilization in Lupinus perennis. Breeding methods involving rapid mass propagation of the X_2 and X_3 offspring with a careful inspection of individual traits and plants according to a planned scheme of selection should be used in further experiments. (TCO)

43777 MUTATIONS AND CROP IMPROVEMENT. III. IPOMOEA BATATAS (L.) POIR. (CONVOLVULACEAE). Gustafsson, Ake; Gadd, Ivar (International Atomic Energy Agency, Vienna; Royal Coll. of Forestry, Stockholm). Hereditas, 53: 77-89(1965).

Research on sweet potatoes is reviewed. Production capacity and quality are the chief objectives in breeding programs of sweet potato. Starch manufacturers would prefer varieties high in starch and low in sugar. Table quality, on the other hand, requires a high sucrose content. Carotene content is also of great importance. Further improvement of sweet potato varieties will benefit from the control of flowering ability and the subsequent possibility of hybridization (F_1 heterosis and gene recombination) and selection work of suitable parent strains and hybrid segregates. Wild hexaploid Ipomoea trifida possesses genes for resistance to nematodes and black rot, which if necessary may be transferred to sweet potato. Vegetative mutations in high-productive varieties having good quality could no doubt be induced advantageously or be selected for in natural materials. X, γ or neutron irradiation of cuttings and roots could easily be carried out on a large scale; in the case of sparsely ionizing radiations by using doses around 4000 R for leaf stalks treated according to method of Nishiyama et al., or 20,000 to 40,000 R if roots are irradiated as outlined by Hernandez et al. In fact, vegetative mutants (sports), high in yield, are commonly distributed in practice and their number may certainly increase through utilization of irradiation methods or, possibly, of chemical mutagens. (TCO)

43778 MUTATIONS AND CROP IMPROVEMENT. IV. POA PRATENSIS L. (GRAMINEAE). Gustafsson, Ake; Gadd, Ivar (International Atomic Energy Agency, Vienna; Royal Coll. of Forestry, Stockholm). Hereditas, 53: 90-102(1965).

Radiation experiments performed indicate that high-apomictic varieties of Poa pratensis may change to partial or complete sexuality by an x irradiation of seeds. The sexual types produced give rise to a great number of chromosome aberrants and to other deviating types, some of which are vigorous. Such vigorous types may appear already in the X_1 generation. In later generations the treated biotypes, often sexual or partially sexual, revert rather rapidly to apomixis. The degree of apomixis (seed constancy) may even be increased as compared to the parent type. Strains were selected that show increased resistance to such fungus diseases as caused by Erysiphe or Puccinia. There are also indications that changes in ecological response may occur. These may widen the cultivation area of a special, high-productive or otherwise suitable variety or adapt the variety to changes in methods of cultivation. The best mutagenic treatment so far analyzed is x irradiation, using a dose of about 20,000 R on dry dormant seeds. (auth)

43779 MUTATIONS AND CROP IMPROVEMENT. V. ARACHIS HYPOGAEA L. (LEGUMINOSAE). Gustafsson, Ake; Gadd, Ivar (International Atomic Energy Agency, Vienna; Royal Coll. of Forestry, Stockholm). Hereditas, 53: 143-64(1965).

Research on Arachis hypogaea is reviewed. Arachis hypogaea is probably an amphidiploid species, with partial homology between chromosomes belonging to different chromosome sets. This is indicated by rare trivalent and quadrivalent formations at the meiotic metaphase. Inheritance of many characteristics studied is of the simple monofactorial type or proceeds by duplicate factors. Morphological mutations are generally recessive. The interesting marker gene Krinkle is a dominant. The population system is characterized by the close autogamy with some exceptional but low degree of outcrossing. The multivalent formation, with crossing over in partially homologous segments, as well as other meiotic disturbances, may give rise to some hereditary instability, of different intensity in different varieties or hybrids of varieties. (Meiosis should be studied more intensively in hybrid and radiation progenies, for instance, in outcrossings of drastic mutant types.) Differences in x-ray sensitivity occur between varieties. Consequently the LD_{50} dose differs with the variety. For dry seeds, with 5 to 10 per cent moisture content, it lies between 10,000 and 35,000 R of x rays. With fast neutrons it apparently lies around 4000 to 5000 reps. The mutation work carried out by Gregory and coworkers is outstanding in methodology and analysis. According to them, the genetical background frequently mutates with x irradiation, giving rise to a series of modifier mutations (micromutations) simultaneously with the origin of drastic morphological mutations (macromutations). Also plants normal in appearance may obtain mutations of the modifier type, with slight effects on morphology, physiology, yield and disease resistance. Of great methodological importance are the mutants resistant to attacks by Cercospora. By selection within the offspring of seemingly normal irradiated plants a strain was obtained, NC 4x, which is high-yielding and of good fruit and seed quality. This strain was released as a trade variety in 1959 as a result of a breeding project lasting ten years. (TCO)

43780 PROCEEDINGS OF THE CONFERENCE ON MECHANISMS OF THE DOSE RATE EFFECT OF RADIATION AT THE GENETIC AND CELLULAR LEVELS, OISO, NOVEMBER 4–7, 1964. Idengaku Zasshi, 40: Suppl., 1-280(1965). (CONF-732).

Separate abstracts were prepared for 16 papers. Two papers were abstracted previously and appeared in NSA Vol. 18 as numbers 43228 and 43229. (C.H.)

For abstracts of individual papers see: 43781–43795, and 43866.

43781 RELATION BETWEEN RADIATION EFFECTS AND DOSE RATES OF X- AND γ-RAYS IN CEREALS. Matsumura, Seiji (National Inst. of Genetics, Misima, Japan). Idengaku Zasshi, 40: Suppl., 1-11(1965).

In order to investigate the relation of radiation effects to dose rates, dry seeds of rice and cinkorn wheat were irradiated with x rays and γ rays from ^{60}Co or ^{137}Cs sources at doses of 4 to 40 kR in experiments with acute (10,000 R/hour) and chronic irradiation (20 to 35.6 R/hour). The germination rate, seedling height, seed fertility in X_1, and chrolophyll mutations in X_2 were investigated. (auth)

43782 COMPARISONS OF THE TOLERANCES OF HIGHER PLANT SPECIES TO ACUTE AND CHRONIC EXPOSURES OF IONIZING RADIATION. Sparrow, Arnold H. (Brookhaven National Lab., Upton, N. Y.). Idengaku Zasshi, 40: Suppl., 12-37(1965). (BNL-8539).

Recent publications have shown that classical concepts concerned with differences in radiosensitivity between species require a more thoroughgoing scrutiny. Calculations of the relative amounts of energy deposited within the chromosome reveal that many of the presumed differences in tolerances merely reflect differences in tar-

get volumes of the genetic material of the species being compared. In seeking to understand the radiobiological consequences of an exposure of tissue to ionizing radiation, it is now clear that one should consider not only the physical parameters of dosimetry, but also certain biological parameters of the cells in which the energy is absorbed. Our results indicate that the most important single biological parameter in comparative radiobiology of the higher plants is interphase chromosome volume which is subject to much variation in different species or tissues. The energy deposited in this volume seems often to be a better index of the ultimate biological effect than is the dose or exposure expressed in rads or roentgens. Data are presented on the radiosensitivity of about 50 species of higher plants that indicate that dose rate needs to be considered in relationship to the nature of the critical targets in the cells being irradiated. It is suggested that dose rate be expressed in terms of energy units (e.g., kev) which will vary with target volume. Results which have a bearing on this and other aspects of comparative radiobiology of woody and herbaceous spermatophytes after acute or chronic exposure to γ radiation from a ^{60}Co source are reported and discussed. (auth)

43783 CYTOLOGICAL STUDIES ON THE RADIOSENSITIVITY OF SPERMATOGONIA OF THE SILKWORM. Nakanishi, Yuh H.; Iwasaki, Tamiko; Kato, Hatao (National Inst. of Radiological Sciences, Chiba, Japan). Idengaku Zasshi, 40: Suppl., 49-67(1965).

A study of morphological features of spermatogonia of about 20,000 silkworm larvae at various developmental stages in relation to their radiosensitivity led to the conclusion that there are some specific types of spermatogonia in the silkworm which exhibit different sensitivities to radiation. Detailed analyses of the radiosensitivity of spermatogonia were undertaken in order to obtain quantitative cytological information concerning radiosensitivity, as well as to supplement some earlier observations by Sado (1961, 1963a, b) for the silkworm on one hand, and on the other hand to confirm the results of Oakberg (1955a, b, 1956a, b, 1957, 1959) and Monsei (1962a, b) for mouse spermatogonia. Careful microscopical examinations of serial sections of the testes made possible the accurate identification of six successive generations or stages of spermatogonia: they are referred to as spermatogonia-I, -II, -III, -IV, -V and -VI, on the basis of the number of the spermatogonia within each gonocyst. The relative radiosensitivity of spermatogonia at different stages was determined by scoring the number of gonocysts containing pycnotic spermatogonia-I to -VI following irradiation with 1000 R of x rays at a dose-rate of 300 R per minute. After irradiation, spermatogonia-VI showed the highest value in pycnotic incidence, while those -V to -I were progressively less in number. An autoradiographic study with tritiated thymidine revealed that there was a significant difference in percentage of labeled gonocysts among different stages of pycnotic spermatogonia. It seems most probable that there is a definite correlation between radiosensitivity of different stages of spermatogonia and degree of DNA synthesis in the cells at the time of irradiation. Furthermore, the spermatogonia-VI were most sensitive, producing chromosome clumping in late prophase, and became progressively less sensitive toward early stages of spermatogonia. Evidence of selective killing of highly radiosensitive spermatogonia was observed in larvae in the late developmental stage, while in newly hatched larvae spermatogonia in the early stages, which form the bulk of the germ cells, are less sensitive. It seems probable that spermatogonia-VI are most sensitive to x rays in producing pycnotic degeneration and chromosome clumping, and that so far as the scope of the present experiments is concerned, the sensitivity to radiation decreases as follows: spermatogonia-VI, -V, -IV, -III, -II and -I. The application of cytological methods and a full understanding of cytological principles are required in order to shed light on the troublesome question of the relationship between radiation and mutation. (auth)

43784 MECHANISMS CONTROLLING TWO TYPES OF DOSE-RATE DEPENDENCE OF RADIATION-INDUCED MUTATION FREQUENCIES IN SILKWORM GONIA. Tazime, Yataro (National Inst. of Genetics, Misima, Japan). Idengaku Zasshi, 40: Suppl., 68-82(1965).

As far as x and γ rays are concerned, the mutational response of young germ cells, mostly gonial stages, of the silkworm is not simple. At least two types of dose-rate dependence, with one being the reverse of the other, have been found in this insect. In one type the mutagenic effectiveness of chronic irradiation (0.1 R/minute) is lower than that of acute irradiation (100 to 300 R/minute) and in the other, mutagenic effectiveness is higher for chronic irradiation than for acute irradiation (Type II). Which type appears is solely dependent upon the developmental stage of the irradiated larva. Irradiation of newly hatched larva result in a Type I dose-rate dependence while irradiation at a later stage, around the time when the larvae are eight days old, gives completely reverse results. The complexity in the feature of the dose-rate effect is entirely due to a drastic change in mutagenic effectiveness of acute irradiation in accordance with the developmental stage. The dose-mutation frequency curve shows the highest peak at hatching time but decreases rapidly thereafter. In contrast, the mutagenic effectiveness of chronic irradiation remains almost the same. In order to interpret the reverse type of dose-rate effect, a hypothesis involving selective cell killing was proposed. The hypothesis was based on the finding that the homogeneous germ cell population which is present at hatching time becomes gradually heterogeneous with the development of the larva and gonial cells at an advanced stage are highly sensitive to cell killing by radiation. It was also assumed that cell killing is more drastic for the acute than for the chronic exposure and that the cells sensitive to killing are also sensitive to having mutations induced in them. However, cytological evidence to support this hypothesis was not obtained. Secondly a differential repopulation hypothesis was proposed but this was again found to be unsatisfactory. The dose-fractionation experiments, however, yielded very suggestive information for the interpretation of the dose-rate effect. When 1000 R acute irradiation was delivered in two fractions, 500 R + 500 R, separated by various time intervals from two to 48 hours, a remarkable increase in mutation frequency was observed throughout the period examined, showing a peak if the second dose was given 12 or 24 hours after the initial exposure. Several possibilities have been considered for interpreting this effect. Among them the most promising was the idea that metastasis produced by the preceding exposure depresses the repair of premutational damage caused by the subsequent exposure. The same idea reasonably explained the drastic change in the mutational response to acute irradiation during the progressive development of the larva. A new hypothesis, based on this idea, is proposed for the interpretation of the complicated features of the dose-rate effect as follows: a large part of the radiation-induced premutational damage is repaired during the post-irradiation recovery process; the degree and extent of repair primarily depends upon the total dose and dose rate; the occurrence of repair also largely depends upon cellular conditions, presumably metabolic activity, of the irradiated cell; and the final magnitude of the observed mutation frequency is determined by both factors in combination. (auth)

43785 MUTAGENIC EFFECTS OF CHRONICALLY AND INTENSELY DELIVERED RADIATION IN DROSOPHILA. Oster, I. I. (Inst. for Cancer Research, Philadelphia). Idengaku Zasshi, 40: Suppl., 83-96(1965).

Results of recent experiments on the effects of varying the dose-rate of γ radiation in Drosophila are presented and discussed in relation to previous findings and those of others. At the present time no clear-cut evidence for a dose-rate effect in the production of mosaically-expressed and whole-body point changes is available although further work is indicated. The latter would be aimed at ruling out

the possibility of complications arising because of differential radiosensitivity masking repair mechanisms. On the other hand, in non-static cells (e.g., those which are more active, metabolically-speaking, and less mature than spermatozoa) processes involving multi-hit phenomena exhibit a distinct dosage dependence. (auth)

43786 RBE OF FAST NEUTRONS TO γ-RAYS FOR MUTATIONS IN RELATION TO REPAIR MECHANISMS. Kondo, Sohei (Osaka Univ.). Idengaku Zasshi, 40: Suppl., 97-106(1965).

A brief review of relative biological effects (RBE) for somatic and genetic damage is given for various organisms. A brief summary is given concerning comparative studies of mutation frequencies with silkworm irradiated with γ rays, 14 Mev neutrons, and fission neutrons. From the analysis of the silkworm data combined with the above mentioned review of RBE data for other organisms, the following hypotheses are proposed: The overall mutation frequency in silkworm gonia depends on the interaction of radiation with the intercellular repair mechanisms connected with certain multi-cellular organs, and the low mutation rate recovered on acute γ irradiation of silkworm larvae at the late gonial stage is due to stimulation of repair by radiation. (auth)

43787 COMPARISONS BETWEEN MUTAGENIC AND CELL-KILLING EFFECTS INDUCED BY RADIATION AND RADIOMIMETIC SUBSTANCES. Nakao, Yoshio (National Inst. of Radiological Sciences, Chiba, Japan). Idengaku Zasshi, 40: Suppl., 107-18(1965).

The mutagenic and cell-killing effects induced by x rays and by chemical mutagens were compared using sex-linked recessive lethal mutation in Drosophila and visible mutation (egg color mutants) detected by specific locus method in the silkworm. In the case of the induction of lethals and translocations by ethylene imine in Drosophila spermatozoa, we have noticed the production of high degree of sterility. And when we compared mutation and translocation frequencies between two groups which showed high and low sterility, we found the existence of parallelism between lethal or translocation frequencies and sterility. In the case of x-ray induced lethal mutations in Drosophila, there was no sign of correlation between mutation frequencies and sterility, even when x ray doses were so high as to produce only a few progeny. There were also no apparent correlations between mutation frequencies and the number of eggs laid, between mutation frequencies and hatchability, and mutation frequencies and the percentages of dead eggs in the early developmental stages in the silkworm, when male moths were x irradiated with the dose of 2 kR. The circumstances were the same as before even when the male moths were irradiated with fairly high dose of x rays (10 kR). When the female moths were irradiated with high dose of x rays (10 kR) (and in this case the lethality amongst eggs was very high), we could not find any difference in the mutation frequencies between two groups which have comparatively high hatchability and those which have low hatchability. The patterns of induction were compared between mutation and lethals at various stages of embryonic development in the silkworm, and it was found that the changes of the percentages of dead eggs at the pigmented egg stages and at the bluish egg stage agreed with those in mutation frequencies. The relationship between mutation induction and the production of cell-killing is discussed. Especially, the relationship of these facts to the hypothesis of selective cell killing is considered to explain the cause of dose rate effect in mutation induction by radiation. (auth)

43788 THE EFFECTS OF DOSE, DOSE RATE AND QUALITY OF RADIATION ON THE DYNAMICS AND SURVIVAL OF THE SPERMATOGONIAL POPULATION OF THE MOUSE. Oakberg, E. F. (Oak Ridge National Lab., Tenn.). Idengaku Zasshi, 40: Suppl., 119-27(1965).

The observation of a dose-rate effect on mutation frequency in late oocyte stages, where no cell killing occurs, is conclusive evidence for intracellular repair of premutational damage. The logical assumption that similar repair occurs in spermatogonia is supported by comparison of mutation frequency and cell killing after 600 R x radiation at ~90, 9.3, and 0.8 R/minute. Mutation frequency in spermatogonia drops by a factor of 3.2 over this range of dose rates, but cell survival is not significantly different. Thus, a dose-rate effect independent of cell selection is demonstrated for mutations in spermatogonia. In investigating the effects of fractionated doses, it was found that most spermatogonia are in interphase, and primarily in G_1, 24 hours after an exposure to 500 R. This supports the hypothesis that cell synchronization by the first dose is an important factor in the increased mutation frequency observed when two 500 R fractions are given 24 hours apart. Relative survival of S and G_2 is less than for G_1 for doses of 500 R or of 500 + 500 R, but survival of G_2 and G_1 are comparable after 1000 R. Furthermore, cell survival is lower, but mutation rate higher after 500 + 500 R than after a single 1000 R exposure. Thus, stage at time of irradiation and differential cell survival are more important than number of survivors per se in the effect of fractionation on mutation frequency. Recovery of post-irradiation DNA synthesis is slower after 1000 R than after either 500 R or 500 + 500 R. The interval between irradiation and initiation of cell division, therefore, is highest for the 1000 R exposure as a result of this greater damage to cellular metabolism. (auth)

43789 THE NATURE OF THE DOSE-RATE EFFECT OF RADIATION ON MUTATION IN MICE. Russell, W. L. (Oak Ridge National Lab., Tenn.). Idengaku Zasshi, 40: Suppl., 128-40(1965). (ORNL-P-681).

Data are reviewed from studies of the dose-rate effect with x, γ, and fission neutrons on mutations in mouse spermatogonia and oocytes irradiated at various dose levels. The finding of an effect of dose rate on mutation, and the experimental evidence leading to the conclusion that this effect is a result of intracellular processes, presumably repair of premutational damage, demonstrate a hitherto unsuspected complexity in the process of induction of mutation by radiation. Further deductions about the nature of the repair process are presented. It is concluded that the dose-rate effect on mutation is probably not due to a process involving the participation of an undamaged strand in the repair of a damaged one. (auth)

43790 KINETIC STUDIES OF THE RECOVERY PROCESSES IN HeLa CELLS DAMAGED BY X-IRRADIATION. Terasima, Toyozo (National Inst. of Radiological Sciences, Chiba, Japan). Idengaku Zasshi, 40: Suppl., 162-75 (1965).

Several responses of HeLa S3 cells to the killing effect of x rays at selected times during the growth cycle are described. Application of metabolic inhibitors such as 5-fluorodeoxyuridine and deoxyadenosine to synchronized population revealed that the most sensitive state of cells during interphase was attained just before the start of DNA synthesis, and that the reduction of sensitivity found in the latter half of interphase was largely correlated with DNA synthesis. Fractionated dose experiments of recovery processes of HeLa S3 cells in culture indicated that at least two mechanisms, repair of sublethal damage and a compartmental shift of cells, operate in the recovery process. (auth)

43791 REPAIR OF X-RAY DAMAGE IN MAMMALIAN CELLS. Elkind, M. M. (National Cancer Inst., Bethesda, Md.). Idengaku Zasshi, 40: Suppl., 176-93(1965).

Results are reported from studies of the recovery from radiation injuries of Chinese hamster cells grown in tissue culture after exposure to fractionated doses of 55 Kv or 2.5 Mv x rays. The influence of oxygen concentration and temperature on recovery of the cells was evaluated. It was concluded that sublethally irradiated cells repair damage rapidly and without delay. In spite of the complexity of the results obtained at 37°C, this conclusion is clear, but it is not possible to state how complete recovery is. It is apparent that in asynchronous Chinese hamster cells, repair is substantial and comes about rapidly. Based on

results at 37°C only, the essential features of the repair-progression model are presented. From the information presented, plus data on the single-dose response as a function of age, a fairly detailed picture of the fractionation response of asynchronous Chinese hamster cells can now be given. From the data presented, we know that both the rate of repair and the rate of progression appear to be weakly dependent on the size of the first dose. As a result, the maximum and the minimum occur at about the same times for a range of first doses. The first dose has the effect, therefore, of selecting a more or less synchronous fraction of the starting population which then proceeds toward division at a rate comparable to that of unirradiated cells. When division starts after the delay period, cell number increases exponentially, but two-dose survival does not. From results obtained after the delay period, we know that it takes about two to three doubling times for synchronization and other transients produced by a first dose (10 to 20% survival) to be damped out. In contrast, repair may be completed during the division delay period or shortly thereafter. Some of the details in the picture described were drawn from studies at reduced temperatures. These results, plus those with hypoxic cells, afford some insight into the mechanism of repair. Repair does not require oxidative metabolism and is weakly dependent on temperature. This suggests that if the process is enzymatic, probably only one or a few enzymes are involved. However, in view of the fact that some repair occurs even at 0.5°C, it is possible that the process is not enzymatic but physical-chemical. Whatever the process of repair may involve, and whatever may be the sites which are repaired, it seems likely that they are common to many types of cells. Fractionation results, qualitatively similar to those described here, have now been observed with other types of cells grown in culture, with mammalian cells assayed in vivo, and with plant cells. It appears that proliferating cells in situ can repair damage in much the same way as cells grown and treated in culture and that the artificial experimental system called cell culture can be used to advantage to study the radiation response of mammalian cells in their normal environment. (auth)

43792 RECUPERATION IN MAMMALIAN CELL SYSTEMS AS REVEALED BY RADIATION DOSE FRACTIONATION. Kallman, Robert F.; Silini, Giovanni; Frindel, Emilia (Stanford Univ., Palo Alto, Calif.). Idengaku Zasshi, 40: Suppl., 207-28(1965).

Mature C57BL and BALB/c mice were whole-body irradiated, with either single 250 kV x ray doses of short duration or with graded series of second doses at different times after one of three constant conditioning doses (D_c). Second doses were administered at two-hour intervals during the first 12 hours and at 6 to 12 hour intervals thereafter up to 48 hours. LD_{50}'s were determined for the 30 days following irradiation, and these data were used for the calculation of residual injury and recovery, or roentgens repaired. The percent residual injury remaining after all D_c's showed characteristic fluctuations, with a first minimum (period of marked second dose refractoriness) falling at 4 to 9 hours and an ensuing maximum at 8 to 10 hours. As shown by additional experiments in which mortality was determined for constant second doses given at 1½ to 3 hour intervals after different conditioning doses, these fluctuations persisted cyclically until at least 48 hours. The period of the radiosensitivity cycle appears to be approximately 11 to 12 hours. The magnitudes of the initial minima and maxima and therefore, presumably, the amplitude of the cycle were independent of the size of the conditioning dose. The decay in percent residual injury in the 12 to 48 hour period could be regarded as an exponential function with superimposed cyclic fluctuations. The rate of decay was strongly first-dose-dependent, proceeding more slowly the higher the D_c. It was also strain-dependent in that mean decay rate of residual injury was slower in the more radiosensitive BALB/c strain. In contrast, however, the two strains did not appear to differ appreciably in either the amplitude or the periodicity of the cyclic fluctuations superimposed over the mean trend of injury decay. When the same C57BL data were analyzed for recovery, in absolute numbers of roentgens repaired per hour, there was no significant difference between the three D_c's during the 12 to 48 hour post-conditioning period; and an arithmetically linear relation between roentgens repaired and time was adequately fitted to the experimental points. The significance and interpretation of the findings are discussed in terms of an hypothesis which relates the observed LD_{50}'s to the probabilities of survival of individual marrow stem cells, and the changes in LD_{50} to the combined effects of cellular depopulation and synchronization in the post-irradiation growth of first dose surviving cells. At the time of conditioning irradiation the cell population is assumed to be heterogeneous with respect to the stages of the generation cycle and therefore with respect to stage-dependent radiosensitivity. The first dose effectively synchronizes the surviving cells so that their net radiosensitivity assumes different levels at different times. Data are presented which show that both DNA synthesis and mitotic activity fall to minimal levels shortly after irradiation. Mitotic activity rises to a maximum at 10 to 12 hours, then DNA synthesis rises to a maximum; and the data are suggestive that these changes are succeeded by a series of regularly spaced peaks in both kinds of activity. These findings therefore tend to support the hypothesis offered to account for the observed radiosensitivity changes. (auth)

43793 MODIFICATION OF THE INACTIVATION OF BACTERIAL SPORES AND THEIR TRANSFORMING DNA BY IONIZING RADIATIONS. Tanooka, Hiroshi (Japan Atomic Energy Research Inst., Tokyo). Idengaku Zasshi, 40: Suppl., 229-41(1965).

Results are reported from studies on the effects of heat treatment on the recovery of transforming DNA and colony-forming ability of Bacillus subtilis vegetative cell and spores exposed to $^{60}Co\gamma$ radiation or 1 Mev electrons. The highly radioresistant nature of B. subtilis spores was found also in their transforming DNA. No dose rate effect was found in the inactivation of the colony-forming ability and the DNA transforming ability of spores in the employed dose region. Comparison between inactivations of the transforming DNA in vivo and in vitro suggested that recovery of the radiation-produced damage occurs by inter-molecular crosslinking. The colony-forming ability of irradiated B. subtilis spores was restored by an anoxic heat-treatment. This recovery was not found in the transforming DNA of spores and in other dry materials, i.e., vegetative B. subtilis cells and their transforming DNA, the pneumococcus transforming DNA, T1 bacteriophages, and diploid yeasts. The free radical concentration measured by the ESR method showed saturation in a high dose region. The radicals exhibited a considerably long half life. An anoxic heat-treatment decreased the radical concentration and prolonged their half life. The relationship of these observed radicals to biological damage and to their thermo-restoration is discussed. (auth)

43794 MODIFICATION OF LETHAL AND MUTAGENIC RADIATION DAMAGES BY GENETIC REPAIR FACTORS IN BACTERIA. Kada, Tsuneo (Inst. of Physical and Chemical Research, Tokyo). Idengaku Zasshi, 40: Suppl., 242-55(1965).

The induction of reversions was studied in E. coli K 12 Hfr thr_T^- by recombination technics. There is no transmission of the induced character either immediately after irradiation with uv or x rays, nor, in most cases, after incubation of exposed cells. The absence of transmission is also seen for the prototrophic character of many mutants derived from F^+ thr_T^- or from various Hfr thr_T^- of different origins of chromosomal injection. Futhermore revertants of F^+ thr_T^- segregated a considerable number of thr^- and the prototrophic character is sensitive to treatment with acridine orange. Secondary irradiation converts prototrophic revertants into auxotrophs with high efficiency. These findings suggest that the radiation-provoked reversion involved a non-chromosomal genetic system and the induced-character can be cured by secondary irradiation, due to loss of this system possessing a greater radio-

sensitivity after mutation. The strain SC of E. coli K 12 brought about, under a condition similar to F-elimination by acridine orange, a high yield of genetically stable new derivatives named AO. If incubated at 37°C after irradiation, the strain AO is more sensitive to low doses of UV and γ rays than the parental strain. At 22°C, AO is as resistant as SC, because of a gradual recovery taking place during several hours after irradiation. The uv-exposed phage T3 gave similar titres on AO and SC, by incubation either at 37°C or 22°C. The uv- or γ-ray-induced chromosomal lesions of Hfr, that were supposed to be transmitted into SC or AO and that would be inhibitory to the marker-incorporation mechanisms, were not influenced by the difference in irradiation sensitivities of these two female strains. The temperature-sensitive recovery in this system is supposed to be related with damages of some specific cellular function involved in the cell replication. (auth)

43795 MOLECULAR MECHANISMS IN THE REPAIR OF IRRADIATED DNA. Howard-Flanders, Paul (Yale Univ., New Haven). Idengaku Zasshi, 40: Suppl., 256-63 (1965).

The molecular mechanisms of repair or recovery in microorganisms, especially E. coli., after exposure to ultraviolet or x radiation are discussed. Radiation effects on cells are intimately concerned with radiation effects on the desoxyribonucleic acid (DNA). It is possible that if we learn enough about radiation effects on DNA in the cell, we shall come to understand the biological effects of radiation at the cellular level. The estimated number of chemical bonds broken in the DNA per lethal hit is about one for single-strand viruses, five to ten for double-strand viruses, fifty to one hundred for haploid microorganisms, and a thousand or more for diploid cells including mammalian cells. We must reconcile this insensitivity to radiation damage in the DNA of cells with the concepts now so successful in molecular genetics, where the detailed structure of DNA is important base by base. The efficient mechanisms that cells have developed for repairing their DNA are discussed. There are two reasons for supposing that DNA repair is closely connected with genetic recombination and may play a part in it. The first is experimental. Certain of the mutants of E. coli K-12 isolated as recombination-defective mutants have proved to be also defective for DNA repair and to be highly sensitive to both ultraviolet and x rays. Moreover, mutants isolated for sensitivity to x rays have also proved defective in genetic recombination. This suggests that one or more common enzymes are employed in genetic recombination and in DNA repair. There is a second reason for associating genetic recombination in DNA repair. It is believed that genetic recombination always proceeds by cutting the DNA strands and then rejoining the ends. It is then necessary to cut the other strands to the correct length and to rejoin them to complete the recombinant molecule. The striking feature of the mechanism proposed for DNA repair is that it can be at once adapted for a mechanism for completing genetic recombination. It is suggested that the region of homologous pairing must be established between single strands to two DNA molecules that terminate with 5′ ends. Then the other ends of the molecules which terminate in 3′ ends are degraded by nucleases and, as in DNA repair are reconstructed to exactly the right length. Thus, once the initial cuts have been made and pairing has been established between the two molecules, this scheme provides satisfactory explanation as to how the remaining strands are cut to the correct length and finally rejoined. (auth)

43796 A NOTE ON PRELIMINARY FIELD STUDIES OF THE USE OF IRRADIATED MALES FOR REDUCTION OF C FATIGANS WIED. POPULATIONS. Krishnamurthy, B. S.; Ray, S. N.; Joshi, G. C. (Central Inst. for Communicable Diseases, Delhi). Indian J. Malariol., 16: 365-73(Dec. 1962).

Irradiation of male pupae of Culex fatigans with γ rays (7700 R) rendered the adults sterile. The proportion of nonviable egg-rafts (embryonated eggs which did not hatch into larvae) increased with a rise in the proportion of sterile males to normal males. Studies were, therefore, undertaken to determine the possibility of the use of the sterile male mosquitoes to achieve reduction in the field in C. fatigans population. The investigations consisted of the following steps: (1) Rearing of large number of mosquitoes in the laboratory. (2) Separation of large number of pupae from the larval cultures and sexing them. (3) Transport of the pupae from the lab to the source of irradiation and back. (4) Exposure of these pupae to γ radiation in batches of 1000 to 1200 pupae. (5) Release of the irradiated sterile male mosquitoes in the experimental village. (6) Collection of data and evaluation of the results. There was high mortality in the irradiated pupae due to repeated handling while separating and transporting them over long distance and effects to minimize pupal mortality were not successful. Male mosquitoes, hatched from the irradiated pupae, were transported to the site of release, the village of Aslatnagar, during the peak period of culicine breeding, but it was only possible to release a total of 24,000 irradiated sterile males during the period of observation. From the data it was seen that the larval, pupal, and adult mosquito density in this experimental village increased similarly to that of the control village during the observation period. The observations also revealed that loss of fertility among the females, determined by the nonviability of the embryonated rafts, was only 6% in the experimental village. Completely unfertilized rafts were obtained from the females in 1.5 and 2.0% in the experimental and control villages, respectively. Thus, the results of this small scale preliminary field trial on the release of irradiated sterile male C. fatigans showed that there was no reduction either in the adult or larval densities, but there was an increase in the percentage of unhatched egg-rafts. This indicated the possibility of using irradiated sterile males to effect reduction of C. fatigans population in the field in more extensive trials. (BBB)

43797 PREVENTION OF LIVER METASTASES BY INTRAVENOUS RADIOISOTOPES: USE OF ^{32}P-LABELED COLLOIDAL CHROMIC PHOSPHATE IN RATS. Ackerman, Norman B.; McFee, Arthur S.; Loken, Merle K. (Univ. of Minnesota, Minneapolis). J. Am. Med. Assoc., 187: 826-8(Mar. 14, 1964).

In Holtzman rats a rapidly growing tumor, the Novikoff hepatoma, was used to simulate liver metastasis by injection of a counted number of cells into the portal vein of the rats. Injection of 100,000 cells of this tumor into the portal vein produced liver tumors in 70% of the rats so treated. In addition to the injection of tumor cells, the experimental animals received intravenously 75 μC of ^{32}P-tagged colloidal chromic phosphate 24 hr before, or one min, 60 min, or 24 hr later. In the control group, 75% of the rats had tumors in the liver at 2 weeks. This decreased to 31%, or eight of 26 animals, in the group receiving colloidal chronic phosphate one min after the tumor cells. Of the 60-min colloidal-chromic-phosphate group 38%, or ten of 26 animals, had liver tumors in two weeks, and the 24-hr colloidal-chromic-phosphate animals 42%, 11 of 26, had liver tumors. Tumor take in animals pretreated with colloidal chromic phosphate was not significantly different from that in the control group. In studies on distribution of colloidal chromic phosphate after intravenous injection it has been shown that about 80% to 90% is concentrated by the liver. Only 2% to 15% is taken up by the spleen and the remainder of the chromic phosphate is distributed in very small quantities among the other tissues of the body. The compound is cleared from the blood within minutes. There is no problem of bone-marrow depression following injection of this material. With massive experimental doses in animals, liver necrosis occurred, but the doses were considerably higher (from 50 to 100 times) than those used here. It was calculated that a dose of 3000 rad was delivered to the livers of the rats used in these studies after the administration of 75 μC of chromic phosphate. This dose was probably in the low therapeutic range. The radiotherapy is, in part, effective because of the almost ideal geometry involved,

that is, radiation directed against single cells or small aggregates of unrooted cells. (BBB)

43798 BEHAVIOR OF LIPASE ACTIVITY OF THE GAMMA-IRRADIATED GROUNDNUT DURING GERMINATION. Patel, G. M.; Vyas, D. N.; Patel, K. C. (Sardar Vallabhbhai Vidyapeeth Univ., Vallabhvidyanagar, India). J. Am. Oil Chemists' Soc., 42: 617-19(July 1965).

Results are reported for changes in lipase activity of peanut seeds germinating 0 to 30 days after exposure to ^{60}Co radiation at doses of 10, 30, 50, 70, 90, and 120 kR. Irradiated seeds showed a comparatively poor rate of germination with increase in radiation dose as compared to control seeds. The increase in lipase activity of the seeds grown in the dark was poor in comparison to that of seeds grown in light. Activity in both irradiated and nonirradiated seeds decreased in the initial stages of germination. This decrease was observed up to the third day of germination; thereafter there was an increase in lipase. Activity of the control seeds attained a maximum on the 12th day of germination and was higher than that obtained for irradiated seeds. The seeds irradiated to 10 kR showed maximum lipase content on 16th day of germination, but variation in activity between the 12- and 20-day periods was low. Other irradiated seeds, except for 30-kR dose level, attained maximum activity on the 12th day. Seeds grown in dark or irradiated at 30 kR reached maximum lipase activity on the 20th day of germination. The lipase activity at maxima observed at 12-day germination had the following trend: control seeds > 10 kR seeds > 50 kR > 70 kR > 90 kR > 120 kR. Maximum activity of the seeds (20-day germination irradiated to 30 kR) was greater than that of seeds grown in darkness. Before germination the lipase activity of control seeds was slightly higher than that of irradiated seeds and there was a regular decrease in lipase with dose. Thus, maximum activity for seeds treated under different conditions was attained at different periods of germination. Plant growth and the behavior of lipase was explained on the basis of metabolic factors such as ascorbic acid oxidase, amino acids, and free fatty acids liberated during germination, and their interactions. (TCO)

43799 EFFECTS OF UNILATERAL THORACIC IRRADIATION ON LUNG FUNCTION. Teates, Charles D. (Univ. of Virginia Hospital, Charlottesville). J. Appl. Physiol., 20: 628-36(July 1965).

Studies were made to eliminate difficulties to better evaluate the pathophysiology of the radiation reaction in the lung. Five mongrel dogs were x irradiated over anterior and posterior portals (7.5 × 15 cm) so that one hemithorax was irradiated from the diaphragm to the apex. Radiation was given with a 200-kv unit to anterior and posterior portals on alternate days for a midlung dose of 4500 R over 23 to 27 days. Pulmonary function was studied prior to irradiation and at intervals up to 207 days after irradiation. With the exception of diffusion capacity (DL_{co}), the mean left-to-right ratios of all functions showed little change until 6 weeks after irradiation, when all indexes of function in the irradiated lung began to gradual reduction until 20 to 29 weeks after irradiation. Function did not return toward normal during the period studied. Each of the dogs had a decreased proportion in all six of the functions measured, and the mean percent change was statistically significant in all functions at 29 weeks. The ratio of DL_{co} in the two lungs showed a statistically significant increase at 1 and 3 weeks after irradiation prior to a steady decline beginning at 6 weeks. Total inspiratory capacity and compliance decreased over the period of study. Beginning 3 to 10 weeks after irradiation, there was a patchy increase in x-ray density in the irradiated lung associated with a shift of the heart toward the irradiated side. Examination of the lungs at autopsy revealed a consistent pattern of lung pathology. (TCO)

43800 EFFECTS OF IRRADIATION UPON LACTATION. Swanson, E. W.; Cragle, R. G.; Miller, J. K. (Univ. of Tennessee, Knoxville). J. Dairy Sci., 48: 563-8(May 1965).

At 60 days before expected parturition one of seven pairs of Jersey or Guernsey cows was exposed to ^{60}Co γ irradiation in a large-animal exposure field to give a total of 400-R calculated air dose. The dose rate varied from 34.5 to 32 R/hr. The average dose to the udder was 288 R. After 18 weeks lactation, seven of the cows originally irradiated prepartum were reirradiated to a dose of 350 R. In addition some cows which had not been irradiated before were given midlactation doses of 400 R. Feed consumption, milk yield, and blood cell changes were compared with paired control cows throughout lactation. Irradiation caused mild to severe reduction in feed intake which, in turn, reduced milk yields significantly. Recovery from the effects of the first irradiation was nearly complete at 15 to 18 wk of lactation, but the cows and their lactation had not recovered from the second irradiation by the end of the lactation. In the additional cows exposed to 400 R once in mid-lactation, milk yields dropped below controls for 5 weeks after irradiation, after which they returned to the normal lactation curves. Weekly tests of milk fat and total solids indicated that milk composition from the irradiated cows was not significantly affected. The responses of cows irradiated with 400 R indicated that it was on the borderline between a survival and a lethal dose; one cow died, probably as the result of radiation-induced weakness but not with a typical radiation syndrome. The second, midlactation irradiation of 350 R caused serious illness of two of the seven cows indicating that 350 R, too, was close to the lethal dose. (BBB)

43801 LACTATION AND RADIONUCLIDE METABOLISM RESPONSES OF DAIRY CATTLE TO LETHAL DOSES OF GAMMA AND NEUTRON RADIATION. Cragle, R. G.; Miller, J. K.; Swanson, E. W.; Brown, D. G. (Univ. of Tennessee, Oak Ridge). J. Dairy Sci., 48: 942-6(July 1965).

Effects of lethal doses of γ or neutron irradiations on lactation and on radioiodine and radiostrontium metabolism were studied. Seven lactating dairy cows were irradiated, four with ^{60}Co γ rays and three with neutrons. The γ exposures were made at the rate of 29.8 rad/hr for a total of 650 rad surface air dose. The neutron exposures were to 649, 671, and 446 rad. The total rad dose of neutron plus γ radiation was 730, 755, and 502. The animals were then given oral doses (200–300 μC) of ^{131}I and ^{89}Sr twice daily. Levels of ^{131}I and ^{89}Sr activity in feces and urine were measured on a 24-hr schedule, and milk was sampled twice a day. γ-Irradiated cows continued to eat and to produce milk of normal composition at moderately reduced rates for 12 to 14 days postirradiation, at which time a general systemic infection occurred, milk secretion and feed intake ceased, and the animals died in three or four days. Immediately after irradiation the neutron-treated cows exhibited a drastically reduced feed intake and milk production dropped sharply. Two of these animals died 20 and 40 days postirradiation, respectively. Passage of ^{131}I and ^{89}Sr into milk was studied only for the γ-irradiated animals, because of low milk production and sporadic eating for neutron-treated animals. Significantly less ^{131}I and ^{89}Sr (as % dose/ml) was found in milk from irradiated cows than in milk from nonirradiated controls. With the beginning of high body temperatures the concentrations of both ^{131}I and ^{89}Sr in urine decreased, despite constant intake of these isotopes, apparently due to kidney failure. Induced radioactivity resulting from neutron irradiation was also measured. Samples of blood taken two hr after termination of neutron irradiation revealed activity from ^{24}Na, with no appreciable contribution from other radioisotopes. The estimated total-body activity for ^{24}Na was 1 to 2 mC. (BBB)

43802 TISSUE-CULTURE STUDIES OF HUMAN ORAL CARCINOMA. II. RADIATION RESPONSES COMPARING PATIENT SURVIVAL, CYTOLOGIC-RADIATION RESPONSE, AND IN VITRO GROWTH CURVES. Silverman, Sol Jr.; Vaeth, Jerome (Univ. of California, San Francisco). J. Dental Res., 44: 554-63(May-June 1965).

Tumor cells were cultured from 17 consecutive patients with squamous-cell carcinomas of the intraoral region. These cultures were x irradiated with 750 and 2000 R, with

various measurements being made at the 4th, 6th, and 8th days. Irradiation of the experimental tubes were performed 24 hr after inoculation. The controls were sham-irradiated. Since these patients were all undergoing radiation therapy for their tumors, cytologic smears from the lesion were obtained before and during treatment. Therapy time varied between 5 and 7 weeks, with a total delivered tissue dose of 6000 to 7000 R for each patient. The radiation response (the number of cells per 100 nonmalignant cells that demonstrate either vacuolization, nuclear and cytoplasmic enlargement, nuclear changes, or multinucleation) was recorded from smears obtained twice a week during radiation therapy. Proliferative capacities up to 8 days in vivo, exfoliative-cytology radiation response counts, and in vitro morphologic changes could not be correlated with varying patient responses and survivals. Proliferative capacities of cells from the same explant varied as much as threefold, and the sterilizing effect in vitro was not uniformly proportional to the amount of irradiation received. It was not possible to quantitate the morphologic changes and compare them with in vivo cytologic radiation responses. Unknown cell factors and nutritional requirements of fresh explants appeared to cause variable results that precluded sufficiently controllable experimental conditions. Therefore, until fresh explants can be more reliably controlled, it is apparent that this system is not useful as a clinical radiosensitivity assay method. The fact that most cultures eventually produced a predominance of fibroblast-like cells, which possibly develop common culture metabolic porperties, may be a factor in not being able to differentiate the response, limited response, and non-response groups. (BBB)

43803 THE EFFECTS OF γ RADIATION ON THE FERTILITY AND LONGEVITY OF HIPPELATES PUSIO. Flint, Hollis M. (North Dakota State Univ., Fargo). J. Econ. Entomol., 58: 555-9(June 1965).

The effect of γ radiation on the gnat was explored preliminary to study of its possible eradication by the sterile male technique. This gnat is an abundant pest of humans and animals in the Southern United States during the summer months. Gnats were irradiated as 24- to 36-hr adults or in the late pupal stage two days prior to expected emergence. A ^{60}Co radiation source was used which delivered 2200 R/min. In tests conducted to determine the radiation level needed to reduce egg hatch to less than 1%, adults and pupae were exposed to doses ranging from 500 to 5000 R. At each level of radiation 20 treated males were crossed with 20 untreated females and 20 untreated males were crossed with 20 treated females. To determine if males treated in either the pupal or adult stage show recovery of fertility postirradiation, gnats were treated in the pupal and adult stage with 500 to 5000 R and after 18 days, the males were crossed with untreated females. In the tests to determine the lethal effects of γ radiation on H. pusio, 50 adults of each sex were given a dose of 5000 R and observed for 7 weeks. Some were exposed to radiation levels proceeding from 0 to 135,000 in 15,000 R increments. Pupae were also subjected to heavy doses of radiation up to a max of 20,000 R. The eye gnat was relatively easy to sterilize without drastic shortening of the life span of the adults. Less than 1% fertility was attained with both sexes when adults were treated with 5000 R and pupae were treated with 4500 R. Females treated in the pupal stage with this dose produced almost no eggs compared with those irradiated as adults where egg production was reduced by only about $\frac{1}{3}$ from that of the controls. The greatest recovery in males was shown after 2500 R where egg hatch went from 7% to 50% of the controls. Although recovery was found at the highest dose of 4500 R, gnats were still 93.5% sterile during the 18- to 26-day test period. Males treated as adults had a significant recovery of fertility at the 2500 and 3000 R levels. When adults are irradiated with 3500 R and higher the process by which fertility was regained is halted. A dose of 5000 R had no significant effect on survival of adults of either sex when held for 7 weeks. The LT_{50} (lethal time in days for 50% of the gnats at each level of treatment) is shown for doses up to 135,000 R. A dose of 15,000 R reduced the LT_{50} of both sexes to about $\frac{1}{2}$ of the control. There was no difference in the LT_{50} and LT_{100} for males and females at doses of 120,000 and 135,000 R. At 105,000 R and lower, the LT_{100} of females was always higher than that of males. When pupae were irradiated there was no difference between the control gnat emergence and emergence from pupae treated with 1000 and 5000 R. At 10,000 R there was a 30% decrease in emergence. The LD_{50} dose was 12,000 R. (BBB)

43804 TAKE-OVER—AN UNUSUAL SELECTION PROCESS IN STEADY-STATE CULTURES OF ESCHERICHIA COLI. Munson, R. J.; Bridges, B. A. (Medical Research Council, Harwell, Berks, Eng.). J. Gen. Microbiol., 37: 411-18(Dec. 1964).

Reversions to tryptophan independence in strain WP 2 of E. coli were studied in cultures grown at 37° in a minimal medium supplemented with 6 μg tryptophan/ml. The proportion of mutants was increased artificially either by exposing the growing culture to γ radiation, or by adding a known number of prototrophs from a culture derived from revertants which had arisen spontaneously. Two cultures were exposed to γ rays from ^{137}Cs during 4 hr to a total dose of 4500 rad, during which time the frequency of prototrophs ($try^+/try^+ + try^-$) increased from 10^{-8} to 2×10^{-7}. After a short pause the try^+ frequency in one culture began to increase again and continued at a steady rate until it reached an apparent max of about 50%. The other culture showed a similar increase after a longer delay. The growth rates of both cultures during the periods of take-over were constant to within 1%. In another experiment which involved two separate irradiations, the first, of 600 rad during 6 hr, increased the proportion of prototrophs to about 3×10^{-6}, at which value it remained constant for 40 hr. The second irradiation (600 rad in 6 hr) increased the value to almost 10^{-7} and, very soon after this, take-over occurred, the proportion of prototrophs increasing during 30 hr to just over 10^{-2}. The constancy of the fraction of prototrophs in the interval between the two radiation exposures confirms the normal absence of selection pressures. Take-over was also initiated after a variable delay when either previously isolated prototrophic revertants or the parent strain E. coli B/r were added to a culture of auxotrophs. The smaller the number of prototrophs added, the greater was the delay observed before take-over started, and when less than 100 prototrophs were added it was not observed at all. Once begun, take-over continued at about the same rate in all experiments. The phenomenon appeared to be correlated with a selective advantage of revertants which became attached, with parent auxotrophs, to the wall of the culture tube. After some hours the film of growth on the wall was composed of $\sim 10^7$ bacteria. It was different from the massive sticky growth sometimes encountered in continuous cultures of E. coli. The experimental observations of this take-over are quantitatively consistent with a hypothesis of wall adsorption of rare and readily attached variant prototrophs. Take-over seems to be a consequence of the detachment rate for variant revertants being less than their rate of multiplication, while for normal prototrophs on the same surface it is greater. (BBB)

43805 DISCRIMINATION LEARNING OF MIRRORED CUES BY RHESUS MONKEYS. Brown, W. Lynn; McDowell, A. A.; Robinson, E. M. (Univ. of Texas, Austin). J. Genet. Psychol., 106: 123-8(Mar. 1965).

On the assumption that the rhesus monkey is capable of learning to discriminate by observing the results of the responses of other monkeys, the question is raised as to whether or not he is likewise capable of learning to discriminate by observing the mirrored results of his own responses. This was studied in three control and seven whole-body irradiated monkeys. These subjects were female survivors of an exposure to nuclear radiation that took place more than five yr earlier. They were sorted into three groups. One group contained the three controls; a second group contained four irradiated monkeys that had been exposed to total radiation doses of 273, 299, or 355

rem; and the third group contained three irradiated monkeys that had been exposed to estimated total radiation dosages of 397, 439, or 512 rem. Their training histories were nearly identical and included numerous Wisconsin General Test Apparatus (WGTA) tasks. The monkeys were first trained to retrieve visible diced apple impaled randomly on the eye screw of one of two identical pieces of Nylong cord. Next they learned, beyond the 0.001 significance level, the mirror discrimination of the baited cord from the nonbaited cord. Lastly they learned, beyond the 0.005 significance level, the mirror discrimination of color cues placed over the baited and nonbaited eye screws of the cords. In each instance, the radiation variable and its interaction with practice failed to approach statistical significance. The results showed that the rhesus monkey is capable of learning to discriminate by observing the mirrored results of his own responses. This capability reflects the complexity of peripheral-cue utilization by the rhesus monkey. During the early trials of mirror discrimination, some monkeys were observed to attempt to reach out directly toward that which was observed in the mirror before responding to one of the two Nylon cords. Gradually, however, they came to utilize the mirrored image as a visual cue for immediate direct response to the appropriate one of the two identical Nylon cords. (BBB)

43806 FURTHER EVIDENCE FOR THE EXCITATORY PROPERTIES OF NONREWARDED CUES. McDowell, A. A.; Brown, W. Lynn (Univ. of Texas, Austin). J. Genet. Psychol., 106: 137-40(Mar. 1965).

Previous evidence argued for the reality of excitation to nonrewarded cues as a mechanism of discrimination learning in studies showing that the prepotent mechanism of learning for rhesus monkeys in response-perseveration learning set to nonrewarded cues is behavioral excitation of response to previously unrewarded cues. Because such findings disagree with the limited role assigned to the results of nonreward by duoprocess theories of learning, it was considered important to demonstrate replication with an independent group of subjects. These were four control and eight whole-body irradiated monkeys which were female survivors of an exposure to nuclear radiations that took place more than four yr earlier. For statistical assay of the radiation variable, the four controls consitituted one group. Four irradiated subjects which had been exposed to total radiation doses of 273, 299, or 355 rem constituted a second group; and four irradiated monkeys which had been exposed to 397, 439, 512 rem constituted the third group. The training histories of the monkeys were nearly identical and included numerous Wisconsin General Test Apparatus (WGTA) tasks. They were trained for 44 days on response-perseveration learning set to nonrewarded cues. Next, followed eight days of testing with two matched groups of six subjects each designed to elucidate the mechanism of learning during the first 44 days of testing. Analysis of results, for eight days of critical testing, showed (beyond the 0.001 significance level) the prepotency of approach to the initially approached but nonrewarded cue over inhibition of approach to the object to which response was not made on the same trial: i.e., nonrewarded cues in response-perseveration learning set possess excitatory properties. (BBB)

43807 SOME RADIATION EFFECTS ON FOOD SATIATION IN THE RHESUS MONKEY. McDowell, A. A.; Brown, W. Lynn (Univ. of Texas, Austin). J. Genet. Psychol., 106: 217-20(June 1965).

Whole-body exposure to radiation produces anorexia in most animals and the degree of anorexia is roughly proportional to the amount of radiation exposure. It is generally assumed that the anorexia dissipates as the animal recovers from the period of acute effects. This study tested the validity of this assumption by food-satiation tests with control monkeys and with irradiated male monkeys more than four years after exposure to neutron radiation. They had been given a 24-hr whole-body exposure every four days at 87.2 mrep/hr until a total dose of 583 rep was achieved. The controls had been sham exposed during the same period. Fourteen adult female rhesus monkeys, ranging in age from 7½ to 8½ years, served as the replication group. The female survivors of an exposure to nuclear radiations more than five years earlier were also tested. The estimated total-radiation doses were 282 to 439 rem. All testing was conducted in a modified version of the Wisconsin General Test Apparatus. Food satiation tests conducted with monkeys exposed to chronic fast-neutron radiation more than four years earlier showed that controls took significantly more trials to food satiation than irradiated monkeys. A replication of the tests with monkeys exposed to nuclear radiations more than five years earlier gave similar results. In the second instance, the controls also ingested to satiation significantly more food (g/lb body weight) than did the irradiated subjects. The results argue for a long-term effect on food consumption of radiation exposure. They may reflect the continuance of conditioned avoidance to food, which avoidance developed during the period of acute radiation effects. They may be due to physical limitations imposed on consumption, due to erosion and scarring of the gastrointestinal tract. Or they may result from limitations imposed upon the digestive processes, due to physiological interference with the cellular secretions associated with digestion. (BBB)

43808 THE EFFECT OF GAMMA RADIATION UPON OPERANT WATER-REINFORCEMENT BEHAVIOR. Wicker, James E.; Brown, W. Lynn (Univ. of Texas, Austin). J. Genet. Psychol., 106: 295-9(June 1965).

Water intake of the rat increases sharply following whole-body x irradiation, whereas food intake measured directly, as well as by operant behavior, decreases following irradiation. A study was therefore made to determine whether rats would continue to work for water in an operant water-reinforcement situation following irradiation or whether water-directed behavior would decrease, as is the case for food. If lever-pressing behavior decreases under these conditions, such behavior might indicate that there is diminution in strength and ability to perform. It is concluded that there is a diminution in strength and ability to perform since nonoperant water intake rises postradiation. Male rats (23) were trained to work a single lever for water reinforcement. After 21 days of baselining, three groups of six rats each were matched on the basis of these 21 days. The remaining five rats were placed in a fourth group. The first (control) group was sham-irradiated. The second group was irradiated with ^{60}Co for a dose of 200 R at a rate of 100 R/min. The third group was given 400 R at this rate. The fourth group (of five rats) was given 800 R at this same rate. Following the day of irradiation, responses were taken for four days. Then, one week following this initial exposure, the radiation treatment was replicated on the same rats, and another four days' of data obtained. A variance analysis was used, with the data grouped into a four-day period prior to irradiation and one four-day period following each radiation exposure. The main effect for periods was significant (beyond the 0.001 level) with responses decreasing from period to period; however, the groups-by-periods interaction was also significant (beyond the 0.05 level), with responses decreasing as dose increases. The results of this study indicate that γ irradiation depresses operant water-reinforcement behavior, and that this depression is proportional to radiation dose. These results are consistent with those obtained for food reinforcement. (BBB)

43809 PIGMENT ACTIVITY IN DERMAL NEVI INDUCED BY ULTRAVIOLET LIGHT: AN ENZYME HISTOCHEMICAL STUDY. Klaus, Sidney N.; Winkelmann, R. K. (Mayo Clinic, Rochester, Minn.). J. Invest. Dermatol., 44: 276-7(Apr. 1965).

Histochemical studies were conducted in two patients with widespread psoriasis. Multiple dermal nevi were removed at the conclusion of the Goeckerman treatment program that includes a daily graduated exposure to uv light to the total body surface. The initial exposure is

within the minimal erythema dose range, and the intensity of light is increased as the patient's tolerance increases. The five lesions studied had received 16 to 21 uv treatments. They were examined for both tyrosinase and nonspecific cholinesterase activity and a portion was fixed in osmium tetroxide for electron microscopy. Nonspecific cholinesterase activity was demonstrated in all lesions. Although some activity appeared within all the nevus cells, a greater activity was observed within the deeper nests of nevus cells. Strong tyrosinase activity was demonstrated in the epidermal melanocytes and in the superficial nests of nevus cells in all specimens. Nests of melanocytes at the pilosebaceous follicles frequently were strongly positive. Normally, dermal nevus cells contain abundant nonspecific cholinesterase activity but do not contain tyrosinase activity. It is evident that sufficient uv light, whether acting directly on the cells or through indirect mediators, can promote an active tyrosinase system. The cholinesterase and tyrosinase activities are not mutually exclusive since nests of cells that showed reactions with both enzymes were present in the midregion of the nevi. These results indicate that dermal nevus cells do not arise from melanocytes but that the nevus cell may originate from a more primitive neuroectodermal precursor. (TCO)

43810 DRUG-INDUCED CHANGES OF THE METABOLISM OF 5-HYDROXYTRYPTAMINE IN THE BRAIN OF X-RAY-TREATED RATS. Palaic, Dj.; Supek, Z. (Inst. Rudjer Boskovic, Zagreb). J. Neurochem., 12: 329-33 (Apr. 1965).

The influence of x rays on the concentration and metabolism of 5-hydroxytryptamine (5-HT) in rat brain after pretreatment with various drugs was studied. Total, basic, and acidic 5-OR indoles (R = H, alkyl, or aryl group) were determined spectrofluorometrically. The basic fraction represents mainly 5-HT and the acidic fraction 5-hydroxyindoleacetic acid (5-HIAA). The determination of 5-HIAA, as the main metabolite of 5-HT, was used as a method of estimating free 5-HT. Pretreatment with 5-hydroxytryptophan (5-HTP) results, normally, in an increase of all three fractions. Irradiation of the experimental animals induced a decrease of 5-HT and an increase of 5-HIAA. Less 5-HT and more 5-HIAA is normally present in brain of reserpinized rats. In reserpinized irradiated rats the increase of 5-HIAA is significantly higher than in non-irradiated rats. In irradiated rats pretreated with α-methyl DOPA, a significant decrease of 5-HT was observed. Brains of rats treated with iproniszid show an increase of 5-HT and a decrease of 5-HIAA. No effect of irradiation on 5-HT and 5-HIAA content was noticed in these animals. These results lend support to the view that 5-HT is liberated by irradiation. (auth)

43811 A CASE OF DOUBLE TRISOMY: TRISOMY NO. 18 AND TRIPLO-X. Uchida, Irene A. (Children's Hospital, Winnipeg, Can.); Lewis, A. J.; Bowman, J. M.; Wang, H. C. J. Pediat., 60: 498-502(Apr. 1962).

Clinical and autopsy findings of an infant who died at 35 days of age with multiple congenital malformations are described. Cytologic studies indicate that the patient was a double trisomic individual: XXX No. 18 trisomy syndrome. There have been three previous reports of double trisomy in man: two cases of mongolism-Klinefelter's syndrome and one mongoloid child with No. 18 trisomy syndrome. In the case reported the combination of chromosomes involved differs from those of the previous cases. Previous radiation exposure of the mother was considered as a possible etiologic factor in this condition in the offspring. The mother had worked as an x-ray technician for 10 yr previously and until she was 4½ months pregnant. There was no known history of congenital anomalies in either the mother's or the father's family. The infant presented multiple congenital malformations. Karyotype analysis showed 3 No. 18 chromosomes, and 17 chromosomes in the C group, following the nomenclature of Patau, or the 6-12 plus X group of the Denver classification. No attempt was made to single-out the X-chromosomes, but the other chromosomes appeared normal in size and distribution. Buccal smears revealed 2 sex chromatin bodies. (TCO)

43812 BIOCHEMICAL STUDIES ON IRRADIATED PROTOZOA. II. THE DEAMINATION OF DEOXYCYTIDINE AND DEOXYCYTIDYLIC ACID BY TETRAHYMENA PYRIFORMIS W. Winicur, Sandra; Roth, Jay S. (Univ. of Connecticut, Storrs). J. Protozool., 12: 166-70(May 1965).

The high speed supernatant fraction obtained from cell-free preparations of Tetrahymena pyriformis W contains an enzyme that deaminates deoxycytidine (dC) readily, but there is no evidence for a specific dCMP deaminase. The supernatant fraction also contains an active dCMP phosphatase which is inhibited by high phosphate concentration. dC deaminase in declining order deaminates BrdC, IdC, dC, MedC, and dCMP. The enzyme does not appear to have a cofactor and is unaffected by Mg^{++} and EDTA. It exhibits a broad pH optimum. Irradiation with 570,000 R of γ-rays did not markedly affect the activity of dC, dG, or dA deamination by Tetrahymena high speed supernatant fraction. (auth)

43813 COMPARATIVE ULTRAVIOLET SENSITIVITY OF REGENERATION IN THE GENUS BLEPHARISMA. Giese, A. C.; McCaw, B. K.; Parker, J. W.; Recher, J. T. (Stanford Univ., Calif.). J. Protozool., 12: 171-7(May 1965).

Earlier tests showed that members of diverse stocks of Blepharisma which vary in size, vigor, and depth of pigmentation, as well as in macronuclear structure, also differed in their uv sensitivity. Since correlations between uv sensitivity and cell characteristics might serve as a background for further analysis of the mechanism of uv action upon cells, the effect of uv upon regeneration of individuals representing several stocks of Blepharisma is reported. An action spectrum for retardation of regeneration was determined in one stock for comparison with that previously determined in another. The blepharismas were irradiated in quartz cells with monochromatic uv ½ hr after cutting, at which time uv action is greatest, the effect declining with lapse of time after cutting. Results showed that degree of regeneration of post-hypostomal portions in different stocks representing several species is retarded to different degrees by identical doses of uv radiation at 2654 Å. The uv susceptibility of regeneration is greater in some small-sized stocks than in some large-sized stocks and in stocks with a lesser amount of pigment than in the more deeply pigmented ones. For the same dose, regeneration is retarded more by low-intensity than by high-intensity short wavelength uv radiation. The uv action spectrum for regeneration delay in the Rao A stock, determined with uv of similar intensity at various short uv wavelengths, resembles absorption by nucleoprotein more than absorption by other cell constituents. Postregeneration division is also retarded by uv, and the action spectrum for division delay resembles that for regeneration delay, except that 2804 Å is relatively more effective in retarding division than regeneration. The specific sensitivity of division to wavelength 2804 Å might be referable to the action of this wavelength on the furrow-forming material. Regeneration may be delayed more than division by such very short wavelength uv (which is absorbed so strongly that it especially damages the surface of the cell) because of the difference in the time scales for the two processes. The greater time lapse before division occurs perhaps allows for more complete recovery from superficial surface injury than is possible in the shorter time before regenerative processes normally begin. (BBB)

43814 SENSITIVITY OF ARTEMIA EGGS TO THE γ-IRRADIATION. III. THE SENSITIVITY AND THE DURATION OF HYDRATION. Iwasaki, Tamiko (National Inst. of Radiological Sciences, Chiba, Japan). J. Radiation Res. (Japan), 5: 91-6(June 1964).

Prior to γ irradiation the water content of Artemia eggs were modified by hydrating at 0 and 27°C for one to seven hours. At three hours after hydration, the water content

reached a plateau at both temperatures. The eggs became more radiosensitive in the wet state than in the dried state. By irradiation with 100 kR, the hatchability of eggs hydrated at 0 and 27°C did not show noticeable difference by prolonged hydration. On the other hand, the radiosensitivity of eggs irradiated with 200 kR steeply increased after one hour hydration at both temperatures. Further hydration at 0°C maintained this level of radiosensitivity, but at 27°C showed the complex pattern. The patterns of increased sensitivity is related to the temperature of the steeping water and may be associated with physiological or developmental stage of the treated eggs. (auth)

43815 SENSITIVITY OF ARTEMIA EGGS TO THE γ-IRRADIATION. IV. AFTER-EFFECT OF IRRADIATION IN COMPARISON WITH THE EFFECT OF HEAT-TREATMENT. Iwasaki, Tamiko (National Inst. of Radiological Sciences, Chiba, Japan). J. Radiation Res. (Japan), 5: 97-101(June 1964).

The change in the extent of biological damage for a given dose by storage after irradiation is called the aftereffect. The purpose of the present study is to compare the after-effect between irradiation and heat-treatment. Artemia dry eggs were exposed to γ rays (120, 240, 360, 480, and 600 kR) or high temperature (at 1000°C for 30, 60, 90, and 120 minutes) and stored at room temperature for varying time (0, 1, 3, 7, and 30 days) after treatment. After the storage period, the eggs were soaked and their hatchabilities were scored after 72 hours. Post-irradiation storage of irradiated eggs resulted in a notable decrease in hatchability, and the rate of decrease was much greater in the eggs given higher doses than in those lower ones. On the contrary, storage of heat-treated eggs did not show such an aftereffect. From this series of experiments, it was concluded that in its nature the damage induced by irradiation is different from that induced by heat-treatment. (auth)

43816 TRANSMUTATION EFFECT OF ^{35}S ON A MYCOBACTERIUM. Tsukamura, Michio (Obuso National Sanatorium, Obu, Japan). Japan. J. Microbiol., 8: 131-7(Dec. 1964).

The effect of ^{35}S irradiation on a Mycobacterium was studied, taking the following points into consideration: (1) Since the half-life period of ^{35}S is relatively long (83 days), long-term observation may be needed to determine its lethal or mutagenic effects. (2) Intracellular irradiation may be more likely to cause death and mutation in bacteria than extracellular irradiation. Thus if ^{35}S irradiation demonstrates lethal or mutagenic effects, these effects may be due to transmutation of ^{35}S to ^{35}Cl in the molecules of the bacteria (^{35}S atoms are incorporated into methionine and cystine of bacterial protein). When the incorporated ^{35}S atoms change into ^{35}Cl atoms in the molecules, ^{35}S-containing amino acids are altered, and protein molecules damaged by the transmutation. Three series of samples were prepared from Mycobacterium smegmatis and stored at −20°C; (a) ^{35}S-labeled cells in 10% glycerol (intracellular irradiation with incorporated ^{35}S); (b) nonradioactive cells in 10% glycerol containing 10 μC/ml ^{35}S (extracellular irradiation with ^{35}S); and (c) nonradioactive cells in 10% glycerol (control). Viable cell numbers and mutation frequency to isoniazid resistance were determined until the 84th day of storage. Bacterial cells maintained their viability up to 84 days of storage when frozen in 10% glycerol containing no radioisotope. Bacterial cells irradiated with extracellular ^{35}S maintained their viability, or viable cells decreased only slightly, even after 84 days of irradiation. Bacterial cells with incorporated ^{35}S lost their viability at a faster rate. It is suggested that this effect is due to the transmutation of ^{35}S to ^{35}Cl in bacterial protein molecules. No significant increase in mutation frequency could be detected in both the samples irradiated with incorporated ^{35}S and with extracellular ^{35}S. (BBB)

43817 IMMUNOLOGICAL ASPECTS OF EXPERIMENTAL PULMONARY SCLEROSIS DUE TO IONIZING RADIATIONS. Mancini, A. M.; Corinaldesi, A.; Tison, V.; Rimondi, C.; Ferracini, R. (Universita, Bologna). Lancet, 1: 1397-8(June 26, 1965).

The possible role of autoantibodies in the pathogenesis of fibrosis of the lung following thoracic irradiation was investigated in rabbits subjected to ^{60}Co γ rays. Irradiation was limited to the right hemi-thorax, 4900 Rad over a 7-day period; 3 months later, some rabbits were exposed at the same site to a second cycle of 5000 Rad, given over 5 days. The rabbits were bled 2-3 months after each cycle. Fragments of the left lung (nonirradiated) and the right (irradiated) lung from each rabbit were examined microscopically and histochemically. Tissue sections were also tested with fluorescein-isothiocyanate (FITC)-labeled γ-globulins, isolated by salting out from the serum of the same animals obtained before and after irradiation. Lung of irradiated rabbits showed thickened periodic acid Schiff-positive alveolar septa infiltrated by lymphocytes and eosinophil cells, with pronounced reticular proliferation; the elastic framework was often disrupted. In rabbits given two cycles of irradiation there were large zones of septal and vascular fibrosis, pronounced changes in the alveolar cells, reticulin and collagen production, and sclero-calcified nodules. FITC-tagged γ-globulins obtained from rabbits long after the irradiation were specifically fixed to the alveolar and septal cells of the treated or untreated lungs of the same or other rabbits. In the irradiated rabbits, whose γ-globulins were fixed in the pulmonary tissue, γ-globulins were found to be increased after the irradiation. Irradiated lungs showed large amounts of globulins, and specific complement-fixation, which were not present in the untreated rabbit lungs. The results demonstrate that pulmonary lesions which progress to sclerosis can be produced in rabbits exposed to high doses of ionizing radiations over the chest. (TCO)

43818 CALCIUM FLUX FROM X-IRRADIATED NITELLA CELLS. Gillet, C.; Klerckx, L. (Universite, Liege). Life Sci., 4: 1561-5(Aug. 1965).

The fresh-water alga Nitella flexilis was cultured in a medium containing 5.5 mC/ml ^{45}Ca. The cells were x irradiated at a dose rate of 100 kR/min to total doses of 250 or 500 kR. The cells were assayed for ^{45}Ca by a G-M counter immediately and for 30 hr postirradiation after being placed in nonradioactive medium. The 250- and 500-kR doses slowed down the speed of the cytoplasmic streaming at about 75 and 50% of the normal rate. The rate of radioactivity loss from control and treated cells was similar; after 10 hr it was a little faster for the irradiated cells. The initial relatively fast ^{45}Ca exchange was followed by a much slower loss of activity. However, the efflux of calcium in Nitella cells was not modified immediately after irradiation. Attempts were also made to detect any changes in the cellular uptake of calcium after irradiation. It was found that the mean amount of ^{45}Ca taken up over a 15-hr period was smaller for the 500-kR irradiated cells than for the controls. But after 20 min the mean activities were about the same for every cell. When these data were plotted against time, no systematic difference appeared between the rate of decreasing activity in irradiated and control cells. Thus, uptake of ^{45}Ca after 15 hr was less in cell walls irradiated with 500 kR (320 counts/sec) or in the controls (587 counts/sec). The main conclusion drawn from these data is the radioresistance of the mechanisms controlling Ca exchange in Nitella for at least two days after irradiation. (BBB)

43819 DISEASES CAUSED OR AGGRAVATED BY SUNLIGHT. Daniels, Farrington, Jr. (Cornell Univ., New York). Med. Clin. N. Am., 49: 565-80(May 1965).

The effects of uv and visible radiations are reviewed, as well as the mechanisms by which radiations can produce disease. The absorption of a photon of visible or uv radiation by a molecule raises its electronic excitation level, making it much more reactive. Absorbed energy may be transferred to another molecule, producing either chemical photosensitization or photosensitization in a biological system. In human skin, photosensitizing chemicals may be exogenous or endogenous. Clinical and epidemiologic evidence indicates that chronic exposure to uv radiation in the poorly pigmented skin produces skin cancer. Senile

elastosis may also be produced in susceptible subjects by uv radiation. Diseases associated with uv or visible light sensitivity or aggravated by sunlight are enumerated. The abnormal responses of skin to uv and visible radiation have varied morphology, including severe sunburn, persistent erythema, urticaria, eczema, and vesicular lesions, also a variety of papular, nodular, and plaque-like lesions (polymorphous light eruptions). Phototoxicity and photoallergy concepts are explained. Many photoallergic reactions are produced by wavelengths between 2850 and 3200 Å; tissue components as well as exogenous drugs can be the primary absorbing molecule. Some differences used clinically to separate light reactions into phototoxic and photoallergic categories are tabulated. Various methods of testing for light sensitivity are outlined. Treatment and management of patients with light-sensitive diseases are considered. Many diseases with a light-sensitive component cannot be treated adequately. Therefore, control of the amount of uv radiation to which the patient is exposed becomes important. Control may be effected by proper use of window glass, plastic filters, sunscreen preparations applied to the skin, and by changing the patient's work pattern. (BBB)

43820 POLYCYTHEMIA, OSTEOMYELOFIBROSIS, AND ACUTE LEUKEMIA. Weissbecker, L.; Gaedtke, Kl. (Universitaet, Kiel). Med. Klin. (Munich), 59: 420-3 (Mar. 13, 1964). (In German).

Metabolic relations between polycythemia and osteomyelofibrosis are obscure. Osteomyelofibrosis may indicate disturbance of an equilibrium between the myeloid and lymphatic system, with failure of the lymphatic tissue. This does not explain the polycythemic state that persists for many years before development of osteomyelofibrosis or osteomyelosclerosis. Increased development of acute leukemia after treatment of polycythemia with x irradiation or radiophosphorus from 2 to as much as 22% is not the result of therapy alone. There are probably close relations between these disorders, but treatment may prevent other complications before the acute leukemia develops. The leukemogenic effects of ionizing irradiations, which triple the number of leukemia cases, is not the accelerated appearance of a pathological trend already present, but is the basic cause of the development of the disease. Often this is a chronic myelogenous type of leukemia. However, it cannot be said that this type of leukemia is the end result of polycythemia while acute leukemia is the result of irradiation treatment. There is no directly linear relation between irradiation dose and occurrence of acute leukemia, although there has been an increase in the incidence of acute leukemia since the introduction of ^{32}P as a treatment of polycythemia. Osteomyelofibrosis has not been observed much in irradiated populations, so that it is not possible to draw any conclusion as to its relation to irradiation. Thus the concept of a single bone marrow disease with differing symptoms may have some significance, but the basic cause of the disease is essentially unknown. (BBB)

43821 A POSSIBLE QUANTITATIVE MECHANISM FOR CARCINOGENESIS BY ULTRA-VIOLET RADIATION. Saslaw, William C. (Princeton Univ., N. J.). Nature, 207: 592-3(Aug. 7, 1965).

By assuming that cells contain two chemical agents, one advancing and one inhibiting growth, it is possible to construct a simple model that quantitatively accounts for the growth-rate of cancers induced by uv radiation. A mechanism based on departures of these chemical agents from equilibrium in the cell is suggested and outlined. The formula is derived by considering the growth to be directly related to the influence ratio, γ, of two chemical substances, A and I, which respectively advance and inhibit cellular growth: $\gamma = A/(I - I_0)$. (P.C.H.)

43822 MIGRATION OF SPLEEN CELLS INTO THE BLOOD STREAM FOLLOWING ANTIGEN STIMULATION OF THE RAT. Cannon, Donald C.; Wissler, Robert W. (Univ. of Chicago). Nature, 207: 654-5(Aug. 7, 1965).

Cell migrations into the blood stream of the rat were investigated by using tritiated thymidine to label the proliferating pyroninophilic or antibody-forming cells of the spleen. For selective labeling of the spleen cells, the spleens were first exteriorized with intact vascular pedicle and protected in a lead shield while the remainder of the body was subjected to x irradiation. The results indicated that during the period of maximal splenic hyperplasia provoked by intravenous particulate antigen, lymphoid cells which are almost certainly formed in the spleen enter the blood stream in significant numbers. The migrating lymphoid cells were morphologically diverse, ranging from forms resembling the large pyroninophilic cells of the splenic red pulp at the one extreme to small lymphocytes at the other. Thus, it appears that the various migrating lymphoid cells are derived directly or by metamorphosis from the antibody-forming cells. (P.C.H.)

43823 THE SIGNIFICANCE OF RADIATION GENETICS IN PRESENT GENETICS. Sobels, F. H. (Rijksuniversiteit, Leiden). Ned. Tijdschr. Geneesk., 107: 2151-8 (Nov. 16, 1963). (In Dutch).

A general introduction to the area of radiation genetics is given. The gonadal dose for different (natural and artificial) radiation sources is discussed. Comparison of the genetically significant dose with x-ray diagnostic doses and the frequency with which the genetically significant dose is exceeded are noted. The effect of genetic components in the etiology of those born with abnormalities or constitutional illnesses is considered. Induction of mutations by radiation includes discussion of the relation between dose and mutation frequency, the influence of dose rate, differential sensitivity to induction of mutations, and chromosomal abnormalities induced by radiation. Genetic damage to man is considered. The doubling dose is defined. Protection from genetic damage is discussed, and approximate values of various genetic effects in a population of 11,000,000 individuals exposed to 400 mR, acute, and chronic radiation per individual per generation are tabulated. (BBB)

43824 IONIZING RADIATION AND LUNG CANCER IN MINERS. New Engl. J. Med., 273: 222-3(July 22, 1965).

The recent report of epidemiologic studies instituted in 1950 by the U. S. Public Health Service among uranium miners in the Colorado Plateau is discussed. The report implicates inhaled radon and its daughter products in these mines as an important factor in the genesis of bronchial cancer in the miners. For the first time, a dose-response relation between exposure to radioactivity in the mines and probability of developing cancer has been demonstrated. The short-lived Rn daughters (isotopes of Po, Pb, and Bi), which are continually produced from Rn decay in air, are the principal source of radiation exposure to the bronchial epithelium. Unlike Rn, they are not gases and are adsorbed readily to dust particles in the air. Their energetic α particles, at least part of which have 13.7-Mev energy, may penetrate to the basal stem cells of the epithelium. Increased incidence of bronchial cancer has also been found associated with radon exposure in mines with little uranium in the ore, as in Newfoundland fluorspar miners. Radon was thought to enter the mine from water seeping from deep sources. Another analysis of causes of death of nonuranium miners has shown an increased mortality from respiratory cancer. The Rn concentration may have been high before institution of adequate ventilation, and these nonuranium miners may have been exposed for 15 years or more to radon daughter products. The three-times greater mortality from bronchial cancer could well be explained, therefore, on the basis of radiation exposure, according to the dose-response relation reported in the U. S. P.H.S. report. Thus, whenever increased concentrations of Rn and its daughters have been measured in underground mines, and when men exposed to this environmental source of α radiation have been adequately studied, an increased incidence of bronchial cancer has been detected, in confirmation of the early studies of uranium miners in Bohemia. (BBB)

43825 CONSEQUENCES OF ULTRAVIOLET RADIATION ON THE DIFFERENTIATION AND GROWTH OF FERN GAMETOPHYTES. Kato, Yukio (Nagoya Univ., Japan). New Phytologist, 63: 22-7(Mar. 1964).

The effects of uv light (principally at 2537 Å) on the differentiation and growth of gametophytes in Pteris vittata, Osmunda japonica, and Dryopteris varia were investigated. It was shown that a single cell may be isolated by uv irradiation and that a normal gametophyte can be regenerated from such a cell. When gametophytes grown under low intensity (150 lux) white light before uv irradiation were irradiated with a high dose, an apicobasal gradient of ability to survive was clearly shown. The survival of each of the cells composing a protonema seems to be related to two different factors; a marked ability for cell division or rapid recovery from the damage of uv at the apical region and a high resistance to uv at the basal region. Under both culture conditions, cells of a definite length alone survive. General effects induced by the uv irradiation include reversal of the polarity in a protonema and modification of the developmental axis. In addition, swelling of the rhizoid and protonema cells, and occurrence of rhizoidal protonema were also described. In fern gametophytes there are apicobasal gradients in permeability, isoelectric point, plasmolytic properties, stainability to dyes, and DNA content. The relation between these gradients and the abilities revealed in the present experiments is still unknown; however, possibly these gradients could play an important role for survival of each cell in a protonema. It is suggested that apical cells have a marked ability to divide and elongate, and might readily recover from partial injury, soon after isolation, and finally regenerate. The length of each cell composing a protonema is an essential factor for survival. In this respect, injury of cells caused by uv irradiation is considerably different from that caused by colchicine or alcohol. In the latter, hypertrophied apical cells can neither develop nor segment further. (BBB)

43826 PSEUDO-AMITOSES PROVOKED BY X RAYS IN ERYTHROPOIETIC CELLS IN VITRO. Rondanelli, E. G.; Trenta, A.; Vannini, V.; Magliulo, E.; Gerna, G. (Universita, Pavia, Italy). Nouvelle Rev. Franc. Hematol., 5: 213-20(Mar.-Apr. 1965). (In French).

Hanging drop cultures of the spleen of the triton Molge vulgaris were exposed to 12 to 15 R of x rays. Thirty-six hr later, the erythropoietic cells were studied under a phase contrast microscope. A large number of cells were observed with the nucleus pinching-in-two, simulating the development of an amitotic division. The cells were large and elongated, and the nucleus constricted. The abnormal nuclei were the result of mitosis stopping at the equatorial plate stage. The chromosomes agglutinated and underwent decondensation. The nuclear membrane reappeared and a polyploid nucleus was formed, constricted along the equatorial plane. The abnormal nuclei were also formed by mitosis stopped in anaphase by the persistence of chromatic bridges. The bridges prevented the complete separation of the chromosomes which had migrated to the poles. The nuclear membrane reformed around the pinching-in-two nucleus. The nuclei were also formed by mitosis stopping in a tripolar anaphase, with two chromosomic stars fused into one, and persistent chromosomic bridges to the third. A very irregular pinching-in-two nucleus resulted. The constricted nucleus in all cases was the result of a stoppage of mitosis, not a stage in direct division. The existence of amitosis in hematopoietic cells is very doubtful. The pinching-in-two nuclei had a remarkable stability. Pseudoamitosis should be used where pinching-in-two follows an abnormal distribution of mitotic chromosomes. If the nuclei eventually seperate, the condition is called binuclearity. (BBB)

43827 SEASONAL VARIATIONS IN THE INCIDENCE OF THE CLINICAL ONSET OF LEUKAEMIA. Lee, J. A. H. (London Hospital, Eng.). Pathol. Microbiol., 27: 772-6(1964).

The possibility that certain etiologic factors, mainly ionizing radiation, may be reflected in the seasonal fluctuations in leukemia incidence was examined. The distribution of the clinical onset of leukemia through the year is bimodal, with peaks in mid-winter and in the early summer. This pattern is found in both sexes, and in children and adults. The present data only extend to age 44, but probably the variation extends beyond this age. Australasian evidence which has been collected suggests that the summer peak in the clinical onset of leukemia of all types is not restricted to England and Wales. Its cause is thus not likely to be found in conditions limited to the latter countries, either in climate or in the system of medical care. The latent period of leukemia after irradiation by x rays is long and variable and it is difficult to explain how a seasonal variation in the beginning of the disease or in its manifestation could persist so as to produce the observed variations in the clinical onset. It may be that most cases of human leukemia develop by different, and much more rapid stages, than does leukemia induced by radiation. Whatever these stages may be, a sharp seasonal variation makes it reasonable to postulate that an infective agent is involved at some point, and adds to the growing body of evidence that leukemia can behave in a variable epidemic way. (BBB)

43828 LEUKEMIAS AND ENVIRONMENT: EPIDEMIOLOGY OF LEUKEMIAS AND STUDIES ON PATHOGENIC EFFECTS OF THE PHYSICAL AND CHEMICAL ENVIRONMENT. Aleksandrowicz, Julian (Academy of Medicine, Krakow). Polski Tygod. Lekar., 19: 1313-15 (Aug. 31, 1964). (In Polish).

The possible influence of radiation and chemical agents on incidence of leukemia in certain parts of Poland was investigated. The records for 1957 to 1959 revealed an incidence of 3.12 per 10,000 for Krakow, 4.09 for Poznan, 3.57 for Lodz, 2.67 for Wroclaw, and 2.48 for Warsaw. Influence of background radiation levels and internal irradiation from radionuclides was studied. Investigation of the physical environment to detect possible anomalies in terrestrial radiation and some possible correlation with the distribution of leukemias revealed no correlation. Investigations of the activity of ^{90}Sr in the bones of deceased leukemic patients (mean value = 0.101 $\mu\mu C$ ^{90}Sr/g Ca) showed that the content of ^{90}Sr was 50% smaller than in the control group (0.089 $\mu\mu C$ ^{90}Sr/g Ca). Standard deviations amounted to 0.135 for the control group and 0.187 for the group with leukemia. Examination of milk, with which the leukemic patients were fed over a long time, showed normal contents of ^{90}Sr(2.7 to 13.5 $\mu\mu C$ ^{90}Sr/g Ca). Investigation of possible chemical contacts as a cause of leukemia revealed that such exposure to chemical agents could be traced in 32.6% of cases with chronic granulocytic leukemia, in 44.9% of cases of lymphatic leukemia, and in 23.3% of cases of myeloid leukemia, in contrast to an incidence of chemical contacts in the nonleukemic controls of only 18.5%. No influence on leukemia morbidity could be traced to carrying or wearing watches with luminescent (Ra-bearing) dials or to exposure from television sets. The possible leukemogenic action of other mutagenic agents which are entering the human environment at an increasing rate is discussed. (BBB)

43829 CHANGES IN ALKALINE PHOSPHATASE IN GRANULOCYTES OF CHEMICAL WORKERS AND RADIOLOGISTS. Pawelski, Slawomir; Wichrzycka, Elzbieta; Mdzewski, Bohdan; Roszkowski, Stanislaw (Inst. of Hematology, Warsaw). Polski Tygod. Lekar., 19: 1433-5(Sept. 21, 1964). (In Polish).

Cytochemical methods were used to assess the activity of alkaline phosphatase in 30 healthy subjects and in 139 persons who had been for many years exposed occupationally to the action of the leukemogenic agents, namely, to x rays (77 persons) and chemical agents (62). Alkaline phosphatase activity of the granulocytes showed no statistically significant decrease in individuals occupationally exposed to the action of such leukemogenic agents as x rays or benzene. However, a statistically significant decrease of alkaline phosphatase activity in the granulocytes was found in a group of 30 persons exposed for a

long time to the action of various chemical substances (toluene, xylene, aniline dyes, and nitrobenzene dyes). The latter group of individuals showed no clinical or hematological evidence of the disease. No correlation was found between the activity of alkaline phosphatase and the length of exposure to the leukemogenic agents or the leukocyte count in peripheral blood. (BBB)

43830 LATE EFFECTS OF RADIOACTIVE MATERIALS DEPOSITED IN MAN. Hasterlik, Robert J. (Univ. of Chicago). Postgrad. Med., 37: 642-9(June 1965).

A survey is made of studies conducted since 1955 on 300 persons who had worked in radium dial factories in Illinois from 1915 to the early 1930's or who had received medical treatment with radium 34 to 45 years ago. These persons were shown to have the characteristic defects and destructive changes in skeletal structure found in Ra poisoning. Radium given intravenously was a popular form of therapy from 1915 to 1930. It was injected in doses of 10 μC per week for many illnesses, including hypertension, rheumatoid arthritis, osteoarthritis, and mental diseases. Therefore, a large group of individuals are available for study in addition to those who worked as dial painters or Ra chemists. Since Ra has a half-life of 1620 yr, the important limiting factor on retention is the life span of the individual. At this time, 35 to 45 years after the ingestion or injection of Ra, these people are excreting in urine and feces between 0.01 and 0.005% per day of what they now retain. This amount retained represents only from 1 to 10% of the amount present when they acquired the Ra in their bodies 35 to 45 years ago. Skeletal defects observed included small areas of bone absorption scattered throughout the skull. Larger areas of bone resorption are seen in the shafts of the humerus, as well as severe destructive changes with secondary osteoarthritic proliferation about the head of the humerus. Among the 300 patients there are 16 with osteosarcomas and 12 with tumors about the head and neck, including eight carcinomas of the mastoid and two squamous carcinomas in either the antrum or the epithelium lining the tooth sockets of the maxilla. Also observed were a large sarcoma (rhabdomyo-sarcoma) of the antrum and another tumor of undetermined type arising in the sphenoid. Two formed Ra dial painters died from myeloid leukemia, but, statistically, incidence of leukemia does not seem to be increased by Ra deposition in bone. Possible carcinogenic mechanisms of Ra are discussed. (BBB)

43831 SIMULTANEOUS ACTION OF ALPHA-RADIATION AND SiO_2 IN ANIMAL EXPERIMENTS. [PART] II. Sevc, Josef. Pracovni Lekar., 17: 177-81(July 1965). (In Czech).

In two separate series of experiments on white mice the model of hepatic silicosis was used to test the effect of the simultaneous action of different amounts of fibroplastic dust and alpha radiation. Apart from histological examinations, in 200 animals the total hydroxyproline content of liver was estimated, and in 150 animals in addition the ratio of soluble collagen proteins was determined. Reduction of the fibroplastic action of SiO_2 was proved again in animals exposed for prolonged periods to alpha radiation. The significance of the effect of radiation depends on the administered amount. After administration of a ten times smaller dose, the significant inhibitory effect was no longer recorded. The higher ratio of soluble collagen proteins seems to be an approach to the explanation of the mechanism of the investigated effect. (auth)

43832 COMPARATIVE LETHALITY RESPONSES OF NEUTRON- AND X-IRRADIATED DOGS: INFLUENCE OF DOSE RATE AND EXPOSURE ASPECT. Ainsworth, E. J.; Leong, G. F.; Kendall, K.; Alpen, E. L. (Naval Radiological Defense Lab., San Francisco). Radiation Res., 26: 32-43(Sept. 1965).

The effect of n/γ dose rate was evaluated by determining the LD_{50}'s for dogs unilaterally exposed at 40 rads/min or 6×10^5 rads/min. The LD_{50}'s differed by only 9 rads, thus indicating no dose-rate effect on acute mortality response. The effect of exposure aspect (unilateral versus bilateral) on LD_{50} was determined with both n/γ- and x-irradiated dogs. In n/γ-irradiated animals, the LD_{50} was not significantly influenced by exposure aspect, but in x irradiated animals, the unilateral LD_{50} was significantly higher than the bilateral LD_{50}. With LD_{50} as the end point, estimates of the relative potency of n/γ-radiation compared with 1-Mvp x radiation depend on the point of dose reference. In terms of exposure (air dose) in space or at the midpoint of the exposure volume, the relative potency is ~1.0. However, in terms of midline tissue doses estimated from phantom studies, the data indicate that n/γ-radiation is significantly more potent in production of acute mortality than is 1-Mvp x radiation. The n/γ relative potency for bilateral exposure is 1.38, and for unilateral exposure is 1.49. At radiation doses ~1.4 times the LD_{50}, comparatively more n/γ-irradiated animals die in less than 7 days than do x irradiated animals. Thus the early-death threshold dose for n/γ-radiation appears to be closer to the midline tissue LD_{50} than is the case with x radiation. The possibility of significant intestinal damage in n/γ-irradiated dogs is discussed. (auth)

43833 HAIR DYSPLASIA INDUCED BY X-RAYS IN MICE UNDER DIFFERENT IRRADIATION CONDITIONS. Van Caneghem, P.; Beaumariage, M. L.; Lachapelle, J. M. (Universite, Liege; Universite, Louvain, Belg.). Radiation Res., 26: 44-53(Sept. 1965).

An attempt was made to observe a previously reported influence of irradiated volume on radioinduced hair dysplasia in mice. A large increase in irradiated volume has no influence on x-ray-induced dysplasia if appropriate precautions are taken to avoid physical error. (P.C.H.)

43834 STUDIES ON SOME RADIATION-INDUCED CHROMOSOME ABERRATIONS IN MAN. Doida, Yukio; Sugahara, Tsutomu; Horikawa, Masakatsu (Kyoto Univ.). Radiation Res., 26: 69-83(Sept. 1965).

The frequency and type of chromosome aberrations induced by ionizing radiations in human peripheral blood were investigated in atomic bomb survivors, in breast cancer patients who had received postoperative radiotherapy, and in radiation personnel who had been exposed to radiation during a long period of working time. Increased frequencies of aneuploid cells and a number of cells with abnormal chromosomes were observed in most of them, especially in the first two groups. However, the frequency of chromatid-type aberrations was at the control level in atomic bomb survivors, highest in radiotherapy patients, and intermediate in radiation personnel. The distributions of missing or additional chromosomes and the ratio of hypodiploid cells to hyperdiploid cells were compared among these three groups. The biological implications are discussed. In atomic bomb survivors, cells having the same types of abnormalities were observed with higher frequency than would be expected on a random basis. In any event, some of the aberrations induced by atomic radiation persisted for as long as 17 or 18 years in peripheral blood. (auth)

43835 THE EFFECTS OF ROENTGEN THERAPY ON THE HOST ACCEPTANCE OF AUTOGENOUS BONE GRAFTS IN DOGS. Hartman, Ted (Cleveland Clinic Foundation); Rapp, Robert. Radiology, 85: 532-6(Sept. 1965).

An experimental study was undertaken to obtain information on the effects of roentgen therapy on autogenous bone grafts in the femoral condyles of 8 dogs. Each right femoral condyl was given 2,000 R; 4 dogs received the radiation at two weeks and the other 4 at six weeks after operation. The left femoral condyles were not irradiated and served as controls. The aorta was injected with a mixture of "Micropaque" and Berlin blue at the time of death. The vascularity of each graft was studied microscopically. It appears that in normal bone and at twelve weeks after irradiation, an orderly progression of vascularity occurred through the grafts whether the time of initiation of irradiation was two or six weeks post-

operatively. Serial roentgenograms confirm the host acceptance of the bone graft after irradiation. (auth)

43836 MIGRATION OF HEMATOPOIETIC BONE MARROW CELLS IN IRRADIATED AND NORMAL MICE. Tubiana, M.; Frindel, E.; Kozinetz, G. I.; Dalle-Chavaudra, N. (Departement des Radiations de l'Institut Gustave-Roussy, Villejuif, Seine, France). Rev. Franc. Etudes Clin. Biol., 9: 742-5(Aug.-Sept. 1964). (In French).

In the rat or mouse exposed to a single dose of lethal radiation, the shielding of the spleen or of one limb suffices to protect the animal. This phenomenon can be explained as resulting from the repopulation of the aplastic area by cells migrating from the nonirradiated area. As proof of this hypothesis, mice, with a single posterior limb protected by a lead shield, were irradiated with 150 R per day for 11 days. Immediately after the eleventh irradiation, 25 μC of ^{3}H-labeled thymidine was injected directly into the bone marrow of the protected limb, the blood supply of which had been cut off from general circulation by a tourniquet. The same procedure was used on mice that had not been irradiated. In addition, some of these received a dose of 4 mg of nonradioactive thymidine. Two hr after the removal of the tourniquet, the mice were killed, and their bone marrow was aspirated from the injected limb to be examined by autoradiography for labeled cells. In both the mice with local aplasia due to partial irradiation, and in the normal mice, ^{3}H-labeled cells were found in the bone marrow at other sites in the body. In the irradiated mice, the percentage of marked cells in the protected and injected limb was 8.7% while in the irradiated, noninjected limb it was 3.6%. In the nonirradiated mice, two hr after the removal of the tourniquet, there were practically no labeled cells in the noninjected limb. However, after about five hr, the percentage of marked cells in the noninjected limb was almost the same as that in the injected limb. This phenomenon suggests the constant migration of marrow hematopoietic cells. Some general remarks on the possible clinical value of these observations are provided. (BBB)

43837 THE EFFECT OF CORTISONE ON GLUCONEOGENESIS IN RATS IRRADIATED WITH X-RAYS. Mazzone, Anna; Rava, Giovanni (Universita, Bari, Italy and Reparto di Radiologia dell'Ospedale Miulli, Bari, Italy). Ric. Sci. Rend., Sez. B, 6: 41-2(Jan.-Mar. 1965). (In Italian).

Rats were irradiated with x rays at 600 R; 48 hrs after the irradiation the rats were injected with cortisone and then with glycine 1-^{14}C. After the sacrifice of the animals the hepatic glycogen was extracted and its specific radioactivity was determined. The results show that in normal rats the incorporation of the glycogen radioactivity increases after treatment with cortisone. The irradiation also causes an increase of the incorporation with respect to the controls, but less than that in the normal rats. The radioactivity of the glycogen from rats irradiated and treated with cortisone was higher than that of the controls and of the rats irradiated alone but not as high as that of normal rats treated with cortisone. (J.S.R.)

43838 SOMATIC IRRADIATION INJURIES. Schlungbaum, W. (Roentgenabteilung, Staedtische Krankenhaus Spandau, Berlin). Roentgenpraxis, 17: 147-59(July 1964). (In German).

Somatic irradiation injuries fall into two major classifications, depending on whether the area irradiated is localized to specific regions or whole-body irradiation is administered. Another factor that is important is the relative radiosensitivity of the organs and tissues irradiated. The most sensitive tissue is the embryo up to the third month of pregnancy, with the fetus following closely in this respect after the third month. Lymphatic organs and blood-forming elements are next most radiosensitive. The zones of bone growth and lens of the eye are relatively less affected by irradiation. The central nervous system and musculature are probably least subject to irradiation damage. Radiodermatitis is one of the most obvious indicators of irradiation damage. Depending on the degree of damage inflicted, ulceration, necrosis, and teleangiectasis may also result. As results of the amounts and nature of the irradiation administered in each case, certain types of injuries appear to be associated with irradiation treatments for various groups of diseases. Thus, after irradiation treatment for tuberculosis, thyrotoxicosis, uterine myoma, neuralgia, osteomyelitis, eczema, herpes, actinomycoses, or lymphogranulomatosis slight injuries such as skin depigmentation, teleangiectasis, or epithelial atrophy with or without destruction of the subepithelial tissues may appear. Mucosal atrophy may also be observed. Only rarely are hyperkeratosis or skin tumors that develop from atrophic skin observed. After treatment for carcinoma, sarcoma, or hypernephroma, slow or nonhealing ulcers may appear, with extensive destruction of deep-lying tissue. (BBB)

43839 PERIPHERAL BLOOD CHANGES CAUSED BY INTERNAL EMITTERS. III. EFFECT OF RADIOIODINE ^{131}I. Dienstbier, Z.; Vitek, F. (Charles Univ., Prague). Sb. Lekar., 67: 33-40(1965). (In Czech).

Adult rats were intravenously injected with 0.19, 0.86, 3.46, 4.33, or 7.22 μC of ^{131}I, as NaI, and four hr to four days later counts were made of peripheral total leukocytes, neutrophils, lymphocytes, reticulocytes, and thrombocytes. The results were compared with those found in the two earlier studies of the effects of ^{32}P and ^{198}Au, and also of x rays. While ^{32}P caused a similar peripheral hematological response to external irradiation, these changes are much less marked after the administration of colloidal ^{198}Au; especially less marked were lymphopenia and neutropenia. Neutrophilia is found after the administration of ^{198}Au, when higher activities are used, apart from the nonspecific initial change, during the third and fourth week. After administration of ^{131}I in even activities of 7.22 μC/g body weight, rats did not show early lymphopenia and only from the second week of the investigation onward was the lymphopenia statistically significant and the lowest values amounted to 60% of the initial number of lymphocytes prior to the experiment. The neutrophilia, persisting for four weeks, was more marked after administration of 4.44 μC/g than after 7.22 μC/g. Similarly as after administration of ^{32}P and ^{198}Au, after the administration of higher ^{131}I activities, reticulocytosis and constant early reticulocytopenia did not develop. These results are interpreted in terms of the nature and energies of the radiations emitted by these three isotopes. (BBB)

43840 LEUKEMIA. Frei III, Emil; Freireich, Emil J. (National Cancer Inst., Bethesda, Md.). Sci. Am., 210: 88-96(May 1964).

The etiology, cellular and clinical characteristics, and treatment of leukemia are reviewed. Although the fundamental cause of human leukemia remains unknown, some contributory factors have been identified. One is ionizing radiation. When the dose of radiation is greater than 200 rad, there is a linear relation between the size of the dose and the frequency of leukemia. The frequency of the disease among those who survived being within 1000 m of ground zero at Hiroshima was 30 times greater than that of unexposed Japanese populations. A relation between the incidence of leukemia and the amount of ionizing radiation has also been found in arthritis patients who had received x-ray treatments of the spine. The leukemia that appears among those who have been exposed to ionizing radiation is myelocytic; the span of time between exposure and clinical detection ranges from two to 15 yr. Radiation, however, is only one factor in leukemia; the large majority of leukemia patients have no history of significant radiation exposure. Heredity also plays a major role in many forms of leukemia. There is no doubt that leukemia has something to do with the hereditary material. The incidence of the disease is high among persons with mongolism, or Down's syndrome. A change or series of changes in a normal immature leukocyte may render it incapable of maturing and of responding to the restraining and directing influences of the body. The genetic hypothesis is consistent with the observation that exposure to ionizing radiation increases the incidence of leukemia; ionizing

radiation can cause mutations. It is also consistent with the chromosome changes observed in Down's syndrome and in chronic myelocytic leukemia. Some clinical and experimental evidence suggest that the cellular transformation that gives rise to leukemia is related to changes in the immune system. Among the treatments of leukemia is the transfusion or grafting of precursor blood cells, which are capable of replication and full maturation into circulating leukocytes, platelets, and red corpuscles. The transfusion of bone marrow has been attempted after first subjecting patients to large doses of ionizing radiation so that their immune response is suppressed and not destroy the foreign bone marrow. Some grafts have functioned for as long as eight months. At the National Cancer Institute grafts were accomplished in 12 patients with acute leukemia by the transfusion of cells from the blood of patients with chronic myelocytic leukemia. The recipients were receiving antileukemic drugs, which like radiation, tend to suppress the immune response. The transfused blood precursor cells seeded the bone marrow and persisted there for as long as three months, producing competent leukocytes, red cells and platelets that circulated in the blood. (BBB)

43841 RADIOLYSIS OF CYSTEINE AND COMPLEX MOLECULES WITH SH LINKAGE III. THE EFFECT OF γ-IRRADIATION ON THE DECOMPOSITION OF S-S LINKAGE IN CHYMOTRYPSINOGEN. Matsuura, Niro (Tokyo Univ.); Muroshima, Kazuko. Sci, Papers Coll. Gen. Educ., Univ. Tokyo, 15: 63-79(June 1965).

From the stoichiometric point of view two molecules of the complex $Co(III)CyS_2$ should be decomposed by each radical H or OH formed by radiolysis of solvent water, if the previous interpretation of the results on the yields are correct. In these lines the deactivation of chymotrypsin caused by γ irradiation was studied by the application of polarographic protein wave or cysteine wave as a measure of S-S linkage destruction. PCMB and UV absorption spectrum methods are also applied since the polarographic protein wave develops not only by the SH group in the protein but also by the S-S bonds. The estimated stoichiometric yields are discussed under the light of the yields obtained for radioinduced oxidation of cysteine and of a cysteine in metallic chelate compound. The experimental procedure is also given. (J.F.P.)

43842 RESUME OF HUMAN STRESSES IN SPACE FLIGHT OPERATIONS AND METHODS OF IMPROVING MAN'S TOLERANCE. Schwichtenberg, A. H.; Lovelace II, W. R. (Lovelace Foundation, Albuquerque, N. Mex.). Southern Med. J., 57: 522-31(May 1964).

Some stresses that pilots would encounter in interplanetary space flights are reviewed, including that of radiation exposure. Radiation in space, along with weightlessness, has usually been considered as the two potentially limiting factors of prolonged manned space flight. Solar flares have by far the greatest known influence upon the varying intensities of cosmic radiation, but recent nuclear tests in space have added one more variable. In the Van Allen belts the radiation levels in the inner area, composed mostly of protons, are estimated at around 10 R per hr and an ~ similar level is reached in the outer belts which are composed mostly of electrons. High-altitude nuclear tests have added some radiation levels below this in the three to four hundred mile level, and more is becoming known of its characteristics and duration. The radiation level usually found in interplanetary space is believed generally low; the altitudes for present orbital flights are around 100 miles. However, with higher altitudes, as in passing through the Van Allen belts enroute to the moon or planets, or with a solar flare, the astronaut may receive considerably higher radiation dosages which could be of significance. From experiences so far, it appears that the hull of the space craft and instruments surrounding the astronauts provide slightly higher shielding effects than were calculated. (TCO)

43843 INTRODUCTION TO CLINICAL EXPERIMENTAL RADIOLOGY. Kaercher, Karl-Heinz. Strahlentherapie, Sonderbaende, 59: 1-457(1964). (In German).

The results of a series of studies in clinical experimental radiology carried out at the Radiation Clinic at the University of Heidelberg are reported. The studies were for the purpose of correlating the results of animal experiments and the reactions of the human body to radiation. Investigations are reported on the reaction of the skin, mucous membrane, and various organs to radiation, radioclinical histology, significance of puncture cytology in radiology, clinical radiohematology, principles and methods of enzyme studies in clinical medicine, practical methods for ferment studies in serum, body fluids, and tissue homogenates, ferment studies in serum and tissues after irradiation, the general radiation reaction in the clinic, the effect of ionizing radiation on organs and systems, and clinical changes on the protein, nitrogen, nucleoprotide, purin, phosphorus, electrolyte, and water content during radiotherapy. (J.S.R.)

43844 MUTAGENIC RESPONSE OF HUMAN SOMATIC CELL LINES. Szybalski, Waclaw; Ragni, G.; Cohn, Naomi K. (Univ. of Wisconsin, Madison). Symp. Intern. Soc. Cell Biol., 3: 209-21(1964).

The studies described were performed with the human somatic cell line D98S, its derivative D98/AG, resistant to 8-azaguanine (AG), and D98/AH, resistant to 8-azahypoxanthine (AH). The cell line D98S descended from a single-cell isolate of the Detroit 98 line. Agents tested for mutagenicity included x ray, uv light, and several other well-known bacterial and viral mutagens, some of which were shown to have mutagenic activity for higher organisms, including the fruit fly and the mouse. A series of aminofluorene derivatives of powerful carcinogens was also included, as were: colchicine, a mitotic inhibitor; Synkavit, a purported radiosensitizer; and strophanthin, a cytotoxic glycoside. The spontaneous mutation rates for this system varied between 10^{-5} to 10^{-6} mutations per cell per generation. Mutagens were tested for mutagenic effects at a concentration permitting 5 to 90% cell survival. No definite or consistent mutagenic effects were observed. Only in the case of x rays was a rather consistent, although still very low, mutagenic effect observed. The most probable basis for this general lack of mutagenic effect might be a mutagen-indifferent mechanism of numerically predominant mutations in the population of somatic mammalian cells. Small intra- or extraciestronic chromosomal rearrangements caused by unequal but homologous synapsis, pairing between normal and inverted regions, or other features of mitotic crossing-over (including nondisjunction) need not necessarily be promoted significantly by any of the toxic agents tested, but still could explain the high frequencies of the spontaneous mutations. Alternative explanations of the mutagen insensitivity of somatic cells, including (1) phenotypic lag, (2) high specificity of the particular reverse (gain) mutations, and (3) failure of the mutagen to penetrate to the immediate vicinity of, and to react with, chromosomal DNA, were experimentally excluded for several of the systems. Treatment with many of the bacterial mutagens actually resulted in a considerable decrease in the frequency of spontaneous mutants. Since the AG-resistant mutants are actually more resistant to several agents tested than the parental D98S cells, the possibility of selective susceptibility of the established mutants to the mutagens was eliminated. On the other hand, the experimental data are consistent with the hypothesis that bacterial mutagens either interfere with the special chromosomal rearrangement leading to the mutation or selectively eliminate the cells undergoing this process. Mutational events based on simple point modifications of the DNA structure, the type prevalent in bacterial and bacteriophage systems, may occur during mitotic replication of human somatic cells. However, this type of relatively rare genetic event (even when stimulated by DNA-specific mutagens) could be overshadowed by much more frequent mutations of a different type caused by chromosomal rearrangements. Some of these arrangements could not be very extensive, since they were not detected cytologically, and since they could be restored by interaction between the chromosomes and purified transforming DNA. (BBB)

43845 A TEST OF A HYPOTHESIS CONCERNING ULTRAVIOLET IRRADIATION DAMAGE AND PHAGE FUNCTIONS. Ebisuzaki, K. (Massachusetts General Hospital, Boston). Virology, 26: 390-3(July 1965).

Infection of Escherichia coli with the T-even bacteriophages results in the formation of two primary classes of proteins, classified on the basis of their temporal appearance as early and late. Synthesis of early proteins is mandatory for the synthesis of late proteins, and synthesis of late proteins is accompanied by a repression of formation of early proteins. However, this regulatory balance is disrupted if the phage are given small doses of uv irradiation; the early proteins are continuously synthesized and synthesis of late proteins is repressed. Stent has suggested a hypothesis whereby this uv effect can be explained on the basis of a clock model of regulation, wherein phage development occurs by a series of consecutive reactions in which inhibition of any one of the reactions prevents a terminal reaction. Stent proposed that uv irradiation inactivates an early cistron and this interrupts the specific induction sequence. In a direct test of the Stent hypothesis, experiments were done to study the ability of uv-irradiated bacteriophage T4 to form a late protein, lysozyme, in cells mixedly infected with an unirradiated nonlysozyme-producing mutant. The formation of the T4 phage-induced lysozyme was shown to be highly sensitive to uv irradiation. The formation of this late protein, in cells infected with nonirradiated, lysozyme-less phage and uv-irradiated, lysozyme-producing phage shows an undiminished, high sensitivity to uv irradiation. These results indicate that the Stent hypothesis does not apply and that the very high uv sensitivity of late phage genes must be explained by other means. Since small doses of uv irradiation are involved, a specific gene such as that of lysozyme is probably not the direct target of the irradiation. Instead, it seems that uv irradiation must invoke damage involving a critical step, which in turn prevents the expression of the lysozyme gene. The formation of late proteins or the cessation of the synthesis of early proteins seems to be regulated by DNA synthesis, and uv irradiation may inhibit late functions by inhibiting DNA synthesis. It follows that the failure to form lysozyme must be due to a failure to replicate the DNA of the irradiated phage, even though the milieu for DNA synthesis is provided. The failure of complementation to appreciably alter the inactivation curves for lysozyme synthesis suggests that a large portion of the phage genome cannot express itself. (BBB)

43846 ON THE EFFECT OF SMALL DOSES OF X RAY ON THE HISTOLOGICAL AND SOME HISTOCHEMICAL CHANGES IN RABBIT LUNGS. Zajusz, Kazimierz; Stoklosa, Edmund (Inst. for Industrial Medicine of the Mining and Steel Industry, Zabrze, Poland). Wiss. Z. Martin-Luther-Univ. Halle-Wittenberg Math.-Natur. Reihe, 13: 431-8(1964). (In German).

The effects of relatively small doses of x irradiation on morphological changes in the rabbit lung during an interval of 4 to 16 days postirradiation were studied. The doses amounted to 25, 50, 100, 150, and 200 R. In order to elucidate the mechanisms of the pathological changes observed, alterations in concentrations of acid and alkaline phosphatase, adenosine triphosphatase, and adenosine monophosphatase were studied histochemically. Single whole-body irradiation with doses of 20 to 25 R produced no detectable changes in the lung tissues. After irradiation with from 25 to 50 R there were circulatory disturbances with hemorrhages into the alveoli. The macrophage system appeared to be extensively stimulated, with proliferation of macrophages. Irradiation dosages of 100 R or more produced additional symptoms of radiation sickness, such as edema, thickening of the alveolar walls, and epithelial and connective tissue proliferation. There was some obliteration of the alveoli. The degree of reaction of the reticuloendothelial system was proportional to the irradiation dose used. In parallel with changes in the reticuloendothelial system the histochemical tests indicated increases in acid phosphatase concentrations. However, in the animals that received from 25 to 50 R the reactions of alkaline phosphatase, adenosine triphosphatase, and adenosine monophosphatase were only moderately increased. At higher irradiation doses the intensity of the histochemical reactions studied was about the same as at the lower doses, and sometimes the reactions even appeared to be reduced. (BBB)

43847 INDUCTION OF PHAGE PRODUCTION AND FORMATION OF CLEAR-PLAQUE MUTATIONS BY UV IRRADIATION OF PROPHAGE AND OF FREE PHAGE KAPPA BY USE OF VARIOUS SERRATIA STRAINS AS HOST. Steiger, H.; Kaplan, R. W. (Universitaet, Frankfurt/Main, Ger.). Z. Allgem. Mikrobiol., 4: 367-89(1964). (In German).

The action of uv light (254 mμ) on phage induction of prophage mutability was studied in three strains (Hy, CN, and EQ) of Serratia marcescens. The lysogenic strain HY(κ) has a 10 times lower rate of uv induction of phage production and lower hit number (n = 2) compared with the strains CN(κ) and EQ(κ)(n = 3). Clear-plaque mutants appear after uv induction of Hy(κ) at very high frequencies, up to 2% after 40 sec uv when uv-irradiated cells are plated before lysis and up to 40% when plated after lysis. In a single-burst experiment 17 ± 7% of the clones after uv-induction contained c-type. The burst size of wild type is about 60; but from c-mutated cells about 200 c-phages were liberated, though the burst size of cells infected with a c-phage is 60 as it is with wild type. The uv-induced bursts with c-type contained none or only a few wild type phages. The c-mutation of prophage is not correlated completely with uv induction. This is shown in experiments where the cells which had not lysed after uv irradiation were cultivated further for 15 generations. Completely clear mutants (c-type) give about 0.02% nonlysed cells among infected cells as is the case with wild- and also 1-type. But these survivors of c-infection are not stably lysogenic and immune as in the case of wild- or 1-type. Photoreactivating light increased the frequency of c-mutants in uv-induced lysate at least at high uv doses. In the strains CN(κ) and EQ(κ) no c-mutations were observed after uv-induction, though c-mutants are phenotypically expressed as clear-plaques on the indicator CN. Thus both strains are unable to turn uv-produced c-premutations to perfect mutations. This hypothesis is supported by the finding that phage uv-irradiated extracellularly gives nearly no increased frequency of clear-plaque mutations on CN though up to 2% of them appear on HY after irradiation for 300 sec. (TCO)

43848 IMMUNIZING EFFECT OF X-IRRADIATED CERCARIAE OF SCHISTOSOMA JAPONICUM IN ALBINO MICE. Hsu, S. Y. Li; Hsu, H. F.; Osborne, J. W. (Univ. of Iowa, Iowa City). Z. Tropenmed. Parasitol., 16: 83-9 (Apr. 1965).

For preparation of immunizing inoculations of Schistosoma japonicum, the cercariae were irradiated in dechlorinated water suspensions. The total exposure dose given to the cercariae used for immunizing the CFW mice varied from 2200 R to 3500 R of 250-kvp x rays at a dose rate of 620 R/min. The cercariae were applied on the abdominal skin of mice, each mouse being immunized twice. For the challenge inoculation, 100 nonirradiated cercariae (50 male and 50 female) were used. In the first experiment, with immunizing cercariae exposed to 3000 R before inoculation, each mouse received 200 x-irradiated cercariae in the first immunizing inoculation, and 61 days later a second immunizing inoculation of 270 x-irradiated cercariae. Eighty days after the second immunizing inoculation each mouse was challenged with 100 nonirradiated cercariae. When these mice were sacrificed on the 34th day of the challenge infection, the number of adult female worms with eggs in their uteri was 31.8 compared with 30 in controls. In subsequent experiments in which the immunization and challenge schedules were varied, no significant immunogenic effect of irradiated cercariae was noted, just as noted in the first experiment. In an earlier study on histopathology in mice infected with x-irradiated cercariae of S. japonicum, the authors reported that with

cercariae exposed to 3000 R, differences in the timing, rate, and site of schistosomulic destruction between mice infected once and those infected twice were not significant. Schistosomulic arrest occurred neither in the skin nor in the lungs, but in the liver. With four infections of cercariae exposed to 3000 R, occasional schistosomulic arrest in lungs was observed, indicating the beginning of a shift of the site of schistosomulic destruction from liver to lungs, this shift being regarded as a manifestation of the degree of acquired immunity. Since the shift of schistosomulic destruction from liver to lungs and skin was not encountered in mice infected twice with cercariae exposed to 3000 R, but only in those infected four times, several repeated infections are necessary in effecting acquired immunity. The fact that no acquired immunity was produced by inoculating mice twice with cercariae exposed to 3000 R was supported by the results of worm recovery in the present experiments. (BBB)

43849 ELECTRON MICROSCOPIC FINDINGS IN THE IRRADIATED SUPRAESOPHAGEAL GANGLION OF ODONATA LARVAE (CALOPTERYX SPLENDENS HAAR). Buchholtz, Christiane (Universitaet Marburg, Lahn, Ger.). Z. Zellforsch., 63: 1-21(June 12, 1964). (In German).

Four types of neurons were observed in the supraesophageal ganglia of odonata larvae x irradiated with 100000 R during the Y and Z developmental stages. These were globular perikaryon, large perikaryon with large round nuclei, large cytoplasm-rich perikaryon with nuclei, and perikaryon with neurosecretory activity. Changes in all except the second type induced by irradiation included increased volume of neuroplasm and reduced size of nuclei. The nucleolus was visible in the karyoplasm of the large round nuclei. High concentrations of chromatin were visible in all four types of perikarya after irradiation. Differences between the perikarya were shown in the endoplasmatic reticulum containing ribosomes, the dictyosomes, and the mitochondria. Very dark granules that suggested ribosomes concentrations were observed particularly in the perikarya with large round nuclei. The secretory vacuoles of the neurosecretory perikarya were reduced and clumped together because of loss of their membranes. Studies with the light microscope indicated increases in cell volume and nuclear swelling after irradiation with 40000 to 50000 R. Usually these changes were reversible, but after 50000 to 150000 R there were irreversible changes. These included localization and accumulation of tigroid material, with appearance of chromatin in the nucleus that shifted the nucleolus to the nuclear edge. Following this the nucleus shifted to the periphery of the cytoplasm, while the tigroid substance separated into five particles and finally disappeared. During this phase there was partial vacuolization of the cytoplasm. Complete necrosis was indicated by appearance of completely pyknotic residual bodies. 76 references. (BBB)

43850 ON A SARCOMA RESULTING AT THE SITE OF ADMINISTRATION FROM PARAVASAL INJECTION OF THOROTRAST. Kemnitz, Peter; Vinz, Heinrich (Institut fuer Pathologie, Magdeburg, Ger.). Zentr. Allgem. Pathol. Pathol. Anat., 106: 502-11(1964). (In German).

Up to now only 2 cases of tumors occurring at the site of paravasal Thorotrast injection have been reported. The 59-yr-old patient reported in this study had received a paravasal injection of Thorotrast at an undeterminable date, but at least 17 yr previously, in the region of the left elbow. X-ray examination revealed an irregularly shaped mass $9 \times 5 \times 4.5$ cm in size at the elbow which contained large amounts of Thorotrast. The axillary lymph nodes also contained Thorotrast. There was clear evidence of tumor metastases in lung, liver, axillary lymph nodes, jejunum, and colon. The tumor in the elbow was a dense, actively growing protoplasmic spindle cell sarcoma. There was no evidence of Thorotrast deposition in the tumor itself. Thorotrastomas occur frequently without inducing tumors of the type reported here. However, they may be transitional stages in the development of tumors, as some experimental animal studies indicate. The 2 other cases of tumors that have been reported after Thorotrast administration were located in the neck after it was administered for carotid angiography. In these cases Thorotrast was found also in spleen, liver, portal lymph nodes, and bone marrow. References cited, 75. (BBB)

43851 STUDIES ON THE PATHOLOGY OF RADIATION DISEASE. Krayevskii, N. A. Oxford, Pergamon Press, 1965. 219p. $15.00.

Translated from Russian by A. Lieberman.

The present state of knowledge on the gross and microscopic anatomy of radiation disease is discussed with reference to about 300 publications, many from Russia. Changes induced by ionizing radiation in the hematopoietic tissue, cardiovascular system, lungs, gastrointestinal tract, endocrine glands, nervous system, and bone are systematically reviewed. A total of 113 microphotographs is illustrated. Two other topics are discussed in detail: characteristics of radiation pathology caused by internally deposited radionuclides, and infectious complications of radiation disease. Other special topics considered include the leukemogenic effect of radiation and the possible mechanisms leading to malignancy, the ability of the organism to recover from prolonged low-dose irradiation, reasons for the differential cellular radiosensitivity of various organs and tissues, and possible toxic factors which may be liberated from radiation-injured cells and be partially responsible for manifestations of the radiation syndrome. (BBB)

43852 AN ASSESSMENT OF THOSE METABOLITES CONSIDERED TO BE OF VALUE IN THE DIAGNOSIS OF EXPOSURE TO RADIATION. Smith, H.; Bates, T. H. (United Kingdom Atomic Energy Authority, Chapelcross, Annan, Scotland). pp 199-215 of STI/PUB/99.

Certain metabolites excreted in urine were examined in cases of human beings exposed to x and γ irradiation for therapeutic reasons. These patients were receiving doses of up to 5000 R over a period of three to five weeks. Urinary excretion of creatinine, creatine, total α-amino-nitrogen, β-amino-isobutyric acid, pyrrole-2-carboxylic acid, 5-hydroxyindoleacetic acid, and indoxyl-sulfate were followed quantitatively during the whole course of treatment. None of the patients were exposed to whole-body irradiation but it is apparent that changes in metabolic function as a result of radioinduced damage can be reflected in urinary excretion. The biochemical rationale and interpretation of these excretion patterns is discussed in relation to that part of the body irradiated, but it was concluded at this stage of investigation that quantitative assessment of biological damage is not possible. However, such tests can be useful as a guide to the clinician on the form of therapy. Preliminary tests on changes in certain plasma metabolites in rats exposed to single sub-lethal doses of x irradiation are worthy of extrapolation to human studies. Plasma concentrations of 5-hydroxytryptamine, uric acid, SGOT, SGPT, globulin fractions of protein, creatine phosphokinase, leucine aminopeptidase, lysyl aminopeptidase, kallikrein, kallidin, zinc, and manganese were measured. Qualitative yet significant changes were observed in plasma levels of uric acid, leucine aminopeptidase, lysyl aminopeptidase, and manganese after irradiation. The significance of these data is discussed. Emphasis in these studies was placed on methods that are simple and quick to perform. 86 references are cited. (auth)

43853 DETERMINATION OF TOTAL ABSORBED DOSE FOLLOWING ACCIDENTAL AND CHRONIC EXPOSURE. Obaturov, G. M. pp 329-47 of STI/PUB/99. (In Russian).

Methods and formulas for calculating the dose absorbed by the critical organs following accidental and chronic (external and internal) exposure are proposed. The doses absorbed by the critical organs upon external exposure are calculated on the basis of the following measurements of internal exposure doses: concentration of radioactive aerosols and period of time during which they enter the body; activity of the excreta; and, activity of the body. Finally, an example is given illustrating the summation of absorbed doses accruing from external and internal exposure. (auth)

43854 ATTEMPT TO ASSESS THE DOSE RECEIVED BY THE BONE MARROW ON EXPOSURE TO A NEUTRON FLUX. Mechali, D.; Dousset, M.; Beau, P.; Le Grand, J. (Centre d'Etudes Nucleaires, Fontenay-aux-Roses, France). pp 483-95 of STI/PUB/99. (In French).

Attempts to calculate the average dose received by bone marrow in the case of whole-body exposure to a neutron flux taking into account its distribution in the organism and the energy of the incident neutrons, are reported. (P.C.H.)

43855 THE EFFECTS OF ^{60}Co ON A DESERT ROOT SYSTEM (TRIBULUS TERRESTRIS L.). Mayes, Mary G. (Lovelace Foundation, Albuquerque, N. Mex.). 11p. (CONF-641219-2). Gmelin, AED-CONF-64-272-1.

From American Association for the Advancement of Science, 131th Annual Meeting, Montreal.

Some of the changes in root meristematic regions undergone by Tribulus terrestris plants grown from seeds irradiated by a ^{60}Co source were described and compared with normal growth and development patterns in control plants. Both control plants and irradiated seed plants displayed four regions in the growing root tip; root cap; apical 300 μ of the meristem zone is characterized by slow elongation, slow cell division, and the presence of typical meristem cells; the adjacent 125 μ at the base of the meristem zone, characterized by rapid elongation, rapid cell division and the presence of vacuolating and dividing cells; and the zone of cell elongation falling between 400 μ and 1000 μ from the base of the root cap, and characterized by relatively slow elongation, absence of cell division, and hence, the presence of vacuolating extending cells. Cell differentiation occurs at different levels within the root, depending upon the particular type of cell involved and whether irradiated seed. The results of the investigation reported here demonstrate the complexity of growth at the meristem. Elongation, cell division, cell enlargement, and differentiation of the various cell types, each of these processes, and a host of others makes its contribution toward building the intricate structure of the mature root. There is usually a simultaneous operation of several of these processes at any particular level in the root tip, while the rate of each undergoes progressive changes in passing along the root. Radiation effects in any particular region are a complex of changes, both structural and morphological in nature. (auth)

43856 THE EFFECT OF RADIATION ON ENZYMATIC ACTIVITY IN SYNCHRONOUSLY DIVIDING TETRAHYMENA PYRIFORMIS GL. Sullivan, Wm. D. (Boston Coll.). 14p. (CONF-641121-1). Gmelin, AED-CONF-64-277-1.

From American Society for Cell Biology, 4th Annual Meeting, Cleveland.

The effects of uv and x radiation on enzyme activity were studied in Tetrahymena pyriformis. Enzymes investigated during different phases of cell division were fumarase, malic dehydrogenase, malic enzyme, isocitric dehydrogenase, and glyceraldehyde-3-phosphate dehydrogenase. X-ray doses were approximately 180,000 R and uv irradiation was at 2537 Å at six in. for 2.5 min. Fumarase, glyceraldehyde-3-phosphate dehydrogenase, malic dehydrogenase, and isocitric dehydrogenase demonstrated an acceleration of activity in all phases of division following x-irradiation, the pattern of activity being almost identical for malic dehydrogenase and fumarase. Glyceraldehyde-3-phosphase dehydrogenase activity was inhibited by uv in all stages with the greatest inhibition demonstrated at 0 to 150 min following removal from the water bath. Activity of uv-irradiated isocitric dehydrogenase followed the same pattern except for the late stages of division when an acceleration activity was noted. (H.G.D.)

43857 THE DEPENDENCE OF DIVISION DELAY ON THE TIME OF IRRADIATION FOR THE IRRADIATED AND POST-IRRADIATED GENERATIONS OF CHINESE HAMSTER CELLS. Froese, G. (Manitoba Cancer Treatment and Research Foundation, Winnipeg, Can.). 6p. (CONF-650219-2). Gmelin, AED-CONF-65-075-2.

From Canadian Association of Radiologists, 28th Annual Meeting, Toronto.

Time-lapse photomicrography was used to demonstrate the dependence of division delay in γ irradiated and post-irradiation generation of hamster cells in culture on the age of the cells at the time of irradiation. Maximum delay occurred in cells irradiated during the middle of their life cycle. It was concluded that the delay exhibited in the post-irradiation generation is the result of a separate non-reversible damage resulting in a permanent change in the affected cells. (C.H.)

Radiation Effects Therapy and Countermeasures

43858 (NP-15310) QUARTERLY PROGRESS REPORT NO. 56. (USAF Radiation Lab., Univ. of Chicago, Ill.). July 15, 1965. Contract AF41(609)-1693. 49p.

Separate abstracts were prepared for four sections of this report. (C.H.)

For abstracts of individual sections see: 43670, 43720, 43859, and 43860.

43859 (NP-15310, pp 1-13) PRELIMINARY STUDIES ON THE MECHANISM OF THE RADIOPROTECTIVE EFFECTS OF DIMETHYLSULFOXIDE (DMSO) IN X-IRRADIATED MICE. Pizak, V.; Doull, J. (USAF Radiation Lab., Univ. of Chicago, Ill.).

Groups of male CF_1 mice were given DMSO (5 gm/kgm, intraperitoneally) and at various intervals thereafter exposed to a lethal dose of whole-body x irradiation (750 R) to establish the time of onset and duration of the radioprotective effect of this agent. The results of these studies demonstrated that the radioprotective effect of DMSO can be detected within the first minute after its administration and that the effect persists for at least 2 hours after administration. Maximal radioprotective activity was obtained between 10 and 60 minutes following DMSO administration. To ascertain the effect of hyperbaric oxygen exposure (60 psig) on the radioprotective effect of DMSO, groups of CF_1 female mice were given DMSO (5 gm/kgm IP) and subsequently exposed to 800 R under conditions of air at 0 psig or 0_2 at 60 psig. The hyperbaric oxygen exposure did not reduce the radioprotective effect of DMSO in these studies. The effect of DMSO alone and in combination with PAPP, MEA, or AET on the survival of mice given x ray doses of 800 R, 1,000 R, and 1,200 R was investigated in groups of CF_1 male mice. The use of these combinations produced an increased number of 30-day survivors over that obtained by administering DMSO or the other protective agents alone. The enhanced protective effect was qualitatively similar at each of the three x ray dosage levels used and with each of the three radioprotective agents (PAPP, MEA, or AET). DMSO in combination with PAPP permitted 60% of a group of mice given 1,200 R of whole-body x irradiation to survive the 30-day post-irradiation period. (auth)

43860 (NP-15310, pp 14-25) STUDIES ON THE EFFECTS OF VARIOUS DRUGS ON THE ADENOSINE TRIPHOSPHATASE ACTIVITY OF THE HEMATOPOIETIC TISSUES OF RATS EXPOSED TO COBALT-60 γ RADIATION. Tardiff, Robert G.; DuBois, Kenneth P. (USAF Radiation Lab., Univ. of Chicago, Ill.).

Adult, female Sprague-Dawley rats were exposed to 21.2 R and several doses from 45 R to 54 R per day of cobalt-60 gamma radiation per day over a 10-hour period each day. At intervals over a considerable period of time, groups each containing four animals were sacrificed and adenosine triphosphatase assays were performed on the spleens. It was found that a progressive increase in the enzyme activity occurred during the first 4 days of irradiation after which time continued exposure resulted in maintenance of the activity at a relatively constant, elevated level. The amount of the increase was dose-dependent in the 21.2 R and 50 R groups. From this response it was felt that drugs could be tested for protective activity against this type of exposure by irradiating animals for

4 days and treating them daily with various drugs. By sacrificing the animals after 4 days of irradiation and drug treatment protection could be measured by determining the extent of the enzyme increase. A protective effect against the increase in enzyme activity was obtained by treatment of the animals with hydrocortisone, cortisone acetate, progesterone, estradiol, thyroid stimulating hormone, thyroxin, adrenal cortex injection, and adrenocorticotrophic hormone. Mercaptoethylamine, aminoethylisothiouronium bromide, hydroxylamine, and cysteine also provided protection against injury of the spleen by daily exposure to gamma radiation at the rate of about 50 R per day. Yeast extract, liver extract, liver fractions, and a liver concentrate all exhibited strong radioprotective properties against the enzyme change in the spleen under the conditions of these radiation exposures. (auth)

43861 (JPRS-31349, pp 1-24) CHEMICAL PREPARATIONS FOR PREVENTION OF RADIATION INJURIES. Yarmonenko, S. P.; Shashkov, V. S.; Kostyanovskii, R. Translated from Farmakol. i Toksikol., 27: 110-36(Mar.-Apr. 1964).

Difficulties encountered in attempts to classify chemical radioprotective compounds are discussed. It is pointed out that the most promising compounds tested belong to two basic large groups, the mercaptoalkylamines and the indolylalkylamines. Recent data are presented on the protective mechanisms of action of these two classes of compounds, as well as several miscellaneous compounds, in a variety of irradiated biological materials ranging from model systems to microorganisms and to man. (C.H.)

43862 HEMATOPORPHYRIN AND WHOLE-BODY IRRADIATION: STUDIES ON THE TIME-EFFECT RELATION AND THE 5 mg/kg DOSE IN THE ALBINO MOUSE. Cittadini, C. (Universita, Siena, Italy). Boll. Soc. Ital. Biol. Sper., 41: 360-3(Apr. 15, 1965). (In Italian).

Forty mice of the NMRI strain, two and one-half months old, were injected intraperitoneally with 5 mg/kg hematoporphyrin at 30 min, one, two, four, or 12 hr before whole-body irradiation. The 200-kv x rays were administered at a dose rate of 46 R/min to total doses of 800 R. The mean survival times (in hr) were: after injection at 30 min pre-irradiation, 170; one hr, 191; two hr, 278; four hr, 274; 12 hr, 296; control (saline-injected), 297. Statistical analysis showed that the 30-min group had a significantly shorter survival time (at the 95% level of confidence). Thus hematoporphyrin when given shortly before irradiation acts as a radiosensitizer in mice. The similarity between the action of this pigment and the radiosensitizing action of oxygen are discussed. (TCO)

43863 RADIOPROTECTIVE ACTIVITY OF NITROGENOUS HETEROCYCLIC COMPOUNDS DERIVED FROM IMIDAZOLE AND BENZIMIDAZOLE. Rinaldi, Renaud; Bernard, Yvette; Guilhermet, Monique (CEN, Grenoble, France). Compt. Rend., 261: 570-2(July 12, 1965). (In French).

The radioprotective action of nitrogenous heterocyclic derivatives of imidazole and benzimidazole was evaluated on mice exposed to a lethal exposure of x rays (DL_{100}/30 days). The reduction in mortality was the evaluation standard. Of the eleven compounds studied, only 1-naphthylmethyl-2-imidazoline, 2-methyl-benzimidazole, and (2,6-dimethyl-4-tertiobutyl-phenyl)methyl-2-imidazoline had an effect. They gave survivals of 100, 60, and 70%, respectively. The activity of 1-naphthyl-methyl-2-imidazoline, which is more significant and regular in females than in males, passes through a maximum at doses very far from the toxic dose. It still has a protective effect if it is injected 1 hr before irradiation. (J.S.R.)

43864 EVALUATION OF THE RADIOPROTECTIVE EFFICACY OF MEXAMINE. Bychkovskaya, I. B.; Bogatyrev, A. V. (Central Scientific Research Inst. of Roentgenology and Radiology, USSR). Dokl. Akad. Nauk SSSR, 161: 704-6(Mar. 21, 1965). (In Russian).

The protective efficacy of mexamine (5-methoxy-tryptamine hydrochloride) against various kinds of radiation death was evaluated by calculating an index called the radiation dose decrease factor. This factor is the degree to which a radioprotective agent decreases the dose, i.e., mitigates the severity, of radiation injury. The average length of life of animals dying within the first 30 days after irradiation and the 30-day survival rate are used to determine LD_{50} (for the 30th day). The ratio of the LD_{50} for the controls to the LD_{50} for the protected animals is the dose decrease factor (DDF). Male white mice weighing 18 to 20 g were exposed to x ray doses ranging from 300 to 1100 R. Half the animals received 75 μg/l gram body weight of mexamine 15 min before irradiation. Two types of radiation deaths were observed: bone-marrow deaths occurring in the controls 8 to 14 days after irradiation with 600 to 700 R, and gastrointestinal deaths occurring 4 to 7 days after irradiation with doses of 900 R and more. The DDF was determined for the entire range of doses used. Mexamine decreased bone-marrow mortality, having a DDF in the corresponding dose range (600 to 700 R) of 1.4 to 1.3. But mexamine was less effective in reducing gastrointestinal mortality, and in the dose range causing death from this type of injury (900 to 1100 R) its DDF was only 1.1 to 1.0. At 800 R, deaths of both kinds were about evenly divided, and the DDF of mexamine was 1.12. Other radioprotective means, hypoxia and amituron (δ-β-aminoethyl isothiuronium), have been shown to have a uniform protective effect against doses of any magnitude, irrespective of the type of injury they cause. The nonuniform effectiveness of mexamine against different doses of radiation shows that its action is not confined to decreasing the effective radiation dose. The reason for its greater effectiveness against bone-marrow mortality remains unknown. The nonuniform efficacy of mexamine also demonstrated the necessity of using a wide range of doses in evaluating the protective effect of any radioprotective agent. (ATD)

43865 pH EFFECT ON THE GAMMA-RAYS SENSITIVITY OF CLOSTRIDIUM SPOROGENES. Milc, G.; Bonotto, S.; De Proost, M. Energia Nucl. (Milan), 12: 422-8(Aug. 1965). (In Italian).

The pH effect was studied on the gamma sensitivity of Clostridium sporogenes PA 3679. The results suggested a probable pH action, which would act varying the relative stability of the biological sites sensitive to the reactions induced by the radiations. A possible radioprotection of spores by inorganic phosphates of the buffer solutions was studied. (auth)

43866 RECOVERY FROM RADIATION DAMAGE AND ITS MODIFICATION IN MAMMALIAN CELLS. Sugahara, Tsutomu (Kyoto Univ.). Idengaku Zasshi, 40: Suppl., 194-206(1965).

Results are reported from studies in mice exposed to 365 R ^{60}Co γ radiation in air at a dose rate of 65 R/min repeated once a week until death occurred and given subcutaneous injections of nucleic acid precursors once or 3 times per week. The data showed that some nucleic acid derivatives are effective in modifying recovery from radiation damage in mammals and mammalian cells, however, the mechanisms underlying these effects seem to be difficult to elucidate. By temporarily classifying various kinds of recovery observed into two classes phenomenologically, a comparative study on the effect of various compounds between these two classes of recovery was undertaken. Class 1 recovery is that observed under physiological conditions, and Class 2 recovery that observed only with special treatment after irradiation. Functionally it seems that the former corresponds to the recovery in sublethally irradiated cells and mammals and the latter to that in lethally irradiated ones. The significance of studying these two recoveries and their modification by chemical agents is stressed, though the data available so far are not yet sufficient for drawing definite conclusions. (auth)

43867 SULFHYDRYL RADIATION PROTECTIVE AGENTS. Shapiro, Bernard; Schwartz, Emanuel E.; Kollmann, George (Albert Einstein Medical Center, Phil-

adelphia). J. Albert Einstein Med. Center, 11: 12-13 (Jan. 1963).

This report concerns attempts to develop radioprotective agents to the point where they can be used to protect man or certain tissues of man against the damaging effects of radiation and also to learn the mechanism of their protective action which may provide insight into the mechanism of action of ionizing radiation. The most effective sulfhydryl protective agent known, S-(2-aminoethyl)thiuronium bromide hydrobromide (AET) was studied in terms of its chemistry, radiation chemistry, interaction with proteins, and metabolism after intraperitoneal and oral routes of administration in normal, irradiated, and tumor-bearing mice. AET, when prepared in aqueous, buffered solutions at pH 7 or above, is converted to the sulfhydryl compound 2-mercaptoethyl-guanidine (MEG) and its disulfide, bis(2-guanidoethyl) disulfide (GED). When irradiated in aqueous buffered solutions, MEG is oxidized to GED which is in turn oxidized to 2-guanido-ethanesulfinic acid (RSO_2H), taurocyamine (RSO_3H), and sulfate. In protein solutions MEG and GED become bound to proteins by forming mixed disulfides with protein sulfhydryl and disulfide groups. Irradiation of these solutions increases the protein binding and produces a new unidentified protein-protective agent bond. In mice, MEG and GED are metabolized to RSO_2H, RSO_3H, sulfate, and a thiolester believed to be S-acetyl-2-mercaptoethyl-guanidine. Most of the protective agent in mice, however, at the time of protection, is in protein-bound form and GED. Distribution and metabolism studies revealed that, by the oral route, MEG is absorbed more rapidly and gives higher tissue levels of the protective agent than GED at 30 min which explains the better protection observed with oral MEG as compared with oral GED when mice are irradiated 30 min after administration. Studies of the chemical forms in the tissues of mice at 20 min after an intraperitoneal dose of GED, when the animals are known to be protected and at 120 min after an intraperitoneal dose of GED when the animal is no longer protected, show that only protein-bound agent and GED consistently decrease in concentration and can be correlated with protection. Other metabolic forms are unchanged or increased in the tissues at 120 min and therefore are not directly involved in protection. Distribution and metabolism studies in tumor-bearing mice showed that subcutaneously transplanted tumors take up very little protective agent and are not protected whereas most normal tissues take up much more of the agent and are protected by oral or intraperitoneal administration of MEG. This suggests a possible future application of sulfhydryl protective agents in x-ray therapy if these agents can ever be made safe for use in man. (BBB)

43868 POTENTIAL ANTIRADIATION COMPOUNDS. II. EXTENSION OF THE NITRO-THIOLACETATE ROUTE. Bhat, K. Venkatramana; McCarthy, Walter C. (Univ. of Washington, Seattle). J. Pharm. Sci., 53: 1545-7(Dec. 1964).

Because of the known high radioprotective activity of compounds containing a mercapto group and an amino group on adjacent carbon atoms, an investigation was made of substituted analogs by addition of thiolacetic acid to ω-nitrostyrene, followed by reduction with lithium aluminum hydride. Ring-substituted ω-nitrostyrenes were also investigated, and those with the 3,4-methylene-dioxy, 3,4-dimethoxy, and 3-methoxy-4-acetoxy groups all gave the expected thiolacetate addition product. 3-Acetoxy-4-methoxy-ω-nitrostyrene underwent an anomalous reaction with thiolacetic acid to give a gum. In the second reaction of the sequence, a typical ring-substituted member of the series, 1-(3′,4′-methylenedioxyphenyl)-1-acetthio-2-nitroethane, was reduced with lithium aluminum hydride to the mercapto-amine, 1-(3′,4′-methylenedioxyphenyl)-1-mercapto-2-aminoethane. Reduction of the sidechain homolog, 1-phenyl-1-acetthio-2-nitropropane, gave cleavage of the carbon chain; none of the expected mercapto-amine was isolated. The reduction products isolated were benzyl disulfide and ethylamine hydrochloride. 1-Phenyl-1-acetthio-2-nitropropane showed some activity in protection of mice against an LD_{100} dose of radiation at a dosage level in the range 151 to 350 mg/kg. The next lower homolog, 1-phenyl-1-acetthio-2-nitroethane. (TCO)

43869 EFFECT OF CYSTEAMINE, CYANIDE AND HIGH-PRESSURE OXYGEN ON SPLENIC OXYGEN TENSION AND SULPHYDRYL CONTENT. Jamieson, Dana. (Cancer Inst. Board, Melbourne). Nature, 207: 541-2 (July 31, 1965).

The mechanism of the radioprotective effect of cysteamine was investigated in rat spleen, a radiosensitive tissue. The effects of cyanide and high pressure oxygen on splenic oxygen tension and sulfhydryl content in the spleen of rats treated with cysteamine were measured. Neither cysteamine or cysteamine plus cyanide had any effect on normal splenic oxygen tension in air or 5 atmospheres of O_2. Results indicated that the radioprotective effect of cysteamine could not be explained as a result of hypoxia. Cysteamine raised the content of sulfhydryl in the spleen while the content of disulfide remained constant. Five atmospheres of O_2 had no effect on the endogenous -SH or -SS- content of rat spleen. However, high-pressure O_2 did significantly reduce the increase of total splenic -SH groups produced by cysteamine, suggesting that O_2 administered under pressure in vivo produces faster oxidation of -SH groups from cysteamine. The administration of cyanide to cysteamine-treated rats failed to alter the changes in splenic -SH or -SS- content produced by cysteamine. It was concluded that the slight reduction of cysteamine radioprotection by high-pressure O_2 may possibly be due to a reduction by the latter of total -SH groups present during irradiation. (C.H.)

43870 MODIFICATION OF THE RADIOMIMETIC EFFICIENCY OF NITROSOAMIDES BY METABOLISM INHIBITORS. Mueller, A. J. (Institut fuer Kulturpflanzenforschung, Deutsche Akademie der Wissenschaften, Berlin). Naturwissenschaften, 52: 213-14(1965). (In German).

The effects of distilled water, sodium azide, potassium cyanide, hydroxylamine, 2,4-dinitrophenol, chloramphenicol, and sulfathiazole on the radiomimetic properties of N-nitroso-N-methyl urea (NMU) and N-nitroso-N-ethyl urea (NEU) were investigated on seeds of Arabidopsis thaliana. The seeds were soaked in water alone, then exposed to the inhibitors, and finally to the mutagenic agents. The effect of the treatment was determined by the relative root length reduction. The results are tabulated and show that sodium azide, potassium cyanide, and hydroxylamine most affect the radiomimetic properties of NEU and NMU. Chloramphenicol and sulfathiazole have no effect. The significance of these results is discussed. (J.S.R.)

43871 ON THE MYORELAXANT EFFECT OF GALLAMINE AND TUBOCURARINE IN IRRADIATED RABBITS. Dostal, M.; Vodicka, I.; Zachvej, J. (Military Medical Research and Postgraduate Inst., Czechoslovakia). Physiol. Bohemoslov., 13: 516-20(1964).

The muscle-relaxant effects of gallamine and tubocurarine were compared in irradiated and nonirradiated rabbits. These myorelaxants were tested during the first ten days after irradiation, with reference to the possibility of their use in anesthesiology for combined surgical and radiological injuries. The rabbits were whole-body x irradiated with a dose of 900 R, corresponding roughly to a median lethal dose, at 180 kv and a dose rate of 17.7 R/min (measured in the air). The myorelaxants were intravenously infused into the hind limb circulation during electrical stimulation of the exposed sciatic nerve, and consumption (the amount required to abolish leg movements) of the infused myorelaxant was measured. Tubocurarine and gallamine consumption from 1 to 12 days after irradiation was compared with consumption in the controls. Consumption of the myorelaxant was taken as the criteria of the change in sensitivity produced by irradiation. Gallamine consumption increased nonsignificantly from the second postirradiation day. On the ninth day it was significantly higher than in the controls. The average values in the control and experimental group on

the first day after irradiation were almost identical. Tubocurarine consumption was significantly raised on the first and third postirradiation day. From the sixth day it was similar to that in the controls. None of the rabbits in any of the irradiated groups was more sensitive to the myorelaxants than the most sensitive individual in the control group. In most rabbits the leg movements disappeared before respiratory movements stopped. In some rabbits, however, the respiratory movements diminished or disappeared during infusion. With prolongation of the interval between irradiation and infusion, the frequency of mild respiratory changes and respiratory arrest increased only in rabbits to which gallamine was administered. (BBB)

43872 UPON THE THERAPEUTIC ACTIVITY OR P.S.E. PREPARATION IN POSTRADIATION PATHOLOGY. Szczeglow, S. M. Polski Przeglad Radiol. i Med. Nuklearnej, 29: 327-35(May-June 1965). (In Polish).

The results of experiments on the influence of P.S.E. preparation on the blood morphology in mice in acute postradiation syndrome, and on the viability of various laboratory animals after multiple high-dose irradiation are reported. Also the results of clinical uses of the P.S.E. administration are included. Therapeutic value, application in the amelioration of hemopoietic action of the bone marrow, and prevention and therapy of infection in postradiation patients treated by irradiation because of neoplastic outgrowths are discussed. (auth)

43873 CHEMICAL PROTECTION AGAINST 440-Mev PROTONS IN MICE PRETREATED WITH MERCAPTOETHYLAMINE (MEA) OR p-AMINOPROPIOPHENONE (PAPP). Oldfield, D. G.; Doull, J.; Plzak, V. (Univ. of Chicago). Radiation Res., 26: 12-24(Sept. 1965).

Mean lethal doses for mice whole-body-irradiated by 440-Mev protons or by 250-kvp x rays with and without preirradiation treatment with 225 mg of 2-mercaptoethylamine hydrochloride (MEA) or 30 mg of p-aminopropiophenone (PAPP) per kilogram were determined by maximum likelihood probit analysis. The mean lethal dose decreased continuously as time of assay increases from 12 to 70 days in all control and treated groups. The dose-reduction factor remained approximately constant from 21 to 70 days. For 30-day assay, values of the factor were: with protons, 1.48 for PAPP, 1.61 for MEA; with x rays, 1.56 for PAPP, 1.39 for MEA. Thus a small but reproducible and time-stable reversal of protector effectiveness was demonstrated in the experimental system used. Possible causes of the reversal effect are discussed on the basis of a simple model for chemical protection. (auth)

43874 CHEMICAL PROTECTION AGAINST ABSORBER-MODERATED PROTONS. Oldfield, D. G.; Doull, J.; Plzak, V. (Univ. of Chicago). Radiation Res., 26: 25-31(Sept. 1965).

Radioprotection in adult CF_1 male mice pretreated with 30 mg of PAPP (p-aminopropiophenone) per kilogram and then whole-body-irradiated at depths in a Masonite phantom corresponding to nominal proton energies of 440, 350, 250, and 150 Mev was measured. Computer probit analysis of 30-day mortality data gave dose-reduction factors of (710/503) = 1.41 at 440 Mev, (847/537) = 1.58 at 350 Mev, (908/583) = 1.56 at 250 Mev, and (702/503) = 1.40 at 150 Mev (all doses in Rads). Comparison of these values with the values (1257/848) = 1.48 for unmoderated 440-Mev protons and (875/561) = 1.56 for 250-kvp x rays, obtained in previous experiments, would indicate that radioprotection by PAPP at the dosage levels used is not strongly dependent on energy or particle type in the ranges of these parameters studied. (auth)

43875 PREFERENTIAL SENSITIZATION OF ANOXIC BACTERIA TO X-RAYS BY ORGANIC NITROXIDE-FREE RADICALS. Emmerson, Peter T.; Howard-Flanders, Paul (Yale Univ., New Haven). Radiation Res., 26: 54-62(Sept. 1965).

The influence of organic nitroxide-free radicals on the sensitivity of E. coli B/r to x rays was studied. Di-t-butyl nitroxide (DTBN), tetramethylpentamethylene nitroxide (TMPMN), and t-butyl-2,6-dimethoxyphenyl nitroxide (TBDMPN) were all found to increase the lethality under anoxia. The variation in sensitivity with concentration was investigated, and it was found that maximum sensitization occurred at 20 mM DTBN, at which concentration the sensitivity was about 75% of that in pure oxygen. The nitroxides do not sensitize aerobic cells, so that the normal oxygen effect is greatly reduced in their presence. Thus, the ratio of the 1% survival doses of anoxic and oxygenated cells is about 3.9 for untreated bacteria, but less than 1.5 in the presence of 20 mM DTBN. (auth)

43876 β-MERCAPTOETHYLAMINE EFFECT ON RADIATION DOSE-RESPONSE CHARACTERISTICS OF GRANULOCYTE AND LYMPHOCYTE COUNTS. Smith, Willie W.; Cornfield, Jerome; Luskus, Carol; Miller, Christine (National Institutes of Health, Bethesda, Md.). Radiation Res., 26: 146-58(Sept. 1965).

Significant protective effects of MEA were demonstrated for lymphocyte counts as early as 2 days after irradiation and for granulocyte counts 3 and 4 days after irradiation. Granulocyte mobilization and MEA toxicity complicated the study of protective effects 1 and 2 days after MEA administration and irradiation. The dose-reduction factors estimated for early granulocyte and lymphocyte counts and for recovery counts 10 to 14 and 16 to 20 days after irradiation were in substantial agreement with each other and with the DRF for 28-day survival. At a time when granulocyte counts had returned to normal, lymphocyte counts in both treated and untreated mice were still far below their initial level, and the difference between treated and untreated mice had essentially disappeared. Without knowledge of the extent to which these counts are dose-dependent, dose-reduction factors could not be computed. (auth)

43877 PROTECTIVE EFFECTS OF CHEMICALS ON RADIATION INDUCED DAMAGES IN SEED-TREATED CROP PLANTS. Biswas, Sudamoy; Yamamoto, Koji; Sato, Yoshimasa; Ukai, Yasuo; Onozawa, Yoshiro; Matsuo, Takane (Tokyo Univ.). Radioisotopes (Tokyo), 14: 411-21(Sept. 1965). (In Japanese).

Experiments on the protective effects of chemicals against radioinduced damages in crop plants were carried out under both temperature and field controlled conditions. Different chemicals from the groups of inorganic and organic reducing substances, sulfhydryl containing compound, amine, vitamin, chelating agent, metabolite, and other compounds were used. It was observed that the x ray induced physiological damage was protected with cysteine, ferrous sulfate, vitamin C or Na-ascorbate, EDTA-2 Na, and K-compounds in the pretreatment only. ATP was also effective in some conditions. Chromosome aberrations induced by radiation was reduced by K-compound, cysteine, and reducing agents in both pre- and post-treatment. Among them, reducing agents and cysteine decreased the number of chromosome bridges proportionally to that of fragments in the state of anaphase to telophase in the 1st mitotic cell divisions. On the other hand, K-compounds decreased the number of fragments more than that of bridges. Most of the chemicals used revealed no protective effects on radioinduced sterility. Radioinduced chlorophyll mutation frequencies were also scarcely affected by the treatment with chemicals in both cases of frequency of streaks on the leaves of X_1 seedlings of heterozygous strains and that of chlorophyll mutations in X_2 generations of homozygous varieties of barley and rice. It was concluded that the physiological damages, chromosomal aberrations, sterility and mutations induced by radiation may be occurred in different processes of the living materials after irradiation. (auth)

Radiation Hazards and Protection

See also HEALTH AND SAFETY.

Refer also to abstracts 44318 and 45655.

43878 APPLICATION OF LIQUID SCINTILLATORS FOR INVESTIGATION OF THE MECHANISM OF RADIATION PROTECTION. Seleznev, A. F.; Pashek, G. M. (Belorussian State Univ., USSR). Dokl. Akad. Nauk BSSR, 9: 331-2(May 1965). (In Russian).

A collimated beam of 661-kev gamma rays from ^{137}Cs was directed at a liquid scintillator consisting of dioxane and 7 g/l of 2,5-diphenyloxazol. The differential distribution spectrum of the pulses due to Compton recoil electrons was determined on a multichannel analyzer. The quenching characteristics were determined on adding beta-aminoethylisothiouronine bromide (AET), 5-methoxytryptamine (MOT), beta-mercaptopropylamine (MPA), or serotonin (ST) to the liquid scintillator. The concentration of radioprotective agent was 20 g/l. Serotonin showed hardly any quenching effect, and also no radioprotective effect, as was expected. On the other hand, the radioprotective agents AET, MOT, and MPA remove 40 to 60% of the available excitation energy. There is a definite correlation between the quenching characteristics of a substance and its radioprotective properties. (TTT)

43879 RADIATION SPECTROMETRY IN SPACE: REQUIREMENTS FOR ACCURATE DOSE DETERMINATIONS. Clark, Benton C. (Air Force Weapons Lab., Kirtland AFB, N. Mex.). 28p. (CONF-720-31). Gmelin, AED-CONF-64-190-36.

From 2nd Symposium on Protection Against Radiation Hazards in Space, Gatlinburg, Tenn., Oct. 1964.

An analysis is performed to find relations between dose calculation errors and radiation measurement errors, for studying the hazard involved in manned space travel. Error dependencies of dose upon spectrum parameters and error dependencies of spectrum parameters upon instrument parameters are treated. (L.B.S.)

Radiotherapy and Radiodiagnosis

43880 (NP-15270) DOSIMETRIA CON PELICULA FOTOGRAFICA PARA BETATERAPIA CUTANEA. Informe No. 155. (Photographic Film Dosimetry in Skin Beta Therapy). Report No. 155. de la Vega Vedoya, Mario; Garcia, Mario E. (Comision Nacional de Energia Atomica, Buenos Aires (Argentina)). 1965. 8p. Dep. mn.

Variation of the depth dose produced by ^{90}Sr-^{90}Y beta sources used in the treatment of various cutaneous diseases, principally hemangiomas and juvenile cheloids was demonstrated using photographic film detectors. The depth dose up to 2000 microns was determined as a per cent of the surface dose. The results showed that the transference factors for any application of ^{90}Sr-^{90}Y of similar geometric characteristics can be determined independently of the activity. The results were compared with determinations made by an ionization chamber. The results were in good agreement. (J.S.R.)

43881 (NP-15271) POSIBILIDADES DEL ^{99m}Tc EN REEMPLAZO DEL RADIOYODO EN EL ESTUDIO DE LA FUNCION TIROIDEA. Informe No. 144. (Possibilities of Using ^{99m}Tc Tracer Instead of Radioiodine in Thyroid Function Investigations). Report No. 144. Chowjnik, Abraham; Degrossi, Osvaldo J.; Gotta, Hector; Olivari, Americo; Pecorini, Victorio (Comision Nacional de Energia Atomica, Buenos Aires (Argentina)). 1965. 15p. Dep. mn.

The efficiency of ^{99m}Tc as a tracer in thyroid function studies was investigated and compared with ^{131}I. The results showed that ^{99m}Tc gives thyroid scintilligrams of excellent resolution comparable to those of ^{131}I and ^{125}I with equipment currently in use. The thyroid uptake of Tc can be used as a rapid index of the thyroid function with respect to its capacity to concentrate iodine. As it is not organically necessary for the thyroid, it can not be used to study the further steps of the glandular function. The body radiation resulting from the use of ^{99m}Tc for diagnostic purposes is a thousand times less than the corresponding radiation from ^{131}I. (J.S.R.)

43882 (UCD-472-112, pp 50-8) ROENTGENOGRAPHIC SURVEY OF EXPERIMENTAL BEAGLES. Parcher, J. W.; Hanson, R. (California Univ., Davis. School of Veterinary Medicine).

The initial whole-body roentgenographic survey technique for dogs that had received ^{90}Sr was modified so as to improve observations with a minimum number of exposures. Highlights are presented from a resume of more than 1300 plates taken over the past year, with photographic illustrations. Of the dogs examined, 76% showed no detectable deviation from normal appearance; 12% had minor changes, such as bowing of certain long bones. Nine of the 174 dogs have radiolucencies, one has an opacity of the tibia, four have anatomical structures missing, and one has a calcified disc. The only soft-tissue change noted was slight splenomegaly in five dogs. (auth)

43883 (UCLA-12-565, pp 65-85) NUCLEAR MEDICINE. (California Univ., Los Angeles. Lab. of Nuclear Medicine and Radiation Biology).

Progress is reported in investigations on renal blood flow, liver blood flow, tracer dilutions in single tube systems, lung scanning following radioisotope inhalation, lung-scanning evaluation of pulmonary blood-flow changes, brain scanning using radioalbumin, interpretation of renograms and scans in kidney disease, lung scanning for pulmonary functions, organ visualization by photo scanning, ^{95}Nb and ^{95}Zr distribution in pregnant rabbit tissue, body burdens of gamma radioactivity in Los Angeles 1960-64, protection from gamma and x radiation, radioprotective chemicals, radioisotopic scanning detection of pulmonary embolism and bronchial obstructions, distribution of intravenously injected radioactive Ca and Sr, radio protective effects of AET and methyl sulfoxide on mice, growth and properties of leukemic cells in mice, effects of thymic epithelial reticular cells on thymectomized mice, and properties of DNA and RNA from mice with virus-induced leukemia. (J.R.D.)

43884 A COMPARISON BETWEEN THE RESULTS OF IRRADIATION THERAPY ALONE AND INDIVIDUALIZED RADIOLOGICAL AND SURGICAL TREATMENT OF CERVICAL CARCINOMA STAGE I. Koller, O. (Norwegian Radium Hospital, Oslo). Acta Obstet. Gynecol. Scand., 43: Suppl. 7, 68-74(1965).

Complications developing as a result of surgical intervention in irradiated tissue are described, and the optimal timing of surgery in relation to radiotherapy is discussed. Two clinical trials were conducted in the treatment of cervical carcinoma Stage I, one with radiation therapy alone and one in a combined radiation and surgical approach. The primary treatment of cervical carcinoma Stage I was intracavitary Ra with a modified Paris technique, delivering a dose of 15,000 to 20,000 R to the cervix, about 6000 R to point A and 800 R to point B during 5 or 10 days. Cases considered as good surgical risks were operated upon 6 to 8 weeks after Ra therapy, either by total hysterectomy with removal of adnexae, or by radical hysterectomy with lymphnodectomy. Of a total of 367 cases, 171 were operated upon, giving an operation rate of 47%. More than half of them were subjected to radical hysterectomy with lymphnodectomy. The 5-yr survival for the operated patients was 85% and for the nonoperated, who received conventional x-ray therapy after Ra application, 69%. A series of 100 unselected cases of Stage I cervical carcinomas was given betatron therapy with 31-Mev x rays, immediately following the Ra treatment, delivering about 4000 R to entire pelvis including the node-bearing areas, during 3 weeks. Two cases developed radiation injuries of the rectum. At 5 yr there were 73% survivors, a cure rate not statistically different from that of the above series. Thus, supervoltage therapy of the type and dose applied, did not effectively control lymph node metastases. Even radical surgery could be performed 6 to 8 weeks after Ra treatment without an undue incidence of complications, but surgical treatment of recurrences after complete external therapy (either with conventional x ray or betatron) gave a very high complication rate and few per-

manent cures. On the other hand, complete courses of external irradiation were given as an adjunct after Ra and surgery without serious complications. (BBB)

43885 DOSAGE TO THE LENS IN RADIOGRAPHY ABOUT THE HEAD AND NECK. Kettunen, Kalevi (Maria Hospital, Helsinki). Acta Ophthalmol., 43: 235-9(1965).

Radiography of the head and neck results in incidental irradiation of various tissues containing important structures, such as the lens. Therefore, a study was made of the magnitude of the dose in lens when standard techniques were applied for radiography of the cranial and facial skull including the pituitary fossa, paranasal sinuses, temporomandibular joints, teeth, and cervical spine. Ionization chambers, used to measure lens doses in various procedures using 60- to 80-kv x rays, recorded doses of 16 to 220 mR during radiography of the cranium (24 × 30 cm field), 9 to 14 mR in maxillary and about 4 mR in cervical spine examinations. Doses to the ipsilateral lens when lateral views were taken were, for various fields: cranium 280, pituitary fossa 46, temporomandibular joint 42, and cervical spine 4 mR/exposure. The contralateral lens received doses of 210, 16, 10, and 2 mR/exposure, respectively, in the same x-ray procedures. Doses to the lens from dental studies of various regions were: lower incisors 2.0, lower canine and premolars 4.0, and lower molars 2.5 mR/exposure. A grid was used in all but the dental studies. The observed doses for these examinations were small compared with the min dose to induce radiation cataracts. It is believed that any amount of radiation energy which is absorbed by living organisms may result in damage to one or more biological systems, although the injury may or may not be detectable during the lifetime of the individuals. Up to a point, many of the acute biological changes resulting from irradiation are reversible and, as such, are subject to recovery and repair. The late effects, at least in part, are the result of the injury which is nonreversible and cumulative in nature. In general, any specific biological system is altered in degree in direct proportion to the amount of the radiation absorbed. (BBB)

43886 THE ROLE OF RADIOISOTOPE SCANNING IN THE EVALUATION OF GASTROINTESTINAL DISEASE. Sodee, D. Bruce; DiStefano, Berardino (Doctors Hospital, Cleveland). Am. J. Gastroenterol., 43: 423-8(May 1965).

Results in a large number of patients whose abdominal organs were scanned with various radioisotopes are reported. These isotopes included: ^{198}Au (100 μC) and ^{131}I-albumin microaggregate (200 μC) for liver scanning, ^{197}Hg-mercury hydroxypropane (100 μC) for spleen scanning, ^{75}Se-methionine (250 μC) for pancreas scanning, and ^{197}Hg (1 mC) for gastrointestinal tract scanning. The scanning procedures were performed on a Magnascanner utilizing a 19-hole collimator. Gross and microaudioradiography were also done using standard technics. Liver scanning was useful in diagnosing liver disease, lesions of about one-in. diameter being visualized, except when on the surface of the liver. Many times it was possible to demonstrate metastatic liver disease and prevent unnecessary surgery. Also, diffuse and infectious hepatic disease showed abnormal scans. Using a 5 × 2-in. crystal with 5-in. focus and 161-hole collimator, lesions ½ cm in size could be seen. In about 400 pancreatic scans with ^{75}Se-methionine and a 5-in. collimator it was possible to see defects about two-cm in size. As the liver also utilizes this radiopharmaceutical, an effort was made to exclude the liver from the pancreatic scan; however, this limited pancreatic scanning in 10% of the patients. In use of ^{197}Hg to locate tumors of the gastrointestinal tract, the surgically removed specimen was autoradiographed and scanned. Individual cases are presented showing the effectiveness of scanning in aiding diagnosis of gastrointestinal disease. (BBB)

43887 THE DETECTION OF MALIGNANT NEOPLASIA OF THE GASTROINTESTINAL TRACT BY THE USE OF RADIOACTIVE PHOSPHORUS AND A MINIATURE GEIGER TUBE. Nelson, Robert S.; Dewey, William C. (Univ. of Texas, Houston). Am. J. Gastroenterol., 44: 9-17(July 1965).

A diagnostic method and instrumentation were developed to detect gastrointestinal cancer with the use of ^{32}P, which is taken up preferentially by rapidly growing tissues. Miniature Geiger counter tubes were passed into the esophagus, stomach, and rectum of patients previously given 500 μC of ^{32}P intravenously to evaluate the method. To test the esophagus and rectum, the counter was placed at the tip of a plastic probe and passed through an esophagoscope and sigmoidoscope. The gastric counter was inserted in the distal end of a controllable tip gastroscope for scanning under direct vision. After considerable experimentation, the largest G-M tubes (25 × 5 mm, with a sensitive area of 5 × 10 mm) that could safely be passed were settled upon as giving optimum results. The G-M tube has an intrinsic efficiency of about 50% for detecting ^{32}P particles and gives a counting rate of about 5500 cpm when placed above a μC/ml solution of ^{32}P. The criterion of accuracy of the test was based, in the case of proven neoplasia, upon the correlation of a histologically proven lesion with at least a 30% increase in counting rate above that seen in the adjacent control area (100 to 200 cpm). There was an accuracy of 94% in cancer, and an overall accuracy of 97%. The accuracy in gastric cancer was only 73%, largely due to technical difficulties, and overall accuracy was 80%. Rectal testing was carried out only in nine patients, eight of whom were correctly evaluated. (TCO)

43888 MODIFICATIONS TO THE ROYAL MARSDEN HOSPITAL GOLD GRAIN IMPLANTATION GUN. Jones, C. H.; Taylor, K. W.; Stedeford, J. B. H. (Royal Cancer Hospital, London). Brit. J. Radiol., 38: 622-4(Aug. 1965).

Radioactive gold (^{198}Au) grains are used extensively as interstitial sources of radiation in the treatment of malignant disease. Usually the grains are implanted by means of a special gun. The grains are contained in aluminum magazines which fit into the barrel of the implantation gun. The original method of loading the gun consisted of the following stages: the aluminum caps of the magazine were removed with a screwdriver; in order to prevent the radioactive gold grains from falling out of the magazine, its ends were dabbed with sterile petroleum jelly; the magazine was inserted into the barrel of the gun, which in turn was screwed onto the shaft and the gun could now be primed ready for use. Exposure to radiation during this procedure was chiefly to the hands, fingers, and eyes. Some simple modifications were made to the magazine and to the gun which eliminate the need for these operations, with a consequent reduction in radiation exposure. (auth)

43889 FILM DOSIMETRY IN RADIODIAGNOSIS TO ASSESS RADIATION BURDEN TO THE POPULATION. Koczkas, Gy; Kiss, I.; Bojtor, I. (Frederic-Joliot Curie National Research Inst. for Radiobiology and Radiohygiene, Budapest; Forte Photochemical Industry, Vac, Hungary). Brit. J. Radiol., 38: 624-5(Aug. 1965).

An important part of medical radiation burden to the population is due to radiodiagnosis. A survey was made to obtain more precise data of the radiation burden to the exposed population in Hungary. The dosimeter of wide measuring range designed for this survey is based on the principle of diagnostic dosimetry: the radiation dose emerging from the x-ray tube is measured by a big surface ionisation chamber set in front of the diaphragm, and the ionisation chamber measures the dose in the field determined by the aperture of the diaphragm. This enables the integral dose to the body to be determined. On the basis of our earlier results with film dosimetry, further experiments were carried out to apply this method in the dosimetry of radiation dose during diagnosis. Certain types of films were found suitable for the measurement of γ radiation in the range of 20 to 1,000 R. Further experiments were aimed at finding different techniques of development to render the films suitable for measurement in the above dose interval in the range of x rays induced by 60 to 200 kv. The assessment of the radiation burden due to diagnostic x ray is of interest from the point of view of the genetical dose to the population. Measurements

were carried out so that about 200 to 300 patients were measured with one and the same dosimeter. Emphasis was placed on gonad dose received during diagnostic x-ray examinations. (C.H.)

43890 MYXEDEMA AFTER X-RAY THERAPY TO THE NECK. McHardy-Young, S.; Lessof, M. H.; Blackburn, G. (Guy's Hospital, London); O'Gorman, P. Brit. Med. J., 2: 230(July 24, 1965).

Data on six cases are presented which confirm previous reports of injury to thyroid function from neck irradiation. Four patients with breast cancer had received estimated doses to the thyroid of 1000 to 1500 rad, and two others, with tuberculous cervical adenitis and Hodgkin's disease, had received 2200 and 1660 rad, respectively, to the thyroid. Myxedema, evaluated by basal metabolic rate, protein-bound iodine, and thyroid ^{131}I uptake tests, was noted six months to 15 yr later. Thyroid antibodies were found in serum in titers of 1:160,000 in two patients, and in titers of 1:40,960 and 1:160 in two others. The total radiation dose to the thyroid in these cases ranged from 1000 to 2200 rad and was less than the 2500 to 6000 rad given in a previously reported series. A direct relation of incidence to radiation dose, therefore, seems unlikely. High antibody titers in 4 out of 6 patients support the view that irradiation of the thyroid gland may be a factor in the initiation of a progressive autoimmune process. However, the alternative possibility that these are patients who would have developed myxedema in the natural course of events cannot be excluded, but in three cases this seemed unlikely because of the rapidity with which myxedema developed within months of irradiation. In view of the purported but ill-defined association of carcinoma of the breast with thyroid disorders, further studies of thyroid function are planned in radiotherapy patients before and after treatment to compare the incidence of naturally occurring hypothyroidism with that which follows radiation treatment. (BBB)

43891 PREGNANCY AFTER PRIMARY IRRADIATION FOR CARCINOMA OF CERVIX. Francis, O. (Madras Medical Coll.; Government Hospital for Women and Children, Madras); Stevens, R. D. Brit. Med. J., 2: 342-3 (Aug. 7, 1965).

A case study of a successful pregnancy after radiotherapy for carcinoma of the cervix is described. The patient was treated with 7000 R to point A, which was followed by an extraperitoneal pelvic lymphoadenectomy. (P.C.H.)

43892 TUMORS OF THE THYROID AND PARATHYROID GLANDS. Ward, Robertson; Lindsay, Stuart; Sheline, Glenn E.; Goldman, Leon (Univ. of California, San Francisco). Calif. Med., 101: 462-9(Dec. 1965).

The use of ^{131}I in the diagnosis and treatment of thyroid tumors is considered, and the effectiveness of external irradiation of these tumors is compared with surgery and other therapy. A scintiscan obtained after the ingestion of a test dose of ^{131}I may be useful in detecting malignant change in a nodular goiter. The finding of a cold nodule by this method is consistent with but not diagnostic of cancer. However, the only way to determine malignancy positively is by microscopic examination. Iodine avidity of tumors, making ^{131}I therapy feasible can probably be established in about half of all patients with differentiated thyroid carcinoma. Therapy consists of ^{131}I, either in a single dose of 200 or more mC, or in several doses at intervals of one to two months. The tumor may regress in from one-third to one-half of the patients so treated, and occasionally evidence of carcinoma will disappear entirely. Not enough time has elapsed to assure with certainty that any patient has been cured by ^{131}I therapy; however, many patients are free of the disease five and ten yr after ^{131}I treatment and usefulness of the method in the selected patient is well established. It is estimated, though, that whole-body irradiation from several hundred millicuries of ^{131}I will cause leukemia in from 3 to 5% of the treated patients. This represents a relatively small risk for the patient with advancing, uncontrolled carcinoma but it rules out the use of ^{131}I as prophylactic therapy. (BBB)

43893 RADIATION, GENES AND CHILDHOOD. Mitchell, Thomas G.; Pearson, Howard A.; McIlraith, James D. (U. S. Naval Hospital, Bethesda, Md.). Clin. Proc. Children's Hosp., 19: 263-77(Oct. 1963).

Genetic and somatic effects of ionizing radiation are reviewed, particularly from the point of view of the exposure of children to medical sources of radiation and the attendant hazards. Natural background radiation levels are compared with doses estimated for average individuals in the United States exposed to radiation for diagnostic medical purposes. Some means of reducing radiologic exposure of children are pointed out. A marked reduction in dose can be made by the use of collimation or cones. It is a simple expedient to tie a lead apron around the waist or place an apron between the tube head and the patient to cut out the radiation which would normally strike the gonadal area. Another measure is to convert to high speed screens and film. This can reduce the dose by one half. It is necessary to use the highest kv consistent with the examination. In fluoroscopy it is important to use small fields, the smallest field consistent with satisfactory examination. It is concluded that ionizing radiation is a potentially deleterious agent for all persons, but particularly so for the young child who has his entire physical and reproductive life ahead of him. However, diagnostic and therapeutic uses of radiation are indispensable in modern medical practice; the accurate diagnosis permitted by x ray has prevented considerable mortality and morbidity in all groups of patients. By the simple expedient of shielding the gonads with a lead apron and directing the x-ray beam away from the gonads, even with no change in indications for fluoroscopy, no change in frequency, and no change in x-ray equipment, it is estimated that the average annual dose to the gonads could be cut from 15 to 5 mR. (BBB)

43894 TELECOBALT TREATMENT OF CARCINOMA OF THE BLADDER. Van Der Werf-Messing, B. (Radio-Therapeutisch Instituut, Rotterdam). Clin. Radiol., 16: 176-72(Apr. 1965).

Radiation doses, clinical results, and complications of treatment are reported for 326 patients, with bladder cancers too large to treat with Ra, subjected to ^{60}Co radiation. Initial exposure was a bladder tumor dose of 5000 R over 5 weeks. This was followed by a period of tumor dose of about 5500 R over 5 weeks. Later the tumor dose was raised to about 6000 R over 6 weeks; the dose then was again increased to 6500 R over 6 weeks. The proportion of patients who experienced subjective improvement after treatment decreased with advancing stage. Radiation damage usually consisted of fibrotic induration, mainly at the site of the anterior field, and usually was symptomless. In a few instances serious radiation damage was encountered. The results suggested that cure is unusual from telecobalt treatment, but it's palliative value is definite. For stage II tumors, survival after one yr was mainly determined by dose given, less than 6000 R yielding a significantly lower survival than 6000 R and 6500 R. Patients of 70 years or more had a worse prognosis than younger ones. For more advanced tumors a dose of at least 6000 R was required in order to have a chance of even temporary growth restraint. All factors investigated (age, sex, primary or secondary treatment of the patient, tumor dose, and histology) had no significant relation to 5-yr survival in any stage group. The incidence of postradiation fibrosis in relation to tumor dose and to the number of skin fields used is described, and serious complications are enumerated. It was seen that with increasing dose clinically demonstrable fibrosis became more frequent, but increasing dose also gave more prolonged survival during which fibrosis could become apparent. Induration appeared more common after 2- than after 3-field treatment, even though 2-field treatment was mainly used for stage IV cases with a very poor survival rate. Fibrosis and other complications were not associated with previous cystotomy. It is concluded that the long-term

results of telecobalt treatment of bladder cancer are discouraging. The prognosis is slightly better in less advanced cases but this treatment can be considered to be only palliative for most patients. The best palliation was achieved after a tumor dose of at least 6000 R over 6 weeks, and preferably 6500 R over 6 weeks. After this treatment, survival after one yr, local cure, and subjective improvement are optimal. Radiation damage increased proportionately with the dose given, and it is suggested that higher doses than 6500 R over 6 weeks are unsafe. (BBB)

43895 TREATMENT OF HYPERTHYROIDISM WITH A FIXED INITIAL DOSE OF RADIOIODINE. Kalliomaki, J. L.; Seppala, P. O. (Univ. of Turku, Finland). Current Therap. Res., 7: 351-4(June 1965).

Previous methods of estimating ^{131}I dose in treatment of hyperthyroidism are reviewed, and the use of a fixed dose is discussed. In the series described here particular attention was given to the development of hypothyroidism as a late complication of ^{131}I therapy. Results are reported for 122 patients treated from 1960 to 1962 for hyperthyroidism with a fixed initial dose, 10 mC, of radioiodine; the follow-up was performed in 1964. Seventy-three of the patients had nodular goiter and, in 49 cases, the thyroid gland was diffusely enlarged or nonpalpable. Thirty patients received two doses and 9 three doses. After a follow-up period of 26 months, 41% of the patients treated with this fixed initial dose were euthyroid, 20% were hypothyroid and 39% had received new doses or were still hyperthyroid. After the third dose of radioiodine, 73% were euthyroid, 25% hypothyroid, and 2% hyperthyroid. The total incidence of hypothyroidism in this series was 31/122 (25.4%); in the patients with nodular goiter it was 15/73 (21%); and in the patients with diffuse goiter or nonpalpable thyroid it was 16/49 (33%). The incidence of hypothyroidism in this series treated with a fixed initial dose is of the same magnitude as in some larger published series where more elaborate methods of determining the dose of radioiodine were used. The fixed dose scheme has the advantage of saving lab work and also hospital beds. Although the hypothyroidism which developed was slight and easily corrected with small doses of thyroid hormone, the relatively high incidence of hypothyroidism after ^{131}I treatment of uncomplicated thyrotoxicosis is unsatisfactory, and further controlled clinical trials of different methods of therapy are needed. The incidence of hypothyroidism is 3.8% after a surgical treatment of hyperthyroid patients at this university. (BBB)

43896 RADIATION PROTECTION DEBATES. Glauner, R. Fortschr. Gebiete Roentgenstrahlen Nuklearmed., 102: 457-9(1965). (In German).

The necessity of protecting patients and the population as much as possible from radiation in its medical applications is emphasized. The responsibility of the doctor in this respect is outlined. The value of the doctors' setting their own standards and enforcement procedure in this respect is discussed. (J.S.R.)

43897 THE PLASTIC REPAIR OF RADIOGENIC DEFECTS OF THE LARYNX AND TRACHEA. Ploner, Luis (Ospedale Maggiore, Bolzano, Italy). Fortschr. Kiefer Gesichtschir., 8: 187-92(1962). (In German).

Despite improvements in irradiation techniques and protection, the skin and associated structures, and the cartilage of the trachea and epiglottis, may be extensively damaged during irradiation treatment of the neck region. Radiation injuries of this type include skin atrophy, ulcerations, and tissue necrosis, but deep-lying cartilaginous or bony structures may also be involved. Sometimes these effects may not appear for 10 or 20 yr after irradiation. Bone becomes necrotic only after a rather long time interval, but destruction is then rapid. Once the protective skin layer is destroyed, cartilage quickly become infected, but disappears very slowly. Damage to the tissues may be sufficient enough to result in a laryngotracheal fistula which requires repair. Because of the anatomical arrangement of the laryngeal and tracheal structures, it is not possible to repair them sufficiently to restore function. What can be done is to repair the area grossly with rotation and pediciled tube flaps. The technique for this is relatively simple, but it will serve as a suitable method of repair. Because the reconstructed tubes are somewhat loose and impede respiration considerably, they should be stiffened by insertion and implantation of cartilage tissue from the ear or ribs. (BBB)

43898 COMPARATIVE USE OF SULFUR-32 AND BROMINE-82 FOR DETERMINATION OF THE EXTRACELLULAR FLUID VOLUME. Lacroix, M.; Busset, R.; Mach, R. S. (Hopital Cantonal, Geneva). Helv. Med. Acta, 32: 87-134(June 1965). (In French).

The use of thiocyanate, sulfate, chloride, bromide, and sodium chloride, bromide, and sodium ions, and their radioisotopic forms, to measure extracellular fluid space is reviewed preliminary to a report of clinical studies with some of these isotopes. The volumes of distribution of $^{35}SO_4$ and ^{82}Br were measured to establish a practical method for the determination of extracellular fluid volume in man. In some cases, distribution of ^{24}Na was compared with these volumes. Determinations in 27 normal males showed that diffusion equilibrium is achieved 50 min after a single intravenous injection. There was good correlation between the volumes of distribution of $^{35}SO_4$ calculated from the extrapolated curve of plasma concentrations and from the concentration measured 50 min after injection. The radiosulfate space measured by extrapolation at time zero in 29 normal males and in 10 normal females was respectively 22.4(±3.2)% and 18.9(±3.4)% of body weight. These values are higher than those for $^{35}SO_4$ space measured 20 min after administration. It equals inulin space and represents the physiological fluid volume. A significant correlation was established between radiosulfate space and theoretical weight and also between this space expressed as percentage of body weight and corpulence index. The equilibration time of $^{35}SO_4$ was studied in cases with fluid retention (cirrhosis of the liver, heart disease, and renal insufficiency). In two cases of cirrhosis of the liver, 8 hr was necessary to achieve equilibrium. The equilibration time of ^{82}Br in normal subjects was achieved after 6 hr; 8 hr was needed to reach equilibrium between plasma and pathological liquids in cases of high fluid retention. The ^{82}Br space measured 24 hr after injection in normal males and in normal females was respectively 26.9(±2.0) and 23.2(±1.3)% of body weight. The ratio of $^{35}SO_4$ volume to simultaneously determined ^{82}Br volume was 0.85(±0.096) with values between 0.71 and 0.95. This result is explained by cellular penetration of ^{82}Br. In spite of this, ^{82}Br is still considered to be the ideal tracer for measurement of extracellular fluid volume and also for the determination of total exchangeable chloride. The volume of distribution of $^{35}SO_4$ is unstable after equilibration because of its rapid urinary excretion and continuous escape from the extracellular pool. In normal subjects, the 50-min volume may be used, but in cases of fluid retention, extrapolation at time zero is required. (BBB)

43899 THE MECHANISM OF EFFECT OF ENERGETIC RADIATION. Pohlit, Wolfgang (Max-Planck-Institut fuer Biophysik, Frankfurt am Main). Internist, 5: 263-71 (July 1964). (In German).

The great advantage of energetic electrons over conventional x irradiation is that the irradiation dose can be administered with a better distribution over the target area, and with greater protection of surrounding tissues. However, in the future it may be possible to improve the dose distribution pattern and also obtain a more selective irradiation effect on tumor cells by high-energy protons. Protons are much heavier than electrons, and so they are scattered less by collision with atoms that comprise the tissues. Thus their paths are essentially linear, and transfer most of their energy to the tissues at the termination of their path. Energy transfer is relatively constant over the entire path, with maximum energy transfer at a depth of 12 or 15 cm in tissue. This compares with the optimal depth of effect of fast electrons which is from

about 6 to 8 cm. The depth of tissue penetrated is proportional to the proton energy. Because of this the nontumor tissue can be better protected. From the fact that the protons are scattered so little in tissue, very small irradiation beams can be used to irradiate very limited areas of the body, such as in the brain. It may also be possible by this means to replace some surgical operations using this type of irradiation. Experimental studies are underway to establish proton irradiation as a method of irradiation therapy. For the present, because of the greater financial costs of proton accelerators as compared to electron accelerators, research in this field has been limited. (BBB)

43900 METHODS OF IRRADIATION WITH LOCALIZED LIMITED RADIATION EFFECT (CLASSICAL RADIUM TREATMENT, CLOSE IRRADIATION, IRRADIATION WITH ARTIFICIAL RADIOACTIVE ISOTOPES). Schlungbaum, W.; Krokowski, E.; Ernst, H. (Universitaet, Berlin). Internist, 5: 284-92(July 1964). (In German).

There are two methods for the application of irradiation from Ra sources. In contact therapy the irradiation source is brought to the tumor surface and is in immediate contact with the lesion. In interstitial therapy the irradiation source is introduced directly into the tumor area itself. Both of these methods are used in treatment with artificial radioisotopes. Close irradiation with x rays is another method used which is analogous to the methods used with Ra. Irradiation with artificially produced radioisotopes has several advantages. Some of these are that tumors may be selectively irradiated with radionuclides best suited with respect to localization and type of radiation, the radioisotopes are much less expensive than Ra, and pure emitters may be used to limit the area irradiated. Also, artificial radioisotopes may be selectively administered in solid, liquid, or gaseous forms to suit the treatment needs. Contact irradiations may be carried out using β or γ emitters, or solid or liquid forms of the radioisotopes may be injected or introduced into hollow organs or spaces in organs. Interstitial irradiations may be carried out by implantation of solid radioisotopes, for limited times or permanently, or by infiltration. Selective irradiations can be carried out to treat thyroid disorders or hemoblastoses. "Paraselective" irradiations can be carried by injection of large radioactive particles or by endolymphatic injection of radioactive solutions. The type of treatment desired and the specific radioisotope used must be adapted to the characteristics and nature of each tumor or disorder to obtain the maximum curative effect. (BBB)

43901 EFFECT OF FILTRATION IN DIAGNOSTIC RADIOLOGY. Beique, R. A.; Rotenberg, A. D. (Montreal General Hospital, Canada). J. Can. Assoc. Radiologists, 16: 59-65(Mar. 1965).

Spectrum of the x-ray beam produced by the target, and how it is modified by filtration and by different body tissues, is discussed, and an analytical study describing the complete spectrum mathematically for any combination of absorbers and accelerating voltage is reported. It is a direct method of evaluating the effect of voltage, filter, and absorber on the intensity and spectral distribution of an x-ray beam. The analytical study of beam properties is based on empirical relations from which a general equation is derived. The equation was solved numerically to give a table from which particular solutions involving any set of parameters can be obtained. As an application of this analytical study, the effects of filtration and accelerating voltage on the sensitivity of x-ray procedures and on the skin dose to the patient are considered. The quality or spectral distribution of an x-ray beam can be modified by changes in kv setting or filtration. The selection of beam quality should be based primarily on the consideration of what is to be visualized on the x-ray film used. Values of kv and filtration appropriate for given procedures will vary. Consideration should also be given to skin dose and exposure multiplier. Filtration should be selected for each procedure. Consideration of the effects of kv value and filtration showed that increasing the kv or filtration has little effect on the min detectable amount of water, as shown by water phantom experiments, once the accelerating voltage exceeds 80 kv. Only the skin dose and exposure factors are changed. The min detectable amount of bone, contrary to that of water, is modified by both voltage and filtration, throughout the entire diagnostic range. Low voltage produces high sensitivity to both water and bone with the penalty of large skin dose and tube loading. The skin dose produced by a given beam is very dependent on the low-energy (soft) component of the beam and therefore on the amount of filtration. The skin dose also depends on the thickness of the object because a given intensity must emerge from it to expose the film. When the skin dose is plotted against filtration, showing the effect of removal of the low-energy part of the spectrum, it is seen that the dose-reduction effect is greatest at low values of filtration when the beam still contains a large fraction of low-energy photons. With 9 mm of aluminum or 0.2 mm of copper the beam is sufficiently hardened with respect to water that further filtration has little effect on the skin dose. (BBB)

43902 THYROID ANTIBODIES AFTER ^{131}I TREATMENT FOR HYPERTHYROIDISM. Einhorn, J.; Fagraeus, Astrid; Jonsson, J. (Radiumhemmet and Statens Bakteriologiska Laboratorium, Stockholm). J. Clin. Endrocrinol. Metab., 25: 1218-24(Sept. 1965).

Antibodies to thyroglobulin and cytoplasmic antigen were studied by immunofluorescence, tanned cell hemagglutination and complement fixation methods in 115 patients before ^{131}I treatment for hyperthyroidism, in 439 patients after such therapy, and in 29 patients after surgical treatment for hyperthyroidism. During the first year after the radioiodine therapy there was a significant increase in the cytoplasmic antibodies; no such rise was observed for the thyroglobulin antibodies. Subsequently, the thyroid antibody titers fell steadily below the pretreatment level. Surgical treatment for hyperthyroidism was found to result in a significant decrease in humoral thyroid antibodies within one year. At the examination carried out during the year after the radioiodine therapy, thyroid antibodies were found in a greater proportion of patients who developed hypothyroidism than in others. At a later examination no such difference was found. Thyroid antibodies were found in a greater proportion of patients cured by one radioiodine treatment than in those requiring several treatments, and more often in younger than older patients of the age group studied. There was no evidence that ^{131}I therapy initiates a progressive autoimmune process. (P.C.H.)

43903 RADIOTHERAPY FOR HEAD AND NECK CANCER: TEAMWORK: PROBLEMS COMMON TO PHYSICIAN AND DENTIST. Delclos, Luis (M. D. Anderson Hospital, Houston, Tex.). J. Prosthetic Dentistry, 15: 157-67 (Jan.-Feb. 1965).

Use of various types of radiation on intraoral cancer is described, with emphasis on the prevention of radionecrosis of healthy tissue. Extraction of the teeth after irradiation is often followed by osteomyelitis of the mandible, but there is controversy as to the advisability of systematically removing the teeth before irradiation. Each patient should be considered individually, according to the condition of the teeth, number to be extracted, and length of time that the treatment can be delayed depending upon the histologic type, site, and extension of the lesion. Systematic removal of teeth near Ra implants or within the beam of external irradiation is not advocated. Precautions are taken to improve the condition of the teeth by the use of a dental spray and antibiotics. Teeth within the tumor area which have sockets so diseased that they are already loose can be extracted, as can teeth which interfere with fitting of an intraoral cone. If extraction is decided upon, a short time interval should be allowed to elapse before beginning therapy. Before a Ra implant is placed in the lateral border of the tongue, one week's interval is enough, since little irradiation reaches the bone. For lesions of the floor of the mouth, if heavy doses of irradiation are contemplated, a delay of two to three weeks

is required before cicatrization of the gum is complete. Prevention of radiation necrosis is also discussed. Although the mucosa of the mouth is more tolerant to irradiation than skin, necrosis occurs in some patients. It may be caused by unusually low tolerance of normal tissue, poor oral hygiene, errors in technique, or retreatment. By systematic underdosage, necrosis could be avoided, but this complication will occur in a small proportion of patients if a cancerocidal dose of radiation is given. Conservative treatment of soft tissue necrosis consists of daily sprays, and frequent irrigations with salt and soda solution. When bone is involved, toothache may occur before any break appears in the mucous membrane. Eventually, the membrane becomes infected, a sequestrum may form, and resection of the mandible becomes necessary. The intraoral route is advised with a tracheostomy. No attempt should be made to close the tissues of the operated area. Also, there should be no attempt made to repair the defect resulting from the resection of the mandible by any type of bone graft or prosthetic appliance. Such a repair might result in the further breakdown in this irradiated tissue. Construction of intraoral applicators is described. With the use of such intraoral applicators loaded with radioactive sources, intraoral plastic devices can be used to protect normal tissue. (BBB)

43904 DETECTION OF PORTAL SYSTEMIC SHUNTS BY HEPATOPULMONARY SCANNING USING ^{131}I MAA: STUDY AND APPLICATION OF MACROAGGREGATED ALBUMIN (MAA) LABELLED WITH ^{131}I. [PART] III. Ueda, Hideo; Kitani, Kenichi; Kameda, Haruo; Yamada, Hideo; Iio, Masahiro (Tokyo Univ.). Japan. Heart J., 6: 115-27(Mar. 1965).

Hepatopulmonary scintiscanning performed following the intrasplenic injection of ^{131}I-MAA (macroaggregated albumin) was shown to be a useful method for the study of the portal circulation. To evaluate the reliability and sensitivity of this method, intrasplenic injection of radioactive rare gas (^{85}Kr and ^{133}Xe) in saline solution with expiratory air monitoring, as well as x-ray examination of esophageal varices, was performed on the same patients. In addition, hepatic blood flow measurements were accomplished by the external monitoring of hepatic clearance of radioactive gas after intrasplenic injection. Previous to scintigram study with MAA, 0.5 to 1.5 ml of ^{85}Kr in saline solution was injected into the spleen and the washout curve of the radioactivity over the liver was recorded externally and appearance of radioactivity in the expiratory air was also detected. In some patients the ^{133}Xe solution was mixed with ^{85}Kr solution before injection to obtain washout curves of both gases by double isotope technique. The appearance time of radioactive gas in the expiratory air was compared with the peak time over the liver. If the former is faster than the latter, this is an indication of the presence of abnormal flow which bypasses the hepatic vascular bed. Then 200 to 300 μC of ^{131}I-MAA in 1.0 ml saline was injected into the spleen percutaneously. Scintiscanning of liver, spleen, and lungs was performed immediately after injection. The accumulation of MAA in the lung, compared with liver, was used to estimate the grade of portal systemic shunting. The results suggests that this technique is a more sensitive means to detect the presence of shunts than roentgenologic study for esophageal varices and the previous methods using radioactive gas. (BBB)

43905 PROSPECTS IN RADIOSURGERY. Lancet, 1: 1373(June 26, 1965).

Present status of the use of protons, neutrons, and α particles to destroy small volumes of tissue, particularly in brain, is reviewed. One advantage which charged-particle beams have is the Bragg peak effect, wherein the amount of energy per unit of track length that such particles deposit in the tissue increases to two or three fold in the last millimeter of their path where ionizations become more frequent. This peaking of the dose enhances the ratio of the target dose to the entrance dose at the skin, and there is no exit dose. Also, at the end of their range in the Bragg peak region, where the particles are slowing down, the form of the energy absorbed is more biologically effective than at the point of entry where they are traveling faster. One problem with the Bragg-peak method is that, although beams of fast particles scatter very little, when the particles are slowed down by energy attenuators for focusing and by tissue on the way to the target, they begin to scatter. The beam profile at the end of the track is then less sharp, and this poor geometry makes the sharp focusing of the peak on to a small target almost impossible. With broader beams for larger targets the Bragg peak, being confined to the last millimeter or two of the beam track, fails to confer its advantages over most of the volume of a large tumor. If this drawback is overcome by graded wedges in the beam path to scan the Bragg peak through the tumor volume, any peaking effect of dose at the end of the beam is almost completely lost. In radiosurgery of the hyperactive pituitary gland, these difficulties have made it impossible to eliminate pituitary function completely with Bragg-peak irradiation without at the same time seriously endangering neighboring structures. Similarly, attempts to focus the Bragg peak of small beams on the ventrolateral nucleus of the thalamus in the radiosurgery of Parkinson's disease encounter difficulty because of the necessarily high dose to the surrounding diencephalon. Broader beams of particles for stereotactic Bragg-peak therapy of cerebral tumors probably cannot replace the more versatile methods of conventional x and γ rays. The possible use of other accelerated particles in radiosurgery is also discussed. Research on such heavy charged particles continues, and a beam of negative pions, particles predicted to have great potential for radiation therapy, is now being examined for therapeutic applications. In addition to producing straight beams, the larger accelerators can supply an increasing number of new isotopes which, together with new radiation camera techniques, provide opportunities for expanding nuclear medicine. The projected omnetron, a machine proposed to accelerate all ions (even uranium ions) to massive energy levels, such as 500 Mev per nucleon, and thus produce densities of ionization that will eliminate all anoxic protection and recovery of cells, represents the latest attempt in the radiation therapy of cancer. (BBB)

43906 RADIOISOTOPES IN OTOLARYNGOLOGY. Goodman, Merrill (Mayo Clinic, Rochester, Minn.). Laryngoscope, 75: 639-61(Apr. 1965).

Applications of radioisotopes in the diagnosis and treatment of diseases of the head and neck are reviewed, including a discussion of the historical aspects and of the biological and physical properties of radioisotopes. Case histories are given to illustrate the uses of various isotopes, particularly ^{131}I. The effectiveness of ^{131}I as a therapeutic agent in hyperthyroidism depends upon its concentration in functioning thyroid tissue. Since the maximum range in tissue of the β particle is 2 mm, and the average range is less than 0.5 mm, and because the β rays contribute at least 90% of the total radiation delivered to the thyroid gland, there is no significant extrathyroidal radiation. It is the accepted opinion that almost every case of hyperthyroidism can be controlled with ^{131}I; however, there are certain contraindications; absolute contraindications are pregnancy and lactation. Relative contraindications are the type of goiter and age of the patient. Large toxic nodular goiters with marked mechanical or cosmetic problems should be handled surgically, as the ^{131}I will not eliminate these factors. In addition, large nodular goiters often have large areas with low uptake of ^{131}I. The use of ^{131}I should be restricted to patients over 35 years of age. It is most useful in elderly patients with thyrocardiac disease. Therapy of thyroid cancer with ^{131}I has been carried out for 15 years with reported results varying from useless to excellent. The primary drawback is that probably not more than 10% of thyroid cancers show appreciable uptake of ^{131}I. In addition, therapeutic response will depend upon the sensitivity of the tumor to irradiation. The use of Ra, Rn, ^{60}Co, ^{198}Au, and ^{90}Y, interstitially implanted, for radiotherapy is also described. Filaments containing ^{90}Y can

be produced by the neutron bombardment of yttrium oxide. The activated yttrium oxide powder is mixed with methyl cellulose and propylene glycol and extruded from a heated stainless steel press into rods or filaments. These are self-sterilizing, may be easily handled and cut by scissors to any convenient length for implanting in tissue. The ^{90}Y is a pure β emitter, having a maxiumum β emission at 2.0 Mev. Penetration in tissue is theoretically a maximum of 1.2 cm, but practically the tissue effect is lethal to a radius of 6 mm around the filament, with a cutoff only 6 to 10 cells thick between complete tissue destruction and no cytologically demonstrable damage. Radiation exposure of the surgeon and the technician is negligible in preparing and implanting these filaments. The surgeon receives up to 50 and the technician 100-150 mR to his hands. There is little or no foreign-body reaction induced by the ^{90}Y filaments, and tissue repair at the radiation site is always complete. No additional surgical trauma is necessary for removal of the radioactive source as in the case with long-lived γ emitters. Use of radioisotopes in otolaryngological research is also discussed. (BBB)

43907 ON THE RECTAL INJURY RESULTING FROM ^{60}Co IRRADIATION TREATMENT FOR CERVICAL CARCINOMA. Watanabe, Myohei (Kumamoto Univ., Japan). Nippon Sanka Fujinka Gakkai Zasshi, 13: 595-604(May 1961). (In Japanese).

Rectal complications following ^{60}Co irradiation were examined in 123 patients with cervical cancer. Radiation therapy consisted of a combination of external radiation and intracavitary implantation of a small source. Rectal symptoms as immediate complications appeared in 68 out of 123 cases. These symptoms were diarrhea and tenesmus, that is, symptoms of proctitis. In most cases they healed spontaneously within a month. If they did not heal, rectal application of hydrocortisone in doses of 100 to 150 mg relieved them without requiring interruption of radiation therapy. Rectal bleeding and ulcers as late complications occurred in 27 and 10 cases, respectively. In three of the latter cases the ulcer developed into recto-vaginal fistulas. Direct measurement of the radiation doses in the rectum with scintillation probes during treatment showed that the average value of the maximum dose in 51 cases given intracavital radiation was 4587 R and reached 6046 R in combination of teleradiation. The minimum dose to the rectum of one case having a rectal ulcer was 7100 R. Therefore, if the total dose of radiation in the rectum was limited to 7000 R, estimated by direct measurements, late complications might not occur. The topical application of cod liver oil aided the relief of late complications. (BBB)

43908 NURSING IN A RADIOTHERAPY UNIT. Parker, B. (Holt Radium Inst., Manchester, Eng.). Nursing Times, 60: 500-2(Apr. 17, 1964).

The nursing care required by patients suffering from the ill effects of radiation following radiotherapy is explained. Most patients are ambulant and in reasonably good general condition and will be receiving treatment for three to four weeks. Minimum nursing care is called for but supervision of diet is vital. This should be of high nutritious standard supplemented as necessary by high-protein beverages. Patients with more advanced stages of malignancy, and some with brain and spinal cord tumors may be only partially ambulant or totally incapacitated. More will be required from the nursing staff to meet psychological and physical needs in these cases. The patient's progress through treatment is outlined. Thus, after x-ray therapy to abdomen there will be: (1) Lassitude due to boredom, anxiety, and disease. (2) Lowering white cell count producing a consequent lowering of resistance to infection. (3) Nausea and vomiting causing weakness and other effects of inadequate nourishment. (4) Diarrhea, with frequent fluid stools producing dehydration. (5) Proctitis, tenesmus, pain, loss of rest, and frequently constipation. After x-ray therapy to mouth, throat, and chest there may be loss of taste, dryness and inflammation of mucosa, and dysphagia. The last three can quickly lead to malnutrition. In all patients there will be erythema of the skin, but with high-voltage machines and modern methods of treatment, this rarely develops beyond a dry, desquamatous stage. It is the duty of nurses in a radiotherapy unit to prevent x-ray reactions from becoming intolerable. (BBB)

43909 CONTEMPORARY RADIATION PROTECTION IN X-RAY LABORATORIES. Bisztray-Balku, Sandor (Orszagos Frederic Joilot-Curie Sugarbiologiai Kutato Intezet, Budapest). Orv. Hetilap, 105: 1219-22(June 28, 1964). (In Hungarian).

Recommendations are made for modernizing obsolete equipment and using adequate filters, sensitive film, proper exposure time, and adequate gonad protection. The smaller the area included in the beam, the smaller the absorbed radiation; therefore, the x ray beam should be adjusted to the smallest possible field. (BBB)

43910 RADIATION RESPONSE AS AN AID IN THE TREATMENT OF CERVICAL CANCER. Morton, Daniel G.; Chang, Norman; Moore, Jerry G. (Univ. of California, Los Angeles). Pacific Med. Surg., 73: 157-60(May-June 1965).

Graham and associates have reported good correlations with certain changes in the normal cells of the vagina before treatment, their SR (sensitization response), but most other observers have not been able to duplicate these results. Graham also reported even better correlations with the presence of specific changes in the vaginal cells obtained by smear following radiation, the RR (radiation response). A modification of the RR test as a method of predicting radiation responsiveness is presented with evaluations one week after a first Ra treatment (comparable to a test dose). It was hoped that this initial radiation response (IRR) might serve as a guide to therapy, if its reliability could be established. The cellular changes indicative of radiation reaction consist of: (1) enlargement of the cells; (2) nuclear hyperchromatism; (3) multinucleation; and (4) vacuolization. If 75% of 100 counted cells show any of these changes, this was rated as a good RR. If less than 75% of the cells show one or more of the changes, the RR was rated as poor. Of the 106 patients studied, two-thirds showed a good RR; and of these 70 patients, 56 (or 80%), were still living at the end of one yr. Of the 36 patients with poor RR, only 12 (or 33.3%) were still living at the end of one yr. The comparable survival figures for the Stage I and II cases were 85.7% one-yr survival for the patients with good RR, and 41.7% for those with poor RR. Within 3 to 4 weeks following the completion of therapy an estimate of clinical response was made independently of the cytological evaluation and resulted in similar figures. To estimate RR at an early period in therapy, calculations were made of the IRR one week after the first Ra treatment and before the initiation of external therapy. These results were almost the same as those after complete radiation. The most striking finding was that at the end of one yr more than one-half of the patients with Stage I and II cancers exhibiting poor IRR had already died of cancer. The comparable figure for the 3-yr cases was 71.4%. The survival rate for those with good IRR was much better than those with poor IRR but may decrease somewhat with time. Thus, it may be advisable to use radical surgery in patients with poor IRR in Stage I and II cervical cancers. While the results obtained by combining RR and CR (clinical response) were even more significant, doubts were expressed as to the advisability of radical operation after full irradiation unless definite persistence or recurrence can be demonstrated locally in the cervix. (BBB)

43911 NUTRITIONAL PROBLEMS WITH MALIGNANT DISEASES. PART 2. SEQUELAE OF TREATMENT FOR CANCER. Shils, Maurice E. (Sloan-Kettering Inst. for Cancer Research, New York). Postgrad. Med., 37: A103-6(Mar. 1965).

Nutritional problems arising from treatment of cancer with radiation, surgery, and chemotherapy are discussed.

All three treatments may affect taste, decrease gastrointestinal absorption, modify the appetite-satiety pattern, and disturb acid-base balance, among other undesirable effects. Examples are cited to emphasize the complexity of nutritional management in cancer. A list of the effects of radiation, surgery, and chemotherapy which may create nutritional problems in patients with cancer is tabulated. As an example, the subjective reactions to loss of the sense of taste following radiotherapy for cancer of the pharynx are described to illustrate the profound psychologic, physiologic, and nutritional problems that may arise in association with different forms of treatment for cancer. With the resulting anorexia and reduced food acceptance, improper selection and unpleasing preparation and serving of foods may create a serious situation. When the sense of taste is lost, the appearance and aroma of food become much more important, as do supplementary liquid feedings. Radiation damage of the intestine creates nutritional problems. The small intestine is particularly susceptible to ionizing radiation, which initially produces edema and congestion with altered peristalsis (underactivity or overactivity). Endarteritis of small vessels, necrosis, ulceration, fibrosis, and stenosis of the intestinal wall may occur in varying degrees. In addition to localized radionecrosis, there may be a more widespread reaction so that indurated bowel is surrounded by fibrous tissue. The late reactions may become apparent in a few months or occasionally years after treatment. The cancer may be cured, but there may be ulceration with hemorrhage, obstruction, fistula formation, diarrhea, and malabsorption. The use of specific vitamins for cancer patients undergoing various treatments is outlined. (BBB)

43912 PROSTHESIS CARCINOMA OF THE HARD PALATE. PROBLEMS AND TREATMENT. von Salis-Samaden, Rudolf (Zentral Roentgeninstitut des Landeskrankenhauses, Salzburg, Austria). Radiol. Austriaca, 14: 191-5(1963). (In German).

Tumor development in the hard palate is relatively rare. A causal connection between tumors of this type and irritation from prostheses has not been definitely established. Even the presence of such a tumor can be demonstrated histologically, it often appears to be relatively benign. Tumors of this type appear to be the result of mechanical trauma rather than any chemical effect of the substances of which the prosthesis may be constructed. However, some exceptions to this may be the result of allergic reactions to the prosthesis material. Diseases which affect the resistance of the mucosa, such as anemia, hypovitaminoses, or diabetes may predispose the oral epithelium to injury. Although a few cases have been reported where cancerous changes occurred in patients who had worn their prostheses for less than 5 yr, early appearance of this tumor is rare. Contact irradiation with a radiostrontium applicator is suitable for treatment of this tumor. An activity of 50 mC, giving 3000 rep at the surface, is adequate. Individual dosages used amount to between 1000 and 1500 rep, given at 24 hr intervals. The total dose required for healing is between 12000 and 15000 rep. Cure is effected within 2 months. This method is easier to use and less irritating to the patient than ^{60}Co or x irradiation treatments. (BBB)

43913 FEDERAL RADIATION PROTECTION LEGISLATION. THE OBLIGATION OF DOCTORS TO REDUCE THE MEDICAL RADIATION BURDEN. Wagner, G. (Universitaet, Zurich). Radiol. Clin. Biol., 34: 101-12 (1965). (In German).

The federal regulations on radiation protection in Germany applicable in diagnostic and therapeutic uses of radiation and personnel monitoring for persons professionally exposed are summarized. The reduction of the bone marrow burden by improved methods of chest x rays is used as an example of methods of possible dose reductions. The radiation burden from shoe fluoresent devices is discussed, and the prohibition of their use for children under 10 years of age is reported. (J.S.R.)

43914 GENETIC HAZARDS OF MEDICAL RADIOLOGY. Schultz, Everett H. Jr. (Univ. of North Carolina School of Medicine, Chapel Hill). Radiol. Clin. N. Am., 3: 243-7(Aug. 1965).

Some new data relating to human genetically controlled defects arising from ionizing irradiation are reviewed which tend to dispel the earlier pessimistic views of the hazards of diagnostic radiology. Some estimates are made of the extent of genetic damage to populations from this source. For estimates of the genetic impact of diagnostic radiology for a population the size of that of the United States (radiation therapy for benign lesions has been largely abandoned in this country), the following assumptions are made for recessive mutations in spermatogonia and resting oocytes: (1) the doubling dose for intermittent x-ray exposures is 100 R; (2) the population gene pool already contains 50 times as many recessive mutant genes, inherited from prior generations, as occur spontaneously in each generation; and (3) a generation is 30 yr. Since 20 mR/yr for 30 yr (the present estimate of diagnostic exposure) is 0.6 R, diagnostic radiology would add mutations equal to 0.6/100, or 0.6% of the number of spontaneous mutations per generation. The number of spontaneous mutations is $\frac{1}{50}$th the number of existing mutations in the gene pool, and the population dose from 30 yr of diagnostic radiology would increase the existing number of mutant genes in premeiotic gametes by 0.006/50, or 0.012%. Mutations induced in meiotic gametes calculated, using a double dose of 40 R and a $\frac{1}{40}$th probability that pregnancy will occur within 8 weeks of any x-ray exposure. These mutations would effectively add about 10% to the number induced in premeiotic gametes, making a total increase of 0.013%. Of 150,000,000 infants to be born in the next 30 yr, about 0.3% will have diseases due to homozygous recessive mutant genes, or 450,000 affected children. Diagnostic radiology, at the current rate of use, for the entire U.S. over a 30-yr interval, would change this number by (1.00013), giving an increase of about 120 cases. This number will be higher at genetic equilibrium as radiation exposure continues. The continuous addition of 0.6% to the spontaneous rate will, after several thousand years, increase the mutant gene pool by about 0.6%. The number of affected individuals would then be increased from 450,000 to 455,400 per 150 million births. Similar calculations are made for dominant mutations. About 1,000,000 children will carry dominant afflictions in the next generation, and diagnostic radiology in the U.S. will increase this number by about 500. It is concluded that the available data do not indicate any need for reduction in the number or types of clinically indicated roentgen examinations on the basis of genetic hazards. (BBB)

43915 PROBLEMS IN RADIATION THERAPY IN THE AGED. Gunn, Walter G. (Milwaukee County General Hospital). Radiol. Clin. N. Am., 3: 263-75(Aug. 1965).

Clinical and experimental data indicate that the aging (as well as the immature) organism is more sensitive to ionizing radiation than the mature or middle-aged organism. Special precautions in the use of radioisotopes and external radiotherapy in older patients are discussed. There appears to be a definite advantage in the use of supervoltage over medium voltage for geriatric patients. Apart from the still controversial aspect of increased cure rate, the main advantages of skin- and bone-sparing effects are most important in the aged. The split-course technique is advised in geriatric therapy, particularly with the use of medium voltage equipment. Many elderly patients are unable to tolerate doses of upwards of 5000 R (skin) to pelvic, abdominal, or chest portals in six weeks. Above age 80, radical treatments are seldom worth while. In old and poor-risk patients limited surgery may be the best treatment, because it is less taxing. For advanced tumors in old patients a short palliative course of radiation is preferable to an attempt at cure, with rare exceptions. It is pointless to inflict considerably more radiation morbidity with only remote chance of long-term survival. The hazard of pneumonitis consequent to radiation for bronchus carcinoma is greater in the elderly patient because of greater debility and increased likelihood of infections. The risks of combining chemotherapy and radiation for breast and

bronchus lesions outweigh their benefits, and radiation should precede any planned chemotherapy. Aged patients are even less suitable for these bone marrow damaging combinations than are younger patients. Two illustrative cases are described in detail to indicate some of the problems encountered in irradiating cancer in elderly patients. Use of radioisotopes (especially ^{51}Cr, ^{85}Sr, ^{131}I, ^{198}Au, and ^{203}Hg) for diagnostic tests in older subjects is also discussed, as well as use of some of these and other isotopes in radiotherapy. Radioiodine can be used effectively for ablating the thyroid in old patients with intractable atrial fibrillation, angina pectoris and congestive failure, inducing a state of hypometabolism. (BBB)

43916 ELECTRON-BEAM TREATMENT PLANNING IN INHOMOGENEOUS TISSUE. Laughlin, J. S.; Lundy, A.; Phillips, R.; Chu, F.; Sattar, A. (Memorial Hospital for Cancer and Allied Diseases, New York). Radiology, 85: 524-31(Sept, 1965).

The influence of inhomogeneities in tissue on the distribution of dose produced by the absorption of electrons was investigated. The effects of relatively lower density material as well as higher density material with a higher atomic number have been studied to evaluate the influence of lung and bone of different dimensions and locations embedded in tissue. On the basis of such data and their analysis specific conclusions covering these effects may be reached. It has further been possible to quantitate the amount of dose modification and to arrive at values of the absorption equivalence thickness (A.E.T.) factor which is inserted in the special correction procedure. This procedure was developed to provide a systematic method of allowing for inhomogeneities. Although the value of this factor depends on the depth, extent, and nature of the inhomogeneity, a formula is given for a single factor which has been found to be adequate in practice. The application of the correction system with the use of the A.E.T. factor is given for specific instances of lesions in different locations. These applications illustrate the flexibility of treatment planning with electrons of adjustable energies, including the use of polystyrene wedges. (auth)

43917 SCATTERED RADIATION IN A PHANTOM FROM DIAGNOSTIC QUALITY RADIATION. Trout, E. Dale (Oregon State Univ., Corvallis); Kelley, John P. Radiology, 85: 546-54(Sept, 1965).

Results are reported from measurements of scattered x radiation from diagnostic quality radiation. A water phantom 40-in. long, 20-in. wide, and 14-in. deep was used with ionization chambers mounted over the phantom. An effort was made to evaluate the contribution made by radiation scattered laterally through tissue from the defined field, leakage radiation from the tube housing, scattered radiation from the filters and beam definer, and radiation scattered from the air column between the defining system and the surface of the phantom or patient. (C.H.)

43918 ON THE TREATMENT OF THYROID CANCER WITH RADIOIODINE. Martz, G.; Meier, E. (Haematologisch-Onkologische Station der Medizinischen Klinik, Kantonsspitals, Zurich). Schweiz. Med. Wochschr., 94: 852-5(June 20, 1964). (In German).

There are four primary methods of treatment of thyroid carcinoma. These are surgery, external irradiation therapy, irradiation therapy with ^{131}I, and thyrotropic hormone. Cystostatic agents may be administered to patients who are resistant to these treatments, but they are relatively ineffective. Hypophysectomy should be effective because of the reduced thyrotropic hormone production, but it is rarely performed. Proper treatment consists of timely and quantitatively adjusted coordination of the four treatments mentioned. The principal treatment is the optimal use of localized irradiation effects of ^{131}I. A number of histologically differentiated thyroid tumors will take up ^{131}I, but the avidity of the normal tissue is usually greater. Another characteristic of thyroid carcinomas and their metastases is that they are endocrinologically dependent, so that their growth and function is governed by thyrotropic hormone. Stimulation of these tumors may be caused by endogenous or exogenous thyrotropic hormone. Production of endogenous hormone can be stimulated by removal of the normal gland tissue, but administration of thyrotropic preparations is less effective. Surgical removal of the primary tumor enhances uptake of ^{131}I by neoplastic metastases. The ^{131}I is administered several weeks after thyroidectomy, while the thyrotropic hormone concentration is still high. The patient should not receive any thyroid hormone prior to treatment. After treatment thyroid hormone is given at maximal levels. The need for additional treatment can be ascertained by scintigraphy. (BBB)

43919 ADRENAL IRRADIATION IN CHRONIC CARDIAC DECOMPENSATION. Ivanyi, Janos (Community Hospital, Gyula, Hungary). Therap. Gegenwart, 103: 311-16(Mar. 1964). (In German).

Ten patients with cardiac decompensation who had become edematous and resistant to treatment with drugs were each irradiated 3 times with 200 R of x irradiation in the region of the adrenal glands. This amount of irradiation was far less than the total of 2000 R fractionated over 5 weeks that has been shown previously to produce kidney damage. No evidence of kidney damage was observed in at least 4 of the patients who were followed up for 1 or 2 yr after irradiation. The patients reacted satisfactorily to the irradiation; only one showed signs of nausea. Diuresis was increased in all of the patients after irradiation, and they became less refractory to drug treatments. In 2 of them drainage of ascites fluid became less necessary than it had been before irradiation. The serum concentrations of K were not altered in any particular direction, and urinary excretion of Na remained essentially unchanged from normal. These results suggested that a combination of x irradiation and medication with the more effective diuretics, such as spirolactones and heterocyclic sulfonamides, might possibly be most beneficial for the more intractable clinical signs of edema induced by cardiac decompensation. (BBB)

43920 ON RADIOGOLD HYPOPHYSECTOMY IN METASTASIZING MAMMARY CARCINOMA. Gromoll, Heinz-Wilhelm; Ott, Joachim; Richter, Hans-Heinrich (Universitaet, Griefswald, Ger.). Wiss. Z. Ernst-Moritz Arndt-Univ. Griefswald, Math.-Naturw. Reihe, 13: 31-5 (1964). (In Germany).

The purpose of endocrine therapy is the palliative treatment of metastasizing mammary carcinoma by removal of the ovaries and adrenals. This has a temporary inhibitory effect on the growth of tumors and their metastases. Complete surgical hypophysectomy for this purpose cannot be attained, but implantation of radiogold seeds is often a more successful procedure. With proper surgical technique implantation need take no longer than 15 min. Depending on the dose to be administered two or three ^{198}Au seeds with a total activity of about 40 mC of γ activity are sufficient. The weak β emission is absorbed by the Pt shell of the gold seeds. The total dose required for complete necrosis of the hypophyseal tissue is between 70,000 and 80,000 R. Higher dosages may injure the optic nerve, or produce diabetes insipidus, fluid fistula, or meningitis, especially in patients with extensive skeletal metastases. In the 20 patients where this technique has been used, subjective improvement and feelings of well being have been observed, and pain has disappeared. For protection of personnel from the irradiation a Pb shield that reduces the exposure by a factor of 10 at a distance of about 50 cm from the irradiation source has been used. Irradiation control is also checked by means of dosimeters. In no instance has the dose to personnel exceeded 100 mR/week. (BBB)

43921 COMPLICATIONS IN THE URINARY ORGANS RESULTING FROM UTERINE CARCINOMA AND ITS TREATMENT. Olanescu, Gheorghe; Bocancea, D.; Ionescu, C.; Calin, Gheorghe (Fundevi Hospital, Bucharest). Wiss. Z. Humboldt-Univ. Berlin, Math.-Natur. Reihe, 12: 159-61(1963). (In German).

In advanced cases of uterine carcinoma, the invasion of the lymphatic bed and the connective tissue of the pelvic wall may cause compression of the ureters. Occasionally the ureters may be obliterated by parietal metastases. Irradiation treatment may increase the frequency of occurrence of severe urological complications. Some of these are adhesions of the ureters, ureteral fistulas of various types and extent, contraction of the bladder, pseudotumoral lesions, and anuria caused by bilateral obliteration of the ureter. Other complications observed are irradiation cystitis with relative good bladder capacity, partial ureteral stenoses, and ureteral hydronephroses. There also may be a generalized radioepithelitis and sclerosis. (BBB)

43922 COMPUTER TREATMENT PLANNING IN RADIATION THERAPY. VOLUME 1. A MONOGRAPH IN THE SERIES IN COMPUTER APPLICATIONS AND INSTRUMENTATION IN RADIOLOGY. Fitzgerald, Lawrence T.; Mauderli, Walter (Gainesville, Fla., Univ. of Florida). 1965. 129p.

Computational methods are presented for use with multiple nonconvergent stationary radiation fields, rotational fields, as well as program for the plotting of isodose curves. A program for the evaluation of transit dose measurements is discussed. The programs are written in Fortran II for an IBM-709 digital computer. The computer programs are set up to use data which are given at points $\frac{1}{2}$ in. apart. When the only data available are in forms of isodose curves, it is necessary to digitize such graphical information. How this can be accomplished is shown. By locating the point of the calculated dose value at the center digit of the three digits printed out (100 or 052), it is possible to print to scale on a rectangular grid. The computer is programmed to calculate the depth dose at each point of this dose grid within the cross section and to print the results to scale. The depth dose value at any point can be closely approximated by considering 24 fields spaced around the cross section at angular intervals of 15°. Each field has a weight of $\frac{1}{24}$. The 24 fields are summed to find the total dose. An illustration of different types of output is included. (TCO)

CHEMISTRY

General

Refer also to abstracts 43708 and 45260.

43923 (ORNL-tr-743) ON THE MODEL LAW FOR FILTRATION AND DETERMINATION OF THE FILTRATION RATE ON THE BASIS OF PERMEABILITY TESTS. Robel, Heinz; Guentzschel, Peter. Translated for Oak Ridge National Lab., Tenn. from Chem. Tech. (Berlin), 17: No. 1, 17-21(1965). 18p. Dep. mn; JCL $1.60 fs, $0.80 mf.

Six dimensionless characteristic factors are calculated from a formal dimensional analysis with nine of the most important influential values for the hydrodynamic process of filtration, where the porosity and specific surface of the cake were selected as structural values. By dropping two values which can be neglected and further recalculation of the remaining values, the problem of the filtrate flow through a cake of constant thickness can be reduced to a function f (Re; λ) = 0. Kafarow and Malinowskaja arrived at this function by a different method and obtained λ = 160/Re; tests confirm this result. The method of modeling the filtration process suggested by the Soviet authors is explained and discussed. (auth)

Analytical Procedures

See also Separation Processes and Procedures.

Refer also to abstracts 44296, 44458, and 44901.

43924 (AERE-R-4990) THE PERFORMANCE OF A DIRECT CURRENT PLASMA JET WITH PARTICULAR REFERENCE TO THE ELIMINATION OF THE MATRIX EFFECTS DUE TO PHOSPHATE AND ALUMINIUM. Webb, M. S. W.; Wildy, P. C.; Wordingham, M. L. (Atomic Energy Research Establishment, Harwell (England)). July 1965. 13p. Dep.; BIS $0.50; HMSO 2s. 6d.

The d-c plasma jet has been found to have advantages over conventional flame photometry and atomic absorption spectrophotometry in that it is free from the matrix effects which cause suppression of the spectra of calcium and strontium in the presence of phosphate and aluminum. The coefficients of variation for the determination of calcium and strontium in tissues, urine, milk and vegetation are 3%, while calcium can be determined in aluminum-containing rocks and ores with a coefficient of variation of 4%. Aqueous solutions of a calcium or strontium salt are used for standardization, and the source is so stable that no internal standard is required. (auth)

43925 (ANL-6956) THE CHEMICAL ANALYSIS OF Pu, Pu ALLOYS, AND Pu COMPOUNDS: METHODS, TECHNIQUES, SEPARATIONS PROCEDURES, AND PHYSICAL DATA. An Annotated Bibliography of the Literature. Evans, H. B.; Karttunen, J. O. (Argonne National Lab., Ill.). Oct. 1964. Contract W-31-109-eng-38. 110p. Dep. mn; CFSTI $4.00 cy, $0.75 mn.

A bibliography of 1172 references with abstracts is presented on all aspects of analytical methods for plutonium. The literature from 1947 through March 1964 is covered, and a keyword subject index is included. (D.L.C.)

43926 (CEA-R-2800) LA DETECTION DU TRITIUM PAR CHROMATOGRAPHIE GAZEUSE DANS LE CO_2 DES PILES G2/G3. (Detection of Tritium in the CO_2 of the G2/G3 Reactors Using Gas Chromatography). Guillermin, Pierre; Rossi, Jacky (Commissariat a l'Energie Atomique, Chusclan (France). Centre de Production de Plutonium de Marcoule). June 1965. 15p. Dep. mn.

The gas-phase chromatographic method, based on the principle of the decomposition of a gas mixture into its pure constituents, makes it possible to identify and rapidly measure the tritium present in the heat-carrying fluid of the reactors G2/G3. The sensitivity limit corresponds to 5×10^{-6} $\mu C/cm^3$ of tritiated gas, whereas the threshold reading of the D.C.C.A. is 10^{-3} $\mu C/cm^3$ in the presence of ^{41}Ar. The apparatus has interesting applications in the conditions where certain β emitters (products of fission or of activation) interfere with the measurement of the tritium. It can easily be adapted to the detection of tritiated steam on condition that a reducing chemical treatment is applied for the atmospheric humidity. In fact, although the method is not as sensitive for the measurement of tritiated vapor as β-spectrometry in a scintillating medium, it may be set up very easily for measuring the C. M. A. of tritium in air and is not affected by the presence of radioactive gases. (auth)

43927 (CONF-650405-16) THE NON-DESTRUCTIVE DETERMINATION OF SILICON AND OXYGEN IN METEORITES BY FAST NEUTRON ACTIVATION ANALYSIS. Vogt, Hames R.; Ehmann, William D. (Kentucky Univ., Lexington). Apr. 19, 1965. Contract AT(40-1)-2670. 20p. Dep. mn; CFSTI $1.00 cy, $0.50 mn.

From International Conference on Modern Trends in Activation Analysis, College Station, Tex.

A fast neutron activation analysis system was developed which permits the rapid and non-destructive analysis of large numbers of samples with good accuracy and precision. A 250 kv Cockcroft-Walton accelerator with a four-Curie tritium target is used to provide a neutron flux in excess of 4×10^9 n cm^{-2} sec^{-1}. An automated irradiation control system was built to control the irradiation and counting processes. The system includes a solenoid operated beam-stop assembly for turning the neutron beam on and off, and two solenoid operated spinner assemblies for rotating the sample container in the neutron beam and in front of the scintillation detector. As many as 60 analyses per hour have been run using this system. Methods for the non-destructive determination of silicon and oxygen in meteorites were developed. New abundance data for these elements in over 100 chondrites and achondrites have been obtained. The samples are irradiated with 14-Mev neutrons and counted using a 3 in. × 3 in. NaI(Tl) crystal and a 400-channel T.M.C. analyzer. An IBM 1410 computer is used to normalize the data for dead time, neutron flux, irradiation time, delay time, and counting time, and to calculate the weight, percentage, and ppm of silicon and oxygen in each sample. The methods used in sample preparation, irradiation, data accumulation, and data reduction are summarized. In addition, sources of error due to sample positioning, self-shielding, instability of the accelerator beam, and target deterioration are reviewed. (D.L.C.)

43928 (EUR-2290.f) DOSAGE DE L'OXYGENE DANS LES PRODUITS ORGANIQUES ET LES METAUX PAR ACTIVATION AUX NEUTRONS DE 14 Mev. (The Determination of Oxygen in Organic Compounds and Metals by Activation with 14 Mev Neutrons). Girardi, F.; Pauly, J.; Sabbioni, E. (European Atomic Energy Community, Ispra (Italy). Joint Nuclear Research Center). 1965. 36p. Dep. mn.

The determination of oxygen was carried out with the reaction $^{16}O(n,p)^{16}N$ by means of 14 Mev neutrons obtained from a neutron generator. This method was applied to routine analysis of organic materials (hydrocarbons of the terphenyl type) and to the determination of oxygen in metals. The effect of the various experimental parameters on sensitivity and precision was considered. Thus the influence of neutron flux inhomogeneity, sample dimensions, and variations of positioning during irradiation was studied. The comparison of two different types of detectors for measuring ^{16}N and the methods used to calculate the oxygen concentration were described. By these studies the experimental conditions which are necessary to obtain

a good precision and accuracy were established. In routine operating conditions, a detection limit of 40 ppm for 10 g samples was obtained. Modifications of the procedure which can lead to lower detection limits are discussed. (auth)

43929 (IS–1237) PURIFICATION OF MATERIALS. OPTICAL EMISSION SPECTROSCOPY AS AN ANALYTICAL TOOL. DeKalb, Edward L.; Kniseley, Richard N.; Fassel, Velmer A. (Ames Lab., Iowa State Univ. of Science and Tech.). Aug. 23, 1965. Contract W-7405-eng-42. 52p. (CONF-650521–2). Dep. mn; CFSTI $3.00 cy, $0.50 mn.

From the Conference on Purification of Materials, New York.

The characteristic line spectra emitted by the elements in flames and discharges can be used for the detection and determination of trace impurities. A review is presented of special problems encountered in applying these spectra to the quantitative determination of trace impurities at lower and lower concentration levels. Detection limits, excitation by arc and spark, carrier distillation, controlled atmospheres, liquid samples, enrichment, and analysis of residues are considered. (D.L.C.)

43930 (JEN–145-DQ/I-46) ANALISIS ESPECTROQUIMICO DE LECTURA DIRECTA DE GRAFITO NUCLEAR. (Direct-Reading Spectrochemical Analysis of Nuclear Graphite). Roca Adell, M.; Becerro Ruiz, E.; Alvarez Gonzalez, F. (Junta de Energia Nuclear, Madrid (Spain). Division de Quimica). 1964. 16p. Dep. mn.

A description is given about the application of a direct-reading spectrometer, the Quantometer, to the determination of boron, calcium, iron, titanium, and vanadium in nuclear grade graphite. For boron, the powdered sample is mixed with 1% cupric fluoride and excited in a 10-amperes direct current arc and graphite electrodes with a crater 7 mm wide and 10 mm deep. For the other elements, a smaller crater was used and dilution with a number of matrices was investigated; the best results are achieved by employing 25% cupric fluoride. The sensitivity limit for boron is 0.15 ppm. (auth)

43931 (K-1650) THE SEPARATION OF POTASSIUM ISOTOPES BY MOLECULAR DISTILLATION. McGill, R. M.; Browell, R. W.; Grisard, J. W.; Blumkin, S.; Von Halle, E.; Janney, D. B. (Oak Ridge Gaseous Diffusion Plant, Tenn.). Sept. 29, 1965. Contract W-7405-eng-26. 133p. Dep. mn; CFSTI $4.00 cy, $1.00 mn.

The technical feasibility of accomplishing the separation of the principal potassium isotopes ^{39}K and ^{41}K on a large scale by the molecular distillation of potassium metal was established. Following preliminary tests, a 10-stage experimental molecular still was designed, constructed, and operated to locate the optimum operating temperature and to investigate the effect on the separation factor of several process variables. The experiment was successful and led to the design and construction of a 15-stage Prototype cascade unit for operation at the optimum evaporating temperature of 270°C. This equipment is now in operation. Conceptual design of a molecular distillation cascade to produce one ton per year of potassium enriched to 99.93% ^{39}K was completed; analysis of the cascade construction and annual operating costs leads to an estimated unit cost of product of about $420/lb. Economic effects of operating this cascade at other ^{41}K depletion factors and other production rates are discussed. (auth)

43932 (LA–3343) DETERMINATION OF TRACE AMOUNTS OF OXYGEN ADDED TO METALLIC SODIUM. Bergstresser, K. S.; Waterbury, G. R.; Metz, C. F. (Los Alamos Scientific Lab., Univ. of California, N. Mex.). May 1965. Contract W-7405-eng-36. 32p. Dep. mn; CFSTI $2.00 cy, $0.50 mn.

Development and evaluation of a method for determining 1 to 10 ppm of oxygen in sodium metal is described. A system was designed for maintaining a supply of low-oxygen sodium and for quantitatively separating, by vacuum distillation, metallic sodium from oxygen-containing impurities in portions of this metal. The nonvolatile residue was dissolved in dilute hydrochloric acid and analyzed with a flame spectrophotometer for sodium as an indirect measurement of the oxygen concentration, assuming that the distillation residue was sodium monoxide. To determine the reliability of the method, samples prepared by adding controlled quantities of oxygen, as water, to sodium metal were analyzed by the described method. The recovery of the added oxygen was quantitative, and the standard deviation of a single measurement was 0.5 ppm in the oxygen concentration range of 1 to 10 ppm. The method requires a minimum of transfer operations and has potential applications, and limitations, in connection with sodium reactor technology. (auth)

43933 (LA–3344) AN INERT ATMOSPHERE ENCLOSURE FOR THE PREPARATION OF SAMPLES PRIOR TO THE DETERMINATION OF OXYGEN. Smith, Maynard E.; Hansel, James M.; Waterbury, Glenn R. (Los Alamos Scientific Lab., Univ. of California, N. Mex.). May 20, 1965. Contract W-7405-eng-36. 11p. Dep. mn; CFSTI $1.00 cy, $0.50 mn.

An inert atmosphere enclosure was assembled by equipping a commercial glove box, constructed from acrylate and methacrylate resin, with a gas purifying and circulating system designed to remove water, oxygen, nitrogen, and carbon dioxide from the argon atmosphere. Linde Molecular Sieve 5A is used as the desiccant and carbon dioxide trap, and uraninum turnings, heated to 640°C, serve as a getter. The water and oxygen concentrations are continually monitored, and an atmosphere containing less than 2 ppm of either constituent can be readily maintained while the box is in use; the concentrations decrease slowly when the box is not being used and the glove covers are in place. Nitrogen and carbon dioxide also are removed effectively by the purification system. Relative efficiencies of anhydrous magnesium perchlorate and molecular sieve as desiccants, and of heated copper and uranium turnings as getters, were investigated. A device is described that prevents atmospheric contamination of samples during transfer from the enclosure to an apparatus for determining oxygen. (auth)

43934 (LA–3345) THE CONTROLLED POTENTIAL ELECTRODEPOSITION OF COBALT FROM PLUTONIUM–CERIUM–COBALT ALLOY SOLUTIONS. Dahlby, Joel W.; Waterbury, Glenn R. (Los Alamos Scientific Lab., Univ. of California, N. Mex.). May 1965. Contract W-7405-eng-36. 11p. Dep. mn; CFSTI $1.00 cy, $0.50 mn.

A method was developed for the determination of 25 to 200 mg of cobalt in plutonium–cerium–cobalt alloys. The cobalt is electro-deposited from basic ammonium sulfate solution containing sulfite ion at a controlled potential of −1.00 to −1.05 volts vs a saturated calomel electrode and at a temperature in the range of 70 to 90°C. The plutonium and cerium are complexed and held in solution by citrate ion. Recoveries of 27-, 54-, 109-, and 221-mg quantities of cobalt were 99.3, 99.7, 99.9, and 100.0% with relative standard deviations of 0.57, 0.30, 0.13, and 0.12%, respectively. Of 35 added ions, 17 did not cause a deviation in the cobalt recovery greater than 0.5%. (auth)

43935 (NIJS-R–447) THE DETERMINATION OF CADMIUM IN URANIUM COMPOUNDS BY ATOMIC ABSORPTION SPECTROPHOTOMETRY. Stupar, J.; Podobnik, B.; Korosin, J. (Nuklearni Institut Jozef Stefan, Ljubljana (Yugoslavia)). Mar. 1965. 11p. Dep. mn.

A method is described for rapid, accurate and very sensitive determination of cadmium in uranium and its compounds. Uranium is removed from cadmium by the extraction with tributyl phosphate in kerosene in a continuously operating device. Cadmium is determined from the water phase after the appropriate preparing of sample solution by measuring: (1) (for solution ranging from 0.05 to 1.5 μg Cd/ml) cadmium absorption in 15 cm long acetylene air–nitrogen flame where 80% methanol solution is atomized. (2) (for solution ranging from 0.003 to 0.1 μg Cd/ml) cadmium absorption in 70 cm absorption cell, where the hydrogen–air flame with sample solution is blown in. The sensitivity and the coefficient of variation of the first arragnement are 0.015 μg Cd/ml and ±1.5%

(at 0.5 μg ml) respectively; the corresponding values of the absorption cell are 0.001 μg Cd/ml and ±8.0% (at 0.007 μg/ml) respectively. (auth)

43936 (ORNL-P-1533) ANALYTICAL LABORATORY HOT-CELL EQUIPMENT. II. A REMOTELY CONTROLLED CORROSION RESISTANT PIPETTER. Maddox, W. L.; Haga, F. E.; Fisher, D. J. (Oak Ridge National Lab., Tenn.). [nd]. Contract W-7405-eng-26. 9p. (CONF-651101-13). Dep. mn; CFSTI $1.00 cy, $0.50 mn.

For presentation at 13th Conference on Remote Systems Technology, Washington, D. C.

A remotely controlled servo pipetter (model Q-1348C) was designed for accurately delivering 0.1 to 1.0 ml portions of liquids which may contain acids, bases, oxidants, or radioactivity. The pipet consists of a syringe having a nonporous Graphitar plunger and a Teflon liner within an Al shell. A Fluorothene side arm and delivery tip are included. The pipet is attached to a driving position servo mechanism, and a single cable connects the remote and control units. The motor and/or pipet may be replaced remotely and simply. (D.L.C.)

43937 (ORNL-TM-1263) THE ASSAY, CHARACTERISTICS, COMPOSITION, AND ORIGIN OF OPIUM. I. THE PRELIMINARY STUDY ON THE USE OF ACTIVATION ANALYSIS IN THE DETERMINATION OF THE ORIGIN OF OPIUM. Leddicotte, G. W.; Emery, J. F.; Bate, L. C. (Oak Ridge National Lab., Tenn.). Sept. 7, 1965. Contract [W-7405-eng-26]. 22p. Dep. mn; CFSTI $1.00 cy, $0.50 mn.

The method of neutron activation analysis was used in a preliminary research study on the general composition of a series of opium samples from a variety of sources. The objects of this work were (1) to show by a unique analysis method what variations existed in each specimen; (2) to show the differences in the amounts of individual constituents; and (3) to also show the relationships between some of these constituents so that some criteria could be established and used to determine the origin of samples of opium. Raw opium samples from at least ten different sources were analyzed in this study by a nondestructive analysis method involving an irradiation and a measurement of the gamma radioactivity by means of a multichannel gamma scintillation spectrometer. Neutron-induced radionuclides were observed for both the major and minor elements found in each sample. The data obtained in this work showed some significant differences not only in the radioactive species observed but also in the relative concentrations of each stable element found. It is believed that these differences can be used to demonstrate how elemental composition may be used to identify the origin of a sample of opium. (auth)

43938 (PG-Report-665) ANALYTICAL METHOD FOR THE ABSORPTIOMETRIC DETERMINATION OF COPPER IN ENRICHED URANIUM METAL (2.2′ DIQUINOLYL METHOD). (Production Group, United Kingdom Atomic Energy Authority, Sellafield (England)). 1965. 5p. Dep.; BIS $0.20; HMSO 1s. 2d.

Copper is determined absorptiometrically as the copper (I) 2,2′ diquinolyl complex after extraction into amyl alcohol. The accuracy (bias) is negligible; the precision (three times standard deviation) is ±15%; the concentration range is 5–150 μg; and the limit of detection is 5 μg. The method is designed for the routine inspection of enriched uranium ingots; it is of value where the amount of available sample is strictly limited. (auth)

43939 (UCD-472-112, pp 59-72) THE DETERMINATION OF ZINC AND IRON IN BIOLOGIC MATERIALS BY X-RAY FLUORESCENCE SPECTROMETRY. Goldman, M.; Hui, C. K.; Anderson, R. P. (California Univ., Davis. School of Veterinary Medicine).

Quantitative determination of Zn and Fe in ashed specimens of dog food, a milk substitute, bone, and hair is described. A method was developed which provides direct corrections for fluorescence attenuation of specimens briquetted with soap. Transmittance of characteristic wavelengths is directly measured and related to fluorescence sensitivity as a means of quantitating sample fluorescence intensity. The method indirectly provides a measure of the mass absorption coefficients of samples which permits rapid quantitation of trace elements without prior knowledge of the matrix composition. (auth)

43940 EXTERNALLY APPLIED PROBE FOR SCANNING RADIOACTIVITY IN COUNTERCURRENT DISTRIBUTION MACHINES. Strickler, Herbert S.; Nechaj, Joseph; Grauer, Robert C. (Allegheny General Hospital, Pittsburgh). Anal. Biochem., 12: 271-4(Aug. 1965).

A modified β-γ scintillation probe with special shielding was developed for the detection of radioactivity in countercurrent distribution work. This semiautomated system was used primarily for localizing an internal standard of 1 μC ^{131}I-thyroxine in studies on the removal of exogenous serum iodine. Its applicability to other areas of exploration, where the isotope energies are sufficient, is considered. Time was saved by the use of this equipment. (auth)

43941 NEUTRON ACTIVATION ANALYSIS OF COPPER IN BISMUTH BY γ,γ-COINCIDENCE MEASUREMENT. Kim, J. I.; Speecke, A.; Hoste, J. (Univ. of Ghent). Anal. Chim. Acta, 33: 123-30(Aug. 1965).

Copper was determined nondestructively by neutron activation analysis in high-purity bismuth down to concentrations of 30 ppb. By using γ-γ coincidence counting of the annihilation photons of ^{64}Cu, interferences from the bremsstrahlung of the matrix could be completely suppressed, together with the interferences due to the induced γ-activities of other impurities such as Zn, Cd, Au, Ag, Sb, and As. The accuracy of the method was tested by spectrophotometry and by destructive activation analysis. The technique was applied to the analysis of a high-purity bismuth rod. (auth)

43942 THE DETERMINATION OF NIOBIUM IN STEEL BY NEUTRON ACTIVATION. Verbeek, A. A. (Atomic Energy Research Establishment, Harwell, Eng.). Anal. Chim. Acta, 33: 131-7(Aug. 1965).

A method was described for determination of niobium in steels by neutron activation analysis. It is applicable to samples containing down to 3 μg of niobium; but this sensitivity may be improved by a factor of 10 by use of a thin beryllium window crystal for counting. The time necessary for the analysis is about 1 hr. (auth)

43943 THE RADIOMETRIC-SPECTROPHOTOMETRIC DETERMINATION OF MICROGRAM AMOUNTS OF NIOBIUM IN ROCKS AND MINERALS. Esson, J. (Univ. of Manchester, Eng.). Analyst, 90: 488-91(Aug. 1965).

An improved method for the determination of 0.5 to 150 ppM of niobium in silicate rocks and minerals is described. Niobium-95 is used to determine the yield of the chemical separation. The thiocyanate complex is extracted into ethyl acetate and the concentration is measured spectrophotometrically. The standard deviation of replicate analyses is less than 2% at the 20 ppM level, but increases at lower concentrations and reaches 20% at 1 ppM. (auth)

43944 DETERMINATION OF CHLORIDE IN BEER BY RADIOACTIVATION ANALYSIS. Souliotis, A. G.; Grimanis, A. P.; Tsanos, N. A. (Nuclear Research Center Democritus, Athens). Analyst, 90: 499-501(Aug. 1965).

The determination of chloride in beer by using radiochemical separations is described. The reaction used is ^{37}Cl(n,γ)^{38}Cl. Radioactivity measurements are made by using a well-type scintillation crystal connected to a single-channel analyzer adjusted to count γ rays of energy greater than 1 Mev. The method results in remarkable purity of the isolated precipitate of silver chloride. Experimental values are reproducible with a relative error of less than ±2%. The sensitivity reaches a value of 0.001 ppM if a neutron flux of 10^{13} neutrons per cm^2 per sec is used. (P.C.H.)

43945 HIGH-EFFICIENCY LIQUID-SCINTILLATION COUNTING OF ^{14}C-LABELLED MATERIAL IN AQUEOUS SOLUTION AND DETERMINATION OF SPECIFIC ACTIVITY

OF LABELLED PROTEINS. Hall, T. C.; Cocking, E. C. (Univ. of Nottingham, Eng.). Biochem. J., 96: 626-33 (Sept. 1965).

Inexpensive scintillation mixtures are described, which make possible the detection of as little as 40 $\mu\mu$C of ^{14}C in aqueous solutions with an efficiency of counting of over 80%. A rapid method for counting alkaline, acidic, and neutral aqueous solutions of up to one ml is described. Ethanol or 2-ethoxyethanol is used as blending agent. The scintillation counting of alkaline solutions can be applied to the accurate determination of the specific activity of ^{14}C-labeled proteins from plant tissues. Attention was paid to the importance of a standardized washing procedure for the removal of all traces of radioactive material from glassware. (auth)

43946 DETERMINATION OF OXYGEN IN STEELS BY AN ISOTOPE DILUTION METHOD. Furuya, Keiichi; Kamada, Hitoshi (Tokyo Univ.). Bunseki Kagaku, 14: 540-4(June 1965). (In Japanese).

An isotope dilution method using ^{18}O-labeled carbon monoxide was applied to the determination of oxygen in NBS standard steel samples. The results were compared with those obtained by the vacuum fusion method. About 10 ppm difference because of gas adsorption in the furnace found in #1040, and #1047 NBS standard samples containing 0.3 and 0.4% manganese, respectively. The isotope dilution determination not using a metal bath technique often failed in samples containing more than 0.5% manganese where all of the carbon monoxide in the system was adsorbed during the gas circulation and the isotope concentration could not be measured. It was known, from the adsorbed quantities of carbon monoxide and gas circulation curves, that carbon monoxide was adsorbed by the vapor and/or films established immediately after melting the sample in the crucible, and that the adsorption was not reproducible when there was insufficient melted metal in the crucible. (auth)

43947 ON DETERMINATION OF OXYGEN IN STAINLESS STEELS. Furuya, Keiichi; Kamada, Hitoshi (Tokyo Univ.). Bunseki Kagaku, 14: 544-7(June 1965). (In Japanese).

Oxygen in stainless steels was determined by fast neutron activation analysis, vacuum fusion analysis, and isotope dilution analysis using $C^{18}O$. The results obtained by the isotope dilution method using a platinum bath agreed well with those by the activation analysis. In vacuum fusion analysis, about 140 ppm and 10 ppm negative differences in the results for 18Cr-8Ni steel and 16Cr steel, respectively, were found, which resulted from gas adsorption in the furnace. That the gas extraction temperature of 1850°C was sufficient to digest the sample in the crucible was known from the results of the isotope dilution analysis. When the ratio of sample to platinum was larger than 0.15, the gas extraction from the crucible became incomplete in the analysis of H-alloy (11%Cr steel). The isotope dilution data are useful for setting optimum experimental condition for accurate vacuum fusion analysis. (auth)

43948 THE ANALYTICAL CHEMISTRY OF THE TRANSURANIUM ELEMENTS. Taylor, B. L. (United Kingdom Atomic Energy Authority, Harwell, Eng.). Chem. Brit., 1: 418-20(Sept. 1965).

The various physical and chemical factors that influence the analytical chemistry of the transuranium elements are discussed. Many methods are available for determining neptunium and plutonium but the chemistry of the heavier elements is restricted by the smaller quantities available, their higher specific activities, and the smaller number of stable oxidation states exhibited by these elements. The heaviest elements, 103 and 104, have not yet been identified chemically. (auth)

43949 AUTOMATIC CONTINUOUS MEASUREMENT OF THE ^{14}C RADIOACTIVITY IN FRACTIONS FROM CHROMATOGRAPHIC COLUMNS. Tykva, Richard; Gruenberger, Desider (Inst. of Chemistry and Biochemistry, Czechoslovak Academy of Sciences, Prague). Chem. Listy, 59: 732-7(1965). (In Czech).

The parameters of a continuous automatic measurement of the radioactivity of ^{14}C in a liquid current, that is used for fractions from chromatographic columns, are described. The measurement is carried out in a simple system in an uncooled photomultiplier. The measurement probe consists of a polyethylene tube filled with anthracene. The effects of the construction method and material of the tubes, their filling, reflectors, lighting layer, grain size of the anthracene filling, and the purified outlet tube material for the preparation of the single crystals were determined. (tr-auth)

43950 NON-DESTRUCTIVE RADIOMETRIC DETERMINATION OF BROMINE IN SEVERAL PHARMACEUTICAL PREPARATIONS. Schiller, P.; Jombik, J. (Univerzity Komenskeho, Bratislava). Chem. Zvesti, 17: 685-8(1963). (In Slovak).

A radiometric method for the rapid determination of Br in the pharmaceutical preparations, Bromisoval, Veralgin, and Bromadal, is described. The Br determination is based on the analytical determination of the reflection of β radiation. A sealed ^{90}Sr emitter was used as source of radiation; a Geiger-Mueller counting tube served to measure the reflected β radiation. The preparations analyzed contained, in addition to Br, only organic components with elements of low at. no. The relatively large difference between the at. no. of Br and the average at. no. of the other components permitted the determination of Br with adequate accuracy. Results of the radiometric method differ from those obtained by the argentometric method used as comparison by a maximum of 1.89%; the results were tabulated for each of the three preparations. (BBB)

43951 DETERMINATION OF IODINE IN ORGANIC POLYMERS BY ACTIVATION ANALYSIS. Simkova, M.; Kukula, F.; Slunecko, J. (Ustav Jaderneho Vyzkumu Ceskoslovenske Akademie ved, Rez, Czechoslovakia). Chem. Zvesti, 19: 115-19(1965). (In Czech).

The γ activity of ^{128}I, produced by neutron irradiation of the sample in the active zone of the reactor, was measured. The samples with a weight of 0.2 to 0.5 g were introduced into polyethylene capsules together with solid KI as a standard and irradiated for 20 min with a neutron flux of 10^{13} n/cm^2 sec. ^{128}I was identified by the γ quanta energy and by the half life that was determined from the time variation of the photopeak surface at 0.45 Mev energy. It was experimentally established that the photopeak corresponds to ^{128}I without interferences with radioisotopes, since the trace masses of Cu and Br that were also identified in the sample, exert no effect with respect to the varying values of the half lives. In the samples investigated iodine was determined in a mass of 10^{-4} g. (tr-auth)

43952 RADIOCOULOMETRIC TITRATION USING A NON-ISOTOPIC INDICATOR IN THE SOLID PHASE. Toelgyessy, J.; Jesenak, V.; Braun, T.; Hradil, M. (Slovenskej Vysokej Skoly Technickej, Bratislava; Eoetvoes Lorand Tudomanyegyetem Szervetlen es Analitikai Kemiai Tanszeke, Budapest). Chem. Zvesti, 19: 465-8(1965). (In Czech).

A new method of radiocoulometric titration, in which a non-isotopic indicator in the solid phase is used, was developed. The cation to be determined forms, during the titration, a soluble complex with the electrogenerated anion. The radioactive indicator that is present in the titrating medium in the form of a weakly soluble precipitate can form a soluble complex simultaneously with a generating anion, however with a higher stability constant than the cation to be determined. After the quantitative formation of the ions to be determined, the radioactive indicator passes into solution, and its activity therefore gradually increases. In this manner Ni was determined, i.e., by titration with coulometric CN^- ions using ^{110m}Ag as indicator. (tr-auth)

43953 CONTRIBUTION TO THE DETERMINATION OF ^{131}I BY AN EXTRACTION METHOD. Brutovsky, M.; Zaduban, M.; Banas, J.; Liptakova, G. (Radiobiologicke Oddeline Ustavu Experimentalnej Biologie Slovenskej Akademie Vied, Kosice, Czechoslovakia; Katedra Biologie University P. J. Safarika, Kosice, Czechoslovakia). Chem Zvesti, 19: 470-4(1965). (In Czech).

The extraction determination of ^{131}I with subsequent precipitation of the reextracted iodide as AgI and its solution in NaCN was reexamined. A quantitative evaluation of the yield was made for the individual steps. Modification of the iodide yield in the extraction of the ions IO_4^-, IO_3^-, SO_4^{2-}, SiO_3^{2-}, Cl^-, and Br^- was determined; the yield in the presence of these ions is 93.3% on an average. This method makes it possible to obtain a total yield of 90% and to determine the activity of ^{131}I at 10^{-11} c/l. (tr-auth)

43954 NEW METHOD FOR THE ISOTOPIC ANALYSIS OF ZIRCONS IN THE NATURAL STATE. Kosztolanyi, Charles (Centre de Recherches Radiogeologiques, Nancy). Compt. Rend., 260: 5849-51(May 31, 1965). (In French).

A new method for the isotopic analysis of zircons based on the activator character of the zircons was developed. It makes it possible, after a direct acid attack on a microamount of the sample placed on the filament of a source with thermionic effect, to obtain the emission spectra of lead, Th, U, and their oxides. Because of the absence of a preliminary chemical treatment, the risks of contamination by common lead are much reduced. (tr-auth)

43955 SPECTROPHOTOMETRIC DETERMINATION OF ZIRCONIUM WITH 7,8,3',4'-TETRAHYDROXY FLAVONOL. Katyal, Mohan; Gupta, B. P.; Singh, R. P. (Univ. of Delhi). Current Sci. (India), 34: 456-7(Aug. 5, 1965).

The use of 7,8,3',4'-tetrahydroxy flavonol in the spectrophotometric determination of Zr is described. The reagent was used in 1.5 N HCl solution. The complex formed was found to obey Beer's law from 0 to 3 ppM of Zr in 1 N HCl. Sensitivity of the reaction was found to be 0.003 μg $Zr/cm^2 = \log I_0/I = 0.001$. Average value of stability constant of the complex with metal ligand ratio as 1:1 was calculated to be 3.65×10^5 in 1 N HCl at 20°C. (P.C.H.)

43956 RECENT DEVELOPMENTS OF ANALYSIS AND SEPARATION OF RARE EARTH ELEMENTS. I. OUTLINE OF THE ANALYSIS FOR RARE EARTH ELEMENTS. Kaneko, Keiji; Okada, Hiroko. Denki Shikensho Iho, 29: 172-9(Feb. 1965). (In Japanese).

More than 500 references on analysis and separation of rare earths published from 1945 to 1961 are classified according to procedures, year published, and countries where investigations were made. Developments and prevailing methods of determination of rare earth elements based on the literature investigation are discussed. (auth)

43957 RECENT DEVELOPMENTS OF ANALYSIS AND SEPARATION OF RARE EARTH ELEMENTS. II. OUTLINE OF THE SEPARATION FOR RARE EARTH ELEMENTS. Kaneko, Keiji; Okada, Hiroko. Denki Shikensho Iho, 29: 180-6(Feb. 1965). (In Japanese).

Recent developments in analysis of rare earths are reviewed with emphasis on such separation as requires advanced techniques in their preparation and determination. Recent tendencies in separation are described. (auth)

43958 DETERMINATION OF ^{131}I BY THE USE OF ACTIVATED CARBON. Garcia Orcoyen, S.; Monleon, J. L.; Velilla, A. (Junta de Energia Nuclear, Madrid). Energia Nucl. (Madrid), 9: 201-7(May-June 1965). (In Spanish).

A method is given for the determination of ^{131}I in air by passing the air across activated carbon granules with large contact surfaces. The I_2 is fixed on the activated carbon, and the activity is determined directly by measurement using a scintillation counter. The details of construction of the activated carbon filter cartridge and the calibration of the detection equipment are given. The operational procedure is indicated. (J.S.R.)

43959 APPLICATION OF ACTIVATION ANALYSIS TO CRIMINAL INVESTIGATION. Travesi Jimenez, A. (Junta de Energia Nuclear, Madrid). Energia Nucl. (Madrid), 9: 217-25(May-June 1965). (In Spanish).

The use of activation analysis in criminal investigation is considered. Its applications to the determination of the origin of samples, determination of gun-powder residues, uses in toxicology, and for analysis of hairs found at scenes of crimes are reviewed. The present and future role of activation analysis in criminal investigation is briefly indicated. (J.S.R.)

43960 USE OF ^{15}N AS AN INTERNAL STANDARD FOR DETERMINING THE QUANTITIES OF RADIOGENIC ARGON. Dmitriev, A. N.; Doil'nitsyn, E. F.; Klyarovskii, V. M.; Pertseva, A. P. (Inst. of Geology and Geophysics, Novosibirsk, USSR). Geokhimiya, No. 7, 874-8(July 1965). (In Russian).

In the determination of radiogenic Ar by the isotopic dilution method, atmospheric Ar or a mixture enriched in ^{36}Ar is used as internal reference. The method requires the use of a complex vacuum system and elaborate instrumentation; in addition, the determination of the $^{36}Ar/^{40}Ar$ ratio is accompanied by the consumption of $^{40}Ar(K_2)$, which reduces the precision of age estimation by this method. A method was therefore developed for the removal of α radiogenic Ar, using ^{15}N as the internal reference. It was assumed that the isotopic concentration of N present in the mineral is that of atmospheric N_2. For a N content of 10^{-4} wt %, the $^{15}N_2$ concentration would be 1.06×10^{-4} mm^3/g. In the case of a 0.5 g sample, 14.9 mm^3/g of $^{15}N_2$ are introduced into the system. The required isotopic ratios were determined on the basis of the mass spectroscopic peak intensities. A family of curves was derived, correlating the K content of the mineral and the flow rate per second of the sample, allowing the age of the mineral to be read directly in millions of years. The age of microcline and muscovite specimens was thus determined. The method is still in the development stage and is expected to be ready soon for carrying out routine determinations. (TTT)

43961 FLOTATION AND COORDINATION CHEMISTRY. ON A METHOD FOR ENRICHMENT OF Ga^{3+}. Seiler, H.; Erlenmeyer, H. (Universitaet, Basel). Helv. Chim. Acta, 48: 1039-42(1965). (In German).

Gallium was enriched by a factor of 3 in aluminum ores by flotation using 2-methyl-8-hydroxyquinoline as collector. The gallium content was determined by colorimetry and activation analysis. (auth)

43962 SIMPLIFIED PROCEDURE FOR DETERMINING AMOUNTS OF TWO MUTUALLY INTERFERING RADIOISOTOPES IN MIXED SAMPLES. Miller, J. K. (Univ. of Tennessee, Oak Ridge); Miller, Geraldine. J. Dairy Sci., 48: 988-9(July 1965).

The described procedure can be applied to any two radioisotopes counted under conditions where one predominates with a minimum contribution from the other, followed by a second counting under conditions where the reverse situation prevails. To test the method, solutions of ^{65}Zn, ^{85}Sr, ^{134}Cs, and ^{144}Ce, each containing 1 $\mu C/100$ ml, were prepared. Cerium-144 was mixed with each of the other radioisotopes in proportions ranging from 0 to 100% of the total mixture by increments of 10%. One- and three-ml portions of each isotope mixture were counted in a γ spectrometer in that portion of the spectrum which yielded maximum ^{144}Ce counts with a minimum contribution from ^{65}Zn, ^{85}Sr, or ^{134}Cs. This was followed by a second counting in that portion of the spectrum where the other radioisotope predominated. Equations, which were derived, were then used to calculate percentages of each radioisotope in each mixture based on the solutions containing only ^{65}Zn, ^{85}Sr, ^{134}Cs, or ^{144}Ce. Total counts for radioisotopes, each mixed with different percentages of ^{144}Ce, did not differ significantly from calculated values, and counts for ^{144}Ce agreed with calculated values. These results were reproducible with an average coefficient of variation of 1.6%. Thus reliable determinations of most pairs of mutually interfering radio-

isotopes can be made in mixtures. It is important that the volume of all samples be constant. (BBB)

43963 THE HIGH-PRECISION ISOTOPIC ANALYSIS OF OXYGEN AND CARBON IN CARBON DIOXIDE. Shackleton, N. J. (Univ. Sub-Dept. of Quaternary Research, Cambridge, Eng.). J. Sci. Instr., 42: 689-92(Sept. 1965).

Modifications are described which enable a commercially available British mass spectrometer to measure small differences in oxygen and carbon isotope ratios with a precision of ±0.01% using as little as 0.1 ml carbon dioxide sample. This precision is needed for geological work but might also find application in the use of stable isotopes of oxygen, nitrogen, or carbon as tracers in biological systems, where substantial isotopic enrichment could be detected in samples as small as 0.001 ml. It is shown that a viscous inlet system is not a necessary requirement for precise isotope ratio work. (auth)

43964 ROLE OF EXCHANGEABLE POTASSIUM AND MAGNESIUM ON CAESIUM ABSORPTION ON MARINE SEDIMENTS. Cheng, Hwa-sheng (National Tsing Hua Univ., Taiwan, China). Nature, 207: 1010(Aug. 28, 1965).

The effects of exchangeable potassium and magnesium on cesium adsorption on Pacific pelagic and terrigenous sediments, containing illite, chlorite, and montmorillonite were investigated. Samples were fractionated into 3 portions according to particle size. The plot of the distribution coefficients versus the ratio of exchangeable potassium to the total K (R_K) resulted in straight lines intercepting at the origin. Assignments were also made as to which clay mineral was worked. The results were consistent with ones showing that K fixation occurs in montmorillonite and Mg fixation occurs in degraded chlorite. It was concluded that exchangeable K and Mg play an important part in the adsorption of Cs in montmorillonite and chlorite, respectively. (P.C.H.)

43965 DETERMINATION OF SILICON IN IRON AND STEEL BY NONDESTRUCTIVE ACTIVATION ANALYSIS WITH 14 Mev NEUTRONS. Kusaka, Yuzuru; Tsuji, Haruo (Konan Univ., Kobeshi, Japan). Nippon Kagaku Zasshi, 86: 733-6(July 1965). (In Japanese).

Minute amounts of silicon in iron and steel were determined by the radioactivities produced by (n,p) reactions of 14-Mev neutrons. Using a Cockcroft-Walton type neutron generator, in which neutrons were generated by the T-d reaction, samples were irradiated and measured as follows: sample weight, 6 to 10 g; neutron flux, 2 to 7×10^6 neutrons/cm^2-sec; irradiation time, 5.0 min; scintillation detector, 1.75 × 2.00 in. well-type NaI; and measurement, γ spectrometry for 1.78-Mev ^{28}Al photopeak using a multichannel pulse height analyzer. Since the 1.78-Mev photopeak in the spectra obtained was overlapped with a small 1.80-Mev photopeak of ^{56}Mn produced by the ^{56}Fe(n,p) reaction, corrections were made by subtracting the long-lived component or by a instrumental compliment-subtraction method. In a neutron flux of 1.0×10^7 neutrons/cm^2-sec, the detection limit was about 5 mg for silicon, or ~0.05% for a 10 g sample. The analysis was interfered with by phosphorus through the ^{31}P(n,α)^{28}Al reaction, but the coexistence of phosphorus at less than 10% of silicon content was permissible. (auth)

43966 THE APPLICATION OF THE ELECTRON MICROPROBE TO THE IDENTIFICATION AND QUANTITATIVE DETERMINATION OF CARBON. Manzione, A. V.; Fornwalt, D. E. (United Aircraft Corp., Middletown, Conn.). Norelco Reptr., 12: 3-6(Jan.-Mar. 1965). (CNLM-6085).

Application of the electron microprobe for identification and quantitative determination of carbon in uranium and other metal carbides is described. A calibration curve for the determination of carbon in the U-C system is presented. The variation of C count rates as a function of the atomic number of the metal component of the various carbides is discussed. The materials studied included B_4C, SiC, TiC, VC, Cr_3C_2, ZrC, NbC, Mo_2C, HfC, TaC, WC, UC, U_2C_3, and UC_2. A plot of the carbon x-ray intensity, in counts/sec, obtained from standards of UC, U_2C_3, and UC_2 vs the carbon content of the compounds in weight percent yielded a calibration, which was successfully applied to the analysis of carbon in two phase specimens in the U-C system. An optical photomicrograph of a typical U-C specimen analyzed by microprobe using the conditions described is shown. The point count data obtained from this specimen indicated that the light etching areas are UC_2 and the dark etching second phase is hyperstoichiometric UC whose composition corresponds to the compound $UC_{1.2}$. This was in agreement with the reported high solubility of carbon in UC in the presence of UC_2. By plotting the count rate of carbon as measured in the various carbides vs the atomic number of the metal constituent of the carbides the discontinuities were obtained. As expected, an increase of carbon content from 21.7% in B_4C to 30.0% in SiC caused an increase in the carbon x-ray intensity. However, as the carbon content decreased from 30.0% in SiC to 20.0% in TiC, the count rate, rather than decreasing as expected, showed an increase by a factor of four. It was postulated that a discontinuity in the mass absorption coefficients in this region is the major cause of the observed increase in carbon x-ray intensity observed between TiC and VC, in which case the decrease is more than can be accounted for by the decrease in carbon content alone. (BBB)

43967 SOME ASPECTS OF THREE METHODS OF RADIUM DETERMINATION. Przytycka, Roza (Inst. for Nuclear Research, Polish Academy of Sciences, Warsaw). Nukleonika, 10: 155-63(1965). (In Polish).

Three methods of determination of radium were compared: the direct, rapid method by means of coprecipitation of radium with a carrier of barium chloride or barium sulfate; the emanation method using ionization chambers and a rotating electrometer; and the emanation method using scintillation flasks, a photomultiplier, and a counting circuit. It was found that the last method is the most convenient and gives the best accuracy. (auth)

43968 DETERMINATION OF CARBON AND HYDROGEN IN HYDROCARBONS BY NEUTRON SCATTERING. Braga, C. Lloyd; Conte, J. C.; da Silva, J. Lopes; Thomaz, M. Fernandes (Centro de Estudos de Quimica Nuclear, Lisbon). Rev. Port. Quim. (Lisbon), 7: 13-16(1965). (In Spanish).

A method is proposed for carbon and hydrogen determination in liquid hydrocarbons, based on the moderation of fast neutrons by the liquid hydrocarbon to be analyzed. The method can be adapted to analysis of mixtures of liquid hydrocarbons flowing in pipes. The error of the determination is of the order of 3%. (auth)

43969 THE VARIATION OF THE INDEX OF REFRACTION OF AQUEOUS SOLUTIONS OF $UO_2(NO_3)_2$. Ripan, R.; Szekely, Z.; Kiss-Imreh, G. (Inst. of Chemistry, Cluj). Rev. Roumaine Chim., 10: 399-405(May 1965). (In French).

The applicability of the refractometric (interferometric) method for aqueous solutions of $UO_2(NO_3)_2$ was studied by following the variation of the index of refraction as a function of the concentration of the uranyl nitrate in the $UO_2(NO_3)_2-H_2O$ system, as a function of the concentration of the NO_3^- ion in the $UO_2(NO_3)_2-NaNO_3-H_2O$ system, as a function of temperature, and as a function of the pH of the acidified solution of $UO_2(NO_3)_2$. The variation of the molar refraction was also studied in the $UO_2(NO_3)_2-H_2O$ system. It was concluded that the interferometric method can be used for determination of $UO_2(NO_3)_2$ and for determination of the free acid in the solution. The formation of complexes between UO_2^{2+} and NO_3^-, the hydrolysis of UO_2^{2+}, and the transition point of crystallohydrates in the aqueous solutions was not detected, in the case of the titration by NaOH. The formation of a single ion, probably the diuranate, was shown. (tr-auth)

43970 ANALYTICAL APPLICATION OF FLUORINE ION. I. DIRECT TITRATION OF THORIUM WITH SODIUM

FLUORIDE. Seki, Jisuke (Inst. of Physical and Chemical Research, Tokyo). Rika Gaku Kenkyusho Hokoku, 37: 464-9(1961). (In Japanese).

Thorium in 50% alcohol solution, at pH 2.4 and 45°C, was directly titrated with 0.1N sodium fluoride, using a few drops of 0.1% solution of alizarine red S and 4 drops of 0.1% solution of pyrocatechol violet as indicator. Accurate results were obtained for 1 to 50 mg Th in 100 ml solution within an error of ±0.5%. Thus, the determination of thorium in monazite could be made under these conditions of titration. (BBB)

43971 RADIOMETRICAL METHODS OF ORE ANALYSIS. PART II. THE FLUORESCENCE ANALYSIS. Dziunikowski, Bohdan. Rudy Metale Niezelazne, 10: 309-13 (1965). (In Polish).

Methods of fluorescence analysis are described, with particular reference to fluorescent excitation by isotopic sources of x radiation. Fluorescence methods and equipment developed for determination of zinc and iron in domestic zinc-lead ores are described. The advantage of the method is its rapidity; the disadvantages are less accuracy as compared to classical methods, the necessity of continual checking of the apparatus, and special calibration required for different kinds of ores. (auth)

43972 THE EXTRACTION OF MICROGRAM AMOUNTS OF ZIRCONIUM WITH N-BENZOYL-N-PHENYLHYDROXYLAMINE. Nee, Che-ming; Chu, Chung-fun; Liang, Shu-chuan (Inst. of Chemistry, Academia Sinica, Peking). Sci. Sinica (Peking), 14: 992-7(July 1965).

The conditions for separation of microgram amounts of zirconium (5 to 100 μg) by means of N-benzolyl-N-phenylhydroxylamine (BPHA) extraction and for zirconium determination in the organic layer were investigated. At least 97% of zirconium was extracted from 0.3 to 1N HCl solutions with BPHA concentrations of less than 6 mg per ml. For BPHA concentrations of 6 mg per ml, zirconium could be quantitatively extracted from 0.3 to 10N hydrochloric acid solutions. The same held for lower BPHA concentration (for example 2 mg per ml), provided ammonium thiocyanate or nitrate (0.1 gm) was also present in the aqueous phase. The addition of these ammonium salts was advantageous to the subsequent photometric determination of zirconium. In the photometric determination, both the amounts of BPHA used in extraction and those of xylenol orange should be kept constant. Large amounts of aluminum, cobalt, copper (after being masked with thiourea), iron(III) (after being reduced with ascorbic acid) thorium, uranium, sulfate, and tartrate did not interfere. Milligram amounts of fluoride and oxalate interfered seriously. (auth)

43973 SUBSTOICHIOMETRIC DETERMINATION OF COPPER IN HIGH-PURITY METALS BY ACTIVATION ANALYSIS. Krivanek, Miloslav; Kukula, Frantisek; Slunecko, Jaroslav (Czechoslovak Academy of Sciences, Prague). Talanta, 12: 721-6(Aug. 1965).

A selective and simple substoichiometric determination of copper in high-purity aluminum, silicon, iron, gallium, zinc, and tin by activation analysis was developed. The radiochemical procedure is based on the extraction of copper diethyldithiocarbamate into chloroform from an aqueous alkaline medium. The only interfering elements are mercury, palladium, silver, osmium, and gold. (auth)

43974 THE DETECTION OF RADIOACTIVE SUBSTANCES IN WATER. Vogler, Peter (Laboratorium der Wasserwirtschaftsdirektion Havel, Potsdam, Ger.). Wiss. Z. Karl-Marx-Univ. Leipzig, Math.-Naturw. Reihe, 13: 7-11(1964). (In German).

A general introduction to the terminology of radioactivity is given and the problems of contamination are discussed with respect to human life. The procedure used for determining water activity at the Wasserwirtschaftsdirektion Havel in Potsdam is described. About 0.5 l water is concentrated to 50 ml by distillation after lowering the pH to 1-2 with H_2SO_4. The residue is placed in a quartz evaporating dish and evaporated to dryness with an ir lamp. The organic residue is ashed at 500°C, weighed, removed from the dish, and homogenized; 150 mg are transferred to an Al capsule and silted with acetone, which is then evaporated. The sample is then placed under a Geiger-Müller counter, previously calibrated; null effects are measured day and night; the two recordings differ by less than 0.4 cpm. Four apparatuses are used; calibration is with ^{40}K, $^{90}Sr/^{90}Y$, and ^{137}Cs preparations. Discussion of procedures for α and γ radiation used by other groups is given. Several recent studies on biological effects of radiation are reviewed. (BBB)

43975 ACTIVATION ANALYTICAL INVESTIGATIONS OF POLYETHYLENES. Sorantin, H.; Patek, P. (Oesterreichische Studiengesellschaft fuer Atomenergie GmbH, Seibersdorf, Austria). Z. Anal. Chem., 211: 99-113(1965). (In German).

After neutron activation of different polyethylenes radioisotopes of 17 elements were identified by γ spectrometry and determined with simultaneously irradiated standards. In samples of the same charge no differences could be detected. Low-pressure polyethylene contained more trace elements and changed more easily to yellow colors after exposure to neutrons than high-pressure polyethylene. (auth)

43976 CONTINUOUS MEASUREMENT OF ^{14}C-LABELED AMINO ACID MIXTURES WITH THE HELP OF A SCINTILLATOR TUBE AFTER SEPARATION ON ION EXCHANGE COLUMNS. Schormueller, J.; Stan, H.-J. (Technische Universitaet, Berlin). Z. Anal. Chem., 211: 274-81(1965). (In German).

A method is described for the continuous measurement of ^{14}C-labeled amino acids during automatic separation by ion-exchanger columns. Immediately after emerging from the column the single fractions are passed through a measuring device consisting of a plastic scintillator between two photomultipliers in a coincidence circuit. Subsequently the eluate is reacted with ninhydrin. The limit of detection is 2×10^{-3} μC. The procedure is simple and the measuring device is commercially available. (auth)

43977 INDUSTRIAL DEVELOPMENT OF ACTIVATION ANALYSIS EQUIPMENT AND ITS APPLICATIONS. Vernin, E. pp 209-21 of Giornate dell'Energia Nucleare 1964. Milan, Federazione delle Associazioni Scientifiche e Tecniche, 1965. (In French).

The development of rugged, simple, and accurate devices for neutron-activation analyses in industrial applications is described. Some industrial uses of such devices are noted. The apparatus consists of a neutron source, a sample transfer system, and a gamma spectrometer. The devices can perform qualitative and/or quantitative analyses. (T.F.H.)

43978 MASS SPECTROSCOPY AS AN ANALYTICAL TOOL. Honig, Richard E. (RCA Labs., Princeton, N. J.). 42p. (CONF-650521-4). Gmelin, AED-CONF-65-113-1, From Conference on Purification of Materials, New York.

The mass spectrometers available today will detect with essentially constant sensitivity all impurities present in the bulk or on the surface of a sample, except near the mass of the major constituent, which may partially mask neighboring impurities. For bulk impurities, detection sensitivities down to the level of parts per billion atomic can be achieved on a routine basis, provided the instrument is operated under adequate vacuum conditions. The major problem remaining relates to the quantitative accuracy and reproducibility of analysis. Even under optimum conditions it is difficult to quote impurity concentrations in homogeneous samples to better than ±30%. Different types of sources available for the production of ions from solids are described, and suitable mass analyzers and ion detectors are discussed. The analytical problems encountered are illustrated by typical results obtained with r-f spark source instruments. (auth)

43979 CHARACTERISTICS OF ION-SENSITIVE EMULSIONS FOR MASS SPECTROGRAPHY. [PART] II. McCrea, J. M. (United States Steel Corp., Monroeville, Pa.). 29p. (CONF-650519-3). Gmelin, AED-CONF-65-120-3.

From 13th Annual Conference of American Society of Testing Materials, St. Louis.

An earlier investigation of the properties of ion-sensitive plates was extended to include additional types of spectrographic emulsions and to obtain more extensive data on the widely used Ilford Type Q2 emulsion. Log-probability response plots are used to compare the different emulsions and emulsion batches. The effects of variations in exposure and processing conditions on the Type Q2 plates were investigated. These effects were correlated, where possible, with the coating analyses and microstructure of the plate emulsion. (auth)

43980 A REVIEW OF EQUIPMENT FOR ANALYZING FOR OXYGEN IN COMBUSTION SYSTEMS. Thompson, A. L. (McGill Univ., Montreal). 5p. (CONF-650444-1). Gmelin, AED-CONF-65-119-1.

From Western States Combustion Inst., 1965 Spring Meeting, Hollywood, Calif.

A comparison was made of commercially available oxygen analyzers with emphasis on: basic principle of operation; accuracy of measurement; portability; and possibility of improvements in design. It was concluded that the paramagnetic properties of oxygen serve very well as a means to detect and measure its presence in a mixture of gases. Abstracts of 5 papers on oxygen analyzers are included. (P.C.H.)

43981 AN ANALYSIS OF THE TECHNIQUE OF LEAST SQUARES AS RELATED TO GAMMA-RAY SCINTILLATION SPECTROSCOPY. Wolberg, John R. (Israel Inst. of Tech., Haifa). 29p. (CONF-650405-15). Gmelin, AED-CONF-65-040-1.

From International Conference on Modern Trends in Activation Analysis, College Station, Tex.

The analysis of gamma scintillation spectra by the method of least squares is discussed. For a given set of data, the method of least squares is shown to provide the solution that minimizes the statistically weighted sum of the square of the differences between the observed and calculated valves of the dependent variable. Gamma spectra can be classified into two categories: those in which the energies of the gamma rays are known but amplitudes are unknown, and those in which neither the energies nor the amplitudes are known. Least square methods can be used for the determination of either amplitudes or amplitudes and energies of the gamma rays. The fundamental concepts associated with least-square analysis are discussed. (F.J.H.)

43982 METHOD FOR THE SEPARATION OF NUCLEAR FUELS. Baehr, Werner; Vogg, Hubert; Ochsenfeld, Wilhelm (to Gesellschaft fuer Kernforschung m.b.H.). German Patent 1,197,630. July 29, 1965. Filed May 9, 1964.

The separation of uranium from plutonium or uranium from thorium is described. The method includes rendering soluble the nuclear fuels in an oxidizing alkaline melt, lixiviating the solidified melted material with water, and separating the precipitate with alkaline solution. The precipitate is absorbed with an acid such as diluted nitric acid. (Gmelin Inst.)

43983 METHOD FOR THE DETERMINATION OF THE HEAVY WATER CONTENT IN WATER SAMPLES. Spies, J. (to Gesellschaft fuer Kernforschung m.b.H.). German Patent 1,198,588. Aug. 12, 1965. Filed Apr. 12, 1961.

The heavy water content in water samples is determined by the measurement of the specific weight of the samples which is proportional to the content of heavy water. The specific weight is determined by measuring the height of rise of the water in capillary tubes of circular cross-section. (Gmelin Inst.)

43984 MEASUREMENT OF RADIOACTIVITY ON PAPER CHROMATOGRAMS. Moses, Vivian; Lonberg-Holm, Knud Karl (to Eckhoff and Slick). U. S. Patent 3,200,252. Aug. 10, 1965. Filed July 9, 1962.

An automatic counting mechanism is patented for measuring the radioactivity of paper chromatograms after the areas of interest are located and excised. The excised areas are mounted between two strips of Mylar film. An arrangement consisting essentially of a pair of parallel rotatable spools spaced apart and carrying the strip of film is used to pass the film between a pair of radiation counters. The film is automatically stopped and started again as each chromatogram segment moves between the counters, and the data are fed to a suitable storage device. (A.G.W.)

Inorganic and Physical Chemistry

43985 (ANL-7000, pp 85-110) DEVELOPMENT OF CERAMIC FUELS. (Argonne National Lab., Ill.).

Results of studies on the preparation and properties of Pu and U monosulfides, Pu, Th, and U monophosphides, and binary compounds of these materials are reported. Measurements were made of the mechanical properties and sintering behavior of UO_2, evaporation rates of MgO, and thermal properties of UC, UO_2, UP, and US. (W.L.G.)

43986 (ANL-7000, pp 201-4) NUCLEAR MAGNETIC RESONANCE STUDIES. (Argonne National Lab., Ill.).

Progress is reported on NMR studies in Al-V alloys, H-V systems, Tc-V alloys, $PuAl_2$, Np metal, and Ti metal. A brief description is given of the components in a coherent pulsed NMR apparatus. (W.L.G.)

43987 (CEA-R-2817) PREPARATION DE CATALYSEURS OXYDES A BASE D'URANIUM [Theses]. (Preparation of Uranium-based Oxide Catalysts [Thesis]). Bressat, Rene (Commissariat a l'Energie Atomique, Fontenay-aux-Roses (France). Centre d'Etudes Nucleaires). 1965. 67p.

The thermal decomposition of uranyl and uranium(IV) oxalates was studied as a means of producing uranium dioxide. The main intermediate phases of the decompositions were isolated and the lines of their x-ray-diffraction patterns were indexed. The oxides produced by the decomposition are ill-defined and unstable: they strongly absorb atmospheric oxygen with modification of the composition and, in certain cases, of the structure (pyrophoric oxide). With a view to obtaining stable oxides, mixed uranium-thorium oxalates were prepared. In order to prepare an oxalate having a homogeneous composition, it is necessary to adopt a well-defined preparation method: the addition of solutions of thorium and uranium(IV) nitrates to a continually saturated oxalic acid solution. The mixed oxide obtained from the thermal decomposition of an oxalate $U_xTh_{1-x}(C_2O_4)_2$, 2 H_2O at 500°C for 24 hours in a current of oxygen leads to a cubic structure which is well-defined both in the bulk and superficially when x is less than 0.35. Above this atomic concentration of uranium, some uranium moves out of the lattice in the form of UO_3 or U_3O_8 according to the temperature. The mixed oxide is not stoichiometric ($U_xTh_{1-x}O_{2+y}$) and the average degree of oxidation of the uranium varies with the temperature and partial oxygen pressure. The oxides thus formed have a high surface area. By dissolving the mixed oxalates in a concentrated solution of ammonium oxalate, it is possible to deposit the catalyst on a support, but the differences in solubilities of thorium and uranium(IV) oxalates in ammonium oxalate make it impossible to prepare double salts formed either of thorium and uranium and of ammonium. (auth)

43988 (CONF-650804-7) PREPARATION AND PROPERTIES OF PROMETHIUM AND SOME OF ITS COMPOUNDS. Weigel, Fritz (Munich Univ. (West Germany). Institut fuer Anorganische Chemie). [1963]. 22p. Dep. mn.

From 5th Rare Earth Research Conference, Ames, Iowa.

Metallic promethium was prepared by reduction of PmF_3 with lithium in vacuo at 750° and annealing at 1200°C. The metal is silvery white; its x-ray diffraction pattern has not yet been fully interpreted. An attempt was made to determine the melting point by means of McWhan's "sol-

der-rupture" method. A value of 852 ± 41°C was found as the average of four determinations. The following compounds of promethium were prepared to date: PmF_3, $PmCl_3$, $PmCl_3 \cdot xH_2O$, PmOF, Pm_2O_3 (A-, B-, and C-type), $Pm(OH)_3$, $Pm(NO_3)_3 \cdot xH_2O$, $PmPO_4 \cdot (0..0,5)H_2O$, $PmPO_4$, $PmAsO_4$, $Pm(IO_3)_3 \cdot xH_2O$, $Pm_2(C_2O_4)_3 \cdot 10H_2O$, $Pm_2(CrO_4)_3$, $PmCrO_3$, $Pm_2(MoO_4)_3$, and $Pm_2(WO_4)_3$. The lattice constants of most of these compounds were determined. In the case of $Pm_2(WO_4)_3$ the tungsten bremsstrahlung excited by the 223 kev β's of ^{147}Pm was studied. The internal target yield in the system $Pm_2O_3-WO_3$ was measured. With increasing WO_3-concentration, this yield increases steadily. The possible application of $Pm_2O_3-WO_3$ phases as –sources with defined spectrum is discussed. (auth)

43989 (MIT-905-20) EFFECTS OF STERIC HINDRANCE AND OF BOND TYPE ON ELECTRONIC ABSORPTION SPECTRA OF CERTAIN 8-QUINOLINOLATES. Popovych, O.; Rogers, L. B. (Massachusetts Inst. of Tech., Cambridge). [Nov. 10, 1964]. Contract AT(30-1)-905. 16p. Dep. mn; CFSTI $1.00 cy, $0.50 mn.

Blue shifts in the spectral maxima of the 2-methyl-8-quinolinolates relative to the 8-quinolinolates of gallium, indium, and thallium(III) appear to be due to steric hindrance and vary in the expected inverse relationship with respect to the size of the metal ion. In the absence of steric hindrance, large red shifts of the low-frequency band are found for a chelate when compared to the ligand itself. From a comparison of spectra for zinc and magnesium chelates, it appears that a large red shift and an enhanced intensity of the low-frequency band are associated with a strong metal-nitrogen (predominantly covalent) bond, whereas a stronger metal-oxygen (predominantly ionic) bond is associated with a smaller shift and, particularly, a small absorptivity of the low-frequency band. (auth)

43990 (MIT-1965-15) SOME NEW DERIVATIVES OF THE $[Mo_6Cl_8]^{4+}$ ION. Cotton, F. A.; Curtis, N. F. (Massachusetts Inst. of Tech., Cambridge. Dept. of Chemistry). Oct. 30, 1964. Contract AT(30-1)-1965. 21p. Dep. mn; CFSTI $1.00 cy, $0.50 mn.

Attempts to prepare new compounds in which the six centrifugally directed Mo orbitals of $[Mo_6Cl_8]^{4+}$ are occupied by various ligands are described. Only in relatively few cases were stoichiometrically well-defined products obtained. These products were: $[Mo_6Cl_8L_6](ClO_4)_4$, $[Mo_6Cl_8L_2(CH_3SO_3)_4]$, and $[Mo_6Cl_{12}L_2]$, where L, in each type of compound, is either $(CH_3)_2SO$ or $HCON(CH_3)_2$. The infrared spectra of these compounds were studied and the assignments show that the ClO_4^- ions do not become coordinated while all $(CH_3)_2SO$ and $HCON(CH_3)_2$ molecules and the $CH_3SO_3^-$ ions are coordinated to Mo atoms through their oxygen atoms. From the composition and infrared evidence regarding coordination, it appears that in all cases the Mo_6Cl_8 group binds just six additional ligands. (auth)

43991 (N64-26433) THE CRYSTALLOGRAPHY OF SOME TRANSITION METAL MOLYBDATES. Carlston, R. C.; Rodier, D. (Grumman Aircraft Engineering Corp., Bethpage, N. Y. Research Dept.). Mar. 1964. 38p. (RM-229).

The formation of transition metal molybdates in the binary $MO-MoO_3$ with M = Mn, Ni, Co, Mg was investigated. Magnesium, although not a transition metal, was included because of the structural similarity of many magnesium and manganese compounds. Only molybdate (VI) compounds were studied. In a standard procedure the materials were weighed, blended in a P-K blender, and fired. The blending was done dry or in alcohol. In the latter the alcohol was dried off at 110°C. Grinding was not done, since the powders were generally 200 mesh. The firings were mostly done in sealed Vycor tubes, although some early firings were done in platinum crucibles. The pseudo binaries (assuming oxygen balance constant) have not yet been completely investigated, and the results are preliminary. Low symmetries seem to characterize this type of molybdate, and the powder patterns described were not deciphered. Single crystals were not grown in this program. (auth)

43992 (NP-15339) UNTERSUCHUNGEN AN BINAEREN UND TERNAEREN OXIDEN DES PROMETHIUMS. (Research on Binary and Ternary Oxides of Promethium (thesis)). Scherer, Volker (Munich Univ. (West Germany). Institut fuer Anorganische Chemie). 1965. 48p. Dep. mn.

The existence of three crystal modifications of promethium sesquioxide was investigated. The methods used for the preparation of the pure Pm^{3+} solutions, for the preparation of the oxides, for the determination of the lattice constants from the powder diagrams, and for the determination of the ion radius of Pm(III) are described. The results showed the existence of all three modifications – a cubic system, a monoclinic system, and a hexagonal system. The colors of the three modifications are all different with the A modification being violet blue, the B modification being violet rose, and the C modification being coral red. The volumes of the elementary cells, calculated from the lattice constants, obey the lanthanide contraction in all three modifications. The ion radius of Pm^{3+} of 0.978 Å agrees very well with the proposed value of 0.979 Å. A supplementary study was made on pseudobinary systems of Pm oxide and tungsten oxide in various mass ratios. The preparation of the samples and the methods used for the x-ray analysis were described. The γ spectrum was measured and evaluated. It was shown that the γ emission in $Pm_2O_3-WO_3$ system depends upon the ratio of the components. A possible structure anomaly in promethium tungstate was indicated. The evaluation of the x-ray diagram was compared with that of the tungstates of Nd and Sm. (J.S.R.)

43993 (NP-15379) BIBLIOGRAPHY ON THE HIGH TEMPERATURE CHEMISTRY AND PHYSICS OF GASES AND GAS-CONDENSED PHASE REACTIONS. Brewer, L. (comp.) (California Univ., Berkeley). June 30, 1965. 28p.

A total of 144 references is presented on spectroscopy of interest to high temperature chemistry and on reactions between gases and condensed phases. (D.L.C.)

43994 (NP-15381) BIBLIOGRAPHY ON THE HIGH TEMPERATURE CHEMISTRY AND PHYSICS OF MATERIALS IN THE CONDENSED STATE. Volume 1965, Number 2, April–June 1965. Diamond, J. J. (ed.) (National Bureau of Standards, Washington, D. C.). 66p.

A total of 656 references is presented of the following subjects: devices for achieving, measuring, and controlling temperatures above 1500°C; devices for physical measurements above 1000°C; properties below and above 1000°C of materials melting above 1500°C; properties above 1000°C of materials melting below 1500°C; phase equilibria; and reactions above 1000°C. (D.L.C.)

43995 (RFP-503) PROPERTIES OF PLUTONIUM DIOXIDE. Moseley, J. D.; Wing, R. O. (Rocky Flats Div., Dow Chemical Co., Denver, Colo.). Aug. 24, 1965. Contract AT(29-1)-1106. 33p. Dep. mn; CFSTI $2.00 cy, $0.50 mn.

Selected physical and chemical properties of plutonium dioxide were investigated. Plutonium dioxide was prepared from the following plutonium salts: oxalate, nitrate, hydroxide, and peroxide. Calcination temperatures used were 240°C, 400°C, 600°C, 800°C, and 1000°C. The density, plutonium content, relative solubility, hygroscopicity, surface area, crystallite size, and thermogravimetric behavior of the oxides were measured. (auth)

43996 (UCRL-11699) CARBOTHERMIC REDUCTION OF ALUMINA: A THERMODYNAMIC ANALYSIS. Worrell, Wayne L. (Lawrence Radiation Lab., Univ. of California, Berkeley). Oct. 7, 1964. Contract W-7405-eng-48. 17p. Dep. mn; CFSTI $1.00 cy, $0.50 mn.

Using new thermodynamic data for Al_4C_3, stability relationships in the Al-C-O system were determined. A Pourbaix-Ellingham diagram was constructed and is used to evaluate the equilibrium carbothermic-reduction process. The analysis indicates that liquid aluminum can never be obtained and that appreciable amounts of $Al_2O(g)$ are present in the vapor. An analysis is also made of an alternate

reduction path in which aluminum vapor is produced by the decomposition of aluminum carbide. The Al_4O_4C and Al_2OC oxycarbide phases are considered to be metastable, but their possible influence on the equilibrium reduction process is briefly discussed. (auth)

43997 (UCRL–11889) INORGANIC MATERIALS RESEARCH DIVISION ANNUAL REPORT, 1964. (Lawrence Radiation Lab., Univ. of California, Berkeley). Feb. 1965. Contract W-7405-eng-48. 171p. Dep. mn; CFSTI $5.00 cy, $1.00 mn.

Summaries are presented of current staff research interest, research recently completed, and general activities. The summaries are arranged under the following headings: chemistry, metallurgy, and physical ceramics. An author index is included. (D.L.C.)

43998 (UCRL–12396) ROLE OF OXYGEN IN SOLID-SOLID REACTIONS. Holt, J. Birch (Lawrence Radiation Lab., Univ. of California, Livermore). July 23, 1965. Contract W-7405-eng-48. 25p. (CONF-650644–1). Dep. mn; CFSTI $1.00 cy, $0.50 mn.

From International Conference on Sintering and Related Phenomena, Notre Dame, Ind.

An understanding of the mechanism of spinel formation from solid-solid reactions remains incomplete, mainly because of the lack of data on the role of oxygen in the overall reaction. Oxygen diffusion along grain boundaries, through pores, in the gas phase or through the lattice has been postulated. To clarify the part oxygen plays in these reactions, the formation of $CoAl_2O_4$ from CoO and Al_2O_3 was studied using single and polycrystalline samples in which oxygen-18 was incorporated. The heat treatments were carried out in various atmospheres. The oxygen mobility was followed by activation of the oxygen-18 by proton bombardment to yield the radioisotope, fluorine-18. The oxygen distribution in the product phase is indicated by autoradiography. It was found that CoO and Al_2O_3 react to form the spinel by the Wagner mechanism. (auth)

43999 (ZFK-PHA–12, pp 7-9) TECHNOLOGY OF MANUFACTURE OF p-n JUNCTIONS BY MEANS OF DIFFUSION OF PHOSPHORUS IN SILICON. Pshiborski, V.

In Russian.

A method for the fabrication of p-n junctions by the thermal diffusion of phosphorus in monocrystalline silicon pellets is described. Results of measurements of the current-voltage characteristics of the detectors are shown for different samples at various times after preparation and for various coatings. (M.J.T.)

44000 (ZFK-PHA–12, pp 33-9) THE PREPARATION OF LARGE-SURFACE pn BARRIER-LAYER ELEMENTS BY LITHIUM DIFFUSION IN p-SILICON. Ulrich, H.

In German.

By diffusion from the liquid phase of lithium, large-surface p-n transitions were prepared in p-silicon. Experimental values of the limiting solubility and the concentration distribution of the lithium in Si were given for various temperatures and compared with theoretical results. From some barrier layers, the current–voltage curves were described and their dependence on the volume and surface properties of the Si was discussed. (tr-auth)

44001 (ZFK-PHA–12, pp 40-9) ION-DRIFT INVESTIGATIONS OF LITHIUM IN p-SILICON. Ulrich, H.; Rehak, K.

In German.

The p-i-n transitions were prepared by the ion-drift method, starting with p-n transitions in p-silicon. The material used had specific resistances of 300 to 500 ohm cm. The dependence given by Pell of the drift depth on the temperature, voltage, and time, which was formulated by Blankenship–Borkowski and Mayer in the equation $W = (2\,\mu Vt)^{\frac{1}{2}}$, can be verified in the limits of the measurement accuracy. Plating studies and capacity measurements by a simple resonance circuit measurement principle was used for evaluation. The arrangement used for carrying out the drift operation and the maximum permissible output of the diode in these conditions were given. (tr-auth)

44002 (AEC-tr-6572) POLARIZATION DURING ION REDOX PROCESSES. RECHARGINGS. IONS OF IRON, THALLIUM, CERIUM AND VANADIUM. Antropov, L.; Mizgireva, E. Translated from Zh. Fiz. Khim., 15: 776-92(1941). 22p. Dep.(mn); $1.00(cy), 1(mn) CFSTI $2.60 (fs), $0.86(mf) JCL.

The possible operation of ion oxidation-reduction process was analyzed and the possible reasons for redox-polarization were explained. It was established that chemical polarization can be explained by slow discharge or slow desorption. Based on the assumption that redox-polarization depends on secondary ion accumulation occurring on the surface of the electrode, an equation was derived for slow desorption. The validity of the derived equation is quantitatively confirmed by the example of the discharged ions of the rare elements — thallium, cerium, vanadium, and iron. In line with the hypothesis of slow desorption requirements, the absolute value of polarization and the nature of its change with respect to current intensity, are determined by the nature of the primary and secondary ions. The maximum polarization, which changes most during the increase of current intensity, should be observed and actually is observed for the ion systems of the 116 type, the minimum and slightly changing polarization during the current increase, is observed for the systems of the IIa type; for the Ia and I6 system it is not very high. The viewpoint developed here makes it possible to predict the more probable type of polarization for the given redox system provided the nature of its primary and secondary ions is known. Scrutiny of Ferster's data on recharge of $V^{v} \rightarrow V^{iv}$ and $V^{III} \rightarrow V^{II}$ and also $Mo^{vi} \rightarrow Mo^{v}$ shows that the relations found with it are well described by the equation for polarization associated with slow desorption. (auth)

44003 (BNL-tr–5) SOLUBILITY OF LITHIUM BROMATE AND OF ITS HYDRATES. Communication II. Averko-Antonovich, I. N. Translated for Brookhaven National Lab., Upton, N. Y. from Zh. Obshch. Khim., 13: 272-8(1943). 11p. Dep. mn; CFSTI $1.00 cy, $0.50 mn; JCL $1.60 fs, $0.80 mf.

The solubility of $LiBrO_3$ in water was determined at temperatures from –45 to 143°, the latter being the boiling point of a saturated $LiBrO_3$ solution (84.6%). At room temperature, $LiBrO_3 \cdot H_2O$ crystallizes; above 52°, the anhydrous form is formed. $LiBrO_3 \cdot H_2O$ easily gives up water when heated in an oven, without melting in its water of crystallization. The eutectic point was found to be –47° and 54.5% $LiBrO_3$. Upon cooling, $LiBrO_3$ easily forms viscous supersaturated solutions down to –70°. (D.L.C.)

44004 STUDIES ON METAL COMPLEXES IN AQUEOUS SOLUTION BY INFRARED SPECTROPHOTOMETRY. V. AN INVESTIGATION OF SOME GLYCOLATE COMPLEXES. Larsson, Ragnar (Univ. of Lund, Sweden). Acta Chem. Scand., 19: 783-90(1965).

Infrared spectra in the wave number range from 1400 to 800°K (cm^{-1}) were recorded for aqueous solutions of glycolate ($HOCH_2COO^-$) complexes of the following metal ions: UO_2^{2+}, Cu^{2+}, Ni^{2+}, Co^{2+}, Gd^{3+}, and Nd^{3+}. The extinction coefficients of the C–O stretching vibration of the C–OH group of the different systems were determined. Three types of bonding of the ligand were deduced from these data: pure chelates (Cu^{2+}, first UO_2^{2+} complex); chelates formed via a water molecule bonded to the metal (Ni^{2+}, Co^{2+}, Gd^{3+}, Nd^{3+}, and the second and third UO_2^{2+}-complexes); and the ligand bonded through the carboxylate group only (UO_2^{2+}). For the UO_2^{2+}-system the contribution of the third type was estimated to be about 15% of the total. (auth)

44005 SCANDIUM MANGANESE(III) OXIDE, A COMPOUND ISOTYPIC WITH $LuMnO_3$. Norrestam, Rolf (Univ. of Stockholm). Acta Chem. Scand., 19: 1009-10 (1965).

A new type of structure of ferroelectric ABO_3 compounds was previously reported. B is trivalent manganese and A is the trivalent ion of the set yttrium, holmium, erbium, thulium, ytterbium, and lutetium. The structure is hexagonal and the unit cell parameters are, e.g., for LuMnO, a =

6.042 and c = 11.37 Å. In order to determine if this structure type is stable for even smaller ions, x-ray powder photographs were taken of scandium manganese (III) oxide. The powder pattern could be interpreted assuming a hexagonal unit cell with the unit-cell parameters a = 5.830 ± 0.001 and c = 11.179 ± 0.002 Å. (F.J.H.)

44006 STUDIES ON RARE EARTH 1,3-DIKETONATES. Purushotham, D.; Rao, V. Ramachandra; Rao, Bh. S. V. Raghava. (Andhra Univ., Waltair, India). Anal. Chim. Acta, 33: 182-97(Aug. 1965).

The chelates of various rare earths with acetylacetone, benzoylacetone, dibenzoylmethane, 2-thenoyltrifluoroacetone, and dithenoylmethane were prepared and some of their physical properties noted. The ultraviolet absorption spectra in various nonaqueous solvents were measured. Absorption measurements in the visible region showed alterations in absorption intensities and resolution in some of the principal bands, depending on the solvent. The infrared spectra were measured and compared with literature data. (auth)

44007 STATISTICAL CALCULATION OF THE ^{18}O AND ^{17}O EQUILIBRIUM DISTRIBUTION IN THE SYSTEM CO_2/H_2O AND CO_2/D_2O FROM MOLECULAR SPECTROSCOPIC DATA. Staschewski, Dieter (Kernforschungszentrum, Karlsruhe, Ger.). Ber. Bunsenges. Physik. Chem., 69: 426-40(1965). (In German).

The theoretical relations required in the calculation of molecular constants from spectroscopic data were examined and supplemented, with particular reference to the Fermi resonance of isotopic CO_2 and water molecules. An approximate formula was derived for the isotope effect of the Fermi resonance constants W_{122}, which agreed with experimental results for CO_2 and which was used for the prediction of the vibrational levels of isotopic water molecules. The dependence of the anharmonicity constants on the resonance parameter, due to the common potential constants, can be approximately included and plays a significant role, especially in the evaluation of the D_2O constants. All constants of isotopic water molecules were determined on the basis of a new vibrational analysis of light water vapor. The separation factors calculated by statistical thermodynamics were compared with previously determined experimental values. (auth)

44008 THERMODYNAMIC PROPERTIES OF HEAVY WATER. Lundqvist, Bengt (Chalmers Technische Hochschule, Goteborg); Persson, Torsten. Brennstoff-Waerme-Kraft, 17: 356-62(July 1965). (In German).

Data for the thermodynamic properties of heavy water are assembled. Values determined experimentally exist for the liquid phase. Measured values for the heat of evaporation exist for temperatures below 220°C; several methods of extrapolation for temperatures over 220°C are examined critically. Entropy and enthalpy values for the vapor are calculated from existing formulas for the specific heat of the ideal gas and from data for light water vapor. The law of the corresponding states was used. The calculated values were compared with Russian measured values for the specific volume and the specific heat. The values for the steam phase are presented in an enthalpy/entropy-diagram the exactness of which is estimated. (auth)

44009 NEUTRON DIFFRACTION STUDY OF URANIUM OXYTELLURIDE (UOTe). Marasik, A.; Niemiec, J. (Inst. for Nuclear Research, Swierk, Poland; Technical Univ., Wroclaw, Poland). Bull. Acad. Polon. Sci., Ser. Sci. Chim., 13: 291-6(1965).

Powder samples of uranium oxytelluride were prepared from pure components, U, Te, and UO_2. Neutron diffraction measurements were made using neutron crystal spectrometers. The specimen was placed in a special cryostat and neutron diffraction patterns were obtained for temperatures of 78 and 293°K within the scattering angle (2θ) range from 5 to 30° using a monochromatic neutron beam of 1.12 Å wavelength. The neutron diffraction patterns obtained at room temperature were used for redetermination of the crystallographic structure. The values of the integrated intensities observed are given and discussed. (F.J.H.)

44010 THE ORTHORHOMBIC SULFIDES, SELENIDES, AND TELLURIDES L_2X_3 OF THE RARE EARTHS, YTTRIUM, AND SCANDIUM OF THE Sc_2S_3 TYPE. Flahaut, Jean; Laruelle, Pierre; Pardo, Marie Paule; Guittard, Micheline (Universite, Paris). Bull. Soc. Chim. France, No. 5, 1399-1404(May 1965). (In French).

The crystal structure of the tellurides of Tb, Dy, Ho, Er, Tm, Lu, Y, and Sc, and the selenides of Ho, Er, Tm, Yb, Lu, and Y, and the sulfide of Sc were determined. All the compounds studied had the same crystalline type, orthorhombic, described previously for Sc_2S_3. This structure is a superstructure of a lattice with fcc base of the NaCl type, with cation lacunae. For Sc_2S_3, the selenides of the rare earths from Dy to Lu, and Y_2Se_3, the base lattice was very lightly deformed. For the tellurides of the rare earths from Tb to Lu, Y_2Te_3, and Sc_2Se_3 no deformation was found in this base lattice. (J.S.R.)

44011 STUDY OF THE HYDROLYSIS IN ACID MEDIUM OF LINEAR AND CYCLIC ACIDS. III. HYDROLYSIS OF 4-METHYL-1,3-DIOXANE AND 1,3-DIOXANE IN WATER. SOLVENT ISOTOPIC EFFECT IN HEAVY WATER. Aftalion, Florin; Lumbroso, Daniel; Hellin, Michel; Coussemant, Fernand (Institut Francais du Petrole, Rueil-Malmaison, France). Bull. Soc. Chim. France, No. 7, 1950-7(July 1965). (In French).

The results of the thermochemical and kinetic studies of the hydrolysis equilibrium reactions of 4-methyl-1-3-dioxane and 1,3-dioxane are reported. The kinetic isotopic effects in heavy water, relative to the hydrolysis of 4,4-dimethyl-1,3-dioxane and 1,3-dioxane, were measured. The results indicated that the mechanism of these reactions is identical to that of the hydrolysis of the linear acetals. (tr-auth)

44012 STUDY OF THE IONIC SPECIES OF PROTACTINIUM IN AQUEOUS SOLUTION. IV. HYDROLYSIS AND POLYMERIZATION OF THE PENTAVALENT PROTACTINIUM. Guillaumont, Robert (Universite, Paris). Bull. Soc. Chim. France, No. 7, 2106-12(July 1965). (In French).

The partition at 25°C of Pa^{5+} between aqueous solutions of $HClO_4 - LiClO_4$ with an ionic force of 3 and benzene solutions of thenoyltrifluoroacetone was studied as a function of the concentration in the element for different acidities. The spectrophotometric absorption of aqueous solutions was also studied in the spectral region from 210 to 350 mμ. The effects of aging of the solutions on partition and absorption were examined. In perchloric medium with an ionic force μ = 3 and an acidity of 1 to 3N, the ions $Pa(OH)_3^{2+}$ or $PaO(OH)^{2+}$ were stable and did not polymerize. In the acidity region from 1 to 10^{-3}N, the appearance of monovalent ions of the type $Pa(OH)_4^+$ led to the reversible formation of polymers in freshly prepared solutions. If these solutions were aged, the polymerization became irreversible. (tr-auth)

44013 THE COMPLEXES OF THE URANYL CATION WITH THE o-MERCAPTOBENZOATE COORDINANT. Israeli, Yigal (Julius) (Hebrew Univ., Jerusalem). Bull. Soc. Chim. France, No. 8, 2187-9(Aug. 1965). (In France).

The complexes of the uranyl cation with the o-mercaptobenzoate coordinant(L) were studied. The results showed that the stability constant of the complex $UO_2(L)_2$ is 1.9×10^{11} and the stability constant of the dimer $(UO_2OH)_2(L)_2$ is 1.2×10^{31}. (tr-auth)

44014 THE HYDRATES OF URANYL SULFATE. Leroy, Jean-Marie; Tudo, Joseph; Tridot, Gabriel (Faculte des Sciences, Lille). Compt. Rend., 260: 5802-5(May 31, 1965). (In French).

Uranyl sulfate hydrates are classified into two series, A and B, including respectively, those with 4.3 and 1 H_2O for the series A and those with 3.5, 3, and 1 H_2O for the series B. Each hydrate was studied to determine its range of stability, its vapor pressure, and its x-ray diffraction spectrum. (tr-auth)

44015 UPPER LIMITS OF GLASS FORMATION AND GLASS STRUCTURE IN THE BINARY SYSTEMS $BeO–SiO_2$, $MgO–SiO_2$, $CaO–SiO_2$, $SrO–SiO_2$, AND $BaO–SiO_2$. Marinov, M.; Dimitriev, J. (Chemischtechnologisches Institut, Sofia-Darvenitza, Bulgaria). Compt. Rend. Acad. Bulgare Sci., 17: 929-31(1964). (In German).

The valence number is shown to play a role in the limit of glass formation for oxides of alkaline earth metals. An expression was developed for S, the upper limit in weight % of the modified oxide: S–C(Mm.100)/(Mm + Ms), where Mm is the molecular weight of the modified oxide and Ms that of the vitrifying oxide. The factor C takes into account radius, charge, and coordination number of the ions; several expressions are considered. The simpler is C = (exp (–1/Rm.Km))–1/Nm, where Rm is the ionic radius, Km the coordination number, and Nm the atomic number, all of the modified oxide. Experimental and calculated S for the series are as follows: Be, 4.8%, 6.4%; Mg, 32.8%, 33.4%; Ca, 55.0%, 52.9%; Sr, 58.2%, 58.2%; and Ba, 62.2%, 62.6%. Good agreement was also found with published data. The similarities and differences between these systems and those of the alkali metals are discussed; the latter four alkaline earth glasses must have a chain structure. (BBB)

44016 ON THE CALCULATION OF THE UPPER GLASS FORMATION LIMITS IN THE BINARY SYSTEMS $BeO–GeO_2$, $MgO–GeO_2$, $CaO–GeO_2$, $SrO–GeO_2$, AND $BaO–GeO_2$. Marinov, M.; Dimitriev, J. (Chemischtechnologisches Institut, Sofia-Darvenitza, Bulgaria). Compt. Rend. Acad. Bulgare Sci., 17: 1095-7(1964). (In German).

For a constant vitrifying oxide component, GeO_2, the upper glass formation limit in weight % of the metal oxides, is governed principally by the parameters of the metal ion. Thus these factors appear as a coefficient C in the expression S = CMm.100/(Mm + Ms), where Mm and Ms are the molecular weights of the metal oxide and vitrifying oxide, respectively. The factor C is given by (exp (–1/(RmKm)))–1/Nm, where Rm is the ionic radius, Km the coordination number, and Nm the atomic number of the metal. For the systems $MO–GeO_2$, calculated values and observed values from other investigations were compared. The observed and calculated values for M are as follows: Be, 6.0, 4.4; Mg, 20.30, 19.9; Ca, 29.90, 29.2; Sr, 44.45, 43.6; Ba, 59.40, 59.4. These results supported the general theory developed for glasses of alkaline earths and alkali metals; they also indicated that glasses do not have the same structure, but that there are a series of structures. (BBB)

44017 PARAMAGNETIC RESONANCE OF CERIUM IN SINGLE-CRYSTAL $PbMoO_4$. Kurkin, I. N.; Morozov, A. M.; Shekun, L. Ya. (Kazan State Univ.). Dokl. Akad. Nauk SSSR, 161: 322-3(Mar. 11, 1965). (In Russian).

Results are presented of an investigation of electron paramagnetic resonance of the simplest of the rare-earth ions (Ce^{3+}, $4f^1$, $^2F_{\frac{5}{2}}$) in a single crystal of $PbMoO_4$ (scheelite structure). The measurements were made with a sample drawn from a melt and containing nominally 0.3 mol % of Ce^{3+} and Yb^{3+} each, introduced into the melt in the form of CeO_2 and Yb_2O_3. The excess charge was compensated with a suitable amount of Na_2MoO_4. The magnetic resonance of Ce^{3+} and Yb^{3+} was reliably observed at 4.2K. One intense line belonged to Ce^{3+}, indicating that only one of the doublets is populated at 4.2K. The parallel and perpendicular g-factors were found to be 2.684 ± 0.005 and 1.514 ± 0.015, respectively. This is within 4% of the values obtained if it was assumed that the wave function of the principal doublet was transformed in accordance with the irreducible representation $\Gamma_{7\tau}$. Certain data derived on the quality of the investigated crystals and on the character of their imperfections, based on the EPR results, are summarized. (CFSTI)

44018 GENERAL PURPOSE INSTALLATION FOR THE HANDLING OF PYROPHORIC MATERIALS UNDER AN INERT ATMOSPHERE. Dequidt Alfeiran, E.; Diaz Diaz, J. Energia Nucl. (Madrid), 9: 166-76(May-June 1965). (In Spanish).

Dry cells for the processing of U powder are described. The cells have an atmosphere of argon and nitrogen with only trace impurities of oxygen, hydrogen, gaseous hydrocarbons, and water vapor. A general description is given of the cells, together with a description of the method used for the determination of the leak velocity. The purification system, measurement of impurities, pressure control, and safety systems are also considered. Some of the operations performed in the cells are summarized. (J.S.R.)

44019 INFRARED AND RAMAN SPECTRA AND VALENCE FORCE CONSTANTS OF IODINE OXIDE PENTAFLUORIDE (IOF_5). Smith, D. F. (Oak Ridge Gaseous Diffusion Plant, Tenn.); Begun, G. M. J. Chem. Phys., 43: 2001-6(Sept. 15, 1965). (K-L-6044).

The infrared and Raman spectra of IOF_5 were recorded. The data are tabulated, and assignments made on the basis of an octahedral structure with a fourfold symmetry axis. Valence force constants were calculated. The bond angles are close to 90°, and there is an indication that the equatorial I-F bond lengths are about the same as the axial I-F bond length. (auth)

44020 ELECTRONIC GROUND STATE AND WAVEFUNCTIONS FOR SCANDIUM MONOXIDE. Carlson, K. Douglas (Case Inst. of Tech., Cleveland); Ludena, Eduardo; Moser, Carl. J. Chem. Phys., 43: 2408-15(Oct. 1, 1965).

Approximate wavefunctions for ScO were calculated by the method of Roothaan to establish the ground-state assignment of the molecule. Experimental analysis leads to a $^4\Sigma$ ground state, but this assignment has been questioned. The wavefunctions were calculated with a limited basis in the matrix Hartree–Fock approximation at three internuclear distances about the minimum in the binding-energy curve. Basis functions of Slater type were selected to include effects of distortion and polarization. Preliminary and final calculations at every stage of computation yielded a $^2\Sigma^+$ ground state of configuration which is largely $\sigma^2\pi^4\sigma$. No other states were found to be near degenerate with this in the region of equilibrium separation reported for the experimental $^4\Sigma$ ground state. It was concluded from this and discussions of possible refinements to the present calculations that $^2\Sigma^+$ is the ground state of the molecule. It seems reasonable that the observed band structure can be explained as arising from a $^2\Sigma^+$ ground state with a large hyperfine splitting, possibly owing to the fact that at equilibrium separation ScO is approximately $Sc^{2+}(4s^2S)O^{2-}(^1S)$. Ground-state parameters calculated here are $D_e \geq 6.5$ ev, $r_e = 1.615$ Å, $\omega_e = 1373$ cm^{-1}, compared with the experimental values $D_e = 6.9$ ev, $r_e = 1.668$ Å, $\omega_e = 971.55$ cm^{-1} reported for the apparent $^4\Sigma$ state. (auth)

44021 REACTIONS OF LIQUID SODIUM WITH TRANSITION-METAL OXIDES. PART I. THE DIOXIDES OF MOLYBDENUM, TUNGSTEN, AND URANIUM. Addison, C. C.; Barker, M. G.; Pulham, R. J. J. Chem. Soc., 4483-9(Aug. 1965).

A description is given of products (which often include ternary oxides) formed by reaction of liquid sodium with oxides of transition metals in a range of valency states, and at temperatures up to 600°C. Liquid sodium does not react with uranium dioxide, but reacts with both MoO_2 and WO_2 in a very similar manner at temperatures about 295 and 320°C, respectively, to give the transition metal and an oxide $Na_3M_2O_6$. From the x-ray diffraction patterns the two ternary oxides are indexed on the basis of a hexagonal unit cell, and cell dimensions are recorded. The composition of the ternary oxide of molybdenum was determined by x-ray phase analysis; the mechanism of its formation and its reactions with water and alcohol are discussed. (auth)

44022 ISOTOPIC EFFECTS DURING VOLTAMETRIC OXIDATION WITH VARIABLE CONTROLLED POTENTIAL OF THE PALLADIUM-HYDROGEN MICROELECTRODE IN DEUTERIC ACID SOLUTIONS. Bucur, Romulus V. (Inst. of Atomic Physics, Cluj). J. Electroanal. Chem., 9: 486-7(May-June 1965). (In French).

The voltametric method with linearly variable potential was used to study the isotope effects during the process of anodic oxidation of hydrogen and deuterium dissolved in palladium. The current-time curves obtained had the shape of a bell. The variation of the peak current with the temperature depends essentially on the presence of deuterium and on the nature of the anions. Experimental results on the variation of the peak current with temperature in H_2SO_4, D_2SO_4, H_3PO_4, and D_3PO_4 solutions at 15 to 45° showed clearly that the activation energy is very sensitive to the deuterium concentration of the solution and to the nature of the anion. (J.S.R.)

44023 CATALYTIC ACTIVITY OF PRASEODYMIUM OXIDE IN DEHYDROGENATION AND DEHYDRATION OF ALCOHOLS AND DEHYDROGENATION OF TETRALIN. Tolstopyatova, A. A.; Chuan, Yu-chi; Gorshkova, L. A. (Zelinskii Inst. of Organic Chemistry, Academy of Sciences, USSR). Kinetika i Kataliz, 6: 466-70(May-June 1965). (In Russian).

The dehydrogenating capacity of praseodymium oxides in reactions of ethyl, n-propyl, isobutyl, and isopropyl alcohols was greater than the dehydrating capacity. For the primary alcohols with increased molecular weight the dehydrogenating capacity increased. At the activation energy of the dehydrogenation and dehydration of alcohols and the C, H, and O bonding energy with praseodymium oxide, and alkyl substitution on the α carbon atom is greater than on the β carbon atom. The activation energy for the dehydrogenation of tetralene on praseodymium oxide was found. (tr-auth)

44024 A SULFIDE FLUORIDE OF THE RARE EARTHS. Hahn, H.; Schmid, R. (Landwirtschaftliche Hochschule, Stuttgart). Naturwissenschaften, 52: 475(1965). (In German).

By conversion of the sesquisulfide with the corresponding fluorides at temperatures from 450 to 500°C the compounds LaSF, CeSF, and EuSF were prepared. For the preparation of EuSF a slight excess of sulfur was necessary. The three compounds are isotypes and crystallized as the corresponding oxide halogenides in the PbFCl type, space group D^7_{4h} – P 4-nnm. The x-ray data for the three compounds are tabulated. (J.S.R.)

44025 SPECIFIC CATION SEQUENCE IN THE INTERFUSION EFFECTS IN MEMBRANE KINETICS. Plonka, Andrzej (Technical Univ., Lodz, Poland; Military Academy of Medicine, Lodz, Poland). Nukleonika, 10: 187-8(1965).

Studies previously showed that in a two-compartment system, phase 1-membrane-phase 2, the tracer movement against the concentration gradient of the traced substance exceeds that along with the gradient. The phenomenological origin of this effect was studied. The dependence of coefficients of tracer transfer rate from water into alkali metal chloride solutions as a function of solution concentration is shown. In all cases the coefficients of tracer transfer rate against concentration of alkali metal chlorides reached a constant value at a concentration of 1 to 2 mmoles per liter. (M.C.G.)

44026 ELECTROLYTIC OXIDATION OF CERIUM(III) TO CERIUM(IV). Jankowska, Helena. Przemysl Chem., 44: 235-43(May 1965). (In Polish).

Electrolytic oxidation of cerium (III) to cerium (IV), in ~3 to 6M HNO_3 solutions in the presence of rare earths and in pure solutions of cerous nitrate, was examined. As the anode Pt net was used as cathodes and graphite rods in sintered glass casings were used. The normal redoxy potential, determined in the system Ce (III) to Ce (IV), was +1.27 v, in relation to the saturated calomel electrode. Depending on the concentration of cerium, electrolyses of solutions, carried out at constant current density in the range from 0.48 to 2.54 amp/dm^2, occurred with a current yield of 62 to 56% for 100% cerium oxidation. The energy consumption was between 0.95 and 2.30 erg/g Ce (IV), depending on the current density used. Electrolyses of the same solutions, carried out at a controlled anode potential, occurred with current yield of 90 to 98% for 100% cerium oxidation. Energy consumption was ~0.8 erg/g Ce (IV). (auth)

44027 COMPLEX SALTS WITH 5-NITROBARBITURIC ACID. III. COMPLEXES OF 5-NITROBARBITURIC ACID WITH CERIUM AND PYRIDINE BASES. Poni, Margareta P.; Iorga, Nicolae; Bostan, Marcel; Gabe, Iulian (Inst. of Chemistry, Iasi). Rev. Roumaine Chim., 10: 429-37 (May 1965). (In French).

Complexes of 5-nitrobarbituric acid with Ce and pyridine bases, α-, β-, and γ-picoline, 2,4- and 2,6-lutidine, and 2,4,6-collidine, were synthesized. The range of stability of the complexes was established using thermogravimetric and thermodifferential analyses. From the data obtained in thermogravimetric analyses, the reaction order and the activation energies of the reactions occurring during the thermal treatment were calculated. (tr-auth)

44028 SOME COMPOUNDS OF SAMARIUM, GADOLINIUM, AND ERBIUM WITH VARIOUS ORGANIC ACIDS. Spacu, P.; Antonescu, Elena; Plostinaru, Silvia (Organic Chemistry Research Center, Bucharest). Rev. Roumaine Chim., 10: 507-13(June 1965). (In German).

Nine new compounds of Sm, Gd, and Er with various organic acids (monobasic acids, two derivatives of benzoic acid, and the dibasic mucic acid) were synthesized. The compounds were chemically tested, and determination and separation methods were worked out on the basis of their properties. (tr-auth)

44029 THE COMPOSITION OF HYDRATED URANIUM PEROXIDE. Kobayashi, Ichiro (Inst. of Physical and Chemical Research, Tokyo). Rika Gaku Kenkyusho Hokoku, 37: 349-53(1961). (In Japanese).

Samples of hydrated uranium peroxide precipitated under various conditions were studied by x-ray diffraction, thermogravimetric, and infrared absorption methods. Hydrated uranium peroxide was prepared by the reaction of hydrogen peroxide with an aqueous solution of uranyl salts (nitrate, sulfate, chloride, acetate, and tartrate), followed by removal of water in air. The samples prepared at temperatures below 87°C differed markedly in x-ray diffraction patterns from those obtained at temperatures above 87°C. The difference in pattern depended only on the temperature at which the precipitate was formed, other conditions of formation, such as pH, concentration of uranyl salt, and concentration of hydrogen peroxide, were found to have no effect. Thermogravimetric curves showed that the precipitate formed at 20°C was 4-hydrate while that formed at 95°C was 2-hydrate. Dehydration in uranium peroxide 4-hydrate by adding alcohol or treating in vacuo yielded the 2-hydrate. (BBB)

44030 OPTICAL AND SPECTRAL PROPERTIES OF RARE EARTH OXIDES IN INORGANIC GLASSES. Kan, Fu-hsi; Jeung, Chung-hung; Chai, Ying-shih (Academia Sinica, Peking). Sci. Sinica (Peking), 14: 1159-70(Aug. 1965).

The structural state of various rare earth oxides in silicate glasses are discussed on the basis of investigations on the optical properties of glasses. Absorption spectra of 12 kinds of rare earth ions in glasses were measured and interpreted. With further analyses of the absorption spectra of rare earth-doped glasses, the influence of base glasses on the activated ions was determined and explained in the light of ligand field conception. Luminescent spectra of glasses activated by 10 kinds of rare earth ions were obtained. Experimental results showed that the transition process and transition probability among various energy levels were affected by base glasses. The possible energy-transferring process occurring at the eigen absorption band of base glasses were considered. (auth)

44031 CHANGES IN THE DOMAIN STRUCTURE OF ROCHELLE SALT CRYSTALS EXPOSED TO X RAYS. Romanyuk, N. A.; Zheludev, I. S. (L'vov State Univ.). Soviet Phys.-Cryst. (English Transl.), 9: 738-9(May-June 1965).

Translated from Kristallografiya, 9: 876-8(Nov.-Dec. 1964).

The successive changes occurring in the domain structure of Rochelle salt crystals when exposed to increasing doses of x rays are described. Irradiation of the salt crystals was carried out at about 20°C and the power of the source in the irradiation zone was about 400 R/min. The domain structure was observed by means of a polarizing microscope. The formation of defects in the salt crystals is discussed. (F.J.H.)

44032 CRYSTALLOGRAPHIC AND OPTICAL CHARACTERISTICS OF THE VANADATES OF CERTAIN RARE EARTH ELEMENTS. Glazyrin, M. P.; Ivakin, A. A. (Inst. of Chemistry, Academy of Sciences, USSR). Soviet Phys.-Cryst. (English Transl.), 9: 779-80(May-June 1965). Translated from Kristallografiya, 9: 927-8(Nov.-Dec. 1964).

Optical and crystallographic characteristics of aqueous decavanadates ($Me_2V_{10}O_{18} \cdot 28H_2O$, where Me = La, Ce, Pr, or Nd) were studied. It was established that all of these compounds crystallize in the monoclinic system and that the angular parameters of the crystals are very similar and the optical properties identical. (F.J.H.)

44033 PRELIMINARY CLASSIFICATION IN THE PLUTONIUM I SPECTRUM. Richards, E. W. T.; Ridgeley, A. (Atomic Energy Research Establishment, Harwell, Eng.). Spectrochim. Acta, 21: 1449-66(Sept. 1965).

Some 119 even and 165 odd levels were identified in the Pu(1) spectrum and about 1200 line assignments were made. The lower configurations $5f^67s^2$, $5f^66d7s$ on the even side of the spectrum, and $5f^56d7s^2$ and $5f^56d^27s$ on the odd side are known. Excitation was primarily to the configurations $5f^67s7p$ and $5f^56d7s7p$. Serious differences were noted between the observed and predicted isotope shifts. (auth)

44034 DIFFUSE REFLECTANCE SPECTRA OF SOME URANIUM(IV) COMPLEXES. Gans, P. (London Univ.); Hathaway, B. J.; Smith, B. C. Spectrochim. Acta, 21: 1589-95(Sept. 1965).

The diffuse reflectance spectra (25000 to 4000 cm^{-1}) of some uranium (IV) complexes involving different coordination numbers of the central uranium are reported. The spectra can be divided into three classes on the basis of the band intensities. The "weak" intensity spectra occurred when the coordination number of uranium was six and the environment was centrosymmetrical. The "strong" intensity spectra occurred when the co-ordination number was higher than six and a center of symmetry was absent. The frequencies of the "medium" intensity spectra could be correlated more closely with those of the "strong" than the "weak" intensity spectra. This indicated the absence of a center of symmetry, and it was suggested that "medium" intensity spectra occur when octahedral or cubic symmetry is destroyed by the presence of nonequivalent ligands. The use of the three classes of spectra in predicting the environment of uranium (IV) ions in complexes is discussed. (auth)

44035 CHEMICAL APPLICATIONS OF THE MOESSBAUER EFFECT. PART 2. OXIDATION STATES OF IRON IN CROCIDOLITE AND AMOSITE. Gibb, T. C.; Greenwood, N. N. (Univ. of Newcastle-upon-Tyne, Eng.). Trans. Faraday Soc., 61: 1317-23(July 1965).

Mössbauer spectra of natural, oxidized, and reduced crocidolite and of amosite were obtained. These indicated that the blue color of crocidolite is not due to the rapid oscillation of electrons between ferrous and ferric ions. The changes in quadrupole splitting, which were observed after chemical treatment, were interpreted in terms of changes in site symmetries of the iron nuclei. No evidence was found for oxidation states of iron below 2+. (auth)

44036 ADSORPTION AND DESORPTION OF HYDROGEN ON POLYCRYSTALLINE TUNGSTEN. Ricca, F.; Medana, R.; Saini, G. (Universita, Turin). Trans. Faraday Soc., 61: 1492-1510(July 1965).

Adsorption and desorption processes for hydrogen on a tungsten sheet were studied in a uhv system employing Alpert gages and an omegatron head, all provided with lanthanum hexaboride cathodes and operated, respectively, at 10 and 1 μA, in order to minimize the secondary effects due to the hot cathodes and to the ionizing electron currents. Initial sticking probabilities were measured; they ranged from 0.135 at 77°K to 0.020 at 473°K. Measured adsorbed quantities, referred to the apparent surface area of the tungsten sheet, corresponded to surface concentrations ranging from 11×10^{14} atoms cm^{-2} at 77°K to 2.3×10^{14} atoms cm^{-2} at 473°K; the surface concentration at 298°K was 8.3×10^{14} atoms cm^{-2}. Desorption spectra revealed six different peaks, grouped two by two in the three temperature regions from 77 to 190°K (γ_1 and γ_2), from 190 to 300°K (α_1 and α_2), and from 300 to 600°K (β_1 and β_2). Room temperature chemisorption gave only β_1 and β_2 states: β_2 sites appeared to be practically filled before the β_1 state was significantly populated, while at saturation the ratio between β_1 and β_2 chemisorbed forms was approximately 2 : 1. (auth)

44037 PROTON MOTIONS IN ACID AQUEOUS SOLUTIONS. Stiller, H. (Kernforschungsanlage, Juelich, Ger.; Centre d'Etude de l'Energie Nucleaire, Mol, Belg.). pp 179-89 of STI/PUB/92(Vol.II).

The incoherent scattering function is measured for liquid and solid aqueous solutions of HF and NH_4F in the region $0.8\ Å^{-1} < Q < 1.6\ Å^{-1}$ and $-0.9\ Mev < \hbar\omega < +1.2\ Mev$. Discrete energy transfers, corresponding to frequencies of the order of $2 \times 10^{11}\ sec^{-1}$, are found in all HF solutions and in the solid solution of NH_4F. The results are compared with results obtained with water. The observed transitions are interpreted as fluctuations of protons between equivalent hydrogen bonding sites. (auth)

44038 STUDIES OF THE SOLID AND LIQUID PHASES OF HF, HCl, AND HBr BY SLOW NEUTRON INELASTIC SCATTERING. Boutin, H. (Picatinny Arsenal, Dover, N. J.; Brookhaven National Lab., Upton, N. Y.); Safford, G. J. pp 393-406 of STI/PUB/92(Vol.II).

The liquid and solid phases of HF, HCl, and HBr were studied between 30 and 1200 cm^{-1} using the inelastic scattering of cold neutrons (0.005 ev). These measurements were made in order to examine systematically the influence of an increasing degree of electronegativity and anion size on the low frequency molecular motions in both the solid and liquid phases. HF was studied because it was known from x-ray diffraction data to form long zigzag hydrogen-bonded chains in the solid state. The spectra of neutrons inelastically scattered from the liquid and solid phase of HF emphasize the high degree of association that exists through the liquid phase owing to hydrogen bonding. The data for HF were compared for purposes of interpretation with similar scattering data for HF_2^- and $H_2F_3^-$ ions which have structures similar to those units which comprise the zigzag hydrogen bonded chains in HF. The data were also compared with Raman and infrared measurements on HF_2 ions. These comparisons allowed frequencies characteristic of a single unit to be differentiated from those characteristics of the entire chain and from the low frequency lattice modes. A line observed at 0.067 ev has been associated with the deformation frequency ν_2 of the F-H...F group in solid HF and has been correlated with similar frequencies in $H_2F_3^-$ and HF_2^- ions as a function of the F-F distance. In addition, a broad peak observed at 0.007 ev has been attributed to a rotational motion of the F-H...F unit around the F-F bond. The spectrum of liquid HF is also discussed with respect to these motions. The spectra of liquid HCl (180°K), solid HCl Phases I and III (143 and 85°K respectively), liquid HBr (193°K), and solid HBr Phases I and II (153 and 103°K respectively) are compared with the data for HF. Those spectra show an increasing complexity compared to that of HF. This can be attributed to a weaker degree of association, which is expected from the decreasing electronegativity of the anion. The systematic study of these spectra in the various phases and at various temperatures allows a distinction to be made between the low frequency motions characteristic of the lattice or of a hydrogen-bonded chain and those low fre-

quency motions which involve nearest-neighbor interactions or short-range forces. The results of these measurements are in agreement with previous infrared data and indicate that hydrogen bonding is an influential factor in explaining the spectra of the solid phases of both HCl and HBr. These data are not in agreement, however, with theories that account for the solid phases of these compounds only in terms of simple dipole arrays or in terms of long-range interactions involving the dipole moment of one single unit interacting with an average electric field. (auth)

44039 DYNAMICS OF LIQUIDS AND SOLIDS BY OPTICAL SPECTROSCOPY. Krishnan, R. S. (Indian Inst. of Science, Bangalore, India). pp 537-51 of STI/PUB/92(Vol.II).

When a beam of monochromatic light traverses any medium, be it a liquid or a crystal, a portion of the radiation is scattered. This scattering of light arises from two distinct processes. One is the thermal scattering of light and the other is Raman effect. The former involves an interaction of the radiation with the optical stratifications in the medium associated with the thermally excited phonons of the acoustic type. The latter arises from an interaction of the vibrations of the atoms and molecules of the medium with the radiation, and is therefore closely linked with its optical vibration spectrum. The theory of thermal scattering by Brillouin ascribes the diffusion of light to the equispaced time-periodic stratifications of density in the medium characteristic of acoustic waves and evisages a Doppler shift of frequency. The experimental observation of well-defined Doppler components in the interferograms of light scattered by liquids and amorphous solids is therefore of fundamental importance in understanding the mechanism of light scattering and the structure of liquids. The presence of such fine structure in the scattered light of liquids was established experimentally. An important outcome of this result is the observation of a strong dependence of the intensity of the central component, the continuum, and the Brillouin components on the viscosity of the medium and the inadequacy of Landau-Placzek theory. The Brillouin components are for fused silica. A precise study of the second-order Raman spectra of alkali halides has significance in view of the conflicting theories of vibration spectra of crystals due to Raman and Born. Hence, with the Rasetti technique, a systematic investigation is carried out of the Raman spectra of alkali halides and other simple crystals, such as diamond and alumina. The available data on the spectra of these crystals cannot be fully explained by the Raman theory, based on the atomistic standpoint and according to which the observed spectrum is due to the finite number of allowed combinations and overtones of the discrete vibrations of the supercell. On the other hand, the occurrence of only a finite and relatively sharp maxima in the Raman spectra of alkali halides, which cannot be explained if the frequency distribution in each branch has only broad maxima in the Born's picture, has led to the concept of the critical points by Van Hove and their activity in optical processes has been worked out by Birman and Loudon. The experimental results in the case of the alkali halides are discussed in the light of these theories and the Lyddane-Sachs-Teller relation. (auth)

44040 CATION-EXCHANGE EQUILIBRIA WITH FUSED SALTS. Freiling, E. C. (Naval Radiological Defense Lab., San Francisco). Vienna, International Atomic Energy Agency, 1965, Preprint No. SM-66/86, 31p. (CONF-650704-29). ORINS.

From IAEA Symposium on Thermodynamics, Vienna.

Solute distributions of alkali metal, alkaline earth, rare earth, transition metal, and actinide ions were studied in fused salt cation exchanger systems. The fused salts employed were alkali halides and nitrates. The cation exchangers used were natural zeolite, synthetic zeolite, high-porosity glasses, and molten oxide mixtures. The molten exchangers were composed of Na_2O and B_2O_3 in various proportions. The relative quantities not only determined the exchanger capacity and electrolyte penetration but also produced distribution coefficients for a given solute, which varied over several orders of magnitude. Moreover, they produced marked reversals in the selectivity series. Studies on anion distributions, miscibility diagrams, vapor pressures, and diffusion rates in these systems elucidated the mechanisms involved and the relation of selectivity to solute properties, system thermodynamics, exchanger structure, and available functional groups. In the region of high Na_2O composition, the distribution coefficients for mono-, di-, and trivalent cations in NaCl not only had the same order of selectivity found in Dowex 50-HCl systems but also similar values for the distribution coefficients. The results are summarized qualitatively and compared to behavior in aqueous systems. (auth)

44041 CHEMICAL REACTIONS DURING RAPID QUENCHING OF O_2-N_2 MIXTURES FROM VERY HIGH TEMPERATURES. Ammann, P. R.; Timmins, R. S. (Avco Corp., Wilmington, Mass.). 26p. (CONF-650444-4). Gmelin, AED-CONF-65-119-4.

From Western States Combustion Inst., 1965 Spring Meeting, Hollywood, Calif.

A model was developed to study chemical reactions that occur in O_2-N_2 mixtures during very rapid cooling in small diameter tubes. The system considers both homogeneous gas phase reactions and surface reactions based upon a simplified mass transfer mechanism. Using an energy balance to determine the rate of quenching, the mole fractions of N_2, O_2, NO, N, and O were calculated as a function of temperature. Air and an equimolal O_2-N_2 mixture were cooled from temperatures which ranged between 3000 and 7300°. The calculations showed that when the gases were cooled at rates exceeding ten million degrees per second, the species did not follow a chemical equilibrium path during the quenching process. In cooling from 4000 to 7000°K, the data show that consideration of surface reactions predicts greater NO yields in the quenched gas than for homogeneous reactions alone. In fact, by comparison with experimental data, the heterogeneous reactions must contribute to the overall chemistry of quenching air. The composition of the quenched gas is strongly dependent upon the temperature-time history of the gas in the probe, and upon the composition of the hot gas before it is quenched. Above 3500°K, the reaction chemistry is influenced strongly by the so-called shuttle reactions. (auth)

44042 METHODS AND APPARATUS IN WHICH A MASS OF SOLID MATERIAL IS SUBJECTED TO TWO SUCCESSIVE TREATMENTS BY GASES. Delange, Maurice; Huet, Henri; Vertes, Paul (to Commissariat a l'Energie Atomique). U. S. Patent 3,198,598. Aug. 3, 1965. Priority date Nov. 5, 1957, France.

A method of preparing uranium fluoride from uranium oxides, UO_3 and U_3O_8, includes continuously feeding the pellets of uranium oxide into a vertical reduction zone having a base of reduced diameter and being heated to 600 to 700°C. A stream of reducing gas is passed upward through the reduction zone in countercurrent to the downward movement of the pellets. A vertical fluorination zone is provided below the reduction zone, and the pellets of uranium oxide obtained from the reduction zone continuously pass into the fluorination zone that is heated to a temperature of 400 to 500°C. Hydrofluoric acid vapor is passed upward through the fluorination zone in countercurrent to the movement of the uranium oxide pellets, and the uranium fluoride pellets are recovered from the bottom of the fluorination zone. A blanket of nitrogen between the reduction and fluorination zones is maintained at a pressure higher than the pressure of the gases in the two zones so as to prevent the energy of the reduction gas into the fluorination zone or the fluorination gas into the reduction zone. The method and apparatus are applicable to other solid-gas two step reactions. (B.L.M.)

44043 MIXED ANTIMONY OXIDE-URANIUM OXIDE OXIDATION CATALYST. Callahan, James L.; Gertisser,

Berthold (to Standard Oil Co.). U. S. Patent 3,198,750. Aug. 3, 1965. Filed Dec. 26, 1962.

An oxidation catalyst consisting essentially of oxides of Sb and U is useful not only in the oxidation of olefins to oxygenated hydrocarbons, such as unsaturated aldehydes and acids, but also in the catalytic oxidative dehydrogenation of olefins to diolefins. The nature of the chemical compounds composing the catalyst is not known, and the proportions of Sb and U in the catalyst can vary widely. The Sb: U atomic ratio can range from 1: 50 to 99: 1; however, optimum activity is obtained at ratios of 1: 1 to 25: 1. The catalyst may be employed without support or combined with any of the known support materials. The catalyst is prepared by heating and drying a mixture of the oxides, and then heating the mixture to a temperature of from 500 to 1150°F for from 2 to 24 hr. (B.L.M.)

Organic Chemistry

44044 (AECL-2218) THE PYROLYSIS OF THE POTENTIAL POWER REACTOR COOLANT, SANTOWAX O-M. Mackintosh, W. D.; Miller, O. A. (Atomic Energy of Canada Ltd., Chalk River (Ontario). Chalk River Nuclear Labs.). June 1965. 23p. Dep.; $1.50.

Work was conducted to demonstrate the suitability of unirradiated Santowax O-M (a mixture of biphenyl and terphenyl) in respect to thermal stability and to aid in the study of the part played by pyrolysis in the degradation of the material by radiation at high temperatures. The effect of some impurities was also investigated, and for comparison with other work pure ortho- and meta-terphenyl were pyrolyzed. It was concluded that when the commercially produced material Santowax O-M is thermally degraded the disappearance of the components and the production of high molecular weight products exhibit first order kinetics while gas evolution is zero order. The activation energies for all these processes are essentially identical, viz. 60 kcal/mole. It was also demonstrated that the disappearance rate for the ortho-isomer is twice that of the meta-. The presence of chlorine increases the rate for ortho- by 15% but the meta-isomer is not affected. Adding 1% HB40(Santowax R 40% hydrogenated) to the mixture increases the disappearance rates of both isomers by 25%, and 10% HB40 almost doubles the rates. (auth)

44045 (JEN-151-DQ/I-52) DETERMINACION DE MASAS MOLECULARES MEDIAS EN REFRIGERANTES NUCLEARES ORGANICOS. I. CRIOSCOPIA DE DISOLUCIONES BENCENICAS. (Determination of Average Molecular Weights of Organic Reactor Coolants. I. Freezing-Point Depression Method for Benzene Solutions). Carreira, M. (Junta de Energia Nuclear, Madrid (Spain). Division de Quimica). 1965. 8p. Dep. mn.

As a working method for determination of changes in molecular mass that may occur by irradiation (pyrolytic-radiolytic decomposition) of polyphenyl reactor coolants, a cryoscopic technique was developed which combined the basic simplicity of Beckmann's method with some experimental refinements taken from the equilibrium methods. A total of 18 runs was made on samples of naphthalene, biphenyl, and the commercial mixtures OM-2 (Progil) and Santowax-R (Monsanto), with an average deviation from the theoretical molecular mass of 0.6%. The average standard deviation (external consistency) is about 0.75%. (auth)

44046 (JEN-152-DQ/I-53) DETERMINACION DE MASAS MOLECULARES MEDIAS EN REFRIGERANTES NUCLEARES ORGANICOS. II. CRIOSCOPIA DE DISOLUCIONES EN ETER DIFENILICO. (Determination of Average Molecular Weights of Organic Reactor Coolants. II. Freezing-Point Depression Method for Diphenyl-Ether Solutions). Carreira, M. (Junta de Energia Nuclear, Madrid (Spain). Division de Quimica). 1965. 13p. Dep. mn.

In order to reduce limitations of solubility, the cryoscopic method developed for benzene solutions of polyphenyl mixtures was extended to diphenyl-ether solutions by introducing some modifications imposed by the physico-chemical properties of this solvent. The Nernsto theory of Beckmann's method was revised, taking into account the heat-transfer characteristics of the system, and the results of that analysis were used to determine the design parameters of a cryoscopic apparatus for measurements on diphenyl-ether solutions. The freezing-point depression constant of diphenyl ether was determined from measurements on three molecular-mass standards: naphthalene (M = 128.16), 1,3-diphenyl-1,3-propanedione (M = 234.26), and tri-n-octylphosphine oxide (M = 380.65). The weighted average value from 20 runs is: K = (7.34 ± 0.05)°C molal. Molecular-mass determinations were carried out on samples of pure o-terphenyl and the commercial mixtures "Progil OMP" and "Santowax OMP," the average deviation of 18 runs from the theoretical values being about 0.7%. The average standard deviation (external consistency) is about 1.3%. (auth)

44047 (NP-15268) SINTESIS DE AMINOACIDOS MARCADOS. II. SINTESIS DE DL GLICINA 1C14 Y DL ALANINA-1C14. Informe No. 142. (Synthesis of Labelled Amino Acids. II. Synthesis of DL Glycine-1-C-14 and DL Alanine-1-C-14. Report No. 142.) Buehler, Mauricio F.; Mitta, Aldo E. A.; de Lezerovich, Juana B. (Comision Nacional de Energia Atomica, Buenos Aires (Argentina)). 1965. 6p. Dep. mn.

The synthesis of glycine and alanine labelled with ^{14}C in the carboxyl group is described. Both acids are prepared by the aminolysis of the corresponding α-bromo acid. The synthesis of the intermediate compound is described. Particular emphasis is given to the problems relative to the purification of the amino acids in order to produce radiochemically pure products. Chromatographic and autoradiographic methods as well as radiation calibrations are used to insure product purity. (J.S.R.)

44048 (TID-21309) PENTAMETHYLDISILANE AND 1,1,2,2-TETRAMETHYLDISILANE, AND THEIR ADDITION TO OLEFINS. Urenovitch, Joseph V.; West, Robert (Wisconsin Univ., Madison. Dept. of Chemistry). [1964]. Contract AT(11-1)-1164. 18p. Dep. mn; CFSTI $1.00 cy, $0.50 mn.

The compounds pentamethyldisilane and 1,1,2,2-tetramethyldisilane were prepared and characterized. Pentamethyldisilane adds to 1-octene and methylcyclohexene in the presence of peroxides or ultraviolet light in the normal way to give high yields of alkylpentamethyldisilanes. 1,1,2,2-tetramethyldisilane also adds to 1-octene in the presence of peroxides to give the normal 1:1 addition product and a mixture of telomers. Chloroplatinic acid-catalyzed reaction of pentamethyldisilane with olefins resulted in much cleavage of the Si–Si bond and yielded only traces of the expected addition product. (auth)

44049 ISOTROPIC ^{17}O COUPLING CONSTANT IN THE NITROBENZENE ANION RADICAL. Gulick, Wilson M. Jr.; Geske, David H. (Cornell Univ., Ithaca, N. Y.). J. Am. Chem. Soc., 87: 4049-52(Sept. 20, 1965).

Synthesis of ^{17}O-nitrobenzene was accomplished from benzene and nitrogen dioxide enriched in ^{17}O. It was thus possible to measure the ^{17}O isotropic coupling constant, a_0, in the nitrobenzene anion radical. In acetonitrile a_0 was 8.86 gauss; in dimethylformamide a_0 increased from 8.84 to 8.99 gauss as the water content was increased from 0 to 10%. These results were compared to earlier molecular orbital calculations of nitrogen and oxygen spin densities, ρ_N^π and ρ_O^π. The possibility is considered that a_0 may be described in terms of the equation $a_0 = Q_{1O}\rho_O^\pi + Q_{2\rho N}\rho_N^\pi$. (auth)

44050 STUDY OF THE LOW-FREQUENCY MOLECULAR MOTIONS IN POLYETHYLENE AND THE N-PARAFFINS BY SLOW NEUTRON INELASTIC SCATTERING. Boutin, H. (Picatinny Arsenal, Dover, N. J.); Prask, H.; Trevino, S. F.; Danner, H. pp 407-19 of STI/PUB/92 (Vol.II).

The time-of-flight spectra of slow neutrons inelastically

scattered from samples of highly crystalline polyethylene at room temperature have been measured. A comparison has been made between the observed structure in the spectra and calculations of intra- and intermolecular motions of crystalline polyethylene. With the exception of a peak at 300 cm^{-1}, all of the structure is accounted for in this manner. The possible origin of this peak is also discussed. The time-of-flight spectra of slow neutrons scattered from samples of solid butane, pentane, hexane and heptane were also obtained. Tentative identification of the observed frequencies on the basis of a normal mode calculation of intramolecular vibrations is made. In addition, a simple explanation for the behavior of the melting temperature as a function of chain length is proposed. (auth)

Radiation Chemistry

See also BIOLOGY AND MEDICINE — Radiation Effects.

Refer also to abstracts 43878 and 45679.

44051 (AE-192) RADIOLYSIS OF AQUEOUS BENZENE SOLUTIONS IN THE PRESENCE OF INORGANIC OXIDES. Christensen, Hilbert C. (Aktiebolaget Atomenergi, Stockholm (Sweden)). July 1965. 15p. Dep. mn.

Aqueous 0.1 N alkaline solutions of benzene were irradiated with ^{60}Co γ rays in the presence of various inorganic oxides. The addition to the solution of silica gel, copper(II) oxide, and chromium(III) oxide did not increase the yield of phenol. When chromium(III) oxide gel, zinc oxide, or titanium dioxide were added, a 9–13 percent increase was obtained, and the addition of uranium dioxide and thorium dioxide caused a 31 and 39 percent increase, respectively. The increase of the phenol yield was related to the energy absorbed by the solid, and G_{ox} values defined in this way were calculated as follows: $G_{ZnO} = 4.0$; $G_{TiO_2} = 3.7$; $G_{UO_2} = 6.4$, and $G_{ThO_2} = 8.0$. The specific surface areas of the oxides were determined and the possibility that the increase of the phenol yield may be dependent on this quantity is discussed. (auth)

44052 (AE-193) RADIOLYSIS OF AQUEOUS BENZENE SOLUTIONS AT HIGHER TEMPERATURES. Christensen, Hilbert C. (Aktiebolaget Atomenergi, Stockholm (Sweden)). July 1965. 15p. Dep. mn.

Aqueous solutions of benzene were irradiated with ^{60}Co γ rays with doses of up to 2.3 Mrad in the temperature region 100–200°C. At 100°C a linear relationship between the phenol concentration and the absorbed dose was obtained, but at 150°C and at higher temperatures, the rate of the phenol formation increased significantly after an initial constant period. With higher doses, the rate decreased again, falling almost to zero at 200°C after a dose of 2.2 Mrad. The G value of phenol in the initial linear period increased from 2.8 at 100°C to 8.0 at 200°C. The reaction mechanism is discussed and reactions constituting a chain reaction are suggested. The result of the addition of iron ions and of a few inorganic oxides to the system is presented and briefly discussed. (auth)

44053 (AFML-TR-65-166) RESEARCH ON ORGANIC RADIATION CHEMISTRY. Swan, G. A.; Allan, L. T. (Newcastle-upon-Tyne Univ. (England)). Jan. 1965. 46p. CFSTI.

The report is divided into four parts. Part I is a gas chromatographic study of the radiolyses products of diethylamine, triethylamine, n-butylamine, and 1-methylpiperidine. Part II is a discussion of the extent of the γ-radiation-induced addition of tertiary amines to alkenes. Part III deals with the photolysis of diethylamine and triethylamine. Part IV discusses the irradiation of o-bromoaniline. (auth)

44054 (COO-1365-7) RADIOLYSIS STUDIES OF FLUOROCARBONS AND ON REACTIVE INTERMEDIATES. Technical Progress Report, October 15, 1964–July 31, 1965. Kevan, Larry (Chicago Univ., Ill. Dept. of Chemistry). Aug. 13, 1965. Contract AT(11-1)-1365. 31p. Dep. mn; CFSTI $2,00 cy, $0.50 mn.

Experimental results are presented on the SO_2 yields and organic products formed by γ-radiolysis of diparatolyl sulfone, diphenyl sulfone, and dibenzthiophene sulfone. A large number of oxyanions was examined for their ability to trap hydrogen atoms in gamma-irradiated frozen solutions at 77°K; effects of added electron scavenger and optical bleaching were also studied. Evidence was found for the following hydrogen atoms precursors: $H_2PO_4^-$, HSO_4^-, and ClO_4^-. Energy transfer in the γ-radiolysis of rare gas–C_2F_6 mixtures was studied, and a recombination energy-transfer efficiency correlation was found. (D.L.C.)

44055 (IAE-788) K VOPROSU O RADIATSIONNOI USTOICHIVOSTI IONOOBMENNYKH SMOL. SOOBSHCHENIE II. O RADIATSIONNOM POVREZHDENII NEKOTORYKH POLIMERIZATSIONNYKH ANIONITOV. (Problem of Radiation Stability of Ion Exchange Resins. II. Radiation Damage to Certain Polymerization Anionites). Novikov, P. D. (Institut Atomnoi Energii, Gosudarstvennyi Komitet po Ispol'zovaniyu Atomnoi Energii SSSR, Moscow). 1964. 36p. Dep. mn.

Comparative data are presented on the radiation stability of strongly basic anion resins of polymerization type AV-19, AV-21, and AV-27, differing in the chemical structure of the three-dimensional form and of the functional groups. It is shown that the anion resin AV-21 has a large radiation stability based on the acenaphthylene and divinylbenzene copolymer. Results of studies of the nature of water-soluble products of radiolysis of the above anion resins and the anion resin AV-17 are also presented. (tr-auth)

44056 (INR-579/XVII/C) RADIOLITYCZNE REAKCJE UTLENIANIA I REDUKCJI JONOW ZELAZA W ROZTWORACH WODNYCH ZAWIERAJACYCH ZWIAZKI ORGANICZNE. BEZPOSREDNIE OBSERWACJE W STALYM POLU PROMIENIOWANIA GAMMA. (The Radiation Induced Reactions of the Oxidation and Reduction of the Iron Ions in the Aqueous Solutions Containing the Organic Substances. Direct Observations in the Constant Gamma-Field). Broszkiewicz, Roman (Institute of Nuclear Research, Warsaw (Poland)). 1964. 91p. Dep. mn.

The effect of the quality and concentration of an organic compound and of the concentration of the iron ions and sulphuric acid on the course of the radiation-induced reactions proceeding in the non-deoxygenated aqueous solutions was investigated. The observations were done with the method of continuous measurements in a constant gamma field. Analysis of results was done and conclusions on the mechanism of the proceeding processes are proposed. (auth)

44057 (IS-T-23) RECOIL CHEMISTRY OF ^{11}C IN LIQUID HYDROCARBONS (thesis). Clark, Donald Eldon (Ames Lab., Iowa State Univ. of Science and Tech.). July 1965. Contract W-7405-eng-82. 97p. Dep. mn; CFSTI $3.00 cy, $0.75 mn.

The chemical behavior of recoil carbon-11 atoms in various C_5-C_7 hydrocarbons was investigated. The recoil atoms were produced by the $^{12}C(\gamma,n)^{11}C$ reaction with the bremsstrahlung beam of an electron synchrotron. Standard gas chromatographic methods coupled with scintillation flow counting techniques were used for radioassay of the labeled products. This study was principally concerned with the product yields of ethane, ethylene, and acetylene from the different target compounds, although methane yields were also determined in all cases. The initial phase of the investigation established the effects of iodine as a radical scavenger and radiation dose on the product yields. Iodine affected the yields of all of the volatile products except for acetylene. Radiation dose had the effect of changing the yields; the changes appeared to be primarily due to radiolytically produced hydrogen which was able to reduce some of the labeled species. When irradiation times of about five minutes or less were used, the results were

approximately the same as would have been obtained for the idealized "zero dose" case. The two-carbon product yields, as well as the $(C_2H_6 + C_2H_4)/C_2$ ratios, were shown to be dependent upon the structure of the target molecules. These results are discussed in terms of the decomposition modes available to the assumed activated complexes resulting from insertion-type reactions of three primary species ^{11}C, ^{11}CH, and $^{11}CH_2$. Mixtures of benzene and methylcyclopentane were irradiated and the yields of volatile products were determined. Within experimental error, the yields were shown to be strictly dependent upon the molar concentrations of the two components. This was interpreted as being an indication that the reaction cross sections for equivalent labeled species with the two different molecules have similar energy dependences. This study appears to confirm that three neutral species, ^{11}C, ^{11}CH, and $^{11}CH_2$, are responsible for the products formed in these systems. The reactions by which the products are formed seem to proceed via mechanisms involving the insertion of these three recoil fragments into C–H and C=C bonds of the parent compounds. (auth)

44058 (LFEN-23) RADIOLISE DA AGUA PURA POR PROTOES DE 1 A 2 MEV. II. FEIXE PULSADO DE 1.57 MEV. (Radiolysis of H_2O by 1 to 2 Mev Protons. II. Production by Pulsed 1.57 Mev Protons). Namorado Rosa, Rui (Laboratorio de Fisica e Engenharia Nucleares, Junta de Energia Nuclear, Sacavem (Portugal)). 1964. 13p. Dep. mn.

The yield of H_2O_2 production by a pulsed 1.57 Mev proton beam is measured in pure aerated water. The pulses are 3.5, 6, 13, and 25 μ sec in width, whereas the dose per pulse lies in the range of 1.5 to 11×10^{17} ev/cm^3. The repetition frequence lies in the range of 250 to 3800 pulses per second. Conclusions are drawn concerning the decay time of molecular products in the interaction zone radiation-water, and the H_2O_2 yield per pulse. (auth)

44059 (NYO–2949–1) A STUDY OF LIQUIDS UNDER OPTICAL AND IONIZING EXCITATION WITH EMPHASIS ON EXCITATION IN THE VACUUM ULTRAVIOLET. Final Report. Weinreb, A. (Division of Biology and Medicine (AEC), Washington, D. C.). [1965]. Contract AT(30-1)-2949. 25p. Dep. mn; CFSTI $1.00 cy, $0.50 mn.

Research on the absorption and luminescence properties of organic systems is described briefly. Work done in the visible and near uv regions is outlined. Extreme vacuum uv was found to produce current oscillations in polystyrene, and experiments were conducted which showed that the currents occurred in the bulk. The effects of guardrings, fields, pressure, and alcohol vapor on the current oscillations were studied. (D.L.C.)

44060 (UCRL-16353) SOME ASPECTS OF THE PHOTOCHEMISTRY AND RADIATION CHEMISTRY OF THYMINE (thesis). Newmark, Joan F. (Lawrence Radiation Lab., Univ. of California, Berkeley). Aug. 23, 1965. Contract W-7405-eng-48. 94p. Dep. mn; CFSTI $3.00 cy, $0.75 mn.

Three problems in the radiation chemistry of thymine were investigated in this work: (1) The mechanism of photodimerization by uv in frozen aqueous solution, (2) the mechanism of energy transfer that might effect the visible light reversal of dimerization, and (3) the sensitivity of thymine to γ radiation as affected by its physical state (solid, solution, frozen solution) and by the presence of ethanol in aqueous deaerated solution. Since dimerization takes place very much more efficiently in ice than in aqueous solution, the role of ice was tested by irradiating slowly and quickly frozen solutions, dry films, and hexane suspensions. Thymine-^{14}C was used in all these experiments, and the products were separated by paper chromatography. The effect of oxygen on the rate of dimer formation in ice was also studied. Results of these experiments and those performed elsewhere suggest that upon freezing, local concentrations of the solute are formed, perhaps in the form of the known monohydrate crystal lattice, which facilitate dimerization. The ice matrix also effectively disperses the local concentrations of solute, allowing more light penetration than possible in thin films. The lack of an observable oxygen effect upon dimerization in ice is probably the result of slow diffusion of the oxygen through the ice lattice, rather than absence of a triplet, diradical intermediate. A model for the phenomenon of photoreactivation, which in some cases has been connected with reversal of thymine dimerization in DNA by the action of visible light, was tested. Acridine orange (AO), a dye which binds to DNA and absorbs in the visible, was used as a model chromophore. The fluorescence yield from AO when irradiated in the visible was increased by the presence of thymine and thymine dimer, indicating formation of a loose complex. However, no reversal of thymine dimer back to the original thymine was observed by irradiation of AO plus the dimer in the visible, either in liquid aerated or deaerated, frozen solution. Thymine is much less resistant to decomposition by ionizing radiation (in liquid solution) than as a dry solid or in frozen aqueous solution. A small concentration of ethanol increases the rate of decomposition of thymine in aqueous, deaerated solution by adding across the 5,6-double bond to form 6-(α-hydroxyethyl)-5,6-dihydrothymine (cis and trans) in yields up to 75%. The isomers were isolated in milligram amounts using silica gel columns and analyzed by standard techniques. Similar adducts are formed in even higher yield when 1,3-dimethylthymine is irradiated. Preliminary experiments with combinations of various alcohols and dihydroxypyrimidines suggest that the reaction is a general one, involving abstraction by the radicals formed by the action of ionizing radiation on water of an α-hydrogen of ethanol. The α-hydroxyethyl radical adds to the electron-deficient 6-position of the dihydroxypyrimidine. The resulting tertiary radical then abstracts a proton from another molecule of alcohol to complete saturation of the double bond. (auth)

44061 (AEC-tr-6567) FLOW METHOD OF IRRADIATION WITH IONIZING RAYS. Zimin, A. V.; Frolov, F. Y. Translated from Tr. Nauchn. Issled. Fiz.-Khim. Inst., [No. 3], 130-3(1963). 8p. Dep. mn; CFSTI $1.00 cy, $0.50 mn; JCL $1.10 fs, $0.80 mf.

A unit for the irradiation of a material in flow comprises an evaporator, condenser, irradiation container, and a flow-measuring device. In the irradiation process, the condensed vapors are allowed to fall from the condenser into the irradiation container and thence into the evaporator. Calculations of the maximum allowable concentration of radiolysis product in the irradiation zone are made for the following radiolyses: $2H_2O \rightarrow H_2O_2$, $2CCl_4 \rightarrow C_2Cl_6 + Cl_2$, $C_6H_6 + CCl_4 \rightarrow C_6H_5CCl_3 + HCl$, and $C_6H_6 + C_2F_3Cl_3 \rightarrow C_6H_5C_2F_3Cl_2 + HCl$. Another unit using a bellows compressor is also described. (D.L.C.)

44062 SYNTHESIS AND PROPERTIES OF NICOTINAMIDE-ADENINE-N^1-OXIDE-DINUCLEOTIDE. Goehring, I.; Wacker, Adolf; Pfleiderer, G. (Institut fuer Therapeutische Biochemie der Universitaet, Frankfurt a.M., Ger.). Biochem. Z., 339: 514-20(June 16, 1964). (In German).

Solutions of nicotinamide adenine dinucleotide in concentrations of 0.5 and 2.5 mg/ml were x irradiated with doses that varied between 500 and 2000 kR. Decomposition of this compound was measured as a function of the irradiation dose by its extinction at 260 mμ. The formation of nicotinamide-adenine-N^1-oxide-dinucleotide was measured by its absorption maximum at 232 mμ. With a dose of 500 kR adenosine-5^1-monophosphate-N-oxide and some adenine-N^1-oxide was formed in the 0.5 mg/ml solutions of nicotinamide adenine dinucleotide. At higher concentrations, 1500 kR was necessary to obtain any significant oxidation effects. Chemical studies indicate that it is unlikely that radiochemically produced peroxides can oxidize nicotinamide adenine dinucleotide to the N^1-oxide at the cellular level. The fact that the nicotinamide adenine dinucleotide levels of animal cells are reduced after irradiation does not necessarily indicate formation of the N^1-oxide. In this instance it is more important that the oxide, if it produced at all, has almost the same enzymatic activity of the parent compound. (BBB)

44063 EFFECT OF NUCLEAR-RADIATIONS ON CELLULOSIC FIBRES. Gupta, A. B. Bombay Technologist, 15: 63-8(1965).

A review is presented on improvements in cellulosic fiber properties by irradiations. Molecular and structural properties, chemical properties, and mechanism are discussed. The use of additives and graft polymerization are briefly discussed. (P.C.H.)

44064 EFFECT OF γ RAYS ON PYRIMIDINE BASES IN AQUEOUS SOLUTION. I. DIHYDROURACIL. Vincendon, Guy; Cier, Andre; Nofre, Claude (Centre du Recherches du Service de Sante des Armees, Lyon). Bull. Soc. Chim. France, No. 7, 1997-2000(July 1965). (In French).

The products formed by γ irradiation of dihydrouracil in aqueous solution in the presence of air or nitrogen atmosphere made it possible to show that the attack by homolytic substitution is made essentially on the sixth position of the pyrimidine nucleus. (tr-auth)

44065 ADDITION REACTIONS INITIATED UNDER RADIATION. II. ADDITION OF CARBON TETRABROMIDE ON ALKENES. Rabilloud, Guy (Centre d'Etudes Nucleaires, Grenoble, France). Bull. Soc. Chim. France, No. 8, 2149-52(Aug. 1965). (In French).

The irradiation of an ethylene hydrocarbon solution in a mixture of carbon tetrachloride and carbon tetrabromide by ^{60}Co γ radiation led to the addition of carbon tetrabromide to the ethylene double bond. The speed of the addition reaction was closely connected to the structure of alkene. (tr-auth)

44066 ADDITION REACTIONS INITIATED UNDER RADIATION. III. ADDITION OF SILANES ON ALKENES. Rabilloud, Guy (Centre d'Etudes Nucleaires, Grenoble, France). Bull. Soc. Chim. France, No. 8, 2152-8(Aug. 1965). (In French).

The radiolysis of silicon hydrides and the further addition of radiolysis fragments to the carbon–carbon double bond of an ethylene hydrocarbon was studied. This addition reaction is a chain reaction that leads to alkyl silanes with a very good yield and high selectivity. (tr-auth)

44067 A L.E.T. INDEPENDENT DOSIMETER BASED ON THE CHEMILUMINESCENT DETERMINATION OF H_2O_2. Armstrong, W. A.; Humphreys, W. G. (Dept. of National Defence, Ottawa). Can. J. Chem., 43: 2576-84(Sept. 1965).

A sensitive method for the determination of H_2O_2 based on the copper-catalyzed chemi-luminescent reaction between luminol and H_2O_2 was developed. The integral luminescence measured with a modified spectrophotofluorometer was found to increase linearly with concentration for 3×10^{-9} to 1.5×10^{-5} M H_2O_2 solutions. This method was applied to the determination of H_2O_2 formed in irradiated water and it was found that this system may be used as a dosimeter in the range 30 to 3000 rads. The following values were obtained for the initial H_2O_2 yields: $G(H_2O_2) = 1.22 \pm 0.07$ for ^{60}Co γ radiation, 1.28 ± 0.09 for 250 kvcp (105 kev effective) x radiation, and 1.31 ± 0.04 for 14 Mev neutrons. These results and those of others demonstrate that the initial yield of H_2O_2 in aerated water increases only by about 15% for an increase in radiation LET of 0.02 to 14 ev/Å. (auth)

44068 RADIOCHEMICAL DEPARTMENT AT THE CZECHOSLOVAK NUCLEAR RESEARCH INSTITUTE. Holub, Frantisek. Czech. Heavy Ind., No. 3, 2-8(1964).

The radiochemical department unites various laboratories for chemical and physico-chemical research and working rooms for handling radioactive materials. The equipment and operating procedures are described. The transport system is shown in diagrams. (M.C.G.)

44069 THERMOELECTRON IRRADIATION OF POLYETHYLENE FILMS. Sakae, Takao; Toriyama, Yotsuo (Musashi Inst. of Tech., Japan). Denki Gakkai Zasshi, 84: 1600-7(Oct. 1964). (In Japanese).

Theories proposed to explain the corona erosion mechanism of insulating materials, such as those involving thermal degradation, erosion by electronic and ionic impacts, sputtering, oxidation and electrochemical reactions, are discussed. No conclusion was reached as to the most important factor of the mechanism. Apart from corona discharge in air, in this consideration, the effects of slow electron irradiation on the surface of polyethylene films were of interest in understanding the effect of impact of charged particles on the sample surface. In comparison with the improvement of insulating properties of polyethylene by high-energy electron beams (β-ray irradiation), the effect of slow electron beams was considered. To correlate corona erosion and charged particle bombardment, thermoelectrons with an energy of 10^2 ev, in atmospheres of N_2 or air at 10^{-3} torr, were used to irradiate polyethylene films. One of the problems encountered when the slow electron beam was projected on dielectrics was the counter electric field from the stored charge on the sample. This field was liable, not only to alter the net irradiation energy, but to dissipate the irradiation beam. Even in a vacuum of 10^{-5} torr, the irradiation marks could be found on the material after irradiation for a few hours. The marks moved in a direction corresponding to the electromagnetic deflection of the beam, and this deflected distance was inversely proportional to the electron velocity. Using this relation, the radiation energy could be measured. Small qualitative changes were detected by surface resistance measurements, infrared absorption spectrography, and observation of irradiated surface by electromicrography. Decreases of the activation energy were found for the samples irradiated in air and a thin oxidized layer was observed. Deterioration was not as great as that with a corona discharge in air, but it had a larger corona resistance than nonirradiated polyethylene films. (BBB)

44070 LOW-TEMPERATURE RADIATION POLYMERIZATION OF ACROLEIN. Finkel'shtein, E. I.; Abkin, A. D. (Karpov Inst. of Physics and Chemistry, Moscow). Dokl. Akad. Nauk SSSR, 161: 1098-1101(Apr. 11, 1965). (In Russian).

Studies were made of low-temperature polymerization of acrolein by gamma rays and of possible production of carbon chain and heterochain polyacrolein. Acrolein was subjected to vacuum distillation; the distilled monomer was filtered through glass at –78°C, and was then dried in a vacuum over calcium hydride for several days at room temperature. Polymerization was carried out in mass and in various solutions at –78 and –196°C. The radiation source was ^{60}Co and dosage was about 200 r/sec. Irradiation of acrolein at –78°C and its solutions in methanol, ethanol, ethyl chloride, and acetone yielded polymers soluble in the monomers or the initial solution at low temperatures. But within 10 to 30 minutes (depending on the nature of the solvent), after warming to room temperature, the transparent solution grew turbid and a flocculent insoluble polymer precipitated. This polymer formed a white powder soluble in dimethylformamide and was basically insoluble in other organic solvents. Infrared spectra coincided with spectra of polyacrolein obtained in other ways. They indicated dominance of polymerization according to the C=O bond. Gamma irradiation of acrolein at –196°C with no acetaldehyde or propionic aldehyde gave a solid, soluble polymer that did not change with time. This indicated that polymers of different structures may be produced during low-temperature radioinduced polymerization of acrolein. (CFSTI)

44071 PULSE RADIOLYSIS OF GASEOUS ARGON–OXYGEN SOLUTIONS. RATE CONSTANT FOR THE OZONE FORMATION REACTION. Sauer, Myran C. Jr.; Dorfman, Leon M. (Argonne National Lab., Ill.). J. Am. Chem. Soc., 87: 3801-6(Sept. 5, 1965).

Pulseradiolysis was used to study the kinetics of ozone formation in gaseous argon-oxygen solutions. The absolute rate constant for the reaction $O + O_2 + Ar = O_3 + Ar$ was found to be $(0.83 \pm 0.08) \times 10^9$ M^{-2} $sec.^{-1}$ at 23°C. (auth)

44072 THE CHEMICAL EFFECTS OF γ-RADIATION ON ORGANIC SYSTEMS. PART XI. THE ACTION OF

RADIATION ON TRIETHYLAMINE, DIETHYLAMINE, n-BUTYLAMINE, AND 1-METHYLPIPERIDINE. Allan, L. T.; Swan, G. A. J. Chem. Soc., 4434-8(Aug. 1965).

Gas-chromatographic studies of the radiolysis products of diethylamine showed the presence of 1,3-diethyl-2,4,5-trimethylimidazolidine(III) and tetraethylhydrazine(IV). The radiolysis products of n-butylamine include N-butylidenebutylamine(VIII), N-(2-ethyl-2-hexenylidene)butylamine(X), 1,2-dibutylhydrazine(XII), meso- and racemic octane-4,5-diamine(VI), and 2,4,5-tripropylimidazolidine (IX). (auth)

44073 EXISTENCE OF LONG-LIVED RADICALS IN THE γ-RADIATION INDUCED POLYMERIZATION OF ETHYLENE. Machi, Sueo; Hagiwara, Miyuki; Gotoda, Masao; Kagiya, Tsutomu (Takasaki Radiation Chemistry Research Establishment, Japan). J. Polymer Sci., Pt. A, 3: 2931-4(Aug. 1965).

In the γ-radiation-induced bulk polymerization of ethylene under high pressure, the growing polymer radical is shown to have a long lifetime at low temperatures (30°C). Separation of the propagation reaction from other elementary reactions is possible. During the propagation reaction the molecular weight of the polymer increased with polymer yield when irradiated with an extremely low dose rate. At elevated temperatures (100°C), the lifetime of the growing polymer radical was not prolonged. (auth)

44074 SPECIFIC INFLUENCE OF TEMPERATURE ON γ-RAY RADIATION INDUCED POLYMERIZATION OF ETHYLENE. Machi, Sueo; Hagiwara, Miyuki; Gotoda, Masao; Kagiya, Tsutomu (Takasaki Radiation Chemistry Research Establishment, Japan). J. Polymer Sci., Pt. A, 3: 3029-30(Aug. 1965).

The rate of polymerization and molecular weight of the ethylene polymer increased continously with reaction time during polymerization of ethylene induced by γ radiation at 20 to 30°C. The temperature effects on the life of the polymer radical and the rate of polymerization are discussed. Temperature effects on radioinduced polymerization from 20 to 45°C and 100 to 140°C were studied. (F.J.H.)

44075 THE MECHANISM OF RADIATION-INDUCED OXIDATION OF ORGANIC COMPOUNDS BY MOLECULAR OXYGEN. Saraeva, V. V. (Moscow State Univ.). Kinetika i Kataliz, 6: 537-40(May-June 1965). (In Russian).

The characteristic pattern of radio-induced oxidation of individual organic compounds with molecular oxygen is shown: radiation, radiation-thermal, and thermal radiation processes. Conditions for the transitions from one process to another were determined. From the transition from radiation to radiation-thermal process the effect of the dose output was found which makes it possible to understand the possibility of development of chain processes at low temperatures and low dose output. Utilization of the proposed method makes it possible to treat limited quantities of given compounds in the range of low, average, and high temperatures and to construct all curves of the dependence of the yield on temperature at different dose outputs. (tr-auth)

44076 FADING IN THERMOLUMINESCENT LITHIUM FLUORIDE USED FOR RADIATION DOSIMETRY. Fowler, J. F. (Hammersmith Hospital, London); Shuttleworth, E.; Svarcer, Vesna; White, J. T.; Karzmark, C. J. Nature, 207: 997-8(Aug. 28, 1965).

Fading in radiation dosimeters of lithium fluoride powders was investigated. Capsules containing 1-2 g LiF powder were irradiated to 1000 Rads, using 15-Mev electrons, 15- or 5-Mv x rays, or ^{60}Co γ rays. The powder was stored in the dark at room temperature unless otherwise stated. One experiment showed that fading was closely similar for doses of 5, 50, 500, and 5000 Rads. The results showed that fading appears to be independent of dose from 5 to 5000 Rads, and depends less on temperature of storage (between 37°C and −18°C) than on the particular batch. The temperature of annealing was also investigated. However, fading was not eliminated if the temperature was somewhat less than 400°C. (P.C.H.)

44077 SEMICONDUCTIVE BEHAVIOR OF ANTHRACENE AND GAMMA-RAY IRRADIATION EFFECTS. Kim, Hi Gyu (Kyung Hee Univ., Korea); Koh, Byung Jyun. New Phys. (Korea), 5: No. 1, 2-8(May 1965).

The activation energy of single crystals of anthracene was evaluated by d-c method, with the change of temperature from 20 to 140°C. The intrinsic and extrinsic conduction mechanism was discussed and compared with the result of photoconductive method. In order to determine the impurity effects, anthracene was irradiated with a high dose of gamma radiation. The charge polarization effect and dielectric relaxation effect were compared, by examining the current decay mode. Activation energies of 2.79 ev in an intrinsic region and 1.69 ev in an extrinsic region were obtained. (auth)

44078 THE EFFECTS OF METAL IONS ON THE AUTOXIDATION OF BENZENE IN AQUEOUS SOLUTIONS. Hotta, Hiroshi; Suzuki, Nobutake (Japan Atomic Energy Research Inst., Tokyo). Nippon Kagaku Zasshi, 86: 651-60(July 1965). (In Japanese).

It was found that the oxidation of benzene in aqueous solutions of ferrous, ferric, and cupric sulfates leads to phenol with good yield at temperatures above 150°C and this yield was effected remarkably by various factors such as purity of the benzene, nature of the metal ions, concentration of sulfuric acid added to the system, irradiation of ^{60}Co gamma rays, etc. It was also found that the phenol produced in ^{18}O-enriched water contains considerable amounts of ^{18}O. Investigations showed the isotope effect for deuterium to hydrogen to be about 1.2 for autoxidation. A reaction scheme was proposed to explain consistently these experimental results. (auth)

44079 RADIOLYSIS OF CHLOROAURIC ACID IN AQUEOUS SOLUTION AND THE NATURE OF THE GOLD-COLLOID PRODUCED. Fujita, Hitoshi; Izawa, Masami; Yamazaki, Hideo (National Inst. of Radiological Sciences, Chiba, Japan). Nippon Kagaku Zasshi, 86: 723-8(July 1965). (In Japanese).

When the aqueous solution of $HAuCl_4$ was irradiated with ^{60}Co γ rays at a dose rate of 9300 to 9800 r/min, colloidal gold particles were produced. The reaction was followed by measurements of the absorption spectrum in the visible region, the turbidity, and the specific conductivity of the solution. The G-value was calculated to be 2.13, which did not depend on the initial concentration of $HAuCl_4$ up to 1×10^{-3} mol/l, nor on the oxygen content dissolved in the solution. The dependence of this reaction on the temperature was small; the apparent activation energy was about 1 kcal/mol. It is possible to use this solution as a chemical dosimeter for high doses of the order of 10^5 r by measuring the specific conductivity. In addition to the investigation described above, the formation of gold-sol in the presence of protective colloids was studied. (auth)

44080 THE RADIOLYSIS OF AQUEOUS METHYLAMMONIUM ION. Riesz, Peter; Morris, Theodore (National Cancer Inst., Bethesda, Md.). Radiation Res., 26: 1-11(Sept. 1965).

Hydrogen yields from the radiolysis of aqueous air-free solutions of methylammonium sulfate and perchlorate were measured as a function of concentration (10^{-2} to 1 N) and pH(0.4 to 4.0). For 0.01 N sulfate and perchlorate, $G(H_2) \approx 1.3$ at pH 1 and increases in a sigmoidal fashion with increasing pH. At high solute concentrations (1 N) the hydrogen yields from sulfate and perchlorate solutions differ with respect to their dependence on concentration and pH. The $G(H_2)$ values from sulfate and perchlorate solutions increase with decreasing dose rate. The $G(D_2)$ value from 99.5% D_2O solutions of 0.01 N $(CH_3\overset{+}{N}D_3)_2SO_4^{=}$ at pD 1.4 is equal to 1.2 ± 0.5, compared to the molecular D_2 yield of 0.4, and G(HD) = 0.14 ± 0.04. The concentration and dose-rate dependence of $G(H_2)$ and the results obtained in D_2O solutions are consistent with a mechanism involving competition between H atom recombination to give H_2, the reaction of H atoms with $\dot{C}H_2\overset{+}{N}H_3$ to give methylammonium

ions, and the reaction of H atoms with methylammonium ions to produce H_2. The rate constant of the latter process was estimated to be about 5×10^3 M^{-1} sec^{-1}, or slower than the corresponding reaction of H atoms with CH_3OH by a factor of about 300. It was shown by pulse radiolysis experiments that the rate constant for the conversion of e^-_{aq} to H by $CH_3\dot{N}H_3$ is 2×10^6 M^{-1} sec^{-1} at zero ionic strength. The hydrogen yields from 1 N methylammonium perchlorate solutions are lower than those from 0.1 N solutions above pH 2. Addition of 1 N sodium perchlorate to 0.01 N methylammonium perchlorate reduces the H_2 yield from 1.9 to 0.1. This behavior appears to be due to the reaction of H atoms with chlorate ions which are a direct radiolysis product of the perchlorate ions. It is suggested that the effect of pH on the hydrogen yields can be understood in terms of the ionization of the $\dot{C}H_2\overset{+}{N}H_3$ radical with a pK value of about 2. (auth)

44081 REDUCED PYRIDINE COENZYMES AS HYDROGEN DONORS IN REPAIR OF RADIATION DAMAGE. Sanner, Tore (Norwegian Radium Hospital, Oslo). Radiation Res., 26: 95-106(Sept. 1965).

The protective effect of reduced and oxidized pyridine coenzymes on the radiation inactivation of tryspin was studied. The reduced coenzymes protected tryspin against inactivation to a greater extent than did the oxidized coenzymes, both in dilute solution and in the dry state. The protective effect of the oxidized coenzymes was almost independent of oxygen, whereas the protective effect of the reduced coenzymes was much greater in the absence than in the presence of oxygen. Electron spin resonance spectroscopy showed that the radicals formed when the reduced coenzymes were irradiated in the dry state were more stable than those induced in the oxidized coenzymes. When molecular mixtures of macromolecules and $NADH_2$ were irradiated at 77°K and heat-treated to room temperature, the total number of radicals in the mixture was higher than calculated from the number of radicals stabilized in the components irradiated separately. The data indicated that a transfer of unpaired spins may occur from macromolecules to $NADH_2$. The data are compatible with the view that $NADH_2$ and $NADPH_2$ may participate in the repair of target radicals in irradiated cells by a hydrogen transfer mechanism. (auth)

44082 THE RADIOLYSIS OF ACETYLENE IN SOLUTION. II. THE EFFECT OF GAMMA RADIATIONS ON AQUEOUS SOLUTIONS OF ACETYLENE: THE EFFECT OF FOREIGN IONS. Fiti, Maria (Inst. of Atomic Physics, Bucharest). Rev. Roumaine Chim., 10: 377-82(Apr. 1965). (In French).

The effect of ^{60}Co γ radiation on aqueous solutions of acetylene was studied in the presence of the foreign ions Fe^{2+}, Cu^+, NO_3^-, SO_4^{2-}, and Cl^-. The variation of radiochemical yields of glyoxal and polymers as a function of the dose intensity, the concentration of the foreign ions, and the pH were found. The behavior of the metallic ions in the radiolytic process at doses of 0.65×10^{19} to 2.2×10^{19} ev/ml-hr was found to be very complex. The effects depended on the radiation dose and on the concentration of the ions used. (tr-auth)

44083 γ-INITIATED GRAFT COPOLYMERIZATION IN THE PRESENCE OF MONOMER VAPOR TO POLYMER FILMS. 2. GRAFTING IN MONOMER VAPOR. Takamatsu, Toshiaki (Inst. of Physical and Chemical Research, Tokyo). Rika Gaku Kenkyusho Hokoku, 37: 1-5(1961). (In Japanese).

When polyethylene and polyvinyl chloride films were irradiated in the presence of monomer vapor, graft copolymers were produced. As monomers, methyl acrylate, ethyl acrylate, methyl methacrylate, and 4-vinyl pyridine were used. The method offers a good technique for graft copolymer formation. It appeared that as the degree of crystallinity of polymer increases, the efficiency of the grafting decreases. The results of x-ray diffraction measurements showed that the crystalline part of polymer is not affected by grafting, the branches occurring primarily in the amorphous region of polymer. (BBB)

44084 γ-INITIATED GRAFT COPOLYMERIZATION OF POLYMER FILMS IN THE PRESENCE OF MONOMER VAPOR. 3. EFFECT OF IRRADIATION TEMPERATURE TO GRAFTING. Takamatsu, Toshiaki; Shinohara, Kenichi (Inst. of Physical and Chemical Research, Tokyo). Rika Gaku Kenkyusho Hokoku, 37: 285-9(1961). (In Japanese).

When polyethylene and polyvinyl chloride films were irradiated in styrene vapor by γ rays from ^{60}Co, graft copolymers were readily produced. To study the effects of temperature of irradiation to grafting, two series of experiments were carried out. In one series, the monomer was kept at room temperature and the polymer was irradiated at various elevated temperatures. In the other, both monomer and polymer were kept at the same temperature during irradiation. For polyethylene, the efficiency of grafting decreased monotonously in the first series of experiments as the temperature was raised. In the second series of experiments, the efficiency increased at first, but reached a maximum at about 60°C and decreased again at higher temperatures, probably because of the onset of thermal polymerization of the monomer. More complicated behaviors were displayed in the polyvinyl chloride-styrene system than in the other system studied. (BBB)

44085 RADIATION-INDUCED OXIDATION OF Sb(III) IN AQUEOUS SOLUTION. 2. Matsuura, Niro; Kurimura, Yoshimi; Takizawa, Masao (Inst. of Physical and Chemical Research, Tokyo). Rika Gaku Kenkyusho Hokoku, 37: 345-8(1961). (In Japanese).

Radiation oxidation of 10^{-4}M Sb(III) in 0.8N H_2SO_4 and in 0.8N HCl by γ rays from ^{60}Co was studied. The samples were irradiated at a dose rate of 2.6×10^4 R/hr at about 20°C. In the presence of oxygen, the G value for the oxidation of Sb(III) in sulfuric acid was 2.6 to 3.3 and dependent on the concentration of Sb(III). In the case of hydrochloric acid, the G value was 3.4 and independent of the Sb(III) concentration. In the absence of oxygen, the G value was 0.43 for the sulfuric acid and 0.36 for the hydrochloric acid. Slow continuation of oxidation of Sb(III) after irradiation was found only in the system with hydrochloric acid in the presence of oxygen. This was considered probably due to hydrogen peroxide produced by irradiation. From the G values observed, a mechanism for the oxidation of Sb(III) is suggested as follows: for the presence of oxygen, $G^{O_2} = \frac{1}{2}(G_{OH} + G_H)$; for the absence of oxygen, $G^{N_2} = \frac{1}{2}(G_{OH} - G_H) + G_{H_2O_2}$. (BBB)

44086 IRRADIATION OF POLYVINYL CHLORIDE IN WATER. II. Takamatsu, Toshiaki; Shinohara, Kenichi (Inst. of Physical and Chemical Research, Tokyo). Rika Gaku Kenkyusho Hokoku, 37: 366-74(1961). (In Japanese).

Effects of temperature on the irradiation of polyvinyl chloride in water by γ rays and electrons were studied, and the results were compared with those of similar experiments carried out in air and in vacuum. Calculations were made on these results to get G values of crosslinking using a previous theory. When polyvinyl chloride was irradiated in air by γ rays, main-chain scission occurred predominantly, and only a decrease of the molecular weight was observed in the range of dose investigated. When it was irradiated in vacuum or in water, molecular weight, in most cases, showed a decrease at the early stage of the irradiation, reached a minimum and then increased. The decrease was slower and the dose for the minimum was smaller when irradiation was done at higher temperatures. The difference in behavior in in-vacuum and in-water irradiation were not large, but in-water irradiation seemed to be more effective in producing crosslinking at room temperature, and in-vacuum irradiation at higher temperatures. It was found that when the polymer was irradiated in water with γ rays at different dose rates and also with electrons from a Van de Graaff generator, more crosslinking was produced, for the same total dose, with lower dose rates. It was also found that when the polymer was irradiated in vacuum and then immersed in water without exposing it to air, an increase of the molecular weight was obtained. These results were interpreted as showing that the small amount of water that penetrated into the polymer

served as plasticizer to increase molecular motion and thus help crosslinking. When polyvinyl chloride was irradiated in water at room temperature and then subjected to heat treatment, the molecular weight was found to increase and this increase was larger at higher temperatures. The increase was especially large when the temperature was higher than the second-order transition temperature. This phenomenon is presumably due to increased molecular motion. (BBB)

44087 EFFECT OF γ-RADIATION ON PORPHYRIN-METAL COMPLEXES. I. γ-IRRADIATION OF CHLOROPHYLL AND ITS COBALT AND COPPER SUBSTITUTION PRODUCTS. Yamamoto, Kiyoko; Araki, Chiroru; Tonomura, Shizu (Inst. of Physical and Chemical Research, Tokyo). Rika Gaku Kenkyusho Hokoku, 37: 458-63(1961). (In Japanese).

Chlorophyll, its cobalt and copper substitution products, and pheophytin in ethereal solution (10^{-4} mole/l) were irradiated by γ rays from a ^{60}Co source. Effects of γ radiation on these substances were studied by spectroscopic changes in the visible region and by analysis of liberated metal ions in the irradiated solutions. The ring in these compounds was opened at doses of $< 10^5$ R of γ radiation. The Cu–N, Co–N, and Mg–N bonds were not broken before opening of the ring. When the ring was opened, reduced compounds with intact metal complex bonds were produced and decomposed in the order of Mg, Co, Cu by increasing γ-radiation doses. (BBB)

44088 EVALUATION OF THERMAL INSULATORS FOR NUCLEAR REACTORS. Crispino, Enrico. Rivoluzione Ind., No. 146, 23-6(May-June 1965). (In Italian).

Insulating material in nuclear reactors is principally exposed to neutron and γ irradiation. The material can absorb neutrons causing a negative effect on the fission processes or inducing radioactivity of the material itself. Radiation damage to the material resulting in a modification of the chemical and physical characteristics can also occur. The occurrence of these two processes in organic and inorganic materials is discussed. It was concluded that the inorganic insulators are the most stable with respect to radiation. (J.S.R.)

44089 DECOMPOSITION OF TERTIARY BUTYL PEROXIDES BY GAMMA-IRRADIATION. Tanaka, Toyosuke; Nakamura, Jiro; Oniyama, Fusayo; Itoh, Novuhiro (Saitama Univ., Urawa, Japan). Sci. Rept. Saitama Univ., Ser. A., 4: 99-102(1964).

Kinetic features of decomposition of tert-butyl peracetate, tert-butyl hydroperoxide, di-tert-butyl peroxide and benzoyl peroxide in some solutions under gamma irradiation from ^{60}Co are discussed. It was evident that the decomposition of these peroxides is the first-order reaction up to 40% of decomposition. (auth)

44090 REACTIONS OF THE HYDROXYL RADICAL. PART 2. DETERMINATION OF ABSOLUTE RATE CONSTANTS. Adams, G. E.; Boag, J. W.; Michael, B. D. (Mount Vernon Hospital, Northwood, Eng.). Trans. Faraday Soc., 61: 1417-24(July 1965).

Absolute rate constants were measured for the reaction of OH with the thiocyanate ion and with selenite ion by measuring the rate of formation of the transient absorptions produced in oxygenated solutions of the respective anions following irradiation by a 0.2 μsec pulse of electrons. The transient absorptions produced in these systems together with that produced in oxygenated solutions of carbonate ion were used as independent reference systems in order to determine, by competition kinetic methods, the absolute reactivity of OH with some organic and inorganic solutes. Good agreement was obtained when the rate constants for the reaction of OH with methanol and with ethanol were measured by three independent methods confirming the validity of competition kinetic methods in pulse radiolysis. (auth)

44091 NEUTRON IRRADIATION OF LINDE MOLECULAR SIEVE 13X. Rees, L. V. C.; Williams, C. J. (Imperial Coll. of Science and Tech., London). Trans. Faraday Soc., 61: 1481-9(July 1965).

The sorption of argon at 90°K in Linde Molecular Sieve 13X was used to determine the damage developed in the sorbent after irradiation with fast neutrons. Damage was first observed at an integrated dose of 6.2×10^{17} neutrons cm^{-2}, and collapse of the lattice occurred when the dose was 7×10^{19} neutrons cm^{-2}. An attempt was made to detect fine changes in the characteristics of the sorption sites due to the irradiation by careful measurements of the sorption of krypton in the range from 25 to –150°C. Sorption, x-ray powder diffraction and density measurements indicated an initial gradual lattice contraction with increasing dose. Exchange isotherms for the pairs of ions $Na^+ \rightleftharpoons Cs^+$, $2Na^+ \rightleftharpoons Ba^{2+}$, and $2Na^+ \rightleftharpoons UO_2^{2+}$ in Linde Sieve 13X were determined, from which ΔG_θ and the activity coefficients of the cations in the exchanger were calculated. The effect of neutron irradiation on the isotherms was studied. An attempt was made to calculate the number of displaced atoms produced in the solid by the fast neutrons and to correlate this with the loss in sorption capacity. It was found that % loss in capacity $\propto$ (dose)$^{\frac{1}{3}}$, suggesting that two oxygens had to be displaced from a silicon or aluminum atom before the sorption capacity was affected. If this assumption were correct, then the calculated displacements had to be reduced by a factor of three to allow for replacements. (auth)

44092 THE FRICTION AND DEFORMATION PROPERTIES OF IRRADIATED POLYTETRAFLUOROETHYLENE (PTFE). McLaren, K. G.; Tabor, D. (Cavendish Lab., Cambridge, Eng.). Wear, 8: 3-7(1965).

Specimens of PTFE (~76% crystalline) sealed under nitrogen in polyethylene bags were irradiated in the electron beam of a linear accelerator at a dose rate of 1-Mrad/min. After a 20-Mrad dose the PTFE was faintly yellow and noticeably brittle; 50-Mrad produced marked yellowing and brittleness. The bulk hardness increased from its original value of 4 kg/mm^2 to a maximum of 5.3 kg/mm^2 after a 5-Mrad dose, then reached a steady value of 5 kg/mm^2 for doses of 20 to 50-Mrad. Both the bulk shear strength and shear energy (estimated from the area under stress-strain curves) were severely reduced by irradiation. The shear strength fell from its initial value of 3.1 kg/mm^2 to 2.0, 1.4, and 1.2 kg/mm^2 for polymer given doses of 1, 5, and 20-Mrad, respectively. When strong adhesion between materials occurred, friction was due mainly to the force required to shear the juntions. For a wide range of materials the ratio (R) of bulk shear strength to bulk hardness gave a reasonable approximation of the observed coefficient of friction, but for unirradiated PTFE these values showed little correlation, indicating that it was not possible to equate the strength of the interface with the bulk shear strength of the polymer. However, if the ratio R varied in the same way as the coefficient of friction, a decrease in the coefficient of friction of PTFE after irradiation would be expected. On the contrary, irradiation caused the reverse effect as shown by friction measurements made with a PTFE pin rubbing continuously on a rotating PTFE disc at speeds from 0.25 to 366 cm/sec. Thus, there was a marked increase in the low-speed friction and in the friction-velocity dependence of the PTFE. For sliding speeds up to about 140 cm/sec the friction increased with increasing radiation dose up to 5-Mrad. At higher speeds with specimens that received 20-Mrad or more, the maximum friction reached ($\mu = 0.24$) was significantly lower than for unirradiated PTFE or PTFE, which had received smaller doses ($\mu = 0.32$). The stiffening of the chain structure by irradiation was offered as a possible explanation of the surprising increase in the friction at low speeds. (BBB)

44093 CHEMICAL DOSIMETRY OF HIGH-ENERGY PARTICLES. Bonet-Maury, P.; Bagno, O.; Weill-Cohen, A. (Universite, Paris). pp 109-13 of STI/PUB/99. (In French).

The effects of 152- and 592-Mev protons and of 50- and 950-Mev electrons on ferrous sulfate solution, radiological

films, and dosimetry glasses were studied. The response of the three dosimeters is fully proportional to the dose absorbed throughout the range investigated, i.e., from 5 to 50 rad for the films and from 100 to 1000 rad for the ferrous sulfate and the glass. The indications are stable for at least several days. Generally speaking, the response of these dosimeters to high-energy particles is similar to their response to gamma rays, in accordance with the fact that for these radiations with low linear energy transfer (LET) the response of chemical systems does not vary much with the LET. The chemical dosimeters studied are quite suitable for measuring high-energy radiation doses and could be used in the event of an accident. (auth)

44094 POST-IRRADIATION GRAFTED VINYL-CELLULOSE COPOLYMERS. Blouin, Florine A.; Arthur, Jett C. Jr. (Dept. of Agriculture, New Orleans). 9p. (CONF-650401-11). Gmelin, AED-CONF-65-041-17.

From American Chemical Society, Detroit.

Purified cotton fibers, yarns, and fabrics were irradiated dry and in nitrogen to a dosage of 10^6 R with gamma rays from ^{60}Co. The irradiated cottons were treated at 23°C with 15% monomer solution in 70, 75, or 80% aqueous $ZnCl_2$. The rates of the grafting reactions of irradiated cotton fibers with vinyl acetate, acrylonitrile, and methyl methacrylate were determined. Tensile properties of the grafted fibers were studied. (F.J.H.)

44095 THE EFFECTS OF REACTOR RADIATION ON THREE HIGH-TEMPERATURE SOLID-FILM LUBRICANTS. McDaniel, R. H. (General Dynamics Corp., Fort Worth, Tex.). Park Ridge, Ill., American Society of Lubrication Engineers, 1965, Preprint No. 65AM 5C4, 29p. (CONF-650547-2). ORINS.

From American Society of Lubrication Engineers, 20th Annual Meeting, Detroit.

Experiments were performed to determine the effects of reactor radiation on the wear life of three high-temperature solid-film lubricants, PbS + MoS_2 + B_2O_3, CaF_2 + oxide frit, and MoS_2 + graphite + sodium silicate. Test specimens were irradiated under static conditions to an average gamma dose of 2.2×10^{11} ergs/gm(C) plus associated neutrons of 5.2×10^{16} n/cm^2 (E > 2.9 Mev). Subsequent tests with a double rub shoe-type sliding-wear tester were made with a load of 110 lb/rub shoe and at a sliding speed of 128 ft/min. Tests were performed at several temperatures up to 1500°F. Based on the data obtained in this experiment and the statistical treatment employed (Weibull plots and ranking of data), it was concluded that static exposure to reactor radiation had no significant effect on the wear life of the PbS + MoS_2 + B_2O_3 film, nor on the CaF_2 coating. The MoS_2 + graphite + sodium silicate film suffered a decrease in wear life at 80°F, but it displayed improved wear life at 600 and 1200°F after irradiation. (auth)

44096 SPACE CHARGE IN PLASTICS PRODUCED BY 2 Mev ELECTRONS. Atchison, G. J. (Dow Chemical Co., Midland, Mich). 10p. (CONF-650401-13). Gmelin, AED-CONF-65-041-7.

From American Chemical Society, Detroit.

The plastic sample to be investigated was in the form of a disk 2 inches in diameter and 0.5 inch thick. It served as the bottom of the irradiation cell. A beam of 2-Mev electrons enters the cell from the top through a thin aluminum window and impinges on the top surface of the plastic sample. The sample thickness is greater than the range of the electrons. A population of trapped electrons is built up within the sample. The trapped electrons produce a negative space charge within the sample. (F.J.H.)

44097 GRAFT POLYMERIZATION UTILIZING IONIZING RADIATION. Magat, Michel; Chapiro, Adolphe; Danon, Jeanne Sebban (to Centre National de la Recherche Scientifique Ministere de l'Education Nationale). U. S. Patent 3,201,336. Aug. 17, 1965. Priority date July 27, 1956, France.

A method is patented for production of graft copolymers having a polymer trunk with graft branches of at least two different polymers. A polymer, preferably in solid form, is subjected to ionizing radiation in the presence of oxygen to form active centers and then contacted with a monomer polymerizable by free radicals to form a graft copolymer. Contact with the monomer is interrupted before all the active centers are utilized, and the irradiated polymer is contacted with a second monomer. This contact may again be interrupted and the polymer may be contacted with a third monomer. The successive grafting is controlled by choice of monomers or by temperature control. (A.G.W.)

Radiochemistry

See also Separation Processes and Procedures.

Refer also to abstract 45542.

44098 (NAS-NS-3057) THE RADIOCHEMISTRY OF RADIUM. Kirby, H. W. (Mound Lab., Miamisburg, Ohio); Salutsky, Murrell L. (Grace (W. R.) and Co., Clarksville, Md. Washington Research Center). Dec. 1964. Contract AT(33-1)-Gen-53. 210p. Dep. mn; CFSTI $2.25 cy, $1.25 mn.

The nuclear and chemical properties of radium which are of interest in radiochemistry are reviewed. Methods for dissolution of radium samples and counting techniques are considered. Detailed radiochemical procedures are compiled. A bibliography of 115 references is also included. (D.L.C.)

44099 PRODUCTION OF ^{26}Al DURING IRRADIATION OF Mg WITH 20-Mev DEUTERONS. Krasnov, N. N.; Dmitriev, P. P.; Sevast'yanov, Yu. G.; Bezmalternykh, S. A. At. Energ. (USSR), 19: 62-3(July 1965).

High specific-activity ^{26}Al was obtained in the reactions ^{25}Mg(d,n) and ^{26}Mg(d,2n) by irradiating Mg with a 20-Mev deuteron beam. The steps involved in the separation of the radiochemically pure Al are listed. The ^{26}Al gamma spectrum, measured on a scintillation spectrometer, is presented. The activity of the ^{26}Al source was measured by comparison of the 511-kev gamma line intensity with a ^{22}Na standard and of the 1830-kev intensity with a ^{88}Y standard. (M.J.T.)

44100 SEPARATION OF ^{22}Na FROM MAGNESIUM TARGET IRRADIATED WITH DEUTERONS. Sevast'yanov, Yu. G.; Bezmaternyh, A. S. At. Energ. (USSR), 19: 63-4(July 1965).

Radioactive ^{22}Na was obtained in the reaction ^{24}Mg(d,α) ^{22}Na by irradiation of the Mg alloy MA8 with 20-Mev deuterons. A method is described for discharging the bulk of the Mg (94 to 97%) by precipitation in the form of $MgSO_4$ from water-acetone solutions. The remaining purification of the ^{22}Na is carried out by ion exchange. The efficiency of the separation is discussed for various solution concentrations and volumes. (M.J.T.)

44101 INTERNATIONAL COMPARISONS OF THE SPECIFIC ACTIVITY OF ^{32}P, ^{60}Co, AND ^{204}Tl SOLUTIONS AND THE ACTIVITY OF ^{60}Co SOLID SOURCES. Konstantinov, A. A.; Perepelkin, V. V.; Kochin, A. E. At. Energ. (USSR), 19: 65-7(July 1965).

Work on the international standardization of the specific activity of ^{32}P, ^{60}Co, and ^{204}Tl dissolved sources and ^{60}Co solid sources (i.e., specially prepared ^{60}Co sources on thin films), carried out in Jan. 1961 and in March and April 1963 in national laboratories of several countries, is described. Results are presented for ^{32}P, ^{60}Co solutions and ^{60}Co solid sources. (M.J.T.)

44102 TRITIATED STARCH GRANULES. Nordin, P.; Moser, H. C.; Senne, J. K. (Kansas State Univ., Manhattan). Biochem. J., 96: 336-9(Aug. 1965).

A technique for surface labeling of starch granules by tritiation is described that could be useful in structure determination. The impurities that are produced must be taken into account but the fact that a high polymer can be successfully tritiated seems very promising. The surfaces of corn-starch granules must contain both amylose and amylopectin. (auth)

44103 SYNTHESIS OF LABELED ORGANIC COMPOUNDS. Otto, P. Ph. H. L. Chem. Weekblad, 60: 59-68(1964).

The determination of the radiochemical purity of labeled compounds and the problems connected with the storage of these compounds are described. A survey is given concerning research at the Radioisotope Department of the Central Laboratory of TNO. (TCO)

44104 EFFECT OF HEAT TREATMENT OF MANGANESE DIOXIDE OF THE RATE OF OXYGEN ISOTOPE EXCHANGE. Kasatkina, L. A.; Zuev, A. P. (Mendeleev Inst. of Chemistry and Tech., Moscow). Kinetika i Kataliz, 6: 476-85(May-June 1965). (In Russian).

The activity of manganese dioxide samples, heated in a vacuum to 350, 450, and 550°, was investigated in the temperature interval from 25 to 350° with respect to the isotopic exchange of oxygen of acids with molecular oxygen, homomolecular exchange of oxygen, and oxidation reactions of CO. It was found that the increase of temperature leads increased activity of the preparation with respect to the isotopic exchange and a decrease of the degree of its heterogeneity. In monolayers the velocity of the isotopic exchange of the acid oxygen drops exponentially with the increase of the degree of exchange. At 300° the oxygen exchange proceeds with less velocity and greater activation energy than the oxidation of CO. The two regions of homomolecular exchange of the oxygen differ from each other: the high temperature range and close to room temperature. The speed of the homomolecular exchange at 25 to 34° on newly treated catalyst is greater than the speed of exchange at 200°, comparable to the velocity of CO oxidation, and is decreased with the time of the aging of the preparation in O_2. (tr-auth)

44105 IMMUNOLOGIC STUDIES OF OCTAPEPTIDES. I. RADIOIODINATION OF OXYTOCIN. Gilliland, Paul F.; Prout, Thaddeus E. (Johns Hopkins Univ., Baltimore). Metab. Clin. Exptl., 14: 912-17(Aug. 1965).

A method is described for radioiodination of oxytocin as a model for other octapeptides. Synthetic oxytocin was added to radioiodine solution containing 0.1 to 1.05 mC of $Na^{131}I$ in a plastic test tube. At one min intervals, reagents were added with gentle shaking in sequence as follows: 25 μl of Chloramine-T (352 mg/100 ml) solution, 100 μl of sodium metabisulfite (240 mg/100 ml) solution, and 200 μl of potassium iodide (1 g/100 ml) solution. The mixture was then transferred to a 10 × 1.2 cm column of Amberlite IRA 400 to separate free ^{131}I from labeled oxytocin. Approximately 20% of the total radioiodine in the iodinating solution was associated with the peptides and 80% remained on the Amberlite column. Labeled peptides did not remain on the column during repassage, and efficiency of iodination was 20%. Ten μg of oxytocin with 1.04 mC ^{131}I in 2.4 μg of carrier iodide with a 20% efficiency of the reactants produced a maximum specific activity of 20.8 mC ^{131}I per mg oxytocin. Based on a molecular weight of 1007 (oxytocin) there were then 0.415 atoms total iodine or 0.0012 atoms of ^{131}I per molecule of oxytocin. It was shown that a preparation of synthetic oxytocin having a biologic activity of 430 units/ml can be successfully labeled with radioiodine by Chloramine-T. (TCO)

44106 REACTIONS OF HOT TRITIUM ATOMS WITH THE SYSTEM, ETHANE AND OXYGEN. Urch, D. S.; Welch, M. J. (London Univ.). Trans. Faraday Soc., 61: 1411-16(July 1965).

Hot tritium atoms, produced by the $^3He(n,p)^3He$ reaction, were reacted with ethane in the presence of varying amounts of oxygen. The experimental results are explained by considering the hot tritium reaction as being composed of hot and "epithermal" contributions, the epithermal part of which disappears above 60% oxygen concentration. A Wolfgang–Estrup kinetic theory analysis of the results confirmed this idea and, from the analysis, values of the reactivity integral and logarithmic energy decrement were calculated. (auth)

44107 PROCESS FOR THE PREPARATION OF COMPOUNDS TAGGED BY RADIOACTIVE TRACERS. Herr, Wilfried (to Max Planck Institut fuer Chemie). British Patent 1,000,760. Aug. 11, 1965. Priority date Sept. 20, 1960, Germany.

A process is described for the preparation of compounds tagged in a predetermined position by radioactive tracers comprises contacting the compound to be tagged in a stream of carrier gas with an absorbent having absorbed on it a tagged isotope in the form of negative ions or with a metal having combined with it a tagged isotope to effect exchange with an exchangable atom in the compound with that of the isotope. The exchange is best effected in a gas chromatographic column since this facilitates the separation of the products resulting from the exchange. The exchange is best effected at elevated temperatures, not more than 50°C below the boiling point of the compound being tagged. The process is described for tagging halogen-substituted organic compounds, but may also be applied to tritium, deuterium, radiosulfur, and radiophosphorus either absorbed in the form of negative ions or chemically bound to a metal surface. (B.L.M.)

Separation Processes and Procedures

See *also* Analytical Procedures
ISOTOPE TECHNOLOGY — Separation and Production

Refer also to abstracts 44156, 44607, 44638, and 45612.

44108 (AERE-R-4440(Pt.3)) REPROCESSING WITH AMINE ETHER SYSTEMS. PART 3. COUNTER-CURRENT TRIALS WITH ALAMINE 336–DIBUTYL CELLOSOLVE. Streeton, R. J. W.; Holdoway, M. J. (Atomic Energy Research Establishment, Harwell (England)). Aug. 1965. 28p. Dep.; BIS $0.80; HMSO 4s.

15% (0.30M) Alamine 336/DBC was tested in the reprocessing of fast reactor fuel (75% uranium; 25% plutonium), for the separation of plutonium from uranium and fission products. Miniature mixer-settler runs, using either uranium(IV) as a stand-in for plutonium, or plutonium(IV) were carried out. Good separations of uranium(IV) and uranium (VI) can be achieved, without using excessive volumes of solvent and scrub, because concentrations up to 16–17 g uranium(IV)/l in the amine phase can be obtained. With plutonium(IV), however, owing to formation of a third phase, the limiting concentration in the amine phase is only 10.5 g plutonium(IV)/l, which is rather low for a satisfactory flowsheet. The behaviour of zirconium/niobium and ruthenium was investigated, and it has been found for ruthenium that only the tetranitratonitrosylruthenium cannot be scrubbed out of the solvent. Decontamination factors of 240 and 42 were obtained for zirconium/niobium and ruthenium, respectively. Backwashing of uranium(IV) or plutonium(IV) from the amine phase was satisfactorily carried out with 1M acetic acid containing 0.05M HNO_3. The solvent was reconditioned by contacting it with 1M HNO_3. (auth)

44109 (BLG-331) SOME ASPECTS OF VOLATILITY PROCESSES FOR REACTOR FUEL ELEMENTS CONTAINING CARBON. Pierini, G.; Schmets, J. (Centre d'Etude de l'Energie Nucleaire, Brussels (Belgium)). June 1965. 14p. (CONF-650606-9). Dep. mn.

From EURATOM Symposium on Fuel Cycles of High-Temperature Gas-Cooled Reactors, Brussels.

Experimental results related to processing of high-temperature gas-cooled reactor fuels containing carbon are discussed. Various reagents, such as nitric acid vapor, oxygen, carbon dioxide, and steam have been used to treat this fuel type. It was also possible to halogenate directly uncoated uranium carbide by means of hydrogen fluoride or chloride. The compounds so formed

can be further converted to volatile halides and especially to hexafluorides achieving a high decontamination. Of the processes investigated, the use of the nitric acid vapor opens a new way for both dry and aqueous reprocessing of carbon coated fuels. (auth)

44110 (BNWL-114) THERMAL EFFECTS IN ANION EXCHANGE RESIN–NITRIC ACID SYSTEMS. Van Slyke, W. J.; Jansen, G. Jr.; Swift, W. H. (Battelle-Northwest, Richland, Wash. Pacific Northwest Lab.). Aug. 1965. Contract AT(45-1)-1830. 68p. Dep. mn; CFSTI $3.00 cy, $0.75 mn.

An analysis of the instability conditions when operating with Permutit SK anion exchange resin in 7M HNO_3 was made. The reaction kinetics for the system were investigated by externally heated pipe pressurization tests and by calorimeter experiments. The chemical and physical properties of the system were correlated by mathematical models for batch and flow cases to predict the conditions that permit self-accelerating chemical reactions. Uncontrolled reaction conditions are favored by: increasing vessel radius, low vessel wall heat transfer coefficients to the surroundings, low thermal conductivity of the vessel contents, high ambient and operating temperatures, and chromium(VI) loaded on the resin. The relations between these variables for the chemical system are graphically presented. The theory, based on the concepts originally proposed by Frank-Kamenetskii, is generally applicable to cylindrical shapes which generate heat with an exponential dependence on temperature. The Redox 233-S incident is discussed briefly in terms of this analysis. (auth)

44111 (BNWL-121) PERFORMANCE EVALUATION OF SLAG AND CRUCIBLE DISSOLVER. Dunn, J. (Battelle-Northwest, Richland, Wash. Pacific Northwest Lab). July 1965. Contract AT(45-1)-1830. 12p. Dep. mn; CFSTI $1.00 cy, $0.50 mn.

A glass mock-up of the liquid portion of a continuous dissolver was satisfactorily operated under stringent process conditions. Dissolution of simulated slag and crucible residues was accomplished at rates two to three times greater than present plant production rates. The ability of the system to maintain or restore circulation, while containing solids equivalent to the insoluble material resulting from about six months' normal production, was demonstrated. The addition of metered steam through sparge distributors to obtain required dilution of the production provides agitation, reduces feed storage requirements and simplifies feed make-up. (auth)

44112 (CONF-651103-4) APPLICATIONS OF NUCLEAR SAFETY CRITERIA TO PLANT OPERATIONS. Ketzlach, Norman (Atomics International, Canoga Park, Calif.). [1964]. Contract AT(11-1)-Gen-8. 26p. Dep. mn; CFSTI $2.00 cy, $0.50 mn.

For Presentation at IAEA Symposium on Criticality Control of Fissile Materials, Stockholm.

Criticality parameters, developed by the use of conservative calculational methods, are presented for uranium carbide fuels. The method of analysis is outlined, together with the application of the criteria developed to plant processing conditions. A method is also presented for applying uranium metal-water data to other uranium fuels when no other criticality data are available. (D.C.W.)

44113 (COO-748-1) RESOLUTION IN CHROMATOGRAPHY. Final Report. Giddings, J. Calvin (Utah Univ., Salt Lake City. Dept. of Chemistry). [1965]. Contract AT(11-1)-748. 14p. Dep. mn; CFSTI $1.00 cy, $0.50 mn.

Research was conducted on: basic chromatographic processes, optimum parameters in chromatography, effects of temperature and temperature programming, and preparative scale operation. Results obtained in each area are described. (D.L.C.)

44114 (NAA-SR-11375) SECOND-CYCLE AIROX REPROCESSING AND PELLET REFABRICATING OF HIGHLY IRRADIATED URANIUM DIOXIDE. Bodine, J. E.; Guon, J.; Sullivan, R. J. (Atomics International, Canoga Park, Calif.). Aug. 31, 1965. Contract AT(11-1)-Gen-8. 45p. Dep. mn; CFSTI $2.00 cy, $0.50 mn.

Uranium dioxide (UO_2) irradiated to burnups from 5,700 to 21,000 Mwd/MTU, and AIROX reprocessed and refabricated into pellets, was reirradiated for an additional 10,000 Mwd/MTU. Postirradiation examination has shown that the second-cycle irradiated UO_2 behaved similarly to production grade UO_2. Some reduction in thermal conductivity may have occurred, however. The second-cycle irradiated UO_2 was AIROX reprocessed and refabricated into pellets. Pellet densities, calculated from gas displacement and geometrical measurements, varied from 92 to 97, and from 92 to 95% of theoretical. Water displacement densities were 96 to 97% of theoretical. Radiochemical analyses indicated that, except for cesium and noble gases, little or no decontamination occurred. (auth)

44115 (ORNL-P-1577) BEHAVIOR OF THE TRANSPLUTONIUM ELEMENTS IN SOLVENT EXTRACTION SYSTEMS. Leuze, R. E.; Baybarz, R. D.; Kappelmann, F. A.; Weaver, Boyd (Oak Ridge National Lab., Tenn.). Aug. 13, 1965. Contract W-7405-eng-26. 34p. (CONF-650918-3). Dep. mn; CFSTI $2.00 cy, $0.50 mn.

From International Conference on the Chemistry of the Solvent Extraction of Metals, Harwell, Berks., Eng.

Very high activity levels were encountered during the separation of multigram amounts of ^{244}Cm–^{243}Am and ^{242}Cm–^{241}Am from fission products by the Tramex process, in which actinides are extracted into a tertiary amine from concentrated lithium chloride solution. Rapid loss of acid and formation of a strong oxidant in the lithium chloride feed solution were the principal effects of the high activity level. Methanol was added to control acid loss and thus prevent precipitation of americium and curium hydroxides. The presence of a strong oxidant makes it impossible to obtain good decontamination from cerium, since tetravalent cerium that is formed extracts with the actinides. Addition of stannous chloride to feed containing 170 Curies of ^{242}Cm per liter (6 w/liter) destroyed the oxidant, kept cerium in the unextractable trivalent state, and resulted in good cerium decontamination. In solutions at twice this activity level, stannous chloride was rapidly consumed, and poor cerium decontamination was obtained. Formation of complexes to preferentially suppress actinide extraction is the basis of a proposed method for actinide-lanthanide group separation, TALSPEAK (an acronym for Trivalent Actinide-Lanthanide Separation by Phosphorus Reagent Extraction from Aqueous Complexes). Group separation was not obtained by extraction into monoacidic organophosphates or -phosphonates from mineral acid solutions. Even though conditions are shifted in favor of lanthanide extraction by the addition of water soluble carboxylic acids and adjustment of pH, it is necessary to decrease actinide extractability by the formation of strong complexes with polyaminocarboxylic acids in order to obtain conditions favorable for complete group separation. Optimum results were obtained by extraction with di(2-ethylhexyl) phosphoric acid from lactic acid solutions containing diethylenetriamine pentaacetic acid. Separations obtained for americium-curium from the lanthanides approach those given by the Tramex process. (auth)

44116 (ORNL-TM-1062) ION EXCHANGE PURIFICATION OF GRAM QUANTITIES OF FISSION-PRODUCED SAMARIUM WITH DIETHYLENETRIAMINEPENTAACETIC ACID AS THE ELUANT. Orr, P. B. (Oak Ridge National Lab., Tenn.). Sept, 1965. Contract W-7405-eng-26. 11p. Dep. mn; CFSTI $1.00 cy, $0.50 mn.

By use of feed material saved from ^{147}Pm separations done in 1959, a total of 11.4 g of >99.9% purity fission-produced Sm_2O_3 was obtained in four runs through Dowex 50W-X4 hydrogen-form resin, with diethylenetriaminepentaacetic acid as eluant. This is the largest amount of samarium yet separated at ORNL. The only rare earth contaminant detected by spectrographic analyses was a maximum of 0.05% europium. Radiochemical analyses showed that no ^{147}Pm was present, and only traces of ^{241}Am and ^{154}Eu were detected. The percentages of each samarium isotope were determined by mass spectrographic

analyses. Procedures and equipment used to purify samarium are given. (auth)

44117 (ORNL-TM-1256) EVALUATION OF SMALL MODIFIED CEN MIXER-SETTLERS FOR THE EXTRACTION OF URANIUM AND THORIUM IN A HOT CELL FACILITY. Klitgaard, J.; Goode, J. H. (Oak Ridge National Lab., Tenn.). Aug. 30, 1965. Contract W-7405-eng-26. 19p. Dep. mn; CFSTI $1.00 cy, $0.50 mn.

In a study of a small modified version of the mixer-settlers used at the Centre d'Etude de l'Energie Nucleaire, at Mol, Belgium, a cascade of three mixer-settlers was made and tested with nonradioactive, simulated feeds adjusted to meet conditions for their purification by the Acid Thorex and Purex processes. The mixer-settlers were constructed from molded Homalite plastic and had 8 extraction, 8 scrub, 8 partitioning, 8 back-extraction, and 16 stripping stages. The chief objective of the study was to acquire performance data (throughput, stage efficiencies, and operating limitations, such as losses) before the equipment is used in a process demonstration with highly radioactive feed. Results indicated that this type of mixer-settler should be satisfactory for hot-cell studies of aqueous nitrate solvent extraction systems. The uranium losses during a Purex run totalled 0.007%, and the overall stage efficiencies were 65 and 77% for extraction and stripping, respectively. In an Acid Thorex run, the uranium losses totalled 0.19% and the thorium losses 0.33%. The separation factors were: thorium from uranium, 360; uranium from thorium, 555. Methods were developed for adjusting the impellers (paddles) to ensure proper hydraulic performance of the units. (auth)

44118 (UCRL-16015) DEVELOPMENT OF SOME HIGH-SPEED CHROMATOGRAPHIC METHODS (thesis). Ajuria-Garza, Sergio (Lawrence Radiation Lab., Univ. of California, Berkeley). June 8, 1965. Contract W-7405-eng-48. 66p. Dep. mn; CFSTI $3.00 cy, $0.75 mn.

A thin-layer chromatography method was developed using as stationary phase a fine mesh ion exchange resin without any admixture, thus eliminating the effects due to binding materials. The plates can be developed by the ascending, descending, horizontal, or centrifugal technique. The spots obtained can be removed mechanically by several methods. An apparatus and a method of operation were developed for the centrifugal acceleration of thin-layer chromatography on 5 × 30 cm glass plates with a substantial reduction in the time of development. A universal chromatographic chamber equally suitable for horizontal, centrifugal, ascending, or descending chromatography either of paper strips or thin-layer plates is described in detail. A comparison was made of the rate of progress of the solvent front in the different chromatographic methods. The speed of the front decreases sharply as the distance from the origin increases except in the centrifugal case in which the speed remains constant. A method of tandem horizontal or centrifugal chromatography is described which permits one to increase the length of a chromatogram in order to separate two substances with very similar R_f values. The length of the chromatogram is only limited by the diffusion of the spots. The above methods are applied to the separation of ^{95}Zr-^{181}Hf, ^{95}Zr-^{95}Nb, and ^{241}Am-^{244}Cm. The radiochromatograms were evaluated by direct scanning and autoradiography. These methods are also discussed. (auth)

44119 FIXATION OF URANYL ACETATE IN AN ANION EXCHANGE RESIN. Vaissiere, Michele; Tremillon, Bernard (E.N.S.C.P., Paris; I.N.S.T.N., Saclay, France). Bull. Soc. Chim. France, No. 7, 2099-2103(July 1965). (In French).

Of a group of 13 elements (Mg, Ca, Ba, Zn, Cd, Hg, Cu, Pb, Mn, Fe, Ni, Co, and U^{6+}), only the last manifests a strong fixation in a Dowex-1 × 8 resin in the acetate form. This fixation was studied quantitatively by the determination of the partition curves and the variations of the partition coefficient of U^{6+} as a function of the concentration of an acetate-buffered solution. The interpretation of the experimental results made it possible to derive the partial dissociation constants of the three complexes, $UO_2(AcO)_3^-$ ($pk_3 = 2.1 \pm 0.3$), $UO_2(AcO)_2$ ($pk_2 = 1.6 \pm 0.3$), and $UO_2(AcO)^+$ ($pk_1 = 2.5 \pm 0.1$), in agreement with the values determined earlier. Formation in the resin of the complex $UO_2(AcO)_3^-$ (exchange constant with AcO^-, $K_3 = 19 \pm 2$) and $UO_2(AcO)_4^{--}$ (partial dissociation constant $pk_4 = -0.6 \pm 0.1$) was established. This selective fixation of U^{6+} made it possible to predict separations of this element. A purification and concentration of U^{6+} in the presence of Cd, Cu, Mn, Ni, and Fe^{3+} are described. (tr-auth)

44120 CHROMATOGRAPHIC SEPARATION OF RADIOCHEMICALLY PURE ^{90}Y FROM THE PARENT ISOTOPE ^{90}Sr. Macasek, F.; Cech, R. (University Komenskeho, Bratislava). Chem. Zvesti, 19: 107-14(1965). (In Slovak).

The coefficient for the chromatographic separation of ^{90}Y and ^{90}Sr in the 10^{-2}M EDTA solutions at pH 4 to 4.5 reached a value of 10^3 to 10^4. In distinction to the effect observed in the separation of macro-quantities of the ions, the use of EDTA complexes with average stability constants did not improve but actually affected the separation adversely. Conditions for chromatographic separation of ^{90}Y and ^{90}Sr, on Dowex 50 X2 in the ammonium form (200 to 230 mesh, column 30 cm × 0.44 cm^2) by elution with 10^{-2}M EDTA at pH 5.11, are as follows: for a flow rate of 0.8 ml/min, at least a 33-fold elution of ^{90}Y from equilibrium ^{90}Sr with a radiochemical purity of >99.9998% is possible. The procedure is simple and requires about 2 hr. The influence of metal-EDTA complexes on the separation was related to the influence on adsorption of Sr by competing ions. (BBB)

44121 ^{90}Sr, SUBPRODUCT OF THE TREATMENT OF IRRADIATED FUEL. Salvador, Leonardo Ramos; Perez, Baldomero Lopez. (Junta de Energia Nuclear, Madrid). Energia Nucl. (Madrid), 9: 209-14(May-June 1965). (In Spanish).

The laboratory methods previously used for the recovery of ^{90}Sr are briefly summarized. These methods were based essentially on typical separations of analytical chemistry. Methods developed for the recovery of ^{90}Sr based on solvent extraction are summarized. The effect of these methods on the cost of fission-product radiation sources is indicated. (J.S.R.)

44122 ION EXCHANGE RESIN SEPARATION AND FLAME PHOTOMETRIC DETERMINATION OF SODIUM, POTASSIUM, MAGNESIUM, CALCIUM, AND STRONTIUM. Breault, Eugene A. (Food and Drug Administration, San Francisco). J. Assoc. Offic. Agr. Chemists, 48: 719-28 (Aug. 1965).

The cation exchange separation of metallic chlorides by hydrochloric acid on an Amberlite CG-120 resin (200 to 400 mesh) column was investigated. Commercially available resin was used in the experiments after "fines" were removed by several water washings. A resin column (24 cm long by 12 mm diameter) gave excellent separation of sodium and potassium, with a total volume of 500 ml of 0.5N HCl at a flow rate of 0.55 ml/min. The recovery of each metal was 100%. Elution of the other three metals required 1100 ml of 1N HCl; separation was very good but recoveries were poor. All of the metals were determined by photometry. (auth)

44123 ION EXCHANGE OF RADIOACTIVE ION WITH ZEOLITIC TUFF. Nishidoi, Mutsumi (Kurita Industry Co., Ltd., Japan). Nippon Genshiryoku Gakkaishi, 7: 298-305(May 1965). (In Japanese).

Study was directed to finding an economical ion exchanger for removing Cs and Sr from radioactive waste. It was found that the ion-exchange capacity of aluminosilicate mineral is closely related to its crystal structure. Work was carried out on zeolitic tuff possessing the three dimensional clay structure. The zeolitic tuff consisted of moldenite crystal and noncrystallized volcanic glass, and these components had different selectivity and exchange capacity. Pretreatment of the zeolitic tuff modified its exchange capacity and selectivity, and this can be attributed to a change in its crystal structure and in some cases in its

solid-state properties. Natural zeolitic tuff was successfully applied to the decontamination of radioactive solutions, and it was found that it has good selectivity for Cs ions. (auth)

44124 PAPER CHROMATOGRAPHIC SEPARATION OF TANTALUM, NIOBIUM, AND HAFNIUM. Nascutiu, T.; Grigorovici, Aurora (Inst. for Atomic Physics, Bucharest). Rev. Roumaine Chim., 10: 449-56(May 1965).

Paper chromatographic separation of tantalum, niobium, and hafnium by using mixtures composed of organic solvent–40% hydrofluoric acid–H_2O or 0.5M organic (oxalic or tartaric) acid (35:2:3) was studied. The most effective separations were obtained by using mixtures containing acetylacetone or dioxane. The radiochemical purity of the separated spots was checked by using a γ spectrometer. (auth)

44125 SEPARATION OF THORIUM, SCANDIUM, AND YTTRIUM EARTHS BY MEANS OF REVERSED-PHASE CHROMATOGRAPHY. Ma, Hui-chang; Nee, Che-ming; Liang, Shu-chuan (Inst. of Chemistry, Academia Sinica, Peking). Sci. Sinica (Peking), 14: 1176-83(Aug. 1965).

By means of tri-n-butyl phosphate (TBP) supported on poly(tetrafluoroethylene) of 50 to 150 mesh as the stationary phase, and mineral acids of different concentrations or water as the mobile phase, it was feasible to separate thorium, scandium, and yttrium earths from each other. Two columns, 0.9 and 2 cm in diameter, were used, and both were packed to a height of 15 cm. Except for samples containing more than 10 mg of thorium, the smaller column was usually used. A two-elution procedure was devised, with which mixtures containing 1 to 99 mg of thorium, 1 to 100 μg of scandium, and 1 to 5 mg of yttrium earths were separated satisfactorily. Using 4N nitric acid as eluant, scandium and yttrium earths were eluted from the column, while thorium remained. The latter could then be washed out with water. After removal of TBP with carbon tetrachloride extraction, the eluate containing scandium and yttrium earths was evaporated to dryness and the residue was taken up with 8N hydrochloric acid. The solution was transferred to the column and eluted with 8N hydrochloric acid to remove yttrium earths, while scandium remained on the column. The latter was finally removed with 2N hydrochloric acid. Flow rate was regulated to 1 cm per minute for all elutions. (auth)

44126 DESIGN OF A CHOP AND LEACH REPROCESSING PLANT FOR THE JAPANESE ATOMIC FUEL CORPORATION. Bloomfield, Donald E.; Ehrman, Chester S.; Vassil, Lefter K. (American Machine and Foundry Co., York, Pa.). 33p. (CONF-650602-51). Gmelin, AED-CONF-65-125-85.

From American Nuclear Society, 11th Annual Meeting, Gatlinburg, Tenn.

A general description of the equipment and systems being considered for use in the Chop and Leach Facility of the Japanese Atomic Fuel Corporation (JAFC) Reprocessing Plant to be built in Tokai-Mura, Japan, is presented. The Chop and Leach Facility is designed to mechanically disassemble spent nuclear fuel elements removed from operating power reactors and to leach the fuel from the clad. Each major component of processing equipment is described in addition to the auxiliary cells and areas surrounding the three process cells. A block flow diagram and chemical process flow diagram are provided to show the flow of materials and chemicals throughout the Chop and Leach Facility. (P.C.H.)

44127 IMPROVEMENTS RELATING TO CHEMICAL EXTRACTION PROCESSES. Hartley, Kenneth; Lindley, John; Bleazard, John Malcolm Bailey (to United Kingdom Atomic Energy Authority). British Patent 1,000,120. Aug. 4, 1965. Filed Dec. 13, 1961.

A method is described for processing reactor fuels by exchange between contacting media, particularly extraction from a solid to a liquid phase. The fuel is finely divided, fed as a solid phase to a first mixer section of a series of mixer sections containing the leaching liquid phase. The contents of the mixer section are agitated, and a quantity of the mixed phases is lifted from a mixer section to a settler section at a higher level. The separation of the phases is allowed to take place in the settler section; and the settled phases are discharged from the settler section, the liquid back to the same mixer section, and the solid forward to the following mixer section in the series. The cyclic repetition of the lifting, settling, and discharging operations processes the solid phase through the series of mixer sections. At the end of the series of sections, the solid phase represents the insoluble residue that can be drained off with only a small amount of the accompanying liquid phase. Detailed description of the mixer-settler apparatus is given. (B.L.M.)

44128 IMPROVEMENTS IN OR RELATING TO THE DISSOLUTION OF URANIUM. Rateau, Arthur (to Commissariat a l'Energie Atomique). British Patent 1,001,431. Aug. 18, 1965. Priority date June 6, 1962, France.

A process for the dissolution of uranium allows a considerably increased velocity of attack under continuous conditions with respect to standard processes with constant rates of introduction of U and HNO_3 into the dissolver while the velocity of attack is maintained at a substantially constant value. Neither high pressure nor elevated temperature are necessary for the process. The U metal or U compound is continuously attack by a solution of HNO_3 containing a controlled and substantially constant concentration of uranyl ions, 2 to 5 moles/l. The HNO_3 concentration is from 1 N to 11 N, preferably 3 N to 5 N. (B.L.M.)

44129 RECOVERY OF URANIUM AND/OR VANADIUM VALUES FROM ORES CONTAINING THE SAME. Lewis, Clifford J.; Dunn, William S. (to Allied Chemical Corp.). U. S. Patent 3,198,599. Aug. 3, 1965. Filed Sept. 15, 1961.

A process for recovering U and V values from their ores consists of contacting the ores with a solubilizing and extracting solution containing either NO_2 or nitrogen tetroxide, a water insoluble organophosphate, and a water-insoluble inert organic solvent. The amount of nitrogen oxide in the solution is at least stoichiometrically equivalent to the U and V values in the ore and generally is adequate to produce a pH of about 0.5 to 2.0. The use of a controlled low amount of water in the system is particularly critical. Use of water in amounts of more than 6 wt % of the extracting solution results in the solubilizing of undesirable metals, while efficient solubilizing of the U and V values is not obtained using less than 1 wt % of water. The preferred composition of the solubilizing and extracting solution is 1 to 5 wt % nitrogen oxide; 5 to 20 wt % of organophosphate, di-2-ethyl-hexyl-phosphoric acid; and 75 to 94 wt % of organic solvent, CCl_4. (B.L.M.)

44130 APPARATUS FOR THE CONTINUOUS ELECTROLYTIC REGENERATION OF ION EXCHANGE RESINS. Chagnon, Pierre; Platzer, Roger (to Commissariat a l'Energie Atomique). U. S. Patent 3,198,723. Aug. 3, 1965. Priority date June 16, 1959, France.

An ion exchange resin is caused to flow as a compact bed continuously through an electrolytic regeneration cell while a regeneration solution is passed through the cell either co-current or countercurrent to the ion exchange resin. The electrolytic cell may be a vertical column through which the resin flows from top to bottom, or it may be a casing mounted around a porous moving double cloth through which the resin passes as a monogranular layer between two bands of cloth. The regeneration cell may be combined with a fixation circuit to provide a purification installation operating continuously in an automatic manner and adaptable to remote control. (A.G.W.)

ENGINEERING

General

44131 (ACNP-65003) STEAM SEPARATION TECHNOLOGY UNDER THE EURATOM PROGRAM. PART 2. PRIMARY AND SECONDARY SEPARATION OF STEAM FROM WATER BY MECHANICAL MEANS. (Allis-Chalmers Mfg. Co., Milwaukee, Wis. Atomic Energy Div.). July 30, 1965. Contract AT(11-1)-1186. 426p. (EURAEC-1452). Dep. mn; CFSTI $7.26 cy, $2.00 mn.

Work Performed under United States-Euratom Joint Research and Development Program.

Three types of mechanical primary separators were developed and tested. Analytical techniques were developed which can be used in the designing of the separators. Type 1. The downcomer centrifugal separator was developed and tested in air-water and steam-water. Total flow rates of 870,000 lb/hr steam-water were achieved in the 10-in. diameter separator. Steam test pressure varied from 600 to 2000 psig. Analytical techniques for separator design are reported. Type 2. Upcomer type centrifugal separators were developed and tested in air-water and steam-water. Total flow rates of 790,000 lb/hr steam-water were achieved in a separator with a 10-in. diameter separating zone and 18-in. diameter shroud. Analytical techniques were developed to facilitate separator design. Type 3. A low pressure drop cross flow separator was developed and tested in both air-water and steam-water. This separator permits higher recirculation flows within a reactor for equal carryunder when compared to a natural-separation design. Test data and design techniques are reported. Limiting capacities of chevron and mesh type dryers were determined by testing in steam at pressures from 600 to 2000 psig at flow rates from 5000 to 60,000 lb/hr. (auth)

44132 (AECL-2249) HIGH PRESSURE ROTARY FACE-TYPE SHAFT SEALS FOR WATER APPLICATIONS. Watson, R. D. (Atomic Energy of Canada Ltd., Chalk River (Ontario)). Dec. 1964. 24p. Dep.; AECL $0.50.

Information resulting from development work performed by AECL was used to explain the operation and failure of rotary face-type shaft seals in high pressure water. Several types of hydrostatic and hydrodynamic seals were investigated and two, the orifice-type controlled leakage hydrostatic seal and elliptical seal, show great promise for the future. A number of different combinations of materials were used in testing shaft seals, but not one has proved entirely satisfactory. (auth)

44133 (BAW-1280-31) MATERIALS EXAMINATION OF A MODEL SODIUM HEATED STEAM GENERATOR. Progress Report. Research Report No. 5131. Fortner, E.; Kovach, P. J. (Babcock and Wilcox Co., Alliance, Ohio. Research Center). Aug. 27, 1965. Contract AT(11-1)-1280. 44p. Dep. mn; CFSTI $2.00 cy, $0.50 mn.

The purpose of this test program is to assess the compatibility of Croloy 2¼ and TP 316 SS in a liquid sodium system, particularly with reference to the design parameters of a full-size sodium-heated steam generator. The samples were as-received commercial pipe and sections of pipe removed from the model steam generator after 1000, 2000, and 4000 hours of operation. The Croloy 2¼ was at 1000°F. TP 316 SS pipe was removed from two positions, one at 1000°F and the other at 1100°F. Metallographic and microhardness studies were made of each sample. As-received and 4000 hour samples of Croloy 2¼ and 316 SS (1100°F) were analyzed with the electron microprobe x-ray analyzer. Two special heat treatments were used with selected specimens to substantiate conclusions based on examination of the loop material. The as-received Croloy 2¼ was slightly decarburized and contained surface depletions of chromium and silicon. Nickel and copper were piled up near the surfaces. These initial gradients (attributed to oxidation during mill treatment) and tempering effects complicate assessment of mass transfer processes. Slight decarburization (detectable to about 15-20 mils after 4000 hours), copper depletion, and nickel pickup occurred during exposure. No preferential mass transfer was indicated by the examination of the TP 316 SS samples although a general attack is probable. The material is characterized by sensitization during exposure and by persistent banding. (auth)

44134 (EUR-2434.d) FLANSCHVERBINDUNGEN MIT STROMISOLIERENDEM DICHTUNGSKOERPER. (Flange Connections Featuring an Insulating Sealing Element). Schupp, W. (European Atomic Energy Community, Ispra (Italy). Joint Nuclear Research Center). 1965. 8p. Dep. mn.

For the operation of test circuits for the examination of heat transfer on tubes and tube bundles with organic coolants or pressurized and boiling water, direct electrical heating is used. This means that the heated test section, must be insulated against the whole circuit. Test circuits operate at approximately 50 atm and 450°C (organic coolants), resp. at 250 atm and 450°C (boiling and pressurized water). The construction described resolves the above problem by means of two ceramic rings (Al_2O_3), the inner ring serving as insulator and as gasket against the coolant. The results achieved with it have been satisfactory up to this date. (auth)

44135 (IA-1033) SEALING FACTORS—THEIR MEASUREMENT AND USE IN THE DESIGN OF VACUUM GASKET SEALS. Roth, A.; Amilani, A. (Israel Atomic Energy Commission, Yavne. Soreq Nuclear Research Center). Apr. 1965. 27p. (CONF-650643-1). Dep. mn.

From 3rd International Vacuum Congress, Stuttgart.

A general method for designing vacuum gasket seals and predicting their performance is described. The method is based on determining the sealing factor, by using a "sealometer" which performs measurements using a regularly shaped model simulating the sealing surface. Equations predicting the idealized sealing process for the model surfaces are derived, results are compared with those obtained in actual seals, and correction factors are derived for the deviations. The possibilities of developing this method for the design of special seals are discussed. (auth)

44136 (LA-3234) THE DEVELOPMENT OF AN INTERLEAVED, FRACTIONAL-TURN COIL. Dike, Robert S.; Kemp, Edwin L.; Marshall, John (Los Alamos Scientific Lab., Univ. of California, N. Mex.). Apr. 1, 1965. Contract W-7405-eng-36. 6p. Dep. mn; CFSTI $1.00 cy, $0.50 mn.

An interleaved, fractional-turn coil design is explained, and the current flow in the coil is discussed. A quarter-turn, 9-in. ID., 11 in. long coil was built and connected to four 25 kv banks with a combined energy of 25 kJ. The system produced 63-kv theta voltage around the coil and generated 13 kG rising in 1.6 μsec. This coil is shown, and the mechanical and electrical advantages are discussed. (auth)

44137 (N64-24017) RIFT SYSTEMS ANALYSIS. VOLUME 3. AERODYNAMICS. Report 201. (Lockheed Missiles and Space Co., Sunnyvale, Calif.). Nov. 1963. Contract NAS 8-5600. 117p. (NASA-CR-56646; NSP-63-96(Vol.3)). CFSTI $9.60 cy.

The results are presented of aerodynamic analyses for the Saturn VN launch vehicles, both RIFT and operational, which are applicable to the 176,000-lb impulse propellant capacity S-N stage. The aerodynamic characteristics are obtained by a combination of theoretical methods and available scale-model experimental test data. The information included covers aerodynamic data for the areas of stability and control, performance, and drag; data for structural de-

sign; data for ground transporter design; and jet-wake characteristics of secondary propulsion systems. (auth)

44138 (NYO-3363-4) AN EXPERIMENTAL STUDY OF FILM RUPTURE IN JOURNAL BEARINGS WITH LOW KINEMATIC VISCOSITY LUBRICANTS. Period Covered: May 1964–February 1965. Orcutt, F. K.; Pan, C. H. T. (Mechanical Technology Inc., Latham, N. Y.). Mar. 1965. Contract AT(30-1)-3363. 63p. (MTI-65TR13). Dep. mn; CFSTI $3.00 cy, $0.75 mn.

Studies of film rupture and cavitation in bearing film were extended to lubrication with fluids of low kinematic viscosity whose surface forces (surface tension and wettability) are different from those of hydrocarbon oils and closer to those of liquid metals. The study consisted of visual observations of the film rupture region, using high-speed still and motion picture records. Local film boiling in the film-rupture region was induced by de-aeration and reduction of ambient pressures. The visual studies and a parallel theoretical analysis indicated that the surface forces greatly affect the details of the film-rupture region. Unstable film-rupture regions as well as entrainment of bubbles and their carry-over to the high pressure regions of the lubricant film are much more prevalent when the lubricant has high surface tension and poor wettability. Since these conditions are at least a prerequisite to cavitation damage, it is particularly desirable in such cases to design bearings so as to avoid generation of large negative pressure gradients which can reduce the hydrodynamic pressures to the vapor pressure of the lubricant. (auth)

44139 (ORNL-TM-1174) ELECTROPLATING OF ^{109}Cd ON COPPER WIRES. Wamanacharya, G. S. (Oak Ridge National Lab., Tenn.). Sept. 1965. Contract W-7405-eng-26. 8p. Dep. mn; CFSTI $1.00 cy, $0.50 mn.

Soft x-ray sources for thickness gages were prepared by electroplating ^{109}Cd onto copper wires from an acid fluoroborate bath. Thin, adherent deposits of cadmium were obtained from a bath containing ~1.7 mC ^{109}Cd/ml, 6-10 mg of cadmium/ml as $Cd(BF_4)_2$, and 5-6 mg of NH_4BF_4 at a pH of 3. A current of one to two ma was passed for about an hour. (auth)

44140 (ORNL-TM-1244) FLASH: AN IBM-7090 CODE FOR COMPUTING MULTI-STAGE FLASH EVAPORATOR PLANT DESIGNS FOR THE DESALINATION OF SEAWATER. Easterday, R. J. (Oak Ridge National Lab., Tenn.). Sept. 1965. Contract W-7405-eng-26. 87p. Dep. mn; CFSTI $3.00 cy, $0.75 mn.

An IBM-7090 code, FLASH, was written to optimize the design of a multi-stage flash evaporator saline water conversion plant. For an assigned water production, successive heat and material balance solutions and associated costs are computed to determine the optimum design. The output consists of listings of the heat and material balance results and of the comparative cost data. The code was originally written by the Bechtel Corporation. (auth)

44141 (RFP-573) AN EXPERIMENTAL HYDROSTATIC JOURNAL BEARING. Rains, A. E. (Rocky Flats Div., Dow Chemical Co., Denver, Colo.). Aug. 27, 1965. Contract AT(29-1)-1106. 33p. Dep. mn; CFSTI $2.00 cy, $0.50 mn.

A description is given of the design, fabrication, and testing of a typical hydrostatic spindle bearing. An extension of classic design to account for shaft angularity is presented. (auth)

44142 (SC-RR-65-286) PROJECT SAND FINAL PROGRAM REPORT. VOLUME III. DYNAMIC ANALYSIS OF THE SAND SAMPLER FLIGHT. Vaughn, H. R.; Matejka, D. Q. (Sandia Corp., Albuquerque, N. Mex.). Sept. 1965. Contract AT(29-1)-789. 63p. Dep. mn; CFSTI $3.00 cy, $0.75 mn.

A dynamic analysis of flight RY-15 of the SAND sampler is presented. The structural failure of the sampling vanes is shown to have resulted from resonance of the first bending mode with the payload oscillatory motion. (auth)

44143 (SC-RR-65-306) SHORT CUT METHOD FOR DIMENSIONAL ANALYSIS. Houghton III, A. V.; Kitzinger, David G. (Sandia Corp., Albuquerque, N. Mex.). Sept. 1965. Contract AT(29-1)-789. 10p. Dep. mn; CFSTI $1.00 cy, $0.50 mn.

Generalized matrix methods for the solution of dimensional analysis problems are described. A simplified method for producing dimensionless products is illustrated by a sample problem. By the simplification method, complete sets of dimensionless products are obtained almost by inspection. (auth)

44144 (TID-22134) EXPERIMENTAL STRESS ANALYSIS OF THE ATTACHMENT REGION OF HEMISPHERICAL SHELLS WITH RADIALLY ATTACHED NOZZLES. Maxwell, R. L.; Holland, R. W.; Cofer, J. A. (Tennessee Univ., Knoxville, Dept. of Mechanical and Aerospace Engineering). June 1965. Contract W-7405-eng-26; Subcontract w7405-Eng-26(2203). 541p. (ME-7-65-1). Dep. mn; CFSTI $8.41 cy, $3.25 mn.

Stress patterns were determined for six nozzle configurations for the following five types of loadings: internal pressure, axial load on nozzle, pure bending moment on nozzle, shear load on nozzle, and pure torque on nozzle. The nozzle radius-to-thickness ratio was varied from 4.75 to 21, but the hemisphere ratio was kept constant at 40.85. (D.L.C.)

44145 (TID-22138) IBM 7090 BOLTED CLOSURE STRESS ANALYSIS PROGRAM. McLaughlin, E. R. (Kaiser Engineers, Oakland, Calif.). July 1, 1962. Contract AT(10-1)-925. 52p. Dep. mn; CFSTI $3.00 cy, $0.50 mn.

The program is written in Fortran II language for the IBM 7090 computer and is divided into two chain links. The first chain link computes the various terms for the edge forces if two or more components are involved, while the second chain link calculates the edge forces, influence coefficients, and stresses. Operating instructions, preparation of input data, flow chart, and sample input data sheets are included. (D.L.C.)

44146 (TIM-874) OVERHUNG ROTOR DYNAMICS TESTS USING HYDROSTATIC WATER BEARINGS. Newey, D. A. (Pratt and Whitney Aircraft, Middletown, Conn. Connecticut Advanced Nuclear Engineering Lab.). June 24, 1965. Contract AT(30-1)-2789. 51p. Dep. mn; CFSTI $3.00 cy, $0.50 mn.

Results are reported of a rotor dynamics test with an overhung mass system using water as a lubricant, which is part of a liquid metal pump development program. Most of the work was directed toward finding a means of predicting and optimizing the conditions required to maintain stable rotation of the shaft. Bearing stiffness was evaluated by use of a hydraulic loading device. The relation between bearing stiffness and stability was studied by observing shaft whirl patterns. Low clearances were found to produce low whirl ratios and considerable hydrodynamic action at high speeds. Higher whirl ration up to six were obtained by increasing the bearing clearance. The dynamic assembly consisted of a relatively stiff shaft supported by orifice compensated hydrostatic bearings. The amplitude of the synchronous whirl pattern at the system critical speed was found to be negligible due to high fluid damping characteristics. (auth)

44147 (TIM-917) SUMMARY OF FLUID FILM BEARING ANALYSIS. Groll, D. (Pratt and Whitney Aircraft, Middletown, Conn. Connecticut Advanced Nuclear Engineering Lab.). June 17, 1965. Contract AT(30-1)-2789. 30p. Dep. mn; CFSTI $2.00 cy, $0.50 mn.

A summary is presented of analytical work done in support of the experimental water and liquid metal bearing program at CANEL. The work included large pool hydrostatic orifice-compensated fluid-film journal bearings, annular orifice-compensated hydrostatic thrust bearings, and rotor dynamics tests in water. (D.L.C.)

44148 (TIM-918) CENTRIFUGAL PUMP IMPELLER DESIGN SYSTEM. Lamers, R. P. (Pratt and Whitney

Aircraft, Middletown, Conn. Connecticut Advanced Nuclear Engineering Lab.). June 24, 1965. Contract AT(30-1)-2789. 58p. Dep. mn; CFSTI $3.00 cy, $0.75 mn.

A summary is presented of the centrifugal pump impeller design system developed at CANEL. The system includes an analysis-design effort and a fabrication-inspection effort. The system is part of the technology which has been developed for the design and development of high speed turbomachinery for pumping high temperature liquid metals. (auth)

44149 (TIM-921) STRADDLE BEARING ROTOR DYNAMICS TESTS WITH STEP BEARING IN WATER. Merz, C. A. (Pratt and Whitney Aircraft, Middletown, Conn. Connecticut Advanced Nuclear Engineering Lab). July 21, 1965. Contract AT(20-1)-2789. 48p. Dep. mn; CFSTI $2.00 cy, $0.50 mn.

Preliminary results are reported of the second of a series of straddle rotor dynamics tests designed to evaluate and develop various types of journal bearings for the SNAP-50/SPUR liquid metal pump development program. The test unit consisted of a vertical rigid rotor supported by two non-uniform clearance journal bearings (step bearings) using demineralized, deaerated water for the bearing lubricant. A single pool hydrostatic thrust bearing was used to support the rotating shaft assembly. The test results indicate that the rigid rotor shaft bearing resonance (critical speed) is highly damped which permits the pump to be designed for operation above the critical speed. However, operation through and above the bending critical speed of the shaft bearing system (flexible shaft design) has not yet been determined. Experimental data are presented for the onset of unstable self-excited whirl. The onset of unstable self-excited whirl always occurred at speeds greater than the first critical speed of the shaft bearing system. Whirl ratios at the onset of unstable self-excited whirl were measured. The effects of journal bearing supply pressure, water inlet temperature, shaft unbalance, and bearing housing flexibility are shown. The data indicates the bearing housing flexibility can influence the onset of unstable self-excited whirl. A model is presented which shows all of the forces acting on a shaft during synchronous whirl which allows estimates of the dynamic journal bearing performance parameters. Comparison of the stability data for the step bearing with that of the hydrostatic journal bearings reported in TIM 836 shows the four pool orifice compensated hydrostatic journal bearing to exhibit a much greater stable region of operation for all journal bearing supply pressures and temperatures tested. (auth)

44150 (TIM-923) BALL BEARING TEST IN LITHIUM. Richards, W. D. (Pratt and Whitney Aircraft, Middletown, Conn. Connecticut Advanced Nuclear Engineering Lab.). July 15, 1965. Contract AT(30-1)-2789. 25p. Dep. mn; CFSTI $1.00 cy, $0.50 mn.

Results are reported of a liquid metal 40 mm bore ball bearing test which was part of a liquid metal pump development program. The test was conducted for 102 hours in 600°F lithium at a maximum rotational speed of 2600 rpm and under a maximum radial load of 40 pounds. Results of this experiment are limited because of a retainer failure after 102 test hours had been obtained. (auth)

44151 (TIM-925) SINGLE HYBRID JOURNAL BEARING TESTS IN WATER. Knudsen, L. (Pratt and Whitney Aircraft, Middletown, Conn. Connecticut Advanced Nuclear Engineering Lab.). July 15, 1965. Contract AT(30-1)-2789. 27p. Dep. mn; CFSTI $2.00 cy, $0.50 mn.

An orifice compensated hybrid hydrostatic journal bearing was tested in water. The test results followed the zero speed theoretical trends with slightly greater load capacity which increased as the journal speed was increased. The lubricant flow rate remained constant for all speeds at constant supply pressure differentials. The 1.5 inch bearing was tested at a diametral journal clearance of 0.0036 inch with orifices of 0.030 to 0.052 inch diameter under differential supply pressures from 12.5 to 80 psi, at speeds from zero to 10,000 rpm and radial loads from zero to 40 pounds. (auth)

44152 (TIM-926) THRUST BEARING TESTS IN WATER. Knudsen, L. (Pratt and Whitney Aircraft, Middletown, Conn. Connecticut Advanced Nuclear Engineering Lab.). July 15, 1965. Contract AT(30-1)-2789. 24p. Dep. mn; CFSTI $1.00 cy, $0.50 mn.

An orifice compensated double-acting hydrostatic thrust bearing was tested in water. The load carrying capacity was lower than the values predicted by an analysis based on flat plate laminar flow theory. Increases in load carrying capacity resulted with increase of speed at all bearing differential supply pressures below 50 psi. The test bearing laminar region flow rates were within 1.3% of the theoretically predicted values. The 3.2 inch diameter thrust bearing was tested with a 0.050 inch diameter orifice under differential supply pressures from 25 to 50 psi at speeds from zero to 11,500 rpm and radial loads from zero to 80 pounds. (auth)

44153 (JPRS-31361) CURRENT STATUS OF THE PROBLEM OF SEA-WATER DISTILLATION. Churin, A. I.; Klyachko, V. A. Translated from Vestn. Akad. Nauk SSSR, No. 6, 34-47 (June 1965). 18p. (TT-65-31858). CFSTI $1.00 cy, $0.50 mn.

Water supply problems are considered. Possible ways for increasing the efficiency in distillation installations are discussed. Methods for preventing scale formation in the evaporators are described. The plants at Shevchenko and elsewhere are described. Other methods for freshening water are considered. The advantages of using dual-purpose atomic power plants to freshen water are discussed in some detail, and plans for such use in USSR are described. (D.L.C.)

44154 SALINE WATER CONVERSION REPORT FOR 1964. (Office of Saline Water, Washington, D. C.). 304p. GPO $2.00.

A detailed summary is presented of the 1964 desalting operations of the Department of the Interior. Research, processes, and demonstration plants are covered. (D.L.C.)

44155 THE CHEMICAL INDUSTRY—A TRAINING GROUND FOR NUCLEAR POWER ENGINEERS. Hoyle, Alex C. (Canadian General Electric Co. Ltd., Peterborough, Ont.). 28p. (CONF-650559-2). Gmelin, AED-CONF-65-086-12.

From American Inst. of Chemical Engineers, 56th National Meeting, San Francisco.

Similarity in the design, steady state operation, and transient behavior of the major heat transport systems of a nuclear reactor to chemical engineering are discussed. A parallel exists in the range of unit operations appropriate to the two industries and the design engineering techniques and training programs are practically the same. The design and operation of a nuclear power reactor matches the definition of chemical engineering. A description of the NPD (Nuclear Power Demonstration) Reactor process systems are given to illustrate the conventional chemical engineering and special engineering knowledge applicable to this type of reactor. (P.C.H.)

Applications of Nuclear Explosions

44156 (DP-956) RECOVERY OF ACTINIDES PRODUCED BY A NUCLEAR DETONATION IN SALT FORMATIONS. Karraker, David G.; Perkins, William C. (Du Pont de Nemours (E. I.) and Co., Aiken, S. C. Savannah River Lab.). June 1965. Contract AT(07-2)-1. 47p. Dep. mn; CFSTI $3.00 cy, $0.50 mn.

A chemical process was developed for the recovery of actinide elements produced by the explosion of a nuclear device in impure salt. The process includes separation of salt by dissolution in water, metathesis of sulfate minerals to carbonates with ammonium carbonate solution, dissolution of the metathesized solids in 6M nitric acid, precipitation of silica from the solution by gelatin, and

two alternating solvent extraction and evaporation steps to produce a concentrated product solution. Developmental tests of the process with samples of debris from the Gnome test indicated that gram quantities of actinides could be recovered in greater than 85% yield from 3×10^4 tons of debris. The two solvent extraction cycles demonstrated a separation of actinides from major cationic impurities—Ca^{2+}, Mg^{2+}, and Fe^{3+}—by a factor of $>10^5$ and, combined with evaporation, gave a product solution equivalent to 100 gallons per 10^4 tons of original salt debris. (auth)

44157 (LA-DC-7304) NEUTRON EXPERIMENTS WITH UNDERGROUND NUCLEAR EXPLOSIONS. Diven, B. C. (Los Alamos Scientific Lab., Univ. of California, N. Mex.). [1965]. Contract W-7405-eng-36. 18p. (CONF-650706-22). Dep. mn; CFSTI $1.00 cy, $0.50 mn.

From International Conference on the Study of Nuclear Structure with Neutrons, Antwerp.

Techniques were developed that use nuclear explosions as pulsed neutron sources for time-of-flight experiments. Measurements of capture and fission cross sections were made. Some preliminary results are presented. (auth)

44158 (UCRL-14311) SOME CALCULATIONS FOR EFFECTING OILFIELD STIMULATION BY NUCLEAR MEANS. Higgins, Gary H.; Rodean, Howard C. (Lawrence Radiation Lab., Univ. of California, Livermore). Aug. 5, 1965. Contract W-7405-eng-48. 16p. (CONF-651007-1). Dep. mn; CFSTI $1.00 cy, $0.50 mn.

From Society of Petroleum Engineers, 40th Annual Fall Meeting, Denver.

Nuclear explosions in underground rock formations form large cavities surrounded by a substantial region of crushed and fractured rock. The cavity generally collapses to form a rubble-filled chimney that is very porous and highly permeable. The surrounding crushed and fractured zone is also increased in permeability to such a degree that the effective well radius of a natural-gas well stimulated by a nuclear explosion may be several times the chimney radius. The relations between yield, depth of burial, and the geometry of chimneys and fractured regions indicate that the effect of explosion yield on the number of wells required in a given region should be investigated from the standpoint of economics. Similarly, the relations between thermal energy deposition and yield indicate that heating of the chimney rubble (and, therefore, the natural gas) is independent of yield, but the thermal time constant of the chimney rubble varies directly with yield and inversely with production rate. A representative value for this time constant is eight years. The radioactivity concentration present in natural gas from a well stimulated by a nuclear explosion is independent of yield only if the design parameters such as fission-to-fusion ratio are held constant. The radionuclides which might be product contaminants are tritium, carbon-14, and krypton-85. These materials will be concentrated in the rubble-filled chimney, so as production proceeds, the contaminants will be purged from the reservoir and the contamination will continuously decrease. The initial concentration of ^{85}Kr might be about 100 pC/cm^3 of gas. After a few hundred million standard cubic feet of gas have been removed (equivalent to about two to five chimney volumes of gas), ninety percent of the contaminants will have been removed from the well. The average contamination for the entire production period will be about 3 pC/cm^3. When these values are compared to stated standards for the general population, these average concentrations do not lead to air contamination in excess of permissible levels. (auth)

44159 THE PARTICLE STATISTICS OF RUBBLE PRODUCED BY UNDERGROUND NUCLEAR EXPLOSIONS. Rodean, Howard C. (Univ. of California, Livermore). Geophysics, 30: 616-23(Aug. 1965). (UCRL-12129).

Underground nuclear explosions produce cavities into which the overburden may collapse, forming a rubble-filled chimney. The particle statistics, especially mean surface-volume diameter, are important to various potential applications of nuclear explosives. The available rubble statistics are rather limited, even with the best data obtained from post-shot exploration of the Hardhat event. Two sets of Hardhat data are presented: one based on photographs of relatively undisturbed rubble, and another obtained from visual estimates of what would be obtained by screening. The method of obtaining particle statistics must be consistent with the intended use of the statistics, because the method of measurement, such as handling for sieving, affects the statistics. It was long established that crushing and grinding (which occur during chimney collapse) force particle statistics toward the lognormal frequency distribution. Both sets of Hardhat data fit the lognormal distribution in a satisfactory manner. The volume-surface mean particle diameter for the undisturbed Hardhat rubble is 1.33 ft, and the estimate for the volume-surface mean particle diameter obtained by screening is 0.433 ft. Additional statistics from the field plus a better understanding of rock-fracture phenomena are required to develop statistical relations for use in prediction and control of underground nuclear explosion effects. (auth)

Facilities and Equipment

Refer also to abstract 45507.

44160 (ANL-7000, pp 278-86) PLANT MODIFICATIONS AND NEW FACILITIES. (Argonne National Lab., Ill.).

A plant recirculating water system for cooling scientific equipment, a He atmosphere system for a single vacuum drybox, a recirculating Ar atmosphere for a glovebox system, the alpha-gamma hot cell, tube fabricating equipment, and extrusion press testing and modification are described. (W.L.G.)

44161 (APDA-174, pp 25-32) SMALL LEAK Na-WATER REACTION. Project Agreement No. 10. Muenchow, H. O. (Atomic Power Development Associates, Inc., Detroit, Mich.).

A program was established to study the effect of a small leak of water into Na on tube wastage for use in the design of future liquid metal-heated steam generators. All of the components of the reaction system were erected in the test stand. The procedure for tube bundle inspection was established, and the methods for obtaining the desired information within the scope of the project using the test data were defined. (auth)

44162 (APDA-174, pp 33-55) SODIUM TECHNOLOGY LOOP. Project Agreement No. 11. Hill, E. F. (Atomic Power Development Associates, Inc., Detroit, Mich.).

Work was continued on establishing the accuracy and precision of the response of three modified Rhometers to typical Na impurities at 450 to 900°F. Water was injected into the loop and changes in Rhometer readings, plugging temperature, cover gas constituents, and chemical analyses were recorded. In addition, the responses of four newly installed O_2 meters were studied up to temperatures of 650°F. During this period, two sample tube cleaning procedures were evaluated and a relatively simple procedure was selected as being adequate. Chemical analyses of samples taken from sample stations RM-1 and RM-2 were compared and no significant difference was found between the two stations. Four types of Rhometer temperature compensation were investigated, and it was determined that Au wire offers a substantial improvement over Pt. Two methods for the determination of H in Na are being investigated. Both methods are potentially quantitative and will enable the identification of the H species. (auth)

44163 (BNL-9502) ALPHA-GAMMA FACILITY FOR METALLURGICAL EXAMINATIONS. Richards, P.; Banslaben, A.; Chow, J. (Brookhaven National Lab., Upton, N. Y.). Sept. 2, 1965. Contract AT-30-2-GEN-16. 13p. Dep. mn; CFSTI $1.00 cy, $0.50 mn.

The design and operation of a facility for cutting, polishing, and testing the metallurgical properties of irradiated in-pile loops and capsules are described. (W.L.G.)

44164 (CEA-R-2755) RACCORD ETANCHE POUR CONDUCTEUR ELECTRIQUE CHAUFFANT A GAINE COAXIALE. (Sealed Coupling for an Electrical Heating Conductor with Coaxial Sheath). Arragon, Philippe; Aubert-Chevallier, Robert; Gentil, Jean; Seguin, Maurice; Vilcot, Marc; Villiers, Jacques (Commissariat a l'Energie Atomique, Grenoble (France). Centre d'Etudes Nucleaires). Mar. 1965. 14p. Dep. mn.

Many irradiation devices call for supplementary electrical heating which can provide a constant temperature. A coupling is described whose high performance makes it possible for the sheathed electrical resistance to provide maximum power. Since this coupling is sealed and does not require special cooling, it may be placed in any position on the irradiation device. (auth)

44165 (CERN-65-29) A HIGH PRECISION AIR CORE MAGNET. Gygi, E.; Schneider, F. (European Organization for Nuclear Research, Geneva (Switzerland)). Aug. 4, 1965. 17p. Dep. mn.

The realization of an axial symmetric field is described. The air-core coil with an over-all length of 50 cm and an inner diameter of 13 cm produces on the axis, over a length of 30 cm, a field which is constant to $\pm 4 \times 10^{-4}$. At a distance of 4 cm from the axis, over the same length, the precision is $\pm 9 \times 10^{-4}$. The method of calculation, the production of the oxidized aluminum bands from which the coil is wound, and the construction of the coil assembly are described. (auth)

44166 (NP-15472) PROPOSED FILTERED SHIELDED CONNECTOR FOR PROTECTION OF WEAPONS FROM ELECTROMAGNETIC RADIATION. No. W-7/65. Walther, M. F. (Naval Weapons Lab., Dahlgren, Va.). June 1965. 13p.

A shielded connector is designed whose purpose is the isolation of the circuitry of a nuclear weapon from the intense r-f fields produced by nuclear explosions. (T.F.H.)

44167 (ORNL-P-1521) THE THORIUM-URANIUM RECYCLE FACILITY. Irvine, A. R.; Lotts, A. L.; Olsen, A. R. (Oak Ridge National Lab., Tenn.). [1965]. Contract W-7405-eng-26. 21p. (CONF-651101-9). Dep. mn; CFSTI $1.00 cy, $0.50 mn.

For Presentation at 13th Conference on Remote Systems Technology, Washington, D. C.

The Thorium-Uranium Recycle Facility provides sufficient space and other facilities for the simultaneous testing and demonstration of two processes for the remote processing of fuel elements, fuel reconstitution, and refabrication into fuel assemblies. Process equipment will be located in two large remotely maintained cells, and two smaller directly maintained cells. An unshielded cell and a shielded service cell with a special remote crane and manipulator system are provided to achieve easy removal and installation of remotely maintained equipment. Special provisions have been made for future conversion of these cells to inert atmosphere, for replacement of the viewing window gas seal plates, and for extinguishing cell fires. (auth)

44168 (ORNL-P-1532) ANALYTICAL LABORATORY HOT-CELL EQUIPMENT. I. SAMPLE PREPARATION APPARATUS FOR THE MOLTEN SALT REACTOR EXPERIMENT. Maddox, W. L.; Haga, F. E. (Oak Ridge National Lab., Tenn.). [1963]. Contract W-7405-eng-26. 13p. (CONF-651101-12). Dep. mn; CFSTI $1.00 cy, $0.50 mn.

For Presentation at 13th Conference on Remote Systems Technology, Washington, D. C.

Samples will be taken for chemical analysis from the MSRE by dipping from the reactor fuel pump bowl with ladles; they will then be cut from the ladles, pulverized, and mixed preparatory to analyses. Descriptions are given of the following apparatus which were developed: transport container machine, ladle cutter, mixer/mill, and powder-transfer shaker. (D.L.C.)

44169 (Y-1478) COMPENDIUM OF GAS AUTOCLAVE ENGINEERING STUDIES. Muzzall, C. E. (ed.) (Union Carbide Corp., Oak Ridge, Tenn. Y-12 Plant). Nov. 2, 1964. Contract W-7405-eng-26. 233p. Dep. mn; CFSTI $6.00 cy, $1.25 mn.

A compendium of nine articles on engineering studies has been prepared by the Engineering Division of the Oak Ridge Y-12 Plant. These studies deal with two basic objectives: (1) the modification of an existing isostatic pressure vessel to permit the use of heated argon gas as the pressure fluid, and (2) the choice of design parameters for a new future facility which will include a large pressure vessel to be operated as a gas autoclave. (auth)

44170 (Y-DA-921) PRODUCTION-SIZE LATHE HYDROSTATIC COMPONENTS. Steger, P. J. (Union Carbide Corp., Oak Ridge, Tenn. Y-12 Plant). May 21, 1965. Contract W-7405-eng-26. 14p. (CONF-650651-1). Dep. mn; CFSTI $1.00 cy, $0.50 mn.

From American Society of Mechanical Engineers, Spring Lubrication Symposium, New York.

Two lathe components using hydrostatic air bearings are described: a hydrostatic boring bar and a production-size spindle. Porous graphite bearing pads are used in both components. The accuracy and performance of the components are discussed. (D.L.C.)

44171 ISOTOPE GAMMA IRRADIATION UNIT UKP-30000. P'yankov, G. N.; Barashkin, M. A.; Kulyupina, N. V. At. Energ. (USSR), 19: 75-6(July 1965).

The UKP-30000 apparatus (Kiev underwater apparatus, 30,000 gn equivalent Ra) is described. The ^{60}Co source is kept in a tank of water, which serves as a biological shield and as a stabilizer of temperature for long irradiations. The sample to be irradiated is positioned near the source by a pulley system. Results of chemical dosimetric measurements of the dose field in the irradiation cassette are given. The temperature environment of the source and cassette was found to be constant up to doses on the order of 10^8 to 10^9 rad. (M.J.T.)

44172 HIGH-DOSE-RATE ISOTOPE GAMMA IRRADIATION UNIT UK-70000. P'yankov, G. N.; Kulyupina, N. V. At. Energ. (USSR), 19: 77-8(July 1965).

The high-dose-rate irradiation facility UK-70000 (Kiev apparatus, 70,000 gn equivalent Ra), using a ^{60}Co source, was constructed for radiation-chemistry research. The hot chamber with water basins, the irradiator, the source remote-handling system, the shielding, and the control and ventilation systems are described. Diagrams of the dose-rate field of the apparatus are presented. The temperature conditions in the facility are discussed. (M.J.T.)

44173 A HALL EFFECT STABILIZER FOR EXPERIMENTAL MAGNETS. Grant, D.; Jones, T. W.; McFarlane, W. K. (Birmingham Univ., Eng.). Nucl. Instr. Methods, 36: 277-82(Oct. 1965).

A "Hall effect" magnetic field stabilizer is described which combines precision with ease of operation. The system, which is simple, economical, and of wide application, is used to stabilize the fields of beam transport magnets at the Birmingham synchrotron. Fields are controlled to a long term stability of 1 gauss and the system corrects for the effect of the pulsed stray field of the synchrotron which rises, at the orbit radius, to 12 kG in 1 sec every 6 sec. It is also possible to change the field to any value between 0.5 kG and 11 kG in a matter of seconds with a resettable accuracy of 0.2 G. The range of the instrument may be extended beyond 11 kG by altering one circuit component. (auth)

44174 IMPROVEMENTS IN OR RELATING TO MANIPULATING TOOLS. Gerard, Bernard (to Commissariat a l'Energie Atomique). British Patent 1,001,652. Aug. 18, 1965. Priority date Sept. 18, 1961, France.

A device is described for controlling manipulating tongs of the type including a body or casing onto which is attached a pair of gripping jaws and a push rod movable within the body or casing in such a manner as to act on the jaws by the intermediary of suitable cam surfaces in order to bring about their opening and closing movements. The body of the tool is supported in the loop of a driving chain by a support pinion that may be translated in an upward and down-

ward direction and rotated by the operation of a differential winch over which the driving chain passes. The translation movement of the support pinion determines the amplitude of the movement of the body, while the rotary movement of the pinion is adapted to control a locking member. The position of the locking member is governed by the movement of the push rod, and the jaws are successively locked in the open and closed positions. A differential winch is provided to cause the tong body to adopt a translatory movement by simultaneously driving the two planetary pinions in the same direction or to cause the locking member only to rotate while the tongs body remains immobile by driving the two pinions in opposite direction. (B.L.M.)

44175 HEAD FOR REMOTE MANIPULATORS. Pesenti, Pierre (to Commissariat a l'Energie Atomique). Canadian Patent 707,662. Apr. 13, 1965. Priority date Aug. 31, 1959, France.

A remote manipulator of radioactive materials is described, which consists essentially of a driving control head and of a receptive or driven head that carries a holder or other device intended to grip. The movements of the holder are identical with the movements of the operator's hands. The improved head of the "knuckle-joint" type has a tubular element carried by an oscillating support and traversed axially by a cable arranged to connect a control member to a holder or other receptor device. (F.S.A.)

44176 TIGHTNESS JOINT. Charrault, Jean-Claude; Cogez, Paul; Guiducci, Lino (to European Atomic Energy Community-EURATOM). Canadian Patent 708,782. May 4, 1965. Priority date Mar. 1, 1963, Belgium.

A tightness joint is described, which involves a change in the physical state, from liquid to solid, of the packing material. A joint between two parts that move relative to one another is realized by a thin metallic partition secured on one part and sliding on the other. This joint finds particular use in organic cooled reactors. Reduced friction, simple construction, and efficient operation are the advantages claimed. (F.S.A.)

44177 REMOTE-CONTROLLED MACHINE TOOL FOR HOT CHAMBERS OF NUCLEAR ENERGY PLANTS. Hermann, Horst (to European Atomic Energy Community-Euratom). U. S. Patent 3,196,718. July 27, 1965. Filed June 11, 1962.

A remote-controlled machine tool is provided with which rotationally symmetrical radioactive elements, such as reactor fuel rods or material testing tubes, can be worked by remote control with removal of chips or without chip formation. Particularly, the tool is intended to cut off the heads and ends of the elements or to cut open their welded seams by means of turning tools, so as to provide access to the radioactive or activated materials. A cylindrical body of the machine is open at both ends and acts at the same time as a base for the machine and as a chuck for the workpiece clamping members or teeth disposed inside it. Peripherally about the base is located a drive cylinder that carries the tool table and the tool support. The conventional displacing mechanism is provided on the base and table and consists of pine and star wheel for producing the radial feed of the tool. The machine has a controllable planetary drive between the tool table and the driving cylinder for obtaining axial feed of the tool with one drive shaft for each of the drive cylinders, the planet cage, and the clamping teeth. The three drive shafts are bundled together and disposed on the same side of the machine. All the parts are mounted on the machine in such a way that the machine can operate either in standing or in suspended position and swings freely with and secured to the workpiece. (B.L.M.)

44178 MANIPULATOR APPARATUS. (to European Atomic Energy Community). U. S. Patent 3,197,041. July 27, 1965. Priority date Jan. 23, 1962, France.

A manipulator arm is constructed of a pair of chain-like assemblies each consisting of a series of interpivoted link members and each substantially flexible when separated from the other. The assemblies are stored when not in use in separate coils. A feed mechanism synchronously feeds out the two assemblies toward mutual coincidence; the two assemblies interlock automatically as they reach their coincident condition and form a rigid arm of variable length. A structure for supporting and wielding the arm in a plurality of directions including overhead is provided. (A.G.W.)

44179 RADIOACTIVE SOURCE HOLDER. Stone, Leonard R.; Radcliffe, Thomas J.; Sower, George W. (to Republic Steel Corp.). U. S. Patent 3,197,639. July 27, 1965. Filed Sept. 25, 1961.

A radioactive source holder is designed to provide adequate shielding against uncontrolled radiation and yet be sufficiently light and convenient for installation at a substantial height at the exterior of a blast furnace. The holder is a lead-lined container equipped with a lever-operated shutter. When the shutter is open, a narrow radiation beam emerges from the front of the holder and passes through the related beam port. When the shutter is closed, the beam is blocked by Pb, and the holder is a safe storage and shipping container. The holder is intended as part of a system for detecting the position of stock within a blast furnace. (A.G.W.)

44180 REMOTE CONTROL APPARATUS. Wallet, Philippe; Taverne, Henri (to Commissariat a l'Energie Atomique). U. S. Patent 3,198,347. Aug. 3, 1965. Priority date Jan. 12, 1961, France.

An apparatus is provided for maneuvering members within an inaccessible sealed enclosure, particularly for maneuvering radioactive objects or receptacles containing such objects. The apparatus includes a tubular member passing in hermetically sealed relationship through the wall of the enclosure, and a support swingably mounted on a tubular member and carrying gripping members. The hermetic sealing means are arranged between the swingable support and the inside of the tubular member. Motor means control the swinging movement of the support in relation to the tubular member and the rotation of the tubular member around its axis. Control means are provided outside the enclosure for displacing the gripping means. (B.L.M.)

Heat Transfer and Fluid Flow

See also PHYSICS — General.

Refer also to abstracts 44813, 45494, 45572, and 45652.

44181 (APDA–174 pp 56-60) FUEL ELEMENT FLOW STABILITY STUDIES. Project Agreement No. 12. Edwards, J. J. (Atomic Power Development Associates, Inc., Detroit, Mich.).

Static pressure distributions were completed for rod bundles with 6-in., 18-in., and 36-in.-wire wrapped pitch, and 0.050-in. and 0.125-in.-dia wires. Work was initiated on 0.250-in.-dia-wire-spaced bundles. Tubes simulating creep-induced deformations between support planes were also introduced into the tube array, and the resulting pressure distributions measured. Data from the bundles tested were processed into a more convenient form for analysis using a specially written data reduction code. (auth)

44182 (BAW-1280-29) MODEL TESTS OF THE SODIUM DISTRIBUTOR FOR THE SODIUM HEATED STEAM GENERATOR. Research Report No. 4475. Lindstrom, G. D. (Babcock and Wilcox Co., Alliance, Ohio. Research Center). Aug. 5, 1965. Contract AT(11-1)-1280. 55p. Dep. mn; CFSTI $3.00 cy, $0.50 mn.

Performance tests were conducted with water in a 1/3.23 scale plastic model. Water flow distribution and pressure drop were determined. A distributor arrangement was developed which performed satisfactorily in the water model and which will meet the requirements (uniform flow distribution and no impinging jets) for the prototype steam generator. (D.L.C.)

44183 (BAW-3238-8) NONUNIFORM HEAT GENERATION EXPERIMENTAL PROGRAM. Quarterly Progress

Report No. 8, April–June 1965. (Babcock and Wilcox Co., Lynchburg, Va. Atomic Energy Div.). Contract AT(30-1)-3238. 50p. (EURAEC–1423). Dep. mn; CFSTI $2.00 cy, $0.50 mn.

Work Performed under United States–Euratom Joint Research and Development Program.

A research program is being conducted to determine the effects of nonuniform heat generation rates in tubular and annular flow channels on burnout under conditions representative of water reactor systems. The work during this report period includes data from two annular test sections. In the first case the inside surface was heated, but in the second case the outside surface was heated. The data tabulated have been reviewed, and a preliminary analysis is presented. For the same conditions of pressure, mass velocity, and inlet temperature the annular test sections produce higher critical heat fluxes than the fluxes in the tubular test sections. (D.L.C.)

44184 (EURAEC–1281) RESEARCH ON THE CRITICAL HEAT FLUX (BURNOUT) IN BOILING WATER. Report No. 09,02,05. Quarterly Progress Report No. 13, October 1–December 31, 1964. Mayinger, F.; Schad, O.; Weiss, E. (Maschinenfabrik Augsburg-Nuernberg A. G., Nuremberg (West Germany)). Jan. 1965. Contract 057-61-RDD. 52p. Dep. mn; CFSTI $3.00 cy, $0.50 mn.

Work Performed under United States–Euratom Joint Research and Development Program.

Measurements were made of the critical heat flux in boiling in round, internally cooled channels with a view to determining the effect of the length/diameter ratio of the test channel on the burnout phenomenon. The tests were made with L/D ratios of 10, 40, and 80 and pressures of 70 and 100 atms. The thermodynamic state at the outlet of the test channel ranged from 55°C sub-cooling up to 20% steam content. The results showed a definite influence of the L/D ratio on the critical heat flux in boiling. With the same thermodynamic state and equal mass flow the heat flux obtainable with L/D ratios of 10 were 4 times those with a ratio of 80. It can be inferred from measurements of the rate of change of the temperature of the heated wall of the test channel at the moment of transition to film boiling that on the hydrodynamic side, too, there are factors which depend on the L/D ratio. (auth)

44185 (GEAP–4910) A PROGRAM OF TWO-PHASE FLOW INVESTIGATION. Ninth Quarterly Report, April–June 1965. Staub, F. W.; Zuber, N.; Bijwaard, G. (General Electric Co., San Jose, Calif. Atomic Power Equipment Dept.). June 1965. Contract AT(04-3)-189. 76p. (EURAEC–1459). Dep. mn; CFSTI $3.00 cy, $0.75 mn.

Work Performed under United States–Euratom Joint Research and Development Program.

Modification of the experimental loop for high pressure operation was initiated. It is anticipated that the experimental equipment will be ready for high pressure operation by the middle of August 1965. Various aspects and characteristics of the void propagation equation derived previously are discussed and analyzed. This equation can be used to predict the transient response of the volumetric concentration to perturbations of 1) power input, 2) inlet flow, 3) system pressure, 4) thermodynamic nonequilibrium, 5) compressibilities of the vapor and of the liquid, and 6) body forces acting on the two-phase mixture. It is noted that since the void propagation equation can be used to predict the void response as function of space and function of time, it is suitable to analyses of transients in fast, power reactors which use a liquid metal for coolant. Solutions of the void propagation equation are presented for operating conditions such as 1) constant power and inlet flow, 2) oscillatory power, 3) oscillatory flow and 4) oscillatory power and flow. Solutions are presented for axially uniform and axially nonuniform power input. The results obtained with these two-power distributions are compared and discussed. It is shown that perturbations of mixture density are propagated through the two-phase mixture by the velocity of kinematic waves. Expressions which predict the rate of propagation of these waves and which are applicable to the operating conditions listed above are presented. The finite rate of propagation of kinematic waves introduces a delay time which characterizes the response of the volumetric concentration to various perturbations. The delay times, appropriate to the operating condition enumerated above, are also presented. The predicted results are compared with experimental data. (J.R.D.)

44186 (LA-DC–7148) FURTHER EXPERIMENTAL STUDY OF H_2O–LH_2 HEAT EXCHANGERS. Bartlit, J. R.; Williamson, K. D. Jr. (Los Alamos Scientific Lab., Univ. of California, N. Mex.). [1965]. Contract W-7405-eng-26. 19p. (CONF-650802–6). Dep. mn; CFSTI $1.00 cy, $0.30 mn.

From Cryogenic Engineering Conference, Houston, Tex.

The results reported are an extension of a study of heat transfer and ice formation during the steady-state operation of countercurrent H_2O-LH_2 heat exchangers which was reported at the 1964 Cryogenic Engineering Conference. In addition to further data obtained on the 1-in. OD model previously described, data were also obtained on a full-scale 5.5-in. OD exchanger. The full-scale exchanger had a 4-in. ID, finned, hydrogen line, 160 feet long, enclosed in a 9½-in. ID outer water jacket. Both exchangers incorporated a twisted tape swirl inducer inside the inner pipe (for the full 47 feet in the model and for 80 feet in the full-scale unit). The full-scale unit was operated at pressures up to 1000 psia while the model was limited to 220 psia. The results from both exchangers indicated that where the swirl inducer was present, heat transfer coefficients approached the values predicted by the Dittus-Boelter equation over the temperature range from 50 to 500°R. These data are in contrast to previously reported coefficients from the model without a swirl inducer. Under these conditions coefficients as low as 11% of Dittus-Boelter were found at low temperatures. Ice thicknesses in both exchangers were calculated to be less than 0.1 inch. The effluent from the full-scale unit was used to drive the turbine of a liquid hydrogen pump. This system was operated without troublesome pressure oscillations. (auth)

44187 (NASA-CR–54405) ALKALI METALS BOILING AND CONDENSING INVESTIGATIONS. Quarterly Progress Report 11, January 1, 1965–March 31, 1965. Tippets, F. E.; Converse, G. L. (eds.) (General Electric Co., Cincinnati, Ohio. Space Power and Propulsion Section). Apr. 23, 1965. Contract NAS 3-2528. 677p.

A research program is being conducted to obtain two-phase heat transfer and fluid flow data for potassium under boiling and condensing conditions. The 300-, 100-, and 50-kw projects are discussed, and the obtained data are given in detail. Facilities, instrumentation, and materials support are also considered. Analysis of instabilities was initiated. (D.L.C.)

44188 (NASA-TN-D–2965) ELECTRODYNAMIC MERCURY PUMP. Vary, A. (National Aeronautics and Space Administration, Cleveland, Ohio. Lewis Research Center). Sept. 1965. 18p. CFSTI $1.00 cy, $0.50 mn.

Problems associated with high-pressure, electromagnetic pumping of mercury were investigated. Electromagnetic pressure development with mercury was difficult to achieve because of two factors: first, mercury wetting of the flow passage surface was not readily attained; second, induction heating of the mercury resulted in vapor formation in the pump flow channel causing loss of developed pressure. Satisfactory results were obtained by chemical and thermal conditioning techniques developed to induce mercury wetting. The problem of overheating was resolved by means of a novel pump cell design that assured better electrical continuity and efficient heat removal. The resultant pump cell had a developed pressure capability of approximately 500 pounds per square inch and was able to meet the following design requirements: output pressure, 350 pounds per square inch; mercury flow rate, 150 pounds per hour; and operating temperature, 600°F. The pump was operated for over 400 hours of which over 200 hours were accumulated in a two-phase corrosion

loop under SNAP-8 conditions of pressure and temperature. (auth)

44189 (NP-15332) SUPERCRITICAL PRESSURE LIQUID HYDROGEN HEAT TRANSFER DATA COMPILATION. Miller, W. S.; Seader, J. D.; Trebes, D. M. (Rocketdyne, Canoga Park, Calif.). Apr. 21, 1965. Contract NAS 8-19. 75p. (R-6129).

A compilation of experimental supercritical pressure liquid hydrogen heat transfer data obtained for turbulent flow inside electrically heated tubes is presented. In all cases the tubes were straight and had a circular cross section. A total of 62 experiments is reported. A pressure range from 400 to 2500 psi was covered and local heat fluxes to 24 Btu/in.^{2}-sec were attained. (auth)

44190 (NYO-2404-67) EFFECTS OF ELECTRICAL FIELDS ON BOILING HEAT TRANSFER. Quarterly Progress Report, October 1, 1964–December 31, 1964. Nichols, Charles R.; Spurlock, Jack M.; Markels, Michael Jr. (Atlantic Research Corp., Alexandria, Va.). Contract AT(30-1)-2404. 27p. Dep. mn; CFSTI $2.00 cy, $0.50 mn.

Boiling burnout is studied in two-phase annular flows of water at 20 to 115 psia, in transverse electric fields produced by alternating voltages of 0 and 1 kv. (T.F.H.)

44191 (NYO-2404-73) EFFECTS OF ELECTRICAL FIELDS ON BOILING HEAT TRANSFER. Quarterly Progress Report, April 1–June 30, 1965. Nichols, Charles R.; Spurlock, Jack M.; Markels, Michael Jr. (Atlantic Research Corp., Alexandria, Va.). Contract AT(30-1)-2404. 21p. Dep. mn; CFSTI $2.00 cy, $0.50 mn.

The effects of electric fields on the boiling burnout characteristics of water flows at 1500 psia in annular cylindrical test sections are studied. The electric fields are produced by 60-cps alternating voltages of 0 to 3000 v, applied perpendicular to the fluid flow. (T.F.H.)

44192 (NYO-3114-9) TWO-PHASE FLOW AND BOILING HEAT TRANSFER. Quarterly Progress Report, April–June 1965. Wallis, G. B.; Turner, J. M.; Meyer, P. E.; Runge, D. E. (Thayer School of Engineering, Dartmouth Coll., Hanover, N. H.). Contract AT(30-1)-3114. 13p. (EURAEC-1451). Dep. mn; CFSTI $1.00 cy, $0.50 mn.

Work Performed Under United States–Euratom Joint Research and Development Program.

Work on co-current upwards annular flow is continuing. An investigation of upwards annular-mist vertical flow was undertaken. A summary is given of work on the rise velocity of cylindrical bubbles in inclined tubes. (auth)

44193 (NYO-3304-5) INVESTIGATION OF BOILING FLOW REGIMES AND CRITICAL HEAT FLUX. Quarterly Progress Report, March 6, 1965–June 15, 1965. Report No. 582. Bergles, A. E.; Clawson, L. G.; Goldberg, P.; Suo, M.; Bourne, J. G. (Dynatech Corp., Cambridge, Mass.). Aug. 1, 1965. Contract AT(30-1)-3304. 25p. Dep. mn; CFSTI $1.00 cy, $0.50 mn.

Completed and anticipated modifications to the experimental facility are described. Recent experimental results for flow regimes in a 2-ft, 0.4-in. ID test section are discussed. The oscillatory instability associated with this test section is considered in detail. The general effects of pressure and length on flow regimes are also considered. (auth)

44194 (SGAE-RE-2/1965) DYNAMISCHE UNTERSUCHUNG DES WAERMEAUSTAUSCHERS. 3. ARBEITSBERICHT. (Dynamic Study of Heat Transfer. 3. Work Report). (Oesterreichische Studiengesellschaft fuer Atomenergie G.m.b.H., Seibersdorf). 1964. 132p. Dep. mn.

Studies are being conducted on the dynamic heat-transfer behavior of individual fuel elements in a reactor plant, with the aim of reducing the safety factors in boiling-water and pressurized-water reactor design. The problems of measuring the radial temperature profile and of temperature noise in the presence of liquid turbulence are discussed. Measurements of the transfer function of the heat exchanger were started. A larger plant for testing steam–water mixtures is being developed. (D.L.C.)

44195 (TID-21256) P AND WA FORCED CONVECTION BOILING POTASSIUM HEAT TRANSFER DATA. Bernstein, E.; Randall, D. (Pratt and Whitney Aircraft, Middletown, Conn. Connecticut Advanced Nuclear Engineering Lab.). [Sept. 1964]. Contract AT(30-1)-2789. 9p. Dep. mn; CFSTI $1.00 cy, $0.50 mn.

A series of forced-convection high-temperature (1725°F) tests were conducted in a gravity-inducing serpentine boiler tube. The data, presented in the form of graphs of local boiling heat transfer and pressure coefficients vs local vapor quality, can be used in the design of once-through alkali metal boilers. A Serpentine Tube Boiler mock-up is described, along with the experimental technique and apparatus. (D.L.C.)

44196 (TID-22145) TWO-PHASE FLOW THROUGH APERTURES. Final Report. Chen, Ping Chien (Minnesota Univ., Minneapolis. Dept. of Chemical Engineering). July 29, 1965. Contract AT(11-1)-926. 168p. Dep. mn; CFSTI $5.00 cy, $1.50 mn.

A test facility was designed and constructed for making blowdown tests of saturated water through a variety of apertures with initial pressures up to 250 psig. The objectives of the experiments were to establish criteria for developing predictive methods for the flow of flashing water through apertures. Problems of this type become important factors in the design of nuclear power safety systems. The apertures used had inlet diameters of $\frac{1}{2}$ and $\frac{1}{4}$ inches, with sharp leading edges. They are of three different geometries; one is with a 12° diverging section, another is with a 60° diverging section which diverges to $D_e/D_a = 3$ followed by a section with constant cross-sectional area, and the third group represents short tubes. The L/D_a values vary from 2 to 4.6. The test results with saturated water indicate no vaporization occurred in the immediate upstream neighborhood of the openings. Saturated water becomes superheated and flows into the apertures as a metastable water jet. Flashing, however, occurs to a certain extent within the apertures causing a back-pressure higher than the downstream pressure. Using the pressure differences between the initial pressure and the backpressure in the single-phase orifice equation with the contraction coefficient of 0.61, the mass flow rates can be predicted. For the diverging apertures, the backpressure phenomena are consistent with the theory of free turbulent jets and the analyses on the thrusts created by the flows. (auth)

44197 (TIM-895) CAVITATION TESTS OF COATED RI-16 IMPELLER. Altieri, J. V. Jr. (Pratt and Whitney Aircraft, Middletown, Conn. Connecticut Advanced Nuclear Engineering Lab.). Jan. 1965. Contract AT(30-1)-2789. 27p. Dep. mn; CFSTI $2.00 cy, $0.50 mn.

A visual study was conducted to investigate the cavitation damage phenomenon on a rotating impeller. A heavy walled plexiglass impeller housing was used and provided excellent viewing. The tests were conducted in 90F de-aerated, demineralized water. The impeller was sprayed with acrylic lacquer which was readily removed by the cavitation pitting action and provided a pattern which indicated the areas of attack on the vane. This method of testing permitted the repeated use of the impeller since the test durations were too brief to inflict damage on the stainless steel impeller. Test results indicate that the suction specific speed of an impeller is not a valid parameter to predict the onset of cavitation damge. These tests also demonstrated that the distance from the visually observed cavitation collapse point to the blade surface is critical, and if increased only slightly, on the order of $\frac{1}{16}$ inch, coating damage could be prevented. In several instances, where there was coating damage, the amount of damage did not depend solely on the volume of cavitation present. At certain operating conditions, large amounts of damage were inflicted on the coating from small amounts of high intensity rear channel tip vortex cavitation. (auth)

44198 (TIM-913) DISSERTATION OF JET PUMP ANALYSIS. Daley, D. P. (Pratt and Whitney Aircraft, Middletown, Conn. Connecticut Advanced Nuclear Engineer-

ing Lab.). June 18, 1965. Contract AT(30-1)-2789. 101p. Dep. mn; CFSTI $4.00 cy, $0.75 mn.

The existing experimental data taken at CANEL are evaluated and compared with those from other sources. An extensive design procedure is discussed to optimize a jet-centrifugal pump combination under specific constraints. The analysis is made general in that it applies to various cases involving different initial assumptions. By a number of iterative steps, these assumptions are validated. The result is a completely sized jet pump and its corresponding dimensionless head-flow and efficiency curves. Finally, the results of the theoretical development are compared with the existing experimental data. Using the CDC computer program, the following conclusions are drawn concerning the theoretical development: (1) the theory behind the numerical method is excellent in predicting a jet pump performance curve; (2) it is good for low to medium flow rates (with respect to the design point – 260 gpm) for the individual components; and (3) it is pessimistic in its prediction of values for the individual components at high flow rates. The theory, when it comes to predicting the various friction factors, leaves much to the conjecture of the designer. It is realized that this is not desirable, yet presently the numerical method is the most accurate and consistent in development. Additional testing of the jet pump, particularly at different area ratios, would aid in developing a better over-all design. (auth)

44199 (UCRL-12045) QUALITATIVE EXPERIMENTAL INVESTIGATIONS ON VARIOUS VORTEX TUBE CONFIGURATIONS. Collins, J. C.; Stubbs, T. F. (Lawrence Radiation Lab., Univ. of California, Livermore). Aug. 1964. Contract W-7405-eng-48. 49p. Dep. mn; CFSTI $2.00 cy, $0.50 mn.

Similarities are considered between the standard vortex tube (upon which most of the past work has been done) and two variations; the tapered vortex tube and the vortex cooler. It is shown that all three variations contain no fundamental differences, and the variation of tube performance with respect to the setting of the exit gas "hot" valve is explained in terms of compressible flow. Mathematical treatment is kept to a minimum; emphasis is placed upon the experimental results obtained from the tests performed on the variations of the standard vortex tube. (auth)

44200 (SC-T-65-756) NUMERICAL SOLUTION OF SOME PROBLEMS OF GAS FLOWS. Chushkin, P. I. Translated by Marcel I. Weinreich (Sandia Corp., Albuquerque, N. Mex.) from Arch. Mech. Stosowanej, 16: 577-96 (1964). 28p. Dep. mn; CFSTI $2.00 cy, $0.50 mn; JCL $2.60 fs, $1.04 mf.

Numerical solutions are presented for the following problems: potential flow in the subsonic and transonic portion of the Laval jet, unstable one-dimensional flow during an explosion in a gas, circumfluence of blunt bodies by hypersonic flow in a magnetic field, and a method for characteristics on the basis of strata. (D.L.C.)

44201 BOILING HEAT TRANSFER AND PEAK NUCLEATE BOILING FLUXES IN SATURATED LIQUID HELIUM BETWEEN THE λ AND CRITICAL TEMPERATURES. Lyon, D. N. (Bell Telephone Labs., Inc., Murray Hill, N. J.). Intern. Advan. Cryog. Eng., 10: 371-9 (1965).

Boiling heat transfer between a flat polished platinum surface in liquid helium was measured for angles of inclination of the surface with respect to the horizontal through 180° at bulk liquid temperatures between 1.765 and 5.130°K. Both the film-boiling and nucleate-boiling regimes were studied. Peak nucleate-boiling fluxes were measured above the lambda point. (D.C.W.)

44202 HEAT EXCHANGE IN TRANSVERSE HOMOGENEOUS MAGNETIC FIELD. Mikhailov, Yu. A.; Ozols, R. Ya. (Inst. of Power Engineering, Academy of Sciences, Latvian SSR). Latvijas PSR Zinatnu Akad. Vestis, Fiz. Tek. Zinatnu Ser., No. 2, 19-26(1965). (In Russian).

Heat exchange in a flat channel filled with a non-compressible electroconducting liquid moving in a stable laminar regime was considered. The walls of the channel were isothermal and the laminar regime was ensured by parallel laminae. The influence of the transverse homogeneous magnetic field on the heat exchange at a constant liquid flow rate and at a constant pressure gradient in the direction of the liquid motion is shown. The value of the outer magnetic field and the electroconductivity of the walls were found to exercise a great influence upon the liquid temperature and Nusselt's number characterizing the heat exchange. (auth)

44203 POWER SUPPLY PLANT FOR THERMAL TEST STANDS IN THE NUCLEAR RESEARCH STATION AT JUELICH IN NORTH RHINE-WESTPHALIA. Neumann, Manfred; Vieten, Manfred. Siemens-Z., 39: 68-73(Jan. 1965). (In German).

To carry out model tests for the investigation of heat transfer conditions on fuel elements and heat exchangers it is necessary to simulate reactor operating conditions. This calls for high low-ripple-content d-c currents with accurate regulation of the voltage. At Jülich, in the Institute for Reactor Components, the d-c is supplied by four three-phase/d-c convertor sets each rated at 5,000 A, 100 v. These can be operated individually, in parallel or in series. (auth)

44204 FACTORS INFLUENCING THE PERFORMANCE OF A FAST-RESPONSE, TRANSPIRATION-COOLED, HIGH TEMPERATURE PROBE. Cheng, Dah Yu; Blackshear, P. L. Jr. (Univ. of Minnesota, Minneapolis). New York, American Inst. of Aeronautics and Astronautics, 1965, Preprint No. 65-359, 11p., $1.00. (CONF-650711-29). ORINS.

From AIAA 2nd Annual Meeting and Technical Demonstration, San Francisco.

A description is given of a dilution type temperature probe, which measures enthalpy by first diluting adiabatically the very high temperature gas with a cool inert diluent, then measures the mixing ratio and the resulting mixture temperature. Measurements were made in argon in a ¼ in. diameter 12 kw plasma torch. Attention is given to the nature of the dilution process, the time response of the probe, the influence of changes in diluent flow rate on enthalpy, and a comparison of the overall accuracy of the instrument with a Greyrad probe and with an integrating calorimeter. (L.B.S.)

44205 WORKING GAS SELECTION FOR THE CLOSED BRAYTON CYCLE. Mason, John L. (Airesearch Mfg. Co., Los Angeles). 36p. (CONF-663-2). ORINS.

From 6th Agard Combustion and Propulsion Colloquium on Energy Sources and Energy Conversion, Cannes, France, Mar. 1964.

Brayton cycle applications to space power were examined and evaluated. All major components except the alternator are shown to be directly influenced by the properties of the cycle working gas. Selection of working gas for low power levels, for which single-stage centrifugal turbocomponents appear preferable, is considered. The Brayton cycle as applied to space power will be designed for minimum system weight, minimum radiator area, or maximum conversion efficiency. The advantage of xenon-helium mixtures over pure monatomic gases is illustrated. (M.C.G.)

44206 IMPROVEMENT IN FINNED HEAT EXCHANGE TUBES. (to Nihon Genshiryoku Kenkyujo). British Patent 1,001,630. Aug. 18, 1965. Priority date Apr. 23, 1962, Japan.

An externally finned heat tube is described that has a number of longitudinal heat transfer fins. Numerous grooves are cut in the longitudinal fins so as to divide each of the fins into a number of unit fins each provided with a pair of diagonally opposite sharp edges. Each of the grooves extend spirally through adjacent longitudinal fins arranged around the periphery of the tube. (B.L.M.)

Materials Testing

Refer also to abstract 45500.

44207 (ANL-7000, pp 146-52) DEVELOPMENT OF NONDESTRUCTIVE METHODS. (Argonne National Lab., Ill.).

Progress in the development of nondestructive methods of materials testing is reported. Effort was directed in the areas of: correlation of the sound transmission properties, heat transfer properties, and strength of a bond; ultrasonic instrument and transducer development; ultrasonic imaging; determination of elastic moduli of high-temperature materials by ultrasonics; development of a neutron image intensification system; development of infrared systems; and investigation of the quality of brazed joints. (W.L.G.)

44208 (BMI-X-346) DEVELOPMENT OF A TRACER SYSTEM FOR IN-PLACE FILTER EVALUATION. Final Report, October 1, 1962–June 30, 1965. Mitchell, Ralph I. (Battelle Memorial Inst., Columbus, Ohio). June 30, 1965. Contract W-7405-eng-92. 29p. Dep. mn; CFSTI $2.00 cy, $0.50 mn.

A tracer system composed of an aerosol generator and a high volume sampler was developed which will enable the determination of holes or tears in absolute filter media. The aerosol generator consists of an "aerosol can" containing a highly fluorescent oil soluble tracer and a fluorinated hydrocarbon. Defects in absolute filters can be detected by challenging them with the fluorescent aerosol and sampling the effluent from the filter with a large area high volume sampler containing a low-pressure-drop filter media. The fluorescent tracer which penetrates the defects in the absolute filter is deposited on the sampling filter media and the area of the stain is proportional to the size of the defect. It is also possible to detect these defects in the absolute filter by the use of a black light thus eliminating the need of sampling the effluent from the filter. (auth)

44209 (EURAEC-1422) NON-DESTRUCTIVE WELDING RESEARCH. Quarterly Report No. 16, April 1–June 30, 1965. (Roentgen Technische Dienst N. V., Rotterdam (Netherlands)). July 22, 1965. Contract 045-61-5 RDH. 15p. (EUR-2370). Dep. mn; CFSTI $1.00 cy, $0.50 mn.

Work Performed under United States–Euratom Joint Research and Development Program.

The use of dynamic screen images for the ultrasonic testing of welds in thick steel plates is described. Cu, Pb, Ag, Ta, and Sn were evaluated as screens for radiographs of steel using a ^{60}Co and a 5 Mev linear accelerator as radiation sources. (W.L.G.)

44210 (KAPL-M-6484) SURFACE CRACK DETECTOR. Krystyan, K. J. (Knolls Atomic Power Lab., Schenectady, N. Y.). July 2, 1965. Contract W-31-109-Eng-52. 14p. Dep. mn; CFSTI $1.00 cy, $0.50 mn.

A feasibility experiment to determine whether or not commercially available diamond phonograph styli used in conjunction with strain gages and appropriate readout equipment could be used to detect surface cracks on metals was completed. The results obtained indicate that surface cracks, of the type investigated, approximately 0.0005 to 0.001 inch wide and less than 0.001 inch deep could be detected if the diamond styli passed over them. (auth)

44211 (ORNL-P-1543) NONDESTRUCTIVE TESTING OF SMALL-DIAMETER REFRACTORY-ALLOY TUBING. Cook, K. V.; McClung, R. W. (Oak Ridge National Lab., Tenn.). Apr. 21, 1965. Contract W-7405-eng-26. 43p. (CONF-650411-6). Dep. mn; CFSTI $2.00 cy, $0.50 mn.

From Joint NASA–AEC Liquid Metals Corrosion Meeting, Gatlinburg, Tenn.

A discussion is given of nondestructive methods used at ORNL to detect flaws and to measure dimensions of refractory metal tubes. The methods include ultrasonics, eddy currents, penetrants, radiography, and air gaging. The principles, equipment used, and applications of each method are discussed. (D.L.C.)

44212 (TIM-878) CAVITATION SENSITIVE COATING EVALUATION. Noell, G. (Pratt and Whitney Aircraft, Middletown, Conn. Connecticut Advanced Nuclear Engineering Lab.). June 15, 1965. Contract AT(30-1)-2789. 44p. Dep. mn; CFSTI $2.00 cy, $0.50 mn.

A summary of tests conducted on surface coatings that can be applied to an impeller in order to locate probable areas of cavitation damage are presented. Various coatings of epoxies, paints, dyes, and platings were tested using a rotating disk with inducer holes as a cavitation producing device. Tests were conducted in demineralized, degassed water at 90 to 100°F. Coating materials were applied to the stainless steel disk and these coatings were screened for their adhesion qualities, response time and the degree of definition. The results indicated that gold acrylic lacquer spray, when applied to a cleaned and degreased surface, produced cavitation damage indications under ten minutes test time. (auth)

44213 DEVICE FOR HIGH-TEMPERATURE TESTING OF TUNGSTEN WIRES. Andrejeff, P. N.; Napolova, G. A. Microtecnic, 29: 69-70(Apr. 1965).

One of the important criteria characterizing the quality of a tungsten wire is working and residual strain at high temperatures. For the measuring of these values, an instrument permitting such parameters to be checked was developed. The determination is effected as a function of time and of the longitudinal mechanical forces. (P.C.H.)

44214 BACKSCATTER FLAW DETECTION SYSTEM. Sinclair, Kenneth F. (to U. S. Navy). U. S. Patent 3,197,638. July 27, 1965. Filed Jan. 21, 1963.

A nondestructive method and apparatus for detecting and locating material flaws require access to only one side of the test object and provides both uniform sensitivity and adequate resolution for various flaw depth locations. The technique employs backscatter radiation resulting from Compton interactions in the test medium and a unique detector-collimator. The detector-collimator is formed with a series of concentric annular passageways running the length of its longitudinal dimension. It functions in such a fashion that the operative detecting area, as seen from a point in the test medium, increases with depth in the medium so that the loss in sensitivity with depth is just offset by the increase in detector area. (A.G.W.)

Protective Structures

44215 (ORNL-3865) PANEL DISCUSSION ON CIVIL DEFENSE, AMERICAN NUCLEAR SOCIETY ANNUAL MEETING, WEDNESDAY EVENING, JUNE 23, 1965, GATLINBURG, TENNESSEE. (Oak Ridge National Lab., Tenn.). Sept. 1965. Contract W-7405-eng-26. 46p. Dep. mn; CFSTI $2.00 cy, $0.50 mn.

The merits of an extensive civil defense program with respect to nuclear warfare are discussed. The economic, political, and technical ramifications of such a program are considered. (D.C.W.)

44216 BASEMENT RADIATION FROM AN INFINITE-PLANE GAMMA SOURCE. Kaplan, A. L. (Technical Operations Research, Burlington, Mass.). 15p. (CONF-650602-49). Gmelin, AED-CONF-65-125-83.

From American Nuclear Society, 11th Annual Meeting, Gatlinburg, Tenn.

Experiments were performed using steel cylinders, 2 ft. in diameter and 2 ft. high, with a 4-ft. deep basement, to explore the discrepancy between theory and experiment for basement shielding. The results are given for a basement location of 1 ft. below the floor on the central axis of the cylinder. (L.B.S.)

44217 EVALUATION OF SHAPE FACTOR IN STRUCTURE SHIELDING CALCULATIONS. Waldman, Jerry (Technical Operations Research, Burlington, Mass.). 11p. (CONF-650602-50). Gmelin, AED-CONF-65-125-84.

From American Nuclear Society, 11th Annual Meeting, Gatlinburg, Tenn.

Experiments were performed to test the validity of the engineering manual approach to changes in dose rate from a fallout field due to variation in structure shape. Four types of roofless steel structures were used: a cylinder, a square, and two rectangles with length to width ratios of 2 and 4. The experiment was run with 20, 40, and 60 psf walls for each structure shape. The results are discussed. (L.B.S.)

44218 PROTECTIVE WINDOWS OR SKYLIGHTS FOR FALLOUT SHELTERS. Larkin, Joseph P. U. S. Patent 3,197,641. July 27, 1965. Filed Feb. 12, 1962.

A suitable window for a fallout shelter consists of a steel drum having transparent sealed ends and filled with a transparent dense liquid. The drum ends are held in place by an arrangement of flanges and clamps so that they can be removed from inside the shelter to provide an emergency exit. Four feet of water in the window is required for adequate protection; denser liquids permit use of thinner windows. (A.G.W.)

Space Propulsion

See also REACTOR TECHNOLOGY — Propulsion and Space.

Refer also to abstract 45448.

44219 (ACF-8) AXISYMMETRIC THIN SHELLS OF REVOLUTION. Ney, L. A. (ACF Industries, Inc., Albuquerque, N. Mex.). [1962]. Contract AT(29-1)-1352. 36p. (CONF-650648-1). Dep. mn; CFSTI $2.00 cy, $0.50 mn.

From IBM User's Conference, Portland, Ore.

An analysis of axisymmetric linear elastic shell theory is presented. The procedure used by the S-126 code was to divide the shell into a multi-regional shell where each region is chosen so as to have no discontinuities of load or geometry within the region. Regions are joined by appropriate boundary equations which include the effects of exterior loading which may be introduced at that point. Multi-layers are allowed in each region. However, their principal function is in defining the thermal condition. The temperature gradient across a layer is taken as linear; therefore, the thinner the layer, the more accurate is the thermal gradient approximation. Inter-laminar shear is neglected. A description of the code is given. (M.O.W.)

44220 (N64-31011) ELECTROTHERMAL ENGINE RESEARCH AND DEVELOPMENT. Summary Report. Phase I. (Research and Advanced Development Div., Avco Corp., Wilmington, Mass.). July 20, 1964. Contract NAS 3-4104. 135p. (NASA-CR-54104; RAD-TR-64-12). CFSTI $4.00 cy, $0.75 mn.

A 3-kw resistojet thrustor based on a wire-coil heat exchanger was developed. In a 293-hr endurance test, the thrustor used a propellant flow rate of 0.065 g/sec of hydrogen and produced a specific impulse of 840 sec at an overall efficiency of 67% with an input power of 3 kw. Data are presented on the compatibility of tungsten, molybdenum, and boron nitride in a hydrogen flow at temperatures in the range 2,000 to 3,000°K. The thrustor supersonic nozzle design was based on an analytical study that included the effects of boundary-layer growth. An area ratio of 30 at a conical expansion total angle of 30° was chosen. (auth)

44221 (N64-31088) RESEARCH ON PROBLEMS OF ION BEAM FORMATION FROM ELECTRON BOMBARDMENT ION SOURCES. Summary Report. King, H. J. (Hughes Research Labs., Malibu, Calif.). Aug. 18, 1964. Contract NAS 3-4118. 39p. (NASA-CR-54143; HRL-4118-S). CFSTI $2.00 cy, $0.50 mn.

Cathode life in Kaufman type mercury electron bombardment ion thrustors was limited by sputtering erosion caused by ions from the plasma accelerated through the cathode sheath. The development of a cathode in which this problem is eliminated by operating the discharge in an arc mode, using the surface of liquid mercury as the cathode and utilizing the removal of liquid mercury atoms from the cathode by the discharge as the propellant feed mechanism, is reported. This also eliminates the need for a liquid-vapor phase separator in the feed system. To provide a stable equilibrium position independent of gravitational forces for the mercury surface, the mercury is forced through a porous tungsten plug or small orifice and held as a thin film or drop by surface tension forces and arc pressure. Cathodes of this design yield a ratio of electrons to atoms leaving the cathode of >25, and they were successfully operated in ion thrustors of the above type. Research is continuing to establish optimum operating conditions for stable efficient operation in a practical thrustor. (auth)

44222 (NP-15068) ANALYSIS OF ELECTRON-ION MIXING IN ION ENGINES. Quarterly Report No. 3, November 1, 1964–January 31, 1965. Wadhwa, R. P.; Brauch, D. F. (Litton Industries, San Carlos, Calif. Research Lab.). Feb. 20, 1965. Contract NAS3-5757. 91p.

The two-dimensional electron-ion mixing program is used to investigate the neutralization mechanism in a practical ion engine. The input conditions—namely, the ion velocity and potential distributions across the injection plane—are fixed according to the results obtained for the ion-gun configuration. For this configuration, the potential difference between the electron emitter and a portion of the injection plane is not enough to prevent electrons from escaping toward the injection plane when the problem is simulated for the reduced ion-mass case. Some solutions to this problem and their physical implications are discussed. Results for various test cases in establishing the requirements on the primary electron emission are discussed. The neutralization mechanism is studied for ion-to-electron mass ratios of 64, 144 and 256, and the results are extrapolated for the actual case. It is found that the ship potential varies with time at the electron plasma frequency and that the fluctuations are reduced as the value of the ion mass is increased. A virtual cathode surrounds the complete emitter although electrons are emitted from half the surface only. Electrons oscillate back and forth resulting in macroscopic neutralization of the ion beam. Because of poor coupling between the ion beam and the electron emitter (in the studies discussed), there is a positive potential build-up in the central region, so that the electrons gain energy. Because of this large potential difference, the regulation on the demand and supply of electrons is not very satisfactory. There is a great tendency to establish thermodynamic equilibrium between ions and electrons. The gain or loss in electron temperature depends upon the potential in a specific region. Electron temperatures four times as high as the electron-emitter temperature are noticed in the high positive potential regions. Lower temperatures result at locations far from the emitter. Ion temperature is increased. Some initial tests on the simulation of the general four-sided electron emitter are discussed. (auth)

44223 (NP-15438) CYCLOTRON RESONANCE PROPULSION SYSTEM. Ninth Monthly Progress Report, July 1965. Miller, David B.; Bethke, George W. (General Electric Co., Philadelphia, Pa. Missile and Space Div.). Aug. 6, 1965. Contract NAS3-6266. 14p.

Further development in the following areas is presented; magnetic probe (Mark V-S accelerator), Mark VIII (screen waveguide) accelerator, thrust stand, microwave probe, and energy analyzer and potential probes. (M.O.W.)

44224 ENERGY STORAGE CAPACITORS FOR PULSED PLASMA THRUSTORS. Hayworth, B. R.; White, C. W.; Miller, A. R. (General Dynamics/Convair, San Diego, Calif.). New York, American Inst. of Aeronautics and

Astronautics, 1965, Preprint No. 65-337, 8p., $1.00. (CONF-650711-36). ORINS.

From AIAA 2nd Annual Meeting and Technical Demonstration, San Francisco.

The capacitor requirements for two types of pulsed plasma accelerators, the coaxial gun and the pulsed arc gun, are discussed. Recent advances in film capacitors have enabled low loss, low impedance pulse-lines to be built for use with the coaxial gun. For example, a 50 μF, 8 kv capacitor with 1.2 nH internal inductance behaves as a distributed element pulse-line with an impedance of 4.7 milliohms and pulse-time of 0.5 microseconds. For the pulsed arc gun the optimum energy-storage system consists of a high impedance, high voltage pulse-line and a step-down transformer. The design criteria for the transformer is presented. The state-of-the-art in capacitor technology is summarized for film-foil, electrolytic, and ceramic capacitors. Film-foil capacitors, with an energy density of 4.3 joules/in.^{3} and 75 joules/lb have been life tested to over 10^6 discharges. The results presented demonstrate that the energy-storage capacitor does not represent a major problem in the development of pulsed plasma thrustors. (auth)

44225 STUDIES OF A SWITCH-TRIGGERED PULSED PLASMA ACCELERATOR. Guman, William J. (Republic Aviation Corp., Farmingdale, N. Y.). New York, American Inst. of Aeronautics and Astronautics, 1965, Preprint No. 65-339, 12p., $1.00. (CONF-650711-34). ORINS.

From AIAA 2nd Annual Meeting and Technical Demonstration, San Francisco.

The impulse behavior of a pulsed plasma accelerator which incorporates a low-pressure pinch-type switch in the electric discharge circuit was studied experimentally on a reaction-type thrust stand, and a brief discussion is presented of some considerations of switch-triggered operation of a pulsed plasma accelerator. Two types of experimental investigations were carried out: application of voltage was delayed relative to propellant injection in cases for which the interelectrode spacing was evacuated prior to gaseous propellant injection, voltage is switched across electrodes containing a uniformly distributed gas. In the latter case, tests were carried out with the initial pressure level of the gas encompassing the entire portion of the Paschen curve where a discharge would normally occur. Measured impulse data and time-of-arrival data of the plasma front at the exit of the accelerator are compared with simplified gasdynamical considerations and blast wave theory. (auth)

44226 HIGH CURRENT DENSITY THRUSTOR EXPERIMENTS. Forbes, S. G.; Beynon, J. C. (TRW Space Tech. Labs., Redondo Beach, Calif.). New York, American Inst. of Aeronautics and Astronautics, 1965, Preprint No. 65-376, 41p., $1.00. (CONF-650711-32). ORINS.

From AIAA 2nd Annual Meeting and Technical Demonstration, San Francisco.

The design, fabrication and testing of a two module cesium contact ion engine capable of 20 millipounds of thrust and a power to thrust ratio below 200 kw/lb is treated. To achieve these objectives thrustor operation at ion current densities from 20 to 40 ma/cm^2 was investigated. To overcome limitations on accelerator durability at these high current densities an electrode replacement device was developed. With the emitter material available for this work representative operational characteristics were: at 4600 sec I_s, 62% electrical efficiency and 163 kw/lb; at 6950 sec I_s, 80% electrical efficiency and 190 kw/lb. Propellant utilization was 0.94 or greater. The grid replacement weight is equivalent to the propellant utilization of not less than 90%. Engine weight is 1 kg/ampere of ion beam. Emitter material currently developed should permit operation with this same engine design at 80% electrical efficiency at 5000 sec with periodic replacement of the accelerator structure. By derating the engine to 70% electrical at 5000 sec at 10,000 hour life on the accelerator structure becomes feasible. Operated in this manner the specific weight is about 2.5 kg/amp of ion beam. (auth)

44227 PERFORMANCE OF ION THRUSTORS AND SYSTEMS FOR SATELLITE CONTROL. Anderson, J. Robert (Hughes Aircraft Co., Malibu, Calif.). New York, American Inst. of Aeronautics and Astronautics, 1965, Preprint No. 65-417, 60p., $1.00. (CONF-650711-9). ORINS.

From AIAA 2nd Annual Meeting and Technical Demonstration, San Francisco.

Recent results achieved in a continuing program for the development of an ion engine satellite control system are described. The correction forces are generated by single, linear-strip, cesium-contact ion rockets of the 0.5 mlb class designed for long life, high thermal efficiency and low mass. Steady state performance tests approaching 2000 hour duration have been conducted satisfactorily. Since attitude control requires pulse operation of the ion thrustors, several thrustors have been cycled more than 50,000 times and life tests totaling over 200,000 temperature cycles have been completed successfully. A novel feature of this linear strip thrustor is the use of a very low mass ionizer which can be heated to 1100°C in less than 15 sec with a warmup energy of only 0.5 W-hr. A laboratory demonstration system has been built which provides two-axis attitude control and station keeping functions. The system is undergoing extensive laboratory testing at the NASA-Lewis Research Center. Included in this system is the necessary power conditioning, controls, propellant feed system, and six ion thrustors in early configurations. The testing consists of prolonged operation in vacuum to determine general system behavior, and testing on the vacuum air bearing facility to determine system performance and demonstrate feasibility. (auth)

44228 PRELIMINARY INVESTIGATIONS TO DETERMINE NUCLEAR-ELECTRIC SPACECRAFT CONFIGURATIONS FOR HIGH-ENERGY MISSIONS. Volkoff, J. J.; Womack, J. R. (California Inst. of Tech., Pasadena). New York, American Inst. of Aeronautics and Astronautics, 1965, Preprint No. 65-413, 31p., $1.00. (CONF-650711-11). ORINS.

From AIAA 2nd Annual Meeting and Technical Demonstration, San Francisco.

It is determined how the mass of spacecraft systems is affected by changes in spacecraft configuration for a conceptual 300-kw(e) nuclear-electric space-craft designed for a Jupiter orbital mission. The powerplant employed a reactor-turbo-generator system. The nuclear-radiation shield, heat-rejection radiators, spacecraft structure, booster-spacecraft adapter, and aerodynamic shroud are considered as subsystems most likely to vary appreciably in mass with changes of space-craft configuration. The two selected spacecraft configuration concepts feature the heat-rejection radiator systems assembled in the flat plane configuration and the cylindrical configuration. The flat plane radiator configuration was found to be the more favorable concept. (auth)

44229 CYCLOTRON RESONANCE THRUSTOR DESIGN AND DIAGNOSTICS TECHNIQUES. Miller, D. B.; Bethke, G. W. (General Electric Co., Philadelphia). New York, American Inst. of Aeronautics and Astronautics, 1965, Preprint No. 65-301, 39p., $1.00. (CONF-650711-39). ORINS.

From AIAA 2nd Annual Meeting and Technical Demonstration, San Francisco.

The most successful cyclotron-resonance accelerator designs have been of the longitudinal-interaction type. Quartz, alumina, sapphire and beryllia have been employed at medium power (to 540 watts, S-band) and high power (to 4150 watts, X-band) to separate the evacuated plasma chamber from the remainder of the waveguide circuit. Sizable wall losses have been encountered, but the accelerator may be made sufficiently short so that an appreciable percentage of the r-f power (up to 65% at X-band) ultimately appears in the accelerated plasma stream. Peripheral gas injection has yielded better results than injection through a hole in the window because of window structure and r-f coupling problems. A diode type of sampling probe has been employed to

measure both power density and ion flux density. Three-, sixteen- and twenty-eight-channel arrays of these probes have been used. Power density and ion flux density mappings across the plasma exhaust stream are shown and interpreted. A multi-electrode, retarding-potential probe is used to study the ion energy characteristics. Energies obtained with this probe are correlated with the diode ion flux and power measurements. This type of accelerator is assessed to have propulsion potentialities, particularly if the space system into which it is to be incorporated already has substantial r-f capacity for communications purposes. (auth)

44230 CESIUM FUELED MPD ARC JET ENGINE PERFORMANCE. Bennett, S.; Enos, G.; John, R. R.; Tuchman, A. (Avco Corp., Wilmington, Mass.). New York, American Inst. of Aeronautics and Astronautics, 1965, Preprint No. 65-296, 16p., $1.00. (CONF-650711-44). ORINS.

From AIAA 2nd Annual Meeting and Technical Demonstration, San Francisco.

Recent experimental results are presented on the performance of an MPD arc thrustor operated with cesium at input power levels between 5 and 10 kilowatts and external magnetic field strengths of the order of 1 kilogauss. The use of condensible cesium permitted engine operation at ambient pressure levels (~0.10 microns) considerably below the ambient pressures (~100 microns) previously obtained with the gaseous propellants, hydrogen and ammonia. The objective of running at the lower pressure levels was to reduce the possible effects of gas entrainment on engine propulsion performance. The over-all electric to thrust power efficiency appears to be primarily a function of the specific impulse, and is quite insensitive to the absolute value of either the input power or the applied external magnetic field. Visual observations strongly suggest that the cesium acceleration process occurs within a magnetically confined volume located outside the physical engine. The estimated ion current, based on the measured cesium flow rate, is almost an order of magnitude less than the actual current. Finally, the apparent MPD arc jet exhaust velocities, based on thrust and mass flow measurements, are larger by a factor of approximately 2 than the velocities that would be obtained by a singly charged cesium ion falling through the arc potential. This conclusion is, however, still tentative because of uncertainty in the measurement of the pressure level of the cesium ambient environment. (auth)

44231 A 100-kv, 10-w HEAVY-PARTICLE THRUSTOR. Cohen, E.; Somol, C. J.; Gordon, D. A. (TRW Space Tech. Labs., Redondo Beach, Calif.). New York, American Inst. of Aeronautics and Astronautics, 1965, Preprint No. 65-377, 33p., $1.00. (CONF-650711-50). ORINS.

From AIAA 2nd Annual Meeting and Technical Demonstration, San Francisco.

The efficiency of an electric thrustor can be expressed as the ratio, $1/(1 + V_d/V_b)$, where the dissipative energy/charge is expressed as V_d and the acceleration voltage applied to the ions as V_b. A fixed parameter of any mission is the specific impulse, a function of V_b. For I_{sp} in the regime of 1000–5000 secs, a large value of V_b can be used with a low value of q/m. The charged heavy particle or colloid shows some promise in obtaining high efficiencies in the lower specific impulse range. The electric thrustor under development makes use of the electrical dispersion of liquids to obtain the required charge/mass ratio. Work began initially with a single capillary tube which could emit a peaked distribution of charged liquid particles when the tip of the tube was exposed to a high electric field. The next step was the paralleling of individual tubes in a module in order to extract greater beam current. Finally a 100 μa beam of charged liquid droplets was accelerated with 100 KV. The problems encountered and the partial solution of these problems are discussed. (auth)

44232 ECONOMICS OF ELECTRICAL PROPULSION FOR EARTH-ORBIT TO LUNAR-ORBIT CARGO TRANSFER. Larson, John W. (General Electric Co., Philadelphia). New York, American Inst. of Aeronautics and Astronautics, 1965, Preprint No. 65-415, 22p., $1.00. (CONF-650711-10). ORINS.

From AIAA 2nd Annual Meeting and Technical Demonstration, San Francisco.

The use of electric propulsion for providing logistic support of advanced lunar operations is examined. The mission is analyzed from the viewpoint of cost effectiveness. Both development and manufacture cost of the nuclear power supply are considered in a parametric manner. Using these criteria for selection, a number of operating modes for electric propulsion are examined and compared, which show that the single-trip mode is more promising than the multiple trip, or shuttle, modes. Thus, a set of specifications can be described for the nuclear power supply which are more reasonable from the standpoint of life qualification, specific weight, and operational complexity. (L.B.S.)

44233 PERFORMANCE OF A TWO-STAGE REPETITIVELY PULSED COAXIAL PLASMA ENGINE. Gorowitz, B.; Karras, T.; Gloersen, P. (General Electric Co., Philadelphia). New York, American Inst. of Aeronautics and Astronautics, 1965, Preprint No. 65-342, 21p., $1.00. (CONF-650711-28). ORINS.

From AIAA 2nd Annual Meeting and Technical Demonstration, San Francisco.

As a result of a succession of changes in propellant loading, electrode geometry and mode of discharge initiation, the overall efficiency of a repetitively pulsed coaxial plasma engine was determined to vary from 35 to 70% in the specific impulse range of 3000–9000 seconds. The values reported are based on direct measurements of engine thrust and total mass flow. Eroded mass was credited toward increasing the effective propellant load. Operation of the engine in the two-stage triggered mode with axial propellant injection has permitted greater control over the pre-firing propellant distribution and time of discharge initiation than could be achieved previously. The result has been a substantial increase in propellant mass utilization accompanied by a lowering of the specific impulse range to values deemed more suitable for presently contemplated missions. The results obtained from the above thrust balance and mass flow measurements were compared with the results from calorimetry of the engine exhaust stream. (auth)

Vacuum Engineering

Refer also to abstract 44357.

44234 (MATT-345) TRANSMITTING MOTION THROUGH A VACUUM WALL. Christie, Robert S. (Princeton Univ., N. J. Plasma Physics Lab.). June 1965. Contract AT(30-1)-1238. 21p. (CONF-650547-3). Dep. mn; CFSTI $1.00 cy, $0.50 mn.

From American Society of Lubrication Engineers, 20th Annual Meeting, Detroit.

Mechanisms for transmitting motion through a vacuum wall and utilizing metal bellows as a vacuum seal are discussed and illustrated. Tests run on the mechanisms are described and the results related. The conclusion is drawn that metal bellows are satisfactory as a vacuum seal for all types of motions illustrated. (auth)

GEOLOGY AND MINERALOGY

General

44235 (DPSPU-64-30-23) THE IMPORTANCE OF CAPILLARY PORES IN RAINWATER PERCOLATION TO THE GROUND WATER TABLE. Horton, J. H.; Hawkins, R. H. (Du Pont de Nemours (E. I.) and Co., Aiken, S. C. Savannah River Plant). Sept. 1964. Contract AT(07-3)-1. 14p. Dep. mn; CFSTI $1.00 cy, $0.50 mn.

Results are reported from a laboratory study of the percolation of rain water through soil to the ground table. Four 5-ft length Plexiglas columns of sandy clay soil; packed to a uniform density of 1.40 g/cc with coarse sand used to create a continuous series of large pores extending throughout the length of the columns were used. Water was added rapidly at the top of the columns until drainage began from both the soil and the sand. Results indicated that the percolation of rain water through the soil to the ground water table is through capillary pores by the displacement of capillary water downward. (C.H.)

44236 (TID-22086) GEOLOGICAL AND GEOCHEMICAL STUDIES OF THE ROSKRUGE RANGE, PIMA COUNTY, ARIZONA (thesis). Bikerman, Michael (Arizona Univ., Tucson). 1965. Contract AT(11-1)-689. 133p. Dep. mn; CFSTI $4.00 cy, $1.00 mn.

A combined field and laboratory investigation of the primarily volcanic Roskruge range, Pima County, Arizona, produced the following results: The rocks in the area fall into three major and several minor divisions. The major groups are: (1) The pre-Laramide dark-colored andesites and sediments that floor the range. A K-Ar date on one of the andesites produced a number, 108 My, on a whole rock analysis. (2) The brightly colored and widespread Laramide volcanics and an associated hypabyssal pluton at Cocoraque Butte, which gave K-Ar mineral ages in the 74 to 66 My spread. (3) The mid-Tertiary potassic basaltic andesites found on an eroded plain that is cut into the Laramide volcanics. These dark-colored extrusives were dated at 23 My by whole rock K-Ar. Amongst the minor units in distribution is the petrographically unusual Recortado ash flow, a small 13 My old unit that preserves a vitrophyre just above its base. Also included in the miscellaneous group of units are the post-orogenic true basalts, which appear as dikes and as a flow(?) at Brawley Wash and which gave whole rock K-Ar dates of about 10 My. Initial strontium 87/86 ratios indicate that the Laramide and mid-Tertiary rocks (including the Recortado ash flow) have values ranging from 0.7056 to 0.7092, while the Brawley Wash basalt has a true deep-seated basalt ratio of 0.7038. The combination of radiochemical assay, petrographic and field study, and isotopic data has established good gross correlation with the already known sequence of formations and plutons in the Tucson Mountains. (auth)

44237 A COMPARISON OF FEATURES CHARACTERISTIC OF NUCLEAR EXPLOSION CRATERS AND ASTROBLEMES. Short, Nicholas M. (Univ. of California, Livermore). Ann. N. Y. Acad. Sci., 123: 573-616 (July 15, 1965). (UCRL-7928-T).

It is shown that underground nuclear explosions at shallow depths in many respects simulate the mechanisms by which impact craters are formed and under appropriate conditions can lead to end results bearing a strong resemblance to Astroblemes. It was found that a detailed study of nuclear explosion craters can be used as an approach to understanding the genesis of impact craters. The general character of underground and cratering nuclear explosions is considered. Shock melt and glass, shock-induced phase transformations, shock metamorphism, shatter cones, physical properties around an explosion, petrographic characteristics, large fracture patterns, and solid-state changes are described. (M.C.G.)

44238 OXYGEN ISOTOPIC STUDIES OF AMPHIBOLITES. Schwarcz, H. P. (McMaster Univ., Hamilton, Ont.); Clayton, R. N. Can. J. Earth Sci., 2: 72-84(Apr. 1965).

Significance of the $^{18}O/^{16}O$ ratios of amphibolites was investigated in relation to the problem of their origin and to their metamorphic history. The oxygen isotopic content of a metamorphic rock is equal to that of its protolith except if it has lost oxygen-bearing compounds (especially H_2O and CO_2) during metamorphism or exchanged with some external oxygen-reservoir either through dry diffusion or by interaction with a mobile fluid phase. If the effect of isotopic composition of the protolith on that of the rock is invariably overwhelming, it should be possible to use the total-rock $^{18}O/^{16}O$ ratio as an index of the protolith. However, if the magnitudes of the effects of the other factors are as great in their influence on the isotopic composition as the difference between a sedimentary and igneous protolith, it would be impossible to use $^{18}O/^{16}O$ ratios unequivocally in all cases. The whole-rock $^{18}O/^{16}O$ ratios of amphibolites from a variety of localities were studied in an attempt to distinguish para-amphibolites from ortho-amphibolites. If para-amphibolites were derived from a pelite-carbonate mixture or any carbonate-bearing sedimentary rock, they should be enriched in ^{18}O relative to basaltic parents. Exchange with an external oxygen reservoir acting as an isotopic buffer during metamorphism would, however, tend to obliterate initial differences between basaltic and metasedimentary parent rocks. It was found that, except for feather amphibolites from the Grenville subprovince of Ontario, rocks from a given area which are geologically distinguishable as para- or ortho-amphibolites do not display the predicted differences in $^{18}O/^{16}O$ ratios. Large differences in isotopic composition between localities are attributed in part to difference in grade of metamorphism and consequent differences in temperature of exchange with an external oxygen isotopic buffer. All samples appear to have exchanged to some extent. (BBB)

44239 XENON, ARGON AND HELIUM IN SOME NATURAL GASES. Shukolyukov, Yu. A.; Tolstikhin, I. N. (Lab. of the Geology of Precambrian, Leningrad). Geokhimiya, No. 7, 801-12(July 1965). (In Russian).

The most probable value of radiogenic He/Ar in gases studied is 12. Variations in the value of radiogenic He/Ar may be accounted for either by helium and argon release from rocks of different composition, or by physico-chemical separation of gases during their migration. Between the helium and the nitrogen content a proportionality was observed as well as between the content of air argon and nitrogen. Only a part of nitrogen in gases has an aerial origin. In the formation of gases from nitrogen thermae the juvenile do not play a great role as the argon isotopic composition is near the aerial. Only a small part of the radiogenic argon under observation may have originated at the expense of the radioactive decay of K, being contained in water. The ratio of Xe isotopes, as well as ^{38}Ar and ^{36}Ar approaches the aerial. This means that the processes leading to an enrichment of xenon in radiogenic isotopes and to a decrease of the $^{38}Ar/^{36}Ar$ ratio, play an unimportant role compared to the migration of atmospheric gases into pore spaces of rocks. (auth)

44240 ISOTOPIC COMPOSITION OF THE CRYSTALLIZATION WATER OF SALINE MINERALS. Borshchevskii, Yu. A.; Khristianov, V. K. Geokhimiya, No. 7, 844-50(July 1965). (In Russian).

The D_2O content in the crystallization water of carnallite, kainite, and other minerals was determined. The analysis showed that the deuterium content, contrary to expectations, is equal to the deuterium in normal oceanic water. The data do not coordinate with calculations assuming that the deuterium content in saline minerals must be considerably

higher than the obtained values for any of the variants of sea water condensation. The discrepancy of theoretical and experimental data is accounted for by the assumption that in a highly mineralized aqueous solution the heavy hydrogen molecules of the water possess higher volatility than light hydrogen molecules while in the water pores of D the bonds will by stronger. An analysis of two water samples taken in an arid zone of salt lakes and saline soils—mother brine of the saltproducing lake Inder (0.0145 ± 0.0003 at. % of D_2O) and rainwater collected in this region (0.0172 + 0.0004 at. % of D_2O) and data of others confirm the assumptions made. (auth)

44241 OXYGEN ISOTOPE FRACTIONATION BETWEEN COEXISTING CALCITE AND DOLOMITE IN THE FRESHWATER UPPER CARBONIFEROUS FREEPORT FORMATION. **Weber, Jon N. (Pennsylvania State Univ., University Park). Nature, 207: 972-3(Aug. 28, 1965).**

Fine-grained dolomitic limestones of the Freeport formation (Upper Carboniferous) outcropping over an area of about 100 square miles in central Pennsylvania were examined. To obtain the values of $\delta^{18}O_{ct}$ and $\delta^{18}O_{dol}$, a number of samples from each collecting site were analyzed to obtain $\delta^{18}O$ for the bulk carbonate, which was a mixture of calcite, dolomite, and siderite. Invariably the dolomite was found to be enriched in ^{18}O. Mean values for 6 collecting sites where the coefficient of multiple correlation was highest were: $\delta^{18}O_{ct} = 7.87$ per mil; $\delta^{18}O_{dol} = 3.04$ per mil; $\delta^{18}O_{dol} - \delta^{18}O_{ct} = 4.83$. The dolomite is relatively enriched in ^{18}O with respect to modern and tertiary calcites. (P.C.H.)

44242 ON THE VARIATIONS IN THE ISOTOPIC COMPOSITIONS OF NATURALLY OCCURRING MOLYBDENUM. **Crouch, E. A. C.; Tuplin, T. A. (Atomic Energy Research Establishment, Harwell, Berks, Eng.). 26p. (CONF-650519-5). Gmelin, AED-CONF-65-120-21.**

From 13th Annual Conference of American Society of Testing Materials, St. Louis.

The isotopic composition of 10 samples of Mo each extracted from an ore sample was determined. The results expressed as isotopic atom ratios were examined in groups of five and the mean and its standard deviation of each group was plotted against time to ensure that the ratios were invariable during the life of the ion source. The isotopic compositions of Mo from the sources were not constant. The procedure used is described. (P.C.H.)

Natural Radioactivity and Fallout

See also HEALTH AND SAFETY.

Refer also to abstracts 43960 and 44292.

44243 (AD-619902) FALLOUT MODELS AND RADIOLOGICAL COUNTERMEASURE EVALUATIONS. **Miller, Carl F. (Stanford Research Inst., Menlo Park, Calif.). May 1965. Contract N228-(62479)65702. 30p.**

A fallout model and other submodels are described that have been formulated to assist in the assessment of radiological defense problems and in the evaluation of radiological countermeasures. The design of the model system emphasizes application of both short-term and long-term radiological problems of interest to civil defense. The types of input data that are utilized, the various important independent parameters that are considered in the models and submodels, and the types of output information are listed. Also, the major assumptions, constraints, and concepts involved in the mathematical construction of each model are summarized. The purpose of the report is to provide researchers on other civil defense investigations general background information on the composition and outputs of these models. The report does not include any of the mathematical formulations of the models. (auth)

44244 (AEET/AM/40) ^{90}Sr CONTENT OF FOOD SAMPLES IN INDIA—DATA SUMMARY THROUGH 1963. **Anand, S. J. S.; Chandrasekaran, V. R.; Hingorani, S. B.; Joshi, L. U.; Khandekar, R. N.; Lalit, B. Y. (Atomic Energy Establishment, Trombay (India). Air Monitoring Section). Sept. 1964. 16p. Dep. mn.**

Data are presented on the ^{90}Sr content of milk, grain, vegetables, meat, and other foods sampled in India from 1959 through 1963. The Ca content of milk and other food samples was also determined. The ^{90}Sr activity of milk samples collected during 1959, 1962, and 1963 was higher than that of samples collected in 1960 and 1961. Milk samples collected in areas of high-rainfall and during the monsoon season contained more ^{90}Sr than other samples. (C.H.)

44245 (BNL-914, pp 125-32) DEPOSITION. **Chamberlain, Arthur C. (Atomic Energy Research Establishment, Harwell (England)).**

The importance and nature of deposition are discussed. The mathematics of deposition and surface resistances are described and equations given. Wind tunnel tests were made using ThB vapor and various surfaces, and the results are shown in plots of various parameters. Some work was also done on evaporation of water, deposition of micron-sized particles, and deposition of 30-μ spores to grass. (D.L.C.)

44246 (BNL-914, pp 133-8) THE CURRENT STATUS OF DEPOSITION RESEARCH. **Raynor, Gilbert S. (Brookhaven National Lab., Upton, N. Y.).**

A review is presented of research on deposition processes, characterization, measurement, and theory. Laboratory and field experiments are summarized. Areas in which further research is needed are outlined. An extensive bibliography is included. (D.L.C.)

44247 (BNL-914, pp 139-40) THE MEASUREMENT OF DEPOSITION. **Islitzer, Norman F. (Weather Bureau, Idaho Falls, Idaho).**

The possible relation of deposition to meteorological variables is discussed. Theoretical treatments of deposition do not clarify the relation, and it appears that, if meteorological factors are important, they should be measured very close to the surface. The simulation of deposition on natural surfaces and the effects of tracer depletion on concentrations are considered. Experiments needed to solve these problems are described. (D.L.C.)

44248 (BNL-914, pp 141-3) DEPOSITION MEASUREMENTS AT HANFORD. **Simpson, Charles L. (General Electric Co., Richland, Wash. Hanford Atomic Products Operation).**

Three experiments were done; the first one involved indirect deposition calculations from mass flux of zinc sulfide releases through arcs. The second one was direct deposition measurements of zinc sulfide on a dried cheat grass, and the results are shown as a plume depletion vs time graph. The final experiment was the release of iodine into a stable atmosphere and the measurement of deposition on rye grass, geraniums, and artificial flowers. The observed distribution of the deposition is discussed. A group discussion is included. (D.L.C.)

44249 (BNL-914, pp 144-5) DEPOSITION CALCULATIONS AT OAK RIDGE. **Hilsmeier, William F. (Weather Bureau, Oak Ridge, Tenn.).**

In the evaluation of maximum washout, an equation was obtained which is independent of the washout and time coefficients. The equation gives a linear area vs maximum washout graph, which can be used to calculate the maximum release in cases where washout is the determining factor. (D.L.C.)

44250 (NP-15269) RADIOESTRONCIO Y ESTRONCIO ESTABLE EN LOS HUESOS Y DIETAS DE LOS NINOS. Informe No. 149. **(Radiostrontium and Strontium Fixation in Bones and Children's Diets). Report No. 149. Beninson, D.; Ramos, E.; Touzet, R. (Comision Nacional de Energia Atomica, Buenos Aires (Argentina)). 1965. 14p. (CONF-765-12). Dep. mn.**

From 2nd Conference on Radioactive Fallout from Nuclear Weapons Tests, Germantown, Md., Nov. 1964.

The results of measurements of ^{90}Sr and natural Sr in the bones of children and the food products of the corresponding diets are presented and discussed. The data show that the levels of $^{90}Sr/Ca$ in the total diet are very close of that of milk for children during the first year of life. Typical incorporations in very small children, during the last three years in Argentina, were of the order of several pC of ^{90}Sr and about a mg of natural Sr per day. Results of measurements of ^{90}Sr in bone samples of distinct age groups, for which detailed information on the dietetic history can be obtained, are presented. The typical levels were of the orders of one pC/g Ca. Natural strontium in the bone appears to increase slowly with age. The factors of discrimination were estimated for various age groups, using a simple model and data on the diet and bones. The evaluations of ^{90}Sr and natural Sr agree adequately and suggest that babies discriminate less between the strontiums than older children and adults. (tr-auth)

44251 (NP–15519, pp 23-51) CANADIAN FALLOUT DATA FOR JUNE, 1965. Samuels, E. R.; Mohindra, V. K. (Department of National Health and Welfare, Ottawa (Ontario). Radiation Protection Div.).

Data are presented on radioactivity due to fallout in samples of air particulates, precipitation, milk, water, wheat, soil, and human bone collected in Canada during June 1965. Data for 1964 are included for comparison. (C.H.)

44252 (NRL–6305) FILTER PACK TECHNIQUE FOR CLASSIFYING RADIOACTIVE AEROSOLS BY PARTICLE SIZE. PART 3. THE SIZE DISTRIBUTION OF AIRBORNE FISSION PRODUCTS DURING 1963 AND 1964. Lockhart, L. B. Jr.; Patterson, R. L. Jr.; Saunders, A. W. Jr. (Naval Research Lab., Washington, D. C.). June 2, 1965. Contract AT(49-7)-2435. 18p. Dep. mn; CFSTI $1.00 cy, $0.50 mn.

Some 60-odd collections of radioactive particulate matter dispersed in the atmosphere have been made during the past two years by use of a filter pack technique utilizing four superimposed filters. The distribution of radioactivity among the filters was analyzed mathematically by means of four simultaneous linear algebraic equations which relate the particle size of the retained material to the filter characteristics so as to permit the assignment of radioactivity in each collection to four major size groupings: 1.1μ, 0.6μ, 0.3μ, and 0.15μ particle diameter. The fission-product radioactivity collected at ground level is associated with particles having an "average" diameter between 0.3 and 1.1μ (assuming spherical particles of 1.8 g/cc density). The conclusion is reached that the extremely small radioactive particulates characteristic of nuclear bomb debris which have resided for an extended period in the stratosphere become attached to the larger nonradioactive aerosols typical of troposphere air by the time they arrive at ground level. A comparison of the relative amounts of various long-lived fission products (^{144}Ce, ^{147}Pm, ^{90}Sr, ^{137}Cs) and of the natural isotope RaD (^{210}Pb) in month-long collections by four-filter packs shows no significant evidence of fractionation effects among the long-lived fission products. This confirms the importance of the attachment process to the size of radioactive fission product conglomerates detected at ground level. Fresh debris from the Chinese nuclear test, however, exhibited a different isotopic distribution with size than did the older bomb debris. Proportionately more of the shorter-lived radioactive fission products collected during transit of debris from the Chinese test appeared in the largest particle size grouping. (auth)

44253 (NYO–2174-36) GENERAL SUMMARY OF PROGRESS [ON RADIOACTIVE FALLOUT DISTRIBUTION], 1964–1965. Appendix A. (New York Operations Office (AEC), N. Y.). Contract AT(30-1)-2174. 72p. Dep. mn; CFSTI $3.00 cy, $0.75 mn.

Progress is reported in studies of radioactive fallout distribution in surface waters and shore sediments of the Atlantic Ocean from 1964 to 1965. Samples of surface water collected by U. S. and European weather ships were analyzed for total radioactivity and ^{137}Cs and ^{90}Sr content, measurements were also made of the fallout in air over sea surfaces. Procedures used for sample collection are described and the callibration of a flame photometer for use in the radiochemical analysis of samples is discussed. Sediments collected at various locations were analyzed for ^{91}Y and ^{140}La and plankton samples from the North Atlantic, Sargasso Sea, and Caribbean were analyzed for beta radioactivity. A procedure is described for the determination of stable Ca in samples after neutron activation. (C.H.)

44254 (RRA–M51) SIMULATION OF FALLOUT GAMMA RADIATION FIELDS BY MONOENERGETIC PLANE ISOTROPIC SOURCES. French, R. L. (Radiation Research Associates, Inc., Fort Worth, Tex.). June 21, 1965. Contract DA-49-146-XZ-254. 28p.

Monte Carlo techniques were used in a study of the gamma radiation environment three feet in air above plane sources of monoenergetic and fission-product gamma radiation. The scattered and direct-beam fluxes were computed in each of ten receiver energy intervals between 0.04 and 3.5 Mev and eighteen 10° receiver angle intervals between 0 (nadir) and 180° (zenith). Source energies of 0.10, 0.67, and 1.25 Mev, which are representative of the gamma rays from ^{144}Ce, ^{137}Cs, and ^{60}Co, respectively, were used in the calculations. Additional calculations were performed for source energies of 0.14, 0.25, 0.40, 0.85, 1.75, 2.50, and 3.50 Mev, and the results were weighted with the gamma spectra from fallout of various ages. Detailed comparisons of the results show that the angular distribution of the dose from a fallout field is simulated with reasonable accuracy over most angles by a plane source of ^{137}Cs or ^{60}Co and over all angles by a mixture of ^{144}Ce, ^{137}Cs, and ^{60}Co. The simulation of the fallout energy spectra is quite poor, however, even if combinations of the three isotopes are employed. Comparisons of the Monte Carlo data with measured data for monoenergetic plane sources show good agreement. (auth)

44255 (RT/PROT(65)–10) DETERMINAZIONE DELLE CONCENTRAZIONI DI UNA NUBE RADIOATTIVA E DELLE CONTAMINAZIONI DEL SUOLO SECONDO IL METODO DI PASQUILL-GIFFORD. (Determination of the Concentration of a Radioactive Cloud and the Contamination of Soil by the Pasquill-Gifford Method). Cucoco, A.; Galvagni, R.; Pucciarelli, L.; Scafe, R. (Comitato Nazionale per l'Energia Nucleare, Rome (Italy)). Mar. 1965. 41p. Dep. mn.

The generalized Gaussian cloud formulas for atmospheric diffusion in the absence of precipitation and in the presence of precipitation are applied in calculations of the concentrations of radioactive clouds and of soil contamination by fission products. The values for ground-level sources as a function of wind velocity and for various source heights and minimum wind are calculated. The results are shown graphically. (J.S.R.)

44256 (ORNL-tr–708) REMARKS TO THE DISCOURSES OF J. JOLY ON THE RADIOACTIVITY OF ROCKS. Hirschi, H. Translated for Oak Ridge National Lab., Tenn., from Naturwissenschaften, No. 45, 939–40 (Nov. 7, 1924). 6p. Dep. mn; JCL $1.10 fs, $0.80 mf.

The remarks are made on the subjects of radioactive halos, uranium-thorium ratios, radioinduced chemical changes, distribution of radioactive materials in nuclei, and overexposed halos. (D.L.C.)

44257 LOW ABUNDANCE OF ^{87}Sr IN ONTARIO CARBONATITES. Powell, J. L. (Oberlin Coll., Ohio). Am. Mineralogist, 50: 1075-9(July–Aug. 1965).

Specimens of 10 Ontario carbonatites were analyzed for ^{87}Sr and ^{86}Sr. Each of the 10 specimens were analyzed once on one of two mass spectrometers. Seven analyses were made on a mass spectrometer that gave a value of $^{87}Sr/^{86}Sr = 0.7081$ for the interlaboratory Sr standard. Three analyses were performed on a second instrument that gave a value of $^{87}Sr/^{86}Sr = 0.7089$ for the standard. The $^{87}Sr/^{86}Sr$ ratios obtained on the second instrument were corrected by -0.0008 to express them relative to

the value of the standard obtained on the first instrument. The $^{87}Sr/^{86}Sr$ ratios varied between 0.7019 and 0.7037 and averaged 0.7028 ± 0.0006. It was concluded that the $^{87}Sr/^{86}Sr$ ratio may be used as an empirical criterion for identifying carbonate rocks of uncertain classification as carbonatite. (F.J.H.)

44258 ON ALPHA AND BETA RADIATION METHOD FOR DETERMINING CONCENTRATIONS OF SHORT-LIVED RADON DAUGHTERS IN AIR. Labushkin, V. G.; Ruzer, L. S. At. Energ. (USSR), 19: 24-8(July 1965).

A new method of measuring the concentrations of ^{218}Po, ^{214}Pb, and ^{214}Bi in air, based on the measurement of alpha and beta activities of a filter directly after pumping through air, is presented. This method gives the possibility of obtaining more accurate results, shortening the measurement time, and calculating the effect of self-absorption of alpha radiation. (tr-auth)

44259 RADIOACTIVE FALLOUT OVER THE USSR AREA IN 1963. Polyakova, T. V.; Pervunina, R. I.; Svitcheva, V. I.; Churkin, V. N. At. Energ. (USSR), 19: 28-35(July 1965).

Reduced data on the radioactive fallout of fission products and their content in the soil in the USSR in 1963 are presented. On the basis of a study of the isotopic content of radioactive fallout, assumptions about its association with concrete series of tests are made. An estimate is given of the general quantity of ^{90}Sr deposited in the northern hemisphere in 1962 and 1963. (tr-auth)

44260 STORAGE OF RADIOACTIVE DEBRIS IN THE POLAR VORTEX. Barcus, J. R. (Univ. of California, Berkeley). J. Atmospheric Sci., 22: 460-2(July 1965).

Observations were made on the storage of radioactive debris in the polar stratosphere in March 1963. A considerable and nearly constant excess, over normal atmospheric contents, was found in the polar atmosphere. Estimates were made of the specific and total activities in the polar vortex. By Sept. and Oct. 1963 the radiation levels in the polar atmosphere had returned to normal. (M.C.G.)

44261 RADIOACTIVE FALLOUT IN SOUTHERN AUSTRALIA DURING THE YEARS 1958–1964. Dyer, A. J.; Hicks, B. B. (Commonwealth Scientific and Industrial Research Organization, Aspendale, Victoria, Australia). J. Geophys. Res., 70: 3879-83(Aug. 15, 1965).

Measurements of total β activity in rainfall at Melbourne during the years 1958 to 1964 show a pronounced seasonal effect with a maximum in November and December, two months after a similar maximum in stratospheric ozone. The rate of transfer of fission debris from the equator to 38°S after the 1958 and 1962 tests is found to be consistent with either a mean poleward circulation in the stratosphere of the order 1 m/sec or an eddy transfer coefficient of 3×10^9 cm^2 sec^{-1}. Verification of these transfer rates is provided by observations by other workers of volcanic dust from the 1963 Bali eruption. (auth)

44262 TRITIUM IN MT. EVEREST ICE—ANNUAL GLACIER ACCUMULATION AND CLIMATOLOGY AT GREAT EQUATORIAL ALTITUDES. Miller, Maynard M. (Michigan State Univ., East Lansing); Leventhal, Joel S.; Libby, W. F. J. Geophys. Res., 70: 3885-8(Aug. 15, 1965).

The tritium content of Mt. Everest ice (Khumbu glacier) shows the annual accumulation to average some 1.7 meters of water equivalent. A layer structure exists in the glacier. The layers down to 20 meters were sampled (Dyhrenfurth expedition), and the tritium peaks due to the nuclear weapons test series Castle (1954), Hardtack (1958), and the U.S.S.R. tests of 1961 and 1962 were identified. The samples were not taken deep enough to reach the pretest level for measurement of the natural tritium content, which was the original intent. The layers occur about two per year. (auth)

44263 $^{234}U/^{238}U$ RATIOS IN COASTAL MARINE WATERS AND CALCIUM CARBONATES. Blanchard, Richard L. (Robert A. Taft Sanitary Engineering Center, Cincinnati). J. Geophys. Res., 70: 4055-61(Aug. 15, 1965).

Water and live molluscan shell samples were collected simultaneously at seven locations on the seacoast of the United States. Samples of silt, water, and shells from an estuary were also included in the study. The water samples were analyzed for ^{238}U, ^{234}U, calcium, and salinity; the shell samples were analyzed for ^{238}U, ^{234}U, calcium, and crystal structure. All water samples, regardless of salinity or total uranium content, were found to have uranium activity ratios, $A_{^{234}U}/A_{^{238}U}$, within the experimental uncertainty of the 1.15 value accepted for an oceanic environment. The results indicate that the normally higher uranium activity ratio of rivers does not increase the ratio of coastal waters above the 1.15 oceanic value. The activity ratios of all except two shell samples analyzed were similar to those of the surrounding seawater and to the oceanic 1.15 value. The application of the results of the study to the determination of geologic age via uranium-uranium daughter equilibrium is discussed. (auth)

44264 JAPANESE DIETARY HABITS AND THE FALLOUT PROBLEM. [PART] II. Hiyama, Yoshio (Tokyo Univ.); Hayami, Hiroshi; Yamagata, Noboru; Asari, Tamiya. J. Radiation Res. (Japan), 5: 102-12(June 1964).

Two types of survey on the contamination of food by fallout in Japan were carried out. The first is the standard diet survey, in which food materials were purchased at 4 localities according to the same standard recipe 4 times a year and radioassayed for ^{90}Sr and ^{137}Cs. Since the autumn of 1961, the food materials collected were divided into 7 groups including cereals; pulses, nuts and fruits; leafy vegetables; root vegetables; sea weeds; fish and shellfish; and milk, meat, eggs, and poultry. Information was collected on the role of these food groups in human body contamination. The other is the daily diet survey, in which one day's amount of diet of 10 to 20 families is selected at random in each of 7 to 10 localities in Japan twice a year. The results obtained by the two methods were compared with each other. Both showed similar tendency as general. However the values were always higher in daily diet survey than standard diet survey. The results of both surveys show generally that vegetables are major sources of both ^{90}Sr and ^{137}Cs in Japan in most cases and the milk is a minor source of contamination. Results of both surveys were always higher in the Japan sea side than in the Pacific side in regard to contamination level. No difference was found between urban and rural. The relationships between the contamination level of diet and that of fallout rate and deposited were estimated, using the values of standard diet in Tokyo. (auth)

44265 RADIOACTIVE CONTAMINATION OF RICE IN JAPAN WITH REFERENCE TO Sr-90 AND Cs-137 CONTENT IN RICE UNTIL 1962. Kodaira, Kiyoshi (National Inst. of Agricultural Sciences, Tokyo). J. Radiation Res. (Japan), 5: 116-19(June 1964).

In Japan, ^{90}Sr in brown rice showed two peaks at October 1959 and October 1962, whereas ^{90}Sr in polished rice showed almost constant level, and less contamination. Cs-137 contamination was roughly 10 times that of ^{90}Sr in polished rice. The ratio is higher than that of fallout itself, which has been estimated as around 3. A discussion on the mechanisms is included, which can be important factors in such a high ^{137}Cs contamination of polished rice: characteristic effect of NH_4^+ ion on the liberation of Cs^+ ion from flooded rice soil, rate of absorption of Cs and Sr in plants. (auth)

44266 ASSAY OF STRONTIUM-90 IN HUMAN BONE IN JAPAN, 1961-1963. Saiki, Massamichi; Koyanagi, Taku; Tanaka, Giichiro; Tomikawa, Akio (National Inst. of Radiological Sciences, Chiba, Japan). J. Radiation Res. (Japan), 5: 120-3(June 1964).

Measurements were made on the ^{90}Sr content in human bone samples from subjects who died during the period from 1961 to October 1963 in Japan. The most remarkable accumulation of ^{90}Sr in human bone was found in 0 to 4 year age group. Considerable increases with time in the

S.U. (^{90}Sr pC/g Ca) value was also found in this group. (auth)

44267 RECENT VARIATION OF ATMOSPHERIC CONTENTS OF C-14 IN TOKYO AND TRANSFER PROBLEM OF ATMOSPHERIC CARBON DIOXIDE. Kigoshi, Kunihiko (Gakushuin Univ., Tokyo). J. Radiation Res. (Japan), 5: 124-30(June 1964).

Data are presented on the variation of atmospheric carbon-14 concentration in Tokyo since the end of 1959. The observed results show big random fluctuation compared with those obtained by Fergusson (1963) in California. This fluctuation is discussed from the view of the nature of air mass on Honshu Island. Based on the variation of the tropospheric content of carbon-14 since 1955, the transport of carbon dioxide from the atmosphere into sea water is discussed using a parallelism between the supplies of carbon-14 and other radionuclides produced by nuclear tests from the stratosphere into the troposphere. (auth)

44268 RADIOACTIVE CONTAMINATION OF MILK IN JAPAN (1961–1963). Tsugo, Tomikichi (Tokyo Univ.); Nozaki, Hiroshi; Asari, Tamiya; Yamagata, Noboru. J. Radiation Res. (Japan), 5: 131-7(June 1964).

Measurements of ^{90}Sr, ^{137}Cs, and ^{131}I concentrations in milk were carried out in order to evaluate the range of the radioactive contamination of milk in Japan since 1961. Farm milks collected from various districts of Japan monthly from 1961 to 1963 were used for radioactivity assay. The results of observation show the ^{90}Sr concentration in milk is higher than that in the previous years (1957 to 1960) all over the country and there is regional variation in ^{90}Sr and ^{137}Cs concentrations. (auth)

44269 FALLOUT RADIOACTIVITY AT GENEVA FOR THE YEAR 1963. Wenger, P.; Soucas, K. (Service Cantonal de Controle des Irradiations, Geneva). Radiol. Clin. Biol., 34: 64-6(1965). (In French)

Data are presented on the content of ^{137}Cs in residents of Geneva during 1963 as determined by whole-body scintillation counting. Data are included from measurements of the ^{137}Cs content in milk samples during 1963. (C.H.)

Site Survey and Selection

Refer also to abstracts 44761 and 45498.

44270 (BNL-914, pp 178-9) THE APPLICATION OF METEOROLOGY TO THE REGULATORY PROGRAM OF THE AEC. Newell, John F. (Atomic Energy Commission, Washington, D. C.).

The problems of a reactor facility from the accidental or routine release standpoint are discussed. The criteria of Part 100 and Part 20, Title 10 of the Code of Federal Regulations are discussed briefly. The effects of terrain and other meteorological variables are considered. It is pointed out that the meteorological data determine the design of safeguards systems for nuclear facilities. A question is raised, whether the margin of safety can be reduced by more accurate diffusion studies. (D.L.C.)

Techniques and Equipment

Refer also to abstract 44526.

44271 COMPARISON OF ^{230}Th AND ^{14}C AGES FOR CARBONATE MATERIALS FROM LAKES LAHONTAN AND BONNEVILLE. Kaufman, Aaron; Broecker, Wallace (Columbia Univ., Palisades, N. Y.). J. Geophys. Res., 70: 4039-54(Aug. 15, 1965).

The reliabilities of the radiocarbon and uranium series in equilibrium methods of absolute age determination as applied to lacustrine carbonates were evaluated. Fifty samples of gastropods, chara, tufa, marl, and ostracods from the Pleistocene deposits of Lakes Lahontan and Bonneville were analyzed for ^{14}C, ^{238}U, ^{234}U, ^{232}Th, ^{230}Th, and ^{226}Ra. The results indicate that samples in which ^{226}Ra is at equilibrium with ^{230}Th and where the ^{232}Th concentration is not unusually large, satisfactory agreement between the two methods generally exists. Whereas a common thorium correction is required, evidence is given that for the basins studied the ^{230}Th–^{232}Th ratio has a nearly constant value of 1.70. Where disagreement between the two methods occurs, the lower age appears to be in error. The anomalies appear to reflect U addition (low ^{230}Th age) or contamination with young carbon (low ^{14}C age). Samples beyond the range of radiocarbon yield ^{230}Th ages consistent with stratigraphic information, offering the possibility of extending the absolute chronology of the fluctuation in the size of these lakes back to 200,000 years ago. Independent age estimates based on the disappearance of the excess ^{234}U incorporated into these samples are clearly invalid. Samples with ^{230}Th ages of more than 100,000 years show excesses of ^{234}U comparable to or even greater than those for samples less than 20,000 years old. Support for Attree's (1962) estimate of 75,200 years for the ^{230}Th half life was obtained (opposed to the previously accepted estimate of 80,000 years). (auth)

44272 URANIUM–THORIUM LEAD TIME CLOCKS. Cook, Melvin A. (Univ. of Utah, Salt Lake City). 32p. (CONF-650422-12). Gmelin, AED-CONF-65-118-33.

From American Geophysical Union, Program for Section of Seismology Annual Meeting, Washington, D. C.

A statistical analysis of common leads (where Pb/U is much greater than unity) shows that the theoretical time index of the conventional theory of the U–Th–Pb time clocks is overshadowed by other factors contributing to alterations. Alterations in U, Th minerals are important as seen by such facts as the large flux of uranium into the oceans in river waters. Apparently, all gradations of physical chemical alteration from U-rich or Th-rich to Pb-rich minerals are possible and actually occur in nature. It is suggested that (n,γ) reactions play an important role in all lead-isotope geochronometry. This suggestion is supported by the following facts: The $^{14}N/^{15}N$ ratio in radioactive minerals is strongly influenced by radioactivity; it is 269 in air and around 174 ± 12 in radioactive minerals. This implies that lead-isotope ratios are also strongly modified by factors outside the normal time clock scheme. Observed age differences between $^{206}Pb/^{238}U$ and $^{207}Pb/^{235}U$ (where no physical chemical differentiation is actually involved) are qualitatively consistent with the suggested influence of neutron-promoted transmutations on the $^{206}Pb/^{207}Pb$ ratio. The presence of ^{208}Pb with too little Th and ^{204}Pb in the samples to explain it, e.g., in ore bodies like those of the Saskatchewan Goldfields and Martin Lake of the Canadian "Shield," the Shinkolobwe, Kantanga are easily explained by the transmutation mechanism. The observed results in these cases permit one to correct for the influence of these transmutation reactions on apparent age. The corrected ages turn out to be small compared with the half-life of ^{235}U and, therefore, these corrections effectively wipe out most of the age in these examples. In general t_2/t_1 averages about 0.87, t_3/t_1 averages about 0.83 and t_4/t_1 about 0.74 where t_1 is the $^{206}Pb/^{207}Pb$ age, t_2 is the $^{207}Pb/^{235}U$ age, t_3 is the $^{206}Pb/^{238}U$ age and t_4 is the $^{208}Pb/Th$ age. If these systematic differences may be interpreted as due to neutron-promoted transmutations, they imply a fatal weakness in the conventional theory of the U–Th–Pb time clocks; they effectively wipe out geologic time. (auth)

Thorium and Uranium Minerals

44273 (RME-4557(Rev.)) RECONNAISSANCE FOR URANIUM IN THE AISEN AREA, PROVINCE OF AISEN, CHILE. Bowes, William A.; Knowles, Paul H.; Maraga B., Aldo; Serrano C., Mario (Division of Raw Materials (AEC), Washington, D. C.; Instituto de Investigaciones Geologicas, Santiago (Chile)). Oct. 1962. 25p. Dep. mn; CFSTI $2.00 cy, $0.50 mn.

In a general reconnaissance for uranium in the Aisén area of southern Chile, the radioactive Rio Correntoso occurrence, a small pitchblende-galena vein in highly radioactive Cretaceous-Tertiary pink granite which crops out spatially above pendants of Paleozoic metasediments near its faulted contact with Jurassic tuffs. One-third of the total field time was spent on supplementary geologic studies in that sector of the Aisen area. Sufficient additional geologic work is proposed to outline structures for physical exploration of the occurrences. (auth)

44274 A UNIQUE OCCURRENCE OF URANIUM MINERALS, MARSHALL PASS, SAGUACHE COUNTY, COLORADO. **Gross, Eugene B. (California Div. of Mines and Geology, San Francisco). Am. Mineralogist, 50: 909-23 (July–Aug. 1965).**

In 1956 several unusual uranium deposits were uncovered in the Marshall Pass district, Saguache County, Colorado. Two of the ore bodies occurred in alluvium at an elevation of about 10,000 feet. The largest of these, on the Lookout No. 22 claim, produced about five tons of high-grade uranium ore. The bedrock at the deposit is a quartzbiotite-feldspar-schist which was altered adjacent to a fault zone. Small areas of the schist were completely replaced by uranium and sulfide minerals, producing rich ore bodies that were found in situ in the alluvium above the fault. Ore pieces are tabular to rounded yellow masses measuring from a few inches in diameter to large slabs 2′ × 1′ × 8″ thick and weighing as much as 140 pounds. Nearly all contained a yellow oxidized coating around a black interior of pitchblende and sulfides. Geochemical sampling of soils surrounding the deposit indicated that uranium had migrated less than 100 feet downslope from the ore body. Radioactive minerals include pitchblende, schoepite, ianthinite, epi-ianthinite, becquerelite, soddyite, boltwoodite, uranophane, zeunerite, metazeunerite, and a hydrated autunite. Other minerals are tetrahedrite, chalcopyrite, sphalerite, chalcocite, covellite, galena, pyrite, and marcasite. Pitchblende occurred in concentrically banded and colloform masses showing fractures and microfaults rehealed by later pitchblende. Secondary uranium minerals and sulfides transected the pitchblende and occurred interstitially between banded masses. The uranium deposit was probably formed under epithermal conditions during early Tertiary time. (auth)

44275 ON THE EXPEDIENCY OF RADIOMETRIC URANIUM ORE DRESSING AND THE CHOICE OF THE OPTIMUM LEVEL OF SEPARATION DURING DRESSING. **Andryushin, I. A.; Roshchin, Yu. V.; Chebotareva, L. D.; Erivanskii, Yu. A. At. Energ. (USSR), 19: 79-80(July 1965).**

Equations are derived for computing the economic effect of ore concentration, the conditions for expedient and optimum concentration, the optimum level of separation, and the condition for expediency of concentration for optimum technological indices. (M.J.T.)

44276 OPTIMUM INDICES OF RADIOMETRIC CONCENTRATION AND CONDITIONS OF EXPEDIENCY OF ITS EXECUTION FOR A LOGNORMAL URANIUM-CONTENT DISTRIBUTION OF VOLUME ELEMENTS OF ORE. **Roshchin, Yu. V. At. Energ. (USSR), 19: 80-2 (July 1965).**

The indices of contrast of U ores and the conditions for their radiometric concentration are considered for the case of a lognormal distribution. Properties of a lognormal distribution are reviewed. The basic indices of grading are expressed in terms of the parameters of the distribution, and the determination of the grading parameters for optimum level of the distribution is discussed. The problem on the expediency of performance of grading is solved. (M.J.T.)

44277 ISOTOPIC COMPOSITION OF LEAD ORE FROM DIFFERENT TYPE DEPOSITS IN THE EASTERN TRANSBAIKAL. **Esikov, A. D.; Tomson, I. N.; Konstantinov, R. M.; Polyakova, O. P. (Inst. of Geology of Ore Deposits, Petrography, Mineralogy and Geochemistry, Moscow). Geokhimiya, No. 7, 791-800(July 1965). (In Russian).**

The isotopic composition of most deposits of different type proved quite similar. Two groups of deposits stood out distinctly by the thorium and uranium isotope ratio. To one of them belong deposits of quartz-cassiterite and quartz-wolframite formation, to the other deposits of gold-galena-sphalerite, molybdenite-galena-sphalerite, galena-sphalerite, and other polysulfide formations. The differences in the thorium and uranium isotope ratio reflect some differences in the character of the ore-forming chambers. Variations in the content of the isotope ^{206}Pb in lead ores of various deposits of galena-sphalerite and other formations were noted. The age of the deposits of various ore formations of the Eastern Transbaikal, calculated as an average of all data obtained is 140 million years. (auth)

44278 ON THE SILICATE FORM OF URANIUM TRANSPORT IN AQUEOUS SOLUTIONS. **Ermolaev, N. P.; Zhidikova, A. P.; Zarinskii, V. A. (Vernadskii Inst. of Geochemistry and Analytical Chemistry, Moscow). Geokhimiya, No. 7, 813-26(July 1965). (In Russian).**

One of the transportation forms of uranium under certain natural conditions in the silicate aqueous solutions appears to be a hydroxyuransilicate compound with the approximate formula $(UO_2OH)(HSiO_3)$. The hydrosilicate complex ion is considered as a group that is stabilizing hydroxyuran in a solution or the former as the addendum of a weak complex. The size of these particles (in solution) is between that of colloid and ionic particles. The established form of uranium migration in solution exists in the near-neutral and weak basic range of pH and temperatures till 200°C, the concentrations of strong electrolytes in a solution being relatively low (i.e., not higher than the equilibrium concentration with uranyl or silicate). The silicate form of uranium transport in carbonate aqueous solutions is destroyed and uranium forms a complex with carbonate. (auth)

44279 VIRGINIA METAMICT MINERALS: COMMENTS ON A URANIUM–NIOBIUM OXIDE FROM POWHATAN COUNTY. **Mitchell, Richard S. (Univ. of Virginia, Charlottesville). Southeastern Geol., 6: 79-85(Mar. 1965).**

The occurrence of a metamict olive-brown uranium-niobium mineral at the old White Peak No. 1 mica mine, Powhatan County, Virginia, is reported. At least 10 lb of the mineral were collected. It occurs as irregular masses and rough tabular crystals. Although it was not possible to establish the crystal morphology with accuracy, because of the altered and rough condition of the faces, it was assumed that the crystals are orthorhombic, flattened parallel to the (010) and elongated slightly along (001). The habit is simple, consisting of (010), (100), and a well-developed macrodome (h01). The interfacial angle between (100) and (h01) is from 130° to 135°. The habit is analogous to samarskite crystals. The mineral is brittle and has a conchoidal fracture which is resinous to adamantine. The hardness is about 5, and the specific gravity ~3.8. The mineral is essentially isotropic and has an index of refraction near 1.83. It is strongly radioactive. Most specimens have a thin, moderate orange-pink alteration crust. After heating to 300°, samples showed strong x-ray reflection for a hexagonal UNb_2O_8 phase. Although the UNb_2O_8 structure dominated all x-ray patterns of heated material, the crystals have habits which are not compatible with the hexagonal structure of UNb_2O_8. Semiquantitative spectrographic analyses showed that the principal constituents are U and Nb, but also considerable amounts of Y, Si, and Fe. The mineral is probably an oxide of uranium and niobium, containing considerable yttrium rare earths. Although this mineral could be distinguished from others of the U–Nb family, a definite name was not assigned to it. Its similarities to as well as differences from samarskite are discussed. (TCO)

HEALTH AND SAFETY

See also BIOLOGY AND MEDICINE — Radiation Hazards and Protection
GEOLOGY AND MINERALOGY — Natural Radioactivity and Fallout

Refer also to abstracts 43853, 43854, 43896, 43913, 44112, 44532, and 44534–44537.

44280 (ABCC–63–64) ATOMIC BOMB CASUALTY COMMISSION ANNUAL REPORT, JULY 1, 1963–JUNE 30, 1964. (Atomic Bomb Casualty Commission, Hiroshima (Japan)). Contract [AT(49-1)-Gen-72]. 97p. Dep. mn; CFSTI $3.00 cy, $0.75 mn.

Progress is reported in epidemiologically-oriented studies on a closed sample population in Hiroshima and Nagasaki exposed to radiation from atomic bombs in 1945. Emphasis is placed on the problems of cancers, aging, and adult diseases, and the growth and development of adolescents exposed in utero or as infants. A list is included of 112 technical reports issued during the period covered by this report. (C.H.)

44281 (AEET–202) UNIT FOR TESTING HIGH EFFICIENCY FILTERS. Kotrappa, P., Jauhri, G. S.; Dua, S. K. (Atomic Energy Establishment, Trombay (India)). 1965. 23p. Dep. mn.

A unit which uses sodium-24 as a tracer was developed to test high efficiency ventilation filters used in radioactive installations. The test aerosols consist of 0.2 micron MMD particles produced by an aerosol generator which uses 5% activated sodium chloride solution. The method of testing consists in isokinetic sampling of air for radioactivity upstream and downstream of the test filter using inline samplers. A study of variation of penetration with velocity indicated no appreciable change when the face velocity was varied from 20 to 275 fpm. Detailed evaluation of the method for reproducibility, sensitivity, and associated hazards was made. The possible improvements (the development work under progress) are also suggested. (auth)

44282 (AHSB(RP)M-35) COMPARATIVE REVIEW OF THE PRINCIPAL NON-STATUTORY UNITED KINGDOM CODES OF PRACTICE FOR PROTECTION AGAINST IONISING RADIATIONS AND RADIOACTIVE MATERIALS. Bennellick, E. J. (Authority Health and Safety Branch, United Kingdom Atomic Energy Authority, Harwell (England)). July 1965. 29p. Dep.; BIS $0.80; HMSO 4s.

A comparison is made of the main provisions of five Codes of Practice for radiation protection comprising two issued by the United Kingdom Atomic Energy Authority and one each by the Medical Research Council, the Ministry of Health, and the Ministry of Labor. (auth)

44283 (AWRE-E–1/65) THE HAZARDS TO THE HUMAN EAR FROM SHOCK WAVES PRODUCED BY HIGH ENERGY ELECTRICAL DISCHARGES. Golden, Pamela M.; Clare, R. (Atomic Weapons Research Establishment, Aldermaston (England)). Aug. 1965. 24p. Dep.; BIS $1.20; HMSO 6s. 0d.

Recent years have produced a proliferation of multiple condenser banks in connection with plasma physics and other research. Examples of other electrical discharges at high energy are spark gaps and exploding wire devices, all of which are liable to produce shock waves which constitute a further possible hazard. Hitherto the energy from such sources has been regarded as being of the same level as that from small arms fire, and no particular precautions, other than using conventional ear muffs, defenders or keeping at an arbitrary safe distance, have been considered necessary. The blast pressures developed by a high energy electrical discharge as received by a transducer mounted in a large baffle normal to the blast were measured and compared with those received by a model ear. It is shown that the pressures developed at the drum of the ear are in excess of those in air and can cause damage to the ear unless precautions are taken. There is a high proportion of large amplitude noise at audio frequencies present which many protective devices transmit. Measurements with samples of these show that there is some attenuation of pressure and it is probable that a muff protector is more efficient than an ear defender which consists of a solid plug with a small axial air channel. (auth)

44284 (AWRE-O–24/65) PROTECTION AGAINST FIRE HAZARDS IN THE DESIGN OF FILTERED VENTILATION SYSTEMS OF RADIOACTIVE AND TOXIC PROCESS BUILDINGS. Smith, S. E.; Hall, F. J.; Holmes, W. E.; George, A. F. (Atomic Weapons Research Establishment, Aldermaston (England)). July 1965. 125p. Dep. mn; BIS $3.40; HMSO 17s.

A number of safety aspects of the design of filtered ventilation systems for radioactive and toxic buildings are considered. These include theoretical and experimental assessments of the heat release from fires of various kinds in workrooms, fume cupboards, glove boxes, and extract systems, the use of spark and flame arrestors, the ignitability of dust deposits in extract systems and filters and the cooling of hot gases in exhaust ducts. As a result of this work, it is possible to formulate principles which should be followed in the layout and design of such systems, in the future; older systems, which are already being modified to include glass paper filters where necessary, have been found not to require any other serious modification as a result of this work. (auth)

44285 (BNWL-SA–29) NATURAL REMOVAL OF FISSION PRODUCTS RELEASED FROM UO_2 FUEL IN CONDENSING STEAM ENVIRONMENTS. McCormack, J. D.; Hilliard, R. K. (Battelle-Northwest, Richland, Wash. Pacific Northwest Lab.). Mar. 24, 1965. Contract AT(45-1)-1830. 22p. (CONF-650407–11). Dep. mn; CFSTI $1.00 cy, $0.50 mn.

From International Symposium on Fission Product Release and Transport Under Accident Conditions, Oak Ridge, Tenn.

The behavior of fission product I, Te, Cs, and Ba and U in aerosols generated from the melting in air and steam of ½-in. diameter by 3 in. long stainless steel-clad UO_2 fuel elements is presently under study. The fumes evolved from melting elements irradiated to 10^{17} to 10^{18} nvt are conducted to a 1.5 cu meter painted tank which contains a condensing steam and air mixture. Samples are taken at intervals during a 5 hour holding period to determine concentrations in the condensate and air, deposition velocities to various surfaces, and the physical form of iodine. Electron micrographs provide particle size information. (auth)

44286 (BNWL-SA–30) FISSION-PRODUCT SIMULATION IN THE CONTAINMENT SYSTEMS EXPERIMENT. Hilliard, R. K.; McCormack, J. D. (Battelle-Northwest, Richland, Wash. Pacific Northwest Lab.). Mar. 22, 1965. Contract AT(45-1)-1830. 20p. (CONF-650407–12). Dep. mn; CFSTI $1.00 cy, $0.50 mn.

From International Symposium on Fission Product Release and Transport Under Accident Conditions, Oak Ridge, Tenn.

One of the major objectives of the Containment Systems Experiment (CSE) is to measure the transport characteristics of fission-product aerosols and vapors which would be released during a reactor loss-of-cooling accident. For several reasons "real" fission-product aerosols will not be used. Simulated fission-product aerosols will be generated and discharged into the simulated reactor primary

vessel. The suitability of the fission-product simulant is being established by comparison with "real" fission products released from irradiated fuels in laboratory and pilot scale experiments being conducted at Hanford and elsewhere. Some considerations in selecting the simulants are: (1) physical and chemical properties similar to real fission products, (2) capability for generation in known reproducible, and suitably large amounts, (3) water solubility and wettability, (4) influence of missing components, (5) suitability for inexpensive and rapid analyses, and (6) post-test cleanup and preparation for the next test. A large number (500–1500) of individual samples will be taken during each CSE test. To reduce analytical cost and to increase accuracy, a relatively simple mixture will be established as the basic aerosol. This will provide a means for evaluating various containment systems and parameters. Present plans are for use of steam or a steam–air mixture sweep gas carrying iodine (in all its forms), fuel material (UO_2 and cladding fumes), a water soluble oxide (K_2O), and a rare gas (xenon). Additional selected components will be added in some tests to obtain information on behavior of specific fission-product elements. Analyses will be performed by gamma spectrometry for short-lived tracers and by fluorometric analysis of uranium. (auth)

44287 (CEA-R-2799) PROBLEMES DE RADIOPROTECTION POSES PAR L'IMPLANTATION DE DISPOSITIFS EXPERIMENTAUX AUPRES D'UNE PILE ATOMIQUE. (Radioprotection Problems Resulting From the Presence of Experimental Devices Around an Atomic Reactor). Fitoussi, Lucien; Lebouleux, Philippe (Commissariat a l'Energie Atomique, Saclay (France). Centre d'Etudes Nucleaires). Apr. 1965. 20p. Dep. mn.

The setting up of experimental devices around a reactor produces dangers of irradiation and radioactive contamination which can become very great in the case of an accident, especially if the in-pile portion contains fissile matter. This may result in irradiation of personnel, prohibition of access to the experimental zones until the sources of irradiation and contamination have been eliminated, and a prolonged stoppage of the reactor. The plans for an in-pile experiment should take into account radioprotection factors; the aim of these is to reduce to a minimum the radioactive risks normally encountered during the experiment and to eliminate any risks of bad accidents and their consequences. The various types of experiments requiring installations outside the pile itself are classified; for each of these experiments the particular radioprotection factors are given. In order to make possible a study of the radioactive dangers likely to arise during a projected experiment, a summary is given of the physical and technical data required by radioprotection specialists, and rules and general advice concerning radioprotection are given which should be useful during the planning of an in-pile experiment and the setting-up of the equipment. (auth)

44288 (DPST-65-30-2) EFFECT OF THE SAVANNAH RIVER PLANT ON ENVIRONMENTAL RADIOACTIVITY. Semiannual Report, January 1–June 30, 1965. (Du Pont de Nemours (E. I.) and Co., Aiken, S. C. Savannah River Lab.). Aug. 1965. Contract [AT(07-2)-1]. 16p. Dep. mn; CFSTI $1.00 cy, $0.50 mn.

Results of the environmental monitoring program for the period January 1 through June 30, 1965, for the atmosphere, vegetation and food, and water are presented. The quantity of radioactive waste released by the Savannah River Plant to its environs was, for the most part, too small to be distinguished from natural background radiation, or was obscured by world-wide fallout from nuclear weapons testing during past years. Fallout from the Chinese nuclear test on May 13, 1965, was detected at SRP on air filters. Beta activity in air, which showed no relationship with Plant operations, was about one-fifth of that for the same period of 1964. Radioactive materials in fish flesh continued to be far below levels considered significant from a health standpoint. The average concentration of radionuclides in river water did not exceed 3.1% of the Maximum Permissible Concentrations. (auth)

44289 (HW-SA-3750) MEASUREMENTS OF RADIOACTIVITY IN ALASKAN NATIVES IN 1964. Palmer, H. E.; Hanson, W. C.; Griffin, B. I.; Braby, L. A. (General Electric Co., Richland, Wash. Hanford Atomic Products Operation). [Oct. 14, 1964]. Contract AT(45-1)-1350. 7p. Dep. mn; CFSTI $1.00 cy, $0.50 mn.

Whole body counting measurements were made on northern Alaskan natives again during the summer of 1964. The adults of the interior village of Anaktuvuk Pass continued to show the highest average body burden, 1280 nanocuries of ^{137}Cs. This is an increase of 200 per cent over the average in the summer of 1962, and 100 per cent over the average in the summer of 1963. The maximum burden found in a native was 2.4 microcuries, but the highest ^{137}Cs body burden, 3.0 microcuries, was measured in a nonnative living on a diet consisting mostly of caribou meat. Sodium-22 was found in Eskimo urine samples and subsequently in reindeer and caribou meat. (auth)

44290 (JAERI–1079) MEASUREMENTS AND CONSIDERATIONS OF THE ENVIRONMENTAL RADIATION AND RADIOACTIVITIES ABOUT THE SITE OF THE JAERI (1956–1963). Ishihara, Toyohide; Tsunokawa, Masayoshi; Sasaki, Satoshi; Kasai, Atushi; Hitomi, Seiich; Moriuchi, Shigeru; Katagiri, Hiroshi; Matsushita, Kozo (Japan Atomic Energy Research Inst., Tokyo). Mar. 1965. 73p. Dep. mn.

In Japanese.

The methods of environmental radiation and radioactivity measurement, radionuclide analyses, and the results of environmental monitoring, about the Japan Atomic Energy Research Institute site from 1956 to 1963 are presented. The radiations and the concentrations of radioactivity in air, fallout, soil, plants, and water, were measured and analyzed. The levels and fluctuations of radiation and radioactivity, the relationships in the radioactivity between environmental samples, the velocity of deposition, and sampling error are discussed. No unusual concentrations of radioactivity and radiation levels due to JAERI facilities were found. (auth)

44291 (JAERI–1081) RADIOLOGICAL MONITORING POINT. PHOTOGRAPHIC DOSIMETER AND GUMMED PAPER STATION. Ishihara, Toyohide; Sasaki, Satoshi; Moriuchi, Shigeru (Japan Atomic Energy Research Inst., Tokyo). July 1965. 13p. Dep. mn.

A description is presented of a simple and economical environmental monitoring device used in the vicinity of an atomic energy facility. The device consists of a photographic (and/or glass) dosimeter for cumulative radiation dose measurements, and gummed paper for measurements of the integrated concentration of particulate radioactivity in the air. Experiments were performed on the latent image fading and growth for periods up to 12 months in order to find the possibility of using photographic dosimeters in which a badge film is used for the environmental gamma radiation measurement. It was shown that if the badge film is suitably packaged and is free from humidity and light, it may be used successfully for the environmental monitoring. The integrated concentration of particulate radioactivity in the air can be evaluated by measuring the total deposited activity and the velocity of deposition. The environmental radiation monitoring program at the Japan Atomic Energy Research Institute is also described. (auth)

44292 (NP–15173) DEPOSITION OF INHALED FISSION PRODUCTS IN LUNGS AND PULMONARY LYMPH NODES OF HUMAN BEINGS. Summary Report on the Research Project. Schoenfeld, T.; Friedmann, Christina (Vienna Univ. (Austria). Institut fuer Anorganische Chemie; Vienna Univ. (Austria). Institut fuer Physikalische Chemie). Feb. 1965. Contract 156/RB. 54p. Dep. mn.

Measurements were made of fission products deposited in human lungs through inhalation. Lungs excised in postmortem examinations from persons who had lived in the Vienna area and died between 1961 and 1964 were ashed and analyzed by γ spectroscopy. Data are presented on the content of ^{144}Ce, ^{95}Zr, and ^{95}Nb in 317 lungs. Data are in-

cluded on the content of these fission products in pulmonary lymph nodes. The data are compared with predicted levels based on measurements of fission products in air samples. Results showed there were large variations in individual ^{144}Ce lung burdens during only one month and that maximum values were found during the summer months. Concentration ratios of 10 to 20 were frequently found in pulmonary lymph nodes. The ^{144}Ce lung burdens were used to calculate the radiation dose to the lungs due to radioactive fission products inhaled by inhabitants of the Vienna area. From Sept. 1961, to Sept. 1962, the average increase in radiation dose to the lungs was about 24 mRem/yr. (C.H.)

44293 (NP-15519) DATA FROM RADIATION PROTECTION PROGRAMS. Volume 3, Number 7. (Department of National Health and Welfare, Ottawa (Ontario). Radiation Protection Div.). July 1965. 118p. Dep. mn.

Separate abstracts were prepared for three sections of this report. A list of publications during the period is included. (C.H.)

For abstracts of individual sections see: 44251, 44294, and 44295.

44294 (NP-15519, pp 3-22) REACTOR ENVIRONMENTAL MONITORING, 1964. Samuels, E. R.; Mohindra, V. K. (Department of National Health and Welfare, Ottawa (Ontario). Radiation Protection Div.).

Results are reviewed from monitoring studies at Canadian reactor sites during 1964. Samples of water and biota were analyzed for radioactivity. Samples of rabbits and fish collected in the Spring and Fall in the vicinity of the reactors were analyzed. (C.H.)

44295 (NP-15519, pp 52-60) REACTOR ENVIRONMENT MONITORING FOR JUNE, 1965. Samuels, E. R.; Mohindra, V. K. (Department of National Health and Welfare, Ottawa (Ontario). Radiation Protection Div.).

The Radiation Protection Division, in collaboration with the Industrial Hygiene Branch of the Ontario Department of Health, conducted monitoring studies on surface waters and biota near the sites of the Chalk River reactors, the Nuclear Power Demonstration reactor, and the Candu reactor. Data collected in June, 1965, are presented. (C.H.)

44296 (NYO-4700(Rev.)(Suppl.II)) HEALTH AND SAFETY LABORATORY ANALYTICAL MANUAL. (Health and Safety Lab., New York Operations Office (AEC), N. Y.). Aug. 1963. Revised Aug. 1965. 99p. Dep. mn; CFSTI $4.00 cy, $0.75 mn.

Additions and corrections made to the Health and Safety Laboratory Manual of Standard Procedures include: analytical data on fission yield and fission product decay; sampling principles, sample handling, and sampling types; the application of air sampling in the evaluation and control of the occupational environment; principles of air sampling; radiochemical determination of Pu and ^{226}Ra in water, urine, and feces; radiochemical determination of Pu in air filters; the determination of ^{90}Sr and ^{137}Cs in large volume sea water samples; and specifications for polyethylene syringe bottles, improved plating cells, and microsorbent filter paper. (H.G.D.)

44297 (ORNL-TM-1251) DESCRIPTION OF FACILITY RADIATION AND CONTAMINATION ALARM SYSTEMS INSTALLED IN THE HIGH RADIATION LEVEL EXAMINATION LABORATORY BUILDING 3525. Inman, J. E.; Knowles, D. J. (Oak Ridge National Lab., Tenn.). Aug. 26, 1965. Contract [W-7405-eng-26]. 19p. Dep. mn; CFSTI $1.00 cy, $0.50 mn.

Alarm systems were installed to continuously and automatically monitor the beta-gamma radiation level, air-contamination level, and neutron level in the entire facility and to report this information to a central control panel in the first-level operating area. Six monitrons, four air monitors, one exhaust duct monitor, seven beta-gamma radiation monitors, and three neutron monitors are connected to the instrument network. Operating personnel are first given warning when a "caution level" of radiation or contamination is detected by a monitron or air monitor, and again when a "high level" is detected. The building evacuation system operates automatically when two or more selected monitrons or two or more selected air monitors detect a "high level" of radiation or air contamination, or when two or more neutron monitors detect a neutron burst or a "high-rate" level, or both. This building is automatically "contained" when two or more monitrons, air monitors, or neutron monitors detect a "caution" level of radiation or air contamination. The evacuation and the containment systems can also be actuated by manual controls. (auth)

44298 (SC-RR-65-9) CONTAINMENT CAPSULE IMPACT SAFETY STUDY PHASE A, PROGRESS REPORT. Young, C. W.; Stoneking, C. E.; Colp, J. L. (Sandia Corp., Albuquerque, N. Mex.). July 1965. Contract AT(29-1)-789. 66p. Dep. mn; CFSTI $3.00 cy, $0.75 mn.

A study was conducted to obtain engineering information on parameters that affect the structural integrity of radioisotope containment capsules which are subjected to impact loading. Cylindrical capsule parameters investigated include (1) the effect of L/D ratio on V_{10}, and (2) the effect of tube wall thickness on V_{10} (V_{10} is that velocity at which 10% of the capsules rupture upon impact). It was found that the rupture velocity decreases with increasing L/D ratio up to a point, and then levels off. Also, the rupture velocity increases with increasing wall thickness. Other important test results are presented in the report along with recommendations on the reorientation of the test program to coincide more closely with the present aerospace nuclear safety philosophy. (auth)

44299 (SZS-2(1965)) DIE BESTIMMUNG DER EINDRINGTIEFE VON AEROSOLEN IN FILTERN. (The Determination of Penetration of Aerosols in Filters). Loessner, Volkhard (Staatliche Zentrale fuer Strahlenschutz, Berlin (East Germany)). Apr. 1965. 35p. Dep. mn.

A procedure for the determination of the depth of penetration of a radioactive marked monodisperse aerosol in membrane and fiber filters is given. On a largely monodisperse SiO_2 aerosol of 0.55 μ, secondary products of thoron were deposited. This aerosol was deposited in membrane and fiber filters. The residual range of the alpha rays from the ThC' which was emitted from the filter surface was determined. Under certain conditions, the measured curves for the number of alpha particles, when subjected to graphical differentiation, yield a picture of the depth of penetration of the aerosol. On the basis of the results obtained with membrane and fiber filters, three different forms of the deposition can be derived. Two of them can be explained by the filtration theory (experimental law for filtration). For the third, a possible explanation is given. It is shown that the differential equation for filtration has no general validity. The aerosol, its size distribution, its radioactive tagging, its deposition in the filter, the measuring process, and the measuring chamber are described. (auth)

44300 (TID-22171) ENVIRONMENTAL RADIOACTIVITY AT ARGONNE NATIONAL LABORATORY, JANUARY-JUNE 1965. (Argonne National Lab., Ill.). Contract W-31-109-eng-38. 26p. Dep. mn; $2.00 cy, $0.50 mn.

Information on the level of radioactivity in the environment and on the amounts of radioactive materials, if any, added to the environment as a result of Argonne operations is presented. The radioactivity of the environment is determined on a continuing basis by measuring the radioactivity in naturally occurring materials collected both on and off the Argonne site. Since radioactivity is usually spread by air and water, the environmental monitoring program at Argonne has concentrated on these materials. Air-filter samples were collected continuously at seven locations on the Argonne site and at five locations off the site. Sampling on charcoal for radioactive iodine was conducted on the site only. Iodine activity in excess of the minimum detectable concentration of 0.2 pC/m^3 (0.2% of the MPC) was not detected. The total alpha and beta ac-

tivities in the air-filter samples are tabulated. No activity attributable to Argonne operations was found in any of these samples. The alpha activities were normal both on and off the site and were in the range found in previous years. The beta activity did not vary significantly at the different sampling locations sampled on the Des Plaines and Illinois Rivers, as was the case for other nuclides. Apparently as a result of dilution, the activity in Sawmill Creek had no detectable effect on the radioactivity in the Des Plaines River. The alpha activities in the Des Plaines and Illinois Rivers were in the normal range and similar to earlier values. The natural beta activity in the Des Plaines and Illinois Rivers varies between 5 and 10 pC/l. The additional beta activity in these streams was due to fallout. There was no indication of activity from Argonne operations in either stream. Three samples of raw milk produced in the area were analyzed monthly for a number of fission products. The long-lived fission products, cesium-137 and strontium-90, were present in all samples. Their average concentrations were 80 and 14 pC/l, respectively. The shorter-lived fission products, barium-140 and strontium-89, were found only in the samples collected June 4, and are attributed to the Chinese test of May 14. The concentrations of these fission products in the June samples were 24 and 14 pC/l, respectively. Fallout activity was present in all types of samples and at all locations throughout the year, but in lower concentration than in 1964. Argonne's contribution to the environment was confined to Sawmill Creek below the waste-water discharge. Radioactivity originating at Argonne was not found in any other material or at any other location off the site. The concentrations of radioactive substances added to the environment during the year by Argonne were considerably less than the MPC's and did not constitute a health hazard. (H.G.D.)

44301 (TID-22172) ENVIRONMENTAL CONCENTRATIONS OF RADIOACTIVE MATERIALS NEAR THE PADUCAH PLANT. Report for the First Half of 1965. (Paducah Gaseous Diffusion Plant, Ky.). Contract W-7405-eng-26. 9p. Dep. mn; CFSTI $1.00 cy, $0.50 mn.

Data summarizing the environmental concentrations of radioactive materials in air and water and the gamma radiation levels in the vicinity of the Paducah Gaseous Diffusion Plant are tabulated. Air monitoring was done by continuous filters, and water samples were taken weekly from the Big Bayou. Alpha counts from air sampling averaged 1.9% of the Radioactivity Concentration Guide (RCG) maximum, and mean beta counts were 0.04% of the RCG value. The average uranium content of water samples was 0.04% of the applicable RCG value for water beyond a controlled area. Uranium content in water samples from the Ohio River below the plant averaged less than 0.01% of the RCG value. The concentration of beta emitters in the Big Bayou averaged 1% of the RCG value for the decay products of ^{238}U, and the beta activity of all samples from the Ohio River averages less than 3% of the RCG value. (H.G.D.)

44302 (TID-22173) SURVEY OF ENVIRONMENTAL RADIOACTIVITY FOR PERIOD JANUARY 1–JUNE 30, 1965. (Ames Lab., Iowa State Univ. of Science and Tech.). Contract W-7405-eng-42. 16p. Dep. mn; CFSTI $1.00 cy, $0.50 mn.

The environmental monitoring report of the Ames Laboratory of the USAEC is the pre-operational program for the Ames Laboratory Research Reactor (ALRR). The program consists of air samples, soil, vegetation, river water, bottom sediment, precipitation and well water samples, and covers the period from January 1, 1965 to June 30, 1965. As soil and vegetation samples are collected later in the year (usually August) that data will be reported in the annual report. The ALRR was not in operation as of 6–30–65. There are no other known contributors to environmental radioactivity levels. It is concluded that radioactivity levels recorded represent background conditions for the above stated period. Average levels of radioactivity were recorded for this period in $\mu\mu c/M^3$ for air, $\mu\mu c/l$ for river water, precipitation, and well water, and $\mu\mu c/g$ for bottom sediment. The ALRR went critical on February 17, 1965, and had not reached full power (5MW) July 12, 1965. It has not been in routine operation. (H.G.D.)

44303 (TRG-Report-888) A HIGH-ACTIVITY IODINE RELEASE FROM IRRADIATED FUEL AND ITS SUBSEQUENT CLEAN-UP. Hillary, J. J.; Taylor, J. C. (Reactor Group, United Kingdom Atomic Energy Authority, Sellafield (England)). Mar. 23, 1965. 18p. Dep.; BIS $0.60; HMSO 3s.

A test at kilocurie level of activity was performed, based on the most stringent conditions postulated in reactors of the advanced gas-cooled type and clean-up effected with a filter-charcoal bed-filter system. Iodine penetration of the treatment system was greater than previously experienced as a result of excessive loading of the charcoal bed by methyl iodide, produced from the iodine released by the fuel. Another type of charcoal was found to give satisfactory retention of methyl iodide. (auth)

44304 (CEA-tr-R-1836) EFFETS NOCIFS DU POLONIUM SUR LES OUVRIERS. (Harmful Effects of Polonium on Workers). Parkomenko, A. Translated into French from Chapter I, pp 6-16 of Hygiene du Travail Utilisant le Polonium. 17p. Dep. mn; JCL $1.60 fs, $0.80 mf.

In working with sealed polonium preparations the only hazard is neutron irradiation. The induced radioactivity that can be caused in the tissues by this irradiation is shown. In working with open sources the hazardous factors are the polonium aerosols, contamination of the skin and clothing, and surface contamination. Each of these is discussed. (J.S.R.)

44305 DIET OF THE FINNISH LAPPS AND ITS ^{137}Cs AND POTASSIUM CONTENTS. Jokelainen, Aili (Univ. of Helsinki). Acta Agral. Finnica, 103: 1-140(1965).

Studies were made on the composition of the Lappish diet, the main sources of ^{137}Cs and potassium, and their total content in the diet. The investigation was carried out in 1960–62 in the communes of Enontekio, Inari, and Utsjoki. For the male reindeer-breeding Lapps and the reindeer-breeding fisher Lapps, the average intake of ^{137}Cs was 4,707–7,262 pC and for the female members of the same groups 1,783–2,068 pC per person per day in spring 1962. For Lappish men of other occupations the corresponding figures were 980–1,682 and for the women of the same group 960–1,907 pC per person per day. On the average the contribution of meat and meat products to the ^{137}Cs content of the diet was 74.7%, fish 12.1%, milk and milk products 10.7%, cereal products 1.5%, potatoes and other vegetables 0.2%, berries and fruits 0.7%, and coffee and tea 0.1%. On the average the intake of potassium was 6.3 g for Lappish men and 5.0 g for Lappish women per person per day. 191 references are cited. (P.C.H.)

44306 FEDERAL RADIATION COUNCIL GUIDES AND OTHER EXPOSURE STANDARDS. Grendon, Alexander (Univ. of California, Berkeley). Am. J. Public Health, 55: 738-47(May 1965).

The first staff report of the Federal Radiation Council, published in May 1960, dealt with basic radiation protection standards applicable to the normal peacetime uses of radiation that affect the exposure of the civilian population. The concepts on which this report is based are reviewed, with emphasis on recommendations of the International Council of Radiation Protection and AEC standards of radiation exposure and the corresponding allowable concentration of radioisotopes in air and water. Recommendations as to the control of the intake of certain isotopes, such as Ra, ^{89}Sr, ^{90}Sr, and ^{131}I, are discussed. (C.H.)

44307 INDUSTRIAL USES OF IONIZING RADIATION. Eisenbud, Merril (New York Univ., New York). Am. J. Public Health, 55: 748-59(May 1965).

Industrial uses of nuclear energy are discussed in terms of the current status and future possibilities. It is pointed out that more is known about the safe handling of nuclear materials, processes, and products than is known about many other substances and processes in our environment.

Applications of radioisotopes, such as ^{238}Pu, ^{90}Sr, and ^{137}Cs as sources of heat for the generation of small amounts of electrical power and possible applications of isotopic power units are reviewed. The present status of nuclear energy as a source of power is reviewed and the operation of the 29 nuclear power plants in use at present is discussed. Emphasis is placed on standards of safety in modern technology. (C.H.)

44308 SOLID PHANTOM WITH ADAPTABLE FORM AND DENSITY PERMITTING A DOSIMETRY THROUGH-CUT ITS VOLUME. Abbatucci, J.-S.; Bloquel, J. Ann. Radiol., 8: 241-2(1965). (In French).

A phantom is described composed of elements in the form of rods piled one on the other. Each element is interchangeable and can be held in position by a perforated support. The elements are 25-cm long and have a cross section of 2 × 2 cm or 4 × 4 cm. Some have a triangular or rectangular cross section in order to permit the contours of the body studied to be followed as closely as possible. The elements are made of Plexiglas (for soft tissues), poplar wood (for the lungs), and specially prepared resin bars for bone. Some elements are perforated to receive an ionization chamber. (J.S.R.)

44309 CONCENTRATION OF ^{137}Cs IN AUSTRALIAN MILK DURING 1963. Alsop, R. J. L.; Bonnyman, J.; Keam, D. W.; Molina-Ramos, J. (Commonwealth X-ray and Radium Lab., Melbourne). Australian J. Sci., 27: 219-22(Feb. 1965).

Results are reported of ^{137}Cs levels in milk samples from seven Australian cities. The pC/l values are tabulated on a monthly basis for all seven cities and compared with values found elsewhere in the world. The radioassay technics used are described in detail. Liquid milk was obtained from each of the cities: Brisbane, Sydney, Melbourne, Hobart, Launceston, Adelaide, and Perth. A specimen was obtained on one day each week, by continuous sampling of milk being processed for consumption in each city. The monthly average value for all the centers, the yearly average value for each center, and the yearly average value for all centers are given. The yearly averages for the various cities were: Brisbane 18, Sydney 26, Melbourne 34, Hobart-Launceston 28, Adelaide 27, and Perth 63 pC ^{137}Cs/l milk. The overall 1963 average for these cities was 33 pC/l. For comparison, yearly average values for 1963 are given for countries in which systematic surveys of ^{137}Cs in whole milk have been carried out. The National Radiation Laboratory, New Zealand, has reported for July to December 1963, results of the measurement of ^{137}Cs in whole milk sampled monthly at eight stations. The average value for all the stations for the six months period was 40 pC/g K. Accepting the average potassium content of milk as 1.4 g/l, this six-monthly average corresponds to 29 pC ^{137}Cs/l milk. The values for Australia and New Zealand are similar magnitude and are much lower than those for countries in the northern hemisphere. (BBB)

44310 ROLE OF THE ARMY MEDICAL SERVICE IN A NUCLEAR WAR. Thieblemont, P. Gaz. Med. France, 71: 2191-2200(June 10, 1964). (In French).

The nature of the health risks to troops in the event of a thermonuclear war demands a new approach to treatment from the army medical services. Exposure to radiation, the huge number of wounded and burned victims involved, and the need for vast supplies of blood, all present particular problems. Two types of radiation danger, external irradiation and inner radionuclide contamination, demand special consideration. Irradiation is due to γ rays and neutrons from the detonation, the early radioactive fallout, and the later fallout of fission products. These combine to produce external burns and cellular lesions. The most effective means in the French Medical Services for detection of contamination is by the use of Chassende-Barox dosimeter with sensitized film. External contamination as treated by ordinary decontamination procedures is described. Internal contamination is avoided by careful delineation of the danger areas, control of water and food supplies, and the use of gas masks. Treatment may be long and demand close and constant surveillance of the victims. In order to protect themselves against direct exposure and to allow immediate mobilization, the medical staff must remain at the rear of the army. To meet these new demands, the army is divided into two forces, a battle corps, which may be armed with nuclear weapons, and defense units distributed over the country, each served by its own medical corps with facilities for decontamination of casualties of thermonuclear weapons. (BBB)

44311 ON MAXIMUM PERMISSIBLE LEVELS OF RADIOACTIVE CONTAMINATION OF SURFACES. Khvostov, N. N. (Central Inst. for Medical Graduate Work, Moscow). Gigiena i Sanit., No. 4, 98-102(Apr. 1965). (In Russian).

The present tolerances for surface contamination are set too low because of the danger of ingesting the radioactive material. A study of the transfer of contamination from the hands and clothes to various surfaces showed that the spread of contamination depended on the level of contamination, type of surface, and contact time. The activity may be free (readily transferred) or fixed (not readily transferred). The maximum allowable skin dose of 1 r/week is obtained at a beta contamination level of 150,000 to 250,000 beta particles/150 cm^2 · min, or at a level of 2000 to 3000 alpha particles/150 cm^2 · min. However, because of the danger of ingesting the radioactive material, the tolerances were set at 100,000 disintegrations/150 cm^2 · min for Class III radioactivities (the least dangerous because of short half-life etc.), 10,000 for Class II radioactivities (intermediate in danger), and 1000 for Class I radioactivities (the most dangerous group). The tolerances were increased a factor of ten, if only a limited surface area were contaminated. These tolerances are for buildings where activity is handled routinely. The tolerances are reduced by a factor of 10 for buildings that do not handle activity routinely, but a tolerance of 1000 disintegrations/150 cm^2 · min is retained for Class I substances (the most dangerous group). The tolerances to the hand are 1000, 500, and 100 disintegrations/150 cm^2 · min respectively for the three classes of radioactivities. The allowable surface contamination on protective clothing is 1000, 500, and 200 disintegrations/150 cm^2 · min respectively for the three classes of radioactivity with a significant area of the clothes being contaminated. The tolerances are a factor of 2 higher with a limited area of the clothes being contaminated (<150 cm^2). (TTT)

44312 EVALUATION OF FILM BADGE DOSIMETERS FOR OCCUPATIONAL RADIATION EXPOSURE. Menker, Donald F.; Dauer, Maxwell (Univ. of Miami, Fla.). (Ind. Med. Surg., 34: 700-4(Sept. 1965).

Sixteen commercial film badge suppliers were contacted and asked to participate in a test. A total of 145 badges were exposed to radium-226 and cobalt-60 gamma rays, x-rays from 80 kvp (2.7 mm Al HVL) and 250 kvcp (3.0 mm Cu HVL) generators, and phosphorus-32 beta particles. After irradiation all badges were returned to the film badge services for processing and reporting. Results were tabulated and compared with the actual measured value and the companies rated without reference to company name. An attempt was made to correlate the reported dose with the films and filters used. There was considerable variation in accuracy among the companies. Although many companies claim an accuracy of better than 10%, only 2.7 to 43% of the reports were within this range. The greatest accuracy occurred with the radium exposures, while the least was with the 80 kvp x radiations. (P.C.H.)

44313 ON THE ^{90}Sr CONTAMINATION OF TISSUE AND A STANDARD DIET. Pribilla, O.; Mutschke, U. (Universitaet, Kiel). Klin. Wochschr., 43: 690-4(June 15, 1965). (In German).

Extensive data are given on radioassays for Sr in human bone and soft tissue (including placenta, testis, and blood) and of diets covering the period from 1958 to present. Since July, 1962 a standard diet, including beverages and milk, has been analyzed for its ^{90}Sr and ^{89}Sr content. A considerable increase of ^{90}Sr contamination in the diet was

observed. A ^{90}Sr level of 60 pC/day was found to be the average for 1963. The increase of the ^{90}Sr content in the diet has, after resumption of the atomic bomb tests in the autumn of 1962, been accompanied by a considerable increase of the ^{90}Sr content in human bones and tissues. At the commencement of 1964 the values for placenta were over 4 pC/g Ca and for bones of newborn 3 pC/g Ca. In radioassays of human plasma made in Kiel, the ^{90}Sr content rose from 0.10 pC/l (0.9 pC/g Ca) in Oct., 1961 to 0.35 pC/l (4.2 pC/g Ca) in Oct., 1963. In the same period the ^{90}Sr content of human testis rose from 0.15 pC/kg fresh weight (1.6 pC/g Ca) to 0.61 pC/kg (3.3 pC/g Ca). Considerable amounts of other data are also tabulated. (BBB)

44314 RADIATION AS THE CAUSE OF LUNG CANCER AMONG URANIUM MINERS. Wagoner, Joseph K. (National Cancer Inst., Bethesda, Md.); Archer, Victor E.; Lundin, Frank E. Jr.; Holaday, Duncan A.; Lloyd, J. William. New Engl. J. Med., 273: 181-8(July 22, 1965).

A study of mortality experience was conducted among 3415 white underground uranium miners, and cause-specific comparisons were made with the general white male population of the Colorado Plateau. A higher total mortality was observed among this group of miners. This excess mortality was attributed to respiratory neoplasms (22 observed as compared with 5.7 expected), violent deaths particularly in mines, and all other causes, a reflection of pulmonary fibrosis and its sequelae. A study of the quantitative relation between airborne radiation and respiratory cancer showed that the age-standardized incidence increased from 3.10 per 10,000 miners per year at the lowest to 116.12 at the highest cumulative-exposure category. An evaluation was also made of the evidence for a causal relation between airborne radiation and respiratory cancer among uranium miners in the United States. (auth)

44315 EVALUATION OF THE VARIABILITY IN THE NUMBER OF LEUKOCYTES IN THE DIAGNOSIS OF HAEMATOPOIESIS IMPAIRED BY IONIZING RADIATION. David, Alois; Roth, Zdenek. Pracovni Lekar., 17: 184-8 (July 1965). (In Czech).

The number of leukocytes was determined in 12 healthy subjects on five consecutive weeks and during ten consecutive months, in order to ascertain the extent of physiological variations of the number of leukocytes. No difference was found in the daily, weekly, and monthly variations. In 11 subjects the variation coefficient of leukocytes reached a maximum of 15% and the variation coefficient of the number of neutrophil leukocytes and lymphocytes a maximum of 25%. It is recommended that for investigations of hematological changes in persons exposed to ionizing radiation four hemograms should be made at weekly intervals before starting work. The average of these can be taken as the normal initial value used for comparison with subsequent examinations. The difference between the assessed values is significant if the total number of leukocytes declines, as compared with the initial normal value by at least 29% (and the number of neutrophil leukocytes or lymphocytes by 48%) or the average value of three consecutive leukocyte counts by 20%, as compared with the initial value (and the value of neutrophil leukocytes and lymphocytes by 33%). This method of evaluation of hemograms helps to differentiate normal drops of leukocyte numbers below the conventional lower borderline of the normal range from pathological leukopenias. (auth)

44316 CLINICAL EXAMINATION OF PERSONS SUSPECTED OF MAJOR EXPOSURE TO IONIZING RADIATION. Klener, Vladislav. Pracovni Lekar., 17: 200-3(July 1965). (In Czech).

After inadequately insured manipulation of a closed ^{60}Co emitter with an activity of 2000 g equivalent Ra, 13 subjects suffered excessive exposure to a single dose. Although the size of the dose was not known, it was essential to evaluate the danger involved in the exposed subjects by means of clinical and hematological tests. In the leukogram of several subjects a temporary non-specific leukocytosis and mild activation of lymphoreticular elements was observed. From the results it was concluded that the dose did not exceed 20 to 50 R, an estimate that was later confirmed by results of individual film dosimetry. (auth)

44317 PROBLEMS OF MEDICAL PHYSICS DURING THE DISMANTLING OF RADON PUMPING STATIONS. Minarik, Frantisek; Hrabovcova, Alojzia; Manca, Jozef; Nikodemova, Denisa; Minarik, Augustin. Pracovni Lekar., 17: 206-10(July 1965). (In Czech).

Problems and hazards involved during dismantling of radon pumping stations are described. Protective measures against surface contamination are discussed. During dismantling of the vacuum portion of the apparatus, contamination of the working atmosphere with ^{222}Ra was recorded. The concentration assessed by membrane filters varied from $0.76 \cdot 10^{-10}$ C/m^3 to $1.54 \cdot 10^{-7}$ C/m^3. Safety and hygienic standards required for this type of work are reviewed. (H.G.D.)

44318 THE RECENT PRESIDENTIAL DECREE ON SAFETY AND HEALTH PROTECTION AGAINST RADIATIONS: ASPECTS AND CONSIDERATIONS REGARDING MEDICAL RADIOLOGY ACTIVITIES. Polvani, C. Radiol. Med., 51: 337-55(Apr. 1965). (In Italian).

The Decree issued by the President of the Italian Republic, and published on April 16th, 1964, concerning the regulations governing nuclear safety and health protection against radiations is evaluated. After reviewing the measures in general, special attention is given to the articles of the Decree most closely concerning medical radiology activities: professional qualifications required for practicing in radiology; conditions to be met for opening and operating radiological departments and cabinets; supervision of staff operating radiological services; and collaboration with the provincial protection Commissions. (auth)

44319 (STI/PUB/99) PERSONNEL DOSIMETRY FOR RADIATION ACCIDENTS. Proceedings Series. Proceedings of a Symposium Held in Vienna, 8-12 March 1965. (International Atomic Energy Agency, Vienna). June 1965. 716p. (CONF-650302). IAEA $14.00; $294,-; £4.40; F.Fr. 56,-; DM 49,-cy.

Fifty articles are included; separate abstracts were prepared for 28. The remaining 22 articles were previously abstracted in NSA as 19: 9477, 18195, 18269, 22589, 22593, 26279, 26579, 26620, 26621, 26622, 26623, 26624, 26625, 26653, 28278, 28693, 30477, 30587, 30588, 31316, 33958, and 36699. (P.C.H.)

For abstracts of individual papers see: 43852–43854, 44093, 44320–44336, and 44532–44538.

44320 THE WHY AND HOW OF NUCLEAR ACCIDENT DOSIMETRY. Vallario, E. J.; Wasson, H. R. (Atomic Energy Commission, Washington, D. C.). pp 31-44 of STI/PUB/99.

The objective of an effective nuclear accident dosimetry program is to ensure that a means is provided for estimating the gamma neutron dose from a nuclear accident. In this connection, the limitation of the film badge is discussed. In addition to certain accident experiences which demonstrate the need for an effective accident dosimetry program at facilities having a potential for nuclear accidents. Certain basic parameters should be considered in the development of an effective nuclear accident dosimetry program. These are a method for screening personnel involved in nuclear accidents; a fixed system (primary unit) capable of determining first collision dose within some established degree of accuracy as its point of location; the need for secondary units; and the need for a device worn by personnel which would afford spectrum and flux information to assist in dose extrapolation from the fixed unit to the location of man. The neutron component of the system should permit flux and spectral information in order to arrive at appropriate quality factors in the dose estimation. Accuracies should be established based upon the current state of the art. The gamma component of the system should permit measuring gamma radiation within the biological area of interest, i.e., from 10 to 10^3 R. Consideration for the number, placement and ease of recovery

of accident units are indeed an integral part of an effective system of accident dosimetry. These considerations should enable reasonable data collection across the entire fission spectrum. (auth)

44321 THE DETECTION OF CRITICALITY ACCIDENTS AT THE COMMISSARIAT A L'ENERGIE ATOMIQUE. Candes, P.; Desneiges, P.; Lavie, J.-M.; Pradel, J.; Baron, H.; Debrie, G.; Planque, M.; Barthoux, A. (Commissariat a l'Energie Atomique, Paris). pp 53-65 of STI/PUB/99. (In French).

As the physical phenomena accompanying a nuclear excursion are inadequate to give warning and may cause confusion, it is necessary to possess special instrumentation to detect criticality accidents and to disclose rapidly any acute exposure of personnel. Bearing in mind the nature of accidents that have occurred and the part detectors are expected to play, the system chosen is based on a dose integrating device for the detector unit proper, and on the principle of coincidence of several items of data for triggering the alarm. The minimum physical and electronic requirements for equipment ensuring reliable operation and the least possible risk of false alarms, established at the request of the Sub-Committee on Critical Masses, are set forth in some detail. Equipment constructed on these lines by the Commissariat à l'Énergie Atomique has undergone systematic trials under actual nuclear excursion conditions at the Health Physics Research Reactor of Oak Ridge National Laboratory. These trials have led to the adoption of two basic detection units, which are described and which consist of a powered photo-multiplication detector and a semiconductor detector. In conclusion, a specific example of construction of a complete installation for detection of criticality accidents at a fissile-materials processing plant is given. (auth)

44322 BIOLOGICAL DOSIMETRY AFTER EXPOSURE TO A HIGH FLUX OF THERMAL AND FAST NEUTRONS. Chanteur, J.; Arnaud, Y.; Pellerin, P. (Commissariat a l'Energie Atomique, Paris). pp 235-50 of STI/PUB/99. (In French).

Experimental procedures for assessing the dose of thermal and fast neutrons received during an accident are defined by describing a method proposed previously which makes use of the (n,γ) and (n,p) activation reactions of the phosphorus in bone. In this way it is possible to pick out the respective fluxes of neutrons with energies lower and higher than 1.8 Mev. The method gives excellent sensitivity, permitting the detection of doses of the order of one rad. Several series of experiments were run on the activation of tricalcium phosphate, of dry or fresh isolated bone, and of the whole animal. Graphic analysis of the decay shows the most favorable moments for measuring the activities, and gives details of the part due to derivatives of the phosphorus activation. The natural phosphorus content of the bone samples is chemically checked, and makes it possible to determine the mass activity, which forms the basis for calculating neutron fluxes. The validity of the results was confirmed by exposure to known fluxes, and a definite procedure for measurement after accidents is suggested. (auth)

44323 ESTABLISHMENT OF NEUTRON FLUXES AND DOSES AFTER A CRITICALITY ACCIDENT USING THE MULTI-SPHERE TECHNIQUE. Benezech, G.; Zaborowski, H. (and others). Commissariat a l'Energie Atomique, Cadarache, France). pp 349-68 of STI/PUB/99. (In French).

The multi-sphere technique can be used to establish neutron fluxes and doses over an energy range between thermal and about 7 Mev. This technique consists of using thermal neutron detectors at the center of polyethylene spheres of various diameters. The responses, for monoenergetic incidental fluxes, are interpolated from experimental data obtained by others with 2-, 2.5-, 10-, and 12-in. spheres. Direct addition of the responses of certain units to neutron fluxes of unknown spectra provides: neutron flux values with an estimated accuracy of ±10%; and kerma and absorbed doses with an estimated accuracy of ±15%. Two detection units were developed. The first is a unit whose thermal neutron detector consists of a 4 mm × 4 mm ^{6}Li crystal, for measuring fluxes of the order of 2 n $cm^{-2}s^{-1}$ and dose rates of ~0.5 mrem/h. The second is a unit whose thermal neutron detector consists of a 6 mm × 6 mm gold cylinder, for measuring integrated fluxes of the order of 10^{6} n/cm^{2} and integrated doses of the order of 0.5 Rem. A spectrometric method applicable to neutrons in the intermediate energy range was devised from the responses with various spheres. Data obtained from trials with these units using an unmoderated fission source are included. (auth)

44324 ROLE OF THE LABORATORY AND THE METHODS TO BE USED IN THE EVENT OF AN ACCIDENT. Jeanmaire, L. (Centre d'Etudes Nucleaires, Fontenay-aux-Roses, France). pp 413-18 of STI/PUB/99. (In French).

The laboratory that measures the radioactivity of personnel after a contamination or radiation accident has a very important part to play. For the measurement to be effective, direct or indirect contamination of the laboratory must as far as possible be avoided. In view of the impossibility of drawing up a valid general plan for all the measurement methods to be employed in the event of an accident, only indications regarding the principles to be followed are given. As in the general case of contamination measurement, both direct and indirect methods are employed. Nevertheless, before resorting to the standard routine techniques it is necessary to use very simple methods, which are less sensitive and sometimes less selective, but are in some cases perfectly adapted to the needs of the situation. Thus contamination of the facilities is reduced to a minimum; the simplicity of operation makes it possible to obtain very rapidly results permitting rough assessment of the seriousness of personnel contamination, followed by appropriate medical action. (auth)

44325 BACKGROUND AND MEASURABILITY OF TEST SAMPLES IN AN EMERGENCY SITUATION. Widell, C.-O. (Aktiebolaget Atomenergi, Studsvik, Sweden). pp 465-70 of STI/PUB/99.

Background radiation levels in the vicinity of a reactor, after a maximum credible accident, were calculated. Based on this the measurability of test samples from air and of human bodies was studied. It was found possible to analyze radiometrically air-filter samples from 0.1 m^{3} air contaminated to 100 MPC (40 hr) β-activity, 100 MPC (40 hr) iodine-131 activity, and 10 MPC (40 hr) α-activity in a gamma background of 2 R/hr. These measurements were carried out in the normal equipments in the counting-room 400 m away from the actual reactor. It is, however, necessary to use well-shielded counters (e.g., 10-cm lead shield). It was also found satisfactory to make rapid β-analyses with an end-window G-M tube ordinarily used in routine control in a 10-cm lead shield. The analyses of iodine-131 had to be carried out in a gamma spectrometer but measuring times of 100 s were found to be satisfactory. Also the spectrometers need to be shielded with at least 10 cm of lead. It might be difficult to investigate body burden of the order of one permissible quarterly intake in an ordinary human body counter if the gamma background is increased to very high levels. In such instances it would be useful either to be able to move the human body counter off the site or to have a transportable counter available. The influence of a raised background is illustrated with figures for an iron-room with 16-cm walls and a 4 in. × 8 in. NaI crystal. All the figures above are calculated with large errors due to large fluctuations in the gamma fields. It is necessary to count the background before as well as after the counting of the sample if no monitor is available. (auth)

44326 EXCESSIVE DOSE LEVELS: REPORTS AND STATISTICS. Venier, A. (Institut National pour la Prevention des Accidents de Travail (ENPI) Rome). pp 471-9 of STI/PUB/99. (In French).

Attention is directed to the absolute necessity of adopting a special emergency procedure for communicating to the

parties concerned the values either of very high doses or of doses exceeding maximum permissible levels. The cases allowing evaluation of the absorption of high and excess doses are much more numerous than might be thought, especially in the field of medical diagnosis. Accordingly, the statistical data for such doses, recorded monthly by the Ionizing Radiation Control Centre of ENPI (Ente Nazionale per la Prevenzione deglie Infortuni) from 1958 to the present time, out of a total of 350,000 evaluations carried out by the film-dosimeter method, are given. From answers received in response to urgent requests it was possible to establish that the high doses recorded were most often the result of irregular or accidental exposure of the dosimeters, and consequently had no bearing upon the doses actually absorbed by the personnel using the dosimeters. Descriptions are also given on what is done at the Centre in cases of contamination and of absorption of high and excess doses, and also the measures taken to speed up the operations of development and evaluation in order to reduce to a minimum the interval between the arrival of the films and the dispatch of documents communicating to the parties concerned the doses absorbed. (auth)

44327 DOSIMETRY OF HIGH-ENERGY PROTONS BY MEASUREMENT OF ^{7}Be FORMED IN THE TISSUES. Legeay, G. (Commissariat a l'Energie Atomique, [Paris]; Centre d'Etudes Nucleaires, Fontenay-aux-Roses, France); Court, L.; Prat, L.; Jeanmaire, L.; Daburon, M. L.; De Kerviler, H.; Tardy-Joubert, P. pp 507-23 of STI/PUB/99. (In French).

In the course of biological experiments at the CERN cyclotron at Geneva (using 600 Mev protons) and the Saturne synchrotron at the Saclay Nuclear Studies Center, the radioactivity induced in living beings was investigated by gamma spectrography. Whereas most of the induced radioisotopes (gamma emitters) are short-lived, the beryllium-7 produced by spallation reactions on, in particular, oxygen, carbon, and nitrogen atoms, has an activity peak which stands out abruptly from the spectrum as a whole at the 479-kev level. As its half life is 54.5 d, it can be recorded for a sufficiently long time. An experiment carried out with Whitsar rats given whole-body exposures of between 400 and 800 rad with 600-Mev protons and of 2000 to 1000 rad with 3-Bev protons, disclosed a linear response of the ^{7}Be activity in relation to the dose absorbed per gram of tissue. Experimental results were compared with the activities calculated in terms of energy on the basis of published cross-sections. The accidental exposure of human beings to proton beams can only be local. Exposure of the heads of Fauve de Bourgogne rabbits weighing approximately 2 kg show that the activity measured on the head, in relation to the rest of the body, is of the order of 1.8 ± 5. ^{7}Be can be detected during the first days in spite of some diffusion. Relative dosimetry, indicating the scale of the accidental exposure received, is therefore possible. (auth)

44328 CRITICAL CONSIDERATION OF THE METHODS OF CALCULATION USED IN THE EVALUATION OF THE ABSORBED DOSE TO THE SKIN IN CASES OF EXTERNAL CONTAMINATION. Casnati, E.; Breuer, F. (CNEN; Centro di Studi Nucleari della Casaccia, Rome). pp 525-39 of STI/PUB/99.

Studies were made in the case of cutaneous contamination, the use of an exponential formula (like the formula of Rossi and Ellis), and whether a similar formula might be considered as satisfactory, for calculation of the beta and the gamma dose, respectively in the case of cutaneous contamination. With this aim the results obtained for this particular type of geometry by the Rossi and Ellis formula and by the Loevinger formula for beta particles were compared; for gamma radiation the values obtained by the exponential formula and by two more elaborated formulas, suitable for the conditions of maximum photonic build-up and of null photonic build-up, were compared. From the results it was concluded that, for the geometric conditions considered, both the dose from beta radiation and that from gamma radiation to the basal layer of the skin can be determined by the exponential type formula: the results in fact are acceptable from a health protection standpoint. (auth)

44329 DOSE ABSORPTION BY TISSUE ON ACCIDENTAL EXPOSURE TO VERY HIGH-ENERGY γ-RADIATION. Ladu, M.; Pelliccioni, M.; Roccella, M. (Comitato Nazionale per l'Energia Nucleare, Rome). pp 541-5 of STI/PUB/99. (In French).

The residual activity in a plastic tissue-equivalent material exposed to a γ-ray beam of 1000 Mev was studied. When examined with a scintillation counter, the plastic showed a γ-activity of 0.5 Mev with a half life of 20.5 min due to activation of the carbonium present in the tissue. While other measurements were made to assess the activation of oxygen and nitrogen in tissue exposed to a high-energy γ-beam, the biological dose which would be absorbed by the organism in the event of an accidental exposure to the same beam was calculated. The total dose was assumed to be given by the sum of the dose absorbed during exposure and the dose resulting from residual activity. (auth)

44330 THE HANFORD CRITICALITY ACCIDENT: DOSIMETRY TECHNIQUES, INTERPRETATIONS AND PROBLEMS. Parker, H. M.; Newton, C. E. Jr. (General Electric Co., Richland, Wash.). pp 567-82 of STI/PUB/99.

The number and integrity of dosimetry techniques used for dose interpretations for the twenty-two personnel involved in the 1962 criticality accident occurring at the Hanford Project were unusually complete. Personnel who received excessive exposures were immediately detected and segregated by monitoring personnel using portable instrumentation for quick-sort procedures which rely on in vivo measurements of ^{24}Na activation. The close correlation between this rapid method of dose interpretation and subsequent sophisticated laboratory procedures was noted. Primary reliance, however, was placed upon film-badge interpretations, as all persons involved were wearing film badges. An area threshold detector, located within twenty-six feet of the critical vessel, furnished data upon which the neutron spectrum and the gamma to neutron ratios were established. Even with sophisticated and complete dosimetry techniques which were available and which are discussed, including blood and whole-body ^{24}Na activity, excreta and ^{32}P analyses, and gold activation, many practical problems became evident. Described are methods or alternatives used to cope with or minimize actual problems including those which could have but did not arise. The quick-sort in vivo procedures successfully used could have become worthless if interfering external contamination were encountered. The support provided by fixed detectors still presents the problems that scattering, moderation, and geometrical factors are not the same between exposed personnel and detector. The unidirectional nature of the heterogeneous gamma-neutron flux, although providing expected variations, presents unique complications in organ dose interpretations. Finally, the problems and delays that can be encountered in the selection and agreement of dose-related conversion factors, methods of calculation, probable applicable spectrums and other necessary supplemental data are covered. (P.C.H.)

44331 DOSIMETRIC AND CLINICAL STUDY OF AN ACCIDENTAL EXPOSURE RECEIVED FROM AN ELECTRON LINEAR ACCELERATOR AS A RESULT OF MALFUNCTIONING. Joffre, H. (Centre d'Etudes Nucleaires, Saclay, France); Vialettes, H.; Rocchesani, J.; Vial, R. pp 583-95 of STI/PUB/99. (In French).

Conditions in which two investigators sustained accidental irradiation of the fingers as a result of an unforseen emission of radiation are described. The presence of a residual beam of 7-Mev electrons led to considerable localized irradiation. The energy of the incident radiation was determined by the method of absorption in various materials. The absorbed dose was determined by a number of radiation detectors, including ionization chambers, radio-photoluminescent glass, and film dosimeters. The victims remained under surveillance for 15 months after

irradiation, which made it possible to study the initial lesions and their development up to the present time. As a result of this incident, new safety rules have been introduced for operating particle accelerators. (auth)

44332 PERSONNEL DOSIMETRY CONTROL AT THE BORIS KIDRIC INSTITUTE, VINCA. Miric, I.; Markovic, P.; Miric, P. (Inst. of Nuclear Science Boris Kidrich, Belgrade). pp 597-606 of STI/PUB/99.

The organization of control and methods which are usually applied in the determination of individual external doses received from gamma rays and neutrons in normal and accidental conditions is discussed. A description is also given of a film dosimeter used under normal conditions for the determination of doses and methods used to measure gamma rays and thermal-neutron doses. The use of activation detectors in estimating neutron doses for accidental irradiations in the Institute at Vinca is also described. (auth)

44333 ACCIDENTAL EXTERNAL EXPOSURE DOSIMETRY AT THE COMMISSARIAT A L'ENERGIE ATOMIQUE. Candes, P.; Lavie, J.-M. (Commissariat a l'Energie Atomique, Saclay, France). pp 607-22 of STI/PUB/99. (In French).

During the past few years, the putting into circulation of increasing quantities of fissile materials has led the Commissariat à l'Énergie Atomique (CEA) to investigate the risks of criticality accidents and especially to assess the doses likely to be received by personnel when such accidents occur. The CEA departments responsible for personnel monitoring have directed their efforts to the development of a simplified neutron and gamma dosimetry system, using both threshold and resonance detectors and detectors equipped with moderators, and dosimetric films and glasses. The system devised, which is suitable for the dosimetry of all acute external exposures, at the high dose-levels and rates such as those occasioned by accidents of various types, includes: primary fixed dosimeters consisting of two gold-detector moderating spheres and gold, copper, sulfur, magnesium, cadmium-shielded, and bare copper activation detectors; secondary fixed dosimeters consisting of activation detectors alone; and personal dosimeters equipped with sulfur, gold, and cadmium-shielded gold, glass, films, and indium discs. The characteristics of the radiation fields in the areas involved will be defined in the light of data obtained from the fixed dosimeters. The personal dosimeters will permit rapid identification of seriously exposed persons and the necessary adjustments in accordance with the location and orientation of each individual. Used together, these data will indicate the fluxes and doses received in each case. The system described has undergone trials under true criticality excursion conditions and, with the exception of the moderator-equipped dosimeters, is already in service at CEA plants or at private industrial establishments working with fissile materials under contract to the CEA. (auth)

44334 TESTS OF A DOSIMETRIC SYSTEM FOR CRITICALITY ACCIDENTS AT A FAST-CRITICAL ASSEMBLY. Bricka, M.; Benezech, G. (and others). (Centre d'Etudes Nucleaires, Cadarache, France). pp 623-31 of STI/PUB/99. (In French).

At the French Commissariat à l'Énergie Atomique, the dosimetry of criticality accidents is carried out by means of a dosimetric system consisting of primary and secondary fixed dosimeters and personal dosimeters equipped with threshold and resonance detectors and moderators, plus dosimetric films and glasses. The system has undergone systematic tests at a bare fast-critical assembly. The tests related to dose evaluation, both under conditions of direct exposure to the source and behind shielding. The personal dosimeters were fixed on phantoms consisting of water-filled polyethylene cylinders. The main purpose of these tests was to appraise the system and its efficiency under the most realistic conditions possible, in order to disclose any weaknesses and make the necessary modifications. The tests also provided excellent practice for the personnel involved. The tests showed the significance of the disturbances close to a moderating mass, which complicate correct determination of the flux, spectrum, and dose when using only personal dosimeter data, thus confirming the value of primary or secondary fixed dosimeters. The orientation of the person exposed proved to be an important factor. (auth)

44335 PERSONNEL MONITORING PRACTICES AT THE NATIONAL REACTOR TESTING STATION. Cipperley, F. V.; Henry, R. W.; Cusimano, J. P. (Atomic Energy Commission, Idaho Falls, Idaho). pp 633-44 of STI/PUB/99.

The film badge utilized in the personnel monitoring programme at the National Reactor Testing Station (NRTS) enables the determination of the type of radiation, estimation of the average energy of the gamma component, and evaluation of the dose to the badge in the range of ~30 mRad to 800 Rad. This range is adequate for most accidental as well as routine exposure monitoring. In emergency situations, an estimated beta-gamma exposure dose can be provided in less than 30 minutes following receipt of the film by the Dosimetry Branch. A personnel neutron threshold detector (PNTD) in each badge provides the capability of rapid field screening of personnel following a criticality incident. The PNTD offers a sensitive and reliable method for the detection and estimation of thermal (<0.4 ev) and fast (>2.5 Mev) neutrons under a variety of conditions. Modifications currently under way should also provide for estimation of epithermal (0.4−1.4 ev) neutrons and provide a detection limit at time-zero of <0.2 mRad thermal or epithermal. Fixed nuclear accident dosimeters (NAD) are strategically located throughout the various operating areas. These contain elemental foils for determination of neutron flux and estimation of the spectrum and chemical dosimeters for measuring the gamma flux. Normalization of the PNTD to the NAD can be accomplished to assist in determining orientation of personnel and calculation of dose. The data obtained during the recent SPERT I and SNAPTRAN-3A reactor destruct series indicated good correlation between the PNTD and similar data obtained from the NAD system. A computer and associated peripheral punched-card equipment are utilized at the NRTS for the dose determinations, maintenance of accurate health-physics records and the rapid retrieval of radiation exposure information in emergency situations such as the SL-1 reactor accident. During a six-week period complete updated exposure lists were furnished the control group each morning at 8 a.m. covering all exposures received at SL-1 through 9 p.m. the preceding day. These lists showed the exposure received on each entry into the SL-1 as well as the accumulated NRTS total for each individual as of that date and proved invaluable for exposure control and work assignment purposes. (auth)

44336 PLANNED PROCEDURES FOR FAST DETERMINATION OF RADIATION LEVELS AND PERSONNEL DOSIMETRY IN CONNECTION WITH RADIOLOGICAL ACCIDENTS. Edvardsson, K.-A.; Wahlberg, T. (Aktiebolaget Atomenergi, Studsvik, Sweden). pp 665-72 of STI/PUB/99.

AB Atomenergi, Sweden, has an emergency organization which starts to function as soon as an alarm indicates that an extraordinary situation with considerable radiation hazards has occurred. This organization is operating from a headquarters where equipment is stored and different types of internal and external communications are available. As to determination of exposures, it is desirable both to obtain rough preliminary values for external and internal exposure rates as soon as possible and to get fairly accurate values for the exposure of each individual involved in the accident within reasonable time. Dose reconnaissance patrols make rapid surveys of the site to get a general estimate of the risks. These patrols start out immediately after the alarm equipped with portable instruments and go by car along fixed routes on the site. Practical tests have shown that results from these patrols

reach the headquarters within 10 to 15 minutes after the alarm and make it possible to get a good picture of radiation levels inside and outside different buildings. The portable equipment includes air sampling equipment with very short sampling time working on the principle of the air ejector. Individual external doses are evaluated on the basis of film exposures, criticality dosimeter activation and analyses of hair and blood activity. Internal contamination is determined by whole-body counting and radiometric analyses of excreta. In order to determine the radiation fields created by an accident a number of fixed control points are equipped with different types of dosimeters which also are evaluated as soon as possible after the hypothetical accident. (auth)

INSTRUMENTATION

General

Refer also to abstract 44366.

44337 (AD-425708) ELECTRON TUBES RADIATION RESISTANT PILOT LINE PRODUCTION. First Quarterly Progress Report, May 21, 1963-August 31, 1963. Grimm, J.; Parks, F. B. (Chatham Electronics Div., Tung-Sol Electric Inc., Livingston, N. J.). Sept. 30, 1963. Contract DA-36-039-AMC-01476(E). 78p. CFSTI $7.60.

A work station was designed and constructed for the purpose of making stems. Carbon molds for each of the four tube types were designed and fabricated. All material such as Corning Alumino-Silicate #1720 and 1723 glass and nickel-moly-nickel leads for use in the production of the stems was ordered. Upon receipt of the glass and leads, the work station and forming molds were successfully evaluated and the feasibility established of the stem design as well as the equipment. Indicated improvements such as higher power at the r-f work, better quality of stems, and closer control over sealing techniques, were made to both equipment and tube fabrication as a result of continued efforts. (auth)

44338 (AD-608496) ALPHA RADIATION HYGROMETER. VOLUME II. FROST-POINT HYGROMETER FOR W-47 AIRCRAFT. Final Report. Crowley, John E.; Konar, Ahmet F. (Honeywell, Inc., Minneapolis, Minn. Aeronautical Div.). Aug. 15, 1964. Contract AF19(604)-8418. 96p. (AFCRL-64-690(II)). CFSTI $4.00.

A frost-point hygrometer for use on W-47 aircraft was designed utilizing alpha radiation techniques to measure the condensate thickness on cooled surfaces. A study of the problems associated with making frost-point measurements from high-speed aircraft was made as part of the design program. (auth)

44339 (AD-608503) ALPHA RADIATION HYGROMETER. VOLUME III. CURRENT PROBLEMS IN STRATOSPHERIC WATER-VAPOR MEASUREMENTS MADE WITH AUTOMATIC FROST-POINT HYGROMETERS. Final Report. Ballinger, J. G.; Fricke, M. P.; Murphy, R. D. (Honeywell, Inc., Minneapolis, Minn. Aeronautical Div.). Aug. 15, 1964. Contract AF19(604)-8418. 33p. (AFCRL-64-690(Vol.III)). CFSTI $2.00 cy, $0.50 mn.

Two basic problems inherent in the stratospheric application of all automatic frost-point hygrometers are examined. In particular, instrument inadequacy due to low rates of mass transfer is found to be a highly probable explanation of the current controversy about upper-atmosphere water-vapor content. The second problem is that of contamination of the moist-air sample by water vapor desorbed from the instrument package and vehicle. The magnitude of this effect precludes a simple accommodation of low mass transfer rates by use of long sampling times. Measures to increase the reliability of future stratospheric data are recommended. (auth)

44340 (AERE-M-1361) AN IMPROVED FURNACE ASSEMBLY FOR HIGH-TEMPERATURE DIFFRACTOMETERS. Baker, T. W.; Spindler, W. E.; Baldock, P. J. (Atomic Energy Research Establishment, Harwell (England)). July 1965. 10p. Dep.; BIS $0.70; HMSO 3s. 6d.

The furnace element in a high-temperature attachment to a Philips x-ray diffractometer was redesigned to give higher specimen temperatures and longer furnace life. The assembly and replacement of the furnace element was also greatly simplified. Arcing, which has proved highly destructive at times, was also eliminated. (auth)

44341 (AERE-R-4962) A RECORDING MICROBALANCE FOR REMOTE THERMOGRAVIMETRIC EXAMINATION OF IRRADIATED MATERIALS. Harrison, K. T.; Scott, K. T. (Atomic Energy Research Establishment, Harwell (England)). June 1965. 22p. Dep.; BIS $0.90; HMSO 4s. 6d.

An assembly is described for the adaptation of the Cahn RM recording microbalance for the thermogravimetric investigation of the oxidation of irradiated uranium dioxide in a preferred form. A 4-in. lead shielding system is employed, enabling specimens up to 20 mg in wt and about 1 Mev Curie in activity to be examined. A description of the operating procedure and the results of trail runs is also given. The system could be used for any irradiated material in the form of small (10-1000 μ) spheroids or chips. (auth)

44342 (APDA-174, pp 67-70) UNDER Na SCANNER. Project Agreement No. 14. Ying, Shuh-pan (Atomic Power Development Associates, Inc., Detroit, Mich.).

The transducers used for ultrasonic attenuation measurements have operated satisfactorily in liquid Na at temperatures up to 500°F. Preliminary attenuation data were obtained and compared with values derived from classical theory. (auth)

44343 (EUR-1918.f) NOMBRE MINIMUM D'INVERSEURS DANS UN SCHEMA ANALOGIQUE. (Minimum Number of Inverters in an Analogue Network). Camion, P. (European Atomic Energy Community, Ispra (Italy). Joint Nuclear Research Center; European Atomic Energy Community, Ispra (Italy). European Scientific Data Processing Center). 1964. 41p. Dep. mn.

The problem treated is to find the non-zero elements, in a matrix with elements 1, −1, 0, whose signs have to be changed in order to minimize the number of columns with elements of opposite signs. The procedure has to obey the rule that if the sign of an element in a line is changed, the signs of all elements in this line are changed. A property of totally unimodular matrices and properties of cycles and cocycles of graphs to which they are connected are given. (auth)

44344 (K-L-1944) FABRICATION OF CALORIMETER ELEMENTS. COMPLETION REPORT ON SANDIA CORPORATION ORDER NUMBER 95-3066. McLaughlin, J. F.; Nolan, T. A.; Burke, T. G.; Wilcox, W. J. Jr. (Oak Ridge Gaseous Diffusion Plant, Tenn.). Jan. 29, 1965. Contract W-7405-eng-26. 73p. Dep. mn; CFSTI $3.00 cy, $0.75 mn.

A process was developed for fabrication of a calorimeter element using a nickel resistance path. The element has a reproducible temperature coefficient of resistance in the temperature range 75 to 200°F. The process consists of the following steps: machining of the substrates, cleaning, anodizing, sealing of the anodized layer, evaporation of the resistance path, attachment of electrical leads, sealing of the resistance path, and testing procedures. Several materials were used as substrates for the calorimeters in the development program. Tantalum was the most extensively used material, and glass, aluminum, and fiberglass laminate were also employed. Several different metals were investigated for use as resistance paths. They were: tellurium, nickel, platinum, copper, iron, and chemically deposited nickel. Tellurium elements were not satisfactory because of their erratic behavior. Platinum could be used if the resistance paths were sealed from the atmosphere, but it has the lowest temperature coefficient of resistance of any of the materials studied. Copper films were not extensively studied, but electrical measurements disclosed some short-term noise. All efforts to make an iron calorimeter failed. Electroless nickel films exhibit a somewhat erratic behavior. Vacuum evaporated nickel films, when successfully sealed from the atmosphere, exhibit reproducible temperature-resistance curves from 75 to 200°F. The resistance of the nickel films was found to be independent of the applied current in the range 0.1 ma to 4.0 ma. (auth)

44345 (LA-DC-6719) POLARIZATION ON THE ENERGY BEAM IN INFRARED GRATING SPECTROPHOTOMETERS. George, Raymond S. (Los Alamos Scientific Lab., Univ. of California, N. Mex.). [1963]. Contract W-7405-eng-36. 32p. Dep. mn; CFSTI, $2.00 cy, $0.50 mn.

An account is given of the polarization occurring within the Perkin-Elmer Model 421 and 521 infrared grating spectrophotometers. It is shown that the use of gratings in these instruments results in considerable polarization of the energy beam. The efficiency curves and the degree of polarization curves for the two components of polarization are given as a function of frequency. The polarization properties of the microsampling unit and the attenuated total reflectance accessory are also investigated. (auth)

44346 (N64-30522) [DESIGN AND DEVELOPMENT OF A TEN NANOSECOND SEMICONDUCTOR SWITCH]. Quarterly Report No. 1. (Bendix Semiconductor Div., Bendix Corp., Holmdel, N. J.). [1964]. Contract NAS 8-11611. 52p. (NASA-CR-58794). CFSTI $3.00 cy, $0.50 mn.

The first phase of the project, concerned primarily with the determination of the design details, was completed. The determination of epitaxial starting material specifications, design of surface geometry, determination of concentrations and depths of diffused regions, and package design are discussed. (D.C.W.)

44347 (ORNL-P-1545) COLLIMATORS FOR LOW-ENERGY GAMMA RAYS. Harris, C. Craig (Oak Ridge National Lab., Tenn.). [1964]. Contract W-7405-eng-26. 4p. (CONF-650313-4). Dep. mn; CFSTI $1.00 cy, $0.50 mn.

From Symposium on Nuclear Medicine, Philadelphia.

The design of collimators for low gamma energies, particularly for energies below 160 kev, is briefly discussed, together with difficulties in the construction of such collimators. (D.C.W.)

44348 (PWAC-473) STATUS OF INSTRUMENT DEVELOPMENT FOR THE SNAP-50 REACTOR TEST PROGRAM. Bliss, P. (Pratt and Whitney Aircraft, Middletown, Conn. Connecticut Advanced Nuclear Engineering Lab.). July 16, 1965. Contract AT(30-1)-2789. 138p. Dep. mn; CFSTI $4.00 cy, $1.00 mn.

Summaries of the acquisition and evaluation of instruments for liquid metal level measurement, neutron flux sensors, gas analysis, process sensors, and vacuum systems are presented. The endurance and drift of Nb-1 Zr alloy sheathed, alumina insulated Chromel/Alumel, Mo/Nb, and W-5 Re/W-26 Re thermocouples was measured to 2300°F. Test results show that Chromel/Alumel thermocouples can be used successfully for long durations at 2200°F and that Mo/Nb and W-5 Re/W-26 Re thermocouples can be used at 2300°F. The design of thermocouples intended for use in Li was varied in order to attain compatibility with the Li. (W.L.G.)

44349 (RT/EL(65)-3) DIZIONARIO DELLA STRUMENTAZIONE NUCLEARE E DELLA TERMINOLOGIA AD ESSA RELATIVA. (Dictionary of Nuclear Instrumentation and Relative Terminology). (Comitato Nazionale per l'Energia Nucleare, Rome (Italy)). Feb. 1965. 284p. Dep. mn.

Terms and words associated with nuclear instrumentation and related fields are defined, and the corresponding English and French expressions are given. An index in English and French with reference to the corresponding Italian terms is also included. (D.C.W.)

44350 (SC-R-65-959) A PRECISION ANALOG MEMORY WITH NONDESTRUCTIVE READOUT USING MULTIAPERTURE FERRITE CORES. Wilken, Andrew C. (Sandia Corp., Albuquerque, N. Mex.). Aug. 1965. Contract AT(29-1)-789. 15p. Dep. mn; CFSTI $1.00 cy, $0.50 mn.

The utilization of a square-loop multiaperture ferrite core in conjunction with solid-state switches results in a device that is capable of nondestructively interrogating the flux content about the core's minor aperture. The minor aperture flux can be controlled by a signal applied to the major aperture. The minor aperture flux quantity is the frequency controlling element of a readout oscillator which is the interrogator. There is, therefore, an analog input to frequency output which can be easily calibrated. The circuit can be operated in a completely passive mode at all times except during the interrogation cycle. The information, once stored as a flux reversal in the multiaperture core, can be maintained for an infinite time interval or until reset. (auth)

44351 (SGAE-E-4/1965) AUSDRUCKVERFAHREN FUER ELEKTRONISCHE IMPULSZAEHLER. (Express Method for Electronic Pulse Counters). Attwenger, W.; Petreczek, K. (Oesterreichische Studiengesellschaft fuer Atomenergie G.m.b.H., Seibersdorf). Mar. 1965. 21p. Dep. mn.

For automatic measurements in nuclear research, scalers with printout units are used. An electronic circuit is described, which allows the print-out of collected data from one or more scalers. The printer is a common adding machine. (auth)

44352 (UJV-1339/65) MERICE A STABILISATORY MAGNETICKYCH POLI. (Magnetic Field Gage and Stabilizer). Kulhanek, J.; Dobias, F. (Ustav Jaderneho Vyzkumu, Ceskoslovenska Akademie Ved, Rez). May 1965. 20p. Dep. mn.

For the accurate measurement of the magnetic fields of a spectrometer and deflection magnet, a series of instruments were developed that make possible not only measurement but also stabilization to more than 5×10^{-5}. The instruments work on the principle of magnetic resonance. The field measurement device is designed for the measurement of homogeneous magnetic fields in the area from 0.1 to 1.9 T. It consists of 5 exchange probes, and the signal is observed on an oscillograph. The stabilizer, with a range of 0.23 to 0.73 T, is built into the multispectrograph. It is remotely operated and controlled with a stable generator of step-wise harmonic oscillations. The long-term stability is better than 10^{-6}. The stabilizer works in the range from 0.77 to 1.22 T. In the mechanical part, it possesses some improvements such as a simple control of the field stabilization. It is provided with an instrument that makes possible the reading of the function break. (tr-auth)

44353 (SLAC-Trans-22) APPLICATION OF PROTON RESONANCE TO THE MEASUREMENT OF INHOMOGENEOUS MAGNETIC FIELDS. Zhernovoy, A. I.; Egorov, Yu. S.; Latyshev, G. D. Translated by J. M. Silberstein (Stanford Linear Accelerator Center, Stanford Univ., Calif.) from Inzh.-Fiz. Zh., Akad. Nauk Belorussk. SSR, No. 9, 123-7(Sept. 1965). 8p. Dep. mn; CFSTI $1.00 cy, $0.50 mn; JCL $1.10 fs, $0.80 mf.

A description is given of nuclear resonance equipment which makes it possible to use the phenomenon of nutation of the resultant magnetic moment of protons of water for the measurement of inhomogeneous magnetic fields. The choice of optical parameters is considered and accuracy of the measurement is estimated. (M.O.W.)

44354 A THEORETICAL ASSESSMENT OF THE POSSIBILITY OF SELECTED-AREA MASS-SPECTROMETRIC ANALYSIS USING A FOCUSED ION BEAM. Long, J. V. P. (Cambridge Univ., Eng.). Brit. J. Appl. Phys., 16: 1277-84(Sept. 1965).

The possibility of making selected area mass-spectrometric measurements on plane specimens of metals and rocks, with a resolution of a few micrometres, by means of a focused ion probe and a conventional mass spectrometer is discussed. The ion beam intensities expected at the detector of the mass spectrometer and the current obtainable in the primary ion beam used for bombardment of the specimen are calculated. The results obtained suggest that ratios of isotopic abundance should be measurable to a reproducibility of approximately 0.1% on areas of a few micrometers diameter when the mass concentration of the element in the specimen and the abundance of its isotopes are greater than about 10%. (auth)

44355 THE INVESTIGATION OF THE EFFECT OF SMOKE ADMIXTURES ON THE CURRENT INTENSITY IN IONIZATION CHAMBERS. Terlecki, J. (Medical University, Gdansk, Poland); Figwer, J. Exptl. Tech. Physik, 13: 204-9(1965). (In German).

The results of a study on the effects of smoke admixtures on the current intensity in ionization chambers are reported. The purpose was to establish data for the development of ionization fire alarms. The working mechanism of the ionization fire alarm depends upon the charging of the aerosols forming the smoke by the collision with light ions in an ionizing medium. The heavy ions formed on both signs have a low mobility which leads to a significant reduction of the ionization current. An ionization and a photoelectric method for smoke detection are compared. (tr-auth)

44356 A SYSTEM TO CONTROL THE EXCITING CURRENT OF ELECTROMAGNETS OF NUCLEAR MAGNETIC-RESONANCE (NMR) SPECTROMETERS. Dekabrun, L. L.; Mkrtchyan, A. R. (Inst. of Chemical Physics, Academy of Sciences, USSR). Izv. Akad. Nauk Arm. SSR, Ser. Fiz. Mat. Nauk, 18: 140-52(1965). (In Russian).

In order to investigate crystal order-disorder by NMR spectroscopy methods, a source of the main magnetic field H_0 which meets all the requirements was developed. The power-supply system for the electromagnet is described. An electronic current stabilizer of the series type is used. The effect of line voltage oscillations is neutralized by the use of an electromechanical transducer with relatively coarse electronic stabilization of output voltage. The initial value of the exciting current of the electromagnet and the law of its scanning in time are established by means of two independent reference voltage sources in the current stabilization system. Since the scanning time may exceed two hours, mechanical scanning by means of a synchronous motor is employed. A specially developed reference voltage source is used: silicon stabilitron tubes with temperature-compensating dividers. The stabilization system uses 6S18S high-power triodes, with an optimal operational mode assured. The special design of the interruptor and error signal amplifier assures reliable amplification of microvolt signals. The control resistance is made of manganin wire in the form of a bifilar loop. A lack of correspondence was found between the actual behavior of the stabilization system and the behavior which might be expected on the basis of the generally accepted electromagnet substitution circuit. As a result, the pass band of the amplifier has to be limited, which operation is accomplished by increasing the time constant of the synchronous detector. (CFSTI)

44357 DEVELOPMENTS IN THE INSTRUMENTATION FOR PHYSICS RESEARCH. Quercia, I. F. (Comitato Nazionale per l'Energia Nucleare, Rome). Nuovo Cimento (1), 2: Suppl., 602-51(1964). (In Italian).

A review is given of the recent developments in the instrumentation in various fields of physics: ultrahigh vacuum techniques; cryogenic apparatus; high magnetic fields; the microtron, an electron accelerator; optical instrumentation applied to the diagnosis and spectroscopy of plasmas; image intensifiers; electronic automation in high-energy physics; and detection of elementary particles at high energies. 88 references. (J.S.R.)

44358 CONTROL SYSTEM FOR PULSED ELECTRON-OPTICAL TRANSFORMERS. Korobkin, V. V.; Malyavkin, L. P.; Shchelev, M. Ya. (Inst. of Physics, Moscow). Pribory i Tekhn. Eksperim., No. 4, 129-33(July-Aug. 1965). (In Russian).

The diagram of the pulsed electron-optical transformer control system with increased image intensity, that makes it possible to obtain single copies and linear scanning of fast processes, was described. The time for the exposure of one frame and the duration of the scanning smoothly covers the range from 0.3 μsec to 10 msec. The startup is produced immediately from the process investigated or with delays of 3 μsec to 3 msec. During tuning periodic operational regimes with frequencies of 50 Hz were used. The committed capacity in dynamic regime is 30 strokes/min in the central frame and 20 strokes/min at the border. The maximum speed of scanning on a screen is 10^8 mm/sec, which with length of scanning on electron optical transformer screens is equal to 20 mm, corresponds to resolution times of 5×10^{-10} sec. (tr-auth)

44359 COAXIAL MERCURY RELAY (Engineering Materials). (Lawrence Radiation Lab., Univ. of California, Berkeley). (CAPE-1258).

20 drawings.

The device described is an electronically operated SPDT switch capable of high voltage applications. The unit was designed to be switched with the high voltage turned off. It consists of a shielded coaxial mercury relay capsule and a relay driver circuit. The mercury relay capsule is used to handle high voltage pulses to 3 kv at less than 1 ma. The relay driver circuit requires a power input of +12 v and a signal level of +4 v to actuate the relay. A system, which uses 50 to 75 of these units, is used as a test setup to check the output of several photomultiplier tubes in connection with a multichannel scaler system. (For Details, See TID-4100) (F.J.H.)

44360 OSCILLOSCOPE (Engineering Materials). (Lawrence Radiation Lab., Univ. of California, Livermore). (CAPE-1072).

124 drawings.

The oscilloscope described provides a high-resolution method of measuring time intervals in the range of 0.5 to 100 μsec. A raster display obtained high resolution, using a technique similar to that used in reproducing a television picture, by having the electron beam move in a vertical and horizontal direction simultaneously. The raster display gave a sweep length equivalent to the number of lines times the interval of a single line, and made optimum use of the tube face for displaying data. The cathode ray tube contained 3 sets of deflection plates: two were used to sweep the beam to present the raster display and the remaining set was used to deflect the beam with pulses that were timed. A second indicator, also a cathode ray tube was used to measure a pulse that may occur during the retrace time of the master display. A separate horizontal sweep circuit was used to provide the sweep for the slave. The timing generator, used for the master, was also used to provide a delayed sweep trigger for the slave. The same vertical sweep, intensifier generator, and marker generator, and marker generator were used for the slave and the master. (For Details, See TID-4100) (F.J.H.)

44361 RHODA—RAPID HAND-OPERATED DIGITIZING APPARATUS. Frisch, O. R. (Cambridge Univ., Eng.). 2p. (CONF-650510-15). Gmelin, AED-CONF-65-110-11.

From Purdue Conference on Instrumentation for High Energy Physics, Lafayette, Ind.

A brief report is presented on the construction and operation of the RHODA hand-operated digitizing apparatus used for scanning and measurement of particle track pictures. (L.B.S.)

44362 SAFETY FLUOROSCOPE WITH AN ALERTING DEVICE OF CONTRASTING COLOR SURROUNDING THE SCREEN. Wyatt, Samuel B.; Alexander, Sidney; Masi, Frank J. (to United States Radium Corp.). U. S. Patent 3,197,636. July 27, 1965. Filed Dec. 28, 1962.

In order to minimize exposure of an x-ray fluoroscopist to x-rays passing beyond the edges of the fluoroscope, the fluoroscope is provided with an indicating border that produces continuous visible warning to the fluoroscopist whenever the x-ray beam diverges beyond the working area of the fluoroscope screen even at very low levels of radiation or screen brightness. This border can be incorporated in the screen itself, in the frame around the screen, or in both. (A.G.W.)

44363 APPARATUS FOR PRODUCING VISUAL IMAGES OF X-RAYED OBJECTS. Arrison, Robert A. Jr.; van der Velden, Cornelius G. (to Laboratory for Electronics, Inc.). U. S. Patent 3,198,947. Aug. 3. 1965. Filed Feb. 21, 1961.

In a system for controlling the brightness of a fluoroscopic image produced by x-rays, the image intensifier element is used as a transducer to derive an electrical signal indicative of the brightness of the produced image. This signal is compared with a preset reference signal, and the difference is fed through a control circuit to vary the high voltage applied to the x-ray tube. (A.G.W.)

44364 TIMING CIRCUITRY INCORPORATING RADIOACTIVE BATTERIES. Wallack, Stanley (to Leesona Corp.). U. S. Patent 3,200,300. Aug. 10, 1965. Filed Nov. 9, 1955.

An electrical device includes a timing unit energized by a first radioactive battery and a fail-safe circuit connected to the timing unit and energized by a second radioactive battery. The power supply for the timing unit periodically energizes an impulse counter by a timed sequence of pulses applied from a timing network. The impulse counter preferably has at least a pair of contacts, of which one is actuated in response to each energizing pulse applied to the counter and the other is actuated in response to a predetermined number of pulses applied to the counter. The fail-safe circuit is designed to operate in response to an interruption in the periodic actuation of the first contact. (A.G.W.)

Radiation Detection

Refer also to abstracts 44321, 44332, 44333, 44335, 44966, 45289, 45291, and 45560.

44365 (AECL–2219) A CONTROL AND READ-OUT SYSTEM FOR THE CHALK RIVER DOUBLE CRYSTAL γ-SPECTROMETER. Howell, W. D.; Shorey, W. R. J. (Atomic Energy of Canada Ltd., Chalk River (Ontario)). Apr. 1965. 107p. Dep.; AECL $1.00.

The Chalk River Double Crystal γ-Spectrometer designed for precision measurement of gamma ray energies requires, as part of its automatic positioning system, a control unit to program the direction and running time of three motors. Two of these motors control the rotation of the two diffracting crystals and the third controls the angular measuring device which tracks the movement of the crystals. The motors are operated in incremental steps which are measured by microswitches riding on the teeth of spur gears in the drive mechanism. On completion of a required spectrometer increment a coupling operation is performed on the gamma beam for a preselected time. The read-out system then records the accumulated data on a Brown recorder, an IBM typewriter and, if desired, on a tape punch in either IBM (8 hole) or Datatron (7 hole) code. The spectrometer is programmed to scan back and forth across a gamma line, reading the data as it proceeds. The spectrometer motor control system and the operating instructions for the associated General Purpose read-out system are described. (auth)

44366 (AED-C–06-12) INSTRUMENTS AND MEASURING TECHNIQUES IN NUCLEAR PHYSICS. Series C. Bibliographies. Debertin, K. (comp.) (Institut fuer Kernphysik, Universitaet Frankfurt (West Germany)). Mar. 1965. 217p. Dep. mn.

A bibliography on instruments and measuring techniques in nuclear physics is presented. The instrumentation covers a wide range of electronic equipment for nuclear physics applications. A considerable number of reports on radiation detection instruments are listed. Reports on various bubble chamber measuring techniques are also listed. (M.O.W.)

44367 (AEEW-M–650) CALCULATED ENERGY RESPONSE OF LITHIUM FLUORIDE FINGER-TIP DOSIMETERS. Johns, T. F. (Atomic Energy Establishment, Winfrith (England)). July 1965. 14p. Dep.; BIS $0.50; HMSO 2s. 6d.

Calculations were made of the energy response of the lithium fluoride thermoluminescent dosimeters being used at A.E.E. Winfrith for the measurement of radiation doses to the finger-tips of people handling radioactive materials. It is shown that the energy response is likely to be materially affected if the sachet in which the powder is held contains elements with atomic numbers much higher than 9 (e.g., if the sachet is made from polyvinyl chloride). (auth)

44368 (AERE-M–633) PULSE SHAPE DISCRIMINATORS FOR SCINTILLATORS CONTAINING ZnS(Ag). Wraight, L. A. (Atomic Energy Research Establishment, Harwell (England)). Aug. 1965. 17p. Dep.; BIS $0.70; HMSO 3s. 6d.

Pulse shapes in ZnS(Ag) for alpha and electron excitation were observed and were found to be different. The nature of the short electron pulses was investigated. On the basis of the observations, efficient pulse-shape discriminators were devised and tested. (D.C.W.)

44369 (AERE-R–4552) REPORT ON DEVELOPMENTS IN HEALTH PHYSICS INSTRUMENTS IN ELECTRONICS DIVISION, A.E.R.E. Abson, W.; Loosemore, W. R. (comps. and eds.) (Atomic Energy Research Establishment, Harwell (England)). Feb. 1964. 73p. (CONF-640304–1). Dep.; BIS $2.80; HMSO 14s. 0d.

From Second Health Instrument Users Symposium, Harwell, Berks, Eng.

A general summary and review of research and development work on topics related to Radiological Protection and Health Physics instrumentation are presented. Separate topics are discussed concerning the following: external β–γ monitoring instruments, neutron monitoring instruments, monitoring instruments for surface contamination, personal beta/gamma dose and dose-rate measurements, gamma spectrometers for district survey, monitoring instruments for radioactive air particulates, and some additional instrumentation topics. (M.O.W.)

44370 (AERE-R–4883) NEW METHODS OF MEASURING NEUTRON DOSE EQUIVALENT RATE AROUND PULSED NEUTRON GENERATORS. Leake, J. W. (Atomic Energy Research Establishment, Harwell (England)). June 1965. 20p. Dep.; BIS $0.60; HMSO 3s.

Two methods of measuring neutron Dose Equivalent (DE) around pulsed machines are described. Both methods employ the moderator system of the neutron counter assembly T. 1940A (which is based on the Andersson–Braun counter), with either the standard T. 1940A boron trifluoride pulse counter or a BF_3 ion chamber mounted at the center. The limitations of the T. 1940A with the pulse-type counter and the advantages of the ion chamber version are discussed. It is shown that under favorable conditions the T. 1940A with a pulse-type counter is able to measure pulsed radiation, with less than 2% count loss, up to a mean DE rate of 1 rem/hr. The response of both systems is proportional to DE rate (as recommended by the I.C.R.P. 1963) within ±50% for neutrons of all energies from thermal to 12 Mev. (auth)

44371 (AERE-R–4921) THE PREPARATION OF LITHIUM-DRIFTED GERMANIUM DIODES AND THEIR USE AS GAMMA RAY DETECTORS. Hooton, B. W. (Atomic Energy Research Establishment, Harwell (England)). July 1965. 15p. Dep.; BIS $0.50; HMSO 2s. 6d.

The advantages of Ge over Si for γ spectroscopy are described. The operation principle and preparation stages of Li-drifted Ge reverse-biased p-i-n junctions are described. During the evaluation of detector characteristics, the effective detector volume, resolution, and γ-ray spectra characteristics were determined. (D.L.C.)

44372 (AFCRL–65–470) FERROUS AMMONIUM SULFATE–CUPRIC CHLORIDE SOLUTIONS FOR DOSIMETRY OF A KILOCURIE ^{60}Co SOURCE. Physical Sciences Research Papers, No. 116. Burke, E. A.; Jimenez, C. M.; Lowe, L. F.; Mulligan, M. (Air Force Cambridge Research Labs., L. G. Hanscom Field, Mass.). June 1965. 24p. CFSTI.

Aqueous solutions of ferrous ammonium sulfate with cupric chloride were studied as a means for determining

the uniformity of the dose rate around a multi-kilocurie cylindrical array of cobalt-60. Reagent grade chemicals and ordinary distilled water were used in all solutions tested. Ferric ion was measured spectrophotometrically at 305 millimicrons. The solution selected to satisfy the requirements for dosimetry contained 5×10^{-4} M ferrous ammonium sulfate and 5×10^{-3} M cupric chloride in 10^{-3} N sulfuric acid. At higher ferrous and cupric ion concentrations, spurious oxidation of the ferrous ion occurred within a short time. At higher acid concentrations, the solutions were not only unstable but also yielded a non-linear production of ferric ion with dose. Spectrophotometric measurements of ferric ion were made in solutions brought to 0.15 N acid concentration, instead of the conventional 0.8 N, in order to minimize spurious oxidation. The molar extinction coefficient at this normality proved to be the same as that in 0.8 N solutions. The G value, as compared to the standard ferrous-ferric dosimeter, was 0.65. Using these solutions, no detectable variation in dose rate was found at symmetrically equivalent positions at the center of the cobalt-60 source. The average dose rate at each end of the cylindrical array proved to be 12 percent lower than that at the center. The dose rate was also less uniform at the ends, varying by ±4 percent from point-to-point. At a distance of fifteen inches from the center of the source array, the dose rate decreased as the square of the distance. (auth)

44373 (ANL-6877, pp 15-20) ELECTRON-NEUTRON INTERACTION. Krohn, Victor E. Jr. (Argonne National Lab., Ill.).

In connection with an experiment on the electron-neutron interaction, some mixtures of ^{3}He, neon, and methane were investigated and found to have advantages as fillings for proportional counters to detect thermal neutrons. Mixture ratios are given. (auth)

44374 (AROD-3347:6) PARTICLE PHYSICS AND NUCLEAR DECAY. CANCELLATION OF PHOTOMULTIPLIER GAIN DRIFT FOLLOWING SOURCE INTENSITY CHANGE. Technical Report No. 1. Brimhall, James E.; Page, Lorne A. (Sarah Mellon Scaife Radiation Lab., Univ. of Pittsburgh, Pa.). July 31, 1965. 83p. CFSTI.

A set of tests performed on several representative tubes (Du Mont type 6292 and RCA type 6342-A) is reported. A principal result is that a cancellation method is evolved which uses a deliberate change in the high voltage to immediately erase the memory of each source intensity change. For several tubes the empirical characteristic curves, relating anode current to high voltage subject to zero gain drift, were determined and extensively tested. The range of validity of the cancellation method in terms of ambient temperature, spectrum, intensity level, was studied. Although a limitation was found at higher temperatures (~50°C), the characteristic curves are valid down to 0°C. It is established that the seat of these gain drifts is neither in the photocathode region nor in the anode region and seems most likely to be distributed over the ten dynode surfaces. Included are a number of connecting topics, each important to an understanding of the main tests, such as: temperature sensitivities of photomultipliers, of NaI scintillators, of light-pipers, NaI afterglow, and grid control of tube current. Grid control, itself a method of preventing gain drift, was validated by a set of tests. (auth)

44375 (BNL-9425) NEON-HYDROGEN BUBBLE CHAMBERS. Albert, R. C.; Goodzeit, C. L.; Pechar, F. C.; Prodell, A. G. (Brookhaven National Lab., Upton, N. Y.). Aug. 1965. Contract AT(30-2)-Gen-16. 15p. (CONF-650802-7). Dep. mn; CFSTI $1.00 cy, $0.50 mn.

From Cryogenic Engineering Conference, Houston, Tex.

Tracks were observed in various liquid neon-liquid hydrogen mixtures in the 20-inch Brookhaven National Laboratory Bubble Chamber. Neon-hydrogen mixtures were used whose radiation lengths varied from that of pure hydrogen to values less than that of propane. Separation of some of the mixtures into two liquid phases was also observed. Properties of the liquid-vapor system and operating conditions of the bubble chamber are discussed. (auth)

44376 (BNL-9466) A THRESHOLD GAS ČERENKOV COUNTER FOR USE AT THE BROOKHAVEN A.G.S. Rubinstein, R. (Cornell Univ., Ithaca, N. Y. Lab. of Nuclear Studies). [1965]. Contract AT(30-2)-Gen-16. 11p. Dep. mn; CFSTI $1.00 cy, $0.50 mn.

A threshold gas Cherenkov counter is described that has a fast (56 UVP) photomultiplier for use with high counting rates (on the order of 10^7 cps). The use of the detector for discriminating pions from heavier particles in momentum-analyzed beams having momenta of 4 to 12 Bev/c is described. (T.F.H.)

44377 (CERN-65-4(Vol.I)) Vth INTERNATIONAL CONFERENCE ON NUCLEAR PHOTOGRAPHY HELD AT CERN, GENEVA, 15-18 SEPTEMBER 1964. Lock, W. O. (ed.) (European Organization for Nuclear Research, Geneva (Switzerland)). Jan. 1965. 121p. (CONF-787 (Vol.I)). Dep. mn.

Separate abstracts were prepared for five of the eight papers included. Two other papers were abstracted previously in NSA (19: 4485 and 15859). The remaining paper, in summary form, deals with charged particle tracks in solids and their applications in nuclear physics and geophysics. (D.C.W.)

For abstracts of individual papers see: 44378-44382.

44378 (CERN-65-4(Vol.I), pp 1-15) RADIATION DETECTION IN LARGE CRYSTALS OF SILVER CHLORIDE: A SURVEY AND REPORT OF RECENT EXPERIMENTS. Childs, Charles B.; Slifkin, Lawrence M.

The use of large single crystals of silver chloride in the detection of charged particles is discussed. A brief survey of radiation damage phenomena and of the decoration process is given, and some results obtained with silver chloride detectors are reviewed. Unsolved problems and experiments now in progress are also discussed. (D.C.W.)

44379 (CERN-65-4(Vol.I), pp 29-41) NOUVEAUX MATERIAUX PHOTOGRAPHIQUES POUR LES RECHERCHES NUCLEAIRES. (New Photographic Materials for Nuclear Research). Bogomolov, C. S.

Some studies made in the development of new photographic materials for nuclear studies are examined. A detailed review is given of the properties of NIKFI emulsions. (J.S.R.)

44380 (CERN-65-4(Vol.I), pp 45-63) QUELQUES PROPRIETES DES EMULSIONS NUCLEAIRES. (Some Properties of Nuclear Emulsions). Cueer, P.

A summary is given of the emulsion characteristics most neglected in the literature. The characteristics discussed are optical and mechanical properties, the latent image in corpuscular photography, sensitivity threshold, topography of the latent image, edification of the latent image, spontaneous evolution of the image, and dating of the events. The varieties of ionographic emulsions are also considered. The tendencies to be encouraged are indicated, and fine measurements with the electron microscope are mentioned. (J.S.R.)

44381 (CERN-65-4(Vol.I), pp 79-87) MEASUREMENTS IN NUCLEAR EMULSIONS--INTRODUCTORY TALK FOR SESSION IX. Herz, A. J.

The suitability of nuclear emulsions for investigations of elementary particles is briefly discussed, with specific consideration of some sources of errors in emulsion measurements. (D.C.W.)

44382 (CERN-65-4(Vol.I), pp 105-10) THE FUTURE PERSPECTIVES FOR EMULSION WORK AT CERN--CLOSING TALK. Gregory, B. P.

Some of the more successful, recent applications of emulsion techniques in high-energy physics are outlined, and the immediate future of these experiments is considered. (D.C.W.)

44383 (CERN-65-4(Vol.II)) Vth INTERNATIONAL CONFERENCE ON NUCLEAR PHOTOGRAPHY HELD AT CERN, GENEVA, 15–18 SEPTEMBER 1964. Dahl-Jensen, E. (ed.) (European Organization for Nuclear Research, Geneva (Switzerland)). Jan. 1965. 387p. (CONF-787 (Vol.II)). Dep. mn.

Seventy-one papers are presented on various aspects of nuclear photography. Separate abstracts were prepared for 63 of the included papers. Four papers appeared previously in NSA as 19: 3029, 14209, 16858, and 27501. Four papers appeared only as summaries and were not abstracted for NSA. (M.O.W.)

For abstracts of individual papers see: 44384–44445, and 45474.

44384 (CERN-65-4(Vol.II), pp I1-8) ENREGISTREMENTS DE TRACES INDIVIDUELLES DANS DIVERS MATERIAUX SOLIDES. (Recordings of Individual Tracks in Various Solid Materials). Debeauvais, Monique.

The recording of α tracks in different types of nitrocelluloses and, in particular, in the commercial product celluloid (nitrocellulose plastified with camphor) was studied. Po α sources were used, and the experimental apparatus is described. The effects of the reagent selective etching and the temperature on the registration sensitivity were determined. The results show that all of the nitrocelluloses could be used to detect low-energy α particles. The conditions for the registration of the particles were defined. (J.S.R.)

44385 (CERN-65-4(Vol.II), I12-19) DOSIMETRIE DE NEUTRONS LENTS PAR ENREGISTREMENT DES TRACES DE FISSION DANS LES ISOLANTS. (Dosimetry of Slow Neutrons by Recording the Fission Tracks in Insulators). Mory, J.; Walker, R. M.

When an insulator is irradiated with particles sufficiently heavy and energetic, these particles damage the material leaving tracks visible to the microscope after an appropriate chemical attack. The fact that the tracks are hollow channels after chemical attack was investigated to determine the usefulness of this phenomenon for the detection of slow neutrons. The variation of the resistance of the insulator after chemical attack is a function of the number of hollow channels. Mica and plastic membranes were tested as neutron detectors. Neither gave reproducible results and absolute values; however the neutron flux can be measured to more than 50%. The limits of utilization of the method are discussed. (J.S.R.)

44386 (CERN-65-4(Vol.II), pp I21-5) DECORATION DES TRACES DE PARTICULES CHARGEES DANS DES MONOCRISTAUX DE CHLORURE D'ARGENT. (Decoration of Tracks of Charged Particles in Silver Chloride Monocrystals). Bilwes-Girardin, L.; Schmitt, R.

Studies on the decoration of tracks of charged particles in silver chloride monocrystals were investigated using an apparatus designed by Childs. The quality of the decoration and the intensity of the granular cloud differ from a cloud of decorated dislocations and vary to a great degree from one sample to another. No difference in structure of the zones decorated with α particles could be detected with respect to neighboring zones where only the dislocations were decorated. It was noted that the α tracks are located in a surface layer of the crystal where the decoration mechanism can be different from that of the internal mass of the crystal. The nature and the concentration of impurities in the crystal and probably the method used for the crystal anneal seem to be predominant factors in the decoration of particle tracks. (J.S.R.)

44387 (CERN-65-4(Vol.II), pp II1-10) INVESTIGATIONS ON THE TOPOGRAPHY OF THE LATENT IMAGE. Moisar, E.

A study is made on the concept that upon particle exposure a latent image is formed predominantly at the surface of the silver bromide grains of a photographic emulsion. The experimental results for the photographic response of a set of four AgBr-emulsions with grain sizes ranging from .15 to 1.0 μ are presented. Conclusions from the study are: the topography and dispersity of the latent image varies according to the intensity and the duration of the exposure, an even distribution of latent image specks throughout the grain is obtained after low-intensity light exposure, and that particle exposure and very short light exposure lead to a preferential formation of a surface image and the absence of an internal image. (M.O.W.)

44388 (CERN-65-4(Vol.II), pp II11-16) SUR LA DISPERSION RELATIVE DE L'IMAGE LATENTE. (The Relative Dispersion of the Latent Image). Nicolae, M.

The relative dispersion of the latent image under the action of α particles, electrons, and light were studied using the method of redox potential. The results were interpreted from the viewpoint of the chemical kinetics by the relation existing between the dimension of the development center and its autocatalytic action. For this purpose the kinetics of development for these three images were followed in the emulsions NIKFI R and IFA EN_2. For the relations established between the speed of development and the redox potential of the detector it was possible to characterize the relative dispersion of the latent images in the following series: α particles, electrons, and light. (J.S.R.)

44389 (CERN-65-4(Vol.II), pp II17-18) DIFFERENCIATION AU MICROSCOPE ELECTRONIQUE D'EMULSIONS D'ORIGINES DIVERSES AYANT SUBI DES IRRADIATIONS α OU β. (Electron Microscopic Differentiation of Emulsions Having Different Origins Exposed to α or β Irradiations). Riedel, G.

Three emulsions (Agfa, Ilford L4, and Gevaert) were exposed to α or β irradiation and the advantages of each for microscopic observation were determined. During development the Ilford emulsion showed the worst adhesion to the support. The grain size of the silver was varied by reducing the time of development. The results are tabulated for the three emulsions with respect to the number of grains per micron of the length of the track and the length of the track in microns for two types of developers. (J.S.R.)

44390 (CERN-65-4(Vol.II), pp II19-28) METHOD FOR INCREASING THE STABILITY OF SENSITIVITY AND LATENT IMAGE OF NUCLEAR EMULSIONS. Romanovskaya, C. M.; Bogomolov, C. S.; Deberdeev, M. Yu.

It was previously suggested that an increase in photosensitivity was stated to occur in the course of storage of emulsion layers capable of recording minimum ionization particles under low humidity (conditioned over dry calcium chloride) and higher temperature conditions. A detailed study of this phenomenon in view of its practical application is presented. (M.O.W.)

44391 (CERN-65-4(Vol.II), pp II29-42) LATENSIFICATION DE L'IMAGE LATENTE DANS LES EMULSIONS IONOGRAPHIQUES. (Latensification of the Latent Image in Ionographic Emulsions). Schmitt, R.; Demoulin, R.; Bilwes-Giradin, L.

The parallelism existing between the latent images caused by exposure to particles and to a brief illumination with light was studied in parallel using Ilford ionographic emulsions. The particles used were α particles from ^{210}Po and β radiation from ^{204}Tl. The results obtained on the reinforcement of light were reported with particular emphasis on the effect of the wavelength of the post irradiation and the effect of the type of emulsion. It appears from the study that there is a continuity between the latensification and the Herschel effect. A maximum of latensification for all the light used for the post exposure was observed; the value of this maximum decreases when the light passes from the near ultraviolet to the region of the Herschel effect. The reinforcement by latensification of the latent image of particles is comparable to that of the brief illumination when the difference of the distribution of the energy given to the grains for the two types of exposure are taken into consideration. However, the practical utilization of the latensification of the latent images of particles is handicapped by the strong absorption of light in the aged emulsion. (J.S.R.)

44392 (CERN-65-4(Vol.II), pp II44-9) THE SENSITIVITY CENTRES AND LATENT IMAGE DISTRIBUTION

AS FACTORS OF NUCLEAR EMULSION PROPERTIES. Zizic, B.; Vukovic, J.

The effect of active impurities on AgBr microcrystals is investigated in order to synthesize ultrafine ionographic high sensitivity emulsions. Substances whose ions can form solid solutions in AgBr crystals are used as the active impurities. The distribution of inner sensitivity centers is adjusted according to the method of additional crystallization of emulsions. A discussion is given of the method of study and the results obtained. (M.O.W.)

44393 (CERN-65-4(Vol.II), pp II50-63) A STUDY OF THRESHOLD OXIDATION AND DEVELOPMENT OF LATENT IMAGE FORMED BY CHARGED PARTICLES IN NUCLEAR EMULSIONS. Kocherov, N. P.

The influence of the size of haloid silver grains and gold concentration in an emulsion upon the value ΔE_{min} (difference between the oxidation-reduction potential of the developer and the silver electrode) as well as on the relation between characteristics of charged particle tracks and the magnitude of the oxidation-reduction potential of the developer is discussed. (M.O.W.)

44394 (CERN-65-4(Vol.II), pp II65-74) SUR LES CENTRES DE SENSIBILITE ET LES CENTRES DE DEVELOPPEMENT DE L'EMULSION NUCLEAIRE NONSENSIBILISEE. (The Centers of Sensitivity and the Centers of Development of Nonsensitized Nuclear Emulsions). Samoilovich, D. M.

The processes for the increase of the sensitivity in nonsensitized emulsions were studied. The sensitivity limit as a function of the conditions of chemical maturation was determined. The results obtained were compared with the known data for emulsions sensitized with gold. The sizes of the sensitivity centers and of the latent image centers were evaluated. The studies were made on nonammoniacal emulsions, the synthesis of which is given. (J.S.R.)

44395 (CERN-65-4(Vol.II), pp II75-87) SUR LES CENTRES DE SENSIBILITE DES EMULSIONS NUCLEAIRES SENSIBILISEES SUCCESSIVEMENT D'OR ET DE TRIETHANOLAMINE. (The Sensitivity Centers of Nuclear Emulsions Sensitized Successively with Gold and Triethanolamine). Samoilovich, D. M.; Ardachev, I. V.; Barinova, E. S.

The composition of the sensitivity centers of nuclear emulsions sensitized during chemical maturation successively with gold salts and triethanolamine before irradiation was analyzed. The analysis of the results showed the augmentation of the sensitivity due to the formation of the adsorbed layers on the surface of the microcrystals of silver halogenide is not confirmed when the sensitivity of the irradiated emulsion in a solution of triethanolamine is not increased. The reduction mechanism of the sensitization which includes the accumulation of atomic silver in the sensitivity centers is no longer confirmed because of the hypersensitization effect. It is assumed that the treatment of the emulsion by triethanolamine before irradiation leads to the formation of two combinations; the first, a very high solubility combination and the second, the formation of an insoluble combination in the water which leads to the increase of the sensitivity and the increase of the size. These two combinations can be present simultaneously. The state of the sensitivity center of the emulsion in all the stages of hypersensitization is described. (J.S.R.)

44396 (CERN-65-4(Vol.II), pp III1-4) SUR LA PREPARATION ET LES CARACTERISTIQUES D'UNE EMULSION NUCLEAIRE TRES CONCENTREE. (The Preparation and the Characteristics of a Very Concentrated Nuclear Emulsion). Apostol, A.; Nicolae, M.

The method for the preparation of an ionographic emulsion having a AgBr concentration of 93 to 94% is described. The sensitivity of the emulsion to particles and to electrons in comparison to the usual emulsions was evaluated by the method of counting the grains on the tracks as well as by the method of direct blackening. Although the grain density on the tracks was superior for the concentrated emulsions, the density of the grain was not superior. (J.S.R.)

44397 (CERN-65-4(Vol.II), pp III5-11) PREPARATION OF EMULSION STACKS FOR UNDERGROUND COSMIC RAY EXPERIMENTS. Cottrell, Don M.; Kirk, J. A.; Lord, J. J.; Piserchio, R. J.

The preparation of emulsion stacks as large as one liter is reported. The emulsion stacks are made completely underground for use in study of cosmic radiation. The detailed descriptions of the materials and the procedure for preparing the emulsion stacks are included. (M.O.W.)

44398 (CERN-65-4(Vol.II), pp III12-16) LOADING OF EMULSIONS WITH DIAMONDS AND POLYSTYRENE FOR EXPERIMENTS WITH STOPPING K-PARTICLES. Davis, Dianne M.; Lord, J. J.; Piserchio, R. J.; Behroozi-Toosi, Fereidoon.

Two experiments are presented which may give considerable insight into the properties of certain hyperfragments and hyperon resonances which are produced in meson (K) stopping, loaded emulsions. In the two experiments described; first, carbon was introduced into the emulsion in the form of diamond powder, and in the second experiment thin sheets of polystyrene were placed between two layers of ordinary nuclear track emulsions. (M.O.W.)

44399 (CERN-65-4(Vol.II), pp III17-20) LOADING OF NUCLEAR EMULSION WITH LIGHT AND HEAVY ELEMENTS. Ganguli, S. N.; Kajarekar, P. J.; Swami, M. S.

The details of an experiment to load electron sensitive emulsions with salts of lithium and bismuth, and diamond in crystal form, are presented. The procedure for mixing the solution directly with the emulsion liquid gel is outlined. (M.O.W.)

44400 (CERN-65-4(Vol.II), pp III31-56) APPLICATION OF SYNTHETIC POLYMERS IN PREPARATION OF FINE-GRAIN NUCLEAR EMULSIONS. I. PROPERTIES OF FINE-GRAIN EMULSION IN CASE OF PARTIAL SUBSTITUTION OF GELATINE WITH POLYVINYLACETALS. II. COAGULATION OF FINE-GRAIN NUCLEAR EMULSION BY A SYNTHETIC POLYMER. Novikova, N. P.; Zakharov, V. I.; Fadina, E. V.

In view of the advantages of polyvinylacetals as compared with other synthetic polymers for photographic nuclear emulsion, they were used for partially substituting gelatin in fine-grain nuclear emulsions. The physical, mechanical, and registration properties of these photographic layers were investigated. The study of optimum conditions for coagulation of fine-grain nuclear emulsion, for washing and sediment peptizing, and also for investigating the possibilities of creating a system which will be colloid-stable after peptizing at any value of pH, is presented. (M.O.W.)

44401 (CERN-65-4(Vol.II), pp IV1-4) TESTS ON EMULSION SENSITIVITY AT LIQUID H_2 TEMPERATURE.

Results referring to the sensitivity of Ilford K5 and G5 emulsions which were exposed at liquid N_2 and H_2 temperatures are included. The procedure for the experimental test is outlined. (M.O.W.)

44402 (CERN-65-4(Vol.II), pp IV5-15) REGRESSION OF SENSITIVITY AND LATENT IMAGE IN NUCLEAR AND LIGHT-SENSITIVE PHOTOGRAPHIC EMULSIONS. Kartuzhanskii, A. L.; Yurchenko, A. F.; Shur, L. I.; Martysh, G. G.

Several experiments were carried out in an attempt to gain information on the aging of nuclear and light-sensitive photographic emulsions. The effects of artificially aging an emulsion by means of high- or low-controlled temperatures are considered. The similarity and dissimilarity of sensitivity specks and latent image specks are examined. Results from the experiments are presented. (M.O.W.)

44403 (CERN-65-4(Vol.II), pp IV16-22) PROPERTIES OF NEW NIFKI AND ORWO NUCLEAR EMULSIONS. Krecker, U.

The development of two high sensitivity nuclear emul-

sions is reported. The composition of the ORWO-K5 is: 4.5 g amidol, 14 g sodium sulfite, 35 g boric acid, 0.8 potassium bromide, and pH = 6.6. The new NIKFI-BR2 is compared and stated to be better than NIKFI-R. Some properties of the new emulsions are presented. (M.O.W.)

44404 (CERN-65-4(Vol.II), pp IV23-31) THE PROPERTIES OF FINE-GRAINED NUCLEAR EMULSION TYPE PR-2. Perfilov, N. A.; Novikova, N. R.; Zakharov, V. I.; Fadina, E. V.

The development of nuclear emulsion type PR-2 is reported. This emulsion contains a high dispersity of microcrystals and a high sensitivity of individual emulsion crystals. For the purpose of selection of developers, tests were made with phenidon, as well as a series of quick-acting developers containing high concentrations of such developing substances as pyrocatechol, pyrogallol, or amidol. Results from these tests are presented. (M.O.W.)

44405 (CERN-65-4(Vol.II), pp IV33-40) SENSIBILITE DES EMULSIONS ILFORD K5 NORMALES ET HYPERSENSIBILISEES AUX BASSES TEMPERATURES. (Sensitivity of Normal and Hypersensitive Ilford K5 Emulsions at Low Temperatures). Ben Sedrine, T.; Weill, R.

It is observed that normal Ilford K5 emulsions exposed at –196°C keep 70% of their sensitivity at 20°C if the processing starts immediately after the warming. The sensitivity decreases when the delay between warming and processing increases. The sensitivity of hypersensitized K5 emulsion is found to remain about 70% even after 28 hours. The same experiment was repeated at liquid helium temperatures. The sensitivity is found to be so low it is difficult to get unbiased measurements. (M.O.W.)

44406 (CERN-65-4(Vol.II), pp IV41-5) HYPERSENSIBILISATION COMPARATIVE A TRIETHANOLAMINE ET AUX AUTRES SENSIBILISATEURS ALCALINS DE L'EMULSION NUCLEAIRE. (Comparative Hypersensitization with Triethanolamine and with Other Alkaline Sensitizers for Nuclear Emulsions). Samoilovich, D. M.; Ardachev, I. V.; Barinova, E. S.

A comparative study was made of the hypersensitization of nuclear emulsions by triethanolamine and by other alkalies, specifically ammonium hydroxide, sodium hydroxide, and sodium carbonate. The mechanism of hypersensitization proposed previously was investigaged. The interaction of different alkaline solutions with the silver halogenide microcrystals was studied, and the grain density and the size density were determined. The results were tabulated and showed that neither the sensitivity nor the fogging of the emulsion treated could be differentiated among the different sensitizers. The studies confirmed that the specific action of triethanolamine consists only in its buffering effect. (J.S.R.)

44407 (CERN-65-4(Vol.II), pp V1-8) UN REVELATEUR POUR LA PHOTOGRAPHIE NUCLEAIRE. (A Developer for Nuclear Photography). Bogomolov, C. S.; Krestovnikova, T. I.; Khaikin, M. S.; Levkoev, I. I.; Koukhtin, V. A.

The photographic properties of derivatives of 4-aminopyrazolone were studied. The layers were irradiated by electrons at 12 to 14 Mev. The results were tabulated and showed that the capacity of the derivatives of 4-aminopyrazolone to develop nuclear emulsions depends upon the electronic character of substituted compounds in the one position of the pyrazolone nucleus. The hydrochloride of 1-phenyl-3-methyl-4-aminopyrazolone was studied in detail with respect to its photographic characteristics. It was studied without support and with a support on glass. The results are tabulated. They show that the granular darkening of the surface parts of the developed layers is 30 to 40% less than in layers developed in amidol. (J.S.R.)

44408 (CERN-65-4(Vol.II), pp V9-15) THEORETICAL GROUNDS FOR THE SELECTION OF DEVELOPING AGENT FOR INTRODUCING IT INTO THE NUCLEAR EMULSION. Veprik, Ya. M.; Zhdanov, A. P.; Martysh, G. G.; Shur, L. I.

A discussion on the creation of a nuclear emulsion with a developing agent (p-oxyphenylglycin) included in its composition is presented. Experiments were made for investigating optimum conditions necessary for introducing the developing agent and also for determining the pH values of the developing alkaline water solution and finding out the possibilities of shifting the equilibrium towards the development process by decreasing the concentration of the oxidized developing agent. Results from these experiments are presented. (M.O.W.)

44409 (CERN-65-4(Vol.II), pp V17-21) L'AUTOMATISATION DU PROCESSUS DE DEVELOPPEMENT ISOTHERMIQUE DE L'EMULSION NUCLEAIRE. (The Automation of the Processes of Isothermal Development of Nuclear Emulsions). Ryabov, V. D.

The automatic equipment designed for the isothermal development of nuclear emulsions is described. The control table is illustrated and the scheme of the development installation is outlined. The electronic block scheme of the control of the development system is given and briefly discussed. (J.S.R.)

44410 (CERN-65-4(Vol.II), pp V22-33) L'ETUDE DES FACTEURS, INFLUANT SUR LA QUALITE DU DEVELOPPEMENT A L'ELECTRODIALYSEUR. (The Study of the Factors Affecting the Quality of the Development with the Electrodialyser). Samoilovich, D. M.; Kondrachina, A. A.; Tarassenkov, V. G.

The electrodialyzer used for the study of the influence of various factors on the density of tracks, the fogging level in the emulsion, and the effect of these factors on the uniformity of development across a level is described. Curves obtained with this electrodialyzer are given which show the typical results obtained and the regime of development that assures the uniformity of development with a satisfactory grain density and with a low fogging level. (J.S.R.)

44411 (CERN-65-4(Vol.II), pp VI1-8) ON CORRELATION BETWEEN DISTORTION IN NUCLEAR EMULSIONS AND SUCCESSIVE DIFFERENCES USED IN MULTIPLE SCATTERING MEASUREMENTS. Aditya, P. K.

An analysis of successive differences of coordinate readings taken for multiple scattering measurements was made in terms of the distortion observed in nuclear emulsions. It was shown that there is a strong correlation between the ratio of successive differences and the distortion contours. (auth)

44412 (CERN-65-4(Vol.II), pp VI11-21) DISTORTION AND SPURIOUS SCATTERING IN NIKFI-R NUCLEAR EMULSION. Krecker, U.

The nuclear emulsion NIKFI-R was irradiated by 10-Bev protons and the spurious scattering was measured. Distortion vectors are given for various treatments of the emulsions. Diagrams showing the distortions and spurious scattering in various treated emulsions are included. (M.O.W.)

44413 (CERN-65-4(Vol.II), pp VI23-30) ON THE PROBLEM OF SPURIOUS SCATTERING IN NUCLEAR EMULSIONS. Fenyves, E.; Gombosi, E.; Janossy, L.; Kiraly, P.; Lee, A.; Rozsa, P.

A method is given for the estimation of the energy of a particle from the sagittas measured on its track in nuclear emulsion in the presence of noise and spurious scattering. The joint probability distribution of Coulomb scattering, noise, and spurious scattering are considered. (M.O.W.)

44414 (CERN-65-4(Vol.II), pp VI31-6) ON THE MEASUREMENT OF COULOMB SCATTERING IN THE PRESENCE OF TRACK DISTORTION AND SPURIOUS SCATTERING. Friedlaender, E. M.; Marcu, M.; Friedlaender, J.

An attempt is made to obtain an estimate for the Coulomb signal on tracks scattered in nuclear emulsions in the presence of spurious scattering and/or C-shaped track curvature due to emulsion distortion and/or to magnetic deflection. (M.O.W.)

44415 (CERN-65-4(Vol.II), pp VI37-52) SOME RESULTS ON SPURIOUS SCATTERING IN PHOTOGRAPHIC EMULSIONS. Rao, G. K.; Kamal, A. A.

Spurious scattering was investigated in 5 pellicles of G_5 emulsions (600 μ thick), one pellicle of L_4 emulsion exposed to 27-Bev/c protons, and one pellicle of K_5 emulsion exposed to 24-Bev/c protons. Results are tabulated. (M.O.W.)

44416 (CERN-65-4(Vol.II), pp VI53-62) AN INVESTIGATION INTO SPURIOUS SCATTERING IN PHOTOGRAPHIC EMULSIONS. Rao, Y. Venkateswar; Kamal, A. A.

From multiple scattering measurements made on 17-Bev/c meson (π^-) beam tracks in G_5 emulsions, it is found that the correlation coefficient ρ_s for spurious scattering between second and third difference, has a value of the order of unity, in the pellicles investigated. This is attributed to the distortion component of spurious scattering. The effect of randomization on higher differences was investigated. Variation of $\bar{D}_s$ with cell length was investigated, and various methods for the elimination of spurious scattering were examined from the point of view of their relative merit. (auth)

44417 (CERN-65-4(Vol.II), pp VII1-14) DISPOSITIF SEMI-AUTOMATIQUE DE MESURE DE LARGEUR DE TRACES. SEMI-AUTOMATION EN PHOTOGRAPHIE CORPUSCULAIRE. (Semiautomatic Apparatus for the Measurement of Track Lengths. Semiautomation in Corpuscular Photography). Annoni, H.; Baumann, G.; Braun, H.; Christophel, E.; Volmer, P.

The general design and performance of apparatus developed for the semiautomatic processing in corpuscular photography are described. The characteristics of the apparatus for the measurement of track lengths are given in diagrams and graphs. A synoptic scheme of its electronics are also given. A device under construction for the measurement of the Coulomb scattering is briefly described. (J.S.R.)

44418 (CERN-65-4(Vol.II.), pp VII15-19) DEVICE FOR MEASUREMENTS OF MULTIPLE SCATTERING AND OF TRACK CURVATURES IN NUCLEAR EMULSIONS. Bott-Bodenhausen, M.

The design and performance of a transistorized device for obtaining measurements of multiple scattering and of track curvatures are discussed. The calculating program is made of three processes: transfer from one store to another, subtraction, and transfer from the binary into the decimal system. A brief discussion of each is included. (M.O.W.)

44419 (CERN-65-4(Vol.II), pp VII20-7) A SEMIAUTOMATIC DEVICE FOR ANALYZING TRACKS IN NUCLEAR EMULSIONS. Breuer, K.; Roessle, E.

The semiautomatic device allows the measurement of length, ionization and geometrical orientation of the tracks of ionizing particles. The track to be measured is steered by the operator along a fixed marking in the field of view. The driving along the three directions of motion of the microscope stage is done by pulse driven motors. These motors are controlled by linear frequency generators so that the resulting speed along the track is constant. Thus the length of the track is determined by the time spent for steering the track along the marking. The components of the length of the stage axis are also measured, yielding the spatial orientation of the track. The specific ionization is measured by grain counting photoelectrically by photomultipliers. Track length, orientation of the track and number of grains are recorded. (auth)

44420 (CERN-65-4(Vol.II), pp VII28-34) A MECHANICAL ANALOG-COMPUTER FOR RANGE AND ANGLE MEASUREMENTS IN NUCLEAR EMULSIONS. Hitzeroth, W.

The main features of a mechanical analog computer which is linked to a Koristka R-4 microscope for the purpose of making measurements of ranges and space angles as they occur in connection with experiments using nuclear emulsions inside gas targets are discussed. (M.O.W.)

44421 (CERN-65-4(Vol.II), pp VII35-7) AUTOMATIC FOLLOWING IN NUCLEAR EMULSIONS. Duff, M. J.

An automatic following microscope with a comprehensive logical control circuit is discussed. The complete system consists of five main sections: the digitized coordinate stage and projection optics, the servo control sampling optics, the servo control electronics, the logical control circuits and the digitizing electronics and readout. A brief discussion of each, and some applications for the system as a whole are presented. (M.O.W.)

44422 (CERN-65-4(Vol.II), pp VII39-42) FURTHER DEVELOPMENT OF THE APPARATUS FOR MEASUREMENTS OF THE PARTICLE TRACKS IN PHOTOEMULSIONS BY THE TELEVISION METHOD. Belovitskii, G. E.; Voronkov, A. E.; Zhdanov, G. B.; Kolesnikova, L. N.; Marenkov, V. S.; Sukhov, L. V.; Soloveva, M. F.; Tretyakova, M. I.; Chernyavskii, M. M.

Further development in the automatic following device for carrying out studies of the track structure in nuclear emulsions is reported. Modifications were made for improvement of the device. New characteristics from these modifications are discussed. (M.O.W.)

44423 (CERN-65-4(Vol.II), pp VIII8) AMELIORATION DE LA RESOLUTION DE MARQUAGES RADIOACTIFS PAR PRISE DE VUES STEREOSCOPIQUES EN MICROSCOPIE ELECTRONIQUE. (Improvement of the Resolution of Radioactive Markings by Stereoscopic Picture Taking in Electron Microscopy). Riedel, G.

Stereoscopic picture taking with the electron microscope makes it possible to separate two tracks whose axes are separated by less than 0.1 μ in vertical projection. The presence of fogging grains reinforce the stereoscopic effect. The use of stereoscopic pictures in the resolution of tritium-labeled dust from silver grains is indicated. The modification made of the cuvette method to improve the stereoscopic pictures is indicated. (J.S.R.)

44424 (CERN-65-4(Vol.II), pp VIII9-16) MOMENTUM DETERMINATION OF LOW MOMENTUM PARTICLES IN EMULSIONS EXPOSED TO A STRONG MAGNETIC FIELD. Villar, E.; Llosa, R.; Gil, D.; Tarrega, P.; Lleo, A.

A new method to determine the momentum of particles with D_s/D_m high values was worked out. This method was checked by means of 14 Bev/c proton reactions, for which the curvature method becomes insufficient. (auth)

44425 (CERN-65-4(Vol.II), pp VIII17-26) REGISTRATION OF α-PARTICLE STARS PRODUCED BY RADIOACTIVE NUCLEI AND TIME DISCRIMINATION OF α-PARTICLE TRACKS IN NUCLEAR EMULSIONS. Berkovich, I. B.; Zhdanov, A. P.; Shur, L. I.

A technique was developed which allows one not only to register alpha particles emitted by radioactive nuclei on a collector, but also to introduce the nuclei themselves directly into the emulsion. Some results for radium-223 and 224 are presented. (M.O.W.)

44426 (CERN-65-4(Vol.II), pp VIII27-33) UTILISATION DU MICROSCOPE ELECTRONIQUE EN VUE DE L'OBSERVATION DES TRACES DANS LES EMULSIONS IONOGRAPHIQUES. (Utilization of the Electron Microscope with the Purpose of the Observation of Tracks in Ionographic Emulsions). Schmitt, R.; Bilwes-Girardin, L.; Nicolae, M.

The thickness of emulsion observable with the electron microscope is limited by only two factors: the diffusion of the beam electrons and the excessive heating of the emulsion layer. It was determined that the second factor is predominant. As the essential problem is the form of the developed grain, examples are given of the grain form using different developers and techniques. (J.S.R.)

44427 (CERN-65-4(Vol.II), pp VIII34-7) ON A METHOD OF MEASUREMENT AND CALCULATION OF FAST PARTICLE MOMENTA IN EMULSIONS EXPOSED IN STRONG MAGNETIC FIELDS. Shahbazian, B. A.

A method of measurement and calculation of fast particle momenta by means of first differences of coordinates taken in two and three points of the track is proposed. In the last case the mean weighted values of momenta, obtained on two parts of the track are calculated. The method is checked on meson (π^-) tracks of 3.85 Bev/c momentum in a magnetic field of 48 kilogauss. (M.O.W.)

44428 (CERN-65-4(Vol.II), pp IX9-13) EMULSION GRAIN DENSITY IN THE EXTREME RELATIVISTIC REGION. Buskirk, F. R.; Dyer, J. N.; Hanson, H. D.; Seng, R.; Weidman, R. H.

Nuclear emulsion measurements of the blob density of meson (π) and electron tracks in the range $\gamma = 2$ to 4000 ($\gamma = 1/\sqrt{1-\beta^2}$) are reported. Data were gathered from four pellicles of 600 μ Ilford K-5 emulsion. The experimental procedure is given. (M.O.W.)

44429 (CERN-65-4(Vol.II), pp IX14-22) ON THE SCATTERING CONSTANT IN NUCLEAR EMULSIONS. Sood, P. M.; Chohan, V. S.

The scattering constant (K) was determined in G_5 nuclear emulsions by Fowler's coordinate method for cell lengths 3 mm to 4 cm by coordinate displacement method for cell lengths 4 mm to 8 cm. Whereas the former method gives satisfactory results at all the cell lengths investigated, the latter method was found to be useful for cell lengths greater than 3 cm. Results, within statistical errors, agree with the theoretically expected values. (auth)

44430 (CERN-65-4(Vol.II), pp IX23-31) RELATIVISTIC INCREASE IN THE TRACK BLOB DENSITY IN VARIOUS NUCLEAR EMULSIONS. Herz, A. J.; Stiller, B.

The emulsions Ilford G5, K5, and L4, Kodak NTB4, NIKFI-BR, and -BM, and Gevaert 715 were examined for the purpose of obtaining information on the ratio g_{pl}/g_{min} (normalized blob density). Data were obtained for the study of the magnitude of the ratio for different emulsions. (M.O.W.)

44431 (CERN-65-4(Vol.II), pp IX32-40) STUDY OF THE MULTIPLE SCATTERING CONSTANT IN EMULSION AT GREAT CELL LENGTHS. Bozoki, G.; Gombosi, E.; Jenik, L.; Nagy, E.; Sahini, M.

The dependence of the scattering constant on cell length is determined from t = 0.5 to 10 cm by two different methods. In the interval 0.5 cm $\leq$ t $\leq$ 3 cm, the coordinate method of multiple scattering measurements and for higher cell lengths the angular dispersion method are used. At t = 3 cm K is determined with both methods to check the consistency of the two methods. Present measurements permit one to investigate the behavior of the spurious scattering as a function of cell length. (M.O.W.)

44432 (CERN-65-4(Vol.II), pp IX41-3) IONIZATION-MOMENTUM DEPENDENCE FOR ELECTRONS AND POSITRONS OF HIGH ENERGY. Zhdanov, G. B.; Tretyakova, M. I.; Shcherbakova, M. N.

In order to clear up a possible difference between the ionizing capacity of particles with a different sign, a series of measurements on electron-positron pairs in the photoemulsions exposed in the pulsed magnetic field of 18 kOE in the CERN proton beam with a momentum of 24 Bev/c was carried out. Results of the ionization measurements are given. (M.O.W.)

44433 (CERN-65-4(Vol.II), pp IX44-7) ARTIFICIAL CONSTRUCTION OF PARTICLE TRACKS BY A MONTE CARLO METHOD. Smith, Francis M.; Shwe, Hla; Barkas, Walter H. (UCRL-11624).

A Monte Carlo method is described for successively generating the grain coordinates of particle tracks in emulsion. For such a calculation one needs to know three parameters of the distribution functions of the grain variables. These are the parameters of multiple scattering, grain noise, and grain spacing. To generate equivalent tracks, the parameters for the distributions of these three random variables may be experimentally determined from a fair sample of real tracks. The method was developed for an emulsion application, but it is readily adapted to other instruments such as the bubble chamber, and to problems of the spatial distribution of ionization in a beam of particles penetrating matter. A brief description of the IBM 7094 program for performing such Monte Carlo calculations of particle track grains is given. (auth)

44434 (CERN-65-4(Vol.II), pp IX48-61) ON THE WIDTH OF HEAVY ION TRACKS IN EMULSION. Katz, Robert; Butts, J. J.

The track width in an emulsion is considered for the complete track length. This was done by projecting the image of the track onto a screen by means of an Ortholux microscope and a xenon lamp, and by tracing the outline of 50μ segments to obtain the area. The model of Bizzeti and Della Corte was modified to assert that a photographic grain will be activated if it is in a region where the energy deposited per unit volume by electrons exceeds a threshold value. Results from this modification are presented. (M.O.W.)

44435 (CERN-65-4(Vol.II), pp IX62-5) IONIZATION DENSITY IN EMULSIONS ENRICHED WITH HYDROGEN. Tolstov, K. D.; Bokova, L. N.; Krivenzova, L. G.; Popova, L.

In order to investigate the ratio of plateau blob density to that of relativistic minimum (I_{pl}/I_{min}), blob density measurements were performed in NIKFI-BR emulsions enriched with H, C, and O nuclei. The emulsion pellicles were loaded with ethylene glycol $(CH_2OH)_2$, which allowed one to double the number of hydrogen nuclei, keeping the blob density of relativistic tracks sufficient. (M.O.W.)

44436 (CERN-65-4(Vol.II), pp X13-18) NUCLEAR EMULSION EXPERIMENTS ON SOUNDING ROCKETS AND SATELLITES. Guss, D. E.; Fichtel, C. E.; Kniffen, D. A.

The application of nuclear emulsions for the study of particle populations in space is discussed. A brief discussion on the emulsion flown with the Aerobee rocket for study of charge distribution and energy spectrum of galactic cosmic low-energy heavy nuclei is given. It is concluded that nuclear emulsions can be successfully flown on rocket vehicles and recovered in good condition. (M.O.W.)

44437 (CERN-65-4(Vol.II), pp X19-32) EMULSION EXPERIMENTS IN ORIENTED POLAR-ORBITING SATELLITES. Heckman, H. H.; Nakano, G. H.

A series of emulsion experiments was made on polar-orbiting satellites (orbit inclination $\geq$65°) whose purpose was to study geomagnetically trapped protons E > 58 Mev. The results from these experiments are described. (M.O.W.)

44438 (CERN-65-4(Vol.II), pp X33-6) THE USE OF GAS TARGETS FOR SCATTERING EXPERIMENTS. Hitzeroth, W.

The application of nuclear emulsions for scattering experiments in which the physically interesting recoil particle has too low an energy to leave feasible liquid hydrogen targets and/or to get into a counter arrangement is discussed. In such cases the use of a gas target plus nuclear emulsions avoids many detection difficulties. Such a target consists of a cylindrical gas container, usually with small annexes for large separations of the windows for beam entry and exit. Some experimental arrangements and results are discussed. (M.O.W.)

44439 (CERN-65-4(Vol.II), pp X36-43)) COMPARISON OF π^0 INTENSITY MEASUREMENTS IN EMULSIONS AND BUBBLE CHAMBERS. King, D. T.

The π^0 intensity from π^- collisions with nuclei was measured at a number of π^- energies by the direct method, i.e., through observations on the conversion of the decay photons, both in emulsion and in bubble chambers. The emulsion experiments were performed with π^- beams of 3.5 and 1.7 Bev/c while corresponding results were obtained in propane-xenon, freon, and propane bubble chambers with π^- beams of 2.8, 7.0, 8.4, and 9.0 Bev/c. The experiments measure the average π^0 intensity per nuclear collision and include, in addition to direct π^0 production, those π^0's which originate through decay of short-lived resonance states such as f_0 and η. (M.O.W.)

44440 (CERN-65-4(Vol.II), pp X44-6) FILM DOSIMETRY WITH INHIBITED DEVELOPMENT. Kubal, Josef.

A method for film development is described using stabilizing additions in the developer which inhibit the reduction process in higher concentration. Results are given for benzotriazole which was the only stabilizer available in the pure state. (M.O.W.)

44441 (CERN-65-4(Vol.II), pp X47-53)) MEASUREMENT OF THE β-PARTICLE DISTRIBUTION OF MASS SELECTED FISSION FRAGMENTS WITH NUCLEAR EMULSIONS. Opower, H.; Konecny, E.; Gunther, H.

The experimental procedure and associated problems in measuring the beta particle distributions from fission fragments are discussed. Results are given for fission fragments of mass 134. (M.O.W.)

44442 (CERN-65-4(Vol.II), pp X57-60) USING PHOTOEMULSION IN PROTON DYNAMIC POLARIZATION CONDITIONS. Luschikov, V. I.; Tolstov, K. D.

In a previously reported method for obtaining polarized protons, it is necessary to put the emulsion in direct contact with a special crystal inside the cavity in a helium cryostat. It is pointed out that dielectric losses in emulsions damage the cavity Q. Experiments were made to determine the modification of Q in the presence of the emulsion inside the cavity. The results are presented. (M.O.W.)

44443 (CERN-65-4(Vol.II), pp X61-6) ON PHOTOEMULSION EXPERIMENTS WITH A HYDROGEN-JET TARGET. Tolstov, K. D.

A brief discussion of several photoemulsion experiments with a hydrogen-jet target is presented. Considered are: elastic p-p scattering, the investigation of isobar excitation in p-p collisions, experiments with a deuteron target, and the investigation of p, k, Λ, and γ spectra in p-p and p-D collisions. (M.O.W.)

44444 (CERN-65-4(Vol.II), pp X67-73)) LE FACTEUR DE CONTRACTION DES EMULSIONS NUCLEAIRES ILFORD G5 EMPLOYEES EN SPECTROMETRIE α. (The Contraction Factor of Ilford G5 Nuclear Emulsions Used in α Spectrometry). Romero, C.; Zamora, M.; Gandia, V.

A new technique for the measurement of the contraction factor of thin nuclear plates used in α spectrometry is presented. This technique was indicated in the method of autoradiography of α emitters. The variation of the contraction factor with the depth in the layers of the plate was studied. (tr-auth)

44445 (CERN-65-4(Vol.II), pp X74-83) THE LOCATION OF TRACKS IN NUCLEAR EMULSION WITH THE AID OF SPARK CHAMBERS. Burhop, E. H. S.; Busza, W.; Davis, D. H. (and others).

The use of a technique in which tracks of particles associated with rare processes are first located in spark chambers is described. From the position and direction of the tracks in the spark chamber it was found possible to locate them in the emulsion stack. The method was applied to the location of very rare neutrino interactions in nuclear emulsion. (M.O.W.)

44446 (COO-1018-1050) ORDER CODE FOR THE FILM SCANNERS OF ILLIAC III. Report No. 176. Breeding, K. J.; McCormick, B. H.; Witsken, J. R. (Illinois Univ., Urbana. Dept. of Computer Science). Mar. 22, 1965. Contract AT(11-1)-1018. 21p. Dep. mn; CFSTI $1.00 cy, $0.50 mn.

To permit efficient usage of an IBM 1302 Disk Storage Unit within the ILLIAC III System, the control and data transmission formats of the Film File Control were remodeled upon those accepted by the IBM 2841-4 Storage Control Unit. Discussions on the following are given: Film File Control—address and format conventions, Film Scanners—modes of operation, and picture display parameters. (M.O.W.)

44447 (EUR-2444.I) SISTEMA MODULARE DI CONTEGGIO DELLA SEZIONE ELETTRONICA. (Modular Counting System in the Electronic Section). Colombo, C.; Stanchi, L. (European Atomic Energy Community, Ispra (Italy). Joint Nuclear Research Center). June 1965. 13p, Dep. mn.

The modular counting system used in nuclear detection measurement is briefly described. The instruments are built according to Esone System; they are designed with the aim to allow many different connections for the particular experiments in a very general way. Some types of lay-out are shown and the main characteristics of all the units are given. (auth)

44448 (HASL-162) NUCLEAR EMULSION SPECTROMETRY AT LOW AND INTERMEDIATE NEUTRON ENERGIES. Sanna, R.; O'Brien, K.; Alberg, M.; Rothenberg, S.; McLaughlin, J. (Health and Safety Lab., New York Operations Office (AEC), N. Y.). July 1964. 99p, Dep. mn; CFSTI $4.00 cy, $0.75 mn.

The use of nuclear emulsions by the AEC Health and Safety Laboratory to measure neutron spectra is described. The experimental procedure is outlined, and the method of processing thick nuclear emulsions using an extended isothermal development is explained, followed by an explanation of the scanning technique used to measure the recoil-proton track length. The analysis of the data to obtain the recoil-proton spectrum is outlined, together with the analysis of the recoil spectrum to obtain the neutron spectrum. The Fortran programs used in these analyses are summarized, and some results indicating the quality of the method are presented. (D.C.W.)

44449 (IAE-704) ZARYADNOE USTROISTVO DLYA PITANIYA USTANOVKI IMPUL'SNYE MAGNITNYE POLYA. (Charging Device for Pulsed Magnetic Field Power Supply). Makar'in, V. K.; Martem'yanov, V. P. (Institut Atomnoi Energii, Gosudarstvennyi Komitet po Ispol'zovaniyu Atomnoi Energii SSSR, Moscow). 1964. 16p. Dep. mn.

A power supply is described for the production of pulsed magnetic fields in bubble, spark, and emulsion chambers used with high-energy particle accelerators. The pulsed magnetic field is produced by discharging a capacitor bank through an inductance coil. The equipment is capable of high-energy storage (~6950 kJ). Because of the use of ignitrons in the rectifier circuit and because of the inductive properties of the circuit, the battery is never discharged completely. It is recharged between the accelerator discharges, which are produced at intervals from 2 to 10 sec. The circuit, the operating principle, the automatic control, and the protective devices are described. The rectifier was used to charge a capacitor bank of 0.162-F capacitance to 4.5 kv. With the battery discharged to 3.5 kv, the rectifier is able to restore the initial 4.5-kv voltage within approximately 5 sec. (ATD)

44450 (IBK-120a) ABSOLUTE MEASUREMENT OF NEUTRON FLUXES INSIDE THE REACTOR CORE. Progress Report. Ajdacic, Vladimir S. (Institut za Nuklearne Nauke Boris Kidric, Belgrade (Yugoslavia)). Oct. 1964. IAEA Contract TB/RI/179. 118p. Dep. mn.

Construction and applications of semiconductor counters for neutron measurements are examined. Neutron measurements in reactors using long-tube equipment is described along with design and operation of ^{6}Li cylindrical neutron spectrometers. (J.R.D.)

44451 (IITRI-578P26-8) A STUDY OF THE FEASIBILITY OF USING SCINTILLATING FIBERS FOR LOW ENERGY BETA COUNTING. Hardie, G.; Preston, C. C.; Ezop, J. J. (IIT Research Inst., Chicago, Ill.). Mar. 5, 1965. Contract AT(11-1)-578. 59p. Dep. mn; CFSTI $3.00 cy, $0.75 mn.

A study was made of various scintillating fiber configurations, suitable for counting low energy betas, which could be easily and reproducibly emptied and filled and yet which would have a reasonably high counting efficiency. A detector was constructed which offered advantages in terms of low cost and simplicity of construction. Procedures were developed for filling and emptying this detector in a reproducible manner. The sample volume of the detector was 11 ml and it had a 1% efficiency for count-

ing the betas from carbon-14. Much higher efficiencies were obtained by closer spacing of the fibers, with some sacrifice in the ease with which the detector is emptied and filled. The problem of detecting the very low energy tritium betas with this type of detector was investigated. It was shown that counting the tritium betas was not feasible with an unselected photomultiplier tube operated at room temperature. However tritium was counted with this type of detector by cooling the photomultiplier tube to -70°C and by a coincidence counting technique. For highest efficiency in tritium counting it is recommended that both cooling and the coincidence technique be employed. Construction details of this detector type as well as guidance in its use are given in this report. The fiber beta detector is compared with the liquid scintillation detector, and the types of experiments in which the fiber beta detector can be used to advantage are considered. As a specific example, a medical experiment involving an external blood loop with a live kidney is discussed. In this particular experiment the liquid scintillation counting technique cannot be used but the fiber beta detector is suitable. (auth)

44452 (K-1642) AN IMPROVED FAST NEUTRON MONITOR. Seaborn, G. B. (Oak Ridge Gaseous Diffusion Plant, Tenn.). Aug. 27, 1965. Contract W-7405-eng-26. 28p. Dep. mn; CFSTI $2.00 cy, $0.50 mn.

An improved fast-neutron monitor was developed, superseding the instrument presently in use for estimating the weights of solid uranium-fluorine deposits in plant process equipment. The new unit is superior in processing a two-thirds greater sensitivity with one-half the weight of the original device. It also contains a ratemeter, a built-in battery charger, and several other improvements. These features, together with the electronic circuits employed, are described in detail. (auth)

44453 (LA-DC-7316) GAMMA SCANNING OF LAMPRE FUEL ELEMENTS WITH A NaI ANTICOINCIDENCE SPECTROMETER. Holm, Dale M.; Sanders, Wm. Mort (Los Alamos Scientific Lab., Univ. of California, N. Mex.). [nd]. Contract W-7405-eng-36. 4p. (CONF-651101-30). Dep. mn; CFSTI $1.00 cy, $0.50 mn.

For Presentation at 13th Conference on Remote Systems Technology, Washington, D. C.

The fission product distributions in molten Pu fuel capsules are measured using a NaI anticoincidence spectrometer. The fuel elements are moved past the detector by a precision scanner. Both continuous and discrete scans can be carried out. (T.F.H.)

44454 (LA-DC-7323) THE SINGLE-SPHERE NEUTRON MONITORING INSTRUMENT. Hankins, Dale E. (Los Alamos Scientific Lab., Univ. of California, N. Mex.). [1965]. Contract W-7405-eng-26. 4p. (CONF-651109-1). Dep. mn; CFSTI $1.00 cy, $0.50 mn.

For Presentation at 1st Symposium on Accelerator Radiation Dosimetry and Experience, Upton, N. Y.

The Bonner sphere technique of measuring neutron spectra consists of a LiI crystal which is placed in the center of 2, 3, 5, 8, and 12 inch spheres. A summary of recent developments concerning a single sphere neutron monitoring instrument, which consists of placing the LiI crystal in the center of a 10 inch sphere, is given. (M.O.W.)

44455 (NP-15047) VYBOR SPEKTROMETRICHESKOGO REZHIMA, FEU-49, NO. 2. (Selection of a Spectrometric Operating Mode of FEU-49, No. 2). Kononov, V. N.; Shorin, V. S. (Gosudarstvennyi Komitet po Ispol'zovaniyu Atomnoi Energii SSSR, Obninsk. Fiziko-Energeticheskii Institut). 1965. 6p. Dep. mn.

A spectrometric operating mode of the FEU-49 photomultiplier, permitting the inherent resolution to be improved by 20% in comparison with the recommended resolution in the photomultiplier ratings, was found. The mode was chosen by regulation of the potential distribution in the photomultiplier input. The improved resolution is reached at a potential difference of 10 v between the photocathode and the modulator. (tr-auth)

44456 (NP-15258) SOVREMENNOE SOSTOYANIE I PUTI RAZVITIYA MNOGOKANAL'NYKH ANALIZATOROV (Status and Means for Development of Multi-Channel Analyzers). Report No. 79. Krasheninnikov, I. S. (Gosudarstvennyi Komitet po Ispol'zovaniyu Atomnoi Energii SSSR). 1964 23p. Dep. mn.

The state of the art is reviewed for multichannel analyzers (MA) having 50 to 100, 200 to 500, and 1000 to 100,000 channels. Various transitorized circuits such as a triggering scheme, and various time and amplitude converters are briefly described. The characteristics of ferrite core memories are given. Data are given on six multichannel analyzers of Russian origin with 50, 100, 128, 256, and 2048 channels. The counting time varied from 16 to 1000 μsec. The integral nonlinearity was 0.5 to 2%. The maximum initial count rate was 5000 to 50,000 counts/sec. Most of the counters had ferrite core memories. The units had one or more of the following features: automatic correction for dead time, typewriter readout, automatic plotter, magnetic tape recorder, or oscilloscope display. The errors due to scale shift and the amplitude converters could be eliminated to improve the operation of the analyzers. (TTT)

44457 (NP-15475) FAST NEUTRON SPECTRUM MEASUREMENTS WITH A ^{6}Li SEMICONDUCTOR NEUTRON SPECTROMETER. Cierjacks, S.; Stegemann, D. (Kernforschungszentrum, Karlsruhe (West Germany)). [1963]. 18p. (INR-68/64). Dep. mn.

A ^{6}Li semiconductor neutron spectrometer is described which can be used for fast neutron spectrum measurements. The resolution was determined using thermal, 3 and 14 Mev neutrons and was found to be around 200-250 kev. The set up of the spectrometer and the equipment used are described. The spectrometer was tested by a measurement of the neutron spectrum originating from the bombardment of ^{238}U with 45 Mev deuterons of the Karlsruhe Cyclotron. For comparison the same spectrum was also measured by threshold activation detectors. Conclusions are drawn from the experiments as to the applicability of the spectrometer in critical fast reactor assemblies. (auth)

44458 (NYO-2767) AN SO_2 MONITOR FOR AIR POLLUTION STUDIES: DESIGN OF THE INSTRUMENT AND FIELD TESTING. Final Report. Hommel, Carlton O.; Bersin, Richard L.; Filipov, Alexander M.; Brousaides, Frederick J. (Tracerlab, Inc., Waltham, Mass.). Aug. 1962. Includes: PRELIMINARY EVALUATION OF THE TRACERMETRIC GAS MONITOR FOR SO_2. Final Report, March 23-May 3, 1962. SUPPLEMENTARY EVALUATION OF THE TRACERMETRIC GAS MONITOR FOR SO_2, June 25-August 22, 1962. Tokiwa, Yoshiro (California. Dept. of Public Health. Air and Industrial Hygiene Lab., Berkeley). Contract AT(30-1)-2525. Dep. mn; CFSTI $3.00 cy, $0.75.

The design and testing of a monitoring device for atmospheric traces of SO_2 is described. SO_2 is caused to react with sodium chlorite, yielding ClO_2 gas, which then reacts with a ^{85}Kr quinol clathrate, thus giving off radioactive ^{85}Kr gas. The radioactive gas is then counted using a G-M tube. (T.F.H.)

44459 (PPAD-2137-561) BUBBLE CHAMBER REPORT. DESIGN AND OPERATION OF A FAST CYCLING LIQUID HYDROGEN BUBBLE CHAMBER. Bazin, M.; Blumenfeld, H.; Liverios, D.; Lloyd, B.; Sanders, H.; Scheibner, M.; Seidlitz, L. (Princeton-Pennsylvania Accelerator, Princeton, N. J.). Aug. 10, 1965. Contract AT(30-1)-2137. 20p. (CONF-650923-3). Dep. mn; CFSTI $1.00 cy, $0.50 mn.

From 5th International Conference on High Energy Accelerators, Frascati, Italy.

A 30-liter cylindrical bubble chamber, 15 in. in diameter and 10 in. deep, is designed for fast (19/sec) cycle operation using liquid H_2. The chamber, cooling column, tem-

perature control system, expansion system, chamber operation, photographic system, and magnet for the chamber are described. (T.F.H.)

44460 (RT/FI(65)8) AN APPARATUS FOR INVESTIGATIONS ON SCINTILLATOR PROPERTIES IN THE TEMPERATURE RANGE −100 deg C TO +50 deg C. de'Munari, G. M.; Mambriani, G.; Giusiano, F. (Comitato Nazionale per l'Energia Nucleare, Rome (Italy)). Mar. 1965. 17p. Dep. mn.

A high sensitivity apparatus for measuring the properties of a scintillator is described. The scintillator temperature may be varied in the range −100 to +50°C. The scintillation light is detected by two Philips 56 AVP photomultipliers in fast coincidence: thus pulses, at the phototube noise level, can be examined. Fast pulses of light, roughly monochromatic, is sent to both phototubes. In this way it is possible to get for each phototube, as a function of the temperature, both the sensitivity and the spectral response. These measurements are rather reproducible (10%) for a given phototube, but there are remarkable differences between different phototubes. (auth)

44461 (TID-22205) THE MEASUREMENT OF ENVIRONMENTAL RADIATION. Annual Report. (New York Univ., N. Y. Dept. of Physics). July 1, 1965. Contract AT(30-1)-1480. 49p. Dep. mn; CFSTI $2.00 cy, $0.50 mn.

The design and calibration of spherical ionization chambers that utilize highly electronegative fillings and low field strengths are reported. Results are included from measurements of cosmic radiation at sea level made on Long Island Sound. A new value was obtained for the cosmic ray barometric correction coefficient. (C.H.)

44462 (TIM-922) 10,000-HOUR TEMPERATURE TEST OF FISSION-COUNTER PREAMPLIFIERS. Atkinson, G. F. (Pratt and Whitney Aircraft, Middletown, Conn. Connecticut Advanced Nuclear Engineering Lab.). June 17, 1965. Contract AT(30-1)-2789. 35p. Dep. mn; CFSTI $2.00 cy, $0.50 mn.

Sixteen preamplifiers amplifying the pulse outputs of irradiated fission counters and possessing high-temperature and radiation-resistant properties were tested at elevated temperatures in a program lasting over 10,000 hr. Five preamplifiers were operated at 250°F, and the remaining eleven were tested, five in operation at a given time, at 350°F. Three preamplifiers at 250°F operated for 10,100 hours without failure. Two preamplifiers at 250°F each suffered a single failure during a similar period, one failing after 7700 hr and the other after 1400 hr. After repair each operated without further failure for the remainder of the test. The original five preamplifiers at 350°F operated for 6400, 6400, 6400, 3000, and 72 hr, respectively, before first failures. Four replacement preamplifiers at 350°F operated for 3000, 2900, 2100, and 500 hr, respectively, before first failures. Two replacement preamplifiers at 350°F each operated 3600 hr without failure. The principal mechanism of failure was the degradation of capacitor insulation resistance. A thorough post-test examination was given all test items. It was concluded that the preamplifier design is suitable for long-term 250°F service but not at 350°F, although modifications to increase reliability at both temperatures are suggested. (auth)

44463 (TRG-Report-1005) IRRADIATED FUEL ELEMENT GAMMA SCANNING RIG: OPERATION AND INSTRUMENTATION. Bridges, C. E.; Mounsey, J. A. (Reactor Group, United Kingdom Atomic Energy Authority, Sellafield (England)). June 17, 1965. 40p. Dep.; BIS $1.20; HMSO 6s.

The gamma scanning rig is used to measure the long- and short-term burnup and power production over the length of fuel elements primarily irradiated in the WAGR. This information is derived from the measurement of the total gamma activities of all fission products together with the measurement of the activities of specific fission products using gamma spectrometry techniques. The gamma activity may be presented as an analog display on a recorder with the element continuously scanned and also in digital form on a strip printer and tape puncher with the element stationary at preselected points of the scan. The methods adopted to control the scanning operations and the instrumentation used to obtain the measurements are described. The general construction of the rig, and the control and measuring instrumentation, are described. The specially constructed position control unit used to program the cycle of operations automatically when spectrometry measurements are made at pre-selected points of the scan is also described. The elements constructed at Windscale are described in sufficient detail for use by maintenance personnel. (auth)

44464 (UCRL-11703) SAMPLING BIAS IN SCANNING PROTON-RECOIL TRACKS IN NUCLEAR EMULSION. Lehman, Richard L.; Fekula, Olga M.; Wayland, J. Robert Jr. (Lawrence Radiation Lab., Univ. of California, Berkeley). Oct. 7, 1964. Contract W-7405-eng-48. 36p. Dep. mn; CFSTI $2.00 cy, $0.50 mn.

A new rapid method, suitable for use with automatic coordinate readout microscope, of sampling track distributions in nuclear emulsion was tested for bias. Length and angular distributions of track samples taken using this method from emulsions exposed edge-normal to single-energy neutron beams were compared with those predicted by s-wave scattering theory. No significant sampling bias was found. (auth)

44465 (UCRL-12020) BACKGROUND EVENTS IN PHOTOMULTIPLIER TUBES AT HIGH ALTITUDES. Anderson, K. A.; Chodil, G.; Hearn, David; Jopson, R. C.; Mark, Hans; Swift, C. D. (Lawrence Radiation Lab., Univ. of California, Livermore). Sept. 24, 1964. Contract W-7405-eng-48. 8p. Dep. mn; CFSTI $1.00 cy, $0.50 mn.

A package carrying a standard type of NaI crystal assembly, lacking only the NaI crystal itself, was flown on a balloon at an altitude of 110,000 feet. The phototube output went to a five-channel pulse-height analyzer, and the counts in each channel were transmitted to the ground station after suitable scaling. The channels were calibrated to correspond to the following equivalent energy intervals if the NaI crystal were mounted in the holder: channel 1, 5 to 15 kev; channel 2, 15 to 25 kev; channel 3, 25 to 35 kev; channel 4, 35 to 45 kev; channel 5, >45 kev. The counts recorded in each channel as a function of altitude are given. It is also shown that the observed counting rates correspond closely to the rates calculated for Cherenkov radiation in the glass of the phototube and crystal holder. (M.O.W.)

44466 (UCRL-16231) SEMICONDUCTOR DETECTORS FOR NUCLEAR SPECTROMETRY. Goulding, Fred S. (Lawrence Radiation Lab., Univ. of California, Berkeley). July 30, 1965. Contract W-7405-eng-48. 178p. Dep. mn; CFSTI $5.00 cy, $1.00 mn.

Four included lectures constitute a collection of essential information on semiconductor detectors and associated systems. The lectures concern; the descriptive theory of semiconductors, semiconductor detector technology and manufacture, factors determining the energy resolution in measurements with semiconductor detectors, and miscellaneous detector topics. Very few experimental results are given. (M.O.W.)

44467 (ZFK-PHA-12) INTERNATIONALE ARBEITSTAGUNG HERSTELLUNG UND ANWENDUNG VON HALBLEITERDETEKTOREN, 23-28 SEPTEMBER 1963 IN ROSSENDORF. (International Conference on the Preparation and Utilization of Semiconductor Detectors, September 23-28, 1963, Rossendorf). (Zentralinstitut fuer Kernphysik, Rossendorf bei Dresden (East Germany)). Oct. 1963. 225p. (CONF-630914). Dep. mn.

The conference included 33 papers. Separate abstracts are prepared for 28 papers. Abstracts of 5 papers previously appeared in NSA as 17: 41930, 18: 4058, 20395, 26606, and 39620. (C.E.S.)

For abstracts of individual papers see: 43999–44001, 44468–44489, and 45289–45291.

44468 (ZFK-PHA-12, pp 10-15) THE STATE OF DEVELOPMENT OF SEMICONDUCTOR DETECTORS IN THE CENTRAL INSTITUTE FOR NUCLEAR PHYSICS AT ROSSENDORF. Kaufmann, C.

In German.

The surface barrier detectors prepared from p-Si were described. The initial material and the properties of these detectors were discussed. A special aging phenomenon was detected. The electronics, especially the preamplifier used, were described. Future developments to be expected were mentioned. (tr-auth)

44469 (ZFK-PHA-12, pp 16-24) SURFACE-BARRIER SILICON DETECTORS WITH GUARD RINGS AND POSSIBILITY OF THEIR UTILIZATION. Khvashchevskaya, Ya.; Dakowski, M. (and others). In Russian.

Using a guard-ring silicon surface-barrier, nuclear radiation detectors with a depletion layer thickness of about 1 mm were obtained. These detectors were used for charged particle spectrometry. The resolution for 8.78-Mev α particles was 16 to 20 kev with a stability of 0.2 to 0.5%/8 hrs. A spectrometer with this type of detector can be used for α particles up to 50 Mev, for protons up to 12 Mev, for deuterons up to 16 Mev, and β rays up to 700 kev. It can also be used for the identification of charged particles such as protons, deuterons, and α particles. (auth)

44470 (ZFK-PHA-12, pp 25-9) METHOD FOR THE PRODUCTION OF SILICON SPECTROMETRIC DETECTORS WITH A WIDE RANGE OF SENSITIVITY. Tszen' Va, Van; Sidorov, A. I.; Sidorova, L. P.; Simonova, L. I.

In Russian.

A method for the production of silicon spectrometric detectors with a wide range of volume charge was described. The method is based on newly observed phenomenon produced by the electric drift of Li and Si ions. Explanations of these phenomena were proposed. (tr-auth)

44471 (ZFK-PHA-12, pp 30-2) USE OF SILICON SURFACE-BARRIER DETECTORS COMPENSATED BY LITHIUM FOR MEASUREMENTS OF ENERGIES OF PROTONS AND DEUTERONS UP TO ENERGIES OF 13 Mev. Wang, Chien-Wa; Osetinskii, G. M.; Sidorov, A. I.; Chieng, Nai-Kung.

In Russian.

The stability and linearity of the amplitude of the output signla of Si surface-barrier Li detectors were investigated as functions of the energies of incident particles. Protons (4 to 9.5 Mev) and deuterons (8 to 13 Mev) from triton reactions with ^{3}He were used. Al cylinders of different thicknesses were placed between the gas target and the detector to vary the particle energy. The dependence of the pulse amplitude on the incident proton and deuteron energies is shown and compared with that for pulses from Pu alpha particles. (M.J.T.)

44472 (ZFK-PHA-12, pp 52-63) SILICON SPECTROMETRIC DETECTORS WITH THE WIDE RANGE OF SENSITIVITY. Matveev, O. A.

In Russian.

The construction and technological manufacture of spectrometric n-i-p detectors, having the capacity to detect β particles of ^{137}Cs at 1 to 1.5% (approximately 8 kev) and gamma radiation of ^{137}Cs at 1.5 to 2% (11 kev) were described. The detectors have high resolution capacities and along with other qualities such measuring devices have uses in many areas of study and technology. (tr-auth)

44473 (ZFK-PHA-12, pp 64-5) GERMANIUM GAMMA COUNTER. Matveev, O. A.

In Russian.

Germanium p-i-n junction detectors can be used as gamma spectrometric counters with much higher efficiency than silicon detectors, because of the higher atomic number of Ge. Si detectors also require cooling for beta and gamma spectrometry. The preparation of the Ge p-i-n junctions is described. The gamma spectrum of ^{137}Cs measured using the Ge detector is presented. (M.J.T.)

44474 (ZFK-PHA-12, pp 66-9) THE STANDARDIZATION OF SEMICONDUCTOR DETECTORS. Kaufmann, C.

In German.

Proposals are made for the standardization of semiconductor detectors, especially surface barrier detectors, so that the conditions of preparation and coupling would be the same. The suggestions are intended only as the basis for discussion among the users of semiconductor detectors and not as rigid guidelines. (J.S.R.)

44475 (ZFK-PHA-12, pp 84-97) PARTICLE DISCRIMINATION WITH SEMICONDUCTOR DETECTORS. Fuelle, R.; Netzband, D.; Schlott, K.

In German.

The principle of the method of thin detectors was explained. Special semiconductor detectors are appropriate for this method. The applicability of the method in nuclear reactions was discussed in general. It appeared that the range of applicability was significantly enlarged when a combination of dE/dx counters and thin semiconductor detectors was used. The electronics were described and practical experiences and measurement results in the reaction ^{10}B(d,t$_0$)^{9}B were reported. (tr-auth)

44476 (ZFK-PHA-12, pp 123-5) APPLICATION OF SEMICONDUCTOR DETECTORS IN THE ASSOCIATED PARTICLE METHOD. Mittenbacher, J.

In Russian.

The associated particle method was applied to the study of the reaction ^{12}C(n,α)^{9}Be and to the detection of ^{3}He particles from the reaction D(d,n)^{3}He. The spectrum obtained is graphed for three detector voltages; the clarification of the α spectra is obtained from the energy dependence of the effective cross section of the reaction T(d,n)^{4}He. The experimental arrangement is shown. (J.S.R.)

44477 (ZFK-PHA-12, pp 126-32) UTILIZATION OF SEMICONDUCTOR DETECTORS IN POLARIZATION EXPERIMENTS. Bem, P.; Gabanets, I.; Karban, O.; Presperin, V.

In Russian.

Si detectors with surface barrier areas of 50 mm^2 were used for the registration of protons by measurement of the polarization in elastic scattering in the energy interval from 5.0 to 6.7 Mev. The detectors were placed in a C polarization analyzer by means of which the asymmetry of the angular distribution was measured after secondary scattering. The stability of operation of the detector during many days was guaranteed by cooling it to temperatures of −20 to −30°C. A reduction of the reverse current of the detector to less than 10^{-7} amps was obtained and simultaneously the ratio of signal to noise was improved. (tr-auth)

44478 (ZFK-PHA-12, pp 133-9) NEUTRON SPECTROSCOPY WITH SEMICONDUCTOR DETECTORS. Regel, K.

In German.

A brief review is given of the various types of semiconductor neutron spectrometers. The suitable experimental investigations concerned semiconductor spectrometers with a radiator foil or specially with the vapor-desposited ^{6}LiF convertor. The introduction of semiconductor detectors with a radiator foil for neutron spectroscopy suffers especially from the too high background effect. Some experiments on the special problems of ^{6}LiF coincidence spectrometers were reported. The resolution of the spectrometer was measured in dependence of various parameters on the spectrometer and detector. (tr-auth)

44479 (ZFK-PHA-12, pp 140-3) SEMICONDUCTOR DETECTORS WITH URANIUM SALTS FOR THE ABSOLUTE MEASUREMENT OF THERMAL NEUTRON BEAMS. Biro, Ya.; Deme, S.; Fekher, I.; Pushkash, L.

In Russian.

The preparation of detectors for thermal neutrons, operating satisfactorily in γ fields with intensities of several hundred R/hr, was described. Semiconductor detectors, combined with convertors of fertile materials, were described. A detector for thermal neutrons

with 50 mm^2 surface was developed. The efficiency of the detector for specific α activities was determined absolutely. The degree of uranium enrichment was $1.02 \times 10^{-5} \pm 5\%$. Some measurements made with this detector were described. (tr-auth)

44480 (ZFK-PHA-12, pp 144-6) STUDY OF A SEMICONDUCTOR DETECTOR FOR THE DETECTION OF THERMAL NEUTRONS IN CONDITIONS OF INTENSE PULSED GAMMA RADIATION. Ishmaev, S. N.; Sedikov, I. P.; Chernyshev, A. A.

In Russian.

The operation of double surface-barrier p-n-p semiconductor detector, using n-type Si with two Au layers, is described for the detection of particles arising upon the fission of ^{235}U by neutrons. The detector circuit is designed so that gamma quanta, which are detected simultaneously in both sensitive layers, give rise to two pulses which cancel each other. (M.J.T.)

44481 (ZFK-PHA-12, pp 149-53) INTERACTION OF HEAVY FISSION PARTICLES WITH SEMICONDUCTOR DETECTORS. Buras, B.; Dakowski, M.; Sowinski, M.; Khvashchevskaya, Ya.

In Russian.

The interaction of heavy fission products with semiconductor detectors of homogeneous (300 ± 20 ohm cm) and nonhomogeneous (280 ± 100 ohm cm) silicon was investigated. It was discovered that with increased voltage on the detector ionization defects decreased and for nonhomogeneous Si in the fission particle spectrum "tails" appeared at very high energies. Preliminary interpretations of the effects observed were suggested. (tr-auth)

44482 (ZFK-PHA-12, pp 154-62) A MONITOR FOR THE READING OF THE d/p RATIOS IN THE CYCLOTRON BEAM. Deutscher, M.

In German.

At the obtainable magnetic current and frequency of the cyclotron at Rossendorf, the separated acceleration of deuterons and hydrogen atoms leads to considerable difficulties. An instrument is described that makes it possible to have a continuing control of the ratios of both types of particles and to permit a correction of the cyclotron parameter. The particle registration is done with a surface barrier detector. (tr-auth)

44483 (ZFK-PHA-12, pp 172-88) A LOW NOISE PREAMPLIFIER FOR SEMICONDUCTOR DETECTORS WITH IMPROVED CONSTANCY. Gaertner, R.

In German.

Two properties are of great significance for the characterization of preamplifiers for semiconductor detectors: the sensitivity and the constancy of the amplification. A summary is presented of the work done in the production of preamplifiers with particular attention given to these two characteristics. Circuits and performance graphs of the preamplifier designed are given. (J.S.R.)

44484 (ZFK-PHA-12, pp 189-95) CHARGE-SENSITIVE PREAMPLIFIER WITH LOW NOISE LEVEL FOR OPERATION WITH SEMICONDUCTOR DETECTORS. Dakowski, M.; Sowinski, M.

In Russian.

The design and properties of the preamplifier circuit, consisting of a cascade section with charge coupling, a triode with strong reverse voltage coupling, shaping circuit, voltage divider, and cathode follower, are described. The method for measuring the preamplifier noise is discussed. (M.J.T.)

44485 (ZFK-PHA-12, pp 196-200) ON COINCIDENCES OF PULSES OF SEMICONDUCTOR DETECTORS, CONNECTED IN A DELAY LINE. Akimov, Yu. K.

In Russian.

A comparison of two devices for selection of coincidences in systems where semiconductor detectors are included as capacitance elements of the line delay is presented. A calculation of the recording inefficiency of the detector on line is given. (tr-auth)

44486 (ZFK-PHA-12, pp 201-5) VARIANT SCHEME OF FAST COINCIDENCES FOR LOW-AMPLITUDE PULSES. Akimov, Yu. K.; Kuznetsov, A. S.

In Russian.

Methods for the registration of fast coincidences of low-amplitude pulses was investigated. Coincidences were obtained on pulses of primary amplitude with subsequent discrimination by a differential device after intensification with a not very wide band intensifier. (tr-auth)

44487 (ZFK-PHA-12, pp 206-14) THEORETICAL AND EXPERIMENTAL STUDIES ON THE FREQUENCY BEHAVIOR AND THE NOISE OF TRANSISTORIZED CHARGED AMPLIFIERS. Richter, W.

In German.

Pulse amplifiers whose input sizes are a predictable charge mass are considered. The equivalent circuit diagram, the limiting frequency, amplification, and minimum noise charge were investigated. The greatest amplification comes from the cascade boot-strap circuit. The smallest measured noise charge is at 2200 e without signal noise. (tr-auth)

44488 (ZFK-PHA-12, pp 215-18) THE SUITABILITY OF A SENSITIVE TIME-PULSE HEIGHT CONVERTOR FOR SEMICONDUCTOR DETECTORS. Meiling, W.

In German.

The basic requirements on time-pulse height convertor circuits for the nanosecond range were discussed. In the apparatus considered the input pulse should operate in the millivolt range. The convertor circuits suitable for application with scintillation counters are not sufficiently accurate for the millivolt pulse. Investigations on a sensitive convertor which corresponds to pulse heights of several decades of millivolts and attains apparatus resolution times of several nanoseconds are reported. (tr-auth)

44489 (ZFK-PHA-12, pp 219-23) THE EFFECT OF THE INPUT RESISTANCE OF AN AMPLIFIER ON THE SIGNAL-TO-NOISE RATIO. Kalinin, A. I.

In Russian.

The signal-to-noise ratio in amplifiers of pulses from semiconductor detectors was studied. In particular, the behavior of the signal-to-noise ratio for changes in the input resistance of the amplifier was considered, and the optimum band of the amplifier corresponding to each input resistance was determined. (tr-auth)

44490 (BNL-tr-1) CONCERNING THE POSSIBILITY OF DETERMINING THE KINEMATIC CHARACTERISTICS OF PARTICLES IN THE SPARK CHAMBER EMPLOYING MULTIPLE SCATTERING AND ADDITIONAL SPARKS. Bayukov, Y. D.; Vorobev, L. S. (Gosudarstvennyi Komitet po Ispol'zovaniyu Atomnoi Energii SSSR, Moscow. Institut Teoreticheskoi i Eksperimental'noi Fiziki). Translated by Stephen Amoretty (Brookhaven National Lab., Upton, N. Y.) from Report N-310. 5p. Dep.mn; CFSTI $1.00 cy, $0.50 mn; JCL $1.10 fs, $0.80 mf.

New methods for measuring the kinematic characteristics of particles in spark chambers (energy, impulse, velocity, etc.,) are discussed. These methods are similar to previous methods of identifying the particles by their angle of multiple scattering and the number of S electrons produced in other track detectors. The methods of multiple scattering and additional sparks are discussed. (M.O.W.)

44491 (CEA-tr-R-1866) METHODE SPECTRALE DE DETERMINATION DES DOSES DES EMETTEURS β. (Spectral Method of Determination of Doses from β Emitters). Aglintsev, K. K.; Maksimova, M. P.; Uryaev, I. A. Translated into French from Recherche Dans le Domaine de Mesure Des Rayonnements Ionisants, 1961. 17p. Dep. mn; JCL, $1.60 fs, $0.80 mf.

The method of dose determination from flat β emitters, based on the use of the real spectrum of electrons, is studied. A scintillation spectrometer with a stilbene crystal was used for the spectral analysis. (tr-auth)

44492 ON MATRIX TREATMENT OF DATA OBTAINED BY FAST NEUTRON SINGLE CRYSTAL SCINTILLATION

SPECTROMETER. Doroshenko, G. G.; Zolotukhin, V. G.; Efimenko, B. A. At. Energ. (USSR), 19: 51-6(July 1965).

Matrices are calculated for the treatment of results of measurements of fast-neutron spectra. The counting efficiencies of a stilbene crystal (height 30 mm and diameter 30 mm) in the energy range 1 to 18 Mev taking into account energy resolution were calculated on the basis of the line shapes $K(E_p,E)$, found by the Monte-Carlo method for 55 values of the initial neutron energy. Calculations were performed for 4 values of the resolution parameter (standard deviation). The direct and inverse transposed matrices are presented. (M.J.T.)

44493 ANALYSIS OF THE SYSTEMATIC ERROR DUE TO DIFFERENTIATION OF APPARATUS SPECTRA MEASURED BY FAST NEUTRON SINGLE CRYSTAL SCINTILLATION SPECTROMETER. Zolotukhin, V. G.; Doroshenko, G. G.; Efimenko, B. A. At. Energ. (USSR), 19: 56-9(July 1965).

The error introduced in the line shape of neutron spectra obtained in a neutron-proton recoil scintillation spectrometer due to the use of the differentiation method in the single-scattering approximation is considered. Monte-Carlo calculations using this approximation were performed. A histogram of the line shape of a detector with a cylindrical stilbene crystal is given for incident neutron energies of 1.0 and 4.15 Mev, and the deviation of the derived differential spectra from the ideal values is shown as a function of neutron energy from 1 to 5 Mev for 1.05- and 2.05-Mev protons, for three different sizes of cylindrical stilbene crystal. It is found that for slowly changing spectra the errors associated with line-shape distortion are within a few percent, but for quickly changing neutron spectra, the error of the differentiation method can reach significant values. (M.J.T.)

44494 A HIGH PRESSURE DIFFUSION CLOUD CHAMBER WITH MACHINE COOLING. Greiner, E. (Friedrich-Schiller-Universitaet, Jena, Ger.). Exptl. Tech. Physik, 13: 191-203(1965). (In German).

A high-pressure diffusion cloud chamber, that operates with various gases up to a pressure of 65 atm, is described. The cloud chamber was installed at the 1 Mv cascade generator at Jena for the study of the elastic scattering of 14.1-Mev neutrons on protons. The apparatus for the photometric registration of the cloud chamber tracks and the construction of a stereocamera are described. (tr-auth)

44495 A PRECISION DOSIMETER ACCORDING TO KUESTNER-PYCHLAU. Pychlau, H.; Pychlau, P. (Physikalisch-Technische Werkstaetten Dr. Pychalu KG, Freiburg i. B.). Fortschr. Gebiete Roentgenstrahlen Nuklearmed., 103: 91-5(1965). (In German).

An account is given of a further development in the large standard dosimeter devised by Küstner. The new precision dosimeter after Küstner-Pychlau is suitable to serve as secondary standard for the calibration of practical dosimeters used and to carry out comparative measurements between standards of the various national laboratories. (auth)

44496 THE HOUGH-POWELL DEVICE FOR AUTOMATIC ANALYSIS OF PLATES OF TRACK CHAMBERS. Benot, M. (CERN, Geneva). Neue Tech., 7: 218-29 (July 1965). (In German).

The analysis of bubble chamber photographs increasingly calls for modern techniques of data handling with digital electronic computing. As it is necessary to analyze a very large number of pictures, automatic measuring instruments such as the HPD described here, were designed and constructed so that the part played by the operator becomes gradually less important. The HPD which was working for some months, gives a better accuracy in the measurements than the manual devices, and from the progress made in the field of programming, it is hoped that it will become an entirely automatic device for the scanning of track chamber pictures. (auth)

44497 DIRECT-RECORDING MEGACHANNEL ANALYZER THROUGH ASSOCIATIVE PROGRAMMING OF A SMALL COMPUTER. Soucek, B. (Brookhaven National Lab., Upton, N. Y.). Nucl. Instr. Methods, 36: 181-91 (Oct. 1965). (BNL-9124).

The need for real-time accumulating analyzers in the megachannel range has become very apparent in recent years, though excessive cost has prevented their construction. Recently, various investigations have suggested that a solution lay in the utilization of the associative memory technique. A megachannel analyzer employing this technique has been designed. This paper deals with the programming and extending of the on-line computer into a megachannel, multidimensional, direct-recording associative analyzer. The features of the system are ultimately determined by the list format used. The random-tree list format, while useful during the experiment, has the disadvantage that all items on the list are interconnected. A megachannel analyzer employing double list technique has been designed to overcome this limitation and is now in successful operation. Experiments are presented which have become possible for the first time due to the associative analyzer technique. It is shown that there is a considerable difference between spectra based on first arrived events and those based on most probable events. (auth)

44498 CIRCULAR SPARK CHAMBERS WITH ELECTRIC LOCALIZATION. Gouanere, M.; Feuvrais, L. (Institut de Physique Nucleaire, Lyon). Nucl. Instr. Methods, 36: 197-201(Oct. 1965). (In French).

The design and the construction of flat, circular, fifteen-gap spark chambers using automatic analysis with current method are described. Their effective angle is twice 165°, and one can measure with them angular distributions of 28 Mev protons, with an energy resolution of 2% and an angular resolution of 3°. The fast localization pulse (30 nsec) enables the triggering of other spark chambers. (auth)

44499 A DETECTOR FOR NEUTRAL AND CHARGED PARTICLES. Daly, N. R.; Powell, R. E.; Ridley, R. G. (Atomic Weapons Research Establishment, Aldermaston, Berks, Eng.). Nucl. Instr. Methods, 36: 226-8(Oct, 1965).

A type of scintillation detector is described that counts low- and high-energy charged particles with high efficiency. Its application to the detection of low energy neutral particles has also been investigated. The use of glass scintillators in a bakeable version of the device is also discussed. (auth)

44500 A FRESH APPROACH TO READOUT COUNTING SYSTEMS. McGinnis, G. A.; Pecina, R. J.; Prucha, L. L. (Argonne National Lab., Ill.). Nucl. Instr. Methods, 36: 255-60(Oct. 1965).

A true readout counter using the systems approach is developed. A gated readout counting decade allows for readout into any serial or parallel output device. (auth)

44501 INTERNAL CONVERSION COEFFICIENTS EMPLOYING INTERNAL-EXTERNAL-CONVERSION TECHNIQUE USING A SCINTILLATION SPECTROMETER. Raja Rao, M.; Jnanananda, S. (Andhra Univ., Waltair, India). Nucl. Instr. Methods, 36: 261-8(Oct. 1965).

A beta scintillation spectrometer with a well-type plastic phosphor is assembled for the measurement of total internal conversion coefficients employing the internal-external-conversion technique. With foils of elements ranging from lead to copper as external converters, measurements were made and the values obtained for the total ICC are 0.112 ± 0.011 and 0.21 ± 0.03 for the 661- and 279-kev transitions of ^{137}Ba and ^{203}Tl isotopes respectively. The deduced α_K values are in satisfactory agreement with the theoretical values. (auth)

44502 SPARK CHAMBER USING HELIUM OR HYDROGEN AT HIGH DENSITY. Schnurmacher, G. L. (Univ. of California, Berkeley). Nucl. Instr. Methods, 36: 269-76 (Oct. 1965). (UCRL-16010).

Efficiency data and threshold voltages are given for a four-gap helium spark chamber in which the pressure was

varied from 1 to 30 atm while the voltage was varied from 13 to 30 kv. Data are also presented for the same spark chamber using unadulterated hydrogen gas up to 6 atm. (auth)

44503 THE OPTIMIZATION OF HALF-LIFE COUNTING EXPERIMENTS. Grant, I. S. (Atomic Energy Centre, Lahore). Nucl. Instr. Methods, 36: 289-92(Oct. 1965).

The accuracy of the decay constant estimated from a least squares analysis of a counting experiment conducted with a multichannel scaler is discussed. The effects of correlations between the counts in different channels, counter efficiency, deadtime, and background, are included. The conditions are easily satisfied for a close approach to the best possible accuracy in the measurement of the decay constant of a source of given strength. (auth)

44504 A TUNNEL DIODE DISCRIMINATOR WITH FIXED DEAD TIME. Diamond, J. M. (Atomenergikommissionens Forsoegsanlaeg, Risoe, Denmark). Nucl. Instr. Methods, 36: 293-301(Oct. 1965).

A solid state discriminator for the range 0.4 to 10 v is described. Tunnel diodes are used for the discriminator element and in a special fixed dead time circuit. An analysis of temperature stability is presented. The regulated power supplies are described, including a special negative resistance feature in the bias supply. (auth)

44505 EFFICIENCY CALCULATIONS FOR A CIRCULAR DETECTOR VIEWING A CIRCULAR RADIATOR. Konijn, J.; Lauber, A.; Tollander, B. (Aktiebolaget Atomenergi, Studsvik, Sweden). Nucl. Instr. Methods, 36: 302-8(Oct. 1965).

Neutrons emanating from an isotropic point source hit a circular target. The secondary particles produced are counted by a circular detector. The planes of the radiator and the detector are both perpendicular to the line through their centers and through the point source. The resulting total and differential detection efficiencies are investigated for different types of angular emission distributions of the secondary particles. Both infinitely thin radiators and radiators of finite thickness are considered. Numerical results are obtained for different values of the radiator thickness, radiator diameter, detector diameter, target-detector distance, and target-neutron source distance. (auth)

44506 THE DESIGN OF A SIMPLE BUT ACCURATE LOW ENERGY BETA LIQUID SCINTILLATION COUNTER. Heiberg, E. (Institut for Atomenergi, Kjeller, Norway). Nucl. Instr. Methods, 36: 314-16(Oct. 1965).

Two coincidence-coupled Philips AVP 153 photomultiplier tubes are employed. The system is mechanical, manually operated. The perspex light-guide is designed for maximum optical efficiency and has a center-hole for placing the sample to be investigated. (auth)

44507 OBSERVATION OF VERTEX EVENTS IN A WIDE-GAP SPARK CHAMBER. Catura, R. C.; Chen, K. W. (Princeton Univ., N. J.). Nucl. Instr. Methods, 36: 317-19(Oct. 1965). (PPAD-2137-552).

The detection of vertex events produced by neutral beam particles in a single-gap spark chamber is studied. The chamber used has a 40 cm gap between the electrodes, which are comprised by 0.001-in.-thick Al sheets. The filler gas is a Ne–10% He mixture at a total pressure of 7 μHg. The chamber is operated in the spark mode. Mechanisms by which the sparks move from the vertex to the upstream electrode are studied. The performance of the spark chamber under these operating conditions is shown. (T.F.H.)

44508 A WIDE RANGE HIGH RESOLUTION TIME-TO-AMPLITUDE CONVERTER. Bell, J. (Univ. of New South Wales, Kensington, Australia); Green, J. H.; Tao, S. J. Nucl. Instr. Methods, 36: 320-2(Oct. 1965).

The design of a wide-range (about 360 nsec), high-resolution (1.2 nsec), high-stability time-to-amplitude converter is described. The circuits are transistorized, and the device utilizes the pulse overlap principle. (T.F.H.)

44509 A NEW DOSIMETER GLASS WITH IMPROVED PROPERTIES. Becker, K. (Julich Nuclear Research Establishment, Ger.). Nucl. Instr. Methods, 36: 323-4 (Oct. 1965).

A glass is described that contains approximately 1% $AgPO_3$, 91% $LiPO_3$, 3% B_2O_3, and 5% $Al(PO_3)_3$, which has a very low predose and energy sensitivity and a higher radiation-dose radiophotoluminescence sensitivity than any commercially available glass. The glass is very sensitive to thermal neutrons, as well as the more easily detectable particles. (T.F.H.)

44510 A GERMANIUM LITHIUM-DRIFT DIODE WITH GUARD-RING FOR γ-RAY SPECTROSCOPY. Tavendale, A. J. (Atomic Energy of Canada Ltd., Chalk River, Ont.). Nucl. Instr. Methods, 36: 325-7(Oct. 1965).

The fabrication of deep-depletion-layer (greater than about 7 mm) Li-drifted Ge p-i-n diodes is described. The starting material is p-type 10-ohm·cm Ga-doped Ge. These diodes are used for gamma spectroscopy. A guard ring technique is used to reduce the surface leakage current below 0.1 mA. (T.F.H.)

44511 AN EFFICIENT DEWAR FOR LITHIUM-DRIFTED GERMANIUM DETECTORS. Kraner, H. W.; Sovka, J. A.; Breckenridge, R. W. Jr. (Massachusetts Inst. of Tech., Cambridge). Nucl. Instr. Methods, 36: 328-30(Oct. 1965).

The design of a simple liquid-nitrogen dewar for use with Li-drifted Ge detectors is described. The "hold" time required for the coolant to boil off is 24 to 65 hr, depending on the reflecting material used. The vessel uses 1.35 liter of liquid nitrogen. (T.F.H.)

44512 ACCELERATION METHOD FOR DETECTION OF SOFT BETA PARTICLES. St. Charalambus; Theodossiou, A. (Univ. of Athens). Nucl. Instr. Methods, 36: 331-2(Oct. 1965).

Soft beta particles emitted by a sample are passed through an accelerating electric field (up to about 25 kv) in vacuum, in order to make possible the passage of these beta particles through the window of a sealed ionization chamber. The background increases rapidly above 25 kv accelerating potential. (T.F.H.)

44513 A REACTION-FREE DYNODE GATE FOR PHOTOMULTIPLIERS. Roose, U. J. (Institut fuer Reine und Angewandte Kernphysik, Kiel). Nucl. Instr. Methods, 36: 333-4(Oct. 1965). (In German).

For measurements at high background a bistable dynodegate was considered following development of a pulsed dynodegate. Diagrams are presented showing voltage dividers for dynodegates for pulsed and bistable operation. Both dynodegates allow a fast electronic intensifying switch of the photomultiplier. (M.C.G.)

44514 THE DEVIATION BETWEEN SPARK AND TRACK IN A WIDE GAP SPARK CHAMBER. Brookes, G. R.; Garvey, J. (Glasgow Univ.). Nucl. Instr. Methods, 36: 335-6(Oct. 1965).

A coherent shift of particle tracks along the electric field direction in wide-gap spark chambers can result from the movement of primary ions under the influence of the leading edge of the high-voltage pulse and the clearing field. This coherent shift is measured as a function of track–field angle (from 5 to 45°) and clearing field (from −0.8 to +0.8 kv). Results are shown graphically. (T.F.H.)

44515 EXPERIMENTAL PHOTOPEAK EFFICIENCIES FOR NaI(Tl) CRYSTALS. Coop, K. L.; Grench, H. A. (Lockheed Palo Alto Research Lab., Calif.). Nucl. Instr. Methods, 36: 339-40(Oct. 1965).

The photopeak efficiencies of 4" × 4" and 3" × 3" NaI(Tl) crystals are measured in several geometries, for gamma energies of 0.15 to 3 Mev. The efficiencies range between 0.15 and 40%. (T.F.H.)

44516 AN EXTENSION OF THE LABEN 512-CHANNEL ANALYSER FOR USE IN MULTIPARAMETER EXPERIMENTS. Gangas, N.; Katselis, V.; Kouvaras, N.; Kossion-

ides, S. (Greek Atomic Energy Commission, Athens). Nucl. Instr. Methods, 36: 341-2(Oct. 1965).

An external auxiliary circuit is added to a 512-channel analyzer, in order to print out numbers N = 100 X + Y, where X and Y represent a coincident event having coordinates channel X and channel Y. The auxiliary circuit consists of a bidirectional scaler, composed of five decade counter units and appropriate logic circuitry. The performance of the assembly in the analysis of the reactions ^{6}Li(d,2α) and ^{7}Li(d,2αn) on natural Li is described. (T.F.H.)

44517 PARTICLE IDENTIFICATION USING A SINGLE COUNTER. Legg, J. C. (Rice Univ., Houston, Tex.). Nucl. Instr. Methods, 36: 343-4(Oct. 1965).

The feasibility of particle identification using a single detector is investigated, using a silicon detector with a 3-mm-deep lithium-drifted layer. The method is based on the observation of the rise times of the pulses produced by the particles in the detector. The technique studied is found to be feasible, and the optimum results are found to be obtainable using an amplifier having 0.05 μsec rise time and 0.2 to 0.35 μsec clipping time. (T.F.H.)

44518 THE BEHAVIOR OF A WIDE GAP SPARK CHAMBER WHEN TWO PARTICLE TRACKS ARE PRESENT. Garvey, J.; Brookes, G. R.; Smith, I. L.; Rutherglen, J. G. (Glasgow Univ.). Nucl. Instr. Methods, 36: 347-9(Oct. 1965).

A single-gap spark chamber having a 15-cm electrode spacing is filled with a Ne–2% He mixture. The response of this chamber to the passage of particles, during the "memory" time of several μsec following the occurrence of a previous spark, is studied. (T.F.H.)

44519 AN ANTICOINCIDENCE-SHIELDED Ge(Li) GAMMA-RAY SPECTROMETER. Hill, M. W. (Pacific Northwest Lab., Richland, Wash.). Nucl. Instr. Methods, 36: 350-2(Oct. 1965).

A lithium-drifted germanium detector is used at the center of a large plastic scintillation detector that acts as an anticoincidence shield and as a gamma spectrometer. The performance of the detector with and without the anticoincidence shield is shown. The shield reduces the Compton background in the measured spectra. (T.F.H.)

44520 ELECTRON EXCITATION OF ZnS(Ag). De Volpi, A.; Porges, K. (Argonne National Lab., Ill.). Nucl. Instr. Methods, 36: 354(Oct. 1965).

The effects of external sources on the apparent response of Ag-activated ZnS to 70-kev electrons are shown. The sources of error discussed include gamma-ray-induced electrons absorbed by the ZnS, pile-up pulses resulting from the high absorption efficiency of transparent media incorporated in most detection systems, and intermediate decay luminescence produced in several transparent materials. (T.F.H.)

44521 NUCLEAR PULSE AMPLIFIERS—FUNDAMENTALS AND DESIGN PRACTICE. Fairstein, E. (Tennelec Instrument Co., Inc., Oak Ridge, Tenn.); Hahn, J. Nucleonics, 23: No. 9, 81-6; 88(Sept. 1965).

Current-mode vs. voltage-mode amplification is discussed. Various sources of pulse-height distortion are considered. Pulse shaping and pile-up effects are described. (M.C.G.)

44522 A NEW ELECTRON DETECTOR WITH HIGH REJECTION POWER AGAINST PIONS. Massam, T.; Muller, Th.; Schneegans, M.; Zichichi, A. (CERN, Geneva). Nuovo Cimento (10), 39: 464-73(Sept. 16, 1965).

An electron detector, which consists of five elements, each one being made of a lead layer followed by a plastic scintillation counter and a two-gap spark chamber, is described. The rejection power of this new detector against pions is of the order of $4 \cdot 10^{-4}$, the efficiency for electron detection varies from 75% to 85%, and the energy resolution can be as good as 10%, in the energy range 1.1 to 2.5 Bev. (auth)

44523 HYDRODYNAMICS OF A RESONANCE BUBBLE CHAMBER. Budagov, Yu. A.; Dzhelepov, V. P.; Lomakin, Yu. F.; Flyagin, V. B.; Shlyapnikov, P. V. (Joint Inst. for Nuclear Research, Dubna, USSR). Pribory i Tekhn. Eksperim., No. 4, 42-5(July-Aug. 1965). (In Russian).

On the basis of a general approach to bubble chambers as in resonance systems, the hydrodynamics of the process of the excitation in liquids of continuous periodic oscillations of pressure were determined with the purpose of developing high efficiency chambers. The possibility of the application of such chambers to experiments at the synchrophasotron was indicated. The relations which represent the practical utilization and combined the basic construction and hydrodynamic parameters of the resonance chambers were investigated. (J.S.R.)

44524 MULTIDIMENSIONAL ANALYZER WITH A PRELIMINARY TREATMENT OF DATA AND COMBINED-TYPE MEMORY. Ekatov, A. B.; Ivchenko, V. E.; Matalin, L. A.; Meshkov, N. V.; Smirnov, V. I.; Chernukhin, V. L. (Inst. of Physics and Power Engineering, Obninsk, USSR). Pribory i Tekhn. Eksperim., No. 4, 94-100(July–Aug. 1965). (In Russian).

A multidimensional analyzer, designed for measurement of the double differential cross section of slow neutrons, was described. The recording device was calculated on the basis of a 16,000 channel spectra and consists of memory on ferritic cores (2048 channels) and magnetic strips. The analyzer can receive data simultaneously from 16 detectors, and the dead time of the apparatus for each entry is 4 μsec. A preliminary classification and leveling of the data before recording on magnetic tape guarantees the reception of information of a mean velocity of 320 pulses/sec. The analyzer does some mathematical processing of a given experiment for decrease of its volume and reduction in form, convenient to introduce into the usual computer. The functional scheme of the device in various operational regimes is described and the characteristics of its individual sections are given. (tr-auth)

44525 STUDIES ON HIGH DOSE RATE-METER BASED ON MEASUREMENT OF THE ELECTRIC RESISTANCE OF LIQUID ORGANIC COMPOUNDS. Kitahara, Kazuta (Kumamoto Univ., Japan); Tanaka, Yoshimasa; Koyano, Akira; Yagisawa, Toshi. Radioisotopes (Tokyo), 14: 377-81(Sept. 1965). (In Japanese).

A study was carried out to devise a new dose rate-meter based on the measurement of electric resistance of liquid organic compounds. A 16,000 C Co-60 source was used as the radiation source. Electric resistance during irradiation was measured with a special type of measuring cell possessing wide electrodes and glass tape as insulator. It was found that a correlation between the dose rate I(R/hr) and the electric resistance R(MΩ) of the measuring cell enclosing liquid paraffin during irradiation could be expressed by the formula, $I = K/R^n$ (where K is a constant) at a constant temperature within a range of dose rate of 10^4 to 10^6 R/hr, but that electric resistance returned to the pre-irradiation level within a few hours upon the removal of the irradiation source, and re-irradiation gave the same electric resistance. From these facts it is considered that the special cell enclosing liquid paraffin could be applied for measuring a high dose rate. (auth)

44526 PROPORTIONAL COUNTING TECHNIQUE FOR LOW LEVEL ^{14}C ACTIVITIES. Moreno y Moreno, Augusto (Comision Nacional de Energia Nuclear, Mexico City). Rev. Mex. Fis., 14: 1-16(1965).

Preliminary work performed for dating archaeological samples and determining the contents of ^{14}C at low level using proportional counting techniques is reported. Descriptions are given of the acetylene method, electronic equipment, counter, and breakdown tests. (L.B.S.)

44527 THE THREE-AXES SPECTROMETER OF THE INSTITUTE FOR ATOMIC PHYSICS, BUCHAREST. Bally, D.; Todireanu, S.; Birsan, I.; Pirlogea, P.; Tarina, E. (Inst. for Atomic Physics, Academy of the R.P.R., Bucharest). Rev. Roumaine Phys., 10: 445-53(1965).

The mechanical unit of a three axes spectrometer is

described. An analytical criterion of the spectrometer resolution vs the transmissions of the monochromator and analyzing units is given. The criterion permits, for a given resolution, the choice of the most convenient divergence of the fourth collimator. When cadmium sheets are used for the third collimator, instead of iron ones, the background measured for scattering angles smaller than 30 degrees, is substantially reduced. The measured differential and differential partial cross-section of hydrogen and vanadium, are presented. (auth)

44528 LOW-LEVEL γ-RAY DOSIMETRY WITH SCINTILLATION COUNTERS. Okano, Masaharu (Inst. of Physical and Chemical Research, Tokyo). Rika Gaku Hokoku, 37: 355-65(1961). (In Japanese).

The applicability of the following three currently used methods of γ-ray dosimetry using a scintillation counter for a very low-level γ-ray dose rate is discussed: (1) absorbed dose rate of a specified scintillator material is measured with direct anode current of a photomultiplier, (2) absorbed dose rate is obtained by integration of the pulse height distribution curve, and (3) exposure dose is calculated from the γ-ray spectrum measured with a scintillation γ-ray spectrometer. It was concluded that the first of these methods is less sensitive and the other two are rather cumbersome and time-consuming. A new and simple method is proposed which uses an ordinary scintillation counter having a NaI(Tl) scintillator covered with a shield for correcting its energy-dependent characteristics. The shield consists of a brass cylinder of 3.5 cm thick fitted to the scintillation crystal and having 25 holes of 8 mm in diameter, which direct to the center of the crystal. With this device, a dose rate of as low as 0.1 μR/hr in the energy range of 0.1 to 2 Mev could be measured by simply reading its counting rate. As an example of this method, data on terrestrial background γ-ray dose rate are illustrated. (BBB)

44529 ON TRANSISTORIZED AIRBORNE APPARATUS FOR DETECTION OF EXTENSIVE AIR SHOWERS. Imai, Takashi; Kamata, Koichi; Kawasaki, Shinkichi; Murakami, Kazuaki (Inst. of Physical and Chemical Research, Tokyo). Rika Gaku Kenkyusho Hokoku, 37: 73-8(1961). (In Japanese).

A new airborne device was constructed for experiments on the altitude variation of air showers. The instrumentation consists of eight scintillation counters, a multichannel synchroscope, and a triggering circuit of a recording camera. To minimize weight, to economize total power consumption, and to facilitate maintenance, almost all electronic circuits are transistorized. Each scintillation counter contains a plastic scintillator (25 × 25 × 5 cm), a photomultiplier, a transistorized logarithmic amplifier, and power supply. Five scintillation counters are used to measure, with recording, the particle density at different points in the air shower to get the information on the lateral structure of shower. The transition meter is composed of three scintillation counters placed on one another with two lead plates inserted between them. By measuring the transition effect occurring in each counter, information on the energy of incident particles can be obtained. The pulses from the eight counters are fed through the logarithmic amplifier to the synchroscope and are photographically recorded. Electric power is supplied mostly from dry batteries, and the total weight of the whole apparatus including dry batteries is about 260 kg. (BBB)

44530 TABLES TO CORRECT FOR RESOLVING TIME COUNTING LOSSES OF NUCLEONIC APPARATUS. Marais, P. G.; deV. Smit, W. B. (Fruit and Food Technology Research Inst., Stellenbosch, South Africa). Tech. Commun., Dept. Agr. Tech. Serv. (S. Africa), No. 37, 49(1965).

Since resolving times of nucleonic apparatus range from a few microseconds in the case of scintillation counters to several hundred for G-M counters, it is impractical to calculate tables containing counting rate corrections (ΔN) for individual resolving times (τ). However, this problem has been solved here by compiling tables in such a way that each table covers a range of resolving times. This was achieved by making use of the fact that for a certain range of τ the value of ΔN may be taken as proportional to τ up to certain counting rates, while for higher counting rates the increase in ΔN (ΔΔN) may be taken as proportional to the increase in τ (Δτ). In calculating the corrections a nonextendable resolving time was assumed; experience has shown that this assumption is valid for most nucleonic apparatus normally in routine use in agricultural research. This includes proportional and scintillation counters where the associated electronic circuits determine the resolving time, as well as G-M counters used with or without external quenching units. Each table covers a range of resolving times and the main figures in each table are the corrections (ΔN) for the initial τ value of each table. These corrections must be added to the observed counting rates, and for τ = 1.0, 2.5, 5.0 ... 550 μsec, they are obtained directly from the tables. Corrections for the higher τ values of each table are obtained in two ways, depending on the counting rate (Ne). For those sections of the tables where ΔN values alone are given, the overall corrections (ΔN′) are given by an equation. Using the principles outlined it was possible to cover a range of resolving times from 1 to 650 μsec with only 22 tables and all these tables are presented. (BBB)

44531 PERFORMANCE OF A THREE-AXIS SPECTROMETER IN EXPERIMENTS OF ELASTIC DIFFRACTION OF NEUTRONS. Caglioti, G. (EURATOM, Ispra, Italy); Tocchetti, D. pp 505-12 of STI/PUB/92(Vol.II).

The method of elastic diffraction of neutrons can be advantageously utilized both in the study of liquid dynamics and in the analysis of some problems in the field of crystal physics. The main features of the experimental technique of elastic neutron diffraction are recalled, and its possible applications are reviewed. Furthermore, a study is presented concerning the instrumental energy resolution of a three-axis spectrometer in experiments of coherent elastic diffraction. (auth)

44532 INDIVIDUAL ALARM DOSIMETERS FOR WORK IN OR ENTRY INTO RADIATION FIELDS. Fitoussi, L. (Centre d'Etudes Nucleaires, Fontenay-aux-Roses, France); Ganouna-Cohen, G.; Rage, P.; Amardeil, P. J. pp 67-76 of STI/PUB/99. (In French).

Studies were made of integrating dosimeters which give an audible alarm when a pre-set dose limit is reached. This means that personnel need not devote any of their attention to dosimetry. The various problems arising out of the use of this technique are discussed. Three pieces of equipment are described. They have certain attributes in common such as: ease of use owing to light weight and small bulk (pocket equipment); variable thresholds; and audible alarm. Some points of difference are: detector used (Geiger counter or ionization chamber); electronic system; thresholds used (a few Rem); and maximum dose rates for which they can be used (from a few tens of Rem/h to 10^4 Rem/hr). (P.C.H.)

44533 HIGH-DOSE IONIZING RADIATION PHOTOGRAPHIC DOSIMETRY. Trousil, J.; Bucina, I. (Inst. for Research, Production, and Application of Radioisotopes, Prague). pp 85-99 of STI/PUB/99.

Film dosimetry of ionizing radiation in the range of 10 mR to 1000 R (for γ and higher energy x rays) is described. Two films with different emulsions, worn simultaneously in the same badge, are used. An essential feature of the technique is that the doses in the given range may be evaluated without knowing whether a higher exposure has taken place with an accuracy better than ±25% over the whole dose range (confidence interval 95%). The radiation energy to which the film has been exposed can also be estimated to a good approximation. The equipment, film types, and chemical processing facilitating these measurements are described, along with the principle of the densitometer construction, which permits measurement of film blackening with the same accuracy in the range from D = 0 to D = 6. By this method the whole range of applicable film blackening may be utilized. The parameters of a dosimeter film suitable for high-dose detection are given, and the properties of high-level

dosimeter FOMA and ORWO films are compared. In the emulsions used for high-level dose measurement and processed in a developer with the addition of inhibitors, the effects of energy dependence and latent image fading on the accuracy of exposure measurement was determined. The errors in film dosimetry of high-level doses, which were observed on the basis of experimental work with the aid of mathematical statistics, are also described. (P.C.H.)

44534 MONOBATH FILMS FOR DETERMINING ACCIDENTAL HIGH-LEVEL EXPOSURES. Wachsmann, F. (Institut fuer Strahlenschutz der Gesellschaft fuer Strahlenforschung mbH, Neuherberg, Ger.). pp 101-8 of STI/PUB/99.

For remote reactor plants and others not provided with a permanent monitoring team to measure the dose to the personnel, the monobath method is recommended for handling film dosimeters. With this method it is possible to determine on the spot and without any loss of time whether persons have received a critical dose calling for medical care. The films recommended enable doses from about 10 to 2000 R to be detected by subjecting the films to an extremely simple monobath process. The density curves, their dependence on the radiation energy and on the temperature of the monobath developer, are shown. The films are processed in daylight in a small device the size of a cigarette packet. By means of this device, which is described in detail, 40 film dosimeters can be processed and evaluated by one person in about one hour. The dose is determined by comparing the film blackening with that of a strip fitted into the device for this purpose. The monobath films are conveniently worn in small sturdy film badges which are insensitive to external influences. Film evaluation is made only if the exposure to radiation is likely to have caused a substantial personnel dose. The films have a lifetime of at least two years. The badges contain a lead filter rendering the film blackening largely independent of the radiation energy over the range from about 75 kev up to 3 Mev and more. If desired, the lead filter can be provided with a window so that part of the radiation can reach the film unattenuated. In this way it is possible to draw conclusions as to the type (gamma or beta rays) and energy of the radiation, both essential factors for a correct evaluation of the hazards. The described monobath film dosimeters can be used alone in the event of an incident or together with other film dosimeters of high sensitivity or with pocket dosimeters based on ionization under normal monitoring conditions. (auth)

44535 UTILITY OF ACTIVATION DETECTORS FOR THE ASSESSMENT OF LARGE DOSES FROM HIGH-ENERGY PARTICLES. Sklavenitis, L. (Centre d'Etudes Nucleaires, Fontenay-aux-Roses, France). pp 279-95 of STI/PUB/99. (In French).

The possibility of using activation detectors for approximate spectral analysis of the radiation field and for flux calculations is discussed. Although present knowledge of very high-energy reactions and the values of the corresponding cross-sections is inadequate, particularly as regards neutrons and relativistic particles, it is nevertheless sufficient to enable a preliminary choice to be made of activation detectors providing, with sufficient accuracy for radiological protection purposes, an estimate of the mean fluxes of particles in various energy ranges and thus the doses absorbed. (P.C.H.)

44536 MULTIPLE-PURPOSE PERSONAL DOSIMETER SUITABLE FOR DOSIMETRY OF HIGH ACCIDENTAL EXPOSURES. Francois, H.; Bourbigot, Yveline; Grand-Clement, Anne-Marie; Portal, G.; Soudain, G. (Centre d'Etudes Nucleaires, Fontenay-aux-Roses, France). pp 319-28 of STI/PUB/99. (In French).

Evaluation of doses received by workers liable to high accidental exposures is given. It consists of a film dosimeter plus a glass, threshold and activation detector pack. The film dosimeter consists of a case fitted with screens demarcating seven different areas of the film. The latter, which provides density measurements by reflection, consists of three emulsions of different sensitivities on a common base, so that a single development covers the dose range between 20 mR and 800 R. An NTA nuclear-emulsion, fast-neutron dosimeter can be added. Two glass dosimeters of different characteristics are included to permit separate evaluation of gamma and thermal neutron radiation. The unit also possesses conventional threshold and activation detectors. (auth)

44537 THE ACTIVATION NEUTRON SPECTROMETER (SNAC) AND ITS RESPONSE TO MODERATION. Bricka, M.; Cercy, J. (Centre d'Etudes Nucleaires, Cadarache, France). pp 381-92 of STI/PUB/99. (In French).

For the purpose of criticality accident dosimetry, simplified spectrometers using activation detectors were studied. These consist of a cadmium case surrounding sulfur, magnesium, gold, and copper discs, and there are copper discs on the two faces of the case to measure thermal fluxes. The diameters used are: 19, 30, 50, 60, and 100 mm. Sensitivity is of the order of 1 Rem. Applying the spectral index method, the measurement data obtained can be utilized with sufficient ease and accuracy. Trials were carried out with a fast critical assembly from which it was possible to establish the spectral pattern in the neighborhood of the reactor and the disturbances caused by the presence of a moderator. The trials showed that personal activation dosimeter data alone cannot be used without large corrections. Orientation of the exposed person has a vital bearing on the correction needed. (auth)

44538 DETECTION AND MEASUREMENT OF ACTIVITY IN WOUNDS. Fessler, H.; Kiefer, H.; Maushart, R. (Nuclear Research Center, Karlsruhe, Ger.). pp 419-26 of STI/PUB/99.

For the proper medical treatment of wounds containing radioactive materials, the physician has to know not only type and amount of activity, but also the location and extent as exactly as possible. The necessary accuracy of detection and measurement can only be achieved with special radiation detectors. They must be very small, insensitive to light and humidity, mechanically robust, electrically safe, and must endure heating to about 200°C for sterilizing purposes. Several possibilities of building such detectors are discussed. The design and construction of some instruments developed and used at the Karlsruhe Nuclear Research Centre are shown, and a comparison of the performance of the different types of counters is given. (auth)

44539 CRYOSTAT (Engineering Materials). (Brookhaven National Lab., Upton, N. Y.). (CAPE-1257). 12 drawings.

The cryostat described is used with a lithium-drifted, germanium γ detector in the study of γ rays produced in nuclear reactions. It requires a minimum of routine maintenance, allows easy portability and maximum counting efficiency. A polyethylene enclosure protects the detector against vapor contamination and clamps the germanium securely against the Al pedestal of a Cu cold finger. Materials of low atomic number are used to reduce γ scattering, and the Al cap is thinned for improved transmission of low-energy γ rays. The lower end of the evacuated assembly is immersed in liquid N, and the operating temperature at the detector is lower than 100°K within an hour of immersion in N. With a low noise, thermionic preamplifier, and a germanium detector of 6 cm^2 area and 6 mm drifted depth, the total capacity presented to the preamplifier is about 20 picofarads, which results in a line width of 3.5 kev. This line width is obtained with the first stage of the preamplifier connected directly to the vacuum feed. With a connecting cable, the lines are broadened in proportion to the added capacity. The effective capacity can also be reduced by the use of a preamplifier with a cooled first stage interior to the vacuum chamber. (For Details, See TID-4100) (F.J.H.)

44540 POSSIBLE ERRORS IN THE FERROUS SULPHATE DOSIMETER. Holloway, A. F.; Froese, G. (Manitoba Cancer Treatment and Research Foundation, Winnipeg, Can.). 5p. (CONF-650219-3). Gmelin, AED-CONF-65-075-3.

From Canadian Association of Radiologists, 28th Annual Meeting, Toronto.

An investigation was made of the discrepancies observed in the results obtained in the calibrating procedure for the electron beam of a betatron, using a ferrous-sulfate dosimeter. It was found that a precipitate forms in ferrous sulfate dosimeter solution, independent of irradiation, which forms a suspension on shaking. The amount of suspension depends on the surface area, time of standing, and nature of the surface. For most dosimetry procedures the effect of any precipitate formed would be very small. (L.B.S.)

44541 A STUDY OF A THERMOLUMINESCENT DOSIMETER. Worton, R. G.; Holloway, A. F. (Manitoba Cancer Treatment and Research Foundation, Winnipeg, Can.). 10p. (CONF-650219-4). Gmelin, AED-CONF-65-075-1.

From Canadian Association of Radiologists, 28th Annual Meeting, Toronto.

A study is made of a thermoluminescent dosimeter using a commercially available system which consists of a LiF phosphor, a read-out instrument, and a dispenser. The results of energy response, sensitivity, and precision studies are presented. It is concluded that because of its small size and ease of handling, its tissue equivalence, and its property of storing absorbed energy, LiF is potentially an ideal dosimeter for in vivo measurements as well as for calibration purposes. (L.B.S.)

44542 PORTABLE, BATTERY-OPERATED MEASURING APPARATUS FOR DETECTION OF RADIATION. Jordan, Kurt; Kuehnert, Hans (to Frieseke and Hoepfner G.m.b.H.). German Patent 1,196,304. July 8, 1965. Filed Mar. 15, 1963.

The instrument is provided with a cylindrical, removable measuring probe comprising a radiation detector which is inserted into the housing of the instrument. This probe has a slotted counter window which can be shielded by an axially movable, cylindrical beta-shield comprising slotted openings. The beta-shield is operated by the range selector. (Gmelin Inst.)

44543 NEUTRON DOSIMETER FOR THE MEASUREMENT OF THE BIOLOGICAL NEUTRON DOSE EFFECT. Kiefer, Hans; Maushart, Rupprecht (to Gesellschaft fuer Kernforschung m.b.H.). German Patent 1,197,180. July 22, 1965. Filed Dec. 11, 1961.

The neutron dosimeter for measuring biological dose effect is combined with activation, threshold, and/or resonance probes. The quantity and/or geometry of these probes is chosen in such a way that the effect of the radiation emitted by the activated probes on a radiation instrument is about proportional to the biological neutron dose effect. (Gmelin Inst.)

44544 HIGH INTENSITY GAMMA INSENSITIVE NEUTRON DOSIMETER. Kronenberg, Stanley (to U. S. Army). U. S. Patent 3,197,637. July 27, 1965. Filed July 2, 1962.

A γ-insensitive neutron dosimeter consists essentially of three spaced parallel metallic plates of equal area and disposed in registered alignment. The plates are electrically insulated from each other. One outer plate is charged negatively and the other positively. The center plate is faced on one side with neutron sensitive material and is electrically connected to a readout device. Neutrons reaching the neutron-sensitive face of the center plate produce high-energy charged particles that escape from the plate and produce low-energy secondary electrons in proportion to the incident neutron flux. The electrons are collected by the positively charged outer plate. A sealed envelope structure provides for maintaining a high vacuum in the space between the plates. (A.G.W.)

44545 X-RAY EMISSION ANALYZER WITH STANDARDIZING SYSTEM AND NOVEL SWITCH MEANS. Furbee, Avery, D. (to General Electric Co.). U. S. Patent 3,198,944. Aug. 3, 1965. Filed Nov. 6, 1961.

A standardizing apparatus and procedure for a continuous readout on-line x-ray gage is patented. Standardization is achieved by temporarily discontinuing regular gage operation and interposing a standard known specimen in the x-ray beam, deriving a pulse output signal for a preset time from a detector responding to intensity of radiation emitted by each element in the standard specimen, converting the pulsed signals from each channel to a voltage analog of the quantity of each element present, electrically comparing this voltage with a standard voltage or memory representative of what the output voltage should be, and then introducing a suitable correction in the system if needed. After termination of the standardizing interval, all channels of the gage are quickly restored to operation at near whatever output level prevailed in each of them before standardization began. (A.G.W.)

44546 RADIATION DOSIMETER PROVIDING A VISUAL REPRESENTATION OF TOTAL DOSE. Dewes, Roger A.; Goodale, Edmund E. (to General Electric Co.). U. S. Patent 3,198,945. Aug. 3, 1965. Filed May 16, 1961.

In a dosimeter suitable for carrying by a person, a phosphor crystal is positioned adjacent a photovoltaic cell. The output of the photovoltaic cell is serially connected to a visual current integrator, which may be a vial having electrodes and containing a chemical solution that changes color in response to electric current passing through it. A predetermined color standard may be positioned adjacent the visual current integrator so that an inspection shows immediately the total radiation dosage. (A.G.W.)

44547 APPARATUS FOR MEASURING ACTIVITY LEVELS OF RADIOACTIVE SAMPLES. Olson, Robert E. (to Packard Instrument Co.). U. S. Patent 3,198,948. Aug. 3, 1965. Filed Apr. 15, 1963.

An elevator mechanism is patented for lowering vials containing a liquid scintillator and radioactive isotope to be measured into a detection chamber and for ejecting the vial upon completion of counting. A sealing arrangement between the elevator and elevator shaft is characterized by the fact that the sealing means employed does not rub against or contact the elevator shaft during passage of the elevator through it; spurious light responses incident to rubbing contact between sealing material and the shaft walls are thus eliminated. The apparatus may be used for manual or semi-automatic operation or with a wide range of automatic sample changers now commercially available. (A.G.W.)

Radiation Effects

44548 (NP-15422) COMPONENTS IRRADIATION TEST NO. 4—2N1132 TRANSISTORS. (Lockheed-Georgia Co., Marietta). July 10, 1964. 76p. (ER-7483).

Fifty specimens of the type 2N1132 transistor from each of three manufacturers were tested to determine the effect of nuclear radiation on the h_{FE}, I_{CBO} and V_{BE} parameters. The three manufacturers were Motorola, Texas Instruments, and Hughes. The specimens, except the control groups, were exposed to a total average radiation exposure of 1.5×10^6 R and 9.1×10^{13} n/cm^2. All irradiated specimens experienced a decrease in h_{FE}, an increase in I_{CBO}, and a decrease in V_{BE}. Under the failure criteria selected (50% reduction in h_{FE}), the Motorola specimens showed the greatest tolerance to radiation failing at 7×10^{12} n/cm^2. The Texas Instruments specimens were next at 4.4×10^{12} n/cm^2, and the Hughes specimens were last at 2×10^{12} n/cm^2. (auth)

44549 EFFECTS OF LOW-ENERGY ELECTRON IRRADIATION ON Si-INSULATED GATE FETS. Speth, A. J.; Fang, F. F. (IBM Watson Research Center, Yorktown

Heights, N. Y.). Appl. Phys. Letters, 7: 145-6(Sept. 15, 1965).

The effects of electron irradiation on the Si-insulated gate FET particularly the functional dependence of device characteristics after bombardment on the gate electrode bias during electron bombardment. The N-channel IGFETs had an oxide thickness of approximately 6000 Å. A 5-kev beam in a vacuum of about 10^{-5} ton was used. The low beam voltage assured that no electron penetrated the silicon. During electron irradiation the gate of the sample was positively biased with respect to the silicon substrate. After irradiation, the channel conductance and transconductance of the device were measured as a function of gate voltage at a small source-to-drain voltage. The sample was then biased for further irradiation. It was found that for each gate bias voltage the threshold voltage of the device shifted to a stable value after a sufficient exposure. Typical behavior of the steady state characteristics measured after beam exposure are shown. (J.F.P.)

44550 SPACE RADIATION: ITS INFLUENCE ON SATELLITE DESIGN. Holmes-Siedle, A. G. (Radio Corp. of America, Princeton, N. J.). RCA Engr., 11: 8-14(June-July 1965).

Problems in the design of electronic equipment to withstand the damaging effect of radiation are discussed in terms of spacecraft design. Each part must be considered separately, taking into account not only the expected radiation dose but also the application and criticality of the component. Some of the currently known information about this complex environment is reviewed and recommendations given for designing electronic equipment for reliable operation in space. (TCO)

ISOTOPE TECHNOLOGY

General

44551 RADIOISOTOPE SELECTION. Taylor, Denis (University Coll., Nairobi, Kenya). EuroNucl., 2: 379-82 (Aug. 1965).

An attempt is made to provide potential radioisotope users with some of the more essential data and the method needed to select a radioisotope for a specific task. Radiation characteristics are discussed. Equations are given for calculating beta and gamma attenuation and gamma dose rates at any given distance. Determining the amount of radioisotope required is discussed. (M.C.G.)

Industrial Applications

Refer also to abstract 44094.

44552 (BLG-327) THE POSSIBILITY OF USING RADIOSENSITIZERS IN THE PRESERVATION OR STERILIZATION OF FOOD, DRUGS AND MEDICAL SUPPLIES BY IRRADIATION. De Proost, M. (Centre d'Etude de l'Energie Nucleaire, Brussels (Belgium)). Nov. 1964. 9p. Dep. mn.

A survey is given of the different chemical products quoted in the literature as compounds enhancing radiation inactivation of bacteria. These compounds are oxygen, vitamin K5 and its analogues, N-ethylmaleimide, alkali halides, halogenophenols and iodoacetamide. The possible technological importance of radiosensitizers in the radiation processing of foods is discussed. (23 references.) (auth)

44553 (EUR-2284.I) DETERMINAZIONE DI PERDITE IN RETI DI DISTRIBUZIONE PER GAS MEDIANTE TRACCIANTI RADIOATTIVI. (Detection of Leakage in Gas-Distribution Networks by Means of Radioactive Tracers). Bruna, A.; Caldera, P. G. (Societa Ricerche Impianti Nucleari, Sluggia (Italy). Centro Ricerche Nucleari). 1965. 38p. Dep. mn.

A description is given of the experiments relating to the study on the applicability of a method for the location by radioactive tracers of leaks in town-gas mains which may be temporarily put out of commission. Since the pinpointing of leaks is based on the possibility of detecting on the surface the radiations emitted by the radioisotope which has escaped from the leakage points in the piping, it was confirmed that the radioisotope concentration in the joints, the foulings, and the condensates was not heavy enough to simulate leakage points. The next step was to establish the influence of certain parameters on the detection efficiency (max/μc ground-infiltration signal). The parameters considered are the nature, compactness, humidity, and depth of the ground above the mains, the extent and location of the leaks, the duration of the radioactive-gas infiltration into the ground, and the gas pressure in the piping. Finally, some leak-location experiments were carried out on sections of mains in operation, of varying lengths, belonging to various distribution facilities and put out of action for the duration of the test. The results of these experiments are promising. (auth)

44554 (IA-1015) THE EFFECT OF ^{60}Co GAMMA RAYS APPLIED AT LOW DOSE RATES ON SOME JUICE CONSTITUENTS AND THE PEEL COLOUR OF GREEN AND RIPE FRUITS OF SEVERAL CITRUS VARIETIES. Kahan, R. S.; Goren, R.; Monselise, S. P. (Israel Atomic Energy Commission, Yavne. Soreq Nuclear Research Center). Apr. 1965. 12p. Dep. mn.

Green Shamouti and Washington navel oranges and Clementines were treated with γ radiation at doses of 28 to 80 krad, and ripe Shamouti oranges with 93 to 184 krad, at low dose rates (less than 2 krad/hour). Irradiation caused degreening within 6 days. There were no significant changes in the acid, vitamin C, soluble solids and hesperidin contents in the juice of the irradiated fruits, except in the case of near-ripe, green Washington navel oranges where 80 krad caused a loss of more than 10% vitamin C. No macro-damage was caused to the pulp or skin of any of the fruits. (auth)

44555 (NP-15373) DEVELOPMENT OF RADIATION STERILIZED FISH ITEMS FOR ARMED FORCES FEEDING. Sinnhuber, R. O. (Oregon State Univ., Corvallis). Aug. 1965. Contract DA19-129-AMC-155(N). 21p. (FD-15).

Five radiation-sterilized (4.5 Mrad) seafood products, including breaded prefried cod patties, breaded prefried halibut patties, enzyme-inactivated cod patties, enzyme-inactivated halibut patties, and halibut steaks, processed with and without antioxidants, were evaluated periodically during 12-month storage at 72°F by subjective and objective methods. Preference panels of 132 to 210 tasters indicated all five products had acceptable flavor after 9-month storage. After 12-month storage, the panels preferred the non-irradiated frozen control samples to the irradiated samples; however, the irradiated samples received flavor scores in the acceptable range with the exception of the prefried halibut patties without antioxidant and halibut steaks with and without antioxidants. The antioxidants had little or no effect on flavor scores. Color reflectance values seemed to be the most reliable method of all the methods studied for measuring length of storage and degree of browning. Sauces, served with enzyme-inactivated halibut patties, proved to be an acceptable alternate method for serving. (auth)

44556 (NP-15464) DEVELOPMENT OF IRRADIATION STERILIZED SHELF-STABLE FISH AND SEAFOOD PRODUCTS. Schultz, H. W.; Sinnhuber, R. O.; Yu, T. C.; Landers, M. (Oregon State Univ., Corvallis. Dept. of Food Science and Tech.). Aug. 1965. Contract DA 19-129-QM-1356. 23p. (FD-16). CFSTI.

Results of a series of experiments have led to the development of five radiation processed (4.5 Mrad) seafood products. These include prefried and enzyme-inactivated codfish patties, prefried and enzyme-inactivated halibut patties, and halibut steak. Large consumer panels judged these products acceptable initially, shortly after irradiation, and after 6 months of shelf storage at 21°C. The study included investigation of a large number of variables including thirty commercial brands of breaded seafood products; enzyme-inactivation technique; a large variety of breadings, batter, and binders; methods for preparing the various types of patties; effects of several different anti-browning and antioxidizing agents; and effects of seasoning and flavor intensifiying agents. Both subjective and objective analytical techniques were used for determining the effects of the various factors on acceptability and stability of the products. (auth)

44557 (NYO-3426-1) STUDY OF THE ECONOMICS OF CONTROLLING SALMONELLAE IN FOODS BY THE USE OF IONIZING RADIATION. (Little (Arthur D.) Inc., Cambridge, Mass.). Apr. 30, 1965. Contract AT(30-T)-3426. 71p. Dep. mn; CFSTI $3.00 cy, $0.75 mn.

The economic feasibility of using ionizing radiation to control salmonellae in poultry products is discussed. Work included the consideration of products ranging from meat meal, fish meal, poultry meat, shell eggs, and processed egg to cake mixes. The technical feasibility of using ionizing radiation in pasteurizing doses to control salmonellae in foods was proven. The necessary sources of radiation are available, and tests have shown the wholesomeness of the irradiated products. On the other hand, Food and Drug Administration approval for irradiation of these materials has not yet been obtained. Further, when irradiating conditions were not properly controlled, undesirable flavors developed. Radiation for pasteurizing

purposes is available by three different methods: ^{60}Co gamma rays, x rays, and electron beams. Exploratory estimates were prepared for evaluating available methods of irradiation at three levels of production. These estimates are based on the assumption that the irradiation step would be part of a process operating for additional purposes (in contrast to a separate facility established for only this function) and that material would be treated in packages or in bulk on a conveyor. (Deviations from these assumed conditions will obviously affect costs.) The figures are derived on the basis that a minimum dose of approximately 500,000 rads would be required for pasteurization. Nominal plant capacities at 2,000, 5,000, and 15,000 lb/hr were derived from annual capacities, under a full-time operation. Anticipated actual hourly capacities would be somewhat higher to provide allowance for down-time for maintenance and repairs. The gamma-ray facilities were priced with cobalt-60 included at 70¢ per curie encapsulated, delivered, and installed. The use of cobalt-60 was shown to be at an economic disadvantage in comparison with machine-produced radiation. This method faces more potent competition, moreover, from other sources. If adequately utilized, existing techniques available to the food industry offer promise of bringing salmonellae under control. Appropriate sanitary measures of a general nature can be more broadly practiced at small expense. In addition, thermal pasteurization can be more extensively used for liquid egg, and the microbiological quality of feeds can be improved by the use of pelleting under controlled conditions. (H.G.D.)

44558 (TID–22139) SIMULTANEOUS RADIATION-HEATING TREATMENT OF HADDOCK. Monthly Progress Letter, July 1–31, 1965. (Massachusetts Inst. of Tech., Cambridge. Dept. of Nutrition and Food Science). Contract AT(30-1)-3343. 6p. Dep. mn; CFSTI $1.00 cy, $0.50 mn.

Bacterial counts on lobster meat irradiated at 32 or 140°F with 125,000 or 250,000 rad doses showed that storage life at 36 to 40°F was extended considerably when irradiation was carried out at the higher temperature. Clostridial counts were negative on material irradiated at 32°F. Results from bacterial counts on scallops and fish sticks irradiated prior to storage at 36 to 40°F were inconclusive at the time of reporting. (H.G.D.)

44559 PRODUCTION EXPERIENCES WITH RADIATION STERILIZATION. Artandi, Charles (Ethicon, Inc., Somerville, N. J.). Bull. Parenteral Drug Assoc., 18: 2-9(Sept.-Oct. 1964).

The seven-yr experience of using radiation to sterilize medical supplies on an industrial scale is recounted. Advantages of radiosterilization over heat sterilization are enumerated. Irradiation does not affect, or may only slightly alter, heat-sensitive or easily degradable materials. Enzymes and many other products like vitamin solutions in oil, antibiotic aerosols and complex salt solutions could be sterilized by radiation. Another important advantage of radiation sterilization is that new, convenient and inexpensive packaging material may be used. Heat sterilization requires use of metal or heavy glass containers to maintain pressures and to protect the materials. In radiation processing a variety of materials may be used, such as thermoplastic films, paper-plastic, foil-plastic laminates, molded, pressure or vacuum-formed plastic containers. It also allows the hermetic sealing of products before sterilization. While radiation sterilization is recommended for many materials, for a large number radiation is contraindicated because of its varied effects on the materials. The radiation facility is described. Its main product is sutures packaged in aluminum-foil plastic laminate packets. The product is fed via a conveyor under the source and back on an output conveyor system. There are two 6-Mev linear accelerators in use. A closed circuit television system allows the observation of the product moving under the radiation source. At a quality control station samples are taken for sterility and physical properties testing. Dose measurements are made using rigid vinyl slides underneath the product to assure that the accelerator delivers a sterilizing dose through the product. The relative advantages of accelerators and radioisotope sources, such as ^{60}Co and ^{137}Cs, for radiosterilization are discussed. The great saving of an isotope facility is in labor and maintenance costs. (BBB)

44560 APPLICATIONS OF RADIOACTIVE NUCLIDES PRODUCED IN NUCLEAR REACTORS. Amphlett, C. B. Chem. Brit., 1: 371-4(Aug. 1965).

The uses of radioisotopes produced in reactors are discussed. Sterilization, pasteurization, polymerization and other chemical reactions, and power production using radioisotopes are described. (M.C.G.)

44561 PRESERVATION OF FOODS BY IRRADIATION. I. EVOLUTION AND PRESENT STATE IN THE WORLD. Del Val Cob, Manuel; Sune, Nicasio Ortin (Junta de Energia Nuclear, Madrid). Energia Nucl. (Madrid), 9: 95-111(Mar.-Apr. 1965). (In Spanish).

The history of preservation and conservation of foods is briefly summarized by a discussion of the problems of preservation, the useful time of storage, the necessity of preservation, the traditional methods used, and preservation of foods by irradiation. The principal developments in the field of food irradiation are discussed with respect to the practical application of radiation for food preservation and the changes produced in the foods by ionizing radiation. Some major bibliographic sources on food preservation by irradiation are given. (J.S.R.)

44562 INDUSTRIAL APPLICATIONS FOR RADIOISOTOPES. Lindhout, A. H. EuroNucl., 2: 387(Aug. 1965).

Applications of radioisotopes in the starch, dairy, and sugar industries discussed at a meeting of the Nederlands Atoomforum are summarized. (M.C.G.)

44563 ADVANCES IN STERILIZATION TECHNIQUES. Ehrlen, I. R. (AB Astra, Soedertaelje, Sweden). Pharm. Weekblad, 99: 1430-8(Dec. 18, 1964).

The use of ionizing radiation and other agents to sterilize pharmaceutical products is reviewed. (BBB)

44564 ADVANCES IN STERILIZATION TECHNIQUES. Ehrlen, I. R. (AB Astra, Soedertaelje, Sweden). Svensk Farm. Tidskr., 68, 818-24(1964).

Recent developments in the technology of thermal, chemical, and radiation sterilization are reviewed. Developments in the ionizing radiation sterilization field have been mainly concerned with practical applications in industry. Of the particle types of radiation, only β rays or megavoltage electrons, from linear accelerators or Van de Graaff generators, have been used. Among electromagnetic radiations, γ rays have been given most attention at present, ^{60}Co and spent fuel elements from atomic reactors being used as radiation sources. That γ radiation is very penetrating is its main advantage as a sterilizing agent, but at the same time offers serious hazards to its use; to exploit it safely and effectively, heavy and expensive shielding precautions have to be combined with a complicated conveyor system. β radiation is very much less penetrating and even radiation from 3-Mev electrons does not penetrate more than about 1 cm of water. This is comparable to the dimensions of a small ampoule. For low-density material or where the material to be irradiated can be spread out in thin layers, fast electrons offer a commercially acceptable solution. The amount of radiation required for effective sterilization is currently 2.5 Mrad, which is considered comparable to autoclaving at 120°C for 20 min. Even viruses, with higher resistance to radiation than bacteria, should be destroyed by this dose. However, when various pharmaceuticals were systematically submitted to 2.5 Mrad ^{60}Co radiation, many drugs showed discoloration and off-odors as well as decreases in potency. In general, dry substances withstand treatment better than in aqueous solutions. The discoloration produced in glass in another unsatisfactory effect, so that possibilities for γ ray sterilization of pharmaceuticals

do not seem very favorable. On the other hand, ionizing radiations offer notable advantages for the sterilization of such biological materials as surgical sutures and arterial, bone, and other tissue grafts. The field in which most progress is being made at present, and where the biggest potential future for radiation sterilization is found, is that of disposable medical supplies. Sterilization of plastic items or similar materials for hospitals, syringes, adhesive dressing, and catheters by radiation methods is rapidly increasing. Plastic is the material of choice for inexpensive single-use items and this can rarely be heat sterilized. Cost, however, is higher for radiation sterilization. Possible technics, whereby radionuclides with short half-lives are added to injectable materials for radiosterilization, are also discussed. (BBB)

44565 GIORNATE DELL'ENERGIA NUCLEARE 1964. Applicazioni Industriali dell'Energia Nucleare: Stato Attuale e Prospettive. (Advances in Nuclear Energy, 1964. Industrial Applications in Nuclear Energy: Present Status and Prospects). Milan, Federazione delle Associazioni Scientifiche e Tecniche, 1965. 348p. (CONF-641221).

Sixteen papers are included; separate abstracts have been prepared for all. Ten papers are in Italian, 4 in English, and 2 in French. (T.F.H.)

For abstracts of individual papers see: 43977, 45610–45622, 45723, and 45724.

44566 DEVELOPMENT OF PROGRAMS ON THE RADIATION PRESERVATION OF FOODS. Schmeigert, B. S.; Markakis, Perialas; Nicholas, R. C. (Michigan State Univ., East Lansing). 8p. (CONF-650552-2). Gmelin, AED-CONF-65-111 4.

From Inst. of Food Technologists, 25th Annual Meeting, Kansas City, Mo.

The use of radiation as a basic or supplemental method for food preservation is reviewed. From intense enthusiasm in the early '50s supporters of the program progressed through phases of cautiousness, international cooperation in research, redefinition to establish two separate goals—preservation or pasteurization and sterilization, and attempts to attain public acceptance through approval by appropriate agencies. Research and development programs are currently shifting emphasis from scientific feasibility to commercial feasibility. (H.G.D.)

44567 IMPROVEMENTS IN OR RELATING TO THE ILLUMINATION OF LEVELLING BUBBLES. Ault, John Douglas (to Saunders-Roe and Nuclear Enterprises Ltd.). British Patent 1,001,771. Aug. 18, 1965. Filed May 1, 1963.

Illumination of the bubble of a level or of a level indicator is provided by one or more self-luminous light sources that utilize a phosphor excited by a gaseous radionuclide. The light source(s) is contained within a chamber containing the bubble or is sealed by a transparent material to a chamber containing the bubble. At least a part of the light sources is coated with reflective material, and the sources are provided with a shockproof mounting that is reflective. The level, the light sources, and any mounting means are protected by an abrasive resistant sheath that is transparent or is provided with one or more windows to view the bubble. Means are provided to attach the level, light sources, or any shockproof mounting to any form of housing. (B.L.M.)

44568 HOT BEARING DETECTOR. Baughman, George W. (to Westinghouse Air Brake Co.). U. S. Patent 3,197,632. July 27, 1965. Filed July 20, 1959.

A hot bearing detector for railway cars utilizes a radioactive pellet enclosed in the journal box adjacent the bearing. The pellet is held by a fusible link in a position such that no radioactivity is detected outside the box. When the bearing, and consequently the link, is overheated, the pellet drops into a position such that radioactivity is detected by a wayside detector. A wheel detector adjacent to and controlled by the radiation detector indicates the position of the overheated bearing. (A.G.W.)

Power Application

Refer also to abstracts 44298, 45654, and 45662.

44569 (AGN-8122) RADIOISOTOPES IN HYDROSPACE. PRELIMINARY SURVEY REPORT. Durham, Laird (Aerojet-General Nucleonics, San Ramon, Calif.). Oct. 1964. Contract AT(04-3)-368. 24p. Dep. mn; CFSTI $1.00 cy, $0.50 mn.

Potential applications for radioisotopes as heat and power sources in the ocean are briefly discussed. (D.C.W.)

44570 RADIOISOTOPE POWER SUBSYSTEMS FOR SPACE APPLICATIONS. Mahefkey, E. T. Jr.; Manikowski, A. F. Jr. (Air Force Aero Propulsion Lab., Wright-Patterson AFB, Ohio). 20p. (CONF-650442-1). Gmelin, AED-CONF-65-072-1.

From 2nd Space Congress, Cocoa Beach, Fla.

The radioisotope power subsystem is potentially an excellent space power subsystem. The radioisotope (thermoelectric) power subsystems of today, SNAP 3, SNAP 9A, SNAP 11, are characterized by high specific weight (1 watt/lb), low operating temperature (~1000°F), and low conversion efficiency (~5%). The radioisotope (thermionic) SNAP 13 operates at 7% generator efficiency (3.1 watt/lb). The major constraints that will ultimately limit the utility of isotope power subsystems are isotope availability and radiation hazard problems. As power requirements and capabilities increase to the .5–10 Kw(e) range, isotope economy becomes a stringent necessity, demanding high thermal-electrical conversion efficiency. Radiation hazard problems are of equal importance in considering application of isotope power subsystems. The problem is that of effectively designing a safe subsystem and still retaining favorable weight and volume characteristics. The most serious safety problems occur between the time of launch and insertion in orbit and re-entry upon completion of the mission. This study includes a survey of the current technologies of energy converters, isotopic fuel form and cladding material compatibility, and launch and operational safety requirements. Converter device performance is presented parametrically, with tabulated data on current laboratory and/or hardware development devices. Thermoelectric generator efficiency (3–5%) appears to be insufficient to warrant consideration for power applications over a few hundred watts. Thermionic devices become attractive efficiency-wise as operating temperatures approach 1500°C. Containment and isotopic fuel form technology have not reached this temperature to date but current development programs, designed to establish this high temperature compatibility in the near future, make the application of thermionic-isotope subsystems attractive from weight and volume considerations. The Rankine (inorganic and liquid metal working fluids) and Brayton (inert gas working fluids) thermodynamic cycles were studied. The Brayton cycle was judged unattractive due to high subsystem weight. The Rankine biphenyl subsystem appears to be the most attractive power conversion scheme for power levels of 1.5 Kw or greater. A comparison of Rankine biphenyl and high temperature thermionic subsystems indicated the latter has more potential for space application, due to lower converter and radiator weight. Data on isotope availability and cost are presented, and various isotope suitability for each conversion device is discussed. Cladding material properties are discussed and related to launch handling and operational hazards problems. Considerations of ablative versus intact re-entry of the isotopic sources are reviewed, and intact re-entry is found to be more suitable, since trends toward high temperature fuel forms make the ablative approach impractical. (auth)

44571 RADIOISOTOPE POWER-GENERATING SYSTEM FOR A MANNED SPACE LABORATORY. Tonelli, A. Duane; Regnier, Edward P. (Douglas Aircraft Co., Santa Monica, Calif.). New York, American Society of Mechanical Engineers, 1965, Preprint No. 65-AV-18, 19p., $1.00. (CONF-650324-2). ORINS.

From American Society of Mechanical Engineers Aviation and Space Conference, Los Angeles.

The results of a study of radioisotope secondary power-generating systems for space applications are presented. The study results are applicable to various space vehicles and missions requiring 4 kw or more of electrical power. The first generation of manned vehicles where a radioisotope power system is potentially applicable include the Extended Apollo and MOL type earth-orbiting laboratories. For this reason, the study results were applied to selecting a radioisotope power system for a small manned orbiting laboratory. The laboratory considered is capable of being launched in the post-1968 time period by a Titan 3C booster. An argon Brayton cycle, Dowtherm A Rankine cycle, and thermoelectric systems were investigated as possible secondary power systems capable of generating 4 kw of electrical power for the vehicle subsystems. Tradeoffs in weight, radiator area requirement, development risk and isotope availability and cost were performed for the various systems. On the basis of the tradeoffs and the 4-kw design load, the argon Brayton-cycle system was recommended. (auth)

44572 SMALL UNDERWATER VEHICLE PROPULSION WITH RADIOISOTOPE POWER. Finkle, Earl (Aerojet-General Corp., Azusa, Calif.). New York, American Inst. of Aeronautics and Astronautics, 1965, Preprint No. 65-484, 15p., $1.00. (CONF-650711-18). ORINS.

From AIAA 2nd Annual Meeting and Technical Demonstration, San Francisco.

Radioisotope propulsion power at the 5–20 kilowatt (6.7–26.8 horsepower) level is considered compatible with a number of manned and unmanned small underwater vehicle-mission combinations. These include the glide vehicle, the hovering platform, the moored-ascending and descending platform, the bottom crawler and the free-running vehicle. The free-running vehicle is chosen for further study because of the accelerating activity in the small submersible area and because preliminary vehicle-mission considerations indicate practical mission possibilities with a nominal 10 kilowatts (13.4 horsepower) of long duration propulsion power. A detailed analysis is presented of the performance of a cerium-144 energized thermal expansion engine propulsion plant in comparison with more conventional plants when applied to an unmanned torpedo-like vehicle. This example clearly demonstrates how radioisotope propulsion power permits the significant extension of missions presently limited by conventional power methods and offers the promise of the achievement of new mission objectives which, until now, have been considered infeasible due to energy density limitations. (auth)

Separation and Production

See also CHEMISTRY — Separation Processes and Procedures.

Refer also to abstract 45612.

44573 (ORNL-P-515) ISOTOPIC CONTAMINATION IN ELECTROMAGNETIC SEPARATORS. Bell, W. A.; Veach, A. M.; Shipley, E. D.; Newman, L. T.; Yonts, O. C.; Lee, J. V.; Spainhour, K. A.; Goslin, R. N. (Oak Ridge National Lab., Tenn.). [Sept. 23, 1964]. Contract W-7405-eng-26. 9p. Dep. mn; CFSTI $1.00 cy, $0.50 mn.

The cross contamination of isotopes resulting in a calcium separation carried out with a highly stabilized ion beam at an unusually low environmental gas pressure is reported. A segmented boundary wall treatment contacting the beam was used to produce an unusually well focused stabilized beam. The degree of contamination produced in this separation is compared to that experienced in the conventional calutron for many years experience with many elements. A general procedure for graphing contamination data is used in making the comparison. (auth)

44574 ENRICHMENT OF DEUTERIUM BY COUNTER-CURRENT ISOTOPE EXCHANGE BETWEEN HYDROGEN AND AMMONIA IN A HOT-AND-COLD PLANT. Walter, S. (Friedrich Uhde GmbH, Dortmund, Ger.); Schindewolf, U. Angew. Chem. Intern. Ed. Engl., 4: 597(July 1965).

Enrichment data and an apparatus are described for a D_2O production system which replaces the usual system of hydrogen sulfide/water by ammonia/water with dissolved potassium amide as catalyst. Here the isotope exchange is much larger and is more dependent upon the temperature and there is the thermodynamically favorable possibility of using hydrogen as starting material. The plant described consists of two cold columns in series with a total length of 28 m and a hot column with a total length of 17.5 m. Each column has an ID of 120 mm and contains about 200 sieve plates. The upper and lower plates of the hot column act as direct heat exchangers. At a pressure of 200 atm and temperature of 60°C in the hot column and –20°C in the cold column, with a potassium amide concentration of 50 g/kg of ammonia, and with a throughput of 450 m^3 of synthesis gas and 50 to 100 kg of ammonia per hr, a six- to seven-fold enrichment of the D was achieved in the H at the top of the hot column and greater than 20-fold enrichment in the ammonia, based on the original D content of the H introduced at the foot of the hot column. The enrichment is expressed by the ratio of the relative D contents in the original H_2, i.e. (n_D/n_H) product: (n_D/n_H) starting hydrogen, where n_D and n_H are the mole fractions of HD and H_2, or NH_2D and NH_3, respectively. (BBB)

44575 RELATIVE DIFFERENCE OF VAPOR PRESSURE IN $^{11}BF_3$–$^{10}BF_3$. Amirkanova, I. B.; Borisov, A. V.; Gverdtsiteli, I. G.; Karamyan, A. T. At. Energ. (USSR), 19: 20-4(July 1965).

The relative differences of vapor pressures of the isotopic molecules $^{11}BF_3$ and $^{10}BF_3$ at temperatures of 147 to 247.7°K were measured by a differential method. The coefficient of enrichment is reduced from 20×10^{-3} (147.0°K) to 1.1×10^{-3} (247.7°K). Within the limits of error of the experiment (2 to 4%), the liquids of the $^{11}BF^3$–$^{10}BF_3$ solutions are ideal. In the measured interval of temperatures, corrections to the coefficient of enrichment associated with the nonideality of the gas phase are calculated. Data obtained in the presence of other parameters of the process of fractionation of BF_3 (the height of the theoretical plate, the throughput of the adapter, etc.) allow the efficiency of the process of separation of $^{11}BF_3$ and $^{10}BF_3$ at various pressures to be calculated. (tr-auth)

44576 STUDIES ON THE PRODUCTION OF HEAVY WATER. II. PILOT PLANT FOR ELECTROLYSIS AND BURNERS. Otero, J. L.; Gispert, M.; Rojas, J. L. Energia Nucl. (Madrid), 9: 90-4(Mar.-Apr. 1965). (In Spanish).

The objectives and characteristics of electrolytic cascades provided with H burners are given. The studies planned in connection with the pilot plant are indicated. (J.S.R.)

44577 SEPARATION OF GASEOUS ISOTOPE MIXTURE IN A SUPERSONIC JET. I. ESTIMATION OF SEPARATION EFFECT. Mikami, Hisashi; Takashima, Yooichi (Tokyo Inst. of Tech.). Nippon Genshiryoku Gakkaishi, 7: 342-51(July 1965). (In Japanese).

The separation effect of the nozzle process was analyzed numerically based on the assumption that the gaseous flow from a nozzle outlet could be regarded as a continuum and that the pressure diffusion in the jet caused isotope separation. An approximate expression was derived for the separation effect, as a function of cut and Mach number. In order to estimate the separation effect, it was necessary to solve the equation of motion expressed by a modified hadograph, using an analog computer. The calculated results gave the fundamental characteristics of this separation process, for example, the relation between the separation effect and the cut whose value was dependent on Mach number. It was indicated that the separation effect was maximum when the Mach number was infinite. (auth)

44578 METHODS FOR THE RAPID RECOVERY OF HEAVY WATER AND OTHER PRODUCTS. Ruskin, Simon Lyon; Ruskin, Dan; Reder, Milton; Farhi, Carol. U. S. Patent 3,197,402. July 27, 1965. Filed Nov. 20, 1957.

In a process for concentrating heavy water, ordinary water is allowed to flow at high velocity through a tube having as its core a permanent magnet of the order of 10,000 G. A magnetohydrodynamic effect is produced, which causes the more common para form of light water and the less common ortho form of heavy water to be propelled outward from the main stream to the periphery of the liquid to form a light-water-enriched layer. This peripheral layer is drained off through a series of outlet tubes as waste, and the heavy-water-enriched main stream is collected for further utilization. The process may also be used for concentrating salts from seawater. (A.G.W.)

MATHEMATICS AND COMPUTERS

44579 (AEEW-R-439) THE FLIC CONVERSION CODES. Basher, J. C. (Atomic Energy Establishment, Winfrith (England)). May 1965. 30p. Dep.; BIS $1.10; HMSO 5s. 6d.

The FORTRAN programs, FLIC 1 and FLIC 2 are described. These programs convert programs coded in one dialect of FORTRAN to another dialect of the same language. FLIC 1 is a general pattern recognition and replacement program whereas FLIC 2 contains extensions directed towards the conversion of FORTRAN II and S2 programs to EGTRAN 1—the dialect now in use on the Winfrith KDF9. FII or S2 statements are replaced where possible by their E1 equivalents; other statements which may need changing are flagged. (auth)

44580 (AERE-R-4964) TABLES FOR THE BINARY ENCODING OF ANGLES. Newson, P. A. (Atomic Energy Research Establishment, Harwell (England)). June 1965. 15p. Dep.; BIS $0.50; HMSO 2s. 6d.

Tables are presented to facilitate working with and conversion between shaft position encoder outputs and angles expressed in degree and radian measures. (auth)

44581 (KAPL-M-6469) MIRAGE-III: MATRIX INTERPRETIVE ROUTINE. Guillette, R. W.; Lechliter, G. L. (Knolls Atomic Power Lab., Schenectady, N. Y.). July 1, 1965. Contract W-31-109-eng-52. 36p. Dep. mn; CFSTI $2.00 cy, $0.50 mn.

The computer program MIRAGE-III, a FORTRAN-IV program which can perform over thirty types of matrix operations, is described. The maximum dimension for any matrix is 54. Operations can be performed in any sequence. (D.C.W.)

44582 (ORNL-3646) RELATED TWO POINT BOUNDARY VALUE PROBLEMS AND ASSOCIATED HARMONIC MATRICES (thesis). Zettl, Anton (Oak Ridge National Lab., Tenn.). Sept. 1965. Contract W-7405-eng-26. 64p. Dep. mn; CFSTI $3.00 cy, $0.75 mn.

Submitted to Univ. of Tennessee, [Knoxville].

The conditions for the Green's function of a two-point boundary value problem to be Hermitian or anti-Hermitian with respect to the Green's function of a related two-point boundary value problem are studied. A method for studying boundary value problems is developed. The method is based on the construction of the Green's function in terms of harmonic matrices and the matrices defining the boundary conditions. (D.C.W.)

44583 INTRINSIC THEORY OF SPINORS. CASE OF THE SPINOR WITH TWO COMPONENTS; INTRINSIC PROPERTIES AND PROPERTIES OF THE INDICES. Cavailles, Paul (Institut Henri Poincare, Paris). Compt. Rend., 260: 5711-14(May 31, 1965). (In French).

By considering that the spinor space relative to a Euclidean vectorial space is a minimum left ideal of the Clifford algebra of this vectorial, the space S_2 of the spinors with two components was studied without utilizing representations: the invariant forms, the conjugations, the isomorphism of the Clifford group reduced from Minkowski space in the Clifford algebra of C^2; in a very general manner the formalism of the point and nonpoint indices are developed. (tr-auth)

44584 TENSORIAL MATRICES. Plebanski, Jerzy (Instituto Politecnico Nacional, Mexico City). Rev. Mex. Fis., 13: 145-262(1964).

The methods of linear algebra are applied to the algebraic analysis of the structure of objects possessing arbitrary sets of indices. With the help of the methodics of analytic functions, general relationships are established between invariants of various types (similar to Rodríguez' formula). The theory of meromorphic functions on generalized matrices is developed, and the theory of canonical forms of generalized matrices is outlined. The theory developed can be used in the study of the algebraic structure and of the algebraic types of the arbitrary spinor-tensor fields, (e.g., spinorial fields with arbitrary number of indices, lorentzian and isotopical, various curvature objects, etc.). Thus, possible applications can be found in field theory (classical and quantum), and in particular in general relativity. (auth)

44585 NORMALIZATION-COEFFICIENTS OF THE LOWERING AND RAISING OPERATORS AND MATRIX-ELEMENTS OF THE GENERATORS OF U_n. Nagel, John G.; Moshinsky, Marcos (Universidad Nacional de Mexico, Mexico City). Rev. Mex. Fis., 14: 29-56(1965).

The normalization-coefficients of the lowering and raising operators of U_n introduced previously are derived in a self-contained way. The normalization-coefficients are then used to derive in an abstract way the matrix-elements of the generators of U_n with respect to basis-vectors characterized by the canonical chain $U_n \supset U_{n-1} \supset \ldots \supset U_2 \supset U_1$. (auth)

METALS, CERAMICS, AND OTHER MATERIALS

General

Refer also to abstracts 43994, 44133, 45572, and 45577.

44586 (ANL-7000) METALLURGY DIVISION ANNUAL PROGRESS REPORT FOR 1964. (Argonne National Lab., Ill.). Contract W-31-109-eng-38. 296p. Dep. mn; CFSTI $7.00 cy, $1.75 mn.

Progress in basic and engineering metallurgical research at Argonne National Laboratory is reported. Separate abstracts were prepared for each of the 19 sections in the report. (W.L.G.)

For abstracts of individual sections see: 43985, 43986, 44160, 44207, 44587, 44616, 44617, 44633, 44674–44680, 44737–44739, and 45559.

44587 (ANL-7000, pp 3-63) FAST REACTOR FUEL ELEMENT DEVELOPMENT AND FABRICATION. (Argonne National Lab., Ill.).

Results of studies on the properties of metallic fuels and their jacket materials, properties of carbide fuels, corrosion of Ti–V alloys in sodium, irradiation of EBR-II fuel elements and structures, development of remote fabrication methods and equipment for metallic fuel elements, development and fabrication of reactor fuel rods and elements, development of fabrication for ZPR-III fuel elements, reactor jacket and component development, nondestructive tests of reactor components, materials used in the liquid-metal seal of EBR-II, selection of the structural material for the FARET liquid-metal system, and economics of plutonium fabrication systems are presented. (W.L.G.)

44588 (BM-RI-6661) ELECTRON-BEAM MELTING OF YTTRIUM. Anable, Wallace E.; Beall, R. A. (Bureau of Mines, Washington, D. C.). 1965. 14p. Bureau of Mines Free.

A study was made of the purification of commercially available yttrium by melting in a 100-kw electron-beam furnace. Button-scale melts were made to determine the ultimate purification that could be attained by melting yttrium at 1,733 to 1,770°C at low pressure (0.05 to 0.1 micron) for 1 to 120 minutes. In addition, numerous melts were made to study the effect of doping yttrium with carbon, 17 selected metallic additions, and 3 compounds. Except for nickel and zirconium, the metallic impurities in yttrium were lowered significantly on extended treatment; silicon was lowered only slightly. The nonmetallic impurities, oxygen, nitrogen, and carbon, were not lowered except on short exposures. In isolated instances, the oxygen content was lowered from 5,860 ppm to about 5,000 ppm. In most instances the carbon content was lowered from 545 to about 220 ppm in 20 minutes and then increased again. It was concluded that yttrium cannot be purified by direct heating or by the doping technique employed. (auth)

44589 (BNWL-102) THERMAL STUDIES [ON] HASTELLOY X METALLIC INSULATION. Hickerson, J. P. (Battelle-Northwest, Richland, Wash. Pacific Northwest Lab.). Aug. 1965. Contract AT(45-1)-1830. 11p. Dep. mn; CFSTI $1.00 cy, $0.50 mn.

In the search for insulation material for ATR gas loop piping, 2000°F helium gas loop through the core, Hastelloy X wire wool had been considered by the Architect Engineer. To determine its suitability, thermal conductivity measurements were made under loop operating conditions. (auth)

44590 (CEA-R-2803) PREPARATION DE FILMS MINCES DE VYNS. (Preparation of Thin VYNS Films). Blanc, Rene; Chedin, Paul; Gizon, Andree (Commissariat a l'Energie Atomique, Grenoble (France). Centre d'Etudes Nucleaires). June 1965. 14p. Dep. mn.

Thin films of VYNS resin (density 3 to 50 $\mu g/cm^2$) are deposited from cyclohexanone solutions. VYNS is a vinyl chloride–vinylacetate copolymer. (T.F.H.)

44591 (CEND-3107-228) BURNABLE POISON ADDITIONS TO UO_2. Progress Report, October 1–December 31, 1964. Brayer, R. C.; Chernock, W. P. (Combustion Engineering, Inc., Windsor, Conn. Nuclear Div.). Feb. 1965. Contract AT(30-1)-3107. 37p. (EURAEC-1306). Dep. mn; CFSTI $2.00 cy, $0.50 mn.

Work Performed Under United States–Euratom Joint Research and Development Program.

Metallographic evaluation of the UO_2–0.05 wt% B_4C element which was thermally tested under both radial and axial thermal gradients, indicated the formation of columnar grains, thus substantiating the estimated fuel centerline temperature of about 2400°C. No boron migration was detected in this element. Attempts to obtain additional information on the influence of temperatures in excess of 1800°C in inducing boron migration in closed systems, operating with an axial thermal gradient for times in excess of 100 hours, were unsuccessful as a result of observed cracks in the tungsten cladding after test. Additional tests using a tungsten liner in more ductile cladding were planned. The enrichment for the fuel rod irradiations in Saxton was fixed at 6% and is based on anticipated fuel centerline temperature of 2200°C and a power rating of 17.8 kw/ft. Orders for fuel cladding and structural materials were placed and are scheduled for delivery in January 1965. Rods for the irradiation test program will be fabricated in February and inserted in Saxton in March 1965 for irradiation to target burnups of 2000 and 5000 MWD/MTU. Additional development of fabrication processes for the irradiation test elements indicated that a loss of 1% in theoretical density may be encountered as a result of heat treatment of the UO_2 particles to reduce the nitrogen content. (auth)

44592 (CLM-R-43) THE PREPARATION AND PROPERTIES OF SINTERED Nb_3Sn. Walker, C. H.; Hancox, R. (Culham Lab., United Kingdom Atomic Energy Authority, Abingdon (England)). May 1965. 14p. Dep. mn; BIS $0.50; HMSO 2s. 6d.

Sintered Nb_3Sn was formed that is capable of supporting current densities greater than 10^5 amps/cm^2 at 50 kG, and is stable against field changes of at least 55 kG. The factors that affect stability are discussed, including the importance of the structure of the sintered material. (auth)

44593 (CONF-650908-4) URANIUM OXIDE FUEL FOR NUCLEAR THERMIONIC CONVERTERS. Grossman, L. N.; Ekvall, R. A.; Hill, H. W. (General Electric Co., Pleasanton, Calif. Atomic Power Equipment Dept.). [1965]. Contract AT(04-3)-189. 10p. Dep. mn; CFSTI $1.00 cy, $0.50 mn.

From International Conference on Thermionic Electrical Power Generation, London.

Long-term, high-temperature compatibility and thermal cycling tests of UO_2 with Mo, Re–W, and W were performed. The results show that Mo, Re–W, and W are suitable emitter cladding materials for nuclear-thermionic energy conversion. (D.C.W.)

44594 (DP-983) REDUCTION OF PLUTONIUM DIOXIDE TO PLUTONIUM METAL. Thompson, Major C. (Du Pont de Nemours (E. I.) and Co., Aiken, S. C. Savannah River Lab.). July 1965. Contract AT(07-2)-1. 10p. Dep. mn; CFSTI $1.00 cy, $0.50 mn.

Attempts were unsuccessful to reduce PuO_2 with calcium or barium to form a coalesced mass of plutonium metal. Molten fluoride fluxes to dissolve CaO or BaO were not effective in promoting the reaction, nor was mechanical agitation. The major difficulty was the rapid separation of the reactant phases. (auth)

44595 (EURAEC-1338) SINTERED URANIUM OXIDE—SINTERING TECHNOLOGY—BEHAVIOR UNDER IRRADIATION. Final Report No. 1, October 1, 1960–December 31, 1963. (Commissariat a l'Energie Atomique, Saclay (France). Centre d'Etudes Nucleaires). Contract 031-60-10 RDF. 145p. (EUR-2314). Dep. mn; CFSTI $4.00 cy, $1.00 mn.

Work Performed under United States-Euratom Joint Research and Development Program.

Direct reduction of UO_3 was performed in a continuously fed rotary tube furnance under a constant counter flow of reducing gas to yield high-surface-area UO_2 powders that were suitable for sintering in H_2. The surface area of the powders was controlled by the H_2-N_2 reducing gas composition, the operating temperature, and the length of the reaction zone or number of calcining cycles. The sintering properties of the powders were investigated for two different conditions: heating at a rate of 100°C/hr to 1400°C and holding for 5 hrs, and heating at a rate of 400°C/hr to 1650°C and holding for 30 min. In both cases, the powders obtained a density of about 95% of theoretical. By using a H_2 sintering atmosphere containing 40 mg/l water, a density increase of 0.1 g/cm³ resulted. A density increase of 0.15 g/cm³ resulted from the use of 3% zinc behenate as a lubricant instead of camphor as a binder when pressing pellets. The oxidation of pellets during the sintering cycle of large-scale operations was investigated. The pellets oxidized on the surface during cooling if the sintering atmosphere contained small amounts of O_2. Micrographic and x-ray examinations of the surfaces provided a means for very close control of the oxidation. Tests to relate the thermal shock resistance to the density of the pellets were unsuccessful; however, it was found to be inversely proportional to the diameter of the cylinder. The apparent thermal conductivity of sintered UO_2 pellets was measured to 2400°C. Interpretation of the data revealed the effects of additional thermal resistivity due to circumferential cracks. The kinetics of grain growth under isothermal conditions between 1400 to 1800°C for compacts from powders of high-specific-surface-area followed the relation: $D^2 - D_0^2 = b_0 t^n \exp(Q/RT)$, where n varies from 0.8 to 1.3 according to the surface area. An attempt to measure the accumulation of fission gases during irradiation at a given burnup rate and center temperature was unsuccessful. Information was obtained on the in-pile variation of the thermal conductivity with temperature to 1250°C. Measurements of the apparent diffusion coefficients of Xe in previously irradiated sintered UO_2 were conducted. Non-diffusion mechanisms, such as evaporation, were also investigated. A method for measuring specific surface areas of the order of a few square centimeters was developed. It consists of applying the BET adsorption method and using a mixture of natural Xe and ^{133}Xe as the adsorbed gas. The gas pressure over the sample is measured with a γ-spectrometer. (W.L.G.)

44596 (EURAEC-1392) COATING UO_2 PARTICLES. Special Report No. 20. Sari, C.; Pivato, J. (Centre d'Etude dell'Energie Nucleaire, Brussels (Belgium); Societe Belge pour l'Industrie Nucleaire, Brussels). [nd]. Contract 27-60-7 RDB. 23p. (EUR-2351; BN-6212-01). Dep. mn; CFSTI $1.00 cy, $0.50 mn.

Work Performed under United States–Euratom Joint Research and Development Program.

Spheroidal particles of UO_2 with a diameter between 100 and 200 microns were coated by different methods with chromium, molybdenum, nickel, iron, copper, molybdenum disulfide, and graphite. The methods used included either evaporation or chemical, electrochemical, and mechanical deposition. The quality of the coatings was investigated by metallography and acid leaching. Thicknesses between 2 and 20 microns can be obtained easily. (auth)

44597 (GEAP-4679) INTERFACIAL REACTION BETWEEN UO_2 AND ZIRCALOY-2. Grossman, L. N.; Rooney, D. M. (General Electric Co., San Jose, Calif. Atomic Power Equipment Dept.). Apr. 1965. Contract AT(04-3)-189. 21p. (EURAEC-1463). Dep. mn; CFSTI $1.00 cy, $0.50 mn.

Work Performed Under United States–Euratom Joint Research and Development Program.

The interfacial reaction between UO_2 and Zircaloy-2 was studied at temperatures between 950 and 1575°K. The reaction proceeds with the formation of oxygen-saturated alpha Zircaloy-2 and a gamma uranium–beta zirconium solid solution. The solid solution transforms on cooling to UZr_2 plus some gamma–beta solid solution; some alpha uranium with Zr in solution forms on cooling from the higher temperatures. The interaction between Zircaloy-2 and UO_2 differs from that between Zr and UO_2 principally in the microstructure of the metallic reaction product. The extent of interaction is limited by oxygen diffusion in alpha Zircaloy-2; the oxygen diffusion rates are essentially identical to those in alpha zirconium. (auth)

44598 (GEMP-49A) HIGH-TEMPERATURE PROGRESS REPORT NO. 49. PART A. (General Electric Co., Cincinnati, Ohio. Nuclear Materials and Propulsion Operation). July 28, 1965. Contract AT(40-1)-2847. 80p. Dep. mn; CFSTI $3.00 cy, $0.75 mn.

Laboratory testing of Fe–Cr–Al–Y-clad fueled specimens exceeded 7000 hours at 950 and 1100°C in air with indication of excellent stability. The first in-pile test of a 2541-clad Fe–40 UO_2 specimen completed 1007 hours at 1100°C in air. Steady-state fission product release during this time did not exceed 10^{-7}. Weight gain data on a series of eight alloys were obtained at 900 and 1100°C for times up to 8000 hours in air. The 2541 and 1541 alloys showed lower oxidation rates than any commercial alloy. Preoxidation at 980°C of Fe–Cr–Al–Y alloys of low Cr content showed promise of enhancing corrosion resistance in steam. Up to 4% strain in preoxidized specimens can be tolerated without reducing the steam corrosion resistance of these alloys. Creep-rupture tests of arc-cast W were performed to provide stress-rupture and creep curves from 1600 to 2800°C for time periods ranging from approximately 5 to 300 hours. Tests at 2000 and 2200°C with special preannealed specimens indicate that a change in the creep mechanism for W occurs between 2000 and 2200°C. First stage creep analyses of the arc-cast W data from 1600 to 2800°C led to a general equation. Creep-rupture tests of arc-cast W–25 Re at 2000°C revealed that this material has a greater rupture life and is more creep resistant than arc-cast W for stresses greater than 1.0 kg/mm². The creep curves for the arc-cast W–25 Re at 2000°C exhibited no primary or secondary creep. W–Re–Mo alloys ranging from W–26 Re to W–29 Re, with 0, 10, and 20% Mo, creep-rupture tested at 1600°C and 4.22 kg/mm², exhibited a grain refinement as the Re content was increased and an increase in grain size as the Mo was increased. The variations in the creep-rupture properties for the alloys are not related to the structure. Creep-rupture data for the W–Re–Mo alloys tested at 2200°C and 0.56 kg/mm² reveal that W–27 Re–20 Mo has the greatest rupture life and is the most creep resistant. Creep data for arc-cast Mo were obtained with an electro-optical extensometer in tests from 1600 to 2200°C. First-stage creep analyses gave results similar to those obtained for arc-cast W. Metallurgical evaluations revealed that W–25 Re–30 Mo alloy is resistant to excess grain growth whether thermal-cycled between 260 and 2150°C, or held isothermally at 2200°C. Both W–25 Re–30 Mo and W–30 Re–30 Mo alloys withstood 90-degree room temperature bend tests after the above treatments. The purification technology developed for W–Re alloys was applied to unalloyed Mo and to Mo alloys with additions of 1, 3, or 5 at. % Re. These alloys resisted room temperature embrittlement when heated to 2200°C. Weldability was better than with the commercial powder metallurgy Mo sheet, but slightly poorer than with the arc-cast product. Procedures for producing seamless tubing of W–25 Re–30 Mo by extruding, hot-working, and predraw cleanup were tentatively identified using carbide "plug" mandrels and sacrificial core fillers. Creep-rupture testing of irradiated W–25 Re specimens at 800 and 900°C indicated that a significant change in flow properties may occur at some temperature between these two temperature levels. The mechanism ap-

pears to be an interaction of dislocations with the irradiation-induced defects, which is much stronger at the 800°C test temperature than at the 900°C level, rather than the possibility of the annealing out of those defects at the higher temperature. Measurement of the recovery of irradiation-induced resistivity yielded good results for specimens tested at elevated temperature in isothermal anneals. Hot-hardness measurements of worked and of neutron-irradiated Mo specimens show very similar recovery behavior. In particular, the apparent small increase in the hardness value at temperatures of about 150°C (0.15 T_m) are observed to occur in both types of specimens. Creep-rupture testing of irradiated Hastelloy N specimens at 815°C shows about a factor of 3.5 reduction in the time to rupture when tested at relatively high stresses. There is a tendency for some recovery to occur when testing at the lower stresses, resulting in about a factor of 1.6 reduction compared to the control data. The times to rupture approach those of the control specimens in a manner observed for irradiated Hastelloy X specimens tested at a slightly higher temperature (870°C). The thermoelectric properties as a function of temperature for Cr, Nb–10 Mo, Nb–20 Mo, and Nb–40 Mo were measured to 1800°C. The alloys of Nb–20 Mo and Nb–40 Mo showed good potential as negative thermoelement materials. BeO, MgO, and HfO_2 were evaluated for use as thermocouple electrical insulators in systems for measuring temperatures up to 2450°C in graphite and hydrogen environments. Mo, Re, and Mo–50 Re were evaluated for use as high-temperature thermocouple sheath materials in a graphite–hydrogen environment. These tests showed Re to be the best potential sheathing material. Of the three insulator materials tested, HfO_2 exhibited the best stability. (W.L.G.)

44599 (GEMP–50A) HIGH-TEMPERATURE MATERIALS PROGRAM. Progress Report No. 50, Part A. (General Electric Co., Cincinnati, Ohio. Nuclear Materials and Propulsion Operation). Aug. 20, 1965. Contract AT(40-1)-2847. 81p. Dep. mn; CFSTI $3.00 cy, $0.75 mn.

Results of creep-rupture testing of W–25Re between 800 and 900°C indicate that the creep activation energy is approximately 125 kcal/g-mole in this temperature range. Hot hardness measurements of W single crystals irradiated to two fast neutron dosage levels (4.6×10^{18} and 2.4×10^{19} nvt) indicate that the hardness is retained to a higher temperature at the higher dosage. The hardness of both specimens was the same at room temperature, but the hardness of the higher dosage specimen was approximately 20% higher at 500°C. This effect is believed to be caused by the greater percentage of Re formed during irradiation. Studies of the transmutation of W atoms into Re and Os atoms as a result of thermal neutron (n,γ) reactions indicated that a considerable number of Re atoms and only a small number of Os atoms are produced. A thermal neutron dose of 2×10^{20} nvt results in 0.19% Re atoms and 0.0012% Os atoms; the quantity of these elements increases as the long half-life (65 and 74 days) W isotopes decay. Preliminary radiochemical analysis indicates that the cross section for the $^{187}W(n,\gamma)^{188}W$ reaction may be larger than published values. Computer studies indicate that the displacement spike density model shows better agreement with experimental irradiation hardening data than the more conventional models based on total displacement density or on only those atoms displaced by neutrons with energies above 1 Mev. Irradiated Hastelloy N specimens were creep-rupture tested at temperatures of 815 and 650°C. Annealing irradiated Hastelloy N specimens at a temperature of 870°C for 4 hours resulted in a slight increase in the creep-rupture life when tested at 650°C and about a factor of two decrease at 815°C when compared to corresponding as-irradiated data. This additional heat treatment on the control specimens did not change the time to rupture at the lower test temperature but did increase the time to rupture about a factor of two at the higher temperature. Modulus-of-rupture measurements on unirradiated BeO indicated that 1 to 2 wt% concentrations of glass-phase additives decrease the strength of materials of 5-μ grain size. A silica glass additive increased the strength of 20-μ grain size material throughout the range from room temperature to 1200°C. BeO specimens irradiated at 1000°C to dosages of 3.5 to 4.7×10^{21} nvt (≥ 1 Mev) appeared in good condition. Although open porosity measurements indicate that some microcracking occurred, the strength of the specimens of 5-μ grain sizes was equal to that of the unirradiated material while the strength of EBOR specimens appeared to have decreased about 40%. Expansion of the specimens of 5-μ grain size was 2 to 3%. Thermal diffusivity measurements were completed on UOX-MgO specimens of 4-μ grain size and 2.9 g/cm³ over the temperature range from 300 to 1000°C. The diffusivity of a specimen irradiated at 1000°C to 2.6×10^{21} nvt (≥ 1 Mev) decreased in comparison to the unirradiated specimen by amounts ranging from approximately 15% at 400°C to 4% at 1000°C. Kr was concurrently dissolved and diffused in arc-cast Ta cathode samples that were self-resistively heated at various temperatures, pressures, and discharge voltages while under glow discharge. Sections of 100 and 200 Å thicknesses were taken in order to establish the distribution profile of Kr in the various samples. The distribution profiles for various temperatures and grain sizes (via high-temperature annealing) gave strong indication that some complex short-circuiting mechanisms are responsible for the bulk transport of the diffusant even in the region near the surface of the sample (<500Å). The release of fission products that are solid in their standard reference states (^{137}Cs, ^{140}Ba, ^{131}I, ^{89}Sr, ^{144}Ce, ^{95}Zr) was determined for a W–Mo–Re canned fuel sample irradiated for 1015 hours at 2000°C by means of leach data taken from the capsule and off-gas ducting. The release values of these fission products were in good agreement with those measured for ^{133}Xe and $^{88,89}Kr$ during the test. These results indicate that the release occurred via recoil from fuel contamination of the specimen surface. The initial tests of Zr–UO_2 reaction show that the Zr goes through a 3-mm thick UO_2 container within 30 minutes at 2200°C in an Ar atmosphere. An LITR irradiation test of BeO-coated BeO-base fuel elements containing 25 vol % UO_2–ThO_2–Y_2O_3 operated at temperatures up to 1500°C at a fission product release level of 20 to 100 less than uncoated fuel elements. (W.L.G.)

44600 (LA–3356) PREPARATION OF ULTRA-HIGH PURITY PLUTONIUM. Leary, J. A.; Mullins, L. J. (Los Alamos Scientific Lab., Univ. of California, N. Mex). July 21, 1965. Contract W-7405-eng-36. 7p. Dep. mn; CFSTI $1.00 cy, $0.50 mn.

A method for eliminating essentially all of the detectable metallic impurities from electrorefined Pu is presented. The method involves the use of carburized Ta cathodes in the electrorefining process. Results indicate that Pu with less than 50 ppm metallic impurities can be prepared routinely. (D.L.C.)

44601 (LA-DC–6407) ALTERNATING CURRENT POLISHING AND ELECTROETCHING OF METALS. Johnson, Kaye Allan (Los Alamos Scientific Lab., Univ. of California, N. Mex.). [1964]. Contract W-7405-eng-36. 18p. Dep. mn; CFSTI $1.00 cy, $0.50 mn.

A-c electropolishing and electroetching, which were applied successfully to Pu allotropes, were extended to other metals. Using only four solutions, the following metals and alloys were etched: Cd, In, Co, Sn, Cu, Bi, Ge, Mg, Cr, Zn, Ag, Th, alpha Pu, pearlytic steel, austenitic steel, Sm, Sc, Ni–Ta, U–V, and Al–U. Micrographs and etching conditions are given for each. (D.L.C.)

44602 (LA-DC–6691) THE ALTERNATING CURRENT ELECTROETCHING OF ALPHA, DELTA AND BETA PLUTONIUM. Johnson, K. Allan (Los Alamos Scientific Lab., Univ. of California, N. Mex.). [nd]. Contract W-7405-eng-36. 14p. Dep. mn; CFSTI $1.00 cy, $0.50 mn.

A new method of etching plutonium was developed which uses alternating current electrolysis. The technique produces etched surfaces on alpha, delta, and beta plutonium and allows the microstructures to be revealed under bright field illumination. The method also preserves the form of

alpha microcracks and delineates coring in stabilized delta and beta allotropes. (auth)

44603 (NAA-SR-10929) THE NATURE AND PROPERTIES OF THE CARBIDES OF URANIUM. Gamba, O. O. (Atomics International, Canoga Park, Calif.). Aug. 31, 1965. Contract AT(11-1)-Gen-8. 61p. Dep. mn; CFSTI $3.00 cy, $0.75 mn.

This report is an evaluation of the literature on the technology of the carbides of uranium. It summarizes the information on their preparation and their physical and mechanical properties, and discusses their chemical behavior in environments related to their application as nuclear fuel. It also describes the fabrication of uranium carbide products, and the compatibility of these products with cladding materials. (auth)

44604 (NUMEC-3428-12) GROWTH OF SINGLE CRYSTALS OF PLUTONIUM. Quarterly Progress Report, April 1-June 30, 1965. (Nuclear Materials and Equipment Corp., Apollo, Pa.). Contract AT(30-1)-3428. 13p. Dep. mn; CFSTI $1.00 cy, $0.50 mn.

Work was conducted towards the objective growing single crystals of stabilized Pu allotropes. During the high pressure studies of alpha Pu, measurements were made of the electric resistivity of alpha Pu at 15 to 45 kilobars from room temperature to 580°C, and the breaks in the curves were observed. Rods of Ga-stabilized delta Pu were subjected to an extensive treatment including homogenization at 425°C for 24 hr and annealing at 450°C for 100 hr; micrography showed that coring was still present. (D.L.C.)

44605 (PWAC-464) DEVELOPMENT OF Cb-Zr-C ALLOYS. Delgrosso, E. J.; Carlson, C. E.; Kaminsky, J. J. (Pratt and Whitney Aircraft, Middletown, Conn. Connecticut Advanced Nuclear Engineering Lab.). Sept. 1965. Contract AT(30-1)-2789. 60p. Dep. mn; CFSTI $3.00 cy, $0.75 mn.

A series of high-strength niobium alloys was developed during a study of the strengthening of niobium by fine particles of oxide or carbide. These alloys were developed by adding stoichiometric concentrations of zirconium and carbon at the one to three atomic percent level. The alloys are characterized by good strength at elevated temperatures and a high degree of fabricability. Sheet, rod, and wire material was produced by extruding consumably arc-cast ingots, followed by cold rolling, swaging, or drawing with reductions in area as great as 95%. The mechanical strength of the alloys was determined from room temperature to 2600°F. The effects of cold working, warm working, and heat treating upon elevated temperature tensile and rupture properties of some alloys were investigated. Three alloys were found to be particularly promising: Nb-1 Zr-0.1 C (PWC-11), Nb-3 Zr-0.34 C (PWC-33), and Nb-3 Zr-0.4 C (PWC-34). Rupture data demonstrated these alloys were strongest in the warm extruded condition, exhibiting a duration limit of 150 to 400 hours at 1315°C under a 9000 psi loading stress, which is equivalent to a 100-hour rupture stress of 10,000 to 14,000 psi. Subsequent extensive cold working reduced this strength, but it was regained almost completely by proper heat treatment. Typical alloy structures are presented in terms of electron transmission metallography and some tentative correlations between strength properties and structure are suggested, in terms of precipitate pinned dislocation tangles or pinned grain boundaries. Debye-Scherrer XRD techniques were utilized to identify the carbide precipitates extracted from the PWC-11 and PWC-33 alloy. On the basis of the evaluations conducted, alloys in this series compared favorably with the strongest currently available niobium base alloys. The PWC-11 alloy was selected as first choice for application to the SNAP-50 program because of its promising strength advantages and favorable working characteristics compared to the Nb-1 Zr alloy. (auth)

44606 (PWAC-483) SPACE RADIATOR FABRICATION DEVELOPMENT. Status Report. Stewart, J. R. (Pratt and Whitney Aircraft, Middletown, Conn. Connecticut Advanced Nuclear Engineering Lab.). Aug. 25, 1965. Contract AT(30-1)-2789. 21p. Dep. mn; CFSTI $1.00 cy, $0.50 mn.

Silver was found to be the only material with which beryllium could be joined to Nb-1 Zr alloy or type 316 stainless steel for extended service in the temperature range 540 to 760°C. These results are based on lap-shear strength tests and on 3000-hour compatibility data. Further, even silver bonded joints are limited to a maximum service temperature of somewhat less than 760°C since beryllium and silver form a brittle intermetallic phase at 760°C. Service temperatures exceeding 760°C thus require the use of a barrier coating to prevent beryllium diffusion. Without a barrier the operating temperature, for times greater than 1000 hours, may be below 650°C. Carbon and silicon coatings, predeposited on the Nb-1 Zr alloy, show promise of reducing beryllium diffusion above 650°C. No effective means of coating the beryllium was developed. (auth)

44607 (RL-SEP-508) INVESTIGATION OF CD_4M Cu AS A HANFORD MALE CONNECTOR (NOZZLE) MATERIAL. Kingsley, Paul S. (General Electric Co., Richland, Wash. Hanford Atomic Products Operation). July 15, 1965. Contract AT(45-1)-1350. 11p. Dep. mn; CFSTI $1.00 cy, $0.50 mn.

It was demonstrated that a casting of stainless steel (ACI# CD4M Cu) has adequate strength and corrosion resistance when properly heat treated to become a capable substitute for the stellite-faced 304-L male connector (nozzle) employed at Hanford for a number of years. (auth)

44608 (TID-22125) STUDIES OF HIGH-CURRENT METALLIC ARCS. Wood, Floyd W.; Beall, R. A. (Bureau of Mines, Albany, Oreg. Albany Metallurgy Research Center). Feb. 1964. 90p. (BM-Bull.-625). Dep. mn; GPO $0.75.

Original experimentation in specially designed arc-melting furnaces and a comprehensive review of technical literature have helped with an understanding of electric arcs as used in metallurgical applications. Results relevant to the distribution of electric potentials and currents, temperatures, pressures, the consumption of electrodes, the identities of particles participating in electrical conduction, and the modes and mechanisms of discharge are presented and discussed. Present knowledge of high-current arcs is insufficient to test pertinent theoretical suggestions. However, the chief doubts concern the identities and the liberation or formation of current-carrying particles. It seems that either novel formulations of existing concepts are needed, or essentially new concepts must be recognized to explain observations. An analysis of the situation leads one to favor the latter possibility and to suggest the existence of supplementary conducting particles. The conduction of current by the streaming of charged agglomerates is postulated. Another outgrowth of analysis is an equation for the arc potential as a function of current densities in the arc. In lieu of conclusions, the potentialities of practical applications and specific needs for fundamental clarification are summarized. (auth)

44609 (TIM-927) CARBURIZATION OF Cb-1 Zr ALLOY. Bornstein, N. S.; Hirakis, E. C.; Friedrich, L. A. (Pratt and Whitney Aircraft, Middletown, Conn. Connecticut Advanced Nuclear Engineering Lab.). Aug. 1965. Contract AT(30-1)-2789. 22p. Dep. mn; CFSTI $1.00 cy, $0.50 mn.

Methods for producing carbide coatings on Nb-1Zr alloy were investigated in an effort to improve the anti-galling characteristics of the alloy. Three carburization techniques were developed based on reaction with one of the following materials: 1) a slurry coating of oil-graphite, 2) a methane-argon atmosphere, or 3) a lithium-carbon solution. The coating thickness could be varied within the range of 0.0001 to 0.0006 inch depending upon the choice of technique and process conditions. Encouraging results were obtained in limited performance tests of threaded assemblies and

simulated bearings. Based upon the kinetic data obtained as a result of the slurry oil–graphite study, it was tentatively concluded that the mechanism controlling the rate of growth of the carbide layer is the same in all three processes. Analysis of the data provided values for the activation energy for NbC film growth (–72.7 ± 3 kcal/mol) and for Nb_2C film growth (–68.8 ± 3 kcal/mol). (auth)

44610 (TIM–943) ELECTRON METALLOGRAPHY TECHNIQUES APPLIED TO BODY CENTERED CUBIC METALS AND ALLOYS. Keegan, W. A.; Karg, A. V.; Fornwalt, D. E. (Pratt and Whitney Aircraft, Middletown, Conn. Connecticut Advanced Nuclear Engineering Lab.). July 30, 1965. Contract AT(30-1)-2789. 21p. Dep. mn; CFSTI $1.00 cy, $0.50 mn.

Equipment, etchants, and techniques used in preparing specimens of body centered cubic metals for examination by transmission electron microscopy are described. Transmission electron photomicrographs of thin foils prepared by the method described are presented. (auth)

44611 (UCRL-16232) KINETICS OF THE DISSOLUTION AND DIFFUSION OF THE OXIDES OF IRON IN SODIUM DISILICATE GLASS (thesis). Borom, Marcus Preston (Lawrence Radiation Lab., Univ. of California, Berkeley). Aug. 4, 1965. Contract W-7405-eng-48. 53p. Dep. mn; CFSTI $3.00 cy, $0.50 mn.

The dissolution of the three oxides of iron by sodium disilicate glass was studied in the temperature range 900 to 1100°C. Diffusion anneals were conducted at several times for each temperature, and the concentration distributions in the iron oxide–glass diffusion couples were analyzed by means of an electron microprobe. The variation of the concentration profiles with time established that the dissolution is controlled by diffusion in the molten glass. The diffusion kinetics were determined by two methods, which employed in one case the mathematics for binary diffusion and in the other case the mathematics for ternary diffusion. The application of the mathematics for binary diffusion permitted only the determination of an apparent diffusivity for the oxides of iron; however, the mathematics of ternary diffusion yielded information regarding the self-diffusion coefficients of each of the individual cations. The relation between the diffusivities is given by $D_{Na} \gg D_{Fe^{2+}} > D_{Si^{4+}} \geq D_{Fe^{3+}}$. The concentration dependence of the diffusion coefficients of the various cations is interpreted on the basis of composition-dependent structural changes in the glass. An activation energy of 30.4 kcal was determined for the diffusion of each of the valences of iron, and the activation energy was found to be independent of glass composition. (auth)

44612 (USBM-RC–1199) QUARTERLY METALLURGY PROGRESS REPORT NO. 27, APRIL 1–July 31, 1965. (Bureau of Mines, Albany, Oreg. Albany Metallurgy Research Center). Contract AT(11-1)-599. 33p. Dep. mn; CFSTI $2.00 cy, $0.50 mn.

Progress is reported on research on HfC, Th–ThO_2 dispersions, cold-mold induction melting equipment and techniques, UC–UN–UO system, and fabrication of W–25 Re alloy. (W.L.G.)

44613 (Y-1476) PREPARING AND SINTERING TUNGSTEN POWDER. Schmitt, C. R.; Phillips, L. R.; Googin, J. M.; Piper, C. F. (Union Carbide Corp., Oak Ridge, Tenn. Y-12 Plant). Mar. 26, 1965. Contract W-7405-eng-26. 93p. Dep. mn; CFSTI $3.00 cy, $0.75 mn.

Variables affecting the production of a sinterable, high-purity, tungsten metal powder by the hydrogen reduction of tungsten oxides were studied; and ultra-fine tungsten powder, submicron in size, with high surface areas ranging from 5 to 15 square meters per gram, were prepared. Sintering tests on isostatically pressed compacts made from these powders showed that a density that is 95–98% of the theoretical density can be obtained by sintering for three hours at 1500°C in a flowing hydrogen atmosphere. This level is much better than the approximately 80–85% of the theoretical density obtained from compacts made from a typical, fine, commercially available tungsten powder having a surface area of 0.2 square meter per gram sintered under equivalent conditions. Studies show that when tungsten oxides are reduced with hydrogen under increasing reduction temperatures in the range between 700–850°C, a decrease occurs in the surface area of the resulting tungsten powders. Sintering tests on pressed compacts made with these powders also showed that a high reduction temperature has an adverse effect on the sintered density. (auth)

44614 (JPRS–24761) STUDIES IN THE METALLURGY OF VARIOUS ALLOYS. Translations from Tr. Inst. Met. im. A. A. Barkova, Akad. Nauk SSSR, No. 14, 78–89; 120–38(1963). 51p. CFSTI $1.50 cy, $0.50 mn.

Five articles are included; separate abstracts have been prepared for four. The paper not abstracted treats structural and property changes in alloys resulting from low-melting components. (D.L.C.)

For abstracts of individual papers see: 44645, and 44708–44710.

44615 RARE EARTHS METALS—METALS OF THE FUTURE. Czerniak, Raisa. Rudy Metale Niezelazne, 10: 215-19(1965). (In Polish).

The possibilities of applying rare earth metals in various industrial, technical, and economic fields were reviewed. The application of lanthanides in the production of steel and cast iron, in the working of non-ferrous metals, in the glass and ceramic industries, in optics and medicine are discussed. Examples are given of the use of rare earth metals as catalysts in some chemical processes. The prospects of applying lanthanides in electrical engineering, electronics, and nuclear engineering are considered. (auth)

Corrosion

44616 (ANL–7000, pp 122-37) DEVELOPMENT OF CORROSION RESISTANT JACKETING AND STRUCTURAL MATERIALS. (Argonne National Lab., Ill.).

Results of studies of the aluminum alloy corrosion in the Borax V reactor, development of corrosion resistant zirconium alloys, effects of alloy additions on the stainless steel corrosion by steam, corrosion of stainless steel and nickel-base alloys by steam at 750°C, inhibiting effects of additions to mercury on the corrosion of titanium, corrosion of molybdenum and tantalum by lithium, corrosion of stainless steel by bismuth–tin eutectic alloy, and the effects of polarization upon the zirconium corrosion by oxygenated sodium are presented. (W.L.G.)

44617 (ANL–7000, pp 213-26) CORROSION RESEARCH. (Argonne National Lab., Ill.).

Progress is reported on research on the mechanism of aqueous corrosion of Al, electron optical studies of corrosion films, mechanism of high temperature corrosion of Al alloys, oxidation of Zr, and polarization studies. (W.L.G.)

44618 (AWRE–O–42/65) THE WATER VAPOUR CORROSION OF URANIUM AND ITS PREVENTION. Corcoran, V. J.; Johnston, C.; Metcalfe, W. J.; Thorpe, J. (Atomic Weapons Research Establishment, Aldermaston (England)). July 1965. 20p. Dep. mn; BIS $0.60; HMSO 3s.

The reaction between uranium and atmospheres containing water vapor in the presence of nitrogen and oxygen was studied at 25 and 40°C. The steady production of hydrogen from uranium and moist nitrogen was suppressed by the presence of gaseous oxygen, which itself was slowly consumed. The ability of sulfide and arsenic coatings to suppress hydrogen production from uranium in moist nitrogen was also investigated. (auth)

44619 (AWRE–O–66/65) URANIUM CORROSION STUDIES. PART I. AN OPTICAL METHOD FOR FOLLOWING OXIDE FORMATION. Grimes, J. H.; Morris, J. R. (Atomic Weapons Research Establishment, Aldermaston (England)). Aug. 1965. 24p. Dep.; BIS $0.80; HMSO 4s. 0d.

An apparatus was developed to measure the growth rates of oxide films on polished uranium surfaces in controlled atmospheres. The rate of oxidation of polished uranium surfaces in the presence of water vapor at 50°C and 70°C was determined, and the results are compared with those of other workers. (auth)

44620 (CNLM-6344) APPLICATION OF INTERNAL FRICTION METHODS TO CORROSION STUDY IN COLUMBIUM ALLOYS. Schenck, G. F. (Pratt and Whitney Aircraft, Middletown, Conn. Connecticut Advanced Nuclear Engineering Lab.). July 30, 1965. Contract AT(30-1)-2789. 20p. (CONF-650646-1). Dep. mn; CFSTI $1.00 cy, $0.50 mn.

From American Society for Testing and Materials, 68th Annual Meeting, Lafayette, Ind.

Lithium corrodes niobium and niobium–zirconium alloys intergranularly and on the (110) crystallographic planes when these alloys are contaminated with oxygen. In certain heat treated conditions, however, niobium–zirconium alloys are not attacked by the alkali metal even though they contain relatively large concentrations of oxygen. The internal friction behavior of oxygenated Nb–1 Zr alloy was studied to determine the physical situation of oxygen in the alloy at various heat treatment conditions. From this investigation it became apparent that lithium is only able to corrode the niobium metal or alloy if the oxygen is in interstitial solid solution. Heat treatment of the Nb–1 Zr alloy at temperatures near 2200°F permits corrosion stabilization of the alloy with oxygen concentrations as great as 2 : 1 atom fraction of the zirconium. The corrosion stabilization is achieved by precipitation of the oxygen as zirconium dioxide. (auth)

44621 (CONF-651006-1) BASIC MECHANISMS OF STRESS CORROSION CRACKING OF TITANIUM. Rideout, S. P.; Louthan, M. R. Jr.; Selby, C. L. (Du Pont de Nemours (E. I.) and Co., Aiken, S. C. Savannah River Lab.). Aug. 1965. Contract AT(07-2)-1. 23p. Dep. mn; CFSTI $1.00 cy, $0.50 mn.

For Presentation at American Society for Testing Materials, 5th Pacific Area National Meeting, Seattle.

Experiments with prepolished, salt-coated strips of Ti–8Al–1Mo–1V exposed under stress in air at high temperatures indicated that stress corrosion cracking was related to hydrogen embrittlement. A wide variety of halogen salts were shown to be effective in causing such cracking. Autoradiographic techniques with radiotracers ^{3}H, ^{36}Cl, and ^{22}Na were used to study the distribution of those elements in salt-coated samples and the results suggested that HCl and NaOH were produced by salt-water reactions. Exposure of stressed, prepolished samples to either HCl or NaOH individually showed that anhydrous HCl caused cracking similar to that observed during hot-salt exposures, while no cracking was produced by NaOH exposures. (auth)

44622 (EURAEC-1433) IMPERFECTIONS IN METALS. II. CORROSION AND OXIDATION. Quarterly Report No. 9, October 1–December 31, 1964. (Centre d'Etude de l'Energie Nucleaire, Mol (Belgium)). Contract 082-62-7 RDB. 17p. (EUR-2375). Dep. mn; CFSTI $1.00 cy, $0.50 mn.

Work Performed under United States–Euratom Joint Research and Development Program.

A study by transmission electron microscopy of stripped oxide films formed on zirconium by oxidation in air showed that uniform film growth does not occur. A large volume of structural heterogeneities was found in the monoclinic zirconia films which replicated the general grain structure of the metal. Regions of fine-grain polycrystalline oxide, formed within the general grain structure, covered almost 5% of the film area. It was observed that those regions oxidized preferentially, resulting in the formation of massive mounds of oxide at longer times. Pseudo-amorphous areas were also observed frequently, especially at lower temperatures and shorter times. Pustules were formed after continued oxidation of the amorphous patches. The pseudo-amorphous areas contained substructure in the form of an apparent grain boundary net and small crystals. A tentative explanation for the presence of these boundaries is presented. (auth)

44623 (NAA-SR-10487) EFFECT OF CARBURIZATION ON THE LOW STRAIN RATE BEHAVIOR OF TYPE 304 STAINLESS STEEL. Interim Report. Stone, D. H.; Schwartz, A. D. (Atomics International, Canoga Park, Calif.). Aug. 31, 1965. Contract AT(11-1)-Gen-8. 32p. Dep.mn; CFSTI $2.00 cy, $0.50 mn.

Pressure stress-rupture specimens of thin walled type 304 stainless steel tubing were tested at temperatures to 1300°F in the presence of an internal diffusion-limited carbon source. The tests determined the effect of simultaneous carburization on the low strain rate behavior of type 304 stainless steel. The stress-rupture life of a tube tested in sodium with a carbon source is over twice as great as the tube life in the absence of the carbon source. All failures occurred in the longitudinal seam weld of the tubing due to the more favorable creep characteristics of the fine grained weld over the coarser grain parent metal. Failures were intergranular and were less than 0.0005-in. diameter. Indications are that total carbon increase of 0.20 wt % during test were not detrimental to the strain behavior of the cladding. (auth)

44624 (NAA-SR-Memo-4887) CARBURIZATION OF TYPE 304 STAINLESS STEEL IN SODIUM–CARBON SYSTEMS. Gill, J. J. (Atomics International, Canoga Park, Calif.). Nov. 16, 1961. Contract AT-11-1-GEN-8. 24p. Dep. mn; CFSTI $1.00 cy, $0.50 mn.

Carburization of Type 304 stainless steel will result from exposure to a sodium–carbon system at 950°F. The rate of carburization does not become significant until a temperature of 1050°F is reached. The carburization process strengthens the 304 stainless steel at elevated temperatures and produces a decrease in the ductility. The stress-rupture life is unaffected by the presence of the carbide layer. At a deflection of 0.076 inches producing a stress of 32,600 psi, the flexural fatigue life is significantly increased by the carburization. (auth)

44625 (TIM-894) CAVITATION DAMAGE TESTS WITH ROTATING DISK IN WATER. Knudsen, L. K. (Pratt and Whitney Aircraft, Middletown, Conn. Connecticut Advanced Nuclear Engineering Lab.). July 1965. Contract AT(30-1)-2789. 126p. Dep. mn; CFSTI $4.00 cy, $1.00 mn.

The cavitation damage resistance of alloys of aluminum, niobium, tantalum, molybdenum, and stainless steel were evaluated in water using a rotating disk apparatus that simulated the cavitation vortex patterns encountered in pumps operating at high suction specific speed. The alloys in decreasing order of cavitation resistance were Ta–8W–2Hf, Nb–18W–8Hf, Ta–10W, type 316 stainless steel, Mo–0.5Ti, Al–4Cu–0.7Mn–0.5Mg, and Al–2.5Mg–0.25Cr. The damage resistance order does not follow a single concept of strain energy, yield point or hardness but appears to be a combination of physical properties and phase structure. Photomicrographs show predominant intergranular cracking for the molybdenum alloy and transgranular cracking for the remaining alloys tested. The second phase precipitate in the aluminum alloy appears to hinder the erosion of material. The small variation in grain size of the heat treated Nb–1 Zr alloy showed small variation in damage resistance with the largest grain structure providing the least erosion. Correlation curves of volume loss as a function of velocity are presented for all materials tested. (auth)

44626 (TIM-896) INTERACTIONS IN A TYPE 316 STAINLESS STEEL–NaK–Cb-1 Zr ALLOY SYSTEM. Lymperes, C. J.; Chapman, J. D.; Schenck, G. F. (Pratt and Whitney Aircraft, Middletown, Conn. Connecticut Advanced Nuclear Engineering Lab.). June 23, 1965. Contract AT(30-1)-2789. 23p. Dep. mn; CFSTI $1.00 cy, $0.50 mn.

A forced circulation, type 316 stainless steel corrosion loop was operated isothermally at 1250°F with K–Na and Nb–1 Zr alloy specimens for a scheduled 3094 hours to study the kinetics of the interaction of the Nb–1 Zr alloy

with C, N_2, and O_2 in the stainless steel-alkali metal system. A carbide–nitride surface reaction layer formed within 250 hours and grew to a maximum thickness of 0.0001 inch in 1000 hours. Carbon contamination (300-400 ppm max.), which occurred during the test, remained isolated near the surface. Nitrogen contamination (600-700 ppm maximum in the outer 0.005 inch region), which occurred throughout the test, diffused to a depth of at least 0.010 inch. There was no significant contamination by oxygen. There was no significant difference between the behavior of specimens in the low velocity flow surge tank and those exposed to a higher flow velocity. (auth)

44627 CORROSION OF CARBON STEEL IN SIMULATED BOILING WATER AND SUPERHEAT REACTOR ENVIRONMENTS. Pearl, W. L.; Wozadlo, G. P. (Vallecitos Atomic Lab., General Electric Co., Pleasanton, Calif.). Corrosion, 21: 260-7(Aug. 1965).

Results are reported on extensive corrosion testing of carbon steel exposed in a dynamic test loop simulating the various environments found in a boiling-water reactor. Water and steam conditions were based on 20 ppm oxygen and 2.5 ppm hydrogen in the 546°F (285°C) saturated steam, a condition representative of the radiolytic water decomposition in boiling-water reactors. The pH of the high-purity water was neutral with no chemicals added to the water. Tests were conducted to study the total corrosion and corrosion product released into the system from isothermal and heat-transfer surfaces as a function of operating conditions. Results of the investigation showed that: the corrosion of carbon steel in such an environment is characterized by an initially rapid filming period governed by nonlinear kinetics followed by an essentially linear corrosion rate. Once the system was properly brought to the oxygen and hydrogen contents typical of BWR conditions, essentially no iron was lost to the system in further exposure to such conditions. A theory describing the formation of the protective oxide is proposed. Additional test results are included for carbon steel exposed to superheated steam at temperatures up to 932°F (500°C). (auth)

44628 RESISTANCE OF YTTRIUM METAL TO HYDROFLUORIC ACID MIXTURES AND HIGH TEMPERATURE OXIDATION. Provow, Douglas M.; Fisher, Ray W. (Iowa State Univ., Ames). Corrosion, 21: 268-73(Aug. 1965). (IS-955).

Acid resistance of yttrium metal is discussed. Though it is highly electropositive and readily dissolves in most acids, it showed excellent resistance in most concentrations of hydrofluoric acid and most mixtures of this acid with other acids. Exposure of yttrium to concentrated hydrofluoric acid produced a fluoride coat, which protected it from further attack. A typical yttrium trifluoride coating nine microns thick was produced by an $HF-HNO_3$ mixture in fourteen days at 50°C (122°F). This was an average of 0.029 mg/cm²-day. (auth)

44629 THE EFFECT OF PRODUCTION ROUTE, AGEING TIME AND OXYGEN CONTENT ON THE PROPERTIES OF Zr-2.5 wt. % Nb. Lees, D. G. (Imperial Metal Industries Ltd., Birmingham, Eng.). Corrosion Sci., 5: 565-77(Aug. 1965).

The effect of varying solution treatment temperature, rolling temperature, aging time and temperature, and oxygen content on the corrosion resistance in steam, and the mechanical properties of Zr-2.5% Nb was investigated. As the aging time was increased, the corrosion resistance in both steam and CO_2 improved continuously, but the percentage of hydrogen picked up during corrosion did not change significantly. The strength at 300°C was raised by cold rolling but then decreased with increasing aging time. Material with high oxygen content possessed better corrosion resistance than that with low. Air cooling after solution treatment did not give as good a combination of strength and corrosion resistance as water quenching. (auth)

44630 THE CORROSION OF URANIUM AND ITS PREVENTION BY ORGANIC COATINGS. Orman, S.; Walker, P. (U. K. Atomic Energy Authority, Aldermaston, Eng.), J. Oil Colour Chemists' Assoc., 48: 233-55(Mar. 1965).

Coatings representative of three of the major curing mechanisms were selected, and various systems falling within the categories, solvent evaporation, oxidative, and two pack systems, were investigated. The coatings tested included: solvent evaporation with chlorinated rubber, styrene-butadiene, ethyl cellulose/phenolic, polystyrene, and natural rubber; oxidative cure with alkyls of various oil lengths, epoxide esters, and styrenated epoxide esters; and reaction coatings with amine-cured epoxide, adduct cured epoxide, polyamide cured epoxide, and polyester/isocyanate adduct. All coatings were evaluated as single and multiple coats on discs formed from the magnesium-reduced unadjusted uranium. Specimens were examined daily for visible signs of corrosion, loose oxide, and film detachment. None of the coatings were protective under the conditions of testing, and several, notably the chlorinated rubber lacquer and the reaction coatings were actively corrosive towards uranium. In spite of this lack of protection, styrene-butadiene, ethyl cellulose, and natural rubber were considered worthy of more detailed examination over a wider range of temperatures. The periodic weight increase of the coated U rods was somewhat variable over the first 100 hr. After this period the specimens coated with the materials, which were not actually corrosive, exhibited a linear rate of weight increase. Consideration of the uranium-water reaction reveals that for every 238 g of uranium consumed only 32 g of oxygen enter into the reaction. It was therefore considered that weight increase determinations, particularly over the initial test period, when uptake figures are low, will be less accurate, and hence less reliable. Where a coating vehicle was intrinsically corrosive towards uranium, the incorporation of inhibitive pigments did not prevent this enhanced corrosion. Visual and gravimetric tests indicated that two coatings (styrene-butadiene and natural rubber) offered marginal protection of uranium under condensation conditions up to 70°C. Further experiments indicated that uranium can be protected by an aluminum pigmented styrene-butadiene lacquer at temperatures up to 40°C. The major reason for the failure of the coatings to afford protection to uranium is that the water permeability of the materials was too high to become a rate-determining stage in the corrosion process. Thus water vapor reached the uranium surface at a rate at least equal to the rate at which it was being consumed by the uranium. (BBB)

44631 OXIDATION OF THE URANIUM–COPPER INTERMETALLIC COMPOUNDS UCu_5 IN CARBON DIOXIDE BETWEEN 350 deg and 850 deg C. Stobbs, J. J.; Pearce, R. J.; Whittle, I. (Central Electricity Generating Board, Glouchestershire, Eng.). Trans. Met. Soc. AIME, 233: 1676-82(Sept. 1965).

The oxidation kinetics of UCu_5 in carbon dioxide were studied over the temperature range from 350 to 850°C. At any one temperature, two successive parabolic rate constants were obtained. Up to 650°C, the temperature dependence of the reaction was small and the first parabolic rate constant was higher than the second. At temperatures of 690°C and above, there was a very marked temperature dependence and the second rate constant was the higher. Metallographic examination showed that attack proceeds via internal oxidation. (auth)

44632 ESTIMATION OF FISSION GAS RELEASE FROM INTENTIONALLY PUNCTURED CALDER HALL TYPE FUEL ELEMENT. Taketani, K.; Ikawa, K. (Japan Atomic Energy Research Inst., Tokyo). 19p. (CONF-650407-13). Gmelin, AED-CONF-65-044-7.

From International Symposium on Fission Product Release and Transport Under Accident Conditions, Oak Ridge, Tenn.

To estimate fission gas release from failed fuel elements in the Calder Hall type Tokai-mura reactor, three experiments were carried out separately. Oxidation in air and in carbon dioxide was observed and the rate of weight increase was measured using miniature fuel ele-

ments with a pin hole of 1.0, 0.5, and 0.2 mm dia. In case of carbon dioxide oxidation, weight increased linearly with heating time at the rate of 100 mg/day and 7 mg/day at 550 and 450°C, respectively. Not much swelling of the cladding was observed. Correlation of fission gas released with the extent of oxidation of uranium by carbon dioxide was investigated. The fractions of fission gas released to completion of oxidation were about 10, 22, and 40% at 500, 600, and 700°C, respectively. This activation energy was calculated to be 5.1 kcal/mol. This temperature dependence indicated that the diffusion in the oxide powder produced by the oxidation is not the controlling factor in the release of fission gas during the oxidation. Diffusion coefficients of fission gas in the uranium dioxide powder formed on carbon dioxide oxidation of uranium were measured in the temperature range 450 to 750°C by post-irradiation isothermal heating technique. The fraction of released fission gas was apparently proportional to the square root of the heating time as can be explained by the general diffusion mechanism. The values for activation energy obtained were considerably smaller than those reported previously. From the results obtained by these measurements, it was found that contamination of the reactor coolant, carbon dioxide, by activity of fission gas released during oxidation is not a significant problem if the fuel concerned is not badly damaged. (auth)

Fabrication

Refer also to abstract 45569.

44633 (ANL–7000, pp 138-45) DEVELOPMENT OF FABRICATION METHODS. (Argonne National Lab., Ill.).

Fabrication of tungsten tubing was attempted by extrusion followed by drawing, rolling, or swaging. General observations on the processes are given; specific criteria were not established due to a lack of high-quality starting material. Preliminary fabrication of W–25 Re tubing by extrusion produced radiographically sound tubing, but additional extrusions are considered necessary to establish reproducibility. Th–U castings were canned in copper and extruded at 500 or 850°C. The extrusion constant decreased with increased extrusion temperature and increased with increasing uranium content. The microstructure consisted of free uranium in a thorium matrix. (W.L.G.)

44634 (DPST–65-83-7) USAEC–AECL COOPERATIVE PROGRAM MONTHLY PROGRESS REPORT, JULY 1965. Hilborn, H. S. (comp.) (Du Pont de Nemours (E. I.) and Co., Aiken, S. C. Savannah River Lab.). Aug. 10, 1965. Contract AT(07-2)-1. 7p. Dep. mn; CFSTI $1.00 cy, $0.50 mn.

A comparison of the stress-orientation behavior of cold-reduced tubing with its opposite form, cold-expanded tubing revealed significant relations between the stress-orientation phenomenon and the fabrication history of the material. Stress orientation of hydride platelets was observed only when the major strains during fabrication were contractile in the test stress direction. When the major strains were tensile, no stress-orientation susceptibility was exhibited. For reduced tubing (and presumably also for expanded tubing) the magnitude of stress orientation susceptibility is related to fabrication temperature. Higher temperatures promote high stress-orientation susceptibilities. In cold-reduced tubing, i.e., diameter continuously reduced at room temperature, stress orientation in the circumferential tubing direction is constant at 1% increase in "f_{48}" (platelets 48 to 90° to the stress axis) per 1000 psi applied tensile stress. In hot-reduced tubing, the stress-orientation effect is about four times as great. Stress orientation in reactor tubing that is fabricated by conventional cold reducing techniques, i.e., drawn, swaged, tube reduced, or tube rolled, is a characteristic of that material and cannot be controlled by the normal fabrication variables of reduction sequences, tool design, and type of cold-reducing process. (auth)

44635 (INR–695/IA/PL) A METHOD OF TARGET PREPARATION BY ELECTRO-SPRAYING DIRECTLY ON SEMICONDUCTOR DETECTORS. Dakowski, M.; Piekarz, H.; Sowinski, M. (Institute of Nuclear Research, Warsaw (Poland)). Jan. 1965. 15p. Dep.

A method of preparing thin (2 $\mu g/cm^2$ to 1.5 mg/cm^2) and uniform ^6Li and ^{235}U targets by electro-spraying directly on semiconductor detectors was used. No changes in the resolutions, active areas, and volt-ampere characteristics of the detectors were observed. (auth)

44636 (IS-1031) EXTRUSION OF CLAD AND UNCLAD YTTRIUM FOR ROD AND TUBING. Owen, C. V.; Scott, T. E.; Carlson, O. N. (Ames Lab., Iowa State Univ. of Science and Tech.). Aug. 1965. Contract W-7405-eng-82. 19p. Dep. mn; CFSTI $1.00 cy, $0.50 mn.

The extrusion of yttrium metal into rods and seamless tubing was studied. Extrusions were made using both as arc-cast and recrystallized starting billets. The results of these extrusions are discussed and criteria for obtaining good tubing are suggested. (auth)

44637 (LA–3340) FORMING OF TEFLON SHEET BY POWDER ROLLING. Sheinberg, H. (Los Alamos Scientific Lab., Univ. of California, N. Mex.). Nov. 29, 1964. Contract W-7405-eng-36. 9p. Dep. mn; CFSTI $1.00 cy, $0.50 mn.

A description is given of the equipment and process used to form high density Teflon sheet by powder rolling. Data on roll opening and rolled and sintered density for three Teflon powders are presented. (auth)

44638 (ORNL–3681) SUMMARY OF THE KILOROD PROJECT. A SEMIREMOTE 10-KG/DAY DEMONSTRATION OF $^{233}UO_2$–ThO_2 FUEL-ELEMENT FABRICATION BY THE ORNL SOL-GEL VIBRATORY-COMPACTION METHOD. Haws, C. C.; Matherne, J. L.; Miles, F. W.; Van Cleve, J. E. (Oak Ridge National Lab., Tenn.). Aug. 1965. Contract W-7405-eng-26. 169p. Dep. mn; CFSTI $5.00 cy, $1.00 mn.

An economical thorium-^{233}U fuel cycle requires rapid, simple chemical and mechanical processes easily adaptable by nature to remote operation. The ORNL-developed sol-gel process for preparing granular, mixed oxides of thorium and uranium uniquely meets this requirement. A complete system for making fuel elements is obtained by coupling the sol-gel process with vibratory-compaction loading of fuel tubes. During the past year an intermediate-scale demonstration (10 kg a day) showed the feasibility of this combination of sol-gel and vibratory compaction. During this demonstration, more than 1 metric ton of 3% $^{233}UO_2$–97% ThO_2 solids were prepared. In the preparation of feed materials, the ^{232}U daughter products were removed from the ^{233}U by a single-cycle solvent extraction process, and thorium nitrate crystals were converted to a dispersible ThO_2 under a superheated steam atmosphere at 450 to 500°C. In the sol-gel process, $UO_2(NO_3)_2$ and ThO_2 feed stocks are blended at 80°C to form a stable sol (3% $^{233}UO_2$–97% ThO_2). The sol is dried to a gel at 80°C and then calcined and reduced at 1150°C to produce a sintered, fragmented UO_2–ThO_2 product. Fuel rods are then fabricated by crushing the sintered solids and screening the solids through a 6-mesh onto a 16-mesh screen. The remainder of the solids are ball-milled to a powder of "smeared" size distribution. These powders are then blended in proper proportions, loaded into Zircaloy tubes by vibratory compaction, and the rod end-fixture is welded into place. The completed fuel rod is then inspected to ensure concentricity, straightness, weld integrity; finally it is decontaminated. All mechanical and chemical processes behaved as expected. After the startup period, equipment-repair frequency was low. Both feed-preparation operations realized 100% on-stream efficiency. On-stream efficiency was 90% for the sol-gel operation for the entire operating period and 80% for the rod-fabrication equipment after startup. Nine hundred rods, each containing 890 g of mixed oxide, and 200 rods, each containing 310 g of the same mixed oxide were prepared. The fuel column in these rods averaged 89.6% of theoretical density, and variations of density were held to within ±2% of a median value along the active length of the fuel column. Experi-

ence was obtained in the handling of large quantities of ^{233}U, and radiation data necessary for the design of larger facilities and higher activity levels were collected. Radiation exposure to workers in routine operations was limited to a tenth of the permissible levels. A single batch, approximately 100 times more radioactive than the routine Kilorod batch, was prepared to measure exposures to workers at extreme levels of activity. In this safety test, aged ^{233}U was used to simulate 14-day-old feed solution containing 800 ppm of ^{232}U. The resulting exposures, using normal Kilorod operating procedures, were at worst eight times higher than when the customary Kilorod ^{233}U feed solutions had been used. Thus, the present equipment, procedures, and working areas can provide radiological safety at much higher concentrations of ^{232}U than that used in the present program. (D.L.C.)

44639 (ORNL-3740) TIME STUDY OF FUEL ROD FABRICATION IN THE KILOROD FACILITY. Van Cleve, J. E. Jr.; Varagona, J. J.; Lotts, A. L. (Oak Ridge National Lab., Tenn.). Oct. 1965. Contract W-7405-eng-26. 66p. Dep. mn; CFSTI $3.00 cy, $0.75 mn.

A time and motion study of fuel rod fabrication in the ORNL Kilorod Facility was performed to aid in the understanding of the process system and to serve as a guide in the extrapolation of data to larger and more sophisticated facilities. The Kilorod operation was divided into 28 operational subroutines composed of over 200 production work elements for which time values were determined. The maximum throughput of the system was determined to be 15.5 rods/day and the maximum crew effectiveness to be 87%. (auth)

44640 (ORNL-P-1446-1) THERMOCHEMICAL DEPOSITION OF REFRACTORY METALS, ALLOYS, AND COMPOUNDS FOR APPLICATION IN THERMIONIC DEVICES. Federer, J. I.; Heestand, R. L.; Patterson, F. H.; Leitten, C. F. Jr. (Oak Ridge National Lab., Tenn.). [1965]. Contract W-7405-eng-26. 13p. (CONF-650908-9). Dep. mn; CFSTI $1.00 cy, $0.50 mn.

From International Conference on Thermionic Electrical Power Generation, London.

Thermionic devices impose rigid requirements on refractory materials technology in relation to fabrication, purity, and physical characteristics. Thermochemical deposition of refractory metals, alloys, and compounds was investigated as a technique for solving these materials problems. Tubular and sheet deposits of W, Re, Mo, and W–Re alloys were prepared by H_2 reduction of the metal hexafluorides in the temperature range 500 to 1000°C at pressures of 5 to 20 torr. Factors affecting deposition rates, purity, and grain orientation were studied. High-purity W sheet of uniform thickness was prepared at about 570°C. W deposited below 800°C is highly oriented with {100} parallel to the deposition surface. Joining of thermochemically deposited and wrought W by deposition was demonstrated by the preparation of joints in sheet and tubing. W–Re alloys deposited in a static hot zone at temperatures of 450 to 700°C are inherently nonuniform in composition and deposition rates due to relative differences in the stabilities of WF_6 and ReF_6. A moving hot-zone technique shows promise of alleviating this problem. UO_2 having oxygen-to-uranium ratios ranging from 2.001 to 2.166 was deposited by reaction of UF_6 with H_2 and water vapor or O_2 at 1250 and 1300°C and pressures of 3 to 6 torr. Both bulk solids and extremely fine powder (60 to 200 Å) were prepared. Stoichiometric SiC was deposited at a rate of 10 mils/hr by H_2 reduction of $SiCl_4$ in the presence of methane at 1300°C and a pressure of 100 torr. In general, thermochemical deposition is a unique method for fabricating many refractory materials of high density and purity and requiring a minimum of finishing operations. (auth)

44641 (ORNL-TM-1193) CALCULATIONS OF CHARGE AND CONTOUR DIMENSIONS OF POWDER-LOADING ASSEMBLY USED IN THE PRODUCTION OF HFIR COMPOSITE FUEL COMPACTS. Watts, T. D.; Werner, W. J.; Hammond, J. P. (Oak Ridge National Lab., Tenn.). Sept. 1965. Contract W-7405-eng-26. 15p. Dep. mn; CFSTI $1.00 cy, $0.50 mn.

Fuel plates for the compact high performance HFIR fuel element are of a complex sandwich construction composed of a fuel-containing cermet clad with type 6061 aluminum. These cermets are unique in that the fuel density must vary in a specified nonlinear manner in the dimension corresponding to plate width. The development of powder metallurgy procedures for producing composite fuel compacts of the proper configuration in a single cold-pressing operation represents a major advancement in the field of fuel-plate technology. Rectangular compacts amenable to standard fabrication procedures are obtained through the combination of a constant-composition dispersion with a varying thickness profile with a mating aluminum filler section. The dimensions of the powder-loading assembly used for loading the fuel and filler sections into the die prior to compacting were calculated. The geometry and dimensions of these sections were back calculated from the final plate specification by use of the rolling reduction, the compact spread during rolling, the pressed density of the two sections of the compact, and the powder compressibilities. Cores pressed with satisfactory contours verified the adequacy of the calculations. (auth)

44642 (RFP-570) FEED RATE CHECKS ON NUMERICAL CONTROLLED MACHINES. Durbin, C. E. (Rocky Flats Div., Dow Chemical Co., Denver, Colo.). Aug. 25, 1965. Contract AT(29-1)-1106. 12p. Dep. mn; CFSTI $1.00 cy, $0.50 mn.

The effects of various feed rates on the intended tool path of numerically controlled boring and turning machines were investigated. The tests were conducted on several types of precision machines at Rocky Flats Plant. The amount of tool overshoot and vibration was recorded. (auth)

44643 (RSIC-410) NONDESTRUCTIVE MEASUREMENT OF RESIDUAL STRESSES IN METALS AND METAL STRUCTURES. Masubuchi, Koichi (Battelle Memorial Inst., Columbus, Ohio). Apr. 30, 1965. Contract DA-01-021-AMC-11706(Z). 128p.

A survey of the methods for nondestructive measurement and evaluation of residual stresses produced during the fabrication of structures made of high-strength aluminum alloys is presented. The fundamental information on residual stresses that is needed to understand measurement techniques; methods of measuring residual stresses, including stress-relaxation techniques, x-ray diffraction technique, the ultrasonic technique, the hardness technique, and cracking techniques; measurement of residual stresses during fabrication of metal structures; and the selection and use of appropriate measurement techniques and evaluation of results are discussed. Recommendations are given for future research on nondestructive measurement of residual stresses produced during fabrication of metal structures. (auth)

44644 (SC-TM-65-276) A SEMICONTINUOUS HOT PRESS TUNNEL KILN. Haertling, G. H. (Sandia Corp., Albuquerque, N. Mex.). June 1965. Contract AT(29-1)-789. 11p. Dep. mn; CFSTI $1.00 cy, $0.50 mn.

A kiln was designed for the fabrication of high quality ceramics by hot pressing. The kiln includes a heated tunnel, a means for moving the parts in molds through the tunnel, and rams for pressing and then ejecting the parts. The kiln was operated to produce ferroelectric ceramics, and the results are described. (D.L.C.)

44645 (JPRS-24761, pp 12-16) INVESTIGATION OF DIFFUSION PROCESSES IN BRAZING RHENIUM-COATED TITANIUM. Bondarev, V. V.; Shinyaev, A. Ya. Translated from Tr. Inst. Met. im. A. A. Barkova, Akad. Nauk SSSR, No. 14, 86-9(1963).

Brazing Ti is difficult because Ti tends to form brittle compounds with the brazing alloy. In order to investigate the possibility of using Re to protect the Ti during brazing, a study was made of the diffusion processes between Ti and a Re galvanic coating at different brazing tem-

peratures. Re-coated samples were brazed with Cu–Ag braze alloys in vacuum at 740 to 850°C. The optimum Re thickness was found to be 6–12 microns. Mechanical tests and metallography show that: a diffusion zone forms which is 3–7 microns wide at the lower temperatures; the braze joint strength reaches its maximum at a zone width of 7–18 microns, reached at 780 to 820°C; at the higher temperatures, the zone widens up to 40 microns, and the joint becomes brittle. (D.L.C.)

44646 A CONTRIBUTION TO THE STUDY OF THE EFFECT OF TiO_2 ADDITIVE ON THE SINTERING OF URANIUM DIOXIDE. Manojlovic, Lj. M.; Herak, R. M.; Malcic, S. S.; Ristic, M. M. Bull. Boris Kidrich Inst. Nucl. Sci., 16: 81-7(Apr. 1965).

The effect of TiO_2-additive on the sintering of uranium dioxide in an argon atmosphere was studied. The sintered samples were investigated by x-ray diffraction. It was shown that at temperatures of 1100, 1200, 1300 and 1400°C a chemical reaction takes place. This reaction is probably the main reason for the beneficial effect of TiO_2-additive on the sintering of uranium dioxide. (auth)

44647 THE REFRACTORY METALS SHEET ROLLING PROGRAM. Lane, J. R.; Ault, G. Mervin. (National Research Council, Washington, D. C.). Metals Eng. Quart., 5: 23-9(Aug. 1965).

The Refractory Metals Sheet Rolling Program, which was started about five years ago, will be concluded as a coordinated activity at the end of this year. The need for the program, its objectives, method of attack, progress to date, and what remains to be done are reviewed. (auth)

44648 ULTRASONIC GRINDING OF NATURAL GRAPHITE. Matuyama, Eitaro (Yamaguchi Univ., Ube, Japan). Nature, 207: 1189-90(Sept. 11, 1965).

Experiments carried out with Madagascar graphite ground in a cell excited with ultrasonic waves are reported. Under an optical microscope ultrasonically ground particles revealed flat glancing faces often exhibiting clear twin boundaries. The surfaces of particles ground in a mortar with a pestle were commonly rougher, showing close fringes of laminated steps on the basal plane. Apparently ultrasonic treatment de-laminates each particle and removes surface roughness. (P.C.H.)

44649 PARTICLE BONDING OF SWAGED URANIUM DIOXIDE COMPACTS. Honda, Yutaka; Takahashi, Shuichiro (Mitsubishi Atomic Power Industry, Inc., Japan). Nippon Genshiryoku Gakkaishi, 7: 351-8(July 1965). (In Japanese).

Bonding of UO_2 particles composing compacts which were swaged at room temperature or at temperatures up to 1,100°C and annealed at temperatures up to 1,100°C for 20 min after swaging, is discussed in relation to swaged UO_2 density, dissolution time in nitric acid solution, specific surface area, and microphotographic observations. UO_2 particles were bonded leaving closed pores by repeated compressive stress and temperature rises resulting from plastic deformation during hot swaging above 800°C. Annealing above 800°C for 20 min after swaging was effective for further particle bonding, an effect, which is associated with atom diffusion accompanied by relief of stress induced in the UO_2 particles by the swaging. This also occurred gradually at room temperature. (auth)

44650 PREPARATION OF SELF-SUPPORTING THIN SILICON TARGETS BY REDUCTIVE EVAPORATION. Karolyi, J.; Szalay, A. (ATOMKI, Debrecen, Hungary). Nucl. Instr. Methods, 36: 353(Oct. 1965).

Si films 20 to 50 $\mu g/cm^2$ thick are deposited by reductive evaporation onto an optically polished stainless steel substrate. The substrate is coated with a monomolecular layer of household detergent prior to the deposition of the Si. After deposition, the Si layer is floated off the substrate by immersion in water. The Si layer can be cut and mounted on frames while it is floating on the water. (T.F.H.)

44651 HYDROSTATIC EXTRUSION OF DIFFICULT METALS. Pugh, H. Ll. D.; Low, A. H. (National Engineering Lab., Glasgow). Sheet Metal Ind., 42: 572-94 (Aug. 1965).

Hydrostatic extrusion as a forming process is discussed. The apparatus used to investigate some aspects of the process is described, and consideration is given to the properties and behavior of high-pressure fluids and lubricants in this work. While some of the features of fluid extrusion can be exploited with common engineering materials, it is in the field of "difficult" materials that the full potential of the process may be seen. With these materials, an extension of the technique, fluid-to-fluid extrusion, is used; this enables brittle materials to be worked cold. An account is given, of the range of materials extruded by this method with a brief statement of the properties of the extruded products, where they were determined. (auth)

44652 ROLLING CAST BERYLLIUM BETWEEN 500 deg AND 1000 deg C. Cheer, D. A.; Evans, R. E.; Lowe, J. N. (Atomic Weapons Research Establishment, Aldermaston, Eng.). Sheet Metal Ind., 42: 595-600(Aug. 1965).

Improvements in casting techniques enabled beryllium sheet to be rolled from cast metal. This material was of near random texture and subsequently formable at relatively low temperatures (200°C). Sheet was produced by both hot sheet rolling and warm bore rolling. However, such material was characterized by a coarse grain-size resulting in low strength. Rolling difficulties are discussed in terms of surface quality, texture, grain refinement, mechanical properties, and formability. Correlation of forming and mechanical properties is shown. (M.C.G.)

44653 SOME TECHNIQUES USED IN THE MACHINING AND WORKING OF CAST TUNGSTEN. Gilbert, J. R. B.; Goold, D.; Thacker, R. J. (Imperial Metal Industries (Kynoch) Ltd., Birmingham, Eng.). Sheet Metal Ind., 42: 601-10; 22(Aug. 1965).

Properties of cast tungsten are described. Methods of machining cast ingots either to billets or to test specimens are discussed. Turning, drilling, grinding, spark machining, and electrochemical machining are considered. The initial breaking down of the cast structure, which is an essential preliminary to further fabrication, is described. Hot extrusion, electrostatic extrusion, hot forging, and cold forging are discussed as methods of forming cast tungsten. (M.C.G.)

44654 PLUTONIUM SHEET FABRICATION. TENSILE PROPERTIES AND CUPPING EXPERIMENTS. Orme, J. T.; Ward, B. J. (Atomic Weapons Research Establishment, Aldermaston, Eng.). Sheet Metal Ind., 42: 611-22 (Aug. 1965).

It was found that good-quality plutonium sheet, of fine grain size, and free from distortion and surface veining effects, can be produced by rolling at β- or γ-phase temperatures, and chill cooling through the transformation to the α phase between loaded platens. The sheet tensile properties varied markedly with the cooling rate after rolling. Rapid cooling increased the strength in the α phase but decreased the strength and increased the elongation in the β phase. All these effects were thought to result from the initial grain refinement produced by rapid cooling. The β-phase properties were highly sensitive to strain rate. Although the β-phase tensile properties suggest poor formability by conventional punch and die techniques, cupping tests showed that the metal can be successfully formed at temperatures around 150°C in the β phase using a rubber forming technique based on the Hydroform principle. (auth)

44655 AUTOMATIC MACHINE FOR MILLING FINS ON CYLINDRICAL PARTS. Tetart, Emile; Juzon, Louvie; Pyrenees, B. (to Commissariat a l'Energie Atomique). British Patent 1,000,237. Aug. 4, 1965. Priority date June 7, 1963, France.

An automatic machine is described for milling parallel helical fins in adjacent sectors in a cylindrical work-piece. The machine includes a support frame, two clamping spindles, and at least one set of milling cutters provided with rotary drive means for producing predetermined relative

movement between the work-piece and the milling cutters. The work-piece to be machined is placed between the clamping spindles, and one of the spindles is movable axially while the other is fixed. The means for producing the relative movements are constituted on the one hand by a motor unit that drives the work-piece in rotation and on the other hand by a reproducing unit that initiates the displacement of the milling cutters in a direction parallel to the axis of the workpiece in a first direction for the purpose of machining the fins in a first sector, then in the opposite direction for the purpose of machining the work-piece in the adjacent sector. The machine is equipped with an automatic control mechanism that controls the complete machining of one piece from the positioning of the milling cutters in contact with the work-piece to the stoppage of the machine on completion of the final machining cycle and the disengagement of the finished machine part. The control mechanism also starts and stops the ancillary devices that control the cooling of the milling cutters and the removal of the swarf. In its preferred form the machine includes two identical work-stations that are located on each side of a central control unit that includes the various parts of the automatic control mechanism. (B.L.M.)

44656 PROCESS FOR MACHINING TUBULAR ELEMENTS WITH FINS FOR HEAT EXCHANGERS. Maillet, Ennemond (to Commissariat a l'Energie Atomique). British Patent 1,000,270. Aug. 4, 1965. Priority date Mar. 21, 1963.

A process is described for machining tubular elements for heat exchangers of the type having adjacent rows of oblique and parallel fins forming a herringbone pattern on the surface. The process is particularly applicable to the fabrication of fuel element cans and consists of machining the fins of each row by means of milling-cutter teeth having the shape of the transverse cross section of the unitary channels formed between two successive fins in the same row. The teeth are parallel to each other and grouped together in such a manner as to form a hollow end-mill. The axis of the end-mill makes a constant angle with the axis of the tubular element. The constant angle is so determined that the fins are inclined towards the downstream end of the fluid flow, and the angle is preferably between 60 and 80°. (B.L.M.)

44657 IMPROVEMENTS IN AND RELATING TO HOT-FORGING APPARATUS. Kaufmann, Jean; Thome, Paul (to Commissariat a l'Energie Atomique). British Patent 1,000,658. Aug. 11, 1965. Priority date May 31, 1961, France.

A hot-forging apparatus is described that is particularly applicable for the hot-forging of a groove, for example a crimping groove, for fixing the end stopper to a can for a fuel element by crimping. The device includes a conducting support adapted to serve as a self-induction coil. The conducting support is a metallic annular member and includes means displaceable radially towards the part to be forged. The displaceable means are jaws movably mounted on the support, and means are also provided for returning the jaws to their initial position after forging. The forging is effected continuously on the tubular members that are passed through the device. Cooling means are provided. (B.L.M.)

44658 IMPROVEMENTS IN OR RELATING TO PROCESSES FOR APPLYING ALLOYS TO METAL SURFACES. Levandowsky, Jean; Mauguen, Pierre; Hainzenlin, Jean Louis; Jacob, Philippe (to Commissariat a l'Energie Atomique). British Patent 1,001,301. Aug. 11, 1965. Priority date Apr. 14, 1961, France.

A process for securing or sticking a readily liquefiable alloy to a metal surface, a portion of which is formed from a non-oxidizing metal, is particularly applicable to providing a liquefiable annular packing as a seal between the vessel of a reactor and a rotatable cover. The alloy is formed of a Bi-Sn alloy, the composition of which is within ±2% of the composition of the eutectic. The metal surface is tinned with a thin layer of the alloy (0.5 to 0.7 mm) in the presence of a chemically active or strong flux. Then the tinned surface is covered with a thin layer of a soft flux (0.3 to 0.4 mm), and the surface is preheated to 80°C. The alloy is poured onto the prepared and preheated surface at a temperature of about 200°C, and the whole is slowly heated to about 150°C to homogenize the various substances of the alloy and to remove the soft flux. The whole is then cooled. (B.L.M.)

44659 REFRACTORY CARBIDES. Sowman, Harold G.; Johnson, James R. (to Minnesota Mining and Mfg. Co.). British Patent 1,001,359. Aug. 18, 1965. Filed July 21, 1961.

A process for the production of solid spherules of uranium carbide, uranium–thorium carbide, and thorium carbide consists of mixing discrete particles of these substances with an inert particulate isolating material, rapidly heating the mixture in a suitable refractory container in a furnace in an inert atmosphere to a temperature of about 2300 to 2700°C, and then cooling the mixture to solidify the molten carbide in spherical shape. Alternatively, discrete irregular particles of U or Th metals or oxides may be mixed with and heated in the presence of an isolating medium containing sufficient carbon to form the carbide(s) in the non-reactive atmosphere. Suitable isolating medium are carbon or boron nitride. The carbide spherules may be coated with a cladding that is impervious to fission products and is non-absorptive of neutrons. (B.L.M.)

44660 BORON CARBIDE SPHERULES. Sowman, Harold G.; Johnson, James R. (to Minnesota Mining and Mfg. Co.). British Patent 1,001,360. Aug. 18, 1965. Filed July 21, 1961.

Solid spherules of boron carbide can be formed by mixing finely divided boron carbide with a finely divided solid isolating medium, rapidly heating the mixture in a suitable refractory container in a furnace in an inert atmosphere to a temperature of about 2300 to 2700°C, and then cooling the mixture to solidify the molten carbide in its spherical shape. Alternatively, discrete particles of boron or the oxide may be mixed with and heated in the presence of an isolating medium containing sufficient carbon to form the carbide in the non-reactive atmosphere. Suitable isolating media are amorphous carbon, graphite, or boron nitride. The carbide spherules may be coated with a cladding that is impervious to fission products and is non-absorptive of neutrons. (B.L.M.)

44661 IMPROVEMENTS IN OR RELATING TO NUCLEAR FUEL ELEMENTS. Boothroyd, Milton Woodall (to United Kingdom Atomic Energy Authority). British Patent 1,001,874. Aug. 18, 1965. Filed Aug. 28, 1961.

A composite nuclear fuel element can is formed of at least two layers of material in which the inner layer (aluminum) has a low creep resistance at high temperatures at which the outer layer (aluminum oxide) has a high creep strength. Both layers have a low absorption cross section for neutrons. A fuel body is arranged in a length of the composite tubing, ceramic spacers are placed at either end of the body, and composite end caps are applied simultaneously to both ends by flash butt welding. A thin ring composed of the same material as the inner layer of the can is shrunk onto the periphery of the spacers before welding. (B.L.M.)

44662 METHOD FOR THE PRODUCTION OF SPHERICAL FUEL ELEMENTS FOR NUCLEAR REACTORS. Greiner, Herbert. German Patent 1,194,992. June 16, 1965. Filed May 10, 1961.

Fuel elements of spherical shape are produced by pressing high-purity graphite around compact fuel spheres by means of two hemispherically shaped press dies. The whole quantity of the powdery graphite which is necessary for the generation of the graphite casing is pressed at the same time by two opposing press dies. The fuel sphere is at the beginning of the pressing procedure supported by means of thin spokes which are introduced into the pressing room through bore-holes in the mantle of the die. As soon as the graphite is sufficiently compact the spokes are retracted. (Gmelin Inst.)

44663 PRESSED BLOCK FOR THE PREPARATION OF ROD-SHAPED NUCLEAR FUEL ELEMENTS. Steinkopff, Horst; Loeffler, Lotar (to Deutsche Akademie der Wissenschaften zu Berlin). German Patent 1,195,879. July 1, 1965. Filed Mar. 21, 1963.

The pressed block for the fabrication of nuclear fuel elements by extrusion according to patent 1 185 308 comprises a fuel dispersion (U_3O_8, Al) sheathed by means of an Al–Si alloy casing which has a closure plate with a plane surface. (Gmelin Inst.)

44664 METHOD FOR THE PRODUCTION OF Al–U ALLOYS. Blomeyer, Walter; Schneider, Guenther. German Patent 1,199,004. Aug. 19, 1965. Filed Oct. 22, 1964.

The method for the production of Al–U-alloys with homogeneous uranium distribution comprises the steps of spraying the molten alloy through a nozzle by means of a gas stream, and of quenching the molten, finely divided particles in water so that a granulation is obtained. (Gmelin Inst.)

44665 URANIUM–CHROMIUM–ALUMINUM TERNARY ALLOY. Layne, Gilbert S.; Huml, James O. (to Dow Chemical Co.). U. S. Patent 3,198,626. Aug. 3, 1965. Filed June 13, 1963.

A ternary intermetallic compound of U–Cr–Al corresponding to the formula UCr_2Al_{21} is reported. On a weight composition basis, the alloy is comprised of 26.2% U, 11.4% Cr, and 63.4% Al. The alloy is particularly suitable for use as a nuclear reactor fuel composition. The alloy has a melting point of above 800°C is chemically less reactive than is a simple U–Al alloy. (B.L.M.)

44666 URANIUM–TUNGSTEN–ALUMINUM TERNARY ALLOY. Layne, Gilbert S.; Huml, James O. (to Dow Chemical Co.). U. S. Patent 3,198,627. Aug. 3, 1965. Filed June 13, 1963.

A ternary intermetallic compound of U–W–Al corresponding to the formula UW_2Al_{21} is reported. On a weight composition basis, the alloy is comprised of 20.3% U, 31.4% W, and 48.3% Al. The alloy is particularly suitable for use as a reactor fuel element composition. The alloy has a melting point of above 800°C and is chemically less reactive than the simple U–Al alloy. (B.L.M.)

44667 URANIUM–TANTALUM–ALUMINUM ALLOY. Layne, Gilbert S.; Huml, James O. (to Dow Chemical Co.). U. S. Patent 3,198,628. Aug. 3, 1965. Filed June 13, 1963.

A ternary intermetallic compound of U–Ta–Al corresponding to the formula UTa_2Al_{21} is reported. On a weight composition basis, the alloy is comprised of 20.4% U, 31% Ta, and 48.6% Al. The alloy is particularly suitable for use as a reactor fuel element composition. The alloy has a melting point above 800°C and is chemically less reactive than the simple U–Al alloy. (B.L.M.)

44668 URANIUM–VANADIUM–ALUMINUM TERNARY ALLOY. Layne, Gilbert S.; Huml, James O. (to Dow Chemical Co.). U. S. Patent 3,198,629. Aug. 3, 1965. Filed June 13, 1963.

A ternary intermetallic compound of U–V–Al corresponding to the formula UV_2Al_{21} is reported. On a weight composition basis, the alloy is comprised of 26.3% U, 11.2% V, and 62.5% Al. The alloy is particularly suitable for use as a reactor fuel element composition. The alloy has a melting point above 800°C and is chemically less reactive than the simple U–Al alloy. (B.L.M.)

44669 PROCESS FOR MAKING CARBON ARTICLES FROM CARBON PARTICLES AND FURANE DERIVATIVES. Johnson, William; Watt, William (to United Kingdom Atomic Energy Authority). U. S. Patent 3,198,714. Aug. 3, 1965. Priority date Dec. 5, 1957, Great Britain.

A process of manufacturing a shaped carbon article having a high density and a low permeability is reported. A mixture is formed of carbon particles and up to about 20 wt % of a liquid binder material consisting essentially of furfuryl alcohol, and a charge of the mixture is shaped to article form. The binder material in the shaped article is polymerized to yield a thermosetting resinous material by heating the shaped article in air to a temperature not in excess of 200°C for a period of time sufficient to effect complete resinification of the binder. After the polymerization of the binder, the shaped article is heated in nonoxidizing conditions at a linear rate of increase of temperature over a period of about three days to a temperature in the range of 1000 to 1350°C and then heated to a temperature in the range of 2000 to 3000°C. (B.L.M.)

44670 RADIATION BARRIER MATERIAL AND METHOD OF MAKING THE SAME. Guglielmo, Richard J. (to Barber, Arthur L. Jr.). U. S. Patent 3,200,085. Aug. 10, 1965. Filed Mar. 2, 1959.

A radiation-attenuating film suitable for making clothing, coverings, and coatings consists essentially of heavy metal particles such as Pb suspended in a resin dispersion of controlled rheology. Resin particles, preferably vinyl chloride polymers or copolymers, are dispersed in a mixture of liquid plasticizers, which may contain also one or more monomers or prepolymers and/or a gelling agent, and the heavy metal particles are then added. A dipping procedure for use with the suspension is described, which eliminates difficulties arising from flowing or dripping of the material. The material may also be formed by brushing, spraying, casting, or molding. (A.G.W.)

44671 PROCESS OF FORMING A CARBON ARTICLE FROM FURFURAL ALCOHOL AND CARBON PARTICLES. Price, Michael Stuart Thomas (to United Kingdom Atomic Energy Authority). U. S. Patent 3,201,330. Aug. 17, 1965. Priority date Nov. 17, 1958, Great Britain.

Shaped articles of carbon can be manufactured by mixing carbon particles with a liquid binder material consisting essentially of furfuryl alcohol and extruding the mixture at room temperature and a pressure of 8–17 tsi. The binder material is then polymerized by heating the article to about 150°C in air and carbonized by heating in nonoxidizing conditions at a rate of increase of about 60°C/hr to a temperature of 800°C. Subsequent graphitizing at a temperature of 2000–3000°C produces an article having relatively low permeability and a density of about 1.8 g/cm^3. (A.G.W.)

Properties and Structure

Refer also to abstracts 43997, 44979, and 45503.

44672 (AD–619201) RESEARCH ON THE SAMARIUM-TYPE INTERMEDIATE PHASES OF INTRA-RARE-EARTH BINARY SYSTEMS. Lundin, C. E. (Denver Research Inst., Univ. of Denver, Colo.). June 1965. Contract Nonr-3661(02). 41p. CFSTI $2.00 cy, $0.50 mn.

Four new binary intra-rare earth systems were investigated by metallography, hardness, and density measurements to confirm the presence of the intermediate samarium-type phase. The systems were: La–Lu, Nd–Lu, Sc–Gd, and Sc–La. The lutetium systems exhibited isomorphism with previous binary intra-rare earth systems, whereas the scandium systems did not. Thermal analysis and resistivity techniques were employed to determine the temperature at which the samarium phase forms in representative intra-binary systems. The thermal analysis and resistivity curves did not indicate reproducible thermal arrests or inflections. The thermodynamics of the intra-binary rare earth systems are being studied by liquid metal solution calorimetry. It was found that the solution of light rare earths were relatively easy in tin, whereas the heavy rare earths were very slow. Other liquid metal calorimeter baths are presently being investigated such as bismuth and indium. Indium shows much more promise for the solution of heavy rare earths. (auth)

44673 (AECL–2268) THE DISSOLUTION AND DIFFUSION OF OXYGEN IN ZIRCONIUM. Doerffler, W. W. (Atomic Energy of Canada Ltd., Chalk River (Ontario)). May 1965. 27p. Dep.; AECL $1.00.

Measurement of the diffusion coefficients of oxygen in α-zirconium by two methods confirmed the results of

Pemsler (for measurements of the dissolution rates of anodic oxides) and the results of Davis (by microhardness measurements on specimens from prolonged thermal oxidation). Repeated dissolution of anodic films and dissolution of thin thermal films gave higher values for the diffusion coefficient and suggested that this may be a function of the oxygen content. Oxidation in air gave anomalous microhardness curves showing a much longer "tail" than expected from the rate of oxygen diffusion. This may be indicative of some interaction between oxygen and nitrogen, with nitrogen diffusing ahead of the oxygen gradient. In the absence of oxygen, the diffusion coefficient for nitrogen is much smaller than that for oxygen. (auth)

44674 (ANL-7000, pp 69-83) DEVELOPMENT OF ALLOY FUELS AND JACKET MATERIALS. (Argonne National Lab., Ill.).

Results of studies on the properties of Pu-Th-U alloys and their compatibility with potential cladding materials, the effects of heat treatments and oxygen on the lattice spacings of high-purity Th, the high-temperature mechanical properties of refractory metals and alloys, and the metallographic specimen preparation of Pu alloys are presented. (W.L.G.)

44675 (ANL-7000, pp 155-75) METALLURGY OF ACTINIDE METALS. (Argonne National Lab., Ill.).

Progress is reported in studies on the preparation of high-purity Pu and U, elastic moduli of single crystal α-U, crystallographic structure of α-U, self-diffusion in α-U, tracer element diffusion in γ-U, metallography of Pu, preferred orientation in sheets of rolled α-Pu, preparation of single crystals of α-Pu and stabilized δ-Pu alloy, effects of pressure on transformation behavior of Pu, electronic structure of Pu, and the electronic structure of Np. (W.L.G.)

44676 (ANL-7000, pp 176-82) METALLURGY OF HCP METALS. (Argonne National Lab., Ill.).

Progress is reported on studies of the effects of H_2 and O_2 on plastic behavior of Zr, dispersion strengthening of Zr by La_2O_3, ThO_2, and Y_2O_3, habit plane of the hydride in hcp metals, and the temperature dependence of the elastic moduli in single crystals of hcp metals. (W.L.G.)

44677 (ANL-7000, pp 183-5) DIFFUSION STUDIES. (Argonne National Lab., Ill.).

Progress is reported for studies on the diffusion of Pd in Cu, Pd, and Ag, diffusion and conductivity in the NaCl-$ZnCl_2$ system, and the effect of magnetic order on diffusion. (W.L.G.)

44678 (ANL-7000, pp 186-200) ALLOYING PROPERTIES. (Argonne National Lab., Ill.).

Progress is reported for studies on the magnetization of Fe alloys, calibration of twin solution calorimeter, thermodynamic properties of Pd-Ag alloys from vapor pressure measurements, intermediate phases in binary systems containing Tc, a scheme for correlating the occurrence of intermediate phases, atomic size in XFe_2 Laves phases by means of the Mossbauer effect, magnetic susceptibility measurements of actinide carbides, and superconductivity in alloys of transition metals. (W.L.G.)

44679 (ANL-7000, pp 205-12) X-RAY AND NEUTRON DIFFRACTION STUDIES. (Argonne National Lab., Ill.).

Progress is reported on neutron diffraction instrumentation, crystallographic computer programs, neutron diffraction structure determination of uranyl nitrate hexahydrate, structure determination of $MnSi_2$, atomic distributions in liquid Na-K alloys, crystal structure of YD_3, neutron and x-ray diffraction study of LiRh, neutron diffraction study of chemical order-disorder in $PtMn_3$, magnetic structures in $PtMn_3$, chemical order in Mn-Co-C carbide system, and ordering in FeV. (W.L.G.)

44680 (ANL-7000, pp 227-32) CERAMIC MATERIALS RESEARCH. (Argonne National Lab., Ill.).

Progress is reported on research on defect equilibria of PuO_2 and the effects of surface structure on catalytic activity of Co_3O_4 and MgO. (W.L.G.)

44681 (AWRE-O-65/65) THE FATIGUE OF URANIUM. Tilbury, P. D. (Atomic Weapons Research Establishment, Aldermaston (England)). Aug. 1965. 19p. Dep. mn; BIS $1.00; HMSO 5s.

Tests were performed on a push-pull machine at zero mean stress. The fatigue limit of worked and annealed uranium was 30000 psi at 10^8 cycles of alternating stress, which is equivalent to the tensile strength $\times$ 0.39. Cold working and decreasing the test temperature increased the fatigue limit. Hydrogen atmospheres had little effect, but the notch effect of a crack in the protective plating lowered the fatigue limit seriously. (auth)

44682 (BDX-613-75) EFFECT OF MOLECULAR STRUCTURE ON THE THERMAL AGING PROPERTIES OF FLEXIBLE URETHANE FOAMS. Smith, C. H.; DeGisi, S. L. (Bendix Corp., Kansas City, Mo.). Sept. 15, 1965. Contract AT(29-1)-613. 18p. (CONF-651107-1). Dep. mn; CFSTI $1.00 cy, $0.50 mn.

For Presentation at American Chemical Society, 1st Midwest Regional Meeting, Kansas City, Mo.

A series of flexible urethane foams was formulated from diisocyanate terminated polyether prepolymers, using both a polyether diol and an ethylenediaminetetraglycol as extenders. The long term compression set characteristics and the compression deflection properties of these foams were studied. The swelling effect in a solvent, the free isocyanate content, and the role of a carbon black filler on the flexible urethane foam formulation were also evaluated. It was concluded that the total amount of diisocyanate used in the formulation, rather than a variation in the type of isocyanate, has the greatest influence on molecular structure. (auth)

44683 (CEA-R-2789) OBSERVATION DE LAMES MINCES MONOCRISTALLINES DE BERYLLIUM EN MICROSCOPIE ELECTRONIQUE. (Electron Microscope Observation of Single-Crystal Beryllium Thin Foils). Antolin, Jacqueline; Poirier, Jean-Paul; Dupouy, Jean-Michel (Commissariat a l'Energie Atomique, Saclay (France). Centre d'Etudes Nucleaires). May 1965. 51p. Dep. mn.

Thin foils prepared from single crystalline beryllium samples deformed at room temperature, were observed by transmission electron microscopy. The various deformation modes were investigated separately from their early stages and their characteristic dislocation configurations were observed. Basal slip is characterized at the outset by the presence of numerous dipoles and elongated prismatic loops. More pronounced cold work leads to the formation of dislocation tangles and bundles which eventually give a cellular structure. Prismatic slip begins by the cross-slip of dislocations from the basal plane into the prismatic plane. A cellular structure is equally observed in heavily deformed samples. Sessile dislocations were observed in twin boundaries; they are pronounced by reactions between slip dislocations and twin dislocations. Finally, the study of samples quenched from 1100°C and annealed at 200°C showed that the observed loops lie in prismatic planes and have a Burgers vector $\vec{b} = \frac{1}{3}\langle 11\bar{2}0\rangle$. (auth)

44684 (CEND-3336-241) DEVELOPMENT AND TESTING OF A TEMPERATURE TRANSIENT METHOD FOR PERFORMING IN-PILE THERMAL CONDUCTANCE TESTING. Progress Report, April 1-June 30, 1965. (Combustion Engineering, Inc., Windsor, Conn. Nuclear Div.). July 1965. Contract AT(30-1)-2379. 24p. (EURAEC-1437). Dep. mn; CFSTI $1.00 cy, $0.50 mn.

Work Performed under United States-Euratom Joint Research and Development Program.

The concept being investigated is one whereby measurement of the transient temperature response at the surface of an operating fuel element, following a reactor power change, will yield thermal conductance values. This two-phase investigation consists first of out-of-pile demon-

strations of feasibility followed by in-pile confirmation of the method. Concurrent mathematical analyses of the thermal model will provide the bases for data interpretation, as well as guides for the design of the experimental portions of the program. Exploratory tests of an out-of-pile element, using ZrO_2 to simulate the fuel, have led to the conclusion that the presence of random thermal disturbances at the element cladding are sufficient to preclude obtaining accurate measurements of temperature-time relations using simple recording equipment. Tests performed with cyclic power inputs in the frequency range from 0.0348 to 0.503 radians/second demonstrated that trends in the response characteristics are as predicted analytically, but the analytical values could not be confirmed. (auth)

44685 (CONF-650908-5) INSULATOR MATERIALS FOR NUCLEAR THERMIONIC POWER CONVERSION. Grossman, Leonard N. (General Electric Co., Pleasanton, Calif. Atomic Power Equipment Dept.). [1965]. Contract AT(04-3)-189. 6p. Dep. mn; CFSTI $1.00 cy, $0.50 mn.

From International Conference on Thermionic Electrical Power Generation, London.

The compatibility of Al_2O_3, BeO, ThO_2, Y_2O_3, and ZrO_2 insulators with cenium vapor and with refractory metals at high temperatures was studied, together with the electric conductivity, thermal expansion and mechanical stability of these materials. (D.C.W.)

44686 (EURAEC-1362) STUDY OF WELDED JOINTS FOR VERY THICK STEEL PLATES. Quarterly Report No. 3, January 1-March 31, 1965. (Institut de Soudure, Paris (France)). June 23, 1965. Contract 007-64-TEEF(RD). 14p. Dep. mn; CFSTI $1.00 cy, $0.50 mn.

Work Performed under United States-Euratom Joint Research and Development Program.

Progress in attempts to cut a 100 mm deep single J groove in a 200 mm thick Mn-Mo steel plate with an oxyacetylene torch is reported. Results of hardness tests in the heat-affected zones and studies of the hydrogen embrittlement cracks in welds produced in Super Elso steel by cold manual arc and submerged arc welding techniques are presented. (W.L.G.)

44687 (EURAEC-1434) IMPERFECTIONS IN METALS. II. CORROSION AND OXIDATION. Quarterly Report No. 10, January 1-March 31, 1965. (Centre d'Etude de l'Energie Nucleaire, Mol (Belgium)). Contract 082-62-7 RDB. 30p. (EUR-2376). Dep. mn; CFSTI $2.00 cy, $0.50 mn.

Work Performed under United States-Euratom Joint Research and Development Program.

A previous report dealt with the formation and behavior of anti-phase boundaries in rutile. Since these defects are characterized by a phase angle ($\alpha = \pi$) deviating from that for usual stacking faults ($\alpha = 2\pi/3$), a study is made of the patterns by which these are revealed in transmission electron microscopy. Use is made of the dynamic theory including anomalous absorption. The specific properties of the fringe patterns at π boundaries are discussed analytically and compared with those at $2\pi/3$ boundaries. From these considerations, criteria can be established which distinguish π boundaries by their contrast features. Some computed profiles illustrate the agreement of this theory with observations on rutile. A discussion is included of the fringe charactieristics at the intersection of bend faults. (auth)

44688 (LA-3359) THE SOLUBILITIES OF SELECTED ELEMENTS IN LIQUID PLUTONIUM. VI. RHENIUM. Bowersox, D. F.; Leary, J. A. (Los Alamos Scientific Lab., Univ. of California, N. Mex.). June 30, 1965. Contract W-7405-eng-36. 9p. Dep. mn; CFSTI $1.00 cy, $0.50 mn.

The solubility of Re in liquid Pu was studied over the range 700 to 950°C from 0 to 4 percent Re. The apparent solubility is given by the equation $\log N_{Re} = 0.1945 - 1.960 \times 10^3 T^{-1}$, where N_{Re} is the solubility of Re expressed as the mole fraction, and T is the temperature in degrees Kelvin. The solubility increased from 1.23 percent Re (by weight) at 700°C to 3.19 percent Re at 950°C. (auth)

44689 (LA-DC-7351) THE BAND STRUCTURE, SPECIFIC HEAT, MAGNETIC SUSCEPTIBILITY, AND ANOMALOUS THERMAL EXPANSION OF DELTA PLUTONIUM. Kmetko, E. A. (Los Alamos Scientific Lab., Univ. of California, N. Mex.). [1964]. Contract W-7405-eng-36. 33p. (CONF-651102-8). Dep. mn; CFSTI $2.00 cy, $0.50 mn.

For Presentation at Royal Commonwealth Society, 3rd International Conference on Plutonium, London.

A rigid, multiple band model, some features of which were suggested by the calculated eigenvalue of the plutonium atom, was assumed for delta plutonium. By finding conditions under which the model accounts for various properties of the metal, some details of the band structure were determined. The outstanding feature is the small breadth of the $5f^{5}/_{2}$ band, around 0.4 ev. The system consisting of this narrow band superimposed upon a much broader 6d band accounts for the negative expansion coefficient as well as for its dependence upon electron concentration as alterable by alloying, the most satisfactory agreement occurring for a 5f-band population of no more than four or five electrons per atom. The contraction is the result of atomic size reduction due to the loss of 5f electrons. The high electronic specific heat (3 cal/mole-°K) and the large magnetic susceptibility, assumed to consist entirely of spin paramagnetic and diamagnetic terms, are also accounted for by the model. (auth)

44690 (LA-DC-7360) MAGNETIC SUSCEPTIBILITY OF DELTA PLUTONIUM-ALLOYS. Lunsford, J. L.; Kmetko, E. A. (Los Alamos Scientific Lab., Univ. of California, N. Mex.). [1965]. Contract W-7405-eng-36. 12p. (CONF-651102-10). Dep. mn; CFSTI $1.00 cy, $0.50 mn.

For Presentation at Royal Commonwealth Society, 3rd International Conference on Plutonium, London.

The magnetic susceptibilities χ of two series of δ-phase alloys made of high-purity Pu and Al or Ga were measured from ~6°K to room temperature. The dependence of χ upon both solute concentration and temperature are weakly negative, the behavior being monotonic in both cases. On the assumption that χ consists only of a Pauli spin paramagnetic term and a diamagnetic one associated with the radon-like core (the Landau term is considered to be negligible by virtue of the apparently high effective carrier mass), the density of states at the Fermi level, at 0°K, is very nearly 20 states/atom-ev. The results are discussed in terms of a two-band model for the electronic structure of δ-Pu. (auth)

44691 (NASA-TN-D-3015) TUNGSTEN-NICKEL-COPPER TERNARY ALLOYS FOR HIGH-TEMPERATURE APPLICATIONS. McIntyre, Ruluff D. (National Aeronautics and Space Administration, Cleveland, Ohio. Lewis Research Center). Sept. 1965. 22p. CFSTI $1.00 cy, $0.50 mn.

Ternary tungsten-nickel-copper alloys were investigated to develop a fabricable alloy which could be sintered at low temperatures and used at temperatures above 3000°F. An effort was made to relate mechanical properties to composition over a range of $\frac{1}{2}$ to 10 total weight percent nickel and copper in tungsten. The result was a tungsten-0.3 percent nickel-0.2 percent copper ternary alloy that exhibited strength and ductility comparable to wrought, recrystallized powder-metallurgy and arc-cast tungsten at temperatures in the vicinity of 3000 to 4000°F, while retaining its capacity for sintering at temperatures as low as 2200°F. Elongation values were comparable to values normally shown for recrystallized tungsten over the temperature interval 3000 to 4000°F. Heat treatment of this alloy following sintering increased the elongation before fracture at 3000°F from 4.0 to 20.0 percent with little loss of strength. In the heat-treated condition, the tungsten-0.3 percent nickel-0.2-percent-copper alloy could be rolled to a 50-percent reduction in thickness at tempera-

tures of approximately 3000°F. The rolled tungsten–0.3 percent nickel–0.2 percent-copper alloy 4 T bend transition temperature compared favorably to that of conventional, unalloyed, worked tungsten sheet material. It is felt that an alloy such as this might be used to prepare tungsten composite materials strengthened by ultrafine dispersoids or strong fibers. Two other alloy compositions investigated, tungsten–1.5 percent nickel–1 percent copper and tungsten–6 percent nickel–4 percent copper, lost almost all their useful strength and elongation at 2500°F. Both of these alloys, however, could be rolled at temperatures near 2000°F in the as-sintered condition. Rolling the tungsten–6 percent nickel–4 percent copper alloy to a 50-percent reduction in thickness imparted to it a strength comparable to wrought, recrystallized tungsten at 1000°F and increased the elongation from 2.0 to 26.0 percent relative to the as-sintered material. (auth)

44692 (NASA-TN-D-3018) HYPERVELOCITY IMPACT DAMAGE CHARACTERISTICS IN BERYLLIUM AND GRAPHITE PLATES AND TUBES. Diedrich, James H.; Loeffler, Irvin J. (National Aeronautics and Space Administration, Cleveland, Ohio. Lewis Research Center); McMillan, A. R. (General Motors Corp., Santa Barbara, Calif. Defense Research Labs.). Sept. 1965. 29p. CFSTI $2.00 cy, $0.50 mn.

Experiments were conducted on beryllium and graphite to determine their behavior under hypervelocity impact. Both materials were impacted with $^1/_8$- and $^3/_{32}$-inch-diameter spherical projectiles of pyrex and aluminum accelerated to a nominal velocity of 25,000 fps by an accelerated reservoir light gas gun. The targets were in the form of flat plates and tubes and were generally tested at temperatures of 70, 700, or 1300°F. Beryllium metal was tested as hot-pressed disks and as tubes fabricated from sintered-powder, cast, and extruded material. All beryllium tubular targets had high-strength inner liners. The various graphite compositions that were tested included flat blocks of ATJ, ZTA, and pyrolytic graphite. A tubular target of AGSR graphite was also tested. These selections reflected a range of densities for the graphite and a range of purities and processing methods for the beryllium. Each material exhibited characteristic brittle crater damage and supplementary cracking damage. The cracking damage was influenced by target size and shape and for beryllium by the processing method of the armor material. The projectile penetration depths were correlated with a frequently used empirical penetration criterion based on target modulus of elasticity. The beryllium crater data exhibited a correlation within the range of experience for other metals while the graphite exhibited penetration depths below the values for metals. Design implications of the results for space radiator applications were discussed. (auth)

44693 (NP-15411) FLOW AND FRACTURE STUDIES OF HIGH PURITY AND ALLOYED BERYLLIUM. Quarterly Progress Report, July 7, 1964–October 6, 1964. Herman, M.; Hoover, D.; Damiano, V.; Pyle, R. (Franklin Inst. Research Labs., Philadelphia, Pa.). Contract NOw 64-0437-d. 14p. (F-B2205-2).

Progress in the development of a beryllium single-crystal grinder-orienter and compression shear dies is reported. Suitably oriented crystals will be sheared along two parallel prism planes for studies of slip in systems having Burgers vectors noncoincident with the basal plane. (W.L.G.)

44694 (NP-15432) FLOW AND FRACTURE STUDIES OF HIGH PURITY AND ALLOYED BERYLLIUM. Final Report. Herman, M.; Hoover, D.; Damiano, V.; Pyle, R.; Tint, G. S.; London, G. J. (Franklin Inst. Research Labs., Philadelphia, Pa.). Aug. 1965. Contract NOw-64-0437-d. 58p. (F-B2205).

A summary is presented of the following studies: single-crystal deformation of pure Be and Be–Cu, zone refining, preparation of polycrystalline Be, calculation of the stresses required to move dislocations on the basal and prism planes of Be, and development of a single-crystal orienter and grinder. (D.L.C.)

44695 (ORNL-P-1506) LOW-TEMPERATURE DUCTILITY AND STRENGTH OF VAPOR-DEPOSITED TUNGSTEN. Schaffhauser, A. C. (Oak Ridge National Lab., Tenn.). [1965]. Contract W-7405-eng-26. 4p. (CONF-651101-19). Dep. mn; CFSTI $1.00 cy, $0.50 mn.

From 13th Conference on Remote Systems Technology, Washington, D. C.

Data are presented on the effects of heat treatment on the ductility and yield strength of vapor-deposited and powder-metallurgy W. Annealing at 1000 to 1800°C is found to decrease greatly the ductile-to-brittle transition temperature of vapor-deposited W to values lower than these for powder-metallurgy W. As-received powder-metallurgy W is stronger than vapor-deposited W, but after annealing at 1800°C and above, the situation is reversed. (D.L.C.)

44696 (ORNL-TM-1188) STUDIES OF THE THORIUM–URANIUM DICARBIDE PSEUDOBINARY SYSTEM IN THE PRESENCE OF EXCESS GRAPHITE (thesis). Cook, Jackie Lee (Oak Ridge National Lab., Tenn.). Sept. 1965. Contract W-7405-eng-26. 200p. Dep. mn; CFSTI $6.00 cy, $1.25 mn.

Submitted to Univ. of Tennessee, Knoxville.

This study combined dilatometry, x-ray diffraction, metallography, thermal analysis, and chemical analysis to provide a better understanding of the phase relationships for the UC_2–ThC_2 pseudobinary system. Thermal expansion as a function of temperature up to 1000°C was determined for UC_2, ThC_2, and the $(U,Th)C_2$ alloys using drop-cast and machined specimens. The microstructural features of all as-cast alloys were similar and all contained excess graphite. Only the anneals above 1500°C for extended periods of time caused significant changes in the microstructure of the carbide or the morphology of the graphite. Microhardness tended to increase slowly with annealing time at 1900°C but did not change significantly for lower temperature anneals. Powder x-ray diffraction patterns were generally diffuse and did not improve appreciably with annealing for material that contained much excess graphite. Specimens of ThC_2 that contained only a trace of free graphite gave sharp diffraction patterns after annealing at 1400°C and below. X-ray diffraction revealed that two distinctly different body-centered tetragonal structures coexisted for alloys in the composition range from 35 to 42 mole per cent ThC_2. Dilatometry and thermal analysis clearly showed two phase transformations in ThC_2 [1500 ± 25°C and 1430 ± 10°C], and the results indicated that the higher temperature transformation was diffusionless. Two similar transformations were observed for ThC_2-rich alloys containing up to 25 mole per cent UC_2. One phase transformation was observed for UC_2 at 1768 ± 25°C. One solid-state transformation occurred for the $(U,Th)C_2$ alloys in the composition range from 25 to 75 mole per cent ThC_2. The transformation temperatures in this composition range passed through a minimum (approximately 1100°C) at approximately 46 mole per cent ThC_2. Two phase diagrams, either of which is consistent with experimental observations, were proposed for the UC_2–ThC_2 pseudobinary system. The mean coefficients of expansion for the $(U,Th)C_2$ alloys between room temperature and 1000°C varies from 8.6×10^{-6} °C^{-1} for ThC_2 to 13.5×10^{-6} °C^{-1} for UC_2. (auth)

44697 (ORNL-TM-1239) PRECIPITATION OF HYDRIDES IN ZIRCALOY-2 AS AFFECTED BY PREFERRED ORIENTATION, ELASTIC STRESS, AND HYDROGEN CONTENT. Rittenhouse, P. L.; Picklesimer, M. L. (Oak Ridge National Lab., Tenn.). Sept. 1965. Contract W-7405-eng-26. 21p. Dep. mn; CFSTI $1.00 cy, $0.50 mn.

Hydride plates in Zircaloy-2 that are oriented perpendicular to a stress direction can drastically reduce ductility. Work was performed to determine the factors that influence directional precipitation of the hydride. Zircaloy-2 specimens were hydrided to three hydrogen levels and the hydrides were precipitated while the specimens were subjected to an elastic stress in either the rolling or transverse direction. Stresses applied during precipitation

cause a reorientation of the hydrides which is dependent on stress level, the direction of stress relative to crystallographic features of the texture of Zircaloy-2, and hydrogen content. (auth)

44698 (PWAC–465) RECOVERY AND RECRYSTALLIZATION OF COLUMBIUM AND SEVERAL COLUMBIUM–ZIRCONIUM ALLOYS. Carlson, C. E.; Delgrosso, E. J. (Pratt and Whitney Aircraft, Middletown, Conn. Connecticut Advanced Nuclear Engineering Lab.). Sept. 1965. Contract AT(30-1)-2789. 29p. Dep. mn; CFSTI $2.00 cy, $0.50 mn.

The recovery and recrystallization characteristics of cold worked Nb and Nb–Zr alloys having nominal compositions of Nb–1 Zr, Nb–3 Zr, and Nb–5 Zr were studied. Activation energies for recovery were determined for the Nb–1 Zr, Nb–3 Zr, and Nb–5 Zr alloys. The activation energies for the initiation of recrystallization were calculated for Nb (2 interstitial levels), Nb–1 Zr (2 interstitial levels), Nb–3 Zr, and Nb–5 Zr. Electron transmission metallography of Nb–1 Zr alloy indicated that during recrystallization, complex dislocation interactions occurred which were strongly influenced by precipitates of ZrO_2. (auth)

44699 (R63FPD33) 1400 deg F WELDABLE SHEET PROGRAM. Barker, J. F.; McHenry, H. T. (General Electric Co., Evendale, Ohio). July 5, 1963. 132p.

The development and properties of René 62, a Ni-based alloy containing Cr, Fe, and Mo and hardened with Al, Nb, and Ti, are described. (W.L.G.)

44700 (TID–22117) MECHANICAL BEHAVIOR OF DILUTE ALLOYS OF NIOBIUM. Final Report. Sinclair, G. M. (Illinois Univ., Urbana. Dept. of Theoretical and Applied Mechanics). July 27, 1965. Contract AT(11-1)-1046. 10p. Dep. mn; CFSTI $1.00 cy, $0.50 mn.

Preliminary measurements of the cyclic stress induced creep in Nb revealed that the amount of plastic deformation at constant load amplitude and low temperatures is dependent on the number of cycles of load. Abstracts of papers written as a result of prior research on the contract are also included in the report. (W.L.G.)

44701 (TID–22144) HIGH TEMPERATURE INORGANIC CHEMISTRY. Annual Progress Report No. 7. Grosse, A. V.; Cahill, J. A. (Temple Univ., Philadelphia, Pa. Research Inst.). Aug. 30, 1965. Contract AT(30-1)-2082. 55p. Dep. mn; CFSTI $3.00 cy, $0.50 mn.

The relationships between the electric conductivities, thermal conductivities, and temperature of liquid metals over their entire liquid range are discussed, and some results are given for Hg and the alkali metals. The work on the correlation of densities, volumes, expansion coefficients, and atomic cell dimensions of Hg from 0 to 1733°K is reported on briefly. Some results are reported for the kinematic viscosities of Hg, Na, and K over their liquid range. Preliminary electric resistivity measurements were made on liquid Sn up to 2000°K. Viscosity studies are described, and results are given for liquid Sn and Ag. The surface tension of liquid salts near the critical temperature is discussed briefly. Data are presented on the solubility of C in liquid Zr to 4000°K. The behavior of a liquid ZrC–C solution on liquid W_2C at 3250°K in a graphite crucible was studied. (D.L.C.)

44702 (TID–22200) GOVERNING FACTORS IN THE FORMATION OF Cr_3O-TYPE STRUCTURES. Final Report. Wilcox, Roy C.; Bull, Fred W.; Eckel, John F. (Virginia Polytechnic Inst., Blacksburg. Dept. of Metals and Ceramic Engineering). June 30, 1965. Contract AT(40-1)-2564. 29p. Dep. mn; CFSTI $2.00 cy, $0.50 mn.

Results are presented of the six ternary systems investigated. All systems have been completed and the results analyzed. Complete ternary solid solubility was found in the V–Si–Sn and V–Rh–Si systems between the Cr_3O-structures. There is some evidence of solubility between Nb_3Al and Nb_3Sn in the Nb–Al–Sn system. However, no solubility was found in the Cr–Si–Sn, the Nb–Rh–Si, and the Cr–Rh–Si systems. These results were unexpected in the Cr–Rh–Si system because both Cr_3Rh and Cr_3Si exist. (auth)

44703 (TIM–844) THE VAPOR PRESSURE OF LITHIUM BETWEEN 1307 AND 1806K. Rigney, D. V.; Kapelner, S. M.; Cleary, R. E. (Pratt and Whitney Aircraft, Middletown, Conn. Connecticut Advanced Nuclear Engineering Lab.). Sept. 1965. Contract AT(30-1)-2789. 14p. Dep. mn; CFSTI $1.00 cy, $0.50 mn.

The vapor pressure of lithium was determined in the temperature range from 1307 to 1806°K. The results of a regression analysis of the data are given by the equation: $\log_{10} P(atm) = 4.8831 - (7877.9/T(°K))$. The calculated heat of vaporization is 36,049 ± 132 calories per mole. (auth)

44704 (TIM–849) THE VISCOSITY OF LITHIUM. Rigney, D. V.; Kapelner, S. M.; Cleary, R. E. (Pratt and Whitney Aircraft, Middletown, Conn. Connecticut Advanced Nuclear Engineering Lab.). July 1965. Contract AT(30-1)-2789. 14p. Dep. mn; CFSTI $1.00 cy, $0.50 mn.

The viscosity of lithium was determined in the temperature range from 600 to 1180°C. The results of a regression analysis of the data are given by the equation: $\log_{10} \eta$ (centipoise) = $(726.07/T(°K)) - 1.3380$. The activation energy required for viscous flow was determined as −3320 calories/mole over the range of investigation. (auth)

44705 (UCRL–11653) THE EFFECT OF SIZE ON THE PLASTIC PROPERTIES OF ALUMINUM SINGLE CRYSTALS. Rosen, A.; Ahmadieh, A. (Lawrence Radiation Lab., Univ. of California, Berkeley). June 9, 1965. Contract W-7405-eng-48. 8p. Dep. mn; CFSTI $1.00 cy, $0.50 mn.

Single crystals of high-purity Al were prepared with final diameters of 0.231, 0.387, and 0.550 in. They were tested at 77°K with a strain rate of 1.67×10^{-4}/sec; after yielding, the strain rate was changed to 1.37×10^{-5}/sec, and the change was repeated several times during straining. The resulting stress-shear strain curves were almost identical, but the stress vs $\beta(= \partial \ln \dot{\gamma}/\partial \tau$, where $\dot{\gamma}$ is the strain rate and τ is the stress) curves show that the dependence of β on the flow stress is influenced by the size. It is concluded that the activation volume of the dislocations is greater for large specimens at the same stress. (D.L.C.)

44706 (UCRL–12264(Rev.1)) THE INFLUENCE OF STRAIN RATE ON MECHANICAL PROPERTIES OF 6061-T6 ALUMINUM UNDER UNIAXIAL AND BIAXIAL STATES OF STRESS. Hoge, K. G. (Lawrence Radiation Lab., Univ. of California, Livermore). Aug. 5, 1965. Contract W-7405-eng-48. 31p. (CONF-650912-2). Dep. mn; CFSTI $2.00 cy, $0.50 mn.

From Society for Experimental Stress Analysis, 2nd International Congress on Experimental Mechanics, Washington, D. C.

A technique is presented for determining mechanical properties of materials under dynamic tensile loads. A Dynapak metalworking machine was modifield into a test fixture capable of producing the required dynamic loads for uniaxial and certain biaxial tensile tests. Results from uniaxial dynamic tests on 6061-T6 aluminum alloy are presented and compared to "static" data obtained from a universal testing machine. The dependence of tensile strength on strain rate and the augmenting effect of temperature on this dependence can be seen. The results of biaxial tests are described in terms of a modified form of the distortion-energy failure theory. (auth)

44707 (WVT–6523) A SURVEY OF ALLOY-EUTECTIC SOURCES FOR ALIGNED STRUCTURES. Harrington, Richards H. (Watervliet Arsenal, N. Y. Benet R and E Labs.). July 1965. 34p. CFSTI $1.00.

A nearly complete evaluation of known binary alloy eutectic systems has been made with the exceptions of incomplete listing of Rare Earth Metals and of Refractory Metals. Seventy-seven eutectic systems are listed as unfavorable

for production of useful whisker (or aligned) structures. Twenty-eight binary eutectic systems are listed as being possible sources for beneficially aligned structures. Some limitations are discussed. The relative value of using high pressure to increase yield quantities is indicated for specific systems. The high cost for high pressure yields does not appear warranted in any case, at least for some time to come. (auth)

44708 (JPRS-24761, pp 1-11) ACTIVATION ENERGY AND MECHANISM OF SELF-DIFFUSION OF NICKEL. Shinyaev, A. Ya. Translated from Tr. Inst. Met. im. A. A. Barkova, Akad. Nauk SSSR, No. 14, 78-85(1963).

^{63}Ni was used in the tracer study of self diffusion of Ni in electrolytic Ni(99.98% pure). Diffusion coefficients were determined for cast and forged samples at 930 to 1300°C. Coefficients of grain boundary diffusion were also determined. The constants in the equation $D = D_0 e \exp -(E/RT)$ were calculated to be $D_0 = 2.59 \pm 0.45$ cm^2/sec and $E = 69.5 \pm 0.5$ kcal/mole, and the entropy change $\Delta S = 13.17$ kcal/deg-mole. The vacany mechanism of diffusion is studied; the total energy of formation and motion of vacancies in Ni, 2.4 ev, is lower than the experimental activation energy of diffusion, 3.01 ev. The possible formation of double vacancies and other complex vacancy groups is considered. (D.L.C.)

44709 (JPRS-24761, pp 17-28) EFFECT OF ADDITIONAL ALLOYING ON THE PROPERTIES OF MAGNESIUM-NEODYMIUM ALLOYS. Drits, M. E.; Sviderskaya, Z. A.; Rokhlin, L. L. Translated from Tr. Inst. Met. im. A. A. Barkova, Akad. Nauk SSSR, No. 14, 120-9(1963).

In an attempt to increase further the high mechanical properties of Mg-Nd alloys at 200-300°C, the effects of 13 alloying elements on these properties after deformation were investigated. The initial alloys contained 2.5% Nd. The effects on the strength were small; these effects and the microstructures are discussed. (D.L.C.)

44710 (JPRS-24761, pp 29-40) RECRYSTALLIZATION OF Mg-Ce ALLOYS. Kadaner, E. S.; Oreshkina, A. A. Translated from Tr. Inst. Met. im. A. A. Barkova, Akad. Nauk SSSR, No. 14, 130-8(1963).

The recrystallization of binary alloys of magnesium and cerium, which are the base materials for a number of heat-resistant industrial alloys, was investigated by microscopic and x-ray methods and by hardness measurements. It was found that adding minute quantities of cerium to magnesium strongly retards development of recrystallization. Increasing cerium content in the alloy retards grain growth, especially at high annealing temperatures. An increase in activation energy for recrystallization of pure magnesium containing only cerium is observed only up to 0.23% Ce. Further increase of cerium content to 1.8% does not affect magnitude of activation energy. At increased temperatures, the role of recrystallization in processes of weakening Mg-Ce alloys was distinctly revealed in hardness measurements made with varying holding times and also in creep tests. The results of these tests are included. (CFSTI)

44711 SYSTEMS BETWEEN NIOBIUM OXIDES AND THE OXIDES OF NICKEL AND COBALT. Burdese, Aurelio; Borlera, Maria Lucco; Rolando, Piero (Istituto di Chimica Generale e Applicata e di Metallurgia del Politecnico, Turin). Atti Accad. Sci. Torino: I. Classe Sci. Fis., Mat. Nat., 99: 565-75(1964-65). (In Italian).

The phase diagrams of Nb_2O_5-NiO and Nb_2O_5-CoO were studied. In both the systems in the zone richest in Nb_2O_5 three phases occurred analogous to those of the type $NbO_{2.43}$, $NbO_{2.48}$, and $NbO_{2.40}$. The three phases contained 2.8, 5.3, and 12.5 mole %, respectively, of NiO and CoO and had incongruent fusion. $NiNb_2O_6$ and $CoNb_2O_6$ existed in three crystalline forms (monoclinic, rhombic, and hexagonal). The high-temperature hexagonal form melts at 1505 and 1470°C. The phases $Ni_4Nb_2O_9$ and $Co_4Nb_2O_9$ melt and decompose at 1510 and 1410°C. The system Nb_2O_5-NiO has two eutectics between the hexagonal form of the nickel niobate (NiO-Nb_2O_5) and the phases NiO-$7Nb_2O_5$ and 4NiO-Nb_2O_5 (1430 and 1490°C). In the system Nb_2O_5-CoO, in correspondence to the eutectics CoO-$7Nb_2O_5$-CoO-Nb_2O_5 and CoO-Nb_2O_5-4CoO-Nb_2O_5, the liquid formed at a lower temperature than that at which the transformation between the rhombic and hexagonal forms of CoO-Nb_2O_5 occurred. (tr-auth)

44712 THERMOELECTRIC CAPACITIES OF THE LIQUID ALLOYS SELENIUM-TELLURIUM. Perron, Jean-Claude (Laboratoire Central des Industries Electriques, Fontenay-aux-Roses, France). Compt. Rend., 260: 5760-3(May 31, 1965). (In French).

The thermoelectric capacity of the liquid mixtures Se-Te_x with the composition $Te_{1-x}Se_x$ with $0 \leq x \leq 0.3$ was studied up to ~750°C. All the compounds were of the type p. The different measurements made on these liquids suggested an interaction where a band structure of the semiconductor type with two types of carriers was considered. (tr-auth)

44713 INTERATOMIC DISTANCES OF LANTHANIDES IN METALLIC CRYSTALS. Sarkisov, E. S. (Moscow State Univ.). Dokl. Akad. Nauk SSSR, 161: 1093-5(Apr. 11, 1965). (In Russian).

Cerium, praseodymium, and terbium are reported in the literature to have smaller interatomic distances than expected on the basis of lanthanide contraction. An attempt was made to relate the interatomic distance of these elements to the state of the tetravalent metal, since these metals form tetravalent as well as trivalent compounds. Europium and ytterbium had larger interatomic distances than expected, possibly because these rare earths behave like bivalent metals with double bonds $6s^2$ outside the subgroups $4f^75s^25p^6$ and $4f^{14}5s^25p^6$, respectively. Starting with equations derived previously an expression was developed for interatomic distance that permits its accurate determination: $d = d_{H-H_{MET(k=1)}} (2\sqrt[3]{1/2}[(Z-f)^{5/3} - z_k^{5/3}]^{3/5} + k^{3/5} f^{3/5})$, where $d_{H-H_{MET(k=1)}}$ is the proportionality factor, numerically equal to the "metallic" interatomic distance of hydrogen with a coordination number $k = 1(d_{H-H_{MET(k=1)}}) = 0.965$ Å, Z is the atomic number, f is the metallic valence, z is the number of 4f electrons participating in the contraction effect, and k is the coordination number of the lattice. With this equation the interatomic distances for all the rare earths in metallic crystals were computed and tabulated. The interatomic distance for these elements in the metallic state was determined by triple bonds ($5d6s^2$ or $4f6s^2$). Only europium and ytterbium were exceptions; for them the double bond ($6s^2$) was responsible. Results showed that the interatomic distance clearly depends on the atomic number, and the indicated equation permits accurate determination of valence electrons in the metallic state for all lanthanides. The equation makes it possible to compute the interatomic distance for promethium, hitherto unknown, assuming a triple bond ($4f6s^2$). The valence computed for this element is 3.589 Å. (CFSTI)

44714 PHASE DIAGRAM OF THE $TiCr_2$-$ZrCr_2$ SYSTEM. Kornilov, I. I.; Budberg, P. B.; Shakhova, K. I.; Alisova, S. P. (Inst. of Metallurgy, USSR). Dokl. Akad. Nauk SSSR, 161: 1378-81(Apr. 21, 1965). (In Russian).

The phase composition and microstructure of pure $TiCr_2$ and $ZrCr_2$ compounds and nine $TiCr_2$-$ZrCr_2$ systems containing from 10 to 90% $TiCr_2$, melted and homogenized at 1250 to 1300°C for 50 hr, were determined by thermal and x-ray-phase analysis. Thermal analysis showed that the alloy liquidus temperatures increased with increasing $ZrCr_2$ content, e.g., from 1480 to 1675°C for pure $TiCr_2$ and $ZrCr_2$, respectively. An analogous increase occurred in the lattice constants. The phase diagram of the $TiCr_2$-$ZrCr_2$ system based on the obtained data is characterized by the formation of a continuous series of solid solutions between both the low-temperature and the high-temperature modifications of $TiCr_2$ and $ZrCr_2$ compounds. The appearance of the two-phase ($\beta + \delta$) and three-phase ($L + \beta + \delta$) regions in the $TiCr_2$-rich alloys is explained by the fact that the $TiCr_2$ compound is formed in the binary Ti-Cr system in the solid state. (CFSTI)

44715 THE SOLUTION OF PRECIPITATES IN VERY DILUTE URANIUM-IRON-ALUMINIUM ALLOYS. Dixon, P. H.; Fern, F. H.; Butcher, B. R. (Atomic Energy Re-

search Establishment, Harwell, Eng.). J. Inst. Metals, 93: 423-8(Aug. 1965). (AERE-R-4636).

The nature of the precipitates occurring in uranium-iron-aluminum alloys and their solution in the β and γ phases were studied by measurements of electrical resistance and by metallography. Iron dissolved rapidly in the β phase. Some UAl_2 precipitates also dissolved and those that did not do so became coarser. Both iron and aluminium dissolved very rapidly in γ-uranium. The γ phase is shown to exist in equilibrium down to 710°C in adjusted uranium. The implications of these results with regard to grain refinement and swelling-resistance of adjusted uranium are discussed. (auth)

44716 THE ROLE OF HYDRIDE PRECIPITATE IN THE FRACTURE OF ZIRCONIUM AND ITS ALLOYS. Erickson, W. H.; Hardie, D. (Univ. of Newcastle-upon-Tyne, Eng.). J. Inst. Metals, 93: 444-6(Aug. 1965).

The presence of hydrogen in zirconium and its alloys causes embrittlement because of the tendency of hydride precipitate to shear, or undergo cleavage, and produce microcracks under the influence of stress concentrations. At 300°C vacuum-annealed and furnace-cooled zirconium–niobium alloy gave an impact value of ~80 ft-lb. If sufficient hydrogen were added to yield 100 ppm as hydride, the impact value would be reduced to ~73 ft-lb. The diminishing effectiveness of the hydride platelets in causing embrittlement in zirconium gave rise to an energy transition and was attributed to one or more of the following factors: increased ductility with better matrix accommodation of cracks and voids formed in the hydride phase; less brittleness and a less effective barrier to dislocation motion; strengthening effects of the hydrogen in solution; and changes of the deformation mechanism with temperature. Nucleation of fracture and propagation of fraction are discussed. (F.J.H.)

44717 THE IDENTIFICATION AND DISTRIBUTION OF INTERMETALLIC COMPOUNDS IN ADJUSTED URANIUM. Smith, A. F. (Berkeley Nuclear Labs., Gloucester, Eng.). J. Inst. Metals, 93: 454-5(Aug. 1965).

Studies were made of as-cast, and as-cast and β-quenched adjusted uranium. The precipitate consisted of a network of particles ~0.1 μm in dia and of smaller particles 0.01 to 0.05 μm in dia distributed fairly uniformly throughout the matrix. Patterns of zones were obtained, which were consistent with a fcc structure. A technique was developed for extracting precipitates for x-ray diffraction. At the edge of a specimen of adjusted uranium soaked in the γ phase and furnace-cooled over a period of several days, two intersecting networks were observed, neither of which was associated with the α-uranium structure. It was considered likely that the coarser network results from a eutectoid reaction at the γ-β phase transformation. The network of smaller particles coincided with β grain boundaries. (M.C.G.)

44718 THE CRYSTAL STRUCTURES OF β-$TaNi_3$, $Ta(Cu_2Al)_2$, $Nb(Cu,Al)_2$, AND $Ta_6(Cu,Al)_7$. Nowotny, H.; Oesterreicher, H. (Universitaet, Vienna). Monatsh. Chem., 95: 982-9(1964). (In German).

Powder mixtures were cold pressed and sintered under Ar in a tungsten oven. Samples of Ta–Ni–Cu were held 20 hr at 1300°C, Ta–Cu–Al samples 2 to 20 hr at 1000 to 1100°C, and Nb–Cu–Al samples 2 hr at 1000°C; all were cooled in the oven. The Ta–Ni–Cu samples were homogenized 20 hr at 950°C or 200 hr at 700°C; several Ta–Ni samples were fused in an arc. A new $TaNi_3$, to be distinguished from the older $TaNi_3$ with $TiCu_3$ structure, was observed; it had the $TiAl_3$ structure, a = 3.627, c = 7.455 Å, and c/a = 2.055. In the μ phase the parameters for a mixture corresponding to $Ta(Ni_{\sim 0.5}Cu_{\sim 0.5})$ are a = 4.95, c = 27.00 Å, and c/a = 5.450. In the region 30 to 50% Nb, 15 to 50% Cu, 25 to 50% Al, a phase $Nb(Cu,Al)_2$ was found with $MgZn_2$ structure; parameters for an Al-rich mixture are a = 5.028, c = 8.300 Å, and c/a = 1.650. A similar Laves phase was also found in the Ta–Cu–Al system; the parameters for $Ta(Cu,Al)_2$ ranged between 4.96 to 5.04 Å for a, 8.37 to 8.11 Å for c, and 1.69 to 1.61 for c/a. A μ phase, $TaNi(Ta_6Ni_7)$, has a = 5.07, c = 27.47 Å, and c/a = 5.47 (hexagonal arrangement) for a sample with 50% Ta, 25% Cu, and 25% Al; the rhomohedric cell has a = 9.603 Å and α = 30°15′40″. (BBB)

44719 INVESTIGATIONS IN THE SYSTEMS: TRANSITION METAL–BORON–ALUMINUM. Rieger, W.; Nowotny, H.; Benesovsky, F. (Universitaet, Vienna). Monatsh. Chem., 95: 1417-23(1964). (In German).

Samples in the series (Ti, Zr, Hf)–B–Al were prepared by hot pressing and homogenization, or by reaction of the cold pressed samples at 1200°C. Structure at temperatures near this may be represented through the equilibria between the diborides of the transition metals and AlB_2, Al, or the aluminides. The compound $Zr_5Al_3B_x$ is of the D 8_8 structure and has a = 8.28 and c = 5.69 Å and c/a = 0.687; these parameters are larger than those of the B-free sample, where a = 8.16 and c = 5.66 Å and c/a = 0.694. In the Hf–B–Al system, $Hf_5Al_3B_x$ is also of the D 8_8 structure and has a = 8.09 and c = 5.70 Å and c/a = 0.704_5 for the Al-rich side; the Hf-rich side has a = 8.10 and c = 5.69 Å and c/a = 0.702. Both sets of values are greater than the B-free compound parameters. A μ-phase $HfAlB_x$ is shown to have a rhombohedric cell; the parameters for $Hf_{0.45}Al_{0.50}B_{0.05}$ are a = 10.20_2 Å, α = 30°7′30″; the intensities are similar to those of Ta(Cu,Al) or TaNi. No solubility in the binary phases was observed. (BBB)

44720 THE CRYSTAL STRUCTURE OF $Zr(Sn,Sb)_2$. Boller, H.; Nowotny, H. (Universitaet, Wien). Monatsh. Chem., 96: 563-4(1965). (In German).

At a low valence electron concentration the $TiSi_2$ structure is found in disilicides; at a high concentration, the $MoSi_2$ structure; and at an intermediate concentration, the $TaSi_2$ structure. This rule was also found applicable in the distannides provided that the transition metal had a large enough radius. The phase $ZrSn_2$ crystallized with the $TiSi_2$ structure; the exchange of Sn by Sb was examined. The material of the $TiSi_2$ structure dissolved almost no antimonide. At a ratio of Sb : Sn = 0.03, the structure changed to the $TaSi_2$ type. Observed and calculated intensities (Cr–K radiation) for the C-40 type were tabulated for a powder pattern. The quasicubic type extended to about $Zr(Sn_{0.73}Sb_{0.27})_2$; the lattice parameters changed from a = 5.507 to 5.521 Å and from c = 7.646 to 7.610 Å. The axis ratio changed from 1.388 to 1.379. This structural modification with small amounts of Sb could be explained as a quasi-dimorphy of $ZrSn_2$. The phase $Zr(Sn,Sb)_2$ thus resembled $HfSn_2$ with the $TaSi_2$ structure; a higher valence in its intermediate phases was suggested for Hf relative to Zr. The extended homogeneous region of the phase with a $TaSi_2$ type was in agreement with the behavior of many other examples. (BBB)

44721 LORENZ NUMBER OF PLUTONIUM METAL. Powell, R. F. (Royal Military Coll. of Science, Shrivenham, Berks, Eng.). Nature, 207: 965(Aug. 28, 1965).

The magnitude of the Lorenz number $L(= k/\sigma T)$ is discussed. The amended form of the Weidemann-Franz law: $(k(\rho + \bar{\rho}_0)/T) = L$ where ρ is the electrical resistivity and $\bar{\rho}_0$ the intercept obtained by extrapolating back the linear low temperature part of the resistivity-temperature curve to zero temperature was tested, and a value of 2.48×10^{-8} V^2 deg^{-2} was obtained for L. (P.C.H.)

44722 DETERMINATION OF LATTICE CONSTANTS WITH GEIGER-COUNTER X-RAY DIFFRACTOMETER. LATTICE CONSTANTS OF UC AND UC_2. Higashi, Iwami (Inst. of Physical and Chemical Research, Tokyo). Rika Gaku Kenkyusho Hokoku, 37: 271-5(1961). (In Japanese).

The accuracy of the lattice constants determined with a Geiger-counter x-ray diffractometer, of which the optical system is aligned and adjusted for use in qualitative identification of crystalline powder, is examined. The zero point of the goniometer used is adjusted with an accuracy of ±0.01° of 2θ. The soller slit, divergence slit, and receiving slit used are set at 0.085 Rad, 2.5°, and 0.2 mm, respectively. Diffraction lines between 90 and 150° (2θ) are recorded with a scanning speed of 0.5° per min. Lat-

tice constants calculated from various diffraction angles measured on the standard substance, Si, are plotted vs $\cos^2\theta$. The plot gives a straight line. The value obtained by extrapolating the straight line to $\cos^2\theta = 0$ is smaller by 0.0005 Å than that published in an earlier paper. Standard deviation of the determined lattice constants of UC is ±0.0002 Å, the constants being measured ten times and corrected for the standard. In the case of UC_2, lattice constants were determined without correction for the standard. Variation of determined values was within 0.002 Å for a_0 and 0.004 Å for c_0. Lattice constants of UC and UC_2 measured on uranium carbides containing different amounts of combined carbon are also presented. (BBB)

44723 THE TRANSFORMATION OF THE ROLLING TEXTURES AND ITS CORRELATION WITH THE STACKING FAULT FREQUENCY IN NICKEL–MOLYBDENUM ALLOYS. Chang, Sin-yu; Sun, Hsui-fan. Sci. Sinica (Peking), 14: 1090-6(July 1965).

The different percentages of molybdenum by weight in the alloys were 1.19, 3.37, 7.11, 11.10, and 14.87%. After hot and cold rolling (the percentage of cold reduction was 96.6%) the textures in the specimens were determined using an x-ray diffractometer and the (111) pole figures were plotted. The movement of the positions of the peaks of diffracted lines were measured, and the stacking fault frequency calculated. The rolling textures in the alloys containing 1.19% Mo, after cold rolling, were found to be (3, 7, 11) [9, 4, $\bar{5}$], (011) [21$\bar{1}$], (112) [11$\bar{1}$], (001) [100], and (110) [001]. They resembled those in pure nickel. Only the (3, 7, 11) [9, 4, $\bar{5}$] texture component was in better conformity than the (123) [412] texture component in pure nickel. The distribution of slip traces in the specimens containing 1.19% Mo and 14.87% was confirmed. The results showed that the cross slip traces occurred in the specimens with the lower percentage of Mo or with the copper-type textures and that single slip traces occurred in most of the specimens containing higher percentages of molybdenum or with the brass-type texture. As the content of molybdenum increased, the sharpness of the cubic texture decreased. (F.J.H.)

44724 THE HAFNIUM–CARBON SYSTEM. Sara, R. V. (Parma Technical Center, Cleveland). Trans. Met. Soc. AIME, 233: 1683-91(Sept. 1965).

Determination of the Hf-C phase diagram was conducted primarily by metallographic and x-ray diffraction studies on appropriate alloys. The only intermediate phase observed in this binary system was HfC. This phase was found to be homogeneous between 34.0 and 48.0 at. % C at 2200°C and between 36.0 and 49.3 at. % C at 3150°C. The lattice-parameter variation was also determined for HfC 1-x compositions prepared at 2200 and 3150°C. The most refractory composition, with a melting point of 3830°C, was established at 47.5 at. % C from melting-point data. Solidus temperatures of 2240 and 3150°C occurred on the high-hafnium and high-carbon sides of the monocarbide, respectively. The invariant point between HfC and carbon was located at 66.0 at. % C, whereas the 2240°C solidus corresponded to the peritectic temperature at which hafnium was formed from HfC and hafnium-rich liquid. Hafnium had a melting temperature of 2208°C and was capable of taking carbon into solution to the extent of 10.5 at. % at this temperature. (auth)

44725 A QUANTITATIVE MEASUREMENT OF THE FRACTION OF TENSILE STRAIN DUE TO TWINNING IN POLYCRYSTALLINE ZIRCONIUM AT 77 deg K. Reed-Hill, R. E.; Buchanan, E. R.; Caldwell, F. W. Jr. (Univ. of Florida, Gainesville). Trans. Met. Soc. AIME, 233: 1716-18(Sept. 1965). (TID-21747).

Polycrystalline zirconium tensile specimens containing a sizable fraction of grains unfavorably oriented for slip were deformed at 77°K to strains as high as 9%. The contributions of the various twinning modes to the observed strain were determined quantitatively using measured twin volume fractions and Schmid orientation factors. The results indicated that at very small strains twinning can account for almost all of the observed strain. At higher strains slip became the dominant means of deformation. The most significant form of twinning was $\{11\bar{2}1\}$. (auth)

44726 DISLOCATION SUBSTRUCTURE AND THE DEFORMATION OF POLYCRYSTALLINE BERYLLIUM. Bonfield, W. (Honeywell Research Center, Hopkins, Minn.). Trans. Met. Soc. AIME, 233: 1719-26(Sept. 1965).

A study was made of the dislocation substructures produced in hot-pressed beryllium specimens strained to various levels in the range from 800×10^{-6} in. per in. to fracture. A number of distinctive dislocation configurations were observed in this region that were not noted at lower levels of strain. These included dislocation-dislocation interactions to form networks, dislocation "walls", subgrain boundaries and complex arrays, interactions between dislocations and large beryllium oxide particles, and the generation of dislocations from certain particles. The nature of these differences in substructure and their relation to the stress-strain characteristics of polycrystalline beryllium are discussed. (auth)

44727 TRANSFORMATIONS IN UAl_4 AND $PuAl_4$. Runnalls, O. J. C.; Boucher, R. R. (Atomic Energy of Canada Ltd., Chalk River, Ont.). Trans. Met. Soc. AIME, 233: 1726-32(Sept. 1965).

A pronounced thermal effect was observed on heating or cooling aluminum-rich Al–U and Al–Pu alloys. From microscopic and X-ray diffraction studies, the effect was attributed to transformations in the intermetallic phases UAl_4 and $PuAl_4$ involving rearrangement or clustering of vacancies. The transformation observed in Al-20 wt % U alloys occurred near the α-Al-UAl_4 eutectic temperature of 646°C making it difficult to detect from heating curves. When cooling, however, thermal and X-ray analyses indicated that the high-temperature phase labeled β-UAl_4 precipitated initially during eutectic solidification. As solidification continued and after an induction period of 5 to 20 min the nucleation and growth of the low-temperature phase, α-UAl_4, produced an evolution of energy, which raised the observed alloy temperature by 1 to 2°C. In Al-Pu alloys the transformation occurred at 645°C, 5 degrees below the eutectic solidification temperature. The estimated latent heat of transformation was 25 ± 5 cal per g $PuAl_4$. The high-temperature forms of UAl_4 and $PuAl_4$ were easily retained by chill casting Al–U and Al–Pu alloys and on reheating the alloys the transformation to the α phase was sluggish even above 600°C. Separated single crystals of UAl_4, for example, showed no evidence of transformation after heating for 16 hr at 620°C. The transformation rates increased rapidly enough with increasing temperature, however, that a spontaneous liberation of energy was observed on occasion when heating cast Al-20 wt % U to near the eutectic temperature. (auth)

44728 SOME ANELASTIC EFFECTS IN ZIRCONIUM AT ROOM TEMPERATURE RESULTING FROM PRESTRAIN AT 77 deg K. Reed-Hill, R. E.; Dahlberg, E. P.; Slippy, W. A. Jr. (Univ. of Florida, Gainesville). Trans. Met. Soc. AIME, 233: 1766-71(Sept. 1965). (TID-21748).

A large room-temperature mechanical-hysteresis effect under cyclic tensile loading was observed in zirconium specimens prestrained at 77°K so as to form large numbers of $\{11\bar{2}1\}$ twins. The observed hysteresis loss was a maximum when the prestrain was just under 1%. It also depended strongly on the maximum applied cyclic stress, but only moderately on loading rate and temperature (−72 to 100°C). The phenomena were also studied in terms of the elastic aftereffect where the data were found to conform closely to the functional relationship between strain and time, $\epsilon = -RT/\alpha \ln \tanh (t + t_0)/2\tau$, for strains as large as about 10^{-4}. This equation can be derived directly from the strain-rate equation $\dot{\epsilon} = A [e^{-}(Q - \alpha\epsilon/RT) - e^{-}(Q + \alpha\epsilon/RT)]$. It appears that within rather wide limits it may be possible to obtain any desired magnitude of damping capacity in zirconium metal. The damping properties may also be given directional characteristics. It is shown that the observed anelastic phenomena can be explained on the assumption that they are the result of stress-induced twin-

boundary movements in which the average twin increases its thickness by only a few percent. (auth)

44729 DIFFUSION OF ^{181}Hf IN Bcc HAFNIUM. Winslow, F. R.; Lundy, T. S. (Oak Ridge National Lab., Tenn.). Trans. Met. Soc. AIME, 233: 1790-1(Sept. 1965). (ORNL-P-1275).

Diffusion coefficients of ^{181}Hf in high-temperature bcc-phase reactor-grade hafnium were determined by standard lathe-sectioning techniques. In all cases, except for specimens annealed at temperatures below 1795°C, normal Gaussian penetration behavior resulted. At lower temperatures, plots of ln A(x) vs x^2 were nonlinear (A(x) = relative activity at a distance x from the original isotope layer). This abrupt change in penetration behavior served to locate the temperature of phase transformation in hafnium. (M.C.G.)

44730 ENVIRONMENTAL INFLUENCES ON THE FATIGUE OF MOLYBDENUM. Roberson, James A. (Aerospace Research Lab., Wright-Patterson AFB, Tex.). Trans. Met. Soc. AIME, 233: 1799-1800(Sept. 1965).

The effects of variations in environment on the fatigue of molybdenum stressed in fully reversed axial tension compression were studied. Data are presented in graphs. The fatigue behavior of warm-worked molybdenum was sensitive to very small quantities of water vapor in air. Water vapor in nitrogen had a very small effect if any. The fatigue life of this material at a given stress was greater in vacuum than in normal air. The amount of improvement increased with decreasing stress levels. (M.C.G.)

44731 REMARKS ON THE ALLOTROPIC TRANSFORMATIONS OF THE SESQUIOXIDES OF THE RARE EARTHS. Foex, Marc. Z. Anorg. Allgem. Chem., 337: 313-24(June 1965). (In German).

Thermal transformations of the Me_2O_3 oxides of rare-earths occurring in the temperature range from 1800 to 2400°C were studied using a special method of thermal analysis. Attempts were made to stabilize high-temperature Me_2O_3 modifications at room temperature by means of CaO or SrO doping and by very rapidly quenching the molten oxides. (auth)

44732 STUDY OF THE DYNAMICS OF LITHIUM HYDRIDE AND DEUTERIDE IN THE INELASTIC SCATTERING OF COLD NEUTRONS. Zemlyanov, M. G.; Brovman, E. G.; Chernoplekov, N. A.; Shitikov, Yu. L. (Inst. of Atomic Energy, Moscow). pp 431-51 of STI/PUB/92(Vol.II). (In Russian).

Experimental investigations are reported on the inelastic scattering of cold neutrons in polycrystalline samples of ^7LiH and ^7LiD. The measurements are carried out by the time-of-flight method, using a beryllium filter and mechanical chopper. In processing the data, allowance is made for the instrumental resolution and the statistical accuracy of the experimental data. A detailed theory is described for LiH and LiD crystals in models of stable ions. Calculations are made of frequency distribution functions and the energy dependence of the polarization vectors, and the Debye–Waller factor is found. The behavior of the neutron inelastic scattering cross section resulting from the presence of two atoms in the elementary nucleus is discussed. The phonon spectra for lithium hydride and deuteride are established using the values computed from the experimental results. The paper includes a comparison of the experimental and theoretical results. (auth)

44733 THE ACTIVITY OF URANIUM IN DILUTE SOLUTION IN LIQUID BISMUTH. Tien, L. C.; Guion, K. J.; Pehlke, R. D. (Univ. of Michigan, Ann Arbor). Vienna, International Atomic Energy Agency, 1965, Preprint No. SM-66/4, 17p. (CONF-650704-13). ORINS.

From IAEA Symposium on Thermodynamics, Vienna.

The activity of uranium was measured in dilute solutions in liquid bismuth. The study employed a galvanic cell with a liquid chloride electrolyte in the temperature range from 400 to 600°C. The activity of uranium was shown to follow Henry's Law, and the activity coefficient in this range was determined. The activity of uranium in UBi_2 was measured over this temperature range, and previous measurements of the solubility of uranium in liquid bismuth were corroborated. Coulometric titration was used to determine the ionic valence in the electrolyte, and the concentration of uranium in the liquid bismuth alloys was determined by chemical sampling of the electrodes. (auth)

44734 RARE EARTH METALS AT HIGH PRESSURES AND TEMPERATURES. Jayaraman, A. (Bell Telephone Labs., Inc., Murray Hill, N. J.). 20p. (CONF-650423-4). Gmelin, AED-CONF-65-058-11.

From International Conference on Physics of Solids and High Pressures, Tucson, Ariz.

The fusion behavior and solid-solid transformations of rare earth metals at high pressures and temperatures are discussed. Phase diagrams of Ce, Eu, and Yb are given. The effects of pressure on crystal structure, melting slopes, critical phenomena, and high-pressure properties are described. (F.J.H.)

44735 REFRACTORY METALS AND ALLOYS. [PART] II. Metallurgical Society Conferences, Volume 17, Chicago, April 12-13, 1962. Semchyshen, M.; Perlmutter, I. (eds.). New York, Interscience Publishers, 1963. 456p. (CONF-620405).

Information is included on: fracture transitions in refractory metals; effects of solutes on ductile-to-brittle transition; effects of mechanical and structural variables on ductile-to-brittle transition; substructure; mechanisms of alloy strengthening; diffusion; effects of alloying elements on oxidation; protective coatings; joining; consolidation; conversion of refractory metals; and refractory metals for glide re-entry vehicles. (P.C.H.)

Radiation Effects

See also CHEMISTRY — Radiation Chemistry.

Refer also to abstracts 44052, 44168, and 45558.

44736 (ANL-6883) EXAMINATION OF IRRADIATED Ag–In–Cd ALLOYS. Reinke, C. F. (Argonne National Lab., Ill.). May 1965. Contract W-31-109-eng-38. 18p. Dep. mn; CFSTI $1.00 cy, $0.50 mn.

Extruded cast and extruded powder specimens of Ag–15 wt.% In–5 wt.% Cd alloy, plated with 25 μ of nickel or 25 μ each of copper plus nickel, were irradiated for 47 effective full-power days at approximately 300°C in a lattice position of the Engineering Test Reactor. The extruded cast alloys exhibited 0.2% yield strengths, ranging from 114 to 140 kg/cm² in the unirradiated condition, and 96 to 150 kg/cm² after irradiation. The percent elongation and reduction in area in both cases normally ranged from 50 to 60%. The 0.2% yield strength for the extruded powder alloys ranged from 190 to 228 kg/cm² in the unirradiated condition, and 214 to 242 kg/cm² after irradiation. There was a noticeable improvement in both the percent elongation and reduction in area of the extruded powder specimens, the postirradiation values being approximately twice the unirradiated values of 10%. Recrystallization and grain growth occurred in all specimens during irradiation. The ASTM grain size on the extruded cast specimens changed from 7 to 4-5.5. Hardness measurements of the extruded cast specimens indicated that softening had occurred. Unirradiated material had DPH values ranging from 55 to 76, with corresponding values after irradiation of 36 to 52. Metallographic examinations indicated that the microstructures had remained a single phase during irradiation. (auth)

44737 (ANL-7000, pp 111-18) EXPERIMENTAL IRRADIATIONS OF FUEL AND CONTROL MATERIALS. (Argonne National Lab., Ill.).

The results of temperature excursions during irradiation of Th–U alloys, radiation effects on thermal ratcheting in Al alloy clad UO_2 fuel elements, and radiation

effects on the structure of US with UOS inclusions are reported. (W.L.G.)

44738 (ANL-7000, pp 119-21) EXAMINATION OF FULL-SCALE REACTOR FUEL ELEMENTS. (Argonne National Lab., Ill.).

Results of examinations of irradiated EBWR prototype fuel plates, fuel element after 100 Mw operation, and a Core 1A spike element are reported. (W.L.G.)

44739 (ANL-7000, pp 233-77) IRRADIATION EFFECTS. (Argonne National Lab., Ill.).

Progress is reported on research on the swelling and growth in U, theoretical study of the migration and coalescence of gas bubbles in solids, fission tracks in evaporated Au films, the effects of fast neutron irradiation on metals and alloys, recovery of lattice parameter and electric resistivity in low-temperature neutron-irradiated Cu, low-temperature energy release in irradiated Cu, irradiation and solid solution strengthening, displacements cascades, studies of lattice defects in quenched and irradiated metals, and theoretical studies of lattice defects in fcc metals. (W.L.G.)

44740 (BMI-1737) IN-PILE STUDIES OF EXPERIMENTAL PYROLYTIC-CARBON-COATED UC_2 AND UO_2 FUEL PARTICLES. Ritzman, Robert L.; Martin, Robert L.; Miller, Neil E.; Townley, Charles W. (Battelle Memorial Inst., Columbus, Ohio). July 28, 1965. Contract W-7405-eng-92. 52p. Dep. mn; CFSTI $1.25 cy, $0.50 mn.

The irradiation performance of pyrolytic-carbon-coated UC_2 and UO_2 particles was studied at temperatures ranging from 100 to 1300°C and to fuel burnups of 12 at. % of the ^{235}U. It was found that coatings on high-density UC_2 particles must be greater than 110 μ thick in order to survive low-temperature irradiation, and in order to exhibit high integrity at elevated temperatures, the coatings must be multilayered as well. However, by using porous UO_2 fuel particles (~80 per cent dense), pyrolytic-carbon coatings as thin as 50 μ performed without failure at low temperature, and a 73 μ columnar coating exhibited only slight failure when irradiated to a ^{235}U burnup of 8.4 at. % at 1300°C. Large (460 μ in diameter) porous UO_2 particles with 113-μ laminar pyrolytic-carbon coatings, currently under study sustained burnups of over 7.5 at. % at 815°C with no indication of coating fracture. Failure at both low and high temperatures is believed to be due primarily to changes induced by fission-fragment recoil in both the fuel-core and coating materials, resulting in stresses in the pyrolytic carbon sufficient to crack the coatings. The in-pile studies were performed in both static and sweep-gas capsules with the particles held in a graphite matrix or in the unsupported condition. Postirradiation examinations included fission-gas-release measurements, determination of the fraction of exposed uranium, and metallographic examination. (auth)

44741 (EURAEC-1383) INFLUENCE OF NITROGEN IN IRON AND STEEL UNDER FAST NEUTRON IRRADIATION. Quarterly Report No. 6, January 1-March 31, 1965. Rossi, F. (Societa Ricerche Impianti Nucleari, Saluggia (Italy). Centro Ricerche Nucleari). Apr. 1965. Contract 004-63-10-TEEI(RD). 14p. (EUR-2346). Dep. mn; CFSTI $1.00 cy, $0.50 mn.

Work Performed under United States-Euratom Joint Research and Development Program.

Resilience, tensile tests, and internal friction measurements were begun on the specimens irradiated during the last quarter. A second irradiation of a larger set of specimens was done under the same conditions as in the first case; the irradiated specimens are now in the reactor pool for a decay period. Annealing measurements on irradiated specimens were also begun and a first group of data, jointly with results obtained before annealing, have been reported. A new series of magnetic measurements by means of a new special apparatus set up in IENGF was performed to check out the viscosity field, its dependence on temperature, and its recovery on the high permeability pure iron specimens previously irradiated. (D.L.C.)

44742 (EURAEC-1430) INFLUENCE OF NITROGEN IN IRON AND STEEL UNDER FAST NEUTRON IRRADIATION. Quarterly Report No. 7, April 1-June 30, 1965. Rossi, F. (Societa Ricerche Impianti Nucleari, Sluggia (Italy). Centro Ricerche Nucleari). July 1965. Contract 004-63-10-TEEI. 15p. (EUR-2373). Dep. mn; CFSTI $1.00 cy, $0.50 mn.

Work Performed under United States-Euratom Joint Research and Development Program.

Work done in SORIN was especially devoted to compare the yield strain/grain size correlation in iron melts of different composition. Tests were made on unirradiated, irradiated and irradiated plus annealed materials. An anomalous behavior, observed in iron-titanium alloys, was confirmed with three different sets of tests. Tests on nitrogen-enriched iron, before and after irradiation, gave a good agreement with literature results. Hardness recovery was studied during isochronal annealing and will be completed with isothermal treatments. Two other irradiations are planned and preliminary tests (to check the new irradiation condition at the higher power level of the reactor) are running. Work done at IENGF was particularly devoted to preliminary magnetic measurements of unirradiated silicon-iron alloy and to the evaluation of the magnetic viscosity effects in pure iron due to irradiation and to their recovery. A short description of the results is reported with particular regard to the better quality of the tests which are now performed with the new hysteresis loop automatic recorder, set up in the laboratory; with this apparatus, magnetic viscosity field was also measured in quenched specimens. (auth)

44743 (GEAP-3634) THE TENSILE PROPERTIES OF IRRADIATED TYPE 304 STAINLESS STEEL STRIP. Van Torne, L. I. (General Electric Co., San Jose, Calif. Atomic Power Equipment Dept.). Feb. 10, 1961. 24p. (R61APE7).

The tensile properties of irradiated type 304 stainless steel strip were obtained. The neutron exposure was 9.08×10^{20} nvt thermal and 9.08×10^{20} nvt fast. The test results were compared to those obtained from unirradiated material and the changes were determined. The 0.2 percent offset yield strength and ultimate tensile strength increased from the annealed condition values by 67,100 psi and 31,500 psi, respectively. The corresponding percentage increase for the yield strength was 130, and for the ultimate strength, 32. The neutron exposure decreased the percent elongation by 12.3 points, or a 35% reduction from the original value. However, the ductility remaining is high as compared to other structural materials. The tensile properties after irradiation are similar to those obtained from type 304 stainless steel in the ¼ hard cold-worked condition. (auth)

44744 (HW-SA-3592) THE EFFECT OF TENSILE STRESS ON THE RADIATION-INDUCED CONTRACTION OF GRAPHITE. Jackson, J. L. (General Electric Co., Richland, Wash. Hanford Atomic Products Operation). Sept. 17, 1964. Contract AT(45-1)-1350. 15p. Dep. mn; CFSTI $1.00 cy, $0.50 mn.

The effect of tensile stresses of 600 and 800 psi on the contraction of EGCR graphite during neutron irradiation at 485°C was studied at exposures up to 1.5×10^{21} neutrons/cm^2, E > 0.18 Mev. Stress-dependent restrained contraction was found, and "irradiation creep" rates comparable to those determined by other investigators for a different graphite were calculated. Results suggest that only a limited amount of the normal contraction can be restrained without fracture of the sample. The relationship between irradiation creep and this restraint limit must be determined before any valid predictions on graphite-core integrity can be stated. (auth)

44745 (LA-DC-6725) RADIATION DAMAGE TO IONIC CRYSTALS AT LOW TEMPERATURES. I. X-RAY DIFFRACTION STUDIES. Pretzel, F. E.; Anderson, J. L. (Los Alamos Scientific Lab., Univ. of California, N. Mex.). [1964]. Contract W-7405-eng-36. 48p. Dep. mn; CFSTI $2.00 cy, $0.50 mn.

Low-temperature x-ray diffraction was used to study lattice changes in crystallites of ionic materials resulting from low-energy β-particle bombardment at 80°K. The mechanism for radiation damage by the production of interstitial-vacancy pairs is found to apply to eleven ionic halides despite variations in structure, colorability, or ionic conduction, but the process appears to be restricted to halogen-containing crystals. Lattice expansion results show that interstitials are produced efficiently by cooperative processes at low temperature, and that most of the vacancies that are also formed do not trap electrons to become F centers. The self-trapped hole has the properties required of an intermediate in a stepwise radiation-damage process. Thermal annealing and deformation studies show that interstitial mobility is relatively high in the alkali halides. It is proposed that the interaction of mobile interstitial defects or self-trapped holes with impurities and lattice imperfections can account for many observations on the coloration of alkali halides near room temperature. (auth)

44746 (NAA-SR-Memo-10626) THE PRODUCTION OF HYDROGEN AND HELIUM IN REACTOR FUEL-CLADDING MATERIALS. Alter, Harry (Atomics International, Canoga Park, Calif.). Nov. 16, 1964. Contract AT-11-1-GEN-8. 27p. Dep. mn; CFSTI $2.00 cy, $0.50 mn.

The amounts of hydrogen and helium gas produced by the constituents of several reactor fuel-cladding materials were calculated. In all instances it is assumed that the fuel-cladding material has been exposed to a fast neutron flux of 10^{16}n/cm^2/sec for a period of two years. The preliminary results permit the calculation of hydrogen and helium production for other fuel clad materials. The final results for the six fuel clad materials of interest appear below:

Alloy	Atoms Hydrogen 10^6 Atoms Alloy	Atoms Helium 10^6 Atoms Alloy
316 SS	8600	400
304 SS	6875	350
Nb	1130	70
V–10% Ti	770	140
V–20% Ti	920	175
Zircaloy 2	350	175

(auth)

44747 (NP-15463) A CALCULATION OF PROTON INDUCED DAMAGE IN GERMANIUM AND SILICON (thesis). Saunders, Edward A. (Rensselaer Polytechnic Inst., Troy, N. Y.). Oct. 1964. 202p.

Experimental work on high-energy proton irradiation of germanium and silicon did not agree with calculations, particularly for proton energies above about 40 Mev. An attempt was made to account for the observed results by means of a complete optical-model calculation of elastic and inelastic cross sections and the use of the "channeling" theory of Oen and Robinson in the treatment of the displacement cascade. The reactions which occur in the energy range of concern are predominantly the (p,n), (p,2n), and (p,pn) reactions. The Hauser-Feshbach theory for the prediction of (p,p') reactions is used. The resulting reaction cross sections are reduced by a factor more than sufficient to account for the increased Q value of the actual reactions over that of the (p,p') reactions used. The result is an estimate of a lower limit on the number of displacements which can be expected. Differential cross sections, both elastic and inelastic, are calculated for silicon and germanium for proton energies through 180 Mev and 140 Mev respectively. The cascade model of Oen and Robinson, which takes into account the inhomogeneity of the crystal, is applied to these cross sections to calculate total numbers of displacements in a crystal as a function of the energy of the incident protons. The results of these calculations on germanium are compared with recently published experimental data obtained using both conductivity and minority carrier lifetime as damage probes. Excellent agreement is obtained using reasonable values of cutoff energy between elastic and inelastic reactions of the primary knockon and of the channeling probability parameter of Oen and Robinson. Calculated results on silicon are in only fair agreement with available experimental data. The poorest agreement is found for proton energies above 40 Mev. It is concluded that the reduction in mass of the recoiling nuclei resulting from the loss of spallation products is the most likely cause for this discrepancy. (D.L.C.)

44748 (ORNL-P-1505) MATHEMATICAL MODEL FOR PREDICTING COATED-PARTICLE BEHAVIOR. Prados, J. W.; Scott, J. L. (Oak Ridge National Lab., Tenn.). [1964]. Contract W-7405-eng-26. 4p. (CONF-651101-18). Dep. mn; CFSTI $1.00 cy, $0.50 mn.

From 13th Conference on Remote Systems Technology, Washington, D. C.

A model was developed for predicting stresses and strains in pyrolytic-carbon coatings on fuel microspheres during irradiation. Calculations with this model lead to the following predictions: coating failure may occur at the inner or outer surface, the former being more likely for enriched-uranium-based particles; a free volume of 2–3% of the fuel volume per at. % burnup ensures adequate coating life; isotropic outer coatings may be provided to prevent failure at the outer surface; increasing the outer-coating thickness beyond an inner dia/outer dia ratio of $\frac{2}{3}$ will not increase its life; and the use of low-density fuel particles should have little adverse effect on coated-particle life. (D.L.C.)

44749 (ORNL-P-1507) IRRADIATION EVALUATION OF FUEL ELEMENTS FOR THE PBRE AND AVR REACTORS. Scott, J. L.; Morgan, J. G.; DeCarlo, V. A. (Oak Ridge National Lab., Tenn.). [1964]. Contract W-7405-eng-26. 4p. (CONF-651101-20). Dep. mn; CFSTI $1.00 cy, $0.50 mn.

From 13th Conference on Remote Systems Technology, Washington, D. C.

Results are summarized of an irradiation test program carried out on spherical fueled-graphite elements containing pyrolytic carbon-coated fuel microspheres. The elements had either machined-graphite shells, molded-unfueled shells, or no shells. Maximum burnups were 9 and 27 at. % for the 6.0- and 3.8-cm-dia spheres, respectively. Good irradiation stabilities were obtained; duplex and triplex, but not laminar, coatings on the fuel particles survived the maximum burnups. Fission gas releases, thermal conductivity, and shrinkages are discussed briefly. (D.L.C.)

44750 (ORNL-TM-1216) EFFECT OF IRRADIATION ON THE MECHANICAL PROPERTIES OF STAINLESS STEEL AT 750 deg C UNDER CONSTANT STRESS RATE CONDITIONS. Venard, J. T.; Kennedy, C. R.; Weir, J. R. (Oak Ridge National Lab., Tenn.). Sept. 1965. Contract W-7405-eng-26. 12p. Dep. mn; CFSTI $1.00 cy, $0.50 mn.

Tube-burst tests in which the loading is controlled to produce a predetermined constant stress rate, after a given neutron exposure, were performed to study the strength and ductility of a 20% Cr–25% Ni–Nb–stabilized stainless steel as a function of neutron dose at 750°C. Total thermal neutron doses ranged from about 6×10^{16} to 3×10^{20} neutrons/cm^2. Approximate stress rates employed were 5×10^3, 3×10^4, and 2×10^3 psi/hr, and corresponding rupture times were 4 to 5 min, 50 min to 1 hr, and 9.5 hr. No loss in strength occurred as the result of neutron irradiation, and at the highest strain rate there was no loss in fracture ductility, even at large doses. At lower strain rates a significant loss in fracture ductility was observed at thermal neutron doses greater than 10^{19} neutrons/cm^2. (auth)

44751 (TID-22110) EFFECTS OF NEUTRON DAMAGE ON THE MECHANICAL PROPERTIES OF PYROLYTIC AND SINGLE CRYSTAL GRAPHITE. Quarterly Progress Report No. 3, October 1, 1964–December 31, 1964. Meers,

J. T. (Union Carbide Corp., Parma, Ohio. Carbon Products Div.; Union Carbide Corp., Parma, Ohio. Research Lab.). July 26, 1965. Contract AT(40-1)-3237. 46p. Dep. mn; CFSTI $2.00 cy, $0.50 mn.

Materials for the test program have been prepared; these include natural graphite crystals and compression-annealed pyrolytic graphite. The shear strength of compression-annealed pyrolytic graphite has been measured, and values ranging from 150 to 350 psi were observed. An apparatus for the static torsion testing of compression-annealed pyrolytic graphite has been constructed. Work has been continued on the measurement of the elastic stiffness and compliance constants. Timoshenko's equation for the flexural vibrations of a long thin bar has been solved, and the solution is being used to compute the value of one modulus from the measured resonant frequency and a known value of the other modulus. To make this computation economical for a large number of bars, a program was written for a digital computer. One plane of vibration yields a value of Young's modulus $1/s_{11}$; the other plane of vibration gives the shear modulus $1/s_{44}$. (auth)

44752 (CEA-tr-A-1818) LA TENUE SOUS RADIATION DES METAUX LEGERS. (The Radiation Behavior of Light Metals). Lintner, K. Translated into French by G. Cen from Aluminium, 37: 645-7(1961). 17p. Dep. mn.; JCL $1.60 fs, $0.80 mf.

A brief review is made of the radiation behavior of aluminum and aluminum–magnesium alloys. The effects of radiation on the mechanical and corrosion behavior are discussed. (J.S.R.)

44753 THE EFFECT OF FAST NEUTRON DAMAGE ON THE DEFORMATION OF COPPER–TIN ALLOYS. Russell, B. (Univ. of Queensland, Brisbane). Acta Met., 13: 999-1009(Sept. 1965).

The deformation behavior of several copper–tin alloys was examined before and after irradiation with fast neutrons. It was found that the first measurable change in all of the alloys occurred at a dose between 10^{16} and 10^{17} nvt and, although the initial flow stress of unirradiated alloys decreased with tin content, all of the alloys reached the same maximum flow stress at a saturation dose of approximately 3×10^{19} nvt. The dependence of the flow stress on grain size was examined and it was found that the friction stress of irradiated alloys decreased linearly with strain and that the initial dislocation sources were heavily jogged. The jogged sources were eliminated by a few percent of strain. A simple theory for irradiation hardening, which predicts a complex relationship between stress and fast neutron dose and between stress and temperature, is proposed. The agreement of the experimental results with this theory is good. (auth)

44754 DETERMINATION OF THE MEAN DIMENSION OF HOLES OR FAULTS IN GERMANIUM IRRADIATED BY FAST NEUTRONS AT 80 deg K. Nguyen Van Dong (CENS, Gif-sur-Yvette, France). Compt. Rend., 260: 5512-15 (May 24, 1965). (In French).

The variations of the thermal conductivity of germanium bombarded at 80°K by fast neutrons were measured by utilizing the formula of Callaway. It was established that the variations of thermal conductivity are connected to the mean dimensions of the faults and to their concentration by a simple expression. From the experimental results, the average radius of the faults was found to be approximately equal to 60 Å. (tr-auth)

44755 STUDY, IN NEUTRON-IRRADIATED ALUMINUM, OF THE ELIMINATION OF FAULTS AS A FUNCTION OF THEIR INITIAL CONCENTRATION. Frois, Colette; Dimitrov, Omourtague (CNRS, Vitry-sur-Seine, France). Compt. Rend., 260: 6883-6(June 28, 1965). (In French).

Samples of very pure aluminum containing approximately 3 ppm of residual impurities were irradiated at doses from 1.5×10^{16} to 10^{18} nR/cm^2. The radiated wires were exposed to successive isochronic anneals. The results showed that a variation of the initial concentration of faults modifies the characteristics of the two principal restoration stages of Al. The first, of relatively low amplitude, decreases for increasing radiation doses. The structure of the second stage is more complex and is subdivided into two substages that become more apparent when the dose is low. The first substage seems to correspond to the existence of several processes for the elimination of faults and the second is represented by a restoration kinetics of the second order. It appears that this stage corresponds to the elimination of the imperfections of Lacunal type. (J.S.R.)

44756 ANOMALOUS TRANSMISSION OF X-RAYS THROUGH GERMANIUM SINGLE CRYSTALS CONTAINING DISLOCATIONS AND IMPURITIES. Maruyama, Susumu (Nippon Telegraph and Telephone Public Corp., Tokyo). J. Phys. Soc. Japan, 20: 1399-1405(Aug. 1965).

The anomalous transmission of x-rays was studied on non- and γ-irradiated germanium single crystals with antimony and arsenic concentrations from 10^{13} to 10^{19}/cm^3 and with dislocation densities from $<10^2$ to 2×10^5/cm^2. The ratios of the anomalous absorption coefficient to the mean absorption coefficient, μ'/μ were determined before and after irradiations. The variations, $\Delta(\mu'/\mu)$, for antimony doped specimens increase appreciably with impurity concentration, while for arsenic negligibly. The variations for arsenic doped ones would be the same as for an antimony doped one with sufficiently low concentration. These results are explained in terms of the differences in atomic radii. The imaginary parts of the structure factors before and after irradiations were also determined from the observed values of μ'/μ. (auth)

44757 RADIATION QUENCHING OF RADIO- AND RADIOTHERMO-LUMINESCENCE OF ZnS PHOSPHORS. II. TRAPPING PROCESS. Huzimura, Ryoitiro (Government Industrial Research Inst., Nagoya, Japan). J. Phys. Soc. Japan, 20: 1417-24(Aug. 1965).

The thermoluminescence of ZnS:Cu:Cl phosphors after irradiation by 4.5 Mev electrons from a linear accelerator or by γ-rays of ^{60}Co was compared with that obtained by near uv light. Three main peaks appear usually. It was found that the ratio of the green peak height at 120–160°K to one at 190–220°K are little dependent on the kind and intensity of radiation and on the excitation time, while for the blue component, the ratio obtained after excitation by γ-rays or 4.5 Mev electrons is smaller than that obtained after uv-excitation. A reduction of the ratio of the blue component to the green one is also observed in the spectra of radio-thermoluminescence of the hexagonal and hexagonal-like phosphors. The results are explained by employing the model on radiation quenching formerly proposed and the nature of traps is discussed. (auth)

44758 ESR STUDIES OF RADIOPHOTOLUMINESCENT CENTERS IN SILVER-ACTIVATED PHOSPHATE GLASS. Yokota, Ryosuke; Imagawa, Hiroshi (Tokyo Shibaura Electric Co., Ltd.). J. Phys. Soc. Japan, 20: 1537-8 (Aug. 1965).

An investigation was made of the ESR spectra of silver-activated phosphate glasses after irradiation with ^{60}Co gamma rays. An analysis of the initial transient behavior of several paramagnetic centers and their simultaneous change in optical properties was made by taking into account Ag^{++}, Ag^0, and Ag^0 pairs acting as radiophotoluminescent centers. (L.B.S.)

44759 ON THE TEMPERATURE DEPENDENCE OF THE RADIATION SATURATION IN SiC. Balarin, M. (Zentralinstitut fuer Kernforschung, Berlin). Phys. Status Solidi, 11: K67-71(Sept. 1, 1965). (In German).

Experimental results on the volume expansion of α-SiC after isothermal irradiation in the temperature range from 130 to 600°C were used to show the temperature dependence of the radiation saturation. The saturation concentration, precipitation rate, and the relative annealing rate were graphed as a function of the temperature. The interpretation of the data to explain the temperature dependence of the radioinduced phenomena is given. (J.S.R.)

44760 THE EFFECTS OF LOW-ENERGY NEUTRON IRRADIATION ON AGE HARDENING IN THE ALLOY Cu-Be. Eggert, Gilbert L. (Sandia Corp., Albuquerque, N. Mex.). Trans. Met. Soc. AIME, 233: 1733-7(Sept. 1965).

The effects of reactor irradiation on age hardening in a Cu-2 wt % Be alloy were investigated in two neutron energy ranges. During some of the irradiations, specimens were exposed to high-energy fission neutrons, which passed through a ^{10}B shield; during other bombardments, the ^{10}B was omitted and specimens were irradiated in a reactor thermal column, or the fuel configuration was modified to increase the thermal-neutron flux at a location in the core. Differences in length, x-ray diffraction angle, and hardness indicated that low-energy neutron irradiation made a small contribution to changes in the measured properties. The influence of defects generated by knock-ons with less than the Brinkman critical energy or by prompt (n,γ) recoil is suggested as the cause of this effect. (auth)

METEOROLOGY

See also GEOLOGY AND MINERALOGY — Site Survey and Selection.

Refer also to abstract 44339.

44761 (BNL-914) CONFERENCE ON AEC METEOROLOGICAL ACTIVITIES, MAY 19–22, 1964. Singer, Irving A.; Smith, Maynard E.; Bierly, Eugene W. (eds.) (Brookhaven National Lab., Upton, N. Y.). Contract AT(30-2)-Gen-16. 189p. (CONF-640511). Dep. mn; CFSTI $5.00 cy, $1.00 mn.

A total of 45 papers, with group discussions, is presented which gives descriptions of site meteorological programs and which discusses major technical problems. Separate abstracts were prepared for 43 of the papers. (D.L.C.)

For abstracts of individual papers see: 44245–44249, 44270, and 44762–44798.

44762 (BNL-914, pp 1-3) THE BROOKHAVEN METEOROLOGICAL PROGRAM. Smith, Maynard E. (Brookhaven National Lab., Upton, N. Y.).

A brief account is given of the meterological work at Brookhaven in three areas: studies of low-level atmospheric structure and wind flow, diffusion-deposition experiments, and development of instruments and techniques. (D.L.C.)

44763 (BNL-914, pp 4-13) THE ARGONNE METEOROLOGY PROGRAM. Moses, Harry (Argonne National Lab., Ill.).

Measurements in the climatological program are described. Soil and rainfall data are given. The possible use of a high-energy proton beam as a meteorological tool is discussed. Some results are presented on radon tracer, smoke plume rise, and wind profile studies. (D.L.C.)

44764 (BNL-914, pp 14-17) SCALE MODEL DIFFUSION EXPERIMENTS. Strom, Gordon (New York Univ., N. Y. School of Engineering and Science).

Experiments are being conducted on a model smoke stack in the Air Pollution Wind Tunnel at New York University, in order to model the atmospheric motions which are significant to diffusion including convective turbulence. It was found that the turbulence in the tunnel was inadequate, and roughness plates were used to remedy this problem. Similarity criteria are discussed. Plume characteristic data are presented for a few of the experiments. (D.L.C.)

44765 (BNL-914, pp 18-19) THE OAK RIDGE METEOROLOGICAL PROGRAM. Hilsmeier, William F. (Weather Bureau, Oak Ridge, Tenn.).

Some results of uranine dye tracer diffusion experiments are described. The climatological network and the Theta-N wind statistics instruments are described. The functions of the Nuclear Safety Information Center are discussed briefly. (D.L.C.)

44766 (BNL-914, pp 20-3) CONTINUOUS POINT SOURCE DIFFUSION IN THE SURFACE LAYER. Gifford, Frank A. Jr. (Weather Bureau, Oak Ridge, Tenn.).

Theories of atmospheric diffusion are discussed. The application of Lagrangian similarity to the problem of atmospheric surface layer diffusion is shown to involve a weak point in the diabatic case, and an alternative derivation is proposed which avoids the difficulty. (D.L.C.)

44767 (BNL-914, pp 24-5) THE METEOROLOGY PROGRAM AT THE HANFORD ATOMIC PRODUCTS OPERATION. Fuquay, James J. (General Electric Co., Richland, Wash. Hanford Atomic Products Operation).

A brief description is given of a study on the prediction of exposures from ground sources, and of a comparison of diffusion experiments from sources near ground level. Tracer development and studies are also discussed. (D.L.C.)

44768 (BNL-914, pp 26-7) DIFFUSION FROM ELEVATED SOURCES. Elderkin, Charles E. (General Electric Co., Richland, Wash. Hanford Atomic Products Operation).

Results from the 8 best tests conducted in 1962 are presented in the form of graphs of standard deviation of crosswind exposure distribution, normalized peak exposure, and normalized crosswind-integrated exposure versus time. (D.L.C.)

44769 (BNL-914, pp 28-32) PRECIPITATION SCAVENGING. Engelmann, Robert J. (General Electric Co., Richland, Wash. Hanford Atomic Products Operation).

Previous work on washout of particles by raindrops is reviewed. Outdoor experiments in scavenging are being done at Hanford using one diffusion tower. The results so far indicate that the smaller raindrops are the best scavengers. Possible errors and further research are discussed. During the group discussion, normalized peak exposure graphs were given which shows that the stable, slightly stable, and unstable regions can be distinguished using travel time. (D.L.C.)

44770 (BNL-914, pp 33-43) THE U. S. WEATHER BUREAU METEOROLOGY PROGRAM. Pack, Donald H. (Weather Bureau, Washington, D. C.).

The program on transport and diffusion in the atmosphere is described, with emphasis on the very small-scale and meso-scale studies. Radon measurements and tetroon flights are discussed in detail. (D.L.C.)

44771 (BNL-914, pp 44-50) AEROSPACE METEOROLOGICAL PROBLEMS AND DIFFUSION CLIMATOLOGY. Van der Hoven, Isaac (Division of Reactor Development (AEC), Washington, D. C.).

A program is being conducted on the transport and diffusion of nuclear materials from a launch pad abort of a missile with a nuclear stage or component. Research on three problem areas are discussed: height of rise of fireball, effects of sea breezes on transport, and diffusion outward to tens of miles of puffs. Studies of low-level inversions and mean mixing depths in U. S. are described, and diffusion frequency data are given for 18 months at Cape Kennedy. Wind direction persistences are compared for Denver and Laredo. Diffusion graphs for Southern California are presented. (D.L.C.)

44772 (BNL-914, pp 51-4) TURBULENCE CHARACTERISTICS NEAR THE GROUND AND SONIC ANEMOMETRY. Bernstein, Abram B. (Weather Bureau, Washington, D. C.).

Research is being done to develop a physical model for micrometeorology, using dimensional analysis. The nature of the dimensional analysis method is discussed, and an exercise in the use of the method is described. Drag coefficients, correlation coefficients, gustiness ratios, and the effects of stability are discussed. The factors involved in planning an experimental program are considered. The sonic anemometer work is discussed briefly. (D.L.C.)

44773 (BNL-914, pp 57-64) PROGRAM REVIEW AND SUMMARY OF RECENT ACCOMPLISHMENTS AT NRTS. Islitzer, Norman F. (Weather Bureau, Idaho Falls, Idaho).

Some of the results of diffusion studies from an elevated source and a ground level continuous point source are reviewed. A discussion is given of present research projects: studies of meso-scale transport using tetroons and radar-transponders, meteorological support of reactor distract tests, monitoring of ^{106}Ru from the Waste Calciner, Controlled Environmental Radioiodine Test, and tracer studies of boundary layer turbulence and diffusion. Operations and service of the U. S. Weather Bureau are also considered. (D.L.C.)

44774 (BNL-914, pp 65-8) THE METEOROLOGY PROGRAM AT THE NEVADA TEST SITE. Allen, Philip W. (Weather Bureau Research Station, Las Vegas, Nev.).

The meteorological activities in support of the AEC Nevada Operations Office are described. The responsibilities include: design of new facilities, scheduling of nuclear events, control of work areas and camp areas, and safety of off-site populations. The difficulties in collecting and interpreting radiation data are considered. The prediction of radiation levels for nuclear rocket engines is discussed. (D.L.C.)

44775 (BNL-914, pp 69-74) THE U. S. PUBLIC HEALTH SERVICE METEOROLOGY PROGRAM. McCormick, Robert A. (Robert A. Taft Sanitary Engineering Center, Cincinnati, Ohio).

The activities of the Weather Bureau Research Station, which functions as the meteorological group in the Division of Air Pollution, are discussed. Four research projects are described: diffusion experiments in St. Louis, SO_2 diffusion project, urban pollutants, and vertical exchange of heat and aerosol matter over a city. (D.L.C.)

44776 (BNL-914, pp 75-84) THE METEOROLOGY PROGRAM AT THE AIR FORCE CAMBRIDGE RESEARCH LABORATORIES. Haugen, Duane A. (Air Force Cambridge Research Labs., L. G. Hanscom Field, Mass.).

The Ocean Breeze-Dry Gulch program was conducted in order to study the Titan II toxicity problem at Cape Kennedy and Vandenberg AFB. The prediction equations and the agreement between observed and predicted normalized centerline concentrations are discussed; the most important meteorological parameter was found to be the bulk stability parameter. The SAND STORM program (firing rocket motors and sampling exhaust products downwind) is described briefly, and some data on normalized centerline exposures are given. The development of the computer-controlled micrometeorological observation system is discussed briefly. (D.L.C.)

44777 (BNL-914, pp 85-90) THE METEOROLOGICAL PROGRAM AT FORT HUACHUCA. Appleby, James F. (Army Electronics Research and Development Activity, Fort Huachuca, Ariz.).

The meteorology group at Fort Huachuca has the responsibilities for basic research in micrometeorology for the Army. The objective is to develop models for the four-dimensional state of the atmospheric boundary layer. The research projects being conducted by external groups and the effort of the internal group are described. (D.L.C.)

44778 (BNL-914, pp 91-2) THE METEOROLOGY PROGRAM AT DUGWAY PROVING GROUND. Carlson, Paul (Dugway Proving Ground, Utah).

Meteorological support is provided for testing chemical and biological weapons at Dugway, and a program on turbulence and diffusion is also being conducted. The program includes modeling studies, studies of complex terrain and vegetation, and in-house studies. Data collection in the instrumentation system is discussed. (D.L.C.)

44779 (BNL-914, pp 93-4) ELEVATED LINE SOURCE PROGRAMS. Vaughan, Leland M. (Metronics Associates, Inc., Palo Alto, Calif.).

Studies using aerial releases of colored tracers and vertical sampling techniques are described. The accuracy of the roto-rod samplers and the collection efficiency of filters are considered. (D.L.C.)

44780 (BNL-914, pp 95-8) TECHNICAL AREAS IN THE FIELD OF METEOROLOGY THAT ARE LIMITING PROGRESS IN THE NUCLEAR INDUSTRY. Gifford, Frank A. Jr. (Weather Bureau, Oak Ridge, Tenn.).

A discussion is presented of meteorology with respect to reactor site selection, hazards analysis, and related problems, such as processing plants and cratering shots. It is stated that meteorology research must be continued. Medium- to long-range dispersion, source strength, and legal aspects of accidents and routine gaseous emission are discussed. (D.L.C.)

44781 (BNL-914, pp 99-102) MESO-SCALE AND MEAN TRANSPORT PROBLEMS. Fuquay, James J. (General Electric Co., Richland, Wash. Hanford Atomic Products Operation).

A discussion is presented of difficulties in meso-scale meteorology problems. Some diffusion work on the complex terrain of Hanford and Vandenberg AFB are described. Tetroon data on eddy motions are considered. (D.L.C.)

44782 (BNL-914, pp 103-6) FUNDAMENTAL PROBLEMS ON THE MESO-SCALE. Vaughan, Leland M. (Metronics Associates, Inc., Palo Alto, Calif.).

A discussion is presented of fundamental problems in meso-scale meteorology: momentum and heat, stability, statistical theory, turbulence, and similarity theory. A group discussion is included. (D.L.C.)

44783 (BNL-914, pp 107-9) IMPORTANCE OF THE TETROON TO MESO-SCALE METEOROLOGY. Angell, James K. (Weather Bureau, Washington, D. C.).

Among the advantages of tetroons are their use to follow air motion and to estimate dispersion over long downwind distances. The use of tetroons in determining a reactor site and for following a release is considered. A group discussion is included. (D.L.C.)

44784 (BNL-914, pp 110-12) MESO-SCALE STUDIES IN THE >100-km RANGE. List, Robert (Weather Bureau, Washington, D. C.).

Data are given on a release of gaseous effluent from a stack, which was monitored by aircraft at ~300 and 600 miles from the stack. An effective horizontal coefficient of eddy diffusion of $\sim 4 \times 10^8$ cm^2/sec was obtained. Data from experiments in the literature on dispersion over long periods of time are plotted. Radioactivity isopleths in the Dominic cloud stem 3 to 6 hr after detonation are given. A group discussion is included. (D.L.C.)

44785 (BNL-914, pp 113-14) AIR POLLUTION IN AN URBAN ENVIRONMENT. McCormick, Robert A. (Robert A. Taft Sanitary Engineering Center, Cincinnati, Ohio).

The complexities of air pollution in the city are discussed, and the results of the St. Louis experiments are considered briefly. A group discussion is included. (D.L.C.)

44786 (BNL-914, pp 115-18) EFFECTS OF VARIABLE SOURCE CONFIGURATIONS IN SPACE AND TIME. Van der Hoven, Isaac (Division of Reactor Development (AEC), Washington, D. C.).

The initial forces and effects involved in the spatial framework of source configuration are considered. A discussion is presented of the parameters which have to be measured in order to obtain information on the source configuration: emission point data, cloud height, emission duration, and atmospheric conditions. The effects of the source configuration on downwind concentrations are discussed, with some example calculations. A group discussion is included. (D.L.C.)

44787 (BNL-914, pp 119-22) CLOUD RISE EXPERIMENTS AT BROOKHAVEN. Frizzola, John A. (Brookhaven National Lab., Upton, N. Y.).

Experiments were made on burning rocket propellant cylinders. Lapse time movies and visual observations of the resulting clouds were analyzed for height of top of plume, elapsed time, and distance downwind. The results for inversion and very light wind-convective cases are described. A group discussion is included. (D.L.C.)

44788 (BNL-914, pp 123-4) THE AIR POLLUTION PROGRAM IN THE PUBLIC HEALTH SERVICE. Pooler, Francis (Robert A. Taft Sanitary Engineering Center, Cincinnati, Ohio).

The three major city studies (Louisville, Nashville, and St. Louis) are discussed. Data treatment and intercity transport of pollution are considered. (D.L.C.)

44789 (BNL-914, pp 146-8) MEASUREMENT AND PREDICTION OF DISPERSION. Slade, David H. (Weather Bureau, Washington, D. C.).

The results of diffusion experiments with release times of a few min to a few hr and travel times on the order of

1 hr, are summarized in order to enable one to construct a diffusion climatology using simple meteorological data. The $\sigma_\theta \bar{u}$ term is used as a predictor of χ/Q in a travel time framework, and conservative curves are given. A group discussion is included. (D.L.C.)

44790 (BNL-914, pp 149-50) DIFFUSION STUDIES IN CANADA. Munn, R. E. (Department of Transport, Toronto (Ontario). Meteorological Branch).

The mobile unit and equipment for conducting diffusion experiments anywhere, and some of these experiments, are described. Some questions are asked on the subjects of air turbulence on the micro- or meso-scales and of internal boundary layers. (D.L.C.)

44791 (BNL-914, pp 151-2) DISPERSION IN URBAN AREAS. Turner, Donald B. (Robert A. Taft Sanitary Engineering Center, Cincinnati, Ohio).

The measurement and prediction of dispersion in urban areas are discussed. The difference of urban and level terrain are described, and some of the problems in estimating concentrations for the longer travel times and distances are given. It is shown that the most important meso-meteorological parameter to forecast is wind direction. (D.L.C.)

44792 (BNL-914, pp 153-5) DIFFUSION STUDIES AT HANFORD. Simpson, Charles L. (General Electric Co., Richland, Wash. Hanford Atomic Products Operation).

The exposure data from 46 experiments are presented in the form of plots of normalized peak exposure vs time. The curves are grouped, according to the Richardson number and the lateral growth parameter, into stable, slightly stable, and unstable groups. The Hanford curves are compared with curves from other ground source experiments. (D.L.C.)

44793 (BNL-914, pp 156-7) TURBULENCE AND LOW-LEVEL STRUCTURE. Davidson, Ben (New York Univ., N. Y.).

The information available about low-level wind structure is discussed, and the statistics of turbulence structure are considered. The validity of Taylor's theory near the ground is questioned. The diffusion equation for different vertical and horizontal atmospheric scales is given, and the diagonalization of the diffusion tensor is suggested. A group discussion is included in which the K theory and diagonalization are considered. (D.L.C.)

44794 (BNL-914, pp 158-60) WIND PROFILE. Arnold, Abraham (Brookhaven National Lab., Upton, N. Y.).

The state of knowledge of wind profiles (speed vs height) is reviewed. The interactions between the fluid mechanics and meteorology disciplines are considered briefly. The logarithmic and power profiles are discussed, and it is concluded that the statement "in an adiabatic atmosphere, the wind profile is logarithmic" may have to be qualified. A group discussion is included. (D.L.C.)

44795 (BNL-914, pp 161-2) TEMPERATURE PROFILES. Bernstein, Arthur B. (Weather Bureau, Washington, D. C.).

Some of the problems of studying turbulent structure are discussed; they include the selection of conditions and the limited range of variables on earth. The problems encountered in the use of dimensionless products to describe the temperature profile are described. (D.L.C.)

44796 (BNL-914, pp 163-72) DIFFUSION EXPERIMENTS. Frenzen, Paul (Argonne National Lab., Ill.).

The idealized diffusion equation $\bar{x}^2 = 2\,\bar{u}^2 \int_0^T \int_0^t R(\xi)d\xi\,dt$ is discussed, and two different experiments with the above equation as a starting point are described. The first one investigates the idealized Taylor diffusion problem; hydrodynamic model studies are used to study the influence of gravitational stability on the Lagrangian autocorrelation function. The other experiment uses Eulerian records of turbulent velocity fluctuations as seen by a fixed anemometer. (D.L.C.)

44797 (BNL-914, pp 173-4) MICROMETEOROLOGY. Barad, Morton L. (Air Force Cambridge Research Labs., L. G. Hanscom Field, Mass.).

The problem of communication between micrometeorologists and macrometeorologists is discussed briefly. It is suggested that conferences be held. A group discussion is included. (D.L.C.)

44798 (BNL-914, pp 175-7) STRUCTURE OF TURBULENCE. Panofsky, Hans A. (Pennsylvania State Univ., University Park).

The state of knowledge of wind structure is surveyed. The area of application of similarity theory is discussed. Wind profile, temperature profile, and Richardson number are discussed. The structure of turbulence is considered in some detail. It is pointed out that further research is needed between 1000 and 5000 ft. (D.L.C.)

44799 (BNL-8516) VERTICAL STRUCTURE OF TURBULENCE. Panofsky, H. A. (Pennsylvania State Univ., University Park); Singer, Irving A. (Brookhaven National Lab., Upton, N. Y.). [Mar. 1964]. Contract AT(30-2)-Gen-16. 21p. Dep. mn; CFSTI $1.00 cy, $0.50 mn.

Based on fluctuation statistics from the Brookhaven tower, statistical models are presented which permit estimation of cross spectra between wind components at various heights. It is shown that a similarity hypothesis proposed by Davenport seems to be valid. The turbulent eddies slope into the wind, with slopes of order unity, probably dependent on wind shear. In free convection, eddies are taller than wide, but in mechanical turbulence and forced convection the reverse is true. (auth)

44800 (BNWL-103) FIELD TESTING OF A FLUORESCEIN-ZINC SULFIDE DUAL ATMOSPHERIC TRACER TECHNIQUE. Nickola, P. W. (Battelle-Northwest, Richland, Wash. Pacific Northwest Lab.). Aug. 1965. Contract AT(45-1)-1830. 29p. Dep. mn; CFSTI $2.00 cy, $0.50 mn.

Four field experiments were conducted in investigation of the compatibility of fluorescein and fluorescent zinc sulfide as dual atmospheric tracers. The two tracers were emitted simultaneously from a common source and collected on common filters. Qualitative and quantitative comparisons of the sampled tracer distributions are presented. The agreement is good. (auth)

44801 (NYO-2363-3) DEL ELECTRONICS CORPORATION RESEARCH, DEVELOPMENT, AND TEST PROGRAM FOR STRATOSPHERIC ELECTROSTATIC PRECIPITATOR AND ASSOCIATED DEVICES. Semi-Annual Progress Report, September 1964-February 1965. Solon, L. R. (comp.) (Del Electronics Corp., Mount Vernon, N. Y.). May 10, 1965. Contract AT(30-1)-2363. 26p. Dep. mn; CFSTI $2.00 cy, $0.50 mn.

The 37-tube Model II Electrostatic Precipitator was developed for sampling stratospheric aerosols at a rate of 1850 ambient cfm at altitudes of 105,000 to 150,000 feet. Work on the following equipment is described: ion-tracer flowmeter, sample recovery system, and self-regulating d-c power supply. A proposed flight program for testing the precipitator is described. (D.L.C.)

PHYSICS

General

44802 (ANL-6877) PHYSICS DIVISION SUMMARY REPORT, JANUARY-MARCH 1964. (Argonne National Lab., Ill.). Contract W-31-109-eng-38. 53p. Dep. mn; CFSTI $3.00 cy, $0.50 mn.

Five papers are included; separate abstracts were prepared for 4. The other paper was previously abstracted for NSA; see 18: 28693. (M.O.W.)

For abstracts of individual papers see: 44373, 44803, 45246, and 45247.

44803 (ANL-6877, pp 21-7) MASS SPECTROMETRIC STUDIES OF THE LASER-PRODUCED GRAPHITE JET. Chupka, W. A.; Berkowitz, J. (Argonne National Lab., Ill.).

The emission spectra of the molecules C_2, C_3, and CN present in laser-produced graphite jets ejected into vacuum and into various ambient gases were studied. The spectral intensities were found to be strongly dependent on the identity of the ambient gas. Mechanisms are proposed to explain the observations. (auth)

44804 (ARL-65-105) RADIATION FROM AN ALTERNATING CURRENT NITROGEN ARC. Schreiber, P. W. (Aerospace Technical Intelligence Center, Wright-Patterson AFB, Ohio). May 1965. 75p. CFSTI.

An experimental investigation of the total power radiated per unit length from a nitrogen arc operating on alternating and direct current is outlined and sample results are given. The measured results include average and instantaneous radiant power, average electric power, root mean square and instantaneous current and voltage, arc radii, spectra, and average absorption as well as the flow parameters such as total mass flow rate and vortex strength. In addition, radiometer calibration techniques and the sources of error are discussed. In order to compare measured quantities with analytical calculations, an approximate solution of the single fluid time-dependent energy equation and Kirchhoff's voltage law was obtained. The solution is based on a simplified model of the arc column, and approximate equations are obtained for arc voltage, current, radius, temperature, and radiation in terms of the root mean square voltage gradient which remains as an unknown. The important parameters include line frequency and voltage, inductance, thermal diffusivity, and approximate slopes of electrical conductivity and radiant power per unit volume as a function of the heat conductivity potential. In general, measured results compare favorably with the analytical calculations based on the simple arc model. The measured radiation tends to be higher than calculated values if recent radiation data for nitrogen are used. However, the errors associated with the measured and calculated radiant power are too great to draw definite conclusions. (auth)

44805 (CEA-R-2769) MESURES DE CHAMPS MAGNETIQUES PULSES RAPIDES A L'AIDE DE L'EFFET FARADAY (theses). (High Speed Pulsed Magnetic Fields Measurements, Using the Faraday Effect (thesis)). Dillet, Alain (Commissariat a l'Energie Atomique, Saclay (France). Centre d'Etudes Nucleaires). 1965. 61p. Dep. mn.

Submitted to Universite, Paris.

A method for measuring pulsed magnetic fields is described in which the rotation of the plane of rotation of light under the influence of the magnetic field in a glass probe is observed. The experimental equipment is described, and some experimental results are included. (D.C.W.)

44806 (IS-T-19) THEORY OF MANY-BOSON SYSTEMS (thesis). Etters, Richard David (Ames Lab., Iowa State Univ. of Science and Tech.). May 1965. Contract W-7405-eng-82. 67p. Dep. mn; CFSTI $3.00 cy, $0.75 mn.

A many-boson theory is developed that is applicable to systems with intermediate as well as weak coupling strength. A transformation of basis from the single-particle representation to an independent collection of quasi-particles, which represent the normal modes of the system, is accomplished in an approximate way. The results are in the form of coupled, non-linear, integral equations for the ground-state energy, the excitation energy, the quasi-particle excitation operator, and the momentum distribution function. No a priori assumptions concerning the population in any single low-lying momentum state is required nor is any artificial separation of the single-particle zero-momentum state from states of higher momentum necessary. Contact with the results of weak-coupling theories is established by imposing additional restrictions on the interaction potential and on the momentum distribution of particles. It is shown that the weak-coupling equations are valid under more general circumstances than was previously apparent. A general theorem is provided that requires the existence of a zero in the excitation spectrum at zero momentum. It is also shown that the low-lying excitations follow a dispersion rule that is linear in momentum, independent of the form of the interaction. The theory is applied to the charged boson gas problem, where it is found that the resulting excitation spectrum is not in agreement with previous calculations at low momenta, but is elsewhere. For systems with interaction potentials similar to that of helium II, it is shown that the weak-coupling equations may be valid at sufficiently low temperatures provided that depletion effects are completely ignored. (auth)

44807 (LA-DC-6556) SYMMETRY OF THE STRESS TENSOR. McLennan, James A. (Los Alamos Scientific Lab., Univ. of California, N. Mex.). [1964]. Contract W-7405-eng-36. 9p. Dep. mn; CFSTI $1.00 cy, $0.50 mn.

The stress tensor for a medium with internal angular momentum is considered, and it is shown how a symmetric stress tensor can be formed. Construction of the symmetric tensor requires that the contribution to the linear momentum of a distribution of internal angular momentum be taken into account. (auth)

44808 (LA-DC-6636) ON THE PROPER USE OF TRANSFORMATIONS OF LOG NORMAL FUNCTIONS IN SMALL-PARTICLE STATISTICS. Goldman, A.; Lewis, H. D.; Moore, R. H. (Los Alamos Scientific Lab., Univ. of California, N. Mex.). [1963]. Contract W-7405-eng-36. 27p. Dep. mn; CFSTI $2.00 cy, $0.50 mn.

A standard notation is suggested for use in all fields concerned with small-particle data analysis. The representation of particle size data by various forms of the log normal function is discussed and related to methods of particle-size measurement. Transformation among parameters defining the functions are discussed, and the general functional relations are developed and listed in tabular form. The use of the proper parameters for data comparisons or for distribution definition is emphasized. (auth)

44809 (SC-DR-65-291) COMPUTATIONAL STUDIES ON THE RECONSTRUCTION OF AN ANALOG SIGNAL FROM NON-UNIFORMLY SPACED SAMPLES. Freeman, J. R. (Sandia Corp., Albuquerque, N. Mex.). July 1965. Contract [AT(29-1)-789]. 56p. Dep. mn; CFSTI $3.00 cy, $0.75 mn.

The reconstruction of an analog signal from non-uniformly spaced samples is investigated; four band-limited composing function approaches and two low-order polynomial approaches to reconstruction are used. These methods are applied both to a non-uniformly sampled test waveform and to a non-uniformly sampled waveform which has been approximately band-limited by numerical prefiltering with a fifth-order Butterworth filter. Graphs of

the reconstructed waveforms and the rms error are shown. (auth)

44810 (TPJU-8/65) A PROOF OF THEOREM ABOUT GENERAL FORM OF ISOTROPIC TENSORS. Kotanski, Andrzej (Jagellonian Univ., Krakow (Poland). Dept. of Theoretical Physics). Apr. 1965. 4p. Dep. mn.

A simple proof of a theorem generalizing the Eckart-Wigner formula is given. The proof is valid for compact groups. (D.C.W.)

44811 (UCRL-7784-T(Rev.1)) MAGNETIC FIELD CALCULATIONS IN AN IRREGULAR TRIANGLE MESH. Winslow, Alan M. (Lawrence Radiation Lab., Univ. of California, Livermore). Aug. 23, 1965. Contract W-7405-eng-48. 36p. (CONF-650922-5). Dep. mn; CFSTI $2.00 cy, $0.50 mn.

From 1st International Symposium on Magnet Technology, Stanford, Calif.

A method is described for the numerical solution of the non-linear magnetostatic equation for the vector potential over an arbitrary polygonal region using a distorted triangle mesh. The equations are solved by successive over-relaxation with automatic optimization of the overrelaxation parameter. Based on this method, a general purpose two-dimensional magnet code was developed which will calculate magnetic fields in any plane arrangement of air, iron, and currents, with speed and accuracy comparable to that obtained with rectangular meshes. (auth)

44812 (UCRL-16099) PHYSICS DIVISION SEMI-ANNUAL REPORT, NOVEMBER 1964 THROUGH APRIL 1965. (Lawrence Radiation Lab., Univ. of California, Berkeley). May 10, 1965. Contract W-7405-eng-48. 71p. Dep. mn; CFSTI $3.00 cy, $0.75 mn.

Summaries of both experimental and theoretical work carried out at the Lawrence Radiation Laboratory during the period Nov. 1964 through April 1965 are presented. Abstracts of published literature during this period are also presented. The summaries include extensive elementary particle studies, research with bubble chambers, and work done in data processing. (M.O.W.)

44813 (NP-tr-1307) NUCLEAR MAGNETIC RESONANCE IN A FLOWING LIQUID. Zhernovoi, Aleksandr Ivanovich; Latyshev, Georgii Dmitrievich. Translation. 17p. Consultants Bureau $22.50.

A review of published data is presented. The results of theoretical and experimental investigations of NMR in flowing liquids and of flow detectors are examined. Applications of NMR in flowing liquids are considered; they include measurement and stabilization of weak magnetic fields, flow rate measurements, relaxation time determinations, etc. (D.L.C.)

44814 RUBIDIUM VAPOR ATOMIC CLOCKS. Gourber, J. P. Ann. Radioelec., 20: 191-211(July 1965). (In French).

A detailed examination is made of the action and performance of optical pumped rubidium vapor clocks. A first limit of the frequency stability of the clocks is defined on the basis of the values of line widths and of the signal/noise ratio. The influence of the various parameters on the resonance signals is examined as well as the signal/noise ratio obtained for optimum adjustments. Examination of the control loop gives the short term stability characteristics. The value of the control gain is fixed and the choice of the cut-off frequency is discussed on the basis of the use to which the clock is put. Long term stability is related to the shifts of the resonance frequency. The effects are divided into two groups according to whether or not they depend on the optical pumping and are examined separately. Lastly, the performance of the two clocks is given. (auth)

44815 DIFFUSION IN THE 4-BODY SYSTEMS. Weyers, J. (Centre de Physique Nucleaire, Louvain, Belg.). Ann. Soc. Sci. Bruxelles, Ser. I, 79: 76-86(1965). (In French).

The possible asymptotic states in the 4-body system are enumerated. Kinematic considerations of the system are outlined. The equations which should satisfy the transition amplitudes are established. (J.S.R.)

44816 ON THE SYMMETRICAL MOTIONS WITH RESPECT TO AN AXIS OF AN INCOMPRESSIBLE VISCOUS FLUID IN MAGNETOFLUIDDYNAMICS. Mattei, Giulio. Atti Accad. Sci. Torino: I. Classe Sci. Fis., Mat. Nat., 99: 181-97(1964-65). (In Italian).

The nonapproximate differential equations which satisfy the functions of current and of the magnetic field are summarized. The form assumed within the framework of the linear approximation is written for the case of slow motion and of weak induced magnetic fields. The nonviscous fluid is examined as a particular case. The hypothesis in which the velocity of the fluid is always parallel to the magnetic field is analyzed. The distribution of the system of total forces of the mechanical and magnetic forces is studied and leads to the conclusion that the plane of the motion constitutes a principal plane for the forces relative to any point. (J.S.R.)

44817 THE THERMAL MOTION OF SIMPLE LIQUIDS. Egelstaff, P. A. (Atomic Energy Research Establishment, Harwell, Eng.). Brit. J. Appl. Phys., 16: 1219-45(Sept. 1965). (AERE-R-4641).

The microscopic behavior of liquids can be studied by radiation scattering techniques. All such data may be reduced to a scattering function, which is the probability S of exchanging an energy $\hbar\omega$ between the radiation and the system if a momentum transfer $\hbar Q$ has taken place. A discussion of some properties of this function and of recent measurements of it by neutron scattering is given. The relation between the Van Hove space-time correlation functions, the velocity and stress correlation functions and the macroscopic physical properties are discussed. Measurements of the incoherent and coherent neutron scattering by liquids will be interpreted on the basis of this discussion. Particular emphasis is given to the scattering for values of the wave number less than the reciprocal of the interatomic distance. In this range of wave numbers the diffusive properties of the medium and the propagation of longitudinal sound waves can be studied. These effects show clearly the difference between thermal motion in solids and liquids and, for example, provide some evidence for the existence of long-range aggregates of atoms in a liquid. It is concluded that the microscopic behavior is understood in a phenomenological sense, but that current techniques are giving a wealth of new information which requires a quantitative theoretical explanation. (auth) explanation. (auth)

44818 TRANSMISSION OF MONOENERGETIC ELECTRON BEAMS THROUGH FOILS. Somogyi, G.; Boedy, Z. T. (Inst. for Experimental Physics, Debrecen, Hungary). Brit. J. Appl. Phys., 16: 1285-90(Sept. 1965).

Theoretical calculations are presented for the transmission of monoenergetic electron beams through foils. Numerical results were obtained for aluminium at 100, 150 and 200 kev incident energies, where the agreement between the theoretical curves and experimental points is found to be good. The effect of geometry on the transmission coefficient is discussed. (auth)

44819 CATALOG OF METEOROLOGICAL DATA RECEIVED DURING THE IGY AND IGC. WORLD DATA AND ITALIAN DATA. Giorgi, Maurizio. CICIG (Comm. Ital. Comit. Intern. Geofis.), Pubbl., IGC (Intern. Geophys. Comm.), No. 43, 1-79(1965). (In Italian).

The data collected during the International Geophysical Year from July 1, 1957 to December 31, 1958, and during the International Geophysical Corporation from January 1, 1959 to December 31, 1959, are cataloged. The synoptic observations on the surface at ground and maritime stations, the observations from radioprobes, wind observations, measurements of the solar and terestrial radiation observations on the ozone, data of the chemical composition of the atmosphere, data on evaporation and transpiration, and data relative to the atmospheric electricity are tabulated. A list of the participating Italian institutions is given. (J.S.R.)

44820 THE STIMULATED EMISSION AND ABSORPTION IN QUANTUM AND CLASSICAL ELECTROMAGNETISM. Convert, Guy (Laboratoires de la C.S.F.,

a Corbeville, Orsay, France). Compt. Rend., 260: 5719-22(May 31, 1965). (In French).

It has been shown for some time that it is possible to define a passage at the classical limit on the purely quantum a priori concepts of stimulated absorption and emission. The classical demonstrations seem however only to have been established in incoherent excitation. A classical calculation is presented valid in coherent fields that attempts to show the basic continuity that exists between the phenomena of stimulated emission and absorption and the more classical mechanism of the energy exchange (plasmas and electron beams). (J.S.R.)

44821 TIME EVOLUTION OF DISCHARGES INDUCED IN GASES BY A LASER. Breton, Claude; Capet, Maurice; Chalmeton, Vincent; Nguyen, Quang Dong; Papoular, Renard (EURATOM-CEA, Fontenay-aux-Roses, France). Compt. Rend., 260: 5731-4(May 31, 1965). , (In French).

Experiments are described which have made it possible to define the concepts of breakdown and threshold, to measure the characteristics of the light emitted, and to establish the nonlinear character of the light-discharge interaction. (tr-auth)

44822 VELOCITY OF SOUND IN LIQUID HYDROGEN. Van Dael, W.; Van Itterbeek, A.; Cops, A.; Thoen, J. Cryogenics, 5: 207-12(Aug. 1965).

The velocity of ultrasonic pulses was measured in liquid normal and parahydrogen between 20 and 32°K at saturated vapor pressure. For normal hydrogen, results on six isotherms up to 250 kg/cm^2 are reported. Some thermodynamic properties, e.g., the compressibilities and the specific heats, are derived. The systematic difference between the data for normal and parahydrogen is shown to be in agreement with a corresponding states treatment. (auth)

44823 LOSS MECHANISM OF ELECTRONS FROM A MAGNETIC BOTTLE. Fukui, Shuji; Hayakawa, Satio; Honzawa, Tadao; Nishimura, Hiroyuki; Obayashi, Haruo (Nagoya Univ., Japan). J. Phys. Soc. Japan, 20: 1487-96 (Aug. 1965).

The motion of electrons in a static magnetic field of mirror geometry was investigated by injecting a beam of kev electrons with a small electron gun in the central region of the magnetic bottle. The first order orbit theory was well verified by high vacuum experiment. The mirror loss of kev electrons was studied by filling the vacuum chamber with helium and argon gases. The mean lifetime of trapped electrons was measured by making use of the azimuthal drift of electrons as a function of gas pressure. The elastic scattering of single or plural type is concluded to be the most responsible for the mirror loss at pressure of 10^{-4} mm Hg or higher. (auth)

44824 LAMINAR FLOW OF CONDUCTING FLUID IN PIPES AND CHANNELS IN THE PRESENCE OF A MAGNETIC FIELD. Regirer, S. A. Magnitn. Gidrodin., No. 1, 5-17(1965). (In Russian).

A review of exact and approximate solutions of magnetohydrodynamic equations for the flow of viscous conducting liquids and gases in pipes and channels in the presence of a magnetic field is submitted. (auth)

44825 FLOW OF CONDUCTING FLUID PAST CIRCULAR CYLINDER IN THE PRESENCE OF TRANSVERSE MAGNETIC FIELD. Kalis, Zh. E.; Tsinober, A. B.; Shtern, A. G.; Shcherbinin, E. V. Magnitn. Gidrodin., No. 1, 18-28(1965). (In Russian).

The flow of a conducting viscous fluid past a circular cylinder in the presence of a transverse magnetic field is investigated on the basis of the numerical solution of the precise Navier-Stokes equations. The perturbation of the magnetic field is supposed to be negligible, i.e., $Re_m = 1$. Results of the calculation are compared with the experimental data. Reynolds number is taken as 40. Stuart number takes values from 0 to 4. (auth)

44826 INFLUENCE OF RELATIVE ROUGHNESS ON ELECTRICALLY CONDUCTING FLUID FLOW IN THE PRESENCE OF A MAGNETIC FIELD. Dukure, R. K. Magnitn. Gidrodin., No. 1, 29-32(1965). (In Russian).

The influence of relative roughness on the friction coefficient of the electrically conducting fluid flow in the presence of a transverse magnetic field is considered. The friction coefficient was determined by measurements of pressure gradients. The range of calculation of friction coefficient by means of M/Re and a formula are found to be dependent on the relative roughness. The analysis of the range of application of different friction coefficient formulas suggests that an increase of the relative roughness causes a decrease of the laminar and transient zones and an increase of the turbulent one. (auth)

44827 SOME RESULTS OF MEASURING TURBULENT PULSATIONS OF VELOCITY IN THE FLOW OF MERCURY IN THE PRESENCE OF A TRANSVERSE MAGNETIC FIELD. Branover, G. G.; Slyusarev, N. M.; Shcherbinin, E. V. Magnitn. Gidrodin., No. 1, 33-6(1965). (In Russian).

Oscillograms of the turbulent pulsations of velocity in the flow of mercury are obtained for various values of the magnetic field intensity. The effect of turbulence suppression was observed. (auth)

44828 THREE-DIMENSIONAL BOUNDARY LAYER OF CONDUCTING FLUID NEAR THE LINE OF INTERSECTION OF TWO SURFACES IN THE PRESENCE OF ELECTROMAGNETIC FIELD. Kitanin, E. L. Magnitn. Gidrodin., No. 1, 37-42(1965). (In Russian).

The influence of electric and magnetic fields on the conducting liquid boundary layer near the intersection line of two surfaces is discussed. The results obtained by means of Oseen's method are compared and found in good agreement with previous results. (auth)

44829 SOME PROBLEMS OF TWO-DIMENSIONAL INCOMPRESSIBLE FLUID CHANNEL FLOW IN THE PRESENCE OF ELECTRIC AND MAGNETIC FIELDS. Koukin, I. K.; Smolin, G. G. Magnitn. Gidrodin., No. 1, 43-54(1965). (In Russian).

A two-dimensional steady laminar incompressible conducting fluid flat channel flow of variable cross section in the presence of electric and magnetic fields is discussed. The approximate equations applied are similar to those for the boundary layer. Similar solutions are obtained by means of Jacobian elliptic functions. (auth)

44830 QUASI-ONE-DIMENSIONAL APPROXIMATION OF AXIS-SYMMETRICAL STEADY MOTION OF CONDUCTING GAS IN EXTERNAL ELECTRIC AND MAGNETIC FIELDS. Filippov, S. S. Magnitn. Gidrodin., No. 1, 55-60 (1965). (In Russian).

A steady conducting gas flow in a coaxial channel with constant or slightly variable cross-section is discussed. Electrical and magnetic fields are assumed to be given. Viscous friction and heat-exchange are neglected. The system of non-linear differential equations in nondimensional variables characterizing the flow is defined. (auth)

44831 LONGITUDINAL ELECTROMOTIVE FORCES AND HALL EFFECT IN A CHANNEL FLOW OF IONIZED GAS. Yantovskii, E. I. Magnitn. Gidrodin., No. 1, 61-6 (1965). (In Russian).

Estimates of electric fields caused by thermoelectricity, electron pressure gradient, large ion slip and Hall effect along the channel with moving ionized gas are presented. Some formulas describing the energy conversion in a channel of fixed direction electric field are evolved. (auth)

44832 OPTIMUM CONDITIONS OF MAGNETO-GAS DYNAMIC CHANNEL FLOWS ACCOUNTING FOR HALL EFFECT. Zelichenko, E. N.; Milleryan, T. E.; Pol'skii, N. I. Magnitn. Gidrodin., No. 1, 67-72(1965). (In Russian).

A one-dimensional problem is considered in order to find geometrical, gas dynamic and electromagnetic parameters of a conducting gas channel flow with the maximum power to be collected from the channel electrodes. The problem is simplified by certain admissible assumptions and some qualitative results are obtained. A detailed analysis and comparison are made of cases when continuous and segmented electrodes are used for different

kinds of circuiting of the electrodes and with external load. The limits of applicability of the one-dimensional idealization are discussed. (auth)

44833 INVESTIGATION OF THE SPATIAL DISTRIBUTION OF MAGNETIC FIELDS AND ELECTROMAGNETIC PHENOMENA IN INDUCTION PUMPS. Okhremenko, N. M. Magnitn. Gidrodin., No. 1, 97-109(1965). (In Russian).

The results of analytical studies of the spatial distribution of electromagnetic field in a flat linear induction pump are given. The limitations of the inductor and channel width, metallic walls of the channel and heat-insulation are taken into account. The efficiency of a device is characterized by demagnetizing factor, determined as a ratio of the normal components of induction on the inductor surface under load and under no load, when the currents of the inductor windings are constant. An approximate expression for the penetration depth of traveling magnetic field in the presence of transverse fringe effect is suggested. The expressions of magnetomotive force and current density components in the liquid metal were obtained. (auth)

44834 IMPULSE METHOD OF MEASUREMENTS OF THE FLOW RATE OF CONDUCTING FLUID. Zheigur, B. D.; Sermons, G. Ya. Magnitn. Gidrodin., No. 1, 141-6 (1965). (In Russian).

A method of measuring the rate of conducting fluid is described, based on the utilization of propagation property of the electromagnetic field impulse in a moving conducting medium. Experimental data on rate measurements by the method are reported. (auth)

44835 ON THE STABILIZING EFFECT OF LONGITUDINAL MAGNETIC FIELD ON NON-UNIFORM TURBULENT FLOWS OF CONDUCTING FLUID. Levin, V. B. Magnitn. Gidrodin., No. 2, 3-10(1965). (In Russian).

The method of calculation of turbulent shear flow characteristics previously described is extended to the flow of conducting fluid in the longitudinal magnetic field. Considerable attention is devoted to the investigation of increase of critical Reynolds' number in pipe flow. A simple analytical correlation is obtained for the effect of Hartmann's number on the critical Reynolds' number, which can be used for evaluation in preparing experimental research and for extrapolation of experimental results. (auth)

44836 APPLICATION OF THE HYPOTHESIS OF LOCALISM IN THE TURBULENT FLOW OF A CONDUCTING FLUID IN MAGNETIC FIELD. Kovner, D. S. Magnitn. Gidrodin., No. 2, 11-18(1965). (In Russian).

The hypothesis of the local mechanism of turbulent transfer taking into account the effect of viscosity is extended—with certain assumptions—to the magnetohydrodynamic flow near the smooth wall or in a flat tube in the presence of longitudinal and transverse magnetic field. Theoretical results are compared with experimental data. (auth)

44837 THE CHAPMAN-JOUGET THEOREM IN MAGNETOHYDRODYNAMICS. Polovin, R. V. Magnitn. Gidrodin., No. 2, 19-22(1965). (In Russian).

It is proved that in a magnetohydrodynamic detonation the speed of the reaction products is equal to the phase velocity of small disturbances (in normal direction), the frame of reference moving with the detonation front and the duct being closed from one end by a perfectly conducting wall. If the detonation occurs in a fast (or slow) shock wave, the speed of the reaction products is equal to the velocity of fast (or slow) magnetosonic waves. The conductivity of the medium in front and behind the discontinuity is supposed to be infinite. The direction and magnitude of the magnetic field, the energy of reaction, as well as the equation of state are supposed to be arbitrary. (auth)

44838 PROFILING OF CHANNELS FOR TURBULENT FLOWS OF SLIGHTLY IONIZED GASES IN THE PRESENCE OF TRANSVERSE MAGNETIC FIELD. Bertinov, A. I.; But, D. A.; Vasyukevich, P. V.; Kalugin, V. N. Magnitn. Gidrodin., No. 2, 55-66(1965). (In Russian).

The vortex flow of a conducting gas delayed by a transverse magnetic field is treated. Differential equations concerning the processes in the channel were derived. Finite solutions of these equations for the cases of constant temperature, constant tangential velocity and constant Mach's number are presented. (auth)

44839 THEORETICAL AND EXPERIMENTAL INVESTIGATION OF SELF-EXCITATION REGIMES IN THE CASE OF INTERACTION BETWEEN THE TRAVELING WAVES MAGNETIC FIELD AND THE IONIZED GAS FLOW. Kushnir, V. S.; Novikov, I. I.; Pichakhchi, L. D.; Fokin, V. N. Magnitn. Gidrodin., No. 2, 67-79(1965). (In Russian).

The interaction between plasma flow and the magnetic field of a traveling wave along the line with concentrated inductances and capacitances is treated. Mathematical expressions for the amplification coefficient, power delivered in the load resistance, electrical efficiency and the magnitude of the positive feedback are obtained, taking into consideration the leakage flux and the finite value of the ratio of channel width to wave length. (auth)

44840 FRINGE EFFECTS IN MAGNETOGASDYNAMICAL CONVERTER. Benenson, E. B.; Genkin, A. L. Magnitn. Gidrodin., No. 2, 80-8(1965). (In Russian).

The problem of fringe effects in the MHD converter channel is considered in the case of finite length insulators separating the uniform electrodes from the earthed part of the device. Potential and current distribution in the channel were obtained and losses due to the back currents and the earth leakage currents were estimated according to the dimensions of the insulator. (auth)

44841 CONDUCTING SLAB IN TRAVELLING MAGNETIC FIELD OF DOUBLE-SIDE INDUCTOR. Valdmanis, Ya. Ya.; Kunin, P. E.; Mikel'son, Ya. Ya.; Taksar, I. M. Magnitn. Gidrodin., No. 2, 101-10(1965). (In Russian).

The expressions for current density and magnetic induction in a conducting slab are obtained, the latter being placed in the traveling magnetic field of different flat double-side inductors. The conditions under which maximum of average force density is obtained were studied in respect of the higher field harmonics. Tables and graphs of the results of numerical calculations are presented. (auth)

44842 FLUIDS AND SUPERFLUIDS. Careri, G. (Universita, Rome). Nuovo Cimento (1), 2: Suppl., 517-20(1964). (In Italian).

The common elements of fluids and superfluids are identified and described in elementary form for the non-specialist. (J.S.R.)

44843 LORENTZ TRANSFORMATIONS OF THERMODYNAMIC QUANTITIES. Sutcliffe, W. G. (Univ. of Delaware, Newark). Nuovo Cimento (10), 39: 683-6(Sept. 16, 1965).

The transformation formulas for basic thermodynamic quantities are derived within phenomenological thermodynamics by use of three assumptions or from relativistic mechanics and statistical thermodynamics. It is found that the transformation for thermodynamic pressure is different from that for mechanical pressure, the two pressures being the same only in the center-of-mass frame. (auth)

44844 ON SOME GENERAL PROPERTIES OF THE DEGENERATE FERMI SYSTEMS. Bonch-Bruevich, V. L. (Moscow State Univ.). Phys. Letters, 18: 260-1(Sept. 1, 1965).

Since there are disordered systems whose stationary states are not describable in terms of the momentum, such as the charge carriers in heavily doped semiconductors or in liquid conductors, the notion of density of states is used to describe such systems. The results demonstrate the theorem that the electric conductivity of the macroscopically homogeneous system at zero temperature is non-zero if and only if the Fermi level lies in the region where the density of states is non-zero and continuous. This theorem is demonstrated without the use of the dispersion law. (J.F.P.)

44845 MAGNETOHYDRODYNAMICAL INSTABILITIES IN ELECTRICAL EXPLOSION. Abramova, K. B.; Valitskii, V. P.; Yandakurov, Yu. V.; Peregood, B. P. (Ioffe Inst. of Physics and Tech., Leningrad). Phys. Letters, 18: 286-8(Sept. 1, 1965).

It is shown that magnetohydrodynamical instabilities occur and develop in a conductor when a high-density current pulse is passing. Momentary shadow photos of wire and explosion products made in different stages of phenomenon development, by using a pulsed x-ray device, are shown. The energy necessary for the wire to be stretched and curved is approximately one third as large as that necessary for the occurrence of the observed number of breaks. But this energy for the solid wire at room temperature is substantially greater than the threshold energy, the strength exceeding the electrodynamical forces by at least two orders of magnitude. The yield point decreases with temperature increasing. Both screw-type and sausage-type instabilities are discussed and analyzed. (J.F.P.)

44846 DENSITY EXPANSION OF THE VISCOSITY OF A MODERATELY DENSE GAS. Sengers, J. V. (National Bureau of Standards, Washington, D. C.). Phys. Rev. Letters, 15: 515-17(Sept. 20, 1965).

Since the divergence of the phase volume implies that the corresponding terms in the density series, both of the pair distribution function and of the transport coefficients, become infinite, unless special cancellations occur, e.g., between contributions from different dynamical events which would lead to an essential reduction of the available phase space, as was previously pointed out, the latter point is investigated in more detail. For this purpose the first density correction to the viscosity of a gas of rigid spheres in two dimensions (rigid disks) is investigated. (J.F.P.)

44847 TEMPERATURE DEPENDENCE OF THE MOESSBAUER EFFECT IN THIN FILMS. Motoc, Cornelia; Corciovei, A. (Inst. for Atomic Physics, Academy of the R.P.R., Bucharest). Rev. Roumaine Phys., 10: 149-67(1965).

The thin film Debye-Waller factor for the recoilless gamma-ray emission for different temperatures is studied as a function of the thickness of the film. It is shown that, by increasing the temperature, the Debye-Waller factor rapidly decreases. This factor, for a small thickness of the film, is also anisotropic with respect to the direction of radiation; for increasing thickness, the anisotropy rapidly decreases. In the case of the temperature T = 0, using a plausible approximation, the same results for the anisotropy of the Debye-Waller factor are obtained, as in a previous paper. (auth)

44848 REFLECTION AND TRANSMISSION IN A SLIGHTLY SCATTERING PLATE. Mockel, Andre. Univ. Bruxelles, Inst. Phys., Bull. No. 14, 1-28(June 1964). (In French).

The problem of the total reflection and transmission of monoenergetic particles with known incident distribution in a plate of slightly scattering material was studied from the viewpoint of its numerical solution. Several approximation methods based on known theoretical solutions of the problem are proposed. They are compared with the results obtained by numerical integration of the tables edited by Bellman, Kalaba, and Prestrud. Another approximation of the same form as the P_1 approximation but with adjusted coefficients is also proposed. This last proposal has the advantage of a very satisfactory precision for the values of the parameters (the error is less than 2%) and a great simplicity of calculation. (tr-auth)

44849 NONLINEAR OSCILLATIONS OF AN ELECTRONIC GAS IN THE MAGNETIC FIELD. Levin, V. A. Vestn. Mosk. Univ., Ser. II: Khim., 20: 62-6(1965). (In Russian).

Cylinder-type oscillations of electrons in cold plasma when the outer magnetic field is present are treated. A class of motions is also described with the pressure under homogeneous deformation taken into account. (auth)

44850 SOME REDUCIBLE MAGNETOGASDYNAMIC FLOWS. Power, G.; Walker, D. (Univ. of Nottingham, Eng.). Z. Angew. Math. Mech., 45: 87-93(May 1965).

Certain steady, rotational, three-dimensional, compressible flows of a gas with infinite electrical conductivity are considered. It is shown that these magnetogasdynamic flows can be linked to associated two-dimensional gasdynamic flows with zero magnetic field which in turn are linked by reciprocal relations to four-parameter classes of rotational gas flows. Simple examples are given showing the relation between the magnetogasdynamic and the associated two-dimensional gasdynamic flows. (auth)

44851 THEORETICAL INVESTIGATIONS ON THE POSSIBILITY OF STIGMATIC CORPUSCULAR-OPTICAL FOCUSING BY RANDOM STATIONARY SPACE-LIMITED ELECTRIC-MAGNETIC FIELDS. Kasper, Erwin (Universitaet, Tuebingen, Ger.). Z. Angew. Phys., 19: 112-20 (1965). (In German).

A general paraxial orbital equation for particles of uniform mass, charge, and energy in space-charge free field was established. A (in general curved) particle orbit was selected as "axis." The two-parametric totality of the orbits going out from a point of the axis (source point) was not stigmatically focused in the general case. A variation of the place of the source point along the axis leads, in general, not to a fulfillment of the conditions for stigmatic focusing. In order to obtain such an image and therefore a paraxial affine image, at least two suitable, independent of each other, continuously variable parameters (source point coordinates, field strength parameter, field form parameter, etc.) must be available. The geometric site of all stigmatic focusing source point is in the rule as a space curve. (tr-auth)

44852 ON CYLINDRICAL IMPLODING SHOCK WAVES. Lee, John H.; Lee, Benedict H. K. (McGill Univ., Montreal). 21p. (CONF-650435-3). Gmelin, AED-CONF-65-097-16.

From 5th Shock Tube Symposium, Silver Spring, Md.

A technique for producing imploding cylindrical shock waves through imploding detonation waves is described. It is found that using the present method of initiation, symmetrical cylindrical imploding detonation waves can be produced in equi-molar acetylene-oxygen mixtures at initial pressures above 150 mm Hg. Due to the effect of area convergence, the detonation wave becomes increasingly overdriven as it implodes towards the center. In the limit, the highly overdriven detonation wave approaches a strong shock wave. Pressure measurements at different radii from the center of symmetry indicate this self-amplifying characteristic of imploding detonation waves. Close agreement between the experimentally measured detonation pressures and those calculated by the Chester-Chisnell-Whitham method is obtained. (auth)

44853 SHOCK FRONT CURVATURE AT INITIAL PRESSURES UP TO 700 mm Hg. Mazzella, A. T. (Univ. of Maryland, College Park); de Boer, P. C. T. 16p. (CONF-650435-6). Gmelin, AED-CONF-65-097-7.

From 5th Shock Tube Symposium, Silver Spring, Md.

Axial extents of curved shock fronts in argon were measured using thin film heat transfer gauges mounted on a plate perpendicular to the axis of a 1½" diameter shock tube. In interpreting the data, use was made of the theoretical shock shape. This shape was determined from previously derived formulas which apply when the boundary layer behind the shock is either laminar or turbulent, and which account in an approximate way for the influence of the flow at the foot of the shock. At low initial pressures the experimental data obtained agree well with theory and with results of other investigators. For initial pressures above 100 mm Hg the data showed appreciable scatter, which is taken to indicate that the shock is oscillating in curvature. The scatter has the order of magnitude which follows from Freeman's theory for the damping of perturbations in shock shape, with the assumption that somewhere near the diaphragm the shock is strongly curved.

Variations in shock tilt were generally less than 0.003 radian. (auth)

44854 TRANSPORT PROPERTIES OF PARTIALLY IONIZED MONATOMIC GASES. De Voto, R. S. (Stanford Univ., Calif.). New York, American Inst. of Aeronautics and Astronautics, 1965, Preprint No. 65-540, 12p., $1.00. (CONF-650711-23). ORINS.

From AIAA 2nd Annual Meeting and Technical Demonstration, San Francisco.

Information on the methods used to determine the collision cross sections between the various particles in a partially ionized gas is given, calculations are made of the transport properties for argon in thermodynamic equilibrium, and the results for the viscosity, thermal conductivity, and diffusion coefficients are plotted. The possibility of carrying out the computations of the transport coefficients in the third and fourth approximation is also shown. The results are discussed. (L.B.S.)

44855 INTERFEROMETRIC MEASUREMENT OF THE VIBRATIONAL RELAXATION TIME IN HYDROGEN–ARGON MIXTURES. Wachsler, Emanuel (Cornell Univ., Ithaca, N. Y.). 12p. (CONF-650435-5). Gmelin, AED-CONF-65-097-5.

From 5th Shock Tube Symposium, Silver Spring, Md.

High resolution of the relaxation zone behind an incident shock wave was obtained by the use of a laser light source in conjunction with a Mach-Zehnder interferometer. The experimental setup consisted of a square, pressure-driven shock tube, 15 feet long and 1.654 inches across. The interferometer was set up in a double pass mode. The ruby laser, cooled to liquid nitrogen temperature, produced a continuous light pulse of 200 microsec. duration. A beam splitter was inserted to provide two pictures of the flow field with different time resolutions. A 0.1 microsec. Kerr cell shutter permitted direct photography of the density distribution in the relaxation zone. The image of the test section was also focused onto a 0.001 inch slit and then into a drum camera. The drum camera picture resolved the relatively slow density changes, and permitted us to measure the shock velocity and to check on the presence of disturbances. This setup was developed principally to study diatomic dissociation reactions. The vibrational relaxation time in hydrogen–argon mixtures was measured over the temperature range of 1300–1900°K. The values obtained for H_2–H_2 collisions, assuming that argon is completely ineffective as a collisional partner, are in good agreement with theoretical calculations by M. Salkoff and E. Bauer. (auth)

44856 EQUATIONS OF MOTION IN NONEQUILIBRIUM STATISTICAL MECHANICS. Robertson, Baldwin (Cornell Univ., Ithaca, N. Y.). 38p. (CONF-641210-23). Gmelin, AED-CONF-64-236-40.

From American Physical Society Meeting, Berkeley, Calif.

Exact equations of motion for the space- and time-dependent thermodynamic coordinates of a many-body system are derived directly from the Liouville equation. This is done by defining a generalized canonical density operator depending only upon present values of the thermodynamic coordinates. This operator is used no matter how far the system is from equilibrium. An explicit expression for the entropy of a system possibly not in equilibrium is given in terms of this operator. The equation of motion for the operator is derived, and the coupled, nonlinear, integro-differential equations of motion for the thermodynamic coordinates follow immediately. (auth)

44857 IONIZING SHOCK STUDIES IN AN ELECTROMAGNETICALLY DRIVEN SHOCK TUBE. Miller, B.; Levine, L.; Gross, R. A. (Columbia Univ., New York). 17p. (CONF-650435-4). Gmelin, AED-CONF-65-097-6.

From 5th Shock Tube Symposium, Silver Spring, Md.

A description is given of a one-meter long coaxial electromagnetic shock tube, the associated components and instrumentation used in ionizing shock studies which include photomultipliers, magnetic field probes, and electric field probes. Some typical experimental results are briefly discussed. (L.B.S.)

Accelerators

Refer also to abstracts 44482, 44635, and 45674.

44858 (BNL-9480) THE HIGH MAGNETIC FIELD LIMIT IN SYNCHROTRONS. Dahl, P. F.; Parzen, G. (Brookhaven National Lab., Upton, N. Y.). [1965]. Contract AT(30-2)-Gen-16. 11p. Dep. mn; CFSTI $1.00 cy, $0.50 mn.

The SIBYL program is used to compute the magnetic field shapes for the Brookhaven AGS at field levels of 13, 14, and 15 kOe. The particle orbits at these levels are then investigated with the PARMESH program. From the computer results, it is found that fields as high as 15 kOe may be used with no sextupole correction and very little quadrupole correction, and that the beam radius under these conditions is about 0.3 in. These results are based on several assumptions. (T.F.H.)

44859 (BNL-9496) COUPLING ELEMENTS IN EQUIVALENT CIRCUIT FOR CAVITY CELLS. Gluckstern, R. L. (Brookhaven National Lab., Upton, N. Y.). Aug. 20, 1965. Contract AT-30-2-GEN-16. 13p. Dep. mn; CFSTI $1.00 cy, $0.50 mn.

For the treatment of fields in a cavity consisting of a chain of coupled cells in the presence of losses, drive input, bunched beam, and cell-to-cell errors, an equivalent circuit was derived from Maxwell's equations which were set up to satisfy the power relations and to give the correct Q. Approximate values for the coupling reactances in the small coupling hole approximation were obtained from this equivalent circuit. Approximate expressions were also obtained for the losses, including coupling effects, for various modes. (M.O.W.)

44860 (IAE-614) REKONSTRUKTSIYA LINEINOGO USKORITELYA ELEKTRONOV INSTITUTA ATOMNOI ENERGII. (Redesign of the IAE Linear Electron Accelerator). Flerov, N. N.; Lipatov, V. P.; Aref'ev, A. V. (Institut Atomnoi Energii, Gosudarstvennyi Komitet po Ispol'zovaniyu Atomnoi Energii SSSR, Moscow). 1964. 24p. Dep. mn.

The redesign of the electron linear accelerator, resulting in an increase in the average neutron yield by a factor of 10, is described. The operational reliability of the machine and the stability of yield were significantly increased. The accelerator operates 10 to 12 hr/day with maximum pulse frequency 100/sec in the triode mode with pulse length 0.6 and 0.2 μsec. A uranium target with water moderator serves as the neutron source. The capacity of the neutron source is at the present time about 10^{12} n/sec. Increasing the source yield enabled a series of physical experiments, which formerly could not be performed, to be set up and carried through. (tr-auth)

44861 (IAE-795) USTANOVKA IMPUL'SNYE MAGNITNYE POLYA. (Pulsed Magnetic Fields Apparatus). Makar'in, V. K.; Martem'nov, V. P. (Institut Atomnoi Energii, Gosudarstvennyi Komitet po Ispol'zovaniyu Atomnoi Energii SSSR, Moscow). 1965. 21p. Dep.mn.

Apparatus for obtaining pulsed magnetic fields in the operating conditions at contemporary elementary-particle accelerators is described. The apparatus consists of a charging device, an energy storage device, a discharge mechanism, and pulsed magnets. Pulsed magnetic fields of $\overline{H}$ = 65 kOe in a volume of 12 liters and $\overline{H}$ = 100 kOe in a volume of 8 liters were obtained using the apparatus described. (tr-auth)

44862 (IAE-867) PUCHOK NEITRONOV DLYA IZMERENIYA SECHENII RASSEYANIYA NA MALYE UGLY (Neutron Beam for Measuring Scattering Cross Sections at Small Angles). Gorlov, G. V.; Kirillov, A. I.; Lebedeva, N. G. (Institut Atomnoi Energii Gosudarstvennyi Komitet po Ispol'zovaniyu Atomnoi Energii SSSR, Moscow). 1965. 9p. Dep. mn.

The construction of a cooled rotating target and a collimator with variable aperture angle is described, intended for obtaining a narrow beam of medium-energy neutrons suitable for measuring differential scattering cross sec-

tions of neutrons at small angles (to angles of ~0.5°). A graph is presented of results of measuring the shape of a collimated neutron beam of energy $E_n = 4$ Mev at a collimator aperture angle of 1° (solid angle $\sim 4 \times 10^{-4}$ sterad). The distribution obtained for the neutron flux density in the beam has practically a right-angle shape; the total neutron flux from the collimator is 4×10^5 neutrons/sec. (The deuteron energy $E_d = 1400$ kev; the energy loss in the layer of heavy ice $\Delta E = 400$ kev; the deuteron current is 40 μamp; the total emission of the target is 1.7×10^9 neutrons/sec.) (tr-auth)

44863 (JINR-P-2231) OTSENKA UROVNEI IONIZIRUYUSHCHEGO IZLUCHENIYA VBLIZI SINKHROFAZOTRONA JINR Na 10 Gev. (An Estimation of Ionizing Radiation Levels Near the 10 Gev Synchrophasotron of the Joint Institute for Nuclear Research). Komochkov, M. M.; Lebedev, V. N. (Joint Inst. for Nuclear Research, Dubna (USSR)). 1965. 12p. Dep. mn.

The levels of different radiation components around the JINR 10 Bev synchrophasotron were estimated. The results of these estimates are presented. Possible sources of radiations are considered with account of some specific characteristics of the shielding geometry. The results of the calculation are in good agreement with experimental data. (auth)

44864 (JINR-P-2253) KINETIKA PROTSESSA MNOGOKRATNOGO USKORENIYA CHASTITS S PERMENNYM ZARYADOM V POTENTSUALNOM ELEKTRICHESKOM POLE. (Kinetics of the Multiple Acceleration of Particles with Variable Charge in a Potential Electric Field). Vyalov, G. N.; Fiks, M. M. (Joint Inst. for Nuclear Research, Dubna (USSR). Lab. of Nuclear Reactions). 1965. 10p. Dep. mn.

The kinetic equation was obtained as a function of the particle distribution during multiple acceleration in a potential electrical field. Using the Fokker- Planck approximation a solution was found for the kinetic equation. The coefficient of particle capture into the multiple acceleration regime is calculated. (auth)

44865 (LAL-1134) ETUDE DE QUELQUES PHENOMENES STOCHASTIQUES DANS LES ANNEAUX DE STOCKAGE (THESE). (Study of Some Stochastic Phenomena in Storage Rings (thesis)). Le Duff, J. (Paris Univ., Orsay (France). Faculte des Sciences). Apr. 1965. 105p. Dep. mn.

The different phenomona of an uncertain character which create an enlargement of the beams and diffusion losses in the stability region are studied. The general method of study used is that used in the theory of Brownian motion, in the kinetic theory of gases, and in plasma physics. An evolution equation is deduced by extension of the Liouville theorem to the case where there is a Hamiltonian disturbed by a non-conservative force which corresponds to a fluctuation term. A stationary solution of the Fokker-Planck equation and the dimensions of the beam in an electron storage ring are deduced by superposing the quantum fluctuations of the radiation of the dampening due to classical radiation. The Kramers' resolution method is used to define the rate of the particle loss. Among the different random phenomona concerned with the fluctuations of the longitudinal energy, the Toucheck effect is emphasized. This is caused by multiple collisions at the interior of one bundle, and it is preponderant at low energies although the quantum effects become sensitive only at higher energies. The multiple bremsstrahlung with the residual gas and during the beam-beam interaction is then studied. (J.S.R.)

44866 (LNF-65/21) PRODUZIONE E SCARICO DI GAS TOSSICI E RADIOATTIVI NEL TUN NEL DEL LINAC DI FRASCATI. (Production and Discharge of Toxic and Radioactive Gas in the Tunnel of the Frascati Linac). Note No. 282. Ladu, M.; Pelliccioni, M.; Roccella, M. (Laboratori Nazionali di Frascati, Comitato Nazionale per l'Energia Nucleare (Italy)). June 28, 1965. 12p. Dep. mn.

Among the other safety problems associated with high-power linear accelerators is that of the production of the toxic gases NO_2 and O_3 and of the nuclides ^{15}O, ^{13}N, and ^{38}Cl. The production in the tunnel of the Frascati linear accelerator of these toxic or radioactive gases is calculated. The results obtained seem to exclude the creation of dangerous situations. (J.S.R.)

44867 (MURA-713) THE DESIGN OF PROTON LINEAR ACCELERATORS FOR ENERGIES UP TO 200 Mev. Austin, B.; Edwards, T. W.; O'Meara, J. E.; Palmer, M. L.; Swenson, D. A.; Young, D. E. (Midwestern Universities Research Assn., Stoughton, Wis.). July 1, 1965. Contract AT(11-1)-384. 164p. Dep. mn; CFSTI $5.00 cy, $1.00 mn.

A study of proton linear accelerators of energy up to 200 Mev using drift tube loaded cavities resonant at 200 Mc is described. Such an accelerator is useful as an injector for a high-energy synchrotron. Two computer programs were used extensively in this study; one was used to calculate the resonant frequency and r-f fields in the appropriate linear accelerator geometry, and the other was used to calculate particle motion in the accelerator. From the field computational program a variety of resonant cavity configurations was investigated, and an optimum structure was chosen on the basis of minimizing the r-f power costs and the structure length costs. Several optimized sets of parameters for a linear accelerator are given. More detailed studies were done on one of the sets of parameters including particle dynamics studies. Tables of drift tube dimensions are given. From the specification of parameters, mechanical engineering studies were made to evolve a design which can be fabricated and from which realistic construction costs can be estimated. Some details of mechanical models constructed to test design features are given. (auth)

44868 (NIRL/R/86) DESIGN OF THE BEAM DEFLECTION SYSTEM FOR THE HARWELL VARIABLE ENERGY CYCLOTRON. Randle, T. C. (National Inst. for Research in Nuclear Science, Chilton (England). Rutherford High Energy Lab.). Mar. 1965. 19p. Dep.; BIS $0.60; HMSO 3s.

The various factors considered during the design of the electrostatic deflector for the VEC are described. The deflector has vertical shaped electrodes to control the radial dispersion of the beam. Further focusing is required after the beam leaves the deflector, and for this purpose a magnetic channel and wedge are compared. (auth)

44869 (NIRL/R/87) THE CENTRAL REGION OF THE VARIABLE ENERGY CYCLOTRON MAGNET. Trew, D. H. (National Inst. for Research in Nuclear Science, Chilton (England). Rutherford High Energy Lab.). Mar. 1965. 13p. Dep.; BIS $0.50; HMSO 2s. 6d.

A rotatable, slotted plug with three fold symmetry is used at the center of each pole piece; this permits the axially inserted ion-source to be located off-center. Measurements show that the first harmonic from the plug system is less than 0.5 Oe, and from the pole piece is less than 3.5 Oe for radii less than 10 inches. Small differences were found between the model and the V.E.C. magnet measurements of the mean field and flutter; these are described and discussed. Field fitting calculations show that satisfactory phase and focusing characteristics exist over the field range 5,000–17,000 Oe. (auth)

44870 (NP-15388) FOKUSIROVKA INTENSIVNOGO ELEKTRONNOGO PUCHKA V USKORITEL'NOI TRUBKE. (Intensive Electron Beam Focusing in an Accelerator Tube). Meshkov, I. N.; Chirikov, B. V. (Akademiya Nauk SSSR, Novosibirsk. Institut Yadernoi Fiziki). 1965. 25p. Dep. mn.

Correct focusing is the most important task when allowing an electron beam to pass through a straight accelerator tube, in order to keep the diameter of the tube as small as possible and to reduce the angular scatter of the beam. Although the general problem of beam focusing has been studied to a great extent, the dynamics of relativistic beams under consideration of its own field and in the presence of a longitudinal accelerating field has not been examined before. The calculations were based on the equa-

tion of motion, considering axially symmetric and band geometry. It was thereby assumed that the beam possesses a laminar character, i.e., the trajectory is not intersected and is sufficiently sharply confined in the transversal direction. Thus, only the motion of the boundary electron had to be considered. Calculations were carried out for the unaccelerated beam, for acceleration in a homogeneous field and for focusing by a periodic field. An expression was obtained for the limiting current that may be accelerated in a given tube without spreading. For $E_0 \sim 10^4$ v/cm and a tube radius of 1 cm, this value was found to be ~2 amp. (TTT)

44871 (PPAD-2137-556) THE EXTERNAL PROTON BEAM FOR THE PRINCETON–PENNSYLVANIA ACCELERATOR. Kirchgessner, J.; Benoit, J. W.; Shoemaker, F. C. (Princeton–Pennsylvania Accelerator, Princeton, N. J.). Aug. 1, 1965. Contract AT(30-1)-2137. 20p. (CONF-650923-1). Dep. mn; CFSTI $1.00 cy, $0.50 mn.

From 5th International Conference on High Energy Accelerators, Frascati, Italy.

The proton beam from the Princeton-Pennsylvania Accelerator was extracted by a method similar to that used on the Electron Synchrotron at Frascati. In this method the $\nu_r = 2/3$ betatron resonance is excited by a second harmonic in the synchrotron field gradient. Both the excitation of the $\nu_r = 2/3$ oscillations and the tuning of the synchrotron magnet to this resonance are accomplished with four modified "hexapole" magnets placed in short straight sections around the machine. These magnets are programmed to control the beam spill. A betatron "oscillation driver" is used to ease the precision requirements on the tune of the synchrotron to resonance. After the beam oscillations have reached sufficient amplitude, the final extraction is accomplished with a plunged septum magnet. This magnet has a peak field of 14 kilogauss. The beam will be led from the machine with a series of DC and programmed, dipole and quadrupole magnets. Some diagrams of the apparatus are presented. (auth)

44872 (PPAD-2137-565) OPERATING EXPERIENCE AND IMPROVEMENTS ON THE PRINCETON–PENNSYLVANIA ACCELERATOR. Allen, H. L.; Awschalom, M.; Droege, T.; Isaila, M.; Kang, C. L.; Kirchgessner, J.; Riedel, J.; Shoemaker, F. C.; Tomlinson, E. P.; White, M. G. (Princeton–Pennsylvania Accelerator, Princeton, N. J.). Aug. 24, 1965. Contract AT(30-1)-2137. 17p. (CONF-650923-2). Dep. mn; CFSTI $1.00 cy, $0.50 mn.

From 5th International Conference on High Energy Accelerators, Frascati, Italy.

Previous applications of the Princeton-Pennsylvania Accelerator PPA are briefly discussed. New developments for the PPA are reported. Future developments for new applications are proposed. (M.O.W.)

44873 (UCRL-16000(Summ.)) 200 Bev ACCELERATOR DESIGN STUDY. (Lawrence Radiation Lab., Univ. of California, Berkeley). June 1965. Contract W-7405-eng-48. 26p. Dep. mn; CFSTI $2.00 cy, $0.75 mn.

A design study for a 200-Bev strong-focusing proton synchrotron is summarized. The accelerator, designed to provide 3×10^{13} protons/pulse, is described, together with the associated facilities. (D.C.W.)

44874 (UCRL-16203) BEVATRON OPERATION AND DEVELOPMENT. 44. [Quarterly Progress Report], October–December 1964. Allison, Robert W. Jr.; Crebbin, Kenneth C.; Everette, William L.; Lothrop, Fred H. G.; Zajec, Emery (Lawrence Radiation Lab., Univ. of California, Berkeley). June 23, 1965. Contract W-7405-eng-48. 20p. Dep. mn; CFSTI $1.00 cy, $0.50 mn.

The Bevatron provided beam for physics research 85% of the scheduled operating time. The only shutdowns were during the normal weekly maintenance periods and holiday periods. Most of the Bevatron study periods were devoted to injection and alignment studies of the injection system. A beam-spilling device using feedback from the beam-induction-electrode system to control the r-f voltage was put into operation. (auth)

44875 (UCRL-16229) DERIVATION OF CORRECTIONS TO CONTROL THE CLOSED ORBIT IN AN ALTERNATING-GRADIENT SYNCHROTRON. Lambertson, G. R.; Laslett, L. Jackson (Lawrence Radiation Lab., Univ. of California, Berkeley). Aug. 31, 1965. Contract W-7405-eng-48. 22p. (CONF-650923-4). Dep. mn; CFSTI $1.00 cy, $0.50 mn.

From 5th International Conference on High Energy Accelerators, Frascati, Italy.

The control of the position of the closed orbit in an alternating-gradient synchrotron by displacement of the magnet structure was studied using a 200-Bev proton synchrotron as a model. (D.C.W.)

44876 (UCRL-16287) ON THE CALCULATION OF NONLINEAR MAGNETOSTATIC FIELDS. Concus, Paul (Lawrence Radiation Lab., Univ. of California, Berkeley). July 21, 1965. Contract W-7405-eng-48. 9p. (CONF-650922-7). Dep. mn; CFSTI $1.00 cy, $0.50 mn.

From 1st International Symposium on Magnet Technology, Stanford, Calif.

The numerical solution of the second-order, elliptic, quasi-linear, partial differential equations that arise in two-dimensional magnetostatic field problems where the permeability varies with the field is considered. A method for solving these problems is outlined, which is based on the iterative solution, by nonlinear successive overrelaxation, of a set of nonlinear difference equations approximating the original differential equation. (D.C.W.)

44877 (UCRL-16346) THE FEASIBILITY OF A LOW-FIELD SUPERCONDUCTING THIN-SEPTUM MAGNET. Green, Michael A. (Lawrence Radiation Lab., Univ. of California, Berkeley). Aug. 16, 1965. Contract W-7405-eng-48. 11p. (CONF-650922-1). Dep. mn; CFSTI $1.00 cy, $0.50 mn.

From 1st International Symposium on Magnet Technology, Stanford, Calif.

Stability and design criteria for a superconducting thin-septum magnet operating at fields up to 15 kOe are outlined. The effects of beam impingement on magnet performance are discussed. (T.F.H.)

44878 (UCRL-16375) COLLINS QUADRUPOLE MAGNETS AND SEXTUPOLE MAGNETS FOR A 200-Gev PROTON SYNCHROTRON. Kilpatrick, Robert A. (Lawrence Radiation Lab., Univ. of California, Berkeley). Aug. 26, 1965. Contract W-7405-eng-48. 10p. (CONF-650922-6). Dep. mn; CFSTI $1.00 cy, $0.50 mn.

From 1st International Symposium on Magnet Technology, Stanford, Calif.

The quadrupole and sextupole magnet designs developed for a 200-Bev proton synchrotron are described. (D.C.W.)

44879 (AEC-tr-6607) THE EFFECT OF MAGNETIC SCREENS WITHIN THE INTERBLOCK GAPS ON THE ITEP (INSTITUTE OF THEORETICAL AND EXPERIMENTAL PHYSICS) PROTON SYNCHROTRON. Simonov, B. I.; Skachkov, S. V.; Shchegolev, V. A. (Gosudarstvennyi Komitet po Ispol'zovaniyu Atomnoi Energii SSSR, Moscow. Institut Teoreticheskoi i Eksperimental'noi Fiziki). Translated from report No. 270. 10p. Dep. mn; CFSTI $1.00 cy, $0.50 mn; JCL $1.10 fs, $0.80 mf.

The influence of screening the beam from the stray magnetic field within the straight sections between the adjacent blocks of the ITEP proton synchrotron on the acceleration process was investigated. It is shown that the screening of two gaps mutually separated by 4 blocks, does not significantly affect the operation of the accelerator. (auth)

44880 ELECTRON CURRENT RELEASE CHARACTERISTICS OF A HIGH FREQUENCY ION SOURCE WITH MESH GRID. Tsuchimoto, Takashi (Hitachi Central Research Lab., Tokyo). Japan. J. Appl. Phys., 4: 458-60 (June 1965).

Electron current was observed from a high frequency ion source with mesh grid in a similar way to get ion beam current. The experimental results suggest that the main cause is the extraction of electrons by the convergence electrode from a plasma, which is formed by an ion beam in the extraction canal and in the convergence pipe. (auth)

44881 SELF-ABSORPTION AND SELF-SCATTERING EFFECTS IN THE BETA PARTICLES SOURCES. Oldano, C.; Pasquarelli, A. (Istituto di Fisica Sperimentale del Politecnico, Turin). Nucl. Instr. Methods, 36: 192-6(Oct. 1965).

A formula is suggested that allows the evaluation of self-absorption and self-scattering in wide sources of beta particles. This formula takes account of the anisotropy in the angular distribution of beta particles emitted by wide sources. Therefore the formula given the possibility of determining the absolute activity of the source when to detect beta particles a counter is used having geometry lower than 2π, such as the end-window Geiger-Müller counter. (auth)

44882 PROPOSED METHODS FOR PRODUCING INTENSE PULSED BEAMS OF MONO-ENERGETIC NEUTRONS. Grodzins, L. (Massachusetts Inst. of Tech., Cambridge); Rose, P. H.; Van de Graaff, R. J. Nucl. Instr. Methods, 36: 202-12(Oct. 1965).

The methods described utilize time-of-flight and extended targets to produce bunched beams of mono-energetic neutrons. It would appear that bunching, factors of several hundred could be achievable by combinations of these techniques. (auth)

44883 AN IMPROVED STRIP SEALED CONTINUOUS ROTATION SCATTERING CHAMBER. Hawrylak, R. A.; Cline, D.; Grube, D. F. (Univ. of Rochester, N. Y.). Nucl. Instr. Methods, 36: 237-40(Oct. 1965).

An improved design is described of an evacuated chamber having two ports in a horizontal plane. The angle between these ports can be changed continuously through an angular range of 180° from −10° to +170° without disturbing the high vacuum maintained inside. A flexible-strip sealed slot is employed, with refinements that result in reliable operation. (auth)

44884 ELECTRONIC REGULATION OF EMISSION CURRENT OF A PULSED INJECTOR FOR 200kv. Heinz, W.; Einenkel, H. (Universitaet, Berlin). Nucl. Instr. Methods, 36: 337-8(Oct. 1965). (In German).

An injector for a FFAG electron synchrotron with a pulse current of 10 amp for a duration of ~1 μsec with a pulse voltage of 200 kv was developed. The beam production system of the injector is a space-charge-limited Pierce gun. A schematic representation of the possible working points of the beam production system is presented, and two possibilities for its control are discussed. Changes in primary voltage cause coarse control and changes in the shock voltage between the cathode and spiral cause fine control. Electronic equipment for bringing about this control is discussed. (M.C.G.)

44885 PRELIMINARY RESULTS FROM A SINGLE GAP PREINJECTOR. Wroe, H. (Rutherford High Energy Lab., Chilton, Eng.). Nucl. Instr. Methods, 36: 345-6(Oct. 1965).

A preinjector for a proton linear accelerator is described in which hydrogen ions are accelerated to several hundred kv across a single gap from a large area of plasma. The plasma is produced by a PIG discharge. (T.F.H.)

44886 STATE OF CONSTRUCTION OF THE RELATIVISTIC CYCLOTRON FOR PROTONS AT 45 Mev. Acerbi, E.; Castiglioni, M.; Fois, M.; Luccio, A.; Merzagora, N.; Resmini, F.; Succi, C.; Tagliaferri, G. (Universita, Milan; Istituto Nazionale di Fisica Nucleare, Milan). Nuovo Cimento (1), 2: Suppl., 567-83(1964). (In Italian).

The relativistic cyclotron of the University of Milan belongs to the category of fixed-frequency cyclotrons with variable azimuthal field and to the Thomas strong focusing type. The fabrication of the most important components of the cyclotron, the methods of measurement, and the calculations made for the realization of the magnetic field are described. (J.S.R.)

44887 THE RESULTS OF ADJUSTMENT OF THE 1.5-M CYCLOTRON, FEI. Krasnov, N. N.; Mozhin, A. N.; Ognev, A. A.; Ponomarev, A. A. (Inst. of Physics and Power Engineering, State Atomic Energy Commission, USSR). Pribory i Tekhn. Eksperim., No. 4, 22-5(July-Aug. 1965). (In Russian).

A brief description is given of the FEI cyclotron of the U-150 type and its operational regime. The methods for the calculation of the phase motion of the particles and the focusing intensity are explained. (tr-auth)

44888 A DEVICE FOR DEVELOPING PULSED MAGNETIC FIELDS UP TO 150 kG. Akhmanov, V. V.; Barkov, L. M.; Bobikov, R. S.; Dobretsov, Yu. P.; Zamolodchikov, B. I.; Nikol'skii, B. A.; Sokolov, B. V.; Khakimov, S. Kh.; Shestakov, V. D. (Inst. of Nuclear Energy, Moscow). Pribory i Tekhn. Eksperim., No. 4, 182-7(July-Aug. 1965). (In Russian).

A device for the production of pulsed magnetic fields at voltages of 146 kgauss in a volume of approximately 600 cm^3 was described. For supply of the pulsed magnets manufactured of Be bronze, battery condensors with surface area of 0.1 f were used; these batteries across a limited resistance were charged from thyratron rectifiers to 2 kv. Synchronization and control systems for combined work with pulsed magnets and synchrocyclotrons were described. (tr-auth)

44889 VERTICAL SHIFT OF A BEAM IN A CYCLOTRON WITH INCONGRUENT MAGNETIC AND ELECTRIC PLANES. Krasnov, N. N.; Mozhin, A. N.; Ognev, A. A.; Ponomarev, A. A. (Inst. of Physics and Power Engineering, Obninsk, USSR). Pribory i Tekhn. Eksperim., No. 4, 219-21(July-Aug. 1965). (In Russian).

It was shown that a small displacement of the mean magnetic plane with respect to the electric plane leads to a substantial vertical shift of the beam if this takes place on the radius where the particles pass through accelerating apertures at negative values of the voltage. The theoretical values were compared to the experimental results. One method for the elimination of this effect—nonsymmetrical external shimming—is indicated. (tr-auth)

44890 PRODUCING HIGH VELOCITY CHARGED PARTICLES. Van de Graaff, Robert Jemison (to High Voltage Engineering Corp.). British Patent 1,000,811. Aug. 11, 1965. Filed July 17, 1961.

An apparatus provided for the acceleration of charged particles includes an accelerator arranged in a single tank and at least two high voltage terminals, at least one of which includes a charge transfer device. The high voltage terminals are supported centrally within a column having a multiplicity of insulating annuli inserted between apertured electrically conductive disks forming equipotential planes. The apertures within the annuli and within the disks are aligned with each other to form an acceleration tube, and the space within the tube is evacuated. The annuli and disks form the sole support of the column, and a single endless insulated charge-carrying belt is arranged to pass through the column to operate between pulleys at each end. The three principal advantages derived from the use of the charge transfer process are (1) multiple use of the available d-c voltage, (2) external and grounded ion injector, and (3) the use of multiple charged positive ions. (B.L.M.)

44891 METHOD AND APPARATUS FOR PRODUCING HIGH VELOCITY CHARGED PARTICLES. Van de Graaff, Robert Jemison (to High Voltage Engineering Corp.). British Patent 1,000,812. Aug. 11, 1965. Filed July 17, 1961.

A method and apparatus are described for producing high velocity charged particles by producing and directing into a region of high positive potential low velocity positive ions, neutralizing some of the positive particles to form low velocity neutral particles of approximately the same velocity and direction, stripping electrons from some of the neutral particles within the region at positive high potential so as to form positive ions, and accelerating the positive ions away from the region of high positive potential. The apparatus includes a source of positive ions, a charge transfer device, a high positive voltage terminal having an electron stripping device within it, and means for directing positive ions from

the positive ion sources successively through the charge transfer and electron stripping devices. (B.L.M.)

44892 APPARATUS FOR THE ACCELERATION OF CHARGED PARTICLES. Van de Graaff, Robert Jemison (to High Voltage Engineering Corp.). British Patent 1,000,813. Aug. 11, 1965. Filed July 17, 1961.

An apparatus is provided for the acceleration of charged particles by means of high voltage and multiple stripping of electrons from the charged particles. Three charge states, negative, positive, or neutral, may occur in the present apparatus. The apparatus includes a high voltage positive terminal and a first stripping device adapted to remove a sufficient number of electrons from some of the particles so that they are left with at least a single electronic net positive charge. At least one further stripping device disposed posterior to and outside of the first stripping device removes additional electrons after the particles have acquired additional energy. A source of negative particles may also be provided. (B.L.M.)

Astrophysics and Cosmology

Refer also to abstracts 43927, 44970, 45176, and 45178.

44893 (NASA-CR-294) ENGINE OPERATING PROBLEMS IN SPACE. THE SPACE ENVIRONMENT. Christensen, D. (Aerojet-General Corp., Azusa, Calif.). Sept. 1965. Contract NAS 7-98. 226p. CFSTI $6.00 cy, $1.25 mn.

A comprehensive definition is presented of the space environment as it is presently known. For the purposes of this program, this environment consists of the solar system, excluding the earth and its inner atmosphere. Special emphasis is given to data on electromagnetic and particulate radiation, meteoroid flux, and the structure and composition of the planetary atmospheres. A list of 405 references is included, many of which are annotated. (auth)

44894 (AD-424481) X-RAY EMISSION OF FLARES ORIGINATING BEHIND THE SOLAR DISK. Solar Research Note No. 47. Vinogradov, Y. I.; Eryushev, N. N. Translated by Alice B. Dunn (Sacramento Peak Observatory, Sunspot, N. Mex.) from Izv. Krymsk. Astrofiz. Observ., 29: 141-5(1963). 6p.

It is noted that some sudden ionospheric disturbances have occurred at times when there were no visible flares on the solar disk. An explanation in terms of flares originating behind the limb of the solar disk is proposed. (D.C.W.)

44895 ON THE CREATION OF LARGE PARTICLE NUMBERS. Eder, G. (Universitaet Giessen, Ger.). Acta Phys. Austriaca, 19: 301-7(1965).

Two possibilities for the creation of large particle numbers within the order of magnitude as they are found in cosmic dimensions are discussed. These possibilities are creation by a direct interaction between two particles of high energy and creation by vacuum fluctuations. In conclusion, it is found that the creation of particles by the collision of elementary particles cannot be important within cosmic dimensions. But the observable universe seems to be one of very many subsystems which has an extraordinarily large effective baryon number, whereas nearly all other subsystems contain mainly neutrinos and photons. (J.F.P.)

44896 EFFECTS OF A SIMULATED SOLAR WIND ON THE PHOTOMETRIC PROPERTIES OF ROCKS AND POWDERS. Hapke, Bruce (Cornell Univ., Ithaca, N. Y.). Ann. N. Y. Acad. Sci., 123: 711-21(July 15, 1965).

The effects of solar wind on the photometric properties of rocks and rock powders were simulated by prolonged bombardment by 2-kv hydrogen ions. Each specimen was irradiated for a time sufficient to deposit of the order of 100 coulomb/cm^2 or approximately equivalent to 2×10^5 years on the moon. All of the naturally occurring rocks and powders were affected. Darkening was believed to be due to 3 separate mechanisms: chemical reduction by monatomic hydrogen, differential collection of sputtered material, and differential sputtering of heterogeneous materials. It was demonstrated that solar wind bombardment will drastically affect the color and albedo of rocky materials. Proton irradiation of fine rock powders changed their photometric characteristics to more closely resemble lunar characteristics. (M.C.G.)

44897 MAGNETOHYDROSTATIC RADIATIVE EQUILIBRIUM OF A GASEOUS MASS, OF PERFECT ELECTRICAL CONDUCTIVITY, WITH CYLINDRICAL SYMMETRY (SUN SPOTS). Ferrero, Giorgio M. Atti. Accad. Sci. Torino: I. Classe Sci. Fis., Mat. Nat., 99: 431-44 (1964-65). (In Italian).

The behavior of the pressure and the temperature of a sun spot that is assumed in magnetohydrostatic equilibrium under the action of a vertical magnetic field is studied. The effect produced on the same sun spot by a poloidal field is also studied. (tr-auth)

44898 OBSERVATIONS FOLLOWED AT THE ASTROPHYSICS OBSERVATORY OF ARCETRI DURING THE YEAR OF 1962. CICIG (Comm. Ital. Comit. Intern. Geofis.), Pubbl., IGC (Intern. Geophys. Comm.), No. 44, 1-65(1965). (In Italian).

The observations made at the Arcetri Astrophysics Observatory during 1962 included the visual observations of the the sun spots in white radiation, spectroscopic studies in Hα of the perturbations, visual and photographic observations in Hα_3 with monocromatic filter, observations of the solar radio emission at 225 MHz, and intensity of the atmospherics. The data on these observations are tabulated. (J.S.R.)

44899 OBSERVATIONS MADE AT THE ASTROPHYSICS OBSERVATORY OF ARCETRI DURING THE YEAR OF 1963. CICIG (Comm. Ital. Comit. Intern. Geofis.), Pubbl., IGC (Intern. Geophys. Comm.), No. 45, 1-64(1965). (In Italian).

The observations made at the Arcetri Astrophysics Observatory during 1963 included the visual observations of the sun spots in white radiation, spectroscopic studies in Hα of the perturbations, visual and photographic observations in Hα_3 with monochromatic filter, observations of the solar radio emission at 225 MHz, and intensity of the atmospherics. The data on these observations are tabulated. (J.S.R.)

44900 GALLIUM IN CHONDRITIC METEORITES. Greenland, L. (Univ. of California, San Diego, La Jolla). J. Geophys. Res., 70: 3813-17(Aug. 15, 1965).

Gallium was determined in ten carbonaceous, six enstatite, and six ordinary chondrites by a neutron activation technique. The following averages (ppm Ga) were obtained: enstatite chondrites, 15.6; type I carbonaceous chondrites, 13.3; type II carbonaceous chondrites, 10.0; type III carbonaceous chondrites, 8.9; ordinary chondrites, 5.4. The fractionation of gallium among these chondrite groups is very similar to that of germanium, and the fractionation of gallium between the sun and the carbonaceous type I chondrites is the same as that of iron. (auth)

44901 INTERPRETATION OF LUNAR ALPHA-SCATTERING DATA. Loomis, Alden A. (California Inst. of Tech., Pasadena). J. Geophys. Res., 70: 3841-9(Aug. 15, 1965).

Many ambiguities are inherent in the interpretation of chemical analyses if such analyses are used alone to interpret a rock genetically. Furthermore, rocks at the surface of the moon may differ from rocks below the surface because of contamination by meteoritic infall, bombardment by charged particles, and extensive mixing by impact. Nevertheless, the broad categories of igneous rocks and meteorites which are familiar on the earth are the best compositional models for rocks on the moon. Anhydrous igneous rocks and meteorites may be categorized on the basis of the atomic percentage of oxygen: (1) below 50%, sputtered rocks and those with free metal in excess of that in chondrites; (2) 50 to 56%, chondritic meteorites; (3) 57 to 58½%, dunites and olivine-rich peridotites; (4)

58½ to 60%, peridotites and pyroxenites; (5) 60 to 61%, basalts, some alkalic derivatives; (6) 61 to 64%, siliceous derivatives, some alkalic rocks. The Si/Na ratio is another reliable chemical parameter on which to base further subdivisions of genetic importance; terrestrial anhydrous igneous rocks and meteorites occupy well-defined fields in a plot of oxygen percentage versus Si/Na. The best parameter for resolving ambiguities in such a plot is the Mg/Si ratio. The concurrence of high Mg/Si and Mg/Na ratios with oxygen contents of over 59 to 60% will indicate water in the sample. The amount of water can be estimated by balancing the cations and anions in the actual analysis. (auth)

44902 HIGH-ENERGY SOLAR NEUTRONS. I. PRODUCTION IN FLARES. Lingenfelter, R. E. (Univ. of California, Los Angeles); Flamm, E. J.; Canfield, E. H.; Kellman, S. J. Geophys. Res., 70: 4077-86(Sept. 1, 1965).

The intensity and energy spectrum of neutrons above 1 Mev produced in the solar photosphere by flare-accelerated protons and α particles is calculated. The solar neutron yield from accelerated particles on helium is found to exceed the yield from evaporation and spallation in heavier elements for incident energies above about 30 Mev and continues to dominate until about 1 Bev. At higher bombarding energies, the p, π^+n reaction in hydrogen is the main neutron source. More than 90% of the total solar neutron production is from knock-on reactions by protons in hydrogen and helium. Owing to this relatively high ratio of knock-on to evaporation neutrons, the solar neutron spectrum is much higher in energy than the spectrum of secondary neutrons produced in the earth's atmosphere by galactic cosmic rays. A Monte Carlo calculation is performed to determine the solar neutron flux escaping into space. (auth)

44903 HIGH-ENERGY SOLAR NEUTRONS. II. FLUX AT THE EARTH. Lingenfelter, R. E. (Univ. of California, Los Angeles); Flamm, E. J.; Canfield, E. H.; Kellman, S. J. Geophys. Res., 70: 4087-95(Sept. 1, 1965).

The intensity and energy spectrum of solar neutrons at the earth relative to the flux of solar protons observed during the last solar cycle is calculated, using the solar neutron production spectrum obtained previously. The time-average solar neutron flux above 10 Mev at 1 AU over the last solar cycle is found to be 3×10^{-3} neutron/cm^2 sec, with a peak intensity at 30 to 40 Mev. This solar neutron flux is comparable to the neutron leakage flux above 10 Mev produced by interactions of galactic cosmic rays with the earth's atmosphere, indicating that solar neutrons may be competitive with leakage neutrons as a source of high-energy decay protons and electrons in the earth's radiation belts. Several anomalous features of the radiation belts are qualitatively consistent with a solar neutron source of the calculated intensity and spectral shape. Following individual major flares, essentially monochromatic bursts of solar neutrons should be observable at high altitudes and latitudes, but no sea-level effects are expected. The search for solar neutrons should be pursued with a counter sensitive above 10 Mev, carried in a satellite in equatorial orbit during the first hour after a major flare. (auth)

44904 AN INVISCID MODEL OF THE SOLAR WIND. Whang, Y. C.; Chang, C. C. (Catholic Univ. of America, Washington, D. C.). J. Geophys. Res., 70: 4175-80(Sept. 1, 1965).

The inviscid model of the solar wind is studied under the assumption that the total energy is transported entirely by convection of kinetic energy at infinity. The exact solution is obtained for all values of the heliocentric distance r, and the quantitative physical implication of this solution is discussed. (auth)

44905 A SEARCH FOR GAMMA-RAY POINT SOURCES. Fichtel, C. E.; Kniffen, D. A. (Goddard Space Flight Center, Greenbelt, Md.). J. Geophys. Res., 70: 4227-34 (Sept. 1, 1965).

A search for point sources of γ rays was made using oriented nuclear emulsions flown on high altitude balloons. The energy range examined was from 10 to 2×10^3 Mev, and the detection efficiency in the 10- to 50-Mev region averaged about 10%, which is almost a factor of 10 greater than that of previous experiments with counter systems. No measurable flux of γ radiation was observed for the regions of the sky examined, which included Cygnus A, the Spiral Arm In, Taurus A, Gemini, the Sun, and the Galactic Anticenter. A summary of the results of this and other experiments and theoretical considerations strongly suggest the need for further research in γ-ray astronomy. (auth)

44906 FURTHER EVIDENCE ON THE ORIGIN OF TRAPPED GASES IN THE METEORITE KHOR TEMIKI. Eberhardt, P.; Geiss, J.; Groegler, N. (Univ. of Berne). J. Geophys. Res., 70: 4375-8(Sept. 1, 1965).

A concentration profile for the trapped gases in the grains of the Khor Temiki meteorite was established by removing the surface layer of individual grains in a homogeneous grain size fraction with hydrofluoric acid and measuring the remaining rare gas contents. The profile shows a strong enrichment of the trapped gases in the surface layer (outermost 5000 A) of the grains. This result is in agreement with the recently established anticorrelation between grain size and trapped gas content. The most likely emplacement mechanism leading to such a pronounced surface effect is ion bombardment. From our experiments, an upper limit of 100 kev is deduced for the energy of the incident ^{4}He ions. (auth)

44907 CHROMIUM ISOTOPES IN METEORITES. Murthy, V. Rama; Sandoval, P. (Univ. of California San Diego, La Jolla). J. Geophys. Res., 70: 4379-82(Sept. 1, 1965).

The isotopic composition of Cr was measured in 4 chondrules, 8 whole chondrite samples, and 2 iron meteorites in a search for the effects of high energy spallation processes affecting the nonvolatile component of the early solar system material. No isotopic variations within the limits of measurement errors of about 1% were found, either among these objects or between the meteorites and the earth. From the constancy of the isotopic composition of Cr in all these objects, it is concluded either that there has been no significant high energy proton irradiation in the early solar system or that chondrules, chondrites, and iron meteorites are all secondary objects derived from a primordial condensate after complete isotopic homogenization. (auth)

44908 A SENSITIVE TEST FOR THE PRESENCE OF ATOMIC HYDROGEN IN INTERGALACTIC SPACE. Scheuer, P. A. G. (Cambridge Univ., Eng.). Nature, 207: 963(Aug. 28, 1965).

It is pointed out that the scattering of Lyman-α quanta on hydrogen atoms in determining the spin temperature of intergalactic hydrogen provides an extraordinarily sensitive indication of the presence of atomic hydrogen. (P.C.H.)

44909 HIGH ENERGY ASTROPHYSICS. Gratton, L. (Laboratorio di Astrofisica e Laboratorio Gas Ionizzati, Frascati, Italy). Nuovo Cimento (1), 2: Suppl., 584-601 (1964). (In Italian).

A review is given on the recent studies in high-energy astrophysics. The experimental results on supernova, radiogalaxies, explosion of the core of the M 82 galaxies, theory of supernova, the problem of hyperdense material, nature of intense radio sources, and invisible matter are discussed. (J.S.R.)

44910 GRAVITATIONAL EFFECTS OF LUMINOSITY. Michel, F. Curtis (Rice Univ., Houston, Tex.). Phys. Rev., 140: B514-15(Oct. 25, 1965).

It is shown that the gravitational effects of the photons (or neutrinos) radiated from a point mass are accurately treated in the newtonian approximation. Contrary to implication elsewhere, such luminosity does not lead to a new inward force (which is shown to violate causality), the only significant effect being the monotonic reduction of the gravitational attraction due to the energy loss via the radiation. (auth)

44911 HIGH-ENERGY PHOTONS FROM THE COMPTON-SYNCHROTRON PROCESS IN THE CRAB NEBULA. Gould, Robert J. (Univ. of California, San Diego). Phys. Rev. Letters, 15: 577-9(Oct. 4, 1965).

For the purposes of comparison with observations at high photon energies, the Compton-synchrotron spectrum of the Crab nebula is computed on the assumption that there exists therein production of a synchrotron spectrum extending from the radio to the optical to the x-ray region. The assumed synchrotron spectrum consists essentially of two branches which are shown. To compute the Compton-synchrotron spectrum, it is necessary to know essentially the spectral densities of synchrotron electrons and photons in the Crab. The differential Compton-synchrotron flux is then computed. The results of the calculations from the model described are given, with the spectral energy flux plotted against the frequency. The observed assumed synchrotron spectrum is shown and the calculated total Compton-synchrotron spectrum is given. (J.F.P.)

44912 ABSENCE OF MARTIAN RADIATION BELTS AND IMPLICATIONS THEREOF. Van Allen, J. A.; Frank, L. A.; Krimigis, S. M.; Hills, H. K. (Univ. of Iowa, Iowa City). Science, 149: 1228-33(Sept. 10, 1965).

A system of sensitive particle detectors on Mariner IV showed the presence of electrons of energy (E_e) less than 40 kiloelectron volts out to a radial distance of 165,000 kilometers in the morning fringe of the earth's magnetosphere but failed to detect any such electrons during the close encounter with Mars on 14-15 July 1965, at the time when the minimum aerocentric radial distance was 13,200 kilometers. This result can mean that the ratio of the magnetic dipole moment of Mars to that of the earth (M_M/M_E) is surely less than 0.001 and probably is less than 0.0005. The corresponding upper limits on the equatorial magnetic field at the surface of Mars are 200 and 100 gammas, respectively. It appears possible that the solar wind interacts directly with the Martian atmosphere. (auth)

44913 SEARCH FOR TRAPPED ELECTRONS AND A MAGNETIC MOMENT AT MARS BY MARINER IV. O'Gallagher, J. J.; Simpson, J. A. (Univ. of Chicago). Science, 149: 1233-9(Sept. 10, 1965).

The Mariner IV spacecraft on 14-15 July 1965 passed within 9850 kilometers of Mars, carrying a solid-state charged-particle telescope which could detect electrons greater than 40 kiloelectron volts and protons greater than 1 million electron volts. The trajectory could have passed through a bow shock, a transition region, and a magnetospheric boundary where particles could be stably trapped for a wide range of Martian magnetic moments. No evidence of charged-particle radiation was found in any of these regions. In view of these results, an upper limit is established for the Martian magnetic moment provided it is assumed that the same physical processes leading to acceleration and trapping of electrons in Earth's magnetic field would be found in a Martian magnetic field. On this basis, the upper limit for the Martian magnetic moment is 0.1% that of Earth for a wide range of postulated orientations with respect to the rotational axis of Mars. The implications of these results for the physical and biological environment of Mars are briefly discussed. (auth)

44914 ENHANCEMENT OF IONIZATION EQUILIBRIUM IN A STELLAR ATMOSPHERE. Kolesnik, I. G. (Main Astronomical Observatory, Academy of Sciences, Ukrainian SSR). Soviet Astron. AJ (English Transl.), 9: 50-63(July-Aug. 1965).

Translated from Astron. Zh., 42: 67-73(Jan.-Feb. 1965).

Observations suggest that the ejection of plasma bunches into the outer layers of the star should occur in T Tau and UV Cet type stars. This may lead to the formation of nonequilibrium plasma in which the electron density is higher than that calculated from Saha's formula for given temperature and density. The interpretation of a plasma bunch in the atmosphere as one of the possible mechanisms responsible for the appearance of a nonequilibrium medium is discussed. Since the expansion of the bunch proceeds much faster than the formation of ionization equilibrium, the final result is the appearance of a medium with excess electron density. Formulas are derived for the departure of the degree of ionization from equilibrium values and it is shown that small dense plasma bunches should be effective in producing the nonequilibrium medium. (auth)

44915 OBSERVATIONS OF THE SPECTRUM OF SPICULES AND THE FINE STRUCTURE OF THE SOLAR CHROMOSPHERE. Nikol'skii, G. M. (Inst. of Terrestrial Magnetism, Ionosphere, and Radiowave Propagation, Academy of Sciences, USSR). Soviet Astron. AJ (English Transl.), 9: 64-72(July-Aug. 1965).

Translated from Astron. Zh., 42: 86-95(Jan.-Feb. 1965).

Various two-component models of the solar atmosphere are critically reviewed. In particular, the picture put forward by Zirin and Dietz, in which there is practically no transition region between the corona and the chromosphere, is shown to be unacceptable. The coronograph at IZMIRAN was used to obtain photographs of chromospheric spicules in hydrogen and helium lines. Helium line profiles were determined in the spicules. The mean width of the line λ 5876 was found to be 0.35 Å, which is appreciably lower than that obtained by other investigators (~0.5-0.6 Å). The discrepancy is explained by radial velocity dispersion of spicules, which is about 10 km/sec on the average. The width of the line λ 10,830 Å, corrected for self-absorption, is in agreement with that found for λ 5876 Å. Hydrogen and helium emission originates in spicules of various types with temperatures of 25,000 and 6000°, respectively. Weak, diffuse helium emission in λ 5876 is observed between spicules up to altitudes of about 20,000 km. The temperature and concentration of helium in these regions is estimated. The distribution of "turbulent velocity" with height is found for the solar atmosphere. The model of the structure of the solar atmosphere, which is in agreement with optical, radio, and rocket observations of the sun, is put forward. Two types of elements dominate up to a height of 7000 km in the chromosphere, namely, "hot helium" spicules and "cold hydrogen" spicules. The relative area of "helium" spicules falls rapidly as one approaches the photosphere. The "helium" elements occupy practically the entire space at a height of 7500 km. (auth)

44916 ON THE MECHANISM OF γ-RAY EMISSION BY SOLAR FLARES. Zheleznyakov, V. V. (Gorkii State Univ., USSR). Soviet Astron. AJ (English Transl.), 9: 73-6(July-Aug. 1965).

Translated from Astron. Zh., 42: 96-101(Jan.-Feb. 1965).

Possible mechanisms which may be responsible for the emission of hard electromagnetic radiation by solar flares are discussed. It is shown that the pulse of γ rays with energies of 0.25-0.5 Mev per photon which was observed on March 20, 1958, may have been due to the "inverse" Compton effect in the neighborhood of flares, i.e., to a process of energy transfer from 4×10^{30} relativistic electrons with energies $E \sim 2 \times 10^{8}$ ev to light photons emitted by the solar surface. Synchrotron emission by these electrons is lower by only an order of magnitude as compared with the microwave burst recorded simultaneously with the γ-ray pulse. On the other hand, if the γ rays are identified with bremsstrahlung (assuming that they are generated in the inner corona) then the resulting flux of radio emission is higher by 5 orders than the observed flux. The discrepancy of one order of magnitude may be reduced by a suitable choice of the electron velocity distribution, since the synchrotron radiation and the Compton γ rays depend in different ways on the particle energy. (auth)

44917 MEASUREMENT OF JUPITER'S INTRINSIC DECIMETER-WAVELENGTH RADIATION. Rzhiga, O. N.; Trunova, Z. G. (Inst. of Radio Engineering and Electronics, Academy of Sciences, USSR). Soviet Astron. AJ (English Transl.), 9: 93-5(July-Aug. 1965).

Translated from Astron. Zh., 42: 121-3(Jan.-Feb. 1965).

The results of measurements of the intrinsic Jovian radiation at a frequency near 700 Mc are presented. The mean equivalent Jovian temperature at that frequency was found to be 12,000 ± 2000°K. The measurement tech-

niques and radiometer calibration technique are described. (auth)

44918 THE NATURE OF SOLAR MAGNETIC FIELDS (THE FINE STRUCTURE OF THE FIELD). Severnii, A. B. (Crimean Astrophysical Observatory, Academy of Sciences, USSR). Soviet Astron. AJ (English Transl.), 9: 171-82 (Sept.-Oct. 1965).
Translated from Astron. Zh., 42: 217-32(Mar.-Apr. 1965).

Observational data on the fine structure of strong magnetic fields on the sun obtained at high resolution are discussed. Topics include purely transverse fields in regions occupied by strong longitudinal fields of a single polarity, the formation of peaks in the field with dimensions of 2 to 5 in., strong rotations of the vector of the transverse field across the surface and with depth in the solar atmosphere, the concentration of sunspot force lines in separate bundles extending radially from the sunspot center, which is revealed by the characteristic pattern of electric current loops around these bundles, the occurrence of adjacent regions in a sunspot with $\partial H_{||}/\partial Z$ and convection of opposite signs. The results of a study of the general solar magnetic field are also discussed. The absence of any coherent or uniform field is noted. (J.F.P.)

44919 POSSIBLE MODELS OF CHROMOSPHERIC SPICULES. Kononovich, E. V. (Shternberg State Astronomical Inst., USSR). Soviet Astron. AJ (English Transl.), 9: 183-90(Sept.-Oct. 1965).
Translated from Astron. Zh., 42: 233-43(Mar.-Apr. 1965).

An attempt is made to construct a model of a spicule on the basis of available data on the H, He, O, and Ca^+ spectral-line widths in individual spicules. In accordance with the observational results, it is assumed that all of the observed emission originates within the confines of one and the same spicule, the diameter of which is taken to be about 10^3 cm. Self-absorption is taken into account through the use of the dependence of the line half-width on the optical thickness at the line center. The use of this method in the case of hydrogen and helium lines leads to an estimate of the popoulation of the second quantum state of hydrogen $n_2 \sim 10^7$ cm^{-3} and that of the metastable triplet level of helium $n_2{}^3S \sim 6 \times 10^4$ cm^{-3}, and the following Doppler velocities of motion of the atoms emitting the observed lines: $V_{Ca^+} \sim V_H \sim 12$ km/sec, $V_{He} \sim 10$ km/sec, and $V_0 \sim 7$ km/sec. From a computation of the dependence of n_2 and $n_2{}^3S$ on temperature and density, together with some assumptions concerning the thermal velocities, it is possible to construct a model of a spicule. In principle, two variants are possible. In both of these the spicule is represented as an extremely dense formation with a mean concentration of hydrogen atoms of 10^{13}-10^{14} cm^{-3}. In the denser layers of the spicule the kinetic temperature can increase, as the density decreases, from $T_e \sim 6000°$ to $T_e \sim 15{,}000°$. The main part of the line emission from hydrogen originates in these parts. In the more rarefied layers of the spicule (probably its outer regions), the temperature is $T_e \sim 15{,}000$-$20{,}000°$ and helium-line emission predominates. Lines of ionized calcium should originate in all regions, including the interspicular space directly adjacent to the spicule, where the velocity of the nonthermal motion may increase to ~12 km/sec. (auth)

44920 ON THE ORIGIN OF SOLAR RADIO BURSTS IN THE METER-WAVELENGTH RANGE. Zheleznyakov, V. V. (Gorkii State Univ., USSR). Soviet Astron. AJ (English Transl.), 9: 191-7(Sept.-Oct. 1965).
Translated from Astron. Zh., 42: 244-52(Mar.-Apr. 1965).

The problem of the origin of various components of radio emission typical of the meter wavelength range, such as type I and type II bursts and reverse drift pairs associated with type III emission, is discussed. The peculiarities of reverse drift pairs are accounted for in a natural way when these phenomena are the result of combination scattering of excited plasma waves on the same plasma waves after being reflected from a local irregularity in the corona. In the interpretation of the type II bursts, the characteristic "splitting" of the harmonic bands is related to the Doppler effect in the transformation of plasma waves excited in the shock front in radio emission. Various ways by which type I bursts might be generated are considered in the summary. (auth)

44921 QUASISTATIONARY CORPUSCULAR STREAMS ON THE DESCENDING BRANCH OF THE 19th SOLAR ACTIVITY CYCLE. Mustel, E. R. (Astronomical Council, Academy of Sciences, USSR). Soviet Astron. AJ (English Transl.), 9: 215-18(Sept.-Oct. 1965).
Translated from Astron. Zh., 42: 276-80(Mar.-Apr. 1965).

It is shown that for the descending branch of the current 19th solar activity cycle the existence of recurrent geomagnetic disturbances is associated with the passage of active regions across the apparent center of the solar disk or near the latter. For the period 1959-1960 the corresponding results were presented. For the period June 1962-June 1963 similar results are presented and are confirmed statistically. Some specific characteristics of the extremely long geomagnetic sequence G, represented by the ten disturbances G_1-G_{10}, are discussed and it is shown that the origin of these characteristics can be related to the presence of intensive and relatively continuous processes of the escape of gases of a nonthermal character from the sun. (auth)

44922 PROBABILITY OF QUASAR PRODUCTION. Zel'dovich, Ya. B. Soviet Astron. AJ (English Transl.), 9: 221-3(Sept.-Oct. 1965).
Translated from Astron. Zh., 42: 283-6(Mar.-Apr. 1965).

Expressions are derived from statistical treatment of the distribution of quasars. At the present time there exist no grounds for assuming the formation of quasars in a remote epoch to be any more probable than in the present epoch. (auth)

44923 REMARKS ON THE NATURE OF X-RAY SOURCES. Shklovskii, I. S. (Shternberg State Astronomical Inst., USSR). Soviet Astron. AJ (English Transl.), 9: 224-5(Sept.-Oct. 1965).
Translated from Astron. Zh., 42: 287-9(Mar.-Apr. 1965).

The "supernova" and "neutron star" hypotheses of the nature of x-ray sources in space are discussed. (auth)

44924 THE PROPAGATION OF SHOCK WAVES IN THE OUTER LAYERS OF A STAR. Nadezhin, D. K.; Frank-Kamenetskii, D. A. Soviet Astron. AJ (English Transl.), 9: 226-32(Sept.-Oct. 1965).
Translated from Astron. Zh., 42: 290-8(Mar.-Apr. 1965).

The ejection of an envelope by a shock wave in the case of explosions on the scale of novas is considered on the basis of a numerical solution of the gas dynamic equations. It is shown that the main mass of gas joins the envelope during the stage of expansion of the outer layers after the shock wave emerges to the surface and that the properties of the envelope are independent of the way in which the shock wave was generated in the deeper layers. The propagation of the shock wave is also calculated by the approximate methods of Chisnell-Whitham and Brinkley-Kirkwood. The latter method is first of all generalized to the case of a nonuniform medium and the gravitational force is taken into account. Conclusions are drawn on the effectiveness of the approximate methods and the automodel solution. In particular, the above approximate methods are not applicable for the determination of the mass of the ejected envelope. (auth)

44925 THE RELATIVISTIC INSTABILITY OF POLYTROPIC SPHERES. Kaplan, S. A.; Lupanov, G. A. (Gorkii State Univ., USSR). Soviet Astron. AJ (English Transl.), 9: 233-7(Sept.-Oct. 1965).
Translated from Astron. Zh., 42: 299-304(Mar.-Apr. 1965).

The problem of general relativistic effects in the theory of the structure of polytropic spheres is discussed. An analytical relation between the mass of the sphere M and

the central density ρ_c is obtained in the approximation of weak relativity. It is shown that it consists of two branches: ascending ($dM/d\rho_c > 0$) and descending ($dM/d\rho_c < 0$). With the help of equations for spherically symmetric disturbances, it is shown that the states corresponding to the descending branch are unstable and the growth increment of this instability is found (the time for the growth of the disturbances is approximately c/a times as large as the time for free fall, where a is the velocity of sound). (auth)

44926 A POSSIBLE MECHANISM OF FORMATION OF GALACTIC BRIDGES. Gershberg, R. E. (Crimean Astrophysical Observatory, Academy of Sciences, USSR). Soviet Astron. AJ (English Transl.), 9: 259-62(Sept.-Oct. 1965).

Translated from Astron. Zh., 42: 330-3(Mar.-Apr. 1965).

The formation of filamentary structures by the twisting of magnetic force lines or the "mechanical pinch effect" is used to explain intergalactic "bridges." It is shown that there is an effective interaction between rotating galactic bodies and the intergalactic medium if there is a reasonable intergalactic magnetic field and a high degree of ionization of the intergalactic medium. As the result of this interaction, a filamentary condensation connecting two galaxies may be formed. The recombination and cooling rates in such condensations are higher than in the surrounding intergalactic medium. Therefore, after an appreciable decrease of ionization and termination of the magnetic interaction, subsequent compression of matter can be maintained by hydrodynamic forces. It is shown that such an intergalactic filament can be brought into a state of gravitational instability, after which the process of stellar formation may begin in it. The proposed model explains a number of observed features of intergalactic bridges. (auth)

44927 THE NEUTRINO LUMINOSITY OF STARS. Masevich, A. G.; Kotok, E. V.; Dluzhnevskaya, O. B.; Mazani, A. (Astronomical Council, Academy of Sciences, USSR; Di Brera Observatory, Italy). Soviet Astron. AJ (English Transl.), 9: 263-73(Sept.-Oct. 1965).

Translated from Astron. Zh., 42: 334-6(Mar.-Apr. 1965).

Physical processes leading to the creation of neutrino-antineutrino pairs in the interiors of stars and their possible significance for stellar evolution are discussed. Eight processes of neutrino pair creation are considered: $e^- + Z \rightarrow e^- + Z + \nu + \tilde{\nu}$; $e^-_{free} \rightarrow e^-_{bound} + \nu + \tilde{\nu}$; $\gamma + Z \rightarrow Z + \nu + \tilde{\nu}$; $\gamma + \gamma \rightarrow \nu + \tilde{\nu}$; $\gamma + e^- \rightarrow e^- + \nu + \tilde{\nu}$; $e^- + e^+ \rightarrow \nu + \tilde{\nu}$; $\gamma + \gamma \rightarrow \nu + \tilde{\nu} + \gamma$; and collective plasma effects. The neutrino luminosity L_ν is calculated for stars with reliable models: Main-sequence stars, giants, supergiants, helium and hydrogen stars, and population II stars (70 evolutionary sequences in all for stars with masses between 0.8 $M_\odot$ and 200 $M_\odot$). The results show that for most of the models discussed the photon luminosity is so far in excess of the neutrino luminosity that the latter can be neglected for the calculation of evolutionary paths. Only during the last stages of evolution of massive stars (the C, O, and Ne burning stage) and during the period of the helium flash in population II stars may L_ν become comparable with or even greater than L_{ph}. In stellar interiors the most efficient process is the photoneutrino process. All calculations were carried out for stable and quasi-stable stages of stellar evolution. (auth)

44928 ON THE THEORY OF STELLAR EVOLUTION AND SOME PROPERTIES OF STAR CLUSTERS. Kholopov, P. N. (Shternberg State Astronomical Inst., USSR). Soviet Astron. AJ (English Transl.), 9: 290-6(Sept.-Oct. 1965).

Translated from Astron. Zh., 42: 369-76(Mar.-Apr. 1965).

The theory of stellar evolution proposed by Schwarzschild and Sandage contradicts observational data indicating that there is a difference between the masses of giants and supergiants in globular clusters. Star clusters with M_V, B–V diagrams which combine the properties of both galactic and globular clusters should be considered to be intermediate between galactic and globular clusters. The comparison of the diagram of these clusters with those of typical galactic and globular clusters leads to the following hypotheses which are alternative to the hypotheses of Schwarzschild and Sandage. There is no unique initial luminosity function for all clusters. A star can remain in the red-giant stage for a long time. Different sections of subgiant and red-giant sequences are formed by stars initially belonging to different sections of the main sequence. The brighter stars of the main sequence become brighter red giants. Red giants during their evolution can lose mass and not become white dwarfs. The bright main-sequence stars observed in some clusters to lie above the point at which the main sequence tends into the region of subgiants have the same age as the other members of the cluster, but for some still unknown reason they evolve in a different manner than the majority of the cluster stars. It is possible that these stars in time become white dwarfs. (auth)

44929 THE INITIAL STAGE OF AN EXPANDING UNIVERSE AND THE APPEARANCE OF A NONUNIFORM DISTRIBUTION OF MATTER. Sakharov, A. D. Zh. Eksperim. i Teor. Fiz., 49: 345-58(July 1965). (In Russian).

An hypothesis of the creation of astronomical bodies as a result of gravitational instability of the expanding universe is investigated. It is assumed that the initial inhomogeneities arise as a result of quantum fluctuations of a cold baryon-lepton matter at densities of the order of 10^{38} baryons/cm^3. It is suggested that at such densities gravitational effects are of decisive importance in the equation of state and the dependence of energy density ϵ on baryon density n can qualitatively be described by graphs. At a certain density $n = n_0$ ϵ vanishes. A theoretical estimation (containing some vague points) yields such initial inhomogeneities in distribution of matter which can explain the origin of clusters of 10^{62} to 10^{63} baryons (10^5 to 10^6 $M_\odot$). The calculated mass is smaller than that of the galaxies by 10^5 to 10^6 times; it is in fact closer to the masses of spherical clusters. The hypothesis is proposed that galaxies are produced as a result of increase of nonuniformities in the motion and distribution of the gas formed during gravitational collapses of the primary stellar clusters. According to this hypothesis the plane component of the galaxy is produced from the gas whereas the spherical component mainly consists of clusters of primary stars captured by the gravitational field of the rotating gas cloud. (auth)

44930 NUCLEAR GAMMA RAYS FROM SUPERNOVA REMNANTS. Haymes, R. C.; Craddock, W. L.; Clayton, D. D. (Rice Univ., Houston, Tex.). 18p. (CONF-650422-9). Gmelin, AED-CONF-65-118-30.

From American Geophysical Union, Program for Section of Seismology Annual Meeting, Washington, D. C.

It is found from calculations that, if the ^{254}Cf-hypothesis of Burbidge et al., is correct, the Crab Nebula presently has a radioactive energy input of 1.2×10^{36} erg/sec, of which 92% is in the form of kinetic energy of alpha particles and fission fragments. That much energy would be significantly related to observed properties of the Crab. To clarify the source of supernova light curves, location and mechanism of heavy-element nucleo-synthesis by rapid neutron captures, and present-day energy balance in supernova remnants, the possibility of experimentally testing the Cf-hypothesis was evaluated by searching for 2.7×10^{34} erg/sec radiated by the Crab in gamma-ray lines associated with trans-bismuth radioactivity. The anticipated line spectrum is complex. The strongest line flux from the Crab is 9.7×10^{-5} cm^{-2} sec^{-1} for the 390 kev line of ^{249}Cf. Stronger line fluxes may come from the x-ray source in Scorpius if it is also a Type I remnant. The requirements for a gamma-ray telescope capable of resolving the lines from the continuous background are discussed. The chance of detection appears favorable from a satellite and may be possible from balloons. (auth)

44931 THERMAL AND NON-THERMAL PROCESSES IN SOLAR FLARES. Acton, Loren W. 6p. (CONF-650422-5). Gmelin, AED-CONF-65-118-23.

From American Geophysical Union, Program for Section of Seismology Annual Meeting, Washington, D. C.

Two models are presented for interpreting the x-ray and microwave emissions observed from solar flares. The thermal model attempts to account for the radiation on the basis of purely thermal emission. Evidence is presented which suggests that energetic, nonthermal electrons are responsible for the observed radiation. It is believed that the x-ray burst is due to bremsstrahlung from sub-relativistic electrons, and the impulsive microwave burst are probably due to synchrotron emission from relativistic electrons. (L.B.S.)

44932 STELLAR AND SOLAR MAGNETIC FIELDS. International Astronomical Union Symposium No. 22 held in Rottach-Egren near Munich, Germany, 3–10 September 1963. Luest, R. (ed.). New York, John Wiley and Sons, 1965. 466p. $17.50. (CONF-630911).

Observations and theories of stellar and solar magnetic fields are analyzed and compared. Observational methods and results, and theoretical aspects for stellar magnetic fields are considered; large scale solar magnetic fields, small scale solar magnetic fields, plages, filaments, sunspots, and solar flares (observations and theory) are also considered. The general aspects of stellar and solar magnetic fields are discussed. It is proposed that the phenomena on the solar surface are gradually becoming clearer. But the magnetic stars remain obscure; and a solution will probably not only require more observations, but also a better interpretation of them. (J.F.P.)

Atomic Physics

Refer also to abstracts 45098, 45270, and 45327.

44933 (COO-1277-12) ENERGY AND ANGULAR DISTRIBUTIONS OF ELECTRONS EJECTED FROM HYDROGEN AND HELIUM BY 100- TO 300-Kev PROTONS. Final Report, April 1, 1963–July 31, 1965. Rudd, M. Eugene; Sautter, Chester A.; Bailey, Carl L. (Concordia Coll., Moorhead, Minn.). Aug. 1, 1965. Contract AT(11-1)-1277. 29p. Dep. mn; CFSTI $2.00 cy, $0.50 mn.

The differential cross sections for electron ejection from He and H_2 by protons at 100 to 300 kev were measured as functions of angle and of the energy of the ejected electrons. The results were compared with theoretical (quantum and classical) predictions. The Born approximation yields good values for total ionization cross sections at high energies and reproduces certain features of the energy and angular distributions, but close quantitative agreement is lacking. (D.C.W.)

44934 (COO-1277-13) AUTOIONIZATION OF GASES BY ION IMPACT. Final Report, March 15, 1965–August 31, 1965. Rudd, M. Eugene; Sautter, Chester A. (Concordia Coll., Moorhead, Minn.). Sept. 1, 1965. Contract AT(11-1)-1277. 9p. Dep. mn; CFSTI $1.00 cy, $0.50 mn.

Measurements were made of the energies of the characteristic lines in the energy spectrum of electrons emitted by He, Ne, Ar, and Kr gases when bombarded by protons. The more prominent lines in He and Ne and their identifications are tabulated. Recommendations are made for further research. (D.L.C.)

44935 (NP-15168) MEASUREMENT OF CESIUM EXCITATION CROSS SECTION NEAR THRESHOLD BY A SWARM TECHNIQUE. Technical Report No. 28. Project DEFENDER. Nolan, J. F.; Phelps, A. V. (Westinghouse Research Labs., Pittsburgh, Pa.). Apr. 15, 1965. Contract NONR-2584(00). 38p.

Electron drift velocities were measured in Ar-Cs mixtures for E/N values between 3×10^{-19} and 5×10^{-18} v-cm^2 and Cs to Ar concentration ratios between 10^{-8} and 10^{-5}. The drift velocity was obtained from measurements of the electron transit time using an ac technique which is a modification of a technique developed originally by Rutherford for ion drift velocity measurements. Numerical solutions of the Boltzmann transport equation were used to determine an excitation cross section which is consistent with the experimental drift velocity data. For a single excitation threshold at 1.386 ev, the best slope for a linear cross section is 7.1×10^{-15} cm^2/ev. If excitation to the 6 $P_\frac{3}{2}$ and 6 $P_\frac{1}{2}$ states is considered separately, with thresholds at 1.386 and 1.454 ev, respectively, the linear cross sections obtained have a slope of 2.5×10^{-15} cm^2/ev for 6 $P_\frac{3}{2}$ excitation and 5.0×10^{-15} cm^2/ev for 6 $P_\frac{1}{2}$ excitation. The range of validity of these values is from threshold up to about 1.8 ev. Other shapes for the cross section are investigated. The experimental cross section is in reasonable agreement with extrapolations of theoretical cross sections. (auth)

44936 (TID-21692) CONTINUOUS REPRESENTATIONS IN THE STATISTICAL THEORY OF ELECTRONIC ENERGIES. THE H_2^+ ION. Technical Report No. 15. Handler, George S. (California Univ., La Jolla, San Diego. Dept. of Chemistry); Golden, Sidney (Brandeis Univ., Waltham, Mass. Dept. of Chemistry). [1964]. Contracts AT(30-1)-2968; Nonr-1677(01). 13p. Dep. mn; CFSTI $1.00 cy, $0.50 mn.

A version of the statistical theory of electron energies, arising from a consideration of alternative partitionings of the Hamiltonian, was applied to the H_2^+ ion, yielding electron energies ~6% greater in magnitude than the exact theoretical values at several values of the internuclear separation. The binding energy at the theoretical equilibrium separation was calculated to be 0.1024 au compared to the experimental value of 0.1026 au. (auth)

44937 (TID-22140) FINAL REPORT [ON ION SPUTTERING]. (Houston Univ., Tex.). Aug. 12, 1965. Contract AT-(40-1)-2573. 16p. Dep. mn; CFSTI $1.00 cy, $0.50 mn.

The yields in sputtering of polycrystalline Cu, Ni, and Ag by argon ions at 30 to 170 kev were measured. The angular distributions of the sputtered particles were also obtained, together with the dependence of the total yield and the distributions on the angle of incidence of the Ar ions. Single crystals of Cu were used to investigate lattice effects on sputtering. The sputtering rate at the beginning of sputtering and the velocity distributions of sputtered atoms were also studied, together with temperature effects on single-crystal spot patterns and yields. (D.C.W.)

44938 (UCRL-14117) SURFACE IONIZATION OF THE ALKALI METALS BY HEATED TUNGSTEN. McFarland, Robert H.; Kinney, John D. (Lawrence Radiation Lab., Univ. of California, Livermore). July 21, 1965. Contract W-7405-eng-48. 8p. (CONF-650806-4). Dep. mn; CFSTI $1.00 cy, $0.50 mn.

From 7th International Conference on Phenomena in Ionized Gases, Belgrade.

Direct measurements of the surface ionization efficiency of lithium and sodium beams on hot tungsten were made. This involved monitoring the hot wire ion signal over tens of hours for known oven loads of metal. The results indicate that the reflection coefficient of the incident atom is zero and that the ratio, $1 - r_a/1 - r_+$, involving reflection coefficients of the temperature equilibrium atom and ion, is unity. Evidence in support of these results exists in terms of the observation that classically computed absolute ionization cross sections agree with measured ones, providing the above conditions on reflection coefficients are assumed. (auth)

44939 Nd ION BOMBARDED CdS. Anderson, W. W. (Stanford Univ., Calif.). Appl. Phys. Letters, 7: 197-9 (Oct. 1, 1965).

In order to obtain rare earth ion concentrations, two samples of CdS were bombarded at 200-kev Nd ion energies for 15 minutes each. Beam current and substrate temperature are given. The different substrate temperatures influenced annealing of radiation damage during bombardment. The total rare-earth content was very small and located within about 1000 Å of the surface. By comparing the photoluminescence of the ion bombarded CdS with that of a vapor-phase-grown CdS:Nd crystal, it was found that the

Nd^{3+} ions are the same in the two crystals. The illustration that replacement collision doping and defect annealing does occur in semiconductors suggests device possibilities. (J.F.P.)

44940 AN INVESTIGATION OF THE OHLIN STRUCTURE NEAR THE QUANTUM LIMIT OF THE CONTINUOUS X-RAY SPECTRUM. Bergwall, Staffan; Tyagi, Rohtash K. (Uppsala Univ.). Arkiv Fysik, 29: 439-54(1965).

The fine structure near the short wavelength limit of the continuous x-ray spectrum was studied by the isochromat method. By use of a vacuum spectrometer provided with a curved crystal and water cooled targets quite reproducible isochromat curves of the transition elements Sc, Ti, V, Cr, and Y (oxide), Zr, Nb, Mo were obtained. The reference wavelength was 2285 X.U. ($CrK\alpha_1$). Characteristic energy loss values for Sc and Y (oxide) are presented for the first time. It is found that a "foot structure" near the limit exists in the isochromat curves of the elements of the first group of transition metals but is missing in the curves of the second group. This difference may be attributed to the different level density in the conduction bands of the actual metal groups. It is further found that the first two peaks in the isochromat curves of all the published elements reappear after equal intervals. This displacement is found to be in a qualitative agreement with the theoretical values as given by the plasma oscillation theory, assuming all d and s electrons to be free. An attempt was also made to explain the different shapes of the isochromats by comparison with the L-absorption curves available. (auth)

44941 FORBIDDEN LINES IN THE L-EMISSION SPECTRUM OF Pb 82. Srivastava, K. S. (Lucknow Univ., India). Indian J. Pure Appl. Phys., 3: 236-7(July 1965).

The L-emission spectrum of lead was investigated using a 40-cm curved mica crystal spectrograph of the transmission type. Three lines at 1062.2, 1030.2 and 836.5 XU were observed for the first time, corresponding to the forbidden transitions $L_{II}M_{II}$, L_IM_I and $L_{II}N_V$ respectively. The presence of the forbidden transition $L_{II}N_{II}$ (λ = 856.7 XU) was conclusively established. (auth)

44942 INELASTIC ELECTRON SCATTERING FROM ATOMS AT MEDIUM ENERGIES. II. POLARIZATION EFFECTS. Bonham, R. A. (Tokyo Univ.; Indiana Univ., Bloomington). J. Chem. Phys., 43: 1933-40(Sept. 15, 1965).

The effects of inelastic electron scattering on the elastic, total, and discrete inelastic differential scattering cross sections were investigated in the second Born approximation. It is shown that in this approximation the polarization corrections can be written as a function of the Coulomb phase shift and other auxiliary functions to within an additive constant in the Coulomb phase. This constant is chosen by imposing the physically reasonable condition that the polarization correction must tend to zero with increasing scattering angle. The results of the calculation of polarization effects on the elastic scattering amplitudes for Ar and U are given for an incident energy of 40 kv. (auth)

44943 FREE-ION AND CRYSTALLINE SPECTRA OF Pr^{3+} (Pr IV). Crosswhite, H. M.; Dieke, G. H.; Carter, Wm. J. (Johns Hopkins Univ., Baltimore). J. Chem. Phys., 43: 2047-54(Sept. 15, 1965).

The spectrum of the free tripositive praseodymium ion (Pr IV) was obtained under high resolution between 1200 Å and the infrared. The analysis yielded all 49 levels of the four lowest configurations $4f^2$, 4f5d, 4f6s, 4f6p. A comparison with the crystal levels of Pr^{3+} in various lattices showed a depression of up to 5% in the anhydrous chlorides. (auth)

44944 EFFECT OF CHEMICAL COMBINATION ON THE SOFT X-RAY K EMISSION BANDS OF NITROGEN AND CARBON. Fischer, David W.; Baun, William L. (Air Force Materials Lab., Wright-Patterson AFB, Ohio). J. Chem. Phys., 43: 2075-8(Sept. 15, 1965).

Chemical combination has a marked effect on the shape of the x-ray K emission bands of nitrogen and carbon. Nitrogen bands from a few nitrides and carbon bands from graphite, diamond, lampblack, and some metallic carbides are shown. The wavelengths of the most prominent parts of the bands are listed as are the half-bandwidths and full bandwidths. Results were obtained using electron excitation, a lead stearate crystal, and flow proportional counter. (auth)

44945 STRONG COUPLING IN NUCLEAR RESONANCE SPECTRA. V. PERTURBATION THEORY FOR THE EXTREME COUPLING CASE. Waugh, J. S.; Wei, E. L. (Massachusetts Inst. of Tech., Cambridge). J. Chem. Phys., 43: 2308-11(Oct. 1, 1965).

The perturbation theory of NMR spectra is given for the case in which the relative chemical shift $\nu_0\delta$ between two groups is much smaller than the coupling constant J. Results are given for the systems AB, AB_2, AB_3, A_2B_2, and A_2B_3 from which it is possible to obtain the parameters from the appropriate spectra without detailed analysis. The proton spectra of methylacetylene is discussed as an example. (auth)

44946 POTENTIAL-ENERGY CURVES FOR THE X $^1\Sigma_g^+$, $b^3\Sigma_u^+$, AND C $^1\Pi_u$ STATES OF THE HYDROGEN MOLECULE. Kolos, W.; Wolniewicz, L. (Univ. of Chicago). J. Chem. Phys., 43: 2429-41(Oct. 1, 1965).

Previous calculation of the ground-state energy of H_2 was extended to include large internuclear distances and accurate potential-energy curve for $0.4 \leq R \leq 10.0$ au is presented. For $0.4 \leq R \leq 4.0$ au expectation values of several operators were also calculated. The calculation was made using a wavefunction in the form of an expansion in elliptic coordinates. The wavefunction depends on the interelectronic distance but, in contrast to the James-Coolidge expansion, is flexible enough to describe properly the dissociation of the molecule. Extensive calculations were also made for the repulsive $^3\Sigma_u^+$ state ($1.0 \leq R \leq 10.0$) and for the $^1\Pi_u$ state ($1.0 \leq R \leq 10.0$). In the former case a van der Waals minimum was found at R = 7.85 au and 4.3 cm^{-1} below the dissociation limit. For the $^1\Pi_u$ state the computed binding energy D_e = 20,490.0 cm^{-1} and the equilibrium internuclear distance R_e = 1.0330 Å are in a satisfactory agreement with the experimental values D_e = 20,488.5 cm^{-1} and R_e = 1.0327 Å. In this case a van der Waals potential maximum was found to occur at R = 9.0 au and 105.5 cm^{-1} above the dissociation limit. Preliminary results for the $^1\Sigma_g^+$ state at $R \approx R_e$ are also given. (auth)

44947 CALCULATION OF INELASTIC ELECTRON-MOLECULE COLLISION CROSS SECTIONS BY CLASSICAL METHODS. Bauer, Ernest; Bartky, Charlotte Decker (Philco Corp., Newport Beach, Calif.). J. Chem. Phys., 43: 2466-76(Oct. 1, 1965).

Thomson's, Gryzinski's, and Ochkur's classical methods for energy transfer in electronic collisions were used together with the quantum-mechanical Franck-Condon factor for the overlap of nuclear wavefunctions to compute inelastic electron-molecule collision cross sections. Specific application is to ionization and to direct and exchange electronic excitation. After first extending previous applications of the classical energy-transfer methods to atoms, calculations were made for ionization, direct and exchange (spin-change) excitation involving air molecules (N_2, N_2^+, NO, O_2, also CO). The results are applied to the near-threshold domain as well as to the overall behavior of the cross section. Agreement with the very few absolute experimental data available is to within better than a factor of 2 to 3. These methods must be regarded as useful when it is considered that there exist hardly any experimental data on excitation and that quantum-mechanical calculations would be prohibitively lengthy to carry out while the present calculations are very simple to perform. (auth)

44948 ENERGY DEPENDENCE OF CROSS SECTIONS FOR COLLISION-INDUCED DISSOCIATION AND ENDOTHERMIC ION-MOLECULE REACTIONS. Refaey, K. M.; Chupka, W. A. (Argonne National Lab., Ill.). J. Chem. Phys., 43: 2544-5(Oct. 1, 1965).

The energy dependence of cross sections for collision-induced dissociation in ion-molecule reactions was studied at 35 to 2000 ev. Cross sections for dissociation of the

propane ion $C_3H_8^+$ into $C_2H_3^+$ and $C_2H_4^+$ by collision with several rare gases, were measured over the energy range V_1 = 50 to 2000 ev. The results showed that the cross section increased at lower energies. It is suggested that the effect in which at least some cross sections do increase again with increasing energy in the kilovolt range is due to electronic excitation. The collision-induced dissociation of O_2^+ on collision with helium was also studied. The cross section remained large at energies well below the threshold for dissociation of the $^2\pi_g$ ground state. (P.C.H.)

44949 ROLE OF EXCHANGE IN ELECTRON SCATTERING BY HELIUM ATOMS. Peterkop, R. K. (Inst. of Physics, Academy of Sciences, Latvian SSR). Latvijas PSR Zinatnu Akad. Vestis, Fiz. Tek. Zinatnu Ser., No. 3, 47-52(1965). (In Russian).

Direct and exchange amplitudes for scattering of electrons by helium atoms were determined in a distorted wave approximation. The calculated exchange cross section constitutes about 10% and the interference part—to 60% of the direct cross section. Considering the mutual interaction between the direct and the exchange scatterings the direct cross-section at zero-energy is reduced by about six times. (auth)

44950 INELASTIC COLLISIONS OF FAST ELECTRONS AND IONS WITH ATOMS. de Heer, F. J. (FOM-Laboratorium voor Massascheiding, Amsterdam). Ned. Tijdschr. Natuurk., 30: 353-82(Nov. 1964). (In Dutch).

A bibliographic review is given of the present state of knowledge of collisions of fast electrons, ions, and atoms with other atoms or molecules. The collision cross sections, experiments with electron beams, experiments with ion beams, and experiments with crossed beams are summarized. 57 references. (J.S.R.)

44951 POLARIZATION CONTRIBUTION TO THE HYDROGEN HYPERFINE STRUCTURE AND PHENOMENOLOGY OF THE ELECTRON-PROTON INTERACTION. Verganelakis, A. (CERN, Geneva); Zwanziger, D. Nuovo Cimento (10), 39: 613-34(Sept. 16, 1965).

In order to understand the significance of the well-known discrepancy of 45 ppm in the hydrogen hyperfine structure the polarization correction is calculated using an isobar model for the proton, and the sensitivity to electron-proton forces of the analysis of the hyperfine splitting is compared with that of the Lamb shift and of electron-proton scattering. A methodological innovation of the calculation is the avoidance of the Rarita-Schwinger formalism for spin $\frac{3}{2}$ by the construction of a covariant analytic amplitude from the familiar nonrelativistic partial-wave amplitude. It is found that the 3-3 isobar, and by extension higher resonances, are more than an order of magnitude too small to be significant and that the discrepancy is genuine. The introduction of a phenomenological electron-proton interaction term, representing unknown or neglected forces, is considered to account for the discrepancy, and it is found that this would not necessarily lead to a contradiction with Lamb shift or electron-proton scattering data. It is pointed out that, whatever the cause of the discrepancy, it is likely to be proportional, in percent, to the electron mass, so that it would be roughly 200 times greater in μ-mesic hydrogen (μ^-,p) than in hydrogen. A measurement of the hyperfine splitting of μ-mesic hydrogen, of sufficient accuracy to determine whether the discrepancy is common to both systems and proportional to the lepton mass, is strongly urged. (auth)

44952 CHEMICAL SHIFT OF THE PROTON IN THE H_2 MOLECULE BY THE M.S.E. Di Giacomo, A. (Universita, Pisa, Italy). Nuovo Cimento (10), 39: 692-6 (Sept. 16, 1965).

A recently developed perturbation method for diatomic molecules, the modified Schroedinger equation, is applied to the calculation of the chemical shift of the proton in H_2. The result agrees to within a few percent with the results obtained by other methods, giving a new demonstration of the efficiency of the method. (auth)

44953 NON-ITERATIVE APPROACH TO THE ELASTIC SCATTERING OF ELECTRONS BY COMPLEX ATOMS. Myerscough, Valerie P. (Univ. of Durham, Eng.). Phys. Letters, 18: 262-3(Sept. 1, 1965).

Most previous calculations on elastic scattering of electrons by complex atoms, including exchange, made use of an iterative solution of the relevant integro-differential equations. An example of noniterative procedure for s-wave elastic scattering by $C(^3P)$ is presented. The variational method of Hulthén, ignoring coupling to other channels, but including exchange, yields for the $L^T = 1$, $S^T = \frac{3}{2}$, ^4P state, the single radial integro-differential equation. Results of this method, applied to s-wave scattering of electrons, are tabulated. (J.F.P.)

44954 THE MECHANISM OF THERMAL RELEASE OF INJECTED INERT GAS FROM TUNGSTEN. Corkhill, D. P.; Carter, G. (Univ. of Liverpool). Phys. Letters, 18: 264-5(Sept. 1, 1965).

Further evidence is presented to support a previous hypothesis regarding the mechanism of thermal release of injected inert gas from tungsten. Polycrystalline tungsten was bombarded with 6×10^{16}, 2-kev Kr^+ ions/cm^2 derived from an r-f source in a high-vacuum system which included a mass spectrometer. After bombardment the tungsten was pulse heated in 100°K steps up to 2300°K, and the quantity of injected gas recovered in each interval determined from the mass spectrometer response is shown. The procedure was then repeated with a dose of Kr^+ ions followed by a dose of Ar^+ ions. Then the tungsten was bombarded with krypton ions, then with argon ions and the procedure repeated individually for each bombardment. The results indicate that the lower energy release portion of trapped inert gases from tungsten can be directly related to their surface proximity, and it is extremely probable that this release is in some way conditioned by the damage induced by the bombardment. The higher energy release portion is associated with deeply penetrating ions, including those which have channeled. (J.F.P.)

44955 FORMATION OF EXCITED HYDROGEN ATOMS BY CHARGE-EXCHANGE IN LITHIUM. Lodge, J. G.; May, R. M. (Univ. of Sydney). Phys. Letters, 18: 268-9(Sept. 1, 1965).

The ratio of the cross section is estimated for the formation of excited hydrogen atoms by charge exchange in lithium. In calculating the cross sections for this reaction, with lithium as the ionizing atom, the lithium wave functions in the relevant matrix elements were approximated by wave functions with an effective charge of Z = 1.25. Using the Born approximation, the cross section can then be computed. The resulting cross-section ratio is plotted as a function of the energy of the incident H atom relative to a stationary Li atom. (J.F.P.)

44956 POLARIZATION OF ALKALI LINE RADIATION EXCITED BY ELECTRON IMPACT. Hafner, H.; Kleinpopen, H.; Krueger, H. (Universitaet, Tuebingen, Ger.). Phys. Letters, 18: 270-1(Sept. 1, 1965).

Experimental investigations on the polarization of several alkali lines are reported. These lines are suited to check some theoretical results on polarization of impact radiation. The crossed beam technique was used in the experiment. The gun producing the electron beam consisted of an oxide-coated cathode, a Pierce electrode system, a collision chamber and a collector electrode. The polarization of the following alkali lines were measured as a function of the electron energy: the first resonance lines with the following main contributions in its isotope compositions, lithium-6, lithium-7, and sodium-23, the λ ($4^2S \rightarrow 2^2P$) = 4971 Å line, and the λ ($3^2D \rightarrow 2^2P$) = 6103 Å line of natural lithium. The polarizations of the three resonance lines investigated increase monotonously from higher energies to the excitation threshold. Within an energy width of the electron beam of about 0.3 ev no minimum or decrease of the polarization was observed for these resonance lines near the excitation threshold. On account of a pressure depolarization observed each polarization value of the resonance lines was obtained by extrapolation to the particle density zero in the atomic beam. These values are given and interpreted. (J.F.P.)

44957 OBSERVATION OF UNDULATIONS OF THE TOTAL ELASTIC SCATTERING CROSS SECTION FOR THE SCATTERING OF HELIUM ATOMIC BEAMS IN Xe, Kr AND Ar. Beier, H.-J. (Technische Universitaet, Berlin). Phys. Letters, 18: 285-6(Sept. 1, 1965).

The velocity dependence of the total elastic scattering cross sections of He–Xe, He–Kr, and He–Ar was investigated. The measurements were performed with the beam-gas attenuation method. The He beam started from a source, which could be cooled down with liquid helium from room temperature to 4.8°K. By this means the mean velocity of the beam was varied continuously in the range of 12.5×10^4 to 1.6×10^4 cm/sec. The beam showed a Maxwellian distribution with a minor modification caused by the applied beam pulsing. The attenuation of the beam up to attenuations larger than 1/e shows linearity in semilogarithmic plotting. The scattering cross sections were calculated from the slopes. (J.F.P.)

44958 PRODUCTION OF HIGHLY POLARIZED ELECTRON BEAMS BY LOW-ENERGY SCATTERING. Jost, K.; Kessler, J. (Technische Hochschule, Karlsruhe, Ger.). Phys. Rev. Letters, 15: 575-7(Oct. 4, 1965).

In order to check the Mott theory of scattering by the screened and by the unscreened Coulomb field, an experiment was performed in which the angular resolution was sufficient to demonstrate the high polarization values concentrated in the peaks which are plotted and shown. In this way electron beams of about 80% polarization were produced, and essential features of the theory were confirmed. A monoenergetic electron beam of some 100 μamp crosses a mercury-atom beam which scatters part of the electron beam. The electron energy can be varied between 100 and 1000 ev. By rotating the electron gun the scattering angles can be varied continuously between 0 and 155°. The angular resolution is about ±1° (half-amplitude). The scattered electron beam is expected to be polarized, the direction of the polarization vector being perpendicular to the plane of scattering. The scattered electrons were accelerated to 120 kev, in order to use the previously reported Mott scattering method of analysis. It was found that the theoretical results were confirmed and that scattering of low-energy electrons represents a convenient method of producing electron beams of high polarization. (J.F.P.)

44959 NEW AUTOIONIZING LEVELS IN HELIUM. Rudd, M. E. (Concordia Coll., Moorhead, Minn.). Phys. Rev. Letters, 15: 580-1(Oct. 4, 1965). (COO-1277-11).

With somewhat increased resolution additional levels were observed in helium including parts of two series not previously reported. Electrons ejected at a 160° angle with respect to the ion beam were observed. The helium pressure in the collision chamber was five to six microns. The bombarding ions were 75-kev H^+ or H_2^+. Three runs at different recorder sensitivities are shown. Two peaks are identified, one of which was not previously observed. The new series are the $(2sns)^1S$ and the $(2snp)^3P$, the first terms of which were previously reported. Both series converge to the same limit as the sp,2n series. A summary of the measured and calculated values of the energies of the two series is given. Identification of the two series was aided by the fact that triplet levels are not excited by proton bombardment but show up strongly under H_2^+ bombardment. (J.F.P.)

44960 THE TIME-INDEPENDENT SCHROEDINGER WAVE EQUATION FOR A PARTICLE IN A CENTRAL POTENTIAL FIELD AS A SPATIAL INTEGRAL EQUATION. Thor, Anders J. Trans. Roy. Inst. Tech. Stockholm, No. 244, 1-12(1965).

The time-independent Schroedinger wave equation for a particle in a general potential field is written as a three-dimensional spatial integral equation. From this equation the corresponding radial integral equation is deduced, on the assumption that the potential is that of a central field. The radial equation is given with two different, but equivalent, expressions of the kernel. The former is the more suitable one for computer integration, while the latter is often preferable for analytic investigations. Finally it is shown that the well-known wave function of a hydrogen-like atom satisfies the integral equation. (auth)

44961 PLASMA OSCILLATIONS OF BOUND ELECTRONS: THE CHARACTERISTIC ENERGY LOSS OF 3.6 ev IN THIN SILVER FOILS. Otto, Andreas (Universitaet, Munich). Z. Physik, 185: 232-62(1965). (In German).

It was experimentally shown that the characteristic energy loss of 3.6 ev in silver foils is composed of a surface loss and the volume-plasma loss of 3.75 ev suggested by Froehlich and Pelzer. The dependence of the contribution of the surface loss on the silver layer thickness and on the velocity of the incident electrons and the displacement or disappearance in covering of the foil with carbon or Al can be theoretically explained by a surface plasma oscillation. After suppression of the surface loss by covering of the silver foil with Al, the remaining volume loss can be clearly detected; the quantitative comparison with theory is satisfactory. (tr-auth)

44962 INTENSITY OF NONRADIATIVE TRANSITIONS IN Ta AND ^{239}Pu MESIC ATOMS. Balats, M. Ya.; Karapetyan, V. V.; Kondrat'ev, L. N.; Obukhov, Yu. V. (Inst. of Theoretical and Experimental Physics, Moscow). Zh. Eksperim. i Teor. Fiz., 49: 3-9(July 1965). (In Russian).

The 2p–1s mesic x-ray transitions in Ta, Pb, and ^{239}Pu are investigated with a scintillation spectrometer. The fraction of nonradiative 2p–1s transitions in Ta and ^{239}Pu is determined by comparing the intensity of radiative transitions per μ^- meson stopped in Ta and ^{239}Pu. (auth)

44963 OPTICAL ORIENTATION OF ATOMS IN A MAGNETIC FIELD PERPENDICULAR TO THE BEAM. Aleksandrov, E. B.; Konstantinov, O. V.; Perel, V. I. (Vavilov State Optical Inst., USSR). Zh. Eksperim. i Teor. Fiz., 49: 97-106(July 1965). (In Russian).

It is demonstrated theoretically and experimentally that an appreciable orientation of atoms can be attained in a magnetic field perpendicular to the orientating light ray. To achieve this a variable magnetic field was imposed on the stationary field. If the directions of these two fields form a small angle, the resulting moment will precess about the stationary field. In this case large time independent components of the moment directed along the magnetic field and light arise. The experiment was carried out in cesium vapor. The orienting ray was circularly polarized and consisted of one of the long wave components of the resonance doublet. (auth)

44964 MEASUREMENT OF CESIUM SPUTTERED COPPER YIELD AND ANGULAR DISTRIBUTION BY A RADIOACTIVE TRACER TECHNIQUE. Olson, N. Thomas; Smith, Harold P. Jr. (Univ. of California, Berkeley). New York, American Inst. of Aeronautics and Astronautics, 1965, Preprint No. 65-379, 12p., $1.00. (CONF-650711-15). ORINS.

From AIAA 2nd Annual Meeting and Technical Demonstration, San Francisco.

A radioactive tracer technique was developed and successfully applied to the measurement of the yield and angular distribution of copper sputtered from a monocrystalline target under bombardment by a 1 to 10 kev cesium ion beam with the beam parallel to the ⟨100⟩ crystallographic vector. The yield is seen to reach a maximum of 7.8 at 7 kev and is considerably lower than that reported for polycrystalline targets. The relative openness of the (100) face is the probable reason for the significant reduction. A possible application of this effect to ion rocket electrode design is noted. Measurement of the absolute angular distribution as a function of energy indicates that increased incident ion energy leads to increased preferred ejection along the ⟨100⟩ and ⟨110⟩ directions. Ejection along the ⟨110⟩ direction is skewed to greater polar angles than that associated with the close-packed direction in copper. This effect is interpreted as suggesting that long focused collision chains are not of primary influence in causing a sputtering event. (auth)

Cosmic Radiation

See also Elementary Particles and Radiations. Nuclear Properties and Reactions.

Refer also to abstract 44437.

44965 MODULATION OF THE PRIMARY SPECTRUM DURING THE RECENT SOLAR CYCLE FOR RIGIDITIES BETWEEN 4 AND 12 BILLION VOLTS. Manzano, J. R.; Winckler, J. R. (Univ. of Minnesota, Minneapolis). J. Geophys. Res., 70: 4097-4106(Sept. 1, 1965).

To get an empirical expression for $\delta D/D_0$, the variation of the differential primary spectrum, the data of four neutron monitors accumulated during most of the solar cycle are used in the expression $\delta D/D_0 = [d/dP(\Delta I/I_0)]/[(1/I_0)(dI_0/dP)]$ where $(d/dP)(\Delta I/I_0)$ is the slope of the percentage variation-rigidity curve, and $(1/I_0)(dI_0/dP)$ is the neutron monitor response curve. The reference level is always June 1955. For statistical convenience, all data are smoothed by 12-mouth moving averages and normalized to sea level. The rather small sensitivity of the neutron monitors below 4 bv rigidity and the lack of information for rigidities above 12 bv allow us to analyze only the interval between those rigidities. It is shown that no hysteresis is significant for the two principal periods of the solar cycle; June 1955 to February 1958 and March 1958 to March 1962 or 1963, according to the data available up to the moment of the analysis. The formula $\delta D/D_0 = -0.036\,(t-5)^{\frac{1}{2}}\,P^{-1.55}$ for $4 \le P \le 12$ bv is obtained for the decrease period, where t is given in months from June 1955. The previous expression is valid for $5 \le t \le 32$. For $t \le 5$, $\delta D/D_0$ must be zero in order to keep the constancy of the counting rate for almost the complete year of 1955. For the recovery period, $\delta D/D_0 = -0.0083\,(115-t)^{\frac{1}{2}}\,P^{-1.55}$ is obtained for the same interval of rigidities. This expression is valid for $33 \le t \le 115$. Here it is assumed that at the beginning of 1965 the solar cycle is recovered to the 1954–1955 level. The difference in the percentage variation of the counting rate for the Climax–Mt. Norikura and Hermanus–Buenos Aires pairs of stations is shown to agree with the calculated values obtained with the empirical laws. It is shown that the variational primary spectrums, obtained with the Japanese neutron monitor latitude surveys from the end of 1956 until April 1962, follow a power law with exponent near 1.6 for three cases and greater than 2 for one case for the interval $4 \le P \le 12$ bv. (auth)

44966 RESPONSE OF ION CHAMBERS IN FREE SPACE TO THE LONG-TERM COSMIC-RAY VARIATION FROM 1960 TO 1965. Kane, S. R.; Winckler, J. R.; Arnoldy, R. L. (Univ. of Minnesota, Minneapolis). J. Geophys. Res., 70: 4107-15(Sept. 1, 1965).

Differential response curves and mean rigidity of response are computed for an ion chamber in free space using the cosmic-ray spectrum at solar minimum and maximum observed by independent cosmic-ray measurements. The response is found to be confined predominantly to the rigidity interval 1.5–2.5 bv during the entire solar cycle and is consistent with the observed modulation of He nuclei at these rigidities. The corresponding rigidity intervals for ion chambers flown on balloons at high latitudes and at Minneapolis are 2.5–3.5 bv and 3.0–4.0 bv, respectively. Using these results and the measurements made with ion chambers aboard the Pioneer 5 (1960), Mariner 2 (1962), and Ogo A (1964–1965) spacecrafts, ion chambers flown on balloons at high latitudes and at Minneapolis, and the He nuclei detectors, the rigidity dependence of the long-term variation during 1960–1965 is found to be consistent with the form $P^{-\beta}$, where $\beta \approx 0.8$. For the subperiods 1960–1962 and 1962–1964, β is about 0.8 and 1.4, respectively. (auth)

44967 SPECTRAL DATA FROM THE COSMIC X-RAY SOURCES IN SCORPIUS AND NEAR THE GALACTIC CENTRE. Giazconi, R.; Gursky, H.; Waters, J. R. (American Science and Engineering, Inc., Cambridge, Mass.). Nature, 207: 572-5(Aug. 7, 1965).

During two rocket flights conducted from White Sands Missile Range on August 28, 1964, (flight I), and October 26, 1964 (flight II), information regarding the spectral composition of the x-ray source in Scorpium (Sco X-1) and those along the Galactic equator in the vicinity of the Galactic center was obtained. Spectral data obtained by placing absorbers in front of the Geiger counters during flight I and by performing a pulse height analysis of the output of a sodium iodide scintillation counter during flight II are reported. The results indicate that the ratio of the counting rate in the Geiger counters to that in the NaI detector is not consistent with a single thermal spectrum. The NaI detector did not detect significant radiation from Sco X-1 beyond about 15 kev, whereas radiation was observed from the Galactic center region to beyond 20 kev. The minimum detectable flux density at 20 kev (defined as equivalent to 1 above background) is about 3×10^{-27} ergs/cm^2-sec (c/s). For both source regions the attenuation of the counting rate in the Geiger counters by the filters indicated that the x-ray flux below 2.5 kev is comparable with that above 2.5 kev. (P.C.H.)

44968 POSITIONS OF THREE COSMIC X-RAY SOURCES IN SCORPIO AND SAGITTARIUS. Clark, G. (Massachusetts Inst. of Tech., Cambridge); Garmire, G.; Oda, M.; Wada, M.; Giacconi, R.; Gursky, H.; Waters, J. R. Nature, 207: 584-7(Aug. 7, 1965). (MIT-2098-157).

The positions of three cosmic x-ray sources were determined in the constellations of Scorpio and Sagittarius within uncertainty areas of 1.2-3 square degrees. The data were obtained with a rocket that was launched from White Sands, New Mexico, on Oct. 26, 1964, at a sidereal time of 20 hr 20 min, and reached an apogee of 224 km. The rocket carried a variety of instruments, among which were several x-ray detectors and two star sensors. The actual orientations of the detectors and star sensors were determined in the rocket frame of reference to accuracies of ±0.3° in elevation and azimuth by optical measurements on the ground before and after the flight. (P.C.H.)

44969 RECENT DEVELOPMENTS IN THE FIELD OF COSMIC PHYSICS: X RAYS OF NON-SOLAR ORIGIN. Bonetti, A. (Universita, Bari, Italy). Nuovo Cimento (1), 2: Suppl., 492-504(1964). (In Italian).

The present state of knowledge on the x rays of non-solar origins is summarized briefly. The characteristics of the x rays in interstellar space, the experimental results, and the mechanism for the production of non-solar x rays are discussed. (J.S.R.)

44970 SPARK-CHAMBER EXPERIMENT ON COSMIC GAMMA RAYS. Cobb, R.; Duthie, J. G.; Stewart, J. (Univ. of Rochester, N. Y.). Phys. Rev. Letters, 15: 507-11(Sept. 20, 1965).

A new upper limit is reported for the flux of gamma rays from the Crab Nebula. The measurements were made by means of a balloon-borne spark chamber flown over India during recent cosmic-ray studies. The flux of gamma rays of energy greater than 100 Mev from the Crab Nebula is estimated to be no larger than 7×10^{-5} cm^{-2} sec^{-1}. Several other objects were also studied and upper limits to the fluxes from these are given. No sources of cosmic gamma rays were identified; and no finite fluxes are claimed. The detector used in the experiment consists of a scintillation-Cherenkov-counter system in conjunction with two spark chambers. The gamma rays observed under 6.5 grams of residual atmosphere showed an east-west asymmetry; the ratio of those rays arriving from the western hemisphere to those arriving from the eastern hemisphere was 1.33 ± 0.19. (J.F.P.)

44971 ORIGIN OF COSMIC X RAYS. Gould, Robert J. (Univ. of California, San Diego, La Jolla). Phys. Rev. Letters, 15: 511-12(Sept. 20, 1965).

A correction is given of the impression given recently by Hoyle (Phys. Rev. Letters, 15: 131(1965)) that the observed diffuse component of cosmic x rays can be accounted for by Compton scattering of low-energy photons by the (presumed) galactic relativistic electrons responsible for

the nonthermal radio background radiation. As Hoyle showed, for radiation density due to the low-energy cosmic photons, the total energy-loss rate from Compton scattering for relativistic electrons is very large. For electrons moving in a magnetic field of 3×10^{-6} G, the energy loss due to Compton scattering equals the energy loss due to synchrotron radiation. However, to compare with the x-ray observations, the associated spectrum of Compton-scattered photons should be considered. The Compton (C) spectrum due to scattering by a distribution of relativistic electrons is essentially the same as the synchrotron (S) spectrum except that it is in a different frequency or energy region. An objection is also raised to Hoyle's conclusion that the density of high-energy electrons in intergalactic space is very small. Although these electrons may decrease in energy in a time much less than the cosmic expansion time, a considerable density of these electrons could still exist in the intergalactic medium if there is continuous production therein via charge-meson (π) production and decay in cosmic-ray nuclear collisions. (J.F.P.)

44972 CHARGE RATIO OF COSMIC-RAY ELECTRONS. Jones, Frank C. (Goddard Space Flight Center, Greenbelt, Md.). Phys. Rev. Letters, 15: 512-14(Sept. 20, 1965).

It is pointed out that the assumption that the ratio of the number of positrons to the number of electrons is approximately 1 at high energies is probably not true. It is shown that at high energies the ratio is considerably larger than one. There is considerable evidence that there are isobars excited in collisions up to 23-Bev/c primary momentum and that retention of a fixed average fraction of the initial energy by the primary particle holds true for very high energies ($\sim 10^{15}$ ev) and for as many as 10 collisions in succession. Furthermore, it appears evident that as higher energies are approached the well-known ($^3/_2$,$^3/_2$) isobar fades out of the picture and the excitation of isobars proceeds with no exchange of isospin or strangeness; that is, the isobars excited in a p-p collision are predominantly of the $T = ½$, $T_3 = ½$, nonstrange variety at ~23 Bev/c. Since the decay of such isobars is via the strong interactions and hence is isotopic-spin conserving, this severely constrains the charge ratio of the resulting secondaries. An estimate is derived for the value of this ratio at high energies based on these considerations. It is expected that this ratio is of the order of 10 rather than one, from the experimental data alone; and it is seen that any possible admixture of other channels cannot reduce the ratio below about five. (J.F.P.)

44973 RECEPTION OF TELEMETERING SIGNALS FROM THE SATELLITE EXPLORER VII: HIGH ENERGY RADIATION MEASUREMENT IN THE EXOSPHERE. Miyazaki, Yukio; Takeuchi, Hajime; Imai, Takashi; Yoshizawa, Tadayoshi; Kaneko, Kayo (Inst. of Physical and Chemical Research, Tokyo). Rika Gaku Kenkyusho Hokoku, 38: 145-52(1962). (In Japanese).

Telemetering signals from the U. S. satellite Explorer VII were received during the period from March to August, 1960, in Tokyo. The methods and progress of the reception of these signals are reported. Analysis of a part of the decoded data showed that the latitude distribution of high energy radiation was not as complex as that obtained by observations in 1958. An indication was seen that the satellite entered the inner radiation belt at the latitude 20°N, at an altitude higher than 1050 km and longitude greater than 140°E. An unusual enhancement of the high energy radiation intensity was observed in April, 1960, at higher latitudes, which is interpreted as due to the shift of the outer radiation belt to lower latitudes. However, in this event, little change was observed at lower latitudes. (BBB)

44974 ON THE COSMIC-RAY INDEX. Wada, Masami; Kodama, Masahiro; Kaneko, Kayo (Inst. of Physical and Chemical Research, Tokyo). Rika Gaku Kenkyusho Hokoku, 38: 589-96(1962). (In Japanese).

As a means of indicating the magnitudes of the various cosmic-ray disturbances, such as the Forbush decrease and 27-day recurrence variation, the cosmic-ray J index, which is analogous to magnetic K index, is introduced. The J index was calculated by using cosmic-ray-neutron data from three stations situated at different longitudes and latitudes, namely, Mt. Norikura, Zugspitze, and Sulphur Mountain, during the IGY 1957/58 period. Numerical values obtained are tabulated throughout the whole IGY period. The relation between the J index and both solar and geomagnetic phenomena is examined. (BBB)

44975 PLASMA-TURBULENCE MECHANISMS AND THE ACCELERATION OF COSMIC RAYS. Tsytovich, V. N. (Inst. of Physics, Academy of Sciences, USSR). Soviet Astron. AJ (English Transl.), 9: 24-30(July-Aug. 1965).

Translated from Astron. Zh., 42: 33-41(Jan.-Feb. 1965).

Mechanisms are considered for the generation of turbulence in a plasma by gravitational instability and by cosmic rays. The influence of nonlinear effects on the turbulence spectrum is discussed. (auth)

44976 JOURNEES D'ETUDES SUR LA PHYSIQUE NUCLEAIRE COSMIQUE 27 ET 28 MAI 1963. (Study Sessions on Cosmic Nuclear Physics. Organized at Saclay May 27 and 28, 1963). [Paris], Presses Universitaires de France, 1965. 144p.

The presentations at the study sessions on cosmic nuclear physics are compiled together with the discussion following each paper. The papers appear to be directed to nonspecialists. The subjects discussed were old and recent data on cosmic radiation, nuclear physics of stars, cosmic radiation in meteorites, study of the energy in the galaxies by radioastronomy, program of the cosmic physics laboratory of the C.N.R.S. during the International Year of the Calm Sun, state of development of studies at very high energies, the experiments in space physics of the C.E.A., solar and cosmic x rays and γ rays, and the study of the electrons of primary cosmic radiation. (J.S.R.)

Criticality Studies

See also REACTOR TECHNOLOGY — Criticality Studies.

44977 (IDO-17095) A CORRELATION OF INTERACTION DATA WITH CALCULATIONS USING THE GELLER MODEL. Fox, J. K. (Phillips Petroleum Co., Idaho Falls, Idaho. Atomic Energy Div.). Aug. 1965. Contract AT (10-1)205. 25p. Dep. mn; CFSTI $2.00 cy, $0.50 mn.

A simple model is described for calculating the critical separation of regular arrays of identical fissile units. The units must be separated mainly by air. The model used is one first derived by Geller. Use is made of the fact that for a critical system the material buckling is equal to the geometric buckling. The model assumes that the total interaction probability, ψ, is simply related to the ratio of the geometric buckling, B_g^2, of the critical isolated unit to that of one unit in the array: $B_g^2 = B_1^2 (1 - \psi)$ where B_1^2 is the geometric buckling of a single unit in the array. The total interaction probability depends mainly upon the solid angle between two units and the total number of units in the array. Normalization to experiment is used to determine the proportionality constant relating the solid angle to the interaction probability. Thus, the calculation is reduced to a simple geometrical problem. To determine the total interaction probability as a function of number of units in an array a determinant is set up based on symmetry. A major difficulty with this method is in how to treat shadow effects. These become important for large arrays. Hence, extrapolations are used to estimate the coupling coefficients of large arrays. The results of extensive comparisons of the model with data obtained at ORNL are presented. These results show that, in general, the calculated separations agree well with the data, except at very close spacings. The concept of a reflector saving applied in the calculation of the geometric buckling of units allows the estimation of the effect of thin reflectors around units and that of a reflecting vault around the array. Two methods are noted whereby conservatism may be introduced and its degree estimated.

The fact that the same model gives good results for both dilute solutions and metal systems indicates that the interaction probability is essentially independent of the leakage neutron energy spectrum. (auth)

Direct Energy Conversion

Refer also to abstract 44640.

44978 (AED-C-15-08) DIRECT CONVERSION OF NUCLEAR ENERGY INTO ELECTRIC ENERGY. Series C: Bibliographies. (Battelle Institut e.V., Frankfurt am Main (West Germany)). Apr. 1965. 120p. Dep. mn.

References (390) are presented for documents on direct conversion of nuclear energy into electric energy. An author index and a report number index are included. (D.C.W.)

44979 (NP-15419) THERMIONIC CONVERSION OF HEAT TO ELECTRICITY. Fourth Quarter Report of Research and Development Program. (General Electric Co., Pleasanton, Calif. Special Purpose Nuclear Systems Operation). June 29, 1965. Contract NObs-90496. 6p.

The diffusion of uranium, from urania, through tungsten at 1800 and 2000°C and of oxygen in molybdenum at 1500 and 1800° was studied, together with the reaction of alumina with niobium at 1550 to 1900°C. Techniques for the fabrication of cesium-resistant, ceramic-to-metal seals were investigated; seals were tested at high temperatures both in cesium and in vacuum. (D.C.W.)

44980 (NP-15433) THE DEVELOPMENT OF AN INSULATED THERMIONIC CONVERTER-HEAT PIPE ASSEMBLY. Quarterly Technical Report No. 1. Harbaugh, W. E. (Radio Corp. of America, Lancaster, Pa. Direct Energy Conversion Dept.). June 1965. Contract AF33 (615)-2617. 48p.

The effort applied during the first three months toward the development of a long-life insulated thermionic converter integrated with an efficient, constant-temperature, heat-transfer device is summarized. Specifically, the cylindrical converter, RCA Type A-1198B will be adapted for heating by means of a heat pipe to operating temperatures of 1500°C. The module available from prior work was life tested for more than 1000 hr. Irreparable damage was caused by equipment failure, and the test was halted. Progress was made in the development of high-temperature, ceramic-metal seals. A program was detailed for the production of ultrapure cesium and for the accurate analysis of the result. New approaches toward lowering the collector work function are being investigated. The promising results of adding xenon to the operating converter are being further investigated to optimize performance. The heat-pipe test vehicle was designed for the evaluation of processing techniques. The process of insulating the emitter from the heat pipe at high temperatures is proceeding on schedule. The converter design was modified to facilitate the use of a heat pipe as the prime source of heat. (auth)

44981 (NP-15435) RESEARCH ON NEW CONCEPTS IN ENERGY CONVERSION. Quarterly Technical Progress Report No. 7, March 1-May 31, 1965. Jackson, W. D.; Brown, G. A.; Kerrebrock, J. L.; Stickney, R. E. (Massachusetts Inst. of Tech., Cambridge. Research Lab. of Electronics). June 15, 1965. Contract AF33(615)-1083. 35p.

The construction of a test facility for research on high-performance condensing ejectors for liquid-metal MHD power systems was begun, and the preliminary experimental study of the MHD induction generator was completed. A boundary-layer analysis of turbulent MHD channel flows was made, and flow measurements with the pilot tube probe were completed. The performance potential of a potassium-vapor MHD generator was studied, and the design parameters for the large segmented-electrode generator experiment were selected. The dependence of thermionic emission from a tungsten crystal upon the crystal orientation was studied, and a quantum-mechanical analysis of alkali atom-metal interactions was undertaken. An optical pumping experiment was performed to measure the importance of the autoionization reaction of excited cesium. A coil system for an MHD induction generator was also designed and tested. (D.C.W.)

44982 ELECTRON DISTRIBUTION AND DENSITY FUNCTION IN AN IONIZED MAGNETOHYDRODYNAMIC CONVERSION GAS. Archambault, Y. Ann. Radioelec., 20: 183-90(July 1965). (In French).

In an ionized gas subjected to an electric field the mean electron energy can be greater than the mean energy of neutral particles, and the degree of ionization increased as compared to that to be expected for thermal ionization at the temperature of the gas. The electron distribution function for such a gas not in thermodynamic equilibrium is examined and it is shown that it is in fact a Maxwell distribution under temperature and density conditions which are those of magnetohydrodynamic conversion. The electron density in a gas of this kind is next examined: it may be distinctly less than that predicted by Saha's law applied to the electron temperature in the case of a gas assumed to be optically thin. (auth)

44983 BINARY INSTALLATION FOR THE PRODUCTION OF ENERGY USING THERMIONIC CONVERTORS. Pandolfi, Maurizio. Atti Accad. Sci. Torino: I. Classe Sci. Fis., Mat. Nat., 99: 233-55(1964-65). (In Italian).

A brief discussion is given of the equations governing the functions of thermionic converters. The yield predictable from the coupling of thermionic converters with conventional installations using gas turbines and water vapor turbines is derived. (tr-auth)

44984 RAYLEIGH-TAYLOR INSTABILITY IN THE STRIATED LAYER MAGNETOHYDRODYNAMIC GENERATOR. Fraidenraich, N. (Univ. of Sheffield, Eng.). Brit. J. Appl. Phys., 16: 1265-75(Sept. 1965).

The flow stability of the striated layer magnetohydrodynamic generator is studied. This problem reduces to the analysis of the Rayleigh-Taylor instability in the case of a finite conducting fluid bound by non-conducting ones when a uniform horizontal magnetic field and vertical electric field (crossed configuration) are applied; the vertical interface is uniformly decelerated in a direction perpendicular both to electric and magnetic fields. Waves propagating across and along the magnetic field are separately analyzed. In the first case, after concluding that there is no influence of the magnetic field on the stability problem, a survey of different influencing factors is made where nonviscous and viscous fluids are considered and finite thickness of the conducting fluid is taken into account. This leads to the conclusion that, for the deceleration occurring in the impulse-type striated layer magnetohydrodynamic generator, a range of wavelengths exists for which the rate of growth of the disturbance is fast enough to destroy the equilibrium configuration. Similar results are found in the case of waves propagating along the magnetic field. (auth)

44985 EFFORTS TO INCREASE THERMIONIC CONVERTER OUTPUT AND EFFICIENCY. Wilson, V. C.; Webster, H. F.; Lawrence, J. (General Electric Co., Schenectady, N. Y.). 13p. (CONF-650908-8). ORINS.

From International Conference on Thermionic Electrical Power Generation, London.

The output characteristics of three converters are presented. All had Ni collectors. Two had 0.002 inch spacings and W or Re emitters. The third was 0.005 inch spaced with a W-25% Re emitter. Under similar conditions the converter with the Re emitter generated slightly higher powers. The W-25% Re emitter operated more nearly like a W emitter. The W-Ni, 0.002 inch spaced converter at $T_E = 2263°K$ generated a usable output of 25 watts/cm^2 at 20 amperes per cm^2 and a calculated efficiency of 22.5%. Electron cooling measurements coupled with a study of the variations in the plasma potential drops indicated that roughly 40% of the power put into the plasma is returned to the emitter. A discussion is given of the possibility of improving converter performance by the use of emitter

surfaces with particular crystallographic orientation. The results of the test of a converter which had a tungsten emitter consisting of 16 cm^2 of 110 crystal face are presented. A calculation was made to find under what conditions the performance of a converter might be improved by operating it in the unignited mode. (auth)

44986 APPLICATION OF NUCLEAR THERMIONICS TO UNDERSEA TECHNOLOGY. Van Hoomissen, J. E.; Case, J. M. (General Electric Co., Pleasanton, Calif.). New York, American Society of Mechanical Engineers, 1965, Preprint No. 65-UNT-4, 9p. $1.00. (CONF-650550-1). ORINS.

From American Society of Mechanical Engineers, Underwater Technology Conference, New London, Conn.

The basic principles of thermionic energy conversion are presented and general considerations in the application of nuclear thermionic technology are discussed. The present state of the thermionic art is reviewed including: laboratory data on the thermionic-converter performance, ex-reactor life testing of conceptual converter designs for nuclear application, and experimental results from materials development programs. Two conceptual power-plant designs, based on present state of the art, are introduced as possible candidates for undersea application. Nuclear thermionic generators are shown to be simple, long life, reliable and maintenance-free systems, that are well adapted to undersea environment and application. (auth)

44987 DESIGN APPLICATIONS OF DIRECT ENERGY CONVERTERS. Henderson, R. E. (General Motors Corp., Indianapolis). New York, American Society of Mechanical Engineers, 1965, Preprint No. 65-MD-50, 6p. $1.00. (CONF-650546-2). ORINS.

From American Society of Mechanical Engineers, Design Engineering Conference and Show, New York.

Although direct-conversion systems of the electrochemical type have been used in a practical manner for many decades, the general application of these systems has come about very slowly. The recent success of the photovoltaic converter for space applications has been the center of a strong upsurge in research. This is resulting in the development of several interesting electrical power supplies which will undoubtedly find uses in this decade. The trend thus appears to be setting in toward direct conversion—warranting interest on the part of design engineers in the basic principles and operating characteristics of these devices. (auth)

44988 INVESTIGATION OF A THERMIONIC CONVERTER OPERATING WITH A HIGH TEMPERATURE COLLECTOR. Blue, E.; Ingold, J. H. (General Electric Co., Pleasanton, Calif.). 6p. (CONF-650908-7). ORINS.

From International Conference on Thermionic Electrical Power Generation, London.

The results of a study to determine the effects of high collector temperature on the current-voltage characteristics of a high pressure Cs thermionic converter are described. The emitter electrode was machined from arc-cast W bar stock and was brazed with Nb to a Ta support cylinder. The collector was made of Ta and had a thick wall to enhance conduction cooling. The variation of peak power with T_C for T_E = 2225°K and spacings of 5, 10 and 15 mils was determined from the data, and is shown along with other data curves. (L.B.S.)

44989 THE DEVELOPMENT OF A RESERVOIRLESS THERMIONIC ENERGY CONVERTER. Harbaugh, W. E.; Block, F. G.; Basiulis, A. (Radio Corporation of America, Lancaster, Pa.). New York, American Inst. of Aeronautics and Astronautics, 1965, Preprint No. 65-472, 8p., $1.00. (CONF-650711-16). ORINS.

From AIAA 2nd Annual Meeting and Technical Demonstration, San Francisco.

An experimental program was established to determine the feasibility of achieving satisfactory performance from a thermionic converter which does not have a reservoir of liquid cesium. Effort was concentrated on finding solutions for two principal problem areas: the establishment of proper cesium pressure initially, and the maintenance of cesium pressure during life. The processing, testing program, life tests, and analysis of the reservoirless converters are discussed. (L.B.S.)

44990 IMPROVEMENTS IN OR RELATING TO MAGNETO-HYDRODYNAMIC GENERATORS. (to Westinghouse Electric Corp.). British Patent 1,000,052. Aug. 4, 1965. Priority date July 13, 1962.

A MHD generator is described that includes means for supplying a thermally ionized working fluid, means for providing a magnetic field in the generator transverse to the direction of the flow of the working fluid, and electrode means for extracting the electrical energy from the fluid. Through sustained internal combustion, a continuous reheating of the working medium is effected throughout its passage through the generator for maintenance of the electrical conductivity of the generator. (B.L.M.)

44991 IMPROVEMENTS IN OR RELATING TO MAGNETO-HYDRODYNAMIC GENERATOR APPARATUS. (to Westinghouse Electric Corp.). British Patent 1,000,300, Aug. 4, 1965. Priority date June 15, 1962, United States.

An apparatus for the conversion of thermal energy to electrical energy includes a plurality of MHD generator stages. Means are provided for supplying ionized working fluid to the stages and for causing the working fluid to flow through the generator stages. Heat is supplied to the working fluid between each immediately succeeding pair of generator stages. Each generator stage includes means for maintaining a magnetic field transverse to the direction of flow of the working fluid, and electrode means for extracting the electrical energy are disposed transverse to the direction of the magnetic field and the flow of the working fluid. A seeding material, e.g., an alkali metal, is supplied to the working fluid to cause it to ionize more readily. The seeding material is reclaimed from the working fluid that has passed through the generator stages and returned to the first generator stage. (B.L.M.)

44992 ELECTROCHEMICAL FUEL CELL OPERATION WITH ANTIPOLAR ION EXCHANGE MEMBRANE. Grueneberg, Gerhard; Jung, Margarete (to Varta AG and Siemens-Schuckert-Werke, AG). U. S. Patent 3,198,666. Aug. 3, 1965. Priority date May 7, 1960, Germany.

A fuel cell for the utilization of fluid fuels comprises means defining a fuel fed electrode and a fluid fed oxygen electrode with a pair of hydrated ion exchange membranes in abutting contact with one another between the electrodes. The pair of membranes include a hydrogen transferring cation exchange membrane in abutting contact with the fuel electrode and a hydroxyl transferring anion exchanger in abutting contact with the oxygen electrode with the membranes serving as electrolyte for the electrodes. The fuel electrode contains as an active catalytic component a member selected from the group consisting of Pt, Pd, and mixtures of the two. The oxygen electrode consists of a member selected from the group consisting of Ag, Pt, and mixtures of the two. The catalytic component is in finely divided form and is embedded substantially into the corresponding surface of the ion exchange membrane in contact with it. The individual particles of the catalytic component are in electrically conductive contact with one another. During operation of the cell, the fuel electrochemically dissolved at the fuel electrode and the oxygen electrochemically dissolved at the oxygen electrode will electrochemically combust at the combined membrane electrolyte with the generation of an electric current. (B.L.M.)

Elementary Particles and Radiations

Refer also to abstracts 44438, 44443, 44951, 45280, 45354, and 45360.

44993 (CEA-R-2778) CALCUL DE LA CONTAMINATION EN MUONS D'UN FAISCEAU DE MESONS π. (Calcu-

lation of the Muon Contamination in a π-Meson Beam). Tran, Anh Ha (Commissariat a l'Energie Atomique, Saclay (France). Centre d'Etudes Nucleaires). 1965. 17p. Dep. mn.

A method is presented for calculating the μ contamination of a π meson beam which is parallel and of cylindrical symmetry. The CONTAMU program used in carrying out this calculation is also given. An evaluation of the μ contamination is necessary for correcting the experimental values of the cross sections of various reactions using the π meson beam as the incident particle beam. The two following cases are treated: (1) the beam is defined by an S_1 counter and the μ contamination is calculated when the beam passes through this counter and (2) the beam is defined by two counters S_1 and S_2 and the μ contamination is calculated when the beam passes through the two counters successively. The calculation is given in detail following the order of the program. A table of results for a few of the parameters defined is given as an example. (tr-auth)

44994 (CERN-65-26) QUANTUM THEORY AND ELEMENTARY PARTICLES. Weisskopf, Victor F. (European Organization for Nuclear Research, Geneva (Switzerland)). July 2, 1965. 23p. Dep. mn.

The quantum structure of matter is discussed with specific consideration of the symmetries of elementary particles. (D.C.W.)

44995 (COO-30-97) A TECHNIQUE FOR STUDYING THE PHYSICAL SCATTERING MATRIX. Rubin, M. H. (Wisconsin Univ., Madison. Dept. of Physics). [1963]. Contract AT(11-1)-30. 15p. Dep. mn; CFSTI $1.00 cy, $0.50 mn.

The Fredholm theory of integral equations is used in a Hilbert space of functions which are square integrable on a contour in order to discuss the Lippmann-Schwinger equation. By exploiting the analyticity of the potential matrix in its indices, a simple proof of the existence of the physical scattering matrix is given. The high-energy behavior of the physical scattering matrix is also discussed. (auth)

44996 (COO-1195-39) SYSTEMATICS OF BARYON STATES. Technical Report No. 143. Hill, R. D. (Illinois Univ., Urbana. Dept. of Physics). Aug. 1965. Contract AT(11-1)-1195. 3p. Dep. mn; CFSTI $1.00 cy, $0.50 mn.

The systematic progression of baryon states with the same J^P values ($\frac{1}{2}^+$, $\frac{3}{2}^+$, $\frac{3}{2}^-$, and $\frac{5}{2}^+$) to higher masses with decreasing values of hypercharge was used to predict the excitations of $\frac{5}{2}^+$, $\frac{7}{2}^+$, and $\frac{9}{2}^+$ states with lower hypercharge values. (D.C.W.)

44997 (COO-1428-14) SINGLE PARTICLE EXCHANGE IN N^{*++} PRODUCTION IN π^+p COLLISIONS. Tautfest, G. W.; Willmann, R. B. (Purdue Univ., Lafayette, Ind.). [1965]. Contract AT(11-1)-1428. 30p. (CONF-650619-3) Dep. mn; CFSTI $2.00 cy, $0.50 mn.

From 2nd Topical Conference on Resonant Particles. Athens, Ohio.

Due to the discrepancy of previous work on the reaction $\pi^+N \rightarrow \pi^0N^{*++}$, an analysis of N^{*++} production at 1.11 and 1.265 Bev/c and a comparison with data at 0.94 and 1.43 Bev/c are presented. The analysis contains 21 diagrams of past and present work on the above reaction. (M.O.W.)

44998 (CU-1932-247) A MEASUREMENT OF THE K^0 MASS AND THE K^0-K^- MASS DIFFERENCE. Kim, J. K.; Kirsch, L.; Miller, D. (Nevis Labs., Columbia Univ., Irvington-on-Hudson, N. Y.). July 1965. Contract AT (30-1)-1932. 13p. (NEVIS-141; R-513). Dep. mn; CFSTI $1.00 cy, $0.50 mn.

From the decay of the K_1^0 in a hydrogen bubble chamber, the mass of the K^0 was measured to be 497.44 ± 0.33 Mev. From the interaction

$$K^-p \rightarrow K^0n$$
$$\quad\quad\quad

It is shown that predictions from certain subgroups of $\tilde{U}(12)$ remain valid for appropriately chosen sets of processes to any order in such symmetry-breaking terms. Predictions based on the subgroups $U(6) \times U(6)$ are shown to be valid in broken $\tilde{U}(12)$ to all orders in kinetons and simple derivative coupling. Examples of new predictions which follow from the W-spin collinear subgroups are given. (M.O.W.)

45003 (IC/65/60) THEORY OF CORRECTIONS TO UNITARY SYMMETRY FORMULAE. Furlan, G.; Lannoy, F.; Rossetti, C.; Segre, G. (International Centre for Theoretical Physics, Trieste (Italy)). 1965. 44p. Dep. mn.

A systematic analysis of the equal time commutation relations of the generators of an algebra with certain physical operators is made. A method is then introduced whereby considering matrix elements of such commutators between physical one-particle states and using completeness and invariance under space-time translations, corrections to broken symmetry group theoretical formulas are obtained. Several applications to weak, electromagnetic, and strong interactions are made. (auth)

45004 (IC/65/66) MASS SPECTRUM FROM NON-COMPACT GROUPS. Barut, A. O. (International Centre for Theoretical Physics, Trieste (Italy)). July 1965. 25p. (CONF-650553-1). Dep. mn.

From Seminar on High Energy Physics and Elementary Particles, Trieste, Italy.

Due to the failure of SU(3) symmetry for particle scattering, it is necessary to find a way to take the mass differences into account to see if then the S-matrix is invariant under SU(3). Some non-compact groups of quantum mechanical systems are discussed. Vibrational and rotational levels of the groups are investigated. Applications of these levels to strongly interacting particles are discussed. (M.O.W.)

45005 (IC/65/68) RELATIVISTIC SYMMETRIES. Fronsdal, C. (International Centre for Theoretical Physics, Trieste (Italy)). July 1965. 31p. (CONF-650553-2). Dep. mn.

From Seminar on High Energy Physics and Elementary Particles, Trieste, Italy.

A theory is described which allows the calculation of a complete set of vertex functions and scattering amplitudes for strong interactions (for every energy and momentum transfer). The structure and representations of generalized Poincaré groups are discussed. The application of SL(6,c) to elementary particles is considered. (M.O.W.)

45006 (IS-1214) PHASE SPACE CONSIDERATIONS FOR THREE-PARTICLE AND FOUR-PARTICLE FINAL STATES. Nyborg, Per; Song, Hi Sung; Kernan, William J.; Good, Roland H. Jr. (Ames Lab., Iowa State Univ. of Science and Tech.). July 1965. Contract W-7405-eng-82. 43p. Dep. mn; CFSTI $2.00 cy, $0.50 mn.

This report gives a detailed and explicit discussion of four-particle phase space in terms of invariant mass variables. The distribution of final states, after taking account of energy and momentum conservation, is integrated over orientations of the entire system and then expressed in terms of the squares of the invariant masses M_{12}, M_{34}, M_{14}, M_{124}, and M_{134}. The results permit analysis for two- and for three-particle resonances. Formulas are given for the boundary of the allowed region in the five dimensions and for the distribution of final states inside. The simpler distributions which result when integrations can be made over some of the invariant masses are derived. The phase space properties of a three-particle system are reviewed also since they provide a guide to the discussion of the four-particle problem. (auth)

45007 (JINR-E-2228) ELEKTROMAGNITNYI RASPAD I ELECTROROZHDENIE $3/2^+$-REZONANSA. (Electromagnetic Decay and Electroproduction of $3/2^+$ Resonances). Belyaev, V. B.; Tik, Tao-Wong; Nguyen Van Hieu (Joint Inst. for Nuclear Research, Dubna (USSR). Lab of Theoretical Physics). 1965. 8p. Dep. mn.

Exact expressions are given for the probability of gamma decay and electroproduction of the decuplet. Expressions for the probabilities are also presented with account of the $\tilde{U}(12)$ symmetry. The latter ones are in agreement with experiment. (auth)

45008 (JINR-E-2246) BARYON ANNIHILATION IN BROKEN U(12) SYMMETRY. Winternitz, P.; Makarov, A. A.; Nguyen Van Hieu; Tkachev, L. G.; Uhlir, M. (Joint Inst. for Nuclear Research, Dubna (USSR). Lab. of Theoretical Physics). 1965. 8p. Dep. mn.

The cross sections of the annihilations $p + \bar{p} \rightarrow M + M$ and $n + \bar{p} \rightarrow M + M$ into pseudoscalar and vector mesons are predicted on the basis of the intrinsically broken $\tilde{U}(12)$ symmetry, taking all possible invariant amplitudes into account. (auth)

45009 (JINR-E-2247) ON THE UNITARITY OF THE S-MATRIX IN THE BROKEN SYMMETRY SL(6). Nguyen Van Hieu; Tavkhelidze, A. N. (Joint Inst. for Nuclear Research, Dubna (USSR). Lab. of Theoretical Physics). June 29, 1965. 7p. Dep. mn.

It is shown that if the internal breakdown of the SL(6) symmetry is taken into account, the S-matrix satisfies the unitarity condition. (auth)

45010 (JINR-E-2259) DETERMINATION OF PARITY IN REACTIONS INDUCED BY GAMMA QUANTA. Bilenkii, S. M.; Ryndin, R. M. (Joint Inst. for Nuclear Research, Dubna (USSR). Lab. of Theoretical Physics). July 8, 1965. 7p. Dep. mn.

A method is proposed to determine the parity in the reactions $\gamma + a \rightarrow b + c$. It is based on invariance under reflections in the reaction plane. (auth)

45011 (JINR-E-2294) THE CURRENT GENERATED ALGEBRAS AND FORM-FACTORS. Bogolubov, N. N.; Makarov, A. A.; Matveev, V.; Nguyen Van Hieu; Smorodinsky, J. A.; Tkachev, L. G.; Uhlir, M.; Winternitz, P. (Joint Inst. for Nuclear Research, Dubna (USSR). Lab. of Theoretical Physics). 1965. 9p. Dep. mn.

A method for studying the algebra of currents is proposed. Relations are obtained for the form factors that describe the electromagnetic and weak interactions of mesons and quarks. (D.C.W.)

45012 (JINR-E-2353) FALLIBILITY OF USING χ^2 CRITERION IN THE PHASE SHIFT ANALYSIS FOR CHOOSING STATISTICALLY PERMISSIBLE AMBIGUOUS SOLUTIONS. Tyapkin, A. A. (Joint Inst. for Nuclear Research, Dubna (USSR). Lab. of Nuclear Problems). 1965. 10p. Dep. mn.

The incorrectness of using the χ^2-criterion for defining the statistical reliability of ambiguous solutions of the phase-shift analysis is shown. A correct method for comparing the reliabilities of various solutions is given. The comparison of methods shows that in the case of the large number of degrees of freedom of the χ^2-distribution, the over-estimation of the solution reliability corresponding to the relative minima of the functional takes place. (auth)

45013 (JINR-P-2230) K VOPROSY O PROKHOZHDENII SPINOVYKH I BESSPINOVYKH CHASTITS CHEREZ VESHCHESTVO. (On Passage of Spin and Spinless Particles Through Matter). Baryshevskii, V. G.; Lyuboshits, V. L.; Podgoretskii, M. I. (Joint Inst. for Nuclear Research, Dubna (USSR). Lab. of Theoretical Physics; Joint Inst. for Nuclear Research, Dubna (USSR). Lab. of High Energy). 1965. 13p. Dep. mn.

The passage of S-state particles through a system of fixed scattering is considered. An integral equation describing a coherent wave in a crystal and amorphous media was obtained. The expressions are given for the waves passed through and reflected from an infinitely wide plate of arbitrary thickness. The results are generalized to the case of the passage of spin particles through a polarized target. (auth)

45014 (JINR-P-2237) RASPADY $3/2^+ \rightarrow 1/2^+ + 0^-$ V NARUSHENNOI SIMMETRII U(12). (The Decays $3/2^+ \rightarrow 1/2^+ + 0^-$ in Broken Symmetry U(12)). Tao Wong Tik (Joint

Inst. for Nuclear Research, Dubna (USSR). Lab. of Theoretical Physics). 1965. 9p. Dep. mn.

Relations between the coupling constants and the decay amplitudes $3/2^+ \rightarrow 1/2^+ + 0^-$ in the symmetry scheme U(12) with account of breakdown were found. (auth)

45015 (JINR-P-2241) ZAVISIMOST VELICHIN IZMERYAEMYKH V POLNOM OPYTE PRI RASSEYANII NUKLONOV NYKLONAMI OT UGLA RASSEYANIYA. (Angular Dependence of Quantities Measured in a Total Set of Experiments on Nucleon-Nucleon Scattering). Kazarinov, Yu. M.; Kiselev, V. S.; Simonov, Yu. N. (Joint Inst. for Nuclear Research, Dubna (USSR). Lab. of Nuclear Problems). 1965. 51p. Dep. mn.

The angular dependences of experimental quantities calculated according to the phase shifts of the most probable solutions are presented. The solutions were found in the phase-shift analysis of the data on nucleon-nucleon scattering at 23, 40, 52, 66, 95, 147, 210, 310, 400, and 630 Mev. (auth)

45016 (JINR-P-2257) UPRUGOE RASSEYANIE Λ-GIPERONOV SO SREDNIM IMPULSOM 2.7 Gev/C Na PROTONAKH. (The Elastic Scattering of Λ-Hyperons with the Average Momentum (2.7 ±/∓ respectively 1.2) Gev/c on Protons). Vishnevskii, V. F.; Tu, Yuan-tsai; Moroz, V. I.; Nikitin, A. V.; Troyan, Yu. A.; Chiang, Shao-Chiung, Wen Yu.; Shakhbazyan, B. A.; Yen, Wu-kuang (Joint Inst. for Nuclear Research, Dubna (USSR). Lab. of High Energy). 1965. 11p. Dep. mn.

The elastic scattering total cross section of Λ-hyperons with the average momentum $\overline{P}_\Lambda = (2.7 \pm 1.2)$ Bev/c on protons is experimentally found to be (1.5 ± 4) mb. This result is compared with the known theoretical and experimental data. (auth)

45017 (JINR-P-2267) O VOSSTANOVLENII AMPLITUDY REAKTSII N + N → π + d. (On Reconstruction of the N + N → π + d Reaction Amplitude). Shekhter, L. Sh. (Joint Inst. for Nuclear Research, Dubna (USSR). Lab. of Theoretical Physics). 1965. 20p. Dep. mn.

The procedure is discussed of reconstructing the N + N → π + d reaction amplitude at the given values of energy and angle. It is shown that for a direct reconstruction of the amplitude up to a common phase factor it is necessary to measure the following quantities: the differential cross section for the unpolarized beam and target, the asymmetry e_1^{LR} for the polarized beam, and e_1^{LR} for the polarized target, an addition to the cross section at different orientations of the beam and target polarization, the deuteron polarization when the beam of initial protons is either unpolarized, or normally, or longitudinally polarized. (auth)

45018 (JINR-P-2283) NARUSHENNAYA SIMMETRIYA U(12) I USLOVIE UNITARNOSTI S-MATRITSY. (Broken Symmetry U(12) and the Unitarity Condition for the S-Matrix). Bokov, O. G.; Nguygen Van Hieu; Rerikh, K. V.; Khelashvili, A. A. (Joint Inst. for Nuclear Research, Dubna (USSR). Lab. of Theoretical Physics). 1965. 12p. Dep. mn.

The problem as to whether the broken symmetry U(12) is consistent with the S-matrix unitarity condition is treated. In terms of the S-matrix elements obtained under the theory of broken symmetry U(12), an account is taken of contributions from the nonregular amplitudes containing momenta explicitly. It is shown that if in the righthand side of $1/i(T - T^+) = TT^+$ the expression for the matrix element of the operator T is substituted, then after summing up over the intermediate states, there appear new amplitudes which are not allowed in the theory of broken symmetry U(12). (auth)

45019 (JINR-P-2286) O SDVIGE ρ-MEZONNOGO PIKA V DVOINOM FOTOROZHDENII. (On the ρ-Meson Peak Shift in Double Photoproduction). Solov'ev, L. D. (Joint Inst. for Nuclear Research, Dubna (USSR). Lab. of Theoretical Physics). 1965. 8p. Dep. mn.

It is shown that the shift of the meson (ρ) peak in double photoproduction may have a dynamical origin. The importance of an experimental study of the $\gamma\pi \rightarrow \pi\pi$ reaction is emphasized. (auth)

45020 (JINR-P-2330) FOTON I NOTOF. (Photon and Notoph). Ogievetskii, V. I.; Polubarinov, I. V. (Joint Inst. for Nuclear Research, Dubna (USSR). Lab. of Theoretical Physics). 1965. 9p. Dep. mn.

In contrast to the case of massive particles, for massless particles the spin component in the direction of the spatial momentum (helicity) is relativistically invariant. The massless particle with helicity 0, the properties of which are complementary to those of the photon (helicity ± 1) and which is therefore named notoph, is discussed. The interacting notoph has spin 1 like the photon. The notoph is described by the antisymmetric tensor-potential, and the field 4-vector serves as the field intensity of the notoph (instead of the vector-potential and the intensity tensor in the case of electromagnetic field). Zero-zero transitions with the emission of the notoph are allowed. (auth)

45021 (JINR-P-2336) VESHCHESTVENNAYA CHAST AMPLITUDY UPRUGOGO p-p-RASSEYANIYA PRI ENERGIYAKH 2,4,6,8 I 10 Gev. (Real Part of the Elastic p-p Scattering Amplitude at 2,4,6,8, and 10 Gev). Dalkhazhav, N.; Zlateva, A.; Kirillova, L. F. (and others) (Joint Inst. for Nuclear Research, Dubna (USSR). Lab. of High Energy). 1965. 5p. Dep. mn.

The results of measurements of the real part of elastic p-p scattering at 4 Bev are presented, as well as more accurate data at energies of 2, 6, 8, and 10 Bev (the data were analyzed with account of the relativistic corrections). The differential cross section was measured in the range $0.003 < |t| < < 0.2$ Bev/c^2. (auth)

45022 (LNF-65/7) VECTOR AND AXIAL CURRENTS UNDER FIRST ORDER SYMMETRY BREAKING. Note No. 273. Gatto, R. (Laboratori Nazionali di Frascati, Comitato Nazionale per l'Energia Nucleare (Italy)). Feb. 22, 1965. 16p. Dep. mn.

Weak and electromagnetic currents in the eightfold way with first order symmetry breaking are discussed. Upon two general assumptions it is shown that up to first order in the symmetry breaking interaction all the vector coupling constants are not renormalized. If applied to strangeness-violating leptonic decays of baryon and mesons, this result allows one to predict uniquely the vector coupling constants up to first order in symmetry breaking. (M.O.W.)

45023 (LNF-65/8) RECENT CALCULATIONS ON ELECTRON-POSITRON COLLIDING BEAM EXPERIMENTS. Note No. 274. Gatto, R. (Laboratorio Nazionali di Frascati, Comitato Nazionale per l'Energia Nucleare (Italy)). Feb. 27, 1965. 14p. Dep. mn.

A summary of recent work carried out in Frascati and in Florence, and of previous work related to experiments of colliding e^+-e^- beams, is presented. Radiative corrections are given for colliding electron and positron beams. Radiative corrections are also given for antiproton-proton collisions. The total cross section for $e^+ + e^- \rightarrow \pi^+ + \pi^- + \eta^0$ as a function of the beam energy is included. (M.O.W.)

45024 (MIT-2098-163) PHOTOPRODUCTION OF MESONS IN THE Gev RANGE. Osborne, L. S. (Massachusetts Inst. of Tech., Cambridge. Lab. for Nuclear Science). Aug. 3, 1965. Contract AT(30-1)-2098. 38p. (CONF-650916-1).

From International Symposium on Electron and Photon Interactions at High Energies, Hamburg.

Some experimental observations on meson photoproduction at high energies are reviewed and are discussed in terms of various models. (D.C.W.)

45025 (N64-26265) TRILINEAR COUPLINGS FORBIDDEN BY NONET SYMMETRY FOR VECTOR MESONS. Sakurai, J. J. (Paris Univ., Orsay (France). Laboratoire de Physique Theorique et Hautes Energies). [1964]. 8p. (CONF-550-100). Dep. mn.

From the International Conference on High-Energy Physics, Dubna, USSR, Aug. 1964.

It is demonstrated that any symmetry that makes the degeneracy of the vector singlet and the vector octet nonaccidental forbids a number of trilinear couplings that not only are known to exist but are also known to play vital

roles in high-energy inelastic processes. It is also shown that for the validity of the mass relations: $m^2(\rho) = m^2(\omega)$ and $m^2(\rho) + m^2(\phi) = 2m^2(K^*)$, which are satisfied rather well and give a value of the ω ϕ mixing angle λ: $\lambda = \cos^{-1}(\frac{2}{3})^{\frac{1}{2}}$, it is essential that the SU(3) invariant interactions that violate nonet symmetry are much weaker than the SU(3) violating interactions responsible for the mass differences among the vector mesons. (auth)

45026 (N64–19243) ON THE K_1^0-2π TRANSITION IN THE UNITARY SYMMETRY SCHEME. Gourdin, Michel (Paris Univ., Orsay (France). Laboratoire de Physique Theorique et Hautes Energies). Feb. 1964. 2p.

The decay $K_1^0 \rightarrow 2\pi$ is studied in the unitary symmetry scheme. It is concluded that U-spin considerations are sufficient to forbid the decay $K_1^0 \rightarrow 2\pi^0$ and, together with the $|\Delta I| = \frac{1}{2}$ rule, forbid the $K_1^0 \rightarrow \pi^+ + \pi^-$ decay. (D.C.W.)

45027 (NP–15199) NEKOTORYE VOPROSY TEORII SLABOGO VZAIMODEISTVIYA (DISSERTATSIYA). (Some Questions on the Theory of Weak Interaction (thesis)). Shabalin, E. P. (Gosudarstvennyi Komitet po Ispol'zovaniyu Atomnoi Energii SSSR, Moscow. Institut Teoreticheskoi i Eksperimental'noi Fiziki). 1965. 108p. Dep. mn.

In the Sakata model the fundamental particles are assumed to be the proton (p), neutron (n), the Λ-hyperon, and their antiparticles. The π-meson and K^+-meson with a strangeness S = 1 are bound states. In the Sakata model lepton decays of π-meson and K-mesons should be considered as an annihilation transfer of a bound state to a corresponding lepton pair. Three rules for lepton decays taking place with a change in strangeness are: $|\Delta S| = 1$, $\Delta Q = \Delta S$, and $\Delta T = \frac{1}{2}$. The discovery of $K_{e\nu}$ and $K_{\mu\nu}$ decays, in which K-mesons decay to two π-mesons and a pair of leptons (electron neutrinos or muon neutrinos) would be of interest in verifying the Sakata model. If the rule $\Delta Q = \Delta S$ is valid, the following decays should exist: 1) $K^+ \rightarrow \pi^+ + \pi^- + e^+ + \nu$, and 2) $K^+ \rightarrow \pi^0 + \pi^0 + e^+ + \nu$. The energy spectrum of the electrons and of the π-mesons, the angular π-e correlation and the probabilities of the $K_{e\nu}$ and $K_{\mu\nu}$ decays are derived. The cross section for the creation of a lepton pair of neutrinos is calculated for neutrino scattering in the Coulomb field of the nucleus for the process: $\nu + Z \rightarrow \nu' + Z + \mu^+ (e^+) + \mu^- (e^-)$. At an energy of 2 Bev the cross section for the creation of electron pairs is a factor of 100 greater than that involving the creation of muon pairs, and attains a value of 8×10^{-41} cm^2 (in lead). It is shown that the reaction $\gamma + \gamma \rightarrow \gamma + \nu + \bar{\nu}$ is not an important source of neutrinos in stars having a temperature of $\sim 10^9$ degrees Kelvin and a density of $\sim 10^6$ g/cm^3. (TTT)

45028 (NP–15207) NERELYATIVISTSKIE TRAEKTORII REDZHE (DISSERTSIYA). (Non-Relativistic Regge Trajectories (thesis)). Report No. 304. Kolkunov, V. A. (Gosudarstvennyi Komitet po Ispol'zovaniyu Atomnoi Energii SSSR, Moscow. Institut Theoreticheskoi i Eksperimental'noi Fiziki). 1964. 189p. Dep. mn.

A potential of the form $V(r) = (g/2m)\, r^{2\epsilon-2} \exp -(\mu r)^{2\tau}$ is taken for substitution in the Schroedinger wave equation. The parameters τ and ϵ are positive. This potential contains the potential well ($\tau = \infty$, $\epsilon = 1$), the Coulomb potential ($\tau = 0$, $\epsilon = \frac{1}{2}$), and the Yukawa potential ($\tau = \epsilon = \frac{1}{2}$). The behavior of Regge trajectories at zero and at infinity are investigated as a function of the character of the potential with distance r. First order and second order perturbation theory are used in transforming the equations of the Regge poles, and in determining the trajectories of the Regge poles at low and at high energies. (TTT)

45029 (NP–15382) VERTEX FUNCTION POLES AND ONE-PARTICLE STATES ORTHOGONALIZATION. Geshkenbein, B. V.; Ioffe, B. L. (Gosudarstvennyi Komitet po Ispol'zovaniyu Atomnoi Energii SSSR, Moscow. Institut Teoreticheskoi i Eksperimental'noi Fiziki). 1964. 7p. Dep. mn.

The vertex function Γ (κ^2) of a spin-zero interaction of three bosons is considered. It is shown that a certain proof that Γ must have a pole in the complex plant is in error. (T.F.H.)

45030 (NP–15390) A SCHEME OF MULTIPLICATION OF SU_3-REPRESENTATIONS. Okun, L. B. (Gosudarstvennyi Komitet po Ispol'zovaniyu Atomnoi Energii SSSR, Moscow. Institut Teoreticheskoi i Eksperimental'noi Fiziki). 1964. 6p. Dep. mn.

A scheme is presented for decomposing a product of two SU(3) representations into irreducible representations. (T.F.H.)

45031 (NP–15391) OPERATORY KAZIMIRA DLYA ORTOGONAL'NOI I SIMPLEKTICHESKOI GRUPPY. (Casimir Operators for an Orthogonal and Symplectic Group). Report No. 352. Perelomov, A. M.; Popov, V. S. (Gosudarstvennyi Komitet po Ispol'zovaniyu Atomnoi Energii SSSR, Moscow. Institut Teoreticheskoi i Eksperimental'noi Fiziki). 1965. 36p. Dep. mn.

Explicit expressions for the eigenvalues of invariant operators of arbitrary order (Casimir operators) in the case of orthogonal and symplectic group were obtained. (auth)

45032 (NP–15452) O NEISTVITEL'NOI CHASTI BESSPINOVOI AMPLITUDY S T = 0 I SPINOZAVISYASHCHIKH AMPLITUDAKH NUKLON-NUKLONNOGO RASSEYANIYA VPERED PRI VYSOKIKH ENERGIYAKH. (Real Part of the Spin-Zero Amplitude for T = 0 and Spin-Dependent Amplitudes of Nucleon-Nucleon Forward Scattering at High Energies). Report No. 325. Kabavets, V. P. (Gosudarstvennyi Komitet po Ispol'zovaniyu Atomnoi Energii SSSR, Moscow. Institut Teoreticheskoi i Eksperimental'noi Fiziki). 1965. 16p. Dep. mn.

On the basis of experimental data on nucleon-nucleon interactions within the framework of isotopic invariance, it is shown that at energies up to 2 or 3 Bev the contribution into the isotopic amplitude A of a state with T = 0 is given by the real part of the spinless amplitude Re A or by spin-dependent amplitudes. $|A|^2/|\mathrm{Im}\ A|^2 \geq 1.14 \pm 0.07$ at $E_{kin} = 2$ Bev. The value Re A at 2.85 Bev obtained from n-p charge exchange data, assuming negligible contribution of spin-dependent amplitudes, is not unique, and equals either (0.35 ± 0.12) Im A or (-0.8 ± 0.12) Im A. Arguments in favor of the second solution are given. The information about Re A and spin-dependent amplitudes that can be obtained from experiments on elastic n-p scattering is considered. (auth)

45033 (NP–15468) PRYAMYE REAKTSII VYBIVANIYA I NEUPRUGOGO RASSEYANIYA. (Direct Knockout and Inelastic Scattering Reactions). Report No. 327. Timashev, S. F. (Gosudarstvennyi Komitet po Ispol'zovaniyu Atomnoi Energii SSSR, Moscow. Institut Teoreticheskoi i Eksperimental'noi Fiziki). 1965. 18p. Dep. mn.

The formulas were obtained for the amplitude of the triangle graph of the knock-out reaction in the general case of particles with arbitrary masses and spin. (auth)

45034 (NP–15470) YAVLENIYA REGENERATSII I POLNYI OPYT V PUCHKE K_0 MEZONOV. (Regeneration Phenomena and Combined Experiments in a Neutral K-Meson Beam). Report No. 323. Vladimirskii, V. V.; Terent'ev, M. V. (Gosudarstvennyi Komitet po Ispol'zovaniyu Atomnoi Energii SSSR, Moscow. Institut Teoreticheskoi i Eksperimental'noi Fiziki). 1965. 15p. Dep. mn.

Regeneration phenomena in the meson(K^0) beam are studied without any assumptions about CP and CPT parity conservation. The combination of experiments is studied to determine a series of parameters characterizing regeneration and character of CP (and may be CPT) parity non-conservation. (auth)

45035 (NP–15471) SIMMETRIYA SIL'NYKH VZAIMODEISTVII I GRUPPA SU_4. (Symmetry of Strong Interactions and the SU_4 Groups). Report No. 290. Vladimirskii, V. V. (Gosudarstvennyi Komitet po Ispol'zovaniyu Atomnoi Energii SSSR, Moscow. Institut Teoreticheskoi i Eksperimental'noi Fiziki). 1964. 64p. Dep. mn.

Representations of SU_4 group are considered and possibility of construction of strongly interacting particles compound model using four baryons as a basis is investigated.

It is shown that the known unitary supermultiplets can be parts of the more complex families of particles and resonances satisfying the higher symmetry SU_4. Symmetry violation and mass formulas are investigated. The tables of the main representations are given. (auth)

45036 (NP-15476) O VOZMOZHNOSTI ISPOL'ZOVANIYA YADERNOGO REAKTORA V KOSMICHESKOGOM PROSTRANSTVE DLYA PRYAMOGO IZMERENIYA SECHENIYA (n-n)-RASSEYANIYA. NO. 7. (On the Possibility of Using Nuclear Reactor in Cosmic Space for Measuring Cross Sections of n-n Scattering. No. 7). Bondarenko, I. I.; Kovalev, V. P.; Zolotukhin, V. G. (Gosudarstvennyi Komitet po Ispol'zovaniyu Atomnoi Energii SSSR, Obninsk. Fiziko-Energeticheskii Institut). 1965. 11p. Dep. mn.

An evaluation of an experiment on the direct measurement of the cross section of n-n scattering in the S-state is presented. It is proposed that a pulsed nuclear reactor with negative temperature coefficient, introduced into cosmic space at a height of 400 to 500 km, be used for the cross-section measurement. It is shown that the n-n scattering length can be measured with an error of ±10%. (tr-auth)

45037 (TID-21316) PERIPHERAL PRODUCTION AND DECAY CORRELATIONS OF RESONANCES. Jackson, J. D. (Illinois Univ., Urbana. Dept. of Physics). [1964]. Contract AT(11-1)-182. 66p. Dep. mn; CFSTI $3.00 cy, $0.75 mn.

Peripheral reactions at incident momenta of a few Bev/c involving the production of one or more unstable particles or resonances are discussed. The prominence of quasi-two-body channels is established, and the peripheral nature of the production process is emphasized. The need for strong form factors in the one-meson-exchange model is noted. The search for ways to test the peripheral model independently of the momentum-transfer distributions leads to consideration of angular correlations of the decay products of the resonances. It is deduced that there is strong experimental evidence for the exchange of definite angular momenta and isospin in the t-channel, most readily interpreted as the exchange of pseudoscalar and vector mesons. Absorption of the lower partial waves due to competing processes is discussed as a mechanism for producing collimation of the reaction products. A specific model that is a high energy-version of the distorted-wave Born approximation is then presented and applied with considerable success to specific reactions yielding decay correlations, angular dependences of production, and absolute cross sections in agreement with experiment. Some failures and limitations of the model are discussed, as well as prospects for improvement. (auth)

45038 (TPJU-7/65) QUANTUM STATISTICS IN THE STATISTICAL MODEL OF MULTIPLE PRODUCTION OF PARTICLES. Zalewski, Kacper (Jagellonian Univ., Krakow (Poland). Dept. of Theoretical Physics). Mar. 1965. 18p. Dep. mn.

It is shown that the normalization volume (V_3) which is arbitrary when using the standard versions of the statistical model can be determined from experiment, when quantum statistics are applied to the particles. $V_3 \to \infty$ corresponds to the classical limit of quantum statistics. Then in the thermodynamic limit Boltzmann's formula should be used. The use of Planck's formula is unjustified. If V_3 is finite and such that Planck's formula applies for average multiplicities, Einstein's condensation should be observed for high multiplicities. The absence of a significant surplus of very low energy pions in high multiplicity events yields a lower bound for V_3. The isospin factor can be separated from the phase space factor only in the classical limit. (auth)

45039 (TPJU-10/65) NEW RESTRICTION ON THE FORWARD SCATTERING AMPLITUDE IN LOCAL FIELD THEORY. Wit, Romuald (Jagellonian Univ., Krakow (Poland). Dept. of Theoretical Physics). June 1965. 8p. Dep. mn.

An integral condition is obtained that must be satisfied by the forward scattering amplitude in local field theory. (T.F.H.)

45040 (TPJU-11/65) LOWER BOUND OF THE FORWARD UNSYMMETRIZED SCATTERING AMPLITUDE. Wit, Romuald (Jagellonian Univ., Krakow (Poland). Dept. of Theoretical Physics). June 1965. 5p. Dep. mn.

It is shown that the forward scattering amplitude of charged pions on protons does not approach zero more rapidly than $1/E^2$ as the energy (E) of the pion becomes unbounded. (T.F.H.)

45041 (TPJU-12/65) CLASSICAL PHASE-SPACE INTEGRAL IN THE STATISTICAL MODEL WITH ANGULAR MOMENTUM CONSERVATION. Kotanski, Andrzej; Zalewski, Kacper (Jagellonian Univ., Krakow (Poland). Dept. of Theoretical Physics). June 1965. 10p. Dep. mn.

The classical nonrelativistic phase-space integral of the statistical model of multiple production is evaluated by the steepest-descents method. The conservation laws for energy-momentum, angular momentum, and center-of-mass position are taken into account. Explicit formulas for the first (thermodynamic) and second approximations are given. The corresponding relativistic phase-space integral diverges for a Gaussian cutoff, so that a sharper cutoff must be applied. (auth)

45042 (UCID-2608) SPIN ANALYSIS FOR THE I = 0 3 PION SYSTEM. Goldhaber, G. (Lawrence Radiation Lab., Univ. of California, Berkeley). July 8, 1965. Contract W-7405-eng-48. 25p. Dep. mn; CFSTI $1.00 cy, $0.50 mn.

The I = 0 states of the 3-pion system having J^{PG} 0^{--}, 1^{--}, 1^{+-}, 2^{--}, and 2^{+-} are considered. For the "simplest" matrix elements for these states, a method denoted "general symmetry analysis" is used to find a graphical representation of the density distributions for the states. (T.F.H.)

45043 (UCRL-16070) MEASUREMENT OF THE POLARIZATION PARAMETER IN PROTON-PROTON SCATTERING FROM 1.7 TO 6.1 Bev (thesis). Grannis, Paul Dutton (Lawrence Radiation Lab., Univ. of California, Berkeley). Aug. 20, 1965. Contract W-7405-eng-48. 109p. Dep. mn; CFSTI $4.00 cy, $0.75 mn.

The polarization parameter in proton-proton scattering is measured at incident proton kinetic energies of 1.7, 2.85, 3.5, 4.0, 5.05, and 6.15 Bev for four-momentum-transfer squared between 0.1 and 1.0 $(Bev/c)^2$. The experiment was done with an unpolarized proton beam from the Bevatron striking a polarized proton target. Both final state protons were detected in coincidence and the asymmetry in counting rate for target protons polarized parallel and antiparallel to the scattering normal was measured. The maximum polarization was observed to decrease from 0.4 at 1.7 Bev to 0.2 at 6.1 Bev. The maximum of the polarization at all energies studied occurs at a four-momentum-transfer squared of 0.3 to 0.4 $(Bev/c)^2$. (auth)

45044 (UCRL-16185) HIGH ENERGY POLARIZATION EXPERIMENTS AND REGGE POLES. Phillips, Roger J. N.; Rarita, William (Lawrence Radiation Lab., Univ. of California, Berkeley). June 10, 1965. Contract W-7405-eng-48. 31p. Dep. mn; CFSTI $2.00 cy, $0.50 mn.

A survey is presented of the various types of polarization experiments that can be performed and of the predictions of Regge pole models. Specifically, π-N, K-N, $\bar{K}$-N, N-N, and $\bar{N}$-N scattering and polarization tensors of the first and second ranks only are considered. (D.C.W.)

45045 (UCRL-16288) K^-p CHARGE-EXCHANGE SCATTERING FROM 1200 TO 1700 Mev/c (thesis). Wohl, Charles Gordon (Lawrence Radiation Lab., Univ. of California, Berkeley). July 13, 1965. Contract W-7405-eng-48. 67p. Dep. mn; CFSTI $3.00 cy, $0.75 mn.

The 72-inch hydrogen bubble chamber was exposed to a beam of mesons (K^-) having laboratory momenta of 1.22, 1.42, 1.51, 1.60, and 1.70 Bev/c. The K^-p charge-exchange-scattering differential cross sections were measured. The cross sections are, from low to high momentum, 2.83 ± 0.14, 1.90 ± 0.12, 1.83 ± 0.09, 1.93 ± 0.13, and 1.66 ± 0.10

mb. The differential cross sections are peaked at the ends ($\cos\theta = \pm 1$); there are two intermediate maxima. As the momentum increases, the peaking shifts rapidly from the backward to the forward direction. Though the forward (low-momentum-transfer) peaking at the higher momenta is considerable a peripheral mechanism is by itself insufficient to reproduce the angular distribution. The differential cross sections are fit to Legendre polynomial series. At 1.22 Bev/c, the series including $P_6(\cos\theta)$ is necessary and sufficient; at the higher momenta, $P_7(\cos\theta)$ is required. The $F_{\frac{5}{2}}$ and $G_{\frac{5}{2}}$ partial-wave amplitudes are both present. At 1.60 and 1.70 Bev/c, the J = 7/2 partial waves account for at least a third of the cross section. The behavior as a function of energy of some of the coefficients of the Legendre-polynomial expansion suggests, though does not definitely establish, the existence of an $F_{\frac{7}{2}}$ $Y_1^*(2065)$. This has the quantum numbers of the recurrence of the $Y_1^*(1385)$ and belongs to the decuplet containing the $N_{\frac{5}{2}}^*(1920)$. (auth)

45046 (UCRL-16295) A REVIEW OF RECENT BOSON RESONANCES. Goldhaber, Sulamith (Lawrence Radiation Lab., Univ. of California, Berkeley). May 1965. Contract W-7405-eng-48. 61p. (CONF-650558-1). Dep. mn; CFSTI $3.00 cy, $0.75 mn.

From 5th Session of the Spring School of Experimental and Theoretical Physics, Nor-Hambert, Erevan, Armenia.

A review is given of boson resonances, with attention to spin determinations, the A_1 and A_2 resonances, the B meson, $K\pi\pi$ resonances, $K\bar{K}\pi$ resonances, the E meson, $\pi\pi(700)$, the M_1 meson, ω decay modes, and boson resonances in K^+-d reactions. (T.F.H.)

45047 (UCRL-16315) STATISTICAL MODEL CALCULATIONS OF HIGH ENERGY REACTIONS (thesis). Campbell, Graham H. (Lawrence Radiation Lab., Univ. of California, Berkeley). Aug. 10, 1965. Contract W-7405-eng-48. 73p. Dep. mn; CFSTI $3.00 cy, $0.75 mn.

Calculations based on a covariant version of the Fermi statistical model were made in an attempt to fit the known gross features of elementary particle reactions at energies presently accessible to accelerators. The object was to provide an extrapolation of these data to the higher energies of future accelerators. The n-fold phase space integration required for the model was reduced to a single contour integral which was approximated by a saddle point technique. Resonance states were included as final state particles. The initial predictions of this model were not in agreement with experiments and although modifications of the model were found to improve the situation, it is shown that none of these modifications yield a reliable method of extrapolation to higher energy. (auth)

45048 (ANL-Trans-217) REAL PART OF THE FORWARD SCATTERING AMPLITUDE OF CHARGED PARTICLES. Levintov, I. I. (Gosudarstvennyi Komitet po Ispol'zovaniyu Atomnoi Energii SSSR, Moscow. Institut Teoreticheskoi i Eksperimental'noi Fiziki). Translated by Elmar K. Wilip (Argonne National Lab., Ill.) from p.1-10 of Preprint No. 316. 7p. Dep. mn; CFSTI $1.00 cy, $0.50 mn; JCL $1.10 fs, $0.80 mf.

A method for calculation of the forward scattering amplitude real part from the data on differential cross section in the region (t) where interference with Coulomb scattering appears is proposed. This method is free of arbitrary assumptions on the properties of scattering amplitudes at small (t). The method gives also the possibility to estimate the contribution of spin terms of the amplitude in differential cross section at t = 0. (auth)

45049 A HERETIC MODEL OF THE NUCLEON. Hautot, A. Bull. Soc. Roy. Sci. Liege, 34: 97-109(1965). (In French).

An arbitrary model of the nucleon in which the nucleon is derived from a neutral particle analogous to the electron is described. It assumes that at the interior of the nucleon region the energy is present under a form bound to the nucleon mass and proposes a definite value for this energy of intranucleon bonding of 1,200 Mev. It attributes to the nucleon an internal structure controlled by two laws with no equivalent in the rest of the atom: a numerical law defining a shell structure and an association law of these shells into two groups. It compares a neutron to a doublet and derives a proton from another doublet. The model proposed is used to calculate the abnormal magnetic moment of the deuteron with a satisfactory precision. (J.S.R.)

45050 ON POLARIZATION PROPERTIES OF MUONS IN ELASTIC NEUTRINO PROCESSES ($\bar{\nu}_\mu + p \rightarrow n + \mu^+$, $\nu_\mu + n \rightarrow p + \mu^-$). Shishkin, G. V. (Inst. of Heat and Mass Exchange, Academy of Sciences, Belorussian SSR). Dokl. Akad. Nauk BSSR, 9: 160-3(Mar. 1965). (In Russian).

To distinguish the two kinds of neutrino and antineutrino a relation is established between the polarization s_ν and the polarization vector of muons in the elastic neutrino reactions $\bar{\nu}_\mu + p \rightarrow n + \mu^+$ and $\nu_\mu + n \rightarrow p + \mu^-$. It is assumed that the neutrino and antineutrino are always completely polarized longitudinally, that is, $s_\nu = \pm 1$. Wave functions of the free fermions are determined by simultaneously solving the Dirac equation and an equation with a projection operator. The hamiltonian of a weak four-fermion interaction is then written with only the vector and axial-vector terms being retained. An expression is written for the matrix element of the reaction $\nu + N \rightarrow N' + \nu$. Here N and N' are nucleons. By using perturbation theory an expression is obtained for the spatial components of the polarization vector of the muons. The probability of muon neutrinos reacting with a proton or neutron and the polarization-vector components of the resulting muons depends strongly on the longitudinal polarization of the neutrino, that is, on s_ν. The neutrino imposes its polarization on the muon that is formed. The polarization vector component depends only on the energy and emergence angle of the muon. The polarization vector of the muons lies in the plane of the reaction, that is, in the momentum plane of the neutrino and the muon. (TTT)

45051 DISPERSION THEORY OF LOW-ENERGY SCATTERING. Serebryakov, V. V.; Shirkov, D. V. (Inst. for Mathematics, Novosibirsk, USSR). Fortschr. Physik, 13: 227-76(1965).

A review is presented which is based largely on the lectures delivered at the Dubna International Winter School of Theoretical Physics on March 1964. Some materials on kinematics, isotopic structure and unitarity of the π-π scattering are given. The original papers by Chew and Mandelstam which have, in fact, given rise to the systematic theoretical studies in this field are included. The works of theoretists of Dubna and Novosibirsk which led to the consistent approach to the theory of strong interactions at low energies are treated. Comparisons are made with experiments. (auth)

45052 FORCED β DECAY OF PROTONS INDUCED BY ELECTROMAGNETIC RADIATION. Gazazyan, A. D. (Erevan State Univ.; Academy of Sciences, Armenian SSR). Izv. Akad. Nauk Arm. SSR, Ser. Fiz. Mat. Nauk, 18: 126-33(1965). (In Russian).

The beta decay induced from a proton by intense electromagnetic radiation with either linear or circular polarization is considered. The interaction between the proton and the electromagnetic radiation is taken into account rigorously, while weak interaction is regarded as a perturbation. The beta decay $p \rightarrow n + e^+ + \nu$ is energy-forbidden for the free proton. Equations are derived for the differential probability of induced beta decay of the proton following absorption of a given number of photons, for the case of both types of polarizations. The results show that at the presently attainable laser fields ($\sim 10^8$V/cm), the effect of induced beta decay of the proton is very small, being of the order of 10^{-6s} sec^{-1} (s is the number of absorbed photons). (ATD)

45053 PHASE SHIFTS AND THE QUANTUM-MECHANICAL HAMILTON-JACOBI EQUATION. Kouri, Donald J.; Curtiss, C. F. (Univ. of Wisconsin, Madison). Chem. Phys., 43: 1919-26(Sept. 15, 1965).

A method of obtaining absolute phase shifts by integration of the quantum-mechanical Hamilton–Jacobi equation was developed and applied to the example of particles interacting through a Lennard-Jones potential. A new ex-

pression for the absolute phase shift is obtained in terms of an irregular solution of the Schrödinger equation. (auth)

45054 A STUDY OF AZIMUTHAL ANISOTROPY IN THE MULTIPLE MESON EMISSION. Teranaka, Masahiko (Shimane Univ., Matsue, Japan). J. Phys. Soc Japan, 20: 1297-1302(Aug. 1965).

The azimuthal anisotropy in the multiple meson emission was studied with the nuclear photographic emulsions exposed to the proton beam of the energy of 30.5 Bev. Forty five events with $n_s \geq 6$ and $N_h \leq 1$ were analyzed. The anisotropy was investigated for the forward and the backward directions respectively in the center of mass system. An effort was made to discriminate the tracks of colliding protons from the relevant meson tracks. The χ^2-test between the experiment and the Monte Carlo computation on the azimuthal distribution did not show any significant difference beyond the significance level, P, of 0.05. (auth)

45055 $K_2^0 \rightarrow \pi^- + \pi^+$, A STRANGE DECAY OF A STRANGE PARTICLE. Nefkens, B. M. K. (Univ. of Illinois, Urbana). Ned. Tijdschr. Natuurk., 30: 383-91(Nov. 1964). (In Dutch).

Theoretical investigations show that K_2^0 cannot decay into two pions when PC is conserved in weak interactions. Therefore the indications of the decay $K_2^0 \rightarrow \pi^- + \pi^+$ detected in two experiments at Brookhaven were surprising. A brief sketch is given of these two experiments. The speculative theoretical explanation of the decay can be divided into two groups: one, theories in which PC is not conserved and the other in which PC is conserved. Summaries of both are given. (J.S.R.)

45056 RESONANCE OF NUCLEAR PARTICLES. Ferro-Luzzi, M. (CERN, Geneva). Nuovo Cimento (1), 2: Suppl., 428-70(1964). (In Italian).

A review is given of the most recent studies on the resonance of nuclear particles. The common characteristics and the experimental methods used in the study of elementary particle resonances are summarized. The individual resonances are reviewed with emphasis on the most important experimental and theoretical studies made. 117 references. (J.S.R.)

45057 THE REACTION $KN\pi\pi$ AT 3 Gev/c AND THE PRODUCTION MECHANISM OF K^*N^*. Ferro-Luzzi, M.; George, R.; Goldschmidt-Clermont, Y.; Henri, V. P.; Jongejans, B.; Leith, D. W. G.; Lynch, G. R.; Muller, F.; Perreau, J.-M. (CERN, Geneva). Nuovo Cimento (10), 39: 417-41(Sept. 16, 1965).

In a study of the four-particle states $K^+p \rightarrow KN\pi\pi$ at 3 Bev/c, it is found that the quasi-two-body process $K^+p \rightarrow K^*N^*$ occurs in large proportion. The cross sections for the various charge and decay modes of K^*N^* are in good agreement with the predictions based on isotopic-spin invariance. The sharply peaked cms production angular distribution suggests peripheralism. Within the framework of a simple one-meson-exchange model the decay angular distributions of K^* and N^* are consistent with the assumption that the reaction proceeds predominantly through the exchange of a single pion. Such a model is unable to explain the nonzero value of the interference parameter Re $q_{1,0}$ (-0.13 ± 0.02). In addition, the model requires the inclusion of a drastic ad-hoc form factor, similar to the one used at 1.96 Bev/c, in order to fit the observed production angular distribution. A modified one-meson-exchange model taking into account the absorption due to competing processes and developed by Jackson, Donohue, Gottfried, Keyser, and Svensson does not explain the absolute value of the cross section but predicts, with a minimum of assumptions, a production angular distribution and decay correlations in reasonable accord with experiment. (auth)

45058 POLARIZATION OF RECOIL PROTONS IN e-p ELASTIC SCATTERING AT 20 FERMI^{-2}. Di Giorgio, G. V.; Ganssauge, E.; Gomez, R.; Gorini, G.; Penner, S.; Serbassi, S.; Vincelli, M. L. (Laboratori Nazionali di Frascati, Rome); Amaldi, E.; Stoppini, G. Nuovo Cimento (10), 39: 474-85(Sept. 16, 1965).

An experiment is described aiming to measure a possible polarization P of the protons recoiling in e-p collisions for a four-momentum transfer $q^2 = 20$ fermi^{-2}. The e-p elastic collisions were detected by observing the scattered electrons and the recoiling protons in coincidence; the polarization P was deduced by measuring the left-right asymmetry in the scattering of the recoiling protons in the carbon plates of a spark chamber. The result of $P = 0.024 \pm 0.050$ is consistent with theoretical estimates that the imaginary part of the scattering amplitude arising from the exchange of two photons between the electron and the proton is negligible. (auth)

45059 ON THE BROKEN SYMMETRY AND POSSIBILITY OF SUPERFORBIDDEN PROCESSES. Yoshimura, T. (Univ. of Nijmegen). Nuovo Cimento (10), 39: 486-93(Sept. 16, 1965).

A mechanism of breakdown of symmetries is suggested which is not compatible with the perturbation theory but is free from the appearance of mass bosons as well as from the possibility of superforbidden processes. Some remarks are made about the unwanted weak processes in which the muon partakes. (auth)

45060 COVARIANT AND HERMITIAN SEMI-CLASSICAL LIMIT OF QUANTUM DYNAMICAL EQUATIONS FOR SPIN-1/2 PARTICLES. Kolsrud, M. (Univ. of Oslo). Nuovo Cimento (10), 39: 504-18(Sept. 16, 1965).

The Dirac equation—with a Pauli term—is transformed to a covariant and hermitian two-component form to first order in $\hbar$. The Bargmann-Michel-Telegdi equations are deduced as equations of motion for spin operators. Corresponding operators in the Dirac and the semiclassical picture are discussed. (auth)

45061 CLEBSCH-GORDAN COEFFICIENTS FOR THE GROUP SU_6. Cook, C. L.; Murtaza, G. (Imperial Coll., London). Nuovo Cimento (10), 39: 531-50(Sept. 16, 1965).

Tables of reduction coefficients for the direct products $\underline{35} \otimes \underline{35}$, $\underline{56} \otimes \underline{35}$, $\underline{56} \otimes \overline{\underline{56}}$ of irreducible representations of SU_6 are presented, and the method of calculation is outlined briefly. (auth)

45062 EXTRAPOLATION OF THE S-MATRIX FROM LEHMANN'S REPRESENTATION. Limic, N. (International Atomic Energy Agency, Trieste). Nuovo Cimento (10), 39: 551-6(Sept. 16, 1965).

The extrapolation of the S-matrix to complex angular momenta is obtained using Lehmann's representation of the amplitude for the elastic scattering. The S-matrix obtained is an analytic regular function in the half-plane Re $l > l_0$. (auth)

45063 LIMITING PROCEDURES FOR SINGULAR POTENTIALS. II. Cornille, H. (CERN, Geneva). Nuovo Cimento (10), 39: 557-80(Sept. 16, 1965).

A method was given previously to construct explicitly the zero-energy physical solution of the Schrödinger equation for singular potentials where the most singular part is repulsive. The previous results are extended both for the physical solution in co-ordinate space and for the solution of the Lippman-Schwinger equation. An arbitrary cutoff, $\theta(r - \epsilon)$, is introduced, and the Fredholm type of solution is studied. It is shown that: both the numerator and the denominator diverge in the same way when the cutoff goes to zero and the limit of their ratio is indeed the right solution; if all variables and constants are considered fixed and the cutoff going to zero is taken, then the solution is the limit of convergent sequences if the cutoff going to zero and the order of Fredholm's determinants going to infinity are connected in a certain manner, both in the numerator and in the denominator. (auth)

45064 A-A POTENTIAL STRENGTH FROM HYPERNUCLEI AND UNITARY SYMMETRY. Panchapakesan, N. (Univ. of Delhi). Nuovo Cimento (10), 39: 581-90(Sept. 16, 1965).

The A-A potential strength is estimated from the binding energy of $^4H_{\Lambda\Lambda}$ as predicted by an extension of the unitary symmetry argument to bound states of baryons. All the potentials are assumed to have gaussian shapes, and

a modification of a method due to Green is used for the calculations. The values obtained are larger than those obtained by Dalitz and others from the binding energy of $^{10}Be_{\Lambda\Lambda}$. (auth)

45065 DETERMINATION OF NEUTRON FORM FACTORS FROM PION ELECTROPRODUCTION. Loubaton, J.-P. (Laboratoire de Physique Theorique et Hautes, Orsay). Nuovo Cimento (10), 39: 591-612(Sept. 16, 1965).

The isobaric model is applied to the study of pion electroproduction on protons. The interpretation of experimental results gives a small negative value for the electric form factor of the neutron. Then it is shown how coincidence experiments would yield information about $\mu^v = G_M^p - G_M^n$. (auth)

45066 TWO-PRONG PROTON-ANTIPROTON ANNIHILATION WITH FORMATION OF A PAIR OF CHARGED MESONS. Jalla, E.; Wataghin, G. (Universita, Torino, Italy). Nuovo Cimento (10), 39: 635-40(Sept. 16, 1965).

The cross section for the two-prong proton–antiproton annihilation with formation of a pair of charged mesons ($\pi^\pm$ or $K^\pm$) is calculated, starting from the Sakurai theory of strong interactions and introducing the vector mesons ρ, φ etc. in the intermediate state. Agreement with experiments can be obtained if convenient form factors are introduced in the interactions. (auth)

45067 ON KINEMATIC CONTRIBUTIONS TO FORM FACTORS. Resnick, L. (Brookhaven National Lab., Upton, N. Y.). Nuovo Cimento (10), 39: 641-9(Sept. 16, 1965). (BNL-9102).

The procedure of calculating kinematic contributions to form factors is examined. Off-shell effects in $\pi N \to \pi N$ scattering and a model problem are calculated. It is shown that some approximations previously used to describe such effects are not generally valid. (auth)

45068 A REMARK ON THE COMPOSITENESS CRITERIA IN THE LEE MODEL. Srivastava, P. K.; Choudhury, S. Rai (Univ. of Delhi). Nuovo Cimento (10), 39: 650-7(Sept. 16, 1965).

The compositeness criteria of Salam are investigated in a Lee model with two V-particles. It is shown that in the presence of two stable particles with identical quantum numbers the concept of compositeness loses its absolute meaning. (auth)

45069 ABSORPTIVE EFFECTS IN PERIPHERAL PRODUCTION PROCESSES: THE REACTION $\bar{p}p \to \bar{N}^*N^*$. Svensson, B. E. Y. (CERN, Geneva). Nuovo Cimento, 39: 667-82(Sept. 16, 1965).

The production of $N^*(1237)$, the nucleon $\frac{3}{2}$-$\frac{3}{2}^+$ isobar, in pair with its antiparticle in proton-antiproton collisions in the laboratory momentum range 3.25 to 7 Bev/c is considered in the one-pion exchange model, modified to take into account absorption in the initial and final state due to competition from other open channels according to the theory by Gottfried and Jackson. It is found that this model reproduces well the slope of the differential cross section, the decay distribution, including an observed small correlation in the decay of the isobar and the anti-isobar, and the energy dependence of the cross section, although the absolute magnitude of the cross section is about a factor of five too big. The production of $Y^*(1382)$ and its antiparticle from the same initial state is also briefly discussed. (auth)

45070 MULTIPLE POLES AND DECAY LAWS. Baracca, A.; Minguzzi, A. (Universita, Bologna). Nuovo Cimento (10), 39: 687-91(Sept. 16, 1965).

The time dependence of the flux of the scattered wave is investigated as a function of the order of the pole of the S-matrix. (auth)

45071 A GENERAL PROOF OF THE POMERANCHUK THEOREM AND RELATED THEOREMS. Martin, A. (CERN, Geneva). Nuovo Cimento (10), 39: 704-15(Sept. 16, 1965).

It is shown that under general analyticity properties recently demonstrated from the LSZ formalism for all forward scattering amplitudes of stable particles by Bros, Epstein, and Glaser, the Pomeranchuk theorem on total cross sections can be proved if the following additional assumptions are made: Inside the analyticity domain, the forward scattering amplitude is bounded by $C(\epsilon) \exp[\epsilon|s|]$ for arbitrarily small ϵ, where $|s|$ is the square of the cms energy in one channel; for physical energies, $s \to \pm\infty$, $|F(s,0)|/|s|\log|s| \to 0$; the difference between particle-particle and particle-antiparticle cross sections has a limit. If any of these three assumptions is released, counter-examples can be found. For the real parts of the amplitudes, similar results can be found. Extensions to the moduli of the amplitudes are also considered. It is shown that if $|F(s,0)|$ is bounded by s^N and if $\lim|F(s,0)/F(-s,0)|$ exists, it is unity. A similar result holds for fixed transfer if the additional assumption is made that $\mathrm{Im}F(s,t)$ has a finite number of oscillations for $s > s_0$ and $s < -s_0$. (auth)

45072 CHARGED SCALAR THEORY AND BROKEN CHARGE SYMMETRY. Schnitzer, H. J. (Brandeis Univ., Waltham, Mass.; Laboratoire de Physique Theorique et Hautes Energies, Orsay). Nuovo Cimento (10), 39: 727-30(Sept. 16, 1965).

Static charged scalar meson theory with broken charge symmetry is solved in the one-meson approximation. It is argued that spontaneous symmetry breakdown does not appear possible in this model with these approximations. Solutions are given for the scattering amplitude and also the isobar mass difference in terms of the n-p mass difference without a perturbation expansion in the symmetry-breaking parameters. (auth)

45073 THE INFLUENCE OF THE NEUTRON-NEUTRON FINAL-STATE INTERACTION ON THE CAPTURE OF MUONS BY DEUTERONS. Dosch, H. G. (CERN, Geneva). Nuovo Cimento (10), 39: 731-8(Sept. 16, 1965).

The influence of the neutron-neutron final-state interaction on the μ capture in deuterium is calculated. It is shown that this process allows from the theoretical point of view a determination of the neutron-neutron scattering length with an accuracy of about 5%. (auth)

45074 APPROXIMATE ONE-TRAJECTORY EXCHANGE. Abers, E. S.; Teplitz, V. L. (CERN, Geneva). Nuovo Cimento (10), 39: 739-57(Sept. 16, 1965).

A version of the one-particle-exchange approximation was suggested by Chew in which the Regge-trajectory nature of the exchanged particle is taken into account. The prescription is explained in detail, and applied to the $\pi\pi$, πN, and $\pi\omega$ amplitudes. Comparison is made with earlier one-particle-exchange calculations in which the amplitude, even though analytic in the direct-channel angular momentum, comes from a force which represents the exchange of an elementary particle. The corrections to $\pi\pi$ and πN scattering are found to be insignificant on the scale of accuracy of such models; but for $\pi\omega$ scattering, the Regge-trajectory nature of the exchanged ρ-meson may be sufficient to change the sign of the force in the 1^+ channel from a repulsion into an attraction, sufficient to create a resonance. Some kinematical properties of unequal-mass scattering amplitudes are discussed, especially the poles of the partial waves at the origin. (auth)

45075 $\tilde{U}_{12}$, UNITARITY AND CROSSING. Alles, W. (CERN, Geneva); Amati, D. Nuovo Cimento (10), 39: 758-65 (Sept. 16, 1965).

It is shown with a simple counterexample (quark-quark and quark-antiquark elastic scattering) that U_{12} is incompatible with unitarity and crossing even when all possible irregular amplitudes or breaking by kineton spurions are included. (auth)

45076 ON THE BOOTSTRAPPING OF PARTICLES WITH SPIN GREATER THAN UNITY. Smith, J. (Univ. of Copenhagen). Nuovo Cimento (10), 39: 766-8(Sept. 16, 1965).

The bootstrapping of particles by the N/D method with the exchange of a spin-2 meson is examined. An explicit expression for the partial-wave amplitude is obtained. The result can be generalized to higher-spin cases; the integrals in the resulting equations are convergent when

the order of the partial wave is equal to, or greater than, the spin of the exchanged particle. A table comparing the high-energy behavior of typical potential terms and of the integral in the equation for the partial-wave amplitude is given for potential theory, spin-1 exchange, and spin-2 exchange. (M.J.T.)

45077 ON THE CONNECTION BETWEEN THE BARYON AND MESON MASS SPECTRA. Freund, P. G. O (Univ. of Chicago). Nuovo Cimento (10), 39: 769-71 (Sept. 16, 1965).

A mass relation between $K^2 - \pi^2$ and $\Xi^2 - N^2$ is obtained from a bound-state equation for mesons incorporating the Gell-Mann-Okubo mass splittings of quarks. The relation is in agreement with a formula derived previously assuming the compatibility of the universal strong interactions in M(12) symmetry and the bound-state picture of hadrons. The Gell-Mann-Okubo splittings of quarks is estimated numerically. (M.J.T.)

45078 NORMALIZATION OF BETHE-SALPETER AMPLITUDE. Ohnuki, Y.; Watanabe, K. (Nagoya Univ., Japan). Nuovo Cimento (10), 39: 772-5(Sept. 16, 1965).

The general formula for the norm of the Bethe-Salpeter bound state is obtained for the fixed-source model and for the Wick-Cutkovsky solution. Restrictions on the spectral representations for the odd and even solutions for the Bethe-Salpeter amplitudes are considered. (M.J.T.)

45079 STUDY OF THE QUENCHING OF MUON DEPOLARIZATION IN SEVERAL MATERIALS AS A FUNCTION OF EXTERNALLY APPLIED MAGNETIC FIELDS. Buhler, A.; Massam, T.; Muller, Th.; Schneegans, M.; Zichichi, A. (CERN, Geneva). Nuovo Cimento (10), 39: 812-23(Oct. 1, 1965).

The results of a systematic study on the quenching of muon depolarization as a function of a variable magnetic field parallel to the original muon polarization are reported. The data obtained are relative to values of the magnetic field which range from 0 to 4 kG and are compared with predictions of the various muonium formation theories. (auth)

45080 MEASUREMENTS OF MUON DEPOLARIZATION IN SEVERAL MATERIALS. Buhler, A.; Massam, T.; Muller, Th.; Schneegans, M.; Zichichi, A. (CERN, Geneva). Nuovo Cimento (10), 39: 824-8(Oct. 1, 1965).

A study of the depolarization of positive muons was made which shows that the muon is not affected by depolarization in the slowing down process and that the residual polarization is due to free muons. The accuracy of the results on the muon depolarization in ten different materials is an order of magnitude better than previously existing data. (auth)

45081 PROTON POLARIZATION IN $\pi^- + p$ ELASTIC SCATTERING AT 8.5 Gev/c. Focardi, S.; Giacomelli, G.; Monari, L.; Serra, P. (Universita, Bologna; Istituto Nazionale di Fisica Nucleare, Bologna). Nuovo Cimento (10), 39: 829-34(Oct. 1, 1965).

An experiment is described on proton polarization in $\pi^- + p$ elastic scattering at 8.5 Bev/c. The experiment was performed using the spark chamber technique. In the four-momentum transfer interval $0.15 \leq |t| \leq 0.8$ $(Bev/c)^2$ the polarization was found to be $P = 0.33 \pm 0.15$. (auth)

45082 SOME CONSIDERATIONS ON THE SCATTERING OF UNSTABLE PARTICLES BY STABLE PARTICLES IN THE STRONG INTERACTIONS. Barshay, S.; Rockmore, R. (Rutgers State Univ., New Brunswick, N. J.). Nuovo Cimento (10), 39: 867-79(Oct. 1, 1965).

The scattering of three stable particles into three stable particles through the intermediary of an unstable particle or resonant state in both the initial and final states is investigated. The incoming unstable particle may be different from the outgoing unstable particle. Two cases are discussed: 1) the scattering interaction between unstable and stable particles is not singular, and in the limit of vanishing widths the expression for the cross section reduces to that describing the collision of two stable particles; 2) the interaction between unstable and stable particles is singular because of the exchange of a real particle (Peierls' mechanism). In case 2), in the limit of vanishing widths, the cross section is singular in the physical region. Further, in this case, the manner of preparation of the initial three-particle state is found to be significant in discussing the process. (auth)

45083 VECTOR INVARIANTS OF SU_3/Z. Esteve, A.; Tiemblo, A. (Instituto de Quimica Fisica Rocasolano, Consejo Superior de Investigaciones Cientificas, Madrid). Nuovo Cimento (10), 39: 880-5(Oct. 1, 1965).

The number and tensor symmetry of the typical vector invariants of SU_3/Z are calculated starting from the inclusions $SU_3/Z \subset O_8 \subset SU_8$. The typical vector invariants of 3rd and 4th orders are given explicitly. (auth)

45084 LOW ANGULAR MOMENTUM NUCLEON-NUCLEON SCATTERING. Dosch, H. G. (Universitaet, Heidelberg); Mueller, V. F. Nuovo Cimento (10), 39: 886-904 (Oct. 1, 1965).

The two states of elastic nucleon-nucleon scattering containing S-waves—the single channel $J^P = 0^+$, $I = 1$ state and the two-channel $J^P = 1^+$, $I = 0$ state—are treated within the framework of relativistic partial-wave dispersion relations. An ND^{-1} ansatz is used for the partial-wave amplitudes, where the left-hand singularities are generated by one-boson exchange. A technique suggested by Schmidt's treatment of Fredholm integral equations is used for solving the integral equations. (auth)

45085 THE LOW-ENERGY PION-KAON INTERACTION. Martin, A. D. (Univ. of Durham, Eng.); Vick, L. L. J. Nuovo Cimento (10), 39: 905-27(Oct. 1, 1965).

An attempt is made to find a self-consistent solution of the πK partial-wave and fixed-momentum-transfer dispersion relations. The existence of the K^* resonance is assumed at the outset of the calculation. The solution is found to predict a reasonable value for the kaon form factor, to give a value of the $\rho K\bar{K}$ coupling constant comparable to that predicted by unitary symmetry, and to be in good agreement with an analysis of the data for K^-p inelastic scattering. Although an attractive $I = \frac{1}{2}$ s-wave πK phase shift is found, no $\varkappa$ (725 Mev) resonance is generated in this channel. In particular it is found hard to determine the value of the isospin plus combination of the s-wave πK scattering lengths; the value most favored by this calculation is in disagreement with that predicted from an analysis of K^+p elastic scattering data. The forces that give rise to the πK interaction are given, and in particular it is found that short-range forces are extremely important in producing the K^* resonance. (auth)

45086 K-MATRIX MODEL OF PERIPHERAL INTERACTIONS. II. NUMERICAL RESULTS FOR K^+p REACTIONS. Dietz, K.; Pilkuhn, H. (CERN, Geneva). Nuovo Cimento (10), 39: 928-40(Oct. 1, 1965).

A previously introduced K-matrix model is used to calculate differential cross sections and decay distributions for 3 Bev/c K^+p reactions. Good agreement with experimental results is found for all measured quantities of two-body inelastic reactions and for the cross section of three- and more-particle production. The calculated elastic cross section agrees in shape, but is too big by a factor of eight. (auth)

45087 THE ABSORPTION MODEL AT HIGH ENERGY AND ITS APPLICATION TO MESON-NUCLEON CHARGE-EXCHANGE SCATTERING. Hoegaasen, H.; Hoegaasen, J. (CERN, Geneva). Nuovo Cimento (10), 39: 941-55(Oct. 1, 1965).

Some general features of the absorption model or distorted-wave Born approximation (DWBA) for high-energy production processes are discussed. It is shown that for constant elastic diffraction peaks the model inherits the high-energy behavior of the Born approximation and further that unitarity is still violated in general as $s \to \infty$. As an example, meson-exchange scattering is calculated and compared with experiment. (auth)

45088 THE N/D METHOD AND THE DIFFRACTION PICTURE. Olesen, P. (Universitet, Copenhagen); Squires, E. J. Nuovo Cimento (10), 39: 956-66(Oct. 1, 1965).

Elastic spin 0-spin 0 scattering is considered, and it is argued that, in order to have a simple connection between the total amplitude and the partial-wave amplitude in the high-energy region, the latter has to satisfy the boundary condition corresponding to the diffraction picture. If the amplitude can be written in the conventional $N_l(\nu)/D_l(\nu)$ form, where $N_l(\nu)$ has only a left-hand cut and $D_l(\nu)$ only a right-hand cut, and where there are no arbitrary subtraction constants, it follows that the imaginary part of $D_l(\nu)$ behaves like $\nu^{-\frac{1}{2}}$ for $\nu \to \infty$ (apart from possible logarithmic factors). (auth)

45089 POSSIBLE S-WAVE $\pi\pi$ FINAL-STATE INTERACTION IN THE REACTION $\pi^- p \to \pi^0\pi^0 n$. Corbett, I. F. (Oxford Univ.); Damerell, C. J. S.; Middlemas, N.; Newton, D.; Clegg, A. B.; Williams, W. S. C.; Carroll, A. S. Nuovo Cimento (10), 39: 979-83(Oct. 1, 1965).

Measurements of the reaction $\pi^- p \to \pi^0\pi^0 n$ at 1.72 to 2.46 Bev/c are presented. Results are consistent with a relatively strong S-wave, T = 0, $\pi\pi$ interaction over a broad range of dipion masses but give no indication of the resonances previously suggested at $\pi\pi$ masses around 400 and 700 Mev. Procedures for kinematical analysis of the decay into two neutral pions and for the subtraction of events containing more than four photons are described. The mass distribution deduced from the decay of 400- and 700-Mev dipions is shown. The production angular distributions for the $\pi\pi$ system for events not due to N* (1238) production and with $\pi\pi$ mass between 280 and 1000 Mev are presented. The pion-nucleon mass distribution for all 4γ events is given. A cross section for the reaction proceeding via the nucleon isobar is deduced. (M.J.T.)

45090 A COMMENT ON THE BOOTSTRAP MECHANISM. Yoshimura, T. (Universiteit, Nijmegen, Netherlands). Nuovo Cimento (10), 39: 984-5(Oct. 1, 1965).

A formulation of the bootstrap mechanism in the framework of the conventional quantum field theory using the Bethe-Salpeter equation and implying the introduction of a field corresponding to the exchanged particle—the particle appearing in the interaction kernel—is discussed. The requirement that the exchanged particle have the same behavior as the particle generated dynamically by the bootstrap mechanism in off-the-mass-shell amplitudes as well as at energies far from the pole is considered. It is shown that, in this case, not only does the equation become nonlinear but also the criterion on permissible approximations for the interaction kernel is violated—the criterion that no diagram may appear twice or more if the equation is iterated. (M.J.T.)

45091 ON ELASTIC SCATTERING AND MULTIPLE PRODUCTION AT HIGH ENERGY. Hama, M. (Osaka Univ.). Nuovo Cimento (10), 39: 988-90(Oct. 1, 1965).

The behavior of elastic amplitudes at finite angle is investigated as the shadow scattering of inelastic processes by the use of information on multiple productions in cosmic-ray scattering. The equation for the elastic amplitude is written, and expressions for the amplitudes of emission of secondaries from two centers corresponding to the two primary interacting particles are found. The equation for the angular distribution of secondaries is then derived. Applications to p-p and π-N elastic scattering amplitudes are considered. (M.J.T.)

45092 EFFECT OF PEAK BROADENING OF STRUCTURE IN THE REGION OF THE ρ^0-MESON. Caldwell, D. O. (Univ. of California, Berkeley); Weinstein, R. Nuovo Cimento (10), 39: 991-5(Oct. 1, 1965).

It is pointed out that experimental results indicating alternatively a single peak and more than one peak in the mass spectrum of the ρ^0 meson may not be conflicting. Differences in the mass resolution of the apparatus involved—spark chambers and bubble chambers—are reviewed. Discrepancies due to the possible processes of pre-decay resonance mixing and post-decay scattering are discussed. (M.J.T.)

45093 TRUNCATION OF THE UNITARY SUM. Kowalski, K. L. (Argonne National Lab., Ill.; Case Inst. of Tech., Cleveland). Nuovo Cimento (10), 39: 1002-4(Oct. 1, 1965).

It is pointed out that it can be ambiguous to study the consequences of the unitarity of S on a subspace H_p on which (1-P)T is not zero by neglecting the contributions from intermediate states lying in H_{1-p} in the equation (1) $A = T^\dagger PT + T^\dagger(1-P)T$ or (2) $A = TPT^\dagger + T(1-P)T^\dagger$. Here, S is the scattering operator, T is the transition operator, $T^\dagger$ is its adjoint, and P is a projection operator onto a subspace H_p of the space H on which S is defined. This ambiguity arises because $T^\dagger PT$ and $TPT^\dagger$ are not necessarily equal on an arbitrary subspace of H. When the scattering is time-reversal invariant, the ambiguity is resolved by using the symmetrical unitary equation (3) $A = \frac{1}{2}(T^\dagger T + TT^\dagger)$. Truncation using equations (1) and (3) is considered on a two-article subspace of H in a representation in which the total angular momentum is diagonal with phases chosen so that the partial-wave amplitudes are symmetric. It is remarked that the same difficulties arise in the K-matrix formalism. (M.J.T.)

45094 REMARKS ON A CONSISTENCY PROBLEM IN HEISENBERG'S NONLINEAR THEORY. Montaldi, E.; Paganoni, L. (Universita, Milan; Istituto Nazionale di Fisica Nucleare, Milan). Nuovo Cimento (10), 39: 1005-11(Oct. 1, 1965).

Spectral formulas for the four-point function for the cases $\tau_0(xx|yy)$ and $\tau_0(xy|xy)$ are considered. The problem is discussed of proving that the spectral functions $A^{(1)}(m^2)$ and $A^{(2)}(m^2)$ exhibit a δ-like singularity corresponding to the mass of a Bose particle. A plausibility argument is presented, showing that this property does not contradict a reasonable assumption regarding the asymptotic behavior of $\tau_0(xx|yy)$ and $\tau_0(xy|xy)$ for $z^2 \to +\infty$. (M.J.T.)

45095 ON THE GREEN FUNCTION FOR THE ITERATED KLEIN-GORDON EQUATION. Montaldi, E. (Universita, Milan; Istituto Nazionale di Fisica Nucleare, Milan). Nuovo Cimento (10), 39: 1012-14(Oct. 1, 1965).

A simple and concise technique for studying the Sonine-Gegenbauer integral is described, in order to gain insight into the problem of the origin of the singularities that the Green's functions for the iterated Klein-Gordon operator may have on the light cone. (M.J.T.)

45096 A SHARPENING OF O'RAIFEARTAIGH'S THEOREM. Roman, P.; Koh, C. J. (Boston Univ.). Nuovo Cimento (10), 39: 1015-16(Oct. 1, 1965).

The possibility of combining Lorentz invariance and internal symmetries within a single group G is discussed. It is proved that in any irreducible representation of G the mass operator $P^2 = P_\mu P^\mu$ cannot have more than one eigenvalue, assuming G is a Lie group of finite order which contains the local inhomogeneous Lorentz group as a subgroup. Thus, if particles in a multiplet are represented by vectors in the representation space considered, all particles in the same multiplet must have the same mass. (M.J.T.)

45097 PROTON-PROTON BREMSSTRAHLUNG CROSS SECTIONS AT 48 Mev. Warner, R. E. (Univ. of Manitoba, Winnipeg). Phys. Letters, 18: 289-90(Sept. 1, 1965).

Proton-proton bremsstrahlung cross section measurements at 48 Mev are reported. These events were identified by measuring the energies of both final protons, which were detected by plastic scintillation counter telescopes at equal angles on opposite sides of the beam and coplanar with the beam. Results are given and interpreted. (J.F.P.)

45098 THE ELECTRON-NEUTRON INTERACTION FROM THE SCATTERING OF NEUTRONS BY NOBLE GASES. Krohn, V. E.; Ringo, G. R. (Argonne National Lab., Ill.). Phys. Letters, 18: 297-9(Sept. 1, 1965).

The low-energy electron-neutron interaction was remeasured by a method used previously. This method depends upon the fact that in the scattering of thermal neutrons the interference between the scattering from the nucleus and the scattering from the electrons of an atom leads to an asymmetric angular distribution. Noble gases at moderate pressures are used in order to avoid diffraction and magnetic moment effects. In the laboratory system, the motion of the center of mass contributes an

asymmetry. Hence, the measurement is a determination of the difference between the observed asymmetry and the asymmetry caused by the motion of the center of mass. The latter was calculated in great detail, which is an important improvement over the approximations used in the past. From the results the effective potential for the electron-neutron interaction is found and given from the argon, krypton, and xenon data. (J.F.P.)

45099 MEASUREMENT OF THE ABSOLUTE VALUE OF THE $K_1^0 \rightarrow K_2^0$ MASS DIFFERENCE. Vishnevskii, M. E.; Galanina, N. D.; Semenov, Yu. A.; Krupchitskii, P. A.; Berezin, V. M.; Murisov, V. A. (Inst. for Theoretical and Experimental Physics, Moscow). Phys. Letters, 18: 339-41(Sept. 1, 1965).

The mass difference between the meson (K_1^0) and the meson (K_2^0) is measured by means of coherent regeneration. A meson (K^0) beam, at a large distance from its point of origin, consists only of mesons (K_2^0). If a plate of some material is placed in the path of such a beam an admixture of mesons (K_1^0) is produced. A certain fraction of this meson (K_1^0) admixture is produced as a result of coherent regeneration by the nuclei in the material of the plate; and in this case there is an interference between the amplitudes of the mesons (K_1^0) components from which the change in mass can be determined. The experiment was carried out with a 7-Bev accelerator. The beam of neutral particles was produced from an internal target. The meson (K_2^0) beam intensity on the surface of the regenerators from which the mesons (K_1^0) were detected was 300K_2^0/pulse for a mean flux of 3×10^{10} protons/pulse in the accelerator. The mean value for the change in mass was found to be $0.82 \pm 0.14\ \hbar/\tau_1 c^2$ where $\tau_1 = 0.92 \times 10^{-10}$ sec. (J.F.P.)

45100 PION-NUCLEON PHASE SHIFT ANALYSIS BELOW 1 Gev. Bareyre, P.; Brickman, C.; Stirling, A. V.; Villet, G. (CEN, Saclay, France). Phys. Letters, 18: 342-5(Sept. 1, 1965).

A new analysis was made at 310 Mev of the meson (π)-nucleon phase shift using the π^-p polarization data previously obtained. For all other energies no selection was made in the experimental data except for slightly increasing the errors in π^0N differential cross sections also given previously. For each energy, starting from a random set of phase shift and varying it in order to minimize the total chi square of the various experimental data, a set of phase shifts corresponding to a relative minimum of the chi square; this operation was repeated many times. (J.F.P.)

45101 PARITY TEST FOR Ω^- USING POLARIZED HYDROGEN TARGET. Bilenkii, S. M.; Ryndin, R. M. (Joint Inst. for Nuclear Research, Dubna, USSR). Phys. Letters, 18: 346-7(Sept. 1, 1965).

A possible method is discussed for determining the Ω^--hyperon parity. Since the decays of Ω^--particles are due to weak interactions, the Ω^- parity can only be determined by investigating the strong and electromagnetic process for their production. Strangeness conservation in strong and electromagnetic interactions and the large value of the Ω^- strangeness lead to the fact that the processes of Ω^- production will involve, as a rule, three and more particles in the final state. A determination of the parity in these reactions can be made only by analyzing those cases in which the momenta of all particles lie in the same plane. The existence of the boson resonance (KK), having strangeness 2, isotopic spin 1, zero spin and positive parity permits consideration, for Ω^- parity determination, a reaction involving two particles in the final state. $K^- + p \rightarrow \Omega^- + 0^+(K + K^0)$. In order to determine the Ω^--hyperon parity unambiguously, the relations are used connecting the asymmetry in this reaction on a polarized proton target with the polarization characteristics of the Ω^- when the protons are unpolarized. (J.F.P.)

45102 A MEASUREMENT OF THE BRANCHING RATIO FOR THE DECAY $\omega^0 \rightarrow e^+ + e^-$. Binnie, D. M. (Imperial Coll. of Science and Tech., London); Duane, A.; Jane, M. R. (and others). Phys. Letters, 18: 348-51(Sept. 1, 1965).

The results of a spark chamber experiment to measure the branching ratio for the decay $\omega^0 \rightarrow e^+ + e^-$ are reported. The main theoretical interest of the ratio is its relevance to the ω^0-ϕ^0 mixing hypothesis previously given. This hypothesis was introduced to account for the failure of the Gell-Mann-Okubo mass-splitting formula to fit the masses of the mesons in the SU(3) octet. An independent check of the hypothesis can be obtained by comparing the decay rates $\omega^0 \rightarrow e^+ + e^-$ and $\phi^0 \rightarrow e^+ + e^-$. The measurement of the first of these rates is not alone sufficient for this check to be made. It does, however, allow a prediction to be made about the second, if the mixing hypothesis is assumed to be correct. In the experiment mesons (ω^0) were produced in the reaction $\pi^- + p \rightarrow n + \omega^0$ using a meson (π) momentum only slightly above the threshold. The neutron time-of-flight spectra is given showing clearly the strong production of mesons (ω^0). The branching ratio for this decay studied is found to be 3/14,000 and with 95% confidence limits the ratio lies between 5×10^{-5} and 6×10^{-4}. (J.F.P.)

45103 SINGLE π^0 PRODUCTION BY 8 Gev/c POSITIVE PIONS AND POSSIBLE ENHANCEMENTS IN THE ($\pi^+\pi^0$) SYSTEM. Deutschmann, M. (Technische Hochschule, Aachen); Schulte, R.; Steinberg, R. (and others). Phys. Letters, 18: 351-4(Sept. 1, 1965).

In order to investigate single meson (π^0) production and possible enhancements in the ($\pi^+\pi^0$) system, a hydrogen bubble chamber was exposed to a beam of 8-Bev/c positive mesons (π) from a proton synchrotron. On 140,000 photographs 9173 two-pronged events were measured. Preliminary results were reported using various computer programs. It was found that 738 events fit the reaction $\pi^+ + p \rightarrow p + \pi^+ + \pi^0$. The Dalitz plot for the reaction is shown. The striking features are the concentration of events in three bands along the edges of the plot and scarcity of events in the middle. The bands correspond to ($\pi^+\pi^0$) enhancement as ρ^+ resonance, ($p\pi^+$) enhancement as N_{33}^{*++} and ($p\pi^0$) enhancements in T = 3/2 and 1/2 isobars. Possible biases and contaminations were studied in detail. (J.F.P.)

45104 EVIDENCE FOR TRIANGLE SINGULARITIES. Month, M. (Univ. of Illinois, Urbana). Phys. Letters, 18: 357-9(Sept. 1, 1965).

It is observed that the mass values and decay characteristics of three-particle enhancements are generally consistent with the properties expected of singularities in triangle diagrams. The triangle graphs produce nearby singularities for mass values given by the Nauenberg-Pais formula do not suffer from a previous objection, and yield distinctive distributions on the three-body Dalitz plots. (J.F.P.)

45105 PION-PION SCATTERING. [PART] III. Saperstein, A. (Wayne State Univ., Detroit); Uretsky, J. Phys. Rev., 140: B352-9(Oct. 25, 1965).

The left-hand partial-wave discontinuities are calculated in fourth-order perturbation theory. The s-wave and p-wave dispersion relations are solved by standard N/D techniques. It is found that the relative contributions arising from the double-spectral terms and the inelastic single-spectral functions are negligible. As a perturbation theory the procedure appears to be sensible for coupling constants $|\lambda|$ less than about 0.1. High-energy p-wave resonances can be made to occur for $|\lambda|$ of about 0.2, but with very large widths. It is suggested that the physical pion-pion system may not be describable in terms of a one-parameter theory, and this notion is given experimental meaning. (auth)

45106 EXACT BOOTSTRAP SOLUTIONS TO THE LOW EQUATION. Huang, Kerson; Mueller, Alfred H. (Massachusetts Inst. of Tech., Cambridge). Phys. Rev., 140: B365-74(Oct. 25, 1965). (MIT-2098-156).

It is inquired whether the Low equation for meson-baryon scattering in the static one-meson approximation possesses bootstrap solutions, defined to be those solutions satisfying Levinson's theorem of potential scattering. The Low equation is allowed to have arbitrary subtractions and arbitrary bound states, except that the baryon must be the lowest bound state. A two-parameter family of cutoff functions, including the case of no cutoff, is introduced. Some 2×2 and 4×4 crossing matrices of certain general forms are considered with the Chew-Low theory included as a special

case of the latter. To answer the question raised, a simple technique is used based on the crossing relation on the imaginary energy axis. It is shown that for all the crossing matrices considered the unsubtracted Low equation does not possess a bootstrap solution, regardless of the choice of bound states and cutoff function. The case of one subtraction for 2×2 crossing matrices is studied, and some necessary bootstrap conditions are found. These restrict the crossing matrix, determine the form of the cutoff junction, and require that in the baryon channel the baryon be the only bound state, while in the other channel there be at most one bound state. These results are generalizations of those obtained earlier by Huang and Low. (auth)

45107 THREE-BODY N/D EQUATIONS. I. INTEGRAL ANGULAR MOMENTA. Mandelstam, Stanley (Univ. of California, Berkeley). Phys. Rev., 140: B375-96(Oct. 25, 1965).

Equations are derived for calculating three-body partial-wave amplitudes once all singularities other than the unitarity discontinuity are known. The equations can easily be reduced to Fredholm equations. They have a similar structure to the two-body equations, but are more complicated owing to the presence of disconnected diagrams. The D function is related to the form factor in the usual way, and it has the expected zeros and cuts on the unphysical sheet. A subsidiary problem which is treated is the determination of a function with kinematical branch points when the discontinuities across the dynamical cuts on all sheets are known. Also, a brief discussion is given of the many-channel analog of the Omnès equation. (auth)

45108 ANOMALOUS MAGNETIC MOMENT OF THE ELECTRON, MUON, AND NUCLEON. Drell, S. D.; Pagels, H. R. (Stanford Univ., Calif.). Phys. Rev., 140: B397-407(Oct. 25, 1965).

The anomalous magnetic moment of the electron, $\frac{1}{2}(g-2)$, is computed using dispersion theory. The analytic continuation is made in the mass of one of the external electron lines, and only the one-electron one-photon states are retained in the absorptive amplitude. In this way g-2 is related to the Compton amplitude which has a known exact threshold behavior. The approximation is an expansion in the low-energy behavior rather than a perturbation expansion in powers of 1/137, and it is shown that a major contribution to g-2 comes from the low-mass region of the electron-photon system near the threshold of the absorptive amplitude. First, in a purely nonrelativistic calculation, it is found that a major part of the $\alpha/2\pi$ correction is accounted for by the Thomson limit. By further refining the calculation by including the exact residue of the pole terms in the Compton amplitude in accord with the low-energy theorem on Compton scattering, it is found that electron-photon states below $2.5mc^2$ in the absorptive amplitude reproduce 90% of the $-0.328\alpha^2/\pi^2$ contribution, and a value of $\sim+0.15\alpha^3/\pi^3$ for the sixth-order term is predicted. A simple physical interpretation of the difference of the muon and electron g-2 values is also given. Finally with this approach the anomalous magnetic moments of the proton and neutron are calculated, with the Kroll-Ruderman theorem on meson photoproduction providing the low-energy anchor in this case. Again when only the low-mass region of the absorptive amplitude is retained, fair agreement with the magnitude and the isovector character of the moments is obtained, finding $\Delta\mu^P \approx 0.7(\Delta\mu_{exp})$ and $\Delta\mu^N \approx 0.9(\Delta\mu_{exp})$. (auth)

45109 REPRODUCTION OF TWO-BODY SCATTERING PHASE SHIFTS BY A PHENOMENOLOGICAL POTENTIAL. Lovitch, L. (Istituto Nazionale di Fisica Nucleare, Pisa, Italy); Rosati, S. Phys. Rev., 140: B408-9(Oct. 25, 1965).

A systematic, rapidly converging process for achieving the best fit to a set of phase shifts by means of a phenomenological potential of a given analytic form is described. The discussion is limited, in the main, to the case of central forces. A corrector formula is given for the simultaneous adjustment of the parameters of the potential. As an example of its efficiency the results obtained after a small number of iterations in trying to fit the p-wave phase shifts of elastic proton-alpha scattering at low energy are presented. (auth)

45110 RELATIVISTIC TREATMENT OF LOOSELY BOUND SYSTEMS IN SCATTERING THEORY. Gross, Franz (Cornell Univ., Ithaca, N. Y.). Phys. Rev., 140: B410-21(Oct. 25, 1965).

An approximate method for treating loosely bound systems is discussed, with the deuteron form factor in the impulse approximation treated as an example. Major advantages of the method are that it is simple and unambiguous, and leads to a quantitative estimate of its accuracy. The principal physical assumption behind the method is that the bound system can be regarded as coupled to only one channel at low energies. This method can be used to obtain simple, relativistically invariant expressions for scattering amplitudes in which the bound state is described by a relativistic wave function. For the deuteron this wave function is related to the d-np vertex with one nucleon off the mass shell. A method by which this wave function can be determined from phenomenological nonrelativistic wave functions is discussed. (auth)

45111 UNITARITY AND ANALYTICITY FOR A SIXTH-ORDER DIAGRAM. Minnaert, Pierre; Seneor, Roland (Ecole Polytechnique, Paris). Phys. Rev., 140: B422-31 (Oct. 25, 1965).

The study of a sixth-order Feynman diagram with an unstable internal particle is worked out. It is proved that, for this diagram and a certain class of diagrams, the unitarity condition is meaningful, in the sense that the absorptive part of the amplitude given by this process is a real function. By analytic continuation out of the physical region, it is shown that the complex singularities of the different terms of the absorptive part cancel out. Consequently, the amplitude admits a Mandelstam representation. An explicit expression of the spectral function is given. (auth)

45112 MESON AND BARYON RESONANCES IN RELATIVISTIC SU(6). Harari, H. (Israel Atomic Energy Commission, Yavne); Horn, D.; Kugler, M.; Lipkin, H. J.; Mishkov, S. Phys. Rev., 140: B431-3(Oct. 25, 1965).

The relativistic SU(6) supermultiplets which can be constructed from two quarks and two antiquarks, three quarks, or four quarks and one antiquark are examined as possible candidates for the classification of meson and baryon resonances. The multiplets can be labeled either by the SU(12) formalism or by the $U(6) \times U(6)$ group of Dashen and Gell-Mann; the two groups lead to equivalent classifications. Those static SU(6) multiplets within a given SU(12) multiplet which represent physical particles (i.e., satisfy Bargmann-Wigner equations) are just the states having the maximal eigenvalue of γ_0 in the SU(12) multiplet. These constitute a representation of the Dashen-Gell-Mann $U(6) \times U(6)$ subgroup of U(12) which commutes with γ_0. Applications to specific resonances are discussed. (auth)

45113 GENERAL SU(3) CROSSING MATRICES AND THE PROJECTION OPERATORS OF 3×8. Nieto, Michael M. (Cornell Univ., Ithaca, N. Y.; California Inst. of Tech., Pasadena). Phys. Rev., 140: B434-42(Oct. 25, 1965).

Expressions are obtained for the SU(3) (u) and (t) crossing matrices in terms of isoscalar factors and Racah coefficients (6-j symbols). Careful attention is given to the question of phases and states. The cases of 3×8 and 8×8 are considered as examples. Methods for obtaining crossing matrices by means of projection operators are illustrated by examining the case of 3×8 in detail. (auth)

45114 REGGE POLES IN QUANTUM ELECTRODYNAMICS WITH MASSIVE PHOTONS. Cheng, Hung; Wu, Tai Tsun (Harvard Univ., Cambridge, Mass.). Phys. Rev., 140: B465-9(Oct. 25, 1965).

The lagrangian theory of quantum electrodynamics with massive photons is used to find that the lowest order radiative corrections to the fourth order box diagram of the Compton scattering amplitude contribute terms proportional to $(\ln t)^2$ for large t, violating the Regge behavior if uncanceled. The sixth-order ladder diagram and two others ob-

tained from it by interchanging one of the external photon vertices with a virtual photon vertex are re-evaluated. It is found that the unwanted terms contributed by all these diagrams exactly cancel, proving that in this theory the fermion lies on a Regge trajectory, up to the sixth-order perturbation. (auth)

45115 A PARITY FOR VERY WEAK INTERACTIONS. Peaslee, D. C. (Massachusetts Inst. of Tech., Cambridge). Phys. Rev., 140: B470-2(Oct. 25, 1965).

Relevance of the charge-parity quantum number A to very weak interactions is studied. It appears that nonleptonic decays conserve AP, when P is real parity; a similar rule is postulated for the hadron currents in leptonic decays. Observed relations between $\Lambda \to p\pi$ and $\Xi^- \to \Lambda\pi$ verify the AP rule with a deviation of order 15% from A symmetry in the baryon octet. Simple relations are predicted between $\Xi \to (\Lambda,\Sigma)$ and $(\Lambda,\Sigma) \to N$ leptonic decays. The structure of nonleptonic decays. The structure of nonleptonic baryon decays is almost completely specified by introduction of one further symmetry postulate, which does not fit readily into the SU_3 framework. The AP rule sheds no light on $K_2^0 \to 2\pi$ decay. (auth)

45116 ALGEBRA OF CURRENTS AND GETTING SU(6) RESULTS FROM SU(4). Ryan, C. (Univ. of Rochester, N. Y.). Phys. Rev., 140: B480-2(Oct. 25, 1965). (UR-875-89).

Within the framework of the algebra-of-currents approach of Lee, it is shown that apart from a slight complication the SU(6) results for the ratios G_A/G_V and μ_p/μ_n are still obtained when the assumption of SU(3) invariance is relaxed and only isospin [SU(2)] symmetry is required. (auth)

45117 UNSTABLE-PARTICLE SCATTERING AND THE STRIP APPROXIMATION. Drummond, Ian T. (Univ. of California, Berkeley). Phys. Rev., 140: B482-99(Oct. 25, 1965).

The problem of formulating a bootstrap calculation when one of the scattering particles is unstable is examined. The unstable-particle scattering amplitude is defined, as an S-matrix pole residue, its analytic structure is discussed, and it is pointed out that it may be determined from the usual Landau rules. It is concluded that although the instability of the external particle complicates the structure it does not do so too severely. Therefore, it can be postulated that, in analogy with the stable case, the unstable-particle amplitude exhibits Regge asymptotic behavior. This assumption leads to the construction of a strip approximation to the amplitude which is a crossing-symmetric superposition of Regge pole terms. It is pointed out that this approximation exhibits, in some respects, satisfactory analytic structure. In particular it takes quite well into account certain anomalous threshold effects. It satisfies a quasi-Mandelstram representation which is used to explore the analytic structure of the corresponding partial-wave amplitudes and their continuation to arbitrary angular momentum. Certain simple discontinuity formulas are employed to obtain dynamical equations for the partial-wave amplitudes, and consequently a complete bootstrap scheme can be constructed formally. Finally, some difficulties and unsolved problems are mentioned. (auth)

45118 POSITION OPERATORS IN RELATIVISTIC SINGLE-PARTICLE THEORIES. Sankaranarayanan, A.; Good, R. H. Jr. (Ames Lab., Ames, Iowa). Phys. Rev., 140: B509-13(Oct. 25, 1965). (IS-1164).

Formulas for position operators that apply uniformly for all spins of particle are given. The three-vector X, of the Newton-Wigner and Foldy type, is treated first. Then it is shown that, although X has complicated Lorentz transformation properties, it is linearly related to a certain four-vector Y_μ which is built up from the Poincaré group generators. The four-vector is the generalization of the classical notion of the component of the position four-vector in the direction perpendicular to the world line of the particle. (auth)

45119 GENERALIZED GOLDSTONE THEOREM. Streater, R. F. (Imperial Coll. of Science and Tech., London). Phys. Rev. Letters, 15: 475-6(Sept. 13, 1965).

A significant generalization is given of a previous theorem. The theorem states that if $\phi_1(x) \to \phi_2(x)$ is a transformation of fields such that $\langle\phi_2(x)\rangle_0 = n \neq 0$ and such that the transformation is generated by a conserved current, then there must be zero-mass particles in the theory with the quantum numbers of ϕ_1. The proof depends on the absence of states of negative norm. The generalization is proven that if a local conserved current generates a transformation $\phi_1(x) \to \phi_2(x)$ between fields corresponding to particles of different mass, then there must be states in the theory with arbitrarily small mass. The absence of states of negative norm is also a condition for the proof. The result shows that any mass differences between particles, one of which is stable, must be caused by a symmetry breaking which is not of the spontaneous type. This theorem can be applied to the proton-neutron mass difference. It is seen that there must exist charge-one particles with arbitrarily small mass, which have never been seen. Similarly, the breaking of the SU(3) mass multiplets may not be explained by spontaneous breakdown. (J.F.P.)

45120 COHERENT K* PRODUCTION IN THE K^+d REACTION AT 2.3 Bev/c. Butterworth, Ian; Brown, John L.; Goldhaber, Gerson; Goldhaber, Sulamith; Hirata, Allan A.; Kadyk, John A.; Trilling, George H. (Univ. of California, Berkeley). Phys. Rev. Letters, 15: 500-3(Sept. 13, 1965).

In a study of K^+d interactions at 2.3 Bev/c the following reactions were observed in which there is single- and double meson(π) production and in which the deuteron does not break up, $K^+ + d \to K^0 + \pi^+ + d$, and $K^+ + d \to K^+ + \pi^- + \pi^+ + d$. These reactions proceed almost entirely through K* production. It is further noted that there is a broad enhancement in the π^+ d mass distribution in the second reaction. This mass distribution is interpreted to be the result of N^{*++} production without deuteron breakup, i.e., $(d\pi^+) = (N^{*++}n)$. It is shown that the results can be interpreted in terms of coherent K* production on the deuteron, the survival of which in the final state imposes a strong restriction on the maximum possible momentum that can be transferred to it. The deuteron thus acts effectively like a momentum transfer filter. The work described is based on an analysis of 100,000 pictures taken with a 20-in bubble chamber filled with deuterium and exposed in a 2.3 Bev/c meson (K^+) beam. (J.F.P.)

45121 EXPERIMENTAL EVIDENCE FOR A RESONANT STATE IN THE $\pi^+\pi^0$p SYSTEM AT 1.71 Bev. Schumann, Thomas G. (Univ. of California, Berkeley). Phys. Rev. Letters, 15: 531-2(Sept. 20, 1965).

Evidence is reported for an enhancement in the $\pi^+\pi^0$p system with a mass of 1.71 Bev and width <50 Mev. A beam of negative mesons (π) with a momentum of 3.9 Bev/c was directed into a 72-in liquid-hydrogen bubble chamber. Four-prong events were investigated. Those events with strange particles were rejected. A mass plot of the $\pi^+\pi^0$p system is shown; the mass plots of the other $\pi\pi$p systems are also shown for comparison. Two other strong enhancements occur in this reaction. One is due to the ω in the $\pi^-\pi^+\pi^0$ system, and one is due to the N_{33}^* in the π^+p system. The enhancement at 1.7 Bev in the $\pi^+\pi^0$p system is not a decay product of a four-body resonance and does not decay dominantly into any lower mass resonance. The Dalitz plots of the kinetic energy of the meson (π^0) versus the kinetic energy of the proton and the meson (π^0) versus the meson (π^+) were plotted for the events with a $\pi^+\pi^0$p mass in the enhancement region. But no sudden change was observed when passing through this region, as was expected due to the complexity of the final state. (J.F.P.)

45122 ANNIHILATIONS OF ANTIPROTONS IN HYDROGEN AT REST INTO TWO MESONS. Baltay, C. (Columbia Univ., New York); Barash, N.; Franzini, P. (and others). Phys. Rev. Letters, 15: 532-3(Sept. 20, 1965).

A tabulation of the rates for the annihilation of antiprotons at rest in hydrogen into various two-body channels is presented. The tabulation is based on an analysis of 9301 two-pronged and 16,700 four-pronged meson (π) annihilations, and 6768 meson (K) annihilations obtained from an exposure of a 30-in hydrogen bubble chamber to a

separated low-energy antiproton beam. In this exposure, one $\bar{p}p$ annihilation into two neutral mesons (K) was observed with both mesons (K^0) decaying into $\pi^+\pi^-$; this is compared to 239 $K^0\bar{K}^0$ events observed with one visible meson (K^0) decay only. This leads to an S state of the $\bar{p}p$ system. (J.F.P.)

45123 NEW NONSINGULAR INTEGRAL EQUATION FOR TWO-PARTICLE SCATTERING. Noyes, H. Pierre (Stanford Univ., Calif.). Phys. Rev. Letters, 15: 538-40 (Sept. 20, 1965).

A new representation is presented for the two-particle scattering amplitude which avoids two previously encountered difficulties simultaneously, while preserving the unitarity of the two-particle scattering matrix. A further advantage of this approach is that it leads to a nonsingular integral equation for the behavior of the scattering matrix off the energy shell, whose kernel is explicitly determined by the (off-shell) Born approximation for the interaction, and which is equivalent to the Schrödinger equation in the nonrelativistic case. It is hoped that this representation will provide a good first approximation for at least some aspects of the three-body problem. (J.F.P.)

45124 TEST OF CHARGE-CONJUGATION INVARIANCE IN $\bar{p}-p$ ANNIHILATIONS AT REST. Baltay, C.; Barash, N.; Franzini, P.; Gelfand, N.; Kirsch, L.; Luetjens, G.; Severiens, J. C.; Steinberger, J.; Tycko, D.; Zanello, D. (Columbia Univ., New York). Phys. Rev. Letters, 15: 591-3 (Oct. 4, 1965).

A search is reported for C violation invariance in the strong interactions. In this experiment the energy and invariant-mass distributions of charge-conjugate channels in a sample of annihilation at rest of antiprotons stopped in liquid hydrogen. The sample which is tested consists of 34811 meson (π) annihilations and 4663 annihilations in which one or more mesons (K^0) are emitted. It is concluded that this search for possible C-invariance violation in $\bar{p}-p$ annihilations at rest gives no indication of violation either in mesons (π) or in mesons (K) annihilations, and that a reasonable upper limit for C-nonconserving amplitudes in the two cases is 1 and 2% respectively. (J.F.P.)

45125 THE STRUCTURE OF NUCLEONS. Foldy, L. L. (Case Inst. of Tech., Cleveland). Phys. Today, 18: 26-30; 32; 34; 36; 38; 40; 42; 44(Sept. 1965).

With the examination of the structure of the proton and neutron a new hierarchical level in the material organization of the physical universe is investigated. At this level of atomic and nuclear structure, the proton and neutron are just two examples of a variety of entities which seem to be closely related and which by custom are called elementary particles. That another hierachy in the structure of matter may underlie the elementary particles is strongly urged by the desire for greater economy in the number of truly fundamental entities and by indications of sufficient symmetries to make such an underlying structural basis an attractive possibility. Discoveries and speculations, the meaning of structure, electromagnetic structure, gravitational and weak interactions, and strong interactions are discussed. There seem little doubt that approximate symmetries among elementary particles exist and probably have some significance. (J.F.P.)

45126 WEAK INTERACTIONS AND HIGHER SYMMETRIES. Cocho, G. (Universidad Nacional Autonoma, Villa Obregon, Mexico). Rev. Mex. Fis., 14: 17-28(1965).

Assuming the weak currents belong to the $T^1 = 1$ (rotated basis in U-space) components of the regular representation of SU_3 and R_8 it is found that the $\Delta T = 1/2$, $\Delta T = 3/2$ relative phase may be nearly 90° without predicting a $\Delta T = 3/2$ rate incompatible with the experimental evidence. It is also found that even a rather small $\Delta T = 3/2$ contribution may give us a sizeable CP violation in the Σ, Λ leptonic decays. (auth)

45127 A CONTRIBUTION TO DISPERSION THEORY OF PION-PION SCATTERING. Fischer, Jan. Rozpravy Cesk. Akad. Ved, Rada Mat. Prirod. Ved, 74: No. 12, 1-59 (1964). (In Czech).

Elastic scattering of pions on pions in the low-energy region is studied on the basis of the unitary condition and the Mandelstam integral representation of the scattering amplitude A. A historical survey of the dispersion theory is presented. Fundamental relations following from the Mandelstam representation are obtained in general form. The derivation of a set of integral equations for A is given. This set is obtained from the Mandelstam representation and unitarity by expanding the angular dependence of A in powers of a special function w, which represents by itself a conformal mapping of the complex cosine plane. An approximative resonant solution of the set of equations is given and relations between resonance parameters are derived. In Appendix A, the isotopic structure of A is derived. In Appendix B, it is shown that from the Mandelstam representation the one-dimensional dispersion relations may be derived for an arbitrary straight line lying in the s, u, t plane. Two special cases thereof, the so-called fixed-momentum-transfer and fixed-cosine dispersion relations are frequently used in the literature. In Appendix C, properties of different conformal mappings of the complex cosine plane are summarized. (auth)

45128 ELECTRON-POSITRON PAIR FORMATION BY A STRONG ELECTROMAGNETIC WAVE IN THE FIELD OF A NUCLEUS. Yakovlev, V. P. Zh. Eksperim. i Teor. Fiz., 49: 318-28(July 1965). (In Russian).

An exact expression is obtained for the differential cross section for electron-positron formation by a strong electromagnetic wave in the field of a nucleus. The partial and total cross sections for a circularly polarized wave are derived by taking into account nonlinearity. It is shown that the energy of the particles produced depends on the angles, but not unambiguously. (auth)

45129 ORIGINS OF THE LEE TRIANGLE. Rosen, S. P. (Purdue Univ., Lafayette, Ind.). 16p. (CONF-650410-37). Gmelin, AED-CONF-65-073-70.

From American Physical Society, Washington, D. C.

The Lee triangle, $\sqrt{3}\,\langle\Sigma^+|p\pi^0\rangle - \langle\Lambda|p\pi^-\rangle = 2\,\langle\Xi^-|\Lambda\pi^-\rangle$, is shown to be a consequence of any Hamiltonian which transforms as a member of an SU(3) octet, and which satisfies one simple constraint. If the Hamiltonian is constructed in the form $\Sigma\, g_n\,[(\bar{B}\times B)_{(n)}\times\pi]_{(8)}$ where $n = 8_D, 8_F, 10, 10^*, 27$, the required constraint is $g_{10} = g_{10^*}$. Thus the baryon-anti-baryon decuplets must appear with equal weights, but the octets and (27)-plet are placed under no restrictions. This result is used to explain why some dynamical models and symmetry arguments predict the Lee triangle, while others do not. Within the framework of SU(6), it also correlates the orbital angular momentum in $\Sigma^+ \to n\pi^+$ with the Lee triangle. (auth)

45130 GENERALIZED CAUCHY REPRESENTATIONS AND RESONANCE PHENOMENA. Dilley, J. (Ohio Univ., Athens). 21p. (CONF-650410-29). Gmelin, AED-CONF-65-083-53.

From American Physical Society, Washington, D. C.

It is well known that if the analytically continued partial wave scattering amplitude has a pole lying near the physical region, then a resonance occurs in the region $E \simeq E_R$, where $E_n = E_R + i\gamma$ is the position of the pole. In practical calculations, the scattering amplitude can be approximated by a single pole term $f_1(E) = B_n g(E_n,E)/(E-E_n)$. In the resonance region, where β is the residue of $f_1(E)$ and $g(E',E)$ is an arbitrary analytic function of E' and E such that $g(E,E) = 1$. The fact that many choices of the function $g(E',E)$ are possible leads to an ambiguity in the representation. The relationship between the observed amplitude and the corresponding pole parameters is discussed, and it is shown that for a class of good representations, the position, height, and width of the resonance are independent of the choice of g to order γ^2/E_R^2. The corresponding situation for complex angular representations using Regge trajectories is also discussed. (auth)

Field Theory and Quantum Mechanics

45131 (JEN-154-DF/I-47) CAMPOS CUANTICOS LOCALES RELATIVOS A PARTICULAS DE MASA NO

NULA. (Relativistic Local Quantum Field Theory for $m \neq 0$ Particles). Morales Villasevil, Angel (Junta de Energia Nuclear, Madrid (Spain). Division de Fisica Teorica). 1965. 252p. Dep. mn.

A method is introduced to deal with relativiltic quantum field theory for particles with $m \neq 0$. Two mappings I and J, giving rise respectively to particle and antiparticle states, are defined between a test space and the physical Hilbert space. The intrinsic field operator is then defined as the minimal causal linear combinations of operators belonging to the annihilation-creation algebra associated to the germ and antigerm parts of the element. Local elements are introduced as improper test elements and local field operators are constructed in the same way as the intrinsic ones. Commutation rules are given. Transformation properties of field operators are easily derived in an original and simple way. Ordinary Dirac theory is obtained as a particular case. New easier realizations are studied in detail for spin ½ particles. The method is generalized to include isotopic spin. (auth)

45132 (JINR-E-2225) A NEW DEFINITION OF TRANSLATIONS IN THE INHOMOGENEOUS SL(6) GROUP. Kadyshevskii, V. G.; Todorov, I. T. (Joint Inst. for Nuclear Research, Dubna (USSR). Lab. of Theoretical Physics). June 19, 1965. 9p. Dep. mn.

A scheme is proposed for introducing a reflection operator and for simplifying the invariant equations of the scalar and spinor fields in SL(6) field theory. (T.F.H.)

45133 (NP-15341) SUR L'UTILISATION DES METRIQUES INDEFINIES POUR LA DETERMINATION DES PROPAGATEURS EN THEORIE QUANTIQUE DES CHAMPS (THESE). (On the Utilization of Indefinite Metrics for the Determination of Propagators in Quantum Field Theory (thesis)). Goldberg, Joseph (Lyon Univ. (France) Faculte des Sciences). 1965. 32p. Dep. mn.

A Hilbert space of infinite dimension with indefinite metrics is defined. The definition of the unitary representations of the Lorentz group is reviewed. The free fields, described as usual in positive definite metrics, but having an indefinite metrics when the fields are in interaction, are examined. The interaction is calculated using an indefinite metrics and perturbation theory. The second order and higher approximations are presented as functional integrals with their nuclei being constituted by the mean values on the vacuum state of commutators of field operators. It is shown that these mean values can be modified by the metrics used. The hypothesis that the field operator commute with the metric operator is discussed. (J.S.R.)

45134 (NP-15397) SPIN PRECESSION IN GRAVITATIONAL FIELD. Zakharov, V. I.; Kobsarev, I. Yu. (Gosudarstvennyi Komitet po Ispol'zovaniyu Atomnoi Energii SSSR, Moscow. Institut Teoreticheskoi i Eksperimental'noi Fiziki). 1965. 12p. Dep. mn.

The equality of precession frequencies of electron spins and classical gyroscopes in gravitational field is discussed. It is shown to follow from the linearized interaction as well as from the iterated Dirac equation in four-leg formulation. (auth)

45135 (NP-15436) GAUGE PROBLEMS IN CANONICALLY QUANTIZED ELECTRODYNAMICS WITHOUT SUBSIDIARY CONDITIONS. Technical Report No. 397. Lam, C. S. (Maryland Univ., College Park. Dept. of Physics and Astronomy). Aug. 1964. 40p.

Relations between time ordered functions of quantum electrodynamics quantized in different gauges are discussed. It is shown that electromagnetic fields may be quantized in any gauge by the functional method. In order to eliminate the asymmetry associated with the usual canonical method, matrix elements are extended beyond the physically realizable charge shell. The discussion concerns; general properties of gauge invariant lagrangians, quantum theory of the uncoupled fields, spinor electrodynamics, and scalar electrodynamics. (M.O.W.)

45136 FOURTH ORDER RENORMALIZATION CONSTANTS IN QUANTUM ELECTRODYNAMICS. Bialynicka-Birula, Z. (Inst. of Physics, Academy of Sciences, Poland). Bull. Acad. Polon. Sci., Ser. Sci., Math., Astron. Phys., 13: 369-72(1965).

An evaluation is made of the divergent parts of the renormalization constants in quantum electrodynamics in the fourth order of perturbation theory. The renormalization constant of the photon propagator and the electromagnetic mass of the electron are investigated, since these are the only renormalization constants with the gauge invariant meaning. The calculation of the electromagnetic mass is repeated according to a renormalization previously given. The results show a possibility that the exact electromagnetic mass of the electron is finite, but that it cannot be expanded into a power series at $e^2 = 0$. (J.F.P.)

45137 SINGULAR SOLUTIONS OF DIRAC EQUATIONS AND THEORY OF THE DE BROGLIE DOUBLE SOLUTION. Thiounn, Mumm. Cahiers Phys., 19: 53-103(Feb. 1965). (In French).

An attempt was made to find, for Dirac equations, point singular solutions whose singularity is displaced on a given trajectory at a given velocity and then with the solutions to determine for what conditions the De Broglie guide theorem corresponding to the Dirac equations can be satisfied. The method of resolution used in the consideration of the guide theorem for the scalar wave equation and for the Dirac equations are justified. The possibility for satisfying the guide theory in the case of Dirac equations is shown by choosing two singular solutions of these equations. In order to understand the profound significance of this guide theorem the lines that at each of their points are tangent to the vector current passing by this point and to the environs of the singular point itself are studied. From the results of this study a more complete interpretation of the guide theorem was developed and the fact that the eigenvalues of the operators representing the components of the vector current are equal to c was interpreted. It was found, that by studying the singular solutions of the Dirac equations without exterior field and by imposing a closed trajectory of being, that the eigenfrequency of the free particle is equal to the rotation frequency of a torus. (J.S.R.)

45138 PSEUDO POTENTIALS. Gombas, P. (Univ. of Budapest). Fortschr. Physik, 13: 137-56(1965). (In German).

Simplifications to the approximation methods used for the solution of quantum mechanical multiparticle problems are necessary because of the extensive calculation time. The utilization of pseudo potentials as simplifications are discussed. Exchange potentials and exclusion potentials are described and their use is illustrated. (J.S.R.)

45139 NOTE ON THE WIGNER REPRESENTATION OF QUANTUM OPERATORS. Hirota, R.; Tosima, S. (Labs. RCA, Inc., Tokyo). J. Phys. Soc. Japan, 20: 1523(Aug. 1965).

It is noted that the Wigner representation of the Heisenberg equation of motion of a dynamical variable $A(p_t, q_t)$ which was developed by Kubo is incorrect. The proof is repeated, and the source of error is pointed out. (L.B.S.)

45140 ON THE POSSIBILITY OF SPLITTING OF ELECTROMAGNETIC SPECTRUM BY GRAVITATIONAL FIELD. [PART] I. Biswas, P. K. (Indian Assn. for the Cultivation of Science, Jadavpur). Nuovo Cimento (10), 39: 190-4(Sept. 1, 1965).

A partial investigation of the role of gravitation in the process of splitting the electromagnetic spectrum is presented. The space-time metric for a weak gravitational field is given in terms of the Newtonian potential. The case where the Newtonian potential is time-dependent and periodic is considered in order to obtain conditions for electromagnetic splitting, and the problem of checking the splitting prediction against the gravitational field equations is posed. (M.J.T.)

45141 TENSOR LAGRANGIANS AND GENERALIZED CONSERVATION LAWS FOR FREE FIELDS. Morgan,

T. A. (Syracuse Univ., N. Y.); Joseph, D. W. Nuovo Cimento(10), 39: 494-503(Sept. 16, 1965).

The existence of tensor lagrangians for noninteracting massless fields of arbitrary spin is demonstrated. In particular, for spin one, the Euler-Lagrange equations for a vector lagrangian are equivalent to Maxwell's equations. Conserved quantities are derived in the usual fashion from these generalized lagrangians by means of Noether's theorem. A tensor Lagrangian and corresponding conserved quantities are also exhibited for the Dirac field with nonzero mass. A very natural quantization assumption which applies to all massless fields is made, and the physical interpretation of the generalized conserved quantities in terms of number operators is given. (auth)

45142 ON THE VOIGT-PALACIOS-GORDON TRANSFORMATION AND THE KINEMATICS IMPLIED BY IT. Strauss, M. (Deutsche Akademie der Wissenschaften, Berlin). Nuovo Cimento (10), 39: 658-66(Sept. 16, 1965).

The kinematics implied by the VPG transformations is developed as the special case $g(\beta) = K(\beta)^{-1}$ of the kinematics implied by the asymmetric transformations $L_g^*(\beta) = g(\beta)L(\beta)$, $L(\beta)$ being the ordinary 1-parametric Lorentz transformation. It is shown that the 1-parametric transformations L_g^*, which do not form a group, give rise to two (formally identical) 2-parametric groups $\hat{g} = \{\hat{G}^{ik}\}$ and $\check{g} = \{\check{G}^{\rho\sigma}\}$ connecting frames of two distinct classes $\hat{C} = \{\Sigma^i\}$ and $\check{C} = \{\Sigma^\rho\}$, respectively, each Σ^i being connected with any Σ^ρ by an asymmetrical transformation L_g^*. It is concluded that this theory is the mathematical model of a hypothetical world possessing two uniform motion equivalences represented by $\hat{C}$ and $\check{C}$, respectively. Some misconceptions that have arisen in connection with the work of Palacios and Gordon are resolved. (auth)

45143 THE INTERPOLATION OF THE WAVE FUNCTION AND THE JOST FUNCTIONS IN THE ENERGY PLANE. Chadan, K. (Laboratoire de Physique Theorique et Hautes Energies, Orsay). Nuovo Cimento (10), 39: 697-703(Sept. 16, 1965).

Some interpolation formulas in energy for the wave function and the Jost functions are derived in the case of central potentials having a finite radius. These formulas provide uniformly convergent series expansions, valid in the entire energy plane, for each function, when its value on a discrete set of the real axis is known. (auth)

45144 PHOTON BOUND STATES AND GRAVITONS. Papini, G. (Univ. of North Carolina, Chapel Hill). Nuovo Cimento (10), 39: 716-26(Sept. 16, 1965).

The possibility that a nonlinear photon-photon interaction gives rise to gravitons is investigated. At first photons are treated as neutral vector particles of small finite mass; then as zero-mass particles in the frame of usual gauge-invariant quantum electrodynamics. The corresponding Bethe-Salpeter equations are solved in the chain approximation. Bound states exist which have the required symmetry properties and correspond to particles with spin two or zero. Of these, only one has zero mass, and its phenomenological coupling to photons is, in the approximation considered, entirely dynamical. (auth)

45145 NUMERICAL EVALUATION OF THE UNCERTAINTY RELATION FOR ANGULAR VARIABLES. Schotsmans, L.; Van Leuven, P. Nuovo Cimento (10), 39: 776-9 (Sept. 16, 1965).

The uncertainties $\Delta\theta$ and ΔL in an angle θ and the corresponding angular momentum component L are considered; it is pointed out that the wave functions lying exactly on the boundary of the physically permissible region in the $\Delta\theta$, ΔL plane are obtained as nodeless solutions of a second-order wave equation. Expressions for the true uncertainty relation for angular variables are obtained, and tables are given of numerically computed values of $\Delta\theta$ and ΔL. (M.J.T.)

45146 SOME REMARKS ABOUT COULOMB EFFECTS ON VERTEX PARTS. Klarsfeld, S. (Universite de Paris, Orsay, France). Nuovo Cimento (10), 39: 975-8(Oct. 1, 1965).

The analytic properties of the vertex part associated with a loosely bound system, decaying virtually into two fragments, are obtained for the case when a long-range force, like a Coulomb repulsion, is acting as well as the usual short-range nuclear forces. Only a preliminary study is made, considering nonrelativistic potential theory, spinless particles, and S-states. An iterative procedure, consisting essentially in applying the Laplace transform method, is used to solve the Schroedinger equation with the Coulomb potential and a short-range Yukawa potential. (M.J.T.)

45147 A CLASS OF AXIALLY SYMMETRIC SOLUTIONS OF COMBINED MAXWELL-EINSTEIN-KLEIN-GORDON'S FIELD. De, N. (Jadavpur Univ., Calcutta). Nuovo Cimento (10), 39: 986-90(Oct. 1, 1965).

A class of solutions of the combined Maxwell-Einstein-Klein-Gordon field is found in the axially symmetric case by the use of Weyl's canonical coordinates only when the mass parameter equals the charge parameter, so that the electrostatic and gravitational forces on matter balance each other. (M.J.T.)

45148 GAUGE SUBTRACTION METHOD FOR EINSTEIN'S PSEUDOTENSOR. Tangherlini, F. R. (George Washington Univ., Washington, D. C.). Phys. Letters, 18: 271-3(Sept. 1, 1965).

It is the customary viewpoint that meaningful calculations cannot be made with Einstein's pseudotensor except in coordinate systems that are asymptotically flat and quasi-rectangular. It is shown that the divergent results for the energy can be eliminated for static or stationary closed systems by using a gauge subtraction technique. As a test of the method, it is used to calculate Bondi's expression for mass aspect for the time-dependent case. A restrictive condition that is needed to obtain Bondi's expression for mass loss or news in the time-dependent case by the method shown, is given and discussed. (J.F.P.)

45149 SECOND METHOD OF IDENTIFYING FAST MONOPOLES. Tompkins, Donald R. (Louisiana State Univ., Baton Rouge). Phys. Rev., 140: B443-5(Oct. 25, 1965).

The ionization and Cherenkov emission from fast monopoles is expected to be nearly uniform. Based on this and an observed similar behavior of fast charges, a method of identifying fast monopoles is proposed which compares the total energy loss rate to the Cherenkov emission. This comparison is useful because for charges (monopoles) the total energy loss and Cherenkov emission are both proportional to the charge (monopole) strength squared. This method could be particularly useful in a search for small-pole-strength monopoles. (auth)

45150 MODEL HAMILTONIANS FOR LOCAL QUANTUM FIELD THEORY. Wilson, Kenneth G. (Cornell Univ., Ithaca, N. Y.). Phys. Rev., 140: B445-57(Oct. 25, 1965).

The problem of renormalization for the interaction of a charged scalar meson field with a fixed two-level point source is studied. Special attention is given to coupling-constant renormalization. In particular, the problem of obtaining eigenstates and eigenvalues of the hamiltonian for the fixed-source theory is studied. A model is proposed for the fixed-source theory, in which mesons exist only if their momenta (k) lie within an infinite set of intervals: $0 < k < k_0$, $\frac{1}{2}\Lambda < k < \Lambda$, $\frac{1}{2}\Lambda^2 < k < \Lambda^2$, etc., where k_0 is of the order of the meson mass, and Λ is much larger. This model is solved by treating the mesons in the nth interval (or lower) as a perturbation on mesons in the (n + 1)st interval (and higher). This reduces the problem to the solution of two strongly cut-off hamiltonians, one of which must be solved for an infinite sequence of coupling constants $\{g_n\}$, one for each momentum interval. It is shown that even if the low-momentum coupling constants g_1, g_2, etc., are small, the sequence goes to infinity as $n \to \infty$. The Lee model is analyzed similarly; here the sequence is undefined

above some finite value of n. A close analogy is shown between this analysis and the analysis of quantum electrodynamics of Gell-Mann and Low. Then the full fixed-source hamiltonian is analyzed qualitatively. The meson field is expanded in terms of a complete set of wave-packet states, the coefficients being discrete oscillator variables. The states are so chosen that the self-interactions of oscillators dominate the coupling between oscillators. For each order of magnitude for the meson momentum, there is one pair of oscillators coupled to the source; this coupling can be analyzed analogously to the model. The full fixed-source hamiltonian is thereby reduced to the solution of a hamiltonian for two oscillators coupled to a two-level source. (auth)

45151 ACCURACY OF MEASUREMENT FOR COUNTING AND INTENSITY-CORRELATION EXPERIMENTS. Goldberger, Marvin L. (Princeton Univ., N. J.); Watson, Kenneth M. Phys. Rev., 140: B500-9(Oct. 25, 1965).

A quantum-mechanical analysis is made of the experimental accuracy to be expected for particle-counting and intensity-correlation experiments. The mean-square fluctuation for an ensemble, consisting of a large number of experiments each conducted over a time interval T, is calculated. (auth)

45152 REGGE POLES IN A POTENTIAL OF THE COULOMB WELL TYPE. Kolkunov, V. A.; Lobov, G. A. (Inst. of Theoretical and Experimental Physics, Moscow). Zh. Eksperim. i Teor. Fiz., 49: 306-14(July 1965). (In Russian).

The energy dependence of the motion of Regge poles is studied on basis of an exact solution of the Schroedinger equation for a potential of the type of a Coulomb well which is identical with a Coulomb potential at short distances and at large distances breaks off as a potential of the rectangular well type. It is shown that at small and intermediate energies the pole trajectories are of the Regge type. At high energies the asymptote of the pole trajectories is the same as that for the Coulomb case. (auth)

45153 NEW FOUNDATIONS OF QUANTUM MECHANICS. Lande, Alfred. Cambridge, Eng., Cambridge University Press, 1965. 178p. $7.50.

The problem of deriving the laws of quantum mechanics from a nonquantal basis without ad hoc assumptions is treated. It is pointed out that there are serious faults in the purely physical arguments which have led to the current dualistic doctrine of matter. It is shown, by making use of the quantum rule for the exchange of linear momentum, that matter diffraction, coherence and other wave-like phenomena can be fully explained on a unitary particle theory of matter. The more fundamental problem of the origin of the quantum laws themselves are discussed, arguing that the laws of quantum mechanics are natural consequences of the same general postulates of symmetry and invariance which are known from deterministic mechanics. (L.B.S.)

45154 SNAP 10A DESIGN, DEVELOPMENT, AND FLIGHT TEST. Wilson, R. F.; Dieckamp, H. M.; Cockeram, D. J. (Atomics International, Canoga Park, Calif.). New York, American Inst. of Aeronautics and Astronautics, 1965, Preprint No. 65-467, 12p., $1.00. (CONF-650711-7). ORINS.

From AIAA 2nd Annual Meeting and Technical Demonstration, San Francisco.

A description is given of the design characteristics of the SNAP 10A system, including the reactor selection, the power conversion system, mechanical components and electrical subsystems. The development program included the normal elements of component, subsystem, and system effort. The various phases of the test program and experience are described. The performance of the system during the flight test is also discussed. (L.B.S.)

Geophysics

45155 (AD-609015) THE DEVELOPMENT OF A PROBE SYSTEM FOR THE MEASUREMENT OF PLASMAS IN THE UPPER ATMOSPHERE. Final Report, April 1, 1959–September 30, 1962. Bettinger, Richard T. (Maryland Univ., College Park. Dept. of Physics and Astronomy). Sept. 1963. Contract AF 19(604)-5575. 64p. (AFCRL-64-102). Dep. mn; CFSTI $3.00 cy, $0.75 mn.

The problem of the measurement of ionospheric parameters, particularly under unusual or extreme conditions, was approached by means of a unique in situ probe system consisting of: a thermal equalization probe to measure the potential of the carrier platform; a pulse probe to measure the electron concentration and energy distribution; and a Langmuir probe to measure positive ion temperatures. In addition, the requisite support systems including telemetry and flight vehicles were developed. The entire system was proven by flight tests. (auth)

45156 (AFCRL-64-768) LABORATORY INVESTIGATION OF GEOMAGNETIC DYNAMOS. Technical Final Report, Lowes, F. J.; Wilkinson, I. (Newcastle-upon-Tyne Univ. (England). Dept. of Physics). Feb. 1964. Contract AF 61(052)-213. 51p. (AD-606831). CFSTI $3.00.

It is likely that the Earth's magnetic field is maintained by a self-exciting dynamo mechanism in the liquid conducting core. An attempt to build a self-exciting homogeneous dynamo in the laboratory is described. By rotating two cylindrical ferromagnetic conductors in cylindrical holes in a stationary block of the same material (with a thin layer of mercury to give electrical contact), evidence was obtained of the existence of a critical velocity of rotation above which the system would be self-exciting. To reduce this critical velocity to an attainable value, some inhomogeneity had to be introduced in the form of thin insulating layers. The behavior of the model in its steady-state self-exciting condition is described; large induced electric currents and magnetic fields were produced and appreciable power was dissipated as Joule heating. Qualitative explanations are suggested, but the behavior is complicated by the saturation of the ferromagnetic conductor. Possible instability oscillations of the system could not be investigated because of the very large viscous damping of the mercury. Methods of reducing this damping are suggested. (auth)

45157 (NP-15386) A LIMIT ON STABLY TRAPPED PARTICLE FLUXES. Research Report 219. Kennel, C. F.; Petschek, H. E. (Avco-Everett Research Lab., Everett, Mass.). July 1965. Contract Nonr-2524(00). 61p.

Whistler mode noise leads to electron pitch angle diffusion. Similarly, ion cyclotron noise couples to ions. This diffusion results in particle precipitation into the ionosphere and creates a pitch angle distribution of trapped particles which is unstable to further wave growth. Since excessive wave growth leads to rapid diffusion and particle loss, the requirement that the growth rate be limited to the rate at which wave energy is depleted by wave propagation allows an estimate of an upper limit to the trapped equatorial particle flux. Electron fluxes >40 kev and proton fluxes >120 kev observed on Explorers XIV and XII respectively obey this limit with occasional exceptions. Beyond L = 4, the fluxes are just below their limit, indicating that an unspecified acceleration source sufficient to keep the trapped particles near their precipitation limit exists. Limiting proton and electron fluxes are roughly equal, suggesting a partial explanation for the existence of larger densities of high energy protons than electrons. Observed electron pitch angle profiles correspond to a diffusion coefficient in agreement with observed lifetimes. The required equatorial whistler mode wide band noise intensity, 10^{-2} γ, is not obviously inconsistent with observations, and is consistent with the lifetime and limiting trapped particle intensity. (auth)

45158 (NP-15424) A SIMPLE EXPLANATION FOR THE SEMI-ANNUAL EFFECT APPEARING IN SATELLITE ORBITAL DECAY DATA. Anderson, Albert D. (Lockheed Missiles and Space Co., Palo Alto, Calif.). Aug. 1965. 32p.

A semi-annual effect was previously found in satellite

orbital decay data. The cause of this effect was interpreted to be a world-wide semi-annual density variation in the upper atmosphere. An analysis is presented which reveals that this effect is correlated definitely with the difference in latitude between satellite perigee and the subsolar point. This relation is explained by inferring that the prominent minimums in orbital decay values near the solstices result from a marked latitude variation in density existing in the winter hemisphere at this time, with the density at the winter pole indicated to be much lower than at the subsolar point (or equator). A contributing factor is that the perigee of a given satellite, which changes latitude regularly from north to south of the subsolar point and vice versa, reaches its maximum distance north or south of the subsolar point near the solstices. This hypothesis is able to explain qualitatively all of the observed features of the semi-annual effect. More important, it strongly indicates the existence of a strong latitudinal density variation in the winter hemisphere. (auth)

45159 (UCRL-14374) SOURCES OF ARTIFICIAL RADIATION BELTS. Christofilos, N. (Lawrence Radiation Lab., Univ. of California, Livermore). Aug. 10, 1965. Contract W-7405-eng-48. 8p. (CONF-650816-1). Dep. mn; CFSTI $1.00 cy, $0.50 mn.

From Conference on Radiation Trapped in the Earth's Magnetic Field, Bergen, Norway.

Since nuclear explosions in outer space have been banned, the discussion concerns other possible sources of artificial radiation belts. The placing of electron accelerators and radioactive isotopes in orbit is considered. It is concluded that the best possible method is the positron emitters. (M.O.W.)

45160 ON THE LOCAL-TIME DEPENDENCE OF OUTER RADIATION ZONE ELECTRON (E > 1.6 Mev) INTENSITIES NEAR THE MAGNETIC EQUATOR. Frank, L. A. (Univ. of Iowa, Iowa City). J. Geophys. Res., 70: 4131-8(Sept. 1, 1965).

A study of approximately 10 months of Explorer 14 observations of energetic electrons (E > 1.6 Mev) in the outer radiation zone near the geomagnetic equator $|\lambda_m| < 25°$ shows that, if the omnidirectional intensity measurements are organized in a B-L system based on surface measurements of the geomagnetic field, a large local-time dependence of intensities on a given L shell is observed beyond $L \simeq 6$. The "average" isoflux contour $J_0 = 10^2$ $(cm^2\ sec)^{-1}$ in an L-local time coordinate system is at $L \simeq 10$ (maximum L) near the local noon meridian and at $L \simeq 8$ (minimum L) near the local midnight meridian. For the contours of higher intensities (and hence smaller radial distances), this local-time variation weakens; for $J_0 = 10^4$ $(cm^2\ sec)^{-1}$, maximum $L \simeq 7$ near local noon, minimum $L \simeq 6$ near local midnight. A geostationary satellite at $6.6R_E$ (earth radii) should observe an average diurnal variation in electron (E > 1.6 Mev) intensity by a factor ~50. At higher magnetic latitudes, $|\lambda_m| > 25°$, near local noon the electron (E > 1.6 Mev) intensity profiles were often not monotonically decreasing with increasing radial distance beyond $\sim 5R_E$ as were the profiles at lower magnetic latitudes but displayed frequent secondary peaks of intensity from 5 to $12R_E$, which may be indicative of an acceleration mechanism for energetic electrons $E \gtrsim 1$ Mev in the local day part of the magnetosphere. The diurnal variations of electron (E > 1.6 Mev) intensities observed near the geomagnetic equatorial plane are consistent with the expected distortion of the geomagnetic field in these regions by the solar wind. (auth)

45161 LOSS AND REPLENISHMENT OF ELECTRONS AT MIDDLE LATITUDES AND HIGH B VALUES. Williams, D. J.; Kohl, J. W. (Johns Hopkins Univ., Silver Spring, Md.). J. Geophys. Res., 70: 4139-50(Sept. 1, 1965).

Using data from the satellite 1963 38C, the spatial characteristics of electrons trapped at high B values in the region $1.4 \leq L \leq 3.4$ were measured. The data were obtained from an integral electron spectrometer sensitive to electrons of energy $E_e \geq 280$ kev, ≥ 1.2 Mev, ≥ 2.4 Mev, and ≥ 3.6 Mev. An intense peak of electrons at $E_e \geq 280$ kev and a corresponding lack of high energy ($E_e \geq 1.2$ Mev) electrons were observed at $L \sim 2.5$. Fluxes of $1.5(10)^6$ electrons $(E_e \geq 280\ kev)/cm^2$ sec ster were observed. A longitude dependence of the observed electron intensity was measured, and plots of the fractional electron transmission through the South Atlantic anomaly were obtained as a function of B value on various L shells. It was found that electrons mirroring at B values which remain above ~350 km in altitude over the South Atlantic anomaly are not disturbed by the anomaly; about 90% of those that reach the 100- to 250-km region over the anomaly are lost, and all those electrons reaching an altitude of ≤100 km over the anomaly are lost. The data indicate that particles are injected into the depleted regions at all longitudes, and that the resulting longitudinal intensity distribution is quite stable during magnetically quiet periods. The data further suggest that the loss of electrons in the anomaly and their subsequent replenishment is a general effect, occurring throughout the radiation cavity. (auth)

45162 A SUDDEN CHANGE IN THE SOLAR WIND PRESSURE AND THE OUTER REGION OF THE MAGNETOSPHERE. Sugiura, Masahisa (Goddard Space Flight Center, Greenbelt, Md.). J. Geophys. Res., 70: 4151-8 (Sept. 1, 1965).

The motions of the magnetic field lines and of the plasma in the outermost region of the magnetosphere that are caused by a sudden change in the solar wind pressure are studied. Using Mead's model for the initial and the final configurations of the magnetic field in the magnetosphere, the field line displacements due to a sudden solar wind pressure change are numerically computed. It is shown that the displacements for high latitude field lines have an appreciable azimuthal component. Thus a solar wind pressure change normal to the magnetospheric boundary surface is partially converted into tangential motions of the plasma inside the boundary, the momentum transfer being accomplished via the magnetic field. The mechanism can be described as a toothpaste-tube effect. The polarization in the magnetic field perturbation expected from this process qualitatively agrees with that observed in sudden commencements. It is suggested that the rise time of a sudden commencement is determined mainly by the time required for the outermost region of the magnetosphere to reach the final equilibrium state. If the field lines in this region are assumed to move with the local Alfvén velocity, the observed rise times of sudden commencements can be explained. According to the above view, the rise time is expected to be the same everywhere in the magnetosphere; this is in agreement with the observations of sudden impulses made by Explorer 12. (auth)

45163 THE RELATIONSHIP BETWEEN SOLAR WIND VELOCITIES AND SURFACE MAGNETIC DISTURBANCES DURING SUDDEN COMMENCEMENT STORMS. Hirshberg, Joan (Ames Research Center, Moffet Field, Calif.). J. Geophys. Res., 70: 4159-63(Sept. 1, 1965).

The relation between the solar wind velocity and the surface magnetic disturbance index is examined at high levels of disturbance through the use of sudden commencement data. It is shown that the results are not in agreement with an extension of those for low values of disturbance from Mariner 2, unless account is taken of the standoff distance between the flare plasma and the shock it causes. This correction will only be large enough to bring about agreement if the front of the plasma cloud is very broad. (auth)

45164 THE INTERACTION OF THE SOLAR PLASMA WITH THE GEOMAGNETIC FIELD. Sozou, C. (Queen Mary Coll., London). J. Geophys. Res., 70: 4165-74 (Sept. 1, 1965).

The interaction of a uniform plasma stream in the joint interplanetary and geomagnetic field when there is a magnetic field along the stream lines is considered. The discussion is restricted to two dimensions. It is assumed that in front of the stream and outside the geomagnetic field boundary a shock wave develops as in the case of supersonic flow past blunt-nosed bodies. The magnetic

field is found to be proportional to the particle flux density. The magnetohydrodynamic equations in the transition layer between the shock and the body are solved numerically, and the effect of the magnetic field on the stand-off distance of the shock is considered. The body causing the assumed shock is obtained and related to the equatorial cross section of the geomagnetic field boundary. (auth)

45165 MAGNETOHYDRODYNAMIC SHOCKS OF GEOPHYSICAL INTEREST. Beard, David B. (Univ. of Kansas, Lawrence; Goddard Space Flight Center, Greenbelt, Md.). J. Geophys. Res., 70: 4181-9(Sept. 1, 1965).

With a view to understanding the physical processes occurring in collisionless magnetohydrodynamic shocks, collisionless shocks are examined from an individual particle point of view, and the results obtained from more standard treatments are re-obtained and illuminated. The transfer of energy from protons to electrons that is obtained by including charge separation effects in the individual particle treatment, is a new result of vital significance to magnetospheric and other geophysical phenomena. (auth)

45166 VERY LOW FREQUENCY PHASE PERTURBATIONS AND THE SOVIET HIGH-ALTITUDE NUCLEAR BURSTS OF OCTOBER 22 AND 28, 1962. I. OBSERVATIONS AND INFERRED RADIATION BELTS. Haave, C. R.; Zmuda, A. J.; Shaw, B. W. (Johns Hopkins Univ., Silver Spring, Md.). J. Geophys. Res., 70: 4191-4206(Sept. 1, 1965).

On October 22 and 28, 1962, nuclear explosions over central Asia produced ionospheric D-layer perturbations as monitored on various VLF paths in the northern hemisphere. Delayed VLF effects due to trapped particles averaged 53% of the normal diurnal change for the burst of October 22, and 29% for the burst of October 28. The types of particles and their energies were the same for both detonations, but differences existed in the spatial extent of the radiation belts producing the VLF phase perturbations. The trapped particles were electrons with $E \lesssim 4$ Mev and protons in the range 2.3 to 4.6 Mev. The electron spectrum is composed of fission and neutron-decay β particles, the latter predominating for $E < 0.78$ Mev. Protons <2.3 Mev may have also been present, but those with $E < 1$ Mev cannot penetrate into the D region and are of no direct VLF interest. With the dipole field approximation, for the detonation of October 22, fission and neutron-decay β particles were trapped in a region bounded by field lines intersecting the earth's surface in a range extending at least from 36.5° to 56° geomagnetic (for the real field the shells are $1.75 \leq L \leq 3.76$). For October 28, fission β particles were confined to areas <49°N ($L < 2.32$) and probably to field lines around that passing through the burst point (at 36.5°N and $L = 1.75$); this type of confinement also existed for 2.3- to 4.6-Mev protons after both nuclear bursts. For October 28, effects due to neutron-decay β particles were found at 49°–51°N ($2.32 \leq L \leq 2.79$), a region which formed the outer boundary for these trapped particles. For the burst of October 22, a prompt effect was observed on the GBR to APL transmission. (auth)

45167 VERY LOW FREQUENCY PHASE PERTURBATIONS AND THE SOVIET HIGH-ALTITUDE NUCLEAR BURSTS OF OCTOBER 22 AND 28, 1962. II. COMPARISON WITH SATELLITE PARTICLE DATA. Zmuda, A. J.; Haave, C. R.; Shaw, B. W. (Johns Hopkins Univ., Silver Spring, Md.). J. Geophys. Res., 70: 4207-18(Sept. 1, 1965).

Energy and spatial characteristics of artificial radiation belts were deduced previously where the temporal histories of the VLF phase perturbations produced by the two Soviet high-altitude nuclear bursts of October 1962 were examined. For both bursts the trapped electrons have energies $\lesssim 4$ Mev, the electron spectrum $\lesssim 0.78$ Mev resembling that from the radioactive decay of neutrons. This dichotomy of fission and neutron-decay β particles in the electron spectrum was not achieved in the satellite particle data so far analyzed, where the energy ranges are either too broad or above 0.78 Mev. For the burst of October 22, the VLF characteristic that electrons $\lesssim 4$ Mev are trapped in the region encompassing at least $1.75 \lesssim L \lesssim 3.76$ is compatible with the trapped particle flux observed by Explorer 14, Alouette, and Telstar 1. For the burst of October 28, the VLF shows that fission β particles $\gtrsim 0.78$ Mev are not present in $L > 2.32$ and are confined on shells <2.32. This characteristic agrees with the results for Alouette electrons $\gtrsim 3.9$ Mev, but not with the Explorer 14 results for $E > 1.6$ Mev or the Explorer 15 results for electrons >1.9 Mev. The Alouette results also show that the energy spectrum extends to about 10 Mev, but that there is a rapid decrease in flux for $E > 4$ Mev. For the burst of October 28, the VLF shows that neutron-decay β particles have an outer trapping boundary at $2.32 \leq L \leq 2.79$, which is compatible with the Explorer 14 results for $E > 230$ kev but not with the Telstar data for $E > 390$ kev, where the outer boundary extends to $L \sim 4$. The VLF result that protons $2.3 < E < 4.6$ Mev are trapped in shells <2.32 complements the Explorer 14 finding that the Soviet bursts produced no discernible changes in the equatorial intensities of protons >500 kev at $L = 2.8$ and 3.2. The characteristics of protons from nuclear explosions are reviewed, and the electron results are consolidated to form at least a model for additional investigations of the artificial radiation belts formed by the Soviet bursts of October 22 and 28, 1962. (auth)

45168 PARTICLE TRAJECTORIES IN MODEL CURRENT SHEETS. I. ANALYTICAL SOLUTIONS. Speiser, T. W. (Goddard Space Flight Center, Greenbelt, Md.). J. Geophys. Res., 70: 4219-26(Sept. 1, 1965).

Approximate analytical solutions are found for two model current sheets. In the first the magnetic field is linear and reverses across a neutral sheet, and the electric field is everywhere uniform, perpendicular to the magnetic field and parallel to the neutral sheet. Charged particles of either sign never come out of the neutral sheet, and their energies increase without bound. In the second model a small component of the magnetic field perpendicular to the neutral sheet is added. This component not only serves to bring particles out of the sheet, but turns protons and electrons toward the same direction, 90° away from the accelerating electric field. The particles are accelerated and then ejected when they have been turned 90°, and the emergent pitch angles to a magnetic line of force will be small if the perpendicular magnetic field component is small. (auth)

45169 SIMULTANEOUS VERY HIGH FREQUENCY AND ULTRA HIGH FREQUENCY OBSERVATIONS OF THE AURORA AT FRASERBURGH, SCOTLAND. Leadabrand, R. L.; Schlobohm, J. C.; Baron, M. J. (Stanford Research Inst., Menlo Park, Calif.). J. Geophys. Res., 70: 4235-84 (Sept. 1, 1965).

Detailed results on the position in space of the aurora indicate that most echoes arise from a layerlike form of auroral scatterers whose thickness is about 10–20 km. The distribution of the auroral return was peaked at about 100 to 120 km, but heights as great as 200 km were observed. Interpretation of results in terms of the Booker scattering formula indicates that the size of the irregularities is 45 to 90 meters along the magnetic field lines and 0.7 meter across the field lines. Detailed comparison of magnetic activity auroral Doppler shifts and auroral echo amplitude indicates that the auroral Doppler spectra and the amplitude of the echoes have a close relation to the auroral current system. The data indicate that the present theories for auroral scattering are insufficient to explain all the experimental characteristics observed. The plasma acoustic-wave model developed for equatorial field-aligned irregularities appears to fit most of the auroral data obtained but warrants further investigation. (J.F.P.)

45170 ON THE RELATION BETWEEN AURORAL RADIO ABSORPTION AND VERY LOW FREQUENCY EMISSIONS. Ecklund, W. L.; Hargreaves, J. K.; Pope, J. H. (National Bureau of Standards, Boulder, Colo.). J. Geophys. Res., 70: 4285-92(Sept. 1, 1965).

Recent ground-based observations of VLF emissions and of 30-Mc/s cosmic noise absorption over an extended area

are compared for a geomagnetic latitude of 59°. The occurrence of VLF emissions is observed to increase with increasing absorption, if there is an area of low absorption within about 150 km of the observation site. If the absorption is widespread, the occurrence of VLF emissions decreases with increasing absorption. The absorption is shown not to change the time of the diurnal maximum of VLF emissions substantially at this latitude. VLF emissions detected while absorption is present near the site tend to be chorus, and those detected while absorption is absent tend to be hiss. In the latter case, absorption is usually present in the auroral zone, some 900 km to the north. The detailed relation between emission generation and absorption production changes diurnally. Some implications are discussed. (auth)

45171 LONG-PERIOD VERY LOW FREQUENCY EMISSION PULSATIONS. Carson, W. B.; Koch, J. A.; Pope, J. H.; Gallet, R. M. (National Bureau of Standards, Boulder, Colo.). J. Geophys. Res., 70: 4293-4303(Sept. 1, 1965).

Pulse trains with periods of the order of a minute occur in the natural VLF signals emitted in the exosphere. Composed of otherwise ordinary VLF emissions, the long-period pulses always rise in frequency. At magnetically conjugate points the long-period pulse signals are received simultaneously. The period of the pulsation events exhibits a latitude dependence, becoming longer at higher altitudes. On the basis of available data, a hypothesis associating hydromagnetic waves with emitting particles is offered to account for the observed properties of the pulsations. (auth)

45172 PHYSICAL SIGNIFICANCE OF INHOMOGENEITIES IN POLAR CAP ABSORPTION EVENTS. Michel, F. C.; Dessler, A. J. (Rice Univ., Houston, Tex.). J. Geophys. Res., 70: 4305-11(Sept. 1, 1965).

Polar cap absorption (PCA) events are caused by the bombardment of the atmosphere over the polar caps by solar flare cosmic rays. The morphology of PCA events is controlled in large part by the configuration of the magnetospheric tail. It is argued that the tail must be longer than about 1 AU in order to account for observed spatial and time inhomogeneities for PCA events due to low-energy (~5 Mev) protons. A magnetosphere whose polar cap field lines are directly connected to the interplanetary field should result in rather homogeneous PCA events with irregularities and inhomogeneities lasting only a few minutes. For a magnetospheric model in which there is a magnetospheric tail longer than about 1 AU and little merging between geomagnetic and interplanetary magnetic field lines, the low-energy (~5 Mev) PCA events should take several hours to become homogeneous over the polar caps. It is concluded that available experimental data support the long magnetospheric tail in which there is negligible direct connection between geomagnetic and interplanetary fields. (auth)

45173 POSITIVE ION-NEUTRAL REACTIONS IN THE IONOSPHERE. Ferguson, E. E.; Fehsenfeld, F. C.; Goldan, P. D.; Schmeltekopf, A. L. (National Bureau of Standards, Boulder, Colo.). J. Geophys. Res., 70: 4323-29(Sept. 1, 1965).

Daytime positive ion densities calculated using recently measured laboratory ion-neutral reaction rate constants are compared with the NRL rocket results between 120 and 220 km. The calculated O^+ densities and N_2^+ densities are found to be in good agreement with the ionospheric observations. The main N_2^+ loss process in this region is the reaction $N_2^+ + O \rightarrow NO^+ + N$. This reaction is also the major source of NO^+ at 140 km. The charge-transfer reaction $O_2^+ + NO \rightarrow NO^+ + O_2$ appears to be a significant source of NO^+ at 120 km and indeed may be the major source. The reaction $O_2^+ + N \rightarrow NO^+ + O$ will be significant at 120 km if the ratio of atomic to molecular nitrogen is as large as 10^{-4}. The fast O_2^+ loss in reaction with NO at 120 km at night requires a local ionization source greater than 1 O_2^+ ion/cc sec to maintain the observed O_2^+ concentration. (auth)

45174 CAUSE OF THE MIDLATITUDE WINTER NIGHT INCREASE IN f_0F_2. Evans, J. V. (Massachusetts Inst. of Tech., Lexington). J. Geophys. Res., 70: 4331-45(Sept. 1, 1965).

Electron density measurements and determinations of the electron and ion temperatures throughout the F region have been made at midlatitudes by the incoherent backscatter technique at Millstone Hill. Results of this work are presented for the hours 1800–0600 EST for the months November and December 1963 and January 1964. The early morning increase in f_0F_2 observable at this station near 0200–0400 EST in these months is accompanied by density increases at all the other altitudes that could be investigated, i.e., up to 600 km. Hence this phenomenon cannot be accounted for by changes only in the shape of the layer. Further, the electron and ion temperatures tended to decrease as the density increased, indicating that freshly produced ionization caused, for example, by particle precipitation cannot be invoked as an explanation. It is concluded that additional ionization must have diffused from great altitudes in the exosphere. It is suggested that this downward motion may occur at this time as a result of a lowering of the exospheric electron temperature after sunset in the southern (summer) hemisphere. (auth)

45175 THE INFLUENCE OF FOCUSING ON THE APPARENT REFLECTION COEFFICIENT OF THE F REGION. Petrie, L. E.; Hagg, E. L.; Warren, E. S. (Defense Research Telecommunications Establishment, Ottawa, Ontario). J. Geophys. Res., 70: 4347-56(Sept. 1, 1965).

The apparent reflection coefficients of the ionosphere for high frequency radio waves were studied using vertical incidence pulse amplitude data obtained at Prince Rupert. The F-layer first-hop reflection coefficient increases in magnitude as the degree of spread F increases. This increase in magnitude can be explained by focusing of the energy scattered from an irregular surface or by propagation of the energy along field-aligned ducts. Revised methods for obtaining calibration constants for ionospheric absorption measurements are required. (auth)

45176 RADAR MEASUREMENTS OF THE TOTAL CISLUNAR ELECTRON CONTENT. Howard, H. T.; Eshleman, V. R.; Barry, G. H.; Fenwick, R. B. (Stanford Univ., Calif.). J. Geophys. Res., 70: 4357-63(Sept. 1, 1965).

During three nights and two mornings at the end of December 1964, two lunar radars were used to make the first measurements of the total integrated electron density between the earth and the moon. The measurements were accomplished by determining the difference in time delay between 25- and 50-Mc/s moon-reflected signals to an accuracy of 10 μsec. The experiment was made possible by the use of FM radar transmissions with time-bandwidth products of 10^5. Subtraction of ionospheric electron contents from the totals determined from the differential group delay measurements suggests that there are two distinct regions beyond the ionosphere. Within the solar wind wake of the earth, in the quadrant opposite the sun, the average cislunar electron density beyond the ionosphere is approximately (300 ± 50) cm^{-3}. In the general direction of the sun, where most of the radar path is beyond the shock wave boundary, the average density is much lower, $(100 \pm 70/150)$ cm^{-3}. Ionospheric and magnetospheric contents and experimental uncertainty are discussed. Though only a few measurements were made, the initial results clearly show a marked effect, which is interpreted here as an average density inside the shock front, in a magnetospheric wake extending at least as far as the lunar orbit, which exceeds the solar wind density by about 200 cm^{-3}. (auth)

45177 A COMPARISON OF ROCKET, SATELLITE, AND RADAR DETERMINATIONS OF ELECTRON TEMPERATURE AT MIDLATITUDES. Evans, J. V. Massachusetts Inst. of Tech., Lexington). J. Geophys. Res., 70: 4365-74(Sept. 1, 1965).

The three principal methods of determining the electron temperature T_e at ionospheric F-region heights are briefly reviewed and their relative merits discussed. Satellite observations suffer because of the difficulty in separately determining time and height dependencies, and rockets cannot be launched on a scale required to follow diurnal

and seasonal changes. The radar backscatter technique has none of these disadvantages, but, in the case of the Millstone Hill radar, suffers from poor height resolution and difficulties arising in the interpretation of some of the observations. Results reported for the year 1963 from rocket soundings from Wallops Island, Virginia, the satellite Explorer 17, and ionospheric backscatter observations from Millstone Hill, Westford, Massachusetts, are compared. These data are particularly well suited for intercomparison, since they all relate to roughly the same geographic location. There is only fair agreement between the height dependence of T_e obtained by backscatter and rocket techniques, but there is good agreement between the satellite and backscatter results for T_e at a fixed altitude. It is believed that the limitations of the three techniques in part account for these differences, and hence the three methods complement one another well. All three techniques indicate that at midlatitudes the electron temperature exceeds the ion temperature both by day and by night. Differing estimates of the magnitude of the nighttime heat flux required to maintain this temperature difference make it difficult at present to establish the source. The backscatter results would, however, be consistent with the amount of heat expected to arise from the cooling of the protonosphere. (auth)

45178 GEOMAGNETIC AND SOLAR DATA. Lincoln, J. Virginia (ed.) (National Bureau of Standards, Boulder, Colo.). J. Geophys. Res., 70: 4383-4(Sept. 1, 1965).

Data are presented for the principal geomagnetic storm sudden commencements for the period February to March 1965. Maximum activity and ranges of the storms are presented. Solar activity characteristics are given for April 1965. (J.F.P.)

45179 SOLAR PLASMA VELOCITY, EXOSPHERIC TEMPERATURE, AND GEOMAGNETIC ACTIVITY. Jacchia, Luigi G. (Smithsonian Institution, Cambridge, Mass.). J. Geophys. Res., 70: 4385-6(Sept. 1, 1965).

The parallel behavior of solar plasma velocities and exospheric temperatures with respect to geomagnetic indices, found in previous work, leads to the conclusion that exospheric temperatures vary with solar wind velocities in a nearly linear fashion. The wind velocity required to cause a temperature increase ΔT for any given value of the geomagnetic index is calculated. A graph of this relation is shown. (J.F.P.)

45180 SEASONAL VARIATION OF AURORA. Schroeder, W. J. Geophys. Res., 70: 4387(Sept. 1, 1965).

The frequency of aurora is given as a function of season from 1957 to 1963. Since previous work shows well-defined minima in May, June, and July and maxima in March-April, and September-October, the maximum shown in July is considered accidental, although such an effect was also observed previously. (J.F.P.)

45181 PROPAGATION OF Pi 2 MICROPULSATIONS THROUGH THE IONOSPHERE. Rostoker, G. (Univ. of British Columbia, Vancouver, Can.). J. Geophys. Res., 70: 4388-90(Sept. 1, 1965).

By further modifying a previously derived equation for waves propagating perpendicular to the field lines, two possible phase velocities are obtained. From results obtained it is inferred that Pi 2 micropulsations can be described by a weak coupling of fluid and electromagnetic disturbances in which the electromagnetic contribution is dominant. Any variations in the values of the parameters which may occur in the course of propagation of the waves over the earth's surface may cause one or the other of the coupled modes to become dominant. Thus alterations in ionospheric conductivity caused by the precipitation of auroral particles will cause the waves to acquire irregular phase velocities during the course of their propagation from the source of the pulsations to the field points. In the case of auroras, different phase shifts are expected between two stations for different sets of peaks in a chain of pulsations. This effect was observed. (J.F.P.)

45182 FARADAY ROTATION AND VOLUME SCATTERING. Flood, W. A.; Camnitz, H. G. (Cornell Aeronautical Lab., Buffalo). J. Geophys. Res., 70: 4391-3 (Sept. 1, 1965).

The correlation between two circularly polarized waves backscattered by electron density fluctuations is determined. If little or no correlation exists between the two magneto-ionic components, it is expected that the resultant polarization at the ground will in general be nonlinear and that when the signal in one linearly polarized receiving channel is maximized the energy in the cross-polarized channel will not be at a minimum as it would in the usual Faraday rotation experiment. From the results it is expected that the fields of two magneto-ionic components are partially uncorrelated, and the sum of the two magneto-ionic components in general gives rise to polarization other than linear. It is thus expected that when the signal on the ground is maximized in one linearly polarized channel, the orthogonal linearly polarized receiving channel will not be zero. (J.F.P.)

45183 INFRASONIC WAVES OF THE AURORAL ZONE. Iyengar, R. S. (Mount Allison Univ., Sackville, New Brunswick, Can.). Nature, 207: 848-9(Aug. 21, 1965).

Discussion is presented on the suggestion that it is possible to account for the energy fluctuations from the atmospheric dynamics, specifically turbulence near 100 km, which can generate infrasonic waves via the pressure fluctuations. Thus it is concluded that turbulence near the 100 km level can be easily considered as an atmospheric source of energy modulation and for the generation of infrasonic waves. (P.C.H.)

45184 THE APPLETON ANOMALY. Kendall, P. C. (Goddard Space Flight Center, Greenbelt, Md.). Nature, 207: 964-5(Aug. 28, 1965).

A possible explanation in terms of horizontal motion of the neutral air caused by ion drag was investigated in order to determine what the drift in the F2 layer should be. It was concluded that account may have to be taken of production, loss, diffusion, electrodynamic drift, horizontal air motions, and temperature variations in assessing quantitatively the grosser features of the F_2 layer at low latitudes. (P.C.H.)

45185 TERRESTRIAL CONTROL IN THE PRODUCTION OF AURORA. Stagg, J. M. Nature, 207: 969-70 (Aug. 28, 1965).

Examples are given which seem to provide evidence for a terrestrial control in the mechanism of aurora production. In view of these examples it is difficult to accept any mechanism for the production of aurora which has not one constituent at least partially within the earth's control. Auroral activity is also discussed. (P.C.H.)

45186 SOME POSSIBLE INSTABILITIES DUE TO THE TAIL WAGGING EFFECT. Lomanitz, Ross. 9p. (CONF-650116-1). Gmelin, AED-CONF-65-021-1.

From American Geophysical Union, Southwestern Regional Meeting, Socorro, N. Mex.

The equations of motion for longitudinal oscillations of a plasma with no streaming velocity are treated. A parallel treatment of Stix's linearized developments for cyclotron damping in a plasma with streaming velocities is presented, assuming, instead of a static unperturbed magnetic field, a magnetic field whose magnitude is constant but whose direction varies harmonically in time. A search was made in particular for instabilities in the results of the linearized treatment; some were found which is assumed to be related to the transfer of energy from the tail-wagging magnetosphere to the plasma with the magnetosphere. (L.B.S.)

45187 HYDROMAGNETIC INSTABILITY OF THE SUB-ALFVEN EQUATIONS. Malkus, Willem V. R. (Univ. of California, Los Angeles). 26p. (CONF-650440-2). Gmelin, AED-CONF-65-095-2.

From American Mathematical Society, 622nd Meeting, New York.

A class of magneto-hydrodynamical instabilities is found which may be responsible for the observed secular variations of the earth's magnetic field. It is observed that steady precession induces zonal flows with sharp discon-

tinuities in slope. Within a part of the laboratory range of parameters, quasi two-dimensional wave-like instabilities occur on these discontinuities. Here, appropriate equations are derived for velocities and frequencies which are small compared to those of Alfvén waves. The conditions for the growth of a small disturbance on a zonal magnetic and velocity field are explored. The problem proves to be non-singular in those terms responsible for electrical dissipation. The characteristic equation for marginal stability sets bounds on the basic zonal fields and determines a dispersion relation for the disturbances. (auth)

45188 A MATHEMATICAL FUNCTION DESCRIBING THE SPACIAL DISTRIBUTION OF PROTONS WITH ENERGIES ABOVE 50 Mev IN THE EARTH'S RADIATION BELTS AS MEASURED BY TELSTAR I IN 1962–1963. Gabbe, John D. (Bell Telephone Labs., Inc., Murray Hill, N. J.). 15p. (CONF-650422-3). Gmelin, AED-CONF-65-118-3.

From American Geophysical Union, Program for Section of Seismology Annual Meeting, Washington, D. C.

The data from the high-energy proton detector on Telstar I within the spatial region defined by $L < 3$, $R < 2$ are fitted by a parametric function for the omnidirectional counting rate, which has the proper boundary conditions and can be transformed in closed form into an equatorial pitch-angle distribution. The estimates for the coefficients determined from the data by fitting the square root of the omnidirectional counting rate using the least-squares criterion on the two-dimensional model. The analysis is described, the coefficients are given, and the quality of the fit is discussed. (L.B.S.)

45189 A SURVEY OF INNER ZONE PROTONS. Fillius, R. W.; McIlwain, C. E. (Univ. of California, San Diego, La Jolla). 50p. (CONF-650422-15). Gmelin, AED-CONF-65-118-26.

From American Geophysical Union, Program for Section of Seismology Annual Meeting, Washington, D. C.

Detailed data are presented from a survey of trapped protons made by Relay I. Six energy channels from 1.1 to 63 Mev are analyzed to determine the stationary distribution of trapped protons as of January 1, 1963. These data are presented as the observed flux of locally mirroring particles plotted as a function of /B/ on each shell of force, and in the form of contour maps in B, L space. (auth)

Low Temperature Physics

Refer also to abstract 44186.

45190 (LA-3319) MEASUREMENT OF HELIUM AND HYDROGEN VISCOSITIES TO 2340 deg K. Guevara, F. A.; Wageman, W. E. (Los Amamos Scientific Lab., Univ. of California, N. Mex.). Jan. 1965. Contract W-7405-eng-36. 39p. Dep. mn; CFSTI $2.00 cy, $0.50 mn.

An apparatus used to measure the viscosities of helium and hydrogen in the temperature range from room temperature to 2340°K is described. A capillary viscometer with a relatively short channel was used to make the measurements. A series of corrections is detailed, and the experimental technique of eliminating the effects of some of them is given. The results are presented as viscosity ratios relative to the viscosities at 283°K. (auth)

45191 (LNF-65/15) CORRENTI PERSISTENTI INDOTTE DA UN ONDA POLARIZZATA CIRCOLARMENTE IN UN ANELLO SUPERCONDUTTORE. (Persistent Currents Induced by Circularly Polarized Waves in a Superconducting Ring). Note No. 278. Guaraldo, C.; Sacerdoti, G.; Susanna, A. (Laboratori Nazionali di Frascati, Comitato Nazionale per l'Energie Nucleare (Italy)). May 7, 1965. 10p. Dep. mn.

The possibility of inducing persistent currents in superconducting rings using circularly polarized electromagnetic waves was examined. The possible physical data that can be obtained from the measurement of the persistent currents thus induced are discussed. (tr-auth)

45192 (ORNL-TM-1266) EXPERIMENTAL SIMULATION OF LARGE, HIGH FIELD, SUPERCONDUCTING MAGNET OPERATION. Gauster, W. F.; Coffey, D. L.; Efferson, K. R.; Luton, J. N.; Ullmaier, H. A. (Oak Ridge National Lab., Tenn.). Sept. 7, 1965. Contract W-7405-eng-26. 40p. Dep. mn; CFSTI $2.00 cy, $0.50 mn.

Diversified work was directed toward a more thorough understanding of the complex performance of superconducting coils. Tests with sample coils wound of 0.005-in. copper-clad Nb(25%)-Zr wire showed very different results from those made previously with 0.010-in. wire coils. The 0.005-in. Nb-Zr wire was used for short sample stabilization experiments which will be continued in order to clarify several newly observed phenomena. A comparison calculation between stabilized coils and conventional superconducting coils was made. Micro Hall Probe measurements were performed on Nb-Zr cylinders and sample coils. Calculations concerning flux distribution in hard superconductors under adiabatic field change were made. (auth)

45193 (TID-21307) CURRENT QUENCHING IN THIN Pb FILMS BY MULTIPLE BOUNDARY PROPAGATION. Stewart, W. C. (Duke Univ., Durham, N. C. Dept. of Electrical Engineering). Aug. 1964. Contract AT(40-1)-2430. 25p. Dep. mn; CFSTI $1.00 cy, $0.50 mn.

The difficulty of determining whether the thermal propagation process originates at a single site or at numerous sites in thin films having high critical currents and correspondingly high thermal propagation velocities is considered. Switching speed measurements at 4.2°K for 400 to 700 A thick Pb films of varying lengths show that the initial normal bridges occur in proportion to film length with current pulses higher than about 1.2 I_c. The dependence of transition rate on I/I_c does not vary with thickness in these films. (auth)

45194 THE CRYSTAL STRUCTURES OF SOLID HYDROGEN AND SOLID DEUTERIUM IN THIN FILMS. Curzon, A. E.; Mascall, A. J. (Imperial Coll. of Science and Tech., London). Brit. J. Appl. Phys., 16: 1301-9(Sept. 1965).

Reflection electron diffraction patterns obtained from thin films of solid hydrogen at approximately 5°K contain sharp rings from a face-centered cubic phase with $a_0 = 5.29 \pm 0.05$ Å, and broader rings which are consistent within experimental error with the hexagonal close-packed structure reported previously. Reflection and transmission diffraction patterns obtained from solid deuterium at about 5 and 7°K respectively contain sharp rings from a face-centered cubic phase with $a_0 = 5.07 \pm 0.05$ Å at approximately 5°K. The atomic positions in the structures were not determined. If it is assumed that there are eight atoms of hydrogen or deuterium per face-centered cubic unit cell, then the calculated densities for the solid elements are in accord with published data. (auth)

45195 RESIDUAL MAGNETIC MOMENTS OF SOME ELEMENTARY SUPERCONDUCTING SPHERES. Carrol, J. Cryogenics, 5: 199-204(Aug. 1965).

Remanent magnetic moments due to an incomplete Meissner effect in crystalline spheres of pure tin, lead, and niobium were studied using a torsion pendulum arrangement. The amount of flux retained in the tin sphere is independent of orientation of the sphere, but the reproducibility of the results and the direction of the moment with respect to that of the external field at the transition are strongly orientation dependent. Near T_c, the damping of the pendulum increases sharply when the sphere has a trapped moment. In the lead and niobium spheres, the trapped moment is highly reproducible, and is always in the direction of the external field at the transition. Rotation of these spheres at speeds up to 30 rev/min during the transition generally causes a reproducible speed-dependent reduction in the magnetic moment. A partial explanation for these phenomena is sought in terms of crystal structure, flaws, normal-superconducting interface surface tension, and eddy-current effects. (auth)

45196 A THREE-PHASE MOTOR WITH SUPERCONDUCTIVE BEARINGS. Buchhold, T. A. Cryogenics, 5: 216-19(Aug. 1965).

A developed three-phase induction motor working at 4.2°K with superconductive windings and superconductive bearings is described. The rotor consists of a thin shell of pure aluminum that rotates in the gap between the outside and the inside part of a stator made of iron laminations. The motor has no wear and avoids the difficulties connected with conventional bearings at 4.2°K. Such a motor will be useful as a laboratory tool and could be applied to drive a pump in a cryotron computer to circulate the liquid helium to keep the temperature everywhere very constant. (auth)

45197 PROXIMITY EFFECT BETWEEN A SUPERCONDUCTING AND A FERROMAGNETIC FILM. Hauser, J. J.; Theuerer, H. C.; Werthamer, N. R. (Bell Telephone Labs., Inc., Murray Hill, N. J.). Phys. Letters, 18: 222-3(Sept. 1, 1965).

Data from experiments on the proximity effect of a ferromagnetic film on a superconducting film are analyzed. New experimental results of the depression of the transition temperature of a superconductor by a ferromagnet which is very large as compared to a nonmagnetic material with the same coherence length were observed. The experimental results can be fitted theoretically by combining previous theories of the proximity effect with the spin scattering theory. (J.F.P.)

45198 CRITICAL FIELDS OF SUPERCONDUCTING BISMUTH AT HIGH PRESSURE. Compy, E. M. (Naval Research Lab., Washington, D. C.). Phys. Letters, 18: 228-9(Sept. 1, 1965).

Measurements of the critical fields of superconducting bismuth III from 1.8 to 4.2°K and the transition temperature in zero magnetic field are reported. The high pressure apparatus is essentially a piston-cylinder device employing silver chloride as a pressure transmitting medium. Temperatures were measured with a carbon resistor calibrated against the vapor pressure of liquid helium. The magnetic field was supplied by a calibrated solenoid magnet. Pressures were applied at 77°K and held constant as the temperature was lowered. Then the electric resistance of the sample was measured as a function of temperature or magnetic field. The measuring current was 500 mamp. Due to the broadness of the transition, two critical fields are used in describing the results. These are plotted against a function of temperature for pressures of approximately 37 kilobar. There were undoubtedly strains in the samples due to pressure inhomogeneities, and therefore these results are considered preliminary. Measures on unstrained samples would probably yield lower critical fields. (J.F.P.)

45199 OBSERVATION OF THE SPEED OF FLUX JUMPS IN SUPERCONDUCTING NIOBIUM. Goodman, B. B.; Wertheimer, M. (Centre de Recherches sur les Tres Basses Temperatures, Grenoble, France). Phys. Letters, 18: 236-8(Sept. 1, 1965).

A high-speed cine-camera was used to study the kinetics of flux jumps in several niobium discs, in an increasing perpendicular magnetic field, at temperatures between 1.4 and 1.9°K, using the Faraday effect technique. A tentative explanation of the results in terms of the critical current density is proposed. The specimens were all 13 mm in diameter. Two typical flux jumps are shown where the position of the boundary between the superconducting and mixed states is indicated for successive frames. The time interval between consecutive frames was 103 μs. The reluctance of flux jumps to coalesce, which is sometimes observed, is illustrated by the concavity of the boundary for the later frames of the second jump. These results are discussed and interpreted. (J.F.P.)

45200 ANALYSIS OF A MAGNETIZATION CURVE OF A SUPERCONDUCTOR OF THE SECOND KIND. Fournet, G.; Baixeras, J. (Lcie, Fontenay-aux-Roses, France). Phys. Letters, 18: 244-5(Sept. 1, 1965). (In French).

A single crystal of niobium with resistivity of the order of 100, in the form of a cylinder 25 mm long and 3 mm in diameter was studied. The sample was cooled to 4.2°K in a zero field. The flux was measured by the deviation of a meter connected to a 5000-turn coil when the bar of niobium was placed in this coil. The value of the flux is proportional to the deviation of the meter; and the coefficient of proportionality was determined by supposing that in the diamagnetic part of the curve, the flux is equal to the negative field. The magnetic field is created by a superconducting coil coaxial with the coil used for the measurement, and much longer than this coil. The curve so obtained is shown. The results were analyzed and the function of free energy arrived at by purely experimental determinations. (J.F.P.)

45201 DISSIPATIVE NORMAL FLUID PRODUCTION BY GRAVITATIONAL SUPERFLUID FLOW. Vermeer, W.; Van Alphen, W. M.; Oljhoek, ᵀ. F.; Taconis, K. W.; De Bruyn Ouboter, R. (Kamerlingh Onnes Lab., Leiden). Phys. Letters, 18: 265-6(Sept. 1, 1965).

Two experiments are performed which demonstrate the conversion of the potential energy of a superfluid, that is the difference in chemical potential, into normal fluid. In the first experiment normal fluid is produced by the potential energy due to a pressure head. The apparatus consists mainly of a copper chamber mounted in vacuum and carrying a thermometer and a heater. This chamber is connected at one side through a superleak with He bath and at the other side again through a superleak to a glass vessel surrounded by the bath in which the height of the liquid level can be changed. A sudden rise or lowering of this level by means of a brass block in the vessel produces a level difference. The corresponding potential energy is equal to 2360 erg and effects a difference in the chemical potential somewhere in the chamber, giving rise to energy dissipation which can be measured by following the temperature rise. Two runs are shown; and the temperature of the copper block is plotted as a function of time. It is concluded that apparently all the available potential energy is dissipated during the flow into heat, developed in the chamber. In the second experiment, in which the results are not yet analyzed, one of the superleaks is replaced by a capillary and a much higher pressure head applied at the entrance of the other superleak. In a stationary state of flow more information is obtained from velocity flow through the superleak. (J.F.P.)

45202 AN ANALOG OF d.c. JOSEPHSON EFFECT IN HELIUM II. Cheishvili, O. D.; Mamaladze, Yu. G. (Inst. of Physics, Academy of Sciences, Tbilissi, Georgian SSR). Phys. Letters, 18: 278-80(Sept. 1, 1965).

A discussion is given of an analogous Josephson effect in helium II. Although the parameter in helium II which corresponds to penetration of the wave field of the condensate into a dielectric, does not very much exceed interatomic distances, it was shown earlier that the depth of penetration of the wave field from the bulk of helium II into a medium with fine pores filled with helium can strongly exceed those distances for pores of different shapes. The flow of the superfluid through a porous partition dividing two infinite volumes of liquid helium II is considered with the flow of the normal component excluded due to narrow pores. A modified Ginzburg-Pitaevski equation is used for this. It determines the modulus of the wave function averages over the volume containing many pores. (J.F.P.)

45203 PSEUDOSPIN MODEL OF LIQUID ^{4}He. Zilsel, P. R. (Princeton Univ., N. J.; Stanford Univ., Calif.). Phys. Rev. Letters, 15: 476-9(Sept. 13, 1965).

It is pointed out that a simple pseudospin model for a gas of hard-core bosons can be applied with a slight modification, to liquid helium-4. It appears to account, at least semiquantitatively, for the liquid-vapor equilibrium as well as for the transition, the off-diagonal long-range order, superfluidity of the low-temperature liquid phase, and the nature of the elementary excitation spectrum. The states for any one cell are those of a Fermi oscillator. But the amplitudes for different cells commute since the underlying field is Bose. (J.F.P.)

45204 INFLUENCE OF ZERO SOUND ON THE THERMODYNAMICS OF ^{3}He. Balian, R.; Fredkin, D. R. (Centre d'Etudes Nucleaires, Saclay, France). Phys. Rev. Letters, 15: 480-2(Sept. 13, 1965).

The possibility is discussed of a finite coupling between helium-3 atoms and collective excitations of the zero-sound type at zero wave number. It is shown that this leads to an infrared type of singularity for the quasi-particle self energy, and noted that this singularity has physically observable consequences, among which are a nonlinear temperature dependence of the specific heat, in agreement with experiment, and a possible lowering of the predicted critical temperature for superfluid helium-3. It is assumed that there exists, for energies less than a maximum value, a boson, with a propagator coupled to the fermions with a constant effective coupling. (J.F.P.)

45205 DIELECTRIC CONSTANT OF ^{3}He IN THE CRITICAL REGION. Chase, C. E. (Massachusetts Inst. of Tech., Cambridge); Zimmerman, G. O. Phys. Rev. Letters, 15: 483-5(Sept. 13, 1965).

A systematic study was made of the equation of state of helium-3, for the purpose of investigating some quantum corrections in detail. A dielectric-constant technique was employed in which the density of a very thin layer of fluid, contained between the plates of a condenser, is derived from the measured change in capacitance as the condenser is filled. Measurements are reported of the density along the critical isotherm. These measurements are believed to be substantially free from the objections mentioned. The measurements show that $\delta = 3.49 \pm 0.1$ over a very wide range of pressure, confirming the existence of substantial deviations from the law of corresponding states. Considerable asymmetry is also found between the high-density and low-density sides of the critical isotherm. (J.F.P.)

45206 METASTABLE CURRENT-CARRYING STATES OF WEAKLY COUPLED SUPERCONDUCTORS. Goldman, A. M. (Stanford Univ., Calif.); Kreisman, P. J.; Scalapino, D. J. Phys. Rev. Letters, 15: 495-9(Sept. 13, 1965).

Experimental and theoretical observations are reported relating to the metastable current-carrying states of weakly coupled superconducting loops. The nature of these metastable states can be illustrated by considering a thick superconducting loop containing one insulating junction. The zero-temperature results given may be simply generalized to finite T. If the junction is characterized by the critical current I_1 which it can support, then the energy coupling the phases across the junction is $-(\hbar I_1/2e)\cos\phi$. Throughout the discussion it is assumed that the junction dimensions are small compared to the Josephson penetration depth so that the current is uniform over the junction area. In the experiment a lead ring with two Josephson junctions was momentarily warmed above its transition temperature with a light pulse from a xenon flash tube and then allowed to cool. The current through the parallel combination of the two junctions was increased from zero at a uniform rate. The I-V curve was then traced on an X-Y recorder. Initially there was no voltage until at some I_c a finite voltage appeared. A range of values of I_c was recorded, indicating that finite ring currents occurred even though the loop was cooled in a d-c magnetic field smaller than that producing one-half of a flux unit through the ring. A histogram of these values is shown. (J.F.P.)

45207 ANOMALOUS BEHAVIOR OF SUPERCONDUCTING MICROGEOMETRIES IN THE PRESENCE OF HIGH CURRENT DENSITIES. Groff, R. P.; Mochel, J. M.; Parks, R. D. (Univ. of Rochester, N. Y.). Phys. Rev. Letters, 15: 517-19(Sept. 20, 1965).

Two striking effects are reported in the behavior of superconducting microgeometries in magnetic fields and in the presence of high current densities. The microgeometry is described and results observed are given. The most striking feature of these results is that the resistance of the microbridge has a nonzero value only at unique values of the magnetic field, which are of the order of one percent of the critical field. There is no complete or self-consistent explanation for this phenomenon. The results described are quite different from those observed in superconducting bridges in simply connected circuits where large d-c currents are produced by constant current sources. A second anomalous effect which is called the "inverse hysteresis effect" occurs in every type of superconducting microgeometry studied, regardless of whether a constant-voltage or constant-current source is used to supply current to the microbridge, or whether a d-c or a-c current is used. It is found that the resistance in decreasing fields is smaller than the resistance in increasing fields. This is exactly opposite to the hysteretic resistive behavior observed in macroscopic geometries. (J.F.P.)

45208 NEW MECHANISM FOR SUPERCONDUCTIVITY. Kohn, W. (Univ. of California, San Diego, La Jolla); Luttinger, J. M. Phys. Rev. Letters, 15: 524-6(Sept. 20, 1965).

A new mechanism is pointed out which provides an instability against Cooper-pair formation. It is found that a weakly interacting system of fermions cannot remain normal down to the absolute zero of temperature, no matter what the form of the interaction. This mechanism has nothing to do with the conventional electron-phonon attractive interaction in metals, or the long-range attractive van der Waals forces in helium-3. It is present even in the case of purely repulsive forces between the particles, and is due to the sharpness of the Fermi surface for the normal system. It is plausible to suppose that the effective interaction between the fermions themselves will have a long-range oscillatory part. By taking advantage of the attractive regions, Cooper pairs can form thus giving rise to superconductivity. To investigate this possibility more systematically the following model is considered: an isotropic system of spin-$\frac{1}{2}$ fermions with weak short-range forces between them. The criterion used for the onset of superconductivity is that the scattering amplitude for pairs of quasiparticles of equal and opposite momenta and total energy corresponding to two particles on the Fermi surface has a pole at a certain temperature. It can be shown that this criterion is exactly the same as can be obtained from the general theory of Cooper-pair formation in the limit as the gap approaches zero. (J.F.P.)

45209 JOSEPHSON TUNNELING AND QUANTUM MECHANICAL PHASE. Ferrell, Richard A. (Univ. of California, Berkeley). Phys. Rev. Letters, 15: 527-9 (Sept. 20, 1965).

An important aspect of Josephson tunneling for the study of field penetration in superconducting films is pointed out. In the case of films thinner than the penetration depth, which were previously studied, the electrodynamic properties of such films are completely specified by two parameters, instead of simply the one parameter relevant for thick films. A previous coordinate notation is used for a film of thickness τ filling the region between the planes $z = 0$ and $z = \tau$, the boundary condition of a vanishing magnetic field at $z = \tau$ is imposed. The quantum mechanical phase question arising in the previous experiment is answered completely by a derived equation. This equation expresses the gauge-invariant connection between the current which produces a phase shift of 2π and the new gauge-invariant parameter. It is necessary to supplement the conventional penetration length with this new parameter, the transfer length, in order to have a complete description of the electrodynamics of a metallic film. (J.F.P.)

45210 ACOUSTIC ATTENUATION IN A TYPE-II SUPERCONDUCTOR. Cooper, L. N.; Houghton, A.; Lee, H. J. (Brown Univ., Providence). Phys. Rev. Letters, 15: 584-6(Oct. 4, 1965).

A brief outline is given of the theory of response of a type-II superconductor in a static magnetic field to an externally applied sound wave. It is shown that the detailed information on the structure of the mixed state of type-II superconductivity can be obtained by examining the nature of ultrasonic attenuation in type-II material. For simplicity, a restriction is made to the case of a longitudinal sound wave with impurity effects neglected. If the effects pre-

dicted are accessible to experiment, ultrasonic attenuation could become a very valuable tool for probing the detailed characteristics of the mixed state of type-II superconductivity. (J.F.P.)

45211 CRYSTAL STRUCTURE OF SOLID DEUTERIUM FROM NEUTRON-DIFFRACTION STUDIES. Mucker, K. F.; Talhouk, S.; Harris, P. M.; White, David; Erickson, R. A. (Ohio State Univ., Columbus). Phys. Rev. Letters, 15: 586-8(Oct. 4, 1965).

A major problem in powder diffraction studies of the solid hydrogens is the preparation of randomly orientated crystal samples. Such solid samples were successfully prepared in the case of ortho-deuterium (97.8% ortho, J = 0; 2.2% para, J = 1) and normal deuterium (66⅔% ortho, 33⅓% para). These yielded reproducible neutron-diffraction data with respect to both line position and intensities from which an unequivocal assignment of the structure of these solids can be made. The solid deuterium samples were prepared by the rapid freezing of the liquid in a thin walled aluminum cell. To test whether random orientation was achieved, the angular dependence of the most intense reflection was measured. In the experiments reported the maximum variation of intensity on a 360° rotation was less than ±20%. Furthermore, the line positions and intensities were reproducible on successive melting and recrystallization of a given deuterium sample. The neutron-diffraction data for a sample of ortho deuterium are shown, and such data were also obtained for a solid sample of normal deuterium. Within experimental error these data are the same, both with respect to line positions and intensities. It is therefore concluded that the crystal structures of ortho and normal deuterium are the same. (J.F.P.)

45212 SUPERCONDUCTIVE MAGNETS. Bogner, Guenther. Siemens-Z., 39: 357-9(Apr. 1965). (In German).

Soon after the discovery of superconductivity in 1911 consideration was given to the possibility of superconductive magnets. However, it was not until recent years, following advances made in refrigeration techniques and the discovery of a number of high-field super-conductors, that the idea was made a reality on a broader basis. Since then, superconductive magnets have been developed with field strengths of up to 100 kG. Their advantage over conventional magnets lies in the reduced power requirements. (auth)

45213 HIGH-TEMPERATURE CRITICAL CURRENT OF VAPOR DEPOSITED Nb_3Sn. Cody, G. D.; Cullen, G. W. 13p. (CONF-650317-3). Gmelin, AED-CONF-65-039-27.

From American Physical Society Meeting, Kansas City, Mo.

Measurements were made in the temperature range 14.5 to 17.5°K using pumped hydrogen. The normal residual resistance of the sample would be about 0.2Ω. Measurements were made at constant field and temperature although the onset of the superconducting transition was determined to be 18.2 ± 0.1°K. Data are presented in graphs. The field dependence of the critical current for Nb_3Sn was found to be in excellent agreement with the theory. (M.C.G.)

Neutron Physics

See also REACTOR TECHNOLOGY — Criticality Studies.

Refer also to abstracts 44527, 45458, and 45674.

45214 (ANL-7024) TABLES OF RESONANCE INTEGRAL FUNCTIONS, L'(Z', ξ). Pennington, Edwin M. (Argonne National Lab., Ill.). Mar. 1965. Contract W-31-109-eng-38. 19p. Dep. mn; CFSTI $1.00 cy, $0.50 mn.

Tables of the function L'(Z', ξ), which occurs in the calculation of resonance integrals for absorbers without admixed moderator in the NRIA approximation, were computed by use of the CDC-3600. The values are calculated in slab, cylindrical, and spherical geometry for ξ = 0.02, (0.01), 0.05, (0.05), 0.50, and ∞, and for j = −2, (0.5), 14 where $Z' = 2^{-j} \times 10^4$. (auth)

45215 (CEA-R-2780) ANALYSE DES RESONANCES DUES AUX NEUTRONS S DANS LES EXPERIENCES DE TRANSMISSION PAR TEMPS DE VOL. II. AVEC TERME D'INTERFERENCE. (Analysis of Resonances Due to s Wave Neutrons in Transmission Time-of-Flight Experiments. II. With An Interference Term). Corge, Charles R. (Commissariat a l'Energie Atomique, Saclay (France). Centre d'Etudes Nucleaires). Apr. 1965. 98p. Dep. mn.

Various methods of analyzing resonances induced by wave neutrons in transmission time-of-flight experiments are described. Interference between resonant and potential scattering is not neglected. A single program is described, where one can find the partial-areas method and also the so-called method of the width at depth f of the dip. (auth)

45216 (CEA-R-2804) METHODE DE MONTE-CARLO POUR L'ETUDE DU RALENTISSEMENT DES NEUTRONS DANS UNE PLAQUE MINCE DE MATIERE HYDROGENEE. (Monte-Carlo Method for Studying the Slowing Down of Neutrons in a Thin Plate of Hydrogenated Matter). Ribon, Pierre; Michaudon, Andre (Commissariat a l'Energie Atomique, Saclay (France). Centre d'Etudes Nucleaires). June 1965. 31p. Dep. mn.

A Monte Carlo method for the study of the slowing down of neutrons, particularly the intensity and time distribution of the slowed-down neutrons, is described. (D.C.W.)

45217 (COO-7-0363) THE ANALYZING POWER OF NEUTRONS FOR HELIUM. Hoop, B. Jr.; Barschall, H. H. (Wisconsin Univ., Madison). [1965]. Contract AT(11-1)-Gen-7. 6p. (CONF-650928-3). Dep. mn; CFSTI $1.00 cy, $0.50 mn.

From International Conference on Polarization Phenomena of Nucleons, Karlsruhe, Ger.

A set of phase shifts for neutron-alpha scattering is proposed for use in the determination of the polarization of neutrons. (D.C.W.)

45218 (DP-938) A COMPUTER CODE FOR ONE-GROUP FLUX CALCULATIONS IN THREE DIMENSIONS. English, Julius C. (Du Pont de Nemours (E. I.) and Co., Aiken, S. C. Savannah River Lab.). May 1965. Contract AT(07-2)-1. 27p. Dep. mn; CFSTI $2.00 cy, $0.50 mn.

A computer code, 3D-HEXLAX, was written in FORTRAN II to solve the one-group neutron diffusion equation over a triangular network of points in two- or three-space dimensions by relaxation methods. The network can contain up to 817 grid points in the R-θ plane and up to 16 horizontal levels. Typical computation time on the IBM 704 ranges from 43 to 255 minutes as the number of grid points vary from 3,500 to 13,000. (auth)

45219 (EUR-2410.I) RISOLUZIONE NUMERICA DELL'EQUAZIONE INTEGRALE DEL TRASPORTO NELLA APPROSSIMAZIONE AD UNA VELOCITA' E SCATTERING ISOTROPO IN SIMMETRIA PIANA E CILINDRICA. (Numerical Solution of the Integral Transport Equation in Approximation to One Velocity and Isotropic Scattering in Plane and Cylindrical Symmetry). Inzaghi, A.; Montagnini, B.; Pomentale, T. (European Atomic Energy Community, Ispra (Italy). European Scientific Data Processing Center). 1965. 110p. Dep. mn.

The code solves the one velocity integral transport equation, under the assumption of isotropic scattering, in plane and cylindrical geometry. Homogeneous (eigenvalue) and nonhomogeneous problems are considered. The difficulties which are usually encountered when it is sought to introduce the reflection boundary condition (of standard use in lattice cell calculations) in an integral formulation of the transport equation are eliminated by representing the angular density of the neutrons entering the cell from the neighboring ones by means of a rapidly converging spherical harmonics expansion. (auth)

45220 (EUR-2411.f) RISOLUZIONE NUMERICA DELL'EQUAZIONE INTEGRALE DEL TRASPORTO NELLA APPROSSIMAZIONE A UNA VELOCITA' E SCATTERING ISOTROPO (TEORIA GENERALE). (A Method of Numerical Solution of the Integral Transport Equation in the One Velocity and Isotropic Scattering Approximation). Montagnini, B. (European Atomic Energy Community, Ispra (Italy). European Scientific Data Processing Center). 1965. 52p. Dep. mn.

The general theory of a method of numerical solution of the integral transport equation, in the one-velocity and isotropic scattering approximation, is developed. One-, two-, and three-dimensional problems are considered. Attention is given to the reflection boundary condition (of standard use in lattice cell calculations). Such a condition is substituted, in the integral formulation, by a suitable distribution of neutron sources placed on the cell boundary, which describes the angular density of the neutrons entering the cell from the neighboring ones. This angular density is written in the form of a rapidly converging spherical harmonics expansion. (auth)

45221 (GEAP-4913) TRANSPORT EQUIVALENT DIFFUSION THEORY. Quarterly Progress Report No. 5, April 1-June 30, 1965. Final Report. Kear, G. H.; Robinson, A. H. (General Electric Co., San Jose, Calif. Atomic Power Equipment Dept.). June 30, 1965. Contract AT(04-3)-189. 50p. (EURAEC-1462). Dep. mn; CFSTI $2.00 cy, $0.50 mn.

Work Performed under United States-Euratom Joint Research and Development Program.

A review of the work done under this contract during the past year is given. Averaging techniques which preserve transport properties are applied to one-group cell calculations and compared with elementary methods. Multi-group considerations lead to a new type of numerical solution for the diffusion equation. (auth)

45222 (INR-624/IX-A/R) THE USE OF THE CHOPPER FOR PULSE NEUTRON MEASUREMENTS. Graffstein, A.; Ogrzewalski, Z.; Rzeszot, T.; Warda, E. (Institute of Nuclear Research, Warsaw (Poland)). Apr. 1965. 12p. (CONF-650504-42). Dep.

From IAEA Symposium on Pulsed Neutron Methods, Karlsruhe, Germany.

The diffusion parameters of the organic glass were measured using the pulsed neutron technique. A neutron pulse introduced into the moderating medium of certain dimensions (geometrical buckling) generates a time-dependent neutron flux, the asymptotic decay constant of which is measured. As a neutron detector the BF_3 miniature proportional counter was used. The pulses from the counter were recorded by a 256-channel time analyzer using a channel width of 4-16 μs. The exponential decay curves were elaborated by means of digital computer GIER. The chopper operating at the horizontal channel of the EWA reactor was used as a pulsed-neutron source. The rotor of the chopper is constructed of the steel and its diameter is 43 cm. The rotor was rotated at a speed of 6,000 rpm. The width of the neutron pulse was about 160 μsec and the repetition rate of 200 sec^{-1}. The sample was placed before the rotor slit. Since the neutron beam from horizontal channel of the reactor was chopped by the rotor, the neutron pulses used for measurements consisted of neutrons of near thermal energy. Due to small leakage of neutrons from the investigated sample during the slowing down process, this method permitted measurement of asymptotic decay constants even for great bucklings. The measurements were carried out for rectangular geometry, and the asymptotic decay constant as a function of buckling was obtained. (auth)

45223 (JAERI-1084) MANUAL OF FREE GAS MODEL-CODE (FREE-CODE). Katuragi, Satoru; Ishiguro, Yukio; Tutui, Tuneo (Japan Atomic Energy Research Inst., Tokyo). Dec. 1964. 9p. Dep. mn. (In Japanese).

The code FREE is prepared to calculate, by the free gas model, the thermal neutron scattering law, Legendre moments of the scattering kernel and the thermal neutron source spectrum. The analytical expressions for the scattering law and for the Legendre moments of the scattering kernel, which are derived from the Van Hove's formula for the differential cross section are given. It is shown how the thermal neutron source spectrum, dependent on the moderator temperature, is calculated numerically. Finally, the formats for the input and output are illustrated. (auth)

45224 (JEN-133-DF/I-43) PROMETEO I, PROGRAMA PARA PROMEDIAR LAS CONSTANTES TERMICAS CON EL ESPECTRO WIGNER-WILKINS EN LA UNIVAC UCT DE LA J.E.N. (PROMETEO I. A Program for Averaging Thermal Constants Over a Wigner-Wilkins Flux Spectrum on the UNIVAC UCT of J.E.N.). Corella, M. R.; Iglesias, T. (Junta de Energia Nuclear, Madrid (Spain). Division de Fisica). 1964. 59p. Dep. mn.

The Prometeo I program for the UNIVAC UCT of J.E.N., determines the spectrum of thermal neutrons in equilibrium with a hydrogen-moderated homogeneous mixture from the Wigner-Wilkins differential equation and averages various cross sections over the spectrum. The cross section libraries available for the Prometeo I are tabulated. (auth)

45225 (JEN-135-DF/I-44) PROMETEO II, PROGRAMA PARA PROMEDIAR LAS CONSTANTES TERMICAS CON EL ESPECTRO WILKINS, EN LA UNIVAC UCT DE LA J.E.N. (PROMETEO II. A Program for Averaging the Thermal Constants From Wilkins Spectrum on the UNIVAC UCT of J.E.N.). Corella, M. R.; Iglesias, T. (Junta de Energia Nuclear, Madrid (Spain). Division de Fisica). 1964. 32p. Dep. mn.

Prometeo II calculates the spectrum of thermal neutrons in equilibrium with a homogeneous mixture, even when the absortion cross section of the constituents vary arbitrarily with energy from the Wilkins differential equation for heavy moderators, and provides microscopic and macroscopic cross sections averaged over that spectrum. (auth)

45226 (KFK-294) ZUR HAERTUNG THERMISCHER NEUTRONENSPEKTREN IN WASSER UND BORSAEURELOESUNG. (On the Hardening of Thermal Neutron Spectra in Water and Boric Acid Solution). Burkart, K. (Kernforschungszentrum, Karlsruhe (West Germany). Institut fuer Neutronenphysik und Reaktortechnik). Jan. 1965. 12p. Dep. mn.

The thermal neutron spectra in water and aqueous boric acid solution were investigated by the integral method using the activation of Lu and Cu probes, and the results were compared with the measurements from the time-of-flight method and the assumptions of the Nelkin model for the thermalization of neutrons. The agreement with the time-of-flight measurements and the assumptions of the Nelkin model was good, whereas the hardening of the spectra appears sharper than given in many earlier publications. (tr-auth)

45227 (NIJS-R-449) REGULAR EIGENFUNCTIONS OF TIME AND VELOCITY DEPENDENT TRANSPORT EQUATION FOR SLABS. Copic, M. (Nuklearni Institut Jozef Stefan, Ljubljana (Yugoslavia)). Apr. 1965. 17p. (CONF-650504-44). Dep. mn.

From IAEA Symposium on Pulsed Neutron Methods, Karlsruhe, Germany.

The regular eigensolutions of the transport equation for slabs of finite half-thickness are decomposed into two terms: the eigensolutions of the infinite medium and the transition functions, needed for the proper description of the boundary conditions. The infinite medium solutions are found by the expansion method of Nelkin using the truncated kernel approximation with linearly anisotropic scattering kernel. The boundary transition functions are obtained in the first order approximation from the inhomogeneous integral equation, derived from the integral form of the transport equation. The results for the free proton gas are obtained by the expansion method, using orthonormal polynomials of velocity on the interval $(0, \infty)$ with the Maxwellian velocity distribution as the weight function. The expansion of the neutron density as function of velocity gives better convergence than the usual expansion of neutron flux into Laguerre polynomials of energy or into odd Hermite polynomials of velocity. (auth)

45228 (NP–15469) VYCHISLENIE DIFFERENTSIAL'-NYKH SECHENII MEDLENNYKH NEITRONOV S POMOSHCH'YU INTEGRIROVANIYA PO VREMENI. (Calculating Differential Cross Sections of Slow Neutrons by Means of Integration With Respect to Time). Report No. 6. Turchin, V. F. (Gosudarstvennyi Komitet po Ispol'zovaniyu Atomnoi Energii SSSR, Obninsk. Fiziko-Energeticheskii Institut). 1965. 17p. Dep. mn.

A method is described for calculating the differential crosss sections of scattering of slow neutrons by crystalline and liquid materials in the noncoherent approximation, using direct integration with respect to time. The algorithm on the basis of which the programs for the calculation of $d^2\sigma/dEd\Omega$ and $d\sigma/dE$ are set up is described. An explanation is proposed for the effect of the spasmodic change of the total scattering cross section of slow neutrons during the transition of ice into water. It is shown that the increase of the cross section proceeds at the expense of additional inelastic scattering in water. The calculation of the effect agrees satisfactorily with the experiments of Heinloth. (tr-auth)

45229 (UJV–1324/65) POUZITI METODY PRAVDEPODOBNOSTI SPAZEK PRO VYPOCET KOEFICIENTU STEPENI RYCHLYMI NEUTRONY. (Collision Probability Method for Calculating Fast Neutron Fission Factor). Kujal, J.; Kujal, B. (Ustav Jaderneho Vyzkumu, Ceskoslovenska Akademie Ved, Rez). 1965. 27p. Dep. mn.

The application of the collision probability method to the calculation of the fast fission factor and the fast fission ratio R is studied. Bases of this method and calculations using two fundamental types of definitions are introduced. The program is coded in Autocode for the National Elliott 803 B computer. Results are given for clustered rod elements with unenriched ceramic fuel, cooled by organic liquid or air, and for a bundle of natural uranium pins with air coolant. (auth)

45230 ABSOLUTE MEASUREMENTS OF 24-kev NEUTRON ABSORPTION CROSS SECTION. Belanova, T. S.; Van'kov, A. A.; Mikailus, F. F.; Stavisskii, Yu. Ya. At. Energ. (USSR), 19: 3-7(July 1965).

The absolute absorption cross sections of neutrons from an Sb-Be source were measured for a series of elements by the method of transmission in spherical geometry. A long counter and a water tank with a system of fission chambers were used independently for an all-wave detector. The effect of resonance blocking on the cross-section values was investigated. The results obtained were processed on the basis of calculations of transmission by the Monte-Carlo method. (tr-auth)

45231 ASYMPTOTIC BEHAVIOR OF LAW OF SLOW NEUTRON SCATTERING. Maiorov, L. V. At. Energ. (USSR), 19: 67-9(July 1965).

A general asymptotic formula of the law of scattering of slow neutrons $S(\alpha,\beta)$ is found, valid in all planes α, β and applicable to a variety of physical problems, in order to improve formulas derived previously, which either did not satisfy the principle of detailed equilibrium or did not have a clear physical sense. The general formula is derived starting from the noncoherent gaussian approximation of the scattering. The range of application of this formula and the use of the formula for calculating the scattering law are discussed. (M.J.T.)

45232 FAST NEUTRON CAPTURE THROUGH CHARGED PARTICLE REACTIONS IN WATER AND IN CONCENTRATED MANGANESE SULPHATE SOLUTION FROM RADIOACTIVE NEUTRON SOURCES. Ryves, T. B.; Harden, D. (National Physical Lab., Teddington, Middx., Eng.). J. Nucl. Energy: Pts. A and B, 19: 607-17 (Aug. 1965).

The fast neutron captures through charged-particle reactions in water and in concentrated manganese sulphate solution were measured for a Ra–α–Be neutron source. The fraction of the total source neutrons captured in water was (1.69 ± 0.25)% and in concentrated manganese sulphate solution (3.05 ± 0.30)%. Calculations for the fast neutron capture for some other neutron sources are given. (auth)

45233 NEUTRON TRANSMISSION OF PALLADIUM IN THE ENERGY RANGE 1.2–100 ev. Constantinescu, M.; Cristea, G.; Dobrescu, S.; Mateiciuc, V.; Stadnicov, T. (Inst. for Atomic Physics, Academy of the R.P.R., Bucharest). Rev. Roumaine Phys., 10: 251-3(1965).

Evidence was found for a resonance at 1.61 ± 0.04 ev in the neutron transmission spectrum of palladium, along with several previously observed resonances. The maximum total cross section was found to be about 120 barns. (L.B.S.)

45234 INELASTIC SCATTERING OF NEUTRONS. VOL. II. Proceedings Series. Proceedings of the Symposium Held at Bombay, 15–19 December 1964. (International Atomic Energy Agency, Vienna). Apr. 1965. 576 p. (CONF-804(Vol.II)). IAEA $11.50; S 241.50; £ 3.9.0; F.Fr. 46.-; DM 40.25 cy. (STI/PUB/92(Vol.II))

Thirty-four papers are included; 27 are in English and 7 in Russian. Separate abstracts have been prepared for 16. Eighteen of the papers were previously abstracted in: NSA, 19: 4740, 9095, 9480, 9481, 11137, 11603, 12099, 12104, 12457, 12473, 12474, 12475, 12478, 13401, 14075, 19413, 21200, and 23255. (T.F.H.)

For abstracts of individual papers see: 44037–44039, 44050, 44531, 44732, 45235–45243, and 45492.

45235 LIQUID DYNAMICS. Larsson, K.-E. (Royal Inst. of Tech., Stockholm). pp 3-34 of STI/PUB/92(Vol.II).

The neutron scattering results obtained from liquids may be divided into at least two classes: those obtained from simple liquids such as liquid metals and condensed noble gases such as argon; and those obtained from polyatomic liquids such as the liquid hydrocarbons. From an analysis of the quasi-elastically and inelastically scattered spectrum for the simple liquids, very direct information is obtained on the local order of the atomic arrangements as a function of time. The existence of interference scattering in the inelastic scattering region clearly indicates that local order is maintained in the simple liquids for a length of time of the order of 10^{-12} sec or longer, allowing a development of vibratory motions of period shorter than 10^{-12} sec. The studies of the more complex hydrogenous liquids lead to an increased insight into the relaxational phenomena in these liquids. Applying the principle of division of the scattered neutron spectrum into an inelastic and a quasi-elastic part, one obtains from the analysis of the inelastic part detailed information about the rotational, librational, and vibrational levels in the molecule as well as in the intermolecular hydrogen bonds. The analysis of the quasi-elastic peak leads in several cases to a determination of a self-diffusion coefficient typical for the proton motion. It is also possible to derive a mean lifetime for the hydrogen bond or for a hindered rotation in some cases. The nature of diffusive motions in the hydrogenous H-bonded liquids is also rather clearly illustrated as a kind of step-wise rotational motion hindered by the H-bond. There seems to exist a universal limiting relaxation time of about 10^{-12} sec in all the hydrogenous liquids investigated at temperatures such that the viscosity of the liquid is of the order of 1 cP or smaller. From a comparison with the ultrasonic data on glycerol it seems clear that the neutron does not observe all the existing relaxational effects present in glycerol but rather selects those mechanisms which occur on the right time scale of 10^{-11} to 10^{-13} sec. It seems that conglomerates of molecules, the size of which is strongly temperature-dependent, may very well exist for the case of glycerol. In such cases the true diffusion mechanism seems to be a very complicated one occurring on various scales of which the neutron experiments give information only on the faster parts. If the technique of exchanging the proton against a deuteron is applied to the hydrogenous samples a considerable increase is gained in the amount of information obtained from the neutron data. This will be exemplified for glycerol which has been investigated both in a partially, $C_3H_5(OD)_3$, and fully, $C_3D_5(OD)_3$, deuterated form. (auth)

45236 THE VAN HOVE SCATTERING FUNCTION FOR WATER. Pope, N. K.; Nation, R. (Royal Military Coll., Kingston, Ont.). pp 141-56 of STI/PUB/92(Vol.II).

Measurements, using the Chalk River rotating crystal spectrometer at a resolution of 2×10^{-4} ev, of the energy distributions of neutrons scattered by water at 25 and 75°C have been reported previously. From the results the Van Hove scattering function, $S(Q,\epsilon)$, was formed for wave vector transfer in the range $0.4 \leq Q \leq 2.0$ Å^{-1} at 75°C and $0.4 \leq Q \leq 2.6$ Å^{-1} at 25°C. Since, for the smaller values of Q used, the energy distributions for fixed Q show quasi-elastic peaks of widths much less than the resolution of the spectrometer, the results were analyzed without constructing a scattering function which had been corrected for resolution. The previously reported $S(Q,\epsilon)$ have been corrected for resolution. The correction has been carried out by assuming that $S(Q,\epsilon)$ can be represented by the quotient of a slowly varying function of ϵ and a Lorentz function. It is found that in the region of the quasi-elastic peak $S(Q,\epsilon)$ can be represented by a Lorentzian form $AW/(\epsilon^2 + W^2)$ where A is slightly Q-dependent and W deviates only slightly from the value DQ^2. D is a constant having values in good agreement with the values of the diffusion constant of water measured at the appropriate temperature. The resolution-corrected $S(Q,\epsilon)$ has been used to construct the frequency spectra of the velocity autocorrelation function. No evidence has been found for a dip near the origin caused by a partial separation of diffusive modes of motion from other types of modes. (auth)

45237 COLD NEUTRON SCATTERING BY METHANE. Dasannacharya, B. A.; Venkataraman, G.; Usha Deniz, K. (Atomic Energy Establishment, Trombay, India). pp 157-66 of STI/PUB/92(Vol.II).

Preliminary measurements are reported on the scattering of 4.1-Å neutrons by liquid methane using a rotating crystal spectrometer. The quasi-elastic width follows the simple diffusion model up to $Q_0 = 1.5$ Å^{-1}. The inelastic parts of the distributions have been compared with an extension, to the liquid state, of Griffing's theory for gaseous methane. The calculations show that free rotational states, if they exist in the liquid state, can be seen as peaks in the scattered neutron spectra at small angles. The distribution at 30° angle of scattering does not show any such peak. It is therefore, consistent with spectroscopic measurements, that the rotational states should be split due to intermolecular interactions. (auth)

45238 COLD NEUTRON SCATTERING BY POLYPHENYLS. Zemlyanov, M. G.; Chernoplekov, N. A.; Shitikov, Yu. L. (Inst. of Atomic Energy, Moscow). pp 221-40 of STI/PUB/92(Vol.II). (In Russian).

The time-of-flight method was used for spectrometric measurements of the inelastic scattering of slow neutrons in samples of benzene, diphenyl and monoisopropyldiphenyl at ambient temperature and in samples of diphenyl at various temperatures from ambient to 362°K. The experimentally measured scattering cross sections are compared with the calculations carried out on models both of monatomic heavy gas with various effective mass values and monatomic gas where allowance is made for the internal vibrational degrees of freedom. The data on the cold neutron inelastic scattering cross section were used in a computer to restore the distribution functions for the square of displacement of hydrogen atoms from positions of equilibrium when there is vibration in the crystal lattice. The nature of the change in the distribution function of the square of displacement as the crystal passes through the melting point is studied by reference to the temperature-dependence of the scattering cross section. The restored displacement distribution functions for benzene and solid diphenyl are compared with the results of optical investigations. (auth)

45239 LATTICE DYNAMICS OF SOLID METHANE. Dorner, B.; Stiller, H. (Kernforschungsanlage, Juelich, Ger.; Centre d'Etudes de l'Energie Nucleaire, Mol, Belg.). pp 291-304 of STI/PUB/92(Vol.II).

Solid methane seems a comparatively simple example of a molecular crystal. Yet the internal dynamics of the system are not understood. Specific heat measurements reveal a phase transformation at 20.4°K; another phase change is found at 8°K. Both transitions are of the second kind. X-ray investigations have indicated that the first transition does not affect the fcc lattice positions of the carbon atoms. The energy distribution of scattered slow neutrons is measured for the γ-phase ($T < 8$°K). The experiments are carried out with the filtered detector technique. Frequency distributions, derived from the assembly of experimental results, are compared to theoretical predictions, which are based on a model proposed by James and Keenan for the orientation structure. The comparison confirms the model for the γ-phase. The observed maximum frequency of acoustic vibrations, $\hbar\omega_D \simeq 4$ Mev, corresponds to that expected for the assumed octopole-octopole interactions. In addition, two optical bands are observed. The ratio of their mean frequencies is found to be 1.25, which under the assumption of harmonic librations corresponds exactly to the value calculated from the proposed orientational structure. Again for octopole-octopole interaction the absolute values of these frequencies indicate $q = 0.16$ e for the effective proton charge. Thermodynamic considerations, applied by James and Keenan to CD_4, give $q = 0.13$ e. The experimental results contradict, however, the orientational structure proposed for the β-phase. For the α-phase the theory predicts the absence of long-range orientational order. The neutron investigations show that yet the rotational motions are not entirely unhindered, but a quantitative interpretation of the spectrum observed in this phase has not been attempted. (auth)

45240 STUDY OF INELASTIC SCATTERING OF SLOW NEUTRONS IN ZIRCONIUM HYDRIDE. Liforov, V. G.; Nikolaev, M. N.; Nozik, V. A.; Parfenov, V. A.; Lemenov, V. A.; Turchin, V. F. pp 317-24 of STI/PUB/92(Vol.II). (In Russian).

The double differential scattering cross section for slow neutrons in zirconium hydride at 490 and 20°C is measured. The experimental results are compared with those obtained from theory. (auth)

45241 STUDY OF LOW-FREQUENCY MOTIONS IN SEVERAL FERROELECTRIC SALTS BY THE INELASTIC SCATTERING OF COLD NEUTRONS. Rush, J. J. (National Bureau of Standards, Washington, D. C.; Argonne National Lab., Ill.); Taylor, T. I. pp 333-45 of STI/PUB/92(Vol.II).

Energy-gain spectra for the inelastic scattering of cold neutrons by ferroelectric $K_4Fe(CN)_6 \cdot 3H_2O$, NH_4HSO_4, $(NH_4)_2SO_4$, and $(NH_4)_2BeF_4$ have been measured above and below T_C, their respective Curie points, using the Argonne cold-neutron facility. For $K_4Fe(CN)_6 \cdot 3H_2O$ ($T_C = 249$°K) scattered spectra were obtained at 121, 175, and 296°K. The results were similar in both the high temperature and ferroelectric phases. A broad band centered at an energy gain 435 ± 40 cm^{-1}(54 ± 5 Mev) is observed at all three temperatures and assigned to the librations of the water molecules. A second broad peak around 165 cm^{-1} is possibly due to the translational motions of the water molecules in the lattice. The room-temperature spectra for NH_4HSO_4(T_C at 154 and 270°K) and $(NH_4)_2SO_4$ ($T_C = 224$°K) show broad bands peaked at about 260 cm^{-1} and 300 cm^{-1}, respectively, which are primarily due to the torsional motions of the ammonium ions. The NH_4HSO_4 spectrum at 177°K shows an indication of splitting, with little shift in the center of the band. At 125°K the spectrum is clearly split, with peaks at 290 ± 25 and 190 ± 16 cm^{-1}. The $(NH_4)_2SO_4$ results at 172°K also exhibit a split band, with peaks centered at 335 ± 25 and 200 ± 16 cm^{-1}. In both cases the higher-energy peaks are assigned to torsional vibrations. The $(NH_4)_2BeF_4$ spectra also show broad "torsional" bands with several indicated maxima in the 175 to 290 cm^{-1} range. No great differences were observed in the spectra above and below the ferroelectric transitions for any of the ammonium salts. The results for all of the compounds studied indicate that the ferroelectric transitions are not related to any large change in the average rotational freedom of the ammonium ions and water molecules. In addition the measurements show that the average barriers to reorientation are relatively small ($V_0 \gtrsim 4$ kcal/mole) in every case. These conclusions do not preclude changes in the ordering of the protons at the transitions. The results

are compared with total cross section data and with data obtained by other techniques. (auth)

45242 STUDY OF ELASTIC INCOHERENT SCATTERING BY AMMONIUM SALTS. Venkataraman, G.; Usha Deniz, K.; Iyengar, P. K.; Vijayaraghavan, P. R.; Roy, A. P. (Atomic Energy Establishment, Trombay, India). pp 347-53 of STI/PUB/92(Vol.II).

The angular distribution of incoherent elastic scattering from several ammonium salts has been studied using a triple-axis spectrometer giving neutrons of energy 0.07 ev and having a window of 0.012 ev at the incident energy. In the case of NH_4Cl(300°K), NH_4Br(300°K), and NH_4I(220°K), the form factor was found to be Gaussian and values for the mean square amplitude were derived. In NH_4I, $(NH_4)_2SnCl_6$, and $(NH_4)_2SnBr_6$ (all at room temperature), the form factor, besides being non-Gaussian, is much sharper, indicating greater freedom of motion for the NH_4^+ ion. The latter results are compared with calculations based on the uniaxial and the free-rotation model for the ion. (auth)

45243 SUMMARY OF THE SYMPOSIUM ON INELASTIC SCATTERING OF NEUTRONS. Egelstaff, P. A. (Atomic Energy Research Establishment, Harwell, Berks, Eng.). pp 553-63 of STI/PUB/92(Vol.II).

An outline is presented of the conference, including discussions of papers on experimental equipment, studies on solids and liquids, and investigations of magnetism. (T.F.H.)

Nuclear Properties and Reactions

Refer also to abstracts 44157, 44439, 45064, 45232, 45259, 45522, 45679, and 45696.

45244 (AEEW-M-472) A NINETEEN GROUP EXTENSION TO THE YIFTAH, OKRENT AND MOLDAUER CROSS-SECTION SET. Rowlands, J. L.; Wardleworth, D. (Atomic Energy Establishment, Winfrith (England)). Mar. 1965. 30p. Dep. mn.

A nineteen group extension to the first fourteen groups of the Yiftah, Okrent and Moldauer corss-section set was produced. The thirty-three groups cover the energy range 0.414 ev to 10 Mev, the highest energy group being of unit lethargy width and the remainder of half-lethargy width. Resonance self-shielding factors at 300°K for ^{235}U, ^{238}U, ^{239}Pu and ^{240}Pu are included. They are cast as a simple formula relating the shielded cross section in each group g to the cross section at infinite dilution via σ_s, the total cross section per atom, and two parameters, α_g and β_g. (auth)

45245 (AFWL-TR-65-95) DELAYED GAMMA RAYS FROM FISSION. Walton, R. B.; Sund, R. E. (General Atomic, San Diego, Calif. John Jay Hopkins Lab. for Pure and Applied Science). Sept. 1965. Contract AF29(601)-6358. 68p.

Studies of delayed gamma rays from fission at early times were conducted, using the pulsed beams of neutrons and bremsstrahlung x rays from an electron linear accelerator to produce fissions. Measurements of the energy spectrum of isomeric gamma rays from the neutron fission of ^{239}Pu and ^{235}U were performed with a NaI detector at a number of time intervals between 50 μsec and 600 μsec. These measurements showed six prominent gamma rays which probably resulted from the decay of three different fission product isomers. The energies of the gamma rays range from 250 to 1260 kev, and the half lives range from 29 to 78 μsec. The intensities of delayed gamma rays from the neutron fission of ^{235}U and ^{239}Pu were measured as a function of time between 60 μsec and 30 msec. The data were normalized at 20 msec to the intensities derived from the theoretical work of Griffin and the data of Fisher and Engle. Results of the spectrum and intensity measurements gave a complete description of delayed gamma rays from ^{235}U (n,F) and ^{239}Pu (n,F) for the time interval from 50 μsec to 30 msec. The intensities of delayed gamma rays from photofission of ^{235}U, ^{239}Pu, and ^{238}U were measured at early times, starting at 2 μsec after fission. An intense short-lived component with an apparent half-life of a few μsec was observed for all three cases of photofission. Although the photofission data for the various target nuclei are qualitatively similar in the time region extending from 2 μsec into the plateau region, some distinct differences in the shapes and magnitudes of the decay curves do exist. For both ^{235}U and ^{239}Pu, the intensity of delayed gamma rays in the isomeric time region from photofission is almost the same as that from neutron fission but is appreciably lower in the plateau region. (auth)

45246 (ANL-6877, pp 5-14) RADIATIVE CAPTURE OF NEUTRONS. Mooring, F. P.; Segel, R. E. (Argonne National Lab., Ill.).

The $^{11}B(n,\gamma)^{12}B$ cross section was measured for neutrons with energies near 20 kev. A resonance in the cross section was observed near this energy. The reaction was identified by observing the half life of its beta-active product. (auth)

45247 (ANL-6877, pp 29-31) S-STATE INTERACTIONS AND NUCLEAR COUPLING SCHEMES. Pandya, S. P. (Argonne National Lab., Ill.).

A simple SU_3 model for effective nuclear interactions, which has many of the features of the realistic interaction between two nucleons as observed in scattering experiments, is considered. This model force operates only in $l = 0$ states of the relative motion of two nucleons. The model is able to give both "pairing" and "rotational" spectra. (auth)

45248 (AWRE-O-23/65) NEUTRON CROSS SECTIONS OF THE PROTON IN THE ENERGY RANGE 0.0001 ev-20 Mev. Horsley, A. (Atomic Weapons Research Establishment, Aldermaston). July 1965. 27p. Dep. mn; BIS $0.80; HMSO 4s.

Recommended values are given for neutron total and partial cross sections of H-1 in the energy range 0.0001 ev to 20 Mev. The available experimental data are supplemented where necessary by estimates based on nuclear theory. Details of energy and angular distributions are given so that the data are complete for the purposes of neutronics calculations. The recommended data were written on punched cards (3A/H data, data file number DFN = 211, for the cross sections of free hydrogen atoms, and 3B/H data, data file number DFN = 212, for the cross sections per hydrogen atom of a water molecule) as part of the UKAEA Nuclear Data Library. (auth)

45249 (AWRE-O-65/65) LIST OF DATA FILES AVAILABLE IN THE UKAEA NUCLEAR DATA LIBRARY AS OF 15TH APRIL 1965. Miller, Susan M.; Parker, K. (Atomic Weapons Research Establishment, Aldermaston). July 1965. 31p. Dep. mn; BIS $0.90; HMSO 4s, 6d.

The data files in the UKAEA library as of April 15, 1965, are summarized. The data consist primarily of cross sections and related data for neutrons at energies between 0.0001 ev and 15 Mev, but some photon cross sections are also included. (D.C.W.)

45250 (BNL-325(2nd Ed.)(Suppl.2)(Vol.III)) NEUTRON CROSS SECTIONS. VOLUME III. Z = 88 to 98. Stehn, John R.; Goldberg, Murrey D.; Wiener-Chasman Renate; Mughabghab, Said F.; Magurno, Benjamin A.; May, Victoria M. (Brookhaven National Lab., Upton, N. Y.). Feb. 1965. Contract AT(30-2)-Gen-16. 282p. Dep. mn; CFSTI $3.00 cy, $1.50 mn.

Neutron cross sections are tabulated and shown graphically for elements having Z = 88 to 98. (T.F.H.)

45251 (BNL-9108) ABSTRACTS OF COMPUTER CODES. A COMPILATION OF COMPUTER CODES USEFUL IN NUCLEAR STRUCTURE PHYSICS. Raz, B. James; Bockelman, Charles K. (Brookhaven National Lab., Upton, N. Y.). [1965]. Contract [AT(30-2)-Gen-16]. 93p. Dep. mn; CFSTI $3.00 cy, $0.75 mn.

Computer programs (175) for calculations on nuclear structure, nuclear reactions, electromagnetic radiation, alpha decay, and beta decay are described in abstract form. Some of the programs deal with instruments and methods. (D.C.W.)

45252 (CEA-R-2734) SPECTROMETRIE DE NEUTRONS RAPIDES A DOUBLE TEMPS-DE-VOL ET ETUDE DE LA REACTION ^{9}Be(n,2n) (theses). (Double Time-of-Flight Fast Neutron Spectrometry and Study of the Reaction ^{9}Be(n,2n) (thesis)). Gondrand, Jean-Claude (Commissariat a l'Energie Atomique, Grenoble (France). Centre d'Etudes Nucleaires). 1965. 52p. Dep. mn.

Submitted to Grenoble Univ. (France).

The interaction between 14.5-Mev neutrons and ^{9}Be was studied by a double time-of-flight method. Energies of the (n,2n) reaction were measured with the two neutrons being in the same plane with the incident neutron and scattering angle 30°. The events were identified by the electronic method (with photographic control) and by the kinematics corresponding principally to formation of resonance states between particles 2α and 2n of the final state: ^{8}Be(0)$\sigma \simeq$ 170 mb, ^{8}Be(2.9 Mev)$\sigma \simeq$ 165 mb, and ^{9}Be(6.67 Mev)^{8}Be(0) $\sigma \simeq$ 95 mb. (M.O.W.)

45253 (COO-7-0362) POLARIZATION OF PROTONS FROM THE D(d,p)T REACTION. Porter, L. E.; Haeberli, W. (Wisconsin Univ., Madison). [1963]. Contract AT(11-1)-Gen-7. 5p. (CONF-650928-2). Dep. mn; CFSTI $1.00 cy, $0.50 mn.

From International Conference on Polarization Phenomena of Nucleons, Karlsruhe, Ger.

The angular dependence of the polarization of protons from the D(d,p)T reaction was determined for eight deuteron energies between 2.1 and 14.1 Mev. Observations were made at nine laboratory angles between 10 and 70° for each deuteron energy. (D.C.W.)

45254 (CRT-1213) NUSTAT—AN APEX PROGRAM FOR FULLY MECHANIZED SHELL MODEL CALCULATIONS. Newton, T. D. (Atomic Energy of Canada Ltd., Chalk River (Ontario)). Mar. 1965. 41p. (AECL-2223). Dep.; AECL $1.00.

The computer program NUSTAT, developed for the solution of shell model problems on the G-20 computer, is described. The program works entirely within the machine memory. The range of problems that can be solved by this program is indicated. (D.C.W.)

45255 (EANDC-45(U)) COMPILATION OF EANDC PRIORITY I REQUESTS. (European-American Nuclear Data Committee). May 1965. 21p. Dep. mn.

A list of requests for nuclear data is presented. Most of the requests are for neutron cross sections. The desired energy ranges and accuracies are included. (D.C.W.)

45256 (HUX-2752-4) WIDE ANGLE ELECTRON PAIR PRODUCTION (thesis). Blumenthal, Ralph Berthold (Harvard Univ., Cambridge, Mass. Dept. of Physics). Jan. 1965. Contract AT(30-1)-2752. 146p. Dep. mn; CFSTI $4.00 cy, $1.00 mn.

An experiment, wide angle electron pair production, which tests quantum electrodynamics at high energies and small distances is described. The photoproduction from carbon of electron-positron pairs was measured at laboratory angles of 4.75, 6.26, and 7.5°. Symmetrical electron-positron pairs in the energy range from 1 to 5 Bev were detected with a magnet-counter system which consisted of two identical but mirror-image arms. The apparatus was checked extensively and the results were reproducible. The differential cross section for the Bethe-Heitler pair production has a deep dip for symmetrical pairs. The cross section was integrated over the acceptance of the apparatus by an IBM 7094 computer using a Monte Carlo technique to obtain theoretical values for the electron pair yields. (auth)

45257 (IAE-811) RASCHET ENERGETICHESKIKH UROVNEI SLABODEFORMIROVANNYKH YADER. (Calculating Energy Levels of Weakly Deformed Nuclei). Krainov, V. P. (Institut Atomnoi Energii, Gosudarstvennyi Komitet po Ispol'zovaniyu Atomnoi Energii SSSR, Moscow). 1965. 8p. Dep. mn.

The Schroedinger equation for the single-particle levels of weakly deformed nuclei is used to obtain an expression for the diagonal matrix element of excitation in the first-order perturbation theory in the deformation parameter. A parameter involved in this expression is evaluated for A ~ 200 and A ~ 150, using radial wave functions. (M.J.T.)

45258 (IAE-833) POROG SIMMETRICHNOGO DELENIYA ^{237}Np. (Threshold of Symmetrical Fission of ^{237}Np). Borisova, N. I.; Novgorodtseva, V. I.; Pchelin, V. A.; Shigin, V. A. (Institut Atomnoi Energii, Gosudarstvennyi Komitet po Ispol'zovaniyu Atomnoi Energii SSSR, Moscow). 1965. 13p. Dep. mn.

The neutron fission of ^{237}Np was studied. The threshold of symmetric fission was measured and found to coincide with the threshold of asymmetric fission. Results obtained are compared with predictions of existing models for fission. (tr-auth)

45259 (IAE-834) POLYARIZATSIYA V n-α RASSEYANNI PRI E_n = 25, 28 I 34 Mev. (Polarization in n-α Scattering at E_n = 25, 28, and 34 Mev). Arifkhanov, V. R.; Vlasov, N. A.; Davydov, V. V.; Samoilov, L. N. (Institut Atomnoi Energii, Gosudarstvennyi Komitet po Ispol'zovaniyu Atomnoi Energii SSSR, Moscow). 1965. 12p. Dep. mn.

Polarized neutrons with energies 25, 28, and 34 Mev were obtained in the T(d,n)^{4}He reaction at 30°. Measurements were carried out of the asymmetry of scattering of these neutrons on helium at various angles from 45 to 150°. The results obtained were compared with the angular dependence of the polarization in p-α scattering, interpolated to the same values of proton energy according to existing data for other energies (22, 29, and 40 Mev). Satisfactory agreement was found of the angular dependence of the asymmetry of n-α and p-α scattering, and the same divergence of them from the predictions of the phase analysis, extrapolated from the energy range <20 Mev, was observed. An initial estimate of the polarization in n-α scattering is given on the basis of the agreement with the polarization in p-α scattering. (tr-auth)

45260 (IDO-14660) BURNUP DETERMINATION OF NUCLEAR FUELS. Project Report for the Quarter, January 1–March 31, 1965. Maeck, W. J.; Rein, J. E. (eds.) (Phillips Petroleum Co., Idaho Falls, Idaho. Atomic Energy Div.). June 1965. Contract AT(10-1)-205. 39p. Dep. mn; CFSTI $2.00 cy, $0.50 mn.

Accurate measurements are carried out of the ^{235}U thermal fission yields of stable and long-lived isotopes of Kr, Xe, Cs, Ce, Nd, and Sm. The analyses are carried out using mass spectrometric and isotope-dilution means. Separation methods are developed for the alkali metals, the alkaline earths, and ruthenium. (T.F.H.)

45261 (IDO-17016) A NONLINEAR LEAST-SQUARE PROGRAM FOR THE DETERMINATION OF PARAMETERS OF PHOTOPEAKS BY THE USE OF A MODIFIED-GAUSSIAN FUNCTION. Putnam, Marie; Helmer, R. G.; Gipson, D. H.; Heath, R. L. (Phillips Petroleum Co., Idaho Falls, Idaho. Atomic Energy Div.). Aug. 1965. Contract AT (10-1)-205. 88p. Dep. mn; CFSTI $3.00 cy, $0.75 mn.

A computer program was written to perform a nonlinear, least-squares fit to a set of data points with one or more Gaussian, or "modified-Gaussian," functions. This program was designed for the analysis of gamma spectra obtained with NaI(Tl) scintillation detectors and lithium-drifted germanium detectors. It is used to determine the photopeak positions (gamma-ray energies) and areas for peaks which contain one or more unresolved photopeaks. Several options are included in the program to facilitate its application to different problems. The input subroutine was arranged so that a minimal amount of input information is needed when a series of similar fits are to be carried out in succession. Complete listings of the FORTRAN IV program are included along with samples of input to the program and complete instructions for preparing input. (auth)

45262 (IS-T-29) AVERAGE HALF-LIFE DETERMINATION OF THE SHORT-LIVED PRODUCTS OF THE PHOTONUCLEAR REACTIONS OF ^{40}Ca (thesis). Kadlecek, John Alfred (Ames Lab., Iowa State Univ. of Science and Tech.). July 1965. Contract W-7405-eng-82. 85p. Dep. mn; CFSTI $3.00 cy, $0.75 mn.

A detailed description of the experimental apparatus and procedure for determining the average half life of the products from high energy photonuclear reactions with ^{40}Ca. Results from two computations are presented. (M.O.W.)

45263 (JAERI-1078) EXCITATION CROSS SECTIONS OF THE (n,n′γ) REACTIONS ON Fe, Co, Ni, Cu, Zn, Mo, Ag, Cd AND Sn. Kikuchi, Shiroh; Okano, Kotoyuki; Nishimura, Kazuaki (Japan Atomic Energy Research Inst., Tokyo). Jan. 1965. 16p. Dep. mn.

Excitation cross sections of (n,n′γ) reactions were measured on the low-lying levels of nuclei of mass number around 60 to 100, by using a ring-geometry arrangement for gamma detection. Numerical values of the cross sections obtained for Fe, Co, Ni, Cu, Zn, Mo, Ag, Cd, and Sn are tabulated. Correction factors for finite angular resolution of the detecting system are calculated and listed. The equations used in calculating theoretical (n,n′γ) cross sections are explicitly presented, and the calculated excitation curves and angular distributions of gamma rays are illustrated. (auth)

45264 (JINR-E-2243) LITHIUM-INDUCED REACTIONS AND THE STRUCTURE OF LIGHT NUCLEI. Rotter, I. (Joint Inst. for Nuclear Research, Dubna (USSR). Lab. of Theoretical Physics). 1965. 17p. Dep. mn.

It is shown that the preponderant reaction mechanism in reactions of the type (Li^6,d), (Li^6,α), (Li^7,t), (Li^7,α) is the stripping-like one. Effects of nuclear structure are seen to play an important role in the angular distributions and in the spectra of the deuterons, alphas, and tritons, respectively. (auth)

45265 (JINR-E-2244) ON THE OBSERVED ISOSPIN VIOLATION IN THE $^{10}B(^6Li,d)^{14}N$ REACTION. Rotter, I. (Joint Inst. for Nuclear Research, Dubna (USSR). Lab. of Theoretical Physics). 1965. 5p. Dep. mn.

An explanation of the "violation of the isospin selection rule" observed in the B(Li-6,d)^{14}N reaction is suggested in terms of mixing of the T = 1 level at 9.17 Mev with α–threshold levels. (auth)

45266 (JINR-E-2285) THE ORBITAL FRACTIONAL PARENTAGE COEFFICIENTS FOR TWO AND THREE NUCLEONS IN THE 2s-1d SHELL IN THE SU(3) CLASSIFICATION SCHEME. Pluhar, Z. (Joint Inst. for Nuclear Research, Dubna (USSR). Lab. of Theoretical Physics). 1965. 9p. Dep. mn.

Tables are given for the orbital fractional parentage coefficients for 2 and 3 nucleons in the SU(3) scheme and for the matrix elements of central Wigner force between two-nucleon states. (auth)

45267 (JINR-P-2161) ISSLEDOVANIE SKHEMY RASPADA ^{147}Eu. (An Investigation of the Decay Mode of ^{147}Eu). Dzhelepov, B., Zhelev, Zh.; Kalimnikov, V.; Kudryavtseva, A.; Lebedev, N.; Mareev, Yu.; Yazvitskii, Yu. (Joint Inst. for Nuclear Research, Dubna (USSR). Lab. of Neutron Physics; Joint Inst. for Nuclear Research, Dubna (USSR). Lab. of Nuclear Problems). 1965. 31p. Dep. mn.

Positrons from the ^{147}Eu decay were observed. Their energy is 630 ± 15 kev. The number of positrons per decay is determined. Six new transitions: 856, 932, 1199, 1256, 1332 and 1454 kev were found. The γ–γ coincidences and the conversion electron spectra were studied. A decay mode is proposed. (auth)

45268 (JINR-P-2235) NOVYE DANNYE O RASPADE ^{135}Ce. (New Data on ^{135}Ce Decay). Abdumalikov, A. A.; Abdurazakov, A. A.; Buribaev, S.; Gromov, K. Ya.; Lebedev, N. A. (Joint Inst. for Nuclear Research, Dubna (USSR). Lab. of Nuclear Problems). 1965. 10p. Dep. mn.

The spectrum of conversion electrons arising in the decay of ^{135}Ce was studied with the aid of a β-spectrograph in a constant magnetic field. Twenty-one γ transitions were found, out of which γ transitions with energies 86.80, 146.0, 200.7, and 267.5 kev are new. The multipoles of seven γ transitions were determined. The decay mode $^{135}Ce \rightarrow {}^{135}La$ is proposed. (auth)

45269 (JINR-P-2236) SPEKTRY KONVERSIONNYKH ELEKTRONOV EZOTOPOV ^{133}Ce I ^{132}Ce. (Spectra of Conversion Electrons of ^{133}Ce and ^{132}Ce Isotopes). Abdumalikov, A. A.; Abdurazakov, A. A.; Gromov, K. Ya.; Lebedev, N. A. (Joint Inst. for Nuclear Research, Dubna (USSR). Lab. of Nuclear Problems). 1965. 6p. Dep. mn.

Using a β-spectrograph in a constant magnetic field the spectra of conversion electrons arising in the decay of ^{133}Ce and ^{132}Ce isotopes were studied in the energy region from 20 to 800 kev. The following new γ transitions were observed in the decay of ^{133}Ce: 87.8 (M1), 123.7, 127.8, 130.7 (M1 + E2), 137.6, 142.3, 155.5 (M1 or E1), 177.1, 178.6, 182.2 (E1 or M1 + E2), 190.1 (M1), 216.8, 251.5, 261.3, and 329.5 kev. In the decay of ^{132}Ce: 76.8 (M1) 97.1 (M1), and 174.0 kev were observed. It is supposed that in the nucleus of ^{132}La the levels with energies 97.1 kev and 174.0 kev are excited. (auth)

45270 (JINR-P-2248) NEKOTORYE INTERFERENTSIONNYE YAVLENIYA VOZNIKAYUSHCHIE PRI SMESHIVANII KVANTOVYKH VROVNEI VNESHNIMI POLYAMI. (Some Interference Phenomena Arising by Mixing Quantum Levels in External Fields). Lyuboshits, V. L.; Onishchuk, V. A.; Podgoretskii, M. I. (Joint Inst. for Nuclear Research, Dubna (USSR). Lab. of High Energy). 1965. 22p. Dep. mn.

Interference phenomena arising in external fields by mixing the quantum-mechanical levels of atomic and nuclear systems are considered. It is shown, in particular, that in the magnetic field the unpolarized nuclei may emit γ-quanta which are polarized along the circle. The influence of the external fields on the dynamical properties of the electric and magnetic sensitivity of the gas at low pressures is considered. (auth)

45271 (JINR-P-2265) OB ODNOI ZAKONOMERNOSTI V SPONTANNOM DELENII YADER. (On a Regularity in a Spontaneous Nuclear Fission). Mekhedov, V. N. (Joint Inst. for Nuclear Research, Dubna (USSR). Lab. of Nuclear Problems). 1965. 8p. Dep. mn.

The dependence of the ratios of the spontaneous fission lifetime to the α-decay lifetime is described as a function of the number of neutrons of heavy isotopes. (auth)

45272 (JINR-P-2270) γ-SPEKTR IZOMERA ^{160m}Ho. (γ Spectrum of ^{160m}Ho Isomer). Grigor'ev, E. P.; Kun Hsian-Chin; Muziol, G.; Kherrmann, E. (Joint Inst. for Nuclear Research, Dubna (USSR). Lab. of Nuclear Problems). 1965. 8p. Dep. mn.

It is shown that hard γ-rays ($E_\gamma > 1$ Mev) arising by the ^{160m}Ho + ^{160}Ho decay follow, in the main, the β decay of ^{160m}Ho isomeric state; the strongest γ-transitions with energy from 0.5 up to 1.0 Mev follow the β-decay of the ^{160}Ho ground state. Investigations were made with the ^{160}Er source immediately after its purification from the daughter isotope of ^{160}Ho. (auth)

45273 (JINR-P-2356) KATALIZ OTRITSATEL'NYMI MYUONAMI YADERNYKH REAKTSII d μ + p → ^{3}He + μ⁻ I d μ + d → p + t + μ⁻ I OBRAZOVANIE μ-MOLEKUL pd μ I dd μ V GAZOOBRAZNOM VODORODE. (Negative Muon Catalysis of the Fusion Reactions d μ + p → ^{3}He + μ⁻ and d μ + d → t + p + μ⁻ and pd μ and dd μ MU-Molecule Production in Gaseous Hydrogen). Dzhelepov, V. P.; Ermolov, P. F.; Moskalev, V. I.; Fil'chenkov, V. V. (Joint Inst. for Nuclear Research, Dubna (USSR). Lab. of Nuclear Problems). 1965. 48p. Dep. mn.

The yields of nuclear reactions dμ + p → ^{3}He + μ⁻ and dμ + d → p + t + μ⁻ were measured with a diffusion cloud chamber filled with hydrogen and deuterium at 7 to 23 atm. The muon transfer rate from the dμ-atom to carbon and oxygen was found from experimental dμ-atom range distributions and Auger electron yields. The formation rates of the pdμ and ddμ molecules (reduced to the density of normal liquid hydrogen and deuterium) were found to be $\lambda_{pd\mu} = 1.8 + 0.6 \times 10^6$ sec^{-1} and $\lambda_{dd\mu} = 0.75 \pm 0.11 \times 10^6$ sec^{-1}. The analysis of the experimental data on the reactions leads to the conclusion that the resonance mechanism of ddμ-molecule formation and the nuclear reaction in-flight is most likely to be the reason for the large yield of the two

deuteron fusion reactions under the conditions of the experiments. (auth)

45274 (NEVIS–136) ASYMMETRY IN ANGULAR DISTRIBUTION OF NEUTRONS FROM MUON CAPTURE IN SPIN 0 NUCLEI (thesis). Anderson, E. Walter (Nevis Labs., Columbia Univ., Irvington-on-Hudson, N. Y.). May 1965. Contract Nonr-266(72). 80p. (CU–242; R–505).

When muons are captured by protons in the process $\mu^- + p \rightarrow n + \nu$, there exists a correlation between the momentum of the neutron and the spin of the muon. With a polarized muon beam, this correlation establishes a spatial asymmetry in the direction of emission of the neutron relative to the direction of muon polarization. An experiment designed to measure this asymmetry was performed at the Nevis Laboratory of Columbia University. A pure muon beam from the Nevis synchrocyclotron was stopped in ^{40}Ca and ^{12}C targets located in a uniform transverse magnetic field. The resulting uniform precession of the muon spin transforms the spatial asymmetry to a time interval distribution as recorded by a fixed detector. The time interval distributions were measured both with a digital time analyzer and with photographs of an oscilloscope trace. The muon polarization was determined from measurements on the muon-electron decay asymmetry, and neutron-gamma ray discrimination was performed by a pulse shape analysis technique. Measurements were made at several neutron energy threshold levels, with the expectation that at high neutron energies, the complications due to nuclear physics effects would be less significant. The results for ^{40}Ca at high neutron energies give a value of the asymmetry which is significantly larger than the theoretical value calculated for a V-A, G and T invariant form of the interaction. The results for ^{12}C suggest a similar behavior but because of a lower statistical level, the results are consistent with zero asymmetry. (auth)

45275 (NP–15138) ETUDE DE QUELQUES NOYAUX DE LA COUCHE D PAR DIFFUSION D'ELECTRONS (THESES). (Study of the d Layer of Some Nuclei by Electron Scattering (thesis)). Lombard, Roselyne (Paris Univ. (France). Faculte des Sciences). 1964. 135p. Dep. mn.

The nuclear structure of ^{27}Al, ^{31}P, and ^{32}S was investigated by electron scattering at 100 to 190 Mev over angles from 40 to 135°. The parameters that define the charge density distributions for these nuclei were determined by elastic scattering. The multipolarities of transitions, reduced transition probabilities, and lifetimes of energy levels were determined by inelastic scattering. The results were interpreted in terms of various models. (D.C.W.)

45276 (NP–15304) BEITRAGE ZUR INDIREKTEN BESTIMMUNG DER HALBWERTSZEITEN KURZLEBIGER SPALTEDELGASE. (Report on the Indirect Determination of the Half-life of Short-lived Fission Rare Gases). Patzelt, Paul (Mainz Univ. (West Germany). Naturwissenschaftliche Fakultaet). 1965. 266p. Dep. mn.

The flow-through method, in which the radioactive rare gas in a carrier gas current is driven through a tube in which an electrically charged wire is introduced axially symmetrically was used for the indirect determination of the short lived rare gas isotopes ^{138}Xe, ^{139}Xe, ^{89}Kr, ^{90}Kr, ^{137}Xe, ^{91}Kr, ^{140}Xe, ^{92}Kr, ^{141}Xe, ^{143}Xe, ^{142}Xe, ^{93}Kr, ^{94}Kr, ^{95}Kr, ^{97}Kr, and ^{144}Xe. The apparatus used for the determination is described. The reproducible intensities and selectivity of the method was determined and the interfering reactions were analyzed. The results obtained were compared with direct decay measurements. The results are discussed with respect to the systematics of the half life and the effect of the half lives on the calculation of the fission yields. (J.S.R.)

45277 (NP-15363) LEVELS IN ^{21}Ne USING THE $^{18}O(\alpha,n\gamma)^{21}Ne$ REACTION. Pronko, J. G.; Olsen, W. C.; Sample, J. T. (Alberta Univ., Edmonton. Nuclear Research Centre). [1965]. 28p. Dep. mn.

The method of triple angular correlations was used to determine the spins of the 0.35-, 1.75- and 2.87-Mev levels as well as the multipole mixing ratios of the gamma rays emitted from these states. The $^{18}O(\alpha,n\gamma)^{21}Ne$ reaction was used with the target approximately 20 kev thick at an alpha-particle beam energy of 2.50 Mev. At a beam energy of 4.43 Mev the gamma rays from the 0.35- and 1.75-Mev levels were observed and three types of angular correlation experiments performed; neutron-gamma-ray angular correlations with the neutron counter at zero degrees, gamma-ray angular distributions with the intermediate radiation unobserved, and gamma-gamma angular correlations. These yielded spin assignments of $J = 5/2$ and $7/2$ for the 0.35- and 1.75-Mev levels respectively and multipole mixing ratios $\delta_{0.35} = +0.08 \pm 0.02$, $\delta_{1.40} = +0.18 \pm 0.02$, and $\delta_{1.75} = +0.03 \pm 0.04$. The 1.75-Mev level was found to decay 4.6% ± 2.0% to the ground state. At a bombarding energy of 5.50 Mev, neutron-gamma-ray correlations yielded a spin of $J = 9/2$ as most probable for the 2.87-Mev level with $\delta_{1.12} = +0.12 \pm 0.06$ and $\delta_{2.82} = +0.035 \pm 0.045$. This level was found to decay at least 63% to the 1.75 Mev level. Positive parities are implied for all the levels studied. (auth)

45278 (NP–15389) O KHIMICHESKIKH REAKTSIYAKH MYUONIYA. IDENTIFIKATSIYA PRODUKTOV VZAIMODEISTVIYA S VESHCHESTVOM. (On the Chemical Reactions of Muonium. Identification of Reaction Products). Report No. 292. Firsov, V. G. (Gosudarstvennyi Komitet po Ispol'zovaniyu Atomnoi Energii SSSR, Moscow. Institut Teoreticheskoi i Eksperimental'noi Fiziki). 1964. 12p. Dep. mn.

The dependence of the μ^+ spin precession on the chemical compound in whose composition the muon appears is considered for various magnetic fields. It is shown that identification according to classes of compounds, and also finer distinction according to the precession frequencies of meson-nucleus spin systems, is possible. (tr-auth)

45279 (NP–15415) LA DISTRIBUTION DES IMPULSIONS DANS LE NOYAU ET LA DIFFUSION DES ELECTRONS (THESES). (The Distribution of Momenta in the Nucleus and the Scattering of Electrons (thesis)). Potter, John (Centre National de la Recherche Scientifique, Paris (France)). 1963. 92p. Dep. mn.

Submitted to Paris Univ., France.

The distribution of nuclear impulses was studied using the reactions (e,e′) and (e,d′p). An attempt is made to explain the high components in the nuclear impulse distribution by a calculation of the high components induced in a Fermi gas by a soft-core interaction. The results showed that electron-proton coincidence experiments can be analyzed in the impulse approximation and should give for the relatively heavy nuclei the same detailed information on the shell structure that (p,2p) experiments have given for light nuclei. Quasi-elastic scattering of electrons can be used to obtain information on the total distribution of impulses even for the heaviest nuclei. The nuclear correlations can be determined. Results obtained on ^{12}C can be explained to a great extent by the soft-core correlations between nucleons. (J.S.R.)

45280 (NP–15457) O NESOKHRANENII VREMENNOI CHETNOSTI V SIL'NYKH VZAIMODEISTVIYAKH. (On the T-Parity Nonconservation in Strong Interactions). Report No. 340. Lobov, G. A. (Gosudarstvennyi Komitet po Ispol'zovaniyu Atomnoi Energii SSSR, Moscow. Institut Teoreticheskoi i Eksperimental'noi Fiziki). 1965. 7p. Dep. mn.

The correlation between two cascade γ-quanta emitted by an excited polarized nucleus is calculated. This correlation is considered taking into account the phenomenon of the time reversion noninvariance in strong interactions for an arbitrary case of mixed γ-transitions. The expected effect of the T-violation in strong interactions is discussed. (auth)

45281 (ORNL-3850) ELASTIC SCATTERING OF 12.0- AND 14.0-Mev DEUTERONS FROM ^{90}Zr AND THE REACTION $^{90}Zr(d,p)^{91}Zr$: TABULATED DIFFERENTIAL CROSS SECTIONS. Dickens, J. K.; Perey, F. G.; Silva, R. J. (Oak Ridge National Lab., Tenn.). Sept. 1965.

Contract W-7405-eng-26. 22p. Dep. mn; CFSTI $2.00 cy, $0.50 mn.

Numerical values of differential cross sections for elastic scattering of 12.0- and 14.0-Mev deuterons from ^{90}Zr are presented in tabular form. Cross sections were determined at 5° intervals between laboratory angles of 20 and 165°. Differential cross sections for proton groups from the ^{90}Zr(d,p)^{91}Zr reaction are reported: for E_d = 12.0 Mev, data are tabulated for 11 proton groups (Q = 4.981, 3.77, 3.55, 3.09, 2.91, 2.79, 2.42, 1.93, 1.73, 1.53, and 1.33 Mev), and for E_d = 14.0 Mev, data are tabulated for 9 proton groups (Q = 4.981, 3.77, 2.91, 2.79, 2.42, 1.93, 1.73, 1.53, and 1.33 Mev). (auth)

45282 (ORNL-TM-1180) MUFFLE—A CODE FOR THE MULTILEVEL ANALYSIS OF NEUTRON CROSS SECTIONS. Preskitt, C. A. (Oak Ridge National Lab., Tenn.). Apr. 28, 1965. Contract W-7405-eng-26. 10p. Dep. mn; CFSTI $1.00 cy, $0.50 mn.

A description is given of a code which computes the neutron cross sections for a fissile nuclide in which one to three reaction channels are open for the fission process. Provision is made for two independent spin states with interfering levels as well as a set of non-interfering levels. The cross sections are integrated over a specified group structure to yield resonance integrals, and, if requested, a tape is written for plotting the results using the Benson-Lehner Electroplotter. (auth)

45283 (SGAE-PH-23/1965) MESSUNG DES BETA-SPEKTRUMS VON ^{90}Y. (Measurement of the ^{90}Y Beta Spectrum). Riehs, Peter (Oesterreichische Studiengesellschaft fuer Atomenergie G.m.b.H., Seibersdorf). [1965]. 7p. Dep. mn.

The beta spectrum of ^{90}Y is measured by means of an intermediate image beta spectrometer and compared with the theoretical unique-first-forbidden spectrum form. The endpoint energy of the spectrum was determined to be 2280 ± 5 kev. (auth)

45284 (TID-22169) BETAS AND BREMSSTRAHLUNG FROM ^{90}Sr-^{90}Y (thesis). Bustard, Thomas Stratton (Martin Co., Baltimore, Md. Nuclear Div.). 1965. Contract AT(30-1)-3062. 116p. Dep. mn; CFSTI $4.00 cy, $0.75 mn.

The beta particles and bremsstrahlung of the radionuclide system ^{90}Sr-^{90}Y were characterized from an engineering standpoint. A thin, point source of ^{90}Sr-^{90}Y was used in conjunction with nuclear pulse height spectrometric techniques to obtain beta absorption and bremsstrahlung formation in targets of atomic number up to 73 and mass thicknesses up to 2.5 gm/cm^2. Particular emphasis was placed upon measurement of the bremsstrahlung spectra produced in targets with a mass thickness less than the range of the ^{90}Y maximum energy beta particle. The ^{90}Sr-^{90}Y spectrum was measured using a collimated anthracene crystal in conjunction with a 512-channel pulse-height analyzer. Kurie plot analysis showed linearity to 65 kev and resulted in maximum beta energy determinations of 0.55 ± 0.01 and 2.19 ± 0.04 Mev for ^{90}Sr and ^{90}Y respectively. Spectrum integration yielded a specific power of 6.81 ± 0.10 watts per kilocurie of ^{90}Sr for the system. This compares with the 6.35 watts per kilocurie measured calorimetrically at the Martin Company. Measurements were made on the attenuation of the betas through targets of varying atomic number. They show the wide variation of the average energy of the transmitted beta particles with absorber thickness. The backscattering characteristics were measured using various backing materials. The fractional increase in the number of betas and total beta particle energy as well as the spectra of the backscattered components are presented. As expected from previously reported results, the backscatter measurements were very sensitive to the experiment configuration. This sensitivity is explained in terms of the Cauchy statistical distribution of beta particles impinging on the scatterer. Bremsstrahlung formation was measured for various target materials using a NaI(Tl) scintillator in the same experimental arrangement as employed for the determination of the beta particle characteristics. Results were obtained as a function of target thickness allowing observation of how the bremsstrahlung spectrum is produced as the beta spectrum is attenuated. The measurements show that the low-energy portion of the bremsstrahlung spectrum accumulates rapidly and is for the most part well established in the thinnest target thicknesses used. The high energy portion accumulates much more slowly and requires approximately one half the ^{90}Y beta particle range to reach the steady state distribution. The k constant present in Evans approximation to thick target bremsstrahlung theory was determined and found to be 0.34×10^{-3} or 0.24×10^{-3} Mev^{-1} for photon number and energy, respectively. The constants were calculated by considering incremental target thicknesses and performing a photon number and energy balance over each increment. The photon number and energy produced in each increment were then summed over the entire target thickness up to the range of the ^{90}Y beta particle to obtain the total bremsstrahlung produced. The significant difference in the k constant between photon number and energy suggests that the Evans approximation does not predict the correct shape for thick target bremsstrahlung spectra. Measured bremsstrahlung spectra shown for various target thicknesses depict the accumulation and subsequent attenuation of the spectra as the target thickness is increased. Average bremsstrahlung energies for the different target materials are also presented. (auth)

45285 (UCRL-16040) COLLECTIVE EXCITATION OF NEUTRON-DEFICIENT BARIUM, XENON, AND CERIUM ISOTOPES: CENTRIFUGAL STRETCHING TREATMENT OF NUCLEI (thesis). Clarkson, Jack E. (Lawrence Radiation Lab., Univ. of California, Berkeley). May 1965. Contract W-7405-eng-48. 78p. Dep. mn; CFSTI $3.00 cy, $0.75 mn.

The collective excitation of various neutron-deficient barium, xenon, and cerium isotopes by the "in-beam" method using lithium-drifted germanium counters was obtained. The (heavy ion, xn) reaction was used to produce ^{126}Ba, ^{124}Ba, ^{122}Xe, ^{120}Xe, and ^{134}Ce. The decay of ^{134}Pr to ^{134}Ce was also observed, with a half life of 17 ± 2 min. Partial level schemes for the ground-state rotational bands to spin 8+ or 10+ are proposed for the nuclides investigated. The lifetime of the first excited state in ^{126}Ba was determined as an in-beam experiment to be 2.7 ± 0.5×10^{-10} seconds and, hence, gives the deformation of ^{126}Ba as $\beta = 0.24 \pm 0.02$. The implications of the rotational energies and spacings as related to deformation in this region are discussed. A classical centrifugal stretching treatment employing realistic nuclear potentials is developed, and the results of this and other works are compared to the calculated energy levels from this treatment. (auth)

45286 (UJV-1293/65) O VOZMOZHNOSTI POLUCHENIYA NEVOZBUZHDENNYKH SOSTAVNYKH YADER TYAZHELYKH TRANSURANOVYKH ELEMENTOV. (Possibility of Obtaining Non-Excited Compound Nuclei of Heavy Transuranium Elements). Maly, Jaromir (Ustav Jaderneho Vyzkumu, Ceskoslovenska Akademie Ved, Rez). 1965. 23p. Dep. mn.

The excitation energies $E_B^X = E_B - Q$ of the same compound nucleus, (Z_c,A_c), (in the first approximation) are calculated. This compound nucleus is assumed to be formed by the nuclear reactions of accelerated heavy ions—at several combinations of a target nucleus (Z_2,A_2) with a heavy ion (Z_1,A_1). The calculations are performed for an initial heavy ion energy equal to the energy of the classical Coulomb barrier (E_B) and for increasing (Z_1,A_1) from H$^1_1$ to $(Z_1,A_1) = [(Z_c,A_c)/2]$. The calculations in the case of compound nuclei of Zr$^{90}_{40}$ or Hf$^{178}_{72}$ show that E_B^X initially grows quickly with increasing (Z_1,A_1) and at large (Z_1,A_1) slowly reaches its maximum value near $(Z_1,A_1) = [(Z_c,A_c/2)]$. On the other hand, a similar calculation of E_B^X performed for the compound nucleus 104^{264}, shows that E_B^X has a maximum at $Z_1 = 10 - 12$, while at higher (Z_1,A_1) it drops to the zero values and near $(Z_1,A_1) = [(Z_c,A_c)/2]$ has nega-

tive values. A similar dependence of E_B^X on the (Z_1,A_1) (with maximum near $Z_1 = 10 - 14$ and zero or negative values of E_B^X at $(Z_1,A_1) = [(Z_c,A_c)/2)]$ appears for all elements from $Z = 100$ to $Z = 116$. For synthesis of heavy elements (Z_c,A_c) with $Z_c \geq 100$, the use of a nuclear reaction reversed to fission of a compound nucleus is proposed: $(Z_1,A_1) + (Z_2,A_2) = (Z_c,A_c)$ where $(Z_1,A_1) \doteq (Z_2,A_2) \doteq [(Z_c,A_c)/2]$ (e.g., $Te_{52}^{130} + Te_{52}^{130} = 104^{260}$ or $Sn_{50}^{124} + Xe_{54}^{136} = 104^{260}$). The calculation of E_B^X for this kind of nuclear synthesis of heavy elements yields the compound nucleus with zero (or near zero) excitation energy. It is supposed that a compound nucleus with $Z_c \geq 100$ and with zero excitation energy will originate with an order of cross section not far from the well-known cross sections σ_c for compound nucleus formation ($\sigma_c \approx 10^{-25}cm^2$). The error of such calculations of E_B^X is discussed in connection with the errors of calculations of Q (Q = exothermic energy of the reaction of compound nucleus formation) calculated with Seeger tables (6) as well as the errors of calculation of E_B. The magnitude of the maximum error in E_B calculations ($\Delta_{E_B^X} \leq 18$ Mev) in the region of $Z_c \geq 104$ shows that the possibility of obtaining a non-excited compound nucleus remains at $(Z_1,A_1) = [(Z_c,A_c)/2]$, even when the maximum error is added to the calculated E_B^X. (auth)

45287 (USNRDL-TR-868) HALF-LIVES OF ^{156}Eu AND ^{157}Eu. Carnahan, C. L.; Bunney, L. R. (Naval Radiological Defense Lab., San Francisco, Calif.). Apr. 29, 1965. Contract AT(49-2)-1167. 19p. Dep. mn; CFSTI $1.00 cy, $0.50 mn.

The half lives of ^{156}Eu and ^{157}Eu were remeasured. Values of 15.21 ± 0.24 days and 15.23 ± 0.03 hours, respectively, were obtained by following the beta decay. A number of gamma energies and relative abundances were obtained for the decay of ^{157}Eu. These were 314(0.05), 369(0.30), 407(1.00), 482(0.34), 629(0.16) and 702(0.06) kev. (auth)

45288 (WASH-1056) REPORTS TO THE AEC NUCLEAR CROSS SECTIONS ADVISORY GROUP MEETING HELD AT NATIONAL BUREAU OF STANDARDS, GAITHERSBURG LABORATORY AND ATOMIC ENERGY COMMISSION HEADQUARTERS, MARCH 8-9, 1965. Smith, A. B. (comp.) (Nuclear Cross Sections Advisory Group (AEC)). 147p. (EANDC(US)-72(U); CONF-650323). Dep. mn; CFSTI $4.00 cy, $1.00 mn.

Research reports which were presented to the AEC Nuclear Cross Sections Advisory Group are included. These reports contain an informal statement of recent developments, changes of emphasis, and preliminary data which are of importance to the cross section measurement program of the AEC. (M.O.W.)

45289 (ZFK-PHA-12, pp 99-105) MEASUREMENT OF THE ANGULAR DISTRIBUTION FOR THE REACTION $^{12}C(d,\alpha)^{10}B$ WITH A SEMICONDUCTOR DETECTOR. Bredel, V.; Klabes, R.; Kuehn, B.; Stiller, G.

In German.

The angular distribution for α particles from the reaction $^{12}C(d,\alpha)^{10}B$ at energies of 12.9, 11.5, and 10.2 Mev were measured using a surface-barrier detector. By suitable selection of the detector voltage the barrier depth could be so selected that the high-energy part of the α-particle spectrum could be separated from the scattered deuterons. (tr-auth)

45290 (ZFK-PHA-12, pp 110-12) EXCITATION FUNCTION FOR THE $^{29}Si(n,\alpha)^{26}Mg$ REACTION IN THE ENERGY RANGE 13.6 TO 15.6 Mev. Jaskola, M.; Turkiewicz, I; Turkiewicz, J.

The excitation function for the $^{29}Si(n,\alpha)^{26}Mg$ reaction going to the ground state of ^{26}Mg was measured in the energy range from 13.6 to 15.6 Mev. The measurements were made using surface barrier Si detectors as both the target and the detector. The spectrum obtained is graphed and the preliminary results are presented. (J.S.R.)

45291 (ZFK-PHA-12, pp 117-22) STUDY OF THE REACTIONS $^{18}O(p,\alpha)^{15}N$ AND $^{11}B(p,\alpha)^{8}Be$ USING SEMICONDUCTOR COUNTERS. Karadzhev, K. V.; Man'ko, V. I.; Chukreev, F. E. In Russian.

N-type Si surface-barrier semiconductor counters were used to study (p,α) reactions on a gaseous O target enriched (60%) in ^{18}O and on a solid ^{11}B target. The variation of the reverse current of the counter with the bias voltage for various radiation doses is shown. The method of amplifying the signal from the alpha particles is described. Results are given of alpha angular distributions from ^{18}O at proton energies from 360 to 2680 kev and of angular distributions from ^{11}B at 1950 to 2800 kev. (M.J.T.)

45292 (BNL-tr-16) NEUTRON-^{235}U NUCLEAR INTERACTION IN THE 0.002-30 kev ENERGY REGION. Van, Shi-di; Van, Yun-chan; Dermendzhiev, E.; Ryabov, Yu. V. (Joint Inst. for Nuclear Research, Dubna (USSR)). Translated by S. Amoretty (Brookhaven National Lab., Upton, N. Y.). 28p. Dep. mn; CFSTI $2.00 cy, $0.50 mn; JCL $2.60 fs, $1.04 mf.

A new experimental method is employed to study the neutron-U-235 nuclear interaction in the 0.002-30 kev energy region in order to obtain the parameters of the levels and to determine the average fission cross sections and the radiation capture. (auth)

45293 (ORNL-tr-696) LONG-RANGE α-PARTICLES OF RADIUM C. Phillipp, K.; Donat, K. Translated for Oak Ridge National Lab., Tenn. from Z. Physik, 52: 759-66(1928). 10p. Dep. mn; JCL $1.10 fs, $0.80 mf.

The investigation of the long-range alpha-particles of RaC, according to the Wilson cloud method, was continued in order to be able to make more accurate statements on the range and frequency of these rays. A movie camera which had been equipped for stereoscopic single frames was used in place of the still camera previously utilized. (auth)

45294 TIME DELAYS IN K X-RAY EMISSION DURING THERMAL FISSION OF ^{235}U. Bridwell, L.; Wehring, B. W.; Wyman, M. E. (Univ. of Illinois, Urbana). Appl. Phys. Letters, 7: 161-3(Sept. 15, 1965).

The time delays in K x ray emission during thermal fission of ^{235}U were measured using equipment having good resolution in both time and energy. A 1-mg/cm^2 foil of uranium enriched to 93.5% ^{235}U was put in contact with a thin plastic scintillation detector which was placed directly in a narrowly collimated beam of thermal neutrons from the thermal column of a reactor. The thinness of the detector allows selective detection of fission fragments in a background of Compton electrons and alpha particles. The energy resolution of an NaI(Tl) crystal allowed time spectrum measurements for both light and heavy fragment x rays the peaks of which occurred at 16 and 32 kev respectively. The prompt spectrum was obtained by choosing sources with suitable energy. Results are shown. (J.F.P.)

45295 THE DECAY OF ^{56}Co. Pettersson, H.; Bergman, O.; Bergman, C. (Uppsala Univ.). Arkiv Fysik, 29: 423-37(1965).

The decay of ^{56}Co to ^{56}Fe was investigated using an iron yoke double focussing spectrometer of 50 cm radius. A total of 18 transitions with energies from 734 kev to 3452 kev were ascribed to the decay from careful internal conversion studies. The gamma ray intensities were determined by photoelectron experiments. The standard error in the energy determinations was generally less than 2 parts in 10^4. The positron investigation showed one intense branch (18.1% of the total decay rate) with an end point energy of 1459 ± 2 kev. Although based on more precise energy data, the scheme of levels which was obtained resembles that suggested by previous investigators; the essential difference is the triplet character of the state previously described as occurring at 4.10 Mev. Multipolarity data, obtained from the absolute measurement of conversion coefficients, were utilized for assigning possible spins and parities to the levels. It is noted that the majority of the transitions are of M1 or/plus E2 character. (auth)

45296 STUDY OF INTERACTION BETWEEN RESONANCE NEUTRONS AND NUCLEI IN THE SACLAY LINEAR ACCELERATOR. Netter, F. At. Energ. (USSR), 19: 8-14(July 1965).

Work is described on the study of the interaction of

resonance neutrons with nuclei, performed on the Saclay linear accelerator. Nuclei of the following elements were studied: Al, V, Mn, Co, Cu, Zn, Ga, As, Se, Br, Y, Zr, Nb, Mo, Ag, Ba, La, Pr, Nd, Tm, W, Pt, Au, Hg, and ^{238}U. The basic purpose of the work is the study of the statistical properties of the resonance parameters. Apparatus is described with which the total cross sections, capture cross sections, and partial radiative transitions are measured. A resolution of 0.3 nsec/m is achieved for a flight distance of 103 m, allowing studies for neutron energies up to 80 kev to be carried out. The method of treating the results is described briefly, and methods for identifying resonances with spins are considered. On the basis of the results obtained, an analysis of the statistical properties of the scattering widths is carried out, and the statistical properties of the radiative widths are surveyed. (tr-auth)

45297 MEASUREMENT OF AVERAGE NUMBER OF FISSION NEUTRONS EMITTED IN A SINGLE CAPTURE EVENT OF 24-Kev NEUTRONS FOR ^{235}U AND ^{239}Pu. Van'kov, A. A.; Stavisskii, Yu. Ya. At. Energ. (USSR), 19: 41-2(July 1965).

The average number of secondary fission neutrons was determined from the balance of the absorbed source neutrons and the emitted fission neutrons by measuring the diffusion lengths of the two neutron groups in water. The count rates of ^{235}U and ^{239}Pu fission chambers were measured as functions of the change of count rate for a changing from a photoneutron source to a fission source of equal intensity. The effective number of neutrons emitted per fission was found from the photoneutron and fission cross sections derived from the measurements. (M.J.T.)

45298 FAST NEUTRON CAPTURE CROSS SECTION FOR RHENIUM. Stavisskii, Yu. Ya.; Shapar, A. V.; Krasnokutskii, R. N. At. Energ. (USSR), 19: 42-3 (July 1965).

The energy dependence of the radiative-capture cross sections of fast neutrons at 20 to 1000 kev was measured for a natural mixture of rhenium isotopes, by the method of recording the prompt capture gamma radiation. Results are presented and compared with previous experiment. (M.J.T.)

45299 ^{235}U FISSION CROSS SECTION FOR RESONANCE NEUTRONS. Wang, Shih-ti; Wang, Yung-chang; Dermendzhiev, E.; Ryabov, Yu. V. At. Energ. (USSR), 19: 43-7(July 1965).

Measurements of the fission cross sections of ^{235}U for neutrons from 2 to 70 ev were carried out for the purpose of obtaining additional information on the parameters of the resonance energy levels. The fission cross section was measured using the time-of-flight method. The detector layout is described. Values of $\sigma_0\Gamma_f$ are presented for neutron resonances from 2 to 73 ev. (M.J.T.)

45300 DELAYED NEUTRON RELATIVE YIELDS DURING ^{235}U AND ^{238}U FISSION. Maksyutenko, B. P. At. Energ. (USSR), 19: 46(July 1965).

Relative yields of delayed neutrons in the neutron fission of ^{235}U at maximum incident energy 6.0 Mev and of ^{238}U at maximum energy 1.75 Mev were studied. Results of the relative yields for groups with various half lives are given. (M.J.T.)

45301 RELATION BETWEEN THE (α,n) REACTION YIELD AND ALPHA PARTICLE ENERGY. Tsenter, E. M.; Silin, A. B. At. Energ. (USSR), 19: 48-50(July 1965).

Empirical formulas obtained previously are used to calculate the neutron yield as a function of alpha energy in (α,n) reactions at 2 to 5.4 Mev with O, Be, B, C, and Mg. Correlations with previous experiments and calculations are discussed. (M.J.T.)

45302 ANALYSES OF PROMPT NEUTRON SPECTRA FOR ^{252}Cf SPONTANEOUS FISSION. Savel'ev, A. E. At. Energ. (USSR), 19: 59-61(July 1965).

An analysis is made of previous measurements of the spectrum of neutrons from spontaneous fission of ^{252}Cf at various angles with respect to the direction of the light fragments. It is assumed that the neutron fission spectrum is isotropic in the cms of the fragments. The neutron spectra from light and heavy fragments are calculated in the cms. By transforming these spectra to the laboratory system and comparing calculated and experimental values, it is seen that the deviation of the calculated spectra from the experimental ones lies practically within the limits of the experimental and calculational errors. Thus it is concluded that in the cms of the light and heavy fragments the neutron spectra are isotropic within 10 to 15%. The cms spectra from light and heavy fragments are also compared with calculations based on the statistical theory of the nucleus. (M.J.T.)

45303 EXPERIMENTAL APPARATUS FOR THE STUDY OF THE ENERGY SPECTRA AND THE POLARIZATION OF PHOTONEUTRONS. De Marco, A.; Garfagnini, R.; Piragino, G. Atti. Accad. Sci. Torino: I. Classe Sci. Fis., Mat. Nat., 99: 445-55(1964-65). (In Italian).

The experimental apparatus constructed near the 100-Mev synchrotron of the Istituto di Fisica, Turin, for the study at 45°, 90°, and 135°, with respect to the γ-ray direction, of the energy spectra and polarization of photoneutrons from various neutrons is described. The technique used is that of the analysis of elastic scattering events of neutrons on He nuclei contained in a scattering chamber. The preliminary results from the operation of the system with a RaD–Be neutron source is reported. (tr-auth)

45304 A PHENOMENOLOGICAL AND QUANTITATIVE DESCRIPTION OF NONELASTIC INTERACTIONS AT LOW ENERGY. APPLICATION TO THE INTERACTION ^{27}Al(p). Hautot, A. Bull. Soc. Roy. Sci. Liege, 34: 110-17(1965). (In French).

The arbitrary nucleon model proposed previously is applied to the study of the interactions ^{27}Al(p,γ) and ^{27}Al (p,α) in order to determine if this model can describe interactions between nucleons. By using a very simple hypothesis for the mechanism of the interaction between ^{27}Al and p, all of the energies observed previously were found with a great exactitude. For the (p,α) reaction only the most intense resonance peaks were considered. The results showed that nonelastic interactions at low and average energy between a nucleus and an incident particle can be described by the following process. During the reaction, unstable associations of electron shells or associations of such shells with one or two nucleons are formed. The resonance energies of the incident particle are the bonding energies of these associations; when the reaction includes a γ emission, the energy of the γ quantum emitted is the energy released by the association at the moment when the associated shells return to their normal state. The probability for the formation of an unstable association in one or several nucleons during an interaction varies with the number and the species (p or n) of nucleons forming the nucleus. (J.S.R.)

45305 STUDY OF THE INELASTIC SCATTERING OF PROTONS AT 155 Mev ON LIGHT NUCLEI. Jacmart, Jean-Claude. Cahiers Phys., No. 173, 1-52(Jan. 1965). (In French).

The experimental method and the characteristic of the apparatus used in the measurement of the inelastic scattering of protons is described. The theory of inelastic scattering is then summarized. The spectra obtained and the differential cross sections for the excitation of the different levels were reported for ^{6}Li, ^{7}Li, ^{9}Be, ^{10}B, ^{11}B, and ^{12}C. (J.S.R.)

45306 THE ELECTRON CONVERSION SPECTRUM EMITTED DURING THE DECAY OF ^{227}Th (RdAc) TO ^{223}Ra (AcX). Briancon, Chantal (CNRS, Orsay, France). Compt. Rend., 260: 5764-6(May 31, 1965). (In French).

A study was made with a semicircular magnetic spectrograph with and without preacceleration on the conversion electron spectrum emitted during the decay ^{227}Th → ^{223}Ra. At least 110 new conversion lines were observed. These are tabulated. (tr-auth)

45307 SIGNALS AT $2\omega_2-\omega_1$ IN NUCLEAR MAGNETIC DOUBLE RESONANCE. Anders, Leslie R.; Baldeschwieler, John D. (Harvard Univ., Cambridge, Mass.). J. Chem. Phys., 43: 2147-8(Sept. 15, 1965).

Analysis of the double-resonance of a single nucleus of spin $\frac{1}{2}$ indicated that the experiment should yield four signals, two signals for each of two distinct values of the stimulating frequency, ω_1. If the resonances occur at values of $\omega_1 = \omega_1'$ and ω_1'', additional signals at $2\omega_2 - \omega_1'$ and $2\omega_2 - \omega_1''$ should be present in the output of the spectrometer when $\omega_1 = \omega_1'$ and ω_1'', respectively. The signals at $2\omega_2 - \omega_1$ in the output of a spectrometer are confirmed by stimulating the spin system at frequency ω_1, but referencing the synchronous detector to a third frequency ω_3. By sweeping ω_3 for fixed values of ω_1 and ω_2, it is possible to scan the output of the spectrometer for all the signals present with any stimulating frequency ω_1. (P.C.H.)

45308 QUASI-FREE ALPHA-ALPHA COLLISIONS IN ^{9}Be AND ^{12}C AT 28 Mev. Yanabu, Takuji (Kyoto Univ.); Yamashita, Sukeaki; Takimoto, Kiyohiko; Ogino, Kouya. J. Phys. Soc. Japan, 20: 1303-12(Aug. 1965).

In the reactions ^{9}Be$(\alpha,2\alpha)^{5}$He and ^{12}C$(\alpha,2\alpha)^{8}$Be at 28 Mev, the single and summed energy spectra of emitted alpha-particles were measured at several pairs of angle in order to investigate the quasi-free collision between incident alpha-particles and alpha-clusters in ^{9}Be and ^{12}C. The summed energy spectrum of the alpha-particles from the reaction ^{9}Be$(\alpha,2\alpha)^{5}$He shows a peak corresponding to the ground state of ^{5}He at the angles at which the emitted particles come from the collision between incident alpha-particles and nearly zero-momentum alpha-clusters in ^{9}Be. The momentum spread of the alpha-cluster in ^{9}Be coupled with ^{5}He (ground state) is estimated to be 0.3 fm^{-1} from the angular correlation of the peak in the summed energy spectrum, and the probability of finding an alpha-cluster in this state is 0.12, if a plane wave impulse approximation is assumed. In the reaction ^{12}C$(\alpha,2\alpha)^{8}$Be$_{g.s.}$, the yield has a minimum at the angles expected from the quasi-free collision between incident alpha-particles and nearly zero-momentum alpha-clusters in ^{12}C. The state in which an alpha-cluster is bound to ^{8}Be (ground state) in ^{12}C seems to be very different from that for ^{9}Be. (auth)

45309 PHOTOPRODUCTION OF DEUTERONS FROM CARBON AT SEVERAL HUNDRED Mev. Kihara, Motohiro (Kyoto Univ.). J. Phys. Soc. Japan, 20: 1313-21 (Aug. 1965).

The yield curve of deuterons of 45 Mev produced at 57° from carbon exposed to the bremsstrahlung of the maximum energy between 400 Mev and 720 Mev and the energy distributions of deuterons by the bremsstrahlung of 650 Mev and 720 Mev were measured. The excitation function of deuterons of 45 Mev and the energy distribution of deuterons at the proton energy of 685 Mev were reduced from the data by the method of photon difference. The identification of deuterons was made by the time-of-flight method with an analyzing magnet. The measurement was analyzed in terms of the independent pair model. The results show that the cross section of the (γ,d) reaction is consistent with the independent pair model with the mesonic process. (auth)

45310 PHOTOREACTIONS IN ^{28}Si NUCLEUS BY MONOCHROMATIC GAMMA-RAYS. Matsumoto, Shinji; Yamashita, Hiroshi; Kamae, Tsuneyoshi; Nogami, Yozo (Tokyo Univ.). J. Phys. Soc. Japan, 20: 1321-32(Aug. 1965).

The structure of the giant resonance in ^{28}Si was studied using monochromatic gamma-rays ($\Delta E_\gamma/E_\gamma \approx 1\frac{1}{2}\%$) from proton capture reactions. A silicon solid-state detector served both as target and detector. Total cross sections for the ^{28}Si (γ,p_0), (γ,p_1), (γ,p_2), (γ,α_0), and (γ,α_1) reactions were obtained from 17.4 to 22.3 Mev and the integrated cross sections were 34.4, 18.9, 17.6, 1.6, and 2.7 mb·Mev, respectively. The excitation functions of proton emission showed many discernible fine structures. Most of the peaks of the cross sections for different exit channels occurred at the same gamma-ray energy and the number of resonance states involved in a peak seems to be a few. The (γ,α_0)-reaction excitation functions revealed several humps which are possibly caused by an E1 absorption. Isotopic-spin selection rule seems no longer to be valid for the present (γ,α_0) reaction. Comparisons were made with the calculated absorption probability from the Nilsson model. (auth)

45311 ENERGY LEVELS OF ^{92}Mo WITH SOFT CORE POTENTIAL. Kumar, Naresh; Kumar, Vijay; Bhanot, V. B. (Panjab Univ., Chandigarh, India). J. Phys. Soc. Japan, 20: 1515(Aug. 1965).

Calculations were made of the low-lying energy levels of ^{92}Mo due to the configuration $(g_{\frac{9}{2}})^2$, using a soft core potential. The results are tabulated along with observed levels. The $(p_{\frac{1}{2}})^2$ and $(p_{\frac{1}{2}})\,(g_{\frac{9}{2}})$ configurations are also considered. (L.B.S.)

45312 ELASTIC AND INELASTIC SCATTERING OF 22.2 Mev ALPHA PARTICLES FROM SOME MEDIUM-WEIGHT NUCLEI. Takahashi, Noriaki; Kato, Syohei; Takeda, Minoru; Yamazaki, Takashi; Yasukawa, Satoshi (Osaka Univ.). J. Phys. Soc. Japan, 20: 1544-5(Aug. 1965).

Angular distributions for elastic and inelastic scattering of 22.2 Mev alpha particles from Ca, Ti, ^{55}Mn, Fe, ^{59}Co, ^{58}Ni, ^{60}Ni, ^{63}Cu, and ^{65}Cu were measured from 15 to 90° in 2.5° intervals, using a solid-state alpha detector. The elastic distributions were analyzed in terms of the optical model with a complex Woods-Saxon potential, and the inelastic distributions were analyzed in terms of the diffraction model. Some preliminary DWBA computations were also made. The parameters are tabulated, and an example of the experimental and calculated distributions is given for ^{58}Ni. (L.B.S.)

45313 STATISTICAL FLUCTUATIONS IN THE EXCITATION FUNCTIONS FROM ^{12}C(^{12}C,α)^{20}Ne. Bondorf, J. P.; Leachman, R. B. Kgl. Danske Videnskab. Selskab, Mat.-Fys. Medd., 34: No. 10, 1-28(1965).

The theory of statistical fluctuations in the cross sections for the energy region of completely overlapping levels is developed for the case of incident particles being zero spin and identical. To facilitate analysis of data, the development is in terms of the correlation coefficient, which is proportional to the difference between the mean square cross section and the square of the mean cross section. Simple expressions are derived relating the correlation coefficient with the number of degrees of freedom in the probability distribution of the cross section. For the differential cross sections, the number of degrees of freedom is twice the effective number of magnetic quantum substates; for the cross section integrated over angle, the number of degrees of freedom depends upon the number of compound spins, the size of the compound spin, and the spin of the final nucleus. Special cases are cited for which selection rules and spherical harmonics reduce the number of degrees of freedom. Cross section data from the reaction ^{12}C(^{12}C,α)^{20}Ne are analyzed. Level densities and widths calculated from statistical theories of levels for all energies but the lowest confirm that the populated levels are completely overlapping. Satisfactory agreement is found between the number of degrees of freedom in the cross section distribution as determined from the data and from theory. (auth)

45314 EFFECT OF THE DIPOLE-QUADRUPOLE INTERACTION ON THE WIDTH AND THE STRUCTURE OF THE GIANT DIPOLE LINE IN SPHERICAL NUCLEI. Le Tourneux, Jean. Kgl. Danske Videnskab. Selskab, Mat.-Fys. Medd., 34: No. 11, 1-27(1965).

A phenomenological study is made of the effect of a dipole-quadrupole interaction on the width and the structure of the giant dipole line in spherical nuclei. The broadening of the line is evaluated through the method of moments. The effect of the interaction on the structure of the line is also studied by constructing the interaction matrix and diagonalizing it. A classical limit is derived for the case of strong coupling. An attempt to correlate the calculated widths with those observed experimentally is presented. (auth)

45315 RACAH ALGEBRA AND NUCLEAR SPECTROSCOPY. Kim, Jin Hum (Korean Univ., Seoul). New Phys. (Korea), 3: No. 2, 60-5(1963). (In Korean).

Racah's method of angular momentum algebra and its

use in the spectroscopy of nuclear states are examined, considering first the coupling of two angular momenta and the wave function of a 2-spin ½ particle system, the method of coupling many angular momenta and many nucleon wave functions. The Racah coefficients, the 6_i and 9_i symbols are defined, reviewing the transformation from the j-j to the L-S coupling. This is followed by a brief examination of the spherical harmonic tensor, defining Wigner-Eckart's reduced matrix element and its use in nuclear spectroscopy. The fractional parentage coefficient and the seniority quantum number of a nuclear state concepts are then mentioned, introducing the Young Tableau scheme for many-nucleon systems. (TTT)

45316 A MOTION DEVICE FOR MOESSBAUER SPECTROMETRY. Miller, C. A.; Broadhurst, J. H. (Birmingham Univ., Eng.). Nucl. Instr. Methods, 36: 283-8(Oct. 1965).

A servo-controlled electromagnetic transducer has been made for studies of the Mössbauer effect. The device operates at velocities up to 30 cm/sec, with a precision between 0.1 and 1% depending upon the waveform and mode of operation used. (auth)

45317 CALCULATION OF THE NUCLEAR CASCADE IN STEEL INITIATED BY 10- AND 19.2-Gev/c PROTONS AND COMPARISON WITH EXPERIMENT. Alsmiller, R. G. Jr. (Oak Ridge National Lab., Tenn.); Barish, J. Nucl. Instr. Methods, 36: 309-13(Oct. 1965). (ORNL-TM-1072).

One-dimensional nucleon-meson cascade calculations have been carried out for the cases of 10- and 19.2-Bev/c protons incident on steel. The star density and track intensity from the 19.2-Bev/c beam and the track intensity from the 10-Bev/c beam are compared with experimental values. In general, the calculated star density is higher than the experimental values and the calculated track intensities are lower than the experimental values. (auth)

45318 EXCITATION OF THE UNNATURAL PARITY 3^+ STATE IN ^{24}Mg IN THE INELASTIC SCATTERING OF α-PARTICLES. Tamura, Taro (Oak Ridge National Lab., Tenn.). Nucl. Phys., 73: 241-55(1965). (ORNL-P-896).

As an example of the excitation of unnatural-parity states in even nuclei by the inelastic scattering of α particles, an analysis is made of data of $^{24}Mg(\alpha,\alpha')^{24}Mg^*$ processes for E_α = 28.5 Mev. The theoretical cross sections are obtained through the coupled-channel calculation, in which 0^+, 2^+, 4^+, 6^+, 2^+, and 3^+ states are coupled together, where the first four states are assumed as members of the K = 0 ground band, while the last two as members of the K = 2 γ-vibrational band. Reasonably good agreement with experiment is obtained, allowing it to be concluded that the multiple-excitation processes can account for the excitation of the unnatural parity states. (auth)

45319 MEASUREMENTS OF THE A AND R PARAMETERS IN PROTON-PROTON SCATTERING AT 47.8 AND 27.6 Mev. Ashmore, A. (Queen Mary Coll., Univ. of London); Davies, B. W.; Devine, M.; Hoey, S. J.; Litt, J.; Shepherd, M. E.; Hanna, R. C.; Robertson, L. P. Nucl. Phys., 73: 256-66(1965).

Measurements are reported of the A and R parameters in proton-proton scattering at five angles at a proton energy of 47.8 Mev and three angles at 27.6 Mev using a proton linear accelerator. The values are used in phase shift analyses with the result that the phase shifts are as well defined near 27 Mev as near 50 Mev. The behavior of the $^3P_0$ phase shift which previously had the largest uncertainty is defined as precisely as at higher energies. (auth)

45320 GAMMA TRANSITIONS IN ^{65}Cu FROM THE DECAY OF ^{65}Ni. Spring, E.; Jungner, H.; Holmberg, P. (Univ. of Helsinki). Nucl. Phys., 73: 267-72(1965).

The gamma radiation following the beta decay of 2.55 hr ^{65}Ni was studied with NaI(Tl) and Ge(Li) detectors. A level scheme is presented with the energies and relative intensities of gamma transitions observed for ^{65}Cu. The directional correlation measurements agree with spin $^7/_2$ for the 1483 kev level and give spin $^5/_2(^5/_2)$ for the 1625 kev level and spin $^5/_2$ for the 1725 kev level. All these levels have negative parity according to the log ft values calculated from the gamma-ray intensities observed. (auth)

45321 COULOMB EXCITATION OF VIBRATIONAL STATES IN DEFORMED EVEN NUCLEI. Yoshizawa, Y.; Elbek, B.; Herskind, B.; Olesen, M. C. (Univ. of Copenhagen). Nucl. Phys., 73: 273-311(1965).

Low lying states in deformed even rare-earth nuclei were studied by Coulomb excitation with 43.5 Mev oxygen ions. Gamma rays from thin oxide targets (≈0.3 mg/cm^2) or thin metal targets (0.5 to 1.2 mg/cm^2) were observed in coincidence with backscattered ions. The yields were normalized on the intensity of the scattered particles. Double groups of gamma rays ascribed to the $2^{+\prime} \rightarrow 0^+$ and the $2^{+\prime} \rightarrow 2^+$ transitions from K = 2 states were observed in ^{150}Nd(1.07 Mev), ^{152}Sm(1.09 Mev), ^{154}Sm(1.44 Mev), ^{156}Gd, ^{158}Gd, ^{160}Gd(1.02 Mev), ^{160}Dy, ^{162}Dy(0.89 Mev), ^{164}Dy(0.77 Mev), ^{164}Er(0.86 Mev), ^{166}Er, ^{168}Er, ^{170}Er(0.93 Mev), and ^{176}Yb(1.27 Mev), where the energies in the parentheses are given for $2^{+\prime}$ states not observed earlier. Gamma rays ascribed to the $0^{+\prime\prime} \rightarrow 2^+$, $2^{+\prime\prime} \rightarrow 0^+$, and $2^{+\prime\prime} \rightarrow 2^+$ transitions from K = 0 states were observed in ^{150}Nd(0.69 Mev), ^{152}Sm, and ^{154}Gd(0.68 Mev), where the energies are for the $0^{+\prime\prime}$ states. Gamma rays in ^{154}Sm and ^{156}Gd suggest K = 0 states at 1.10 and 1.06 Mev, respectively. The B(E2) values determined from the yields range from 2 to 8 single-particle units, being roughly inversely proportional to the excitation energies for the levels. The theory of multiple Coulomb excitation for the different bands is in qualitative agreement with the experimental observations. (auth)

45322 SPECTRUM OF γ-RAYS FROM THE ^{54}Fe(n,γ)^{55}Fe REACTION. Firsov, E. I.; Loskutova, N. G.; Rudak, E. A. (Byelorussian Academy of Sciences, USSR). Nucl. Phys., 73: 312-20(1965).

The γ rays from the ^{54}Fe(n,γ)^{55}Fe reaction on thermal neutrons were investigated with a magnetic Compton γ spectrometer with a resolution of 2% and lower energy limit of the measured γ rays of 0.3 Mev. The sample was prepared from iron enriched to 78.1% in ^{54}Fe. The experiment revealed γ rays of the following energies and intensities (in parentheses): 9.31(61), 8.89(12), doublet 7.27(3.0), 6.82(2.0), 6.27(3.0), 5.75(2.5), 5.50(2.0), 5.37(1.3), doublet 4.73(3.0), 4.55(1.4), 4.46(1.5), 4.17(1.5), 3.79(1.7), 3.38(1.5), doublet 3.07(4.0), 2.90(1.0), 2.67(1.5), 2.63(1.0), 2.47(2.4), 2.05(2.5), 1.92(2.5), 1.63(1.5), 1.5(1.5), 1.32(1.0), 1.24(1.0), groups of lines 0.93(10.0), and 0.41(29.0) Mev. A level scheme of the ^{55}Fe is proposed and the main characteristics of this scheme are discussed. (auth)

45323 ANGULAR DISTRIBUTIONS FROM SHELL-MODEL FORBIDDEN (d,p) TRANSITIONS TO SPIN ½ STATES IN ^{43}Ca, ^{45}Ca AND ^{47}Ti. Belote, T. A.; Dorenbusch, W. E.; Hansen, Ole; Rapaport, J. (Massachusetts Inst. of Tech., Cambridge). Nucl. Phys., 73: 321-7(1965). (MIT-2098-140).

The (d,p) transitions to the ground state and first excited states of ^{43}Ca, ^{45}Ca, and ^{47}Ti were measured at deuteron energies near 7 Mev. The similarity between the shapes of the angular distributions to the weak 374-kev $^1/_2^-$ level in ^{43}Ca, the 176-kev level in ^{45}Ca, and the $^1/_2^-$ ground state of ^{47}Ti suggests that these transitions proceed through a direct-reaction mechanism. (auth)

45324 THE ENERGY LEVELS OF ^{129}I. Hurley, J. P.; Mathiesen, J. M. (Naval Radiological Defense Lab., San Francisco). Nucl. Phys., 73: 328-48(1965).

The radiations from ^{129}I were restudied using a Ge(Li) detector, scintillation detectors, and coincidence and sum-coincidence techniques. The ^{129m}Te source was prepared by the irradiation of enriched ^{128}Te with thermal neutrons, followed by chemical separation. A 4-kev resolution Ge(Li) detector was used to find gamma rays at energies of 27, 208, 250, 278, 280, 343, 345, 460, 487, 532, 557, 573, 624, 673, 697, 730, 742, 804, 819, 837, 848, 982, 1022, 1050, 1083, 1112, 1233, 1262, and 1400 kev. From coincidence and sum-coincidence studies on these transitions, it was concluded that excited levels are populated at 27, 278, 343, 487, 557, 697, 730, 831, 846, 1022, 1050, 1083, 1112, 1262,

1378, 1404, and 1427 kev. Gamma-ray intensities were calculated from the Ge(Li) spectra. (auth)

45325 CROSS SECTION OF SOME REACTIONS OF ^{99}Tc WITH 14.1 Mev NEUTRONS. Golchert, Norbert W. (Illinois Inst. of Technology, Chicago; Argonne National Lab., Ill); Gardner, Donald G.; Sedlet, Jacob. Nucl. Phys., 73: 349-52(1965).

An activation method was employed to determine the cross sections of reactions of ^{99}Tc with 14.1 Mev neutrons. The following cross sections were measured: $\sigma(n,p)$ = 7.0 ± 1.1 mb, $\sigma(n,\alpha)$ = 2.02 ± 0.22 mb, and $\sigma(n,n')$ = 41.3 ± 6.6 mb. Upper limits were placed on the following cross sections: $\sigma(n,p\alpha) < 1.0$ mb, and $\sigma(n,n'\alpha) < 1.0$ mb. A value of 7.2 ± 2.2 mb was obtained for the cross section for the (n,2n) reaction on ^{14}N. The nitrogen was present along with technetium in the target material ammonium pertechnetate. The observed $\sigma(n,p)$ agrees well with the value of 6.3 mb, from the semi-empirical predictions of Gardner, Yu, and Rosenblum, but the predicted value for $\sigma(n,\alpha)$ is 5.4 mb. It is suggested that the observed $\sigma(n,\alpha)$ of ^{99}Tc represents a partial cross section to the ground state of ^{96}Mo, and that there exists a so far unobserved isomeric state of ^{96}Nb with a short half life that primarily decays by β^- emission to ^{96}Mo. The (n,α) cross section to this state is estimated to be about 3 mb. (auth)

45326 EXPERIMENTAL OBSERVATIONS OF ELECTRIC QUADRUPOLE EFFECTS IN THE MUONIC SPECTRA OF ^{238}U, ^{181}Ta AND ^{239}Pu. Raboy, S. (Argonne National Lab., Ill.); Trail, C. C.; Bjorkland, J. A.; Ehrlich, R. D.; Powers, R. J.; Telegdi, V. L. Nucl. Phys., 73: 353-67 (1965).

The spectra of the 2p → 1s and 3d → 2p transitions in the muonic atoms of ^{238}U, ^{181}Ta, and ^{239}Pu were studied using a NaI(Tl) scintillation spectrometer with an anticoincidence annulus of NaI(Tl). The effects caused by the electric quadrupole interaction between the muon and these nuclei were detected, and the intrinsic quadrupole moments Q_0 of ^{181}Ta and ^{238}U were measured. The intrinsic quadrupole moment of ^{239}Pu was found to be large and positive. (auth)

45327 MEASUREMENT OF Z DEPENDENCE OF ELASTIC SCATTERING CROSS SECTION OF GAMMA RAYS. Anand, S.; Sood, B. S. (Punjabi Univ., Patiala, India). Nucl. Phys., 73: 368-78(1965).

The Z dependence of the elastic scattering cross section of gamma rays was investigated below 1 Mev at different angles. The results show that the index to the power of Z on which the cross section depends increases with the momentum transfer involved in scattering; this agrees with the predictions of modified form factor calculations of Brown and Mayers but contradicts the nonrelativistic form factor calculations of Franz. The observed Z dependence and the refined calculations of Rayleigh scattering from the K electrons of mercury by Brown and Mayers are used to estimate the coherent scattering cross sections of 1.33 Mev gamma rays from uranium, lead, and tin. The estimated values are found to show a fair agreement with the available experimental data. (auth)

45328 ^{124}Sb SPECTRUM SHAPE. Hsue, S. T.; Langer, L. M.; Tang, S. M.; Zollman, D. A. (Indiana Univ., Bloomington). Nucl. Phys., 73: 379-84(1965).

The beta ^{124}Sb spectrum above 1.0 Mev was measured with a magnetic spectrometer employing a solid state device as detector. The emphasis was on the detailed shape of the highest energy group. The use of the solid state detector resulted in much lower background and helped in the precise determination of the end point and the shape. Attempts to check on the possible existence of a 1.658-Mev beta group and on the shape of the 1.59-Mev group were also made. The experimental shape of the highest energy group was found to be best fitted with an empirical shape factor $S\alpha q^2 + \lambda_1 p^2 + D$, with D = 16 ± 2. The shape is also fitted very well by $S = k(1 + aW + b/W + cW^2)$ with a = −0.250, b = −0.060 and c = 0.041. The end point of this group was found to be 2.305 ± 0.005 Mev, which is somewhat lower than previous determinations. The data suggest the existence of the 1.658-Mev group, or, that if there is no such group, the shape of the 1.59-Mev group differs from the statistical shape. (auth)

45329 PHOTOFISSION OF U AND Th BETWEEN 300 AND 1000 Mev. Carbonara, F. (Universita, Naples; Istituto Nazionale di Fisica Nucleare, Naples); de Carvalho, H. G.; Rinzivillo, R.; Sassi, E.; Murtas, G. P. Nucl. Phys., 73: 385-97(1965).

Loaded nuclear emulsions were exposed to the bremsstrahlung beam of a 1-Bev electron synchrotron to measure natural uranium and thorium fission cross sections in the energy range 300 to 1000 Mev. The cross sections per photon are constant within the experimental errors, and amount to 67 ± 7 and 37 ± 4 mb for U and Th, respectively. These results are briefly discussed. (auth)

45330 PHOTONEUTRON SPECTRA AND CROSS SECTIONS FOR ^{12}C AND ^{16}O. Verbinski, V. V.; Courtney, J. C. (Oak Ridge National Lab., Tenn.). Nucl. Phys., 73: 398-412(1965). (ORN–TM–1158).

Partial (γ,n) cross sections were measured for two self-conjugate nuclei ^{12}C and ^{16}O by measuring the spectral intensity of emitted neutrons in conjunction with a determination of the time-integrated absolute photon flux. The maximum-energy photoneutrons which leave the residual nuclei in their ground state were isolated from other transitions, making it possible to study individual excited levels in ^{12}C and ^{16}O. By measuring the neutron spectra at several angles and taking advantage of the use of self-conjugate target nuclei, these isolated levels in ^{12}C and ^{16}O were found to be due to electric dipole photoabsorption with subsequent emission of d-wave neutrons. (auth)

45331 DECAY OF ^{86}Rb. Gupta, U. C.; Srivastava, P. K.; Khera, G. D. (Atomic Energy Establishment Trombay, Bombay). Nucl. Phys., 73: 413-16(1965).

The number of gamma rays per disintegration in the decay of ^{86}Rb was measured by a NaI(Tl) scintillation spectrometer and a $4\pi\beta$-gamma coincidence counting set-up. The 1.08-Mev gamma rays were found to be 8.9 ± 0.3% of the total disintegration rate. (auth)

45332 EXCHANGE MAGNETIC MOMENT IN THREE-BODY NUCLEI. [PART] I. Padgett, Doran W. (Catholic Univ. of America, Washington, D. C.); Frank, William M.; Brennan, James G. Nucl. Phys., 73: 424-44(1965).

Meson exchange effects are considered in an attempt to explain the nuclear magnetic moment anomaly of the three-body system. The exchange magnetic moments were calculated for the case of two-body one-meson exchange and three-body two-meson exchange in the ground state of the three-body system by the methods of static Chew-Low Theory. The ground state was assumed to be a pure space symmetric $^2S_{\frac{1}{2}}$ state. An adjustable hard core radius r_c was used in the form of a cut-off of the radial integrals for interparticle distance less than r_c. The absolute value of the total exchange moment was found to be 0.4, 0.3, and 0.2 nm for hard core radii 0.3, 0.4, and 0.5 f, respectively. The two-body one-meson exchange process for the hard core radius of 0.4 f accounts for 0.2 nm which is ⅔ of the value reported by Villars. The remaining 0.1 nm results from the three-body two-meson exchange process. (auth)

45333 EXCHANGE MAGNETIC MOMENT IN THREE-BODY NUCLEI. [PART] II. Brennan, James G. (Catholic Univ. of America, Washington, D. C.); Frank, William M.; Padgett, Doran W. Nucl. Phys., 73: 445-8(1965).

Meson exchange effects which arise in static Chew-Low theory include terms which can connect S state to D state components of the three-body wave function. A modified Pease-Feshbach three-body wave function is used to determine such meson exchange contributions. The result, −0.03 nuclear magnetons, is of the right sign and magnitude to bring the total meson exchange moment into close agreement with that predicted by Sachs. (auth)

45334 COMPOSITION OF THE GIANT DIPOLE STATE. Young, J. E. (Los Alamos Scientific Lab., N. Mex.). Nucl. Phys., 73: 449-60(1965). (LA-DC-6882).

The structure of the giant dipole state is studied within

the framework of the many-particle Green function theory. It is found that the configuration mixing from two-particle, two-hole states influences all particle-hole matrix elements. As this is believed small from general nuclear structure evidence, the particle-hole model of Brown and collaborators ought to be substantially correct for the dipole state. A specific exception might occur for the low-lying T = 0, 3^- states. (auth)

45335 GAMMA-GAMMA DIRECTIONAL CORRELATIONS IN ^{129}I. Gupta, S. L.; Saha, N. K. (Univ. of Delhi). Nucl. Phys., 73: 461-72(1965).

Coincidence and gamma-gamma angular correlation measurements were made for five cascades of ^{129}I, namely, 455-27, 275-275, 205-275, 720-695, and 555-830 kev. The corresponding correlation functions obtained are $W(\theta) = 1 - (0.160 \pm 0.033)P_2(\cos\theta) + (0.022 \pm 0.060)P_4(\cos\theta)$, $W(\theta) = 1 + (0.039 \pm 0.007)P_2(\cos\theta) - (0.009 \pm 0.008)P_4(\cos\theta)$, $W(\theta) = 1 - (0.104 \pm 0.012)P_2(\cos\theta) - (0.010 \pm 0.021)P_4(\cos\theta)$, $W(\theta) = 1$ (within 1%), and $W(\theta) = 1 - (0.167 \pm 0.036)P_2(\cos\theta) + (0.060 \pm 0.080)P_4(\cos\theta)$. The results indicate spins of 3/2 (or 5/2), 1/2, 3/2, 11/2, 3/2, 9/2, and 9/2 (or 13/2) for the levels at 275, 482, 550, 695, 830, 1385, and 1415 kev, respectively. The E2/M1 mixing ratio for the 27-kev 1-forbidden M1 transition is discussed. (auth)

45336 THE REACTION $^{10}B(d,p_0)^{11}B$. Barz, H. W.; Fuelle, R.; Netzband, D.; Reif, R.; Schlott, K.; Slotta, J. (Zentralinstitut fur Kernforschung, Rossendorf). Nucl. Phys., 73: 473-80(1965).

The angular distribution and the absolute cross section of the reaction $^{10}B(d,p_0)^{11}B$ were measured at $E_d = 13.5$ Mev. The results are compared with the predictions of the Butler, diffraction, and DWBA theories. A good fit was obtained. The reduced width and the spectroscopic factor are deduced and compared with the results obtained by other authors at different energies. (auth)

45337 EXPERIMENTAL DEVELOPMENTS IN THE STUDY OF THE POLARIZATION IN NUCLEAR REACTIONS. Poiani, G. (Universita, Trieste, Italy; Istituto Nazionale di Fisica Nucleare, Trieste, Italy). Nuovo Cimento (1), 2: Suppl., 355-82(1964). (In Italian).

The experimental developments of the last year in the field of polarization in nuclear reactions are illustrated. The emphasis is on the polarization in nuclear reactions following the use of polarized charged particle beams or of polarized targets. The construction of the polarized source is considered. 57 references. (J.S.R.)

45338 FISSION PHYSICS. Cortini, G. (Universita, Naples). Nuovo Cimento (1), 2: Suppl., 383-99(1964). (In Italian).

A brief review is given of the studies on fission being undertaken in Italian laboratories. The experimental techniques used to study fission physics are discussed. A synthesis of the most important experimental results with a comment on the internal coherence of these results is given. The problems that each give from the theoretical viewpoint are examined. Some recent attempts on the theoretical interpretation of the results are summarized. 35 references. (J.S.R.)

45339 NUCLEAR STRUCTURE INVESTIGATION BY MEANS OF PION-NUCLEUS INTERACTION. Jean, M. (Universite de Paris, Orsay, France). Nuovo Cimento (1), 2: Suppl., 400-14(1964).

The information that can be learned from nuclear interactions with pions is sketched briefly. The discussion is limited to a consideration of energies less than 200 Mev. The absorption and then the scattering of pions by nuclei are considered. (J.S.R.)

45340 METHODS OF ANALYTICITY AND UNITARITY IN NUCLEAR PHYSICS: ATTEMPTS OF NEW LOW-ENERGY PHENOMENOLOGY. Bosco, B. (Universita, Turin; Istituto Nazionale di Fisica Nucleare, Turin). Nuovo Cimento (1), 2: Suppl., 415-27(1964). (In Italian).

The general methods developed recently in the study of strong interactions between elementary particles can be in some cases applied to nuclear interactions. Two types of phenomena that present a very simple manner for the analysis of nuclear interactions are the processes of direct interaction and electromagnetic interactions that induce two-body decay of nuclei. After a brief review of the principles of analyticity and unitarity, the analysis of direct nuclear reactions are described. The two-body decay of nuclei is also considered. (J.S.R.)

45341 INVESTIGATION OF THE ^{96}Nb DISINTEGRATION SCHEME BY MEANS OF A HIGH-RESOLUTION LITHIUM-ION DRIFT GERMANIUM GAMMA-RAY SPECTROMETER. Monaro, S. (Brookhaven National Lab., Upton, N. Y.). Nuovo Cimento (10), 39: 442-63(Sept. 16, 1965).

The decay of the 24-hr ^{96}Nb was the subject of an extensive investigation in order to obtain more detailed information about the level structure of the even-even nucleus ^{96}Mo. A high-resolution lithium drifted germanium γ spectrometer was used. The existence of several previously unreported γ rays was revealed, and their energies and intensities were measured with high accuracy. For instance, the composite peak at about 800 kev in the spectrum of the ^{96}Nb decay was very well resolved in its 779, 811, and 851 kev components. Moreover, from the precision energy measurements of the transitions appearing in the decay of ^{96}Nb, it could be established that the 459.5, 569.3, and 811 kev γ rays do not de-excite a single level of the even-even ^{96}Mo as previously reported, but the 459.5 kev transition de-excites a level at 2438.5 kev, whereas the 569.3 and 811 kev transitions de-excite a 2440.5 kev level. Furthermore, the existence of the second 2^+ vibrational level at 1499 kev in ^{96}Mo, excited in the ^{96}Nb decay, was shown, and the value of the radio cascade/crossover was measured and found equal to 2.27 ± 0.55. From the measured value of the cascade/crossover ratio and from the known $\epsilon B(E2)_{exp}$ quantity, found by means of Coulomb excitation experiments, the $B(E2, 2^{+\prime} \rightarrow 0^+)_d$ and $B(E2, 2^{+\prime} \rightarrow 2^+)_d$ reduced electromagnetic transition rates for the second two plus state were determined together with the ratio $R = (B(E2, 2^{+\prime} \rightarrow 2^+)_d)/(B(E2, 2^+ \rightarrow 0^+)_d)$. The results are $B(E2, 2^{+\prime} \rightarrow 0^+)_d = (0.32 \pm 0.08) \cdot 10^{-50}$, $B(E2, 2^{+\prime} \rightarrow 2^+)_d = (3 \pm 0.95) \cdot 10^{-48}$, and $R = 0.97 \pm 0.30$. These results support a collective model interpretation for the two 2^+ levels in question. (auth)

45342 A STUDY OF SHORT-RANGE HYPERFRAGMENTS PRODUCED BY K^- CAPTURES IN EMULSIONS. Evans, D. A.; Goodhead, D. T.; Ismail, A. Z. M.; Prakash, Y. (Oxford Univ.). Nuovo Cimento (10), 39: 785-811 (Oct. 1, 1965).

A study of about 1000 short-range (≤ 10 μm) hyperfragments produced by K^- captures in emulsions is presented. The experimental data indicate that the production characteristics of 0 to 3 μm hyperfragments are different from those of 5 to 10 μm; the hyperfragments of range 0 to 3 μm seem to be predominantly heavy spallation products from Ag and Br, while the 5 to 10 μm group are of lighter species ($A < 15$) produced mainly from the light emulsion nuclei. These results are in good agreement with the calculated range and mass distributions obtained by a Monte Carlo procedure. It is further shown that the discrepancy between the calculated and observed F/B ratios of the black prongs with respect to the hyperfragment track can be explained by the effects of a contribution to the hyperfragment momentum from the scatterings and interactions of particles created in the initial cascade stage. An estimate of the Λ^0 binding energy in nuclear matter ($D_\Lambda \approx 30$ to 32 Mev) is made from the mesonic decay of heavy spallation hyperfragments of range ≤ 3 μm. (auth)

45343 LEVEL WIDTHS OF NUCLEI AT HIGH EXCITATION ENERGY: SOME CONSIDERATIONS ON THE ANALYSIS OF EXPERIMENTAL DATA. Gadioli, E. (Universita, Milan); Iori, I.; Marini, A. Nuovo Cimento (10), 39: 996-1001(Oct. 1, 1965).

The procedure is discussed for analyzing experimental data to obtain a correct value of the coherence energy Γ', which characterizes the energy variations of the cross sections of compound-nucleus reactions and is directly associated with the widths of the compound-nucleus levels.

Two methods are considered: Ericson's method of studying the correlation functions of experimental points and the method of Brink and Stephen of relating the coherence energy to the average number of maxima of the excitation function in a unit energy interval. Results are shown of Monte-Carlo calculations of the behavior of the cross section as a function of energy, simulating a nonstatistical effect besides a statistical one. (M.J.T.)

45344 RADIATIVE LIFETIME OF THE FIRST EXCITED STATE OF ^{41}Sc. Youngblood, D. H.; Aldridge, J. P.; Class, C. M. (Rice Univ., Houston, Tex.). Phys. Letters, 18: 291-2(Sept. 1, 1965). (TID-22121).

A determination of the lifetime of the state in ^{41}Sc is derived from a measurement of its radiative width. The 1.72-Mev state of ^{41}Sc can be excited by means of resonance capture occurring in the ^{40}Ca(p,γ)^{41}Sc reaction at a proton energy of 648 kev. The radiative width of the state is related to the cross section of the reaction. The quantity most conveniently measured in this reaction is the positron activity of scandium-41, occurring after the gamma transition to the ground state. The thin and thick target yields of positrons in the neighborhood of the 648-kev resonance are shown. These data were obtained using targets about 10- and 50-kev thick prepared in the target chamber by evaporating natural calcium metal onto gold backings. The positron activity was detected by a pair of scintillation counters operating in coincidence. The experimental results confirm the spin assignment of $\frac{3}{2}^-$ for the state and strengthen its identification as the analog of the $\frac{3}{2}^-$ state in calcium-41 at 1.95 Mev. The lifetime derived is 4.3×10^{-13} sec. (J.F.P.)

45345 AN INVESTIGATION OF THE INTERNAL BREMSSTRAHLUNG SPECTRUM ACCOMPANYING THE ELECTRON CAPTURE PROCESS OF ^{36}Cl CLOSE TO THE END-POINT ENERGY. Berenyi, D. (Inst. of Nuclear Research, Hungarian Academy of Sciences, Debrecen); Ujhelyi, Cs.; Feher, I. Phys. Letters, 18: 293-5(Sept. 1, 1965).

The shape of the internal bremsstrahlung spectrum accompanying the chlorine-36 electron capture decay was studied only close to the end point. But this was done very precisely. The measurements were carried out using a whole body counter with a very low background. Also the crystal used had a high sensitivity. These techniques made it possible to improve appreciably on former measurements. From these studies a new value was obtained for the end-point energy of the spectrum; for the total disintegration energy of this decay, Q = 1158 ± 18 kev. An additional result is a more accurate determination of the shape factor of the internal bremsstrahlung spectrum in the energy range near the end point. (J.F.P.)

45346 DEUTERON EXCITATION OF TWO-PHONON STATES IN ^{60}Ni. Tamura, T. (Oak Ridge National Lab., Tenn.); Jolly, R. K. Phys. Letters, 18: 295-7(Sept. 1, 1965). (ORNL-P-1476).

The deuteron inelastic scattering data in which the excitation cross sections of all the triad of two-phonon states were observed are reported. The elastic and inelastic scattering cross sections were taken of 15-Mev deuterons from a cyclotron on rolled metallic nickel targets of thickness 1 mg/cm^2. The elastic deuteron scattering data were obtained with a specially designed triple Cs(I) scintillation detector arrangement placed at the focal plane of a magnetic spectrograph. The data to the 0_0^+, 2_1^+, 0_2^+, 2_2^+, and 4_1^+ states are given. They are compared with the prediction of the coupled-channel calculations. (J.F.P.)

45347 STRIPPING ANALYSIS OF THE ^{138}Ba(d,p)^{139}Ba REACTIONS. Rapaport, J. (Universidad de Chile, Santiago); Buechner, W. W. Phys. Letters, 18: 299-301(Sept. 1, 1965).

The ^{138}Ba(d,p)^{139}Ba reaction was obtained with 7.5-Mev deuterons; and the ^{139}Ba groups were followed according to kinematics in the gaps of the magnetic spectrograph between 30 and 172.5°. At the forward angles the ^{139}Ba groups are rather weak. A natural barium target was made by vacuum evaporation of $BaCl_2$ onto a thin Formvar backing. Deuterons were accelerated by an electrostatic generator, deflected 90° in an analyzing magnet, and allowed to enter the target chamber of the multiple-gap magnetic spectrograph. A summary is given of the results obtained corresponding to states in ^{139}Ba. Both the incident deuteron energy and the outgoing proton energy are lower than the Coulomb barrier, indicating that Coulomb stripping should play an important role in this case. The distorted wave code was used to fit the experimental angular distributions, to assign l_n values, and to extract spectroscopic factors. (J.F.P.)

45348 A NEW EXCITED STATE OF ^{8}Li. Watson, J. W. (Haverford Coll., Penna.); Ajzenberg-Selove, F.; Middleton, R. Phys. Letters, 18: 302-4(Sept. 1, 1965).

The ^{9}Be(t,α)^{8}Li reaction was studied to investigate further the excitation region between 2.28 and 8 Mev. A self-supported ^{9}Be target ~80 μg/cm^2 thick was bombarded with 13-Mev tritons. The resultant alphas were detected with 25 μ-thick nuclear emulsion plates. The plates were placed at 24 angles relative to the incident triton beam, between 5 and 175°. The magnetic field setting in the multigap spectrograph was 9.395 kilogauss. The exposure was of 864 microcoulomb. An alpha-particle group not identifiable in terms of known states in ^{8}Li, or in terms of carbon and oxygen contamination, was observed at 9 angles between 12.5 and 72.5° to the incident beam. The new group is labeled ^{8}Li(6.53) in both spectra shown. The ground and first two excited states of ^{8}Li are also observed. The excitation energy is found to be 6.532 ± 0.025 Mev. The width of this state is also calculated. Various alternative explanations of the observed phenomenon are also discussed. (J.F.P.)

45349 PROTON SCATTERING FROM A TUNGSTEN SINGLE CRYSTAL. Tulinov, A. F.; Kulikauskas, V. S.; Malov, M. M. (Moscow State Univ.). Phys. Letters, 18: 304-7(Sept. 1, 1965).

A study is made of the influence of different factors on the dips in the direction of the crystalline axes which appear in the angular distribution of charged reaction products from proton scattering from a tungsten single crystal. The measurements were carried out using a 120 cm cyclotron. The proton energy was changed with absorbers; and a 2 mm thick tungsten single crystal was used as a target. The crystalline axis corresponding to the shortest distance between lattice sites was used. It was found that the width of the dip increases with the depth of the scattering layer. This may be explained by protons emerging from the internal part of the sample and passing through a thick layer, then suffering multiple scattering. It is not quite clear yet how the depth of the dip depends on the position of the reflecting layer. (J.F.P.)

45350 NUCLEAR GROUND STATE PROPERTIES OF ^{16}O BY AN EXTENSION OF THE EDEN-EMERY METHOD. MacKellar, A. D.; Becker, R. L. (Oak Ridge National Lab., Tenn.). Phys. Letters, 18: 308-10(Sept. 1, 1965).

The approximations contained in the calculation of Eden et al. (Proc. Roy. Soc. (London) A248, 266(1958)) of the binding energy per nucleon in oxygen-16 are investigated, and the method is generalized to remove those approximations which appeared the most serious. Calculations for oxygen-16 were performed with two different potentials in order to determine the quantitative importance of the improvements in the computational method, and to obtain a better account of the two-nucleon data. All terms in the nucleon-nucleon potential are retained. The retention of the two-body spin-orbit potential is important because, even though it is of short range, it has a depth just outside the hard core which is appreciably greater than the central potential. The tensor force is handled accurately by solving coupled equations. This gives rise to the main increase in complexity in the calculation. The rms radius of the shell model ground state obtained from either potential is about half way between the experimental value and the value of Eden et al. (J.F.P.)

45351 MUON CAPTURE AND ELECTRIC DIPOLE EXCITATION FOR LITHIUM. Lodder, A.; Jonker, C. C.

(Vrije Universiteit, Amsterdam). Phys. Letters, 18: 310-13(Sept. 1, 1965).

The total meson (μ) capture probabilities for lithium-6 and -7, which were measured previously, are calculated. The two capture probabilities are calculated in two ways, by means of the closure approximation, and by extracting the dipole part of the main meson (μ) capture-matrix elements from the cross section for the giant resonance gamma excitation. It is shown that a previous proposal for double magic nuclei can be extended to a greater class of nuclei. (J.F.P.)

45352 ANISOTROPY OF CONVERSION ELECTRONS FROM (p,2n) AND (α,4n) REACTIONS. Ejiri, H. (Tokyo Univ.); Ishihara, M.; Sakai, M.; Katori, K.; Inamura, T. Phys. Letters, 18: 314-16(Sept. 1, 1965).

The anisotropy of the conversion electrons from vibrational and rotational states excited by the (p,2n) and (α,4n) reactions on medium heavy nuclei are reported. The 14-Mev proton beam and the 40-Mev alpha beam from the cyclotron were used to bombard targets. The conversion electrons from the reactions were analyzed by a sector type β spectrometer and were detected with a surface barrier silicon detector. Conversion electrons of the transitions between rotational levels were observed in the reactions ^{187}Re(p,2n)^{186}Os and ^{154}Sm(α,4n)^{154}Gd. The anisotropy of the K conversion electrons is shown. The observed anisotropies increase smoothly with increasing spins of the associated rotational states in both reactions. The anisotropy for the alpha induced reaction is clearly larger than that for the proton induced reaction. The anisotropic distribution of the conversion electrons can be qualitatively accounted for in terms of the spin alignment of the excited state. (J.F.P.)

45353 PHOTODISINTEGRATION OF ^{4}He. Clerc, H. G. (Technische Hochschule, Darmstadt, Ger.); Stewart, R. J.; Morrison, R. C. Phys. Letters, 18: 316-18(Sept. 1, 1965).

The reaction ^{4}He(γ,p) was observed in the gamma-ray energy range from 24 to 56 Mev. The experiment was performed by placing a ^{4}He gas target in the bremsstrahlung beam from the electron linac. Charged particles emitted at 90° with respect to the direction of the incident beam were focused by a quadrupole triplet onto a semiconductor detector. This arrangement allows the separation of particles with different masses. For ^{4}He(γ,p)^{3}H there is a breakup into two particles which do not have excited states. The measured angle and energy of only one of the emitted particles therefore determine the energy of the γ quantum that produced the reaction. The electric dipole cross section was obtained from the differential measurement. Over the whole energy range no pronounced fine structure could be found. (J.F.P.)

45354 NEUTRON-NEUTRON SCATTERING LENGTH BY PION ABSORPTION IN ^{3}He. Khanna, F.; Bonner, B. E.; Duck, I. (Rice Univ., Houston, Tex.). Phys. Letters, 18: 318-19(Sept. 1, 1965). (TID-22101).

The final state interaction idea is used for the reaction $\pi^- + {}^3\text{He} \rightarrow p + n + n$. Assuming that the capture takes place from the Bohr 1s-orbit, the three nucleons are left in a state with the parity and spin of $\frac{1}{2}^-$. The enhancement in the proton spectrum is due to the strong s-wave correlation between the two neutrons since the p-wave to s-wave enhancement is less than 1% for small relative momenta between the two neutrons. The proton is in a p-wave relative to the center of mass of the two neutrons. With these assumptions the differential cross section is plotted as a function of s for several values of the scattering length, which is assumed negative. A careful examination on the proton spectrum near the maximum energy of protons will yield information on the neutron-neutron scattering length. (J.F.P.)

45355 ENERGY LEVELS OF ^{30}S, ^{26}Si AND ^{8}B FROM (^{3}He,n) REACTIONS. McMurray, W. R.; Van der Merwe, P.; Van Heerden, I. J. (Southern Universities Nuclear Inst., Faure, S. Africa). Phys. Letters, 18: 319-22 (Sept. 1, 1965).

New information about levels in sulfur-30, silicon-26, and boron-8 was obtained from neutron time-of-flight studies of the (He-3,n) reaction on silicon-28, magnesium-24, and lithium-6. All the targets were evaporated onto tantalum backings and mounted on a wobbler, cooled externally by a jet of compressed air. Neutron spectra obtained from each of these reactions are shown. Time-of-flight spectra were obtained from the pulsed beam from a Van de Graaff accelerator. Pulse shape discrimination was applied to reject γ events in the scintillator. Neutron yields were measured relative to integrated beam current and long-counter counts. (J.F.P.)

45356 NEUTRON RESONANCE CAPTURE IN 2s-1d SHELL NUCLEI. Bergqvist, I.; Biggerstaff, J. A.; Gibbons, J. H.; Good, W. M. (Oak Ridge National Lab., Tenn.). Phys. Letters, 18: 323-5(Sept. 1, 1965).

A neutron resonance capture gamma-ray spectrum experiment on nuclei in the 2s-1d shell, that is in the mass region 19–40, was performed. The apparatus consists of a NaI spectrometer and neutron time-of-flight equipment. Gamma spectra from capture in two resonances in ^{24}Mg (n,γ) are shown. Strong transitions are observed to the ground state ($^{5}/_{2}^{+}$), the first excited state at 0.58 Mev ($^{1}/_{2}^{+}$), and to levels at 1.96($^{5}/_{2}^{+}$) and 2.57 Mev ($^{1}/_{2}^{+}$). The 50-kev resonance was not previously reported from neutron measurements. Results tend to favor an assignment of $^{3}/_{2}^{-}$ to the observed resonance. A possible explanation for observed systematic differences in various data, namely, the apparent enhancement of M1 transition strengths over E1, could be the presence of M1 giant resonance transitions due to spin flip of $d_{5/2}$ nucleons. (J.F.P.)

45357 K ISOMERISM IN ^{176}Yb. Vergnes, M.; Rotbard, G.; Ronsin, G.; Kalifa, J. (Universite de Paris, Orsay, France). Phys. Letters, 18: 325-6(Sept. 1, 1965). (In French).

An activity of period $T^{1}/_{2} = 11.7 \pm 0.5$ was found by Kantele (Physics Letters, 2: 293(1962)) and assigned to a new isomeric state of ^{176}Yb. The gamma rays associated with this activity formed a triple de-excitation cascade from the rotational level 8^+ of ^{176}Yb, coming from the new isomeric state. Since the energy, the angular momentum, and the parity of the new isomeric level are unknown, the experiment is repeated. Deuterons of 4 Mev produced by a Van de Graaff accelerator were used to produce thermal neutrons, which were filtered by cadmium. An enriched target containing 96.5% ^{176}Yb was used. It was concluded in agreement with Kantele that the activity is produced by the reaction (n,n') on ^{176}Yb and corresponds to a new isomeric level of ^{176}Yb. The energy levels found in this experiment are shown schematically. (J.F.P.)

45358 O^0-YIELD OF GAMMA RAYS IN THE T(p,γ)^{4}He REACTION. Schrack, R.; Kohler, D.; Puttaswamy, N. G.; Meyerhof, W. E. (Stanford Univ., Calif.). Phys. Letters, 18: 327-9(Sept, 1, 1965).

The O^0 yield of the T(p,γ) reaction was determined as a means of studying higher lying states of ^{4}He, since it selects the triplet T + p interactions. Previous studies indicated that the capture in this reaction proceeds mainly by electric dipole emission, with some electric quadrupole admixture, through singlet T + p interactions. Both these types of radiation would have zero yield at a O^0 emission angle. But it was previously shown that triplet T + p interactions would produce gamma emission at O^0. A 14-kev thick T-Zr target on 0.025-cm thick silver backing was bombarded with protons from a 3-Mev Van de Graaff accelerator. The yield was determined at 8.6, 46.4, and O^0 in order to calibrate the O^0 cross section and to compute the singlet contribution. The differential cross section for the T(p,γ) reaction at O^0 is shown as a function of proton energy in the laboratory system. (J.F.P.)

45359 EXPERIMENTAL EVIDENCE FOR COMPETING SPHERICAL AND DEFORMED SHAPES IN N = 89 NUCLEI. Sheline, R. K.; Kenefick, R. A.; Nealy, C. L.; Udagawa, T. (Florida State Univ., Tallahassee). Phys. Letters, 18: 330-2(Sept. 1, 1965).

A survey was made of (d,p) and (p,p′) reactions of the spectroscopic levels depicting the transition from the closed shell nucleus ^{144}Sm through the sequence of Sm isotopes to the highly deformed nucleus ^{152}Sm. Preliminary results are also found for the reactions ^{148}Nd(d,p)^{149}Nd and ^{150}Nd(d,t)^{149}Nd. The most striking conclusion of this study is the suggestion that relatively independent spherical and deformed nuclear shapes are clearly in evidence close to the ground state in the transition region, particularly in ^{151}Sm. Three pieces of experimental evidence are presented for the greater complexity which results from the greater richness of spectra and structure in this transition region. Data presented suggest that generally spherical, prolate, and probably oblate shapes are found in each nucleus. The energetic threshold for the appearance of these shapes will vary from nucleus to nucleus, making a series of complex surfaces on a three-dimensional plot of neutron number, proton number, and energy. (J.F.P.)

45360 A MEASUREMENT OF THE π LIFETIME VIA THE INVERSE DECAY PROCESS. Bellettini, G. (Istituto Nazionale di Fisica Nucleare, Pisa, Italy; Universita, Pisa, Italy); Bemporad, C.; Braccini, P. L.; Foa, L. Phys. Letters, 18: 333-8(Sept. 1, 1965).

The lifetime of the neutral meson (π) was measured by studying meson (π^0) photoproduction on a heavy nucleus. The basic principle is that around the forward direction the coherent photoproduction is more predominant than the incoherent production and that the amplitude for the coherent process contains together with a nuclear part, an electromagnetic part which describes neutral meson (π) photoproduction in the interaction of the incident photon with a virtual photon associated with the Coulomb field of the target nucleus. This process can be considered the inverse of the meson (π^0) disintegration into two photons, and the resulting cross section is inversely proportional to the meson (π^0) lifetime. The coherent photoproduction of neutral mesons (π) on lead around the forward direction was measured with an angular resolution of the order of $\pm 0.5°$ using a meson (π^0) detector containing 10 independent counting channels. The lifetime obtained is $\tau^0 = (0.74 \pm 0.105)\ 10^{-16}$ sec. (J.F.P.)

45361 A DETERMINATION OF THE Λ-NUCLEAR POTENTIAL WELL-DEPTH. Lemonne, J. (Universite Libre, Brussels); Mayeur, C.; Sacton, J. (and others). Phys. Letters, 18: 354-7(Sept. 1, 1965).

The total number of nucleons ejected during the primary evaporation phase was calculated separately for each hypernuclei decay event from the number of charged baryonic particles seen at the primary star, using previous results. These values are given. According to Walecka's formula it is found that the lowest observed value of the potential well depth (22.8 Mev) leads to an estimate of the upper limit of the Λ-nuclear potential in the range 26.1 to 28.3 Mev for values of nuclear mass between 60 and 100. It is concluded that the Λ nuclear potential well depth is not greater than 27.2 + 1.3 Mev. (J.F.P.)

45362 MEASUREMENT AND STATISTICAL THEORY ANALYSIS OF ^{56}Fe(^{3}He,p) AND ^{63}Cu(^{3}He,p) ENERGY AND ANGULAR DISTRIBUTIONS-NUCLEAR SHELL EFFECTS. Hazan, Jean-Pierre; Merkel, George (Univ. of Rochester, N. Y.). Phys. Rev., 139: B835-45(Aug. 23, 1965).

Thin ^{56}Fe and ^{63}Cu targets (approximately 1.5 mg/cm^2) were bombarded with 10-Mev ^{3}He particles. The proton energy and angular distributions produced by the ^{56}Fe(^{3}He,p) and ^{63}Cu(^{3}He,p) reactions were measured by the E − ΔE particle identification technique. In the statistical theory interpretation of the experimental cross sections both the shape and magnitude of the angular and energy distributions were calculated. Contributions from the (^{3}He,np) and (^{3}He,2p) reactions were also calculated. Large sections of the measured proton energy and angular distributions (about 90% of the total cross sections) are consistent with the predictions of the statistical theory of compound-nucleus reactions. A conventional statistical theory calculation of the ^{63}Cu(^{3}He,p) cross sections is generally consistent with the experimental cross sections; however, a similar conventional calculation of the ^{56}Fe(^{3}He,p) cross sections yields values 50% smaller than the experimental results. Rosenzweig has derived an expression for nuclear level densities which indicates that level densities of nuclei in the immediate vicinity of the doubly closed shell ^{56}Ni nucleus can be influenced by nuclear shell structure at excitation energies as high as 15 Mev. A second statistical theory calculation of the magnitude and shape of the ^{56}Fe(^{3}He,p) cross sections, based on the Rosenzweig level density expression, yields calculated cross sections generally consistent with the measured ^{56}Fe(^{3}He,p) cross sections. (auth)

45363 EXCHANGE ELECTRICAL MOMENTS FOR NUCLEAR BETA AND GAMMA TRANSITIONS. Fujii, Yasunori (Stanford Univ., Calif.); Fujita, Jun-Ichi. Phys. Rev., 140: B239-44(Oct. 25, 1965).

The relative importance of exchange electric currents in nuclear beta and gamma transitions is estimated by using their relation to the Van Vleck potential and to the sum rule for the nuclear photoabsorption cross section. Though the exchange electric currents are not experimentally observable because of the Siegert theorem, the estimates give an idea of the difference between a free nucleon and a nucleon inside a nucleus. It is found that the magnitude of the exchange electric current relative to the convection current is more than 40% at the Fermi surface. (auth)

45364 COLLECTIVE MOTION IN FINITE MANY-PARTICLE SYSTEMS. III. FOUNDATIONS OF A THEORY OF ROTATIONAL SPECTRA OF DEFORMED NUCLEI. Klein, Abraham (Univ. of Pennsylvania, Philadelphia); Celenza, Louis; Kerman, Arthur K. Phys. Rev., 140: B245-63(Oct. 25, 1965).

The generalized Hartree-Fock approximation developed previously is applied to provide a microscopic and fully quantum-mechanical self-consistent theory of the rotational spectra of deformed nuclei. By starting from a rotation- and inversion-invariant hamiltonian, the equations of the method are derived, including the effect of pairing correlations. The equations of motion yield the description of a quasiparticle (hole) self-consistently coupled to a rotator. Within a consistent approximation, all the usual observables associated with the notion of deformed nuclei — moments of inertia, collective gyromagnetic ratios, quadrupole moments, and transition probabilities — can be obtained in terms of the solutions of these equations, which are developed as a power series in the reciprocal of the moment of inertia. The zero-order theory is equivalent to the best current theory of nuclear shapes and also describes, therefore, the quadrupolar properties of the nucleus. The first-order solution suffices for the calculation of the moment of inertia and the collective gyromagnetic ratio. Here again familiar results are obtained in the only case considered in detail, that of a single band with unlimited angular-momentum states available. The second-order solution is also found and used to study the spectrum of the neighboring odd nuclei. The main results are contained in the formulas for the moment of inertia and decoupling parameter for odd-particle or hole-based bands, where the self-consistency requirements yield terms not hitherto noticed in the case of an odd nucleus. (auth)

45365 STRUCTURAL SIGNIFICANCE OF THE PRINCIPAL QUANTUM NUMBER OF NUCLEONIC ORBITAL WAVE FUNCTIONS. Pauling, Linus (Center for the Study of Democratic Institutions, Santa Barbara, Calif.). Phys. Rev. Letters, 15: 499(Sept. 13, 1965).

An interpretation is formulated of the principal quantum of nucleonic orbital wave functions. The study is based on the assumption that nucleons in nuclei are for the most part clustered into spherons. A spheron consists of nucleons in a localized 1$_s$ orbital. The principal spherons are the helion (alpha particle) and the triton. A property of radial wave functions led to the following interpretation of the subshells of the shell model of the atomic nucleus. Those subshells that occur (are occupied) with only the value 1 for the principal quantum number n contribute only the outer layer of the nucleus (the mantle). Those subshells that occur with two values of n contribute to the mantle and

the next inner layer, and so on. For given n, the subshells are filled in the order of increasing l, and for given l in the order of increasing n. (J.F.P.)

45366 PHOTON ABSORPTION CROSS SECTION OF SPHERICAL NUCLEI. Huber, Max G. (Universitaet, Frankfurt am Main); Weber, Hans J.; Danos, Michael; Greiner, Walter. Phys. Rev. Letters, 15: 529-31(Sept. 20, 1965).

The gamma absorption cross sections are calculated for vanadium-51, manganese-55, and arsenic-75. The results are plotted with the experimental results. Within uncertainties it is concluded that the structure of the giant dipole resonance for spherical nuclei as well as for deformed nuclei is described by the collective hamiltonian. The influence of the odd particle is as unimportant in the spherical nuclei as it is in the deformed nuclei. (J.F.P.)

45367 EXCITED STATE OF $_{\Lambda}Be^{9}$ AND THE Λ-N INTERACTION. Ali, S. (Univ. of Manchester, Eng.); Murphy, J. W.; Bodmer, A. R. Phys. Rev. Letters, 15: 534-7 (Sept. 20, 1965).

Results are reported of calculating B_{Λ}^{*} with a three-body model consisting of two α particles and the Λ. The excited state is taken as built on the first excited state (J = 2) of ^{8}Be by, in effect, coupling the Λ(in an s state) to the excited ^{8}Be core. The long lifetime is then readily understood as a consequence of the decay into an l = 2 final state of $_{\Lambda}He^{5}$ + ^{4}He together with the small Q value. The results obtained for B_{Λ}^{*} are shown. It is seen that only a fairly small increase in B_{Λ}^{*} is obtained by use of the three-parameter function. The rms radius and rearrangement energy of the ^{8}Be core are also shown. It is believed that the results for B_{Λ}^{*} are the first rather definite confirmation of such a short range for the attractive part of the Λ-N interaction. (J.F.P.)

45368 POSSIBLE EVIDENCE FOR NUCLEAR INTERACTION OF MUON ABOVE 3 x 10^{14} ev. Matano, T. (Tokyo Univ.); Nagano, M.; Shibata, S.; Suga, K.; Kameda, T.; Toyoda, Y.; Maeda, T.; Hasegawa, H. Phys. Rev. Letters, 15: 594-6(Oct. 4, 1965).

An almost horizontal air shower was observed which suggests the nuclear interaction of a meson (μ) or (neutrino) with an energy of more than 3×10^{14} ev. The spark-chamber picture is shown in which the many parallel tracks imply that the zenith angle is very large. The measurement of this angle shows that the shower was observed at an atmospheric thickness of 12000 g/cm^2. The total energy of the shower is estimated from the reasonable assumption that the shower is a nucleonic air shower. This assumption can be made from the presence of the nuclear active particle of large energy whose interaction is shown. The cross section could depend on the energy as $E^{\frac{1}{2}}$ or E^{2}. (J.F.P.)

45369 INTERNAL CONVERSION COEFFICIENTS OF E2 TRANSITIONS. Swarnagowri, S.; Ramaswamy, M. K. (Karnatak Univ., Dharwar, India). Proc. Indian Acad. Sci., Sect. A, 62: 34-55(July 1965).

An analysis of K-conversion coefficients of E2 transitions of the type $2^{+} \rightarrow 0^{+}$, $0^{+} \rightarrow 2^{+}$, $4^{+} \rightarrow 2^{+}$, $6^{+} \rightarrow 4^{+}$, and $8^{+} \rightarrow 6^{+}$ together with their methods of determination was carried out. The ratios of experimental to theoretical α_{k} values are plotted against the atomic weights and it is seen that there is no similar behavior among these transitions. (auth)

45370 TENSOR FORCE IN THE NUCLEUS ^{18}F. Fosado P., Mario E.; Wolf B., K. Bernardo (Universidad Nacional de Mexico, Mexico City). Rev. Mex. Fis., 14: 57-66(1965).

The energy levels of ^{18}F are calculated when one adds a tensor force to a central interaction with and without exchange. No significant improvement of the levels is obtained which suggests that a purely central interaction, plus spin orbit coupling, could account for the properties of nuclei in the 2s-1d shell. (auth)

45371 HALF-LIFE OF ^{32}P. Marais, P. G.; Deist, J. (Western Province Fruit Research Inst., Stellenbosch, S. Africa). S. African J. Agr. Sci., 4: 627-9(Dec. 1961).

The half life of ^{32}P, produced by the reaction ^{32}S(n,p)^{32}P, was investigated. Liquid G-M counters were used for the radiometric measurements. These were thin glass-wall β counters with a wall thickness of ~0.2 mm. Because of the low maximum counting rate of these counters, namely 20,000 cpm, and the known quick decrease in activity of the ^{32}P, a stock solution of high initial activity was prepared, from which suitable dilutions were made for measurement at frequent intervals. Sufficient carrier (100 ppm P) was added to eliminate the possibility of ^{32}P adsorption on the walls of the glass containers. The decay was followed, using two counters, for a period of 160 days, and 120 decay points were taken with each counter during this time. Standard readings were taken with uranium. The regression equations, together with the standard errors of the regression coefficients, were as follows: Counter 1: Y = −(0.021,072 ± 0.000,008) X ± 4.1476; and Counter 2: Y = −(0.021,082 ± 0.000,009) X ± 4.1811. The pooled regression coefficient (b), together with its standard error, were calculated, giving a value of −(0.021,077 ± 0.000,007). Using this value the half life of ^{32}P (T) was calculated from the relation $T = \log_{10}2/b$. Thus the half life is 14.282 ± 0.005 days. (TCO)

45372 NUCLEAR PHYSICS: A STATUS REPORT. Zucker, A. (Oak Ridge National Lab., Tenn.); Bromley, D. A. Science, 149: 1197-1205(Sept. 10, 1965). (ORNL-P-995).

The development of nuclear physics, its present position, and future prospects are reviewed. Topics discussed include nuclear models, nuclear reactions, the present status, and the impact of nuclear physics. (J.F.P.)

45373 RESTORATION OF COMPLEX GAMMA SPECTRA. Renard, A. Univ. Bruxelles, Inst. Phys., Bull. No. 1, 1-17(Apr. 1965). (In French).

A general and objective method of the resolution of complex γ spectra that necessitates the determination of the response matrix of the spectrometer under an explicit form and the resolution of a system of linear equations is described. The different aspects of this problem are summarized. The method used for the determination of the response matrix is given and the iteration method for the restoration of the complex spectra is discussed. The method is applied to the analysis of γ spectra of known components. (J.S.R.)

45374 PHOTOTRITONS FROM ^{6}Li. Sherman, N. K.; Baglin, J. E.; Morrison, R. C.; Owens, R. O.; Stewart, J. R.; Schultz, H. L. (Yale Univ., New Haven). 20p. (CONF-650410-31). Gmelin, AED-CONF-65-073-51.

From American Physical Society, Washington, D. C.

Charged disintegration products of ^{6}Li which were irradiated with 40 or 32 Mev bremsstrahlung were momentum analyzed by a quadrupole triplet magnet system and detected by a silicon barrier system. Evidence was found that tritons are produced in the photodisintegration. (L,B,S.)

45375 THE MEASUREMENT AND UTILIZATION OF NEUTRON-CAPTURE GAMMA RADIATION. Lussie, William G.; Brownlee, James L. Jr. (Univ. of Illinois, Urbana). 22p. (CONF-650405-18). Gmelin, AED-CONF-65-040-25.

From International Conference on Modern Trends in Activation Analysis, College Station, Tex.

In accordance with the Bohr theory of nuclear reactions, a highly excited state—the compound nucleus—is formed on the absorption of a bombarding particle by a target nucleus. This de-excites almost immediately, usually by means of gamma ray emission. The emission usually takes place through a cascade of two or more gamma photons via intermediate levels to the ground state. Relationships are reviewed which permit calculation of the excitation energy of the compound nucleus, and a relationship is derived for calculating the total number of compound nuclei formed during an irradiation period, t. Techniques for the measurement of capture gamma ray spectra are reviewed, and the sum-coincidence and fast/slow sum-coincidence methods, as applied to the measurement of capture gamma ray spectra, are discussed. Brief discussions on the application of capture gamma measurements to elemental and iso-

topic analyses, and to angular correlation–decay scheme studies are included. (auth)

45376 $^{89}Y(n,\gamma)^{90m}Y$ AND $^{89}Y(n,\gamma)^{90}Y$ CROSS SECTIONS BETWEEN 0.145 AND 1.225 Mev. Grench, H. A.; Coop, K. L.; Menlove, H. O.; Vaughn, F. J. 10p. (CONF-650410-27). Gmelin, AED-CONF-65-073-61.

From American Physical Society, Washington, D. C.

The isomer ratio for the $^{89}Y(n,\gamma)$ reaction at 0.145 to 1.225 Mev was measured in order to determine the spin cutoff factor in the spin dependence of the level density. The Hauser–Feshbach statistical theory was used for comparison with experiment and the Fermi gas model was used for obtaining the energy dependence of the level density. A value of 3.26 was obtained for the spin cutoff factor, which corresponds to an effective nuclear moment of inertia about half that of a rigid body. (L.B.S.)

45377 DIFFERENTIAL CROSS SECTIONS OF ALPHA PARTICLES FROM $^{16}O(d,\alpha)^{14}N$. Jobst, J. E. 12p. (CONF-650410-28). Gmelin, AED-CONF-65-073-55.

From American Physical Society, Washington, D. C.

Silicon surface-barrier detectors were used in a differentially-pumped gas scattering chamber to study the excitation functions of the $^{16}O(d,\alpha)^{14}N$ reaction from 5 to 9 Mev, and at angles of 30, 90, 135, 150, and 168°. The ground and second excited-state cross sections are presented. The group correlation function for α_0 and α_2 was evaluated in order to compare systematically the excitation functions. Preliminary studies were also made of the yield of α_2 particles up to deuteron energies of 15 Mev which was found to be uniformly small. (L.B.S.)

45378 POLARIZATION OF 39-Mev PROTONS ELASTICALLY SCATTERED FROM ^{58}Ni AND ^{60}Ni. Poppe, C. H.; Boyd, R.; Liers, H.; Williams, J. H. (Univ. of Minnesota, Minneapolis). 12p. (CONF-650410-30). Gmelin, AED-CONF-65-073-52.

From American Physical Society, Washington, D. C.

An optical model-analysis was made of the results of the 39 Mev proton elastic scattering from ^{58}Ni and ^{60}Ni. An attempt was made to determine the parameters of the central well by fitting the cross section data, and to determine the spin-orbit potential parameters by fitting the polarization data. The results are obtained for pure surface or volume absorption. It is concluded that a strong interrelation at 40 Mev exists between the differential cross section and the polarization, such that simultaneous fitting of both is required, varying both central-potential and spin-orbit potential parameters. (L.B.S.)

45379 THE ANGULAR DISTRIBUTION OF GAMMA RAYS FROM THE 62 ev NEUTRON RESONANCE IN ^{124}Sn. McNeill, K. G.; McConnell, D. B.; Firk, F. W. K. (Atomic Energy Research Establishment, Harwell, Berks, Eng.). 15p. (CONF-650410-32). Gmelin, AED-CONF-65-073-49.

From American Physical Society, Washington, D. C.

Measurements were made of the spectra and the angular distribution of gamma rays following the capture of 62 ev neutrons by ^{124}Sn. Evidence was found that the capturing state is a $P_{1/2}$ state, and that it decays predominantly to the $S_{1/2}$ state at 0.19 Mev. (L.B.S.)

Plasma Physics and Thermonuclear Processes

Refer also to abstract 44975.

45380 (AD-426192) COOPERATIVE EFFECTS AND PLASMA LOSSES IN A MAGNETIC FIELD. Final Report, March 1, 1962–February 28, 1963. Kursunoglu, Behram (Miami Univ., Coral Gables, Fla. Dept. of Physics). Contract AF19(604)-8082. 21p. (AFCRL-63-775). CFSTI $2.60.

Diffusion of electrons and ions in a plasma across a magnetic field with the interplay of an anisotropic dynamical friction is formulated in terms of the methods of Brownian motion. For a special symmetry of the dynamical friction matrix, it is found that for Larmor periods of the order of the relaxation time across the magnetic field, the diffusion takes place as an ordinary Brownian motion uninhibited by the external magnetic field. (auth)

45381 (ARL-65-115) PLASMA RESONANCE PROBE CHARACTERISTICS IN A MAGNETIC FIELD. Crawford, F. W. (Stanford Univ., Calif.). Apr. 1965. Contract AF33(616)-8121. 19p. CFSTI.

The operation of the plasma resonance probe in the absence of a magnetic field is now well understood, and the resonant frequency can be interpreted to give the electron density in the plasma. In many potential applications of this diagnostic technique to laboratory and space plasmas, a static magnetic field is present. The resulting modifications to the resonance are studied. The analysis is based on the simplified model of the probe behavior that was validated for the zero magnetic field case by the work of Harp and Crawford. It is concluded that the technique can be applied to obtain the electron plasma frequency, ω_p, and the electron density for $\omega_c^2 \ll \omega_p^2$, and the electron cyclotron frequency, ω_c, and hence the local magnetic field when $\omega_c^2 \gg \omega_p^2$. An approximate correction formula is derived for the intermediate range, $\omega_c^2 \approx \omega_p^2$. (auth)

45382 (BRL-MR-1644) ON THE USE OF VACUUM ULTRAVIOLET ABSORPTION AS A MEASURE OF TEMPERATURE IN RARE GAS PLASMAS. Rudd, R. A. (Ballistic Research Labs., Aberdeen Proving Ground, Md.). Apr. 1965. 36p.

An extension of the theory of plasma temperature measurement by vacuum u-v absorption is made which makes this technique useful in obtaining time-resolved temperatures. A survey of available photoionization cross sections is given, and improvements which lead to better time resolution are suggested. (auth)

45383 (D1-82-0419) SOME RELATED PHENOMENA IN PLASMAS IN SOLIDS AND IN GASES. Drummond, James E. (Boeing Scientific Research Labs., Seattle, Wash. Plasma Physics Lab.). Mar. 1964. 38p.

A review of some examples of plasma phenomena in solids which are related to those in gases is presented. Extensive discussions on the helical instability and helicons are presented. It is also pointed out how the relation of plasma phenomena in gases and solids has extended plasma research and enlarged its area of application. (M.O.W.)

45384 (D1-82-0436) THE PRODUCTION OF DENSE BEAMS OF LOW-ENERGY IONS. Kofoid, M. J.; Braams, C. M.; Zieske, P. (Boeing Scientific Research Labs., Seattle, Wash. Plasma Physics Lab.). June 1965. 17p.

Dense beams of positive ions of less than 1.0-kev energy have been produced using a duoplasmatron with an extraction voltage of 20 kV as a source. Outward radial electrostatic forces due to space charge impose a restriction upon the intensity of an ion beam while it is being formed in vacuum. The problem of designing the electrostatic lens system for decreasing the energy of the ions while simultaneously focusing them to produce a maximum-density parallel beam is discussed. The system consisted of a unipotential lens, which was integral with the source (Radiation Dynamics Type DY-1), and two additional immersion lenses. Most of the deceleration and beam compression was accomplished in the last lens. Its design was the major problem. Because a fairly exact analysis would have been very complicated, a simple approximate method for designing this lens was devised. The design values of current in the final low-energy beam checked well with those from experiment. (auth)

45385 (D1-82-0437) COMPOSITION OF NOBLE GAS ION BEAMS PRODUCED WITH A DUOPLASMATRON. Braams, C. M.; Zieske, P.; Kofoid, M. J. (Boeing Scientific Research Labs., Seattle, Wash. Plasma Physics Lab.). June 1965. 22p.

Beams of noble gas ions produced with a duoplasmatron ion source were magnetically analyzed, while the gas pressure in the source was varied. At high pressures, the beam consisted primarily of singly charged ions. With decreasing pressure, the yield of multiply ionized ions increased and

was finally limited by the rising arc voltage which caused overheating of the anode. No measurable amount of He^{2+} or Ne^{2+} was detected. In the other gases, the following maximum yields were measured for the more highly ionized species: 63% Ar^{2+}, 54% Kr^{2+}, 16% Kr^{3+}, 24% Xe^{2+}, and 1.2% Xe^{3+}. Traces of molecular ions were detected in all the noble gases studied. (auth)

45386 (D1-82-0439) THE EXCITATION OF HIGHER MODES BY THE HELICAL INSTABILITY. Johnson, Roy R. (Boeing Scientific Research Labs., Seattle, Wash. Plasma Physics Lab.). Apr. 1965. 47p.

The conditions whereby the helical instability can excite higher modes in the plasma column are investigated. As the amplitude of the helical instability increases, it changes the radial distribution of the averaged charge density. The finite amplitude theory of the helical or m = 1 instability is employed to determine the averaged charged density which is then used to determine the conditions for the onset of the m = 2 instability. The onset of the m = 2 instability is thus determined as a function of the amplitude of the helical instability for specified conditions within the plasma column. These results are then combined with the energy balance relation of the positive column. The wavelengths and frequencies of the helical and m = 2 modes are determined for the conditions at the onset of the m = 2 mode. The wavelength of the m = 2 mode is found to be shorter than for the helical mode, whereas the frequency is found to be greater. (auth)

45387 (D1-82-0442) PERMANENTLY MAGNETIZED FERRITE ANTENNA WINDOWS FOR IMPROVING ELECTROMAGNETIC WAVE TRANSMISSION THROUGH A PLASMA. Kofoid, Melvin J. (Boeing Scientific Research Labs., Seattle, Wash. Plasma Physics Lab.). June 1965. 15p.

A longitudinal magnetic field (B_z) can be employed to increase the transmission through a plasma of a right-hand polarized electromagnetic (EM) wave at below the natural plasma frequency. The B_z field can be produced by permanently magnetized ferrite material in the form of a thick sheet placed as a window in front of the radiator and directly adjacent to the plasma. The crucial point is that it has been shown by test that h-f EM waves can be transmitted with only reasonable attenuation through a thick sheet of ferrite which is producing a B_z >1500 gauss longitudinal field at the sheet surface. Further, due to its rotational field-displacement properties, there exists the possibility that the magnetized ferrite sheet serving as the antenna window may be so constructed as to be simultaneously an isolator and thereby reduce the changes in load impedance seen by the radiator with varying plasma sheath conditions. (auth)

45388 (GA-6432) FLUTE CHARACTERISTICS OF AND MICROWAVE EMISSION FROM A PLASMA IN A MIRROR. Scott, F. R.; Jensen, T. H.; Wharton, C. B.; Fleischmann, H.; Tuckfield, R. G. Jr. (General Atomic, San Diego, Calif. John Jay Hopkins Lab. for Pure and Applied Science). June 15, 1965. 33p. (CONF-650911-10).

From 2nd Conference on Plasma Physics and Controlled Nuclear Fusion Research, Abingdon, Berks, England.

A pulsed mirror was constructed to study the stability of a plasma of modest energy. The 70 ev plasma is piped from a gun to the mirror by a linear octopole guide field. The mirror field is turned on in a plasma transit time. Plasma densities of 10^{13} electrons/cm^3 are observed in the central plane of the mirror. Two distinct modes of operation are observed and depend only on conditions established in the guide field. In the first mode the plasma in the mirror appears flute stable, most of the plasma escapes axially, a slow anomalous radial diffusion is observed and microwave emission occurs at the electron cyclotron harmonics ranging from n = 1 to at least n = 19. The microwave emission is not compatible with the electron branch of the Harris instability. The stability of this mode is attributed to line tying by cold plasma effusing from the guide field region. Densities above 10^{11} electrons/cm^3 were observed for 200 μsec in the region between the mirror and the guide field. With the addition of an axially symmetric cylinder in the guide field, this density is decreased. Measurements show plasma densities below 10^{11} after 40 μsec in this region. The resulting plasma trapped in the mirror exhibits flute instabilities, radial plasma loss, intense erratic microwave emission and rapid density decay. The m = 1 flute is identified and its phase is followed through 4π. The phase velocity is in the direction of the electron grad B drift. The sign of this phase velocity may be explained by the theory of Krall if the electron energy exceeds the ion energy sufficiently. The addition of conducting plates in the downstream mirror region tempered the violence of the flute instability. This tempering depends only on the surface resistance of these plates. This effect was examined by measuring the frequency spectrum of signals from coated scintillator probes placed near the vacuum envelope. (auth)

45389 (GA-6513) LANDAU DAMPING AND GROWTH OF ELECTROSTATIC MODES WITH FINITE SYSTEM EFFECTS. Book, David L. (General Atomics, San Diego, Calif. John Jay Hopkins Lab. for Pure and Applied Science). June 29, 1965. Contracts NAS7-275 and AF49(638)-1546. 22p.

For a plasma with finite cross section of the sort which occurs typically in laboratory plasma wave experiments, in a constant magnetic field, the Landau damping (or growth) is obtained by a variational procedure in terms of the plasma velocity distribution function and potential and density profiles. The result is applied to the damping associated with the upper and lower branches of the dispersion curve for longitudinal electron plasma waves in the case of a Maxwellian velocity distribution in slab and cylindrical geometries. Application is also made to the growth rates resulting from a low-density electron beam with radially dependent energy superposed on a Maxwellian. (auth)

45390 (IAE-780) NEUSTOICHIVOST RAZRYADA S NAKALENNYM KATODOM V MAGNITNOM POLE PRI NIZKIKH DAVLENIYAKH. (Discharge Instability With a Heated Cathode in a Magnetic Field at Low Pressures). Vlasov, M. A.; Dobrokhotov, E. I.; Zharinov, A. V. (Institut Atomnoi Energii, Gosudarstvennyi Komitet po Ispol'zovaniyu Atomnoi Energii SSSR, Moscow). 1964. 44p. Dep. mn.

Results are presented of a study of a gas discharge with heated cathode in an equipotential volume in a magnetic field of intensity up to 2000 Oe. In the range of pressures investigated, from 2×10^{-6} to 10^{-4} mm Hg, a plasma column is formed, negatively charged with respect to the surrounding walls. It was established that such a discharge becomes unstable with an increase of the pressure of the neutral gas. A plasma torch, stationarily rotating into the electron side, is formed, escaping from the region of the primary beam. The appearance of the torch is the result of the polarization of the plasma in the beam of primary electrons in the presence of azimuthal nonhomogeneity in the density and the difference in the drift velocities of the ions and electrons. For further increase of pressure, the stationary rotation disappears, and intensive oscillations with a continuous frequency spectrum develop in the discharge. An explanation of the basic laws of behavior of the discharge is given. On the basis of a simplified model, an expression for the frequency of rotation of the torch, which is qualitatively confirmed by experiment, is obtained. (tr-auth)

45391 (INR-612/IXA/PR) VZAIMODEISTVIE VYSTRYKH PLASMOIDOV S BAR'EROM POSTOYANNOGO MAGNITNOGO POLYA. (Interactions of Fast Plasmoids With a Constant Magnetic Field Barrier). Khvashchevski, S. (Institute of Nuclear Research, Warsaw (Poland)). Mar. 1965. 21p.

The effect of plasma displacement by an external magnetic field was studied by injecting plasmoids into a magnetic field and measuring the vortex electric currents excited in them by an electric field. The variation of maximum plasmoid density with position in the measuring chamber is described. Results of measurements are given

for the dependence of the double-probe current and the diamagnetic signal on the maximum magnetic field, the probe characteristics of the plasmoids in the presence and absence of the magnetic barrier, and the variations of E/E_∞ (ratio of magnetic current displaced by plasma to total unexcited plasma current) and of H_z/H_0 (ratio of magnetic field intensity on axis of cylinder to unexcited field) with the screening coefficient. (M.J.T.)

45392 (IPP-1/39) ELEKTROMAGNETISCHE STRAHLUNG AUS PLASMEN HOHER TEMPERATUR UND DICHTE. (Electromagnetic Radiation From Plasmas of High Temperature and Density). Eberhagen, A. (Institut fuer Plasmaphysik, G.m.b.H. Garching (West Germany)). July 1965. 45p. Dep. mn.

A survey on the electromagnetic radiation from plasmas of high temperature and density is presented. Bremsstrahlung radiation and line emission from these plasmas are treated. Also a short review is given on radiation losses from these plasmas. (auth)

45393 (IPP-2/38) INFLUENCE OF PROBE LOSSES ON THE ION DENSITY OF THERMAL ALKALI PLASMA IN A MAGNETIC FIELD. Guilino, E.; Hashmi, M. (Institut fuer Plasmaphysik, G.m.b.H., Garching (West Germany)). June 1965. 34p. Dep. mn.

According to the "Equilibrium Theory" the ion density on the axis of a thermal alkali plasma in a strong magnetic field should be mainly determined by the end plate losses and hence described by the SAHA equation. However, measurements of the ion density with Langmuir single probes in a cesium plasma show discrepancies up to more than one order of magnitude, depending on density and plate temperature. A modification of the "Equilibrium Theory" is described which takes into account the particle losses at the probe surface. The calculations yield agreement with the experiments. (auth)

45394 (IPP-6/37) CONNECTION BETWEEN CORRELATIONS AND FLUCTUATIONS IN A PLASMA. Feix, Marc R.; von Hagenow, Karl U. (Institut fuer Plasmaphysik, G.m.b.H. Garching (West Germany)). June 1965. 11p. Dep. mn.

The space-time fluctuations of the density in a plasma is obtained by introducing in the Vlasov equation an initial distribution describing the microscopic fluctuations at a given time. The statistical description of this initial condition is entirely provided by the two particles correlation function H(k,u) of the Bogoliubov-Lenard theory. The result can be considered as a generalization of the Nyquist theorem: A static description of a fluctuating microscopic quantity plus a macroscopic equation describing a time evolution–gives the frequency spectrum of the microscopic quantity. (auth)

45395 (IPP-6/38) ON THE DYNAMICS OF A TOROIDAL θ-PINCH. Schlueter, A. (Institut fuer Plasmaphysik, G.m.b.H. Garching (West Germany)). July 1965. 13p. Dep. mn.

The equation of motion of the meridional center of mass of a toroidal θ-pinch is derived. It is shown that the equation $d^2S/dt^2 = 2c^2/S$ (S = distance of the meridional center of mass from the axis; c = Newtonian speed of sound) is a good approximation. It gives an outward acceleration independent of the ratio p/B^2. The right hand side contains contributions of about equal magnitude due to the gas pressure and due to the diamagnetic behavior of the plasma. Corrections to this relation due to "geometrical" effects are of second order in the aspect ratio $A(A \ll 1)$ while dynamical corrections due to compression or expansion of the plasma are of first order in A. Both are of minor importance in practical applications. (auth)

45396 (LA-DC-7120) THETA-PINCH SOURCES OF VACUUM ULTRAVIOLET RADIATION. Peacock, N. J.; Cowan, R. D.; Sawyer, G. A. (Los Alamos Scientific Lab., Univ. of California, N. Mex.). [1965]. Contract W-7405-eng-36. 13p. (CONF-650806-12). Dep. mn; CFSTI $1.00 cy, $0.50 mn.

From 7th International Conference on Phenomena in Ionized Gases, Belgrade.

Theta-pinch plasmas have demonstrated the highest known laboratory temperatures and are thus a convenient source for exciting the spectra of highly stripped ions. Grazing incidence spectrographs were used to study the spectra of highly excited rare gases and of Fe. Some of the iron lines were classified as transitions in Fe VIII–Fe XVI. (auth)

45397 (MATT-282) PLASMA CONFINEMENT IN THE MODEL C STELLARATOR. Yoshikawa, S.; Young, K. M.; Sinclair, R. M.; Harries, W. L. (Princeton Univ., N. J. Plasma Physics Lab.). June 1964. Contract AT(30-1)-1238. 100p. Dep. mn; CFSTI $3.00 cy, $0.75 mn.

The confinement of the plasma in the Model C Stellarator was studied as a function of various parameters. The loss seems to be proportional to the ohmic heating current density $j_{||}$, when $j_{||}$ is high. This agrees with the theory of the drift mode "universal" instability of Kadomtsev and Kuckes, which is caused by both $j_{||}$ and the density gradient perpendicular to the main confining field, B. Even when $j_{||}$ is small, a rapid plasma loss is still observed. The cause for this loss may be connected with an imperfect toroidal equilibrium due to the effects of finite resistivity and finite ion Larmor radius ρ_i. The resistive MHD instabilities are not ruled out especially in the low current regime, but the observed increase in confining time with the application of a radial electric field favors the idea that imperfect equilibrium is involved. (auth)

45398 (MATT-332) PLASMA HEATING AT 500 MEGAHERTZ. Ellis, Robert A. Jr.; Rye, Barry J. (Princeton Univ., N. J. Plasma Physics Lab.). June 1965. Contract AT(30-1)-1238. 54p. Dep. mn; CFSTI $3.00 cy, $0.50 mn.

The production and heating of deuterium and helium plasmas in the B-3 stellarator by a 25 kw 500 MHz generator are investigated. The efficiency for plasma production by r-f is found to be comparable with ohmic heating at similar power levels. The confinement of the plasma produced is in order of magnitude agreement with the Bohm formula as well as the predictions of the so-called lack of equilibrium theory. Measurements were also obtained at mw power levels in order to identify the plasma wave interaction involved. Although data are not conclusive, the plasma generation and heating at ion densities greater than 10^{12} cm^{-3} are tentatively attributed to collisional damping of the whistler mode. The range of conditions included the lower hybrid resonance but there was no experimental evidence for this resonance. An interesting feature of the wave propagation was the observation of a sharp onset of wave propagation around the stellarator for densities less than some critical value. Some possible explanations for this phenomenon are presented. (auth)

45399 (NASA-CR-54451) INVESTIGATION OF COLLISION PROBABILITY OF ELECTRONS AND IONS WITH ALKALI METAL ATOMS. Semiannual Report, October 22, 1964–May 11, 1965. Bullis, R. H.; Nighan, W. L. (United Aircraft Corp., East Hartford, Conn. Research Labs.). May 1965. Contract NAS 3-4171. 85p. (UACRL-C-920243-12).

A cesium arc discharge was used in conjunction with electrostatic and r-f conductivity probe techniques to determine the collision probability of electrons with cesium atoms over the energy range from 0.2 to 0.6 ev. Further cesium ion-cesium atom collision probability measurements were made in the existing modified Ramsauer beam experiment in an attempt to extend the energy range of these measurements below 0.1 ev. Ion beam energy distributions were obtained at 0.1 ev. Ion beams with energies of 0.058 ev have been successfully detected; preliminary collision cross-section data are reported. Experiments are continuing to refine and further analyze these data. A knowledge of both the collision probability of electrons and cesium ions with cesium atoms is essential in the analysis of the neutralization plasma existing in the thermionic converter as well as being important in the analysis of other devices that employ cesium vapor in an ionized state. (auth)

45400 (NASA-TN-D-2982) ENERGY ADDITION TO AN ATOMIC HYDROGEN PLASMA AT OFF-RESONANT

CONDITIONS. Woollett, Richard R. (National Aeronautics and Space Administration, Cleveland, Ohio. Lewis Research Center). Sept. 1965. 44p. CFSTI $2.00 cy, $0.50 mn.

The efficiency of energy addition to a plasma by means of a Stix coil was determined for off-resonant conditions. The results included effects of cyclotron damping and axial temperature. The coupling resonance was found to be much sharper than had been predicted previously. Additional maxima in power absorption were found at slightly higher magnetic fields. These off-resonant maxima exhibited magnitudes and breadths that made them appear well suited to plasma heating. These new maxima appeared because of a beat phenomenon between the forced and natural plasma waves. (auth)

45401 (NP-15196) METOD OPREDELENIYA KOEFFITSIENTOV OTRAZHENIYA V PLAZMENNOM VOLNOVODE. (Method for Determining Coefficients of Reflection in a Plasma Waveguide). Ivanov, B. I. (Akademiya Nauk Ukrainskoi SSR, Kharkov. Fiziko-Tekhnicheskii Institut). 1964. 10p. Dep. mn.

A local change in magnetic field is applied to one end of a plasma waveguide as a perturbing force. The modulation coefficients of the wave are measured to the right and to the left of the perturbed region. Equations are developed that give the reflection coefficients in a plasma waveguide by measuring a modulated amplitude in the region of the ion cyclotron resonance. The signal frequency was 1×10^6 cycles/sec. The magnetic field strength was 500 to 1000 gauss. The plasma density was 10^9 to 10^{10}/cm^3. The hydrogen pressure was 10^{-5} to 10^{-4} mm Hg std, and the amplitude of the signal at the waveguide inlet was 10 to 200 v. The left end of the waveguide was open, and the right end was cooled with a water jacket for a length of about 30 cm (the waveguide length was about 150 cm). The reflection coefficients were found to be about 1.0 for the open end, and 0.1 to 0.3 for the loaded end of the waveguide. The value of the reflection coefficient did not depend on the amplitude of the wave either in the linear case, or in the case of a small nonlinearity. (TTT)

45402 (NP-15200) NELINELNAYA STABILIZATSIYA PUCHKOVYKH NEUSTOICHIVOSTEI PLAZMY. (Non-Linear Stabilization of Beam Instabilities in Plasma). Tsytovich, V. N.; Shapiro, V. D. (Akademiya Nauk Ukrainskoi SSR, Kharkov. Fiziko-Tekhnicheskii Institut). 1964. 15p. Dep. mn.

On passing a low-density beam through a plasma it is possible that the effects of the nonlinear interaction of the waves are small, that is, they show up within a time interval much greater than the quasilinear relaxation time of the beam. The energy of the oscillations excited by the beam is comparable with the initial beam energy, and can be used for turbulent heating, the generation of microwaves etc. It is shown that within a definite range of plasma parameters beam stabilities can be stabilized because of nonlinear effects, that is, the beam can pass through the plasma without substantial energy losses, and is effectively accelerated by an external field. The oscillations react by an induced scattering mechanism with the plasma particles, and go to the non-resonant region of the spectrum, where they cannot react directly with the beam. If the condition $T_i > T_e\,(m_i/m_e)(V_e/V_f)^2$ is fulfilled, the nonlinear interaction stabilizes the beam even in the absence of extraneous noise. Otherwise, a source of external intensive noise is required for stabilization. Here V_e is the thermal velocity of the plasma electrons, and V_f is the phase velocity of the interacting waves. (TTT)

45403 (NP-15445) NOTES ON LOW FREQUENCY PLASMA OSCILLATIONS (ANODE OSCILLATIONS AND FORCED RELAXATION OSCILLATIONS). Rijnhuizen Report 65-24. Terlouw, J. C. (Stichting voor Fundamenteel Onderzoek der Materie, Jutphaas (Netherlands). Instituut voor Plasma-Fysica). Apr. 1965. 16p. Dep. mn.

A study of cesium plasma instabilities in front of the anode in a gas discharge is presented. The following discussions are presented; the anode fall in potential, periodicity of the anode oscillations, influence of anode cooling, relaxation oscillations, and the cathode region during a relaxation oscillation. (M.O.W.)

45404 (ORNL-P-1557) A STUDY OF THE PROPERTIES OF IONIC SOUND WAVES. Jones, W. D.; Alexeff, I. (Oak Ridge National Lab., Tenn.). Aug. 3, 1965. Contract W-7405-eng-26. 24p. (CONF-650806-5). Dep. mn; CFSTI $1.00 cy, $0.50 mn.

From 7th International Conference on Phenomena in Ionized Gases, Belgrade.

Extensive studies were made of the properties of ionic sound waves using a time-of-flight technique. The waves were propagated in collisionless plasmas formed by rare-gas discharges, with $T_e \gg T_i$. The following plasma and wave properties were investigated: wave velocity dependence upon ion mass, frequency and electron temperature; wave reflection; wave interference phenomena; wave gas damping; wave focusing; plasma sheaths; plasma ion temperature; and the adiabatic compression coefficient of the electron gas. (auth)

45405 (ORNL-P-1576) ION CYCLOTRON HARMONIC SPECTRUM GENERATED IN AN ENERGETIC ION PLASMA. Bell, P. R.; Kelley, G. G.; Lazar, N. H.; Stratton, R. F. (Oak Ridge National Lab., Tenn.). [1965]. Contract W-7405-eng-26. 15p. (CONF-650806-9). Dep. mn; CFSTI $1.00 cy, $0.50 mn.

From 7th International Conference on Phenomena in Ionized Gases, Belgrade.

Measurements were made of the electric and magnetic fields produced in a plasma of 3×10^9 ions/cc density with a mean ion energy of about 700 kev. Spectral analysis of the signals show oscillations at the ion cyclotron frequency and its harmonics up to at least the 70th harmonic. The intensity ratio to an electrostatic probe is less than 30 db between the 3rd harmonic (usually the strongest) and the 60th harmonic. The plasma is contained in a nearly uniform magnetic field between mirror coils spaced 4 meters apart. As a result of the strong anisotropy of the particle velocities, most of the plasma is further restricted axially by a very small magnetic mirror to a region ~ ±30 cm about the midplane. The plasma diameter is 30 cm. The electric field is strongly absorbed by the plasmas. Probes axially spaced by more than 10 cm show almost complete lack of phase correlation, although the spectral distributions are not very different. When the plasma decays, some of the fields persist for density reductions of more than an order of magnitude. In particular, the fundamental, whose width at full density is ~ 150 kc (f = 18.3 Mc), lasts for several seconds and shows a frequency shift of ~ 50 kc as well. (auth)

45406 (SIT-2852-17) EXPERIMENTAL INVESTIGATION OF CUSPED CONTAINMENT GEOMETRIES. Annual Report, 1964-1965. Yevick, George J. (Stevens Inst. of Tech., Hoboken, N. J. Dept. of Physics). Contract AT(30-1)-2582. 122p. (SIT-164). Dep. mn; CFSTI $4.00 cy, $0.75 mn.

A summary is presented of performance tests and evaluation of the Chalice main bank Mark II, radiation detection instruments for measuring neutrons from Chalice, magnetic fields and coil parameters for Chalice, and initial experimental efforts in Chalice. A theoretical study is included of the supercollective modes of one-dimensional plasma systems. (T.F.H.)

45407 (SU-AA217) ARGON PLASMA TRANSPORT PROPERTIES. de Voto, R. Stephen (Stanford Univ., Calif. Inst. for Plasma Research). Feb. 1965. 58p.

The transport properties of equilibrium argon plasma were calculated for pressures of 1, 10, 100, 760 and 1900 mm Hg and temperatures from 5000 to 20000°K. In addition to the usual viscosity and thermal conductivity, the thermal and multicomponent diffusion coefficients have also been computed. Two problems not occurring in computations of properties of un-ionized gases are examined. The first concerns the rate of convergence of the approximations to the transport coefficients. It is found that at least the third approximation to the thermal conductivity must be used

down to very low degrees of ionization to ensure the accuracy of the results. Very slow convergence is also observed for the electron-atom, atom-electron and electron-ion diffusion coefficients at very low degrees of ionization. The source of this behavior is apparently the Ramsauer minimum in the electron-argon atom cross sections. The second problem occurs in the charged particle cross sections. In the present report the shielded Coulomb potential is used to bypass the divergence occurring in this cross section when the unshielded potential is used. Inclusion of terms of order unity in these cross sections increases the transport coefficients by appreciable amounts. Computations of electric conductivity are also compared with some measured values here. (auth)

45408 (SU-IPR-11) WAVE PROPAGATION ALONG A WARM NONUNIFORM PLASMA COLUMN. Crawford, F. W.; Tataronis, J. A. (Stanford Univ., Calif. Inst. for Plasma Research). May 1965. Contract AT(04-3)-326. 30p. Dep. mn; CFSTI $2.00 cy, $0.50 mn.

The dipolar resonances that occur when an axially uniform plasma column is subjected to a transverse r-f electric field have received much study, and can be predicted accurately from a hydrodynamic description of the plasma perturbation and knowledge of the transverse electron density profile. These frequencies may be interpreted as the cutoffs of series of modes propagating along the column. Such propagation is studied in infinite planar geometry for a number of basic cases. Dispersion curves and descriptions of the plasma parameters at cutoff are given for modes with axially symmetric and axially asymmetric potential distributions in three different geometries: first for plasma filling the plates, and then for plasma separated from the plates either by one or two dielectric layers. The feasibility of observing these waves experimentally is discussed, and experimental evidence for their propagation is cited. (auth)

45409 (TID-22132) HIGH TEMPERATURE PLASMAS BY LASER HEATING. Quarterly Progress Report No. 3, April 6–July 5, 1965. Phelps, A. V. (Westinghouse Research Labs., Pittsburgh, Pa.). July 15, 1965. Contract AT(30-1)-3472. 14p. Dep. mn; CFSTI $1.00 cy, $0.50 mn.

The behavior and properties of laser-produced plasmas were investigated using diamagnetic loops, electrostatic probes, framing camera photography, and plasma energy absorption. Particles were successfully suspended electrostatically, but the emphasis remained on the retracting-pedestal approach. (D.C.W.)

45410 (TID-22183) THE STUDY OF PLASMA DIFFUSION ACROSS MAGNETIC FIELDS. Quarterly Status Report No. 13, May 1–July 31, 1965. (Stanford Univ., Calif. Inst. for Plasma Research). July 1965. Contract AT(04-3)-326. 15p. Dep. mn; CFSTI $1.00 cy, $0.50 mn.

A theoretical investigation was made on the growth of plasma fluctuations in a plasma which is subjected to an external electric field. A study was made of diffusion in a cylindrical discharge in a strong axial magnetic field. A theoretical and experimental study of some of the possible instabilities in such a discharge and their effects on diffusion rates is presented. Conclusions from the above investigations are presented. (M.O.W.)

45411 (UCRL-7935) INVESTIGATION OF A PLASMA FROM AN OCCLUDED GAS, COLD PLASMA SOURCE. Steinhaus, James F.; Oleson, Norman L.; Barr, William L. (Lawrence Radiation Lab., Univ. of California, Livermore). Jan. 13, 1964. Contract W-7405-eng-48. 57p. Dep. mn; CFSTI $3.00 cy, $0.50 mn.

Plasma was generated in a source using a hydrogen-loaded titanium washer with power supplied by a variable-length square-wave pulse line (15-635 μsec). The source was mounted on the axis at one of two coils forming a magnetic mirror geometry. Spectroscopic studies were made to: identify the types of ions present (H, Ti^{+}, Ti^{++}, Ti^{+++}, O^{+}, O^{++}, Al, Al^{+}, Al^{++}, Ta^{+}), measure ion velocities by Doppler shift (from 5×10^{5} to 2×10^{6} cm/sec), and record the variation of light intensity with time. Microwave cutoff measurements made simultaneously with various frequencies provided time history curves of the plasma densities, which exceeded 1 to 3×10^{14} electrons per cm^{3}. Parameters affected by the age of the hydrogen-loaded washer were examined. Studies of the electron density decay after the end of the pulse revealed that the decay time is determined by the rate of cross-field diffusion and is intermediate between the rates calculated simply for ion diffusion and those calculated for ambipolar diffusion. Microwave interferometer fringe shift measurements provided information on the plasma charge-density profile. Profile measurements were also made using a thermistor located close to the gun to measure the relative energy contributions of the intercepted neutral and charged particles. This allowed an evaluation of the percentage of neutrals present in the plasma column (≈10%). The floating double probe technique was used to measure electron temperatures and time of flight. Electron temperatures were found to decrease with time during the pulse the variation being from 15 to 1 ev and 3 to <1 ev for old and new source washers, respectively. Results of these various investigations are presented together with a discussion of the probable mechanisms involved. (auth)

45412 (UCRL-7978) A NULL METHOD OF MEASURING MICROWAVE PHASE SHIFTS. Gardner, Andrew L. (Lawrence Radiation Lab., Univ. of California, Livermore). Aug. 6, 1964. Contract W-7405-eng-48. 22p. Dep. mn; CFSTI $1.00 cy, $0.50 mn.

A companion paper by Gardner and Hawke described a microwave phase shifter, with constant output, capable of rapid phase control by the bias voltage applied to varactor diodes. The application of this device to measure phase shifts in a c-w microwave system by a null method is described. If phase and amplitude variations are not too fast, standard oscilloscope components can provide most of the required circuitry. Examples are given, including the measurement of 0.003° phase shift at 9 Gc in a plasma experiment. (auth)

45413 (UCRL-12456) EXPERIMENTAL STUDIES WITH THE ASTRON FACILITY. Briggs, R. J.; Christofilos, N.; Hester, R. E.; Lauer, E. J.; Weiss, P. B. (Lawrence Radiation Lab., Univ. of California, Livermore). July 19, 1965. Contract W-7405-eng-48. 20p. (CONF-650911-11). Dep. mn; CFSTI $1.00 cy, $0.50 mn.

From 2nd Conference on Plasma Physics and Controlled Nuclear Fusion Research, Abingdon, Berks, Eng.

In relation to the Astron facility, the trapping efficiency, lifetime of the E-layer, radial and axial density distribution, and measurements on the strong r-f fields generated during the injection phase are discussed. The overlapping of a sequence of electron pulses injected at intervals of 2.8 msec, which demonstrates the feasibility of a steady state E-layer, is discussed. (M.O.W.)

45414 (UCRL-12480) THEORY OF THE ELECTROSTATIC PROBE AND ITS IMPROVED USE AS A DIAGNOSTIC TOOL. Hall, Laurence S.; Freis, Robert P. (Lawrence Radiation Lab., Univ. of California, Livermore). July 29, 1965. Contract W-7405-eng-48. 14p. (CONF-650806-3). Dep. mn; CFSTI $1.00 cy, $0.50 mn.

From 7th International Conference on Phenomena in Ionized Gases, Belgrade.

The steady-state electrostatic probe problem is studied in a theoretical model similar to that of Bernstein and Rabinowitz, but differing in that the methods used are applicable to systems in which the undisturbed distributions of attracted and repelled particles at infinity are arbitrary. Computations are made in which these distributions are both Maxwellian (but at different temperatures). The results for cylindrical probes are presented in graphical form in a manner which permits the simple determination of unknown plasma parameters in terms of easily measured properties of empirical current-voltage characteristics. (auth)

45415 (UCRL-14137) LOW-TEMPERATURE PLASMA COLUMN CONFINEMENT BY MAGNETIC FIELDS WITH

SHEAR. Hartman, Charles W.; Munger, Richard H. (Lawrence Radiation Lab., Univ. of California, Livermore). July 29, 1965. Contract W-7405-eng-48. 15p. (CONF-650806-8). Dep. mn; CFSTI $1.00 cy, $0.50 mn.

From 7th International Conference on Phenomena in Ionized Gases, Belgrade.

The effect of magnetic shear on the stability of a low-temperature potassium-plasma column is investigated in a single-ended "Q"-type device. Shear is provided by a conducting rod placed along the axis of the column, which adds B_θ field to the uniform B_z confining field. With no shear, a spectrum of drift waves is observed with $k_\perp \approx m/R \gg k_z$, m = 1-10. Propagation is with the electron-diamagnetic drift. Under "weak" radial gradient conditions $a_i\nabla \ln N \lesssim 1$, stabilization against drift waves is obtained for $B_\theta/B_z \gtrsim 0.4$. With a strong density gradient $a_i\nabla \ln N \approx 1$, high m number modes were found to be preferentially damped by shear, while m ≈ 1, 2 modes remained unstable up to $B_\theta/B_z = 0.5$. (auth)

45416 (UCRL-16263) ELECTROLYTIC CAPACITOR BANKS. Hopkins, Donald B. (Lawrence Radiation Lab., Univ. of California, Berkeley). July 12, 1965. Contract W-7405-eng-48. 15p. (CONF-650815-1). Dep. mn; CFSTI $1.00 cy, $0.50 mn.

From Symposium on Engineering Problems of Controlled Thermonuclear Research, Livermore, Calif.

A series string of electrolytic capacitors was proven to be a reliable energy-storage unit. Electrolytic capacitor banks were providing magnetic field energy for Berkeley rotating plasma experiments in 1958. Considerations in the theory, design, and usage of low- and high-voltage banks are discussed. Basic electrolytic capacitor properties are reviewed, several particular banks are discussed, then possibilities for future development are examined. (auth)

45417 THERMODYNAMICS OF A MHD-PLASMA WITH INFINITE ELECTRICAL CONDUCTIVITY. Cap, F. (Univ. of Innsbruck). Acta Phys. Austriaca, 19: 333-8(1965).

If the thermodynamic properties are known, the methods of potential flow of compressible fluids can be used for describing the flow in an inviscid plasma with infinite electric conductivity and frozen-in magnetic fields. The so obtained solutions of flow problems represent asymptotic cases since real plasmas have high but not infinite conductivity. It is important to know these solutions because they make it possible to evaluate certain extremum values, and, with the help of perturbation theory, to proceed to the yet unknown solutions for plasmas of very high but not infinite electric conductivity. A fluid with peculiar thermodynamic properties is investigated. (J.F.P.)

45418 CONTRIBUTION TO THE INTERACTION BETWEEN A RADIATION FIELD AND A PLASMA. Mangeney, A. (Institut d'Astrophysique, Paris). Ann. Phys. (Paris)(13), 10: 191-229(Mar.-Apr. 1965). (In French).

The interaction between a radiation field and a plasma is theoretically studied by considering the system as composed of two coupled substances: the oscillation of the field and the charged particles. This system is represented by a statistical ensemble described in the phase space of the total system by a distribution density dependent on the microscopic state of the electromagnetic fields and of the charged particle fluid. As the evolution of this distribution density obeys a Liouville equation, the situation is identical to that existing in statistical hydrodynamics. The methods of statistical hydrodynamics are considered within the framework of the description of the interaction between a radiation field and a plasma. The effective application of this formalism is shown. At the lowest approximation the particles evolve independently of the electromagnetic field. The energy exchange between charged particles and radiation is considered. A general method for the calculation of the coefficients of emission and absorption that does not rest on any hypothesis of local thermodynamic equilibrium is established. The radiation of plasma during equilibrium can then be studied. This method is applied to problems of Thomson scattering and bremsstrahlung. (J.S.R.)

45419 NONLINEAR PLASMA WAVE INTERACTION IN AN ARC DISCHARGE. Kerzar, B.; Abrahamsen, K.; Weissglas, P. (Royal Inst. of Tech., Stockholm). Appl. Phys. Letters, 7: 155-6(Sept. 15, 1965).

The results of an experimental study of the modulation of plasma parameters at lower powers by the propagating wave are presented. The plasma used in the experiments is the positive column of a low-pressure mercury arc enclosed in a circular waveguide. The dispersion curve of the symmetric surface mode, and the dispersion curves of the first two symmetric temperature modes are shown. The three curves were all measured at a frequency of 1.2 Bc by varying the discharge current. The dispersion of the first two temperature modes at 2.4 Bc are also shown. At the intersection of two curves the nonlinearity of the interaction was established by exciting one mode at 1.2 Bc by an azimuthally symmetric coupling system outside the discharge tube. A probe was used to pick up waves propagating along the column at 1.2 and 2.4 Bc. To locate the intersection, the discharge current was swept from 0.1 to 1 amp. The probe signal is plotted versus the discharge current. A comparison with the other curves shows that one of the peaks is due to nonlinear coupling. (J.F.P.)

45420 NON-LINEAR CHARACTERISTICS IN HIGH-FREQUENCY GAS DISCHARGE. Ahlbom, S.; Neuhaus, H. (Universitaet, Stockholm). Arkiv Fysik, 29: 455-8(1965). (In German).

Based on experiments made by Swan and Kino and Krenz some further experiments concerning the nonlinear characteristics of a plasma were carried out. In a helium plasma at a pressure of about 2 mm Hg, excited by a microwave field of 2.4 GHz, harmonics of this frequency up to the eighth were detected without difficulty in our apparatus, which is described. A qualitative relation between gas pressure, consumed microwave power and efficiency of the harmonic generation was established. With a similar equipment, helium plasma was used as the nonlinear component in a mixer where one of the harmonics of the excitation frequency is mixed with a signal of about 1 GHz. A further development of these experiments was made by coupling a comparatively weak microwave signal to a plasma excited by another microwave source of high power. The signal is then observed to generate harmonics with an efficiency not correlated to the signal power. The presence of the subharmonic frequency could not be detected, however, although several experiments with helium, neon, and mercury were made. (auth)

45421 SCHLIEREN PHOTOGRAPHY OF THE FIRST HALF-CYCLE OF A THETA PINCH DISCHARGE. Rye, R. J.; Waller, J. W.; McKenzie, A. S. V.; Irving, J. (Univ. of Strathclyde, Glasgow). Brit. J. Appl. Phys., 16: 1404-6(Sept. 1965).

The plasma formed during the first half-cycle of a theta pinch was studied and the electron density measured using Schlieren methods. (auth)

45422 STRUCTURE AND THE STABILITY OF SHOCK WAVES IN ELECTROMAGNETIC MEDIA. Golden, Kenneth I. (Actuellement Williamson Development Co., Inc., West Concord, Mass.). Cahiers Phys., 18: 409-60(Nov-Dec. 1964). (In French).

The structures of stationary shock waves in electromagnetic media and the stability of their flow are studied. The macroscopic equations controlling the movement of a plasma were developed from successive moments of the Boltzmann equation. The structures of stationary shock waves in a two-fluid scheme are determined when the magnetic field is always parallel to the surface of the shock plane (parallel shock). The stability of all the couples of possible stationary states separated by hypothetical shock discontinuities are studied. Discontinuities parallel to the magnetic field in a two-fluid scheme are first considered and then the discontinuities that are always perpendicular to the magnetic field are treated for the case where the Hall effects are very important in fluid magnetodynamics. (J.S.R.)

45423 THE RELATION BETWEEN COLUMN STRATIFICATION AND NEGATIVE ION CONTENT IN AN IMPURE Ar DISCHARGE. Drost, H.; Klotz, H.-D.; Timm, U.; Pupke, H. (Forschungsgemeinschaft, Deutsche Akademie der Wissenschaften, Berlin; Institut fuer Biophysik, Berlin). Exptl. Tech. Physik, 13: 170-4(1965). (In German).

By using a sensitive ion detector, column negative ions can be extracted from a stratified Ar discharge. Their presence is conditioned by the impurities contained in the discharge tube (principally H_2O and O_2). Just as in a stratified O_2 discharge, the ion intensities measured along the column indicate an increased concentration of negative ions in the strata and a strict relation between ion current pattern and character of the column stratification. The necessity of the existence of negative ions for strata formation is discussed. (tr-auth)

45424 CROSS-POLARIZED ELECTROMAGNETIC BACKSCATTER FROM TURBULENT PLASMAS. Ruffine, R. S.; De Wolf, D. A. (RCA Labs., Princeton, N. J.). J. Geophys. Res., 70: 4313-21(Sept. 1, 1965).

The cross section for the backscattering of cross-polarized electromagnetic radiation by an underdense plasma is calculated by means of the second Born approximation. It is shown that when the dimensions of the scattering volume are much greater than the wavelength of the radiation and the correlation length of the plasma, the major contribution to the cross section arises from the asymptotic part of the four-point correlation function. The assumption that $kV^3 \gg 1$ also makes it possible to reduce the 6-dimensional integral to an integral over the direction of the intermediate scattering. This integral is carried out explicitly for some assumed correlation functions and some scattering volumes. (auth)

45425 LINEARIZED NON-EQUILIBRIUM FLOW OF A PARTIALLY IONIZED GAS WITH A RADIATIVE LOSS. Murasaki, Toshimitsu; Morioka, Shigeki (Osaka Univ.). J. Phys. Soc. Japan, 20: 1476-87(Aug. 1965).

Simply approximated expressions for collisional-radiative reaction rate and radiative loss in a partially ionized gas are discussed. The linearized equations describing non-equilibrium flow of an ionized gas with a radiative loss are derived for the two cases, in one of which radiative recombination and de-excitation probabilities are dominant and in the second collisional probabilities are dominant. As an illustration the axial velocity distribution in a two-dimensional supersonic jet is considered. The methods of analysis and the solutions are discussed for the two cases above and for the possible values of the parameters characterizing reaction rate and radiative loss. The profile in general consists of two parts: One is due to the pressure difference between a jet and its surrounding fluid and the other due to the radiative loss. The latter profile is characterized by a modified triangular wave starting immediately after the exit. (auth)

45426 SOME REMARKS ON THE COLLISIONLESS PLASMA FLOW. Tajiri, Masayoshi (Osaka Univ.). J. Phys. Soc. Japan, 20: 1497-1502(Aug. 1965).

The flow of a collisionless plasma with an aligned magnetic field is discussed on the basis of the Chew-Goldberger-Low approximation. It is shown that the fundamental equations can be reduced to the ordinary gasdynamic equations by making use of a suitable transformation. In the hodograph plane of the reduced variables, a family of exact solutions are obtained in a similar way to the case of ordinary gasdynamics. As examples, both the flow through a de Laval nozzle and the spiral flow are studied extensively. (auth)

45427 OSCILLATIONS IN A PLASMA IN A MAGNETIC FIELD. Kato, Kiyoe (Electrotechnical Lab., Tokyo); Kawasaki, Eiichi. J. Phys. Soc. Japan, 20: 1521(Aug. 1965).

An experiment was performed which is similar to previous experiments in which the electron oscillations of the hybrid mode, the cyclotron mode, and the plasma mode in a plasma were observed. Some new modes were found and the profile of interaction between modes was observed. (L.B.S.)

45428 HIGHER HARMONICS AND SUB-HARMONICS OF ELECTRON PLASMA OSCILLATIONS. Kawabe, Takaya (Tokyo Univ.); Kojima, Shoji; Takayama, Kazuo. J. Phys. Soc. Japan, 20: 1539-40(Aug. 1965).

Observations are reported of three higher harmonics and a subharmonic of the fundamental plasma frequency in a mercury-filled discharge tube. The discharge current was varied from 5 to 100 mA, and the oscillations were measured with three sets of field intensity meters over the frequency range between 375 and 2350 Mc/s. Fine structures were also observed in the fundamental plasma oscillation and its harmonics. Other phenomena were observed at high discharge currents which suggest the existence of some parametric mechanism in a plasma. (L.B.S.)

45429 EXTENSION OF RANGE OF ELECTRON DENSITY IN PLASMAS MEASURABLE BY MICROWAVES. Takeda, Susumu; Masumi, Motoshi (Nagoya Univ., Japan). Japan. J. Appl. Phys., 4: 471-2(June 1965).

The lowest electron density measurable by microwaves through plasma is limited by a phase angle detectable in the equipment used. This small phase difference can be expanded by an impedance transformation which is realized by using a dielectric plate of a quarter wave length put before a collisionless plasma. In contrast to the cavity method which is sensitive only in the low electron density region, this method has an advantage of a broad range of measurable electron density. The electron density decay of an afterglow plasma in argon is shown, in which the electron density is calculated by the method given. (J.F.P.)

45430 ACCELERATION OF PULSATING PLASMA CLOT. Kolesnikov, P. M. Magnitn. Gidrodin., No. 1, 73-9(1965). (In Russian).

The acceleration of pulsating plasma clot in a high current impulse accelerator is considered. The pulses of the plasma clot are caused by the magnetic forces of interior currents and the gas-kinetic forces in the clot. These pulses are decreasing and they can disappear altogether with increasing gas-kinetic pressure. In this case, only an increase of the clot width occurs. Strong pulses caused by rapid variation of inductance may result in excess voltages in the system which causes instability of pinch type. The movement of the mass center of the clot caused by the magnetic forces was examined. (auth)

45431 PARAMETERS OF PLASMA BUNCHES OF A COAXIAL INJECTOR. Kruglyakov, E. P.; Malinovskii, V. K.; Nesterikhin, Yu. E. Magnitn. Gidrodin., No. 1, 80-6(1965). (In Russian).

A coaxial plasma accelerator is considered. The parameters of plasmoids: the velocity of the front, the distribution of density as a function of time, temperature, are presented for different regimes of acceleration. It is shown that the plasmoid is preceded by moving neutral gas but the tail part of the plasma is of a thermal character. The results are discussed. (auth)

45432 ON WAVE TRANSFORMATION IN MAGNETO-HYDRODYNAMICS. Moiseev, S. S.; Smilyanski, V. R. Magnitn. Gidrodin., No. 2, 23-30(1965). (In Russian).

The problem of the transformation of waves in ideal magnetohydrodynamics is investigated and various ways to solve the problem are discussed. Plasma has been treated in a magnetohydrodynamic approximation. (auth)

45433 ON THE POSSIBILITY OF TEMPERATURE AND DENSITY DETERMINATION OF NON-STATIONARY PLASMA BY MEANS OF OPTICAL INTERFEROMETRY. Kruglyakov, E. P.; Malinovskii, V. K.; Nesterikhin, Yu. E. Magnitn. Gidrodin., No. 2, 31-4(1965). (In Russian).

An application of Michelson interferometer for the nonstationary plasma diagnostics is reported. Data for determining the electron density, the degree of ionization and the temperature of plasma are presented. (auth)

45434 ON SOME PECULIARITIES OF THE BEHAVIOR OF PLASMA HEATED BY COLLISIONLESS SHOCK WAVES. Iskoldskii, A. M.; Kurtmullaev, R. Kh.; Luk'yanov, V. N.; Nesterikhin, Yu. E.; Ponomarenko, A. G. Magnitn. Gidrodin., No. 2, 35-43(1965). (In Russian).

Preliminary results of investigations concerning the process of excitation of collisionless plasma shock waves are reported. Data about the numerous effects in plasma placed in a magnetic field are obtained by means of optical magnetic measurements. It is shown, that the captured magnetic field can exist much longer than the duration of current in the shock circuit. It is believed that this can be explained by the formation of a cylindrical plasma layer. (auth)

45435 INVESTIGATION OF RELSOTRON ACCELERATION OF PLASMA IN PRESENCE OF THE TRANSVERSE MAGNETIC FIELD. Fedorov, V. M. Magnitn. Gidrodin., No. 2, 44-54(1965). (In Russian).

The acceleration of plasma in a relsotron with the flat electrodes in the presence of transverse magnetic field is treated. Image convertors were used for observation of plasma. Speed obtained by image convertors was compared with the one calculated from the voltage measurements at the end of the rails. Data obtained by using the above mentioned methods are discussed. (auth)

45436 INCOHERENT MICROWAVE SCATTERING FROM RESONANT PLASMA OSCILLATIONS. Stern, R. A.; Tzoar, N. (Bell Telephone Labs., Inc., Whippany, N. J.). Phys. Rev. Letters, 15: 485-8(Sept. 13, 1965).

Microwave scattering was observed at the plasma line from controlled electron-plasma oscillations generated in a laboratory plasma. In the experiment, the scattering cross section is greatly enhanced by exciting in the plasma large-amplitude oscillation modes, using the Tonks-Dattner resonances, previously reported. These are radial electron-plasma oscillation modes strongly coupled to transverse electromagnetic waves. By this means the scattering at the plasma line becomes easily detectable. It is found that the plasma is driven strongly out of equilibrium by a relatively low-frequency resonance signal, which generates an electron-density wave whose amplitude is proportional to the strength of the resonance signal. By this means, the amplitude of the fluctuation spectrum can be made as large as required simply by increasing the resonance power level. Because plasma resonance provides effective coupling between transverse and longitudinal waves, resonance field strengths of 0.1 v/cm suffice to bring the scattering cross section up to levels at which the scattering is easily detectable. (J.F.P.)

45437 INDUCTION-FIELD CALCULATIONS AND THEIR APPLICATION TO MEASUREMENTS OF CONDUCTIVITY DISTRIBUTIONS IN CYLINDRICAL PLASMAS. Stokes, A. D. (Univ. of Sydney). Proc. Inst. Elec. Engrs., (London), 112: 1583-8(Aug. 1965).

The problem of determining conductivity distributions from measurements on magnetic loops (induction coils) is examined. Maxwell's equations are written for a cylindrically symmetric system allowing for radial variations in conductivity, and solved numerically for specific types of distribution similar to those found in plasma experiments. Methods are described by which the field impedance (E/H) at the boundary of the medium can be found and used to characterize the distribution. (auth)

45438 THE FLUTE INSTABILITY OF A PLASMA CONFINED IN AN AXI-SYMMETRIC WAVE FORM MAGNETO-STATIC FIELD. Matsuda, Kyoko; Kihara, Taro (Inst. of Physical and Chemical Research, Tokyo). Rika Gaku Kenkyusho Hokoku, 37: 79-82(1961). (In Japanese).

The flute instability is investigated of a plasma confined in a magneto-static field of axi-symmetric wave form. Numerical calculations were made for various conditions to verify the formula obtained by Rosenbluth and Longmire, and it was shown that the plasma is unstable under these conditions. (BBB)

45439 QUASILINEAR THEORY OF A WEAKLY TURBULENT PLASMA WITH ACCOUNT OF CORRELATION OF ELECTRIC FIELDS. Bass, F. G.; Fainberg, Ya. B.; Shapiro, V. D. Zh. Eksperim. i Teor. Fiz., 49: 329-34 (July 1965). (In Russian).

Equations of quasilinear theory are derived by taking into account the finite time of electric and magnetic microfield correlation in the plasma. Cases of electrostatic oscillations and an electromagnetic wave moving along an external magnetic field are considered. Heating of the plasma by an external random field is investigated with aid of obtained equations. (auth)

45440 SINGULAR EIGENFUNCTIONS AND PLASMA PROBLEMS. Case, K. M. (Univ. of Michigan, Ann Arbor). 34p. (CONF-650440-1). Gmelin, AED-CONF-65-095-1.

From American Mathematical Society, 622nd Meeting, New York.

It is shown that many initial value and boundary value plasma problems can be solved by the analog of a normal mode expansion technique. General properties of solutions of equations involving operators are proved. (L.B.S.)

45441 QUASI-STEADY-STATE PULSED PLASMA THRUSTORS. Ashby, D. E. T. F.; Gooding, T. J.; Larson, A. V. (General Dynamics/Convair, San Diego, Calif.). New York, American Inst. of Aeronautics and Astronautics, 1965, Preprint No. 65-338, 8p., $1.00. (CONF-650711-35). ORINS.

From AIAA 2nd Annual Meeting and Technical Demonstration, San Francisco.

It is proposed that in d-c plasma thrustors which accelerate plasma by the interaction of the discharge current and its magnetic field, the input power is proportional to the cube of the exhaust velocity. For velocities of 10^4 to 10^5 m/sec powers of the order of 10^2 to 10^4 kw are indicated. The mean power level can be reduced and the thrustor can be operated into a hard vacuum (10^{-6} torr) without a gigantic pumping system if the discharge current and propellant are pulsed. Experiments with a pulsed arc thrustor are described. The thrustor is powered by a lumped parameter pulse-line of several hundred microseconds period; hydrogen, nitrogen, and argon propellants have been used. The arc characteristics are similar to the d-c magnetoplasmadynamic arcs. Exhaust velocities between 1 and 5×10^4 m/sec and thermal efficiencies between 15% and 25% are typical. Experimental difficulties arising from currents external to the thrustor and from propellant adsorbed on the electrodes are discussed. The addition of an external magnetic field improves the symmetry of the discharge, reduces localized anode erosion, increases the arc impedance of a factor of two, but does not alter the thermal efficiency significantly. The azimuthal Hall currents constitute only 5% of the total current. (auth)

45442 LINEAR PINCH DRIVEN BY A HIGH-CURRENT PULSE-FORMING NETWORK. Black, Neville A. (Princeton Univ., N. J.). New York, American Inst. of Aeronautics and Astronautics, 1965, Preprint No. 65-336, 7p., $1.00. (CONF-650711-37). ORINS.

From AIAA 2nd Annual Meeting and Technical Demonstration, San Francisco.

Most pulsed plasma experiments have been performed using a parallel-connected capacitor bank which delivers a damped sine-wave current to the discharge, producing secondary "self-crowbarring" breakdowns shortly after the first quarter cycle of current. These secondary breakdowns complicate the interpretation of various diagnostic observations and invalidate simple theoretical models. Rectangular current pulses can be produced by low impedance pulse-forming networks consisting of lumped capacitances connected across the distributed inductance associated with two parallel conducting plates. For example, using 60 microfarads total capacitance at 10 kv, a flat-topped pulse of 250,000 amperes and 5 microseconds duration rising in about 0.6 microseconds is readily achieved. When this pulse is applied to a large-radius linear pinch discharge, a single current sheet is driven completely to its center without secondary breakdown.

Pinch behavior under sinusoidal and rectangular pulse operation is studied by means of streak photographs and magnetic probe records for discharges in argon in the 100 micron regime. These observations are correlated with Rosenbluth's snowplow model. The pulse-driven current sheets are of greater amplitude, decay more slowly, and achieve terminal velocities four times greater than the sine wave cases. (auth)

45443 EXPERIMENTS IN A HOLLOW CATHODE HALL CURRENT ACCELERATOR. Weinstein, Richard H.; Hoell, James M. (Langley Research Center, Hampton, Va.). New York, American Inst. of Aeronautics and Astronautics, 1965, Preprint No. 65-299, 8p., $1.00. (CONF-650711-40). ORINS.

From AIAA 2nd Annual Meeting and Technical Demonstration, San Francisco.

Experiments were performed in a coaxial Hall current plasma accelerator utilizing a hollow tungsten cathode and a concentric carbon ring anode to produce an argon arc discharge in a diverging magnetic field. Argon is injected through each electrode separately to assess the effect of the mode of gas injection on accelerator operation. The thrust produced by the accelerator is measured with an external balance, and electrostatic probes are used to measure potential profiles, temperatures, and densities in the jet. The discharge power is up to 15 kw, with argon mass flows from 0.0009 to 0.016 gram per second and magnetic fields from 0.035 to 0.10 weber/meter^2. The rate of gas injection through the anode is shown to critically effect the entire accelerator behavior and when this rate becomes too low, electrode erosion gives spurious, high thrust results. (auth)

45444 PRELIMINARY DESIGN CONSIDERATIONS OF A HIGH PERFORMANCE HALL-CURRENT ACCELERATOR. Pinsley, Edward A. (United Aircraft Corp., East Hartford, Conn.). New York, American Inst. of Aeronautics and Astronautics, 1965, Preprint No. 65-300, 16p., $1.00. (CONF-650711-41). ORINS.

From AIAA 2nd Annual Meeting and Technical Demonstration, San Francisco.

Recent experiments with a low density annular accelerator have shown that the Hall-current acceleration process involving a radial magnetic field and an axial electric field can be employed with cesium as a propellant to produce moderate thrust densities, high efficiencies, and values of specific impulse in the 1500–5000 sec regime. The relatively simple geometry of this accelerator, and the low density feature which decouples gross ion and electron motions, permits extrapolation of the results of the model experiments to performance regimes required by large prototype configurations. It is shown that the reduction in over-all thrustor efficiency due to ion swirl and to the leakage of electrons across the magnetic field can be minimized by the proper selection of the ratio of ion cyclotron radius to accelerator length. Constraints on thrustor design imposed by fluctuations due to the onset of a two-stream instability and by magnet and cathode requirements are discussed. Design parameters for a large, prototype, cesium Hall-current thrustor are presented. (auth)

45445 INVESTIGATION OF CURRENT SHEET MICROSTRUCTURE. Lovberg, R. H. (Univ. of California, San Diego, La Jolla). New York, American Inst. of Aeronautics and Astronautics, 1965, Preprint No. 65-335, 16p., $1.00. (CONF-650711-38). ORINS.

From AIAA 2nd Annual Meeting and Technical Demonstration, San Francisco.

Experiments were performed using a theta pinch device to investigate electron-ion current partitioning in hydrogen, which influences the viscous drag which occurs when ions, which have been given propulsive momentum parallel to the electrode surfaces, are also required to carry current to the cathode in the event of inadequate electron emission. Studies of nitrogen current sheets were also carried out. The results are discussed. (L.B.S.)

45446 DIAGNOSTIC STUDIES IN A HALL ACCELERATOR AT LOW EXHAUST PRESSURE. Brockman, P.; Hess, R.; Bowen, F.; Jarrett, O. (Langley Research Center, Hampton, Va.). New York, American Inst. of Aeronautics and Astronautics, 1965, Preprint No. 65-297, 12p., $1.00. (CONF-650711-43). ORINS.

From AIAA 2nd Annual Meeting and Technical Demonstration, San Francisco.

The influence of mass entrainment from the vacuum tank or of mass eroded from the electrodes on the velocity determination from thrust and mass flow in coaxial Hall current accelerators is evaluated. Changes in potential distribution and Hall currents in the plasma exhaust stream where some part of the acceleration may take place are also studied. Double probe velocity measurements were performed; electron temperatures, ion currents, and ion densities were also determined. The velocities show good agreement with those obtained from thrust measurements. (L.B.S.)

45447 COMPRESSIBILITY AND NON-EQUILIBRIUM EFFECTS ON THE RESPONSE OF A LANGMUIR PROBE IN A FLOWING PLASMA. Lam, S. H. (Princeton Univ., N. J.). New York, American Inst. of Aeronautics and Astronautics, 1965, Preprint No. 65-543, 9p., $1.00. (CONF-650711-25). ORINS.

From AIAA 2nd Annual Meeting and Technical Demonstration, San Francisco.

The general theory for a continuum Langmuir probe in a flowing, weakly ionized plasma is treated following the analytical developments of Lam, and is extended to include compressibility and non-equilibrium effects. (L.B.S.)

45448 ELECTRON DENSITY AND TEMPERATURE MEASUREMENTS IN THE EXHAUST OF A MPD SOURCE. Kelly, A. J.; Nerheim, N. M.; Gardner, J. A. (California Inst. of Tech., Pasadena). New York, American Inst. of Aeronautics and Astronautics, 1965, Preprint No. 65-298, 12p., $1.00. (CONF-650711-42). ORINS.

From AIAA 2nd Annual Meeting and Technical Demonstration, San Francisco.

Electron density and temperature profiles were measured in the exhaust of a magnetoplasmadynamic (MPD) source, operated in a vacuum facility which provides background pressures of from ~100 to ~1,000 μ. Electron density profile measurements, made at several stations downstream of the source by using a Langmuir probe (flashed prior to each measurement) and a 24-Gc/sec microwave swinging arm probe, show agreement to within a factor of two over their common range of measurement (2×10^{12}cm$^{-3} \rightarrow 7 \times 10^{12}$cm^{-3}). Spectroscopic measurements, utilizing relative ion line intensities at the exit plane of the source, yield electron temperatures in the range 16,000 to 20,000°K for argon mass flows of 0.2 to 0.5 g/sec and currents of 750 to 2,000 amp. Electron temperature profiles, measured 56 cm downstream of the source, have maximums of 6,000 to 7,000°K which are consistent with collision frequency data obtained with the microwave probe at this station. It is concluded that the plasma generated by the MPD source is in a highly non-equilibrium state. The degree of ionization at the exit of the source is lower than the equilibrium value based on the measured electron temperature. In the fully developed plume, electron temperature and density measurements show that the degree of ionization is higher than equilibrium. (auth)

45449 NEUTRAL MASS DENSITY MEASUREMENTS IN A REPETITIVELY PULSED COAXIAL PLASMA ACCELERATOR. Karras, T.; Gorowitz, B.; Gloersen, P. (General Electric Co., Philadelphia). New York, American Inst. of Aeronautics and Astronautics, 1965, Preprint No. 65-341, 18p., $1.00. (CONF-650711-48). ORINS.

From AIAA 2nd Annual Meeting and Technical Demonstration, San Francisco.

A pulsed coaxial accelerator is discussed which uses an axial feed engine. The design of the two stage Med A-7D engine is shown. Early gas density measurements were performed using a modified 6AH6 vacuum tube as an ionization gage in order to determine the amount of mass in the A4-T gun at the time of discharge; the results are summarized. Measurements on high conduc-

ance feed nozzles, A7-D and A9-D which showed improvement in mass utilization, are discussed. (L.B.S.)

45450 COLLISIONAL-DISSOCIATIVE RECOMBINATION OF ELECTRONS WITH MOLECULAR IONS. Collins, C. B. (Southwest Center for Advanced Studies, Dallas). 42p. (CONF-650220-1). Gmelin, AED-CONF-65-022-4.

From American Physical Society, Southwest Meeting, Norman, Okla.

The recombination rate of electrons in a hypothetical plasma containing ions of a molecule having both repulsive and bound neutral states is calculated for electron densities between 10^{10} and $10^{14}/cm^3$ and temperatures ranging from 250 to 2000°K. It is found that if the molecule has a dissociative state located sufficiently close in energy to the molecular ion, values are obtained considerably in excess of the collisional-radiative recombination rate for systems possessing only bound states. (auth)

45451 THE EFFECT OF A NEUTRAL PLASMA ON ION TRAJECTORIES. Seitz, W.; Eilenberg, S. (Electro-Optical Systems, Inc., Pasadena, Calif.). New York, American Inst. of Aeronautics and Astronautics, 1965, Preprint No. 65-381, 29p., $1.00. (CONF-650711-12). ORINS.

From AIAA 2nd Annual Meeting and Technical Demonstration, San Francisco.

Experimental results indicate that, under certain conditions, the ion beam in an ion engine undergoes severe deflection in the region where neutralization of the beam is supposed to occur. It is believed that this effect is in some manner related to the existence of a neutral plasma surface. The results of a quantitative attempt to examine this effect in terms of one- and three-dimensional models are presented. The plasma is simulated by assigning appropriate boundary conditions at the plasma surface. It is required that the sheath be an equipotential and that the gradient of the potential, ∇V, be zero at the plasma boundary, i.e., the Cauchy conditions are specified. The shape of the plasma is not known a priori, but rather must be determined by finding a boundary for which these conditions are satisfied. The numerical technique consists of specifying the electric field on a trial boundary, then examining the resulting potential distribution for a unipotential surface on this boundary. A sequence of numerical solutions is found in which the trial boundary is perturbed for each iterate until the Cauchy conditions are satisfied. (auth)

45452 THEORY OF ELECTROSTATIC DOUBLE PROBE COMPRISED OF TWO PARALLEL PLATES. Chung, Paul M.; Blankenship, Victor D. (Aerospace Corp., San Bernardino, Calif.). New York, American Inst. of Aeronautics and Astronautics, 1965, Preprint No. 65-542, 20p., $1.00. (CONF-650711-24). ORINS.

From AIAA 2nd Annual Meeting and Technical Demonstration, San Francisco.

The difficulties with continuum single probes in plasma diagnostics may arise from the uncertainties surrounding the other electrode (ground), which usually does not assume the plasma potential at the point of interest, and from the fact that the probe disturbs the plasma to a much greater extent than that predicted by classical theories. In order to circumvent these difficulties, the double-probes comprised of two parallel plates are analyzed. Because of the simple geometry, the complete flow region between the two electrodes, comprised of two boundary layers and an inviscid layer, can be analyzed in detail. The governing equations for the electrical and flow properties of the continuum, weakly ionized plasma are solved. The cases of electron temperature in frozen state, with respect to the neutral gas temperature, and in equilibrium are considered. From the solution, simple equations are derived which can be used to translate the potential-current characteristics of the probe into the electron temperature and number density of the free stream plasma. The analysis also shows the detailed mechanism by which electricity is conducted between two plates across a flowing plasma. (auth)

45453 CONTINUUM RADIATION FROM PARTIALLY IONIZED ARGON. Barzelay, Martin E. (Syracuse Univ., N. Y.). New York, American Inst. of Aeronautics and Astronautics, 1965, Preprint No. 65-546, 20p., $1.00. (CONF-650711-27). ORINS.

From AIAA 2nd Annual Meeting and Technical Demonstration, San Francisco.

Experimental measurements of the total thermal radiation from an argon plasma arc of the wall-stabilized type with Poiseuille flow are compared with theoretical predictions. The magnitude of radiation is of importance both for reentry calculations and for use in the Heller-Elenbas energy balance equation when transport properties are to be determined. The experimentally measured radiation (utilizing a carefully-calibrated novel radiation meter) was compared with predictions from semi-classical quantum theory (cum experimental constants) based on recombination and bremsstrahlung. A simple equation for the total radiated power (in watts/cc) as a function of temperature was developed and corroborated by experiment. In making the comparisons spectrographically determined temperature distributions from a similar arc in the same laboratory were utilized. The plasma arc was operated at one atmosphere over a range of argon flow rates from 0.02 to 0.415 grams/sec and currents from 35 to 500 amperes for three different column lengths. Steady state total radiation as high as 5500 watts/cm of column length, representing over 30 percent of the power input to the arc, was measured. (auth)

45454 COMPUTER STUDIES OF PLASMA BOUNDARIES AND LENS EFFECTS CREATED BY IMMERSED AND WITHDRAWN NEUTRALIZERS. Brauch, D. F.; Buneman, O.; Wadhwa, R. P. (Litton Industries, Inc., San Carlos, Calif.). New York, American Inst. of Aeronautics and Astronautics, 1965, Preprint No. 65-380, 12p., $1.00. (CONF-650711-13). ORINS.

From AIAA 2nd Annual Meeting and Technical Demonstration, San Francisco.

The results of a computer study using two extremes of neutral configurations for a given ion gun are presented, which yield information on the plasma sheath formed by the neutralizer and on the lens effect due to the sheath. It is found that the dominant effect of the neutralized geometry seems to pull the equipotentials straight across the beam and thus to create less lens effect than takes place in the absence of plasma. The withdrawn neutralizer configuration does not seem substantially worse than the immersed neutralizer configuration, which introduces a slight lens effect, creating cross-overs. (L.B.S.)

45455 METHOD FOR THE GENERATION AND CONTAINMENT OF A HIGH-ENERGY PLASMA. Koller, Alois; Michel, Alfred (to Siemens-Schuckertwerke Aktiengesellschaft). German Patent 1,196,801. July 15, 1965. Filed June 14, 1963.

A method for the generation and containment of a high-energy plasma by means of alternating z- and Θ-pinches in a cylindrical or toroidal discharge vessel is characterized in that two succeeding z- and Θ-pinch phases are separated by an inertia phase which is free from magnetic fields. (Gmelin Inst.)

45456 METHOD AND APPARATUS FOR PRODUCING A PLASMA. Carter, Arlen F. (to National Aeronautics and Space Administration). U. S. Patent 3,201,635. Aug. 17, 1965. Filed Mar. 7, 1962.

An apparatus is patented for producing a highly conductive plasma having an electron concentration on the order of 10^{16} electrons/cc and homogeneous temperature and pressure distribution. An electrical arc is struck and maintained between two electrodes. A fluid, such as compressed gas, is fed through the arc and heated to form a high temperature gaseous jet, which passes into a settling chamber adjacent the electrodes. There the jet is seeded with an ionizing agent, preferably an alkali metal. (A.G.W.)

Shielding

Refer also to abstract 45575.

45457 (AD-462614) THE VARIATION OF DOSE ATTENUATION OF TWO-LEGGED CONCRETE DUCTS WITH INCIDENT GAMMA-RAY ENERGY. Chapman, J. M. (Naval Civil Engineering Lab., Port Hueneme, Calif.). Apr. 16, 1965. 12p. (N-707). CFSTI.

Gamma dose attenuation factors were measured in a 3-foot square and an 11-inch square duct using ^{198}Au (.412 Mev), ^{137}Cs (.662 Mev), and ^{60}Co (1.25 Mev) gamma sources. Attenuation factors for given geometries were compared as a function of the incident gamma energy. It was found that the attenuation factor decreases monotonically with increasing energy. Measured attenuation factors were compared with values obtained using a computer code based on the albedo concept. It was found that calculated attenuation factors are high by as much as 78% for ^{198}Au in the 11-inch duct. (auth)

45458 (AE-190) ON THE USE OF IMPORTANCE SAMPLING IN PARTICLE TRANSPORT PROBLEMS. Eriksson, Bo (Aktiebolaget Atomenergi, Stockholm (Sweden)). June 1965. 28p. Dep. mn.

The idea of importance sampling is applied to the problem of solving integral equations of Fredholm's type. Especially Bolzmann's neutron transport equation is taken into consideration. For the solution of the latter equation, an importance sampling technique is derived from some simple transformations at the original transport equation into a similar equation. Examples of transformations are given, which were used with great success in practice. (auth)

45459 (EUR-2488.e) A NUMERICAL SOLUTION OF THE GAMMA TRANSPORT EQUATION APPLIED TO CONCRETE SLABS. Penkuhn, H. (European Atomic Energy Community, Ispra (Italy). Joint Nuclear Research Center). Aug. 1965. 18p. Dep. mn.

The gamma transport equation is solved numerically in plane multislab geometry. A monoenergetic source is assumed on one surface, with isotropic or collimated angular distribution. After computing the unscattered flux, the fluxes at lower energies are calculated using those at higher energies without iteration. Integration of the differential fluxes gives the energy spectra and buildup factors. Source energies $\geq$ 10 Mev and thicknesses of some dozen mfp can be handled with the present program BIGGI 3. As application, buildup factors for normal and heavy concretes are calculated and compared with those of Al, A, and Fe. The so-called Z_{eff} results for heavy concretes to be a function of the source energy. (auth)

45460 (LA-3377) THE NON-EQUILIBRIUM DIFFUSION EQUATION. Freeman, B. E. (Los Alamos Scientific Lab., Univ. of California, N. Mex.). Sept. 1, 1965. Contract W-7405-eng-36. 18p. Dep. mn; CFSTI $1.00 cy, $0.50 mn.

The system of equations describing the diffusion of radiation through material is discussed from the point of view of the formulation for numerical solution. These equations, which are more general than the equilibrium diffusion equation, contain terms describing (a) cooling of material by radiation in optically thin systems, (b) diffusion of radiation through material with or without energy exchange with the material, and (c) an approximation to the free streaming of radiation. Consequently, they are applicable to a much wider range of radiation transport phenomena than the equilibrium diffusion equation. The several regions of applicability are examined from the point of view of the structure of the equations and the frequency dependence. Finally, the general non-equilibrium diffusion equations are discussed regarding appropriate mean absorption coefficients for frequency groups. Spatial and time dependences of the difference equations are also considered. (auth)

45461 (N64-25922) THEORETICAL ASPECTS OF NEUTRON ACTIVATION OF STRUCTURES. Favale, A. J.; D'Agostino, M. D.; Rossi, M. L. (Grumman Aircraft Engineering Corp., Bethpage, N. Y. Research Dept.). Feb. 1964. 43p. (RM-227).

The major theoretical aspects that must be considered before the neutron activation properties of structures (nuclear reactors for space flight) can be determined are discussed. Factors considered are the irradiation schedule of the reactor, the derivation of neutron activity due to cyclic and noncyclic irradiation, the geometry of the facility housing the reactor, and chain disintegrations. Also recommended procedures for neutron cross-section calculations, in the energy regions E < 0.0 Mev and E > 0.1 Mev, are described. (auth)

45462 (NP-15163) A MONTE CARLO PROCEDURE FOR CALCULATING THE MIGRATION OF PROTONS TAKING ACCOUNT ONLY OF ELECTROMAGNETIC INTERACTIONS. Johansson, C.; Leimdoerfer, M. (Forsvarets Forskiningsanstalt, Stockholm (Sweden)). Jan. 1965. 18p. Dep. mn.

A method is described for investigating the penetration and slowing-down of protons due to proton-atom interactions of non-nuclear type. A "continuous slowing-down" model was applied which moves the protons down in energy between a set of predefined energy points. A sample result shows the expected energy distribution of 187 Mev protons after penetrating aluminum slabs of various thicknesses. (auth)

45463 (NP-15425) COMPUTATIONAL METHODS FOR SPACE RADIATION SHIELDING ANALYSIS. Douglas Paper No. 3525. Billings, M. P.; Langley, R. W. (Douglas Aircraft Co., Inc., Santa Monica, Calif. Missile and Space Systems Div.). May 1965. 43p.

Analytical methods and computer programs were developed at Douglas for use in establishing the radiation shielding requirements of space vehicle systems. Current techniques for performing space radiation shielding analyses are reviewed in the context of the digital computer programs in which they were incorporated. Calculations dealing with the transport of primary charged particles and secondary reaction products through matter are performed by the CHARGE program for geometrically simple systems. The calculation of radiation levels in geometrically complex vehicle-shield configurations is accomplished by the SIGMA program, using the QUAD generalized quadratic surface geometry package. Procedures for ascertaining the optimal distribution of shield mass subject to specific dose design criteria are presently under development. (auth)

45464 (ORNL-TM-1167) CALCULATIONS OF CONCRETE SHIELDS FOR FISSION SOURCES. Nichols, J. P. (Oak Ridge National Lab., Tenn.). June 17, 1965. Contract W-7405-eng-26. 21p. Dep. mn; CFSTI $1.00 cy, $0.50 mn.

The spatial dose rates from point isotropic fission sources in normal concrete and seven concretes with high iron-ore content were calculated using four IBM-7090 codes for fast neutrons, low-energy neutrons, primary gamma rays, and secondary gamma rays, respectively. The effect of the source neutron spectrum on the fast-neutron dose rate in water and in hydrous iron-ore concrete was studied. (D.C.W.)

45465 NEUTRON DISTRIBUTION IN STRAIGHT CYLINDRICAL CHANNEL. Kramer-Ageev, E. A.; Markov, V. N.; Mashkovich, V. P.; Saharov, V. K.; Saharov, V. M. At. Energ. (USSR), 19: 46-8(July 1965).

Energy and spatial distributions of neutrons in a straight cylindrical channel passing through water shielding were studied, using a Po-Be source. Results are given of fast-neutron spectra for disk isotropic sources and for fast- and intermediate-neutron fluxes as functions of distance along the channel from the source and distance from the center axis of the channel. (M.J.T.)

45466 PENETRATION OF GAMMA QUANTA THROUGH SHIELDING BARRIER. Ermakov, S. M.; Petrov, E. E. At. Energ. (USSR), 19: 71-3(July 1965).

The effect associated with the passage of gamma quanta through a flat shielding barrier consisting of a primary layer of water and a secondary layer of lead is described. The effect involves the possible increase of intensity of transmitted gamma radiation incident at large angles to the normal with increasing thickness of the water layer. Monte-Carlo calculations were carried out using a statistical model. Results for 8-Mev gamma quanta incident at 85° for water-layer thicknesses from 0 to 20 cm are given for the variation of transmission probability as a function of water-layer thickness for lead layers of 3 to 30 mm, the variation of the transmission, reflection, and absorption probabilities as a function of water-layer thickness, and the changes of the spectral shape of the transmitted and reflected radiation and of the shape of the angular distribution of the transmitted radiation as functions of the thickness of the water layer. (M.J.T.)

45467 CALORIMETRIC DETERMINATION OF ABSORBED DOSE OF IONIZING RADIATION OF A REACTOR BY THE METHOD OF COMPENSATION OF HEAT PRODUCTION IN THE SAMPLE. Karasev, V. S.; Kolyada, V. M. At. Energ. (USSR), 19: 74-5(July 1965).

A method is described, allowing high rates of absorbed dose to be measured with great accuracy without requiring calculations using the thermal-physical constants of the materials. A method of electric compensation of heat production in the investigated sample was used in the isothermal calorimeter. The calorimeter performance was investigated, and an error of measurement of absorbed energy of 3 to 5% was found. Results of measurements of the absorbed dose rates in tin, lead, and steel samples are given. (M.J.T.)

45468 HEAVY AND SPECIAL CONCRETES IN NUCLEAR INDUSTRY. Launay, Pierre. Bull. Inform. A.T.E.N. (Assoc. Tech. Energie Nucl.), No. 53, 44-52(May-June 1965). (In French).

The mechanism and the biological effects of radiation are briefly reviewed as an introduction to a description of the principal characteristics of heavy concretes and of some special concretes. The characteristics and the construction methods for baryte concretes, baryte concretes with scrap metal incorporation, baryte concrete with pig iron tailings, and iron-ore based concretes are discussed. The properties of concretes containing B ores or serpentine and magnetite are briefly indicated. (J.S.R.)

45469 REACTOR SHIELDING CALCULATIONS BY THE MONTE CARLO METHOD. Jordan, T. M. (Douglas Aircraft Co., Inc., Santa Monica, Calif.). 29p. (CONF-650501-15). ORINS.

From The Application of Computing Methods to Reactor Problems, Argonne, Ill.

Monte Carlo techniques are outlined for the numerical solution of the energy-dependent Boltzmann equation for neutrons or gamma rays, which significantly reduce the computer time required for Monte Carlo shielding calculations. This reduction is a maximum for calculations involving multi-energy source and/or interaction spectra and complicated source, shield, and system geometries. The Monte Carlo techniques include the use of energy independent biasing functions, energy-dependent samples which span the entire energy range of interest, and analytic integrations of the energy dependence of the differential angular-energy interaction cross sections. Typical numerical results obtained from the Monte Carlo computer program SOBER are presented to demonstrate the accuracy, flexibility, and computational speed achieved through the use of these techniques. (auth)

45470 THE ERD CONCEPT IN SPACE RADIATION SHIELDING. Haffner, J. W. (North American Aviation, Inc., Downey, Calif.). New York, American Inst. of Aeronautics and Astronautics, 1965, Preprint No. 65-497, 18p., $1.00. (CONF-650711-19). ORINS.

From AIAA 2nd Annual Meeting and Technical Demonstration, San Francisco.

A study was made to determine the effects of the use of the ERD (effective residual dose) concept on space shielding thicknesses. The ERD equation was applied for two classes of missions—deep space missions and earth orbital missions. Point doses were calculated in order to avoid the problem of nonuniform irradiation of the body. The extension of these point doses to skin and blood forming doses is discussed. (L.B.S.)

Solid State Physics

See also CHEMISTRY — Inorganic and Physical Chemistry
METALS, CERAMICS, AND OTHER MATERIALS — Properties and Structure

Refer also to abstracts 44954 and 45383.

45471 (AECL-2309) THE ROLE OF DIFFUSION MEASUREMENTS IN THE STUDY OF CRYSTAL LATTICE DEFECTS. Kidson, G. V. (Atomic Energy of Canada Ltd., Chalk River (Ontario)). July 1965. 23p. (CONF-650704-32). Dep., AECL $0.50.

From IAEA Symposium on Thermodynamics, Vienna.

A review is presented of some recent diffusion studies conducted that provide, in addition to data of interest in nuclear technology, a means of gaining some insight into the more fundamental nature of the lattice defects occurring in the materials. The systems discussed are (i) self diffusion in the high temperature phase of pure zirconium, (ii) solute diffusion in lead, and (iii) interdiffusion of aluminum and zirconium. The unusual and at present incompletely understood results described in (i) are briefly reviewed. Evidence is given to suggest that diffusion occurs either through a dense dislocation network produced as a result of a martensitic phase transformation, or, alternatively, by excess vacancies introduced into the crystal by impurities. In (ii) the extraordinarily rapid diffusion of noble metal solutes in high purity lead single crystals is discussed in terms of the state of solution of the solute atoms. It will be shown that their diffusion behavior can be understood by assuming that a fraction f_i of the dissolved solute atoms occupy interstitial sites. The measured diffusion coefficient D_m is related to the interstitial diffusion coefficient by $D_m = f_i D_i$. In (iii) the formation and rapid growth of a single intermetallic compound $ZrAl_3$ in the diffusion zone formed between pure zirconium and pure aluminum is described and the diffusion mechanism is interpreted in terms of the structure of the compound lattice. The results indicate that $ZrAl_3$ forms a defect lattice, leading to the relatively rapid migration of aluminum atoms. (auth)

45472 (AERE-M-1605) THE FERMI SURFACE OF PALLADIUM. Lomer, W. M. (Atomic Energy Research Establishment, Harwell (England)). July 1965. 8p. Dep.; BIS $0.30; HMSO 1s. 9d.

An attempt is made to dimension the sketch of the d-hole Fermi surface in palladium. Hybridization between the s and d bands is considerable and affects the transport properties, but probably does not affect the Fermi surface. (D.C.W.)

45473 (BLG-329) DISCUSSION OF THE PRINCIPAL METHODS OF POLARON THEORY. Evrard, R.; Devreese, J. (Centre d'Etude de l'Energie Nucleaire, Brussels (Belgium)). Sept. 1963. 20p. (CONF-630910-1). Dep. mn.

From 8th Summer Meeting of Physicists, Hercegnovi, Yugoslavia.

The concept of a polaron is introduced in a qualitative way and the most important theories are briefly discussed. The results on the self-energy of the polaron derived by Lee, Low and Pines are obtained by generalizing the treatment of the interaction between a particle with an infinite mass and a scalar field. It is shown that in the Feynman theory of the polaron implicitly a coordinate defining approximately the center of the polaron is incorporated. The validity of the different methods is then discussed on the basis of an exactly soluble polaron model. (auth)

45474 (CERN-65-4(Vol.II), pp III21-30) FUNDAMENTAL ASPECTS OF GROWTH AND SHAPE OF PHOTOGRAPHIC SILVER HALIDE CRYSTALS. Klein, E.; Moisar, E.

A brief review of the growth and shape of silver halide crystals is presented. Discussions are given on the following: recrystallization in stationary systems, growth during double-jet precipitations, mechanism of crystal growth, and crystal shape. (M.O.W.)

45475 (IAE-750) VLIYANIE ANGARMONIZMA NA SPEKTR FONONOV VBLIZI TOCHKI VYROZHDENIYA. (Anharmonism Influence on the Phonon Spectrum Near the Point of Origin). Kagan, Yu.; Zhernov, A. P. (Institut Atomnoi Energii, Gosudarstvennyi Komitet po Ispol'zovaniyu Atomnoi Energii SSSR, Moscow). 1964. 12p. Dep. mn.

Green's function method is used for the analysis of anharmonism influence on phonon spectrum near a degeneracy point. The independent effects in harmonic approximation of phonon branches on each other in contrast to the usual case makes it necessary the solving of the Dyson equation system. The cases of essential and accidental degeneracy are considered. It is shown that at accidental degeneracy the occurring excitations may have strongly differing lifetimes and frequency renormalizations both in value and in temperature dependence. The cross section of single-phonon coherent neutron scattering near the degeneracy point is especially analyzed. (auth)

45476 (IDO-17106) A PROPOSAL TO INVESTIGATE THE PHYSICAL PROPERTIES OF SAMPLES UNDER VERY HIGH PRESSURES BY TIME-OF-FLIGHT NEUTRON DIFFRACTION METHODS. Brugger, R. M. (Phillips Petroleum Co., Idaho Falls, Idaho. Atomic Energy Div.). Aug. 1965. Contract AT(10-1)-205. 20p. Dep. mn; CFSTI $1.00 cy, $0.50 mn.

The possibility of investigating the properties of solids under very high pressures by neutron diffraction measurements on powdered samples was proposed and investigated. To explore the difficulties that might arise in neutron diffraction experiments on high-pressure samples, a double-axis spectrometer was assembled at the MTR and was used in measurements on Bi and KNO_3. The preliminary data showed that the resolution and intensities were superior to those for x-ray methods. Calculations indicated that a resolution improvement of X5 could be obtained over conventional diffractometers with a time-of-flight system. A simplified time-of-flight system was assembled at the MTR, and some measurements were made on Al and KNO_3. Pressure systems were proposed. (D.C.W.)

45477 (NIJS-R-444) NUCLEAR SPIN RELAXATION BY FIXED DAMAGE CENTERS IN IRRADIATED $NaH_3(SeO_3)_2$. Blinc, R.; Zupancic, I. (Nuklearni Institut Jozef Stefan, Ljubljana (Yugoslavia)). Dec. 1964. 4p. Dep. mn.

A single crystal of $NaH_3(SeO_3)_2$ was exposed to ^{60}Co gamma rays at room temperature. The proton spin-lattice relaxation time in the $NaH_3(SeO_3)_2$ was measured as a function of irradiation time and of temperature. (D.C.W.)

45478 (NP-15110) LUMINESCENCE DU SULFURE DE CADMIUM SOUS BOMBARDEMENT ELECTRONIQUE (THESES). (Luminescence of Cadmium Sulfide under Electron Bombardment (thesis)). Bombre, Francois (Paris Univ. (France). Faculte des Sciences). 1965. 124p. Dep. mn.

Cathode luminescence was used to study the luminescence of cadmium sulfide in the vicinity of the absorption limit. The essential points acquired in cathode luminescence are first reviewed. The properties and the electron structure of cadmium sulfide are reviewed and a brief survey is made of the experimental results obtained previously on the luminescence at 4 and 77°K and at room temperature. The experimental apparatus used to study the radiation emitted and the various results obtained after a variation of the experimental parameters are described. It is shown how the results obtained can be interpreted within the framework of the present theories. (J.S.R.)

45479 (TID-21301) THE ELECTRICAL CONDUCTIVITY OF THIN-METALLIC FILMS WITH UNLIKE SURFACES. Lucas, M. S. P. (Duke Univ., Durham, N. C. Dept. of Electrical Engineering). Oct. 1964. Contract AT(40-1)-2430. 13p. Dep. mn; CFSTI $1.00 cy, $0.50 mn.

A theoretical analysis, based on the Fuchs-Sondheimer formalism, is given of the conductivity of single-layer, thin-metallic films in which the scattering of the conduction electrons is different at each surface. The electron-surface scattering is described by the parameters P and Q which represent the fractions of conduction electrons specularly scattered at each surface. Tables of normalized resistivity as a function of thickness divided by mean free path are given for various combinations of P and Q. (auth)

45480 (UCRL-10771) THE UV ABSORPTION SPECTRUM OF TRAPPED S_2. Brewer, L.; Brabson, G. D.; Meyer, B. (Lawrence Radiation Lab., Univ. of California, Berkeley). Sept. 1964. Contract W-7405-eng-48. 23p. Dep. mn; CFSTI $1.00 cy, $0.50 mn.

The u-v absorption spectrum of trapped S_2 was studied in N_2, Ar, Kr and Xe matrices at 4° and 20°K. Up to 26 vibrational bands of the $v'' = 0$ progression of the $^3\Sigma_u^- \leftarrow {}^3\Sigma_g^-$ system were observed. In each of the matrices, the origin of the transition was shifted by an amount characteristic of the particular matrix; red shifts were observed for Xe, Kr and Ar, while N_2 yielded a blue shift. The vibrational spacing indicated distortion of the potential energy curve under the influence of the matrix field. The absorption bands were slightly shaded towards the blue and had a half width of about 150 cm^{-1}. At low v', doublet structure was observed. (auth)

45481 (UCRL-12470) STUDIES OF BAND STRUCTURE AND ELECTRON SCATTERING IN ALUMINUM BY PHOTOEMISSION. Wooten, F.; Huen, T.; Stuart, R. N. (Lawrence Radiation Lab., Univ. of California, Livermore). Aug. 23, 1965. Contract W-7405-eng-48. 17p. (CONF-650929-1). Dep. mn; CFSTI $1.00 cy, $0.50 mn.

From International Conference on Optical and Electronic Properties of Metals and Alloys, Paris.

The energy distribution of electrons emitted from aluminum was measured as a function of photon energy in the energy range from 5 to 11.5 ev. The emitted electron energy distribution is almost a replica of the density of occupied states. There is only a small contribution to the energy distribution from electrons which have undergone electron–electron scattering, and some structure in the density of states near the Fermi energy can be resolved. The results are in agreement with both soft x-ray emission data and theoretical calculations. Monte Carlo calculations of the energy distribution and quantum yield were made. The calculations include both electron-electron scattering and electron-phonon scattering. By filtering calculations to experimental results, information on electron scattering cross sections was obtained. The mean free path for electron-electron scattering is about 1000 Å for electrons 6 ev above the Fermi energy. (auth)

45482 INELASTIC NEUTRON SPECTRA AND THE VIBRATIONAL MODES OF THE HYDROGEN LAYER IN ALKALI AND ALKALINE-EARTH HYDROXIDES. Pelah, I.; Krebs, K.; Imry, Y. (EURATOM-C.C.R., Ispra, Italy). J. Chem. Phys., 43: 1864-9(Sept. 15, 1965).

Inelastic neutron scattering spectra of pure and deuterated lithium hydroxides and of $Ca(OH)_2$, $Ca(OD)_2$, and $Mg(OH)_2$ are presented. These spectra are explained by the interaction of neutrons with lattice vibrations in the scatterers. Special emphasis is given to the part of the spectra that is predominantly influenced by vibrations of the hydrogen layer atoms. (auth)

45483 NUCLEAR QUADRUPOLE RESONANCE AND BONDING IN CRYSTALLINE AMMONIA. Lehrer, S. S.; O'Konski, C. T. (Univ. of California, Berkeley). J. Chem. Phys., 43: 1941-9(Sept. 15, 1965).

Nuclear quadrupole coupling constants (eQq) of ^{14}N were

determined as a function of temperature for each of the isotopic species NH_3, NH_2D, NHD_2, and ND_3 in the crystalline state. The temperature dependences are explained, following a theory proposed by Bayer, in terms of an averaging of the electric field gradient (q) by torsional lattice motions. Frequencies and moments of inertia known from other spectroscopic studies of NH_3 and ND_3 were employed in the calculations, which also led to values for the quadrupole coupling constants without zero-point vibrations. These values turned out to be the same (–3.47 Mc/sec) within 1% for NH_3 and ND_3, showing that the different field gradients for the various isotopic species in the crystalline solid as well explained in terms of lattice motions. Comparison of the vibrationless, or quasistatic values, with the coupling constants of the gaseous molecules (–4.08 Mc/sec) then gave the shift produced by the crystalline field, here called the quasistatic shift. This is large relative to the changes produced by isotopic substitution in the gaseous molecule. Calculations of the electric field and the field gradient produced at a given ^{14}N nucleus by surrounding molecules in the known crystal structure were made to explain the quasistatic shift. Molecules containing the nearest hydrogen were treated as a distribution of four point charges, and the others, to a total of about 100, were taken as point dipoles. Both models were consistent with a crystalline dipole moment evaluated from the gaseous value and the known molecular polarizability, taking into account the reaction field of the lattice. The quasistatic shift was orders of magnitude too large to be accounted for by the direct field gradient of surrounding neighbors; it is better described in terms of a redistribution of electrons in the nitrogen p orbitals by polarization of the molecule in the crystal field. (auth)

45484 ENERGY LEVELS OF Pr^{3+} IN LaF_3. Caspers, H. H.; Rast, H. E.; Buchanan, R. A. (Naval Ordnance Lab., Corona, Calif.). J. Chem. Phys., 43: 2124-8(Sept. 15, 1965).

The absorption and fluorescence spectra of $Pr^{3+}(4f^2)$ in LaF_3 were investigated in the spectral region 4,000 to 60,000 Å. From the results and previously published data, all of the 2J + 1 Stark components of the $^3H_{4,5,6}$, $^3F_{2,3,4}$, $^1G_4$, $^1D_2$, $^3P_{0,2}$, levels are identified. By means of a least-squares method, the Slater and spin-orbit parameters were calculated that give a theoretical free-ion spectrum in close agreement with the observed spectrum of $Pr^{3+}(4f_2)$ in LaF_3 crystals. When the electrostatic interaction between $4f^2$ and $5d^2$ electronic configurations is taken into account, the average deviation between the calculated and the observed spectrum is 58 cm^{-1}. The values of the parameters giving the best fit are F_2 = 312.7 cm^{-1}, F_4 = 50.99 cm^{-1}, F_6 = 4.778 cm^{-1}, and ζ = 757.0 cm^{-1}. (auth)

45485 NUCLEAR MAGNETIC SHIELDING OF ALKALI IONS IN CRYSTALS AND DILUTE AQUEOUS SOLUTIONS. Ikenberry, Dennis; Das, T. P. (Univ. of California, Riverside). J. Chem. Phys., 43: 2199-2202(Oct. 1, 1965).

The formulation for the Kondo-Yamashita overlap mechanism for the nuclear magnetic shielding in alkali halides developed earlier, is applied to the rubidium nucleus in RbCl, RbBr, and RbI crystals. The pertinent average energy denominators of perturbation theory are obtained using experimental pressure data on the magnetic shielding. Using these energy denominators, the calculated values of σ_{Rb}, the chemical shifts for the rubidium nucleus in the crystal with respect to the free ion, are -2.17×10^{-4}, -2.14×10^{-4}, and -2.11×10^{-4} for RbCl, RbBr, and RbI, respectively. When combined with Baron's experimental data on the chemical shifts with respect to dilute aqueous solutions, σ_{Rb}^{aq} was obtained, which represents the chemical shift between the Rb^+ ion in aqueous solution and the free ion, the values -0.88×10^{-4}, -0.63×10^{-4}, and -0.60×10^{-4} from the RbCl, RbBr, and RbI data, respectively. These values are in fair agreement with the result $\sigma_{Rb}^{aq} = -0.65 \times 10^{-4}$ that was derived using a model of six oriented water molecules around the Rb^+ ion in dilute aqueous solutions. (auth)

45486 INDUCED PARASITIC FERROMAGNETISM IN $(La_{0.9}Bi_{0.1})CrO_3$. Iwahashi, Katsutoshi; Iida, Shuichi (Tokyo Univ.). J. Phys. Soc. Japan, 20: 1526(Aug. 1965).

The results of magnetization measurements of a synthetic single crystal of $(La_{0.9}Bi_{0.1})CrO_3$ are presented and are explained by the presence of induced parasitic ferromagnetism. The explanations are supported by an analysis using the thermodynamic potential expanded in terms of sublattice magnetizations. (L.B.S.)

45487 AN OBSERVATION ON THE FERMI SURFACE OF COPPER BY POSITRON ANNIHILATION. Fujiwara, Kunio (Tokyo Univ.). J. Phys. Soc. Japan, 20: 1533 (Aug. 1965).

An improved measurement was carried out of the angular correlation of annihilation photons in a copper single crystal, which directly demonstrated the anisotropic feature of the Fermi surface. The ^{64}Cu positron source (~1 C) was produced inside the single crystal specimen by neutron bombardment, thus obtaining a counting rate as high as in previous experiments. More detailed measurements on copper and some copper alloys are in preparation. (L.B.S.)

45488 LUMINESCENCE OF ALKALI HALIDE CRYSTALS DOPED WITH HEAVY HALIDE IONS UNDER X IRRADIATION. Valbis, Ya. A. (Latvian State Univ., (USSR). Latvijas PSR Zinatnu Akad. Vestis, Fiz. Tek. Zinatnu Ser., No. 2, 65-71(1965). (In Russian).

The luminescence of alkali halide crystals with small (less than several mol %) admixtures of heavy halide ions under x irradiation was investigated at temperatures 90 and 295°K. The most probable models of luminescence centers and their correspondence to the observed luminescence bands are discussed on the grounds of observed luminescence spectra and their dependence upon concentrations of heavy halide ion admixtures and temperature. (auth)

45489 CRYSTAL EFFECTS IN THE SCATTERING OF NEUTRONS WITH ENERGY FROM 30 TO 1000 ev. Drittler, K.; Biel, W.; Komenda, W.; Nohadani, H. (Universitaet, Kiel). Naturwissenschaften, 52: 205(1965). (In German).

The total microscopic effective cross section of neutrons on chemically bound nuclei can be expressed by $\sigma = 4\pi|a|^2 f$, where a is the scattering length. The function f is dependent on the direction of the incident neutrons as long as the atoms are in the bound state. Variation of the direction of the incident neutron changes the attenuated neutron intensity. The ratios of the neutron intensities in scattering studies on copper single crystals were graphed in experimental verifications of the dependence of f on the incident angle. (J.S.R.)

45490 TEMPERATURE DEPENDENCE OF CHARACTERISTIC ENERGY LOSSES IN KBr. Creuzburg, M.; Raether, H. (Universitaet, Hamburg). Phys. Letters, 18: 231(Sept. 1, 1965).

Further investigations of the energy loss spectra of 50 kev electrons having passed through thin films of KBr were carried out at different temperatures. The first three peaks in the energy loss spectra of KBr at 20 and –196°C are shown. A shift to higher energies with decreasing temperature is observed with the first two peaks, but none for the third. This energy shift is given together with data obtained by optical measurements. There is a fairly good agreement within the limits of accuracy. It is apparent that the temperature dependence of these energy loss peaks, which were optically identified as transitions into exciton states is due to the change of the energy levels by the variation of atomic distances with temperature. These energy losses do not show the energy shift characteristic for volume plasma losses. The 13.4 ev loss of KBr is attributed to volume plasma excitation. (J.F.P.)

45491 MOESSBAUER RESONANCE OF ^{127}I IN FERROMAGNETIC CrI_3. Kalvius, G. M.; Oppliger, L. D.; Ruby, S. L. (Argonne National Lab., Ill.). Phys. Letters, 18: 241-2(Sept. 1, 1965).

The hyperfine splitting was studied in ferromagnetic CrI_3 in order to find a large field for Mössbauer effect determination of the quadrupole moment of the first excited ($^7/_2^+$) state of ^{127}I. The iodine magnetic field in CrI_3 is also of interest. The measurements were performed with an electromechanical velocity spectrometer. Spectra at 4.2°K

show only a single absorption dip. It is appreciably broader than the line width obtained from cubic NaI which gives nearly the natural line width. Therefore, the magnetic field in CrI_3 is not large enough to resolve the individual lines. The Curie point for CrI_3 is 70°K. At 78°K the resonance sharpens but is still broader than in NaI. This indicates the presence of an unresolved quadrupole hyperfine interaction which is anticipated in this crystal lattice. Since there is practically no structure in the observed resonance line, the full width at half maximum is used as the characteristic quantity for further evaluation. Spectra are calculated over a wide range of parameters. (J.F.P.)

45492 LATTICE VIBRATIONS IN MOLECULAR CRYSTALS AND NEUTRON SCATTERING. Hahn, H. (Kernforschungsanlage, Juelich, Ger.). pp 279-89 of STI/PUB/92(Vol.II).

A description of the vibrations of a lattice of quasi-rigid molecules in terms of molecular translations and rotations is given in the harmonic approximation valid for small amplitudes. The neutron incoherent one-phonon scattering cross section is investigated for the case in which there is little or no mixture between rotational and translational vibrations. This is true either if the coupling parameters between the rotations and the translations are small, or if the mass involved in rotation about the molecule's center of gravity is small compared to the total molecular mass, i.e., if the mass is concentrated in the middle of the molecule as in solid methane. Simple results are obtained only for the case of cubic lattice symmetry and of circular symmetry of the librational parts of the thermal clouds of the atoms. In this case, as with incoherent scattering from simple cubic lattices, the energy distribution of the scattered neutrons gives (after division by some known function of temperature and frequency) directly the frequency distribution function of the molecular crystal. However, the spectra of the center of mass and rotational vibrations enter the cross section with different scale factors. The coherent one-phonon cross section is also given and examined as to how, from the variations in intensity along the scattering surfaces and from their shape, one can infer the character (rotational, translational, degree of mixing) of the vibrations contributing to them. (auth)

REACTOR TECHNOLOGY

General

Refer also to abstracts 44155 and 44270.

45493 (APDA-174) QUARTERLY TECHNICAL PROGRESS REPORT ON AEC-SPONSORED ACTIVITIES, APRIL-JUNE 1965. (Atomic Power Development Associates, Inc., Detroit, Mich.). Contract AT(11-1)-865. 80p. Dep. mn; CFSTI $3.00 cy, $0.75 mn.

Progress is reported under the headings fast reactor meltdown studies, paste concept for fast reactor blanket application, small-leak sodium-water reaction, sodium technology loop, fuel element flow stability studies, development of EOCR as a fast fuel test facility, under-sodium scanner, compilation of Fermi experience, and fast flux test facility. Separate abstracts were prepared for each project except fast reactor meltdown studies. (J.R.D.)

For abstracts of individual sections see: 44161, 44162, 44181, 44342, 45499, 45562, 45669, and 45670.

45494 (NAA-SR-11008) TRANS-FUGUE-I—A DIGITAL CODE FOR TRANSIENT TWO-PHASE FLOW AND HEAT TRANSFER. Noyes, R. C.; Morgan, J. G.; Cappel, H. H. (Atomics International, Canoga Park, Calif.). July 25, 1965. Contract AT(11-1)-Gen-8. 51p. Dep. mn; CFSTI $3.00 cy, $0.50 mn.

To provide a tool for analysis of postulated reactor incidents involving boiling, a transient single-channel, two-phase-flow, and heat-transfer digital code was developed. Called "TRANS-FUGUE-I," this code is based on a homogeneous hydrodynamic model which assumes equal phase temperatures and velocities. It assumes vapor generation to be heat-transfer-limited only, and calculates axial distribution of velocity, void fraction, pressure, coolant temperature, and fuel temperature. Transients simulating power excursions, loss of flow, loss of pressure and channel plugging can be studied. Calculations with the code for typical sodium-cooled fast reactor situations have revealed that in many accidents void growth is not heat-transfer-limited but rather limited by self-pressurization. For these cases, the TRANS-FUGUE-I calculations were found to overestimate the void growth rate; however, a method of approximate correction for this effect was developed. Studies indicate that the code is most useful for studying transient boiling in high pressure, stable systems, and boiling in fast reactors during power transients caused by large reactivity insertions. It also is useful in determining which parameters determine void growth rate for a wide range of accidents. (auth)

45495 (WAPD-T-1653) EFFECT OF LOW COBALT IMPURITY STAINLESS STEEL ON COOLANT ACTIVITY OF PRESSURIZED WATER REACTORS. Bergmann, C. A. (Bettis Atomic Power Lab., Pittsburgh, Pa.). Apr. 5, 1964 Contract AT(11-1)-Gen-14. 9p. (CONF-179-19). Dep. mn; CFSTI $1.00 cy, $0.50 mn.

From American Chemical Society, Radionuclidic Exchange on Soils, Minerals, and Resins, Philadelphia, Apr. 1964.

Data were obtained on the long-lived activity of the coolant and primary system components after shutdown of the SM-1 and PM-2A reactors, which are identical to each other except for the low cobalt content of the stainless steel in the PM-2A core. The observed $^{58}Co/^{60}Co$ ratios were compared with these calculated from assumptions that the activity was due to activation of in-flux and/or out-of-flux materials. The results show that the use of low-cobalt stainless steel in in-flux does not significantly reduce ^{60}Co activity levels and hence is of questionable value. (D.L.C.)

45496 (WCAP-3269-30) A STUDY OF THE ZIRCALOY-STEAM REACTION IN A SIMULATED REACTOR LOSS-OF-COOLANT ACCIDENT. Kubit, C. J.; Stanutz, R. N.; Fultonberg, D. N. (Westinghouse Electric Corp., Pittsburgh, Pa. Atomic Power Div.). [nd]. Contract AT(30-1)-3269. 29p. Dep. mn; CFSTI $2.00 cy, $0.50 mn.

An experiment was performed to study the kinetics and extent of reaction between Zircaloy-2 and steam under conditions of a simulated pressurized water reactor loss-of-coolant accident. Prior to the experiment, the expected temperature transients of the clad surface of stainless steel fuel rods after a loss-of-coolant accident were obtained from computer code runs. An attempt was made to duplicate the calculated transients by means of a programmed heat input to the specimens in an autoclave containing 150 psi, 600°F steam. A comparison of the experimental temperature transient of the Zircaloy-2 specimen with that of a stainless steel control sample indicates that there was no autocatalytic effect and that the Zircaloy-steam reaction was negligible up to 1750°F, the highest temperature reached in the experiment. (auth)

45497 (ORNL-tr-652) THE NEW INSTITUTE FOR REACTOR SAFETY. Karr, H. Translated for Oak Ridge National Lab., Tenn., from Atomwirtschaft, 10: 140-1(Mar. 1965). 11p. Dep. mn; JCL $1.60 fs, $0.80 mf.

The Institute for Reactor Safety will collect and evaluate information related to safety in nuclear engineering and will participate in the approval and supervision of nuclear plants. The activities and organization of the Institute are outlined. (D.C.W.)

45498 SITES FOR THE CONSTRUCTION OF NUCLEAR REACTORS. Vinck, W.-F. Bull. Inform. Assoc. Belge Develop. Pacifique Energie At., No. 56, 7-11(June 1965). (In French).

A review is given of the principles that in Europe guide the selection of sites for nuclear reactors with respect to public health and safety. The weight given to the population density in site selection in the various European countries is indicated. The parameters for the safety and estimation of the site conditions are discussed with respect to the possibility of an accident by leak to the heat transfer system, liberation and retention of fission products, efficiency of the injection system for the safety of the core, theoretical efficiency of the vessel, possible cases of inefficiency of the vessel, mechanisms for the retention and controlled ventilation of the fission products, and maximum conceivable accident in gas-cooled reactors. The site parameters to be considered in the case of an accident and for normal operation of the reactor are discussed. The general factors applied throughout Europe are briefly summarized. (J.S.R.)

Auxiliaries and Components

45499 (APDA-174, pp 10-24) PASTE CONCEPT FOR FAST REACTOR BLANKET APPLICATIONS. Project Agreement No. 8. Kovacic, E. C.; Chamberlain, H. V.; Moore, C. R. (Atomic Power Development Associates, Inc., Detroit, Mich.).

The high-temperature Na-U paste loop was operated on an initial charge of approximately 260 cc of stainless steel particles in Na for 230 hours. During this period, paste flow rates were measured for a range of Na flow rates to the eductor, demonstrating the flexibility of the operation. The loop was subsequently charged with an additional 1900 cc of stainless steel particles and was circulated for about 140 hours. Using a simulant paste loop containing Cu shot and water, several tests were conducted to provide solutions to some of the problems encountered in the high-temperature loop. (auth)

45500 (HW-65756) A DATA RECORDING SYSTEM FOR THE FUEL CORE TESTER. Waldkoetter, G. L. (General Electric CO., Richland, Wash. Hanford Atomic

Products Operation). June 20, 1960. Contract AT(45-1)-1350. 19p. Dep. mn; CFSTI $0.75 cy, $0.50 mn.

An automatic data recording system developed for use in the inspection of the grain structure and surface quality of fuel cores with the UT2 fuel core tester is described. (D.C.W.)

45501 (IAE-611) ISSLEDOVANIYA PO PRIMENENIYU ORGANICHESKIKH TEPLONOSITELEI-ZAMEDLITELEI V YADERNYKH REAKTORAKH. (Studies on the Use of Organic Coolant-Moderators in Nuclear Reactors). Aleksenko, Yu. N.; Brodskii, A. M.; Zvonov, N. V. (and others) (Institut Atomnoi Energii, Gosudarstvennyi Komitet po Ispol'zovaniyu Atomnoi Energii SSSR, Moscow). 1964. 36p. Dep. mn.

A survey of basic studies on the use of high-boiling organic liquids as coolants and moderators in nuclear reactors is presented. Results of radiation-chemistry, thermophysical, corrosion, and neutron-physics investigations are considered. Data on the use of the process of destructive hydrogenation for the detection of the products of radiolysis of the organic coolants are included. (tr-auth)

45502 (RL-REA-2120) STRAP-ON RTD TEST PLAN. MODEL FOUR TESTING. Green, J. W.; Hildreth, N. T.; Kaveckis, J. E. (General Electric Co., Richland, Wash. Hanford Atomic Products Operation). May 19, 1965. Contract AT(45-1)-1350. 17p. Dep. mn; CFSTI $1.00 cy, $0.50 mn.

The tests to which strap-on reactor thermocouple devices are to be subjected are outlined, together with the limits that the devices must meet. (D.C.W.)

45503 (SWRI-1228-69) STUDIES OF THE FATIGUE STRENGTH OF PRESSURE VESSELS. 1. CYCLIC PRESSURE TESTS OF LARGE SIZE PRESSURE VESSELS. 2. LOW CYCLE FATIGUE TESTING OF ONE-HALF SCALE MODEL PRESSURE VESSELS. 3. EFFECT OF WELD DEFECTS ON THE FATIGUE STRENGTH OF A302B STEEL. Pickett, A. G.; Grigory, S. C.; Whiting, A. R. (Southwest Research Inst., San Antonio, Tex.). July 18, 1965. Contract AT(11-1)-1228. 21p. (SWRI-1228-70; SWRI-1228-71). Dep. mn; CFSTI $1.00 cy, $0.50 mn.

The fatigue cracks that occurred in the nozzles of the A201B Vessel No. 7 during 0-2650 psig internal pressure cycling up to 147,665 cycles are described. Out-of-roundness measurements were made on Penn State One-Half Scale Vessel, Nozzle S. Fatigue data are plotted for sound-weld and weld-defect specimens of A302B steel. (D.L.C.)

45504 PRESTRESSED CONCRETE PRESSURE VESSELS FOR NUCLEAR REACTORS. Courbon, M. (Etudes de la Societe des Grands Travaux, Marseille). Bull. Inform. A.T.E.N. (Assoc. Tech. Energie Nucl.), No. 53, 29-43 (May-June 1965). (In French).

The principles of prestressed concrete and its use for the construction of reactor vessels were examined. Its application is described and the future of this technique is predicted. (J.S.R.)

45505 PRESTRESSED CONCRETE PRESSURE VESSELS. I. REVIEW OF EXPERIENCE TO DATE. Marsh, Roland O.; Melese, Gilbert B. (General Atomic Div., General Dynamics Corp., San Diego, Calif.). Nucleonics, 23: No. 9, 63-7(Sept. 1965).

The design and construction of prestressed-concrete pressure vessels is discussed. Advantages of concrete are considered. Thermal insulation, loading conditions, design analysis and testing, and vessel models for studying design concepts are discussed. Some existing vessels are described. (M.C.G.)

45506 PRESTRESSED CONCRETE VESSELS. II. AN APPLICATION TO BOILING D_2O REACTORS. Margen, Peter (Aktiebolaget Atomenergi, Stockholm); Beliaev, Gunnar; Lindbo, Tord. Nucleonics, 23: No. 9, 68-9; 78 (Sept. 1965).

The question of thermally insulating the D_2O-water and steam from the concrete is considered. A proposed design for a 400-Mw(e) boiling-heavy-water reactor with a prestressed concrete pressure vessel is described. (M.C.G.)

45507 RULES FOR CONSTRUCTION OF NUCLEAR VESSELS. ASME Boiler and Pressure Vessel Code, Section III, 1965 Edition. Report of Subcommittee of Boiler and Pressure Vessel Committee. New York, The American Society of Mechanical Engineers, 1965. 154p.

Included, Summer 1965 Addenda, ASME Boiler and Pressure Vessel Code, Nuclear Vessels, 1965 Edition, date of Issuance June 30, 1965. 14p.

45508 IMPROVEMENTS IN OR RELATING TO METHODS OF AND APPARATUS FOR MEASURING THE PERIOD OF A NUCLEAR REACTOR. Passe, Jean (to Commissariat a l'Energie Atomique). British Patent 1,000,843, Aug. 11, 1965. Priority date May 17, 1963, France.

A method and apparatus for measuring the period of a reactor consists in integrating a value of current produced by at least one ionization chamber located near the core of the reactor during two equal and successive time intervals and relating the two results. The apparatus consists of the ionization chamber or a member providing a current representing a flux connected alternately during a period equal to the period of time, θ, chosen, by means of two identical electronic circuits to a measuring apparatus directly giving the period to be measured in relation to two successive readings. Each electronic circuit is made up of an integrator connected by means of a time-base generator to an amplifier connected to the input of the ionization chamber. A converter transforms the ionization current into a series of pulses of a frequency proportional to the current, and the pulses are counted alternately during the equal periods by scalers. (B.L.M.)

45509 IMPROVEMENTS IN NUCLEAR REACTORS. (to Atomic Energy of Canada Ltd.). British Patent 1,001,118. Aug. 11, 1965. Priority date July 8, 1963, United States.

A reactor fuel channel lattice is provided for a right circular cylindrical reactor core having a central axis. The lattice includes a number of fuel channels each having a reference position. Each of the fuel channels are skewed at an angle to the central axis. Each reference position is at the same radius from the central axis as the ends of the fuel channel and is located on the bisector of an angle subtended by the ends of the fuel channel at the central axis in a plane normal to the axis. The reference positions form a uniform reference lattice by which the fuel channels are nonuniformly spaced at any cross section intermediate the ends of the reactor. The fuel channels are more closely spaced radially and longitudinally at the center of the core than at the edges. The fuel channels may all be skewed at the same angle; or the lattice may be divided into regions, and the fuel channels within a region skewed at the same angle but at different angles within different regions. The regions are concentric about the axis of the core. If the lattice is divided into two regions, the skew angle in the outer region is greater than in the inner region. (B.L.M.)

45510 PLUG AND PLUG INSERTION MEANS FOR NUCLEAR REACTOR PRESSURE VESSELS. (to Groupement Atomique Alsacienne Atlantique). British Patent 1,001,580. Aug. 18, 1965. Priority date Aug. 7, 1961, France.

A plug and plug insertion means are provided for the tank-bottom apertures of reactors, particularly heavy-water reactors. Means are provided for inserting, locking and unlocking, and removing the plugs. The plug is hollow, has a wall, a bottom, and an open top. It is adapted to slide into and plug an aperture. A locking means inside the plug serving to lock the plug in the aperture consists of a number of bolts controlled by a resilient element. Openings are provided in the walls to allow passage of the bolts, and means are provided in the wall of the aperture for receiving the bolts. Inserting means grip the plug for insertion into the aperture, and extracting means grip and unlock the plug for removal from the aperture. A carrier is adapted to receive the inserting and extracting means and serves to support the plug for its positioning and removal. The carrier also provides for the symmetrical operation of the locking means. The plug itself may be of hollow aluminum consisting of a band of cold worked

aluminum vertically folded so as to form a spring. The two ends of the spring are shaped to act as bolts that radially extend beyond the wall of the plug and horizontally engage a circular groove provided in the wall of the aperture. (B.L.M.)

45511 MODERATOR STRUCTURES FOR NUCLEAR REACTORS. Rose, Walter (to English Electric Co., Ltd.). British Patent 1,001,621. Aug. 18, 1965. Filed Feb. 9, 1962.

A moderator structure is described for a reactor that includes a number of vertical columns disposed on a square lattice. Each column is formed of co-axially arranged graphite bricks. The bricks constitute horizontally extending layers in the core. Each alternate brick in each column and each alternate brick in each layer comprise a key brick at each end of which is an axially extending end portion of generally square cross section. Each end portion overlaps vertically the corresponding end portions of the key bricks of the next adjacent layer in the next adjacent columns. The key bricks are taken along the axes of the lattice so as to locate the layers relatively to each other. The remaining bricks are spacer bricks each arranged to be in contact with other bricks only at its ends. In each layer the key bricks of each column are keyed to the key bricks in the next adjacent columns taken along the diagonals of the lattice so as to locate the columns relatively to each other. (B.L.M.)

45512 REFUELLING DEVICE FOR NUCLEAR REACTORS. Aubert, Michel; Brouard, Daniel; Rouge, Pierre (to Commissariat a l'Energie Atomique). British Patent 1,001,926. Aug. 18, 1965. Priority date July 31, 1963, France.

A fuelling device is described for a gas-cooled reactor of the type including a moderator structure through which are formed channels for accommodating fuel elements. The handling device is placed within the reactor pressure vessel and the biological shield inside a compartment that is separated from the core chamber by a wall provided with openings for providing access to the channels. A system is provided for the insertion and withdrawal of fuel element magazines into and out of the compartment. The handling system is provided with means for effecting a transfer of fuel elements between a magazine and a channel, and a storage system is located in the compartment and includes a number of magazine storage stations. The system for the insertion and withdrawal into and out of the servicing chamber of the handling device comprises a lock-chamber disposed within a horizontal tunnel that provides access to the servicing chamber and that separates the servicing chamber from those portions of the system maintained at atmospheric pressure. Within the tunnel a seating having a horizontal axis is formed in the tunnel wall, and a longitudinal rail carried by the wall has a gap in the vicinity of the seating. A rotary system consists of a base-plate that is rotatably mounted on a vertical pivot supported by the bottom portion of the tunnel wall, and a door is provided that is capable of being applied against the seating by jacks. The rotary system performs a movement of rotation about the pivot between a closed position in which the door is opposite to the seating and an open position in which the door is moved away from the seating. A rail segment secured to this base plate is adapted to span the gap in the rail secured to the tunnel wall when the door is in the open position. (B.L.M.)

45513 HANDLING APPARATUS FOR AN INSTALLATION FOR RELOADING A NUCLEAR REACTOR WITH FUEL ELEMENTS. Lemesle, Georges; Martin, Roger; Rouge, Pierre; Vivien, Jean (to Commissariat a l'Energie Atomique). British Patent 1,002,006. Aug. 18, 1965. Priority date Oct. 6, 1962, France.

A fuel handling apparatus for a gas cooled reactor includes a beam mounted rotatably about a vertical axis in a garret that is formed inside the biological shield and pressure vessel of the reactor. The garret is separated from a chamber occupied by the core by a wall reducing the radiation from the core and having orifices permitting access to vertical channels in the core accommodating the fuel elements. Means are provided for rotating the beam, and an assembly is movable along the beam carrying a vertically movable gripping device. First and second driving means are arranged outside the shield in a chamber in communication with the garret, and first and second flexible means extend through the shield substantially on the axis of rotation of the beam and connect the movable assembly to the first driving means and the gripping device to the second driving means, respectively. The garret offers numerous advantages, such as exchange between the fuel elements, and the irradiated elements may be stored in the garret until they have cooled sufficiently for removal. Since it may be necessary to enter the garret to repair the handling machinery, a slight pressure differential between the garret and the core chamber is maintained during normal operation in order to limit the pollution of the apparatus situated in the garret. (B.L.M.)

45514 NUCLEAR REACTOR REFUELLING FACILITY. Lemesle, Georges; Martin, Roger; Rouge, Pierre; Vivien, Jean (to Commissariat a l'Energie Atomique). British Patent 1,002,007. Aug. 18, 1965. Priority date Dec. 11, 1962, France.

A refueling facility is provided for the insertion and withdrawal of fuel elements into and out of a servicing chamber of a gas cooled reactor. The device includes a lock-chamber occupied by a conveyor that is provided with fuel element compartments. The conveyor is movable so as to displace the fuel element compartments between a position in which the compartments are located opposite an inlet providing admission to the lock-chamber from the servicing chamber and a position in which the compartments are located opposite an outlet from the lock-chamber to the exterior. The inlet and outlet are provided with isolating valves. First fuel-element magazines are provided for transfer between a location opposite the inlet of the lock-chamber and storage locations within the servicing chamber, and second fuel-element magazines are provided for disposal in a location opposite the outlet of the lock-chamber. Means are provided for the exchange of fuel elements between the compartments of the conveyor and compartments of the first and second magazines. (B.L.M.)

45515 SHUT-OFF DEVICE FOR NUCLEAR REACTORS. Dosch, Peter (to Gesellschaft fuer Kernforschung m.b.H.). German Patent 1,196,306. July 8, 1965. Filed Dec. 18, 1962.

The shut-off device for nuclear reactors comprises a collision momentum generating device which accelerates the safety elements and the accelerating force of which is much higher than the holding force of a holding device holding the safety elements. This shut-off device is improved in that the safety elements are subdivided the adjacent parts of the elements being held together by suited holding devices until a collision momentum is imparted to the free end of the element. (Gmelin Inst.)

45516 CONTROL ROD LIFT-COUPLING MECHANISM. Fortescue, Peter (to General Dynamics Corp.). U. S. Patent 3,197,378. July 27, 1965. Filed Nov. 8, 1961.

A mechanism for releasably coupling a lifting or regulating means to a movable element in a nuclear reactor is particularly adapted to handling of control rods. The mechanism is so arranged that, when the control rod is dropped in an emergency situation, a minimum of associated equipment is dropped with it. The coupling mechanism may be readily disconnected when the control rod is at rest within the reactor core, but cannot be disconnected while the control rod is suspended above the reactor. (A.G.W.)

45517 GUIDE TUBES FOR NUCLEAR REACTORS. Alfille, Lucien; Ropers, Jean; Gewiss, Claude (to Commissariat a l'Energie Atomique). U. S. Patent 3,197,379. July 27, 1965. Priority date May 2, 1961, France.

A composite guide tube for a fuel element housed in a pressure tube of a fluid-cooled, liquid-moderated reactor includes an inner metal tubular element for guiding the fuel element and a metallic structure having a low apparent

density surrounding the tubular element and serving as heat insulation. The metallic structure consists of helically wound strips of thin permanently bent metal covering the surface of the tubular element. The structure contacts the outer surface of the tubular element and the inner surface of the pressure tube in such a manner that it also serves to hold the tubular element in position in the pressure tube. The strips located in the hot inner zone of the reactor may be of a different material from those in the cold outer zone. (A.G.W.)

45518 NUCLEAR REACTOR CONTROL ROD ASSEMBLY WITH IMPROVED DRIVING MECHANISM. Macomber, John W. (to National Aeronautics and Space Administration). U. S. Patent 3,198,709. Aug. 3, 1965. Filed May 1, 1963.

A number of elongated control rod assemblies, forming both regulator and shim rods, extend vertically through the reactor core and are arranged in substantial juxtaposition with the fuel elements of the core. Each of the control rod assemblies has either a reflector section or a fuel section interposed between a poison section and a guide section. Provision is made for easy assembly so that these sections may be joined together. Driving apparatus is mounted below the reactor core to extend or retract the control rods into and out of the core to alter the reactor power level. Means are provided for operatively connecting the driving apparatus to the control rods, and each shim-rod has a drive-release mechanism incorporating members that are movable into and out of engagement with the guide sections of the shim rods. Provision is also made for disassembling the sections independently of the operation of the connecting devices so that sections of the control rods can be readily replaced. (B.L.M.)

45519 REACTOR COOLANT SYSTEM. Long, Robert B. (to Esso Research and Engineering Co.). U. S. Patent 3,198,710. Aug. 3, 1965. Filed Nov. 12, 1958.

A method is patented for transferring heat from a nuclear reactor by carrying out an endothermic dehydrogenation process within the reactor and then regenerating the reactant by hydrogenation outside the reactor. The surfaces of the reactor fuel elements are coated with a suitable dehydrogenation catalyst, and cyclohexane is supplied to the fuel region. The cyclohexane is converted to benzene, which is withdrawn from the core and passed through a steam plant in which cyclohexane is regenerated. About 1200 Btu per pound of cyclohexane can be removed from an operating reactor in this manner. (A.G.W.)

45520 LIQUID COOLED NUCLEAR REACTOR WITH IMPROVED FLOW DISTRIBUTION MEANS. Vendryes, Georges; Duport, Jacques (to Commissariat a l'Energie Atomique). U. S. Patent 3,200,045. Aug. 10, 1965. Priority date Mar. 10, 1961, France.

The neutronic portion of a liquid-metal-cooled breeder reactor is surrounded by a tank supplied with coolant axially from beneath through a single supply conduit. Different flow rates to different regions of the reactor are provided by a system of diaphragms and concentric sleeves attached to the conduit. An outlet in the top portion of the tank conveys the hot liquid metal to heat exchangers. (A.G.W.)

Criticality Studies

See also PHYSICS — Criticality Studies.

Refer also to abstracts 45244 and 45572.

45521 (AAEC/TM-118) RESONANCE ABSORPTION IN SMALL HOMOGENEOUS CRITICAL ASSEMBLIES. Keane, A.; McKay, M. H. (Australian Atomic Energy Commission Research Establishment, Lucas Heights). Dec. 1961. 12p. Dep. mn.

A theoretical investigation is made of the effects of resonance fission on the effective reproduction constant and the fuel temperature coefficient of a nuclear reactor. Then, taking account of epithermal leakage from a small homogeneous critical assembly, formulas are derived for the resonance escape probability using both the narrow-resonance and the infinite-mass approximations. (auth)

45522 (AE-195) EXPERIMENTAL STUDIES ON ASSEMBLIES 1 AND 2 OF THE FAST REACTOR FRO. PART 1. Andersson, T. L.; Hellstrand, E.; Londen, S-O.; Tiren, L. I. (Aktiebolaget Atomenergi, Stockholm (Sweden)). Aug. 1965. 48p. Dep. mn.

FRO is a fast zero power reactor built for experiments in reactor physics. It is a split table machine containing vertical fuel elements. 120 kg of ^{235}U are available as fuel, which is fabricated into metallic plates of 20% enrichment. The control system comprises 5 spring-loaded safety elements and 3 + 1 elements for startup operations and power control. The reactor went critical in February 1964. The first assemblies studied were made up of undiluted fuel into a cylindrical and a spherical core, respectively, surrounded by a reflector made of copper. Some experiments made on these systems are described. Primarily, critical mass determinations, flux distribution measurements and studies of the conversion ratio are dealt with. The measured quantities were compared with theoretical predictions using various transport theory programs (DSN, TDC) and cross section sets. The experimental results show that the neutron spectrum in the copper reflector is softer than predicted, but apart from this discrepancy agreement with theory was generally obtained. (auth)

45523 (AEEW-R-425) ZADOC—A TWO GROUP, TWO DIMENSIONAL FUEL MANAGEMENT PROGRAMME FOR IBM 7090 OR STRETCH. Allen, F. R. (Atomic Energy Establishment, Winfrith (England)). Apr. 1965. 58p. Dep.; BIS $1.60; HMSO 8s.

ZADOC is a Fortran 2 or S2 language program for assessment calculations of fuel management on a two-group, two space dimension (x-y) model of a reactor core. The code allows automatic computation of a variety of fuel management schemes ranging from batch operation to on-line refuelling. (auth)

45524 (AEEW-R-428) AN ANALYSIS OF SOME TWO-ZONE EXPONENTIAL EXPERIMENTS ON GRAPHITE MODERATED LATTICES. King, D. C.; Gibson, M. (Atomic Energy Establishment, Winfrith (England)). July 1965. 26p. Dep.; BIS $0.80; HMSO 4s.

Two methods for deriving the buckling of the test lattice from two-zone heterogeneous graphite exponential experiments are demonstrated. These are based on (a) one group perturbation theory and (b) two-group diffusion theory. It is shown that, although the two group method has wider applicability, both methods are sufficiently accurate when the lattice parameters are matched within certain limits. With sufficient test fuel available to load one half of the stack the analysis error is small compared with full stack systematic experimental uncertainties and an accuracy of ±0.35% in reactivity is possible for A.G.R. type lattices. (auth)

45525 (EUR-2470.e) PIN-TO-PIN INTERACTIONS IN FUEL CLUSTERS. PART I. Amyot, L. (European Atomic Energy Community, Ispra (Italy). Joint Nuclear Research Center). Aug. 1965. 15p. Dep. mn.

The pin-to-pin collision probability is important for the calculation of the hyperfine structure of the flux distribution in heterogeneous fuel elements. Previous methods of calculation require long machine time. An analytical approach for a routine-type calculation (requiring less time than previous methods) is presented. Starting from the exact expression, an approximate formula is derived for the pin-to-pin collision probability which will be asymptotically rigorous when the optical distance and target pins does not vary with the direction of the neutron path. (M.O.W.)

45526 (GA-6633) PRECRITICAL CALCULATIONS FOR THE 2.9 IN. PITCH, TWMR CRITICAL ASSEMBLY. Peak, J. C.; Lovallo, J. M. (General Atomic, San Diego,

Calif. John Jay Hopkins Lab. for Pure and Applied Science). Aug. 1, 1965. Contract SNPC-27. 24p. (NASA-CR-54644).

The critical loadings for the 2.9-in.-pitch core are given, and the precritical calculations for the water-reflected core are summarized. The calculations include thermal and high-energy disadvantage factors, thermal and fast spectra, thermal disadvantage factors for cadmium, and the effective multiplication factor. The measurement of the asymptotic decay constant is briefly considered; theoretical values of the decay constant are included, together with axial and radial flux distributions. (D.C.W.)

45527 (IDO-17078) SPORT—A SYSTEM FOR PROCESSING REACTOR TRANSIENT DATA ON THE IBM-7040 COMPUTER. Power, B. J.; Hagen, R. N.; Johnson, S. O. (Phillips Petroleum Co., Idaho Falls, Idaho. Atomic Energy Div.). July 1965. Contract AT(10-1)-205. 209p. Dep. mn; CFSTI $6.00 cy, $1.25 mn.

To facilitate the processing and analysis of data recorded during transient tests in the Spert reactors, a system of programs for the IBM-7040 computer was developed to smooth and store data so they are readily accessible, calculate from the power history the reactivity and energy release as functions of time, and provide a means by which frequency response analyses of data can be made. The mathematics employed in the various programs in the system and the procedures necessary to process data with the system are described. Test and sample problems are presented, and a complete listing of the source program is included. (auth)

45528 (IDO-17097) SPERT PROJECT QUARTERLY TECHNICAL REPORT, JANUARY-MARCH 1965. Crocker, J. G. (ed.) (Phillips Petroleum Co., Idaho Falls, Idaho. Atomic Energy Div.). July 1965. Contract AT(10-1)-205. 28p. Dep. mn; CFSTI $2.00 cy, $0.50 mn.

A series of tests was performed with the Spert III plate-type core to investigate the effects of the initial reactor power level on the dynamic response of the core. One of the primary purposes for these tests was to provide a basis for evaluating one of the more widely used computer programs for calculating reactor kinetic behavior, the ART-04 program. Comparisons of calculated and experimental results were made for the following types of transient tests: (a) power excursions initiated by one-dollar stepwise reactivity insertions from initial power levels ranging from 0.01 to 28 MW, (b) power excursions initiated by ramp reactivity insertions of 0.05 dollars/sec from power levels of 1 and 25 MW, and (c) partial and total losses-of-flow from power levels of 10 and 28 MW. The initial conditions for most of the transients were 500°F core inlet coolant temperature, 2500-psig system pressure, and 20 ft/sec core coolant flow. Fuel plate surface temperature measurements were made with MgO-insulated, stainless-steel-sheathed thermocouples. Tests, however, show that the use of these thermocouples can result in substantial errors in the measurements. Using a transfer function approach, a technique was developed whereby the originally recorded temperature data from these thermocouples can be corrected to agree within approximately 10 percent at the time of peak temperature with that which would be given by the faster-response thermocouples. A brief report on recent coolant pump failure is presented. A portion of the subassembly test program with the Capsule Driver Core (CDC) in Spert IV includes the planned destruction of test fuel samples. In preparation for such testing, a series of out-of-pile capsule and instrumentation tests is being conducted. In the tests, chemical explosives were used to mock up rapid releases of nuclear energy within capsules or cylinders made of 6061-T6 aluminum, 304 stainless steel, and A106 grade B carbon steel. From the results which were obtained from these out-of-pile tests, a design for the capsule to be used in in-pile tests of the CDC fuel was established. (M.O.W.)

45529 (INR-600/IX-A/PR) WATER REACTIVITY EFFECTS IN THE ANNA CRITICAL ASSEMBLY. Bouzyka, Jacek; Kubowski, Jerzy; Latek, Stanislaw; Suwalski, Witold (Institute of Nuclear Research, Warsaw (Poland)). Feb. 1965. 22p. Dep.

The results of reactivity measurements on the loss of water from the fuel and graphite (experimental) channels of the ANNA critical assembly are presented. The shadowing effect, as well as the opposed effect of the water removal from the core and the side reflector, respectively, was observed. The results are very important for the reactor operation. (auth)

45530 (JAERI-1082) MULTIGROUP CALCULATIONS OF KINETICS PARAMETERS IN FAST REACTORS (KPARAM-CODE). Moriguchi, Kinichi; Suzuki, Tomoo (Japan Atomic Energy Research Inst., Tokyo). Feb. 1965. 41p. Dep. mn.

The KPARAM code, which calculates the effective delayed neutron fraction, β_{eff}, the prompt neutron lifetime, l_p, and other related kinetics parameters for the kinetics analysis of large, fast, plutonium-fueled reactors, is described. These reactors have different kinetics behaviors from fast reactors fueled with ^{235}U, due to the much smaller delayed-neutron fraction emitted in the fissioning of plutonium. As the model, the IBM-704 Code 1188/RE was used, but the KPARAM calculates the real and adjoint fluxes case by case, in its one-dimensional multigroup diffusion equation subroutine. The program was written in the Fortran II language for the IBM 7090 first, and then rewritten in the Fortran IV language for the IBM 7044. (auth)

45531 (N64-29786) SUMMARY OF DIFFUSION THEORY FOR HOMOGENEOUS AND HETEROGENEOUS NUCLEAR REACTORS. Lectures 3 and 4. Beeler, J. R. Jr. (General Electric Co., Cincinnati, Ohio. Nuclear Materials and Propulsion Operation). [1963]. Contract NAS8-5215. 56p. (NASA-CR-52959; GEMP-190c). CFSTI $9.60.

Two lectures on diffusion theory in reactors are included. The important concepts in reactor theory are discussed and classical references for better understanding of these concepts are pointed out. The ideas on which elementary reactor theory is based and results for the one-group and two-group diffusion theory approximations are presented. Theory is presented for the following: a homogeneous infinite system, a homogeneous bare reactor, and non-uniform reactors. (M.O.W.)

45532 (ORNL-TM-1219) A SURVEY OF DOPPLER COEFFICIENTS FOR UO_2 FUEL. Preskitt, C. A. (Oak Ridge National Lab., Tenn.). Apr. 27, 1965. Contract W-7405-eng-26. 10p. Dep. mn; CFSTI $1.00 cy, $0.50 mn.

Four experimental and two theoretical studies of the Doppler coefficient of UO_2 fuel were compared. The results appear to divide into two distinct groups with about the same dependence on surface-to-mass ratio, but separated by a difference of ~15%. (auth)

45533 (WCAP-3269-33) CONTROL ROD WORTH IN A HETEROGENEOUS MOCKUP OF A LARGE PRESSURIZED WATER REACTOR CORE. Lacey, P. G. (Westinghouse Electric Corp., Pittsburgh, Pa. Atomic Power Div.). July 1964. Contract AT(30-1)-3269. 104p. Dep. mn; CFSTI $4.00 cy, $0.75 mn.

The analytic methods and procedures used to calculate control rod worth in large PWR cores were applied to the analysis of critical experiment configurations in which control rod worth was measured. The results of this correlation are given along with complete descriptions of the analytic and experimental methods. Reactivity worths are given for cruciform-shaped control rods of Ag-In-Cd and B_4C in a simulated hot-core fuel assembly mockup. (auth)

45534 (WCAP-3269-35) LOCAL FISSION POWER DISTRIBUTIONS AROUND CONTROL RODS AND CONTROL ROD FOLLOWERS IN SIMULATED PWR CORES. Lacey, P. G. (Westinghouse Electric Corp., Pittsburgh, Pa. Atomic Power Div.). Sept. 1964. Contract AT(30-1)-3269. 89p. Dep. mn; CFSTI $3.00 cy, $0.75 mn.

Local fission power distributions around cruciform

shaped control rods and control rod followers are given for a typical pressurized water reactor fuel assembly design. Experimental data taken by gamma scanning typical fuel rods around the control rod channel in a simulated core cross section are compared with calculated fission power distributions. All cores were critical experiments using Type 304 stainless steel clad UO_2 fuel rods. A majority of the data apply to fully inserted or fully withdrawn, centrally located control rods, however, some of the data apply to an off-center control rod inserted half way into the core to permit observation of axial power shape as a function of radial position from the control rod channel. Discussion of the analytic and experimental techniques as well as the correlation between experiment and theory is given. (auth)

45535 (WCAP-3269-47) AN ANALYSIS OF REACTIVITY WORTH OF THE ROD CLUSTER CONTROL (RCC) ELEMENTS AND LOCAL WATER-HOLE POWER DENSITY PEAKING. Sha, William T. (Westinghouse Electric Corp., Pittsburgh, Pa. Atomic Power Div.). May 1965. Contract AT(30-1)-3269. 120p. Dep. mn; CFSTI $4.00 cy, $0.75 mn.

The reactivity worth and local power disturbances associated with a reactivity control system consisting of clusters of small cylindrical poison elements is investigated. The results of the experimental program of RCC evaluation are presented. In the rod worth computation a method to specify the boundary condition of the rod cluster (RCC) elements in two-group, two-dimensional diffusion theory is presented. A semi-empirical design procedure is developed for the extrapolation in size and temperature to the operating PWR core. It appears that rod worth can be correlated within 3.5% for the practical RCC arrangement by using this method. A comparison is also made between the calculated values of power-peaking and experimental measurements. It is concluded that RCC local water-hole power density can be predicted within ±2%. The proposed procedure is compared to a technique which attempts to eliminate the consequence of empiricism in extrapolation in order to establish the probable accuracy of the extrapolation. (auth)

45536 HETEROGENEOUS ABSORBER EFFICIENCY IN HOMOGENEOUS URANIUM-WATER REACTORS. Vladykov, G. M.; Dubovskii, B. G.; Kamaev, A. V.; Sviridenko, V. Ya.; Kuznetsov, F. M.; Popov, G. A.; Palamarchuk, Yu. D. At. Energ. (USSR), 19: 14-19(July 1965).

Results are presented of experiments on the determination of the efficiency of absorbers in homogeneous uranium-water reactors. The efficiency of single rods and of groups of cylindrical rods of boron and cadmium carbide was studied as a function of the dimensions of the absorbers and the U concentration in the active zone. The effect of steel jackets on the efficiency of the rods is shown. A comparison of results of a two-group calculation of efficiency of the central BC rod with the experimental data was carried out. (tr-auth)

45537 PHYSICAL CHARACTERISTIC OF CRITICAL ASSEMBLY WITH BeO MODERATOR. Lomakin, S. S. At. Energ. (USSR), 19: 69-71(July 1965).

Studies intended for the determination of the neutron-physics characteristics of a critical assembly with BeO moderator are discussed. The geometry of the assembly, using flat ^{235}U fuel elements, is described. Results of measurements are given for the dependence of the length of the active zone with three layers of fuel elements on the geometry, the variation of the geometrical parameter χ^2 on the number of elements in a layer at constant fuel concentration, and the distribution of thermal neutron density in a layer with three vertical fuel elements. The coefficient of fuel self-screening was calculated by various methods, including the Monte-Carlo method and the P_3 approximation, and compared with measurements. (M.J.T.)

45538 EFFECT OF A VOIDED GAP ON REACTIVITY COEFFICIENT FOR VOIDING CORE SODIUM IN A FAST REACTOR, FOR VARIOUS GEOMETRIES. Noderer, L. C.; Visner, Sidney (Combustion Engineering, Inc., Windsor, Conn.). 13p. (CONF-654-94). Gmelin, AED-CONF-64-219-138.

From American Nuclear Society Meeting, San Francisco, Nov.-Dec. 1964.

It is shown that a permanently voided gap between the core and blanket in a fast reactor substantially increases the leakage effect when sodium is removed from the core by decreasing the return probability of neutrons from the blanket to the core so that a negative voiding coefficient for the core sodium can be attained. Since the neutrons which are not returned to the core are nearly all absorbed in the blanket, there is no loss in overall breeding ratio. (L.B.S.)

45539 XENON-INDUCED OSCILLATIONS. Canosa, Jose; Brooks, Harvey (Harvard Univ., Cambridge, Mass.). 5p. (CONF-650602-55). Gmelin, AED-CONF-65-125-54.

From American Nuclear Society, 11th Annual Meeting, Gatlinburg, Tenn.

The xenon-induced oscillations in the power level (fundamental mode) and in the power distribution (first harmonic) were studied for a slab reactor with prompt power reactivity feedback, using one-group space-dependent kinetic equations and linearized theory. The influence of the equilibrium power distribution is studied for two extreme cases when this distribution has a pure sine shape and a flat shape. (L.B.S.)

Design and Feasibility

45540 PROCESS AND APPARATUS FOR PRODUCING NUCLEAR ENERGY. (to Deutsche Forschungsanstalt fuer Luft und Raumfahrt e.V.). British Patent 1,000,050, Aug. 4, 1965. Priority date Aug. 29, 1961, Germany.

A method for utilizing nuclear energy consists of providing a stabilized confined plasma of a gaseous fissionable material, producing a nuclear reaction in the plasma, passing a gaseous working medium over the surface of the confined plasma, and using the working medium for power generation. The reactor for carrying out this process comprises a reaction chamber adapted to contain the gaseous fissionable material, UF_6; means to spontaneously ionize the material entering the chamber; an electromagnetic field system for confining and stabilizing the ionized fissionable material; and tubes terminating in an inwardly arcuate portion and united parallel to each other to form a pressure tight hollow cylinder. The cylinder is open at one end, closed at the other by the inwardly arcuate portions, and contains the working medium, hydrogen, introduced by pumping means into the tubes. An enclosure of moderator material surrounds the hollow cylinder and serves as moderator and reflector or is associated with a separate reflector surrounding the cylinder. (B.L.M.)

45541 NUCLEAR POWER REACTOR. Borst, Lyle B. (to Dow Chemical Co.). U. S. Patent 3,197,375. July 27, 1965. Filed Oct. 28, 1958.

The reactor patented has a core of fissile material of concentration and composition insufficient for a divergent neutronic chain reaction. The multiplication factor of the core approximates unity but does not exceed the prompt criticality of the material. Neutrons are provided from an external source in quantity sufficient to replace neutrons lost by leakage. A steady-state subcritical neutronic chain reaction is thus produced and sustained in the core, but the reactor may be operated without the precautions required for supercritical reactors. (A.G.W.)

Fuels

Refer also to abstracts 44453 and 44684.

45542 (BAW-272) RADIOCHEMISTRY OF NUCLEAR FUELS. Quarterly Progress Report No. 2, November 1, 1964-January 31, 1965. Mueller, J. J.; Dewell, E. H. (Babcock and Wilcox Co., Lynchburg, Va.). Contract AT(30-1)-3376. 53p. Dep. mn; CFSTI $3.00 cy, $0.50 mn.

Six aluminum capsules containing three samples each of uranium dioxide and mixed uranium dioxide and thorium dioxide were prepared for exposure in the BAWTR. The first capsule was used as a dry-run test dummy, and the other five were exposed in the reactor for approximately 2 hours at fluxes of about 7×10^{13} n/cm^2-sec. The capsules contained cobalt–aluminum alloy and iron flux wires, which were subsequently removed, cut into small lengths, and assayed for ^{60}Co and ^{54}Mn; the ^{60}Co monitored thermal neutrons, and the ^{54}Mn monitored fast neutrons. Thermal fluxes were calculated for all five of the exposed capsules. Fast flux calculations and fission product ^{137}Cs burnup data were essentially completed for the first exposed capsule. (auth)

45543 (EUR–2480.f) ETUDE DES PERTURBATIONS CIRCONFERENTIELLES ET AXIALES DANS UNE GAINE CYLINDRIQUE D'ELEMENT COMBUSTIBLE (METHODES MATHEMATIQUE ET RHEOANALOGIQUE). (Study of Circumferential and Axial Temperature Perturbations in a Cylindrical Fuel Element Canning (Mathematical and Rheoanalogical Methods)). Aranovitch, E.; Labarre, E.; Reynen, J. (European Atomic Energy Community, Ispra (Italy). Joint Nuclear Research Center). Aug. 1965. 76p. Dep. mn.

The effect on the local canning temperature of circumferential perturbations in the fuel heat generation, the heat transfer coefficients between fuel and canning on one side and between canning and fluid on the other side were studied mathematically by the decomposition of the perturbations into Fourier series. Several numerical cases are considered. (auth)

45544 (HW–79951(Pt.1)) FUEL CYCLE ANALYSIS CHAINED COMPUTER PROGRAMS GUIDE. A FORTRAN II, VERSION 2 MONITOR SYSTEM. McConiga, A. F. (comp.) (General Electric Co., Richland, Wash. Hanford Atomic Products Operation). Dec. 1, 1963. Contract AT(45-1)-1350. 55p. Dep. mn; CFSTI $3.00 cy, $0.50 mn.

A guide for preparing input data for reactor fuel cycle analysis chained computer programs based upon the MELEAGER-ALTHAEA burnup code is presented. A demonstration of program output using a simulated pressurized water reactor concept is included, together with a listing of effective cross sections as a function of neutron temperature. (D.C.W.)

45545 (HW–79951(Pt.2)) FUEL CYCLE ANALYSIS CHAINED COMPUTER PROGRAMS GUIDE. A FORTRAN II, VERSION 2 MONITOR SYSTEM. (General Electric Co., Richland, Wash. Hanford Atomic Products Operation). Dec. 1, 1963. Contract AT(45-1)-1350. 422p. Dep. mn; CFSTI $7.22 cy, $2.00 mn.

45546 (HW–79951(Pt.3)) FUEL CYCLE ANALYSIS CHAINED COMPUTER PROGRAMS GUIDE. A FORTRAN II, VERSION 2 MONITOR SYSTEM. (General Electric Co., Richland, Wash. Hanford Atomic Products Operation). Dec. 1, 1963. Contract AT(45-1)-1350. 90p. Dep. mn; CFSTI $3.00 cy, $0.75 mn.

45547 (INR–585/XIV/R) EK-10 DISPERSION FUEL ELEMENTS FOR EXPERIMENTAL AND UNIVERSITY REACTORS. Rutkowski, W.; Szteke, W.; Wieczorkowski, M. (Institute of Nuclear Research, Warsaw (Poland)). Dec. 1964. 29p. Dep.

In connection with investigation work on dispersion type fuels for experimental and university reactors, it appeared necessary to study EK-10 elements with UO_2-Mg dispersion cores. An informatory batch of such fuel rods was necessary for further testing experiments. Investigation and production data for the fuel rods mentioned above are described. (auth)

45548 (WAPD-TM-498) THE STEADY CREEP SWELLING OF A CLAD NUCLEAR FUEL PLATE. Small, W. C. (Bettis Atomic Power Lab., Pittsburgh, Pa.). July 1965. Contract AT-11-1-GEN-14. 20p. Dep. mn; CFSTI $1.00 cy, $0.50 mn.

An analysis is presented for the steady creep swelling of a long clad nuclear fuel plate due to fission gases. The effect of this gas pressure is represented by a dilatation term in the equations which also allow for the inelastic compressibility resulting from external constraints (cladding). The problem is idealized as a semi-infinite clad plate on a dilatating foundation (fuel). Alternative one-dimensional strain and stress models are presented for the foundation, and emphasis is placed on the cladding deformation in the vicinity of the edge. An approximate solution is obtained for the stress model utilizing a combination of the collocation and minimum potential energy methods. The results show that, for the range of parameters considered, the cladding reaches its maximum lateral displacement at about three cladding thicknesses from the edge. (auth)

45549 HEAT TRANSFER AND PRESSURE DROP OF A GAS-COOLED REACTOR FUEL ELEMENT CAN MODEL WITH INCLINED POLYZONAL SPIRAL FINNING. Dokmanovic, B.; Spasojevic, D. Bull. Boris Kidrich Inst. Nucl. Sci., 16: 100-23(Apr. 1965).

Heat transfer, pressure drop and flow pattern of a gas-cooled reactor fuel element model with inclined polyzonal spiral finning were investigated. A brief description of the apparatus, the method of measurement and the calculation of the results is given. Axial temperature distribution in the fin root and local values of St_x are given. Correlations for St_{kmin}, St_{kaver}, and f_{aver} as a function of Re are derived. (auth)

45550 NUCLEAR FUEL ASSEMBLY END SUPPORTS. Dodd, John Alan (to Societe Anglo-Belge Vulcain, S.A.). British Patent 1,000,339. Aug. 4, 1965. Filed Apr. 25, 1963.

An end fitting is described that is particularly suited to secure a fuel assembly to a support grid in a marine reactor in which movement of fuel assemblies with respect to the support grid under the effect of the movement of the ship is to be restrained. The end fitting comprises a threaded spindle to penetrate an aperture in the grid, a shoulder to limit this penetration, and a threaded nut to be screwed into the spindle. The co-operating threads on the nut and the spindle are discontinuous and capable of disengagement by partial rotation of the nut to permit axial displacement of the nut. Locking means to counter the rotation of the nut comprise a deformable ring formed as an integral axial extension of the nut. The ring is reversibly deformable into locking engagement with a recess in the spindle. (B.L.M.)

45551 IMPROVEMENTS IN OR RELATING TO FUEL ELEMENTS. Pickman, David Openshaw (to United Kingdom Atomic Energy Authority). British Patent 1,001,534. Aug. 18, 1965. Filed Aug. 1, 1963.

A reactor fuel element has a sheath provided with groups of antibowing lugs spaced along the length of the sheath. At least one of the antibowing lugs situated in a group of the lugs at the end of the sheath is provided with radially extensible means that are capable of being reduced in effective radial length from an extended position against the action of resilient means tending to hold it in the extended position. The radially extensible means is made up of a lever arm pivoted at one end on one of the groups of lugs at the one end of the sheath and spring means acting between the lug and the lever arm tending to push the arm outwardly in an extended position from the lug. (B.L.M.)

45552 IMPROVEMENTS IN OR RELATING TO HEAT-EXTRACTING DEVICES AND NUCLEAR FUEL ELEMENT SHEATHS INCORPORATING SAME. (to Commissariat a l'Energie Atomique). British Patent 1,001,975. Aug. 18, 1965. Priority Nov. 18, 1960, France.

A heat-exchanger arrangement of the type in which a heat exchange wall is in contact with the transfer fluid is described. The wall is provided with a plurality of fins arranged on the heat exchange surface in a chevron or herringbone pattern and inclined to the surface. The inclination of each fin varies along its length. At least the downstream or outlet ends of the fins are inclined out of the normal to the exchange surface. (B.L.M.)

45553 NUCLEAR REACTOR FUEL ELEMENTS. Blake, Leslie Reginald (to United Kingdom Atomic En-

ergy Authority). U. S. Patent 3,197,381. July 27, 1965. Priority date Oct. 4, 1960, Great Britain.

A fuel element, particularly for fast reactors, is composed of a string of individually sheathed fuel sections arranged end to end in a common outer sheath with thermally bonding material between the sheaths. In each of the fuel sections the fuel occupies only 50–90% of the volume provided, leaving space for expansion of the fuel and for liberated gaseous fission products. The outer sheaths of the elements are preferably formed with projections that can engage with projections of adjacent elements to form an assembly that can be charged into a reactor as a single unit. (A.G.W.)

45554 INTERNALLY STRENGTHENED FLAT FUEL PLATE. Zambrow, John L. (to Sylvania Electric Products Inc.). U. S. Patent 3,197,382. July 27, 1965. Filed Aug. 11, 1960.

Flat, metal-clad ceramic-core fuel plates are intended to provide improved thermal conductivity and resistance to internal pressure from gaseous fission products. The fuel plates consist essentially of a metal tray containing coplanar square flat UO_2 ceramic fuel slabs. A metal dowel is inserted into a hole in each fuel slab, the assembly is covered with a metal sheet, and the edges are hermetically sealed. The metal dowels within the slabs are metallurgically bonded to both the top and bottom plates and act as structural columns that strengthen the assembly. (A.G.W.)

45555 NUCLEAR REACTOR FUEL ELEMENT. Maillet, Ennemond (to Commissariat a l'Energie Atomique). U. S. Patent 3,197,383. July 27, 1965. Priority date Feb. 9, 1962, France.

The reactor fuel element patented consists essentially of a rod of fissile material enclosed in a can and disposed within a casing. The external surface of the can and the internal surface of the casing are formed with opposed concave surfaces that cooperate to form cooling-gas passages between them. Each concavity on the external surface of the can is provided with oblique fins that cooperate with the concavity of the casing to impart a helical flow to gas moving along the passage. Projections between adjacent concavities engage to center the can with respect to the casing. (A.G.W.)

45556 NUCLEAR THERMIONIC CONVERTER. Gleason, Charles H.; Feaster, Gene R. (to Westinghouse Electric Corp.). U. S. Patent 3,201,619. Aug. 17, 1965. Filed June 7, 1960.

A reactor fuel element is combined with a thermionic converter to form a device for converting thermal energy developed by a nuclear reactor directly into electrical energy. A cathodic cladding tube spaced inside a generally tubular anodic envelope is capable of electron emission and is electrically insulated from the envelope. A mass of fissile material in the cladding tube is capable of fissioning so as to sustain a chain reaction when placed in a lattice array of similar fuel element-converters. Electrical contacts to the tube and the envelope are provided. Material capable of ionization by the γ radiation normally associated with a reactor is contained in the space between the tube and the envelope. An arrangement is suggested for mounting and operating a relatively large number of such converters to obtain usable quantities of electrical energy. (A.G.W.)

Power and Power-Breeder Reactors

Refer also to abstract 44463.

45557 (ACNP–65557) PATHFINDER ATOMIC POWER PLANT TECHNICAL PROGRESS REPORT, JULY 1964–SEPTEMBER 1964. (Allis-Chalmers Mfg. Co., Bethesda, Md. Atomic Energy Div.). June 1965. Contract AT(11-1)-589. 24p. Dep. mn; CFSTI $1.00 cy, $0.50 mn.

Test 302 (Full Boiler Core Loading and Criticality) was completed for the boiler core of 96 2.2 w/o elements. In this test, control-rod bank and group critical heights rod-differential worths, and total and most reactive single-rod-full-out shutdown margins were determined as a function of the number of boron-stainless-steel poison shims in the core. The pre-test analysis and experimental data taken during this test are presented. The pre-test analysis of test 303 (Full Core Loading and Criticality) is presented. (M.O.W.)

45558 (AGN-TM-409) ARMY GAS-COOLED REACTOR SYSTEMS PROGRAM. IB-17R-2 IN-PILE TEST. (Aerojet-General Nucleonics, San Ramon, Calif.). Feb. 1965. Contract AT(10-1)-880. 146p. Dep. mn; CFSTI $4.00 cy, $1.00 mn.

An instrumented prototype fuel element of the design proposed for the second core loading for the reactor of the demonstration mobile, nuclear power plant (ML-1) was tested in-pile. The test element, designated for the IB-17R-2, operated in the General Electric Test Reactor for 5819 hr in air at ML-1 reference flow and temperature conditions. The objectives of the test included the development of data for comparison with earlier results; for evaluation of fluid flow characteristics to verify engineering calculations and tests; for evaluation of the neutronic performance; and for confirmation of the design by long-term in-pile irradiation. Evaluation of data indicated the following: the pressure drop was slightly less than predicted by the engineering calculations; the turbulence promoters provided on the cladding increased the heat transfer coefficient sufficiently to reduce the nominal cladding operating temperature 35 to 50°F (compared with smooth cladding); and the neutronic performance and other parameters were essentially as predicted. Post irradiation examination revealed minor oxidation of the Hastelloy X fuel pin cladding; slight reduction in ultimate and tensile strengths of the cladding; the presence of a second phase on the inside surface of some fuel pins; cracking in the fuel particles and beryllia matrix; and higher than anticipated release of fission product gas. (auth)

45559 (ANL–7000, pp 64-8) PLUTONIUM RECYCLE DEMONSTRATION EXPERIMENT IN EBWR. (Argonne National Lab., Ill.).

The fabrication of the control rods and fuel elements is described. (W.L.G.)

45560 (ANL–7011) METHOD FOR NEUTRON-FLUX STUDIES IN AN OPERATING POWER REACTOR USING BASE AND CADMIUM-COVERED RADIOACTIVANTS. Knapp, W. G. (Argonne National Lab., Ill.). Mar. 1965. Contract W-31-109-eng-38. 26p. Dep. mn; CFSTI $2.00 cy, $0.50 mn.

A method of study of neutron-flux distributions and energy spectra in the core of an operating nuclear power reactor was developed. The foil-activation technique, including the use of cadmium absorber covers, was adapted in a way that overcomes the access limitations of most power reactors. Small spherical foils are inserted through the tube irradiation facilities having a $^3/_{16}$-in. OD into selected locations in the core without affecting the reactor operation. Both insertion and removal are performed with pneumatic transfer methods. The small ($^1/_{16}$-in.-diameter) spherical foils can be fabricated from a variety of detector materials and are particularly adapted to automatic analysis techniques. An automatic sample changer is described that was used extensively during the initial demonstration of the method in the Experimental Boiling Water Reactor (EBWR). Modifications and recommendations based on actual experience with the method in the EBWR are given. (auth)

45561 (APDA–172) A PASTE CONCEPT FOR FAST REACTOR BLANKET APPLICATIONS. Kovacic, E. C.; Chamberlain, H. V.; Klickman, A. E.; Moore, C. R. (Atomic Power Development Associates, Inc., Detroit, Mich.). May 1965. Contract AT(11-1)-865. 96p. Dep. mn; CFSTI $3.00 cy, $0.75 mn.

Results of previous investigations (e.g., bed density under static and flowing conditions, dimensionless paste flow correlations, disengagement of escaped fission gases, particle

stitching by fission fragment thermal spikes, particle sintering and attrition, particle-container compatibility, mechanical and engineering design studies, etc.) on the applications of pastes for fast reactor core applications are shown to be applicable to the paste blanket concept and to support its basic feasibility. Application of the concept to future fast reactor designs is exemplified by the conceptual design study of a paste blanket for use in a modular-type reactor utilizing a molten plutonium fuel alloy core concept. Physics analyses show that in such a reactor, breeding ratios (i.e., ratio of plutonium produced to fissile material destroyed) as high as 1.9 may be attained. The effect on breeding ratio of variations in the blanket thickness and composition is reported; in all cases it has been shown that breeding ratios of 1.5 or greater may be obtained. Consideration of the thermal and mechanical engineering problems indicates no basic feasibility problems and reveals no difficulties unique to the modular blanket concept. The pertinent design and performance data for the blanket are presented and the general arrangement of the core and blanket is illustrated. A conceptual design study has been made of an inpile test loop of the re-entry type that is intended as a proof-of-principle demonstration of the basic concept. The study shows that a meaningful experiment could be conducted in the reflector region of the Fast Reactor Core Test Facility. The general arrangements of the test loop in the FRCTF and of the inpile test assembly are illustrated, and the pertinent design and performance data for the mockup blanket test section are presented. The experimental program which is being conducted in support of the overall program is reviewed. Results of studies made utilizing simulant pastes of copper particles in water contained in plastic components have demonstrated the long-term, unattended operability of the paste system, have extended the basic knowledge of paste density and paste flow beyond the simple geometries to geometries of interest to the conceptual paste blanket, and have provided necessary information for the design of actual paste systems. One such system, a stainless steel loop which will permit testing actual pastes of fertile material particles in sodium, has been built and is described. (auth)

45562 (APDA-174, pp 71-3) COMPILATION OF FERMI EXPERIENCE. Project Agreement No. 15. Ball, G. L.; Hess, J. W.; Kovacic, E. C.; Lindsey, P. S.; Mueller, R. E.; Peters, N. T.; Reicks, G. H.; Siegel, S. (Atomic Power Development Associates, Inc., Detroit, Mich.).

Work was initiated on the preparation of eight reports covering the experience gained from the Enrico Fermi Atomic Power Plant project. Important components and systems are being treated in individual reports. A final draft was completed for the report covering the Na system level detectors. Brief, narrative descriptions of 26 proposed additional reports on the Fermi plant were written. (auth)

45563 (BNWL-106) MINIMIZED FUEL CYCLE COST FOR A SIMULATED HEAVY WATER REACTOR. PART I. Deonigi, D. E.; Horton, P. A.; McConiga, A. F. (Battelle-Northwest, Richland, Wash. Pacific Northwest Lab.). Apr. 1965. Contract AT(45-1)-1830. 90p. Dep. mn; CFSTI $3.00 cy, $0.75 mn.

The minimum fuel costs for a heavy-water-moderated power reactor were calculated over a series of changing economic conditions, assuming that the lattice spacing will remain fixed. The results are presented in graphical form. (D.C.W.)

45564 (BNWL-SA-85) TRANSPORT AND BUILDUP OF RADIOACTIVE MATERIALS IN REACTOR SYSTEMS AS DETERMINED BY SHUTDOWN RADIATION MEASUREMENTS. Perrigo, Lyle D. (Battelle-Northwest, Richland, Wash. Pacific Northwest Lab.). Mar. 5, 1965. Contract AT(45-1)-1830. 14p. Dep. mn; CFSTI $1.00 cy, $0.50 mn.

A program for measuring the radiation shutdown levels on the Plutonium Recycle Test Reactor is reported. The shutdown radiation measurement technique is described in detail with reference to criteria and techniques, site locations, and measurement devices. The results of the PRTR shutdown radiation measurement program are presented by considering past PRTR operation composed of three phases: reactor startup and operation to the rupture, the rupture and decontamination, and post decontamination operation. (M.O.W.)

45565 (CEA-R-2781) RADIOPROTECTION ET OPERATIONS DE DECONTAMINATION SUR LE COULOIR VIBRANT CENTRAL DE LA PILE G.3. (Radioprotection and Decontamination Operation on the Central Vibrating Channels of the Reactor G 3). Chassany, Jean-Philippe; Cohendy, Gerard; Rodier, Jean (Commissariat a l'Energie Atomique, Chusclan (France). Centre de Production de Plutonium de Marcoule). May 1965. 19p. Dep. mn.

The dose rate in the vibrating channels room of the discharge system, which is due to the contamination of one of the channels by a ruptured can, was high. It was necessary to intervene in order that normal maintenance could be carried out on this equipment. The operation was carried out from a neighboring room using cleaning tubes, and then directly, after numerous precautions were taken. Radioprotection was made very difficult because of the irradiation and of the powdery state of the contamination. The average individual integrated dose for the 122 persons having taken part in this 2-month operation was 362 MRem. (auth)

45566 (CEA-R-2785) MESURE DE RADIOACTIVITE A L'INTERIEUR DU CAISSON DE LA PILE G.3 APRES 4 ANS DE FONCTIONNEMENT. (Radioactivity Measurements Inside the Pressure Vessel of the Reactor G3 After 4 Years Operation). Chassany, Jean-Philippe; Guillermin, Pierre; Delmar, Jean (Commissariat a l'Energie Atomique, Chusclan (France). Centre de Production de Plutonium de Marcoule). Apr. 1965. 9p. Dep. mn.

At the end of the piping coming into the vessel, the dose rate reached 75 mR/hr and 100 mR/hr near the deflector. On the other side of this deflector, it was still 100 mR/hr and then increased rapidly to over 1 R/hr at 1 meter from the startup chambers. On the sides, the flux tended to decrease (80 mR/hr) and was 2 R/hr at a height of 3 meters. This dose rate could certainly have been decreased by discharging the peripheral zone of the reactor. Consequently, it should be possible to enter the vessel, if necessary, if great care is taken to avoid contamination and if the total dose is followed as precisely as possible during the operations. (auth)

45567 (CVNA-235) RESEARCH AND DEVELOPMENT PROGRAM. Quarterly Progress Report, October-December 1964. (Westinghouse Electric Corp., Pittsburgh, Pa. Atomic Power Div.). Contract AT(30-1)-2289. 65p. Dep. mn; CFSTI $3.00 cy, $0.75 mn.

Most of the design effort during this quarter was concentrated on the 65 Mw study. DNB ratios were evaluated for rod withdrawal taking into account local conditions in the hot pressure tube. Data were gathered on coolant system corrosion product spectra and radiation in the side shielding. Data are included on thermal and hydraulic core design for 65.0 Mw gross fission power. Results of shutdown nuclear tests are included along with those from flux wire irradiation measurements, and the core follow program for the quarter. Results of ultrasonic inspection of pressure tubes are included followed by a hazards report. (J.R.D.)

45568 (CVNA-238) CVTR—HIGH pD TESTS. Post-Construction Research and Development Program. Cameron, W. Wayne (Carolinas Virginia Nuclear Power Associates, Inc., Parr, S. C.). Aug. 1965. Contract AT(30-1)-2289. 29p. Dep. mn; CFSTI $2.00 cy, $0.50 mn.

The tests and the test results obtained from operation of the Primary Coolant System of the Carolinas Virginia Tube Reactor (CVTR) at high pD are described. These tests were performed in April and May of 1965 as part of the Post Construction Research and Development Program, AEC Contract No. AT(30-1)-2289. Ammonia was injected into the previously neutral primary coolant and data were obtained on system chemistry, reactivity, flows, pressure drops, and primary and moderator temperatures,

during changing pD levels and at high pD operation. After removing the ammonia from the system by ion exchange, lithium hydroxide was injected into the coolant, and similar test data were obtained. No significant changes in loop flow rate, flow redistribution, or reactivity were noted. (auth)

45569 (DP-976) METAL FUEL TUBE MANUFACTURE. Nemeth, Stephen R. (comp.) (Du Pont de Nemours (E. I.) and Co., Aiken. S. C. Savannah River Lab.). July 1965. Contract AT(07-2)-1. 87p. Dep. mn; CFSTI $3.00 cy, $0.75 mn.

Development and fabrication of tubular coextruded Zircaloy-clad uranium metal fuel elements for a heavy water-moderated-and-cooled power reactor is described. Approximately 200 experimental uranium tubular elements, 10 feet long, were fabricated of which 36 were irradiated. The remainder were used for evaluation of fabrication techniques and flow tests. Although the majority of tubes had cores of unalloyed uranium, uranium alloys with 2 wt % Zr and with Fe, Si, Al, and Mo (approximately 0.2% total) were also included. Some 24 short-length (12-inch) elements were fabricated using brazed end seals rather than the integral end seals used for the long tubes. Fabrication techniques were developed for manufacture of 80 Zircaloy-clad Zr–^{235}U alloy tubular driver elements, 10 feet long, for the HWCTR. Utilizing the techniques developed for uranium fuel tubes, a number of Th–^{235}U metal fuel tubes were coextruded to pilot the manufacture of Th–^{233}U breeder reactor fuel. (auth)

45570 (EUR-2422.i) APPARECCHIATURA DI CONTROLLO AUTOMATICO DEL REATTORE DRAGONE. (Dragon Reactor Automatic Control Equipment). Franchi, M.; Garroni, A.; Sciuto, F. (European Atomic Energy Community, Ispra (Italy). Joint Nuclear Research Center). 1965. 53p. Dep. mn.

The DRAGON reactor automatic control equipment, regulating the cooling gas outlet temperature and the power is described. This special purpose electronic controller is entirely made with solid state devices. (auth)

45571 (EUR-2431.f) ANALYSEUR DE FONCTIONS DE TRANSFERT POUR LE REACTEUR DRAGON. (Transfer Functions Analyser for Dragon Reactor). Bredael, I.; Sciuto, F. (European Atomic Energy Community, Ispra (Italy). Joint Nuclear Research Center). 1965. 61p. Dep. mn.

The description of a transfer functions analyzer is given. The interest of this realization resides in the measurement accuracy and in the flexibility on use. The equipment, completely transistorized, is based on digital techniques. (auth)

45572 (GEAP-4755) NUCLEAR SUPERHEAT PROJECT TWENTY-FIRST QUARTERLY REPORT, AUGUST–OCTOBER 1964. Fiock, W. L. (General Electric Co., San Jose, Calif. Atomic Power Equipment Dept.). Nov. 1964. Contract AT(04-3)-189. 136p. Dep. mn; CFSTI $4.00 cy, $1.00 mn.

Work was completed on the post-irradiation examination of ESH-1.1 and ESH-4 fuel elements. Test results on Type 304 stainless steel-to-Zircaloy and Incoloy-to-Zircaloy process tube joints showed that these joints perform satisfactorily. Examination of the SC-8 coupon capsule indicated that a worn filler block permitted excessive vibration, leading to failure of a coolant tube. The capsule was removed from the reactor after 1½ cycles (1.1×10^{20} nvt) and the coupons prepared for testing at RML. The thermal aging characteristics of Incoloy-801, Incoloy-825, Inconel-625, René-62, Hastelloy-X and Inconel-718 were determined at 1000 to 1300°F. The ultimate strength and ductility were evaluated at room temperature and elevated temperatures. Iconel-625, Incoloy-801, and Incoloy-825 indicated favorable characteristics with regard to strength and ductility. Work was initiated on the evaluation of B content in Incoloy-800 with respect to reduction in tensile properties due to irradiation. Results obtained from the controlled-environment strain cycler were inconclusive and testing with this device was discontinued. The corrosion data for Incoloy-800 were re-evaluated on the basis of the combined results from commercial Incoloy-800 and the low Al-Ti Incoloy-800. A corrosion model makes a general corrosion allowance of 0.0022 in. in three years at the upper 95% confidence level. Testing of superheat cladding materials in the CL-4 loop was discontinued for programmatic reasons. All dynamic corrosion testing of superheat cladding materials is now being done in the CL-1 facility with five heater positions. Inconel-600 testing was completed with results that indicate that this material could experience heavy scaling within a few months at 1300°F. Testing in depth of Inconel-625 was initiated. Three heater sheaths were exposed for 14 days in CL-4 to the cycle run using 0.5 ppm Cl^- as $FeCl_3$. No detectable post-operation damage has been noted. Heat transfer tests were made in steam with Reynolds numbers up to 10^6 to obtain correlation with variable fluid properties. Preliminary tests conducted with boundary layer turbulence promoters in the steam test section (tubular section with steam flow on the inside) confirm that such devices improve the heat transfer and that smooth tube correlation methods can be used for the turbulence promoter data. Multi-rod tests were conducted with smooth rods in the air test facility in preparation for investigations of turbulence promoters with rod geometries. Results of studies indicate that substantial savings in fuel cost and capital costs can be realized through the use of turbulence promoters. The ESH-3A fuel bundle was fabricated and it is available for hot-fuel loading. Results of RML examination of the BONUS velocity tube (Type 347 or 348 stainless steel) indicate that this material performed satisfactorily. Peak exposures were on the order of 1.8×10^{20} nvt (energy >1 Mev). Shielding necessary for operation of mixed spectrum critical facility at 2000 watts without interference to nearby counting facilities was installed. Reconstitution of the fast core enrichment from 23.6 to 23.1% accomplished by exchanging one 26.5% enriched rod for a natural enriched rod in 30 bundles, decreased the fast core power from 40 to approximately 33% of the total power. Additional Doppler measurements were made. Flooding effect measurements were made with one and four bundles, with and without poison materials. Polyethylene was the hydrogeneous material, and Hf, Eu_2O_3, and B_4C were the poisons used. Results of the four-bundle experiments indicate that the flooding reactivity could be reduced to a negligible amount through the utilization of epithermal poisons, and that the reactivity penalty for the required amounts of these poisons would be small. Fast core control worth was evaluated by both the differential period and pulsed neutron techniques. Power distribution mapping was completed for both the 23.6 and 23.1% U-235 enriched fast core. Uranium foils were irradiated at selected locations throughout the core and then counted to establish local power levels. Calculations utilizing new cross section data were found to over-predict fast core reactivity by about 3%. (J.R.D.)

45573 (GEAP-4902) PERFORMANCE OF FUEL RODS TO INVESTIGATE INCREASED THERMAL OUTPUT CAPABILITIES. Hoffmann, J. P.; Ogawa, S. Y.; Williamson, H. E. (General Electric Co., San Jose, Calif. Atomic Power Equipment Dept.). June 1965. Contract AT(04-3)-189. 87p. Dep. mn; CFSTI $3.00 cy, $0.75 mn.

Fuel rods were designed to investigate increased thermal output capabilities and were irradiated in two VBWR test fuel assemblies. One design was to test and evaluate the long-term behavior of UO_2 fuel rods operated at high power densities associated with UO_2 centerline temperatures near the UO_2 melting point. The second design was to test and evaluate the improvement in the fuel bulk thermal conductivity by the use of molybdenum additions to the UO_2. Both fuel rod designs used 0.508-mm wall, 1.308-cm OD stainless steel cladding. Irradiation test experiences and the results of postirradiation examinations performed are reported. (auth)

45574 (GEAP-4914) RADIAL VANE STEAM SEPARATOR DEVELOPMENT. Fourth Quarterly Report, April–June 1965. Moen, R. H. (General Electric Co., San Jose, Calif. Atomic Power Equipment Dept.). July 1965. Contract AT(04-3)-189. 69p. (EURAEC-1450). Dep. mn; CFSTI $3.00 cy, $0.75 mn.

Work Performed Under United States–Euratom Joint Research and Development Program.

Tests of the two-vane adjustable nozzle unit were completed. These tests showed good performance, but led to the discovery of a major problem — the movement of the separated air or steam with the water is much greater than thought in the past. This problem is being attacked by tests of the FCRV-3 separator which was built in anticipation of the problem. Testing of the two-vane clear plastic unit has begun and is giving useful information. The Large Air-Water Test Facility modification was completed and the FCRV-3 installed for testing. Useful design graphs for wall water layer thickness were prepared. (auth)

45575 (GMAD–3078-28) MCR SMALL SOURCE EXPERIMENTS. Schamberger, R.; Celnik, J. (United Nuclear Corp., White Plains, N. Y. Development Div.). May 3, 1965. Contract AT(30-1)-3078. 103p. (EDR-4195). Dep. mn; CFSTI $4.00 cy, $0.75 mn.

For Allison Div., General Motors Corp., Indianapolis, Ind.

Military Compact Reactor (MCR) shield design analytical techniques and cross sections were tested by comparing calculations with measurements for experiments emphasizing the secondary gamma production in specific test materials. Measurements were made with a gamma spectrometer behind a configuration consisting of a layer of gamma shielding material (the test sample) adjacent to a small polonium-beryllium neutron source, followed by neutron and gamma shielding material to reduce extraneous detector response. Calculations of spectrometer response for samples of lead, tungsten, and titanium hydride were performed with a three-dimensional Monte Carlo code, derived from the one-dimensional Monte Carlo codes used in the MCR preliminary design shield analysis. The calculations generally gave satisfactory predictions of the measurements. Differences between the measured and calculated responses indicated that some of the cross sections used, particularly for lead, were low and should be revised. It is estimated that these revisions would lead to a 10% increase in predicted total dose rate external to the MCR shield. (auth)

45576 (IA–1039) CALCULATION OF THE DOPPLER EFFECT IN FAST REACTORS. Szwarcbaum (Shaviv), G.; Yiftah, S. (Israel Atomic Energy Commission, Yavne. Soreq Nuclear Research Center). May 1965. 85p. Dep. mn.

Methods and parameters used in the calculation of the Doppler effect in typical 800 to 2500 liter fast reactors are described. The influence of the chemical composition of the fuel and the plutonium isotopic composition on the total Doppler effect are examined. (auth)

45577 (IDO–28645) ARMY GAS-COOLED REACTOR SYSTEMS PROGRAM. Quarterly Progress Report, January 1–March 31, 1965. (Aerojet-General Nucleonics, San Ramon, Calif.). May 14, 1965. Contract AT(10-1)-880. 133p. Dep. mn; CFSTI $3.00 cy, $1.00 mn.

The technical progress of the Army Gas-Cooled Reactor Systems Program is summarized. The ML-1 power plant was operated for about 350 hr during the report period. A leak between the process gas system and the shield solution system was discovered late in January. The reactor skid was uncoupled from the power conversion skid and transferred in the fully fueled condition to the Gas-Cooled Reactor Facility. The repair of the leak was essentially complete by the end of March. The data developed in the afterheat experiment, during which the maximum fuel element temperature observed following a reactor scram from sustained operation at 3.1 Mw(t) was 1475°F with no coolant flow except that provided by the coastdown of the t-c set, was evaluated and the ANASIM (transient temperature prediction) computer program was normalized to the experimental results. The permissible fuel element cladding hot spot temperature was revised upward from 1750 to 1800°F for 10,000-hr operation based on recent materials evaluation and thermal analysis. The design of a partial replacement core, designated ML-1-IM, was initiated. These fuel elements will be used to "spike" the ML-1-I core; it is anticipated that this procedure will increase the reactivity lifetime of the original core loading to 15,000 hr. The improved ML-1 precooler, the new fans for the precooler air-side cooling assembly and the alternator speed reducer were received. Fabrication of the alternator continued and the design and fabrication of an improved lubrication system was initiated. The investigation of the cladding failure in the IB-17R-3 test element continued. Hot cell examination revealed a small crack in the turbulence promoter section of the cladding; the metallographic examination was complete at the end of March and the results were being evaluated. Evaluation of the performance limits of Hastelloy X as a fuel element cladding material continued. A series of photoelastic stress experiments were conducted to verify the design and calculational procedures for an ML-1-type calandria. Optimization of the ML-1A radiation shielding continued as did modification of the GCR Facility. The conceptual design of a closed-cycle test facility (GDF) was completed. (auth)

45578 (JAERI–1080) NUCLEAR PARAMETRIC STUDY OF THE PRESSURE TUBE-TYPE D_2O MODERATED LATTICES. Furuhashi, Akira; Shindo, Ryuichi (Japan Atomic Energy Inst., Tokyo). Sept. 1965. 61p. Dep. mn. (In Japanese).

The results of nuclear parametric studies of pressure tube-type D_2O moderated lattices, which were carried out using the computer code WATCH TOWER-II (a point burnup code for D_2O moderated power reactors), are presented. Results of survey calculations connected with the conceptual design works of 300Mw(e) D_2O moderated power reactors using five kinds of cooling systems are presented. Also included are results of the optimization studies on lattice structure, enrichment and other parameters with respect to the fuel burnup; and emphasis is on the boiling H_2O- and CO_2-cooled systems. Nuclear fuel economy and the utilization of plutonium fuel are also briefly discussed. (auth)

45579 (NAA-SR-11414) SRE HEAT TRANSFER SYSTEM DEMOLITION. Nicholson, J. O. (Atomics International, Canoga Park, Calif.). Aug. 31, 1965. Contract AT(11-1)-Gen-8. 25p. Dep. mn; CFSTI $1.00 cy, $0.50 mn.

Demolition operations were carried out on the heat transfer systems as part of the SRE Power Expansion Program. The preparation for the demolition and the removal and disposal of the heat transfer systems are discussed. The radiation experience is considered briefly. (D.L.C.)

45580 (NP-15283) RAPPORT SUR LES PERSPECTIVES DE DEVELOPPEMENT DES CENTRALES NUCLEAIRES EN FRANCE. (Report on Prospects for Development of Nuclear Power Stations in France). (Commission Consultative pour la Production d'Electricite d'Origine Nucleaire (France)). 1964. 74p. Dep. mn.

Includes ANNEXES AU RAPPORT DE LA COMMISSION. (Addenda to the Report of the Commission).

The evolution of the production of electricity and of the corresponding needs in primary energy is discussed. The present economic data and the future prospects of classical nuclear power stations are given. The major technical uncertainties are discussed. The possible development of nuclear power and the eventual difficulties with respect to the industrial plan and to the supplies of nuclear fuels are indicated. The priority to be accorded to the development of nuclear power plants in France for the period of 1965 to 1970 is given. (tr-auth)

45581 (NP–15291) DESIGN STUDY OF A SMALL NUCLEAR POWER PLANT FOR AUSTRIA. Gruemm, H.; Erbacher, W. (Arbeitsgemeinschaft Kernkraftwerk der Elektrizitaetswirtschaft, Vienna (Austria)). Sept. 1964. 19p. Dep. mn.

The detailed design study of a small (15 Mw(e)) nuclear power plant with a PWR of advanced design for a site in Austria is included. In addition a study of a competitive 250 Mw(e)-nuclear power plant will be evaluated for reasons of comparison. (auth)

45582 (NP-15320) OUTLOOK ON THE UTILIZATION OF THORIUM IN POWER REACTORS IN ITALY. (Ente Nazionale per l'Energia Elettrica, Rome (Italy)). Feb. 1964. 102p. Dep. mn.

The results of an economic analysis aimed at examining the prospects of employing thorium in Italian nuclear power plants are presented. A survey of the general features and main components of fuel cost of the U-Th cycle, as well as a brief review of the thorium reactors operating or being built today are presented. The results of an economic comparison of the uranium cycle with thorium cycles in graphite-gas, pressurized water, and boiling water reactors, with special reference to the SIMEA, SELNI, and SENN reactors are included. (M.O.W.)

45583 (NP-15365) PROJEKT SCHNELLER BRUETER KARLSRUHE. JAHRESBERICHT 1963. (Karlsruhe Fast Breeder Project. Annual Report, 1963). (Kernforschungszentrum, Karlsruhe (West Germany)). May 1964. 80p. Dep. mn.

The Karlsruhe breeder project is the result of an association between the Karlsruhe research center and Euratom. The present annual report, the first issued since the inception of the project, gives a brief review of the development of the project. The present stages of component development are described in some detail. Publications of results obtained are tabulated in an appendix. (J.S.R.)

45584 (NYO-3379-1) DEVELOPMENT OF REALISTIC REQUIREMENTS FOR PM-TYPE REACTOR INSTRUMENTATION. Task 1 Topical Report. Lenk, Pedro R.; Wurster, D. E.; McCreary, Joseph C. (Bailey Meter Co., Wickliffe, Ohio). July 30, 1965. Contract AT(30-1)-3379. 164p. Dep. mn; CFSTI $5.00 cy, $1.00 mn.

Reactor instrumentation philosophy and implementation are reviewed to develop realistic instrumentation requirements for PM-type reactors. An instrumentation system that completely satisfies both the functional and integrity requirements is described. (D.C.W.)

45585 (ORNL-P-1502) APPLICATION OF AN ON-LINE DIGITAL COMPUTER TO A REACTOR EXPERIMENT. Engel, J. R. (Oak Ridge National Lab., Tenn.). [nd]. Contract W-7405-eng-26. 4p. (CONF-651101-15). Dep. mn.; CFSTI $1.00 cy, $0.50 mn.

For Presentation at 13th Conference on Remote Systems Technology, Washington, D. C.

It is reported that an on-line digital computer (Bunker-Ramo Model 340) is now being used in conjunction with the Molten-Salt Reactor Experiment. The expectations and some routine calculations performed by the computer are discussed. (M.O.W.)

45586 (ORNL-P-1503) PREDICTED AND OBSERVED NUCLEAR CHARACTERISTICS OF THE MOLTEN SALT REACTOR EXPERIMENT. Engel, J. R.; Haubenreich, P. N.; Prince, B. E. (Oak Ridge National Lab., Tenn.). [nd]. Contract W-7405-eng-26. 3p. (CONF-651101-16). Dep. mn; CFSTI $1.00 cy, $0.50 mn.

From 13th Conference on Remote Systems Technology, Washington, D. C.

Experiments previously carried out in the MSRE are reviewed. The combination of results from these experiments tend to demonstrate the nuclear characteristics of the MSRE. Conclusions are presented. (M.O.W.)

45587 (ORNL-P-1504) THERMAL STRESS CONSIDERATIONS IN THE MOLTEN SALT REACTOR EXPERIMENT. Gabbard, Charles H. (Oak Ridge National Lab., Tenn.). [1962]. Contract W-7405-eng-26. 4p. (CONF-651101-17). Dep. mn; CFSTI $1.00 cy, $0.50 mn.

From 13th Conference on Remote Systems Technology, Washington, D. C.

It is reported that the fuel and coolant pumps, the freeze flanges, and the coolant piping penetrations through the containment vessel wall in the MSRE were found to have relatively high thermal stresses. A brief discussion of these thermal stresses is given. (M.O.W.)

45588 (ORNL-TM-1060) MOLTEN SALT CONVERTER REACTOR. DESIGN STUDY AND POWER COST ESTIMATES FOR A 1000 MWE STATION. Alexander, L. G.; Carter, W. L.; Craven, C. W.; Janney, D. B.; Kerlin, T. W.; Van Winkle, R. (Oak Ridge National Lab., Tenn.). Sept. 1965. Contract W-7405-eng-26. 351p. Dep. mn; CFSTI $7.00 cy, $1.75 mn.

The MSCR is a one-region, one-fluid, graphite-moderated converter reactor fueled with a mixture of the fluorides of thorium-uranium, lithium-7, and beryllium which is circulated through the 20-ft-diam core to an external heat exchanger. Heat is transferred through an intermediate salt-coolant to steam at 2400 psi, 1000°F in a Loeffler boiler system having a net thermal efficiency of 41.5%. Spent fuel is processed by fluorination (at 0.08 mill/kwhe) for recycle of isotopes of uranium. The stripped salt is discarded. A capital investment of $143/kwe (3.0 mills/kwhe), an operation and maintenance annual expense of $2.1 million (0.3 mill/kwhe), and a minimum fuel cycle cost of 0.7 mill/kwhe (optimum conversion ratio is ~0.9) were estimated, giving a net power cost of 4.0 mills/kwhe. All costs were based on 1962 bases ground rules. Second generation plants may have capital costs as low as $125/kwe. Conversion ratios slightly greater than one can be obtained in advanced designs. (auth)

45589 (ORNL-TM-1197) EGCR CONTROL-ROD-DRIVE ENDURANCE TEST. Ferguson, W. F. (Oak Ridge National Lab., Tenn.). Sept. 1965. Contract W-7405-eng-26. 38p. Dep. mn; CFSTI $2.00 cy, $0.50 mn.

A rod-drive mechanism purchased for use in the Experimental Gas-Cooled Reactor was subjected to an endurance test under simulated reactor environmental conditions except for neutron radiation. The drive mechanism with a control rod attached was operated through numerous cycles of each of the mechanism's normal operating functions. It is concluded that the rod drive meets the performance requirements of the design specifications and is satisfactory for use in the EGCR. (auth)

45590 (TID-3584) NUCLEAR ENERGY FOR WATER DESALTING. A Bibliography. Kuhns, Helen F. (Oak Ridge National Lab., Tenn.); Raleigh, Henry D. (comps.) (Division of Technical Information Extension (AEC), Oak Ridge, Tenn.). Sept. 1965. 25p. Dep. mn; CFSTI $2.00 cy, $0.50 mn.

Included are 107 references to publications on the use of nuclear energy in the production of potable water from saline or brackish waters. The uses of nuclear reactors, radioisotopic heat sources, and nuclear explosives are covered in relation to the various possible desalination methods available. Author and report number-availability indexes are included. (auth)

45591 (TID-22129) HALLAM NUCLEAR POWER FACILITY MONTHLY OPERATING REPORT NO. 34, MAY 1965. (Consumers Public Power District, Hallam, Nebr.). Contract AT(11-1)-513. 42p. Dep. mn; CFSTI $2.00 cy, $0.50 mn.

The reactor remained shutdown for the moderator replacement program. The status of the replacement program is summarized, together with significant operating activities during the month and plant performance through May, 1965. (D.C.W.)

45592 (TID-22135) HALLAM NUCLEAR POWER FACILITY MONTHLY OPERATING REPORT NO. 35, JUNE 1965. (Consumers Public Power District, Hallam, Nebr.). Contract AT(11-1)-513. 52p. Dep. mn; CFSTI $3.00 cy, $0.50 mn.

The reactor remained shutdown for the moderator replacement program, under which five more ruptured moderator elements were removed and inspected. Other significant activities during the month are summarized, together with plant performance through June, 1965. (D.C.W.)

45593 (TID-22168) PATHFINDER ATOMIC POWER PLANT. Monthly Operating Report No. 1, March-December 1964. Bjeldanes, M. N. (Northern States Power Co., Minneapolis, Minn.). Contract AT(11-1)-589. 46p. Dep. mn; CFSTI $2.00 cy, $0.50 mn.

Plant operations from the initial core loading until the end of 1964 are summarized. Core loading and performance, startup tests, cooling-water chemistry, radiation-monitor calibration, waste disposal, and training activities are covered. (D.C.W.)

45594 (TRG-Report-864) REACTIVITY FEEDBACK IN THE DOUNREAY FAST REACTOR, AUGUST 1962–DECEMBER 1963. Wheeler, R. C.; Tait, D. (Reactor Group, United Kingdom Atomic Energy Authority, Dounreay (Scotland)). Jan. 11, 1965. 75p. Dep.; BIS $2.00 cy, HMSO 10s.

The measurements of reactivity feedback during charges B3, B4, and C4 are described. These include the isothermal temperature coefficients, the steady-state power coefficients (as functions of power and flow), the responses to oscillating reactivity input, and some responses to negative ramp reactivity changes. A significant decrease in the negative core feedback for small changes was observed between the first measurements at low burnup and the later measurements on charges B4 and C4, when the reactor was first run at full power. This decrease is attributed partly to the change to non-interlocked fuel (in the type 3A and 3B elements) and partly to the cracking of fuel on burnup. The overall fast-acting feedback was found to be positive (although small) during part of the period considered. The reasons why the negative feedback for small changes is different from the feedback calculated for large changes are discussed. The calculations of the feedback are outlined, and the main uncertainties which remain are concerned with the blanket flow rates (and thus blanket temperatures), the bowing of control rod elements and the axial expansion of the fuel. (auth)

45595 (TRG-Report-976) ODYSSEUS—A TWO-GROUP, TWO-DIMENSIONAL FUEL CYCLE COMPUTER PROGRAMME SUITABLE FOR ADVANCED GAS-COOLED REACTORS. PART A. GENERAL DESCRIPTION OF THE PROGRAMME. Buckler, A. N. (Reactor Group, United Kingdom Atomic Energy Authority, Sellafield (England)). Apr. 15, 1965. 16p. Dep.; BIS $0.50; HMSO 2s. 6d.

ODYSSEUS is a Fortran II program for assessment calculations of fuel management in advanced gas cooled reactors. A variety of automatic and semi-automatic fuel management schemes may be studied. The reactor power output may be shaped to a desired form by differential absorber control or fuel manipulation. Batch refueling, axial and radial shuffling, and on-line refueling may all be simulated. (auth)

45596 (WCAP–2042) 1000 MWe SUPERCRITICAL PRESSURE NUCLEAR REACTOR PLANT STUDY. SELECTION OF PREFERRED REACTOR CONCEPT. Tower, S. N. (Westinghouse Electric Corp., Pittsburgh, Pa. Atomic Power Dept.). July 1962. Contract AT(30-1)-2948. 236p. Dep. mn; CFSTI $6.00 cy, $1.25 mn.

Conceptual reactor design studies were performed on a 1000-Mwe SCOTT-R and 1000-Mwe FBGR to determine the preferred supercritical pressure concept for continued development. The SCOTT-R concept is graphite moderated employing fuel inside pressure tubes, while the FBGR concept employs fuel dispersed in graphite external to the pressure tubes. As a result of the study, it is concluded that the SCOTT-R possesses a relative economic advantage of about 1 mill/kwh, and continued development of the SCOTT-R concept is recommended. (auth)

45597 (WCAP–3269-31) LARGE CLOSED-CYCLE WATER REACTOR RESEARCH AND DEVELOPMENT PROGRAM. DEVELOPMENT OF AUXILIARY SYSTEMS. Cordle, H. J. (Westinghouse Electric Corp., Pittsburgh, Pa. Atomic Power Div.) Feb. 1965. Contract AT(30-1)-3269. 169p Dep. mn; CFSTI $5.00 cy, $1.00 mn.

This report contains the results of the development of auxiliary systems for a 395-Mwe closed-cycle water reactor with chemical shim control. Significant areas of development are discussed and descriptions of the system conceptual designs are included for the chemical and volume control system, the sampling system, the auxiliary coolant system and the safety injection system. Requirements for waste disposal and vapor container ventilation for the reference plant are included. (auth)

45598 (WCAP–3269-44) SAXTON CHEMICAL SHIM KINETIC EXPERIMENTS. Rajagopal, V.; Swen, G. E. (Westinghouse Electric Corp., Pittsburgh, Pa. Atomic Power Div.). June 1965. Contract AT(30-1)-3269. 113p. Dep. mn; CFSTI $4.00 cy, $0.75 mn.

Experimental studies of the inherent fluctuations (noise) and response to forced reactivity modulations (oscillation tests) in a nuclear power reactor were conducted, with a view to determine applications to characterize the dynamics of power reactors, and to study the effects of chemical shim control on the dynamic behavior of a reactor. Measurements of the power density spectra and cross-power density spectra of the fluctuations in nuclear power, coolant flow, and temperatures have been performed at various reactor operating conditions. Oscillation tests consisted of producing pseudo-random, random, or sinusoidal changes in reactivity through an oscillator, and measuring the reactor flux and temperature responses at different operating conditions by correlation techniques. For analysis, an analog power and cross-power density spectrum analyzer was employed. Applications of noise analysis techniques to monitor nucleate boiling and other operational characteristics of reactors are discussed. Techniques for obtaining frequency response characteristics and analysis of the data to obtain gross and local kinetic parameters in a power reactor are also discussed. The transfer functions determined at a power level of 20 Mwt under both chemical shim and rodded shim control operations show no evidence of any power reversible boron hideout at the test conditions. The transfer functions in both cases had the same shape except for small changes in time constants. The kinetic parameters determined during synthetic crud injection and pH tests give some indication of the possible mechanisms that produce a reactivity effect when pH level of the main coolant is changed. (auth)

45599 (WCAP–3269-49) OPTIMUM CORE LATTICE PARAMETERS FOR THE SAN ONOFRE NUCLEAR GENERATING STATION. Strawbridge, L. E.; Barry, R. F. (Westinghouse Electric Corp., Pittsburgh, Pa. Atomic Power Div.). Feb. 1965. Contract AT(30-1)-3269. 74p. Dep. mn; CFSTI $3.00 cy, $0.75 mn.

An optimization study, applicable to large steel clad pressurized water reactors, was completed. This study uses the extensive physics data reported earlier, coupled with detailed fuel cost equations, to determine the core parameters corresponding to minimum fuel costs. An optimization code (LOCK) was written for the IBM-7094 to facilitate the study. Up to three parameters (W/U, pellet size, and enrichment) can be optimized simultaneously by the code. The LOCK code is described in detail. Many results obtained with the code are presented. Relatively loose lattices were found to be economically attractive with the optimum W/U generally greater than 4.5. (W/U is defined as the volume of water in the active core divided by the volume of uranium, if the uranium existed in metallic form.) The optimum pellet diameter was found to be approximately 0.36 inches, and the optimum burnup was in the range of 25,000 to 30,000 Mwd/Mtu. It should be noted that the detailed consideration of plant components and burnout heat fluxes (which are beyond the scope of this study) tend to reduce the optimum water-to-fuel ratio. The effect on the optimum lattice parameters was determined for changes in such parameters as fabrication costs, reprocessing cost, separative work charge, load factor and kw/ft limit. In addition, the effect of a nuclear economy based on private fuel ownership was evaluated. The results are presented in graphical form. (auth)

45600 (WCAP–3385-4) SAXTON PLUTONIUM PROGRAM. Quarterly Progress Report for the Period Ending June 30, 1965. (Westinghouse Electric Corp., Pittsburgh, Pa. Atomic Power Div.). July 1965. Contract AT(30-1)-3385. 92p. (EURAEC–1420). Dep. mn; CFSTI $3.00 cy, $0.75 mn.

Work Performed under United States–Euratom Joint Research and Development Program.

Activities in a program to develop information concerning the utilization of Pu-enriched fuel in pressurized water reactor systems are summarized. The program is being carried out by designing and operating a partial core of PuO_2-UO_2 in the Saxton reactor. Developmental work is summarized in sections on fuel design, performance and analysis of critical experiments, fuel fabrication, shipping container design, safeguards analysis, alpha protection system, and nuclear analysis of operation performance. (J.R.D.)

45601 (WCAP-3750) LARGE CLOSED-CYCLE WATER REACTOR RESEARCH AND DEVELOPMENT PROGRAM. Progress Report, October 1-December 31, 1963. (Westinghouse Electric Corp., Pittsburgh, Pa. Atomic Power Div.). Contract AT(30-1)-3269. 241p. Dep. mn; CFSTI $6.00 cy, $1.25 mn.

Progress is reported in sections on project administration, reactor physics development, chemical shim development, plant development, reactor hazards analysis, and critical experiments. (J.R.D.)

45602 (WCAP-6493) EFFECT OF FUEL BURNUP ON THE MODERATOR TEMPERATURE COEFFICIENT IN A PWR. Poncelet, C. G. (Westinghouse Electric Corp., Pittsburgh, Pa. Atomic Power Div.). [1964]. Contract AT(30-1)-3017. 5p. (CONF-650602-6). Dep. mn; CFSTI $1.00 cy, $0.50 mn.

From American Nuclear Society 11th Annual Meeting, Gatlinburg, Tenn.

An analysis of the variation of the moderator temperature coefficient with burnup in terms of ^{235}U depletion, Pu buildup, fission-product buildup, and control-rod removal is summarized. (D.C.W.)

45603 (Y-1491) REVIEW OF HYDRAULIC PROBLEMS ON THE BONUS REACTOR PRESSURE CONTROL SYSTEM. Speas, I. G.; Cobb, J. S.; Groothuis, S. E. (Union Carbide Corp., Oak Ridge, Tenn. Y-12 Plant). June 14, 1965. Contract W-7405-eng-26. 29p. Dep. mn; CFSTI $2.00 cy, $0.50 mn.

A study was made of the BONUS reactor pressure control system to determine the cause of the malfunction of the hydraulic controls on the major steam valves. It was concluded that the principal contributor to the valve trouble was the high moisture content of the phosphate-ester hydraulic fluid. This excessive moisture reacted with the hydraulic fluid to produce an acid which, in turn, corroded the steel components of the system and produced fine abrasive particles that eroded the servo metering surfaces. Modifications were recommended that should alleviate the current problems. (auth)

45604 (JPRS-31245) EXPERIMENTAL STUDY ON MODELS OF THE TEMPERATURE FIELDS OF FUEL ELEMENTS IN THE ACTIVE ZONE AND SHIELD OF THE BN-350 REACTOR. Subbotin, V. I.; Ushakov, P. A.; Zhukov, A. V.; Talanov, V. D.; Kudryavtseva, L. K.; Sviridenko, E. Ya.; Vasil'eva, L. V. (Gosudarstvennyi Komitet po Ispol'zovaniyu Atomnoi Energii SSSR, Obninsk. Fiziko-Energeticheskii Institut). Translation of Eksperimental'noe Issledovanie na Modelyakh Poley Temperatury Teplovydelyayushchikh Elementov Aktivnoy Zony i Ekrana Reaktora BN-350. Apr. 1965. 22p. (TT-65-31742). CFSTI $1.00 cy, $0.50 mn.

The temperature fields of the heat-exchange elements of the BN-350 reactor were investigated under different conditions of heat transfer (central and peripheral heat-exchange elements) using models of the active zone and shielding of the reactor. (D.C.W.)

45605 (ORNL-tr-788) AN INVESTIGATION OF THE POSSIBILITY OF USING THORIUM IN HIGH-ENERGY REACTORS. Leipunskii, A. I.; Kazachkovskii, O. D.; Shikhov, S. B.; Murogov, V. M. Translated for Oak Ridge National Lab., Tenn. from At. Energ. (USSR), 18: 342-50(1965). 19p. Dep. mn; CFSTI $1.00 cy, $0.50 mn; JCL $1.60 fs, $0.80 mf.

A description is given of the results of an investigation of the possibility of using ^{233}U and thorium in a system of breeder reactors. It is shown that the most promising from the point of view of doubling time is the joint use of $^{233}U-Th$ and $^{239}Pu-^{238}U$ in a combined fuel cycle of fast reactors, provided the thorium is arranged in the shields and the ^{233}U, ^{239}Pu and ^{238}U are in the cores. The burnup and conversion of ^{233}U and ^{239}Pu in a combined fuel cycle is done in such a way that their quantitative ratio remains constant. The doubling time of a system of fast reactors working under conditions of a combined fuel cycle is substantially less than the doubling time of reactors using only ^{233}U and thorium. Thorium is the main raw material in the combined fuel cycle. A method is pointed out for the production of isotopically pure ^{233}U with a ^{233}U content of $10^{-4}\%$. (auth)

45606 THE POSSIBLE ROLE OF NUCLEAR ENERGY FOR SEA WATER DESALINATION. Ertaud, Andre. Bull. Inform. A.T.E.N. (Assoc. Tech. Energie Nucl.), No. 53, 5-19(May-June 1965). (In French).

A cost comparison was made of nuclear and conventional power plants for the desalination of sea water. The simultaneous production of electricity and desalinated water, the efficiency of the natural uranium-graphite-gas reactor, the development of mixed nuclear power plants, and the types of reactor are considered. (J.S.R.)

45607 THE CONTROL OF THE NUCLEAR FUEL OF A CHINON POWER PLANT. Cordier, Gilbert. Bull. Inform A.T.E.N. (Assoc. Tech. Energie Nucl.), No. 54, 26-31(July-Aug. 1965). (In French).

A system of permanent control of the fuel elements at the reactor was developed to account for the location of presence of each fuel element. The method for identification adopted for the fuel elements is described. The control system used at the reactor (arrival, storage, receipt, reactor loading, period in the reactor, discharge and storage in the pool, and shipment to the reprocessing plant) is summarized. (J.S.R.)

45608 ACHIEVEMENT OF CLEAN CONDITIONS IN GAS-COOLED NUCLEAR REACTORS. Anderson, E. (Nuclear Power Group, Knutsford, Cheshire, Eng.). Proc. Inst. Mech. Engrs. (London), 179: Pt. 1, No. 3, 67-80(1964-65).

Precautions taken to ensure clean conditions in the first civil nuclear power stations resulted in excessive costs and delays. These precautions are aimed at the elimination of materials which could poison the core, create a maintenance hazard, affect the fuel elements, or increase the fire risk in the core. The subject is reviewed in the light of the considerable experience of constructing and running reactors now available, and an attempt is made to assess the importance of the various precautions. (auth)

45609 A 300-MW ATOMIC POWER STATION WITH A SIEMENS PRESSURIZED-WATER REACTOR AT OBRIGHEIM IN GERMANY. Frewer, Hans. Siemens-Z., 39: 323-5(Apr. 1965). (In German).

In March 1964 Siemens-Schuckertwerke were awarded the order for the construction of what will be Germany's largest atomic power station. This power station, located at Obrigheim on the Neckar, will have a gross electric output of 300 Mw. The reactor will be of the Siemens pressurized-water type. The plant, which is scheduled to go into service at the end of 1968, is being constructed entirely by Siemens-Schuckertwerke acting in the capacity of general contractor. (auth)

45610 EUROPEAN SITUATION IN THE AREA OF NUCLEAR ENERGY PRODUCTION. Baruffa, A. pp 25-48 of Giornate dell'Energia Nucleare 1964. Milan, Federazione delle Associazioni Scientifiche e Tecniche, 1965. (In Italian).

An hypothesis on the evolution of the energy needs of Europe was constructed in order to define the magnitude of the problem and to indicate the most important technical options that must be considered in attaining the fundamental objectives of sufficient power for an industrial section. On the basis of the characteristics of this hypothesis, the actual state and conditions of development of the principal industrial sectors for an increasing utilization of nuclear energy were examined. (J.S.R.)

45611 GAS-COOLED REACTOR EXPERIENCE IN THE UNITED KINGDOM. MacRae, W. pp 49-63 of Giornate dell'Energia Nucleare 1964. Milan, Federazione delle Associazioni Scientifiche e Tecniche, 1965.

The experience of constructing and operating gas cooled reactor power plants over the last 8 years have shown that: they are safe and reliable; they can operate at high load factors; they are suitable for operation in large power networks; their capital and generating cost has been halved in that period; there is considerable scope for developments in design, leading to higher ratings and temperatures, which will result in further reductions in cost; and the reactor unit sizes can match those of quite large turbo-generating plants. (auth)

45612 THE GROWTH OF AN INTEGRATED FUELLING SERVICE FOR POWER REACTORS. Norman, K. J. pp 65-76 of Giornate dell'Energia Nucleare 1964. Milan, Federazione delle Associazioni Scientifiche e Tecniche, 1965.

Facilities for reprocessing and fabricating Magnox-reactor fuel elements, AGR fuel elements, and fuel elements for a steam-generating heavy-water power reactor using UO_2 fuel are described. Facilities for enriching uranium by gaseous diffusion, and for fabricating and processing plutonium, are discussed. The operation of the British fuel-cycle-service system is outlined. (T.F.H.)

45613 CURRENT NUCLEAR SITUATION IN THE UNITED KINGDOM. Cartwright, H. pp 77-85 of Giornate dell'Energia Nucleare 1964. Milan, Federazione delle Associazioni Scientifiche e Tecniche, 1965.

The state of Calder Hall reactors, the Windscale AGR, the DFR, and the British steam-generating heavy-water power reactor is outlined, as is the status of nuclear power for use in civil electrical networks in Britain. (T.F.H.)

45614 THE ELECTRONUCLEAR POWER PLANTS IN FRANCE. Roux, J. P. pp 87-92 of Giornate dell'-Energia Nucleare 1964. Milan, Federazione delle Associazioni Scientifiche e Tecniche, 1965. (In French).

A description is given of the status of EDF 1,2,3, and 4 (natural U fuel, graphite moderator, carbon-dioxide coolant), EL 4 (natural U fuel, heavy-water moderator, carbon-dioxide coolant), and CHOOZ (enriched UO_2 fuel, water moderator and coolant) French nuclear power plants. (T.F.H.)

45615 OUTLOOK FOR THE UNITED STATES NUCLEAR POWER. Staebler, U. M.; Giambusso, A. pp 93-105 of Giornate dell'Energia Nucleare 1964. Milan, Federazione delle Associazioni Scientifiche e Tecniche, 1965.

An outline is given of the development programs, economics, and applications of nuclear power plants in the U.S.A. (T.F.H.)

45616 EXPERIENCE IN TEST AND USE OF THREE ITALIAN NUCLEAR POWER PLANTS. Sani, L.; Campiani, A.; Gualtieri, G.; Velona, F. pp 107-89 of Giornate dell'Energia Nucleare 1964. Milan, Federazione delle Associazioni Scientifiche e Tecniche, 1965. (In Italian).

The experience gained in the testing and operation of three Italian nuclear power plants, the graphite-gas Latina Power Plant, the Garigliano Boiling Water Power Plant, and the Trino Vercellese Pressurized Water Power Plant, is discussed. An attempt was made to give a synthesis of the most salient points of these experiences and to compare and contrast the results obtained with power plants of three different types. The study was limited to the test of the nuclear parts of the plant. The pre-operational test and nuclear tests including zero power studies and the power studies, are reported. Functional tests at power were also performed. The inconveniences encountered during operation of the power test are indicated. The results of the first period of power operation of the Latina power plant (for a year) and of the Garigliano power plant (for 5 months) are reported and compared. (J.S.R.)

45617 EXPERIENCE IN DESIGNING THE NUCLEAR SECTION OF THE S.El.N.I. INSTALLATION. CONSIDERATIONS FOR THE DEVELOPMENT OF LINES FOR PRESSURIZED WATER REACTORS. Casini, R. pp 191-207 of Giornate dell'Energia Nucleare 1964. Milan, Federazione delle Associazioni Scientifiche e Tecniche, 1965. (In Italian).

The original design concept of the S.El.N.I. nuclear power plant was a copy of the Yankee power plant. The design modifications introduced, principally the adoption of chemical shim and the subdivision of the core into zones of various enrichment, to increase the nominal power of the first core are described. The characteristics that future pressurized water reactors may have are indicated and the principal design problems that remain to be solved are summarized. (J.S.R.)

45618 OUTLOOK FOR THE USE OF NUCLEAR ENERGY FOR THE PRODUCTION OF HEAT AT LOW TEMPERATURE. Baldetti, S.; Biondi, L.; Cerullo, N.; Di Menza, R.; Guerrini, B.; Lazzarino, L.; Pierazzi, L.; Vaudo, A. pp 223-51 of Giornate dell'Energia Nucleare 1964. Milan, Federazione delle Associazioni Scientifiche e Tecniche, 1965. (In Italian).

Vapor at relatively low temperatures and pressures can be used in industrial plants (principally chemical), for domestic heating, and for the desalination of sea water. The utilization of nuclear power plants for the production of vapor at low temperature at a competitive cost was examined. In the power area and the vapor characteristics that best satisfy the utilizations discussed, organic-cooled reactors seemed of special interest. After a preliminary examination of the most promising lines of development of an organic reactor for production of heat at low temperature, preliminary results in a design study of this type of reactor are presented. (J.S.R.)

45619 APPLICATION OF NUCLEAR ENERGY FOR DESALINATION. Dall'Asta, G.; Bortone, C. pp 253-71 of Giornate dell'Energia Nucleare 1964. Milan, Federazione delle Associazioni Scientifiche e Tecniche, 1965. (In Italian).

Needs for desalination, the systems used, the proposed utilization of nuclear reactors for this purpose, and the principles of the multi-flash evaporation system are reviewed, and the coupling of reactors and desalinators is discussed. In the coupling of nuclear reactors and desalinators various problems are presented. The use of a reactor for water alone or for the simultaneous production of electrical energy is considered. The conditions under which a nuclear reactor would be more economical as a heat source than a conventional fuel power plant are considered. In the case of electricity production the use of controlled pressure turbines is compared with the use of condensation turbines. The advantages of reactors producing vapor at high temperatures or low temperatures are considered. (J.S.R.)

45620 SOME ALTERNATES FOR THE UTILIZATION OF ORGANIC LIQUID REACTORS FOR DESALINATION OF SALT WATER. Di Menze, R.; Pittori, S.; Pierazzi, L.; Valant, P. pp 273-84 of Giornate dell'Energia Nucleare 1964. Milan, Federazione delle Associazioni Scientifiche e Tecniche, 1965. (In Italian).

An economic comparison was made of water and organic nuclear reactors for the simultaneous production of electrical energy and vapor and of organic reactors for vapor production and of water reactors for the simultaneous production of electrical energy and vapor. The water reactors considered were the PWR and the BWR. The results showed that the dual-purpose organic reactors could not be competitive with the water reactors for powers of the order of 150 Mw(t). At 1700 Mw(t) however the two reactors would be competitive. The unit cost of thermal energy at 1500 Mw(t) was decidedly higher for the vapor-producing organic reactor. At powers below 150 Mw(t), however, the situation was reversed. (J.S.R.)

45621 EFFICIENT UTILIZATION OF NUCLEAR FUELS. Rollier, M. A. pp 285-313 of Giornate dell'-

Energia Nucleare 1964. Milan, Federazione delle Associazioni Scientifiche e Tecniche, 1965. (In Italian).

The economics of nuclear reactors is indicated by a summary of the future energy needs and sources of the United States. The cost reduction available by improvement of existing reactor types is indicated. As the availability of U is not unlimited, the development of reactors not based on a uranium cycle is necessary. The development of advanced types of converter reactors and of breeder reactors is discussed. Thorium thermal generators, fast breeder reactors, and the type of thorium converter best suited for the nuclear system are discussed. The use of thorium as the initial fissionable material in thorium reactors is considered. A nuclear electrical system with a minimum investment in ^{235}U enriched fuel is proposed. (J.S.R.)

45622 PROSPECTS AND ASPECTS OF THE DEVELOPMENT OF NUCLEAR ENERGY IN ITALY. Salvetti, C. pp 335-48 of Giornate dell'Energia Nucleare 1964. Milan, Federazione delle Associazioni Scientifiche e Tecniche, 1965. (In Italian)

The prospects of developing a nuclear market in Italy are summarized, and the activities of the C.N.E.N. (Comitato Nazionale Energia Nucleare) in the development of this nuclear market are indicated. The role of the C.N.E.N. in the development and construction of tested reactors and of prototype reactors is briefly considered. (J.S.R.)

45623 FAST REACTOR CORE DESIGN AND SAFETY STUDIES IN FRANCE AND IN THE FEDERAL REPUBLIC OF GERMANY. Zaleski, C. P. (EURATOM-CEA Association, Cadarache, France); Smidt, D. 17p. (CONF-650417-3). Gmelin, AED-CONF-65-074-9.

From American Nuclear Society, National Topical Meeting on Fast Reactor Tech., Detroit.

The main features of the development program which is considered desirable in the field of fast reactors in France and in the Federal Republic of Germany are indicated, and justification for the program is given. A description is given of the reference cores which were developed within the scope of the conceptual studies on large fast breeder reactors, which is completed by comments on the methods and calculations which were used to determine accurately their characteristics. Some considerations on the dynamic behavior the reference cores are also given. (L.B.S.)

45624 CHEMICAL ENGINEERING ASPECTS OF BOILING WATER REACTORS. McNelly, M. J.; Huntley, H. W.; Burley, E. L. (General Electric Co., San Jose, Calif.). 20p. (CONF-650559-4). Gmelin, AED-CONF-65-086-11).

From American Inst. of Chemical Engineers, 56th National Meeting, San Francisco.

The principles of design and operation of the boiling water reactor are described, with particular reference to those aspects which are dependent on various unit operations. In this way, the importance of the chemical engineering contribution to nuclear power development is stressed. (auth)

45625 THE TECHNOLOGY OF INCORPORATING A THERMAL NEUTRON SPECTRUM OR A FAST NEUTRON SPECTRUM CENTRAL SUPERHEATING REGION TO IMPROVE BWR PERFORMANCE AS EVALUATED THROUGH THREE 600 Mwe PLANT DESIGNS. Imhoff, D. H. 6p. (CONF-650602-52). Gmelin, AED-CONF-65-125-15.

From American Nuclear Society, 11th Annual Meeting, Gatlinburg, Tenn.

Two approaches which were investigated for adding nuclear superheat to a BWR led to three 600 Mw(e) plant studies, which include a modified boiling water reactor, an integral thermal spectrum superheat reactor, and an integral fast spectrum superheat reactor. The plant designs are described and comparisons are made on both technical and economic bases. (L.B.S.)

45626 SOME PHYSICS ASPECTS OF PRESSURE TUBE AND PRESSURE VESSEL TYPE HEAVY WATER REACTORS. Jirlow, K.; Persbagen, B. (Aktiebolaget Atomenergi, Stockholm). 16p. (CONF-650602-53). Gmelin, AED-CONF-65-125-12.

From American Nuclear Society, 11th Annual Meeting, Gatlinburg, Tenn.

A comparison of some physics characteristics of pressure tube and pressure vessel reactors led to the following conclusions: the neutron economy is as good in the pressure vessel as well as in tube reactors; continous refuelling is essential for the preservation of good neutron economy and can be achieved in vessel as well as tube reactors; fuel transposition in the out-in direction is shown to be the most effective way of obtaining radial power flattening; and pressure vessel reactors have more freedom than pressure tube reactors in the choice of a proper void coefficient of reactivity. (L.B.S.)

45627 UNDERWATER THERMOELECTRIC REACTOR PLANT. Dufrane, Kenneth (Martin Co., Baltimore). New York, American Inst. of Aeronautics and Astronautics, 1965, Preprint No. 65-447, 16p., $1.00. (CONF-650711-8). ORINS.

From AIAA 2nd Annual Meeting and Technical Demonstration, San Francisco.

The basic requirements or mission specifications imposed upon the concept and the resulting design and performance characteristics on an underwater thermoelectric reactor plant are outlined. The power plant is a self-pressurized, natural circulation, pressurized water reactor which develops electric power directly from heat by means of a thermoelectric generator. A description is given of the system, including the arrangement, pressure vessels, core mechanical design, nuclear design, thermoelectric elements, power conditioning and storage, shielding, water chemistry, operation, and safety. In addition, the special features of the design which contribute especially to the underwater application are summarized. Technology assessment and the potential of the system are discussed. (L.B.S.)

45628 NUCLEAR REACTORS. (to Hitachi Ltd.). British Patent 1,001,745. Aug. 18, 1965. Priority date May 10, 1963, Japan.

A nuclear reactor includes a pressurized-water type reactor core, a pressure vessel including a closed loop of passage for recirculation of pressurized water as a coolant-moderator, and a once-through secondary coolant system. The secondary coolant system includes a boiling region and a superheating region arranged in the loop of passage. The boiling region is located about the periphery of the pressurized-water type reactor core and is coupled with the core to provide neutron reflection. (B.L.M.)

45629 EPITHERMAL THORIUM POWER-BREEDER NUCLEAR REACTOR. Balent, Ralph; Beeley, Raymond J. (to North American Aviation, Inc.). U. S. Patent 3,197,376. July 27, 1965. Filed Dec. 16, 1960.

A thorium power breeder reactor has a moderator of beryllium arranged to form channels for fuel elements. The fuel elements supported within the channels contain ^{232}Th and ^{233}U. A liquid metal coolant is passed through the channels but does not contact the moderator. A reflector surrounding the core consists of moderator material and ^{232}Th rods. The coolant and moderator are present in sufficient quantity to provide a neutron spectrum in the core having a mean energy of about $1-10^5$ ev. (A.G.W.)

45630 POWER PLANT FOR SUPERHEATING THE STEAM ORIGINATING FROM THE STEAM GENERATOR OF A NUCLEAR PRESSURIZED WATER REACTOR. Dahlgren, Joens Arthur. U. S. Patent 3,197,380. July 27, 1965. Priority date Feb. 23, 1962, Sweden.

A method for superheating steam originating from the steam generator of a pressurized reactor is intended to reduce the risk of transfer of radioactive products from the reactor to the superheated steam. A minor portion of the pressurized water is passed through a first heat exchanger in which it is allowed to heat an auxiliary liquid, and the auxiliary liquid thus heated is passed through a second heat exchanger in which it is allowed to superheat the steam.

The auxiliary liquid may then be passed to an intermediate superheater between two turbine elements. The auxiliary liquid may be circulated in a separate system, or feed water may be used. (A.G.W.)

Process Heat Reactors

45631 (COO–283) DEEP-POOL REACTOR FOR WATER DESALTING. (Bechtel Corp., San Francisco, Calif.). June 30, 1965. Contract AT(11-1)-1444. 164p. Dep. mn; CFSTI $5.00 cy, $1.00 mn.

The results of an engineering design study performed to investigate the potential and feasibility of a deep-pool reactor concept for ultimate use as an economic heat source for a single-purpose water desalting plant are presented. Detailed information is given concerning: the site, reactor plant, water plant, electrical system, safety considerations, 10- and 200-mgd plants, and an economic evaluation. (M.O.W.)

45632 (HPR–63) NOISE EXPERIMENTS WITH THE HBWR SECOND FUEL CHARGE. Eurola, T. (Institutt for Atomenergi, Halden (Norway). OECD Halden Reaktor Prosjekt). Dec. 1964. 82p. Dep. mn.

The HBWR experience in the study of boiling water reactor dynamics by the noise technique is summarized. This experience is based on measurements of fluctuations of a number of local in-core and integral parameters at various operational conditions and on studies of a simplified analogue simulation of the HBWR plant. The noise technique is quite useful both as a parallel and a supplementary tool to the other experimental techniques in dynamic studies. It gives information on the tendency of the system to oscillations and a quantitative measure of the nature of oscillations in terms of magnitude and frequency band. It can be useful in stability limit estimations and give information on coupling effects in the coolant circulation within the core. However, care has to be exercised in applying the technique to dynamic studies through transfer function measurements, if any nonlinearities are expected. (auth)

45633 (HPR–62) DYNAMICS MODEL OF THE HBWR HEAT REMOVAL CIRCUITS. Eurola, T. (Institutt for Atomenergi, Halden (Norway). OECD Halden Reaktor Prosjekt). Dec. 1964. 78p. Dep. mn.

A dynamics model of the heat removal circuits of the HBWR plant for small perturbations is presented. In derivation of the model, a lumped parameter single-point description, instead of the distribution parameter description, was used whenever possible. The model was applied in a simplified form to both the HBWR first charge and second charge circuits. The simplification was to include only the circuits containing saturated steam and water. A parametric study was performed on the simplified model to find out the effect of uncertainties in various important parameters, such as heat transfer coefficients, masses of water at saturation and pressure drops, which are not easy to determine theoretically. The strongest influence on the reactor pressure to primary steam flow transfer function, which is the most important one for the overall reactor dynamics, was caused by the primary side parameters. A good agreement with the experiments was obtained in the second charge case with a proper choice of these parameters using the simplified model. The used values are physically justifiable, and even though they may not be quite correct ones, the study indicates the importance of taking into account the structural and fluid masses in a proper way. (auth)

45634 WHY NOT SINGLE-PURPOSE REACTORS FOR DESALTING. Baron, S.; Zizza, M. (Burns and Roe, Inc., New York). Nucleonics, 23: No. 9, 44-7(Sept. 1965).

The development of large single-purpose reactor-powered water plants is discussed. It was concluded that for a 100×10^6 gpd plant, water would cost ~40¢/1000 gal. The disadvantages of dual-purpose plants include production of large blocks of power, limits to flexibility of plant location due to power transmission costs, lower plant efficiency under certain operating conditions, and higher costs than single-purpose plants. A reactor design is proposed in which brine temperature is limited to 190°F. The reactor can be either light-water cooled and moderated with slightly enriched uranium fuel, or heavy-water cooled and moderated with natural or slightly enriched uranium fuel. Selected as basic design was an aluminum-clad natural UO_2 fuel, with D_2O as coolant and moderator. Multistage flash evaporator designs were studied and evaluated. (M.C.G.)

45635 THE PROSPECTS FOR DUAL-PURPOSE PLANTS. Crever, Frederick E. (General Electric Co., San Jose, Calif.). Nucleonics, 23: No. 9, 48-50(Sept. 1965).

Dual-purpose nuclear desalting plants are considered in the light of fundamental thermodynamics and economics. The effects of size and duality are discussed, and the cost of steam considered. It was concluded that in areas requiring both power and water, dual-purpose plants with ~10^8 gpd capacities can be economical if designed for fixed rather than flexible product ratio and tailored to particular applications. (M.C.G.)

45636 NUCLEAR DESALTING FOR AGRICULTURAL WATER. Hammond, R. Philip (Oak Ridge National Lab., Tenn.). Nucleonics, 23: No. 9, 51-3; 55(Sept. 1965).

The role of nuclear desalination plants in solving the problem of agricultural water is discussed. Controlling factors, such as population growth, food requirements, and land and its use are discussed. The amount of water needed for food production is considered. Data on the cost of desalting are reviewed. It was concluded that, combined with improved agricultural techniques, nuclear desalting may add as little as 2.5 cents per day to the cost of man's food. (M.C.G.)

Production Reactors

Refer also to abstract 44303.

45637 (DP–999) THE SAVANNAH RIVER HIGH FLUX DEMONSTRATION. Papers Presented at The Eleventh Annual Meeting, The American Nuclear Society, Gatlinburg, Tennessee, June 21, 1965. Crandall, J. L. (comp.) (Du Pont de Nemours (E. I.) and Co., Aiken, S. C. Savannah River Lab.). June 1965. Contract AT(07-2)-1. 81p. Dep. mn; CFSTI $3.00 cy, $0.75 mn.

Separate abstracts were prepared for the six papers included. (D.C.W.)

For abstracts of individual papers see: 45638–45643.

45638 (DP–999, pp 7-17) A DESCRIPTION OF THE SAVANNAH RIVER HIGH FLUX CHARGE. Crandall, J. L.; Smith, J. A.; Towler, O. A. (Du Pont de Nemours (E. I.) and Co., Aiken, S. C. Savannah River Lab.). (CONF-650602–42).

From American Nuclear Society 11th Annual Meeting, Gatlinburg, Tenn.

The Savannah River production reactor that is currently operating with a high-flux demonstration lattice at thermal-neutron fluxes up to 5×10^{15}/cm^2-sec is described, together with the particular lattice used for the high-flux loadings. (D.C.W.)

45639 (DP-999, pp 19-28) ISOTOPE PRODUCTION IN A SAVANNAH RIVER REACTOR AT FLUX LEVELS ABOVE 10^{15} n/(cm^2)(sec). Smith, J. A.; Hennelly, E. J.; Ice, C. H.; Allen, H. F. (Du Pont de Nemours (E. I.) and Co., Aiken, S. C. Savannah River Lab.). (CONF-650602-43).

From American Nuclear Society 11th Annual Meeting, Gatlinburg, Tenn.

The general benefits that can be derived from high-flux charges, the specific purposes of the Savannah River charge, and the characteristics of the charge that are pertinent to production programs are reviewed. (D.C.W.)

45640 (DP-999, pp 29-42) PHYSICS DESIGN OF THE SAVANNAH RIVER HIGH FLUX CHARGE. Graves, W. E.; O'Neill, G. F.; Dunklee, A. E.; Topp, S. V. (Du Pont de Nemours (E. I.) and Co., Aiken, S. C. Savannah River Lab.). (CONF-650602-44).

From American Nuclear Society 11th Annual Meeting, Gatlinburg, Tenn.

The experimental and theoretical activities by which the lattice design was fixed are summarized. These include measurements of core bucklings in an exponential pile, mockup experiments of the whole core in a critical facility, critical experiments on the first core, a theoretical determination of the optimum method of control-rod withdrawal, and calculations of burnup and spatial flux. (D.C.W.)

45641 (DP-999, pp 43-64) ENGINEERING ASPECTS OF THE SAVANNAH RIVER HIGH FLUX CHARGE. Nelson, E. C.; Baker, D. Jr.; Mirshak, S.; Peters, A. H. (Du Pont de Nemours (E. I.) and Co., Aiken, S. C. Savannah River Lab.). (CONF-650602-45).

From American Nuclear Society 11th Annual Meeting, Gatlinburg, Tenn.

The high neutron flux in the Savannah River reactor was obtained with a combination of low fuel concentration and high specific power. Design and operating considerations for high specific power are discussed, together with some other engineering aspects of a high-flux core. Calculation of core size, mechanical design, hydraulics, and heat transfer are covered. (D.C.W.)

45642 (DP-999, pp 65-71) TEMPERATURE COEFFICIENTS OF REACTIVITY IN THE SAVANNAH RIVER HIGH FLUX CHARGE. Bailey, C. E.; Baumann, N. P.; Jewell, C. E. (Du Pont de Nemours (E. I.) and Co., Aiken, S. C. Savannah River Lab.). (CONF-650602-4).

From American Nuclear Society 11th Annual Meeting, Gatlinburg, Tenn.

Calculations of the temperature coefficients of reactivity in the high-flux charge are compared with measurements of the coefficients in both a subcritical facility and a zero-power critical facility and with measurements in the reactor. (D.C.W.)

45643 (DP-999, pp 73-86) OPERATING EXPERIENCE WITH THE FIRST SAVANNAH RIVER HIGH FLUX CHARGE. Towler, O. A.; Hilley, J. R.; Fox, L. W.; Anderson, R. F. (Du Pont de Nemours (E. I.) and Co., Aiken, S. C. Savannah River Lab.). (CONF-650602-47).

From American Nuclear Society 11th Annual Meeting, Gatlinburg, Tenn.

Observations in the first six fuel cycles of the high-flux charge are summarized. Neutron flux distributions and magnitudes, power, temperature coefficients of reactivity, xenon worth, and reactivity change with exposure are covered. (D.C.W.)

45644 (ORNL-P-1501) HFIR PREOPERATIONAL VIBRATION AND HYDRAULIC TEST PROGRAM. Dixon, G. J. (Oak Ridge National Lab., Tenn.). July 28 and 29, 1965. Contract W-7405-eng-26. 16p. (CONF-650710-7). Dep. mn; CFSTI $1.00 cy, $0.50 mn.

From American Nuclear Society, Meeting on Reactor Operating Experience, Jackson Lake Lodge, Wyo.

After a general description of the design and uses of HFIR, the preoperational tests carried out to ensure mechanical integrity of the core assembly and the primary coolant system and to determine the detailed flow characteristics in various regions are reviewed. (T.F.H.)

45645 (ORNL-TM-1259) A SECOND GENERATION OF REACTOR CONTROL SYSTEMS AS APPLIED TO THE HIGH FLUX ISOTOPE REACTOR. Oakes, L. C. (Oak Ridge National Lab., Tenn.). Sept. 1, 1965. Contract W-7405-eng-26. 29p. Dep. mn; CFSTI $2.00 cy, $0.50 mn.

A safety system, a startup instrument covering 10 decades, and a multiple-channel regulating system (all transistorized and employing modular construction) are described, as applied to the HFIR. (auth)

45646 CLAMP-ON PROCESS TUBE TEMPERATURE DETECTOR FOR MONITORING NUCLEAR REACTOR OPERATION. Greenberg, H. J. Engelhard Inc., Tech. Bull., 4: 101-4 (Dec. 1963).

A description is given of the clamp-on resistance temperature detectors (RTD) which are installed on the external surfaces of the discharge end of each of 1004 process tubes in the primary coolant loop for control of the NPR. The design, construction, testing, and functional specifications are presented. (L.B.S.)

Propulsion and Space

See also ENGINEERING — Space Propulsion.

Refer also to abstract 44219.

45647 (AED-C-22-04) NUCLEAR SHIP PROPULSION, Series C, Bibliographies. Paro, J. N. (comp.) (Reactor Centrum Nederland, The Hague). July 1965. 75p. Dep. mn.

References (245) for documents on nuclear ship propulsion are presented. An author index is included, together with a report number index. (D.C.W.)

45648 (GA-6478) SYNTHESIS OF THERMIONIC POWER CONVERSION TO NUCLEAR REACTORS FOR SPACE POWER APPLICATIONS. Perry, L. W.; Homeyer, W. G. (General Atomic, San Diego, Calif. John Jay Hopkins Lab. for Pure and Applied Science). June 28, 1965. Contract AT(04-3)-167. 8p. (CONF-650908-3). Dep. mn; CFSTI $1.00 cy, $0.50 mn.

From International Conference on Thermionic Electrical Power Generation, London.

The three general concepts for incorporating thermionic cells into a reactor are briefly compared in terms of the performance of individual thermionic cells. The in-core cell concept is discussed in more detail, with consideration of two arrangements of fuel and coolant. It is shown that a configuration in which the fuel is contained within the emitter allows higher power densities over a broad range of cell diameters. The effects of cell parameters on reactor performance are considered. (D.C.W.)

45649 (N64-32637) PARAMETRIC PERFORMANCE ANALYSIS FOR INTERPLANETARY MISSIONS UTILIZING FIRST-GENERATION NUCLEAR STAGES. Stafford, Walter H.; Harlin, Sam H.; Catalfamo, Carmen R. (National Aeronautics and Space Administration, Huntsville, Ala. George C. Marshall Space Flight Center). Oct. 1964. 210p. (NASA-TN-D-2160). CFSTI $3.50 cy, $1.25 mn.

A method for determining the effects of earth thrust-to-weight ratios and specific impulses on interplanetary transfer trajectory parameters is described. These effects were investigated for hyperbolic escape from, and braking into, an orbit about each of the planets Mars and Venus, and for escape from Earth. The approach used for the escape trajectories was to determine the trajectory parameters at burnout and convert the characteristic velocity to a hyperbolic excess velocity. A single stage, with constant thrust directed along the velocity vector, was used. The approach used for the braking trajectories was to determine the arrival velocity for a given transfer trajectory and initiate burning such that circular orbit conditions are attained at burnout. The characteristic velocity was then converted to a hyperbolic excess velocity. A single stage, with constant thrust directed against the velocity vector, was used. Specific impulses of 600 to 1000 seconds and thrust-to-weight ratios of 0.05 to 0.5 were used in all instances. The data derived from this study are presented graphically. (auth)

45650 (NAA-SR-10997) DEVELOPMENT, ACCEPTANCE AND QUALIFICATION TESTING OF THE SNAP 10A EJECTABLE HEAT SHIELD. Sperow, H. L. (Atomics International, Canoga Park, Calif.). Aug. 31, 1965. Contract AT(11-1)-Gen-8. 69p. Dep. mn; CFSTI $3.00 cy, $0.75 mn.

The development, acceptance, and qualification tests performed on the SNAP-10A ejectable heat shield and components, the results of those tests, and the conclusions drawn from the results are summarized. (auth)

45651 (NAA-SR-11103) DISINTEGRATION AND DISPERSION OF THE SNAP 10A REACTOR UPON RETURN FROM SATELLITE ORBIT. Elliott, R. D. (Atomics International, Canoga Park, Calif.). Sept. 1, 1965. Contract AT(11-1)-Gen-8. 45p. Dep. mn; CFSTI $2.00 cy, $0.50 mn.

A study of the disintegration and dispersion of the SNAP (Systems for Nuclear Auxiliary Power) 10A reactor upon atmospheric reentry from a satellite orbit is described. The flight configuration is that of the SNAP 10A reactor containing NaK coolant and mated to the forward end of the Agena-D vehicle. It is shown that the SNAP 10A/Agena system will be oscillating in an approximately nose-first attitude at the time of reentry. It is concluded that the reactor components will have disintegrated and dispersed at an altitude of not less than 237,000 ft. (auth)

45652 (NASA-TN-D-2696) STABILITY OF TWO-FLUID WHEEL FLOWS. Reshotko, Eli; Monnin, Carl F. (National Aeronautics and Space Administration, Cleveland, Ohio. Lewis Research Center). Aug. 1965. 25p. CFSTI $1.00 cy, $0.50 mn.

The stability of an incompressible two-fluid wheel flow to infinitesimal helical disturbances is considered for the case where the inner fluid is heavy and the outer fluid is light. This situation may be viewed as a Rayleigh-Taylor problem in the frame of the rotating fluid and is dynamically unstable. As the density ratio of inner to outer fluid increases, the calculated growth rates increase and approach a limiting value as the density ratio becomes infinite. Growth rates also increase with increasing axial as well as azimuthal wave number. Furthermore, the presence of a fixed boundary outside the light fluid tends to have negligible influence on the growth rates as the density ratio becomes very large. (auth)

45653 (NAA-SR-11430) PRELIMINARY SNAPSHOT-1 PERFORMANCE—SUMMARY. Galantine, R. M. (ed.) (Atomics International, Canoga Park, Calif.). Aug. 1, 1965. Contract AT-11-1-GEN-8. 101p. Dep. mn; CFSTI $4.00 cy, $0.75 mn.

This report presents the preliminary evaluation of test results from the SNAPSHOT flight test of the SNAP 10A system. The SNAP 10A/Agena spacecraft was launched into a near circular, polar orbit at 13:24 PST on April 3, 1965. After verification of a near nominal orbit, the reactor startup command was given and full power was achieved about 12 hr from launch at 01:45 PST on April 4, 1965. After six days of active control, to compensate for short-term reactivity effects, the control system was deactivated and the power system was operated in a self-regulating manner for 43 days. During this period, all systems functioned normally and performance data were as anticipated. On May 16, 1965, after 43 days of continuous operation, premature shutdown of the SNAP 10A system occurred. At the time of this report, evaluation of the data and circumstances surrounding the shutdown was incomplete. The program has demonstrated that reactor space power systems can be integrated into a typical spacecraft, that the factory-through-flight sequence can be routinely programmed, that no special ground handling equipment or launch base procedures are necessary, that safety questions can be handled in an objective manner, and that public acceptance of nuclear power in space is readily obtainable. The flight provided information on the effects of hard vacuum and zero-gravity operation, verification of component performance and methods of predicting performance in space using ground test data, invaluable data on radiation shielding, information on the effective neutron source strength of space, and related technical data. (auth)

45654 (NASA-TN-D-2968) THERMODYNAMIC AND TURBOMACHINERY CONCEPTS FOR RADIOISOTOPE AND REACTOR BRAYTON-CYCLE SPACE POWER SYSTEMS. Glassman, Arthur J. (National Aeronautics and Space Administration, Cleveland, Ohio. Lewis Research Center). Aug. 1965. 31p. CFSTI $2.00 cy, $0.50 mn.

A study was made for the purpose of exploring thermodynamic and turbomachinery concepts for low-power (2- to 10-kw) radioisotope and intermediate-power (100- to 300-kw) reactor Brayton-cycle systems. The effects of intercooling and reheating on the system were examined. Turbomachinery characteristics for one single- and two dual-shaft arrangements were determined parametrically as a function of rotative speed and included the effects of varying molecular weight, pressure level, and pressure ratio. Several favorable configurations were selected and presented as examples of geometries suitable for these systems. For a low-power radioisotope system, where the achievement of high cycle efficiency is of prime importance, the maximum increase in cycle efficiency achievable by the use of both intercooling and reheating was about 0.05 out of a total of about 0.35 to 0.40. For a typical intermediate-power reactor system, where the achievement of minimum radiator area is of prime importance, intercooling offers no area reduction but reheating results in about a 15 percent reduction in minimum area. Comparable size and specific speed designs can be evolved for the radioisotope- and reactor-system turbomachinery when a constant ratio of pressure to power is used. Rotative speeds, however, are considerably higher for the reactor system designs, but these can be reduced, if desired, by reducing the pressure to power ratio. For both systems, suitable turbomachinery can be evolved that will not be significantly different from those currently under experimental investigation for solar Brayton-cycle systems. (auth)

45655 (NUS-229) DOSE CALCULATION MODELS FOR RE-ENTERING NUCLEAR ROCKET DEBRIS. DeAgazio, Albert W. (Nuclear Utility Services, Inc., Washington, D. C.). May 12, 1965. 47p.

An investigation of the hazards to man which may result from nuclear rocket engine flight failures is made. The external dose functions and external and internal dose probability functions are derived. External whole body gamma and beta dose relations are derived for receptors who are not fixed in a given location for the entire exposure period. The probability of receiving a given external dose, the number of people receiving at least a given dose and the overall population dose are also derived for external gamma radiation exposures. Internal dose probability functions are derived for both ingestion and inhalation. (M.O.W.)

45656 (PWAC-474) DETERMINATION OF ABSOLUTE POWER IN SNAP-50 CRITICAL ASSEMBLIES BY ^{140}Ba FISSION PRODUCT MEASUREMENTS. Welsh, W. F. (Pratt and Whitney Aircraft, Middletown, Conn. Connecticut Advanced Nuclear Engineering Lab.). July 30, 1965. Contract AT(30-1)-2789. 75p. Dep. mn; CFSTI $3.00 cy, $0.75 mn.

The absolute power of a critical assembly for a given critical experiment is obtained by combining the results of measurements of the core center power density and the relative power distribution normalized to the core center. An enriched uranium metal strip is used to measure the core center power density. During operation of the assembly, fissions take place within the strip causing a buildup of fission products. A known percentage of the fissions produce the fission product ^{140}Ba. This decays by β^- emission to ^{140}La which in turn decays by β^- emission to ^{140}Ce. The ^{140}La decay is accompanied by the emission of a 1.60 Mev gamma ray. The parent-daughter relationship and the half-lives of ^{140}Ba and ^{140}La are such that the 1.60 Mev ^{140}La activity reaches its maximum at several days after shutdown. At this time the gamma activity of other fission products has been substantially reduced, so that the ^{140}La activity stands prominently above the background. This activity is measured using a scintillation spectrometer, and the number of ^{140}Ba nuclei produced in the strip by fission is calculated. Then the core center power density, in units of fission rate per unit mass, can

be obtained from the number of ^{140}Ba nuclei produced, the known fission yield of ^{140}Ba, the ^{235}U mass of the measurement strip and the period and duration at power of the critical assembly. The relative power distribution is measured using catcher foil techniques. When the absolute power of the critical assembly during the calibration run is known, this power level is associated with the neutron level of the run as recorded by neutron monitors of fixed geometry. Since the reading of each neutron monitor is directly proportional to the power level, the absolute power of subsequent runs can be determined from the corresponding readings of the linear neutron monitors. (auth)

45657 (TID–22088) ECONOMICS OF A 47,000 DWT TANKER. Blumberg, B. (General Electric Co., Cincinnati, Ohio. Nuclear Materials and Propulsion Operation). [nd]. Contract AT(40-1)-2847. 7p. (TM–64-9-7). Dep. mn; CFSTI $1.00 cy, $0.50 mn.

An economic comparison is presented for a nuclear system (the 630A) and a conventionally powered tanker on a route between Kuwait and Philadelphia. A comparison of the 630A and a pressurized water reactor is also included. Both capital and operating costs are considered. (D.C.W.)

45658 (TID-22097) NUCLEAR ROCKETS BASED ON GRAPHITE REACTOR TECHNOLOGY. THEIR APPLICATIONS AND DEVELOPMENT STATUS. Finger, Harold B.; Johnson, Paul G.; Morrissey, John E.; Siegel, Alan R. (National Aeronautics and Space Administration). Sept. 28, 1964. 127p. (X65-10546; NASA-TM-X-54858). Dep. mn; CFSTI $4.00 cy, $0.75 mn.

Nuclear rocket propulsion based upon solid-core graphite reactor technology is discussed. The requirements for various types of missions are considered; and the design and development status of the NERVA engine is summarized. Advanced research and technology are also discussed including the Phoebus reactor. (D.C.W.)

45659 (TIM–807) THE REACTOR WEIGHT OPTIMIZATION PARAMETRIC CODE—WOP. Fish, R. W.; Killen, R. E. (Pratt and Whitney Aircraft, Middletown, Conn. Connecticut Advanced Nuclear Engineering Lab.). July 22, 1965. Contract AT(30-1)-2789. 68p. Dep. mn; CFSTI $3.00 cy, $0.75 mn.

The methods used for conducting detailed reactor parametric design studies are described. In general, the purpose of the parametric methods used is to optimize reactors on the basis of minimum weight, while matching desired operating conditions and remaining within imposed operating limitations. The Weight Optimization Parametric Code (WOP) is given which calculates reactor weights and dimensions from input physics data, desired operating conditions and material properties for all reactors within the input ranges of up to four independent physics variables. The code then selects the minimum weight reactor satisfying all input operating limitations from all the reactors considered. (M.O.W.)

45660 (TIM–919) MOTOR CAVITY EVACUATION STUDY. Cygnor, J. (Pratt and Whitney Aircraft, Middletown, Conn. Connecticut Advanced Nuclear Engineering Lab.). May 28, 1965. Contract AT(30-1)-2789. 23p. Dep. mn; CFSTI $1.00 cy, $0.50 mn.

Cavitation induced between a rotating and stationary cylinder was used as a means of vaporizing the liquid within the gap. The cavitation was induced by centrifugal type dynamic seals attached to each end of the rapidly accelerated rotating cylinder. Five versions of the basic test model were investigated. Successful liquid displacements were attained with water within four seconds. Visual observations and high speed movie studies were made of the displacement mechanism. In addition, oscillograph records were made of pressure and temperature gradients in the gap. (auth)

45661 MISSION INTEGRATION OF NUCLEAR DYNAMIC POWER SYSTEMS. Duchon, Paul; Finch, W. C. (Aerojet-General Corp., Azusa, Calif.). New York, American Society of Mechanical Engineers, 1965, Preprint No. 65-AV-32, 12p., $1.00. (CONF-650324–1). ORINS.

From American Society of Mechanical Engineers, Aviation and Space Conference, Los Angeles.

The nuclear dynamic electric power generating system, because of its wide application to space missions, is considered in the light of its integration with earth orbiting, planetary base, and deep space missions, manned and unmanned. The need for mission integration development to either parallel or follow the development of the power system is demonstrated. The variables which translate across the interfaces between the power system and the mission are described, as are the parametric effects they have upon the system and the mission. These include such items as environment, radioactivity, thermal conditions, reliability, gravity field, electrical duty cycle, maintenance, emergency power, vehicle dynamics, and configuration. To exemplify the task of mission-power system integration, manned earth orbiting, manned planetary base and unmanned mission systems are described. Several major areas of study prerequisite to the subject task are described. Among these are nuclear shielding, redundancy, radiator, hazards, and thermal management. Finally, a list of specific studies is recommended. (auth)

45662 THE APPLICATION OF NUCLEAR REACTORS AND RADIOISOTOPES TO UNDERWATER-VEHICLE PROPULSION. Jaffee, H. (Aerojet-General Nucleonics, San Ramon, Calif.); Buck, K.; McCluer, H.; Montgomery, H.; Finkle, E. New York, American Society of Mechanical Engineers, 1965, Preprint No. 65-UNT-6, 11p. $1.00. (CONF-650550–2). ORINS.

From American Society of Mechanical Engineers, Underwater Technology Conference, New London, Conn.

The application of radioisotope power plants and small gas-cooled reactors to underwater vehicle propulsion was examined. A radioisotope-powered engine using a reciprocating-steam power conversion system is described for the power range of tens of shaft horsepower. Three nuclear reactor systems based upon essentially the same compact, fast spectrum gas-cooled reactor but employing a Brayton, Rankine (dual) and Loeffler power conversion cycle, respectively, are described for the power range of thousands of shaft horsepower. Plants of both general types are applicable to the increasing requirements for undersea propulsion power for scientific, military, and commercial missions. (auth)

45663 NUCLEAR VEHICLE TECHNOLOGY AND TESTING—ENGINE SYSTEMS. White, L. E. (Aerojet-General Corp., Jackass Flats, Nev.) New York, American Inst. of Aeronautics and Astronautics, 1965, Preprint No. 65-529, 27p., $1.00. (CONF-650711–33). ORINS.

From AIAA 2nd Annual Meeting and Technical Demonstration, San Francisco.

The testing portion of the NERVA development program is described. The new major facilities, the engine test stand (ETS-1) and the engine, maintenance, assembly, and disassembly (E-MAD) complex, is discussed. The ETS-1 provides the means for performing controlled static firing of the engine. The E-MAD complex provides the means for assembly of the engine, its final checkout, and its transportation to ETS-1; and, following the test firing at ETS-1, further provides for the remote disassembly of the engine, its extensive post-operative examination, and the disposal of radioactive engine hardware. (L.B.S.)

45664 THERMOELECTRIC TECHNOLOGY FOR SPACE-POWER SYSTEMS. Klem, R. L.; Helwig, W. J. (Radio Corp. of America, Harrison, N. J.). New York, American Inst. of Aeronautics and Astronautics, 1965, Preprint No. 65-469, 8p., $1.00. (CONF-650711–6). ORINS.

From AIAA 2nd Annual Meeting and Technical Demonstration, San Francisco.

Design considerations and performance data are described for silicon-germanium thermoelectric converters which can be used in nuclear applications with either reactor or isotope heat sources. Extensive life tests have demonstrated the suitability of these converters for use in space power systems. The SNAP 10A system characteristics are considered as an example. (L.B.S.)

45665 NERVA PROGRESS REPORT. Arnold, W. H. Jr. (Westinghouse Electric Corp., Pittsburgh). New York, American Inst. of Aeronautics and Astronautics, 1965, Preprint No. 65-528, 8p., $1.00. (CONF-650711-20). ORINS.

From AIAA 2nd Annual Meeting and Technical Demonstration, San Francisco.

The status of the NERVA reactor program is described in terms of the NRX–A2 and NRX–A3 tests. The test objectives and performance data are given. (L.B.S.)

45666 SNAP 8 REACTOR AND SHIELD DESIGNS AND OPERATING EXPERIENCE. Johnson, C. E.; Mason, D. G. (Atomics International, Canoga Park, Calif.). New York, American Inst. of Aeronautics and Astronautics, 1965, Preprint No. 65-473, 23p., $1.00. (CONF-650711-17). ORINS.

From AIAA 2nd Annual Meeting and Technical Demonstration, San Francisco.

The SNAP 8 reactor is a heat source suitable for long-endurance 10- to 50-kw space electric power supplies. Two tests have demonstrated the feasibility of the reactor: the SNAP 8 Experimental Reactor (S8ER) and the SNAP 8 Developmental Reactor Mockup (S8DRM). The S8ER demonstrated reliable long-term operation of the reactor core and reflector. During 500 days of nuclear operation, it operated one year in the power range 400 to 600 kwt with a 1300°F coolant outlet temperature and continuously for over 5000 hours, thus establishing what is believed to be a new record for continuous reactor operation in the United States. Automatic control system performance and structural capabilities of the reactor design were verified in nonnuclear testing of the S8DRM. The reactor and shield design is summarized for manned and unmanned space applications. Curves are provided allowing spacecraft designers to rapidly estimate shield weight for both applications as a function of payload diameter, payload separation distance, dose rate for manned applications, and total dose for unmanned applications. The design approach to high reliability is described and the validity indicated by the S8ER 5000-hour continuous run. (auth)

Research and Test Reactors

Refer also to abstract 44287.

45667 (AE–194) THEORETICAL WORK FOR FAST ZERO-POWER REACTOR FRO. Haeggblom, Hans (Aktiebolaget Atomenergi, Stockholm (Sweden)). Aug. 1965. 45p. Dep. mn.

The theoretical part of the fast reactor physics work in Sweden has mainly been connected with the FRO reactor. The principal features of this reactor, evaluation of cross sections, calculations of critical masses, reactivity of the air gap and of control rods, and calculations of neutron generation time and effective beta values are described. Carlson codes in spherical and in cylindrical geometry are used to evaluate critical masses and fluxes. In cases when reactivity changes are calculated, complementary methods are perturbation theory and variational calculus. The agreement with experiments is in some cases good, especially the determination of critical mass; but in other cases discrepancies are observed (the activation of ^{238}U in the reflector is much larger than the theoretical spectrum predicts). (auth)

45668 (ANL–7026) THERMAL-NEUTRON FLUXES FOR CP-5 VERTICAL IRRADIATION FACILITIES. Frazier, D. S. (Argonne National Lab., Ill.). Mar. 1965. Contract W-31-109-eng-38. 30p. Dep. mn; CFSTI $2.00 cy, $0.50 mn.

Thermal-neutron fluxes measured in the CP-5 reactor at Argonne National Laboratory over a two-year period are presented graphically. The method used in measuring the fluxes is described briefly. (auth)

45669 (APDA–174, pp 61–6) DEVELOPMENT OF EOCR AS A FAST FUEL TEST FACILITY. Project Agreement No. 13. Shoudy, A. A.; Huebotter, P. R. (Atomic Power Development Associates, Inc., Detroit, Mich.).

The extension of Project Agreement No. 13 was phased out during this quarter. During the period, work was initiated on all of the items listed under the scope of the contract; however, very few quantitative conclusions could be drawn. In those instances where there are no results to report, a discussion of the method of approach is given. (auth)

45670 (APDA–174, pp 74–6) FAST FLUX TEST FACILITY. Project Agreement No. 16. Amorosi, A.; Duffy, J. G.; MacLeod, R. A. (Atomic Power Development Associates, Inc., Detroit, Mich.).

APDA has provided engineering and consulting assistance to Battelle Northwest (BNW) for the design of the Fast Flux Test Facility. Several meetings were held with BNW personnel on various conceptual design features, problem areas, and definitions of the areas in which APDA would assist BNW. Conceptual design studies were initiated on core cross sections, reactor configurations, and bottom reentry loop design. (auth)

45671 (BAW–1195-4) BLOWDOWN MODELS APPLICABLE TO THE LOSS-OF-FLUID TEST FACILITY (LOFT). EVALUATION. Parks, Charles E. (Babcock and Wilcox Co., Lynchburg, Va. Atomic Energy Div.). June 1965. Contract AT(10-1)-1195. 42p. Dep. mn; CFSTI $2.00 cy, $0.50 mn.

LOFT is a pressurized-water loss-of-fluid test facility. An investigation is carried out of existing blowdown models and associated experiments, and of the relative merits of these models in analyzing coolant-loss accidents in systems such as LOFT. (T.F.H.)

45672 (BNWL–89) FAST NEUTRON FLUX CHARACTERISTICS OF THE ETR, G-7 HOT WATER LOOP. Bement, A. L.; Irvin, J. E.; Dahl, R. E. (Battelle-Northwest, Richland, Wash. Pacific Northwest Lab.). Aug. 1965. Contract AT(45-1)-1830. 78p. Dep. mn; CFSTI $3.00 cy, $0.75 mn.

In the course of conducting irradiations on reactor structural materials in the ETR hot-water G-7 loop, dosimeters of Fe, Ni, Ti, and Al-0.1 wt% Co were activated, counted, and analyzed. From these measurements, the mean spatial neutron flux distribution in the G-7 position was mapped, and variations in the flux intensity and configuration of this distribution from cycle to cycle were determined. The greatest reliability in flux measurement was obtained with iron detectors counted nondestructively. Iron detectors subjected to chemical isotopic separation gave values as much as 20% lower than companion samples counted nondestructively. Flux values measured from nickel dosimeters were often erratic, particularly after long exposures where corrections of the thermal neutron burnout of cobalt are expectantly inaccurate. Contributing factors in the erratic response for nickel were thermal flux perturbations caused by adjacent experiments and from materials inserted into the loop. The accuracy in measured flux was estimated to be within 10%, and flux maps and spatial coefficients were derived which permitted calculating the flux at any position within the loop within 20% accuracy. A 4 to 8% correction resulted in normalizing the effective cross sections for iron and nickel, respectively, over the slightly moderated ETR spectrum compared to a fission spectrum for energies above 1 Mev. (auth)

45673 (EIR–85) TEMPERATUR-KOEFFIZIENT DES SAPHIR. (Temperature-Coefficient of SAPHIR). Huerlimann, T.; Beusch, R. (Eidgenoessisches Institut fuer Reaktorforschung, Wuerenlingen (Switzerland)). Aug. 1965. 15p. Dep. mn.

The reactivity perturbations occurring in the heating up of the entire reactor by 1°C was calculated for initial temperatures of 10, 20, and 30°C. These perturbations can be traced back to 2 categories: alteration of the volume of the various reactor zones and alteration of the neutron temperature and the material constants within the zones. The calculations are based on the perturbation calculation and use the weight functions for the quadratic 5 × 5 core SAPHIR. The integral of the reactivity influence is extended over the core and the reflector. The values of the perturbation functions were calculated. (J.S.R.)

45674 (GA-6168) REPETITIVELY PULSED ACCELERATOR BOOSTERS. Beyster, J. R.; Russell, J. L. (General Atomic, San Diego, Calif. John Jay Hopkins Lab. for Pure and Applied Science). Feb. 15, 1965. Contract AT(04-3)-167. 41p. (CONF-650217-2). Dep. mn; CFSTI $2.00 cy, $0.50 mn.

From Symposium on Pulsed High Intensity Fission Neutron Sources, Washington, D. C.

A research program for building a very high peak power level short burst reactor by bombarding a supercritical fast reactor with an electron beam from a high current linear accelerator is reported. The experimental and theoretical results obtained from this program are summarized. This is followed by a general discussion of repetitively pulsed accelerator boosters and the potentialities of a thermal flux booster. (M.O.W.)

45675 (IAE-725) OBORUDOVANIE NEKOTORYKH EKSPERIMENTAL'NYKH KANALOV NAUCHNO-ISSLEDOVATEL'SKIKH REAKTOROV SOVETSKOGO SOYUZA. (Instrumentation of Certain Experimental Channels in USSR Research Reactors). Demidov, A. M. (Institut Atomnoi Energii, Gosudarstvennyi Komitet po Ispol'zovaniyu Atomnoi Energii SSSR, Moscow). 1964. 33p. Dep. mn.

The devices and physical characteristics of some channels of the research reactors of the Soviet Union are described. The reactor types involved are VVRM, IRT, Riga, VVR-2, VVRS, TVR, and SM-2. In addition to data on the channels and their equipment, auxiliary equipment such as neutron spectrometers and monochromators, neutron polarizers, dosimeters, the indium-gallium loop, and transporters for radioactive substances are considered. It is pointed out that the preferred future trend in research reactor design should follow the path of increasing the channels and specializing their design in accordance with their ultimate purpose. (ATD)

45676 (IDO-16871-4) FUNDAMENTALS IN THE OPERATION OF NUCLEAR TEST REACTORS. VOLUME 4. ENGINEERING AND DESIGN CONSIDERATIONS FOR IN-PILE TESTS. (Phillips Petroleum Co., Idaho Falls, Idaho. Atomic Energy Div.). July 1965. Contract AT(10-1)-205. 319p. Dep. mn; CFSTI $7.00 cy, $1.50 mn.

The various aspects of the experimental programs at the MTR, the ETR, and the ATR are discussed, and some of the engineering and design principles associated with these programs are reviewed. Fluid flow, heat transfer, shielding, in-pile tube design, out-of-pile equipment design, instrumentation, decontamination, specific types of experiments, and hazards are covered. (D.C.W.)

45677 (INR-614/IXA/P) POMIAR PARAMETRU β-/l GRAFITOWO-WODNEGO REAKTORA MOCY ZEROWEJ ANNA PRZY POMOCY IMPULSOWEGO GENERATORA NEUTRONOW. (Measurements of β-/l Parameters in the Water-Graphite Zero Power Anna Reactor Using the Pulse Neutron Source). Khvashchevski, S.; Dybovski, K. (Institute of Nuclear Research, Warsaw (Poland)). 1965. 20p Dep.

The β/l crit. and reactivities of the control and safety rods of the ANNA reactor were measured utilizing pulse neutron source. Because the prompt and delayed neutron lifetimes in the ANNA reactor are comparable, corrections had to be introduced into the relations of the β/l crit. and reactivities with the prompt neutron decay constant. The method of the results of processing are also given. (auth)

45678 (JEN-149-DQ/I-50) WATER TREATMENT PROCESS IN THE JEN-1 RESEARCH REACTOR. Urgel, M.; Perez-Bustamanate, J. A.; Batuecas, T. (Junta de Energia Nuclear, Madrid (Spain). Division de Fisica). 1965. 31p. (CONF-213-2). Dep. mn.

From Symposium on Water Chemistry in Reactors, Rome, May 1963.

The main characteristics and requirements which must be met by waters to be used for nuclear reactors were studied with emphasis on those used in primary and secondary circuits and the purification systems to be employed in each case. The experiments carried out for the initial pretreatment of water and the ion-exchange deionization processes including a number of systems consisting of separated and mixed beds loaded with a variety of different commercially available resins are described. A parallel physico-chemical investigation of the resin characteristics was carried out in order to select those showing optimal features in regards to their ulterior adoption in connection with a light-water cooled reactor. Results are included referring to the performance of the water-deionization unit built for the supply of the swimming-pool of the J.E.N.-1 reactor. (auth)

45679 (NYO-1859-11) TENTH ANNUAL PROGRESS REPORT, JULY 1, 1964-JUNE 30, 1965. Remick, Forrest J. (Pennsylvania State Univ., University Park. Dept. of Nuclear Engineering). June 1965. Contract AT(30-1)-1859. 61p. Dep. mn; CFSTI $3.00 cy, $0.75 mn.

Work at Pennsylvania State University nuclear reactor facility is summarized in sections on administration, and usage of the facility for research, education, and training. A list of publications, reports, talks, and theses associated with work at the facility is included. (J.R.D.)

45680 (ORNL-TM-1190) DESCRIPTION OF THE LITR REACTOR CONTROL AND INSTRUMENTATION SYSTEMS. Bates, A. E. G. (Oak Ridge National Lab., Tenn.). July 16, 1965. Contract W-7405-eng-26. 47p. Dep. mn; CFSTI $2.00 cy, $0.50 mn.

The reactor control and instrumentation systems for the LITR were modernized and upgraded. The process hardware was completely replaced with the most modern and versatile all-electronic equipment. The nuclear system assemblies were rebuilt and improved so that they would be interchangeable directly, or following minor modification, with comparable Oak Ridge Research Reactor (ORR) assemblies. All control system hardware was replaced with new assemblies and components that are standard in current design practices. These systems are described, and their operation is discussed. (auth)

45681 (RCN-36) COMPILATION OF NEUTRON FLUX DENSITY DATA IN THE H.F.R. Zijp, W. L. (Reactor Centrum Nederland, Petten). May 1965. 37p. Dep. mn.

A compilation of thermal and fast flux density values is presented referring to the extended fuel core, the reflector region, the poolside facility, and the pneumatic post system. The data are based upon several measurements and are sometimes supplemented with best estimates for those positions where no experimental data are available. As the actual flux density values are dependent upon the core configuration, the irradiation experiments installed, and the degree of burn-up, the quoted values must be handled very cautiously and must be considered as giving only orders of magnitude. (auth)

45682 (RT/ING(64)-15) ANALISI DEL SISTEMA DI REGOLAZIONE NON LINEARE PER IL REATTORE RTM. (Analysis of a Nonlinear Control System for Reactor RTM). Giordano, P.; Mathis, A.; Scandellari, G. (Comitato Nazionale per l'Energia Nucleare, Rome (Italy)). Nov. 1964. 73p. Dep. mn.

The design procedure for a nonlinear reactor control system is described. The control system contains two nonlinearities, separated by a linear section: a dead-band, normally used to reduce the noise excitation of the control system, and a gear backlash, which in this case is particularly important, due to the fact that the control elements are cylinders with limited effective angular range. The type of electrical motors was also defined (Slo-Syn motors, which can operate as synchronous or stepping motors). The work was developed using analog and analytical methods in parallel, and the final control scheme (a velocity servo with stepping motors) was thoroughly tested on the analog computer with noisy inputs, and theoretically studied with a describing function method extended to the case of systems with multiple nonlinearities connected by linear sections. (auth)

45683 THE LONDON UNIVERSITY NUCLEAR REACTOR CONSORT. Grant, P. J. (Imperial Coll. of Science and Tech., London). Nature, 207: 911-13(Aug. 28, 1965).

The design and construction of the reactor Consort is described. Consort is a water-cooled and moderated reactor fuelled with enriched uranium (80% ^{235}U) and has a power of 100 kw (thermal). The purpose of the reactor is to provide experimental facilities for research and training in nuclear engineering and applied nuclear science for the London University and other educational institutions in the London area. The main reactor parameters and fluxes available in the experimental facilities are tabulated. (P.C.H.)

45684 INVESTIGATIONS INVOLVING THE USE OF FAST NEUTRONS FROM A REACTOR. Kim, Kee Hyun (Atomic Energy Research Inst., Korea). New Phys. (Korea), 3: No. 2, 51-5(1963). (In Korean).

Current studies based on the use of fast neutrons from a typical reactor are reviewed, discussing the reactor's neutron energy spectrum and the methods employed to detect fast neutrons. The four methods considered are: nuclear emulsion, threshold reaction, proton recoil and radiation damage in solids, as indicated by changes in electric conductivity. The research areas covered include fast-neutron spectroscopy, nuclear reactions induced by recoil protons, using water as moderator, tritium induced reactions based on tritium produced from lithium irradiated in the reactor, inelastic neutron scattering, energetic γ ray sources formed by neutron capture and radiation damage. (TTT)

45685 A STUDY OF THE DYNAMICS OF A TRIGA TYPE REACTOR. Hornyik, K.; Wyman, M. E. (Univ. of Illinois, Urbana). 32p. (CONF-650413-12). Gmelin, AED-CONF-65-042-20.

From Symposium on Neutron Dynamics and Control, Tucson, Ariz.

A number of measurements of coolant flow and coolant temperatures were performed on a TRIGA Mark II pulsing reactor under both steady state and transient conditions. Based on these measurements as well as on other pertinent information, a simple analytical model was developed and found to be in good agreement over the whole range of operations including the transients following fast insertion of reactivity in excess of one dollar. A non-uniform heat source distribution over the radius of the fuel rod causing a temporary peaking of the fuel temperature near the surface of the rod during a pulse transient as well as the natural circulation-cooling conditions require an adequate treatment of the heat transfer model in order to describe the temperature feedback phenomena with sufficient accuracy. (auth)

45686 HYDRAULIC TRANSFER FACILITY FOR IRRADIATION CONTAINERS. Mitault, Gerard; Puychevrier, Jean (to Commissariat a l'Energie Atomique). British Patent 1,000,680. Aug. 11, 1965. Priority date June 20, 1963, France.

A facility is described for the hydraulic transfer of irradiation containers between an irradiation station located within a body of water, for example the water of a swimming pool type reactor, and a charge and discharge station, which is located outside the body of water. The installation is designed to prevent the passage of activated water into that portion of the circulating system located outside the reactor tank while transfer operations are in progress. The installation includes a transit tube for transferring containers and connecting the charge station to a first extremity of the irradiation station, a circulator tube permanently connected to the charge station, and a distributor. The distributor includes means for providing a communication between the first extremity of the irradiation station and the body of water or for isolating the first extremity from the body of water and for connecting the circulating tube either to one or the other extremity of of the irradiation station, a circulating pump for the purpose of causing water to circulate either in one direction or the other within the circulating tube, and a compensating tank that serves to supply the tubes with a quantity of purified water corresponding to the quantity of water delivered to the body of water through the distributor. (B.L.M.)

WASTE DISPOSAL AND PROCESSING

See also BIOLOGY AND MEDICINE — Ecology.
CHEMISTRY — Radiochemistry.
CHEMISTRY — Separation Processes and Procedures.
HEALTH AND SAFETY.

45687 (DP-966) TAFI-II, A COMPUTER CODE FOR MANAGEMENT OF RADIOACTIVE WASTE. Tharin, Catherine R. (Du Pont de Nemours (E. I.) and Co., Aiken, S. C. Savannah River Lab.). Aug. 1965. Contract AT(07-2)-1. 42p. Dep. mn; CFSTI $2.00 cy, $0.50 mn.

A computer program, TAFI-II, was written in FORTRAN II to assist in the regulation and inventory control of radioactive fission products that are stored in waste tanks at the Savannah River Plant. The inventories and heat generation rates are computed for thirteen isotopes in each of twenty-four waste tanks. The program prepares a report that summarizes the data and provides an up-to-date status of the conditions in the waste tanks. (auth)

45688 (NP-15367) CHEMICAL ENGINEERING STUDIES ON THE PROCESSING OF RADIOACTIVE LIQUID WASTES BY EVAPORATION. Progress Report, January 1–June 30, 1964. Yamamoto, Yutaka; Miyauchi, T.; Kunii, D.; Kiyose, R. (Tokyo Univ. (Japan). Faculty of Engineering). Contract 250/RB. 24p. Dep. mn.

The operational characteristics of fluidized-bed spray evaporator for processing radioactive liquid wastes were investigated. Although the principal idea of the process is almost the same as the double-effect evaporator, by using the spray evaporator for final evaporation and solidification, it becomes possible to get the product directly from the evaporator as solid particles and thus to minimize the cost of disposal of radioactive liquid wastes. (P.C.H.)

45689 (ORNL-P-1568) DEMONSTRATION OF DISPOSAL OF HIGH-LEVEL RADIOACTIVE SOLIDS IN SALT. Empson, F. M.; Boegly, W. J. Jr.; Bradshaw, R. L.; McClain, W. C.; Parker, F. L.; Schaffer, W. F. Jr. (Oak Ridge National Lab., Tenn.). [1964]. Contract W-7405-eng-26. 33p. (CONF-650554-1). Dep. mn; CFSTI $2.00 cy, $0.50 mn.

From 2nd Symposium on Salt, Cleveland.

A description is given of Project Salt Vault, a demonstration using irradiated ETR fuel assemblies and the inactive mine of the Carey Salt Company at Lyons, Kansas. The engineering and scientific objectives of Project Salt Vault are outlined. The instrumentation and the canning and shipment of the ETR fuel assemblies are described. The status of Project Salt Vault is given. (D.L.C.)

45690 (RL-SA-40) STATUS OF FISSION PRODUCT RECOVERY AT HANFORD. Beard, S. J.; Smith, P. W. (General Electric Co., Richland, Wash. Hanford Atomic Products Operation). Aug. 16, 1965. Contract AT(45-1)-1350. 20p. (CONF-650902-11). Dep. mn; CFSTI $1.00 cy, $0.50 mn.

From American Chemical Society, 150th National Meeting, Atlantic City.

The recovery of fission products was initiated at Hanford in August 1960 with the production of strontium-90 and cesium-137. The program has since included production of custom quantities of cerium-144 and promethium-147. The current program involves separation of strontium and rare earths from Purex acid waste by lead carrier sulfate precipitation and subsequent separation of rare earths from strontium by oxalate precipitation. Strontium is further purified by di(2-ethylhexyl)phosphoric acid solvent extraction. Cesium-137 is recovered from aged alkaline wastes by processing the alkaline supernatant solution through a bed of alumino-silicate resin. Several other processes have been demonstrated with full level process solutions in plant equipment. Cesium has been recovered from alkaline wastes by zeolite ion exchange and nickel ferrocyanide precipitation and from acid wastes by phosphotungstic acid precipitation. Technetium-99 has been recovered and purified by anion exchange. Cerium-144 has been separated from the rare earths by di(2-ethylhexyl)phosphoric acid solvent extraction using silver catalyzed persulfate oxidation of cerium(III) to cerium(IV). Promethium-147 was subsequently separated from the cerium-free rare earths by chromatographic ion exchange. Future plans include the recovery of megacurie quantities of Sr, Cs, Ce, and Pm in a waste processing plant scheduled for startup in 1967. (auth)

45691 (RL-SA-41) OPERATING EXPERIENCE ON IN-TANK SOLIDIFICATION OF RADIOCHEMICAL WASTES. Shefcik, J. J. (General Electric Co., Richland, Wash. Hanford Atomic Products Operation). Aug. 17, 1965. Contract AT(45-1)-1350. 18p. (CONF-650902-10). Dep. mn; CFSTI $1.00 cy, $0.50 mn.

From American Chemical Society, 150th National Meeting, Atlantic City.

The initial operation of the First In-Tank Solidification Unit is described. Alkaline radiochemical waste solutions are evaporated within a 750,000-gallon underground tank by sparging with compressed air electrically heated to 1200°F. The air sparger also serves as an air-lift circulator to agitate the solution and as a heat exchanger. To avoid the high entrainment normally associated with hot air sparging, more than half of the available heat is transferred to the solution by passing the hot air down the hollow wall of the 40-inch diameter, 12-foot long, circulator-sparger. Stud fins are used to improve the heat transfer coefficient. The off-gas vapors are filtered and dehumidified, producing condensate and effluent air streams very low in residual radioactivity. Solution decontamination factors of greater than 10^5 are obtained. As evaporation occurs, additional radiochemical waste solutions are added. After wastes have been boiled down by a factor of 4 to 6, the concentrate will be allowed to cool and solidify. (auth)

45692 (UCD-472-112, pp 141-7) ION EXCHANGE REMOVAL OF ^{90}Sr FROM BIOLOGIC WASTES. Anderson, R. P.; Goldman, M.; Taie, M. (California Univ., Davis. School of Veterinary Medicine).

The fourth year of operation of the Sr-90 waste decontamination plant is reported. The average concentration of radioactivity per batch, 50 pC/ml, remained approximately the same as for 1963. The waste influent rate of 700 gal/day totalling 250,000 gallons during 1964 more than doubled that of 1963. Forty-eight mC were removed by ion exchange with an average decontamination factor exceeding 3000. A total discharge of 50 μC Sr-90 was made to the underground leaching field. (auth)

45693 PLANT FOR TREATMENT OF RADIOACTIVE WASTES OF THE CZECHOSLOVAK INSTITUTE OF NUCLEAR RESEARCH. Jenicek, A.; Kortus, J. Czech. Heavy Ind., No. 3, 9-14(1964).

A central station of comparatively high capacity was erected for treatment of low-level effluents from various sources, chiefly from decontamination of surfaces of laboratory equipment contaminated in radiochemical work. The station was designed for processing 3.6 m^3 of effluents per hour. It was assumed that the maximum specific ac-

tivity would be 10^{-5} C/l with an average activity lower by about two orders of magnitude. The radioactive solutions are mixed with precipitants and, in coagulation, the predominant part of the activity is retained in flakes. The sludge is placed in asphalt-lined metal barrels. Waste waters with higher activity or those not efficiently deactivated by a chemical method are evaporated. Radiation protection procedures are described. (M.C.G.)

GENERAL AND MISCELLANEOUS

45694 (AECL-2251) ANNUAL REPORT, 1964-65. (Atomic Energy of Canada Ltd., Chalk River (Ontario)). 40p. Dep. mn; AECL Free.

Activities at AECL directed toward scientific research and development in atomic energy are described. Efforts devoted to development of economic nuclear power, operation of reactors, production of radioisotopes, and development of associated equipment are also described. The information is presented in sections on nuclear power programs, Chalk River Nuclear Laboratories, Whiteshell Nuclear Research Establishment, commercial products, finance, and administration. (J.R.D.)

45695 (BNL-912) MECHANISM OF THE IMMUNE RESPONSE. Brookhaven Lecture Series, No. 42. Koshland, Marian Elliott (Brookhaven National Lab., Upton, N. Y.). Dec. 9, 1964. Contract [AT(30-2)-Gen-16]. 18p. Dep. mn; CFSTI $1.00 cy, $0.50 mn.

Mechanisms of antibody formation and specificity of action are discussed, and a simplified scheme of the methods used for the preparation and purification of the antibody is presented. Rabbit antibodies were analyzed for amino acid content by several methods in order to guarantee purity. When standard errors of individual determinations were calculated for arsonic, phenyltrimethylammonium, and phenyl-β-lactoside antibodies, it was found that $\frac{2}{3}$ of the time an individual result did not differ from the average by more than 2%. The overall similarity of compositions was demonstrated by the fact that the amount of lipine found in arsonic antibody was 69.6 residues and in ammonium antibody 69.4 residues. However, a few small but significant differences did appear. For example, the arsonic antibody had a higher arginine and isoleucine content while the ammonium antibody had a higher aspartic acid and leucine content. The differences in amino acid content were too large to be accounted for by impurities in the preparation. Therefore, it was suggested that each of the rabbits used, genetically produced two kinds of γ-globulin. Further amino acid analyses demonstrated that the amino acid content of one antibody was not affected by the simultaneous production of another antibody. Results indicate that the instructive theory of antibody formation is incorrect and support the basic tenet of the selective theory, namely that antibody synthesis is a genetically controlled process. (H.G.D.)

45696 (CALT-221-12) EFFECTS OF LIQUID QUENCHING ON THE CONSTITUTION AND STRUCTURE OF SILVER-SILICON AND GOLD-SILICON ALLOYS. Report No. 37. Luo, H. L.; Klement, W. Jr.; Anantharaman, T. R. (California Inst. of Tech., Pasadena. W. M. Keck Lab. of Engineering Materials). July 1965. Contract AT(04-3)-221. 16p. Dep. mn; CFSTI $1.00 cy, $0.50 mn.

Rapid quenching from the liquid state is shown to lead to amorphous solidification of gold-silicon alloys around the eutectic composition and to the formation of three silver-silicon and gold-silicon intermediate phases. The β Ag-Si phase is hexagonal close-packed and may be considered a Hume-Rothery phase. The β and γ Au-Si phases have complex face-center cubic structures and may be looked upon as superlattices built of 8 and 125 unit cells, respectively, of the simple face-centered cubic structure of gold. The construction of the liquid-quenched alloys in both binary systems is discussed with reference to the rate of cooling from the melt. (auth)

45697 (COO-330-11) [PROGRESS REPORT ON CARBOHYDRATE CATABOLISM IN PLANTS] JULY 1965. Beevers, Harry (Purdue Research Foundation, Lafayette, Ind.). Contract AT(11-1)-330. 16p. Dep. mn; CFSTI $1.00 cy, $0.50 mn.

Research on routes of carbohydrate breakdown in higher plants is reviewed. Areas of carbohydrate metabolism discussed include: initial phases of carbohydrate breakdown; pyruvate and acetate utilization; relationships with amino acid metabolism; sugar uptake; and regulation of respiration. A bibliography of 23 publications resulting from research carried out on the contract is presented. (H.G.D.)

45698 (CU-2663-18) EXPERIMENTS AND HYDROGRAPHIC SURVEYS OFF SANDY HOOK, NEW JERSEY (1963). Ichiye, Takashi (Columbia Univ., Palisades, N. Y. Lamont Geological Observatory). July 1965. Contract AT(30-1)-2663. 29p. (CU-266(48)-11). Dep. mn; CFSTI $2.00 cy, $0.50 mn.

Dye diffusion experiments carried out off Sandy Hook, New Jersey on August 7 and October 15 through 18 in 1963 are described. Aerial photographs from a low flying airplane in October experiments showed fine structures of dye patches, such as striations, owing to calm weather. A shipborne fluorometer indicated that dye was thinly spread vertically only above seven meters in October although thermocline was located at about 25 meters. Hydrographic data off Sandy Hook Bay were collected at three different tidal stages on August 6 to 7. These data indicate that advection of the water in the bay by tidal currents occurred independently at each level without much vertical mixing. Relationships between spectrum of mean square deviations of concentration and that of turbulent energy are discussed in relation to dye diffusion process. (auth)

45699 (CU-2663-21) GEOSTROPHIC EDDIES IN THE OCEAN. PART I. Ichiye, T. (Columbia Univ., Palisades, N. Y. Lamont Geological Observatory). Aug. 1965. Contract AT(30-1)-2663. 28p. (CU-1806-4; CU-266(48)-14). Dep. mn; CFSTI $2.00 cy, $0.50 mn.

The results of observations of eddies with dimensions of several kilometers to a few hundred kilometers are reviewed. Detailed measurements of an eddy off California revealed the quasi-geostrophic structure of the eddy of intermediate size. Eddies in the eastern half of the Gulf of Mexico are described from hydrographic data collected since 1950. Case histories and dynamical structure of eddies generated by cutoff of increasing meanders of the Gulf Stream and the Kuroshio are discussed. Generation of eddies and perturbations in the ocean due to moving meteorological disturbances are explained from examples in case of extra-tropical cyclones in the ocean polar front of the North Pacific and the one in case of hurricane in the central Gulf of Mexico. Dynamics on development of eddies due to a shearing instability are briefly reviewed. (auth)

45700 (DP-970) A COMPUTER PROGRAM FOR CIRCULATION OF LIBRARY JOURNALS. Skelton, Margaret W.; Haefner, Richard R. (Du Pont de Nemours (E. I.) and Co., Aiken, S. C. Savannah River Lab.). June 1965. Contract AT(07-2)-1. 54p. Dep. mn; CFSTI $3.00 cy, $0.50 mn.

A computer program, JURN, was written in FORTRAN II which automates the repetitive paperwork needed to circulate technical journals. The program reduces to a minimum the time and effort required to prepare and maintain current records. The program provides printed distribution slips for each circulating journal, notification of reorder dates, listings of circulating and reference journals, and complete listings of library holdings. A maximum of 1000 people and 750 separate journals (titles) can be accommodated by this program. Up to 50 copies of each journal may be circulated to a maximum of 16 people per copy. (auth)

45701 (LA-3324) HASTI—A NUMERICAL CALCULATION OF TWO-DIMENSIONAL LAGRANGIAN HYDRODYNAMICS UTILIZING THE CONCEPT OF SPACE-DEPENDENT TIME STEPS. Browne, Phillip L.; Hoyt,

Martha S. (Los Alamos Scientific Lab., Univ. of California, N. Mex.). May 5, 1965. Contract W-7405-eng-36. 24p. Dep. mn; CFSTI $2.00 cy, $0.50 mn.

A numerical experiment is described in which an attempt was made to reduce the calculation time of a two-dimensional, Lagrangian, hydrodynamics code, without loss of accuracy. The reduction was accomplished by utilizing a space-dependent time step; i.e., the frequency with which a point is calculated depends on the rate at which changes are occurring in the vicinity of the point. This system permitted savings to be made by eliminating calculations in regions undergoing relatively slow changes. (auth)

45702 (LA-DC-6558) DEVELOPMENT OF THE MAPPING FUNCTION AT A CORNER. Wigley, Neil M. (Los Alamos Scientific Lab., Univ. of California, N. Mex.). [1964]. Contract W-7405-eng-36. 47p. Dep. mn; CFSTI $2.00 cy, $0.50 mn.

Let D be a domain in the plane which is partially bounded by two curves Γ_1 and Γ_2 which meet at the origin and form there an interior angle $\pi\tau > 0$. Let N be an integer ≥ 2 and let α be a real number such $0 < \alpha < 1$. Suppose that for i = 1, 2, Γ_i admits a parameterization $x = x_i(t)$, $y = y_i(t)$, $0 \leq t \leq 1$, where x_i and y_i have N-th derivatives which are uniformly α-Hölder continuous, and $|x_i'(t)| + |y_i'(t)| > 0$. Let G(z) map the sector $0 < \arg z < \pi\tau$ conformally onto D in such a way that G(O) = O. Then if τ is irrational G(z) has an asymptotic expansion in powers of z and $z^{1/\tau}$, with error term $o(z^{N-\epsilon})$. If $\tau = p/q$, a reduced fraction, then G(z) has an asymptotic expansion in powers of z, $z^{1/\tau}$, and $z^q \log z$, with error term $o(z^{N-\epsilon})$. In both cases ϵ is an arbitrarily small positive number. Furthermore expansions for derivatives of G(z) of order $\leq$ N may be obtained by differentiating formally. (auth)

45703 (LA-DC-6667) COMMENTS ON A FLOATING-POINT VERSION OF NORDSIECK'S SCHEME FOR THE NUMERICAL INTEGRATION OF DIFFERENTIAL EQUATIONS. Lewis, H. R. Jr.; Stovall, E. J. Jr. (Los Alamos Scientific Lab., Univ. of California, N. Mex.). [1963]. Contract W-7405-eng-36. 13p. Dep. mn; CFSTI $1.00 cy, $0.50 mn.

Modifications of Nordsieck's scheme for numerical integration of differential equations are described which allow satisfactory operation with floating-point arithmetic. (D.C.W.)

45704 (LA-DC-6717) THE EFFECT OF OPTICAL PUMP PULSE SHAPE ON RUBY INVERSION. Mace, P. N.; McCall, G. H. (Los Alamos Scientific Lab., Univ. of California, N. Mex.). [1961]. Contract W-7405-eng-36. 4p. Dep. mn; CFSTI $1.00 cy, $0.50 mn.

The effect of the shape of the optical pump pulse on population inversion in ruby was investigated. Calculations were performed for five pulse shapes. (D.C.W.)

45705 (NP-15193) NUCLEAR ENERGY DEVELOPMENT IN THE RUMANIAN PEOPLE'S REPUBLIC. Brief Survey. (Institutul de Fizica Atomica, Academia R. P. R., Bucharest (Romania)). 1964. 111p. Dep. mn.

Research projects on cosmic rays and elementary particles, low-energy nuclear physics, reactor physics, neutron scattering, radiation effects on matter, radiation chemistry, radioisotopes, applications of stable isotopes, and use of radioisotopes in agriculture, biology, and medicine are discussed. Research techniques and results in basic research are described. (P.C.H.)

45706 (ORNL-TM-1254) CHRNØGRM—A COMPUTER PROGRAM FOR ANALYSIS OF CHRONOPOTENTIOGRAMS. Savage, Serena; Shults, W. D. (Oak Ridge National Lab., Tenn.). Aug. 31, 1965. Contract W-7405-eng-26. 14p. Dep. mn; CFSTI $1.00 cy, $0.50 mn.

A computer program is given which computes the "least squares" straight line, the slope, the quarter-wave potential, and the standard deviations for the latter two parameters for the conventional semi-log (Karaoglanoff) plot of potential-time data taken from experimental chronopotentiograms. These results, plus the input data and the value of the logarithm term in the Karaoglanoff equation, are printed out to facilitate comparison between theory and experiment. Detailed instructions for the use of the program are given. The program is written in Fortran 63 for the ORNL CDC 1604-A computer. (auth)

45707 (SC-DR-65-261) THE U1627 (A G-SECOND INTEGRATOR). Sirwinski, V. (Sandia Corp., Albuquerque, N. Mex.). Aug. 1965. Contract AT(29-1)-789. 18p. Dep. mn; CFSTI $1.00 cy, $0.50 mn.

The mechanical and electrical characteristics of the U1627, which is capable of integrating any shaped volt-second curve and providing a digital readout is described. (auth)

45708 (SC-R-65-915) BASIC PRINCIPLES OF FUNCTIONAL GAGING. Roth, Edward S. (Sandia Corp., Albuquerque, N. Mex.). July 1965. Contract AT(29-1)-789. 8p. (CONF-650327-1). Dep. mn; CFSTI $1.00 cy, $0.50 mn.

From American Society of Tool and Mfg. Engineers, Annual Conference, Cleveland.

Two kinds of functional gages are briefly discussed. The first is a feature relation gage and the second a feature location and relation gage. Ten basic design principles of these gages are reviewed. A brief discussion of basic interchangeability gage forms is presented. (M.O.W.)

45709 (SC-R-65-963) ON INTEGER LINEAR PROGRAMMING IN COMBINATORIAL ANALYSIS (thesis). Woolsey, R. E. D. (Sandia Corp., Albuquerque. N. Mex.). Aug. 1965. Contract AT(29-1)-789. 81p. Dep. mn; CFSTI $3.00 cy, $0.75 mn.

Submitted to Univ. of Texas, [Austin].

Certain classes of problems in combinatorial analysis are easily expressible in forms suitable for linear programming. However, linear programming is not used extensively in problems of this type. The principal difficulty is the common restriction in such problems that some (or all) of the solution variables are required to take on only integer values. A computer-oriented method is defined for attacking a problem of the above type. (auth)

45710 (SC-TM-64-1772) TRANSIENT RESPONSE OF LINEAR DAMPED LUMPED SPRING-MASS SYSTEMS BY EXPERIMENTALLY DERIVED TRANSFER FUNCTIONS. Kelley, R. W. (Sandia Corp., Albuquerque, N. Mex.). Mar. 1965. Contract AT(29-1)-789. 58p. Dep. mn.

The application of experimentally derived transfer functions to purely mechanical systems is investigated. The transfer function for a mechanical model, intended to represent a viscously damped single-degree system, is experimentally derived by subjecting the mechanical model to steady-state sinusoidal vibration and utilizing the resulting Bode plots. This experimental transfer function is used to predict the transient response to a mechanical shock pulse. The suitability of this experimental transfer function is investigated by comparing the response with the theoretical response of the idealized system and with the actual response of the model to a mechanical shock pulse. A discussion is presented on methods of improving the experimental transfer function by utilizing the amplitude and phase plots. (auth)

45711 (SC-TM-65-81) DYNAMIC RESPONSES OF CYLINDRICAL SHELLS UNDER LATERAL LOADS. Murfin, W. B. (Sandia Corp., Albuquerque, N. Mex.). July 1965. Contract AT(29-1)-789. 10p. Dep. mn; CFSTI $1.00 cy, $0.50 mn.

A solution for the dynamic response of ring structures compatible with the equilibrium equations is discussed. The response to a time-varying pressure pulse is calculated by Duhamel's integral. (auth)

45712 (SC-TM-65-82) AN APPROACH TO THE STIFFNESS OF LATERALLY LOADED CONICAL SHELLS. Leineweber, A. J. (Sandia Corp., Albuquerque, N. Mex.). Aug. 1965. Contract AT(29-1)-789. 12p. Dep. mn; CFSTI $1.00 cy, $0.50 mn.

Beginning with the equilibrium equations for a shell of revolution in which general lateral loading and bending

stresses are considered, force-displacement relations for a conical shell are obtained and expressed in finite difference form. From this set of equations, the stiffnesses for the conical shell are determined. (auth)

45713 (SC-TM-65-279) A FREON TF SOLVENT RESIDUE ANALYZER. Preliminary Report. (Sandia Corp., Albuquerque, N. Mex.). June 1965. Contract AT(29-1)-789. 10p. Dep. mn; CFSTI $1.00 cy, $0.50 mn.

A description is given of the design and development of an instrument which will measure the nonvolatile residue content of Freon TF Solvent. The instrument is capable of measuring residue content as low as one part per million and will give an instantaneous and continuous read-out from a volume of the solvent. The instrument is suitable for production line usage and when used in conjunction with a recirculating cleaning system it will give a continuous reading of the condition of the solvent in the system. The instrument may also be used for an indirect in-process cleanliness test of the components being cleaned. Preliminary test data and calibration curves are included as well as a discussion of future improvements which are anticipated. (auth)

45714 (SC-TM-65-349) DECISION ORDER TECHNIQUE. Brautigam, D. P. (Sandia Corp., Albuquerque, N. Mex.). July 1965. Contract [AT(29-1)-789]. 51p. Dep. mn; CFSTI $3.00 cy, $0.50 mn.

Decision Order Technique (DOT) integrates decision concepts into system analysis. The principal phases of decision making and the basic theories of decision making are discussed. Using the total systems concept, the business or industrial organization can be thought of as a complex network of information channels established for the purpose of accomplishing certain objectives. Every action point in a system is backed by a decision point with each action generating information that may be used at other decision points, which in turn will result in additional action. A conceptual framework is established and quantitative scales are created to evaluate three factors considered in analyzing the decision processes at each decision point. The contribution that each factor makes to systems analysis and business management are discussed, and DOT is developed further as an analytical instrument through the investigation of relations between the factors and the development of mathematical and analog techniques to evaluate these relations and compare them to real world situations. The conclusions delineate the contributions that DOT makes to systems analysis and business management along with criticism of assumptions and methodology used in the development of Decision Order Technique. (auth)

45715 (SC-TM-65-359) SOME TEMPERATURE CONSIDERATIONS IN TRANSISTOR CIRCUIT DESIGN. Espenshade, D. L. (Sandia Corp., Albuquerque, N. Mex.). Aug. 1965. Contract AT(29-1)-789. 27p. Dep. mn; CFSTI $2.00 cy, $0.50 mn.

Transistor heating is analyzed to derive algebraic relations which assure satisfactory temperature equilibrium in transistor circuits. Two rather simple relations are adequate for circuits in which the transistor power dissipation is maintained below the rated maximum. The procedure for analyzing circuits in which the dissipation exceeds the rated maximum for short-time durations is explained. Several sample circuits are analyzed to derive relations describing bias and stability conditions. These relations are applicable, or can be easily modified to apply, to nearly all biasing schemes. (auth)

45716 (TID-4043(Rev.2)) INDEX TO CONFERENCES RELATING TO NUCLEAR SCIENCE. Clark, Willie E.; Greene, Alden G.; Pflueger, Margaret L. (eds.) (Division of Technical Information Extension (AEC) Oak Ridge, Tenn.). June 1965. 204p. DTI Extension. Free.

This index provides access to information on conferences in subject indexes of NSA Vols. 11-18, the announcement series TID-19000 Nos. 1-6, and the files of the AEC Division of Technical Information Extension. The index, which is of the keyword-in-context kind, consists of the following parts: permuted titles and cities, dates, numbered conferences, report number, and title list. (D.L.C.)

45717 (UCRL-7850(Rev.1)) ECONOMICS OF GROUND WATER RECHARGE. Todd, David K. (Lawrence Radiation Lab., Univ. of California, Livermore). Sept. 28, 1964. Contract W-7405-eng-48. 37p. Dep. mn; CFSTI $2.00 cy, $0.50 mn.

Costs and benefits of artificially recharging ground water are reviewed to form a basis for economic evaluation of the technique. Alternative procedures, institutional and financial arrangements, and cost components are considered. Selected cost data, mostly from California projects, are summarized. (auth)

45718 (UCRL-11662) THE DILATION CONTRIBUTION TO THE HEAT CAPACITY OF COPPER AND ALPHA BRASS AT ELEVATED TEMPERATURES. Chang, Y. Austin; Hultgren, Ralph (Lawrence Radiation Lab., Univ. of California, Berkeley). Sept. 1964. Contract W-7405-eng-48. 22p. Dep. mn; CFSTI $1.00 cy, $0.50 mn.

The compressibility as a function of temperature was measured for copper and brass (9.7 at. percent zinc) from sonic velocities. With the aid of these data the dilational contribution to the heat capacity, $C_p - C_v$, was calculated from 77 to 800°K. This term amounts to less than 3 percent of the total heat capacity at room temperature and below, but becomes much more important at elevated temperatures. The Nernst-Lindemann empirical equation satisfactorily predicts the dilational term for copper and the brass. For other substances, it gives a result considerably too high. (auth)

45719 (UCRL-12012) DESIGN OF MODULO-N COUNTERS FOR ANY CODE. Werner, R. (Lawrence Radiation Lab., Univ. of California, Livermore). Aug. 7, 1965. Contract W-7405-eng-48. 15p. Dep. mn; CFSTI $1.00 cy, $0.50 mn.

A step-by-step procedure is developed to design a flip-flop counter which will count to any number in any sequence. The logical properties of various flip-flops are used to minimize the circuitry required. (auth)

45720 (UCRL-12055-T) FIVE-MILLION POUND SHOCK TESTING FACILITY. Phelan, R. M. (Cornell Univ., Ithaca, N. Y.; Lawrence Radiation Lab., Univ. of California, Livermore). [nd]. Contract W-7405-eng-48. 58p. Dep. mn; CFSTI $3.00 cy, $0.75 mn.

A description is given of one approach for upgrading a shock testing facility from 250,000 to 5,000,000 lb when acceleration pulses are desired with levels up to 10,000 g and rise times measured in tenths of a millisecond. The system uses the transfer of momentum between a carriage and a reaction device, or pulse shaper, to provide a degree of control over the shape of the shock signature. Basis design philosophy and practical limitations are presented. Modifications in operating theory and procedure that have resulted from experience with the system at levels up to 3,300,000 lb and 8,300 g are discussed. (auth)

45721 (UCRL-14254) A SCHEMATIC VIEW OF THE ORIGIN OF LIFE. Hart, Roger G. (Lawrence Radiation Lab., Univ. of California, Livermore). June 11, 1965. Contract W-7405-eng-48. 16p. Dep. mn; CFSTI $1.00 cy, $0.50 mn.

A 6-stage scheme for the origin of life is presented. It begins with a catalyst-polymer and proceeds as an evolution by a series of rare, but nearly inevitable, accidents and a continual screening of the accidental products by natural selection. The first 4 stages are assumed to occur in shallow water where a variety and abundance of monomer molecules exist in energetic states, activated by solar radiation or otherwise, that favor polymerization. In the 5th and 6th stages, the supply of activated monomers in free solution has been depleted and the polymers acquire means of obtaining them from other sources. It is postulated that the first self-replicating molecules arose by chance polymerization and that from this single origin there was a proliferation and wide dispersal of such molecules, that replication appeared as one of many chance

modifications and involved 2 catalysts and 2 templates, with auxiliary products eventually being formed including a gelling substance that led to the formation of protoplasm and resulted in large masses of thin, pigmented jelly containing autocatalysts floating in the open sea. After the jelly acquired an outer membrane, the interior composition diverged further from that of the environment and permitted complex processes of metabolism and replication to evolve. (C.H.)

45722 (UCRL-16188) WATER TUNNEL WITH MOVING WALLS (thesis). **Atkins, Thomas (Lawrence Radiation Lab., Unv. of California, Berkeley). June 1965. Contract W-7405-eng-48. 53p. Dep. mn; CFSTI $3.00 cy, $0.50 mn.**

The design of a recirculating water tunnel is described. The tunnel has a square cross section, six inches on a side. It makes use of a system of moving walls as a calming section to allow the damping out of velocity fluctuations without permitting a boundary layer growth. The moving wall system is described in detail. The tunnel is designed to obtain turbulence levels as low as 0.0008% at Reynolds numbers up to 10,000 with a flat velocity profile. A technique to allow photographic study of the flow using tellurium electrodes is outlined. These electrodes emit a black colloidal suspension of tellurium which is very suitable for photographing. A typical experiment to be performed in the tunnel is also described. It is the flow past a rectangular cutout, or notch, resulting in the formation of a stable eddy. In particular, the experiment would attempt to confirm the existence of secondary eddies in the corners of the notch. (auth)

45723 POSSIBILITIES AND CONDITIONS FOR THE DEVELOPMENT OF NUCLEAR INDUSTRIAL COMMUNITIES. Lepore, R. pp 315-24 of Giornate dell'Energia Nucleare 1964. Milan, Federazione delle Associazioni Scientifiche e Tecniche, 1965. (In Italian).

The nuclear branch of industry can be considered as composed of the following tightly interconnecting sectors: basic and applied research, design of components of both a nuclear and conventional character, design of nuclear plants, construction of components of both a nuclear and conventional character, construction and assembly of the plant, testing and start-up of a nuclear plant, and operation of nuclear installations. These sectors were examined in order to illustrate how the countries of the European community are developing a nuclear industry. (J.S.R.)

45724 CONJECTURES FOR THE DEVELOPMENT OF INDUSTRIAL ACTIVITY IN THE NUCLEAR FIELD. Terra, L. pp 325-34 of Giornate dell'Energia Nucleare 1964. Milan, Federazione delle Associazioni Scientifiche e Tecniche, 1965. (In Italian).

The conditions for the development and maintenance of a nuclear market are indicated. The assumptions made of the public and private resources available for the development of nuclear energy in Italy are summarized. (J.S.R.)

45725 FORECAST OF THE ENERGY FUTURE. Young, J. F. (General Electric Co., Cincinnati). 13p. (CONF-650429-15). ORINS.

From American Power Conference, Chicago.

Energy consumption and sources are discussed. It is postulated that the efficient use of low-yield uranium will provide an almost infinite source of power. The forecast growth of electrical power generation by 1980 is toward some 25,000 trillion Btu's. It was estimated that coal use will grow from 2,000 to 12,500 trillion Btu's between 1947 and 1980 and that nuclear power will reach 4,500 trillion Btu's usage in 1980. Forecasts tend toward a 1980 nuclear generation economy of over 80,000 Mw(e). A future nuclear economy made up of boiling water reactors and fast breeder reactors is considered. The nuclear power industry does not appear to be uranium-limited. Application of nuclear energy can help keep electrical energy use growing at a faster rate than total energy used. (F.J.H.)

CORPORATE AUTHOR INDEX

This index contains entries for this period for all report literature and, in addition, for certain published literature items for which it is felt that a corporate approach is especially desirable, e.g., symposia, conference proceedings, and meetings.

Each entry under a corporate author is a shortened version of the title of the publication, followed by the *NSA* volume and abstract number. Report numbers are given in parentheses.

The phrase "Progress report" is abbreviated as "Prog. rpt.," permitting a more rapid and complete alphabetical arrangement of the titles without changing the location of the progress report titles in relation to the other titles.

A

ACF INDUSTRIES, INC., ALBUQUERQUE, N. MEX.
Axisymmetric thin shells of revolution, 19: 44219 (ACF-8)

AEROJET-GENERAL CORP., AZUSA, CALIF.
Engine operating problems in space, 19: 44893 (NASA-CR-294)

AEROJET-GENERAL NUCLEONICS, SAN RAMON, CALIF.
Army Gas-Cooled Reactor systems program, 19: 45558 (AGN-TM-409)
Prog. rpt. on AGCR, 1–3/65, 19: 45577 (IDO-28645)
Radioisotopes in hydrospace. Preliminary survey report, 19: 44569 (AGN-8122)

AEROSPACE RESEARCH LABS., WRIGHT-PATTERSON AFB, OHIO.
Radiation from an a-c nitrogen arc, 19: 44804 (ARL-65-105)

AIR FORCE CAMBRIDGE RESEARCH LABS., L. G. HANSCOM FIELD, MASS.
Ferrous ammonium sulfate-cupric chloride solutions for dosimetry of a kilocurie ^{60}Co source, 19: 44372 (AFCRL-65-470)
Meteorology program at the Air Force Cambridge Research Laboratories, 19: 44776 (BNL-914, pp 75-84)
Micrometeorology, 19: 44797 (BNL-914, pp 173-4)

AKADEMIYA NAUK SSSR, NOVOSIBIRSK. INSTITUT YADERNOI FIZIKI.
Intensive electron beam focusing in an accelerator tube, 19: 44870 (NP-15388)

AKADEMIYA NAUK UKRAINSKOI SSR, KHARKOV. FIZIKO-TEKHNICHESKII INSTITUT.
Method for determining coefficients of reflection in a plasma waveguide, 19: 45401 (NP-15196)
Nonlinear stabilization of beam instabilities in plasma, 19: 45402 (NP-15200)

AKTIEBOLAGET ATOMENERGI, STOCKHOLM (SWEDEN).
Experimental studies on assemblies 1 and 2 of the fast reactor FRO. I., 19: 45522 (AE-195)
Radiolysis of aqueous benzene solutions in the presence of inorganic oxides, 19: 44051 (AE-192)
Radiolysis of aqueous benzene solutions at higher temperatures, 19: 44052 (AE-193)
Theoretical work for fast zero-power reactor FRO, 19: 45667 (AE-194)
Use of importance sampling in particle transport problems, 19: 45458 (AE-190)

ALBERTA UNIV., EDMONTON. NUCLEAR RESEARCH CENTRE.
Levels in ^{21}Ne using ^{18}D(α,nγ)^{21}Ne reaction, 19: 45277 (NP-15363)

ALLIS-CHALMERS MFG. CO., BETHESDA, MD. ATOMIC ENERGY DIV.
Prog. rpt. on Pathfinder power plant, 7–9/64, 19: 45557 (ACNP-65557)

ALLIS-CHALMERS MFG. CO., MILWAUKEE, WIS. ATOMIC ENERGY DIV.
Primary and secondary separation of steam from water by mechanical means, 19: 44131 (ACNP-65003)

ALLISON DIV., GENERAL MOTORS CORP., INDIANAPOLIS, IND.
Military Compact Reactor small source experiments, 19: 45575 (GMAD-3078-28)

AMES LAB., IOWA STATE UNIV. OF SCIENCE AND TECH.
Average half-life determination of the short-lived products of the photonuclear reactions of ^{40}Ca, 19: 45262 (IS-T-29)
Extrusion of clad and unclad yttrium for rod and tubing, 19: 44636 (IS-1031)
Optical emission spectroscopy as an analytical tool, 19: 43929 (IS-1237)
Phase space considerations for three-particle and four-particle final states, 19: 45006 (IS-1214)
Recoil chemistry of ^{11}C in liquid hydrocarbons, 19: 44057 (IS-T-23)
Survey of environmental radioactivity for period January 1–June 30, 1965, 19: 44302 (TID-22173)
Theory of many-boson systems, 19: 44806 (IS-T-19)

ARBEITSGEMEINSCHAFT KERNKRAFTWERK DER ELEKTRIZITAET-SWIRTSCHAFT, VIENNA (AUSTRIA).
Design study of small nuclear power plant for Austria, 19: 45581 (NP-15291)

ARGONNE NATIONAL LAB., ILL.
Alloying properties, 19: 44678 (ANL-7000, pp 186-200)
Argonne meterology program, 19: 44763 (BNL-914, pp 4-13)
Bibliography on chemical analysis of Pu, Pu alloys and Pu compounds, 19: 43925 (ANL-6956)
Ceramic materials research, 19: 44680 (ANL-7000, pp 227-32)
Corrosion research, 19: 44617 (ANL-7000, pp 213-26)
Development of alloy fuels and jacket materials, 19: 44674 (ANL-7000, pp 69-83)
Development of ceramic fuels, 19: 43985 (ANL-7000, pp 85-110)
Development of corrosion-resistant jacketing and structural materials, 19: 44616 (ANL-7000, pp 122-37)
Development of fabrication methods, 19: 44633 (ANL-7000, pp 138-45)
Development of nondestructive methods, 19: 44207 (ANL-7000, pp 146-52)
Diffusion experiments, 19: 44796 (BNL-914, pp 163-72)
Diffusion studies, 19: 44677 (ANL-7000, pp 183-5)
Electron-neutron interaction, 19: 44373 (ANL-6877, pp 15-20)
Environmental radioactivity at Argonne National Laboratory, January–June 1965, 19: 44300 (TID-22171)
Examination of full-scale reactor fuel elements, 19: 44738 (ANL-7000, pp 119-21)
Examination of irradiated Ag–In–Cd alloys, 19: 44736 (ANL-6883)
Experimental irradiations of fuel and control materials, 19: 44737 (ANL-7000, pp 111-18)
Fast reactor fuel element development and fabrication, 19: 44587 (ANL-7000, pp 3-63)
Irradiation effects, 19: 44739 (ANL-7000, pp 233-77)
Mass spectrometric studies of laser-produced graphite jet, 19: 44803 (ANL-6877, pp 21-7)
Metallurgy of actinide metals, 19: 44675 (ANL-7000, pp 155-75)
Metallurgy of HCP metals, 19: 44676 (ANL-7000, pp 176-82)
Method for neutron-flux studies in an operating power reactor using base and cadmium-covered radioactivants, 19: 45560 (ANL-7011)
Nuclear magnetic resonance studies, 19: 43986 (ANL-7000, pp 201-4)
Plant modifications and new facilities, 19: 44160 (ANL-7000, pp 278-86)
Plutonium recycle demonstration experiment in EBWR, 19: 45559 (ANL-7000, pp 64-8)
Prog. rpt. on metallurgy, annual, 1964, 19: 44586 (ANL-7000)
Prog. rpt. on physics, 1–3/64, 19: 44802 (ANL-6877)
Radiative capture of neutrons, 19: 45246 (ANL-6877, pp 5-14)
S-state interactions and nuclear coupling schemes, 19: 45247 (ANL-6877, pp 29-31)
Tables of resonance integral functions, $L'(Z', \xi)$, 19: 45214 (ANL-7024)

Thermal-neutron fluxes for CP-5 vertical irradiation facilities, 19: 45668 (ANL-7026)
X-ray and neutron diffraction studies, 19: 44679 (ANL-7000, pp 205-12)

ARIZONA UNIV., TUCSON.
Geological and geochemical studies of the Roskruge Range, Pima County, Arizona, 19: 44236 (TID-22086)

ARMY ELECTRONICS RESEARCH AND DEVELOPMENT ACTIVITY, FORT HUACHUCA, ARIZ.
Meteorological program at Fort Huachuca, 19: 44777 (BNL-914, pp 85-90)

ASSOCIATION CLAUDE BERNARD, PARIS (FRANCE).
Radiation effects on the functions and enzymatic potential of platelets, 19: 43714 (EUR-2438.f)

ATLANTIC RESEARCH CORP., ALEXANDRIA, VA.
Prog. rpt. on effects of electrical fields on boiling heat transfer, 12/64, 19: 44190 (NYO-2404-67)
Prog. rpt. on effects of electrical fields on boiling heat transfer, 4–6/65, 19: 44191 (NYO-2404-73)

ATOMIC BOMB CASUALTY COMMISSION, HIROSHIMA (JAPAN).
Active tuberculosis in malignant disease of reticuloendothelial origin, Hiroshima, 1949–62, 19: 43710 (ABCC-16-64)
Prog. rpt. of Atomic Bomb Casualty Commission, annual, 7/63–6/64, 19: 44280 (ABCC-63-64)

ATOMIC ENERGY COMMISSION, WASHINGTON, D. C.
Application of meteorology to the regulatory program of the AEC, 19: 44270 (BNL-914, pp 178-9)

ATOMIC ENERGY ESTABLISHMENT, TROMBAY (INDIA).
Unit for testing high-efficiency filters, 19: 44281 (AEET-202)

ATOMIC ENERGY ESTABLISHMENT, TROMBAY (INDIA). AIR MONITORING SECTION.
Strontium-90 content of food samples in India—data summary through 1963, 19: 44244 (AEET/AM/40)

ATOMIC ENERGY ESTABLISHMENT, WINFRITH (ENGLAND).
Analysis of some two-zone exponential experiments on graphite moderated lattices, 19: 45524 (AEEW-R-428)
Calculated energy response of lithium fluoride finger-tip dosimeters, 19: 44367 (AEEW-M-550)
FLIC conversion codes, 19: 44579 (AEEW-R-439)
Nineteen-group extension to the Yiftah, Okrent and Moldauer cross-section set, 19: 45244 (AEEW-M-472)
ZADOC—two-group two dimensional fuel management program, 19: 45523 (AEEW-R-425)

ATOMIC ENERGY OF CANADA LTD., CHALK RIVER (ONTARIO).
Control and read-out system for Chalk River double crystal spectrometer, 19: 44365 (AECL-2219)
Dissolution and diffusion of oxygen in zirconium, 19: 44673 (AECL-2268)
High-pressure rotary face-type shaft seals for water applications, 19: 44132 (AECL-2249)
NUSTAT—program for fully mechanized shell model calculations, 19: 45254 (CRT-1213)
Prog. rpt. annual, 1964-65, 19: 45694 (AECL-2251)
Role of diffusion measurements in study of crystal lattice defects, 19: 45471 (AECL-2309)

ATOMIC ENERGY OF CANADA LTD., CHALK RIVER (ONTARIO). CHALK RIVER NUCLEAR LABS.
Pyrolysis of the potential power reactor coolant, Santowax O-M, 19: 44044 (AECL-2218)

ATOMIC ENERGY RESEARCH ESTABLISHMENT, HARWELL (ENGLAND).
Deposition of fallout, 19: 44245 (BNL-914, pp 125-32)
Fermi surface of palladium, 19: 45472 (AERE-M-1605)
Health physics instruments, AERE, 19: 44369 (AERE-R-4552)
Improved furnace assembly for high-temperature diffractometers, 19: 44340 (AERE-M-1361)
New methods of measuring neutron dose equivalent rate around pulsed neutron generators, 19: 44370 (AERE-R-4883)
Performance of plasma jet in elimination of matrix effects due to phosphate and Al, 19: 43924 (AERE-R-4990)
Preparation of lithium-drifted germanium diodes and their use as γ detectors, 19: 44371 (AERE-R-4921)
Pulse shape discriminators for scintillators containing ZnS(Ag), 19: 44368 (AERE-M-833)
Recording microbalance for remote thermogravimetric examination of irradiated materials, 19: 44341 (AERE-R-4962)
Reprocessing with amine ether systems. III., 19: 44108 (AERE-R-4440 (Pt.3))
Tables for binary encoding of angles, 19: 44580 (AERE-R-4964)

ATOMIC POWER DEVELOPMENT ASSOCIATES, INC., DETROIT, MICH.
Compilation of Fermi experience, 19: 45562 (APDA-174, pp 71-3)
Development of EOCR as fast fuel test facility, 19: 45669 (APDA-174, pp 61-6)
Fast flux test facility, 19: 45670 (APDA-174, pp 74-6)
Fuel element flow stability studies, 19: 44181 (APDA-174 pp 56-60)
Na technology loop, 19: 44162 (APDA-174 pp 33-55)
Paste concept for fast reactor blanket applications, 19: 45499 (APDA-174, pp 10-24)
Paste concept for fast reactor blanket applications, 19: 45561 (APDA-172)
Prog. rpt., 4–6/65, 19: 45493 (APDA-174)
Small leak Na–H_2O reaction, 19: 44161 (APDA-174 pp 25-32)
Under Na scanner, 19: 44342 (APDA-174, pp 67-70)

ATOMIC WEAPONS RESEARCH ESTABLISHMENT, ALDERMASTON (ENGLAND).
Fatigue of uranium, 19: 44681 (AWRE-O-65/65)
Hazards to human ear from shock waves produced by high-energy electrical discharges, 19: 44283 (AWRE-E-1/65)
List of data files available in the UKAEA nuclear data library as of 15th April 1965, 19: 45249 (AWRE-O-55/65)
Neutron cross sections of the proton in the energy range 0.0001 ev to 20 Mev, 19: 45248 (AWRE-O-23/65)
Protection against fire hazards in the design of filtered ventilation systems of radioactive and toxic process buildings, 19: 44284 (AWRE-O-24/65)
Uranium corrosion. I. Optical method for following oxide formation, 19: 44619 (AWRE-O-66/65)
Water vapor corrosion of uranium and its prevention, 19: 44618 (AWRE-O-42/65)

ATOMICS INTERNATIONAL, CANOGA PARK, CALIF.
Applications of nuclear safety criteria to plant operations, 19: 44112 (CONF-651103-4)
Carburization of type 304 stainless steel in sodium–carbon systems, 19: 44624 (NAA-SR-Memo-4887)
Development, acceptance and qualification testing of the SNAP-10A ejectable heat shield, 19: 45650 (NAA-SR-10997)
Disintegration and dispersion of the SNAP-10A reactor upon return from satellite orbit, 19: 45651 (NAA-SR-11103)
Effect of carburization on low strain rate behavior of type 304 stainless steel, 19: 44623 (NAA-SR-10487)
Nature and properties of carbides of uranium, 19: 44603 (NAA-SR-10929)
Preliminary SNAPSHOT-1 performance—summary, 19: 45653 (NAA-SR-11430)
Second-cycle AIROX reprocessing and pellet refabricating of highly irradiated UO_2, 19: 44114 (NAA-SR-11375)
SRE heat transfer system demolition, 19: 45579 (NAA-SR-11414)
TRANS-FUGUE-I—digital code for transient two-phase flow and heat transfer, 19: 45494 (NAA-SR-11008)

AUSTRALIAN ATOMIC ENERGY COMMISSION RESEARCH ESTABLISHMENT, LUCAS HEIGHTS.
Resonance absorption in small homogeneous critical assemblies, 19: 45521 (AAEC/TM-118)

AUTHORITY HEALTH AND SAFETY BRANCH, UNITED KINGDOM ATOMIC ENERGY AUTHORITY, HARWELL (ENGLAND).
Review of UK codes of practice for protection radiations, 19: 44282 (AHSB(RP)M-35)

AVCO-EVERETT RESEARCH LAB., EVERETT, MASS.
Limit on stably trapped particle fluxes, 19: 45157 (NP-15386)

B

BABCOCK AND WILCOX CO., ALLIANCE, OHIO. RESEARCH CENTER.
Model tests of the sodium distributor for the sodium-heated steam generator, 19: 44182 (BAW-1280-29)
Prog. rpt. on materials of Na heated steam generator, 8/27/65, 19: 44133 (BAW-1280-31)

BABCOCK AND WILCOX CO., LYNCHBURG, VA.
Prog. rpt. on radiochemistry of nuclear fuels, 11/64–1/65, 19: 45542 (BAW-272)

BABCOCK AND WILCOX CO., LYNCHBURG, VA. ATOMIC ENERGY DIV.
Blowdown models applicable to the loss-of-fluid test facility (LOFT). Evaluation, 19: 45671 (BAW-1195-4)
Prog. rpt. on nonuniform heat generation experimental program, 4–6/65, 19: 44183 (BAW-3238-8)

BAILEY METER CO., WICKLIFFE, OHIO.
Development of realistic requirements for PM-type reactor instrumentation, 19: 45584 (NYO-3379-1)

BALLISTIC RESEARCH LABS., ABERDEEN PROVING GROUND, MD.
On the use of vacuum ultraviolet absorption as a measure of temperature in rare gas plasmas, 19: 45382 (BRL-MR-1644)

BATTELLE INSTITUT E. V., FRANKFURT AM MAIN (WEST GERMANY).
Bibliography on direct conversion of nuclear energy, 19: 44978 (AED-C-15-08)

BATTELLE MEMORIAL INST., COLUMBUS, OHIO.
In-pile studies of experimental pyrolytic-carbon-coated UC_2 and UO_2 fuel particles, 19: 44740 (BMI-1737)

Nondestructive measurement of residual stresses in metals and metal structures, 19: 44643 (RSIC-410)
Prog. rpt. on tracer system for in-place filter evaluation, final, 10/62–6/65, 19: 44208 (BMI-X-346)

BATTELLE-NORTHWEST, RICHLAND, WASH. PACIFIC NORTHWEST LAB.
A selected list of references (1960–May 1965) on swine in biomedical research, 19: 43713 (BNWL-115)
Fast neutron flux characteristics of the ETR, G-7 hot water loop, 19: 45672 (BNL-89)
Field testing of a fluorescein–ZnS dual atmospheric tracer technique, 19: 44800 (BNWL-103)
Fission-product simulation in containment systems experiment, 19: 44286 (BNWL-SA-30)
Minimized fuel cycle cost for simulated heavy water reactor, 19: 45563 (BNWL-106)
Natural removal of fission products released from UO_2 fuel in condensing steam environments, 19: 44285 (BNWL-SA-29)
Performance evaluation of slag and crucible dissolver, 19: 44111 (BNWL-121)
Thermal effects in anion exchange resin-nitric acid systems, 19: 44110 (BNWL-114)
Thermal studies [on] Hastelloy X metallic insulation, 19: 44589 (BNWL-102)
Transport and buildup of radioactive materials in reactor systems as determined by shutdown radiation measurements, 19: 45564 (BNWL-SA-85)

BECHTEL CORP., SAN FRANCISCO, CALIF.
DEEP—pool reactor for water desalting, 19: 45631 (COO-283)

BENDIX CORP., KANSAS CITY, MO.
Effect of molecular structure on the thermal aging properties of flexible urethane foams, 19: 44682 (BDX-613-75)

BENDIX SEMICONDUCTOR DIV., BENDIX CORP., HOLMDEL, N. J.
Prog. rpt. on design of ten-nanosecond semiconductor switch, 1964, 19: 44346 (N64-30522)

BETTIS ATOMIC POWER LAB., PITTSBURGH, PA.
Effect of low cobalt impurity stainless steel on coolant activity of pressurized water reactors, 19: 45495 (WAPD-T-1653)
Steady creep swelling of a clad nuclear fuel plate, 19: 45548 (WAPD-TM-498)

BOEING SCIENTIFIC RESEARCH LABS., SEATTLE, WASH. PLASMA PHYSICS LAB.
Composition of noble gas ion beams produced with a duoplasmatron, 19: 45385 (D1-82-0437)
Excitation of higher modes by the helical instability, 19: 45386 (D1-82-0439)
Permanently magnetized ferrite antenna windows for improving electromagnetic wave transmission through a plasma, 19: 45387 (D1-82-0442)
Production of dense beams of low-energy ions, 19: 45384 (D1-82-0436)
Some related phenomena in plasmas in solids and in gases, 19: 45383 (D1-82-0419)

BRANDIES UNIV., WALTHAM, MASS. DEPT. OF CHEMISTRY.
Continuous representations in the statistical theory of electronic energies, 19: 44936 (TID-21692)

BROOKHAVEN NATIONAL LAB., UPTON, N. Y.
Abstracts of computer codes. A compilation of computer codes useful in nuclear structure physics, 19: 45251 (BNL-9108)
Aerospace meteorological problems and diffusion climatology, 19: 44771 (BNL-914, pp 44-50)
Air pollution in an urban environment, 19: 44785 (BNL-914, pp 113-14)
Air pollution program in the Public Health Service, 19: 44788 (BNL-914, pp 123-4)
Alpha–gamma facility for metallurgical examinations, 19: 44163 (BNL-9502)
Application of meteorology to the regulatory program of the AEC, 19: 44270 (BNL-914, pp 178-9)
Argonne meteorology program, 19: 44763 (BNL-914, pp 4-13)
Brookhaven meteorological program, 19: 44762 (BNL-914, pp 1-3)
Cloud rise experiments at Brookhaven, 19: 44787 (BNL-914, pp 119-22)
Conference on AEC meteorological activities, May 19–22, 1964, 19: 44761 (BNL-914)
Continuous point source diffusion in the surface layer, 19: 44766 (BNL-914, pp 20-3)
Coupling elements in equivalent circuit for cavity cells, 19: 44859 (BNL-9496)
Current status of fallout deposition research, 19: 44246 (BNL-914, pp 133-8)
Deposition calculations at Oak Ridge, 19: 44249 (BNL-914, pp 144-5)
Deposition of fallout, 19: 44245 (BNL-914, pp 125-32)
Diffusion experiments, 19: 44796 (BNL-914, pp 163-72)
Diffusion from elevated sources, 19: 44768 (BNL-914, pp 26-7)
Diffusion studies in Canada, 19: 44790 (BNL-914, pp 149-50)
Diffusion studies at Hanford, 19: 44792 (BNL-914, pp 153-5)
Dispersion in urban areas, 19: 44791 (BNL-914, pp 151-2)
Effects of variable source configurations in space and time, 19: 44786 (BNL-914, pp 115-18)
Elevated line source programs, 19: 44779 (BNL-914, pp 93-4)
Fallout deposition measurements at Hanford, 19: 44248 (BNL-914, pp 141-3)
Fundamental problems on the meso-scale, 19: 44782 (BNL-914, pp 103-6)
Galvani, Volta and bioelectricity, 19: 43664 (BNL-9337)
High magnetic field limit in synchrotrons, 19: 44858 (BNL-9480)
Importance of the tetroon to meso-scale meteorology, 19: 44783 (BNL-914, pp 107-9)
Material transfer, membranes and metabolism, 19: 43665 (BNL-9338)
Measurement and prediction of dispersion, 19: 44789 (BNL-914, pp 146-8)
Measurement of fallout deposition, 19: 44247 (BNL-914, pp 139-40)
Mechanism of the immune response, 19: 45695 (BNL-912)
Meso-scale and mean transport problems, 19: 44781 (BNL-914, pp 99-102)
Meso-scale studies in the >100-km range, 19: 44784 (BNL-914, pp 110-12)
Meteorological program at Fort Huachuca, 19: 44777 (BNL-914, pp 85-90)
Meteorology program at Hanford Atomic Products Operation, 19: 44767 (BNL-914, pp 24-5)
Meteorology program at the Nevada Test site, 19: 44774 (BNL-914, pp 65-8)
Meteorology program at the Air Force Cambridge Research Laboratories, 19: 44776 (BNL-914, pp 75-84)
Meteorology program at Dugway Proving Ground, 19: 44778 (BNL-914, pp 91-2)
Micrometeorology, 19: 44797 (BNL-914, pp 173-4)
Neon-hydrogen bubble chambers, 19: 44375 (BNL-9425)
Neutron cross sections, III., Z = 88 to 98, 19: 45250 (BNL-325(2nd Ed.) (Suppl.2)(Vol.III))
Oak Ridge meteorological program, 19: 44765 (BNL-914, pp 18-19)
Precipitation scavenging, 19: 44769 (BNL-914, pp 28-32)
Program review and summary of recent accomplishments at NRTS, 19: 44773 (BNL-914, pp 57-64)
Radiation and the patterns of nature, 19: 43711 (BNL-924)
Relative biological effectiveness of different types of ionizing radiations: cytogenetic effects in maize, 19: 43712 (BNL-9383)
Scale-model diffusion experiments, 19: 44764 (BNL-914, pp 14-17)
Technical areas in meteorology that are limiting progress in nuclear industry, 19: 44780 (BNL-914, pp 95-8)
Temperature profiles, 19: 44795 (BNL-914, pp 161-2)
Transfer rates of gamma globulin between cerebrospinal fluid and blood plasma in multiple sclerosis, 19: 43666 (BNL-9406)
Turbulence and low-level structure, 19: 44793 (BNL-914, pp 156-7)
Turbulence characteristics near the ground and sonic anemometry, 19: 44772 (BNL-914, pp 51-4)
U.S. Public Health Service meteorology program, 19: 44775 (BNL-914, pp 69-74)
U.S. Weather Bureau meteorology program, 19: 44770 (BNL-914, pp 33-43)
Vertical structure of turbulence, 19: 44799 (BNL-8516)
Wind profile, 19: 44794 (BNL-914, pp 158-60)

BRUSSELS UNIV. (BELGIUM).
Experimental basis of quantitative interpretation of the renogram, 19: 43667 (EUR-1890.f)

BUREAU OF MINES, ALBANY, OREG. ALBANY METALLURGY RESEARCH CENTER.
Prog. rpt. on metallurgy research, 4–7/65, 19: 44612 (USBM-RC-1199)
Studies of high-current metallic arcs, 19: 44608 (TID-22125)

BUREAU OF MINES, WASHINGTON, D. C.
Electron-beam melting of yttrium, 19: 44588 (BM-RI-6661)

C

CALIFORNIA DEPT. OF PUBLIC HEALTH, BERKELEY. AIR AND INDUSTRIAL HYGIENE LAB.
Design of SO_2 monitor for air pollution studies, 19: 44458 (NYO-2767)

CALIFORNIA INST. OF TECH., PASADENA. W. M. KECK LAB. OF ENGINEERING MATERIALS.
Effects of liquid quenching on the constitution and structure of silver–silicon and gold–silicon alloys, 19: 45696 (CALT-221-12)

CALIFORNIA UNIV., BERKELEY.
Bibliography on high-temperature chemistry and physics of gases and gas-condensed phase reactions, 19: 43993 (NP-15379)

CALIFORNIA UNIV., DAVIS. SCHOOL OF VETERINARY MEDICINE.
Absorption and deposition of ^{89}Sr and ^{47}Ca from ligated intestinal segments of adult beagles, 19: 43677 (UCD-472-112, pp 86-96)

Clinical blood chemistry studies in beagles, 19: 43674 (UCD-472-112, pp 36-43)
Hematology report on beagles, 19: 43725 (UCD-472-112, pp 44-9)
Ion exchange removal of ^{90}Sr from biologic wastes, 19: 45692 (UCD-472-112, pp 141-7)
Kennel report on beagle colony, 19: 43645 (UCD-472-112, pp 10-22)
Pathology report on beagles, 19: 43727 (UCD-472-112, pp 126-40)
Procedures for maintaining an outbred beagle colony, 19: 43646 (UCD-472-112, pp 23-35)
Prog. rpt. on effects of Sr-90 ingestion on growth of beagle, annual, 1964, 19: 43644 (UCD-472-112)
Quality control of ^{90}Sr-containing food, 19: 43675 (UCD-472-112, pp 73-9)
Radium metabolism by beagles following single and multiple injections, 19: 43678 (UCD-472-112, pp 97-108)
Roentgenographic survey of experimental beagles, 19: 43882 (UCD-472-112, pp 50-8)
Skeletal dosimetry and exposure status of beagle colony, 19: 43726 (UCD-472-112, pp 120-5)
Status of experimental ^{90}Sr–^{226}Ra beagle colony as of 31 January 1965, 19: 43680 (UCD-472-112, pp 148-74)
Strontium deposition in bone and teeth of beagle puppies, 19: 43676 (UCD-472-112, pp 80-5)
Strontium-90 uptake and retention in labeled beagles, 19: 43679 (UCD-472-112, pp 109-19)
The determination of zinc and iron in biologic materials by x-ray fluorescence spectrometry, 19: 43939 (UCD-472-112, pp 59-72)

CALIFORNIA UNIV., LA JOLLA, SAN DIEGO. DEPT. OF CHEMISTRY.
Continuous representations in the statistical theory of electronic energies, 19: 44936 (TID-21692)

CALIFORNIA UNIV., LOS ANGELES. LAB OF NUCLEAR MEDICINE AND RADIATION BIOLOGY.
Biochemistry, 19: 43681 (UCLA-12-565, pp 17-31)
Biophysics, 19: 43648 (UCLA-12-565, pp 87-96)
Environmental radiation, 19: 43662 (UCLA-12-565, pp 97-128)
Nuclear medicine, 19: 43883 (UCLA-12-565, pp 65-85)
Pharmacology and toxicology, 19: 43728 (UCLA-12-565, pp 59-64)
Prog. rpt. on biophysics and nuclear medicine, semiannual, 6/65, 19: 43647 (UCLA-12-565)
Radiobiology, 19: 43682 (UCLA-12-565 pp 33-57)

CAROLINAS VIRGINIA NUCLEAR POWER ASSOCIATES, INC., PARR, S. C.
CVTR—high pD tests, 19: 45568 (CVNA-238)

CENTRAL UTILITIES ATOMIC POWER ASSOCIATES.
Prog. rpt. on Pathfinder power plant, 7–9/64, 19: 45557 (ACNP-65557)

CENTRE D'ETUDE DE L'ENERGIE NUCLEAIRE, BRUSSELS (BELGIUM).
Coating UO_2 particles, 19: 44596 (EURAEC-1392)
Possibility of using radiosensitizers in preservation or sterilization of food, drugs and medical supplies by irradiation, 19: 44552 (BLG-327)
Principal methods of polaron theory, 19: 45473 (BLG-329)
Volatility processes for reactor fuel elements containing carbon, 19: 44109 (BLG-331)

CENTRE D'ETUDE DE L'ENERGIE NUCLEAIRE, MOL (BELGIUM).
Prog. rpt. on imperfections in metals. II., 10–12/64, 19: 44622 (EURAEC-1433)
Prog. rpt. on imperfections in metals. II., 1–3/65, 19: 44687 (EURAEC-1434)

CENTRE NATIONAL DE LA RECHERCHE SCIENTIFIQUE, PARIS (FRANCE).
Distribution of momenta in the nucleus and the scattering of electrons, 19: 45279 (NP-15415)

CHEMICAL RESEARCH AND DEVELOPMENT LABS., EDGEWOOD ARSENAL, MD. EXPERIMENTAL MEDICAL DIV.
Prog. rpt. on radiation-resistant electron tubes, 5/21–8/31/63, 19: 44337 (AD-425708)

CHICAGO UNIV., ILL. DEPT. OF CHEMISTRY.
Prog. rpt. on radiolysis studies on fluorocarbons and on reactive intermediates, 10/64–7/65, 19: 44054 (COO-1365-7)

COLUMBIA UNIV., PALISADES, N. Y. LAMONT GEOLOGICAL OBSERVATORY.
Experiments and hydrographic surveys off Sandy Hook, New Jersey (1963), 19: 45698 (CU-2663-18)
Geostrophic eddies in the ocean. I., 19: 45699 (CU-2663-21)

COMBUSTION ENGINEERING, INC., WINDSOR, CONN. NUCLEAR DIV.
Production of hydrogen and helium in reactor fuel-cladding materials, 19: 44746 (NAA-SR-Memo-10626)
Prog. rpt. on burnable poison additions to UO_2, 10–12/64, 19: 44591 (CEND-3107-228)
Prog. rpt. on in-pile thermal conductance testing, 4–6/65, 19: 44684 (CEND-3336-241)

COMISION NACIONAL DE ENERGIA ATOMICA, BUENOS AIRES (ARGENTINA).
Photographic film dosimetry in skin β-therapy, 19: 43880 (NP-15270)
Possibilities of using ^{99m}Tc tracer instead of radioiodine in thyroid function investigations, 19: 43881 (NP-15271)
Radiostrontium and strontium fixation in bones and children's diets, 19: 44250 (NP-15269)
Synthesis of dl glycine-1-C-14 and dl alanine-1-C-14, 19: 44047 (NP-15268)

COMITATO NAZIONALE PER L'ENERGIA NUCLEARE, ROME (ITALY).
Analysis of nonlinear control system for reactor RTM, 19: 45682 (RT/ING(64)-15)
Apparatus for investigations on scintillator properties in the temperature range –100°C to +50°C, 19: 44460 (RT/FI(65)8)
Determination of concentration of a radioactive cloud and contamination of soil by Pasquill–Gifford method, 19: 44255 (RT/PROT(65)-10)
Dictionary of nuclear instrumentation and relative terminology, 19: 44049 (RT/EL(65)-3)

COMMISSARIAT A L'ENERGIE ATOMIQUE, CHUSCLAN (FRANCE). CENTRE DE PRODUCTION DE PLUTONIUM DE MARCOULE.
Detection of tritium in the CO_2 of the G2/G3 reactors using gas chromatography, 19: 43926 (CEA-R-2800)
Radioactivity measurements inside pressure vessel of reactor G-3 after 4 years operation, 19: 45566 (CEA-R-2785)
Radioprotection and decontamination operation on the central vibrating channels of the Reactor G3, 19: 45565 (CEA-R-2781)

COMMISSARIAT A L'ENERGIE ATOMIQUE, FONTENAY-AUX-ROSES (FRANCE). CENTRE D'ETUDES NUCLEAIRES.
Preparation of uranium-based oxide catalysts, 19: 43987 (CEA-R-2817)

COMMISSARIAT A L'ENERGIE ATOMIQUE, GRENOBLE (FRANCE). CENTRE D'ETUDES NUCLEAIRES.
Double time-of-flight fast neutron spectrometry and study of the reaction $^9Be(n,2n)$, 19: 45252 (CEA-R-2734)
Preparation of thin VYNS films, 19: 44590 (CEA-R-2803)
Sealed coupling for an electrical heating conductor with coaxial sheath, 19: 44164 (CEA-R-2755)

COMMISSARIAT A L'ENERGIE ATOMIQUE, SACLAY (FRANCE). CENTRE D'ETUDES NUCLEAIRES.
Analysis of resonances due to s wave neutrons in transmission time of flight experiments. II., 19: 45215 (CEA-R-2780)
Calculation of the muon contamination in a π-meson beam, 19: 44993 (CEA-R-2778)
Electron microscope observation of single-crystal beryllium thin foils, 19: 44683 (CEA-R-2789)
High-speed pulsed magnetic fields measurements, using the Faraday effect, 19: 44805 (CEA-R-2769)
Monte-Carlo method for studying slowing down of neutrons in thin plate of hydrogenated matter, 19: 45216 (CEA-R-2804)
Prog. rpt. on irradiation behavior of sintered U oxide, 10/60–12/63, 19: 44595 (EURAEC-1338)
Radioprotection problems resulting from the presence of experimental devices around a reactor, 19: 44287 (CEA-R-2799)

COMMISSION CONSULTATIVE POUR LA PRODUCTION D'ELECTRICITE D'ORIGINE NUCLEAIRE (FRANCE).
Prospects for nuclear power stations in France, 19: 45580 (NP-15283)

CONCORDIA COLL., MOORHEAD, MINN.
Prog. rpt. on autoionization of gases by ion impact, 3–3/65, 19: 44934 (COO-1277-13)
Prog. rpt. on energy and angular distribution of electrons ejected from H and He by 100- to 300-Kev protons, 4/63–7/65, 19: 44933 (COO-1277-12)

CONSUMERS PUBLIC POWER DISTRICT, HALLAM, NEBR.
Prog. rpt. on Hallam Facility operation, 5/65, 19: 45591 (TID-22129)
Prog. rpt. on Hallam Facility operation, 6/65, 19: 45592 (TID-22135)

CORNELL UNIV., ITHACA, N. Y.
Five-million pound shock testing facility, 19: 45720 (UCRL-12055-T)

CORNELL UNIV., ITHACA, N. Y. LAB. OF NUCLEAR STUDIES.
A threshold gas cherenkov counter for use at the Brookhaven A.G.S., 19: 44376 (BNL-9466)

CULHAM LAB., UNITED KINGDOM ATOMIC ENERGY AUTHORITY, ABINGDON (ENGLAND).
Preparation and properties of sintered Nb_3Sn, 19: 44592 (CLM-R-43)

D

DEL ELECTRONICS CORP., MOUNT VERNON, N. Y.
Prog. rpt. on stratospheric electrostatic precipitator and associated devices, semiannual, 9/64–2/65, 19: 44801 (NYO-2363-3)

DENVER RESEARCH INST., UNIV. OF DENVER, COLO.
Samarium-type intermediate phases of intra-rare-earth binary systems, 19: 44672 (AD-619201)

DEPARTMENT OF NATIONAL HEALTH AND WELFARE, OTTAWA (ONTARIO). RADIATION PROTECTION DIV.
Canadian fallout data for June 1965, 19: 44251 (NP-15519, pp 23-51)
Data from Radiation Protection Programs. Vol. 3, No. 7, 19: 44293 (NP-15519)
Reactor environmental monitoring, 1964, 19: 44294 (NP-15519, pp 3-22)
Reactor environment monitoring for June 1965, 19: 44295 (NP-15519, pp 52-60)
DEPARTMENT OF TRANSPORT, TORONTO (ONTARIO). METEOROLOGICAL BRANCH.
Diffusion studies in Canada, 19: 44790 (BNL-914, pp 149-50)
DEUTSCHES ELEKTRONEN-SYNCHROTRON, HAMBURG (WEST GERMANY).
Photoproduction of mesons in hydrogen bubble chamber at energies up to 5.5 Bev, 19: 44999 (DESY-65/5)
DIVISION OF BIOLOGY AND MEDICINE (AEC), WASHINGTON, D. C.
Study of liquids under optical and ionizing excitation with emphasis on excitation in the vacuum ultraviolet, 19: 44059 (NYO-2949-1)
DIVISION OF RAW MATERIALS (AEC), WASHINGTON, D. C.
Reconnaissance for uranium in the Aisen Area, Aisen, Chile, 19: 44273 (RME-4557(Rev.))
DIVISION OF REACTOR DEVELOPMENT (AEC), WASHINGTON, D. C.
Aerospace meteorological problems and diffusion climatology, 19: 44771 (BNL-914, pp 44-50)
Effects of variable source configurations in space and time, 19: 44786 (BNL-914, pp 115-18)
DIVISION OF TECHNICAL INFORMATION EXTENSION, (AEC), OAK RIDGE, TENN.
Index to conferences relating to nuclear science, 19: 45716 (TID-4043(Rev.2))
Nuclear energy for water desalting, 19: 45590 (TID-3584)
DOUGLAS AIRCRAFT CO., INC., SANTA MONICA, CALIF. MISSILE AND SPACE SYSTEMS DIV.
Computational methods for space radiation shielding analysis, 19: 45463 (NP-15425)
DU PONT DE NEMOURS (E. I.) & CO., AIKEN, S. C. SAVANNAH RIVER LAB.
Basic mechanisms of stress corrosion cracking of titanium, 19: 44621 (CONF-651006-1)
Computer code for one-group flux calculations in three dimensions, 19: 45218 (DP-938)
Computer program for circulation of library journals, 19: 45700 (DP-970)
Description of the Savannah River high flux charge, 19: 45638 (DP-999, pp 7-17)
Engineering aspects of the Savannah River high flux charge, 19: 45641 (DP-999, pp 43-64)
Isotope production in a Savannah River reactor at flux levels above 10^{15} n/(cm^2)(sec), 19: 45639 (DP-999, pp 19-28)
Metal fuel tube manufacture, 19: 45569 (DP-976)
Operating experience with the first Savannah River high flux charge, 19: 45643 (DP-999, pp 73-86)
Physics design of the Savannah River high flux charge, 19: 45640 (DP-999, pp 29-42)
Prog. rpt. on effect of SRP on environmental radioactivity, semiannual, 1–6/65, 19: 44288 (DPST-65-30-2)
Prog. rpt. on properties of thin-walled Zy tubing, 7/65, 19: 44634 (DPST-65-83-7)
Recovery of actinides produced by a nuclear detonation in salt formations, 19: 44156 (DP-956)
Reduction of plutonium dioxide to plutonium metal, 19: 44594 (DP-983)
Savannah River high flux demonstration, 19: 45637 (DP-999)
TAFI-II, computer code for management of radioactive waste, 19: 45687 (DP-966)
Temperature coefficients of reactivity in the Savannah River high flux charge, 19: 45642 (DP-999, pp 65-71)
DU PONT DE NEMOURS (E. I.) & CO., AIKEN, S. C. SAVANNAH RIVER PLANT.
Importance of capillary pores in rainwater percolation to the ground water table, 19: 44235 (DPSPU-64-30-23)
DUGWAY PROVING GROUND, UTAH
Meteorology program at Dugway Proving ground, 19: 44778 (BNL-914, pp 91-2)
DUKE UNIV., DURHAM, N. C. DEPT. OF ELECTRICAL ENGINEERING.
Current quenching in thin Pb films by multiple boundary propagation, 19: 45193 (TID-21307)
Electrical conductivity of thin-metallic films with unlike surfaces, 19: 45479 (TID-21301)
DYNATECH CORP., CAMBRIDGE, MASS.
Prog. rpt. on boiling flow regimes and critical heat flux, 3/6–6/15/65, 19: 44193 (NYO-3304-5)

E

EIDGENOESSISCHES INSTITUT FUER REAKTORFORSCHUNG, WUERENLINGEN (SWITZERLAND).
Temperature-coefficient of SAPHIR, 19: 45673 (EIR-85)
EMORY UNIV., ATLANTA, GA.
Effect of weightlessness and radiation on growth of wheat coleoptile, 19: 43717 (NASA-CR-303)
ENTE NAZIONALE PER L'ENERGIA ELETTRICA, ROME (ITALY).
Outlook on the utilization of thorium in power reactors in Italy, 19: 45582 (NP-15320)
EUROPEAN-AMERICAN NUCLEAR DATA COMMITTEE.
Compilation of EANDC priority I requests, 19: 45255 (EANDC-45(U))
EUROPEAN ATOMIC ENERGY COMMUNITY.
Detection of leakage in gas-distribution networks by means of radioactive tracers, 19: 44553 (EUR-2284.i)
Determination of O in organic compounds and metals by activation with neutrons, 19: 43928 (EUR-2290.f)
Dragon reactor automatic control equipment, 19: 45570 (EUR-2422.i)
Experimental basis of quantitative interpretation of the renogram, 19: 43667 (EUR-1890.f)
Method of numerical solution of the integral transport equation in the one-velocity and isotropic scattering approximation, 19: 45220 (EUR-2411.i)
Minimum number of inverters in an analog network, 19: 44343 (EUR-1918.f)
Modular counting system in the electronic section, 19: 44447 (EUR-2444.i)
Numerical solution of integral transport equation in approximation to one-velocity and isotropic scattering in plane and cylindrical symmetry, 19: 45219 (EUR-2410.i)
Numerical solution of the γ transport equation applied to concrete slabs, 19: 45459 (EUR-2488.e)
Pin-to-pin interactions in fuel clusters. I., 19: 45525 (EUR-2470.e)
Radiation effects on the functions and enzymatic potential of platelets, 19: 43714 (EUR-2438.f)
Study of circumferential and axial temperature perturbations in a cylindrical fuel element canning (mathematical and rheoanalogical methods), 19: 45543 (EUR-2480.f)
Transfer functions analyzer for Dragon Reactor, 19: 45571 (EUR-2431.f)
EUROPEAN ATOMIC ENERGY COMMUNITY, ISPRA (ITALY). EUROPEAN SCIENTIFIC DATA PROCESSING CENTER.
Method of numerical solution of the integral transport equation in the one-velocity and isotropic scattering approximation, 19: 45220 (EUR-2411.i)
Minimum number of inverters in an analog network, 19: 44343 (EUR-1918.f)
Numerical solution of integral transport equation in approximation to one-velocity and isotropic scattering in plane and cylindrical symmetry, 19: 45219 (EUR-2410.i)
EUROPEAN ATOMIC ENERGY COMMUNITY, ISPRA (ITALY). JOINT NUCLEAR RESEARCH CENTER.
Determination of O in organic compounds and metals by activation with neutrons, 19: 43928 (EUR-2290.f)
Dragon reactor automatic control equipment, 19: 45570 (EUR-2422.i)
Flange connections featuring an insulating sealing element, 19: 44134 (EUR-2434.d)
Minimum number of inverters in an analog network, 19: 44343 (EUR-1918.f)
Modular counting system in the electronic section, 19: 44447 (EUR-2444.i)
Numerical solution of the γ transport equation applied to concrete slabs, 19: 45459 (EUR-2488.e)
Pin-to-pin interactions in fuel clusters. I., 19: 45525 (EUR-2470.e)
Study of circumferential and axial temperature perturbations in a cylindrical fuel element canning (mathematical and rheoanalogical methods), 19: 45543 (EUR-2480.f)
Transfer functions analyzer for Dragon Reactor, 19: 45571 (EUR-2431.f)
EUROPEAN ORGANIZATION FOR NUCLEAR RESEARCH, GENEVA (SWITZERLAND).
A developer for nuclear photography, 19: 44407 (CERN-65-4(Vol.II), pp V1-8)
A mechanical analog computer for range and angle measurements in nuclear emulsions, 19: 44420 (CERN-65-4(Vol.II), pp VII28-34)
A semiautomatic device for analyzing tracks in nuclear emulsions, 19: 44419 (CERN-65-4(Vol.II), pp VII20-7)
Application of synthetic polymers in preparation of fine-grain nuclear emulsions. I. and II., 19: 44400 (CERN-65-4(Vol.II), pp III31-56)
Artificial construction of particle tracks by a Monte Carlo method, 19: 44433 (CERN-65-4(Vol.II), pp IX44-7)
Automatic following in nuclear emulsions, 19: 44421 (CERN-65-4(Vol.II),

pp VII 35-7)
Automation of the processes of isothermal development of nuclear emulsions, 19: 44409 (CERN-65-4(Vol.II), pp V17-21)
Centers of sensitivity and the centers of development of nonsensitized nuclear emulsions, 19: 44394 (CERN-65-4(Vol.II), pp II65-74)
Comparative hypersensitization with triethanolamine and with other alkaline sensitizers for nuclear emulsions, 19: 44406 (CERN-65-4 (Vol.II), pp IV41-5)
Comparison of π^0 intensity measurements in emulsions and bubble chambers, 19: 44439 (CERN-65-4(Vol.II), pp X37-43)
Conference on nuclear photography, 5th, Geneva, 9/64, 19: 44377 (CERN-65-4(Vol.I))
Conference on nuclear photography, 5th, Geneva, 9/64, 19: 44383 (CERN-65-4(Vol.III))
Contraction factor of Ilford G5 nuclear emulsions used in α spectrometry, 19: 44444 (CERN-65-4(Vol.II), pp X67-73)
Correlation between distortion in nuclear emulsions and successive differences used in multiple scattering measurements, 19: 44411 (CERN-65-4(Vol.II), pp VI1-8)
Decoration of tracks of charged particles in silver chloride monocrystals, 19: 44386 (CERN-65-4(Vol.II), pp 121-5)
Device for measurements of multiple scattering and of track curvatures in nuclear emulsions, 19: 44418 (CERN-65-4(Vol.II), pp VII15-19)
Distortion and spurious scattering in NIKFI-R nuclear emulsion, 19: 44412 (CERN-65-4(Vol.II), pp VI11-21)
Dosimetry of slow neutrons by recording the fission tracks in insulators, 19: 44385 (CERN-65-4(Vol.II), 112-19)
Electron microscopic differentiation of emulsions having different origins exposed to α or β irradiations, 19: 44389 (CERN-65-4(Vol.II), pp II17-18)
Emulsion experiments in oriented polar-orbiting satellites, 19: 44437 (CERN-65-4(Vol.II), pp X19-32)
Emulsion grain density in the extreme relativistic region, 19: 44428 (CERN-65-4(Vol.II), pp IX9-13)
Film dosimetry with inhibited development, 19: 44440 (CERN-65-4 (Vol.II), pp X44-6)
Fundamental aspects of growth and shape of photographic silver halide crystals, 19: 45474 (CERN-65-4(Vol.II), pp III21-30)
Further development of apparatus for measurements of particle tracks in photoemulsions by television method, 19: 44422 (CERN-65-4(Vol.II), pp VII39-42)
Future perspectives for emulsion work at CERN, 19: 44382 (CERN-65-4(Vol.I), pp 105-10)
High precision air core magnet, 19: 44165 (CERN-65-29)
Improvement of the resolution of radioactive markings by stereoscopic picture taking in electron microscopy, 19: 44423 (CERN-65-4(Vol.II), pp VII18)
Investigation into spurious scattering in photographic emulsions, 19: 44416 (CERN-65-4(Vol.II), pp VI58-62)
Investigations on the topography of the latent image, 19: 44387 (CERN-65-4(Vol.II), pp 111-10)
Ionization density in emulsions enriched with hydrogen, 19: 44435 (CERN-65-4(Vol.II), pp IX62-5)
Ionization-momentum dependence for electrons and positrons of high energy, 19: 44432 (CERN-65-4(Vol.II), pp IX41-3)
Latensification of the latent image in ionographic Emulsions, 19: 44391 (CERN-65-4(Vol.II), pp II29-42)
Loading of emulsions with diamonds and polystyrene for experiments with stopping K particles, 19: 44398 (CERN-65-4(Vol.II), pp III12-16)
Loading of nuclear emulsion with light and heavy elements, 19: 44399 (CERN-65-4(Vol.II), pp III17-20)
Location of tracks in nuclear emulsion with aid of spark chambers, 19: 44445 (CERN-65-4(Vol.II), pp X74-83)
Measurement of Coulomb scattering in the presence of track distortion and spurious scattering, 19: 44414 (CERN-65-4(Vol.II), pp VI31-6)
Measurement of the β-particle distribution of mass selected fission fragments with nuclear emulsions, 19: 44441 (CERN-65-4(Vol.II), pp X47-53)
Measurements in nuclear emulsions, 19: 44381 (CERN-65-4(Vol.I), pp 79-87)
Method for increasing the stability of sensitivity and latent image of nuclear emulsions, 19: 44390 (CERN-65-4(Vol.II), pp III19-28)
Method of measurement and calculation of fast particle momenta in emulsions exposed in strong magnetic fields, 19: 44427 (CERN-65-4 (Vol.II), pp VIII34-7)
momentum determination of low-momentum particles in emulsions exposed to strong magnetic field, 19: 44424 (CERN-65-4(Vol.II), pp VIII9-16)
Multiple scattering constant in emulsion at great cell lengths, 19: 44431 (CERN-65-4(Vol.II), pp IX32-40)
New photographic materials for nuclear research, 19: 44379 (CERN-65-4(Vol.I), pp 29-41)

Nuclear emulsion experiments on sounding rockets and satellites, 19: 44436 (CERN-65-4(Vol.II), pp X13-18)
Photoemulsion experiments with a hydrogen-jet target, 19: 44443 (CERN-65-4(Vol.II), pp X61-6)
Preparation and characteristics of a very concentrated nuclear emulsion, 19: 44396 (CERN-65-4(Vol.II), pp III1-4)
Preparation of emulsion stacks for underground cosmic-ray experiments, 19: 44397 (CERN-65-4(Vol.II), pp III5-11)
Properties of new NIKFI and ORWO nuclear emulsions, 19: 44403 (CERN-65-4(Vol.II), pp IV16-22)
Quantum theory and elementary particles, 19: 44994 (CERN-65-26)
Radiation detection in large crystals of silver chloride, 19: 44378 (CERN-65-4(Vol.I), pp 1-15)
Recordings of individual tracks in various solid materials, 19: 44384 (CERN-65-4(Vol.II), pp 11-8)
Registration of α-particle stars produced by radioactive nuclei and fine discrimination of α-particle tracks in nuclear emulsions, 19: 44425 (CERN-65-4(Vol.II), pp VIII17-26)
Regression of sensitivity and latent image in nuclear and light-sensitive photographic emulsions, 19: 44402 (CERN-65-4(Vol.II), pp IV5-15)
Relative dispersion of the latent image, 19: 44388 (CERN-65-4(Vol.II), pp III1-16)
Relativistic increase in the track blob density in various nuclear emulsions, 19: 44430 (CERN-65-4(Vol.II), pp IX23-31)
Results on spurious scattering in photographic emulsions, 19: 44415 (CERN-65-4(Vol.II), pp VI37-52)
Scattering constant in nuclear emulsions, 19: 44429 (CERN-65-4 (Vol.II), pp IX14-22)
Semiautomatic apparatus for measurement of track lengths. Semiautomation in corpuscular photography, 19: 44417 (CERN-65-4(Vol.II), pp VIII1-14)
Sensitivity centers and latent image distribution as factors of nuclear emulsion properties, 19: 44392 (CERN-65-4(Vol.II), pp II44-9)
Sensitivity centers of nuclear emulsions sensitized successively with gold and triethanolamine, 19: 44395 (CERN-65-4(Vol.II), pp II75-87)
Sensitivity of normal and hypersensitive Ilford K5 emulsions at low temperatures, 19: 44405 (CERN-65-4(Vol.II), pp IV33-40)
Some properties of nuclear emulsions, 19: 44380 (CERN-65-4(Vol.I), pp 45-63)
Spurious scattering in nuclear emulsions, 19: 44413 (CERN-65-4(Vol.II), pp VI23-30)
Study of the factors affecting the quality of the development with the electrodialyser, 19: 44410 (CERN-65-4(Vol.II), pp V22-33)
Tests on emulsion sensitivity at liquid H_2 temperature, 19: 44401 (CERN-65-4(Vol.II), pp IV1-4)
The properties of fine-grained nuclear emulsion type PP-2, 19: 44404 (CERN-65-4(Vol.II), pp IV23-31)
Theoretical grounds for the selection of developing agent for introducing it into the nuclear emulsion, 19: 44408 (CERN-65-4(Vol.II), pp V9-15)
Threshold oxidation and development of latent image formed by charged particles in nuclear emulsions, 19: 44393 (CERN-65-4(Vol.II), pp II50-63)
Use of gas targets for scattering experiments, 19: 44438 (CERN-65-4 (Vol.II), pp X33-6)
Using photoemulsion in proton dynamic polarization conditions, 19: 44442 (CERN-65-4(Vol.II), pp X57-60)
Utilization of the electron microscope with the purpose of the observation of tracks in ionographic emulsions, 19: 44426 (CERN-65-4(Vol.II), pp VIII27-33)
Width of heavy ion tracks in emulsion, 19: 44434 (CERN-65-4(Vol.II), pp IX48-61)

F

FORSVARETS FORSKNINGSANSTALT, STOCKHOLM (SWEDEN).
Monte Carlo procedure for calculating migration of protons, 19: 45462 (NP-15163)
FRANKLIN INST. RESEARCH LABS., PHILADELPHIA, PA.
Prog. rpt. on flow and fracture studies of alloyed Be, 7/7--10/64, 19: 44693 (NP-15411)
Prog. rpt. on flow and fracture studies of alloyed Be, final, 8/65, 19: 44694 (NP-15432)

G

GENERAL ATOMIC, SAN DIEGO, CALIF. JOHN JAY HOPKINS LAB. FOR PURE AND APPLIED SCIENCE.
Delayed γ rays from fission, 19: 45245 (AFWL-TR-65-95)
Flute characteristics of and microwave emission from a plasma in a mirror, 19: 45388 (GA-6432)
Landau damping and growth of electrostatic modes with finite system

effects, 19: 45389 (GA-6513)
Precritical calculations for the 2.9-in. pitch, TWMR critical assembly, 19: 45526 (GA-6633)
Repetitively pulsed accelerator boosters, 19: 45674 (GA-6168)
Synthesis of thermionic power conversion to nuclear reactors for space power applications, 19: 45648 (GA-6478)
GENERAL ELECTRIC CO., CINCINNATI, OHIO. NUCLEAR MATERIALS AND PROPULSION OPERATION.
Diffusion theory for homogeneous and heterogeneous reactors, 19: 45531 (N64-29786)
Economics of a 47,000-DWT tanker, 19: 45657 (TID-22088)
Prog. rpt. on high-temperature materials, 7/65, 19: 44598 (GEMP-49A)
Prog. rpt. on high-temperature materials, 8/20/65, 19: 44599 (GEMP-50A)
GENERAL ELECTRIC CO., CINCINNATI, OHIO. SPACE POWER AND PROPULSION SECTION.
Prog. rpt. on alkali metals boiling and condensing, 1–3/65, 19: 44187 (NASA-CR-54405)
GENERAL ELECTRIC CO., EVENDALE, OHIO.
1400°F weldable sheet program, 19: 44699 (R63FPD33)
GENERAL ELECTRIC CO., PHILADELPHIA, PA. MISSILE AND SPACE DIV.
Prog. rpt. on cyclotron resonance propulsion system, 7/65, 19: 44223 (NP-15438)
GENERAL ELECTRIC CO., PLEASANTON, CALIF. ATOMIC POWER EQUIPMENT DEPT.
Insulator materials for nuclear thermionic power conversion, 19: 44685 (CONF-650908-5)
Prog. rpt. on thermionic conversion of heat to electricity, 4–6/65, 19: 44979 (NP-15419)
Uranium oxide fuel for nuclear thermionic converters, 19: 44593 (CONF-650908-4)
GENERAL ELECTRIC CO., RICHLAND, WASH. HANFORD ATOMIC PRODUCTS OPERATION.
Data recording system for fuel core tester, 19: 45500 (HW-65756)
Differential responses of germ cells in flour beetles due to x-ray dose, hypotherma, sex-exposed and age, 19: 43715 (HW-SA-3747)
Diffusion from elevated sources, 19: 44768 (BNL-914, pp 26-7)
Diffusion studies at Hanford, 19: 44792 (BNL-914, pp 153-5)
Effect of tensile stress on the radiation-induced contraction of graphite, 19: 44744 (HW-SA-3592)
Fallout deposition measurements at Hanford, 19: 44248 (BNL-914, pp 141-3)
Fuel cycle analysis chained computer programs guide, 19: 45544 (HW-79951(Pt.1))
Fuel cycle analysis chained computer programs guide, 19: 45545 (HW-79951(Pt.2))
Fuel cycle analysis chained computer programs guide, 19: 45546 (HW-79951(Pt.3))
Instrument for automatic regulation of inhaled aerosols, 19: 43668 (HW-SA-3618)
Investigation of CD_4M Cu as Hanford male connector (nozzle) material, 19: 44607 (RL-SEP-508)
Measurements of radioactivity in Alaskan natives in 1964, 19: 44289 (HW-SA-3750)
Meso-scale and mean transport problems, 19: 44781 (BNL-914, pp 99-102)
Meteorology program at Hanford Atomic Products Operation, 19: 44767 (BNL-914, pp 24-5)
Operating experience on in-tank solidification of radiochemical wastes, 19: 45691 (RL-SA-41)
Precipitation scavenging, 19: 44769 (BNL-914, pp 28-32)
Reproductive performance of x-rayed single-species and mixed-species cultures of Tribolium confusum and T. castaneum reared at different temperatures, 19: 43716 (HW-SA-3748)
Status of fission product recovery at Hanford, 19: 45690 (RL-SA-40)
Snap-on RTD test plan, model four testing, 19: 45502 (RL-REA-2120)
GENERAL ELECTRIC CO., SAN JOSE, CALIF. ATOMIC POWER EQUIPMENT DEPT.
Interfacial reaction between UO_2 and zircaloy-2, 19: 44597 (GEAP-4679)
Performance of fuel rods to investigate increased thermal output capabilities, 19: 45573 (GEAP-4902)
Prog. rpt. on nuclear superheat project, 8–10/64, 19: 45572 (GEAP-4755)
Prog. rpt. on radial vane steam separator, 4–6/65, 19: 45574 (GEAP-4914)
Prog. rpt. on transport equivalent diffusion theory, 4–6/65, 19: 45221 (GEAP-4913)
Prog. rpt. on two-phase flow, 4–6/65, 19: 44185 (GEAP-4910)
Tensile properties of irradiated type 304 stainless steel strip, 19: 44743 (GEAP-3634)
GENERAL MOTORS CORP., SANTA BARBARA, CALIF. DEFENSE RESEARCH LABS.
Hypervelocity impact damage characteristics in beryllium and graphite plates and tubes, 19: 44692 (NASA-TN-D-3018)
GOSUDARSTVENNYI KOMITET PO ISPOL'ZOVANIYU ATOMNOI ENERGII SSSR.
Development of multichannel analyzers, 19: 44456 (NP-15258)
GOSUDARSTVENNYI KOMITET PO ISPOL'ZOVANIYU ATOMNOI ENERGII SSSR, MOSCOW. INSTITUT TEORETICHESKOI I EKSPERIMENTAL'NOI FIZIKI.
A scheme of multiplication of SU_3-representations, 19: 45030 (NP-15390)
Casimir operators for an orthogonal and symplectic group, 19: 45031 (NP-15391)
Chemical reactions of muonium. Identification of reaction products, 19: 45278 (NP-15389)
Direct knockout and inelastic scattering reactions, 19: 45033 (NP-15468)
Non-relativistic Regge trajectories, 19: 45028 (NP-15207)
Possibility of determining kinematic characteristics of particles in spark chamber employing multiple scattering and additional sparks, 19: 44490 (BNL-tr-1)
Rate of spontaneous and radiation-induced chromonone re-arrangements in medulla ossium of mice of different age, 19: 43729 (BNL-tr-12)
Real part of the spin-zero amplitude for T = 0 and spin-dependent amplitudes of nucleon-nucleon forward scattering at high energies, 19: 45032 (NP-15452)
Real part of the forward scattering amplitude of charged particles, 19: 45048 (ANL-Trans-217)
Regeneration phenomena and combined experiments in K^0 meson beam, 19: 45034 (NP-15470)
Spin precession in gravitational fields, 19: 45134 (NP-15397)
Symmetry of strong interactions and the SU_4 groups, 19: 45035 (NP-15471)
T-parity nonconservation in strong interactions, 19: 45280 (NP-15457)
Theory of weak interaction, 19: 45027 (NP-15199)
Vertex function poles and one-particle states orthogonalization, 19: 45029 (NP-15382)
GOSUDARSTVENNYI KOMITET PO ISPOL'ZOVANIYU ATOMNOI ENERGII SSSR, OBNINSK. FIZIKO-ENERGETICHESKII INSTITUT.
Calculating differential cross sections of slow neutrons by means of integration with respect to time, 19: 45228 (NP-15469)
Models of the temperature fields of fuel elements in the active zone and shield of the BN-350 reactor, 19: 45604 (JPRS-31245)
Possibility of using nuclear reactor in cosmic space for measuring cross sections of n-n scattering, 19: 45036 (NP-15476)
Spectrometric operating mode of FEU-49, 19: 44455 (NP-15047)
GRACE (W. R.) AND CO., CLARKSVILLE, MD. WASHINGTON RESEARCH CENTER.
Radiochemistry of radium, 19: 44098 (NAS-NS-3057)
GRENOBLE UNIV. (FRANCE).
Double time-of-flight fast neutron spectrometry and study of the reaction $^9Be(n,2n)$, 19: 45252 (CEA-R-2734)
GRUMMAN AIRCRAFT ENGINEERING CORP., BETHPAGE, N. Y. RESEARCH DEPT.
Crystallography of some transition metal molybdates, 19: 43991 (N64-26433)
Theoretical aspects of neutron activation of structures, 19: 45461 (N64-25922)

H

HARVARD UNIV., CAMBRIDGE, MASS. DEPT. OF PHYSICS.
Photoproduction of charged pion pairs, 19: 45000 (HUX-2752-7)
Scattering (e,p) at high momentum transfers and proton EM form factors, 19: 45001 (HUX-2752-8)
Wide-angle electron pair production, 19: 45256 (HUX-2752-4)
HEALTH AND SAFETY LAB., NEW YORK OPERATIONS OFFICE (AEC), N. Y.
Health and safety laboratory analytical manual, 19: 44296 (NYO-4700 (Rev.)(Suppl.II))
Nuclear emulsion spectrometry at low and intermediate neutron energies, 19: 44448 (HASL-162)
HONEYWELL, INC., MINNEAPOLIS, MINN. AERONAUTICAL DIV.
Alpha radiation hygrometer. II., 19: 44338 (AD-608496)
Alpha radiation hygrometer. III., 19: 44339 (AD-608503)
HOUSTON, UNIV., TEX.
Prog. rpt. [on ion sputtering], final, 8/12/65, 19: 44937 (TID-22140)
HUGHES RESEARCH LABS., MALIBU, CALIF.
Research on problems of ion beam formation from electron bombardment ion sources, 19: 44221 (N64-31088)

I

IIT RESEARCH INST., CHICAGO, ILL.

Possibility of using scintillating fibers for low-energy β counting, 19: 44451 (IITRI-578P26-8)

ILLINOIS UNIV., URBANA. DEPT. OF COMPUTER SCIENCE.
Order code for the film scanners of ILLIAC III, 19: 44446 (COO-1018-1050)

ILLINOIS UNIV., URBANA. DEPT. OF PHYSICS.
Peripheral production and decay correlations of resonances, 19: 45037 (TID-21316)
Systematics of baryon states, 19: 44996 (COO-1195-39)

ILLINOIS UNIV., URBANA. DEPT. OF THEORETICAL AND APPLIED MECHANICS.
Prog. rpt. on mechanical behavior of dilute alloys of Nb, final, 7/65, 19: 44700 (TID-22117)

INDIANA UNIV. FOUNDATION. RESEARCH DIV., BLOOMINGTON, IND.
Prog. rpt. on effect of radiation in altering incidence of mutations in Drosophila, 1963–64, 19: 43724 (TID-22160)

INSTITUT ATOMNOI ENERGII, GOSUDARSTVENNYI KOMITET PO ISPOL'ZOVANIYU ATOMNOI ENERGII SSSR, MOSCOW.
Anharmonism influence on the phonon spectrum near the point of origin, 19: 45475 (IAE-750)
Calculating energy levels of weakly deformed nuclei, 19: 45257 (IAE-811)
Charging device for pulsed magnetic field power supply, 19: 44449 (IAE-704)
Discharge instability with a heated cathode in a magnetic field at low pressures, 19: 45390 (IAE-780)
Instrumentation of certain experimental channels in USSR research reactors, 19: 45675 (IAE-725)
Neutron beam for measuring scattering cross sections at small angles, 19: 44862 (IAE-867)
Polarization in n-α scattering at E_n equals 25, 28, and 34 Mev, 19: 45259 (IAE-834)
Pulsed magnetic fields apparatus, 19: 44861 (IAE-795)
Radiation stability of ion exchange resins. II., 19: 44055 (IAE-788)
Redesign of IAE linear electron accelerator, 19: 44860 (IAE-614)
Threshold of symmetrical fission of ^{237}Np, 19: 45258 (IAE-833)
Use of organic coolant-moderators in nuclear reactors, 19: 45501 (IAE-611)

INSTITUT DE SOUDURE, PARIS (FRANCE).
Prog. rpt. on study of welded joints for very thick steel plates, 1–3/65, 19: 44686 (EURAEC-1362)

INSTITUT FUER KERNPHYSIK, UNIVERSITAET FRANKFURT (WEST GERMANY).
Bibliography on instruments and measuring techniques in nuclear physics, 19: 44366 (AED-C-06-12)

INSTITUT FUER PLASMAPHYSIK, G.M.B.H. GARCHING (WEST GERMANY).
Connection between correlations and fluctuations in a plasma, 19: 45394 (IPP-6/37)
Dynamics of a toroidal theta pinch, 19: 45395 (IPP-6/38)
Electromagnetic radiation from plasmas of high temperature and density, 19: 45392 (IPP-1/39)
Influence of probe losses on the ion density of a thermal alkali plasma in a magnetic field, 19: 45393 (IPP-2/38)

INSTITUT ZA NUKLEARNE NAUKE "BORIS KIDRIC," BELGRADE (YUGOSLAVIA).
Prog. rpt. on absolute measurement of neutron fluxes inside reactor core, final, 1/63–1/65, 19: 44450 (IBK-120a)

INSTITUTE OF NUCLEAR RESEARCH, WARSAW (POLAND).
Dispersion fuel elements for experimental and university reactors, 19: 45547 (INR-585/XIV/R)
Interactions of fast plasmoids with constant magnetic field barrier, 19: 45391 (INR-612/IXA/PR)
Measurements of β/1 parameters in ANNA, 19: 45677 (INR-614/1XA/P)
Radiation-induced reactions of oxidation and reduction of iron ions in aqueous solutions, 19: 44056 (INR-579/XVII/C)
Target preparation by electro-spraying directly on semiconductor detectors, 19: 44635 (INR-595/IA/PL)
Use of the chopper for pulse neutron measurements, 19: 45222 (INR-624/IX-A/R)
Water reactivity effects in the Anna critical assembly, 19: 45529 (INR-600/IX-A/PR)

INSTITUTO DE INVESTIGACIONES GEOLOGICAS, SANTIAGO (CHILE).
Reconnaissance for uranium in the Aisen Area, Aisen, Chile, 19: 44273 (RME-4557(Rev.))

INSTITUTT FOR ATOMENERGI, HALDEN (NORWAY). OECD HALDEN REAKTOR PROSJEKT.
Dynamics model of the HBWR heat removal circuits, 19: 45633 (HPR-62)
Noise experiments with the HBWR second fuel charge, 19: 45632 (HPR-53)

INSTITUTUL DE FIZICA ATOMICA, ACADEMIA R. P. R., BUCHAREST (ROMANIA).
Nuclear energy development, 1964, 19: 45705 (NP-15193)

INTERNATIONAL ATOMIC ENERGY AGENCY, VIENNA (AUSTRIA).
Conference on inelastic scattering of neutrons, Bombay, 12/64, IL., 19: 45234
Dosimetry for radiation accidents, Vienna, 3/65, 19: 44319 (STI/PUB/99)

INTERNATIONAL CENTRE FOR THEORETICAL PHYSICS, TRIESTE (ITALY).
Experimental tests of broken $\bar{U}(12)$ and approximate $U(6) \times U(6)$, 19: 45002 (IC/65/59)
Mass spectrum from noncompact groups, 19: 45004 (IC/65/66)
Relativistic symmetries, 19: 45005 (IC/65/68)
Theory of corrections to unitary symmetry formulae, 19: 45003 (IC/65/60)

ISRAEL ATOMIC ENERGY COMMISSION, YAVNE. SOREQ NUCLEAR RESEARCH CENTER.
Calculation of Doppler effect in fast reactors, 19: 45576 (IA-1039)
Effect of ^{60}Co gamma rays applied at low dose rates on some juice constituents and peel color of green and ripe citrus fruits, 19: 44554 (IA-1015)
Sealing factors—their measurement and use in design of vacuum gasket seals, 19: 44135 (IA-1033)

J

JAGELLONIAN UNIV., KRAKOW (POLAND). DEPT. OF THEORETICAL PHYSICS.
Classical phase-space integral in the statistical model with angular momentum conservation, 19: 45041 (TPJU-12/65)
Lower bound of the forward unsymmetrized scattering amplitude, 19: 45040 (TPJU-11/65)
New restriction on the forward scattering amplitude in local field theory, 19: 45039 (TPJU-10/65)
Proof of theorem about general form of isotropic tensors, 19: 44810 (TPJU-8/65)
Quantum statistics in statistical model of multiple production of particles, 19: 45038 (TPJU-7/65)

JAPAN ATOMIC ENERGY RESEARCH INST., TOKYO.
Environmental radiation and radioactivities about site of JAERI, 1956–1963, 19: 44290 (JAERI-1079)
Excitation cross sections of the (n,n'γ) reactions on Fe, Co, Ni, Cu, Zn, Mo, Ag, Cd, and Sn, 19: 45263 (JAERI-1078)
Manual of free gas model-code (FREE code), 19: 45223 (JAERI-1084)
Multigroup calculations of kinetics parameters in fast reactors (KPARAM code), 19: 45530 (JAERI-1082)
Nuclear parametric study of the pressure tube-type D_2O moderated lattices, 19: 45578 (JAERI-1080)
Radiological monitoring point. Photographic dosimeter and gamma paper station, 19: 44291 (JAERI-1081)

JOINT INST. FOR NUCLEAR RESEARCH, DUBNA (USSR).
Estimation of ionizing radiation levels near 10-Bev synchrophasotron, 19: 44863 (JINR-P-2231)
Neutron-^{235}U nuclear interaction in the 0.002 to 30 kev energy region, 19: 45292 (BNL-tr-16)

JOINT INST. FOR NUCLEAR RESEARCH, DUBNA (USSR). LAB OF HIGH ENERGY.
Elastic scattering of Λ hyperons on protons, 19: 45016 (JINR-P-2257)
Passage of spin and spinless particles through matter, 19: 45013 (JINR-P-2230)
Real part of the elastic p-p scattering amplitude at 2, 4, 6, 8, and 10 Bev, 19: 45021 (JINR-P-2336)
Some interference phenomena arising by mixing quantum levels in external fields, 19: 45270 (JINR-P-2248)

JOINT INST. FOR NUCLEAR RESEARCH, DUBNA (USSR). LAB. OF NEUTRON PHYSICS.
Decay mode of ^{147}Eu, 19: 45267 (JINR-P-2161)

JOINT INST. FOR NUCLEAR RESEARCH, DUBNA (USSR). LAB OF NUCLEAR PROBLEMS.
Angular dependence of quantities measured in total set of experiments on nucleon-nucleon scattering, 19: 45015 (JINR-P-2241)
Catalysis by μ^- of $d\mu + p \rightarrow {}^3He + \mu^-$ and $d\mu + d \rightarrow t + p + \mu^-$, 19: 45273 (JINR-P-2356)
Decay mode of ^{147}Eu, 19: 45267 (JINR-P-2161)
Fallibility of using χ^2 criterion in phase-shift analysis for choosing statistically permissible ambiguous solutions, 19: 45012 (JINR-E-2353)
γ Spectrum of ^{160m}Ho isomer, 19: 45272 (JINR-P-2270)
New data on ^{135}Ce decay, 19: 45268 (JINR-P-2235)
Regularity in spontaneous nuclear fission, 19: 45271 (JINR-P-2265)
Spectra of conversion electrons of ^{139}Ce and ^{132}Ce isotopes, 19: 45269 (JINR-P-2236)

JOINT INST. FOR NUCLEAR RESEARCH, DUBNA (USSR). LAB OF NUCLEAR REACTIONS.
Kinetics of multiple acceleration of particles with variable charge in a potential electric field, 19: 44864 (JINR-P-2253)

JOINT INST. FOR NUCLEAR RESEARCH, DUBNA (USSR). LAB OF THEORETICAL PHYSICS.
Baryon annihilation in broken U(12) symmetry, 19: 45008 (JINR-E-2246)
Broken symmetry U(12) and unitarity condition for the S matrix, 19: 45018 (JINR-P-2283)
Current-generated algebras and form factors, 19: 45011 (JINR-E-2294)
Decays $\frac{3}{2}^+ \rightarrow \frac{1}{2}^+ + 0^-$ in broken symmetry U(12), 19: 45014 (JINR-P-2237)
Determination of parity in reactions induced by γ quanta, 19: 45010 (JINR-E-2259)
Electromagnetic decay and electroproduction of $^3/_2^+$ resonances, 19: 45007 (JINR-E-2228)
Lithium-induced reactions and the structure of light nuclei, 19: 45264 (JINR-E-2243)
New definition of translations in the inhomogeneous SL(6) group, 19: 45132 (JINR-E-2225)
On the observed isospin violation in the $^{10}B(^6Li,d)^{14}N$ reaction, 19: 45265 (JINR-E-2244)
On the ρ-meson peak shift in double photoproduction, 19: 45019 (JINR-P-2286)
Orbital fractional parentage coefficients for two and three nucleons in the 2s-1d shell in SU(3) classification scheme, 19: 45266 (JINR-E-2285)
Passage of spin and spinless particles through matter, 19: 45013 (JINR-P-2230)
Photon and notoph, 19: 45020 (JINR-P-2330)
Reconstruction of $N + N \rightarrow \pi + d$, 19: 45017 (JINR-P-2267)
Unitarity of the S matrix in the broken symmetry SL(6), 19: 45009 (JINR-E-2247)
JUNTA DE ENERGIA NUCLEAR, MADRID (SPAIN). DIVISION DE FISICA.
PROMETEO I—program for averaging thermal constants over Wigner-Wilkins flux spectrum, 19: 45224 (JEN-133-DF/I-43)
PROMETEO II—program for averaging thermal constants from Wilkins spectrum, 19: 45225 (JEN-135-DF/I-44)
JUNTA DE ENERGIA NUCLEAR, MADRID (SPAIN). DIVISION DE FISICA TEORICA.
Relativistic local quantum field theory for m = 0 particles, 19: 45131 (JEN-154-DF/I-47)
JUNTA DE ENERGIA NUCLEAR, MADRID (SPAIN). DIVISION DE QUIMICA.
Determination of average molecular weights of organic reactor coolants. I., 19: 44045 (JEN-151-DQ/I-52)
Determination of average molecular weights of organic reactor coolants. II., 19: 44046 (JEN-152-DQ/I-53)
Direct-reading spectrochemical analysis of nuclear graphite, 19: 43930 (JEN-145-DQ/I-46)
Water treatment process in JEN-1 research reactor, 19: 45678 (JEN-149-DQ/I-50)

K

KAISER ENGINEERS, OAKLAND, CALIF.
IBM 7090 bolted closure stress analysis program, 19: 44145 (TID-22138)
KENTUCKY UNIV., LEXINGTON.
The non-destructive determination of silicon and oxygen in meteorites by fast neutron activation analysis, 19: 43927 (CONF-650405-16)
KERNFORSCHUNGSZENTRUM, KARLSRUHE (WEST GERMANY).
Fast neutron spectrum measurements with a ^6Li semiconductor neutron spectrometer, 19: 44457 (NP-15475)
Prog. rpt. on fast breeder project, annual, 1963, 19: 45583 (NP-15365)
KERNFORSCHUNGSZENTRUM, KARLSRUHE (WEST GERMANY). INSTITUT FUER NEUTRONENPHYSIK UND REAKTORTECHNIK.
Hardening of thermal neutron spectra in water and boric acid solution, 19: 45226 (KFK-294)
KNOLLS ATOMIC POWER LAB., SCHENECTADY, N. Y.
MIRAGE-III: matrix interpretive routine, 19: 44581 (KAPL-M-6469)
Surface crack detector, 19: 44210 (KAPL-M-6484)

L

LABORATORI NAZIONALI DI FRASCATI, COMITATO NAZIONALE PER L'ENERGIA NUCLEARE (ITALY).
Persistent currents induced by circularly polarized waves in a superconducting ring, 19: 45191 (LNF-65/15)
Production and discharge of toxic and radioactive gas in tunnel of Frascati linac, 19: 44866 (LNF-65/21)
Recent calculations on electron-positron colliding beam experiments, 19: 45023 (LNF-65/8)
Vector and axial currents under first-order symmetry breaking, 19: 45022 (LNF-65/7)
LABORATORIO DE FISICA E ENGENHARIA NUCLEARES, JUNTA DE ENERGIA NUCLEAR, SACAVEM (PORTUGAL).
Radiolysis of H_2O by 1- to 2-Mev protons. II., 19: 44058 (LFEN-23)
LAWRENCE RADIATION LAB., UNIV. OF CALIFORNIA, BERKELEY.
Carbothermic reduction of alumina: a thermodynamic analysis, 19: 43996 (UCRL-11699)
Collective excitation of neutron-deficient Ba, Xe, and Ce isotopes: centrifugal stretching treatment of nuclei, 19: 45285 (UCRL-16040)
Collins quadrupole magnets and sextupole magnets for a 200-Bev proton synchrotron, 19: 44878 (UCRL-16375)
Derivation of corrections to control closed orbit in an alternating-gradient synchrotron, 19: 44875 (UCRL-16229)
Development of some high-speed chromatographic methods, 19: 44118 (UCRL-16015)
Dilation contribution to the heat capacity of copper and alpha brass at elevated temperatures, 19: 45718 (UCRL-11662)
Effect of size on plastic properties of aluminum single crystals, 19: 44705 (UCRL-11653)
Electrolytic capacitor banks, 19: 45416 (UCRL-16263)
Growth curve for mammary fibroadenoma in female rat, 19: 43649 (UCRL-16177)
High-energy polarization experiments and Regge poles, 19: 45044 (UCRL-16185)
K^-p charge-exchange scattering from 1200 to 1700 Mev/c, 19: 45045 (UCRL-16288)
Kinetics of dissolution and diffusion of oxides of iron in sodium disilicate glass, 19: 44611 (UCRL-16232)
Measurement of polarization parameter in proton-proton scattering from 1.7 to 6.1 Bev, 19: 45043 (UCRL-16070)
On the calculation of nonlinear magnetostatic fields, 19: 44876 (UCRL-16287)
Prog. rpt. on Bevatron operation and development, 10–12/64, 19: 44874 (UCRL-16203)
Prog. rpt. on inorganic materials research, annual, 1964, 19: 43997 (UCRL-11889)
Prog. rpt. on physics, semiannual, 11/64–4/65, 19: 44812 (UCRL-16099)
Review of recent boson resonances, 19: 45046 (UCRL-16295)
Sampling bias in scanning proton-recoil tracks in nuclear emulsion, 19: 44464 (UCRL-11703)
Semiconductor detectors for nuclear spectrometry, 19: 44466 (UCRL-16231)
Some aspects of the photochemistry and radiation chemistry of thymine, 19: 44060 (UCRL-16353)
Spin analysis for I = 0 3-pion system, 19: 45042 (UCID-2608)
Statistical model calculations of high energy reactions, 19: 45047 (UCRL-16315)
The feasibility of a low-field superconducting thin-septum magnet, 19: 44877 (UCRL-16346)
Uv absorption spectrum of trapped S_2, 19: 45480 (UCRL-10771)
Water tunnel with moving walls, 19: 45722 (UCRL-16188)
200 Bev accelerator design study, 19: 44873 (UCRL-16000(Summ.))
LAWRENCE RADIATION LAB., UNIV. OF CALIFORNIA, LIVERMORE.
Background events in photomultiplier tubes at high altitudes, 19: 44465 (UCRL-12020)
Design of Modulo-N counters for any code, 19: 45719 (UCRL-12012)
Economics of ground water recharge, 19: 45717 (UCRL-7850(Rev.1))
Experimental studies with the Astron facility, 19: 45413 (UCRL-12456)
Five-million pound shock testing facility, 19: 45720 (UCRL-12055-T)
Influence of strain rate on mechanical properties of 6061-T6 aluminum under uniaxial and biaxial states of stress, 19: 44706 (UCRL-12264 (Rev.1))
Investigation of plasma from an occluded gas, cold plasma source, 19: 45411 (UCRL-7935)
Low-temperature plasma column confinement by magnetic fields with shear, 19: 45415 (UCRL-14137)
Magnetic field calculations in an irregular triangle mesh, 19: 44811 (UCRL-7784-T(Rev.1))
Null method of measuring microwave phase shifts, 19: 45412 (UCRL-7978)
Qualitative experimental investigations on various vortex tube configurations, 19: 44199 (UCRL-12045)
Role of oxygen in solid–solid reactions, 19: 43998 (UCRL-12396)
Schematic view of the origin of life, 19: 45721 (UCRL-14254)
Some calculations for effecting oilfield stimulation by nuclear means, 19: 44158 (UCRL-14311)
Sources of artificial radiation belts, 19: 45159 (UCRL-14374)
Studies of band structure and electron scattering in Al by photoemission, 19: 45481 (UCRL-12470)
Surface ionization of alkali metals by heated tungsten, 19: 44938 (UCRL-14117)
Theory of the electrostatic probe and its improved use as a diagnostic tool, 19: 45414 (UCRL-12480)

LITTLE (ARTHUR D.) INC., CAMBRIDGE, MASS.
Economics of controlling Salmonellae in foods by use of ionizing radiation, 19: 44557 (NYO-3426-1)
LITTON INDUSTRIES, SAN CARLOS, CALIF. RESEARCH LAB.
Prog. rpt. on analysis of electron-ion mixing in ion engines, 11/64–1/65, 19: 44222 (NP-15068)
LOCKHEED AIRCRAFT CORP., PALO ALTO, CALIF.
Semi-annual effect appearing in satellite orbital decay data, 19: 45158
LOCKHEED–GEORGIA CO., MARIETTA.
Components irradiation test No. 4—2N1132 transistors, 19: 44548 (NP-15422)
LOCKHEED MISSILES AND SPACE CO., SUNNYVALE, CALIF.
RIFT systems analysis. III. Aerodynamics, 19: 44137 (N64-24017)
LOS ALAMOS SCIENTIFIC LAB., UNIV. OF CALIFORNIA, N. MEX.
Alternating current polishing and electroetching of metals, 19: 44601 (LA-DC-6407)
Alternating current electroetching of α, ∂, and β plutonium, 19: 44602 (LA-DC-6691)
Band structure, specific heat, magnetic susceptibility, and anomalous thermal expansion of delta Pu, 19: 44689 (LA-DC-7351)
Determination of trace amounts of oxygen added to metallic sodium, 19: 43932 (LA-3343)
Development of an interleaved, fractional-turn coil, 19: 44136 (LA-3234)
Development of the mapping function at a corner, 19: 45702 (LA-DC-6558)
Effect of optical pump pulse shape on ruby inversion, 19: 45704 (LA-DC-6717)
Floating-point version of Nordsieck's scheme for numerical integration of differential equations, 19: 45703 (LA-DC-6667)
Forming of Teflon sheet by powder rolling, 19: 44637 (LA-3340)
Further experimental study of H_2O–LH_2 heat exchangers, 19: 44186 (LA-DC-7148)
Gamma scanning of LAMPRE fuel elements with a NaI anticoincidence spectrometer, 19: 44453 (LA-DC-7316)
HASTI—a numerical calculation of two-dimensional lagrangian hydrodynamics utilizing the concept of space-dependent time steps, 19: 45701 (LA-3324)
Inert atmosphere enclosure for the preparation of samples prior to determination of oxygen, 19: 43933 (LA-3344)
Magnetic susceptibility of delta plutonium alloys, 19: 44690 (LA-DC-7360)
Measurement of helium and hydrogen viscosities to 2340°K, 19: 45190 (LA-3319)
Neutron experiments with underground nuclear explosions, 19: 44157 (LA-DC-7304)
Non-equilibrium diffusion equation, 19: 45460 (LA-3377)
Polarization on energy beam in infrared grating spectrophotometers, 19: 44345 (LA-DC-6719)
Preparation of ultra-high purity plutonium, 19: 44600 (LA-3356)
Proper use of transformations of log normal functions in small-particle statistics, 19: 44808 (LA-DC-6636)
Radiation damage to ionic crystals at low temperatures. I., 19: 44745 (LA-DC-6725)
Single-sphere neutron monitoring instrument, 19: 44454 (LA-DC-7323)
Solubilities of selected elements in liquid plutonium, 19: 44688 (LA-3359)
Symmetry of the stress tensor, 19: 44807 (LA-DC-6556)
The controlled potential electrodeposition of cobalt from plutonium–cerium–cobalt alloy solutions, 19: 43934 (LA-3345)
Theta-pinch sources of vacuum ultraviolet radiation, 19: 45396 (LA-DC-7120)
LYON UNIV. (FRANCE).
Preparation of uranium-based oxide catalysts, 19: 43987 (CEA-R-2817)
LYON UNIV. (FRANCE). FACULTE DES SCIENCES.
Utilization of indefinite metrices for the determination of propagators in quantum field theory, 19: 45133 (NP-15341)

M

MAINZ UNIV. (WEST GERMANY). NATURWISSENSCHAFTLICHE FAKULTAET.
Indirect determination of half life of short-lived fission rare gases, 19: 45276 (NP-15304)
MARINE BIOLOGICAL LAB., WOODS HOLE, MASS.
Galvani, Volta and bioelectricity, 19: 43664 (BNL-9337)
Material transfer, membranes and metabolism, 19: 43665 (BNL-9338)
MARTIN CO., BALTIMORE, MD. NUCLEAR DIV.
Betas and bremsstrahlung from ^{90}Sr–^{90}Y, 19: 45284 (TID-22169)
MARYLAND UNIV., COLLEGE PARK.
Acute depletion of Ca, P, and Sr from the bovine calf by hemodialysis, 19: 43673 (TID-22147)
Betas and bremsstrahlung from ^{90}Sr–^{90}Y, 19: 45284 (TID-22169)
MARYLAND UNIV., COLLEGE PARK. DEPT. OF PHYSICS AND ASTRONOMY.
Gauge problems in canonically quantized electrodynamics without subsidiary conditions, 19: 45135 (NP-15436)
Prog. rpt. on probe system for upper atmosphere plasmas, 4/59–9/62, 19: 45155 (AD-609015)
MASCHINENFABRIK AUGSBURG-NUERNBERG A. G., NUREMBERG (WEST GERMANY).
Prog. rpt. on critical heat flux (burnout) in boiling H_2O, 10–12/64, 19: 44184 (EURAEC-1281)
MASSACHUSETTS INST. OF TECH., CAMBRIDGE.
Effects of steric hindrance and of bond type on electronic absorption spectra of certain 8-quinolinolates, 19: 43989 (MIT-905-20)
MASSACHUSETTS INST. OF TECH., CAMBRIDGE. DEPT. OF CHEMISTRY.
Some new derivatives of the $[Mo_6Cl_8]^{4+}$ ion, 19: 43990 (MIT-1955-15)
MASSACHUSETTS INST. OF TECH., CAMBRIDGE. DEPT. OF NUTRITION AND FOOD SCIENCE.
Prog. rpt. on simultaneous radiation-heating of treatment of haddock, 7/61, 19: 44558 (TID-22139)
MASSACHUSETTS INST. OF TECH., CAMBRIDGE. DEPT. OF PHYSICS.
Prog. rpt. on radium and mesothorium poisoning and dosimetry and instrumentation, 1950–65, 19: 43672 (TID-22131)
MASSACHUSETTS INST. OF TECH., CAMBRIDGE. LAB. FOR NUCLEAR SCIENCE.
Photoproduction of mesons in the Bev range, 19: 45024 (MIT-2098-162)
MASSACHUSETTS INST. OF TECH., CAMBRIDGE. RESEARCH LAB. OF ELECTRONICS.
Prog. rpt. on energy conversion, 3–5/65, 19: 44981 (NP-15435)
MECHANICAL TECHNOLOGY INC., LATHAM, N. Y.
Prog. rpt. on film rupture in journal bearings, 5/64–2/65, 19: 44138 (NYO-3363-4)
METRONICS ASSOCIATES, INC., PALO ALTO, CALIF.
Elevated line source programs, 19: 44779 (BNL-914, pp 93-4)
Fundamental problems on the meso-scale, 19: 44782 (BNL-914, pp 103-6)
MIAMI UNIV., CORAL GABLES, FLA. DEPT. OF PHYSICS.
Prog. rpt. on cooperative effects and plasma losses in magnetic field, final, 3/62–2/63, 19: 45380 (AD-426192)
MIDWESTERN UNIVERSITIES RESEARCH ASSN., STOUGHTON, WIS.
Design of proton linear accelerators for energies up to 200 Mev, 19: 44867 (MURA-713)
MINNESOTA UNIV., MINNEAPOLIS. DEPT. OF CHEMICAL ENGINEERING.
Prog. rpt. on two-phase flow through apertures, final, 7/65, 19: 44138 (TID-22145)
MOUND LAB., MIAMISBURG, OHIO.
Radiochemistry of radium, 19: 44098 (NAS-NS-3057)
MUNICH UNIV. (WEST GERMANY). INSTITUT FUER ANORGANISCHE CHEMIE.
Binary and ternary oxides of Pm, 19: 43992 (NP-15339)
Preparation and properties of promethium and some of its compounds, 19: 43988 (CONF-650804-7)

N

NATIONAL ACADEMY OF SCIENCES–NATIONAL RESEARCH COUNCIL, WASHINGTON, D. C.
Radiochemistry of radium, 19: 44098 (NAS-NS-3057)
NATIONAL AERONAUTICS AND SPACE ADMINISTRATION, CLEVELAND, OHIO. LEWIS RESEARCH CENTER.
Electrodynamic mercury pump, 19: 44188 (NASA-TN-D-2965)
Energy addition to an atomic hydrogen plasma at off-resonant conditions, 19: 45400 (NASA-TN-D-2982)
Hypervelocity impact damage characteristics in beryllium and graphite plates and tubes, 19: 44692 (NASA-TN-D-3018)
Stability of two-fluid wheel flows, 19: 45652 (NASA-TN-D-2696)
Thermodynamic and turbomachinery concepts for radioisotope and reactor Brayton-cycle space power systems, 19: 45654 (NASA-TN-D-2968)
Tungsten–nickel–copper ternary alloys for high-temperature applications, 19: 44691 (NASA-TN-D-3015)
NATIONAL AERONAUTICS AND SPACE ADMINISTRATION, HUNTSVILLE, ALA. GEORGE C. MARSHALL SPACE FLIGHT CENTER.
Parametric performance analysis for interplanetary missions utilizing first-generation nuclear stages, 19: 45649 (N64-32637)
NATIONAL AERONAUTICS AND SPACE ADMINISTRATION, WASHINGTON, D. C.
Bibliography on aerospace medicine and biology, 19: 43719 (NASA-SP-

7011(13))
Nuclear rockets based on graphite reactor technology, 19: 45658 (TID-22097)
NATIONAL AERONAUTICS AND SPACE ADMINISTRATION, WASHINGTON, D. C. SCIENTIFIC AND TECHNICAL INFORMATION DIV.
Bibliography on aerospace medicine and biology, 19: 43718 (NASA-SP-7011(12))
NATIONAL BUREAU OF STANDARDS, WASHINGTON, D. C.
Bibliography on high-temperature chemistry and physics of materials in the condensed state, 19: 43994 (NP-15381)
NATIONAL INST. FOR RESEARCH IN NUCLEAR SCIENCE, CHILTON (ENGLAND). RUTHERFORD HIGH ENERGY LAB.
Central region of the variable-energy cyclotron magnet, 19: 44869 (NIRL/R/87)
Design of beam deflection system for the Harwell variable energy cyclotron, 19: 44868 (NIRL/R/86)
NAVAL CIVIL ENGINEERING LAB., PORT HUENEME, CALIF.
Variation of dose attenuation of two-legged concrete ducts with incident γ energy, 19: 45457 (AD-462614)
NAVAL RESEARCH LAB., WASHINGTON, D. C.
Filter pack technique for classifying radioactive aerosols by particle size. III., 19: 44252 (NRI-6305)
NAVAL WEAPONS LAB., DAHLGREN, VA.
Proposed filtered shielded connector for protection of weapons from electromagnetic radiation, 19: 44166 (NP-15472)
NEVIS LABS., COLUMBIA UNIV., IRVINGTON-ON-HUDSON, N. Y.
Asymmetry in angular distribution of neutrons from muon capture in spin 0 nuclei, 19: 45274 (NEVIS-136)
Measurement of the K^0 mass and the K^0–K^- mass difference, 19: 44998 (CU-1932-247)
NEWCASTLE-UPON-TYNE UNIV. (ENGLAND).
Research on organic radiation chemistry, 19: 44053 (AFML-TR-65-166)
NEWCASTLE-UPON-TYNE UNIV. (ENGLAND). DEPT. OF PHYSICS.
Laboratory investigation of geomagnetic dynamos, 19: 45156 (AFCRL-64-768)
NEW YORK OPERATIONS OFFICE (AEC), N. Y.
Prog. rpt. on radioactive fallout distribution, 1964–65, 19: 44253 (NYO-2174-36)
NEW YORK UNIV., N. Y.
Turbulence and low-level structure, 19: 44793 (BNL-914, pp 156-7)
NEW YORK UNIV., N. Y. DEPT. OF PHYSICS.
Prog. rpt. on measurement of environmental radiation, annual, 6/64–6/65, 19: 44461 (TID-22205)
NEW YORK UNIV., N. Y. SCHOOL OF ENGINEERING AND SCIENCE.
Scale-model diffusion experiments, 19: 44764 (BNL-914, pp 14-17)
NORTHERN STATES POWER CO., MINNEAPOLIS, MINN.
Prog. rpt. on Pathfinder power plant, 7–9/64, 19: 45557 (ACNP-65557)
Prog. rpt. on Pathfinder power plant operation, 3–12/64, 19: 45593 (TID-22168)
NUCLEAR CROSS SECTIONS ADVISORY GROUP (AEC).
Reports to AEC Nuclear Cross Sections Advisory Group meeting, March 8–9, 1965, 19: 45288 (WASH-1056)
NUCLEAR MATERIALS AND EQUIPMENT CORP., APOLLO, PA.
Prog. rpt. on growth of single crystals of Pu, 4–6/65, 19: 44604 (NUMEC-3428-12)
NUCLEAR UTILITY SERVICES, INC., WASHINGTON, D. C.
Dose calculation models for re-entering nuclear rocket debris, 19: 45655 (NUS-229)
NUKLEARNI INSTITUT "JOZEF STEFAN," LJUBLJANA (YUGOSLAVIA).
Nuclear spin relaxation by fixed damage centers in irradiated $NaH_3(SeO_3)_2$, 19: 45477 (NIJS-R-444)
Regular eigenfunctions of time and velocity dependent transport equation for slabs, 19: 45227 (NIJS-R-449)
The determination of cadmium in uranium compounds by atomic absorption spectrophotometry, 19: 43935 (NIJS-R-447)

O

OAK RIDGE GASEOUS DIFFUSION PLANT, TENN.
Fabrication of calorimeter elements, 19: 44344 (K-L-1944)
Improved fast neutron monitor, 19: 44452 (K-1642)
Separation of potassium isotopes by molecular distillation, 19: 43931 (K-1650)
OAK RIDGE NATIONAL LAB., TENN.
Application of online digital computer to a reactor experiment, 19: 45585 (ORNL-P-1502)
Behavior of the transplutonium elements in solvent extraction systems, 19: 44115 (ORNL-P-1577)
Calculations of charge and contour dimensions of powder-loading assembly used in the production of HFIR composite fuel compacts, 19: 44641 (ORNL-TM-1193)
Calculations of concrete shields for fission sources, 19: 45464 (ORNL-TM-1167)
CHRNOGRM—computer program for analysis of chronopotentiograms, 19: 45706 (ORNL-TM-1254)
Collimators for low-energy γ rays, 19: 44347 (ORNL-P-1545)
Demonstration of disposal of high-level radioactive solids in salt, 19: 45689 (ORNL-P-1568)
Description of facility radiation and contamination alarm systems installed in High Radiation Level Examination Laboratory Building, 19: 44297 (ORNL-TM-1251)
Description of the LITR reactor control and instrumentation systems, 19: 45680 (ORNL-TM-1190)
Effect of irradiation on the mechanical properties of stainless steel at 750°C under constant stress rate conditions, 19: 44750 (ORNL-TM-1216)
EGCR control-rod-drive endurance test, 19: 45589 (ORNL-TM-1197)
Elastic scattering of 12.0- and 14.0-Mev deuterons from ^{90}Zr and the reaction $^{90}Zr(d,p)^{91}Zr$, 19: 45281 (ORNL-3850)
Electroplating of ^{109}Cd on copper wires, 19: 44139 (ORNL-TM-1174)
Evaluation of small modified CEN mixer-settlers for extraction of uranium and thorium in a hot cell facility, 19: 44117 (ORNL-TM-1256)
Experimental simulation of large, high field, superconducting magnet operation, 19: 45192 (ORNL-TM-1266)
FLASH: an IBM-7090 code for computing multi-stage flash evaporator plant designs for desalination of seawater, 19: 44140 (ORNL-TM-1244)
High flux isotope reactor preoperational vibration and hydraulic test program, 19: 45644 (ORNL-P-1501)
Ion cyclotron harmonic spectrum generated in an energetic ion plasma, 19: 45405 (ORNL-P-1576)
Ion exchange purification of fission-produced Sm, 19: 44116 (ORNL-TM-1062)
Irradiation evaluation of fuel elements for PBRE and AVR reactors, 19: 44749 (ORNL-P-1507)
Isotopic contamination in electromagnetic separators, 19: 44573 (ORNL-P-515)
Low-temperature ductility and strength of vapor-deposited tungsten, 19: 44695 (ORNL-P-1506)
Mathematical model for predicting coated-particle behavior, 19: 44748 (ORNL-P-1505)
Molten salt converter reactor. Design study and power cost estimates for a 1000-Mwe station, 19: 45588 (ORNL-TM-1060)
MUFFLE—code for multilevel analysis of neutron cross sections, 19: 45282 (ORNL-TM-1180)
Nondestructive testing of small-diameter refractory-alloy tubing, 19: 44211 (ORNL-P-1543)
Nuclear energy for water desalting, 19: 45590 (TID-3584)
Panel discussion on civil defense, ANS annual meeting, June 23, 1965, Gatlinburg, Tennessee, 19: 44215 (ORNL-3865)
Precipitation of hydrides in Zircaloy-2 as affected by preferred orientation, elastic stress, and hydrogen content, 19: 44697 (ORNL-TM-1239)
Predicted and observed nuclear characteristics of the Molten Salt Reactor Experiment, 19: 45586 (ORNL-P-1503)
Prog. rpt. on space biology, annual, 7/1/64–6/30/65, 19: 43721 (ORNL-TM-1217)
Properties of ionic sound waves, 19: 45404 (ORNL-P-1557)
Related two-point boundary value problems and associated harmonic matrices, 19: 44582 (ORNL-3646)
Remotely controlled corrosion-resistant pipetter, 19: 43936 (ORNL-P-1533)
Sample preparation apparatus for MSRE, 19: 44168 (ORNL-P-1532)
Second generation of reactor control systems as applied to the HFIR, 19: 45645 (ORNL-TM-1259)
Summary of the Kilorod Project, 19: 44638 (ORNL-3681)
Survey of Doppler coefficients for UO_2 fuel, 19: 45532 (ORNL-TM-1219)
Thermal stress considerations in the Molten Salt Reactor Experiment, 19: 45587 (ORNL-P-1504)
Thermochemical deposition of refractory metals, alloys, and compounds for application in thermionic devices, 19: 44640 (ORNL-P-1446-1)
Thorium–uranium dicarbide pseudobinary system in the presence of excess graphite, 19; 44696 (ORNL-TM-1188)
Thorium–uranium recycle facility, 19: 44167 (ORNL-P-1521)
Time study of fuel rod fabrication in the Kilorod facility, 19: 44639 (ORNL-3740)
Use of activation analysis in determination of origin of opium, 19: 43937 (ORNL-TM-1263)
OESTERREICHISCHE STUDIENGESELLSCHAFT FUER ATOMENERGIE G.M.B.H., SEIBERSDORF.
Dynamic study of heat transfer. III., 19: 44194 (SGAE-RE-2/1965)
Express method for electronic pulse counters, 19: 44351 (SGAE-E-4/1965)

OESTERREICHISCHE STUDIENGESELLSCHAFT FUER ATOMENERGIE G.M.B.H., SEIBERSDORF. INSTITUT FUER CHEMIE.
Measurement of β spectrum ^{90}Y, 19: 45283 (SGAE-PH-23/1965)
OFFICE OF SALINE WATER, WASHINGTON, D. C.
Saline water conversion report for 1964, 19: 44154
OREGON STATE UNIV., CORVALLIS.
Development of radiation-sterilized fish items for armed forces feeding, 19: 44555 (NP-15373)
OREGON STATE UNIV., CORVALLIS. DEPT. OF FOOD SCIENCE AND TECH.
Irradiation-sterilized shelf-stable fish and seafood products, 19: 44556 (NP-15464)

P

PADUCAH GASEOUS DIFFUSION PLANT, KY.
Environmental concentrations of radioactive materials near the Paducah Plant, 1–6/65, 19: 44301 (TID-22172)
PARIS UNIV. (FRANCE).
Distribution of moments in the nucleus and the scattering of electrons, 19: 45279 (NP-15415)
High-speed pulsed magnetic fields measurements, using the Faraday effect, 19: 44805 (CEA-R-2769)
PARIS UNIV. (FRANCE). FACULTE DES SCIENCES.
Luminescence of CdS under electron bombardment, 19: 45478 (NP-15110)
Study of the d layer of some nuclei by electron scattering, 19: 45275 (NP-15138)
PARIS UNIV., ORSAY (FRANCE). FACULTE DES SCIENCES.
Some stochastic phenomena in storage rings, 19: 44865 (LAL-1134)
PARIS UNIV., ORSAY (FRANCE). LABORATOIRE DE PHYSIQUE THEORIQUE ET HAUTES ENERGIES.
$K^0 \rightarrow 2\pi$ transition in unitary symmetry, 19: 45026 (N64-19243)
Trilinear couplings forbidden by nonet symmetry for vector mesons, 19: 45025 (N64-26265)
PAVIA UNIV. (ITALY). ISTITUTO DI GENETICA.
Prog. rpt. on mutation rates and mutational loads in man, annual, 9/64–8/65, 19: 43642 (NYO-2280-8)
PENNSYLVANIA STATE UNIV., UNIVERSITY PARK.
Structure of turbulence, 19: 44798 (BNL-914, pp 175-7)
Vertical structure of turbulence, 19: 44799 (BNL-8516)
PENNSYLVANIA STATE UNIV., UNIVERSITY PARK. DEPT. OF NUCLEAR ENGINEERING.
Prog. rpt., annual, 7/64–5/65, 19: 45679 (NYO-1859-11)
PHILLIPS PETROLEUM CO. IDAHO FALLS, IDAHO., ATOMIC ENERGY DIV.
Correlation of interaction data with calculations using the Geller model, 19: 44977 (IDO-17095)
Fundamentals in operation of test reactors. IV., 19: 45676 (IDO-16871-4)
Nonlinear least-square program for the determination of parameters of a modified-Gaussian function, 19: 45261 (IDO-17016)
Prog. rpt. on burnup determination of nuclear fuels, 1–3/65, 19: 45260 (IDO-14660)
Prog. rpt. on Spert Project, 1–3/65, 19: 45528 (IDO-17097)
Proposal to investigate physical properties of samples under very high pressures by time-of-flight neutron diffraction methods, 19: 45476 (IDO-17106)
SPORT—system for processing reactor transient data, 19: 45527 (IDO-17078)
PRATT AND WHITNEY AIRCRAFT, MIDDLETOWN, CONN. CONNECTICUT ADVANCED NUCLEAR ENGINEERING LAB.
Application of internal friction methods to corrosion study in Nb alloys, 19: 44620 (CNLM-6344)
Ball bearing test in lithium, 19: 44150 (TIM-923)
Carburization of Nb–1 Zr alloy, 19: 44609 (TIM-927)
Cavitation damage tests with rotating disk in water, 19: 44625 (TIM-894)
Cavitation-sensitive coating evaluation, 19: 44212 (TIM-878)
Cavitation tests of coated RI-16 impeller, 19: 44197 (TIM-895)
Centrifugal pump impeller design system, 19: 44148 (TIM-918)
Determination of absolute power in SNAP-50 critical assemblies by ^{140}Ba fission product measurements, 19: 45656 (PWAC-474)
Development of Cb–Zr–C alloys, 19: 44605 (PWAC-464)
Dissertation of jet pump analysis, 19: 44198 (TIM-913)
Electron metallography techniques applied to bcc metals and alloys, 19: 44610 (TIM-943)
Forced convection boiling potassium heat transfer data, 19: 44195 (TID-21256)
Interactions in type 316 stainless steel–NaK–Nb-1 Zr alloy system, 19: 44626 (TIM-896)
Motor cavity evacuation study, 19: 45660 (TIM-919)
Overhung rotor dynamics tests using hydrostatic water bearings, 19: 44146 (TIM-874)
Reactor weight optimization parametric code—WOP, 19: 45659 (TIM-807)
Recovery and recrystallization of Nb and several Nb–Zr alloys, 19: 44698 (PWAC-465)
Single hybrid journal bearing tests in water, 19: 44151 (TIM-925)
Space radiator fabrication development, 19: 44606 (PWAC-483)
Status of instrument development for the SNAP-50 reactor test program, 19: 44348 (PWAC-473)
Straddle bearing rotor dynamics tests with step bearing in water, 19: 44149 (TIM-921)
Summary of fluid film bearing analysis, 19: 44147 (TIM-917)
The vapor pressure of lithium between 1307 and 1806°K, 19: 44703 (TIM-844)
Thrust bearing tests in water, 19: 44152 (TIM-926)
Viscosity of lithium, 19: 44704 (TIM-849)
10,000-hour temperature test of fission-counter preamplifiers, 19: 44462 (TIM-922)
PRINCETON–PENNSYLVANIA ACCELERATOR, PRINCETON, N. J.
Design of fast-cycling liquid-H_2 bubble chamber, 19: 44459 (PPAD-2137-561)
External proton beam for the Princeton–Pennsylvania accelerator, 19: 44871 (PPAD-2137-556)
Operating experience and improvements on the Princeton–Pennsylvania accelerator, 19: 44872 (PPAD-2137-565)
PRINCETON UNIV., N. J.
Plasma heating at 500 megahertz, 19: 45398 (MATT-332)
PRINCETON UNIV., N. J. PLASMA PHYSICS LAB.
Plasma confinement in the model C stellarator, 19: 45397 (MATT-282)
Transmitting motion through a vacuum wall, 19: 44234 (MATT-345)
PRODUCTION GROUP, UNITED KINGDOM ATOMIC ENERGY AUTHORITY, ANNON (SCOTLAND).
Metabolism of radioactive strontium in rats, I., 19: 43671 (PG-Report 662)
PRODUCTION GROUP, UNITED KINGDOM ATOMIC ENERGY AUTHORITY, SELLAFIELD (ENGLAND).
Analytical method for the absorptiometric determination of copper in enriched uranium metal, 19: 43938 (PG-Report-665)
PURDUE RESEARCH FOUNDATION, LAFAYETTE, IND.
Prog. rpt. on carbohydrate catabolism in plants, 7/65, 19: 45697 (COO-330-11)
PURDUE UNIV., LAFAYETTE, IND.
Single-particle exchange in N^{*++} production in $\pi^+ p$ collisions, 19: 44997 (COO-1428-14)

R

RADIATION RESEARCH ASSOCIATES, INC., FORT WORTH, TEX.
Simulation of fallout gamma radiation fields by monoenergetic plane isotropic sources, 19: 44254 (RRA-M51)
RADIO CORP. OF AMERICA, LANCASTER, PA. DIRECT ENERGY CONVERSION DEPT.
Prog. rpt. on insulated thermionic converter-heat pipe assembly, 6/65, 19: 44980 (NP-15433)
REACTOR CENTRUM NEDERLAND, PETTEN.
Compilation of neutron flux density data in the HFR, 19: 45681 (RCN-36)
REACTOR CENTRUM NEDERLAND, THE HAGUE.
Bibliography on nuclear ship propulsion, 19: 45647 (AED-C-22-04)
REACTOR GROUP, UNITED KINGDOM ATOMIC ENERGY AUTHORITY, DOUNREAY (SCOTLAND).
Reactivity feedback in the Dounreay fast reactor, August 1962–December 1963, 19: 45594 (TRG-Report-864)
REACTOR GROUP, UNITED KINGDOM ATOMIC ENERGY AUTHORITY, SELLAFIELD (ENGLAND).
High-activity iodine release from irradiated fuel and its subsequent clean-up, 19: 44303 (TRG-Report-888)
Irradiated fuel element gamma scanning rig: operation and instrumentation, 19: 44463 (TRG-Report-1005)
ODYSSEUS—two-group, two-dimensional fuel cycle computer program suitable for advanced gas-cooled reactors, 19: 45595 (TRG-Report-976)
RENSSELAER POLYTECHNIC INST., TROY, N. Y.
Calculation of proton-induced damage in germanium and silicon, 19: 44747 (NP-15463)
RESEARCH AND ADVANCED DEVELOPMENT DIV., AVCO CORP., WILMINGTON, MASS.
Electrothermal engine research and development, 19: 44220 (N64-31011)
ROBERT A. TAFT SANITARY ENGINEERING CENTER, CINCINNATI, OHIO.
Air pollution in an urban environment, 19: 44785 (BNL-914, pp 113-14)
Air pollution program in the Public Health Service, 19: 44788 (BNL-914, pp 123-4)
Dispersion in urban areas, 19: 44791 (BNL-914, pp 151-2)

U.S. Public Health Service meteorology program, 19: 44775 (BNL-914, pp 69-74)
Supercritical pressure liquid hydrogen heat transfer data compilation, 19: 44189 (NP-15332)

ROCKY FLATS DIV., DOW CHEMICAL CO., DENVER, COLO.
Experimental hydrostatic journal bearing, 19: 44141 (RFP-573)
Feed-rate checks on numerical-controlled machines, 19: 44642 (RFP-570)
Properties of plutonium dioxide, 19: 43995 (RFP-503)

ROENTGEN TECHNISCHE DIENST N. V., ROTTERDAM (NETHERLANDS).
Prog. rpt. on non-destructive welding research, 4–6/65, 19: 44209 (EURAEC-1422)

S

SANDIA CORP., ALBUQUERQUE, N. MEX.
A precision analog memory with nondestructive readout using multi-aperture ferrite cores, 19: 44350 (SC-R-65-959)
Approach to stiffness of laterally loaded conical shells, 19: 45712 (SC-TM-65-82)
Basic principles of functional gaging, 19: 45708 (SC-R-65-915)
Computational studies on the reconstruction of an analog signal from non-uniformly spaced samples, 19: 44809 (SC-DR-65-291)
Decision order technique, 19: 45714 (SC-TM-65-349)
Dynamic responses of cylindrical shells under lateral loads, 19: 45711 (SC-TM-65-81)
Freon TF solvent residue analyzer, 19: 45713 (SC-TM-65-279)
Numerical solution of some problems of gas flows, 19: 44200 (SC-T-65-756)
On integer linear programming in combinatorial analysis, 19: 45709 (SC-R-65-963)
Prog. rpt. on containment capsule impact safety, Phase A, 7/65, 19: 44298 (SC-RR-65-9)
Project SAND final program report. III., 19: 44142 (SC-RR-65-286)
Semicontinuous hot-press tunnel kiln, 19: 44644 (SC-TM-65-276)
Short cut method for dimensional analysis, 19: 44143 (SC-RR-65-306)
Some temperature considerations in transistor circuit design, 19: 45715 (SC-TM-65-359)
Transient response of linear damped lumped spring-mass systems by experimentally derived transfer functions, 19: 45710 (SC-TM-64-1772)
U1627 (A g-second integrator), 19: 45707 (SC-DR-65-261)

SARAH MELLON SCAIFE RADIATION LAB., UNIV. OF PITTSBURGH, PA.
Particle physics and nuclear decay. Cancellation of photomultiplier gain drift following source intensity change, 19: 44374 (AROD-3347:6)

SOCIETA RICERCHE IMPIANTI NUCLEARI, SLUGGIA (ITALY). CENTRO RICERCHE NUCLEARI.
Detection of leakage in gas-distribution networks by means of radioactive tracers, 19: 44553 (EUR-2284.i)
Prog. rpt. on influence of N in Fe and steel under fast neutron irradiation, 1–3/65, 19: 44741 (EURAEC-1383)
Prog. rpt. on influence of N in Fe and steel under fast neutron irradiation, 19: 44742 (EURAEC-1430)

SOCIETE BELGE POUR L'INDUSTRIE NUCLEAIRE, BRUSSELS.
Coating UO_2 particles, 19: 44596 (EURAEC-1392)

SOUTHWEST RESEARCH INST., SAN ANTONIO, TEX.
Prog. rpt. on fatigue strength of pressure vessels, 7/15/65, 19: 45503 (SWRI-1228-69)

STAATLICHE ZENTRALE FUER STRAHLENSCHUTZ, BERLIN (EAST GERMANY).
Determination of penetration of aerosols in filters, 19: 44299 (SZS-2(1965))

STANFORD LINEAR ACCELERATOR CENTER, STANFORD UNIV., CALIF.
Application of proton resonance to the measurement of inhomogeneous magnetic fields, 19: 44353 (SLAC-Trans-22)

STANFORD RESEARCH INST., MENLO PARK, CALIF.
Fallout models and radiological countermeasure evaluations, 19: 44243 (AD-619902)

STANFORD UNIV., CALIF.
Plasma resonance probe characteristics in a magnetic field, 19: 45381 (ARL-65-115)

STANFORD UNIV., CALIF. INST. FOR PLASMA RESEARCH.
Argon plasma transport properties, 19: 45407 (SU-AA217)
Prog. rpt. on plasma diffusion across magnetic fields, 5–7/65, 19: 45410 (TID-22183)
Wave propagation along a warm nonuniform plasma column, 19: 45408 (SU-IPR-11)

STEVENS INST. OF TECH., HOBOKEN, N. J. DEPT. OF PHYSICS.
Prog. rpt. on cusped containment geometries, annual, 1964–65, 19: 45406 (SIT-2852-17)

STICHTING VOOR FUNDAMENTEEL ONDERZOEK DER MATERIE, JUTPHAAS (NETHERLANDS). INSTITUUT VOOR PLASMA-FYSICA.
Low-frequency plasma oscillations (anode oscillations and forced relaxation oscillations), 19: 45403 (NP-15445)

T

TEMPLE UNIV., PHILADELPHIA, PA. RESEARCH INST.
Prog. rpt. on high-temperature inorganic chemistry, annual, 6/64–6/65, 19: 44701 (TID-22144)

TENNESSEE UNIV., KNOXVILLE. DEPT. OF MECHANICAL AND AEROSPACE ENGINEERING.
Experimental stress analysis of attachment region of hemispherical shells with radially attached nozzles, 19: 44144 (TID-22134)

THAYER SCHOOL OF ENGINEERING, DARTMOUTH COLL., HANOVER, N. H.
Prog. rpt. on two-phase flow and boiling heat transfer, 4–6/65, 19: 44192 (NYO-3114-9)
Prog. rpts. on uptake of radioisotopes by edible marine products, 1960–62, 19: 43669 (NP-15159)

TOKYO UNIV. (JAPAN). FACULTY OF ENGINEERING.
Prog. rpt. on processing radioactive liquid wastes by evaporation, 1–6/64, 19: 45688 (NP-15367)

TRACERLAB, INC., WALTHAM, MASS.
Design of SO_2 monitor for air pollution studies, 19: 44458 (NYO-2767)

U

UNION CARBIDE CORP., OAK RIDGE, TENN. Y-12 PLANT.
Compendium of gas autoclave engineering studies, 19: 44169 (Y-1478)
Hydraulic problems on BONUS reactor pressure control system, 19: 45603 (Y-1491)
Preparing and sintering tungsten powder, 19: 44613 (Y-1476)
Production-size lathe hydrostatic components, 19: 44170 (Y-DA-921)

UNION CARBIDE CORP., PARMA, OHIO. CARBON PRODUCTS DIV.
Prog. rpt. on effects of neutron damage on mechanical properties of graphite, 10–12/64, 19: 44751 (TID-22110)

UNION CARBIDE CORP., PARMA, OHIO. RESEARCH LAB.
Prog. rpt. on effects of neutron damage on mechanical properties of graphite, 10–12/64, 19: 44751 (TID-22110)

UNITED AIRCRAFT CORP., EAST HARTFORD, CONN. RESEARCH LABS.
Prog. rpt. on collision probability of electrons and ions with alkali metal atoms, semiannual, 10/22/64–5/11/65, 19: 45399 (NASA-CR-54451)

UNITED NUCLEAR CORP., WHITE PLAINS, N. Y. DEVELOPMENT DIV.
Military Compact Reactor small source experiments, 19: 45575 (GMAD-3078-28)

UNITED STATES–EURATOM JOINT RESEARCH AND DEVELOPMENT PROGRAM.
Coating UO_2 particles, 19: 44596 (EURAEC-1392)
Interfacial reaction between UO_2 and zircaloy-2, 19: 44597 (GEAP-4679)
Prog. rpt. on critical heat flux (burnout) in boiling H_2O, 10–12/64, 19: 44184 (EURAEC-1281)
Prog. rpt. on imperfections in metals. II., 10–12/64, 19: 44622 (EURAEC-1433)
Prog. rpt. on imperfections in metals. II., 1–3/65, 19: 44687 (EURAEC-1434)
Prog. rpt. on influence of N in Fe and steel under fast neutron irradiation, 1–3/65, 19: 44741 (EURAEC-1383)
Prog. rpt. on non-destructive welding research, 4–6/65, 19: 44209 (EURAEC-1422)
Prog. rpt. on radial vane steam separator, 4–6/65, 19: 45574 (GEAP-4914)
Prog. rpt. on Saxton Pu program, 6/65, 19: 45600 (WCAP-3385-4)
Prog. rpt. on study of welded joints for very thick steel plates, 1–3/65, 19: 44686 (EURAEC-1362)
Prog. rpt. on transport equivalent diffusion theory, 4–6/65, 19: 45221 (GEAP-4913)
Prog. rpt. on two-phase flow, 4–6/65, 19: 44185 (GEAP-4910)
Prog. rpt. on two-phase flow and boiling heat transfer, 4–6/65, 19: 44192 (NYO-3114-9)

USAF RADIATION LAB., UNIV. OF CHICAGO, ILL.
Effects of various drugs on ATP activity of hematopoietic tissues of rats exposed to γ radiation, 19: 43860 (NP-15310, pp 14-25)
Inhibitory effect of x radiation on development of n-demethylase activity in livers of young male rats, 19: 43720 (NP-15310, pp 26-35)
Mechanism of action of 2-mercaptoethyl-amine, 19: 43670 (NP-15310, pp 36-47)
Prog. rpt. on biological and medical aspects of atomic energy, 7/15/65, 19: 43858 (NP-15310)
Radioprotective effects of DMSO in x-irradiated mice, 19: 43859 (NP-15310, pp 1-13)

USTAV JADERNEHO VYZKUMU, CESKOSLOVENSKA AKADEMIE VED, REZ.
Collision probability method for calculating fast neutron fission factor, 19: 45229 (UJV-1324/65)
Magnetic field gage and stabilizer, 19: 44352 (UJV-1339/65)
Possibility of obtaining non-excited compound nuclei of heavy transuranium elements, 19: 45286 (UJV-1293/65)
UTAH UNIV., SALT LAKE CITY. DEPT. OF CHEMISTRY.
Prog. rpt. on resolution in chromatography, final, 4/59–3/65, 19: 44113 (COO-748-1)

V

VIENNA UNIV. (AUSTRIA). INSTITUT FUER ANORGANISCHE CHEMIE.
Prog. rpt. on deposition of inhaled fission products in lungs, final, 10/62–10/64, 19: 44292 (NP-15173)
VIENNA UNIV. (AUSTRIA). INSTITUT FUER PHYSIKALISCHE CHEMIE.
Prog. rpt. on deposition of inhaled fission products in lungs, final, 10/62–10/64, 19: 44292 (NP-15173)
VIRGINIA POLYTECHNIC INST., BLACKSBURG. DEPT. OF METALS AND CERAMIC ENGINEERING.
Governing factors in the formation of Cr_3O-type structures, 19: 44702 (TID-22200)

W

WATERVLIET ARSENAL, N. Y. BENET R AND E LABS.
Survey of alloy-eutectic sources for aligned structures, 19: 44707 (WVT-6523)
WEATHER BUREAU, IDAHO FALLS, IDAHO.
Measurement of fallout deposition, 19: 44247 (BNL-914, pp 139-40)
Program review and summary of recent accomplishments at NRTS, 19: 44773 (BNL-914, pp 57-64)
WEATHER BUREAU, OAK RIDGE, TENN.
Continuous point source diffusion in the surface layer, 19: 44766 (BNL-914, pp 20-3)
Deposition calculations at Oak Ridge, 19: 44249 (BNL-914, pp 144-5)
Oak Ridge meteorological program, 19: 44765 (BNL-914, pp 18-19)
Technical areas in meteorology that are limiting progress in nuclear industry, 19: 44780 (BNL-914, pp 95-8)
WEATHER BUREAU, WASHINGTON, D. C.
Importance of the tetroon to meso-scale meteorology, 19: 44783 (BNL-914, pp 107-9)
Measurement and prediction of dispersion, 19: 44789 (BNL-914, pp 146-8)
Meso-scale studies in the >100-km range, 19: 44784 (BNL-914, pp 110-12)
Temperature profiles, 19: 44795 (BNL-914, pp 161-2)
Turbulence characteristics near the ground and sonic anemometry, 19: 44772 (BNL-914, pp 51-4)
U.S. Weather Bureau meteorology program, 19: 44770 (BNL-914, pp 33-43)
WEATHER BUREAU RESEARCH STATION, LAS VEGAS, NEV.
Meteorology program at the Nevada Test Site, 19: 44774 (BNL-914, pp 65-8)
WESTINGHOUSE ELECTRIC CORP., PITTSBURGH, PA. ATOMIC POWER DEPT.
1000-Mwe supercritical pressure nuclear reactor plant study, 19: 45596 (WCAP-2042)
WESTINGHOUSE ELECTRIC CORP., PITTSBURGH, PA. ATOMIC POWER DIV.
Control rod worth in heterogeneous mockup of large PWR core, 19: 45533 (WCAP-3269-33)
Effect of fuel burnup on moderator temperature coefficient in a PWR, 19: 45602 (WCAP-5493)
Large closed-cycle water reactor auxiliary systems, 19: 45597 (WCAP-3269-31)
Local fission power distributions around control rods and control rod followers in simulated PWR cores, 19: 45534 (WCAP-3269-35)
Optimum core lattice parameters for the San Onofre nuclear generating station, 19: 45599 (WCAP-3269-49)
Prog. rpt. on CVTR, 10–12/64, 19: 45567 (CVNA-235)
Prog. rpt. on large closed-cycle water reactor, 19: 45601 (WCAP-3750)
Prog. rpt. on Saxton Pu program, 6/65, 19: 45600 (WCAP-3385-4)
Reactivity worth of rod cluster control elements and local water hole power density peaking, 19: 45535 (WCAP-3269-47)
Saxton chemical shim kinetic experiments, 19: 45598 (WCAP-3269-44)
Zircaloy-steam reaction in a simulated reactor loss-of-coolant accident, 19: 45496 (WCAP-3269-30)
WESTINGHOUSE RESEARCH LABS., PITTSBURGH, PA.
Measurement of Cs excitation cross section near threshold by swarm technique, 19: 44935 (NP-15168)
Prog. rpt. on plasmas by laser heating, 4/6–7/5/65, 19: 45409 (TID-22132)
WISCONSIN UNIV., MADISON.
Analyzing power of neutrons for helium, 19: 45217 (COO-7-0363)
Polarization of protons from the D(d,p)T reaction, 19: 45253 (COO-7-0362)
WISCONSIN UNIV., MADISON. DEPT. OF CHEMISTRY.
Pentamethyldisilane and 1,1,2,2-tetramethyldisilane, and their addition to olefins, 19: 44048 (TID-21309)
WISCONSIN UNIV., MADISON. DEPT. OF PHYSICS.
Technique for studying the physical scattering matrix, 19: 44995 (COO-30-97)

Y

YALE UNIV., NEW HAVEN, CONN.
Prog. rpt. on effects of radiation on biological molecules and on cells in tissue culture, annual, 1964, 19: 43723 (TID-22128)
Prog. rpt. on embryogenesis and histogenesis in Pinus lambertiana., 4/65, 19: 43643 (TID-22143)
YALE UNIV., NEW HAVEN, CONN. SCHOOL OF FORRESTRY.
Prog. rpt. on effect of ionizing radiation on forest trees, 11/64–10/65, 19: 43722 (TID-22108)

Z

ZENTRALINSTITUT FUER KERNPHYSIK, ROSSENDORF BEI DRESDEN (EAST GERMANY).
Angular distribution for reaction $^{12}C(d,\alpha)^{10}B$ with a semiconductor detector, 19: 45289 (ZFK-PHA-12, pp 99-105)
Application of semiconductor detectors in the associated particle method, 19: 44476 (ZFK-PHA-12, pp 123-5)
Charge-sensitive preamplifier with low noise level for operation with semiconductor detectors, 19: 44484 (ZFK-PHA-12, pp 189-95)
Coincidences of pulses of semiconductor detectors, connected in delay line, 19: 44485 (ZFK-PHA-12, pp 196-200)
Conference on preparation and utilization of semiconductor detectors, Rossendorf, 9/63, 19: 44467 (ZKF-PHA-12)
Development of semiconductor detectors in Central Institute for Nuclear Physics at Rossendorf, 19: 44468 (ZFK-PHA-12, pp 10-15)
Effect of input resistance of an amplifier on the signal-to-noise ratio, 19: 44489 (ZFK-PHA-12, pp 219-23)
Excitation function for the $^{29}Si(n,\alpha)^{26}Mg$ reaction in energy range 13.6 to 15.6 Mev, 19: 45290 (ZFK-PHA-12, pp 110-12)
Germanium gamma counter, 19: 44473 (ZFK-PHA-12, pp 64-5)
Interaction of heavy fission particles with semiconductor detectors, 19: 44481 (ZFK-PHA-12, pp 149-53)
Ion-drift investigations of lithium in p-silicon, 19: 44001 (ZFK-PHA-12, pp 40-9)
Low-noise preamplifier for semiconductor detectors with improved constancy, 19: 44483 (ZFK-PHA-12, pp 172-88)
Method for production of silicon spectrometric detectors with wide range of sensitivity, 19: 44470 (ZFK-PHA-12, pp 25-9)
Monitor for reading of d/p ratios in the cyclotron beam, 19: 44482 (ZFK-PHA-12, pp 154-62)
Neutron spectroscopy with semiconductor detectors, 19: 44478 (ZFK-PHA-12, pp 133-9)
Particle discrimination with semiconductor detectors, 19: 44475 (ZFK-PHA-12, pp 84-97)
Preparation of large-surface p-n barrier-layer elements by lithium diffusion in p-silicon, 19: 44000 (ZFK-PHA-12, pp 33-9)
Semiconductor detectors with uranium salts for absolute measurement of thermal neutron beams, 19: 44479 (ZFK-PHA-12, pp 140-3)
Semiconductor detector for detection of thermal neutrons in conditions of intense pulsed γ radiation, 19: 44480 (ZFK-PHA-12, pp 144-6)
Silicon spectrometric detectors with wide range of sensitivity, 19: 44472 (ZFK-PHA-12, pp 52-63)
Standardization of semiconductor detectors, 19: 44474 (ZFK-PHA-12, pp 66-9)
Study of reactions $^{18}O(p,\alpha)^{15}N$ and $^{11}B(p,\alpha)^{8}Be$ using semiconductor counters, 19: 45291 (ZFK-PHA-12, pp 117-22)
Suitability of sensitive time-pulse height convertor for semiconductor detectors, 19: 44488 (ZFK-PHA-12, pp 215-18)
Surface-barrier silicon detectors with guard rings and possibility of their utilization, 19: 44469 (ZFK-PHA-12, pp 16-24)
Technology of manufacture of p-n junctions by means of diffusion of phosphorus in silicon, 19: 43999 (ZFK-PHA-12, pp 7-9)
Theoretical and experimental studies on frequency behavior and the noise of transistorized charged amplifiers, 19: 44487 (ZFK-PHA-12, pp

206-14)
Use of silicon surface-barrier detectors compensated by lithium for measurements of energies of protons and deuterons up to energies of 13 Mev, 19: 44471 (ZFK-PHA-12, pp 30-2)

Utilization of semiconductor detectors in polarization experiments, 19: 44477 (ZFK-PHA-12, pp 126-32)
Variant scheme of fast coincidences for low-amplitude pulses, 19: 44486 (ZFK-PHA-12, pp 201-5)

PERSONAL AUTHOR INDEX

Each entry after an author's name is a shortened version of the title of the report or article, followed by the *NSA* volume and abstract number. Report numbers are given in parentheses.

The phrase "Progress report" is abbreviated as "Prog. rpt.," permitting a more rapid and complete alphabetical arrangement of the titles without changing the location of the progress report titles in relation to the other titles.

Because of problems involving the mechanical preparation of this index, all accent marks are omitted. The following changes in spelling have been introduced to reduce some of the confusion which might result from omitting the accents:

Æ	becomes	ae
Ö		oe
ø		oe
Ü		ue (except in transliterated Chinese names)

A

ABBATUCCI, J.-S., Solid phantom with adaptable form and density permitting a dosimetry throughout its volume, 19: 44308

ABDUMALIKOV, A. A., New data on ^{135}Ce decay, 19: 45268 (JINR-P-2235)

ABDUMALIKOV, A. A., Spectra of conversion electrons of ^{133}Ce and ^{132}Ce isotopes, 19: 45269 (JINR-P-2236)

ABDURAZAKOV, A. A., New data on ^{135}Ce decay, 19: 45268 (JINR-P-2235)

ABDURAZAKOV, A. A., Spectra of conversion electrons of ^{133}Ce and ^{132}Ce isotopes, 19: 45269 (JINR-P-2236)

ABERS, E. S., Approximate one-trajectory exchange, 19: 45074

ABKIN, A. D., Low-temperature radiation polymerization of acrolein, 19: 44070

ABRAHAMS, C., Quality control of ^{90}Sr-containing food, 19: 43675 (UCD-472-112, pp 73-9)

ABRAHAMSEN, K., Nonlinear plasma wave interaction in an arc discharge, 19: 45419

ABRAMOVA, K. B., Magnetohydrodynamic instabilities in electrical explosion, 19: 44845

ABSON, W., Health physics instruments, AERE, 19: 44369 (AERE-R-4552)

ACERBI, E., State of construction of the relativistic cyclotron for protons at 45 Mev, 19: 44886

ACKERMAN, Norman B., Prevention of liver metastases by intravenous radioisotopes, 19: 43797

ACTON, Loren W., Thermal and non-thermal processes in solar flares, 19: 44931

ADAMS, G. E., Reactions of the hydroxyl radical. II., 19: 44090

ADDISON, C. C., Reactions of liquid sodium with transition-metal oxides. I., 19: 44021

ADITYA, P. K., Correlation between distortion in nuclear emulsion and successive differences used in multiple scattering measurements, 19: 44411 (CERN-65-4(Vol.II), pp VII-8)

AFTALION, Floris, Hydrolysis in acid medium of linear and cyclic acids. III., 19: 44011

AGLINTSEV, K. K., Spectral method of determination of doses from β-α emitters, 19: 44491 (CEA-tr-R-1866)

AHLBOM, S., Non-linear characteristics in high-frequency gas discharge, 19: 45420

AHMADIEH, A., Effect of size on plastic properties of aluminum single crystals, 19: 44705 (UCRL-11653)

AHNSTROEM, G., Tritium labeling of cells in vitro, 19: 43651

AINSWORTH, E. J., Comparative lethality responses of neutron- and x-irradiated dogs, 19: 43832

AJDACIC, Vladimir S., Prog. rpt. on absolute measurement of neutron fluxes inside reactor core, final, 1/63–1/65, 19: 44450 (IBK-120a)

AJURIA-GARZA, Sergio, Development of some high-speed chromatographic methods, 19: 44118 (UCRL-16015)

AJZENBERG-SELOVE, F., New excited state of ^{9}Li, 19: 45348

AKHMANOV, V. V., Device for developing pulsed magnetic fields up to 150 kG, 19: 44888

AKIMOV, Yu. K., Coincidences of pulses of semiconductor detectors, connected in delay line, 19: 44485 (ZFK-PHA-12, pp 196-200)

AKIMOV, Yu. K., Variant scheme of fast coincidences for low-amplitude pulses, 19: 44486 (ZFK-PHA-12, pp 201-5)

ALBERG, M., Nuclear emulsion spectrometry at low and intermediate neutron energies, 19: 44448 (HASL-162)

ALBERT, R. C., Neon-hydrogen bubble chambers, 19: 44375 (BNL-9425)

ALDRIDGE, J. P., Radiative lifetime of the first excited state of ^{41}Sc, 19: 45344

ALEKSANDROV, E. B., Optical orientation of atoms in a magnetic field perpendicular to the beam, 19: 44963

ALEKSANDROWICZ, Julian, Leukemias and environment, 19: 43828

ALEKSENKO, Yu. N., Studies on the use of organic coolant-moderators in nuclear reactors, 19: 45501 (IAE-611)

ALEXANDER, L. G., Molten salt converter reactor. Design study and power cost estimates for a 1000-Mwe station, 19: 45588 (ORNL-TM-1060)

ALEXANDER, Sidney, Safety fluoroscope with an alerting device of contrasting color surrounding the screen, 19: 44362

ALEXEFF, I., Properties of ionic sound waves, 19: 45404 (ORNL-P-1557)

ALFILLE, Lucien, Guide tubes for nuclear reactors, 19: 45517

AL-HINDAWI, A. Y., Effect of irradiation on function and survival of rat thyroid cells, 19: 43757

ALI, S., Excited state of $_{4}$Be^{9} and the Λ-N interaction, 19: 45367

ALISOVA, S. P., Phase diagram of the $TiCr_2$–$ZrCr_2$ system, 19: 44714

ALLAN, L. T., Chemical effects of γ radiation on organic systems. XI., 19: 44072

ALLAN, L. T., Research on organic radiation chemistry, 19: 44053 (AFML-TR-65-166)

ALLEN, F. R., ZADOC—two group, two dimensional fuel management program, 19: 45523 (AEEW-R-425)

ALLEN, H. F., Isotope production in a Savannah River reactor at flux levels above 10^{15} n/(cm^2)(sec), 19: 45639 (DP-999, pp 19-28)

ALLEN, H. L., Operating experience and improvements on the Princeton–Pennsylvania accelerator, 19: 44872 (PPAD-2137-565)

ALLEN, Philip W., Meteorology program at the Nevada Test Site, 19: 44774 (BNL-914, pp 65-8)

ALLES, W., U_{12}, unitarity and crossing, 19: 45075

ALLISON, Robert W. Jr., Prog. rpt. on Bevatron operation and development, 10–12/64, 19: 44874 (UCRL-16203)

ALPEN, E. L., Comparative lethality responses of neutron- and x-irradiated dogs, 19: 43832

ALSMILLER, R. G. Jr., Nuclear cascade in steel initiated by 10- and 19.2-Bev/c protons, 19: 45317

ALSOP, R. J. L., Concentration of cesium-137 in Australian milk during 1963, 19: 44309

ALTER, Harry, Production of hydrogen and helium in reactor fuel-cladding materials, 19: 44746 (NAA-SR-Memo-10626)

ALTIERI, J. V. Jr., Cavitation tests of coated RI-16 impeller, 19: 44197 (TIM-895)

ALVAREZ GONZALEZ, F., Direct-reading spectrochemical analysis of

nuclear graphite, 19: 43930 (JEN-145-DQ/I-46)
AMALDI, E., Polarization of recoil protons in e-p elastic scattering at 20 Fermi^{-2}, 19: 45058
AMARDEIL, P. J., Individual alarm dosimeters for work in or entry into radiation fields, 19: 44532
AMATI, D., U_{12}, unitarity and crossing, 19: 45075
AMLANI, A., Sealing factors—their measurement and use in design of vacuum gasket seals, 19: 44135 (IA-1033)
AMIRKANOVA, I. B., Relative difference of vapor pressure in $^{11}BF_3$–$^{10}BF_3$, 19: 44575
AMMANN, P. R., Chemical reactions during rapid quenching of O_2–N_2 mixtures from very high temperatures, 19: 44041
AMORETTY, S., Neutron-^{238}U nuclear interaction in the 0.002 to 30 kev energy region, 19: 45292 (BNL-tr-16)
AMORETTY, S., Rate of spontaneous and radiation-induced chromosome re-arrangements in medulla ossium of mice of different age, 19: 43729 (BNL-tr-12)
AMORETTY, Stephen, Possibility of determining kinematic characteristics of particles in spark chamber employing multiple scattering and additional sparks, 19: 44490 (BNL-tr-1)
AMOROSI, A., Fast flux test facility, 19: 45670 (APDA-174, pp 74-6)
AMPHLETT, C. B., Applications of radioactive nuclides produced in reactors, 19: 44560
AMYOT, L., Pin-to-pin interactions in fuel clusters. I., 19: 45525 (EUR-2470.e)
ANABLE, Wallace E., Electron-beam melting of yttrium, 19: 44588 (BM-RI-6661)
ANAND, S., Measurement of Z dependence of elastic scattering cross section of γ rays, 19: 45327
ANAND, S. J. S., Strontium-90 content of food samples in India—data summary through 1963, 19: 44244 (AEET/AM/40)
ANANTHARAMAN, T. R., Effects of liquid quenching on the constitution and structure of silver–silicon and gold–silicon alloys, 19: 45696 (CALT-221-12)
ANDERS, Leslie R., Signals at $2\omega_2-\omega_1$ in nuclear magnetic double resonance, 19: 45307
ANDERSEN, A. C., Hematology report on beagles, 19: 43725 (UCD-472-112, pp 44-9)
ANDERSEN, A. C., Pathology report on beagles, 19: 43727 (UCD-472-112, pp 126-40)
ANDERSEN, A. C., Prog. rpt. on effects of Sr-90 ingestion on growth of beagle, annual, 1964, 19: 43644 (UCD-472-112)
ANDERSON, Albert D., Semi-annual effect appearing in satellite orbital decay data, 19: 45158 (NP-15424)
ANDERSON, E., Achievement of clean conditions in gas-cooled nuclear reactors, 19: 45608
ANDERSON, E. Walter, Asymmetry in angular distribution of neutrons from neon capture in spin 0 nuclei, 19: 45274 (NEVIS-136)
ANDERSON, J. L., Radiation damage to ionic crystals at low temperatures. I., 19: 44745 (LA-DC-6725)
ANDERSON, J. Robert, Performance of ion thrustors and systems for satellite control, 19: 44227
ANDERSON, K. A., Background events in photomultiplier tubes at high altitudes, 19: 44465 (UCRL-12020)
ANDERSON, R. F., Operating experience with the first Savannah River high flux charge, 19: 45643 (DP-999, pp 73-86)
ANDERSON, R. P., Ion exchange removal of ^{90}Sr from biologic wastes, 19: 45692 (UCD-472-112, pp 141-7)
ANDERSON, R. P., The determination of zinc and iron in biologic materials by x-ray fluorescence spectrometry, 19: 43939 (UCD-472-112, pp 59-72)
ANDERSON, Robert E., Active tuberculosis in malignant disease of reticuloendothelial origin, Hiroshima, 1949–62, 19: 43710 (ABCC-16-64)
ANDERSON, W. W., Neodymium-ion bombarded CdS, 19: 44939
ANDERSSON, T. L., Experimental studies on assemblies 1 and 2 of the fast reactor FRO. I., 19: 45522 (AE-195)
ANDREJEFF, P. H., Device for high-temperature testing of tungsten wires, 19: 44213
ANDRYUSHIN, I. A., Expediency of radiometric uranium ore dressing and the choice of the optimum level of separation during dressing, 19: 44275
ANGELL, James K., Importance of the tetroon to meso-scale meteorology, 19: 44783 (BNL-914, pp 107-9)
ANNONI, H., Semiautomatic apparatus for measurement of track lengths. Semiautomation in corpuscular photography, 19: 44417 (CERN-65-4 (Vol.II), pp VII1-14)
ANTOLIN, Jacqueline, Electron microscope observation of single-crystal beryllium thin foils, 19: 44683 (CEA-R-2789)
ANTONESCU, Elena, Some compounds of samarium, gadolinium, and erbium with various organic acids, 19: 44028
ANTROPOV, L., Polarization during ion redox processes. Ions of Fe, Tl, Ce, and V, 19: 44002 (AEC-tr-6572)
APOSTOL, A., Preparation and characteristics of a very concentrated nuclear emulsion, 19: 44396 (CERN-65-4(Vol.II), pp III1-4)
APPLEBY, James F., Meteorological program at Fort Huachuca, 19: 44777 (BNL-914, pp 85-90)
ARAKI, Chiroru, Effect of γ-radiation on porphyrin-metal complexes. I., 19: 44087
ARANOVITCH, E., Study of circumferential and axial temperature perturbations in a cylindrical fuel element canning (mathematical and rheonalogical methods, 19: 45543 (EUR-2480.f)
ARCHAMBAULT, Y., Electron distribution and density function in an ionized MHD conversion gas, 19: 44982
ARCHER, Victor E., Radiation as cause of lung cancer among uranium miners, 19: 44314
ARDACHEV, I. V., Comparative hypersensitization with triethanolamine and with other alkaline sensitizers for nuclear emulsions, 19: 44406 (CERN-65-4(Vol.II), pp IV41-5)
ARDACHEV, I. V., Sensitivity centers of nuclear emulsions sensitized successfully with gold and triethanolamine, 19: 44395 (CERN-65-4 (Vol.II), pp II75-87)
AREF'EV, A. V., Redesign of IAE linear electron accelerator, 19: 44860 (IAE-614)
ARIFKHANOV, V. R., Polarization in n-α scattering at E_n = 25, 28, and 34 Mev, 19: 45259 (IAE-834)
ARMSTRONG, W. A., LET-independent dosimeter based on chemiluminescent determination of H_2O_2, 19: 44067
ARNAUD, Y., Biological dosimetry after exposure to a high flux of thermal and fast neutrons, 19: 44322
ARNOLD, Abraham, Wind profile, 19: 44794 (BNL-914, pp 158-60)
ARNOLD, James S., Growth curve for mammary fibroadenoma in female rat, 19: 43649 (UCRL-16177)
ARNOLD, W. H. Jr., NERVA progress report, 19: 45665
ARNOLDY, R. L., Response of ion chambers in free space to long-term cosmic-ray variation from 1960 to 1965, 19: 44966
ARRAGON, Philippe, Sealed coupling for an electrical heating conductor with coaxial sheath, 19: 44164 (CEA-R-2755)
ARRISON, Robert A. Jr., Apparatus for producing visual images of x-rayed objects, 19: 44363
ARTANDI, Charles, Production experiences with radiation sterilization, 19: 44559
ARTHUR, Jon C. Jr., Post-irradiation grafted vinyl cellulose copolymers, 19: 44094
ASARI, Tomiya, Japanese dietary habits and the fallout problem. II., 19: 44264
ASARI, Tomiya, Radioactive contamination of milk in Japan (1961–1963), 19: 44268
ASCHBACHER, P. W., Total body water estimations in dairy cattle using tritiated water, 19: 43694
ASHBY, D. E. T. F., Quasi-steady-state pulsed plasma thrustors, 19: 45441
ASHMORE, A., Measurements of the A and R parameters in proton-proton scattering at 47.8 and 27.6 Mev, 19: 45319
ATCHISON, G. J., Space charge in plastics produced by 2-Mev electrons, 19: 44096
ATKINS, Thomas, Water tunnel with moving walls, 19: 45722 (UCRL-16188)
ATKINSON, G. F., 10,000-hour temperature test of fission-counter preamplifiers, 19: 44462 (TIM-922)
ATTWENGER, W., Express method for electronic pulse counters, 19: 44351 (SGAE-E-4/1965)
AUBERT, Michel, Refueling device for nuclear reactors, 19: 45512
AUBERT-CHEVALLIER, Robert, Sealed coupling for an electrical heating conductor with coaxial sheath, 19: 44164 (CEA-R-2755)
AULT, G. Marvin, Refractory metals sheet rolling program, 19: 44647
AULT, John Douglas, Improvements in or relating to illumination of leveling bubbles, 19: 44567
AUPECLE, P., Thorotrast disease concerning one observation, 19: 43738
AUSTIN, B., Design of proton linear accelerators for energies up to 200 Mev, 19: 44867 (MURA-713)
AVERKO-ANTONOVICH, I. N., Solubility of lithium bromate and of its hydrates, 19: 44003 (BNL-tr-5)
AVRAMENKO, B. I., Sterility of male plants due to penetrating radiation, 19: 43767
AWSCHALOM, M., Operating experience and improvements on the Princeton–Pennsylvania accelerator, 19: 44872 (PPAD-2137-565)

B

BAEHR, Werner, Method for separation of nuclear fuels, 19: 43982
BAGLIN, J. E., Phototritons from ^{6}Li, 19: 45374
BAGNO, O., Chemical dosimetry of high-energy particles, 19: 44093
BAILEY, C. E., Temperature coefficients of reactivity in the Savannah River high flux charge, 19: 45642 (DP-999, pp 65-71)
BAILEY, Carl L., Prog. rpt. on energy and angular distribution of electrons

ejected from H and He by 100- to 300-Kev protons, 4/63–7/65, 19: 44933 (COO-1277-12)
BAIXERAS, J., Analysis of a magnetization curve of superconductor of the second kind, 19: 45200
BAKER, D. Jr., Engineering aspects of the Savannah River high flux charge, 19: 45641 (DP-999, pp 43-64)
BAKER, T. W., Improved furnace assembly for high-temperature diffractometers, 19: 44340 (AERE-M-1361)
BALARIN, M., Temperature dependence of radiation saturation in SiC, 19: 44759
BALATS, M. Ya., Intensity of nonradiative transitions in Ta and ^{239}Pu mesic atoms, 19: 44962
BALDESCHWIELER, John D., Signals at $2\omega_2-\omega_1$ in nuclear magnetic double resonance, 19: 45307
BALDETTI, S., Outlook for use of nuclear energy for production of heat at low temperature, 19: 45618
BALDOCK, P. J., Improved furnace assembly for high-temperature diffractometers, 19: 44340 (AERE-M-1361)
BALENT, Ralph, Epithermal thorium power-breeder nuclear reactor, 19: 45629
BALIAN, R., Influence of zero sound on the thermodynamics of ^{3}He, 19: 45204
BALL, G. L., Compilation of Fermi experience, 19: 45562 (APDA-174, pp 71-3)
BALLINGER, J. G., Alpha radiation hygroneter. III., 19: 44338 (AD-608503)
BALLY, D., Three-axes spectrometer of Institute for Atomic Physics, Bucharest, 19: 44527
BALTAY, C., Annihilations of antiprotons in hydrogen at rest into two mesons, 19: 45122
BALTAY, C., Test of charge-conjugation invariance in $\bar{p}p$ annihilations at rest, 19: 45124
BANAS, J., Contribution to the determination of ^{131}I by an extraction method, 19: 43953
BANSLABEN, A., Alpha-gamma facility for metallurgical examinations, 19: 44163 (BNL-9502)
BARACCA, A., Multiple poles and decay laws, 19: 45070
BARAD, Morton L., Microneteorology, 19: 44797 (BNL-914, pp 173-4)
BARASH, N., Annihilations of antiprotons in hydrogen at rest into two mesons, 19: 45122
BARASH, N., Test of charge-conjugation invariance in $\bar{p}p$ annihilations at rest, 19: 45124
BARASHKIN, M. A., Isotope gamma irradiation unit UKP-30000, 19: 44171
BARCUS, J. R., Storage of radioactive debris in the polar vortex, 19: 44260
BAREYRE, P., Pion-nucleon phase shift analysis below 1 Bev, 19: 45100
BARINOVA, E. S., Comparative hypersensitization with triethanolamine and with other alkaline sensitizers for nuclear emulsions, 19: 44406 (CERN-65-4(Vol.II), pp IV41-5)
BARINOVA, E. S., Sensitivity centers of nuclear emulsions sensitized successfully with gold and triethanolamine, 19: 44395 (CERN-65-4 (Vol.II), pp II75-87)
BARISH, J., Nuclear cascade in steel initiated by 10- and 19.2 Bev/c protons, 19: 45317
BARKAS, Walter H., Artificial construction of particle tracks by a Monte Carlo method, 19: 44433 (CERN-65-4(Vol.II), pp IX44-7)
BARKER, J. F., 1400°F weldable sheet program, 19: 44699 (R63FPD33)
BARKER, M. G., Reactions of liquid sodium with transition-metal oxides. I., 19: 44021
BARKOV, L. M., Device for developing pulsed magnetic fields up to 150 kG, 19: 44888
BARON, H., Detection of criticality accidents, CEA, France, 19: 44321
BARON, M. J., Simultaneous vhf and uhf observations of the aurora at Fraserburgh, Scotland, 19: 45169
BARON, S., Why not single-purpose reactors for desalting, 19: 45634
BARR, William L., Investigation of plasma from an occluded gas, cold plasma source, 19: 45411 (UCRL-7935)
BARRY, G. H., Radar measurements of total cislunar electron content, 19: 45176
BARRY, R. F., Optimum core lattice parameters for the San Onofre nuclear generating station, 19: 45599 (WCAP-3269-49)
BARSCHALL, H. H., Analyzing power of neutrons for helium, 19: 45217 (COO-7-0063)
BARSHAY, S., Scattering of unstable particles by stable particles in strong interactions, 19: 45082
BARTHOUX, A., Detection of criticality accidents, CEA, France, 19: 44321
BARTKY, Charlotte Decker, Calculation of inelastic electron-molecule collision cross sections by classical methods, 19: 44947
BARTLIT, J. R., Further experimental study of H_2O-LH_2 heat exchangers, 19: 44186 (LA-DC-7148)
BARUFFA, A., European situation in the area of nuclear energy production, 19: 45610
BARUT, A. O., Mass spectrum from noncompact groups, 19: 45004 (IC/65/66)
BARYSHEVSKII, V. G., Passage of spin and spinless particles through matter, 19: 45013 (JINR-P-2230)
BARZ, H. W., Reaction $^{10}B(d,p_0)^{11}B$, 19: 45336
BARZELAY, Martin E., Continuum radiation from partially ionized argon, 19: 45453
BASHER, J. C., FLIC conversion codes, 19: 44579 (AEEW-R-439)
BASIULIS, A., Development of a reservoirless thermionic energy converter, 19: 44989
BASS, F. G., Quasilinear theory of weakly turbulent plasma with account of correlation of electric fields, 19: 45439
BATE, L. C., Use of activation analysis in determination of origin of opium, 19: 43937 (ORNL-TM-1263)
BATES, A. E. G., Description of the LITR reactor control and instrumentation systems, 19: 45680 (ORNL-TM-1190)
BATES, T. H., Metabolism of radioactive strontium in rats. I., 19: 43671 (PG-Report 662)
BATES, T. H., Metabolites considered to be of value in diagnosis of exposure to radiation, 19: 43852
BATES, T. H., Removal of radionuclides from the body, 19: 43700
BATUECAS, T., Water treatment process in JEN-1 research reactor, 19: 45678 (JEN-149-DQ/I-50)
BAUER, Ernest, Calculation of inelastic electron-molecule collision cross sections by classical methods, 19: 44947
BAUGHMAN, George W., Hot bearing detector, 19: 44568
BAUMANN, G., Semiautomatic apparatus for measurement of track lengths. Semiautomation in corpuscular photography, 19: 44417 (CERN-65-4 (Vol.II), pp VIII-14)
BAUMANN, N. P., Temperature coefficients of reactivity in the Savannah River high flux charge, 19: 45642 (DP-999, pp 65-71)
BAUN, William L., Effect of chemical combination on soft x-ray K emission bands of nitrogen and carbon, 19: 44944
BAYBARZ, R. D., Behavior of the transplutonium elements in solvent extraction systems, 19: 44115 (ORNL-P-1577)
BAYUKOV, Y. D., Possibility of determining kinematic characteristics of particles in spark chamber employing multiple scattering and additional sparks, 19: 44490 (BNL-tr-1)
BAZIN, M., Design of fast-cycling liquid-H_2 bubble chamber, 19: 44459 (PPAD-2137-561)
BEALL, R. A., Electron-beam melting of yttrium, 19: 44588 (BM-RI-6661)
BEALL, R. A., Studies of high-current metallic arcs, 19: 44608 (TID-22125)
BEARD, David B., Magnetohydrodynamic shocks of geophysical interest, 19: 45165
BEARD, S. J., Status of fission product recovery at Hanford, 19: 45690 (RL-SA-40)
BEAU, P., Attempt to assess the dose received by bone marrow on exposure to neutron flux, 19: 43854
BEAUMARIAGE, M. L., Hair dysplasia induced by x rays in mice under different irradiation conditions, 19: 43833
BECERRO RUIZ, E., Direct-reading spectrochemical analysis of nuclear graphite, 19: 43930 (JEN-145-DQ/I-46)
BECKER, K., New dosimeter glass with improved properties, 19: 44509
BECKER, R. L., Nuclear ground state properties of ^{18}O by an extension of Eden-Emery method, 19: 45350
BEELER, J. R. Jr., Diffusion theory for homogeneous and heterogeneous reactors, 19: 45531 (N64-29786)
BEELEY, Raymond J., Epithermal thorium power-breeder nuclear reactor, 19: 45629
BEEVERS, Harry, Prog. rpt. on carbohydrate catabolism in plants, 7/65, 19: 45697 (COO-330-11)
BEGUN, G. M., Infrared and Raman spectra and valence force constants of IOF_5, 19: 44019
BEHROOZI-TOOSI, Foreidoon, Loading of emulsions with diamonds and polystyrene for experiments with stopping K particles, 19: 44398 (CERN-65-4(Vol.II), pp III12-16)
BEIER, H.-J., Observation of undulations of the total elastic scattering cross section for the scattering of He atomic beams in Xe, Kr, and Ar, 19: 44957
BEIQUE, R. A., Effect of filtration in diagnostic radiology, 19: 43901
BELANOVA, T. S., Absolute measurements of 24-kev neutron absorption cross section, 19: 45230
BELIAEV, Gunnar, Prestressed concrete vessels. II., 19: 45506
BELL, J., Wide-range high-resolution time-to-amplitude converter, 19: 44501
BELL, P. R., Ion cyclotron harmonic spectrum generated in an energetic ion plasma, 19: 45405 (ORNL-P-1576)
BELL, W. A., Isotopic contamination in electromagnetic separators, 19: 44573 (ORNL-P-515)
BELLETTINI, G., Measurement of π lifetime via the inverse decay

process, 19: 45360
BELOTE, T. A., Angular distributions from shell-model forbidden (d,p) transitions to spin 5/2 states in ^{43}Ca, ^{45}Ca, and ^{47}Ti, 19: 45323
BELOVITSKII, G. E., Further development of apparatus for measurements of particle tracks in photoemulsions by television method, 19: 44422 (CERN-65-4(Vol.II), pp VII39-42)
BELYAEV, V. B., Electromagnetic decay and electroproduction of 3/2+ resonances, 19: 45007 (JINR-E-2228)
BEM, P., Utilization of semiconductor detectors in polarization experiments, 19: 44477 (ZFK-PHA-12, pp 126-32)
BEMENT, A. L., Fast neutron flux characteristics of the ETR, G-7 hot water loop, 19: 45672 (BNWL-89)
BEMPORAD, C., Measurement of π lifetime via the inverse decay process, 19: 45360
BENENSON, E. B., Fringe effects in magnetogasdynamical converter, 19: 44840
BENESOVSKY, F., Investigations in transition metal–boron–aluminum, 19: 44719
BENEZECH, G., Establishment of neutron fluxes and doses after criticality accident, 19: 44323
BENEZECH, G., Tests of dosimetric system for criticality accidents at a fast-critical assembly, 19: 44334
BENINSON, D., Radiostrontium and strontium fixation in bones and children's diets, 19: 44250 (NP-15269)
BENNELLICK, E. J., Review of UK codes of practice for protection radiations, 19: 44282 (AHSB(RP)M-35)
BENNETT, S., Cesium-fueled MPD arc-jet engine performance, 19: 44230
BENOIT, J. W., External proton beam for the Princeton–Pennsylvania accelerator, 19: 44871 (PPAD-2137-556)
BENOT, M., Hough-Powell device for automatic analysis of plates of track chambers, 19: 44496
BEN SEDRINE, T., Sensitivity of normal and hypersensitive Ilford K5 emulsions at low temperatures, 19: 44405 (CERN-65-4(Vol.II), pp IV33-40)
BERENYI, D., Internal bremsstrahlung spectrum accompanying the electron capture process of ^{36}Cl close to the end-point energy, 19: 45345
BEREZIN, V. M., Measurement of the absolute value of the $K_1^0 - K_2^0$ mass difference, 19: 45099
BERGER, G.-B., Biological indicators to evaluate radioactive damage, 19: 43753
BERGLES, A. E., Prog. rpt. on boiling flow regimes and critical heat flux, 3/6–6/15/65, 19: 44193 (NYO-3304-5)
BERGMAN, C., Decay of ^{56}Co, 19: 45295
BERGMAN, O., Decay of ^{56}Co, 19: 45295
BERGMANN, C. A., Effect of low cobalt impurity stainless steel on coolant activity of pressurized water reactors, 19: 45495 (WAPD-T-1653)
BERGQVIST, I., Neutron resonance capture in 2s-1d shell nuclei, 19: 45356
BERGSTRESSER, K. S., Determination of trace amounts of oxygen added to metallic sodium, 19: 43932 (LA-3343)
BERGWALL, Staffan, Ohlin structure near quantum limit of the continuous x-ray spectrum, 19: 44940
BERKOVICH, I. B., Registration of α-particle stars produced by radioactive nuclei and time discrimination of α-particle tracks in nuclear emulsions, 19: 44425 (CERN-65-4(Vol.II), pp VIII17-26)
BERKOWITZ, J., Mass spectrometric studies of laser-produced graphite jet, 19: 44803 (ANL-6877, pp 21-7)
BERLYN, Graeme P., Prog. rpt. on embryogenesis and histogenesis in Pinus lambertiana, 4/65, 19: 43643 (TID-22143)
BERNARD, Yvette, Radioprotective activity of nitrogenous heterocyclic compounds derived from imidazole and benzimidazole, 19: 43863
BERNARDO, K., Tensor force in the nucleus ^{18}F, 19: 45370
BERNICK, Sol, Response of liver to target irradiation, 19: 43735
BERNSTEIN, Abram B., Turbulence characteristics near the ground and sonic anemometry, 19: 44772 (BNL-914, pp 51-4)
BERNSTEIN, Arthur B., Temperature profiles, 19: 44795 (BNL-914, pp 161-2)
BERNSTEIN, E., Forced convection boiling potassium heat transfer data, 19: 44195 (TID-21256)
BERSIN, Richard L., An SO_2 monitor for air pollution studies: design of the instrument and field testing, 19: 44458 (NYO-2767)
BERTINOV, A. I., Profiling channels for flows of ionized gases in transverse magnetic field, 19: 44838
BETHKE, G. W., Cyclotron resonance thrustor design and diagnostics techniques, 19: 44229
BETHKE, George W., Prog. rpt. on cyclotron resonance propulsion system, 7/65, 19: 44223 (NP-15438)
BETTINGER, Richard T., Prog. rpt. on probe system for upper atmosphere plasmas, 4/59–9/62, 19: 45155 (AD-609015)
BEUSCH, R., Temperature-coefficient of SAPHIR, 19: 45673 (EIR-85)
BEVACQUA, V., Radioiodine metabolism in patients affected by a simple sporadic goiter, 19: 43691
BEYNON, J. C., High current density thrustor experiments, 19: 44226
BEYSTER, J. R., Repetitively pulsed accelerator boosters, 19: 45674 (GA-6168)
BEZMALTERNYKH, S. A., Production of ^{28}Al during irradiation of Mg with 20-Mev deuterons, 19: 44099
BEZMATERNYH, A. S., Separation of ^{22}Na from magnesium target irradiated with deuterons, 19: 44100
BHANOT, V. B., Energy levels of ^{92}Mo with soft core potential, 19: 45311
BHAT, K. Venkatramana, Potential antiradiation compounds. II., 19: 43868
BIALYNICKA-BIRULA, Z., Fourth-order renormalization constants in quantum electrodynamics, 19: 45136
BIEL, W., Crystal effects in the scattering of neutrons with energy from 30 to 1000 ev, 19: 45489
BIERLY, Eugene W., Conference on AEC meteorological activities, May 19–22, 1964, 19: 44761 (BNL-914)
BIGGERSTAFF, J. A., Neutron resonance capture in 2s-1d shell nuclei, 19: 45356
BIJWAARD, G., Prog. rpt. on two-phase flow, 4–6/65, 19: 44185 (GEAP-4910)
BIKERMAN, Michael, Geological and geochemical studies of the Roskruge Range, Pima County, Arizona, 19: 44236 (TID-22086)
BILENKII, S. M., Determination of parity in reactions induced by γ quanta, 19: 45010 (JINR-E-2259)
BILENKII, S. M., Parity test for Ω^- using polarized hydrogen target, 19: 45101
BILLEN, Daniel, X-ray-induced perturbations in replication of bacterial chromosome, 19: 43741
BILLINGS, M. P., Computational methods for space radiation shielding analysis, 19: 45463 (NP-15425)
BILWES-GIRADIN, L., Latensification of the latent image in ionographic emulsions, 19: 44391 (CERN-65-4(Vol.II), pp II29-42)
BILWES-GIRARDIN, L., Decoration of tracks of charged particles in silver chloride monocrystals, 19: 44386 (CERN-65-4(Vol.II), pp I21-5)
BILWES-GIRARDIN, L., Utilization of the electron microscope with the purpose of the observation of tracks in ionographic emulsions, 19: 44426 (CERN-65-4(Vol.II), pp VIII27-33)
BINNIE, D. M., Measurement of branching ratio for decay $\omega^0 \rightarrow e^+ + e^-$, 19: 45102
BIONDI, L., Outlook for use of nuclear energy for production of heat at low temperature, 19: 45618
BIRO, Ya., Semiconductor detectors with uranium salts for absolute measurement of thermal neutron beams, 19: 44479 (ZFK-PHA-12, pp 140-3)
BIRSAN, I., Three-axes spectrometer of Institute for Atomic Physics, Bucharest, 19: 44527
BISERTE, Gerard, Combination of radioactive gamma aminobutyric acid in the cerebral tissue of the rat, 19: 43690
BISWAS, P. K., Splitting of electromagnetic spectrum by gravitational fields. I., 19: 45140
BISWAS, Sudamoy, Protective effects of chemicals on radiation induced damages in seed-treated crop plants, 19: 43877
BISZTRAY-BALKU, Sandor, Contemporary radiation protection in x-ray laboratories, 19: 43909
BJELDANES, M. N., Prog. rpt. on Pathfinder power plant operations, 3–12/64, 19: 45593 (TID-22168)
BJORKLAND, J. A., Experimental observations of electric quadrupole effects in the muonic spectra of ^{235}U, ^{181}Ta, and ^{239}Pu, 19: 45326
BLACK, Neville A., Linear pinch driven by a high-current pulse-forming network, 19: 45442
BLACKBURN, G., Myxedema after x-ray therapy to the neck, 19: 43890
BLACKSHEAR, P. L. Jr., Factors influencing the performance of fast-response, transpiration-cooled, high temperature probe, 19: 44204
BLAKE, Leslie Reginald, Nuclear reactor fuel elements, 19: 45553
BLANC, Rene, Preparation of thin VYNS films, 19: 44590 (CEA-R-2803)
BLANCHARD, Richard L., Ratios of ^{234}U/^{238}U in coastal marine waters and calcium carbonates, 19: 44263
BLANKENSHIP, Victor D., Theory of electrostatic double probe comprised of two parallel plates, 19: 45452
BLEAZARD, John Malcolm Bailey, Improvements relating to chemical extraction processes, 19: 44127
BLINC, R., Nuclear spin relaxation by fixed damage centers in irradiated $NaH_3(SeO_3)_2$, 19: 45477 (NIJS-R-444)
BLISS, P., Status of instrument development for the SNAP-50 reactor test program, 19: 44348 (PWAC-473)
BLIXT, Stig, Induced mutations in peas. VI., 19: 43732
BLIXT, Stig, Induced mutations in peas. V., 19: 43734
BLOCK, F. G., Development of a reservoirless thermionic energy converter, 19: 44989
BLOMEYER, Walter, Method for the production of Al–U alloys, 19: 44664
BLOOMFIELD, Donald E., Design of a chop and leach reprocessing plant, 19: 44126

BLOQUEL, J., Solid phantom with adaptable form and density permitting a dosimetry throughout its volume, 19: 44308

BLOUIN, Florise A., Post-irradiation grafted vinyl cellulose copolymers, 19: 44094

BLUE, E., Thermionic converter operating with a high temperature collector, 19: 44988

BLUMBERG, B., Economics of a 47,000-dwt tanker, 19: 45657 (TID-22088)

BLUMENFELD, H., Design of fast-cycling liquid-H_2 bubble chamber, 19: 44459 (PPAD-2137-561)

BLUMENTHAL, Ralph Barthold, Wide-angle electron pair production, 19: 45256 (HUX-2752-4)

BLUMKIN, S., Separation of potassium isotopes by molecular distillation, 19: 43931 (K-1650)

BOAG, J. W., Reactions of the hydroxyl radical. II., 19: 44090

BOBIKOV, R. S., Device for developing pulsed magnetic fields up to 150 kG, 19: 44838

BOCANCEA, D., Complications in the urinary organs resulting from uterine carcinoma and its treatment, 19: 43921

BOCCI, V., Physico-chemical and biological alterations induced by γ irradiation of ^{131}I-labeled rabbit serum γ-globulin, 19: 43686

BOCHAROV, Yu. S., Rate of spontaneous and radiation-induced chromosome re-arrangements in medulla ossium of mice of different age, 19: 43729 (BNL-tr-12)

BOCKELMAN, Charles K., Abstracts of computer codes. A compilation of computer codes useful in nuclear structure physics, 19: 45251 (BNL-9108)

BODINE, J. E., Second-cycle AIROX reprocessing and pellet refabricating of highly irradiated UO_2, 19: 44114 (NAA-SR-11375)

BODMER, A. R., Excited state of $_4Be^9$ and the A-N interaction, 19: 45367

BOEDY, Z. T., Transmission of monoenergetic electron beams through foils, 19: 44818

BOEGLY, W. J. Jr., Demonstration of disposal of high-level radioactive solids in salt, 19: 45689 (ORNL-P-1568)

BOGATYREV, A. V., Evaluation of the radioprotective efficacy of mexamine, 19: 43864

BOGNER, Guenther, Superconductive magnets, 19: 45212

BOGOLUBOV, N. N., Current-generated algebras and form factors, 19: 45011 (JINR-E-2294)

BOGOMOLOV, C. S., A developer for nuclear photography, 19: 44407 (CERN-65-4(Vol.II), pp VI-8)

BOGOMOLOV, C. S., Method for increasing the stability of sensitivity and latent image of nuclear emulsions, 19: 44390 (CERN-65-4(Vol.II)), pp II19-28)

BOGOMOLOV, C. S., New photographic materials for nuclear research, 19: 44379 (CERN-65-4(Vol.I), pp 29-41)

BOJTOR, I., Film dosimetry in radiodiagnosis to assess radiation burden to the population, 19: 43889

BOKOV, O. G., Broken symmetry U(12) and unitarity condition for the S matrix, 19: 45018 (JINR-P-2283)

BOKOVA, L. N., Ionization density in emulsions enriched with hydrogen, 19: 44435 (CERN-65-4(Vol.II), pp IX62-5)

BOLLER, H., Crystal structure of $Zr(Sn,Sb)_2$, 19: 44720

BOMBRE, Francois, Luminescence of CdS under electron bombardment, 19: 45478 (NP-15110)

BONCH-BRUEVICH, V. L., General properties of degenerate Fermi systems, 19: 44844

BONDARENKO, I. I., Possibility of using nuclear reactor in cosmic space for measuring cross sections of n-e scattering, 19: 45036 (NP-15476)

BONDAREV, V. V., Investigation of diffusion processes in brazing rhenium-coated titanium, 19: 44645 (JPRS-24761, pp 12-16)

BONDORF, J. P., Statistical fluctuations in the excitation functions from $^{12}C(^{12}C,\alpha)^{20}Ne$, 19: 45313

BONET-MAURY, P., Chemical dosimetry of high-energy particles, 19: 44093

BONETTI, A., Recent developments in field of cosmic physics, 19: 44969

BONFIELD, W., Dislocation substructure and deformation of polycrystalline Be, 19: 44726

BONHAM, R. A., Inelastic electron scattering from atoms at medium energies. II., 19: 44942

BONNER, B. E., Neutron-neutron scattering length by pion absorption in ^{3}He, 19: 45354

BONNYMAN, J., Concentration of cesium-137 in Australian milk during 1963, 19: 44309

BONOTTO, S., pH effect on γ sensitivity of Clostridium sporogenes, 19: 43865

BONSIGNORE, D., Uridine diphosphate glucose pyrophosphorylase activity in liver of irradiated rats, 19: 43747

BOOK, David L., Landau damping and growth of electrostatic modes with finite system effects, 19: 45389 (GA-6513)

BOOTHROYD, Milton Woodall, Improvements in or relating to nuclear fuel elements, 19: 44661

BORISOV, A. V., Relative difference of vapor pressure in $^{11}BF_3$–$^{10}BF_3$, 19: 44575

BORISOVA, N. I., Threshold of symmetrical fission of ^{237}Np, 19: 45258 (IAE-833)

BORLERA, Maria Lucca, Systems between niobium oxides and oxides of nickel and cobalt, 19: 44711

BORNSTEIN, N. S., Carburization of Nb–1 Zr alloy, 19: 44608 (TIM-927)

BOROM, Marcus Preston, Kinetics of dissolution and diffusion of oxides of iron in sodium disilicate glass, 19: 44611 (UCRL-16232)

BORSHCHEVSKII, Yu. A., Isotopic composition of the crystallization water of saline minerals, 19: 44240

BORST, Lyle B., Nuclear power reactor, 19: 45541

BORTONE, C., Application of nuclear energy for desalination, 19: 45619

BOSCO, B., Methods of analyticity and unitarity in nuclear physics: attempts of new low-energy phenomenology, 19: 45340

BOSTAN, Marcel, Complex salts with 5-nitrobarbituric acid. III., 19: 44027

BOTT-BODENHAUSEN, M., Device for measurements of multiple scattering and of track curvatures in nuclear emulsions, 19: 44418 (CERN-65-4 (Vol.II), pp VIII5-19)

BOUCHER, R. R., Transformations in UAl_4 and $PuAl_4$, 19: 44727

BOULANGER, Paul, Combination of radioactive gamma aminobutyric acid in the cerebral tissue of the rat, 19: 43690

BOURBIGOT, Yvelise, Multiple-purpose personal dosimeter, 19: 44536

BOURNE, J. G., Prog. rpt. on boiling flow regimes and critical heat flux, 3/6–6/15/65, 19: 44193 (NYO-3304-5)

BOUTIN, H., Studies of the solid and liquid phases of Hf, HCl, and HBr by slow neutron inelastic scattering, 19: 44038

BOUTIN, H., Study of low-frequency molecular motions in polyethylene and the n-paraffins by slow neutron inelastic scattering, 19: 44050

BOUZYKA, Jacek, Water reactivity effects in the Aana critical assembly, 19: 45529 (INR-600/IX-A/PR)

BOWEN, F., Diagnostic studies in a Hall accelerator at low exhaust pressure, 19: 45446

BOWERSOX, D. F., Solubilities of selected elements in liquid plutonium. VI. Rhenium, 19: 44688 (LA-3359)

BOWES, William A., Reconnaissance for uranium in the Aisen Area, Aisen, Chile, 19: 44273 (RME-4557(Rev.))

BOWMAN, J. M., Case of double trisomy: trisomy No. 18 and triplo-z, 19: 43811

BOYD, R., Polarization of 39-Mev protons elastically scattered from ^{58}Ni and ^{60}Ni, 19: 45378

BOZOKI, G., Multiple scattering constant in emulsion at great cell length, 19: 44431 (CERN-65-4(Vol.II), pp IX32-40)

BRAAMS, C. M., Composition of noble gas ion beams produced with a duoplasmatron, 19: 45385 (D1-82-0437)

BRAAMS, C. M., Production of dense beams of low-energy ions, 19: 45384 (D1-82-0436)

BRABSON, G. D., Uv absorption spectrum of trapped S_2, 19: 45480 (UCRL-10771)

BRABY, L. A., Measurements of radioactivity in Alaskan natives in 1964, 19: 44289 (HW-SA-3750)

BRACCINI, P. L., Measurement of π lifetime via the inverse decay process, 19: 45360

BRADSHAW, R. L., Demonstration of disposal of high-level radioactive solids in salt, 19: 45689 (ORNL-P-1568)

BRAGA, C. Lloyd, Determination of carbon and hydrogen in hydrocarbons by neutron scattering, 19: 43968

BRALL, U., Photoproduction of mesons in hydrogen bubble chamber at energies up to 5.5 Bev, 19: 44999 (DESY-65/5)

BRANOVER, G. G., Results of measuring turbulent pulsations of velocity in flow of mercury in presence of transverse magnetic field, 19: 44827

BRAUCH, D. F., Computer studies of plasma boundaries and loss effects created by immersed and withdrawn neutralizers, 19: 45454

BRAUCH, D. F., Prog. rpt. on analysis of electron-ion mixing in ion engine, 11/64–1/65, 19: 44222 (NP-15068)

BRAUN, H., Semiautomatic apparatus for measurement of track lengths. Semiautomation in corpuscular photography, 19: 44417 (CERN-65-4 (Vol.II), pp VIII1-14)

BRAUN, T., Radiocoulometric titration using non-isotopic indicator in solid phase, 19: 43952

BRAUTIGAM, D. P., Decision order technique, 19: 45714 (SC-TM-65-349)

BRAYER, R. C., Prog. rpt. on burnable poison additions to UO_2, 10–12/64, 19: 44591(R) (CEND-3107-228)

BREAULT, Eugene A., Ion exchange resin separation and flame photometric determination of Na, K, Mg, Ca, and Sr, 19: 44122

BRECKENRIDGE, R. W. Jr., Efficient dewar for lithium-drifted germanium detectors, 19: 44511

BREDAEL, I., Transfer functions analyzer for Dragon reactor, 19: 45571 (EUR-2431. f)

BREDEL, V., Angular distribution for reaction $^{12}C(d,\alpha)^{10}B$ with a semiconductor detector, 19: 45289 (ZFK-PHA-12, pp 99-105)

BREEDING, K.J., Order code for the film scanners of Illiac III, 19: 44446 (COO-1018-1050)
BRENNAN, James G., Exchange magnetic moment in three-body nuclei. I., 19: 45332
BRENNAN, James G., Exchange magnetic moment in three-body nuclei. II., 19: 45333
BRESSAT, Rene, Preparation of uranium-based oxide catalysts, 19: 43987 (CEA-R-2817)
BRETON, Claude, Time evolution of discharges induced in gases by a laser, 19: 44821
BREUER, F., Evaluation of the absorbed dose to the skin, 19: 44328
BREUER, K., A semiautomatic device for analyzing tracks in nuclear emulsions, 19: 44419 (CERN-65-4(Vol.II), pp VII20-7)
BREWER, L., Bibliography on high-temperature chemistry and physics of gases and gas-condensed phase reactions, 19: 43993 (NP-15379)
BREWER, L., Uv absorption spectrum of trapped S_2, 19: 45480 (UCRL-10771)
BRIANCON, Chantal, Electron conversion spectrum emitted during the decay of ^{227}Th(RdAc) to ^{223}Ra(AcX), 19: 45306
BRICKA, M., Activation neutron spectrometer and its response to moderation, 19: 44537
BRICKA, M., Tests of dosimetric system for criticality accidents at a fast-critical assembly, 19: 44334
BRICKMAN, C., Pion-nucleon phase shift analysis below 1 Bev, 19: 45100
BRIDGES, B. A., Take-over--an unusual selection process in steady-state cultures of E. coli, 19: 43804
BRIDGES, C. E., Irradiated fuel element gamma scanning rig: Operation and instrumentation, 19: 44463 (TRG-Report-1005)
BRIDWELL, L., Time delays in K x-ray emission during thermal fission of ^{235}U, 19: 45294
BRIGGS, R. J., Experimental studies with the Astron facility, 19: 45413 (UCRL-12456)
BRINHALL, James E., Particle physics and nuclear decay. Cancellation of of photomultiplier gain drift following source intensity change, 19: 44374 (AROD-3347:6)
BROADHURST, J. H., Motion device for Moessbauer spectrometry, 19: 45316
BROCKMAN, P., Diagnostic studies in a Hall accelerator at low exhaust pressure, 19: 45446
BRODSKII, A. M., Studies on the use of organic coolant-moderators in nuclear reactors, 19: 45501 (IAE-611)
BROECKER, Wallace, Comparison of ^{230}Th and ^{14}C ages for carbonate materials from Lakes Lahontan and Bonneville, 19: 44271
BROMLEY, D. A., Nuclear physics: a status report, 19: 45372
BROOKES, G. R., Behavior of a wide-gap spark chamber when two particle tracks are present, 19: 44518
BROOKES, G. R., Deviation between spark and track in wide-gap spark chamber, 19: 44514
BROOKS, Harvey, Xenon-induced oscillations, 19: 45539
BROSZKIEWICZ, Roman, Radiation-induced reactions of oxidation and reduction of iron ions in aqueous solutions, 19: 44056 (INR-579/XVII/C)
BROUARD, Daniel, Refueling device for nuclear reactors, 19: 45512
BROUSAIDES, Frederick J., An SO_2 monitor for air pollution studies: design of the instrument and field testing, 19: 44458 (NYO-2767)
BROWMAN, E. G., Dynamics of LiH and LiD in inelastic scattering of cold neutrons, 19: 44732
BROWELL, R. W., Separation of potassium isotopes by molecular distillation, 19: 43931 (K-1650)
BROWN, A. C., Fate of ThO_2 injected into the pedal sinus of Bullia, 19: 43695
BROWN, D. G., Lactation and radionuclide metabolism responses of dairy cattle to lethal doses of γ and neutron radiation, 19: 43801
BROWN, D. P., Instrument for automatic regulation of inhaled aerosols, 19: 43668 (HW-SA-3618)
BROWN, G. A., Prog. rpt. on energy conversion, 3-5/65, 19: 44981 (NP-15435)
BROWN, John L., Coherent K* production in the K+d reaction at 2.3 Bev/c, 19: 45120
BROWN, Rosalind J., Fate of ThO_2 injected into the pedal sinus of Bullia, 19: 43695
BROWN, W. Lynn, Discrimination learning of mirrored cues by rhesus monkeys, 19: 43805
BROWN, W. Lynn, Effect of γ radiation upon operant water-reinforcement behavior, 19: 43808
BROWN, W. Lynn, Further evidence for excitatory properties of non-rewarded cues, 19: 43806
BROWN, W. Lynn, Radiation effects on food satiation in the rhesus monkey, 19: 43807
BROWN, W. O., Partition of certain mineral nutrients in colostomized laying pullet, 19: 43693
BROWNE, Phillip L., HASTI--a numerical calculation of two-dimensional Lagrangian hydrodynamics utilizing the concept of space-dependent time steps, 19: 45701 (LA-3324)
BROWNLEE, James L. Jr., Measurement and utilization of neutron-capture γ radiation, 19: 45375
BRUENGER, Friedrich W., Interactions of Pu(IV) with blood proteins, 19: 43705
BRUGGER, R. M., Proposal to investigate physical properties of samples under very high pressures by time-of-flight neutron diffraction methods, 19: 45476 (IDO-17106)
BRUNA, A., Detection of leakage in gas-distribution networks by means of radioactive tracers, 19: 44553 (EUR-2284.1)
BRUTOVSKY, M., Contribution to the determination of ^{131}I by an extraction method, 19: 43953
BUCHANAN, E. R., Measurement of fraction of tensile strain due to twinning in polycrystalline Zr at 77°K, 19: 44725
BUCHANAN, R. A., Energy levels of Pr^{3+} in LaF_3, 19: 45484
BUCHHOLD, T. A., Three-phase motor with superconductive bearings, 19: 45196
BUCHHOLTZ, Christiane, Irradiated supraesophageal ganglion of odonata larvae (calopteryx splendens haar), 19: 43849
BUCINA, I., High-dose ionizing radiation photographic dosimetry, 19: 44533
BUCK, K., The application of nuclear reactors and radioisotopes to underwater-vehicle propulsion, 19: 45662
BUCKLER, A. N., ODYSSEUS--two-group, two-dimensional fuel cycle computer program suitable for advanced gas-cooled reactors, 19: 45595 (TRG-Report-976)
BUCUR, Romulus V., Isotopic effects during voltametric oxidation with variable controlled potential of the palladium--hydrogen microelectrode in deuteric acid solutions, 19: 44022
BUDAGOV, Yu. A., Hydrodynamics of a resonance bubble chamber, 19: 44523
BUDBERG, P. B., Phase diagram of the $TiCr_2$--$ZrCr_2$ system, 19: 44714
BUECHNER, W. W., Stripping analysis of the ^{138}Ba(d,p)^{139}Ba reactions, 19: 45347
BUEHLER, Mauricio F., Synthesis of DL glycine-1-C-14 and DL alanine-1-C-14, 19: 44047 (NP-15268)
BUHLER, A., Measurements of muon depolarization in several materials, 19: 45080
BUHLER, A., Quenching of muon depolarization in several materials as function of externally applied magnetic fields, 19: 45079
BULL, Fred W., Governing factors in the formation of Cr_3O-type structures, 19: 44702 (TID-22200)
BULLIS, R. H., Prog. rpt. on collision probability of electrons and ions with alkali metal atoms, semiannual, 10/22/64-5/11/65, 19: 45399 (NASA-CR-54451)
BUNEMAN, O., Computer studies of plasma boundaries and lens effects created by immersed and withdrawn neutralizers, 19: 45454
BUNNEY, L. R., Half lives of ^{150}Eu and ^{157}Eu, 19: 45287 (USNRDL-TR-868)
BURAS, B., Interaction of heavy fission particles with semiconductor detectors, 19: 44481 (ZFK-PHA-12, pp 149-53)
BURDESE, Aurelio, Systems between niobium oxides and oxides of nickel and cobalt, 19: 44711
BURG, C., Permanent and transmissible modification of virulence of solid isologous tumor after x irradiation, 19: 43762
BURHOP, E. H. S., Location of tracks in nuclear emulsion with aid of spark chambers, 19: 44445 (CERN-65-4(Vol.II), pp X74-83)
BURIBAEV, S., New data on ^{138}Ce decay, 19: 45268 (JINR-P-2235)
BURKART, K., Hardening of thermal neutron spectra in water and boric acid solution, 19: 45226 (KFK-294)
BURKE, E. A., Ferrous ammonium sulfate-cupric chloride solutions for dosimetry of a kilocurie ^{60}Co source, 19: 44372 (AFCRL-65-470)
BURKE, T. G., Fabrication of calorimeter elements, 19: 44344 (K-L-1944)
BURLEY, E. L., Chemical engineering aspects of boiling water reactors, 19: 45624
BURNET, MacFarlane, Somatic mutation and chronic disease, 19: 43749
BUSKIRK, F. R., Emulsion grain density in the extreme relativistic region, 19: 44428 (CERN-65-4(Vol.II), pp IX9-13)
BUSSET, R., Comparative use of S-32 and Br-82 for determination of extracellular fluid volume, 19: 43898
BUSTAD, L. K., A selected list of references (1960--May 1965) on swine in biomedical research, 19: 43713 (BNWL-115)
BUSTARD, Thomas Stratton, Betas and bremsstrahlung from ^{90}Sr--^{90}Y, 19: 45284 (TID-22169)
BUSZA, W., Location of tracks in nuclear emulsion with aid of spark chambers, 19: 44445 (CERN-65-4(Vol.II), pp X74-83)
BUT, D. A., Profiling channels for flows of ionized gases in transverse magnetic field, 19: 44838
BUTCHER, B. R., Solution of precipitates in very dilute uranium--iron--aluminium alloys, 19: 44715

BUTTERWORTH, Ian, Coherent K* production in the K+d reaction at 2.3 Bev/c, 19: 45120
BUTTS, J. J., Width of heavy ion tracks in emulsion, 19: 44434 (CERN-65-4(Vol.II), pp IX48-61)
BYCHKOVSKAYA, I. B., Evaluation of the radioprotective efficacy of mexamine, 19: 43864

C

CAEN, J., Radiation effects on the functions and enzymatic potential of platelets. Annual report, 1963/64, 19: 43714 (EUR-2438.f)
CAHILL, J. A., Prog. rpt. on high-temperature inorganic chemistry, annual, 6/64–6/65, 19: 44701 (TID-22144)
CALDERA, P. G., Detection of leakage in gas-distribution networks by means of radioactive tracers, 19: 44553 (EUR-2284.1)
CALDWELL, D. O., Effect of peak broadening on structure in the region of the ρ^0 meson, 19: 45092
CALDWELL, F. W. Jr., Measurement of fraction of tensile strain due to twinning in polycrystalline Zr at 77°K, 19: 44725
CALIN, Gheorghe, Complications in the urinary organs resulting from uterine carcinoma and its treatment, 19: 43921
CALLAHAN, James L., Mixed antimony oxide–uranium oxide oxidation catalyst, 19: 44043
CALVERT, S., Strontium deposition in bone and teeth of beagle puppies, 19: 43676 (UCD-472-112, pp 80-5)
CAMERON, W. Wayne, CVTR—high pD tests, 19: 45568 (CVNA-238)
CAMION, P., Minimum number of inverters in an analog network, 19: 44343 (EUR-1918.f)
CAMNITZ, H. G., Faraday rotation and volume scattering, 19: 45182
CAMPBELL, Graham M., Statistical model calculations of high energy reactions, 19: 45057 (UCRL-16315)
CAMPLANI, A., Experience in test and use of Italian nuclear power plants, 19: 45616
CANDES, P., Detection of criticality accidents, CEA, France, 19: 44321
CANFIELD, E. H., High-energy solar neutrons. I., 19: 44902
CANFIELD, E. H., High-energy solar neutrons. II., 19: 44903
CANNON, Donald C., Migration of spleen cells into blood stream following antigen stimulation, 19: 43822
CANONICA, C., Uridine diphosphate glucose pyrophosphorylase acitivity in liver of irradiated rats, 19: 43747
CANOSA, Jose, Xenon-induced oscillations, 19: 45539
CANTALAMESSA, L., Radioiodine metabolism in patients affected by a simple sporadic goiter, 19: 43691
CAP, F., Thermodynamics of a MHD plasma with infinite electrical conductivity, 19: 45417
CAPET, Maurice, Time evolution of discharges induced in gases by a laser, 19: 44821
CAPLAN, Arnold I., Effect of Sr^{2+} on swelling and ATP-linked contraction of mitochondria, 19: 43688
CAPPEL, H. H., TRANS-FUGUE-1—digital code for transient two-phase flow and heat transfer, 19: 45494 (NAA-SR-11008)
CARAFOLI, Ernesto, Effect of Sr^{2+} on swelling and ATP-linked contraction of mitochondria, 19: 43688
CARBONARA, F., Photofission of U and Th between 300 and 1000 Mev, 19: 45329
CARERI, G., Fluids and superfluids, 19: 44842
CARLSON, C. E., Development of Cb–Zr–C alloys, 19: 44605 (PWAC-464)
CARLSON, C. E., Recovery and recrystallization of Nb and several Nb–Zr alloys, 19: 44698 (PWAC-465)
CARLSON, K. Douglas, Electronic ground state and wave functions for scandium monoxide, 19: 44020
CARLSON, O. N., Extrusion of clad and unclad yttrium for rod and tubing, 19: 44636 (IS-1031)
CARLSON, Paul, Meteorology program at Dugway Proving Ground, 19: 44778 (BNL-914, pp 91-Z)
CARLSTON, R. C., Crystallography of some transition metal molybdates, 19: 43991 (N64-26433)
CARNAHAN, C. L., Half lives of ^{156}Eu and ^{157}Eu, 19: 45287 (USNRDL-TR-868)
CARRAI, M., Uridine diphosphate glucose pyrophosphorylase activity in liver of irradiated rats, 19: 43747
CARREIRA, M., Determination of average molecular weights of organic reactor coolants. I., 19: 44045 (JEN-151-DQ/I-52)
CARREIRA, M., Determination of average molecular weights of organic reactor coolants. II., 19: 44046 (JEN-152-DQ/I-53)
CARROL, J., Residual magnetic moments of some elementary superconducting spheres, 19: 45195
CARROLL, A. S., S-wave π-σ final-state interactions in $\pi^- + p \to \pi^0 + n^0$, 19: 45089
CARSON, W. B., Long-period vlf emission pulsations, 19: 45171
CARTER, Arlen F., Method and apparatus for producting a plasma, 19: 45456
CARTER, G., Mechanism of thermal release of injected inert gas from tungsten, 19: 44954
CARTER, W. L., Molten salt converter reactor. Design study and power cost estimates for a 1000-Mwe station, 19: 45588 (ORNL-TM-1060)
CARTER, Wm. J., Free-ion and crystalline spectra of Pr(III), 19: 44943
CARTWRIGHT, H., Current nuclear situation in the United Kingdom, 19: 45613
CASE, J. M., Application of nuclear thermionics to undersea technology, 19: 44986
CASE, K. M., Singular eigenfunctions and plasma problems, 19: 45440
CASINI, R., Experience in designing nuclear section ofthe SENI installation, 19: 45617
CASNATI, E., Evaluation of the absorbed dose to the skin, 19: 44328
CASPERS, H. H., Energy levels of Pr^{3+} in LaF_3, 19: 45484
CASTIGLIONI, M., State of construction of the relativistic cyclotron for protons at 45 Mev, 19: 44886
CATALFAMO, Carmen R., Parametric performance analysis for interplanetary missions utilizing first-generation nuclear stages, 19: 45649 (N64-32637)
CATURA, R. C., Observation of vertex events in wide-gap spark chamber, 19: 44507
CAVAILLES, Paul, Spinor with two components. Intrinsic properties and properties of the indices, 19: 44583
CAVALLI-SFORZA, L. L., Prog. rpt. on mutation rates and mutational loads in man, annual, 9/64–8/65, 19: 43642 (NYO-2280-8)
CECH, R., Chronstographic separation of radiochemically pure ^{90}Y from the parent isotope ^{90}Sr, 19: 44120
CELENZA, Louis, Collective motion in finite many-particle systems. III., 19: 45364
CELNIK, J., Military Compact Reactor small source experiments, 19: 45575 (GMAD-3078-28)
CERCY, J., Activation neutron spectrometer and its response to moderation, 19: 44537
CERULLO, N., Outlook for use of nuclear energy for production of heat at low temperature, 19: 45618
CHADAN, K., Interpolation of wave function and the Jost functions in the energy plane, 19: 45143
CHAGNON, Pierre, Apparatus for continuous electrolytic regeneration of ion exchange resins, 19: 44130
CHAI, Ying-shih, Optical and spectral properties of rare earth oxides in inorganic glasses, 19: 44030
CHALMETON, Viscount, Time evolution of discharges induced in gases by a laser, 19: 44821
CHAMBERLAIN, Arthur C., Deposition [of fallout], 19: 44245 (BNL-914, pp 125-32)
CHAMBERLAIN, H. V., Paste concept for fast reactor blanket applications, 19: 45561 (APDA-172)
CHAMBERLAIN, H. V., Paste concept for fast reactor blanket applications, 19: 45499 (APDA-174, pp 10-24)
CHANDRASEKARAN, V. R., Strontium-90 content of food samples in India–data summary through 1963, 19: 44244 (AEET/AM/40)
CHANG, C. C., Inviscid model of the solar wind, 19: 44904
CHANG, Norman, Radiation response as aid in treatment of cervical cancer, 19: 43910
CHANG, Sin-yu, Stacking fault frequency in Ni–Mo alloys, 19: 44723
CHANG, Wen Yu., Elastic scattering of Λ hyperons on protons, 19: 45016 (JINR-P-2257)
CHANG, Y. Austin, Dilation contribution to the heat capacity of copper and alpha brass at elevated temperatures, 19: 45718 (UCRL-11662)
CHANTEURR, J., Biological dosimetry after exposure to a high flux of thermal and fast neutrons, 19: 44322
CHAPIRO, Adolphe, Graft polymerization utilizing ionizing radiation, 19: 44097
CHAPMAN, I. V., Metabolism of radioactive strontium in rats. I., 19: 43671 (PG-Report 662)
CHAPMAN, J. D., Interactions in type 316 stainless steel–NaK–Nb–1 Zr alloy system, 19: 44626 (TIM-896)
CHAPMAN, J. M., Variation of dose attenuation of two-legged concrete ducts with incident γ energy, 19: 45457 (AD-462614)
CHARRAULT, Jean-Claude, Tightness joint, 19: 44176
CHASE, C. E., Dielectric constant of ^{3}He in the critical region, 19: 45205
CHASSANY, Jean-Philippe, Radioprotection and decontamination operation on the central vibrating channels of the Reactor G 3, 19: 45565 (CEA-R-2781)
CHASSANY, Jean-Philippe, Radioactivity measurements inside pressure vessel of Reactor G 3 after 4 years operation, 19: 45566 (CEA-R-2785)
CHEBOTAREVA, L. D., Expediency of radiometric uranium ore dressing and the choice of the optimum level of separation during dressing, 19: 44275
CHEDIN, Paul, Preparation of thin VYNS films, 19: 44590 (CEA-R-2803)
CHEER, D. A., Rolling cast beryllium between 500 and 1000°C, 19: 44652

CHEISHVILI, O. D., Analog of d-c Josephson effect in He II, 19: 45202
CHEN, K. W., Observation of vertex events in wide-gap spark chamber, 19: 44507
CHEN, Kao-wei Wendell, Electron-proton scattering at high momentum transfers. II., 19: 45001 (HUX-2752-8)
CHEN, Ping Chien, Prog. rpt. on two-phase flow through apertures, final, 7/65, 19: 44196 (TID-22145)
CHENG, Dah Yu, Factors influencing the performance of fast-response, transpiration-cooled, high temperature probe, 19: 44204
CHENG, Hung, Regge poles in quantum electrodynamics with massive photons, 19: 45114
CHENG, Hwa-sheng, Role of exchangeable potassium and magnesium on cesium absorption on marine sediments, 19: 43964
CHERNOCK, W. P., Prog. rpt. on burnable poison additions to UO_2, 10–12/64, 19: 44591(R) (CEND-3107-228)
CHERNOPLEKOV, N. A., Cold neutron scattering by polyphenyls, 19: 45238
CHERNOPLEKOV, N. A., Dynamics of LiH and LiD in inelastic scattering of cold neutrons, 19: 44732
CHERNUKHIN, V. L., Multidimensional analyzer with a preliminary treatment of data and combined-type memory, 19: 44524
CHERNYAVSKII, M. M., Further development of apparatus for measurements of particle tracks in photoemulsions by television method, 19: 44422 (CERN-65-4(Vol.II), pp VIII39-42)
CHERNYSHEV, A. A., Semiconductor detector for detection of thermal neutrons in conditions of intense pulsed γ radiation, 19: 44480 (ZFK-PHA-12, pp 144-6)
CHEVALIER, P., Growth in the CBA mouse of J sarcoma irradiated in vitro, 19: 43763
CHIANG, Shao-Chiang, Elastic scattering of Λ hyperons on protons, 19: 45016 (JINR-P-2257)
CHIENG, Hai-Kung, Use of silicon surface-barrier detectors compensated by lithium for measurements of energies of protons and deuterons up to energies of 13 Mev, 19: 44471 (ZFK-PHA-12, pp 30-2)
CHILDS, Charles B., Radiation detection in large crystals of silver chloride, 19: 44378 (CERN-65-4(Vol.I), pp 1-15)
CHIRIKOV, B. V., Intensive electron beam focusing in an accelerator tube, 19: 44870 (NP-15388)
CHISTYAKOVA, T. I., Changes in concentration of nucleic acids in gonads of Leucaspius delineatus after exposure to uranium, 19: 43769
CHODIL, G., Background events in photomultiplier tubes at high altitudes, 19: 44465 (UCRL-12020)
CHOHAN, V. S., Scattering constant in nuclear emulsions, 19: 44429 (CERN-65-4(Vol.II), pp IX14-22)
CHONE, B., Method of ^{3}H-thymidine incorporation in fractionally irradiated bone marrow, 19: 43731
CHOUDHURY, S. Rai, Remark on compositeness criteria in the Lee model, 19: 45068
CHOW, J., Alpha-gamma facility for metallurgical examinations, 19: 44163 (BNL-9502)
CHOWNIK, Abraham, Possibilities of using ^{99m}Tc tracer instead of radioiodine in thyroid function investigations, 19: 43881 (NP-15271)
CHRISTENSEN, D., Engine operating problems in space. The space environment, 19: 44893 (NASA-CR-294)
CHRISTENSEN, Hilbert C., Radiolysis of aqueous benzene solutions in the presence of inorganic oxides, 19: 44051 (AE-192)
CHRISTENSEN, Hilbert C., Radiolysis of aqueous benzene solutions at higher temperatures, 19: 44052 (AE-193)
CHRISTIE, Robert S., Transmitting motion through a vacuum wall, 19: 44234 (MATT-345)
CHRISTOFILOS, N., Experimental studies with the Astron facility, 19: 45413 (UCRL-12456)
CHRISTOFILOS, N., Sources of artificial radiation belts, 19: 45159 (UCRL-14374)
CHRISTOPHEL, E., Semiautomatic apparatus for measurement of track lengths. Semiautomation in corpuscular photography, 19: 44417 (CERN-65-4(Vol.II), pp VIII1-14)
CHRISTOV, G., Influence of ionizing radiations on normal volutin and volutin induced by means of sulfonamides in certain bacteria, 19: 43759
CHU, Chung-fun, Extraction of microgram amounts of zirconium with n-benzoyl-n-phenylhydroxylamine, 19: 43972
CHU, F., Electron-beam treatment planning in inhomogeneous tissue, 19: 43916
CHUAN, Yu-chi, Catalytic activity of praseodymium oxide in dehydrogenation and dehydration of alcohols and dehydrogenation of tetralin, 19: 44023
CHUKREEV, F. E., Study of reactions $^{18}O(p,\alpha)^{15}N$ and $^{11}B(p,\alpha)^{8}Be$ using semiconductor counters, 19: 45291 (ZFK-PHA-12, pp 117-22)
CHUNG, Paul M., Theory of electrostatic double probe comprised of two parallel plates, 19: 45452
CHUPKA, W. A., Energy dependence of cross sections for collision-induced dissociation and endothermic ion-molecule reactions, 19: 44948
CHUPKA, W. A., Mass spectrometric studies of laser-produced graphite jet, 19: 44803 (ANL-6877, pp 21-7)
CHURIN, A. I., Current status of the problem of sea-water distillation, 19: 44153 (JPRS-31361)
CHURKIN, V. N., Radioactive fallout over the USSR area in 1963, 19: 44259
CHUSHKIN, P. I., Numerical solution of some problems of gas flows, 19: 44200 (SC-T-65-756)
CIER, Andre, Effect of γ rays on pyrimidine bases in aqueous solution. I., 19: 44064
CIERJACKS, S., Fast neutron spectrum measurements with a ^{6}Li semiconductor neutron spectrometer, 19: 44457 (NP-15475)
CIPPERLEY, F. V., Personnel monitoring practices at the National Testing Station, 19: 44335
CITTADINI, C., Hematoporphyrin and whole-body irradiation, 19: 43862
CITTADINI, G., Total-body x irradiation and subsequent administration in single or repeated dose of hematoporphyrin, 19: 43748
CLARK, Benton C., Radiation spectrometry in space: requirements for accurate dose determinations, 19: 43879
CLARK, Donald Eldon, Recoil chemistry of ^{11}C in liquid hydrocarbons, 19: 44057 (IS-T-23)
CLARK, G., Positions of three cosmic x-ray sources in Scorpio and Sagittarius, 19: 44968
CLARK, Willie E., Index to conferences relating to nuclear science, 19: 45716 (TID-4043(Rev.2))
CLARKSON, Jack E., Collective excitation of neutron-deficient Ba, Xe, and Ce isotopes: centrifugal stretching treatment of nuclei, 19: 45285 (UCRL-16040)
CLASS, C. M., Radiative lifetime of the first excited state of ^{41}Sc, 19: 45344
CLAWSON, L. G., Prog. rpt. on boiling flow regimes and critical heat flux, 3/6–6/15/65, 19: 44193 (NYO-3304-5)
CLAYTON, D. D., Nuclear gamma rays from supernova remnants, 19: 44930
CLEARY, R. E., The vapor pressure of lithium between 1307 and 1806°K, 19: 44703 (TIM-844)
CLEARY, R. E., Viscosity of lithium, 19: 44704 (TIM-849)
CLEEMPOEL, H., Experimental basis of quantitative interpretation of the renogram, 19: 43667 (EUR-1890.f)
CLEGG, A. B., S-wave π-π final-state interactions in $\pi^{-} + p \rightarrow \pi^{0} + n^{0}$, 19: 45089
CLERC, H. G., Photodisintegration of ^{4}He, 19: 45353
CLINE, D., Improved strip-sealed continuous rotation scattering chamber, 19: 44883
CLOSON, Jacques, Early effects of irradiations at low doses, 19: 43752
COBB, J. S., Hydraulic problems on BONUS reactor pressure control system, 19: 45603 (Y-1491)
COBB, R., Spark-chamber experiment on cosmic γ rays, 19: 44970
COCHO, G., Weak interactions and higher symmetries, 19: 45126
COCKERAM, D. J., SNAP-10A design, development, and flight test, 19: 45154
COCKING, E. C., High-efficiency liquid-scintillation counting of ^{14}C-labeled material in aqueous solution, 19: 43945
CODY, G. D., High-temperature critical current of vapor deposited Nb_3Sn, 19: 45213
COFER, J. A., Experimental stress analysis of attachment region of hemispherical shells with radially attached nozzles, 19: 44144 (TID-22134)
COFFEY, D. L., Experimental simulation of large, high field, superconducting magnet operation, 19: 45192 (ORNL-TM-1266)
COGEZ, Paul, Tightness joint, 19: 44176
COHEN, E., 100-Kv, 10-w heavy-particle thrustor, 19: 44231
COHENDY, Gerard, Radioprotection and decontamination operation on the central vibrating channels of the Reactor G 3, 19: 45565 (CEA-R-2781)
COHN, M. L., Effect of near-ultraviolet light on staphlococci and mycobacteria in droplet nuclei, 19: 43736
COHN, M. L., Effect of near-ultraviolet light on culture media, 19: 43737
COHN, Naomi K., Mutagenic response of human somatic cell lines, 19: 43844
COHN, S. H., Metabolism of ^{46}Sc in man, 19: 43692
COLIN, F., Experimental basis of quantitative interpretation of the renogram, 19: 43667 (EUR-1890.f)
COLLINS, C. B., Collisional-dissociative recombination of electrons with molecular ions, 19: 45450
COLLINS, J. C., Qualitative experimental investigations on various vortex tube configurations, 19: 44199 (UCRL-12045)
COLOMBO, C., Modular counting system in the electronic section, 19: 44447 (EUR-2444.i)
COLP, J. L., Prog. rpt. on containment capsule impact safety, 19: 44298 (SC-RR-65-9)
COMPY, E. M., Critical fields of superconducting bismuth at high pressure,

19: 45198
CONCUS, Paul, On the calculation of nonlinear magnetostatic fields, 19: 44876 (UCRL-16287)
CONSTANTINESCU, M., Neutron transmission of Pd in energy range 1.2 to 100 ev, 19: 45233
CONTE, J. C., Determination of carbon and hydrogen in hydrocarbons by neutron scattering, 19: 43968
CONVERSE, G. L., Prog. rpt. on alkali metals boiling and condensing, 1–3/65, 19: 44187 (NASA-CR-54405)
CONVERT, Guy, Stimulated emission and absorption in quantum and classical electromagnetism, 19: 44820
COOK, C. L., Clebsch-Gordan coefficients for group SU_6, 19: 45061
COOK, Jackie Lee, Thorium–uranium dicarbide pseudobinary system in the presence of excess graphite, 19: 44696 (ORNL-TM-1188)
COOK, K. V., Nondestructive testing of small-diameter refractory-alloy tubing, 19: 44211 (ORNL-P-1543)
COOK, Melvin A., Uranium–thorium–lead time clocks, 19: 44272
COOP, K. L., Cross sections for $^{89}Y(n,\gamma)^{90m}Y$ and $^{89}Y(n,\gamma)^{90}Y$ between 0.145 and 1.225 Mev, 19: 45376
COOP, K. L., Experimental photopeak efficiencies for NaI(Tl) crystals, 19: 44515
COOPER, L. N., Acoustic attenuation in type II superconductor, 19: 45210
COPIC, M., Regular eigenfunctions of time and velocity dependent transport equation for slabs, 19: 45227 (NIJS-R-449)
COPS, A., Velocity of sound in liquid hydrogen, 19: 44822
CORBETT, I. F., S-wave π-π final-state interactions in $\pi^- + p \to \pi^0 + \pi^0$, 19: 45089
CORCIOVEI, A., Temperature dependence of Moessbauer effect in thin films, 19: 44847
CORCORAN, Cornelia, Transfer rates of gamma globulin between cerebrospinal fluid and blood plasma in multiple sclerosis, 19: 43666 (BNL-9406)
CORCORAN, V. J., Water vapor corrosion of uranium and its prevention, 19: 44618 (AWRE-O-42/65)
CORDIER, Gilbert, Control of the nuclear fuel of a Chinon power plant, 19: 45607
CORDLE, H. J., Large closed-cycle water reactor auxiliary systems, 19: 45597 (WCAP-3269-31)
CORELLA, M. R., PROMETEO I—program for averaging thermal constants over Wigner-Wilkins flux spectrum, 19: 45224 (JEN-133-DF/I-43)
CORELLA, M. R., PROMETEO II—program for averaging thermal constants from Wilkins spectrum, 19: 45225 (JEN-135-DF/I-44)
CORGE, Charles R., Analysis of resonances due to a wave neutrons in transmission time of flight experiments. II., 19: 45215 (CEA-R-2780)
CORINALDESI, A., Immunological aspects of experimental pulmonary sclerosis due to ionizing radiations, 19: 43817
CORKHILL, D. P., Mechanism of thermal release of injected inert gas from tungsten, 19: 44954
CORNFIELD, Jerome, MEA effect on radiation dose-response characteristics of granulocyte and lymphocyte counts, 19: 43876
CORNILLE, H., Limiting procedures for singular potentials, 19: 45063
CORTINI, G., Fission physics, 19: 45338
COTTON, F. A., Some new derivatives of the $(Mo_6Cl_8)^{4+}$ ion, 19: 43990 (MIT-1965-15)
COTTRELL, Don M., Preparation of emulsion stacks for underground cosmic-ray experiments, 19: 44397 (CERN-65-4(Vol.II), pp III5-11)
COURBON, M., Prestressed concrete pressure vessels for nuclear reactors, 19: 45504
COURT, L., Dosimetry of high-energy protons by measurement of beryllium-7 formed in the tissues, 19: 44327
COURTNEY, J. C., Photoneutron spectra and cross sections for ^{12}C and ^{16}O, 19: 45330
COUSINEAU, Gilles Herve, Macromolecule synthesis in developing sea urchin eggs, 19: 43709
COUSSEMANT, Fernand, Hydrolysis in acid medium of linear and cyclic acids. III., 19: 44011
COWAN, R. D., Theta-pinch sources of vacuum uv radiation, 19: 45396 (LA-DC-7120)
COWLEY, Ray G., Inhalant allergy to the screwworm fly, 19: 43652
CRADDOCK, W. L., Nuclear gamma rays from supernova remnants, 19: 44930
CRAGLE, R. G., Effects of irradiation upon lactation, 19: 43800
CRAGLE, R. G., Lactation and radionuclide metabolism responses of dairy cattle to lethal doses of γ and neutron radiation, 19: 43801
CRAGLE, R. G., Total body water estimations in dairy cattle using tritiated water, 19: 43694
CRANDALL, J. L., Description of the Savannah River high flux charge, 19: 45638 (DP-999, pp 7-17)
CRANDALL, J. L., Savannah River high flux demonstration, 19: 45637 (DP-999)
CRAVEN, C. W., Molten salt converter reactor. Design study and power cost estimates for a 1000-Mwe station, 19: 45588 (ORNL-TM-1060)
CRAWFORD, F. W., Plasma resonance probe characteristics in a magnetic field, 19: 45381 (ARL-65-115)
CRAWFORD, F. W., Wave propagation along a warm nonuniform plasma column, 19: 45408 (SU-IPR-11)
CREBBIN, Kenneth C., Prog. rpt. on Bevatron operation and development, 10–12/64, 19: 44874 (UCRL-16203)
CREUZBURG, M., Temperature dependence of characteristic energy losses in KBr, 19: 45490
CREVER, Frederick E., Prospects for dual-purpose plants, 19: 45635
CRISPINO, Enrico, Evaluation of thermal insulators for nuclear reactors, 19: 44088
CRISTEA, G., Neutron transmission of Pd in energy range 1.2 to 100 ev, 19: 45233
CROCKER, J. G., Prog. rpt. on Spert Project, 1–3/65, 19: 45528 (IDO-17097)
CROSSWHITE, H. M., Free-ion and crystalline spectra of Pr(III), 19: 44943
CROUCH, E. A. C., Variations in isotopic compositions of naturally occurring molybdenum, 19: 44242
CROWLEY, John E., Alpha radiation hygrometer. II., 19: 44338 (AD-608498)
CUEER, P., Some properties of nuclear emulsions, 19: 44380 (CERN-65-4 (Vol.I), pp 45-63)
CULLEN, G. W., High-temperature critical current of vapor deposited Nb_3Sn, 19: 45213
CUOCO, A., Determination of concentration of radioactive cloud and contamination of soil by Pasquill-Gifford Method, 19: 44255 (RT/PROT(65)-10)
CUPERLOVIC, K., Vaccination against Dictyocaulus filaria with irradiated larvae, 19: 43750
CURTIS, Howard J., Somatic mutations and carcinogenesis, 19: 43754
CURTIS, N. F., Some new derivatives of the $(Mo_6Cl_8)^{4+}$ ion, 19: 43990 (MIT-1965-15)
CURTISS, C. F., Phase shifts and the quantum-mechanical Hamilton-Jacobi equation, 19: 45053
CURZON, A. E., Crystal structures of solid H and solid D in thin films, 19: 45194
CUSIMANO, J. P., Personnel monitoring practices at the National Testing Station, 19: 44335
CYGNOR, J., Motor cavity evacuation study, 19: 45660 (TIM-919)
CZERNIAK, Roisa, Rare earth metals—metals of the future, 19: 44615

D

DABURON, M. L., Dosimetry of high-energy protons by measurement of beryllium-7 formed in the tissues, 19: 44327
D'AGOSTINO, M. D., Theoretical aspects of neutron activation of structures, 19: 45461
DAHL, P. F., High magnetic field limit in synchrotrons, 19: 44858 (BNL-9480)
DAHL, R. E., Fast neutron flux characteristics of the ETR, G-7 hot water loop, 19: 45672 (BNWL-89)
DAHLBERG, E. P., Anelastic effects in Zr at room temperature resulting from prestrain at 77°K, 19: 44728
DAHLBY, Joel W., The controlled potential electrodeposition of cobalt from plutonium–cerium–cobalt alloy solutions, 19: 43934 (LA-3345)
DAHLGREN, Jones Arthur, Power plant for superheating the steam originating from the steam generator of a nuclear pressurized water reactor, 19: 45630
DAHL-JENSEN, E., Conference on nuclear photography, 5th, Geneva, 9/64, 19: 44383 (CERN-65-4(Vol.II))
DAKOWSKI, M., Charge-sensitive preamplifier with low noise level for operation with semiconductor detectors, 19: 44484 (ZFK-PHA-12, pp 189-95)
DAKOWSKI, M., Interaction of heavy fission particles with semiconductor detectors, 19: 44481 (ZFK-PHA-12, pp 149-53)
DAKOWSKI, M., Surface-barrier silicon detectors with guard rings and possibility of their utilization, 19: 44469 (ZFK-PHA-12, pp 16-24)
DAKOWSKI, M., Target preparation by electro-spraying directly on semiconductor detectors, 19: 44635 (JNR-595/IA/PL)
DALEY, D. P., Dissertation of jet pump analysis, 19: 44198 (TIM-913)
DALKHAZHAV, N., Real part of the elastic p-p scattering amplitude at 2, 4, 6, 8, and 10 Bev, 19: 45021 (JINR-P-2336)
DALL'ASTA, G., Application of nuclear energy for desalination, 19: 45619
DALLE-CHAVAUDRA, N., Migration of hematopoietic bone marrow cells in irradiated and normal mice, 19: 43836
DALY, N. R., Detector for neutral and charged particles, 19: 44499
DAMERELL, C. J. S., S-wave π-π final-state interactions in $\pi^- + p \to \pi^0 + \pi^0$, 19: 45089
DAMIANO, V., Prog. rpt. on flow and fracture studies of alloyed Be, 7/7–10/64, 19: 44693 (NP-15411)
DAMIANO, V., Prog. rpt. on flow and fracture studies of alloyed Be, final,

8/65, 19: 44694 (NP-15432)
DANIELS, Farrington Jr., Diseases caused or aggravated by sunlight, 19: 43819
DANNER, H., Study of low-frequency molecular motions in polyethylene and the n-paraffins by slow neutron inelastic scattering, 19: 44050
DANON, Joanne Sobhan, Graft polymerization utilizing ionizing radiation, 19: 44097
DANOS, Michael, Photon absorption cross section of spherical nuclei, 19: 45366
DARDEN, E. B. Jr., Prog. rpt. on space biology, annual, 7/1/64–6/30/65, 19: 43721 (ORNL-TM-1217)
DAS, T. P., Nuclear magnetic shielding of alkali ions in crystals and dilute aqueous solutions, 19: 45485
DASANNACHARYA, B. A., Cold neutron scattering by methane, 19: 45237
DA SILVA, J. Lopes, Determination of carbon and hydrogen in hydrocarbons by neutron scattering, 19: 43968
DAUER, Maxwell, Evaluation of film badge dosimeters for occupational radiation exposure, 19: 44312
DAVID, Alois, Leukocytes in the diagnosis of hematopoiesis impaired by ionizing radiation, 19: 44315
DAVIDSON, Ben, Turbulence and low-level structure, 19: 44793 (BNL-914, pp 156-7)
DAVIES, B. W., Measurements of the A and R parameters in proton-proton scattering at 47.8 and 27.6 Mev, 19: 45319
DAVIS, D. H., Location of tracks in nuclear emulsion with aid of spark chambers, 19: 44445 (CERN-65-4(Vol.II), pp X74-83)
DAVIS, Dianne M., Loading of emulsions with diamonds and polystyrene for experiments with stopping K particles, 19: 44398 (CERN-65-4(Vol.II), pp III12-16)
DAVRIL, Monique, Combination of radioactive gamma aminobutyric acid in the cerebral tissue of the rat, 19: 43690
DAVYDOV, V. V., Polarization in n-α scattering at E_n = 25, 28, and 34 Mev, 19: 45259 (IAE-834)
DE, N., Class of axially symmetric solutions of combined Maxwell-Einstein-Klein-Gordon's field, 19: 45147
DE AGAZIO, Albert W., Dose calculation models for re-entering nuclear rocket debris, 19: 45655 (NUS-229)
DEBEAUVAIS, Monique, Recordings of individual tracks in various solid materials, 19: 44384 (CERN-65-4(Vol.II), pp II-8)
DEBERDEEV, M. Yu., Method for increasing the stability of sensitivity and latent image of nuclear emulsions, 19: 44390 (CERN-65-4(Vol.II)), pp II19-28)
DEBERTIN, K., Bibliography on instruments and measuring techniques in nuclear physics, 19: 44366 (AED-C-06-12)
DE BOER, P. C. T., Shock front curvature at initial pressures up to 700 mm Hg, 19: 44853
DEBRIE, G., Detection of criticality accidents, CEA, France, 19: 44321
DE BRUYN OUBOTER, R., Dissipative normal fluid production by gravitational superfluid flow, 19: 45201
DE CARLO, V. A., Irradiation evaluation of fuel elements for PBRE and AVR reactors, 19: 44749 (ORNL-P-1507)
DE CARVALHO, H. G., Photofission of U and Th between 300 and 1000 Mev, 19: 45329
DE GIRARDIER, J., Thorotrast disease concerning one observation, 19: 43738
DE GISI, S. L., Effect of molecular structure on the thermal aging properties of flexible urethane foams, 19: 44682 (BDX-613-75)
DEGROSSI, Osvaldo J., Possibilities of using ^{99m}Tc tracer instead of radioiodine in thyroid function investigations, 19: 43881 (NP-15271)
DE HEER, F. J., Inelastic collisions of fast electrons and ions with atoms, 19: 44950
DEIST, J., Half life of ^{32}P, 19: 45371
DEKABRUN, L. L., System to control the exciting current of electromagnets of nuclear magnetic resonance spectrometers, 19: 44356
DE KALB, Edward L., Optical emission spectroscopy as an analytical tool, 19: 43929 (IS-1237)
DE KERVILER, H., Dosimetry of high-energy protons by measurement of beryllium-7 formed in the tissues, 19: 44327
DELANGE, Maurice, Methods and apparatus in which a mass of solid material is subjected to two successive treatments by gases, 19: 44042
DE LA VEGA VEDOYA, Mario, Photographic film dosimetry in skin β therapy, 19: 43880 (NP-15270)
DELCLOS, Luis, Radiotherapy for head and neck cancer, 19: 43903
DE LEZEROVICH, Juana B., Synthesis of DL glycine-1-C-14 and DL alanine-1-C-14, 19: 44047 (NP-15268)
DELGROSSO, E. J., Development of Cb–Zr–C alloys, 19: 44605 (PWAC-464)
DELGROSSO, E. J., Recovery and recrystallization of Nb and several Nb–Zr alloys, 19: 44698 (PWAC-465)
DELLA ROSA, R. J., Absorption and deposition of ^{85}Sr and ^{47}Ca from ligated intestinal segments of adult beagles, 19: 43677 (UCD-472-112, pp 86-96)
DELLA ROSA, R. J., Quality control of ^{90}Sr-containing food, 19: 43675 (UCD-472-112, pp 73-9)
DELLA ROSA, R. J., Radium metabolism by beagles following single and multiple injections, 19: 43678 (UCD-472-112, pp 97-108)
DELLA ROSA, R. J., Strontium deposition in bone and teeth of beagle puppies, 19: 43676 (UCD-472-112, pp 80-5)
DELMAR, Jean, Radioactivity measurements inside pressure vessel of Reactor G 3 after 4 years operation, 19: 45566 (CEA-R-2785)
DEL VAL COB, Manuel, Preservation of foods by irradiation. I., 19: 44561
DE MARCO, A., Apparatus for study of energy spectra and polarization of photoneutrons, 19: 45303
DEME, S., Semiconductor detectors with uranium salts for absolute measurement of thermal neutron beams, 19: 44479 (ZFK-PHA-12, pp 140-3)
DEMIDOV, A. M., Instrumentation of certain experimental channels in USSR research reactors, 19: 45675 (IAE-725)
DE MIGNARD, Valentin A., Response of liver to target irradiation, 19: 43735
DEMOULIN, R., Latensification of the latent image in ionographic emulsions, 19: 44391 (CERN-65-4(Vol.II), pp II29-42)
DE'MUNARI, G. M., Apparatus for investigations on scintillator properties in the temperature range −100°C to +50°C, 19: 44460 (RT/FI(65)8)
DENEFLE, J. P., Effect of spinal cord fragments on culture growth of marrow of graft carrier, 19: 43761
DEONIGI, D. E., Minimized fuel cycle cost for simulated heavy water reactor. I., 19: 45563 (BNWL-106)
DE PROOST, M., pH effect on γ sensitivity of Clostridium sporogenes, 19: 43865
DE PROOST, M., Possibility of using radiosensitizers in preservation or sterilization of food, drugs and medical supplies by irradiation, 19: 44552 (BLG-327)
DEQUIDT ALFEIRAN, E., Installation for the handling of pyrophoric materials under an inert atmosphere, 19: 44018
DERMENDZHIEV, E., Neutron-^{235}U nuclear interaction in the 0.002 to 30 kev energy region, 19: 45292 (BNL-tr-16)
DERMENDZHIEV, E., Uranium-235 fission cross section for resonance neutrons, 19: 45299
DESNEIGES, P., Detection of criticality accidents, CEA, France, 19: 44321
DESSLER, A. J., Physical significance of inhonogeneities in polar cap absorption events, 19: 45172
DEUTSCHER, M., Monitor for reading of d/p ratios in the cyclotron beam, 19: 44482 (ZFK-PHA-12, pp 154-62)
DEUTSCHMANN, M., Single π^0 production by 8-Bev/c positive pions, 19: 45103
DEVANI, Muljibhai, Catalytic effect of Th and Zr ions on the hydrolysis of nucleotides, 19: 43708
DEVINE, M., Measurements of the A and R parameters in proton-proton scattering at 47.8 and 27.6 Mev, 19: 45319
DE VOLPI, A., Electron excitation of ZnS(Ag), 19: 44520
DE VOTO, R. S., Transport properties of partially ionized monatomic gases, 19: 44854
DE VOTO, R. Stephen, Argon plasma transport properties, 19: 45407 (SU-AA217)
DEVREESE, J., Principal methods of polaron theory, 19: 45473 (BLG-329)
DE V. SMIT, W. B., Tables to correct for resolving-time counting losses of nucleonic apparatus, 19: 44530
DEWELL, E. H., Prog. rpt. on radiochemistry of nuclear fuels, 11/64–1/65, 19: 45542 (BAW-272)
DEWES, Roger A., Radiation dosimeter providing visual representation of total dose, 19: 44546
DEWEY, William C., Detection of malignant neoplasia of the gastrointestinal tract by use of radioactive phosphorus and a miniature Geiger tube, 19: 43887
DE WOLF, D. A., Cross-polarized electromagnetic backscatter from turbulent plasmas, 19: 45424
DIAMOND, J. J., Bibliography on high-temperature chemistry and physics of materials in the condensed state, 19: 43994 (NP-15381)
DIAMOND, J. M., Tunnel diode discriminator with fixed dead time, 19: 44504
DIAZ, J. Diez, Installation for the handling of pyrophoric materials under an inert atmosphere, 19: 44018
DICKENS, J. K., Elastic scattering of 12.0- and 14.0-Mev deuterons from ^{90}Zr and the reaction ^{90}Zr(d,p)^{91}Zr, 19: 45281 (ORNL-3850)
DIECKAMP, H. M., SNAP-10A design, development, and flight test, 19: 45154
DIEDRICH, James H., Hypervelocity impact damage characteristics in beryllium and graphite plates and tubes, 19: 44692 (NASA-TN-D-3018)
DIEKE, G. H., Free-ion and crystalline spectra of Pr(III), 19: 44943
DIENSTBIER, Z., Peripheral blood changes caused by internal emitters. III., 19: 43839
DIETZ, K., K-matrix model of peripheral interactions. II., 19: 45086

DI GIACOMO, A., Chemical shift of the proton in the H_2 molecule, 19: 44952
DI GIOGIO, G. V., Polarization of recoil protons in e-p elastic scattering at 20 Fermi^{-2}, 19: 45058
DIKE, Robert S., Development of an interleaved, fractional-turn coil, 19: 44136 (LA-3234)
DILLE, J. Robert, Inhalant allergy to the screwworm fly, 19: 43652
DILLET, Alain, High-speed pulsed magnetic fields measurements, using the Faraday effect, 19: 44805 (CEA-R-2769)
DILLEY, J., Generalized Cauchy representations and resonance phenomena, 19: 45130
DI MENZA, R., Outlook for use of nuclear energy for production of heat at low temperature, 19: 45618
DI MENZE, R., Some alternates for the utilization of organic liquid reactors for desalination of salt water, 19: 45620
DIMITRIEV, J., Upper limits of glass formation and glass structure in binary systems BeO–SiO_2, MgO–SiO_2, CaO–SiO_2, SrO–SiO_2, and BaO–SiO_2, 19: 44015
DIMITRIEV, J., Upper glass formation limits in the binary systems BeO–GeO_2, MgO–GeO_2, CaO–GeO_2, SrO–GeO_2, and BaO–GeO_2, 19: 44016
DIMITROV, Omourtague, Study in neutron-irradiated Al of elimination of faults, 19: 44755
DISKO, N. A., Blood serum proteinographic chart during chronic x irradiation, 19: 43766
DI STEFANO, Berardino, Role of radioisotope scanning in the evaluation of gastrointestinal disease, 19: 43886
DIVEN, B. C., Neutron experiments with underground nuclear explosions, 19: 44157 (LA-DC-7304)
DIXON, G. J., High flux isotope reactor preoperational vibration and hydraulic test program, 19: 45644 (ORNL-P-1501)
DIXON, P. H., Solution of precipitates in very dilute uranium–iron–aluminium alloys, 19: 44715
DLUZHNEVSKAYA, O. B., Neutrino luminosity of stars, 19: 44927
DMITRIEV, A. N., Use of ^{15}N as internal standard for determining quantities of radiogenic argon, 19: 43960
DMITRIEV, P. P., Production of ^{26}Al during irradiation of Mg with 20-Mev deuterons, 19: 44099
DOBIAS, F., Magnetic field gage and stabilizer, 19: 44352 (UJV-1339/65)
DOBRESCU, S., Neutron transmission of Pd in energy range 1.2 to 100 ev, 19: 45233
DOBRETSOV, Yu. P., Device for developing pulsed magnetic fields up to 150 kG, 19: 44888
DOBROKHOTOV, E. I., Discharge instability with a heated cathode in a magnetic field at low pressures, 19: 45390 (IAE-780)
DODD, John Alan, Nuclear fuel assembly end supports, 19: 45550
DOERFFLER, W. W., Dissolution and diffusion of oxygen in zirconium, 19: 44673 (AECL-2268)
DOIDA, Yukio, Radiation-induced chromosome aberrations in man, 19: 43834
DOIL'NITSYN, E. F., Use of ^{15}N as internal standard for determining quantities of radiogenic argon, 19: 43960
DOKMANOVIC, B., Heat transfer and pressure drop of a gas-cooled reactor fuel element can model with inclined polyzonal spiral finning, 19: 45549
DONAT, K., Long-range α-particles of radium C, 19: 45293 (ORNL-tr-696)
DORENBUSCH, W. E., Angular distributions from shell-model forbidden (d,p) transitions to spin $^5/_2$ states in ^{49}Ca, ^{49}Ca, and ^{47}Ti, 19: 45323
DORFMAN, Leon M., Pulse radiolysis of gaseous argon–oxygen solutions. Rate constant for the ozone formation reaction, 19: 44071
DORNER, B., Lattice dynamics of solid methane, 19: 45239
DOROSHENKO, G. G., Analysis of systematic error due to differentiation of spectra measured by fast neutron single crystal scintillation spectrometer, 19: 44493
DOROSHENKO, G. G., Matrix treatment of data obtained by fast neutron single-crystal scintillation spectrometer, 19: 44492
DOSCH, H. G., Low angular momentum nucleon-nucleon scattering, 19: 45084
DOSCH, H. G., The influence of the neutron-neutron final-state interaction on the capture of muons by deuterons, 19: 45073
DOSCH, Peter, Shut-off device for nuclear reactors, 19: 45515
DOSTAL, M., Myorelaxant effect of gallamine and tubocurarine in irradiated rabbits, 19: 43871
DOULL, J., Chemical protection against 440-Mev protons in mice pretreated with MEA or PAPP, 19: 43873
DOULL, J., Chemical protection against absorber-moderated protons, 19: 43874
DOULL, J., Radioprotective effects of DMSO in x-irradiated mice, 19: 43859 (NP-15310, pp 1-13)
DOUSSET, M., Attempt to assess the dose received by bone marrow on exposure to neutron flux, 19: 43854
DOWNEY, Harry Fred, Acute depletion of Ca, P, and Sr from the bovine calf by hemodialysis, 19: 43673 (TID-22147)

DRELL, S. D., Anomalous magnetic moment of the electron, muon, and nucleon, 19: 45108
DRITS, M. E., Effect of additional alloying on properties of magnesium–neodymium alloys, 19: 44709 (JPRS-24761, pp 17-28)
DRITTLER, K., Crystal effects in the scattering of neutrons with energy from 30 to 1000 ev, 19: 45489
DROEGE, T., Operating experience and improvements on the Princeton–Pennsylvania accelerator, 19: 44872 (PPAD-2137-565)
DROST, H., Relation between column stratification and negative ion content in an impure Ar discharge, 19: 45423
DRUMMOND, Ian T., Unstable-particle scattering and the strip approximation, 19: 45117
DRUMMOND, James E., Some related phenomena in plasmas in solids and in gases, 19: 45383 (D1-82-0419)
DUA, S. K., Unit for testing high-efficieacy filters, 19: 44281 (AEET-282)
DUANE, A., Measurement of branching ratio for decay $\omega^0 \rightarrow e^+ + e^-$, 19: 45102
DUBININ, N. P., Analysis of delayed effects of γ rays and 660-Mev protons on chromosomes, 19: 43770
DU BOIS, Kenneth P., Effects of various drugs on ATP activity of hematopoietic tissues of rats exposed to γ radiation, 19: 43860 (NP-15310, pp 14-25)
DU BOIS, Kenneth P., Inhibitory effect of x radiation on development of N-demethylase activity in livers of young, male rats, 19: 43720 (NP-15310, pp 26-35)
DU BOIS, Kenneth P., Mechanism of action of 2-mercaptoethylamine, 19: 43670 (NP-15310, pp 36-47)
DUBOVSKII, B. G., Heterogeneous absorber efficiency in homogeneous uranium–water reactors, 19: 45536
DUCHON, Paul, Mission integration of nuclear dynamic power systems, 19: 45661
DUCK, I., Neutron-neutron scattering length by pion absorption in ^3He, 19: 45354
DUFF, M. J., Automatic following in nuclear emulsions, 19: 44421 (CERN-65-4(Vol.II), pp VIII35-7)
DUFFY, J. G., Fast flux test facility, 19: 45670 (APDA-174, pp 74-6)
DUFRANE, Kenneth, Underwater thermoelectric reactor plant, 19: 45627
DUKURE, R. K., Influence of relative roughness on electrically conducting fluid flow in presence of a magnetic field, 19: 44826
DUNKLEE, A. E., Physics design of the Savannah River high flux charge, 19: 45640 (DP-999, pp 29-42)
DUNN, Alice B., X-ray emission of flares originating behind the solar disk, 19: 44894 (AD-424481)
DUNN, J., Performance evaluation of slag and crucible dissolver, 19: 44111 (BNWL-121)
DUNN, William S., Recovery of uranium and/or vanadium values from ores containing the same, 19: 44129
DUPLAN, J. F., Prenatal and neonatal mortalities induced in mice by x irradiation of fetus alone or of mother alone, 19: 43760
DUPORT, Jacques, Liquid cooled nuclear reactor with improved flow distribution means, 19: 45520
DUPOUY, Jean-Michel, Electron microscope observation of single-crystal beryllium thin foils, 19: 44683 (CEA-R-2789)
DURBIN, C. E., Feed-rate checks on numerical-controlled machines, 19: 44642 (RFP-570)
DURBIN, Patricia W., Growth curve for mammary fibroadenoma in female rat, 19: 43649 (UCRL-16177)
DURHAM, Laird, Radioisotopes in hydrospace. Preliminary survey report, 19: 44569 (AGN-8122)
DUSSERRE, L., Thorotrast disease concerning one observation, 19: 43738
DUTHIE, J. G., Spark-chamber experiment on cosmic γ rays, 19: 44970
DYBOVSKI, K., Measurement of β/l parameters in ANNA, 19: 45677 (INR-614/IXA/P)
DYER, A. J., Radioactive fallout in Southern Australia during years 1958–1964, 19: 44261
DYER, J. N., Emulsion grain density in the extreme relativistic region, 19: 44428 (CERN-65-4(Vol.II), pp IX9-13)
DYMOND, B., Metabolism of radioactive strontium in rats. I., 19: 43671 (PG-Report 662)
DZHELEPOV, B., Decay mode of ^{147}Eu, 19: 45267 (JINR-P-2161)
DZHELEPOV, V. P., Catalysis by μ^- of $d\mu + p \rightarrow {}^3He + \mu^-$ and $d\mu + d \rightarrow t + p + \mu^-$, 19: 45273 (JINR-P-2356)
DZHELEPOV, V. P., Hydrodynamics of a resonance bubble chamber, 19: 44523
DZIUNIKOWSKI, Bohdan, Radiometrical methods of ore analysis. II., 19: 43971

E

EASTERDAY, R. J., FLASH: an IBM-7090 code for computing multi-stage flash evaporator plant designs for desalination of seawater, 19: 44140

(ORNL-TM-1244)
EBERHAGEN, A., Electromagnetic radiation from plasmas of high temperature and density, 19: 45392 (IPP-1/39)
EBERHARDT, P., Further evidence on the origin of trapped gases in the meteorite Khor Temiki, 19: 44906
EBISUZAKI, K., Test of hypothesis concerning uv irradiation damage and phage functions, 19: 43845
ECKEL, John F., Governing factors in the formation of Cr_3O-type structures, 19: 44702 (TID-22200)
ECKLUND, W. L., Relation between auroral radio absorption and vlf emissions, 19: 45170
EDER, G., Creation of large particle numbers, 19: 44895
EDVARDSSON, K.-A., Planned procedures for fast determination of radiation levels and personnel dosimetry in connection with radiological accidents, 19: 44336
EDWARDS, Betty F., Effect of weightlessness and radiation on growth of wheat coleoptile, 19: 43717 (NASA-CR-303)
EDWARDS, J. J., Fuel element flow stability studies, 19: 44181 (APDA-174 pp 56-60)
EDWARDS, T. W., Design of proton linear accelerators for energies up to 200 Mev, 19: 44867 (MURA-713)
EFFERSON, K. R., Experimental simulation of large, high field, superconducting magnet operation, 19: 45192 (ORNL-TM-1266)
EFIMENKO, B. A., Analysis of systematic error due to differentiation of spectra measured by fast neutron single crystal scintillation spectrometer, 19: 44493
EFIMENKO, B. A., Matrix treatment of data obtained by fast neutron single-crystal scintillation spectrometer, 19: 44492
EGELSTAFF, P. A., Summary of symposium on inelastic scattering of neutrons, 19: 45243
EGELSTAFF, P. A., Thermal motion of simple liquids, 19: 44817
EGGERT, Gilbert L., Effects of low-energy neutron irradiation on age hardening in Cu–Be, 19: 44760
EGOROV, Yu. S., Application of proton resonance to the measurement of inhomogeneous magnetic fields, 19: 44353 (SLAC-Trans-22)
EHMANN, William D., The non-destructive determination of silicon and oxygen in meteorites by fast neutron activation analysis, 19: 43927 (CONF-650405-16)
EHRENBERG, L., Tritium labeling of cells in vitro, 19: 43651
EHRLEN, I. R., Advances in sterilization techniques, 19: 44563
EHRLEN, I. R., Advances in sterilization techniques, 19: 44564
EHRLICH, R. D., Experimental observations of electric quadrupole effects in the muonic spectra of ^{235}U, ^{181}Ta, and ^{239}Pu, 19: 45326
EHRMAN, Chester S., Design of a chop and leach reprocessing plant, 19: 44126
EILENBERG, S., Effect of neutral plasma on ion trajectories, 19: 45451
EINENKEL, H., Electronic regulation of emission current of a pulsed injector for 200 kv, 19: 44884
EINHORN, J., Thyroid antibodies after ^{131}I treatment for hyperthyroidism, 19: 43902
EISENBUD, Merril, Industrial uses of ionizing radiation, 19: 44307
EJIRI, H., Anisotropy of conversion electrons from (p,2n) and (α,4n) reactions, 19: 45352
EKATOV, A. B., Multidimensional analyzer with a preliminary treatment of data and combined-type memory, 19: 44524
EKVALL, R. A., Uranium oxide fuel for nuclear thermionic converters, 19: 44593 (CONF-650908-4)
ELBEK, B., Coulomb excitation of vibrational states in deformed even nuclei, 19: 45321
ELDERKIN, Charles E., Diffusion from elevated sources, 19: 44768 (BNL-914, pp 26-7)
ELKIND, M. M., Repair of x-ray damage in mammalian cells, 19: 43791
ELLIOTT, R. D., Disintegration and dispersion of the SNAP-10A reactor upon return from satellite orbit, 19: 45651 (NAA-SR-11103)
ELLIS, Robert A. Jr., Plasma heating at 500 megahertz, 19: 45398 (MATT-332)
EMERY, J. F., Use of activation analysis in determination of origin of opium, 19: 43937 (ORNL-TM-1263)
EMMERSON, Peter T., Preferential sensitization of anoxic bacteria to x rays by organic nitroxide-free radicals, 19: 43875
EMMERT, Fred H., Forces involved in retention and movement of non-metabolic Sr in phaseolus vulgaris, 19: 43703
EMPSON, F. M., Demonstration of disposal of high-level radioactive solids in salt, 19: 45689 (ORNL-P-1568)
ENGEL, J. R., Application of on-line digital computer to a reactor experiment, 19: 45585 (ORNL-P-1502)
ENGEL, J. R., Predicted and observed nuclear characteristics of the Molten Salt Reactor Experiment, 19: 45586 (ORNL-P-1503)
ENGELMANN, Robert J., Precipitation scavenging, 19: 44769 (BNL-914, pp 28-32)
ENGLISH, Julies C., Computer code for one-group flux calculations in three dimensions, 19: 45218 (DP-938)
ENOS, G., Cesium-fueled MPD arc-jet engine performance, 19: 44230
ERBACHER, W., Design study of small nuclear power plant for Austria, 19: 45581 (NP-15291)
ERDMAN, Howard E., Differential responses of germ cells in flour beetles due to x-ray dose, hypotherma, $t_{.5}$x-exposed and age, 19: 43715 (HW-SA-3747)
ERDMAN, Howard E., Reproductive performance of x-rayed single-species and mixed-species cultures of Tribolium confusum and T. castaneum reared at different temperatures, 19: 43716 (HW-SA-3748)
ERICKSON, R. A., Crystal structure of solid deuterium from neutron-diffraction studies, 19: 45211
ERICKSON, W. H., Role of hydride precipitate in fracture of Zr and its alloys, 19: 44716
ERIKSSON, Bo, Use of importance sampling in particle transport problems, 19: 45458 (AE-190)
ERIVANSKII, Yu. A., Expediency of radiometric uranium ore dressing and the choice of the optimum level separation during dressing, 19: 44275
ERLENMEYER, H., Flotation and coordination chemistry. Method for enrichment of Ga^{3+}, 19: 43961
ERMAKOV, S. M., Penetration of γ quanta through shielding barrier, 19: 45466
ERMOLAEV, N. P., Silicate form of uranium transport in aqueous solutions, 19: 44278
ERMOLOV, P. F., Catalysis by μ^- of $d\mu + p \rightarrow {}^3He + \mu^-$ and $d\mu + d \rightarrow t + p + \mu^-$, 19: 45273 (JINR-P-2356)
ERNST, H., Methods of irradiation with localized limited radiation effect, 19: 43900
ERTAUD, Andre, Possible role of nuclear energy for sea water desalination, 19: 45606
ERYUSHEV, N. N., X-ray emission of flares originating behind the solar disk, 19: 44894 (AD-424481)
ESHLEMAN, V. R., Radar measurements of total cislunar electron content, 19: 45176
ESIKOV, A. D., Isotopic composition of lead ore from different type deposits in Eastern Transbaikal, 19: 44277
ESPENSHADE, D. L., Some temperature considerations in transistor circuit design, 19: 45715 (SC-TM-65-359)
ESSON, J., The radiometric-spectrophotometric determination of microgram amounts of niobium in rocks and minerals, 19: 43943
ESTEVE, A., Vector invariants of SU_3/Z, 19: 45083
ETIENNE-MARTIN, P., Thorotrast disease concerning one observation, 19: 43738
ETTERS, Richard David, Theory of many-boson systems, 19: 44806 (IS-T-19)
EUROLA, T., Dynamics model of the HBWR heat removal circuits, 19: 45633 (HPR-62)
EUROLA, T., Noise experiments with the HBWR second fuel charge, 19: 45632 (HPR-53)
EVANS, D. A., Short-range hyperfragments produced by K^- captures in emulsions, 19: 45342
EVANS, H. B., Bibliography on chemical analysis of Pu, Pu alloys and Pu compounds, 19: 43925 (ANL-6956)
EVANS, J. V., Cause of the midlatitude winter night increase in f_0F_2, 19: 45174
EVANS, J. V., Comparison of rocket, satellite, and radar determinations of electron temperature at midlatitudes, 19: 45177
EVANS, R. E., Rolling cast beryllium between 500 and 1000°C, 19: 44652
EVERETT, Mark Allen, Biochemical changes induced by uv light, 19: 43764
EVERETTE, William L., Prog. rpt. on Bevatron operation and development, 10–12/64, 19: 44874 (UCRL-16203)
EVRARD, R., Principal methods of polaron theory, 19: 45473 (BLG-329)
EZOP, J. J., Feasibility of using scintillating fibers for low-energy β counting, 19: 44451 (IITRI-578P26-8)

F

FADINA, E. V., Application of synthetic polymers in preparation of fine-grain nuclear emulsions. I. and II., 19: 44400 (CERN-65-4(Vol.II), pp III31-56)
FADINA, E. V., The properties of fine-grained nuclear emulsion type PR-2, 19: 44404 (CERN-65-4(Vol.II), pp IV23-31)
FAGRAEUS, Astrid, Thyroid antibodies after ^{131}I treatment for hyperthyroidism, 19: 43902
FAINBERG, Yu. B., Quasilinear theory of weakly turbulent plasma with account of correlation of electric fields, 19: 45439
FAIRSTEIN, E., Nuclear pulse amplifiers, 19: 44521
FANG, F. F., Effects of low-energy electron irradiation on Si-insulated gate field-effect transistors, 19: 44549
FARNI, Carol, Methods for rapid recovery of heavy water and other products,

19: 44578
FASSEL, Velmer A., Optical emission spectroscopy as an analytical tool, 19: 43929 (IS-1237)
FAVALE, A. J., Theoretical aspects of neutron activation of structures, 19: 45461 (N64-25922)
FEASTER, Gene R., Nuclear thermionic converter, 19: 45556
FEDERER, J. I., Thermochemical deposition of refractory metals, alloys, and compounds for application in thermionic devices, 19: 44640 (ORNL-P-1446-1)
FEDOROV, V. M., Investigation of relsotron acceleration of plasma in presence of the transverse magnetic field, 19: 45435
FEDOROVA, A. V., Changes of cholinesterase activity in chronic administration of certain isotopes, 19: 43775
FEHER, I., Internal bremsstrahlung spectrum accompanying the electron capture process of ^{36}Cl close to the end-point energy, 19: 45345
FEHSENFELD, F. C., Positive ion-neutral reactions in the ionosphere, 19: 45173
FEIX, Marc R., Connection between correlations and fluctuations in a plasma, 19: 45394 (IPP-6/37)
FEKHER, I., Semiconductor detectors with uranium salts for absolute measurement of thermal neutron beams, 19: 44479 (ZFK-PHA-12, pp 140-3)
FEKULA, Olga M., Sampling bias in scanning proton-recoil tracks in nuclear emulsion, 19: 44464 (UCRL-11703)
FENWICK, R. B., Radar measurements of total cislunar electron content, 19: 45176
FENYVES, E., Spurious scattering in nuclear emulsions, 19: 44413 (CERN-65-4(Vol.II), pp VI23-30)
FERGUSON, E. E., Positive ion-neutral reactions in the ionosphere, 19: 45173
FERGUSON, W. F., EGCR control-rod-drive endurance test, 19: 45589 (ORNL-TM-1197)
FERN, F. H., Solution of precipitates in very dilute uranium–iron–aluminium alloys, 19: 44715
FERRACINI, R., Immunological aspects of experimental pulmonary sclerosis due to ionizing radiations, 19: 43817
FERRELL, Richard A., Josephson tunneling and quantum mechanical phase, 19: 45209
FERRERO, Giorgio M., Magnetohydrostatic radiative equilibrium of a gaseous mass, of perfect electrical conductivity, with cylindrical symmetry (sun spots), 19: 44897
FERRO-LUZZI, M., Reaction $KN\pi\pi$ at 3 Bev/c and production mechanism of K^*N^*, 19: 45057
FERRO-LUZZI, M., Resonance of nuclear particles, 19: 45056
FESSLER, H., Detection and measurement of activity in wounds, 19: 44538
FEUVRAIS, L., Circular spark chambers with electric localization, 19: 44498
FICHTEL, C. E., Nuclear emulsion experiments on sounding rockets and satellites, 19: 44436 (CERN-65-4(Vol.II), pp X13-18)
FICHTEL, C. E., Search for gamma-ray point sources, 19: 44905
FIKS, M. M., Kinetics of multiple acceleration of particles with variable charge in a potential electric field, 19: 44864 (JINR-P-2253)
FIL'CHENKOV, V. V., Catalysis by μ^- of $d\mu + p \rightarrow {}^3He + \mu^-$ and $d\mu + d \rightarrow t + p + \mu^-$, 19: 45273 (JINR-P-2356)
FILIPOV, Alexander M., Au SO_2 monitor for air pollution studies: design of the instrument and field testing, 19: 44458 (NYO-2767)
FILIPPOV, S. S., Axis-symmetrical steady motion of conducting gas in external electric and magnetic fields, 19: 44830
FILLIUS, R. W., Survey of inner-zone protons, 19: 45189
FINCH, W. C., Mission integration of nuclear dynamic power systems, 19: 45661
FINGER, Harold B., Nuclear rockets based on graphite reactor technology. Their applications and development status, 19: 45658 (TID-22097)
FINKEL'SHTEIN, E. I., Low-temperature radiation polymerization of acrolein, 19: 44070
FINKLE, E., The application of nuclear reactors and radioisotopes to underwater-vehicle propulsion, 19: 45662
FINKLE, Earl, Small underwater vehicle propulsion with radioisotope power, 19: 44572
FIOCK, W. L., Prog. rpt. on nuclear superheat project, 8–10/64, 19: 45572 (GEAP-4755)
FIRK, F. W. K., Angular distribution of γ rays from 62-ev neutron resonance in ^{124}Sn, 19: 45379
FIRSOV, E. I., Spectrum of γ rays from $^{54}Fe(n,\gamma)^{55}Fe$ reaction, 19: 45322
FIRSOV, V. G., Chemical reactions of muonium. Identification of reaction products, 19: 45278 (NP-15389)
FISCHER, David W., Effect of chemical combination on soft x-ray K emission bands of nitrogen and carbon, 19: 44944
FISCHER, Jan, Contribution to dispersion theory of pion-pion scattering, 19: 45127
FISH, R. W., Reactor weight optimization parametric code—WOP, 19: 45659 (TIM-807)

FISHER, D. J., Remotely controlled corrosion-resistant pipetter, 19: 43936 (ORNL-P-1533)
FISHER, Ray W., Resistance of Y metal to HF mixtures and high-temperature oxidation, 19: 44628
FITA, Mario, Radiolysis of acetylene in solution. II., 19: 44082
FITOUSSI, L., Individual alarm dosimeters for work in or entry into radiation fields, 19: 44532
FITOUSSI, Lucien, Radioprotection problems resulting from the presence of experimental devices around a reactor, 19: 44287 (CEA-R-2799)
FITZGERALD, Lawrence T., Computer treatment planning in radiation therapy. I., 19: 43922
FLAHAUT, Jean, Orthorhombic sulfides, selenides, and tellurides L_2X_3 of the rare earths, yttrium, and scandium of the Sc_2S_3 type, 19: 44010
FLAMM, E. J., High-energy solar neutrons. I., 19: 44902
FLAMM, E. J., High-energy solar neutrons. II., 19: 44903
FLEISCHMANN, H., Flute characteristics of and microwave emission from a plasma in a mirror, 19: 45388 (GA-6432)
FLEROV, N. N., Redesign of IAE linear electron accelerator, 19: 44860 (IAE-614)
FLINT, Hollis M., Effects of γ radiation on fertility and longevity of Hippelates pusio, 19: 43803
FLOOD, W. A., Faraday rotation and volume scattering, 19: 45182
FLYAGIN, V. B., Hydrodynamics of a resonance bubble chamber, 19: 44921
FOA, L., Measurement of π lifetime via the inverse decay process, 19: 45360
FOCARDI, S., Proton polarization in $\pi^- + p$ elastic scattering at 8.5 Bev/c, 19: 45081
FOEX, Marc, Allotropic transformations of sesquioxides of rare earths, 19: 44731
FOIS, M., State of construction of the relativistic cyclotron for protons at 45 Mev, 19: 44886
FOKIN, V. N., Self-excitation regimes in interaction between traveling wave magnetic field and ionized gas flow, 19: 44839
FOLDY, L. L., Structure of nucleons, 19: 45125
FOMICHENKO, K. V., Blood serum proteinographic chart during chronic x irradiation, 19: 43766
FORBES, I. J., Studies of cytotoxicity using ^{32}P, 19: 43740
FORBES, S. G., High current density thrustor experiments, 19: 44226
FORNWALT, D. E., Application of the electron microprobe to the identification and quantitative determination of carbon, 19: 43966
FORNWALT, D. E., Electron metallography techniques applied to bcc metals and alloys, 19: 44610 (TIM-943)
FORTESCUE, Peter, Control rod lift-coupling mechanism, 19: 45516
FORTNER, E., Prog. rpt. on materials of Na heated steam generator, 8/27/65, 19: 44133 (BAW-1280-31)
FOSADO P., Tensor force in the nucleus ^{18}F, 19: 45370
FOURNET, G., Analysis of a magnetization curve of superconductor of the second kind, 19: 45200
FOWLER, J. F., Fading in thermoluminescent lithium fluoride used for radiation dosimetry, 19: 44076
FOX, J. K., Correlation of interaction data with calculations using the Geller model, 19: 44977 (IDO-17095)
FOX, L. W., Operating experience with the first Savannah River high flux charge, 19: 45643 (DP-999, pp 73-86)
FRAIDENRAICH, N., Rayleigh-Taylor instability in striated layer MHD generator, 19: 44984
FRANCHI, M., Dragon Reactor automatic control equipment, 19: 45570 (EUR-2422.i)
FRANCIS, O., Pregnancy after primary irradiation for carcinoma of cervix, 19: 43891
FRANCOIS, H., Multiple-purpose personal dosimeter, 19: 44536
FRANK, L. A., Absence of Martian radiation belts and implications thereof, 19: 44912
FRANK, L. A., Local-time dependence of outer radiation zone electron ($E > 1.6$ Mev) intensities near the magnetic equator, 19: 45160
FRANK, William M., Exchange magnetic moment in three-body nuclei. I., 19: 45332
FRANK, William M., Exchange magnetic moment in three-body nuclei. II., 19: 45333
FRANK-KAMENETSKII, D. A., Propagation of shock waves in outer layers of a star, 19: 44924
FRANZINI, P., Annihilations of antiprotons in hydrogen at rest into two mesons, 19: 45122
FRANZINI, P., Test of charge-conjugation invariance in $\bar{p}p$ annihilations at rest, 19: 45124
FRAZIER, D. S., Thermal-neutron fluxes for CP-5 vertical irradiation facilities, 19: 45668 (ANL-7026)
FREDKIN, D. R., Influence of zero sound on the thermodynamics of ^3He, 19: 45204
FREEMAN, B. E., Non-equilibrium diffusion equation, 19: 45460 (LA-3377)
FREEMAN, J. R., Computational studies on the reconstruction of an analog

signal from non-uniformly spaced samples, 19: 44809 (SC-DR-65-291)
FREI III, Emil, Leukemia, 19: 43840
FREILING, E. C., Cation-exchange equilibria with fused salts, 19: 44040
FREIREICH, Emil J., Leukemia, 19: 43840
FREIS, Robert P., Theory of the electrostatic probe and its improved use as a diagnostic tool, 19: 45414 (UCRL-12480)
FRENCH, R. L., Simulation of fallout gamma radiation fields by monoenergetic plane isotropic sources, 19: 44254 (RRA-M51)
FRENZEN, Paul, Diffusion experiments, 19: 44796 (BNL-914, pp 163-72)
FREUND, P. G. O., Connection between baryon and meson mass spectra, 19: 45077
FREWER, Hans, 300-Mw atomic power station with a Siemens pressurized water reactor at Obrigheim in Germany, 19: 45609
FRICKE, M. P., Alpha radiation hygrometer. III., 19: 44338 (AD-608503)
FRIEDLAENDER, E. M., Measurement of Coulomb scattering in the presence of track distortion and spurious scattering, 19: 44414 (CERN-65-4(Vol.II) pp VI31-6)
FRIEDLAENDER, J., Measurement of Coulomb scattering in the presence of track distortion and spurious scattering, 19: 44414 (CERN-65-4(Vol.II), pp VI31-6)
FRIEDMANN, Christine, Prog. rpt. on deposition of inhaled fission products in lungs, final, 10/62–10/64, 19: 44292 (NP-15173)
FRIEDRICH, L. A., Carburization of Nb–1 Zr alloy, 19: 44609 (TIN-927)
FRINDEL, E., Migration of hematopoietic bone marrow cells in irradiated and normal mice, 19: 43836
FRINDEL, Emilie, Recuperation in mammalian cell systems as revealed by radiation dose fractionation, 19: 43792
FRISCH, O. R., RHODA—rapid hand-operated digitizing apparatus, 19: 44361
FRIZZOLA, John A., Cloud rise experiments at Brookhaven, 19: 44787 (BNL-914, pp 119-22)
FROESE, G., Dependence of division delay on time of irradiation for irradiated and post-irradiated generations of Chinese hamster cells, 19: 43857
FROESE, G., Possible errors in the ferrous sulfate dosimeter, 19: 44540
FROIS, Colette, Study in neutron-irradiated Al of elimination of faults, 19: 44755
FROLOV, F. Y., Flow method of irradiation with ionizing rays, 19: 44061 (AEC-tr-6567)
FRONSDAL, C., Relativistic symmetries, 19: 45005 (IC/65/68)
FUELLE, R., Particle discrimination with semiconductor detectors, 19: 44475 (ZFK-PHA-12, pp 84-97)
FUELLE, R., Reaction $^{10}B(d,p_0)^{11}B$, 19: 45336
FUJII, Yasunori, Exchange electrical moments for nuclear β and γ transitions, 19: 45363
FUJITA, Hitoshi, Radiolysis of chloroauric acid in aqueous solution, 19: 44079
FUJITA, Jun-Ichi, Exchange electrical moments for nuclear β and γ transitions, 19: 45363
FUJIWARA, Kunio, Observation on Fermi surface of copper by positron annihilation, 19: 45487
FUKUI, Shuji, Loss mechanism of electrons from a magnetic bottle, 19: 44823
FULTONBERG, D. N., Zircaloy-steam reaction in a simulated reactor loss-of-coolant accident, 19: 45496 (WCAP-3269-30)
FUQUAY, James J., Meso-scale and mean transport problems, 19: 44781 (BNL-914, pp 99-102)
FUQUAY, James J., Meteorology program at Hanford Atomic Products Operation, 19: 44767 (BNL-914, pp 24-5)
FURBEE, Avery D., X-ray emission analyzer with standardizing system and novel switch means, 19: 44545
FURLAN, G., Theory of corrections to unitary symmetry formulae, 19: 45003 (IC/65/60)
FURUHASHI, Akira, Nuclear parametric study of the pressure tube-type D_2O moderated lattices, 19: 45578 (JAERI-1080)
FURUYA, Keiichi, Determination of O in steels, 19: 43946
FURUYA, Keiichi, Determination of oxygen in stainless steels, 19: 43947

G

GABANETS, I., Utilization of semiconductor detectors in polarization experiments, 19: 44477 (ZFK-PHA-12, pp 126-32)
GABBARD, Charles H., Thermal stress considerations in the Molten Salt Reactor Experiment, 19: 45587 (ORNL-P-1504)
GABBE, John D., Mathematical function describing spacial distribution of protons in earth's radiation belts, 19: 45188
GABE, Iulian, Complex salts with 5-nitrobarbituric acid. III., 19: 44027
GADD, Ivar, Mutations and crop improvement. I., 19: 43656
GADD, Ivar, Mutations and crop improvement. II., 19: 43776
GADD, Ivar, Mutations and crop improvement. III., 19: 43777
GADD, Ivar, Mutations and crop improvement. IV., 19: 43778
GADD, Ivar, Mutations and crop improvement. V., 19: 43779
GADIOLI, E., Level widths of nuclei at high excitation energy, 19: 45343
GAEDTKE, Kl., Polycythemia, osteomyelofibrosis, and acute leukemia, 19: 43820
GAERTNER, R., Low-noise preamplifier for semiconductor detectors with improved constancy, 19: 44483 (ZFK-PHA-12, pp 172-88)
GAGLIOTI, G., Performance of three-axis spectrometer in experiments of elastic diffraction of neutrons, 19: 44531
GALANINA, N. D., Measurement of the absolute value of the $K_1^0 \rightarrow K_1^0$ mass difference, 19: 45099
GALANTINE, R. M., Preliminary SNAPSHOT-1 performance–summary, 19: 45653 (NAA-SR-11430)
GALLET, R. M., Long-period vlf emission pulsations, 19: 45171
GALVAGNI, R., Determination of concentration of radioactive cloud and contamination of soil by Pasquill-Gifford method, 19: 44255 (RT/PROT(65)-10)
GAMBA, O. O., Nature and properties of carbides of uranium, 19: 44603 (NAA-SR-10929)
GANDIA, V., Contraction factor of Ilford G5 nuclear emulsions used in α spectrometry, 19: 44444 (CERN-65-4(Vol.II), pp X67-73)
GANGAS, N., Extension of Laben 512-channel analyzer for use in multiparameter experiments, 19: 44516
GANGULI, S. N., Loading of nuclear emulsion with light and heavy elements, 19: 44399 (CERN-65-4(Vol.II), pp III17-20)
GANOUNA-COHEN, G., Individual alarm dosimeters for work in or entry into radiation fields, 19: 44532
GANS, P., Diffuse reflectance spectra of some uranium(IV) complexes, 19: 44034
GANSSAUGE, E., Polarization of recoil protons in e-p elastic scattering at 20 Fermi^{-2}, 19: 45058
GARCIA, Marie E., Photographic film dosimetry in skin β therapy, 19: 43880 (NP-15270)
GARCIA ORCOYEN, S., Determination of ^{131}I by use of activated carbon, 19: 43958
GARDNER, Andrew L., Null method of measuring microwave phase shifts, 19: 45412 (UCRL-7978)
GARDNER, Donald G., Cross section of some reactions of ^{99}Tc with 14.1-Mev neutrons, 19: 45325
GARDNER, J. A., Electron density and temperature measurements in exhaust of a MPD source, 19: 45448
GARFAGNINI, R., Apparatus for study of energy spectra and polarization of photoneutrons, 19: 45303
GARMIRE, G., Positions of three cosmic x-ray sources in Scorpio and Sagittarius, 19: 44968
GARRONI, A., Dragon Reactor automatic control equipment, 19: 45570 (EUR-2422.i)
GARVEY, J., Behavior of a wide-gap spark chamber when two particle tracks are present, 19: 44518
GARVEY, J., Deviation between spark and track in wide-gap spark chamber, 19: 44514
GATTO, R., Recent calculations on electron-positron colliding beam experiments, 19: 45023 (LNF-65/8)
GATTO, R., Vector and axial currents under first-order symmetry breaking, 19: 45022 (LNF-65/7)
GAUSTER, W. F., Experimental simulation of large, high field, superconducting magnet operation, 19: 45192 (ORNL-TM-1266)
GAZAZYAN, A. D., Forced β decay of protons induced by electromagnetic radiation, 19: 45052
GEE, W., Hematology report on beagles, 19: 43725 (UCD-472-112, pp 44-9)
GEISS, J., Further evidence on the origin of trapped gases in the meteorite Khor Temiki, 19: 44906
GELFAND, N., Test of charge-conjugation invariance in $\bar{p}p$ annihilations at rest, 19: 45124
GENAZZANI, E., Intracellular enzyme variations from x rays. I., 19: 43739
GENKIN, A. L., Fringe effects in magnetogasdynamical converter, 19: 44840
GENTIL, Jean, Sealed coupling for an electrical heating conductor with coaxial sheath, 19: 44164 (CEA-R-2755)
GEORGE, A. F., Protection against fire hazards in the design of filtered ventilation systems of radioactive and toxic process buildings, 19: 44284 (AWRE-O-24/65)
GEORGE, R., Reaction $KN\pi\pi$ at 3 Bev/c and production mechanism of K^*N^*, 19: 45057
GEORGE, Raymond S., Polarization on energy beam in infrared grating spectrophotometers, 19: 44345 (LA-DC-6719)
GERARD, Bernard, Improvements in or relating to manipulating tools, 19: 44174
GERNA, G., Morphogenesis of binucleated erythropoietic cells by action of x rays, 19: 43730
GERNA, G., Pseudo-amitoses provoked by x rays in erythropoietic cells in

vitro, 19: 43826
GERSHBERG, R. E., Possible mechanism of formation of galactic bridges, 19: 44926
GERTISSER, Berthold, Mixed antimony oxide–uranium oxide oxidation catalyst, 19: 44043
GESHKENBEIN, B. V., Vertex function poles and one-particle states orthogonalization, 19: 45029 (NP-15382)
GESKE, David H., Isotropic ^{17}O coupling constant in the nitrobenzene anion radical, 19: 44049
GEWISS, Claude, Guide tubes for nuclear reactors, 19: 45517
GIACCONI, R., Positions of three cosmic x-ray sources in Scorpio and Sagittarius, 19: 44968
GIACCONI, R., Spectral data from cosmic x-ray sources in Scorpius and near the galactic center, 19: 44967
GIACOMELLI, G., Proton polarization in $\pi^- + p$ elastic scattering at 8.5 Bev/c, 19: 45081
GIAMBUSSO, A., Outlook for United States nuclear power, 19: 45615
GIBB, T. C., Chemical applications of the Moessbauer effect. II., 19: 44035
GIBBONS, Harry L., Inhalant allergy to the screwworm fly, 19: 43652
GIBBONS, J. H., Neutron resonance capture in 2s-1d shell nuclei, 19: 45356
GIBSON, M., Analysis of some two-zone exponential experiments on graphite moderated lattices, 19: 45524 (AEEW-R-428)
GIDDINGS, J. Calvin, Prog. rpt. on resolution in chromatography, final, 4/59–3/65, 19: 44113 (COO-748-1)
GIESE, A. C., Comparative uv sensitivity of regeneration in the genus blepharisma, 19: 43812
GIFFORD, Frank A. Jr., Continuous point source diffusion in the surface layer, 19: 44766 (BNL-914, pp 20-3)
GIFFORD, Frank A. Jr., Technical areas in meteorology that are limiting progress in nuclear industry, 19: 44780 (BNL-914, pp 95-8)
GIL, D., Momentum determination of low-momentum particles in emulsions exposed to strong magnetic field, 19: 44424 (CERN-65-4(Vol.II), pp VIII9-16)
GILBERT, J. R. B., Techniques in machining and working of cast tungsten, 19: 44653
GILL, J. J., Carburization of type 304 stainless steel in sodium–carbon systems, 19: 44624 (NAA-SR-Memo-4887)
GILLET, C., Calcium flux from x-irradiated Nitella cells, 19: 43818
GILLILAND, Paul F., Immunologic studies of octapeptides. II., 19: 43658
GILLILAND, Paul F., Immunologic studies of octapeptides. I., 19: 44105
GIORDANO, P., Analysis of nonlinear control system for reactor RTM, 19: 45682 (RT/ING(64)-15)
GIORGI, Maurizio, Catalog of meteorological data received during the IGY and IGC. World data and Italian data, 19: 44819
GIPSON, D. H., A nonlinear least-square program for the determination of parameters of photopeaks by the use of a modified-Gaussian function, 19: 45261 (IDO-17016)
GIRARDI, F., Determination of O in organic compounds and metals by activation with neutrons, 19: 43928 (EUR-2290.f)
GISPERT, M., Studies on production of heavy water. II., 19: 44576
GIUSIANO, F., Apparatus for investigations on scintillator properties in the temperature range −100°C to +50°C, 19: 44460 (RT/FI(65)8)
GIUSTINA, G., Radioiodine metabolism in patients affected by a simple sporadic goiter, 19: 43691
GIZON, Andree, Preparation of thin VYNS films, 19: 44590 (CEA-R-2803)
GLASSMAN, Arthur J., Thermodynamic and turbomachinery concepts for radioisotope and reactor Brayton-cycle space power systems, 19: 45654 (NASA-TN-D-2968)
GLAUNER, R., Radiation protection debates, 19: 43896
GLAZYRIN, M. P., Crystallographic and optical characteristics of vanadates of certain rare earth elements, 19: 44032
GLEASON, Charles H., Nuclear thermionic converter, 19: 45556
GLOERSEN, P., Neutral mass density measurements in a repetitively pulsed coaxial plasma accelerator, 19: 45449
GLOERSEN, P., Performance of two-stage repetitively pulsed coaxial plasma engine, 19: 44233
GLUCKSTERN, R. L., Coupling elements in equivalent circuit for cavity cells, 19: 44859 (BNL-9496)
GOEHRING, I., Synthesis and properties of nicotinamide-adenine-N^1-oxide-dinucleotide, 19: 44062
GOLCHERT, Norbert W., Cross section of some reactions of ^{99}Tc with 14.1-Mev neutrons, 19: 45325
GOLDAN, P. D., Positive ion-neutral reactions in the ionosphere, 19: 45173
GOLDBERG, Joseph, Utilization of indefinite metrics for the determination of propagators in quantum field theory, 19: 45133 (NP-15341)
GOLDBERG, Murray D., Neutron cross sections. Z = 88 to 98, 19: 45250 (BNL-325(2nd Ed.)(Suppl. 2)(Vol.III))
GOLDBERG, P., Prog. rpt. on boiling flow regimes and critical heat flux, 3/6–6/15/65, 19: 44193 (NYO-3304-5)
GOLDBERGER, Marvin L., Accuracy of measurement for counting and intensity-correlation experiments, 19: 45151
GOLDEN, Kenneth I., Structure and the stability of shock waves in electromagnetic media, 19: 45422
GOLDEN, Pamela M., Hazards to human ear from shock waves produced by high-energy electrical discharges, 19: 44283 (AWRE-E-1/65)
GOLDEN, Sidney, Continuous representations in the statistical theory of electronic energies, 19: 44936 (TID-21692)
GOLDFEDER, Anna, Determination of cell cycle and time of synthesis of DNA using tritated thymidine and autoradiography, 19: 43698
GOLDHABER, G., Spin analysis for I = 0 3-pion system, 19: 45042 (UCID-2608)
GOLDHABER, Gerson, Coherent K* production in the K+d reaction at 2.3 Bev/c, 19: 45120
GOLDHABER, Sulamith, Coherent K* production in the K+d reaction at 2.3 Bev/c, 19: 45120
GOLDHABER, Sulamith, Review of recent boson resonances, 19: 45046 (UCRL-16295)
GOLDMAN, A., Proper use of transformations of log normal functions in small-particle statistics, 19: 44808 (LA-DC-6636)
GOLDMAN, A. M., Metastable current-carrying states of weakly coupled superconductors, 19: 45206
GOLDMAN, Leon, Tumors of thyroid and parathyroid glands, 19: 43892
GOLDMAN, M., Ion exchange removal of ^{90}Sr from biologic wastes, 19: 45692 (UCD-472-112, pp 141-7)
GOLDMAN, M., Radium metabolism by beagles following single and multiple injections, 19: 43678 (UCD-472-112, pp 97-108)
GOLDMAN, M., Skeletal dosimetry and exposure status of beagle colony, 19: 43726 (UCD-472-112, pp 120-5)
GOLDMAN, M., The determination of zinc and iron in biologic materials by x-ray fluorescence spectrometry, 19: 43939 (UCD-472-112, pp 59-72)
GOLDMAN, Marvin, Strontium-90 uptake and retention in labeled beagles, 19: 43679 (UCD-472-112, pp 109-19)
GOLDSCHMIDT-CLERMONT, Y., Reaction $KN\pi\pi$ at 3 Bev/c and production mechanism of K*N*, 19: 45057
GOMBAS, P., Pseudo potentials, 19: 45138
GOMBOSI, E., Multiple scattering constant in emulsion at great cell length, 19: 44431 (CERN-65-4(Vol.II), pp IX32-40)
GOMBOSI, E., Spurious scattering in nuclear emulsions, 19: 44413 (CERN-65-4(Vol.II), pp VI23-30)
GOMEZ, R., Polarization of recoil protons in e-p elastic scattering at 20 Fermi-a, 19: 45058
GONDRAND, Jean-Claude, Double time-of-flight fast neutron spectrometry and study of the reaction $^9Be(n,2n)$, 19: 45252 (CEA-R-2734)
GOOD, R. H. Jr., Position operators in relativistic single-particle theories, 19: 45118
GOOD, Roland H. Jr., Phase space considerations for three-particle and four-particle final states, 19: 45006 (IS-1214)
GOOD, W. M., Neutron resonance capture in 2s-1d shell nuclei, 19: 45356
GOODALE, Edmund E., Radiation dosimeter providing visual representation of total dose, 19: 44546
GOODE, J. H., Evaluation of small modified CEN mixer-settlers for extraction of uranium and thorium in a hot cell facility, 19: 44117 (ORNL-TM-1256)
GOODHEAD, D. T., Short-range hyperfragments produced by K⁻ captures in emulsions, 19: 45342
GOODING, T. J., Quasi-steady-state pulsed plasma thrustors, 19: 45441
GOODMAN, B. B., Observation of speed of flux jumps in superconducting Nb, 19: 45199
GOODMAN, Merrill, Radioisotopes in otolaryngology, 19: 43906
GOODZEIT, C. L., Neon-hydrogen bubble chambers, 19: 44375 (BNL-9425)
GOOGIN, J. M., Preparing and sintering tungsten powder, 19: 44613 (Y-1476)
GOOLD, D., Techniques in machining and working of cast tungsten, 19: 44653
GORDON, D. A., 100-Kv, 10-w heavy-particle thruster, 19: 44231
GOREN, R., Effect of ^{60}Co gamma rays applied at low dose rates on some juice constituents and peel color of green and ripe citrus fruits, 19: 44554 (IA-1015)
GORINI, G., Polarization of recoil protons in e-p elastic scattering at 20 Fermi-a, 19: 45058
GORLOV, G. V., Neutron beam for measuring scattering cross sections at small angles, 19: 44862 (IAE-867)
GOROWITZ, B., Neutral mass density measurements in a repetitively pulsed coaxial plasma accelerator, 19: 45449
GOROWITZ, B., Performance of two-stage repetitively pulsed coaxial plasma engine, 19: 44233
GORSHKOVA, L. A., Catalytic activity of praseodymium oxide in dehydrogenation and dehydration of alcohols and dehydrogenation of tetralin, 19: 44023

GOSLIN, R. N., Isotopic contamination in electromagnetic separators, 19: 44573 (ORNL-P-515)
GOTODA, Masao, Existence of long-lived radicals in γ radiation induced polymerization of ethylene, 19: 44073
GOTODA, Masao, Specific influence of temperature on γ-radiation induced polymerization of ethylene, 19: 44074
GOTTA, Hector, Possibilities of using ^{99m}Tc tracer instead of radioiodine in thyroid function investigations, 19: 43881 (NP-15271)
GOUANERE, M., Circular spark chambers with electric localization, 19: 44498
GOULD, Robert J., High-energy photons from compton-synchrotron process in the Crab Nebula, 19: 44911
GOULD, Robert J., Origin of cosmic x rays, 19: 44971
GOULDING, Fred S., Semiconductor detectors for nuclear spectrometry, 19: 44466 (UCRL-16231)
GOURBER, J. P., Rubidium vapor atomic clocks, 19: 44814
GOURDIN, Michel, $K_1^0 \to 2\pi$ transition in unitary symmetry, 19: 45026 (N64-19243)
GRADY, J. E., Polarizing microscopy of abnormal destine produced by injections of strontium or fluoride, 19: 43687
GRAFFSTEIN, A., Use of the chopper for pulse neutron measurements, 19: 45222 (INR-624/IX-A/R)
GRAND-CLEMENT, Ann-Marie, Multiple-purpose personal dosimeter, 19: 44536
GRANNIS, Paul Dutton, Measurement of polarization parameter in proton-proton scattering from 1.7 to 6.1 Bev, 19: 45043 (UCRL-16070)
GRANT, D., Hall effect stabilizer for experimental magnets, 19: 44173
GRANT, I. S., Optimization of half-life counting experiments, 19: 44503
GRANT, P. J., London University reactor Consort, 19: 45683
GRATTON, L., High energy astrophysics, 19: 44909
GRAUER, Robert C., Externally applied probe for scanning radioactivity in countercurrent distribution machines, 19: 43940
GRAVES, W. E., Physics design of the Savannah River high flux charge, 19: 45640 (DP-999, pp 29-42)
GREEN, J. H., Wide-range high-resolution time-to-amplitude converter, 19: 44508
GREEN, J. W., Strap-on RTD test plan, model four testing, 19: 45502 (RL-REA-2120)
GREEN, Michael A., The feasibility of a low-field superconducting thin-septum magnet, 19: 44877 (UCRL-16346)
GREENBERG, H. J., Clamp-on process tube temperature detector for monitoring nuclear reactor operation, 19: 45646
GREENE, Alden G., Index to conferences relating to nuclear science, 19: 45716 (TID-4043(Rev.2))
GREENLAND, L., Gallium in chondritic meteorites, 19: 44900
GREENWOOD, N. N., Chemical applications of the Moessbauer effect. II., 19: 44035
GREGORY, B. P., Future perspectives for emulsion work at CERN, 19: 44382 (CERN-65-4(Vol.I), pp 105-10)
GREINER, E., High-pressure diffusion cloud chamber with machine cooling, 19: 44494
GREINER, Herbert, Method for production of spherical fuel elements for nuclear reactors, 19: 44662
GREINER, Walter, Photon absorption cross section of spherical nuclei, 19: 45366
GRENCH, H. A., Cross sections for ^{89}Y(n,γ)^{90m}Y and ^{89}Y(n,γ)^{90}Y between 0.145 and 1.225 Mev, 19: 45376
GRENCH, H. A., Experimental photopeak efficiencies for NaI(Tl) crystals, 19: 44515
GRENDON, Alexander, Federal Radiation Council guides and other exposure standards, 19: 44306
GREY, Stephen, Effect of weightlessness and radiation on growth of wheat coleoptile, 19: 43717 (NASA-CR-303)
GRIFFIN, B. I., Measurements of radioactivity in Alaskan natives in 1964, 19: 44289 (HW-SA-3750)
GRIGOR'EV, E. P., Gamma spectrum of ^{160m}Ho isomer, 19: 45272 (JINR-P-2270)
GRIGOROVICI, Aurora, Paper chromatographic separation of tantalum, niobium, and hafnium, 19: 44124
GRIGORY, S. C., Prog. rpt. on fatigue strength of pressure vessels, 7/15/65, 19: 45503 (SWRI-1228-69)
GRIMANIS, A. P., Determination of chloride in beer by radioactivation analysis, 19: 43944
GRIMES, J. H., Uranium corrosion. I. Optical method for following oxide formation, 19: 44619 (AWRE-O-66/65)
GRIMM, J., Prog. rpt. on radiation-resistant electron tubes, 5/21–8/31/63, 19: 44337 (AD-425708)
GRISARD, J. W., Separation of potassium isotopes by molecular distillation, 19: 43931 (K-1650)
GRODZINS, L., Proposed methods for producing intense pulsed beams of monoenergetic neutrons, 19: 44882
GROEGLER, N., Further evidence on the origin of trapped gases in the meteorite Khor Temiki, 19: 44906
GROFF, R. P., Anomalous behavior of superconducting microgeometries in presence of high current densities, 19: 45207
GROLL, D., Summary of fluid film bearing analysis, 19: 44147 (TIM-917)
GROMOLL, Heinz-Wilhelm, On radiogold hypophysectomy in metastasizing mammary carcinoma, 19: 43920
GROMOV, K. Ya., New data on ^{135}Ce decay, 19: 45268 (JINR-P-2235)
GROMOV, K. Ya., Spectra of conversion electrons of ^{138}Ce and ^{132}Ce isotopes, 19: 45269 (JINR-P-2236)
GROOTHUIS, S. E., Hydraulic problems on BONUS reactor pressure control system, 19: 45603 (Y-1491)
GROSS, Eugene B., Unique occurrence of uranium minerals, Marshall Pass, Saguache County, Colorado, 19: 44274
GROSS, Franz, Relativistic treatment of loosely bound systems in scattering theory, 19: 45110
GROSS, R. A., Ionizing shock studies in electromagnetically driven shock tube, 19: 44857
GROSSE, A. V., Prog. rpt. on high-temperature inorganic chemistry, annual, 6/64–6/65, 19: 44701 (TID-22144)
GROSSMAN, L. N., Interfacial reaction between UO_2 and Zircaloy-2, 19: 44597 (GEAP-4679)
GROSSMAN, L. N., Uranium oxide fuel for nuclear thermionic converters, 19: 44593 (CONF-650908-4)
GROSSMAN, Leonard N., Insulator materials for nuclear thermionic power conversion, 19: 44685 (CONF-650908-5)
GRUBE, D. F., Improved strip-sealed continuous rotation scattering chamber, 19: 44883
GRUEMM, H., Design study of small nuclear power plant for Austria, 19: 45581 (NP-15291)
GRUENBERGER, Desider, Automatic continuous measurement of the ^{14}C radioactivity in fractions from chromatographic columns, 19: 43949
GRUENEBERG, Gerhard, Electrochemical fuel cell operation with antipolar ion exchange membrane, 19: 44992
GUALTIERI, G., Experience in test and use of Italian nuclear power plants, 19: 45616
GUARALDO, C., Persistent currents induced by circularly polarized waves in a superconducting ring, 19: 45191 (LNF-65/15)
GUENTZSCHEL, Peter, Model law for filtration and determination of the filtration rate on the basis of permeability tests, 19: 43923 (ORNL-tr-743)
GUERRIN, J., Thorotrast disease concerning one observation, 19: 43738
GUERRINI, B., Outlook for use of nuclear energy for production of heat at low temperature, 19: 45618
GUEVARA, F. A., Measurement of helium and hydrogen viscosities to 2340°K, 19: 45190 (LA-3319)
GUGLIELMO, Richard J., Radiation barrier material and method of making the same, 19: 44670
GUIDUCCI, Lino, Tightness joint, 19: 44176
GUILHERMET, Monique, Radioprotective activity of nitrogenous heterocyclic compounds derived from imidazole and benzimidazole, 19: 43863
GUILINO, E., Influence of probe losses on the ion density of a thermal alkali plasma in a magnetic field, 19: 45393 (IPP-2/38)
GUILLAUMONT, Robert, Ionic species of protactinium in aqueous solutions. IV., 19: 44012
GUILLERMIN, Pierre, Detection of tritium in CO_2 of G2/G3 reactors using gas chromatography, 19: 43926 (CEA-R-2800)
GUILLERMIN, Pierre, Radioactivity measurements inside pressure vessel of Reactor G 3 after 4 years operation, 19: 45566 (CEA-R-2785)
GUILLETTE, R. W., MIRAGE-III: matrix interpretive routine, 19: 44581 (KAPL-M-6469)
GUION, K. J., Activity of uranium in dilute solution in liquid bismuth, 19: 44733
GUITTARD, Michelina, Orthorhombic sulfides, selenides, and tellurides L_2X_3 of the rare earths, yttrium, and scandium of the Sc_2S_3 type, 19: 44010
GULICK, Wilson M. Jr., Isotropic ^{17}O coupling constant in the nitrobenzene anion radical, 19: 44049
GUMAN, William J., Studies of a switch-triggered pulsed plasma accelerator, 19: 44225
GUNN, Walter G., Problems in radiation therapy in the aged, 19: 43915
GUNTHER, H., Measurement of the β-particle distribution of mass selected fission fragments with nuclear emulsions, 19: 44441 (CERN-65-4(Vol.II), pp X47-53)
GUON, J., Second-cycle AIROX reprocessing and pellet refabricating of highly irradiated UO_2, 19: 44114 (NAA-SR-11375)
GUPTA, A. B., Effect of nuclear radiations on cellulosic fibres, 19: 44063
GUPTA, B. P., Spectrophotometric determination of zirconium with 7,8,3',4'-tetrahydroxy flavonol, 19: 43955
GUPTA, S. L., Gamma-gamma directional correlations in ^{128}I, 19: 45335
GUPTA, U. C., Decay of ^{86}Rb, 19: 45331

GURSKY, H., Positions of three cosmic x-ray sources in Scorpio and Sagittarius, 19: 44968
GURSKY, H., Spectral data from cosmic x-ray sources in Scorpius and near the galactic center, 19: 44967
GUSMANO, E. A., Metabolism of ^{46}Sc in man, 19: 43692
GUSS, D. E., Nuclear emulsion experiments on sounding rockets and satellites, 19: 44436 (CERN-65-4(Vol.II), pp X13-18)
GUSTAFSSON, Ake, Mutations and crop improvement. I., 19: 43656
GUSTAFSSON, Ake, Mutations and crop improvement. II., 19: 43776
GUSTAFSSON, Ake, Mutations and crop improvement. III., 19: 43777
GUSTAFSSON, Ake, Mutations and crop improvement. IV., 19: 43778
GUSTAFSSON, Ake, Mutations and crop improvement. V., 19: 43779
GVERDTSITELI, I. G., Relative difference of vapor pressure in $^{11}BF_3$–$^{10}BF_3$, 19: 44575
GYGI, E., High precision air core magnet, 19: 44165 (CERN-65-29)

H

HAAVE, C. R., Vlf phase perturbations and the Soviet high-altitude nuclear bursts of October 22 and 28, 1962. I., 19: 45166
HAAVE, C. R., Vlf phase perturbations and the Soviet high-altitude nuclear bursts of October 22 and 28, 1962. II., 19: 45167
HAEBERLI, W., Polarization of protons from the D(d,p)T reaction, 19: 45253 (COO-7-0362)
HAEFNER, Richard R., Computer program for circulation of library journals, 19: 45700 (DP-970)
HAEGGBLOM, Hans, Theoretical work for fast zero-power reactor FRO, 19: 45667 (AE-194)
HAERTLING, G. H., Semicontinuous hotpress tunnel kiln, 19: 44644 (SC-TM-65-276)
HAFFNER, J. W., ERD concept in space radiation shielding, 19: 45470
HAFNER, H., Polarization of alkali line radiation excited by electron impact, 19: 44956
HAGA, F. E., Remotely controlled corrosion-resistant pipetter, 19: 43936 (ORNL-P-1533)
HAGA, F. E., Sample preparation apparatus for MSRE, 19: 44168 (ORNL-P-1532)
HAGEN, R. N., SPORT—system for processing reactor transient data, 19: 45527 (IDO-17078)
HAGG, E. L., Influence of focusing on the apparent reflection coefficient of the F region, 19: 45175
HAGIWARA, Miyuki, Existence of long-lived radicals in γ radiation induced polymerization of ethylene, 19: 44073
HAGIWARA, Miyuki, Specific influence of temperature on γ-radiation induced polymerization of ethylene, 19: 44074
HAHN, H., Lattice vibrations in molecular crystals and neutron scattering, 19: 45492
HAHN, H., Sulfide fluoride of the rare earths, 19: 44024
HAHN, J., Nuclear pulse amplifiers, 19: 44521
HAINZENLIN, Jean Louis, Improvements in or relating to processes for applying alloys to metal surfaces, 19: 44658
HALL, F. J., Protection against fire hazards in the design of filtered ventilation systems of radioactive and toxic process buildings, 19: 44284 (AWRE-O-24/65)
HALL, Lawrence S., Theory of the electrostatic probe and its improved use as a diagnostic tool, 19: 45414 (UCRL-12480)
HALL, T. C., High-efficiency liquid-scintillation counting of ^{14}C-labeled material in aqueous solution, 19: 43945
HAMA, M., Elastic scattering and multiple production at high energy, 19: 45091
HAMMOND, J. P., Calculations of charge and contour dimensions of powder-loading assembly used in the production of HFIR composite fuel compacts, 19: 44641 (ORNL-TM-1193)
HAMMOND, R. Philip, Nuclear desalting for agricultural water, 19: 45636
HANCOX, R., Preparation and properties of sintered Nb_3Sn, 19: 44592 (CLM-R-43)
HANDLER, George S., Continuous representations in the statistical theory of electronic energies, 19: 44936 (TID-21692)
HANKINS, Dale E., Single-sphere neutron monitoring instrument, 19: 44454 (LA-DC-7323)
HANNA, R. C., Measurements of the A and R parameters in proton-proton scattering at 47.8 and 27.6 Mev, 19: 45319
HANSEL, James M., Inert atmosphere enclosure for the preparation of samples prior to determination of oxygen, 19: 43933 (LA-3344)
HANSEN, Ole, Angular distributions from shell-model forbidden (d,p) transitions to spin 5/2 states in ^{43}Ca, ^{45}Ca, and ^{47}Ti, 19: 45323
HANSON, H. D., Emulsion grain density in the extreme relativistic region, 19: 44428 (CERN-65-4(Vol.II), pp IX9-13)
HANSON, R., Roentgenographic survey of experimental beagles, 19: 43882 (UCD-472-112, pp 50-8)
HANSON, W. C., Measurements of radioactivity in Alaskan natives in 1964, 19: 44289 (HW-SA-3750)
HAPKE, Bruce, Effects of simulated solar wind on photometric properties of rocks and powders, 19: 44896
HARADA, Y., Base composition of messenger RNA of Pseudomonas effus irradiated with uv light, 19: 43744
HARARI, H., Experimental tests of broken U(12) and approximate U(6) × U(6), 19: 45002 (IC/65/59)
HARARI, H., Meson and baryon resonances in relativistic SU(6), 19: 45112
HARBAUGH, W. E., Development of a reservoirless thermionic energy converter, 19: 44989
HARBAUGH, W. E., Prog. rpt. on insulated thermionic converter-heat pipe assembly, 6/65, 19: 44980 (NP-15433)
HARDEN, D., Fast neutron capture through charged particle reactions in water and in concentrated manganese sulfate solution from radioactive neutron sources, 19: 45232
HARDIE, D., Role of hydride precipitate in fracture of Zr and its alloys, 19: 44716
HARDIE, G., Feasibility of using scintillating fibers for low-energy β counting, 19: 44451 (IITRI-578P26-8)
HARGREAVES, J. K., Relation between auroral radio absorption and vlf emissions, 19: 45170
HARLIN, Sam H., Parametric performance analysis for interplanetary missions utilizing first-generation nuclear stages, 19: 45649 (N64-32637)
HARRIES, W. L., Plasma confinement in the model C stellarator, 19: 45397 (MATT-282)
HARRINGTON, Richards H., Survey of alloy-eutectic sources for aligned structures, 19: 44707 (WVT-6523)
HARRIS, C. Craig, Collimators for low-energy γ rays, 19: 44347 (ORNL-P-1545)
HARRIS, P. M., Crystal structure of solid deuterium from neutron-diffraction studies, 19: 45211
HARRISON, K. T., Recording microbalance for remote thermogravimetric examination of irradiated materials, 19: 44341 (AERE-R-4962)
HART, Roger G., Schematic view of the origin of life, 19: 45721 (UCRL-14254)
HARTLEY, Kenneth, Improvements relating to chemical extraction processes, 19: 44127
HARTMAN, Charles W., Low-temperature plasma column confinement by magnetic fields with shear, 19: 45415 (UCRL-14137)
HARTMAN, Ted, Effects of roentgen therapy on host acceptance of autogenous bone grafts in dogs, 19: 43835
HASEGAWA, H., Possible evidence for nuclear interaction of μ above 3×10^{14} ev, 19: 45368
HASHMI, M., Influence of probe losses on the ion density of a thermal alkali plasma in a magnetic field, 19: 45393 (IPP-2/38)
HASTERLIK, Robert J., Late effects of radioactive materials deposited in man, 19: 43830
HATHAWAY, B. J., Diffuse reflectance spectra of some uranium(IV) complexes, 19: 44034
HAUBENREICH, P. N., Predicted and observed nuclear characteristics of the Molten Salt Reactor Experiment, 19: 45586 (ORNL-P-1503)
HAUGEN, Duane A., Meteorology program at the Air Force Cambridge Research Laboratories, 19: 44776 (BNL-914, pp 75-84)
HAUSER, J. J., Proximity effect between a superconducting and a ferromagnetic film, 19: 45197
HAUTOT, A., Description of nonelastic interactions at low energy. Application to the interaction $^{27}Al(p)$, 19: 45304
HAUTOT, A., Heretic model of the nucleon, 19: 45049
HAWKINS, R. H., Importance of capillary pores in rainwater percolation to the ground water table, 19: 44235 (DPSPU-64-30-23)
HAWRYLAK, R. A., Improved strip-sealed continuous rotation scattering chamber, 19: 44883
HAWS, C. C., Summary of the Kilorod Project, 19: 44638 (ORNL-3681)
HAYAKAWA, Satio, Loss mechanism of electrons from a magnetic bottle, 19: 44823
HAYAMI, HIROSHI, Japanese dietary habits and the fallout problem. II., 19: 44264
HAYMES, R. C., Nuclear gamma rays from supernova remnants, 19: 44930
HAYWORTH, R. R., Energy storage capacitors for pulsed plasma thrustors, 19: 44224
HAZAN, Jean-Pierre, Analysis of $^{56}Fe(^3He,p)$ and $^{63}Cu(^3He,p)$ energy and angular distributions-nuclear shell effects, 19: 45362
HEARN, David, Background events in photomultiplier tubes at high altitudes, 19: 44465 (UCRL-12020)
HEATH, R. L., A nonlinear least-square program for the determination of parameters of photopeaks by the use of a modified-Gaussian function, 19: 45261 (IDO-17016)
HECHMAN, H. H., Emulsion experiments in oriented polar-orbiting satellites, 19: 44437 (CERN-65-4(Vol.II), pp X19-32)
HEESTAND, R. L., Thermochemical deposition refractory metals, alloys,

and compounds for application in thermionic devices, 19: 44640 (ORNL-P-1446-1)

HEIBERG, E., Design of simple but accurate low-energy β liquid scintillation counter, 19: 44506

HEINZ, W., Electronic regulation of emission current of a pulsed injector for 200 kv, 19: 44884

HELLIN, Michel, Hydrolysis in acid medium of linear and cyclic acids. III., 19: 44011

HELLSTRAND, E., Experimental studies on assemblies 1 and 2 of the fast reactor FRO. I., 19: 45522 (AE-195)

HELMER, R. G., A nonlinear least-square program for the determination of parameters of photopeaks by the use of a modified-Gaussian function, 19: 45261 (IDO-17016)

HELWIG, W. J., Thermoelectric technology for space-power systems, 19: 45664

HENDERSON, R. E., Design applications of direct energy converters, 19: 44987

HENNELLY, E. J., Isotope production in a Savannah River reactor at flux levels above 10^{15} n/(cm²)(sec), 19: 45639 (DP-999, pp 19-28)

HENRI, V. P., Reaction $KN\pi\pi$ at 3 Bev/c and production mechanism of K^*N^*, 19: 45057

HENRY, R. W., Personnel monitoring practices at the National Testing Station, 19: 44335

HERAK, R. M., Contribution to study of effect of TiO_2 additive on sintering of UO_2, 19: 44646

HERMAN, M., Prog. rpt. on flow and fracture studies of alloyed Be, 7/7–10/64, 19: 44693 (NP-15411)

HERMAN, M., Prog. rpt. on flow and fracture studies of alloyed Be, final, 8/65, 19: 44694 (NP-15432)

HERMANN, Horst, Remote-controlled machine tool for hot chambers of nuclear energy plants, 19: 44177

HERR, Wilfried, Process for the preparation of compounds tagged by radioactive tracers, 19: 44107

HERSKIND, B., Coulomb excitation of vibrational states in deformed even nuclei, 19: 45321

HERZ, A. J., Measurements in nuclear emulsions, 19: 44381 (CERN-65-4 (Vol.I), pp 79-87)

HERZ, A. J., Relativistic increase in the track blob density in various nuclear emulsions, 19: 44430 (CERN-65-4(Vol.II), pp IX23-31)

HESS, J. W., Compilation of Fermi experience, 19: 45562 (APDA-174, pp 71-3)

HESS, R., Diagnostic studies in a Hall accelerator at low exhaust pressure, 19: 45446

HESTER, R. E., Experimental studies with the Astron facility, 19: 45413 (UCRL-12456)

HEWITT, Roger, X-ray-induced perturbations in replication of bacterial chromosome, 19: 43741

HICKERSON, J. P., Thermal studies on Hastelloy X metallic insulation, 19: 44589 (BNWL-102)

HICKS, B. B., Radioactive fallout in Southern Australia during years 1958–1964, 19: 44261

HIGASHI, Iwami, Determination of lattice constants with Geiger-counter x-ray diffractometer. Lattice constants of UC and UC_2, 19: 44722

HIGGINS, Gary H., Some calculations for effecting oilfield stimulation by nuclear means, 19: 44158 (UCRL-14311)

HILBORN, H. S., Prog. rpt. on properties of thin-walled Zy tubing, 7/65, 19: 44634 (DPST-65-83-7)

HILDRETH, N. T., Strap-on RTD test plan, model four testing, 19: 45502 (RL-REA-2120)

HILL, E. F., Na technology loop, 19: 44162 (APDA-174 pp 33-55)

HILL, H. W., Uranium oxide fuel for nuclear thermionic converters, 19: 44593 (CONF-650908-4)

HILL, M. W., Anticoincidence-shielded Ge(Li) γ spectrometer, 19: 44519

HILL, R. D., Systematics of baryon states, 19: 44996 (COO-1195-39)

HILLARY, J. J., High-activity iodine release from irradiated fuel and its subsequent clean-up, 19: 44303 (TRG-Report-888)

HILLEY, J. R., Operating experience with the first Savannah River high flux charge, 19: 45643 (DP-999, pp 73-86)

HILLIARD, R. K., Fission-product simulation in containment systems experiment, 19: 44286 (BNWL-SA-30)

HILLIARD, R. K., Natural removal of fission products released from UO_2 fuel in condensing steam environments, 19: 44285 (BNWL-SA-29)

HILLS, H. K., Absence of Martian radiation belts and implications thereof, 19: 44912

HILSMEIER, William F., Deposition calculations at Oak Ridge, 19: 44249 (BNL-914, pp 144-5)

HILSMEIER, William F., Oak Ridge meteorological program, 19: 44765 (BNL-914, pp 18-19)

HINGORANI, S. B., Strontium-90 content of food samples in India—data summary through 1963, 19: 44244 (AEET/AM/40)

HIRAKIS, E. C., Carburization of Nb–1 Zr alloy, 19: 44609 (TIM-927)

HIRATA, Allen A., Coherent K* production in the K⁺d reaction at 2.3 Bev/c, 19: 45120

HIROTA, R., Wigner representation of quantum operators, 19: 45139

HIRSCHI, H., Remarks to discourses of J. Joly on radioactivity of rocks, 19: 44256 (ORNL-tr-708)

HIRSHBERG, Joos, Relationship between solar wind velocities and surface magnetic disturbances during sudden commencement storms, 19: 45163

HITOMI, Soiichi, Environmental radiation and radioactivities about site of JAERI, 1956–1963, 19: 44290 (JAERI-1079)

HITZEROTH, W., A mechanical analog computer for range and angle measurements in nuclear emulsions, 19: 44420 (CERN-65-4(Vol.II), pp VII28-34)

HITZEROTH, W., Use of gas targets for scattering experiments, 19: 44438 (CERN-65-4(Vol.II), pp X33-6)

HIYAMA, Yoshio, Japanese dietary habits and the fallout problem. II., 19: 44264

HIYAMA, Yoshio, Prog. rpts. on uptake of radioisotopes by edible marine products, 1960–62, 19: 43669 (NP-15159)

HOEGAASEN, H., Absorption model at high energy and its application to meson-nucleon charge-exchange scattering, 19: 45087

HOEGAASEN, J., Absorption model at high energy and its application to meson-nucleon charge-exchange scattering, 19: 45087

HOELL, James M., Experiments in a hollow cathode Hall current accelerator, 19: 45443

HOEY, S. J., Measurements of the A and R parameters in proton-proton scattering at 47.8 and 27.6 Mev, 19: 45319

HOFFMANN, J. P., Performance of fuel rods to investigate increased thermal output capabilities, 19: 45573 (GEAP-4902)

HOGE, K. G., Influence of strain rate on mechanical properties of 6061-T6 aluminum under uniaxial and biaxial states of stress, 19: 44706 (UCRL-12264(Rev.1))

HOLADAY, Duncan A., Radiation as cause of lung cancer among uranium miners, 19: 44314

HOLDOWAY, M. J., Reprocessing with amine ether systems. II., 19: 44108 (AERE-R-4440(Pt.3))

HOLLAND, R. W., Experimental stress analysis of attachment region of hemispherical shells with radially attached nozzles, 19: 44144 (TID-22134)

HOLLOWAY, A. F., Possible errors in the ferrous sulfate dosimeter, 19: 44540

HOLLOWAY, A. F., Thermoluminescent dosimeter, 19: 44541

HOLM, Dale M., Gamma scanning of LAMPRE fuel elements with a NaI anticoincidence spectrometer, 19: 44453 (LA-DC-7316)

HOLMBERG, P., Gamma transitions in ^{65}Cu from decay of ^{65}Ni, 19: 45320

HOLMES, W. E., Protection against fire hazards in the design of filtered ventilation systems of radioactive and toxic process buildings, 19: 44284 (AWRE-O-24/65)

HOLMES-SIEDLE, A. G., Space radiation: its influence on satellite design, 19: 44550

HOLT, J. Birch, Role of oxygen in solid-solid reactions, 19: 43998 (UCRL-12396)

HOLUB, Frantisek, Radiochemical department at Czechoslovak Nuclear Research Institute, 19: 44068

HOMEYER, W. G., Synthesis of thermionic power conversion to nuclear reactors for space power applications, 19: 45648 (GA-6478)

HONMEL, Carlton O., An SO_2 monitor for air pollution studies: design of the instrument and field testing, 19: 44458 (NYO-2767)

HONDA, Yutaka, Particle bonding of swaged UO_2 compacts, 19: 44649

HONIG, Richard E., Mass spectroscopy as an analytical tool, 19: 43978

HONJO, I., Base composition of messenger RNA of Pseudomonas effusa irradiates with uv light, 19: 43744

HONZAWA, Todao, Loss mechanism of electrons from a magnetic bottle, 19: 44823

HOOP, B. Jr., Analyzing power of neutrons for helium, 19: 45217 (COO-7-0363)

HOOTON, B. W., Preparation of lithium-drifted germanium diodes and their use as γ detectors, 19: 44371 (AERE-R-4921)

HOOVER, D., Prog. rpt. on flow and fracture studies of alloyed Be, 7/7–10/64, 19: 44693 (NP-15411)

HOOVER, D., Prog. rpt. on flow and fracture studies of alloyed Be, final, 8/65, 19: 44694 (NP-15432)

HOPKINS, Donald B., Electrolytic capacitor banks, 19: 45416 (UCRL-16263)

HORIE, Kenya, Histopathological studies on transplanted experimental osteogenic sarcoma, 19: 43772

HORIKAWA, Masakatsu, Radiation-induced chromosome aberrations in man, 19: 43834

HORN, D., Meson and baryon resonances in relativistic SU(6), 19: 45112

HORNYIK, K., Dynamics of a Triga-type reactor, 19: 45685

HORSLEY, A., Neutron cross sections of the proton in the energy range

0.0001 ev to 20 Mev, 19: 45248 (AWRE-O-23/65)
HORTON, J. H., Importance of capillary pores in rainwater percolation to the ground water table, 19: 44235 (DPSPU-64-30-23)
HORTON, P. A., Minimized fuel cycle cost for simulated heavy water reactor. I., 19: 45563 (BNWL-106)
HOSTE, J., Neutron activation analysis of copper in bismuth by (γ-γ) coincidence measurement, 19: 43941
HOTTA, Hiroshi, Effects of metal ions on autoxidation of benzene in aqueous solutions, 19: 44078
HOUGHTON, A., Acoustic attenuation in type II superconductor, 19: 45210
HOUGHTON III, A. V., Short cut method for dimensional analysis, 19: 44143 (SC-RR-65-306)
HOWARD, H. T., Radar measurements of total cislunar electron content, 19: 45176
HOWARD-FLANDERS, Paul, Molecular mechanisms in repair or irradiated DNA, 19: 43795
HOWARD-FLANDERS, Paul, Preferential sensitization of anoxic bacteria to x rays by organic nitroxide-free radicals, 19: 43875
HOWELL, W. D., Control and read-out system for Chalk River double crystal γ spectrometer, 19: 44365 (AECL-2219)
HOYLE, Alex C., Chemical industry—a training ground for nuclear power engineers, 19: 44155
HOYT, Martha S., HASTI—a numerical calculation of two-dimensional Lagrangian hydrodynamics utilizing the concept of space-dependent time steps, 19: 45701 (LA-3324)
HRABOVCOVA, Alojzia, Dismantling of Rn pumping stations, 19: 44317
HRADIL, M., Radiocoulometric titration using non-isotopic indicator in solid phase, 19: 43952
HSU, H. F., Immunizing effect of x-irradiated cercariae of Schistosoma japonicum in albino mice, 19: 43848
HSU, Jong M., Manganese (^{54}Mn) distribution in scorbutic guinea pigs, 19: 43697
HSU, S. Y. Li, Immunizing effect of x-irradiated cercariae of Schistosoma japonicum in albino mice, 19: 43848
HSUE, S. T., Antimony-124 spectrum shape, 19: 45328
HUANG, Kerson, Exact bootstrap solutions to the Low equation, 19: 45106
HUBER, Max G., Photon absorption cross section of spherical nuclei, 19: 45366
HUDNIK-PLEVNIK, Tamara A., Effect of x irradiation on pulse-labeling of RNA in Salmonella typhimurium, 19: 43743
HUEBOTTER, P. R., Development of EOCR as fast fuel test facility, 19: 45669 (APDA-174, pp 61-6)
HUEN, T., Studies of band structure and electron scattering in Al by photoemission, 19: 45481 (UCRL-12470)
HUERLIMANN, T., Temperature-coefficient of SAPHIR, 19: 45673 (EIR-85)
HUET, Henri, Methods and apparatus in which a mass of solid material is subjected to two successive treatments by gases, 19: 44042
HUI, C. K., The determination of zinc and iron in biologic materials by x-ray fluorescence spectrometry, 19: 43939 (UCD-472-112, pp 59-72)
HULTGREN, Ralph, Dilation contribution to the heat capacity of copper and alpha brass at elevated temperatures, 19: 45718 (UCRL-11662)
HUML, James O., Uranium–chromium–aluminum ternary alloy, 19: 44665
HUML, James O., Uranium–tungsten–aluminum ternary alloy, 19: 44666
HUML, James O., Uranium–tantalum–aluminum alloy, 19: 44667
HUMPHREYS, W. G., LET-independent dosimeter based on chemiluminescent determination of H_2O_2, 19: 44067
HUNTLEY, H. W., Chemical engineering aspects of boiling water reactors, 19: 45624
HURLEY, J. P., Energy levels of ^{130}I, 19: 45324
HUZIMURA, Ryoitiro, Radiation quenching of radio- and radiothermoluminescence of ZnS phosphors. II., 19: 44757

I

ICE, C. H., Isotope production in a Savannah River reactor at flux levels above 10^{15} n/(cm^2)(sec), 19: 45639 (DP-999, pp 19-28)
ICHIYE, T., Geostrophic eddies in the ocean. I., 19: 45699 (CU-2663-21)
ICHIYE, Takashi, Experiments and hydrographic surveys off Sandy Hook, New Jersey (1963), 19: 45698 (CU-2663-18)
IGLESIAS, T., PROMETEO I—program for averaging thermal constants over Wigner-Wilkins flux spectrum, 19: 45224 (JEN-133-DF/I-43)
IGLESIAS, T., PROMETEO II—program for averaging thermal constants from Wilkins spectrum, 19: 45225 (JEN-135-DF/I-44)
IIDA, Shoichi, Induced parasitic ferromagnetism in $(La_{0.9}Bi_{0.1})CrO_3$, 19: 45486
IIO, Masahiro, Detection of portal systemic shunts by hepatopulmonary scanning using ^{131}I MAA. III., 19: 43904
IKAWA, K., Estimation of fission gas release from punctured Calder Hall type fuel element, 19: 44632
IKENBERRY, Dennis, Nuclear magnetic shielding of alkali ions in crystals and dilute aqueous solutions, 19: 45485

IMAGAWA, Hiroshi, ESR studies of radiophotoluminescent centers in silver-activated phosphate glass, 19: 44758
IMAI, Takashi, High-energy radiation measurement in the exosphere by Explorer VII, 19: 44973
IMAI, Takashi, Transistorized airborne apparatus for detection of extensive air showers, 19: 44529
IMHOFF, D. H., Incorporating a superheating region to improve BWR performance, 19: 45625
IMRY, Y., Inelastic neutron spectra and vibrational modes of the hydrogen layer in alkali and alkaline-earth hydroxides, 19: 45482
INAMURA, T., Anisotropy of conversion electrons from (p,2n) and (α,4n) reactions, 19: 45352
INGOLD, J. H., Thermionic converter operating with a high temperature collector, 19: 44988
INMAN, J. E., Description of facility radiation and contamination alarm installed in High Radiation Level Examination Laboratory Building 19: 44297 (ORNL-TM-1251)
INZAGHI, A., Numerical solution of integral transport equation in approximation to one-velocity and isotropic scattering in plane and cylindrical symmetry, 19: 45219 (EUR-2410.i)
IOFFE, B. L., Vertex function poles and one-particle states orthogonalization, 19: 45029 (NP-15382)
IONESCU, C., Complications in the urinary organs resulting from uterine carcinoma and its treatment, 19: 43921
IORGA, Nicolae, Complex salts with 5-nitrobarbituric acid. III., 19: 44027
IORI, I., Level widths of nuclei at high excitation energy, 19: 45343
IPATEV, A. N., Sterility of male plants due to penetrating radiation, 19: 43767
IRVIN, J. E., Fast neutron flux characteristics of the ETR, G-7 hot water loop, 19: 45672 (BNWL-89)
IRVINE, A. R., Thorium–uranium recycle facility, 19: 44167 (ORNL-P-1521)
IRVING, J., Schlieren photography of first half cycle of a theta pinch discharge, 19: 45421
ISAILA, M., Operating experience and improvements on the Princeton–Pennsylvania accelerator, 19: 44872 (PPAD-2137-565)
ISHIGURO, Yukio, Manual of free gas model-code (FREE code), 19: 45223 (JAERI-1084)
ISHIHARA, M., Anisotropy of conversion electrons from (p,2n) and (α,4n) reactions, 19: 45352
ISHIHARA, Toyohide, Environmental radiation and radioactivities about the site of JAERI, 1956–1963, 19: 44290 (JAERI-1079)
ISHIHARA, Toyohide, Radiological monitoring point. Photographic dosimeter and gammed paper station, 19: 44291 (JAERI-1081)
ISHMAEV, S. N., Semiconductor detector for detection of thermal neutrons in conditions of intense pulsed γ radiation, 19: 44480 (ZFK-PHA-12, pp 144-6)
ISKOLDSKII, A. M., Peculiarities of plasma heated by collisionless shock waves, 19: 45434
ISLITZER, Norman F., Measurement of [fallout] deposition, 19: 44247 (BNL-914, pp 139-40)
ISLITZER, Norman F., Program review and summary of recent accomplishments at NRTS, 19: 44773 (BNL-914, pp 57-64)
ISMAIL, A. Z. M., Short-range hyperfragments produced by K$^-$ captures in emulsions, 19: 45342
ISRAELI, Yigal (Julius), Complexes of the uranyl cation with the o-mercaptobenzoate coordinant, 19: 44013
ITOH, Hovuhiro, Decomposition of tertiary butyl peroxides by γ irradiation, 19: 44089
IVAKIN, A. A., Crystallographic and optical characteristics of vanadates of certain rare earth elements, 19: 44032
IVANOV, B. I., Method for determining coefficients of reflection in a plasma waveguide, 19: 45401 (NP-15196)
IVANYI, Janos, Adrenal irradiation in chronic cardiac decompensation, 19: 43919
IVCHENKO, V. E., Multidimensional analyzer with a preliminary treatment of data and combined-type memory, 19: 44524
IWAHASHI, Katsutoshi, Induced parasitic ferromagnetism in $(La_{0.9}Bi_{0.1})CrO_3$, 19: 45486
IWASAKI, Tomiko, Cytological studies on radiosensitivity of spermatogonia of the silkworm, 19: 43783
IWASAKI, Tomiko, Sensitivity of Artemia eggs to irradiation. III., 19: 43814
IWASAKI, Tomiko, Sensitivity of Artemia eggs to irradiation. IV., 19: 43815
IYENGAR, P. K., Study of elastic incoherent scattering by ammonium salts, 19: 45242
IYENGAR, R. S., Infrasonic waves of the auroral zone, 19: 45183
IZAWA, Masami, Radiolysis of chloroauric acid in aqueous solution, 19: 44079

J

JACCHIA, Luigi G., Solar plasma velocity, exospheric temperature, and geomagnetic activity, 19: 45179

JACKSON, J. D., Peripheral production and decay correlations of resonances, 19: 45037 (TID-21316)

JACKSON, J. L., Effect of tensile stress on the radiation-induced contraction of graphite, 19: 44744 (HW-SA-3592)

JACKSON, W. D., Prog. rpt. on energy conversion, 3–5/65, 19: 44981 (NP-15435)

JACMART, Jean-Claude, Inelastic scattering of protons at 155 Mev on light nuclei, 19: 45305

JACOB, Philippe, Improvements in or relating to processes for applying alloys to metal surfaces, 19: 44658

JAFFEE, H., The application of nuclear reactors and radioisotopes to underwater-vehicle propulsion, 19: 45662

JALLA, E., Two-prong proton-antiproton annihilation with formation of a pair of charged mesons, 19: 45066

JAMIESON, Dana, Effect of cysteamine, cyanide and high-pressure oxygen on splenic oxygen tension and sulfhydryl content, 19: 43869

JANE, M. R., Measurement of branching ratio for decay $\omega^0 \rightarrow e^+ + e^-$, 19: 45102

JANKOWSKA, Helena, Electrolytic oxidation of cerium(III) to cerium(IV), 19: 44026

JANNEY, D. B., Molten salt converter reactor. Design study and power cost estimates for a 1000-Mwe station. 19: 45588 (ORNL-TM-1060)

JANNEY, D. B., Separation of potassium isotopes by molecular distillation, 19: 43931 (K-1650)

JANOSSY, L., Spurious scattering in nuclear emulsions, 19: 44413 (CERN-65-4(Vol.II), pp VI23-30)

JANSEN, G. Jr., Thermal effects in anion exchange resin–nitric acid systems, 19: 44110 (BNWL-114)

JARRETT, O., Diagnostic studies in a Hall accelerator at low exhaust pressure, 19: 45446

JASKOLA, M., Excitation function for the $^{29}Si(n,\alpha)^{26}Mg$ reaction in energy range 13.6 to 15.6 Mev, 19: 45290 (ZFK-PHA-12, pp 110-12)

JAUHRI, G. S., Unit for testing high-efficiency filters, 19: 44281 (AEET-202)

JAYARAMAN, A., Rare earth metals at high pressures and temperatures, 19: 44734

JEAN, M., Nuclear structure investigation by means of pion-nucleus interaction, 19: 45339

JEANMAIRE, L., Dosimetry of high-energy protons by measurement of beryllium-7 formed in the tissues, 19: 44327

JEANMAIRE, L., Role of laboratory and methods to be used in event of an accident, 19: 44324

JENSON, Robert, Producing high-velocity charged particles, 19: 44890

JENICEK, A., Plant for treatment of radioactive wastes of the Czechoslovak Institute of Nuclear Research, 19: 45693

JENIK, L., Multiple scattering constant in emulsion at great cell lengths, 19: 44431 (CERN-65-4(Vol.II), pp IX32-40)

JENSEN, T. H., Flute characteristics of and microwave emission from a plasma in a mirror, 19: 45388 (GA-6432)

JESENAK, V., Radiocoulometric titration using non-isotopic indicator in solid phase, 19: 43952

JEUNG, Chung-hung, Optical and spectral properties of rare earth oxides in inorganic glasses, 19: 44030

JEUNG, Nylon, Growth curve for mammary fibroadenoma in female rat, 19: 43649 (UCRL-16177)

JEWELL, C. E., Temperature coefficients of reactivity in the Savannah River high flux charge, 19: 45642 (DP-999, pp 65-71)

JIMENEZ, C. M., Ferrous ammonium sulfate-cupric chloride solutions for dosimetry of a kilocurie ^{60}Co source, 19: 44372 (AFCRL-65-470)

JIRLOW, K., Physics aspects of pressure tube and pressure vessel type heavy water reactors, 19: 45626

JNANANANDA, S., Internal conversion coefficients employing internal-external-conversion technique using a scintillation spectrometer, 19: 44501

JOBST, J. E., Differential cross sections of α particles from $^{16}O(d,\alpha)^{14}N$, 19: 45377

JOFFRE, H., Accidental exposure received from an electron linear accelerator, 19: 44331

JOHANSSON, C., Monte Carlo procedure for calculating migration of protons, 19: 45462 (NP-15163)

JOHN, R. R., Cesium-fueled MPD arc-jet engine performance, 19: 44230

JOHNS, T. F., Calculated energy response of lithium fluoride finger-tip dosimeters, 19: 44367 (AEEW-M-550)

JOHNSON, C. E., SNAP-8 reactor and shield designs and operating experience, 19: 45666

JOHNSON, C. L., Thyroid function in rainbow trout. I., 19: 43773

JOHNSON, James R., Boron carbide spherules, 19: 44660

JOHNSON, James R., Refractory carbides, 19: 44658

JOHNSON, K. Allen, Alternating current electroetching of α, δ, and β plutonium, 19: 44602 (LA-DC-6691)

JOHNSON, Kay Allen, Alternating current polishing and electroetching of metals, 19: 44601 (LA-DC-6507)

JOHNSON, Paul G., Nuclear rockets based on graphite reactor technology. Their applications and development status, 19: 45658 (TID-22097)

JOHNSON, Roy R., Excitation of higher modes by the helical instability, 19: 45386 (D1-82-0439)

JOHNSON, S. O., SPORT—aystem for processing reactor transient data, 19: 45527 (IDO-17078)

JOHNSON, William, Process for making carbon articles from carbon particles and furane derivatives, 19: 44669

JOHNSTON, C., Water vapor corrosion of uranium and its prevention, 19: 44618 (AWRE-O-42/65)

JOKELAINEN, Aili, Diet of Finnish Lapps and its ^{137}Cs and potassium contents, 19: 44305

JOLLY, R. K., Deuteron excitation of two-phonon states in ^{60}Ni, 19: 45346

JOMBIK, J., Nondestructive radiometric determination of bromine in several pharmaceutical preparations, 19: 43950

JONES, C. H., Modifications to Royal Marsden Hospital gold grain implantation gun, 19: 43888

JONES, Frank C., Charge ratio of cosmic-ray electrons, 19: 44972

JONES, T. W., Hall effect stabilizer for experimental magnets, 19: 44173

JONES, W. C., Properties of ionic sound waves, 19: 45404 (ORNL-P-1557)

JONGEJANS, B., Reaction $KN\pi\pi$ at 3 Bev/c and production mechanism of K^*N^*, 19: 45057

JONKER, C. C., Muon capture and electric dipole excitation for lithium, 19: 45351

JONSSON, J., Thyroid antibodies after ^{131}I treatment for hyperthyroidism, 19: 43902

JOPSON, R. C., Background events in photomultiplier tubes at high altitudes, 19: 44465 (UCRL-12020)

JORDAN, Kurt, Portable, battery-operated measuring apparatus for detection of radiation, 19: 44542

JORDAN, T. M., Reactor shielding calculations by Monte Carlo method, 19: 45469

JORGENSEN, George, X-ray-induced perturbations in replication of bacterial chromosome, 19: 43741

JOSEPH, D. W., Tensor Lagrangians and generalized conservation laws for free fields, 19: 45141

JOSHI, G. C., Use of irradiated males for reduction of C. fatigans populations, 19: 43796

JOSHI, L. U., Strontium-90 content of food samples in India—data summary through 1963, 19: 44244 (AEET/AM/40)

JOST, K., Production of highly polarized electron beams by low-energy scattering, 19: 44958

JOVANOVIC, M., Vaccination against Dictyocaulus filaria with irradiated larvae, 19: 43750

JUNG, Margarete, Electrochemical fuel cell operation with antipolar ion exchange membrane, 19: 44992

JUNGNER, H., Gamma transitions in ^{65}Cu from decay of ^{65}Ni, 19: 45320

JUZON, Louvie, Automatic machine for milling fins on cylindrical parts, 19: 44655

K

KABAVETS, V. P., Real part of the spin-zero amplitude for T = 0 and spin-dependent amplitudes of nucleon-nucleon forward scattering at high energies, 19: 45032 (NP-15452)

KADA, Tsuneo, Modification of lethal and mutagenic radiation damages by genetic repair factors in bacteria, 19: 43794

KADANER, E. S., Recrystallization of Mg–Ce alloys, 19: 44710 (JPRS-24761, pp 29-40)

KADLECEK, John Alfred, Average half-life determination of the short-lived products of the photonuclear reactions of ^{40}Ca, 19: 45262 (IS-T-29)

KADYK, John A., Coherent K^* production in the K^+d reaction at 2.3 Bev/c, 19: 45120

KADYSHEVSKII, V. G., New definition of translations in the inhomogeneous SL(6) group, 19: 45132 (JINR-E-2225)

KAERCHER, Karl-Heinz, Introduction to clinical experimental radiology, 19: 43843

KAGAN, Yu., Anharmonism influence on the phonon spectrum near the point of origin, 19: 45475 (IAE-750)

KAGIYA, Tsutomu, Existence of long-lived radicals in γ radiation induced polymerization of ethylene, 19: 44073

KAGIYA, Tsutomu, Specific influence of temperature on γ-radiation induced polymerization of ethylene, 19: 44074

KAHAN, R. S., Effect of ^{60}Co gamma rays applied at low dose rates on some juice constituents and peel color of green and ripe citrus fruits,

19: 44554 (IA-1015)
KAJAREKAR, P. J., Loading of nuclear emulsion with light and heavy elements, 19: 44399 (CERN-65-4(Vol.II), pp III17-20)
KALIFA, J., K isomerism in ^{176}Yb, 19: 45357
KALIMNIKOV, V., Decay mode of ^{147}Eu, 19: 45267 (JINR-P-2161)
KALININ, A. I., Effect of input resistance of an amplifier on the signal-to-noise ratio, 19: 44489 (ZFK-PHA-12, pp 219-23)
KALIŠ, Zh. E., Flow of conducting fluid past circular cylinder in presence of transverse magnetic field, 19: 44825
KALLIOMAKI, J. L., Treatment of hyperthyroidism with fixed initial dose of radioiodine, 19: 43895
KALLMAN, Robert F., Recuperation in mammalian cell systems as revealed by radiation dose fractionation, 19: 43792
KALUGIN, V. N., Profiling channels for flows of ionized gases in transverse magnetic field, 19: 44838
KALVIUS, G. M., Moessbauer resonance of ^{127}I in ferromagnetic CrI_3, 19: 45491
KAMADA, Hitoshi, Determination of O in steels, 19: 43946
KAMADA, Hitoshi, Determination of oxygen in stainless steels, 19: 43947
KAMAE, Tsuneyoshi, Photoreactions in ^{28}Si nucleus by monochromatic γ rays, 19: 45310
KAMAEV, A. V., Heterogeneous absorber efficiency in homogeneous uranium–water reactors, 19: 45536
KAMAL, A. A., Investigation into spurious scattering in photographic emulsions, 19: 44416 (CERN-65-4(Vol.II), pp VI53-62)
KAMAL, A. A., Results on spurious scattering in photographic emulsions, 19: 44415 (CERN-65-4(Vol.II), pp VI37-52)
KAMAL, T. H., Total body water estimations in dairy cattle using tritiated water, 19: 43694
KAMATA, Keiichi, Transistorized airborne apparatus for detection of extensive air showers, 19: 44529
KAMEDA, Haruo, Detection of portal systemic shunts by hepatopulmonary scanning using ^{131}I MAA. III., 19: 43904
KAMEDA, T., Possible evidence for nuclear interaction of μ above 3×10^{14} ev, 19: 45368
KAMINSKY, J. J., Development of Cb–Zr–C alloys, 19: 44605 (PWAC-464)
KAN, Fu-hsi, Optical and spectral properties of rare earth oxides in inorganic glasses, 19: 44030
KANE, S. R., Response of ion chambers in free space to long-term cosmic-ray variation from 1960 to 1965, 19: 44966
KANEKO, Kayo, Cosmic-ray index, 19: 44974
KANEKO, Kayo, High-energy radiation measurement in the exosphere by Explorer VII, 19: 44973
KANEKO, Keiji, Analysis and separation of rare earth elements. I., 19: 43956
KANEKO, Keiji, Analysis and separation of rare earth elements. II., 19: 43957
KANG, C. L., Operating experience and improvements on the Princeton–Pennsylvania accelerator, 19: 44872 (PPAD-2137-565)
KAPELNER, S. M., The vapor pressure of lithium between 1307 and 1806°K, 19: 44703 (TIM-844)
KAPELNER, S. M., Viscosity of lithium, 19: 44704 (TIM-849)
KAPLAN, A. L., Basement radiation from an infinite-plane γ source, 19: 44216
KAPLAN, R. W., Induction of phage production and formation of clear-plaque mutations by uv irradiation of prophage and of free-phage kappa, 19: 43847
KAPLAN, S. A., Relativistic instability of polytropic spheres, 19: 44925
KAPPELMANN, F., Behavior of the transplutonium elements in solvent extraction systems, 19: 44115 (ORNL-P-1577)
KARADZHEV, K. V., Study of reactions $^{18}O(p,\alpha)^{15}N$ and $^{11}B(p,\alpha)^{8}Be$ using semiconductor counters, 19: 45291 (ZFK-PHA-12, pp 117-22)
KARAMYAN, A. T., Relative difference of vapor pressure in $^{11}BF_3$–$^{10}BF_3$, 19: 44575
KARAPETYAN, V. V., Intensity of nonradiative transitions in Ta and ^{230}Pu mesic atoms, 19: 44962
KARASEV, V. S., Calorimetric determination of absorbed dose of ionizing radiation of a reactor by the method of compensation of heat production in the sample, 19: 45467
KARBAN, O., Utilization of semiconductors in polarization experiments, 19: 44477 (ZFK-PHA-12, pp 126-32)
KARG, A. V., Electron metallography techniques applied to bcc metals and alloys, 19: 44610 (TIM-943)
KAROLYI, J., Preparation of self-supporting thin silicon targets by reductive evaporation, 19: 44650
KARR, H., New institute for reactor safety, 19: 45497 (ORNL-tr-652)
KARRAKER, David G., Recovery of actinides produced by a nuclear detonation in salt formations, 19: 44156 (DP-956)
KARRAS, T., Neutral mass density measurements in a repetitively pulsed coaxial plasma accelerator, 19: 45449
KARRAS, T., Performance of two-stage repetitively pulsed coaxial plasma engine, 19: 44233
KARTTUNEN, J. O., Bibliography on chemical analysis of Pu, Pu alloys and Pu compounds, 19: 43925 (ANL-6956)
KARTUZHANSKII, A. L., Regression of sensitivity and latent image in nuclear and light-sensitive photographic emulsions, 19: 44402 (CERN-65-4(Vol.II), pp IV5-15)
KARZMARK, C. J., Fading in thermoluminescent lithium fluoride used for radiation dosimetry, 19: 44076
KASAI, Atsushi, Environmental radiation and radioactivities about site of JAERI, 1956–1963, 19: 44290 (JAERI-1079)
KASATKINA, L. A., Effect of heat treatment of MnO_2 on rate of oxygen isotope exchange, 19: 44104
KASPER, Erwin, Theoretical investigations on possibility of stigmatic corpuscular-optical focusing by random stationary space-limited electric-magnetic fields, 19: 44851
KATAGIRI, Hiroshi, Environmental radiation and radioactivities about the site of JAERI, 1956–1963, 19: 44290 (JAERI-1079)
KATO, Hotuo, Cytological studies on radiosensitivity of spermatogonia of the silkworm, 19: 43783
KATO, Kiyoe, Oscillations in a plasma in a magnetic field, 19: 45427
KATO, Syohei, Scattering of alpha particles from medium-weight nuclei, 19: 45312
KATO, Yukio, Consequences of uv radiation on differentiation and growth of fern gametophytes, 19: 43825
KATORI, K., Anisotropy of conversion electrons from (p,2n) and (α,4n) reactions, 19: 45352
KATSELIS, V., Extension of Laben 512-channel analyzer for use in multiparameter experiments, 19: 44516
KATURAGI, Satoru, Manual of free gas model-code (FREE code), 19: 45223 (JAERI-1084)
KATYAL, Mohan, Spectrophotometric determination of zirconium with 7,8,3',4'-tetrahydroxy flavonol, 19: 43955
KATZ, Robert, Width of heavy ion tracks in emulsion, 19: 44434 (CERN-65-4(Vol.II), pp IX48-61)
KAUFMAN, Aaron, Comparison of ^{230}Th and ^{14}C ages for carbonate materials from Lakes Lahontan and Bonneville, 19: 44271
KAUFMANN, C., Development of semiconductor detectors in Central Institute for Nuclear Physics at Rossendorf, 19: 44468 (ZFK-PHA-12, pp 10-15)
KAUFMANN, C., Standardization of semiconductor detectors, 19: 44474 (ZFK-PHA-12, pp 66-9)
KAUFMANN, Jean, Improvements in and relating to hot-forging apparatus, 19: 44657
KAVECKIS, J. E., Strap-on RTD test plan, model four testing, 19: 45502 (RL-REA-2120)
KAWABE, Tokuya, Higher harmonics and sub-harmonics of electron plasma oscillations, 19: 45428
KAWASAKI, Eiichi, Oscillations in a plasma in a magnetic field, 19: 45427
KAWASAKI, Shinkichi, Transistorized airborne apparatus for detection of extensive air showers, 19: 44529
KAWIN, Bergene, Manganese (^{54}Mn) distribution in scorbutic guinea pigs, 19: 43697
KAZACHKOVSKII, O. D., Possibility of using thorium in high-energy reactors, 19: 45605 (ORNL-tr-788)
KAZARINOV, Yu. M., Angular dependence of quantities measured in total set of experiments on nucleon-nucleon scattering, 19: 45015 (JINR-P-2241)
KEAM, D. W., Concentration of cesium-137 in Australian milk during 1963, 19: 44309
KEANE, A., Resonance absorption in small homogeneous critical assemblies, 19: 45521 (AAEC/TM-118)
KEAR, G. H., Prog. rpt. on transport equivalent diffusion theory, 4–6/65, 19: 45221 (GEAP-4913)
KEEGAN, W. A., Electron metallography techniques applied to bcc metals and alloys, 19: 44610 (TIM-943)
KELLEY, G. G., Ion cyclotron harmonic spectrum generated in an energetic ion plasma, 19: 45405 (ORNL-P-1576)
KELLEY, John P., Scattered radiation in phantom from diagnostic quality radiation, 19: 43917
KELLEY, R. W., Transient response of linear damped lumped spring-mass systems by experimentally derived transfer functions, 19: 45710 (SC-TM-64-1772)
KELLMAN, S., High-energy solar neutrons. I., 19: 44902
KELLMAN, S., High-energy solar neutrons. II., 19: 44903
KELLY, A. J., Electron density and temperature measurements in exhaust of a MPD source, 19: 45448
KEMNITZ, Peter, Sarcoma resulting at site of administration from paravasal injection of Thorotrast, 19: 43850
KEMP, Edwin L., Development of an interleaved, fractional-turn coil, 19: 44136 (LA-3234)
KENDALL, K., Comparative lethality responses of neutron- and x-

irradiated dogs, 19: 43832
KENDALL, P. C., Appleton anomaly, 19: 45184
KENEFICK, R. A., Experimental evidence for competing spherical and deformed shapes in N = 89 nuclei, 19: 45359
KENNEDY, C. R., Effect of irradiation on the mechanical properties of stainless steel at 750°C under constant stress rate conditions, 19: 44750 (ORNL-TM-1216)
KENNEL, C. F., Limit on stably trapped particle fluxes, 19: 45157 (NP-15386)
KERLIN, T. W., Molten salt converter reactor. Design study and power cost estimates for a 1000-Mwe station, 19: 45588 (ORNL-TM-1060)
KERMAN, Arthur K., Collective motion in finite many-particle systems. III., 19: 45364
KERMAN, William J., Phase space considerations for three-particle and four-particle final states, 19: 45006 (IS-1214)
KERREBROCK, J. L., Prog. rpt. on energy conversion, 3–5/65, 19: 44981 (NP-15435)
KERZAR, B., Nonlinear plasma wave interaction in an arc discharge, 19: 45419
KESSLER, J., Production of highly polarized electron beams by low-energy scattering, 19: 44958
KETTUNEN, Kalevi, Dosage to lens in radiography about the head and neck, 19: 43885
KETZLACH, Norman, Applications of nuclear safety plant operations, 19: 44112 (CONF-651103-4)
KEVAN, Larry, Prog. rpt. on radiolysis studies on fluorocarbons and on reactive intermediates, 10/64–7/65, 19: 44054 (COO-1365-7)
KHAIKIN, M. S., A developer for nuclear photography, 19: 44407 (CERN-65-4(Vol.II), pp V1-8)
KHAKIMOV, S. Kh., Device for developing pulsed magnetic fields up to 150 kG, 19: 44888
KHANDEKAR, R. N., Strontium-90 content of food samples in India—data summary through 1963, 19: 44244 (AEET/AM/40)
KHANNA, F., Neutron-neutron scattering length by pion absorption in ^{3}He, 19: 45354
KHELASHVILI, A. A., Broken symmetry U(12) and unitarity condition for the S matrix, 19: 45018 (JINR-P-2283)
KHERA, G. D., Decay of ^{86}Rb, 19: 45331
KHERRMANN, E., Gamma spectrum of ^{160m}Ho isomer, 19: 45272 (JINR-P-2270)
KHOLOPOV, P. N., Theory of stellar evolution and some properties of star clusters, 19: 44928
KHRISTIANOV, V. K., Isotopic composition of the crystallization water of saline minerals, 19: 44240
KHVASHCHEVOKAYA, Yo., Surface-barrier silicon detectors with guard rings and possibility of their utilization, 19: 44469 (ZFK-PHA-12, pp 16-24)
KHVASHCHEVSKAYA, Yo., Interaction of heavy fission particles with semiconductor detectors, 19: 44481 (ZFK-PHA-12, pp 149-53)
KHVASHCHEVSKI, S., Interactions of fast plasmoids with a constant magnetic field barrier, 19: 45391 (INR-612/IXA/PR)
KHVASHCHEVSKI, S., Measurements of β/1 parameters in ANNA, 19: 45677 (INR-614/IXA/P)
KHVOSTOV, N. N., Maximal permissible levels of radioactive contamination of the surfaces, 19: 44311
KHVOSTOVA, V. V., Analysis of delayed effects of γ rays and 660-Mev protons on chromosomes, 19: 43770
KIDSON, G. V., Role of diffusion measurements in study of crystal lattice defects, 19: 45471 (AECL-2309)
KIEFER, H., Detection and measurement of activity in wounds, 19: 44538
KIEFER, Hans, Neutron dosimeter for measurement of biological neutron dose effect, 19: 44543
KIGOSHI, Koshiko, Recent variation of atmospheric contents of C-14 in Tokyo and transfer problem of atmospheric carbon dioxide, 19: 44267
KIHARA, Motohiro, Photoproduction of deuterons from carbon at several hundred Mev, 19: 45309
KIHARA, Toru, Flute instability of plasma confined in axi-symmetric wave form magneto-static field, 19: 45438
KIKUCHI, Shiroh, Excitation cross sections of the (n,n'γ) reactions on Fe, Co, Ni, Cu, Zn, Mo, Ag, Cd and Sn, 19: 45263 (JAERI-1078)
KILLEN, R. E., Reactor weight optimization parametric code—WOP, 19: 45659 (TIM-807)
KILPATRICK, Robert A., Collins quadrupole magnets and sextupole magnets for a 200-Bev proton synchrotron, 19: 44878 (UCRL-16375)
KIM, Ni Gyu, Semiconductive behavior of anthracene and γ irradiation effects, 19: 44077
KIM, J. I., Neutron activation analysis of copper in bismuth by (γ-γ) coincidence measurement, 19: 43941
KIM, J. K., Measurement of the K^0 mass and the K^0–K^- mass difference, 19: 44998 (CU-1932-247)
KIM, Jin Hum, Racah algebra and nuclear spectroscopy, 19: 45315
KIM, Koo Hyun, Investigations involving use of fast neutrons from a reactor, 19: 45684
KING, D. C., Analysis of some two-zone exponential experiments on graphite moderated lattices, 19: 45524 (AEEW-R-428)
KING, D. T., Comparison of π^0 intensity measurements in emulsions and bubble chambers, 19: 44439 (CERN-65-4(Vol.II), pp X37-43)
KING, H. J., Research on problems of ion beam formation from electron bombardment ion sources, 19: 44221 (N64-31088)
KINGSLEY, Paul S., Investigation of CD_4M Cu as Hanford male connector (nozzle) material, 19: 44607 (RL-SEP-508)
KINNEY, John D., Surface ionization of alkali metals by heated tungsten, 19: 44938 (UCRL-14117)
KINOSHITA, Florence, Inhibitory effect of x radiation on development of N-demethylase activity in livers of young, male rats, 19: 43720 (NP-15310, pp 26-35)
KIRALY, P., Spurious scattering in nuclear emulsions, 19: 44413 (CERN-65-4(Vol.II), pp VI23-30)
KIRBY, H. W., Radiochemistry of radium, 19: 44098 (NAS-NS-3057)
KIRCHGESSNER, J., External proton beam for the Princeton–Pennsylvania accelerator, 19: 44871 (PPAD-2137-556)
KIRCHGESSNER, J., Operating experience and improvements on the Princeton–Pennsylvania accelerator, 19: 44872 (PPAD-2137-565)
KIRILLOV, A. I., Neutron beam for measuring scattering cross sections at small angles, 19: 44862 (IAE-867)
KIRILLOVA, L. F., Real part of the elastic p-p scattering amplitude at 2, 4, 6, 8, and 10 Bev, 19: 45021 (JINR-P-2336)
KIRK, J. A., Preparation of emulsion stacks for underground cosmic-ray experiments, 19: 44397 (CERN-65-4(Vol.II), pp III5-11)
KIRSCH, L., Measurement of the K^0 mass and the K^0–K^- mass difference, 19: 44998 (CU-1932-247)
KIRSCH, L., Test of charge-conjugation invariance in $\bar{p}p$ annihilations at rest, 19: 45124
KISELEV, V. S., Angular dependence of quantities measured in total set of experiments on nucleon-nucleon scattering, 19: 45015 (JINR-P-2241)
KISS, I., Film dosimetry in radiodiagnosis to assess radiation burden to the population, 19: 43889
KISS-IMREH, G., Variation of the index of refraction of aqueous solutions of $UO_2(NO_3)_2$, 19: 43969
KITAHARA, Kazuto, High-dose ratemeter based on measurement of electric resistance of liquid organic compounds, 19: 44525
KITANI, Kenichi, Detection of portal systemic shunts by hepatopulmonary scanning using ^{131}I MAA. III., 19: 43904
KITANIN, E. L., Boundary layer of conducting fluid near intersection of two surfaces in presence of electromagnetic field, 19: 44828
KITZINGER, David G., Short cut method for dimensional analysis, 19: 44143 (SC-RR-65-306)
KIYOSE, R., Prog. rpt. on processing radioactive liquid wastes by evaporation, 1–6/64, 19: 45688 (NP-15367)
KLABES, R., Angular distribution for reaction $^{12}C(d,\alpha)^{10}B$ with a semiconductor detector, 19: 45289 (ZFK-PHA-12, pp 99-105)
KLARSFELD, S., Coulomb effects on vertex parts, 19: 45146
KLAUS, Sidney N., Pigment activity in dermal nevi induced by uv light: an enzyme histochemical study, 19: 43809
KLEIN, Abraham, Collective motion in finite many-particle systems. III., 19: 45364
KLEIN, E., Fundamental aspects of growth and shape of photographic silver halide crystals, 19: 45474 (CERN-65-4(Vol.II), pp III21-30)
KLEINPOPEN, H., Polarization of alkali line radiation excited by electron impact, 19: 44956
KLEM, R. L., Thermoelectric technology for space-power systems, 19: 45664
KLEMENT, W. Jr., Effects of liquid quenching on the constitution and structure of silver–silicon and gold–silicon alloys, 19: 45696 (CALT-221-12)
KLENER, Vladislav, Clinical examination of persons suspected of major exposure to ionizing radiation, 19: 44316
KLEPPING, Cl., Thorotrast disease concerning one observation, 19: 43738
KLERCKX, L., Calcium flux from x-irradiated Nitella cells, 19: 43818
KLICKMAN, A. E., Paste concept for fast reactor blanket applications, 19: 45561 (APDA-172)
KLITGAARD, J., Evaluation of small modified CEN mixer-settlers for extraction of uranium and thorium in a hot cell facility, 19: 44117 (ORNL-TM-1256)
KLOTZ, H.-D., Relation between column stratification and negative ion content in an impure Ar discharge, 19: 45423
KLYACHKO, V. A., Current status of the problem of sea-water distillation, 19: 44153 (JPRS-31361)
KLYAROVSKII, V. M., Use of ^{15}N as internal standard for determining quantities of radiogenic argon, 19: 43960
KMETKO, E. A., Band structure, specific heat, magnetic susceptibility, and anomalous thermal expansion of delta Pu, 19: 44689 (LA-DC-7351)

KMETKO, E. A., Magnetic susceptibility of delta plutonium alloys, 19: 44690 (LA-DC-7360)
KNAPP, W. G., Method for neutron-flux studies in an operating power reactor using bare and cadmium-covered radioactivants, 19: 45560 (ANL-7011)
KNIFFEN, D. A., Nuclear emulsion experiments on sounding rockets and satellites, 19: 44436 (CERN-65-4(Vol.II), pp X13-18)
KNIFFEN, D. A., Search for gamma-ray point sources, 19: 44905
KNISELEY, Richard N., Optical emission spectroscopy as an analytical tool, 19: 43929 (IS-1237)
KNOWLES, D. J., Description of facility radiation and contamination alarm systems installed in High Radiation Level Examination Laboratory Building, 19: 44297 (ORNL-TM-1251)
KNOWLES, Paul H., Reconnaissance for uranium in the Aisen Area, Aisen, Chile, 19: 44273 (RME-455 7(Rev.))
KNUDSEN, L., Single hybrid journal bearing tests in water, 19: 44151 (TIM-925)
KNUDSEN, L., Thrust bearing tests in water, 19: 44152 (TIM-926)
KNUDSEN, L. K., Cavitation damage tests with rotating disk in water, 19: 44625 (TIM-894)
KOBAYASHI, Ichiro, Composition of hydrated uranium peroxide, 19: 44029
KOBSAREV, I. Yu., Spin precession in gravitational fields, 19: 45134 (NP-15397)
KOCH, J. A., Long-period vlf emission pulsations, 19: 45171
KOCHEROV, N. P., Threshold oxidation and development of latent image formed by charged particles in nuclear emulsions, 19: 44393 (CERN-65-4 (Vol.II), pp II50-63)
KOCHIN, A. E., International comparisons of the specific activity of ^{32}P, ^{60}Co, and ^{204}Tl solutions and the activity of ^{60}Co solid sources, 19: 44101
KOCZKAS, Gy, Film dosimetry in radiodiagnosis to assess radiation burden to the population, 19: 43889
KODAIRA, Kiyoshi, Radioactive contamination of rice in Japan with reference to Sr-90 and Cs-137 content in rice until 1962, 19: 44265
KODAMA, Masahiro, Cosmic-ray index, 19: 44974
KOFOID, M. J., Composition of noble gas ion beams produced with a duoplasmatron, 19: 45385 (D1-82-0437)
KOFOID, M. J., Production of dense beams of low-energy ions, 19: 45384 (D1-82-0436)
KOFOID, Melvin J., Permanently magnetized ferrite antenna windows for improving electromagnetic wave transmission through a plasma, 19: 45387 (D1-82-0442)
KOH, Byung Jyun, Semiconductive behavior of anthracene and γ irradiation effects, 19: 44077
KOH, C. J., Sharpening of O'Raifeartaigh's theorem, 19: 45096
KOHL, J. W., Loss and replenishment of electrons at middle latitudes and high B values, 19: 45161
KOHLER, D., ^{60}O yield of gamma rays in T(p,γ)^{4}He reaction, 19: 45358
KOHN, W., New mechanism for superconductivity, 19: 45208
KOJIMA, Shoji, Higher harmonics and sub-harmonics of electron plasma oscillations, 19: 45428
KOLESHIK, I. G., Enhancement of ionization equilibrium in a stellar atmosphere, 19: 44914
KOLESNIKOV, P. M., Acceleration of pulsating plasma clot, 19: 45430
KOLESNIKOVA, L. N., Further development of apparatus for measurements of particle tracks in photoemulsions by television method, 19: 44422 (CERN-65-4(Vol.II), pp VII39-42)
KOLKUNOV, V. A., Non-relativistic Regge trajectories, 19: 45028 (NP-15027)
KOLKUNOV, V. A., Regge poles in a potential of the Coulomb well type, 19: 45152
KOLLER, Alois, Method for generation and containment of a high-energy plasma, 19: 45455
KOLLER, O., Comparison between results of irradiation therapy alone and individualized radiological and surgical treatment of cervical carcinoma, 19: 43884
KOLLIOPOULOU, Helena, Qualitative biological effects variation after irradiation of partition tissue, 19: 43745
KOLLMANN, George, Sulfhydryl radiation protective agents, 19: 43867
KOLOS, W., Potential-energy curves for $X^1\Sigma_g^+$, $b^3\Sigma_u^+$, $C^1\pi_u$ states of the hydrogen molecule, 19: 44946
KOLSRUD, M., Covariant and hermitian semi-classical limit of quantum dynamical equations for spin-½ particles, 19: 45060
KOLYADA, V. M., Calorimetric determination of absorbed dose of ionizing radiation of a reactor by the method of compensation of heat production in the sample, 19: 45467
KOMENDA, W., Crystal effects in the scattering of neutrons with energy from 30 to 1000 ev, 19: 45489
KOMOCHKOV, M. M., Estimation of ionizing radiation levels near 10-Bev synchrophasotron, 19: 44863 (JINR-P-2231)
KONAR, Ahmet F., Alpha radiation hygrometer. II., 19: 44338 (AD-608496)
KONDO, Sohei, RBE of fast neutrons to γ rays for mutations in relation to repair mechanisms, 19: 43786
KONDRACHINA, A. A., Study of the factors affecting the quality of the development with the electrodialyser, 19: 44410 (CERN-65-4(Vol.II), pp V22-33)
KONDRAT'EV, L. N., Intensity of nonradiative transitions in Ta and ^{239}Pu mesic atoms, 19: 44962
KONECNY, E., Measurement of the β-particle distribution of mass selected fission fragments with nuclear emulsions, 19: 44441 (CERN-65-4(Vol.II), pp X47-53)
KONEV, S. V., Effect of glycolysis rate increase of a yeast cell by uv light of mitogenetic intensity, 19: 43765
KONIJN, J., Efficiency calculations for a circular detector viewing a circular radiator, 19: 44505
KONONOVICH, E. V., Possible models of chromospheric spicules, 19: 44919
KONOPLYANNIKOV, A. G., Effectiveness of recovery of mice following their exposure to 660-Mev protons, 19: 43771
KONOV, V. N., Selection of spectrometric operating mode of FEU-49, No. 2, 19: 44455 (NP-15047)
KONSTANTINOV, A. A., International comparisons of the specific activity of ^{32}P, ^{60}Co, and ^{204}Tl solutions and the activity of ^{60}Co solid sources, 19: 44101
KONSTANTINOV, O. V., Optical orientation of atoms in a magnetic field perpendicular to the beam, 19: 44963
KONSTANTINOV, R. M., Isotopic composition of lead ore from different type deposits in Eastern Transbaikal, 19: 44277
KORMAN, Samuel, Transfer rates of gamma globulin between cerebrospinal fluid and blood plasma in multiple sclerosis, 19: 43666 (BNL-9406)
KORNILOV, I. I., Phase diagram of the $TiCr_2$–$ZrCr_2$ system, 19: 44714
KORNITZER, F., Experimental basis of quantitative interpretation of the renogram, 19: 43667 (EUR-1890.f)
KOROBKIN, V. V., Control system for pulsed electron-optical transformer, 19: 44358
KOROSIN, J., The determination of cadmium in uranium compounds by atomic absorption spectrophotometry, 19: 43935 (NIJS-R-447)
KORTUS, J., Plant for treatment of radioactive wastes of the Czechoslovak Institute of Nuclear Research, 19: 45693
KOSHLAND, Marian Elliott, Mechanism of the immune response, 19: 45695 (BNL-912)
KOSSIONIDES, S., Extension of Laben 512-channel analyzer for use in multiparameter experiments, 19: 44516
KOSTYANOVSKII, R., Chemical preparations for prevention of radiation injuries, 19: 43861 (JPRS-31349, pp 1-24)
KOSZTOLANYI, Charles, New method for isotopic analysis of zircons in natural state, 19: 43954
KOTANSKI, Andrzej, Classical phase-space integral in the statistical model with angular momentum conservation, 19: 45041 (TPJU-12/65)
KOTANSKI, Andrzej, Proof of theorem about general form of isotropic tensors, 19: 44810 (TPJU-8/65)
KOTOK, E. V., Neutrino luminosity of stars, 19: 44927
KOTRAPPA, P., Unit for testing high-efficiency filters, 19: 44281 (AEET-202)
KOUKHTIN, V. A., A developer for nuclear photography, 19: 44407 (CERN-65-4(Vol.II), pp V1-8)
KOUKIN, I. K., Two-dimensional incompressible fluid channel flow in presence of electric and magnetic fields, 19: 44829
KOURI, Donald J., Phase shifts and the quantum-mechanical Hamilton-Jacobi equation, 19: 45053
KOUVARAS, N., Extension of Laben 512-channel analyzer for use in multiparameter experiments, 19: 44516
KOVACH, P. J., Prog. rpt. on materials of Na heated steam generator, 8/27/65, 19: 44133 (BAW-1280-31)
KOVACIC, E. C., Compilation of Fermi experience, 19: 45562 (APDA-174, pp 71-3)
KOVACIC, E. C., Paste concept for fast reactor blanket applications, 19: 45561 (APDA-172)
KOVACIC, E. C., Paste concept for fast reactor blanket applications, 19: 45499 (APDA-174, pp 10-24)
KOVALEV, V. P., Possibility of using nuclear reactor in cosmic space for measuring cross sections of n-e scattering, 19: 45036 (NP-15476)
KOVNER, D. S., Application of hypothesis of localism in turbulent flow of conducting fluid in magnetic field, 19: 44836
KOWALSKI, K. L., Truncation of the unitary sum, 19: 45093
KOYANAGI, Take, Assay of strontium-90 in human bone in Japan, 1961–1963, 19: 44266
KOYANO, Akira, High-dose ratemeter based on measurement of electric resistance of liquid organic compounds, 19: 44525
KOZINETZ, G. I., Migration of hematopoietic bone marrow cells in irradiated and normal mice, 19: 43836
KRAINOV, V. P., Calculating energy levels of weakly deformed nuclei, 19: 45257 (IAE-811)

KRAMER, H. W., Efficient dewar for lithium-drifted germanium detectors, 19: 44511
KRAMER-AGEEV, E. A., Neutron distribution in straight cylindrical channel, 19: 45465
KRASHENINNIKOV, I. S., Development of multichannel analyzers, 19: 44456 (NP-15258)
KRASHOKUTSKII, R. N., Fast neutron capture cross section for Re, 19: 45298
KRASNOV, N. N., Production of ^{28}Al during irradiation of Mg with 20-Mev deuterons, 19: 44099
KRASNOV, N. N., Results of adjustment of 1.5-m cyclotron, FEI, 19: 44887
KRASNOV, N. N., Vertical shift of a beam in a cyclotron with incongruent magnetic and electric planes, 19: 44889
KRAYEVSKII, N. A., Pathology of radiation disease, 19: 43851
KREBS, K., Inelastic neutron spectra and vibrational modes of the hydrogen layer in alkali and alkaline-earth hydroxides, 19: 45482
KRECKER, U., Distortion and spurious scattering in NIKFI-R nuclear emulsion, 19: 44412 (CERN-65-4(Vol.II), pp VI11-21)
KRECKER, U., Properties of new NIKFIAN ORWO nuclear emulsions, 19: 44403 (CERN-65-4(Vol.II), pp IV16-22)
KREISMAN, P. J., Metastable current-carrying states of weakly coupled superconductors, 19: 45206
KRESTOVNIKOVA, T. I., A developer for nuclear photography, 19: 44407 (CERN-65-4(Vol.II), pp V1-8)
KRIMIGIS, S. M., Absence of Martian radiation belts and implications thereof, 19: 44912
KRISHNAMURTHY, B. S., Use of irradiated males for reduction of C. fatigans populations, 19: 43796
KRISHNAN, R. S., Dynamics of liquids and solids by optical spectroscopy, 19: 44039
KRIVANEK, Miloslav, Substoichiometric determination of copper in high-purity metals by activation analysis, 19: 43973
KRIVENZOVA, L. G., Ionization density in emulsions enriched with hydrogen, 19: 44435 (CERN-65-4(Vol.II), pp IX62-5)
KROHN, V. E., Electron-neutron interaction from scattering of neutrons by noble gases, 19: 45098
KROHN, Victor E. Jr., Electron-neutron interaction, 19: 44373 (ANL-6877, pp 15-20)
KROKOWSKI, E., Methods of irradiation with localized limited radiation effect, 19: 43900
KRONENBERG, Stanley, High-intensity γ insensitive neutron dosimeter, 19: 44544
KRUEGER, H., Polarization of alkali line radiation excited by electron impact, 19: 44956
KRUGLYAKOV, E. P., Parameters of plasma bunches of a coaxial injector, 19: 45431
KRUGLYAKOV, E. P., Temperature and density determination of non-stationary plasma, 19: 45433
KRUPCHITSKII, P. A., Measurement of the absolute value of the $K_1^0 \rightarrow K_2^0$ mass difference, 19: 45099
KRYSTYAN, K. J., Surface crack detector, 19: 44210 (KAPL-M-6484)
KUBAL, Joseph, Film dosimetry with inhibited development, 19: 44440 (CERN-65-4(Vol.II), pp X44-6)
KUBENA, K., Chromatographic investigation of some important substances in aqueous humor of the sound eye, after x irradiation, and in traumatic cataract, 19: 43755
KUBIT, C. J., Zircaloy-steam reaction in a simulated reactor loss-of-coolant accident, 19: 45496 (WCAP-3269-30)
KUBOWSKI, Jerzy, Water reactivity effects in the Anna critical assembly, 19: 45529 (INR-600/IX-A/PR)
KUDRYASHOV, Yu. B., Effectiveness of recovery of mice following their exposure to 660-Mev protons, 19: 43771
KUDRYAVTSEVA, A., Decay mode of ^{147}Eu, 19: 45267 (JINR-P-2161)
KUDRYAVTSEVA, L. K., Models of the temperature fields of fuel elements in the active zone and shield of the BN-350 reactor, 19: 45604 (JPRS-31245)
KUEHN, B., Angular distribution for reaction $^{12}C(d,\alpha)^{10}B$ with a semiconductor detector, 19: 45289 (ZFK-PHA-12, pp 99-105)
KUENNERT, Hans, Portable, battery-operated measuring apparatus for detection of radiation, 19: 44542
KUGLER, M., Meson and baryon resonances in relativistic SU(6), 19: 45112
KUHNS, Nelson F., Nuclear energy for water desalting. A bibliography, 19: 45590 (TID-3584)
KUJAL, B., Collision probability method for calculating fast neutron fission factor, 19: 45229 (UJV-1324/65)
KUJAL, J., Collision probability method for calculating fast neutron fission factor, 19: 45229 (UJV-1324/65)
KUKULA, F., Determination of iodine in organic polymers by activation analysis, 19: 43951
KUKULA, Frantisek, Substoichiometric determination of copper in high-purity metals by activation analysis, 19: 43973
KULHANEK, J., Magnetic field gage and stabilizer, 19: 44352 (UJV-1339/65)
KULIKAUSKAS, V. S., Proton scattering from a tungsten single crystal, 19: 45349
KULYUPINA, N. V., High-dose-rate isotope gamma irradiation unit UK-70000, 19: 44172
KULYUPINA, N. V., Isotope gamma irradiation unit UKP-30000, 19: 44171
KUMAR, Naresh, Energy levels of ^{92}Mo with soft core potential, 19: 45311
KUMAR, Vijay, Energy levels of ^{92}Mo with soft core potential, 19: 45311
KUN HSIAN-CHIN, Gamma spectrum of ^{160m}Ho isomer, 19: 45272 (JINR-P-2270)
KUNII, D., Prog. rpt. on processing radioactive liquid wastes by evaporation, 1-6/64, 19: 45688 (NP-15367)
KUNIN, P. E., Conducting slab in traveling magnetic field of double-side inductor, 19: 44841
KURIMURA, Yoshimi, Radiation-induced oxidation of Sb(III) in aqueous solution. II., 19: 44085
KURKIN, I. N., Paramagnetic resonance of cerium in single-crystal $PbMoO_4$, 19: 44017
KURSANOV, A. L., Metabolism and transport of organic substances in the phloem, 19: 43685
KURSUNOGLU, Behram, Prog. rpt. on cooperative effects and plasma losses in magnetic field, final, 3/62-2/63, 19: 45380 (AD-426192)
KURTMULLAEV, R. Kh., Peculiarities of plasma heated by collisionless shock waves, 19: 45434
KUSAKA, Yuzuru, Determination of Si in Fe and steel by activation analysis, 19: 43965
KUSHNIR, V. S., Self-excitation regimes in interaction between traveling waves magnetic field and ionized gas flow, 19: 44839
KUZNETSOV, A. S., Variant scheme of fast coincidences for low-amplitude pulses, 19: 44486 (ZFK-PHA-12, pp 201-5)
KUZNETSOV, F. M., Heterogeneous absorber efficiency in homogeneous uranium-water reactors, 19: 45536

L

LABARRE, E., Study of circumferential and axial temperature perturbations in a cylindrical fuel element canning (mathematical and rheoanalogical methods), 19: 45543 (EUR-2480.f)
LABUSHKIN, V. G., Alpha and β radiation method for determining concentrations of short-lived radon daughters in air, 19: 44258
LACEY, P. G., Control rod worth in heterogeneous mockup of large PWR core, 19: 45533 (WCAP-3269-33)
LACEY, P. G., Local fission power distributions around control rods and control rod followers in simulated PWR cores, 19: 45534 (WCAP-3269-35)
LACHAPELLE, J. M., Hair dysplasia induced by x rays in mice under different irradiation conditions, 19: 43833
LACROIX, M., Comparative use of S-32 and Br-82 for determination of extracellular fluid volume, 19: 43898
LADU, M., Dose absorption by tissue on accidental exposure to very high-energy γ radiation, 19: 44329
LADU, M., Production and discharge of toxic and radioactive gas in tunnel of Frascati linac, 19: 44866 (LNF-65/21)
LALIT, B. Y., Strontium-90 content of food samples in India—data summary through 1963, 19: 44244 (AEET/AM/40)
LAM, C. S., Gauge problems in canonically quantized electrodynamics without subsidiary conditions, 19: 45135 (NP-15436)
LAM, S. H., Compressibility and non-equilibrium effects on the response of a Langmuir probe in flowing plasma, 19: 45447
LAMBERTSON, G. R., Derivation of corrections to control closed orbit in an alternating-gradient synchrotron, 19: 44875 (UCRL-16229)
LAMERS, R. P., Centrifugal pump impeller design system, 19: 44148 (TIM-918)
LANDE, Alfred, New foundations of quantum mechanics, 19: 45153
LANDERS, M., Irradiation-sterilized shelf-stable fish and seafood products, 19: 44556 (NP-15464)
LANE, J. R., Refractory metals sheet rolling program, 19: 44647
LANE-PETTER, W., Observations on autoclaved, fumigated and irradiated diets for breeding mice, 19: 43654
LANGER, L. M., Antimony-124 spectrum shape, 19: 45328
LANGLEY, R. W., Computational methods for space radiation shielding analysis, 19: 45463 (NP-15425)
LANIUS, K., Photoproduction of mesons in hydrogen bubble chamber at energies up to 5.5 Bev, 19: 44999 (DESY-65/5)
LANNOY, F., Theory of corrections to unitary symmetry formulae, 19: 45003 (IC/65/60)
LANZEROTTI, Louis John, Photoproduction of charged pion pairs, 19: 45000 (HUX-2752-7)
LARKIN, Joseph P., Protective windows or skylights for fallout shelters,

19: 44218
LA ROCHE, Gilles, Thyroid function in rainbow trout. I., 19: 43773
LARSON, A. V., Quasi-steady-state pulsed plasma thrustors, 19: 45441
LARSON, John W., Economics of electrical propulsion for earth-orbit to lunar-orbit cargo transfer, 19: 44232
LARSSON, K.-E., Liquid dynamics, 19: 45235
LARSSON, Rognar, Metal complexes in aqueous solution by infrared spectrophotometry. V., 19: 44004
LARUELLE, Pierre, Orthorhombic sulfides, selenides, and tellurides L_2X_3 of the rare earths, yttrium, and scandium of the Sc_2S_3 type, 19: 44010
LASLETT, L. Jackson, Derivation of corrections to control closed orbit in an alternating-gradient synchrotron, 19: 44875 (UCRL-16229)
LATEK, Stanislaw, Water reactivity effects in the Anna critical assembly, 19: 45529 (INR-600/IX-A/PR)
LATYSHEV, G. D., Application of proton resonance to the measurement of inhomogeneous magnetic fields, 19: 44353 (SLAC-Trans-22)
LATYSHEV, Georgii Dmitrievich, Nuclear magnetic resonance in a flowing liquid, 19: 44813 (NP-tr-1307)
LAUBER, A., Efficiency calculations for a circular detector viewing a circular radiator, 19: 44505
LAUER, E. J., Experimental studies with the Astron facility, 19: 45413 (UCRL-12456)
LAUGHLIN, J. S., Electron-beam treatment planning in inhomogeneous tissue, 19: 43916
LAUNAY, Pierre, Heavy and special concretes in nuclear industry, 19: 45468
LAVIE, J.-M., Accidental external exposure dosimetry at the Commissariat a l'Energie Atomique, 19: 44333
LAVIE, J.-M., Detection of criticality accidents, CEA, France, 19: 44321
LAWRENCE, J., Efforts to increase thermionic converter output and efficiency, 19: 44985
LAX, Louis C., Transfer rates of gamma globulin between cerebrospinal fluid and blood plasma in multiple sclerosis, 19: 43666 (BNL-9406)
LAYNE, Gilbert S., Uranium–chromium–aluminum ternary alloy, 19: 44665
LAYNE, Gilbert S., Uranium–tungsten–aluminum ternary alloy, 19: 44666
LAYNE, Gilbert S., Uranium–tantalum–aluminum alloy, 19: 44667
LAYNE, Gilbert S., Uranium–vanadium–aluminum ternary alloy, 19: 44668
LAZAR, N. H., Ion cyclotron harmonic spectrum generated in an energetic ion plasma, 19: 45405 (ORNL-P-1576)
LAZZARINO, L., Outlook for use of nuclear energy for production of heat at low temperature, 19: 45618
LEACHMAN, R. B., Statistical fluctuations in the excitation functions from $^{12}C(^{12}C,\alpha)^{20}Ne$, 19: 45313
LEADABRAND, R. L., Simultaneous vhf and uhf observations of the aurora at Fraserburgh, Scotland, 19: 45169
LEAKE, J. W., New methods of measuring dose equivalent rate around neutron generators, 19: 44370 (AERE-R-4883)
LEARY, J. A., Preparation of ultra-high purity plutonium, 19: 44600 (LA-3356)
LEARY, J. A., Solubilities of selected elements in liquid plutonium. VI. Rhenium, 19: 44688 (LA-3359)
LEBEDEV, N., Decay mode of ^{147}Eu, 19: 45267 (JINR-P-2161)
LEBEDEV, N. A., New data on ^{135}Ce decay, 19: 45268 (JINR-P-2235)
LEBEDEV, N. A., Spectra of conversion electrons of ^{133}Ce and ^{139}Ce isotopes, 19: 45269 (JINR-P-2236)
LEBEDEV, V. N., Estimation of ionizing radiation levels near 10-Bev synchrophasotron, 19: 44863 (JINR-P-2231)
LEBEDEVA, N. G., Neutron beam for measuring scattering cross sections at small angles, 19: 44862 (IAE-867)
LEBOULEUX, Philippe, Radioprotection problems resulting from the presence of experimental devices around a reactor, 19: 44287 (CEA-R-2799)
LECHLITER, G. L., MIRAGE-III: Matrix interpretive routine, 19: 44581 (KAPL-M-6469)
LEDDICOTTE, G. W., Use of activation analysis in determination of origin of opium, 19: 43937 (ORNL-TM-1263)
LE DUFF, J., Some stochastic phenomena in storage rings, 19: 44865 (LAL-1134)
LEE, A., Spurious scattering in nuclear emulsions, 19: 44413 (CERN-65-4 (Vol.II), pp VI23-30)
LEE, Benedict H. K., Cylindrical imploding shock waves, 19: 44852
LEE, H. J., Acoustic attenuation in type II superconductor, 19: 45210
LEE, J. A. H., Seasonal variations in incidence of clinical onset of leukemia, 19: 43827
LEE, J. V., Isotopic contamination in electromagnetic separators, 19: 44573 (ORNL-P-515)
LEE, John H., Cylindrical imploding shock waves, 19: 44852
LEES, D. G., Effect of production route, ageing time and oxygen content on properties of Zr–2.5 wt.% Nb, 19: 44629
LEGEAY, G., Dosimetry of high-energy protons by measurement of beryllium-7 formed in the tissues, 19: 44327
LEGG, J. C., Particle identification using a single counter, 19: 44517
LE GRAND, J., Attempt to assess the dose received by bone marrow on exposure to neutron flux, 19: 43854
LEHMAN, Richard L., Sampling bias in scanning proton-recoil tracks in nuclear emulsion, 19: 44464 (UCRL-11703)
LEHRER, S. S., Nuclear quadrupole resonance and bonding in crystalline ammonia, 19: 45483
LEIMDOERFER, M., Monte Carlo procedure for calculating migration of protons, 19: 45462 (NP-15163)
LEINEWEBER, A. J., Approach to stiffness of laterally loaded conical shells, 19: 45712 (SC-TM-65-82)
LEIPUNSKII, A. I., Possibility of using thorium in high-energy reactors, 19: 45605 (ORNL-tr-788)
LEITH, D. W. G., Reaction $KN\pi\pi$ at 3 Bev/c and production mechanism of K^*N^*, 19: 45057
LEITTEN, C. F. Jr., Thermochemical deposition of refractory metals, alloys, and compounds for application in thermionic devices, 19: 44640 (ORNL-P-1446-1)
LEMENOV, V. A., Study of inelastic scattering of slow neutrons in zirconium hydride, 19: 45240
LEMESLE, Georges, Handling apparatus for an installation for reloading a nuclear reactor with fuel elements, 19: 45513
LEMESLE, Georges, Nuclear reactor refueling facility, 19: 45514
LEMONNE, J., A determination of the Λ nuclear potential well depth, 19: 45361
LENK, Pedro R., Development of realistic requirements for PM-type reactor instrumentation. Task 1 topical report, 19: 45584 (NYO-3379-1)
LENZERINI, L., Uridine diphosphate glucose pyrophosphorylase activity in liver of irradiated rats, 19: 43747
LEONG, G. F., Comparative lethality responses of neutron- and x-irradiated dogs, 19: 43832
LEPORE, R., Possibilities and conditions for development of nuclear industrial communities, 19: 45723
LEROY, Jean-Marie, Hydrates of uranyl sulfate, 19: 44014
LESSOF, M. H., Myxedema after x-ray therapy to the neck, 19: 43890
LE TOURNEUX, Jean, Structure of giant dipole line in spherical nuclei, 19: 45314
LEUZE, R. E., Behavior of the transplutonium elements in solvent extraction systems, 19: 44115 (ORNL-P-1577)
LEVANDOWSKY, Jean, Improvements in or relating to processes for applying alloys to metal surfaces, 19: 44658
LEVENTHAL, Joel S., Tritium in Mt. Everest ice—annual glacier accumulation and climatology at great equatorial altitudes, 19: 44262
LEVIN, V. A., Nonlinear oscillations of electronic gas in magnetic field, 19: 44849
LEVIN, V. B., Stabilizing effect of longitudinal magnetic field on flows of conducting fluid, 19: 44835
LEVINE, L., Ionizing shock studies in electromagnetically driven shock tube, 19: 44857
LEVINTOV, I. I., Real part of the forward scattering amplitude of charged particles, 19: 45048 (ANL-Trans-217)
LEVKOEV, I. I., A developer for nuclear photography, 19: 44407 (CERN-65-4(Vol.II), pp VI-8)
LEWIS, A. J., Case of double trisomy: trisomy No. 18 and triplo-x, 19: 43811
LEWIS, Clifford J., Recovery of uranium and/or vanadium values from ores containing the same, 19: 44129
LEWIS, H. D., Proper use of transformations of log normal functions in small-particle statistics, 19: 44808 (LA-DC-6636)
LEWIS, H. R. Jr., Floating-point version of Nordsieck's scheme for numerical integration of differential equations, 19: 45703 (LA-DC-6667)
LIANG, Shu-chuan, Extraction of microgram amounts of zirconium with n-benzoyl-n-phenylhydroxylamine, 19: 43972
LIANG, Shu-chuan, Separation of Th, Sc, and Y earths, 19: 44125
LIBBY, W. F., Tritium in Mt. Everest ice—annual glacier accumulation and climatology at great equatorial altitudes, 19: 44262
LIERS, H., Polarization of 39-Mev protons elastically scattered from ^{58}Ni and ^{60}Ni, 19: 45378
LIFOROV, V. G., Study of inelastic scattering of slow neutrons in zirconium hydride, 19: 45240
LIMIC, N., Extrapolation of the S matrix from Lehmann's representation, 19: 45062
LINCOLN, J. Virginia, Geomagnetic and solar data, 19: 45178
LINDBO, Tord, Prestressed concrete vessels. II., 19: 45506
LINDHOUT, A. H., Industrial applications for radioisotopes, 19: 44562
LINDLEY, John, Improvements relating to chemical extraction processes, 19: 44127
LINDSAY, Stuart, Tumors of thyroid and parathyroid glands, 19: 43892
LINDSEY, P. S., Compilation of Fermi experience, 19: 45562 (APDA-174, pp 71-3)
LINDSTROM, G. D., Model tests of the sodium distributor for the sodium-

heated steam generator, 19: 44182 (BAW-1280-29)
LINGENFELTER, R. E., High-energy solar neutrons. I., 19: 44902
LINGENFELTER, R. E., High-energy solar neutrons. II., 19: 44903
LINTNER, K., Radiation behavior of light metals, 19: 44752 (CEA-tr-A-1818)
LIPATOV, V. P., Redesign of IAE linear electron accelerator, 19: 44860 (IAE-614)
LIPKIN, H. J., Experimental tests of broken $\bar{U}(12)$ and approximate $U(6) \times U(6)$, 19: 45002 (IC/65/59)
LIPKIN, H. J., Meson and baryon resonances in relativistic SU(6), 19: 45112
LIPPINCOTT, Stuart W., Transfer rates of gamma globulin between cerebrospinal fluid and blood plasma in multiple sclerosis, 19: 43666 (BNL-9406)
LIPTAKOVA, G., Contribution to the determination of ^{131}I by an extraction method, 19: 43953
LIST, Robert, Meso-scale studies in the >100-km range, 19: 44784 (BNL-914, pp 110-12)
LITT, J., Measurements of the A and R parameters in proton-proton scattering at 47.8 and 27.6 Mev, 19: 45319
LIVERIOS, D., Design of fast-cycling liquid-H_2 bubble chamber, 19: 44459 (PPAD-2137-561)
LLED, A., Momentum determination of low-momentum particles in emulsions exposed to strong magnetic field, 19: 44424 (CERN-65-4(Vol.II), pp VIII9-16)
LLOSA, R., Momentum determination of low-momentum particles in emulsions exposed to strong magnetic field, 19: 44424 (CERN-65-4(Vol.II), pp VIII9-16)
LLOYD, B., Design of fast-cycling liquid-H_2 bubble chamber, 19: 44459 (PPAD-2137-561)
LLOYD, J. William, Radiation as cause of lung cancer among uranium miners, 19: 44314
LOBOV, G. A., Regge poles in a potential of the Coulomb well type, 19: 45152
LOBOV, G. A., T-parity nonconservation in strong interactions, 19: 45280 (NP-15457)
LOCK, W. O., Conference on nuclear photography, 5th, Geneva, 9/64, 19: 44377 (CERN-65-4(Vol.I))
LOCKHART, L. B. Jr., Filter pack technique for classifying radioactive aerosols by particle size. III., 19: 44252 (NRL-6305)
LODER, A., Muon capture and electric dipole excitation for lithium, 19: 45351
LO DESERTO, A., Radioiodine metabolism in patients affected by a simple sporadic goiter, 19: 43691
LODGE, J. G., Formation of excited hydrogen atoms by charge-exchange in lithium, 19: 44955
LOEFFLER, Irvin J., Hypervelocity impact damage characteristics in beryllium and graphite plates and tubes, 19: 44692 (NASA-TN-D-3018)
LOEFFLER, Lotar, Pressed block for preparation of rod-shaped nuclear fuel elements, 19: 44663
LOESSNER, Volkhard, Determination of penetration of aerosols in filters, 19: 44299 (SZS-2(1965))
LOKEN, Merle K., Prevention of liver metastases by intravenous radioisotopes, 19: 43797
LOMAKIN, S. S., Physical characteristic of critical assembly with BeO moderator, 19: 45537
LOMAKIN, Yu. F., Hydrodynamics of a resonance bubble chamber, 19: 44523
LOMANITZ, Ross, Instabilities due to the tail-wagging effect, 19: 45186
LOMBARD, Rosalyne, Study of the d layer of some nuclei by electron scattering, 19: 45275 (NP-15138)
LOMER, W. M., Fermi surface of palladium, 19: 45472 (AERE-M-1605)
LOMBERG-HOLM, Knud Karl, Measurement of radioactivity on paper chromatograms, 19: 43984
LONDON, G. J., Prog. rpt. on flow and fracture studies of alloyed Be, final, 8/65, 19: 44694 (NP-15432)
LONDON, S-O., Experimental studies on assemblies 1 and 2 of the fast reactor FRO. I., 19: 45522 (AE-195)
LONG, J. V. P., Theoretical assessment of the possibility of selected-area mass-spectrometric analysis using focused ion beam, 19: 44354
LONG, Robert B., Reactor coolant system, 19: 45519
LOONIS, Aldea A., Interpretation of lunar α-scattering data, 19: 44901
LOOSEMORE, W. R., Health physics instruments, AERE, 19: 44369 (AERE-R-4552)
LORD, J. J., Loading of emulsions with diamonds and polystyrene for experiments with stopping K particles, 19: 44398 (CERN-65-4(Vol.II), pp III12-16)
LORD, J. J., Preparation of emulsion stacks for underground cosmic-ray experiments, 19: 44397 (CERN-65-4(Vol.II), pp III5-11)
LORIAK, A. Ya., Effect of climatic conditions on chronic irradiation with ultra-high frequency energy, 19: 43774
LOSKUTOVA, N. G., Spectrum of γ rays from $^{54}Fe(n,\gamma)^{55}Fe$ reaction, 19: 45322
LOTHROP, Fred H. G., Prog. rpt. on Bevatron operation and development, 10–12/64, 19: 44874 (UCRL-16203)
LOTTS, A. L., Thorium–uranium recycle facility, 19: 44167 (ORNL-P-1521)
LOTTS, A. L., Time study of fuel rod fabrication in the Kilorod facility, 19: 44639 (ORNL-3740)
LOUBATON, J. P., Determination of neutron form factors from pion electroproduction, 19: 45065
LOUTHAN, M. R. Jr., Basic mechanisms of stress corrosion cracking of titanium, 19: 44621 (CONF-651006-1)
LOVALLO, J. M., Precritical calculations for the 2.9-in. pitch, TWNR critical assembly, 19: 45526 (GA-6633)
LOVBERG, R. H., Investigation of current sheet microstructure, 19: 45445
LOVELACE II, W. R., Human stresses in space flight operations and methods of improving man's tolerance, 19: 43842
LOVITCH, L., Reproduction of two-body scattering phase shifts by a phenomenological potential, 19: 45109
LOW, A. H., Hydrostatic extrusion of difficult metals, 19: 44651
LOWE, J. N., Rolling cast beryllium between 500 and 1000°C, 19: 44652
LOWE, L. F., Ferrous ammonium sulfate-cupric chloride solutions for dosimetry of a kilocurie ^{60}Co source, 19: 44372 (AFCRL-65-470)
LOWES, F. J., Laboratory investigation of geomagnetic dynamos, 19: 45156 (AFCRL-64-768)
LUCAS, M. S. P., Electrical conductivity of thin-metallic films with unlike surfaces, 19: 45479 (TID-21301)
LUCCIO, A., State of construction of the relativistic cyclotron for protons at 45 Mev, 19: 44886
LUDENA, Eduardo, Electronic ground state and wave functions for scandium monoxide, 19: 44020
LUEST, R., Stellar and solar magnetic fields, 19: 44932
LUETJENS, G., Test of charge-conjugation invariance in $\bar{p}p$ annihilations at rest, 19: 45124
LUK'YANOV, V. N., Peculiarities of plasma heated by collisionless shock waves, 19: 45434
LUMBROSO, Daniel, Hydrolysis in acid medium of linear and cyclic acids. III., 19: 44011
LUNDIN, C. E., Samarium-type intermediate phases of intra-rare-earth binary systems, 19: 44672 (AD-619201)
LUNDIN, Frank E. Jr., Radiation as cause of lung cancer among uranium miners, 19: 44314
LUNDQVIST, Bengt, Thermodynamic properties of heavy water, 19: 44008
LUNDY, A., Electron-beam treatment planning in inhomogeneous tissue, 19: 43916
LUNDY, T. S., Diffusion of ^{181}Hf in bcc hafnium, 19: 44729
LUNSFORD, J. L., Magnetic susceptibility of delta plutonium alloys, 19: 44690 (LA-DC-7360)
LUO, H. L., Effects of liquid quenching on the constitution and structure of silver–silicon and gold–silicon alloys, 19: 45696 (CALT-221-12)
LUPANOV, G. A., Relativistic instability of polytropic spheres, 19: 44925
LUPULESCU, A., Autoradiography of the thyroid gland, 19: 43683
LUSCHIKOV, V. I., Using photoemulsion in proton dynamic polarization conditions, 19: 44442 (CERN-65-4(Vol.II), pp X57-60)
LUSKUS, Carol, MEA effect on radiation dose-response characteristics of granulocyte and lymphocyte counts, 19: 43876
LUSSIE, William G., Measurement and utilization of neutron-capture γ radiation, 19: 45375
LUTON, J. N., Experimental simulation of large, high field, superconducting magnet operation, 19: 45192 (ORNL-TM-1266)
LUTTINGER, J. M., New mechanism for superconductivity, 19: 45208
LYMPERES, C. J., Interactions in type 316 stainless steel–NaK–Nb–1 Zr alloy system, 19: 44626 (TIM-896)
LYNCH, G. R., Reaction $KN\pi\pi$ at 3 Bev/c and production mechanism of K^*N^*, 19: 45057
LYON, D. N., Boiling heat transfer and peak nucleate boiling fluxes in saturated liquid helium between the λ and critical temperatures, 19: 44201
LYSKOVA, T. I., Effect of glycolysis rate increase of a yeast cell by uv light of mitogenetic intensity, 19: 43765
LYUBOSHITS, V. L., Passage of spin and spinless particles through matter, 19: 45013 (JINR-P-2230)
LYUBOSHITS, V. L., Some interference phenomena arising by mixing quantum levels in external fields, 19: 45270 (JINR-P-2248)

M

MA, Hoi-chang, Separation of Th, Sc, and Y earths, 19: 44125
MACASEK, F., Chromatographic separation of radiochemically pure ^{90m}Y from the parent isotope ^{90}Sr, 19: 44120
MACE, P. N., Effect of optical pump pulse shape on ruby inversion,

19: 45704 (LA-DC-6717)
MACH, R. S., Comparative use of S-32 and Br-82 for determination of extracellular fluid volume, 19: 43898
MACHI, Sueo, Existence of long-lived radicals in γ radiation induced polymerization of ethylene, 19: 44073
MACHI, Sueo, Specific influence of temperature on γ-radiation induced polymerization of ethylene, 19: 44074
MAC KELLAR, A. D., Nuclear ground state properties of ^{16}O by an extension of Eden-Emery method, 19: 45350
MACKINTOSH, W. D., Pyrolysis of the potential power reactor coolant, Santowax O-M, 19: 44044 (AECL-2218)
MAC LEOD, R. A., Fast flux test facility, 19: 45670 (APDA-174, pp 74-6)
MACOMBER, John W., Nuclear reactor control rod assembly with improved driving mechanism, 19: 45518
MAC RAE, W., Gas-cooled reactor experience in the United Kingdom, 19: 45611
MADDOX, W. L., Remotely controlled corrosion-resistant pipetter, 19: 43936 (ORNL-P-1533)
MADDOX, W. L., Sample preparation apparatus for MSRE, 19: 44168 (ORNL-P-1532)
MAECK, W. J., Prog. rpt. on burnup determination of nuclear fuels, 1–3/65, 19: 45260 (IDO-14660)
MAEDA, T., Possible evidence for nuclear interaction of μ above 3×10^{14} ev, 19: 45368
MAGAT, Michel, Graft polymerization utilizing ionizing radiation, 19: 44097
MAGLIULO, E., Morphogenesis of binucleated erythropoietic cells by action of x rays, 19: 43730
MAGLIULO, E., Pseudo-amitoses provoked by x rays in erythropoietic cells in vitro, 19: 43826
MAGURNO, Benjamin A., Neutron cross sections. Z = 88 to 98, 19: 45250 (BNL-325(2nd Ed.)(Suppl.2)(Vol.III))
MAHEFKEY, E. T. Jr., Radioisotope power subsystems for space applications, 19: 44570
MAILLET, Emmanuel, Nuclear reactor fuel element, 19: 45555
MAILLET, Emmanuel, Process for machining tubular elements with fins for heat exchangers, 19: 44656
MAIOROV, L. V., Asymptotic behavior of law of slow neutron scattering, 19: 45231
MAKAR'IN, V. K., Charging device for pulsed magnetic field power supply, 19: 44449 (IAE-704)
MAKAR'IN, V. K., Pulsed magnetic fields apparatus, 19: 44861 (IAE-795)
MAKAROV, A. A., Baryon annihilation in broken U(12) symmetry, 19: 45008 (JINR-E-2246)
MAKAROV, A. A., Current-generated algebras and form factors, 19: 45011 (JINR-E-2294)
MAKITA, Motoo, Histopathological studies on transplanted experimental osteogenic sarcoma, 19: 43772
MAKSIMOVA, M. P., Spectral method of determination of doses from β-α emitters, 19: 44491 (CEA-tr-R-1866)
MAKSYUTENKO, B. P., Delayed neutron relative yields during ^{235}U and ^{238}U fission, 19: 45300
MALCIC, S. S., Contribution to study of effect of TiO_2 additive on sintering of UO_2, 19: 44646
MALINOVSKII, V. K., Parameters of plasma bunches of a coaxial injector, 19: 45431
MALINOVSKII, V. K., Temperature and density determination of non-stationary plasma, 19: 45433
MALKUS, Willem V. R., Hydromagnetic instability of sub-Alfvén equations, 19: 45187
MALOV, M. M., Proton scattering from a tungsten single crystal, 19: 45349
MALY, Jaromir, Possibility of obtaining non-excited compound nuclei of heavy transuranium elements, 19: 45286 (UJV-1293/65)
MALYAVKIN, L. P., Control system for pulsed electron-optical transformers, 19: 44358
MAMALADZE, Yu. G., Analog of d-c Josephson effect in He II, 19: 45202
MAMBRIANI, G., Apparatus for investigations on scintillator properties in the temperature range −100°C to +50°C, 19: 44460 (RT/FI(65)8)
MANCA, Josef, Dismantling of Rn pumping stations, 19: 44317
MANCINI, A. M., Immunological aspects of experimental pulmonary sclerosis due to ionizing radiations, 19: 43817
MANDELSTAM, Stanley, Three-body N/D equations. I., 19: 45107
MANGENEY, A., Contribution to interaction between a radiation field and a plasma, 19: 45418
MANIKOWSKI, A. F. Jr., Radioisotope power subsystems for space applications, 19: 44570
MAN'KO, V. I., Study of reactions $^{18}O(p,\alpha)^{15}N$ and $^{11}B(p,\alpha)^{8}Be$ using semiconductor counters, 19: 45291 (ZFK-PHA-12, pp 117-22)
MANOJLOVIC, Lj. M., Contribution to study of effect of TiO_2 additive on sintering of UO_2, 19: 44646
MANZANO, J. R., Modulation of primary spectrum during the recent solar cycle for rigidities between 4 and 12 Bev, 19: 44965
MANZIONE, A. V., Application of the electron microprobe to the identification and quantitative determination of carbon, 19: 43966
MARAGA B., Aldo, Reconnaissance for uranium in the Aisen Area, Aisen, Chile, 19: 44273 (RME-4557(Rev.))
MARAIS, P. G., Half life of ^{32}P, 19: 45371
MARAIS, P. G., Tables to correct for resolving-time counting losses of nucleonic apparatus, 19: 44530
MARASIK, A., Neutron diffraction study of uranium oxytelluride (UOTe), 19: 44009
MARCU, M., Measurement of Coulomb scattering in the presence of track distortion and spurious scattering, 19: 44414 (CERN-65-4(Vol.II), pp VI31-6)
MAREEV, Yu., Decay mode of ^{147}Eu, 19: 45267 (JINR-P-2161)
MARENKOV, V. S., Further development of apparatus for measurements of particle tracks in photoemulsions by television method, 19: 44422 (CERN-65-4(Vol.II), pp VII39-42)
MARGEN, Peter, Prestressed concrete vessels. II., 19: 45506
MARIANI, A., Radiomimetic effects of mono- and bi-functional alkylating compounds in triticum monococcum (2x) and triticum durum (4x), 19: 43653
MARINI, A., Level widths of nuclei at high excitation energy, 19: 45343
MARINOV, M., Upper limits of glass formation and glass structure in binary systems $BeO–SiO_2$, $MgO–SiO_2$, $CaO–SiO_2$, $SrO–SiO_2$, and $BaO–SiO_2$, 19: 44015
MARINOV, M., Upper glass formation limits in the binary systems $BeO–GeO_2$, $MgO–GeO_2$, $CaO–GeO_2$, $SrO–GeO_2$, and $BaO–GeO_2$, 19: 44016
MARIO, E., Tensor force in the nucleus ^{18}F, 19: 45370
MARK, Hans, Background events in photomultiplier tubes at high altitudes, 19: 44465 (UCRL-12020)
MARKAKIS, Perielus, Development of programs on radiation preservation of foods, 19: 44566
MARKELS, Michael Jr., Prog. rpt. on effects of electrical fields on boiling heat transfer, 12/64, 19: 44190 (NYO-2404-67)
MARKELS, Michael Jr., Prog. rpt. on effects of electrical fields on boiling heat transfer, 4–6/65, 19: 44191 (NYO-2404-73)
MARKOV, V. N., Neutron distribution in straight cylindrical channel, 19: 45465
MARKOVIC, P., Personnel dosimetry control at Boris Kidrich Institute, Vinca, 19: 44332
MARKUS, Bonno, Qualitative biological effects variation after irradiation of partition tissue, 19: 43745
MARSH, Roland O., Prestressed concrete pressure vessels. I., 19: 45555
MARSHALL, John, Development of an interleaved, fractional-turn coil, 19: 44136 (LA-3234)
MARTEM'NOV, V. P., Pulsed magnetic fields apparatus, 19: 44861 (IAE-795)
MARTEM'YANOV, V. P., Charging device for pulsed magnetic field power supply, 19: 44449 (IAE-704)
MARTIN, A., General proof of Pomeranchuk theorem and related theorems, 19: 45071
MARTIN, A. D., Low-energy pion-kaon interaction, 19: 45085
MARTIN, Robert L., In-pile studies of experimental pyrolytic-carbon-coated UC_2 and UO_2 fuel particles, 19: 44740 (BMI-1737)
MARTIN, Roger, Handling apparatus for an installation for reloading a nuclear reactor with fuel elements, 19: 45513
MARTIN, Roger, Nuclear reactor refueling facility, 19: 45514
MARTYSH, G. G., Regression of sensitivity and latent image in nuclear and light-sensitive photographic emulsions, 19: 44402 (CERN-65-4 (Vol.II), pp IV5-15)
MARTYSH, G. G., Theoretical grounds for the selection of developing agent for introducing it into the nuclear emulsion, 19: 44408 (CERN-65-4 (Vol.II), pp V9-15)
MARTZ, G., Treatment of thyroid cancer with radioiodine, 19: 43918
MARUYAMA, Susumu, Anomalous transmission of x rays through Ge single crystals containing dislocations and impurities, 19: 44756
MASAHARU, Okano, Low-level γ dosimetry with scintillation counters, 19: 44528
MASCALL, A. J., Crystal structures of solid H and solid D in thin films, 19: 45194
MASEVICH, A. G., Neutrino luminosity of stars, 19: 44927
MASHKOVICH, V. P., Neutron distribution in straight cylindrical channel, 19: 45465
MASI, Frank J., Safety fluoroscope with an alerting device of contrasting color surrounding the screen, 19: 44362
MASON, D. G., SNAP-8 reactor and shield designs and operating experience, 19: 45666
MASON, John L., Working gas selection for the closed Brayton cycle, 19: 44205
MASSAM, T., Measurements of muon depolarization in several materials, 19: 45080

MASSAM, T., New electron detector with high rejection power against pions, 19: 44522
MASSAM, T., Quenching of muon depolarization in several materials as function of externally applied magnetic fields, 19: 45079
MASUBUCHI, Koichi, Nondestructive measurement of residual stresses in metals and metal structures, 19: 44643 (RSIC-410)
MASUMI, Motoshi, Extension of range of electron density in plasmas measurable by microwaves, 19: 45429
MATALIN, L. A., Multidimensional analyzer with a preliminary treatment of data and combined-type memory, 19: 44524
MATANO, T., Possible evidence for nuclear interaction of μ above 3×10^{14} ev, 19: 45368
MATEICIUC, V., Neutron transmission of Pd in energy range 1.2 to 100 ev, 19: 45233
MATEJKA, D. Q., Project SAND final program report. III., 19: 44142 (SC-RR-65-286)
MATHERNE, J. L., Summary of the Kilorod Project, 19: 44638 (ORNL-3681)
MATHIESEN, J. M., Energy levels of ^{129}I, 19: 45324
MATHIS, A., Analysis of nonlinear control system for reactor RTM, 19: 45682 (RT/ING(64)-15)
MATSUDA, Kyoko, Flute instability of plasma confined in axi-symmetric wave form magneto-static field, 19: 45438
MATSUMOTO, Shinji, Photoreactions in ^{28}Si nucleus by monochromatic γ rays, 19: 45310
MATSUMURA, Seiji, Relation between radiation effects and dose rates of x and γ rays in cereals, 19: 43781
MATSUO, Takase, Protective effects of chemicals on radiation induced damages in seed-treated crop plants, 19: 43877
MATSUSHITA, Kozo, Environmental radiation and radioactivities about the site of JAERI, 1956–1963, 19: 44290 (JAERI-1079)
MATSUURA, Niro, Effect of γ irradiation on decomposition of S-S linkage in chymotrypsinogen, 19: 43841
MATSUURA, Niro, Radiation-induced oxidation of Sb(III) in aqueous solution. II., 19: 44085
MATTEI, Giulio, Symmetrical motions with respect to axis of incompressible viscous fluid in magnetofluiddynamics, 19: 44816
MATUYAMA, Eitaro, Ultrasonic grinding of natural graphite, 19: 44648
MATVEEV, O. A., Germanium gamma counter, 19: 44473 (ZFK-PHA-12, pp 64-5)
MATVEEV, O. A., Silicon spectrometric detectors with wide range of sensitivity, 19: 44472 (ZFK-PHA-12, pp 52-63)
MATVEEV, V., Current-generated algebras and form factors, 19: 45011 (JINR-E-2294)
MAUDERLI, Walter, Computer treatment planning in radiation therapy. I., 19: 43922
MAUGUEN, Pierre, Improvements in or relating to processes for applying alloys to metal surfaces, 19: 44658
MAUSHART, R., Detection and measurement of activity in wounds, 19: 44538
MAUSHART, Rupprecht, Neutron dosimeter for measurement of biological neutron dose effect, 19: 44543
MAXWELL, R. L., Experimental stress analysis of attachment region of hemispherical shells with radially attached nozzles, 19: 44144 (TID-22134)
MAY, R. M., Formation of excited hydrogen atoms by charge-exchange in lithium, 19: 44955
MAY, Victoria M., Neutron cross sections. Z = 88 to 98, 19: 45250 (BNL-325(2nd Ed.)(Suppl.2)(Vol.III))
MAYES, Mary G., Effects of ^{60}Co on desert root system (Tribulus terrestris), 19: 43855
MAYEUR, C., A determination of the Λ nuclear potential well depth, 19: 45361
MAYINGER, F., Prog. rpt. on critical heat flux (burnout) in boiling H_2O, 10–12/64, 19: 44184 (EURAEC-1281)
MAZANI, A., Neutrino luminosity of stars, 19: 44927
MAZZELLA, A. T., Shock front curvature at initial pressures up to 700 mm Hg, 19: 44853
MAZZONE, Anne, Effect of cortisone on gluconeogenesis in rats irradiated with x rays, 19: 43837
MC CALL, G. H., Effect of optical pump pulse shape on ruby inversion, 19: 45704 (LA-DC-6717)
MC CANCE, R. A., Metabolism of Ca, P, Mg and strontium, 19: 43701
MC CARTER, Anne, Retention of I-131 in blood plasma of molybdate-fed rabbits, 19: 43689
MC CARTHY, Walter C., Potential antiradiation compounds. II., 19: 43868
MC CAW, B. K., Comparative uv sensitivity of regeneration in the genus blepharisma, 19: 43813
MC CLAIN, W. C., Demonstration of disposal of high-level radioactive solids in salt, 19: 45689 (ORNL-P-1568)
MC CLUER, H., The application of nuclear reactors and radioisotopes to underwater-vehicle propulsion, 19: 45662
MC CLUNG, R. W., Nondestructive testing of small-diameter refractory-alloy tubing, 19: 44211 (ORNL-P-1543)
MC CONIGA, A. F., Fuel cycle analysis chained computer programs guide, 19: 45544 (HW-79951(Pt.1))
MC CONIGA, A. F., Minimized fuel cycle cost for simulated heavy water reactor. I., 19: 45563 (BNWL-106)
MC CONNELL, D. B., Angular distribution of γ rays from 62-ev neutron resonance in ^{124}Sn, 19: 45379
MC CORMACK, J. D., Fission-product simulation in containment systems experiment, 19: 44286 (BNWL-SA-30)
MC CORMACK, J. D., Natural removal of fission products released from UO_2 fuel in condensing steam environments, 19: 44285 (BNWL-SA-29)
MC CORMICK, B. H., Order code for the film scanners of Illiac III, 19: 44446 (COO-1018-1050)
MC CORMICK, Robert A., Air pollution in an urban environment, 19: 44785 (BNL-914, pp 113-14)
MC CORMICK, Robert A., U. S. Public Health Service meteorology program, 19: 44775 (BNL-914, pp 69-74)
MC CRACKEN, K. J., Partition of certain mineral nutrients in colostomized laying pullet, 19: 43693
MC CREA, J. M., Characteristics of ion-sensitive emulsions for mass spectrography. II., 19: 43979
MC CREARY, Joseph C., Development of realistic requirements for PM-type reactor instrumentation, 19: 45584 (NYO-3379-1)
MC DANIEL, R. H., The effects of reactor radiation on three high-temperature solid-film lubricants, 19: 44095
MC DOWELL, A. A., Discrimination learning of mirrored cues by rhesus monkeys, 19: 43805
MC DOWELL, A. A., Further evidence for excitatory properties of non-rewarded cues, 19: 43806
MC DOWELL, A. A., Radiation effects on food satiation in the rhesus monkey, 19: 43807
MC FARLAND, Robert H., Surface ionization of alkali metals by heated tungsten, 19: 44938 (UCRL-14117)
MC FARLANE, W. K., Hall effect stabilizer for experimental magnets, 19: 44173
MC FEE, Arthur S., Prevention of liver metastases by intravenous radioisotopes, 19: 43797
MC GILL, R. M., Separation of potassium isotopes by molecular distillation, 19: 43931 (K-1650)
MC GINNIS, G. A., Fresh approach to readout counting systems, 19: 44500
MC HARDY-YOUNG, S., Myxedema after x-ray therapy to the neck, 19: 43890
MC HENRY, H. T., 1400°F weldable sheet program, 19: 44699 (R63FPD33)
MC ILRAITH, James D., Radiation, genes and childhood, 19: 43893
MC ILWAIN, C. E., Survey of inner-zone protons, 19: 45189
MC INTYRE, Ruluff D., Tungsten–nickel–copper ternary alloys for high-temperature applications, 19: 44691 (NASA-TN-D-3015)
MC KAY, M. H., Resonance absorption in small homogeneous critical assemblies, 19: 45521 (AAEC/TM-118)
MC KELVIE, D. H., Clinical blood chemistry studies in beagles, 19: 43674 (UCD-472-112, pp 36-43)
MC KELVIE, D. H., Kennel report on beagle colony, 19: 43645 (UCD-472-112, pp 10-22)
MC KELVIE, D. H., Pathology report on beagles, 19: 43727 (UCD-472-112, pp 126-40)
MC KELVIE, D. H., Procedures for maintaining an outbred beagle colony, 19: 43646 (UCD-472-112, pp 23-35)
MC KENZIE, A. S. V., Schlieren photography of first half cycle of a theta pinch discharge, 19: 45421
MC KIM, F., Clinical blood chemistry studies in beagles, 19: 43674 (UCD-472-112, pp 36-43)
MC LAREN, K. G., The friction and deformation properties of irradiated polytetrafluoroethylene (PTFE), 19: 44092
MC LAUGHLIN, E. R., IBM 7090 bolted closure stress analysis program, 19: 44145 (TID-22138)
MC LAUGHLIN, J., Nuclear emulsion spectrometry at low and intermediate neutron energies, 19: 44448 (HASL-162)
MC LAUGHLIN, J. F., Fabrication of calorimeter elements, 19: 44344 (K-L-1944)
MC LENNAN, James A., Symmetry of the stress tensor, 19: 44807 (LA-DC-6556)
MC MILLAN, A. R., Hypervelocity impact damage characteristics in beryllium and graphite plates and tubes, 19: 44692 (NASA-TN-D-3018)
MC MURRAY, W. R., Energy levels of ^{30}S, ^{28}Si, and ^{8}B from (^{3}He,n) reactions, 19: 45355
MC NEILL, K. G., Angular distribution of γ rays from 62-ev neutron resonance in ^{124}Sn, 19: 45379
MC NELLY, M. J., Chemical engineering aspects of boiling water reactors, 19: 45624
MDZEWSKI, Bohdan, Changes in alkaline phosphatase in granulocytes of

chemical workers and radiologists, 19: 43829
MECHALI, D., Attempt to assess the dose received by bone marrow on exposure to neutron flux, 19: 43854
MEDANA, R., Adsorption and desorption of hydrogen on polycrystalline tungsten, 19: 44036
MEERS, J. T., Prog. rpt. on effects of neutron damage on mechanical properties of graphite, 10–12/64, 19: 44751 (TID-22110)
MEIER, E., Treatment of thyroid cancer with radioiodine, 19: 43918
MEILING, W., Suitability of sensitive time-pulse height convector for semiconductor detectors, 19: 44488 (ZFK-PHA-12, pp 215-18)
MEKHEDOV, V. N., Regularity in spontaneous nuclear fission, 19: 45271 (JINR-P-2265)
MELESE, Gilbert B., Prestressed concrete pressure vessels. I., 19: 45505
MENKER, Donald F., Evaluation of film badge dosimeters for occupational radiation exposure, 19: 44312
MENLOVE, H. O., Cross sections for $^{89}Y(n,\gamma)^{90m}Y$ and $^{89}Y(n,\gamma)^{90}Y$ between 0.145 and 1.225 Mev, 19: 45376
MERCENIER, P., Experimental basis of quantitative interpretation of the renogram, 19: 43667 (EUR-1890.f)
MERCULIEV, E., Autoradiography of the thyroid gland, 19: 43683
MERGEN, Francois, Prog. rpt. on effect of ionizing radiation on forest trees, 11/64–10/65, 19: 43722 (TID-22108)
MERKEL, George, Analysis of $^{56}Fe(^3He,p)$ and $^{63}Cu(^3He,p)$ energy and angular distributions-nuclear shell effects, 19: 45362
MERZ, C. A., Straddle bearing rotor dynamics tests with step bearing in water, 19: 44149 (TIM-921)
MERZAGORA, M., State of construction of the relativistic cyclotron for protons at 45 Mev, 19: 44886
MESHKOV, I. N., Intensive electron beam focusing in an accelerator tube, 19: 44870 (NP-15388)
MESHKOV, M. V., Multidimensional analyzer with a preliminary treatment of data and combined-type memory, 19: 44524
METCALFE, W. J., Water vapor corrosion of uranium and its prevention, 19: 44618 (AWRE-O-42/65)
METZ, C. F., Determination of trace amounts of oxygen added to metallic sodium, 19: 43932 (LA-3343)
MEYER, B., Uv absorption spectrum of trapped S_2, 19: 45480 (UCRL-10771)
MEYER, P. E., Prog. rpt. on two-phase flow and boiling heat transfer, 4–6/65, 19: 44192 (NYO-3114-9)
MEYERHOF, W. E., ^{90}O yield of gamma rays in T(p,γ)^{4}He reaction, 19: 45358
MICHAEL, B. D., Reactions of the hydroxyl radical. II., 19: 44090
MICHALSKI, T., Radiation-induced mutations in Digitalis Lanata EHRH, 19: 43746
MICHAUDON, Andre, Monte-Carlo method for studying slowing down of neutrons in thin plate of hydrogenated matter, 19: 45216 (CEA-R-2804)
MICHEL, Alfred, Method for generation and containment of a high-energy plasma, 19: 45455
MICHEL, F. C., Physical significance of inhomogeneities in polar cap absorption events, 19: 45172
MICHEL, F. Curtis, Gravitational effects of luminosity, 19: 44910
MIDDLEBROOK, G., Effect of near-ultraviolet light on staphlococci and mycobacteria in droplet nuclei, 19: 43736
MIDDLEBROOK, G., Effect of near-ultraviolet light on culture media, 19: 43737
MIDDLEMAS, H., S-wave π-σ final-state interactions in $\pi^- + p \rightarrow \pi^0 + n^0$, 19: 45089
MIDDLETON, R., New excited state of ^6Li, 19: 45348
MIKAILUS, F. F., Absolute measurements of 24-kev neutron absorption cross section, 19: 45230
MIKAMI, Hisashi, Separation of gaseous isotope mixture in a supersonic jet. I., 19: 44577
MIKEL'SON, Yu. Yu., Conducting slab in traveling magnetic field of double-side inductor, 19: 44841
MIKHAILOV, Yu. A., Heat exchange in transverse homogeneous magnetic field, 19: 44202
MILC, G., pH effect on γ sensitivity of Clostridium sporogenes, 19: 43865
MILLER, A. R., Energy storage capacitors for pulsed plasma thrustors, 19: 44224
MILLER, B., Ionizing shock studies in electromagnetically driven shock tube, 19: 44857
MILLER, C. A., Motion device for Moessbauer spectrometry, 19: 45316
MILLER, Carl F., Fallout models and radiological countermeasure evaluations, 19: 44243 (AD-619902)
MILLER, Christine, MEA effect on radiation dose-response characteristics of granulocyte and lymphocyte counts, 19: 43876
MILLER, D., Measurement of the K^0 mass and the K^0–K^- mass difference, 19: 44998 (CU-1932-247)
MILLER, D. B., Cyclotron resonance thrustor design and diagnostics techniques, 19: 44229
MILLER, David B., Prog. rpt. on cyclotron resonance propulsion system, 7/65, 19: 44223 (NP-15438)
MILLER, Geraldine, Simplified procedure for determining amounts of two mutually interfering radioisotopes in mixed samples, 19: 43962
MILLER, J. K., Effects of irradiation upon lactation, 19: 43800
MILLER, J. K., Lactation and radionuclide metabolism responses of dairy cattle to lethal doses of γ and neutron radiation, 19: 43801
MILLER, J. K., Simplified procedure for determining amounts of two mutually interfering radioisotopes in mixed samples, 19: 43962
MILLER, Maynard M., Tritium in Mt. Everest ice—annual glacier accumulation and climatology at great equatorial altitudes, 19: 44262
MILLER, Neil E., In-pile studies of experimental pyrolytic-carbon-coated UC_2 and UO_2 fuel particles, 19: 44740 (BMI-1737)
MILLER, O. A., Pyrolysis of the potential power reactor coolant, Santowax O-M, 19: 44044 (AECL-2218)
MILLER, Susan M., List of data files available in the UKAEA nuclear data library as of 15th April 1965, 19: 45249 (AWRE-O-55/65)
MILLER, W. S., Supercritical pressure liquid hydrogen heat transfer data compilation, 19: 44189 (NP-15332)
MILLERYAN, T. E., Optimum conditions of magnetogasdynamic channel flows accounting for Hall effect, 19: 44832
MINARIK, Augustin, Dismantling of Rn pumping stations, 19: 44317
MINARIK, Frantisek, Dismantling of Rn pumping stations, 19: 44317
MINGUZZI, A., Multiple poles and decay laws, 19: 45070
MINNAERT, Pierre, Unitarity and analyticity for sixth-order diagram, 19: 45111
MIRIC, I., Personnel dosimetry control at Boris Kidrich Institute, Vinca, 19: 44332
MIRIC, P., Personnel dosimetry control at Boris Kidrich Institute, Vinca, 19: 44332
MIRSHAK, S., Engineering aspects of the Savannah River high flux charge, 19: 45641 (DP-999, pp 43-64)
MISHKOV, S., Meson and baryon resonances in relativistic SU(6), 19: 45112
MITAULT, Gerard, Hydraulic transfer facility for irradiation containers, 19: 45686
MITCHELL, Ralph I., Prog. rpt. on tracer system for in-place filter evaluation, final, 10/62–6/65, 19: 44208 (BMI-X-346)
MITCHELL, Richard S., Virginia metamict minerals: comments on a uranium–niobium oxide from Powhatan County, 19: 44279
MITCHELL, Thomas G., Radiation, genes and childhood, 19: 43893
MITTA, Aldo E. A., Synthesis of DL glycine-1-C-14 and DL alanine-1-C-14, 19: 44047 (NP-15268)
MITTENBACHER, J., Application of semiconductor detectors in the associated particle method, 19: 44476 (ZFK-PHA-12, pp 123-5)
MIYAUCHI, T., Prog. rpt. on processing radioactive liquid wastes by evaporation, 1–6/64, 19: 45688 (NP-15367)
MIZGIREVA, E., Polarization during ion redox processes. Ions of Fe, Tl, Ce, and V, 19: 44002 (AEC-tr-6572)
MKRTCHYAN, A. R., System to control the exciting current of electromagnets of nuclear magnetic resonance spectrometers, 19: 44356
MOCHEL, J. M., Anomalous behavior of superconducting microgeometries in presence of high current densities, 19: 45207
MOCKEL, Andre, Reflection and transmission in slightly scattering plate, 19: 44848
MOEN, R. H., Prog. rpt. on radial vane steam separator, 4–6/65, 19: 45574 (GEAP-4914)
MOHINDRA, V. K., Canadian fallout data for June, 1965, 19: 44251 (NP-15519, pp 23-51)
MOHINDRA, V. K., Reactor environmental monitoring, 1964, 19: 44294 (NP-15519, pp 3-22)
MOHINDRA, V. K., Reactor environment monitoring for June, 1965, 19: 44295 (NP-15519, pp 52-60)
MOISAR, E., Fundamental aspects of growth and shape of photographic silver halide crystals, 19: 45474 (CERN-65-4(Vol.II), pp III21-30)
MOISAR, E., Investigations on the topography of the latent image, 19: 44387 (CERN-65-4(Vol.II), pp II1-10)
MOISEEV, S. S., Wave transformation in magnetohydrodynamics, 19: 45432
MOLINA-RAMOS, J., Concentration of cesium-137 in Australian milk during 1963, 19: 44309
MONARI, L., Proton polarization in $\pi^- + p$ elastic scattering at 8.5 Bev/c, 19: 45081
MONARO, S., Investigation of ^{96}Nb disintegration scheme, 19: 45341
MONLEON, J. L., Determination of ^{131}I by use of activated carbon, 19: 43958
MONNIN, Carl F., Stability of two-fluid wheel flows, 19: 45652 (NASA-TN-D-2696)
MONNOT, P., Prenatal and neonatal mortalities induced in mice by x irradiation of fetus alone or of mother alone, 19: 43760
MONSELISE, S. P., Effect of ^{60}Co gamma rays applied at low dose rates on some juice constituents and peel color of green and ripe citrus fruits,

19: 44554 (IA-1015)
MONTAGNINI, B., Method of numerical solution of the integral transport equation in the one-velocity and isotropic scattering approximation, 19: 45220 (EUR-2411.i)
MONTAGNINI, B., Numerical solution of integral transport equation in approximation to one-velocity and isotropic scattering in plane and cylindrical symmetry, 19: 45219 (EUR-2410.i)
MONTALDI, E., Green function for the iterated Klein-Gordon equation, 19: 45095
MONTALDI, E., Remarks on consistency problem in Heisenberg's nonlinear theory, 19: 45094
MONTEMAGNO, U., Intracellular enzyme variations from x rays. I., 19: 43739
MONTGOMERY, H., The application of nuclear reactors and radioisotopes to underwater-vehicle propulsion, 19: 45662
MONTH, M., Evidence for triangle singularities, 19: 45104
MOORE, C. R., Paste concept for fast reactor blanket applications, 19: 45561 (APDA-172)
MOORE, C. R., Paste concept for fast reactor blanket applications, 19: 45499 (APDA-174, pp 10-24)
MOORE, Jerry G., Radiation response as aid in treatment of cervical cancer, 19: 43910
MOORE, R. H., Proper use of transformations of log normal functions in small-particle statistics, 19: 44808 (LA-DC-6636)
MOORING, F. P., Radiative capture of neutrons, 19: 45246 (ANL-6877, pp 5-14)
MORALES VILLASEVIL, Angel, Relativistic local quantum field theory for m = 0 particles, 19: 45131 (JEN-154-DF/I-47)
MORENO Y MORENO, Augusto, Proportional counting technique for low-level ^{14}C activities, 19: 44526
MORGAN, J. G., Irradiation evaluation of fuel elements for PBRE and AVR reactors, 19: 44749 (ORNL-P-1507)
MORGAN, J. G., TRANS-FUGUE-I—digital code for transient two-phase flow and heat transfer, 19: 45494 (NAA-SR-11008)
MORGAN, T. A., Tensor Lagrangians and generalized conservation laws for free fields, 19: 45141
MORIGUCHI, Kinichi, Multigroup calculations of kinetics parameters in fast reactors (KPARAMCODE), 19: 45530 (JAERI-1082)
MORIOKA, Shigeki, Linearized non-equilibrium flow of a partially ionized gas with a radiative loss, 19: 45425
MORIUCHI, Shigeru, Environmental radiation and radioactivities about site of JAERI, 1956–1963, 19: 44290 (JAERI-1079)
MORIUCHI, Shigeru, Radiological monitoring point. Photographic dosimeter and gamma paper station, 19: 44291 (JAERI-1081)
MOROZ, V. I., Elastic scattering of Λ hyperons on protons, 19: 45016 (JINR-P-2257)
MOROZOV, A. M., Paramagnetic resonance of cerium in single-crystal $PbMoO_4$, 19: 44017
MORRIS, J. R., Uranium corrosion. I. Optical method for following oxide formation, 19: 44619 (AWRE-O-66/65)
MORRIS, Theodore, The radiolysis of aqueous methyl-ammonium ion, 19: 44080
MORRISON, R. C., Photodisintegration of ^4He, 19: 45353
MORRISON, R. C., Phototritons from ^6Li, 19: 45374
MORRISSEY, John E., Nuclear rockets based on graphite reactor technology. Their applications and development status, 19: 45658 (TID-22097)
MORROW, Lewis B., Active tuberculosis in malignant disease of reticuloendothelial origin, Hiroshima, 19: 43710 (ABCC-16-64)
MORTON, Daniel G., Radiation response as aid in treatment of cervical cancer, 19: 43910
MORY, J., Dosimetry of slow neutrons by recording the fission tracks in insulators, 19: 44385 (CERN-65-4(Vol.II), I12-19)
MOSELEY, J. D., Properties of plutonium dioxide, 19: 43995 (RFP-503)
MOSER, Carl, Electronic ground state and wave functions for scandium monoxide, 19: 44020
MOSER, H. C., Tritiated starch granules, 19: 44102
MOSES, Harry, Argonne meteorology program, 19: 44763 (BNL-914, pp 4-13)
MOSES, Vivian, Measurement of radioactivity on paper chromatograms, 19: 43984
MOSHINSKY, Marcos, Matrix-elements of generators of U_n, 19: 44585
MOSKALEV, V. I., Catalysis by μ^- of $d\mu + p \rightarrow {}^3He + \mu^-$ and $d\mu + d \rightarrow t + p + \mu^-$, 19: 45273 (JINR-P-2356)
MOTOC, Cornelia, Temperature dependence of Moessbauer effect in thin films, 19: 44847
MOUNSEY, J. A., Irradiated fuel element gamma scanning rig: Operation and instrumentation, 19: 44463 (TRG-Report-1005)
MOVSESIJAN, M., Vaccination against Dictyocaulus filaria with irradiated larvae, 19: 43750
MOZHIN, A. N., Results of adjustment of 1.5-m cyclotron, FEI, 19: 44887
MOZHIN, A. N., Vertical shift of a beam in a cyclotron with incongruent magnetic and electric planes, 19: 44889
MRAZ, F. R., Iodine-131 uptake in radiothyroidectomized chicks, 19: 43704
MUCKER, K. F., Crystal structure of solid deuterium from neutron-diffraction studies, 19: 45211
MUELLER, A. J., Modification of radiomimetic efficiency of nitrosoamides by metabolism inhibitors, 19: 43870
MUELLER, Alfred H., Exact bootstrap solutions to the Low equation, 19: 45106
MUELLER, J. J., Prog. rpt. on radiochemistry of nuclear fuels, 11/64–1/65, 19: 45542 (BAW-272)
MUELLER, R. E., Compilation of Fermi experience, 19: 45562 (APDA-174, pp 71-3)
MUELLER, V. F., Low angular momentum nucleon-nucleon scattering, 19: 45084
MUENCHOW, H. O., Small leak Na–H_2O reaction, 19: 44161 (APDA-174 pp 25-32)
MUGHABGHAB, Said F., Neutron cross sections. Z = 88 to 98, 19: 45250 (BNL-325(2nd Ed.)(Suppl.2)(Vol.III))
MULLER, F., Reaction $KN\pi\pi$ at 3 Bev/c and production mechanism of K*N*, 19: 45057
MULLER, H. J., Prog. rpt. on effect of radiation in altering incidence of mutations in Drosophila, 1963–64, 19: 43724 (TID-22160)
MULLER, Th., Measurements of muon depolarization in several materials, 19: 45080
MULLER, Th., New electron detector with high rejection power against pions, 19: 44522
MULLER, Th., Quenching of muon depolarization in several materials as function of externally applied magnetic fields, 19: 45079
MULLIGAN, M., Ferrous ammonium sulfate-cupric chloride solutions for dosimetry of a kilocurie ^{60}Co source, 19: 44372 (AFCRL-65-470)
MULLINS, L. J., Preparation of ultra-high purity plutonium, 19: 44600 (LA-3356)
MUNGER, Richard H., Low-temperature plasma column confinement by magnetic fields with shear, 19: 45415 (UCRL-14137)
MUNN, R. E., Diffusion studies in Canada, 19: 44790 (BNL-914, pp 149-50)
MUNSON, R. J., Take-over—an unusual selection process in steady-state cultures of E. coli, 19: 43804
MURAKAMI, Kazuaki, Transistorized airborne apparatus for detection of extensive air showers, 19: 44529
MURASAKI, Toshimitsu, Linearized non-equilibrium flow of a partially ionized gas with a radiative loss, 19: 45425
MURAV'EVA, L. I., Mutation variability of E. coli K-12 λ under influence of neutron irradiation, 19: 43751
MURFIN, W. B., Dynamic responses of cylindrical shells under lateral loads, 19: 45711 (SC-TM-65-81)
MURISOV, V. A., Measurement on the absolute value of the $K^0_1 - K^0_2$ mass difference, 19: 45099
MUROGOV, V. M., Possibility of using thorium in high-energy reactors, 19: 45605 (ORNL-tr-788)
MUROSHIMA, Kazuko, Effect of γ irradiation on decomposition of S-S in chymotrypsinogen, 19: 43841
MURPHY, J. W., Excited state of $_\Lambda Be^9$ and the Λ-N interaction, 19: 45367
MURPHY, R. D., Alpha radiation hygrometer. III., 19: 44338 (AD-608503)
MURTAS, G. P., Photofission of U and Th between 300 and 1000 Mev, 19: 45329
MURTAZA, G., Clebsch-Gordan coefficients for group SU_6, 19: 45061
MURTHY, V. Rama, Chromium isotopes in meteorites, 19: 44907
MUSHINSKAYA, L. G., Sterility of male plants due to penetrating radiation, 19: 43767
MUSTEL, E. R., Quasistationary corpuscular streams on descending branch of the 19th solar activity cycle, 19: 44921
MUTSCHKE, U., Strontium-90 contamination of tissue and a standard diet, 19: 44313
MUZIOL, G., Gamma spectrum of ^{160m}Ho isomer, 19: 45272 (JINR-P-2270)
MUZZALL, C. E., Compendium of gas autoclave engineering studies, 19: 44169 (Y-1478)
MYERSCOUGH, Valerie P., Non-iterative approach to the elastic scattering of electrons by complex atoms, 19: 44953

N

NADEZHIN, D. K., Propagation of shock waves in outer layers of a star, 19: 44924
NAGANO, M., Possible evidence for nuclear interaction of μ above 3×10^{14} ev, 19: 45368
NAGEL, John G., Matrix-elements of generators of U_n, 19: 44585
NAGY, E., Multiple scattering constant in emulsion at great cell lengths, 19: 44431 (CERN-65-4(Vol.II), pp IX32-40)
NAKAMURA, Jiro, Decomposition of tertiary butyl peroxides by γ irradiation, 19: 44089

NAKANISHI, Yuh H., Cytological studies on radiosensitivity of spermatogonia of the silkworm, 19: 43783
NAKANO, G. H., Emulsion experiments in oriented polar-orbiting satellites, 19: 44437 (CERN-65-4(Vol.II), pp X19-32)
NAKAO, Yoshio, Mutagenic and cell-killing effects induced by radiation and radiomimetic substances, 19: 43787
NAMORADO ROSA, Rui, Radiolysis of H_2O by 1- to 2-Mev protons. II., 19: 44058 (LFEN-23)
NAPOLOVA, G. A., Device for high-temperature testing of tungsten wires, 19: 44213
NASCUTIU, T., Paper chromatographic separation of tantalum, niobium, and hafnium, 19: 44124
NATION, R., Van Hove scattering function for water, 19: 45236
NEALY, C. L., Experimental evidence for competing spherical and deformed shapes in N = 89 nuclei, 19: 45359
NECHAJ, Joseph, Externally applied probe for scanning radioactivity in countercurrent distribution machines, 19: 43940
NEE, Cho-ming, Extraction of microgram amounts of zirconium with n-benzoyl-n-phenylhydroxylamine, 19: 43972
NEE, Cho-ming, Separation of Th, Sc, and Y earths, 19: 44125
NEFKENS, B. M. K., $K_1^0 \rightarrow \pi^+ + \pi^-$, strange decay of strange particle, 19: 45055
NELSON, E. C., Engineering aspects of the Savannah River high flux charge, 19: 45641 (DP-999, pp 43-64)
NELSON, Robert S., Detection of malignant neoplasia of the gastrointestinal tract by use of radioactive phosphorus and a miniature Geiger tube, 19: 43887
NEMETH, Stephen R., Metal fuel tube manufacture, 19: 45569 (DP-976)
NERHEIM, N. M., Electron density and temperature measurements in exhaust of a MPD source, 19: 45448
NESTERIKHIN, Yu. E., Parameters of plasma bunches of a coaxial injector, 19: 45431
NESTERIKHIN, Yu. E., Peculiarities of plasma heated by collisionless shock waves, 19: 45434
NESTERIKHIN, Yu. E., Temperature and density determination of non-stationary plasma, 19: 45433
NETTER, F., Study of interaction between resonance neutrons and nuclei in Saclay linear accelerator, 19: 45296
NETZBAND, D., Particle discrimination with semiconductor detectors, 19: 44475 (ZFK-PHA-12, pp 84-97)
NETZBAND, D., Reaction $^{10}B(d,p_0)^{11}B$, 19: 45336
NEUHAUS, H., Non-linear characteristics in high-frequency gas discharge, 19: 45420
NEUMANN, Manfred, Power supply plant for thermal test stands in nuclear research station at Juelich in North Rhine-Westphalia, 19: 44203
NEVZGODINA, L. V., Analysis of delayed effects of γ rays and 660-Mev protons on chromosomes, 19: 43770
NEWEY, D. A., Overhung rotor dynamics tests using hydrostatic water bearings, 19: 44146 (TIM-874)
NEWMAN, L. T., Isotopic contamination in electromagnetic separators, 19: 44573
NEWMARK, Joan F., Some aspects of the photochemistry and radiation chemistry of thymine, 19: 44060 (UCRL-16353)
NEWSOM, P. A., Tables for binary encoding of angles, 19: 44580 (AERE-R-4964)
NEWTON, C. E. Jr., Hanford criticality accident: dosimetry techniques, interpretations, and problems, 19: 44330
NEWTON, D., S-wave π-σ final-state interactions in $\pi^- + p \rightarrow \pi^0 + n^0$, 19: 45089
NEWTON, John F., Application of meteorology to the regulatory program of the AEC, 19: 44270 (BNL-914, pp. 178-9)
NEWTON, T. D., NUSTAT—program for fully mechanized shell model calculations, 19: 45254 (CRT-1213)
NEY, L. A., Axisymmetric thin shells of revolution, 19: 44219 (ACF-8)
NGUYEN, Quang Dong, Time evolution of discharges induced in gases by a laser, 19: 44821
NGUYEN VAN DONG, Determination of mean dimension of holes or faults in germanium irradiated by fast neutrons at 80°K, 19: 44754
NGUYEN VAN HIEU, Baryon annihilation in broken U(12) symmetry, 19: 45008 (JINR-E-2246)
NGUYEN VAN HIEU, Current-generated algebras and form factors, 19: 45011 (JINR-E-2294)
NGUYEN VAN HIEU, Electromagnetic decay and electroproduction of Y_1^* resonances, 19: 45007 (JINR-E-2228)
NGUYEN VAN HIEU, Unitarity of the S matrix in the broken symmetry SL(6), 19: 45009 (JINR-E-2247)
NGUYEN VAN HIEU, Broken symmetry U(12) and unitarity condition for the S matrix, 19: 45018 (JINR-P-2283)
NICHOLAS, R. C., Development of programs on radiation preservation of foods, 19: 44566
NICHOLS, Charles R., Prog. rpt. on effects of electrical fields on boiling heat transfer, 12/64, 19: 44190 (NYO-2404-67)
NICHOLS, Charles R., Prog. rpt. on effects of electrical fields on boiling heat transfer, 4–6/65, 19: 44191 (NYO-2404-73)
NICHOLS, J. P., Calculations of concrete shields for fission sources, 19: 45464 (QRNL-TM-1167)
NICHOLSON, J. O., SRE heat transfer system demolition, 19: 45579 (NAA-SR-11414)
NICKOLA, P. W., Field testing of a fluorescein–ZnS dual atmospheric tracer technique, 19: 44800 (BNWL-103)
NICOLAE, M., Autoradiography of the thyroid gland, 19: 43683
NICOLAE, M., Preparation and characteristics of a very concentrated nuclear emulsion, 19: 44396 (CERN-65-4(Vol.II), pp III1-4)
NICOLAE, M., Relative dispersion of the latent image, 19: 44388 (CERN-65-4(Vol.II), pp III1-16)
NICOLAE, M., Utilization of the electron microscope with the purpose of the observation of tracks in ionographic emulsions, 19: 44426 (CERN-65-4(Vol.II), pp VIII27-33)
NIEMIEC, J., Neutron diffraction study of uranium oxytelluride (UOTe), 19: 44009
NIETO, Michael M., General SU(3) crossing matrices and projection operators of 3 × 8, 19: 45113
NIGHAN, W. L., Prog. rpt. on collision probability of electrons and ions with alkali metal atoms, semiannual, 11/22/64–5/11/65, 19: 45399 (NASA-CR-54451)
NIKITIN, A. V., Elastic scattering of Λ hyperons on protons, 19: 45016 (JINR-P-2257)
NIKODEMOVA, Denise, Dismantling of Rn pumping stations, 19: 44317
NIKOLAEV, M. N., Study of inelastic scattering of slow neutrons in zirconium hydride, 19: 45240
NIKOL'SKII, B. A., Device for developing pulsed magnetic fields up to 150 kG, 19: 44888
NIKOL'SKII, G. M., Spectrum of spicules and fine structure of the solar chromosphere, 19: 44915
NIMS, Leslie F., Galvani, Volta and bioelectricity, 19: 43664 (BNL-9337)
NIMS, Leslie F., Material transfer, membranes and metabolism, 19: 43665 (BNL-9338)
NISHIDOI, Mutsumi, Ion exchange of radioactive ion with zeolitic tuff, 19: 44123
NISHIMURA, Hiroyuki, Loss mechanism of electrons from a magnetic bottle, 19: 44823
NISHIMURA, Kazuoki, Excitation cross sections of the $(n,n'\gamma)$ reactions on Fe, Co, Ni, Cu, Zn, Mo, Ag, Cd and Sn, 19: 45263 (JAERI-1078)
NIX, H., Quality control of ^{90}Sr-containing food, 19: 43675 (UCD-472-112, pp 73-9)
NODERER, L. C., Effect of a voided gap on reactivity coefficient for voiding core sodium in a fast reactor, for various geometries, 19: 45538
NOELL, G., Cavitation-sensitive coating evaluation, 19: 44212 (TIM-870)
NOFRE, Claude, Effect of γ rays on pyrimidine bases in aqueous solution. I., 19: 44064
NOGAMI, Yozo, Photoreactions in ^{28}Si nucleus by monochromatic γ rays, 19: 45310
NOHADANI, H., Crystal effects in the scattering of neutrons with energy from 30 to 1000 ev, 19: 45489
NOLAN, J. F., Measurement of Cs excitation cross section near threshold by swarm technique, 19: 44935 (NP-15168)
NOLAN, T. A., Fabrication of calorimeter elements, 19: 44344 (K-L-1944)
NORDIN, P., Tritiated starch granules, 19: 44102
NORMAN, K. J., The growth of an integrated fueling service for power reactors, 19: 45612
NORRESTAM, Rolf, Scandium manganese(III) oxide, a compound isotypic with $LaMnO_3$, 19: 44005
NOVGORODTSEVA, V. I., Threshold of symmetrical fission of ^{237}Np, 19: 45258 (IAE-833)
NOVIKOV, I. I., Self-excitation regimes in interaction between traveling waves magnetic field and ionized gas flow, 19: 44839
NOVIKOV, P. D., Radiation stability of ion exchange resins. II., 19: 44055 (IAE-788)
NOVIKOVA, N. R., Application of synthetic polymers in preparation of fine-grain nuclear emulsions. I. and II., 19: 44400 (CERN-65-4(Vol.II), pp III31-56)
NOVIKOVA, N. R., The properties of fine-grained nuclear emulsion type PR-2, 19: 44404 (CERN-65-4(Vol.II), pp IV23-31)
NOWOTNY, H., Crystal structures of β–$TaNi_3$, $Ta(Cu,Al)_2$, $Nb(Cu,Al)_2$, and $Ta_6(Cu,Al)_7$, 19: 44718
NOWOTNY, H., Crystal structure of $Zr(Sn,Sb)_2$, 19: 44720
NOWOTNY, H., Investigations in transition metal-boron–aluminum, 19: 44719
NOYES, H. Pierre, New nonsingular integral equation for two-particle scattering, 19: 45123
NOYES, R. C., TRANS-FUGUE-I—digital code for transient two-phase flow and heat transfer, 19: 45494 (NAA-SR-11008)

NOZAKI, Hiroshi, Radioactive contamination of milk in Japan (1961–1963), 19: 44268

NOZIK, V. A., Study of inelastic scattering of slow neutrons in zirconium hydride, 19: 45240

NOZU, K., Base composition of messenger RNA of Pseudomonas effusa irradiated with uv light, 19: 43744

NYBORG, Per, Phase space considerations for three-particle and four-particle final states, 19: 45006 (IS-1214)

O

OAKBERG, E. F., Effects of radiation on spermatogonial population of the mouse, 19: 43788

OAKES, L. C., Second generation of reactor control systems as applied to the HFIR, 19: 45645 (ORNL-TM-1259)

OBATUROV, G. M., Determination of total absorbed dose following accidental and chronic exposure, 19: 43853

OBAYASHI, Haruo, Loss mechanism of electrons from a magnetic bottle, 19: 44823

O'BRIEN, K., Nuclear emulsion spectrometry at low and intermediate neutron energies, 19: 44448 (HASL-162)

OBUKHOV, Yu. V., Intensity of nonradiative transitions in Ta and ^{239}Pu mesic atoms, 19: 44962

OCHSENFELD, Wilhelm, Method for separation of nuclear fuels, 19: 43982

ODA, M., Positions of three cosmic x-ray sources in Scorpio and Sagittarius, 19: 44968

OESTERREICHER, H., Crystal structures of β–$TaNi_3$, $Ta(Cu,Al)_2$, $Nb(Cu,Al)_2$, and $Ta_6(Cu,Al)_7$, 19: 44718

O'GALLAGHER, J. J., Search for trapped electrons and a magnetic moment at Mars by Mariner IV, 19: 44913

OGAWA, Eiichi, Elimination of radioactive strontium deposited in bone, 19: 43706

OGAWA, S. Y., Performance of fuel rods to investigate increased thermal output capabilities, 19: 45573 (GEAP-4902)

OGIEVETSKII, V. I., Photon and notoph, 19: 45020 (JINR-P-2330)

OGINO, Kouya, Quasi-free α-α collisions in ^{9}Be and ^{12}C at 28 Mev, 19: 45308

OGNEV, A. A., Results of adjustment of 1.5-m cyclotron, FEI, 19: 44887

OGNEV, A. A., Vertical shift of a beam in a cyclotron with incongruent magnetic and electric planes, 19: 44889

OGRZEWALSKI, Z., Use of the chopper for pulse neutron measurements, 19: 45222 (INR-624/IX-A/R)

OHNUKI, Y., Normalization of Bethe-Salpeter amplitude, 19: 45078

OKADA, Hiroko, Analysis and separation of rare earth elements. I., 19: 43956

OKADA, Hiroko, Analysis and separation of rare earth elements. II., 19: 43957

OKANO, Kotoyuki, Excitation cross sections of the (n,n′γ) reactions on Fe, Co, Ni, Cu, Zn, Mo, Ag, Cd and Sn, 19: 45263 (JAERI-1078)

OKHREMENKO, M. M., Spatial distribution of magnetic fields and electromagnetic phenomena in induction pumps, 19: 44833

O'KONSKI, C. T., Nuclear quadrupole resonance and bonding in crystalline ammonia, 19: 45483

OKUN, L. B., A scheme of multiplication of SU_3-representations, 19: 45030 (NP-15390)

OLANESCU, Gheorghe, Complications in the urinary organs resulting from uterine carcinoma and its treatment, 19: 43921

OLDANO, C., Self-absorption and self-scattering effects in the β particle sources, 19: 44881

OLDFIELD, D. G., Chemical protection against 440-Mev protons in mice pretreated with MEA or PAPP, 19: 43873

OLDFIELD, D. G., Chemical protection against absorber-moderated protons, 19: 43874

OLESEN, M. C., Coulomb excitation of vibrational states in deformed even nuclei, 19: 45321

OLESEN, P., N/P method and the diffraction picture, 19: 45088

OLESON, Norman L., Investigation of plasma from an occluded gas, cold plasma source, 19: 45411 (UCRL-7935)

OLIVARI, Americo, Possibilities of using ^{99m}Tc tracer instead of radioiodine in thyroid function investigations, 19: 43881 (NP-15271)

OLJHOEK, J. F., Dissipative normal fluid production by gravitational superfluid flow, 19: 45201

OLSEN, A. R., Thorium–uranium recycle facility, 19: 44167 (ORNL-P-1521)

OLSEN, W. C., Levels in ^{21}Ne using $^{18}O(\alpha,n\gamma)^{21}Ne$ reaction, 19: 45277 (NP-15363)

OLSON, N. Thomas, Measurement of Cs-sputtered Cu yield and angular distribution by a radioactive tracer technique, 19: 44964

OLSON, Robert E., Apparatus for measuring activity levels of radioactive samples, 19: 44547

O'MEARA, J. E., Design of proton linear accelerators for energies up to 200 Mev, 19: 44867 (MURA-713)

O'NEILL, G. F., Physics design of the Savannah River high flux charge, 19: 45640 (DP-999, pp 29-42)

ONISHCHUK, V. A., Some interference phenomena arising by mixing quantum levels in external fields, 19: 45270 (JINR-P-2248)

ONIYAMA, Fusuyo, Decomposition of tertiary butyl peroxides by γ irradiation, 19: 44089

ONOZAWA, Yoshiro, Protective effects of chemicals on radiation induced damages in seed-treated crop plants, 19: 43877

OPOWER, H., Measurement of the β-particle distribution of mass selected fission fragments with nuclear emulsions, 19: 44441 (CERN-65-4(Vol.II), pp X47-53)

OPPLIGER, L. D., Moessbauer resonance of ^{127}I in ferromagnetic CrI_3, 19: 45491

ORCUTT, F. K., Prog. rpt. on film rupture in journal bearings, 5/64–2/65, 19: 44138 (NYO-3363-4)

ORESHKINA, A. A., Recrystallization of Mg–Ce alloys, 19: 44710 (JPRS-24761, pp 29-40)

ORMAN, S., Corrosion of uranium and its prevention by organic coatings, 19: 44630

ORME, J. T., Plutonium sheet fabrication, 19: 44654

ORR, P. B., Ion exchange purification of fission-produced Sm, 19: 44116 (ORNL-TM-1062)

OSBORNE, J. W., Immunizing effect of x-irradiated cercariae of Schistosoma japonicum in albino mice, 19: 43848

OSBORNE, L. S., Photoproduction of mesons in the Bev range, 19: 45024 (MIT-2098-163)

OSETINSKII, G. M., Use of silicon surface-barrier detectors compensated by lithium for measurements of energies of protons and deuterons up to energies of 13 Mev, 19: 44471 (ZFK-PHA-12, pp 30-2)

OSTER, I. I., Mutagenic effects of chronically and intensely delivered radiation in Drosophila, 19: 43785

OTERO, J. L., Studies on production of heavy water. II., 19: 44576

OTH, D., Permanent and transmissible modification of virulence of solid isologous tumor after x irradiation, 19: 43762

OTT, Joachim, On radiogold hypophysectomy in metastasizing mammary carcinoma, 19: 43920

OTTO, Andreas, Plasma oscillations of bound electrons: characteristic energy loss of 3.6 ev in thin silver foils, 19: 44961

OTTO, P. Ph. H. L., Synthesis of labeled organic compounds, 19: 44103

OWEN, C. V., Extrusion of clad and unclad yttrium for rod and tubing, 19: 44636 (IS-1031)

OWENS, R. O., Phototritons from ^{6}Li, 19: 45374

OZOLS, R. Yu., Heat exchange in transverse homogeneous magnetic field, 19: 44202

P

PACK, Donald H., U. S. Weather Bureau meteorology program, 19: 44770 (BNL-914, pp 33-43)

PADGETT, Dana W., Exchange magnetic moment in three-body nuclei. I., 19: 45332

PADGETT, Dana W., Exchange magnetic moment in three-body nuclei. II., 19: 45333

PAGANONI, L., Remarks on consistency problem in Heisenberg's nonlinear theory, 19: 45094

PAGE, Lorne A., Particle physics and nuclear decay. Cancellation of photomultiplier gain drift following source intensity change, 19: 44374 (AROD-3347:6)

PAGELS, H. R., Anomalous magnetic moment of the electron, muon, and nucleon, 19: 45108

PALAIC, Dj., Metabolism of 5-hydroxytryptamine in brain of x-ray-tested rats, 19: 43810

PALAMARCHUK, Yu. D., Heterogeneous absorber efficiency in homogeneous uranium–water reactors, 19: 45536

PALMER, H. E., Measurements of radioactivity in Alaskan natives in 1964, 19: 44289 (HW-SA-3750)

PALMER, M. L., Design of proton linear accelerators for energies up to 200 Mev, 19: 44867 (MURA-713)

PAN, C. H. T., Prog. rpt. on film rupture in journal bearings, 5/64–2/65, 19: 44138 (NYO-3363-4)

PANCHAPAKESAN, N., Λ–Λ potential strength from hypernuclei and unitary symmetry, 19: 45064

PANDOLFI, Maurizio, Binary installation for production of energy using thermionic convertors, 19: 44983

PANDYA, S. P., S-state interactions and nuclear coupling schemes, 19: 45247 (ANL-6877, pp 29-31)

PANOFSKY, H. A., Vertical structure of turbulence, 19: 44799 (BNL-8516)

PANOFSKY, Hans A., Structure of turbulence, 19: 44798 (BNL-914, pp 175-7)

PAPINI, G., Photon bound states and gravitons, 19: 45144

PAPOULAR, Renard, Time evolution of discharges induced in gases by a laser, 19: 44821

PARCHER, J. W., Kennel report on beagle colony, 19: 43645 (UCD-472-112, pp 10-22)

PARCHER, J. W., Roentgenographic survey of experimental beagles, 19: 43882 (UCD-472-122, pp 50-8)

PARDO, Mario Paulo, Orthorhombic sulfides, selenides, and tellurides L_9X_3 of the rare earths, yttrium, and scandium of the Sc_2S_3 type, 19: 44010

PARFENOV, V. A., Study of inelastic scattering of slow neutrons in zirconium hydride, 19: 45240

PARKER, B., Nursing in a radiotherapy unit, 19: 43908

PARKER, F. L., Demonstration of disposal of high-level radioactive solids in salt, 19: 45689 (ORNL-P-1568)

PARKER, H. M., Hanford criticality accident: dosimetry techniques, interpretations, and problems, 19: 44330

PARKER, J. W., Comparative uv sensitivity of regeneration in the genus blepharisma, 19: 43813

PARKER, K., List of data files available in the UKAEA nuclear data library as of 15th April 1965, 19: 45249 (AWRE-O-55/65)

PARKOMENKO, A., Harmful effects of polonium on workers, 19: 44304 (CEA-tr-R-1836)

PARKS, Charles E., Blowdown models applicable to the loss-of-fluid test facility (LOFT). Evaluation, 19: 45671 (BAW-1195-4)

PARKS, F. B., Prog. rpt. on radiation-resistant electron tubes, 5/21–8/31/63, 19: 44337 (AD-425708)

PARKS, R. D., Anomalous behavior of superconducting microgeometries in presence of high current densities, 19: 45207

PARO, J. N., Bibliography on nuclear ship propulsion, 19: 45647 (AED-C-22-04)

PARR, Robert M., Measuring radioisotopes in biomedical samples, 19: 43659

PARZEN, G., High magnetic field limit in synchrotrons, 19: 44858 (BNL-9480)

PASHEK, G. M., Application of liquid scintillators for investigation of mechanism of radiation protection, 19: 43878

PASQUARELLI, A., Self-absorption and self-scattering effects in the β particle sources, 19: 44881

PASSE, Jean, Improvements in or relating to methods of and apparatus for measuring the period of a nuclear reactor, 19: 45508

PATEK, P., Activation analytical investigations of polyethylenes, 19: 43975

PATEK, Paul R., Response of liver to target irradiation, 19: 43735

PATEL, G. M., Behavior of lipase activity of γ-irradiated groundnut during germination, 19: 43798

PATEL, K. C., Behavior of lipase activity of γ-irradiated groundnut during germination, 19: 43798

PATTERSON, F. H., Thermochemical deposition of refractory metals, alloys, and compounds for application in thermionic devices, 19: 44640 (ORNL-P-1446-1)

PATTERSON, R. L. Jr., Filter pack technique for classifying radioactive aerosols by particle size. III., 19: 44252 (NRL-6305)

PATZELT, Paul, Indirect determination of half life of short-lived fission rare gases, 19: 45276 (NP-15304)

PAULING, Linus, Structural significance of the principal quantum number of nucleonic orbital wave functions, 19: 45365

PAULY, J., Determination of O in organic compounds and metals by activation with neutrons, 19: 43928 (EUR-2290.f)

PAWELSKI, Slawomir, Changes in alkaline phosphatase in granulocytes of chemical workers and radiologists, 19: 43829

PCHELIN, V. A., Threshold of symmetrical fission of ^{237}Np, 19: 45258 (IAE-833)

PEACOCK, N. J., Theta-pinch sources of vacuum uv radiation, 19: 45396 (LA-DC-7120)

PEAK, J. C., Precritical calculations for the 2.9-in. pitch, TWNR critical assembly, 19: 45526 (GA-6633)

PEARCE, R. J., Oxidation of the U–Cu intermetallic compounds UCu_5 in CO_2 between 350 and 850°C, 19: 44631

PEARL, W. L., Corrosion of carbon steel in simulated boiling water and superheat reactor environments, 19: 44627

PEARSON, Howard A., Radiation, genes and childhood, 19: 43893

PEASLEE, D. C., Parity for very weak interactions, 19: 45115

PECHAR, F. C., Neon-hydrogen bubble chambers, 19: 44375 (BNL-9425)

PECINA, R. J., Fresh approach to readout counting systems, 19: 44500

PECORINI, Victorio, Possibilities of using ^{99m}Tc tracer instead of radioiodine in thyroid function investigations, 19: 43881 (NP-15271)

PEHLKE, R. D., Activity of uranium in dilute solution in liquid bismuth, 19: 44733

PEKAS, J. C., A selected list of references (1960–May 1965) on swine in biomedical research, 19: 43713 (BNWL-115)

PELAH, I., Inelastic neutron spectra and vibrational modes of the hydrogen layer in alkali and alkaline-earth hydroxides, 19: 45482

PELLERIN, P., Biological dosimetry after exposure to a high flux of thermal and fast neutrons, 19: 44322

PELLICCIONI, M., Dose absorption by tissue on accidental exposure to very high-energy γ radiation, 19: 44329

PELLICCIONI, M., Production and discharge of toxic and radioactive gas in tunnel of Frascati linac, 19: 44866 (LNF-65/21)

PENKUHN, H., Numerical solution of the γ transport equation applied to concrete slabs, 19: 45459 (EUR-2488.e)

PENNER, S., Polarization of recoil protons in e-p elastic scattering at 20 Fermi^{-2}, 19: 45058

PENNINGTON, Edwin M., Tables of resonance integral functions, $L'(Z', \delta)$, 19: 45214 (ANL-7024)

PEREGOOD, B. P., Magnetohydrodynamic instabilities in electrical explosion, 19: 44845

PEREL, V. I., Optical orientation of atoms in a magnetic field perpendicular to the beam, 19: 44963

PERELOMOV, A. M., Casimir operators for an orthogonal and symplectic group, 19: 45031 (NP-15391)

PEREPELKIN, V. V., International comparisons of the specific activity of ^{32}P, ^{60}Co, and ^{204}Tl solutions and the activity of ^{60}Co solid sources, 19: 44101

PEREY, F. G., Elastic scattering of 12.0- and 14.0-Mev deuterons from ^{90}Zr and the reaction $^{90}Zr(d,p)^{91}Zr$, 19: 45281 (ORNL-3850)

PEREZ, Baldomero Lopez, Strontium-90, subproduct of treatment of irradiated fuel, 19: 44121

PEREZ-BUSTAMANATE, J. A., Water treatment process in JEN-1 research reactor, 19: 45678 (JEN-149-DQ/I-50)

PERFILOV, N. A., The properties of fine-grained nuclear emulsion type PR-2, 19: 44404 (CERN-65-4(Vol.II), pp IV23-31)

PERKINS, William C., Recovery of actinides produced by a nuclear detonation in salt formations, 19: 44156 (DP-956)

PERLMUTTER, I., Conference on refractory metals and alloys, Chicago, 4/62. II., 19: 44735

PERREAU, J.-M., Reaction $KN_{\pi\pi}$ at 3 Bev/c and production mechanism of K^*N^*, 19: 45057

PERRIGO, Lyle D., Transport and buildup of radioactive materials in reactor systems as determined by shutdown radiation measurements, 19: 45564 (BNWL-SA-85)

PERRON, Jean-Claude, Thermoelectric capacities of Se–Te liquid alloys, 19: 44712

PERRY, L. W., Synthesis of thermionic power conversion to nuclear reactors for space power applications, 19: 45648 (GA-6478)

PERSHAGEN, B., Physics aspects of pressure tube and pressure vessel type heavy water reactors, 19: 45626

PERSSON, Torsten, Thermodynamic properties of heavy water, 19: 44008

PERTSEVA, A. P., Use of ^{15}N as internal standard for determining quantities of radiogenic argon, 19: 43960

PERVUNINA, R. I., Radioactive fallout over the USSR area in 1963, 19: 44259

PESENTI, Pierre, Head for remote manipulators, 19: 44175

PETERKOP, R. K., Role of exchange in electron scattering by hellium atoms, 19: 44949

PETERS, A. H., Engineering aspects of the Savannah River high flux charge, 19: 45641 (DP-999, pp 43-64)

PETERS, N. T., Compilation of Fermi experience, 19: 45562 (APDA-174, pp 71-3)

PETRECZEK, K., Express method for electronic pulse counters, 19: 44351 (SGAE-E-4/1965)

PETRIE, L. E., Influence of focusing on the apparent reflection coefficient of the F region, 19: 45175

PETROV, E. E., Penetration of γ quanta through shielding barrier, 19: 45466

PETSCHEK, H. E., Limit on stably trapped particle fluxes, 19: 45157 (NP-15386)

PETTERSSON, H., Decay of ^{56}Co, 19: 45295

PFLEIDERER, G., Synthesis and properties of nicotinamide-adenine-N^1-oxide-dinucleotide, 19: 44062

PFLUEGER, Margaret L., Index to conferences relating to nuclear science, 19: 45716 (TID-4043(Rev.2))

PHELAN, R. M., Five-million pound shock testing facility, 19: 45720 (UCRL-12055-T)

PHELPS, A. V., Measurement of Cs excitation cross section near threshold by swarm technique, 19: 44935 (NP-15168)

PHELPS, A. V., Prog. rpt. on plasmas by laser heating, 4/6–7/5/65, 19: 45409 (TID-22132)

PHILLIPP, K., Long-range α-particles of radium C, 19: 45293 (ORNL-tr-696)

PHILLIPS, A. J., Mortality study of primary tumors of bone in Canada, 19: 43655

PHILLIPS, L. R., Preparing and sintering tungsten powder, 19: 44613 (Y-

1476)
PHILLIPS, R., Electron-beam treatment planning in inhomogeneous tissue, 19: 43916
PHILLIPS, Roger J. N., High-energy polarization experiments and Regge poles, 19: 45044 (UCRL-16185)
PICHAKHCHI, L. D., Self-excitation regimes in interaction between traveling waves magnetic field and ionized gas flow, 19: 44839
PICKETT, A. G., Prog. rpt. on fatigue strength of pressure vessels, 7/15/65, 19: 45503 (SWRI-1228-69)
PICKLESIMER, M. L., Precipitation of hydrides in Zircaloy-2 as affected by preferred orientation, elastic stress, and hydrogen content, 19: 44697 (ORNL-TM-1239)
PICKMAN, David Openshaw, Improvements in or relating to fuel elements, 19: 45551
PIEKARZ, H., Target preparation by electro-spraying directly on semiconductor detectors, 19: 44635 (INR-595/IA/PL)
PIERAZZI, L., Outlook for use of nuclear energy for production of heat at low temperature, 19: 45618
PIERAZZI, L., Some alternates for the utilization of organic liquid reactors for desalination of salt water, 19: 45620
PIERINI, G., Volatility processes for reactor fuel elements containing carbon, 19: 44109 (BLG-331)
PILKUHN, H., K-matrix model of peripheral interactions. II., 19: 45086
PINSLEY, Edward A., Preliminary design considerations of high-performance Hall current accelerator, 19: 45444
PIOTROWSKI, Feliks, Retention of P-32 in body of the human louse, 19: 43684
PIPER, C. F., Preparing and sintering tungsten powder, 19: 44613 (Y-1476)
PIRAGINO, G., Apparatus for study of energy spectra and polarization of photoneutrons, 19: 45303
PIRLOGEA, P., Three-axes spectrometer of Institute for Atomic Physics, Bucharest, 19: 44527
PISERCHIO, R. J., Loading of emulsions with diamonds and polystyrene for experiments with stopping K particles, 19: 44398 (CERN-65-4(Vol.II), pp III12-16)
PISERCHIO, R. J., Preparation of emulsion stacks for underground cosmic-ray experiments, 19: 44397 (CERN-65-4(Vol.II), pp III5-11)
PITTORI, S., Some alternates for the utilization of organic liquid reactors for desalination of salt water, 19: 45620
PIVATO, J., Coating UO_2 particles, 19: 44596 (EURAEC-1392)
PLANQUE, M., Detection of criticality accidents, CEA, France, 19: 44321
PLATZER, Roger, Apparatus for continuous electrolytic regeneration of ion exchange resins, 19: 44130
PLEBANSKI, Jerzy, Tensorial matrices, 19: 44584
PLONER, Lois, Plastic repair of radiogenic defects of the larynx and trachea, 19: 43897
PLONKA, Andrzej, Specific cation sequence in interfusion effects in membrane kinetics, 19: 44025
PLOSTINARU, Silvia, Some compounds of samarium, gadolinium, and erbium with various organic acids, 19: 44028
PLUNAR, Z., Orbital fractional parentage coefficients for two and three nucleons in the 2s-1d shell in SU(3) classification scheme, 19: 45266 (JINR-E-2285)
PLZAK, V., Chemical protection against 440-Mev protons in mice pre-treated with MEA or PAPP, 19: 43873
PLZAK, V., Chemical protection against absorber-moderated protons, 19: 43874
PLZAK, V., Radioprotective effects of DMSO in x-irradiated mice, 19: 43859 (NP-15310, pp 1-13)
PODGORETSKII, M. I., Passage of spin and spinless particles through matter, 19: 45013 (JINR-P-2230)
PODGORETSKII, M. I., Some interference phenomena arising by mixing quantum levels in external fields, 19: 45270 (JINR-P-2248)
PODOBNIK, B., The determination of cadmium in uranium compounds by atomic absorption spectrophotometry, 19: 43935 (NIJS-R-447)
POHLIT, Wolfgang, Mechanism of effect of energetic radiation, 19: 43899
POIANI, G., Experimental developments in study of polarization in nuclear reactions, 19: 45337
POIRIER, Jean-Paul, Electron microscope observation of single-crystal beryllium thin foils, 19: 44683 (CEA-R-2789)
POLOVIN, R. V., Chapman-Jouget theorem in magnetohydrodynamics, 19: 44837
POL'SKII, N. I., Optimum conditions of magnetogasdynamic channel flows accounting for Hall effect, 19: 44832
POLUBARINOV, I. V., Photon and notoph, 19: 45020 (JINR-P-2330)
POLVANI, C., Recent Presidential decree on safety and health protection against radiation, 19: 44318
POLYAKOVA, O. P., Isotopic composition of lead ore from different type deposits in Eastern Transbaikal, 19: 44277
POLYAKOVA, T. V., Radioactive fallout over the USSR area in 1963, 19: 44259
POMENTALE, T., Numerical solution of integral transport equation in approximation to one-velocity and isotropic scattering in plane and cylindrical symmetry, 19: 45219 (EUR-2410.i)
PONCELET, C. G., Effect of fuel burnup on moderator temperature coefficient in a PWR, 19: 45602 (WCAP-5493)
PONI, Margerete P., Complex salts with 5-nitrobarbituric acid. III., 19: 44027
PONOMARENKO, A. G., Peculiarities of plasma heated by collisionless shock waves, 19: 45434
PONOMAREV, A. A., Results of adjustment of 1.5-m cyclotron, FEI, 19: 44887
PONOMAREV, A. A., Vertical shift of a beam in a cyclotron with incongruent magnetic and electric planes, 19: 44889
POOLER, Francis, Air pollution program in Public Health Service, 19: 44788 (BNL-914, pp 123-4)
POPE, J. H., Long-period vlf emission pulsations, 19: 45171
POPE, J. H., Relation between auroral radio absorption and vlf emissions, 19: 45170
POPE, N. K., Van Hove scattering function for water, 19: 45236
POPOV, G. A., Heterogeneous absorber efficiency in homogeneous uranium–water reactors, 19: 45536
POPOV, V. S., Casimir operators for an orthogonal and symplectic group, 19: 45031 (NP-15391)
POPOVA, L., Ionization density in emulsions enriched with hydrogen, 19: 44435 (CERN-65-4(Vol.II), pp IX62-5)
POPOVYCH, O., Effects of steric hindrance and of bond type on electronic absorption spectra of certain 8-quinolinolates, 19: 43989 (MIT-905-20)
POPPE, C. H., Polarization of 39-Mev protons elastically scattered from ^{58}Ni and ^{60}Ni, 19: 45378
PORGES, K., Electron excitation of ZnS(Ag), 19: 44520
PORTAL, G., Multiple-purpose personal dosimeter, 19: 44536
PORTER, G., Observations on autoclaved, fumigated and irradiated diets for breeding mice, 19: 43654
PORTER, L. E., Polarization of protons from the D(d,p)T reaction, 19: 45253 (COO-7-0062)
PORTER, N. S., Instrument for automatic regulation of inhaled aerosols, 19: 43668 (HW-SA-3618)
POTTER, John, Distribution of momenta in the nucleus and the scattering of electrons, 19: 45279 (NP-15415)
POWELL, J. L., Low abundance of ^{87}Sr in Ontario carbonatites, 19: 44257
POWELL, R. E., Detector for neutral and charged particles, 19: 44499
POWELL, R. F., Lorentz number of plutonium metal, 19: 44721
POWELL, T. J., Skeletal dosimetry and exposure status of beagle colony, 19: 43726 (UCD-472-112, pp 120-5)
POWELL, T. J., Strontium-90 uptake and retention in labeled beagles, 19: 43679 (UCD-472-112, pp 109-19)
POWER, B. J., SPORT—system for processing reactor transient data, 19: 45527 (IDO-17078)
POWER, G., Some reducible magnetogasdynamic flows, 19: 44850
POWERS, R. J., Experimental observations of electric quadrupole effects in the muonic spectra of ^{235}U, ^{181}Ta, and ^{239}Pu, 19: 45326
POWERS, S., Clinical blood chemistry studies in beagles, 19: 43674 (UCD-472-112, pp 36-43)
PRADEL, J., Detection of criticality accidents, CEA, France, 19: 44321
PRADOS, J. W., Mathematical model for predicting coated-particle behavior, 19: 44748 (ORNL-P-1505)
PRAKASH, Y., Short-range hyperfragments produced by K^- captures in emulsions, 19: 45342
PRASK, H., Study of low-frequency molecular motions in polyethylene and the n-paraffins by slow neutron inelastic scattering, 19: 44050
PRAT, L., Dosimetry of high-energy protons by measurement of beryllium-7 formed in the tissues, 19: 44327
PRESKITT, C. A., MUFFLE—code for multilevel analysis of neutron cross sections, 19: 45282 (ORNL-TM-1180)
PRESKITT, C. A., Survey of Doppler coefficients for UO_2 fuel, 19: 45532 (ORNL-TM-1219)
PRESPERIN, V., Utilization of semiconductor detectors in polarization experiments, 19: 44477 (ZFK-PHA-12, pp 126-32)
PRESTON, C. C., Feasibility of using scintillating fibers for low-energy β counting, 19: 44451 (IITRI-578P26-8)
PRETZEL, F. E., Radiation damage to ionic crystals at low temperatures. I., 19: 44745 (LA-DC-6725)
PRIBILLA, O., Strontium-90 contamination of tissue and of standard diet, 19: 44313
PRICE, Michael Stuart Thomas, Process of forming carbon article from furfural alcohol and carbon particles, 19: 44671
PRINCE, B. E., Predicted and observed nuclear characteristics of the Molten Salt Reactor Experiment, 19: 45586 (ORNL-P-1503)
PRODELL, A. G., Neon-hydrogen bubble chambers, 19: 44375 (BNL-9425)
PRONKO, J. G., Levels in ^{21}Ne using ^{18}O(α,nγ)^{21}Ne reaction, 19: 45277 (NP-15363)

PROUT, Theddeus E., Immunologic studies of octapeptides. II., 19: 43658
PROUT, Theddeus E., Immunologic studies of octapeptides. I., 19: 44105
PROVOW, Douglas M., Resistance of Y metal to HF mixtures and high-temperature oxidation, 19: 44628
PRUCHA, L. L., Fresh approach to readout counting systems, 19: 44500
PRZYTYCKA, Rose, Aspects of three methods of radium determination, 19: 43967
PSHIBORSKI, V., Technology of manufacture of p-n junctions by means of diffusion of phosphorus in silicon, 19: 43999 (ZFK-PHA-12, pp 7-9)
PUCCIARELLI, L., Determination of concentration of radioactive cloud and contamination of soil by Pasquill-Gifford method, 19: 44255 (RT/PROT(65)-10)
PUCK, Theodore T., Studies of life cycle of mammalian cells, 19: 43758
PUGH, H. Ll. D., Hydrostatic extrusion of difficult metals, 19: 44651
PULHAM, R. J., Reactions of liquid sodium with transition-metal oxides. I., 19: 44021
PUPKE, H., Relation between column stratification and negative ion content in an impure Ar discharge, 19: 45423
PURUSHOTHAM, D., Studies on rare earth 1,3-diketonates, 19: 44006
PUSHKASH, L., Semiconductor detectors with uranium salts for absolute measurement of thermal neutron beams, 19: 44479 (ZFK-PHA-12, pp 140-3)
PUTNAM, Marie, A nonlinear least-square program for the determination of parameters of photopeaks by the use of a modified-Gaussian function, 19: 45261 (IDO-17016)
PUTTASWAMY, N. G., ^{6}O yield of gamma rays in $T(p,\gamma)^{4}He$ reaction, 19: 45358
PUYCHEVRIER, Jean, Hydraulic transfer facility for irradiation containers, 19: 45686
P'YANKOV, G. N., High-dose-rate isotope gamma irradiation unit UK-70000, 19: 44172
P'YANKOV, G. N., Isotope gamma irradiation unit UKP-30000, 19: 44171
PYCHLAU, H., Precision dosimeter according to Kuestner-Pychlau, 19: 44495
PYCHLAU, P., Precision dosimeter according to Kuestner-Pychlau, 19: 44495
PYLE, R., Prog. rpt. on flow and fracture studies of alloyed Be, 7/7–10/64, 19: 44693 (NP-15411)
PYLE, R., Prog. rpt. on flow and fracture studies of alloyed Be, final, 8/65, 19: 44694 (NP-15432)
PYRENEES, B., Automatic machine for milling fins on cylindrical parts, 19: 44655

Q

QUERCIA, I. F., Developments in the instrumentation for physics research, 19: 44357

R

RABILLOUD, Guy, Addition reactions initiated under radiation. II., 19: 44065
RABILLOUD, Guy, Addition reactions initiated under radiation. III., 19: 44066
RABOY, S., Experimental observations of electric quadrupole effects in the muonic spectra of ^{235}U, ^{181}Ta, and ^{239}Pu, 19: 45326
RADCLIFFE, Thomas J., Radioactive source holder, 19: 44179
RAETHER, H., Temperature dependence of characteristic energy losses in KBr, 19: 45490
RAGE, P., Individual alarm dosimeters for work in or entry into radiation fields, 19: 44532
RAGNI, G., Mutagenic response of human somatic cell lines, 19: 43844
RAINS, A. E., Experimental hydrostatic journal bearing, 19: 44141 (RFP-573)
RAJAGOPAL, V., Saxton chemical shim kinetic experiments, 19: 45598 (WCAP-3269-44)
RAJA RAO, M., Internal conversion coefficients employing internal-external-conversion technique using a scintillation spectrometer, 19: 44501
RALEIGH, Henry D., Nuclear energy for water desalting. A bibliography, 19: 45590 (TID-3584)
RAMASWAMY, M. K., Internal conversion coefficients of E2 transitions, 19: 45369
RAMOS, E., Radiostrontium and strontium fixation in bones and children's diets, 19: 44250 (NP-15269)
RANDALL, D., Forced convection boiling potassium heat transfer data, 19: 44195 (TID-21256)
RANDLE, T. C., Design of beam deflection system for the Harwell variable energy cyclotron, 19: 44868 (NIRL/R/86)
RAO, Bh. S. V. Raghava, Studies on rare earth 1,3-diketonates, 19: 44006
RAO, G. K., Results on spurious scattering in photographic emulsions, 19: 44415 (CERN-65-4(Vol.II), pp VI37-52)
RAO, V. Ramachandra, Studies on rare earth 1,3-diketonates, 19: 44006
RAO, Y. Venkateswar, Investigation into spurious scattering in photographic emulsions, 19: 44416 (CERN-65-4(Vol.II), pp VI53-62)
RAPAPORT, J., Angular distributions from shell-model forbidden (d,p) transitions to spin $^{5}/_{2}$ states in ^{43}Ca, ^{45}Ca, and ^{47}Ti, 19: 45323
RAPAPORT, J., Stripping analysis of the $^{138}Ba(d,p)^{139}Ba$ reactions, 19: 45347
RAPPAPORT, Irving, Some studies of infectious process with MS_2 bacteriophage, 19: 43742
RARITA, William, High-energy polarization experiments and Regge poles, 19: 45044 (UCRL-16185)
RAST, H. E., Energy levels of Pr^{3+} in LaF_3, 19: 45484
RATEAU, Arthur, Improvements in or relating to dissolution of uranium, 19: 44128
RAUBER, G., Permanent and transmissible modification of virulence of solid isologous tumor after x irradiation, 19: 43762
RAVA, Giovanni, Effect of cortisone on gluconeogenesis in rats irradiated with x rays, 19: 43837
RAY, S. N., Use of irradiated males for reduction of C. fatigans populations, 19: 43796
RAYNOR, Gilbert S., Current status of [fallout] deposition research, 19: 44246 (BNL-914, pp 133-8)
RAZ, B. James, Abstracts of computer codes. A compilation of computer codes useful in nuclear structure physics, 19: 45251 (BNL-9108)
RECHER, J. T., Comparative uv sensitivity of regeneration in the genus blepharisma, 19: 43813
REDER, Milton, Method for rapid recovery of heavy water and other products, 19: 44578
REED-HILL, R. E., Anelastic effects in Zr at room temperature resulting from prestrain at 77°K, 19: 44728
REED-HILL, R. E., Measurement of fraction of tensile strain due to twinning in polycrystalline Zr at 77°K, 19: 44725
REES, L. V. C., Neutron irradiation of Linde Molecular Sieve 13X, 19: 44091
REFAEY, K. M., Energy dependence of cross sections for collision-induced dissociation and endothermic ion-molecule reactions, 19: 44948
REGEL, K., Neutron spectroscopy with semiconductor detectors, 19: 44478 (ZFK-PHA-12, pp 133-9)
REGIRER, S. A., Laminar flow of conducting fluid in pipes and channels in presence of magnetic field, 19: 44824
REGNIER, Edward P., Radioisotope power-generating system for manned space laboratory, 19: 44571
REHAK, K., Ion-drift investigations of lithium in p-silicon, 19: 44001 (ZFK-PHA-12, pp 40-9)
REICKS, G. H., Compilation of Fermi experience, 19: 45562 (APDA-174, pp 71-3)
REIF, R., Reaction $^{10}B(d,p_0)^{11}B$, 19: 45336
REIMANN, G., Photoproduction of mesons in hydrogen bubble chamber at energies up to 5.5 Bev, 19: 44999 (DESY-65/5)
REIN, J. E., Prog. rpt. on burnup determination of nuclear fuels, 1–3/65, 19: 45260 (IDO-14660)
REINKE, C. F., Examination of irradiated Ag–In–Cd alloys, 19: 44736 (ANL-6883)
REMICK, Forrest J., Prog. rpt., annual, 7/64–5/65, 19: 45679 (NYO-1859-11)
RENARD, A., Restoration of complex γ spectra, 19: 45373
RERIKH, K. V., Broken symmetry U(12) and unitarity condition for the S matrix, 19: 45018 (JINR-P-2283)
RESHOTKO, Eli, Stability of two-fluid wheel flows, 19: 45652 (NASA-TN-D-2696)
RESMINI, F., State of construction of the relativistic cyclotron for protons at 45 Mev, 19: 44886
RESNICK, L., Kinematic contributions to form factors, 19: 45067
REYNEN, J., Study of circumferential and axial temperature perturbations in a cylindrical fuel element canning (mathematical and rheoanalogical methods, 19: 45543 (EUR-2480.f)
RIBON, Pierre, Monte-Carlo method for studying slowing down of neutrons in thin plate of hydrogenated matter, 19: 45216 (CEA-R-2804)
RICCA, F., Adsorption and desorption of hydrogen on polycrystalline tungsten, 19: 44036
RICHARDS, E. W. T., Preliminary classification in the plutonium I spectrum, 19: 44033
RICHARDS, P., Alpha-gamma facility for metallurgical examinations, 19: 44163 (BNL-9502)
RICHARDS, W. D., Ball bearing test in lithium, 19: 44150 (TIM-923)
RICHTER, Hans-Heinrich, On radiogold hypophysectomy in metastasizing mammary carcinoma, 19: 43920
RICHTER, W., Theoretical and experimental studies on frequency behavior and the noise of transistorized charged amplifiers, 19: 44487 (ZFK-PHA-12, pp 206-14)
RIDDELL, Patricia E., Retention of I-131 in blood plasma of molybdate-

fed rabbits, 19: 43689
RIDEOUT, S. P., Basic mechanisms of stress corrosion cracking of titanium, 19: 44621 (CONF-651006-1)
RIDGELEY, A., Preliminary classification in the plutonium I spectrum, 19: 44033
RIDLEY, R. G., Detector for neutral and charged particles, 19: 44499
RIEDEL, G., Electron microscopic differentiation of emulsions having different origins exposed to α or β irradiations, 19: 44389 (CERN-65-4(Vol.II) pp III7-18)
RIEDEL, G., Improvement of the resolution of radioactive markings by stereoscopic picture taking in electron microscopy, 19: 44423 (CERN-65-4(Vol.II), pp VIII8)
RIEDEL, J., Operating experience and improvements on the Princeton–Pennsylvania accelerator, 19: 44872 (PPAD-2137-565)
RIEGER, W., Investigations in transition metal–boron–aluminum, 19: 44719
RIEHS, Peter, Measurement of β spectrum ^{90}Y, 19: 45283 (SGAE-PH-23/1965)
RIESZ, Peter, The radiolysis of aqueous methyl-ammonium ion, 19: 44080
RIGNEY, D. V., The vapor pressure of lithium between 1307 and 1806°K, 19: 44703 (TIM-844)
RIGNEY, D. V., Viscosity of lithium, 19: 44704 (TIM-849)
RINONDI, C., Immunological aspects of experimental pulmonary sclerosis due to ionizing radiations, 19: 43817
RINALDI, Renaud, Radioprotective activity of nitrogenous heterocyclic compounds derived from imidazole and benzimidazole, 19: 43863
RINGO, G. R., Electron-neutron interaction from scattering of neutrons by noble gases, 19: 45098
RINZIVILLO, R., Photofission of U and Th between 300 and 1000 Mev, 19: 45329
RIPAMONTI, A., Radioiodine metabolism in patients affected by a simple sporadic goiter, 19: 43691
RIPAN, R., Variation of the index of refraction of aqueous solutions of $UO_2(NO_3)_2$, 19: 43969
RISTIC, M. M., Contribution to study of effect of TiO_2 additive on sintering of UO_2, 19: 44646
RITTENHOUSE, P. L., Precipitation of hydrides in Zircaloy-2 as affected by preferred orientation, elastic stress, and hydrogen content, 19: 44697 (ORNL-TM-1239)
RITZMAN, Robert L., In-pile studies of experimental pyrolytic-carbon-coated UC_2 and UO_2 fuel particles, 19: 44740 (BMI-1737)
ROBEL, Heinz, Model law for filtration and determination of the filtration rate on the basis of permeability tests, 19: 43923 (ORNL-tr-743)
ROBERSON, James A., Environmental influences on fatigue of Mo, 19: 44730
ROBERT, J., Permanent and transmissible modification of virulence of solid isologous tumor after x irradiation, 19: 43762
ROBERTSON, Baldwin, Equations of motion in nonequilibrium statistical mechanics, 19: 44856
ROBERTSON, L. P., Measurements of the A and R parameters in proton-proton scattering at 47.8 and 27.6 Mev, 19: 45319
ROBINSON, A. H., Prog. rpt. on transport equivalent diffusion theory, 4–6/65, 19: 45221 (GEAP-4913)
ROBINSON, E. M., Discrimination learning of mirrored cues by rhesus monkeys, 19: 43805
ROBINSON, G. A., Retention of I-131 in blood plasma of molybdate-fed rabbits, 19: 43689
ROCA ADELL, M., Direct-reading spectrochemical analysis of nuclear graphite, 19: 43930 (JEN-145-DQ/I-46)
ROCCELLA, M., Dose absorption by tissue on accidental exposure to very high-energy γ radiation, 19: 44329
ROCCELLA, M., Production and discharge of toxic and radioactive gas in tunnel of Frascati linac, 19: 44866 (LNF-65/21)
ROCCHESANI, J., Accidental exposure received from an electron linear accelerator, 19: 44331
ROCKMORE, R., Scattering of unstable particles by stable particles in strong interactions, 19: 45082
RODEAN, Howard C., Particle statistics of rubble produced by underground nuclear explosions, 19: 44159
RODEAN, Howard C., Some calculations for effecting oilfield stimulation by nuclear means, 19: 44158 (UCRL-14311)
RODIER, D., Crystallography of some transition metal molybdates, 19: 43991 (N64-26433)
RODIER, Jean, Radioprotection and decontamination operation on the central vibrating channels of the Reactor G 3, 19: 45565 (CEA-R-2781)
ROESSLE, E., A semiautomatic device for analyzing tracks in nuclear emulsions, 19: 44419 (CERN-65-4(Vol.II), pp VII20-7)
ROGERS, L. B., Effects of steric hindrance and of bond type on electronic absorption spectra of certain 8-quinolinolates, 19: 43989 (MIT-905-20)
ROJAS, J. L., Studies on production of heavy water. II., 19: 44576
ROKHLIN, L. L., Effect of additional alloying on properties of magnesium–neodymium alloys, 19: 44709 (JPRS-24761, pp 17-28)
ROLANDO, Piero, Systems between niobium oxides and oxides of nickel and cobalt, 19: 44711
ROLLIER, M. A., Efficient utilization of nuclear fuels, 19: 45621
ROMAN, P., Sharpening of O'Raiferartaigh's theorem, 19: 45096
ROMANOVSKAYA, C. M., Method for increasing the stability of sensitivity and latent image of nuclear emulsions, 19: 44390 (CERN-65-4(Vol.)), pp II19-28)
ROMANYUK, N. A., Changes in domain structure of Rochelle salt crystals exposed to x rays, 19: 44031
ROMERO, C., Contraction factor of Ilford G5 nuclear emulsions used in α spectrometry, 19: 44444 (CERN-65-4(Vol.II), pp 67-73)
RONDANELLI, E. G., Pseudo-amitoses provoked by x rays in erythropoietic cells in vitro, 19: 43826
RONDANELLI, G., Morphogenesis of binucleated erythropoietic cells by action of x rays, 19: 43730
RONSIN, G., K isomerism in ^{176}Yb, 19: 45357
ROONEY, D. M., Interfacial reaction between UO_2 and Zircaloy-2, 19: 44597 (GEAP-4679)
ROOSE, U. J., Reaction-free dynode gate for photomultipliers, 19: 44513
ROPERS, Jean, Guide tubes for nuclear reactors, 19: 45517
ROSATI, S., Reproduction of two-body scattering phase shifts by a phenomenological potential, 19: 45109
ROSCHIN, Yu. V., Optimum indices of radiometric concentration and conditions of expediency of its execution for a lognormal uranium-content distribution of volume elements of ore, 19: 44276
ROSE, P. H., Proposed methods for producing intense pulsed beams of monoenergetic neutrons, 19: 44882
ROSE, Walter, Moderator structures for nuclear reactors, 19: 45511
ROSEN, A., Effect of size on plastic properties of aluminum single crystals, 19: 44705 (UCRL-11653)
ROSEN, C.-G., Tritium labeling of cells in vitro, 19: 43651
ROSEN, S. P., Origins of the Lee triangle, 19: 45129
ROSHCHIN, Yu. V., Expediency of radiometric uranium ore dressing and the choice of the optimum level of separation during dressing, 19: 44275
ROSOFF, Betty, Metabolism of ^{46}Sc in man, 19: 43692
ROSOFF, Betty, Tissue distribution of ^{65}Zn in tumor tissue and normal tissue in man, 19: 43699
ROSS, Russell, Autoradiographic localization of lipid- and water-soluble compounds: a new approach, 19: 43696
ROSSETTI, C., Theory of corrections to unitary symmetry formulae, 19: 45003 (IC/65/60)
ROSSI, F., Prog. rpt. on influence of N in Fe and steel under fast neutron irradiation, 1–3/65, 19: 44741 (EURAEC-1383)
ROSSI, F., Prog. rpt. on influence of N in Fe and steel under fast neutron irradiation, 4–6/65, 19: 44742 (EURAEC-1430)
ROSSI, Jacky, Detection of tritium in CO_2 of G2/G3 reactors using gas chromatography, 19: 43926 (CEA-R-2800)
ROSSI, M. L., Theoretical aspects of neutron activation of structures, 19: 45461 (N64-25922)
ROSTOKER, G., Propagation of Pi 2 micropulsations through the ionosphere, 19: 45181
ROSZKOWSKI, Stanislaw, Changes in alkaline phosphatase in granulocytes of chemical workers and radiologists, 19: 43829
ROTBARD, G., K isomerism in ^{176}Yb, 19: 45357
ROTENBERG, A. D., Effect of filtration in diagnostic radiology, 19: 43901
ROTH, A., Sealing factors—their measurement and use in design of vacuum gasket seals, 19: 44135 (IA-1033)
ROTH, Edward S., Basic principles of functional gaging, 19: 45708 (SC-R-65-915)
ROTH, Jay S., Biochemical studies on irradiated protozoa. II., 19: 43812
ROTHENBERG, S., Nuclear emulsion spectrometry at low and intermediate neutron energies, 19: 44448 (HASL-162)
ROTTER, I., Lithium-induced reactions and the structure of light nuclei, 19: 45264 (JINR-E-2243)
ROTTER, I., On the observed isospin violation in the $^{10}B(^6Li,d)^{14}N$ reaction, 19: 45265 (JINR-E-2244)
ROTZSCH, Wolfgang, Use of isotopes in physiological chemistry, 19: 43707
ROUGE, Pierre, Handling apparatus for an installation for reloading a nuclear reactor with fuel elements, 19: 45513
ROUGE, Pierre, Nuclear reactor refueling facility, 19: 45514
ROUGE, Pierre, Refueling device for nuclear reactors, 19: 45512
ROUX, J. P., The electronuclear power plants in France, 19: 45614
ROWLANDS, J. L., Nineteen-group extension to the Yiftah, Okrent and Moldauer cross-section set, 19: 45244 (AEEW-M-472)
ROY, A. P., Study of elastic incoherent scattering by ammonium salts, 19: 45242
ROZSA, P., Spurious scattering in nuclear emulsions, 19: 44413 (CERN-65-4(Vol.II), pp VI23-30)
RUBIN, M. H., Technique for studying the physical scattering matrix,

19: 44995 (COO-30-97)
RUBINSTEIN, R., A threshold gas Cherenkov counter for use at the Brookhaven A.G.S., 19: 44376 (BNL-9466)
RUBY, S. L., Moessbauer resonance of ^{127}I in ferromagnetic CrI_3, 19: 45491
RUDAK, E. A., Spectrum of γ rays from $^{54}Fe(n,\gamma)^{55}Fe$ reaction, 19: 45322
RUDD, M. E., New autoionizing levels in helium, 19: 44959
RUDD, M. Eugene, Prog. rpt. on energy and angular distribution of electrons ejected from H and He by 100- to 300-kev protons, 4/63–7/65, 19: 44933 (COO-1277-12)
RUDD, M. Eugene, Prog. rpt. on autoionization of gases by ion impact, 3–8/65, 19: 44934 (COO-1277-13)
RUDD, R. A., On the use of vacuum uv absorption as a measure of temperature in rare gas plasmas, 19: 45382 (BRL-MR-1644)
RUDNICKI, Tadeusz, Retention of P-32 in body of the human louse, 19: 43684
RUDNICKI, Tadeusz, Total dose and some postirradiation reactions at cellular level, 19: 43733
RUFFINE, R. S., Cross-polarized electromagnetic backscatter from turbulent plasmas, 19: 45424
RUNGE, D. E., Prog. rpt. on two-phase flow and boiling heat transfer, 4–6/65, 19: 44192 (NYO-3114-9)
RUNNALLS, O. J. C., Transformations in UAl_4 and $PuAl_4$, 19: 44727
RUSH, J. J., Low-frequency motions in several ferroelectric salts, 19: 45241
RUSKIN, Dan, Methods for rapid recovery of heavy water and other products, 19: 44578
RUSKIN, Simon Lyon, Methods for rapid recovery of heavy water and other products, 19: 44578
RUSSELL, B., Effect of fast neutron damage on deformation of Cu–Sn alloys, 19: 44753
RUSSELL, J. L., Repetitively pulsed accelerator boosters, 19: 45674 (GA-6168)
RUSSELL, W. L., Nature of dose-rate effect of radiation on mutation in mice, 19: 43789
RUTHERGLEN, J. G., Behavior of a wide-gap spark chamber when two particle tracks are present, 19: 44518
RUTKOWSKI, W., Dispersion fuel elements for experimental and university reactors, 19: 45547 (INR-585/XIV/R)
RUZER, L. S., Alpha and β radiation method for determining concentrations of short-lived radon daughters in air, 19: 44258
RYABOV, V. D., Automation of the processes of isothermal development of nuclear emulsions, 19: 44409 (CERN-65-4(Vol.II), pp V17-21)
RYABOV, Yu. V., Neutron-^{235}U nuclear interaction in the 0.002 to 30 kev energy region, 19: 45292 (BNL-tr-16)
RYABOV, Yu. V., Uranium-235 fission cross section for resonance neutrons, 19: 45299
RYAN, C., Algebra of currents and getting SU(6) results from SU(4), 19: 45116
RYE, Berry J., Plasma heating at 500 megahertz, 19: 45398 (MATT-332)
RYE, R. J., Schlieren photography of first half cycle of a theta pinch discharge, 19: 45421
RYNDIN, R. M., Determination of parity in reactions induced by γ quanta, 19: 45010 (JINR-E-2259)
RYNDIN, R. M., Parity test for Ω^- using polarized hydrogen target, 19: 45101
RYVES, T. B., Fast neutron capture through charged particle reactions in water and in concentrated manganese sulfate solution from radioactive neutron sources, 19: 45232
RZESZOT, T., Use of the chopper for pulse neutron measurements, 19: 45222 (INR-624/IX-A/R)
RZHIGA, O. N., Measurement of Jupiter's intrinsic decimeter-wavelength radiation, 19: 44917

S

SABBIONI, E., Determination of O in organic compounds and metals by activation with neutrons, 19: 43928 (EUR-2290.f)
SACERDOTI, G., Persistent currents induced by circularly polarized waves in a superconducting ring, 19: 45191 (LNF-65/15)
SACTON, J., A determination of the Λ nuclear potential well depth, 19: 45361
SAFFORD, G. J., Studies of the solid and liquid phases of Hf, HCl, and HBr by slow neutron inelastic scattering, 19: 44038
SAHA, N. K., Gamma-gamma directional correlations in ^{126}I, 19: 45335
SAHAROV, V. K., Neutron distribution in straight cylindrical channel, 19: 45465
SAHAROV, V. M., Neutron distribution in straight cylindrical channel, 19: 45465
SAHINI, M., Multiple scattering in emulsion at great cell lengths, 19: 44431 (CERN-65-4(Vol.II), pp IX32-40)
SAIKI, Massamichi, Assay of strontium-90 in human bone in Japan, 1961–1963, 19: 44266
SAINI, G., Adsorption and desorption of hydrogen on polycrystalline tungsten, 19: 44036
ST. CHARALAMBUS, Acceleration method for detection of soft β particles, 19: 44512
SAKAE, Tokuo, Thermoelectron irradiation of polyethylene films, 19: 44069
SAKAI, M., Anisotropy of conversion electrons from (p,2n) and (α,4n) reactions, 19: 45352
SAKHAROV, A. D., Initial stage of an expanding universe and the appearance of a nonuniform distribution of matter, 19: 44929
SAKURAI, J. J., Trilinear couplings forbidden by nonet symmetry for vector mesons, 19: 45025 (N64-26265)
SALUTSKY, Murrell L., Radiochemistry of radium, 19: 44098 (NAS-NS-3057)
SALVADOR, Leonardo Ramos, Strontium-90 subproduct of treatment of irradiated fuel, 19: 44121
SALVETTI, C., Prospects and aspects of the development of nuclear energy in Italy, 19: 45622
SAMOILOV, L. N., Polarization in n-α scattering at E_n= 25, 28, and 34 Mev, 19: 45259 (IAE-834)
SAMOILOVICH, D. M., Centers of sensitivity and the centers of development of nonsensitized nuclear emulsions, 19: 44394 (CERN-65-4(Vol.II), pp II65-74)
SAMOILOVICH, D. M., Comparative hypersensitization with triethanolamine and with other alkaline sensitizers for nuclear emulsions, 19: 44406 (CERN-65-4(Vol.II), pp IV41-5)
SAMOILOVICH, D. M., Sensitivity centers of nuclear emulsions sensitized successfully with gold and triethanolamine, 19: 44395 (CERN-65-4 (Vol.II), pp II75-87)
SAMOILOVICH, D. M., Study of the factors affecting the quality of the development with the electrodialyser, 19: 44410 (CERN-65-4(Vol.II), pp V22-23)
SAMPLE, J. T., Levels in ^{21}Ne using $^{18}O(\alpha,n\gamma)^{21}Ne$ reaction, 19: 45277 (NP-15363)
SAMUELS, E. R., Canadian fallout data for June, 1965, 19: 44251 (NP-15519, pp 23-51)
SAMUELS, E. R., Reactor environmental monitoring, 1964, 19: 44294 (NP-15519, pp 3-22)
SAMUELS, E. R., Reactor environment monitoring for June, 1965, 19: 44295 (NP-15519, pp 52-60)
SANDERS, H., Design of fast-cycling liquid-H_2 bubble chamber, 19: 44459 (PPAD-2136-561)
SANDERS, Wm. Mort, Gamma scanning of LAMPRE spectrometer, 19: 44463 (LA-DC-7316)
SANDOVAL, P., Chromium isotopes in meteorites, 19: 44907
SANI, L., Experience in test and use of Italian nuclear power plants, 19: 45616
SANKARANARAYANAN, A., Position operators in relativistic single-particle theories, 19: 45118
SANNA, R., Nuclear emulsion spectrometry at low and intermediate neutron energies, 19: 44448 (HASL-162)
SANNER, Tore, Reduced pyridine coenzymes as hydrogen donors in repair of radiation damage, 19: 44081
SANTOS, A., Quality control of ^{90}Sr-containing food, 19: 43675 (UCD-472-112, pp 73-9)
SAPERSTEIN, A., Pion-pion scattering. III., 19: 45105
SARA, R. C., Hafnium–carbon system, 19: 44724
SARAEVA, V. V., The mechanism of radiation-induced oxidation of organic compounds by molecular oxygen, 19: 44075
SARI, C., Coating UO_2 particles, 19: 44596 (EURAEC-1392)
SARKISOV, E. S., Interatomic distances of lanthanides in metallic crystals, 19: 44713
SASAKI, Satoshi, Environmental radiation and radioactivities about site of JAERI, 1956–1963, 19: 44290 (JAERI-1079)
SASAKI, Satoshi, Radiological monitoring point. Photographic dosimeter and gammed paper station, 19: 44291 (JAERI-1081)
SASLAW, William C., Possible quantitative mechanism for carcinogenesis by uv radiation, 19: 43821
SASSI, E., Photofission of U and Th between 300 and 1000 Mev, 19: 45329
SATO, Kazuto, Histopathological studies on transplanted experimental osteogenic sarcoma, 19: 43772
SATO, Yoshimasa, Protective effects of chemicals on radiation induced damages in seed-treated crop plants, 19: 43877
SATTAR, A., Electron-beam treatment planning in inhomogeneous tissue, 19: 43916
SAUER, Myron C. Jr., Pulse radiolysis of gaseous argon–oxygen solutions. Rate constant for the ozone formation reaction, 19: 44071
SAUNDERS, A. W. Jr., Filter pack technique for classifying radioactive aerosols by particle size. III., 19: 44252 (NRL-6305)

SAUNDERS, Edward A., Calculation of proton-induced damage in germanium and silicon, 19: 44747 (NP-15463)
SAUTTER, Chester A., Prog. rpt. on autoionization of gases by ion impact, 3-8/65, 19: 44934 (COO-1277-13)
SAUTTER, Chester A., Prog. rpt. on energy and angular distribution of electrons ejected from H and He by 100- to 300-Kev protons, 4/63-7/65, 19: 44933 (COO-1277-12)
SAVAGE, Serena, CHRNOGRM—computer program for analysis of chronopotentiograms, 19: 45706 (ORNL-TM-1254)
SAVCHENKO, A. P., Sterility of male plants due to penetrating radiation, 19: 43767
SAVEL'EV, A. E., Analyses of prompt neutron spectra for ^{252}Cf spontaneous fission, 19: 45302
SAVITSKY, V. F., Rate of spontaneous and radiation-induced chromosome re-arrangements in medulla ossium of mice of different age, 19: 43729 (BNL-tr-12)
SAWYER, G. A., Theta-pinch sources of vacuum uv radiation, 19: 45396 (LA-DC-7120)
SCAFE, R., Determination of concentration of radioactive cloud and contamination of soil by Pasquill-Gifford method, 19: 44255 (RT/PROT(65)-10)
SCALAPINO, D. J., Metastable current-carrying states of weakly coupled superconductors, 19: 45206
SCANDELLARI, G., Analysis of nonlinear control system for reactor RTM, 19: 45682 (RT/ING(64)-15)
SCHAD, O., Prog. rpt. on critical heat flux (burnout) in boiling H_2O, 10-12/64, 19: 44184 (EURAEC-1281)
SCHAFFER, W. F. Jr., Demonstration of disposal of high-level radioactive solids in salt, 19: 45689 (ORNL-P-1568)
SCHAFFHAUSER, A. C., Low-temperature ductility and strength of vapor-deposited tungsten, 19: 44695 (ORNL-P-1506)
SCHAMBERGER, R., Military Compact Reactor small source experiments, 19: 45575 (GMAD-3078-28)
SCHEIBNER, M., Design of fast-cycling liquid-H_2 bubble chamber, 19: 44459 (PPAD-2137-561)
SCHELSKE, Claire L., Ecological implications of fallout radioactivity accumulated by molluscs, 19: 43663
SCHENCK, G. F., Application of internal friction methods to corrosion study in Nb alloys, 19: 44620 (CNLM-6344)
SCHENCK, G. F., Interactions in type 316 stainless steel-NaK-Nb-1 Zr alloy system, 19: 44626 (TIM-896)
SCHERER, Volker, Binary and ternary oxides of Pm, 19: 43992 (NP-15339)
SCHEUER, P. A. G., Sensitive test for presence of atomic hydrogen in intergalactic space, 19: 44908
SCHILLER, P., Nondestructive radiometric determination of bromine in several pharmaceutical preparations, 19: 43950
SCHINDEWOLF, U., Enrichment of deuterium by countercurrent isotope exchange between hydrogen and ammonia in a hot-and-cold plant, 19: 44574
SCHLOBOHM, J. C., Simultaneous vhf and uhf observations of the aurora at Fraserburgh, Scotland, 19: 45169
SCHLOTT, K., Particle discrimination with semiconductor detectors, 19: 44475 (ZFK-PHA-12, pp 84-97)
SCHLOTT, K., Reaction $^{10}B(d,p_0)^{11}B$, 19: 45336
SCHLUETER, A., Dynamics of a toroidal theta pinch, 19: 45395 (IPP-6/38)
SCHLUNGBAUM, W., Methods of irradiation with localized limited radiation effect, 19: 43900
SCHLUNGBAUM, W., Somatic irradiation injuries, 19: 43838
SCHMEIGERT, B. S., Development of programs on radiation preservation of foods, 19: 44566
SCHMELTEKOPF, A. L., Positive ion-neutral reactions in the ionosphere, 19: 45173
SCHMETS, J., Volatility processes for reactor fuel elements containing carbon, 19: 44109 (BLG-331)
SCHMID, R., Sulfide fluoride of the rare earths, 19: 44024
SCHMITT, C. R., Preparing and sintering tungsten powder, 19: 44613 (Y-1476)
SCHMITT, R., Decoration of tracks of charged particles in silver chloride monocrystals, 19: 44386 (CERN-65-4(Vol.II), pp I21-5)
SCHMITT, R., Latensification of the latent image in ionographic emulsions, 19: 44391 (CERN-65-4(Vol.II), pp II29-42)
SCHMITT, R., Utilization of the electron microscope with the purpose of the observation of tracks in ionographic emulsions, 19: 44426 (CERN-65-4 (Vol.II), pp VIII27-33)
SCHNEEGANS, M., Measurements of muon depolarization in several materials, 19: 45080
SCHNEEGANS, M., New electron detector with high rejection power against pions, 19: 44522
SCHNEEGANS, M., Quenching of muon depolarization in several materials as function of externally applied magnetic fields, 19: 45079
SCHNEIDER, F., High precision air core magnet, 19: 44165 (CERN-65-29)
SCHNEIDER, Guenther, Method for the production of Al-U alloys, 19: 44664
SCHNITZER, H. J., Charged scalar theory and broken charge symmetry, 19: 45072
SCHNURMACHER, G. L., Spark chamber using helium or hydrogen at high density, 19: 44502
SCHOENFELD, T., Prog. rpt. on deposition of inhaled fission products in lungs, final, 10/62-10/64, 19: 4492 (NP-15173)
SCHORMUELLER, J., Continuous measurement of ^{14}C-labeled amino acid mixtures with help of scintillator tube after separation on ion exchange columns, 19: 43976
SCHOTSMANS, L., Numerical evaluation of the uncertainty relation for angular variables, 19: 45145
SCHRACK, R., ^{6}O yield of gamma rays in $T(p,\gamma)^{4}He$ reaction, 19: 45358
SCHREIBER, P. W., Radiation from an a-c nitrogen arc, 19: 44804 (ARL-65-105)
SCHROEDER, W., Seasonal variation of aurora, 19: 45180
SCHULTE, R., Single π^0 production by 8-Bev/c positive pions, 19: 45103
SCHULTZ, Everett H. Jr., Genetic hazards of medical radiology, 19: 43914
SCHULTZ, H. L., Phototritons from ^{6}Li, 19: 45374
SCHULTZ, H. W., Irradiation-sterilized shelf-stable fish and seafood products, 19: 44556 (NP-15464)
SCHUMANN, Thomas G., Resonant state in the $\pi^+\pi^0$p system at 1.71 Bev, 19: 45121
SCHUPP, W., Flange connections featuring an insulating sealing element, 19: 44134 (EUR-2434.d)
SCHWARCZ, H. P., Oxygen isotopic studies of amphibolites, 19: 44238
SCHWARTZ, A. D., Effect of carburization on low strain rate behavior of type 304 stainless steel, 19: 44623 (NAA-SR-10487)
SCHWARTZ, Emanuel E., Sulfhydryl radiation protective agents, 19: 43867
SCHWICHTENBERG, A. H., Human stresses in space flight operations and methods of improving man's tolerance, 19: 43842
SCIUTO, F., Dragon reactor automatic control equipment, 19: 45570 (EUR-2422.i)
SCIUTO, F., Transfer functions analyzer for Dragon reactor, 19: 45571 (EUR-2431.f)
SCOTT, F. R., Flute characteristics of and microwave emission from a plasma in a mirror, 19: 45388 (GA-6432)
SCOTT, J. L., Irradiation evaluation of fuel elements for PBRE and AVR reactors, 19: 44749 (ORNL-P-1507)
SCOTT, J. L., Mathematical model for predicting coated-particle behavior, 19: 44748 (ORNL-P-1505)
SCOTT, K. T., Recording microbalance for remote thermogravimetric examination of irradiated materials, 19: 44341 (AERE-R-4962)
SCOTT, T. E., Extrusion of clad and unclad yttrium for rod and tubing, 19: 44636 (IS-1031)
SEABORN, G.B., Improved fast neutron monitor, 19: 44452 (K-1642)
SEADER, J. D., Supercritical pressure liquid hydrogen heat transfer data compilation, 19: 44189 (NP-15332)
SEDIKOV, I. P., Semiconductor detector for detection of thermal neutrons in conditions of intense pulsed γ radiation, 19: 44480 (ZFK-PHA-12, pp 144-6)
SEDLET, Jacob, Cross section of some reactions of ^{99}Tc with 14.1-Mev neutrons, 19: 45325
SEGEL, R. E., Radiative capture of neutrons, 19: 45246 (ANL-6877, pp 5-14)
SEGRE, G., Theory of corrections to unitary symmetry formulae, 19: 45003 (IC/65/60)
SEGUIN, Maurice, Sealed coupling for an electrical heating conductor with coaxial sheath, 19: 44164 (CEA-R-2755)
SEIDLITZ, L., Design of fast-cycling liquid-H_2 bubble chamber, 19: 44459 (PPAD-2137-561)
SEILER, H., Flotation and coordination chemistry. Method for enrichment of Ga^{3+}, 19: 43961
SEITZ, W., Effect of neutral plasma on ion trajectories, 19: 45451
SEKI, Jisuke, Analytical application of fluorine ion. I., 19: 43970
SELBY, C. L., Basic mechanisms of stress corrosion cracking of titanium, 19: 44621 (CONF-651006-1)
SELEZNEV, A. F., Application of liquid scintillators for investigation of mechanism of radiation protection, 19: 43878
SEMCHYSHEN, M., Conference on refractory metals and alloys, Chicago, 4/62. II., 19: 44735
SEMENOV, Yu. A., Measurement of the absolute value of the $K_1^0 \to K_1^+$ mass difference, 19: 45099
SENEOR, Roland, Unitarity and analyticity for sixth-order diagram, 19: 45111
SENG, R., Emulsion grain density in the extreme relativistic region, 19: 44428 (CERN-65-4(Vol.II), pp IX9-13)
SENGERS, J. V., Density expansion of viscosity of moderately dense gas, 19: 44846

SENNE, J. K., Tritiated starch granules, 19: 44102
SEPPALA, P. O., Treatment of hyperthyroidism with fixed initial dose of radioiodine, 19: 43895
SERBASSI, S., Polarization of recoil protons in e-p elastic scattering at 20 Fermi^{-2}, 19: 45058
SEREBRYAKOV, V. V., Dispersion theory of low-energy scattering, 19: 45051
SERMONS, G. Ye., Impulse method of measurements of flow rate of conducting fluid, 19: 44834
SERRA, P., Proton polarization in $\pi^- + p$ elastic scattering at 8.5 Bev/c, 19: 45081
SERRANO C., Mario, Reconnaissance for uranium in the Aisen Area, Aisen, Chile, 19: 44273 (RME-4557(Rev.))
SEVAST'YANOV, Yu. G., Production of ^{26}Al during irradiation of Mg with 20-Mev deuterons, 19: 44099
SEVAST'YANOV, Yu. G., Separation of ^{22}Na from magnesium target irradiated with deuterons, 19: 44100
SEVC, Josef, Simultaneous action of α radiation and SiO_2 in animal experiments. II., 19: 43831
SEVERIENS, J. C., Test of charge-conjugation invariance in $\bar{p}p$ annihilations at rest, 19: 45124
SEVERNII, A. B., Nature of solar magnetic fields (the fine structure of the field), 19: 44918
SHA, William T., Reactivity worth of rod cluster control elements and local water-hole power density peaking, 19: 45535 (WCAP-3269-47)
SHABALIN, E. P., Theory of weak interaction, 19: 45027 (NP-15199)
SHACKLETON, N. J., High-precision isotopic analysis of oxygen and carbon in carbon dioxide, 19: 43963
SHAHBAZIAN, B. A., Method of measurement and calculation of fast particle momenta in emulsions exposed in strong magnetic fields, 19: 44427 (CERN-65-4(Vol.II), pp VIII24-7)
SHAKHBAZYAN, B. A., Elastic scattering of Λ hyperons on protons, 19: 45016 (JINR-P-2257)
SHAKHOVA, K. I., Phase diagram of the $TiCr_2$–$ZrCr_2$ system, 19: 44714
SHAPAR, A. V., Fast neutron capture cross section for Re, 19: 45298
SHAPIRO, Bernard, Sulfhydryl radiation protective agents, 19: 43867
SHAPIRO, V. D., Non-linear stabilization of beam instabilities in plasma, 19: 45402 (NP-15200)
SHAPIRO, V. D., Quasilinear theory of weakly turbulent plasma with account of correlation of electric fields, 19: 45439
SHASHKOV, V. S., Chemical preparations for prevention of radiation injuries, 19: 43861 (JPRS-31349, pp 1-24)
SHAW, B. W., VIf phase perturbations and the Soviet high-altitude nuclear bursts of October 22 and 28, 1962. I., 19: 45166
SHAW, B. W., VIf phase perturbations and the Soviet high-altitude nuclear bursts of October 22 and 28, 1962. II., 19: 45167
SHCHEGOLEV, V. A., Effect of magnetic screens within the interblock gaps on the ITEP proton synchrotron, 19: 44879 (AEC-tr-6607)
SHCHELEV, M. Ya., Control system for pulsed electron-optical transformers, 19: 44358
SHCHERBAKOVA, M. N., Ionization-momentum dependence for electrons and positrons of high energy, 19: 44432 (CERN-65-4(Vol.II), pp IX41-3)
SHCHERBININ, E. V., Flow of conducting fluid past circular cylinder in presence of transverse magnetic field, 19: 44825
SHCHERBININ, E. V., Results of measuring turbulent pulsations of velocity in flow of mercury in presence of transverse magnetic field, 19: 44827
SHEFCIK, J. J., Operating experience on in-tank solidification of radiochemical wastes, 19: 45691 (RL-SA-41)
SHEINBERG, H., Forming of Teflon sheet by powder rolling, 19: 44637 (LA-3340)
SHEKHTER, L. Sh., Reconstruction of $N + N \rightarrow \pi + d$, 19: 45017 (JINR-P-2267)
SHEKUN, L. Ya., Paramagnetic resonance of cerium in single-crystal $PbMoO_4$, 19: 44017
SHELINE, Glenn E., Tumors of thyroid and parathyroid glands, 19: 43892
SHELINE, R. K., Experimental evidence for competing spherical and deformed shapes in N = 89 nuclei, 19: 45359
SHEPHERD, M. E., Measurements of the A and R parameters in proton-proton scattering at 47.8 and 27.6 Mev, 19: 45319
SHERMAN, N. K., Phototritons from ^{6}Li, 19: 45374
SHESTAKOV, V. D., Device for developing pulsed magnetic fields up to 150 kG, 19: 44888
SHIBATA, S., Possible evidence for nuclear interaction of μ above 3×10^{14} ev, 19: 45368
SHIGIN, V. A., Threshold of symmetrical fission of ^{237}Np, 19: 45258 (IAE-833)
SHIKHOV, S. B., Possibility of using thorium in high-energy reactors, 19: 45605 (ORNL-tr-788)
SHILS, Maurice E., Nutritional problems with malignant diseases. II., 19: 43911
SHINDO, Ryuichi, Nuclear parametric study of the pressure tube-type D_2O moderated lattices, 19: 45578 (JAERI-1080)
SHINOHARA, Kenichi, Gamma-initiated graft copolymerization of polymer films in presence of monomer vapor. III., 19: 44084
SHINOHARA, Keqichi, Irradiation of polyvinyl chloride in water. II., 19: 44086
SHINYAEV, A. Ya., Activation energy and mechanism of self-diffusion of Ni, 19: 44708 (JPRS-24761, pp 1-11)
SHINYAEV, A. Ya., Investigation of diffusion processes in brazing rhenium-coated titanium, 19: 44645 (JPRS-24761, pp 12-16)
SHIPLEY, E. D., Isotopic contamination in electromagnetic separators, 19: 44573 (ORNL-P-515)
SHIRKOV, D. V., Dispersion theory of low-energy scattering, 19: 45051
SHISHKIN, G. V., Polarization properties of muons in elastic neutrino processes, 19: 45050
SHITIKOV, Yu. L., Cold neutron scattering by polyphenyls, 19: 45238
SHITIKOV, Yu. L., Dynamics of LiH and LiD in inelastic scattering of cold neutrons, 19: 44732
SHKLOVSKII, I. S., Remarks on nature of x-ray sources, 19: 44923
SHLYAPNIKOV, P. V., Hydrodynamics of a resonance bubble chamber, 19: 44523
SHOEMAKER, F. C., External proton beam for the Princeton–Pennsylvania accelerator, 19: 44871 (PPAD-2137-556)
SHOEMAKER, F. C., Operating experience and improvements on the Princeton–Pennsylvania accelerator, 19: 44872 (PPAD-2137-565)
SHOREY, W. R. J., Control and read-out system for Chalk River double crystal γ spectrometer, 19: 44365 (AECL-2219)
SHORIN, V. S., Selection of spectrometric operating mode of FEU-49, No. 2, 19: 44455 (NP-15047)
SHORT, Nicholas M., Comparison of features characteristic of nuclear explosion craters and astroblemes, 19: 44237
SHOUDY, A. A., Development of EOCR as fast fuel test facility, 19: 45669 (APDA-174, pp 61-6)
SHTERN, A. G., Flow of conducting fluid past circular cylinder in presence of transverse magnetic field, 19: 44825
SHUKOLYUKOV, Yu. A., Xenon, argon and helium in some natural gases, 19: 44239
SHULTS, W. D., CHRNOGRM—computer program for analysis of chronopotentiograms, 19: 45706 (ORNL-TM-1254)
SHULTZ, F. T., Procedures for maintaining an outbred beagle colony, 19: 43646 (UCD-472-112, pp 23-35)
SHUR, L. I., Registration of α-particle stars produced by radioactive nuclei and time discrimination of α-particle tracks in nuclear emulsions, 19: 44425 (CERN-65-4(Vol.II), pp VIII17-26)
SHUR, L. I., Regression of sensitivity and latent image in nuclear and light-sensitive photographic emulsions, 19: 44402 (CERN-65-4(Vol.II), pp IV5-15)
SHUR, L. I., Theoretical grounds for the selection of developing agent for introducing it into the nuclear emulsion, 19: 44408 (CERN-65-4(Vol.II), pp V9-15)
SHUTTLEWORTH, E., Fading in thermoluminescent lithium fluoride used for radiation dosimetry, 19: 44076
SHWE, Hla, Artificial construction of particle tracks by a Monte Carlo method, 19: 44433 (CERN-65-4(Vol.II), pp IX44-7)
SIDOROV, A. I., Method for production of silicon spectrometric detectors with wide range of sensitivity, 19: 44470 (ZFK-PHA-12, pp 25-9)
SIDOROV, A. I., Use of silicon surface-barrier detectors compensated by lithium for measurements of energies of protons and deuterons up to energies of 13 Mev, 19: 44471 (ZFK-PHA-12, pp 30-2)
SIDOROVA, L. P., Method for production of silicon spectrometric detectors with wide range of sensitivity, 19: 44470 (ZFK-PHA-12, pp 25-9)
SIEGEL, Alan R., Nuclear rockets based on graphite reactor technology. Their applications and development status, 19: 45658 (TID-22097)
SIEGEL, H. S., Iodine-131 uptake in radiothyroidectomized chicks, 19: 43704
SIEGEL, S., Compilation of Fermi experience, 19: 45562 (APDA-174, pp 71-3)
SILBERSTEIN, J. M., Application of proton resonance to the measurement of inhomogeneous magnetic fields, 19: 44353 (SLAC-Trans-22)
SILIN, A. B., Relation between the (α,n) reaction yield and α particle energy, 19: 45301
SILINI, Giovanni, Recuperation in mammalian cell systems as revealed by radiation dose fractionation, 19: 43792
SILVA, R. J., Elastic scattering of 12.0- and 14.0-Mev deuterons from ^{90}Zr and the reaction ^{90}Zr(d,p)^{91}Zr, 19: 45281 (ORNL-3850)
SILVERMAN, Sol Jr., Tissue-culture studies of human oral carcinoma. II., 19: 43802
SIMKOVA, M., Determination of iodine in organic polymers by activation analysis, 19: 43951
SIMONOV, B. I., Effect of magnetic screens within the interblock gaps on the ITEP proton synchrotron, 19: 44879 (AEC-tr-6607)
SIMONOV, Yu. N., Angular dependence of quantities measured in total set of

experiments on nucleon-nucleon scattering, 19: 45015 (JINR-P-2241)
SIMONOVA, L. I., Method for production of silicon spectrometric detectors with wide range of sensitivity, 19: 44470 (ZFK-PHA-12, pp 25-9)
SIMPSON, Charles L., Diffusion studies at Hanford, 19: 44792 (BNL-914, pp 153-5)
SIMPSON, Charles L., [Fallout] deposition measurements at Hanford, 19: 44248 (BNL-914, pp 141-3)
SIMPSON, J. A., Search for trapped electrons and a magnetic moment at 6am by Mariner IV, 19: 44913
SINCLAIR, G. M., Prog. rpt. on mechanical behavior of dilute alloys of Nb, final, 7/65, 19: 44700 (TID-22117)
SINCLAIR, Kenneth F., Backscatter flaw detection system, 19: 44214
SINCLAIR, R. M., Plasma confinement in the model C stellarator, 19: 45397 (MATT-282)
SINGER, Irving A., Conference on AEC meteorological activities, May 19–22, 1964, 19: 44761 (BNL-914)
SINGER, Irving A., Vertical structure of turbulence, 19: 44799 (BNL-8516)
SINGH, R. P., Spectrophotometric determination of zirconium with 7,8,3',4'-tetrahydroxy flavonol, 19: 43955
SINNHUBER, R. O., Development of radiation-sterilized fish items for armed forces feeding, 19: 44555 (NP-15373)
SINNHUBER, R. O., Irradiation-sterilized shelf-stable fish and seafood products, 19: 44556 (NP-15464)
SIRVINSKI, V., U1627 (a g-second integrator), 19: 45707 (SC-DR-65-261)
SKACHKOV, S. V., Effect of magnetic screens within the interblock gaps on the ITEP proton synchrotron, 19: 44879 (AEC-tr-6607)
SKELTON, Margaret W., Computer program for circulation of library journals, 19: 45700 (DP-970)
SKLAVENITIS, L., Utility of activation detectors for the assessment of large doses, 19: 44535
SLADE, David H., Measurement and prediction of dispersion, 19: 44789 (BNL-914, pp 146-8)
SLIFKIN, Lawrence M., Radiation detection in large crystals of silver chloride, 19: 44378 (CERN-65-4(Vol.I), pp 1-15)
SLIPPY, W. A. Jr., Anelastic effects in Zr at room temperature resulting from prestrain at 77°K, 19: 44728
SLOTTA, J., Reaction $^{10}B(d,p_0)^{11}B$, 19: 45336
SLUNECKO, J., Determination of iodine in organic polymers by activation analysis, 19: 43951
SLUNECKO, Jaroslav, Substoichiometric determination of copper in high-purity metals by activation analysis, 19: 43973
SLYUSAREV, N. M., Results of measuring turbulent pulsations of velocity in flow of mercury in presence of transverse magnetic field, 19: 44827
SMALL, N. C., Steady creep swelling of a clad nuclear fuel plate, 19: 45548 (WAPD-TM-498)
SMIDT, D., Fast reactor core design and safety studies in France and in the Federal Republic of Germany, 19: 45623
SMILYANSKI, V. R., Wave transformation in magnetohydrodynamics, 19: 45432
SMIRNOV, V. I., Multidimensional analyzer with a preliminary treatment of data and combined-type memory, 19: 44524
SMITH, A. B., Reports to AEC Nuclear Cross Sections Advisory Group Meeting, March 8–9, 1965, 19: 45288 (WASH-1056)
SMITH, A. F., Identification and distribution of intermetallic compounds in adjusted uranium, 19: 44717
SMITH, B. C., Diffuse reflectance spectra of some uranium(IV) complexes, 19: 44034
SMITH, C. H., Effect of molecular structure on the thermal aging properties of flexible urethane foams, 19: 44682 (BDX-613-75)
SMITH, D. F., Infrared and Raman spectra and valence force constants of IOF_5, 19: 44019
SMITH, Francis M., Artificial construction of particle tracks by a Monte Carlo method, 19: 44433 (CERN-65-4(Vol.II), pp IX44-7)
SMITH, H., Metabolism of radioactive strontium in rats. I., 19: 43671 (PG-Report 662)
SMITH, H., Metabolites considered to be of value in diagnosis of exposure to radiation, 19: 43852
SMITH, Harold H., Relative biological effectiveness of different types of ionizing radiations: cytogenetic effects in maize, 19: 43712 (BNL-9383)
SMITH, Harold P. Jr., Measurement of Cs-sputtered Cu yield and angular distribution by a radioactive tracer technique, 19: 44964
SMITH, Hylton, Removal of radionuclides from the body, 19: 43700
SMITH, I. L., Behavior of a wide-gap spark chamber when two particle tracks are present, 19: 44518
SMITH, J., Bootstrapping of particles with spin greater than unity, 19: 45076
SMITH, J. A., Description of the Savannah River high flux charge, 19: 45638 (DP-999, pp 7-17)
SMITH, J. A., Isotope production in a Savannah River reactor at flux levels above 10^{15} n/(cm²)(sec), 19: 45639 (DP-999, pp 19-28)
SMITH, Maynard E., Brookhaven meteorological program, 19: 44762 (BNL-914, pp 1-3)
SMITH, Maynard E., Conference on AEC meteorological activities, May 19–22, 1964, 19: 44761 (BNL-914)
SMITH, Maynard E., Inert atmosphere enclosure for the preparation of samples prior to determination of oxygen, 19: 43933 (LA-3344)
SMITH, P. W., Status of fission product recovery at Hanford, 19: 45690 (RL-SA-40)
SMITH, S. E., Protection against fire hazards in the design of filtered ventilation systems of radioactive and toxic process buildings, 19: 44284 (AWRE-O-24/65)
SMITH, Willie W., MEA effect on radiation dose-response characteristics of granulocyte and lymphocyte counts, 19: 43876
SMOLIN, G. G., Two-dimensional incompressible fluid channel flow in presence of electric and magnetic fields, 19: 44829
SMORODINSKY, J. A., Current-generated algebras and form-factors, 19: 45011 (JINR-E-2294)
SOBELS, F. H., Significance of radiation genetics in present genetics, 19: 43823
SODEE, D. Bruce, Role of radioisotope scanning in the evaluation of gastrointestinal disease, 19: 43886
SOKOLIC, A., Vaccination against Dictyocaulus filaria with irradiated larvae, 19: 43750
SOKOLOV, B. V., Device for developing pulsed magnetic fields up to 150 kG, 19: 44888
SOLON, L. R., Prog. rpt. on stratospheric electrostatic precipitator and associated devices, semiannual, 9/64–2/65, 19: 44801 (NYO-2363-3)
SOLOV'EV, L. D., On the ρ-meson peak shift in double photoproduction, 19: 45019 (JINR-P-2286)
SOLOVEVA, M. F., Further development of apparatus for measurements of particle tracks in photoemulsions by television method, 19: 44422 (CERN-65-4(Vol.II), pp VII39-42)
SOMOGYI, G., Transmission of monoenergetic electron beams through foils, 19: 44818
SOMOL, C. J., 100-Kv, 10-w heavy-particle thrustor, 19: 44231
SONG, Hi Sung, Phase space considerations for three-particle and four-particle final states, 19: 45006 (IS-1214)
SOOD, B. S., Measurement of Z dependence of elastic scattering cross section of γ rays, 19: 45327
SOOD, P. M., Scattering constant in nuclear emulsions, 19: 44429 (CERN-65-4(Vol.II), pp IX14-22)
SORANTIN, H., Activation analytical investigations of polyethylenes, 19: 43975
SOUCAS, K., Fallout radioactivity at Geneva for the year 1963, 19: 44269
SOUCEK, B., Direct-recording megachannel analyzer through associative programming of a small computer, 19: 44497
SOUDAIN, G., Multiple-purpose personal dosimeter, 19: 44536
SOULIOTIS, A. G., Determination of chloride in beer by radioactivation analysis, 19: 43944
SOVKA, I. A., Efficient dewar for lithium-drifted germanium detectors, 19: 44511
SOWER, George W., Radioactive source holder, 19: 44179
SOWINSKI, M., Charge-sensitive preamplifier with low noise level for operation with semiconductor detectors, 19: 44484 (ZFK-PHA-12, pp 189-95)
SOWINSKI, M., Interaction of heavy fission particles with semiconductor detectors, 19: 44481 (ZFK-PHA-12, pp 149-53)
SOWINSKI, M., Target preparation by electro-spraying directly on semiconductor detectors, 19: 44635 (INR-595/IA/PL)
SOWMAN, Harold G., Boron carbide spherules, 19: 44660
SOWMAN, Harold G., Refractory carbides, 19: 44659
SOZOU, C., Interaction of solar plasma with the geomagnetic field, 19: 45164
SPACU, P., Some compounds of samarium, gadolinium, and erbium with various organic acids, 19: 44028
SPAINHOUR, K. A., Isotopic contamination in electromagnetic separators, 19: 44573 (ORNL-P-515)
SPARRMAN, B., Radiomimetic effects of mono- and bi-functional alkylating compounds in triticum monococcum (2x) and triticum durum (4x), 19: 43653
SPARROW, Arnold H., Tolerances of higher plant species to radiation, 19: 43782
SPASOJEVIC, D., Heat transfer and pressure drop of a gas-cooled reactor fuel element can model with inclined polyzonal spiral finning, 19: 45549
SPEAS, I. G., Hydraulic problems on BONUS reactor pressure control system, 19: 45603 (Y-1491)
SPEECKE, A., Neutron activation analysis of copper in bismuth by (γ-γ) coincidence measurement, 19: 43941
SPEISER, T. W., Particle trajectories in model current sheets. I., 19: 45168
SPENCER, Herta, Metabolism of ^{46}Sc in man, 19: 43692
SPENCER, Herta, Tissue distribution of ^{65}Zn in tumor tissue and normal tissue in man, 19: 43699

SPEROW, H. L., Development, acceptance and qualification testing of the SNAP-10A ejectable heat shield, 19: 45650 (NAA-SR-10997)
SPETH, A. J., Effects of low-energy electron irradiation on Si-insulated gate field-effect transistors, 19: 44549
SPIES, J., Method for determination of heavy water content in water samples, 19: 43983
SPINDLER, W. E., Improved furnace assembly for high-temperature diffractometers, 19: 44340 (AERE-M-1361)
SPRING, E., Gamma transitions in ^{65}Cu from decay of ^{65}Ni, 19: 45320
SPURLOCK, Jack M., Prog. rpt. on effects of electrical fields on boiling heat transfer, 12/64, 19: 44190 (NYO-2404-67)
SPURLOCK, Jack M., Prog. rpt. on effects of electrical fields on boiling heat transfer, 4–6/65, 19: 44191 (NYO-2404-73)
SQUIRES, E. J., N/P method and the diffraction picture, 19: 45088
SRIVASTAVA, K. S., Forbidden lines in L-emission spectrum of Pb-82, 19: 44941
SRIVASTAVA, P. K., Decay of ^{86}Rb, 19: 45331
SRIVASTAVA, P. K., Remark on compositeness criteria in the Lee model, 19: 45068
STADNICOV, T., Neutron transmission of Pd in energy range 1.2 to 100 ev, 19: 45233
STAEBLER, U. M., Outlook for United States nuclear power, 19: 45615
STAFFORD, Walter H., Parametric performance analysis for interplanetary missions utilizing first-generation nuclear stages, 19: 45649 (N64-32637)
STAGG, J. M., Terrestrial control in the production of aurora, 19: 45185
STAN, H.-J., Continuous measurement of ^{14}C-labeled amino acid mixtures with help of scintillator tube after separation on ion exchange columns, 19: 43976
STANCHI, L., Modular counting system in the electronic section, 19: 44447 (EUR-2444.i)
STANUTZ, R. N., Zircaloy-steam reaction in a simulated reactor loss-of-coolant accident, 19: 45496 (WCAP-3269-30)
STAPLETON, G. E., Prog. rpt. on space biology, annual, 7/1/64–6/30/65, 19: 43721 (ORNL-TM-1217)
STASCHEWSKI, Dieter, Statistical calculation of the ^{18}O and ^{17}O equilibrium distribution in the system CO_2/H_2O and CO_2/D_2O from molecular spectroscopic data, 19: 44007
STAUB, F. W., Prog. rpt. on two-phase flow, 4–6/65, 19: 44185 (GEAP-4910)
STAVISSKII, Yu. Ya., Absolute measurements of 24-kev neutron absorption cross section, 19: 45230
STAVISSKII, Yu. Ya., Fast neutron capture cross section for Re, 19: 45298
STAVISSKII, Yu. Ya., Measurement of average number of fission neutrons emitted in a single capture event of 24-kev neutrons for ^{235}U and ^{239}Pu, 19: 45297
STEDEFORD, J. B. H., Modifications to Royal Marsden Hospital gold grain implantation gun, 19: 43888
STEGEMANN, D., Fast neutron spectrum measurements with a ^{6}Li semiconductor neutron spectrometer, 19: 44457 (NP-15475)
STEGER, P. J., Production-size lathe hydrostatic components, 19: 44170 (Y-DA-921)
STEHN, John R., Neutron cross sections, Z = 88 to 98, 19: 45250 (BNL-325(2nd Ed.)(Suppl.2)(Vol.III))
STEIGER, H., Induction of phage production and formation of clear-plaque mutations by uv irradiation of prophage and of free-phage kappa, 19: 43847
STEINBERG, R., Single π^0 production by 8-Bev/c positive pions, 19: 45103
STEINBERGER, J., Test of charge-conjugation invariance in $\bar{p}p$ annihilations at rest, 19: 45124
STEINHAUS, James F., Investigation of plasma from an occluded gas, cold plasma source, 19: 45411 (UCRL-7935)
STEINKOPFF, Horst, Pressed block for preparation of rod-shaped nuclear fuel elements, 19: 44663
STERN, R. A., Incoherent microwave scattering from resonant plasma oscillations, 19: 45436
STEVENS, R. D., Pregnancy after primary irradiation for carcinoma of cervix, 19: 43891
STEVENS, Walter, Interactions of Pu(IV) with blood proteins, 19: 43705
STEWART, J., Spark-chamber experiment on cosmic γ rays, 19: 44970
STEWART, J. R., Phototritons from ^{6}Li, 19: 45374
STEWART, J. R., Space radiator fabrication development, 19: 44606 (PWAC-483)
STEWART, R. J., Photodisintegration of ^{4}He, 19: 45353
STEWART, W. C., Current quenching in thin Pb films by multiple boundary propagation, 19: 45193 (TID-21307)
STICKNEY, R. E., Prog. rpt. on energy conversion, 3–5/65, 19: 44981 (NP-15435)
STILLER, B., Relativistic increase in the track blob density in various nuclear emulsions, 19: 44430 (CERN-65-4(Vol.II), pp IX23-31)
STILLER, G., Angular distribution for reaction ^{12}C(d,α)^{10}B with a semiconductor detector, 19: 45289 (ZFK-PHA-12, pp 99-105)
STILLER, H., Lattice dynamics of solid methane, 19: 45239
STILLER, H., Proton motions in acid aqueous solutions, 19: 44037
STIRLING, A. V., Pion-nucleon phase shift analysis below 1 Bev, 19: 45100
STOBBS, J. J., Oxidation of the U–Cu intermetallic compounds UCu_5 in CO_2 between 350 and 850°C, 19: 44631
STOKES, A. D., Induction-field calculations and their application to measurements of conductivity distributions in cylindrical plasmas, 19: 45437
STOKLOSA, Edmund, Effect of x rays on histological and some histochemical changes in rabbit lungs, 19: 43846
STONE, D. H., Effect of carburization on low strain rate behavior of type 304 stainless steel, 19: 44623 (NAA-SR-10487)
STONE, J. M., Radium metabolism by beagles following single and multiple injections, 19: 43678 (UCD-472-112, pp 97-108)
STONE, Leonard R., Radioactive source holder, 19: 44179
STONEKING, C. E., Prog. rpt. on containment capsule impact safety, 19: 44298 (SC-RR-65-9)
STOPPINI, G., Polarization of recoil protons in e-p elastic scattering at 20 Fermi^{-2}, 19: 45058
STOVALL, E. J. Jr., Floating-point version of Nordsieck's scheme for numerical integration of differential equations, 19: 45703 (LA-DC-6667)
STOVER, Betsy J., Interactions of Pu(IV) with blood proteins, 19: 43705
STRATTON, R. F., Ion cyclotron harmonic spectrum generated in an energetic ion plasma, 19: 45405 (ORNL-P-1576)
STRAUSS, M., Voigt-Palacios-Gordon transformation and kinematics implied by it, 19: 45142
STRAWBRIDGE, L. E., Optimum core lattice parameters for the San Onofre nuclear generating station, 19: 45599 (WCAP-3269-49)
STREATER, R. F., Generalized Goldstone theorem, 19: 45119
STREETON, R. J. W., Reprocessing with amine ether systems. II., 19: 44108 (AERE-R-4440(Pt.3))
STRICKLER, Herbert S., Externally applied probe for scanning radioactivity in countercurrent distribution machines, 19: 43940
STROM, Gordon, Scale-model diffusion experiments, 19: 44764 (BNL-914, pp 14-17)
STUART, R. N., Studies of band structure and electron scattering in Al by photoemission, 19: 45481 (UCRL-12470)
STUBBS, T. F., Qualitative experimental investigations on various vortex tube configurations, 19: 44199 (UCRL-12045)
STUPAR, J., The determination of cadmium in uranium compounds by atomic absorption spectrophotometry, 19: 43935 (NIJS-R-447)
SUBBOTIN, V. I., Models of the temperature fields of fuel elements in the active zone and shield of the BN-350 reactor, 19: 45604 (JPRS-31245)
SUCCI, C., State of construction of the relativistic cyclotron for protons at 45 Mev, 19: 44886
SUGA, K., Possible evidence for nuclear interaction of μ above 3×10^{14} ev, 19: 45368
SUGAHARA, Tsutomu, Radiation-induced chromosome aberrations in man, 19: 43834
SUGAHARA, Tsutomu, Recovery from radiation damage and its modification in mammalian cells, 19: 43866
SUGIURA, Masahisa, Sudden change in solar wind pressure and outer region of the magnetosphere, 19: 45162
SUKHOV, L. V., Further development of apparatus for measurements of particle tracks in photoemulsions by television method, 19: 44422 (CERN-65-4(Vol.II), pp VII39-42)
SULLIVAN, R. J., Second-cycle AIROX reprocessing and pellet refabricating of highly irradiated UO_2, 19: 44114 (NAA-SR-11375)
SULLIVAN, Wm. D., Effect of radiation on enzymatic activity in synchronously dividing Tetrahymena pyriformis, 19: 43856
SUN, Hsui-fan, Stacking fault frequency in Ni–Mo alloys, 19: 44723
SUND, R. E., Delayed γ rays from fission, 19: 45245 (AFWL-TR-65-95)
SUNE, Nicasio Ortin, Preservation of foods by irradiation. I., 19: 44561
SUO, M., Prog. rpt. on boiling flow regimes and critical heat flux, 3/6–6/15/65, 19: 44193 (NYO-3304-5)
SUPEK, Z., Metabolism of 5-hydroxytryptamine in brain of x-ray-treated rats, 19: 43810
SUSANNA, A., Persistent currents induced by circularly polarized waves in a superconducting ring, 19: 45191 (LNF-65/15)
SUTCLIFFE, W. G., Lorentz transformations of thermodynamic quantities, 19: 44843
SUWALSKI, Witold, Water reactivity effects in the Anna critical assembly, 19: 45529 (INR-600/IX-A/PR)
SUZUKI, Nobutake, Effects of metal ions on autoxidation of benzene in aqueous solutions, 19: 44078
SUZUKI, Shiro, Elimination of radioactive strontun deposited in bone, 19: 43706
SUZUKI, Tomoo, Multigroup calculations of kinetics parameters in fast reactors (KPARAMCODE), 19: 45530 (JAERI-1082)

SVARCER, Vesna, Fading in thermoluminescent lithium fluoride used for radiation dosimetry, 19: 44076

SVENSSON, B. E. Y., Absorptive effects in $\bar{p}p \rightarrow \bar{N}^*N^*$, 19: 45069

SVIDERSKAYA, Z. A., Effect of additional alloying on properties of magnesium–neodymium alloys, 19: 44709 (JPRS-24761, pp 17-28)

SVIRIDENKO, E. Ya., Models of the temperature fields of fuel elements in the active zone and shield of the BN-350 reactor, 19: 45604 (JPRS-31245)

SVIRIDENKO, V. Ya., Heterogeneous absorber efficiency in homogeneous uranium–water reactors, 19: 45536

SVITCHEVA, V. I., Radioactive fallout over the USSR area in 1963, 19: 44259

SWAMI, M. S., Loading of nuclear emulsion with light and heavy elements, 19: 44399 (CERN-65-4(Vol.II), pp III17-20)

SWAN, G. A., Chemical effects of γ radiation on organic systems. XI., 19: 44072

SWAN, G. A., Research on organic radiation chemistry, 19: 44053 (AFML-TR-65-166)

SWANSON, E. W., Effects of irradiation upon lactation, 19: 43800

SWANSON, E. W., Lactation and radionuclide metabolism responses on dairy cattle to lethal doses of γ and neutron radiation, 19: 43801

SWARNAGOWRI, S., Internal conversion coefficients of E2 transitions, 19: 45369

SWEN, G. E., Saxton chemical shim kinetic experiments, 19: 45598 (WCAP-3269-44)

SWENSON, D. A., Design of proton linear accelerators for energies up to 200 Mev, 19: 44867 (MURA-713)

SWIFT, C. D., Background events in photomultiplier tubes at high altitudes, 19: 44465 (UCRL-12020)

SWIFT, W. H., Thermal effects in anion exchange resin–nitric acid systems, 19: 44110 (BNWL-114)

SZALAY, A., Preparation of self-supporting thin silicon targets by reductive evaporation, 19: 44650

SZCZEGLOW, S. M., Therapeutic activity of P.S.E. preparation in post-radiation pathology, 19: 43872

SZEKELY, Z., Variation of the index on refraction of aqueous solutions of $UO_2(NO_3)_2$, 19: 43969

SZTEKE, W., Dispersion fuel elements for experimental and university reactors, 19: 45547 (INR-585/XIV/R)

SZWARCBAUM (SHAVIV), G., Calculation of Doppler effect in fast reactors, 19: 45576 (IA-1039)

SZYBALSKI, Waclaw, Mutagenic response of human somatic cell lines, 19: 43844

T

TABOR, D., The friction and deformation properties of irradiated polytetrafluoroethylene (PTFE), 19: 44092

TACONIS, K. W., Dissipative normal fluid production by gravitational superfluid flow, 19: 45201

TAGLIAFERRI, G., State of construction of the relativistic cyclotron for protons at 45 Mev, 19: 44886

TAIE, M., Ion exchange removal of ^{90}Sr from biologic wastes, 19: 45692 (UCD-472-112, pp 141-7)

TAIT, D., Reactivity feedback in the Dounreay fast reactor, August 1962–December 1963, 19: 45594 (TRG-Report-864)

TAJIRI, Masayoshi, Some remarks on the collisionless plasma flow, 19: 45426

TAKAHASHI, Noriaki, Scattering of alpha particles from medium-weight nuclei, 19: 45312

TAKAHASHI, Shuichiro, Particle bonding of swaged UO_2 compacts, 19: 44649

TAKAMATSU, Toshiaki, Gamma-initiated graft copolymerization in presence of monomer vapor to polymer films. II., 19: 44083

TAKAMATSU, Toshiaki, Gamma-initiated graft copolymerization of polymer films in presence of monomer vapor. III., 19: 44084

TAKAMATSU, Toshiaki, Irradiation of polyvinyl chloride in water. II., 19: 44086

TAKASHIMA, Yoichi, Separation of gaseous isotope mixture in a supersonic jet. I., 19: 44577

TAKAYAMA, Kazuo, Higher harmonics and sub-harmonics of electron plasma oscillations, 19: 45428

TAKEDA, Minoru, Scattering of alpha particles from medium-weight nuclei, 19: 45312

TAKEDA, Susumu, Extension of range of electron density in plasmas measurable by microwaves, 19: 45429

TAKETANI, K., Estimation of fission gas release from punctured Calder Hall type fuel element, 19: 44632

TAKEUCHI, Hajime, High-energy radiation measurement in the exosphere by Explorer VII, 19: 44973

TAKIMOTO, Kiyohiko, Quasi-free α-α collisions in ^9Be and ^{12}C at 28 Mev, 19: 45308

TAKIZAWA, Masao, Radiation-induced oxidation of Sb(III) in aqueous solution. II., 19: 44085

TAKSAR, I. M., Conducting slab in traveling magnetic field of double-side inductor, 19: 44841

TALANOV, V. D., Models of the temperature fields of fuel elements in the active zone and shield of the BN-350 reactor, 19: 45604 (JPRS-31245)

TALHOUK, S., Crystal structure of solid deuterium from neutron-diffraction studies, 19: 45211

TALMAGE, David W., Erythrocyte chimerism and acquired immunologic tolerance, 19: 43657

TAMURA, T., Deuteron excitation of two-phonon states in ^{60}Ni, 19: 45346

TAMURA, Toro, Excitation of the unnatural parity 3^+ state in ^{24}Mg in inelastic scattering of α particles, 19: 45318

TANAKA, Giichiro, Assay of strontium-90 in human bone in Japan, 1961–1963, 19: 44266

TANAKA, Toyosuke, Decomposition of tertiary butyl peroxides by γ irradiation, 19: 44089

TANAKA, Yoshimasa, High-dose ratemeter based on measurement of electric resistance of liquid organic compounds, 19: 44525

TANG, S. M., Antimony-124 spectrum shape, 19: 45328

TANGHERLINI, F. R., Gauge subtraction method for Einstein's pseudotensor, 19: 45148

TANOOKA, Hiroshi, Modification of inactivation of bacterial spores and their transforming DNA by ionizing radiations, 19: 43793

TAO, S. J., Wide-range high-resolution time-to-amplitude converter, 19: 44508

TARASSENKOV, V. G., Study of the factors affecting the quality of the development with the electrodialyser, 19: 44410 (CERN-65-4(Vol.II), pp V22-33)

TARDIFF, Robert G., Effects of various drugs on ATP activity of hematopoietic tissues of rats exposed to γ radiation, 19: 43860 (NP-15310, pp 14-25)

TARDY-JOUBERT, P., Dosimetry of high-energy protons by measurement of beryllium-7 formed in the tissues, 19: 44327

TARINA, E., Three-axes spectrometer of Institute for Atomic Physics, Bucharest, 19: 44527

TARREGA, P., Momentum determination of low-momentum particles in emulsions exposed to strong magnetic field, 19: 44424 (CERN-65-4 (Vol.II), pp VIII9-16)

TATARONIS, J. A., Wave propagation along a warm nonuniform plasma column, 19: 45408 (SU-IPR-11)

TAUTFEST, G. W., Single-particle exchange in N^{*++} production in π^+p collisions, 19: 44997 (COO-1428-14)

TAVENDALE, A. J., Germanium lithium-drift diode with guard-ring for γ spectroscopy, 19: 44510

TAVERNE, Henri, Remote control apparatus, 19: 44180

TAVKHELIDZE, A. N., Unitarity of the S matrix in the broken symmetry SK(6), 19: 45009 (JINR-E-2247)

TAYLOR, B. L., Analytical chemistry of the transuranium elements, 19: 43948

TAYLOR, Denis, Radioisotope selection, 19: 44551

TAYLOR, J. C., High-activity iodine release from irradiated fuel and its subsequent clean-up, 19: 44303 (TRG-Report-888)

TAYLOR, K. W., Modifications to Royal Marsden Hospital gold grain implantation gun, 19: 43888

TAYLOR, T. I., Low-frequency motions in several ferroelectric salts, 19: 45241

TAZIME, Yutaro, Radiation-induced mutation frequencies in silkworm gonia, 19: 43784

TEATES, Charles D., Effects of unilateral thoracic irradiation on lung function, 19: 43799

TELEGDI, V. L., Experimental observations of electric quadrupole effects in the muonic spectra of ^{238}U, ^{181}Ta, and ^{239}Pu, 19: 45326

TELITCHENKO, M. M., Changes in concentration of nucleic acids in gonads of Leucaspius delineatus after exposure to uranium, 19: 43769

TEPLITZ, V. L., Approximate one-trajectory exchange, 19: 45074

TERANAKA, Masahiko, Study of azimuthal anisotropy in multiple meson emission, 19: 45054

TERASIMA, Toyozo, Recovery processes in HeLa cells damaged by x irradiation, 19: 43790

TERENT'EV, M. V., Regeneration phenomena and combined experiments in K^0 meson beam, 19: 45034 (NP-15470)

TERLECKI, J., Investigation of the effect of smoke admixtures on the current intensity in ionization chambers, 19: 44355

TERLOUW, J. C., Low-frequency plasma oscillations (anode oscillations and forced relaxation oscillations), 19: 45403 (NP-15445)

TERRA, L., Conjectures for development of industrial activity in the nuclear field, 19: 45724

TETART, Emile, Automatic machine for milling fins on cylindrical parts, 19: 44655

THACKER, R. J., Techniques in machining and working of cast tungsten, 19: 44653

THARIN, Catherine R., TAFI-II, computer code for management of radioactive waste, 19: 45687 (DP-966)

THEODOSIOU, A., Acceleration method for detection of soft β particles, 19: 44512

THEUERER, H. C., Proximity effect between a superconducting and a ferromagnetic film, 19: 45197

THIEBLEMONT, P., Role of the army medical service in nuclear war, 19: 44310

THIOUNN, Mme, Singular solutions of Dirac equations and theory of the de Broglie double solution, 19: 45137

THOEN, J., Velocity of sound in liquid hydrogen, 19: 44822

THOMAZ, M. Fernandes, Determination of carbon and hydrogen in hydrocarbons by neutron scattering, 19: 43968

THOME, Paul, Improvements in and relating to hot-forging apparatus, 19: 44657

THOMPSON, A. L., A review of equipment for analyzing for oxygen in combustion systems, 19: 43980

THOMPSON, Major C., Reduction of plutonium dioxide to plutonium metal, 19: 44594 (DP-983)

THOR, Anders J., Time-dependent Schroedinger wave equation for a particle in a central potential field as a spatial integral equation, 19: 44960

THORPE, J., Water vapor corrosion of uranium and its prevention, 19: 44618 (AWRE-O-42/65)

TIEMBLO, A., Vector invariants of SU_3/Z, 19: 45083

TIEN, L. C., Activity of uranium in dilute solution in liquid bismuth, 19: 44733

TIK, Tso-Wong, Decays $\frac{3}{2}^+ \rightarrow \frac{1}{2}^+ + 0^-$ in broken symmetry U(12), 19: 45012 (JINR-P-2237)

TIK, Tso-Wong, Electromagnetic decay and electroproduction of $\frac{3}{2}^+$ resonances, 19: 45007 (JINR-E-2228)

TILBURY, P. D., Fatigue of uranium, 19: 44681 (AWRE-O-65/65)

TIMASHEV, S. F., Direct knockout and inelastic scattering reactions, 19: 45033 (NP-15468)

TIMM, U., Relation between column stratification and negative ion content in an impure Ar discharge, 19: 45423

TIMMINS, R. S., Chemical reactions during rapid quenching of O_2–N_2 mixtures from very high temperatures, 19: 44041

TINT, G. S., Prog. rpt. on flow and fracture studies of alloyed Be, final, 8/65, 19: 44694 (NP-15432)

TIPPETS, F. E., Prog. rpt. on alkali metals boiling and condensing, 1–3/65, 19: 44187 (NASA-CR-54405)

TIREH, L. I., Experimental studies on assemblies 1 and 2 of the fast reactor FRO. I., 19: 45522 (AE-195)

TISON, V., Immunological aspects of experimental pulmonary sclerosis due to ionizing radiations, 19: 43817

TKACHEV, L. G., Baryon annihilation in broken U(12) symmetry, 19: 45008 (JINR-E-2246)

TKACHEV, L. G., Current-generated algebras and form factors, 19: 45011 (JINR-E-2294)

TODD, David K., Economics of ground water recharge, 19: 45717 (UCRL-7850(Rev.I))

TODIREANU, S., Three-axes spectrometer of Institute for Atomic Physics, Bucharest. 19: 44527

TODOROV, I. T., New definition of translations in the inhomogeneous SL(6) group, 19: 45132 (JINR-E-2225)

TOELGYESSY, J., Radiocoulometric titration using non-isotopic indicator in solid phase, 19: 43952

TOKIWA, Yoshiro, An SO_2 monitor for air pollution studies, 19: 44458 (NYO-2767)

TOLLANDER, B., Efficiency calculations for a circular detector viewing a circular radiator, 19: 44505

TOLSTIKHIN, I. N., Xenon, argon and helium in some natural gases, 19: 44239

TOLSTOPYATOVA, A. A., Catalytic activity of praseodymium oxide in dehydrogenation and dehydration of alcohols and dehydrogenation of tetralin, 19: 44023

TOLSTOV, K. D., Ionization density in emulsions enriched with hydrogen, 19: 44435 (CERN-65-4(Vol.II), pp IX62-5)

TOLSTOV, K. D., Photoemulsion experiments with a hydrogen-jet target, 19: 44443 (CERN-65-4(Vol.II), pp X61-6)

TOLSTOV, K. D., Using photoemulsion in proton dynamic polarization conditions, 19: 44442 (CERN-65-4(Vol.II), pp X57-60)

TOMIKAWA, Akio, Assay of strontium-90 in human bone in Japan, 1961–1963, 19: 44266

TOMLINSON, E. P., Operating experience and improvements on the Princeton–Pennsylvania accelerator, 19: 44872 (PPAD-2137-565)

TOMPKINS, Donald R., Second method of identifying fast monopoles, 19: 45149

TOMSON, I. N., Isotopic composition of lead ore from different type deposits in Eastern Transbaikal, 19: 44277

TONELLI, A. Duane, Radioisotope power-generating system for manned space laboratory, 19: 44571

TONOMURA, Shizo, Effect of γ-radiation on porphyrin-metal complexes. I., 19: 44087

TOPP, S. V., Physics design of the Savannah River high flux charge, 19: 45640 (DP-999, pp 29-42)

TORIYAMA, Yotsuo, Thermoelectron irradiation of polyethylene films, 19: 44069

TOSIMA, S., Wigner representation of quantum operators, 19: 45139

TOUZET, R., Radiostrontium and strontium fixation in bones and children's diets, 19: 44250 (NP-15269)

TOWER, S. N., 1000-Mwe supercritical pressure nuclear reactor plant study, 19: 45596 (WCAP-2042)

TOWLER, O. A., Description of the Savannah River high flux charge, 19: 45638 (DP-999, pp 7-17)

TOWLER, O. A., Operating experience with the first Savannah River high flux charge, 19: 45643 (DP-999, pp 73-86)

TOWNLEY, Charles W., In-pile studies of experimental pyrolytic-carbon-coated UC_2 and UO_2 fuel particles, 19: 44740 (BMI-1737)

TOYODA, Y., Possible evidence for nuclear interaction of μ above 3×10^{14} ev, 19: 45368

TRAIL, C. C., Experimental observations of electric quadrupole effects in the muonic spectra of ^{235}U, ^{181}Ta, and ^{239}Pu, 19: 45326

TRAN, Anh Ha, Calculation of the muon contamination in a π-meson beam, 19: 44993 (CEA-R-2778)

TRAPMANN, Heinz, Catalytic effect of Th and Zr ions on the hydrolysis of nucleotides, 19: 43708

TRAVESI JIMENEZ, A., Application of activation analysis to criminal investigation, 19: 43959

TREBES, D. M., Supercritical pressure liquid hydrogen heat transfer data compilation, 19: 44189 (NP-15332)

TREMILLON, Bernard, Fixation of uranyl acetate in an anion exchange resin, 19: 44119

TRENTA, A., Morphogenesis of binucleated erythropoietic cells by action of x rays, 19: 43730

TRENTA, A., Pseudo-amitoses provoked by x rays in erythropoietic cells in vitro, 19: 43826

TRETYAKOVA, M. I., Further development of apparatus for measurements of particle tracks in photoemulsions by television method, 19: 44422 (CERN-65-4(Vol.II), pp VII39-42)

TRETYAKOVA, M. I., Ionization-momentum dependence for electrons and positrons of high-energy, 19: 44432 (CERN-65-4(Vol.II), pp IX41-3)

TREVINO, S. F., Study of low-frequency molecular motions in polyethylene and the n-paraffins by slow neutron inelastic scattering, 19: 44050

TREW, D. H., Central region of the variable-energy cyclotron magnet, 19: 44869 (NIRL/R/87)

TRIDOT, Gabriel, Hydrates of uranyl sulfate, 19: 44014

TRILLING, George H., Coherent K^* production in the K⁺d reaction at 2.3 Bev/c, 19: 45120

TROUSIL, J., High-dose ionizing radiation photographic dosimetry, 19: 44533

TROUT, E. Dale, Scattered radiation in phantom from diagnostic quality radiation, 19: 43917

TROYAN, Yu. A., Elastic scattering of Λ hyperons on protons, 19: 45016 (JINR-P-2257)

TRUNOVA, Z. G., Measurement of Jupiter's intrinsic decimeter-wavelength radiation, 19: 44917

TSANOS, N. A., Determination of chloride in beer by radioactivation analysis, 19: 43944

TSENTER, E. M., Relation between the (α,n) reaction yield and α particle energy, 19: 45301

TSINOBER, A. B., Flow of conducting fluid past circular cylinder in presence of transverse magnetic field, 19: 44825

TSUCHIMOTO, Takeshi, Electron current release characteristics of high-frequency ion source with mesh grid, 19: 44880

TSUGO, Tomokichi, Radioactive contamination of milk in Japan (1961–1963), 19: 44268

TSUJI, Haruo, Determination of Si in Fe and steel by activation analysis, 19: 43965

TSUKAMURA, Michio, Transmutation effect of ^{35}S on a Mycobacterium, 19: 43816

TSUNOKAWA, Masayoshi, Environmental radiation and radioactivities about site of JAERI, 1956–1963, 19: 44290 (JAERI-1079)

TSUZUKI, Hiroshi, Elimination of radioactive strontium deposited in bone, 19: 43706

TSYTOVICH, V. N., Non-linear stabilization of beam instabilities in plasma, 19: 45402 (NP-15200)

TSYTOVICH, V. N., Plasma-turbulence mechanisms and acceleration of cosmic rays, 19: 44975
TSZEN'VA, Van, Method for production of silicon spectrometric detectors with wide range of sensitivity, 19: 44470 (ZFK-PHA-12, pp 25-9)
TU, Yuan-tsai, Elastic scattering of Λ hyperons on protons, 19: 45016 (JINR-P-2257)
TUBIANA, M., Migration of hematopoietic bone marrow cells in irradiated and normal mice, 19: 43836
TUCHMAN, A., Cesium-fueled MPD arc-jet engine performance, 19: 44230
TUCKFIELD, R. G. Jr., Flute characteristics of and microwave emission from a plasma in a mirror, 19: 45388 (GA-6432)
TUDO, Joseph, Hydrates of uranyl sulfate, 19: 44014
TULINOV, A. F., Proton scattering from a tungsten single crystal, 19: 45349
TUPLIN, T. A., Variations in isotopic compositions of naturally occurring molybdenum, 19: 44242
TURCHIN, V. F., Calculating differential cross sections of slow neutrons by means of integration with respect to time, 19: 45228 (NP-15469)
TURCHIN, V. F., Study of inelastic scattering of slow neutrons in zirconium hydride, 19: 45240
TURKIEWICZ, I., Excitation function for the $^{29}Si(n,\alpha)^{26}Mg$ reaction in energy range 13.6 to 15.6 Mev, 19: 45290 (ZFK-PHA-12, pp 110-12)
TURKIEWICZ, J., Excitation function for the $^{29}Si(n,\alpha)^{26}Mg$ reaction in energy range 13.6 to 15.6 Mev, 19: 45290 (ZFK-PHA-12, pp 110-12)
TURNER, Donald B., Dispersion in urban areas, 19: 44791 (BNL-914, pp 151-2)
TURNER, J. M., Prog. rpt. on two-phase flow and boiling heat transfer, 4-6/65, 19: 44192 (NYO-3114-9)
TUTUI, Yuneo, Manual of free gas model-code (FREE code), 19: 45223 (JAERI-1084)
TYAGI, Rohtash K., Ohlin structure near quantum limit of the continuous x-ray spectrum, 19: 44940
TYAPKIN, A. A., Fallability of using χ^2 criterion in phase-shift analysis for choosing statistically permissible ambiguous solutions, 19: 45012 (JINR-E-2353)
TYCKO, D., Test of charge-conjugation invariance in $\bar{p}p$ annihilations at rest, 19: 45124
TYLKA, Richard, Automatic continuous measurement of the ^{14}C radioactivity in fractions from chromatographic columns, 19: 43949
TZOAR, N., Incoherent microwave scattering from resonant plasma oscillations, 19: 45436

U

UCHIDA, Irene A., Case of double trisomy: trisomy No. 18 and triplo-x, 19: 43811
UDAGAWA, T., Experimental evidence for competing spherical and deformed shapes in N = 89 nuclei, 19: 45359
UEDA, Hideo, Detection of portal systemic shunts by hepatopulmonary scanning using ^{131}I MAA. III., 19: 43904
UHLIR, M., Baryon annihilation in broken U(12) symmetry, 19: 45008 (JINR-E-2246)
UHLIR, M., Current-generated algebras and form factors, 19: 45011 (JINR-E-2294)
UJHELYI, Cs., Internal bremsstrahlung spectrum accompanying the electron capture process of ^{36}Cl close to the end-point energy, 19: 45345
UKAI, Yosuo, Protective effects of chemicals on radiation induced damages in seed-treated crop plants, 19: 43877
ULLMAIER, H. A., Experimental simulation of large, high field, superconducting magnet operation, 19: 45192 (ORNL-TM-1266)
ULRICH, H., Ion-drift investigations of lithium in p-silicon, 19: 44001 (ZFK-PHA-12, pp 40-9)
ULRICH, H., Preparation of large-surface pn barrier-layer elements by lithium diffusion in p-silicon, 19: 44000 (ZFK-PHA-12, pp 33-9)
URCH, D. S., Reactions of hot tritium atoms with the system ethane and oxygen, 19: 44106
URENOVITCH, Joseph V., Pentamethyldisilane and 1,1,2,2-tetramethyldisilane, and their addition to olefins, 19: 44048 (TID-21309)
URGEL, M., Water treatment process in JEN-1 research reactor, 19: 45678 (JEN-149-DQ/I-50)
URYAEV, I. A., Spectral method of determination of doses from β-α emitters, 19: 44491 (CEA-tr-R-1866)
USHA DEVIZ, K., Cold neutron scattering by methane, 19: 45237
USHA DEVIZ, K., Study of elastic incoherent scattering by ammonium salts, 19: 45242
USHAKOV, P. A., Models of the temperature fields of fuel elements in the active zone and shield of the BN-350 reactor, 19: 45604 (JPRS-31245)

V

VAETH, Jerome, Tissue-culture studies of human oral carcinoma. II., 19: 43802
VAISSIERE, Michele, Fixation of uranyl acetate in an anion exchange resin, 19: 44119
VALANT, P., Some alternates for the utilization of organic liquid reactors for desalination of salt water, 19: 45620
VALBIS, Ya. A., Luminescence of alkali halide crystals doped with heavy halide ions under x radiation, 19: 45488
VALDMANIS, Ya. Ya., Conducting slab in traveling magnetic field of double-side inductor, 19: 44841
VALENTINI, L., Radioiodine metabolism in patients affected by a simple sporadic goiter, 19: 43691
VALITSKII, V. P., Magnetohydrodynamic instabilities in electrical explosion, 19: 44845
VALLARIO, E. J., Why and how of nuclear accident dosimetry, 19: 44320
VAL'SHTREM, E. A., Restoration of mitotic acitivity in the ependyma of cerebral hemispheres of x-irradiated rat embryos, 19: 43768
VAN, Shi-di, Neutron-^{235}U nuclear interaction in the 0.002 to 30 kev energy region, 19: 45292 (BNL-tr-16)
VAN, Yun-chun, Neutron-^{235}U nuclear interaction in the 0.002 to 30 kev energy region, 19: 45292 (BNL-tr-16)
VAN ALLEN, J. A., Absence of Martian radiation belts and implications thereof, 19: 44912
VAN ALPHEN, W. M., Dissipative normal fluid production by gravitational superfluid flow, 19: 45201
VAN CANEGHEM, P., Hair dysplasia induced by x rays in mice under different irradiation conditions, 19: 43833
VAN CLEVE, J. E., Summary of the Kilorod Project, 19: 44638 (ORNL-3681)
VAN CLEVE, J. E. Jr., Time study of fuel rod fabrication in the Kilorod facility, 19: 44639 (ORNL-3740)
VAN DAEL, W., Velocity of sound in liquid hydrogen, 19: 44822
VAN DE GRAAFF, Producing high-velocity charged particles, 19: 44890
VAN DE GRAAFF, R. J., Proposed methods for producing intense pulsed beams of monoenergetic neutrons, 19: 44882
VAN DE GRAAFF, Robert Jemison, Apparatus for acceleration of charged particles, 19: 44892
VAN DE GRAAFF, Robert Jemison, Method and apparatus for producing high-velocity charged particles, 19: 44891
VAN DER HOVEN, Isaac, Aerospace meteorological problems and diffusion climatology, 19: 44771 (BNL-914, pp 44-50)
VAN DER HOVEN, Isaac, Effects of variable source configurations in space and time, 19: 44786 (BNL-914, pp 115-18)
VAN DER MERWE, P., Energy levels of ^{30}S, ^{26}Si, and ^{8}B from $(^{3}He,n)$ reactions, 19: 45355
VAN DER VELDEN, Cornelius G., Apparatus for producing visual images of x-rayed objects, 19: 44363
VAN DER WERF-MESSING, B., Telecobalt treatment of carcinoma of the bladder, 19: 43894
VAN HEERDEN, I. J., Energy levels of ^{30}S, ^{26}Si, and ^{8}B from $(^{3}He,n)$ reactions, 19: 45355
VAN HOOMISSEN, J. E., Application of nuclear thermionics to undersea technology, 19: 44986
VAN ITTERBEEK, A., Velocity of sound in liquid hydrogen, 19: 44822
VAN'KOV, A. A., Absolute measurements of 24-kev neutron absorption cross section, 19: 45230
VAN'KOV, A. A., Measurement of average number of fission neutrons emitted in a single capture event of 24-kev neutrons for ^{235}U and ^{239}Pu, 19: 45297
VAN LEUVEN, P., Numerical evaluation of the uncertainty relation for angular variables, 19: 45145
VANNINI, V., Morphogenesis of binucleated erythropoietic cells by action of x rays, 19: 43730
VANNINI, V., Pseudo-amitoses provoked by x rays in erythropoietic cells in vitro, 19: 43826
VAN SLYKE, W. J., Thermal effects in anion exchange resin–nitric acid systems, 19: 44110 (BNWL-114)
VAN TORNE, L. I., Tensile properties of irradiated type 304 stainless steel strip, 19: 44743 (GEAP-3634)
VAN WINKLE, R., Molten salt converter reactor. Design study and power cost estimates for a 1000-Mwe station, 19: 45588 (ORNL-TM-1060)
VARAGONA, J. J., Time study of fuel rod fabrication in the Kilorod facility, 19: 44639 (ORNL-3740)
VARY, A., Electrodynamic mercury pump, 19: 44188 (NASA-TN-D-2965)
VASIL'EVA, L. V., Models of the temperature fields of fuel elements in the active zone and shield of the BN-350 reactor, 19: 45604 (JPRS-31245)
VASSIL, Lester K., Design of a chop and leach reprocessing plant, 19: 44126
VASYUKEVICH, P. V., Profiling channels for flows of ionized gases in transverse magnetic field, 19: 44838
VAUDO, A., Outlook for use of nuclear energy for production of heat at low temperature, 19: 45618

VAUGHAN, Leland M., Elevated line source progr ms, 19: 44779 (BNL-914, pp 93-4)
VAUGHAN, Leland M., Fundamental problems on the meso-scale, 19: 44782 (BNL-914, pp 103-6)
VAUGHN, F. J., Cross sections for $^{89}Y(n,\gamma)^{90m}Y$ and $^{89}Y(n,\gamma)^{90}Y$ between 0.145 and 1.225 Mev, 19: 45376
VAUGHN, H. R., Project SAND final program report. III., 19: 44142 (SC-RR-65-286)
VEACH, A. M., Isotopic contamination in electromagnetic separators, 19: 44573 (ORNL-P-515)
VELILLA, A., Determination of ^{131}I by use of activated carbon, 19: 43958
VELONA, F., Experience in test and use of Italian nuclear power plants, 19: 45616
VENARD, J. T., Effect of irradiation on the mechanical properties of stainless steel at 750°C under constant stress rate conditions, 19: 44750 (ORNL-TM-1216)
VENDRYES, Georges, Liquid cooled nuclear reactor with improved flow distribution means, 19: 45520
VENIER, A., Excessive dose levels: reports and statistics, 19: 44326
VENKATARAMAN, G., Cold neutron scattering by methane, 19: 45237
VENKATARAMAN, G., Study of elastic incoherent scattering by ammonium salts, 19: 45242
VEPRIK, Yu. M., Theoretical grounds for the selection of developing agent for introducing it into the nuclear emulsion, 19: 44408 (CERN-65-4 (Vol.II), pp V9-15)
VERBEEK, A. A., Determination of niobium in steel by neutron activation, 19: 43942
VERBINSKI, V. V., Photoneutron spectra and cross sections for ^{12}C and ^{16}O, 19: 45330
VERGANELAKIS, A., Polarization contribution to the hydrogen hyperfine structure and phenomenology of the electron-proton interaction, 19: 44951
VERGNES, M., K isomerism in ^{176}Yb, 19: 45357
VERMEER, W., Dissipative normal fluid production by gravitational superfluid flow, 19: 45201
VERNIN, E., Industrial development of activation analysis equipment and its applications, 19: 43977
VERTES, Paul, Methods and apparatus in which a mass of solid material is subjected to two successive treatments by gases, 19: 44042
VIAL, R., Accidental exposure received from an electron linear accelerator, 19: 44331
VIALETTES, H., Accidental exposure received from an electron linear accelerator, 19: 44331
VICENDON, Guy, Effect of γ rays on pyrimidine bases in aqueous solution. I., 19: 44064
VICK, L. L. J., Low-energy pion-kaon interaction, 19: 45085
VIETEN, Manfred, Power supply plant for thermal test stands in nuclear research station at Juelich in North Rhine-Westphalia, 19: 44203
VIJAYARAGHAVAN, P. R., Study of elastic incoherent scattering by ammonium salts, 19: 45242
VILCOT, Marc, Sealed coupling for an electrical heating conductor with coaxial sheath, 19: 44164 (CEA-R-2755)
VILLAR, E., Monostun determination of low-monostun particles in emulsions exposed to strong magnetic field, 19: 44424 (CERN-65-4(Vol.II), pp VIII9-16)
VILLET, G., Pion-nucleon phase shift analysis below 1 Bev, 19: 45100
VILLIERS, Jacques, Sealed coupling for an electrical heating conductor with coaxial sheath, 19: 44164 (CEA-R-2755)
VINCELLI, M. L., Polarization of recoil protons in e-p elastic scattering at 20 Fermi-², 19: 45058
VINCK, W.-F., Sites for construction of nuclear reactors, 19: 45498
VINOGRADOV, Y. I., X-ray emission of flares originating behind the solar disk, 19: 44894 (AD-424481)
VINZ, Heinrich, Sarcoma resulting at site of administration from paravasal injection of Thorotrast, 19: 43850
VISHNEVSKII, M. E., Measurement of the absolute value of the $K_1^0 \rightarrow K_2^0$ mass difference, 19: 45099
VISHNEVSKII, V. F., Elastic scattering of Λ hyperons on protons, 19: 45016 (JINR-P-2257)
VISNER, Sidney, Effect of a voided gap on reactivity coefficient for voiding core sodium in a fast reactor, for various geometries, 19: 45538
VITEK, F., Peripheral blood changes caused by internal emitters. III., 19: 43839
VIVIEN, Jean, Handling apparatus for an installation for reloading a nuclear reactor with fuel elements, 19: 45513
VIVIEN, Jean, Nuclear reactor refueling facility, 19: 45514
VLADIMIRSKII, V. V., Regeneration phenomena and combined experiments in K^0 meson beam, 19: 45034 (NP-15470)
VLADIMIRSKII, V. V., Symmetry of strong interactions and the SU_4 groups, 19: 45035 (NP-15471)
VLADYKOV, G. M., Heterogeneous absorber efficiency in homogeneous uranium–water reactors, 19: 45536
VLASOV, M. A., Discharge instability with a heated cathode in a magnetic field at low pressures, 19: 45390 (IAE-780)
VLASOV, N. A., Polarization in n-α scattering at E_n = 25, 28, and 34 Mev, 19: 45259 (IAE-834)
VODICKA, I., Myorelaxant effect of gallamine and tubocurarine in irradiated rabbits, 19: 43871
VOGG, Hubert, Method for separation of nuclear fuels, 19: 43982
VOGLER, Peter, The detection of radioactive substances in water, 19: 43974
VOGT, Hames R., The non-destructive determination of silicon and oxygen in meteorites by fast neutron activation analysis, 19: 43927 (CONF-650405-16)
VOLKOFF, J. J., Preliminary investigations to determine nuclear-electric spacecraft configurations for high-energy missions, 19: 44228
VOLMER, P., Semiautomatic apparatus for measurement of track lengths. Semiautomation in corpuscular photography, 19: 44417 (CERN-65-4 (Vol.II), pp VII1-14)
VON HAGENOW, Karl U., Connection between correlations and fluctuations in a plasma, 19: 45394 (IPP-6/37)
VON HALLE, E., Separation of potassium isotopes by molecular distillation, 19: 43931 (K-1650)
VON SALIS-SAMADEN, Rudolf, Prosthesis carcinoma of the hard palate. Problems and treatment, 19: 43912
VOROBEV, L. S., Possibility of determining kinematic characteristics of particles in spark chamber employing multiple scattering and additional sparks, 19: 44490 (BNL-tr-1)
VORONKOV, A. E., Further development of apparatus for measurements of particle tracks in photoemulsions by television method, 19: 44422 (CERN-65-4(Vol.II), pp VII39-42)
VUKOVIC, J., Sensitivity centers and latent image distribution as factors of nuclear emulsion properties, 19: 44392 (CERN-65-4(Vol.II), pp II44-8)
VYALOV, G. N., Kinetics of multiple acceleration of particles with variable charge in a potential electric field, 19: 44864 (JINR-P-2253)
VYAS, D. N., Behavior of lipase activity of γ-irradiated groundnut during germination, 19: 43798

W

WACHSLER, Emanuel, Interferometric measurement of vibrational relaxation time in hydrogen–argon mixtures, 19: 44855
WACHSMANN, F., Monobath films for determining accidental high-level exposures, 19: 44534
WACKER, Adolf, Synthesis and properties of nicotinamide-adenine-N^1-oxide-dinucleotide, 19: 44062
WADA, M., Positions of three cosmic x-ray sources in Scorpio and sagittarius, 19: 44968
WADA, Masumi, Cosmic-ray index, 19: 44974
WADHWA, R. P., Computer studies of plasma boundaries and lens effects created by immersed and withdrawn neutralizers, 19: 45454
WADHWA, R. P., Prog. rpt. on analysis of electron-ion mixing in ion engines, 11/64–1/65, 19: 44222 (NP-15068)
WAGEMAN, W. E., Measurement of helium and hydrogen viscosities to 2340°K, 19: 45190 (LA-3319)
WAGNER, G., Obligation of doctors to reduce the medical radiation burden, 19: 43913
WAGONER, Joseph K., Radiation as cause of lung cancer among uranium miners, 19: 44314
WAHLBERG, T., Planned procedures for fast determination of radiation levels and personnel dosimetry in connection with radiological accidents, 19: 44336
WALDKOETTER, G. L., Data recording system for fuel core tester, 19: 45500 (HW-65756)
WALDMAN, Jerry, Evaluation of shape factor in structure shielding calculations, 19: 44217
WALKER, C. H., Preparation and properties of sintered Nb_3Sn, 19: 44592 (CLM-R-43)
WALKER, D., Some reducible magnetogasdynamic flows, 19: 44850
WALKER, P., Corrosion of uranium and its prevention by organic coatings, 19: 44630
WALKER, R. M., Dosimetry of slow neutrons by recoding the fission tracks in insulators, 19: 44385 (CERN-65-4(Vol.II), 112-19)
WALLACK, Stanley, Timing circuitry incorporating radioactive batteries, 19: 44364
WALLER, J. W., Schlieren photography of first half cycle of a theta pinch discharge, 19: 45421
WALLET, Philippe, Remote control apparatus, 19: 44180
WALLIS, G. B., Prog. rpt. on two-phase flow and boiling heat transfer, 4–6/65, 19: 44192 (NYO-3114-9)
WALTER, S., Enrichment of deuterium by countercurrent isotope exchange between hydrogen and ammonia in a hot-and-cold plant, 19: 44574
WALTHER, M. F., Proposed filtered shielded connector for protection of

weapons from electromagnetic radiation, 19: 44166 (NP-15472)
VALTON, R. B., Delayed γ rays from fission, 19: 45245 (AFWL-TR-65-95)
VAMANACHARYA, G. S., Electroplating of ^{109}Cd on copper wires, 19: 44139 (ORNL-TM-1174)
VANG, Chien-Wu, Use of silicon surface-barrier detectors compensated by lithium for measurements of energies of protons and deuterons up to energies of 13 Mev, 19: 44471 (ZFK-PHA-12, pp 30-2)
VANG, H. C., Case of double trisomy: trisomy No. 18 and triplo-x, 19: 43811
VANG, Shih-ri, Uranium-235 fission cross section for resonance neutrons, 19: 45299
VANG, Yung-chang, Uranium-235 fission cross section for resonance neutrons, 19: 45299
VARD, B. J., Plutonium sheet fabrication, 19: 44654
VARD, Robertson, Tumors of thyroid and parathyroid glands, 19: 43892
VARDA, E., Use of the chopper for pulse neutron measurements, 19: 45222 (INR-624/IX-A/R)
VARDLEWORTH, D., Nineteen-group extension to the Yiftah, Okrent and Moldauer cross-section set, 19: 45244 (AEEW-M-472)
VARNER, R. E., Proton-proton bremsstrahlung cross sections at 48 Mev, 19: 45097
VARREN, E. S., Influence of focusing on the apparent reflection coefficient of the F region, 19: 45175
VASSON, H. R., Why and how of nuclear accident dosimetry, 19: 44320
VATAGHIN, G., Two-prong proton-antiproton annihilation with formation of a pair of charged mesons, 19: 45066
VATANABE, K., Normalization of Bethe-Salpeter amplitude, 19: 45078
VATANABE, Myohei, Rectal injury resulting from ^{60}Co irradiation treatment for cervical carcinoma, 19: 43907
VATERBURY, G. R., Determination of trace amounts of oxygen added to metallic sodium, 19: 43932 (LA-3343)
VATERBURY, Glenn R., Inert atmosphere enclosure for the preparation of samples prior to determination of oxygen, 19: 43933 (LA-3344)
VATERBURY, Glenn R., The controlled potential electrodeposition of cobalt from plutonium–cerium–cobalt alloy solutions, 19: 43934 (LA-3345)
VATERS, J. R., Positions of three cosmic x-ray sources in Scorpio and Sagittarius, 19: 44968
VATERS, J. R., Spectral data from cosmic x-ray sources in Scorpius and near the galactic center, 19: 44967
VATSON, J. W., New excited state of ^{8}Li, 19: 45348
VATSON, Kenneth M., Accuracy of measurement for counting and intensity-correlation experiments, 19: 45151
VATSON, R. D., High-pressure rotary face-type shaft seals for water applications, 19: 44132 (AECL-2249)
VATT, William, Process for making carbon articles from carbon particles and furane derivatives, 19: 44669
VATTS, T. D., Calculations of charge and contour dimensions of powder-loading assembly used in the production of HFIR composite fuel compacts, 19: 44641 (ORNL-TM-1193)
VAUGH, J. S., Strong coupling in nuclear resonance spectra. V., 19: 44945
VAYLAND, J. Robert Jr., Sampling bias in scanning proton-recoil tracks in nuclear emulsion, 19: 44464 (UCRL-11703)
VEAVER, Boyd, Behavior of the transplutonium elements in solvent extraction systems, 19: 44115 (ORNL-P-1577)
VEBB, M. S. W., Performance of plasma jet in elimination of matrix effects due to phosphate and Al, 19: 43924 (AERE-R-4990)
VEBER, Hans J., Photon absorption cross section of spherical nuclei, 19: 45366
VEBER, Jon H., Oxygen isotope fractionation between coexisting calcite and dolomite in the freshwater upper carboniferous Freeport Formation, 19: 44241
VEBSTER, H. F., Efforts to increase thermionic converter output and efficiency, 19: 44985
VEHRING, B. W., Time delays in K x-ray emission during thermal fission of ^{235}U, 19: 45294
VEI, E. L., Strong coupling in nuclear resonance spectra. V., 19: 44945
VEIDMAN, R. H., Emulsion grain density in the extreme relativistic region, 19: 44428 (CERN-65-4(Vol.II), pp IX9-13)
VEIGEL, Fritz, Preparation and properties of promethium and some of its compounds, 19: 43988 (CONF-650804-7)
VEILL, R., Sensitivity of normal and hypersensitive Ilford K5 emulsions at low temperatures, 19: 44405 (CERN-65-4(Vol.II), pp IV33-40)
VEILL-COHEN, A., Chemical dosimetry of high-energy particles, 19: 44093
VEINREB, A., Study of liquids under optical and ionizing excitation with emphasis on excitation in the vacuum ultraviolet, 19: 44059 (NYO-2949-1)
VEINREICH, Marcel I., Numerical solution of some problems of gas flows, 19: 44200 (SC-T-65-756)
VEINSTEIN, R., Effect of peak broadening on structure in the region of the ρ^0 meson, 19: 45092
VEINSTEIN, Richard H., Experiments in a hollow cathode Hall current accelerator, 19: 45443
VEIR, J. R., Effect of irradiation on the mechanical properties of stainless steel at 750°C under constant stress rate conditions, 19: 44750 (ORNL-TM-1216)
VEISS, E., Prog. rpt. on critical heat flux (burnout) in boiling H_2O, 10–12/64, 19: 44184 (EURAEC-1281)
VEISS, P. B., Experimental studies with the Astron facility, 19: 45413 (UCRL-12456)
VEISSBECKER, L., Polycythemia, osteomyelofibrosis, and acute leukemia, 19: 43820
VEISSGLAS, P., Nonlinear plasma wave interaction in an arc discharge, 19: 45419
VEISSKOPF, Victor F., Quantum theory and elementary particles, 19: 44994 (CERN-65-26)
VELCH, M. J., Reactions of hot tritium atoms with the system ethane and oxygen, 19: 44106
VELSH, W. F., Determination of absolute power in SNAP-50 critical assemblies by ^{140}Ba fission product measurements, 19: 45656 (PWAC-474)
VENGER, P., Fallout radioactivity at Geneva for the year 1963, 19: 44269
VERNER, R., Design of Modulo-N counters for any code, 19: 45719 (UCRL-12012)
VERNER, W. J., Calculations of charge and contour dimensions of powder-loading assembly used in the production of HFIR composite fuel compacts, 19: 44641 (ORNL-TM-1193)
VERTHAMER, N. R., Proximity effect between a superconducting and a ferromagnetic film, 19: 45197
VERTHEIMER, M., Observation of speed of flux jumps in superconducting Nb, 19: 45199
VEST, Robert, Pentamethyldisilane and 1,1,2,2-tetramethyldisilane, and their addition to olefins, 19: 44048 (TID-21309)
VEYERS, J., Diffusion in the 4-body systems, 19: 44815
VHANG, Y. C., Inviscid model of the solar wind, 19: 44904
VHARTON, C. B., Flute characteristics of and microwave emission from a plasma in a mirror, 19: 45388 (GA-6432)
VHEELER, R. C., Reactivity feedback in the Dounreay fast reactor, August 1962–December 1963, 19: 45594 (TRG-Report-864)
VHITE, C. W., Energy storage capacitors for pulsed plasma thrustors, 19: 44224
VHITE, David, Crystal structure of solid deuterium from neutron-diffraction studies, 19: 45211
VHITE, J. T., Fading in thermoluminescent lithium fluoride used for radiation dosimetry, 19: 44076
VHITE, L. E., Nuclear vehicle technology and testing—engine systems, 19: 45663
VHITE, M. G., Operating experience and improvements on the Princeton–Pennsylvania accelerator, 19: 44872 (PPAD-2137-565)
VHITING, A. R., Prog. rpt. on fatigue strength of pressure vessels, 7/15/65, 19: 45503 (SWRI-1228-69)
VHITTLE, I., Oxidation of the U–Cu intermetallic compounds UCu_5 in CO_2 between 350 and 850°C, 19: 44631
VICHRZYCKA, Elzbieta, Changes in alkaline phosphatase in granulocytes of chemical workers and radiologists, 19: 43829
VICKER, James E., Effect of γ radiation upon operant water-reinforcement behavior, 19: 43808
VIDDOWSON, E. M., Metabolism of Ca, P, Mg and strontium, 19: 43701
VIDELL, C.-O., Background and measurability of test samples in an emergency situation, 19: 44325
VIECZORKOWSKI, M., Dispersion fuel elements for experimental and university reactors, 19: 45547 (INR-585/XIV/R)
VIENER-CHASMAN, Renate, Neutron cross sections. Z = 88 to 98, 19: 45250 (BNL-325(2nd Ed.)(Suppl.2)(Vol.III))
VIGLEY, Neil M., Development of the mapping function at a corner, 19: 45702 (LA-DC-6558)
VILCOX, Roy C., Governing factors in the formation of Cr_3O-type structures, 19: 44702 (TID-22200)
VILCOX, W. J. Jr., Fabrication of calorimeter elements, 19: 44344 (K-L-1944)
VILDY, P. C., Performance of plasma jet in elimination of matrix effects due to phosphate and Al, 19: 43924 (AERE-R-4990)
VILIP, Elmer K., Real part of the forward scattering amplitude of charged particles, 19: 45048 (ANL-Trans-217)
VILKEN, Andrew C., A precision analog memory with nondestructive readout using multiaperture ferrite cores, 19: 44350 (SC-R-65-959)
VILKINSON, I., Laboratory investigation of geomagnetic dynamos, 19: 45156 (AFCRL-64-768)
VILLIAMS, C. J., Neutron irradiation of Linde Molecular Sieve 13X, 19: 44091
VILLIAMS, D. J., Loss and replenishment of electrons at middle latitudes and high B values, 19: 45161
VILLIAMS, J. H., Polarization of 39-Mev protons elastically scattered

from ^{58}Ni and ^{60}Ni, 19: 45378
WILLIAMS, Marilyn H., Growth curve for mammary fibroadenoma in female rat, 19: 43649 (UCRL-16177)
WILLIAMS, W. S. C., S-wave π-π final-state interactions in $\pi^- + p \to \pi^0 + \pi^0$, 19: 45089
WILLIAMSON, H. E., Performance of fuel rods to investigate increased thermal output capabilities, 19: 45573 (GEAP-4902)
WILLIAMSON, K. D. Jr., Further experimental study of H_2O--LH_2 heat exchangers, 19: 44186 (LA-DC-7148)
WILLMANN, R. B., Single-particle exchange in N^{*++} production in π^+p collisions, 19: 44997 (COO-1426-14)
WILSKE, Kenneth R., Autoradiographic localization of lipid- and water-soluble compounds: a new approach, 19: 43696
WILSON, G. M., Effect of irradiation on function and survival of rat thyroid cells, 19: 43757
WILSON, Kenneth G., Model Hamiltonians for local quantum field theory, 19: 45150
WILSON, R. F., SNAP-10A design, development, and flight test, 19: 45154
WILSON, V. C., Efforts to increase thermionic converter output and efficiency, 19: 44985
WILSON, W. E. C., Erythrocyte chimerism and acquired immunologic tolerance, 19: 43657
WINCKLER, J. R., Modulation of primary spectrum during the recent solar cycle for rigidities between 4 and 12 Bev, 19: 44965
WINCKLER, J. R., Response of ion chambers in free space to long-term cosmic-ray variation from 1960 to 1965, 19: 44966
WING, R. O., Properties of plutonium dioxide, 19: 43995 (RFP-503)
WINICUR, Sandra, Biochemical studies on irradiated protozoa. II., 19: 43812
WINKELMANN, R. K., Pigment activity in dermal nevi induced by uv light: an enzyme histochemical study, 19: 43809
WINSLOW, Alan M., Magnetic field calculations in an irregular triangle mesh, 19: 44811 (UCRL-7784-T(Rev.1))
WINSLOW, F. R., Diffusion of ^{181}Hf in bcc hafnium, 19: 44729
WINTERNITZ, P., Baryon annihilation in broken U(12) symmetry, 19: 45008 (JINR-E-2246)
WINTERNITZ, P., Current-generated algebras and form factors, 19: 45011 (JINR-E-2294)
WISSLER, Robert W., Migration of spleen cells into blood stream following antigen stimulation, 19: 43822
WIT, Romuald, Lower bound of the forward unsymmetrized scattering amplitude, 19: 45040 (TPJU-11/65)
WIT, Romuald, New restriction on the forward scattering amplitude in local field theory, 19: 45039 (TPJU-10/65)
WITSKEN, J. R., Order code for the film scanners of Illiac III, 19: 44446 (COO-1018-1050)
WITTMIER, J., Quality control of ^{90}Sr-containing food, 19: 43675 (UCD-472-112, pp 73-9)
WOHL, Charles Gordon, K-p charge-exchange scattering from 1200 to 1700 Mev/c, 19: 45045 (UCRL-16288)
WOLBERG, John R., Analysis of technique of least squares as related to γ scintillation spectroscopy, 19: 43981
WOLF, B., Tensor force in the nucleus ^{19}F, 19: 45370
WOLF, H., Absorption and deposition of ^{89}Sr and ^{47}Ca from ligated intestinal segments of adult beagles, 19: 43677 (UCD-472-112, pp 86-96)
WOLF, H., Radium metabolism by beagles following single and multiple injections, 19: 43678 (UCD-472-112, pp 97-108)
WOLF, H., Strontium deposition in bone and teeth of beagle puppies, 19: 43676 (UCD-472-112, pp 80-5)
WOLNIEWICZ, L., Potential-energy curves for $X^1\Sigma_g^+$, $b^3\Sigma_u^+$, $C^1\pi_u$ states of the hydrogen molecule, 19: 44946
WOMACK, J. R., Preliminary investigations to determine nuclear-electric spacecraft configurations for high-energy missions, 19: 44228
WOOD, Floyd W., Studies of high-current metallic arcs, 19: 44608 (TID-22125)
WOODALL, A. H., Thyroid function in rainbow trout. I., 19: 43773
WOODWELL, George M., Radiation and the patterns of nature, 19: 43711 (BNL-924)
WOOLLETT, Richard R., Energy addition to an atomic hydrogen plasma at off-resonant conditions, 19: 45400 (NASA-TN-D-2982)
WOOLLEY, Joseph T., Radial exchange of labeled water in intact maize roots, 19: 43702
WOOLSEY, R. E. D., On integer linear programming in combinatorial analysis, 19: 45709 (SC-R-65-963)
WOOTEN, F., Studies of band structure and electron scattering in Al by photoemission, 19: 45481 (UCRL-12470)
WORDINGHAM, M. L., Performance of plasma jet in elimination of matrix effects due to phosphate and Al, 19: 43924 (AERE-R-4990)
WORRELL, Wayne L., Carbothermic reduction of alumina: a thermodynamic analysis, 19: 43996 (UCRL-11699)
WORTON, R. G., Thermoluminescent dosimeter, 19: 44541

WOZADLO, G. P., Corrosion of carbon steel in simulated boiling water and superheat reactor environments, 19: 44627
WRAIGHT, L. A., Pulse shape discriminators for scintillators containing ZnS(Ag), 19: 44368 (AERE-M-833)
WROE, H., Preliminary results from single-gap preinjector, 19: 44885
WU, Tai Tsun, Regge poles in quantum electrodynamics with massive photons, 19: 45114
WURSTER, D. E., Development of realistic requirements for PM-type reactor instrumentation. Task 1 topical report, 19: 45584 (NYO-3379-1)
WYATT, Samuel B., Safety fluoroscope with an alerting device of contrasting color surrounding the screen, 19: 44362
WYMAN, M. E., Dynamics of a Triga-type reactor, 19: 45685
WYMAN, M. E., Time delays in K x-ray emission during thermal fission of ^{235}U, 19: 45294

Y

YAEGER, J. A., Polarizing microscopy of abnormal dentine produced by injections of strontium or fluoride, 19: 43687
YAGISAWA, Toshi, High-dose ratemeter based on measurement of electric resistance of liquid organic compounds, 19: 44525
YAKOVLEV, V. P., Electron-positron pair formation by a strong electromagnetic wave in the field of a nucleus, 19: 45128
YAM, Kai-Ming, Mechanism of action of 2-mercaptoethylamine, 19: 43670 (NP-15310, pp 36-47)
YAMADA, Hideo, Detection of portal systemic shunts by hepatopulmonary scanning using ^{131}I MAA. III., 19: 43904
YAMAGATA, Noboru, Japanese dietary habits and the fallout problem. II., 19: 44264
YAMAGATA, Noboru, Radioactive contamination of milk in Japan (1961-1963), 19: 44268
YAMAMOTO, Kiyoko, Effect of γ-radiation on porphyrin-metal complexes. I., 19: 44087
YAMAMOTO, Koji, Protective effects of chemicals on radiation induced damages in seed-treated crop plants, 19: 43877
YAMAMOTO, Yutaka, Prog. rpt. on processing radioactive liquid wastes by evaporation, 1-6/64, 19: 45688 (NP-15367)
YAMASHITA, Hiroshi, Photoreactions in ^{28}Si nucleus by monochromatic γ rays, 19: 45310
YAMASHITA, Sukeaki, Quasi-free α-α collisions in ^{9}Be and ^{12}C at 28 Mev, 19: 45308
YAMAZAKI, Hideo, Radiolysis of chloroauric acid in aqueous solution, 19: 44079
YAMAZAKI, Takashi, Scattering of alpha particles from medium-weight nuclei, 19: 45312
YANABU, Takuji, Quasi-free α-α collisions in ^{9}Be and ^{12}C at 28 Mev, 19: 45308
YANDAKUROV, Yu. V., Magnetohydrodynamic instabilities in electrical explosion, 19: 44845
YANTOVSKII, E. I., Longitudinal electromotive forces and Hall effect in channel flow of ionized gas, 19: 44831
YARMONENKO, S. P., Chemical preparations for prevention of radiation injuries, 19: 43861 (JPRS-31349, pp 1-24)
YARMONENKO, S. P., Effectiveness of recovery of mice following their exposure to 660-Mev protons, 19: 43771
YASUKAWA, Satoshi, Scattering of alpha particles from medium-weight nuclei, 19: 45312
YAZVITSKII, Yu., Decay mode of ^{147}Eu, 19: 45267 (JINR-P-2161)
YEN, Wu-kuang, Elastic scattering of Λ hyperons on protons, 19: 45016 (JINR-P-2257)
YEVICK, George J., Prog. rpt. on cusped containment geometries, annual, 1964-65, 19: 45406 (SIT-2852-17)
YIFTAH, S., Calculation of Doppler effect in fast reactors, 19: 45576 (IA-1039)
YING, Shuh-pan, Under Na scanner, 19: 44342 (APDA-174, pp 67-70)
YOKOTA, Ryosuke, ESR studies of radiophotoluminescent centers in silver-activated phosphate glass, 19: 44758
YONTS, O. C., Isotopic contamination in electromagnetic separators, 19: 44573 (ORNL-P-515)
YOSHIKAWA, S., Plasma confinement in the model C stellarator, 19: 45397 (MATT-282)
YOSHIMURA, T., Broken symmetry and possibility of superforbidden processes, 19: 45059
YOSHIMURA, T., Comment on the bootstrap mechanism, 19: 45090
YOSHIZAWA, Tadayoshi, High-energy radiation measurement in the exosphere by Explorer VII, 19: 44973
YOSHIZAWA, Y., Coulomb excitation of vibrational states in deformed even nuclei, 19: 45321
YOUNG, C. W., Prog. rpt. on containment capsule impact safety, Phase A, 7/65, 19: 44298 (SC-RR-65-9)
YOUNG, D. E., Design of proton linear accelerators for energies up to 200

Rev, 19: 44867 (MURA-713)
YOUNG, J. E., Composition of the giant dipole state, 19: 45334
YOUNG, J. F., Forecast of the energy future, 19: 45725
YOUNG, K. M., Plasma confinement in the model C stellarator, 19: 45397 (NATT-282)
YOUNG, L. G., Radium metabolism by beagles following single and multiple injections, 19: 43678 (UCD-472-112, pp 97-108)
YOUNG, L. G., Strontium-90 uptake and retention in labeled beagles, 19: 43679 (UCD-472-112, pp 109-19)
YOUNGBLOOD, D. H., Radiative lifetime of the first excited state of ^{41}Sc, 19: 45344
YU, T. C., Irradiation-sterilized shelf-stable fish and seafood products, 19: 44556 (NP-15464)
YUASA, S., Base composition of messenger RNA of Pseudomonas effusa irradiated with uv light, 19: 43744
YUKIO, Miyazaki, High-energy radiation measurement in the exosphere by Explorer VII, 19: 44973
YURCHENKO, A. F., Regression of sensitivity and latent image in nuclear and light-sensitive photographic emulsions, 19: 44402 (CERN-65-4 (Vol.II), pp IV5-15)

Z

ZABOROWSKI, H., Establishment of neutron fluxes and doses after criticality accident, 19: 44323
ZACHVEJ, J., Myorelaxant effect of gallamine and tubocurarine in irradiated rabbits, 19: 43871
ZADUBAN, M., Contribution to the determination of ^{131}I by an extraction method, 19: 43953
ZAJEC, Emery, Prog. rpt. on Bevatron operation and development, 10-12/64, 19: 44874 (UCRL-16203)
ZAJUSZ, Kazimiera, Effect of x rays on histological and some histochemical changes in rabbit lungs, 19: 43846
ZAKHAROV, V. I., Application of synthetic polymers in preparation of fine-grain nuclear emulsions. I. and II., 19: 44400 (CERN-65-4(Vol.II), pp III31-56)
ZAKHAROV, V. I., Spin precession in gravitational fields, 19: 45134 (NP-15397)
ZAKHAROV, V. I., The properties of fine-grained nuclear emulsion type PR-2, 19: 44404 (CERN-65-4(Vol.II), pp IV23-31)
ZALESKI, C. P., Fast reactor core design and safety studies in France and in the Federal Republic of Germany, 19: 45623
ZALEWSKI, Kacper, Classical phase-space integral in the statistical model with angular momentum conservation, 19: 45041 (TPJU-12/65)
ZALEWSKI, Kacper, Quantum statistics in statistical model of multiple production of particles, 19: 45038 (TPJU-7/65)
ZAMBROW, John L., Internally strengthened flat fuel plate, 19: 45554
ZAMOLODCHIKOV, B. I., Device for developing pulsed magnetic fields up to 150 kG, 19: 44888
ZAMORA, M., Contraction factor of Ilford G5 nuclear emulsions used in α spectrometry, 19: 44444 (CERN-65-4(Vol.II), pp X67-73)
ZANELLO, D., Test of charge-conjugation invariance in $\bar{p}p$ annihilations at rest, 19: 45124
ZAPOLSKAYA, N. A., Changes of cholinesterase activity in chronic administration of certain isotopes, 19: 43775
ZARINSKII, V. A., Silicate form of uranium transport in aqueous solutions, 19: 44278
ZDENEK, Roth, Leukocytes in the diagnosis of hematopoiesis impaired by ionizing radiation, 19: 44315
ZEL'DOVICH, Ya. B., Probability of quasar production, 19: 44922
ZELICHENKO, E. N., Optimum conditions of magnetogasdynamic channel flows accounting for Hall effect, 19: 44832
ZEMLYANOV, M. G., Cold neutron scattering by polyphenyls, 19: 45238
ZEMLYANOV, M. G., Dynamics of LiH and LiD in inelastic scattering of cold neutrons, 19: 44732
ZETTL, Anton, Related two-point boundary value problems and associated harmonic matrices, 19: 44582 (ORNL-3646)
ZHARINOV, A. V., Discharge instability with a heated cathode in a magnetic field at low pressures, 19: 45390 (IAE-780)
ZHDANOV, A. P., Registration of α-particle stars produced by radioactive nuclei and time discrimination of α-particle tracks in nuclear emulsions, 19: 44425 (CERN-65-4(Vol.II), pp VIII17-26)
ZHDANOV, G. B., Further development of apparatus for measurements of particle tracks in photoemulsions by television method, 19: 44422 (CERN-65-4(Vol.II), pp VII39-42)
ZHDANOV, G. B., Ionization-momentum dependence for electrons and positrons of high energy, 19: 44432 (CERN-65-4(Vol.II), pp IX41-3)
ZHDANOV, V. P., Theoretical grounds for the selection of developing agent for introducing it into the nuclear emulsion, 19: 44408 (CERN-65-4 (Vol.II), pp V9-15)
ZHEIGUR, B. D., Impulse method of measurements of flow rate of conducting fluid, 19: 44834
ZHELEV, Zh., Decay mode of ^{147}Eu, 19: 45267 (JINR-P-2161)
ZHELEZNYAKOV, V. A., Mechanism of γ emission by solar flares, 19: 44916
ZHELEZNYAKOV, V. V., Origin of solar radio bursts in the meter-wavelength range, 19: 44920
ZHELUDEV, I. S., Changes in domain structure of Rochelle salt crystals exposed to x rays, 19: 44031
ZHERNOV, A. P., Anharmonism influence on the phonon spectrum near the point of origin, 19: 45475 (IAE-750)
ZHERNOVOI, Aleksandr Ivanovich, Nuclear magnetic resonance in a flowing liquid, 19: 44813 (NP-tr-1307)
ZHERNOVOY, A. I., Application of proton resonance to the measurement of inhomogeneous magnetic fields, 19: 44353 (SLAC-Trans-22)
ZHIDIKOVA, A. P., Silicate form of uranium transport in aqueous solutions, 19: 44278
ZHUKOV, A. V., Models of the temperature fields of fuel elements in the active zone and shield of the BN-350 reactor, 19: 45604 (JPRS-31245)
ZICHICHI, A., Measurements of muon depolarization in several materials, 19: 45080
ZICHICHI, A., New electron detector with high rejection power against pions, 19: 44522
ZICHICHI, A., Quenching of muon depolarization in several materials as function of externally applied magnetic fields, 19: 45079
ZIESKE, P., Composition of noble gas ion beams produced with a duoplasmatron, 19: 45385 (D1-82-0437)
ZIESKE, P., Production of dense beams of low-energy ions, 19: 45384 (D1-82-0436)
ZIJP, W. L., Compilation of neutron flux density data in the HFR, 19: 45681 (RCN-36)
ZILSEL, P. R., Pseudospin model of liquid ^4He, 19: 45203
ZIMIN, A. V., Flow method of irradiation with ionizing rays, 19: 44061 (AEC-tr-6567)
ZIMMERMAN, G. O., Dielectric constant of ^3He in the critical region, 19: 45205
ZIZIC, B., Sensitivity centers and latent image distribution as factors of nuclear emulsion properties, 19: 44392 (CERN-65-4(Vol.II), pp II44-9)
ZIZZA, M., Why not single-purpose reactors for desalting, 19: 45634
ZLATEVA, A., Real part of the elastic p-p scattering amplitude at 2, 4, 6, 8, and 10 Bev, 19: 45021 (JINR-P-2336)
ZMUDA, A. J., VIf phase perturbations and the Soviet high-altitude nuclear bursts of October 22 and 28, 1962. I., 19: 45166
ZMUDA, A. J., VIf phase perturbations and the Soviet high-altitude nuclear bursts of October 22 and 28, 1962. II., 19: 45167
ZOLLMAN, D. A., Antimony-124 spectrum shape, 19: 45328
ZOLOTUKHIN, V. G., Analysis of systematic error due to differentiation of spectra measured by fast neutron single crystal scintillation spectrometer, 19: 44493
ZOLOTUKHIN, V. G., Matrix treatment of data obtained by fast neutron single-crystal scintillation spectrometer, 19: 44492
ZOLOTUKHIN, V. G., Possibility of using nuclear reactor in cosmic space for measuring cross sections of n-n scattering, 19: 45036 (NP-15476)
ZUBER, H., Prog. rpt. on two-phase flow, 4-6/65, 19: 44185 (GEAP-4910)
ZUCKER, A., Nuclear physics: a status report, 19: 45372
ZUCKERMAN, Solly, Sensitivity of gonads to radiation, 19: 43756
ZUEV, A. P., Effect of heat treatment of MnO_2 on rate of oxygen isotope exchange, 19: 44104
ZUPANCIC, I., Nuclear spin relaxation by fixed damage centers in irradiated $NaH_3(SeO_3)_2$, 19: 45477 (NIJS-R-444)
ZVONOV, N. V., Studies on the use of organic coolant-moderators in nuclear reactors, 19: 45501 (IAE-611)

SUBJECT INDEX

Main entries in this index are generally specific materials, things, and processes. These are followed by modifiers that describe the properties of, and processes applied to, the main entries.

The number preceding the colon is the *NSA* volume number, and the number following is the abstract number. The designation (R) following the abstract number indicates that the abstract is of a progress report; (P) indicates a patent; and (T) indicates a translation. Abstracts for reports other than progress reports carry no letter designation. References to report numbers, where appropriate, are included after the abstract number of the citation. Published literature (journal article or book) is identifiable by the absence of a report number.

The user should bear in mind that the ideas presented in the original literature, rather than key words, have been indexed. The indexers have tried to select what seemed the most probable and logical place to look for typical information. Since it is not possible to anticipate where a user would look for information, numerous cross references are included to assist him in his search.

Experience in using an index of this type will be the best guide in obtaining the desired information, and a consideration of synonymous or closely related terms will prove valuable.

Information must be so indexed as to be of the greatest use to the greatest number of users. This requires that a topic be indexed to headings that most specifically describe it and not ordinarily to the headings that describe its ultimate use, nor to the general class headings that include the specific headings. For example, information on the treatment of thyroid disease with I-131 would be indexed under Thyroid Diseases and under Iodine Isotopes I-131, but not necessarily under Radiotherapy. A study of the effects of x radiation on hair would be indexed under both X Radiation and Hair.

The broad, general class headings are used only for general information or for comprehensive reports or articles.

Subject Heading Styles

Generally, the direct form of subject entry is used rather than inverted headings or, in some cases, subheadings; e.g., Amino Acids rather than Acids, amino; Helium Isotopes He-4 rather than Helium — isotopes He-4 or Helium — He-4 isotopes. Note, however, that in some cases modifying terms are used parenthetically in preference to a more direct type of entry which would result in the scattering of information. Organic compounds, however, are usually entered in the index in the inverted form so that substituted compounds can be listed near the parent compound; e.g., Benzene, Bromo- rather than Bromobenzene. In general, the style of nomenclature used is that of *Chemical Abstracts*, except that some items listed in that publication as subheadings are elevated to form part of the main heading; e.g., Butyric Acid, Methyl Ester rather than Butyric Acid — methyl ester.

Alphabetization

Main headings are arranged according to the widely accepted word-by-word alphabetic system. A parenthetic qualifier following a main heading is disregarded in alphabetizing unless there are two or more headings identical except for the parenthetic qualifier, in which case the qualifier determines the order. Headings involving Greek letters are arranged as if the names of the letters were spelled out, e.g., Mesons (π), Mesons (ξ).

Nomenclature of Inorganic Compounds

Inorganic compounds are indexed in the direct form, listing cations in the order of increasing valence in the case of polycationic salts of varying valence and in alphabetic order for polycationic salts in which all cations have the same valence; e.g., Sodium Aluminum Silicates and Potassium Sodium Sulfates.

Multicomponent Systems

Multicomponent alloys, except well-known trade names, are indexed under each element in the alloy.

Example: Aluminum–Chromium Alloys are indexed

ALUMINUM ALLOYS
  Al–Cr ...
CHROMIUM ALLOYS
  Al–Cr ...

Well-known alloys such as Hastelloy are indexed directly. Cross references appear in the index cumulations. Multicomponent systems of elements are indexed similarly.

Example: Silicon–Tungsten Systems are indexed

SILICON SYSTEMS
  Si–W ...
TUNGSTEN SYSTEMS
  Si–W ...

Multicomponent systems of compounds are similarly indexed under the compound.

Physical States of Materials

Specification of the physical state of the material, if other than normal, is included in the modifying phrase.

Modifying Phrases (Subheadings)

Whenever it appears that such information would be useful, descriptive phrases (modifiers), rather than ordinary subheadings, are used under the main headings to give a better indication of the material covered in an abstract. Such phrases are written so that the idea considered most important is presented first. However, when using this index, the reader is advised to scan all modifiers under a main heading to determine whether any abstracts in addition to the most obvious should be consulted for the desired information. Many of the modifiers are designed to be read in inverted order or to be read with the main heading inserted at the position of the comma in order to obtain a meaningful phrase; e.g., Uranium–allotropic transformation temperatures of, effect of cooling rate on is read "effect of cooling rate on allotropic transformation temperatures of uranium." In many cases, the prepositions have been

omitted from such phrases provided no ambiguity results from the omission.

For entries concerned with physics, if the modifier does not indicate whether the reference is experimental or theoretical, a symbol E or T or E/T is given.

Conferences

Proceedings of conferences and conference papers are included in the Report Number Index.

A

ABSTRACTS
on analytical methods for plutonium, 19: 43925 (ANL-6956)
on computer programs for calculations in nuclear physics, 19: 45251 (BNL-9108)
on desalination of brackish or saline waters by nuclear energy, 19: 45590 (TID-3584)
on nuclear cross section measurement, reports for AEC program on, 19: 45288 (WASH-1056)
on physics research, 19: 44812(R) (UCRL-16099)
ACCELERATORS
beam focusing in tube for, electron, (T), 19: 44870 (NP-15388)
cavity resonator coupling elements for, equivalent circuit for, 19: 44859 (BNL-9496)
design parameters for high-performance Hall-current plasma, 19: 45444
instrumentation developments for electron, 19: 44357
magnetic field calculations for, method for nonlinear, 19: 44876 (UCRL-16287)
magnets for, feasibility of superconducting thin-septum, 19: 44877 (UCRL-16346)
performance of electron, for artificial radiation belt production, 19: 45159 (UCRL-14374)
performance of quasi-steady-state pulsed plasma, 19: 45441
plasma diagnostic studies in Hall-current, 19: 45446
plasma, gas density measurements in pulsed coaxial, (E), 19: 45449
plasma, performance of hollow cathode Hall current, 19: 45443
storage rings for, beam fluctuations and losses in, 19: 44865 (LAL-1134)
ACCIDENTS
clinical and dosimetric study of linear accelerator, 19: 44331
detection of criticality, alarm system for, 19: 44321
dosimetry of criticality, use of activation detector with spectrometer for, 19: 44537
Hanford criticality, dosimetry problems in, 19: 44330
neutron dose and flux measurements in criticality, using multi-sphere technique, 19: 44323
radiation dosimetry in, clinical and hematologic test for gamma, 19: 44316
radiation dosimetry of personnel in criticality, 19: 44319 (STI/PUB/99)
radiation dosimetry in nuclear, program for, 19: 44320
radiation dosimetry of, use of activation detectors for, 19: 44332
radiation dosimetry of personnel in event of, system for, 19: 44333
radiation dosimetry system for fast-critical assembly criticality, 19: 44334
radiation dosimetry in, program for, 19: 44336
radiation exposure in, use of blood picture in estimating, 19: 44315
radiation exposure to personnel in, role of laboratory and methods used in event of, 19: 44324
radioactivity in vicinity of reactor, background, 19: 44325
ACETAMIDE, IODO-
radiosensitivity effects on bacteria, 19: 44552 (BLG-327)
ACETIC ACID, [(CARBOXYMETHYLIMINO) BIS(ETHYLENENITRILO)] TETRA-
complexes with sodium, effects on strontium-85 elution from mouse bones, 19: 43706
use as eluant in ion exchange purification of fission-produced samarium, 19: 44116 (ORNL-TM-1062)
use in TALSPEAK solvent extraction process for actinide–lanthanide group separation, 19: 44115 (ORNL-P-1577)
ACETIC ACID, (ETHYLENEDIAMINE) TETRA-
complexes with sodium, effects on strontium-85 elution from mouse bones, 19: 43706
solvent properties for strontium and yttrium, 19: 44120
ACETIC ACID, (ETHYLENEDIAMINE)TETRA-, CALCIUM SALTS
complexes with sodium, effects on strontium-85 elution from mouse bones, 19: 43706
ACETIC ACID, (ETHYLENEDIAMINE) TETRA-, SODIUM SALTS
effects on strontium-85 elution from mouse bones, 19: 43706
protective effects against radiation damage in crop plants, 19: 43877
ACETIC ACID, FLUORO-
effectiveness in removal of radioisotopes from body, 19: 43700
ACETIC ACID, IODO-
effects on strontium-85 elution from mouse bones, 19: 43706
ACETIC ACID, VINYL ESTER
polymerization pre-irradiated cotton fibers, 19: 44094
ACETIC ACID, VINYL ESTER POLYMERS
polyvinyl acetate-polyvinyl chloride, preparation of thin films of, (E), 19: 44590 (CEA-R-2803)
ACETONE, THENOYLTRIFLUORO-
complexes with rare earths, preparation and properties, 19: 44006
benzene–thenoyltrifluoracetone, solvent properties for pentavalent protactinium, 19: 44012
ACETYLENE
radiolysis of, effects of foreign ions on, 19: 44082
ACIDS
proton motion in aqueous solutions of, 19: 44037
ACOUSTIC WAVES
propagation of ion, in collisionless plasma, (E), 19: 45404 (ORNL-P-1557)
ACRIDINES
genetic effects of acridine orange in *Escherichia coli*, 19: 43794
ACROLEIN
radioinduced polymerization of, at −78 and −196°C, 19: 44070
ACRYLIC ACID, ETHYL ESTER
radioinduced graft polymerization with polyethylene and polyvinyl chloride, 19: 44083
ACRYLIC ACID, METHYL ESTER
radioinduced graft polymerization with polyethylene and polyvinyl chloride, 19: 44083
ACRYLONITRILES
polymerization pre-irradiated cotton fibers, 19: 44094
ACTINIDES
distribution in fused salt-cation exchanger systems, 19: 44040
separation from debris formed by nuclear explosion in salt formation, 19: 44156 (DP-956)
separation from lanthanides, TALSPEAK process for, 19: 44115 (ORNL-P-1577)
ACTINIUM ISOTOPES
neutron cross sections of, tabulation, (E), 19: 45250 (BNL-325(2nd Ed.) (Suppl.2)(Vol.III))
ACTINOMYCIN
effects on macromolecule synthesis in developing sea urchin eggs, 19: 43709
ACTIVATION ANALYSIS
development for determination of trace elements in organic liquids, 19: 45679(R) (NYO-1859-11)
gamma spectra analysis by method of least squares in, 19: 43981
instruments for industrial neutron-, design of, (E), 19: 43977
use for biomedical samples, 19: 43659
use to determine origin of opium samples, 19: 43937 (ORNL-TM-1263)
uses in criminal investigation, 19: 43959
ACTIVATION DETECTORS
design and fabrication of bead chain, for neutron flux determination, 19: 45560 (ANL-7011)
evaluation of, for assessing high-energy radiation doses, 19: 44535
performance for neutron flux determination in reactors, 19: 45560 (ANL-7011)
use for neutron dosimetry of accidents, 19: 44332
use of aluminum–cobalt and iron, for neutron fluxes in capsule irradiations, 19: 45542(R) (BAW-272)
use with spectrometer for criticality accident dosimetry, 19: 44537
ADDITION COMPOUNDS
radiation effects on argon, neutron, 19: 45679(R) (NYO-1859-11)
uses of krypton-85 quinol clathrates for inverse radiometric analysis of atmospheric sulfur dioxide, (E), 19: 44458 (NYO-2767)
ADENOSINEPHOSPHORIC ACIDS
effects on heartbeat, 19: 43681(R) (UCLA-12-565, pp 17-31)
effects on strontium-85 elution from mouse bones, 19: 43706
hydrolysis of, catalytic effects of thorium and zirconium ions on, 19: 43708
protective effects against radiation damage in crop plants, 19: 43877
ADENYL PYROPHOSPHATASE
effects of strontium on activity of, in rat liver mitochondria, 19: 43688
ADRENAL GLANDS
radiation exposure of, effects on cardiac decompensation, 19: 43919
ADRENAL HORMONES
protective effects of, against radiation injuries in rat spleen, 19: 43860(R) (NP-15310, pp 14-25)
ADRENOCORTICOTROPIC HORMONE
protective effects of, against radiation injuries in rat spleen, 19: 43860(R) (NP-15310, pp 14-25)
AERODYNAMICS
analysis of Saturn VN launch vehicles, 19: 44137 (N64-24017)
AEROSOLS
particle size distribution in radioactive atmospheric, collected in 1963 and 1964, 19: 44252 (NRL-6305)
penetration of filters by radioactive, measurement of depth of, 19: 44299 (SZS-2(1965))
sampling stratospheric, electrostatic precipitator development for, 19: 44801(R) (NYO-2363-3)
use of fluorescent, in in-place evaluation of filters, 19: 44208(R) (BMI-X-346)

use of radioactive, to test high-efficiency filters, 19: 44281 (AEET-202)
use to simulate fission products in Containment System Experiment, 19: 44286 (BNWL-SA-30)
AGE
effects on radiosensitivity of man, 19: 43915
radiosensitivity effects on mouse chromosomes, 19: 43729(T) (BNL-tr-12)
AGE ESTIMATION
argon–potassium method of, using nitrogen-15 as internal standard in argon determination, 19: 43960
methods for, lead–thorium–uranium, 19: 44272
methods of, comparison of radiocarbon and uranium-series-inequilibrium, 19: 44271
potassium–argon dating of rocks in Roskruge range in Pima County, Arizona, 19: 44236 (TID-22086)
AGRICULTURE
mutations in, use of, 19: 43656
water supplies for, use of nuclear desalting for, 19: 45636
AIR
analysis for iodine-131 by sorption on activated carbon and scintillation counting, 19: 43958
analysis for radon daughters, method for, 19: 44258
corrosive effects on A288 and X8001 aluminum alloys, 19: 44616(R) (ANL-7000, pp 122-37)
corrosive effects on plutonium–uranium alloys, effects on additions on, 19: 44587(R) (ANL-7000, pp 3-63)
effects on fatigue of molybdenum, 19: 44730
oxidative effects on aluminum–chromium–iron–yttrium alloy at 900 and 1100°C, 19: 44598(R) (GEMP-49A)
AIRCRAFT
hygrometer design for high-speed, 19: 44338 (AD-608496)
ALANINE
carbon-14 uptake by, in rat cerebral tissue, 19: 43690
synthesis of carbon-14-labeled DL-, 19: 44047 (NP-15268)
ALARM SYSTEMS
description of radiation, in ORNL High Radiation Level Examination Laboratory, 19: 44297 (ORNL-TM-1251)
design of individual, for personnel use, 19: 44532
development of fire, using ionization chamber, 19: 44355
development of, for criticality accident detection at nuclear plants, 19: 44321
ALASKA
cesium-137 content of man in Northern, 19: 44289 (HW-SA-3750)
sodium-22 content of Eskimos in, 19: 44289 (HW-SA-3750)
ALBUMINS
radiation effects on content in rats, x, 19: 43766
radiolysis of bovine serum, decomposition of sulfur linkage in gamma, 19: 43841
reactions with plutonium ions, bovine, 19: 43705
toxic effects of radioactive, on brain tissue, 19: 43883(R) (UCLA-12-565, pp 65-85)
tracer use of iodine-131-labeled macroaggregates of, 19: 43904
ALGAE
metabolism of radionuclides by marine, 19: 43669(R) (NP-15159)
radiation effects on calcium-45 uptake by *Nitella flexilis*, 19: 43818
ALKALI METAL CHLORIDES
diffusion of sodium-22-labeled aqueous solutions of, through membrane, 19: 44025
ALKALI METAL HALIDES
radiation damage at low temperatures to crystals of, x-ray-diffraction studies of beta, 19: 44745 (LA-DC-6725)
radiation effects on luminescence of doped, at 90 and 295°K, 19: 45488
radiosensitivity effects on bacteria, 19: 44552 (BLG-327)
spectra of, theory for Raman, 19: 44039
ALKALI METAL HYDROXIDES
performance as sensitizer for nuclear emulsions, 19: 44406 (CERN-65-4 (Vol.II), pp IV41-5)
ALKALI METAL IONS
photoinduced dissociation energies of gaseous, 19: 43997(R) (UCRL-11889)
ALKALI METALS
distribution in fused salt-cation exchanger systems, 19: 44040
electric and thermal conductivities of liquid, correlation over entire liquid range, 19: 44701(R) (TID-22144)
photoinduced dissociation energies of gaseous, 19: 43997(R) (UCRL-11889)
separation processes for, in spent reactor fuels, (E), 19: 45260(R) (IDO-14660)
sorption on metal surfaces, bonding in, (T), 19: 44981(R) (NP-15435)
use in seeding plasma, 19: 45456(P)
ALKALINE EARTH METALS
distribution in fused salt-cation exchanger systems, 19: 44040
separation processes for, in spent reactor fuels, (E), 19: 45260(R) (IDO-14660)
ALKENES
oxidation of, catalyst for, 19: 44043(P)
preparation of diolefins from olefins, catalyst for, 19: 44043(P)
ALLOYS
eutectics in binary, survey for aligned structures, 19: 44707 (WVT-6523)
research program on, 19: 43997(R) (UCRL-11889)
ALPHA BEAMS
radiosurgical use of, 19: 43905
ALPHA PARTICLES
angular correlations in deuteron reactions (d,α) with oxygen-16 at 5 to 9 Mev, 19: 45377
detection and identification using lithium-drifted silicon detectors, (E), 19: 44517
detection and measurement in atmosphere and body from reactor accident, 19: 44325
detection in nuclear emulsions, 19: 44389 (CERN-65-4(Vol.II), pp II17-18)
detection in nuclear emulsions, track discrimination in, 19: 44425 (CERN-65-4(Vol.II), pp VIII17-26)
detection in presence of deuterons, semiconductor detector for, 19: 45289 (ZFK-PHA-12, pp 99-105)
detection of, performance of nitrocelluloses for, 19: 44384 (CERN-65-4 (Vol.II), pp II-8)
detection of, performance of surface-barrier silicon detectors for, 19: 44469 (ZFK-PHA-12, pp 16-24)
detection of, semiconductor detector for, 19: 44476 (ZFK-PHA-12, pp 123-5)
effects on gonads of fish, 19: 43769
effects on mice, 19: 43831
effects on nuclear emulsions, dispersion of latent images in, 19: 44388 (CERN-65-4(Vol.II), pp III1-16)
effects on nuclear emulsions, latensification of latent image in, 19: 44391 (CERN-65-4(Vol.II), pp II29-42)
emission in lithium-6 and -7 reactions with nuclei, mechanisms for, (T), 19: 45264 (JINR-E-2243)
interactions with protons, phenomenological potential for phase shifts in, 19: 45109
neutron scattering by, phase shifts for, (T), 19: 45217 (COO-7-0363)
pathological effects on, in lungs, 19: 43824
ranges in bismuth-214 decay, (E), 19: 45293(T) (ORNL-tr-696)
reactions (α,nγ) with oxygen-18 at 2.50 Mev, angular correlations and distributions for, (E), 19: 45277 (NP-15363)
reactions (α,n) with nuclei at 2 to 5.4 Mev, neutron yield in, 19: 45301
reactions (α,2n) with beryllium-9 and carbon-12 at 28 Mev, spectra from, (E), 19: 45308
reactions (α,4n) with samarium-154 at 40 Mev, conversion electron anisotropy from, (E), 19: 45352
scattering by intermediate nuclei at 22.2 Mev, angular distributions from elastic and inelastic, (E), 19: 45312
scattering by lunar materials, interpretation of, 19: 44901
scattering by magnesium-24 at 28.5 Mev, excitation of 3+ state in inelastic, (T), 19: 45318
scattering by nickel-58 at 22.2 Mev, angular distributions from elastic and inelastic, (E), 19: 45312
spectra from alpha reactions (α,2n) with beryllium-9 and carbon-12 at 28 Mev, (E), 19: 45308
ALPHA SOURCES
content in air and water around Paducah Gaseous Diffusion Plant, Jan.-June 1965, 19: 44301 (TID-22172)
ALPHA SPECTROMETERS
nuclear emulsion contraction factor in, method for measuring, 19: 44444 (CERN-65-4(Vol.II), pp X67-73)
ALUMINATES
analysis for gallium by activation analysis and colorimetry, 19: 43961
ALUMINUM
analysis for trace amounts of copper by activation methods, 19: 43973
bremsstrahlung production by strontium-90–yttrium-90 beta particles in, (E), 19: 45284 (TID-22169)
corrosion by oxygenated-water, effects of polarizing current on, 19: 44617(R) (ANL-7000, pp 213-26)
deformation of polycrystalline, at high strain rates, 19: 43997(R) (UCRL-11889)
diffusion in zirconium, 19: 45471 (AECL-2309)
dislocation loops in pure, 19: 43997(R) (UCRL-11889)
effects on photonetric determination of zirconium, 19: 43972
effects on steam corrosion of Incoloy 800, 19: 44616(R) (ANL-7000, pp 122-37)

electron beam transmission through foils of, monoenergetic, (T), 19: 44818
electron structure, 19: 45481 (UCRL-12470)
equation of state of, to Debye approximation, 19: 43997(R) (UCRL-11889)
extrusion by hydrostatic methods, 19: 44651
fabrication of inner layer of composite fuel element can of, 19: 44661(P)
mechanical properties of 6061-T6, effects of strain rate on dynamic, 19: 44706 (UCRL-12264(Rev.1))
meson (μ^+) depolarization quenching in, as function of longitudinal magnetic field, (E/T), 19: 45079
meson (μ^+) depolarization in targets of, (E), 19: 45080
neutron cross sections for, from 0.414 ev to 5.5 Mev, 19: 45244 (AEEW-M-472)
neutron scattering by liquid, dynamics of, (E), 19: 45235
photon reactions in Bev range, meson (ρ^0) production in, (E), 19: 45000 (HUX-2752-7)
photon reactions with, electron emission in, (E), 19: 45481 (UCRL-12470)
plastic deformation of single crystals of, effects of size on, 19: 44705 (UCRL-11653)
radiation effects on corrosion and mechanical properties of, neutron, 19: 44752 (CEA-tr-A-1818)
radiation effects on faults in, as function of concentration, 19: 44755
stacking-fault energy of pure, 19: 43997(R) (UCRL-11889)
strain hardening of single crystals of, effects of polyslip on, 19: 43997(R) (UCRL-11889)

ALUMINUM ALLOYS
corrosion by air, boric acid, and water of A288 and X8001, 19: 44616(R) (ANL-7000, pp 122-37)
corrosion mechanisms, 19: 44617(R) (ANL-7000, pp 213-26)
corrosion product films on A288 and X8001, structure of, 19: 44617(R) (ANL-7000, pp 213-26)
extrusion by hydrostatic methods, 19: 44651
fabrication of, nondestructive measurement of residual stresses produced during, 19: 44643 (RSIC-410)
radiation effects on thermal ratcheting between urania and A-288, neutron, 19: 44737(R) (ANL-7000, pp 111-18)
Al–Cr–Fe–Y, corrosion by steam at 550°C of 1041, effects of preoxidation and strain on, 19: 44598(R) (GEMP-49A)
Al–Cr–Fe–Y, corrosion by steam at 730°C, 19: 44598(R) (GEMP-49A)
Al–Cr–Fe–Y, elastic constants at 30 to 1200°C of 2541, dynamic, 19: 44598(R) (GEMP-49A)
Al–Cr–Fe–Y, oxidation by air at 900 and 1100°C, effects of composition on, 19: 44598(R) (GEMP-49A)
Al–Cr–Fe–Y, reactions with iron–urania at 950 and 1100°C in air, 19: 44598(R) (GEMP-49A)
Al–Cr–Mg, erosion by water of rotating disks of, 19: 44625 (TIM-894)
Al–Cr–U, fabrication of reactor fuels of, 19: 44665(P)
Al–Cu, radiation damage in, effects of aluminum content on fast neutron, 19: 44739(R) (ANL-7000, pp 233-77)
Al–Cu, radiation effects on single crystal, effects of aluminum content on strength-annealing of neutron, 19: 44739(R) (ANL-7000, pp 233-77)
Al–Cu, radiation effects on strength of, effects of aluminum content on neutron, 19: 44739(R) (ANL-7000, pp 233-77)
Al–Cu–Mg–Mn, erosion by water of rotating disks of, 19: 44625 (TIM-894)
Al–Cu–Nb, crystal structure, 19: 44718
Al–Cu–Ta, crystal structure, 19: 44718
Al–Fe–U, phase studies, 19: 44715
Al–Hg–Ni, corrosive effects on titanium of mercury-based, 19: 44616(R) (ANL-7000, pp 122-37)
Al–Hg–Zr, corrosive effects on titanium of mercury-based, 19: 44616(R) (ANL-7000, pp 122-37)
Al–Mg, creep at high temperatures, effects of recovery treatment on, 19: 43997(R) (UCRL-11889)
Al–Mg, dislocation loop climb in, negative, 19: 43997(R) (UCRL-11889)
Al–Mg, radiation effects on corrosion and mechanical properties of, neutron, 19: 44752 (CEA-tr-A-1818)
Al–Mo–Ti–V, corrosion cracking of, mechanisms for stress, 19: 44621 (CONF-651006-1)
Al–Nb–Sn, phase study of Cr_3O structures in, 19: 44702 (TID-22200)
Al–Pu, magnetic susceptibility of δ-phase, at 6 to 300°K, 19: 44690 (LA-DC-7360)
Al–Pu, nuclear magnetic resonance in $PuAl_2$, 19: 43986(R) (ANL-7000, pp 201-4)
Al–Pu, phase transformations on heating and cooling in intermetallic compound $PuAl_4$, 19: 44727
Al–Pu–U, corrosion by air at room temperature, 19: 44587(R) (ANL-7000, pp 3-63)
Al–Sb, fusion thermodynamic properties of AlSb, 19: 43997(R) (UCRL-11889)
Al–stainless steel, corrosion by steam at 650°C, 19: 44616(R) (ANL-7000, pp 122-37)
Al–Ta–U, fabrication of reactor fuels of, 19: 44667(P)
Al–Tc, phase studies, 19: 44678(R) (ANL-7000, pp 186-200)
Al–U, fabrication, 19: 44664(P)
Al–U phase studies of distribution of intermetallic compounds in, 19: 44717
Al–U, phase transformations on heating and cooling in intermetallic compound UAl_4, 19: 44727
Al–U–V, fabrication of reactor fuels of, 19: 44668(P)
Al–V, nuclear magnetic resonance, 19: 43986(R) (ANL-7000, pp 201-4)
Al–W–U, fabrication of reactor fuels of, 19: 44666(P)

ALUMINUM ISOTOPES Al-26
gamma spectrum, (E), 19: 44099
production of high-activity, in magnesium (d,n) and (d,2n) reactions at 20 Mev, (E), 19: 44099

ALUMINUM ISOTOPES Al-27
energy level structure of, (E/T), 19: 45275 (NP-15138)
neutron reactions, Q values for, 19: 44450(R) (IBK-120a)
proton reactions (p,α) and (p,γ) with, nucleon model for, 19: 45304

ALUMINUM OXIDES
diffusion of helium through polycrystalline ceramics of, at high temperatures, 19: 43997(R) (UCRL-11889)
effects of additives of, on modulus of rupture of beryllia, 19: 44599(R) (GEMP-50A)
effects of particles of, on strength of sodium borosilicate glass, 19: 43997(R) (UCRL-11889)
fabrication of outer layer of composite fuel element can of, 19: 44661(P)
hot pressing of powdered, densification in, 19: 43997(R) (UCRL-11889)
production of bicrystals of, 19: 43997(R) (UCRL-11889)
properties in in-pile thermionic cells, 19: 44685 (CONF-650908-5)
reactions with cobalt oxide to form spinel, tracer study of mechanism of of solid-state, 19: 43998 (UCRL-12396)
reactions with niobium at high temperatures, 19: 44979(R) (NP-15419)
reduction of, thermodynamic analysis of carbothermic, 19: 43996 (UCRL-11699)
Al_2O_3–CaO–SiO_2, diffusion in, ternary, 19: 43997(R) (UCRL-11889)
Al_2O_3–Nb, seals of, development of high-temperature metal-to-ceramic, 19: 44598(R) (GEMP-49A)

ALUMINUM SILICATES
joining of glasses of, to metals, 19: 44337(R) (AD-425708)

ALUMINUM SYSTEMS
Al–B–Hf, phase studies of, 19: 44719
Al–B–Ti, phase studies, 19: 44719
Al–B–Zr, phase studies, 19: 44719
Al–C–Mo, superconductivity, 19: 43997(R) (UCRL-11889)
Al–C–O, thermodynamic analysis of equilibrium phases in, 19: 43996 (UCRL-11699)
Al–U_3O_8, fabrication of powder compacts of, loading assembly for, 19: 44641 (ORNL-TM-1193)
Al–U_3O_8, pressed block design for fabrication of rod shaped, 19: 44663(P)

AMERICIUM
separation from curium by solvent extraction, 19: 44115 (ORNL-P-1577)

AMERICIUM ISOTOPES
neutron cross sections of, tabulation, (E), 19: 45250 (BNL-325(2nd Ed.) (Suppl. 2)(Vol. III))

AMERICIUM ISOTOPES Am-241
separation from curium-244, chromatographic, 19: 44118 (UCRL-16015)

AMIDOL
performance as developer for nuclear emulsions, 19: 44404 (CERN-65-4 (Vol.II), pp IV23-31)

AMINES
dibutoxyethane, use in reprocessing of fast reactor fuel, 19: 44108 (AERE-R-4440(Pt.3))

AMINO ACIDS
content in rabbit antibodies, 19: 45695 (BNL-912)
determination of carbon-14-labeled, after separation on ion exchange, scintillation method for continuous, 19: 43976
radiation effects on content in rabbit eyes, 19: 43755

AMMONIA
deuterium exchange with hydrogen between water and, in hot-and-cold plant, 19: 44574
nitrogen-14 NQR in deuterated and normal crystalline, (E), 19: 45483
reactions with potassium, equilibrium data on, 19: 43997(R) (UCRL-11889)
spectra of nitrobenzene and nitrosobenzene radical anions in liquid, electron spin resonance, 19: 43997(R) (UCRL-11889)

AMMONIUM ACID SULFATES
spectra of, cold-neutron-scattering analysis of low-frequency vibrational, 19: 45241

AMMONIUM BERYLLIUM FLUORIDES

spectra of, cold-neutron-scattering analysis of low-frequency vibrational, 19: 45241
AMMONIUM BROMIDES
neutron incoherent scattering at 0.07 ev, (E), 19: 45242
AMMONIUM CHLORIDES
effects on strontium-85 elution from mouse bones, 19: 43706
neutron incoherent scattering at 0.07 ev, (E), 19: 45242
AMMONIUM FLUORIDES
proton motion in aqueous solutions of, 19: 44037
AMMONIUM HYDROXIDES
performance as sensitizer for nuclear emulsions, 19: 44406 (CERN-65-4(Vol.II), pp IV41-5)
AMMONIUM IODIDES
neutron incoherent scattering at 0.07 ev, (E), 19: 45242
AMMONIUM IRON(II) SULFATES
$Fe(NH_4)_2(SO_4)_2-CuCl_2-H_2SO_4-H_2O$, properties as gamma dosimeter, 19: 44372 (AFCRL-65-470)
AMMONIUM PERCHLORATES
methyl-, radiolysis effects on hydrogen yields in aqueous, 19: 44080
AMMONIUM SULFATES
methyl-, radiolysis effects on hydrogen yields in aqueous, 19: 44080
spectra of, cold-neutron-scattering analysis of low-frequency vibrational, 19: 45241
AMMONIUM TIN BROMIDES
neutron incoherent scattering at 0.07 ev, (E), 19: 45242
AMMONIUM TIN CHLORIDES
neutron incoherent scattering at 0.07 ev, (E), 19: 45242
AMPLIFIERS
bibliography, 19: 44366 (AED-C-06-12)
design and performance of charge-sensitive, for semiconductor detectors, 19: 44484 (ZFK-PHA-12, pp 189-95)
development of low noise, for semiconductor detectors, 19: 44483 (ZFK-PHA-12, pp 172-88)
performance of fission-chamber pre-, at high temperatures, 19: 44462 (TIM-922)
performance of transistorized, frequency and noise effects on, 19: 44487 (ZFK-PHA-12, pp 206-14)
pulse height distortion in, sources of, 19: 44521
pulse signal-to-noise ratio from semiconductor detectors, effects of input resistance on, 19: 44489 (ZFK-PHA-12, pp 219-23)
ANEMOMETERS
development of sonic, 19: 44772 (BNL-914, pp 51-4)
ANILINE, o-BROMO-
radiolysis products of, gamma, 19: 44053 (AFML-TR-65-166)
ANIMAL CARE
diet for breeding mice, 19: 43654
dog colony maintenance, 19: 43645(R) (UCD-472-112, pp 10-22)
dog colony maintenance, 19: 43646(R) (UCD-472-112, pp 23-35))
status of experimental dog colony, 19: 43680(R) (UCD-472-112, pp 148-74)
ANIMAL CELLS
cytology, tracer study using phosphorus-32, 19: 43740
growth kinetics of tumors of epithelial and spindle, using autoradiography and tritiated thymidine, 19: 43698
labeling with tritium, 19: 43651
mutations in human somatic, in tissue culture, 19: 43844
radiation injuries in, repair mechanisms for HeLa cells in culture, 19: 43790
radiation injuries in, repair mechanisms for hamster cells in tissue culture, 19: 43791
radiation injury and recovery in hamster cells in culture, 19: 43857
radioinduced mutations of, in tissue culture, 19: 43844
radiosensitivity of, in tissue cultures, 19: 43723(R) (TID-22128)
reproduction of, biochemical study of, 19: 43758
use in evaluation of radiation effects, 19: 43753
ANIMAL METABOLISM
in human fetuses, 19: 43701
ANIMAL REPRODUCTION
radiation effects on Tribolium, effects of dose and temperature on, 19: 43715 (HW-SA-3747)
radiation effects on Tribolium, effects of genetics and temperature on x, 19: 43716 (HW-SA-3748)
ANIMALS
ecological and radiation effects, studies at Nevada Test Site on, Jan.–June 1965, 19: 43662(R) (UCLA-12-565, pp 97-128)
radiation effects on, biological indicators for evaluating, 19: 43753
radiation effects on, correlation with studies on man, 19: 43843
ANION EXCHANGE MATERIALS
radiation stability of strongly basic, reactor, 19: 44055 (IAE-788)
reactions of Permutit SK resin with dichromate and nitric acid in contactor, analysis of uncontrolled, 19: 44110 (BNWL-114)
ANIONS
effects of oxy-, on hydrogen atom trapping in frozen irradiated solutions, 19: 44054(R) (COO-1365-7)
ANODES
reaction distribution in porous copper, 19: 43997(R) (UCRL-11889)
ANOXIA
effects on recovery of irradiated hamster cells in tissue culture, 19: 43791
ANTHRACENE
radiation effects on semiconducting properties, 19: 44077
ANTIBIOTICS
radiosterilization of, effects on potency, 19: 44559
ANTIBODIES
amino acid content in rabbit, 19: 45695 (BNL-912)
detection in rabbits of oxytocin, autoradiographic method for, 19: 43658
effects of iodine-131 therapy for hyperthyroidism on cytoplasmic and thyroglobulin, 19: 43902
formation and specificity of, mechanisms for, 19: 45695 (BNL-912)
production in rabbits of oxytocin, 19: 43658
role of, in pathogenesis of radioinduced pulmonary sclerosis in rabbits, 19: 43817
ANTIGENS
effects on spleen cell migration in blood stream of irradiated rats, 19: 43822
ANTIMONY
effect on determination of copper in bismuth by neutron activation methods, 19: 43941
ANTIMONY ALLOYS
Al–Sb, fusion thermodynamic properties of AlSb, 19: 43997(R) (UCRL-11889)
Sb–Ga, fusion thermodynamic properties of GaSb, 19: 43997(R) (UCRL-11889)
Sb–In, fusion thermodynamic properties of InSb, 19: 43997(R) (UCRL-11889)
Sb–Sn–Zr, phase studies, 19: 44720
Sb–Zr, crystal structure of intermetallic compound $ZrSb_2$ in, 19: 44720
ANTIMONY IONS
radioinduced oxidation of trivalent, in hydrochloric acid and sulfuric acid, 19: 44085
ANTIMONY ISOTOPES Sb-124
beta spectrum above 1.0 Mev, shape of, (E), 19: 45328
ANTIMONY ISOTOPES Sb-125
gamma directional correlation, 19: 45679(R) (NYO-1859-11)
ANTIMONY OXIDES
SbO–UO, use as oxidation catalysts, 19: 44043(P)
ANTINEUTRONS
interactions with nucleons at high energies, polarization and Regge poles in, (T), 19: 45044 (UCRL-16186)
ANTINUCLEONS
interactions with nucleons at high energies, resonance production in, (T), 19: 45037 (TID-21316)
production by elementary particle processes in special relativity, 19: 44895
ANTIPROTONS
interactions with protons at high energies, statistical model calculations for, 19: 45047 (UCRL-16315)
interactions with protons at rest, annihilation into two mesons in, (E), 19: 45122
interactions with neutrons and protons, broken U(12) analysis of annihilation, (T), 19: 45008 (JINR-E-2246)
interactions with protons, radiative corrections for, (T), 19: 45023 (LNF-65/8)
interactions with protons, cross sections for charged-meson pair formation in annihilation, (T), 19: 45066
interactions with protons at 3.25 to 7 Bev/c, OPE model for N*N* production in, (T), 19: 45069
interactions with protons at rest, C invariance test from annihilation, (E), 19: 45124
ARCHAEOLOGICAL SPECIMENS
carbon-14 content in, proportional counting technique for, 19: 44526
ARGENTINA
strontium-90 contents in bones and diet in, 19: 44250 (NP-15269)
ARGON
content in natural gases, 19: 44239
electric discharges in, relation between column stratification and negative ion content in impure, 19: 45423
electron density and temperature in plasma jet of, (E), 19: 45448
electron inelastic scattering at 40 kv, polarization in, (T), 19: 44942
electron reactions with, in magnetic bottle, 19: 44823
helium elastic scattering by, total cross section for, (E), 19: 44957

ionization of, electron ejection energies in auto-, 19: 44934(R) (COO-1277-13)
neutron scattering by, effective potential for electron-neutron interactions from, (E), 19: 45098
neutron scattering by liquid, dynamics of, (E), 19: 45235
pinch discharge in plasma of, high-current pulse-driven linear, 19: 45442
plasma of, transport properties of, (T), 19: 45407 (SU-AA217)
properties for use in closed Brayton cycle space power plants, 19: 44205
relaxation of interatomic distances about vacancy in solid, (T), 19: 43997(R) (UCRL-11889)
release from tungsten, mechanism of thermal, (E), 19: 44954
shock front curvature in, (E), 19: 44853
spectra of sulfur molecules in solid, u-v absorption, (E), 19: 45480 (UCRL-10771)
thermal radiation from plasma arc of, (E/T), 19: 45453
transport properties of partially ionized, 19: 44854

ARGON COMPOUNDS
radiation effects on clathrate, neutron, 19: 45679(R) (NYO-1859-11)

ARGON FLUORIDES
sorption on irradiated ion exchanger material at 90°K, 19: 44091

ARGON IONS
reactions with tungsten at 1 to 4 kev, trapping in, (E), 19: 44954
sputtering on copper, nickel, and silver at 30 to 170 kev, (E), 19: 44937(R) (TID-22140)
yields from duoplasmatron ion source, pressure dependence of, (E), 19: 45385 (D1-82-0437)

ARGON ISOTOPES Ar-36
content in meteorite Khor Temiki, (E), 19: 44906
content in natural gases, 19: 44239

ARGON ISOTOPES Ar-38
content in meteorite Khor Temiki, (E), 19: 44906
content in natural gases, 19: 44239

ARGON ISOTOPES Ar-40
content in meteorite Khor Temiki, (E), 19: 44906
content in natural gases, 19: 44239
determination of, in minerals, use of nitrogen-15 as internal standard in, 19: 43960

ARGON ISOTOPES Ar-41
decay of, gamma spectra from, 19: 45679(R) (NYO-1859-11)

ARGON SYSTEMS
Ar–Cs, cesium excitation cross sections from electron drift velocities in, (E), 19: 44935 (NP-15168)
Ar–H, shock waves in, interferometric measurement of vibrational relaxation behind, 19: 44855
Ar–O, radiolysis of, kinetics of ozone formation in pulse, 19: 44071

ARGONNE FAST REACTOR EXPERIMENT TEST
structural material for liquid-metal system in, selection of, 19: 44587(R) (ANL-7000, pp 3-63)

ARGONNE NATIONAL LAB., LEMONT, ILL.
meteorological program, 19: 44763 (BNL-914, pp 4-13)

ARGONNE RESEARCH REACTOR
neutron fluxes in vertical irradiation facilities of, thermal, 19: 45668 (ANL-7026)

ARIZONA (PIMA CO.)
geology of volcanic Roskruge range, 19: 44236 (TID-22086)

ARMY REACTORS
instrumentation for PM-type, design of, 19: 45584 (NYO-3379-1)

ARMY REACTORS (ML-1)
development, 19: 45577(R) (IDO-28645)
fuel element irradiation testing for, in-pile, 19: 45558 (AGN-TM-409)

ARMY REACTORS (PM-2)
coolant contamination by cobalt-60, 19: 45495 (WAPD-T-1653)

ARMY REACTORS (SM-1)
coolant contamination by cobalt-60, 19: 45495 (WAPD-T-1653)

ARSENIC
effect on determination of copper in bismuth by neutron activation methods, 19: 43941

ARSENIC ISOTOPES As-75
gamma absorption cross section, (T), 19: 45366
neutron reactions with, resonances in, (E), 19: 45296

ASCORBIC ACID
effects on strontium-85 elution from mouse bones, 19: 43706
protective effects against radiation damage in crop plants, 19: 43877

ASPARTIC ACID
carbon-14 uptake by, in rat cerebral tissue, 19: 43690

ASTROPHYSICS
cosmic x-ray sources in Sagittarius and Scorpio, positions of three, (E), 19: 44968
hydrogen detection in intergalactic space, sensitive method for, (E), 19: 44908
review of high-energy, 19: 44909
review on research at Arcetri Astrophysics Observatory in 1963, 19: 44899
review on research at Arcetri Astrophysics Observatory in 1962, 19: 44898
review studies in, 19: 44976
x-ray spectra near Galactic center and in Scorpius, (E), 19: 44967

ATLANTIC OCEAN
fallout monitoring, 1964, 19: 44253(R) (NYO-2174-36)

ATMOSPHERE
atmospheric radiation monitoring at Ames, Jan.-June 1965, 19: 44302 (TID-22173)
auroral production in, terrestrial control in, 19: 45185
carbon-14 content of, in Japan, 19: 44267
cloud rise experiments in, 19: 44787 (BNL-914, pp 119-22)
contamination in cities, 19: 44788 (BNL-914, pp 123-4)
contamination of urban, 19: 44785 (BNL-914, pp 113-14)
contamination of, meteorological studies of, 19: 44775 (BNL-914, pp 69-74)
deposition from, by washout, (T), 19: 44249 (BNL-914, pp 144-8)
deposition from, Hanford studies, 19: 44248 (BNL-914, pp 141-3)
deposition from, meteorological aspects of, 19: 44247 (BNL-914, pp 139-40)
deposition from, review of research on, 19: 44246 (BNL-914, pp 133-8)
deposition from, studies, 19: 44245 (BNL-914, pp 125-32)
diffusion and transport in, U. S. Weather Bureau studies, 19: 44770 (BNL-914, pp 33-43)
diffusion and transport in, studies at National Reactor Testing Station on, 19: 44773 (BNL-914, pp 57-64)
diffusion from ground sources, data on, 19: 44792 (BNL-914, pp 153-5)
diffusion in surface layer of, Lagrangian similarity theory of, (T), 19: 44766 (BNL-914, pp 20-3)
diffusion in, aerospace and climatology studies on, 19: 44771 (BNL-914, pp 44-50)
diffusion in, elevated line source tests on, 19: 44779 (BNL-914, pp 93-4)
diffusion in, from elevated sources, (E), 19: 44768 (BNL-914, pp 26-7)
diffusion in, integration of Sutton point-source formula for, (T), 19: 43997(R) (UCRL-11889)
diffusion studies of, Canadian, 19: 44790 (BNL-914, pp 149-50)
dispersion in meso-scale meteorology, studies, 19: 44784 (BNL-914, pp 110-12)
dispersion in urban, 19: 44791 (BNL-914, pp 151-2)
dispersion in, effects of source configuration on, 19: 44786 (BNL-914, pp 116-18)
dispersion in, summary of diffusion experiments for prediction of, 19: 44789 (BNL-914, pp 146-8)
meteorology of, research program on boundary layer, 19: 44777 (BNL-914, pp 85-90)
monitoring Savannah River Plant, Jan. to June 1965, 19: 44288(R) (DPST-65-30-2)
monitoring sulfur dioxide in, instrument design for, (E), 19: 44458 (NYO-2767)
particle scavenging by precipitation in, 19: 44769 (BNL-914, pp 28-32)
plasma diagnostics in upper, probe system for, 19: 45155(R) (AD-609015)
radiation monitoring at Argonne, Jan.-June 1965, 19: 44300 (TID-22171)
radioactivity at Paducah Gaseous Diffusion Plant, Jan.-June 1965, 19: 44301 (TID-22172)
radioactivity from reactor accident in, measurability of, 19: 44325
radioactivity of Canadian, June 1965, 19: 44251 (NP-15519, pp 23-6)
radioactivity over Atlantic Ocean, fallout, 19: 44253(R) (NYO-2174-36)
sampling for nuclear debris in upper, dynamic analysis of SAND flight, 19: 44142 (SC-RR-65-286)
sampling for occupational safety, 19: 44296 (NYO-4700(Rev.)(Suppl.II))
satellite orbital decay in, semi-annual effects in, 19: 45158 (NP-15424)
tracer technique for studies of, tests of fluorescein-zinc sulfide dual, 19: 44800 (BNWL-103)
turbulence in, low-level, 19: 44793 (BNL-914, pp 156-7)

ATMOSPHERE EXPOSURE CHAMBERS
regulator for, automatic, 19: 43668 (HW-SA-3618)

ATOMIC BEAMS
electron scattering from mercury, polarization in, (E), 19: 44958

ATOMIC CLOUDS
fallout from, effects of precipitation on, 19: 44255 (RT/PROT(65)-10)
radioactivity isopleths of, in Dominic test, 19: 44784 (BNL-914, pp 110-12)

ATOMIC ENERGY
development and uses of, in Italy, 19: 45724
uses in industry, conference, 19: 44565

ATOMIC ENERGY COMMISSION
meteorological activities of, conference on, 19: 44761 (BNL-914)
reactor regulatory program, use of meteorology in, 19: 44270 (BNL-914, pp 178-9)

ATOMIC EXPLOSIONS
actinide recovery from debris in salt formation, 19: 44156 (DP-956)
crater formation by, comparison with astroblemes, 19: 44237
effects on chromosome aberrations in humans, 19: 43834
effects on populations, pathological, 19: 44280(R) (ABCC-63-64)
radio waves from, shielding nuclear-weapon circuits from, (E), 19: 44166 (NP-15472)
use of underground, in stimulating oilfields, 19: 44158 (UCRL-14311)
ATOMIC PHYSICS
research on, in Rumania, 19: 45705 (NP-15193)
ATOMIC WEAPONS
circuitry for, shielding from nuclear-blast r-f fields, (E), 19: 44166 (NP-15472)
ATOMS
detection and measurement of neutral, using scintillation detectors, (E), 19: 44499
electron and ion reactions with, review of, 19: 44950
electron elastic scattering by complex, noniterative approach to, (T), 19: 44953
electron inelastic scattering by, polarization in, (T), 19: 44942
energy level mixing in external fields, interference phenomena in, 19: 45270 (JINR-P-2248)
energy level population inversion in optically pumped rubies, pump pulse shape effect on, (T), 19: 45704 (LA-DC-6717)
AUDITORY ORGANS
shock wave effects on, high-energy electric discharge, 19: 44283 (AWRE-E-1/65)
AURORAL STORMS
infrasonic wave generation in, (T), 19: 45183
occurrence frequency of, seasonal variation of, (E), 19: 45180
production of, terrestrial control in, 19: 45185
properties of, radar observations of, (E), 19: 45169
AUSTRALIA
cesium-137 content in milk in, 1963, 19: 44309
AUSTRALIA (SOUTH AUSTRALIA)
fallout deposition in 1958 to 1964, 19: 44261
AUSTRIA
fallout monitoring, 1961 to 1965, 19: 44292(R) (NP-15173)
nuclear power plant for, design study of, 19: 45581 (NP-15291)
AUTORADIOGRAPHY
for localization of tritium-labeled lipids and organic acids, 19: 43696
quantitative aspects of dog kidney, 19: 43667 (EUR-1890.f)
AVR REACTOR
fuel element irradiation evaluation for, 19: 44749 (ORNL-P-1507)

B

BABCOCK AND WILCOX TEST REACTOR
fuel capsule irradiations in, 19: 45542(R) (BAW-272)
BACTERIA
genetic effects in human cells in tissue culture, 19: 43844
properties of desoxyribonucleic acid in *Bacillus subtilis*, 19: 43723(R) (TID-22128)
radiation effects on salmonellae, 19: 44557 (NYO-3426-1)
radiation effects on meat contamination with, 19: 44558(R) (TID-22139)
radiation effects on sulfonamide-induced and normal volutin in, 19: 43759
radiation effects on droplet nuclei staphylocci, uv, 19: 43736
radiation effects on droplet nuclei in mycobacterium, uv, 19: 43736
radiation effects on culture media for tubercle, uv, 19: 43737
radiation effects on base composition of messenger RNA in *Pseudomonas effusa*, 19: 43744
radiation injuries in *Bacillus subtilis*, effects of heat treatment on, 19: 43793
radioinduced mutations of *Mycobacterium smegmatis*, effects of transmutation of incorporated sulfur-35 on, 19: 43816
radioinduced mutations of *Mycobacterium smegmatis*, effects of external exposure to sulfur-35, 19: 43816
radioinduced phage induction in *Serratia marcescens*, uv, 19: 43847
radiosensitivity of, effects of chemicals on, 19: 44552 (BLG-327)
radiosensitivity of *Bacillus subtilis* vegetative spores, 19: 43793
radiosensitivity of *Bacillus subtilis* spores, 19: 43793
radiosensitivity of transforming desoxyribonucleic acid in *Bacillus subtilis* vegetative cells and spores, 19: 43793
BACTERIOPHAGES
genetic effects in human cells in tissue culture, 19: 43844
radiation effects on protein metabolism in, ultraviolet, 19: 43845
radiation effects on infection of *E. coli*, uv, 19: 43742
radiosensitivity of *Escherichia coli*, 19: 43794
BALANCES
design and operation of recording micro-, for remote thermogravimetry of irradiated uranium dioxide, 19: 44341 (AERE-R-4962)
BALLOONS
use of tetroons in meso-scale meteorology, 19: 44783 (BNL-914, pp 107-9)
BARBITURIC ACIDS
complexes with cerium and pyridine bases, preparation and stability, 19: 44027
metabolism in rats of, 19: 43670(R) (NP-15310, pp 36-47)
BARIUM
separation from sodium by ion exchange, 19: 44091
separation from uranium by ion exchange, 19: 44119
BARIUM ISOTOPES Ba-124
energy levels, (E/T), 19: 45285 (UCRL-16040)
BARIUM ISOTOPES Ba-126
energy levels, (E/T), 19: 45285 (UCRL-16040)
BARIUM ISOTOPES Ba-137
gamma transitions of, determination of internal conversion coefficients of, (E), 19: 44501
BARIUM ISOTOPES Ba-138
deuteron reactions (d,p) at 7.5 Mev, barium-139 levels from, (E), 19: 45347
BARIUM ISOTOPES Ba-139
energy levels of, from deuteron reactions (d,p) with barium-138, (E), 19: 45347
BARIUM ISOTOPES Ba-140
diffusion from irradiated molybdenum–rhenium–tungsten alloy, 19: 44599(R) (GEMP-50A)
production in SNAP-50 critical assemblies, absolute power determination by, 19: 45656 (PWAC-474)
BARIUM OXIDES
$BaO–SiO_2$, glass formation and structure in, 19: 44015
BARIUM SULFIDES
sublimation of, mass spectrometric study, 19: 43997(R) (UCRL-11889)
BARLEY
radiation effects on, protective effects of chemicals against seed, 19: 43877
BARYONS
annihilation of, broken $\bar{U}(12)$ symmetry for analysis of, (T), 19: 45008 (JINR-E-2246)
field theory for relativistic quantum, 19: 45131 (JEN-154-DF/I-47)
form factors, (T), 19: 45011 (JINR-E-2294)
interactions with mesons, exact bootstrap solutions to Low equation for, 19: 45106
interactions with electrons, resonance in, (T), 19: 45007 (JINR-E-2228)
mass formulas for mesons and Gell-Mann-Okubo quark splitting for, (T), 19: 45077
BARYONS, RESONANCE
decay of Σ^*, in broken symmetry $\bar{U}(12)$, (T), 19: 45014 (JINR-P-2237)
electro-production and decay, (T), 19: 45007 (JINR-E-2228)
interactions with stable particle, strong, (T), 19: 45082
production in interactions at high energies, peripheral model for, (T), 19: 45037 (TID-21316)
production of N^{*++}, in meson (π^+)-proton interactions at 1.11 and 1.265 Bev/c, 19: 44997 (COO-1428-14)
production of N^*_{33} in meson (π^+)–proton interactions, (E), 19: 45103
production of N^*_{33} in meson (π^-)-proton interactions at 3.9 Bev/c, 19: 45121
production of N^{*++} in deuteron-meson (K^+) interactions at 2.3 Bev/c, 19: 45120
production of N^*, in meson (K^+)–proton interactions at 3 Bev/c, (E/T), 19: 45057
production of $N^*(1237)$ and $\bar{N}^*$ in antiproton–proton interactions at 3.25 to 7 Bev/c, OPE model for, (T), 19: 45069
production of $\pi^+\pi^0 p$ (1710), in meson (π^-)-proton interactions at 3.9 Bev/c, (E), 19: 45121
production of $Y^*(1382)$ and $\bar{Y}^*$ in antiproton–proton interactions at 3.25 to 7 Bev/c, OPE model for, (T), 19: 45069
review, 19: 45056
symmetries for, relativistic SU(6) supermultiplet, 19: 45112
systematics, (T), 19: 44996 (COO-1195-39)
BEAMS
scattering chambers for, description of continuous-rotation vacuum, (E), 19: 44883
BEANS
effects of carbon dioxide on roots of, 19: 43662(R) (UCLA-12-565, pp 97-128)
radiation effects on, protective effects of chemicals against seed, 19: 43877
radioinduced sterility in pollen of, γ, 19: 43767
strontium-89 uptake and deposition in tops of, forces affecting non-metabolic, 19: 43703

BEARINGS
analysis of fluid-film, summary of CANEL work on, 19: 44147 (TIM-917)
overheating of railway-car, radioisotope detector for, 19: 44568(P)
test of ball, in lithium, 19: 44150 (TIM-923)
tests of orifice-compensated double-acting hydrostatic thrust, in water, 19: 44152 (TIM-926)
use of superconducting, in three-phase induction motor, 19: 45196
BEHAVIOR
radiation effects on food satiation in rhesus monkeys, 19: 43807
radiation effects on water intake by rats, 19: 43808
BELLOWS
use as seal in transmitting motion through vacuum wall, 19: 44234 (MATT-345)
BENTONITES
effects of additives of, on modulus of rupture of beryllia, 19: 44599(R) (GEMP-50A)
BENZENE
neutron scattering by, distributions from cold, 19: 45238
oxidation in aqueous solutions, effects of metal ions on phenol yields at 150°C, 19: 44078
oxidation of, deuterium and oxygen-18 isotope effects on phenol yields from, 19: 44078
radiation effects on oxidation of, in presence of metal ions, 19: 44078
radioinduced reactions with carbon tetrachloride and trichlorotrifluoroethane, calculated product accumulation in, 19: 44061(T) (AEC-tr-6567)
radiolysis of aqueous solutions of, effects of oxides on gamma, 19: 44051 (AE-192)
radiolysis of aqueous solutions of, at 100 to 200°C, 19: 44052 (AE-193)
use in cryoscopic method for molecular weight determination in organic reactor coolants, 19: 44045 (JEN-151-DQ/I-52)
benzene–methylcyclopentane, reactions with recoil carbon-11 produced by gamma irradiation, 19: 44057 (IS-T-23)
benzene–thenoyltrifluoracetone, solvent properties for pentavalent protactinium, 19: 44012
BENZENE, NITRO-
labeling with oxygen-17, coupling constant for, 19: 44049
spectra of radical anions of, electron spin resonance, 19: 43997(R) (UCRL-11889)
BENZENE, NITROSO-
spectra of radical anions of, electron spin resonance, 19: 43997(R) (UCRL-11889)
BENZIMIDAZOLE
radiosensitivity effects in mice, 19: 43863
BENZOHYDROXAMIC ACID, *N*-PHENYL-
solvent properties for zirconium, 19: 43972
BENZOIC ACID
complexes with uranyl cations, stability, 19: 44013
compound formation with samarium, gadolinium, and erbium, 19: 44028
BENZOYL PEROXIDE
radiolysis of, kinetics of gamma, 19: 44089
BERKELIUM ISOTOPES
neutron cross sections of, tabulation, (E), 19: 45250 (BNL-325(2nd Ed.) (Suppl.2)(Vol. III))
BERYLLIUM
alpha reactions (α,n) at 2 to 5.4 Mev, neutron yields in, 19: 45301
brazing to niobium–1 zirconium and type 316 stainless steel using silver, 19: 44606 (PWAC-483)
brazing to niobium–1 zirconium with silver alloys, effects of carbon and silicon coatings on, 19: 44606 (PWAC-483)
deformation of single-crystal foils of, electron microscopic study of, 19: 44683 (CEA-R-2789)
deformation of single crystals of, by double shear, 19: 44694(R) (NP-15432)
deformation of, effects of dislocation substructure on, 19: 44726
deformation properties of single crystal, 19: 44693(R) (NP-15411)
dislocation movement on planes of, stress calculations for, 19: 44694(R) (NP-15432)
effects of additives of, on modulus of rupture of beryllia, 19: 44599(R) (GEMP-50A)
effects on plants and soil, 19: 43662(R) (UCLA-12-565, pp 97-128)
extrusion by hydrostatic methods, 19: 44651
hot working of single crystals of, 19: 44694(R) (NP-15432)
impact properties of plates and tubes of, hypervelocity, 19: 44692 (NASA-TN-D-3018)
mechanical properties of rolled cast, 19: 44652
phase transformations in, relation of c/a ratio and elastic moduli temperature dependence with, 19: 44676(R) (ANL-7000, pp 176-82)
reactions with metals at 540 to 760°C *in vacuo*, 19: 44606 (PWAC-483)
rolling of cast, at 500 to 1000°C, 19: 44652
BERYLLIUM ALLOYS
Be–Cu, deformation of single crystals of, by microstrain compression, 19: 44694(R) (NP-15432)
Be–Cu, radiation effects on age hardening, 19: 44760
Be–Fe, magnetization at 295°K, saturation, 19: 44678(R) (ANL-7000, pp 186-200)
Be–Ni, preparation by zone melting, 19: 44694(R) (NP-15432)
BERYLLIUM ISOTOPES Be-7
detection and measurement in animal and human tissues, proton dosimetry by, 19: 44327
BERYLLIUM ISOTOPES Be-9
alpha reactions (α,2α) at 28 Mev, spectra from, (E), 19: 45308
neutron reactions (n,2n) at 14.5 Mev, angular correlations and cross sections for, (E), 19: 45252 (CEA-R-2734)
proton scattering at 155 Mev, cross sections and spectra in inelastic, 19: 45305
triton reactions (t,α) at 13 Mev, lithium-8 excited states from, (E), 19: 45348
BERYLLIUM MODERATED REACTORS
design of epithermal thorium power-breeder, 19: 45629(P)
BERYLLIUM NITRIDES
decomposition of, evaporation study, 19: 43997(R) (UCRL-11889)
BERYLLIUM OXIDES
diffusion of krypton from, at 1100 and 1200°C, 19: 44599(R) (GEMP-50A)
effects of coatings of, on fission gas release from beryllia-based fuels, 19: 44599(R) (GEMP-50A)
modulus of rupture at 30 to 1200°C, effects of glass-phase additives on, 19: 44599(R) (GEMP-50A)
properties in in-pile thermionic cells, 19: 44685 (CONF-650908-5)
radiation effects on mechanical properties of, fast neutron, 19: 44599(R) (GEMP-50A)
reactions with carbon and molybdenum–rhenium at 2450°C, 19: 44598(R) (GEMP-49A)
BeO–GeO_2, glass formation limits in, calculation of upper, 19: 44016
BeO–MgO, radiation effects on thermal diffusivity of, fast neutron, 19: 44599(R) (GEMP-50A)
BeO–SiO_2, glass formation and structure in, 19: 44015
BERYLLIUM OXIDES (IMPREGNATED)
fission gas release from urania–thoria–yttria fuel in, effects of beryllia coating on, 19: 44599(R) (GEMP-50A)
BETA DECAY
electric moments in nuclear, exchange, (T), 19: 45363
BETA PARTICLES
detection and measurement of, using liquid scintillation counter, (E), 19: 44506
detection and measurement of soft, using acceleration method, (E), 19: 44512
detection and measurement of low-energy, performance of scintillation fibers for, 19: 44451 (IITRI-578P26-8)
detection and measurement of, instrumentation for, 19: 44369 (AERE-R-4552)
detection and measurement in atmosphere and body from reactor accident, 19: 44325
detection in nuclear emulsions, 19: 44389 (CERN-65-4(Vol.II) pp II17-18)
detection of, performance of surface-barrier silicon detectors for, 19: 44469 (ZFK-PHS-12, pp 16-24)
dosage to skin from external contamination, evaluation of methods for, 19: 44328
dosimetry of strontium-90, deposited in dog skeleton, 19: 43726(R) (UCD-472-112, pp 120-5)
dosimetry of, spectral method for determining, 19: 44491(T) (CEA-tr-R-1866)
effects in *Mycobacterium smegmatis* of sulfur-35, genetic, 19: 43816
effects on blood picture in dogs, 19: 43725(R) (UCD-472-112, pp 44-9)
effects on ionic crystals at low temperatures, x-ray-diffraction studies, 19: 44745 (LA-DC-6725)
effects on nuclear emulsions, intensification of latent image in, 19: 44391 (CERN-65-4(Vol.II), pp 29-42)
effects on tumor growth in rats of, from phosphorus-32 chromium phosphate colloids, 19: 43797
energy spectra from fission fragments, emulsions for measuring, 19: 44441 (CERN-65-4(Vol.II), pp X47-53)
reactions with metal targets, bremsstrahlung production in, (E), 19: 45284 (TID-22169)
spectra from strontium-90–yttrium-90 sources, (E), 19: 45284 (TID-22169)
BETA SOURCES
content in air and water around Paducah Gaseous Diffusion Plant, Jan.-June 1965, 19: 44301 (TID-22172)
content in air at Savannah River Plant, Jan. to June 1965, 19: 44288(R) (DPST-65-30-2)
dose rates from flat, spectral method for, 19: 44491(T) (CEA-tr-R-1866)

dosimetry of strontium-90-yttrium-90, in skin, 19: 43880 (NP-15270)
effects of ingested, on skeleton of dogs, 19: 43882 (UCD-472-112 pp 50-8)
performance for artificial radiation belt production, 19: 45159 (UCRL-14374)
performance of, effects of self-absorption and self-scattering on, (E), 19: 44881
radioisotope selection for use as, 19: 44551
surface contamination by, maximumum permissible levels for, 19: 44311
therapeutic use of strontium-90, for mouth cancers, 19: 43912
BETA SPECTROMETERS
design and performance of semiconductor, 19: 44472 (ZFK-PHA-12, pp 52-63)
design of scintillation, for internal conversion coefficient determinations, 19: 44501
performance of scintillation, for dosimetry, 19: 44491(T) (CEA-tr-R-1866)
BEVATRON
operation and development of, (E), 19: 44874(R) (UCRL-16203)
BEVERAGES
analysis for chloride in beer, activation, 19: 43944
BIBLIOGRAPHIES
on analytical methods for plutonium, 19: 43925 (ANL-6956)
on carbohydrate catabolism in plants, 19: 45697(R) (COO-330-11)
on cesium-137 and potassium contents in Finnish Lapp diet, 19: 44305
on cross section measurement program of AEC, 19: 45288 (WASH-1056)
on deposition from atmosphere, 19: 44246 (BNL-914, pp 133-8)
on desalination of brackish or saline waters by nuclear energy, 19: 45590 (TID-3584)
on direct conversion of nuclear energy into electric energy, 19: 44978 (AED-C-15-08)
on Doppler effect in fast reactors, 19: 45576 (IA-1039)
on fluid-film bearing analysis and rotor dynamic tests, 19: 44147 (TM-917)
on high-temperature chemistry and physics of gases and gas-condensed phase reactions, 19: 43993 (NP-15379)
on high-temperature chemistry and physics of condensed materials, 19: 43994 (NP-15381)
on instruments and measuring techniques in nuclear physics, 19: 44366 (AED-C-06-12)
on nuclear magnetic resonance in flowing liquids, 19: 44813(T) (NP-tr-1307)
on nuclear ship propulsion, 19: 45647 (AED-C-22-64)
on optical emission spectroscopy for determination of trace impurities, 19: 43929 (IS-1237)
on pathology of radiation sickness, 19: 43851
on physics research, 19: 44812(R) (UCRL-16099)
on plastic fatigue properties of heat resistant alloys, 19: 44599(R) (GEMP-50A)
on radiochemistry of radium, 19: 44098 (NAS-NS-3057)
on radium poisoning, 19: 43672(R) (TID-22131)
on space environment, 19: 44893 (NASA-CR-294)
on space medicine, 19: 43718 (NASA-SP-7011(12))
on space medicine, 19: 43719 (NASA-SP-7011(13))
on technology of uranium carbides, 19: 44603 (NAA-SR-10929)
on theory of Raman spectra, 19: 44039
on use of metabolites in diagnosis of radiation exposure, 19: 43852
radiation effects in swine, 19: 43713 (BNWL-115)
BIOCHEMISTRY
bioelectric forces involved in the thermodynamics of material transfer across biological membranes, 19: 43664 (BNL-9337)
research programs on, 19: 43647(R) (UCLA-12-565)
thermodynamics of material transfer across biological membranes, 19: 43665 (BNL-9338)
BIOLOGICAL MATERIALS
analysis for iron and zinc, x-ray fluorescence spectrometric, 19: 43939(R) (UCD-472-112, pp 59-72)
analysis for radioisotopes, instruments and methods for, 19: 43659
BIOLOGICAL SYSTEMS
bioelectric forces involved in material transfer in, 19: 43664 (BNL-9337)
ion exchange across membranes in, thermodynamics of, 19: 43665 (BNL-9338)
radiation effects on, RBE for proton, 19: 43721(R) (ORNL-TM-1217)
radiation monitoring, 19: 43663
BIOLOGY
origin of life, scheme for, 19: 45721 (UCRL-14254)
research programs on, at AECL, 19: 45694(R) (AECL-2251)
BIOMETRY
equations for thermodynamic processes in biological systems, 19: 43664 (BNL-9337)
growth curve for mammary fibroadenoma in rats, 19: 43649 (UCRL-16177)
mathematical relations for thermodynamics of material transfer across biological membranes, 19: 43665 (BNL-9338)
BIOPHYSICS
bioelectric forces involved in the thermodynamics of material transfer across biological membranes, 19: 43664 (BNL-9337)
research programs on, 19: 43647(R) (UCLA-12-565)
thermodynamics of material transfer across biological membranes, 19: 43665 (BNL-9338)
BIPHENYL
neutron scattering by, distributions from cold, 19: 45238
BIPHENYL, ISOPROPYL-
neutron scattering by, distributions from cold, 19: 45238
properties as reactor coolant and moderator, (E), 19: 45501 (IAE-611)
2,2'-BIQUINOLINE
analytical use in determination of copper in enriched uranium metal, 19: 43938 (PG-Report-665)
BISMUTH
analysis for copper by neutron activation methods using gamma-gamma coincidence, 19: 43941
extrusion by hydrostatic methods, 19: 44651
incorporation in electron sensitive nuclear emulsions, 19: 44399 (CERN-65-4(Vol.II), pp III17-20)
neutron absorption cross sections at 24 kev, (E), 19: 45230
phases at high pressures, 19: 43997(R) (UCRL-11889)
solvent properties for uranium at 400 to 600°C, 19: 44733
superconducting critical fields at high pressures, (E), 19: 45198
BISMUTH ALLOYS
Bi–Sn, corrosive effects on type 304 stainless steel, effects of flow rate and temperature on, 19: 44616(R) (ANL-7000, pp 122-37)
Bi–Sn, use as liquefiable seal for metal surfaces, 19: 44658(P)
BISMUTH CHROMATES
magnetic properties of $(La_{0.9}Bi_{0.1})CrO_3$, (E), 19: 45486
BISMUTH ISOTOPES Bi-214
alpha decay of, particle ranges in, (E), 19: 45293(T) (ORNL-tr-696)
determination in air, filter measurement of, 19: 44258
BLADDER
radiotherapy of carcinomas of, 19: 43894
BLOOD
analysis for chemical constituents in dog, 19: 43674(R) (UCD-472-112, pp 36-43)
flow in kidneys and liver, tracer determination of, 19: 43883(R) (UCLA-12-565, pp 65-85)
flow in pulmonary arteries, tracer patterns of, 19: 43883(R) (UCLA-12-565, pp 65-85)
flow of pulmonary, measurement by lung scanning, 19: 43883(R) (UCLA-12-565, pp 65-85)
radiation effects on spleen cell migration in rat, after antigen stimulation, 19: 43822
radioactivity of dog, following renogram preparation, 19: 43667 (EUR-1890.f)
strontium-90 content in human, in Germany, 19: 44313
BLOOD CELLS
reactions of canine blood, with plutonium ions, 19: 43705
BLOOD CIRCULATION
tracer study of portal systemic shunts, 19: 43904
BLOOD DISEASES
mutation rates for hemophilia, 19: 43642(R) (NYO-2280-8)
BLOOD FORMATION
radiation effects on erythropoiesis and myelopoiesis in bone marrow, 19: 43731
BLOOD PICTURE
radiation dosimetry using human, method for gamma, 19: 44316
radiation effects on dog, ingested strontium-90, 19: 43725(R) (UCD-472-112, pp 44-9)
radiation effects from injected gold-198, phosphorus-32, or iodine-131 on, in rats, 19: 43839
BLOOD PLASMA
iodine-131 uptake and retention by rabbit, effects of dietary molybdenum on, 19: 43689
iodine-131 uptake by chick, age and dose effects on, 19: 43704
radiation effects on metabolites in human and rat, 19: 43852
tritium uptake by cattle, 19: 43694
BLOOD PLATELETS
radiation effects on, biochemical and morphological, 19: 43714 (EUR-2438.f)
BLOOD VOLUME
determination by tracer method, apparatus for, 19: 43661(P)
determination of, tracer technique for, 19: 43660(P)
BODY FLUIDS
measurement in man, tracer methods, 19: 43898

BOILERS
construction of, rules for, 19: 45507
description of mockup of serpentine tube, for potassium, 19: 44195 (TID-21256)
flow distributor model tests for prototype sodium-heated, 19: 44182 (BAW-1280-29)
materials compatibility in sodium-heated, study of Croloy 2¼ and Type 316 stainless steel, 19: 44133(R) (BAW-1280-21)
model of, for San Onofre Plant, 19: 45601(R) (WCAP-3750)

BOILING
burnout in annular flows, effects of electric fields on, (E), 19: 44190(R) (NYO-2404-67)
burnout in annular flows, effects of electric fields on, (E), 19: 44191(R) (NYO-2404-73)
burnout in tubular and annular flow channels, effects of nonuniform heat generation on, 19: 44183(R) (BAW-3238-8)
critical heat flux in water in internally cooled channels at 70 and 100 atm, effects of length/diameter ratio on, 19: 44184(R) (EURAEC-1281)
departure from nucleate, analysis for large closed-cycle reactors, 19: 45601(R) (WCAP-3750)
departure from nucleate, effects of burnout on, 19: 45601(R) (WCAP-3750)
flow regimes in high-pressure water systems, research program on, 19: 44193(R) (NYO-3304-5)
forced-convection heat transfer of potassium in serpentine tube, 19: 44195 (TID-21256)
heat transfer in nucleate, in liquid helium, 19: 44201
of potassium, two-phase heat transfer and fluid flow in, 19: 44187(R) (NASA-CR-54405)

BOILING REACTORS
description of CANDU-type light water, 19: 45694(R) (AECL-2251)
design and operation principles of, chemical engineering aspects of, 19: 45624
design with nuclear superheaters, 19: 45625
design with superheating system, 19: 45628(P)
fuel cycle economics for, 19: 45582 (NP-15320)
pressure vessels for heavy-water, use of prestressed concrete in, 19: 45506
steam separator design and development for, 19: 45574(R) (GEAP-4914)
use for nuclear power production, 19: 45725

BOLTS AND NUTS
stress analysis of bolted closures, 19: 44145 (TID-22138)

BONE DISEASES
etiology of osteomelofibrosis, 19: 43820

BONE MARROW
diseases of, pathology of, 19: 43820
effects of irradiated spinal cord grafts to chorioallantoid on production of, in chickens, 19: 43761
migration of cells of, in mice, 19: 43836
radiation dose to, calculation from neutron flux exposure, 19: 43854
radiation effects on erythropoiesis and myelopoiesis in, 19: 43731
radiation effects on mitotic activity and structural chromosomes in rat, integral dose effects on, 19: 43733
radiosensitivity of, effects of age, 19: 43915
radiosensitivity of, in mice, 19: 43792

BONE TUMORS
electron beam therapy of, dose calculations for, 19: 43916
incidence in Canada of, 1956 to 1961, 19: 43655
radiation effects on transplanted, in rats, 19: 43772
radioinduced by injected Thorotrast, 19: 43850

BONES
phosphorus activation reactions in, use in neutron dosimetry, 19: 44322
plutonium-239 elution from rat, effectiveness of chelating agents and other compounds for, 19: 43700
radiation effects on host acceptance of autogenous grafts of, in dogs, 19: 43835
radioactivity of Canadian, June 1965, 19: 44251 (NP-15519, pp 23-51)
strontium-85 elution from rat, effectiveness of chelating agents and other compounds for, 19: 43700
strontium-85 elution from, by chelating agents and salts, 19: 43706
strontium-90 content in, effects of age on, 19: 44250 (NP-15269)
strontium-90 content in human, in Japan, 1961 through 1963, 19: 44266
strontium-90 content in human, in Germany, 19: 44313

BORIC ACID
corrosive effects on A288 and X8001 aluminum alloys, 19: 44616(R) (ANL-7000, pp 122-37)
boric acid–H_2O, neutron spectra hardening in, thermal, 19: 45226 (KFK-294)

BORON
alpha reactions (α,n) at 2 to 5.4 Mev, neutron yields in, 19: 45301
determination in nuclear grade graphite, spectrochemical, 19: 43930
(JEN-145-DQ/I-46)
diffusion in boron carbide–uranium(IV) oxide fuel rods, 19: 44591(R) (CEND-3107-228)

BORON CARBIDES
analysis for carbon using electron microprobe, 19: 43966
neutron absorption efficiency in homogeneous uranium–water reactors, (E/T), 19: 45536
preparation of spherules of, 19: 44660(P)
reactions with uranium(IV) oxides at high temperatures, 19: 44591(R) (CEND-3107-228)

3269-33)
reactivity worths of rod clusters of, (E/T), 19: 45535 (WCAP-3269-47)
B_4C–UO_2, fabrication and stability for use as reactor fuel, 19: 44591(R) (CEND-3107-228)

BORON FLUORIDES
vapor pressures boron-10 and -11, 19: 44575

BORON ISOTOPES B-8
energy levels of, from helium-3 reactions (He-3,n) with lithium-6, (E), 19: 45355

BORON ISOTOPES B-10
deuteron reactions (d,p) at 13.5 Mev, cross sections for, (E), 19: 45336
lithium-6 reactions (Li-6,d) with, isospin violation in, (T), 19: 45265 (JINR-E-2244)
neutron reactions (n,α), spectra from, 19: 44450(R) (IBK-120a)
proton scattering at 155 Mev, cross sections and spectra in inelastic, 19: 45305
reactions (B-10,3n) with indium-115 at 37 Mev, xenon-122 energy levels from, (E), 19: 45285 (UCRL-16040)
reactions (B-10,5n) with indium-115 at 67 Mev, xenon-120 energy levels from, (E), 19: 45285 (UCRL-16040)
separation from boron-11 using boron trifluorides vapor pressure variation, 19: 44575

BORON ISOTOPES B-11
neutron reactions (n,γ) at 20 kev, cross sections for, (E), 19: 45246(R) (ANL-6877,pp 5-14)
proton reactions (p,α) at 1950 to 2800 kev, angular distributions from, (E), 19: 45291 (ZFK-PHA-12, pp 117-22)
proton scattering at 155 Mev, cross sections and spectra in inelastic, 19: 45305
reactions (B-11,4n) with indium-115, xenon-122 energy levels from, (E), 19: 45285 (UCRL-16040)
reactions (B-11,4n) with indium-127, cerium-134 energy levels from, (E), 19: 45285 (UCRL-16040)
separation from boron-10 using boron trifluorides vapor pressure variation, 19: 44575

BORON ISOTOPES B-12
energy levels of, parity and spin of, (E), 19: 45246(R) (ANL-6877,pp 5-14)

BORON NITRIDES
reactions with molybdenum and tungsten at high temperatures, 19: 44228 (N64-31011)
use as an isolating medium in the preparation of uranium carbide and thorium carbide spherules, 19: 44659(P)
use as isolating medium in production of boron carbide spherules, 19: 44660(P)

BORON OXIDES
B_2O_3–PbS–MoS_2, radiation effects on lubricant wear properties of solid films, 19: 44095

BORON SYSTEMS
Al–B–Hf, phase studies of, 19: 44719
Al–B–Ti, phase studies, 19: 44719
Al–B–Zr, phase studies, 19: 44719

BOROSILICATE GLASS
strengthening by alumina particles, 19: 43997(R) (UCRL-11889)

BOSONS
interactions of spin-0, N/D method and diffraction model in elastic, (T), 19: 45088
interactions of three, vertex functions for spin-zero, 19: 45029 (NP-15382)
properties of liquid helium-4, pseudospin model for, (T), 19: 45203
resonance properties of, review, 19: 45046 (UCRL-16295)
spectral formulas for, in Heisenberg nonlinear theory, 19: 45094
systems of interesting, theory of many-body, 19: 44806 (IS-T-19)

BRAIN
carbon-14 uptake by amino acids in rat, *in vitro*, 19: 43690
radiation effects on myelin from rat, 19: 43682(R) (UCLA-12-565, pp 33-57)
radiation effects on synthesis of proteins in rat, 19: 43682(R) (UCLA-12-565, pp 33-57)
radiation effects on metabolism of 5-hydroxytryptamine in rat, 19: 43810

radiosensitivity of, in rat embryos, 19: 43768
toxic effects of radioalbumin on, 19: 43883(R) (UCLA-12-565, pp 65-85)
BRAIN TUMORS
localization of, development of scanning methods for, 19: 43648(R) (UCLA-12-565, pp 87-96)
BRASS
compressibility and dilatational contribution to thermal capacity at 77 to 800°K, 19: 45718 (UCRL-11662)
extrusion by hydrostatic methods, 19: 44651
BRAZED JOINTS
nondestructive testing of, comparison of methods for, 19: 44207(R) (ANL-7000, pp 146-52)
BRAZING
of titanium, use of rhenium coatings in, 19: 44645 (JPRS-24761, pp 12–16)
BREATH
analysis for radon, 19: 43672(R) (TID-22131)
inhalation of cigarette smoke by dogs, instrument for control of, 19: 43668 (HW-SA-3618)
BREEDER REACTORS
blankets for fast, development of paste, 19: 45561 (APDA-172)
coolant flow distribution system for liquid-metal cooled, 19: 45520(P)
development of fast, in France and Germany, 19: 45623
development of Karlsruhe, 19: 45583(R) (NP-15365)
development of, for fuel production, 19: 45621
fuels for fast, merits of thorium, 19: 45605(T) (ORNL-tr-788)
use for nuclear power production, 19: 45725
BREMSSTRAHLUNG
emission in proton interactions at 48 Mev, cross sections for, (E), 19: 45097
emission in storage rings, (T), 19: 44865 (LAL-1134)
energy spectra of internal, from electron capture decay of chlorine-36, (E), 19: 45345
interactions with protons at 0.6 to 5.5 Bev, meson (π) production in, (E), 19: 44999 (DESY-65/5)
reactions (γ,d) with carbon at 400 to 720 Mev, cross sections for, (E/T), 19: 45309
reactions (γ,f) with thorium and uranium at 300 to 1000 Mev, cross sections for, (E), 19: 45329
reactions (γ,p) and (γ,t) with helium-4 at 24 to 56 Mev, E1 cross section for, (E), 19: 45353
reactions (γ,t) with lithium-6 at 32 and 40 Mev, spectra of, (E), 19: 45374
reactions with carbon, electron pair production in, (E/T), 19: 45256 (HUX-2752-4)
BRITISH REACTORS
description of superheated-steam heavy-water, (E), 19: 45613
fuel fabrication and processing facility for, (E), 19: 45612
BRITTANY POWER REACTOR (EL-4)
description and performance of, (E), 19: 45614
BROMIDE IONS
effects on radiolysis of cytosine and thymine, 19: 43682(R) (UCLA-12-565, pp 33-57)
BROMIDE SPACE
measurement in man, tracer method, 19: 43898
BROMINE
determination in pharmaceutical preparations by radiometric methods, 19: 43950
reactions with linoleic acid, products from, 19: 43681(R) (UCLA-12-565, pp 17-31)
spin precession in compounds of muonium and, (T), 19: 45278 (NP-15389)
spin precession in μ-mesic, 19: 45278 (NP-15389)
BROMINE ISOTOPES Br-79
neutron reactions with, resonances in, (E), 19: 45296
BROMINE ISOTOPES Br-81
neutron reactions with, resonances in, (E), 19: 45296
BROMINE ISOTOPES Br-82
decay of, gamma spectra from, 19: 45679(R) (NYO-1859-11)
diagnostic use for body fluid measurements, 19: 43898
BROOKHAVEN ALTERNATING-GRADIENT SYNCHROTRON
magnetic fields in, high-field limitations on, (T), 19: 44858 (BNL-9480)
BROOKHAVEN NATIONAL LAB., UPTON, N. Y.
meteorological program, 19: 44762 (BNL-914, pp 1-3)
BUBBLE CHAMBERS
bibliography, 19: 44366 (AED-C-06-12)
design of fast-cycling liquid-hydrogen, 19: 44459 (PPAD-2137-561)
hydrodynamics of resonance, 19: 44523
meson (π^-) reactions in, meson (π^0) intensity from, 19: 44439 (CERN-65-4(Vol.II), pp X37-43)
particle track analysis in, order code for computerized, 19: 44446 (COO-1018-1050)
particle track artificial construction in, by Monte Carlo method, 19: 44433 (CERN-65-4(Vol.II), pp IX44-7)
particle tracks in, device for automatic analysis of, 19: 44496
performance of hydrogen–neon mixtures for, 19: 44375 (BNL-9425)
research with, bibliography for, 19: 44812(R) (UCRL-16099)
BUBBLES
illumination of leveling instrument, use of radioactive gases for, 19: 44567(P)
rise velocity in inclined tubes, 19: 44192(R) (NYO-3114-9)
BUTANE
spectra of solid, slow-neutron-scattering analysis of, (E), 19: 44050
1,3-BUTANEDIONE, 1-PHENYL- COMPLEXES
with rare earths, preparation and properties, 19: 44006
***tert*-BUTYL HYDROPEROXIDE**
radiolysis of, kinetics of gamma, 19: 44089
***tert*-BUTYL PEROXIDE**
radiolysis of, kinetics of gamma, 19: 44089
BUTYL PHOSPHATES
solvent properties for thorium and rare earths, 19: 44125
BUTYLAMINE
radiolysis of, yields in gamma, 19: 44072
radiolysis products of, gamma, 19: 44053 (AFML-TR-65-166)

C

CADMIUM
determination in uranium compounds, atomic absorption spectrophotometric, 19: 43935 (NIJS-R-447)
effect on determination of copper in bismuth by neutron activation methods, 19: 43941
neutron absorption cross sections at 24 kev, (E), 19: 45230
neutron reactions (n,n′γ) with, cross section for, 19: 45263 (JAERI-1078)
performance for neutron flux determination in reactors, 19: 45560 (ANL-7011)
phase transformations in, relation of c/a ratio and elastic moduli temperature dependence with, 19: 44676(R) (ANL-7000, pp 176-82)
separation from uranium by ion exchange, 19: 44119
CADMIUM ALLOYS
of rod clusters of, (E/T), 19: 45535 (WCAP-3269-47)
Cd–In–Ag, radiation effects on plated, 19: 44736 (ANL-6883)
Cd–In–Ag, reactivity effects of cruciform rods of, in large PWR, 19: 45533 (WCAP-3269-33)
CADMIUM CARBIDES
neutron absorption efficiency in homogeneous uranium–water reactors, 19: 45536
CADMIUM ISOTOPES Cd-109
deposition on copper wires by electroplating, for use as soft x-ray sources, 19: 44139 (ORNL-TM-1174)
CADMIUM ISOTOPES Cd-115
metabolism by marine organisms, 19: 43669(R) (NP-15159)
CADMIUM SULFIDES
diffusion of copper into, optical absorption study, 19: 43997(R) (UCRL-11889)
evaporation mechanism studies, 19: 43997(R) (UCRL-11889)
neodymium ion reactions at 200 kev, replacement collision doping by, (E), 19: 44939
radioinduced luminescence of, electron, 19: 45478 (NP-15110)
CALCITES
oxygen-18 fractionation between coexisting dolomite and, in Freeport formation, Penn., 19: 44241
CALCIUM
content in experimental dog diet, control of, 19: 43675(R) (UCD-472-112, pp 73-9)
depletion from calves of, by hemodialysis, tracer study, 19: 43673 (TID-22147)
determination by flame photometry using d-c plasma jets, 19: 43924 (AERE-R-4990)
determination by flame photometry, 19: 44122
determination in biological samples, after neutron activation, 19: 44253(R) (NYO-2174-36)
determination in nuclear grade graphite, spectrochemical, 19: 43930 (JEN-145-DQ/I-46)
meson (μ^+) depolarization in targets of, (E), 19: 45080
metabolism in human fetuses of, 19: 43701
metabolism in nursing puppies, effects of strontium content of diet on, 19: 43676(R) (UCD-472-112, pp 80-5)
separation from magnesium, potassium, sodium, and strontium by ion exchange, 19: 44122
separation from uranium by ion exchange, 19: 44119
CALCIUM CARBONATES
uranium-234/-238 ratio in US coastal, 19: 44263
CALCIUM CHLORIDES

corrosive effects on titanium alloys at 650°F, 19: 44621 (CONF-651006-1)
effects on strontium-85 elution from mouse bones, 19: 43706
CALCIUM FLUORIDES
ductility and yield points of crystalline, effects of impurities on, 19: 45679(R) (NYO-1859-11)
radiation effects on lubricant wear properties of solid films, 19: 44095
CALCIUM HYDROXIDES
neutron inelastic scattering spectra of deuterated and normal, vibrational modes in, (E), 19: 45482
CALCIUM ISOTOPES
separation in calutron, effects of low pressure and high stability operation on contamination in, 19: 44573 (ORNL-P-515)
CALCIUM ISOTOPES Ca-39
half life, 19: 45262 (IS-T-29)
CALCIUM ISOTOPES Ca-40
gamma reactions (γ,n) with, half life determination from, 19: 45262 (IS-T-29)
meson (μ^-) capture by, asymmetry in neutron angular distributions from, (E), 19: 45274 (NEVIS-136)
meson (μ^+) depolarization quenching in, as function of longitudinal magnetic field, (E/T), 19: 45079
proton reactions (p,γ) at 648 kev, radiative lifetime of excited scandium-41 from, (E), 19: 45344
CALCIUM ISOTOPES Ca-42
deuteron reactions (d,p) at 7 Mev, cross sections for, (E), 19: 45323
CALCIUM ISOTOPES Ca-44
deuteron reactions (d,p) at 7 Mev, cross sections for, (E), 19: 45323
CALCIUM ISOTOPES Ca-45
distribution of intravenously injected, effects of time on, 19: 43883(R) (UCLA-12-565, pp 65-85)
excretion in feces and urine by colostomized pullets, determination by isotopic dilution method, 19: 43693
radiation effects on uptake of, by *Nitella flexilis*, 19: 43818
CALCIUM ISOTOPES Ca-47
gastrointestinal absorption in dogs, 19: 43677(R) (UCD-472-112, pp 86-96)
CALCIUM OXIDES
effect on allotropic transformations of rare earth sesquioxides, 19: 44731
Al_2O_3–CaO–SiO_2, diffusion in, ternary, 19: 43997(R) (UCRL-11889)
CaO–GeO_2, glass formation limits in, calculation of upper, 19: 44016
CaO–SiO_2, glass formation and structure in, 19: 44015
CALCIUM SULFIDES
sublimation of, mass spectrometric study, 19: 43997(R) (UCRL-11889)
CALDER HALL REACTORS
contamination control, 19: 45608
fuel fabrication and processing facilities for, (E), 19: 45612
operation and performance of, (E), 19: 45613
operation experience of, (E), 19: 45611
CALIFORNIUM ISOTOPES
neutron cross sections of, tabulation, (E), 19: 45250 (BNL-325(2nd Ed.) (Suppl.2)(Vol.III))
production in high-flux Savannah River Production Reactors, 19: 45639 (DP-999, pp 19-28)
CALIFORNIUM ISOTOPES Cf-252
fission of, prompt neutron spectra from spontaneous, (T), 19: 45302
CALORIMETERS
resistor elements for, fabrication of thin-film, 19: 44344 (K-L-1944)
CALUTRONS
contamination in calcium isotope separation, effects of low pressure and high stability operation on, 19: 44573 (ORNL-P-515)
CAMERAS
design of stereo-, for use with cloud chambers, 19: 44494
CANADA
fallout monitoring, June 1965, 19: 44251 (NP-15519, pp 23-51)
CANADIAN REACTORS
environs monitoring, 1964, 19: 44294 (NP-15519, pp 3-22)
environs monitoring, June 1965, 19: 44295 (NP-15519, pp 52-60)
CANDU REACTOR
description of, 19: 45694(R) (AECL-2251)
fuel burnup in, plutonium, 19: 45578 (JAERI-1080)
CARBIDES
spectra of, effects of chemical combination on soft x-ray K emission bands of carbon in, (E), 19: 44944
CARBOHYDRATES
catabolism in higher plants, review of, 19: 45697(R) (COO-330-11)
radiation effects on gluconeogenesis, effects of cortisone in rats, 19: 43837
CARBON
alpha reactions (α,n) at 2 to 5.4 Mev, neutron yields in, 19: 45301
bremsstrahlung reactions with, electron pair production in, (E/T), 19: 45256 (HUX-2752-4)
bremsstrahlung reactions (γ,d) at 400 to 720 Mev, cross sections for, (E/T), 19: 45309
detection and separation from sodium loops, in-line devices for, 19: 44162(R) (APDA-174, pp 33-55)
determination in carbides using electron microprobe, 19: 43966
determination in liquid hydrocarbons by fast neutron moderation, 19: 43968
effects of coatings of, on silver alloy brazing of beryllium to niobium–1 zirconium alloy, 19: 44606 (PWAC-483)
effects on mechanical properties of niobium–zirconium alloys, 19: 44605 (PWAC-464)
effects on stress rupture of type 304 stainless steel, 19: 44623 (NAA-SR-10487)
electron scattering by atomic, noniterative approach to elastic, (T), 19: 44953
fabrication of articles of, having high density and low permeability, 19: 44669(P)
meson (K) stopping by emulsions loaded with, 19: 44398 (CERN-65-4 (Vol.II), pp III12-16)
meson (μ^+) depolarization quenching in, as function of longitudinal magnetic field, (E/T), 19: 45079
meson (μ^+) depolarization in targets of, (E), 19: 45080
neutron cross sections for, from 0.414 ev to 5.5 Mev, 19: 45244 (AEEW-M-472)
photon reactions in Bev range, meson (π) and (ρ) production in, (E), 19: 45000 (HUX-2752-7)
preparation of spherules of, 19: 44659(P)
radiation effects on coatings of pyrolytic, on fuel particles, 19: 44740 (BMI-1737)
radiation effects on pyrolytic coatings of, on fuel particles, 19: 44748 (ORNL-P-1505)
reactions with beryllium, hafnium, and magnesium oxides at 2450°C, 19: 44598(R) (GEMP-49A)
reactions with niobium–zirconium alloy in potassium–sodium environment at 1250°F, 19: 44626 (TIM-896)
solubility in liquid zirconium at 2700 to 4000°K, 19: 44701(R) (TID-22144)
spectra of molecular, in laser-produced graphite jets, (E), 19: 44803(R) (ANL-6877, pp 21-7)
spectra of, effects of chemical combination on soft x-ray K emission bands of, (E), 19: 44944
use as an isolating medium in the preparation of uranium carbide and thorium carbide spherules, 19: 44659(P)
use of amorphous, as isolating medium in production of boron carbide spherules, 19: 44660(P)
CARBON (ACTIVATED)
uses in determination of iodine-131, 19: 43958
CARBON DIOXIDES
analysis for tritium by gas chromatography, 19: 43926 (CEA-R-2800)
carbon and oxygen isotopic ratios in, mass spectrometer for determining, 19: 43963
carbon-14 uptake by, in rat cerebral tissue, 19: 43690
corrosive effects on niobium–zirconium alloys, 19: 44629
corrosive effects on copper–uranium intermetallic compound at 350 to 850°C, 19: 44631
reactions with uranium in fuel elements, fission gas release in, 19: 44632
CO_2–D_2O, oxygen-17 and oxygen-18 equilibrium distribution in, 19: 44007
CO_2–H_2O, oxygen-17 and oxygen-18 distribution equilibrium in, 19: 44007
CARBON ISOTOPES
abundance ratios in carbon dioxide, mass spectrometer for determining, 19: 43963
properties for tracer use in biology, 19: 43707
CARBON ISOTOPES C-11
recoil reactions in liquid hydrocarbons, 19: 44057 (IS-T-23)
CARBON ISOTOPES C-12
alpha reactions (α,2n) at 28 Mev, spectra from, (E), 19: 45308
carbon-12 reactions (C-12,α) with, statistical fluctuations in excitation function for, (T), 19: 45313
deuterium reactions (d,α) at 10.2 to 12.9 Mev, angular distributions for, (E), 19: 45289 (ZFK-PHA-12, pp 99-105)
electron scattering by, nucleon momentum distribution from, (T), 19: 45279 (NP-15415)
gamma reactions (γ,n) in liquid hydrocarbons, recoil reactions of carbon-11 produced by, 19: 44057 (IS-T-23)
meson (μ^-) capture by, asymmetry in neutron angular distributions from, (E), 19: 45274 (NEVIS-136)

photon reactions (γ,n) to 33 Mev cross sections and spectra from, (E), 19: 45330
proton scattering at 155 Mev, cross sections and spectra in inelastic, 19: 45305
reactions (C-12,4n) with tin-116 at 80 Mev, barium-124 energy levels from, (E), 19: 45285 (UCRL-16040)
CARBON ISOTOPES C-14
beta particles from, design and performance of scintillation fibers for detecting, 19: 44451 (IITRI-578P26-8)
content in atmosphere of Japan, 19: 44267
determination in archeological samples, proportional counter technique for, 19: 44526
determination in aqueous solutions by scintillation counting, 19: 43945
determination in amino acids separated by ion exchange, scintillation method for continuous, 19: 43976
incorporation into DL-alanine and DL-glycine, 19: 44047 (NP-15268)
measurement in chromatographic column fractions, use of photomultiplier tube for continuous automatic, 19: 43949
tracer use of, in studies of plant metabolism, 19: 43685
uptake by amino acids in rat cerebral tissue, *in vitro*, 19: 43690
use in carbonate age estimation, 19: 44271
CARBON MONOXIDES
electron reactions with, classical calculation of cross sections for inelastic, (T), 19: 44947
CARBON STEEL
corrosion by boiling water and steam in simulated reactor environment, 19: 44627
production of high-strength, 19: 43997(R) (UCRL-11889)
CARBON SYSTEMS
Al–C–Mo, superconductivity, 19: 43997(R) (UCRL-11889)
Al–C–O, thermodynamic analysis of equilibrium phases in, 19: 43996 (UCRL-11699)
C–Co–Mn, crystal structure studies, 19: 44679(R) (ANL-7000, pp 205-12)
C–Mo–Ti–Zr, mechanical properties at high temperatures, 19: 44674(R) (ANL-7000, pp 69-83)
C–Mo–V, superconductivity, 19: 43997(R) (UCRL-11889)
C–Na, carburization effects on type 304 stainless steel, 19: 44624 (NAA-SR-Memo-4387)
C–Nb–Zr, development of, with high-temperature strength, 19: 44605 (PWAC-464)
C–O–U, density and lattice parameters, effects of composition on, 19: 44612(R) (USBM-RC-1199)
C–Pu–U, corrosion by air at room temperature, 19: 44587(R) (ANL-7000, pp 3-63)
C–Pu–U, lattices parameters as function of composition, 19: 44678(R) (ANL-7000, pp 186-200)
C–Pu–U, preparation, 19: 44587(R) (ANL-7000, pp 3-63)
C–Pu–U, susceptibility at 25°C, 19: 44678(R) (ANL-7000, pp 186-200)
C–W_2C–ZrC, behavior at 3250°K in graphite crucible, 19: 44701(R) (TID-22144)
CARBON TETRABROMIDE
radioinduced addition to ethylene in carbon tetrachloride solutions, 19: 44065
CARBON TETRACHLORIDE
radioinduced reactions with benzene in flow irradiator, calculated product accumulation in, 19: 44061(T) (AEC-tr-6567)
radiolysis in flow irradiator, calculated product accumulation in, 19: 44061(T) (AEC-tr-6567)
CARBONATES
age of Lake-Lahontan and -Bonneville lacustrine, carbon-14 and thorium-230, 19: 44271
uranium transport in aqueous solutions of, complexing in, 19: 44278
CARBONATITES
strontium-87 to strontium-86 ratio in, Ontario, Canada, 19: 44257
CARCINOGENESIS
radiation, quantitative mechanism for uv, 19: 43821
role of radioinduced somatic mutations in, 19: 43754
CARCINOMAS
radiation effects on cell cultures of intraoral, x, 19: 43802
radiotherapy of bladder, 19: 43894
radiotherapy of cervical, pregnancy occurrence after primary, 19: 43891
radiotherapy of thyroid, using iodine-131, 19: 43918
radiotherapy of uterine, combination of surgery with, 19: 43884
radiotherapy of uterine, late pathological effects, 19: 43907
radiotherapy of uterine, complications in urinary tract from, 19: 43921
therapy of metastasizing mammary, with radioinduced pituitary ablation, 19: 43920
zinc-65 uptake and distribution in human, 19: 43699
CAROLINAS-VIRGINIA TUBE REACTOR
cooling system operation at high pD, 19: 45568 (CVNA-238)
development and operation, Oct.–Dec. 1964, 19: 45567 (CVNA-235)
CASCADES
design for potassium isotope separations by molecular distillation, 19: 43931 (K-1650)
CATARACTS
effects on content of amino acids and sugars in rabbit, 19: 43755
CATTLE
calcium depletion from calves by hemodialysis, tracer study, 19: 43673 (TID-22147)
phosphorus depletion from calves by hemodialysis, tracer study, 19: 43673 (TID-22147)
radiation effects on lactation in dairy cows, 19: 43800
radiation effects on lactation in dairy, 19: 43801
radiation effects on metabolism in dairy, 19: 43801
strontium depletion from calves by hemodialysis, tracer study, 19: 43673 (TID-22147)
water content in, tracer technique for determining whole-body, 19: 43694
CAVES
description of Brookhaven alpha-gamma metallurgy hot cell, 19: 44163 (BNL-9502)
description of Thorium–Uranium Recycle Facility, 19: 44167 (ORNL-P-1521)
design of, at Czechoslovak Nuclear Research Institute, 19: 44068
CAVITATION
damage on coated impeller, studies, 19: 44197 (TIM-895)
CELLULOSES
performance of nitro-, for alpha detection, 19: 44384 (CERN-65-4 (Vol.II), pp II-8)
radiation effects on properties of, 19: 44063
CENTRIFUGAL PUMPS
development for SNAP-50, cavity evacuation study for, 19: 45660 (TIM-919)
impeller design system for, 19: 44148 (TIM-916)
CENTRIFUGATION
effects on growth of wheat seedlings, 19: 43717 (NASA-CR-303)
CENTRIFUGES
instrumentation for, design and performance of g-second integrator, 19: 45707 (SC-DR-65-261)
CERAMIC MATERIALS
mechanical properties of composites with brittle matrices, 19: 43997(R) (UCRL-11889)
properties for use in thermionic cells, 19: 44980(R) (NP-15433)
reactions with cesium vapor, 19: 44980(R) (NP-15433)
research program on, 19: 43997(R) (UCRL-11889)
CERIUM
effects on recrystallization of magnesium, 19: 44710(T) (JPRS-24761, pp 29–40)
stability of plasma of, in gas discharges, 19: 45403 (NP-15445)
CERIUM ALLOYS
Ce–Co–Pu, analysis for cobalt by controlled potential electrodeposition, 19: 43934 (LA-3345)
Ce–Cu, crystal structure studies, 19: 44678(R) (ANL-7000, pp 186-200)
Ce–stainless steel, corrosion by steam at 650°C, 19: 44616(R) (ANL-7000, pp 122-37)
CERIUM COMPLEXES
with 5-nitrobarbituric acid and pyridine bases, preparation and stability, 19: 44027
CERIUM FLUORIDES
reactions with cerium sulfides, preparation of cerium sulfide fluoride by, 19: 44024
CERIUM IONS
electron paramagnetic resonance of, in single-crystal lead molybdate, 19: 44017
oxidation of trivalent to tetravalent, electrolytic, 19: 44026
oxidation-reduction reactions of, polarization during, 19: 44002(T) (AEC-tr-6572)
CERIUM ISOTOPES
production in thermal-neutron fission of uranium-235, (E), 19: 45260(R) (IDO-14660)
CERIUM ISOTOPES Ce-132
decay of, conversion electron and gamma spectra from, 19: 45269 (JINR-P-2236)
CERIUM ISOTOPES Ce-133
decay of, conversion electron and gamma spectra from, 19: 45269 (JINR-P-2236)
CERIUM ISOTOPES Ce-134
energy levels, (E/T), 19: 45285 (UCRL-16040)
CERIUM ISOTOPES Ce-135
decay of, conversion electron and gamma spectra from, (E), 19: 45268 (JINR-P-2235)
CERIUM ISOTOPES Ce-144

determination in lung tissues, spectrometric, 19: 44292(R) (NP-15173)
determination in mixture with cesium-134, strontium-90, or zinc-65, method for, 19: 43962
diffusion from irradiated molybdenum–rhenium–tungsten alloy, 19: 44599(R) (GEMP-50A)
metabolism by marine organisms, 19: 43699(R) (NP-15159)
separation from wastes at Hanford, 19: 45690 (RL-SA-40)
uptake by clams, 19: 43663
use as power source for underwater vehicle propulsion, 19: 44572

CERIUM OXIDES
effects on optical properties of silicate glasses, 19: 44030
phase transformations in, at 1800 to 2400°C, 19: 44731

CERIUM SULFIDES
reactions with cerium fluorides, preparation of cerium sulfide fluoride by, 19: 44024

CERIUM VANADATES
crystallographic and optical properties of hydrated, 19: 44032(T)

CESIUM
charge transfer with cesium ions, cross section, 19: 43997(R) (UCRL-11889)
electron reactions with atoms of, excitation cross sections for, (E), 19: 44935 (NP-15168)
ion density of magnetically contained plasma of, Langmuir probe effects on, (E/T), 19: 45393 (IPP-2/38)
ionization of, auto-, (E), 19: 44981 (NP-15435)
optical orientation of atoms of, in magnetic fields, 19: 44963
plasma of, collision probabilities in, (E), 19: 45399(R) (NASA-CR-54451)
reactions with ceramic materials, 19: 44980(R) (NP-15433)
reactions with metal oxides at high temperatures, 19: 44685 (CONF-650908-5)
separation from liquid wastes by ion exchange using zeolite taff, 19: 44123
separation from sodium by ion exchange, 19: 44091
sorption on marine sediments, role of exchangeable magnesium and potassium in, 19: 43964
use in reservoirless thermionic converters, 19: 44989

CESIUM IONS
charge transfer with cesium, cross section, 19: 43997(R) (UCRL-11889)
collision probability with cesium atoms in plasma, (E), 19: 45399(R) (NASA-CR-54451)
copper sputtering by 1 to 10 kev, tracer technique for, (E), 19: 44964

CESIUM ISOTOPES
production in thermal-neutron fission of uranium-235, (E), 19: 45260(R) (IDO-14660)

CESIUM ISOTOPES Cs-134
determination in mixture with cerium-144, method for, 19: 43962
metabolism by marine organisms, 19: 43669(R) (NP-15159)

CESIUM ISOTOPES Cs-137
content in Alaskan natives, 19: 44289 (HW-SA-3750)
content in Australian milk, 1963, 19: 44309
content in diet in Japan, 1961 to 1964, 19: 44264
content in Finnish Lapp diet, 19: 44305
content in irradiated fuel capsule, 19: 45542(R) (BAW-272)
content in man of, in Switzerland, 1963, 19: 44269
content in milk in Japan, 1961 to 1964, 19: 44268
content in milk of, in Switzerland, 1963, 19: 44269
content in rice in Japan, 1959 and 1962, 19: 44265
content of caribou meat, 19: 44289 (HW-SA-3750)
determination in large volumes of seawater, method for, 19: 44296 (NYO-4700(Rev.)(Suppl.II))
determination in sea water, 19: 44253(R) (NYO-2174-36)
diffusion from irradiated molybdenum–rhenium–tungsten alloy, 19: 44599(R) (GEMP-50A)
distribution in farm soil at Nevada Test Site, 19: 43662(R) (UCLA-12-565, pp 97-128)
effects on cholinesterase activity, 19: 43775
effects on Drosophila oogonia, mutagenic, 19: 43724(R) (TID-22160)
effects on Drosophila sperm, mutagenic, 19: 43724(R) (TID-22160)
separation from wastes at Hanford, 19: 45690 (RL-SA-40)
uptake by humans in Los Angeles, 1960–64, 19: 43883(R) (UCLA-12-565, pp 65-85)

CESIUM SYSTEMS
Ar–Cs, cesium excitation cross sections from electron drift velocities in, (E), 19: 44935 (NP-15168)

CHARCOAL
sorptive properties for iodine released by irradiated fuel, 19: 44303 (TRG-Report-888)

CHARGED PARTICLE BEAMS
control in alternating-gradient synchrotrons, by magnet structure displacement, (T), 19: 44875 (UCRL-16229)
focusing by random stationary electric-magnetic field, stigmatic, 19: 44851
particle losses in storage rings, (T), 19: 44865 (LAL-1134)
use of polarized, in nuclear reactions, 19: 45337

CHARGED PARTICLES
detection and measurement of, using scintillation detectors, (E), 19: 44499
detection using large single crystals of silver chloride, 19: 44378 (CERN-65-4(Vol.I), pp 2-15)
effects on nuclear emulsions, latent image formation and threshold oxidation in, 19: 44393 (CERN-65-4(Vol.II), pp II50-63)
interactions of, real part of forward amplitude for, (T), 19: 45048(T) (ANL-Trans-217)
motion in electric fields, kinetic equation for multiple acceleration of, 19: 44864 (JINR-P-2253)
motion in geomagnetic fields, model current sheets for trajectories of, (T), 19: 45168
motion in linear accelerator, computer program for analyzing, 19: 44867 (MURA-713)
reactions in hydrogen-enriched nuclear emulsions, ionization density of, 19: 44435 (CERN-65-4(Vol.II), pp IX62-5)
reactions with silver bromide in emulsions, latent image formation in, 19: 44387 (CERN-65-4(Vol.II), pp III-10)
tracks in silver chloride monocrystals, determination of, 19: 44386 (CERN-65-4(Vol.II), pp I21-5)

CHELATES
effectiveness in removal of radioisotopes from body, 19: 43700

CHEMICAL ANALYSIS
methods for plutonium, bibliography on, 19: 43925 (ANL-6956)
methods for trace impurities, review of emission-spectroscopy, 19: 43929 (IS-1237)

CHEMICAL ENGINEERING
relation to nuclear power engineering, 19: 44155

CHEMICAL RADIATION DETECTORS
calibration of ferrous sulfate dosimeter, 19: 44540
chemiluminescence properties of hydrogen peroxides for use as, 19: 44067
design of high dose rate organic, 19: 44525
fading of thermoluminescent lithium fluoride, 19: 44076
performance of films, glasses, and ion sulfate solutions as, for electron and protons, 19: 44093
properties of ferrous ammonium sulfate–cupric chloride, for kilocurie cobalt-60 sources, 19: 44372 (AFCRL-65-470)

CHEMICALS AND REAGENTS
effects on phosphatase content of granulocytes, of man, 19: 43829
leukemogenic effects in man of, 19: 43828
research program on inorganic, 19: 43997(R) (UCRL-11889)
use of non-isotopic solid, in radiocoulometric titration, 19: 43952

CHEMISTRY
bibliography on gases and gas-condensed phase reactions, 19: 43993 (NP-15379)
bibliography on high-temperature, of condensed materials, 19: 43994 (NP-15381)

CHERENKOV DETECTORS
design for analyzing beams at 4 to 12 Bev/c, 19: 44376 (BNL-9466)

CHICKENS
effects of irradiated spinal cord grafts to chorioallantoid on marrow production in, 19: 43761
excretion of calcium-45 mineral nutrients, and phosphorus-32 in feces and urine by, determination by isotopic dilution method, 19: 43693
iodine-131 uptake by blood plasma, muscle, and thyroid in, age and dose effects on, 19: 43704

CHILE
uranium reconnaissance in Aisen area of southern, 19: 44273 (RME-4557(Rev.))

CHIMERAS
immune reactions in mouse erythrocyte, 19: 43657

CHINON REACTORS
fuel management procedures for, 19: 45607

CHINON REACTORS (EDF-1)
description and performance of, (E), 19: 45614

CHINON REACTORS (EDF-2)
description and performance of, (E), 19: 45614

CHINON REACTORS (EDF-3)
description and performance of, (E), 19: 45614

CHLORAMPHENICOL
effects on radiokinetic effects of nitrofuranides on herb seeds, 19: 43870

CHLORIDE IONS
effects on radiolysis of acetylene, 19: 44082
effects on radiolysis of cytosine and thymine, 19: 43682(R) (UCLA-12-565, pp 33-57)

CHLORIDE SPACE
measurement in man, tracer method, 19: 43898
CHLORIDES
corrosive effects on fuel element cladding, 19: 45601(R) (WCAP-3750)
determination in beer, activation, 19: 43944
CHLORINE
effects on pyrolysis of terphenyls, 19: 44044 (AECL-2218)
spin precession in μ-mesic, 19: 45278 (NP-15389)
spin precession in compounds of muonium and, (T), 19: 45278 (NP-15389)
CHLORINE ISOTOPES Cl-36
decay of, internal bremsstrahlung spectra from electron-capture, (E), 19: 45345
CHLORINE ISOTOPES Cl-38
production in tunnel of Frascati electron linear accelerator, (T), 19: 44866 (LNF-65/21)
CHLORITES
sorptive properties for cesium, role of exchangeable magnesium and potassium in, 19: 43964
CHLOROPHYLLS
genetic factors influencing, in peas, 19: 43734
radiation effects on cobalt and copper substituted and normal, spectra of, 19: 44087
CHOLESTEROL
determination in blood, of dogs, 19: 43674(R) (UCD-472-112, pp 36-43)
CHOLINESTERASES
radiation effects of cesium-137 and strontium-90 on activity of, 19: 43775
CHROMATOGRAPHIC SEPARATIONS
development of high-speed thin-layer, 19: 44118 (UCRL-16015)
CHROMATOGRAPHY
radioactivity measurement in paper, apparatus for, 19: 43984(P)
resolution in, research on, 19: 44113(R) (COO-748-1)
use of thin-layer, for determination of radioisotopes in biomedical samples, 19: 43659
CHROMIUM
deposition on uranium dioxide particles, 19: 44596 (EURAEC-1392)
extrusion by hydrostatic methods, 19: 44651
hyperfine field, 19: 43997(R) (UCRL-11889)
neutron absorption cross sections at 24 kev, (E), 19: 45230
neutron cross sections for, from 0.414 ev to 5.5 Mev, 19: 45244 (AEEW-M-472)
reactions with beryllium, copper, stainless steel, and niobium alloys to 760°C *in vacuo*, 19: 44606 (PWAC-483)
reactions with fissium–plutonium–uranium alloys at 750°C, 19: 44587(R) (ANL-7000, pp 3-63)
reactions with plutonium–thorium–uranium alloys at 650°C, 19: 44674(R) (ANL-7000, pp 69-83)
CHROMIUM ALLOYS
Al–Cr–Fe–Y, corrosion by steam at 550°C of 1041, effects of preoxidation and strain on, 19: 44598(R) (GEMP-49A)
Al–Cr–Fe–Y, corrosion by steam at 730°C, 19: 44598(R) (GEMP-49A)
Al–Cr–Fe–Y, elastic constants at 30 to 1200°C of 2541, dynamic, 19: 44598(R) (GEMP-49A)
Al–Cr–Fe–Y, oxidation by air at 900 and 1100°C, effects of composition on, 19: 44598(R) (GEMP-49A)
Al–Cr–Fe–Y, reactions with iron–uranium at 950 and 1100°C in air, 19: 44598(R) (GEMP-49A)
Al–Cr–Mg, erosion by water of rotating disks of, 19: 44625 (TIM-894)
Al–Cr–U, fabrication of reactor fuels of, 19: 44665(P)
Cr–Ni, corrosion by steam at high temperature, 19: 45572(R) (GEAP-4755)
Cr–Ni, reactions with plutonium–thorium–uranium alloys at 650°C, 19: 44674(R) (ANL-7000, pp 69-83)
Cr–Pt, crystal structure studies, 19: 44678(R) (ANL-7000, pp 186-200)
Cr–Ti, phase studies, 19: 44714
Cr–Ti–V, fabricability of, effects of composition on, 19: 44587(R) (ANL-7000, pp 3-63)
Cr–Ti–Zr, phase studies, 19: 44714
Cr–Zr, phase studies, 19: 44714
CHROMIUM CARBIDES
analysis for carbon using electron microprobe, 19: 43966
CHROMIUM COUPLES
Cr/Re–W, thermoelectric potential to 1600°C, 19: 44598(R) (GEMP-49A)
CHROMIUM IODIDES
iodine-127 Mössbauer resonance in ferromagnetic, (E), 19: 45491
CHROMIUM ISOTOPES
content in meteorites, (E), 19: 44907
CHROMIUM OXIDES
effects on gamma radiolysis of aqueous solutions of benzene, 19: 44051 (AE-192)
spectra at, Ohlin structure near limit of continuous x-ray, (E), 19: 44940
CHROMIUM PHOSPHATES
colloids, distribution in rat tissues, tracer study, 19: 43797
CHROMIUM STEEL
Cr–Mo, compatibility of Croloy 2¼ in sodium-heated boiler containing Type 316 stainless steel, 19: 44133(R) (BAW-1280-21)
Cr–Ni, hardness of heat-affected zones of welded joints in Super Elso, 19: 44686(R) (EURAEC-1362)
CHROMIUM SYSTEMS
Cr–Rh–Si, phase study of Cr_3O structures in, 19: 44702 (TID-22200)
Cr–Si–Sn, phase study of Cr_3O-type structures in, 19: 44702 (TID-22200)
CHROMOSOMES
chemically induced aberrations of, 19: 43844
effects of alkylating compounds on *Triticum durum* and *T. monococcum*, 19: 43653
radiation effects on maize, meson, neutron, proton, and x, 19: 43712 (BNL-9383)
radiation effects on, in erythrocytes of man, 19: 43672(R) (TID-22131)
radiation effects on, tracer study, 19: 43758
radiation effects on XXX No. 18 trisomy syndrome development in baby, etiologic, 19: 43811
radiation effects on rat bone marrow, integral dose effects on, 19: 43733
radiation effects on replication of, in *E. coli*, 19: 43741
radioinduced aberrations in mouse, effects of age on x, 19: 43729(T) (BNL-tr-12)
radioinduced aberrations in pea seed, 19: 43770
radioinduced aberrations in *Escherichia coli*, 19: 43794
radioinduced aberrations in human, 19: 43834
radioinduced aberrations of, 19: 43844
radioinduced aberrations of Allium root tip, 19: 43745
volume in interphase of, effects on radiosensitivity of higher plants, 19: 43782
CHYMOTRYPSINOGEN
radiolysis of, decomposition of sulfur linkage in gamma, 19: 43841
CIRCUITS
design for printing out scaler data, (E), 19: 44351 (SGAE-E-4/1965)
design for use with 512-channel analyzer, for analyzing multiparameter experiments, (E), 19: 44516
design of transistorized, temperature effects on, 19: 45715 (SC-TM-65-259)
inverter requirements for analog networks, 19: 44343 (EUR-1918.i)
shielding nuclear-weapons, from nuclear-blast r-f fields, (E), 19: 44166 (NP-15472)
CIRCULATORY DISEASES
radiodiagnosis of portal systemic shunts, 19: 43904
CIVILIAN DEFENSE
feasibility of, against nuclear attacks, 19: 44215 (ORNL-3865)
radiological countermeasures in, fallout model for planning, 19: 44243 (AD-619902)
CLEANING SOLUTIONS
analysis of Freon TF for nonvolatile residues, instrument for, 19: 45713 (SC-TM-65-279)
CLOSTRIDIUM
radiation effects on lobster contamination with, 19: 44558(R) (TID-22139)
radiosensitivity of spores of, effects of pH and phosphate solutions on, 19: 43865
CLOUD CHAMBERS
bibliography, 19: 44366 (AED-C-06-12)
design of high pressure diffusion, for neutron scattering studies, 19: 44494
CLOUDS
rise in atmosphere, experiments on, 19: 44787 (BNL-914, pp 119-22)
COATINGS
corrosion of fuel-element, by chlorides at high temperatures, 19: 45601(R) (WCAP-3750)
corrosion protection by, on uranium, 19: 44630
fabrication and forming of radiation-attenuating, 19: 44670(P)
indicator, for possible cavitation damage to impellers, 19: 44212 (TIM-878)
properties of Zircaloy-4, mechanical and physical, 19: 45601(R) (WCAP-3750)
radiation effects on pyrolytic carbon, on fuel particles, 19: 44748 (ORNL-P-1505)
testing of metallic, facility for strain fatigue, 19: 45601(R) (WCAP-3750)
testing Zircaloy-4, for ceramic fuel pellets, 19: 45601(R) (WCAP-3750)
COBALT
determination in cerium–cobalt–plutonium alloys by controlled potential electrodeposition, 19: 43934 (LA-3345)
effects on photometric determination of zirconium, 19: 43972
neutron reactions (n,n'γ) with, cross section for, 19: 45263 (JAERI-1078)

phase transformations in, relation of c/a ratio and elastic moduli temperature dependence with, 19: 44676(R) (ANL-7000, pp 176-82)
reactions with beryllium, copper, stainless steel, and niobium alloys to 760°C *in vacuo*, 19: 44606 (PWAC-483)
separation from uranium by ion exchange, 19: 44119

COBALT ALLOYS
Ce–Co–Pu, analysis for cobalt by controlled potential electrodeposition, 19: 43934 (LA-3345)
Co–Rh–U, crystal structure studies, 19: 44678(R) (ANL-7000, pp 186-200)

COBALT COMPLEXES
with glycolic acid, binding energy of, infrared spectrophotometric study of, 19: 44004

COBALT ISOTOPES Co-56
beta decay of, level scheme and conversion coefficients from, (E), 19: 45295

COBALT ISOTOPES Co-59
neutron reactions with, resonances in, (E), 19: 45296

COBALT ISOTOPES Co-60
activity of dissolved and solid sources of, international comparison of specific, 19: 44101
content in coolant of pressurized water reactors, effects of low-cobalt stainless steel on, 19: 45495 (WAPD-T-1653)
metabolism by marine organisms, 19: 43669(R) (NP-15159)
therapeutic use for bladder carcinomas, 19: 43894
therapeutic use of applicators of, 19: 43906

COBALT MOLYBDATES
preparation and structure of, 19: 43991 (N64-26433)

COBALT OXIDES
catalytic effects on nitrous oxides decomposition, 19: 44680(R) (ANL-7000, pp 227-32)
reactions with alumina to form spinel, tracer study of mechanism of solid-state, 19: 43998 (UCRL-12396)
Co_3O–MgO, catalytic effects on nitrous oxides decomposition, 19: 44680(R) (ANL-7000, pp 227-32)
CoO–Nb_2O_5, phase diagram, 19: 44711

COBALT SYSTEMS
C–Co–Mn, crystal structure studies, 19: 44679(R) (ANL-7000, pp 205-12)

COCKCROFT-WALTON ACCELERATORS
use in activation analysis of meteorites for oxygen and silicon, 19: 43927 (CONF-650405-16)

COILS
use of induction, for measuring plasma conductivity distributions, (T), 19: 45437

COINCIDENCE COUNTERS
design of plastic scintillation detectors as anticoincidence shields for germanium gamma spectrometers, (E), 19: 44519
design of scintillation anti-, for gamma spectroscopy of molten-plutonium fuel elements, 19: 44453 (LA-DC-7316)

COLLAGEN
radiation effects on mouse, alpha, 19: 43831

COLLIDINES
complexes with cerium and 5-nitrobarbituric acid, preparation, 19: 44027

COLLIMATORS
design of low-energy gamma, 19: 44347 (ORNL-P-1545)

COLORADO (SAGUACHE CO.)
uranium occurrence in Marshall Pass district, 19: 44274

COMPUTER PROGRAMS
B-106, least-squares method for lattice constants, FORTRAN for CDC 3600, 19: 44679(R) (ANL-7000, pp 205-12)
CANDLE, for refueling SCE, 19: 45601(R) (WCAP-3750)
CHRNOGRM, for analysis of chronopotentiograms, in FORTRAN 63 for CDC 1604-A, 19: 45706 (ORNL-TM-1254)
CINDER, for fission product cross sections, 19: 45601(R) (WCAP-3750)
CONTAMU, for meson (μ) contamination in meson (π) beams, 19: 44993 (CEA-R-2778)
DEFT, for obtaining neutron diffusion coefficients from transport theory, 19: 45221(R) (GEAP-4913)
FLASH, for optimization of design of multi-stage flash evaporator plant for desalination, Fortran II for IBM 7090, 19: 44140 (ORNL-TM-1244)
FLIC-1, for FORTRAN pattern recognition and replacement, in FORTRAN for IBM 7090 or STRETCH, 19: 44579 (AEEW-R-439)
FLIC-2, for FORTRAN conversion to EGTRAN 1, in FORTRAN for IBM 7090 or STRETCH, 19: 44579 (AEEW-R-439)
for calculations in nuclear physics, 19: 45251 (BNL-9108)
for cross sections and lattice displacements in radiation damage calculations, 19: 44747 (NP-15463)
for integer linear programming in combinatorial analysis, (T), 19: 45709 (SC-R-65-963)
for least-squares analysis of gamma spectra, 19: 45261 (IDO-17016)
for neutron transport equations in cylindrical and plane geometry, for IBM 7090, 19: 45219 (EUR-2410.i)
for population studies, IBM 7090, 19: 43642(R) (NYO-2280-8)
for reactor fuel cycle analysis, 19: 45545 (HW-79951(Pt.2))
for reactor fuel cycle analysis, neutron cross sections for, 19: 45546 (HW-79951(Pt.3))
for reactor fuel-cycle analysis, 19: 45544 (HW-79951(Pt.1))
for space radiation shielding analysis, development of, 19: 45463 (NP-15425)
for stress analysis of bolted closures, Fortran II for IBM 7090, 19: 44145 (TID-22138)
for thermal stability of anion exchange resin–nitric acid systems in contactor, Fortran for IBM 7090, 19: 44110 (BNWL-114)
for treatment planning in radiotherapy, FORTRAN II for IBM-709, 19: 43922
FREE, for calculation of thermal neutron scattering law and associated Legendre moments, 19: 45223 (JAERI-1084)
HASTI, for two-dimensional Lagrangian hydrodynamics with space-dependent time steps, 19: 45701 (LA-3324)
JET SET, for analysis of jet pump, CDC, 19: 44198 (TIM-913)
JURN, for circulation of technical journals, FORTRAN II, 19: 45700 (DP-970)
KPARAM, for multigroup calculations of kinetics parameters in fast reactors, in FORTRAN for IBM 7044 and 7090, 19: 45530 (JAERI-1082)
LASER, for criticality studies, 19: 45600(R) (WCAP-3385-4)
LEOPARD, for criticality studies, 19: 45600(R) (WCAP-3385-4)
LOCK, for optimizing core lattice parameters for pressurized-water reactors, 19: 45599 (WCAP-3269-49)
MESSYMESH, for calculation of fields in linear accelerators, 19: 44867 (MURA-713)
MIRAGE-III, for matrix operations, 19: 44581 (KAPL-M-6469)
MUFFLE, for neutron fission cross sections, in FORTRAN IV for IBM 7090, 19: 45282 (ORNL-TM-1180)
NUSTAT, for shell model calculations, 19: 45254 (CST-1213)
ODYSSEUS, fuel cycle analyses for gas-cooled reactors, in FORTRAN II, (T), 19: 45595 (TRG-Report-976)
PARMILA, for analysis of particle motion in linear accelerator, 19: 44867 (MURA-713)
Prometeo I, for Wigner-Wilkins thermal neutron spectra, for UNIVAC UCT, 19: 45224 (JEN-133-DF/I-43)
Prometeo II, for thermal neutron spectra in homogeneous mixtures, for UNIVAC UCT, 19: 45225 (JEN-135-DF/I-44)
S-126, for axisymmetric shell stress analysis, 19: 44219 (ACF-8)
SPORT, for processing transient data from Spert reactors, 19: 45527 (IDO-17078)
TAFI-II, for management of radioactive waste, FORTRAN II for IBM-704, 19: 45687 (DP-966)
TRANS-FUGUE-I, for transient two-phase flow and heat transfer in liquid-metal-cooled reactors, Fortran, 19: 45494 (NAA-SR-11008)
TRIM, for magnetostatic field calculations, 19: 44811 (UCRL-7784-T (Rev.1))
WOP, for rocket reactor weight optimization studies, 19: 45659 (TIM-307)
ZADOC, for reactor fuel management calculations, in FORTRAN II for IBM 7090 or STRETCH, 19: 45523 (AEEW-R-425)
3D-HEXLAX, for one-group neutron flux calculations in three dimensions, (T), 19: 45218 (DP-938)

COMPUTERS
development of order code for film scanners of Illiac III, 19: 44446 (COO-1018-1050)
performance in megachannel pulse analyzers, 19: 44497
performance of analog, for angle and range measurements in nuclear emulsions, 19: 44420 (CERN-65-4(Vol.II), pp VII28-34)
performance of digital, for on-line calculations of MSRE, 19: 45585 (ORNL-P-1502)
use in measuring radioisotopes in biomedical samples, 19: 43659

CONCRETES
gamma dose buildup factors for, 19: 45459 (EUR-2488.e)
gamma dose rates in, from point isotropic fission sources, (T), 19: 45464 (ORNL-TM-1167)
neutron dose rates in, from point isotropic fission sources, (T), 19: 45464 (ORNL-TM-1167)
properties in reactor pressure vessels, 19: 45505
properties of prestressed, for construction of reactor pressure vessels, 19: 45506
shielding properties, 19: 45468
uses of prestressed, for reactor pressure vessels, 19: 45504

CONDENSATION
of potassium, two-phase heat transfer and fluid flow in, 19: 44187(R) (NASA-CR-54405)

CONES
stiffness of laterally loaded shells, (T), 19: 45712 (SC-TM-65-82)

CONFERENCES
see also introduction to Report Number Index
Advances in Nuclear Energy 1964. Industrial Applications of Nuclear Energy: Present Status and Prospects. Milan, Italy, Dec., 1964, 19: 44565
index to, relating to nuclear science, 19: 45716 (TID-4043(Rev.2))
mechanisms of the Dose Rate Effect of Radiation at the Genetic and Cellular Levels, Oiso, 1964, 19: 43780
Nuclear Photography, Fifth International Conference on, Geneva, Sept. 15–18, 1964, 19: 44377 (CERN-65-4(Vol.I))
Nuclear Photography, Fifth International, CERN, Geneva, Jan. 1965, 19: 44383 (CERN-65-4(Vol.II))
Personnel Dosimetry for Radiation Accidents, Vienna, March 8 to 12, 1965, 19: 44319 (STI/PUB/99)
CONNECTORS (ELECTRIC)
design of sealed coupling for heaters in irradiation devices, 19: 44164 (CEA-R-2755)
CONSTANTS AND CONVERSION FACTORS
between binary shaft position encoder outputs and degree and radian measure, (T), 19: 44580 (AERE-R-4964)
CONTAMINATION
atmospheric radon, during pumping station dismantling, 19: 44317
CONVECTION (FORCED)
boiling heat transfer of potassium in serpentine tube, 19: 44195 (TID-21256)
CONVERSION ELECTRONS
spectra from thorium-227 decay, 19: 45306
COPPER
coating of wires of, with cadmium-109 for use as soft x-ray sources, 19: 44139 (ORNL-TM-1174)
compressibility and dilatational contribution to thermal capacity at 77 to 800°K, 19: 45718 (UCRL-11662)
deposition on uranium dioxide particles, 19: 44596 (EURAEC-1392)
determination in bismuth by neutron activation methods using gamma-gamma coincidence, 19: 43941
determination in enriched uranium metal, absorptiometric, 19: 43938 (PG-Report-665)
determination in high-purity metals and silicon by activation methods, 19: 43973
diffusion into cadmium sulfide, optical absorption study, 19: 43997(R) (UCRL-11889)
dislocation mobility and plastic deformation in, 19: 43997(R) (UCRL-11889)
effects on photometric determination of zirconium, 19: 43972
electric conductivity of thin films of, 19: 44344 (K-L-1944)
electrolysis of porous anodes of, reaction distribution, 19: 43997(R) (UCRL-11889)
energy release in irradiated, low-temperature, 19: 44739(R) (ANL-7000, pp 233-77)
exploding were phenomena of, MHD instabilities in, (E), 19: 44845
meson (μ^+) depolarization quenching in, as function of longitudinal magnetic field, (E/T), 19: 45079
neutron absorption cross sections at 24 kev, (E), 19: 45230
neutron cross sections for, from 0.414 ev to 5.5 Mev, 19: 45244 (AEEW-M-472)
neutron reactions (n,n′γ) with, cross section for, 19: 45263 (JAERI-1078)
photon reactions in Bev range, meson (ρ^0) production in, (E), 19: 45000 (HUX-2752-7)
positron annihilation in, anisotropy of Fermi surface from, (E), 19: 45487
radiation effects on electric resistivity at 4°K, fast neutron, 19: 44739(R) (ANL-7000, pp 233-77)
reactions with metals at 540 to 760°C *in vacuo*, 19: 44606 (PWAC-483)
separation from uranium by ion exchange, 19: 44119
sputtering by argon ions at 30 to 170 kev, (E), 19: 44937(R) (TID-22140)
sputtering by cesium ions at 1 to 10 kev, tracer technique for, (E), 19: 44964
use as filter for radiographic inspection of steel, 19: 44209(R) (EURAEC-1422)
vacancy aggregates in quenched single crystals of, 19: 43997(R) (UCRL-11889)
COPPER ALLOYS
extrusion by hydrostatic methods, 19: 44651
Al–Cu, radiation damage in, effects of aluminum content on fast neutron, 19: 44739(R) (ANL-7000, pp 233-77)
Al–Cu, radiation effects on single crystal, effects of aluminum content on strength-annealing of neutron, 19: 44739(R) (ANL-7000, pp 233-77)
Al–Cu, radiation effects on strength of, effects of aluminum content on neutron, 19: 44739(R) (ANL-7000, pp 233-77)
Al–Cu–Mg–Mn, erosion by water of rotating disks of, 19: 44625 (TIM-894)
Al–Cu–Nb, crystal structure, 19: 44718
Al–Cu–Ta, crystal structure, 19: 44718
Be–Cu, deformation of single crystals of, by microstrain compression, 19: 44694(R) (NP-15432)
Be–Cu, radiation effects on age hardening, 19: 44760
Ce–Cu, crystal structure studies, 19: 44678(R) (ANL-7000, pp 186-200)
Cu–Fe–Zr, corrosion by steam at 540°C, effects of pressure on, 19: 44616(R) (ANL-7000, pp 122-37)
Cu–Ga, radiation effects on strength of, effects of gallium content on neutron, 19: 44739(R) (ANL-7000, pp 233-77)
Cu–Ho, crystal structure studies, 19: 44678(R) (ANL-7000, pp 186-200)
Cu–La, crystal structure studies, 19: 44678(R) (ANL-7000, pp 186-200)
Cu–Ni–Ta, crystal structure, 19: 44718
Cu–Ni–W, mechanical properties and microstructure of, 19: 44691 (NASA-TN-D-3015)
Cu–Pr, crystal structure studies, 19: 44678(R) (ANL-7000, pp 186-200)
Cu–Pu–U, corrosion by air at room temperature, 19: 44587(R) (ANL-7000, pp 3-63)
Cu–Rh–Ti, crystal structure studies, 19: 44678(R) (ANL-7000, pp 186-200)
Cu–Sm, crystal structure studies, 19: 44678(R) (ANL-7000, pp 186-200)
Cu–Sn, dislocations and stacking-fault energy of alpha, 19: 43997(R) (UCRL-11889)
Cu–Sn, radiation effects on deformation of, fast-neutron, 19: 44753
Cu–Tb, crystal structure studies, 19: 44678(R) (ANL-7000, pp 186-200)
Cu–Tm, crystal structure studies, 19: 44678(R) (ANL-7000, pp 186-200)
Cu–U, oxidation of intermetallic compound UCu_5 by carbon dioxide at 350 to 850°C, 19: 44631
Cu–Zr, corrosion by steam at 540°C, 19: 44616(R) (ANL-7000, pp 122-37)
COPPER CHLORIDES
$Fe(NH_4)_2(SO_4)_2$–$CuCl_2$–H_2SO_4–H_2O, properties as gamma dosimeter, 19: 44372 (AFCRL-65-470)
COPPER COMPLEXES
with glycolic acid, binding energy of, infrared spectrophotometric study of, 19: 44004
COPPER FLUORIDES
use as matrix in spectrochemical analysis of graphite, 19: 43930 (JEN-145-DQ/I-46)
COPPER IONS
effects on radiolysis of acetylene, 19: 44082
spectra of hydrated, electron spin resonance, 19: 43997(R) (UCRL-11889)
COPPER ISOTOPES Cu-63
helium-3 reactions (He-3,p) at 10 Mev, angular and energy distributions from, (E/T), 19: 45362
helium-3 reactions (He-3,np) and (He-3,2p) at 10 Mev, cross sections for, (E/T), 19: 45362
neutron reactions (n,γ) with, rates for, (E/T), 19: 45522 (AE-195)
COPPER ISOTOPES Cu-65
energy levels and gamma transitions from nickel-65 decay, (E), 19: 45320
COPPER ISOTOPES Cu-66
decay of, gamma spectra from, 19: 45679(R) (NYO-1859-11)
COPPER OXIDES
effects on gamma radiolysis of aqueous solutions of benzene, 19: 44051 (AE-192)
COPPER SULFATES
effects on autoxidation of benzene in aqueous solutions, 19: 44078
CORROSION
radioactive products of cooling system, effects on shielding design, 19: 45601(R) (WCAP-3750)
CORROSION FILMS
deposition in loops, factors affecting, 19: 45601(R) (WCAP-3750)
CORROSION LOOPS
operation for crud deposition studies, 19: 45601(R) (WCAP-3750)
CORTISONE
effects on gluconeogenesis in irradiated rats, 19: 43837
protective effects of, against radiation injuries in rat spleen, 19: 43860(R) (NP-15310, pp 14-25)
COSMIC ELECTRONS
charge ratio of, (T), 19: 44972
COSMIC PARTICLES
detection using nuclear emulsions in rockets and satellites, 19: 44436 (CERN-65-4(Vol.II), pp X13-18)
interactions at high energy, multiple production in elastic, (T), 19: 45091
COSMIC RADIATION
acceleration of, plasma-turbulence mechanism for, (T), 19: 44975(T)
detection and measurement at sea level, 19: 44461(R) (TID-22205)
detection underground, preparation of emulsion stack for, 19: 44397 (CERN-65-4(Vol.II), pp III5-11)
distribution in exosphere, Explorer VII measurement of, 19: 44973
dosimetry for manned space travel, 19: 43879
effects on spacecraft design, 19: 44550

energy spectra of primary, during complete solar cycle, 19: 44965
flux of primary, 19: 44893 (NASA-CR-294)
gamma flux in, measurement of, (E), 19: 44970
intensity variations of, ion chamber response in free space for long-term, 19: 44966
intensity variations of, J-index for, 19: 44974
origin of x radiation in, (T), 19: 44971
production and properties of non-solar x, 19: 44969
review studies of, 19: 44976
sources in Sagittarius and Scorpio, positions of three x-ray, (E), 19: 44968
spectra of x, near Galactic center and in Scorpius, (E), 19: 44967

COSMIC SHOWERS
detection of extensive, design of transistorized airborne apparatus for, 19: 44529

COSMOLOGY
expansion of universe and distribution of matter in, 19: 44929
gravitational effects of stellar neutrino and photon luminosity, (T), 19: 44910
nucleon creation in, (T), 19: 44895

COULOMETRY
radio-, use of non-isotopic solid indicator in titration by, 19: 43952

COUNTING DEVICES
design of gated-readout decade, (E), 19: 44500
design of Modulo-N, for any code, 19: 45719 (UCRL-12012)

CRATERS
properties of astroblemes and nuclear-explosion, 19: 44237

CREATINE
radiation effects on metabolism of, in man, 19: 43852

CREATINEPHOSPHORIC ACID
radiation effects on metabolism of, in rats, 19: 43852

CREATININE
radiation effects on metabolism of, in man, 19: 43852

CRISTOBALITES
sorptive properties for cesium, role of exchangeable magnesium and potassium in, 19: 43964

CRITICAL ASSEMBLIES
criticality accidents at fast-, efficiency of dosimetry system for, 19: 44334
criticality studies of plutonia–urania, 19: 45600(R) (WCAP-3385-4)
criticality studies in FRO, (E/T), 19: 45522 (AE-195)
design of Saxton plutonium, 19: 45600(R) (WCAP-3385-4)
fabrication of oxide fuel pellets for Doppler experiments in ZPR-III, 19: 44587(R) (ANL-7000, pp 3-63)
fabrication of SEFOR-ZPR-III fuel plates, 19: 44587(R) (ANL-7000, pp 3-63)
neutron physics calculations for water-reflected tungsten, 19: 45526 (GA-6633)
neutron physics characteristics of beryllium-oxide moderated, (E/T), 19: 45537
neutron resonance absorption in homogeneous, 19: 45521 (AAEC/TM-118)
reactivity effects of water losses from graphite–uranium, 19: 45529 (INR-600/IX-A/PR)

CRITICALITY STUDIES
critical separation of regular arrays of fissile units, 19: 44977 (IDO-17095)
of clad plutonia and urania lattices, 19: 45600(R) (WCAP-3385-4)

CROSS SECTIONS
calculation of inelastic electron-molecule collision, by classical methods, (T), 19: 44947
measurement program for nuclear, reports for AEC on, 19: 45288 (WASH-1056)

CRUCIBLES
dissolution of plutonium residues from, dissolver performance for, 19: 44111 (BNWL-121)

CRUSTACEA
metabolism of radionuclides by marine, 19: 43669(R) (NP-15159)
radiosensitivity of Artemia eggs, effects of hydration on, 19: 43814
radiosensitivity of Artemia eggs, effects of heat treatment on, 19: 43815

CRYOGENICS
instrumentation developments in, 19: 44357

CRYOSTATS
design for semiconductor gamma detectors, engineering drawings for, 19: 44539
design of liquid-nitrogen dewar vessel for germanium detectors, (E), 19: 44511

CRYSTAL DETECTORS
properties of large silver chloride, 19: 44378 (CERN-65-4(Vol.I), pp 1-15)

CRYSTALLOGRAPHY
lattice constants, computer program for least-squares method of obtaining, 19: 44679(R) (ANL-7000, pp 205-12)

CRYSTALS
elementary particle transmission through s-state, (T), 19: 45013 (JINR-P-2230)
lattice constants of, determination using Geiger-counter x-ray diffractometer, 19: 44722
lattice defects in, diffusion studies of, 19: 45471 (AECL-2309)
neutron scattering cross sections in, slow, (T), 19: 45228 (NP-15469)
neutron scattering in, single-phonon coherent, (T), 19: 45475 (IAE-750)
neutron scattering cross sections at 30 to 1000 ev, (E), 19: 45489
polarons in, principal methods for theory of, 19: 45473 (BLG-329)
radiation damage at low temperatures to ionic, x-ray-diffraction studies of beta, 19: 44745 (LA-DC-6725)
spectra of vibrational modes in molecular, (T), 19: 45492

CULTURE MEDIA
radiation effects on tubercle bacilli, uv, 19: 43737

CUPFERRON
protective effects against radiation damage in crop plants, 19: 43877

CURIUM
separation from americium by solvent extraction, 19: 44115 (ORNL-P-1577)

CURIUM ISOTOPES
neutron cross sections of, tabulation, (E), 19: 45250 (BNL-325(2nd Ed.) (Suppl.2)(Vol.III))
production in high-flux Savannah River Production Reactors, 19: 45639 (DP-999, pp 19-28)

CURIUM ISOTOPES Cm-244
separation from americium-241, chromatographic, 19: 44118 (UCRL-16015)

CUTTING TOOLS
design of remote-control, 19: 44177(P)

CYANIDES
effects on oxygen tension and sulfhydryl content in mouse spleen, 19: 43869

CYCLOHEXANES
dehydrogenation in reactor cooling systems, use for heat transfer, 19: 45519(P)

CYCLOHEXENE, 1-METHYL-
reactions with pentamethyldisilane, addition, 19: 44048 (TID-21309)

CYCLOPENTANE, METHYL-
benzene–methylcyclopentane, reactions with recoil carbon-11 produced by gamma irradiation, 19: 44057 (IS-T-23)

CYCLOTRONS
beam adjustments in 1.5 m, 19: 44887
beam monitor for determining deuteron/proton ratios, semiconductor, 19: 44482 (ZFK-PHA-12, pp 154-62)
beam vertical shift in, with incongruent electric and magnetic planes, 19: 44889
fabrication status of University of Milan relativistic proton, 19: 44886
instrumentation developments for electron, 19: 44357
magnets for variable-energy, performance of central region of, 19: 44869 (NIRL/R/87)

CYLINDERS
critical separation of regular arrays of fissile, 19: 44977 (IDO-17095)
dynamic response of shell, to lateral loads, (T), 19: 45711 (SC-TM-65-81)

CYSTEINE
protective effects of, against radiation injuries in rat spleen, 19: 43860(R) (NP-15310, pp 14-25)
protective effects against radiation damage in crop plants, 19: 43877
radiolysis of, decomposition of sulfur linkage in gamma, 19: 43841

CYSTINE
radiolysis of, decomposition of sulfur linkage in gamma, 19: 43841

CYTIDINE
hydrolysis of 3′-nucleotide of, catalytic effects of thorium and zirconium ions on, 19: 43708

CYTIDINE, 2′-DEOXY-
deamination by *Tetrahymena pyriformis* enzyme, 19: 43812

CYTIDYLIC ACIDS
deoxy-, deamination by *Tetrahymena pyriformis* enzyme, 19: 43812

CYTOLOGY
of spermatogonia in silkworm larvae, 19: 43783
reproduction of animal cells, 19: 43758
tracer study using phosphorus-32, 19: 43740

CYTOPLASM
synthesis of sub-cellular organelles in, mechanisms of, 19: 43682(R) (UCLA-12-565, pp 33-57)

CYTOSINE
radiolysis of aqueous, effects of bromides and chlorides on, 19: 43682(R) (UCLA-12-565, pp 33-57)

D

DATA RECORDING SYSTEMS
design for fuel element testing, 19: 45500 (HW-65756)
design for printing out scaler data, (E), 19: 44351 (SGAE-E-4/1965)

DATA TABULATIONS
compilation of requests for nuclear data, 19: 45255 (EANDC-45(U))
geomagnetic and solar activity parameters, Mar.-April 1965, 19: 45178
heat transfer data for supercritical-pressure liquid hydrogen in turbulent flow through tubes, 19: 44189 (NP-15332)
library of nuclear data, UKAEA, 19: 45249 (AWRE-O-55/65)
neutron cross sections for elements having Z = 88 to 98, (E), 19: 45250 (BNL-325(2nd Ed.)(Suppl.2)(Vol.III))
neutron cross sections for fast reactors, from 0.414 ev to 5.5 Mev, 19: 45244 (AEEW-M-472)
neutron cross sections of free hydrogen at 0.0001 ev to 20 Mev, 19: 45248 (AWRE-O-23/65)
neutron flux densities in High Flux Reactor, 19: 45681 (RCN-36)
tables of resonance integral functions, 19: 45214 (ANL-7024)

DEHYDROGENASES
radiation effects on Tetrahymena, uv and x, 19: 43856

DEUTERIUM
crystal structure of thin films, (E), 19: 45194
crystal structure of, from neutron-diffraction studies, (E), 19: 45211
deuteron reactions (d,p) at 2.1 to 14.1 Mev, proton polarization in, (E), 19: 45253 (COO-7-0362)
effects autoxidation of benzene in aqueous solutions of metal ions, 19: 44078
effects on hydrogen anodic oxidation in acid solutions, 19: 44022
effects on hydrolysis of 4-methyl-1,3-dioxane and 1,3-dioxane in heavy water, 19: 44011
incorporation in haloörganic compounds, 19: 44107(P)
oxidation in acid solutions, isotope effects in voltametric, 19: 44022
production and heating of plasma of, in B-3 stellarator, (E), 19: 45398 (MATT-332)
scattering by nickel-60 at 15 Mev, excitation of two-phonon states by inelastic, (E), 19: 45346
separation by countercurrent exchange between ammonia and water in hot-and-cold plant, 19: 44574
separation from sea water using magnetohydrodynamic effect, 19: 44578(P)
spin precession in μ-mesic, 19: 45278 (NP-15389)
spin precession in compounds of muonium and, (T), 19: 45278 (NP-15389)
tracer use of, in studies of plant metabolism, 19: 43685

DEUTERONS
detection and identification using lithium-drifted silicon detectors, (E), 19: 44517
detection of, performance of surface-barrier silicon detectors for, 19: 44469 (ZFK-PHA-12, pp 16-24)
detection of, silicon surface-barrier detectors for, 19: 44471 (ZFK-PHA-12, pp 30-2)
emission in lithium-6 reactions with nuclei, mechanisms for, (T), 19: 45264 (JINR-E-2243)
interactions with mesons (K^+) at 2.3 Bev/c, coherent K^* production in, (E), 19: 45120
interactions with gamma rays, detection using emulsions, 19: 44438 (CERN-65-4(Vol.II), pp X33-6)
interactions with protons, detection using emulsions, 19: 44443 (CERN-65-4(Vol.II), pp X61-6)
interactions with mesons (μ^-), effect of neutron-neutron final state on, (T), 19: 45073
magnetic moment of, nucleon model for, (T), 19: 45049
production in bremsstrahlung reactions (γ,d) with carbon at 400 to 720 Mev, cross sections for, (E/T), 19: 45309
production in nucleon–nucleon interactions, polarization from, 19: 45017 (JINR-P-2267)
reactions (d,α) with oxygen-16 at 5 to 9 Mev, differential cross sections for, 19: 45377
reactions (d,α) with carbon-12 at 10.2 to 12.9 Mev, angular distributions for, (E), 19: 45289 (ZFK-PHA-12, pp 99-105)
reactions (d,p) with deuterium at 2.1 to 14.1 Mev, proton polarization in, (E), 19: 45253 (COO-7-0362)
reactions (d,p) with zirconium-90 at 12 and 14 Mev, differential cross sections for, (E), 19: 45281 (ORNL-3850)
reactions (d,p) with samarium-150, deformed and spherical nuclei from, (E), 19: 45359
reactions (d,p) with neodymium-148, deformed and spherical nuclei from, (E), 19: 45359
reactions (d,p) with calcium-42, -44, and titanium-46 at 7 Mev, (E), 19: 45323
reactions (d,p) with boron-10 at 13.5 Mev, cross sections for, (E), 19: 45336
reactions (d,p) with barium-138 at 7.5 Mev, barium-139 levels from, (E), 19: 45347
reactions (d,t) with neodymium-150, deformed and spherical nuclei from, (E), 19: 45359
reactions with mesic deuterium atoms, (E), 19: 45273 (JINR-P-2356)
scattering by zirconium-90 at 12 and 14 Mev, differential cross sections for elastic, (E), 19: 45281 (ORNL-3850)
wave function for, as loosely bound system in relativistic scattering theory, 19: 45110

DIALYSIS
use of electro-, for nuclear emulsion processing, 19: 44410 (CERN-65-4(Vol.II), pp V22-32)

DIAMONDS
incorporation in electron sensitive nuclear emulsions, 19: 44399 (CERN-65-4(Vol.II), pp III17-20)
meson (K) stopping by emulsions loaded with, 19: 44398 (CERN-65-4 (Vol.II), pp III12-16)
spectra of, effects of chemical combination on soft x-ray K emission bands of carbon in, (E), 19: 44944

DICHROMATES
reactions with anion exchange resin and nitric acid in contactor, analysis of uncontrolled, 19: 44110 (BNWL-114)

DIELECTRIC FILMS
radiation effects from corona in electric discharges, 19: 44069

DIES
design of compression shear, for beryllium single crystal deformation studies, 19: 44693(R) (NP-15411)

DIET
calcium content of dog, effects on strontium metabolism by nursing puppies, 19: 43676(R) (UCD-472-112, pp 80-5)
cesium-137 content in Finnish Lapp, relation of potassium to, 19: 44305
for mice during breeding, sterilization of, 19: 43654
nutritional management of cancer patients after radiotherapy, 19: 43911
quality control of experimental dog, 19: 43675(R) (UCD-472-112, pp 73-9)
radioactivity from strontium-89 and -90 content in standard German, 19: 44313
radiosterilization of commercial mouse, 19: 43654
strontium content of dog, effects on calcium metabolism by nursing puppies, 19: 43676(R) (UCD-472-112, pp 80-5)
strontium-90 content of, in Argentina, 19: 44250 (NP-15269)

DIETHYLAMINE
photolysis products of, 19: 44053 (AFML-TR-65-166)
radiolysis of, yields in gamma, 19: 44072
radiolysis products of, gamma, 19: 44053 (AFML-TR-65-166)

DIFFERENTIAL EQUATIONS
Green's functions for related two-point boundary value problems, 19: 44582 (ORNL-3646)
integration of, method for numerical, 19: 45703 (LA-DC-6667)
solution for magnetostatic field calculations, method of numerical, 19: 44811 (UCRL-7784-T(Rev.1))
solution for magnetostatic field calculations, method of, 19: 44876 (UCRL-16287)

DIFFUSION
analysis of ternary, (T), 19: 43997(R) (UCRL-11889)
climatology studies of atmospheric, 19: 44771 (BNL-914, pp 44-50)
experiments on, using idealized equation, 19: 44796 (BNL-914, 163-72)
mechanisms in atmospheric, from elevated sources, (E), 19: 44768 (BNL-914, pp 26-7)
theory of atmospheric surface layer, Lagrangian similarity, (T), 19: 44766 (BNL-914, pp 20-3)
use in studies of crystal defects, 19: 45471 (AECL-2309)

DIODES
fabrication and characteristics of lithium-drifted germanium, for gamma spectrometry, 19: 44371 (AERE-R-4921)

DIOXANE
dioxane-2,5-diphenyloxazole, quenching effects of radioprotective compounds on irradiated, 19: 43878
hydrolysis of, in heavy water, deuterium isotope effects on, 19: 44011
solvent properties for hafnium, niobium, and tantalum, 19: 44124
4-methyl-1,3-, hydrolysis of, in heavy water, deuterium isotope effects on, 19: 44011

DIRECT ENERGY CONVERSION DEVICES
bibliography on nuclear-electric, 19: 44978 (AED-C-15-08)
design uses of, 19: 44987

DISEASES
effects of scurvy on manganese metabolism in guinea pigs, 19: 43697
of bone marrow, etiology of, 19: 43820
radioinduced, by ultraviolet or sunlight, 19: 43819
relation of radioinduced somatic mutations to, 19: 43749

DISSOLVERS
performance evaluation of continuous, for plutonium slag and crucible residues 19: 44111 (BNWL-121)
DISTILLATION APPARATUS
design for potassium isotope separations, 19: 43931 (K-1650)
DOGS
blood for chemical constituents in, 19: 43674 (UCD-472-112, pp 36-43)
blood picture in female, 19: 43674 (UCD-472-112, pp 36-43)
calcium-47 absorption by gastrointestinal tract of, 19: 43677(R) (UCD-472-112, pp 86-96)
care of experimental colony, 19: 43645(R) (UCD-472-112, pp 10-22)
care of experimental colony, 19: 43646(R) (UCD-472-112, pp 23-35))
care of experimental colony of, status of, 19: 43680(R) (UCD-472-112, pp 148-74)
diet of experimental, quality control of, 19: 43675(R) (UCD-472-112, pp 73-9,
pathology of experimental colony of, 19: 43727(R) (UCD-472-112, pp 126-40)
radiation dose to skeleton of, from ingested strontium-90, 19: 43726(R) (UCD-472-112, pp 120-5)
radiation effects on blood picture of, after ingestion of strontium-90, 19: 43725(R) (UCD-472-112, pp 44-9)
radiation effects on skeleton of, ingested strontium-90, 19: 43882 (UCD-472-112, pp 50-8)
radiation effects on lungs of, pathophysiology of, 19: 43799
radiation effects on lethality in, dose and exposure effects on neutron and x-ray, 19: 43832
radiation effects on acceptance of autogenous bone grafts by, x, 19: 43835
radiography of, whole-body, 19: 43882 (UCD-472-112, pp 50-8)
radium-226 metabolism in, injected, 19: 43678(R) (UCD-472-112, pp 97-108)
renograms in, quantitative aspects of, 19: 43667 (EUR-1890.f)
strontium metabolism in nursing, effects of calcium content of diet on, 19: 43676(R) (UCD-472-112, pp 80-5)
strontium-85 absorption by gastrointestinal tract of, 19: 43677(R) (UCD-472-112, pp 86-96)
strontium-90 metabolism, 19: 43679(R) (UCD-472-112, pp 109-19)
DOLOMITES
oxygen-18 fractionation between coexisting calcite and, in Freeport formation, Penn., 19: 44241
DOMINIC OPERATION
cloud stem of, radioactivity isopleths, 19: 44784 (BNL-914, pp 110-12)
DOSIMETERS
calibration of ferrous sulfate, 19: 44540
descriptions of fixed and personal, for assessment in event of criticality accident, 19: 44333
design of gamma-insensitive neutron, 19: 44544(P)
design of individual alarm, for personnel use, 19: 44532
design of neutron, for measuring biological dose effect, 19: 44543(P)
design of personal, for evaluation of high accidental exposures, 19: 44536
design of portable, having visual dose representation, 19: 44546(P)
development of large standard, after Kuestner device, 19: 44495
efficiency of system of, for criticality accidents at fast-critical assembly, 19: 44334
fading of thermoluminescent lithium fluoride, 19: 44076
performance of lithium fluoride finger-tip, 19: 44367 (AEEW-M-550)
performance of phosphate-glass, (E), 19: 44509
properties of ferrous ammonium sulfate–cupric chloride, for kilocurie cobalt-60 sources, 19: 44372 (AFCRL-65-470)
properties of lithium fluoride thermoluminescent, 19: 44541
system of, for personnel monitoring at National Reactor Testing Station, 19: 44335
DOUNREAY FAST REACTOR
operation and performance of, (E), 19: 45613
reactivity feedback effects in, (E), 19: 45594 (TRG-Report-864)
DROSOPHILA
effects of radiomimetic substances in, lethal, 19: 43787
effects of radiomimetic substances in, genetic, 19: 43787
radiation effects in, lethal, 19: 43787
radiation effects in, genetic, 19: 43787
radioinduced mutations in, gamma, 19: 43724(R) (TID-22160)
radioinduced mutations in, effects of dose rate, 19: 43785
DRUGS
activation analysis of opium for origin determination, 19: 43937 (ORNL-TM-1263)
effects of metabolic-inhibiting, on metabolism of 5-hydroxytryptamine, in rat brain, 19: 43810
effects of 3-indolyl-ethyl-piperazine, 19: 43728(R) (UCLA-12-565, pp 59-64)
effects on growth of transplanted sarcoma in rats, 19: 43772
radiosterilization of, using radioisotopes, 19: 44560
DYES
diffusion in pine embryos, fluorescent tracing of, 19: 43643(R) (TID-22143)
effects of acridine orange on thymine–thymine dimer in presence of light, 19: 44060 (UCRL-16353)
DYSPROSIUM
elastic moduli at 298°K, 19: 44676(R) (ANL-7000, pp 176-82)
separation from scandium and thorium by reversed-phase chromatography, 19: 44125
DYSPROSIUM ALLOYS
Dy–Ag, crystal structure studies, 19: 44678(R) (ANL-7000, pp 186-200)
Dy–Au, crystal structure studies, 19: 44678(R) (ANL-7000, pp 186-200)
DYSPROSIUM CHLORIDES
pharmacology and toxicology of, 19: 43728(R) (UCLA-12-565, pp 59-64)
DYSPROSIUM ISOTOPES Dy-160
energy levels of, parity and spin of, 19: 45272 (JINR-P-2270)
oxygen-16 inelastic scattering at 43.5 Mev, vibrational-state excitation in, (E), 19: 45321
DYSPROSIUM ISOTOPES Dy-162
oxygen-16 inelastic scattering at 43.5 Mev, vibrational-state excitation in, (E), 19: 45321
DYSPROSIUM ISOTOPES Dy-164
oxygen-16 inelastic scattering at 43.5 Mev, vibrational-state excitation in, (E), 19: 45321
DYSPROSIUM OXIDES
effects on optical properties of silicate glasses, 19: 44030
phase transformations in, at 1800 to 2400°C, 19: 44731
DYSPROSIUM TELLURIDES
crystal structure, 19: 44010

E

EARTH
interplanetary missions from, trajectory parameters for, 19: 45649 (N64-32637)
terrestrial control in the production of aurora, 19: 45185
ECOLOGY
radiation effects on, of field and forest plant communities, 19: 43711 (BNL-924)
research programs at UCLA, 19: 43662(R) (UCLA-12-565, pp 97-128)
EGGS
effects of actinomycin D and heavy water on macromolecule synthesis in developing sea urchin, 19: 43709
radiosensitivity of Artemia, effects of hydration on, 19: 43814
radiosensitivity of Artemia, effects of heat treatment on, 19: 43815
EINSTEINIUM ISOTOPES
production in high-flux Savannah River Production Reactors, 19: 45639 (DP-999, pp 19-28)
ELECTRIC ARCS
development and performance of high-current, 19: 44608 (TID-22125)
radiation from a-c and d-c operated nitrogen, 19: 44804 (ARL-65-105)
ELECTRIC CONDENSERS
performance of energy storage, for pulsed plasma accelerators, 19: 44224
properties of banks of, for rotating plasma experiments, 19: 45416 (UCRL-16263)
ELECTRIC CONDUCTIVITY
theory of, in thin metallic films with unlike surfaces, 19: 45479 (TID-21301)
ELECTRIC CONDUCTORS
current density and magnetic induction in slab of, in magnetic field of inductor, 19: 44841
ELECTRIC CONTROL SYSTEMS
design of Hall-effect, for stabilization of electromagnetics, (E), 19: 44173
ELECTRIC CURRENTS
bioelectric forces involved in the thermodynamics of material transfer across biological membranes, 19: 43664 (BNL-9337)
induction in superconducting rings using polarized electromagnetic waves, (T), 19: 45191 (LNF-65/15)
ELECTRIC DISCHARGE
column stratification and negative ion content on impure argon, relation between, 19: 45423
effects on polyethylene films, corona, 19: 44069
in gases, time evolution of laser induced, 19: 44821
plasma oscillations in, cesium, 19: 45403 (NP-15445)
shock waves from, hazards to human ear of, 19: 44283 (AWRE-E-1/65)
stability of heated-cathode plasma, in magnetic field at low pressures, (E/T), 19: 45390 (IAE-780)
ELECTRIC FIELDS
atomic energy level mixing in external fields, interference phenomena in,

19: 45270 (JINR-P-2248)
charged-particle acceleration in, kinetic equation for multiple, 19: 44864 (JINR-P-2253)
effects on boiling burnout in annular flows, (E), 19: 44190(R) (NYO-2404-67)
effects on boiling burnout in annular flows, (E), 19: 44191(R) (NYO-2404-73)
nuclear energy level mixing in external fields, interference phenomena in, 19: 45270 (JINR-P-2248)
plasma fluctuations in, 19: 45410(R) (TID-22183)
ELECTRIC INSULATORS
performance for slow neutron dosimetry, 19: 44385 (CERN-65-4(Vol.II), pp 112-19)
ELECTRIC POWER
generation by Brayton cycle turboelectric power plants for space applications, 19: 44205
production and uses of, forecast of future, 19: 45725
production of, using radioisotopes, 19: 44560
ELECTRIC PROBES
development, 19: 44223(R) (NP-15438)
effects on ion density of magnetically contained cesium plasma, (E/T), 19: 45393 (IPP-2/38)
performance of resonance, for plasma diagnostics, 19: 45381 (ARL-65-115)
theory of double, for plasma diagnostics, 19: 45452
theory of Langmuir, for plasma diagnostics, 19: 45447
use in plasma diagnostics, (T), 19: 45414 (UCRL-12480)
ELECTRICITY
production by direct conversion of reactor heat, device for, 19: 45556(P)
ELECTROCHEMICAL CORROSION
design of polarization cell for liquid-metal, 19: 44616(R) (ANL-7000, pp 122-37)
polarization apparatus for studies of, 19: 44617(R) (ANL-7000, pp 213-26)
ELECTROCHEMISTRY
bioelectric forces involved in the thermodynamics of material transfer across biological membranes, 19: 43664 (BNL-9337)
current distribution in cells, 19: 43997(R) (UCRL-11889)
optical properties of electrode-electrolyte interfaces, 19: 43997(R) (UCRL-11889)
redox reactions of ions, polarization during, 19: 44002(T) (AEC-tr-6572)
separation of electrolytic solution into double layer and bulk regions, (T), 19: 43997(R) (UCRL-11889)
ELECTRODES
electrolyte films on gas, 19: 43997(R) (UCRL-11889)
polarization of flooded porous, effects of electrode reaction kinetics on, 19: 43997(R) (UCRL-11889)
ELECTROLYTES
transport properties of concentrated solutions of, 19: 43997(R) (UCRL-11889)
ELECTROLYTIC CELLS
current distribution at gas-electrode-electrolyte interface, 19: 43997(R) (UCRL-11889)
design for regeneration of ion-exchange resins, 19: 44130(P)
ELECTROLYTIC POLISHING
use of alternating current in, 19: 44601 (LA-DC-6407)
ELECTROMAGNETIC FIELDS
charged-particle optical stigmatic focusing by random stationary, 19: 44851
effect on boundary layer of conducting fluid, 19: 44828
interactions with plasma, (T), 19: 45418
production in ion plasma, properties of, (E), 19: 45405 (ORNL-P-1576)
ELECTROMAGNETIC PUMPS
design and performance of, for mercury, 19: 44188 (NASA-TN-D-2965)
magnetic field distribution in flat linear induction, 19: 44833
ELECTROMAGNETIC WAVES
emission from plasma of high density and temperature, 19: 45392 (IPP-1/29)
interactions in nuclear field, electron-pair production by, 19: 45128
interactions with superconducting rings, persistent currents from, (T), 19: 45191 (LNF-65/15)
plasma heating by, using Stix coil, (T), 19: 45400 (NASA-TN-D-2982)
scattering by turbulent plasma, cross-polarized back-scatter in, (T), 19: 45424
spectral splitting by gravitational field, (T), 19: 45140
survey on solar, 19: 44893 (NASA-CR-294)
transmission through plasma, magnetized ferrite antenna windows for, 19: 45387 (D1-82-0442)
ELECTROMAGNETISM
absorption and emission in quantum and classical, stimulated, 19: 44820
ELECTRON BEAMS
dose calculations for inhomogeneous tissue, 19: 43916
effects in Allium root tips, genetic, 19: 43745
effects on friction and deformation properties of polytetrafluoroethylene, 19: 44092
effects on luminescence of cadmium sulfide, 19: 45478 (NP-15110)
effects on polyethylene films, 19: 44069
effects on radio- and radiothermo-luminescence of zinc sulfide phosphors, 19: 44757
focusing in accelerator tube, (T), 19: 44870 (NP-15388)
injection in FFAG accelerators, electronic control of 200-kv injector for, 19: 44884
interactions with positron beams, radiative corrections for, (T), 19: 45023 (LNF-65/8)
motion in magnetic bottle, 19: 44823
production of highly polarized, by low-energy scattering, (E), 19: 44958
reactions with supercritical fast reactor cores, neutron flux enhancement from, 19: 45874 (GA-6168)
therapeutic use of, 19: 43899
transmission of monoenergetic, through foils, (T), 19: 44818
use in salmonellae control in meat, economic feasibility of, 19: 44557 (NYO-3426-1)
ELECTRON MICROSCOPES
control systems for increased image intensity in, 19: 44358
specimen holder for, description of liquid-helium, 19: 44739(R) (ANL-7000, pp 233-77)
use for track viewing in ionographic emulsions, 19: 44426 (CERN-65-4 (Vol.II), pp VIII27-33)
ELECTRON MICROSCOPY
fringe patterns of anti-phase boundaries in rutile, 19: 44687(R) (EURAEC-1434)
use of transmission, in examination of bcc metals and alloys, 19: 44610 (TIM-943)
uses for particle track resolution in nuclear emulsions, 19: 44423 (CERN-65-4(Vol.II), pp VIII8)
ELECTRON PAIRS
production by electromagnetic wave in nuclear field, 19: 45128
production in bremsstrahlung reactions with carbon, (E/T), 19: 45256 (HUX-2752-4)
ELECTRON TUBES
fabrication of radiation-resistant, development of pilot line production capability for, 19: 44337(R) (AD-425708)
ELECTRONIC EQUIPMENT
cooling of, plant recirculating water system for, 19: 44160(R) (ANL-7000, pp 278-86)
design for printing out scaler data, (E), 19: 44351 (SGAE-E-4/1965)
design for space environment, influence of radiation on, 19: 44550
design of solid-state fixed-dead-time pulse discriminators, (E), 19: 44504
development for high-energy physics, 19: 44357
inverter requirements for analog networks, 19: 44343 (EUR-1918.i)
ELECTRONS
attachment reactions with sulfur hexafluoride, rates of, 19: 43997(R) (UCRL-11889)
collision probability with cesium atoms in plasma, (E), 19: 45399(R) (NASA-CR-54451)
content in cislunar space, radar measurements of, (E), 19: 45176
density and distribution function in magnetohydrodynamic conversion gas, (T), 19: 44982
density and temperature in plasma from hydrogen-loaded titanium washer source, (E), 19: 45411 (UCRL-7935)
density and temperature in ionosphere, (E), 19: 45174
density and temperature in non-stationary plasma, optical interferometry for, 19: 45433
density and temperature in exhaust of argon MPD source, (E), 19: 45448
density distributions in artificial belts from high-altitude nuclear explosions, 19: 45167
density in plasma, microwave diagnostics of, (E), 19: 45429
density in theta-pinch plasma, Schlieren photography for, (E), 19: 45421
detection and measurement by silver-activated zinc sulfide crystals, (E), 19: 44520
detection with discrimination against mesons (π), scintillation detector–spark chamber for, 19: 44522
dosimetry of, from exposure by linear accelerator malfunction, 19: 44331
dosimetry of, performance of ferrous sulfate detectors for, 19: 44540
effects of low energy, on silicon insulated gate field-effect transistors, 19: 44549
effects of pulsed, on reactions of hydroxyl ions, 19: 44090
effects on dosimetry glasses, iron sulfate solutions, and radiological films at 50 to 950 Mev, 19: 44093
effects on nuclear emulsions, dispersion of latent images in, 19: 44388 (CERN-65-4(Vol.II), pp III1-16)

effects on polyvinyl chloride in water and vacuum, 19: 44086
effects on space charge in plastics at 2 Mev, 19: 44096
effects on thermoluminescence fading in dosimetric lithium fluoride, storage effects on, 19: 44076
emission from h-f ion sources, (E), 19: 44880
emission from tungsten crystals, orientation effects on thermionic, (E), 19: 44981(R) (NP-15435)
emission in ion engines, ion-beam neutralization by, 19: 44222(R) (NP-15068)
emission in photon reactions with aluminum, (E), 19: 45481 (UCRL-12470)
emission in proton reactions with helium and molecular hydrogen, (E), 19: 44933 (COO-1277-12)
energy loss in thin silver foils, (E/T), 19: 44961
energy losses in potassium bromide, temperature dependence, (E), 19: 45490
flux distribution in ionosphere, limitation on, 19: 45157 (NP-15386)
flux of geomagnetically trapped, at middle latitudes and high B values, (E), 19: 45161
intensities in radiation belts near magnetic equator, local-time dependence of, (E), 19: 45160
interactions with phonons in aluminum, (T), 19: 45481 (UCRL-12470)
interactions with protons at high momentum transfers, elastic, (E), 19: 45001 (HUX-2752-8)
interactions with neutrons, effective potential for, (E), 19: 45098
interactions with nucleons in nuclei, (T), 19: 45279 (NP-15415)
interactions with positrons in storage rings, bremsstrahlung from, (T), 19: 44865 (LAL-1134)
interactions with protons, hydrogen hyperfine structure from polarization in, (T), 19: 44951
interactions with baryons, resonance in, (T), 19: 45007 (JINR-E-2228)
interactions with protons at 20 f-s, polarization in elastic, (E), 19: 45058
interactions with protons, neutron form factor from (eN_{2P}), (T), 19: 45065
magnetic moment of, dispersion theory for anomalous, 19: 45108
magnetic trapping on Mars, (E), 19: 44913
mass of, electromagnetic, (T), 19: 45136
oscillations in gases of, in magnetic fields, 19: 44849
oscillations in mercury plasma, higher- and sub-harmonics of, 19: 45428
oscillations in plasma in magnetic fields, (E), 19: 45427
radio-wave backscattering from density fluctuations of ionospheric, polarization in, (T), 19: 45182
reaction with argon and helium gas in magnetic bottle, loss mechanism of, 19: 44823
reactions in nuclear emulsions, ionization losses in, 19: 44428 (CERN-65-4(Vol.II), pp IX9-13)
reactions in nuclear emulsions, ionization losses in, 19: 44432 (CERN-65-4(Vol.II), pp IX41-3)
reactions with alkali metals, polarization of spectra line radiation from, (E), 19: 44956
reactions with argon atoms in plasma, (T), 19: 45407 (SU-AA217)
reactions with atoms and molecules, review of, 19: 44950
reactions with cesium atoms, excitation cross sections for, (E), 19: 44935 (NP-15168)
reactions with mercury cathodes, ion beam formation in, 19: 44221 (N64-31088)
reactions with molecular ions in plasma, collisional-dissociative recombination in, 19: 45450
reactions with molecules, classical calculation of cross sections for inelastic, (T), 19: 44947
scattering by aluminum-27, phosphorus-31, and sulfur-32, nuclear structure from, (E/T), 19: 45275 (NP-15138)
scattering by argon and uranium at 40 kv, polarization in inelastic, (T), 19: 44942
scattering by atoms, polarization in inelastic, (T), 19: 44942
scattering by carbon, noniterative approach to elastic, (T), 19: 44953
scattering by complex atoms, noniterative approach to elastic, (T), 19: 44953
scattering by helium atoms, exchange in, (T), 19: 44949
spin precession frequencies of, in gravitational fields, (T), 19: 45134 (NP-15397)
temperature determinations in midlatitude ionosphere, comparison of radar, rocket, and satellite, (E), 19: 45177

ELECTROPHORESIS
of rabbit lymphocytes from red cells, 19: 43648(R) (UCLA-12-565, pp 87-96)
separations development, 19: 43997(R) (UCRL-11889)

ELECTROSTATIC LENSES
design for production of low-energy ions using duoplasmatron, (E/T), 19: 45384 (D1-82-0436)

ELECTROSTATIC PRECIPITATORS
development for sampling stratospheric aerosols, 19: 44801(R) (NYO-2363-3)

ELEMENTARY PARTICLES
compositeness criteria in Lee model with two V particles, Salam, 19: 45068
decays and interactions of, charge-parity quantum number in very weak, (T), 19: 45115
detection and measurement using nuclear emulsions, 19: 44381 (CERN-65-4(Vol.I), pp 79-87)
detection of, instrumentation development for, 19: 44357
form factors of quarks, (T), 19: 45011 (JINR-E-2294)
interaction amplitudes of, normalization of Bethe-Salpeter bound-state, (T), 19: 45078
interaction amplitudes of, equation for two-body, (T), 19: 45123
interaction amplitudes of, truncation of unitary sum for, (T), 19: 45093
interactions at high energies, resonance production in, (T), 19: 45037 (TID-21316)
interactions at high energy, absorption or DWBA model for production, (T), 19: 45087
interactions at high energy, multiple production in elastic, (T), 19: 45091
interactions in loosely bound system, relativistic scattering theory for, 19: 45110
interactions of, analyticity and unitarity for sixth-order Feynman diagrams for, 19: 45111
interactions of, approximate one-trajectory exchange for amplitudes of, (T), 19: 45074
interactions of, amplitudes and vertex functions for strong, (T), 19: 45005 (IC/65/68)
interactions of, Bethe-Salpeter equation in bootstrap mechanism for, 19: 45090
interactions of, CP violation and higher symmetries for weak, (T), 19: 45126
interactions of, Coulomb effects on vertex parts in, (T), 19: 45146
interactions of, decay laws and S-matrix pole multiplicity in, (T), 19: 45070
interactions of, direct knock-on for inelastic, (T), 19: 45033 (NP-15468)
interactions of, kinematic contributions to form factors in, (T), 19: 45067
interactions of, local field theory for forward scattering amplitudes, 19: 45039 (TPJU-10/65)
interactions of, Lehmann's representation for extrapolation of S-matrix in, 19: 45062
interactions of, limiting procedures for singular potentials in Schroedinger equation for, 19: 45063
interactions of, multiple production in, (T), 19: 45038 (TPJU-7/65)
interactions of, N/D equations for three-body partial-wave amplitudes of, 19: 45107
interactions of, phase spaces of 3- and 4-particle final states, (T), 19: 45006 (IS-1214)
interactions of, phenomenological potential for two-body phase shifts in, 19: 45109
interactions of, Pomeranchuk theorem for amplitudes of, 19: 45071
interactions of, Regge trajectories in nonrelativistic, 19: 45028 (NP-15207)
interactions of resonance and stable, strong, (T), 19: 45082
interactions of spin-0, N/D method and diffraction model in elastic, (T), 19: 45088
interactions of stable and unstable, strip approximation in bootstrap calculation of, 19: 45117
interactions of, spin-2 meson exchange in bootstrapping for p-wave amplitude of, (T), 19: 45076
interactions of, statistical model calculations for, 19: 45047 (UCRL-16315)
interactions of, statistics in phase-shift analysis of, 19: 45012 (JINR-E-2353)
interactions of, Sakata model for weak, 19: 45027 (NP-15199)
interactions of, symmetry for strong, 19: 45035 (NP-15471)
interactions of, statistical model for multiple production in, (T), 19: 45041 (TPJU-12/65)
interactions of, T-parity nonconservation strong, (T), 19: 45280 (NP-15457)
interactions of, 3×8 and 8×8 general SU(3) crossing matrices for, 19: 45113
interactions with potential fields, Schroedinger equation for, (T), 19: 44960
interactions with gamma rays, parity determination in, 19: 45010 (JINR-E-2259)
Klein-Gordon equation for, Green functions for iterated, 19: 45095
mass of, states of small, (T), 19: 45119
methods of analyticity and unitarity for analysis of nuclear reactions, 19: 45340
model for free, position operators for all spins in relativistic, 19: 45118

model for, impossibility of combined internal-symmetry and Lorentz-invariance, 19: 45096
models of, vector invariants of SU(3)/Z group for, 19: 45083
momentum determination in nuclear emulsions, method for, 19: 44424 (CERN-65-4(Vol.II), pp VIII9-16)
momentum determination in nuclear emulsions, method for fast, 19: 44427 (CERN-65-4(Vol.II), pp VIII34-7)
parity of, method for determining, (T), 19: 45010 (JINR-E-2259)
phase shift analysis using Hamilton-Jacobi equation, (T), 19: 45053
polarization experiments at high energies, Regge pole effects in, (T), 19: 45044 (UCRL-16186)
properties of, determination by spark chambers, 19: 44490(T) (BNL-tr-1)
quantum dynamical equations for spin-½, covariant and hermitian semi-classical limit of, 19: 45060
representations in SU(3), method for multiplying, 19: 45030 (NP-15390)
representations in SU(3) theory, methods for multiplying, 19: 45030 (NP-15390)
research on, bibliography for, (E/T), 19: 44812(R) (UCRL-16099)
research on, CERN nuclear emulsion, 19: 44382 (CERN-65-4(Vol.I), pp 105-10)
resonance phenomena of, generalized Cauchy representations and, 19: 45130
resonances of, review of, 19: 45056
scattering from static potential in momentum space, scattering matrix for, (T), 19: 44995 (COO-30-97)
symmetries for, relativistic, 19: 45005 (IC/65/68)
symmetries of, axial and vector currents in broken, (T), 19: 45022 (LNF-65/7)
symmetries of, Casimir operators for orthogonal and symplectic, 19: 45031 (NP-15391)
symmetries of, corrections to unitary, 19: 45003 (IC/65/60)
symmetry breakdown mechanism for, avoidance of superforbidden processes in, 19: 45059
symmetry for, consistency of s-matrix unitarity condition with broken U(12), (T), 19: 45018 (JINR-P-2283)
symmetry for, representations of SU(4), 19: 45035 (NP-15471)
symmetry for, tests of broken $\bar{U}(12)$, 19: 45002 (IC/65/59)
symmetry for, unitarity and crossing in $\bar{U}(12)$, (T), 19: 45075
symmetry groups for, mass spectra from non-compact, 19: 45004 (IC/65/66)
symmetry models for, Lee triangle from, 19: 45129
symmetry of, algebra of currents in Lee model for SU(4), 19: 45116
symmetry of, Clebsch-Gordan coefficients for SU(6), 19: 45061
symmetry of, S-matrix unitarity in SL(6) broken, 19: 45009 (JINR-E-2247)
theory of, in inhomogeneous SL(6) framework, 19: 45132 (JINR-E-2225)
theory of, symmetries in quantum, 19: 44994 (CERN-65-26)
transport in amorphous media and crystals, s-state, (T), 19: 45013 (JINR-P-2230)
transport in matter, use of importance sampling for, 19: 45458 (AE-190)

ELEMENTS
determination of trace impurities by emission spectroscopy, review, 19: 43929 (IS-1237)

EMBRYONIC TISSUES
culturing method for hypocotyl, 19: 43643(R) (TID-22143)

EMBRYOS
growth of excised pine, effects of light on, 19: 43643(R) (TID-22143)
morphology of *Pinus lambertiana*, 19: 43643(R) (TID-22143)
radiosensitivity of brain of rat, 19: 43768

ENGINEERING
method for dimensional analysis, 19: 44143 (SC-RR-65-306)

ENGINEERING TEST REACTOR
neutron flux characteristics of G-7 hot-water, fast, (E), 19: 45672 (BNWL-89)

ENZYMES
activity in chicken livers, effects of estrogen on, 19: 43682(R) (UCLA-12-565, pp 33-57)
activity of N-demethylase, measurement in rat liver, 19: 43720(R) (NP-15310, pp 26-35)
deamination of deoxycytidine and deoxycytidylic acid by *Tetrahymena pyriformis*, 19: 43812
levels in heating rat heart cells, lipid effects on, 19: 43681(R) (UCLA-12-565, pp 17-31)
radiation effects on activity of, in rat brains, 19: 43682(R) (UCLA-12-565, pp 33-57)
radiation effects on activity of, in rat liver, 19: 43747
radiation effects on activity in peanuts of lipase, γ, 19: 43798
radiation effects on cholinesterase and tyrosinase activity in human skin lesions, uv, 19: 43809
radiation effects on metabolism of, in man and rats, 19: 43852
radiation effects on Tetrahymena fumarase, uv and x, 19: 43856
radiation effects on activity of N-demethylase, in rat liver, 19: 43720(R) (NP-15310, pp 26-35)
reactions in substrate complexes, perturbation-type analysis of, 19: 43682(R) (UCLA-12-565, pp 33-57)

EPITHELIUM
reticular cells of, effects on thymectomized mice, 19: 43883(R) (UCLA-12-565, pp 65-85)

ERBIUM
separation from scandium and thorium by reversed-phase chromatography, 19: 44125

ERBIUM ALLOYS
Er–Ag, crystal structure studies, 19: 44678(R) (ANL-7000, pp 186-200)
Er–Fe, isomer shift of iron-57 in $ErFe_2$ at 300 and 800°K, 19: 44678(R) (ANL-7000, pp 186-200)
Er–Ga, crystal structure studies, 19: 44678(R) (ANL-7000, pp 186-200)
Er–Hf–Pd, crystal structure studies, 19: 44678(R) (ANL-7000, pp 186-200)
Er–Pt, crystal structure studies, 19: 44678(R) (ANL-7000, pp 186-200)

ERBIUM CHLORIDES
pharmacology and toxicology of, 19: 43728(R) (UCLA-12-565, pp 59-64)

ERBIUM COMPOUNDS
with organic acids, preparation and properties, 19: 44028

ERBIUM ISOTOPES Er-160
gamma spectra, (E), 19: 45272 (JINR-P-2270)

ERBIUM ISOTOPES Er-164
oxygen-16 inelastic scattering at 43.5 Mev, vibrational-state excitation in, (E), 19: 45321

ERBIUM ISOTOPES Er-166
oxygen-16 inelastic scattering at 43.5 Mev, vibrational-state excitation in, (E), 19: 45321

ERBIUM ISOTOPES Er-168
oxygen-16 inelastic scattering at 43.5 Mev, vibrational state excitation in, (E), 19: 45321

ERBIUM ISOTOPES Er-170
oxygen-16 inelastic scattering at 43.5 Mev, vibrational-state excitation in, (E), 19: 45321

ERBIUM SELENIDES
crystal structure, 19: 44010

ERBIUM TELLURIDES
crystal structure, 19: 44010

ERYTHROCYTES
chimerism and acquired immunologic tolerance in mouse, 19: 43657
hemoglobin synthesis in, parameters of, 19: 43682(R) (UCLA-12-565, pp 33-57)
radiation effects on chromosomes in, of man, 19: 43672(R) (TID-22131)
radiation effects on morphology of, in salamanders, 19: 43730
respiration in chicken, 19: 43682(R) (UCLA-12-565, pp 33-57)
separation from lymphocytes by electrophoresis, 19: 43648(R) (UCLA-12-565, pp 87-96)

ERYTHROPOIESIS
preparation stimulating, protective effects against radiation injuries in animals and man, 19: 43872

ESCHERICHIA COLI
radiation effects on, effects of organic nitroxide-free radicals on sensitization of, 19: 43875
radiation effects on chromosome replication in, 19: 43741
radiation effects on infection of, with bacteriophage MS_2, 19: 43742
radiation effects, genetic, 19: 43751(T)
radiation injuries in, modification by genetic repair factors, 19: 43794
radiation injuries in, repair mechanisms for, 19: 43795
radioinduced mutations of, 19: 43804

ESOPHAGUS
radiodiagnosis of cancer in, using phosphorus-32 and miniature Geiger tube, 19: 43887

ESTRADIOL
protective effects of, against radiation injuries in rat spleen, 19: 43860(R) (NP-15310, pp 14-25)

ESTROGENS
effects on enzyme activity in chicken livers, 19: 43682(R) (UCLA-12-565, pp 33-57)
effects on ribonuclei acid levels in chicken livers, 19: 43682(R) (UCLA-12-565, pp 33-57)

ETHANE
reaction with recoil tritium, effects of oxygen on, 19: 44106
1-phenyl-1-acetthio-2-nitro-, protective effects against radiation lethality in mice, 19: 43868

ETHANE, DIBUTOXY-
dibutoxyethane, use in reprocessing of fast reactor fuel, 19: 44108 (AERE-R-4449(Pt.3))

ETHANE, HEXAFLUORO-
hexafluoroethane–rare gas, radiolysis, energy transfer in gamma, 19: 44054(R) (COO-1365-7)

ETHANE, TRICHLOROTRIFLUORO-
radioinduced reactions with benzene, calculated product accumulation in, 19: 44061(T) (AEC-tr-6567)
ETHANES, HALO-
internal rotation barriers, (T), 19: 43997(R) (UCRL-11889)
ETHANETHIOL, 2-AMINO-
effects on oxygen tension and sulfhydryl content in mouse spleen, 19: 43869
protective effects against proton and x irradiation effects on mice, 19: 43873
protective effects against radiation effects on granulocyte and lymphocyte counts in mice, 19: 43876
protective effects of, against radiation injuries in mice, synergistic effects with dimethyl sulfoxide, 19: 43859(R) (NP-15310, p 1-13)
radioprotective effects of, reaction mechanisms for, 19: 43869
ETHANETHIOLS, 2-AMINO-
protective effects of, against radiation injuries in rat spleen, 19: 43860(R) (NP-15310, pp 14-25)
ETHANOL
dehydration and dehydrogenation of, catalytic effects of praseodymium oxide on, 19: 44023
radiation effects on reactions with hydroxyl ions, 19: 44090
ETHANOL, 2-AMINO-
effects on metabolism of hexobarbital in rats, 19: 43670(R) (NP-15310, pp 36-47)
ETHANOL, 2,2',2''-NITRILOTRI-
performance as sensitizer for nuclear emulsions, 19: 44406 (CERN-65-4(Vol.II), pp IV41-5)
performance for nuclear emulsion sensitization, 19: 44395 (CERN-65-4 (Vol.II), pp II75-87)
ETHYL ETHER
effects on strontium-85 elution from mouse bones, 19: 43706
ETHYLENE
radioinduced addition of carbon tetrabromide to, in carbon tetrachloride solutions, 19: 44065
radioinduced addition of radiolytic fragments from silicon hydrides to, 19: 44066
radioinduced bulk polymerization of, long-lived radicals in, 19: 44073
radioinduced polymerization of, effects of temperature on, 19: 44074
ETHYLENE, CHLORO- POLYMERS
radiation effects on, in water and vacuum, 19: 44086
radioinduced graft polymerization with acrylates, methacrylates, and 4-vinyl pyridine, 19: 44083
radioinduced graft polymerization with styrene, temperature effects on, 19: 44084
polyvinyl acetate-polyvinyl chloride, preparation of thin films of, (E), 19: 44590 (CEA-R-2803)
ETHYLENE POLYMERS
analysis for iodine-128, activation, 19: 43951
analysis for trace impurities by activation methods, 19: 43975
meson (μ^+) depolarization quenching in, as function of longitudinal magnetic field, (E/T), 19: 45079
meson (μ^+) depolarization in targets of, (E), 19: 45080
radiation effects on films of, electron, 19: 44069
radiation effects from corona in electric discharges, 19: 44069
radioinduced graft polymerization with acrylates, methacrylates, and 4-vinyl pyridine, 19: 44083
radioinduced graft polymerization with styrene, temperature effects on, 19: 44084
spectra of, slow-neutron-scattering analysis of, (E), 19: 44050
ETHYLENE, TETRAFLUORO- POLYMERS
fabrication of high-density Teflon sheet, by powder rolling, 19: 44637 (LA-3340)
meson (μ^+) depolarization quenching in, as function of longitudinal magnetic field, (E/T), 19: 45079
meson (μ^+) depolarization in targets of, (E), 19: 45080
radiation effects on friction and deformation properties, 19: 44092
EUROPE
nuclear energy utilization in, 19: 45610
nuclear industry development in, 19: 45723
EUROPIUM FLUORIDES
reactions with europium sulfide, preparation of europium sulfide fluoride by, 19: 44024
EUROPIUM ISOTOPES Eu-147
beta decay, conversion electron spectra and γ-γ coincidences for, (E), 19: 45267 (JINR-P-2161)
EUROPIUM ISOTOPES Eu-154
half life, (E), 19: 45287 (USNRDL-TR-868)
EUROPIUM ISOTOPES Eu-157
decay, (E), 19: 45287 (USNRDL-TR-868)
EUROPIUM OXIDES
effects on optical properties of silicate glasses, 19: 44030
phase transformations in, at 1800 to 2400°C, 19: 44731
EUROPIUM SULFIDES
reactions with europium fluoride, preparation of europium sulfide fluoride by, 19: 44024
EUTECTICS
survey of binary-alloy, for aligned structures, 19: 44707 (WVT-6523)
EVAPORATORS
design optimization of multi-stage flash, for desalination, 19: 44140 (ORNL-TM-1244)
operational characteristics of fluidized-bed spray, for waste processing, 19: 45688(R) (NP-15367)
EVOLUTION
origin of life, scheme for, 19: 45721 (UCRL-14254)
EXCRETORY SYSTEMS
physiology of, in snails, 19: 43695
EXHAUST SYSTEMS
design for radiochemical laboratories, 19: 44284 (AWRE-O-24/65)
EXOSPHERE
electron diffusion from, ionospheric ionization increase from, (E), 19: 45174
hydromagnetic emission from, v-l-f, (E), 19: 45171
radiation measurement in, Explorer VII high-energy, 19: 44973
temperature variation in, with solar wind velocity, (T), 19: 45179
EXPERIMENTAL BOILING WATER REACTOR
control rod fabrication for plutonium recycle tests in, 19: 45559(R) (ANL-7000, pp 64-8)
fuel element fabrication for Plutonium Recycle Demonstration Experiment in, 19: 45559(R) (ANL-7000, pp 64-8)
fuel plate, radioinduced swelling, 19: 44738(R) (ANL-7000, pp 119-21)
neutron flux distributions in, method for determining, 19: 45560 (ANL-7011)
EXPERIMENTAL GAS COOLED REACTOR
control-rod drive for, testing of, 19: 45589 (ORNL-TM-1197)
graphite contraction during irradiation, effects of tensile stresses on, 19: 44744 (HW-SA-3692)
EXPERIMENTAL ORGANIC COOLED REACTOR
development as fast fuel test facility, 19: 45669(R) (APDA-174, pp 61-6)
EXPLODING WIRE PHENOMENA
magnetohydrodynamic instability of copper, (E), 19: 44845
EXPLOSIONS
flow in gas, numerical solution to unstable one-dimensional, 19: 44200(T) (SC-T-65-756)
EXPONENTIAL PILES
neutron buckling in two-zone heterogeneous graphite, (E), 19: 45524 (AEEW-R-428)
EXTRUSION
hydrostatic methods of, review, 19: 44651
EYES
effects of cataracts on content of amino acids and sugars in rabbit, 19: 43755
radiation dose to, during diagnostic radiography of head and neck region, 19: 43885
radiation effects on lens in mouse, protons, 19: 43721(R) (ORNL-TM-1217)
radiation effects on content of amino acids and sugars in rabbit, 19: 43755
radiosensitivity of lens, 19: 43885

F

FALLOUT
animal food-chain kinetics of, following nuclear explosions, 19: 43662(R) (UCLA-12-565, pp 97-128)
content in marine environment, 19: 43663
content in polar stratosphere, 1963, 19: 44260
criticality studies in FRO assembly, (E/T), 19: 45522 (AE-195)
deposition and ground of, meteorological factors in, 19: 44255 (RT/PROT(65)-10)
deposition from atmosphere, review of research on, 19: 44246 (BNL-914, pp 133-8)
deposition from atmosphere, meteorological aspects of, 19: 44247 (BNL-914, pp 139-40)
deposition from atmosphere, studies, 19: 44245 (BNL-914, pp 125-32)
diffusion in atmosphere, integration of Sutton point-source formula for, (T), 19: 43997(R) (UCRL-11889)
gamma radiation from, simulation of, 19: 44254 (RRA-M51)
model of, for civilian defense, 19: 44243 (AD-619902)
monitoring at Argonne, Jan.-June 1965, 19: 44300 (TID-22171)
monitoring at Savannah River Plant, Jan. to June 1965, 19: 44288(R) (DPST-65-30-2)

monitoring in Alaska, 1964, 19: 44289 (HW-SA-3750)
monitoring in Atlantic Ocean, 1964, 19: 44253(R) (NYO-2174-36)
monitoring in Austria, 1961 to 1965, 19: 44292(R) (NP-15173)
monitoring in Canada, June 1965, 19: 44251 (NP-15519, pp 23-51)
monitoring in India, 1959 to 1964, 19: 44244 (AEET/AM/40)
monitoring in Japan, 1961 to 1964, 19: 44264
monitoring in Japan, 1959 through 1962, 19: 44265
monitoring in Japan, 1961 through 1963, 19: 44266
monitoring in Japan, 1961 to 1964, 19: 44268
monitoring in Southern Australia in 1958 to 1964, 19: 44261
monitoring in Soviet Union, 1963, 19: 44259
monitoring in Switzerland, 1963, 19: 44269
particle size distribution in 1963 and 1964, 19: 44252 (NRL-6305)
shelters against, windows for, 19: 44218(P)
uptake by desert shrubs, 19: 43662(R) (UCLA-12-565, pp 97-128)
washout from atmosphere, (T), 19: 44249 (BNL-914, pp 144-8)

FAST REACTORS
blankets for, development paste, 19: 45561 (APDA-172)
coolant transient two-phase flow and heat transfer in liquid-metal-cooled, 19: 45494 (NAA-SR-11008)
development of breeder, in France and Germany, 19: 45623
development of Karlsruhe, 19: 45583(R) (NP-15365)
electron beam reactions with supercritical cores of, neutron flux enhancement from, 19: 45874 (GA-6168)
fuel element design for, 19: 45553(P)
fuels for breeder-type, merits of thorium, 19: 45605(T) (ORNL-tr-788)
neutron cross sections for, from 0.414 ev to 5.5 Mev, 19: 45244 (AEEW-M-472)
neutron Doppler effect in, (T), 19: 45576 (IA-1039)
neutron kinetics of plutonium-fueled, computer program for calculating, 19: 45530 (JAERI-1082)
physics calculations for Swedish FRO, 19: 45667 (AE-194)
reactivity in, Doppler temperature coefficient of, (T), 19: 45576 (IA-1039)
reactivity sodium void coefficient for, 19: 45538

FATIGUE
research program on pressure-vessel, 19: 45503(R) (SWRI-1228-69)
test equipment for metal, design of, 19: 45601(R) (WCAP-3750)

FATTY ACIDS
oxidation of long-chain, cofactor requirements for, 19: 43681(R) (UCLA-12-565, pp 17-31)
radioinduced decarboxylation of saturated, mechanisms of, 19: 43681(R) (UCLA-12-565, pp 17-31)

FECES
analysis for plutonium, radiochemical method for, 19: 44296 (NYO-4700(Rev.)(Suppl.II))
analysis for radium-226, radiochemical method for, 19: 44296 (NYO-4700(Rev.)(Suppl.II))
excretion of calcium-45, mineral nutrients, and phosphorus-32 by colostomized pullets, 19: 43693

FERMI FAST BREEDER REACTOR
operating experience at, 19: 45562(R) (APDA-174, pp 71-3)

FERMIONS
properties of disordered, degenerate systems of, (T), 19: 44844
quantum dynamical equations for spin-½, covariant and hermitian semi-classical limit of, 19: 45060
Regge poles for, in quantum electrodynamics with massive photons, 19: 45114

FERNS
radiation effects on growth and differentiation of gametophytes of, ultraviolet, 19: 43825

FERROMAGNETIC MATERIALS
effects on superconducting films, proximity, (T), 19: 45197

FETUSES
calcium metabolism in human, 19: 43701
magnesium metabolism in human, 19: 43701
phosphorus metabolism in human, 19: 43701
radiation effects on XXX No. 18 trisomy syndrome development in, etiologic, 19: 43811
strontium metabolism in human, 19: 43701

FFAG ACCELERATORS
beam injection system for, electronic control of, 19: 44884

FIELD THEORY
conservation laws and tensor Lagrangians for free fields, generalized, 19: 45141
definitions of translations in inhomogeneous SL(6), 19: 45132 (JINR-E-2225)
formalism of relativistic quantum, for baryons and mesons, 19: 45131 (JEN-154-DF/I-47)
hamiltonians for local quantum model, 19: 45150
propagators in quantum, determination using indefinite metrics, 19: 45133 (NP-15341)
representation of I = 0 states of three-pion resonances in, 19: 45042 (UCID-2608)
representations in SU(3), methods for multiplying, 19: 45030 (NP-15390)
scattering amplitudes in local, restrictions on forward, 19: 45039 (TPJU-10/65)
solutions for combined Maxwell-Einstein-Klein-Gordon equations, axially symmetric, 19: 45147
vertex functions for three-boson spin-zero interactions, 19: 45029 (NP-15382)
wave functions in energy plane, interpolation of Jost and, 19: 45143

FILMS
fabrication and forming of flexible radiation-attenuating, 19: 44670(P)
interference patterns from thin, optical phase changes in, 19: 43997(R) (UCRL-11889)
Mössbauer effect in thin, temperature dependence of, 19: 44847
preparation of thin copolymer polyvinyl acetate–polyvinyl chloride, (E), 19: 44590 (CEA-R-2803)
structure of zirconium oxide, formed on zirconium, 19: 44622(R) (EURAEC-1433)

FILTERS
analysis for plutonium, radiochemical method for, 19: 44296 (NYO-4700(Rev.)(Suppl.II))
fire prevention in radiochemical laboratory systems of, 19: 44284 (AWRE-O-24/65)
penetration by radioactive aerosol, measurement of depth of, 19: 44299 (SZS-2(1965))
testing high-efficiency, using sodium-24 aerosol, 19: 44281 (AEET-202)
testing of high-efficiency, fluorescent aerosol tracer system for in-place, 19: 44208(R) (BMI-X-346)

FILTRATION
rate through filter and cake, tests of model of, 19: 43923(T) (ORNL-tr-743)

FINLAND
cesium-137 content in Lapp diet in, relation of potassium to, 19: 44305

FINNED TUBES
design with chevron or herringbone pattern, 19: 45552(P)
design with grooved longitudinal fins, 19: 44206(P)
fabrication of herringbone, process for, 19: 44656(P)
fabrication of, automatic machine for, 19: 44655(P)

FIRES
prevention of, in radiochemical laboratories, 19: 44284 (AWRE-O-24/65)

FISH
metabolism of radionuclides by marine, 19: 43669(R) (NP-15159)
radiation effects on gonadal nucleic acids in, α, 19: 43769
radiation processing of, effects on wholesomeness when stored at room temperature, 19: 44555 (NP-15373)
radiation processing of codfish and halibut, 19: 44556 (NP-15464)
radioactivity of, at Savannah River Plant, Jan. to June 1965, 19: 44288(R) (DPST-65-30-2)
radioinduced thyroidectomy in trout, after administration of iodine-131, 19: 43773
wax from coelacanth, composition of, 19: 43681(R) (UCLA-12-565, pp 17-31)

FISSION
distributions around PWR control rods, 19: 45534 (WCAP-3269-35)
effects of resonance, in small critical assemblies, 19: 45521 (AAEC/TM-118)
research studies on, Italian, 19: 45338
spectra from, methods for in-core determination of, 19: 44450(R) (IBK-120a)
yields from uranium-235 thermal-neutron, (E), 19: 45260(R) (IDO-14660)

FISSION CHAMBERS
amplifier performance at high temperatures, pre-, 19: 44462 (TIM-922)

FISSION FRAGMENTS
beta distributions from, measurement using emulsions, 19: 44441 (CERN-65-4(Vol.II), X47-53)
detection of heavy, semiconductor detectors for, 19: 44481 (ZFK-PHA-12, pp 149-53)
effects on displacement cascades in gold films, 19: 44739(R) (ANL-7000, pp 233-77)
scattering of, effects on fission spectra, 19: 44450(R) (IBK-120a)
tracks in evaporated gold films, 19: 44739(R) (ANL-7000, pp 233-77)

FISSION PRODUCTS
buildup and transport in PRTR, shutdown radiation measurements for determining, 19: 45564 (BNWL-SA-85)
cross sections of, computer calculation of, 19: 45601(R) (WCAP-3750)
decays and yields of, analytical data on, 19: 44296 (NYO-4700(Rev.)(Suppl.II))
diffusion and coalescence in reactor fuels, theory for gas, 19: 44739(R) (ANL-7000, pp 233-77)
diffusion from irradiated Windscale fuel, 19: 44303 (TRG-Report-888)

diffusion from molten of fuel elements into condensing steam, 19: 44285 (BNWL-SA-29)
diffusion of gaseous, from intentionally punctured Calder Hall type fuel elements, 19: 44632
effects on reactor primary cooling system shielding design, 19: 45601(R) (WCAP-3750)
radiation dose to lungs from inhaled, 19: 44292(R) (NP-15173)
release from containment, simulation study, 19: 44286 (BNWL-SA-30)

FISSIONABLE MATERIAL
critical separation of regular arrays of, 19: 44977 (IDO-17095)

FISSIUM
fissium–Pu–U, burnup in, effects of cladding thickness on attainable, 19: 44587(R) (ANL-7000, pp 3-63)
fissium–Pu–U, enthalpy to 1200°C, 19: 44587(R) (ANL-7000, pp 3-63)
fissium–Pu–U, phases and transformation kinetics, 19: 44587(R) (ANL-7000, pp 3-63)
fissium–Pu–U, properties of, effects of composition on, 19: 44587(R) (ANL-7000, pp 3-63)
fissium–U, radioinduced swelling in, effects of postirradiation annealing temperature on, 19: 44587(R) (ANL-7000, pp 3-63)
fissium–U–Zr, radioinduced swelling in, effects of postirradiation annealing temperature on, 19: 44587(R) (ANL-7000, pp 3-63)
fissium–Pu–U, reactions with vanadium at 1100 to 1400°C, 19: 44587(R) (ANL-7000, pp 3-63)
fissium–Pu–U, reactions with chromium, molybdenum, and niobium at 750°C, 19: 44587(R) (ANL-7000, pp 3-63)
fissium–Pu–U, reactions with niobium–zirconium and titanium–vanadium alloys at 750°C, 19: 44587(R) (ANL-7000, pp 3-63)
fissium–Pu–U, reactions with Hastelloy-X and type 304 stainless steel at 750°C, 19: 44587(R) (ANL-7000, pp 3-63)

FLANGES
connections with insulating sealing element for heated test sections in tubes, 19: 44134 (EUR-2434.d)

FLUID FLOW
boiling burnout in annular, effects of electric fields on, (E), 19: 44190(R) (NYO-2404-67)
boiling burnout in annuli, effects of electric fields on, (E), 19: 44191(R) (NYO-2404-73)
eddy formation in notch, water tunnel experiment on, 19: 45722 (UCRL-16188)
electromagnetic field effect of boundary layer of two surfaces in conducting, 19: 44828
magnetohydrodynamic, symmetric motions of incompressible viscous, 19: 44816
magnetohydrodynamic viscous, past circular cylinders, (T), 19: 44825
magnetohydrodynamic, influence of relative roughness on friction coefficient in, 19: 44826
magnetohydrodynamic, stabilizing effect of magnetic field on, 19: 44835
magnetohydrodynamic localism hypothesis for turbulence in conducting, 19: 44836
oscillations in forced-convection two-phase, analysis of initiating mechanisms for, 19: 44185(R) (GEAP-4910)
past obstacles, equations for, 19: 43997(R) (UCRL-11889)
regimes in high-pressure boiling water systems, research program on, 19: 44193(R) (NYO-3304-5)
stability in striated layer MHD cells, Rayleigh-Taylor, (T), 19: 44984
stability of two-fluid wheel, to helical disturbances, 19: 45652 (NASA-TN-D-2696)
two-phase, in boiling and condensation of potassium, 19: 44187(R) (NASA-CR-54405)
two-phase, in liquid-metal-cooled fast reactors, 19: 45494 (NAA-SR-11008)
two-phase, of saturated water through apertures, (E), 19: 44196(R) (TID-22145)
two-phase, research program on upward annular, 19: 44192(R) (NYO-3114-9)
velocity of conducting, impulse method for, (E), 19: 44834

FLUID FLOW (LAMINAR)
magnetohydrodynamic, in channels and pipes, (T), 19: 44824
of conducting incompressible fluid in flat channel in electric and magnetic fields, 19: 44829
production at high Reynolds numbers, water tunnel with moving walls for, 19: 45722 (UCRL-16188)
production at high Reynolds numbers, moving-wall tunnel for, 19: 43997(R) (UCRL-11889)

FLUID FLOW (TURBULENT)
heat transfer to supercritical-pressure liquid hydrogen in tubes, data compilation, 19: 44189 (NP-15332)
magnetohydrodynamic, boundary-layer analysis of, (T), 19: 44981(R) (NP-15435)
of mercury in magnetic field; velocity pulsations in, (E), 19: 44827
performance of vortex tube, 19: 44199 (UCRL-12045)

FLUIDS
properties common to superfluids and, 19: 44842

FLUORESCEIN
use in dual atmospheric tracer technique, 19: 44800 (BNWL-103)

FLUORIDES
effects on photometric determination of zirconium, 19: 43972
effects on properties of dentin, in rat teeth, 19: 43687

FLUORIMETERS
image-brightness control system for, design, 19: 44363(P)
screen design for, warning border, 19: 44362(P)

FLUORINE
spin precession in μ-mesic, 19: 45278 (NP-15389)
spin precession in compounds of muonium and, (T), 19: 45278 (NP-15389)

FLUORINE ISOTOPES F-18
energy levels in, tensor force for, (T), 19: 45370

FOOD
fallout contamination in Japan, 19: 44264
monitoring Savannah River Plant, Jan. to June 1965, 19: 44288(R) (DPST-65-30-2)
processing of, uses of radioisotopes in industrial, 19: 44562
radiation processing of, evaluation of, 19: 44552 (BLG-327)
radiation processing of fish products, effects on wholesomeness when stored at room temperature, 19: 44555 (NP-15373)
radiation processing of fish products, 19: 44556 (NP-15464)
radiopreservation of, review of, 19: 44561
radiosterilization of, research and development in, 19: 44566
strontium-90 content of Indian, 1959 to 1964, 19: 44244 (AEET/AM/40)
vitamin stability in prepared dog, during storage, 19: 43644(R) (UCD-472-112)

FORESTS
radiation effects on, ecological, 19: 43711 (BNL-924)
radiation effects on pine-oak, gamma, 19: 43722(R) (TID-22108)

FORGING
equipment for hot, of tubular parts, 19: 44657(P)

FORMAMIDE, *N,N*-DIMETHYL-
complexes with molybdenum chlorides, 19: 43990 (MIT-1965-15)

FRANCE
nuclear power plant development in, 19: 45580 (NP-15283)

FREE RADICALS
electron spin resonance spectra of nitrobenzene and nitrosobenzene radical anions in liquid ammonia, 19: 43997 (UCRL-11889)
electron spin resonance spectra of, formed by reduction of sulfur nitride, 19: 43997(R) (UCRL-11889)
electron spin resonance of, in irradiated *Bacillus subtilis*, 19: 43793
reactions of, studies of complex, 19: 43997(R) (UCRL-11889)

FREONS
analysis of TF, for nonvolatile residues, instrument for, 19: 45713 (SC-TM-65-279)

FRUITS
radiation processing of oranges, effects on juice constituents and skin color, 19: 44554 (IA-1015)

FUEL CELLS
design using antipolar ion exchange membrane, 19: 44992(P)

FUNGI
radioinduced sterility in pollen of, γ, 19: 43767

FURFURYL ALCOHOLS
use as binder in forming carbon articles, 19: 44671(P)
use as binder in the manufacture of shaped carbon articles, 19: 44669(P)

FURNACES
design for high-temperature x-ray diffractometers, 19: 44340 (AERE-M-1361)

FUSED SALTS
surface tension near critical temperature, 19: 44701(R) (TID-22144)

G

GADOLINIUM
Curie temperature, effects of pressure on, 19: 43997(R) (UCRL-11889)
elastic moduli at 298°K, 19: 44676(R) (ANL-7000, pp 176-82)
separation from scandium and thorium by reversed-phase chromatography, 19: 44125

GADOLINIUM ALLOYS
Gd–Ag, crystal structure studies, 19: 44678(R) (ANL-7000, pp 186-200)
Gd–Au, crystal structure studies, 19: 44678(R) (ANL-7000, pp 186-200)
Gd–Fe, isomer shift of iron-57 in $GdFe_2$ at 300 and 800°K, 19: 44678(R) (ANL-7000, pp 186-200)
Gd–Sc, phase studies of samarium-type intermediate phases in, 19: 44672 (AD-619201)

GADOLINIUM COMPLEXES
with glycolic acid, binding energy of, infrared spectrophotometric study

of, 19: 44004
GADOLINIUM COMPOUNDS
with organic acids, preparation and properties, 19: 44028
GADOLINIUM IONS
water exchange in solution, nuclear magnetic resonance study, 19: 43997(R) (UCRL-11889)
GADOLINIUM ISOTOPES Gd-154
oxygen-16 inelastic scattering at 43.5 Mev, vibrational-state excitation in, (E), 19: 45321
GADOLINIUM ISOTOPES Gd-156
oxygen-16 inelastic scattering at 43.5 Mev, vibrational-state excitation in, (E), 19: 45321
GADOLINIUM ISOTOPES Gd-158
oxygen-16 inelastic scattering at 43.5 Mev, vibrational-state excitation in, (E), 19: 45321
GADOLINIUM ISOTOPES Gd-161
oxygen-16 inelastic scattering at 43.5 Mev, vibrational-state excitation in, (E), 19: 45321
GADOLINIUM OXIDES
effects on optical properties of silicate glasses, 19: 44030
phase transformations in, at 1800 to 2400°C, 19: 44731
GAGES
design concepts of functional, 19: 45708 (SC-R-65-915)
GALAXIES
evolution of, gravitational instability of expanding universe for, 19: 44929
gamma point sources in Milky Way, search for, (E/T), 19: 44905
magnetic fields of, bridge formation from, (T), 19: 44926(T)
radio emission from, 19: 44909
x-ray spectra near Galactic center and in Scorpius, (E), 19: 44967
GALLIUM
analysis for trace amounts of copper by activation methods, 19: 43973
content in chondritic meteorites, 19: 44900
determination in aluminum ores by activation analysis and colorimetry, 19: 43961
GALLIUM ALLOYS
Cu–Ga, radiation effects on strength of, effects of gallium content on neutron, [illegible]: 44739(R) (ANL-7000, pp 233-77)
Er–Ga, crystal structure studies, 19: 44678(R) (ANL-7000, pp 186-200)
Ga–Fe, magnetization at 295°K, saturation, 19: 44678(R) (ANL-7000, pp 186-200)
Ga–Lu–Ni, crystal structure studies, 19: 44678(R) (ANL-7000, pp 186-200)
Ga–Nd, crystal structure studies, 19: 44678(R) (ANL-7000, pp 186-200)
Ga–Pu, magnetic susceptibility of δ-phase, at 6 to 300°K, 19: 44690 (LA-DC-7360)
Ga–Sn, crystal structure studies, 19: 44678(R) (ANL-7000, pp 186-200)
Sb–Ga, fusion thermodynamic properties of GaSb, 19: 43997(R) (UCRL-11889)
GALLIUM ARSENIDES
fusion thermodynamic properties, 19: 43997(R) (UCRL-11889)
GALLIUM COMPLEXES
with 8-quinolinol derivatives, electronic absorption spectra, 19: 43989 (MIT-905-20)
GALLIUM ISOTOPES Ga-69
neutron reactions with, resonances in, (E), 19: 45296
GAMMA RADIATION
absorbed dose rates of reactor, calorimetric measurement of, 19: 45467
absorption by spherical nuclei, cross section for, (T), 19: 45366
angular distribution from neutron capture by tin-124 at 62 ev, (E), 19: 45379
biochemical effects on globulin *in vitro*, 19: 43686
collimator design for low-energy, 19: 44347 (ORNL-P-1545)
control of populations of gnats, *Hippelates pusio*, by, 19: 43803
detection and measurement of, efficiency of sodium-iodide phosphors for, 19: 44515
detection and measurement in atmosphere and body from reactor accident, 19: 44325
detection and measurement of, instrumentation for, 19: 44369 (AERE-R-4552)
detection using emulsions, 19: 44443 (CERN-65-4(Vol.II), pp X61-6)
distribution in 3-region cores, 19: 45601(R) (WCAP-3750)
dosage to skin from external contamination, evaluation of methods for, 19: 44328
dose attenuation factors in concrete ducts, energy dependence of, (E/T), 19: 45457 (AD-462614)
dose distribution to tissues from accidental exposure to, calculation of, 19: 44329
dose distributions above fallout, simulation of, 19: 44254 (RRA-M51)
dose from re-entering nuclear rocket debris, models for calculating, 19: 45655 (NUS-229)
dose from re-entering nuclear rocket debris, models for calculating, 19: 45655 (NUS-229)
dose rates in concrete and water from point isotropic fission sources, (T), 19: 45464 (ORNL-TM-1167)
dosimetry in accidents, clinical and hematologic tests for, 19: 44316
dosimetry in accidental and normal conditions, methods for, 19: 44332
dosimetry of, performance of scintillation counters for low-level, 19: 44528
dosimetry using photographic films with inhibited development, 19: 44440 (CERN-65-4(Vol.II), pp X44-6)
effects autoxidation of benzene in aqueous solutions of metal ions, 19: 44078
effects in Drosophila, genetic, effects of dose rate on, 19: 43785
effects in *Escherichia coli*, lethal, 19: 43794
effects in *Escherichia coli*, genetic, 19: 43794
effects in mouse oöcytes, genetic, 19: 43789
effects in mouse spermatogonia, genetic, 19: 43789
effects in pea seeds, genetic, 19: 43770
effects in rice seeds, biological, effects of dose rate, 19: 43781
effects in silkworms, genetic, 19: 43784
effects in silkworm gonads, genetic, 19: 43786
effects in wheat seeds, biological, effects of dose rate, 19: 43781
effects of reactor, on radiation stability of strongly basic anion exchange resins, 19: 44055 (IAE-788)
effects on addition of tertiary amines to 1-octene, 19: 44053 (AFML-TR-65-166)
effects on addition of carbon tetrabromide to ethylene in carbon tetrachloride solutions, 19: 44065
effects on adenosine triphosphatase activity in rat spleen, chronic exposure, 19: 43860(R) (NP-15310, pp 14-25)
effects on amines, products of, 19: 44053 (AFML-TR-65-166)
effects on aqueous methyl ammonium perchlorate and sulfate, hydrogen yields in, 19: 44080
effects on aqueous solution of acetylene in presence of foreign ions, 19: 44082
effects on aqueous solutions of benzene, effects of oxides on, 19: 44051 (AE-192)
effects on aqueous solutions of benzene at 100 to 200°C, 19: 44052 (AE-193)
effects on Artemia eggs, 19: 43815
effects on blood formation in bone marrow, 19: 43731
effects on bulk polymerization of ethylene under high pressure, long-lived radicals in, 19: 44073
effects on chemical constituents and color of oranges, 19: 44554 (IA-1015)
effects on chymotrypsinogen, decomposition of sulfur linkage in, 19: 43841
effects on Clostridium spores, 19: 43865
effects on cobalt and copper substituted and normal chlorophyll, spectra of, 19: 44087
effects on decomposition of benzoly peroxide *tert*-butyl peroxides, 19: 44089
effects on diaryl sulfones, 19: 44054(R) (COO-1365-7)
effects on dihydrouracil, 19: 44064
effects on dioxane-2,5-diphenyloxazole phosphor, quenching effects of radioprotective compounds on, 19: 43878
effects on eggs of Artemia, 19: 43814
effects on field plants, ecological, 19: 43711 (BNL-924)
effects on forest trees, ecological, 19: 43711 (BNL-924)
effects on formation of alkyl silanes from addition of radiolytic fragments from silicon hydrides to ethylene, 19: 44066
effects on frozen solutions of oxyanions, 19: 44054(R) (COO-1365-7)
effects on gonads of male mosquitoes, 19: 43796
effects on graft polymerization of polyethylene and polyvinyl chloride with monomers, 19: 44083
effects on graft polymerization of polyethylene and polyvinyl chloride with styrene, temperature effects on, 19: 44084
effects on grafting vinyl acetate acrylonitrile, and methyl methacrylate cotton fibers, 19: 44094
effects on granulocyte and lymphocyte counts in mice, protective effects of MEA against, 19: 43876
effects on growth inhibition and lethality of higher plants, acute and chronic exposure, 19: 43782
effects on Habrobracon sperm, 19: 43721(R) (ORNL-TM-1217)
effects on hamster cells in culture, pathological, 19: 43857
effects on hexafluoroethane–rare gas mixtures, 19: 44054(R) (COO-1365-7)
effects on lactation in dairy cattle, 19: 43801
effects on larvae of sheep lungworm, lethal, 19: 43750
effects on lipase activity in peanuts, 19: 43798
effects on luminescence in silver-activated phosphate glass, ESR spectra

from, (E), 19: 44758
effects on male plant sterility, 19: 43767
effects on metabolism in dairy cattle, 19: 43801
effects on metabolism in man, use in exposure diagnosis, 19: 43852
effects on mice, 19: 43662(R) (UCLA-12-565, pp 97-128)
effects on n-butyl-, diethyl-, and triethyl, amines, and 1-methylpiperidine, yields in, 19: 44072
effects on *Neurospora*, 19: 43648(R) (UCLA-12-565, pp 87-96)
effects on oxidation and reduction of iron ions in oxygenated sulfuric acid solutions, effects of organic compounds on, 19: 44056 (INR-579/XVII/C)
effects on oxidation of trivalent antimony in acid solution, 19: 44085
effects on pine and oak, 19: 43722(R) (TID-22108)
effects on *Pinus thunbergii*, 19: 43682(R) (UCLA-12-565, pp 33-57)
effects on polymerization of acrolein at −78 and −196°C, 19: 44070
effects on polymerization of ethylene at 20 to 45 and 100 to 140°C, 19: 44074
effects on polyvinyl chloride in water and in vacuum, 19: 44086
effects on production of colloidal gold particles in chloroauric acid, 19: 44079
effects on proton spin-lattice relaxation in sodium selenites, (E), 19: 45477 (NIJS-R-444)
effects on pulmonary sclerosis induction in rabbits, role of autoantibodies in pathogenesis of, 19: 43817
effects on radio- and radiothermo-luminescence of zinc sulfide phosphors, 19: 44757
effects on seed germination and seedling growth, 19: 43722(R) (TID-22108)
effects on seed hybridization, 19: 43767
effects on seed of *Digitalis Lanata EHRH*, 19: 43746
effects on semiconducting properties of anthracene, 19: 44077
effects on thermal insulation in reactors, 19: 44088
effects on thermoluminescence fading in dosimetric lithium fluoride, storage effects on, 19: 44076
effects on three high-temperature solid-film lubricants, 19: 44095
effects on thymine, 19: 43682(R) (UCLA-12-565, pp 33-57)
effects on thymine, 19: 44060 (UCRL-16353)
effects on transistors, 19: 44548 (NP-15422)
effects on Tribulus root meristems, 19: 43855
effects on trypsin, protective effects of oxidized and reduced pyridine coenzymes against, 19: 44081
effects on x-ray transmission in doped germanium single crystals, 19: 44756
emission by polarized nuclei, correlation of cascade, (T), 19: 45280 (NP-15457)
emission from galactic point sources, search for, (E/T), 19: 44905
emission from solar flares, mechanism for, (T), 19: 44916(T)
emission from supernova remnants, 19: 44930
emission in fission, delayed, (E), 19: 45245 (AFWL-TR-65-95)
emission in neutron capture reactions, 19: 45375
flux distributions above fallout, simulation of, 19: 44254 (RRA-M51)
flux from Crab Nebula, upper limit for, (E), 19: 44970
genetic effects in *Escherichia coli*, 19: 43804
human body burdens of, in Los Angeles 1960–64, 19: 43883(R) (UCLA-12-565, pp 65-85)
interactions with deuterons and protons, detection using emulsions, 19: 44438 (CERN-65-4(Vol.II), pp X33-6)
interactions with elementary particles, parity determination in, (T), 19: 45010 (JINR-E-2259)
physiological effects on lactation in dairy cows, 19: 43800
production in reactor shielding for, (E/T), 19: 45575 (GMAD-3078-23)
protection against, development of compounds for, 19: 43883(R) (UCLA-12-565, pp 65-85)
radioisotope selection for use as, 19: 44551
reactions (γ,α) and (γ,p) with silicon-28 at 17.4 to 22.3 Mev, cross sections for, (E), 19: 45310
reactions (γ,n) with carbon-40, half life determination from, 19: 45262 (IS-T-29)
reactions (γ,π^0) with lead at 1 Bev, meson (π^0) lifetime from, (E), 19: 45360
scattering cross sections to 1.3 Mev, Z dependence of elastic, (E/T), 19: 45327
shielding against, basement structure for, 19: 44216
shielding calculations for reactors, Monte Carlo method for, 19: 45469
spectra in cobalt-56 decay, (E), 19: 45295
transmission through flat water-lead shielding barrier, as function of shielding thickness, (T), 19: 45466
transport in concrete slabs, solution of equation for, 19: 45459 (EUR-2488.e)
use in salmonellae control in meat, economic feasibility of, 19: 44557 (NYO-3426-1)

GAMMA SOURCES
design modifications for gold-198 grain implantation gun, 19: 43888
dosimetry of multi-kilocurie, 19: 44372 (AFCRL-65-470)
effects on Drosophila oogonia, mutagenic, 19: 43724(R) (TID-22160)
effects on Drosophila sperm, mutagenic, 19: 43724(R) (TID-22160)
for radiosterilization, evaluation of, 19: 44559
therapeutic use of cobalt-60, for bladder carcinoma, 19: 43894
use of gold-198 seeds, for pituitary ablation, 19: 43920

GAMMA SPECTRA
analysis by scintillation spectroscopy and method of least squares, 19: 43981
analysis of complex, iteration method for, 19: 45373
analysis of, computer program for least-squares, 19: 45261 (IDO-17016)

GAMMA SPECTROMETERS
control and read-out system for double-crystal, 19: 44365 (AECL-2219)
design and performance of semiconductor, 19: 44472 (ZFK-PHA-12, pp 52-63)
design for analyzing burnup distributions in spent fuel elements, (E), 19: 44463 (TRG-Report-1005)
design of anticoincidence-shielded germanium, (E), 19: 44519
design of lithium-drifted germanium, (E), 19: 44510
design of scintillation anticoincidence, for scanning molten-plutonium fuel elements, 19: 44453 (LA-DC-7316)
mechanical drive design for Moessbauer, (E), 19: 45316
performance of germanium junction, 19: 44473 (ZFK-PHA-12, pp 64-5)
photopeak efficiencies of thallium-activated sodium-iodide, (E), 19: 44515
properties of lithium-drifted germanium diode, 19: 44371 (AERE-R-4921)
use in determination of radioisotopes in biomedical samples, 19: 43659

GARIGLIANO POWER REACTOR
fuel cycle economics for, thorium–uranium, 19: 45582 (NP-15320)
testing and operation of, comparison with other Italian power reactors, 19: 45616

GAS ANALYZERS
oxygen, review on, 19: 43980

GAS COOLED REACTORS
contamination control, 19: 45608
fast fission factors in natural-uranium-fueled air-cooled, (T), 19: 45229 (UJV-1324/65)
fuel cycles in advanced, computer analysis of, (T), 19: 45595 (TRG-Report-976)
fuel element can model for, heat transfer and pressure drop of, 19: 45549
fuel elements design for, finned, 19: 45555(P)
loading apparatus for, 19: 45512(P)
loading apparatus for, 19: 45513(P)
use as power source for underwater propulsion, 19: 45662

GAS FLOW
electromotive force and Hall effect in conducting channel, 19: 44831
magnetic field interactions with ionized, self-excitation in, 19: 44839
magnetohydrodynamic, in coaxial channel, 19: 44830
magnetohydrodynamic channel, optimum conditions for Hall effect in, 19: 44832
magnetohydrodynamic, channel profiling for turbulent, 19: 44838
magnetohydrodynamic, reduction of three-dimensional compressible, 19: 44850
numerical solutions to problems in, 19: 44200(T) (SC-T-65-756)

GAS FLOW (TURBULENT)
magnetohydrodynamic, channel profiling for, 19: 44838

GASEOUS DIFFUSION PLANTS
description of British, for enriching uranium, (E), 19: 45612
radiation monitoring at Paducah, Jan.-June 1965, 19: 44301 (TID-22172)

GASEOUS FUEL REACTORS
design of, using MHD principle, 19: 45540(P)
fuel flow stability to helical disturbances, gaseous wheel-flow, (T), 19: 45652 (NASA-TN-D-2696)

GASES
bibliography on high-temperature chemistry and physics of, 19: 43993 (NP-15379)
density in pulsed coaxial plasma accelerators, (E), 19: 45449
electric discharges in, time evolution of laser induced, 19: 44821
electron density function and distribution in magnetohydrodynamic conversion, (T), 19: 44982
expansion in stellar envelopes, (T), 19: 44924(T)
flow of partially ionized, linearized nonequilibrium, 19: 45425
oscillations in electron, in magnetic fields, 19: 44849
plasma phenomena in, correlation with solid-state plasma, 19: 45383 (D1-82-0419)
properties of helium-4, pseudospin boson model for, (T), 19: 45203
reactions with solids, apparatus for continuous two-step, 19: 44042(P)
stability of polytropic stellar spheres of, relativistic, (T), 19: 44925(T)
theory of Bose, 19: 44806 (IS-T-19)

viscosity of moderately dense, density expansion of, (T), 19: 44846
GASKETS
performance of vacuum, factor method for predicting, 19: 44135 (IA-1033)
GASTROINTESTINAL TRACT
calcium-47 absorption in dog, 19: 43677(R) (UCD-472-112, pp 86-96)
radiodiagnosis of diseases of, using radioisotopes and external scanning, 19: 43886
radiodiagnosis of cancer in, using phosphorus-32 and miniature Geiger tube, 19: 43887
strontium-85 absorption in dog, 19: 43677(R) (UCD-472-112, pp 86-96)
GEIGER-MUELLER TUBES
design of pocket-size, for use as individual alarm systems by personnel, 19: 44532
development of miniature, for use with phosphorus-32 in radiodiagnosis, 19: 43887
performance for inverse radiometric analysis of atmospheric sulfur dioxide, (E), 19: 44458 (NYO-2767)
GENETICS
radiation effects in man, genetic, 19: 43823
radiosensitivity effects on reproduction in Tribolium, x, 19: 43716 (HW-SA-3748)
GEOMAGNETIC FIELDS
charged-particle trajectories in model current sheets for, (T), 19: 45168
drifts in F2 layer, Appleton anomaly in, (T), 19: 45184
dynamo theory of, model for studying, 19: 45156 (AFCRL-64-768)
effects on exospheric temperature, (T), 19: 45179
interactions with solar plasma, (T), 19: 45164
pulsations of, ionospheric propagation of Pi 2 micro-, (T), 19: 45181
solar wind effects on outer, (T), 19: 45162
variations of, hydromagnetic instability of sub-Alfvén equation for, 19: 45187
GEOMAGNETIC STORMS
data for Feb.-March 1965, 19: 45178
occurrence of, correlation with solar activity cycle, 19: 44921(T)
solar wind effects on surface disturbances during sudden commencements, (T), 19: 45163
GEOPHYSICS
infrasonic wave generation in auroral zone, 19: 45183
GERMAN REACTORS
design of 300-Mw PWR, 19: 45609
GERMANIUM
heat content of pure, at high temperatures, 19: 43997(R) (UCRL-11889)
performance of lithium-drifted, as semiconductor gamma spectrometer, (E), 19: 44510
performance of lithium-drifted, as gamma spectrometer, (E), 19: 44519
radiation damage in, calculations of proton, 19: 44747 (NP-15463)
radiation effects on crystal structure defects and thermal conductivity of, at 80°K, 19: 44754
radiation effects on x-ray transmission in doped single crystals of, γ-, 19: 44756
GERMANIUM JUNCTIONS
performance in gamma spectrometers, 19: 44473 (ZFK-PHA-12, pp 64-5)
GERMANIUM OXIDES
$BeO–GeO_2$, glass formation limits in, calculation of upper, 19: 44016
$CaO–GeO_2$, glass formation limits in, calculation of upper, 19: 44016
$GeO_2–MgO$, glass formation limits in, calculation of upper, 19: 44016
$GeO_2–SrO$, glass formation limits in, calculation of upper, 19: 44016
GERMANIUM SYSTEMS
Ge–Si, use in thermoelectric converters for space power systems, 19: 45664
GERMANIUM TELLURIDES
superconductivity of, 19: 43997(R) (UCRL-11889)
GERMANY
activities of Institute for Reactor Safety of Federal Republic, 19: 45497(T) (ORNL-tr-652)
radiation protection regulations in, 19: 43913
radioactivity from strontium-89 and -90 in human bones, soft tissues, and standard diet in, 19: 44313
GERMINATION
radiation effects on Pinus and Quercus, gamma, 19: 43722(R) (TID-22108)
GIBBSITES
dehydration of, 19: 43997(R) (UCRL-11889)
GLACIERS
tritium accumulation and high-altitude climatology in Mt. Everest, 19: 44262
GLASS
bonding to metals, studies, 19: 43997(R) (UCRL-11889)
formation and structure in binary oxide systems, 19: 44015
formation limits in binary oxide systems, calculation of, 19: 44016
neutron diffusion constants in organic, measurement using neutron chopper, 19: 45222 (INR-624/IX-A/R)
optical properties of, effects of rare earth ions on, 19: 44030
radiation effects on dosimetry, electron and proton, 19: 44093
GLOBINS
radiation effects on content in rats, x, 19: 43766
GLOBULIN
determination in blood, of dogs, 19: 43674(R) (UCD-472-112, pp 36-43)
irradiated, metabolism in rabbits, 19: 43686
radiation effects on metabolism of, in rats, 19: 43852
radiation effects on properties of, *in vitro*, 19: 43686
reactions of canine alpha, beta, and gamma, with plutonium ions, 19: 43705
transfer between cerebrospinal fluid and plasma in multiple sclerosis patients, tracer study of, 19: 43666 (BNL-9406)
GLOVE BOXES
description and operation of recirculating argon atmosphere, 19: 44160(R) (ANL-7000, pp 278-86)
description of helium atmosphere system for vacuum, 19: 44160(R) (ANL-7000, pp 278-86)
design of inert-atmosphere, for preparation of samples for oxygen trace analysis, 19: 43933 (LA-3344)
GLUCOSE
determination in blood, of dogs, 19: 43674(R) (UCD-472-112, pp 36-43)
GLUTAMIC ACID
carbon-14 uptake by, in rat cerebral tissue, 19: 43690
GLYCEROL
neutron scattering by liquid, dynamics of, (E), 19: 45235
GLYCINE
radiation effects on metabolism in rats, effects of cortisone, 19: 43837
synthesis of carbon-14-labeled DL-, 19: 44047 (NP-15268)
uptake by cytoplasms and red cells, 19: 43682(R) (UCLA-12-565, pp 33-57)
GLYCOGEN
radiation effects on content in rat liver of, 19: 43735
GLYCOLIC ACID COMPLEXES
with metal ions, binding energy of, infrared spectrophotometric study of, 19: 44004
GLYCOLYSIS
radiation effects on Saccharomyces, uv, 19: 43765
GLYOXAL
yields from radiolysis of acetylene, 19: 44082
GOITER
iodine-131 metabolism in man with, age effects on, 19: 43691
GOLD
effect on determination of copper in bismuth by neutron activation methods, 19: 43941
effects on determination of copper in high-purity metals by activation methods, 19: 43973
fission fragment tracks in evaporated thin films of, 19: 44739(R) (ANL-7000, pp 233-77)
neutron absorption cross sections at 24 kev, (E), 19: 45230
performance for nuclear emulsion sensitization, 19: 44395 (CERN-65-4 (Vol.II), pp II75-87)
radiation damage displacement cascades in films of, fast neutron, fission fragment, and proton, 19: 44739(R) (ANL-7000, pp 233-77)
radiation effects on electric resistivity at 4°K, fast neutron, 19: 44739(R) (ANL-7000, pp 233-77)
radiation effects on stacking fault annihilation in films of, neutron, 19: 44739(R) (ANL-7000, pp 233-77)
GOLD ALLOYS
Au–Ho, crystal structure studies, 19: 44678(R) (ANL-7000, pp 186-200)
Au–Sc, crystal structure studies, 19: 44678(R) (ANL-7000, pp 186-200)
Au–Sn, heat of solution at 425°C, 19: 44678(R) (ANL-7000, pp 186-200)
Au–Tb, crystal structure studies, 19: 44678(R) (ANL-7000, pp 186-200)
Au–Y, crystal structure studies, 19: 44678(R) (ANL-7000, pp 186-200)
Dy–Au, crystal structure studies, 19: 44678(R) (ANL-7000, pp 186-200)
Gd–Au, crystal structure studies, 19: 44678(R) (ANL-7000, pp 186-200)
GOLD HALIDES
performance in nuclear emulsions, 19: 44393 (CERN-65-4(Vol.II), pp II50-63)
GOLD ISOTOPES Au-179
neutron reactions with, resonances in, (E), 19: 45296
GOLD ISOTOPES Au-197
neutron reactions (n,γ) with, rates for, (E/T), 19: 45522 (AE-195)
GOLD ISOTOPES Au-198
diagnostic tracer use of, for gastrointestinal diseases, 19: 43886
effects of injected, on blood picture in rats, 19: 43839
therapeutic use for treatment of cancers, design of implantation gun for, 19: 43888
therapeutic use of applicators of, 19: 43906
use of seeds of, for pituitary ablation, 19: 43920

GOLD SYSTEMS
Au–Si, phases and structure of, effects of liquid quenching on, 19: 45696 (CALT-221-12)
GONADS
radiation effects in mouse, genetic, 19: 43788
radiation effects in mouse spermatogonia, pathological, 19: 43788
radiation effects in mice, genetic, 19: 43789
radiosensitivity of, 19: 43889
radiosensitivity of, in children, 19: 43893
radiosensitivity of, in man, 19: 43914
radiosensitivity of, 19: 43756
radiosensitivity of *Leucaspius delineatus*, α, 19: 43769
radiosensitivity of spermatogonia in silkworm larvae, effects of developmental stage on, 19: 43783
radiosensitivity of, in silkworms, 19: 43784
radiosensitivity of, 19: 43823
strontium-90 content in human, in Germany, 19: 44313
zinc-65 uptake and distribution in normal and tumorous, in man, 19: 43699
GRAPHITE
analysis of nuclear grade, for boron, calcium, iron, titanium, and vanadium, spectrochemical, 19: 43930 (JEN-145-DQ/I-46)
deposition on urandium dioxide particles, 19: 44596 (EURAEC-1392)
fabrication of shaped articles of, using furfuryl alcohol binder, 19: 44671(P)
grinding of natural, ultrasonic, 19: 44648
impact properties of plates and tubes of, hypervelocity, 19: 44692 (NASA-TN-D-3018)
laser beam reactions with, molecular emission spectra in jets from, (E), 19: 44803(R) (ANL-6877, pp 21-7)
mechanical properties of compression-annealed pyrolytic, 19: 44751(R) (TID-22110)
radiation effects on mechanical properties of pyrolytic and single-crystal, 19: 44751(R) (TID-22110)
radioinduced contraction of EGCR, effects of tensile stresses on neutron, 19: 44744 (HW-SA-3592)
spectra of, effects of chemical combination on soft x-ray K emission bands of carbon in, (E), 19: 44944
use as isolating medium in production of boron carbide spherules, 19: 44660(P)
graphite–MoS_2–$NaSiO_3$, radiation effects on lubricant wear properties of solid films, 19: 44095
GRAPHITE MODERATED REACTORS
fuel cycle economics for gas-cooled, thorium–uranium, 19: 45582 (NP-15320)
GRASS
deposition of iodine and zinc sulfide on, from atmosphere, 19: 44248 (BNL-914, pp 141-3)
GRAVITATION
effects on growth of wheat seedlings, 19: 43717 (NASA-CR-303)
effects on splitting of electromagnetic-wave spectrum, (T), 19: 45140
electron spin precession frequencies in, (T), 19: 45134 (NP-15397)
energy divergence in closed systems, elimination by gauge subtraction, (T), 19: 45148
luminosity effects on, from neutrino and photon radiation, (T), 19: 44910
production of gravitons in nonlinear bound-state photon-photon interactions, (T), 19: 45144
GREAT BRITAIN
radiation protection codes, 19: 44282 (AHSB(RP)M-36)
GROUND
fallout contamination of, effects of cloud height and wind on, 19: 44255 (RT/PROT(65)-10)
GROUND WATERS
recharge of, economics of artificial, 19: 45717 (UCRL-7850(Rev.1))
GROWTH
radiation effects on Tribulus root, γ, 19: 43855
GUANOSINE
hydrolysis of 3′-nucleotide of, catalytic effects of thorium and zirconium ions on, 19: 43708
GUINEA PIGS
manganese metabolism in scorbutic, 19: 43697

H

HAFNIUM
diffusion of hafnium-181 in bcc, 19: 44729
phase transformations in, relation of c/a ratio and elastic moduli temperature dependence with, 19: 44676(R) (ANL-7000, pp 176-82)
separation from niobium and tantalum by paper chromatography, 19: 44124
HAFNIUM ALLOYS
Er–Hf–Pd, crystal structure studies, 19: 44678(R) (ANL-7000, pp 186-200)
Hf–Nb–W, erosion by water of rotating disks of, 19: 44625 (TIM-894)
Hf–Os–Ta, crystal structure studies, 19: 44678(R) (ANL-7000, pp 186-200)
Hf–Ta–W, erosion by water of rotating disks of, 19: 44625 (TIM-984)
HAFNIUM CARBIDES
analysis for carbon using electron microprobe, 19: 43966
phase studies, 19: 44724
HfC–Mo, solidus temperature at 2350°C, 19: 44612(R) (USBM-RC-1199)
HfC–Nb, solidus temperature at 2310°C, 19: 44612(R) (USBM-RC-1199)
HfC–Ta, solidus temperature at 2680°C, 19: 44612(R) (USBM-RC-1199)
HfC–Ti, solidus temperature at 1655°C, 19: 44612(R) (USBM-RC-1199)
HfC–V, solidus temperature at 1790°C, 19: 44612(R) (USBM-RC-1199)
HfC–W, solidus temperature at 2730°C, 19: 44612(R) (USBM-RC-1199)
HfC–Zr, solidus temperature at 1760°C, 19: 44612(R) (USBM-RC-1199)
HAFNIUM ISOTOPES Hf-166
energy levels of, rotational, (T), 19: 45285 (UCRL-16040)
HAFNIUM ISOTOPES Hf-168
energy levels of, rotational, (T), 19: 45285 (UCRL-16040)
HAFNIUM ISOTOPES Hf-170
energy levels of, rotational, (T), 19: 45285 (UCRL-16040)
HAFNIUM ISOTOPES Hf-172
energy levels of, rotational, (T), 19: 45285 (UCRL-16040)
HAFNIUM ISOTOPES Hf-178
energy levels of, rotational, (T), 19: 45285 (UCRL-16040)
HAFNIUM ISOTOPES Hf-181
diffusion in bcc hafnium, 19: 44729
separation from zirconium-95, chromatographic, 19: 44118 (UCRL-16015)
HAFNIUM OXIDES
reactions with carbon, molybdenum, molybdenum–rhenium and rhenium at 2450°C, 19: 44598(R) (GEMP-49A)
HAFNIUM SYSTEMS
Al–B–Hf, phase studies of, 19: 44719
HAIR
radioinduced dysplasia of mouse, local and whole-body, x, 19: 43833
HALDEN BOILING REACTOR
cooling system of, dynamic model for, 19: 45633 (HPR-62)
kinetics of, noise technique for determining, 19: 45632 (HPR-53)
HALIDES
radiation damage at low temperatures to ionic, x-ray-diffraction studies of beta, 19: 44745 (LA-DC-6725)
HALLAM POWER REACTOR
operation, June 1965, 19: 45592(R) (TID-22135)
operation, May 1965, 19: 45591(R) (TID-22129)
HALOGEN ISOTOPES
incorporation of radioactive, in haloorganic compounds, 19: 44107(P)
HALOORGANIC COMPOUNDS
labelling of, process for, 19: 44107(P)
HANDBOOKS AND MANUALS
dictionary of nuclear instrumentation, 19: 44349 (RT/EL(65)-3)
Health and Safety Laboratory Analytical Manual, 19: 44296 (NYO-4700(Rev.)(Suppl.II))
HANDS
radiation doses to, finger-tip dosimeters for determining, 19: 44367 (AEEW-M-550)
HANFORD PRODUCTION REACTORS (N)
temperature monitoring of, clamp-on resistance detectors for, 19: 45646
HANFORD WORKS, RICHLAND, WASH.
fission product recovery from wastes, status, 19: 45690 (RL-SA-40)
meteorological program, 19: 44767 (BNL-914, pp 24-5)
HARWELL SYNCHROTRON
beam deflection system for, design of, 19: 44868 (NIRL/R/86)
HASTELLOY F
corrosion by steam at high temperature, 19: 45572(R) (GEAP-4755)
HASTELLOY X
hardness and tensile properties at 1000 to 1300°F, effects of annealing on, 19: 45572(R) (GEAP-4755)
performance as fuel element cladding material, 19: 45577(R) (IDO-28645)
radiation effects on fuel pin cladding of, in-pile, 19: 45558 (AGN-TM-409)
reactions with fissium–plutonium–uranium alloys at 750°C, 19: 44587(R) (ANL-7000, pp 3-63)
strain effects on, effects of environment on plastic, 19: 45572(R) (GEAP-4755)
thermal conductivity of wire wool of, 19: 44589 (BNWL-102)
HAYNES 25 ALLOY
wear in borated and lithiated water, 19: 45601(R) (WCAP-3750)
HEALTH PHYSICS
instrumentation development for, 19: 44369 (AERE-R-4552)
laboratory manual for, analytical, 19: 44296 (NYO-4700(Rev.)(Suppl.II))
measures for radon pump disassembly, 19: 44317
program for dosimetry in nuclear accidents, 19: 44320

radiation dosage to skin from external contamination, evaluation of methods for beta and gamma, 19: 44328
radiation dosimetry in Hanford criticality accident, problems in, 19: 44330
radiation dosimetry of personnel in accidents, 19: 44319 (STI/PUB/99)
radiation dosimetry of exposure from linear accelerator malfunction, 19: 44331
radiation dosimetry of personnel in accidents, program for, 19: 44336
radiation experience in Kilorod project for fabrication of uranium-233 dioxide–thorium dioxide fuel rods, 19: 44638 (ORNL-3681)
radiation protection, Italian Decree on, 19: 44318
radioisotope measurements in biomedical samples, instruments and methods for, 19: 43659
role of laboratory and methods used in event of accident, 19: 44324
statistics on dosimetry results of high radiation levels, 19: 44326

HEART
cells of rat, effects of lipids on, 19: 43681(R) (UCLA-12-565, pp 17-31)
heating energy for, metabolic sources of, 19: 43681(R) (UCLA-12-565, pp 17-31)
myosin synthesis in, 19: 43681(R) (UCLA-12-565, pp 17-31)

HEART DISEASES
radiotherapy of cardiac decompensation, effects of irradiation of adrenal glands on, 19: 43919

HEAT
conversion to electricity in reactors, device for direct, 19: 45556(P)
coupling for, design of sealed, 19: 44164 (CEA-R-2755)

HEAT EXCHANGERS
design of finned tube, 19: 44206(P)
design of, with finned wall, 19: 45552(P)
fabrication of finned, for use in fuel element cans, 19: 44656(P)
performance of water–liquid hydrogen, 19: 44186 (LA-DC-7148)

HEAT-RESISTING ALLOYS
fuel burnup in pressure tube type, 19: 45578 (JAERI-1080)
plastic fatigue properties of, bibliography of, 19: 44599(R) (GEMP-50A)

HEAT TRANSFER
between platinum surface and liquid helium, boiling, 19: 44201
boiling burnout in annular flows, effects of electric fields on, (E), 19: 44190(R) (NYO-2404-67)
boiling burnout in annular flows, effects of electric fields on, (E), 19: 44191(R) (NYO-2404-73)
dynamic studies of, in water reactors, 19: 44194 (SGAE-RE-2/1965)
effects of nonuniform, on boiling burnout in tubular and annular flow channels, 19: 44183(R) (BAW-3238-8)
from heated tubes to supercritical-pressure liquid hydrogen in turbulent flow, data compilation, 19: 44189 (NP-15332)
in forced-convection two-phase flow, effects of voids on, 19: 44185(R) (GEAP-4910)
in Russian reactor BN-350, 19: 45604(T) (JPRS-31245)
in transverse homogeneous magnetic field, 19: 44202
to superheated steam in tubes, parameters of, 19: 45572(R) (GEAP-4755)
transient, in liquid-metal-cooled fast reactors, 19: 45494 (NAA-SR-11008)

HEAT TRANSFER SYSTEMS
development for thermionic cells, 19: 44980(R) (NP-15433)
heat source for reactor simulation, power supply for, 19: 44203

HEAVY WATER REACTORS
description of British for power, (E), 19: 45613
fuel costs for power, minimum, 19: 45563 (BNWL-106)
fuel fabrication and processing facilities for British, (E), 19: 45612
fuel tube fabrication for power, 19: 45569 (DP-976)
neutron economy of pressure tube and pressure vessel, 19: 45626
pressure vessels for boiling, use of prestressed concrete in, 19: 45506
pressure vessels for, plug for sealing apertures in, 19: 45510(P)

HELIUM
content in natural gases, 19: 44239
diffusion through polycrystalline alumina ceramics at high temperatures, 19: 43997(R) (UCRL-11889)
electron reactions with, in magnetic bottle, 19: 44823
electron scattering by atomic, exchange in, (T), 19: 44949
energy levels of excited, autoionization, 19: 44934(R) (COO-1277-13)
energy levels of, autoionizing, (E), 19: 44959
flow of liquid II, dissipative normal fluid production in gravitational, (E), 19: 45201
flow of liquid II, Josephson effect analog for, (T), 19: 45202
heat transfer in liquid, boiling, 19: 44201
magnetic moment anomaly of, meson exchange effects on, (T), 19: 45332
microwave excitation of plasma of, harmonic generation by, (E), 19: 45420
neutron scattering by, polarization determinations by, (T), 19: 45217 (COO-7-0363)
performance in high-pressure spark chambers, (E), 19: 44502
production and heating of plasma of, in B-3 stellarator, (E), 19: 45398 (MATT-332)
proton reactions at 100 to 300 kev, electron emission in, (E), 19: 44933(R) (COO-1277-12)
reactions with oxygen ions, energy effects on cross sections for dissociation in, (E), 19: 44948
scattering by argon, krypton, and xenon for beams of, total elastic cross sections for, (E), 19: 44957
solubility in uranium dioxide, (T), 19: 43997(R) (UCRL-11889)
viscosity at 280 to 2340°K, (E), 19: 45190 (LA-3319)
yields in fast neutron irradiation of reactor fuel cladding materials, (T), 19: 44746 (NAA-SR-Memo-10626)

HELIUM ISOTOPES He-3
content in meteorite Khor Temiki, (E), 19: 44906
detection of, semiconductor detector for, 19: 44476 (ZFK-PHA-12, pp 123-5)
dielectric constant in critical region, (E), 19: 45205
magnetic moment of, meson exchange effects on wave function for, (T), 19: 45333
meson (π^-) capture by, neutron-neutron scattering length from, (T), 19: 45354
reactions (He-3,np) and (He-3,2p) with copper-63 and iron-56 at 10 Mev, cross sections for, (E/T), 19: 45362
reactions (He-3,n) with silicon-28 at 5.5 Mev, sulfur-30 levels from, (E), 19: 45355
reactions (He-3,n) with magnesium-24 at 5.5 Mev, silicon-26 levels from, (E), 19: 45355
reactions (He-3,n) with lithium-6 at 5.5 Mev, boron-8 levels from, (E), 19: 45355
reactions (He-3,p) with iron-56 at 10 Mev, angular and energy distributions from, (E/T), 19: 45362
reactions (He-3,p) with copper-63 at 10 Mev, angular and energy distributions from, (E/T), 19: 45362
thermodynamic properties of, effects of zero sound on, (T), 19: 45204
He-3–methane–Ne, performance as filling in thermal neutron detectors, 19: 44373(R) (ANL-6877, pp 15-20)

HELIUM ISOTOPES He-4
bremsstrahlung reactions (γ,p) and (γ,t) at 24 to 56 Mev, E1 cross section for, (E), 19: 45353
content in meteorite Khor Temiki, (E), 19: 44906
neutron scattering at 25 to 34 Mev, angular distributions and polarization in, (E), 19: 45259 (IAE-834)
properties of liquid, pseudospin model for, (T), 19: 45203

HELIUM SYSTEMS
He–Xe, properties for use in closed Brayton cycle space power plants, 19: 44205

HEMATOPOIETIC SYSTEM
radiation effects on human, determination of exposure in accidents by, 19: 44315
radiosensitivity of, in mice, 19: 43836
radiosensitivity of, in rats, 19: 43839
radiosensitivity of erythropoiesis and myelopoiesis in, 19: 43731

HEMISPHERES
stress patterns of attachment region of shells with radially attached nozzles, 19: 44144 (TID-22134)

HEMOGLOBIN
synthesis in red cells, parameters of, 19: 43682(R) (UCLA-12-565, pp 33-57)

HEPTENE
spectra of solid, slow-neutron-scattering analysis of, (E), 19: 44050

HETEROGENEOUS REACTORS
neutron diffusion theory for, lectures on, 19: 45531 (N64-29786)

HEXANE
spectra of solid, slow-neutron-scattering analysis of, (E), 19: 44050

HIGH-ALTITUDE EXPLOSIONS
effects on ionospheric D layer, v-l-f perturbations from, 19: 45166
electron production from, geomagnetic trapping of, 19: 45167

HIGH TEMPERATURE GAS COOLED REACTOR EXPERIMENT
control system equipment for Dragon, design of automatic, 19: 45570 (EUR-2422.i)
reactivity transfer functions analyzer for Dragon, design of, 19: 45571 (EUR-2431.i)

HIGH-TEMPERATURE REACTIONS
between gases and condensed phases, bibliography on, 19: 43993 (NP-15379)
bibliography on, 19: 43994 (NP-15381)

HIGH TEMPERATURE SEPARATION PROCESSES
zone refining, automated control system for, 19: 44694(R) (NP-15432)

HIPPURIC ACID, o-IODO-, SODIUM SALTS
diffusion to blood and urine in dogs following renogram preparation, 19: 43667 (EUR-1890.f)

HIROSHIMA

population of, clinical status of radiation-exposed, 19: 44280(R) (ABCC-63-64)
tuberculosis frequency among leukemia patients in, 19: 43710 (ABCC-16-64)
HISTIDINE
protective effects against radiation damage in crop plants, 19: 43877
HOLMIUM
separation from scandium and thorium by reversed-phase chromatography, 19: 44125
HOLMIUM ALLOYS
Au–Ho, crystal structure studies, 19: 44678(R) (ANL-7000, pp 186-200)
Cu–Ho, crystal structure studies, 19: 44678(R) (ANL-7000, pp 186-200)
Ho–Ag, crystal structure studies, 19: 44678(R) (ANL-7000, pp 186-200)
HOLMIUM CHLORIDES
pharmacology and toxicology of, 19: 43728(R) (UCLA-12-565, pp 59-64)
HOLMIUM ISOTOPES Ho-160
decay of metastable, gamma spectra from, (E), 19: 45272 (JINR-P-2270)
HOLMIUM SELENIDES
crystal structure, 19: 44010
HOLMIUM TELLURIDES
crystal structure, 19: 44010
HOMOGENEOUS REACTORS
neutron absorber efficiency in uranium–water, heterogeneous, (E), 19: 45536
neutron diffusion theory for, lectures on, 19: 45531 (N64-29786)
HOSPITALS
nursing care of patients after radiotherapy, 19: 43908
nutritional management of cancer patients after radiotherapy, 19: 43911
HYDRAULICS
of metal flow effects on fuel elements, 19: 44181(R) (APDA-174, pp 56-60)
HYDRAZYL, DIPHENYLPICRYL-
protective effects against radiation damage in trypsin, 19: 44081
HYDROBROMIC ACID
phase studies on solid and liquid, using slow neutrons, (E), 19: 44038
HYDROCARBONS
analysis of liquid, for carbon and hydrogen, by fast neutron moderation, 19: 43968
preparation of oxygenated, from alkenes, 19: 44043(P)
reactions of liquid, with recoil carbon-11 produced by gamma irradiation, 19: 44057 (IS-T-23)
HYDROCHLORIC ACID
corrosive effects on titanium alloys at 650°F, 19: 44621 (CONF-651006-1)
phase studies on solid and liquid, using slow neutrons, (E), 19: 44038
solvent properties for thorium and rare earths, 19: 44125
HYDRODYNAMICS
calculation of two-dimensional Lagrangian, with space-dependent time steps, 19: 45701 (LA-3324)
HYDROFLUORIC ACID
phase studies on solid and liquid, using slow neutrons, (E), 19: 44038
proton motion in aqueous solutions of, 19: 44037
uses in paper chromatographic separation of hafnium, niobium, and tantalum, 19: 44124
$HF–HNO_3$, corrosive effects on yttrium, 19: 44628
HYDROGEN
chemical shift of proton in diatomic, modified Schrödinger equation for, (T), 19: 44952
crystal structure of thin films, (E), 19: 45194
current sheet microstructure in theta-pinch plasma of, (E/T), 19: 45445
detection and separation from sodium loops, in-line devices for, 19: 44162(R) (APDA-174, pp 33-55)
determination in intergalactic space, sensitive method for, (E), 19: 44908
determination in liquid hydrocarbons by fast neutron moderation, 19: 43968
effects on critical resolved shear stress in zirconium, 19: 44676(R) (ANL-7000, pp 176-82)
effects on deuterium anodic oxidation in acid solutions, 19: 44022
effects on fracture of zirconium and zirconium alloys, 19: 44716
effects on mechanical properties of zirconium, 19: 44676(R) (ANL-7000, pp 176-82)
effects on uranium fatigue, 19: 44681 (AWRE-O-65/65)
energy of molecular, potential energy curves for, (T), 19: 44946
exchange with deuterium in ammonia and water in hot-and-cold plant, 19: 44574
heat transfer from water to liquid, in heat exchangers, 19: 44186 (LA-DC-7148)
heat transfer to supercritical-pressure liquid, in turbulent flow through tubes, 19: 44189 (NP-15332)
hyperfine structure of, from polarization in electron-proton interactions, (T), 19: 44951
neutron cross sections of free, from 0.0001 ev to 20 Mev, 19: 45248 (AWRE-O-23/65)
neutron scattering by, performance of three-axis spectrometer for thermal, 19: 44527
ortho-para conversion in solid, effects of molar volume on rate constant of, 19: 43997(R) (UCRL-11889)
oxidation in deuterium-labeled acid solutions, isotope effects in voltametric, 19: 44022
performance in high-pressure spark chambers, (E), 19: 44502
photon reactions in Bev range, meson (π) and (ρ) production in, (E), 19: 45000 (HUX-2752-7)
plasma of, heating by electromagnetic waves using Stix coils, (T), 19: 45400 (NASA-TN-D-2982)
production during uranium corrosion by water vapor, effects on oxygen on, 19: 44618 (AWRE-O-42/65)
proton reactions at 100 to 300 kev, electron emission in, (E), 19: 44933(R) (COO-1277-12)
proton reactions with jets of, detection using emulsions, 19: 44443 (CERN-65-4(Vol.II), pp X61-6)
proton scattering at 27.6 and 47.8 Mev, Wolfenstein A and R parameters from, (E), 19: 45319
sorption by tungsten sheet at 77 to 600°K, 19: 44036
spin precession in μ-mesic, 19: 45278 (NP-15389)
thermodynamic properties of normal and para, (E), 19: 44822
trapping of atomic, in irradiated frozen solutions of oxyanions, 19: 44054(R) (COO-1365-7)
ultrasonic propagation in liquid, velocity of, (E), 19: 44822
viscosity at 280 to 2340°K, (E), 19: 45190 (LA-3319)
wave equations for, time-independent Schroedinger, (T), 19: 44960
yields in fast neutron irradiation of reactor fuel cladding materials, (T), 19: 44746 (NAA-SR-Memo-10626)
yields in gamma radiolysis of aqueous methyl ammonium perchlorate and sulfate, 19: 44080
HYDROGEN IONS
binding energy of molecular, (T), 19: 44936 (TID-21692)
reactions with helium at 75 kev, autoionizing energy levels from, (E), 19: 44959
reactions with lithium, excited atom production in charge-exchange, (T), 19: 44955
HYDROGEN ISOTOPES
properties for tracer use in biology, 19: 43707
HYDROGEN ISOTOPES H-4
binding energy of $^4H_{\Lambda\Lambda}$, Λ–Λ potential strength from, (T), 19: 45064
HYDROGEN PEROXIDES
properties for use as LET independent dosimeter, chemiluminescent, 19: 44067
reactions with uranyl compounds, preparation of uranium peroxide by, 19: 44029
yields in radiolysis of water by pulsed protons, 19: 44058 (LFEN-23)
HYDROGEN SYSTEMS
Ar–H, shock waves in, interferometric measurement of vibrational relaxation behind, 19: 44855
H–Ne, performance in bubble chambers, 19: 44375 (BNL-9425)
H–V, nuclear magnetic resonance, 19: 43986(R) (ANL-7000, pp 201-4)
HYDROGEN TETRACHLOROAURATE(III)
radiolysis of, production of colloidal gold particles in gamma, 19: 44079
HYDROMAGNETIC WAVES
emission of v-l-f, from exosphere, (E), 19: 45171
propagation in solar wind interactions with magnetosphere, (T), 19: 45165
stability of sub-Alfvén, 19: 45187
HYDROQUINONE
uses of krypton-85 quinol clathrates for inverse radiometric analysis of atmospheric sulfur dioxide, (E), 19: 44458 (NYO-2767)
HYDROURACIL
radiolysis of, in aqueous solutions in air or nitrogen, 19: 44064
HYDROXYL IONS
radiation effects on reactions of, with ethanol, methanol, and thiocyanate and selenite ions, 19: 44090
HYDROXYL RADICAL
reactions of, studies of complex, 19: 43997(R) (UCRL-11889)
HYDROXYLAMINE
effects on radiomimetic effects of nitrosoamides on herb seeds, 19: 43870
protective effects of, against radiation injuries in rat spleen, 19: 43860(R) (NP-15310, pp 14-25)
HYGROMETERS
design of alpha-radiation frost-point, for high-speed aircraft, 19: 44338 (AD-608496)
problems of alpha-source automatic frost-point, for water content measurements in stratosphere, 19: 44339 (AD-608503)

HYPERFRAGMENTS
binding energy of ${}^{4}H_{\Lambda\Lambda}$, Λ–Λ potential strength from, (T), 19: 45064
decay of, hyperon (Λ) nuclear potential well depth from, (T), 19: 45361
energy levels of ${}_{\Lambda}Be^{9}$, excited, (T), 19: 45367
hyperon (Λ)-nucleon interactions in ${}_{\Lambda}Be^{9}$, 19: 45367
production of short-range, in meson (K⁻) captures in emulsions, (E/T), 19: 45342
HYPERONS (Λ)
decay of, charge-parity quantum number in leptonic, (T), 19: 45115
decay of, CP violation in leptonic, (T), 19: 45126
detection using emulsions, 19: 44443 (CERN-65-4(Vol.II), pp X61-6)
interactions with protons at 2.7 Bev/c, total cross section for elastic, (E), 19: 45016 (JINR-P-2257)
reactions with nuclei, potential well depth for, (T), 19: 45361
HYPERONS (Λ^0)
binding energy in hyperfragments from meson (K^0) capture in emulsions, (E/T), 19: 45342
decay of, charge-parity quantum number in ($p\pi$), (T), 19: 45115
interactions with hyperons (Λ^0), hypernucleus binding energy and unitary symmetry for potential strength of, 19: 45064
HYPERONS (Ω^-)
production in meson (K^-)–proton interactions for parity test of, (T), 19: 45101
HYPERONS (Σ)
decay of, charge-parity quantum number in leptonic, (T), 19: 45115
decay of, CP violation in leptonic, (T), 19: 45126
HYPERONS (Ξ)
decay of, charge-parity quantum number in leptonic, (T), 19: 45115
HYPERONS (Ξ^-)
decay of, charge-parity quantum number in ($\Lambda\pi$), (T), 19: 45115
HYPERTHYROIDISM
iodine-131 therapy for, effects on cytoplasmic and thyroglobulin antibodies, 19: 43902

I

ICE
neutron scattering cross sections in, slow, (T), 19: 45228 (NP-15469)
IGNEOUS ROCKS
strength of basalt, effects of stress rate and temperature on, 19: 43997(R) (UCRL-11889)
ILLINOIS
fallout monitoring at Argonne, Jan.-June 1965, 19: 44300 (TID-22171)
ILLITES
sorptive properties for cesium, role of exchangeable magnesium and potassium in, 19: 43964
IMAGE BRIGHTNESS INTENSIFIERS
design for fluoroscopy, 19: 44363(P)
development for brain scanners, 19: 43648(R) (UCLA-12-565, pp 87-96)
development for physic research, 19: 44357
IMIDAZOLE
radiosensitivity effects in mice, 19: 43863
IMMUNE REACTIONS
effects of erythrocyte chimerism induction on, in neonatal mice, 19: 43657
of sheep, to vaccine against lungworm prepared for irradiated larvae, 19: 43750
rabbits oxytocin, tracer study, 19: 43658
radiation effects on, to autogenous bone grafts in dogs, 19: 43835
IMMUNIZATION
of mice against Schistosoma, use of irradiated cercariae for, 19: 43848
IMPACT SHOCK
effects of hypervelocity, on beryllium and graphite plates and tubes, 19: 44692 (NASA-TN-D-3018)
effects on radioisotope containment capsules, 19: 44298(R) (SC-RR-65-9)
testing facility, design of pulsed five-million-pound, 19: 45720 (UCRL-12055-T)
IMPELLERS
cavitation damage on coated, studies, 19: 44197 (TIM-895)
damage to, coatings for indicating possible, cavitation, 19: 44212 (TIM-878)
design system for centrifugal-pump, 19: 44148 (TIM-918)
IN-PILE LOOPS
design, 19: 45676 (IDO-16871-4)
fast neutron flux characteristics of G-7, in ETR, (E), 19: 45672 (BNWL-89)
INCOLOY
corrosion by steam at 650°C of type 800, effects of aluminum additions on, 19: 44616(R) (ANL-7000, pp 122-37)
corrosion by steam at 750°C of type 800, 19: 44616(R) (ANL-7000, pp 122-37)
corrosion by steam under nuclear superheat reactor conditions, 19: 45572(R) (GEAP-4755)
corrosion of 800 and 825, by high-temperature steam, 19: 45572(R) (GEAP-4755)
hardness and tensile properties of 801 and 825, at 1000 to 1300°F, 19: 45572(R) (GEAP-4755)
strain effects on, effects of environment on plastic, 19: 45572(R) (GEAP-4755)
INCONEL
corrosion by chemical shim solutions at 600°C, 19: 45601(R) (WCAP-3750)
corrosion by steam at 750°C of types 600, 625, and X750, 19: 44616(R) (ANL-7000, pp 122-37)
corrosion of 600, 625, and 718, by high-temperature steam, 19: 45572(R) (GEAP-4755)
strain effects on, effects of environment on plastic, 19: 45572(R) (GEAP-4755)
tensile properties of 625 and 718, at 1000 to 1300°F, 19: 45572(R) (GEAP-4755)
INDEXES
to conferences relating to nuclear science, 19: 45716 (TID-4043(Rev.2))
INDIA
fallout monitoring, 1959 to 1964, 19: 44244 (AEET/AM/40)
INDIUM
neutron absorption cross sections at 24 kev, (E), 19: 45230
INDIUM ALLOYS
of rod clusters of, (E/T), 19: 45535 (WCAP-3269-47)
Cd–In–Ag, radiation effects on plated, 19: 44736 (ANL-6883)
Cd–In–Ag, reactivity effects of cruciform rods of, in large PWR, 19: 45533 (WCAP-3269-33)
In–Sn, thermal capacity, coefficient of electron, 19: 43997(R) (UCRL-11889)
Sb–In, fusion thermodynamic properties of InSb, 19: 43997(R) (UCRL-11889)
INDIUM ARSENIDES
fusion thermodynamic properties, 19: 43997(R) (UCRL-11889)
INDIUM COMPLEXES
with 8-quinolinol derivatives, electronic absorption spectra, 19: 43989 (MIT-905-20)
INDIUM ISOTOPES In-115
boron-10 reactions (B-10,3n) at 37 Mev, xenon-122 energy levels from, (E), 19: 45285 (UCRL-16040)
boron-10 reactions (B-10,5n) at 67 Mev, xenon-120 energy levels from, (E), 19: 45285 (UCRL-16040)
boron-11 reactions (B-11,4n) at 57 Mev, xenon-122 energy levels from, (E), 19: 45285 (UCRL-16040)
neutron reaction (n,n') with, rates for, (E/T), 19: 45522 (AE-195)
nitrogen-14 reactions (N-14,5n) at 84 Mev, barium-124 energy levels from, (E), 19: 45285 (UCRL-16040)
nitrogen-14 reactions (N-14,3n) at 52 Mev, barium-126 energy levels from, (E), 19: 45285 (UCRL-16040)
INDOLE
determination in brain tissues, spectrofluorometric, 19: 43810
INDOLE,3-(2-AMINOETHYL)-
radiation effects on metabolism of, in rats, 19: 43852
radiosensitivity effects in mice, 19: 43864
5-hydroxy-, radiation effects on metabolism in rat brain, effects of metabolic inhibiting drugs on, 19: 43810
INDOLE, 3-(2-AMINOETHYL)-5-METHOXY-
effects on irradiated dioxane-2,5-diphenyloxazole phosphor, quenching, 19: 43878
3-INDOLEACETIC ACID
radiation effects on metabolism of, in man, 19: 43852
INDOLEACETIC ACID, 5-HYDROXY-
radiation effects on content of, in rat brain, 19: 43810
5-INDOLOL, 3-(2-AMINOETHYL)-
creatinine sulfate of, protective effects against gamma and x radiation, 19: 43883(R) (UCLA-12-565, pp 65-85)
effects on irradiated dioxane-2,5-diphenyloxazole phosphor, quenching, 19: 43878
INDUCTORS
electric conducting slab in magnetic field of double-side, current density and magnetic induction in, 19: 44841
INDUSTRIAL HYGIENE
practice in uranium mines, effects on incidence of lung cancers, 19: 44314
INDUSTRIAL MANAGEMENT
systems analysis for, decision order technique for, 19: 45714 (SC-TM-65-349)
INFECTIONS
radiation effects on *E. coli*, with bacteriophage MS_2, 19: 43742

INOR-8
radiation effects on stress-rupture properties at 816°C of, fast neutron, 19: 44598(R) (GEMP-49A)
radiation effects on creep-rupture properties of, effects of annealing of fast neutron, 19: 44599(R) (GEMP-50A)
INSECTS
population control of *Culex fatigans*, by release of irradiated males, 19: 43796
radiation control of gnats, *Hippelates pusio*, 19: 43803
radiation effects on reproduction in Tribolium, effects of dose and temperature on x, 19: 43715 (HW-SA-3747)
radiation effects on reproduction in Tribolium, effects of genetics and temperature on x, 19: 43716 (HW-SA-3748)
radiation effects on developing nerves in larvae of Odonata, morphological, 19: 43849
radiosensitivity of various developmental stages, 19: 43796
radiosterilization of screwworm flies for aerial dispersion, inhalant allergic response in man to, 19: 43652
INSTRUMENTATION
bibliography, for nuclear physics, 19: 44366 (AED-C-06-12)
design for in-pile tests, 19: 45676 (IDO-16871-4)
design for LITR, 19: 45680 (ORNL-TM-1190)
design for ORNL High Flux Isotope Reactor, 19: 45645 (ORNL-TM-1259)
design for PM-type Army Reactors, 19: 45584 (NYO-3379-1)
design for Russian research reactors, 19: 45675 (IAE-725)
development for fast reactors, 19: 45493(R) (APDA-174)
development of nuclear, for detector locations at Selni and Sena, 19: 45601(R) (WCAP-3750)
dictionary of nuclear, 19: 44349 (RT/EL(65)-3)
response to impurities in sodium loops, 19: 44162(R) (APDA-174, pp 33-55)
testing strap-on reactor thermocouple devices, 19: 45502 (RL-REA-2120)
INSTRUMENTS
design for particle track measurement, 19: 44361
INTERFEROMETERS
use of optical, for plasma diagnostics, 19: 45433
INTERNAL CONVERSION
coefficients and spectra in cobalt-56 decay, (E), 19: 45295
coefficients of E2 transitions in nuclei, (T), 19: 45369
detection and measurement of, using scintillation spectrometers, (E), 19: 44501
INTESTINE
radiation effects on tryptophan sorption from rat, 19: 43728(R) (UCLA-12-565, pp 59-64)
radiation effects on methionine sorption from rat, 19: 43728(R) (UCLA-12-565, pp 59-64)
radiodiagnosis of cancer in, using phosphorus-32 and miniature Geiger tube, 19: 43887
radiosensitivity of, in cancer patients, 19: 43911
IODINE
deposition from atmosphere on vegetation, 19: 44248 (BNL-914, pp 141-3)
diffusion from irradiated Windscale fuel, 19: 44303 (TRG-Report-888)
diffusion from molten fuel elements into condensing steam, 19: 44285 (BNWL-SA-29)
metabolism in trout, 19: 43773
radiative lifetime of excited $B^3\pi$ state of gaseous, 19: 43997(R) (UCRL-11889)
sorption by charcoal, 19: 44303 (TRG-Report-888)
spin precession in compounds of muonium and, (T), 19: 45278 (NP-15389)
spin precession in μ-mesic, 19: 45278 (NP-15389)
IODINE FLUORIDE OXIDES
spectra and valence force constants of IOF_5, 19: 44019
IODINE ISOTOPES I-125
metabolism in thyroid of injected, in rats, 19: 43757
IODINE ISOTOPES I-127
boron-11 reactions (B-11,4n) at 57 Mev, cerium-134 energy levels from, (E), 19: 45285 (UCRL-16040)
Mössbauer resonance in ferromagnetic chromium iodide, (E), 19: 45491
IODINE ISOTOPES I-128
decay scheme,, 19: 45679(R) (NYO-1859-11)
determination in organic polymers, activation, 19: 43951
IODINE ISOTOPES I-129
energy levels and gamma spectra from tellurium-129 decay, (E), 19: 45324
energy levels and gamma-gamma directional correlations, (E), 19: 45335
gamma spectra from, energy levels and spins of, 19: 45679(R) (NYO-1859-11)
IODINE ISOTOPES I-131
determination by extraction, method for, 19: 43953
determination in air by sorption on activated carbon and scintillation counting, 19: 43958
determination in solutions, use of scintillation counter for, 19: 43940
diagnostic and therapeutic uses for thyroid tumors, 19: 43892
diagnostic tracer use of, for gastrointestinal diseases, 19: 43886
diffusion from irradiated molybdenum–rhenium–tungsten alloy, 19: 44599(R) (GEMP-50A)
distribution and localization in rat thyroid with goiter by autoradiography, 19: 43683
effects of injected, on blood picture in rats, 19: 43839
effects on thyroid function in rats of injected, 19: 43757
incorporation in oxytocin, 19: 44105
metabolism by marine organisms, 19: 43669(R) (NP-15159)
metabolism in patients with goiter, age effects on, 19: 43691
metabolism in thyroid of injected, in rats, 19: 43757
radiation effects on metabolism of, in dairy cattle, 19: 43801
therapeutic use for hyperthyroidism of, 19: 43895
therapeutic use for hyperthyroidism, 19: 43906
therapeutic use for thyroid carcinoma, 19: 43918
therapeutic use in hyperthyroidism, effects on cytoplasmic and thyroglobulin antibodies, 19: 43902
thyroidectomy in trout induced by, 19: 43773
tracer use of macroaggregated albumin labeled with, for diagnosis of circulatory shunts, 19: 43904
uptake by blood plasma, muscle, and thyroid in chicks, age and dose effects on, 19: 43704
uptake by rabbit blood plasma and thyroid, effects of dietary molybdenum on, 19: 43689
uptake in food chain, controlled release tests on, 19: 44773 (BNL-914, pp 57-64)
ION BEAMS
neutralization in ion engines, 19: 44222(R) (NP-15068)
neutralizer configurations for, plasma boundaries and lens effect of, 19: 45454
production of low-energy, using duoplasmatron, (E/T), 19: 45384 (D1-82-0436)
production using electron bombardment ion sources, 19: 44221 (N64-31088)
trajectory of, effect of neutral plasma on, (T), 19: 45451
ION EXCHANGE
strontium-90 separation from biological wastes by, 19: 45692 (UCD-472-112, pp 141-7))
ION EXCHANGE MATERIALS
properties of zeolite taff, for separation of cesium and strontium from liquid wastes, 19: 44123
radiation effects on sorptive properties, 19: 44091
ION EXCHANGE PROCESSES
equipment for continuous, with regeneration circuit, 19: 44130(P)
ION SOURCES
design, fabrication, and testing of cesium contact, 19: 44226
electron current release characteristics of h-f, (E), 19: 44880
electrostatic lenses for duoplasmatron, for production of low-energy ions, (E/T), 19: 45384 (D1-82-0436)
ion beam formation from electron bombardment, 19: 44221 (N64-31088)
performance of cesium contact, for satellite control, 19: 44227
plasma properties from hydrogen-labeled titanium washer, (E), 19: 45411 (UCRL-7935)
rare-gas ion yields from duoplasmatron, pressure dependence of, (E), 19: 45385 (D1-82-0437)
IONIZATION CHAMBERS
current intensity in, effects of smoke admixtures on, 19: 44355
design and calibration of spherical, 19: 44461(R) (TID-22205)
design of pocket-size, for use as individual alarm systems by personnel, 19: 44532
performance of, for dosimetry of scattered x radiation, 19: 43889
performance with accelerating fields for detecting soft beta particles, (E), 19: 44512
response in free space to long-term cosmic ray variations, 19: 44966
IONOSPHERE
disturbances in, from solar flares behind solar disk, (T), 19: 44894(T) (AD-424481)
effects of high-altitude nuclear burst on D layer of, 19: 45166
electron density and temperature in F region of, (E), 19: 45174
electron fluxes in, limitation on, 19: 45157 (NP-15386)
electron temperatures in midlatitude, comparison of radar, rocket, and satellite measurements of, 19: 45177
ion densities and reactions in, (T), 19: 45173
ion temperature in F region of, (E), 19: 45174
magnetic drifts in F2 layer, Appleton anomaly in, (T), 19: 45184
microwave propagation in, phase velocities for Pi 2, (T), 19: 45181
plasma diagnostics in, probe system for, 19: 45155(R) (AD-609015)
proton fluxes in, limitation on, 19: 45157 (NP-15386)
radio absorption and v-l-f emission in auroral, (E), 19: 45170
radio wave reflection from F region in, focusing effects on apparent

coefficients for, (T), 19: 45175
radio-wave backscattering from electron density fluctuations in, polarization in, (T), 19: 45182
IONS
cyclotron harmonic spectra from plasma, (E), 19: 45405 (ORNL-P-1576)
electron reactions with molecular, collisional-dissociative recombination in, 19: 45450
reactions with atoms and molecules, review of, 19: 44950
reactions with molecules, energy effects on cross sections for dissociation in, (E), 19: 44948
temperature in ionosphere, (E), 19: 45174
track widths in nuclear emulsions, measurement of, 19: 44434 (CERN-65-4(Vol.II), pp IX48-61)
transfer across biological membranes of, thermodynamics, 19: 43665 (BNL-9338)
IOWA
radiation monitoring at Ames, Jan.-June 1965, 19: 44302 (TID-22173)
IRIDIUM ALLOYS
Ir–Ni–U, crystal structure studies, 19: 44678(R) (ANL-7000, pp 186-200)
Ir–Pt–Y, crystal structure studies, 19: 44678(R) (ANL-7000, pp 186-200)
Ir–U, crystal structure studies, 19: 44678(R) (ANL-7000, pp 186-200)
Ir–Zr, lattice parameters of Zr_2Ir, 19: 44678(R) (ANL-7000, pp 186-200)
IRON
analysis for silicon by activation methods using 14-Mev neutrons, 19: 43965
analysis for trace amounts of copper by activation methods, 19: 43973
creep of alpha, at 375 to 1150°K, 19: 43997(R) (UCRL-11889)
deposition on uranium dioxide particles, 19: 44596 (EURAEC-1392)
determination in biological materials, x-ray fluorescence spectrometric, 19: 43939(R) (UCD-472-112, pp 59-72)
determination in nuclear grade graphite, spectrochemical, 19: 43930 (JEN-145-DQ/I-46)
determination in ores by radiometric fluorescence analysis, 19: 43971
diffusion into sodium disilicate glass, 19: 43997(R) (UCRL-11889)
effects on photometric determination of zirconium, 19: 43972
electric conductivity of thin films of, 19: 44344 (K-L-1944)
extrusion by hydrostatic methods, 19: 44651
hyperfine fields of osmium and platinum nuclei in, 19: 43997(R) (UCRL-11889)
neutron cross sections for, from 0.414 ev to 5.5 Mev, 19: 45244 (AEEW-M-472)
neutron reactions (n,n'γ) with, cross section for, 19: 45263 (JAERI-1078)
phases at high pressures, 19: 43997(R) (UCRL-11889)
radiation effects on electric resistivity at 4°K, fast neutron, 19: 44739(R) (ANL-7000, pp 233-77)
radiation effects on, research program on effects of nitrogen on fast neutron, 19: 44741 (EURAEC-1383)
radiation effects on, research program on effects of nitrogen on fast-neutron, 19: 44742(R) (EURAEC-1430)
reactions with beryllium, copper, stainless steel, and niobium alloys to 760°C *in vacuo*, 19: 44606 (PWAC-483)
separation from uranium by ion exchange, 19: 44119
thermal conductivity of Armco, at 300 to 1000°C, 19: 44599(R) (GEMP-50A)
IRON ALLOYS
Al–Cr–Fe–Y, corrosion by steam at 550°C of 1041, effects of preoxidation and strain on, 19: 44598(R) (GEMP-49A)
Al–Cr–Fe–Y, corrosion by steam at 730°C, 19: 44598(R) (GEMP-49A)
Al–Cr–Fe–Y, elastic constants at 30 to 1200°C of 2541, dynamic, 19: 44598(R) (GEMP-49A)
Al–Cr–Fe–Y, oxidation by air at 900 and 1100°C, effects of composition on, 19: 44598(R) (GEMP-49A)
Al–Cr–Fe–Y, reactions with iron–urania at 950 and 1100°C in air, 19: 44598(R) (GEMP-49A)
Al–Fe–U, phase studies, 19: 44715
Be–Fe, magnetization at 295°K, saturation, 19: 44678(R) (ANL-7000, pp 186-200)
Cu–Fe–Zr, corrosion by steam at 540°C, effects of pressure on, 19: 44616(R) (ANL-7000, pp 122-37)
Er–Fe, isomer shift of iron-57 in $ErFe_2$ at 300 and 800°K, 19: 44678(R) (ANL-7000, pp 186-200)
Fe–Lu, isomer shift of iron-57 in $LuFe_2$ at 300 and 800°K, 19: 44678(R) (ANL-7000, pp 186-200)
Fe–Mn, deformation behavior, effects of interstitials on, 19: 43997(R) (UCRL-11889)
Fe–Mn, thermodynamic properties at 1450°K, 19: 43997(R) (UCRL-11889)
Fe–Mo, magnetization at 295°K, saturation, 19: 44678(R) (ANL-7000, pp 186-200)
Fe–Nb, isomer shift of iron-57 in $NbFe_2$ at 300 and 800°K, 19: 44678(R) (ANL-7000, pp 186-200)
Fe–Ni–Zr, corrosion by steam at 540°C, effects of alloy microstructure on, 19: 44616(R) (ANL-7000, pp 122-37)
Fe–Ni–Zr, corrosion by steam at 540°C, effects of pressure on, 19: 44616(R) (ANL-7000, pp 122-37)
Fe–Pu–U, corrosion by air at room temperature, 19: 44587(R) (ANL-7000, pp 3-63)
Fe–Re, magnetization at 295°K, saturation, 19: 44678(R) (ANL-7000, pp 186-200)
Fe–Sc, isomer shift of iron-57 in $ScFe_2$ at 300 and 800°K, 19: 44678(R) (ANL-7000, pp 186-200)
Fe–Sm, isomer shift of iron-57 in $SmFe_2$ at 300 and 800°K, 19: 44678(R) (ANL-7000, pp 186-200)
Fe–Ta, isomer shift of iron-57 in $TaFe_2$ at 300 and 800°K, 19: 44678(R) (ANL-7000, pp 186-200)
Fe–Ti, isomer shift of iron-57 in $TiFe_2$ at 300 and 800°K, 19: 44678(R) (ANL-7000, pp 186-200)
Fe–U, isomer shift of iron-57 in UFe_2 at 300 and 800°K, 19: 44678(R) (ANL-7000, pp 186-200)
Fe–V, lattice parameter, 19: 44679(R) (ANL-7000, pp 205-12)
Fe–W, isomer shift of iron-57 in WFe_2 at 300 and 800°K, 19: 44678(R) (ANL-7000, pp 186-200)
Fe–Y, isomer shift of iron-57 in YFe_2 at 300 and 800°K, 19: 44678(R) (ANL-7000, pp 186-200)
Fe–Zr, isomer shift of iron-57 in $ZrFe_2$ at 300 and 800°K, 19: 44678(R) (ANL-7000, pp 186-200)
Ga–Fe, magnetization at 295°K, saturation, 19: 44678(R) (ANL-7000, pp 186-200)
Gd–Fe, isomer shift of iron-57 in $GdFe_2$ at 300 and 800°K, 19: 44678(R) (ANL-7000, pp 186-200)
IRON IONS
effects on radiolysis of acetylene, 19: 44082
Mössbauer spectra of divalent and trivalent, in crocidolite and amosite, 19: 44035
oxidation-reduction reactions of, polarization during, 19: 44002(T) (AEC-tr-6572)
radioinduced oxidation and reduction in oxygenated sulfuric acid solutions, effects of organic compounds on, 19: 44056 (INR-579/XVII/C)
spectra in theta-pinch plasma, 19: 45396 (LA-DC-7120)
water exchange in solution, nuclear magnetic resonance study, 19: 43997(R) (UCRL-11889)
IRON ISOTOPES Fe-54
neutron reactions (n,γ) with, gamma spectra from thermal, (E), 19: 45322
IRON ISOTOPES Fe-55
energy levels from iron-54 (n,γ) reactions, (E), 19: 45322
IRON ISOTOPES Fe-56
helium-3 reactions (He-3,p) at 10 Mev, angular and energy distributions from, (E/T), 19: 45362
helium-3 reactions (He-3,np) and (He-3,2p) at 10 Mev, cross sections for, (E/T), 19: 45362
IRON MINERALS
Mössbauer spectra of amosite and crocidolite, determination of oxidation states of iron from, 19: 44035
IRON OXIDES
diffusion in sodium disilicate glass, kinetics, 19: 44611 (UCRL-16232)
stability of galvanic cell studies of, 19: 43997(R) (UCRL-11889)
IRON(II) SULFATES
effects on autoxidation of benzene in aqueous solutions, 19: 44078
performance for electron dosimetry, 19: 44540
protective effects against radiation damage in crop plants, 19: 43877
radiation effects on, electron and proton, 19: 44093
IRON(III) SULFATES
effects on autoxidation of benzene in aqueous solutions, 19: 44078
IRON SYSTEMS
Fe–UO_2, reactions with aluminum–chromium–iron–yttrium alloys at 950 and 1100°C in air, 19: 44598(R) (GEMP-49A)
IRRADIATION FACILITIES
description of, for flowing material, 19: 44061(T) (AEC-tr-6567)
design and performance of UKP-30000 isotope gamma, 19: 44171
design and performance of UK-70000 high-dose-rate gamma, 19: 44171
heater in, sealed coupling for, 19: 44164 (CEA-R-2755)
ISOBUTYRIC ACID
β-amino-, radiation effects on human metabolism of, 19: 43852
ISOTOPE EFFECTS
of deuterium and oxygen-18 on autoxidation of benzene in aqueous solution of metal ions, 19: 44078
on hydrolysis of 4-methyl-1,3-dioxane and 1,3-dioxane in heavy water, 19: 44011
on spectra of plutonium(I), 19: 44033
ISOTOPE SEPARATION METHODS
diffusion, nozzle processes in supersonic jet for, 19: 44577
ISOTOPES
separation of gaseous in supersonic jet, 19: 44577

ISOTOPIC EQUILIBRATION
oxygen-16/18, in metamorphic rocks, 19: 44238
use for determination of age or volume of liquids, 19: 43660(P)
use for determination of liquid volumes, apparatus for, 19: 43661(P)
ITALY
nuclear energy development in, 19: 45724
nuclear power utilization in, prospects for, 19: 45622

J

JAPAN
carbon-14 content of atmosphere of, 1959 to 1964, 19: 44267
environs monitoring at Atomic Energy Institute, 19: 44291 (JAERI-1081)
fallout monitoring, 1961 to 1964, 19: 44264
fallout monitoring, 1959 through 1962, 19: 44265
fallout monitoring, 1961 through 1963, 19: 44266
fallout monitoring, 1961 to 1964, 19: 44268
radiation monitoring at Japan Atomic Energy Research Institute, 19: 44290 (JAERI-1079)
JET PUMPS
analysis of, experimental and theoretical, 19: 44198 (TIM-913)
JETS
flow in subsonic and transonic portion of Laval, numerical solution, 19: 44200(T) (SC-T-65-765)
isotope separation in supersonic, 19: 44577
JOINTS
design of, utilizing change of state from liquid to solid of packing material, 19: 44176(P)
JOURNAL BEARINGS
analysis of fluid-film, summary of CANEL work on, 19: 44147 (TIM-917)
design and performance of hydrostatic spindle, 19: 44141 (RFP-573)
dynamic tests of hydrostatic water, with overhung rotor, 19: 44146 (TIM-874)
dynamic tests of step, with straddle rotors, 19: 44149 (TIM-921)
film rupture and cavitation in, lubricated with low kinematic viscosity fluids, 19: 44138(R) (NYO-3363-4)
tests of orifice-compensated hybrid, in water, 19: 44151 (TIM-925)

K

KAOLINITES
sorptive properties for cesium, role of exchangeable magnesium and potassium in, 19: 43964
KENTUCKY
fallout monitoring at Paducah, Jan.-June 1965, 19: 44301 (TID-22172)
KIDNEYS
blood flow in, tracer determination of, 19: 43883(R) (UCLA-12-565, pp 65-85)
renogram interpretation for diseased, 19: 43883(R) (UCLA-12-565, pp 65-85)
renogram interpretation for dog, 19: 43667 (EUR-1890.f)
KILNS
design and performance of semicontinuous hot press tunnel, for fabrication of ceramic materials, 19: 44644 (SC-TM-65-276)
KRYPTON
diffusion from beryllia and sapphire at 1100 and 1200°C, 19: 44599(R) (GEMP-50A)
helium elastic scattering by, total cross section for, (E), 19: 44957
ionization of, electron ejection energies in auto-, 19: 44934(R) (COO-1277-13)
neutron scattering by, effective potential for electron-neutron interactions from, (E), 19: 45098
release from tungsten, mechanism of thermal, (E), 19: 44954
sorption on irradiated ion exchange material at 25 to −150°C, 19: 44091
spectra of sulfur molecules in solid, u-v absorption, (E), 19: 45480 (UCRL-10771)
KRYPTON IONS
reactions with tungsten at 1 to 4 kev, trapping in, (E), 19: 44954
yields from duoplasmatron ion source, pressure dependence of, (E), 19: 45385 (D1-82-0437)
KRYPTON ISOTOPES
production in thermal-neutron fission of uranium-235, (E), 19: 45260(R) (IDO-14660)
KRYPTON ISOTOPES Kr-85
diffusion from beryllia-coated beryllia-based thoria–urania–yttria fuels, 19: 44599(R) (GEMP-50A)
diffusion into arc-cast tantalum, 19: 44599(R) (GEMP-50A)
tracer use for diagnosis of circulatory shunts, 19: 43904
uses in quinol clathrates for inverse radiometric analysis of atmospheric sulfur dioxide, (E), 19: 44458 (NYO-2767)
KRYPTON ISOTOPES Kr-87
diffusion from beryllia-coated beryllia-based thoria–urania–yttria fuels, 19: 44599(R) (GEMP-50A)
KRYPTON ISOTOPES Kr-88
diffusion from beryllia-coated beryllia-based thoria–urania–yttria fuels, 19: 44599(R) (GEMP-50A)
KRYPTON ISOTOPES Kr-89
half life of, determination of, 19: 45276 (NP-15304)
KRYPTON ISOTOPES Kr-90
half life of, determination of, 19: 45276 (NP-15304)
KRYPTON ISOTOPES Kr-91
half life of, determination of, 19: 45276 (NP-15304)
KRYPTON ISOTOPES Kr-92
half life of, determination of, 19: 45276 (NP-15304)
KRYPTON ISOTOPES Kr-93
half life of, determination of, 19: 45276 (NP-15304)
KRYPTON ISOTOPES Kr-94
half life of, determination of, 19: 45276 (NP-15304)
KRYPTON ISOTOPES Kr-95
half life of, determination of, 19: 45276 (NP-15304)
KRYPTON ISOTOPES Kr-97
half life of, determination of, 19: 45276 (NP-15304)

L

LABORATORIES
design of radiochemical, at Czechoslovak Nuclear Research Institute, 19: 44068
radioactive waste solutions from, central plant for processing, 19: 45693
LABORATORY EQUIPMENT
description of strip-sealed continuous-rotation scattering chamber, (E), 19: 44883
design for handling pyrophoric materials under inert atmosphere, 19: 44018
design of analytical health physics, 19: 44296 (NYO-4700(Rev.) (Suppl.II))
performance of vortex tubes, 19: 44199 (UCRL-12045)
LACTIC ACID
use in TALSPEAK solvent extraction process for actinide–lanthanide group separation, 19: 44115 (ORNL-P-1577)
LANTHANUM ALLOYS
Cu–La, crystal structure studies, 19: 44678(R) (ANL-7000, pp 186-200)
La–Lu, phase studies of samarium-type intermediate phases in, 19: 44672 (AD-619201)
La–Sc, phase studies of samarium-type intermediate phases in, 19: 44672 (AD-619201)
LANTHANUM CHROMATES
magnetic properties of $(La_{0.9}Bi_{0.1})CrO_3$, (E), 19: 45486
LANTHANUM FLUORIDES
praseodymium ion spectra in, energy levels in absorption and fluorescence, (E), 19: 45484
reactions with lanthanum sulfides, preparation of lanthanum sulfide fluoride by, 19: 44024
LANTHANUM ISOTOPES La-135
energy levels of, parity and spin of, (E), 19: 45268 (JINR-P-2235)
LANTHANUM OXIDES
effects on optical properties of silicate glasses, 19: 44030
effects on strength of zirconium, 19: 44676(R) (ANL-7000, pp 176-82)
ground electronic state of gaseous, 19: 43997(R) (UCRL-11889)
phase transformations in, at 1800 to 2400°C, 19: 44731
LANTHANUM SULFIDES
reactions with lanthanum fluoride, preparation of lanthanum sulfide fluoride by, 19: 44024
LANTHANUM VANADATES
crystallographic and optical properties of hydrated, 19: 44032(T)
LARVAE
radiation effects in silkworm, genetic, 19: 43784
radiation effects on developing nerves in Odonata, morphological, 19: 43849
radioinduced mutations of silkworm, 19: 43786
radiosensitivity of sheep lungworm, 19: 43750
radiosensitivity of spermatogonia in silkworm, 19: 43783
LATINA POWER REACTOR
fuel cycle economics for, thorium–uranium, 19: 45582 (NP-15320)
operation experience of, (E), 19: 45611
testing and operation of, comparison with other Italian power reactors, 19: 45616
LEAD
current quenching in superconducting films of, (E/T), 19: 45193 (TID-21307)
current-carrying states of weakly coupled superconductors of, metastable,

(E), 19: 45206
determination in zircons by spectroscopic methods, 19: 43954
diffusion of solutes in single crystals of, 19: 45471 (AECL-2309)
gamma elastic scattering cross sections to 1.33 Mev, (E/T), 19: 45327
gamma production and transport in, (E/T), 19: 45575 (GMAD-3078-23)
gamma reactions (γ,π^0) at 1 Bev, meson (π^0) lifetime from, (E), 19: 45360
magnetic moments of superconducting spheres of, residual, (E), 19: 45195
neutron absorption cross sections at 24 kev, (E), 19: 45230
radiation absorbed dose rates in, calorimetric measurement of reactor, 19: 45467
separation from uranium by ion exchange, 19: 44119
spectra of, forbidden lines in L x-ray, (E), 19: 44941
thermal capacity of normal and superconducting, 19: 43997(R) (UCRL-11889)
use as filter for radiographic inspection of steel, 19: 44209(R) (EURAEC-1422)

LEAD ALLOYS
Pb–Ag, heat of formation of liquid, 19: 43997(R) (UCRL-11889)

LEAD COUPLES
Pb–Ni, superconductivity of film, ferromagnetic effects on, (T), 19: 45197

LEAD ISOTOPES
content in lead deposits in Eastern Transbaikal, 19: 44277

LEAD ISOTOPES Pb-208
content in lead deposits in Eastern Transbaikal, 19: 44277

LEAD ISOTOPES Pb-212
deposition of gaseous, on artificial rough surfaces, 19: 44245 (BNL-914, pp 125-32)

LEAD ISOTOPES Pb-214
determination in air, filter measurement of, 19: 44258

LEAD MINERALS
age estimation by uranium–thorium–lead method, 19: 44272

LEAD MOLYBDATES
cerium and ytterbium electron paramagnetic resonance in, 19: 44017

LEAD ORES
isotopic composition of, in Eastern Transbaikal, 19: 44277

LEAD OXIDES
determination in zircons by spectroscopic methods, 19: 43954

LEAD SULFIDES
B_2O_3–PbS–MoS_2, radiation effects on lubricant wear properties of solid films, 19: 44095

LEAD SYSTEMS
Pb–H_2O, gamma transmission through, as function of thickness, (T), 19: 45466

LEAD TELLURIDES
heat of formation of, 19: 43997(R) (UCRL-11889)

LEAKS
detection in gas mains, using radiotracers, 19: 44553 (EUR-2284.i)

LECTURES
on reactor diffusion theory, 19: 45531 (N64-29786)
on semiconductors detectors for nuclear spectrometry, 19: 44466 (UCRL-16231)

LEUKEMIA
cells from virus-induced, growth and properties of, 19: 43883(R) (UCLA-12-565, pp 65-85)
chemically induced in man, 19: 43828
etiology and treatment of, 19: 43840
radioinduced in man, 19: 43828
radioinduced in man, 19: 43840
radioinduced, etiology of, 19: 43820
radioinduced, in man, etiology, 19: 43827
tuberculosis frequency among Japanese patients with, 19: 43710 (ABCC-16-64)

LEUKOCYTES
growth of, detection of immunological initiation of, 19: 43648(R) (UCLA-12-565, pp 87-96)
radiation effects on mouse, protective effects of MEA against, 19: 43876
radiation effects on, strontium-90, 19: 43882 (UCD-472-112, pp 50-8)
radiation effects on alkaline phosphatase content of granulocytes, 19: 43829
radiation effects in human, determination of exposure in accidents by, 19: 44315
separation from red cells by electrophoresis, 19: 43648(R) (UCLA-12-565, pp 87-96)

LEVEL INDICATORS
design of illumination system for bubble of, 19: 44567(P)

LIBRARIES
journal circulation, computer program for, 19: 45700 (DP-970)

LIFE SPANS
data on dog, experimental colony, 19: 43727(R) (UCD-472-112, pp 126-40)
radiation effects on mouse, protective effects of nitrogenous heterocyclics against x, 19: 43863
radiation effects on mouse, after fetal or maternal exposure, 19: 43760

LIGHT
effects on acridine orange–thymine–thymine dimer, 19: 44060 (UCRL-16353)
effects on culture media for tubercle bacilli, 19: 43737
effects on growth of excised pine embryos, 19: 43643(R) (TID-22143)
effects on nuclear emulsions, dispersion of latent images in, 19: 44388 (CERN-65-4(Vol.II), pp III1-16)
interactions in gases, time evolution of discharges induced by, 19: 44821
interference patterns in thin films, phase changes in, 19: 43997(R) (UCRL-11889)
orientation of cesium atoms in magnetic fields by circularly polarized, 19: 44963
pathological effects in man, 19: 43819
polarization effects in infrared grating spectrophotometers, 19: 44345 (LA-DC-6719)
scattering by liquids and solids, theory of Raman spectra from, 19: 44039

LIMESTONE
oxygen-18 fractionation between coexisting calcite and, in Freeport formation, Penn., 19: 44241

LINEAR ACCELERATORS
design of Soviet IAE electron, for increased yield, 19: 44860 (IAE-614)
design of 200-Mev proton, 19: 44867 (MURA-713)
gas production of radioactive and toxic gases in tunnel of Frascati electron, (T), 19: 44866 (LNF-65/21)
malfunction of, clinical and dosimetric study of exposures from, 19: 44331
proton beam injectors for, design of single-gap, (E), 19: 44885

LINOLEIC ACID
bromination of, products of partial, 19: 43681(R) (UCLA-12-565, pp 17-31)

LIPIDS
autoradiographic localization of tritium-labeled, in rat tissues, 19: 43696
effects on heart cells of rats, 19: 43681(R) (UCLA-12-565, pp 17-31)
radiation effects on content in rat liver of, 19: 43735

LIQUID FLOW
nuclear magnetic resonance in, review, 19: 44813(T) (NP-tr-1307)

LIQUID METAL COOLED REACTORS
coolant flow distribution system for, design of, 19: 45520(P)
coolant transient two-phase flow and heat transfer in, calculation of, 19: 45494 (NAA-SR-11008)
design of epithermal thorium power-breeder, 19: 45629(P)
development, 19: 45493(R) (APDA-174)
reactivity sodium void coefficient for, 19: 45538

LIQUIDS
charge carrier disorder in conducting, (T), 19: 44844
motion of simple, neutron scattering for determination of thermal, (T), 19: 44817
neutron inelastic scattering by, conference, 19: 45243
neutron scattering cross sections in, slow, (T), 19: 45228 (NP-15469)
spectra of, theory for Raman, 19: 44039
use in 100 kv, 10-w heavy-particle thrustor, 19: 44231
volume of, radioactivity detection techniques for measurement of, 19: 43660(P)
volume of, radioactivity dilution techniques for measurement of, 19: 43661(P)

LITHIUM
bearing test in, ball, 19: 44150 (TIM-923)
corrosive effects on molybdenum and tantalum at 1000°C, 19: 44616(R) (ANL-7000, pp 122-37)
corrosive effects on niobium–zirconium alloy, effects of heat treatment and oxygen on, 19: 44620 (CNLM-6344)
effects on deformation of magnesium, 19: 43997(R) (UCRL-11889)
electron reactions with, polarization of spectral line radiation by, (E), 19: 44956
hydrogen ion reactions with, excited atom production in charge-exchange, (T), 19: 44955
incorporation in electron sensitive nuclear emulsions, 19: 44399 (CERN-65-4(Vol.II), pp III17-20)
ionization by hot tungsten, efficiency of surface, 19: 44938 (UCRL-14117)
viscosity at 600 to 1180°C, 19: 44704 (TIM-849)

LITHIUM ALLOYS
Li–Rh, crystal structure studies, 19: 44679(R) (ANL-7000, pp 205-12)

LITHIUM BORIDES
vapor pressure at 1307 to 1806°K, 19: 44703 (TIM-844)

LITHIUM BROMATES

solubility in water, 19: 44003(T) (BNL-tr-6)

LITHIUM DEUTERIDES
crystal properties of, neutron-scattering analysis of, (E), 19: 44732

LITHIUM FLUORIDES
ductility and yield points of crystalline, effects of impurities on, 19: 45679(R) (NYO-1859-11)
performance as finger-tip dosimeters, energy response calculation for, 19: 44367 (AEEW-M-550)
properties for use as thermoluminescent detector, 19: 44541
radiation effects on thermoluminescence fading in dosimetric, storage effects on, 19: 44076

LITHIUM HYDRIDES
crystal properties of, neutron-scattering analysis of, (E), 19: 44732

LITHIUM HYDROXIDES
neutron inelastic scattering spectra of deuterated and normal, vibrational modes in, (E), 19: 45482

LITHIUM IONS
diffusion in p-silicon, 19: 44001 (ZFK-PHA-12, pp 40-9)

LITHIUM ISOTOPES Li-6
bremsstrahlung reactions (γ,t) at 32 and 40 Mev, spectra of, (E), 19: 45374
deposition on semiconductor detectors as targets, by electrospraying, 19: 44635 (INR-595/IA/PL)
electron reactions with, polarization of spectral line radiation by, (E), 19: 44956
helium-3 reactions (He-3,α) at 5.5 Mev, boron-8 levels from, (E), 19: 45355
meson (μ) capture by, E1 excitation in, (T), 19: 45351
neutron reactions (n,α) spectra from, 19: 44450(R) (IBK-120a)
performance in semiconductor spectrometers for measuring fast neutron spectra, 19: 44457 (NP-15475)
proton scattering at 155 Mev, cross sections and spectra in inelastic, 19: 45305
reactions (Li-6,α) and (Li-6,d) with nuclei, mechanisms for, (T), 19: 45264 (JINR-E-2243)
reactions (Li-6,d) with boron-10, isospin violation in, (T), 19: 45265 (JINR-E-2244)
use in semiconductor neutron counters, 19: 44450(R) (IBK-120a)

LITHIUM ISOTOPES Li-7
electron reactions with, polarization of spectral line radiation by, (E), 19: 44956
meson (μ) capture by, E1 excitation in, (T), 19: 45351
properties in lithium deuteride and hydride, (E), 19: 44732
reactions (Li-7,α) and Li-7,t) with nuclei, mechanisms for, (T), 19: 45264 (JINR-E-2243)

LITHIUM ISOTOPES Li-8
energy levels from triton reactions (t,α) with beryllium-9 excited, (E), 19: 45348

LITHIUM PERCHLORATES
$HClO_4$–$LiClO_4$, effects on hydrolysis and polymerization of pentavalent protactinium, 19: 44012

LIVER
blood flow in, tracer determination of, 19: 43883(R) (UCLA-12-565, pp 65-85)
effects of strontium on mitochondria of rat, 19: 43688
enzyme activity in chicken, effects of estrogen on, 19: 43682(R) (UCLA-12-565, pp 33-57)
extracts, protective effects against radiation injuries in rat spleen, 19: 43860(R) (NP-15310, pp 14-25)
radiation effects on uridine diphosphate glucose pyrophosphorylase activity in rat, 19: 43747
radiation effects on N-demethylase activity in rat, 19: 43720(R) (NP-15310, pp 26-35)
radiation effects in rat, pathological, 19: 43735
radiation effects in rat, biochemical, 19: 43735
ribonucleic acid levels in chicken, effects of estrogen on, 19: 43682(R) (UCLA-12-565, pp 33-57)
zinc-65 uptake and distribution in normal and tumorous, in man, 19: 43699

LIVER DISEASES
radiodiagnosis of diseases of, 19: 43886

LOOPS
design and operation of sodium, 19: 44162(R) (APDA-174, pp 33-55)
operation of sodium–uranium paste flow, 19: 45499(R) (APDA-174, pp 10-24)

LOS ALAMOS MOLTEN PLUTONIUM REACTOR EXPERIMENTS
fuel element analysis for fission product distributions, 19: 44453 (LA-DC-7316)

LUBRICANTS
analysis for metallic wear products, activation, 19: 45679(R) (NYO-1859-11)
radiation effects on high-temperature solid-film, 19: 44095

LUMINESCENT DETECTORS
performance of phosphate-glass, for dosimetry, (E), 19: 44509

LUNGS
analysis for cerium-144, spectrometric, 19: 44292(R) (NP-15173)
cancer, incidence in, of uranium miners, 19: 43824
electron beam therapy of lesions in, dose calculations for, 19: 43916
fission product deposition in, 19: 44292(R) (NP-15173)
pulmonary functions of, evaluation by tracer scanning, 19: 43883(R) (UCLA-12-565, pp 65-85)
radiation effects on dog, pathophysiology of, 19: 43799
radiation effects on rabbit, histological, 19: 43846
radioinduced sclerosis in rabbit, role of autoantibodies in pathogenesis of, 19: 43817
tumor incidence in, of uranium miners, 19: 44314
visualization of, by scanning inhaled radioisotopes, 19: 43883(R) (UCLA-12-565, pp 65-85)
zinc-65 uptake and distribution in normal and tumorous, in man, 19: 43699

LUTETIUM
separation from scandium and thorium by reversed-phase chromatography, 19: 44125

LUTETIUM ALLOYS
Fe–Lu, isomer shift of iron-57 in $LuFe_2$ at 300 and 800°K, 19: 44678(R) (ANL-7000, pp 186-200)
Ga–Lu–Ni, crystal structure studies, 19: 44678(R) (ANL-7000, pp 186-200)
La–Lu, phase studies of samarium-type intermediate phases in, 19: 44672 (AD-619201)
Lu–Ag, crystal structure studies, 19: 44678(R) (ANL-7000, pp 186-200)
Lu–Nd, phase studies of samarium-type intermediate phases in, 19: 44672 (AD-619201)

LUTETIUM OXIDES
effects on optical properties of silicate glasses, 19: 44030

LUTETIUM SELENIDES
crystal structure, 19: 44010

LUTETIUM TELLURIDES
crystal structure, 19: 44010

LUTIDINES
complexes with cerium and 5-nitrobarbituric acid, preparation, 19: 44027

LYMPH SYSTEM
zinc-65 uptake and distribution in normal and tumorous, in man, 19: 43699

LYSOZYME
radiolysis of, decomposition of sulfur linkage in gamma, 19: 43841

M

MACHINE TOOLS
description of hydrostatic boring bar and spindle for lathe, 19: 44170 (Y-DA-921)
feed rate checks of numerically controlled, 19: 44642 (RFP-570)

MACHINING
equipment for finned-tube, automatic, 19: 44655(P)

MAGNESIUM
alpha reactions (α,n) at 2 to 5.4 Mev, neutron yields in, 19: 45301
deformation of, effects of lithium on, 19: 43997(R) (UCRL-11889)
determination by flame photometry, 19: 44122
effects on cesium sorption by marine sediments, 19: 43964
extrusion by hydrostatic methods, 19: 44651
metabolism in human fetuses of, 19: 43701
phase transformations in, relation of c/a ratio and elastic moduli temperature dependence with, 19: 44676(R) (ANL-7000, pp 176-82)
recrystallization of, alloying effects of cerium on, 19: 44710(T) (JPRS-24761, pp 29–40)
separation from calcium, potassium, sodium, and strontium by ion exchange, 19: 44122
separation from uranium by ion exchange, 19: 44119
sodium-22 separation from deuteron-irradiated targets of, 19: 44100

MAGNESIUM ALLOYS
extrusion by hydrostatic methods, 19: 44651
Al–Cr–Mg, erosion by water of rotating disks of, 19: 44625 (TIM-894)
Al–Cu–Mg–Mn, erosion by water of rotating disks of, 19: 44625 (TIM-894)
Al–Mg, creep at high temperatures, effects of recovery treatment on, 19: 43997(R) (UCRL-11889)
Al–Mg, dislocation loop climb in, negative, 19: 43997(R) (UCRL-11889)
Al–Mg, radiation effects on corrosion and mechanical properties of, neutron, 19: 44752 (CEA-tr-A-1818)
Mg–Ag, deformation of single crystals of, at 77 to 300°K, 19: 43997(R) (UCRL-11889)

Mg–Hg–Ni, corrosive effects on titanium of mercury-based, 19: 44616(R) (ANL-7000, pp 122-37)
Mg–Hg–Zr, corrosive effects on titanium of mercury-based, 19: 44616(R) (ANL-7000, pp 122-37)
Mg–Nd, mechanical properties of, effects of alloying elements on, 19: 44709(T) (JPRS-24761, pp 17–28)

MAGNESIUM CHLORIDES
corrosive effects on titanium alloys at 650°F, 19: 44621 (CONF-651006-1)
effects on strontium-85 elution from mouse bones, 19: 43706

MAGNESIUM COMPLEXES
with 8-quinolinol derivatives, electronic absorption spectra, 19: 43989 (MIT-905-20)

MAGNESIUM HYDROXIDES
neutron inelastic scattering spectra of deuterated and normal, vibrational modes in, (E), 19: 45482

MAGNESIUM ISOTOPES Mg-23
energy level distributions, (T), 19: 45313

MAGNESIUM ISOTOPES Mg-24
alpha inelastic scattering at 28.5 Mev, excitation of unnatural parity 3⁺ state in, (T), 19: 45318
energy level distributions, (T), 19: 45313
helium-3 reactions (He-3,n) at 5.5 Mev, silicon-26 levels from, (E), 19: 45355
neutron capture by, resonances from, (E), 19: 45356

MAGNESIUM MOLYBDATES
preparation and structure of, 19: 43991 (N64-26433)

MAGNESIUM OXIDES
diffusion of nickel oxide into single crystals of, 19: 43997(R) (UCRL-11889)
dislocations in deformed, 19: 43997(R) (UCRL-11889)
effects of additives of, on modulus of rupture of beryllia, 19: 44599(R) (GEMP-50A)
evaporation rates at 1790 to 2300°K, 19: 43985(R) (ANL-7000, pp 85-110)
plastic deformation of single crystals of, 19: 43997(R) (UCRL-11889)
radiation effects on catalytic properties for nitrous oxides decomposition, neutron, 19: 44680(R) (ANL-7000, pp 227-32)
reactions with carbon, molybdenum, and molybdenum–rhenium at 2450°C, 19: 44598(R) (GEMP-49A)
BeO–MgO, radiation effects on thermal diffusivity of, fast neutron, 19: 44599(R) (GEMP-50A)
Co_3O–MgO, catalytic effects on nitrous oxides decomposition, 19: 44680(R) (ANL-7000, pp 227-32)
GeO_2–MgO, glass formation limits in, calculation of upper, 19: 44016
MgO–SiO_2, glass formation and structure in, 19: 44015

MAGNET COILS
design of interleaved fractional-turn, for high fields with short rise times, 19: 44136 (LA-3234)
performance of superconducting, (E/T), 19: 45192 (ORNL-TM-1266)

MAGNETIC FIELDS
analysis of high-field limits on, in Brookhaven AGS, (T), 19: 44858 (BNL-9480)
atomic energy level mixing in external fields, interference phenomena in, 19: 45270 (JINR-P-2248)
book: *Stellar and Solar Magnetic Fields*, 19: 44932
calculation of nonlinear, method for, 19: 44876 (UCRL-16287)
calculations of, method for, 19: 44811 (UCRL-7784-T(Rev.1))
effect on oscillations in electron gas, 19: 44849
effect on stability of turbulent flows of conducting fluid, 19: 44835
effects of longitudinal, on meson (μ^+) depolarization quenching in targets, (E/T), 19: 45079
effects on electromagnetic wave propagation through plasma, 19: 45387 (D1-82-0442)
electron loss mechanism in, with mirror geometry, 19: 44823
heat exchange in transverse homogeneous, 19: 44202
interactions with ionized gas flow, self-excitation in, 19: 44839
measurement and stabilization of, devices for, 19: 44352 (UJV-1339/65)
measurement of inhomogeneous, using proton resonance, 19: 44353(T) (SLAC-Trans-22)
measurement of rapidly pulsed, method for, 19: 44805 (CEA-R-2769)
nuclear energy level mixing in external fields, interference phenomena in, 19: 45270 (JINR-P-2248)
plasma column, stability in longitudinal, (T), 19: 45386 (D1-82-0439)
plasma containment by, magnetic shear effects on stability of, (E), 19: 45415 (UCRL-14137)
plasma containment in galaxies by, bridge mechanism for, (T), 19: 44926(T)
plasma diffusion and stability in, (E/T), 19: 45380(R) (AD-426192)
plasma diffusion in, 19: 45410(R) (TID-22183)
production of axially symmetric, air-core magnet for, 19: 44165 (CERN-65-29)
production of pulsed, design of apparatus for, 19: 44861 (IAE-795)
production of pulsed, power supply for, 19: 44449 (IAE-704)
properties of solar, fine-structure in, (T), 19: 44918(T)
stabilization of, using Hall-effect control systems, (E), 19: 44173

MAGNETIC MIRROR MACHINES
plasma containment in, magnetic shear effects on, (E), 19: 45415 (UCRL-14137)

MAGNETIC MIRRORS
plasma stability in pulsed, (E), 19: 45388 (GA-6432)

MAGNETIC MONOPOLES
detection of fast, using Cherenkov emission and ionization loss, (T), 19: 45149

MAGNETIC PROBES
development, 19: 44223(R) (NP-15438)

MAGNETIC PROPERTIES
measurement of saturation magnetization of iron alloys by force method, apparatus for, 19: 44678(R) (ANL-7000, pp 186-200)
of x irradiated desoxyribonucleic acid, 19: 43723(R) (TID-22128)

MAGNETIC RESONANCE
of free radicals in irradiated *Bacillus subtilis* cells, 19: 43793

MAGNETIC SUSCEPTIBILITY
measurement as function of pressure, method for, 19: 43997(R) (UCRL-11889)

MAGNETOHYDRODYNAMIC CELLS
design, 19: 44991(P)
design with continuous reheating of the working fluid, 19: 44990(P)
electric current and potential distributions in, fringe effects from, 19: 44840
electron density and distribution function in gases of, 19: 44982
fluid flow instability in striated layer, Rayleigh-Taylor, (T), 19: 44984
performance of potassium-vapor, 19: 44981(R) (NP-15435)
research progress on liquid-metal, 19: 44981(R) (NP-15435)
use with gaseous fuel reactors, 19: 45540(P)

MAGNETOHYDRODYNAMICS
detonation in shock waves, 19: 44837
fluid flow in pipe and channels in, laminar, (T), 19: 44824
fluid flow in, influence of relative roughness on friction coefficient, 19: 44826
fluid flow in, localism hypothesis for turbulence in conducting, 19: 44836
fluid flow in, stabilizing effect of magnetic field on turbulent, 19: 44835
fluid flow in, symmetric motions of incompressible viscous, 19: 44816
fluid flow past circular cylinders in, viscous, (T), 19: 44825
gas flow in coaxial channel in, quasi-one-dimensional approximation of steady, 19: 44830
gas flow in, optimum conditions for Hall effect in channel, 19: 44832
gas flow in, reduction of three-dimensional compressible, 19: 44850
plasma thermodynamics in, infinite-conducting, (T), 19: 45417
theorem in, Chapman-Jouget, 19: 44837
use in heavy-water concentration, 19: 44578(P)
wave transformation in, 19: 45432

MAGNETOMETERS
design for particle spectrometers, 19: 44352 (UJV-1339/65)
design of proton magnetic resonance, for inhomogeneous fields, 19: 44353(T) (SLAC-Trans-22)

MAGNETOSPHERE
plasma instabilities in, 19: 45186
proton distribution at 1.1 to 63 Mev in inner, (E), 19: 45189
solar wind effects on field lines and plasma in outer, (T), 19: 45162
solar wind interactions with, MHD shock propagation from, (T), 19: 45165
structure of, PCA events from tail-like, (T), 19: 45172

MAGNETS
analysis of high-field limits on, in Brookhaven AGS, (T), 19: 44858 (BNL-9480)
control systems for, design of Hall-effect, (E), 19: 44173
current control system for NMR spectrometer, 19: 44356
design for pulsed-field production, 19: 44861 (IAE-795)
design of air-core, for production of axially symmetric fields, 19: 44165 (CERN-65-29)
design of compact inhomogeneous-field, for mass spectrometer, 19: 43997(R) (UCRL-11889)
design of quadrupole and sextupole, for 200-Bev proton synchrotron, 19: 44878 (UCRL-16375)
development of high-field, 19: 44357
development of pulsed, with fields up to 15 k gauss, 19: 44888
development of superconductive, 19: 45212
feasibility of superconducting thin-septum, for accelerators, 19: 44877 (UCRL-16346)
performance of central region of variable energy cyclotron, 19: 44869 (NIRL/R/87)
properties of beam-analyzing, at Princeton synchrotron, 19: 44871

(PPAD-2137-556)
MAIZE
metabolism of tritiated water in roots of *Zea maize*, 19: 43702
radioinduced mutations in meson, neutron, proton, and x, 19: 43712 (BNL-9383)
radioinduced sterility in pollen of, γ, 19: 43767
MALEIMIDE, *N*-ETHYL-
radiosensitivity effects on bacteria, 19: 44552 (BLG-327)
MALIC ACID
radiation effects on Tetrahymena, uv and x, 19: 43856
MAMMALS
radiosensitivity of gonads of, 19: 43756
MAMMARY GLAND
radiation effects on lactation in dairy cows, 19: 43800
tumor growth in rat, 19: 43649 (UCRL-16177)
MAN
allergic reaction in aerial dispersal of radiosterilized screwworm flies, 19: 43652
biological effects of space flight in, bibliography on, 19: 43718 (NASA-SP-7011(12))
biological effects of space flight in, bibliography on, 19: 43719 (NASA-SP-7011(13))
body fluids measurements in, tracer methods, 19: 43898
cesium-137 content in, in Switzerland, 1963, 19: 44269
iodine-131 metabolism in goiterous, age effects on, 19: 43691
leukemia etiology in, 19: 43828
leukemia etiology and treatment in, 19: 43840
mutagenesis in, 19: 43642(R) (NYO-2280-8)
pathological effects of radium deposited in, 19: 43830
pathological effects of injected Thorotrast in, 19: 43738
phosphatase content of leukocytes in, 19: 43829
radiation dose from nuclear rocket debris, external and internal, 19: 45655 (NUS-229)
radiation dose to organs in, formulas and methods for calculating, 19: 43853
radiation dosimetry by beryllium-7 measurements in tissues of, proton, 19: 44327
radiation effects on, protective effects of erythropoiesis stimulating preparation against, 19: 43872
radiation effects on, correlation of animal studies with, 19: 43843
radiation effects on metabolites, use in exposure diagnosis, 19: 43852
radiation effects at low doses, review on, 19: 43752
radiation effects, somatic, 19: 43838
radiation effects, genetic, 19: 43823
radiation hazards of diagnostic radiography in, 19: 43914
radioactive contamination of Alaskan, whole-body measurement of, 19: 44289 (HW-SA-3750)
radioinduced chromosome aberrations in, 19: 43834
radioinduced leukemia in, etiology of, 19: 43827
radiosensitivity of gonads in children, 19: 43893
radiosensitivity of, effects of age, 19: 43915
radiosensitivity of skin of, 19: 43819
radiotherapy of hyperthyroidism using iodine-131, effects on cytoplasmic and thyroglobulin antibodies, 19: 43902
radium poisoning in, research study review, 19: 43672(R) (TID-22131)
scandium-46 metabolism by, 19: 43692
stresses in space flight, methods for improving tolerance to, 19: 43842
zinc-65 uptake and distribution in normal and tumor tissue in, 19: 43699
MANDELIC ACID
compound formation with samarium, gadolinium, and erbium, 19: 44028
MANDELIC ACID, *p*-BROMO-
compound formation with samarium, gadolinium, and erbium, 19: 44028
MANGANESE
effect on determination of oxygen in steel by isotope dilution method, 19: 43946
excretion in feces and urine in colostomized pullets, 19: 43693
radiation effects on metabolism of, in rats, 19: 43852
separation from uranium by ion exchange, 19: 44119
MANGANESE ALLOYS
Al–Cu–Mg–Mn, erosion by water of rotating disks of, 19: 44625 (TIM-894)
Fe–Mn, deformation behavior, effects of interstitials on, 19: 43997(R) (UCRL-11889)
Fe–Mn, thermodynamic properties at 1450°K, 19: 43997(R) (UCRL-11889)
Mn–Pt, crystal structure of $PtMn_3$, chemical order-disorder, in, 19: 44679(R) (ANL-7000, pp 205-12)
Mn–Pt, magnetic structure in $PtMn_3$, 19: 44679(R) (ANL-7000, pp 205-12)
MANGANESE ISOTOPES Mn-54
metabolism in scorbutic guinea pigs, 19: 43697
uptake by scallops, 19: 43663
MANGANESE ISOTOPES Mn-55
gamma absorption cross section, (T), 19: 45366
neutron reactions (n,γ) with, rates for, (E/T), 19: 45522 (AE-195)
MANGANESE MOLYDATES
preparation and structure of, 19: 43991(N64-26433)
MANGANESE OXIDES
oxygen isotope exchange reactions in, temperature effects on rate of, 19: 44104
MANGANESE SILICIDES
crystal lattice parameters, 19: 44679(R) (ANL-7000, pp 205-12)
MANGANESE SULFATES
neutron capture with charged-particle emission in, determination for source calibration, (E), 19: 45232
MANGANESE SYSTEMS
C–Co–Mn, crystal structure studies, 19: 44679(R) (ANL-7000, pp 205-12)
MARCOULE REACTORS (G-3)
fuel element failure in, radioprotection and decontamination operations for, 19: 45565 (CEA-R-2781)
radiation dose rates in pressure vessel of, 19: 45566 (CEA-R-2785)
MARITIME NUCLEAR STEAM GENERATOR
economic analysis of, for 47,000 DWT tanker, 19: 45657 (TID-22088)
MARITIME REACTORS
fuel element securing device for, 19: 45550(P)
MASERS (OPTICAL)
beam reactions with solids, production of hot plasma by pulsed, (E), 19: 45409 (TID-22132)
beam reactions with graphite, molecular emission spectra in jets from, (E), 19: 44803(R) (ANL-6877, pp 21-7)
gas breakdown by light from, time evolution of, 19: 44821
MASS SPECTROGRAPHY
emulsions for use in, properties of ion-sensitive, 19: 43979
equipment and methods for, in determination of trace impurities in inorganic solids, 19: 43978
MASS SPECTROMETERS
design and development for selected area analysis, 19: 44354
uses for analyzing nuclide yields from uranium-235 thermal fission, (E), 19: 45260(R) (IDO-14660)
MATERIALS TESTING
brazed joints, comparison of methods for nondestructive, 19: 44207(R) (ANL-7000, pp 146-52)
cavitation damage to impellers, coatings for indicating, 19: 44212 (TIM-878)
equipment for high-temperature wires, 19: 44213
equipment for reactor fuel core, data recording, 19: 45500 (HW-65756)
loops for design of inpile, 19: 45676 (IDO-16871-4)
methods for tubing, nondestructive pulsed electromagnetic field and radiography, 19: 44587(R) (ANL-7000, pp 3-63)
neutron image intensification system for, development of, 19: 44207(R) (ANL-7000, pp 146-52)
nondestructive flaw detection using backscattered radiation, 19: 44214(P)
nondestructive measurement of residual stresses in metals and metal structures, 19: 44643 (RSIC-410)
nondestructive methods for small-diameter refractory-alloy tubing, 19: 44211 (ORNL-P-1543)
nondestructive methods of, development of, 19: 44207(R) (ANL-7000, pp 146-52)
radiographic inspection of steel, evaluation of filters for use in, 19: 44209(R) (EURAEC-1422)
shock testing facility, design of pulsed five-million-pound, 19: 45720 (UCRL-12055-T)
surface crack detection using diamond stylus and strain gage, 19: 44210 (KAPL-M-6484)
ultrasonic determination of elastic moduli of high-temperature materials, 19: 44207(R) (ANL-7000, pp 146-52)
ultrasonic inspection of steel welds, use of dynamic screen images for, 19: 44209(R) (EURAEC-1422)
ultrasonic radiation images, system for television presentation of, 19: 44207(R) (ANL-7000, pp 146-52)
MATERIALS TESTING REACTOR MOCKUP
instrumentation and control systems of, design of, 19: 45680 (ORNL-TM-1190)
neutron flux densities in, 19: 45681 (RCN-36)
MATHEMATICAL TABLES
conversions between binary shaft position encoder outputs and degree and radian measure, (T), 19: 44580 (AERE-R-4964)
MATHEMATICS
equations for prediction of instabilities in forced-convection two-phase flow, 19: 44185(R) (GEAP-4910)
equations for thermodynamic processes in biological systems, 19: 43665 (BNL-9338)
Green's functions for related two-point boundary value problems,

19: 44582 (ORNL-3646)
integer linear programming in combinatorial analysis, (T), 19: 45709 (SC-R-65-963)
integration of differential equations method for, 19: 45703 (LA-DC-6667)
mapping function at corners, development of, 19: 45702 (LA-DC-6556)
matrices in, theory for tensorial, 19: 44584
matrix elements of generators of U_n, normalization coefficients for, 19: 44585
spinors in, intrinsic theory of two-component, 19: 44583
MATTER
neutron s-wave resonances in, (E/T), 19: 45215 (CEA-R-2780)
MEATS
cesium-137 content of caribou, 19: 44289 (HW-SA-3750)
radiation effects on salmonellae in, 19: 44557 (NYO-3426-1)
radiation effects on bacterial counts in lobster, 19: 44558(R) (TID-22139)
radiation effects on bacterial counts in scallop, 19: 44558(R) (TID-22139)
radiation effects on bacterial counts in haddock, 19: 44558(R) (TID-22139)
radiopasteurization of poultry, economic feasibility of salmonellae control by, 19: 44557 (NYO-3426-1)
sodium-22 content of caribou and reindeer, 19: 44289 (HW-SA-3750)
MECHANICAL DRIVES
design for Moessbauer spectrometer, (E), 19: 45316
MECHANICS
equations of motion in nonequilibrium statistical, 19: 44856
phase spaces for 3- and 4-particle final states in elementary particle interactions, (T), 19: 45006 (IS-1214)
response of linear damped lumped spring-mass systems, transfer function formalism for transient, 19: 45710 (SC-TM-64-1772)
MEDICAL SUPPLIES
radiosterilization of, evaluation, 19: 44559
radiosterilization of, using radioisotopes, 19: 44560
radiosterilization of, evaluation of, 19: 44564
MEDICINE
nursing care of patients after radiotherapy, 19: 43908
nutritional management of cancer patients after radiotherapy, 19: 43911
radiation protection procedures in, 19: 43896
radiation protection in radiological, Italian Decree on, 19: 44318
research programs on nuclear, 19: 43647(R) (UCLA-12-565)
role of army medical service in nuclear warfare, 19: 44310
MEIOSIS
radiation effects on Pinus rigido, gamma, 19: 43722(R) (TID-22108)
MEMBRANE FILTERS
penetration by radioactive aerosol, measurement of depth of, 19: 44299 (SZS-2(1965))
MEMBRANES
bioelectric forces involved in material transfer across biological, 19: 43664 (BNL-9337)
diffusion of tracer against concentration gradient through, 19: 44025
material transfer across biological, thermodynamics of, 19: 43665 (BNL-9338)
MEMORY DEVICES
design of analog, with nondestructive readout, 19: 44350 (SC-R-65-959)
MERCHANT VESSELS
economics of nuclear-powered tanker, 19: 45657 (TID-22088)
propulsion systems for, bibliography on, 19: 45647 (AED-C-22-64)
MERCURY
corrosion effects on titanium, inhibiting effects of dissolved aluminum, nickel, or zirconium on, 19: 44616(R) (ANL-7000, pp 122-37)
corrosive effects on zirconium nitride, effects of dissolved titanium on, 19: 44616(R) (ANL-7000, pp 122-37)
diagnostic tracer use of, for gastrointestinal diseases, 19: 43886
effects on determination of copper in high-purity metals by activation methods, 19: 43973
electric and thermal conductivities of liquid, correlation over entire liquid range, 19: 44701(R) (TID-22144)
electron oscillations in plasma of, higher- and sub-harmonics of, 19: 45428
electron reactions with cathodes of, ion beam production by, 19: 44221 (N64-31088)
electron scattering from atomic beams of, polarization in, (E), 19: 44958
flow in magnetic field, turbulent velocity pulsations in, (E), 19: 44827
gamma elastic scattering cross sections to 1.33 Mev, (E/T), 19: 45327
neutron absorption cross sections at 24 kev, (E), 19: 45230
pumping of liquid, electrodynamic pump for, 19: 44188 (NASA-TN-D-2965)
separation from uranium by ion exchange, 19: 44119
thermal capacity of normal and superconducting, 19: 43997(R) (UCRL-11889)
viscosity of liquid, kinematic, 19: 44701(R) (TID-22144)
MERCURY ALLOYS
Al–Hg–Ni, corrosive effects on titanium of mercury-based, 19: 44616(R) (ANL-7000, pp 122-37)
Al–Hg–Zr, corrosive effects on titanium of mercury-based, 19: 44616(R) (ANL-7000, pp 122-37)
Hg–Ni–Zr, corrosive effects on titanium of mercury-based, 19: 44616(R) (ANL-7000, pp 122-37)
Mg–Hg–Ni, corrosive effects on titanium of mercury-based, 19: 44616(R) (ANL-7000, pp 122-37)
Mg–Hg–Zr, corrosive effects on titanium of mercury-based, 19: 44616(R) (ANL-7000, pp 122-37)
MERCURY ISOTOPES Hg-201
neutron reactions with, resonances in, (E), 19: 45296
MESIC ATOMS
x-ray transitions in μ-mesic tantalum and plutonium-239, 2p–1s, (E), 19: 44962
MESIC MOLECULES
production in reactions of mesic deuterium atoms with deuterons and protons, (E), 19: 45273 (JINR-P-2356)
MESON BEAMS
analysis of 4- to 12-Bev/c pion, using gas Cherenkov counter, 19: 44376 (BNL-9466)
meson (μ) contamination in meson (π), method for calculating, 19: 44993 (CEA-R-2778)
production of (K^0), regeneration phenomena in, (T), 19: 45034 (NP-15470)
MESON PAIRS
photoproduction of (π), on carbon and hydrogen in Bev range, 19: 45000 (HUX-2752-7)
MESON SHOWERS
production of meson–nucleon, by 10- and 20-Bev/c protons in steel, (T), 19: 45317
MESONS
decay of vector, trilinear couplings forbidden by nonet symmetry in, (T), 19: 45025 (N64-26265)
emission in proton interactions in nuclear emulsions at 30.5 Bev, multiple, 19: 45054
field theory for, relativistic quantum, 19: 45131 (JEN-154-DF/I-47)
form factors of, current algebra for studying, (T), 19: 45011 (JINR-E-2294)
interactions of field of charged scalar, with fixed two-level point source, (T), 19: 45150
interactions of T = 2, with nucleons, form factors from off-shell effects in, (T), 19: 45067
interactions with baryons, exact bootstrap solutions to Low equation for, 19: 45106
mass formulas for baryons and, Gell-Mann-Okubo quark splitting for, (T), 19: 45077
model for static charged scalar, with broken charge symmetry, 19: 45072
photoproduction at high energies, (E/T), 19: 45024 (MIT-2098-163)
production in interactions at high energies, peripheral model for, (T), 19: 45037 (TID-21316)
MESONS, RESONANCE
decay of K*, trilinear couplings forbidden by nonet symmetry in, (T), 19: 45025 (N64-26265)
interactions with stable particle, strong, (T), 19: 45082
production in bremsstrahlung-proton interactions at 0.6 to 5.5 Bev, (E), 19: 44999 (DESY-65/5)
production of K* in deuteron-meson (K^+) interactions at 2.3 Bev/c, 19: 45120
production of K*, in meson (K^+)–proton interactions at 3 Bev/c, (E/T), 19: 45057
production of S-wave T = 0 $\pi\pi$, in meson (π^-)-proton interactions at 1.7 to 2.5 Bev/c, (E), 19: 45089
production of, triangle singularities in, (T), 19: 45104
properties of, review, 19: 45046 (UCRL-16295)
representation of I = 0 states of three-pion, (T), 19: 45042 (UCID-2608)
review, 19: 45056
symmetries for, relativistic SU(6) supermultiplet, 19: 45112
MESONS (η)
production in antiproton-proton annihilations at rest, (E), 19: 45122
MESONS (K)
detection using emulsions, 19: 44443 (CERN-65-4(Vol.II), pp X61-6)
interactions with nucleons at high energies, polarization and Regge poles in, (T), 19: 45044 (UCRL-16186)
interactions with mesons (π) at low energy, dispersion relations for, (T), 19: 45085
interactions with nucleons at high energy, absorption model for charge-exchange, (T), 19: 45087
production in antiproton-proton annihilations at rest, (E), 19: 45122
stopping by emulsions loaded with carbon, 19: 44398 (CERN-65-4 (Vol.II), pp III12-14)
MESONS (K^-)

capture in emulsions, short-range hyperfragment production in, (E/T), 19: 45342
interactions with protons at 1.22 to 1.70 Bev/c, charge-exchange, (E/T), 19: 45045 (UCRL-16288)
interactions with protons for hyperon (Ω^-) parity test, 19: 45101
mass difference (K^0-K^-), (E), 19: 44998 (CU-1932-247)
photoproduction at high energies, (E/T), 19: 45024 (MIT-2098-163)
MESONS (K^0)
decay of K_2^0, 2π, (T), 19: 45026 (N64-19243)
decay of K_2^0, 2π PC conservation in, (E/T), 19: 45055
decay of, CP violation in, (T), 19: 45034 (NP-15470)
interactions with nucleons at high energies, polarization and Regge poles in, (T), 19: 45044 (UCRL-16186)
mass, (E), 19: 44998 (CU-1932-247)
mass K_1^0 and K_2^0, difference of, (E), 19: 45099
production of beams of, regeneration phenomena in, (T), 19: 45034 (NP-15470)
MESONS (K^+)
decay of, leptonic, (T), 19: 45027 (NP-15199)
interactions with protons at high energies, resonance production in, (T), 19: 45037 (TID-21316)
interactions with protons at 3 Bev/c, decay distributions and differential cross sections for, (T), 19: 45086
interactions with deuterons at 2.3 Bev/c, coherent K^+ production in, (E), 19: 45120
interactions with protons at 3 Bev/c, K^+N^+ production in (KN_{33}), (E/T), 19: 45057
photoproduction at high energies, (E/T), 19: 45024 (MIT-2098-163)
MESONS (μ)
capture by lithium-6 and -7, E1 excitation in, (T), 19: 45351
contest in meson (π) beams, method for calculating, 19: 44993 (CEA-R-2778)
effects on maize, mutagenic, 19: 43712 (BNL-9383)
magnetic moment of, dispersion theory for anomalous, 19: 45108
reactions with nuclei above 300 Tev, evidence for, (E), 19: 45368
transfer from mesic deuterium atoms to carbon and oxygen, (E), 19: 45273 (JINR-P-2356)
MESONS (μ^-)
capture by spin-0 nuclei asymmetry in neutron angular distributions from, (E), 19: 45274 (NEVIS-136)
interactions with deuterons, effect of neutron–neutron final state on, (T), 19: 45073
polarization from neutrino (ν_μ)–neutron interactions, (T), 19: 45050
MESONS (μ^+)
polarization from antineutrino ($\bar{\nu}_\mu$)–proton interactions, (T), 19: 45050
reactions in targets, depolarization quenching as function of longitudinal magnetic fields in, (E/T), 19: 45079
slowdown in targets, depolarization in, (E), 19: 45080
spin precession in muonium compounds, (T), 19: 45278 (NP-15389)
MESONS (ω)
interactions with mesons (π), one-trajectory exchange for amplitudes of, (T), 19: 45074
production in antiproton-proton annihilations at rest, (E), 19: 45122
production in meson (π^-)-proton interactions at 3.9 Bev/c, (E), 19: 45121
MESONS (ω^0)
decay of, branching ratio for $e^+ + e^-$, (E), 19: 45102
MESONS (π)
beam contamination by meson (μ), method for calculating, 19: 44993 (CEA-R-2778)
effects on maize, mutagenic, 19: 43712 (BNL-9383)
electroproduction on protons, neutron form factor from, (T), 19: 45065
interactions with nucleons at high energies, polarization and Regge poles in, (T), 19: 45044 (UCRL-16186)
interactions with mesons (K) at low energy, dispersion relations for, (T), 19: 45085
interactions with nucleons at high energy, absorption model for charge-exchange, (T), 19: 45087
interactions with nucleons at high energy, multiple production in elastic, (T), 19: 45091
interactions with nucleons below 1 Bev, phase shift analysis of, (T), 19: 45100
interactions with mesons (π), perturbation theory for p-wave amplitudes in, 19: 45105
interactions with meson (π), dispersion theory for elastic low-energy, 19: 45127
interactions with mesons (π), isotopic structure and unitarity of, 19: 45051
interactions with nucleons, form factors from off-shell effects in, (T), 19: 45067
interactions with mesons (π), mesons (ω), and nucleons, one-trajectory exchange for amplitudes of, (T), 19: 45074
photoproduction of, meson (ρ) effects in double, (T), 19: 45019 (JINR-P-2286)
photoproduction on protons at 0.6 to 5.5 Bev, (E), 19: 44999 (DESY-65/5)
production in antiproton-proton annihilations at rest, (E), 19: 45122
reactions with nuclei below 200 Mev, nuclear structure from, 19: 45339
MESONS (π^-)
capture by helium-3, neutron-neutron scattering length from, (T), 19: 45354
interactions of three, analysis of I = 0 states in, (T), 19: 45024 (UCID-2608)
interactions with protons at high energies, statistical model calculations for, 19: 45047 (UCRL-16315)
interactions with protons at 8.5 Bev/c, polarization in elastic, (E), 19: 45081
interactions with protons at 3.9 Bev/c, resonance in $\pi^+\pi^0$p system from, (E), 19: 45121
interactions with protons at 1.7 to 2.5 Bev/c, S-wave final-state $\pi\pi$ in, (E), 19: 45089
interactions with protons, high-energy limits for, 19: 45040 (TPJU-11/65)
momentum determination in nuclear emulsions, method for, 19: 44427 (CERN-65-4(Vol.II), pp VIII34-7)
photoproduction on carbon and hydrogen in Bev range, (E), 19: 45000 (HUX-2752-7)
reactions in bubble chambers and emulsions, meson (π^0) intensity from, 19: 44439 (CERN-65-4(Vol.II), pp X37-43)
scattering in nuclear emulsions at 17 Bev/c, spurious, 19: 44416 (CERN-65-4(Vol.II), pp V153-62)
MESONS (π^0)
interactions with meson (π^0) in meson (π^-)-proton interactions, S-wave T = 0 final-state, (E), 19: 45089
lifetime of, inverse decay process for, (E), 19: 45360
photoproduction at high energies, (E/T), 19: 45024 (MIT-2098-163)
photoproduction on lead at 1 Bev, lifetime from, 19: 45360
photoproduction on deuterons and protons, detection using emulsions, 19: 44438 (CERN-65-4(Vol.II), pp X33-6)
production in meson (π^-) reactions in bubble chambers and emulsions, intensity of, 19: 44439 (CERN-65-4(Vol.II), pp X37-43)
reactions in nuclear emulsions, ionization losses in, 19: 44428 (CERN-65-4(Vol.II), pp IX9-13)
MESONS (π^+)
interactions with protons at high energies, resonance production in, (T), 19: 45037 (TID-21316)
interactions with protons at 1.11 and 1.265 Bev/c, N^{*++} production in, 19: 44997 (COO-1428-14)
interactions with protons at 8 Bev/c, resonance enhancement from, (E), 19: 45103
interactions with protons, high-energy limits for, 19: 45040 (TPJU-11/65)
photoproduction at high energies, (E/T), 19: 45024 (MIT-2098-163)
photoproduction on carbon and hydrogen in Bev range, (E), 19: 45000 (HUX-2752-7)
MESONS (ρ)
decay of, trilinear couplings forbidden by nonet symmetry in, (T), 19: 45025 (N64-26265)
effects in double photoproduction of mesons (π), (T), 19: 45019 (JINR-P-2286)
production in antiproton-proton annihilations at rest, (E), 19: 45122
MESONS (ρ^0)
mass spectrum structure in, peak-broadening effect on, 19: 45092
photoproduction on aluminum, carbon, copper, and hydrogen in Bev range, (E), 19: 45000 (HUX-2752-7)
MESONS (ρ^+)
production in mesons (π^+)–proton interactions at 8 Bev/c, (E), 19: 45103
METABOLISM
radiation effects on human and rat, use in exposure diagnosis, 19: 43852
thermodynamics of material transfer across biological membranes, 19: 43665 (BNL-9338)
use as indicator of radiation effects, 19: 43753
METABOLISM CAGES
design and cost of air conditioned, 19: 43644(R) (UCD-472-112)
design of rat, 19: 43728(R) (UCLA-12-565, pp 59-64)
METAL POWDERS
use of heavy, in radiation-attenuating films, 19: 44670(P)
METALLOGRAPHY
etching using alternating current method, 19: 44601 (LA-DC-6407)
procedures for plutonium alloys, 19: 44674(R) (ANL-7000, pp 69-83)
use of transmission electron microscopy in examination of bcc metals and alloys, 19: 44610 (TIM-943)
METALLURGY

facility for radioactive material, 19: 44163 (BNL-9502)
translations of Russian studies on, 19: 44614 (JPRS-24761)
METALS
analysis for oxygen, activation, 19: 43928 (EUR-2290.f)
bonding to glass, studies, 19: 43997(R) (UCRL-11889)
crystal lattice defects in fcc, theoretical study of, 19: 44739(R) (ANL-7000, pp 233-77)
effects of flowing, on fuel elements, 19: 44181(R) (APDA-174, pp 56-60)
electric conductivity of thin films of, with unlike surfaces, 19: 45479 (TID-21301)
isotope abundance ratios of, selected-area mass spectrometric analysis of, 19: 44354
joining to aluminum silicate glass, techniques for, 19: 44337(R) (AD-425708)
phase transformations in hcp, relation of c/a ratio and elastic moduli temperature dependence with, 19: 44676(R) (ANL-7000, pp 176-82)
preparation of thin foils of, for electron metallography, 19: 44610 (TIM-943)
radiation effects on mechanical properties of, displacement spike density model for neutron, 19: 44599(R) (GEMP-50A)
research program on, 19: 43997(R) (UCRL-11889)
vacancy clustering during quenching in fcc, 19: 44739(R) (ANL-7000, pp 233-77)
METAMICT MINERALS
occurrence and properties of niobium–uranium, in Powhatan County, Virginia, 19: 44279
METEORITES
analysis for oxygen and silicon, fast-neutron activation, 19: 43927 (CONF-650405-16)
chromium isotopic content in, (E), 19: 44907
gallium content in chondritic, 19: 44900
rare gas content in Khor Temiki, (E), 19: 44906
METEOROIDS
fluxes in space, 19: 44893 (NASA-CR-294)
METEOROLOGY
aerospace studies, 19: 44771 (BNL-914, pp 44-50)
atmospheric deposition problems, 19: 44247 (BNL-914, pp 139-40)
atmospheric diffusion studies in Canada, 19: 44790 (BNL-914, pp 149-50)
atmospheric diffusion from ground sources, data on, 19: 44792 (BNL-914, pp 153-5)
atmospheric dispersion in, summary of diffusion experiments for prediction of, 19: 44789 (BNL-914, pp 146-8)
atmospheric dispersion in urban areas, 19: 44791 (BNL-914, pp 151-2)
atmospheric turbulence, low-level, 19: 44793 (BNL-914, pp 156-7)
communication problems in micro-, 19: 44797 (BNL-914, pp 173-4)
conference on AEC activities in, 19: 44761 (BNL-914)
diffusion climatology studies, 19: 44771 (BNL-914, pp 44-50)
diffusion experiments, 19: 44796 (BNL-914, pp 163-72)
diffusion tests in, elevated line source, 19: 44779 (BNL-914, pp 93-4)
dispersion in meso-scale, studies, 19: 44784 (BNL-914, pp 110-12)
fallout rates, 19: 44255 (RT/PROT(65)-10)
measurements during IGY and IGC in, Italian and world, 19: 44819
problems in meso-scale, fundamental, 19: 44782 (BNL-914, pp 103-6)
problems in, meso-scale and mean transport, 19: 44781 (BNL-914, pp 99-102)
program at Air Force Cambridge Research Laboratories, 19: 44776 (BNL-914, pp 75-84)
program at Argonne, 19: 44763 (BNL-914, pp 4-13)
program at Brookhaven, 19: 44762 (BNL-914, pp 1-3)
program at Dugway Proving Ground, 19: 44778 (BNL-914, pp 91-2)
program at Hanford, 19: 44767 (BNL-914, pp 24-6)
program at Nevada Test Site, 19: 44774 (BNL-914, pp 65-8)
program in Oak Ridge, Tennessee, 19: 44765 (BNL-914, pp 18-19)
program of U. S. Public Health Service, 19: 44775 (BNL-914, pp 69-74)
program of U. S. Weather Bureau, 19: 44770 (BNL-914, pp 33-43)
research at National Reactor Testing Station on, 19: 44773 (BNL-914, pp 57-64)
research in, for nuclear industry, 19: 44780 (BNL-914, pp 95-8)
research program on atmospheric boundary layer, 19: 44777 (BNL-914, pp 85-90)
source configuration effects on downwind concentrations, 19: 44786 (BNL-914, pp 116-18)
temperature profiles, problems in, 19: 44795 (BNL-914, pp 161-2)
tetroons in meso-scale, 19: 44783 (BNL-914, pp 107-9)
turbulence characteristics near ground in micro-, dimensional analysis, 19: 44772 (BNL-914, pp 81-4)
turbulence structure in micro-, 19: 44798 (BNL-914, pp 175-7)
use in reactor safety evaluation, 19: 44270 (BNL-914, pp 178-9)
wind profiles, review, 19: 44794 (BNL-914, pp 158-60)
METHACRYLIC ACID, METHYL ESTER
polymerization pre-irradiated cotton fibers, 19: 44094
radioinduced graft polymerization with polyethylene and polyvinyl chloride, 19: 44083
METHANE
crystal lattice dynamics of solid, in alpha, beta, and gamma phases, (E/T), 19: 45239
neutron scattering by, distributions from cold, (E), 19: 45237
He-3–methane–Ne, performance as filling in thermal neutron detectors, 19: 44373(R) (ANL-6877, pp 15-20)
METHANE, CHLOROTRIFLUORO-
heat transfer properties of Refrigerant-22 in two-phase flows, 19: 44185(R) (GEAP-4910)
meson (μ^+) depolarization quenching in, as function of longitudinal magnetic field, (E/T), 19: 45079
meson (μ^+) depolarization in targets of, (E), 19: 45080
METHANE, TRICHLOROFLUORO-
meson (μ^+) depolarization quenching in, as function of longitudinal magnetic field, (E/T), 19: 45079
meson (μ^+) depolarization in targets of, (E), 19: 45080
METHANESULFONIC ACID, BUTYL ESTER
effects on cytology and physiology of *Triticum durum* and *T. monococcum*, 19: 43653
METHANESULFONIC ACID, ETHYL ESTER
labeling with tritium to prepare labeled cells, 19: 43651
METHANEDISULFONIC ACID, 2-METHOXYETHYL ESTER
effects on cytology and physiology of *Triticum durum* and *T. monococcum*, 19: 43653
METHANESULFONIC ACID, TETRAMETHYLENE ESTER
effects on cytology and physiology of *Triticum durum* and *T. monococcum*, 19: 43653
METHANOL
radiation effects on reactions with hydroxyl ions, 19: 44090
METHIONINE
radiation effects on intestinal sorption in rats, 19: 43728(R) (UCLA-12-565, pp 59-64)
METHYL SULFOXIDE
complexes with molybdenum chlorides, 19: 43990 (MIT-1965-15)
protective effects of AET mixtures against gamma radiation, 19: 43883(R) (UCLA-12-565, pp 65-85)
protective effects of, against radiation injuries in mice, 19: 43859(R) (NP-15310, pp 1-13)
MICA
performance for slow neutron dosimetry, 19: 44385 (CERN-65-4(Vol.II), pp 112-19)
MICE
bone marrow cell migration in, 19: 43836
diets for breeding, 19: 43654
epithelial cell graft-effects on thymectomized, 19: 43883(R) (UCLA-12-565, pp 65-85)
erythrocyte chimerism and acquired immunologic tolerance in neonatal, 19: 43657
growth kinetics of epithelial and spindle cell tumors in, using autoradiography and tritiated thymidine, 19: 43698
immunizing effects of irradiated *Schistosoma japonicum* cercariae in, 19: 43848
leukemia induction in, growth and properties of cells from, 19: 43883(R) (UCLA-12-565, pp 65-85)
metabolism of aminoethylisothiuronium in, irradiated, normal, and tumor-bearing, 19: 43867
radiation effects on, protective effects of nitrogenous heterocyclics against x, 19: 43863
radiation effects on, protective effects of erythropoiesis stimulating preparation against, 19: 43872
radiation effects on, protective effects of *p*-aminopropiophenone and MEA against proton and x-ray, 19: 43873
radiation effects on, protective effects of *p*-aminopropiophenone against whole-body proton, 19: 43874
radiation effects on granulocyte and lymphocyte counts in, protective effects of MEA against, 19: 43876
radiation effects on, protective effects of hematoporphyrins against x, 19: 43862
radiation effects on, protective effects of 1-phenyl-1-acetthio-2-nitroethane and -propane against, 19: 43868
radiation effects on, gamma, 19: 43662(R) (UCLA-12-565, pp 97-128)
radiation effects on bone-injection-protected, effects of plethora on, 19: 43682(R) (UCLA-12-565, pp 33-57)
radiation effects on, LET for, 19: 43721(R) (ORNL-TM-1217)
radiation effects on lens opacity in, protons, 19: 43721(R) (ORNL-TM-1217)
radiation effects on neonatal and prenatal mortalities in, by fetal or maternal exposure, 19: 43760
radiation effects on virulence of tumor grafted in successive generations

of, 19: 43762
radiation effects on growth of transplanted sarcoma in, 19: 43763
radiation effects on, combined silicon dioxide and alpha, 19: 43831
radiation effects on hair of, local and whole-body, x, 19: 43833
radiation injuries in, protective effects of tryptamine against, 19: 43864
radiation injuries, protective effects of injected nucleic acid precursors, 19: 43866
radiation injuries in, pathology and recovery, 19: 43771
radiation injuries and recovery in, after exposure to fractionated doses, 19: 43792
radiation injuries, protective effects of dimethyl sulfoxide against, 19: 43859(R) (NP-15310, pp 1-13)
radioinduced chromosomal aberrations in, effects of age on x, 19: 43729(T) (BNL-tr-12)
radioinduced mutations in spermatogonia of, effects of dose, dose rate, and radiation quality on, 19: 43788
radioinduced mutations in, effects of dose rate on, 19: 43789
radiosensitivity of, effects of hematoporphyrin on, 19: 43748
radiosensitivity of, effects of mouse strain, 19: 43792
strontium-85 elution from bones of, by chelating agents and salts, 19: 43706

MICROWAVE EQUIPMENT
reflection coefficients in plasma-filled waveguides, method for determining, 19: 45401 (NP-15196)

MICROWAVES
emission from plasma in magnetic mirrors, (E), 19: 45388 (GA-6432)
emission from solar flares, models for, 19: 44931
interactions with plasma, harmonic generation by, (E), 19: 45420
phase shifts in plasma, null method of measuring, 19: 45412 (UCRL-7978)
propagation of Pi-2 micropulsations through ionosphere, phase velocities for, (T), 19: 45181
reflection in plasma-filled waveguides, 19: 45401 (NP-15196)
scattering from resonant plasma oscillations, incoherent, (E), 19: 45436
use for plasma diagnostics, cross-polarized backscatter in, (T), 19: 45424
use for plasma electron density measurements, (E), 19: 45429

MILITARY COMPACT REACTOR
shielding for, gamma production and transport in, (E/T), 19: 45575 (GMAD-3078-23)

MILK
analysis for calcium and strontium by flame photometry using plasma jets, 19: 43924 (AERE-R-4990)
cesium-137 content in, in Switzerland, 1963, 19: 44269
cesium-137 content in Australian, 1963, 19: 44309
fallout contamination in Japan, 1961 to 1964, 19: 44268
radiation effects on production of, by dairy cows, 19: 43800
radiation monitoring at Argonne, Jan.-June 1965, 19: 44300 (TID-22171)
radioactivity of Canadian, June 1965, 19: 44251 (NP-15519, pp 23-51)
strontium-90 content of Indian, 1959 to 1964, 19: 44244 (AEET/AM/40)
tritium uptake by cattle, 19: 43694

MINERALS
analysis for argon-40, use of nitrogen-15 as internal standard in, 19: 43960
analysis for niobium, radiometric-spectrophotometric, 19: 43943
deuterium content of crystallization water of saline, 19: 44240

MINING
lung cancer incidence in uranium, 19: 44314

MITOCHONDRIA
effect of strontium on contraction and swelling of rat liver, 19: 43688

MITOSIS
effects on radiosensitivity of animal cells, 19: 43790
radiation effects on, in animal cells, 19: 43758
radiation effects on, in brain of rat embryos, 19: 43768
radiation effects on, in bone marrow cells in mice, tracer study, 19: 43792
radiation effects on Tribulus root, y, 19: 43855
radiation effects on rat bone marrow, integral dose effects on, 19: 43733
time intervals of epithelial and spindle cell mouse tumor, using autoradiography and tritiated thymidine, 19: 43698

MIXED SPECTRUM CRITICAL ASSEMBLY
activation measurements in, neutron Doppler, 19: 45572(R) (GEAP-4755)
power distributions in fast and thermal regions of, 19: 45572(R) (GEAP-4755)
reactivity of, effects of flooding and poisons on, 19: 45572(R) (GEAP-4755)

MIXER-SETTLERS
design of series for processing finely divided reactor fuels, 19: 44127(P)
evaluation of small modified CEN, for use in Acid Thorex and Purex processes, 19: 44117 (ORNL-TM-1256)

MOLECULAR WEIGHTS
determination in organic reactor coolants, cryoscopic method for, 19: 44045 (JEN-151-DQ/I-52)
determination in organic reactor coolants, cryoscopic method for, 19: 44046 (JEN-152-DQ/I-53)

MOLECULES
binding energy in statistical theory, 19: 44936 (TID-21692)
detection and measurement of neutral, using scintillation detectors, (E), 19: 44499
dissociation by electron-ion collisional recombination, 19: 45450
electron and ion reactions with, review of, 19: 44950
electron reactions with, classical calculation of cross sections for inelastic, (T), 19: 44947
reactions with ions, energy effects on cross sections for dissociation in, (E), 19: 44948
spectra of vibrational modes of, in crystals, (T), 19: 45492

MOLLUSKS
excretion of foreign particles by, tracer study in Bullia, 19: 43695
metabolism of radionuclides by marine, 19: 43669(R) (NP-15159)
radioisotope content in, ecological implications of, 19: 43663

MOLTEN SALT REACTOR EXPERIMENT
control of, computer for, 19: 45585 (ORNL-P-1502)
cooling system of, thermal stresses in, 19: 45587 (ORNL-P-1504)
criticality studies, 19: 45586 (ORNL-P-1503)
fuel sampling for analysis, apparatus for, 19: 44168 (ORNL-P-1532)

MOLTEN SALT REACTORS
design and economics of power-breeder, 19: 45588 (ORNL-TM-1060)

MOLYBDENUM
corrosion by lithium at 1000°C, 19: 44616(R) (ANL-7000, pp 122-37)
creep properties at 1600 to 2200°C of arc-cast, 19: 44598(R) (GEMP-49A)
deposition method for, thermochemical, 19: 44640 (ORNL-P-1446-1)
deposition on uranium dioxide particles, 19: 44596 (EURAEC-1392)
diffusion of oxygen in, at high temperatures, 19: 44979(R) (NP-15419)
effects of dietary, on iodine-131 uptake and retention by rabbit thyroid, 19: 43689
effects on fabricability of titanium–vanadium alloys, 19: 44587(R) (ANL-7000, pp 3-63)
extrusion by hydrostatic methods, 19: 44651
fatigue of, effects of air, nitrogen, and water vapor on, 19: 44730
isotopic compositions of naturally occurring, variations in, 19: 44242
neutron absorption cross sections at 24 kev, (E), 19: 45230
neutron cross sections for, from 0.414 ev to 5.5 Mev, 19: 45244 (AEEW-M-472)
neutron reactions (n,n′γ) with, cross section for, 19: 45263 (JAERI-1078)
radiation effects on hot hardness of, fast neutron, 19: 44598(R) (GEMP-49A)
reactions with beryllium, copper, stainless steel, and niobium alloys to 760°C *in vacuo*, 19: 44606 (PWAC-483)
reactions with boron nitrides at high temperatures, 19: 44220 (N64-31011)
reactions with fissium–plutonium–uranium alloys at 750°C, 19: 44587(R) (ANL-7000, pp 3-63)
reactions with hafnium and magnesium oxides at 2450°C, 19: 44598(R) (GEMP-49A)
reactions with metal oxides at high temperatures, 19: 44685 (CONF-650908-5)
reactions with uranium dioxide at high temperatures, 19: 44593 (CONF-650908-4)
spectra at, Ohlin structure near limit of continous x-ray, (E), 19: 44940

MOLYBDENUM ALLOY COUPLES
Mo–Nb/Re–W, thermoelectric potential to 1800°C, 19: 44598(R) (GEMP-49A)

MOLYBDENUM ALLOYS
Al–Mo–Ti–V, corrosion cracking of, mechanisms for stress, 19: 44621 (CONF-651006-1)
Fe–Mo, magnetization at 295°K, saturation, 19: 44678(R) (ANL-7000, pp 186-200)
Mo–Nb, microstructures, 19: 44610 (TIM-943)
Mo–Ni, crystal structure stacking faults in, effects of rolling textures on, 19: 44723
Mo–Pu–U, corrosion by air at room temperature, 19: 44587(R) (ANL-7000, pp 3-63)
Mo–Pu–U, properties of cast, 19: 44587(R) (ANL-7000, pp 3-63)
Mo–Re, purification process variables, 19: 44598(R) (GEMP-49A)
Mo–Re, reactions with beryllium, hafnium, and magnesium oxides at 2450°C, 19: 44598(R) (GEMP-49A)
Mo–Re–W, creep-rupture properties, effects of composition on, 19: 44598(R) (GEMP-49A)
Mo–Re–W, fabrication of seamless tubing of, procedures for, 19: 44598(R) (GEMP-49A)
Mo–Re–W, fission product release, 19: 44599(R) (GEMP-50A)
Mo–Ti, erosion by water of rotating disks of, 19: 44625 (TIM-894)

Mo–Ti, microstructures, 19: 44610 (TIN-943)
MOLYBDENUM CARBIDES
analysis for carbon using electron microprobe, 19: 43966
superconductivity, 19: 43997(R) (UCRL-11889)
MOLYBDENUM CHLORIDES
complexes with dimethylformamide and methyl sulfoxide, 19: 43990 (MIT-1965-15)
MOLYBDENUM COUPLES
Mo/Nb, performance to 2300°F, 19: 44348 (PWAC-473)
MOLYBDENUM ISOTOPES Mo-92
energy levels with soft core potential, (T), 19: 45311
MOLYBDENUM ISOTOPES Mo-94
abundance in naturally occurring molybdenum, 19: 44242
MOLYBDENUM ISOTOPES Mo-95
abundance in naturally occurring molybdenum, 19: 44242
MOLYBDENUM ISOTOPES Mo-96
abundance in naturally occurring molybdenum, 19: 44242
energy levels and gamma spectra of, from niobium-96 decay, (E), 19: 45341
MOLYBDENUM ISOTOPES Mo-97
abundance in naturally occurring molybdenum, 19: 44242
MOLYBDENUM ISOTOPES Mo-98
abundance in naturally occurring molybdenum, 19: 44242
MOLYBDENUM ISOTOPES Mo-100
abundance in naturally occurring molybdenum, 19: 44242
MOLYBDENUM OXIDES
reactions with liquid sodium, composition and properties of products in, 19: 44021
MOLYBDENUM STEEL
Cr–Mo, compatibility of Croloy 2¼ in sodium-heated boiler containing Type 316 stainless steel, 19: 44133(R) (BAW-1280-31)
MOLYBDENUM SULFIDES
B_2O_3–PbS–MoS_2, radiation effects on lubricant wear properties of solid films, 19: 44095
graphite–MoS_2–$NaSiO_3$, radiation effects on lubricant wear properties of solid films, 19: 44095
MOLYBDENUM SYSTEMS
Al–C–Mo, superconductivity, 19: 43997(R) (UCRL-11889)
C–Mo–Ti–Zr, mechanical properties at high temperatures, 19: 44674(R) (ANL-7000, pp 69-83)
C–Mo–V, superconductivity, 19: 43997(R) (UCRL-11889)
HfC–Mo, solidus temperature at 2350°C, 19: 44612(R) (USBM-RC-1199)
Mo–UO_2, thermal conductivity of fuel rods of, effects of molybdenum additions on, 19: 45573 (GEAP-4902)
MONAZITES
analysis for thorium by titration with sodium fluoride, 19: 43970
MONKEYS
radiation effects on learning ability of rhesus, 19: 43805
radiation effects on learning ability of rhesus, 19: 43806
radiation effects on food satiation in rhesus, 19: 43807
MONTE CARLO METHOD
for neutron slowing down in thin plates of hydrogenous materials, 19: 45216 (CEA-R-2804)
use for particle track construction in emulsions, 19: 44433 (CERN-65-4 (Vol.II), pp IX44-7)
use in proton migration calculations, 19: 45462 (NP-15163)
MONTMORILLONITES
sorptive properties for cesium, role of exchangeable magnesium and potassium in, 19: 43964
MOON
materials on, alpha-scattering analyses of, 19: 44901
solar wind effects on photometric properties, 19: 44896
MOSQUITOES
control of populations of *Culex fatigans* by release of irradiated males, 19: 43796
MÖSSBAUER EFFECT
in iodine-127 in ferromagnetic chromium iodide for, (E), 19: 45491
in thin films, temperature dependence of, 19: 44847
spectroscopy of, design of drives for, (E), 19: 45316
MOTORS
design of three-phase induction, with superconductive bearings, 19: 45196
MOUNT EVEREST
tritium glacier accumulation and high-altitude climatology in ice of, 19: 44262
MOUTH
radiation effects on carcinoma cells from, x, 19: 43802
radiotherapy of cancers of, 19: 43903
radiotherapy of tumors of, 19: 43912
MUCIC ACID
compound formation with samarium, gadolinium, and erbium, 19: 44028
MULTIPLE SCLEROSIS
gamma globulin transfer between cerebrospinal fluid and plasma in, tracer study of, 19: 43666 (BNL-9406)
MUONIUM
production in polarized meson (μ^+) reactions with targets with longitudinal magnetic field, (E/T), 19: 45079
spin precession in compounds with, (T), 19: 45278 (NP-15389)
MUSCLE RELAXANTS
radiation effects on physiological response of rabbits to, 19: 43871
MUSCLES
iodine-131 uptake by chick, age and dose effects on, 19: 43704
zinc-65 uptake and distribution in normal and tumorous, in man, 19: 43699
MUTAGENS
effects on peas, 19: 43734
genetic effects in human cells in tissue culture, 19: 43844
MUTATIONS
human load of, 19: 43642(R) (NYO-2280-8)
radioinduced, 19: 43823
radioinduced *Digitalis Lanata EHRH*, seed-exposure, 19: 43746
radioinduced in *Arachis hypogea*, review, 19: 43779
radioinduced in Drosophila oogonia, gamma, 19: 43724 (TID-22160)
radioinduced in Drosophila, effects of dose rate on, 19: 43785
radioinduced in Drosophila, 19: 43787
radioinduced in *Escherichia coli*, 19: 43751(T)
radioinduced in *Escherichia coli*, 19: 43794
radioinduced in *Escherichia coli*, 19: 43795
radioinduced in larvae of silkworms, 19: 43786
radioinduced in Lupinus, review, 19: 43776
radioinduced in maize, meson, neutron, proton, and x, 19: 43712 (BNL-9383)
radioinduced in mice, effects of dose, dose rate, and radiation quality on, 19: 43788
radioinduced in mice, effects of dose rate on, 19: 43789
radioinduced in peas, 19: 43732
radioinduced in peas, 19: 43734
radioinduced in *Poa pratensis*, agricultural significance of x, 19: 43778
radioinduced in rice, 19: 43781
radioinduced in silkworms, 19: 43784
radioinduced in silkworms, 19: 43786
radioinduced in silkworms, 19: 43787
radioinduced in sweet potatoes, review, 19: 43777
radioinduced in wheat, 19: 43781
radioinduced phage induction in *Serratia marcescens*, uv, 19: 43847
radioinduced somatic, relation to chronic diseases, 19: 43749
radioinduced somatic, carcinogenesis of, 19: 43754
radioinduced, in *Escherichia coli*, 19: 43804
radioinduced, in man, 19: 43914
radioinduced, in *Mycobacterium smegmatis*, effects of external exposure to sulfur-35, 19: 43816
radioinduced, in *Mycobacterium smegmatis* by transmutation of incorporated sulfur-35, 19: 43816
radioinduced, in silkworm larvae, 19: 43783
radiosensitivity of *Escherichia coli*, 19: 43794
rate in man, 19: 43642(R) (NYO-2280-8)
use of plant, review, 19: 43656
MYOSINS
synthesis in cultured heart cells, 19: 43681(R) (UCLA-12-565, pp 17-31)

N

NAGASAKI
population of, clinical status of radiation-exposed, 19: 44280(R) (ABCC-63-64)
NAPHTHALENE, 1,2,3,4-TETRAHYDRO-
dehydrogenation of, catalytic effects of praseodymium oxide on, 19: 44023
NATIONAL REACTOR TESTING STATION
meteorological research at, 19: 44773 (BNL-914, pp 57-64)
personnel dosimetry system at, 19: 44335
NATURAL GAS
rare gas content in, variations in, 19: 44239
NATURAL WATERS
atmospheric radiation monitoring at Ames, Jan.-June 1965, 19: 44302 (TID-22173)
NEBULAE
gamma flux from Crab, upper limit for, (E), 19: 44970
photon production in Compton-synchrotron process in Crab, high-energy, (T), 19: 44911
NECK

radiation injuries of larynx and trachea resulting from radiotherapy, surgical repair of, 19: 43897
radiotherapy of tumors of, effects on thyroid function, 19: 43890

NEODYMIUM ALLOYS
Ga–Nd, crystal structure studies, 19: 44678(R) (ANL-7000, pp 186-200)
La–Nd, phase studies of samarium-type intermediate phases in, 19: 44672 (AD-619201)
Mg–Nd, mechanical properties of, effects of alloying elements on, 19: 44709 (JPRS-24761, pp 17–28)

NEODYMIUM COMPLEXES
with glycolic acid, binding energy of, infrared spectrophotometric study of, 19: 44004

NEODYMIUM IONS
reactions with cadmium sulfide crystals at 200 kev, replacement collision doping by, (E), 19: 44939

NEODYMIUM ISOTOPES
production in thermal-neutron fission of uranium-235, (E), 19: 45260(R) (IDO-14660)

NEODYMIUM ISOTOPES Nd-143
neutron reactions with, resonances in, (E), 19: 45296

NEODYMIUM ISOTOPES Nd-145
neutron reactions with, resonances in, (E), 19: 45296

NEODYMIUM ISOTOPES Nd-148
deuteron reactions (d,p) with, deformed and spherical nuclei from, (E), 19: 45359

NEODYMIUM ISOTOPES Nd-149
production from deuteron reactions (d,p) with neodymium-148 and (d,t) with neodymium-150, deformed and spherical shapes from, (E), 19: 45359

NEODYMIUM ISOTOPES Nd-150
deuteron reactions (d,t) with, deformed and spherical nuclei from, (E), 19: 45359
oxygen-16 inelastic scattering at 43.5 Mev, vibrational-state excitation in, (E), 19: 45321

NEODYMIUM OXIDES
effects on optical properties of silicate glasses, 19: 44030
phase transformations in, at 1800 to 2400°C, 19: 44731

NEODYMIUM VANADATES
crystallographic and optical properties of hydrated, 19: 44032(T)

NEON
energy levels of excited, autoionization, 19: 44934(R) (COO-1277-13)

NEON ISOTOPES Ne-20
content in meteorite Khor Temiki, (E), 19: 44906
energy level distributions, (T), 19: 45313

NEON ISOTOPES Ne-21
content in meteorite Khor Temiki, (E), 19: 44906
energy levels of, mixing ratios, parities, and spins of, (E), 19: 45277 (NP-15363)

NEON ISOTOPES Ne-22
content in meteorite Khor Temiki, (E), 19: 44906

NEON SYSTEMS
He-3–methane–Ne, performance as filling in thermal neutron detectors, 19: 44373(R) (ANL-6877, pp 15-20)
H–Ne, performance in bubble chambers, 19: 44375 (BNL-9425)

NEPTUNIUM
electric conductivity of alpha, at 5 to 300°K, 19: 44675(R) (ANL-7000, pp 155-75)
Hall coefficient of alpha, at 5 to 420°K, 19: 44675(R) (ANL-7000, pp 155-75)

NEPTUNIUM ISOTOPES
neutron cross sections of, tabulation, (E), 19: 45250 (BNL-325(2nd Ed.) (Suppl. 2)(Vol. III))

NEPTUNIUM ISOTOPES Np-237
neutron fission rates in FRO critical assemblies, (E/T), 19: 45522 (AE-195)
neutron reactions (n,f) at 0.4 to 4.15 Mev, energy dependence of cross sections for, (E), 19: 45258 (IAE-833)

NERVES
radiation effects on, in developing insect larvae, morphological, 19: 43849

NERVOUS SYSTEM
radiation effects at ultra-high frequency energy on, climate effects on, 19: 43774

NEUROSPORA
radiation effects on, gamma, 19: 43648(R) (UCLA-12-565, pp 87-96)

NEUTRINO PAIRS
production in photon interactions, (T), 19: 45027 (NP-15199)
production in stellar evolution, (T), 19: 44927(T)

NEUTRINOS
emission from point mass, effects on gravitation of, (T), 19: 44910
emission in stellar evolution, luminosity of, (T), 19: 44927(T)

NEUTRINOS (ν_μ)
interactions with neutrons, polarization of mesons (μ^-) from, (T), 19: 45050

NEUTRINOS ($\bar{\nu}_\mu$)
interactions with protons, polarization of mesons (μ^+) from, (T), 19: 45050

NEUTRON ACTIVATION CROSS SECTIONS
calculation for structural materials, methods for, (T), 19: 45461 (N64-25922)

NEUTRON BEAMS
energy and spatial distributions in straight cylindrical channel through water, (E), 19: 45465
production of intense monoenergetic, (E/T), 19: 44882
production of narrow medium-energy, for small-angle scattering measurements, (E), 19: 44862 (IAE-867)
radiosurgical use of, 19: 43905

NEUTRON CROSS SECTIONS
library of, UKAEA, 19: 45249 (AWRE-O-55/65)
measurements of, compilation of requests for, 19: 45255 (EANDC-45(U))
tables of, for reactor fuel cycle analysis, 19: 45546 (HW-79951(Pt.3))
tabulation of 19-group, for fast reactor analysis, 19: 45244 (AEEW-M-472)
tabulation of, for elements having Z = 88 to 98, (E), 19: 45250 (BNL-325(2nd Ed.)(Suppl. 2)(Vol. III))

NEUTRON-DIFFRACTION ANALYSIS
spectrometer for, performance of three-axis, (E), 19: 44531

NEUTRON DIFFRACTOMETERS
design of time-of-flight, for studying solids under high pressures, 19: 45476 (IDO-17106)

NEUTRON FISSION CROSS SECTIONS
calculation of, computer program for, 19: 45282 (ORNL-TM-1180)

NEUTRON SOURCES
calibration using concentrated manganese sulfate baths and water, determination of capture with charged-particle emission for, (E), 19: 45232
development of pulsed high-intensity fission, 19: 45874 (GA-6168)
performance of underground nuclear explosions as, 19: 44157 (LA-DC-7304)
research programs on, at AECL, 19: 45694(R) (AECL-2251)
yield of electron-linear-accelerator uranium-target, 19: 44860 (IAE-614)

NEUTRON SPECTRA
hardening of thermal, in boric acid–water solution, 19: 45226 (KFK-294)

NEUTRON SPECTROMETERS
design and operation of semiconductor, for in-core measurements, 19: 44450(R) (IBK-120a)
efficiency of stilbene crystal fast, matrix treatment for, 19: 44492
line-shape errors from differentiation method with single-crystal scintillation, (T), 19: 44493
performance of double time-of-flight, 19: 45252 (CEA-R-2734)
performance of lithium-6 semiconductor, 19: 44457 (NP-15475)
performance of semiconductor, 19: 44478 (ZFK-PHA-12, pp 132-9)
performance of three-axis, for neutron scattering by hydrogen and vanadium, 19: 44527
performance of three-axis, for use in diffraction analyses, (E), 19: 44531
use of fast chopper for diffusion measurements in organic glass, 19: 45222 (INR-624/IX-A/R)

NEUTRONS
absorbed dose rates of reactor, calorimetric measurement of, 19: 45467
absorption cross sections at 24 kev, (E), 19: 45230
absorption in homogeneous critical assemblies, resonance, 19: 45521 (AAEC/TM-118)
activation of structural materials, (T), 19: 45461 (N64-25922)
angular distributions from meson (μ^-) capture by spin 0 nuclei, asymmetry of, (E), 19: 45274 (NEVIS-136)
capture by magnesium-24 and sulfur-33, resonances from, (E), 19: 45356
capture by nuclei, measurement techniques for radiative, 19: 45375
capture by tin-124 at 62 ev, angular distribution from radiative, (E), 19: 45379
correlations in nuclei, (T), 19: 45279 (NP-15415)
density distribution in two-zone heterogeneous graphite exponential pile, buckling, (E), 19: 45525 (AEEW-R-428)
detection and measurement of, gamma-insensitive dosimeter for, 19: 44544(P)
detection and measurement of, instrumentation for, 19: 44369 (AERE-R-4552)
detection and measurement in reactor cores, methods for, 19: 44450(R) (IBK-120a)
detection and measurement of, geometrical efficiencies of detectors for, (T), 19: 44505
detection of, Bonner single-sphere instrument for, 19: 44454 (LA-DC-7323)
diffusion in reactors, lectures on, 19: 45531 (N64-29786)
diffusion theory for, transport-equivalent, 19: 45221(R) (GEAP-4913)

distribution in large closed-cycle reactor primary shields, 19: 45601(R) (WCAP-3750)
distributions in beryllium-oxide moderated critical assemblies, (E/T), 19: 45537
dosimeter design for, 19: 44543(P)
dosimetry around pulsed sources, systems for, 19: 44370 (AERE-R-4883)
dosimetry in accidental and normal conditions, methods for, 19: 44332
effects of reactor, on radiation stability of strongly basic anion exchange resins, 19: 44055 (IAE-788)
effects on age hardening of beryllium–copper alloys, 19: 44760
effects on aluminum–copper single crystals, effects of aluminum content on strength-annealing of, 19: 44739(R) (ANL-7000, pp 233-77)
effects on argon clathrates, 19: 45679(R) (NYO-1859-11)
effects on corrosion and mechanical properties of aluminum and aluminum–magnesium alloys, 19: 44752 (CEA-tr-A-1818)
effects on dimensional changes in thorium–uranium alloys, 19: 44737(R) (ANL-7000, pp 111-18)
effects on dimensions of EGCR graphite, effects of tensile stresses on, 19: 44744 (HW-SA-3592)
effects on faults in aluminum as function of concentration, 19: 44755
effects on fueled graphite spheres, 19: 44749 (ORNL-P-1507)
effects on lactation in dairy cattle, 19: 43801
effects on lethality in dogs, dose and exposure effects on, 19: 43832
effects on maize, mutagenic, 19: 43712 (BNL-9383)
effects on mechanical properties of metals, displacement spike density model for, 19: 44599(R) (GEMP-50A)
effects on metabolism in dairy cattle, 19: 43801
effects on peas, genetic, 19: 43734
effects on pyrolytic carbon-coated uranium carbide and dioxide fuel particles, 19: 44740 (BMI-1737)
effects on pyrolytic-carbon-coated fuel particles, 19: 44748 (ORNL-P-1505)
effects on rupture properties of niobium-stabilized stainless steel under constant stress rate conditions, 19: 44750 (ORNL-TM-1216)
effects on stacking fault annihilation in gold films, 19: 44739(R) (ANL-7000, pp 233-77)
effects on strength of copper alloys, effects of aluminum and gallium on, 19: 44739(R) (ANL-7000, pp 233-77)
effects on thermal ratcheting in aluminum-clad uranio fuel elements, 19: 44737(R) (ANL-7000, pp 111-18)
effects on thermal insulation in reactors, 19: 44088
effects on transformations in uranium oxysulfide–uranium sulfide, 19: 44737(R) (ANL-7000, pp 111-18)
effects on transistors, 19: 44548 (NP-15422)
effects on trimethylsilane, 19: 45679(R) (NYO-1859-11)
emission in plutonium-239 and uranium-235 (n,f) reactions at 24 kev, secondary, (E), 19: 45297
energy and intensity spectra of solar, above 1 Mev, (T), 19: 44902
energy and intensity spectra of solar, near earth, (E/T), 19: 44903
energy and spatial distributions in straight cylindrical channel through water, (E), 19: 45465
flux calculations in three dimensions, computer program for one-group, (T), 19: 45218 (DP-938)
flux distribution in reactors, method for determining, 19: 45560 (ANL-7011)
flux in reactor fuel pin clusters, method for determining, 19: 45525 (EUR-2470.e)
fluxes in reactors, activation measurement of, 19: 45542(R) (BAW-272)
form factor determination from meson (π) electroproduction on protons, (T), 19: 45065
genetic effects in *Escherichia coli*, 19: 43751(T)
interactions with electrons, effective potential for, (E), 19: 45098
interactions with protons, design of high pressure diffusion cloud chamber for studying elastic, 19: 44494
interactions with nucleons in nuclei, (T), 19: 45279 (NP-15415)
interactions with antiprotons, broken U(12) analysis of annihilation, (T), 19: 45008 (JINR-E-2246)
interactions with protons at 23 to 630 Mev, angular dependence of phase shift analysis of, 19: 45015 (JINR-P-2241)
interactions with neutrons in s-state, reactor in space for measuring cross section of, (T), 19: 45036 (NP-15476)
interactions with neutrinos (ν_μ), polarization of mesons (μ^-) from, (T), 19: 45050
kinetics in fast plutonium-fueled reactors, computer program for calculating, 19: 45530 (JAERI-1082)
kinetics in pressure tube and pressure vessel type heavy water reactors, 19: 45626
magnetic moment of, dispersion theory for anomalous, 19: 45108
mass relative to protons, small-mass charged particles from, 19: 45119
momentum distributions in nuclei, 19: 45279 (NP-15415)
multiplication in arrays of fissile units, 19: 44977 (IDO-17095)
photoproduction cross sections and spectra on carbon-12 and oxygen-16 to 33 Mev, (E), 19: 45330
photoproduction of, apparatus for study of energy spectra and polarization in, 19: 45303
polarization of, determination by scattering on helium, (T), 19: 45217 (COO-7-0363)
production in solar flares, (T), 19: 44902
reactions (n,α) with sulfur-32, cross sections and Q values for, 19: 45679(R) (NYO-1859-11)
reactions (n,α) with boron-10, spectra from, 19: 44450(R) (IBK-120a)
reactions (n,α) with lithium-6, spectra from, 19: 44450(R) (IBK-120a)
reactions (n,α) with silicon-29 at 13.6 to 15.6 Mev, excitation function for, 19: 45290 (ZFK-PHA-12, pp 110-12)
reactions (n,f) with plutonium-239 and uranium-235 at 24 kev, secondary-neutron yield from, (E), 19: 45279
reactions (n,γ) with boron-11 at 20 kev, cross sections for, (E), 19: 45246(R) (ANL-6877,pp 5-14)
reactions (n,γ) with uranium-235 at 0.002 to 30 kev, cross sections for, (E), 19: 45292 (BNL-tr-16)
reactions (n,γ) with tungsten-187, cross section for, 19: 44599(R) (GEMP-50A)
reactions (n,γ) with yttrium-89 at 0.145 to 1.225 Mev, cross sections and isomer ratios for, (E), 19: 45376
reactions (n,n'γ) with nuclei for $60 \geq A \geq 100$, cross sections for, 19: 45263 (JAERI-1078)
reactions with aluminum and silicon isotopes, Q values for, 19: 44450(R) (IBK-120a)
reactions with copper-63, gold-197, indium-115, manganese-55, and phosphorus-31, rates for, (E/T), 19: 45522 (AE-195)
reactions with hydrogen at 0.0001 ev to 20 Mev, cross sections for, 19: 45248 (AWRE-O-23/65)
reactions with nuclei having $Z = 88$ to 98, cross sections, (E), 19: 45250 (BNL-325(2nd Ed.)(Suppl.2)(Vol.III))
reactions with nuclei to 80 kev, statistical properties of resonance parameters in, (E), 19: 45296
reactions with plutonium-239 at 20 to 120 ev, fission cross sections for, (E), 19: 44157 (LA-DC-7304)
reactions with uranium-235 at 0.002 to 30 kev, fission cross sections for, (E), 19: 45292 (BNL-tr-16)
reactions with uranium dioxides, Doppler coefficients for, 19: 45532 (ORNL-TM-1219)
scattering by alpha particles, phase shifts for, (T), 19: 45217 (COO-7-0363)
scattering by ferroelectric salts, uses for analysis of low-frequency vibrations, 19: 45241
scattering by helium-4 at 25 to 34 Mev, angular distributions and polarization in, (E), 19: 45259 (IAE-834)
scattering by hydrogen layers in alkali and alkaline earth hydroxides, spectra of inelastic, (E), 19: 45482
scattering by liquids, determination of thermal motion from, (T), 19: 44817
scattering by liquids, dynamics of, (E), 19: 45235
scattering by matter, s-wave resonances in, (E/T), 19: 45215 (CEA-R-2780)
scattering by molecular crystals, (T), 19: 45492
scattering by solid methane, diagnostic uses of, (E/T), 19: 45239
scattering by water, van Hove function for, (E), 19: 45236
scattering in crystals, single-phonon coherent, (T), 19: 45475 (IAE-750)
scattering length from meson (π^-) capture by helium-3, (T), 19: 45354
scattering of slow, asymptotic formula for law of, 19: 45231
scattering of, conference on inelastic, 19: 45234
scattering of, conference on inelastic, 19: 45243
scattering on helium, elastic, 19: 45303
shielding calculations for reactors, Monte Carlo method for, 19: 45469
slowing down in thin plates of hydrogenous material, Monte Carlo method for studying, 19: 45216 (CEA-R-2804)
structure of, general survey of, 19: 45125
tables of resonance integral functions, 19: 45214 (ANL-7024)
transmission in palladium at 1.2 to 100 ev, resonances in, (E), 19: 45233
transport equations in cylindrical and plane geometry, computer program for, 19: 45219 (EUR-2410.i)
transport equation in one-velocity and isotropic-scattering approximation, 19: 45220 (EUR-2411.i)
transport equation for slab geometry, time- and velocity-dependent, (T), 19: 45227 (NIJS-R-449)
transport in matter, use of importance sampling for, 19: 45458 (AE-190)
yields in (a,n) reactions at 2 to 5.4 Mev, 19: 45301

NEUTRONS, COLD

scattering by methane, distributions from, (E), 19: 45237
scattering by polyphenyls, 19: 45238

scattering by zirconium hydrides, distributions from inelastic, (E), 19: 45240
NEUTRONS, FAST
capture in manganese sulfate baths and water with charged-particle emission, (E), 19: 45232
detection and measurement by sulfur-32 activation, 19: 45679(R) (NYO-1859-11)
detection and measurement using fission foils, 19: 45679(R) (NYO-1859-11)
detection and measurement of, system for, 19: 44452 (K-1642)
detection methods for reactor, 19: 45684
dose rates in concrete and water from point isotropic fission sources, (T), 19: 45464 (ORNL-TM-1167)
dosimetry in man, biological method for, 19: 44322
effects in silkworm gonads, genetic, 19: 43786
effects of hot hardness of molybdenum, 19: 44598(R) (GEMP-49A)
effects on aluminum–copper alloys, effects of aluminum content on, 19: 44739(R) (ANL-7000, pp 233-77)
effects on creep-rupture properties of tungsten–25 rhenium alloy, 19: 44598(R) (GEMP-49A)
effects on creep-rupture properties of INOR-8, effects of annealing on, 19: 44599(R) (GEMP-50A)
effects on deformation of copper–tin alloys, 19: 44753
effects on displacement cascades in gold films, 19: 44739(R) (ANL-7000, pp 233-77)
effects on electric resistivity of metals at 4°K, 19: 44739(R) (ANL-7000, pp 233-77)
effects on germanium at 80°K, 19: 44754
effects on hot hardness of tungsten single crystals, 19: 44599(R) (GEMP-50A)
effects on iron and steel, research program on effects of nitrogen on, 19: 44741 (EURAEC-1383)
effects on iron and steel, research program on effects of nitrogen on, 19: 44742(R) (EURAEC-1430)
effects on mechanical properties of beryllia, 19: 44599(R) (GEMP-50A)
effects on resistivity of tungsten, 19: 44598(R) (GEMP-49A)
effects on sorptive properties of, 19: 44091
effects on stress-rupture properties of INOR-8 at 816°C, 19: 44598(R) (GEMP-49A)
effects on tensile properties of type 304 stainless steel, 19: 44743 (GEAP-3634)
effects on thermal diffusivity of beryllium oxides–0.5 magnesium oxides, 19: 44599(R) (GEMP-50A)
energy spectra of, performance of lithium-6 semiconductor spectrometer for measuring, 19: 44457 (NP-15475)
flux densities in High Flux Reactor, 19: 45681 (RCN-36)
measurements of, matrix treatment of spectrometric, 19: 44492
reactions (n,f) at 0.4 to 4.15 Mev, energy dependence of cross sections for, (E), 19: 45258 (IAE-833)
reactions (n,f) with uranium-235 and -238, delayed neutron yields from, (E), 19: 45300
reactions (n,γ) with rhenium at 20 to 1000 kev, cross sections for, (E), 19: 45298
reactions (n,2n) with nitrogen-14 at 14.1 Mev, cross sections for, (E), 19: 45325
reactions (n,2n) with beryllium-9 at 14.5 Mev, angular correlations and cross sections for, (E), 19: 45252 (CEA-R-2734)
reactions with technetium-99 at 14.1 Mev, cross sections for, (E), 19: 45325
reactions with uranium-235 in reactor fuels, measurement of fission, (T), 19: 45229 (UJV-1324/65)
use in activation analysis of meteorites for oxygen and silicon, 19: 43927 (CONF-650405-16)
NEUTRONS, FISSION
effects in mouse oöcytes, genetic, 19: 43789
effects in mouse spermatogonia, genetic, 19: 43789
effects in silkworm gonads, genetic, 19: 43786
NEUTRONS, PROMPT
spectra from californium-252 spontaneous fission, (T), 19: 45302
NEUTRONS, RESONANCE
reactions (n,f) with uranium-235 at 2 to 70 ev, cross sections for, (E), 19: 45299
NEUTRONS, THERMAL
detection in presence of intense gamma background, semiconductor detector for, 19: 44480 (ZFK-PHA-12, pp 144-6)
detection of, performance of helium-3, methane, and neon mixtures for, 19: 44373(R) (ANL-6877, pp 15-20)
detection of, performance of semiconductor detectors with uranium salts for, 19: 44479 (ZFK-PHA-12, pp 140-3)
detection using silver-activated zinc sulfide, pulse-shape discriminator for, 19: 44368 (AERE-M-833)
diffusion constants in organic glass, measurement using neutron chopper, 19: 45222 (INR-624/IX-A/R)
dose and flux measurements in criticality accidents, using multi-sphere technique, 19: 44323
dosimetry in accidental and normal conditions, methods for, 19: 44332
dosimetry in man, biological method for, 19: 44322
dosimetry of, performance of insulators for measurement of, 19: 44385 (CERN-65-4(Vol.II), II2-19)
dosimetry of, using radioluminescent phosphate glass, (E), 19: 44509
effects on magnesium oxides catalytic properties for nitrous oxides decomposition, 19: 44680(R) (ANL-7000, pp 227-32)
effects on plated cadmium–indium–silver alloys, 19: 44736 (ANL-6883)
effects on swelling of uranium, effects of pre- and postirradiation heat treatments on, 19: 44739(R) (ANL-7000, pp 233-77)
effects on tensile properties of type 304 stainless steel, 19: 44743 (GEAP-3634)
effects on uranium single crystal growth, 19: 44739(R) (ANL-7000, pp 233-77)
flux densities in High Flux Reactor, 19: 45681 (RCN-36)
fluxes in concrete and water, from point isotropic fission sources, (T), 19: 45464 (ORNL-TM-1167)
fluxes in vertical irradiation facilities of CP-5, 19: 45668 (ANL-7026)
reactions (n,γ) with tungsten, osmium and rhenium production from, 19: 44599(R) (GEMP-50A)
reactions (n,γ) with iron-54, gamma spectra from, (E), 19: 45322
reactions with uranium-235, yields of isotopes from fission, (E), 19: 45260(R) (IDO-14660)
reactions with uranium-235, K x ray emission during, (E), 19: 45294
scattering by ammonium compounds, distribution from incoherent, 19: 45242
scattering by argon, krypton, and xenon, electron-neutron interaction potential from, (E), 19: 45098
scattering by crystals at 30 to 1000 ev, cross section for, (E), 19: 45489
scattering by halogen acids, distributions from slow inelastic, (E), 19: 44038
scattering by hydrogen and vanadium, performance of three-axis spectrometer for, 19: 44527
scattering by lithium deuteride and hydride, (E), 19: 44732
scattering by ytterbium-176, isomeric states from, (E), 19: 45357
scattering cross sections in crystalline and liquid substances, (T), 19: 45228 (NP-15469)
scattering of, computer program for calculating Legendre moments from, 19: 45223 (JAERI-1084)
spectra in boric acid–water solutions, hardening of, 19: 45226 (KFK-294)
spectra in homogeneous hydrogen-moderated mixture, program for Wigner-Wilkins, 19: 45224 (JEN-133-DF/I-43)
spectra in homogeneous mixtures, computer program for, 19: 45225 (JEN-135-DF/I-44)
NEVADA TEST SITE
ecological and radiation effects, studies on animals and plants in, Jan.–June 1965, 19: 43662(R) (UCLA-12-565, pp 97-128)
meteorological program, 19: 44774 (BNL-914, pp 65-8)
NICHROME
corrosion by steam at 750°C of type V, 19: 44616(R) (ANL-7000, pp 122-37)
NICKEL
bremsstrahlung production by strontium-90–yttrium-90 beta particles in, (E), 19: 45284 (TID-22169)
deposition of substrates, 19: 44344 (K-L-1944)
deposition on uranium dioxide particles, 19: 44596 (EURAEC-1392)
determination by radiocoulometric titration using solid non-isotopic indicator, 19: 43952
diffusion in nickel at 930 to 1300°C, mechanism of self-, 19: 44708(T) (JPRS-24761, pp 1–11)
effects on corrosion by mercury titanium, 19: 44616(R) (ANL-7000, pp 122-37)
electric conductivity of thin films of, 19: 44344 (K-L-1944)
neutron cross sections for, from 0.414 ev to 5.5 Mev, 19: 45244 (AEEW-M-472)
neutron reactions (n,n′γ) with, cross section for, 19: 45263 (JAERI-1078)
radiation effects on electric resistivity at 4°K, fast neutron, 19: 44739(R) (ANL-7000, pp 233-77)
reactions with beryllium, copper, stainless steel, and niobium alloys to 760°C *in vacuo*, 19: 44606 (PWAC-483)
reactions with plutonium–thorium–uranium alloys at 650°C, 19: 44674(R) (ANL-7000, pp 69-83)
separation from uranium by ion exchange, 19: 44119
sputtering by argon ions at 30 to 170 kev, (E), 19: 44937(R) (TID-22140)
NICKEL ALLOY COUPLES
Alumel/Chromel, performance to 2200°F, 19: 44348 (PWAC-473)
NICKEL ALLOYS

extrusion by hydrostatic methods, 19: 44651
Al–Hg–Ni, corrosive effects on titanium of mercury-based, 19: 44616(R) (ANL-7000, pp 122-37)
Be–Ni, preparation by zone melting, 19: 44694(R) (NP-15432)
Cr–Ni, corrosion by steam at high temperature, 19: 45572(R) (GEAP-4755)
Cr–Ni, reactions with plutonium–thorium–uranium alloys at 650°C, 19: 44674(R) (ANL-7000, pp 69-83)
Cu–Ni–Ta, crystal structure, 19: 44718
Cu–Ni–W, mechanical properties and microstructure of, 19: 44691 (NASA-TN-D-3015)
Fe–Ni–Zr, corrosion by steam at 540°C, effects of alloy microstructure on, 19: 44616(R) (ANL-7000, pp 122-37)
Fe–Ni–Zr, corrosion by steam at 540°C, effects of pressure on, 19: 44616(R) (ANL-7000, pp 122-37)
Ge–La–Ni, crystal structure studies, 19: 44678(R) (ANL-7000, pp 186-200)
Hg–Ni–Zr, corrosive effects on titanium of mercury-based, 19: 44616(R) (ANL-7000, pp 122-37)
In–Ni–U, crystal structure studies, 19: 44678(R) (ANL-7000, pp 186-200)
Mg–Hg–Ni, corrosive effects on titanium of mercury-based, 19: 44616(R) (ANL-7000, pp 122-37)
Mo–Ni, crystal structure stacking faults in, effects of rolling textures on, 19: 44723
Ni–Nb–Ru, crystal structure studies, 19: 44678(R) (ANL-7000, pp 186-200)
Ni–Pd–U, crystal structure studies, 19: 44678(R) (ANL-7000, pp 186-200)
Ni–Pt–U, crystal structure studies, 19: 44678(R) (ANL-7000, pp 186-200)
Ni–Rh–U, crystal structure studies, 19: 44678(R) (ANL-7000, pp 186-200)
Ni–Ta, crystal structure, 19: 44718
Ni–Zr, brittleness and fracture of, effects of hydrogen on, 19: 44716
Ni–Zr, corrosion by steam at 540°C, 19: 44616(R) (ANL-7000, pp 122-37)

NICKEL COMPLEXES
with glycolic acid, binding energy of, infrared spectrophotometric study of, 19: 44004

NICKEL COUPLES
Pb–Ni, superconductivity of film, ferromagnetic effects on, (T), 19: 45197

NICKEL ISOTOPES Ni-58
alpha elastic and inelastic scattering at 22.2 Mev, angular distributions from, (E), 19: 45312
proton elastic scattering at 39 Mev, polarization in, 19: 45378

NICKEL ISOTOPES Ni-60
deuteron inelastic scattering at 15 Mev, excitation of two-phonon states by, (E), 19: 45346
proton elastic scattering at 39 Mev, polarization in, 19: 45378

NICKEL ISOTOPES Ni-65
beta decay of, gamma spectra from, (E), 19: 45320

NICKEL MOLYBDATES
preparation and structure of, 19: 43991 (N64-26433)

NICKEL OXIDES
diffusion into magnesium oxide single crystals, 19: 43997(R) (UCRL-11889)
stability of galvanic cell studies of, 19: 43997(R) (UCRL-11889)
NiO–Nb_2O_5, phase diagram, 19: 44711

NICKEL STEEL
Cr–Ni, hardness of heat-affected zones of welded joints in Super Elso, 19: 44686(R) (EURAEC-1362)

NIOBIUM
bremsstrahlung production by strontium-90–yttrium-90 beta particles in, (E), 19: 45284 (TID-22169)
creep in, cyclic stress induced, 19: 44700(R) (TID-22117)
crystallization and recovery of cold worked, 19: 44698 (PWAC-465)
determination in minerals and silicate rocks, radiometric-spectrophotometric, 19: 43943
determination in steel by neutron activation, 19: 43942
effects on fabricability of titanium–vanadium alloys, 19: 44587(R) (ANL-7000, pp 3-63)
extrusion by hydrostatic methods, 19: 44651
magnetic flux jumps in superconducting, speed of, (E/T), 19: 45199
magnetic moments of superconducting spheres of, residual, (E), 19: 45195
magnetization curve of type II superconducting, (E), 19: 45200
microstructures, 19: 44610 (TIM-943)
neutron absorption cross sections at 24 kev, (E), 19: 45230
neutron reactions in, yields of helium and hydrogen produced by fast, 19: 44746 (NAA-SR-Memo-10626)
reactions with aluminum oxides at high temperatures, 19: 44979(R) (NP-15419)
reactions with fissium–plutonium–uranium alloys at 750°C, 19: 44587(R) (ANL-7000, pp 3-63)
reactions with metal oxides at high temperatures, 19: 44685 (CONF-650908-5)
separation from hafnium and tantalum separation from niobium and by paper chromatography, 19: 44124
solvent extraction by Alamine 336–dibutyl cellosolve in contactor, 19: 44108 (AERE-R-4440(Pt.3))
spectra at, Ohlin structure near limit of continuous x-ray, (E), 19: 44940
thermal capacity of normal and superconducting, 19: 43997(R) (UCRL-11889)

NIOBIUM ALLOY COUPLES
Mo–Nb/Re–W, thermoelectric potential to 1800°C, 19: 44598(R) (GEMP-49A)

NIOBIUM ALLOYS
Al–Cu–Nb, crystal structure, 19: 44718
Al–Nb–Sn, phase study of Cr_3O structures in, 19: 44702 (TID-22200)
Fe–Nb, isomer shift of iron-57 in $NbFe_2$ at 300 and 800°K, 19: 44678(R) (ANL-7000, pp 186-200)
Hf–Nb–W, erosion by water of rotating disks of, 19: 44625 (TIM-894)
Mo–Nb, microstructures, 19: 44610 (TIM-943)
Nb–Rh–Zr, superconducting transition temperature, 19: 44678(R) (ANL-7000, pp 186-200)
Nb–Sn, preparation and sintering of Nb_3Sn, 19: 44592 (CLM-R-43)
Nb–Sn, properties of sintered Nb_3Sn, as superconducting magnetic coil, 19: 44592 (CLM-R-43)
Nb–Sn, superconductivity critical currents in intermetallic compound Nb_3Sn, 19: 45213
Nb–Ti, reactions with metals at 540 to 760°C *in vacuo*, 19: 44606 (PWAC-483)
Nb–Ti–V, microstructure of, effects of annealing temperature on, 19: 44587(R) (ANL-7000, pp 3-63)
Nb–Ti–Zr, microstructure of, effects of annealing temperature on, 19: 44587(R) (ANL-7000, pp 3-63)
Nb–Zr, brazing to beryllium using silver, 19: 44606 (PWAC-483)
Nb–Zr, brazing to beryllium with silver alloys, effects of carbon and silicon coatings on, 19: 44606 (PWAC-483)
Nb–Zr, brittleness and fracture of, effects of hydrogen on, 19: 44716
Nb–Zr, carburization of, for prevention of galling, 19: 44609 (TIM-927)
Nb–Zr, corrosion by lithium, effects of heat treatment and oxygen on, 19: 44620 (CNLM-6344)
Nb–Zr, corrosion by potassium–sodium at 1250°F, effects of carbon, nitrogen and oxygen on, 19: 44626 (TIM-896)
Nb–Zr, corrosion resistance of, effects of production method and aging on, 19: 44629
Nb–Zr, crystallization and recovery of cold worked, 19: 44698 (PWAC-465)
Nb–Zr, erosion by water of rotating disks of, 19: 44625 (TIM-894)
Nb–Zr, mechanical properties at high temperatures, 19: 44674(R) (ANL-7000, pp 69-83)
Nb–Zr, mechanical properties of, effects of carbon and oxygen on, 19: 44605 (PWAC-464)
Nb–Zr, mechanical properties of effects of aging, oxygen content, and production method on, 19: 44629
Nb–Zr, microstructures, 19: 44610 (TIM-943)
Nb–Zr, microstructure of, effects of annealing temperature on, 19: 44587(R) (ANL-7000, pp 3-63)
Nb–Zr, reactions with metals at 540 to 760°C *in vacuo*, 19: 44606 (PWAC-483)
Nb–Zr, reactions with fissium–plutonium–uranium alloys at 750°C, 19: 44587(R) (ANL-7000, pp 3-63)
Ni–Nb–Ru, crystal structure studies, 19: 44678(R) (ANL-7000, pp 186-200)

NIOBIUM CARBIDES
analysis for carbon using electron microprobe, 19: 43966
formation by carburization of niobium–zirconium alloy, 19: 44609 (TIM-927)
superconductivity, 19: 43997(R) (UCRL-11889)
NbC–TaC, superconductivity, 19: 43997(R) (UCRL-11889)

NIOBIUM COUPLES
Mo/Nb, performance to 2300°F, 19: 44348 (PWAC-473)

NIOBIUM ISOTOPES Nb-95
content in marine environment, 19: 43663
determination in lung tissues, spectrometric, 19: 44292(R) (NP-15173)
distribution in fetal and maternal rabbit tissues, 19: 43883(R) (UCLA-12-565, pp 65-85)
separation from zirconium-95, chromatographic, 19: 44118 (UCRL-16015)

NIOBIUM ISOTOPES Nb-96
beta decay of, gamma spectra from, (E), 19: 45341

NIOBIUM MINERALS

occurrence and properties of niobium–uranium metamict mineral in Powhatan County, 19: 44279
NIOBIUM OXIDES
effects on sintering of uranio, 19: 43985(R) (ANL-7000, pp 85-110)
stability of galvanic cell studies of, 19: 43997(R) (UCRL-11889)
CoO–Nb_2O_5, phase diagram, 19: 44711
NiO–Nb_2O_5, phase diagram, 19: 44711
NIOBIUM SYSTEMS
Al_2O_3–Nb, seals of, development of high-temperature metal-to-ceramic, 19: 44598(R) (GEMP-49A)
C–Nb–Zr, development of, with high-temperature strength, 19: 44605 (PWAC-464)
HfC–Nb, solidus temperature at 2310°C, 19: 44612(R) (USBM-RC-1199)
Nb–Rh–Si, phase study of Cr_3O-type structures in, 19: 44702 (TID-22200)
NITRIC ACID
reactions with anion exchange resin and dichromate in contactor, analysis of uncontrolled, 19: 44110 (BNWL-114)
solvent properties for thorium and rare earths, 19: 44125
use in uranium dissolution, 19: 44128(P)
use of vapors of, in reprocessing of carbon-containing fuel elements, 19: 44109 (BLG-331)
HF–HNO_3, corrosive effects on yttrium, 19: 44628
NITRIDES
spectra of, effects of chemical combination on soft x-ray K emission bands of nitrogen in, (E), 19: 44944
NITRITE IONS
effects on radiolysis of acetylene, 19: 44082
NITROGEN
content in natural gases, 19: 44239
current sheet microstructure in theta-pinch plasma of, (E/T), 19: 45445
determination in blood, of dogs, 19: 43674 (UCD-472-112, pp 36-43)
effects on fast neutron-irradiated iron and steel, research program on, 19: 44741 (EURAEC-1383)
effects on fast-neutron effects on iron and steel, research program on, 19: 44742(R) (EURAEC-1430)
effects on fatigue of molybdenum, 19: 44730
electron reactions with, classical calculation of cross sections for inelastic, (T), 19: 44947
radiation effects on metabolism of total α-amino-, in man, 19: 43852
radiation from arcs of, analysis of, 19: 44804 (ARL-65-105)
reactions of atoms of, with sulfur compounds, 19: 43997(R) (UCRL-11889)
reactions with niobium–zirconium alloy in potassium–sodium environment at 1250°F, 19: 44626 (TIM-896)
spectra of sulfur molecules in solid, u-v absorption, (E), 19: 45480 (UCRL-10771)
spectra of, effects of chemical combination on soft x-ray K emission bands of, (E), 19: 44944
NITROGEN IONS
content and reactions in ionosphere, (T), 19: 45173
electron reactions with, classical calculation of cross sections for inelastic, (T), 19: 44947
NITROGEN ISOTOPES
properties for tracer use in biology, 19: 43707
NITROGEN ISOTOPES N-13
production in tunnel of Frascati electron linear accelerator, (T), 19: 44866 (LNF-65/21)
NITROGEN ISOTOPES N-14
neutron reactions (n,2n) at 14.1 Mev, cross sections for, (E), 19: 45325
nuclear quadrupole coupling constants in deuterated and normal crystalline ammonia, (E), 19: 45483
reactions (N-14,3α) with indium-115 at 52 Mev, barium-126 energy levels from, (E), 19: 45285 (UCRL-16040)
reactions (N-14,5α) with indium-115 at 84 Mev, barium-124 energy levels from, (E), 19: 45285 (UCRL-16040)
NITROGEN ISOTOPES N-15
use as internal standard in determination of argon-40 in minerals, 19: 43960
NITROGEN ISOTOPES N-16
effects on reactor primary cooling system shielding design, 19: 45601(R) (WCAP-3750)
NITROGEN OXIDES
content and reactions in ionosphere, (T), 19: 45173
decomposition of nitrous, catalytic properties of chromium and magnesium oxides for, 19: 44680(R) (ANL-7000, pp 227-32)
electron reactions with, classical calculation of cross sections for inelastic, (T), 19: 44947
production in tunnel of Frascati electron linear accelerator, (T), 19: 44866 (LNF-65/21)
use for processing uranium and vanadium ores, 19: 44129(P)
NITROGEN SYSTEMS
N–O, chemical reactions during high temperature rapid quenching of, 19: 44041
NITROXIDE
di-*t*-butyl-, radiosensitivity effects on *E. coli* B/r, 19: 43875
t-butyl-2,6-dimethoxyphenyl-, radiosensitivity effects on *E. coli* B/r, 19: 43875
tetramethylpentamethylene-, radiosensitivity effects on *E. coli* B/r, 19: 43875
NOISE
reduction in nuclear magnetic resonance spectra, methods for, 19: 43997(R) (UCRL-11889)
NOZZLES
design for electrothermal thrustor using wire-coil heat exchanger, 19: 44220 (N64-31011)
materials in male connectors for fuel reprocessing, evaluation of ACI CD_4M Cu stainless steel as, 19: 44607 (RL-SEP-508)
stress patterns of radial attachements of, to hemispherical shells, 19: 44144 (TID-22134)
NPD REACTOR
description of, 19: 45694(R) (AECL-2251)
systems in, chemical engineering role in, 19: 44155
NRX REACTOR
description of, 19: 45694(R) (AECL-2251)
NUCLEAR BATTERIES
containers for, impact testing of, 19: 44298(R) (SC-RR-65-9)
use in fail safe timing circuits, 19: 44364(P)
NUCLEAR EMULSIONS
aging by controlled temperatures, effects of, 19: 44402 (CERN-65-4 (Vol.II), pp IV5-15)
alpha-particle track registration and discrimination in, 19: 44425 (CERN-65-4(Vol.II), pp VIII17-26)
charged particle ionization density in carbon-, hydrogen-, and oxygen-enriched, 19: 44435 (CERN-65-4(Vol.II), pp IX62-5)
charged-particle reactions with silver bromide in, latent image formation in, 19: 44387 (CERN-65-4(Vol.II), pp III-10)
coagulation of fine-grain, by synthetic polymers, 19: 44400 (CERN-65-4(Vol.II), pp III31-56)
contraction factor of, method for measuring, 19: 44444 (CERN-65-4 (Vol.II), pp X67-73)
developers for fine-grain, evaluation of, 19: 44404 (CERN-65-4(Vol.II) pp IV23-31)
development, 19: 44379 (CERN-65-4(Vol.I), pp 29-41)
electron and meson (π^0) ionization losses in, 19: 44428 (CERN-65-4 (Vol.II), pp IX9-13)
electron and positron ionization losses in, momentum dependence of, 19: 44432 (CERN-65-4(Vol.II), pp IX41-3)
image formation in, latensification of, 19: 44391 (CERN-65-4(Vol.II), pp II29-42)
ion track widths in, measurement of, 19: 44434 (CERN-65-4(Vol.II), pp IX48-61)
meson (K⁻) capture in, short-range hyperfragment production in, (E/T), 19: 54342
meson (μ^+) depolarization quenching in, as function of longitudinal magnetic field, (E/T), 19: 45079
meson (μ^+) depolarization in targets of, (E), 19: 45080
meson (π^-) reactions in, meson (π^0) intensity from, 19: 44439 (CERN-65-4(Vol.II), pp X37-43)
meson (π^-) spurious scattering at 17 Bev/c, 19: 44416 (CERN-65-4 (Vol.II), pp VI53-62)
particle Coulomb scattering measurements in, effects of spurious scattering and track distortions on, 19: 44414 (CERN-65-4(Vol.II), pp VI31-6)
particle ionization losses in, 19: 44430 (CERN-65-4(Vol.II), pp IX23-31)
particle momentum determination in, method for, 19: 44427 (CERN-65-4 (Vol.II), pp VIII34-7)
particle momentum determination in, method for slow, 19: 44424 (CERN-65-4(Vol.II), pp VIII9-16)
particle scattering measurements in, Coulomb and spurious effects on, 19: 44413 (CERN-65-4(Vol.II), pp VI23-30)
particle scattering measurements in, device for multiple, 19: 44418 (CERN-65-4(Vol.II), pp VIII5-19)
particle scattering constant determination in, method for, 19: 44429 (CERN-65-4(Vol.II), pp IX14-22)
particle scattering constant of cell length dependence of, 19: 44431 (CERN-65-4(Vol.II), pp IX22-40)
particle track analysis in, automatic device for, 19: 44421 (CERN-65-4 (Vol.II), pp VII35-7)
particle track artificial construction in, by Monte Carlo method, 19: 44433 (CERN-65-4(Vol.II), pp IX44-7)
particle track curvatures in, device for measuring, 19: 44418 (CERN-

65-4(Vol.II), pp VIII5-19)
particle track distortion in, successive differences for analyzing, 19: 44411 (CERN-65-4(Vol.II), pp VII-8)
particle track location in, using spark chambers, 19: 44445 (CERN-65-4 (Vol.II), pp X74-83)
particle track measurements in, semiautomatic apparatus for, 19: 44417 (CERN-65-4(Vol.II), pp VIII-14)
particle track measurements in, apparatus development for, 19: 44422 (CERN-65-4(Vol.II), pp VII39-42)
particle track resolution in, electron microscopy for, 19: 44423 (CERN-65-4(Vol.II), pp VIII8)
particle tracks in, semiautomatic device for analyzing, 19: 44419 (CERN-65-4(Vol.II), pp VII20-7)
particle tracks in, computer for angle and range measurements of, 19: 44420 (CERN-65-4(Vol.II), pp VII28-34)
particle tracks in, use of electron microscopes for observing, 19: 44426 (CERN-65-4(Vol.II), pp VIII27-33)
performance for cosmic particle studies in space, 19: 44436 (CERN-65-4(Vol.II), pp X13-18)
performance for detecting geomagnetically trapped protons, 19: 44437 (CERN-65-4(Vol.II), pp X19-32)
performance for gamma, hyperon (Λ), meson (K), and proton detection, 19: 44443 (CERN-65-4(Vol.II), pp X61-6)
performance for low-energy recoil scattering experiments, 19: 44438 (CERN-65-4(Vol.II), pp X33-6)
performance for measuring beta distributions from fission fragments, 19: 44441 (CERN-65-4(Vol.II), pp X47-53)
performance for study of proton reactions with hydrogen jets, 19: 44443 (CERN-65-4(Vol.II), pp X61-6)
performance of Agfa, Gevaert, and Ilford L4 for alpha and beta particles, 19: 44389 (CERN-65-4(Vol.II), pp III7-18)
performance under proton dynamic polarization conditions, 19: 44442 (CERN-65-4(Vol.II), pp X57-60)
preparation for underground cosmic radiation studies, 19: 44397 (CERN-65-4(Vol.II), pp III5-11)
preparation of bismuth, diamond, and lithium loaded, 19: 44399 (CERN-65-4(Vol.II), pp III17-20)
preparation of carbon loaded, for meson (K) stopping, 19: 44398 (CERN-65-4(Vol.II), pp III12-16)
preparation of 94% silver bromide concentration, 19: 44396 (CERN-65-4(Vol.II), pp III1-4)
preparation with self-contained developing agent, 19: 44408 (CERN-65-4(Vol.II), pp V9-16)
processing of, automatic equipment for isothermal, 19: 44409 (CERN-65-4(Vol.II), pp V17-21)
processing of, developers for, 19: 44407 (CERN-65-4(Vol.II), pp V1-9)
processing of, electrodialyser for, 19: 44410 (CERN-65-4(Vol.II), pp V22-32)
properties of fine-grain polyvinylacetals, 19: 44400 (CERN-65-4 (Vol.II), pp III21-56)
properties of fine-grain PR-2, 19: 44404 (CERN-65-4(Vol.II), IV23-31)
properties of gold and silver halide, latent image formation and threshold oxidation in, 19: 44393 (CERN-65-4(Vol.II), pp II50-63)
properties of ion-sensitive, for mass spectrography, 19: 43979
properties of NIKFI and ORWO, 19: 44403 (CERN-65-4(Vol.II), pp IV16-22)
properties of, review of, 19: 44380 (CERN-65-4(Vol.I), pp 45-63)
proton interactions at 30.5 Bev in, anisotropy in multiple meson emission in, 19: 45054
proton recoil tracks in, sampling bias in scanning, 19: 44464 (UCRL-11703)
proton spurious scattering and track distorion in, 19: 44412 (CERN-65-4(Vol.II), pp VII1-21)
proton spurious scattering in, 19: 44415 (CERN-65-4(Vol.II), pp VI37-52)
radiation effects on dispersion of latent images in, alpha particle, electrons, and light, 19: 44388 (CERN-65-4(Vol.II), pp III1-16)
sensitivity at liquid hydrogen and nitrogen temperatures, 19: 44401 (CERN-65-1(Vol.II), pp IV1-4)
sensitivity centers and latent image distributions in, 19: 44392 (CERN-65-4(Vol.II), pp II44-9)
sensitivity of Ilford K5, at low temperatures, 19: 44405 (CERN-65-4 (Vol.II), pp IV33-40)
sensitivity of, materials study for hyper-, 19: 44406 (CERN-65-4 (Vol.II), pp IV41-5)
sensitivity of, method for increasing, 19: 44390 (CERN-65-4(Vol.II), pp II19-28)
sensitivity of, performance of gold and triethanolamine for improvement of, 19: 44395 (CERN-65-4(Vol.II), pp II75-87)
sensitivity of, processes for increasing, 19: 44394 (CERN-65-4(Vol.II), pp II65-74)
use in detection and measurement of elementary particles, 19: 44381 (CERN-65-4(Vol.I), pp 79-87)
use in elementary particle studies at CERN, 19: 44382 (CERN-65-4 (Vol.I), pp 105-10)
use in measurement of neutron spectra, 19: 44448 (HASL-162)

NUCLEAR HEATING PLANTS
developments in, 1965, 19: 44307

NUCLEAR MAGNETIC RESONANCE
analysis of spectra, decomposition of peaks in, 19: 43997(R) (UCRL-11889)
coupling constants in, perturbation theory for extreme, (T), 19: 44945
noise reduction in spectra, 19: 43997(R) (UCRL-11889)
signals at $2\omega_2-\omega_1$ in double, (T), 19: 45307
use for inhomogeneous field measurements, 19: 44353(T) (SLAC-Trans-22)
uses of, in flowing liquids, 19: 44813(T) (NP-tr-1307)

NUCLEAR MATERIALS MANAGEMENT
burnup measurement in fuels, development of techniques for, 19: 45542(R) (BAW-272)
criticality calculations for regular arrays, 19: 44977 (IDO-17095)
procedures at Chinon power plant, 19: 45607

NUCLEAR MODELS
energy-level spectra for deformed, Hartree-Fock approximation for rotational, 19: 45364
statistical, for multiple-production interactions, (T), 19: 45041 (TPJU-12/65)

NUCLEAR MODELS (SHELL)
calculations in, computer program for, 19: 45254 (CST-1213)
nucleon orbital fractional parentage coefficients in 2s-1d shell, SU(3), 19: 45266 (JINR-E-2285)

NUCLEAR PHYSICS
calculations in, computer programs for, 19: 45251 (BNL-9108)
instrumentation for, bibliography, 19: 44366 (AED-C-06-12)
measuring techniques in, bibliography, 19: 44366 (AED-C-06-12)
research in, status of, 19: 45372
research on, bibliography for, (E/T), 19: 44812(R) (UCRL-16099)
research on, in Rumania, 19: 45705 (NP-15193)

NUCLEAR POWER
development and uses of, in Italy, 19: 45724
development in Europe, industrial, 19: 45723
developments in, 1965, 19: 44307
production and uses of, forecast of future, 19: 45725

NUCLEAR POWER PLANTS
criticality accidents in, alarm system for detecting, 19: 44321
design for water desalination, 19: 45635
design of German 300-Mw pressurized-water, 19: 45609
design of thermoelectric, for underwater applications, 19: 45627
design of 15 Mw(e), for Austria, 19: 45581(NP-15291)
development in Europe, review of conditions for, 19: 45610
development in France, 19: 45580 (NP-15283)
development in Italy, prospects for, 19: 45622
development in U.S.A., outline, 19: 45615
development of Canadian, 19: 45694(R) (AECL-2251)
superheaters for, design using auxiliary liquid, 19: 45630(P)
use in sea water desalination, economic aspects of, 19: 45606

NUCLEAR REACTIONS
analysis of direct, methods of analyticity and unitarity for, 19: 45340
cross sections for, AEC program on, 19: 45288 (WASH-1056)
energy-level excitation in compound-nucleus, data analysis for widths in, (T), 19: 45343
neutron-capture gamma radiation from, measurement techniques for, 19: 45375
polarization in, experimental developments on, 19: 45337

NUCLEAR SPECTRA
analysis of, Racah algebra for, 19: 45315
measurement using nuclear emulsions, 19: 44448 (HASL-162)

NUCLEAR STRUCTURE
analysis using meson (π) reactions with nuclei, 19: 45339
energy levels in, many-particle Green function theory for composition of giant-dipole, 19: 45334

NUCLEAR SUBMARINES
propulsion of, radioisotope and reactor, 19: 45662

NUCLEI
alpha elastic and inelastic scattering at 22.2 Mev by intermediate, angular distributions from, (E), 19: 45312
beta and gamma transitions in, exchange electric moments for, (T), 19: 45363
decay of analyticity and unitarity for analysis of two-body, 19: 45340
decay of loosely bound, Coulomb effects on vertex parts in, (T), 19: 45146
decay of, optimization of counters for measuring, (E/T), 19: 44503
energy level interaction effects on shape of giant dipole line in spherical,

dipole-quadrupole, (T), 19: 45314
energy level mixing in external fields, interference phenomena in, 19: 45270 (JINR-P-2248)
energy levels at high excitation energy, data analysis for widths of compound-nucleus, (T), 19: 45343
energy levels of heavy, rotational, (T), 19: 45285 (UCRL-16040)
energy levels of weakly deformed, in first-order perturbation theory, 19: 45257 (IAE-811)
energy levels of, many-particle Green function theory for composition of giant-dipole, 19: 45334
energy-level spectra of deformed, Hartree-Fock approximation for rotational, (T), 19: 45364
fission of, spontaneous, 19: 45271 (JINR-P-2265)
gamma emission by polarized, correlation of cascade, (T), 19: 45280 (NP-15457)
gamma transitions of, determination of internal conversion coefficients of, (E), 19: 44501
internal conversion coefficients of E2 transitions in, (T), 19: 45369
lithium reactions (Li-6,α), (Li-6,d), (Li-7,α), and (Li-7,t) with, mechanisms for, (T), 19: 45264 (JINR-E-2243)
meson (μ) reactions above 300 Mev with, evidence for, (E), 19: 45368
meson (π) reactions below 200 Mev with, nuclear structure from, 19: 45339
neutrino scattering by Coulomb field of, lepton pair production in, (T), 19: 45027 (NP-15199)
neutron reactions to 80 kev, resonance parameters in, (E), 19: 45296
nucleon interactions in, SU(3) model for s-state, (T), 19: 45247(R) (ANL-6877,pp 29-31)
nucleon momentum distribution in, (T), 19: 45279 (NP-15415)
nucleon wave functions for, structural effects of principal quantum number on, (T), 19: 45365
particle reactions with, statistical model for multiple production in, (T), 19: 45041 (TPJU-12/65)
production of compound transuranic, in heavy ion reactions with heavy nuclei, (T), 19: 45286 (UJV-1293/65)
proton reactions at 10 and 20 Bev/c, in steel, (T), 19: 45317
spectra of, signals at $2\omega_0-\omega_1$ in double NMR, (T), 19: 45307

NUCLEI (CELLS)
radiation effects on morphology of erythrocyte, in salamanders, 19: 43730
radiation effects on droplet nuclei in staphylococcus , uv, 19: 43736

NUCLEIC ACIDS
precursors of, protective effects against radiation injuries in mice, 19: 43866
radiation effects on fish gonad, α, 19: 43769

NUCLEON SHOWERS
production of meson–nucleon, by 10- and 20-Bev/c protons in steel, (T), 19: 45317

NUCLEONS
interactions in nuclei, SU(3) model for s-state, (T), 19: 45247(R) (ANL-6877,pp 29-31)
interactions of, spin-dependent amplitudes for, (E/T), 19: 45032 (NP-15452)
interactions with nucleons at high energies, resonance production in, (T), 19: 45037 (TID-21316)
interactions with nucleons at high energies, polarization and Regge poles in, (T), 19: 45044 (UCRL-16186)
interactions with meson (K) and mesons (π) at high energies, polarization and Regge poles in, (T), 19: 45044 (UCRL-16186)
interactions with antinucleons at high energies, polarization and Regge poles in, (T), 19: 45044 (UCRL-16186)
interactions with nucleons, relativistic particle-wave dispersion relations for elastic, 19: 45084
interactions with mesons (K) and (π) at high energy, absorption model for charge-exchange, (T), 19: 45087
interactions with mesons (π) at high energy, multiple production in elastic, (T), 19: 45091
interactions with mesons (π) below 1 Bev, phase shift analysis of, (T), 19: 45100
interactions with protons, amplitudes and deuteron polarization from, (T), 19: 45017 (JINR-P-2267)
interactions with mesons, form factors from off-shell effects in, (T), 19: 45067
interactions with mesons (π), one-trajectory exchange for amplitudes of, (T), 19: 45074
model of, deuteron magnetic moment from, (T), 19: 45049
orbital fractional parentage coefficients in 2s-1d shell, SU(3), 19: 45266 (JINR-E-2285)
production by elementary particle processes in special relativity, 19: 44895
scattering by nuclear Coulomb field, lepton pair production in, (T), 19: 45027 (NP-15199)
wave functions for orbital, structural effects of principal quantum number on, (T), 19: 45365

NUCLEOSIDES
radiation effects on composition of, in messenger RNA in *Pseudomonas effusa*, 19: 43744

NUCLEOTIDES
hydrolysis of, catalytic effects of thorium and zirconium ions on, 19: 43708
nicotinamide adenine di-, radiation effects on formation of N^1-oxide by decomposition of, 19: 44062
nicotinamide-adenine-N^1-oxide-di, preparation by radioinduced decomposition of nicotinamide adenine dinucleotide, 19: 44062
radiation effects on, 19: 43682(R) (UCLA-12-565, pp 33-57)

O

OAK RIDGE
meteorological program, 19: 44765 (BNL-914, pp 18-19)

OAK RIDGE NATIONAL LAB., TENN.
fuel rod fabrication in Kilorod Facility at, efficiency in, 19: 44639 (ORNL-3740)
radiation alarm system in High Radiation Level Examination Laboratory building, 19: 44297 (ORNL-TM-1251)

OBRIGHEIM POWER REACTOR (*Germany*)
design, 19: 45609

OCEANOGRAPHY
circulation in oceans, geostrophic eddies, 19: 45699 (CU-2663-21)
dye diffusion experiments in Sandy Hook Bay, New Jersey, 19: 45698 (CU-2663-18)

1-OCTENE
radioinduced addition of triethylamine and 1-methylpiperidine to, gamma, 19: 44053 (AFML-TR-65-166)
reactions with tetra- and penta-methyldisilane, addition, 19: 44048 (TID-21309)

OHIO RIVER
radioactivity of, Jan.-June 1965, 19: 44301 (TID-22172)

OLEIC ACID
neutron scattering by liquid, dynamics of, (E), 19: 45235

ONIONS
radiation effects on, protective effects of chemicals against seed, 19: 43877

ONTARIO
strontium-87 to strontium-86 ratio in carbonatites in, 19: 44257

OOCYTES
radiation effects in mouse, genetic, 19: 43788
radiation effects in mice, genetic, 19: 43789

OPTICAL SYSTEMS
development for plasma diagnostics, 19: 44357

ORES
analysis by fluorescence methods using radioisotopes as source of x radiation, 19: 43971
analysis for calcium and strontium by flame photometry using plasma jets, 19: 43924 (AERE-R-4990)

ORGANIC ACIDS
autoradiographic localization of tritium-labeled, in rat tissues, 19: 43696
radiation effects on metabolism of pyrrole-2-carboxylic acid in man, 19: 43852

ORGANIC COMPOUNDS
analysis for oxygen, activation, 19: 43928 (EUR-2290.f)
effects on radioinduced oxidation and reduction of iron ions in solutions, 19: 44056 (INR-579/XVII/C)
electric conductivity of liquid, design of high dose rate-meter based on, 19: 44525
preparation, purification, and storage of labeled, review on, 19: 44103
properties for use as corrosion-inhibiting coatings for uranium, 19: 44630
radioinduced oxidation by molecular oxygen, mechanism of, 19: 44075

ORGANIC COOLED REACTORS
cooling systems of, use of tightness joint in, 19: 44176(P)
design for power generation and process heat production, 19: 45618
economic aspects of, for power production and sea water desalination, 19: 45620
fast fission factors in natural-uranium-fueled, (T), 19: 45229 (UJV-1324/65)

ORGANISMS
synthesis of desoxyribonucleic acid in *Stentor coeruleus*, 19: 43682(R) (UCLA-12-565, pp 33-57)
synthesis of ribonucleic acid in *Stentor coeruleus*, 19: 43682(R) (UCLA-12-565, pp 33-57)

ORGANS
radiation dose to, formulas and methods for calculating, 19: 43853

visualization by photoscanning, methods for, 19: 43883(R) (UCLA-12-565, pp 65-85)
ORIFICES
two-phase flow of saturated water through, (E), 19: 44196(R) (TID-22145)
ORNL HIGH FLUX ISOTOPE REACTOR
control systems for, design of, 19: 45645 (ORNL-TM-1259)
fuel element production for, powder loading assembly for, 19: 44641 (ORNL-TM-1193)
testing of, preoperational hydraulic and vibrational, 19: 45644 (ORNL-P-1501)
OSCILLOGRAPHS
design of high-resolution, engineering drawings for, 19: 44360
OSMIUM
effects on determination of copper in high-purity metals by activation methods, 19: 43973
hyperfine fields in iron, 19: 43997(R) (UCRL-11889)
production in thermal neutron reactions with tungsten, 19: 44599(R) (GEMP-50A)
OSMIUM ALLOYS
Hf–Os–Ta, crystal structure studies, 19: 44678(R) (ANL-7000, pp 186-200)
Os–U, crystal structure studies, 19: 44678(R) (ANL-7000, pp 186-200)
OXALATES
effects on photometric determination of zirconium, 19: 43972
OXALIC ACID
uses in paper chromatographic separation of hafnium, niobium, and tantalum, 19: 44124
OXAZOLE, 2,5-DIPHENYL–
dioxane-2,5-diphenyloxazole, quenching effects of radioprotective compounds on irradiated, 19: 43878
OXYGEN
alpha reactions (α,n) at 2 to 5.4 Mev, neutron yields in, 19: 45301
detection and separation from sodium loops, in-line devices for, 19: 44162(R) (APDA-174, pp 33-55)
determination in combustion systems, review of equipment for, 19: 43980
determination in metals and organic compounds, activation, 19: 43928 (EUR-2290.f)
determination in meteorites, fast-neutron activation, 19: 43927 (CONF-650405-16)
determination in steels by isotope dilution methods, 19: 43946
determination in stainless steel by activation, isotope dilution, and vacuum fusion methods, 19: 43947
determination of traces of, in sodium metal, 19: 43932 (LA-3343)
determination of traces of, equipment for preparation and transfer of samples for, 19: 43933 (LA-3344)
diffusion in molybdenum at high temperatures, 19: 44979(R) (NP-15419)
diffusion in zirconium, anodic film dissolution and hardness studies, 19: 44673 (AECL-2268)
effects on hardness of titanium–vanadium alloys, 19: 44587(R) (ANL-7000, pp 3-63)
effects on lattice spacing of thorium, 19: 44674(R) (ANL-7000, pp 69-73)
effects on mechanical properties of zirconium, 19: 44676(R) (ANL-7000, pp 176-82)
effects on mechanical properties of niobium–zirconium alloys, 19: 44605 (PWAC-464)
effects on oxygen tension and sulfhydryl content in mouse spleen, 19: 43869
effects on reaction of recoil tritium with ethane, 19: 44106
effects on thorium phosphides, 19: 43985(R) (ANL-7000, pp 85-110)
effects on urania compacts during sintering, control of, 19: 44595(R) (EURAEC-1338)
effects on uranium corrosion by water vapor at 25 and 40°C, 19: 44618 (AWRE-O-42/65)
effects on uranium phosphides, 19: 43985(R) (ANL-7000, pp 85-110)
electron reactions with, classical calculation of cross sections for inelastic, (T), 19: 44947
neutron cross sections for, from 0.414 ev to 5.5 Mev, 19: 45244 (AEEW-M-472)
photon reactions (γ,n) to 33 Mev cross sections and spectra from, (E), 19: 45330
radioinduced reactions with organic compounds, mechanism of, 19: 44075
radiosensitivity effects on bacteria, 19: 44552 (BLG-327)
reactions with niobium–zirconium alloy in potassium–sodium environment at 1250°F, 19: 44626 (TIM-896)
spectrum of $^1\Delta_g$ state in discharged, paramagnetic resonance, 19: 43997(R) (UCRL-11889)
OXYGEN IONS
content and reactions in ionosphere, (T), 19: 45173
reactions with helium, energy effects on cross sections for dissociation in, (E), 19: 44948
OXYGEN ISOTOPES
abundance ratios in carbon dioxide, mass spectrometer for determining, 19: 43963
properties for tracer use in biology, 19: 43707
OXYGEN ISOTOPES O-15
production in tunnel of Frascati electron linear accelerator, (T), 19: 44866 (LNF-65/21)
OXYGEN ISOTOPES O-16
content in metamorphic rocks, ratio to oxygen-18, 19: 44238
deuteron reactions (d,α) at 5 to 9 Mev, differential cross sections for, 19: 45377
exchange reactions with oxygen-18 in manganese dioxide, temperature effects on rate of, 19: 44104
nucleon binding energies of ground-state, (T), 19: 45350
scattering by deformed even rare-earth nuclei at 43.5 Mev, vibrational-state excitation in inelastic, (E), 19: 45321
OXYGEN ISOTOPES O-17
coupling constant in nitrobenzene anion radical, 19: 44049
distribution equilibrium in carbon dioxide–water and carbon dioxide–water-d_2 systems, 19: 44007
incorporation in nitrobenzene, 19: 44049
nuclear magnetic resonance of, in studies of water exchange with paramagnetic cations in solution, 19: 43997(R) (UCRL-11889)
OXYGEN ISOTOPES O-18
alpha reactions (α,nγ) at 2.50 Mev, angular correlations and distributions for, (E), 19: 45277 (NP-15363)
content in metamorphic rocks, ratio to oxygen-16, 19: 44238
determination in water by activation, 19: 45679(R) (NYO-1859-11)
distribution equilibrium in carbon dioxide–water and carbon dioxide–water-d_2 systems, 19: 44007
effects on oxidation of benzene, 19: 44078
exchange reactions with oxygen-16 in manganese dioxide, temperature effects on rate of, 19: 44104
fractionation between coexisting calcite and dolomite in Freeport formation, Penn., 19: 44241
incorporation in phenol by autoxidation of benzene in oxygen-18 enriched water, 19: 44078
proton activation of, in tracer study of solid-state reactions of oxides, 19: 43998 (UCRL-12396)
proton reactions (p,α) at 360 to 2680 kev, angular distributions from, (E), 19: 45291 (ZFK-PHA-12, pp 117-22)
OXYGEN SYSTEMS
Al–C–O, thermodynamic analysis of equilibrium phases in, 19: 43996 (UCRL-11699)
Ar–O, radiolysis of, kinetics of ozone formation in pulse, 19: 44071
C–O–U, density and lattice parameters, effects of composition on, 19: 44612(R) (USBM-RC-1199)
N–O, chemical reactions during high temperature rapid quenching of, 19: 44041
OXYTOCINS
immunity in rabbits, tracer study, 19: 43658
labeling with iodine-131, 19: 44105
OYSTERS
zinc-65 uptake by, 19: 43663
OZONE
production in tunnel of Frascati electron linear accelerator, (T), 19: 44866 (LNF-65/21)
yields from pulse radiolysis of argon–oxygen solutions, 19: 44071

P

PAIR PRODUCTION
electron, in electromagnetic wave interactions in nuclear field, 19: 45128
PALLADIUM
bremsstrahlung production by strontium-90–yttrium-90 beta particles in, (E), 19: 45284 (TID-22169)
diffusion in, mechanisms for self-, 19: 44677(R) (ANL-7000, pp 183-5)
effects on determination of copper in high-purity metals by activation methods, 19: 43973
Fermi surface of, d-hole, 19: 45472 (AERE-M-1605)
neutron transmission at 1.2 to 100 ev in, resonances in, (E), 19: 45233
radiation effects on electric resistivity at 4°K, fast neutron, 19: 44739(R) (ANL-7000, pp 233-77)
reactions with beryllium, copper, stainless steel, and niobium alloys to 760°C *in vacuo*, 19: 44606 (PWAC-483)
PALLADIUM ALLOYS
Er–Hf–Pd, crystal structure studies, 19: 44678(R) (ANL-7000, pp 186-200)
Ni–Pd–U, crystal structure studies, 19: 44678(R) (ANL-7000, pp 186-200)

Pd–Ag, thermodynamic properties, 19: 44678(R) (ANL-7000, pp 186-200)
Pd–Pt–U, crystal structure studies, 19: 44678(R) (ANL-7000, pp 186-200)
Pd–Rh–U, crystal structure studies, 19: 44678(R) (ANL-7000, pp 186-200)
Pd–Sn, heat of solution at 425°C, 19: 44678(R) (ANL-7000, pp 186-200)
Pd–Tm, crystal structure studies, 19: 44678(R) (ANL-7000, pp 186-200)
PALMITIC ACID
metabolism of carbon-14 labeled, by rats, 19: 43681(R) (UCLA-12-565, pp 17-31)
synthesis of carbon-14 labeled, 19: 43681(R) (UCLA-12-565, pp 17-31)
PANCREAS
radiodiagnosis of diseases of, 19: 43886
zinc-65 uptake and distribution in normal and tumorous, in man, 19: 43699
PAPAVERINE
effects on spasmogenic actions of uridine phosphates, 19: 43728(R) (UCLA-12-565, pp 59-64)
PARAFFIN
properties as radiation dose rate meter, 19: 44525
PARASITES
phosphorus-32 uptake and retention by human louse, 19: 43684
vaccine for sheep lungworms, preparation from irradiated larvae, 19: 43750
PARTICLE COLLECTORS
performance of gummed paper, 19: 44291 (JAERI-1081)
PARTICLE STATISTICS
formalism for multiple particle production, 19: 45038 (TPJU-7/65)
PARTICLE TRACKS
analysis in bubble and spark chambers, device for automatic, 19: 44496
analysis in ionographic emulsions, electron microscopes for, 19: 44426 (CERN-65-4(Vol.II), pp VIII27-33)
analysis in nuclear emulsions, semiautomatic device for, 19: 44419 (CERN-65-4(Vol.II), pp VII20-7)
analysis in nuclear emulsions, automatic device for, 19: 44421 (CERN-65-4(Vol.II), pp VIII35-7)
characteristics in spark chambers, during time of sensitivity to previous spark, (E), 19: 44518
construction in emulsions, Monte Carlo code for artificial, 19: 44433 (CERN-65-4(Vol.II), pp IX44-7)
location in nuclear emulsions using spark chambers, 19: 44445 (CERN-65-4(Vol.II), pp X74-83)
location in wide-gap spark chambers, errors in, (E), 19: 44514
measurement in nuclear emulsions, analog computer for, 19: 44420 (CERN-65-4(Vol.II), pp VII28-34)
measurement in nuclear emulsions, apparatus for, 19: 44422 (CERN-65-4(Vol.II), pp VIII39-42)
measurement in nuclear emulsions, semiautomatic device for, 19: 44417 (CERN-65-4(Vol.II), pp VIII1-14)
measurement of, design of digitizing apparatus for, 19: 44361
resolution in nuclear emulsions, electron microscopy for, 19: 44423 (CERN-65-4(Vol.II), pp VIII8)
width of heavy-ion, in emulsions, 19: 44434 (CERN-65-4(Vol.II), pp IX48-61)
PARTICLE TRAJECTORIES
determination in geomagnetic fields, model current sheets for, (T), 19: 45168
PARTICLES
deposition of small, on artificial rough surfaces, 19: 44245 (BNL-914, pp 125-32)
diffusion in four-body systems, 19: 44815
reflection and transmission in slightly scattering plates, (T), 19: 44848
scavenging by atmospheric precipitation, 19: 44769 (BNL-914, pp 28-32)
size distributions of, representation by log normal functions, 19: 44808 (LA-DC-6636)
stress tensor for systems with internal angular momentum, symmetry of, (T), 19: 44807 (LA-DC-6556)
PATHOLOGY
radiation sickness, review on, 19: 43851
PEAS
radiation effects on seeds of, effects of storage on genetic, 19: 43770
radioinduced mutations in, 19: 43732
PEBBLE BED REACTOR EXPERIMENT (ORNL)
fuel element irradiation evaluation for, 19: 44749 (ORNL-P-1507)
PENNSYLVANIA
oxygen-18 fractionation between coexisting calcite and, in Freeport formation, Penn., 19: 44241
PENNSYLVANIA RESEARCH REACTOR
operation, July 1964–June 1965, 19: 45679(R) (NYO-1859-11)
2,4-PENTANEDIONE
solvent properties for hafnium, niobium, and tantalum, 19: 44124
2,4-PENTANEDIONE COMPLEXES
with rare earths, preparation and properties, 19: 44006
PENTANES
neutron scattering by liquid, dynamics of, (E), 19: 45235
spectra of solid, slow-neutron-scattering analysis of, (E), 19: 44050
PERCHLORIC ACID
$HClO_4$–$LiClO_4$, effects on hydrolysis and polymerization of pentavalent protactinium, 19: 44012
PEROXYACETIC ACID
tert-butyl ester radiolysis of, kinetics of gamma, 19: 44089
PERSONNEL
gamma body burden of Los Angeles, 1960–64, 19: 43883(R) (UCLA-12-565, pp 65-85)
lung cancer incidence in uranium mining, 19: 44314
radiation body burdens from reactor accident, measurability of, 19: 44325
radiation dosimetry in event of criticality accident, system for, 19: 44333
radiation dosimetry of, in accidents, 19: 44319 (STI/PUB/99)
radiation dosimetry in event of nuclear accident, program for, 19: 44320
radiation dosimetry of, biological method for fast and thermal neutron, 19: 44322
radiation dosimetry of, reports and statistics on results of, 19: 44326
radiation dosimetry in Hanford criticality accident, problems in, 19: 44330
radiation dosimetry of, methods for, 19: 44332
radiation dosimetry at fast-critical assembly, efficiency of system for, 19: 44334
radiation dosimetry in accidents, program for, 19: 44336
radiation effects at ultra-high frequency energy on, climate effects on, 19: 43774
radiation effects on chromosome aberrations in, 19: 43834
radiation exposure from linear accelerator malfunction, clinical and dosimetric study of, 19: 44331
radiation exposure in accidents, clinical and hematologic tests for, 19: 44316
radiation exposure in accidents, role of laboratory and methods used in event of, 19: 44324
radiation hazards to workers using open or sealed sources of, 19: 44304(T) (CEA-tr-R-1836)
radiation monitoring of, design of individual alarm systems for, 19: 44532
radiation monitoring of, design of monobath film detectors for, 19: 44534
radiation monitoring of, design of personal dosimeter for, 19: 44536
radiation monitoring of, accuracy of film badges for, 19: 44312
radiation monitoring program at National Reactor Testing Station for, 19: 44335
radiation protection of, during radon pump disassembly, 19: 44317
PERTURBATION THEORY
for extreme coupling in NMR spectra, (T), 19: 44945
radiation dosimetry of, development of film detectors for, 19: 44533
PETROLEUM
properties as reactor coolant and moderator, (E), 19: 45501 (IAE-611)
PHANTOMS
design of solid, with adaptable density and form for dosimetry throughout, 19: 44308
dosimetry of scattered x radiation from diagnostic quality radiation in, 19: 43917
PHARMACEUTICALS
analysis for bromine by radiometric methods, 19: 43950
radiosterilization of, review on techniques in, 19: 44563
radiosterilization of, evaluation of, 19: 44564
PHARMACOLOGY
research programs on, 19: 43647(R) (UCLA-12-565)
PHASE STUDIES
transformations under pressure, method for determination of, 19: 43997(R) (UCRL-11889)
PHENOL
labeling with oxygen-18 by autoxidation of benzene in oxygen-18-enriched water, 19: 44078
yields from oxidation of benzene in aqueous solutions of metal ions, 19: 44078
yields in gamma radiolysis of aqueous solutions of benzene at 100 to 200°C, 19: 44052 (AE-193)
PHENOL, DINITRO-
effects on radiomimetic effects of nitrosoamides on herb seeds, 19: 43870
effects on strontium-85 elution from mouse bones, 19: 43706
PHENOLS
halogeno-radiosensitivity effects on bacteria, 19: 44552 (BLG-327)
PHENYL ETHER
freezing point depression constant of, 19: 44046 (JEN-152-DQ/I-53)
PHONONS
interactions with electrons in aluminum, (T), 19: 45481 (UCRL-12470)

spectra of, anharmonic effects near point of origin of, (T), 19: 45475 (IAE-750)
PHOSPHATASES
effects of chemicals on leukocyte content of, 19: 43829
radiation effects on activity of, in rat spleen, effects of various drugs on, 19: 43860(R) (NP-15310, pp 14-25)
radiation effects on leukocyte content of, 19: 43829
radiation effects on content of, in rat tissues, 19: 43739
PHOSPHATE GLASS
radioinduced luminescence in silver-activated, ESR spectra from γ-, (E), 19: 44758
radioluminescence of, dosimetric uses of, (E), 19: 44509
PHOSPHATES
radioinduced production from carbon disulfide–methanol, 19: 45679(R) (NYO-1859-11)
radiosensitivity effects on Clostridium spores, 19: 43865
PHOSPHORIC ACID
use in TALSPEAK solvent extraction process for actinide–lanthanide group separation, 19: 44115 (ORNL-P-1577)
PHOSPHORIC ACID, BIS(2-ETHYLHEXYL) ESTERS
solvent properties for uranium and vanadium in ores, 19: 44129(P)
PHOSPHORS
meson (μ^+) depolarization quenching in, as function of longitudinal magnetic field, (E/T), 19: 45079
meson (μ^+) depolarization in targets of, (E), 19: 45080
scintillation properties of, apparatus for study of, 19: 44460 (RT/FI (65)8)
use of radioactivity excited, to illuminate bubble of a leveling instrument, 19: 44567(P)
PHOSPHORUS
activation reactions in bone, use in neutron dosimetry, 19: 44322
content in experimental dog diet, control of, 19: 43675(R) (UCD-472-112, pp 73-9)
depletion from calves of, by hemodialysis, tracer study, 19: 43673 (TID-22147)
determination in blood, of dogs, 19: 43674(R) (UCD-472-112, pp 36-43)
effects on determination of silicon in steel by activation methods, 19: 43965
metabolism in human fetuses of, 19: 43701
oxidation of white, anodic, 19: 43997(R) (UCRL-11889)
PHOSPHORUS COMPOUNDS
analysis and separation of, activation and chromatographic methods for, 19: 45679(R) (NYO-1859-11)
PHOSPHORUS ISOTOPES
incorporation of radioactive, in halo organic compounds, 19: 44107(P)
PHOSPHORUS ISOTOPES P-31
energy level structure of, (E/T), 19: 45275 (NP-15138)
neutron reactions (n,p) with, rates for, (E/T), 19: 45522 (AE-195)
PHOSPHORUS ISOTOPES P-32
activity of dissolved sources of, international comparison of specific, 19: 44101
determination in solutions, use of scintillation counter for, 19: 43940
effects of injected, on blood picture in rats, 19: 43839
excretion in feces and urine by colostomized pullets, determination by isotopic dilution method, 19: 43693
half life, 19: 45371
radiation effects on pulse labeling of RNA in *Salmonella typhimurium* by, 19: 43743
therapeutic use of, for polycythemia, 19: 43820
tracer use in cytology, 19: 43740
uptake and retention by human louse, 19: 43684
use with miniature Geiger tube in diagnosis of esophageal, gastric, and rectal cancer, 19: 43887
PHOTOCHEMISTRY
research program on uv excitation of organic liquids, 19: 44059 (NYO-2949-1)
PHOTOGRAPHIC EMULSIONS
aging by controlled temperatures, effects of, 19: 44402 (CERN-65-4 (Vol.II), pp IV5-15)
PHOTOGRAPHIC FILM
radiation effects on, electron and proton, 19: 44093
PHOTOGRAPHIC FILM DETECTORS
description of, for personnel monitoring, 19: 44332
design of monobath, for accidental high-level exposures, 19: 44534
development and characteristics of, for gamma and x-ray activity at 10 mR to 1000 R, 19: 44533
evaluation of accuracy of, for occupational exposures, 19: 44312
performance for environmental monitoring, 19: 44291 (JAERI-1081)
performance for gamma dosimetry, 19: 44440 (CERN-65-4(Vol.II), pp X44-6)
performance of, for dosimetry of scattered x radiation, 19: 43889
performance, for dosimetry of beta sources in skin, 19: 43880 (NP-15270)
processing of, method for inhibited, 19: 44440 (CERN-65-4(Vol.II), pp X44-6)
use at National Reactor Testing Station, 19: 44335
PHOTOGRAPHY
conference on nuclear, 19: 44377 (CERN-65-4(Vol.I))
conference on nuclear, proceedings of, 19: 44383 (CERN-65-4(Vol.II))
use of Schlieren, for plasma diagnostics, (E), 19: 45421
PHOTOMETERS
calibration of flame, for analysis of sea water samples, 19: 44253(R) (NYO-2174-36)
PHOTOMETRY
plasma jet performance in flame, 19: 43924 (AERE-R-4990)
PHOTOMULTIPLIER TUBES
dynode gate for, development of pulsed and bistable, 19: 44513
gain drift cancellation following source intensity variation, 19: 44374 (AROD-3347:6)
operating mode of FEU-49, resolution in spectrometric, 19: 44455 (NP-15047)
performance for determining scintillator properties, 19: 44460 (RT/FI(65)8)
radiation background in, at high altitudes, 19: 44465 (UCRL-12020)
use for continuous automatic measurement of carbon-14 on chromatographic column fractions, 19: 43949
PHOTONS
angular correlations from positron annihilation in copper, (E), 19: 45487
emission from point mass, effects on gravitation of, (T), 19: 44910
emission in stellar evolution, luminosity of, (T), 19: 44927(T)
interactions in nuclear field, electron-pair production by, 19: 45128
interactions of massive, for fermion Regge poles in quantum electrodynamics, 19: 45114
interactions of, neutrino pair production in, (T), 19: 45027 (NP-15199)
interactions with photons, graviton production in nonlinear bound-state, (T), 19: 45144
interactions with protons, induced beta decay in, 19: 45052
reaction cross sections for, UKAEA library of, 19: 45249 (AWRE-O-55/65)
reactions with aluminum and copper in Bev range, meson (ρ^0) production in, 19: 45000 (HUX-2752-7)
reaction with carbon and hydrogen in Bev range, pair production in, (E), 19: 45000 (HUX-2752-7)
PHYSICS
bibliography on gases and gas-condensed phase reactions, 19: 43993 (NP-15379)
bibliography on high-temperature, of condensed materials, 19: 43994 (NP-15381)
form of isotropic tensors, 19: 44810 (TPJU-8/65)
research, 19: 44802(R) (ANL-6877)
research in, instrumentation development for, 19: 44357
research programs on, at AECL, 19: 45694(R) (AECL-2251)
stress tensor for medium with internal angular momentum, symmetry of, (T), 19: 44807 (LA-DC-6556)
PHYSIOLOGY
bioelectric forces involved in the thermodynamics of material transfer across biological membranes, 19: 43664 (BNL-9337)
thermodynamics of material transfer across biological membranes, 19: 43665 (BNL-9338)
PICOLINES
complexes with cerium and 5-nitrobarbituric acid, preparation and stability, 19: 44027
PINCH DEVICES
development of Chalice, (E), 19: 45406(R) (SIT-2852-17)
use of theta, as vacuum u-v source, 19: 45396 (LA-DC-7120)
PINCH EFFECT
plasma containment in galaxies by, bridge mechanism for, (T), 19: 44926(T)
plasma kinetics in toroidal theta, (T), 19: 45395 (IPP-6/38)
PIPERAZINE
properties of 3-indolyl-ethyl derivatives of, psycho-sedative, 19: 43728(R) (UCLA-12-565, pp 59-64)
PIPERIDINE
radiolysis of, yields in gamma, 19: 44072
PIPERIDINE, 1-METHYL-
radioinduced addition to 1-octene, gamma, 19: 44053 (AFML-TR-65-166)
radiolysis products of, gamma, 19: 44053 (AFML-TR-65-166)
PIPES
leak detection in gas, using radiotracers, 19: 44553 (EUR-2284.f)
PIPETTES
design of remotely controlled corrosion-resistant, 19: 43936 (ORNL-P-1533)
PITUITARY GLAND

radioinduced hypophyseal ablation of, 19: 43920
PLACENTA
strontium-90 content in human, in Germany, 19: 44313
PLANETS
atmospheres of, survey on, 19: 44893 (NASA-CR-294)
electron trapping on Mars, (E), 19: 44913
magnetic moment of Mars, (E), 19: 44913
orbits around Mars and Venus, trajectory parameters of entry and escape from, 19: 45649 (N64-32637)
radiation belts of Mars, implications of absence of, (E/T), 19: 44912
radio emission from Jupiter, (E), 19: 44917(T)
PLANKTON
radioactivity of Atlantic Ocean, fallout, 19: 44253(R) (NYO-2174-36)
PLANT CELLS
labeling with tritium, 19: 43651
radioinduced chromosome aberrations in Allium root tips, 19: 43745
PLANT METABOLISM
carbohydrate, in higher plants, review of catabolic, 19: 45697(R) (COO-330-11)
of tritiated water in *Zea maize* roots, 19: 43702
tracer studies of, 19: 43685
PLANTS
atmospheric radiation monitoring at Ames, Jan.-June 1965, 19: 44302 (TID-22173)
deposition of iodine and zinc sulfide on, from atmosphere, 19: 44248 (BNL-914, pp 141-3)
ecological and radiation effects, studies at Nevada Test Site on, Jan.–June 1965, 19: 43662(R) (UCLA-12-565, pp 97-128)
effects of beryllium on, 19: 43662(R) (UCLA-12-565, pp 97-128)
monitoring Savannah River Plant, Jan. to June 1965, 19: 44288(R) (DPST-65-30-2)
mutations in, agricultural use of, 19: 43656
radiation effects on field community of, ecological, 19: 43711 (BNL-924)
radiation effects on seed germination and seedling growth in, 19: 43722(R) (TID-22108)
radiation effects on *Poa pratensis*, mutagenic x, 19: 43778
radiation effects on lipase activity in peanut, y, 19: 43798
radioinduced mutations in Lupinus, review, 19: 43776
radioinduced mutations in sweet potato, review, 19: 43777
radioinduced mutations in *Arachis hypogea*, review, 19: 43779
radioinduced mutations in pea, 19: 43734
radioinduced mutations in *Digitalis Lanata EHRH*, seed-exposure, 19: 43746
radioinduced sterility in pollen of, y, 19: 43767
radiosensitivity of, effects of chromosome size and growth habits on, 19: 43711 (BNL-924)
radiosensitivity of, effects of target volume in various species, 19: 43782
PLASMA
acceleration in transverse magnetic field, relsotron, 19: 45435
acceleration of bunches of, in coaxial injector, 19: 45431
acceleration of pulsating clot of, 19: 45430
accelerator design and diagnostic techniques, cyclotron resonance, 19: 44229
accelerator for, design parameters for Hall-current, 19: 45444
accelerator for, gas density measurements in pulsed coaxial, (E), 19: 45449
accelerators for, performance of switch-triggered pulsed, 19: 44225
accelerators for, performance of hollow cathode Hall current, 19: 45443
accelerators for, diagnostic studies in Hall-current, 19: 45446
acoustic wave propagation in collisionless, ion, (E), 19: 45404 (ORNL-P-1557)
boundaries and loss effect by ion beam neutralizers, computer simulation of, 19: 45454
collision probabilities in cesium, (E), 19: 45399(R) (CR-54451)
containment and generation of high-energy, method for, (E), 19: 45455(P)
containment by stellarator model C, (T), 19: 45397 (MATT-282)
containment in galaxies, bridge mechanism for, (T), 19: 44926(T)
current sheet microstructure in theta pinch hydrogen and nitrogen, (E/T), 19: 45445
density fluctuations in, space-time, (T), 19: 45394 (IPP-6/37)
diagnostics in ionosphere, probe system for, 19: 45155(R) (AD-609015)
diagnostics of, instrumentation development for, 19: 44357
diagnostics of, performance of resonance probes for, 19: 45381 (ARL-65-115)
diagnostics of, theory of Langmuir probe for, 19: 45447
diagnostics of, theory of electrostatic double probe for, 19: 45452
diagnostics using electrostatic probes, (T), 19: 45414 (UCRL-12480)
diffusion across magnetic fields, 19: 45410(R) (TID-22183)
diffusion across magnetic fields, (E/T), 19: 45380(R) (AD-426192)
displacement and vortex currents in, with magnetic-field barrier, (E), 19: 45391 (INR-612/IXA/PR)
effects on ion beam trajectories, (T), 19: 45451
eigenfunctions for initial and boundary value problems in, 19: 45450
ejection from stellar outer layers, (T), 19: 44914(T)
electric conductivity in cylindrical, induction-field calculations for distributions of, (T), 19: 45437
electromagnetic radiation from high density and temperature, 19: 45392 (IPP-1/39)
electromagnetic radiation backscattering from turbulent, cross-polarized, (T), 19: 45424
electromagnetic wave transmission through, magnetized ferrite antenna windows for, 19: 45387 (D1-82-0442)
electron density and temperature of non-stationary, optical interferometry for, 19: 45433
electron density and temperature in argon MPD source, (E), 19: 45448
electron density and refractive index of theta pinch, Schlieren photography for, (E), 19: 45421
electron density in, microwave diagnostics of, (E), 19: 45429
electron oscillations in, in magnetic fields, (E), 19: 45427
electron oscillations in mercury, higher- and sub-harmonics of, (E), 19: 45428
electron reactions with molecular ions in, collisional-dissociative recombination, 19: 45450
electrostatic wave propagation in, in magnetic fields, (T), 19: 45389 (GA-6513)
flow of partially ionized, effect of collisional radiative reaction processes on, 19: 45425
flow with aligned magnetic field, collisionless, 19: 45426
heating by electromagnetic waves using Stix coil, (T), 19: 45400 (NASA-TN-D-2982)
heating in B-3 stellarator, (E), 19: 45398 (MATT-332)
ion cyclotron harmonic spectra from, (E), 19: 45405 (ORNL-P-1576)
ion density of magnetically contained cesium, Langmuir probe effects on, (E/T), 19: 45393 (IPP-2/38)
magnetohydrodynamic approximation for, 19: 45432
microwave emission in magnetic mirrors, (E), 19: 45388 (GA-6432)
microwave excitation of helium, harmonic generation by, (E), 19: 45420
microwave phase shifts in, null method for measuring, 19: 45412 (UCRL-7978)
microwave reflection in plasma-filled waveguides, 19: 45401 (NP-15196)
microwave scattering from resonant oscillations of, (E), 19: 45436
oscillations in, electric field enhancement of, 19: 45410(R) (TID-22183)
oscillations of, supercollective modes in one-dimensional, (T), 19: 45406(R) (SIT-2852-17)
pinch discharge in argon high-current pulse-driven linear, 19: 45442
pinch discharge in, dynamics of toroidal theta, (T), 19: 45395 (IPP-6/38)
production of high-electron-density, 19: 45456(P)
production of hot, using pulsed laser-beam reactions with solids, (E), 19: 45409 (TID-22132)
production of, electrolytic capacitor banks for, 19: 45416 (UCRL-16263)
properties from hydrogen-loaded titanium washer source, (E), 19: 45411 (UCRL-7935)
properties of, in Astron facility, 19: 45413 (UCRL-12456)
radiation field interactions with, (T), 19: 45418
research in gases and solids, review of, 19: 45383 (D1-82-0419)
shock wave heating of, effects of, (E), 19: 45434
shock wave stability and structure in, 19: 45422
solar wind effects in outer magnetosphere, (T), 19: 45162
stability in axi-symmetric magnetic field, (T), 19: 45438
stability in constant magnetic fields, (E/T), 19: 45380(R) (AD-426192)
stability in magnetic mirrors, flute, (E), 19: 45388 (GA-6432)
stability of cesium, in gas discharges, 19: 45403 (NP-15445)
stability of column of, in longitudinal magnetic fields, (T), 19: 45386 (D1-82-0439)
stability of heated-cathode discharge, in magnetic field at low pressures, (E/T), 19: 45390 (IAE-780)
stability of, in magnetosphere, 19: 45186
stability of, magnetic shear effects on, (E), 19: 45415 (UCRL-14137)
temperature measurement in argon, probe for, 19: 44204
temperature of, measurement using vacuum u-v absorption, (T), 19: 45382 (BRL-MR-1644)
theory of weakly turbulent, quasilinear, 19: 45439
thermal radiation from argon, (E/T), 19: 45453
thermodynamics of MHD, with infinite conductivity, (T), 19: 45417
transport properties of argon, (T), 19: 45407 (SU-AA217)
turbulence in, mechanisms for, (T), 19: 44975(T)
wave interactions in arc discharge, non-linear, (E), 19: 45419
wave propagation in warm nonuniform column of, (T), 19: 45408 (SU-IPR-11)
wave propagation in, effects of nonlinear interactions on, (T), 19: 45402 (NP-15200)

PLASMA JETS
acceleration of plasmoids by coaxial, 19: 45431
development of cyclotron resonance, for propulsion, 19: 44223(R) (NP-15438)
development of cyclotron resonance, for propulsion, 19: 44229
electron density and temperature in argon, (E), 19: 45448
energy storage capacitors for pulsed, 19: 44224
performance of cesium fueled MPD arc, for propulsion, 19: 44230
performance of hollow cathode Hall current, 19: 45443
performance of pulsed arc, 19: 45441
performance of switch-triggered pulsed, 19: 44225
performance of two-stage pulsed coaxial, 19: 44233
use in determination of calcium and strontium by flame photometry, 19: 43924 (AERE-R-4990)
velocity distribution in supersonic effect of radiative loss on, 19: 45425
PLASTICIZERS
use in radiation-attenuating films, 19: 44670(P)
PLASTICS
extrusion by hydrostatic methods, 19: 44651
performance for slow neutron dosimetry, 19: 44385 (CERN-65-4(Vol.II), pp 112-19)
PLATES
critical separation of regular arrays of fissile, 19: 44977 (IDO-17095)
particle reflection and transmission in slightly scattering, (T), 19: 44848
PLATINUM
electric conductivity of thin films of, 19: 44344 (K-L-1944)
hyperfine fields in iron, 19: 43997(R) (UCRL-11889)
reactions with beryllium, copper, stainless steel, and niobium alloys to 760°C *in vacuo*, 19: 44606 (PWAC-483)
PLATINUM ALLOYS
Cr–Pt, crystal structure studies, 19: 44678(R) (ANL-7000, pp 186-200)
Er–Pt, crystal structure studies, 19: 44678(R) (ANL-7000, pp 186-200)
Ir–Pt–Y, crystal structure studies, 19: 44678(R) (ANL-7000, pp 186-200)
Mn–Pt, crystal structure of $PtMn_3$, chemical order-disorder, in, 19: 44679(R) (ANL-7000, pp 205-12)
Mn–Pt, magnetic structure in $PtMn_3$, 19: 44679(R) (ANL-7000, pp 205-12)
Ni–Pt–U, crystal structure studies, 19: 44678(R) (ANL-7000, pp 186-200)
Pd–Pt–U, crystal structure studies, 19: 44678(R) (ANL-7000, pp 186-200)
PLATINUM ISOTOPES Pt-195
neutron reactions with, resonances in, (E), 19: 45296
PLOWSHARE PROJECT
actinide recovery from Gnome debris in salt formation, 19: 44156 (DP-956)
use of nuclear explosions in stimulating oilfields, calculations, 19: 44158 (UCRL-14311)
PLUTONIUM
analytical methods for, bibliography on, 19: 43925 (ANL-6956)
burnup in heavy water reactors, 19: 45578 (JAERI-1080)
crystal preferred orientation in sheets of rolled alpha, 19: 44675(R) (ANL-7000, pp 155-75)
determination in air filters, radiochemical, 19: 44296 (NYO-4700 (Rev.)(Suppl.II))
electric conductivity of alpha, effects of pressure on, 19: 44675(R) (ANL-7000, pp 155-75)
electric conductivity of alpha, relation of Hall coefficient to, 19: 44675(R) (ANL-7000, pp 155-75)
electric conductivity of alpha, at high pressures, 19: 44604(R) (NUMEC-3428-12)
electronic structure of, two-band model proposed for, 19: 44675(R) (ANL-7000, pp 155-75)
etching of alpha, beta, and delta, using a-c electrolysis, 19: 44602 (LA-DC-6691)
fabrication of sheet, 19: 44654
fabrication systems for, economic studies of, 19: 44587(R) (ANL-7000, pp 3-63)
Hall coefficient of alpha, at 5 to 300°K, 19: 44675(R) (ANL-7000, pp 155-75)
Hall coefficient of beta, at 5 to 440°K, 19: 44675(R) (ANL-7000, pp 155-75)
Hall coefficient of aluminum-stabilized delta, at 5 to 440°K, 19: 44675(R) (ANL-7000, pp 155-75)
Lorenz number of, (E), 19: 44721
metallographic preparation of, by electropolishing, 19: 44675(R) (ANL-7000, pp 155-75)
microstructure of gallium-stabilized delta, after homogenization and annealing, 19: 44604(R) (NUMEC-3428-12)
phase diagram at high pressures, electric resistivity study, 19: 44604(R) (NUMEC-3428-12)
preparation of single crystals of alpha, 19: 44675(R) (ANL-7000, pp 155-75)
preparation of ultra-high-purity, by electrorefining, 19: 44600 (LA-3356)
processing facility for, description of British, (E), 19: 45612
production by reduction of dioxide, attempts on, 19: 44594 (DP-983)
properties and structure of delta, band model for, 19: 44689 (LA-DC-7351)
properties in thermal reactors, control rod and fuel element fabrication for experiments on, 19: 45559 (ANL-7000, pp 64-8)
separation from fast reactor fuels, using Alamine 336–dibutyl cellosolve, 19: 44108 (AERE-R-4440(Pt.3))
separation from uranium, method for, 19: 43982(P)
solvent properties for rhenium at 700 to 950°C, 19: 44688 (LA-3359)
spectra of, isotope shifts in, 19: 44033
tensile properties of sheet, 19: 44654
PLUTONIUM ALLOYS
analysis of, bibliography on, 19: 43925 (ANL-6956)
metallographic procedures, 19: 44674(R) (ANL-7000, pp 69-83)
Al–Pu, magnetic susceptibility of δ-phase, at 6 to 300°K, 19: 44690 (LA-DC-7360)
Al–Pu, nuclear magnetic resonance in $PuAl_2$, 19: 43986(R) (ANL-7000, pp 201-4)
Al–Pu, phase transformations on heating and cooling in intermetallic compound $PuAl_4$, 19: 44727
Al–Pu–U, corrosion by air at room temperature, 19: 44587(R) (ANL-7000, pp 3-63)
Ce–Co–Pu, analysis for cobalt by controlled potential electrodeposition, 19: 43934 (LA-3345)
Cu–Pu–U, corrosion by air at room temperature, 19: 44587(R) (ANL-7000, pp 3-63)
Fe–Pu–U, corrosion by air at room temperature, 19: 44587(R) (ANL-7000, pp 3-63)
fissium–Pu–U, burnup in, effects of cladding thickness on attainable, 19: 44587(R) (ANL-7000, pp 3-63)
fissium–Pu–U, enthalpy to 1200°C, 19: 44587(R) (ANL-7000, pp 3-63)
fissium–Pu–U, phases and transformation kinetics, 19: 44587(R) (ANL-7000, pp 3-63)
fissium–Pu–U, properties of, effects of composition on, 19: 44587(R) (ANL-7000, pp 3-63)
fissium–Pu–U, reactions with vanadium at 1100 to 1400°C, 19: 44587(R) (ANL-7000, pp 3-63)
fissium–Pu–U, reactions with chromium, molybdenum, and niobium at 750°C, 19: 44587(R) (ANL-7000, pp 3-63)
fissium–Pu–U, reactions with Hastelloy-X and type 304 stainless steel at 750°C, 19: 44587(R) (ANL-7000, pp 3-63)
fissium–Pu–U, reactions with niobium–zirconium and titanium–vanadium alloys at 750°C, 19: 44587(R) (ANL-7000, pp 3-63)
Ga–Pu, magnetic susceptibility of δ-phase, at 6 to 300°K, 19: 44690 (LA-DC-7360)
Mo–Pu–U, corrosion by air at room temperature, 19: 44587(R) (ANL-7000, pp 3-63)
Mo–Pu–U, properties of cast, 19: 44587(R) (ANL-7000, pp 3-63)
PuC–UC, sintering properties, 19: 44587(R) (ANL-7000, pp 3-63)
Pu–Th–U, fabricability and thermal expansion of, 19: 44674(R) (ANL-7000, pp 69-83)
Pu–Th–U, phase studies, 19: 44674(R) (ANL-7000, pp 69-83)
Pu–Th–U, reactions with chromium, nickel, and stainless steel at 650°C, 19: 44674(R) (ANL-7000, pp 69-83)
Pu–Th–U, reactions with chromium–nickel and titanium–vanadium alloys at 650°C, 19: 44674(R) (ANL-7000, pp 69-83)
Pu–Ti–U, corrosion by air at room temperature, 19: 44587(R) (ANL-7000, pp 3-63)
Pu–U, fabrication of, for SEFOR-ZPR-III fuel plates, 19: 44587(R) (ANL-7000, pp 3-63)
Pu–U, reactions with vanadium at 1100 to 1400°C, 19: 44587(R) (ANL-7000, pp 3-63)
Pu–U–V, corrosion by air at room temperature, 19: 44587(R) (ANL-7000, pp 3-63)
Pu–U–Zr, corrosion by air at room temperature, 19: 44587(R) (ANL-7000, pp 3-63)
PLUTONIUM CARBIDES
susceptibility at 4 to 370°K, 19: 44678(R) (ANL-7000, pp 186-200)
PLUTONIUM COMPOUNDS
analysis of, bibliography on, 19: 43925 (ANL-6956)
PLUTONIUM IONS
reactions with bovine and canine blood proteins, binding, 19: 43705
PLUTONIUM ISOTOPES
neutron cross sections of, tabulation, (E), 19: 45250 (BNL-325(2nd Ed.) (Suppl. 2)(Vol.III))
production in high-flux Savannah River Production Reactors, 19: 45639 (DP-999, pp 19-28)
PLUTONIUM ISOTOPES Pu-239

electric quadrupole moment from x-ray spectrum of mesic (μ), (E), 19: 45326
fission of, delayed gamma emission in, (E), 19: 45245 (AFWL-TR-65-95)
neutron cross sections for, from 0.414 ev to 5.5 Mev, 19: 45244 (AEEW-M-472)
neutron fission cross sections at 20 to 120 ev, (E), 19: 44157 (LA-DC-7304)
neutron fission rates in FRO critical assemblies, (E/T), 19: 45522 (AE-195)
neutron fission reactions at 24 kev, secondary neutron yield from, (E), 19: 45297
removal from rat bones, effectiveness of chelating agents and other compounds for, 19: 43700
x-ray transitions in μ-mesic atoms of 2p–1s, 19: 44962

PLUTONIUM ISOTOPES Pu-240
neutron cross sections for, from 0.414 ev to 5.5 Mev, 19: 45244 (AEEW-M-472)

PLUTONIUM(IV) OXIDES
electric conductivity at 1100 to 1600°C, effects of oxygen pressure on, 19: 44680(R) (ANL-7000, pp 227-32)
fabrication of fuel pellets of, for Doppler experiments in ZPR-III, 19: 44587(R) (ANL-7000, pp 3-63)
free energy of oxygen in, partial molar, 19: 44680(R) (ANL-7000, pp 227-32)
oxygen content at 1100 to 1600°C, effects of oxygen pressure on, 19: 44680(R) (ANL-7000, pp 227-32)
properties of, study of chemical and physical, 19: 43995 (RFP-503)
reduction to metal by barium and calcium, attempts on, 19: 44594 (DP-983)
PuO_2–UO_2, fabrication of fuel pellets of, for Doppler experiments in ZPR-III, 19: 44587(R) (ANL-7000, pp 3-63)

PLUTONIUM PHOSPHIDES
crystal lattice constants, 19: 43985(R) (ANL-7000, pp 85-110)
preparation and sintering properties, 19: 43985(R) (ANL-7000, pp 85-110)

PLUTONIUM RECYCLE TEST REACTOR
radioactive material buildup and transport in, shutdown radiation measurements for determining, 19: 45564 (BNWL-SA-85)

PLUTONIUM SULFIDES
crystal lattice constants, 19: 43985(R) (ANL-7000, pp 85-110)
sintering properties and thermal expansion, 19: 43985(R) (ANL-7000, pp 85-110)

PLUTONIUM SYSTEMS
C–Pu–U, corrosion by air at room temperature, 19: 44587(R) (ANL-7000, pp 3-63)
C–Pu–U, lattices parameters as function of composition, 19: 44678(R) (ANL-7000, pp 186-200)
C–Pu–U, preparation, 19: 44587(R) (ANL-7000, pp 3-63)
C–Pu–U, susceptibility at 25°C, 19: 44678(R) (ANL-7000, pp 186-200)

POLARISCOPY
use of ellipsometry for studies of electrodes, 19: 43997(R) (UCRL-11889)

POLARONS
theory of, principal methods for, 19: 45473 (BLG-329)

POLLEN
radioinduced sterility in, γ, 19: 43767

POLONIUM
radiation hazards to workers using open or sealed sources of, 19: 44304(T) (CEA-tr-R-1836)

POLONIUM ISOTOPES Po-212
use in determining aerosol penetration depths in filters, 19: 44299 (SZS-2(1965))

POLONIUM ISOTOPES Po-218
determination in air, filter measurement of, 19: 44258

POLYCYTHEMIA
phosphorus-32 therapy of, 19: 43820

POLYMERIZATION
radioinduced graft, using two or more monomers, 19: 44097(P)
radioinduced, methods using of radioisotopes for, 19: 44560

POLYMERS
analysis for iodine-128, activation, 19: 43951
yields from radiolysis of acetylene, 19: 44082

POLYPHENYL SYSTEMS
pyrolysis of Santowax O-M, 19: 44044 (AECL-2218)

POLYPHENYLS
molecular weight determination, cryoscopic method using benzene solutions, 19: 44045 (JEN-151-DQ/I-52)
molecular weight determination, cryoscopic method using phenyl ether solutions, 19: 44046 (JEN-152-DQ/I-53)
neutron scattering by, distributions from cold, 19: 45238

POPULATIONS
analysis of human, 19: 43642(R) (NYO-2280-8)
control of *Culex fatigans*, by release of irradiated males, 19: 43796
radiation control of gnat, *Hippelates pusio*, 19: 43803
radiation effects on, atomic-bomb, 19: 44280(R) (ABCC-63-64)
radiation effects, genetic, 19: 43823
radiation protection standards for, 19: 44306
survey for bone cancer incidence in Canadian, 1956 to 1961, 19: 43655

POROUS MATERIALS
thermal aging properties of flexible urethane foams, effects of molecular structure on, 19: 44682 (BDX-613-75)

PORPHYRINS
radiosensitivity effects in mice, 19: 43862
radiosensitivity effects of blood, in mice, 19: 43748

POSITRON BEAMS
interactions with electron beams, radiative corrections for, (T), 19: 45023 (LNF-65/8)

POSITRONS
annihilation in copper, anisotropy of Fermi surface from, (E), 19: 45487
interactions with electrons in storage rings, bremsstrahlung from, (T), 19: 44865 (LAL-1134)
reactions in nuclear emulsions, ionization losses in, 19: 44432 (CERN-65-4(Vol.II), pp IX41-3)
spectra in cobalt-56 decay, (E), 19: 45295

POTASSIUM
boiling and condensation of, two-phase heat transfer and fluid flow in, 19: 44187(R) (NASA-CR-54405)
boiling heat transfer in serpentine tube, forced-convection, 19: 44195 (TID-21256)
content in Finnish Lapp diet, 19: 44305
determination by flame photometry, 19: 44122
effects on cesium sorption by marine sediments, 19: 43964
excretion in feces and urine in colostomized pullets, 19: 43693
ionization by hot tungsten, efficiency of surface, 19: 44938 (UCRL-14117)
reactions with ammonia, equilibrium data on, 19: 43997(R) (UCRL-11889)
separation from calcium, magnesium, sodium, and strontium by ion exchange, 19: 44122
stability of plasma of, effects of magnetic shear on, (E), 19: 45415 (UCRL-14137)
viscosity of liquid, kinematic, 19: 44701(R) (TID-22144)

POTASSIUM ALLOYS
K–Na, corrosive effects on niobium–zirconium alloy at 1250°F, effects of carbon, nitrogen and oxygen on, 19: 44626 (TIM-896)

POTASSIUM AMIDE
catalytic effects on deuterium enrichment in ammonia-hydrogen system, 19: 44574

POTASSIUM BROMIDES
electron energy-loss spectra in, temperature dependence of, (E), 19: 45490
protective effects against radiation damage in crop plants, 19: 43877

POTASSIUM CARBONATES
protective effects against radiation damage in crop plants, 19: 43877

POTASSIUM CHLORIDES
corrosive effects on titanium alloys at 650°F, 19: 44621 (CONF-651006-1)
protective effects against radiation damage in crop plants, 19: 43877

POTASSIUM CYANIDES
effects on radiomimetic effects of nitrosoamides on herb seeds, 19: 43870

POTASSIUM FERRICYANIDES
spectra of, cold-neutron-scattering analysis of low-frequency vibrational, 19: 45241

POTASSIUM HALIDES
radiation effects on luminescence of doped, at 90 and 295°K, 19: 45488

POTASSIUM IODATES
protective effects against radiation damage in crop plants, 19: 43877

POTASSIUM IODIDES
protective effects against radiation damage in crop plants, 19: 43877

POTASSIUM ISOTOPES K-39
separation by molecular distillation, cascade unit for, 19: 43931 (K-1650)

POTASSIUM ISOTOPES K-41
separation by molecular distillation, cascade unit for, 19: 43931 (K-1650)

POTASSIUM SODIUM TARTRATES
radiation effects on changes in domain structure, 19: 44031(T)

POTENTIOMETRIC ANALYSIS
computer program for chrono-, 19: 45706 (ORNL-TM-1254)

POWDER COMPACTS
fabrication of fuel elements of, powder loading assembly for, 19: 44641 (ORNL-TM-1193)

packing efficiency for irregular-shaped particles, 19: 44587(R) (ANL-7000, pp 3-63)
POWER BREEDER REACTORS
design and economics of molten-salt, 19: 45588 (ORNL-TM-1060)
design of epithermal thorium, 19: 45629(P)
POWER BURST FACILITY
use in fast fuel meltdown studies, feasibility of, 19: 45493(R) (APDA-174)
POWER CYCLES
thermodynamics and turbomachinery for Brayton, in radioisotope and reactor systems, 19: 45654 (NASA-TN-D-2968)
POWER PLANTS
performance of nuclear-thermionic, for space vehicles, 19: 45648 (GA-6478)
POWER REACTORS
auxiliary systems development for 395-Mwe water-cooled, (E), 19: 45597 (WCAP-3269-31)
contamination control, 19: 45608
description of British superheated-steam, (E), 19: 45613
design for water desalination, economics of, 19: 45620
design of German 300-Mw pressurized water, 19: 45609
design of graphite-moderated, gas-cooled, for sea water desalination, 19: 45606
design of organic-cooled dual-purpose, for process heat production, 19: 45618
design of subcritical, 19: 45541(P)
design of thermoelectric, for underwater applications, 19: 45627
design of 1000-Mwe pressurized-water, 19: 45596 (WCAP-2042)
development of dual-purpose, for desalination of sea water, 19: 45619
developments in, 1965, 19: 44307
fuel burnup in pressure tube type heavy water, (T), 19: 45578 (JAERI-1080)
fuel costs for heavy-water-moderated, minimum, 19: 45563 (BNWL-106)
fuel cycles in advanced gas-cooled, computer analysis of, (T), 19: 45595 (TRG-Report-976)
fuel fabrication and processing facilities for British, (E), 19: 45612
fuel for, economics of, 19: 45621
fuel tube fabrication for heavy-water, 19: 45569 (DP-976)
POWER SUPPLIES
design for production of pulsed magnetic fields, 19: 44449 (IAE-704)
performance for thermal test stands for reactor simulation, 19: 44203
properties of marine radioisotope, 19: 44569 (AGN-8122)
PRASEODYMIUM ALLOYS
Cu–Pr, crystal structure studies, 19: 44678(R) (ANL-7000, pp 186-200)
Pr–Zn, crystal structure studies, 19: 44678(R) (ANL-7000, pp 186-200)
PRASEODYMIUM IONS
energy levels of free trivalent, (E), 19: 44943
spectra in lanthanum fluoride, energy levels in absorption and fluorescence, (E), 19: 45484
PRASEODYMIUM ISOTOPES Pr-134
decay, (E), 19: 45285 (UCRL-16040)
PRASEODYMIUM OXIDES
catalytic effects on dehydration and dehydrogenation of alcohols and tetralin, 19: 44023
effects on optical properties of silicate glasses, 19: 44030
phase transformation in, at 1800 to 2400°C, 19: 44731
PRASEODYMIUM VANADATES
crystallographic and optical properties of hydrated, 19: 44032(T)
PRECIPITATION, ATMOSPHERIC
atmospheric radiation monitoring at Ames, Jan.-June 1965, 19: 44302 (TID-22173)
effects on fallout from atomic clouds, 19: 44255 (RT/PROT(65)-10)
particle scavenging by, 19: 44769 (BNL-914, pp 28-32)
radioactivity of Canadian, June 1965, 19: 44251 (NP-15519, pp 23-51)
PREGNANCY
occurrence after primary radium therapy of cervical carcinoma, 19: 43891
PRESSURE VESSELS
closures in, stress analysis of bolted, 19: 44145 (TID-22138)
construction of, rules for, 19: 45507
conversion of thirty-inch, to gas autoclave, 19: 44169 (Y-1478)
design and performance of prestressed-concrete, 19: 45505
design and performance of prestressed-concrete, in boiling heavy-water reactors, 19: 45506
design and uses of prestressed concrete, 19: 45504
development of Gas Autoclave Facility, 19: 44169 (Y-1478)
fatigue strength of, research program on, 19: 45503(R) (SWRI-1228-69)
fission product release from containment, simulation study, 19: 44286 (BNWL-SA-30)
plug and plug insertion means for apertures in reactor, 19: 45510(P)
seals for, liquefiable bismuth–tin alloy, 19: 44658(P)
stress analysis of Kiwi, computer program for, 19: 44219 (ACF-8)
PRESSURIZED WATER REACTORS
control and stability of large, factors affecting, 19: 45601(R) (WCAP-3750)
control rod clusters for, worth of, (E/T), 19: 45535 (WCAP-3269-47)
control rod worths in large, 19: 45533 (WCAP-3269-33)
control system design for RTM, nonlinear, 19: 45682 (RT/ING(64)-15)
coolant blowdown models for LOFT, 19: 45671 (BAW-1196-4)
coolant loss accident, Zircaloy-2–steam reaction in simulated, 19: 45496 (WCAP-3269-30)
core development for large, 19: 45601(R) (WCAP-3750)
core lattice parameters for, optimization of, 19: 45599 (WCAP-3269-49)
description of British superheated, (E), 19: 45613
design of German 300-Mw, 19: 45609
design of thermoelectric, for underwater applications, 19: 45627
design of 1000-Mwe power, 19: 45596 (WCAP-2042)
design of 15 Mw(e), for Austria, 19: 45581 (NP-15291)
design with superheating system, 19: 45628(P)
fuel cycle analysis for, 19: 45545 (HW-79951(Pt.2))
fuel cycle economics for, thorium–uranium, 19: 45582 (NP-15320)
fuel fabrication and processing facilities for British, (E), 19: 45612
moderator temperature coefficient in, burnup effects on, 19: 45602 (WCAP-5493)
neutron fission power distributions around control rods of, 19: 45534 (WCAP-3269-35)
power distribution in fuel rod cluster control cores of, effects of enrichment on, 19: 45601(R) (WCAP-3750)
stability of, effects of fuel temperature, moderator temperature, and power distribution on, 19: 45601(R) (WCAP-3750)
superheater design for, 19: 45630(P)
PRINCETON SYNCHROTRON
beam extraction from, method for, 19: 44871 (PPAD-2137-556)
development and operation of, 19: 44872 (PPAD-2137-565)
PROCESS HEAT REACTORS
design of dual-purpose, 19: 45618
development for desalination of sea water, 19: 45619
development for sea water desalination, 19: 45634
use for desalting water for agriculture, 19: 45636
PROGESTERONE
protective effects of, against radiation injuries in rat spleen, 19: 43860(R) (NP-15310, pp 14-25)
PROLINE, HYDROXY-
radiation effects on content in mouse liver, alpha, 19: 43831
PROMETHIUM
preparation and properties of, 19: 43988 (CONF-650804-7)
PROMETHIUM COMPOUNDS
preparation and properties of, 19: 43988 (CONF-650804-7)
PROMETHIUM IONS
radius of trivalent, 19: 43992 (NP-15339)
PROMETHIUM ISOTOPES Pm-147
separation from wastes at Hanford, 19: 45690 (RL-SA-40)
PROMETHIUM OXIDES
preparation and properties of binary and ternary, 19: 43992 (NP-15339)
Pm_2O_3–WO_3, properties, 19: 43992 (NP-15339)
PROPANE
1-phenyl-1-acetthio-2-nitro-, protective effects against radiation lethality in mice, 19: 43868
1,3-PROPANEDIONE, 1,3-DIPHENYL-
complexes with rare earths, preparation and properties, 19: 44006
1,3-PROPANEDISULFONIC ACID, DIETHYL ESTER
effects on cytology and physiology of *Triticum durum* and *T. monococcum*, 19: 43653
2-PROPANETHIOL, 1-AMINO-
effects on irradiated dioxane-2,5-diphenyloxazole phosphor, quenching, 19: 43878
1-PROPANOL
dehydration and dehydrogenation of, catalytic effects of praseodymium oxide on, 19: 44023
2-PROPANOL
dehydration and dehydrogenation of, catalytic effects of praseodymium oxide on, 19: 44023
1-PROPANOL, 2-METHYL-
dehydration and dehydrogenation of, catalytic effects of praseodymium oxide on, 19: 44023
PROPIOPHENONE, p-AMINO-
protective effects against proton and x irradiation effects on mice, 19: 43873
protective effects against proton radiation effects on mice, 19: 43874
protective effects of, against radiation injuries in mice, synergistic effects with dimethyl sulfoxide, 19: 43859(R) (NP-15310, pp 1-13)
PROPORTIONAL DETECTORS
design for low-level activity determination of carbon-14, 19: 44526

response of, filled with helium-3, methane, and neon mixtures, 19: 44373(R) (ANL-6877, pp 15-20)

PROPULSION

bibliography on nuclear ship, 19: 45647 (AED-C-22-64)
electric, charged droplet thrustor for, 19: 44231
electric, economics for earth-lunar cargo transfer, 19: 44232
electrothermal systems for space, development of, 19: 44220 (N64-31011)
ion engines for space, ion-beam neutralization in, 19: 44222(R) (NP-15068)
ion, beam formation from electron bombardment sources for, 19: 44221 (N64-31088)
ion, cyclotron resonance thrustor for, 19: 44229
ion, testing of cesium contact engine for, 19: 44226
nuclear, economics for tanker, 19: 45657 (TID-22088)
plasma-jet development for, cyclotron resonance, 19: 44223(R) (NP-15438)
plasma-jet, cesium fueled MPD arc, 19: 44230

PROPYNE

spectra of, perturbation theory for extreme coupling in proton, (T), 19: 44945

PROTACTINIUM IONS

hydrolysis and polymerization of pentavalent, in aqueous solutions at 25°C, 19: 44012

PROTACTINIUM ISOTOPES

neutron cross sections of, tabulation, (E), 19: 45250 (BNL-325(2nd Ed.) (Suppl.2)(Vol.III))

PROTECTIVE CLOTHING

fabrication and forming of flexible radiation-attenuating film for, 19: 44670(P)

PROTEINS

determination of carbon-14-labeled, in plant tissues, by scintillation counting, 19: 43945
labeling with tritium, 19: 43651
radiation effects on synthesis in rat brains, x, 19: 43682(R) (UCLA-12-565, pp 33-57)
radiation effects on metabolism of, in bacteriophage, 19: 43845
reactions of canine blood, with plutonium ions, 19: 43705

PROTON BEAMS

effects on biological systems, RBE for, 19: 43721(R) (ORNL-TM-1217)
effects on displacement cascades in gold films, 19: 44739(R) (ANL-7000, pp 233-77)
effects on lens opacity in mouse eyes, 19: 43721(R) (ORNL-TM-1217)
effects on mice, LET for, 19: 43721(R) (ORNL-TM-1217)
extraction from Princeton synchrotron, method for, 19: 44871 (PPAD-2137-556)
production by single-gap extraction from plasma, (E), 19: 44885
radiosurgical use of, 19: 43905
therapeutic use of, 19: 43899

PROTONS

angular distributions from shell-model forbidden (d,p) transitions, (E), 19: 45323
angular distributions from boron-10 (d,p) reactions at 13.5 Mev, (E), 19: 45336
chemical shift in molecular hydrogen, modified Schrödinger equation for, (T), 19: 44952
detection and identification using lithium-drifted silicon detectors, (E), 19: 44517
detection of, performance of surface-barrier silicon detectors for, 19: 44469 (ZFK-PHA-12, pp 16-24)
detection of, silicon surface-barrier detectors for, 19: 44471 (ZFK-PHA-12, pp 30-2)
detection using emulsions, 19: 44443 (CERN-65-4(Vol.II), pp X61-6)
distribution in inner magnetosphere at 1.1 to 63 Mev, (E), 19: 45189
distribution in radiation belts, analysis of spatial, (E/T), 19: 45188
dosimetry in animals and man by beryllium-7 measurements in tissues, 19: 44327
effects in mice, pathological, 19: 43771
effects in pea seeds, genetic, 19: 43770
effects of 1.57-Mev pulses of, on water, 19: 44058 (LFEN-23)
effects on dosimetry glasses, iron sulfate solutions, and radiological films at 152 to 592 Mev, 19: 44093
effects on germanium and silicon, calculations, 19: 44747 (NP-15463)
effects on maize, mutagenic, 19: 43712 (BNL-9383)
effects on mice, protective effects of *p*-aminopropiophenone and MEA against, 19: 43873
effects on mice, protective effects of *p*-aminopropiophenone against whole-body, 19: 43874
energy spectra of geomagnetically trapped, from emulsion experiments in polar-orbiting satellites, 19: 44437 (CERN-65-4(Vol.II), pp X19-32)
flux distribution in ionosphere, limitation on, 19: 45157 (NP-15386)
form factors of, electromagnetic, (E), 19: 45001 (HUX-2752-8)
interactions at 1.7 to 6.2 Bev, polarization effects in, 19: 45043 (UCRL-16070)
interactions at 48 Mev, cross sections for bremsstrahlung production in, (E), 19: 45097
interactions in nuclear emulsions at 30.5 Bev, anisotropy in multiple meson emission in, 19: 45054
interactions with antiprotons, mesons (π^-), and protons at high energies, statistical model calculations for, 19: 45047 (UCRL-16315)
interactions with mesons (π^+) at 1.11 and 1.265 Bev/c, N^{*++} production in, 19: 44997 (COO-1428-14)
interactions with electrons at high momentum transfers, elastic, (E), 19: 45001 (HUX-2752-8)
interactions with mesons (K^+) and mesons (π^+) at high energies, resonance production in, (T), 19: 45037 (TID-21316)
interactions with mesons (K^-) at 1.22 to 1.70 Bev/c, charge-exchange, (E/T), 19: 45045 (UCRL-16288)
interactions with mesons (π^-) at 8.5 Bev/c, polarization in elastic, (E), 19: 45081
interactions with mesons (K^+) at 3 Bev/c, decay distributions and differential cross sections for, (T), 19: 45086
interactions with mesons (π^-) at 1.7 to 2.5 Bev/c, S-wave final-state $\pi\pi$ in, (E), 19: 45089
interactions with mesons (K^-) for hyperon (Ω^-) parity test, (T), 19: 45101
interactions with mesons (π^+) at 8 Bev/c, resonance enhancement from, (E), 19: 45103
interactions with alpha particles, phenomenological potential for phase shifts in, 19: 45109
interactions with mesons (π^-) at 3.9 Bev/c, resonance in $\pi^+\pi^0$p system from, (E), 19: 45121
interactions with antiprotons at rest, annihilation into two mesons in, (E), 19: 45122
interactions with gamma rays, detection using emulsions, 19: 44438 (CERN-65-4(Vol.II), pp X33-6)
interactions with deuterons and protons, detection using emulsions, 19: 44443 (CERN-65-4(Vol.II), pp X61-6)
interactions with neutron, design of high pressure diffusion cloud chamber for studying elastic, 19: 44494
interactions with protons at high energy, multiple production in elastic, (T), 19: 45091
interactions with antiprotons at rest, C invariance test from annihilation, (E), 19: 45124
interactions with electrons, hydrogen hyperfine structure from polarization in, (T), 19: 44951
interactions with bremsstrahlung, at 0.6 to 5.5 Bev, meson (π) production in, (E), 19: 44999 (DESY-65/5)
interactions with electrons at 20 f^{-2}, polarization in elastic, (E), 19: 45058
interactions with antiprotons, broken $\bar{U}(12)$ analysis of annihilation, (T), 19: 45008 (JINR-E-2246)
interactions with nucleons at 23 to 630 Mev, angular dependence of phase shift analysis of, 19: 45015 (JINR-P-2241)
interactions with hyperons (Λ) at ~2.7 Bev/c, total cross section for elastic, (E), 19: 45016 (JINR-P-2257)
interactions with nucleons, amplitudes and deuteron polarization from, (T), 19: 45017 (JINR-P-2267)
interactions with protons at 2 to 10 Bev, elastic, (E), 19: 45021 (JINR-P-2336)
interactions with antiprotons, radiative corrections for, (T), 19: 45023 (LNF-65/8)
interactions with charged mesons (π), high-energy limits for, 19: 45040 (TPJU-11/65)
interactions with antineutrinos ($\bar{\nu}_\mu$), polarization of mesons (μ^+) from, (T), 19: 45050
interactions with photons, induced beta decay in, 19: 45052
interactions with mesons (K^+) at 3 Bev/c, K^*N^* production in ($KN\pi\pi$), (E/T), 19: 45057
interactions with electrons, neutron form factor from (eNe), (T), 19: 45061
interactions with antiprotons at 3.25 to 7 Bev/c, OPE model for $\bar{N}^*N^*$ production in, (T), 19: 45069
interactions with antiprotons, cross sections for charged-meson pair formation in annihilation, (T), 19: 45066
magnetic moment of, dispersion theory for anomalous, 19: 45108
mass relative to neutrons, small-mass charged particles from, (T), 19: 45119
momentum determination in nuclear emulsions, method for, 19: 44434 (CERN-65-4(Vol.II), pp VIII9-16)
motion in aqueous acid solutions, 19: 44037
motion in linear accelerator, computer program for analyzing, 19: 44867 (MURA-713)
polarization in deuteron reactions (d,p) with deuterium, (E), 19: 45253

(COO-7-0362)
polarization of, performance of semiconductor detectors for measuring, 19: 44477 (ZFK-PHA-12, pp 126-32)
production in Crab Nebula, Compton-synchrotron process for, (T), 19: 44911
reactions (γ,n) with carbon-12 and oxygen-16 to 33 Mev, cross sections and spectra, (E), 19: 45330
reactions (p,α) with boron-11 and oxygen-18 at 360 to 2800 kev, angular distributions from, (E), 19: 45291 (ZFK-PHA-12, pp 117-22)
reactions (p,α) and (p,γ) with aluminum 27, nucleon model for, 19: 45304
reactions (p,γ) with tritium at 3 Mev, yields from, (E), 19: 45358
reactions (p,γ) with calcium-40 at 648 kev, radiative lifetime of excited scandium-41 from, (E), 19: 45344
reactions (p,2n) with rhenium-187 at 14 Mev, conversion electron anisotropy from, (E), 19: 45352
reactions with helium and molecular hydrogen, electron emission in, (E), 19: 44933(R) (COO-1277-12)
reactions with mesic deuterium atoms, (E), 19: 45273 (JINR-P-2356)
reactions with nuclei in steel at 10 and 20 Bev/c, (T), 19: 45317
recoil tracks in emulsions, sampling bias in scanning for, 19: 44464 (UCRL-11703)
scattering by hydrogen at 27.6 and 47.8 Mev, Wolfenstein A and R parameters from, (E), 19: 45319
scattering by nickel-58 and -60 at 39 Mev, polarization in, 19: 45378
scattering by tungsten crystals, angular distribution of charged products from, (E), 19: 45349
scattering in nuclear emulsions at 10 Bev, spurious, 19: 44412 (CERN-65-4(VolII), pp VII1-21)
scattering in nuclear emulsions at 24 and 27 Bev/c, spurious, 19: 44415 (CERN-65-4(Vol.II), pp VI37-52)
scattering on light nuclei at 155 Mev, cross sections and spectra in inelastic, 19: 45305
structure of, general survey of, 19: 45125
theory of zero-helicity, 19: 45020 (JINR-P-2330)
transmission through flat water-lead shielding barrier, as function of shielding thickness, (T), 19: 45466
transport in matter, Monte Carlo method for calculating, 19: 45462 (NP-15163)

PROTOZOA
radiation effects on regeneration in Blepharisma, uv, 19: 43813
radiation effects on enzymes in Tetrahymena, uv and x, 19: 43856
radiosensitivity of *Tetrahymena pyriformis*, effects of, enzyme effects on, 19: 43812

PSEUDOUREA, 2-(2-AMINOETHYL)-2-THIO-
chemical and physiological properties of, 19: 43867
effects on irradiated dioxane-2,5-diphenyloxazole phosphor, quenching, 19: 43878
metabolism in irradiated, normal, and tumor-bearing mice, 19: 43867
protective effects of, against radiation injuries in rat spleen, 19: 43860(R) (NP-15310, pp 14-25)
protective effects against gamma and x radiation, 19: 43883(R) (UCLA-12-565, pp 65-85)
protective effects of methyl sulfoxide mixtures against gamma radiation, 19: 43883(R) (UCLA-12-565, pp 65-85)
protective effects of, against radiation injuries in mice, synergistic effects with dimethyl sulfoxide, 19: 43859(R) (NP-15310, pp 1-13)
radiation chemistry of, 19: 43867

PSYCHOLOGY
radiation effects on learning ability of rhesus monkeys, 19: 43805
radiation effects on learning ability of rhesus monkeys, 19: 43806

PUERTO RICO POWER REACTOR
pressure control system malfunctions, 19: 45603 (Y-1491)

PULSE ANALYZERS
description of megachannel computerized, 19: 44497
design of nsec-range time-to-amplitude converters, (E), 19: 44508
design of shape discriminator for thermal-neutron detection using silver-activated zinc sulfide, 19: 44368 (AERE-M-833)
design of solid-state fixed-dead-time discriminators, (E), 19: 44504
development for semiconductor detectors, 19: 44488 (ZFK-PHA-12, pp 215-18)
development of multichannel, with memory devices for data processing, 19: 44524
development of multichannel, 19: 44456 (NP-15258)
modification of 512-channel, for use in multiparameter experiments, (E), 19: 44516

PULSE INTEGRATORS
design and performance of g-second, for centrifuges, 19: 45707 (SC-DR-65-261)

PULSE MODIFIERS
design of nsec-range time-to-amplitude converters, (E), 19: 44508

PUMPS (LIQUID METAL)
rotor-bearing dynamic tests for SNAP-50/SPUR, 19: 44149 (TIM-921)

PUPAE
radiosensitivity of gonads in male mosquito, 19: 43796
radiosensitivity of gnat, *Hippelates pusio*, 19: 43803

PUREX PROCESS
mixer-settler tests for thorium and uranium separation, 19: 44117 (ORNL-TM-1256)

PYRAZOLONES
performance as developers for nuclear emulsions, 19: 44407 (CERN-65-4 (Vol.II), pp V1-8)

PYRIDINE COMPLEXES
with cerium and 5-nitrobarbituric acid, preparation and stability, 19: 44027

PYRIDINE, 4-VINYL-
radioinduced graft polymerization with polyethylene and polyvinyl chloride, 19: 44083

PYRIDINES
protective effects against radiation damage in trypsin, 19: 44081

PYROGALLOL
performance as developer for nuclear emulsions, 19: 44404 (CERN-65-4 (Vol.II), pp IV23-31)

Q

QUANTUM ELECTRODYNAMICS
gauge problems in canonically quantized, 19: 45135 (NP-15436)
graviton production in nonlinear bound-state photon-photon interactions, (T), 19: 45144
Regge poles in Lagrangian theory of, with massive photons, 19: 45114
renormalization constants in, fourth order, (T), 19: 45136

QUANTUM MECHANICS
book: *New Foundations of Quantum Mechanics*, 19: 45153
Dirac equations in, de Broglie guide theorem for, 19: 45137
electron spin precession frequencies in gravitational fields, (T), 19: 45134 (NP-15397)
Heisenberg nonlinear theory in, consistency in spectral formulas in, 19: 45094
many-body problem in, pseudo potentials in, 19: 45138
operators in, Wigner representation of, 19: 45139
phase shift analysis using Hamilton-Jacobi equation, (T), 19: 45053
Schroedinger equation for Regge poles in Coulomb-type potential, 19: 45152
Schroedinger equation for singular potentials in, limiting procedures for, 19: 45063
statistics in, for analysis of accuracy of intensity-correlation and particle-counting experiments, 19: 45151
uncertainty relation for angular variables, numerical evaluation of, 19: 45145
vertex parts associated with loosely bound system Coulomb effects on analytic properties of, 19: 45146
wave functions in energy plane, interpolation of Jost and, 19: 45143

QUINOLINES
effects on spasmogenic actions of uridine diphosphate, 19: 43728(R) (UCLA-12-565, pp 59-64)

8-QUINOLINOL COMPLEXES
with gallium, indium, magnesium, thallium, and zinc, electronic absorption spectra, 19: 43989 (MIT-905-20)

8-QUINOLINOL, 2-METHYL-
complexes with gallium, indium, magnesium, thallium, and zinc, electronic absorption spectra, 19: 43989 (MIT-905-20)

R

RABBITS
amino acid content in antibodies of, 19: 45695 (BNL-912)
antibody formation in, mechanisms for, 19: 45695 (BNL-912)
fetal and maternal tissues of, niobium-95 and zirconium-95 distribution in, 19: 43883(R) (UCLA-12-565, pp 65-85)
iodine-131 uptake by blood plasma and thyroid in, effects of dietary molybdenum on, 19: 43689
metabolism of irradiated globulin in, tracer study, 19: 43686
oxytocin immunity in, tracer study, 19: 43658
radiation dosimetry by beryllium-7 measurements in tissues of, proton, 19: 44327
radiation effects on response to muscle relaxant drugs, 19: 43871
radiation effects on amino acids and sugars in eyes of, 19: 43755
radiation effects on lungs of, histological, 19: 43846
radioinduced pulmonary sclerosis in, role of autoantibodies in pathogenesis of, 19: 43817

RADAR
performance for ionospheric electron temperature determination, (E),

19: 45177
performance of f-m, in total cislunar electron content measurements, (E), 19: 45176
use in auroral observations, (E), 19: 45169
RADIATION
dosage to critical organs in accidental and chronic exposure, formulas and methods for calculating, 19: 43853
dose levels near 10-Bev synchrophasotron at JINR, 19: 44863 (JINR-P-2231)
dose rates in pressure vessel of Saccoule Reactor (G-3), 19: 45566 (CEA-R-2785)
dose to bone marrow from neutron flux exposure, calculation of, 19: 43854
dosimetry for manned space travel, 19: 43879
dosimetry in Hanford criticality accident, problems in, 19: 44330
dosimetry of high-level, reports and statistics on results of, 19: 44326
dosimetry of, device for, 19: 44536
dosimetry of, evaluation of activation detectors for, 19: 44535
dosimetry of, using radioluminescent phosphate glass, (E), 19: 44509
dosimetry using blood picture, 19: 44315
effects in man, genetic, 19: 43914
effects in man, genetic, 19: 43823
effects in man, somatic, 19: 43838
effects on animal cells, biological, 19: 43758
effects on animals, biological indicators for evaluating, 19: 43753
effects on animals and humans, correlation of, 19: 43843
effects on *Arachis hypogea*, mutagenic, 19: 43779
effects on bone marrow cell migration in mice, 19: 43836
effects on chromosome aberrations in man, 19: 43834
effects on content of amino acids and sugars in rabbit eyes, 19: 43755
effects on decarboxylation of fatty acids, 19: 43681(R) (UCLA-12-565, pp 17-31)
effects on enzyme activity in rat brains, 19: 43682(R) (UCLA-12-565, pp 33-57)
effects on growth of transplanted sarcoma in mice, 19: 43763
effects on induction of somatic mutations, carcinogenesis of, 19: 43754
effects on induction of mutations in peas, 19: 43732
effects on intestinal tryptophan sorption in rats, 19: 43728(R) (UCLA-12-565, pp 59-64)
effects on intestinal methionine sorption in rats, 19: 43728(R) (UCLA-12-565, pp 59-64)
effects on Lupinus, mutagenic, 19: 43776
effects on man at low doses, review on, 19: 43752
effects on mice, effects of plethora on, 19: 43682(R) (UCLA-12-565, pp 33-57)
effects on mice, protective effects of 1-phenyl-1-acetthio-2-nitroethane and -propane against, 19: 43868
effects on mitotic activity and structural chromosomes in rat bone marrow cells, integral dose effects on, 19: 43733
effects on myelin from rat brains, 19: 43682(R) (UCLA-12-565, pp 33-57)
effects on oxidation of organic compounds by molecular oxygen, mechanism of, 19: 44075
effects on personnel at ultra-high frequency energy, climate effects on, 19: 43774
effects on plants at Nevada Test Site, summary for Jan.–June 1965, 19: 43662(R) (UCLA-12-565, pp 97-128)
effects on properties of cellulosic fibers, 19: 44063
effects on reproduction and survival in Pinus and Quercus, 19: 43722(R) (TID-22108)
effects on somatic mutation induction, relation to chronic diseases, 19: 43749
effects on spleen of mice, nodule formation from x, 19: 43682(R) (UCLA-12-565, pp 33-57)
effects on sweet potatoes, mutagenic, 19: 43777
emission from nitrogen ores, analysis of, 19: 44804 (ARL-65-105)
hazards in space flight, methods for improving, 19: 43842
interactions with plasma, (T), 19: 45418
leukemogenic effects in man of, 19: 43827
leukemogenic effects of background, in man, 19: 43828
leukemogenic effects in man, 19: 43840
physiological effects in monkeys of, whole-body, 19: 43807
polymerization induced by, multiple grafting in, 19: 44097(P)
psychological effects in rhesus monkeys, 19: 43805
psychological effects in rhesus monkeys, 19: 43806
research programs on environmental, 19: 43647(R) (UCLA-12-565)
shielding against space, effective residual dose concept for, 19: 45470
transport in matter, non-equilibrium diffusion equation for, (T), 19: 45460 (LA-3377)
use in food preservation, 19: 44561
use of backscattered, in nondestructive flaw detection, 19: 44214(P)
RADIATION CHEMISTRY
research facilities for, at Czechoslovak Nuclear Research Institute, 19: 44068
research on, in Rumania, 19: 45705 (NP-15193)
RADIATION DETECTION INSTRUMENTS
accuracy in intensity-correlation and particle-counting experiments, quantum-mechanical analysis of, 19: 45151
calibration and performance for dosimetry use in space, 19: 43879
counters for, design of gated-readout decade, (E), 19: 44500
design for activity in wounds, 19: 44538
design for fast neutrons, 19: 44452 (K-1642)
design for industrial neutron-activation analysis, (E), 19: 43977
design for neutron dosimetry around pulsed sources, 19: 44360 (AERE-R-4883)
design of portable, battery-operated, 19: 44542(P)
development for health physics, 19: 44369 (AERE-R-4552)
development of, for whole-body counting of man, 19: 43672(R) (TID-22131)
optimization of, for half-life measurements, (E/T), 19: 44503
resolution time counting losses in, correction tables for, 19: 44530
sample transfer device for, 19: 44547(P)
time-to-amplitude converters for, design of, (E), 19: 44508
RADIATION DETECTION INSTRUMENTS (PULSE TYPE)
design of modular counting system for use as, 19: 44447 (EUR-2444.i)
design of transistorized scintillation, for extensive air showers, 19: 44529
development for external detection of radioactivity in countercurrent distribution machines, 19: 43940
modification of 512-channel analyzer for use in multiparameter experiments, (E), 19: 44516
RADIATION DETECTORS
bibliography, 19: 44366 (AED-C-06-12)
development, 19: 44357
development of Bonner single-sphere, for neutrons, 19: 44454 (LA-DC-7323)
efficiency of circular, viewing a circular radiator, (T), 19: 44505
RADIATION INJURIES
anesthesiology after, use of muscle relaxants during surgery, 19: 43871
development in urinary tract from radiotherapy of uterine carcinomas, 19: 43921
in *Escherichia coli*, repair mechanisms for, 19: 43795
in mice, protective effects of aminoethylisothiuronium, 19: 43867
induced by injected Thorotrast, 19: 43850
of *Bacillus subtilis* vegetative cells and spores, effects of heat treatment, 19: 43793
pathology and recovery from, in mice, 19: 43771
pathology of, in hamster cells in culture, 19: 43857
pathology of, in man, 19: 43838
pathology of, in rat liver, 19: 43735
pathology of, induced in thyroid gland of rats by injected iodine-131, 19: 43757
pathology of, induced by deposited Thorotrast, 19: 43738
permanency in Quercus, 19: 43722(R) (TID-22108)
protection against, reaction mechanisms in chemical, 19: 43861(T) (JPRS-51349, pp 1-24)
protection against, effects of tryptamine in, 19: 43864
protection against, effects of various nucleic acid precursors in mice, 19: 43866
protection against, effects of various drugs in rat spleen, 19: 43860(R) (NP-15310, pp 14-25)
protection against, effects of dimethyl sulfoxide in mice, 19: 43859(R) (NP-15310, pp 1-13)
protective effects of erythropoiesis stimulating preparation against, in animals and man, 19: 43872
recovery in Quercus, 19: 43722(R) (TID-22108)
recovery mechanisms in mice, 19: 43866
recovery mechanisms in mammals, 19: 43792
recovery mechanisms for, in hamster cells in culture, 19: 43857
repair mechanisms for, in mammalian cells, 19: 43790
repair mechanisms for, in mammalian cells, 19: 43791
surgical repair of neck, resulting from radiotherapy, 19: 43897
RADIATION MONITORING
alarm system in ORNL High Radiation Level Examination Laboratory, 19: 44297 (ORNL-TM-1251)
data from Canadian reactor sites, 1964, 19: 44294 (NP-15519, pp 3-22)
data from Canadian reactor sites, June 1965, 19: 44295 (NP-15519, pp 52-60)
equipment development for, 19: 44369 (AERE-R-4552)
film badge accuracy for, of personnel, 19: 44312
methods and results of, at JAERI, 19: 44290 (JAERI-1079)
procedures at JAERI, 19: 44291 (JAERI-1081)
program at Ames, Jan.-June 1965, 19: 44302 (TID-22173)

program at ANL, Jan.-June 1965, 19: 44300 (TID-22171)
program at Paducah Gaseous Diffusion Plant, Jan.-June 1965, 19: 44301 (TID-22172)
program at Savannah River Plant, Jan. to June 1965, 19: 44288(R) (DPST-65-30-2)
program for, in event of nuclear accident, 19: 44320
RADIATION PROTECTION
codes of Great Britain, 19: 44282 (AHSB(RP)M-36)
during diagnostic radiography, 19: 43893
during diagnostic radiography, 19: 43909
equipment for Saxton program, 19: 45600(R) (WCAP-3385-4)
in medical radiology, Italian Decree on, 19: 44318
problems with experimental devices around reactors, 19: 44287 (CEA-R-2799)
procedures for, in medical applications of radiation, 19: 43896
regulations for diagnostic radiography, in Germany, 19: 43913
standards for industrial uses of radiation, 19: 44307
standards for protection of population during peacetime, 19: 44306
RADIATION SICKNESS
nutritional management of patients with, induced by radiotherapy of cancer, 19: 43911
pathology of, review on, 19: 43851
protective effects of erythropoiesis stimulating preparation against, in animals and man, 19: 43872
RADIATION SOURCES
container design for, 19: 44179(P)
economic aspects of fission-product, 19: 44121
intensity variations of, effects on gain of photomultiplier tubes, 19: 44374 (AROD-3347:6)
RADIATION TARGET CANS
transfer from pool reactor to experimental areas, hydraulic system for, 19: 45686(P)
transfer from pool reactor to experimental areas, hydraulic system for, 19: 45686(P)
RADIATION TARGETS
neutron yields from uranium, in electron accelerators, 19: 44860 (IAE-614)
preparation by electrospraying on semiconductor detectors, 19: 44635 (INR-595/IA/PL)
preparation of thin-film self-supporting silicon, (E), 19: 44650
use of polarized, in nuclear reactions, 19: 45337
RADIO WAVES
absorption in auroral ionosphere, 19: 45170
emission from solar flares, models for, 19: 44931
emission of decimeter length, from Jupiter, (E), 19: 44917(T)
emission of solar, origin of bursts in, 19: 44920(T)
reflection by ionospheric F region, focusing effects on apparent coefficient for, (T), 19: 45175
scattering by ionospheric electron density fluctuations, correlation between circularly polarized waves from, (T), 19: 45182
RADIOACTIVE CONTAMINATION
levels for surface, maximum permissible, 19: 44311
measurement in Alaskan natives, whole-body, 19: 44289 (HW-SA-3750)
RADIOACTIVE MATERIALS
activity of, sample transfer device for measuring, 19: 44547(P)
buildup and transport in PRTR, shutdown radiation measurements for determining, 19: 45564 (BNWL-SA-85)
content in fish at Savannah River Plant, Jan. to June 1965, 19: 44288(R) (DPST-65-30-2)
handling of, design of remotely controlled manipulators for, 19: 44175(P)
handling of, remote-control equipment for, 19: 44180(P)
RADIOACTIVITY
detection and measurement in wounds, devices for, 19: 44538
determination in water, method for, 19: 43974
halos in rocks, 19: 44256(T) (ORNL-tr-708)
measurement on paper chromatograms, 19: 43984(P)
RADIOAPPLICATORS
design modifications for gold-198 grain implantation gun, 19: 43888
design of radium, 19: 43900
therapeutic use of, 19: 43906
RADIOBIOLOGY
clinical studies on animals and man, correlation of, 19: 43843
research on, in Rumania, 19: 45705 (NP-15193)
research programs on, 19: 43647(R) (UCLA-12-565)
use of swine in medical research, bibliography, 19: 43713 (BNWL-115)
RADIOCHEMICAL PROCESSING PLANTS
description of British, for power-reactor fuels, (E), 19: 45612
description of Thorium–Uranium Recycle Facility, 19: 44167 (ORNL-P-1521)
design of Chop and Leach, in Japan, 19: 44126
fire prevention in, 19: 44284 (AWRE-O-24/65)
performance of Kilorod pilot, for fabrication of uranium-233 dioxide–thorium dioxide fuel rods by sol-gel vibratory-compaction method, 19: 44638 (ORNL-3681)
RADIOCHEMISTRY
methods for health physics, 19: 44296 (NYO-4700(Rev.)(Suppl.II))
methods of, for reactor fuel burnup analysis, 19: 45542(R) (BAW-272)
of radium, review, 19: 44098 (NAS-NS-3057)
RADIODIAGNOSIS
of circulatory shunts, 19: 43904
of gastrointestinal diseases using radioisotopes and external scanning, 19: 43886
of thyroid diseases using technetium-99, 19: 43881 (NP-15271)
of thyroid tumors using iodine-131, 19: 43892
use of phosphorus-32 with miniature Geiger tube for, of cancer in esophagus, gastric tract, and rectum, 19: 43887
RADIOFREQUENCY SPECTROMETERS
magnet current control system for NMR, 19: 44356
RADIOGRAPHY
diagnostic, use of filters for, 19: 43901
filters for steel, evaluation of, 19: 44209(R) (EURAEC-1422)
method of whole-body, minimum exposure, 19: 43882 (UCD-472-112, pp 50-8)
radiation dose from scattered radiation during diagnostic, measurement of, 19: 43917
radiation dose to patients during diagnostic, 19: 43889
radiation hazards to eyes during diagnostic, of head and neck regions, 19: 43885
radiation hazards of diagnostic, in children, 19: 43893
radiation hazards of diagnostic, 19: 43914
radiation hazards of diagnostic, 19: 43823
radiation protection during diagnostic, 19: 43909
radiation protection during diagnostic, 19: 43913
RADIOISOTOPES
containers for, impact testing of, 19: 44298(R) (SC-RR-65-9)
determination in countercurrent distribution machines, β-γ scintillation probe for external, 19: 43940
determination in mixed samples, method for, 19: 43962
development of commercial, by AECL, 19: 45694(R) (AECL-2251)
incorporation in organic compounds, review on, 19: 44103
monitoring in Des Plaines and Illinois Rivers, Jan.-June 1965, 19: 44300 (TID-22171)
performance of positron-emitting, for artificial radiation belt production, 19: 45159 (UCRL-14374)
removal from body, effectiveness of chelating agents and other compounds for, 19: 43700
research and development on food, 19: 44566
solubility in reactor-activated soils, 19: 43662(R) (UCLA-12-565, pp 97-128)
therapeutic use of, for tumor therapy, 19: 43900
use as power source for manned space laboratory, 19: 44571
use as power source for underwater vehicle propulsion, 19: 44572
use as power source for underwater propulsion, 19: 45662
use in dairy starch, and sugar industries in Netherlands, 19: 44562
use in fluorescence analysis of ores, 19: 43971
use in marine heat and power sources, 19: 44569 (AGN-8122)
use in railway-car hot bearing detectors, 19: 44568(P)
use of gaseous, for illumination of bubble of leveling instrument, 19: 44567(P)
use of inhaled, for lung scanning, 19: 43883(R) (UCLA-12-565, pp 65-85)
use to detect leaks in gas mains, 19: 44553 (EUR-2284.i)
uses of, selection methods for, 19: 44551
uses to induce chemical change, sterilize drugs, and medical supplies, and generate electricity, 19: 44560
RADIOLOGICAL DEFENSE
planning of, fallout model for, 19: 44243 (AD-619902)
RADIOLOGICAL WARFARE
medical service in, role of army, 19: 44310
RADIOLOGY
radiation protection in medical, Italian Decree on, 19: 44318
RADIOMETRIC ANALYSIS
methods for health physics, 19: 44296 (NYO-4700(Rev.)(Suppl.II))
uses of inverse, using krypton-85 quinol clathrate for monitoring atmospheric sulfur dioxide, (E), 19: 44458 (NYO-2767)
RADIOMIMETIC SUBSTANCES
effects in Drosophila, genetic, 19: 43787
effects in Drosophila, lethal, 19: 43787
effects in silkworms, genetic, 19: 43787
effects in silkworms, lethal, 19: 43787
RADIOPROTECTIVE COMPOUNDS
effectiveness of sulfhydryl, 19: 43867
effects of nucleic acid precursors in mice, 19: 43866

effects of 1-phenyl-1-acetthio-2-nitroethane and -propane as, in mice, 19: 43868
protective effects of AET and serotonin against gamma and x radiation, 19: 43883(R) (UCLA-12-565, pp 65-85)
reaction mechanisms of, review, 19: 43861(T) (JPRS-51349, pp 1-24)
RADIOSENSITIVITY
effects of heat treatment on Artemia egg, 19: 43815
effects of hematoporphyrin on, of mice, 19: 43748
effects of hydration on Artemia egg, 19: 43814
effects on regeneration in Blepharisma, 19: 43813
enhancement of, chemicals for, 19: 44552 (BLG-327)
of animal cells, effects of mitotic stage on, 19: 43790
of bone marrow, in mice, 19: 43792
of brain of rat embryos, 19: 43768
of erythropoiesis and myelopoiesis in bone marrow, 19: 43731
of gonads, 19: 43889
of gonads, 19: 43756
of mammalian cells in tissue culture, 19: 43723(R) (TID-22128)
of man, effects of age on, 19: 43915
of mice, effects of mouse strain on, 19: 43792
of plants, effects of target volume in various species, 19: 43782
RADIOSTERILIZATION
evaluation of food and drug, 19: 44552 (BLG-327)
methods of, using radioisotopes, 19: 44560
of *Hippelates pusio* males, effects on population control, 19: 43803
of male mosquitoes, population control by, 19: 43796
of medical supplies, evaluation of, 19: 44559
of medical supplies, evaluation of, 19: 44564
of mouse diet, effects on wholesomeness, 19: 43654
of pharmaceuticals, evaluation of, 19: 44564
of screwworm flies for aerial dispersion, inhalant allergic response in man to, 19: 43652
salmonellae control by, economic feasibility of, 19: 44557 (NYO-3426-1)
use in pharmaceutical industry, review on techniques in, 19: 44563
RADIOTHERAPY
cure of patients after, 19: 43908
computer program for treatment planning in, 19: 43922
design modifications for gold-198 grain implantation gun, 19: 43888
development of radioapplicators for, 19: 43906
dose calculations for electron beam in inhomogeneous tissues, 19: 43916
effects of uterine carcinoma, on urinary tract, 19: 43921
effects on chromosome aberrations in humans, 19: 43834
of cancers of mouth, 19: 43903
of cancers, nutritional management of patients after, 19: 43911
of carcinoma of the bladder, 19: 43894
of carcinoma of uterus, late pathological effects, 19: 43907
of carcinomas in aged patients, 19: 43915
of carcinomas of uterus, combination of surgery with, 19: 43884
of cardiac decompensation, effects of irradiation of adrenal glands on, 19: 43919
of hyperthyroidism using iodine-131, 19: 43895
of mouth tumors using beta source, 19: 43912
of neck region, surgical repair of injuries resulting from, 19: 43897
of neck tumors, effects on thyroid function, 19: 43890
of skin lesions using beta source, depth-dose measurements, 19: 43880 (NP-15270)
of thyroid diseases using iodine-131, 19: 43906
of thyroid tumors using iodine-131, 19: 43892
of tumors using radium source, 19: 43900
of uterine cancers, evaluation of results, 19: 43910
use of alpha particles, neutrons, or protons for tissue destruction, 19: 43905
use of proton beams for, 19: 43899
RADIUM
carcinogenic effects of, in man, 19: 43830
determination of, evaluation of three methods for, 19: 43967
radiochemistry of, review, 19: 44098 (NAS-NS-3057)
therapeutic use of, for carcinoma of uterus, 19: 43884
therapeutic use of applicators of, 19: 43906
therapy of cervical carcinoma, pregnancy occurrence after, 19: 43891
use as radiation source for therapy, 19: 43900
RADIUM ISOTOPES
neutron cross sections of, tabulation, (E), 19: 45250 (BNL-325(2nd Ed.) (Suppl. 2)(Vol. III))
RADIUM ISOTOPES Ra-223
alpha decay in nuclear emulsions, track discrimination in, 19: 44425 (CERN-65-4(Vol. II), pp VIII17-26)
RADIUM ISOTOPES Ra-224
alpha decay in nuclear emulsions, track discrimination in, 19: 44425 (CERN-65-4(Vol. II), pp VIII17-26)
RADIUM ISOTOPES Ra-226
metabolism of injected, in dogs, 19: 43678(R) (UCD-472-112, pp 97-108)
RADIUM ISOTOPES Ra-228
pathological effects of deposited, in man, 19: 43672(R) (TID-22131)
RADIUM POISONING
pathology of, in man, 19: 43672(R) (TID-22131)
pathology of, in man, 19: 43830
RADON
detection and measurement of, in breath, 19: 43672(R) (TID-22131)
pathological effects of inhaled, in uranium miners, 19: 43824
pumping stations for, health physics aspects of dismantling, 19: 44317
therapeutic use of applicators of, 19: 43906
RAIN WATER
particle washout by, (T), 19: 44249 (BNL-914, pp 144-8)
percolation through soil, 19: 44235 (DPSPU-64-30-23)
RARE EARTH ALLOYS
phases in intra-rare-earth binary, research program on samarium-type intermediate, 19: 44672 (AD-619201)
RARE EARTH COMPLEXES
diketonate, preparation and properties, 19: 44006
RARE EARTH OXIDES
optical properties of, in silicate glasses, 19: 44030
phase transformations in, at 1800 to 2400°C, 19: 44731
RARE EARTHS
analysis and determination of, review of, 19: 43956
analysis and determination of, review of, 19: 43957
distribution in fused salt-cation exchanger systems, 19: 44040
effects of others, on electrolytic oxidation of cerium(III) to cerium(IV), 19: 44026
interatomic distances of, in metallic crystals, 19: 44713
pharmacology and toxicology of, 19: 43728(R) (UCLA-12-565, pp 59-64)
properties and uses of, review on, 19: 44615
properties at high pressures and temperatures, 19: 44734
separation from actinides, TALSPEAK process for, 19: 44115 (ORNL-P-1577)
separation of, review of, 19: 43956
separation of, review of methods for, 19: 43957
RARE GASES
hexafluoroethane--rare gas, radiolysis, energy transfer in gamma, 19: 44054(R) (COO-1365-7)
plasma of, temperature measurement using vacuum u-v absorption, (T), 19: 45382 (BRL-MR-1644)
spectra in theta-pinch plasma, 19: 45396 (LA-DC-7120)
RATE METERS
design of high dose, based on electric conductivity of liquid organic compounds, 19: 44525
RATS
autoradiographic localization of tritium in tissues of, 19: 43696
carbon-14 uptake by amino acids in cerebral tissue in, *in vitro*, 19: 43690
dentin in teeth of, effects of injected fluoride or strontium on, 19: 43687
effects of strontium on mitochondria of liver of, 19: 43688
iodine-131 distribution and localization in thyroid of goiterous, by autoradiography, 19: 43683
metabolism of hexobarbital in, 19: 43670(R) (NP-15310, pp 36-47)
plutonium-239 elution from bones of, effectiveness of chelating agents and other compounds for, 19: 43700
radiation dosimetry by beryllium-7 measurements in tissues of, proton, 19: 44327
radiation effects on adenosine triphosphatase activity in spleen of, effects of various drugs on, 19: 43860(R) (NP-15310, pp 14-25)
radiation effects on intestinal tryptophan sorption in, 19: 43728(R) (UCLA-12-565, pp 59-64)
radiation effects on intestinal methionine sorption in, 19: 43728(R) (UCLA-12-565, pp 59-64)
radiation effects on uridine diphosphate glucose pyrophosphorylase activity in liver of, 19: 43747
radiation effects on serum proteins in, x, 19: 43766
radiation effects on water intake by, 19: 43808
radiation effects on metabolism of 5-hydroxytryptamine in brain of, 19: 43810
radiation effects on spleen cell migration in blood stream of, after antigen stimulation, 19: 43822
radiation effects on gluconeogenesis in, effects of cortisone on, 19: 43837
radiation effects on blood picture in, from injected gold-198, phosphorus-32, or iodine-131, 19: 43839
radiation effects on metabolites, use in exposure diagnosis, 19: 43852
radiation effects on N-demethylase activity in liver of, 19: 43720(R) (NP-15310, pp 26-35)
radiation effects on mitotic activity and structural chromosomes in

bone marrow in, integral dose effects on, 19: 43733
radiation effects on liver of, pathological, 19: 43735
radiation effects on phosphatase content of spleen, 19: 43739
radioinduced bone sarcomas in, 19: 43772
radiosensitivity of brain of, 19: 43768
splenic oxygen tension and sulfhydryl content, effects of cysteamine on, 19: 43869
strontium-85 elution from bones of, effectiveness of chelating agents and other compounds for, 19: 43700
strontium-85 metabolism in, 19: 43671 (PG-Report-662)
tumor growth in, 19: 43649 (UCRL-16177)

REACTOR BREEDING BLANKETS
development of paste-type, 19: 45493(R) (APDA-174)
development of paste, for fast reactors, 19: 45561 (APDA-172)
development of sodium–uranium paste, 19: 45499(R) (APDA-174, pp 10-24)

REACTOR CONTROL ELEMENTS
performance of chemical shim, in power reactors, 19: 45598 (WCAP-3269-44)

REACTOR CONTROL RODS
coupling to drive, design of releasable, 19: 45516(P)
design with driving mechanism, 19: 45518(P)
development for fuel rod cluster control cores, 19: 45601(R) (WCAP-3750)
drive testing for, 19: 45589 (ORNL-TM-1197)
efficiency of boron- and cadmium-carbide, in homogeneous uranium–water reactors, (E/T), 19: 45536
fabrication for Plutonium Recycle Demonstration Experiment, 19: 45559(R) (ANL-7000, pp 64-8)
neutron fission power distribution around, in PWR, 19: 45534 (WCAP-3269-35)
reactivity worth in pressurized water reactors, 19: 45533 (WCAP-3269-33)
reactivity worths of clusters of, analysis of, (E/T), 19: 45535 (WCAP-3269-47)
worth measurements in Mixed Spectrum Critical Assembly, 19: 45572(R) (GEAP-4755)

REACTOR CONTROL SYSTEMS
design for LITR, 19: 45680 (ORNL-TM-1190)
design for ORNL High Flux Isotope Reactor, 19: 45645 (ORNL-TM-1259)
design for shutdown, 19: 45515(P)
design of transfer function analyzer for Dragon reactor, 19: 45571 (EUR-2431.i)
development for large closed-cycle reactors, 19: 45601(R) (WCAP-3750)
instrumentation design for, 19: 45508(P)

REACTOR COOLANTS
molecular weight determination in organic, cryoscopic method using benzene solutions, 19: 44045 (JEN-151-DQ/I-52)
molecular weight determination in organic, cryoscopic method using phenyl ether solutions, 19: 44046 (JEN-152-DQ/I-53)
performance of high-boiling organic, (E), 19: 45501 (IAE-611)
pyrolysis of Santowax O-M, 19: 44044 (AECL-2218)
radioactivity of aqueous, effects on shielding design, 19: 45601(R) (WCAP-3750)

REACTOR COOLING SYSTEMS
blowdown models for LOFT pressurized-water, 19: 45671 (BAW-1195-4)
design using cyclohexane dehydrogenation, 19: 45519(P)
flow distribution system for liquid-metal, 19: 45520(P)
maintenance of gas-cooled, 19: 45608
materials for gas-cooled, 19: 45608
operation at high pD, 19: 45568 (CVNA-238)
testing for large closed cycle reactor, model, 19: 45601(R) (WCAP-3750)

REACTOR ENGINEERING
core design for high-flux production reactors, 19: 45641 (DP-999, pp 43-64)
heat transfer in water reactors, dynamic studies, 19: 44194 (SGAE-RE-2/1965)
physics methods for light-water cores, 19: 45601(R) (WCAP-3750)
relation to chemical engineering, 19: 44155
research programs on, at AECL, 19: 45694(R) (AECL-2251)

REACTOR FUEL ALLOYS
fabrication of aluminum-chromium-uranium, 19: 44665(P)
fabrication of aluminum–tantalum–uranium, 19: 44667(P)
fabrication of aluminum–uranium–vanadium, 19: 44668(P)

REACTOR FUEL ELEMENTS
burnup distributions in, gamma-spectrometric measurement of, (E), 19: 44463 (TRG-Report-1005)
can design for, composite-tubing, 19: 44661(P)
canning of, hot-forging apparatus for crimping operation during, 19: 44657(P)
cans for, automatic machine for fabrication of finned, 19: 44655(P)
cans for, fabrication of finned, 19: 44656(P)
cladding materials for, performance limits of Hastelloy X, 19: 45577(R) (IDO-28645)
cladding materials for, helium and hydrogen production by fast neutron irradiation of, (T), 19: 44746 (NAA-SR-Memo-10626)
design for gas-cooled reactor, 19: 45549
design of finned, for improved rigidity, 19: 45555(P)
design with double sheath and inside void, 19: 45553(P)
design with sheath unit antibowing lugs, 19: 45551(P)
fabrication for British power reactors, facilities for, (E), 19: 45612
fabrication for rod cluster control experiments, 19: 45601(R) (WCAP-3750)
fabrication of aluminum-tungsten-uranium, 19: 44666(P)
fabrication of ESH-3A, for irradiation in EVESR, 19: 45572(R) (GEAP-4755)
fission gas release from intentionally punctured Calder Hall type, estimation of, 19: 44632
fission product distributions in molten-plutonium, 19: 44453 (LA-DC-7316)
fission product release from molten, into condensing steam, 19: 44285 (BNWL-SA-29)
fission product release from irradiated Windscale, 19: 44303 (TRG-Report-888)
heat transfer and pressure drop of GCR, 19: 45549
management at Chinon reactor, 19: 45607
processing irradiated, design of remote-controlled cutting tool for, 19: 44177(P)
processing of spent, design of Chop and Leach plant for, 19: 44126
radiation effects on advanced prototype, 19: 45601(R) (WCAP-3750)
reprocessing of carbon-containing, volatility processes for, 19: 44109 (BLG-331)
reprocessing of irradiated, evaluation of male connector material for, 19: 44607 (RL-SEP-508)
securing to support grid, end fitting for, 19: 45550(P)
separation of strontium-90 from irradiated, solvent extraction, 19: 44121
temperature distributions in Russian reactor BN-350, 19: 45604(T) (JPRS-31245)
temperature perturbations in cans of, axial and circumferential, (T), 19: 45543 (EUR-2480.f)
testing in liquid metal flows, apparatus for, 19: 44181(R) (APDA-174, pp 56-60)
testing of, data recording system for, 19: 45500 (HW-65756)

REACTOR FUEL ELEMENTS (CERAMIC)
design and fabrication of metal-clad plate, 19: 45554(P)
design of plutonia–urania, 19: 45600(R) (WCAP-3385-4)
fabrication for Plutonium Recycle Demonstration Experiment, 19: 45559(R) (ANL-7000, pp 64-8)
fast fission factors in rods of natural-uranium, (T), 19: 45229 (UJV-1324/65)
thermal conductance measurement in uranium dioxide, development of in-pile transient method for, 19: 44684 (CEND-3336-241)

REACTOR FUEL ELEMENTS (DISPERSION)
development of uranium dioxide–magnesium, for research reactors, 19: 45547 (INR-585/XIV/R)
fabrication of rod-shaped, pressed block design for, 19: 44663(P)
radiation effects on fueled graphite spheres, 19: 44749 (ORNL-P-1507)

REACTOR FUEL ELEMENTS (THERMOELECTRIC)
design of combination thermionic converter and, 19: 45556(P)

REACTOR FUEL PINS
fast fission factors in natural-uranium clustered, (T), 19: 45229 (UJV-1324/65)
neutron flux in clusters of, method for determining, 19: 45525 (EUR-2470.e)
radiation effects on Hastelloy X cladding of, in-pile, 19: 45558 (AGN-TM-409)

REACTOR FUEL PLATES
design and fabrication of ceramic-slab assembly, 19: 45554(P)
fabrication of SEFOR-ZPR-III, 19: 44587(R) (ANL-7000, pp 3-63)
swelling of clad, analysis of steady creep, 19: 45548 (WAPD-TM-498)

REACTOR FUEL RODS
fabrication and loading of RCC, for Saxon reactor tests, 19: 45601(R) (WCAP-3750)
fabrication for ESH-3 clusters, 19: 45572(R) (GEAP-4755)
fabrication in ORNL Kilorod Facility, efficiency in, 19: 44639 (ORNL-3740)
fabrication of boron carbide–uranium(IV) oxide, 19: 44591(R) (CEND-3107-228)
fabrication of uranium-233 dioxide–thorium dioxide, Kilorod demonstration of sol-gel vibratory-compaction process for, 19: 44638 (ORNL-3681)
fast fission factors in ceramic natural-uranium clustered, (T), 19: 45229 (UJV-1324/65)

performance of urania, with centerline temperatures near melting point, 19: 45573 (GEAP-4902)
REACTOR FUEL SPHERES
fabrication by pressing, method for, 19: 44662(P)
radiation effects on fueled graphite, 19: 44749 (ORNL-P-1507)
REACTOR FUEL TUBES
fabrication of Zircaloy-clad uranium metal and alloy, for heavy-water power reactors, 19: 45569 (DP-976)
REACTOR FUELS
burnup and management of, computer program for calculating, 19: 45523 (AEEW-R-425)
burnup of, activation measurement of, 19: 45542 (BAW-272)
cycle studies for, in advanced gas-cooled reactors, (T), 19: 45595 (TRG-Report-976)
design and testing of clustered, for reactor evaluation channel, 19: 45601(R) (WCAP-3750)
fabrication of powder compact, loading assembly for, 19: 44641 (ORNL-TM-1193)
fission gas migration and coalescence in, theory for, 19: 44739(R) (ANL-7000, pp 233-77)
neutron Doppler coefficients for uranium dioxide, 19: 45532 (ORNL-TM-1219)
performance of thorium-bearing, in fast breeder reactors, 19: 45605(T) (ORNL-tr-788)
processing British, facilities for, (E), 19: 45612
processing of, criticality parameters for, 19: 44112 (CONF-651103-4)
processing of, series mixer-settler apparatus for, 19: 44127(P)
radiation effects on pyrolytic carbon-coated uranium carbide and dioxide particles, 19: 44740 (BMI-1737)
radiation effects on pyrolytic carbon coatings on particles, predictions, 19: 44748 (ORNL-P-1505)
reprocessing and refabrication of second-cycle irradiated uranium dioxide, by AIROX process, 19: 44114 (NAA-SR-11375)
reprocessing of fast, using Alamine 336–dibutyl cellosolve, 19: 44108
separation processes for spent, (E), 19: 45260(R) (IDO-14660)
uses of, economics of, 19: 45621
REACTOR MATERIALS
neutron activation of structural, (T), 19: 45461 (N64-25922)
research programs on, at AECL, 19: 45694(R) (AECL-2251)
technology of uranium carbides, literature survey, 19: 44603 (NAA-SR-10929)
REACTOR MATRICES
design for high-flux production reactors, 19: 45638 (DP-999, pp 7-17)
design with skewed channels, 19: 45509(P)
development for high-flux production reactors, 19: 45640 (DP-999, pp 29-42)
fuel representation for cluster and uniform, analysis of homogeneous and shell, 19: 45601(R) (WCAP-3750)
neutron critical buckling measurements for plutonia–urania, 19: 45600(R) (WCAP-3385-4)
neutron disadvantage factors for light-water moderated, calculation of, 19: 45601(R) (WCAP-3750)
power distribution in, effects of core distributions and borated coolant on, 19: 45601(R) (WCAP-3750)
power distribution in slab, xenon-induced oscillations in, 19: 45539
power peaking in, effects of fuel cladding, water holes, and water slots on, 19: 45601(R) (WCAP-3750)
reactivity effects of water losses from graphite–uranium, 19: 45529 (INR-600/IX-A/PR)
REACTOR MODERATORS
design of graphite-brick, 19: 45511(P)
element replacement in Hallam, 19: 45591(R) (TID-22129)
element replacement in Hallam, 19: 45592(R) (TID-22135)
performance of high-boiling organic, (E), 19: 45501 (IAE-611)
REACTOR SAFETY
activities of Institute for Reactor Safety of Federal Republic, 19: 45497(T) (ORNL-tr-652)
analysis for Saxton reactor, 19: 45600(R) (WCAP-3385-4)
hazard analysis for coolant-loss in large closed-cycle reactors, 19: 45601(R) (WCAP-3750)
meteorological research for, 19: 44780 (BNL-914, pp 95-8)
meteorology in, 19: 44270 (BNL-914, pp 178-9)
meteorology research program on, 19: 44771 (BNL-914, pp 44-50)
problems with experimental devices around reactors, 19: 44287 (CEA-R-2799)
REACTOR SAFETY EXPERIMENTS
coolant blowdown models for LOFT pressurized-water, 19: 45671 (BAW-1195-4)
coolant loss accident, Zircaloy-2–steam reaction in simulated, 19: 45496 (WCAP-3269-30)
destruct tests at National Reactor Testing Station, meteorological support of, 19: 44773 (BNL-914, pp 57-64)
fuel destruction test for SPERT IV, out-of-pile, 19: 45528(R) (IDO-17097)
reactivity insertion response of SPERT III plate-type core, 19: 45528(R) (IDO-17097)
transient test data from Spert, computer programs for processing, 19: 45527 (IDO-17078)
REACTOR SHIELDING
calculations for, Monte Carlo computer program for, 19: 45469
radiation distribution in, 19: 45601(R) (WCAP-3750)
temperature distributions in Russian reactor BN-350, 19: 45604(T) (JPRS-31245)
REACTOR TUBES
design of guide, for liquid-moderated reactors, 19: 45517(P)
inspection of CVTR, sonic, 19: 45567(R) (CVNA-235)
REACTORS
development for desalination, deep-pool concept for, 19: 45637 (COO-283)
fuel channels in, lattice design for, 19: 45509(P)
fuel cycle analysis for, computer programs for, 19: 45544 (HW-79951 (Pt.1))
fuel cycle analysis for, computer programs for, 19: 45545 (HW-79951 (Pt.2))
fuel cycle analysis for, neutron cross sections for, 19: 45546 (HW-79951(Pt.3))
loading device for, 19: 45514(P)
neutron flux distributions in, method for determining, 19: 45560 (ANL-7011)
neutron flux measurements in, performance of semiconductor detectors for, 19: 44450(R) (IBK-120a)
radiation absorbed dose rates from, calorimetric measurement of, 19: 45467
reactivity period meter design for, 19: 45508(P)
shutdown of, device for, 19: 45515(P)
site selection in Europe for, principles of, 19: 45498
thermal insulation for, evaluation of, 19: 44088
use for desalination, abstracts of publications on, 19: 45590 (TID-3584)
REFRACTORY MATERIALS
bibliography on high-temperature chemistry and physics of, 19: 43994 (NP-15381)
elastic moduli of, ultrasonic determination of, 19: 44207(R) (ANL-7000, pp 146-52)
properties and uses of, conference on, 19: 44735
sheet rolling program for, developments in, 19: 44647
testing of small-diameter alloy tubing, methods for nondestructive, 19: 44211 (ORNL-P-1543)
REGENERATION
radiation effects on Blepharisma, uv, 19: 43813
RELATIVITY THEORY
Einstein pseudotensor, gauge subtraction method for, (T), 19: 45148
kinematics from Voigt-Palacios-Gordon transformation in, 19: 45142
solutions for combined Maxwell-Einstein-Klein-Gordon equations, axially symmetric, 19: 45147
thermodynamic quantities in, Lorentz transformations for, 19: 44843
RELAYS
design of coaxial mercury, engineering drawings for, 19: 44359
REMOTE-CONTROL EQUIPMENT
cutting tool design for opening fuel elements or material testing tubes, 19: 44177(P)
description of pneumatic grapple for fuel elements, 19: 44587(R) (ANL-7000, pp 3-63)
design for handling radioactive materials, 19: 44180(P)
design for preparation of samples from Molten Salt Reactor Experiment, 19: 44168 (ORNL-P-1532)
design for transmitting motion through vacuum wall, 19: 44234 (MATT-345)
design of balance for thermogravimetry of irradiated uranium dioxide, 19: 44341 (AERE-R-4962)
design of control device for tongs, 19: 44174(P)
design of corrosion-resistant pipetter, 19: 43936 (ORNL-P-1533)
manipulator design with extensible-retractable arm, 19: 44178(P)
manipulator head design for, 19: 44175(P)
RENÉ-41
corrosion by steam at 750°C, 19: 44616(R) (ANL-7000, pp 122-37)
RENÉ-62
corrosion by steam at high temperature, 19: 45572(R) (GEAP-4755)
development and properties, 19: 44699 (R63FPD33)
hardness and tensile properties at 1000 to 1300°F, effects of annealing on, 19: 45572(R) (GEAP-4755)
REPTILES
radiation effects on Nevada Test Site, 19: 43662(R) (UCLA-12-565, pp 97-128)

radiation effects on Puerto Rican forest, 19: 43662(R) (UCLA-12-565, pp 97-128)
RESEARCH REACTORS
control rod worths of ANNA, 19: 45677 (INR-614/IXA/P)
coolant blowdown models for LOFT pressurized-water, 19: 45671 (BAW-1195-4)
design and construction of Consort, 19: 45683
design of Fast Flux Test Facility, 19: 45670(R) (APDA-174, pp 74-6)
experimental facilities for fast neutron studies, 19: 45684
fuel elements for, development of dispersion-type, 19: 45547 (INR-585/XIV/R)
instrumentation of Russian, 19: 45675 (IAE-725)
kinetics of Triga Mark II, model for, (E/T), 19: 45685
loop design for, 19: 45676 (IDO-16871-4)
physics calculations for Swedish FRO, 19: 45667 (AE-194)
radiation protection problems with experimental devices, 19: 44287 (CEA-R-2799)
reactivity of Swiss SAPHIR, temperature coefficient of, 19: 45673 (EIR-85)
RESINS
performance for water deionization, 19: 45678 (JEN-149-DQ/I-50)
radiation stability of strongly basic anion, reactor, 19: 44055 (IAE-788)
regeneration of ion-exchange, apparatus for continuous, 19: 44130(P)
use in radiation-attenuating films, 19: 44670(P)
RESISTORS
fabrication of thin nickel-film, for use as calorimeter elements, 19: 44344 (K-L-1944)
RESPIRATION
in chicken red cells, 19: 43682(R) (UCLA-12-565, pp 33-57)
RHENIUM
deposition method for, thermochemical, 19: 44640 (ORNL-P-1446-1)
effects of coatings of, on brazing of titanium, 19: 44645 (JPRS-24761, pp 12–16)
elastic moduli at 298°K, 19: 44676(R) (ANL-7000, pp 176-82)
neutron reactions (n,γ) at 20 to 1000 kev, cross sections for, (E), 19: 45298
performance as emitter in thermionic cells, 19: 44985
phase transformations in, relation of c/a ratio and elastic moduli temperature dependence with, 19: 44676(R) (ANL-7000, pp 176-82)
production in thermal neutron reactions with tungsten, 19: 44599(R) (GEMP-50A)
reactions with hafnium oxides at 2450°C, 19: 44598(R) (GEMP-49A)
reactions with metal oxides at high temperatures, 19: 44685 (CONF-650908-5)
solubility in liquid plutonium at 700 to 950°C, 19: 44688 (LA-3359)
RHENIUM ALLOY COUPLES
Cr/Re–W, thermoelectric potential to 1600°C, 19: 44598(R) (GEMP-49A)
Mo–Nb/Re–W, thermoelectric potential to 1800°C, 19: 44598(R) (GEMP-49A)
Re–W/Re–W, performance to 2300°F, 19: 44348 (PWAC-473)
RHENIUM ALLOYS
Fe–Re, magnetization at 295°K, saturation, 19: 44678(R) (ANL-7000, pp 186-200)
Mo–Re, purification process variables, 19: 44598(R) (GEMP-49A)
Mo–Re, reactions with beryllium, hafnium, and magnesium oxides at 2450°C, 19: 44598(R) (GEMP-49A)
Mo–Re–W, creep-rupture properties, effects of composition on, 19: 44598(R) (GEMP-49A)
Mo–Re–W, fabrication of seamless tubing of, procedures for, 19: 44598(R) (GEMP-49A)
Mo–Re–W, fission product release, 19: 44599(R) (GEMP-50A)
Re–W, creep-rupture properties at 2000°C of arc-cast, 19: 44598(R) (GEMP-49A)
Re–W, creep-rupture at 800 to 900°C, activation energy for, 19: 44599(R) (GEMP-50A)
Re–W, deposition method for, thermochemical, 19: 44640 (ORNL-P-1446-1)
Re–W, extrusion to sheet bar, arc-melted ingot and powder compact, 19: 44612(R) (USBM-RC-1199)
Re–W, fabrication of tubing of, process development for, 19: 44633(R) (ANL-7000, pp 138-45)
Re–W, performance as emitter in thermionic cells, 19: 44985
Re–W, radiation effects on creep-rupture properties of, fast neutron, 19: 44598(R) (GEMP-49A)
Re–W, reactions with uranium dioxide at high temperatures, 19: 44593 (CONF-650908-4)
Re–W, sintering properties of, effects of prealloyed powders on, 19: 44612(R) (USBM-RC-1199)
Re–W, Young's modulus at 800 to 2200°C, static, 19: 44674(R) (ANL-7000, pp 69-83)
RHENIUM ISOTOPES Re-187
proton reactions (p,2n) at 14 Mev, conversion electron anisotropy from, (E), 19: 45352
RHODIUM ALLOYS
Co–Rh–U, crystal structure studies, 19: 44678(R) (ANL-7000, pp 186-200)
Li–Rh, crystal structure studies, 19: 44679(R) (ANL-7000, pp 205-12)
Ni–Rh–U, crystal structure studies, 19: 44678(R) (ANL-7000, pp 186-200)
Pd–Rh–U, crystal structure studies, 19: 44678(R) (ANL-7000, pp 186-200)
RHODIUM SYSTEMS
Cr–Rh–Si, phase study of Cr_3O structures in, 19: 44702 (TID-22200)
Nb–Rh–Si, phase study of Cr_3O-type structures in, 19: 44702 (TID-22200)
Rh–Si–V, phase study of Cr_3O-type structures in, 19: 44702 (TID-22200)
RIBONUCLEASE
radiolysis of, decomposition of sulfur linkage in gamma, 19: 43841
RIBONUCLEIC ACID
content in chicken livers, effects of estrogen on, 19: 43682(R) (UCLA-12-565, pp 33-57)
hydrolysis of, catalytic effects of thorium and zirconium ions on, 19: 43708
properties of, from mice with virus-induced leukemia, 19: 43883(R) (UCLA-12-565, pp 65-85)
radiation effects on phosphorus-32 pulse labeling of, in *Salmonella typhimurium*, 19: 43743
radiation effects on base composition of messenger, in *Pseudomonas effusa*, 19: 43744
synthesis in developing sea urchin eggs, effects of actinomycin D and heavy water on, 19: 43709
synthesis in *Stentor coeruleus*, 19: 43682(R) (UCLA-12-565, pp 33-57)
RIBONUCLEIC ACID, DESOXY-
hydrolysis of, catalytic effects of thorium and zirconium ions on, 19: 43708
properties of, from mice with virus-induced leukemia, 19: 43883(R) (UCLA-12-565, pp 65-85)
radiation effects on electron spin resonance of, 19: 43723(R) (TID-22128)
radiation effects on metabolism in thyroid gland of, from injected iodine-131 in rats, 19: 43757
radiation effects on metabolism of, in mice, tracer study, 19: 43792
radiation effects on content in rat liver of, 19: 43735
radiation effects on synthesis of, in *E. coli*, 19: 43741
radiation injuries of, repair mechanisms for, 19: 43795
radiosensitivity of, in *Bacillus subtilis* spores and vegetative cells, 19: 43793
synthesis in developing sea urchin eggs, effects of actinomycin D and heavy water on, 19: 43709
synthesis in epithelial and spindle cell tumors in mice, kinetics of, 19: 43698
synthesis in *Stentor coeruleus*, 19: 43682(R) (UCLA-12-565, pp 33-57)
thymine content of complementary strands of, in *Bacillus subtilis*, 19: 43723(R) (TID-22128)
RICE
fallout contamination in Japan, 1959 and 1962, 19: 44265
radiation effects on, protective effects of chemicals against seed, 19: 43877
radiation effects in seeds of, effects of dose rate, 19: 43781
ROCKET MOTOR NOZZLES
stress analysis of Kiwi, computer program for, 19: 44219 (ACF-8)
ROCKET REACTORS
design of, computer program for weight optimization in, 19: 45659 (TIM-307)
design of, effects on spacecraft mass, 19: 44228
fuel flow stability to helical disturbances, gaseous wheel-flow, (T), 19: 45652 (NASA-TN-D-2696)
performance analysis for interplanetary missions, 19: 45649 (N64-32637)
re-entry breakup of, beta and gamma dose calculational models for debris from, 19: 45655 (NUS-229)
ROCKET REACTORS (KIWI)
development of Nerva, status of, 19: 45665
engine system tests of NERVA, 19: 45663
pressure vessel and rocket nozzle stresses in, computer program for analyzing, 19: 44219 (ACF-8)
status, 19: 45658 (TID-22097)
ROCKETS
aerodynamics of Saturn VN, 19: 44137 (N64-24017)
performance for ionospheric electron temperature determination, (E), 19: 45177
radiation detectors for, performance of emulsion, 19: 44436 (CERN-65-4 (Vol.II), pp X13-18)
status and uses of nuclear, using solid-core graphite reactors, 19: 45658 (TID-22097)

ROCKS
analysis for calcium and strontium by flame photometry using plasma jets, 19: 43924 (AERE-R-4990)
analysis for niobium, radiometric-spectrophotometric, 19: 43943
analysis of lunar, alpha-scattering, 19: 44901
geology of volcanic, in Roskruge range in Pima County, Arizona, 19: 44236 (TID-22086)
isotope abundance ratios of, selected-area mass spectrometric analysis of, 19: 44354
oxygen-18/16 ratio in metamorphic, effects of origin and history on, 19: 44238
radioactive halos in, 19: 44256(T) (ORNL-tr-708)
solar wind effects on photometric properties of, simulation of, 19: 44896
ROOTS
metabolism of tritiated water in *Zea maize*, 19: 43702
radiation effects on meristematic regions in *Tribulus terrestris*, γ, 19: 43855
radioinduced chromosome aberrations in Allium, 19: 43745
ROTARY SEALS
development of face-type shaft, for use in water at high pressure, 19: 44132 (AECL-2249)
ROTORS
dynamic tests in water, summary of CANEL, 19: 44147 (TIM-917)
dynamic tests of overhung, using hydrostatic water bearings, 19: 44146 (TIM-874)
dynamic tests of straddle, with step bearings, 19: 44149 (TIM-921)
RUBBER
properties for use as corrosion-inhibiting coating for uranium, 19: 44630
RUBIDIUM
charge transfer with rubidium ions, cross section, 19: 43997(R) (UCRL-11889)
use of vapor of, in atomic clocks, 19: 44814
RUBIDIUM BROMIDES
rubidium ion nuclear magnetic shielding in, (E), 19: 45485
RUBIDIUM CHLORIDES
rubidium ion nuclear magnetic shielding in, (E), 19: 45485
RUBIDIUM IODIDES
rubidium ion nuclear magnetic shielding in, (E), 19: 45485
RUBIDIUM IONS
charge transfer with rubidium, cross section, 19: 43997(R) (UCRL-11889)
nuclear magnetic shielding of, in rubidium halides, (E), 19: 45485
RUBIDIUM ISOTOPES Rb-86
beta decay of, gamma intensity in, (E), 19: 45331
RUBIES
energy level population inversion in optically pumped, pump pulse shape effect on, (T), 19: 45704 (LA-DC-6717)
RUSSIAN REACTORS
temperature distributions in BN-350, 19: 45604(T) (JPRS-31245)
RUTHENIUM
elastic moduli at 298°K, 19: 44676(R) (ANL-7000, pp 176-82)
phase transformations in, relation of c/a ratio and elastic moduli temperature dependence with, 19: 44676(R) (ANL-7000, pp 176-82)
separation processes for, in spent reactor fuels, (E), 19: 45260(R) (IDO-14660)
solvent extraction by Alamine 336–dibutyl cellosolve in contactor, 19: 44108 (AERE-R-4440(Pt.3))
RUTHENIUM ALLOYS
Ni–Nb–Ru, crystal structure studies, 19: 44678(R) (ANL-7000, pp 186-200)
Ru–U, crystal structure studies, 19: 44678(R) (ANL-7000, pp 186-200)
Ru–Zr, lattice parameters of Zr_2Rh, 19: 44678(R) (ANL-7000, pp 186-200)
RUTHENIUM CHLORIDE COMPLEXES
preparation and properties of anionic, 19: 43997(R) (UCRL-11889)
RUTHENIUM ISOTOPES Ru-106
diffusion from waste calciners, 19: 44773 (BNL-914, pp 57-64)
metabolism by marine organisms, 19: 43669(R) (NP-15159)
uptake by clams, 19: 43663
RUTILES
faults in, electron microscopic fringe patterns of anti-phase boundaries of, 19: 44687(R) (EURAEC-1434)

S

SAFETY
standards for industrial uses of radiation, 19: 44307
SAINT LAURENT-DES-EAUX REACTOR (EDF-4)
description and performance of, (E), 19: 45614
SALAMANDERS
radiation effects on morphology of erythrocytes in, 19: 43730
SALMONELLA
radiation effects on phosphorus-32 labeling of RNA in typhimurium, 19: 43743
SALT DEPOSITS
actinide recovery from debris formed by nuclear explosion in, 19: 44156 (DP-956)
waste solid disposal in mine, demonstration of, 19: 45689 (ORNL-P-1568)
SALTS
separation from sea water using magnetohydrodynamic effect, 19: 44578(P)
SAMARIUM
purification of fission-produced, in feed materials from promethium-147 separations, 19: 44116 (ORNL-TM-1062)
separation from scandium and thorium by reversed-phase chromatography, 19: 44125
SAMARIUM ALLOYS
Cu–Sm, crystal structure studies, 19: 44678(R) (ANL-7000, pp 186-200)
Fe–Sm, isomer shift of iron-57 in $SmFe_2$ at 300 and 800°K, 19: 44678(R) (ANL-7000, pp 186-200)
Ga–Sm, crystal structure studies, 19: 44678(R) (ANL-7000, pp 186-200)
SAMARIUM COMPOUNDS
with organic acids, preparation and properties, 19: 44028
SAMARIUM ISOTOPES
production in thermal-neutron fission of uranium-123, (E), 19: 45260(R) (IDO-14660)
SAMARIUM ISOTOPES Sm-147
energy levels of, parity and spin of, (E), 19: 45267 (JINR-P-2161)
SAMARIUM ISOTOPES Sm-150
deuteron reactions (d,p) with, deformed and spherical nuclei from, (E), 19: 45359
SAMARIUM ISOTOPES Sm-151
production in deuteron reactions (d,p) with samarium-150 deformed and spherical shapes from, (E), 19: 45359
SAMARIUM ISOTOPES Sm-152
oxygen-16 inelastic scattering at 43.5 Mev, vibrational-state excitation in, (E), 19: 45321
SAMARIUM ISOTOPES Sm-154
alpha reactions (α,4n) at 40 Mev, conversion electron anisotropy from, (E), 19: 45352
oxygen-16 inelastic scattering at 43.5 Mev, vibrational-state excitation in, (E), 19: 15321
SAMARIUM OXIDES
effects on optical properties of silicate glasses, 19: 44030
phase transformations in, at 1800 to 2400°C, 19: 44731
SAMPLING
electrostatic precipitator development for stratospheric, 19: 44801(R) (NYO-2363-3)
equipment for preparation of samples from Molten Salt Reactor Experiment, 19: 44168 (ORNL-P-1532)
equipment for preparation and transfer of samples for oxygen trace analysis, 19: 43933 (LA-3344)
of upper atmosphere for nuclear debris, dynamic analysis of SAND flight, 19: 44142 (SC-RR-65-286)
principles and types of, 19: 44296 (NYO-4700(Rev.)(Suppl.II))
signals from nonuniformly spaced samples, reconstruction of analog, 19: 44809 (SC-DR-65-291)
SAN ONOFRE POWER REACTOR
boiler model for, 19: 45601(R) (WCAP-3750)
core lattice parameters for, optimization of, 19: 45599 (WCAP-3269-49)
SAPPHIRES
diffusion of krypton from, at 1100 and 1200°C, 19: 44599(R) (GEMP-50A)
SARCOMAS
incidence in Canada of, 19: 43655
radiation effects on growth of transplanted, in mice, 19: 43763
radioinduced by ingested strontium-90, in dogs, 19: 43727(R) (UCD-472-112, pp 126-40)
radioinduced by injected Thorotrast, 19: 43850
radioinduced by phosphorus-32 in bones of rats, 19: 43772
transplantation of radioinduced, in rats, 19: 43772
SATELLITES
control system for, performance of cesium ion engine, 19: 44227
orbital decay of semi-annual effects in, 19: 45158 (NP-15424)
performance for ionospheric electron temperature determination, (E), 19: 45177
power sources for, impact testing of capsules for radioisotopic, 19: 44298(R) (SC-RR-65-9)
radiation detectors for, performance of emulsion, 19: 44436 (CERN-65-4 (Vol.II), pp X13-18)
radiation detectors for, performance of emulsion, 19: 44437 (CERN-65-4 (Vol.II), pp X19-32)

SAVANNAH RIVER COMPONENTS TEST REACTOR
fuel tube fabrication for, 19: 45569 (DP-976)
SAVANNAH RIVER PLANT
radiation monitoring at, Jan. to June 1965, 19: 44288(R) (DPST-65-30-2)
SAVANNAH RIVER PRODUCTION REACTORS
core design and operation for high-flux, 19: 45637 (DP-999)
core design for high-flux, 19: 45638 (DP-999, pp 7-17)
core design for high-flux, engineering aspects of, 19: 45641 (DP-999, pp 43-64)
core development for high-flux, 19: 45640 (DP-999, pp 29-42)
isotope production in high-flux, 19: 45639 (DP-999, pp 19-28)
operation with high-flux core, 19: 45643 (DP-999, pp 73-86)
reactivity in high-flux, temperature coefficients of, 19: 45642 (DP-999, pp 65-71)
SAXTON POWER REACTOR
core fouling in, effects on boron hideout, 19: 45601(R) (WCAP-3750)
fuel assemblies for, fabrication and loading of RCC test, 19: 45601(R) (WCAP-3750)
fuel element testing in, 19: 45600(R) (WCAP-3385-4)
kinetics of, effects of chemical sham control on, (E/T), 19: 45598 (WCAP-3269-44)
operation of, effects of crud deposits on, 19: 45601(R) (WCAP-3750)
SCALERS
printout circuitry for, design of, (E), 19: 44351 (SGAE-E-4/1965)
SCANDIUM
separation from thorium and other rare earths by reversed-phase chromatography, 19: 44125
spectra at, Ohlin structure near limit of continuous x-ray, (E), 19: 44940
SCANDIUM ALLOYS
Au–Sc, crystal structure studies, 19: 44678(R) (ANL-7000, pp 186-200)
Fe–Sc, isomer shift of iron-57 in $ScFe_2$ at 300 and 800°K, 19: 44678(R) (ANL-7000, pp 186-200)
Gd–Sc, phase studies of samarium-type intermediate phases in, 19: 44672 (AD-619201)
La–Sc, phase studies of samarium-type intermediate phases in, 19: 44672 (AD-619201)
Sc–Ag, crystal structure studies, 19: 44678(R) (ANL-7000, pp 186-200)
SCANDIUM ISOTOPES Sc-41
energy levels of, lifetime and radiative width of first excited, (E), 19: 45344
SCANDIUM ISOTOPES Sc-46
metabolism in man, 19: 43692
SCANDIUM MANGANATES
crystal structure of $ScMnO_3$, x-ray-diffraction studies of, 19: 44005
SCANDIUM OXIDES
wavefunctions for, calculation for ground-state assignment, (T), 19: 44020
SCANDIUM SULFIDES
crystal structure, 19: 44010
SCANDIUM TELLURIDES
crystal structure, 19: 44010
SCATTERING
amplitudes for, normalization of Bethe-Salpeter bound-state, 19: 45078
amplitudes in local field theory, restrictions on forward, 19: 45039 (TPJU-10/65)
amplitudes of charged particle, determination of real part of forward, (T), 19: 45048(T) (ANL-Trans-217)
amplitudes of two-body, equation for, (T), 19: 45123
amplitudes of, truncation of unitary sum for, 19: 45093
bound systems in relativistic theory of, loosely, 19: 45110
dispersion theory of low-energy, 19: 45051
Heisenberg nonlinear theory of, consistency problem in spectral formulas in, 19: 45094
of elementary particles from static potential, scattering matrix for, (T), 19: 44995 (COO-30-97)
Regge trajectories in, nonrelativistic, 19: 45028 (NP-15207)
s-matrix for, consistency of unitarity condition with broken U(12) symmetry, (T), 19: 45018 (JINR-P-2283)
wave flux in, decay laws and S-matrix pole multiplicity for, 19: 45070
SCHISTOSOMA
radiation effects on infectivity of cercariae of, in mice, 19: 43848
SCINTILLATION DETECTORS
description of, for charged and neutral particles, (E), 19: 44499
design and performance of scintillating fibers, for low-energy beta particles, 19: 44451 (IITRI-578P26-8)
design for extensive air showers, 19: 44529
design for internal conversion coefficient determinations, (E), 19: 44501
design of anticoincidence, for gamma spectroscopy of molten-plutonium fuel elements, 19: 44453 (LA-DC-7316)
design of liquid, for beta counting, (E), 19: 44506
design of spark-chamber, for electrons, with discrimination against mesons (π), 19: 44522
performance as anticoincidence shields for germanium gamma spectrometers, (E), 19: 44519
performance for beta dosimetry, 19: 44491(T) (CEA-tr-R-1866)
performance for low-level gamma dosimetry, 19: 44528
photomultiplier gain in, effect of source intensity variation on, 19: 44374 (AROD-3347:6)
photopeak efficiencies of thallium-activated sodium-iodide, (E), 19: 44515
pulse shape discriminator design for zinc sulfide, 19: 44368 (AERE-M-833)
response of silver-activated zinc-sulfide, to electrons, (E), 19: 44520
use in determination of radioisotopes in biomedical samples, 19: 43659
SEA URCHINS
effects of actinomycin D and heavy water on macromolecule synthesis in developing eggs of, 19: 43709
metabolism of radionuclides by, 19: 43669(R) (NP-15159)
SEA WATER
analysis for cesium-137, large-volume, 19: 44296 (NYO-4700(Rev.) (Suppl.II))
analysis for strontium-90, large-volume, 19: 44296 (NYO-4700(Rev.) (Suppl.II))
carbon-14 content in, 19: 44267
desalination of, computer code for design of evaporator plant for, 19: 44140 (ORNL-TM-1244)
desalination of, comparison of organic-cooled and water-cooled power reactors for, 19: 45620
desalination of, deep-pool reactor development for, 19: 45631 (COO-283)
desalination of, design of organic-cooled dual-purpose reactor for, 19: 45618
desalination of, development of single-purpose reactors for, 19: 45634
desalination of, design of dual-purpose nuclear power plants for, 19: 45635
desalination of, economics of dual-purpose reactor for, 19: 45606
desalination of, uses of nuclear reactors in, 19: 45619
desalination of, use of nuclear reactors for, 19: 45636
desalination of, 1964 report from Department of Interior, 19: 44154
desalination using nuclear energy, abstracts of publications on, 19: 45590 (TID-3584)
distillation of, survey of status of, 19: 44153(T) (JPRS-31361)
processing for deuterium and salt recovery, magnetohydrodynamic, 19: 44578(P)
radioisotope content of, effects on radioactivity of edible marine organisms, 19: 43669(R) (NP-15159)
uranium-235/-238 ratio in US coastal, 19: 44263
SEALS AND GLANDS
design of insulating, for heated test sections in tubes, 19: 44134 (EUR-2434.d)
design of plug and insertion means for apertures in reactor pressure vessels, 19: 45510(P)
development of ceramic-metal, for nuclear-thermionic cells, 19: 44979(R) (NP-15419)
development of ceramic-metal, for thermionic cells, 19: 44980(R) (NP-15433)
preparation of liquefiable bismuth–tin alloy, for reactor pressure vessels and covers, 19: 44658(P)
SEED
effects of nitrosoamides on, chemical inhibition of radiomimetic, 19: 43870
radiation effects on production of pine, gamma, 19: 43722(R) (TID-22108)
radiation effects on *Digitalis Lanata EHRH*, 19: 43746
radiation effects in pea, genetic, 19: 43770
radiation effects in wheat, biological, 19: 43781
radiation effects in rice, biological, 19: 43781
radioinduced sterility in, γ, 19: 43767
SEEDLINGS
development in Pinus lambertiana, 19: 43643(R) (TID-22143)
growth of wheat, effects of radiation and weightlessness on, 19: 43717 (NASA-CR-303)
radiation effects on cytology and morphology in Pinus, 19: 43722(R) (TID-22108)
radiation effects on growth in Pinus and Quercus, gamma, 19: 43722(R) (TID-22108)
SEIGNETTOELECTRIC MATERIALS
fabrication of ferroelectric ceramics by hot pressing, 19: 44644 (SC-TM-65-276)
spectra of, cold-neutron-scattering analysis of low-frequency vibrational, 19: 45241
SELENITES
radiation effects on reactions of, with hydroxyl ions, 19: 44090
SELENIUM

diagnostic tracer use of, for gastrointestinal diseases, 19: 43886
SELENIUM ISOTOPES Se-77
neutron reactions with, resonances in, (E), 19: 45296
SELENIUM ISOTOPES Se-81
decay of, gamma spectra from, 19: 45679(R) (NYO-1859-11)
SELENIUM SYSTEMS
Se–Te, thermoelectric capacities of liquid, 19: 44712
SEMICONDUCTOR DETECTORS
amplifier signal-to-noise ratio for, effects of input resistance on, 19: 44489 (ZFK-PHA-12, pp 219-23)
amplifiers for, development of low noise, 19: 44483 (ZFK-PHA-12, pp 172-88)
amplifiers for, design and performance of charge-sensitive, 19: 44484 (ZFK-PHA-12, pp 189-95)
coating with lithium-6 and uranium-235 by electrospraying, 19: 44635 (INR-595/IA/PL)
coincidence circuits for, efficiency of, 19: 44485 (ZFK-PHA-12, pp 196-200)
coincidence circuits for, efficiency for low-amplitude pulses, 19: 44486 (ZFK-PHA-12, pp 201-5)
cryostat design for gamma, engineering drawings for, 19: 44539
design and operation of long-tube, for reactor in-core measurements, 19: 44450(R) (IBK-120n)
design and performance of silicon, for beta and gamma rays, 19: 44472 (ZFK-PHA-12, pp 52-63)
design and production of, standards for, 19: 44474 (ZFK-PHA-12, pp 66-9)
development and performance for fission products and neutrons, 19: 44450(R) (IBK-120n)
development and uses of, conference on, 19: 44467 (ZFK-PHA-12)
development of silicon, 19: 44468 (ZFK-PHA-12, pp 10-15)
dewar vessel design for lithium-drifted germanium, (E), 19: 44511
fabrication and characteristics of lithium-drifted germanium diodes for gamma spectrometry, 19: 44371 (AERE-R-4921)
operation mechanisms of, 19: 44450(R) (IBK-120n)
performance for alpha and helium-3 particles, 19: 44476 (ZFK-PHA-12, pp 123-5)
performance for alpha detection in presence of deuterons, 19: 45289 (ZFK-PHA-12, pp 99-105)
performance for alpha particles, 19: 45291 (ZFK-PHA-12, pp 117-22)
performance for determining deuteron/proton ratios in cyclotron beams, 19: 44482 (ZFK-PHA-12, pp 154-62)
performance for heavy fission particles, 19: 44481 (ZFK-PHA-12, pp 149-53)
performance for nuclear spectrometry, lectures on, 19: 44466 (UCRL-16231)
performance for proton polarization measurements, 19: 44477 (ZFK-PHA-12, pp 126-32)
performance for thermal neutrons in intense gamma background, 19: 44480 (ZFK-PHA-12, pp 144-6)
performance for triton discrimination, 19: 44475 (ZFK-PHA-12, pp 84-97)
performance in neutron spectrometers, 19: 44478 (ZFK-PHA-12, pp 132-9)
performance of anticoincidence-shielded germanium, as gamma spectrometers, (E), 19: 44519
performance of germanium, for gamma rays, 19: 44473 (ZFK-PHA-12, pp 64-5)
performance of lithium-drifted germanium, as gamma spectrometers, (E), 19: 44510
performance of lithium-drifted silicon, for particle identification, (E), 19: 44517
performance of lithium-6 loaded, in neutron spectrometers, 19: 44457 (NP-15475)
performance of lithium-compensated silicon, for deuterons and protons, 19: 44471 (ZFK-PHA-12, pp 30-2)
performance of silicon surface barrier, with guard rings, 19: 44469 (ZFK-PHA-12, pp 16-24)
production of silicon, with wide sensitivity range, 19: 44470 (ZFK-PHA-12, pp 25-9)
pulse analyzers for, time-to-pulse height, 19: 44488 (ZFK-PHA-12, pp 215-18)
use in determination of radioisotopes in biomedical samples, 19: 43659
use with uranium salts for thermal neutron detection, 19: 44479 (ZFK-PHA-12, pp 140-3)
SEMICONDUCTORS
charge carrier disorder in, (T), 19: 44844
plasma phenomena in, correlation with gases, 19: 45383 (D1-82-0419)
SENA POWER REACTOR
description and performance of, (E), 19: 45614
SEPARATION PROCESSES
design for alkali metals, alkaline earth metals, and ruthenium, (E), 19: 45260(R) (IDO-14660)
development for processing finely divided reactor fuels, series mixer-settler apparatus for, 19: 44127(P)
use of AIROX, in reprocessing and refabrication of second-cycle irradiated uranium dioxide fuel, 19: 44114 (NAA-SR-11375)
SEPARATORS
design and development of steam, 19: 45574(R) (GEAP-4914)
development for separation of steam from water, 19: 44131 (ACNP-65003)
SHEEP
vaccine for lungworm in, preparation from irradiated larvae, 19: 43750
SHELLS
dynamic response of cylindrical, to lateral loads, (T), 19: 45711 (SC-TM-65-81)
stiffness of laterally loaded conical, (T), 19: 45712 (SC-TM-65-82)
stress analysis of axisymmetric thin, 19: 44219 (ACF-8)
stress patterns of attachment region of hemispherical, with radially attached nozzles, 19: 44144 (TID-22134)
SHELTERS
feasibility of nuclear explosion, 19: 44215 (ORNL-3865)
shielding calculations for fallout, shape factors in, 19: 44217
windows for fallout, design of, 19: 44218(P)
SHIELDED CONTAINERS
design of light, for radiation sources, 19: 44179(P)
SHIELDING
calculations for fallout shelters, shape factor in, 19: 44217
calculations for manned space vehicles, effective residual dose concept for, 19: 45470
calculations for space radiation, methods for, 19: 45463 (NP-15425)
gamma dose attenuation in concrete ducts, energy dependence of, (E/T), 19: 45457 (AD-462614)
radiation absorbed dose rates in, calorimetric measurement of reactor, 19: 45467
SHIELDING MATERIALS
fabrication and forming of flexible film, 19: 44670(P)
radiation transport in, non-equilibrium diffusion equation for, (T), 19: 45460 (LA-3377)
SHOCK TUBES
design and performance of electromagnetic, 19: 44857
SHOCK WAVES
effects of electric discharge, on human ear, 19: 44283 (AWRE-E-1/65)
effects of solar-flare, on geomagnetic disturbances, (T), 19: 45163
interactions with plasma, heating effects of, (E), 19: 45434
magnetohydrodynamic detonation in, 19: 44837
production cylindrical imploding, 19: 44852
propagation in argon, front curvature in, (E), 19: 44853
propagation in gas explosion, numerical solution of unstable one-dimensional flow, 19: 44200(T) (SC-T-65-756)
propagation in outer stellar layers, (T), 19: 44924(T)
propagation in solar wind interactions with magnetosphere, (T), 19: 45165
stability and structure in plasma, 19: 45422
SILANES
alkyl-, yields of, from radiolysis of silicon hydrides in presence of ethylene, 19: 44066
pentamethyldi-, preparation and addition to olefins, 19: 44048 (TID-21309)
radiation effects on, neutron, 19: 45679(R) (NYO-1859-11)
tetramethyldi-, preparation and addition to olefins, 19: 44048 (TID-21309)
SILICATE ROCKS
analysis for niobium, radiometric-spectrophotometric, 19: 43943
SILICON
analysis for trace amounts of copper by activation methods, 19: 43973
defects in solar cells of, 19: 43997(R) (UCRL-11887)
determination in iron and steel by activation analysis using 14-Mev neutrons, 19: 43965
determination in meteorites, fast-neutron activation, 19: 43927 (CONF-650405-16)
diffusion of lithium ions in p-type, 19: 44001 (ZFK-PHA-12, pp 40-9)
effects of coatings of, on silver alloy brazing of beryllium to niobium–1 zirconium alloy, 19: 44606 (PWAC-483)
performance of lithium-drifted, for detection and identification of particles, (E), 19: 44517
preparation for detectors with wide sensitivity range, 19: 44470 (ZFK-PHA-12, pp 25-9)
preparation of self-supporting films of, (E), 19: 44650
radiation damage in, calculations of proton, 19: 44747 (NP-15463)
radiation effects on gate field-effect transistors insulated by, electron, (E), 19: 44549

SILICON CARBIDES
analysis for carbon using electron microprobe, 19: 43966
deposition method for, thermochemical, 19: 44640 (ORNL-P-1446-1)
radiation effects on, temperature dependence of, 19: 44759
SILICON HYDRIDES
radiolysis of, addition to ethylene of fragments from, 19: 44066
SILICON ISOTOPES Si-26
energy levels of, from helium-3 reactions (He-3,n) with magnesium-24, (E), 19: 45355
SILICON ISOTOPES Si-28
gamma reactions (γ,α) and (γ,p) at 17.4 to 22.3 Mev, cross sections for, (E), 19: 45310
helium-3 reactions (He-3,n) at 5.5 Mev, sulfur-30 levels from, (E), 19: 45355
neutron reactions, Q values for, 19: 44450(R) (IBK-120a)
SILICON ISOTOPES Si-29
neutron reactions (n,α) at 13.6 to 15.6 Mev, excitation function for, 19: 45290 (ZFK-PHA-12, pp 110-12)
neutron reactions, Q values for, 19: 44450(R) (IBK-120a)
SILICON ISOTOPES Si-30
neutron reactions, Q values for, 19: 44450(R) (IBK-120a)
SILICON JUNCTIONS
preparation of p-n, by lithium diffusion, 19: 44000 (ZFK-PHA-12, pp 33-9)
preparation of p-n, by phosphorus diffusion, 19: 43999 (ZFK-PHA-12, pp 7-9)
SILICON OXIDES
diffusion in sodium disilicate glass, kinetics, 19: 44611 (UCRL-16232)
effects of additives of, on modulus of rupture of beryllia, 19: 44599(R) (GEMP-50A)
effects on gamma radiolysis of aqueous solutions of benzene, 19: 44051 (AE-192)
Al_2O_3–CaO–SiO_2, diffusion in, ternary, 19: 43997(R) (UCRL-11889)
BaO–SiO_2, glass formation and structure in, 19: 44015
BeO–SiO_2, glass formation and structure in, 19: 44015
CaO–SiO_2, glass formation and structure in, 19: 44015
MgO–SiO_2, glass formation and structure in, 19: 44015
SILICON SYSTEMS
Au–Si, phases and structure of, effects of liquid quenching on, 19: 45696 (CALT-221-12)
Cr–Rh–Si, phase study of Cr_3O structures in, 19: 44702 (TID-22200)
Cr–Si–Sn, phase study of Cr_3O-type structures in, 19: 44702 (TID-22200)
Ge–Si, use in thermoelectric converters for space power systems, 19: 45664
Nb–Rh–Si, phase study of Cr_3O-type structures in, 19: 44702 (TID-22200)
Rh–Si–V, phase study of Cr_3O-type structures in, 19: 44702 (TID-22200)
Si–Ag, phases and structure of, effects of liquid quenching on, 19: 45696 (CALT-221-12)
Si–Sn–V, phase study of Cr_3O-type structures in, 19: 44702 (TID-22200)
Si–stainless steel, corrosion by steam at 650°C, 19: 44616(R) (ANL-7000, pp 122-37)
Si–Tc, phase studies, 19: 44678(R) (ANL-7000, pp 186-200)
SILKWORMS
effects of radiomimetic substances in, lethal, 19: 43787
effects of radiomimetic substances in, genetic, 19: 43787
radiation effects in genetic, 19: 43784
radiation effects in, lethal, 19: 43787
radiation effects in, genetic, 19: 43787
radioinduced mutations of, 19: 43786
radiosensitivity of spermatogonia in larvae of, 19: 43783
SILTS
radioactivity of Atlantic Ocean, fallout, 19: 44253(R) (NYO-2174-36)
SILVER
effect on determination of copper in bismuth by neutron activation methods, 19: 43941
effects on determination of copper in high-purity metals by activation methods, 19: 43973
electron energy loss in thin foils of, (E/T), 19: 44961
gamma elastic scattering cross sections to 1.33 Mev, (E/T), 19: 45327
neutron absorption cross sections at 24 kev, (E), 19: 45230
neutron reactions (n,n′γ) with, cross section for, 19: 45263 (JAERI-1078)
radiation effects on electric resistivity at 4°K, fast neutron, 19: 44739(R) (ANL-7000, pp 233-77)
reactions with beryllium, copper, stainless steel, and niobium alloys to 760°C *in vacuo*, 19: 44606 (PWAC-483)
sputtering by argon ions at 30 to 170 kev, (E), 19: 44937(R) (TID-22140)
use as filter for radiographic inspection of steel, 19: 44209(R) (EURAEC-1422)
viscosity of liquid, 19: 44701(R) (TID-22144)
SILVER ALLOYS
Ag–Sn, heat of solution at 425°C, 19: 44678(R) (ANL-7000, pp 186-200)
Ag–Tb, crystal structure studies, 19: 44678(R) (ANL-7000, pp 186-200)
Ag–Tm, crystal structure studies, 19: 44678(R) (ANL-7000, pp 186-200)
Ag–Y, crystal structure studies, 19: 44678(R) (ANL-7000, pp 186-200)
Ag–Zn, crystal structure studies, 19: 44678(R) (ANL-7000, pp 186-200)
Cd–In–Ag, radiation effects on plated, 19: 44736 (ANL-6883)
Cd–In–Ag, reactivity effects of cruciform rods of, in large PWR, 19: 45533 (WCAP-3269-33)
Cd–In–Ag, reactivity worths, 19: 45535 (WCAP-3269-47)
Dy–Ag, crystal structure studies, 19: 44678(R) (ANL-7000, pp 186-200)
Er–Ag, crystal structure studies, 19: 44678(R) (ANL-7000, pp 186-200)
Gd–Ag, crystal structure studies, 19: 44678(R) (ANL-7000, pp 186-200)
Ho–Ag, crystal structure studies, 19: 44678(R) (ANL-7000, pp 186-200)
Lu–Ag, crystal structure studies, 19: 44678(R) (ANL-7000, pp 186-200)
Mg–Ag, deformation of single crystals of, at 77 to 300°K, 19: 43997(R) (UCRL-11889)
Pb–Ag, heat of formation of liquid, 19: 43997(R) (UCRL-11889)
Pd–Ag, thermodynamic properties, 19: 44678(R) (ANL-7000, pp 186-200)
Sc–Ag, crystal structure studies, 19: 44678(R) (ANL-7000, pp 186-200)
SILVER BROMIDES
charged-particle reactions in emulsions, latent image formation in, 19: 44387 (CERN-65-4(Vol.II), pp III-10)
performance in nuclear emulsions, impurity effects on, 19: 44392 (CERN-65-4(Vol.II), pp II44-9)
preparation for nuclear emulsions, 19: 44396 (CERN-65-4(Vol.II), pp III1-4)
SILVER CHLORIDES
charged-particle tracks in, determination of, 19: 44386 (CERN-65-4 (Vol.II), pp I21-5)
use of large single crystals of, in charged particle detection, 19: 44378 (CERN-65-4(Vol.I), pp 1-15)
SILVER HALIDES
crystal growth and structure, 19: 45474 (CERN-65-4(Vol.II), pp III21-30)
performance in nuclear emulsions, 19: 44393 (CERN-65-4(Vol.II), pp II50-63)
SILVER OXIDES
effects on mice, 19: 43831
SILVER SYSTEMS
Si–Ag, phases and structure of, effects of liquid quenching on, 19: 45696 (CALT-221-12)
SIOUX FALLS POWER REACTOR
criticality studies of boiler core, 19: 45557(R) (ACNP-65557)
operation, March–Dec., 1964, 19: 45593(R) (TID-22168)
SKELETON
radiation dose to dog, from ingested strontium-90, 19: 43726(R) (UCD-472-112, pp 120-5)
radiation effects on dog, ingested strontium-90, 19: 43882 (UCD-472-112, pp 50-8)
strontium-90 metabolism in dog, 19: 43679(R) (UCD-472-112, pp 109-19)
SKIN
beta dosimetry in, 19: 43880 (NP-15270)
radiation dose calculation from external contamination, evaluation of methods for beta and gamma, 19: 44328
radiation effects in, ultraviolet, 19: 43764
radioactive contamination of, tolerance standards for, 19: 44311
radiosensitivity of human, 19: 43819
SKIN LESIONS
radiation effects on cholinesterase and tyrosinase activity in, uv, 19: 43809
radiotherapy using beta source, dosimetry, 19: 43880 (NP-15270)
SLAGS
dissolution of plutonium, dissolver performance for, 19: 44111 (BNWL-121)
SLUG CANS
design of composite aluminum–aluminum oxide, 19: 44661(P)
SMOKES
control of inhaled cigarette, in dogs during iron-59 exposure experiments, instrument for, 19: 43668 (HW-SA-3618)
detection of, comparison of ionization and photoelectric methods for, 19: 44355
diffusion from stacks, wind tunnel scale model experiments on, 19: 44764 (BNL-914, pp 14-17)
effects of admixtures of, on current intensity in ionization chamber, 19: 44355
SNAILS
excretion of foreign particles by, tracer study in Bullia, 19: 43695
radiation effects on spleen cells of *Helix vulgaris*, in tissue culture, 19: 43826
SODIUM
analysis for oxygen traces, 19: 43932 (LA-3343)
corrosive effects on zirconium at 540°C of oxygenated, effects of polarizing current on, 19: 44616(R) (ANL-7000, pp 122-37)

corrosive effects of oxygen contaminated, on titanium–vanadium alloys, 19: 44587(R) (ANL-7000, pp 3-63)
determination by flame photometry, 19: 44122
excretion in feces and urine in colostomized pullets, 19: 43693
ionization by hot tungsten, efficiency of surface, 19: 44938 (UCRL-14117)
neutron cross sections for, from 0.414 ev to 5.5 Mev, 19: 45244 (AEEW-M-472)
neutron scattering by liquid, dynamics of, (E), 19: 45235
purification by in-line methods, design and operation of loop for, 19: 44162(R) (APDA-174, pp 33-55)
radiative lifetime of $^2P–^2S$ transition of gaseous, 19: 43997(R) (UCRL-11889)
reactions of liquid, with molybdenum, tungsten, and uranium oxides, 19: 44021
reactions with water, test loop for, 19: 44161(R) (APDA-174, pp 25-32)
separation from barium, cesium, and uranium by ion exchange, 19: 44091
separation from calcium, magnesium, potassium, and strontium by ion exchange, 19: 44122
sound attenuation by liquid, measuring methods for, 19: 44342(R) (APDA-174, pp 67-70)
viscosity of liquid, kinematic, 19: 44701(R) (TID-22144)

SODIUM ALLOYS
Cs–Rh–Ti, crystal structure studies, 19: 44678(R) (ANL-7000, pp 186-200)
K–Na, corrosive effects on niobium–zirconium alloy at 1250°F, effects of carbon, nitrogen and oxygen on, 19: 44626 (TIM-896)
Nb–Rh–Zr, superconducting transition temperature, 19: 44678(R) (ANL-7000, pp 186-200)

SODIUM ARSENATES
effects on strontium-85 elution from mouse bones, 19: 43706

SODIUM AZIDES
effects on radiomimetic effects of nitrosoamides on herb seeds, 19: 43870

SODIUM BROMIDES
corrosive effects on titanium alloys at 650°F, 19: 44621 (CONF-651006-1)

SODIUM CARBONATES
effects on strontium-85 elution from mouse bones, 19: 43706
performance as sensitizer for nuclear emulsions, 19: 44406 (CERN-65-4(Vol.II), pp IV41-5)

SODIUM CHLORIDES
corrosive effects on titanium alloys at 650°F, 19: 44621 (CONF-651006-1)
diffusion of sodium-22-labeled, in two-compartment system, 19: 44025
effects on strontium-85 elution from mouse bones, 19: 43706
solvent properties for zinc chloride, 19: 44677(R) (ANL-7000, pp 183-5)
NaCl–$ZnCl_2$, diffusion and ionic conductivity in, 19: 44677(R) (ANL-7000, pp 183-5)

SODIUM CITRATES
effectiveness in removal of radioisotopes from body, 19: 43700
effects on strontium-85 elution from mouse bones, 19: 43706

SODIUM COMPLEXES
with calcium and magnesium salts of EDTA, effects on strontium-85 elution from mouse bones, 19: 43706
with DTPA, effects on strontium-85 elution from mouse bones, 19: 43706

SODIUM FLUORIDES
analytical use for thorium determination by titration, 19: 43970
ductility and yield points of crystalline, effects of impurities on, 19: 45679(R) (NYO-1859-11)
effectiveness in removal of radioisotopes from body, 19: 43700
effects on strontium-85 elution from mouse bones, 19: 43706

SODIUM HALIDES
radiation effects on luminescence of doped, at 90 and 295°K, 19: 45488

SODIUM HYDROXIDES
corrosive effects on titanium alloys at 650°F, 19: 44621 (CONF-651006-1)
performance as sensitizer for nuclear emulsions, 19: 44406 (CERN-65-4(Vol.II), pp IV41-5)

SODIUM IODIDES
corrosive effects on titanium alloys at 650°F, 19: 44621 (CONF-651006-1)
efficiency for detecting gamma rays, 19: 44515
protective effects against radiation damage in crop plants, 19: 43877

SODIUM ISOTOPES Na-22
content in caribou and reindeer meat, 19: 44289 (HW-SA-3750)
content in Eskimo urine, 19: 44289 (HW-SA-3750)
separation from deuteron-irradiated magnesium targets, 19: 44100

SODIUM ISOTOPES Na-23
electron reactions with, polarization of spectral line radiation by, (E), 19: 44956
energy level distributions, (T), 19: 45313

SODIUM ISOTOPES Na-24
use in testing high-efficiency filters, 19: 44281 (AEET-202)

SODIUM MOLYBDATES
production, properties, and structure of, 19: 44021

SODIUM OXIDES
diffusion in sodium disilicate glass, kinetics, 19: 44611 (UCRL-16232)

SODIUM PHOSPHATES
effectiveness in removal of radioisotopes from body, 19: 43700

SODIUM REACTOR EXPERIMENT
heat transfer system demolition in Power Expansion Program, 19: 45579 (NAA-SR-11414)

SODIUM SALICYLATES
effectiveness in removal of radioisotopes from body, 19: 43700

SODIUM SELENITES
proton spin lattice relaxation time in irradiated, dose and temperature dependence of, (E), 19: 45477 (NIJS-R-444)

SODIUM SILICATE GLASS
diffusion of iron oxides in di-, kinetics, 19: 44611 (UCRL-16232)
diffusion of iron into di-, 19: 43997(R) (UCRL-11889)

SODIUM SILICATES
graphite–MoS_2–$NaSiO_3$, radiation effects on lubricant wear properties of solid films, 19: 44095

SODIUM SPACE
measurement of, tracer method, 19: 43898

SODIUM SULFATES
effects on strontium-85 elution from mouse bones, 19: 43706
protective effects against radiation damage in crop plants, 19: 43877

SODIUM SYSTEMS
C–Na, carburization effects on type 304 stainless steel, 19: 44624 (NAA-SR-Memo-4387)

SODIUM THIOSULFATES
effects on strontium-85 elution from mouse bones, 19: 43706

SODIUM TUNGSTATES
production, properties, and structure of, 19: 44021

SOILS
atmospheric radiation monitoring at Ames, Jan.-June 1965, 19: 44302 (TID-22173)
content of cesium-137 at Nevada Test Site farm, 19: 43662(R) (UCLA-12-565, pp 97-128)
effects of beryllium on, 19: 43662(R) (UCLA-12-565, pp 97-128)
radioactivity of Canadian, June 1965, 19: 44251 (NP-15519, pp 23-51)
rain water percolation through, 19: 44235 (DPSPU-64-30-23)

SOLAR BATTERIES
defects in silicon cells, 19: 43997(R) (UCRL-11889)

SOLAR FLARES
data for April 1965, 19: 45178
effects on geomagnetic disturbances, (T), 19: 45163
gamma emission from, mechanism for, (T), 19: 44916(T)
microwave and x-ray emissions from, models for, 19: 44931
neutron production in, (T), 19: 44902
x-ray emission from, behind solar disk, (T), 19: 44894(T) (AD-424481)

SOLAR RADIATION
effects on magnetic disturbances at earth surface, during sudden commencements, (T), 19: 45163
effects on outer magnetospheric field lines and plasma, (T), 19: 45162
effects on rocks and rock powders, simulation of, 19: 44896
emission of corpuscular, on descending branch of activity cycle, 19: 44921(T)
emission of gamma, from flares, (T), 19: 44916(T)
emission of γ-f, in meter wavelength range, 19: 44920(T)
energy and intensity spectra of neutron, above 1 Mev, (T), 19: 44902
energy and intensity spectra of neutron, near earth, (E/T), 19: 44903
interactions with geomagnetic fields, (T), 19: 45164
interactions with magnetosphere, MHD shock propagation from, (T), 19: 45165
model of solar wind, inviscid, (T), 19: 44904
role in origin of life, 19: 45721 (UCRL-14254)
spectra of vacuum u-v, 19: 45396 (LA-DC-7120)
velocity of solar wind, exospheric temperature dependence on, (T), 19: 45179

SOLID SOLUTIONS
dislocation pairs in fcc, diffraction analysis, 19: 43997(R) (UCRL-11889)

SOLIDS
analysis for trace impurities using mass spectroscopy, 19: 43978
elementary particle transmission through amorphous, s-state, (T), 19: 45013 (JINR-P-2230)
lattice defects in, diffusion studies of, 19: 45471 (AECL-2309)
neutron inelastic scattering by, conference, 19: 45243

properties under high pressures, measurements using time-of-flight neutron diffractometers, 19: 45476 (IDO-17106)
reactions with gases, apparatus for continuous two-step, 19: 44042(P)
spectra of, theory for Raman, 19: 44039
SOLUTIONS
hydrogen atom trapping in frozen gamma-irradiated, effects of oxyanions on, 19: 44054(R) (COO-1365-7)
transport properties of concentrated electrolyte, 19: 43997(R) (UCRL-11889)
SOLVENT EXTRACTION PROCESSES
development of TALSPEAK, for actinide–lanthanide group separation, 19: 44115 (ORNL-P-1577)
for recovering actinides from debris formed by nuclear explosion in salt formation, 19: 44156 (DP-956)
radiation effects on transplutonium element separation by Clanex, 19: 44115 (ORNL-P-1577)
SONIC INSPECTION
equipment for pressure tube, 19: 45567(R) (CVNA-235)
SOUND
attenuation by liquid sodium, measurement method for, 19: 44342(R) (APDA-174, pp 67-70)
attenuation in type II superconductors, (T), 19: 45210
SOVIET UNION
fallout monitoring, 1963, 19: 44259
isotopic composition of lead ores in Eastern Transbaikal, 19: 44277
SPACE
electron content in cislunar, radar measurements of, (E), 19: 45176
environmental survey, 19: 44893 (NASA-CR-294)
hydrogen detection in intergalactic space, sensitive method for, (E), 19: 44908
SPACE FLIGHT
biological effects in man, bibliography on, 19: 43718 (NASA-SP-7011(12))
biological effects in man, bibliography on, 19: 43719 (NASA-SP-7011(13))
effects of weightlessness on growth of wheat seedlings during, preliminary study, 19: 43717 (NASA-CR-303)
effects on Habrobracon sperm, 19: 43721(R) (ORNL-TM-1217)
human stresses in, methods for improving tolerance to, 19: 43842
nuclear systems for, mission integration of, 19: 45661
orbits around Mars and Venus, trajectory parameters of entry and escape from, 19: 45649 (N64-32637)
radiation effects on growth of wheat seedlings during, preliminary study, 19: 43717 (NASA-CR-303)
SPACE MEDICINE
bibliography on, 19: 43718 (NASA-SP-7011(12))
bibliography on, 19: 43719 (NASA-SP-7011(13))
SPACE VEHICLES
aerodynamics of Saturn VN, 19: 44137 (N64-24017)
design of nuclear-electric, for high-energy missions, 19: 44228
design of, influence of radiation on, 19: 44550
dynamic analysis of Sampler for Aerospace Nuclear Debris flight, 19: 44142 (SC-RR-65-286)
electric power generation in, using closed Brayton cycle, 19: 44205
neutron activation of structural materials in, (T), 19: 45461 (N64-25922)
performance parameters for interplanetary nuclear, 19: 45649 (N64-32637)
power plants for, performance of nuclear-thermionic, 19: 45648 (GA-6478)
propulsion for earth-lunar cargo transfer, economics of electric, 19: 44232
propulsion systems for, development of electrothermal, 19: 44220 (N64-31011)
radioisotope power-generating system for manned space laboratory, 19: 44571
shielding for manned, effective residual dose concept for, 19: 45470
use of refractory materials for, 19: 44735
SPANISH REACTORS (JEN-1)
water deionization in, 19: 45678 (JEN-149-DQ/I-50)
SPARK CHAMBERS
design of high-pressure helium- or hydrogen-filled, (E), 19: 44502
design of scintillation-detector, for electrons, with discrimination against mesons (π), 19: 44522
elementary particles in, method for determining properties of, 19: 44490(T) (BNL-tr-1)
particle tracks in wide-gap, errors in, (E), 19: 44514
particle tracks in, device for automatic analysis of, 19: 44496
performance of circular, using automatic current-method analysis, (E), 19: 44498
performance of wide-gap, for detecting vertex events, (E), 19: 44507
response of wide-gap, during time of sensitivity to previous spark, (E), 19: 44518
use for particle track location in emulsions, 19: 44445 (CERN-65-4 (Vol.II), pp X74-83)
use in cosmic gamma flux studies, (E), 19: 44970
SPECIFIC HEAT
measurement as function of pressure, method for, 19: 43997(R) (UCRL-11889)
SPECTRA
coupling constants in NMR, perturbation theory for extreme, (T), 19: 44945
SPECTROMETERS
development for plasma studies, 19: 44357
magnetic field measurement and stabilization in, devices for, 19: 44352 (UJV-1339/65)
use with activation detector for criticality accident dosimetry, 19: 44537
SPECTROPHOTOMETERS
polarization effects in infrared grating, 19: 44345 (LA-DC-6719)
SPECTROSCOPY
analysis of trace impurities by optical emission, review, 19: 43929 (IS-1237)
bibliography on high-temperature, 19: 43993 (NP-15379)
semiconductors detectors for nuclear, lectures on, 19: 44466 (UCRL-16231)
SPERM
radiation effects on Habrobracon, gamma, 19: 43721(R) (ORNL-TM-1217)
radiation effects on Drosophila, mutagenic gamma, 19: 43724(R) (TID-22160)
SPHERES
stability of polytropic stellar, relativistic, (T), 19: 44925(T)
SPINAL CORD
radiation effects of chorioallantoid grafted, on marrow production in chickens, 19: 43761
SPINELS
formation by solid-state reactions of aluminum and cobalt oxides, tracer study of mechanism of, 19: 43998 (UCRL-12396)
SPLEEN
oxygen tension of mouse, effects of cysteamine, cyanide, and high-pressure oxygen, 19: 43869
radiation effects on adenosine triphosphatase activity in rat, effects of various drugs on, 19: 43860(R) (NP-15310, pp 14-25)
radiation effects on cell migration in blood stream of rats after antigen stimulation, 19: 43822
radiation effects on cells of *Molge vulgaris*, in tissue culture, 19: 43826
radiation effects on phosphatase content of, in rats, 19: 43739
radiodiagnosis of diseases of, 19: 43886
radioinduced nodule formation in mouse, 19: 43682(R) (UCLA-12-565, pp 33-57)
sulfhydryl content in mouse, effects of cysteamine, cyanide, and high-pressure oxygen, 19: 43869
zinc-65 uptake and distribution in normal and tumorous, in man, 19: 43699
SPONTANEOUS FISSION
regularity in, 19: 45271 (JINR-P-2265)
SPORES
radiosensitivity of Clostridium, effects of pH and phosphate solutions on, 19: 43865
radiosensitivity of *Bacillus subtilis*, 19: 43793
SPRINGS
response of linear damped lumped spring-mass systems, transfer function formalism for transient, 19: 45710 (SC-TM-64-1772)
STACK DISPOSAL
diffusion in, wind tunnel scale model experiments on, 19: 44764 (BNL-914, pp 14-17)
STAINLESS STEEL
analysis for oxygen by activation, isotope dilution, and vacuum fusion methods, 19: 43947
brazing type 316, to beryllium using silver, 19: 44606 (PWAC-483)
carburization of type 304 by carbon–sodium, effects on mechanical properties, 19: 44624 (NAA-SR-Memo-4387)
compatibility of Type 316, in sodium-heated boiler containing Croloy 2¼, 19: 44133(R) (BAW-1280-21)
corrosion by bismuth–tin alloy, effects of flow rate and temperature on, 19: 44616(R) (ANL-7000, pp 122-37)
corrosion by chemical shim solutions at 600°C, 19: 45601(R) (WCAP-3750)
corrosion by chlorides, stress, 19: 45601(R) (WCAP-3750)
corrosion by steam at 750°C of types 304, 316, 321, 347, and 406, 19: 44616(R) (ANL-7000, pp 122-37)
corrosion by steam under nuclear superheat reactor conditions, 19: 45572(R) (GEAP-4755)
corrosion by steam at high temperature, 19: 45572(R) (GEAP-4755)
effects of low-cobalt, on cobalt-60 activity in coolant of pressurized

water reactors, 19: 45495 (WAPD-T-1653)
erosion of rotating disks of type 316, by water, 19: 44625 (TIM-894)
evaluation of ACI# CD_4M Cu, as male connector material in fuel reprocessing, 19: 44607 (RL-SEP-508)
neutron reactions in Types 304 and 316, yields of helium and hydrogen produced by fast, 19: 44746 (NAA-SR-Memo-10626)
radiation effects on, in-reactor, 19: 45669(R) (APDA-174, pp 61-6)
radiation effects on constant-stress-rate rupture properties of niobium-stabilized, neutron, 19: 44750 (ORNL-TM-1216)
radiation effects on tensile properties of type 304, fast and thermal neutron, 19: 44743 (GEAP-3634)
reactions with fissium–plutonium–uranium alloys at 750°C of type 304, 19: 44587(R) (ANL-7000, pp 3-63)
reactions with metals at 540 to 760°C *in vacuo* by type 316, 19: 44606 (PWAC-483)
reactions with plutonium–thorium–uranium alloys at 650°C, 19: 44674(R) (ANL-7000, pp 69-83)
rupture of type 304, effects of carburization on stress, 19: 44623 (NAA-SR-10487)
strain effects on 304, effects of environment on plastic, 19: 45572(R) (GEAP-4755)
wear in borated and lithiated water, 19: 45601(R) (WCAP-3750)
Al–stainless steel, corrosion by steam at 650°C, 19: 44616(R) (ANL-7000, pp 122-37)
Ce–stainless steel, corrosion by steam at 650°C, 19: 44616(R) (ANL-7000, pp 122-37)
Si–stainless steel, corrosion by steam at 650°C, 19: 44616(R) (ANL-7000, pp 122-37)
stainless steel–Y, corrosion by steam at 650°C, 19: 44616(R) (ANL-7000, pp 122-37)
stainless steel–Zr, corrosion by steam at 650°C, 19: 44616(R) (ANL-7000, pp 122-37)

STANDARDS
for construction of boilers and pressure vessels, 19: 45507
for radioactive contamination of surfaces, 19: 44311

STARCHES
labeling with tritium, 19: 44102

STARS
book: *Stellar and Solar Magnetic Fields*, 19: 44932
cosmic x-ray sources in Sagittarius and Scorpio, positions of three, (E), 19: 44968
evolution and properties, (T), 19: 44928(T)
evolution of quasars, probability of, (T), 19: 44922(T)
evolution of, neutrino-pair processes in, (T), 19: 44927(T)
gamma emission from supernova remnants, 19: 44930
ionization equilibrium in atmosphere of, enhancement of, (T), 19: 44914(T)
luminosity of, gravitational effects of neutrino and photon, (T), 19: 44910
luminosity of, neutrino and photon, (T), 19: 44927(T)
shock wave propagation in outer layers of, (T), 19: 44924(T)
stability of polytropic spheres for, relativistic, (T), 19: 44925(T)
theory of supernova, 19: 44909
x-ray emission from, (T), 19: 44923(T)
x-ray spectra near Galactic center and in Scorpius, (E), 19: 44967

STATISTICS
accuracy in intensity-correlation and particle-counting experiments, quantum-mechanical analysis of, 19: 45151
in phase-shift analysis of elementary particle interactions, 19: 45012 (JINR-E-2353)
particle size distribution representation by log normal functions, 19: 44808 (LA-DC-6636)
reconstruction of analog signals from nonuniformly spaced samples, 19: 44809 (SC-DR-65-291)

STEAM
corrosive effects on iron–nickel–zirconium alloy, effects of alloy microstructure on, 19: 44616(R) (ANL-7000, pp 122-37)
corrosive effects on copper–zirconium and nickel–zirconium alloys at 540°C, 19: 44616(R) (ANL-7000, pp 122-37)
corrosive effects on zirconium-based alloys, effects of pressure on, 19: 44616(R) (ANL-7000, pp 122-37)
corrosive effects on stainless steel at 650°C, effects of alloy additions on, 19: 44616(R) (ANL-7000, pp 122-37)
corrosive effects on Incoloy 800, effects of aluminum additions on, 19: 44616(R) (ANL-7000, pp 122-37)
corrosive effects at 750°C on Inconel 600, 625, and X750, 19: 44616(R) (ANL-7000, pp 122-37)
corrosive effects at 750°C on Incoloy 8000, Rene 41, and Nichrome V, 19: 44616(R) (ANL-7000, pp 122-37)
corrosive effects at 750°C on types 304, 316, 321, 347, and 406 stainless steels, 19: 44616(R) (ANL-7000, pp 122-37)
corrosive effects on materials for reactor cooling systems, 19: 45572(R) (GEAP-4755)
corrosive effects on carbon steel, 19: 44627
corrosive effects on niobium–zirconium alloys, 19: 44629
corrosive effects on aluminum–chromium–iron–yttrium alloys at 730°C, 19: 44598(R) (GEMP-49A)
corrosive effects on iron-based 1041 alloy, effects of preoxidation and strain on, 19: 44598(R) (GEMP-49A)
fission product release into condensing, from molten fuel elements, 19: 44285 (BNWL-SA-29)
reactions with Zircaloy-2 in simulated reactor loss-of-coolant accident, 19: 45496 (WCAP-3269-30)
separation from water, development of separators for, 19: 44131 (ACNP-65003)
superheating for nuclear power plant, 19: 45630(P)

STEAM ENGINEERING
design and development of radial vane steam separator, 19: 45574(R) (GEAP-4914)

STEAM GENERATING HEAVY WATER MODERATED REACTOR
fuel burnup in, plutonium, 19: 45578 (JAERI-1080)

STEEL
analysis for niobium by neutron activation, 19: 43942
analysis for oxygen by isotope dilution method, 19: 43946
analysis for silicon by activation methods using 14-Mev neutrons, 19: 43965
development of high-yield-strength ductile, 19: 43997(R) (UCRL-11889)
extrusion by hydrostatic methods, 19: 44651
fatigue strength of A302B, effects of weld defects on, 19: 45503(R) (SWRI-1228-69)
proton reactions with nuclei in, at 10 and 20 Bev/c, (T), 19: 45317
radiation absorbed dose rates in, calorimetric measurement of reactor, 19: 45467
radiation effects on, research program on effects of nitrogen on fast neutron, 19: 44741 (EURAEC-1383)
radiation effects on, research program on effects of nitrogen on fast-neutron, 19: 44742(R) (EURAEC-1430)
strain aging of conventional and ausform H-11, 19: 43997(R) (UCRL-11889)
strength of ausformed, 19: 43997(R) (UCRL-11889)

STELLARATORS (B-3)
plasma production and heating in, (E), 19: 45398 (MATT-332)

STELLARATORS (C)
plasma containment in, (T), 19: 45397 (MATT-282)

STRATOSPHERE
fallout content in polar, 1963, 19: 44260
sampling in, electrostatic precipitator development for, 19: 44801(R) (NYO-2363-3)
water content measurements in, problems of automatic frost-point hygrometers for, 19: 44339 (AD-608503)

STRESS ANALYSIS
computer program for axisymmetric thin shells of revolution, 19: 44219 (ACF-8)
of attachment region of hemispherical shells with radially attached nozzles, (E), 19: 44144 (TID-22134)
of bolted closures, computer program for, 19: 44145 (TID-22138)

STRONTIUM
depletion from calves of, by hemodialysis, tracer study, 19: 43673 (TID-22147)
determination by flame photometry using d-c plasma jets, 19: 43924 (AERE-R-4990)
determination by flame photometry, 19: 44122
effects of stable, on non-metabolic strontium-89 uptake and deposition in tops of bean plants, 19: 43703
effects on properties of dentin, in rat teeth, 19: 43687
metabolism in bones, effects of age on, 19: 44250 (NP-15269)
metabolism in human fetuses of, 19: 43701
metabolism in nursing puppies, effects of calcium content of diet on, 19: 43676(R) (UCD-472-112, pp 80-5)
neutron absorption cross sections at 24 kev, (E), 19: 45230
physiological effects in rat liver mitochondria of, 19: 43688
separation from calcium, magnesium, potassium, and sodium by ion exchange, 19: 44122
separation from irradiated fuel by solvent extraction, economics of, 19: 44121
separation from liquid wastes by ion exchange using zeolite taff, 19: 44123
separation from yttrium, chromatographic, 19: 44120

STRONTIUM CHLORIDES
effects on strontium-85 elution from mouse bones, 19: 43706

STRONTIUM ISOTOPES
abundance in rocks in Roskruge range, Pima County, Arizona, 19: 44236 (TID-22086)

STRONTIUM ISOTOPES Sr-85
determination in excreta, radiochemical, 19: 43671 (PG-Report-662)
determination in rats, whole-body counting, 19: 43671 (PG-Report-662)
determination in tissues, radiochemical, 19: 43671 (PG-Report-662)
gastrointestinal absorption in dogs, 19: 43677(R) (UCD-472-112, pp 86-96)
metabolism in rats, 19: 43671 (PG-Report-662)
removal from bone deposited, effects of chelating agents and salts on, 19: 43706
removal from rat bones, effectiveness of chelating agents and other compounds for, 19: 43700
STRONTIUM ISOTOPES Sr-86
content ratio to strontium-87 in carbonatites, Ontario, Canada, 19: 44257
STRONTIUM ISOTOPES Sr-87
content ratio to strontium-86 carbonatites, Ontario, Canada, 19: 44257
STRONTIUM ISOTOPES Sr-89
content in animals and plants in Sedan fallout field, 19: 43662(R) (UCLA-12-565, pp 97-128)
content in standard diet in Germany, 19: 44313
diffusion from irradiated molybdenum–rhenium–tungsten alloy, 19: 44599(R) (GEMP-50A)
metabolism by marine organisms, 19: 43669(R) (NP-15159)
radiation effects on metabolism of, in dairy cattle, 19: 43801
uptake and deposition of non-metabolic, in tops of bean plants, 19: 43703
STRONTIUM ISOTOPES Sr-90
beta particles from, bremsstrahlung production by, (E), 19: 45284 (TID-22169)
content in animals and plants in Sedan fallout field, 19: 43662(R) (UCLA-12-565, pp 97-128)
content in bone in Japan, 1961 through 1963, 19: 44266
content in bones, effects of age on, 19: 44250 (NP-15269)
content in diet in Argentina, 19: 44250 (NP-15269)
content in diet in Japan, 1961 to 1964, 19: 44264
content in experimental dog diet, control of, 19: 43675(R) (UCD-472-112, pp 73-9)
content in food and milk in India, 1959 to 1964, 19: 44244 (AEET/AM/40)
content in milk in Japan, 1961 to 1964, 19: 44268
content in rice in Japan, 1959 and 1962, 19: 44265
determination in large volumes of seawater, method for, 19: 44296 (NYO-4700(Rev.)(Suppl.II))
determination in mixture with cerium-144, method for, 19: 43962
determination in sea water, 19: 44253(R) (NYO-2174-36)
effects of ingested, on weight gain in dogs, 19: 43645(R) (UCD-472-112, pp 10-22)
effects of ingested, on blood picture in dogs, 19: 43725(R) (UCD-472-112, pp 44-9)
effects of ingested, on life spans of dogs, 19: 43727(R) (UCD-472-112, pp 126-40)
effects of ingested, on leukocyte values in beagles, 19: 43882 (UCD-472-112, pp 50-8)
effects of ingested, on skeleton of dogs, 19: 43882 (UCD-472-112, pp 50-8)
effects on cholinesterase activity, 19: 43775
effects on strontium-85 elution from mouse bones, 19: 43706
fallout in northern hemisphere in 1962-3, 19: 44259
human bones, soft tissues, and standard diet in Germany, 19: 44313
metabolism in dogs, 19: 43679(R) (UCD-472-112, pp 109-19)
radiation dose to dog skeleton from ingested, 19: 43726(R) (UCD-472-112, pp 120-5)
separation from biological wastes by ion exchange, 19: 45692 (UCD-472-112, pp 141-7))
separation from wastes at Hanford, 19: 45690 (RL-SA-40)
therapeutic use for mouth tumors, 19: 43912
uptake by dog skeleton after oral administration, 19: 43679(R) (UCD-472-112, pp 109-19)
STRONTIUM ISOTOPES Sr-95
distribution of intravenously injected, effects of time on, 19: 43883(R) (UCLA-12-565, pp 65-85)
STRONTIUM OXIDES
effect on allotropic transformations of rare earth sesquioxides, 19: 44731
GeO_2–SrO, glass formation limits in, calculation of upper, 19: 44016
STRONTIUM SULFIDES
sublimation of, mass spectrometric study, 19: 43997(R) (UCRL-11889)
STYRENE
radioinduced graft polymerization with polyethylene and polyvinyl chloride, temperature effects on, 19: 44084
STYRENE POLYMERS
meson (K) stopping by emulsions loaded with, 19: 44398 (CERN-65-4 (Vol.II), pp III12-16)
radioinduced current oscillations in, extreme vacuum ultraviolet, 19: 44059 (NYO-2949-1)
radioinduced space charge in, by 2-Mev electrons, 19: 44096
SUBMARINES
propulsion of, radioisotope power source for, 19: 44572
SUCROSE
uptake by sugar pine embryos, tracer study of, 19: 43643(R) (TID-22143)
SUGARS
radiation effects on content in rabbit eyes, 19: 43755
SULFANILAMIDE
N-2-thiazolyl-, effects on radiomimetic effects of nitrosoamides on herb seeds, 19: 43870
SULFATE IONS
effects on radiolysis of acetylene, 19: 44082
SULFATE SPACE
measurement in man, tracer method, 19: 43898
SULFATES
effects on photometric determination of zirconium, 19: 43972
indoxyl-, radiation effects on human metabolism of, 19: 43852
SULFONES
radiolysis of diparatolyl, diphenyl, and dibenzthiophene, gamma, 19: 44054(R) (COO-1365-7)
SULFUR
dissociation of gaseous, mass spectrometric study, 19: 43997(R) (UCRL-11889)
meson (μ^+) depolarization in targets of, (E), 19: 45080
spectra of high-temperature diatomic, in inert matrices, 19: 43997(R) (UCRL-11889)
spectra of molecular, in inert gas matrices, u-v absorption, (E), 19: 45480 (UCRL-10771)
SULFUR COMPOUNDS
reactions with nitrogen atoms, 19: 43997 (UCRL-11889)
SULFUR DIOXIDES
detection and measurement in atmosphere, monitor design for, (E), 19: 44458 (NYO-2767)
SULFUR FLUORIDES
electron attachment reactions of hexa-, rates of, 19: 43997(R) (UCRL-11889)
SULFUR ISOTOPES
incorporation of radioactive, in halo0rganic compounds, 19: 44107(P)
SULFUR ISOTOPES S-30
energy levels of, from helium-3 reactions (He-3,n) with silicon-28, (E), 19: 45355
SULFUR ISOTOPES S-32
energy level structure of, (E/T), 19: 45275 (NP-15138)
neutron reactions (n,p), use in determining fast fluxes, 19: 45679(R) (NYO-1859-11)
neutron reactions (n,α), cross sections and Q values of, 19: 45679(R) (NYO-1859-11)
SULFUR ISOTOPES S-33
neutron capture by, resonances from, (E), 19: 45356
SULFUR ISOTOPES S-35
decay to chlorine-35 of, genetic effects, 19: 43816
diagnostic use for body fluid measurements, 19: 43898
SULFUR NITRIDE CHLORIDES
preparation and reactions of S_4N_3Cl, 19: 43997(R) (UCRL-11889)
SULFUR NITRIDES
spectra of radicals produced by reduction of S_4N_4, electron spin resonance, 19: 43997(R) (UCRL-11889)
SULFUR OXIDES
measurement in man, tracer method, 19: 43898
SULFURIC ACID
$Fe(NH_4)_2(SO_4)_2$–$CuCl_2$–H_2SO_4–H_2O, properties as gamma dosimeter, 19: 44372 (AFCRL-65-470)
SUN
activity cycle of, correlation with geomagnetic storms, (E), 19: 44921(T)
activity parameters for April 1965, 19: 45178
book: *Stellar and Solar Magnetic Fields*, 19: 44932
chromosphere of, spectra of spicules and fine structure of, 19: 44915(T)
chromosphere of, spicule models for, (T), 19: 44919(T)
magnetic fields of, fine structure of, (T), 19: 44918(T)
spot temperature and pressure in magnetohydrostatic equilibrium, 19: 44897
SUPERCONDUCTIVITY
induction of currents in rings, using polarized electromagnetic waves, (T), 19: 45191 (LNF-65/15)
mechanism for, instability against Cooper-pair formation in, (T), 19: 45208
research program on, 19: 43997(R) (UCRL-11889)
SUPERCONDUCTORS

acoustic attenuation in type II, (T), 19: 45210
critical fields of bismuth III, at high pressures, (E), 19: 45198
current quenching in thin lead films, (E/T), 19: 45193 (TID-21307)
current-carrying states of weakly coupled, metastable, (E), 19: 45206
development of magnets of, 19: 45212
electron tunneling in thin films of, quantum mechanical phase in Josephson, (T), 19: 45209
ferromagnetic film proximity effects on film, transition-temperature depression by, (T), 19: 45197
magnetic flux distribution in hard, under adiabatic field variations, (T), 19: 45192 (ORNL-TM-1266)
magnetic flux jumps in niobium, speed of, (E/T), 19: 45199
magnetic moments of lead, niobium, and tin spheres, residual, (E), 19: 45195
magnetization curve of niobium type II, (E), 19: 45200
performance in thin-septum magnets for accelerators, 19: 44877 (UCRL-16346)
properties of microgeometries in presence of high current densities, anomalous, (E), 19: 45207
use of bearings of, in three-phase induction motor, 19: 45196

SUPERFLUIDITY
flow of helium II through porous partition, analogous Josephson effect for, (T), 19: 45202
flow of helium II, dissipative normal fluid production in, gravitational, (E), 19: 45201
properties common to fluids, 19: 44842

SUPERHEATERS
design for pressurized water reactor power plant, 19: 45630(P)
development, 19: 45572(R) (GEAP-4755)

SUPERHEATERS (NUCLEAR)
design for boiling water reactors, 19: 45625

SUPERSONIC FLOW
circumfluence of blunt bodies in magnetic field in conducting gas, numerical solution, 19: 44200(T) (SC-T-65-756)

SURFACE WATERS
radiation monitoring at Argonne, Jan.-June 1965, 19: 44300 (TID-22171)
radioactivity at Paducah Gaseous Diffusion Plant, Jan.-June 1965, 19: 44301 (TID-22172)
radioactivity of, at Savannah River Plant, Jan. to June 1965, 19: 44288(R) (DPST-65-30-2)

SURFACES
crack detection on, using diamond stylus and strain gage, 19: 44210 (KAPL-M-6484)
radioactive contamination of, tolerance standards for, 19: 44311

SURGERY
of carcinoma of uterus, combination of radiotherapy with, 19: 43884
repair of radiation injuries of larynx and trachea resulting from radiotherapy by, 19: 43897
using radiation sources, review, 19: 43905

SWIMMING POOL REACTORS
control system design for RTN, nonlinear, 19: 45682 (RT/ING(64)-15)
experimental facilities for hydraulic transfer of irradiated containers, 19: 45686(P)

SWINE
radiation effects on, bibliography, 19: 43713 (BNWL-115)

SWITCHES
design of electronically operated, engineering drawings for, 19: 44359
development of 10-nsec semiconductor, 19: 44346(R) (N64-30522)

SWITZERLAND
fallout monitoring, 1963, 19: 44269

SYNCHROCYCLOTRONS
magnets for, pulsed, 19: 44888

SYNCHROTRONS
beam screening of ITEP proton, effects on operation of, 19: 44879(T) (AEC-tr-6607)
design of 200-Bev strong-focusing proton, 19: 44873 (UCRL-16000 (Summ.))
magnet designs for 200-Bev proton, quadrupole and sextupole, 19: 44878 (UCRL-16375)
orbit control in alternating-gradient, by magnet structure displacement, (T), 19: 44875 (UCRL-16229)
radiation levels near JINR 10-Bev, 19: 44863 (JINR-P-2231)

SYSTEMS FOR NUCLEAR AUXILIARY POWER
development of radioisotope power subsystem, 19: 44570
mission integration of reactor, 19: 45661
power cycles for, thermodynamic and turbomachinery concepts for, 19: 45654 (NASA-TN-D-2968)
use of radioisotope, for manned space laboratory, 19: 44571

SYSTEMS FOR NUCLEAR AUXILIARY POWER (SNAP-8)
mercury pump for, development of electrodynamic, 19: 44188 (NASA-TN-D-2965)
operation experience, 19: 45666
shield design, 19: 45666

SYSTEMS FOR NUCLEAR AUXILIARY POWER (SNAP-10)
design, development, and flight test of SNAP-10A, 19: 45154
flight test of 10A, performance of SNAPSHOT-1, 19: 45653 (NAA-SR-11430)
re-entry disintegration and dispersion of 10A, 19: 45651 (NAA-SR-11103)
shield heat testing for 10A, ejectable, 19: 45650 (NAA-SR-10997)
thermoelectric converter characteristics for 10A, silicon–germanium, 19: 45664

SYSTEMS FOR NUCLEAR AUXILIARY POWER (SNAP-50)
instrument development, 19: 44348 (PWAC-473)
power determination from barium-140 fission product measurements, 19: 45656 (PWAC-474)
pumps for, cavity evacuation study of, 19: 45660 (TIM-919)

T

TANTALUM
bremsstrahlung production by strontium-90–yttrium-90 beta particles in, (E), 19: 45284 (TID-22169)
corrosion by lithium at 1000°C, 19: 44616(R) (ANL-7000, pp 122-37)
diffusion of krypton-85 into arc-cast, 19: 44599(R) (GEMP-50A)
effects on fabricability of titanium–vanadium alloys, 19: 44587(R) (ANL-7000, pp 3-63)
extrusion by hydrostatic methods, 19: 44651
microstructures, 19: 44610 (TIM-943)
reactions with beryllium, copper stainless steel, and niobium alloys to 760°C *in vacuo*, 19: 44606 (PWAC-483)
reactions with metal oxides at high temperatures, 19: 44685 (CONF-650908-5)
separation from niobium and hafnium by paper chromatography, 19: 44124
thermal capacity of normal and superconducting, 19: 43997(R) (UCRL-11889)
use as filter for radiographic inspection of steel, 19: 44209(R) (EURAEC-1422)
x-ray transitions in μ-mesic atoms of 2p–1s, 19: 44962

TANTALUM ALLOYS
Al–Cu–Ta, crystal structure, 19: 44718
Al–Ta–U, fabrication of reactor fuels of, 19: 44667(P)
Cu–Ni–Ta, crystal structure, 19: 44718
Hf–Os–Ta, crystal structure studies, 19: 44678(R) (ANL-7000, pp 186-200)
Hf–Ta–W, erosion by water of rotating disks of, 19: 44625 (TIM-894)
Ni–Ta, crystal structure, 19: 44718
Ta–W, erosion by water of rotating disks of, 19: 44625 (TIM-894)

TANTALUM CARBIDES
analysis for carbon using electron microprobe, 19: 43966
structure of $Ta_{64}C$, 19: 43997(R) (UCRL-11889)
superconductivity, 19: 43997(R) (UCRL-11889)
NbC–TaC, superconductivity, 19: 43997(R) (UCRL-11889)

TANTALUM ISOTOPES Ta-181
electric quadrupole moment from x-ray spectrum of mesic (μ), (E), 19: 45326

TANTALUM OXIDES
stability of galvanic cell studies of, 19: 43997(R) (UCRL-11889)

TANTALUM SYSTEMS
HfC–Ta, solidus temperature at 2680°C, 19: 44612(R) (USBM-RC-1199)

TARTARIC ACID
uses in paper chromatographic separation of hafnium, niobium, and tantalum, 19: 44124

TARTRATES
effects on photometric determination of zirconium, 19: 43972

TECHNETIUM ALLOYS
Al–Tc, phase studies, 19: 44678(R) (ANL-7000, pp 186-200)
Tc–V, nuclear magnetic resonance relaxation times, 19: 43986(R) (ANL-7000, pp 201-4)
Tc–V, superconducting transition temperature, 19: 44678(R) (ANL-7000, pp 186-200)

TECHNETIUM ISOTOPES Tc-99
neutron reactions (n,α), (n,n′), (n,n′α), (n,p), (n,pα) at 14.1 Mev, cross sections for, (E), 19: 45325
separation from wastes at Hanford, 19: 45690 (RL-SA-40)
tracer use of, for thyroid function studies, 19: 43881 (NP-15271)

TECHNETIUM SYSTEMS
Si–Tc, phase studies, 19: 44678(R) (ANL-7000, pp 186-200)

TECHNICAL REPORTS
list of Pennsylvania Reactor facility, 19: 45679(R) (NYO-1859-11)

TEETH
fluoride effects on properties of dentin, in rat, 19: 43687
strontium effects on properties of dentin, in rat, 19: 43687

TELLURIUM
electric conductivity of thin films of, 19: 44344 (K-L-1944)
TELLURIUM ISOTOPES Te-129
beta decay of, gamma spectra in, (E), 19: 45324
beta decay of, gamma-gamma directional correlations in, (E), 19: 45335
TELLURIUM SYSTEMS
Se–Te, thermoelectric capacities of liquid, 19: 44712
TEMPERATURE
climate effects on radiation effects at ultra-high frequency energy on personnel, 19: 43774
effects of cryogenic, on nuclear emulsions, 19: 44401 (CERN-65-4 (Vol.II), pp IV1-4)
effects on nuclear emulsion aging, 19: 44402 (CERN-65-4(Vol.II), pp IV5-15)
effects on recovery of irradiated hamster cells in tissue culture, 19: 43791
measurement in argon plasma, probe for, 19: 44204
profiles in meteorology, 19: 44795 (BNL-914, pp 161-2)
radiosensitivity effects on reproduction in Tribolium, x, 19: 43716 (HW-SA-3748)
radiosinsitivity effects on reproduction in Tribolium, x, 19: 43715 (HW-SA-3747)
TERBIUM
Curie and Neel temperatures, effects of pressure on, 19: 43997(R) (UCRL-11889)
separation from scandium and thorium by reversed-phase chromatography, 19: 44125
TERBIUM ALLOYS
Ag–Tb, crystal structure studies, 19: 44678(R) (ANL-7000, pp 186-200)
Au–Tb, crystal structure studies, 19: 44678(R) (ANL-7000, pp 186-200)
Cu–Tb, crystal structure studies, 19: 44678(R) (ANL-7000, pp 186-200)
TERBIUM OXIDES
phase transformations in, at 1800 to 2400°C, 19: 44731
TERBIUM TELLURIDES
crystal structure, 19: 44010
TERPHENYL
properties as reactor coolant and moderator, (E), 19: 45501 (IAE-611)
pyrolysis of *ortho-* and *meta-*, 19: 44044 (AECL-2218)
TETRACYCLINE
effects on strontium-85 elution from mouse bones, 19: 43706
TEXTILES
radiation effects of pre-irradiation on grafting acrylonitrile, methyl methacrylate, and vinyl acetate on, 19: 44094
THALLIUM
phase transformations in, relation of c/a ratio and elastic moduli temperature dependence with, 19: 44676(R) (ANL-7000, pp 176-82)
THALLIUM COMPLEXES
with 8-quinolinol derivatives, electronic absorption spectra, 19: 43989 (MIT-905-20)
THALLIUM IONS
oxidation-reduction reactions of, polarization during, 19: 44002(T) (AEC-tr-6572)
THALLIUM ISOTOPES Tl-203
gamma transitions of, determination of internal conversion coefficients of, (E), 19: 44501
THALLIUM ISOTOPES Tl-204
activity of dissolved sources of, international comparison of specific, 19: 44101
THERMAL CONDUCTIVITY
measurement in ceramic materials, apparatus for heat pulse, 19: 43985(R) (ANL-7000, pp 85-110)
measurement in uranium dioxide fuel elements, development of in-pile transient method for, 19: 44684 (CEND-3336-241)
THERMAL INSULATION
development for thermionic cells, 19: 44980(R) (NP-15433)
radiation effects on, in reactor environment, 19: 44088
thermal conductivity of Hastelloy X wire wool, 19: 44589 (BNWL-102)
THERMAL RADIATION
emission from partially ionized argon, (E/T), 19: 45453
radiosensitivity effects on Artemia eggs, 19: 43815
THERMIONIC CELLS
cladding materials for uranium dioxide fuel in, 19: 44593 (CONF-650908-4)
current-voltage characteristics of cesium, effect of high collector temperature on, (E), 19: 44988
design of combination reactor fuel element and, 19: 45556(P)
design uses of, 19: 44987
development of nuclear, for undersea applications, 19: 44986
development of reservoirless cesium, 19: 44989
development using heat pipe, 19: 44980(R) (NP-15433)
electric insulation for in-pile, 19: 44685 (CONF-650908-5)
emitter efficiency and performance in, 19: 44985
emitter fabrication by thermochemical deposition, 19: 44640 (ORNL-P-1446-1)
materials for nuclear, 19: 44979(R) (NP-15419)
research progress, 19: 44981(R) (NP-15435)
use with gas and vapor turbine for production of energy, 19: 44983
THERMOCOUPLES
design of clamp-on, for NPD reactor, 19: 45646
performance of fast-response, for SPERT III fuel plate measurements, 19: 45528(R) (IDO-17097)
testing strap-on devices for reactor, 19: 45502 (RL-REA-2120)
THERMODYNAMICS
bioelectric forces involved in material transfer across biological membranes, 19: 43664 (BNL-9337)
of many-body systems, equations of motion for, 19: 44856
of material transfer across biological membranes, 19: 43665 (BNL-9338)
transformations of quantities in, Lorentz, (T), 19: 44843
THERMOELECTRIC CELLS
design and performance of silicon–germanium, for space power systems, 19: 45664
design uses of, 19: 44987
THERMOLUMINESCENCE
radiation effects on, in dosimetric lithium fluorides, 19: 44076
THERMOLUMINESCENT DETECTORS
properties of lithium fluoride, 19: 44541
THERMOMETRY
bibliography on high-temperature, 19: 43994 (NP-15381)
THERMONUCLEAR REACTORS
development of Chalice, (E), 19: 45406(R) (SIT-2852-17)
plasma properties in Astron, 19: 45413 (UCRL-12456)
THIETANE, 3-CHLORO-
nuclear magnetic resonance spectrum, 19: 43997(R) (UCRL-11889)
THIOCYANATE IONS
radiation effects on reactions of, with hydroxyl ions, 19: 44090
THIOPHENE
methylenedi-, complexes with rare earths, preparation and properties, 19: 44006
THOREX PROCESS
mixer-settler tests for thorium and uranium separation, 19: 44117 (ORNL-TM-1256)
THORIUM
crystal lattice spacing of, effects of heat treatments and oxygen content on, 19: 44674(R) (ANL-7000, pp 69-83)
determination in monazite by titration with sodium fluoride, 19: 43970
determination in zircons by spectroscopic methods, 19: 43954
economics of reactor fuel cycles containing, 19: 45582 (NP-15320)
effects on photometric determination of zirconium, 19: 43972
neutron absorption cross sections at 24 kev, (E), 19: 45230
performance as fuel for fast breeder reactors, 19: 45605(T) (ORNL-tr-788)
performance as reactor fuel, economic comparison with uranium, 19: 45582 (NP-15320)
photofission at 300 to 1000 Mev, cross sections for, (E), 19: 45329
separation by Acid Thorex and Purex processes, mixer-settler tests for, 19: 44117 (ORNL-TM-1256)
separation from rare earths by reverse-phase chromatography, 19: 44125
separation from uranium, method for, 19: 43982(P)
THORIUM ALLOYS
Pu–Th–U, fabricability and thermal expansion of, 19: 44674(R) (ANL-7000, pp 69-83)
Pu–Th–U, phase studies, 19: 44674(R) (ANL-7000, pp 69-83)
Pu–Th–U, reactions with chromium, nickel, and stainless steel at 650°C, 19: 44674(R) (ANL-7000, pp 69-83)
Pu–Th–U, reactions with chromium–nickel and titanium–vanadium alloys at 650°C, 19: 44674(R) (ANL-7000, pp 69-83)
Th–U, extrusion of rods of, 19: 44633(R) (ANL-7000, pp 138-45)
Th–U, radiation effects on dimensional changes in, transient temperature and neutron, 19: 44737(R) (ANL-7000, pp 111-18)
THORIUM CARBIDES
ThC_2–UC_2, phase studies and thermal expansion of pseudobinary, 19: 44696 (ORNL-TM-1188)
ThC–UC, preparation of spherules of, 19: 44659(P)
THORIUM IONS
effects on hydrolysis of nucleotides, catalytic, 19: 43708
THORIUM ISOTOPES
content in lead ores in Eastern Transbaikal, 19: 44277
neutron cross sections of, tabulation, (E), 19: 45250 (BNL-325(2nd Ed.) (Suppl. 2)(Vol. III))
THORIUM ISOTOPES Th-227
decay of, conversion electron spectra from, 19: 45306
THORIUM ISOTOPES Th-230

use in carbonate age estimation, 19: 44271
THORIUM ISOTOPES Th-232
energy levels of, rotational, (T), 19: 45285 (UCRL-16040)
photofission at 300 to 1000 Mev, cross sections for, (E), 19: 45329
use in epithermal power-breeder reactor, 19: 45629(P)
THORIUM MINERALS
age estimation by uranium–thorium–lead method, 19: 44272
THORIUM OXIDES
determination in zircons by spectroscopic methods, 19: 43954
properties in in-pile thermionic cells, 19: 44685 (CONF-650908-5)
THORIUM(IV) OXIDES
effects on gamma radiolysis of aqueous solutions of benzene, 19: 44051 (AE-192)
effects on strength of zirconium, 19: 44676(R) (ANL-7000, pp 176-82)
excretion of particles of, by snails, 19: 43695
pathological effects of deposited, in man, 19: 43738
sarcomas induced by injected, 19: 43850
ThO_2–UO_2, fabrication of uranium-233-enriched, into fuel rods by sol-gel vibratory-compaction process, 19: 44638 (ORNL-3681)
ThO_2–UO_2–Y_2O_3, fission gas release from beryllia-based, effects of beryllia coatings on, 19: 44599(R) (GEMP-50A)
THORIUM PHOSPHIDES
oxidation of, differential thermal and thermogravimetric analyses of, 19: 43985(R) (ANL-7000, pp 85-110)
properties, 19: 43985(R) (ANL-7000, pp 85-110)
ThP–UP, preparation and properties, 19: 43985(R) (ANL-7000, pp 85-110)
THORIUM URANIUM OXALATES
preparation and properties for use as catalysts, 19: 43987 (CEA-R-2817)
THULIUM
separation from scandium and thorium by reversed-phase chromatography, 19: 44125
THULIUM ALLOYS
Ag–Tm, crystal structure studies, 19: 44678(R) (ANL-7000, pp 186-200)
Cu–Tm, crystal structure studies, 19: 44678(R) (ANL-7000, pp 186-200)
Pd–Tm, crystal structure studies, 19: 44678(R) (ANL-7000, pp 186-200)
THULIUM SELENIDES
crystal structure, 19: 44010
THULIUM TELLURIDES
crystal structure, 19: 44010
THYMIDINE
metabolism in rat thyroid of, tracer study, 19: 43757
tritiated, use in studies on growth kinetics in epithelial and spindle cell tumors in mice, 19: 43698
THYMINE
content in complementary strands of desoxyribonucleic acid, 19: 43723(R) (TID-22128)
radiation effects on, gamma and ultraviolet, 19: 44060 (UCRL-16353)
radiation effects on, gamma, 19: 43682(R) (UCLA-12-565, pp 33-57)
radiolysis of aqueous, effects of bromides and chlorides on, 19: 43682(R) (UCLA-12-565, pp 33-57)
THYROID DISEASES
radiodiagnosis of, using technetium-99 as tracer, 19: 43881 (NP-15271)
radiotherapy of carcinoma, using iodine-131, 19: 43918
radiotherapy of hyperthyroidism, using iodine-131, 19: 43906
radiotherapy of hyperthyroidism using iodine-131, 19: 43895
THYROID GLAND
iodine-131 distribution and localization by autoradiography in rat, with goiter, 19: 43683
iodine-131 uptake and retention by rabbit, effects of dietary molybdenum on, 19: 43689
iodine-131 uptake by chick, age and dose effects on, 19: 43704
radiation effects on function of, 19: 43890
radiation effects on function of trout, from iodine-131, 19: 43773
radiodiagnosis and therapy of tumors of, using iodine-131, 19: 43892
THYROID HORMONES
protective effects of, against radiation injuries in rat spleen, 19: 43860(R) (NP-15310, pp 14-25)
THYROXINE
protective effects of, against radiation injuries in rat spleen, 19: 43860(R) (NP-15310, pp 14-25)
TIME MEASUREMENT
performance and properties of rubidium vapor atomic clocks for, 19: 44814
TIMING CIRCUITS
design using radioactive batteries, 19: 44364(P)
TIN
analysis for trace amounts of copper by activation methods, 19: 43973
bremsstrahlung production by strontium-90–yttrium-90 beta particles in, (E), 19: 45284 (TID-22169)
electric conductivity of liquid at temperatures to 2000°K, 19: 44701(R) (TID-22144)
gamma elastic scattering cross sections to 1.33 Mev, (E/T), 19: 45327
magnetic moments of superconducting spheres of, residual, (E), 19: 45195
neutron absorption cross sections at 24 kev, (E), 19: 45230
neutron reactions (n,n'γ) with, cross section for, 19: 45263 (JAERI-1078)
phases at high pressures, 19: 43997(R) (UCRL-11889)
radiation absorbed dose rates in, calorimetric measurement of reactor, 19: 45467
superconducting microgeometries in presence of high current densities, anomalous behavior of, (E), 19: 45207
use as filter for radiographic inspection of steel, 19: 44209(R) (EURAEC-1422)
viscosity of liquid, 19: 44701(R) (TID-22144)
TIN ALLOYS
Ag–Sn, heat of solution at 425°C, 19: 44678(R) (ANL-7000, pp 186-200)
Al–Nb–Sn, phase study of Cr_3O structures in, 19: 44702 (TID-22200)
Au–Sn, heat of solution at 425°C, 19: 44678(R) (ANL-7000, pp 186-200)
Bi–Sn, corrosive effects on type 304 stainless steel, effects of flow rate and temperature on, 19: 44616(R) (ANL-7000, pp 122-37)
Bi–Sn, use as liquefiable seal for metal surfaces, 19: 44658(P)
Cu–Sn, dislocations and stacking-fault energy of alpha, 19: 43997(R) (UCRL-11889)
Cu–Sn, radiation effects on deformation of, fast-neutron, 19: 44753
In–Sn, thermal capacity, coefficient of electron, 19: 43997(R) (UCRL-11889)
Nb–Sn, preparation and sintering of Nb_3Sn, 19: 44592 (CLM-R-43)
Nb–Sn, properties of sintered Nb_3Sn, as superconducting magnetic coil, 19: 44592 (CLM-R-43)
Nb–Sn, superconductivity critical currents in intermetallic compound Nb_3Sn, 19: 45213
Pd–Sn, heat of solution at 425°C, 19: 44678(R) (ANL-7000, pp 186-200)
Sb–Sn–Zr, phase studies, 19: 44720
Sn–Zr, crystal structure of intermetallic compound $ZrSn_2$ in, 19: 44720
TIN CHLORIDES
protective effects against radiation damage in crop plants, 19: 43877
TIN ISOTOPES Sn-116
carbon-12 reactions (C-12,4n) at 80 Mev, barium-124 energy levels from, (E), 19: 45285 (UCRL-16040)
TIN ISOTOPES Sn-124
neutron radiative capture at 62 ev, angular distribution from, (E), 19: 45379
TIN ISOTOPES Sn-125
decay scheme, 19: 45679(R) (NYO-1859-11)
TIN SYSTEMS
Cr–Si–Sn, phase study of Cr_3O-type structures in, 19: 44702 (TID-22200)
Si–Se–V, phase study of Cr_3O-type structures in, 19: 44702 (TID-22200)
TIN TELLURIDES
heat of formation of, 19: 43997(R) (UCRL-11889)
TISSUE CULTURES
radiation effects on intracecal carcinoma, z, 19: 43802
radiation effects on spleen cells of *Molge vulgaris* in, 19: 43826
radiation injuries in HeLa cells in, repair mechanisms for, 19: 43790
radiation injuries in hamster cells in, repair mechanisms for, 19: 43791
radiation injury and recovery in hamster cells in, 19: 43857
radioinduced mutations in human somatic cells in, 19: 43844
radiosensitivity of mammalian cells in, 19: 43723(R) (TID-22128)
TISSUES
analysis for calcium and strontium by flame photometry using plasma jets, 19: 43924 (AERE-R-4990)
analysis for carbon-14-labeled protein by scintillation counting, 19: 43945
carbon-14 uptake by amino acids in rat cerebral, *in vitro*, 19: 43690
niobium-95 and zirconium-95 distribution in rabbit fetal and maternal, 19: 43883(R) (UCLA-12-565, pp 65-85)
preparation of, for autoradiography, 19: 43696
radiation dose distribution in, calculation of, 19: 44329
radiation dosimetry in animal and human, by beryllium-7 measurements in, 19: 44327
radiation effects on metabolites in human and rat, use in exposure diagnosis, 19: 43852
radioinduced destruction of, 19: 43905
radiosterilization of grafts, 19: 44564
zinc-65 uptake and distribution in normal and tumor, in man, 19: 43699
TITANIUM
brazing of rhenium-coated, diffusion processes in, 19: 44645 (JPRS-24761, pp 12-16)
corrosion by mercury, inhibiting effects of dissolved aluminum, nickel, or zirconium on, 19: 44616(R) (ANL-7000, pp 122-37)
corrosion by mercury-based ternary alloys with aluminum, magnesium, nickel, and zirconium, 19: 44616(R) (ANL-7000, pp 122-37)

determination in nuclear grade graphite, spectrochemical, 19: 43930 (JEN-145-DQ/I-46)
diffusion in bcc phases of, 19: 45471 (AECL-2309)
effects on zirconium nitride corrosion by mercury, 19: 44616(R) (ANL-7000, pp 122-37)
extrusion by hydrostatic methods, 19: 44651
nuclear magnetic resonance, 19: 43986(R) (ANL-7000, pp 201-4)
phase transformations in, relation of c/a ratio and elastic moduli temperature dependence with, 19: 44676(R) (ANL-7000, pp 176-82)
reactions with beryllium, copper, stainless steel, and niobium alloys to 760°C *in vacuo*, 19: 44606 (PWAC-483)
spectra at, Ohlin structure near limit of continuous x-ray, (E), 19: 44940

TITANIUM ALLOYS
Al–Mo–Ti–V, corrosion cracking of, mechanisms for stress, 19: 44621 (CONF-651006-1)
Cr–Ti, phase studies, 19: 44714
Cr–Ti–V, fabricability of, effects of composition on, 19: 44587(R) (ANL-7000, pp 3-63)
Cr–Ti–Zr, phase studies, 19: 44714
Cu–Rh–Ti, crystal structure studies, 19: 44678(R) (ANL-7000, pp 186-200)
Fe–Ta, isomer shift of iron-57 in $TaFe_2$ at 300 and 800°K, 19: 44678(R) (ANL-7000, pp 186-200)
Fe–Ti, isomer shift of iron-57 in $TiFe_2$ at 300 and 800°K, 19: 44678(R) (ANL-7000, pp 186-200)
Mo–Ti, erosion by water of rotating disks of, 19: 44625 (TIM-894)
Mo–Ti, microstructures, 19: 44610 (TIM-943)
Nb–Ti, reactions with metals at 450 to 760°C *in vacuo*, 19: 44606 (PWAC-483)
Nb–Ti–V, microstracture of, effects of annealing temperature on, 19: 44587(R) (ANL-7000, pp 3-63)
Nb–Ti–Zr, microstructure of, effects of annealing temperature on, 19: 44587(R) (ANL-7000, pp 3-63)
Pu–Ti–U, corrosion by air at room temperature, 19: 44587(R) (ANL-7000, pp 3-63)
Ti–V, corrosion by oxygen-contaminated sodium, 19: 44587(R) (ANL-7000, pp 3-63)
Ti–V, enthalpy, thermal conductivity, and thermal expansion of, 19: 44587(R) (ANL-7000, pp 3-63)
Ti–V, fabricability of TV-20, effects of molybdenum, niobium, and tantalum additions on, 19: 44587(R) (ANL-7000, pp 3-63)
Ti–V, fabrication of TV-20, 19: 44587(R) (ANL-7000, pp 3-63)
Ti–V, hardness of, effects of oxygen and titanium content on, 19: 44587(R) (ANL-7000, pp 3-63)
Ti–V, mechanical properties at high temperatures, 19: 44674(R) (ANL-7000, pp 69-83)
Ti–V, neutron reactions in, yields of helium and hydrogen produced by fast, 19: 44746 (NAA-SR-Memo-10626)
Ti–V, reactions with plutonium–thorium–uranium alloys at 650°C, 19: 44674(R) (ANL-7000, pp 69-83)
Ti–V, reactions with fissium–plutonium–uranium alloys at 750°C, 19: 44587(R) (ANL-7000, pp 3-63)

TITANIUM CARBIDES
analysis for carbon using electron microprobe, 19: 43966

TITANIUM HYDRIDES
gamma production and transport in, (E/T), 19: 45575 (GMAD-3078-23)

TITANIUM ISOTOPES Ti-46
deuteron reactions (d,p) at 7 Mev, cross sections for, (E), 19: 45323

TITANIUM OXIDES
effect on sintering of uranium dioxide, 19: 44646
effects on sintering of urania, 19: 43985(R) (ANL-7000, pp 85-110)

TITANIUM(IV) OXIDES
effects on gamma radiolysis of aqueous solutions of benzene, 19: 44051 (AE-192)
oxygen free energy in, partial molar, 19: 44680(R) (ANL-7000, pp 227-32)

TITANIUM SYSTEMS
Al–B–Ti, phase studies, 19: 44719
C–Mo–Ti–Zr, mechanical properties at high temperatures, 19: 44674(R) (ANL-7000, pp 69-83)
HfC–Ti, solidus temperature at 1655°C, 19: 44612(R) (USBM-RC-1199)

TOMATOES
radioinduced sterility in pollen of, γ, 19: 43767

TOXICOLOGY
research programs on, 19: 43647(R) (UCLA-12-565)
tracer studies using phosphorus-32 in cells, 19: 43740

TRACER TECHNIQUES
aerosol penetration depths in filters, 19: 44299 (SZS-2(1965))
for cytological studies, 19: 43740
for diagnosis of gastrointestinal diseases, 19: 43886
leak detection in gas mains, 19: 44553 (EUR-2284.i)
radioisotope selection for use in, 19: 44551
testing high-efficiency filters, 19: 44281 (AEET-202)
uses in Rumania, 19: 45705 (NP-15193)

TRACER TECHNIQUES (AGRICULTURE)
body water determination in cattle using tritium, 19: 43694

TRACER TECHNIQUES (BIOLOGY)
autoradiographic localization of tritium, 19: 43696
for hemoglobin synthesis in red cells, 19: 43682(R) (UCLA-12-565, pp 33-57)
properties of radioisotopes for, 19: 43707
using thorotrast particles for study of excretory system of mollusk, 19: 43695

TRACER TECHNIQUES (BOTANY)
for plant metabolic studies, 19: 43685

TRACER TECHNIQUES (CHEMISTRY)
study of solid-state reactions of oxides, using proton activation of oxygen-18, 19: 43998 (UCRL-12396)

TRACER TECHNIQUES (ENGINEERING)
development for in-place filter evaluation, 19: 44208(R) (BMI-X-346)

TRACER TECHNIQUES (MEDICINE)
determination of age or volume of liquids, 19: 43660(P)
determination of liquid volumes, 19: 43661(P)
for blood flow evaluation, 19: 43883(R) (UCLA-12-565, pp 65-85)
for blood flow in kidneys and liver, 19: 43883(R) (UCLA-12-565, pp 85-85)
for diagnosis of circulatory shunts, 19: 43904
for dilution studies used in radiocardiography, 19: 43883(R) (UCLA-12-565, pp 65-85)
for measurement of body fluids, 19: 43898
for thyroid function studies, 19: 43881 (NP-15271)

TRACER TECHNIQUES (METEOROLOGY)
tests of fluorescein-zinc sulfide dual, 19: 44800 (BNWL-103)

TRAMEX PROCESS
radiation effects on transplutonium element separation by, 19: 44115 (ORNL-P-1577)

TRANSISTORS
development of 10-nsec switching, 19: 44346(R) (N64-30522)
heating of, effects on circuit design, 19: 45715 (SC-TM-65-359)
radiation effects on, gamma and neutron, 19: 44548 (NP-15422)
radiation effects on silicon-insulated gate field-effect, electron, 19: 44549

TRANSITION METALS
distribution in fused salt-cation exchanger systems, 19: 44040

TRANSURANIC ELEMENTS
analytical chemistry of, review of, 19: 43948
production in heavy ion reactions with heavy nuclei, (T), 19: 45286 (UJV-1293/65)

TREES
embryogenesis in *Pinus lambertiana*, 19: 43643(R) (TID-22143)
histogenesis in *Pinus lambertiana*, 19: 43643(R) (TID-22143)
radiation effects on *Pinus thunbergii*, gamma, 19: 43682(R) (UCLA-12-565, pp 33-57)
radiation injuries in oak, 19: 43722(R) (TID-22108)
radiosensitivity of, 19: 43711 (BNL-924)

TRIETHYLAMINE
photolysis products of, 19: 44053 (AFML-TR-65-166)
radioinduced addition to 1-octene, gamma, 19: 44053 (AFML-TR-65-166)
radiolysis of, yields in gamma, 19: 44072
radiolysis products of, gamma, 19: 44053 (AFML-TR-65-166)

TRINO POWER REACTOR
design and development, 19: 45617
fuel cycle economics for, thorium–uranium, 19: 45582 (NP-15320)
testing of, comparison with other Italian power reactors, 19: 45616

TRITIUM
autoradiographic localization of, in rat tissues, 19: 43696
beta particles from, design and performance of scintillation fibers for detecting, 19: 44451 (IITRI-578P26-8)
determination in carbon dioxide by gas chromatography, 19: 43926 (CEA-R-2800)
incorporation in cells *in vitro*, 19: 43651
incorporation in ethyl methanesulfonate, 19: 43651
incorporation in halo&rganic compounds, 19: 44107(P)
incorpor::tion into starch granules, 19: 44102
magnetic moment anomaly of, meson exchange effects on, (T), 19: 45332
magnetic moment of, meson exchange effects on wave function for, (T), 19: 45333
proton reactions (p,γ) at 3 Mev, yields from, (E), 19: 45358
reactions of recoil, with ethane, effects of oxygen on, 19: 44106
tracer use of, in studies of plant metabolism, 19: 43685
use in determining water content of cattle, 19: 43694

TRITONS
detection of, semiconductor detector discrimination for, 19: 44475 (ZFK-

PHA-12, pp 84-97)
emission in lithium-7 reactions with nuclei, mechanisms for, (T), 19: 45264 (JINR-E-2243)
production in bremsstrahlung reactions (γ,t) with lithium-6 at 32 and 40 Mev, (E), 19: 45374
reactions (t,α) with beryllium-9 at 13 Mev, lithium-8 excited states from, (E), 19: 45348
TRYPSIN
radiation effects on, protective effects of oxidized and reduced pyridine coenzymes against gamma, 19: 44081
TRYPTOPHAN
radiation effects on sorption from rat intestine, 19: 43728(R) (UCLA-12-565, pp 59-64)
TUBERCULOSIS
diagnosis in leukemia patients, frequency in Hiroshima of, 19: 43710 (ABCC-16-64)
TUBES
boiling burnout in, effects of nonuniform heat generation on, 19: 44183(R) (BAW-3238-8)
boiling critical heat flux in water at 70 and 100 atm in internally cooled, effects of length/diameter ratio on, 19: 44184(R) (EURAEC-1281)
boiling heat transfer of potassium in serpentine, forced-convection, 19: 44195 (TID-21256)
bubble rise velocity in inclined, 19: 44192(R) (NYO-3114-9)
heat transfer to supercritical-pressure liquid hydrogen in turbulent flow through, data compilation, 19: 44189 (NP-15332)
testing of small-diameter refractory-alloy, methods for nondestructive, 19: 44211 (ORNL-P-1543)
testing sealed radioisotope-containing, impacting, 19: 44298(R) (SC-RR-65-9)
TUMORS
growth curve for mammary fibroadenoma in rats, 19: 43649 (UCRL-16177)
growth kinetics of epithelial and spindle cell mouse, using autoradiography and tritiated thymidine, 19: 43698
growth of transplanted, in rats, effects of phosphorus-32 colloids on, 19: 43797
incidence of lung, in uranium miners, 19: 44314
metastatic, effects of phosphorus-32 chromium phosphate colloids on, in rats, 19: 43797
radiation effects on virulence of, grafted in successive generations of mice, 19: 43762
radiodiagnosis and therapy of thyroid, using iodine-131, 19: 43892
radiodiagnosis of esophageal, gastric, and rectal, using phosphorus-32 and miniature Geiger tube, 19: 43887
radioinduced in man, by deposited radium, 19: 43830
radioinduced lung, in uranium miners, 19: 43824
radiotherapy of neck, effects on thyroid function, 19: 43890
radiotherapy of oral, 19: 43912
radiotherapy of thyroid, using iodine-131, 19: 43906
radiotherapy of uterine, evaluation of results, 19: 43910
radiotherapy of, nutritional management of patients after, 19: 43911
radiotherapy using radium source, 19: 43900
TUNGSTEN
creep of arc-cast, equation for, 19: 44598(R) (GEMP-49A)
creep-rupture properties of arc-cast, at 1600 to 2800°C, 19: 44598(R) (GEMP-49A)
deposition method for, thermochemical, 19: 44640 (ORNL-P-1446-1)
diffusion of uranium in, from uranium(IV) oxides, 19: 44975(R) (NP-15419)
electron emission from crystals of, orientation effects on thermionic, (E), 19: 44981(R) (NP-15435)
elongation of arc-cast, effects of annealing at 2400°C on, 19: 44598(R) (GEMP-49A)
extrusion by hydrostatic methods, 19: 44651
fabrication of tubing of, process development for, 19: 44633(R) (ANL-7000, pp 138-45)
gamma elastic scattering cross sections to 1.33 Mev, (E/T), 19: 45327
gamma production and transport in, (E/T), 19: 45575 (GMAD-3078-23)
gas thermal release from, mechanism of injected inert, (E), 19: 44954
ionization of alkali metal beams by hot, efficiency of surface, 19: 44938 (UCRL-14117)
machining and working of cast, 19: 44653
mechanical properties of vapor-deposited and powder-metallurgy, 19: 44695 (ORNL-P-1506)
neutron absorption cross sections at 24 kev, (E), 19: 45230
neutron reactions (n,γ) with, osmium and rhenium production from thermal, 19: 44599(R) (GEMP-50A)
performance as emitter in thermionic cells, 19: 44985
preparation of high-surface-area powders of, by hydrogen reduction of tungstic oxide, 19: 44613 (Y-1476)
proton scattering by crystals of, angular distribution of charged products from, (E), 19: 45349
radiation effects on resistivity of, fast neutron, 19: 44598(R) (GEMP-49A)
radiation effects on hot hardness of single crystal, fast neutron, 19: 44599(R) (GEMP-50A)
reactions with beryllium, copper, stainless steel, and niobium alloys to 760°C *in vacuo*, 19: 44606 (PWAC-483)
reactions with boron nitrides at high temperatures, 19: 44220 (N64-31011)
reactions with metal oxides at high temperatures, 19: 44685 (CONF-650908-5)
reactions with uranium dioxide at high temperatures, 19: 44593 (CONF-650908-4)
sintering of high-purity, high-surface-area powders of, 19: 44613 (Y-1476)
sorptive properties for hydrogen at 77 to 600°K, 19: 44036
testing wires of, device for high temperature, 19: 44213
Young's modulus at 800 to 2200°C, static, 19: 44674(R) (ANL-7000, pp 69-83)
TUNGSTEN ALLOY COUPLES
Cr/Re–W, thermoelectric potential to 1600°C, 19: 44598(R) (GEMP-49A)
Mo–Nb/Re–W, thermoelectric potential to 1800°C, 19: 44598(R) (GEMP-49A)
Re–W/Re–W, performance to 2300°F, 19: 44348 (PWAC-473)
TUNGSTEN ALLOYS
development of, with high-temperature strength and low-temperature sinterability, 19: 44691 (NASA-TN-D-3015)
Al–W–U, fabrication of reactor fuels of, 19: 44666(P)
Cu–Ni–W, mechanical properties and microstructure of, 19: 44691 (NASA-TN-D-3015)
Fe–W, isomer shift of iron-57 in WFe_2 at 300 and 800°K, 19: 44678(R) (ANL-7000, pp 186-200)
Hf–Nb–W, erosion by water of rotating disks of, 19: 44625 (TIM-894)
Hf–Ta–W, erosion by water of rotating disks of, 19: 44625 (TIM-894)
Mo–Re–W, creep-rupture properties, effects of composition on, 19: 44598(R) (GEMP-49A)
Mo–Re–W, fabrication of seamless tubing of, procedures for, 19: 44598(R) (GEMP-49A)
Mo–Re–W, fission product release, 19: 44599(R) (GEMP-50A)
Re–W, creep-rupture properties at 2000°C of arc-cast, 19: 44598(R) (GEMP-49A)
Re–W, creep-rupture at 800 to 900°C, activation energy for, 19: 44599(R) (GEMP-50A)
Re–W, deposition method for, thermochemical, 19: 44640 (ORNL-P-1446-1)
Re–W, extrusion to sheet bar, arc-melted ingot and powder compact, 19: 44612(R) (USBM-RC-1199)
Re–W, fabrication of tubing of, process development for, 19: 44633(R) (ANL-7000, pp 138-45)
Re–W, performance as emitter in thermionic cells, 19: 44985
Re–W, radiation effects on creep-rupture properties of, fast neutron, 19: 44598(R) (GEMP-49A)
Re–W, reactions with uranium dioxide at high temperatures, 19: 44593 (CONF-650908-4)
Re–W, sintering properties of, effects of prealloyed powders on, 19: 44612(R) (USBM-RC-1199)
Re–W, Young's modulus at 800 to 2200°C, static, 19: 44674(R) (ANL-7000, pp 69-83)
Ta–W, erosion by water of rotating disks of, 19: 44625 (TIM-894)
TUNGSTEN CARBIDES
analysis for carbon using electron microprobe, 19: 43966
C–W_2C–ZrC, behavior at 3250°K in graphite crucible, 19: 44701(R) (TID-22144)
TUNGSTEN ISOTOPES W-172
energy levels of, rotational, (T), 19: 45285 (UCRL-16040)
TUNGSTEN ISOTOPES W-174
energy levels of, rotational, (T), 19: 45285 (UCRL-16040)
TUNGSTEN ISOTOPES W-176
energy levels of, rotational, (T), 19: 45285 (UCRL-16040)
TUNGSTEN ISOTOPES W-187
neutron reactions (n,γ) with, cross section for, 19: 44599(R) (GEMP-50A)
TUNGSTEN ISOTOPES W-188
production in neutron reactions with tungsten-187, cross section for, 19: 44599(R) (GEMP-50A)
TUNGSTEN OXIDES
hygroscopicity of high-surface-area powders of, 19: 44613 (Y-1476)
preparation of high-surface-area powders of, by precipitation methods, 19: 44613 (Y-1476)
reactions with liquid sodium, composition and properties of products in, 19: 44021
Pm_2O_3–WO_3, properties, 19: 43992 (NP-15339)
TUNGSTEN SYSTEMS

HfC–W, solidus temperature at 2730°C, 19: 44612(R) (USBM-RC-1199)

U

ULTRASONICS
inspection of steel welds by, use of dynamic screen images for, 19: 44209(R) (EURAEC-1422)
propagation in liquid hydrogen, velocity of, (E), 19: 44822
radiation images, system for television presentation of, 19: 44207(R) (ANL-7000, pp 146-52)
use in determining elastic moduli of high-temperature materials, 19: 44207(R) (ANL-7000, pp 146-52)
use in grinding natural graphite, 19: 44648
ULTRAVIOLET RADIATION
carcinogenesis by, quantitative mechanism for, 19: 43821
effects in *Escherichia coli*, lethal, 19: 43794
effects in *Escherichia coli*, genetic, 19: 43794
effects in *Escherichia coli*, 19: 43795
effects in fern gametophytes, biological, 19: 43825
effects in skin, biochemical, 19: 43764
effects of extreme vacuum, on polystyrene, 19: 44059 (NYO-2949-1)
effects on base composition of messenger RNA in *Pseudomonas effusa*, 19: 43744
effects on cholinesterase and tyrosinase activity in skin lesions, 19: 43809
effects on culture media for tubercle bacilli, 19: 43737
effects on diethylamine and triethylamine, 19: 44053 (AFML-TR-65-166)
effects on droplet nuclei in bacteria, 19: 43736
effects on *E. coli* infection with bacteriophage MS_2, 19: 43742
effects on enzyme activity in Tetrahymena, 19: 43856
effects on glycolysis rate in Saccharomyces, 19: 43765
effects on phage induction in *Serratia marcescens*, 19: 43847
effects on radio- and radiothermo-luminescence of zinc sulfide phosphors, 19: 44757
effects on regeneration in Blepharisma, 19: 43813
effects on thymine, 19: 44060 (UCRL-16353)
genetic effects in human cells in tissue culture, 19: 43844
metabolic effects in bacteriophage, 19: 43845
pathological effects in man, 19: 43819
UNDERGROUND EXPLOSIONS
actinide recovery from debris in salt formation, 19: 44156 (DP-956)
neutron release in, use for time-of-flight experiments, 19: 44157 (LA-DC-7304)
particle statistics of rubble from nuclear, 19: 44159
throwout from nuclear, effects on vegetation, 19: 43662(R) (UCLA-12-565, pp 97-128)
use of atomic, in stimulating oilfields, 19: 44158 (UCRL-14311)
UNDERGROUND STRUCTURES
shielding properties of basement, for gamma radiation, 19: 44216
URACIL, 6-PROPYL-2-THIO-
effects on thyroid metabolism in rats injected with iodine-131, 19: 43757
URANIUM
analysis for cadmium, atomic absorption spectrophotometric, 19: 43935 (NIJS-R-447)
analysis of enriched, for copper, absorptiometric, 19: 43938 (PG-Report-665)
content in Ohio River below Paducah, Jan.-June 1965, 19: 44301 (TID-22172)
corrosion by water vapor, effects of oxygen on hydrogen production during, 19: 44618 (AWRE-O-42/65)
corrosion protection of, by organic coatings, 19: 44630
crystallographic structure of alpha, 19: 44675(R) (ANL-7000, pp 155-75)
determination in zircons by spectroscopic methods, 19: 43954
diffusion from uranium(IV) oxides through tungsten, 19: 44979(R) (NP-15419)
diffusion in alpha, self-, 19: 44675(R) (ANL-7000, pp 155-75)
diffusion in gamma, mechanisms for impurity, 19: 44675(R) (ANL-7000, pp 155-75)
dissolution by nitric acid solution containing uranyl ions, 19: 44128(P)
effects on gonadal nucleic acids in fish, 19: 43769
effects on photometric determination of zirconium, 19: 43972
elastic moduli of single crystals of alpha, at 44 to 923°K, 19: 44675(R) (ANL-7000, pp 155-75)
elastic moduli of, relation of specific heat and thermal expansion to, 19: 44675(R) (ANL-7000, pp 155-75)
electron inelastic scattering at 40 kv, polarization in, (T), 19: 44942
fatigue of, effects of cold working, hydrogen, notches, and temperature on, 19: 44681 (AWRE-O-65/65)
fuel element fission gas release in, 19: 44632
gamma elastic scattering cross sections to 1.33 Mev, (E/T), 19: 45327
neutron absorption cross sections at 24 kev, (E), 19: 45230
neutron fission of, time delays in K x ray emission during thermal, 19: 45294
oxidation by carbon dioxide, fission product release in, 19: 44632
oxidation by water vapor, optical measurements of film growth at 50 and 70°C, 19: 44619 (AWRE-O-86/65)
performance as reactor fuel, economic comparison with thorium, 19: 45582 (NP-15320)
phase transition at 41°K, 19: 44675(R) (ANL-7000, pp 155-75)
photofission at 300 to 1000 Mev, cross sections for, (E), 19: 45329
processing of powdered, design of facility with inert atmosphere for, 19: 44018
radioinduced growth in single crystal, thermal neutron, 19: 44739(R) (ANL-7000, pp 233-77)
radioinduced swelling in, effects of pre- and postirradiation heat treatments on neutron, 19: 44739(R) (ANL-7000, pp 233-77)
reactions with vanadium at 1100 to 1400°C, 19: 44587(R) (ANL-7000, pp 3-63)
separation by Acid Thorex and Purex processes, mixer-settler tests for, 19: 44117 (ORNL-TM-1256)
separation from fast reactor fuels, using Alamine 336–dibutyl cellosolve, 19: 44108 (AERE-R-4440(Pt.3))
separation from ores by extraction with organophosphates, 19: 44129(P)
separation from other metal ions by ion exchange, 19: 44119
separation from plutonium and thorium, method for, 19: 43982(P)
separation from sodium by ion exchange, 19: 44091
solubility in liquid bismuth at 400 to 600°C, 19: 44733
transport as silicate in aqueous solutions, complexing in, 19: 44278
URANIUM ALLOYS
Al–Cr–U, fabrication of reactor fuels of, 19: 44665(P)
Al–Fe–U, phase studies, 19: 44715
Al–Pu–U, corrosion by air at room temperature, 19: 44587(R) (ANL-7000, pp 3-63)
Al–Te–U, fabrication of reactor fuels of, 19: 44677(P)
Al–U, fabrication, 19: 44664(P)
Al–U phase studies of distribution of intermetallic compounds in, 19: 44717
Al–U, phase transformations on heating and cooling in intermetallic compound UAl_4, 19: 44727
Al–U–V, fabrication of reactor fuels of, 19: 44668(P)
Al–W–U, fabrication of reactor fuels of, 19: 44666(P)
Co–Rh–U, crystal structure studies, 19: 44678(R) (ANL-7000, pp 186-200)
Cu–Pu–U, corrosion by air at room temperature, 19: 44587(R) (ANL-7000, pp 3-63)
Cu–U, oxidation of intermetallic compound UCu_5 by carbon dioxide at 350 to 850°C, 19: 44631
Fe–Pu–U, corrosion by air at room temperature, 19: 44587(R) (ANL-7000, pp 3-63)
Fe–U, isomer shift of iron-57 in UFe_2 at 300 and 800°K, 19: 44678(R) (ANL-7000, pp 186-200)
fissium–Pu–U, burnup in, effects of cladding thickness on attainable, 19: 44587(R) (ANL-7000, pp 3-63)
fissium–Pu–U, enthalpy to 1200°C, 19: 44587(R) (ANL-7000, pp 3-63)
fissium–Pu–U, phase and transformation kinetics, 19: 44587(R) (ANL-7000, pp 3-63)
fissium–Pu–U, properties of, effects of composition on, 19: 44587(R) (ANL-7000, pp 3-63)
fissium–U, radioinduced swelling in, effects of postirradiation annealing temperature on, 19: 44587(R) (ANL-7000, pp 3-63)
fissium–U–Zr, radioinduced swelling in, effects of postirradiation annealing temperature on, 19: 44587(R) (ANL-7000, pp 3-63)
fissium–Pu–U, reactions with vanadium at 1100 to 1400°C, 19: 44587(R) (ANL-7000, pp 3-63)
fissium–Pu–U, reactions with chromium, molybdenum, and niobium at 750°C, 19: 44587(R) (ANL-7000, pp 3-63)
fissium–Pu–U, reactions with Hastelloy-X and type 304 stainless steel at 750°C, 19: 44587(R) (ANL-7000, pp 3-63)
fissium–Pu–U, reactions with niobium–zirconium and titanium–vanadium alloys at 750°C, 19: 44587(R) (ANL-7000, pp 3-63)
Ir–Ni–U, crystal structure studies, 19: 44678(R) (ANL-7000, pp 186-200)
Ir–U, crystal structure studies, 19: 44678(R) (ANL-7000, pp 186-200)
Mo–Pu–U, corrosion by air at room temperature, 19: 44587(R) (ANL-7000, pp 3-63)
Mo–Pu–U, properties of cast, 19: 44587(R) (ANL-7000, pp 3-63)
Ni–Pd–U, crystal structure studies, 19: 44678(R) (ANL-7000, pp 186-200)
Ni–Pt–U, crystal structure studies, 19: 44678(R) (ANL-7000, pp 186-200)
Ni–Rh–U, crystal structure studies, 19: 44678(R) (ANL-7000, pp 186-200)

Os–U, crystal structure studies, 19: 44678(R) (ANL-7000, pp 186-200)
Pd–Pt–U, crystal structure studies, 19: 44678(R) (ANL-7000, pp 186-200)
Pd–Rh–U, crystal structure studies, 19: 44678(R) (ANL-7000, pp 186-200)
PuC–UC, sintering properties, 19: 44587(R) (ANL-7000, pp 3-63)
Pu–Th–U, fabricability and thermal expansion of, 19: 44674(R) (ANL-7000, pp 69-83)
Pu–Th–U, phase studies, 19: 44674(R) (ANL-7000, pp 69-83)
Pu–Th–U, reactions with chromium, nickel, and stainless steel at 650°C, 19: 44674(R) (ANL-7000, pp 69-83)
Pu–Th–U, reactions with chromium–nickel and titanium–vanadium alloys at 650°C, 19: 44674(R) (ANL-7000, pp 69-83)
Pu–Ti–U, corrosion by air at room temperature, 19: 44587(R) (ANL-7000, pp 3-63)
Pu–U, fabrication of, for SEFOR-ZPR-III fuel plates, 19: 44587(R) (ANL-7000, pp 3-63)
Pu–U, reactions with vanadium at 1100 to 1400°C, 19: 44587(R) (ANL-7000, pp 3-63)
Pu–U–V, corrosion by air at room temperature, 19: 44587(R) (ANL-7000, pp 3-63)
Pu–U–Zr, corrosion by air at room temperature, 19: 44587(R) (ANL-7000, pp 3-63)
Ru–U, crystal structure studies, 19: 44678(R) (ANL-7000, pp 186-200)
Th–U, extrusion of rods of, 19: 44633(R) (ANL-7000, pp 138-45)
Th–U, radiation effects on dimensional changes in, transient temperature and neutron, 19: 44737(R) (ANL-7000, pp 111-18)

URANIUM ARSENIDES
corrosion by water vapor at 25 and 40°C, 19: 44618 (AWRE-O-42/65)

URANIUM CARBIDES
analysis for carbon using electron microprobe, 19: 43966
lattice constants of, 19: 44722
preparation of spherules of, 19: 44659(P)
reprocessing of, volatility processes for, 19: 44109 (BLG-331)
technology of, literature survey, 19: 44603 (NAA-SR-10929)
thermal properties at room temperature, 19: 43985(R) (ANL-7000, pp 85-110)
ThC_2–UC_2, phase studies and thermal expansion of pseudobinary, 19: 44696 (ORNL-TM-1188)
ThC–UC, preparation of spherules of, 19: 44659(P)
UC–H_2O, criticality parameters for, 19: 44112 (CONF-651103-4)
UC–UP, preparation and properties, 19: 43985(R) (ANL-7000, pp 85-110)
UC–US, oxidation of, differential thermal and thermogravimetric analyses of, 19: 43985(R) (ANL-7000, pp 85-110)

URANIUM COMPLEXES
mercaptobenzoate, stability, 19: 44013
spectra of, effects of coordination number on diffuse reflectance, 19: 44034
with glycolic acid, binding energy of, infrared spectrophotometric study of, 19: 44004

URANIUM COMPOUNDS
analysis for cadmium, atomic absorption spectrophotometric, 19: 43935 (NIJS-R-447)
dissolution by nitric acid solution containing uranyl ions, 19: 44128(P)

URANIUM DEPOSITS (CHILE)
reconnaissance in Aisen area, 19: 44273 (RME-4557(Rev.))

URANIUM(IV) FLUORIDES
preparation from uranium oxides by reduction-fluorination in gas-solid contacting, 19: 44042(P)

URANIUM(VI) FLUORIDES
use in gaseous fuel reactor incorporating MHD principle, 19: 45540(P)

URANIUM(IV) IODIDES
ThO_2–UO_2, fabrication of uranium-233-enriched, into fuel rods by sol-gel vibratory-compaction process, 19: 44638 (ORNL-3681)

URANIUM ISOTOPES
content in lead ores in Eastern Transbaikal, 19: 44277
enrichment facility for, description of British gaseous diffusion, (E), 19: 45612
neutron cross sections of, tabulation, (E), 19: 45250 (BNL-325(2nd Ed.) (Suppl.2)(Vol.III))

URANIUM ISOTOPES U-233
processing of, for fabrication into uranium dioxide–thorium dioxide fuel rods, 19: 44638 (ORNL-3681)

URANIUM ISOTOPES U-234
content in US coastal marine waters and calcium carbonates, 19: 44263

URANIUM ISOTOPES U-235
analysis for copper, absorptiometric, 19: 43938 (PG-Report-665)
deposition on semiconductor detectors as targets, by electrospraying, 19: 44635 (INR-595/IA/PL)
electric quadrupole moment from x-ray spectrum of mesic (μ), (E), 19: 45326
fission cross sections, 19: 45601(R) (WCAP-3750)
fission of, delayed gamma emission in, (E), 19: 45245 (AFWL-TR-65-95)
neutron cross sections for, from 0.414 ev to 5.5 Mev, 19: 45244 (AEEW-M-472)
neutron fission cross sections at 0.002 to 30 kev, (E), 19: 45292 (BNL-tr-16)
neutron fission in reactor fuels, measurement of fast, (T), 19: 45229 (UJV-1324/65)
neutron fission of, yields from thermal, (E), 19: 45260(R) (IDO-14660)
neutron fission rates in FRO critical assemblies, (E/T), 19: 45522 (AE-195)
neutron fission reactions at 24 kev, secondary neutron yield from, (E), 19: 45297
neutron fission reactions at 6.0 Mev maximum, delayed neutron yields from, (E), 19: 45300
neutron reactions (n,γ) at 0.002 to 30 kev, cross sections for, (E), 19: 45292 (BNL-tr-16)
neutron reactions (n,f) at 2 to 70 ev, cross sections for, (E), 19: 45299

URANIUM ISOTOPES U-238
content in US coastal marine waters and calcium carbonates, 19: 44263
energy levels of, rotational, (T), 19: 45285 (UCRL-16040)
neutron capture and fission rates in FRO critical assemblies, (E/T), 19: 45522 (AE-195)
neutron cross sections for, from 0.414 ev to 5.5 Mev, 19: 45244 (AEEW-M-472)
neutron fission reactions at 1.75 Mev maximum, delayed neutron yields from, (E), 19: 45300
photofission at 300 to 1000 Mev, cross sections for, (E), 19: 45329
photofission of, delayed gamma emission in, (E), 19: 45245 (AFWL-TR-65-95)

URANIUM MINERALS
age estimation by uranium–thorium–lead method, 19: 44272
occurrence and properties of niobium–uranium metamict mineral in Powhatan County, 19: 44279
occurrence in Marshall Pass, Saguache County, Colo., 19: 44274

URANIUM ORES
miners of, lung cancer incidence in, 19: 44314
pathological effects of inhaled radon from, in miners, 19: 43824
processing with a combined solubilization and extraction solution, 19: 44129(P)
radiometric concentration and optimum separation level of, (T), 19: 44275
radiometric dressing of, for lognormal uranium distribution in ore volume elements, (T), 19: 44276

URANIUM(IV) OXALATES
thermal decomposition of, preparation of uranium dioxide by, 19: 43987 (CEA-R-2817)

URANIUM OXIDES
determination in zircons by spectroscopic methods, 19: 43954
fluorination to uranium(IV) fluoride, gas-solid contacting process for, 19: 44042(P)
formation of films of, on uranium in water vapor, 19: 44619 (AWRE-O-66/65)
SbO–UO, use as oxidation catalysts, 19: 44043(P)

URANIUM(IV) OXIDES
cladding materials for, in nuclear-thermionic cells, 19: 44593 (CONF-650908-4)
coating of particles of, 19: 44596 (EURAEC-1392)
deformation and mechanical properties, 19: 43985(R) (ANL-7000, pp 85-110)
density of sintered, effects of water and zinc behenate on, 19: 44595(R) (EURAEC-1338)
deposition method for, thermochemical, 19: 44640 (ORNL-P-1446-1)
diffusion of uranium from, through tungsten, 19: 44979(R) (NP-15419)
diffusion of xenon in irradiated sintered compacts of, 19: 44595(R) (EURAEC-1338)
evaporation of sintered, at 1800°C, 19: 44595(R) (EURAEC-1338)
fabrication of fuel pellets of, for Doppler experiments in ZPR-III, 19: 44587(R) (ANL-7000, pp 3-63)
grain growth kinetics of sintered compacts of, at 1400 to 1800°C, 19: 44595(R) (EURAEC-1338)
interatomic forces in, (T), 19: 43997(R) (UCRL-11889)
neutron Doppler coefficients for, survey of measurements of, 19: 45532 (ORNL-TM-1219)
oxidation during sintering of, control of, 19: 44595(R) (EURAEC-1338)
preparation by thermal decomposition of uranium(IV) and uranyl oxalates, 19: 43987 (CEA-R-2817)
preparation of high-surface-area powders of, process for, 19: 44595(R) (EURAEC-1338)
pressing high-surface-area powders of, use of zinc behenate as lubricant for, 19: 44595(R) (EURAEC-1338)
radiation effects on thermal ratcheting in aluminum-clad, neutron,

19: 44737(R) (ANL-7000, pp 111-18)
reactions with boron carbides at high temperatures, 19: 44591(R) (CEND-3107-228)
reactions with liquid sodium, 19: 44021
reactions with molybdenum, tungsten, and rhenium–tungsten alloys at high temperatures, 19: 44593 (CONF-650908-4)
reactions with Zircaloy-2 at 950 to 1575°K, interfacial, 19: 44597 (GEAP-4679)
reactions with zirconium at 2200°C, 19: 44599(R) (GEMP-50A)
reprocessing and refabrication of second-cycle irradiatdd, by AIROX process, 19: 44114 (NAA-SR-11375)
sintering of, effect of titanium dioxide additive on, 19: 44646
sintering of, effects of niobium oxide and titanium oxide additions on, 19: 43985(R) (ANL-7000, pp 85-110)
sintering properties of high-surface-area powders of, 19: 44595(R) (EURAEC-1338)
solvent properties for helium, (T), 19: 43997(R) (UCRL-11889)
surface area of powders of, method for measuring, 19: 44595(R) (EURAEC-1338)
swaging and annealing at 0 to 1100°C, particle bonding in, 19: 44649
thermal conductivity to 2400°C of sintered, 19: 44595(R) (EURAEC-1338)
thermal properties at room temperature, 19: 43985(R) (ANL-7000, pp 85-110)
thermal shock resistance of sintered compacts of, 19: 44595(R) (EURAEC-1338)
thermogravimetry of irradiated, balance for remote, 19: 44341 (AERE-R-4962)
B_4C–UO_2, fabrication and stability for use as reactor fuel, 19: 44591(R) (CEND-3107-228)
Fe–UO_2, reactions with aluminum–chromium–iron–yttrium alloys at 950 and 1100°C in air, 19: 44598(R) (GEMP-49A)
Mo–UO_2, thermal conductivity of fuel rods of, effects of molybdenum additions on, 19: 45573 (GEAP-4902)
PuO_2–UO_2, fabrication of fuel pellets of, for Doppler experiments in ZPR-III, 19: 44587(R) (ANL-7000, pp 3-63)
ThO_2–UO_2–Y_2O_3, fission gas release from beryllia-based, effects of beryllia coatings on, 19: 44599(R) (GEMP-50A)

URANIUM(IV-VI) OXIDES
effects on gamma radiolysis of aqueous solutions of benzene, 19: 44051 (AE-192)
Al–U_3O_8, fabrication of powder compacts of, loading assembly for, 19: 44641 (ORNL-TM-1193)
Al–U_3O_8, pressed block design for fabrication of rod shaped, 19: 44663(P)

URANIUM OXYSULFIDES
UOS–US, radiation effects on transformations in, neutron, 19: 44737(R) (ANL-7000, pp 111-18)

URANIUM OXYTELLURIDES
crystal structure of, neutron diffraction studies of, 19: 44009

URANIUM PEROXIDES
preparation and composition of hydrates of, 19: 44029

URANIUM PHOSPHIDES
fabrication of, hot-pressing and sintering in, 19: 43985(R) (ANL-7000, pp 85-110)
oxidation of, differential thermal and thermogravimetric analyses of, 19: 43985(R) (ANL-7000, pp 85-110)
properties of, effects of heating *in vacuo* on, 19: 43985(R) (ANL-7000, pp 85-110)
thermal properties at room temperature, 19: 43985(R) (ANL-7000, pp 85-110)
ThP–UP, preparation and properties, 19: 43985(R) (ANL-7000, pp 85-110)
UC–UP, preparation and properties, 19: 43985(R) (ANL-7000, pp 85-110)
UP–US, properties of, effects of composition on, 19: 43985(R) (ANL-7000, pp 85-110)

URANIUM SALTS
use with semiconductor detectors for thermal neutron detection, 19: 44479 (ZFK-PHA-12, pp 140-3)

URANIUM SILICATES
transport in aqueous solutions, complexing in, 19: 44278

URANIUM SULFIDES
corrosion by water vapor at 25 and 40°C, 19: 44618 (AWRE-O-42/65)
preparation, 19: 43985(R) (ANL-7000, pp 85-110)
thermal properties at room temperature, 19: 43985(R) (ANL-7000, pp 85-110)
UC–US, oxidation of, differential thermal and thermogravimetric analyses of, 19: 43985(R) (ANL-7000, pp 85-110)
UOS–US, radiation effects on transformations in, neutron, 19: 44737(R) (ANL-7000, pp 111-18)
UP–US, properties of, effects of composition on, 19: 43985(R) (ANL-7000, pp 85-110)

URANIUM SYSTEMS
C–O–U, density and lattice parameters, effects of composition on, 19: 44612 (USBM-RC-1199)
C–Pu–U, corrosion by air at room temperature, 19: 44587(R) (ANL-7000, pp 3-63)
C–Pu–U, lattices parameters as function of composition, 19: 44678(R) (ANL-7000, pp 186-200)
C–Pu–U, preparation, 19: 44587(R) (ANL-7000, pp 3-63)
C–Pu–U, susceptibility at 25°C, 19: 44678(R) (ANL-7000, pp 186-200)
U–H_2O, criticality parameters for, 19: 44112 (CONF-651103-4)

URANYL ACETATES
sorption of, on ion exchange resins, 19: 44119

URANYL COMPOUNDS
reactions with hydrogen peroxide, preparation of uranium peroxide by, 19: 44029

URANYL IONS
use in combination with nitric acid solutions in uranium dissolution, 19: 44128(P)

URANYL NITRATES
determination in aqueous solution using refractometric method, 19: 43969
structure of hexahydrate, neutron diffraction determination of, 19: 44679(R) (ANL-7000, pp 205-12)

URANYL OXALATES
thermal decomposition of, preparation of uranium dioxide by, 19: 43987 (CEA-R-2817)

URANYL SULFATES
properties of hydrates of, 19: 44014

UREA
N-nitroso-*N*-ethyl-, chemical inhibition of radiomimetic effects on seeds, 19: 43870
N-nitroso-*N*-methyl-, chemical inhibition of radiomimetic effects on seeds, 19: 43870

URETHAN POLYMERS
thermal aging properties of flexible foams of, effects of molecular structure on, 19: 44682 (BDX-613-75)

URIC ACID
determination in blood, of dogs, 19: 43674(R) (UCD-472-112, pp 36-43)
radiation effects on metabolism of, in rats, 19: 43852

URIDINE
hydrolysis of 3′-nucleotide of, catalytic effects of thorium and zirconium ions on, 19: 43708
properties of phosphates of, effects of papaverine derivatives on spasmogenic, 19: 43728(R) (UCLA-12-565, pp 59-64)
spasmogenic effect actions phosphates of, effects of 3-methylisoquinoline compounds on, 19: 43728(R) (UCLA-12-565, pp 59-64)

URINARY TRACT
radiation injuries of, during radiotherapy of uterine carcinomas, 19: 43921

URINE
analysis for calcium and strontium by flame photometry using plasma jets, 19: 43924 (AERE-R-4990)
analysis for plutonium, radiochemical method for, 19: 44296 (NYO-4700(Rev.)(Suppl.II))
analysis for radium-226, radiochemical method for, 19: 44296 (NYO-4700(Rev.)(Suppl.II))
excretion of calcium-45, mineral nutrients, and phosphorus-45 by colostomized pullets, 19: 43693
radiation effects on substances in, use in evaluating damage, 19: 43753
radiation effects on metabolites in human and rat, 19: 43852
radioactivity of dog, following renogram preparation, 19: 43667 (EUR-1890.f)
sodium-22 content of Eskimo, 19: 44289 (HW-SA-3750)
tritium uptake by cattle, 19: 43694

UTERUS
radiotherapy of carcinomas of, combination of surgery with, 19: 43884
radiotherapy of carcinomas of, late pathological effects, 19: 43907
radiotherapy of cancers of, evaluation of results, 19: 43910
radiotherapy of cervical carcinoma of, pregnancy occurrence after primary, 19: 43891
radiotherapy of, complications in urinary tract from, 19: 43921

V

V PARTICLES
compositeness criteria in Lee model, Salam, 19: 45068

VACCINES
against Schistosoma in mice, use of irradiated cercariae for, 19: 43848
against sheep lungworm, preparation from irradiated larvae, 19: 43750

VACUUM SEALS
description of strip-sealed continuous-rotation scattering chamber, (E),

19: 44883
performance of gaskets, factor method for predicting, 19: 44135 (IA-1033)
use of bellows as, in transmitting motion through vacuum wall, 19: 44234 (MATT-345)
VACUUM SYSTEMS
description of strip-sealed continuous-rotation scattering chamber, (E), 19: 44883
instrumentation development for ultrahigh, 19: 44357
VACUUM TECHNIQUES
instrumentation developments for ultrahigh, 19: 44357
VACUUM VESSELS
description of strip-sealed continuous-rotation scattering chamber, (E), 19: 44883
VALLECITOS BOILING WATER REACTOR
fuel rod design for increased thermal output, testing of, 19: 45573 (GEAP-4902)
VAN ALLEN RADIATION BELTS
effects of artificial, on ionospheric D layer, 19: 45166
electron density distributions in artificial, 19: 45167
electron intensities near magnetic equator in outer, local-time dependence of, (E), 19: 45160
electron loss and replenishment at middle latitudes and high B values, 19: 45161
production of artificial, sources for, 19: 45159 (UCRL-14374)
production of artificial, from high-altitude nuclear explosions, 19: 45166
proton spatial distribution in, analysis of high-energy, (E/T), 19: 45188
radiation measurement in, Explorer VII high-energy, 19: 44973
VAN DE GRAAFF ACCELERATORS
design, 19: 44890(P)
design, 19: 44891(P)
design, 19: 44892(P)
VANADIUM
determination in nuclear grade graphite, spectrochemical, 19: 43930 (JEN-145-DQ/I-46)
extrusion by hydrostatic methods, 19: 44651
neutron scattering by, performance of three-axis spectrometer for thermal, 19: 44527
reactions with beryllium, copper, stainless steel, and niobium alloys to 760°C *in vacuo*, 19: 44606 (PWAC-483)
reactions with uranium, plutonium–uranium, and fission–plutonium–uranium alloys at 1100 to 1400°C, 19: 44587(R) (ANL-7000, pp 3-63)
separation from ores by extraction with organophosphates, 19: 44129(P)
spectra at, Ohlin structure near limit of continuous x-ray, (E), 19: 44940
thermal capacity of normal and superconducting, 19: 43997(R) (UCRL-11889)
VANADIUM ALLOYS
Al–Mo–Ti–V, corrosion cracking of, mechanisms for stress, 19: 44621 (CONF-651006-1)
Al–U–V, fabrication of reactor fuels of, 19: 44668(P)
Al–V, nuclear magnetic resonance, 19: 43986(R) (ANL-7000, pp 201-4)
Cr–Ti–V, fabricability of, effects of composition on, 19: 44587(R) (ANL-7000, pp 3-63)
Fe–V, lattice parameter, 19: 44679(R) (ANL-7000, pp 205-12)
Nb–Ti–V, microstructure of, effects of annealing temperature on, 19: 44587(R) (ANL-7000, pp 3-63)
Pu–U–V, corrosion by air at room temperature, 19: 44587(R) (ANL-7000, pp 3-63)
Tc–V, nuclear magnetic resonance relaxation times, 19: 43986(R) (ANL-7000, pp 201-4)
Tc–V, superconducting transition temperature, 19: 44678(R) (ANL-7000, pp 186-200)
Ti–V, corrosion by oxygen-contaminated sodium, 19: 44587(R) (ANL-7000, pp 3-63)
Ti–V, enthalpy, thermal conductivity, and thermal expansion of, 19: 44587(R) (ANL-7000, pp 3-63)
Ti–V, fabricability of TV-20, effects of molybdenum, niobium, and tantalum additions on, 19: 44587(R) (ANL-7000, pp 3-63)
Ti–V, fabrication of TV-20, 19: 44587(R) (ANL-7000, pp 3-63)
Ti–V, hardness of, effects of oxygen and titanium content on, 19: 44587(R) (ANL-7000, pp 3-63)
Ti–V, mechanical properties at high temperatures, 19: 44674(R) (ANL-7000, pp 69-83)
Ti–V, neutron reactions in, yields of helium and hydrogen produced by fast, 19: 44746 (NAA-SR-Memo-10626)
Ti–V, reactions with plutonium–thorium–uranium alloys at 650°C, 19: 44674(R) (ANL-7000, pp 69-83)
Ti–V, reactions with fission–plutonium–uranium alloys at 750°C, 19: 44587(R) (ANL-7000, pp 3-63)
VANADIUM CARBIDES
analysis for carbon using electron microprobe, 19: 43966
VANADIUM IONS
oxidation-reduction reactions of, polarization during, 19: 44002(T) (AEC-tr-6572)
VANADIUM ISOTOPES V-51
gamma absorption cross section, (T), 19: 45366
VANADIUM ORES
processing with a combined solubilization and extraction solution, 19: 44129(P)
VANADIUM SYSTEMS
C–Mo–V, superconductivity, 19: 43997(R) (UCRL-11889)
HfC–V, solidus temperature at 1790°C, 19: 44612(R) (USBM-RC-1199)
H–V, nuclear magnetic resonance, 19: 43986(R) (ANL-7000, pp 201-4)
Rh–Si–V, phase study of Cr_3O-type structures in, 19: 44702 (TID-22200)
Si–Sn–V, phase study of Cr_3O-type structures in, 19: 44702 (TID-22200)
VENTILATION
system design for radiochemical laboratories, 19: 44284 (AWRE-O-24/65)
VESPIDAE
action effects on, space flight, 19: 43721(R) (ORNL-TM-1217)
radiation effects on sperm in, gamma, 19: 43721(R) (ORNL-TM-1217)
VINYL ALCOHOL POLYMERS
performance in fine-grain nuclear emulsions, 19: 44400 (CERN-65-4 (Vol.II), pp III31-56)
VIRGINIA
occurrence and properties of niobium–uranium metamict mineral in Powhatan County, 19: 44279
VITAMIN C
radiation effects on content in oranges, 19: 44554 (IA-1015)
VITAMIN K
radiosensitivity effects on bacteria, 19: 44552 (BLG-327)
VITAMINS
radiosterilization of, effects on potency, 19: 44559
stability in prepared dog food during storage, 19: 43644(R) (UCD-472-112)
VOLATILITY SEPARATION PROCESSES
development for carbon-containing fuel elements, 19: 44109 (BLG-331)

W

WASTE DISPOSAL
inventory control and regulation of, computer program for, 19: 45687 (DP-966)
methods at Sioux Falls Power Reactor, 19: 45593(R) (TID-22168)
storage of high-level solids in salt mine, demonstration of, 19: 45689 (ORNL-P-1568)
WASTE PROCESSING
calcination, ruthenium-106 release in, 19: 44773 (BNL-914, pp 57-64)
ion exchange, for removal of strontium-90 from biologic waste, 19: 45692 (UCD-472-112, pp 141-7))
ion-exchange methods of, properties of zeolite taff for, 19: 44123
precipitation methods for low-level aqueous solutions, design of plant using, 19: 45693
solidification by evaporation, operating experience on in-tank, 19: 45691 (RL-SA-41)
WASTE SOLUTIONS
evaporation of, operational characteristics of fluidized-bed spray evaporator for, 19: 45688(R) (NP-15367)
separation of fission products from, at Hanford, 19: 45690 (RL-SA-40)
WATER
analysis for oxygen-18 activation, 19: 45679(R) (NYO-1859-11)
analysis for plutonium, radiochemical method for, 19: 44296 (NYO-4700(Rev.)(Suppl.II))
analysis for radioactivity, method for, 19: 43974
analysis for radium-226, radiochemical method for, 19: 44296 (NYO-4700(Rev.)(Supp.II))
analysis for water-d_2 by specific weight measurement, 19: 43983(P)
boiling critical heat flux in internally cooled channels at 70 and 100 atm, effects of length/diameter ratio on, 19: 44184(R) (EURAEC-1281)
boiling flow regimes in high-pressure, research program on, 19: 44193(R) (NYO-3304-5)
cavitation damage on coated impellers, studies, 19: 44197 (TIM-895)
corrosive effects on A288 and X8001 aluminum alloys, 19: 44616(R) (ANL-7000, pp 122-37)
corrosive effects on aluminum, effects of polarizing current on, 19: 44617(R) (ANL-7000, pp 213-26)
corrosive effects of boiling, on carbon steel, 19: 44627
detection and separation from sodium loops, in-line devices for, 19: 44162(R) (APDA-174, pp 33-55)
determination in cattle, tracer technique for whole-body, 19: 43694
deuterium content of crystallization, of saline minerals, 19: 44240
deuterium exchange with hydrogen between ammonia and, in hot-and-cold plant, 19: 44574
effects of borated and lithiated, on wear of cylinders and pistons,

19: 45601(R) (WCAP-3750)
effects on radiomimetic effects of nitrosoamides on herb seeds, 19: 43870
effects on sintered density of urania powders, 19: 44595(R) (EURAEC-1338)
erosive effects on rotating metal disks, 19: 44625 (TIM-894)
evaporation from artificial rough surfaces, 19: 44245 (BNL-914, pp 125-32)
exchange with ferric and gadolinium ions in solution, nuclear magnetic resonance study, 19: 43997(R) (UCRL-11889)
flow of saturated, through apertures, (E), 19: 44196(R) (TID-22145)
gamma dose rates in, from point isotropic fission sources, (T), 19: 45464 (ORNL-TM-1167)
heat transfer to liquid hydrogen from, in heat exchangers, 19: 44186 (LA-DC-7148)
monitoring Savannah River Plant, Jan. to June 1965, 19: 44288(R) (DPST-65-30-2)
neutron capture with charged-particle emission in, determination for source calibration, (E), 19: 45232
neutron dose rates in, from point isotropic fission sources, (T), 19: 45464 (ORNL-TM-1167)
neutron scattering cross sections in, slow, (T), 19: 45228 (NP-15469)
neutron scattering by liquid, dynamics of, (E), 19: 45235
neutron scattering by, van Hove function for, (E), 19: 45236
properties for uses in reactors, 19: 45678 (JEN-149-DQ/I-50)
radioactivity of reactor coolant, effects of low-cobalt stainless steel on cobalt-60, 19: 45495 (WAPD-T-1653)
radiolysis by 1.57-Mev proton pulses, 19: 44058 (LFEN-23)
radiolysis in flow irradiator, calculated product accumulation in, 19: 44061(T) (AEC-tr-6567)
radiosensitivity effects on Artemia eggs, 19: 43814
reactions with sodium, test loop for, 19: 44161(R) (APDA-174, pp 25-32)
separation from steam, development of separators for, 19: 44131 (ACNP-65003)
solvent properties for lithium bromate, 19: 44003(T) (BNL-tr-6)
boric acid–H_2O, neutron spectra hardening in, thermal, 19: 45226 (KFK-294)
CO_2–H_2O, oxygen-17 and oxygen-18 distribution equilibrium in, 19: 44007
$Fe(NH_4)_2(SO_4)_2$–$CuCl_2$–H_2SO_4–H_2O, properties as gamma dosimeter, 19: 44372 (AFCRL-65-470)
Pb–H_2O, gamma transmission through, as function of thickness, (T), 19: 45466
UC–H_2O, criticality parameters for, 19: 44112 (CONF-651103-4)
U–H_2O, criticality parameters for, 19: 44112 (CONF-651103-4)

WATER-*d*,
concentration using magnetohydrodynamic effect, 19: 44578(P)
content in crystallization water of saline minerals, 19: 44240
determination in water by specific weight measurement, 19: 43983(P)
effects on hydrolysis of 4-methyl-1,3-dioxane and 1,3-dioxane, 19: 44011
effects on macromolecule synthesis in developing sea urchin eggs, 19: 43709
production of, pilot plant for electrolytic, 19: 44576
thermodynamic properties of, 19: 44008
CO_2–D_2O, oxygen-17 and oxygen-18 equilibrium distribution in, 19: 44007

WATER-*t*,
plant metabolism of, in *Zea maize* roots, 19: 43702

WATER COOLED REACTORS
auxiliary systems development for 395-Mwe, (E), 19: 45597 (WCAP-3269-31)
economic aspects of, for power production and sea water desalination, 19: 45620
heat transfer in, dynamic studies, 19: 44194 (SGAE-RE-2/1965)
neutron absorber efficiency in homogeneous uranium, heterogeneous, (E/T), 19: 45536

WATER MODERATED REACTORS
design with superheating system, 19: 45628(P)
fuel-element guide tube design for, 19: 45517(P)

WATER SUPPLIES
radioactivity of Canadian, June 1965, 19: 44251 (NP-15519, pp 23-51)
recharge of ground water as, economics of artificial, 19: 45717 (UCRL-7850(Rev.1))

WATER VAPOR
corrosive effects on uranium at 25 and 40°C, effects of oxygen on, 19: 44618 (AWRE-O-42/65)
corrosive effects on uranium arsenides and sulfides at 25 and 40°C, 19: 44618 (AWRE-O-42/65)
effects on fatigue of molybdenum, 19: 44730
reactions with uranium, growth of oxide films in, 19: 44619 (AWRE-O-66/65)

WAXES
composition of coelacanth fish, 19: 43681(R) (UCLA-12-565, pp 17-31)

WEAR
testing cylinder and piston, in reactor shim solutions, 19: 45601(R) (WCAP-3750)

WELDED JOINTS
corrosion of Incaloy-to-Zircaloy, by steam under reactor conditions, 19: 45572(R) (GEAP-4755)
corrosion of stainless steel-to-Zircaloy, by steam under reactor conditions, 19: 45572(R) (GEAP-4755)
hardness of heat-affected zones of, effects of welding technique on, 19: 44686(R) (EURAEC-1362)

WELDING
arc-initiation circuit for remote fuel rod, 19: 44587(R) (ANL-7000, pp 3-63)

WELDS
effects on fatigue strength of steel, 19: 45503(R) (SWRI-1228-69)

WHEAT
effects of alkylating compounds on cytology and physiology of *T. durum* and *T. monococcum*, 19: 43653
growth of seedlings of, effects of radiation and weightlessness on, 19: 43717 (NASA-CR-303)
radiation effects in seeds of, effects of dose rate, 19: 43781
radioactivity of Canadian, June 1965, 19: 44251 (NP-15519, pp 23-51)
radioinduced sterility in pollen of, γ, 19: 43767

WHITESHELL REACTOR NO. 1
research programs on, at AECL, 19: 45694(R) (AECL-2251)

WIND
profiles of, review, 19: 44794 (BNL-914, pp 158-60)
structure of, in micrometeorology, 19: 44798 (BNL-914, pp 175-7)
turbulence in, low-level, 19: 44793 (BNL-914, pp 156-7)
turbulence of components of, vertical structure of, 19: 44799 (BNL-8516)

WIND TUNNELS
use in scale model smoke diffusion experiments, 19: 44764 (BNL-914, pp 14-17)

WINDOWS
design for fallout shelters, 19: 44218(P)

WINDSCALE ADVANCED GAS COOLED REACTOR
fuel element burnup distributions in, analysis of, (E), 19: 44463 (TRG-Report-1005)
fuel element failure, fission product release in, 19: 44303 (TRG-Report-888)
fuel fabrication and processing facilities for, (E), 19: 45612
operation and performance of, (E), 19: 45613

WIRES
testing for residual strain and working at high temperatures, device for, 19: 44213

WORMS
vaccine for sheep lungworms, preparation from irradiated larvae, 19: 43750

WOUNDS
radioactivity in, detection and measurement of, 19: 44538

X

X RADIATION
biological effects in *Schistosoma japonicum* cercariae, 19: 43848
dose measurements for eyes of, during diagnostic radiography of head and neck region, 19: 43885
dosimetry of scattered, during diagnostic radiography, 19: 43917
dosimetry of, during diagnostic radiography, 19: 43889
dosimetry of, for diagnostic use, 19: 43901
effects in Drosophila, lethal, 19: 43787
effects in Drosophila, genetic, 19: 43787
effects in *Escherichia coli*, lethal, 19: 43794
effects in *Escherichia coli*, genetic, 19: 43794
effects in *Escherichia coli*, 19: 43795
effects in mice, fractionated doses, 19: 43792
effects in mice, pathological, 19: 43771
effects in mouse oöcytes, genetic, 19: 43788
effects in mouse oöcytes, genetic, 19: 43789
effects in mouse spermatogonia, genetic, 19: 43788
effects in mouse spermatogonia, pathological, effects of dose, dose rate, and radiation quality on, 19: 43788
effects in mouse spermatogonia, genetic, 19: 43789
effects in rat liver, pathological, 19: 43735
effects in rice seeds, biological, effects of dose rate, 19: 43781
effects in silkworms, genetic, 19: 43784
effects in silkworms, genetic, 19: 43787
effects in silkworms, lethal, 19: 43787
effects in wheat seeds, biological, effects of dose rate, 19: 43781

effects of exposure of adrenal glands to, on recovery from cardiac decompensation, 19: 43919
effects on acceptance of autogenous bone grafts in dogs, 19: 43835
effects on activity of N-demethylase, in rat liver, 19: 43720(R) (NP-15310, pp 26-35)
effects on blood platelets, biochemical, 19: 43714 (EUR-2438.f)
effects on blood platelets, morphological, 19: 43714 (EUR-2438.f)
effects on calcium-45 uptake by *Nitella flexilis*, 19: 43818
effects on carcinoma cell cultures, 19: 43802
effects on changes in domain structures of Rochelle salt crystals, 19: 44031(T)
effects on chromosome replication in *E. coli*, 19: 43741
effects on crop plants, protective effects of chemicals against seed, 19: 43877
effects on developing nerves, in insect larvae, morphological, 19: 43849
effects on dog lungs, pathophysiology of, 19: 43799
effects on *E. coli* B/r, effects of organic nitroxide-free radicals on sensitization of, 19: 43875
effects on enzyme activity in Tetrahymena, 19: 43856
effects on growth of transplanted sarcoma in rats, 19: 43772
effects on growth of wheat seedlings, 19: 43717 (NASA-CR-303)
effects on hair of mice, local and whole-body, 19: 43833
effects on hamster cells in tissue culture, fractionated doses, 19: 43791
effects on HeLa cells in tissue culture, fractionated doses, 19: 43790
effects on larvae of sheep lungworm, lethal, 19: 43750
effects on lethality in dogs, dose and exposure effects on, 19: 43832
effects on luminescence of doped alkali metal halides at 90 and 295°K, 19: 45488
effects on magnetic properties of deoxyribonucleic acid, 19: 43723(R) (TID-22128)
effects on maize, mutagenic, 19: 43712 (BNL-9383)
effects on marrow production in chickens by exposure of spinal cord graft to chorioallantoid, 19: 43761
effects on metabolism in man and rats, use in exposure diagnosis, 19: 43852
effects on mice, protective effects of nitrogenous heterocyclics against, 19: 43863
effects on mice, protective effects of *p*-aminopropiophenone and MEA against, 19: 43873
effects on mice, protective effects of hematoporphyrin against, 19: 43862
effects on mitosis in brain of rat embryos, 19: 43768
effects on mouse chromosomes, effects of age on aberrant, 19: 43729(T) (BNL-tr-12)
effects on neonatal and prenatal mortalities in mice after fetal or maternal exposure, 19: 43760
effects on nicotinamide-adenine-N¹-oxide-dinucleotide formation in nicotinamide adenine dinucleotide decomposition, 19: 44062
effects on peas, genetic, 19: 43734
effects on phosphatase content of granulocytes, of man, 19: 43829
effects on phosphorus-32 pulse labeling of RNA in *Salmonella typhimurium*, 19: 43743
effects on *Poa pratensis*, mutagenic, 19: 43778
effects on protein synthesis in rat brains, 19: 43682(R) (UCLA-12-565, pp 33-57)
effects on rabbit lungs, histological, 19: 43846
effects on reproduction in Tribolium, effects of dose and temperature on, 19: 43715 (HW-SA-3747)
effects on reproductive performance in Tribolium, effects of genetics and temperature on, 19: 43716 (HW-SA-3748)
effects on serum protein content in rats, 19: 43766
effects on sulfonamide-induced and normal volutin in bacteria, 19: 43759
effects on thermoluminescence fading in dosimetric lithium fluoride, storage effects on, 19: 44076
effects on thyroid function, 19: 43890
effects on uridine diphosphate glucose pyrophosphorylase activity in rat liver, 19: 43747
effects on virulence of tumor grafted in successive generations of mice, 19: 43762
effects on XXX No. 18 trisomy syndrome development in baby, etiologic, 19: 43811
emission from flares behind solar disk, (T), 19: 44894(T) (AD-424481)
emission from solar flares, models for, 19: 44931
emission of K, during uranium-235 thermal fission, (E), 19: 45294
genetic effects in human cells in tissue culture, 19: 43844
metabolic effects in rat brain, 19: 43810
metabolic effects in rats, effects of cortisone on, 19: 43837
morphological effects on spleen cells of *Molge vulgaris* in tissue culture, 19: 43826
morphological effects on erythrocytes in salamanders, 19: 43730
origin of cosmic, (T), 19: 44971
physiological effects on response to muscle relaxant drugs, in rabbits, 19: 43871
physiological effects in rats, 19: 43808
physiological effects on phosphatase content in rat tissues, 19: 43739
production and properties of non-solar, in interstellar space, 19: 44969
protection against, development of compounds for, 19: 43883(R) (UCLA-12-565, pp 65-85)
sources of cosmic, neutron-star and supernova, (T), 19: 44923(T)
therapeutic use of, for tumor therapy, 19: 43900
transmission in doped germanium single crystals, γ-radiation effects on, 19: 44756
use in salmonellae control in meat, economic feasibility of, 19: 44557 (NYO-3426-1)

X-RAY DIFFRACTOMETERS
furnace design for high-temperature, 19: 44340 (AERE-M-1361)
goniometer with single-crystal orienter and grinder, 19: 44694(R) (NP-15432)
use of Geiger-counter, in determination of lattice constants, 19: 44722

X-RAY EQUIPMENT
design modifications for obsolete, to improve radiation protection, 19: 43909

X-RAY SOURCES
preparation of soft, by electroplating of cadmium-109 on copper wires, 19: 44139 (ORNL-TM-1174)

X-RAY SPECTRA
effects of chemical bonding on soft, 19: 44944
modification by filtration of, 19: 43901

X-RAY SPECTROMETERS
standardizing continuous readout on-line, apparatus and procedure for, 19: 44545(P)

XENON
content in natural gases, 19: 44239
diffusion of irradiated sintered compacts of urania, 19: 44595(R) (EURAEC-1338)
helium elastic scattering by, total cross section for, (E), 19: 44957
neutron scattering by, effective potential for electron-neutron interactions from, (E), 19: 45098
reactor criticality effects in slab matrices, 19: 45539
spectra of sulfur molecules in solid, u-v absorption, (E), 19: 45480 (UCRL-10771)

XENON IONS
yields from duoplasmatron ion source, pressure dependence of, (E), 19: 45385 (D1-82-0437)

XENON ISOTOPES
production in thermal-neutron fission of uranium-235, (E), 19: 45260(R) (IDO-14660)

XENON ISOTOPES Xe-120
energy levels, (E/T), 19: 45285 (UCRL-16040)

XENON ISOTOPES Xe-122
energy levels, (E/T), 19: 45285 (UCRL-16040)

XENON ISOTOPES Xe-133
diffusion from beryllia-coated beryllia-based thoria–urania–yttria fuels, 19: 44599(R) (GEMP-50A)
tracer use for diagnosis of circulatory shunts, 19: 43904

XENON ISOTOPES Xe-134
content in natural gases, 19: 44239

XENON ISOTOPES Xe-135
diffusion from beryllia-coated beryllia-based thoria–urania–yttria fuels, 19: 44599(R) (GEMP-50A)

XENON ISOTOPES Xe-136
content in natural gases, 19: 44239

XENON ISOTOPES Xe-137
decay scheme, 19: 45679(R) (NYO-1859-11)
half life of, determination of, 19: 45276 (NP-15304)

XENON ISOTOPES Xe-138
half life of, determination of, 19: 45276 (NP-15304)

XENON ISOTOPES Xe-139
half life of, determination of, 19: 45276 (NP-15304)

XENON ISOTOPES Xe-140
half life of, determination of, 19: 45276 (NP-15304)

XENON ISOTOPES Xe-141
half life of, determination of, 19: 45276 (NP-15304)

XENON ISOTOPES Xe-142
half life of, determination of, 19: 45276 (NP-15304)

XENON ISOTOPES Xe-143
half life of, determination of, 19: 45276 (NP-15304)

XENON ISOTOPES Xe-144
half life of, determination of, 19: 45276 (NP-15304)

XENON SYSTEMS
He–Xe, properties for use in closed Brayton cycle space power plants,

19: 44205

Y

YANKEE POWER REACTOR
reactivity coefficients in, burnup effects on, 19: 45602 (WCAP-5493)
YEASTS
extracts, protective effects against radiation injuries in rat spleen, 19: 43860(R) (NP-15310, pp 14-25)
radiation effects on glycolysis rate in, uv, 19: 43765
YTTERBIUM
separation from scandium and thorium by reversed-phase chromatography, 19: 44125
YTTERBIUM ALLOYS
stainless steel–Y, corrosion by steam at 650°C, 19: 44616(R) (ANL-7000, pp 122-37)
YTTERBIUM IONS
electron paramagnetic resonance of, in single-crystal lead molybdate, 19: 44017
YTTERBIUM ISOTOPES Yb-164
energy levels of, rotational, (T), 19: 45285 (UCRL-16040)
YTTERBIUM ISOTOPES Yb-166
energy levels of, rotational, (T), 19: 45285 (UCRL-16040)
YTTERBIUM ISOTOPES Yb-172
oxygen-16 inelastic scattering at 43.5 Mev, vibrational-state excitation in, (E), 19: 45321
YTTERBIUM ISOTOPES Yb-174
oxygen-16 inelastic scattering at 43.5 Mev, vibrational-state excitation in, (E), 19: 45321
YTTERBIUM ISOTOPES Yb-176
energy levels of, isomeric, (E), 19: 45357
oxygen-16 inelastic scattering at 43.5 Mev, vibrational-state excitation in, (E), 19: 45321
YTTERBIUM OXIDES
effects on optical properties of silicate glasses, 19: 44030
YTTERBIUM SELENIDES
crystal structure, 19: 44010
YTTRIUM
corrosion protection by hydrofluoric acid, 19: 44628
extrusion of clad and unclad, into rods and tubing, 19: 44636 (IS-1031)
phase transformations in, relation of c/a ratio and elastic moduli temperature dependence with, 19: 44676(R) (ANL-7000, pp 176-82)
purification by electron-beam melting, 19: 44588 (BM-RI-6661)
separation from scandium and thorium by reversed-phase chromatography, 19: 44125
separation from strontium, chromatographic, 19: 44120
solubility in acids, 19: 44628
YTTRIUM ALLOYS
Ag–Y, crystal structure studies, 19: 44678(R) (ANL-7000, pp 186-200)
Al–Cr–Fe–Y, corrosion by steam at 550°C of 1041, effects of preoxidation and strain on, 19: 44598(R) (GEMP-49A)
Al–Cr–Fe–Y, corrosion by steam at 730°C, 19: 44598(R) (GEMP-49A)
Al–Cr–Fe–Y, elastic constants at 30 to 1200°C of 2541, dynamic, 19: 44598(R) (GEMP-49A)
Al–Cr–Fe–Y, oxidation by air at 900 and 1100°C, effects of composition on, 19: 44598(R) (GEMP-49A)
Al–Cr–Fe–Y, reactions with iron–uranio at 950 and 1100°C in air, 19: 44598(R) (GEMP-49A)
Au–Y, crystal structure studies, 19: 44678(R) (ANL-7000, pp 186-200)
Fe–Y, isomer shift of iron in YFe_2 at 300 and 800°K, 19: 44678(R) (ANL-7000, pp 186-200)
Ir–Pt–Y, crystal structure studies, 19: 44678(R) (ANL-7000, pp 186-200)
YTTRIUM ISOTOPES Y-89
neutron reactions (n,γ) at 0.145 to 1.225 Mev, cross sections and isomer ratios for, (E), 19: 45376
YTTRIUM ISOTOPES Y-90
beta particles from, bremsstrahlung production by, (E), 19: 45284 (TID-22169)
beta spectra of, (E), 19: 45283 (SGAE-PH-23/1965)
therapeutic use of applicators of, 19: 43906
YTTRIUM OXIDES
effects on strength of zirconium, 19: 44676(R) (ANL-7000, pp 176-82)
properties in in-pile thermionic cells, 19: 44685 (CONF-650908-5)
spectra at, Ohlin structure near limit of continuous x-ray, (E), 19: 44940
ThO_2–UO_2–Y_2O_3, fission gas release from beryllia-based, effects of beryllia coatings on, 19: 44599(R) (GEMP-50A)
YTTRIUM SELENIDES
crystal structure, 19: 44010
YTTRIUM TELLURIDES
crystal structure, 19: 44010

Z

ZINC
analysis for trace amounts of copper by activation methods, 19: 43973
deformation of single crystals of, at high strain rates, 19: 43997(R) (UCRL-11889)
determination in biological materials, x-ray fluorescence spectrometric, 19: 43939(R) (UCD-472-112, pp 59-72)
determination in ores by radiometric fluorescence analysis, 19: 43971
effect on determination of copper in bismuth by neutron activation methods, 19: 43941
neutron absorption cross sections at 24 kev, (E), 19: 45230
neutron reactions (n,n'γ) with, cross section for, 19: 45263 (JAERI-1078)
phase transformations in, relation of c/a ratio and elastic moduli temperature dependence with, 19: 44676(R) (ANL-7000, pp 176-82)
separation from uranium by ion exchange, 19: 44119
ZINC ALLOYS
radiation effects on metabolism of, in rats, 19: 43852
Ag–Zn, crystal structure studies, 19: 44678(R) (ANL-7000, pp 186-200)
Pt–Zn, crystal structure studies, 19: 44678(R) (ANL-7000, pp 186-200)
ZINC CHLORIDES
solubility in sodium chloride, 19: 44677(R) (ANL-7000, pp 183-5)
NaCl–$ZnCl_2$, diffusion and ionic conductivity in, 19: 44677(R) (ANL-7000, pp 183-5)
ZINC COMPLEXES
with 8-quinolinol derivatives, electronic absorption spectra, 19: 43989 (MIT-905-20)
ZINC ISOTOPES Zn-65
determination in mixture with cerium-144, method for, 19: 43962
metabolism by marine organisms, 19: 43669(R) (NP-15159)
uptake and distribution in normal and tumor tissue in man, 19: 43699
uptake by oysters, 19: 43663
ZINC OXIDES
effects on gamma radiolysis of aqueous solutions of benzene, 19: 44051 (AE-192)
ZINC SULFIDES
deposition from atmosphere on vegetation, 19: 44248 (BNL-914, pp 141-3)
luminescence response of silver-activated, to electrons, (E), 19: 44520
use in dual atmospheric tracer technique, 19: 44800 (BNWL-103)
Cl–Cu–ZnS, radiation effects on luminescence of, electron, gamma, and uv, 19: 44757
ZIRCALOY-2
corrosion by steam under nuclear superheat reactor conditions, 19: 45572(R) (GEAP-4755)
extrusion by hydrostatic methods, 19: 44651
fabrication of tubing of, stress-orientation developed during, 19: 44634(R) (DPST-65-83-7)
hydride precipitation in, effects of elastic stresses on orientation of, 19: 44697 (ORNL-TM-1239)
neutron reactions in, yields of helium and hydrogen produced by fast, 19: 44746 (NAA-SR-Memo-10626)
reactions with steam in simulated reactor loss-of-coolant accident, 19: 45496 (WCAP-3269-30)
reactions with uranium dioxide at 950 to 1575°K, interfacial, 19: 44597 (GEAP-4679)
testing for SCE fuel cladding, 19: 45601(R) (WCAP-3750)
ZIRCALOY-4
properties of, mechanical and physical, 19: 45601(R) (WCAP-3750)
reactions with steam, facility for testing, 19: 45601(R) (WCAP-3750)
ZIRCONIUM
brittleness and fracture of, effects of hydrogen on, 19: 44716
corrosion by oxygenated sodium at 540°C, effects of polarizing current on, 19: 44616(R) (ANL-7000, pp 122-37)
deformation by strains due to twinning at 77°K, 19: 44725
determination in organic solutions by photometric methods, 19: 43972
determination using 7, 8, 3', 4'-tetrahydroxy flavonol, spectrophotometric, 19: 43955
diffusion in aluminum, 19: 45471 (AECL-2309)
diffusion in bcc phases of, 19: 45471 (AECL-2309)
effects on corrosion by mercury titanium, 19: 44616(R) (ANL-7000, pp 122-37)
elastic properties at room temperature effects of prestrain at 77°K on, 19: 44728
extrusion by hydrostatic methods, 19: 44651
hydride distribution in matrix of, 19: 44676(R) (ANL-7000, pp 176-82)
mechanical properties of, combined effects of hydrogen and oxygen on, 19: 44676(R) (ANL-7000, pp 176-82)
neutron absorption cross sections at 24 kev, (E), 19: 45230
oxidation reaction mechanisms, 19: 44617(R) (ANL-7000, pp 213-26)
oxide film structure on, 19: 44622(R) (EURAEC-1433)

phase transformations in, relation of c/a ratio and elastic moduli temperature dependence with, 19: 44676(R) (ANL-7000, pp 176-82)
reactions with beryllium, copper, stainless steel, and niobium alloys to 760°C *in vacuo*, 19: 44606 (PWAC-483)
reactions with uranium dioxide at 2200°C, 19: 44599(R) (GEMP-50A)
separation from hydrochloric acid solutions by solvent extraction using N-benzoyl-N-phenylhydroxylamine, 19: 43972
shear stress in, effects of hydrogen on critical resolved, 19: 44676(R) (ANL-7000, pp 176-82)
solvent extraction by Alamine 336–dibutyl cellosolve in contactor, 19: 44108 (AERE-R-4440(Pt.3))
solvent properties of liquid, for carbon at 2700 to 4000°K, 19: 44701(R) (TID-22144)
spectra at, Ohlin structure near limit of continuous x-ray, (E), 19: 44940
strengthening by powdered lanthanum, thorium, and yttrium oxide dispersions, 19: 44676(R) (ANL-7000, pp 176-82)

ZIRCONIUM ALLOYS
superconductivity in, 19: 44678(R) (ANL-7000, pp 186-200)
Al–Hg–Zr, corrosive effects on titanium of mercury-based, 19: 44616(R) (ANL-7000, pp 122-37)
Cr–Ti–Zr, phase studies, 19: 44714
Cr–Zr, phase studies, 19: 44714
Cu–Fe–Zr, corrosion by steam at 540°C, effects of pressure on, 19: 44616(R) (ANL-7000, pp 122-37)
Cu–Zr, corrosion by steam at 540°C, 19: 44616(R) (ANL-7000, pp 122-37)
Fe–Ni–Zr, corrosion by steam at 540°C, effects of alloy microstructure on, 19: 44616(R) (ANL-7000, pp 122-37)
Fe–Ni–Zr, corrosion by steam at 540°C, effects of pressure on, 19: 44616(R) (ANL-7000, pp 122-37)
Fe–Zr, isomer shift of iron-57 in $ZrFe_2$ at 300 and 800°K, 19: 44678(R) (ANL-7000, pp 186-200)
fission–U–Zr, radioinduced swelling in, effects of postirradiation annealing temperature on, 19: 44587(R) (ANL-7000, pp 3-63)
Hg–Ni–Zr, corrosive effects on titanium of mercury-based, 19: 44616(R) (ANL-7000, pp 122-37)
Ir–Zr, lattice parameters of Zr_2Ir, 19: 44678(R) (ANL-7000, pp 186-200)
Mg–Hg–Zr, corrosive effects on titanium of mercury-based, 19: 44616(R) (ANL-7000, pp 122-37)
Nb–Rh–Zr, superconducting transition temperature, 19: 44678(R) (ANL-7000, pp 186-200)
Nb–Ti–Zr, microstructure of, effects of annealing temperature on, 19: 44587(R) (ANL-7000, pp 3-63)
Nb–Zr, brazing to beryllium using silver, 19: 44606 (PWAC-483)
Nb–Zr, brazing to beryllium with silver alloys, effects of carbon and silicon coatings on, 19: 44606 (PWAC-483)
Nb–Zr, brittleness and fracture of, effects of hydrogen on, 19: 44716
Nb–Zr, carburization of, for prevention of galling, 19: 44609 (TIM-927)
Nb–Zr, corrosion by lithium, effects of heat treatment and oxygen on, 19: 44620 (CNLM-6344)
Nb–Zr, corrosion by potassium–sodium at 1250°F, effects of carbon, nitrogen and oxygen on, 19: 44626 (TIM-896)
Nb–Zr, corrosion resistance of, effects of production method and aging on, 19: 44629
Nb–Zr, crystallization and recovery of cold worked, 19: 44698 (PWAC-465)
Nb–Zr, erosion by water of rotating disks of, 19: 44625 (TIM-894)
Nb–Zr, mechanical properties at high temperatures, 19: 44674(R) (ANL-7000, pp 69-83)
Nb–Zr, mechanical properties of, effects of carbon and oxygen on, 19: 44605 (PWAC-464)
Nb–Zr, mechanical properties of effects of aging, oxygen content, and production method on, 19: 44629
Nb–Zr, microstructures, 19: 44610 (TIM-943)
Nb–Zr, microstructure of, effects of annealing temperature on, 19: 44587(R) (ANL-7000, pp 3-63)
Nb–Zr, reactions with fissium–plutonium–uranium alloys at 750°C, 19: 44587(R) (ANL-7000, pp 3-63)
Nb–Zr, reactions with metals at 540 to 760°C *in vacuo*, 19: 44606 (PWAC-483)
Ni–Zr, brittleness and fracture of, effects of hydrogen on, 19: 44716
Ni–Zr, corrosion by steam at 540°C, 19: 44616(R) (ANL-7000, pp 122-37)
Pu–U–Zr, corrosion by air at room temperature, 19: 44587(R) (ANL-7000, pp 3-63)
Ru–Zr, lattice parameters of Zr_2Rh, 19: 44678(R) (ANL-7000, pp 186-200)
Sb–Se–Zr, phase studies, 19: 44720
Se–Zr, crystal structure of intermetallic compound $ZrSe_2$ in, 19: 44720
Sb–Zr, crystal structure of intermetallic compound $ZrSb_2$ in, 19: 44702
stainless steel–Zr, corrosion by steam at 650°C, 19: 44616(R) (ANL-7000, pp 122-37)

ZIRCONIUM BORIDES
diffusion of oxygen in alpha, anodic film dissolution and hardness studies, 19: 44673 (AECL-2268)

ZIRCONIUM CARBIDES
analysis for carbon using electron microprobe, 19: 43966
C–W_2C–ZrC, behavior at 3250°K in graphite crucible, 19: 44701(R) (TID-22144)

ZIRCONIUM HYDRIDES
neutron inelastic scattering by, distributions from cold, (E), 19: 45240
precipitation in Zircaloy-2, effects of elastic stresses on orientation of, 19: 44697 (ORNL-TM-1239)

ZIRCONIUM IONS
effects on hydrolysis of nucleotides, catalytic, 19: 43708

ZIRCONIUM ISOTOPES Zr-90
deuteron elastic scattering at 12 and 14 Mev, differential cross sections for, (E), 19: 45281 (ORNL-3850)
deuteron reactions (d,p) at 12 and 14 Mev, differential cross sections for, (E), 19: 45281 (ORNL-3860)

ZIRCONIUM ISOTOPES Zr-95
content in marine environment, 19: 43663
determination in lung tissues, spectrometric, 19: 44292(R) (NP-15173)
diffusion from irradiated molybdenum–rhenium–tungsten alloy, 19: 44599(R) (GEMP-50A)
distribution in fetal and maternal rabbit tissues, 19: 43883(R) (UCLA-12-565, pp 65-85)
separation from niobium-95 and hafnium-181, chromatographic, 19: 44118 (UCRL-16015)

ZIRCONIUM NITRIDES
corrosion by mercury, effects of dissolved titanium on, 19: 44616(R) (ANL-7000, pp 122-37)

ZIRCONIUM OXIDES
effects of additives of, on modulus of rupture of beryllia, 19: 44599(R) (GEMP-50A)
properties in in-pile thermionic cells, 19: 44685 (CONF-650908-5)
structure of films of, formed on zirconium, 19: 44622(R) (EURAEC-1433)
use in development of in-pile method for measuring thermal conductance of fuel elements, 19: 44684 (CEND-3336-241)

ZIRCONIUM SYSTEMS
Al–B–Zr, phase studies, 19: 44719
C–Mo–Ti–Zr, mechanical properties at high temperatures, 19: 44674(R) (ANL-7000, pp 69-83)
C–Nb–Zr, development of, with high-temperature strength, 19: 44605 (PWAC-464)
HfC–Zr, solidus temperature at 1760°C, 19: 44612(R) (USBM-RC-1199)

ZIRCONS
analysis of, spectroscopic, 19: 43954

REPORT NUMBER INDEX

Reports, conference papers and proceedings, numbered translations, and patents abstracted during the period are included in this index. Each item is listed by report number; this is followed by the abstract number and a brief notation regarding public availability. The index entries show, when known, which reports are on file in the depository libraries, which reports have been published in open-literature journals (journal citation given), and which reports can be purchased (source and price). Whenever a report is identified by more than one number, cross references from secondary to primary report numbers are cited.

The report number codes apply to AEC reports unless designated otherwise. Non-AEC reports are identified by parenthetical notes after the report codes; e.g., (non-AEC), (British), (Canadian), (French). The note (Misc.) identifies those codes used for both USAEC and non-AEC reports. Patents are listed under the heading "PATENTS"; the country of origin is included in parentheses.

A comprehensive listing of both AEC and non-AEC report codes is contained in TID-85(3rd Rev.), *Report Number Series Used by the Division of Technical Information in Cataloging Reports*. This information is also included in the Cumulative Report Number Index (issued annually).

Public Availability of USAEC Reports

All USAEC reports abstracted in *NSA* are available to the public through one or more of the following sources:

(1) Depository libraries in the United States, in other countries, and in international agencies. A list of these depositories appears on the inside covers of each issue of *NSA*.

(2) Scientific and technical journals or other publications.

(3) Microcard Editions, Inc., in Microcard and micronegative form. Orders and inquiries should be sent to: Accounting and Shipping Department, West Salem, Wisconsin 54669.

(4) Clearinghouse for Federal Scientific and Technical Information, U. S. Department of Commerce, Springfield, Virginia 22151.

(5) Superintendent of Documents, U. S. Government Printing Office, Washington, D. C. 20402.

Public Availability of Non-AEC Reports

U. S. Reports. Many reports of U. S. Government agencies are available to the public from the Clearinghouse for Federal Scientific and Technical Information (CFSTI). This availability is given when known. Such reports should be ordered by AD number or NASA-N number. If availability is not shown, inquiries may be directed to CFSTI. In the case of NP numbers, inquiries should be by title and author.

Non-U. S. Reports. Many reports of atomic energy establishments of other countries are deposited in the libraries listed on the inside covers of each issue of *NSA*.

Additionally, the following countries have made their reports available as indicated.

AUSTRALIA

Australian Atomic Energy Commission Research Establishment. Available upon request from the Library, Australian Atomic Research Establishment, Private Mail Bag, Sutherland, New South Wales, Australia.

BELGIUM

Centre d'Étude de l'Énergie Nucléaire. Available upon request to individuals and organizations, from the Centre d'Étude de l'Énergie Nucléaire (CEN), 31, Rue Belliard, Bruxelles, Belgium.

CANADA

Atomic Energy of Canada Limited. For sale by the Technical Information Officer, Atomic Energy of Canada Limited, Chalk River, Ontario, Canada. Copies are also deposited in libraries in the United Kingdom.

National Research Council of Canada. Available from the National Research Council of Canada, Ottawa 2, Ontario, Canada.

DENMARK

Atomic Energy Commission Research Establishment, Risø. Available on exchange from the Library, Danish Atomic Energy Commission, Risø, Roskilde, Denmark. Also for sale by Jul. Gjellerup, Booksellers, 87 Sölvgade, København K., Denmark.

Danatom. Available on loan from Research Establishment, Risø, Roskilde, Denmark. Copies are available from Danatom, Aurehøjvej 2, Hellerup, Denmark.

FRANCE

Commissariat à l'Énergie Atomique. Inquiries for reports numbered 1-2199 should be addressed to Commissariat à l'Énergie Atomique, Service Central de Documentation, Centre d'Études Nucléaires de Saclay, Boite Postale No. 2, Gif-sur-Yvette (S. et O.), France. Reports numbered 2200 and above are available from La Documentation Francaise, 16 Rue Lord-Byron, Paris VIII, France.

Service Central de Protection contre les Rayonnements Ionisants. Copies are available from Ministère de la Santé Publique, Service Central de Protection contre les Rayonnements Ionisants, B. P. n° 35–LE VESINET (S. et O.), France.

GERMANY

Deutsches Elektronen-Synchrotron DESY. Copies are available from Deutsches Elektronen-Synchrotron Desy, Dokumentation, 2000 Hamburg-Gr. Flottbek 1, Notkestieg 1, Germany.

Kernforschungsanlage. Copies may be ordered from Zentralbibliothek der Kernforschungsanlage Jülich, Jülich, Bundesrepublik Deutschland.

Hahn-Meitner-Institute für Kernforschung. Available without charge from Hahn-Meitner-Institute für Kernforschung Berlin, Bibliothek, Glienicker Strasse 100, 1 Berlin 39, Germany. Copies are deposited in many national nuclear centers in the world.

Johann-Wolfgang-Goethe Universität, Frankfurt Am Main, Institut für Kernphysik, (IKF). Copies are available from Gmelin Institut, 40-42 Varrentrappstrasse, Frankfurt (Main), West Germany.

ISRAEL

Israel Atomic Energy Commission. Available without charge from Ministry of Defence/Atomic Energy Com-

mission, Soreq Research Establishment, Yavne, Israel. Copies are deposited in libraries in Israel and in other countries.

ITALY

Centro Informazioni Studi Esperienze (CISE). For sale at CISE Press Office, Casella Postale 3986, Milano, Italy. Copies are deposited in libraries in Italy.

Comitato Nazionale per l'Energia Nucleare. Copies are available from Comitato Nazionale per l'Energia Nucleare, Divisione Affari Internazionali e Studi Economici, Ufficio Pubblicazioni, Via Belisario, 15, Roma, Italy.

JAPAN

Japan Atomic Energy Research Institute (JAERI). Available from the Staff Supply Cooperative of Japan Atomic Energy Research Institute (JAERI), 1-1 Tamura-Cho, Shiba, Minato-Ku, Tokyo, Japan. Copies are deposited in depositories in Tokyo, Nagoya, and Osaka.

Nagoya University. Copies are available from Research Information Center, Institute of Plasma Physics, Nagoya University, Nagoya, Japan.

University of Tokyo. Available free of charge from Institute for Nuclear Study, University of Tokyo, Tanashi-Machi, Kitatama-gun, Tokyo, Japan.

NETHERLANDS

Reactor Centrum Nederland. For sale by Reactor Centrum Nederland, 112 Scheveningseweg, 's-Gravenhage, The Netherlands. Copies are deposited in university libraries in Holland and in many national nuclear centers in the world.

NEW ZEALAND

Institute of Nuclear Sciences. Copies are available from Librarian, Institute of Nuclear Sciences, D.S.I.R., Private Bag, Lower Hutt, New Zealand. Copies are deposited in other countries.

NORWAY

Forsvarets Forskningsinstitutt. Copies available from Norwegian Defence Research Establishment, Library, P. O. Box 25, Kjeller, Norway.

Institutt for Atomenergi. "KR" reports are available on an exchange basis from the Library, Institutt for Atomenergi, Box 40, Kjeller, Norway. Other series are not generally available to the public.

Norwegian Reactor School. Copies are available from The Library, Institutt for Atomenergi, P. O. Box 40, Kjeller, Norway.

PAKISTAN

Atomic Energy Center. Copies are available from Atomic Energy Center, P. O. Box 658, Lahore, (West Pakistan).

POLAND

Reports of the Polish nuclear institutes are published by the Nuclear Energy Information Center of the Government Commissioner for Use of Nuclear Energy. Copies are available from Ośrodek Informacji o Energii Jądrowej, Warszawa, PKiN, Poland.

SPAIN

Junta de Energia Nuclear. "JEN" reports are available without charge from Servicio de Documentation, Junta de Energia Nuclear, Ciudad Universitaria, Madrid (3), Spain.

SWEDEN

Aktiebolaget Atomenergi. "AE" reports are for sale from Aktiebolaget Atomenergi, Library Section, Box 43041, Stockholm 43, Sweden. Bibliographies and literature surveys of the VDDIT- series may be obtained from Aktiebolaget Atomenergi, Information Office, Scientific and Technical Information, Box 43041, Stockholm 43, Sweden. Other series are not generally available to the public. Organizations in the atomic energy field may obtain copies from Aktiebolaget Atomenergi. Microcopy of AE reports is available from the International Documentation Centre, Tumba, Sweden.

SWITZERLAND

CERN European Organization for Nuclear Research. Available without charge from CERN European Organization for Nuclear Research, Geneva 23, Switzerland. Copies are deposited in libraries in 13 countries.

Eidgenössisches Institut für Reaktorforschung. "EIR" reports are available from Eidgenössiches Institut für Reaktorforschung, c/o Bibliothek, Würenlingen/Ag, Switzerland.

TURKEY

Turkish Atomic Energy Commission. Copies are available free of charge from T.A.E.C., Çekmece Nuclear Research Center, P. O. Box 1, Airport, İstanbul, Turkey.

UNITED KINGDOM

United Kingdom Atomic Energy Authority. Some reports are for sale in the United States by the British Information Service (BIS), 845 Third Avenue, New York, N. Y. 10022. United Kingdom reports generally may be purchased from Her Majesty's Stationery Office, London. Copies not for sale by Her Majesty's Stationery Office may be purchased in microcopy form from Micro Methods Limited, East Ardsley, Wakefield, Yorks, England. Report copies are deposited in a large number of libraries in England.

Conferences

Published conference proceedings as well as individual unpublished papers from conferences are included in this index. A CONF number is assigned to the conference if published proceedings are received and also if only a single paper is received. The base number used is year-month-sequence. Thus, the number CONF-650101 would indicate that the conference was held in 1965, in January, and that this was the first January 1965 conference so received. This number would be assigned to complete published proceedings, or if individual papers are received, the base number would be extended to include a paper number, i.e., CONF-650101-1. As additional papers are received, they will be assigned consecutive numbers in the series, CONF-650101-1, 2, 3, 4, etc. This numbering system ensures that all papers received from a conference will be associated with that conference in this index.

If published proceedings are received after the receipt of individual papers, the complete proceedings will be abstracted and the abstract number will appear in this index with the base CONF number.

Abbreviations Used in Availability Column

AECL	For sale by Atomic Energy of Canada Ltd., Chalk River, Ontario, Canada.
BIS	For sale by British Information Service, 845 Third Avenue, New York, N. Y. 10022
CFSTI	For sale by the Clearinghouse for Federal Scientific and Technical Information, U.S. Department of Commerce, Springfield, Virginia 22151. The symbol "cy" indicates that the format of the item sold may be either a printed document or a photographic reproduction (two-thirds of original size) depending upon the availability of printed stock. The indicated price is for either format. The symbol "mn" is used to indicate

that copy is available in the form of micronegatives (microfiche). The number preceding the "mn" symbol indicates the number of micronegatives in the set. Micronegatives are available at the following prices: One micronegative, $0.50; each additional micronegative of the set, $0.25. For additional micronegative copies of the same report requested at the time of the original order, $0.25 per micronegative. Prices are reduced on micronegatives if subscription distribution is purchased.

Dep. AEC reports: Full-size copy is on deposit in the depository libraries both inside and outside the United States. These reports are also for sale by Microcard Editions, Inc., Accounting and Shipping Department, West Salem, Wisconsin 54669.
Non-AEC reports: Full-size copy on deposit in the depository libraries in the United States only.

Dep.(mn) Same as for Dep., except copy is in micronegative (microfiche) form.

DSIR For sale by the National Lending Library for Science and Technology (D.S.I.R.), Boston Spa, Yorkshire, England.

DTI Extension Available from the U. S. Atomic Energy Commission, Division of Technical Information Extension, P. O. Box 62, Oak Ridge, Tennessee 37831.

EM Blueprints and Microcopy of AEC engineering drawings are available from Clearinghouse for Federal Scientific and Technical Information, U. S. Department of Commerce, Springfield, Virginia 22151. Current prices of the CAPE- packages may be obtained from this address. TID-4100, available from the Division of Technical Information Extension, P. O. Box 62, Oak Ridge, Tennessee 37831, contains information on all the CAPE- packages for sale.

Gmelin Available at a nominal charge and under the AED- number shown from Atomic Energy Documentation Center, Gmelin Institute, 40-42 Varrentrappstrasse, Frankfurt (Main), West Germany.

GPO For sale by the Superintendent of Documents, Government Printing Office, Washington, D. C. 20402.

HMSO Her Majesty's Stationery Office, London.

IAEA Available from the International Atomic Energy Agency, Vienna, Austria, and from its sales agencies in various countries throughout the world. A list of these agencies is found in each STI/DOC and STI/PUB publication.

JCL For sale by the Special Libraries Association Translation Center, John Crerar Library, 35 West 33rd Street, Chicago, Illinois 60616.

LC For sale by the Library of Congress, Photoduplication Service, Washington, D. C. 20540.

NAS National Academy of Sciences, National Research Council, Washington, D. C. 20418.

NRC For sale by the National Research Council of Canada, Ottawa, Ontario, Canada.

ORINS Available on interlibrary loan from the Library, Oak Ridge Institute of Nuclear Studies, Post Office Box 117, Oak Ridge, Tennessee 37831.

UKAEA, London Available from United Kingdom Atomic Energy Authority, 11 Charles II Street, London, S. W. 1.

UN United Nations Bookshop, United Nations Headquarters, New York, New York.

USGS Available free of charge from the U. S. Geological Survey, Washington, D. C. 20242.

[The symbols "ph," "mf," and "fs" are used to designate that copy is available only in photostat, microfilm, or facsimile form. The symbol "mn" is used to designate that copy is available in micronegative (microfiche) form. The symbol "cy" is used to designate full size or photographically enlarged copy (two-thirds of original size).]

Report No.	Abstract No.	Availability
AAEC-TM–	**(Australian)**	
118	19-45521	Dep. mn
ABCC–		
16-64	19-43710	Dep. mn; CFSTI $1.00 cy, $0.50 mn
63-64	19-44280	Dep. mn; CFSTI $3.00 cy, $0.75 mn
ACF–		
8	19-44219	Dep. mn; CFSTI $2.00 cy, $0.50 mn
ACHP–	**(Misc.)**	
65003	19-44131	Dep. mn; CFSTI $7.26 cy, $2.00 mn
65557	19-45557	Dep. mn; CFSTI $1.00 cy, $0.50 mn
AD–	**(Misc.)**	
424481	19-44894	
425708	19-44337	CFSTI $7.60
426192	19-45380	CFSTI $2.60
462614	19-45457	CFSTI
466108	19-44254	See RRA-M51
468477	19-44980	See NP-15433
606831	19-45156	See AFCRL-64-768
608496	19-44338	CFSTI $4.00
608503	19-44339	CFSTI $2.00 cy, $0.50 mn
609015	19-45155	Dep. mn; CFSTI $3.00 cy, $0.75 mn
618071	19-44981	See NP-15435
619201	19-44672	CFSTI $2.00 cy, $0.50 mn
619379	19-44979	See NP-15419
619902	19-44243	
620882	19-44970	Phys. Rev. Letters, 15: 507-11(1965)
AE–	**(Non-AEC)**	
190	19-45458	Dep. mn
192	19-44051	Dep. mn
193	19-44052	Dep. mn
194	19-45667	Dep. mn
195	19-45522	Dep. mn
AEC-tr–	**(For complete listing see TID-4025)**	
6567	19-44061	Dep. mn; CFSTI $1.00 cy, $0.50 mn; JCL $1.10 fs, $0.80 mf
6572	19-44002	Dep. mn; CFSTI $1.00 cy, 1 mn; JCL $2.60 fs, $0.86 mf
6607	19-44879	Dep. mn; CFSTI $1.00 cy, $0.50 mn; JCL $1.10 fs, $0.80 mf
AECL–	**(Canadian)**	
2218	19-44044	Dep.; $1.50
2219	19-44365	Dep.; AECL $1.00
2223	19-45254	See CRT-1213
2249	19-44132	Dep.; AECL $0.50
2251	19-45694	Dep. mn; AECL Free
2268	19-44673	Dep.; AECL $1.00
2309	19-45471	Dep.; AECL $0.50
AED-C–	**(Non-AEC)**	
06-12	19-44366	Dep. mn
15-08	19-44978	Dep. mn
22-04	19-45647	Dep. mn
AEET–	**(Indian)**	
202	19-44281	Dep. mn
AEET-AM–	**(Indian)**	
40	19-44244	Dep. mn
AEEW-M–	**(British)**	
472	19-45244	Dep. mn
550	19-44367	Dep.; BIS $0.50; HMSO 2s. 6d
AEEW-R–	**(British)**	
425	19-45523	Dep.; BIS $1.60; HMSO 8s.
428	19-45524	Dep.; BIS $0.80; HMSO 4s.
439	19-44579	Dep.; BIS $1.10; HMSO 5s. 6d.
AERE-M–	**(British)**	
833	19-44368	Dep.; BIS $0.70; HMSO 3s. 6d.
1361	19-44340	Dep.; BIS $0.70; HMSO 3s. 6d.
AERE-R–	**(British)**	
1605	19-45472	Dep.; BIS $0.30; HMSO 1s. 9d.
4440(Pt.3)	19-44108	Dep.; BIS $0.80; HMSO 4s.
4552	19-44369	Dep.; BIS $2.80; HMSO 14s. 0d.
4636	19-44715	J. Inst. Metals, 93: 423-8(1965)
4641	19-44817	Brit. J. Appl. Phys., 16: 1219-45(1965)
4883	19-44370	Dep.; BIS $0.60; HMSO 3s.
4921	19-44371	Dep.; BIS $0.50; HMSO 2s. 6d.
4962	19-44341	Dep.; BIS $0.90; HMSO 4s. 6d.
4964	19-44580	Dep.; BIS $0.50; HMSO 2s. 6d.
4990	19-43924	Dep.; BIS $0.50; HMSO 2s. 6d.
AFCRL–	**(Non-AEC)**	
64-102	19-45155	See AD-609015
64-690(II)	19-44338	See AD-608496
64-690(Vol.III)	19-44339	See AD-608503
64-768	19-45156	CFSTI $3.00
65-470	19-44372	CFSTI
AFML-TR–	**(Non-AEC)**	
65-166	19-44053	CFSTI
AFWL-TR–	**(Non-AEC)**	
65-95	19-45245	
AGN–	**(Misc.)**	
8122	19-44569	Dep. mn; CFSTI $1.00 cy, $0.50 mn
AGN-TM–		
409	19-45558	Dep. mn; CFSTI $4.00 cy, $1.00 mn
AHSB(RP)–	**(British)**	
M-35	19-44282	Dep.; BIS $0.80; HMSO 4s.
ANL–		
6877	19-44802	Dep. mn; CFSTI $3.00 cy, $0.50 mn
6883	19-44736	Dep. mn; CFSTI $1.00 cy, $0.50 mn
6956	19-43925	Dep. mn; CFSTI $4.00 cy, $0.75 mn
7000	19-44586	Dep. mn; CFSTI $7.00 cy, $1.75 mn
7011	19-45560	Dep. mn; CFSTI $2.00 cy, $0.50 mn
7024	19-45214	Dep. mn; CFSTI $1.00 cy, $0.50 mn
7026	19-45668	Dep. mn; CFSTI $2.00 cy, $0.50 mn
ANL-Trans–		
217	19-45048	Dep. mn; CFSTI $1.00 cy, $0.50 mn; JCL $1.10 fs, $0.80 mf
APDA–	**(Misc.)**	
172	19-45561	Dep. mn; CFSTI $3.00 cy, $0.75 mn
174	19-45493	Dep. mn; CFSTI $3.00 cy, $0.75 mn
ARL–	**(Non-AEC)**	
65-105	19-44804	CFSTI
65-115	19-45381	CFSTI J. Appl. Phys., 36: 3142-5(1965)
AROD–	**(Misc.)**	
3347:6	19-44374	CFSTI
AWRE-E–	**(British)**	
1/65	19-44283	Dep.; BIS $1.20; HMSO 6s. 0d.
AWRE-O–	**(British)**	
23/65	19-45248	Dep. mn; BIS $0.80; HMSO 4s.
24/65	19-44284	Dep. mn; BIS $3.40; HMSO 17s.
42/65	19-44618	Dep. mn; BIS $0.60; HMSO 3s.
55/65	19-45249	Dep. mn; BIS $0.90; HMSO 4s. 6d.
65/65	19-44681	Dep. mn; BIS $1.00; HMSO 5s.
66/65	19-44619	Dep.; BIS $0.80; HMSO 4s. 0d.
BAW–	**(Misc.)**	
272	19-45542	Dep. mn; CFSTI $3.00 cy, $0.50 mn
1195-4	19-45671	Dep. mn; CFSTI $2.00 cy, $0.50 mn
1280-29	19-44182	Dep. mn; CFSTI $3.00 cy, $0.50 mn
1280-31	19-44133	Dep. mn; CFSTI $2.00 cy, $0.50 mn
3238-8	19-44183	Dep. mn; CFSTI $2.00 cy, $0.50 mn
BDX–		
613-75	19-44682	Dep. mn; CFSTI $1.00 cy, $0.50 mn
BLG–	**(Belgian)**	

Report No.	Abstract No.	Availability
327	19-44552	Dep. mn
329	19-45473	Dep. mn
331	19-44109	Dep. mn
Bkl-Bull.–		
625	19-44608	See TID-22125
Bkl-Rl–	(Misc.)	
6661	19-44588	Bureau of Mines Free
Bml–	(Misc.)	
1737	19-44740	Dep. mn; CFSTI $1.25 cy, $0.50 mn
Bml-X–		
346	19-44208	Dep. mn; CFSTI $2.00 cy, $0.50 mn
BN–	(Misc.)	
6212-01	19-44596	See EURAEC-1392
BNL–		
325(2nd Ed.) (Suppl.2)(Vol.III)	19-45250	Dep. mn; CFSTI $3.00 cy, $1.50 mn
912	19-45695	Dep. mn; CFSTI $1.00 cy, $0.50 mn
914	19-44761	Dep. mn; CFSTI $5.00 cy, $1.00 mn
924	19-43711	Dep. mn; CFSTI $1.00 cy, $0.50 mn
8516	19-44799	Dep. mn; CFSTI $1.00 cy, $0.50 mn
9102	19-45067	Nuovo Cimento (10), 39: 641-9(1965)
9108	19-45251	Dep. mn; CFSTI $3.00 cy, $0.75 mn
9124	19-44497	Nucl. Instr. Methods, 36: 181-91(1965)
9337	19-43664	Dep. mn; CFSTI $2.00 cy, $0.50 mn
9338	19-43665	Dep. mn; CFSTI $3.00 cy, $0.50 mn
9383	19-43712	Dep. mn; CFSTI $1.00 cy, $0.50 mn
9406	19-43666	Dep. mn; CFSTI $1.00 cy, $0.50 mn
9425	19-44375	Dep. mn; CFSTI $1.00 cy, $0.50 mn
9466	19-44376	Dep. mn; CFSTI $1.00 cy, $0.50 mn
9480	19-44858	Dep. mn; CFSTI $1.00 cy, $0.50 mn
9496	19-44859	Dep. mn; CFSTI $1.00 cy, $0.50 mn
9502	19-44163	Dep. mn; CFSTI $1.00 cy, $0.50 mn
BNL-tr–		
1	19-44490	Dep. mn; CFSTI $1.00 cy, $0.50 mn; JCL $1.10 fs, $0.80 mf
5	19-44003	Dep. mn; CFSTI $1.00 cy, $0.50 mn; JCL $1.60 fs, $0.80 mf
12	19-43729	Dep. mn; CFSTI $1.00 cy, $0.50 mn; JCL $1.10 fs, $0.80 mf
16	19-45292	Dep. mn; CFSTI $2.00 cy, $0.50 mn; JCL $2.60 fs, $1.04 mf
BNWL–		
89	19-45672	Dep. mn; CFSTI $3.00 cy, $0.75 mn
102	19-44589	Dep. mn; CFSTI $1.00 cy, $0.50 mn
103	19-44800	Dep. mn; CFSTI $2.00 cy, $0.50 mn
106	19-45563	Dep. mn; CFSTI $3.00 cy, $0.75 mn
114	19-44110	Dep. mn; CFSTI $3.00 cy, $0.75 mn
115	19-43713	Dep. mn; CFSTI $5.00 cy, $1.00 mn
121	19-44111	Dep. mn; CFSTI $1.00 cy, $0.50 mn
BNWL-SA–		
29	19-44285	Dep. mn; CFSTI $1.00 cy, $0.50 mn
30	19-44286	Dep. mn; CFSTI $1.00 cy, $0.50 mn
85	19-45564	Dep. mn; CFSTI $1.00 cy, $0.50 mn
BRL-MR–	(Non-AEC)	
1644	19-45382	
CALT–		
221-12	19-45696	Dep. mn; CFSTI $1.00 cy, $0.50 mn
CAPE–		
1072	19-44360	
1257	19-44539	
1258	19-44359	
CEA-R–	(French)	
2734	19-45252	Dep. mn
2755	19-44164	Dep. mn
2769	19-44805	Dep. mn
2778	19-44993	Dep. mn
2780	19-45215	Dep. mn
2781	19-45565	Dep. mn
2785	19-45566	Dep. mn
2789	19-44683	Dep. mn
2799	19-44287	Dep. mn
2800	19-43926	Dep. mn
2803	19-44590	Dep. mn
2804	19-45216	Dep. mn
2817	19-43987	
CEA-tr–	(French)	
A-1818	19-44752	Dep. mn; JCL $1.60 fs, $0.80 mf
R-1836	19-44304	Dep. mn; JCL $1.60 fs, $0.80 mf
R-1866	19-44491	Dep. mn; JCL $1.60 fs, $0.30 mf
CEND–	(Misc.)	
3107-228	19-44591	Dep. mn; CFSTI $2.00 cy, $0.50 mn
3336-241	19-44684	Dep. mn; CFSTI $1.00 cy, $0.50 mn
CERN–	(European Organization for Nuclear Research)	
65-4(Vol.I)	19-44377	Dep. mn
65-4(Vol.II)	19-44383	Dep. mn
65-26	19-44994	Dep. mn Science, 149: 1181-9(1965)
65-29	19-44165	Dep. mn
CLM-R–	(British)	
43	19-44592	Dep. mn; BIS $0.50; HMSO 2s. 6d.
CNLM–	(Misc.)	
6085	19-43966	Norelco Reptr., 12: 3-6(1965)
6344	19-44620	Dep. mn; CFSTI $1.00 cy, $0.50 mn
CONF-179–	(American Chemical Society Radionuclidic Exchange on Soils, Minerals, and Resins, Philadelphia, Apr. 1964)	
19	19-45495	See WAPD-T-1653
CONF-213–	(Symposium on Water Chemistry in Reactors, Rome, May 1963)	
2	19-45678	See JEN-149-DQ/I-50
CONF-550–	(The International Conference on High-Energy Physics, Dubna, August 5–15, 1964)	
100	19-45025	See N64-26265
CONF-654–	(American Nuclear Society Meeting, San Francisco, Nov. 30–Dec. 3, 1965) Proceedings	
94	19-45538	Gmelin, AED-CONF-64-219-138
CONF-663–	(6th Agard Combustion and Propulsion Colloquium on Energy Sources and Energy Conversion, Cannes, France, Mar. 1964)	
2	19-44205	ORINS
CONF-720–	(2nd Symposium on Protection Against Radiation Hazards in Space, Gatlinburg, Oct. 1964)	
31	19-43879	Gmelin, AED-CONF-64-190-36
CONF-732–	19-43780	(Conference on the Mechanisms of the Dose Rate Effect at the Genetic and Cellular Level, Oiso, Japan, Nov. 1964)
CONF-765–	(2nd Conference on Radioactive Fallout from Nuclear Weapons Tests, Germantown, Md., Nov. 3–6, 1964)	
12	19-44250	See NP-15269
CONF-787(Vol.I)	19-44377	(5th International Conference on Nuclear Photography, Geneva, Sept. 15–18, 1964) See CERN-65-4(Vol.I)
CONF-787(Vol.II)	19-44383	(5th International Conference on Nuclear Photography, Geneva, Sept. 15–18, 1964) See CERN-65-4(Vol.II)
CONF-804(Vol.I)–	19-43262	(Symposium on the Inelastic Scattering of Neutrons, Bombay, Dec. 15–19, 1964) See STI-PUB-92(Vol.I)
CONF-804(Vol.II)	19-45234	(Symposium on the Inelastic Scattering of Neutrons, Bombay, Dec. 15–19, 1964) See STI-PUB-92(Vol.II)

Report No.	Abstract No.	Availability
CONF-620405–	19-44735	(Symposium on Refractory Metals and Alloys, Chicago, Apr. 12–13, 1962)
CONF-630910–		(8th Summer Meeting of Physicists, Herceguovi, Yugoslavia, Sept. 1963)
1	19-45473	See BLG-329
CONF-630911–	19-44932	(Symposium on Stellar and Solar Magnetic Fields, Munich, Sept. 3–10, 1963)
CONF-630914–	19-44467	(International Conference on Preparation and Application of Semiconductor Detectors, Rossendorf, Sept. 23–8, 1963)
CONF-640304–		(Second Health Instrument Users Symposium, Harwell, Berks, England, Mar. 18–19, 1964)
1	19-44369	See AERE-R-4552
CONF-640511–	19-44761	(Conference on AEC Meteorological Activities, Upton, N. Y., May 19–22, 1964)
CONF-640808–		(European Congress on Cardiology, Prague, Aug. 17–22, 1964)
2	19-43667	See EUR-1890.f
CONF-641121–		(American Society for Cell Biology, 4th Annual Meeting, Cleveland, Nov. 11–13, 1964)
1	19-43856	Gmelin, AED-CONF-64-277-1
CONF-641210–		(American Physical Society Meeting, Berkeley, Calif., Dec. 1964)
23	19-44856	Gmelin, AED-CONF-64-236-40
CONF-641219–		(American Assn. for the Advancement of Science, 131th Annual Meeting, Montreal, Dec. 26–31, 1964)
1	19-43663	Gmelin, AED-CONF-64-272-3
2	19-43855	Gmelin, AED-CONF-64-272-1
CONF-641221–	19-44565	(Symposium on Industrial Applications of Nuclear Energy, Milan, Dec. 10–12, 1964)
CONF-650116–		(American Geophysical Union, Southwestern Regional Meeting, Socorro, N. Mex., Jan. 28–30, 1965)
1	19-45186	Gmelin, AED-CONF-65-021-1
CONF-650217–		(Symposium on Pulsed High Intensity Fission Neutron Sources, Washington, D. C., Feb. 18, 1965)
2	19-45674	See GA-6168
CONF-650219–		(Canadian Assn. of Radiologists, 28th Annual Meeting, Toronto, Ont., Canada, Feb. 24–28, 1965)
2	19-43857	Gmelin, AED-CONF-65-075-2
3	19-44540	Gmelin, AED-CONF-65-075-3 Radiology, 85: 729-30(1965)
4	19-44541	Gmelin, AED-CONF-65-075-1
CONF-650220–		(American Physical Society, Northwest Meeting, Norman, Okla., Feb. 25–27, 1965)
1	19-45450	Gmelin, AED-CONF-65-022-4
CONF-650302–	19-44319	(IAEA Symposium on Personnel Dosimetry for Accidental High-Level Exposure to External and Internal Radiation, Vienna, Mar. 1965) See STI-PUB-99
CONF-650313–		(Symposium on Nuclear Medicine, Philadelphia, Mar. 19–20, 1965)
4	19-44347	See ORNL-P-1545
CONF-650317–		(American Physical Society Meeting, Kansas City, Mo., Mar. 25, 1965)
3	19-45213	Gmelin, AED-CONF-65-039-27
CONF-650323–	19-45288	(The AEC Nuclear Cross Sections Advisory Group Meeting, Germantown, Md., Mar. 8–9, 1965) Proceedings See WASH-1056
CONF-650324–		(American Society of Mechanical Engineers, Aviation and Space Conference, Los Angeles, Mar. 14–18, 1965)
1	19-45661	ORINS
2	19-44571	ORINS
CONF-650327–		(American Society of Tool and Mfg. Engineers, Annual Conference, Cleveland, Mar. 29–Apr. 2, 1965)
1	19-45708	See SC-R-65-915
CONF-650401–		(American Chemical Society, Detroit, Apr. 4–9, 1965)
11	19-44094	Gmelin, AED-CONF-65-041-17
13	19-44096	Gmelin, AED-CONF-65-041
CONF-650405–		(International Conference on Modern Trends in Activation Analysis, College Station, Tex., Apr. 19–22, 1965)
15	19-43981	Gmelin, AED-CONF-65-040-1
16	19-43927	Dep. mn; CFSTI $1.00 cy, $0.50 mn
18	19-45375	Gmelin, AED-CONF-65-040-25
CONF-650407–		(International Symposium on Fission Product Release and Transport Under Accident Conditions, Oak Ridge, Tenn., Apr. 1965)
11	19-44285	See BNWL-SA-29
12	19-44286	See BNWL-SA-30
13	19-44632	Gmelin, AED-CONF-65-044-7
CONF-650410–		(American Physical Society, Washington, D. C., Apr. 26–29, 1965)
27	19-45376	Gmelin, AED-CONF-65-073-61
28	19-45377	Gmelin, AED-CONF-65-073-55
29	19-45130	Gmelin, AED-CONF-65-083-53
30	19-45378	Gmelin, AED-CONF-65-073-52
31	19-45374	Gmelin, AED-CONF-65-073-51
32	19-45379	Gmelin, AED-CONF-65-073-49
34	19-45353	Phys. Letters, 18: 316-18(1965)
37	19-45129	Gmelin, AED-CONF-65-073-70 Phys. Rev., 140: B326-9(1965)
CONF-650411–		(Joint NASA–AEC Liquid Metals Corrosion Meeting, Gatlinburg, Tenn., Apr. 21–23, 1965)
6	19-44211	See ORNL-P-1543
CONF-650413–		(Symposium on Neutron Dynamics and Control, Tucson, Ariz., Apr. 5–7, 1965)
12	19-45685	Gmelin, AED-CONF-65-042-20
CONF-650417–		(American Nuclear Society, National Topical Meeting on Fast Reactor Technology, Detroit, Apr. 26–28, 1965)
3	19-45623	Gmelin, AED-CONF-65-074-9
CONF-650422–		(American Geophysical Union, Program for Section of Seismology Annual Meeting, Washington, D. C., Apr. 19–22, 1965)
2	19-45166	J. Geophys. Res., 70: 4191-4206(1965)
3	19-45188	Gmelin, AED-CONF-65-118-3
5	19-44931	Gmelin, AED-CONF-65-118-23
8	19-45161	J. Geophys. Res., 70: 4139-50(1965)
9	19-44930	Gmelin, AED-CONF-65-118-30
12	19-44272	Gmelin, AED-CONF-65-118-33
15	19-45189	Gmelin, AED-CONF-65-118-26
CONF-650423–		(International Conference on Physics of Solids and High Pressures, Tucson, Apr. 19–21, 1965)
4	19-44734	Gmelin, AED-CONF-65-058-11
CONF-650429–		(American Power Conference, Chicago, Apr. 27–29, 1965)
15	19-45725	ORINS
CONF-650435–		(5th Shock Tube Symposium, Silver Spring, Md., Apr. 28–30, 1965)
3	19-44852	Gmelin, AED-CONF-65-097-16
4	19-44857	Gmelin, AED-CONF-65-097-6
5	19-44855	Gmelin, AED-CONF-65-097-5
6	19-44853	Gmelin, AED-CONF-65-097-7
CONF-650440–		(American Mathematical Society, 622nd Meeting, New York, Apr. 12–15, 1965)
1	19-45440	Gmelin, AED-CONF-65-095-1
2	19-45187	Gmelin, AED-CONF-65-095-2
CONF-650442–		(2nd Space Congress, Cocoa Beach, Fla., Apr. 5–7, 1965)

Report No.	Abstract No.	Availability
1	19-44570	Gmelin, AED-CONF-65-072-1
CONF-650444–	(Western States Combustion Inst., 1965 Spring Meeting, Hollywood, Calif., Apr. 21–22, 1965)	
1	19-43980	Gmelin, AED-CONF-65-119-1
4	19-44041	Gmelin, AED-CONF-65-119-4
CONF-650501–	(The Application of Computing Methods to Reactor Problems, Argonne, Ill., May 17–19, 1965)	
15	19-45469	ORINS
CONF-650504–	(IAEA Symposium on Pulsed Neutron Methods, Karlsruhe, Germany, May 10–14, 1965)	
42	19-45222	See INR-624/IX-A/R
44	19-45227	See NIJS-R-449
CONF-650510–	(Purdue Conference on Instrumentation for High Energy Physics, Lafayette, Indiana, May 11–15, 1965)	
15	19-44361	Gmelin, AED-CONF-65-110-11
CONF-650519–	(13th Annual Conference of American Society of Testing Materials, St. Louis, May 16–21, 1965)	
3	19-43979	Gmelin, AED-CONF-65-120-3
5	19-44242	Gmelin, AED-CONF-65-120-21
CONF-650521–	(Conference on Purification of Materials, New York, May 6–8, 1965)	
2	19-43929	See IS-1237
4	19-43978	Gmelin, AED-CONF 65-113-1
CONF-650546–	(American Society of Mechanical Engineers, Design Engineering Conference and Show, New York, May 17–20, 1965)	
2	19-44987	ORINS
CONF-650547–	(American Society of Lubrication Engineers, 20th Annual Meeting, Detroit, May 4–7, 1965)	
2	19-44095	ORINS
3	19-44234	See MATT-345
CONF-650550–	(American Society of Mechanical Engineers, Underwater Technology Conference, New London, Conn., May 5–7, 1965)	
1	19-44986	ORINS
2	19-45662	ORINS
CONF-650552–	(Institute of Food Technologists, 25th Annual Meeting, Kansas City, Mo., May 16–20, 1965)	
2	19-44566	Gmelin, AED-CONF-65-111-4
CONF-650553–	(Seminar on High Energy Physics and Elementary Particles, Trieste, Italy, May 3–June 30, 1965)	
1	19-45004	See IC/65/66
2	19-45005	See IC/65/68
CONF-650554–	(2nd Symposium on Salt, Cleveland, May 3–5, 1965)	
1	19-45689	See ORNL-P-1568
CONF-650558–	(5th Session of the Spring School of Experimental and Theoretical Physics, Nor-Hambert Ervan, Armenia, May 18–27, 1965)	
1	19-45046	See UCRL-16295
CONF-650559–	(American Institute of Chemical Engineers, 56th National Meeting, San Francisco, Calif., May 16–19, 1965)	
2	19-44155	Gmelin, AED-CONF-65-086-12
4	19-45624	Gmelin, AED-CONF-65-086-11
CONF-650602–	(American Nuclear Society 11th Annual Meeting, Gatlinburg, Tenn., June 20–24, 1965)	
4	19-45642	See DP-999, pp 65-71
8	19-45602	See WCAP-5493
42	19-45638	See DP-999, pp 7-17
43	19-45639	See DP-999, pp 19-28
44	19-45640	See DP-999, pp 29-42
45	19-45641	See DP-999, pp 43-64
47	19-45643	See DP-999, pp 73-86
49	19-44216	Gmelin, AED-CONF-65-125-83
50	19-44217	Gmelin, AED-CONF-65-125-84
51	19-44126	Gmelin, AED-CONF-65-125-85
52	19-45625	Gmelin, AED-CONF-65-125-15
53	19-45626	Gmelin, AED-CONF-65-125-12
55	19-45539	Gmelin, AED-CONF-65-125-54
CONF-650606–	(EURATOM Symposium on Fuel Cycles of High-Temperature Gas-Cooled Reactors, Brussels, June 10–11, 1965)	
9	19-44109	See BLG-331
CONF-650619–	(2nd Topical Conference on Resonant Particles, Athens, Ohio, June 10–12, 1965)	
3	19-44997	See COO-1428-14
CONF-650643–	(3rd International Vacuum Congress, Stuttgart, June 28–July 2, 1965)	
1	19-44135	See IA-1033
CONF-650644–	(International Conference on Sintering and Related Phenomena, Notre Dame, Ind., June 21–23, 1965)	
1	19-43998	See UCRL-12396
CONF-650646–	(American Society for Testing and Materials, 68th Annual Meeting, Lafayette, Ind., June 13–18, 1965)	
1	19-44620	See CNLM-6344
CONF-650647–	(Society of Nuclear Medicine, 12th Annual Meeting, Bal Harbour, Fla., June 19, 1965)	
1	19-43666	See BNL-9406
CONF-650648–	(IBM User's Conference, Portland, Ore., June 17–18, 1965)	
1	19-44219	See ACF-8
CONF-650651–	(American Society of Mechanical Engineers, Spring Lubrication Symposium, New York, June 7–9, 1965)	
1	19-44170	See Y-DA-921
CONF-650704–	(IAEA Symposium on Thermodynamics, Vienna, July 22–27, 1965)	
13	19-44733	ORINS
29	19-44040	ORINS
32	19-45471	See AECL-2309
CONF-650706–	(International Conference on the Study of Nuclear Structure with Neutrons, Antwerp, July 19–23, 1965)	
22	19-44157	See LA-DC-7304
CONF-650710–	19-43507	(American Nuclear Society, Meeting on Reactor Operating Experience, Jackson Lake Lodge, Wyo., July 28–30, 1965)
7	19-45644	See ORNL-P-1501
CONF-650711–	(AIAA 2nd Annual Meeting and Technical Demonstration, San Francisco, July 26–29, 1965)	
6	19-45664	ORINS
7	19-45154	ORINS
8	19-45627	ORINS
9	19-44227	ORINS
10	19-44232	ORINS
11	19-44228	ORINS
12	19-45451	ORINS
13	19-45454	ORINS
15	19-44964	ORINS
16	19-44989	ORINS
17	19-45666	ORINS
18	19-44572	ORINS
19	19-45470	ORINS
20	19-45665	ORINS
23	19-44854	ORINS
24	19-45452	ORINS
25	19-45447	ORINS
27	19-45453	ORINS
28	19-44233	ORINS
29	19-44204	ORINS
32	19-44226	ORINS
33	19-45663	ORINS
34	19-44225	ORINS
35	19-45441	ORINS
36	19-44224	ORINS
37	19-45442	ORINS

Report No.	Abstract No.	Availability
38	19-45445	ORINS
39	19-44229	ORINS
40	19-45443	ORINS
41	19-45444	ORINS
42	19-45448	ORINS
43	19-45446	ORINS
44	19-44230	ORINS
48	19-45449	ORINS
50	19-44231	ORINS
CONF-650802–	**(Cryogenic Engineering Conference, Houston, Tex., Aug. 23–25, 1965)**	
6	19-44186	See LA-DC-7148
7	19-44375	See BNL-9425
CONF-650804–	**(5th Rare Earth Research Conference, Ames, Iowa, Aug. 30–Sept. 1, 1965)**	
7	19-43988	Dep. mn
CONF-650806–	**(7th International Conference on Phenomena in Ionized Gases, Belgrade, Aug. 22–27, 1965)**	
3	19-45414	See UCRL-12480
4	19-44938	See UCRL-14117
5	19-45404	See ORNL-P-1557
8	19-45415	See UCRL-14137
9	19-45405	See ORNL-P-1576
12	19-45396	See LA-DC-7120
CONF-650814–	**(Symposium on Mutational Process, Prague, Aug. 9–11, 1965)**	
1	19-43712	See BNL-9383
CONF-650815–	**(Symposium on Engineering Problems of Controlled Thermonuclear Research, Livermore, Calif., Aug. 1965)**	
1	19-45416	See UCRL-16263
CONF-650816–	**(Conference on Radiation Trapped in the Earth's Magnetic Field, Bergen, Norway, Aug. 16–Sept. 3, 1965)**	
1	19-45159	See UCRL-14374
CONF-650902–	**(American Chemical Society, 150th National Meeting, Atlantic City, Sept. 12–17, 1965)**	
10	19-45691	See RL-SA-41
11	19-45690	See RL-SA-40
CONF-650908–	**(International Conference on Thermionic Electrical Power Generation, London, Sept. 20–25, 1965)**	
3	19-45648	See GA-6478
4	19-44593	Dep. mn; CFSTI $1.00 cy, $0.50 mn
5	19-44685	Dep. mn; CFSTI $1.00 cy, $0.50 mn
7	19-44988	ORINS
8	19-44985	ORINS
9	19-44640	See ORNL-P-1446-1
CONF-650911–	**(2nd Conference on Plasma Physics and Controlled Nuclear Fusion Research, Abingdon, Berks., Eng.)**	
10	19-45388	See GA-6432
11	19-45413	See UCRL-12456
CONF-650912–	**(Society for Experimental Stress Analysis, 2nd International Congress on Experimental Mechanics, Washington, D. C., Sept. 28–Oct. 1, 1965)**	
2	19-44706	See UCRL-12264(Rev.1)
CONF-650916–	**(International Symposium on Electron and Photon Interactions at High Energies, Hamburg, Sept. 1965)**	
1	19-45024	See MIT-2098-163
CONF-650918–	**(International Conference on the Chemistry of the Solvent Extraction of Metals, Harwell, Berks., England, Sept. 1965)**	
3	19-44115	See ORNL-P-1577
CONF-650922–	**(1st International Symposium on Magnet Technology, Stanford, Calif., Sept. 8–10, 1965)**	
1	19-44877	See UCRL-16346
5	19-44811	See UCRL-7784-T(Rev.1)
6	19-44878	See UCRL-16375
7	19-44876	See UCRL-16287
CONF-650923–	**(5th International Conference on High Energy Accelerators, Frascati, Italy, Sept. 9–16, 1965)**	
1	19-44871	See PPAD-2137-556
2	19-44872	See PPAD-2137-565
3	19-44459	See PPAD-2137-561
4	19-44875	See UCRL-16229
CONF-650928–	**(International Conference on Polarization Phenomena of Nucleons, Karlsruhe, Germany, Sept. 6–10, 1965)**	
2	19-45253	See COO-7-0362
3	19-45217	See COO-7-0363
CONF-650929–	**(International Conference on Optical and Electronic Properties of Metals and Alloys, Paris, Sept. 13–16, 1965)**	
1	19-45481	See UCRL-12470
CONF-651006–	**(American Society for Testing Materials, 5th Pacific Area National Meeting, Seattle, Oct. 31–Nov. 5, 1965)**	
1	19-44621	Dep. mn; CFSTI $1.00 cy, $0.50 mn
CONF-651007–	**(Society of Petroleum Engineers, 40th Annual Fall Meeting, Denver, Oct. 3–6, 1965)**	
1	19-44158	See UCRL-14311
CONF-651101–	**(American Nuclear Society, Winter Meeting, Washington, D. C., Nov. 15–18, 1965. (Revised 11-8-65))**	
9	19-44167	See ORNL-P-1521
12	19-44168	See ORNL-P-1532
13	19-43936	See ORNL-P-1533
15	19-45585	See ORNL-P-1502
16	19-45586	See ORNL-P-1503
17	19-45587	See ORNL-P-1504
18	19-44748	See ORNL-P-1505
19	19-44695	See ORNL-P-1506
20	19-44749	See ORNL-P-1507
30	19-44453	See LA-DC-7316
CONF-651102–	**(Royal Commonwealth Society, 3rd International Conference on Plutonium, London, Nov. 22–26, 1965)**	
8	19-44689	See LA-DC-7351
10	19-44690	See LA-DC-7360
CONF-651103–	**(IAEA Symposium on Criticality Control of Fissile Materials, Stockholm, Nov. 1–5, 1965)**	
4	19-44112	Dep. mn; CFSTI $2.00 cy, $0.50 mn
CONF-651107–	**(American Chemical Society, 1st Midwest Regional Meeting, Kansas City, Mo., Nov. 4–5, 1965)**	
1	19-44682	See BDX-613-75
CONF-651109–	**(1st Symposium on Accelerator Radiation Dosimetry and Experience, Upton, N. Y., Nov. 3–5, 1965)**	
1	19-44454	See LA-DC-7323
CDO–		
7-0362	19-45253	Dep. mn; CFSTI $1.00 cy, $0.50 mn
7-0363	19-45217	Dep. mn; CFSTI $1.00 cy, $0.50 mn
30-97	19-44995	Dep. mn; CFSTI $1.00 cy, $0.50 mn
283	19-45631	Dep. mn; CFSTI $5.00 cy, $1.00 mn
330-11	19-45697	Dep. mn; CFSTI $1.00 cy, $0.50 mn
748-1	19-44113	Dep. mn; CFSTI $1.00 cy, $0.50 mn
1018-1050	19-44446	Dep. mn; CFSTI $1.00 cy, $0.50 mn
1195-39	19-44996	Dep. mn; CFSTI $1.00 cy, $0.50 mn
1277-11	19-44959	Phys. Rev. Letters, 15: 580-1(1965)
1277-12	19-44933	Dep. mn; CFSTI $2.00 cy, $0.50 mn
1277-13	19-44934	Dep. mn; CFSTI $1.00 cy, $0.50 mn
1365-7	19-44054	Dep. mn; CFSTI $2.00 cy, $0.50 mn
1428-14	19-44997	Dep. mn; CFSTI $2.00 cy, $0.50 mn
CRT–	**(Canadian)**	
1213	19-45254	Dep.; AECL $1.00
CU–	**(Misc.)**	
266(48)-11	19-45698	See CU-2663-18
266(48)-14	19-45699	See CU-2663-21
242	19-45274	See NEVIS-136
1806-4	19-45699	See CU-2663-21

Report No.	Abstract No.	Availability
1932-247	19-44998	Dep. mn; CFSTI $1.00 cy, $0.50 mn
2663-18	19-45698	Dep. mn; CFSTI $2.00 cy, $0.50 mn
2663-21	19-45699	Dep. mn; CFSTI $2.00 cy, $0.50 mn
CVNA–	**(Misc.)**	
235	19-45567	Dep. mn; CFSTI $3.00 cy, $0.75 mn
238	19-45568	Dep. mn; CFSTI $2.00 cy, $0.50 mn
D–	**(Misc.)**	
1-82-0419	19-45383	Also in STI/PUB/89
1-82-0436	19-45384	Rev. Sci. Instr., 36: 1415-17(1965)
1-82-0437	19-45385	Rev. Sci. Instr., 36: 1411-14(1965)
1-82-0439	19-45386	
1-82-0442	19-45387	
DESY–	**(German)**	
65/5	19-44999	Dep. mn
DF–		
938	19-45218	Dep. mn; CFSTI $2.00 cy, $0.50 mn
956	19-44156	Dep. mn; CFSTI $3.00 cy, $0.50 mn
966	19-45687	Dep. mn; CFSTI $2.00 cy, $0.50 mn
970	19-45700	Dep. mn; CFSTI $3.00 cy, $0.50 mn
976	19-45569	Dep. mn; CFSTI $3.00 cy, $0.75 mn
983	19-44594	Dep. mn; CFSTI $1.00 cy, $0.50 mn
999	19-45637	Dep. mn; CFSTI $3.00 cy, $0.75 mn
DPSPU–		
64-30-23	19-44235	Dep. mn; CFSTI $1.00 cy, $0.50 mn
DPST–		
65-30-2	19-44288	Dep. mn; CFSTI $1.00 cy, $0.50 mn
65-83-7	19-44634	Dep. mn; CFSTI $1.00 cy, $0.50 mn
DUBNA REPORTS	**(Russian)**	
See JINR (Russian)		
EANDC–	**(European-American Nuclear Data Committee)**	
45(U)	19-45255	Dep. mn
EANDC-US–	**(European-American Nuclear Data Committee)**	
72(U)	19-45288	See WASH-1056
EDR–	**(Misc.)**	
4195	19-45575	See GMAD-3078-28
EIR–	**(Swiss)**	
85	19-45673	Dep. mn
ER–	**(Misc.)**	
7483	19-44548	See NP-15422
EUR–	**(European Atomic Energy Community)**	
1890.f	19-43667	Dep. mn
1918.f	19-44343	Dep. mn
2284.i	19-44553	Dep. mn
2290.f	19-43928	Dep. mn
2314	19-44595	See EURAEC-1338
2346	19-44741	See EURAEC-1383
2351	19-44596	See EURAEC-1392
2370	19-44209	See EURAEC-1422
2373	19-44742	See EURAEC-1430
2375	19-44622	See EURAEC-1433
2376	19-44687	See EURAEC-1434
2410.i	19-45219	Dep. mn
2411.i	19-45220	Dep. mn
2422.i	19-45570	Dep. mn
2431.f	19-45571	Dep. mn
2434.d	19-44134	Dep. mn
2438.f	19-43714	Dep. mn
2444.i	19-44447	Dep. mn
2470.e	19-45525	Dep. mn
2480.f	19-45543	Dep. mn
2488.e	19-45459	Dep. mn
EURAEC–		
1281	19-44184	Dep. mn; CFSTI $3.00 cy, $0.50 mn
1306	19-44591	See CEND-3107-228
1338	19-44595	Dep. mn; CFSTI $4.00 cy, $1.00 mn
1362	19-44686	Dep. mn; CFSTI $1.00 cy, $0.50 mn
1383	19-44741	Dep. mn; CFSTI $1.00 cy, $0.50 mn
1392	19-44596	Dep. mn; CFSTI $1.00 cy, $0.50 mn
1420	19-45600	See WCAP-3385-4
1422	19-44209	Dep. mn; CFSTI $1.00 cy, $0.50 mn
1423	19-44183	See BAW-3238-8
1430	19-44742	Dep. mn; CFSTI $1.00 cy, $0.50 mn
1433	19-44622	Dep. mn; CFSTI $1.00 cy, $0.50 mn
1434	19-44687	Dep. mn; CFSTI $2.00 cy, $0.50 mn
1437	19-44684	See CEND-3336-241
1450	19-45574	See GEAP-4914
1451	19-44192	See NYO-3114-9
1452	19-44131	See ACNP-65003
1459	19-44185	See GEAP-4910
1462	19-45221	See GEAP-4913
1463	19-44597	See GEAP-4679
F–	**(Misc.)**	
B2205	19-44694	See NP-15432
FD–	**(Non-AEC)**	
15	19-44555	See NP-15373
16	19-44556	See NP-15464
GA–	**(Misc.)**	
6168	19-45674	Dep. mn; CFSTI $2.00 cy, $0.50 mn
6432	19-45388	
6478	19-45648	Dep. mn; CFSTI $1.00 cy, $0.50 mn
6513	19-45389	
6633	19-45526	
GEAP–	**(Misc.)**	
3634	19-44743	
4679	19-44597	Dep. mn; CFSTI $1.00 cy, $0.50 mn
4755	19-45572	Dep. mn; CFSTI $4.00 cy, $1.00 mn
4902	19-45573	Dep. mn; CFSTI $3.00 cy, $0.75 mn
4910	19-44185	Dep. mn; CFSTI $3.00 cy, $0.75 mn
4913	19-45221	Dep. mn; CFSTI $2.00 cy, $0.50 mn
4914	19-45574	Dep. mn; CFSTI $3.00 cy, $0.75 mn
GEMP–	**(Misc.)**	
49A	19-44598	Dep. mn; CFSTI $3.00 cy, $0.75 mn
50A	19-44599	Dep. mn; CFSTI $3.00 cy, $0.75 mn
190c	19-45531	See N64-29786
GMAD–		
3078-28	19-45575	Dep. mn; CFSTI $4.00 cy, $0.75 mn
HASL–		
162	19-44448	Dep. mn; CFSTI $4.00 cy, $0.75 mn
HPR–	**(Norwegian)**	
53	19-45632	Dep. mn
62	19-45633	Dep. mn
HRL–	**(Non-AEC)**	
4118-S	19-44221	See N64-31088
HUX–		
2752-4	19-45256	Dep. mn; CFSTI $4.00 cy, $1.00 mn
2752-7	19-45000	Dep. mn; CFSTI $5.00 cy, $1.00 mn
2752-8	19-45001	Dep. mn; CFSTI $6.00 cy, $1.25 mn
HW–		
65756	19-45500	Dep. mn; CFSTI $0.75 cy, $0.50 mn
79951(Pt.1)	19-45544	Dep. mn; CFSTI $3.00 cy, $0.50 mn
79951(Pt.2)	19-45545	Dep. mn; CFSTI $7.22 cy, $2.00 mn
79951(Pt.3)	19-45546	Dep. mn; CFSTI $3.00 cy, $0.75 mn
HW-SA–		
3592	19-44744	Dep. mn; CFSTI $1.00 cy, $0.50 mn
3618	19-43668	Dep. mn; CFSTI $1.00 cy, $0.50 mn
3747	19-43715	Dep. mn; CFSTI $1.00 cy, $0.50 mn
3748	19-43716	Dep. mn; CFSTI $1.00 cy, $0.50 mn
3750	19-44289	Dep. mn; CFSTI $1.00 cy, $0.50 mn
IA–	**(Non-AEC)**	
1015	19-44554	Dep. mn
1033	19-44135	Dep. mn
1039	19-45576	Dep. mn

Report No.	Abstract No.	Availability
IAE–	**(Non-AEC)**	
611	19-45501	Dep. mn
614	19-44860	Dep. mn
704	19-44449	Dep. mn
725	19-45675	Dep. mn
750	19-45475	Dep. mn
780	19-45390	Dep. mn
788	19-44055	Dep. mn
795	19-44861	Dep. mn
811	19-45257	Dep. mn
833	19-45258	Dep. mn Yadern. Fiz., 2: 243-7(1965)
834	19-45259	Dep. mn Yadern. Fiz., 2: 239-42(1965)
867	19-44862	Dep. mn
IBK–	**(Yugoslavian)**	
120a	19-44450	Dep. mn
IC–	**(Misc.)**	
65/59	19-45002	Dep. mn
65/60	19-45003	Dep. mn
65/66	19-45004	Dep. mn
65/68	19-45005	Dep. mn
IDO–		
14660	19-45260	Dep. mn; CFSTI $2.00 cy, $0.50 mn
16871-4	19-45676	Dep. mn; CFSTI $7.00 cy, $1.50 mn
17016	19-45261	Dep. mn; CFSTI $3.00 cy, $0.75 mn
17078	19-45527	Dep. mn; CFSTI $6.00 cy, $1.25 mn
17095	19-44977	Dep. mn; CFSTI $2.00 cy, $0.50 mn
17097	19-45528	Dep. mn; CFSTI $2.00 cy, $0.50 mn
17106	19-45476	Dep. mn; CFSTI $1.00 cy, $0.50 mn
28645	19-45577	Dep. mn; CFSTI $3.00 cy, $1.00 mn
IITRI–	**(Misc.)**	
578P26-8	19-44451	Dep. mn; CFSTI $3.00 cy, $0.75 mn
INR–	**(Non-AEC)**	
68/64	19-44457	See NP-15475
579/XVII/C	19-44056	Dep. mn
585/XIV/R	19-45547	Dep.
595/IA/PL	19-44635	Dep.
600/IX-A/PR	19-45529	Dep.
612/IXA/PR	19-45391	
614/IXA/P	19-45677	Dep.
624/IX-A/R	19-45222	Dep.
IPP–	**(Non-AEC)**	
1/39	19-45392	Dep. mn
2/38	19-45393	Dep. mn
6/37	19-45394	Dep. mn
6/38	19-45395	Dep. mn
IS–		
955	19-44628	Corrosion, 21: 268-73(1965)
1031	19-44636	Dep. mn; CFSTI $1.00 cy, $0.50 mn
1164	19-45118	Phys. Rev., 140: B509-13(1965)
1214	19-45006	Dep. mn; CFSTI $2.00 cy, $0.50 mn
1237	19-43929	Dep. mn; CFSTI $3.00 cy, $0.50 mn
IS-T–		
19	19-44806	Dep. mn; CFSTI $3.00 cy, $0.75 mn
23	19-44057	Dep. mn; CFSTI $3.00 cy, $0.75 mn
29	19-45262	Dep. mn; CFSTI $3.00 cy, $0.75 mn
JAERI–	**(Japanese)**	
1078	19-45263	Dep. mn
1079	19-44290	Dep. mn
1080	19-45578	Dep. mn
1081	19-44291	Dep. mn
1082	19-45530	Dep. mn
1084	19-45223	Dep. mn
JEN–	**(Spanish)**	
133-DF/I-43	19-45224	Dep. mn
135-DF/I-44	19-45225	Dep. mn
145-DQ/I-46	19-43930	Dep. mn
149-DQ/I-50	19-45678	Dep. mn
151-DQ/I-52	19-44045	Dep. mn
152-DQ/I-53	19-44046	Dep. mn
154-DF/I-47	19-45131	Dep. mn
158-SI/I-15	19-44561	Energia Nucl. (Madrid), 9: 95-111(1965)
JINR–	**(Russian)**	
E-2225	19-45132	Dep. mn
E-2228	19-45007	Dep. mn
E-2243	19-45264	Dep. mn
E-2244	19-45265	Dep. mn
E-2246	19-45008	Dep. mn
E-2247	19-45009	Dep. mn
E-2259	19-45010	Dep. mn
E-2285	19-45266	Dep. mn
E-2294	19-45011	Dep. mn
E-2353	19-45012	Dep. mn
P-2161	19-45267	Dep. mn
P-2230	19-45013	Dep. mn
P-2231	19-44863	Dep. mn
P-2235	19-45268	Dep. mn
P-2236	19-45269	Dep. mn
P-2237	19-45014	Dep. mn
P-2241	19-45015	Dep. mn
P-2248	19-45270	Dep. mn
P-2253	19-44864	Dep. mn
P-2257	19-45016	Dep. mn
P-2265	19-45271	Dep. mn
P-2267	19-45017	Dep. mn
P-2270	19-45272	Dep. mn
P-2283	19-45018	Dep. mn
P-2286	19-45019	Dep. mn
P-2330	19-45020	Dep. mn
P-2336	19-45021	Dep. mn
P-2356	19-45273	Dep. mn
JPRS–	**(Non-AEC)**	
24761	19-44614	CFSTI $1.50
31245	19-45604	CFSTI $1.00 cy, $0.50 mn
31349	19-43650	CFSTI $2.00 cy, $0.50 mn
31361	19-44153	CFSTI $1.00 cy, $0.50 mn
K–		
1642	19-44452	Dep. mn; CFSTI $2.00 cy, $0.50 mn
1650	19-43931	Dep. mn; CFSTI $4.00 cy, $1.00 mn
K-L–		
1944	19-44344	Dep. mn; CFSTI $3.00 cy, $0.75 mn
6044	19-44019	J. Chem. Phys., 43: 2001-6(1965)
KAPL-M–		
6469	19-44581	Dep. mn; CFSTI $2.00 cy, $0.50 mn
6484	19-44210	Dep. mn; CFSTI $1.00 cy, $0.50 mn
KFK–	**(German)**	
294	19-45226	Dep. mn
LA–		
3234	19-44136	Dep. mn; CFSTI $1.00 cy, $0.50 mn
3319	19-45190	Dep. mn; CFSTI $2.00 cy, $0.50 mn
3324	19-45701	Dep. mn; CFSTI $2.00 cy, $0.50 mn
3340	19-44637	Dep. mn; CFSTI $1.00 cy, $0.50 mn
3343	19-43932	Dep. mn; CFSTI $2.00 cy, $0.50 mn
3344	19-43933	Dep. mn; CFSTI $1.00 cy, $0.50 mn
3345	19-43934	Dep. mn; CFSTI $1.00 cy, $0.50 mn
3356	19-44600	Dep. mn; CFSTI $1.00 cy, $0.50 mn
3359	19-44688	Dep. mn; CFSTI $1.00 cy, $0.50 mn
3377	19-45460	Dep. mn; CFSTI $1.00 cy, $0.50 mn
LA-DC–		
6407	19-44601	Dep. mn; CFSTI $1.00 cy, $0.50 mn
6556	19-44807	Dep. mn; CFSTI $1.00 cy, $0.50 mn
6558	19-45702	Dep. mn; CFSTI $2.00 cy, $0.50 mn
6636	19-44808	Dep. mn; CFSTI $2.00 cy, $0.50 mn
6667	19-45703	Dep. mn; CFSTI $1.00 cy, $0.50 mn
6691	19-44602	Dep. mn; CFSTI $1.00 cy, $0.50 mn
6717	19-45704	Dep. mn; CFSTI $1.00 cy, $0.50 mn
6719	19-44345	Dep. mn; CFSTI $2.00 cy, $0.50 mn
6725	19-44745	Dep. mn; CFSTI $2.00 cy, $0.50 mn
6882	19-45334	Nucl. Phys., 73: 449-60(1965)
7120	19-45396	Dep. mn; CFSTI $1.00 cy, $0.50 mn
7148	19-44186	Dep. mn; CFSTI $1.00 cy, $0.50 mn

Report No.	Abstract No.	Availability
7304	19-44157	Dep. mn; CFSTI $1.00 cy, $0.50 mn
7316	19-44453	Dep. mn; CFSTI $1.00 cy, $0.50 mn
7323	19-44454	Dep. mn; CFSTI $1.00 cy, $0.50 mn
7351	19-44689	Dep. mn; CFSTI $2.00 cy, $0.50 mn
7360	19-44690	Dep. mn; CFSTI $1.00 cy, $0.50 mn
LAL–	**(French)**	
1134	19-44865	Dep. mn
LFEN–	**(Portuguese)**	
23	19-44058	Dep. mn
LNF–	**(Italian)**	
65/7	19-45022	Dep. mn
65/8	19-45023	Dep. mn
65/15	19-45191	Dep. mn
65/21	19-44866	Dep. mn
MATT–		
282	19-45397	Dep. mn; CFSTI $3.00 cy, $0.75 mn
332	19-45398	Dep. mn; CFSTI $3.00 cy, $0.50 mn
345	19-44234	Dep. mn; CFSTI $1.00 cy, $0.50 mn
ME–	**(Misc.)**	
7-65-1	19-44144	See TID-22134
MIT–	**(Misc.)**	
905-20	19-43989	Dep. mn; CFSTI $1.00 cy, $0.50 mn
1965-15	19-43990	Dep. mn; CFSTI $1.00 cy, $0.50 mn
2098-140	19-45323	Nucl. Phys., 73: 321-7(1965)
2098-156	19-45106	Phys. Rev., 140: B365-74(1965)
2098-157	19-44968	Nature, 207: 584-7(1965)
2098-163	19-45024	
MTI–	**(Misc.)**	
6STR13	19-44138	See NYO-3363-4
MURA–	**(Misc.)**	
713	19-44867	Dep. mn; CFSTI $5.00 cy, $1.00 mn
N–	**(Misc.)**	
707	19-45457	See AD-462614
64-19243	19-45026	
64-24017	19-44137	CFSTI $9.60 cy
64-25922	19-45461	
64-26265	19-45025	Dep. mn
64-26433	19-43991	
64-29786	19-45531	CFSTI $9.60
64-30522	19-44346	CFSTI $3.00 cy, $0.50 mn
64-31011	19-44220	CFSTI $4.00 cy, $0.75 mn
64-31088	19-44221	CFSTI $2.00 cy, $0.50 mn
64-32637	19-45649	CFSTI $3.50 cy, $1.25 mn
NAA-SR–		
10487	19-44623	Dep. mn; CFSTI $2.00 cy, $0.50 mn
10929	19-44603	Dep. mn; CFSTI $3.00 cy, $0.75 mn
10997	19-45650	Dep. mn; CFSTI $3.00 cy, $0.75 mn
11008	19-45494	Dep. mn; CFSTI $3.00 cy, $0.50 mn
11103	19-45651	Dep. mn; CFSTI $2.00 cy, $0.50 mn
11375	19-44114	Dep. mn; CFSTI $2.00 cy, $0.50 mn
11414	19-45579	Dep. mn; CFSTI $1.00 cy, $0.50 mn
11430	19-45653	Dep. mn; CFSTI $4.00 cy, $0.75 mn
NAA-SR-Memo–		
4887	19-44624	Dep. mn; CFSTI $1.00 cy, $0.50 mn
10626	19-44746	Dep. mn; CFSTI $2.00 cy, $0.50 mn
NAS-NS–	**(Misc.)**	
3057	19-44098	Dep. mn; CFSTI $2.25 cy, $1.25 mn
NASA-CR–	**(Misc.)**	
294	19-44893	CFSTI $6.00 cy, $1.25 mn
303	19-43717	Dep. mn; CFSTI $3.00 cy, $0.75 mn
52959	19-45531	See N64-29786
54104	19-44220	See N64-31011
54143	19-44221	See N64-31088
54405	19-44187	
54451	19-45399	
54644	19-45526	See GA-6633
56646	19-44137	See N64-24017
58794	19-44346	See N64-30522
60585	19-44548	See NP-15422
62681	19-44222	See NP-15068
NASA-SP–	**(Misc.)**	
7011(12)	19-43718	CFSTI $1.00 cy, $0.75 mn
7011(13)	19-43719	CFSTI $1.00 cy, $1.00 mn
NASA-TM–	**(Misc.)**	
X-54858	19-45658	See TID-22097
NASA-TN–	**(Misc.)**	
D-2160	19-45649	See N64-32637
D-2696	19-45652	CFSTI $1.00 cy, $0.50 mn
D-2965	19-44188	CFSTI $1.00 cy, $0.50 mn
D-2968	19-45654	CFSTI $2.00 cy, $0.50 mn
D-2982	19-45400	CFSTI $2.00 cy, $0.50 mn
D-3015	19-44691	CFSTI $1.00 cy, $0.50 mn
D-3018	19-44692	CFSTI $2.00 cy, $0.50 mn
NEVIS–	**(Misc.)**	
136	19-45274	
141	19-44998	See CU-1932-247
NIJS-R–	**(Yugoslavian)**	
444	19-45477	Dep. mn
447	19-43935	Dep. mn
449	19-45227	Dep. mn
NIRL-R–	**(British)**	
86	19-44868	Dep.; BIS $0.60; HMSO 3s.
87	19-44869	Dep.; BIS $0.50; HMSO 2s. 6d.
NP–	**(AEC File No. for Non-AEC Reports)**	
15047	19-44455	Dep. mn
15068	19-44222	
15110	19-45478	Dep. mn
15138	19-45275	Dep. mn
15159	19-43669	Dep. mn
15163	19-45462	Dep. mn
15168	19-44935	Phys. Rev., 140: A792-9(1965)
15173	19-44292	Dep. mn
15193	19-45705	Dep. mn
15196	19-45401	Dep. mn
15195	19-45027	Dep. mn
15200	19-45402	Dep. mn Nucl. Fusion, 5: 228-33(1965)
15207	19-45028	Dep. mn
15258	19-44456	Dep. mn
15268	19-44047	Dep. mn
15269	19-44250	Dep. mn
15270	19-43880	Dep. mn
15271	19-43881	Dep. mn
15283	19-45580	Dep. mn
15291	19-45581	Dep. mn
15304	19-45276	Dep. mn
15320	19-45582	Dep. mn
15332	19-44189	
15339	19-43992	Dep. mn
15341	19-45133	Dep. mn
15363	19-45277	Dep. mn
15365	19-45583	Dep. mn
15367	19-45688	Dep. mn
15373	19-44555	
15379	19-43993	
15381	19-43994	
15382	19-45029	Dep. mn
15386	19-45157	
15388	19-44870	Dep. mn
15389	19-45278	Dep. mn
15390	19-45030	Dep. mn
15391	19-45031	Dep. mn JETP Lett. (USSR) (Engl. Transl.), 2: 20-2(1965)
15397	19-45134	Dep. mn
15411	19-44693	
15415	19-45279	Dep. mn
15419	19-44979	CFSTI $1.00 cy, $0.50 mn
15422	19-44548	
15424	19-45158	

Report No.	Abstract No.	Availability
15425	19-45463	
15432	19-44694	
15433	19-44980	
15435	19-44981	CFSTI $2.00 cy, $0.50 mn
15436	19-45135	
15438	19-44223	
15445	19-45403	Dep. mn
15452	19-45032	Dep. mn
15457	19-45280	Dep. mn
15463	19-44747	
15464	19-44556	CFSTI
15468	19-45033	Dep. mn Yadern. Fiz., 2: 215-22(1965)
15469	19-45228	Dep. mn
15470	19-45034	Dep. mn
15471	19-45035	Dep. mn
15472	19-44166	
15475	19-44457	Dep. mn
15476	19-45036	Dep. mn
15519	19-44293	Dep. mn
NP-tr-	**(AEC File No. for Non-AEC Translations)**	
1307	19-44813	Consultants Bureau $22.50
NRL-	**(Misc.)**	
6305	19-44252	Dep. mn; CFSTI $1.00 cy, $0.50 mn
NSP-	**(Non-AEC)**	
63-96(Vol.3)	19-44137	See N64-24017
NUMEC-		
3428-12	19-44604	Dep. mn; CFSTI $1.00 cy, $0.50 mn
NUS-	**(Misc.)**	
229	19-45655	
NYO-		
1859-11	19-45679	Dep. mn; CFSTI $3.00 cy, $0.75 mn
2174-36	19-44253	Dep. mn; CFSTI $3.00 cy, $0.75 mn
2280-8	19-43642	Dep. mn; CFSTI $1.00 cy, $0.50 mn
2363-3	19-44801	Dep. mn; CFSTI $2.00 cy, $0.50 mn
2404-67	19-44190	Dep. mn; CFSTI $2.00 cy, $0.50 mn
2404-73	19-44191	Dep. mn; CFSTI $2.00 cy, $0.50 mn
2767	19-44458	Dep. mn; CFSTI $3.00 cy, $0.75
2949-1	19-44059	Dep. mn; CFSTI $1.00 cy, $0.50 mn
3114-9	19-44192	Dep. mn; CFSTI $1.00 cy, $0.50 mn
3304-5	19-44193	Dep. mn; CFSTI $1.00 cy, $0.50 mn
3363-4	19-44138	Dep. mn; CFSTI $3.00 cy, $0.75 mn
3379-1	19-45584	Dep. mn; CFSTI $5.00 cy, $1.00 mn
3426-1	19-44557	Dep. mn; CFSTI $3.00 cy, $0.75 mn
4700(Rev.) (Suppl.II)	19-44296	Dep. mn; CFSTI $4.00 cy, $0.75 mn
ORNL-		
3646	19-44582	Dep. mn; CFSTI $3.00 cy, $0.75 mn
3681	19-44638	Dep. mn; CFSTI $5.00 cy, $1.00 mn
3740	19-44639	Dep. mn; CFSTI $3.00 cy, $0.75 mn
3850	19-45281	Dep. mn; CFSTI $2.00 cy, $0.50 mn
3865	19-44215	Dep. mn; CFSTI $2.00 cy, $0.50 mn
ORNL-P-	**(Misc.)**	
515	19-44573	Dep. mn; CFSTI $1.00 cy, $0.50 mn
896	19-45318	Nucl. Phys., 73: 241-55(1965)
995	19-45372	Science, 149: 1197-1205(1965)
1275	19-44729	Trans. Met. Soc. AIME, 233: 1790-1(1965)
1446-1	19-44640	Dep. mn; CFSTI $1.00 cy, $0.50 mn
1476	19-45346	Phys. Letters, 18: 295-7(1965)
1495	19-45350	Phys. Letters, 18: 308-10(1965)
1501	19-45644	Dep. mn; CFSTI $1.00 cy, $0.50 mn
1502	19-45585	Dep. mn; CFSTI $1.00 cy, $0.50 mn
1503	19-45586	Dep. mn; CFSTI $1.00 cy, $0.50 mn
1504	19-45587	Dep. mn; CFSTI $1.00 cy, $0.50 mn
1505	19-44748	Dep. mn; CFSTI $1.00 cy, $0.50 mn
1506	19-44695	Dep. mn; CFSTI $1.00 cy, $0.50 mn
1507	19-44749	Dep. mn; CFSTI $1.00 cy, $0.50 mn
1521	19-44167	Dep. mn; CFSTI $1.00 cy, $0.50 mn
1532	19-44168	Dep. mn; CFSTI $1.00 cy, $0.50 mn
1533	19-43936	Dep. mn; CFSTI $1.00 cy, $0.50 mn
1543	19-44211	Dep. mn; CFSTI $2.00 cy, $0.50 mn
1545	19-44347	Dep. mn; CFSTI $1.00 cy, $0.50 mn
1557	19-45404	Dep. mn; CFSTI $1.00 cy, $0.50 mn
1568	19-45689	Dep. mn; CFSTI $2.00 cy, $0.50 mn
1576	19-45405	Dep. mn; CFSTI $1.00 cy, $0.50 mn
1577	19-44115	Dep. mn; CFSTI $2.00 cy, $0.50 mn
ORNL-TM-		
1060	19-45588	Dep. mn; CFSTI $7.00 cy, $1.75 mn
1062	19-44116	Dep. mn; CFSTI $1.00 cy, $0.50 mn
1072	19-45317	Nucl. Instr. Methods, 36: 309-13(1965)
1158	19-45330	Nucl. Phys., 73: 398-412(1965)
1167	19-45464	Dep. mn; CFSTI $1.00 cy, $0.50 mn
1174	19-44139	Dep. mn; CFSTI $1.00 cy, $0.50 mn
1180	19-45282	Dep. mn; CFSTI $1.00 cy, $0.50 mn
1188	19-44696	Dep. mn; CFSTI $6.00 cy, $1.25 mn
1190	19-45680	Dep. mn; CFSTI $2.00 cy, $0.50 mn
1193	19-44641	Dep. mn; CFSTI $1.00 cy, $0.50 mn
1197	19-45589	Dep. mn; CFSTI $2.00 cy, $0.50 mn
1216	19-44750	Dep. mn; CFSTI $1.00 cy, $0.50 mn
1217	19-43721	Dep. mn; CFSTI $1.00 cy, $0.50 mn
1219	19-45532	Dep. mn; CFSTI $1.00 cy, $0.50 mn
1239	19-44697	Dep. mn; CFSTI $1.00 cy, $0.50 mn
1244	19-44140	Dep. mn; CFSTI $3.00 cy, $0.75 mn
1251	19-44297	Dep. mn; CFSTI $1.00 cy, $0.50 mn
1254	19-45706	Dep. mn; CFSTI $1.00 cy, $0.50 mn
1256	19-44117	Dep. mn; CFSTI $1.00 cy, $0.50 mn
1259	19-45645	Dep. mn; CFSTI $2.00 cy, $0.50 mn
1263	19-43937	Dep. mn; CFSTI $1.00 cy, $0.50 mn
1266	19-45192	Dep. mn; CFSTI $2.00 cy, $0.50 mn
ORNL-tr-		
652	19-45497	Dep. mn; JCL $1.60 fs, $0.80 mf
696	19-45293	Dep. mn; JCL $1.10 fs, $0.80 mf
708	19-44256	Dep. mn; JCL $1.10 fs, $0.80 mf
743	19-43923	Dep. mn; JCL $1.60 fs, $0.80 mf
788	19-45605	Dep. mn; CFSTI $1.00 cy, $0.50 mn; JCL $1.60 fs, $0.80 mf
PATENTS	**(British)**	**4s. 6d. each, U. K. Patent Office**
1,000,050	19-45540	
1,000,052	19-44990	
1,000,120	19-44127	
1,000,237	19-44655	
1,000,270	19-44656	
1,000,300	19-44991	
1,000,339	19-45550	
1,000,658	19-44657	
1,000,680	19-45686	
1,000,760	19-44107	
1,000,811	19-44890	
1,000,812	19-44891	
1,000,813	19-44892	
1,000,843	19-45508	
1,001,118	19-45509	
1,001,301	19-44658	
1,001,359	19-44659	
1,001,360	19-44660	
1,001,431	19-44128	
1,001,534	19-45551	
1,001,580	19-45510	
1,001,621	19-45511	
1,001,630	19-44206	
1,001,652	19-44174	
1,001,745	19-45628	
1,001,771	19-44567	
1,001,874	19-44661	
1,001,875	19-43660	
1,001,876	19-43661	
1,001,926	19-45512	
1,001,975	19-45552	
1,002,006	19-45513	
1,002,007	19-45514	
PATENTS	**(Canadian)**	
707,662	19-44175	
708,782	19-44176	
PATENTS	**(German)**	
1,194,992	19-44662	
1,195,879	19-44663	
1,196,304	19-44542	

Report No.	Abstract No.	Availability
1,196,306	19-45515	
1,196,801	19-45455	
1,197,180	19-44543	
1,197,630	19-43982	
1,198,588	19-43983	
1,199,004	19-44664	
PATENTS	**(U. S.)**	**$0.25 each, U. S. Patent Office**
3,196,718	19-44177	
3,197,041	19-44178	
3,197,375	19-45541	
3,197,376	19-45629	
3,197,378	19-45516	
3,197,379	19-45517	
3,197,380	19-45630	
3,197,381	19-45553	
3,197,382	19-45554	
3,197,383	19-45555	
3,197,402	19-44578	
3,197,632	19-44568	
3,197,636	19-44362	
3,197,637	19-44544	
3,197,638	19-44214	
3,197,639	19-44179	
3,197,641	19-44218	
3,198,347	19-44180	
3,198,598	19-44042	
3,198,599	19-44129	
3,198,626	19-44665	
3,198,627	19-44666	
3,198,628	19-44667	
3,198,629	19-44668	
3,198,666	19-44992	
3,198,709	19-45518	
3,198,710	19-45519	
3,198,714	19-44669	
3,198,723	19-44130	
3,198,750	19-44043	
3,198,944	19-44545	
3,198,945	19-44546	
3,198,947	19-44363	
3,198,948	19-44547	
3,200,045	19-45520	
3,200,085	19-44670	
3,200,252	19-43984	
3,200,300	19-44364	
3,201,330	19-44671	
3,201,336	19-44097	
3,201,619	19-45556	
3,201,635	19-45456	
PG-Report–	**(British)**	
662	19-43671	Dep.; BIS $1.60; HMSO 8s.
665	19-43938	Dep.; BIS $0.20; HMSO 1s. 2d.
PPAD–		
2137-552	19-44507	Nucl. Instr. Methods, 36: 317-19(1965)
2137-556	19-44871	Dep. mn; CFSTI $1.00 cy, $0.50 mn
2137-561	19-44459	Dep. mn; CFSTI $1.00 cy, $0.50 mn
2137-565	19-44872	Dep. mn; CFSTI $1.00 cy, $0.50 mn
PWAC–	**(Misc.)**	
464	19-44605	Dep. mn; CFSTI $3.00 cy, $0.75 mn
465	19-44698	Dep. mn; CFSTI $2.00 cy, $0.50 mn
473	19-44348	Dep. mn; CFSTI $4.00 cy, 1.00 mn
474	19-45656	Dep. mn; CFSTI $3.00 cy, $0.75 mn
483	19-44606	Dep. mn; CFSTI $1.00 cy, $0.50 mn
Q–	**(Misc.)**	
B2205-2	19-44693	See NP-15411
R–	**(Misc.)**	
505	19-45274	See NEVIS-136
513	19-44998	See CU-1932-247
6129	19-44189	See NP-15332
61APE7	19-44743	See GEAP-3634
63FPD33	19-44699	
RAD-TR–	**(Non-AEC)**	
64-12	19-44220	See N64-31011
RCH–	**(Dutch)**	
36	19-45681	Dep. mn
RFP–		
503	19-43995	Dep. mn; CFSTI $2.00 cy, $0.50 mn
570	19-44642	Dep. mn; CFSTI $1.00 cy, $0.50 mn
573	19-44141	Dep. mn; CFSTI $2.00 cy, $0.50 mn
RL-REA–		
2120	19-45502	Dep. mn; CFSTI $1.00 cy, $0.50 mn
RL-SA–		
40	19-45690	Dep. mn; CFSTI $1.00 cy, $0.50 mn
41	19-45691	Dep. mn; CFSTI $1.00 cy, $0.50 mn
RL-SEP–		
508	19-44607	Dep. mn; CFSTI $1.00 cy, $0.50 mn
RM–	**(Misc.)**	
227	19-45461	See N64-25922
229	19-43991	See N64-26433
RME–		
4557(Rev.)	19-44273	Dep. mn; CFSTI $2.00 cy, $0.50 mn
RRA–	**(Misc.)**	
M51	19-44254	
RSIC–	**(Non-AEC)**	
410	19-44643	
RT-EL–	**(Italian)**	
(65)-3	19-44349	Dep. mn
RT-FI–	**(Italian)**	
(65)8	19-44460	Dep. mn
RT-ING–	**(Italian)**	
(64)-15	19-45682	Dep. mn
RT-PROT–	**(Italian)**	
(65)-10	19-44255	Dep. mn
SC-DR–		
65-261	19-45707	Dep. mn; CFSTI $1.00 cy, $0.50 mn
65-291	19-44809	Dep. mn; CFSTI $3.00 cy, $0.75 mn
SC-R–		
65-915	19-45708	Dep. mn; CFSTI $1.00 cy, $0.50 mn
65-959	19-44350	Dep. mn; CFSTI $1.00 cy, $0.50 mn
65-963	19-45709	Dep. mn; CFSTI $3.00 cy, $0.75 mn
SC-RR–		
65-9	19-44298	Dep. mn; CFSTI $3.00 cy, $0.75 mn
65-286	19-44142	Dep. mn; CFSTI $3.00 cy, $0.75 mn
65-306	19-44143	Dep. mn; CFSTI $1.00 cy, $0.50 mn
SC-T–		
65-756	19-44200	Dep. mn; CFSTI $2.00 cy, $0.50 mn; JCL $2.60 fs, $1.04 mf
SC-TM–		
64-1772	19-45710	Dep. mn
65-81	19-45711	Dep. mn; CFSTI $1.00 cy, $0.50 mn
65-82	19-45712	Dep. mn; CFSTI $1.00 cy, $0.50 mn
65-276	19-44644	Dep. mn; CFSTI $1.00 cy, $0.50 mn
65-279	19-45713	Dep. mn; CFSTI $1.00 cy, $0.50 mn
65-349	19-45714	Dep. mn; CFSTI $3.00 cy, $0.50 mn
65-359	19-45715	Dep. mn; CFSTI $2.00 cy, $0.50 mn
SGAE-E–	**(Austrian)**	
4/1965	19-44351	Dep. mn
SGAE-PH–	**(Austrian)**	
23/1965	19-45283	Dep. mn
SGAE-RE–	**(Austrian)**	
2/1965	19-44194	Dep. mn
SIT–	**(Misc.)**	

Report No.	Abstract No.	Availability
164	19-45406	See SIT-2852-17
2852-17	19-45406	Dep. nn; CFSTI $4.00 cy, $0.75 mn
SLAC-PUB-		
124	19-45123	Phys. Rev. Letters, 15: 538-40(1965)
SLAC-Trans-		
22	19-44353	Dep. nn; CFSTI $1.00 cy, $0.50 mn; JCL $1.10 fs, $0.80 mf
STI-PUB-	**(International Atomic Energy Agency)**	
92(Vol.II)	19-45234	IAEA $11.50; $ 241.50; £3.9.0; F.Fr. 46.-; DM 40.25 cy
SU-	**(Misc.)**	
AA217	19-45407	
SU-IPR-		
11	19-45408	Dep. nn; CFSTI $2.00 cy, $0.50 mn
SWRI-		
1228-69	19-45503	Dep. nn; CFSTI $1.00 cy, $0.50 mn
SZS-	**(German)**	
2(1965)	19-44299	Dep. nn
TID-		
3584	19-45590	Dep. nn; CFSTI $2.00 cy, $0.50 mn
4043(Rev.2)	19-45716	DTI Extension Free
21256	19-44195	Dep. nn; CFSTI $1.00 cy, $0.50 mn
21301	19-45479	Dep. nn; CFSTI $1.00 cy, $0.50 mn
21307	19-45193	Dep. nn; CFSTI $1.00 cy, $0.50 mn
21309	19-44048	Dep. nn; CFSTI $1.00 cy, $0.50 mn
21316	19-45037	Dep. nn; CFSTI $3.00 cy, $0.75 mn
21692	19-44936	Dep. nn; CFSTI $1.00 cy, $0.50 mn
21747	19-44725	Trans. Met. Soc. AIME, 233: 1716-18(1965)
21748	19-44728	Trans. Met. Soc. AIME, 233: 1766-71(1965)
22086	19-44236	Dep. nn; CFSTI $4.00 cy, $1.00 mn
22088	19-45657	Dep. nn; CFSTI $1.00 cy, $0.50 mn
22097	19-45658	Dep. nn; CFSTI $4.00 cy, $0.75 mn
22101	19-45354	Phys. Letters, 18: 318-19(1965)
22108	19-43722	Dep. nn; CFSTI $1.00 cy, $0.50 mn
22110	19-44751	Dep. nn; CFSTI $2.00 cy, $0.50 mn
22117	19-44700	Dep. nn; CFSTI $1.00 cy, $0.50 mn
22121	19-45344	Phys. Letters, 18: 291-2(1965)
22125	19-44608	Dep. nn; GPO $0.75
22128	19-43723	Dep. nn; CFSTI $1.00 cy, $0.50 mn
22129	19-45591	Dep. nn; CFSTI $2.00 cy, $0.50 mn
22131	19-43672	Dep. nn; CFSTI $2.00 cy, $0.50 mn
22132	19-45409	Dep. nn; CFSTI $1.00 cy, $0.50 mn
22134	19-44144	Dep. nn; CFSTI $8.41 cy, $3.25 mn
22135	19-45592	Dep. nn; CFSTI $3.00 cy, $0.50 mn
22138	19-44145	Dep. nn; CFSTI $3.00 cy, $0.50 mn
22139	19-44558	Dep. nn; CFSTI $1.00 cy, $0.50 mn
22140	19-44937	Dep. nn; CFSTI $1.00 cy, $0.50 mn
22143	19-43643	Dep. nn; CFSTI $1.00 cy, $0.50 mn
22144	19-44701	Dep. nn; CFSTI $3.00 cy, $0.50 mn
22145	19-44196	Dep. nn; CFSTI $5.00 cy, $1.50 mn
22147	19-43673	Dep. nn; CFSTI $4.00 cy, $1.00 mn
22160	19-43724	Dep. nn; CFSTI $1.00 cy, $0.50 mn
22168	19-45593	Dep. nn; CFSTI $2.00 cy, $0.50 mn
22169	19-45284	Dep. nn; CFSTI $4.00 cy, $0.75 mn
22171	19-44300	Dep. nn; $2.00 cy, $0.50 mn
22172	19-44301	Dep. nn; CFSTI $1.00 cy, $0.50 mn
22173	19-44302	Dep. nn; CFSTI $1.00 cy, $0.50 mn
22183	19-45410	Dep. nn; CFSTI $1.00 cy, $0.50 mn
22200	19-44702	Dep. nn; CFSTI $2.00 cy, $0.50 mn
22205	19-44461	Dep. nn; CFSTI $2.00 cy, $0.50 mn
TM-	**(Misc.)**	
807	19-45659	Dep. nn; CFSTI $3.00 cy, $0.75 mn
844	19-44703	Dep. nn; CFSTI $1.00 cy, $0.50 mn
849	19-44704	Dep. nn; CFSTI $1.00 cy, $0.50 mn
874	19-44146	Dep. nn; CFSTI $3.00 cy, $0.50 mn
878	19-44212	Dep. nn; CFSTI $2.00 cy, $0.50 mn
894	19-44625	Dep. nn; CFSTI $1.00 cy, $1.00 mn
895	19-44197	Dep. nn; CFSTI $2.00 cy, $0.50 mn
896	19-44626	Dep. nn; CFSTI $1.00 cy, $0.50 mn
913	19-44198	Dep. nn; CFSTI $4.00 cy, $0.75 mn
917	19-44147	Dep. nn; CFSTI $2.00 cy, $0.50 mn
918	19-44148	Dep. nn; CFSTI $3.00 cy, $0.75 mn
919	19-45660	Dep. nn; CFSTI $1.00 cy, $0.50 mn
921	19-44149	Dep. nn; CFSTI $2.00 cy, $0.50 mn
922	19-44462	Dep. nn; CFSTI $2.00 cy, $0.50 mn
923	19-44150	Dep. nn; CFSTI $1.00 cy, $0.50 mn
925	19-44151	Dep. nn; CFSTI $2.00 cy, $0.50 mn
926	19-44152	Dep. nn; CFSTI $1.00 cy, $0.50 mn
927	19-44609	Dep. nn; CFSTI $1.00 cy, $0.50 mn
943	19-44610	Dep. nn; CFSTI $1.00 cy, $0.50 mn
TM-	**(Misc.)**	
64-9-7	19-45657	See TID-22088
TPJU-	**(Polish)**	
7/65	19-45038	Dep. nn
8/65	19-44810	Dep. nn
10/65	19-45039	Dep. nn
11/65	19-45040	Dep. nn Acta Phys. Pol., 28: 295-6(1965)
12/65	19-45041	Dep. nn
TRG-Report-	**(British)**	
864	19-45594	Dep.; BIS $2.00 cy, HMSO 10s.
888	19-44303	Dep.; BIS $0.60; HMSO 3s.
976	19-45595	Dep.; BIS $0.50; HMSO 2s. 6d.
1005	19-44463	Dep.; BIS $1.20; HMSO 6s.
TT-	**(Canadian)**	
65-31742	19-45604	See JPRS-31245
65-31846	19-43650	See JPRS-31349
65-31858	19-44153	See JPRS-31361
UACRL-C-	**(Non-AEC)**	
920243-12	19-45399	See NASA-CR-54451
UCD-		
472-112	19-43644	Dep. nn; CFSTI $5.00 cy, $1.00 mn
UCID-		
2608	19-45042	Dep. nn; CFSTI $1.00 cy, $0.50 mn
UCLA-		
12-565	19-43647	Dep. nn; CFSTI $4.00 cy, $0.75 mn
UCRL-		
7784-T(Rev.1)	19-44811	Dep. nn; CFSTI $2.00 cy, $0.50 mn
7850(Rev.1)	19-45717	Dep. nn; CFSTI $2.00 cy, $0.50 mn
7928-T	19-44237	Ann. N. Y. Acad. Sci., 123: 573-616(1965)
7935	19-45411	Dep. nn; CFSTI $3.00 cy, $0.50 mn
7978	19-45412	Dep. nn; CFSTI $1.00 cy, $0.50 mn
10771	19-45480	Dep. nn; CFSTI $1.00 cy, $0.50 mn
11624	19-44433	See CERN-65-4(Vol.II)
11653	19-44705	Dep. nn; CFSTI $1.00 cy, $0.50 mn
11662	19-45718	Dep. nn; CFSTI $1.00 cy, $0.50 mn
11699	19-43996	Dep. nn; CFSTI $1.00 cy, $0.50 mn
11703	19-44464	Dep. nn; CFSTI $2.00 cy, $0.50 mn
11889	19-43997	Dep. nn; CFSTI $5.00 cy, $1.00 mn
12012	19-45719	Dep. nn; CFSTI $1.00 cy, $0.50 mn
12020	19-44465	Dep. nn; CFSTI $1.00 cy, $0.50 mn
12045	19-44199	Dep. nn; CFSTI $2.00 cy, $0.50 mn
12055-T	19-45720	Dep. nn; CFSTI $3.00 cy, $0.75 mn
12129	19-44159	Geophysics, 30: 616-23(1965)
12264(Rev.1)	19-44706	Dep. nn; CFSTI $2.00 cy, $0.50 mn
12396	19-43998	Dep. nn; CFSTI $1.00 cy, $0.50 mn
12456	19-45413	Dep. nn; CFSTI $1.00 cy, $0.50 mn
12470	19-45481	Dep. nn; CFSTI $1.00 cy, $0.50 mn
12480	19-45414	Dep. nn; CFSTI $1.00 cy, $0.50 mn
14117	19-44938	Dep. nn; CFSTI $1.00 cy, $0.50 mn
14137	19-45415	Dep. nn; CFSTI $1.00 cy, $0.50 mn
14254	19-45721	Dep. nn; CFSTI $1.00 cy, $0.50 mn
14311	19-44158	Dep. nn; CFSTI $1.00 cy, $0.50 mn
14374	19-45159	Dep. nn; CFSTI $1.00 cy, $0.50 mn
16000(Summ.)	19-44873	Dep. nn; CFSTI $2.00 cy, $0.75 mn
16010	19-44502	Nucl. Instr. Methods, 36: 269-76(1965)
16015	19-44118	Dep. nn; CFSTI $3.00 cy, $0.75 mn
16040	19-45285	Dep. nn; CFSTI $3.00 cy, $0.75 mn
16070	19-45043	Dep. nn; CFSTI $4.00 cy, $0.75 mn
16099	19-44812	Dep. nn; CFSTI $3.00 cy, $0.75 mn
16177	19-43649	Dep. nn; CFSTI $1.00 cy, $0.50 mn
16185	19-45044	Dep. nn; CFSTI $2.00 cy, $0.50 mn

Report No.	Abstract No.	Availability
16188	19-45722	Dep. nn; CFSTI $3.00 cy, $0.50 mn
16203	19-44874	Dep. nn; CFSTI $1.00 cy, $0.50 mn
16229	19-44875	Dep. nn; CFSTI $1.00 cy, $0.50 mn
16231	19-44466	Dep. nn; CFSTI $5.00 cy, $1.00 mn
16232	19-44611	Dep. nn; CFSTI $3.00 cy, $0.50 mn
16263	19-45416	Dep. nn; CFSTI $1.00 cy, $0.50 mn
16287	19-44876	Dep. nn; CFSTI $1.00 cy, $0.50 mn
16288	19-45045	Dep. nn; CFSTI $3.00 cy, $0.75 mn
16295	19-45046	Dep. nn; CFSTI $3.00 cy, $0.75 mn
16300	19-45120	Phys. Rev. Letters, 15: 500-3(1965)
16315	19-45047	Dep. nn; CFSTI $3.00 cy, $0.75 mn
16346	19-44877	Dep. nn; CFSTI $1.00 cy, $0.50 mn
16353	19-44060	Dep. nn; CFSTI $3.00 cy, $0.75 mn
16375	19-44878	Dep. nn; CFSTI $1.00 cy, $0.50 mn
UJV–	**(Czechoslovakian)**	
1293/65	19-45286	Dep. nn
1324/65	19-45229	Dep. nn
1339/65	19-44352	Dep. nn
UR–		
875-89	19-45116	Phys. Rev., 140: B480-2(1965)
URPA–		
94	19-44970	See AD-620882
USBM-RC–		
1199	19-44612	Dep. nn; CFSTI $2.00 cy, $0.50 mn
USHRDL-TR–	**(Misc.)**	
868	19-45287	Dep. nn; CFSTI $1.00 cy, $0.50 mn
WAPD-T–		
1653	19-45495	Dep. nn; CFSTI $1.00 cy, $0.50 mn
WAPD-TM–	**(Misc.)**	
498	19-45548	Dep. nn; CFSTI $1.00 cy, $0.50 mn
WASH–		
1056	19-45288	Dep. nn; CFSTI, $4.00 cy, $1.00 mn
WCAP–	**(Misc.)**	
2042	19-45596	Dep. nn; CFSTI $6.00 cy, $1.25 mn
3269-30	19-45496	Dep. nn; CFSTI $2.00 cy, $0.50 mn
3269-31	19-45597	Dep. nn; CFSTI $5.00 cy, $1.00 mn
3269-33	19-45533	Dep. nn; CFSTI $4.00 cy, $0.75 mn
3269-35	19-45534	Dep. nn; CFSTI $3.00 cy, $0.75 mn
3269-44	19-45598	Dep. nn; CFSTI $4.00 cy, $0.75 mn
3269-47	19-45535	Dep. nn; CFSTI $4.00 cy, $0.75 mn
3269-49	19-45599	Dep. nn; CFSTI $3.00 cy, $0.75 mn
3385-4	19-45600	Dep. nn; CFSTI $3.00 cy, $0.75 mn
3750	19-45601	Dep. nn; CFSTI $6.00 cy, $1.25 mn
5493	19-45602	Dep. nn; CFSTI $1.00 cy, $0.50 mn
WVT–	**(Non-AEC)**	
6523	19-44707	CFSTI $1.00
X–	**(Misc.)**	
65-10546	19-45658	See TID-22097
65-12152	19-44548	See NP-15422
65-15179	19-44222	See NP-15068
Y–		
1476	19-44613	Dep. nn; CFSTI $3.00 cy, $0.75 mn
1478	19-44169	Dep. nn; CFSTI $6.00 cy, $1.25 mn
1491	19-45603	Dep. nn; CFSTI $2.00 cy, $0.50 mn
Y-DA–		
921	19-44170	Dep. nn; CFSTI $1.00 cy, $0.50 mn
ZFK-PHA–	**(German)**	
12	19-44467	Dep. nn

DEPOSITORIES OF USAEC REPORTS

In Countries Other than the U.S.

ARGENTINA
Buenos Aires, Comisión Nacional de Energía Atómica
AUSTRALIA
Canberra, Australian National Library
Sutherland, New South Wales, Australian Atomic Energy Commission
AUSTRIA
Vienna, Zentral Bibliothek der Physikalischen Institute der Universität
BELGIUM
Mol-Donk, Centre d'Etude de l'Energie Nucleaire
BOLIVIA
La Paz, Comisión Nacional de Energia Nuclear
BRAZIL
Rio de Janeiro, Instituto Brasileiro de Bibliografia e Documentacao
São Paulo, Instituto de Energia Atomica, Cidade Universitaria São Paulo
BURMA
Rangoon, Union of Burma Applied Research Institute, Atomic Energy Center Library
CANADA
Hamilton, McMaster University
Ottawa, National Research Council Library
Vancouver, University of British Columbia
CHILE
Santiago, Instituto de Fisica y Matematicas, Universidad de Chile
CHINA
Hsinchu, Taiwan, Free China, National Tsing Hua University
COLOMBIA
Bogota, Instituto De Asuntos Nucleares
COSTA RICA
San Pedro, University of Costa Rica Library
DENMARK
Risö, Danish Atomic Energy Commission
ECUADOR
Quito, Escuela Politécnica Nacional
EL SALVADOR
San Salvador, Universidad de El Salvador, Biblioteca de Energia Nuclear
FINLAND
Helsinki, Teknillisen Korkeakoulun Kirjasto
FRANCE
Gif-sur-Yvette, Centre d'Etudes Nucléaires de Saclay
Paris, Académie des Sciences
GERMANY
Berlin, Hahn-Meitner-Institut für Kernforschung Berlin
Frankfurt/Main, Gmelin-Institut
Munich, Technische Hochschule, Bibliothek
GHANA
Accra, University College of Ghana
GREECE
Athens, Nuclear Research Center "Democritus"
GUATEMALA
Guatemala, Comisión Nacional de Energía Nuclear
INDIA
Bombay, Department of Atomic Energy
INDONESIA
Djogjakarta, Java, Science Faculty, Gadjah Mada University
IRAN
Tehran, Tehran University Nuclear Centre
IRAQ
Baghdad, Iraqi Atomic Energy Commission
IRELAND
Dublin, University College
ISRAEL
Rehovoth, Israel Atomic Energy Commission
ITALY
Rome, Centro di Studi Nucleari della Casaccia
Rome, Comitato Nazionale per l'Energia Nucleare
JAPAN
Tokyo, National Diet Library
KOREA
Seoul, Office of Atomic Energy
LEBANON
Beirut, Lebanese National Council for Scientific Research
LUXEMBOURG
Luxembourg, Ministry of Transport and Electricity
MALAYSIA
Kuala Lumpur, University of Malaysia
MEXICO
Mexico, D.F., Comisión Nacional de Energía Nuclear
NETHERLANDS
The Hague, Reactor Centrum Nederland
NEW ZEALAND
Lower Hutt, Institute of Nuclear Sciences
NIGERIA
Ibadan, University of Ibadan
NORWAY
Lillestrom, Institutt för Atomenergi
PAKISTAN
Lahore, West Pakistan, Atomic Energy Centre
PERU
Lima, Junta de Control de Energia Atomica
PHILIPPINE REPUBLIC
Manila, Philippine Atomic Energy Commission
POLAND
Warsaw, Biura Pelnomocnika Rzadu do Spraw Wykorzystania Energii Jadrowej
PORTUGAL
Sacavem, Junta de Energía Nuclear
REPUBLIC OF SOUTH AFRICA
Pretoria, Atomic Energy Board Library
REPUBLIC OF THE CONGO
Leopoldville, Université Lovanium
SPAIN
Madrid, Junta de Energía Nuclear, Biblioteca Documentación y Publicaciones, Ciudad Universitaria
SWEDEN
Nyköping, Aktiebolaget Atomenergi
SWITZERLAND
Zürich, Eidgenössische Technische Hochschule, Bibliothek
THAILAND
Bangkok, Office of the Thai Atomic Energy Commission, Department of Science
TURKEY
Ankara, Turkish Atomic Energy Commission, Atomic Energy Library
UNITED ARAB REPUBLIC
Cairo, Atomic Energy Commission
UNITED KINGDOM
Belfast, City Library
Birmingham, Central Library
Boston Spa, National Lending Library for Science and Technology
Bristol, Central Library
Glasgow, Mitchell Library
Kingston upon Hull, Central Library
Leeds, Central Library
Liverpool, Central Library
London, Central Library, Acton
London, Science Museum Library, South Kensington
Manchester, Central Library
Newcastle upon Tyne, Central Library
Nottingham, Central Library
Sheffield, Central Library
URUGUAY
Montevideo, Comision Nacional de Energia Atomica
VENEZUELA
Caracas, Instituto Venezolano de Investigaciones Científicas
VIET-NAM
Saigon, Atomic Energy Office
YUGOSLAVIA
Belgrade, Federal Commission for Nuclear Energy

In International Agencies

AUSTRIA
Vienna, International Atomic Energy Agency
BELGIUM
Brussels, La Bibliotheque EURATOM
FRANCE
Paris, European Nuclear Energy Agency, O.E.C.D.
ITALY
Ispra, EURATOM Research Center
SWITZERLAND
Geneva, United Nations Library

UNITED STATES
GOVERNMENT PRINTING OFFICE
DIVISION OF PUBLIC DOCUMENTS
WASHINGTON, D.C. 20402

OFFICIAL BUSINESS

POSTAGE AND FEES PAID
U.S. GOVERNMENT PRINTING OFFICE

MIAMI UNIVERSITY LIBRARY